NISTIR XXXX Draft

Face Recognition Technology Evaluation (FRTE)

Part 1: Verification

Patrick Grother
Mei Ngan
Kayee Hanaoka
Joyce C. Yang
Austin Hom

Information Access Division
Information Technology Laboratory

This publication is available free of charge from:
https://www.nist.gov/programs-projects/face-recognition-vendor-test-frvt-ongoing

2026/05/08

NATIONAL INSTITUTE OF STANDARDS AND TECHNOLOGY
U.S. DEPARTMENT OF COMMERCE

U.S. Department of Commerce
Howard Lutnick, Secretary

National Institute of Standards and Technology
Craig Burkhardt, Acting Under Secretary of Commerce for Standards and Technology and Acting NIST Director

ACKNOWLEDGMENTS

The authors are grateful for the long-standing support and collaboration of the the Department of Homeland Security's Science & Technology Directorate (S&T) and the Office of Biometric Identity Management (OBIM).

Additionally, the authors are grateful to staff in the NIST Biometrics Research Laboratory for infrastructure supporting rapid evaluation of algorithms.

DISCLAIMER

Specific hardware and software products identified in this report were used in order to perform the evaluations described in this document. In no case does identification of any commercial product, trade name, or vendor, imply recommendation or endorsement by the National Institute of Standards and Technology, nor does it imply that the products and equipment identified are necessarily the best available for the purpose.

INSTITUTIONAL REVIEW BOARD

The National Institute of Standards and Technology's Research Protections Office reviewed the protocol for this project and determined it is not human subjects research as defined in Department of Commerce Regulations, 15 CFR 27, also known as the Common Rule for the Protection of Human Subjects (45 CFR 46, Subpart A).

FNMR(T) "False non-match rate"
FMR(T) "False match rate"

FRTE STATUS

This report is a draft NIST Interagency Report, and is open for comment. It is the thirty seventh edition of the report since the first was published in June 2017. Prior editions of this report are maintained on the FRTE website, and may contain useful information about older algorithms and datasets no longer used in FRTE.

FRTE remains open: All tracks of the FRTE are open to new algorithm submissions.

2026-05-08 changes since 2026-03-30:

- ▹ We have added results for first algorithms from four developers: Ethiopian Labor Market Information System, Face Int, Lishui Shuyan Huirong Technology Co, and YuanLi Technology.
- ▹ We have added results for new algorithms from twenty-one returning developers: Advance.AI, BioID GmbH, Tripleize, Dralmey Solutions, FaceLocate, HyperVerge Inc, InfoCert, ioNetworks Inc, Innov8tif Solutions, Kneron Inc, Mobai, Onfido, PAPIL11 S.R.O., PT Technology Biometric Indonesia, Shanghai Jiao Tong University, TNG Digital Sdn Bhd, TOPPAN Security Co, Unissey, UZINFOCOM, Viante.AI, and Vsoft.

2026-03-30 changes since 2026-03-05:

- ▹ We have added results for first algorithms from three developers: Ice House, Shufti, and Smarg Technologies Pvt Ltd
- ▹ We have added results for new algorithms from four returning developers: AI Implementation Group, Daon, PNPSecure, and Sensetime Group

2026-03-05 changes since 2026-03-02:

- ▹ We have updated the missing results for VisionBox.

2026-03-02 changes since 2026-01-22:

- ▹ We have added results for first algorithms from two developers: FPT Telecom JSC, and Iris ID Systems
- ▹ We have added results for new algorithms from six returning developers: Biometrik Systems Private Limited, GTEL OTS JSC, ID3 Technology, NextMeta Labs, Nominder, and ROC.

2025-01-22 changes since 2025-12-19:

- ▹ We have added results for first algorithms from five developers: CAKE by VPBank, RealSense, Sum and Substance Ltd, Transmit Security Ltd, and Vaidio.
- ▹ We have added results for new algorithms from eleven returning developers: Beijing DeepSense Technologies, Compal Electronics, Candour Biometrics, Clearview AI Inc, IE SARSENOV, Miaxis Biometrics, Onfido, Paravision, Shanghai Jiao Tong University, STCON LLC, and Toshiba.

2025-12-19 changes since 2025-09-30:

- ▷ We have added results for first algorithms from one developers: Sparktek International Pte Ltd.
- ▷ We have added results for new algorithms from 13 returning developers: BioID GmbH, Chunghwa Telecom, Dermalog, Hyundai Motor Company, IDENTY, Innovatrics, InterLink labs, Matrix Comsec Pvt Ltd, Sightropic, Trust Stamp, Viettel Artificial Intelligence and Data Services Center, Viettel High Technology, and Vsoft.

2025-09-30 changes since 2025-08-13:

- ▷ We have added results for first algorithms from three developers: Biometrik Systems Private Limited, OOTO AI, and Toss.
- ▷ We have added results for new algorithms from four returning developers: Jaak IT, Online Mobile Services JSC, Regula Forensics, and Unissey

2025-08-13 changes since 2025-07-15:

- ▷ We have added results for first algorithms from four developers: BTS Digital, IE SARSENOV, UZINFOCOM, and Vsoft.
- ▷ We have added results for new algorithms from seventeen returning developers: 2060.io, Beijing DeepSense Technologies, ID R&D Inc, Innovatrics, IntelliVIX, Metsakuur, Mobai, NextMeta Labs, Neurotechnology, Onfido, QazSmartVision.AI, ROC, STCON LLC, Toshiba, VinBigData, Vision-Box, and Visica AI Solutions.

2025-07-15 changes since 2025-05-28:

- ▷ We have added results for first algorithms from three developers: Matrix Comsec Pvt Ltd, PNPSecure, and Urielsoft Co. Ltd.
- ▷ We have added results for new algorithms from eleven returning developers: Daon, Dermalog, Hyundai Motor Company, Incode Technologies Inc, Intel Research Group, Kloudspot Inc, Omnigarde Ltd, Paravision, Universidade de Coimbra, Viante.AI, and Vietnam Posts and Telecommunications Group.

2025-05-28 changes since 2025-04-25:

- ▷ We have added results for new algorithms from seven returning developers: BioID GmbH, Cubox, DiDi ChuXing Technology, InterLink labs, IDENTY, PAPIL11 S.R.O., and Trust Stamp.

2025-04-25 changes since 2025-03-18:

- ▷ We have added results for first algorithms from seven developers: ArVİs Teknoloji San.Tic.A.Ş., Compal Electronics, FCI Vietnam, GTEL OTS JSC, Shenzhen Polytechnic University, Sightropic, and TNG Digital Sdn Bhd.
- ▷ We have added results for new algorithms from eleven returning developers: Awidit Systems, Cyberextruder, FRP LLC, Kasikorn Labs, NCS Pte Ltd, Nominder, Shanghai Jiao Tong University, STCON LLC, Tech5 SA, Veridas Digital Authentication Solutions S.L., and Viettel High Technology.

2025-03-18 changes since 2025-03-05:

- ▷ We have added results for first algorithms from one developers: FaiceTech Ltd.
- ▷ We have added results for new algorithms from ten returning developers: Beijing DeepSense Technologies, BioID Technologies SA, EI Networks Private Ltd, Hangzhuo AIlu Network Information Technology, Innovatrics, Private Identity LLC, Samsung S1 Corp, TigerIT Bangladesh Ltd, Via Technologies Inc, and Viettel Cyberspace Center.

2025-03-05 changes since 2025-01-30:

- ▷ We have added results for first algorithms from three developers: 2060.io, MB Bank, and Visica AI Solutions
- ▷ We have added results for new algorithms from twelve returning developers: AFR Engine, AI Implementation Group, Authme, Hyundai Motor Company, FacePhi, Inspur (Beijing) Electronic Information Industry Co, LightVision Inc, QazSmartVision.AI, ROC, Toshiba, Techainer, and VinBigData.

2025-01-30 changes since 2024-12-18:

- ▷ We have added results for first algorithms from four developers: Innov8tif Solutions, Maverick Research, PT Technology Biometric Indonesia, and TTI Group.
- ▷ We have added results for new algorithms from ten returning developers: Coretech Knowledge Inc, Intel Research Group, IQSEC, i2v Systems, PAPIL11 S.R.O., Paravision, Taiwan Mobile, Touchless ID, useB, and Viante.AI.

2024-12-18 changes since 2024-11-08:

- ▷ We have added results for first algorithms from six developers: BioID GmbH, InterLink labs, KYB-AI Ltd, Keyless Technologies, Pyramid Cyber Security + Forensic (P),and Syscake S.r.l..
- ▷ We have added results for new algorithms from sixteen returning developers: Alchera Inc, Awidit Systems, Cubox, DeCloak Intellegences, Beijing DeepSense Technologies, Innovatrics, Kasikorn Labs, Mitek Systems, Mukh Technologies, NCS Pte Ltd, NextMeta Labs, Nominder, PT Autentika Digital Indonesia, Sensetime Group, Shanghai Jiao Tong University, and STCON LLC.

2024-11-08 changes since 2024-10-07:

- ▷ We have added results for first algorithms from two developers: Hyderabad-Centre for Development of Advanced Computing, and TAHAKOM.
- ▷ We have added results for new algorithms from ten returning developers: Candour Biometrics, Cyberextruder, DICIO, First Credit Bureau Kazakhstan, Metsakuur, Mobbeel Solutions, Samsung S1 Corp, Vietnam Payment Solution, VinBigData, and Yuan High-Tech Development.

2024-10-07 changes since 2024-09-16:

- ▷ We have added results for first algorithms from three developers: Enqura, Kloudspot, and Penacomp Systemy Informatyczne.
- ▷ We have added results for new algorithms from fourteen returning developers: Chunghwa Telecom, Cyberlink, Dactionable Technologies, Daon, FPT Information System, Hangzhuo AIlu Network Information Technology, Kakao Bank, Panasonic R+D Center Singapore, Paravision, Private Identity, QazSmartVision.AI, Toshiba, Vietnam Posts and Telecommunications Group, and UNICC-Solution Architecture Section.

2024-09-16 changes since 2024-08-09:

- ▷ We have added results for first algorithms from one developer: Taiwan Mobile.
- ▷ We have added results for new algorithms from eleven returning developers: Cognitec Systems GmbH, Coretech Knowledge Inc, FaceOnLive Inc, Idemia, Intel Research Group, Luxand Inc, Ovision, PAPIL11 S.R.O., Unissey, useB, and Vivotek.

2024-08-09 changes since 2024-07-03:

- ▷ We have added results for first algorithms from seven developers: Affinsys AI Ltd, AI Implementation Group, Celloscope Limited, Hyundai Motor Company, ID R&D Inc, LightVision Inc and NextMeta Labs.
- ▷ We have added results for new algorithms from eleven returning developers: AFR Engine, Antheus Technologia, CTBC Bank, Innovatrics, Mitek Systems, Neurotechnology, Nominder, Seventh Sense Artificial Intelligence, Universidade de Coimbra, University of Surrey-CVSSP, Viettel Cyberspace Center, Vision-Box and Yoti.

2024-07-03 changes since 2024-05-30:

- ▷ We have include all algorithms evaluated since the ongoing FRTE evaluation started in 2017. Previously we listed only results for each developer's two most recent implementations. The main results page has been revised with a "by developer" tab which lists only the most accurate algorithm from each developer, where accuracy is defined by the lowest FNMR value for the visa-border dataset.
- ▷ We have added results for first algorithms from two developers: Taiwan Computer Vision and Telexper International.
- ▷ We have added results for new algorithms from fifteen returning developers: Alchera Inc, Beijing DeepSense Technologies, Cyberlink Corp, Dermalog, FacePhi, Facia.ai, FRP LLC, NCS Pte Ltd, Omnigarde Ltd, Online Mobile Services JSC, Qnap Security, ROC, STCON LLC, Videmo Intelligente Videoanalyse, and Viettel Group.

2024-05-30 changes since 2024-04-17:

- ▷ We have added results for first algorithms from three developers: ALTTEKGlobal, Fourthline, and IQSEC
- ▷ We have added results for new algorithms from thirteen returning developers: Candour Biometrics, Chunghwa Telecom, Clearview AI Inc, Cognitec Systems GmbH, Incode Technologies Inc, ioNetworks Inc, HyperVerge Inc, Mobbeel Solutions, Panasonic R+D Center Singapore, QazSmartVision.AI, Vietnam Posts and Telecommunications Group, VinBigData and Yuan High-Tech Development

- ▷ We have retired results for eleven algorithms per our policy to only list results for eleven algorithms per developer. Results for retired algorithms appear in prior versions of this report in the archive.

2024-04-17 changes since 2024-03-26:

- ▷ We have added results for first algorithms from four developers: Ovision, Vietnam National Cyber Security Technology Corporation, Vivotek, and Vocalize.
- ▷ We have added results for new algorithms from four returning developers: Intel Research Group, Kakao Bank, Luxand, and Turkcell Technology.
- ▷ We have retired results for nine algorithms per our policy to only list results for four algorithms per developer. Results for retired algorithms appear in prior versions of this report in the archive.

2024-03-26 changes since 2024-02-21:

- ▷ We have added results for first algorithms from six developers: FaceLocate, FPT Education, FPT Information System, Kogniza Technology, i2v Systems, and Seamfix.
- ▷ We have added results for new algorithms from eleven returning developers: AFR Engine, Aware, Beijing Hisign Technology, Cu-Face, Dactionable Technologies, First Credit Bureau Kazakhstan, Innovatrics, Nominder, Securif AI, Veridium, and Viettel Cyberspace Center.
- ▷ We have retired results for nine algorithms per our policy to only list results for two algorithms per developer. Results for retired algorithms appear in prior versions of this report in the archive.

2024-02-21 changes since 2024-01-22:

- ▷ We discontinued the visa-visa benchmark in FRTE since Feburary 14th 2024. For highly performing algorithms, the only remaining false negative error in that set were in babies and in a few greyscale poor quality half-tone scans of paper photos.
- ▷ We have added results for first algorithms from four developers: Online Mobile Services JSC, Openedge Technologies, TNI Technoology, and Yoti.
- ▷ We have added results for new algorithms from nine returning developers: CMC Institute of Science and Technology, City and County of Honolulu, Dermalog, Euronovate SA, Maxvision Technology, Megvii/Face++, Neurotechnology, Toshiba, useB, and Universidade de Coimbra.
- ▷ We have retired results for nine algorithms per our policy to only list results for two algorithms per developer. Results for retired algorithms appear in prior versions of this report in the archive.

2024-01-22 changes since 2023-12-15:

- ▷ We have added results for first algorithms from six developer: GPS Vietnam Trading, iCOMM Media & Tech, PAPIL11 S.R.O., QazSmartVision.AI, Sparsh CCTV, and VNIS Joint Stock.
- ▷ We have added results for new algorithms from eight returning developers: Cyberlink Corp, Intellivision, Hangzhuo AIlu Network Information Technology, Lebentech Biometrics, Momentum Digital, Regular Biometrics Solutions, ROC, and Via Technologies Inc.
- ▷ We have retired results for six algorithms per our policy to only list results for two algorithms per developer. Results for retired algorithms appear in prior versions of this report in the archive.

2023-12-15 changes since 2023-11-21:

- ▷ We have added results for first algorithms from five developer: CMC University, Element System Solutions Company, Fraud.com, Techainer, and Vietnam Payment Solutions.
- ▷ We have added results for new algorithms from thirteen returning developers: Accurascan, Adera Global, Alchera, Aware, Clearview AI, Cognitec Systems, Incode Technologies Inc, Inspur (Beijing) Electronic Information, IntelliVIX, ioNetworks, NHN Corp, PT Autentika Digital Indonesia, and Qnap Security.
- ▷ We have retired results for twelve algorithms per our policy to only list results for two algorithms per developer. Results for retired algorithms appear in prior versions of this report in the archive.

2023-11-21 changes since 2023-10-27:

- ▷ We have added results for new algorithms from ten returning developers: Coretech Knowledge Inc, Beijing DeepSense Technologies, General Interface Solutions Holding Ltd, Glory, Kakao Brain, Nominder, Smarvist Teknoloji, STCON LLC, Suprema AI Inc, and Yuan High-Tech Development
- ▷ We have retired results for eight algorithms per our policy to only list results for two algorithms per developer. Results for retired algorithms appear in prior versions of this report in the archive.

2023-10-27 changes since 2023-09-29:

- ▷ We have added results for first algorithms from two developer: Authme and Dactionable Technologies.
- ▷ We have added results for new algorithms from twelve returning developers: Intel Research Group, Guangzhou Pixel Solutions, Kasikorn Labs, Kakao Bank, Luxand, Megvii/Face++, Panasonic R+D Center Singapore, Private Identity LLC, Recognito, Seventh Sense Artificial Intelligence, UNICC-Solution Architecture Section, and Universidade de Coimbra.
- ▷ We have retired results for eight algorithms per our policy to only list results for two algorithms per developer. Results for retired algorithms appear in prior versions of this report in the archive.

2023-09-29 changes since 2023-09-09:

- ▷ We have added results for first algorithms from one developer: Intozi Tech.
- ▷ We have added results for new algorithms from seven returning developers: Euronovate, Maxvision Technology, Miaxis Biometrics, Mukh Technologies, Toshiba, University of Surrey-CVSSP, and useB.
- ▷ We have retired results for six algorithms per our policy to only list results for two algorithms per developer. Results for retired algorithms appear in prior versions of this report in the archive.

2023-09-09 changes since 2023-08-16:

- ▷ We have renamed and split FRVT into two sets of technology evaluations: The Face Recognition Technology Evaluation (FRTE) is the umbrella for the ongoing 1:1, 1:N and twins disambiguation tracks; the Face Analysis Technology Evaluation (FATE) holds the morph and attacked detection tracks, the quality assessment tracks, and the new age estimation tracks.

- ▷ We have added results for first algorithms from two developers: Facehawk and Regular Biometrics Solutions.
- ▷ We have added results for new algorithms from eight returning developers: CMC Institute of Science and Technology, Canon, Cu-Face, EI Networks, ICM Airport Technics, Securif AI, Securifai, Vietnam Posts and Telecommunications Group, and Vision Intelligence Center of Meituan
- ▷ We have retired results for six algorithms per our policy to only list results for two algorithms per developer. Results for retired algorithms appear in prior versions of this report in the archive.

2023-08-16 changes since 2023-07-21:

- ▷ We have added results for first algorithms from one developers: Facia.ai.
- ▷ We have added results for new algorithms from fifteen returning developers: Accurascan, Alchera, FOO, Hangzhuo AIlu Network Information Technology, HyperVerge, ioNetworks, Innovatrics, Nominder, Rank One Computing, Neurotechnology, Tech5, Tripleize, Unissey, UX Labs, and Verigram.
- ▷ We have retired results for ten algorithms per our policy to only list results for two algorithms per developer. Results for retired algorithms appear in prior versions of this report in the archive.

2023-07-21 changes since 2023-06-16:

- ▷ We have added results for first algorithms from five developers: DeCloak Intellegences, Innominds Software SEZ India, Trust Stamp, Vcortex Labs, and Viettel Cyberspace Center
- ▷ We have added results for new algorithms from fourteen returning developers: AFR Engine, Alice Biometrics, Euronovate SA, IMDS Software, Idemia, IntelliVIX, Intellivision, NHN, Pangiam, STCON, Samtech InfoNet, Veridium, VinBigData, and Vision-Box
- ▷ We have retired results for eleven algorithms per our policy to only list results for two algorithms per developer. Results for retired algorithms appear in prior versions of this report in the archive.
- ▷ We have stopped using wild images in FRVT since May 1st 2023. All results for that set have been removed from the website, and will be removed from future PDF reports.

2023-06-16 changes since 2023-04-20:

- ▷ We have added results for first algorithms from seven developers: EI Networks Private Ltd, General Interface Solutions Holding Ltd, Recognito, Serendipity Ltd, ST Engineering, and useB.
- ▷ We have added results for new algorithms from eighteen returning developers: Advance.AI, AYF Technology, Cyberlink Corp, Incode Technologies Inc, Intel Research Group, Intellibrain Technological Projects, Maxvision Technology, Megvii/Face++, Omnigarde Ltd, Paravision, Qnap Security, Seventh Sense Artificial Intelligence, Shanghai Jiao Tong University, Veridas Digital Authentication Solutions S.L., Universidade de Coimbra, Yuan High-Tech Development, UNICC-Solution Architecture Section, and Verihubs,verihubs-inteligensia.
- ▷ We have retired results for 15 algorithms per our policy to only list results for two algorithms per developer. Results for retired algorithms appear in prior versions of this report in the archive.

2023-04-20 changes since 2023-04-04:

- ▷ We have added results for first algorithms from one developers: IDENTY.

- ▷ We have added results for new algorithms from three returning developers: Metsakuur, Autentika Digital Indonesia, and Verigram.
- ▷ FRVT will re-open 2023-05-01.
- ▷ We have retired results for 3 algorithms per our policy to only list results for two algorithms per developer. Results for retired algorithms appear in prior versions of this report in the archive.

2023-04-04 changes since 2023-03-09:

- ▷ We have added results for first algorithms from six developers: Aratek Biometrics City and County of Honolulu, FOO, Intelligent Control Technology NCS, and Swsam Solutions.
- ▷ We have added results for new algorithms from nine returning developers: Cubox, Glory, InsightFace AI, Miaxis Biometrics, Mukh Technologies, Turkcell Technology, Samsung S1, Via Technologies, and Vision Intelligence Center of Meituan
- ▷ We have retired results for 7 algorithms per our policy to only list results for two algorithms per developer. Results for retired algorithms appear in prior versions of this report in the archive.

2023-03-09 changes since 2023-02-01:

- ▷ We have added results for first algorithms from eight developers: Biometric LLC (biometric.vision) KZ, Candour Biometrics, Fast Enterprises, KakaoBank, Mitek Systems, Nominder, Private Identity, and UNICC-Solution Architecture Section.
- ▷ We have added results for new algorithms from 22 returning developers: AFR Engine, Biocube Matrics, CMC Institute of Science and Technology, Cloudwalk - Moontime Smart Technology, Cyberlink Corp, Beijing DeepSense Technologies, First Credit Bureau Kazakhstan, Enface, Hangzhuo AIlu Network Information Technology, Herta Security, IMDS Software, Inspur (Beijing) Electronic Information Industry Co, Intellivision, MicroFocus, Neurotechnology, Pangiam, NSENSE Corp, STCON LLC, Touchless ID, University of Surrey-CVSSP, Vision-Box, and YooniK.
- ▷ We have retired results for 14 algorithms per our policy to only list results for two algorithms per developer. Results for retired algorithms appear in prior versions of this report in the archive.
- ▷ We have introduced new set of non-frontal portrait to border comparisons. The new images are described in section 2.3 and their use in seciton 3.2.

2023-02-01 changes since 2022-12-15:

- ▷ We have added results for first algorithms from four developers: CU-Face, Korea ID, Onfido, and TrueID-VNG.
- ▷ We have added results for new algorithms from 21 returning developers: Alchera, Armatura, Cogent-Thales, Dermalog, Didi ChuXing Global Face, Gorilla, Hyperverge, Innovatrics, Intel Research, IntelliVIX, Intema-LGL, Kasikorn Labs, Paravision, Rank One Computing, Sensetime Group, Suprema AI, Tech5, Unissey, U. Coimbra Visteam, Vixvizion (Imagus), and Yuan High-Tech Development.
- ▷ We have retired results for 20 algorithms per our policy to only list results for two algorithms per developer. Results for retired algorithms appear in prior versions of this report in the archive.
- ▷ We have introduced new set of non-frontal portrait to border comparisons. The new images are described in section 2.3 and their use in seciton 3.2.

2022-12-15 changes since 2022-11-06:

- ▷ We have added results for first algorithms from four developers: Miaxis Biometrics, PT Autentika Digital Indonesia, PT Qlue Performa Indonesia, and STCON.
- ▷ We have added results for new algorithms from 14 returning developers: Adera Global, Aiseemu Technology, Chunghwa Telecom,chtface, FRP, Griaule, Line Corporation, Maxvision Technology, Mukh Technologies, Papilon Savunma, Qnap Security, Realnetworks, Securif AI, SQIsoft, and Veridium.
- ▷ We have retired results for 10 algorithms per our policy to only list results for two algorithms per developer. Results for retired algorithms appear in prior versions of this report in the archive.

2022-11-06 changes since 2022-09-26:

- ▷ We have added results for first algorithms from six developers: AFR Engine, CMC Institute of Science and Technology, Saga Densan Center, Turkcell Technology, UXLabs, and Wise AI SDN BHD.
- ▷ We have added results for new algorithms from 14 returning developers: Coretech Knowledge, Cloudwalk - Moontime, Cloudmatrix, Deepglint, Guangzhou Pixel Solutions, Hangzhuo AIlu Network Information Technology, NEO Systems, One More Security, Palit Microsystems, Panasonic R+D Center Singapore, Samsung S1, Seventh Sense Artificial Intelligence, Touchless ID, and Veridas Digital Authentication Solutions S.L.
- ▷ We have retired results for 10 algorithms per our policy to only list results for two algorithms per developer. Results for retired algorithms appear in prior versions of this report in the archive.

2022-09-26 changes since 2022-08-30:

- ▷ We have added results for first algorithms from three developers: Codeline, First Credit Bureau Kazakhstan, and InfoCert.
- ▷ We have added results for new algorithms from 14 returning developers: Advancegroup, Armatura LLC, Beijing Hisign Technology, Cybercore, Cyberlink Corp, Herta Security, ICM Airport Technics, InsightFace AI, Metsakuur, NSENSE Corp, Samsung-SDS, Videmo Intelligente Videoanalyse, Vietnam Posts and Telecommunications Group, and Vision Intelligence Center of Meituan.
- ▷ We have retired results for 11 algorithms per our policy to only list results for two algorithms per developer. Results for retired algorithms appear in prior versions of this report in the archive.

2022-08-30 changes since 2022-07-29:

- ▷ We have added results for first algorithms from two developers: Aximetria, Intellibrain Technological Projects
- ▷ We have added results for new algorithms from twelve returning developers: Alchera Inc, Dermalog, Idemia, Incode Technologies Inc, Intellivision, Kasikorn Labs, Megvii/Face++, Techsign, TuringTech.vip, Universidade de Coimbra, Verijelais, Vixvizon
- ▷ We have retired results for six algorithms per our policy to only list results for two algorithms per developer. Results for retired algorithms appear in prior versions of this report in the archive.

2022-07-29 changes since 2022-06-27:

- ▷ We have added results for first algorithms from seven developers: FRP LLC (Hawaii), IMDS Software, Inspur (Beijing) Electronic Information Industry, Intema - LGL Group, PAPAGO, Qaz Biometric Systems, and VIDA-Digital Identity
- ▷ We have added results for new algorithms from nine returning developers: Cyberextruder, Glory, Maxvision Technology, Rank One Computing, Securif AI, Suprema AI, Suprema ID, Toshiba, and Yuan High-Tech Development.
- ▷ We have retired results for nine algorithms per our policy to only list results for two algorithms per developer. Results for retired algorithms appear in prior versions of this report in the archive.

2022-07-29 changes since 2022-06-27:

- ▷ We have added results for first algorithms from seven developers: FRP LLC (Hawaii), IMDS Software, Inspur (Beijing) Electronic Information Industry, Intema - LGL Group, PAPAGO, Qaz Biometric Systems, and VIDA-Digital Identity
- ▷ We have added results for new algorithms from nine returning developers: Cyberextruder, Glory, Maxvision Technology, Rank One Computing, Securif AI, Suprema AI, Suprema ID, Toshiba, and Yuan High-Tech Development.
- ▷ We have retired results for nine algorithms per our policy to only list results for two algorithms per developer. Results for retired algorithms appear in prior versions of this report in the archive.

2022-06-27 changes since 2022-06-03:

- ▷ We have added results for first algorithms from two developers: Krungthai Bank, and Smartbiometrik.
- ▷ We have added results for new algorithms from thirteen returning developers: Aiseemu, Corsight, Digidata, Griaule, Guangzhou Pixel Solutions, Hangzhuo AI Network Information Technology, Neurotechnology, Real Networks, Samsung S1, Sensetime Group, Smart Engines, Verihubs Inteligensia, and VinBigData.
- ▷ We have retired results for eight algorithms per our policy to only list results for two algorithms per developer. Results for retired algorithms appear in prior versions of this report in the archive.

2022-06-03 changes since 2022-05-05:

- ▷ We have added results for first algorithms from seven developers: Jaak IT, Metsakuur, Palit Microsystems, Smarvist Teknoloji, and Touchless ID.
- ▷ We have added results for new algorithms from sixteen returning developers: Cyberlink, FaceOnLive, Kakao Enterprise, Line Corporation (Line Clova), Multi-Modality Intelligence, NEO Systems, and Unissey
- ▷ We have retired results for four algorithms per our policy to only list results for two algorithms per developer. Results for retired algorithms appear in prior versions of this report in the archive.
- ▷ We have moved the results for the twenty human-difficult pairs used in the May 2018 paper *Face recognition accuracy of forensic examiners, superrecognizers, and face recognition algorithms* by Phillips et al. [1]. to the algorithm-specific report cards (example: PDF).

- ▷ Likewise, we have added figures showing impostor distribution shifts across demographics to the report card.

2022-05-05 changes since 2022-03-18:

- ▷ We have added results for first algorithms from seven developers: Accurascan, DICIO, FacePhi, Pangiam, University of Surrey-CVSSP, and Veridium.
- ▷ We have added results for new algorithms from sixteen returning developers: ACI Software, Canon Inc, Cloudwalk - Moontime Smart Technology, Cybercore,

2022-05-05 changes since 2022-03-18:

- ▷ We have added results for first algorithms from seven developers: Accurascan, DICIO, FacePhi, Pangiam, University of Surrey-CVSSP, and Veridium.
- ▷ We have added results for new algorithms from sixteen returning developers: ACI Software, Canon Inc, Cloudwalk - Moontime Smart Technology, Cybercore, Cyberextruder, Gemalto Cogent, HyperVerge Inc, KuKe3D Technology, Megvii/Face++, Mobbeel Solutions, Panasonic R+D Center Singapore, Qnap Security, Samsung-SDS, Vietnam Posts and Telecommunications Group, Viettel Group, and Vision Intelligence Center of Meituan.
- ▷ We have retired results for 12 algorithms per our policy to only list results for two algorithms per developer. Results for retired algorithms appear in prior versions of this report in the archive.

2022-03-18 changes since 2022-02-23:

- ▷ We have added support for the detection of multiple people in a single image (see Section 1.2). Specifically the API allows an algorithm to extract features from one or more faces it detects in an image. NIST scores such cases as a correct match when any detected face matches the reference photo, and as a false positive when either face matches a non-mated reference photo. The expected effect of doing this will be to improve reported false non-match rates, and to minimally elevate false match rates. This technique was only applied to images of type "border" and "kiosk".
- ▷ We have added results for first algorithms from four developers: IntelliVIX, Kasikorn Labs, Lebentech Biometrics, and Wicket.
- ▷ We have added results for new algorithms from 10 returning developers: Chunghwa Telecom, Cloudmatrix, Beijing DeepSense Technologies, FarBar Inc, Imagus Technology Pty, Intellivision, Maxvision Technology, NHN Corp, Seventh Sense Artificial Intelligence, and Verigram.
- ▷ We have retired results for 4 algorithms per our policy to only list results for two algorithms per developer. Results for retired algorithms appear in prior versions of this report in the archive.

2022-02-23 changes since 2022-01-24:

- ▷ We have added results for first algorithms from four developers: AFIS and Biometrics Consulting, Digidata, Graymatics, Hangzhuo AIlu Network Information Technology, KnowUTech LLC, Sukshi Technology Innovation, T4iSB, and TuringTech.vip

- ▷ We have added results for new algorithms from 18 returning developers: Cognitec Systems GmbH, GeoVision Inc, Glory, Herta Security, Intel Research Group, InsightFace AI, Kakao Enterprise, N-Tech Lab, Omnigarde Ltd, Papilon Savunma, Paravision, Realnetworks Inc, Reveal Media Ltd, Shenzhen Inst Adv Integrated Tech CAS, Suprema AI Inc, Toshiba, Universidade de Coimbra, and Yuan High-Tech Development
- ▷ We have retired results for 14 algorithms per our policy to only list results for two algorithms per developer. Results for retired algorithms appear in prior versions of this report in the archive.

2022-01-24 changes since 2022-01-20:

- ▷ We have added results for new algorithms from one returning developer: Vocord.

2022-01-20 changes since 2021-12-18:

- ▷ We have added results for first algorithms from four developers: Armatura, Beyne.AI, One More Security, and VinBigData
- ▷ We have added results for new algorithms from 19 returning developers: AuthenMetric, BOE Technology Group, Cybercore, Cyberlink, Dahua Technology, FaceTag Co, Innovatrics, Megvii, Mobbeel Solutions, Neurotechnology, Oz Forensics, Rank One Computing, Regula Forensics, Samsung S1, Securif AI, Sensetime Group, TigerIT Americas, Videmo Intelligente Videoanalyse, and YooniK.
- ▷ We have retired results for 14 algorithms per our policy to only list results for two algorithms per developer. Results for retired algorithms appear in prior versions of this report in the archive.

: **2021-12-16** changes since 2021-11-22:

- ▷ We have added results for first algorithms from five developers: Alfabeta, Cloudmatrix, Euronovate SA, FaceOnLive Inc, and Mobipin Technology.
- ▷ We have added results for new algorithms from ten returning developers: ACI Software, ITMO University, NEO Systems, Guangzhou Pixel Solutions, Panasonic R+D Center Singapore, Qnap Security, Scanovate, Tevian, Unissey, and Vietnam Posts and Telecommunications Group.
- ▷ We have retired results for eight algorithms per our policy to only list results for two algorithms per developer. Results for retired algorithms appear in prior versions of this report in the archive.
- ▷ We have revamped the figure showing performance on 20 pairs of open-source images. It now color-codes false negatives and postives against a default threshold value.

2021-11-22 changes since 2021-10-28:

- ▷ We have added results to the website for kiosk-collected images where the design and geometry configuration mean that many images have considerable downward pitch angle. In some images, the face is partially cropped. Some images have other background faces.
- ▷ We have stopped using child exploitation images in FRVT, as we lost access to the imagery. All results for that set have been removed from the website, and will be removed from future PDF reports.
- ▷ We have added results for first algorithms from seven new developers: CUDO Communication, Daon, KuKe3D Technology, Mantra Softech India, Maxvision Technology, Multi-Modality Intelligence, and Samsung-SDS.

- ▷ We have added results for new algorithms from seven returning developers: Acer Incorporated, Cloudwalk-Moontime Smart Technology, Gorilla Technology, ID3 Technology, Incode Technologies, NSENSE Corp., and SQIsoft.
- ▷ We have retired results for six algorithms per our policy to only list results for two algorithms per developer. Results for retired algorithms appear in prior versions of this report in the archive.

2021-10-28 changes since 2021-09-08:

- ▷ We have substantially revised the algorithm-specific report cards that are linked from the FRVT results page. (Example: HTML).
- ▷ We have added results for first algorithms from eight new developers: Beijing Mendaxia Technology, Beijing Hisign Technology, Biocube Matrics, Clearview AI, Reveal Media, Toppan ID Gate, Verigram, and Viettel High Technology.
- ▷ We have added results for new algorithms from thirty returning developers: 20Face, 3divi, Canon Inc Chunghwa Telecom, Corsight, Decatur Industries, Deepglint, Dermalog, FaceTag, Fiberhome Telecommunication Technologies, GeoVision, ICM Airport Technics, Imagus Technology, InsightFace AI, Kakao Enterprise, Kookmin University, Line Corporation, N-Tech Lab, NotionTag Technologies, Realnetworks, Suprema ID, Taiwan-Certificate Authority, Toshiba, Tripleize, Trueface.ai, Veridas Digital Authentication, Visidon, VisionLabs, YooniK, and Yuan High-Tech Development.
- ▷ We have retired results for twenty algorithms per our policy to only list results for two algorithms per developer. Results for retired algorithms appear in prior versions of this report in the archive.

2021-09-08 changes since 2021-08-02:

- ▷ We have added results for first algorithms from seven new developers: Griaule, SQIsoft, Qnap Security, Techsign, Smart Engines, Verihubs, and Wuhan Tianyu Information Industry.
- ▷ We have added results for new algorithms from sixteen returning developers: ADVANCE.AI, Authen-Metric, CloudSmart Consulting, Code Everest Pvt, Cognitec Systems, Thales Gemalto Cogent, Intel Research Group, Omnigarde, Oz Forensics, Rank One Computing, Samsung S1 Corp, Securif AI, Tevian, TigerIT Americas, Universidade de Coimbra, and Vigilant Solutions
- ▷ We have retired results for eleven algorithms per our policy to only list results for two algorithms per developer. Results for retired algorithms appear in prior versions of this report in the archive.

2021-08-02 changes since 2021-06-25:

- ▷ We have added results for first algorithms from eight new developers: Bee the Data, Closeli Inc, Coretech Knowledge Inc, Deepsense (France), ioNetworks Inc, Kakao Pay Corp, Seventh Sense Artificial Intelligence, and SK Telecom.
- ▷ We have added results for new algorithms from fifteen returning developers: Alchera Inc, Adera Global PTE, Aware, Bresee Technology, Cyberlink Corp, Expasoft LLC, Fujitsu Research and Development Center, Gorilla Technology, Idemia, Neurotechnology, NEO Systems, NHN Corp, Paravision, Panasonic R+D Center Singapore, and Shenzhen University-Macau University of Science and Technology.
- ▷ We have retired results for twelve algorithms per our policy to only list results for two algorithms per developer. Results for retired algorithms appear in prior versions of this report in the archive.

2021-06-25 changes since 2021-05-21:

- ▷ We have added results for first algorithms from six new developers: Alice Biometrics, BOE Technology Group, Fincore, Neosecu, Sodec App, and Yuntu Data and Technology.
- ▷ We have added results for new algorithms from seven returning developers: Incode Technologies, HyperVerge, Mobbeel Solutions, Guangzhou Pixel Solutions, Remark Holdings, Sensetime, and Vietnam Posts and Telecommunications Group.
- ▷ We have retired results for four algorithms per our policy to only list results for two algorithms per developer. Results for retired algorithms appear in prior versions of this report in the archive.

2021-05-21 changes since 2021-04-26:

- ▷ We have added results for first algorithms from five new developers: Ekin Smart City Technologies, Suprema ID, Tripleize, Taiwan-Certificate Authority, and Vision Intelligence Center of Meituan.
- ▷ We have added results for new algorithms from eight returning developers: ID3 Technology, Imagus Technology, Momentum Digital, N-Tech Lab, NSENSE, Shanghai Jiao Tong University, Vision-Box, and Yuan High-Tech Development
- ▷ We have retired results for seven algorithms per our policy to only list results for two algorithms per developer. Results for retired algorithms appear in prior versions of this report in the archive.

2021-04-26 changes since 2021-04-16:

- ▷ We have added results for first algorithms from three new developers: Quantasoft, Rendip, and NEO Systems.
- ▷ We have added results for new algorithms from four returning developers: 3Divi, Realnetworks, Veridas Digital Authentication Solutions, and Universidade de Coimbra.
- ▷ We have retired results for three algorithms per our policy to only list results for two algorithms per developer. Results for retired algorithms appear in prior versions of this report in the archive.

2021-04-16 changes since 2021-03-19:

- ▷ We have added results for first algorithms from six new developers: 20Face, Beijing DeepSense Technologies, BitCenter UK, Enface, FaceTag, InsightFace AI, Line Corporation, Lema Labs, Nanjing Kiwi Network Technology, Omnigarde, Regula Forensics, and Suprema.
- ▷ We have added results for new algorithms from ten returning developers: CloudSmart Consulting, Dermalog, GeoVision, Neurotechnology, Panasonic R+D Center Singapore, Samsung S1, Securif AI, Trueface.ai, Vigilant Solutions, and Visidon.
- ▷ We have retired results for ten algorithms per our policy to only list results for two algorithms per developer. Results for retired algorithms appear in prior versions of this report in the archive.

2021-03-19 changes since 2021-03-05:

- ▷ We have added results for first algorithms from six new developers: Ajou University, AuthenMetric, Code Everest, Corsight, Papilon Savunma, and NHN Corp
- ▷ We have added results for new algorithms from seven returning developers: Alchera, Deepglint, Fiberhome Telecommunication Technologies, Kakao Enterprise, Kookmin University, Megvii/Face++, and NotionTag Technologies.
- ▷ We have updated many of the hyperlinked HTML report-cards to include seven figures on demographic dependence. Figures of this kind first appeared, and are documented in, the December 2019 document, NIST Interagency Report 8280 on demographic differentials in face recognition. The figures quantify false negative dependence on demographics using "visa-border" comparisons, and false positive dependence using comparisons of "application" photos that uniformly of quality and similar to visa photos.

2021-03-05 changes since 2021-01-19:

- ▷ We have added results for first algorithms from three new developers: IVA Cognitive, Mobbeel, and MoreDian Technology.
- ▷ We have added results for new algorithms from returning developers: Ability Enterprise - Andro Video, ACI Software, Adera Global, AnyVision, BioID Technologies, China Electronics Import-Export, Cognitec Systems, Fujitsu Research and Development Center, Glory, Guangzhou Pixel Solutions, Hengrui AI Technology, Incode Technologies, Intel Research, iQIYI, Mobai, Oz Forensics, Paravision, VisionLabs, and Xforward AI Technology.
- ▷ We have added a new "resources" tab to the main webpage. It includes sortable columns for data related to speed, model size, storage, and memory consumption.
- ▷ We have retired results for 13 algorithms per our policy to only list results for two algorithms per developer. Results for retired algorithms appear in prior versions of this report in the archive.

2021-01-19 changes since 2020-12-18:

- ▷ This report adds results for first algorithms from four developers: Herta Security, Irex AI, Shenzhen University-Macau University of Science and Technology, and Vietnam Posts and Telecommunications Group. See Table 21 for more information.
- ▷ The report also includes results for thirteen developers who have previously submitted algorithms: Bresee Technology, Canon (previously Canon Information Technology (Beijing)), Cyberlink, CSA IntelliCloud Technology, Dahua Technology, ID3 Technology, Imagus Technology (Vixvizion), Moontime Smart Technology, N-Tech Lab, Thales Cogent, Veridas Digital Authentication Solutions, Vocord, and Yuan High-Tech Development.
- ▷ We have retired results for ten algorithms per our policy to only list results for two algorithms per developer. Results for retired algorithms appear in prior versions of this report in the archive.

2020-12-18 changes since 2020-10-09:

- ▷ This report adds results for first algorithms from ten developers: BitCenter UK, CloudSmart Consulting, Cubox, Institute of Computing Technology, Naver Corp, Minivision, NSENSE Corp, Viettel Group, Visage Technologies, and Xiamen University. See Table 21 for more information.

- ▷ The report also includes results for eighteen developers who have previously submitted algorithms: ADVANCE.AI, Awidit Systems, Chosun University, Dermalog, GeoVision, ICM Airport Technics, Idemia, Institute of Information Technologies, Kakao Enterprise, Neurotechnology, Panasonic R+D Center Singapore, Rank One Computing, Sensetime Group, Shanghai Jiao Tong University, TigerIT Americas LLC, Vigilant Solutions, Winsense, and YooniK
- ▷ We have retired results for twelve algorithms per our policy to only list results for two algorithms per developer. Results for retired algorithms appear in prior versions of this report in the archive.

Changes since September 18, 2020:

- ▷ This report adds results for first algorithms from five developers: Aigen, Cortica, Kookmin University, Securif AI and Vinai.
- ▷ The report also includes results for three developers who have previously submitted algorithms: Fujitsu Laboratories, Hengrui AI, and X-Forward AI.
- ▷ In the per-algorithm report-cards linked from tables and the main webpage, we have added a chart to showing reduction in error rates over the course of FRVT i.e. from 2017 onwards for all algorithms supplied by that developer. Similarly we have added a chart showing error rate reductions for our test of protective face mask verification.
- ▷ We plan to continue evaluating algorithms on various mask datasets. We hold that algorithms should be capable of detecting masks and verifying identity of all combinations of masked and unmasked faces. We have accordingly increased the amount to time allowed to extract those features from 1.0 to 1.5 seconds.

Changes since August 25, 2020:

- ▷ This report adds results for first algorithms from eight new developers. Akurat Satu Indonesia, Cybercore, Decatur Industries, Innef Labs, Satellite Innovation/Eocortex, Expasoft, and Mobai.
- ▷ The report includes results for seven developers who have previously submitted algorithms: 3Divi, BioID Technologies, Incode Technologies, Innovatrics, iSAP Solution, Synology, and Tevian.
- ▷ We have retired results for five algorithms per our policy to only list results for two algorithms per developer. Results for retired algorithms appear in prior versions of this report in the archive.

Changes since July 27, 2020:

- ▷ We have introduced per-algorithm report sheets. These are HTML documents linked from the accuracy tables in this report (i.e. Table 87) and on the FRVT 1:1 homepage. The sheets contain interactive graphics allowing, for example, mouseover exploration of FNMR(T) and FMR(T). Some of their content had previously appeared in this document.
- ▷ This report adds results for algorithms from six new developers. ACI Software, Bresee Technology, Fiberhome Telecommunication Technologies, Imageware Systems, Oz Forensics, and Pensees.
- ▷ The report includes results for thirteen developers who have previously submitted algorithms: Canon Information Technology (Beijing), Cyberlink, Dahua Technology, Gorilla Technology, ID3 Technology, Intel Research Group, iQIYI Inc, Momentum Digital, Netbridge Technology, Tech5 SA, Shenzhen AiMall Tech, Vigilant Solutions, and VisionLabs.
- ▷ We have retired results for nine algorithms per our policy to only list results for two algorithms per developer. Results for retired algorithms appear in prior versions of this report in the archive.

Changes since May 18, 2020:

- ▷ The report is the first FRVT update since the pandemic closed it from March to June 2020.
- ▷ This report includes results for algorithms from nine new developers: GeoVision Inc, Su Zhou NaZhi-TianDi Intelligent Technology, YooniK, AYF Technology, PXL Vision AG, Yuan High-Tech Development, Beihang University-ERCACAT, ICM Airport Technics, and Staqu Technologies
- ▷ This report includes results for algorithms from 15 returning developers Acer Incorporated, Antheus Technologia, Chosun University, Chunghwa Telecom, Idemia, Moontime Smart Technology, Neurotechnology, Guangzhou Pixel Solutions, Panasonic R+D Center Singapore, Rank One Computing, Scanovate, Shanghai Universiy - Shanghai Film Academy, Synesis, Trueface.ai, and Veridas Digital Authentication Solutions
- ▷ We have retired results for ten algorithms per our policy to only list results for two algorithms per developer. Results for retired algorithms appear in prior versions of this report in the archive.
- ▷ We separated timing and other resource consumption from the main participation table. The new Table 54 includes template generation durations for four kinds of images, not just mugshots.
- ▷ We have published a separate report, NIST Interagency Report 8311 on accuracy of pre-pandemic algorithms on subjects wearing face masks. We plan to track improvements in accuracy on masked images going forward. In particular, we invite submission of algorithms that can detect whether a person is wearing a mask, extract features from the full face or the exposed periocular region, and do appropriate comparison. We do not intend to evaluate algorithms that assume 100% of images will be of masked individuals.

Changes since March 25, 2020:

- ▷ The report is a maintenance release - it does not add any new algorithms, and FRVT has been closed to new algorithms since mid March 2020.
- ▷ We modified the primary accuracy summary, Table 87, as follows:
  - ▷▷ For visa images, the column for FNMR at FMR = 0.0001 has been removed. The visa images are so highly controlled that the error rates for the most accurate algorithms are dominated by false rejection of very young children and by the presence of a few noisy greyscale images. For now, two visa columns remain: FNMR at FMR= 10^{-6} and, for matched covariates, FNMR at FMR= 10^{-4}.
  - ▷▷ We have inserted a new column labelled "BORDER" giving accuracy for comparison of moderately poor webcam border-crossing photos that exhibit pose variations, poor compression, and low contrast due to strong background illumination. The accuracies are the worst from all cooperative image datasets used in FRVT.
- ▷ Accordingly, we updated the failure-to-template rates in Table 112.
- ▷ We withdrew a figure showing how false matches are concentrated in certain visa images used in cross-comparison, because it didn't attempt to include demographic information.

Changes since February 27, 2020:

- ▷ The report adds results algorithms from two new developers: Beijing Alleyes Technology, and the Chinese University of Hong Kong. Results for newly submitted algorithms from two other developers will appear in the next report.

- ▷ The report adds results for algorithms from thirteen returning developers: ASUSTek Computer, Aware, Cyberlink Corp, Gorilla Technology, Innovative Technology, Kakao Enterprise, Lomonosov Moscow State University, Panasonic R+D Center Singapore, Shenzhen AiMall Technology, Shenzhen Intellifusion Technologies, Synology, Tech5 SA, and Via Technologies.
- ▷ Per policy to only list results for two algorithms per developer, we have dropped results for algorithms from Aware, Cyberlink, Gorilla Technology, Kakao Enterprise, Lomonosov Moscow State University, Panasonic R+D Center Singapore, and Tech5 SA.

Changes since January 20, 2020:

- ▷ The report adds results for five new developers: Ability Enterprise (Andro Video), Chosun University, Fujitsu Research and Development Center, University of Coimbra, and Xforward AI Technology.
- ▷ The report adds results for algorithms from six returning developers: AlphaSSTG, Incode Technologies, Kneron. Shanghai Jiao Tong University, Vocord, and X-Laboratory.
- ▷ We have corrected template comparison timing numbers for algorithms submitted September 2019 to January 2020. The values reported previously were slower due to a software bug.
- ▷ We have dropped results for algorithms from Vocord and Incode per policy to only list results for two algorithms per developer.
- ▷ The FRVT 1:1 homepage has been updated with latest accuracy results.
- ▷ The FRVT 1:N homepage now includes an update to the September 2019 NIST Interagency Report 8271. The new report adds results for one-to-many search algorithms submitted to NIST from June 2019 to January 2020.

Changes since January 6, 2020:

- ▷ Section 2 has been updated to better describe the Visa and Border images. The caption for Table 87 has been updated to better relate the accuracy values to particular image comparisons.
- ▷ The report adds results for five new developers: Acer, Advance.AI, Expasoft, Netbridge Technology, and Videmo Intelligente Videoanalyse.
- ▷ The report adds results for algorithms from 7 returning developers: China Electronics Import-Export Corp, Intel Research Group, ITMO University, Neurotechnology, N-Tech Lab, Rokid, and VisionLabs.
- ▷ We have dropped results from this edition of the report per policy to only list results for two algorithms per developer: N-Tech Lab, Neurotechnology, ITMO, Visionlabs, and CEIEC.
- ▷ The FRVT homepage has been updated with latest accuracy results.

Changes since November 11, 2019:

- ▷ Table 54 has been updated to include runtime memory usage. This is the first time such a quantity has been reported. The value is the peak size of the resident set size logged during enrollment of single images.
- ▷ We have migrated summary results table to a new platform that supports sortable tables: https://pages.nist.gov/frvt/html/frvt11.html
- ▷ The report adds results for four new developers: Antheus Technologia, BioID Technologies SA, Canon Information Tech. (Beijing), Samsung S1 (listed in the tables as S1), and Taiwan AI Labs.

- ▷ The report adds results for algorithms from 13 returning developers: Anke Investments, Chunghwa Telecom, Deepglint, Institute of Information Technologies, iQIYI, Kneron, Ping An Technology, Paravision, KanKan Ai, Rokid Corporation, Shanghai Universiy - Shanghai Film Academy, Veridas Digital Authentication Solutions, and Videonetics Technology.
- ▷ We have dropped results from this edition of the report per policy to only list results for two algorithms per developer: remarkai-000, veridas-001, sensetime-001, iit-000, anke-003, and everai-002. Results for these are available in prior editions of this report linked from the FRVT page.
- ▷ We issued NIST Interagency Report 8280: FRVT Part 3: Demographics on 2019-12-19. It includes results for many of the algorithms covered by this report.

Changes since October 16, 2019:

- ▷ The report adds results for ten new developers: Ai-Union Technology, ASUSTek Computer, DiDi ChuXing Technology, Innovative Technology, Luxand, MVision, Pyramid Cyber Security + Forensic, Scanovate, Shenzhen AiMall Tech, and TUPU Technology.
- ▷ The report adds results for 12 returning developers: CTBC Bank Glory Gorilla Technology Guangzhou Pixel Solutions Imagus Technology Incode Technologies Lomonosov Moscow State University Rank One Computing Samtech InfoNet Shanghai Ulucu Electronics Technology Synesis, and Winsense.
- ▷ We have dropped results from this edition of the report per policy to only list results for two algorithms per developer: glory-000, gorilla-002, incode-003, rankone-006, and synesis-004.
- ▷ Results for five recently submitted algorithms will appear in the next report.

Changes since September 11, 2019:

- ▷ The report adds results for five new participants: Awidit Systems (Awiros), Momemtum Digital (Sertis), Trueface AI, Shanghai Jiao Tong University, and X-Laboratory.
- ▷ The reports adds results for five new algorithms from returning developers: Cyberlink, Hengrui AI Technology, Idemia, Panasonic R+D Singapore, and Tevian. This causes three algorithm, to be de-listed from the report per policy to list results for two algorithms per developer.

Changes since July 31 2019:

- ▷ The HTML table on the FRVT 1:1 homepage has been updated to include a column for cross-domain Visa-Border verification. Results for this new dataset appeared in the July 29 report under the name "CrossEV" - these are now renamed "Visa-Border".
- ▷ The FRVT 1:1 homepage lists algorithms according to lowest mean rank accuracy:
  Rank($\text{FNMR}_{\text{VISA}}$ at FMR = 0.000001) +
  Rank($\text{FNMR}_{\text{VISA-BORDER}}$ at FMR = 0.000001) +
  Rank($\text{FNMR}_{\text{MUGSHOT}}$ at FMR = 0.00001 after 14 years) +
  Rank($\text{FNMR}_{\text{WILD}}$ at FMR = 0.00001)
  This ordering rewards high accuracy across all datasets.
- ▷ The main results in Table 87 is now in landscape format to accomodate extra columns for the Visa-Border set, and mugshot comparisons after at least 12 years.
- ▷ The report adds results for nine new participants: Alpha SSTG, Intel Research, ULSee, Chungwa Telecon, iSAP Solution, Rokid, Shenzhen EI Networks, CSA Intellicloud, Shenzhen Intellifusion Technologies.

FNMR(T) "False non-match rate"
FMR(T) "False match rate"

- ▷ The reports adds results for six new algorithms from returning developers: Innovatrics, Dahua Technology, Tech5 SA, Intellivision, Nodeflux and Imperial College, London. One algorithm, from Imperial has been retired, per policy to list results for two algorithms per developer.
- ▷ The cross-country false match rate heatmaps have been replotted to reveal more structure by listing countries by region instead of alphabetically.
- ▷ The next version of this report will be posted around October 18, 2019.

Changes since July 3 2019:

- ▷ The HTML table on the FRVT 1:1 homepage has been updated to list the 20 most accurate developers rather than algorithms, choosing the most accurate algorithm from each developer based on visa and mugshot results. Also, the algorithms are ordered in terms of lowest mean rank across mugshot, visa and wild datasets, rewarding broad accuracy over a good result on one particular dataset.
- ▷ This report includes results for a new dataset - see the column labelled "visa-border" in Table 5. It compares a new set of high quality visa-like portraits with a set webcam border-crossing photos that exhibit moderately poor pose variations and background illumination. The two new sets are described in sections 2.2 and 2.4. The comparisons are "cross-domain" in that the algorithm must compare "visa" and "wild" images. Results for other algorithms will be added in future reports as they become available.
- ▷ This report adds results for algorithms from 9 developers submitted in early July 2019. These are from 3DiVi, Camvi, EverAI-Paravision, Facesoft, Farbar (F8), Institute of Information Technologies, Shanghai U. Film Academy, Via Technologies, and Ulucu Electronics Tech. Six of these are new participants.
- ▷ Several other algorithms have been submitted and are being evaluated. Results will be released in the next report, scheduled for September 5. That report will include results for new datasets.
- ▷ Older algorithms from Everai, Camvi and 3DiVi, have been retired, per the policy to list only two algorithms per developer.

Changes since June 20 2019:

- ▷ This report adds results for algorithms from 18 developers submitted in early June 2019. These are from CTBC Bank, Deep Glint, Thales Cogent, Ever AI Paravision, Gorilla Technology, Imagus, Incode, Kneron, N-Tech Lab, Neurotechnology, Notiontag Technologies, Star Hybrid, Videonetics, Vigilant Solutions, Winsense, Anke Investments, CEIEC, and DSK. Nine of these are new participants.
- ▷ Several other algorithms have been submitted and are being evaluated. Results will be released in the next report, scheduled for August 1.
- ▷ Older algorithms from Everai, Thales Cogent, Gorilla Technology, Incode, Neurotechnology, N-Tech Lab and Vigilant Solutions have been retired, per the policy to list only two algorithms per developer.

Changes since April 2019:

- ▷ This report adds results for nine algorithms from nine developers submitted in early June 2019. These are from Tencent Deepsea, Hengrui, Kedacom, Moontime, Guangzhou Pixel, Rank One Computing, Synesis, Sensetime and Vocord.
- ▷ Another 23 algorithms have been submitted and are being evaluated. Results will be released in the next report, scheduled for July 3.
- ▷ Older algorithms for Rank One, Synesis, and Vocord have been retired, per the policy to list only two algorithms per developer.

Changes since February 2019:

- ▷ This report adds results for 49 algorithms from 42 developers submitted in early March 2019.

- ▷ This report omits results for algorithms that we retired. We retired for three reasons: 1. The developer submitted a new algorithm, and we only list two. 2. The algorithm needs a GPU, and we no longer allow GPU-based algorithms. 3. Inoperable algorithms.
- ▷ Previous results for retired algorithms are available in older editions of this report linked here.
- ▷ The mugshot database used from February 2017 to January 2019 has been replaced with an extract of the mugshot database documented in NIST Interagency Report 8238, November 2018. The new mugshot set is described in section 2.5 and is adopted because:
  - ▷▷ It has much better identity label integrity, so that false non-match rates are substantially lower than those reported in FRVT 1:1 reports to date - see Figure 284.
  - ▷▷ It includes images collected over a 17 year period such that ageing can be much better characterized - - see Figure 781.
- ▷ Using the new mugshot database, Figure 781 shows accuracy for four demographic groups identified in the biographic metadata that accompanies the data: black females, black males, white females and white males.
- ▷ The report added a figure (now moved to web) with results for the twenty human-difficult pairs used in the May 2018 paper *Face recognition accuracy of forensic examiners, superrecognizers, and face recognition algorithms* by Phillips et al. [1].
- ▷ The report uses an update to the wild image database that corrects some ground truth labels.
- ▷ Some results for the child exploitation database are not complete. They are typically updated less frequently than for other image sets.

FNMR(T) "False non-match rate"
FMR(T) "False match rate"

Contents

ACKNOWLEDGMENTS 1

DISCLAIMER 1

INSTITUTIONAL REVIEW BOARD 1

1 METRICS 131
1.1 CORE ACCURACY . . . 131
1.2 MULTI-TEMPLATE SCORING METHODOLOGY . . . 131

2 DATASETS 132
2.1 VISA IMAGES . . . 132
2.2 APPLICATION IMAGES . . . 132
2.3 APPLICATION IMAGES WITH HEAD YAW . . . 132
2.4 BORDER CROSSING IMAGES . . . 133
2.5 MUGSHOT IMAGES . . . 133
2.6 KIOSK IMAGES . . . 133
2.7 WILD IMAGES . . . 134

3 RESULTS 134
3.1 TEST GOALS . . . 134
3.2 TEST DESIGN . . . 135
3.3 FAILURE TO ENROLL . . . 138
3.4 RECOGNITION ACCURACY . . . 164
3.5 GENUINE DISTRIBUTION STABILITY . . . 771
3.5.1 EFFECT OF BIRTH PLACE ON THE GENUINE DISTRIBUTION . . . 771
3.5.2 EFFECT OF AGEING . . . 862
3.5.3 EFFECT OF AGE ON GENUINE SUBJECTS . . . 945
3.6 IMPOSTOR DISTRIBUTION STABILITY . . . 1038
3.6.1 EFFECT OF BIRTH PLACE ON THE IMPOSTOR DISTRIBUTION . . . 1038
3.6.2 EFFECT OF AGE ON IMPOSTORS . . . 1041

List of Tables

1 PARTICIPANT INFORMATION . . . 42
2 PARTICIPANT INFORMATION . . . 43
3 PARTICIPANT INFORMATION . . . 44
4 PARTICIPANT INFORMATION . . . 45
5 PARTICIPANT INFORMATION . . . 46
6 PARTICIPANT INFORMATION . . . 47
7 PARTICIPANT INFORMATION . . . 48
8 PARTICIPANT INFORMATION . . . 49
9 PARTICIPANT INFORMATION . . . 50
10 PARTICIPANT INFORMATION . . . 51
11 PARTICIPANT INFORMATION . . . 52
12 PARTICIPANT INFORMATION . . . 53
13 PARTICIPANT INFORMATION . . . 54
14 PARTICIPANT INFORMATION . . . 55
15 PARTICIPANT INFORMATION . . . 56
16 PARTICIPANT INFORMATION . . . 57
17 PARTICIPANT INFORMATION . . . 58
18 PARTICIPANT INFORMATION . . . 59

FNMR(T) "False non-match rate"
FMR(T) "False match rate"

19 Participant Information . . . 60
20 Participant Information . . . 61
21 Participant Information . . . 62
22 Algorithm summary . . . 63
23 Algorithm summary . . . 64
24 Algorithm summary . . . 65
25 Algorithm summary . . . 66
26 Algorithm summary . . . 67
27 Algorithm summary . . . 68
28 Algorithm summary . . . 69
29 Algorithm summary . . . 70
30 Algorithm summary . . . 71
31 Algorithm summary . . . 72
32 Algorithm summary . . . 73
33 Algorithm summary . . . 74
34 Algorithm summary . . . 75
35 Algorithm summary . . . 76
36 Algorithm summary . . . 77
37 Algorithm summary . . . 78
38 Algorithm summary . . . 79
39 Algorithm summary . . . 80
40 Algorithm summary . . . 81
41 Algorithm summary . . . 82
42 Algorithm summary . . . 83
43 Algorithm summary . . . 84
44 Algorithm summary . . . 85
45 Algorithm summary . . . 86
46 Algorithm summary . . . 87
47 Algorithm summary . . . 88
48 Algorithm summary . . . 89
49 Algorithm summary . . . 90
50 Algorithm summary . . . 91
51 Algorithm summary . . . 92
52 Algorithm summary . . . 93
53 Algorithm summary . . . 94
54 Algorithm summary . . . 95
55 False Non-Match Rate . . . 96
56 False Non-Match Rate . . . 97
57 False Non-Match Rate . . . 98
58 False Non-Match Rate . . . 99
59 False Non-Match Rate . . . 100
60 False Non-Match Rate . . . 101
61 False Non-Match Rate . . . 102
62 False Non-Match Rate . . . 103
63 False Non-Match Rate . . . 104
64 False Non-Match Rate . . . 105
65 False Non-Match Rate . . . 106
66 False Non-Match Rate . . . 107
67 False Non-Match Rate . . . 108
68 False Non-Match Rate . . . 109
69 False Non-Match Rate . . . 110
70 False Non-Match Rate . . . 111
71 False Non-Match Rate . . . 112
72 False Non-Match Rate . . . 113
73 False Non-Match Rate . . . 114
74 False Non-Match Rate . . . 115

FNMR(T) "False non-match rate"
FMR(T) "False match rate"

75 False Non-Match Rate . . . 116
76 False Non-Match Rate . . . 117
77 False Non-Match Rate . . . 118
78 False Non-Match Rate . . . 119
79 False Non-Match Rate . . . 120
80 False Non-Match Rate . . . 121
81 False Non-Match Rate . . . 122
82 False Non-Match Rate . . . 123
83 False Non-Match Rate . . . 124
84 False Non-Match Rate . . . 125
85 False Non-Match Rate . . . 126
86 False Non-Match Rate . . . 127
87 False Non-Match Rate . . . 128
88 Failure to Enrol Rates . . . 139
89 Failure to Enrol Rates . . . 140
90 Failure to Enrol Rates . . . 141
91 Failure to Enrol Rates . . . 142
92 Failure to Enrol Rates . . . 143
93 Failure to Enrol Rates . . . 144
94 Failure to Enrol Rates . . . 145
95 Failure to Enrol Rates . . . 146
96 Failure to Enrol Rates . . . 147
97 Failure to Enrol Rates . . . 148
98 Failure to Enrol Rates . . . 149
99 Failure to Enrol Rates . . . 150
100 Failure to Enrol Rates . . . 151
101 Failure to Enrol Rates . . . 152
102 Failure to Enrol Rates . . . 153
103 Failure to Enrol Rates . . . 154
104 Failure to Enrol Rates . . . 155
105 Failure to Enrol Rates . . . 156
106 Failure to Enrol Rates . . . 157
107 Failure to Enrol Rates . . . 158
108 Failure to Enrol Rates . . . 159
109 Failure to Enrol Rates . . . 160
110 Failure to Enrol Rates . . . 161
111 Failure to Enrol Rates . . . 162
112 Failure to Enrol Rates . . . 163

List of Figures

1 performance summary: FNMR vs. template size tradeoff . . . 129
2 performance summary: FNMR vs. template time tradeoff . . . 130
3 example images . . . 134
(a) Visa . . . 134
(b) Mugshot . . . 134
(c) Wild . . . 134
(d) Border . . . 134
4 performance on 20 human-difficult pairs . . . 165
5 performance on 20 human-difficult pairs . . . 166
6 performance on 20 human-difficult pairs . . . 167
7 performance on 20 human-difficult pairs . . . 168
8 performance on 20 human-difficult pairs . . . 169
9 performance on 20 human-difficult pairs . . . 170
10 performance on 20 human-difficult pairs . . . 171

FNMR(T) "False non-match rate"
FMR(T) "False match rate"

11 PERFORMANCE ON 20 HUMAN-DIFFICULT PAIRS . . . 172
12 PERFORMANCE ON 20 HUMAN-DIFFICULT PAIRS . . . 173
13 PERFORMANCE ON 20 HUMAN-DIFFICULT PAIRS . . . 174
14 PERFORMANCE ON 20 HUMAN-DIFFICULT PAIRS . . . 175
15 PERFORMANCE ON 20 HUMAN-DIFFICULT PAIRS . . . 176
16 PERFORMANCE ON 20 HUMAN-DIFFICULT PAIRS . . . 177
17 PERFORMANCE ON 20 HUMAN-DIFFICULT PAIRS . . . 178
18 PERFORMANCE ON 20 HUMAN-DIFFICULT PAIRS . . . 179
19 PERFORMANCE ON 20 HUMAN-DIFFICULT PAIRS . . . 180
20 PERFORMANCE ON 20 HUMAN-DIFFICULT PAIRS . . . 181
21 PERFORMANCE ON 20 HUMAN-DIFFICULT PAIRS . . . 182
22 PERFORMANCE ON 20 HUMAN-DIFFICULT PAIRS . . . 183
23 PERFORMANCE ON 20 HUMAN-DIFFICULT PAIRS . . . 184
24 PERFORMANCE ON 20 HUMAN-DIFFICULT PAIRS . . . 185
25 PERFORMANCE ON 20 HUMAN-DIFFICULT PAIRS . . . 186
26 PERFORMANCE ON 20 HUMAN-DIFFICULT PAIRS . . . 187
27 PERFORMANCE ON 20 HUMAN-DIFFICULT PAIRS . . . 188
28 PERFORMANCE ON 20 HUMAN-DIFFICULT PAIRS . . . 189
29 PERFORMANCE ON 20 HUMAN-DIFFICULT PAIRS . . . 190
30 PERFORMANCE ON 20 HUMAN-DIFFICULT PAIRS . . . 191
31 PERFORMANCE ON 20 HUMAN-DIFFICULT PAIRS . . . 192
32 PERFORMANCE ON 20 HUMAN-DIFFICULT PAIRS . . . 193
33 PERFORMANCE ON 20 HUMAN-DIFFICULT PAIRS . . . 194
34 PERFORMANCE ON 20 HUMAN-DIFFICULT PAIRS . . . 195
35 PERFORMANCE ON 20 HUMAN-DIFFICULT PAIRS . . . 196
36 PERFORMANCE ON 20 HUMAN-DIFFICULT PAIRS . . . 197
37 PERFORMANCE ON 20 HUMAN-DIFFICULT PAIRS . . . 198
38 PERFORMANCE ON 20 HUMAN-DIFFICULT PAIRS . . . 199
39 PERFORMANCE ON 20 HUMAN-DIFFICULT PAIRS . . . 200
40 PERFORMANCE ON 20 HUMAN-DIFFICULT PAIRS . . . 201
41 PERFORMANCE ON 20 HUMAN-DIFFICULT PAIRS . . . 202
42 PERFORMANCE ON 20 HUMAN-DIFFICULT PAIRS . . . 203
43 PERFORMANCE ON 20 HUMAN-DIFFICULT PAIRS . . . 204
44 PERFORMANCE ON 20 HUMAN-DIFFICULT PAIRS . . . 205
45 PERFORMANCE ON 20 HUMAN-DIFFICULT PAIRS . . . 206
46 PERFORMANCE ON 20 HUMAN-DIFFICULT PAIRS . . . 207
47 PERFORMANCE ON 20 HUMAN-DIFFICULT PAIRS . . . 208
48 PERFORMANCE ON 20 HUMAN-DIFFICULT PAIRS . . . 209
49 PERFORMANCE ON 20 HUMAN-DIFFICULT PAIRS . . . 210
50 PERFORMANCE ON 20 HUMAN-DIFFICULT PAIRS . . . 211
51 PERFORMANCE ON 20 HUMAN-DIFFICULT PAIRS . . . 212
52 PERFORMANCE ON 20 HUMAN-DIFFICULT PAIRS . . . 213
53 PERFORMANCE ON 20 HUMAN-DIFFICULT PAIRS . . . 214
54 PERFORMANCE ON 20 HUMAN-DIFFICULT PAIRS . . . 215
55 PERFORMANCE ON 20 HUMAN-DIFFICULT PAIRS . . . 216
56 PERFORMANCE ON 20 HUMAN-DIFFICULT PAIRS . . . 217
57 PERFORMANCE ON 20 HUMAN-DIFFICULT PAIRS . . . 218
58 PERFORMANCE ON 20 HUMAN-DIFFICULT PAIRS . . . 219
59 PERFORMANCE ON 20 HUMAN-DIFFICULT PAIRS . . . 220
60 PERFORMANCE ON 20 HUMAN-DIFFICULT PAIRS . . . 221
61 PERFORMANCE ON 20 HUMAN-DIFFICULT PAIRS . . . 222
62 PERFORMANCE ON 20 HUMAN-DIFFICULT PAIRS . . . 223
63 PERFORMANCE ON 20 HUMAN-DIFFICULT PAIRS . . . 224
64 PERFORMANCE ON 20 HUMAN-DIFFICULT PAIRS . . . 225
65 PERFORMANCE ON 20 HUMAN-DIFFICULT PAIRS . . . 226
66 PERFORMANCE ON 20 HUMAN-DIFFICULT PAIRS . . . 227
67 PERFORMANCE ON 20 HUMAN-DIFFICULT PAIRS . . . 228

FNMR(T) "False non-match rate"
FMR(T) "False match rate"

68 PERFORMANCE ON 20 HUMAN-DIFFICULT PAIRS . . . 229
69 PERFORMANCE ON 20 HUMAN-DIFFICULT PAIRS . . . 230
70 PERFORMANCE ON 20 HUMAN-DIFFICULT PAIRS . . . 231
71 PERFORMANCE ON 20 HUMAN-DIFFICULT PAIRS . . . 232
72 PERFORMANCE ON 20 HUMAN-DIFFICULT PAIRS . . . 233
73 PERFORMANCE ON 20 HUMAN-DIFFICULT PAIRS . . . 234
74 PERFORMANCE ON 20 HUMAN-DIFFICULT PAIRS . . . 235
75 PERFORMANCE ON 20 HUMAN-DIFFICULT PAIRS . . . 236
76 PERFORMANCE ON 20 HUMAN-DIFFICULT PAIRS . . . 237
77 PERFORMANCE ON 20 HUMAN-DIFFICULT PAIRS . . . 238
78 PERFORMANCE ON 20 HUMAN-DIFFICULT PAIRS . . . 239
79 PERFORMANCE ON 20 HUMAN-DIFFICULT PAIRS . . . 240
80 PERFORMANCE ON 20 HUMAN-DIFFICULT PAIRS . . . 241
81 PERFORMANCE ON 20 HUMAN-DIFFICULT PAIRS . . . 242
82 PERFORMANCE ON 20 HUMAN-DIFFICULT PAIRS . . . 243
83 PERFORMANCE ON 20 HUMAN-DIFFICULT PAIRS . . . 244
84 PERFORMANCE ON 20 HUMAN-DIFFICULT PAIRS . . . 245
85 PERFORMANCE ON 20 HUMAN-DIFFICULT PAIRS . . . 246
86 PERFORMANCE ON 20 HUMAN-DIFFICULT PAIRS . . . 247
87 PERFORMANCE ON 20 HUMAN-DIFFICULT PAIRS . . . 248
88 PERFORMANCE ON 20 HUMAN-DIFFICULT PAIRS . . . 249
89 PERFORMANCE ON 20 HUMAN-DIFFICULT PAIRS . . . 250
90 PERFORMANCE ON 20 HUMAN-DIFFICULT PAIRS . . . 251
91 PERFORMANCE ON 20 HUMAN-DIFFICULT PAIRS . . . 252
92 PERFORMANCE ON 20 HUMAN-DIFFICULT PAIRS . . . 253
93 PERFORMANCE ON 20 HUMAN-DIFFICULT PAIRS . . . 254
94 PERFORMANCE ON 20 HUMAN-DIFFICULT PAIRS . . . 255
95 PERFORMANCE ON 20 HUMAN-DIFFICULT PAIRS . . . 256
96 PERFORMANCE ON 20 HUMAN-DIFFICULT PAIRS . . . 257
97 PERFORMANCE ON 20 HUMAN-DIFFICULT PAIRS . . . 258
98 PERFORMANCE ON 20 HUMAN-DIFFICULT PAIRS . . . 259
99 PERFORMANCE ON 20 HUMAN-DIFFICULT PAIRS . . . 260
100 PERFORMANCE ON 20 HUMAN-DIFFICULT PAIRS . . . 261
101 PERFORMANCE ON 20 HUMAN-DIFFICULT PAIRS . . . 262
102 PERFORMANCE ON 20 HUMAN-DIFFICULT PAIRS . . . 263
103 PERFORMANCE ON 20 HUMAN-DIFFICULT PAIRS . . . 264
104 PERFORMANCE ON 20 HUMAN-DIFFICULT PAIRS . . . 265
105 PERFORMANCE ON 20 HUMAN-DIFFICULT PAIRS . . . 266
106 PERFORMANCE ON 20 HUMAN-DIFFICULT PAIRS . . . 267
107 PERFORMANCE ON 20 HUMAN-DIFFICULT PAIRS . . . 268
108 PERFORMANCE ON 20 HUMAN-DIFFICULT PAIRS . . . 269
109 ERROR TRADEOFF CHARACTERISTIC: VISA IMAGES . . . 270
110 ERROR TRADEOFF CHARACTERISTIC: VISA IMAGES . . . 271
111 ERROR TRADEOFF CHARACTERISTIC: VISA IMAGES . . . 272
112 ERROR TRADEOFF CHARACTERISTIC: VISA IMAGES . . . 273
113 ERROR TRADEOFF CHARACTERISTIC: VISA IMAGES . . . 274
114 ERROR TRADEOFF CHARACTERISTIC: VISA IMAGES . . . 275
115 ERROR TRADEOFF CHARACTERISTIC: VISA IMAGES . . . 276
116 ERROR TRADEOFF CHARACTERISTIC: VISA IMAGES . . . 277
117 ERROR TRADEOFF CHARACTERISTIC: VISA IMAGES . . . 278
118 ERROR TRADEOFF CHARACTERISTIC: VISA IMAGES . . . 279
119 ERROR TRADEOFF CHARACTERISTIC: VISA IMAGES . . . 280
120 ERROR TRADEOFF CHARACTERISTIC: VISA IMAGES . . . 281
121 ERROR TRADEOFF CHARACTERISTIC: VISA IMAGES . . . 282
122 ERROR TRADEOFF CHARACTERISTIC: VISA IMAGES . . . 283
123 ERROR TRADEOFF CHARACTERISTIC: VISA IMAGES . . . 284
124 ERROR TRADEOFF CHARACTERISTIC: VISA IMAGES . . . 285

FNMR(T) "False non-match rate"
FMR(T) "False match rate"

125 ERROR TRADEOFF CHARACTERISTIC: VISA IMAGES . . . 286
126 ERROR TRADEOFF CHARACTERISTIC: VISA IMAGES . . . 287
127 ERROR TRADEOFF CHARACTERISTIC: VISA IMAGES . . . 288
128 ERROR TRADEOFF CHARACTERISTIC: VISA IMAGES . . . 289
129 ERROR TRADEOFF CHARACTERISTIC: VISA IMAGES . . . 290
130 ERROR TRADEOFF CHARACTERISTIC: VISA IMAGES . . . 291
131 ERROR TRADEOFF CHARACTERISTIC: VISA IMAGES . . . 292
132 ERROR TRADEOFF CHARACTERISTIC: VISA IMAGES . . . 293
133 ERROR TRADEOFF CHARACTERISTIC: VISA IMAGES . . . 294
134 ERROR TRADEOFF CHARACTERISTIC: VISA IMAGES . . . 295
135 ERROR TRADEOFF CHARACTERISTIC: VISA IMAGES . . . 296
136 ERROR TRADEOFF CHARACTERISTIC: VISA IMAGES . . . 297
137 ERROR TRADEOFF CHARACTERISTIC: VISA IMAGES . . . 298
138 ERROR TRADEOFF CHARACTERISTIC: VISA IMAGES . . . 299
139 ERROR TRADEOFF CHARACTERISTIC: VISA IMAGES . . . 300
140 ERROR TRADEOFF CHARACTERISTIC: VISA IMAGES . . . 301
141 ERROR TRADEOFF CHARACTERISTIC: VISA IMAGES . . . 302
142 ERROR TRADEOFF CHARACTERISTIC: VISA IMAGES . . . 303
143 ERROR TRADEOFF CHARACTERISTIC: VISA IMAGES . . . 304
144 ERROR TRADEOFF CHARACTERISTIC: VISA IMAGES . . . 305
145 ERROR TRADEOFF CHARACTERISTIC: VISA IMAGES . . . 306
146 ERROR TRADEOFF CHARACTERISTIC: VISA IMAGES . . . 307
147 ERROR TRADEOFF CHARACTERISTIC: VISA IMAGES . . . 308
148 ERROR TRADEOFF CHARACTERISTIC: VISA IMAGES . . . 309
149 ERROR TRADEOFF CHARACTERISTIC: VISA IMAGES . . . 310
150 ERROR TRADEOFF CHARACTERISTIC: VISA IMAGES . . . 311
151 ERROR TRADEOFF CHARACTERISTIC: VISA IMAGES . . . 312
152 ERROR TRADEOFF CHARACTERISTIC: VISA IMAGES . . . 313
153 ERROR TRADEOFF CHARACTERISTIC: VISA IMAGES . . . 314
154 ERROR TRADEOFF CHARACTERISTIC: VISA IMAGES . . . 315
155 ERROR TRADEOFF CHARACTERISTIC: VISA IMAGES . . . 316
156 ERROR TRADEOFF CHARACTERISTIC: VISA IMAGES . . . 317
157 ERROR TRADEOFF CHARACTERISTIC: VISA IMAGES . . . 318
158 ERROR TRADEOFF CHARACTERISTIC: VISA IMAGES . . . 319
159 ERROR TRADEOFF CHARACTERISTIC: VISA IMAGES . . . 320
160 ERROR TRADEOFF CHARACTERISTIC: VISA IMAGES . . . 321
161 ERROR TRADEOFF CHARACTERISTIC: VISA IMAGES . . . 322
162 ERROR TRADEOFF CHARACTERISTIC: VISA IMAGES . . . 323
163 ERROR TRADEOFF CHARACTERISTIC: VISA IMAGES . . . 324
164 ERROR TRADEOFF CHARACTERISTIC: VISA IMAGES . . . 325
165 ERROR TRADEOFF CHARACTERISTIC: VISA IMAGES . . . 326
166 ERROR TRADEOFF CHARACTERISTIC: VISA IMAGES . . . 327
167 ERROR TRADEOFF CHARACTERISTIC: VISA IMAGES . . . 328
168 ERROR TRADEOFF CHARACTERISTIC: VISA IMAGES . . . 329
169 ERROR TRADEOFF CHARACTERISTIC: VISA IMAGES . . . 330
170 ERROR TRADEOFF CHARACTERISTIC: VISA IMAGES . . . 331
171 ERROR TRADEOFF CHARACTERISTIC: VISA IMAGES . . . 332
172 ERROR TRADEOFF CHARACTERISTIC: VISA IMAGES . . . 333
173 ERROR TRADEOFF CHARACTERISTIC: VISA IMAGES . . . 334
174 ERROR TRADEOFF CHARACTERISTIC: VISA IMAGES . . . 335
175 ERROR TRADEOFF CHARACTERISTIC: VISA IMAGES . . . 336
176 ERROR TRADEOFF CHARACTERISTIC: VISA IMAGES . . . 337
177 ERROR TRADEOFF CHARACTERISTIC: VISA IMAGES . . . 338
178 ERROR TRADEOFF CHARACTERISTIC: VISA IMAGES . . . 339
179 ERROR TRADEOFF CHARACTERISTIC: VISA IMAGES . . . 340
180 ERROR TRADEOFF CHARACTERISTIC: VISA IMAGES . . . 341
181 ERROR TRADEOFF CHARACTERISTIC: VISA IMAGES . . . 342

FNMR(T) "False non-match rate"
FMR(T) "False match rate"

182 ERROR TRADEOFF CHARACTERISTIC: VISA IMAGES . . . 343
183 ERROR TRADEOFF CHARACTERISTIC: VISA IMAGES . . . 344
184 ERROR TRADEOFF CHARACTERISTIC: VISA IMAGES . . . 345
185 ERROR TRADEOFF CHARACTERISTIC: VISA IMAGES . . . 346
186 ERROR TRADEOFF CHARACTERISTIC: VISA IMAGES . . . 347
187 ERROR TRADEOFF CHARACTERISTIC: VISA IMAGES . . . 348
188 ERROR TRADEOFF CHARACTERISTIC: VISA IMAGES . . . 349
189 ERROR TRADEOFF CHARACTERISTIC: VISA IMAGES . . . 350
190 ERROR TRADEOFF CHARACTERISTIC: VISA IMAGES . . . 351
191 ERROR TRADEOFF CHARACTERISTIC: VISA IMAGES . . . 352
192 ERROR TRADEOFF CHARACTERISTIC: VISA IMAGES . . . 353
193 ERROR TRADEOFF CHARACTERISTIC: VISA IMAGES . . . 354
194 ERROR TRADEOFF CHARACTERISTIC: VISA IMAGES . . . 355
195 ERROR TRADEOFF CHARACTERISTIC: VISA IMAGES . . . 356
196 ERROR TRADEOFF CHARACTERISTIC: VISA IMAGES . . . 357
197 ERROR TRADEOFF CHARACTERISTIC: VISA IMAGES . . . 358
198 ERROR TRADEOFF CHARACTERISTIC: VISA IMAGES . . . 359
199 ERROR TRADEOFF CHARACTERISTIC: VISA IMAGES . . . 360
200 ERROR TRADEOFF CHARACTERISTIC: VISA IMAGES . . . 361
201 ERROR TRADEOFF CHARACTERISTIC: VISA IMAGES . . . 362
202 ERROR TRADEOFF CHARACTERISTIC: VISA IMAGES . . . 363
203 ERROR TRADEOFF CHARACTERISTIC: VISA IMAGES . . . 364
204 ERROR TRADEOFF CHARACTERISTIC: VISA IMAGES . . . 365
205 ERROR TRADEOFF CHARACTERISTIC: VISA IMAGES . . . 366
206 ERROR TRADEOFF CHARACTERISTIC: VISA IMAGES . . . 367
207 ERROR TRADEOFF CHARACTERISTIC: VISA IMAGES . . . 368
208 ERROR TRADEOFF CHARACTERISTIC: VISA IMAGES . . . 369
209 ERROR TRADEOFF CHARACTERISTIC: VISA IMAGES . . . 370
210 ERROR TRADEOFF CHARACTERISTIC: VISA IMAGES . . . 371
211 ERROR TRADEOFF CHARACTERISTIC: VISA IMAGES . . . 372
212 ERROR TRADEOFF CHARACTERISTIC: VISA IMAGES . . . 373
213 ERROR TRADEOFF CHARACTERISTIC: VISA IMAGES . . . 374
214 ERROR TRADEOFF CHARACTERISTIC: VISA IMAGES . . . 375
215 ERROR TRADEOFF CHARACTERISTIC: VISA IMAGES . . . 376
216 ERROR TRADEOFF CHARACTERISTIC: VISA IMAGES . . . 377
217 ERROR TRADEOFF CHARACTERISTIC: VISA IMAGES . . . 378
218 ERROR TRADEOFF CHARACTERISTIC: VISA IMAGES . . . 379
219 ERROR TRADEOFF CHARACTERISTIC: MUGSHOT IMAGES . . . 380
220 ERROR TRADEOFF CHARACTERISTIC: MUGSHOT IMAGES . . . 381
221 ERROR TRADEOFF CHARACTERISTIC: MUGSHOT IMAGES . . . 382
222 ERROR TRADEOFF CHARACTERISTIC: MUGSHOT IMAGES . . . 383
223 ERROR TRADEOFF CHARACTERISTIC: MUGSHOT IMAGES . . . 384
224 ERROR TRADEOFF CHARACTERISTIC: MUGSHOT IMAGES . . . 385
225 ERROR TRADEOFF CHARACTERISTIC: MUGSHOT IMAGES . . . 386
226 ERROR TRADEOFF CHARACTERISTIC: MUGSHOT IMAGES . . . 387
227 ERROR TRADEOFF CHARACTERISTIC: MUGSHOT IMAGES . . . 388
228 ERROR TRADEOFF CHARACTERISTIC: MUGSHOT IMAGES . . . 389
229 ERROR TRADEOFF CHARACTERISTIC: MUGSHOT IMAGES . . . 390
230 ERROR TRADEOFF CHARACTERISTIC: MUGSHOT IMAGES . . . 391
231 ERROR TRADEOFF CHARACTERISTIC: MUGSHOT IMAGES . . . 392
232 ERROR TRADEOFF CHARACTERISTIC: MUGSHOT IMAGES . . . 393
233 ERROR TRADEOFF CHARACTERISTIC: MUGSHOT IMAGES . . . 394
234 ERROR TRADEOFF CHARACTERISTIC: MUGSHOT IMAGES . . . 395
235 ERROR TRADEOFF CHARACTERISTIC: MUGSHOT IMAGES . . . 396
236 ERROR TRADEOFF CHARACTERISTIC: MUGSHOT IMAGES . . . 397
237 ERROR TRADEOFF CHARACTERISTIC: MUGSHOT IMAGES . . . 398
238 ERROR TRADEOFF CHARACTERISTIC: MUGSHOT IMAGES . . . 399

FNMR(T) "False non-match rate"
FMR(T) "False match rate"

239 ERROR TRADEOFF CHARACTERISTIC: MUGSHOT IMAGES . . . 400
240 ERROR TRADEOFF CHARACTERISTIC: MUGSHOT IMAGES . . . 401
241 ERROR TRADEOFF CHARACTERISTIC: MUGSHOT IMAGES . . . 402
242 ERROR TRADEOFF CHARACTERISTIC: MUGSHOT IMAGES . . . 403
243 ERROR TRADEOFF CHARACTERISTIC: MUGSHOT IMAGES . . . 404
244 ERROR TRADEOFF CHARACTERISTIC: MUGSHOT IMAGES . . . 405
245 ERROR TRADEOFF CHARACTERISTIC: MUGSHOT IMAGES . . . 406
246 ERROR TRADEOFF CHARACTERISTIC: MUGSHOT IMAGES . . . 407
247 ERROR TRADEOFF CHARACTERISTIC: MUGSHOT IMAGES . . . 408
248 ERROR TRADEOFF CHARACTERISTIC: MUGSHOT IMAGES . . . 409
249 ERROR TRADEOFF CHARACTERISTIC: MUGSHOT IMAGES . . . 410
250 ERROR TRADEOFF CHARACTERISTIC: MUGSHOT IMAGES . . . 411
251 ERROR TRADEOFF CHARACTERISTIC: MUGSHOT IMAGES . . . 412
252 ERROR TRADEOFF CHARACTERISTIC: MUGSHOT IMAGES . . . 413
253 ERROR TRADEOFF CHARACTERISTIC: MUGSHOT IMAGES . . . 414
254 ERROR TRADEOFF CHARACTERISTIC: MUGSHOT IMAGES . . . 415
255 ERROR TRADEOFF CHARACTERISTIC: MUGSHOT IMAGES . . . 416
256 ERROR TRADEOFF CHARACTERISTIC: MUGSHOT IMAGES . . . 417
257 ERROR TRADEOFF CHARACTERISTIC: MUGSHOT IMAGES . . . 418
258 ERROR TRADEOFF CHARACTERISTIC: MUGSHOT IMAGES . . . 419
259 ERROR TRADEOFF CHARACTERISTIC: MUGSHOT IMAGES . . . 420
260 ERROR TRADEOFF CHARACTERISTIC: MUGSHOT IMAGES . . . 421
261 ERROR TRADEOFF CHARACTERISTIC: MUGSHOT IMAGES . . . 422
262 ERROR TRADEOFF CHARACTERISTIC: MUGSHOT IMAGES . . . 423
263 ERROR TRADEOFF CHARACTERISTIC: MUGSHOT IMAGES . . . 424
264 ERROR TRADEOFF CHARACTERISTIC: MUGSHOT IMAGES . . . 425
265 ERROR TRADEOFF CHARACTERISTIC: MUGSHOT IMAGES . . . 426
266 ERROR TRADEOFF CHARACTERISTIC: MUGSHOT IMAGES . . . 427
267 ERROR TRADEOFF CHARACTERISTIC: MUGSHOT IMAGES . . . 428
268 ERROR TRADEOFF CHARACTERISTIC: MUGSHOT IMAGES . . . 429
269 ERROR TRADEOFF CHARACTERISTIC: MUGSHOT IMAGES . . . 430
270 ERROR TRADEOFF CHARACTERISTIC: MUGSHOT IMAGES . . . 431
271 ERROR TRADEOFF CHARACTERISTIC: MUGSHOT IMAGES . . . 432
272 ERROR TRADEOFF CHARACTERISTIC: MUGSHOT IMAGES . . . 433
273 ERROR TRADEOFF CHARACTERISTIC: MUGSHOT IMAGES . . . 434
274 ERROR TRADEOFF CHARACTERISTIC: MUGSHOT IMAGES . . . 435
275 ERROR TRADEOFF CHARACTERISTIC: MUGSHOT IMAGES . . . 436
276 ERROR TRADEOFF CHARACTERISTIC: MUGSHOT IMAGES . . . 437
277 ERROR TRADEOFF CHARACTERISTIC: MUGSHOT IMAGES . . . 438
278 ERROR TRADEOFF CHARACTERISTIC: MUGSHOT IMAGES . . . 439
279 ERROR TRADEOFF CHARACTERISTIC: MUGSHOT IMAGES . . . 440
280 ERROR TRADEOFF CHARACTERISTIC: MUGSHOT IMAGES . . . 441
281 ERROR TRADEOFF CHARACTERISTIC: MUGSHOT IMAGES . . . 442
282 ERROR TRADEOFF CHARACTERISTIC: MUGSHOT IMAGES . . . 443
283 ERROR TRADEOFF CHARACTERISTIC: MUGSHOT IMAGES . . . 444
284 ERROR TRADEOFF CHARACTERISTIC: MUGSHOT IMAGES . . . 445
285 ERROR TRADEOFF CHARACTERISTIC: WILD IMAGES . . . 446
286 ERROR TRADEOFF CHARACTERISTIC: WILD IMAGES . . . 447
287 ERROR TRADEOFF CHARACTERISTIC: WILD IMAGES . . . 448
288 ERROR TRADEOFF CHARACTERISTIC: WILD IMAGES . . . 449
289 ERROR TRADEOFF CHARACTERISTIC: WILD IMAGES . . . 450
290 ERROR TRADEOFF CHARACTERISTIC: WILD IMAGES . . . 451
291 ERROR TRADEOFF CHARACTERISTIC: WILD IMAGES . . . 452
292 ERROR TRADEOFF CHARACTERISTIC: WILD IMAGES . . . 453
293 ERROR TRADEOFF CHARACTERISTIC: WILD IMAGES . . . 454
294 ERROR TRADEOFF CHARACTERISTIC: WILD IMAGES . . . 455

295 ERROR TRADEOFF CHARACTERISTIC: WILD IMAGES . . . 456
296 ERROR TRADEOFF CHARACTERISTIC: WILD IMAGES . . . 457
297 ERROR TRADEOFF CHARACTERISTIC: WILD IMAGES . . . 458
298 ERROR TRADEOFF CHARACTERISTIC: WILD IMAGES . . . 459
299 ERROR TRADEOFF CHARACTERISTIC: WILD IMAGES . . . 460
300 ERROR TRADEOFF CHARACTERISTIC: WILD IMAGES . . . 461
301 ERROR TRADEOFF CHARACTERISTIC: WILD IMAGES . . . 462
302 ERROR TRADEOFF CHARACTERISTIC: WILD IMAGES . . . 463
303 ERROR TRADEOFF CHARACTERISTIC: WILD IMAGES . . . 464
304 ERROR TRADEOFF CHARACTERISTIC: WILD IMAGES . . . 465
305 ERROR TRADEOFF CHARACTERISTIC: WILD IMAGES . . . 466
306 ERROR TRADEOFF CHARACTERISTIC: WILD IMAGES . . . 467
307 ERROR TRADEOFF CHARACTERISTIC: WILD IMAGES . . . 468
308 ERROR TRADEOFF CHARACTERISTIC: WILD IMAGES . . . 469
309 ERROR TRADEOFF CHARACTERISTIC: WILD IMAGES . . . 470
310 ERROR TRADEOFF CHARACTERISTIC: WILD IMAGES . . . 471
311 ERROR TRADEOFF CHARACTERISTIC: WILD IMAGES . . . 472
312 ERROR TRADEOFF CHARACTERISTIC: WILD IMAGES . . . 473
313 ERROR TRADEOFF CHARACTERISTIC: WILD IMAGES . . . 474
314 ERROR TRADEOFF CHARACTERISTIC: WILD IMAGES . . . 475
315 ERROR TRADEOFF CHARACTERISTIC: WILD IMAGES . . . 476
316 ERROR TRADEOFF CHARACTERISTIC: WILD IMAGES . . . 477
317 ERROR TRADEOFF CHARACTERISTIC: WILD IMAGES . . . 478
318 ERROR TRADEOFF CHARACTERISTIC: WILD IMAGES . . . 479
319 ERROR TRADEOFF CHARACTERISTIC: WILD IMAGES . . . 480
320 ERROR TRADEOFF CHARACTERISTIC: WILD IMAGES . . . 481
321 FALSE MATCH RATES WITHIN AND ACROSS DEMOGRAPHIC GROUPS . . . 482
322 FALSE MATCH RATES WITHIN AND ACROSS DEMOGRAPHIC GROUPS . . . 483
323 FALSE MATCH RATES WITHIN AND ACROSS DEMOGRAPHIC GROUPS . . . 484
324 FALSE MATCH RATES WITHIN AND ACROSS DEMOGRAPHIC GROUPS . . . 485
325 FALSE MATCH RATES WITHIN AND ACROSS DEMOGRAPHIC GROUPS . . . 486
326 FALSE MATCH RATES WITHIN AND ACROSS DEMOGRAPHIC GROUPS . . . 487
327 FALSE MATCH RATES WITHIN AND ACROSS DEMOGRAPHIC GROUPS . . . 488
328 FALSE MATCH RATES WITHIN AND ACROSS DEMOGRAPHIC GROUPS . . . 489
329 FALSE MATCH RATES WITHIN AND ACROSS DEMOGRAPHIC GROUPS . . . 490
330 FALSE MATCH RATES WITHIN AND ACROSS DEMOGRAPHIC GROUPS . . . 491
331 FALSE MATCH RATES WITHIN AND ACROSS DEMOGRAPHIC GROUPS . . . 492
332 FALSE MATCH RATES WITHIN AND ACROSS DEMOGRAPHIC GROUPS . . . 493
333 FALSE MATCH RATES WITHIN AND ACROSS DEMOGRAPHIC GROUPS . . . 494
334 FALSE MATCH RATES WITHIN AND ACROSS DEMOGRAPHIC GROUPS . . . 495
335 FALSE MATCH RATES WITHIN AND ACROSS DEMOGRAPHIC GROUPS . . . 496
336 FALSE MATCH RATES WITHIN AND ACROSS DEMOGRAPHIC GROUPS . . . 497
337 FALSE MATCH RATES WITHIN AND ACROSS DEMOGRAPHIC GROUPS . . . 498
338 FALSE MATCH RATES WITHIN AND ACROSS DEMOGRAPHIC GROUPS . . . 499
339 FALSE MATCH RATES WITHIN AND ACROSS DEMOGRAPHIC GROUPS . . . 500
340 FALSE MATCH RATES WITHIN AND ACROSS DEMOGRAPHIC GROUPS . . . 501
341 FALSE MATCH RATES WITHIN AND ACROSS DEMOGRAPHIC GROUPS . . . 502
342 FALSE MATCH RATES WITHIN AND ACROSS DEMOGRAPHIC GROUPS . . . 503
343 FALSE MATCH RATES WITHIN AND ACROSS DEMOGRAPHIC GROUPS . . . 504
344 FALSE MATCH RATES WITHIN AND ACROSS DEMOGRAPHIC GROUPS . . . 505
345 FALSE MATCH RATES WITHIN AND ACROSS DEMOGRAPHIC GROUPS . . . 506
346 FALSE MATCH RATES WITHIN AND ACROSS DEMOGRAPHIC GROUPS . . . 507
347 FALSE MATCH RATES WITHIN AND ACROSS DEMOGRAPHIC GROUPS . . . 508
348 FALSE MATCH RATES WITHIN AND ACROSS DEMOGRAPHIC GROUPS . . . 509
349 FALSE MATCH RATES WITHIN AND ACROSS DEMOGRAPHIC GROUPS . . . 510
350 FALSE MATCH RATES WITHIN AND ACROSS DEMOGRAPHIC GROUPS . . . 511
351 FALSE MATCH RATES WITHIN AND ACROSS DEMOGRAPHIC GROUPS . . . 512

FNMR(T) "False non-match rate"
FMR(T) "False match rate"

352 FALSE MATCH RATES WITHIN AND ACROSS DEMOGRAPHIC GROUPS . . . 513
353 FALSE MATCH RATES WITHIN AND ACROSS DEMOGRAPHIC GROUPS . . . 514
354 FALSE MATCH RATES WITHIN AND ACROSS DEMOGRAPHIC GROUPS . . . 515
355 FALSE MATCH RATES WITHIN AND ACROSS DEMOGRAPHIC GROUPS . . . 516
356 FALSE MATCH RATES WITHIN AND ACROSS DEMOGRAPHIC GROUPS . . . 517
357 FALSE MATCH RATES WITHIN AND ACROSS DEMOGRAPHIC GROUPS . . . 518
358 FALSE MATCH RATES WITHIN AND ACROSS DEMOGRAPHIC GROUPS . . . 519
359 FALSE MATCH RATES WITHIN AND ACROSS DEMOGRAPHIC GROUPS . . . 520
360 FALSE MATCH RATES WITHIN AND ACROSS DEMOGRAPHIC GROUPS . . . 521
361 FALSE MATCH RATES WITHIN AND ACROSS DEMOGRAPHIC GROUPS . . . 522
362 FALSE MATCH RATES WITHIN AND ACROSS DEMOGRAPHIC GROUPS . . . 523
363 FALSE MATCH RATES WITHIN AND ACROSS DEMOGRAPHIC GROUPS . . . 524
364 FALSE MATCH RATES WITHIN AND ACROSS DEMOGRAPHIC GROUPS . . . 525
365 FALSE MATCH RATES WITHIN AND ACROSS DEMOGRAPHIC GROUPS . . . 526
366 FALSE MATCH RATES WITHIN AND ACROSS DEMOGRAPHIC GROUPS . . . 527
367 FALSE MATCH RATES WITHIN AND ACROSS DEMOGRAPHIC GROUPS . . . 528
368 FALSE MATCH RATES WITHIN AND ACROSS DEMOGRAPHIC GROUPS . . . 529
369 FALSE MATCH RATES WITHIN AND ACROSS DEMOGRAPHIC GROUPS . . . 530
370 FALSE MATCH RATES WITHIN AND ACROSS DEMOGRAPHIC GROUPS . . . 531
371 FALSE MATCH RATES WITHIN AND ACROSS DEMOGRAPHIC GROUPS . . . 532
372 FALSE MATCH RATES WITHIN AND ACROSS DEMOGRAPHIC GROUPS . . . 533
373 FALSE MATCH RATES WITHIN AND ACROSS DEMOGRAPHIC GROUPS . . . 534
374 FALSE MATCH RATES WITHIN AND ACROSS DEMOGRAPHIC GROUPS . . . 535
375 FALSE MATCH RATES WITHIN AND ACROSS DEMOGRAPHIC GROUPS . . . 536
376 FALSE MATCH RATES WITHIN AND ACROSS DEMOGRAPHIC GROUPS . . . 537
377 FALSE MATCH RATES WITHIN AND ACROSS DEMOGRAPHIC GROUPS . . . 538
378 FALSE MATCH RATES WITHIN AND ACROSS DEMOGRAPHIC GROUPS . . . 539
379 FALSE MATCH RATES WITHIN AND ACROSS DEMOGRAPHIC GROUPS . . . 540
380 FALSE MATCH RATES WITHIN AND ACROSS DEMOGRAPHIC GROUPS . . . 541
381 FALSE MATCH RATES WITHIN AND ACROSS DEMOGRAPHIC GROUPS . . . 542
382 FALSE MATCH RATES WITHIN AND ACROSS DEMOGRAPHIC GROUPS . . . 543
383 FALSE MATCH RATES WITHIN AND ACROSS DEMOGRAPHIC GROUPS . . . 544
384 FALSE MATCH RATES WITHIN AND ACROSS DEMOGRAPHIC GROUPS . . . 545
385 FALSE MATCH RATES WITHIN AND ACROSS DEMOGRAPHIC GROUPS . . . 546
386 FALSE MATCH RATES WITHIN AND ACROSS DEMOGRAPHIC GROUPS . . . 547
387 SEX AND RACE EFFECTS: MUGSHOT IMAGES . . . 548
388 SEX AND RACE EFFECTS: MUGSHOT IMAGES . . . 549
389 SEX AND RACE EFFECTS: MUGSHOT IMAGES . . . 550
390 SEX AND RACE EFFECTS: MUGSHOT IMAGES . . . 551
391 SEX AND RACE EFFECTS: MUGSHOT IMAGES . . . 552
392 SEX AND RACE EFFECTS: MUGSHOT IMAGES . . . 553
393 SEX AND RACE EFFECTS: MUGSHOT IMAGES . . . 554
394 SEX AND RACE EFFECTS: MUGSHOT IMAGES . . . 555
395 SEX AND RACE EFFECTS: MUGSHOT IMAGES . . . 556
396 SEX AND RACE EFFECTS: MUGSHOT IMAGES . . . 557
397 SEX AND RACE EFFECTS: MUGSHOT IMAGES . . . 558
398 SEX AND RACE EFFECTS: MUGSHOT IMAGES . . . 559
399 SEX AND RACE EFFECTS: MUGSHOT IMAGES . . . 560
400 SEX AND RACE EFFECTS: MUGSHOT IMAGES . . . 561
401 SEX AND RACE EFFECTS: MUGSHOT IMAGES . . . 562
402 SEX AND RACE EFFECTS: MUGSHOT IMAGES . . . 563
403 SEX AND RACE EFFECTS: MUGSHOT IMAGES . . . 564
404 SEX AND RACE EFFECTS: MUGSHOT IMAGES . . . 565
405 SEX AND RACE EFFECTS: MUGSHOT IMAGES . . . 566
406 SEX AND RACE EFFECTS: MUGSHOT IMAGES . . . 567
407 SEX AND RACE EFFECTS: MUGSHOT IMAGES . . . 568
408 SEX AND RACE EFFECTS: MUGSHOT IMAGES . . . 569

FNMR(T) "False non-match rate"
FMR(T) "False match rate"

409 SEX AND RACE EFFECTS: MUGSHOT IMAGES . . . 570
410 SEX AND RACE EFFECTS: MUGSHOT IMAGES . . . 571
411 SEX AND RACE EFFECTS: MUGSHOT IMAGES . . . 572
412 SEX AND RACE EFFECTS: MUGSHOT IMAGES . . . 573
413 SEX AND RACE EFFECTS: MUGSHOT IMAGES . . . 574
414 SEX AND RACE EFFECTS: MUGSHOT IMAGES . . . 575
415 SEX AND RACE EFFECTS: MUGSHOT IMAGES . . . 576
416 SEX AND RACE EFFECTS: MUGSHOT IMAGES . . . 577
417 SEX AND RACE EFFECTS: MUGSHOT IMAGES . . . 578
418 SEX AND RACE EFFECTS: MUGSHOT IMAGES . . . 579
419 SEX AND RACE EFFECTS: MUGSHOT IMAGES . . . 580
420 SEX AND RACE EFFECTS: MUGSHOT IMAGES . . . 581
421 SEX AND RACE EFFECTS: MUGSHOT IMAGES . . . 582
422 SEX AND RACE EFFECTS: MUGSHOT IMAGES . . . 583
423 SEX AND RACE EFFECTS: MUGSHOT IMAGES . . . 584
424 SEX AND RACE EFFECTS: MUGSHOT IMAGES . . . 585
425 SEX AND RACE EFFECTS: MUGSHOT IMAGES . . . 586
426 SEX AND RACE EFFECTS: MUGSHOT IMAGES . . . 587
427 SEX AND RACE EFFECTS: MUGSHOT IMAGES . . . 588
428 SEX AND RACE EFFECTS: MUGSHOT IMAGES . . . 589
429 SEX AND RACE EFFECTS: MUGSHOT IMAGES . . . 590
430 SEX AND RACE EFFECTS: MUGSHOT IMAGES . . . 591
431 SEX AND RACE EFFECTS: MUGSHOT IMAGES . . . 592
432 SEX AND RACE EFFECTS: MUGSHOT IMAGES . . . 593
433 SEX AND RACE EFFECTS: MUGSHOT IMAGES . . . 594
434 SEX AND RACE EFFECTS: MUGSHOT IMAGES . . . 595
435 SEX AND RACE EFFECTS: MUGSHOT IMAGES . . . 596
436 SEX AND RACE EFFECTS: MUGSHOT IMAGES . . . 597
437 SEX AND RACE EFFECTS: MUGSHOT IMAGES . . . 598
438 SEX AND RACE EFFECTS: MUGSHOT IMAGES . . . 599
439 SEX AND RACE EFFECTS: MUGSHOT IMAGES . . . 600
440 SEX AND RACE EFFECTS: MUGSHOT IMAGES . . . 601
441 SEX AND RACE EFFECTS: MUGSHOT IMAGES . . . 602
442 SEX AND RACE EFFECTS: MUGSHOT IMAGES . . . 603
443 SEX AND RACE EFFECTS: MUGSHOT IMAGES . . . 604
444 SEX AND RACE EFFECTS: MUGSHOT IMAGES . . . 605
445 SEX AND RACE EFFECTS: MUGSHOT IMAGES . . . 606
446 SEX AND RACE EFFECTS: MUGSHOT IMAGES . . . 607
447 SEX AND RACE EFFECTS: MUGSHOT IMAGES . . . 608
448 SEX AND RACE EFFECTS: MUGSHOT IMAGES . . . 609
449 SEX AND RACE EFFECTS: MUGSHOT IMAGES . . . 610
450 SEX AND RACE EFFECTS: MUGSHOT IMAGES . . . 611
451 SEX AND RACE EFFECTS: MUGSHOT IMAGES . . . 612
452 SEX AND RACE EFFECTS: MUGSHOT IMAGES . . . 613
453 SEX EFFECTS: VISA IMAGES . . . 614
454 SEX EFFECTS: VISA IMAGES . . . 615
455 SEX EFFECTS: VISA IMAGES . . . 616
456 SEX EFFECTS: VISA IMAGES . . . 617
457 SEX EFFECTS: VISA IMAGES . . . 618
458 SEX EFFECTS: VISA IMAGES . . . 619
459 SEX EFFECTS: VISA IMAGES . . . 620
460 SEX EFFECTS: VISA IMAGES . . . 621
461 SEX EFFECTS: VISA IMAGES . . . 622
462 SEX EFFECTS: VISA IMAGES . . . 623
463 SEX EFFECTS: VISA IMAGES . . . 624
464 SEX EFFECTS: VISA IMAGES . . . 625
465 SEX EFFECTS: VISA IMAGES . . . 626

FNMR(T) "False non-match rate"
FMR(T) "False match rate"

466 SEX EFFECTS: VISA IMAGES . . . 627
467 SEX EFFECTS: VISA IMAGES . . . 628
468 SEX EFFECTS: VISA IMAGES . . . 629
469 SEX EFFECTS: VISA IMAGES . . . 630
470 SEX EFFECTS: VISA IMAGES . . . 631
471 SEX EFFECTS: VISA IMAGES . . . 632
472 SEX EFFECTS: VISA IMAGES . . . 633
473 SEX EFFECTS: VISA IMAGES . . . 634
474 SEX EFFECTS: VISA IMAGES . . . 635
475 SEX EFFECTS: VISA IMAGES . . . 636
476 SEX EFFECTS: VISA IMAGES . . . 637
477 SEX EFFECTS: VISA IMAGES . . . 638
478 SEX EFFECTS: VISA IMAGES . . . 639
479 SEX EFFECTS: VISA IMAGES . . . 640
480 SEX EFFECTS: VISA IMAGES . . . 641
481 SEX EFFECTS: VISA IMAGES . . . 642
482 SEX EFFECTS: VISA IMAGES . . . 643
483 SEX EFFECTS: VISA IMAGES . . . 644
484 SEX EFFECTS: VISA IMAGES . . . 645
485 SEX EFFECTS: VISA IMAGES . . . 646
486 SEX EFFECTS: VISA IMAGES . . . 647
487 SEX EFFECTS: VISA IMAGES . . . 648
488 SEX EFFECTS: VISA IMAGES . . . 649
489 SEX EFFECTS: VISA IMAGES . . . 650
490 SEX EFFECTS: VISA IMAGES . . . 651
491 SEX EFFECTS: VISA IMAGES . . . 652
492 SEX EFFECTS: VISA IMAGES . . . 653
493 SEX EFFECTS: VISA IMAGES . . . 654
494 SEX EFFECTS: VISA IMAGES . . . 655
495 SEX EFFECTS: VISA IMAGES . . . 656
496 SEX EFFECTS: VISA IMAGES . . . 657
497 SEX EFFECTS: VISA IMAGES . . . 658
498 SEX EFFECTS: VISA IMAGES . . . 659
499 SEX EFFECTS: VISA IMAGES . . . 660
500 SEX EFFECTS: VISA IMAGES . . . 661
501 SEX EFFECTS: VISA IMAGES . . . 662
502 SEX EFFECTS: VISA IMAGES . . . 663
503 SEX EFFECTS: VISA IMAGES . . . 664
504 SEX EFFECTS: VISA IMAGES . . . 665
505 SEX EFFECTS: VISA IMAGES . . . 666
506 SEX EFFECTS: VISA IMAGES . . . 667
507 SEX EFFECTS: VISA IMAGES . . . 668
508 SEX EFFECTS: VISA IMAGES . . . 669
509 SEX EFFECTS: VISA IMAGES . . . 670
510 SEX EFFECTS: VISA IMAGES . . . 671
511 SEX EFFECTS: VISA IMAGES . . . 672
512 SEX EFFECTS: VISA IMAGES . . . 673
513 SEX EFFECTS: VISA IMAGES . . . 674
514 SEX EFFECTS: VISA IMAGES . . . 675
515 SEX EFFECTS: VISA IMAGES . . . 676
516 SEX EFFECTS: VISA IMAGES . . . 677
517 SEX EFFECTS: VISA IMAGES . . . 678
518 SEX EFFECTS: VISA IMAGES . . . 679
519 SEX EFFECTS: VISA IMAGES . . . 680
520 SEX EFFECTS: VISA IMAGES . . . 681
521 SEX EFFECTS: VISA IMAGES . . . 682
522 SEX EFFECTS: VISA IMAGES . . . 683

FNMR(T) "False non-match rate"
FMR(T) "False match rate"

523 SEX EFFECTS: VISA IMAGES . . . 684
524 SEX EFFECTS: VISA IMAGES . . . 685
525 SEX EFFECTS: VISA IMAGES . . . 686
526 SEX EFFECTS: VISA IMAGES . . . 687
527 SEX EFFECTS: VISA IMAGES . . . 688
528 SEX EFFECTS: VISA IMAGES . . . 689
529 SEX EFFECTS: VISA IMAGES . . . 690
530 SEX EFFECTS: VISA IMAGES . . . 691
531 SEX EFFECTS: VISA IMAGES . . . 692
532 SEX EFFECTS: VISA IMAGES . . . 693
533 SEX EFFECTS: VISA IMAGES . . . 694
534 SEX EFFECTS: VISA IMAGES . . . 695
535 SEX EFFECTS: VISA IMAGES . . . 696
536 SEX EFFECTS: VISA IMAGES . . . 697
537 SEX EFFECTS: VISA IMAGES . . . 698
538 SEX EFFECTS: VISA IMAGES . . . 699
539 SEX EFFECTS: VISA IMAGES . . . 700
540 SEX EFFECTS: VISA IMAGES . . . 701
541 SEX EFFECTS: VISA IMAGES . . . 702
542 SEX EFFECTS: VISA IMAGES . . . 703
543 FALSE MATCH RATE CALIBRATION: MUGSHOT IMAGES . . . 704
544 FALSE MATCH RATE CALIBRATION: MUGSHOT IMAGES . . . 705
545 FALSE MATCH RATE CALIBRATION: MUGSHOT IMAGES . . . 706
546 FALSE MATCH RATE CALIBRATION: MUGSHOT IMAGES . . . 707
547 FALSE MATCH RATE CALIBRATION: MUGSHOT IMAGES . . . 708
548 FALSE MATCH RATE CALIBRATION: MUGSHOT IMAGES . . . 709
549 FALSE MATCH RATE CALIBRATION: MUGSHOT IMAGES . . . 710
550 FALSE MATCH RATE CALIBRATION: MUGSHOT IMAGES . . . 711
551 FALSE MATCH RATE CALIBRATION: MUGSHOT IMAGES . . . 712
552 FALSE MATCH RATE CALIBRATION: MUGSHOT IMAGES . . . 713
553 FALSE MATCH RATE CALIBRATION: MUGSHOT IMAGES . . . 714
554 FALSE MATCH RATE CALIBRATION: MUGSHOT IMAGES . . . 715
555 FALSE MATCH RATE CALIBRATION: MUGSHOT IMAGES . . . 716
556 FALSE MATCH RATE CALIBRATION: MUGSHOT IMAGES . . . 717
557 FALSE MATCH RATE CALIBRATION: MUGSHOT IMAGES . . . 718
558 FALSE MATCH RATE CALIBRATION: MUGSHOT IMAGES . . . 719
559 FALSE MATCH RATE CALIBRATION: MUGSHOT IMAGES . . . 720
560 FALSE MATCH RATE CALIBRATION: MUGSHOT IMAGES . . . 721
561 FALSE MATCH RATE CALIBRATION: MUGSHOT IMAGES . . . 722
562 FALSE MATCH RATE CALIBRATION: MUGSHOT IMAGES . . . 723
563 FALSE MATCH RATE CALIBRATION: MUGSHOT IMAGES . . . 724
564 FALSE MATCH RATE CALIBRATION: MUGSHOT IMAGES . . . 725
565 FALSE MATCH RATE CALIBRATION: MUGSHOT IMAGES . . . 726
566 FALSE MATCH RATE CALIBRATION: MUGSHOT IMAGES . . . 727
567 FALSE MATCH RATE CALIBRATION: MUGSHOT IMAGES . . . 728
568 FALSE MATCH RATE CALIBRATION: MUGSHOT IMAGES . . . 729
569 FALSE MATCH RATE CALIBRATION: MUGSHOT IMAGES . . . 730
570 FALSE MATCH RATE CALIBRATION: MUGSHOT IMAGES . . . 731
571 FALSE MATCH RATE CALIBRATION: MUGSHOT IMAGES . . . 732
572 FALSE MATCH RATE CALIBRATION: MUGSHOT IMAGES . . . 733
573 FALSE MATCH RATE CALIBRATION: MUGSHOT IMAGES . . . 734
574 FALSE MATCH RATE CALIBRATION: MUGSHOT IMAGES . . . 735
575 FALSE MATCH RATE CALIBRATION: MUGSHOT IMAGES . . . 736
576 FALSE MATCH RATE CALIBRATION: MUGSHOT IMAGES . . . 737
577 FALSE MATCH RATE CALIBRATION: MUGSHOT IMAGES . . . 738
578 FALSE MATCH RATE CALIBRATION: MUGSHOT IMAGES . . . 739
579 FALSE MATCH RATE CALIBRATION: MUGSHOT IMAGES . . . 740

580 FALSE MATCH RATE CALIBRATION: MUGSHOT IMAGES . . . 741
581 FALSE MATCH RATE CALIBRATION: MUGSHOT IMAGES . . . 742
582 FALSE MATCH RATE CALIBRATION: MUGSHOT IMAGES . . . 743
583 FALSE MATCH RATE CALIBRATION: MUGSHOT IMAGES . . . 744
584 FALSE MATCH RATE CALIBRATION: MUGSHOT IMAGES . . . 745
585 FALSE MATCH RATE CALIBRATION: MUGSHOT IMAGES . . . 746
586 FALSE MATCH RATE CALIBRATION: MUGSHOT IMAGES . . . 747
587 FALSE MATCH RATE CALIBRATION: MUGSHOT IMAGES . . . 748
588 FALSE MATCH RATE CALIBRATION: MUGSHOT IMAGES . . . 749
589 FALSE MATCH RATE CALIBRATION: MUGSHOT IMAGES . . . 750
590 FALSE MATCH RATE CALIBRATION: MUGSHOT IMAGES . . . 751
591 FALSE MATCH RATE CALIBRATION: MUGSHOT IMAGES . . . 752
592 FALSE MATCH RATE CALIBRATION: MUGSHOT IMAGES . . . 753
593 FALSE MATCH RATE CALIBRATION: MUGSHOT IMAGES . . . 754
594 FALSE MATCH RATE CALIBRATION: MUGSHOT IMAGES . . . 755
595 FALSE MATCH RATE CALIBRATION: MUGSHOT IMAGES . . . 756
596 FALSE MATCH RATE CALIBRATION: MUGSHOT IMAGES . . . 757
597 FALSE MATCH RATE CALIBRATION: MUGSHOT IMAGES . . . 758
598 FALSE MATCH RATE CALIBRATION: MUGSHOT IMAGES . . . 759
599 FALSE MATCH RATE CALIBRATION: MUGSHOT IMAGES . . . 760
600 FALSE MATCH RATE CALIBRATION: MUGSHOT IMAGES . . . 761
601 FALSE MATCH RATE CALIBRATION: MUGSHOT IMAGES . . . 762
602 FALSE MATCH RATE CALIBRATION: MUGSHOT IMAGES . . . 763
603 FALSE MATCH RATE CALIBRATION: MUGSHOT IMAGES . . . 764
604 FALSE MATCH RATE CALIBRATION: MUGSHOT IMAGES . . . 765
605 FALSE MATCH RATE CALIBRATION: MUGSHOT IMAGES . . . 766
606 FALSE MATCH RATE CALIBRATION: MUGSHOT IMAGES . . . 767
607 FALSE MATCH RATE CALIBRATION: MUGSHOT IMAGES . . . 768
608 FALSE MATCH RATE CALIBRATION: MUGSHOT IMAGES . . . 769
609 FALSE MATCH RATE CALIBRATION: VISA IMAGES . . . 770
610 EFFECT OF COUNTRY OF BIRTH ON FNMR . . . 772
611 EFFECT OF COUNTRY OF BIRTH ON FNMR . . . 773
612 EFFECT OF COUNTRY OF BIRTH ON FNMR . . . 774
613 EFFECT OF COUNTRY OF BIRTH ON FNMR . . . 775
614 EFFECT OF COUNTRY OF BIRTH ON FNMR . . . 776
615 EFFECT OF COUNTRY OF BIRTH ON FNMR . . . 777
616 EFFECT OF COUNTRY OF BIRTH ON FNMR . . . 778
617 EFFECT OF COUNTRY OF BIRTH ON FNMR . . . 779
618 EFFECT OF COUNTRY OF BIRTH ON FNMR . . . 780
619 EFFECT OF COUNTRY OF BIRTH ON FNMR . . . 781
620 EFFECT OF COUNTRY OF BIRTH ON FNMR . . . 782
621 EFFECT OF COUNTRY OF BIRTH ON FNMR . . . 783
622 EFFECT OF COUNTRY OF BIRTH ON FNMR . . . 784
623 EFFECT OF COUNTRY OF BIRTH ON FNMR . . . 785
624 EFFECT OF COUNTRY OF BIRTH ON FNMR . . . 786
625 EFFECT OF COUNTRY OF BIRTH ON FNMR . . . 787
626 EFFECT OF COUNTRY OF BIRTH ON FNMR . . . 788
627 EFFECT OF COUNTRY OF BIRTH ON FNMR . . . 789
628 EFFECT OF COUNTRY OF BIRTH ON FNMR . . . 790
629 EFFECT OF COUNTRY OF BIRTH ON FNMR . . . 791
630 EFFECT OF COUNTRY OF BIRTH ON FNMR . . . 792
631 EFFECT OF COUNTRY OF BIRTH ON FNMR . . . 793
632 EFFECT OF COUNTRY OF BIRTH ON FNMR . . . 794
633 EFFECT OF COUNTRY OF BIRTH ON FNMR . . . 795
634 EFFECT OF COUNTRY OF BIRTH ON FNMR . . . 796
635 EFFECT OF COUNTRY OF BIRTH ON FNMR . . . 797
636 EFFECT OF COUNTRY OF BIRTH ON FNMR . . . 798

FNMR(T) "False non-match rate"
FMR(T) "False match rate"

637 EFFECT OF COUNTRY OF BIRTH ON FNMR . . . 799
638 EFFECT OF COUNTRY OF BIRTH ON FNMR . . . 800
639 EFFECT OF COUNTRY OF BIRTH ON FNMR . . . 801
640 EFFECT OF COUNTRY OF BIRTH ON FNMR . . . 802
641 EFFECT OF COUNTRY OF BIRTH ON FNMR . . . 803
642 EFFECT OF COUNTRY OF BIRTH ON FNMR . . . 804
643 EFFECT OF COUNTRY OF BIRTH ON FNMR . . . 805
644 EFFECT OF COUNTRY OF BIRTH ON FNMR . . . 806
645 EFFECT OF COUNTRY OF BIRTH ON FNMR . . . 807
646 EFFECT OF COUNTRY OF BIRTH ON FNMR . . . 808
647 EFFECT OF COUNTRY OF BIRTH ON FNMR . . . 809
648 EFFECT OF COUNTRY OF BIRTH ON FNMR . . . 810
649 EFFECT OF COUNTRY OF BIRTH ON FNMR . . . 811
650 EFFECT OF COUNTRY OF BIRTH ON FNMR . . . 812
651 EFFECT OF COUNTRY OF BIRTH ON FNMR . . . 813
652 EFFECT OF COUNTRY OF BIRTH ON FNMR . . . 814
653 EFFECT OF COUNTRY OF BIRTH ON FNMR . . . 815
654 EFFECT OF COUNTRY OF BIRTH ON FNMR . . . 816
655 EFFECT OF COUNTRY OF BIRTH ON FNMR . . . 817
656 EFFECT OF COUNTRY OF BIRTH ON FNMR . . . 818
657 EFFECT OF COUNTRY OF BIRTH ON FNMR . . . 819
658 EFFECT OF COUNTRY OF BIRTH ON FNMR . . . 820
659 EFFECT OF COUNTRY OF BIRTH ON FNMR . . . 821
660 EFFECT OF COUNTRY OF BIRTH ON FNMR . . . 822
661 EFFECT OF COUNTRY OF BIRTH ON FNMR . . . 823
662 EFFECT OF COUNTRY OF BIRTH ON FNMR . . . 824
663 EFFECT OF COUNTRY OF BIRTH ON FNMR . . . 825
664 EFFECT OF COUNTRY OF BIRTH ON FNMR . . . 826
665 EFFECT OF COUNTRY OF BIRTH ON FNMR . . . 827
666 EFFECT OF COUNTRY OF BIRTH ON FNMR . . . 828
667 EFFECT OF COUNTRY OF BIRTH ON FNMR . . . 829
668 EFFECT OF COUNTRY OF BIRTH ON FNMR . . . 830
669 EFFECT OF COUNTRY OF BIRTH ON FNMR . . . 831
670 EFFECT OF COUNTRY OF BIRTH ON FNMR . . . 832
671 EFFECT OF COUNTRY OF BIRTH ON FNMR . . . 833
672 EFFECT OF COUNTRY OF BIRTH ON FNMR . . . 834
673 EFFECT OF COUNTRY OF BIRTH ON FNMR . . . 835
674 EFFECT OF COUNTRY OF BIRTH ON FNMR . . . 836
675 EFFECT OF COUNTRY OF BIRTH ON FNMR . . . 837
676 EFFECT OF COUNTRY OF BIRTH ON FNMR . . . 838
677 EFFECT OF COUNTRY OF BIRTH ON FNMR . . . 839
678 EFFECT OF COUNTRY OF BIRTH ON FNMR . . . 840
679 EFFECT OF COUNTRY OF BIRTH ON FNMR . . . 841
680 EFFECT OF COUNTRY OF BIRTH ON FNMR . . . 842
681 EFFECT OF COUNTRY OF BIRTH ON FNMR . . . 843
682 EFFECT OF COUNTRY OF BIRTH ON FNMR . . . 844
683 EFFECT OF COUNTRY OF BIRTH ON FNMR . . . 845
684 EFFECT OF COUNTRY OF BIRTH ON FNMR . . . 846
685 EFFECT OF COUNTRY OF BIRTH ON FNMR . . . 847
686 EFFECT OF COUNTRY OF BIRTH ON FNMR . . . 848
687 EFFECT OF COUNTRY OF BIRTH ON FNMR . . . 849
688 EFFECT OF COUNTRY OF BIRTH ON FNMR . . . 850
689 EFFECT OF COUNTRY OF BIRTH ON FNMR . . . 851
690 EFFECT OF COUNTRY OF BIRTH ON FNMR . . . 852
691 EFFECT OF COUNTRY OF BIRTH ON FNMR . . . 853
692 EFFECT OF COUNTRY OF BIRTH ON FNMR . . . 854
693 EFFECT OF COUNTRY OF BIRTH ON FNMR . . . 855

694 EFFECT OF COUNTRY OF BIRTH ON FNMR . . . 856
695 EFFECT OF COUNTRY OF BIRTH ON FNMR . . . 857
696 EFFECT OF COUNTRY OF BIRTH ON FNMR . . . 858
697 EFFECT OF COUNTRY OF BIRTH ON FNMR . . . 859
698 EFFECT OF COUNTRY OF BIRTH ON FNMR . . . 860
699 EFFECT OF COUNTRY OF BIRTH ON FNMR . . . 861
700 ERROR TRADEOFF CHARACTERISTIC: MUGSHOT IMAGES . . . 863
701 ERROR TRADEOFF CHARACTERISTIC: MUGSHOT IMAGES . . . 864
702 ERROR TRADEOFF CHARACTERISTIC: MUGSHOT IMAGES . . . 865
703 ERROR TRADEOFF CHARACTERISTIC: MUGSHOT IMAGES . . . 866
704 ERROR TRADEOFF CHARACTERISTIC: MUGSHOT IMAGES . . . 867
705 ERROR TRADEOFF CHARACTERISTIC: MUGSHOT IMAGES . . . 868
706 ERROR TRADEOFF CHARACTERISTIC: MUGSHOT IMAGES . . . 869
707 ERROR TRADEOFF CHARACTERISTIC: MUGSHOT IMAGES . . . 870
708 ERROR TRADEOFF CHARACTERISTIC: MUGSHOT IMAGES . . . 871
709 ERROR TRADEOFF CHARACTERISTIC: MUGSHOT IMAGES . . . 872
710 ERROR TRADEOFF CHARACTERISTIC: MUGSHOT IMAGES . . . 873
711 ERROR TRADEOFF CHARACTERISTIC: MUGSHOT IMAGES . . . 874
712 ERROR TRADEOFF CHARACTERISTIC: MUGSHOT IMAGES . . . 875
713 ERROR TRADEOFF CHARACTERISTIC: MUGSHOT IMAGES . . . 876
714 ERROR TRADEOFF CHARACTERISTIC: MUGSHOT IMAGES . . . 877
715 ERROR TRADEOFF CHARACTERISTIC: MUGSHOT IMAGES . . . 878
716 ERROR TRADEOFF CHARACTERISTIC: MUGSHOT IMAGES . . . 879
717 ERROR TRADEOFF CHARACTERISTIC: MUGSHOT IMAGES . . . 880
718 ERROR TRADEOFF CHARACTERISTIC: MUGSHOT IMAGES . . . 881
719 ERROR TRADEOFF CHARACTERISTIC: MUGSHOT IMAGES . . . 882
720 ERROR TRADEOFF CHARACTERISTIC: MUGSHOT IMAGES . . . 883
721 ERROR TRADEOFF CHARACTERISTIC: MUGSHOT IMAGES . . . 884
722 ERROR TRADEOFF CHARACTERISTIC: MUGSHOT IMAGES . . . 885
723 ERROR TRADEOFF CHARACTERISTIC: MUGSHOT IMAGES . . . 886
724 ERROR TRADEOFF CHARACTERISTIC: MUGSHOT IMAGES . . . 887
725 ERROR TRADEOFF CHARACTERISTIC: MUGSHOT IMAGES . . . 888
726 ERROR TRADEOFF CHARACTERISTIC: MUGSHOT IMAGES . . . 889
727 ERROR TRADEOFF CHARACTERISTIC: MUGSHOT IMAGES . . . 890
728 ERROR TRADEOFF CHARACTERISTIC: MUGSHOT IMAGES . . . 891
729 ERROR TRADEOFF CHARACTERISTIC: MUGSHOT IMAGES . . . 892
730 ERROR TRADEOFF CHARACTERISTIC: MUGSHOT IMAGES . . . 893
731 ERROR TRADEOFF CHARACTERISTIC: MUGSHOT IMAGES . . . 894
732 ERROR TRADEOFF CHARACTERISTIC: MUGSHOT IMAGES . . . 895
733 ERROR TRADEOFF CHARACTERISTIC: MUGSHOT IMAGES . . . 896
734 ERROR TRADEOFF CHARACTERISTIC: MUGSHOT IMAGES . . . 897
735 ERROR TRADEOFF CHARACTERISTIC: MUGSHOT IMAGES . . . 898
736 ERROR TRADEOFF CHARACTERISTIC: MUGSHOT IMAGES . . . 899
737 ERROR TRADEOFF CHARACTERISTIC: MUGSHOT IMAGES . . . 900
738 ERROR TRADEOFF CHARACTERISTIC: MUGSHOT IMAGES . . . 901
739 ERROR TRADEOFF CHARACTERISTIC: MUGSHOT IMAGES . . . 902
740 ERROR TRADEOFF CHARACTERISTIC: MUGSHOT IMAGES . . . 903
741 ERROR TRADEOFF CHARACTERISTIC: MUGSHOT IMAGES . . . 904
742 ERROR TRADEOFF CHARACTERISTIC: MUGSHOT IMAGES . . . 905
743 ERROR TRADEOFF CHARACTERISTIC: MUGSHOT IMAGES . . . 906
744 ERROR TRADEOFF CHARACTERISTIC: MUGSHOT IMAGES . . . 907
745 ERROR TRADEOFF CHARACTERISTIC: MUGSHOT IMAGES . . . 908
746 ERROR TRADEOFF CHARACTERISTIC: MUGSHOT IMAGES . . . 909
747 ERROR TRADEOFF CHARACTERISTIC: MUGSHOT IMAGES . . . 910
748 ERROR TRADEOFF CHARACTERISTIC: MUGSHOT IMAGES . . . 911
749 ERROR TRADEOFF CHARACTERISTIC: MUGSHOT IMAGES . . . 912
750 ERROR TRADEOFF CHARACTERISTIC: MUGSHOT IMAGES . . . 913

FNMR(T) "False non-match rate"
FMR(T) "False match rate"

751 ERROR TRADEOFF CHARACTERISTIC: MUGSHOT IMAGES . . . 914
752 ERROR TRADEOFF CHARACTERISTIC: MUGSHOT IMAGES . . . 915
753 ERROR TRADEOFF CHARACTERISTIC: MUGSHOT IMAGES . . . 916
754 ERROR TRADEOFF CHARACTERISTIC: MUGSHOT IMAGES . . . 917
755 ERROR TRADEOFF CHARACTERISTIC: MUGSHOT IMAGES . . . 918
756 ERROR TRADEOFF CHARACTERISTIC: MUGSHOT IMAGES . . . 919
757 ERROR TRADEOFF CHARACTERISTIC: MUGSHOT IMAGES . . . 920
758 ERROR TRADEOFF CHARACTERISTIC: MUGSHOT IMAGES . . . 921
759 ERROR TRADEOFF CHARACTERISTIC: MUGSHOT IMAGES . . . 922
760 ERROR TRADEOFF CHARACTERISTIC: MUGSHOT IMAGES . . . 923
761 ERROR TRADEOFF CHARACTERISTIC: MUGSHOT IMAGES . . . 924
762 ERROR TRADEOFF CHARACTERISTIC: MUGSHOT IMAGES . . . 925
763 ERROR TRADEOFF CHARACTERISTIC: MUGSHOT IMAGES . . . 926
764 ERROR TRADEOFF CHARACTERISTIC: MUGSHOT IMAGES . . . 927
765 ERROR TRADEOFF CHARACTERISTIC: MUGSHOT IMAGES . . . 928
766 ERROR TRADEOFF CHARACTERISTIC: MUGSHOT IMAGES . . . 929
767 ERROR TRADEOFF CHARACTERISTIC: MUGSHOT IMAGES . . . 930
768 ERROR TRADEOFF CHARACTERISTIC: MUGSHOT IMAGES . . . 931
769 ERROR TRADEOFF CHARACTERISTIC: MUGSHOT IMAGES . . . 932
770 ERROR TRADEOFF CHARACTERISTIC: MUGSHOT IMAGES . . . 933
771 ERROR TRADEOFF CHARACTERISTIC: MUGSHOT IMAGES . . . 934
772 ERROR TRADEOFF CHARACTERISTIC: MUGSHOT IMAGES . . . 935
773 ERROR TRADEOFF CHARACTERISTIC: MUGSHOT IMAGES . . . 936
774 ERROR TRADEOFF CHARACTERISTIC: MUGSHOT IMAGES . . . 937
775 ERROR TRADEOFF CHARACTERISTIC: MUGSHOT IMAGES . . . 938
776 ERROR TRADEOFF CHARACTERISTIC: MUGSHOT IMAGES . . . 939
777 ERROR TRADEOFF CHARACTERISTIC: MUGSHOT IMAGES . . . 940
778 ERROR TRADEOFF CHARACTERISTIC: MUGSHOT IMAGES . . . 941
779 ERROR TRADEOFF CHARACTERISTIC: MUGSHOT IMAGES . . . 942
780 ERROR TRADEOFF CHARACTERISTIC: MUGSHOT IMAGES . . . 943
781 ERROR TRADEOFF CHARACTERISTIC: MUGSHOT IMAGES . . . 944
782 EFFECT OF SUBJECT AGE ON FNMR . . . 946
783 EFFECT OF SUBJECT AGE ON FNMR . . . 947
784 EFFECT OF SUBJECT AGE ON FNMR . . . 948
785 EFFECT OF SUBJECT AGE ON FNMR . . . 949
786 EFFECT OF SUBJECT AGE ON FNMR . . . 950
787 EFFECT OF SUBJECT AGE ON FNMR . . . 951
788 EFFECT OF SUBJECT AGE ON FNMR . . . 952
789 EFFECT OF SUBJECT AGE ON FNMR . . . 953
790 EFFECT OF SUBJECT AGE ON FNMR . . . 954
791 EFFECT OF SUBJECT AGE ON FNMR . . . 955
792 EFFECT OF SUBJECT AGE ON FNMR . . . 956
793 EFFECT OF SUBJECT AGE ON FNMR . . . 957
794 EFFECT OF SUBJECT AGE ON FNMR . . . 958
795 EFFECT OF SUBJECT AGE ON FNMR . . . 959
796 EFFECT OF SUBJECT AGE ON FNMR . . . 960
797 EFFECT OF SUBJECT AGE ON FNMR . . . 961
798 EFFECT OF SUBJECT AGE ON FNMR . . . 962
799 EFFECT OF SUBJECT AGE ON FNMR . . . 963
800 EFFECT OF SUBJECT AGE ON FNMR . . . 964
801 EFFECT OF SUBJECT AGE ON FNMR . . . 965
802 EFFECT OF SUBJECT AGE ON FNMR . . . 966
803 EFFECT OF SUBJECT AGE ON FNMR . . . 967
804 EFFECT OF SUBJECT AGE ON FNMR . . . 968

FNMR(T) "False non-match rate"
FMR(T) "False match rate"

805 EFFECT OF SUBJECT AGE ON FNMR . . . 969
806 EFFECT OF SUBJECT AGE ON FNMR . . . 970
807 EFFECT OF SUBJECT AGE ON FNMR . . . 971
808 EFFECT OF SUBJECT AGE ON FNMR . . . 972
809 EFFECT OF SUBJECT AGE ON FNMR . . . 973
810 EFFECT OF SUBJECT AGE ON FNMR . . . 974
811 EFFECT OF SUBJECT AGE ON FNMR . . . 975
812 EFFECT OF SUBJECT AGE ON FNMR . . . 976
813 EFFECT OF SUBJECT AGE ON FNMR . . . 977
814 EFFECT OF SUBJECT AGE ON FNMR . . . 978
815 EFFECT OF SUBJECT AGE ON FNMR . . . 979
816 EFFECT OF SUBJECT AGE ON FNMR . . . 980
817 EFFECT OF SUBJECT AGE ON FNMR . . . 981
818 EFFECT OF SUBJECT AGE ON FNMR . . . 982
819 EFFECT OF SUBJECT AGE ON FNMR . . . 983
820 EFFECT OF SUBJECT AGE ON FNMR . . . 984
821 EFFECT OF SUBJECT AGE ON FNMR . . . 985
822 EFFECT OF SUBJECT AGE ON FNMR . . . 986
823 EFFECT OF SUBJECT AGE ON FNMR . . . 987
824 EFFECT OF SUBJECT AGE ON FNMR . . . 988
825 EFFECT OF SUBJECT AGE ON FNMR . . . 989
826 EFFECT OF SUBJECT AGE ON FNMR . . . 990
827 EFFECT OF SUBJECT AGE ON FNMR . . . 991
828 EFFECT OF SUBJECT AGE ON FNMR . . . 992
829 EFFECT OF SUBJECT AGE ON FNMR . . . 993
830 EFFECT OF SUBJECT AGE ON FNMR . . . 994
831 EFFECT OF SUBJECT AGE ON FNMR . . . 995
832 EFFECT OF SUBJECT AGE ON FNMR . . . 996
833 EFFECT OF SUBJECT AGE ON FNMR . . . 997
834 EFFECT OF SUBJECT AGE ON FNMR . . . 998
835 EFFECT OF SUBJECT AGE ON FNMR . . . 999
836 EFFECT OF SUBJECT AGE ON FNMR . . . 1000
837 EFFECT OF SUBJECT AGE ON FNMR . . . 1001
838 EFFECT OF SUBJECT AGE ON FNMR . . . 1002
839 EFFECT OF SUBJECT AGE ON FNMR . . . 1003
840 EFFECT OF SUBJECT AGE ON FNMR . . . 1004
841 EFFECT OF SUBJECT AGE ON FNMR . . . 1005
842 EFFECT OF SUBJECT AGE ON FNMR . . . 1006
843 EFFECT OF SUBJECT AGE ON FNMR . . . 1007
844 EFFECT OF SUBJECT AGE ON FNMR . . . 1008
845 EFFECT OF SUBJECT AGE ON FNMR . . . 1009
846 EFFECT OF SUBJECT AGE ON FNMR . . . 1010
847 EFFECT OF SUBJECT AGE ON FNMR . . . 1011
848 EFFECT OF SUBJECT AGE ON FNMR . . . 1012
849 EFFECT OF SUBJECT AGE ON FNMR . . . 1013
850 EFFECT OF SUBJECT AGE ON FNMR . . . 1014
851 EFFECT OF SUBJECT AGE ON FNMR . . . 1015
852 EFFECT OF SUBJECT AGE ON FNMR . . . 1016
853 EFFECT OF SUBJECT AGE ON FNMR . . . 1017
854 EFFECT OF SUBJECT AGE ON FNMR . . . 1018
855 EFFECT OF SUBJECT AGE ON FNMR . . . 1019

FNMR(T) "False non-match rate"
FMR(T) "False match rate"

856 EFFECT OF SUBJECT AGE ON FNMR . . . 1020
857 EFFECT OF SUBJECT AGE ON FNMR . . . 1021
858 EFFECT OF SUBJECT AGE ON FNMR . . . 1022
859 EFFECT OF SUBJECT AGE ON FNMR . . . 1023
860 EFFECT OF SUBJECT AGE ON FNMR . . . 1024
861 EFFECT OF SUBJECT AGE ON FNMR . . . 1025
862 EFFECT OF SUBJECT AGE ON FNMR . . . 1026
863 EFFECT OF SUBJECT AGE ON FNMR . . . 1027
864 EFFECT OF SUBJECT AGE ON FNMR . . . 1028
865 EFFECT OF SUBJECT AGE ON FNMR . . . 1029
866 EFFECT OF SUBJECT AGE ON FNMR . . . 1030
867 EFFECT OF SUBJECT AGE ON FNMR . . . 1031
868 EFFECT OF SUBJECT AGE ON FNMR . . . 1032
869 EFFECT OF SUBJECT AGE ON FNMR . . . 1033
870 EFFECT OF SUBJECT AGE ON FNMR . . . 1034
871 EFFECT OF SUBJECT AGE ON FNMR . . . 1035
872 EFFECT OF SUBJECT AGE ON FNMR . . . 1036
873 IMPOSTOR COUNTS FOR CROSS COUNTRY FMR CALCULATIONS . . . 1040

FNMR(T) "False non-match rate"
FMR(T) "False match rate"

	Location	Developer Name	Short Name	Seq. Num.	Validation Date
1	KR	Urielsoft Co. Ltd	urielsoft-000	000	2025-06-30
2	EE	2060.io	2060io-001	001	2025-01-22
3	EE	2060.io	2060io-002	002	2025-07-23
4	NL	20Face	20face-000	000	2021-04-12
5	NL	20Face	20face-001	001	2021-09-29
6	US	3Divi	3divi-000	000	2017-03-16
7	US	3Divi	3divi-001	001	2017-06-22
8	US	3Divi	3divi-002	002	2017-10-20
9	US	3Divi	3divi-003	003	2018-10-09
10	US	3Divi	3divi-004	004	2019-07-22
11	US	3Divi	3divi-005	005	2020-08-28
12	US	3Divi	3divi-006	006	2021-04-14
13	US	3Divi	3divi-007	007	2021-09-27
14	TH	ACI Software	acisw-003	003	2020-08-03
15	TH	ACI Software	acisw-006	006	2021-02-25
16	TH	ACI Software	acisw-007	007	2021-11-15
17	TH	ACI Software	acisw-008	008	2022-03-22
18	US	AFIS and Biometrics Consulting	afisbiometrics-000	000	2022-01-27
19	US	AFR Engine	afrengine-000	000	2022-09-29
20	US	AFR Engine	afrengine-001	001	2023-01-26
21	US	AFR Engine	afrengine-002	002	2023-06-27
22	US	AFR Engine	afrengine-003	003	2024-03-15
23	US	AFR Engine	afrengine-004	004	2024-07-22
24	US	AFR Engine	afrengine-005	005	2025-02-18
25	UZ	AI Implementation Group	aigroup-000	000	2024-07-17
26	UZ	AI Implementation Group	aigroup-001	001	2025-02-18
27	UZ	AI Implementation Group	aigroup-002	002	2026-03-12
28	VN	ALTTEKGlobal	alttekglobal-000	000	2024-04-12
29	TW	ASUSTek Computer Inc	asusaics-000	000	2019-10-24
30	TW	ASUSTek Computer Inc	asusaics-001	001	2020-02-25
31	CN	AYF Technology	ayftech-001	001	2020-07-06
32	CN	AYF Technology	ayftech-003	003	2023-05-15
33	TW	Ability Enterprise - Andro Video	androvideo-000	000	2021-01-25
34	IN	Accurascan	accurascan-001	001	2023-0-15
35	IN	Accurascan	accurascan-002	002	2023-08-01
36	IN	Accurascan	accurascan-003	003	2023-12-06
37	TW	Acer Incorporated	acer-000	000	2020-01-08
38	TW	Acer Incorporated	acer-001	001	2020-06-30
39	TW	Acer Incorporated	acer-002	002	2021-11-10
40	SG	Adera Global PTE	adera-001	001	2019-06-17
41	SG	Adera Global PTE	adera-002	002	2021-02-16
42	SG	Adera Global PTE	adera-003	003	2021-07-12
43	SG	Adera Global PTE	adera-004	004	2022-11-14
44	SG	Adera Global PTE	adera-005	005	2023-11-17
45	SG	Advance.AI	advance-002	002	2019-12-19
46	SG	Advance.AI	advance-003	003	2021-08-05
47	SG	Advance.AI	advance-004	004	2022-09-06
48	SG	Advance.AI	advance-005	005	2023-05-25
49	SG	Advance.AI	advance-006	006	2026-04-03
50	AE	Affinsys AI Ltd	affinsys-ai-000	000	2024-07-11
51	TH	Ai First	aifirst-001	001	2019-11-21
52	TW	AiUnion Technology	aiunionface-000	000	2019-10-22
53	TH	Aigen	aigen-001	001	2020-10-06
54	TH	Aigen	aigen-002	002	2021-03-15
55	CN	Aiseemu Technology	aiseemu-001	001	2022-06-16
56	CN	Aiseemu Technology	aiseemu-002	002	2022-11-18
57	KR	Ajou University	ajou-001	001	2021-03-08
58	ID	Akurat Satu Indonesia	ptakuratsatu-000	000	2020-09-11
59	KR	Alchera Inc	alchera-000	000	2019-03-01
60	KR	Alchera Inc	alchera-001	001	2019-03-01
61	KR	Alchera Inc	alchera-002	002	2021-03-05
62	KR	Alchera Inc	alchera-003	003	2021-07-13
63	KR	Alchera Inc	alchera-004	004	2022-08-12
64	KR	Alchera Inc	alchera-005	005	2023-01-04
65	KR	Alchera Inc	alchera-006	006	2023-07-18
66	KR	Alchera Inc	alchera-007	007	2023-11-22
67	KR	Alchera Inc	alchera-008	008	2024-06-17
68	KR	Alchera Inc	alchera-009	009	2024-11-14
69	ID	Alfabeta	alfabeta-001	001	2021-12-02
70	ES	Alice Biometrics	alice-000	000	2021-06-15

Table 1: Summary of participant information included in this report.

FNMR(T) "False non-match rate"
FMR(T) "False match rate"

	Location	Developer Name	Short Name	Seq. Num.	Validation Date
71	ES	Alice Biometrics	alice-001	001	2023-07-05
72	RU	Alivia / Innovation Sys	isystems-000	000	2018-01-11
73	RU	Alivia / Innovation Sys	isystems-001	001	2018-06-12
74	RU	Alivia / Innovation Sys	isystems-002	002	2018-10-18
75	IN	AllGoVision	allgovision-000	000	2019-03-01
76	CN	AlphaSSTG	alphaface-001	001	2019-09-03
77	CN	AlphaSSTG	alphaface-002	002	2020-02-20
78	GB	Amplified Group	amplifiedgroup-001	001	2019-03-01
79	CN	Anke Investments	anke-000	000	2018-06-26
80	CN	Anke Investments	anke-001	001	2018-06-26
81	CN	Anke Investments	anke-002	002	2018-10-19
82	CN	Anke Investments	anke-003	003	2019-02-27
83	CN	Anke Investments	anke-004	004	2019-06-27
84	CN	Anke Investments	anke-005	005	2019-11-21
85	BR	Antheus Technologia	antheus-000	000	2019-12-05
86	BR	Antheus Technologia	antheus-001	001	2020-06-25
87	BR	Antheus Technologia	antheus-002	002	2024-07-15
88	GB	AnyVision	anyvision-001	001	2018-01-31
89	GB	AnyVision	anyvision-002	002	2018-01-31
90	GB	AnyVision	anyvision-004	004	2018-06-15
91	GB	AnyVision	anyvision-005	005	2021-02-03
92	TR	ArVIs Teknoloji San.Tic.A.Ş.	arvis-000	000	2025-04-08
93	CN	Aratek Biometrics Co Ltd	aratek-001	001	2023-03-27
94	US	Armatura LLC	armatura-001	001	2022-01-04
95	US	Armatura LLC	armatura-002	002	2022-09-16
96	US	Armatura LLC	armatura-003	003	2023-01-13
97	CN	AuthenMetric	authenmetric-002	002	2021-03-10
98	CN	AuthenMetric	authenmetric-003	003	2021-08-09
99	CN	AuthenMetric	authenmetric-004	004	2022-01-03
100	TW	Authme	authme-001	001	2023-10-17
101	TW	Authme	authme-002	002	2025-02-10
102	US	Aware	aware-000	000	2017-10-27
103	US	Aware	aware-001	001	2017-10-27
104	US	Aware	aware-002	002	2018-06-15
105	US	Aware	aware-003	003	2018-10-19
106	US	Aware	aware-004	004	2019-03-01
107	US	Aware	aware-005	005	2020-02-27
108	US	Aware	aware-006	006	2021-07-03
109	US	Aware	aware-007	007	2023-11-15
110	US	Aware	aware-008	008	2024-03-15
111	IN	Awidit Systems	awiros-001	001	2019-09-23
112	IN	Awidit Systems	awiros-002	002	2020-10-28
113	IN	Awidit Systems	awiros-003	003	2024-11-01
114	IN	Awidit Systems	awiros-004	004	2025-03-31
115	CH	Aximetria	aximetria-001	001	2022-08-10
116	JP	Ayonix	ayonix-000	000	2017-06-22
117	CN	BOE Technology Group	boetech-001	001	2021-06-22
118	CN	BOE Technology Group	boetech-002	002	2021-12-21
119	KZ	BTS Digital	btsdigital-001	001	2025-07-31
120	ES	Bee the Data	beethedata-000	000	2021-07-26
121	CN	Beihang University-ERCACAT	ercacat-001	001	2020-07-06
122	CN	Beijing Alleyes Technology	alleyes-000	000	2020-03-09
123	CN	Beijing DeepSense Technologies	deepsense-000	000	2021-03-19
124	CN	Beijing DeepSense Technologies	deepsense-001	001	2022-03-11
125	CN	Beijing DeepSense Technologies	deepsense-002	002	2023-02-22
126	CN	Beijing DeepSense Technologies	deepsense-003	003	2023-10-23
127	CN	Beijing DeepSense Technologies	deepsense-004	004	2024-06-21
128	CN	Beijing DeepSense Technologies	deepsense-005	005	2024-10-28
129	CN	Beijing DeepSense Technologies	deepsense-006	006	2025-03-07
130	CN	Beijing DeepSense Technologies	deepsense-007	007	2025-07-08
131	CN	Beijing DeepSense Technologies	deepsense-008	008	2026-01-13
132	CN	Beijing Hisign Technology	hisign-001	001	2021-09-24
133	CN	Beijing Hisign Technology	hisign-002	002	2022-09-09
134	CN	Beijing Hisign Technology	hisign-003	003	2024-03-15
135	CN	Beijing Mendaxia Technology	mendaxiatech-000	000	2021-09-15
136	CN	Beijing Vion Technology Inc	vion-000	000	2018-10-19
137	DE	Betaface	betaface-000	000	2018-05-29
138	DE	Betaface	betaface-002	002	2018-05-29
139	KZ	Beyne.AI	beyneai-000	000	2022-01-03
140	DE	BioID GmbH	bioid-001	001	2024-11-13

Table 2: Summary of participant information included in this report.

	Location	Developer Name	Short Name	Seq. Num.	Validation Date
141	DE	BioID GmbH	bioid-002	002	2025-04-25
142	DE	BioID GmbH	bioid-003	003	2025-11-26
143	DE	BioID GmbH	bioid-004	004	2026-04-13
144	CH	BioID Technologies SA	bioidtechswiss-000	000	2019-11-15
145	CH	BioID Technologies SA	bioidtechswiss-001	001	2020-08-28
146	CH	BioID Technologies SA	bioidtechswiss-002	002	2021-02-17
147	CH	BioID Technologies SA	bioidtechswiss-003	003	2025-03-12
148	IN	Biocube Matrics	biocube-001	001	2021-09-08
149	IN	Biocube Matrics	biocube-002	002	2023-02-09
150	KZ	Biometric LLC	biometric-vision-000	000	2023-01-25
151	IN	Biometrik Systems Private Limited	biometrik-001	001	2025-09-18
152	IN	Biometrik Systems Private Limited	biometrik-002	002	2026-01-20
153	UK	BitCenter UK	farfaces-001	001	2021-04-09
154	CN	Bitmain	bm-001	001	2018-10-17
155	CN	Bresee Technology	bresee-000	000	2020-08-07
156	CN	Bresee Technology	bresee-001	001	2020-12-30
157	CN	Bresee Technology	bresee-002	002	2021-06-30
158	VN	CAKE by VPBank	cakevn-001	001	2026-01-12
159	VN	CMC Institute of Science and Technology	cist-001	001	2022-10-20
160	VN	CMC Institute of Science and Technology	cist-002	002	2023-02-09
161	VN	CMC Institute of Science and Technology	cist-003	003	2023-08-14
162	VN	CMC Institute of Science and Technology	cist-004	004	2024-02-15
163	VN	CMC Univerisity	cmcuni-001	001	2023-12-05
164	CN	CSA IntelliCloud Technology	intellicloudai-001	001	2019-08-13
165	CN	CSA IntelliCloud Technology	intellicloudai-002	002	2020-12-17
166	TW	CTBC Bank	ctbcbank-000	000	2019-06-28
167	TW	CTBC Bank	ctbcbank-001	001	2019-10-28
168	TW	CTBC Bank	ctbcbank-002	002	2024-07-10
169	KR	CUDO Communication	cudocommunication-001	001	2021-10-20
170	US	Camvi Technologies	camvi-001	001	2017-09-13
171	US	Camvi Technologies	camvi-002	002	2018-10-19
172	US	Camvi Technologies	camvi-003	003	2019-03-01
173	US	Camvi Technologies	camvi-004	004	2019-07-12
174	FI	Candour Biometrics	candour-001	001	2023-02-10
175	FI	Candour Biometrics	candour-002	002	2024-03-07
176	FI	Candour Biometrics	candour-003	003	2024-10-23
177	FI	Candour Biometrics	candour-004	004	2026-01-08
178	CN	Canon Inc	canon-002	002	2020-12-29
179	JP	Canon Inc	canon-003	003	2021-09-15
180	JP	Canon Inc	canon-004	004	2022-04-25
181	JP	Canon Inc	canon-005	005	2023-09-05
182	CN	Canon Inc	cib-000	000	2019-12-11
183	CN	Canon Inc	cib-001	001	2020-08-05
184	BD	Celloscope Limited	celloscope-001	001	2024-07-15
185	CN	China Electronics Import-Export Corp	ceiec-001	001	2019-03-01
186	CN	China Electronics Import-Export Corp	ceiec-002	002	2019-06-12
187	CN	China Electronics Import-Export Corp	ceiec-003	003	2020-01-06
188	CN	China Electronics Import-Export Corp	ceiec-004	004	2021-01-18
189	CN	China University of Petroleum	upc-001	001	2019-06-05
190	CN	Chinese University of Hong Kong	cuhkee-001	001	2020-03-18
191	KR	Chosun University	chosun-000	000	2020-02-12
192	KR	Chosun University	chosun-001	001	2020-07-01
193	KR	Chosun University	chosun-002	002	2020-11-25
194	TW	Chunghwa Telecom	chtface-001	001	2019-08-06
195	TW	Chunghwa Telecom	chtface-002	002	2019-12-07
196	TW	Chunghwa Telecom	chtface-003	003	2020-06-24
197	TW	Chunghwa Telecom	chtface-004	004	2021-10-08
198	TW	Chunghwa Telecom	chtface-005	005	2022-03-09
199	TW	Chunghwa Telecom	chtface-006	006	2022-11-03
200	TW	Chunghwa Telecom	chtface-007	007	2024-04-23
201	TW	Chunghwa Telecom	chtface-008	008	2024-09-27
202	TW	Chunghwa Telecom	chtface-009	009	2025-10-21
203	US	City and County of Honolulu	cchonolulu-000	000	2023-03-27
204	US	City and County of Honolulu	cchonolulu-001	001	2024-01-18
205	US	Clearview AI Inc	clearviewai-000	000	2021-09-22
206	US	Clearview AI Inc	clearviewai-001	001	2023-12-05
207	US	Clearview AI Inc	clearviewai-002	002	2024-05-22
208	US	Clearview AI Inc	clearviewai-003	003	2026-01-09
209	CN	Closeli Inc	closeli-001	001	2021-07-15
210	US	CloudSmart Consulting LLC	csc-001	001	2020-11-20

Table 3: Summary of participant information included in this report.

	Location	Developer Name	Short Name	Seq. Num.	Validation Date
211	US	CloudSmart Consulting LLC	csc-002	002	2021-03-24
212	US	CloudSmart Consulting LLC	csc-003	003	2021-08-26
213	TW	Cloudmatrix	cloudmatrix-000	000	2021-10-22
214	TW	Cloudmatrix	cloudmatrix-001	001	2022-02-16
215	TW	Cloudmatrix	cloudmatrix-002	002	2022-10-17
216	CN	Cloudwalk - Hengrui AI Technology	cloudwalk-hr-000	000	2019-03-01
217	CN	Cloudwalk - Hengrui AI Technology	cloudwalk-hr-001	001	2019-06-04
218	CN	Cloudwalk - Hengrui AI Technology	cloudwalk-hr-002	002	2019-10-08
219	CN	Cloudwalk - Hengrui AI Technology	cloudwalk-hr-003	003	2020-09-25
220	CN	Cloudwalk - Hengrui AI Technology	cloudwalk-hr-004	004	2021-02-10
221	CN	Cloudwalk - Moontime Smart Technology	cloudwalk-mt-000	000	2019-06-03
222	CN	Cloudwalk - Moontime Smart Technology	cloudwalk-mt-002	002	2020-07-02
223	CN	Cloudwalk - Moontime Smart Technology	cloudwalk-mt-003	003	2020-12-22
224	CN	Cloudwalk - Moontime Smart Technology	cloudwalk-mt-004	004	2021-11-09
225	CN	Cloudwalk - Moontime Smart Technology	cloudwalk-mt-005	005	2022-03-29
226	CN	Cloudwalk - Moontime Smart Technology	cloudwalk-mt-006	006	2022-10-20
227	CN	Cloudwalk - Moontime Smart Technology	cloudwalk-mt-007	007	2023-02-21
228	IN	Code Everest Pvt	facex-001	001	2021-03-08
229	IN	Code Everest Pvt	facex-002	002	2021-08-24
230	KR	Codeline	codeline-000	000	2022-09-13
231	DE	Cognitec Systems GmbH	cognitec-000	000	2018-10-19
232	DE	Cognitec Systems GmbH	cognitec-001	001	2019-03-01
233	DE	Cognitec Systems GmbH	cognitec-002	002	2021-02-24
234	DE	Cognitec Systems GmbH	cognitec-003	003	2021-07-30
235	DE	Cognitec Systems GmbH	cognitec-004	004	2022-02-10
236	DE	Cognitec Systems GmbH	cognitec-005	005	2023-12-01
237	DE	Cognitec Systems GmbH	cognitec-006	006	2024-04-29
238	DE	Cognitec Systems GmbH	cognitec-007	007	2024-08-29
239	TW	Compal Electronics	compal-000	000	2025-03-20
240	TW	Compal Electronics	compal-001	001	2025-12-08
241	TW	Coretech Knowledge Inc	coretech-000	000	2021-07-12
242	TW	Coretech Knowledge Inc	coretech-001	001	2022-09-29
243	TW	Coretech Knowledge Inc	coretech-002	002	2023-11-02
244	TW	Coretech Knowledge Inc	coretech-003	003	2024-08-07
245	TW	Coretech Knowledge Inc	coretech-004	004	2024-12-23
246	IL	Corsight	corsight-001	001	2021-03-11
247	IL	Corsight	corsight-002	002	2021-09-01
248	IL	Corsight	corsight-003	003	2022-06-09
249	IL	Cortica	cor-001	001	2020-09-24
250	TW	Cu-Face	cu-face-002	002	2023-01-05
251	TW	Cu-Face	cu-face-003	003	2023-08-28
252	TW	Cu-Face	cu-face-004	004	2024-03-13
253	KR	Cubox	cubox-001	001	2020-12-07
254	KR	Cubox	cubox-002	002	2021-08-24
255	KR	Cubox	cubox-003	003	2023-03-07
256	KR	Cubox	cubox-004	004	2024-12-05
257	KR	Cubox	cubox-005	005	2025-05-14
258	JP	Cybercore	cybercore-000	000	2020-08-26
259	JP	Cybercore	cybercore-001	001	2021-12-15
260	JP	Cybercore	cybercore-002	002	2022-04-25
261	JP	Cybercore	cybercore-003	003	2022-08-31
262	US	Cyberextruder	cyberextruder-001	001	2017-08-02
263	US	Cyberextruder	cyberextruder-002	002	2018-01-30
264	US	Cyberextruder	cyberextruder-003	003	2022-03-16
265	US	Cyberextruder	cyberextruder-004	004	2022-07-20
266	US	Cyberextruder	cyberextruder-005	005	2024-10-01
267	US	Cyberextruder	cyberextruder-006	006	2025-03-19
268	TW	Cyberlink Corp	cyberlink-000	000	2019-03-01
269	TW	Cyberlink Corp	cyberlink-001	001	2019-03-01
270	TW	Cyberlink Corp	cyberlink-002	002	2019-06-12
271	TW	Cyberlink Corp	cyberlink-003	003	2019-10-07
272	TW	Cyberlink Corp	cyberlink-004	004	2020-02-27
273	TW	Cyberlink Corp	cyberlink-005	005	2020-07-31
274	TW	Cyberlink Corp	cyberlink-006	006	2021-01-08
275	TW	Cyberlink Corp	cyberlink-007	007	2021-07-16
276	TW	Cyberlink Corp	cyberlink-008	008	2022-01-07
277	TW	Cyberlink Corp	cyberlink-009	009	2022-05-12
278	TW	Cyberlink Corp	cyberlink-010	010	2022-09-16
279	TW	Cyberlink Corp	cyberlink-011	011	2023-01-30
280	TW	Cyberlink Corp	cyberlink-012	012	2023-06-02

Table 4: Summary of participant information included in this report.

FNMR(T) "False non-match rate"
FMR(T) "False match rate"

	Location	Developer Name	Short Name	Seq. Num.	Validation Date
281	TW	Cyberlink Corp	cyberlink-013	013	2023-12-15
282	TW	Cyberlink Corp	cyberlink-014	014	2024-05-23
283	TW	Cyberlink Corp	cyberlink-015	015	2024-09-26
284	MX	DICIO	dicio-001	001	2022-03-22
285	MX	DICIO	dicio-002	002	2024-10-03
286	CN	DSK	dsk-000	000	2019-06-28
287	VN	Dactionable Technologies	datech-000	000	2023-10-16
288	VN	Dactionable Technologies	datech-001	001	2024-02-21
289	VN	Dactionable Technologies	datech-002	002	2024-09-11
290	CN	Dahua Technology	dahua-000	000	2018-10-19
291	CN	Dahua Technology	dahua-001	001	2018-10-19
292	CN	Dahua Technology	dahua-002	002	2019-03-01
293	CN	Dahua Technology	dahua-003	003	2019-08-14
294	CN	Dahua Technology	dahua-004	004	2019-12-18
295	CN	Dahua Technology	dahua-005	005	2020-08-13
296	CN	Dahua Technology	dahua-006	006	2020-12-30
297	CN	Dahua Technology	dahua-007	007	2021-12-20
298	IE	Daon	daon-000	000	2021-11-03
299	IE	Daon	daon-001	001	2024-09-26
300	IE	Daon	daon-002	002	2025-07-01
301	IE	Daon	daon-003	003	2026-03-12
302	TW	DeCloak Intellegences	decloakface-001	001	2023-06-13
303	TW	DeCloak Intellegences	decloakface-002	002	2024-10-28
304	US	Decatur Industries Inc	decatur-000	000	2020-08-18
305	US	Decatur Industries Inc	decatur-001	001	2021-09-27
306	CN	Deepglint	deepglint-001	001	2019-06-21
307	CN	Deepglint	deepglint-002	002	2019-11-15
308	CN	Deepglint	deepglint-003	003	2021-03-03
309	CN	Deepglint	deepglint-004	004	2021-09-17
310	CN	Deepglint	deepglint-005	005	2022-10-17
311	FR	Deepsense	dps-000	000	2021-07-16
312	DE	Dermalog	dermalog-001	001	2017-02-22
313	DE	Dermalog	dermalog-002	002	2017-02-22
314	DE	Dermalog	dermalog-003	003	2017-07-10
315	DE	Dermalog	dermalog-004	004	2017-10-26
316	DE	Dermalog	dermalog-005	005	2018-02-02
317	DE	Dermalog	dermalog-006	006	2018-10-18
318	DE	Dermalog	dermalog-007	007	2020-11-25
319	DE	Dermalog	dermalog-008	008	2021-03-25
320	DE	Dermalog	dermalog-009	009	2021-10-06
321	DE	Dermalog	dermalog-010	010	2022-07-25
322	DE	Dermalog	dermalog-011	011	2022-12-12
323	DE	Dermalog	dermalog-012	012	2024-01-19
324	DE	Dermalog	dermalog-013	013	2024-06-18
325	DE	Dermalog	dermalog-014	014	2025-06-17
326	DE	Dermalog	dermalog-015	015	2025-11-26
327	CN	DiDi ChuXing Technology	didiglobalface-001	001	2019-10-23
328	CN	DiDi ChuXing Technology	didiglobalface-002	002	2023-01-09
329	CN	DiDi ChuXing Technology	didiglobalface-003	003	2025-05-01
330	IN	Digidata	digidata-000	000	2022-01-27
331	IN	Digidata	digidata-001	001	2022-06-10
332	GB	Digital Barriers	digitalbarriers-000	000	2017-05-31
333	GB	Digital Barriers	digitalbarriers-001	001	2017-07-20
334	GB	Digital Barriers	digitalbarriers-002	002	2019-03-01
335	UY	Dralmey Solutions	dralmey-001	001	2026-03-27
336	IN	EI Networks Private Ltd	einetworksindia-000	000	2023-05-03
337	IN	EI Networks Private Ltd	einetworksindia-001	001	2023-09-05
338	IN	EI Networks Private Ltd	einetworksindia-002	002	2025-02-21
339	TR	Ekin Smart City Technologies	ekin-002	002	2021-05-04
340	TH	Element System Solutions Company Ltd	element-000	000	2023-11-14
341	AE	Enface	enface-000	000	2021-04-09
342	AE	Enface	enface-001	001	2021-12-17
343	AE	Enface	enface-002	002	2023-02-27
344	GB	Enqura Ltd	enqura-001	001	2024-09-25
345	ET	Ethiopian Labor Market Information System	ethiopianlmis-000	000	2026-03-18
346	CH	Euronovate SA	euronovate-001	001	2021-11-15
347	CH	Euronovate SA	euronovate-002	002	2023-06-28
348	CH	Euronovate SA	euronovate-003	003	2023-09-19
349	CH	Euronovate SA	euronovate-004	004	2024-01-19
350	RU	Expasoft LLC	expasoft-000	000	2020-01-06

Table 5: Summary of participant information included in this report.

	Location	Developer Name	Short Name	Seq. Num.	Validation Date
351	RU	Expasoft LLC	expasoft-001	001	2020-09-03
352	RU	Expasoft LLC	expasoft-002	002	2021-07-26
353	VN	FCI Vietnam	fci-000	000	2025-04-01
354	LB	FOO	foomobi-001	001	2023-03-13
355	LB	FOO	foomobi-002	002	2023-08-07
356	VN	FPT Education	fedu-001	001	2024-03-15
357	VN	FPT Information System	fpt-000	000	2024-02-26
358	VN	FPT Information System	fpt-001	001	2024-09-16
359	VN	FPT Telecom JSC	fpttelecom-000	000	2026-02-03
360	US	FRP LLC	frpkauai-001	001	2022-07-18
361	US	FRP LLC	frpkauai-002	002	2022-11-21
362	US	FRP LLC	frpkauai-003	003	2024-05-30
363	US	FRP LLC	frpkauai-004	004	2025-03-25
364	IL	Face Int	faceint-001	001	2026-03-27
365	CA	FaceLocate	facelocate-001	001	2024-02-22
366	CA	FaceLocate	facelocate-002	002	2026-03-25
367	DE	FaceOnLive Inc	faceonlive-001	001	2021-11-23
368	DE	FaceOnLive Inc	faceonlive-002	002	2022-04-11
369	DE	FaceOnLive Inc	faceonlive-003	003	2024-08-12
370	ES	FacePhi	facephi-000	000	2022-04-06
371	ES	FacePhi	facephi-001	001	2024-05-24
372	ES	FacePhi	facephi-002	002	2025-02-11
373	GB	FaceSoft	facesoft-000	000	2019-07-10
374	KR	FaceTag Co	facetag-000	000	2021-03-22
375	KR	FaceTag Co	facetag-001	001	2021-08-17
376	KR	FaceTag Co	facetag-002	002	2022-01-06
377	UK	Facehawk Ltd	facehawk-000	000	2023-08-22
378	UK	Facia.ai	facia-001	001	2023-07-21
379	UK	Facia.ai	facia-002	002	2024-06-21
380	UK	FaiceTech Ltd	faicetech-000	000	2025-03-11
381	TW	FarBar Inc	f8-001	001	2019-07-11
382	TW	FarBar Inc	f8-002	002	2022-03-02
383	US	Fast Enterprises	fastenterprises-000	000	2023-03-01
384	CN	Fiberhome Telecommunication Technologies	fiberhome-nanjing-002	002	2020-08-10
385	CN	Fiberhome Telecommunication Technologies	fiberhome-nanjing-003	003	2021-03-12
386	CN	Fiberhome Telecommunication Technologies	fiberhome-nanjing-004	004	2021-09-14
387	UK	Fincore Ltd	fincore-000	000	2021-06-07
388	KZ	First Credit Bureau Kazakhstan	firstcreditkz-001	001	2022-08-22
389	KZ	First Credit Bureau Kazakhstan	firstcreditkz-002	002	2023-02-21
390	KZ	First Credit Bureau Kazakhstan	firstcreditkz-003	003	2024-02-20
391	KZ	First Credit Bureau Kazakhstan	firstcreditkz-004	004	2024-10-02
392	NL	Fourthline	fourthlinecom-001	001	2024-04-15
393	UK	Fraud.com	fraudcom-000	000	2023-12-01
394	CN	Fudan University	fdu-000	000	2017-11-22
395	CN	Fudan University	fdu-001	001	2018-01-11
396	CN	Fujitsu Research and Development Center	fujitsulab-000	000	2020-02-04
397	CN	Fujitsu Research and Development Center	fujitsulab-001	001	2020-09-30
398	CN	Fujitsu Research and Development Center	fujitsulab-002	002	2021-02-24
399	CN	Fujitsu Research and Development Center	fujitsulab-003	003	2021-07-12
400	VN	GPS Vietnam Trading	gpstechvn-000	000	2024-01-02
401	VN	GTEL OTS JSC	gtelots-000	000	2025-04-14
402	VN	GTEL OTS JSC	gtelots-001	001	2026-02-02
403	US	Gemalto Cogent	cogent-000	000	2018-01-12
404	US	Gemalto Cogent	cogent-001	001	2018-05-29
405	US	Gemalto Cogent	cogent-002	002	2018-10-19
406	US	Gemalto Cogent	cogent-003	003	2019-03-01
407	US	Gemalto Cogent	cogent-004	004	2019-06-14
408	US	Gemalto Cogent	cogent-005	005	2020-12-29
409	US	Gemalto Cogent	cogent-006	006	2021-07-28
410	US	Gemalto Cogent	cogent-007	007	2022-04-11
411	US	Gemalto Cogent	cogent-008	008	2023-01-03
412	TW	General Interface Solutions Holding Ltd	gistouch-000	000	2023-05-08
413	TW	General Interface Solutions Holding Ltd	gistouch-001	001	2023-11-09
414	TW	GeoVision Inc	geo-000	000	2020-06-29
415	TW	GeoVision Inc	geo-001	001	2020-10-30
416	TW	GeoVision Inc	geo-002	002	2021-04-01
417	TW	GeoVision Inc	geo-003	003	2021-09-15
418	TW	GeoVision Inc	geo-004	004	2022-02-10
419	JP	Glory	glory-000	000	2018-06-06
420	JP	Glory	glory-001	001	2018-06-08

Table 6: Summary of participant information included in this report.

FNMR(T) "False non-match rate"
FMR(T) "False match rate"

	Location	Developer Name	Short Name	Seq. Num.	Validation Date
421	JP	Glory	glory-002	002	2019-11-12
422	JP	Glory	glory-003	003	2021-01-15
423	JP	Glory	glory-004	004	2022-02-08
424	JP	Glory	glory-005	005	2022-07-08
425	JP	Glory	glory-006	006	2023-03-23
426	JP	Glory	glory-007	007	2023-11-10
427	TW	Gorilla Technology	gorilla-000	000	2018-02-13
428	TW	Gorilla Technology	gorilla-001	001	2018-05-25
429	TW	Gorilla Technology	gorilla-002	002	2018-10-17
430	TW	Gorilla Technology	gorilla-003	003	2019-06-19
431	TW	Gorilla Technology	gorilla-004	004	2019-11-04
432	TW	Gorilla Technology	gorilla-005	005	2020-03-11
433	TW	Gorilla Technology	gorilla-006	006	2020-07-31
434	TW	Gorilla Technology	gorilla-007	007	2021-06-28
435	TW	Gorilla Technology	gorilla-008	008	2021-11-08
436	TW	Gorilla Technology	gorilla-009	009	2022-12-14
437	US	Graymatics	graymatics-001	001	2022-01-13
438	US	Griaule	griaule-000	000	2021-08-20
439	US	Griaule	griaule-001	001	2022-05-31
440	US	Griaule	griaule-002	002	2022-12-02
441	CN	Guangzhou Pixel Solutions	pixelall-002	002	2019-06-06
442	CN	Guangzhou Pixel Solutions	pixelall-003	003	2019-10-15
443	CN	Guangzhou Pixel Solutions	pixelall-004	004	2020-07-02
444	CN	Guangzhou Pixel Solutions	pixelall-005	005	2021-02-05
445	CN	Guangzhou Pixel Solutions	pixelall-006	006	2021-06-17
446	CN	Guangzhou Pixel Solutions	pixelall-007	007	2021-12-01
447	CN	Guangzhou Pixel Solutions	pixelall-008	008	2022-06-16
448	CN	Guangzhou Pixel Solutions	pixelall-009	009	2022-10-26
449	CN	Guangzhou Pixel Solutions	pixelall-010	010	2023-10-18
450	CN	Hangzhuo AIlu Network Information Technology	hzailu-001	001	2022-01-27
451	CN	Hangzhuo AIlu Network Information Technology	hzailu-002	002	2022-06-02
452	CN	Hangzhuo AIlu Network Information Technology	hzailu-003	003	2022-10-11
453	CN	Hangzhuo AIlu Network Information Technology	hzailu-004	004	2023-02-27
454	CN	Hangzhuo AIlu Network Information Technology	hzailu-005	005	2023-08-10
455	CN	Hangzhuo AIlu Network Information Technology	hzailu-006	006	2023-12-28
456	CN	Hangzhuo AIlu Network Information Technology	hzailu-007	007	2024-09-06
457	CN	Hangzhuo AIlu Network Information Technology	hzailu-008	008	2025-02-27
458	ES	Herta Security	hertasecurity-000	000	2021-01-05
459	ES	Herta Security	hertasecurity-001	001	2022-01-18
460	ES	Herta Security	hertasecurity-002	002	2022-09-02
461	ES	Herta Security	hertasecurity-003	003	2023-01-27
462	CN	Hikvision Research Institute	hik-001	001	2019-03-01
463	IN	Hyderabad-Centre for Development of Advanced Computing	cdachyd-001	001	2024-10-01
464	IN	HyperVerge Inc	hyperverge-001	001	2020-12-13
465	IN	HyperVerge Inc	hyperverge-002	002	2021-05-27
466	IN	HyperVerge Inc	hyperverge-003	003	2022-04-11
467	IN	HyperVerge Inc	hyperverge-004	004	2022-12-14
468	IN	HyperVerge Inc	hyperverge-005	005	2023-08-08
469	IN	HyperVerge Inc	hyperverge-006	006	2024-05-02
470	IN	HyperVerge Inc	hyperverge-007	007	2026-04-10
471	KR	Hyundai Motor Company	hyundai-roboticslab-000	000	2024-07-12
472	KR	Hyundai Motor Company	hyundai-roboticslab-001	001	2025-02-03
473	KR	Hyundai Motor Company	hyundai-roboticslab-002	002	2025-06-03
474	KR	Hyundai Motor Company	hyundai-roboticslab-003	003	2025-11-14
475	AU	ICM Airport Technics	icm-002	002	2020-11-13
476	AU	ICM Airport Technics	icm-003	003	2021-09-06
477	AU	ICM Airport Technics	icm-004	004	2022-09-07
478	AU	ICM Airport Technics	icm-005	005	2023-09-05
479	US	ID R&D Inc	idrnd-000	000	2024-07-26
480	US	ID R&D Inc	idrnd-001	001	2025-07-31
481	FR	ID3 Technology	id3-001	001	2017-08-04
482	FR	ID3 Technology	id3-002	002	2017-08-04
483	FR	ID3 Technology	id3-003	003	2018-10-05
484	FR	ID3 Technology	id3-004	004	2019-03-01
485	FR	ID3 Technology	id3-005	005	2020-08-04
486	FR	ID3 Technology	id3-006	006	2020-12-17
487	FR	ID3 Technology	id3-007	007	2021-05-17
488	FR	ID3 Technology	id3-008	008	2021-11-10
489	FR	ID3 Technology	id3-009	009	2026-02-05
490	UK	IDENTY	identy-000	000	2023-04-04

Table 7: Summary of participant information included in this report.

	Location	Developer Name	Short Name	Seq. Num.	Validation Date
491	UK	IDENTY	identy-001	001	2025-05-21
492	UK	IDENTY	identy-002	002	2025-11-14
493	KZ	IE SARSENOV	asr-000	000	2025-07-30
494	KZ	IE SARSENOV	asr-001	001	2025-12-01
495	CA	IMDS Software	imds-software-001	001	2022-07-06
496	CA	IMDS Software	imds-software-002	002	2023-02-10
497	CA	IMDS Software	imds-software-003	003	2023-06-20
498	MX	IQSEC	iqsec-001	001	2024-04-12
499	MX	IQSEC	iqsec-002	002	2025-01-08
500	RU	ITMO University	itmo-001	001	2017-06-12
501	RU	ITMO University	itmo-002	002	2017-08-07
502	RU	ITMO University	itmo-003	003	2018-01-23
503	RU	ITMO University	itmo-004	004	2018-06-13
504	RU	ITMO University	itmo-005	005	2018-10-19
505	RU	ITMO University	itmo-006	006	2019-03-01
506	RU	ITMO University	itmo-007	007	2020-01-06
507	RU	ITMO University	itmo-008	008	2021-11-19
508	RU	IVA Cognitive	ivacognitive-001	001	2021-01-29
509	FR	Idemia	idemia-003	003	2018-10-19
510	FR	Idemia	idemia-004	004	2019-03-01
511	FR	Idemia	idemia-005	005	2019-10-11
512	FR	Idemia	idemia-006	006	2020-07-06
513	FR	Idemia	idemia-007	007	2020-12-04
514	FR	Idemia	idemia-008	008	2021-07-07
515	FR	Idemia	idemia-009	009	2022-07-27
516	FR	Idemia	idemia-010	010	2023-06-30
517	FR	Idemia	idemia-011	011	2024-08-06
518	FR	Idemia	morpho-000	000	2017-07-11
519	FR	Idemia	morpho-001	001	2017-07-10
520	FR	Idemia	morpho-002	002	2017-12-28
521	US	Imageware Systems	iws-000	000	2020-08-12
522	GB	Imperial College London	imperial-000	000	2019-03-01
523	GB	Imperial College London	imperial-001	001	2019-03-01
524	GB	Imperial College London	imperial-002	002	2019-08-28
525	US	Incode Technologies Inc	incode-000	000	2018-06-01
526	US	Incode Technologies Inc	incode-001	001	2018-06-13
527	US	Incode Technologies Inc	incode-002	002	2018-10-18
528	US	Incode Technologies Inc	incode-003	003	2019-03-01
529	US	Incode Technologies Inc	incode-004	004	2019-06-12
530	US	Incode Technologies Inc	incode-005	005	2019-10-17
531	US	Incode Technologies Inc	incode-006	006	2020-02-20
532	US	Incode Technologies Inc	incode-007	007	2020-08-25
533	US	Incode Technologies Inc	incode-008	008	2021-01-19
534	US	Incode Technologies Inc	incode-009	009	2021-06-22
535	US	Incode Technologies Inc	incode-010	010	2021-10-22
536	US	Incode Technologies Inc	incode-011	011	2022-08-10
537	US	Incode Technologies Inc	incode-012	012	2023-05-05
538	US	Incode Technologies Inc	incode-013	013	2023-12-08
539	US	Incode Technologies Inc	incode-014	014	2024-04-08
540	US	Incode Technologies Inc	incode-015	015	2025-06-12
541	IT	InfoCert	infocert-001	001	2022-09-08
542	IT	InfoCert	infocert-002	002	2026-03-18
543	IN	Innef Labs	innefulabs-000	000	2020-09-04
544	IN	Innominds Software SEZ India Pvt	innominds-001	001	2023-06-23
545	MY	Innov8tif Solutions	innov8tif-000	000	2024-12-10
546	MY	Innov8tif Solutions	innov8tif-001	001	2026-04-22
547	GB	Innovative Technology	innovativetechnologyltd-001	001	2019-10-22
548	GB	Innovative Technology	innovativetechnologyltd-002	002	2020-02-26
549	SK	Innovatrics	innovatrics-000	000	2017-07-25
550	SK	Innovatrics	innovatrics-001	001	2017-07-25
551	SK	Innovatrics	innovatrics-002	002	2018-02-05
552	SK	Innovatrics	innovatrics-003	003	2018-06-14
553	SK	Innovatrics	innovatrics-004	004	2018-10-19
554	SK	Innovatrics	innovatrics-005	005	2019-03-01
555	SK	Innovatrics	innovatrics-006	006	2019-08-13
556	SK	Innovatrics	innovatrics-007	007	2020-08-19
557	SK	Innovatrics	innovatrics-008	008	2021-12-15
558	SK	Innovatrics	innovatrics-009	009	2022-01-19
559	SK	Innovatrics	innovatrics-010	010	2023-08-03
560	SK	Innovatrics	innovatrics-011	011	2024-03-08

Table 8: Summary of participant information included in this report.

	Location	Developer Name	Short Name	Seq. Num.	Validation Date
561	SK	Innovatrics	innovatrics-012	012	2024-07-10
562	SK	Innovatrics	innovatrics-013	013	2024-11-13
563	SK	Innovatrics	innovatrics-014	014	2025-03-13
564	SK	Innovatrics	innovatrics-015	015	2025-07-24
565	SK	Innovatrics	innovatrics-016	016	2025-11-28
566	CN	InsightFace AI	insightface-000	000	2021-03-17
567	CN	InsightFace AI	insightface-001	001	2021-09-27
568	CN	InsightFace AI	insightface-002	002	2022-01-31
569	CN	InsightFace AI	insightface-003	003	2022-08-23
570	CN	InsightFace AI	insightface-004	004	2023-03-31
571	CN	Inspur (Beijing) Electronic Information Industry Co	inspur-000	000	2022-07-19
572	CN	Inspur (Beijing) Electronic Information Industry Co	inspur-001	001	2023-02-24
573	CN	Inspur (Beijing) Electronic Information Industry Co	inspur-002	002	2023-12-08
574	CN	Inspur (Beijing) Electronic Information Industry Co	inspur-003	003	2025-02-11
575	CN	Institute of Computing Technology	icthtc-000	000	2020-11-29
576	RU	Institute of Information Technologies	iit-000	000	2019-03-01
577	RU	Institute of Information Technologies	iit-001	001	2019-07-05
578	RU	Institute of Information Technologies	iit-002	002	2019-12-04
579	RU	Institute of Information Technologies	iit-003	003	2020-12-01
580	IS	Intel Research Group	intelresearch-000	000	2019-07-08
581	IS	Intel Research Group	intelresearch-001	001	2020-01-14
582	IS	Intel Research Group	intelresearch-002	002	2020-07-24
583	IS	Intel Research Group	intelresearch-003	003	2021-01-18
584	IS	Intel Research Group	intelresearch-004	004	2021-08-24
585	IS	Intel Research Group	intelresearch-005	005	2022-02-13
586	IS	Intel Research Group	intelresearch-006	006	2022-12-19
587	IS	Intel Research Group	intelresearch-007	007	2023-05-30
588	IS	Intel Research Group	intelresearch-008	008	2023-10-03
589	IS	Intel Research Group	intelresearch-009	009	2024-03-26
590	IS	Intel Research Group	intelresearch-010	010	2024-08-20
591	IS	Intel Research Group	intelresearch-011	011	2024-12-24
592	IS	Intel Research Group	intelresearch-012	012	2025-07-03
593	KR	IntelliVIX	intellivix-001	001	2022-02-25
594	KR	IntelliVIX	intellivix-002	002	2022-07-14
595	KR	IntelliVIX	intellivix-003	003	2022-12-12
596	KR	IntelliVIX	intellivix-004	004	2023-06-21
597	KR	IntelliVIX	intellivix-005	005	2023-11-14
598	KR	IntelliVIX	intellivix-006	006	2025-07-31
599	AE	Intellibrain Technological Projects	g42-intellibrain-001	001	2022-07-27
600	AE	Intellibrain Technological Projects	g42-intellibrain-002	002	2023-05-10
601	CN	Intelligent Control Technology Co Ltd - IGearx	igearx-face-000	000	2023-03-28
602	US	Intellivision	intellivision-001	001	2017-10-10
603	US	Intellivision	intellivision-002	002	2019-08-23
604	US	Intellivision	intellivision-003	003	2022-03-07
605	US	Intellivision	intellivision-004	004	2022-07-28
606	US	Intellivision	intellivision-005	005	2023-02-06
607	US	Intellivision	intellivision-006	006	2023-07-14
608	US	Intellivision	intellivision-007	007	2023-12-19
609	LU	Intema-LGL Group	intema-000	000	2022-07-15
610	LU	Intema-LGL Group	intema-001	001	2023-01-11
611	US	InterLink labs	interlinklabs-001	001	2024-11-08
612	US	InterLink labs	interlinklabs-002	002	2025-04-21
613	US	InterLink labs	interlinklabs-003	003	2025-11-18
614	IN	Intozi Tech Pvt Ltd	intozi-001	001	2023-09-25
615	US	IrexAI	irex-000	000	2020-12-17
616	US	Iris ID Systems	irisid-001	001	2026-01-30
617	IL	Is It You	isityou-000	000	2017-06-26
618	MX	Jaak IT	jaakit-001	001	2022-05-20
619	MX	Jaak IT	jaakit-002	002	2025-09-11
620	GB	KYB-AI Ltd	kbyai-000	000	2024-11-29
621	KR	Kakao Bank	kakaobank-000	000	2023-02-27
622	KR	Kakao Bank	kakaobank-001	001	2023-10-10
623	KR	Kakao Bank	kakaobank-002	002	2024-04-01
624	KR	Kakao Bank	kakaobank-003	003	2024-09-30
625	KR	Kakao Brain	kakao-001	001	2019-03-01
626	KR	Kakao Brain	kakao-002	002	2019-06-19
627	KR	Kakao Brain	kakao-003	003	2020-02-26
628	KR	Kakao Brain	kakao-004	004	2020-10-28
629	KR	Kakao Brain	kakao-005	005	2021-03-09
630	KR	Kakao Brain	kakao-007	007	2022-01-12

Table 9: Summary of participant information included in this report.

FNMR(T) "False non-match rate"
FMR(T) "False match rate"

	Location	Developer Name	Short Name	Seq. Num.	Validation Date
631	KR	Kakao Brain	kakao-008	008	2022-05-12
632	KR	Kakao Brain	kakao-009	009	2023-11-07
633	KR	Kakao Pay Corp	kakaopay-001	001	2021-07-06
634	TH	Kasikorn Labs	kasikornlabs-000	000	2022-03-02
635	TH	Kasikorn Labs	kasikornlabs-001	001	2022-07-26
636	TH	Kasikorn Labs	kasikornlabs-002	002	2022-12-13
637	TH	Kasikorn Labs	kasikornlabs-003	003	2023-10-05
638	TH	Kasikorn Labs	kasikornlabs-004	004	2024-11-04
639	TH	Kasikorn Labs	kasikornlabs-005	005	2025-04-04
640	SG	Kedacom International Pte	kedacom-000	000	2019-06-03
641	GB	Keyless Technologies	keyless-000	000	2024-11-21
642	US	Kloudspot Inc	kloudspot-001	001	2024-09-03
643	US	Kloudspot Inc	kloudspot-002	002	2025-06-16
644	US	Kneron Inc	kneron-003	003	2019-07-01
645	US	Kneron Inc	kneron-005	005	2020-02-21
646	US	Kneron Inc	kneron-006	006	2026-04-10
647	US	KnowUTech LLC	knowutech-000	000	2022-02-13
648	US	Kogniza Technology	kogniza-001	001	2024-03-01
649	KR	Kookmin University	kookmin-001	001	2020-09-28
650	KR	Kookmin University	kookmin-002	002	2021-03-05
651	KR	Korea Identification Inc	koreaid-001	001	2022-12-12
652	TH	Krungthai	krungthai-002	002	2022-06-21
653	CN	KuKe3D Technology	kuke3d-001	001	2021-10-28
654	CN	KuKe3D Technology	kuke3d-002	002	2022-04-14
655	MX	Lebentech Biometrics	lebentech-000	000	2022-02-16
656	MX	Lebentech Biometrics	lebentech-001	001	2023-12-12
657	IN	Lema Labs	lemalabs-001	001	2021-04-13
658	KR	LightVision Inc	lightvision-000	000	2024-06-27
659	KR	LightVision Inc	lightvision-001	001	2025-02-18
660	JP	Line Corporation	lineclova-000	000	2021-03-31
661	JP	Line Corporation	lineclova-001	001	2021-09-26
662	JP	Line Corporation	lineclova-002	002	2022-05-18
663	JP	Line Corporation	lineclova-003	003	2022-11-28
664	CN	Lishui Shuyan Huirong Technology Co	lssytech-000	000	2026-03-18
665	RU	Lomonosov Moscow State University	intsysmsu-000	000	2019-06-18
666	RU	Lomonosov Moscow State University	intsysmsu-001	001	2019-10-22
667	RU	Lomonosov Moscow State University	intsysmsu-002	002	2020-03-12
668	IN	Lookman Electroplast Industries	lookman-002	002	2018-06-13
669	IN	Lookman Electroplast Industries	lookman-004	004	2019-06-03
670	US	Luxand Inc	luxand-000	000	2019-11-07
671	US	Luxand Inc	luxand-001	001	2023-10-17
672	US	Luxand Inc	luxand-003	003	2024-03-25
673	US	Luxand Inc	luxand-004	004	2024-08-01
674	VN	MB Bank	mbbankvn-000	000	2025-02-12
675	RU	MVision	mvision-001	001	2019-11-12
676	IN	Mantra Softech India	mantra-000	000	2021-10-28
677	ID	Matrix Comsec Pvt Ltd	matrixcomsec-000	000	2025-06-11
678	ID	Matrix Comsec Pvt Ltd	matrixcomsec-001	001	2025-11-26
679	AE	Maverick Research	maverickresearch-000	000	2024-12-26
680	CN	Maxvision Technology	maxvision-000	000	2021-10-27
681	CN	Maxvision Technology	maxvision-001	001	2022-03-03
682	CN	Maxvision Technology	maxvision-002	002	2022-07-12
683	CN	Maxvision Technology	maxvision-003	003	2022-11-14
684	CN	Maxvision Technology	maxvision-004	004	2023-05-08
685	CN	Maxvision Technology	maxvision-005	005	2023-09-21
686	CN	Maxvision Technology	maxvision-006	006	2024-01-19
687	CN	Megvii/Face++	megvii-000	000	2018-02-13
688	CN	Megvii/Face++	megvii-001	001	2018-06-15
689	CN	Megvii/Face++	megvii-002	002	2018-10-19
690	CN	Megvii/Face++	megvii-003	003	2021-03-08
691	CN	Megvii/Face++	megvii-004	004	2021-11-19
692	CN	Megvii/Face++	megvii-005	005	2022-03-28
693	CN	Megvii/Face++	megvii-006	006	2022-08-08
694	CN	Megvii/Face++	megvii-007	007	2023-05-17
695	CN	Megvii/Face++	megvii-008	008	2023-10-12
696	CN	Megvii/Face++	megvii-009	009	2024-02-12
697	KR	Metsakuur	metsakuurcompany-001	001	2022-05-12
698	KR	Metsakuur	metsakuurcompany-002	002	2022-09-14
699	KR	Metsakuur	metsakuurcompany-003	003	2023-04-04
700	KR	Metsakuur	metsakuurcompany-004	004	2024-10-24

Table 10: Summary of participant information included in this report.

FNMR(T) "False non-match rate"
FMR(T) "False match rate"

	Location	Developer Name	Short Name	Seq. Num.	Validation Date
701	KR	Metsakuur	metsakuurcompany-005	005	2025-07-31
702	CN	Miaxis Biometrics	miaxis-001	001	2022-11-15
703	CN	Miaxis Biometrics	miaxis-002	002	2023-03-22
704	CN	Miaxis Biometrics	miaxis-003	003	2023-09-19
705	CN	Miaxis Biometrics	miaxis-004	004	2025-12-09
706	GB	MicroFocus	microfocus-001	001	2018-06-13
707	GB	MicroFocus	microfocus-002	002	2018-10-17
708	GB	MicroFocus	microfocus-003	003	2023-02-23
709	GB	Microfocus	microfocus-000	000	2018-06-13
710	CN	Minivision	minivision-000	000	2020-10-28
711	UK	Mitek Systems	mitek-000	000	2023-01-27
712	UK	Mitek Systems	mitek-001	001	2024-07-02
713	UK	Mitek Systems	mitek-002	002	2024-11-19
714	NO	Mobai	mobai-000	000	2020-08-26
715	NO	Mobai	mobai-001	001	2021-02-17
716	NO	Mobai	mobai-002	002	2025-07-07
717	NO	Mobai	mobai-003	003	2026-04-13
718	ES	Mobbeel Solutions	mobbl-000	000	2021-01-28
719	ES	Mobbeel Solutions	mobbl-001	001	2021-06-16
720	ES	Mobbeel Solutions	mobbl-002	002	2021-12-16
721	ES	Mobbeel Solutions	mobbl-003	003	2022-04-19
722	ES	Mobbeel Solutions	mobbl-004	004	2024-05-20
723	ES	Mobbeel Solutions	mobbl-005	005	2024-10-15
724	KR	Mobipin Technology	mobipintech-000	000	2021-11-23
725	TH	Momentum Digital	sertis-000	000	2019-10-07
726	TH	Momentum Digital	sertis-001	001	2020-07-30
727	TH	Momentum Digital	sertis-002	002	2021-05-13
728	TH	Momentum Digital	sertis-003	003	2023-12-27
729	CN	MoreDian Technology	moredian-000	000	2021-02-24
730	US	Mukh Technologies	mukh-001	001	2022-03-22
731	US	Mukh Technologies	mukh-002	002	2022-11-01
732	US	Mukh Technologies	mukh-003	003	2023-03-15
733	US	Mukh Technologies	mukh-004	004	2023-09-13
734	US	Mukh Technologies	mukh-005	005	2024-12-05
735	CN	Multi-Modality Intelligence	multimodality-000	000	2021-10-19
736	CN	Multi-Modality Intelligence	multimodality-001	001	2022-05-16
737	RU	N-Tech Lab	ntechlab-000	000	2017-03-13
738	RU	N-Tech Lab	ntechlab-001	001	2017-05-10
739	RU	N-Tech Lab	ntechlab-002	002	2017-08-23
740	RU	N-Tech Lab	ntechlab-003	003	2017-12-29
741	RU	N-Tech Lab	ntechlab-004	004	2018-06-14
742	RU	N-Tech Lab	ntechlab-005	005	2018-10-19
743	RU	N-Tech Lab	ntechlab-006	006	2019-03-01
744	RU	N-Tech Lab	ntechlab-007	007	2019-06-25
745	RU	N-Tech Lab	ntechlab-008	008	2020-01-06
746	RU	N-Tech Lab	ntechlab-009	009	2020-12-30
747	RU	N-Tech Lab	ntechlab-010	010	2021-04-30
748	RU	N-Tech Lab	ntechlab-011	011	2021-09-13
749	RU	N-Tech Lab	ntechlab-012	012	2022-01-20
750	SG	NCS Pte Ltd	ncssg-001	001	2023-03-24
751	SG	NCS Pte Ltd	ncssg-002	002	2024-06-25
752	SG	NCS Pte Ltd	ncssg-003	003	2024-10-30
753	SG	NCS Pte Ltd	ncssg-004	004	2025-04-03
754	CA	NEO Systems	neosystems-001	001	2021-03-02
755	CA	NEO Systems	neosystems-002	002	2021-07-03
756	CA	NEO Systems	neosystems-003	003	2021-11-11
757	CA	NEO Systems	neosystems-004	004	2022-05-02
758	KR	NHN Corp	nhn-001	001	2021-03-15
759	KR	NHN Corp	nhn-002	002	2021-07-15
760	KR	NHN Corp	nhn-003	003	2022-02-22
761	KR	NHN Corp	nhn-004	004	2023-06-26
762	KR	NHN Corp	nhn-005	005	2023-12-06
763	KR	NSENSE Corp	nsensecorp-001	001	2020-10-20
764	KR	NSENSE Corp	nsensecorp-002	002	2021-05-06
765	KR	NSENSE Corp	nsensecorp-003	003	2021-10-29
766	KR	NSENSE Corp	nsensecorp-004	004	2022-09-08
767	KR	NSENSE Corp	nsensecorp-005	005	2023-02-08
768	CN	Nanjing Kiwi Network Technology	kiwitech-000	000	2021-03-19
769	KR	Naver Corp	clova-000	000	2020-10-21
770	KR	Neosecu Co	openface-001	001	2021-06-15

Table 11: Summary of participant information included in this report.

	Location	Developer Name	Short Name	Seq. Num.	Validation Date
771	TW	Netbridge Technology Incoporation	netbridgetech-001	001	2020-01-08
772	TW	Netbridge Technology Incoporation	netbridgetech-002	002	2020-08-11
773	LT	Neurotechnology	neurotechnology-000	000	2017-03-22
774	LT	Neurotechnology	neurotechnology-001	001	2017-08-07
775	LT	Neurotechnology	neurotechnology-002	002	2017-11-02
776	LT	Neurotechnology	neurotechnology-003	003	2018-02-02
777	LT	Neurotechnology	neurotechnology-004	004	2018-10-19
778	LT	Neurotechnology	neurotechnology-005	005	2019-03-01
779	LT	Neurotechnology	neurotechnology-006	006	2019-06-26
780	LT	Neurotechnology	neurotechnology-008	008	2020-01-08
781	LT	Neurotechnology	neurotechnology-009	009	2020-07-07
782	LT	Neurotechnology	neurotechnology-010	010	2020-11-26
783	LT	Neurotechnology	neurotechnology-011	011	2021-03-26
784	LT	Neurotechnology	neurotechnology-012	012	2021-07-26
785	LT	Neurotechnology	neurotechnology-013	013	2022-01-07
786	LT	Neurotechnology	neurotechnology-015	015	2022-06-07
787	LT	Neurotechnology	neurotechnology-016	016	2023-02-01
788	LT	Neurotechnology	neurotechnology-017	017	2023-07-28
789	LT	Neurotechnology	neurotechnology-018	018	2024-02-09
790	LT	Neurotechnology	neurotechnology-019	019	2024-07-31
791	LT	Neurotechnology	neurotechnology-020	020	2025-08-01
792	IN	NextMeta Labs	nextmetalabs-001	001	2024-07-02
793	IN	NextMeta Labs	nextmetalabs-002	002	2024-12-04
794	IN	NextMeta Labs	nextmetalabs-003	003	2025-07-08
795	IN	NextMeta Labs	nextmetalabs-004	004	2026-01-27
796	US	Noblis	noblis-000	000	2017-07-05
797	ID	Nodeflux	nodeflux-000	000	2019-03-01
798	ID	Nodeflux	nodeflux-001	001	2019-03-01
799	ID	Nodeflux	nodeflux-002	002	2019-08-13
800	LT	Nominder	nominder-000	000	2023-02-06
801	LT	Nominder	nominder-001	001	2023-07-19
802	LT	Nominder	nominder-002	002	2023-11-04
803	LT	Nominder	nominder-003	003	2024-03-06
804	LT	Nominder	nominder-004	004	2024-07-11
805	LT	Nominder	nominder-005	005	2024-11-12
806	LT	Nominder	nominder-006	006	2025-04-07
807	LT	Nominder	nominder-007	007	2026-02-10
808	IN	NotionTag Technologies Private Limited	notiontag-000	000	2019-06-12
809	IN	NotionTag Technologies Private Limited	notiontag-001	001	2021-03-04
810	IN	NotionTag Technologies Private Limited	notiontag-002	002	2021-09-17
811	US	OOTO AI	ooto-001	001	2025-09-11
812	US	Omnigarde Ltd	omnigarde-000	000	2021-04-05
813	US	Omnigarde Ltd	omnigarde-001	001	2021-08-23
814	US	Omnigarde Ltd	omnigarde-002	002	2022-01-19
815	US	Omnigarde Ltd	omnigarde-003	003	2023-05-10
816	US	Omnigarde Ltd	omnigarde-004	004	2024-06-24
817	US	Omnigarde Ltd	omnigarde-005	005	2025-06-02
818	KR	One More Security	omface-000	000	2021-12-15
819	KR	One More Security	omface-001	001	2022-10-21
820	UK	Onfido	onfido-000	000	2022-12-13
821	UK	Onfido	onfido-001	001	2025-07-17
822	UK	Onfido	onfido-002	002	2025-12-16
823	UK	Onfido	onfido-003	003	2026-04-22
824	VN	Online Mobile Services JSC	momovn-001	001	2024-01-26
825	VN	Online Mobile Services JSC	momovn-002	002	2024-06-04
826	VN	Online Mobile Services JSC	momovn-003	003	2025-09-19
827	IN	Openedge Technologies Pvt	openedge-000	000	2024-01-29
828	AE	Ovision	ovisionllc-001	001	2024-04-03
829	AE	Ovision	ovisionllc-002	002	2024-08-05
830	RU	Oz Forensics LLC	oz-001	001	2020-07-29
831	RU	Oz Forensics LLC	oz-002	002	2021-01-18
832	RU	Oz Forensics LLC	oz-003	003	2021-08-09
833	RU	Oz Forensics LLC	oz-004	004	2021-12-13
834	TW	PAPAGO Inc	papago-001	001	2022-07-19
835	CZ	PAPIL11 S.R.O.	papil11-000	000	2024-01-04
836	CZ	PAPIL11 S.R.O.	papil11-001	001	2024-08-06
837	CZ	PAPIL11 S.R.O.	papil11-002	002	2025-01-02
838	CZ	PAPIL11 S.R.O.	papil11-003	003	2025-04-29
839	CZ	PAPIL11 S.R.O.	papil11-004	004	2026-03-31
840	KR	PNPSecure	pnpsecure-000	000	2025-06-05

Table 12: Summary of participant information included in this report.

FNMR(T) "False non-match rate"
FMR(T) "False match rate"

	Location	Developer Name	Short Name	Seq. Num.	Validation Date
841	KR	PNPSecure	pnpsecure-001	001	2026-03-03
842	ID	PT Autentika Digital Indonesia	autentika-000	000	2022-12-05
843	ID	PT Autentika Digital Indonesia	autentika-001	001	2023-04-05
844	ID	PT Autentika Digital Indonesia	autentika-002	002	2023-11-21
845	ID	PT Autentika Digital Indonesia	autentika-003	003	2024-11-12
846	ID	PT Ice House	icehouse-000	000	2026-02-27
847	ID	PT Qlue Performa Indonesia	qluevision-001	001	2022-11-15
848	ID	PT Technology Biometric Indonesia	techbiometricid-001	001	2025-01-02
849	ID	PT Technology Biometric Indonesia	techbiometricid-002	002	2026-04-09
850	CH	PXL Vision AG	pxl-001	001	2020-06-30
851	TW	Palit Microsystems	palit-000	000	2022-05-16
852	TW	Palit Microsystems	palit-001	001	2022-09-26
853	SG	Panasonic R+D Center Singapore	psl-000	000	2018-06-18
854	SG	Panasonic R+D Center Singapore	psl-001	001	2018-10-12
855	SG	Panasonic R+D Center Singapore	psl-002	002	2019-02-28
856	SG	Panasonic R+D Center Singapore	psl-003	003	2019-10-01
857	SG	Panasonic R+D Center Singapore	psl-004	004	2020-03-03
858	SG	Panasonic R+D Center Singapore	psl-005	005	2020-07-06
859	SG	Panasonic R+D Center Singapore	psl-006	006	2020-11-13
860	SG	Panasonic R+D Center Singapore	psl-007	007	2021-03-19
861	SG	Panasonic R+D Center Singapore	psl-008	008	2021-07-21
862	SG	Panasonic R+D Center Singapore	psl-009	009	2021-12-08
863	SG	Panasonic R+D Center Singapore	psl-010	010	2022-04-19
864	SG	Panasonic R+D Center Singapore	psl-011	011	2022-10-06
865	SG	Panasonic R+D Center Singapore	psl-012	012	2023-10-13
866	SG	Panasonic R+D Center Singapore	psl-013	013	2024-04-18
867	SG	Panasonic R+D Center Singapore	psl-014	014	2024-09-11
868	US	Pangiam	pangiam-000	000	2022-04-04
869	US	Pangiam	pangiam-001	001	2023-02-21
870	US	Pangiam	pangiam-002	002	2023-06-21
871	TR	Papilon Savunma	papsav1923-001	001	2021-03-10
872	TR	Papilon Savunma	papsav1923-002	002	2022-01-20
873	TR	Papilon Savunma	papsav1923-003	003	2022-11-25
874	US	Paravision	everai-000	000	2018-10-19
875	US	Paravision	everai-001	001	2018-10-19
876	US	Paravision	everai-002	002	2019-03-01
877	US	Paravision	paravision	003	2019-07-01
878	US	Paravision	paravision-004	004	2019-12-11
879	US	Paravision	paravision-006	006	2021-02-01
880	US	Paravision	paravision-008	008	2021-06-30
881	US	Paravision	paravision-010	010	2022-02-02
882	US	Paravision	paravision-011	011	2022-12-12
883	US	Paravision	paravision-013	013	2023-05-08
884	US	Paravision	paravision-015	015	2024-09-09
885	US	Paravision	paravision-017	017	2025-01-13
886	US	Paravision	paravision-018	018	2025-06-12
887	US	Paravision	paravision-020	020	2025-12-11
888	SG	Pensees Pte	pensees-001	001	2020-08-17
889	PL	Pentacomp Systemy Informatyczne	pentacomp-000	000	2024-09-26
890	CN	Ping An Technology	pa-002	002	2017-09-25
891	CN	Ping An Technology	pa-003	003	2017-05-25
892	US	Private Identity LLC	privid-001	001	2023-02-06
893	US	Private Identity LLC	privid-002	002	2023-10-03
894	US	Private Identity LLC	privid-003	003	2024-09-24
895	US	Private Identity LLC	privid-004	004	2025-03-05
896	IN	Pyramid Cyber Security + Forensic (P)	pyramid-000	000	2019-11-04
897	IN	Pyramid Cyber Security + Forensic (P)	pyramid-001	001	2024-11-26
898	KZ	Qaz Biometric Systems	qazbs-000	000	2022-06-22
899	KZ	QazSmartVision.AI	qazsmartvisionai-000	000	2024-01-11
900	KZ	QazSmartVision.AI	qazsmartvisionai-001	001	2024-05-21
901	KZ	QazSmartVision.AI	qazsmartvisionai-002	002	2024-09-25
902	KZ	QazSmartVision.AI	qazsmartvisionai-003	003	2025-01-30
903	KZ	QazSmartVision.AI	qazsmartvisionai-004	004	2025-07-18
904	TW	Qnap Security	qnap-000	000	2021-08-09
905	TW	Qnap Security	qnap-001	001	2021-12-09
906	TW	Qnap Security	qnap-002	002	2022-04-15
907	TW	Qnap Security	qnap-003	003	2022-12-09
908	TW	Qnap Security	qnap-004	004	2023-05-05
909	TW	Qnap Security	qnap-005	005	2023-11-16
910	TW	Qnap Security	qnap-006	006	2024-06-14

Table 13: Summary of participant information included in this report.

	Location	Developer Name	Short Name	Seq. Num.	Validation Date
911	CZ	Quantasoft	quantasoft-003	003	2021-04-19
912	US	ROC	rankone-000	000	2017-03-21
913	US	ROC	rankone-001	001	2017-04-12
914	US	ROC	rankone-002	002	2017-08-18
915	US	ROC	rankone-003	003	2017-11-28
916	US	ROC	rankone-004	004	2018-06-12
917	US	ROC	rankone-005	005	2018-10-09
918	US	ROC	rankone-006	006	2019-02-27
919	US	ROC	rankone-007	007	2019-06-03
920	US	ROC	rankone-008	008	2019-11-12
921	US	ROC	rankone-009	009	2020-06-26
922	US	ROC	rankone-010	010	2020-11-05
923	US	ROC	rankone-011	011	2021-08-27
924	US	ROC	rankone-012	012	2021-12-27
925	US	ROC	rankone-013	013	2022-07-09
926	US	ROC	rankone-014	014	2022-12-21
927	US	ROC	rankone-015	015	2023-07-20
928	US	ROC	roc-016	016	2023-12-19
929	US	ROC	roc-017	017	2024-06-24
930	US	ROC	roc-018	018	2025-01-30
931	US	ROC	roc-019	019	2025-07-21
932	US	ROC	roc-020	020	2026-02-06
933	US	RealSense	realsense-001	001	2025-12-01
934	US	Realnetworks Inc	realnetworks-000	000	2018-05-30
935	US	Realnetworks Inc	realnetworks-001	001	2018-10-19
936	US	Realnetworks Inc	realnetworks-002	002	2019-02-28
937	US	Realnetworks Inc	realnetworks-003	003	2019-06-12
938	US	Realnetworks Inc	realnetworks-004	004	2021-04-15
939	US	Realnetworks Inc	realnetworks-005	005	2021-09-27
940	US	Realnetworks Inc	realnetworks-006	006	2022-02-09
941	US	Realnetworks Inc	realnetworks-007	007	2022-06-14
942	US	Realnetworks Inc	realnetworks-008	008	2022-11-10
943	AE	Recognito	recognito-000	000	2023-05-24
944	AE	Recognito	recognito-001	001	2023-09-27
945	US	Regula Forensics	regula-000	000	2021-04-13
946	US	Regula Forensics	regula-001	001	2021-12-14
947	US	Regula Forensics	regula-002	002	2025-09-15
948	AM	Regular Biometrics Solutions	rebs-000	000	2023-08-22
949	AM	Regular Biometrics Solutions	rebs-001	001	2023-12-22
950	CN	Remark Holdings	remarkai-000	000	2019-03-01
951	CN	Remark Holdings	remarkai-001	001	2019-03-01
952	CN	Remark Holdings	remarkai-002	002	2019-11-21
953	CN	Remark Holdings	remarkai-003	003	2021-06-22
954	SG	Rendip	rendip-000	000	2021-04-19
955	UK	Reveal Media Ltd	revealmedia-005	005	2021-09-24
956	UK	Reveal Media Ltd	revealmedia-006	006	2022-01-26
957	CN	Rokid Corporation	rokid-000	000	2019-08-01
958	CN	Rokid Corporation	rokid-001	001	2019-12-13
959	KR	SK Telecom	sktelecom-000	000	2021-07-09
960	KR	SQIsoft	sqisoft-001	001	2021-07-27
961	KR	SQIsoft	sqisoft-002	002	2021-11-03
962	KR	SQIsoft	sqisoft-003	003	2022-10-26
963	SG	ST Engineering	stengg-000	000	2023-06-06
964	SA	STCON LLC	stcon-000	000	2022-11-02
965	SA	STCON LLC	stcon-001	001	2023-03-03
966	SA	STCON LLC	stcon-002	002	2023-07-05
967	SA	STCON LLC	stcon-003	003	2023-11-07
968	SA	STCON LLC	stcon-004	004	2024-06-18
969	SA	STCON LLC	stcon-005	005	2024-11-13
970	SA	STCON LLC	stcon-006	006	2025-03-17
971	SA	STCON LLC	stcon-007	007	2025-07-18
972	SA	STCON LLC	stcon-008	008	2025-12-30
973	DE	Saffe	saffe-001	001	2018-10-19
974	DE	Saffe	saffe-002	002	2019-03-01
975	JP	Saga Densan Center Co Ltd	sdc-000	000	2022-10-18
976	KR	Samsung S1 Corp	s1-001	001	2019-12-06
977	KR	Samsung S1 Corp	s1-002	002	2021-03-24
978	KR	Samsung S1 Corp	s1-003	003	2021-08-24
979	KR	Samsung S1 Corp	s1-004	004	2022-01-04
980	KR	Samsung S1 Corp	s1-005	005	2022-06-17

Table 14: Summary of participant information included in this report.

	Location	Developer Name	Short Name	Seq. Num.	Validation Date
981	KR	Samsung S1 Corp	s1-006	006	2022-10-17
982	KR	Samsung S1 Corp	s1-007	007	2023-03-20
983	KR	Samsung S1 Corp	s1-008	008	2024-10-16
984	KR	Samsung S1 Corp	s1-009	009	2025-02-25
985	KR	Samsung-SDS	samsungsds-000	000	2021-10-28
986	KR	Samsung-SDS	samsungsds-001	001	2022-04-18
987	KR	Samsung-SDS	samsungsds-002	002	2022-09-16
988	IN	Samtech InfoNet Limited	samtech-000	000	2017-05-02
989	IN	Samtech InfoNet Limited	samtech-001	001	2019-10-15
990	IN	Samtech InfoNet Limited	samtech-002	002	2023-07-06
991	RU	Satellite Innovation/Eocortex	eocortex-000	000	2020-08-26
992	IL	Scanovate	scanovate-001	001	2019-11-12
993	IL	Scanovate	scanovate-002	002	2020-06-26
994	IL	Scanovate	scanovate-003	003	2021-11-15
995	NG	Seamfix	seamfix-001	001	2024-03-08
996	RO	Securif AI	securifai-001	001	2020-10-06
997	RO	Securif AI	securifai-002	002	2021-03-19
998	RO	Securif AI	securifai-003	003	2021-08-03
999	RO	Securif AI	securifai-004	004	2021-12-21
1000	RO	Securif AI	securifai-005	005	2022-05-16
1001	RO	Securif AI	securifai-006	006	2022-11-14
1002	RO	Securif AI	securifai-007	007	2023-08-17
1003	RO	Securif AI	securifai-008	008	2024-02-26
1004	CN	Sensetime Group	sensetime-001	001	2018-10-19
1005	CN	Sensetime Group	sensetime-002	002	2018-10-19
1006	CN	Sensetime Group	sensetime-003	003	2019-06-04
1007	CN	Sensetime Group	sensetime-004	004	2020-11-20
1008	CN	Sensetime Group	sensetime-005	005	2021-05-24
1009	CN	Sensetime Group	sensetime-006	006	2021-12-28
1010	CN	Sensetime Group	sensetime-007	007	2022-06-17
1011	CN	Sensetime Group	sensetime-008	008	2023-01-04
1012	CN	Sensetime Group	sensetime-010	010	2024-12-03
1013	CN	Sensetime Group	sensetime-011	011	2026-03-17
1014	UZ	Serendipity Ltd	serendipity-000	000	2023-05-31
1015	SG	Seventh Sense Artificial Intelligence	seventhsense-000	000	2021-06-29
1016	SG	Seventh Sense Artificial Intelligence	seventhsense-001	001	2022-03-04
1017	SG	Seventh Sense Artificial Intelligence	seventhsense-002	002	2022-10-17
1018	SG	Seventh Sense Artificial Intelligence	seventhsense-003	003	2023-05-31
1019	SG	Seventh Sense Artificial Intelligence	seventhsense-005	005	2023-10-05
1020	SG	Seventh Sense Artificial Intelligence	seventhsense-006	006	2024-07-09
1021	US	Shaman Software	shaman-000	000	2017-12-05
1022	US	Shaman Software	shaman-001	001	2018-01-13
1023	CN	Shanghai Jiao Tong University	sjtu-001	001	2019-09-27
1024	CN	Shanghai Jiao Tong University	sjtu-002	002	2020-02-12
1025	CN	Shanghai Jiao Tong University	sjtu-003	003	2020-11-02
1026	CN	Shanghai Jiao Tong University	sjtu-004	004	2021-05-13
1027	CN	Shanghai Jiao Tong University	sjtu-005	005	2023-05-05
1028	CN	Shanghai Jiao Tong University	sjtu-006	006	2024-12-06
1029	CN	Shanghai Jiao Tong University	sjtu-007	007	2025-04-16
1030	CN	Shanghai Jiao Tong University	sjtu-008	008	2025-12-11
1031	CN	Shanghai Jiao Tong University	sjtu-009	009	2026-04-13
1032	CN	Shanghai Ulucu Electronics Technology	uluface-002	002	2019-07-10
1033	CN	Shanghai Ulucu Electronics Technology	uluface-003	003	2019-11-12
1034	CN	Shanghai University - Shanghai Film Academy	shu-001	001	2019-06-17
1035	CN	Shanghai University - Shanghai Film Academy	shu-002	002	2019-12-10
1036	CN	Shanghai University - Shanghai Film Academy	shu-003	003	2020-06-24
1037	CN	Shanghai Yitu Technology	yitu-000	000	2017-05-23
1038	CN	Shanghai Yitu Technology	yitu-001	001	2018-06-12
1039	CN	Shanghai Yitu Technology	yitu-002	002	2018-10-19
1040	CN	Shanghai Yitu Technology	yitu-003	003	2019-03-01
1041	CN	Shenzhen AiMall Tech	aimall-001	001	2019-11-12
1042	CN	Shenzhen AiMall Tech	aimall-002	002	2020-03-12
1043	CN	Shenzhen AiMall Tech	aimall-003	003	2020-08-12
1044	CN	Shenzhen EI Networks	einetworks-000	000	2019-08-13
1045	CN	Shenzhen Inst Adv Integrated Tech CAS	siat-002	002	2018-06-13
1046	CN	Shenzhen Inst Adv Integrated Tech CAS	siat-004	004	2019-03-01
1047	CN	Shenzhen Inst Adv Integrated Tech CAS	siat-005	005	2022-02-08
1048	CN	Shenzhen Intellifusion Technologies	intellifusion-001	001	2019-08-22
1049	CN	Shenzhen Intellifusion Technologies	intellifusion-002	002	2020-03-18
1050	CN	Shenzhen Polytechnic University	szpu-000	000	2025-03-28

Table 15: Summary of participant information included in this report.

FNMR(T) "False non-match rate"
FMR(T) "False match rate"

	Location	Developer Name	Short Name	Seq. Num.	Validation Date
1051	CN	Shenzhen University-Macau University of Science and Technology	sztu-000	000	2020-12-17
1052	CN	Shenzhen University-Macau University of Science and Technology	sztu-001	001	2021-07-13
1053	UK	Shufti	shufti-001	001	2026-03-17
1054	QA	Sightropic	sightropic-000	000	2025-03-26
1055	QA	Sightropic	sightropic-001	001	2025-11-25
1056	IN	Smarg Technologies Pvt Ltd	smargtech-001	001	2026-03-17
1057	RU	Smart Engines	smartengines-000	000	2021-08-25
1058	RU	Smart Engines	smartengines-001	001	2022-05-31
1059	ES	Smartbiometrik	smartbiometrik-001	001	2022-05-16
1060	TR	Smarvist Teknoloji	smartvist-000	000	2022-05-10
1061	TR	Smarvist Teknoloji	smartvist-001	001	2023-11-02
1062	DE	Smilart	smilart-001	001	2018-02-06
1063	DE	Smilart	smilart-002	002	2018-02-06
1064	DE	Smilart	smilart-003	003	2019-03-01
1065	TR	Sodec App Inc	sodec-000	000	2021-06-02
1066	CN	Sparktek International Pte Ltd	sparktek-000	000	2025-11-24
1067	IN	Sparsh CCTV	sparsh-001	001	2024-01-02
1068	IN	Staqu Technologies	staqu-000	000	2020-07-15
1069	CN	Star Hybrid Limited	starhybrid-001	001	2019-06-19
1070	CN	Su Zhou NaZhiTianDi intelligent technology	nazhiai-000	000	2020-06-25
1071	IN	Sukshi Technology Innovation	sukshi-000	000	2022-02-13
1072	GB	Sum and Substance Ltd	sumsub-000	000	2025-12-15
1073	KR	Suprema AI Inc	suprema-000	000	2021-03-31
1074	KR	Suprema AI Inc	suprema-001	001	2021-09-23
1075	KR	Suprema AI Inc	suprema-002	002	2022-02-11
1076	KR	Suprema AI Inc	suprema-003	003	2022-07-20
1077	KR	Suprema AI Inc	suprema-004	004	2023-01-09
1078	KR	Suprema AI Inc	suprema-005	005	2023-10-25
1079	KR	Suprema ID Inc	supremaid-001	001	2021-05-04
1080	KR	Suprema ID Inc	supremaid-002	002	2022-06-24
1081	UK	Swsam Solutions	swsam-001	001	2023-03-13
1082	RU	Synesis	synesis-000	000	2018-02-09
1083	RU	Synesis	synesis-001	001	2018-05-31
1084	RU	Synesis	synesis-003	003	2018-10-19
1085	RU	Synesis	synesis-004	004	2019-03-01
1086	RU	Synesis	synesis-005	005	2019-06-06
1087	RU	Synesis	synesis-006	006	2019-10-10
1088	RU	Synesis	synesis-007	007	2020-06-24
1089	TW	Synology Inc	synology-000	000	2019-10-23
1090	TW	Synology Inc	synology-001	001	2020-02-26
1091	TW	Synology Inc	synology-002	002	2020-08-20
1092	IT	Syscake S.r.l.	syscake-000	000	2024-11-26
1093	BR	T4iSB	t4isb-000	000	2022-01-28
1094	SA	TAHAKOM	tahakom-001	001	2024-10-17
1095	MY	TNG Digital Sdn Bhd	tngd-001	001	2025-03-17
1096	MY	TNG Digital Sdn Bhd	tngd-002	002	2026-03-18
1097	VN	TNI Tech Co	tnitech-000	000	2024-02-05
1098	AE	TOPPAN Security Co	toppansecurity-001	001	2026-03-30
1099	VN	TTI Group	ttigroup-000	000	2024-12-16
1100	CN	TUPU Technology	tuputech-000	000	2019-10-11
1101	TW	Taiwan AI Labs	ailabs-001	001	2019-12-18
1102	TW	Taiwan Computer Vision	tcv-001	001	2024-05-30
1103	TW	Taiwan Mobile	taiwanmobile-001	001	2024-08-06
1104	TW	Taiwan Mobile	taiwanmobile-002	002	2024-12-11
1105	TW	Taiwan-Certificate Authority Incorporation	twface-000	000	2021-05-14
1106	TW	Taiwan-Certificate Authority Incorporation	twface-001	001	2021-09-14
1107	CH	Tech5 SA	tech5-000	000	2018-10-09
1108	CH	Tech5 SA	tech5-001	001	2018-10-19
1109	CH	Tech5 SA	tech5-002	002	2019-03-01
1110	CH	Tech5 SA	tech5-003	003	2019-08-19
1111	CH	Tech5 SA	tech5-004	004	2020-03-09
1112	CH	Tech5 SA	tech5-005	005	2020-07-24
1113	CH	Tech5 SA	tech5-007	007	2022-12-30
1114	CH	Tech5 SA	tech5-008	008	2023-08-11
1115	CH	Tech5 SA	tech5-009	009	2025-04-17
1116	VN	Techainer	techainer-001	001	2023-11-30
1117	VN	Techainer	techainer-002	002	2025-02-14
1118	SA	Technology Control Company	tcc-000	000	2026-02-10
1119	TR	Techsign	techsign-000	000	2021-08-25
1120	TR	Techsign	techsign-001	001	2022-07-01

Table 16: Summary of participant information included in this report.

	Location	Developer Name	Short Name	Seq. Num.	Validation Date
1121	TW	Telexper International	telexper-000	000	2024-06-21
1122	CN	Tencent Deepsea Lab	deepsea-001	001	2019-06-03
1123	RU	Tevian	tevian-000	000	2017-12-10
1124	RU	Tevian	tevian-001	001	2018-01-19
1125	RU	Tevian	tevian-002	002	2018-06-14
1126	RU	Tevian	tevian-003	003	2018-10-19
1127	RU	Tevian	tevian-004	004	2019-03-01
1128	RU	Tevian	tevian-005	005	2019-09-21
1129	RU	Tevian	tevian-006	006	2020-09-11
1130	RU	Tevian	tevian-007	007	2021-08-06
1131	RU	Tevian	tevian-008	008	2021-12-06
1132	US	TigerIT Bangladesh Ltd	tiger-001	001	2018-01-23
1133	US	TigerIT Bangladesh Ltd	tiger-002	002	2018-06-13
1134	US	TigerIT Bangladesh Ltd	tiger-003	003	2018-10-16
1135	US	TigerIT Bangladesh Ltd	tiger-004	004	2020-12-01
1136	US	TigerIT Bangladesh Ltd	tiger-005	005	2021-07-29
1137	US	TigerIT Bangladesh Ltd	tiger-006	006	2021-12-13
1138	US	TigerIT Bangladesh Ltd	tiger-007	007	2025-03-05
1139	RU	Tinkoff Bank	tinkoff-001	001	2021-05-13
1140	CN	TongYi Transportation Technology	tongyi-004	004	2018-10-19
1141	CN	TongYi Transportation Technology	tongyi-005	005	2019-06-12
1142	CN	TongYi Transportation Technology	tongyitrans-001	001	2017-04-01
1143	CN	TongYi Transportation Technology	tongyitrans-002	002	2017-07-15
1144	CN	TongYi Transportation Technology	tongyitrans-003	003	2018-05-15
1145	TW	Toppan ID Gate	toppanidgate-000	000	2021-09-28
1146	JP	Toshiba	toshiba-000	000	2018-01-11
1147	JP	Toshiba	toshiba-001	001	2018-01-11
1148	JP	Toshiba	toshiba-002	002	2018-10-19
1149	JP	Toshiba	toshiba-003	003	2019-03-01
1150	JP	Toshiba	toshiba-004	004	2021-09-27
1151	JP	Toshiba	toshiba-005	005	2022-02-09
1152	JP	Toshiba	toshiba-006	006	2022-06-29
1153	JP	Toshiba	toshiba-007	007	2023-09-13
1154	JP	Toshiba	toshiba-008	008	2024-02-01
1155	JP	Toshiba	toshiba-009	009	2024-09-16
1156	JP	Toshiba	toshiba-010	010	2025-02-03
1157	JP	Toshiba	toshiba-011	011	2025-07-08
1158	JP	Toshiba	toshiba-012	012	2026-01-09
1159	KR	Toss	toss-000	000	2025-09-22
1160	ES	Touchless ID	touchlessid-000	000	2022-05-02
1161	ES	Touchless ID	touchlessid-001	001	2022-09-21
1162	ES	Touchless ID	touchlessid-002	002	2023-01-23
1163	ES	Touchless ID	touchlessid-003	003	2023-07-12
1164	ES	Touchless ID	touchlessid-004	004	2024-12-27
1165	Il	Transmit Security Ltd	transmitsecurity-001	001	2025-12-04
1166	JP	Tripleize	aize-001	001	2021-04-23
1167	JP	Tripleize	aize-002	002	2021-10-08
1168	JP	Tripleize	aize-003	003	2023-08-10
1169	JP	Tripleize	aize-006	006	2026-04-08
1170	VN	TrueID-VNG	trueidvng-001	001	2023-01-05
1171	US	Trueface.ai	trueface-000	000	2019-10-08
1172	US	Trueface.ai	trueface-001	001	2020-07-20
1173	US	Trueface.ai	trueface-002	002	2021-03-29
1174	US	Trueface.ai	trueface-003	003	2021-09-30
1175	UK	Trust Stamp	truststamp-001	001	2023-07-14
1176	UK	Trust Stamp	truststamp-002	002	2025-05-23
1177	UK	Trust Stamp	truststamp-003	003	2025-11-19
1178	CN	TuringTech.vip	turingtechvip-001	001	2022-02-03
1179	CN	TuringTech.vip	turingtechvip-002	002	2022-07-27
1180	TR	Turkcell Technology	turkcell-000	000	2022-10-11
1181	TR	Turkcell Technology	turkcell-001	001	2023-03-15
1182	TR	Turkcell Technology	turkcell-002	002	2024-03-18
1183	CN	ULSee Inc	ulsee-001	001	2019-07-31
1184	UN	UNICC-Solution Architecture Section	unicc-001	001	2023-02-17
1185	UN	UNICC-Solution Architecture Section	unicc-002	002	2023-06-07
1186	UN	UNICC-Solution Architecture Section	unicc-003	003	2023-10-16
1187	UN	UNICC-Solution Architecture Section	unicc-004	004	2024-09-23
1188	TW	UXLabs	uxlabs-001	001	2022-09-19
1189	TW	UXLabs	uxlabs-003	003	2023-07-28
1190	UZ	UZINFOCOM	uzinfocom-000	000	2025-07-28

Table 17: Summary of participant information included in this report.

	Location	Developer Name	Short Name	Seq. Num.	Validation Date
1191	UZ	UZINFOCOM	uzinfocom-001	001	2026-04-08
1192	HU	Ultinous	ultinous-000	000	2017-12-18
1193	HU	Ultinous	ultinous-001	001	2018-02-02
1194	FR	Unissey	unissey-001	001	2021-11-29
1195	FR	Unissey	unissey-002	002	2022-04-29
1196	FR	Unissey	unissey-003	003	2022-12-19
1197	FR	Unissey	unissey-004	004	2023-07-19
1198	FR	Unissey	unissey-005	005	2024-08-06
1199	FR	Unissey	unissey-006	006	2025-09-11
1200	FR	Unissey	unissey-007	007	2026-03-25
1201	PT	Universidade de Coimbra	visteam-000	000	2020-01-14
1202	PT	Universidade de Coimbra	visteam-001	001	2021-03-16
1203	PT	Universidade de Coimbra	visteam-002	002	2021-08-20
1204	PT	Universidade de Coimbra	visteam-003	003	2022-01-31
1205	PT	Universidade de Coimbra	visteam-004	004	2022-08-01
1206	PT	Universidade de Coimbra	visteam-005	005	2023-01-04
1207	PT	Universidade de Coimbra	visteam-006	006	2023-05-25
1208	PT	Universidade de Coimbra	visteam-007	007	2023-10-18
1209	PT	Universidade de Coimbra	visteam-008	008	2024-02-06
1210	PT	Universidade de Coimbra	visteam-009	009	2024-07-26
1211	PT	Universidade de Coimbra	visteam-010	010	2025-05-28
1212	UK	University of Surrey-CVSSP	surrey-cvssp-000	000	2022-03-25
1213	UK	University of Surrey-CVSSP	surrey-cvssp-001	001	2022-09-22
1214	UK	University of Surrey-CVSSP	surrey-cvssp-002	002	2023-02-16
1215	UK	University of Surrey-CVSSP	surrey-cvssp-003	003	2023-09-13
1216	UK	University of Surrey-CVSSP	surrey-cvssp-004	004	2024-07-11
1217	US	VCognition	vcog-002	002	2017-06-12
1218	VN	VNIS Joint Stock	vnis-000	000	2024-01-08
1219	US	Vaidio	vaidio-001	001	2025-12-10
1220	US	Vcortex Labs	vcortex-001	001	2023-06-14
1221	ES	Veridas Digital Authentication Solutions S.L.	veridas-001	001	2019-03-01
1222	ES	Veridas Digital Authentication Solutions S.L.	veridas-002	002	2019-03-01
1223	ES	Veridas Digital Authentication Solutions S.L.	veridas-003	003	2019-11-27
1224	ES	Veridas Digital Authentication Solutions S.L.	veridas-004	004	2020-07-21
1225	ES	Veridas Digital Authentication Solutions S.L.	veridas-005	005	2020-12-15
1226	ES	Veridas Digital Authentication Solutions S.L.	veridas-006	006	2021-04-15
1227	ES	Veridas Digital Authentication Solutions S.L.	veridas-007	007	2021-09-02
1228	ES	Veridas Digital Authentication Solutions S.L.	veridas-008	008	2022-10-17
1229	ES	Veridas Digital Authentication Solutions S.L.	veridas-009	009	2023-05-08
1230	ES	Veridas Digital Authentication Solutions S.L.	veridas-010	010	2025-03-18
1231	UK	Veridium	veridium-000	000	2022-03-28
1232	UK	Veridium	veridium-001	001	2022-11-03
1233	UK	Veridium	veridium-002	002	2023-06-30
1234	UK	Veridium	veridium-003	003	2024-02-21
1235	KZ	Verigram	verigram-000	000	2021-09-06
1236	KZ	Verigram	verigram-001	001	2022-03-09
1237	KZ	Verigram	verigram-002	002	2023-04-03
1238	KZ	Verigram	verigram-003	003	2023-08-09
1239	ID	Verihubs	verihubs-inteligensia-000	000	2021-07-27
1240	ID	Verihubs	verihubs-inteligensia-001	001	2022-06-16
1241	ID	Verihubs	verihubs-inteligensia-002	002	2023-06-07
1242	ID	Verijelas	verijelas-000	000	2022-08-01
1243	TW	Via Technologies Inc	via-000	000	2019-07-08
1244	TW	Via Technologies Inc	via-001	001	2020-01-08
1245	TW	Via Technologies Inc	via-004	004	2023-02-23
1246	TW	Via Technologies Inc	via-005	005	2023-12-26
1247	TW	Via Technologies Inc	via-006	006	2025-02-24
1248	AE	Viante.AI	viante-000	000	2023-06-09
1249	AE	Viante.AI	viante-001	001	2024-12-30
1250	AE	Viante.AI	viante-002	002	2025-06-17
1251	AE	Viante.AI	viante-003	003	2026-03-27
1252	DE	Videmo Intelligente Videoanalyse	videmo-000	000	2019-12-19
1253	DE	Videmo Intelligente Videoanalyse	videmo-001	001	2021-12-22
1254	DE	Videmo Intelligente Videoanalyse	videmo-002	002	2022-08-31
1255	DE	Videmo Intelligente Videoanalyse	videmo-003	003	2024-06-18
1256	IN	Videonetics Technology Pvt	videonetics-001	001	2019-06-19
1257	IN	Videonetics Technology Pvt	videonetics-002	002	2019-11-21
1258	VN	Vietnam National Cyber Security Technology Corporation	ncsgroup-000	000	2024-03-18
1259	VN	Vietnam Payment Solution	vnpay-000	000	2023-12-05
1260	VN	Vietnam Payment Solution	vnpay-001	001	2024-10-15

Table 18: Summary of participant information included in this report.

FNMR(T) "False non-match rate"
FMR(T) "False match rate"

	Location	Developer Name	Short Name	Seq. Num.	Validation Date
1261	VN	Vietnam Posts and Telecommunications Group	vnpt-001	001	2021-01-08
1262	VN	Vietnam Posts and Telecommunications Group	vnpt-002	002	2021-06-08
1263	VN	Vietnam Posts and Telecommunications Group	vnpt-003	003	2021-12-01
1264	VN	Vietnam Posts and Telecommunications Group	vnpt-004	004	2022-04-15
1265	VN	Vietnam Posts and Telecommunications Group	vnpt-005	005	2022-08-24
1266	VN	Vietnam Posts and Telecommunications Group	vnpt-006	006	2023-08-18
1267	VN	Vietnam Posts and Telecommunications Group	vnpt-007	007	2024-04-29
1268	VN	Vietnam Posts and Telecommunications Group	vnpt-008	008	2024-09-20
1269	VN	Vietnam Posts and Telecommunications Group	vnpt-009	009	2025-06-04
1270	VN	Viettel Artificial Intelligence	viettelai-000	000	2023-06-26
1271	VN	Viettel Artificial Intelligence	viettelai-001	001	2023-11-20
1272	VN	Viettel Artificial Intelligence	viettelai-002	002	2024-07-17
1273	VN	Viettel Artificial Intelligence	viettelai-003	003	2025-02-27
1274	VN	Viettel Artificial Intelligence and Data Services Center	viettelai-004	004	2025-11-26
1275	VN	Viettel Group	vts-000	000	2020-11-04
1276	VN	Viettel Group	vts-001	001	2022-04-20
1277	VN	Viettel Group	vts-002	002	2024-06-04
1278	VN	Viettel High Technology	viettelhightech-000	000	2021-08-04
1279	VN	Viettel High Technology	viettelhightech-001	001	2025-03-18
1280	VN	Viettel High Technology	viettelhightech-002	002	2025-10-15
1281	US	Vigilant Solutions	vigilantsolutions-000	000	2017-03-30
1282	US	Vigilant Solutions	vigilantsolutions-001	001	2017-06-13
1283	US	Vigilant Solutions	vigilantsolutions-002	002	2017-09-28
1284	US	Vigilant Solutions	vigilantsolutions-003	003	2018-01-23
1285	US	Vigilant Solutions	vigilantsolutions-004	004	2018-06-14
1286	US	Vigilant Solutions	vigilantsolutions-005	005	2018-10-11
1287	US	Vigilant Solutions	vigilantsolutions-006	006	2019-03-01
1288	US	Vigilant Solutions	vigilantsolutions-007	007	2019-06-27
1289	US	Vigilant Solutions	vigilantsolutions-008	008	2020-08-03
1290	US	Vigilant Solutions	vigilantsolutions-009	009	2020-12-07
1291	US	Vigilant Solutions	vigilantsolutions-010	010	2021-04-07
1292	US	Vigilant Solutions	vigilantsolutions-011	011	2021-08-07
1293	VN	VinAI Research VietNam	vinai-000	000	2020-09-24
1294	VN	VinBigData	vinbigdata-001	001	2022-01-06
1295	VN	VinBigData	vinbigdata-002	002	2022-06-07
1296	VN	VinBigData	vinbigdata-003	003	2023-06-23
1297	VN	VinBigData	vinbigdata-004	004	2024-05-08
1298	VN	VinBigData	vinbigdata-005	005	2024-10-16
1299	VN	VinBigData	vinbigdata-006	006	2025-02-19
1300	VN	VinBigData	vinbigdata-007	007	2025-07-24
1301	SE	Visage Technologies	visage-000	000	2020-12-09
1302	BR	Visica AI Solutions	visica-001	001	2025-02-14
1303	BR	Visica AI Solutions	visica-002	002	2025-07-15
1304	FI	Visidon	vd-000	000	2018-06-13
1305	FI	Visidon	vd-001	001	2019-02-26
1306	FI	Visidon	vd-002	002	2021-04-12
1307	FI	Visidon	vd-003	003	2021-10-12
1308	CN	Vision Intelligence Center of Meituan	meituan-000	000	2021-05-14
1309	CN	Vision Intelligence Center of Meituan	meituan-001	001	2022-03-25
1310	CN	Vision Intelligence Center of Meituan	meituan-002	002	2022-09-14
1311	CN	Vision Intelligence Center of Meituan	meituan-003	003	2023-03-06
1312	CN	Vision Intelligence Center of Meituan	meituan-004	004	2023-08-16
1313	PT	Vision-Box	visionbox-000	000	2019-02-26
1314	PT	Vision-Box	visionbox-001	001	2019-03-01
1315	PT	Vision-Box	visionbox-002	002	2021-04-29
1316	PT	Vision-Box	visionbox-003	003	2023-02-01
1317	PT	Vision-Box	visionbox-004	004	2023-06-30
1318	PT	Vision-Box	visionbox-005	005	2024-07-29
1319	PT	Vision-Box	visionbox-006	006	2025-07-29
1320	PT	Vision-Box	visionbox-007	007	2026-02-03
1321	RU	VisionLabs	visionlabs-001	001	2017-06-12
1322	RU	VisionLabs	visionlabs-002	002	2017-09-08
1323	RU	VisionLabs	visionlabs-003	003	2018-02-02
1324	RU	VisionLabs	visionlabs-004	004	2018-06-15
1325	RU	VisionLabs	visionlabs-005	005	2018-10-19
1326	RU	VisionLabs	visionlabs-006	006	2019-03-01
1327	RU	VisionLabs	visionlabs-007	007	2019-06-12
1328	RU	VisionLabs	visionlabs-008	008	2020-01-06
1329	RU	VisionLabs	visionlabs-009	009	2020-07-27
1330	RU	VisionLabs	visionlabs-010	010	2021-01-25

Table 19: Summary of participant information included in this report.

FNMR(T) "False non-match rate"
FMR(T) "False match rate"

	Location	Developer Name	Short Name	Seq. Num.	Validation Date
1331	RU	VisionLabs	visionlabs-011	011	2021-10-13
1332	TW	Vivotek	vivotek-001	001	2024-04-03
1333	TW	Vivotek	vivotek-002	002	2024-08-15
1334	AU	Vixvizon	vixvizion-000	000	2019-06-19
1335	AU	Vixvizon	vixvizion-001	001	2019-10-22
1336	AU	Vixvizon	vixvizion-002	002	2020-12-31
1337	AU	Vixvizon	vixvizion-003	003	2021-05-18
1338	AU	Vixvizon	vixvizion-004	004	2021-09-20
1339	AU	Vixvizon	vixvizion-005	005	2022-03-03
1340	AU	Vixvizon	vixvizion-006	006	2022-08-11
1341	AU	Vixvizon	vixvizion-007	007	2023-01-17
1342	US	Vocalize	vocalize-001	001	2024-03-27
1343	RU	Vocord	vocord-001	001	2017-04-21
1344	RU	Vocord	vocord-002	002	2017-06-07
1345	RU	Vocord	vocord-003	003	2018-01-23
1346	RU	Vocord	vocord-004	004	2018-06-15
1347	RU	Vocord	vocord-005	005	2018-10-19
1348	RU	Vocord	vocord-006	006	2019-03-01
1349	RU	Vocord	vocord-007	007	2019-06-06
1350	RU	Vocord	vocord-008	008	2020-01-31
1351	RU	Vocord	vocord-009	009	2020-12-28
1352	RU	Vocord	vocord-010	010	2021-12-20
1353	BR	Vsoft	vsoft-001	001	2025-08-01
1354	BR	Vsoft	vsoft-002	002	2025-11-28
1355	BR	Vsoft	vsoft-003	003	2026-03-30
1356	US	Wicket	wicket-000	000	2022-02-14
1357	CN	Winsense	winsense-000	000	2019-06-17
1358	CN	Winsense	winsense-001	001	2019-10-16
1359	CN	Winsense	winsense-002	002	2020-11-20
1360	MY	Wise AI SDN BHD	wiseai-001	001	2022-10-25
1361	CN	Wuhan Tianyu Information Industry	wuhantianyu-001	001	2021-08-05
1362	CN	X-Laboratory	x-laboratory-000	000	2019-09-03
1363	CN	X-Laboratory	x-laboratory-001	001	2020-01-21
1364	CN	Xforward AI Technology	xforwardai-000	000	2020-02-06
1365	CN	Xforward AI Technology	xforwardai-001	001	2020-09-25
1366	CN	Xforward AI Technology	xforwardai-002	002	2021-02-10
1367	CN	Xiamen Meiya Pico Information	meiya-001	001	2019-03-01
1368	CN	Xiamen University	xm-000	000	2020-10-19
1369	PT	YooniK	yoonik-000	000	2020-06-24
1370	PT	YooniK	yoonik-001	001	2020-10-26
1371	PT	YooniK	yoonik-002	002	2021-09-06
1372	PT	YooniK	yoonik-003	003	2022-01-06
1373	PT	YooniK	yoonik-004	004	2023-02-10
1374	UK	Yoti	yoti-001	001	2024-02-13
1375	UK	Yoti	yoti-002	002	2024-07-03
1376	TW	Yuan High-Tech Development	yuan-000	000	2020-06-30
1377	TW	Yuan High-Tech Development	yuan-001	001	2021-01-08
1378	TW	Yuan High-Tech Development	yuan-002	002	2021-05-17
1379	TW	Yuan High-Tech Development	yuan-003	003	2021-09-17
1380	TW	Yuan High-Tech Development	yuan-004	004	2022-01-14
1381	TW	Yuan High-Tech Development	yuan-005	005	2022-06-22
1382	TW	Yuan High-Tech Development	yuan-006	006	2022-12-14
1383	TW	Yuan High-Tech Development	yuan-007	007	2023-05-11
1384	TW	Yuan High-Tech Development	yuan-008	008	2023-11-06
1385	TW	Yuan High-Tech Development	yuan-009	009	2024-04-24
1386	TW	Yuan High-Tech Development	yuan-010	010	2024-10-22
1387	CN	YuanLi Technology	yuanli-001	001	2026-03-23
1388	CN	Yuntu Data and Technology	ytu-000	000	2021-06-16
1389	CN	Zhuhai Yisheng Electronics Technology	yisheng-000	000	2017-08-17
1390	CN	Zhuhai Yisheng Electronics Technology	yisheng-001	001	2017-08-17
1391	CN	Zhuhai Yisheng Electronics Technology	yisheng-002	002	2018-02-01
1392	CN	Zhuhai Yisheng Electronics Technology	yisheng-004	004	2018-06-12
1393	IN	i2v Systems	i2v-001	001	2024-03-11
1394	IN	i2v Systems	i2v-002	002	2025-01-15
1395	VN	iCOMM Media and Tech	icomm-000	000	2023-12-26
1396	CN	iQIYI Inc	iqface-000	000	2019-06-04
1397	CN	iQIYI Inc	iqface-001	001	2019-12-11
1398	CN	iQIYI Inc	iqface-003	003	2021-02-23
1399	TW	iSAP Solution Corporation	isap-001	001	2019-08-07
1400	TW	iSAP Solution Corporation	isap-002	002	2020-09-01

Table 20: Summary of participant information included in this report.

	Location	Developer Name	Short Name	Seq. Num.	Validation Date
1401	TW	ioNetworks Inc	ionetworks-000	000	2021-07-20
1402	TW	ioNetworks Inc	ionetworks-001	001	2023-08-01
1403	TW	ioNetworks Inc	ionetworks-002	002	2023-12-08
1404	TW	ioNetworks Inc	ionetworks-003	003	2024-05-09
1405	TW	ioNetworks Inc	ionetworks-004	004	2026-04-22
1406	KR	useB	useb-000	000	2023-05-08
1407	KR	useB	useb-001	001	2023-09-12
1408	KR	useB	useb-002	002	2024-01-19
1409	KR	useB	useb-003	003	2024-08-09
1410	KR	useB	useb-004	004	2024-12-23

Table 21: Summary of participant information included in this report.

FNMR(T) "False non-match rate"
FMR(T) "False match rate"

	ALGORITHM	CONFIG	LIBRARY	TEMPLATE							COMPARISON[4]	
	NAME	DATA	DATA	MEMORY	SIZE	GENERATION TIME (ms)[4]					TIME (ns)[5]	
		(KB)[1]	(KB)[2]	(MB)[3]	(B)	MUGSHOT	480x720	960x1440	1600x2400	3000x4500	GENUINE	IMPOSTOR
1	2060io-001	567279	43224	^{230}629	^{1397}10488 ± 0	^{1010}958 ± 22	^{734}983 ± 38	^{740}1045 ± 205	^{1042}1724 ± 310	^{1049}3474 ± 1170	^{1083}7105 ± 42	^{1079}7071 ± 47
2	2060io-002	579607	42980	^{617}1559	^{1396}10488 ± 0	^{345}398 ± 0	^{230}418 ± 1	^{293}525 ± 1	^{479}786 ± 1	-	^{1079}7000 ± 91	^{1073}6965 ± 85
3	20face-000	117155	324083	^{574}1417	^{893}2048 ± 0	^{161}232 ± 1	^{93}223 ± 1	^{74}226 ± 4	^{59}222 ± 1	^{41}224 ± 1	^{1322}44880 ± 134	^{1321}44462 ± 163
4	20face-001	226824	324119	^{599}1512	^{1233}4096 ± 0	^{204}279 ± 2	^{113}266 ± 1	^{87}266 ± 1	^{76}267 ± 1	^{57}267 ± 0	^{1028}5553 ± 54	^{1026}5541 ± 65
5	3divi-000	169360	139460	-	^{117}512 ± 0	^{212}285 ± 52	-	-	-	-	^{108}378 ± 20	^{112}375 ± 19
6	3divi-001	190867	139473	-	^{1261}4096 ± 0	^{196}274 ± 47	-	-	-	-	^{236}636 ± 19	^{247}634 ± 16
7	3divi-002	190867	175117	-	^{1247}4096 ± 0	^{203}279 ± 48	-	-	-	-	^{269}692 ± 22	^{293}707 ± 26
8	3divi-003	191636	55903	-	^{1169}4096 ± 0	^{653}650 ± 90	-	-	-	-	^{225}627 ± 11	^{234}623 ± 32
9	3divi-004	263670	50794	-	^{601}2048 ± 0	^{1038}984 ± 131	-	-	-	-	^{325}794 ± 35	^{337}801 ± 40
10	3divi-005	264098	53870	-	^{520}2048 ± 0	^{1047}993 ± 83	^{848}1136 ± 88	^{952}1309 ± 137	^{903}1348 ± 131	^{933}1671 ± 166	^{323}790 ± 20	^{329}791 ± 23
11	3divi-006	273866	52656	^{515}1252	^{863}2048 ± 0	^{662}654 ± 1	^{443}651 ± 0	^{414}660 ± 1	^{383}678 ± 2	^{372}759 ± 13	^{318}775 ± 19	^{322}770 ± 22
12	3divi-007	483115	24723	^{528}1288	^{811}2048 ± 0	^{610}615 ± 1	^{403}616 ± 1	^{371}623 ± 1	^{348}644 ± 1	^{348}727 ± 5	^{281}707 ± 31	^{299}712 ± 25
13	accurascan-001	14057	24437	^{383}944	^{115}512 ± 0	^{137}204 ± 27	^{88}215 ± 17	^{71}220 ± 16	^{67}237 ± 18	^{80}339 ± 19	^{1202}15634 ± 54	^{1204}15647 ± 77
14	accurascan-002	14057	24437	^{385}945	^{133}512 ± 0	^{97}173 ± 23	^{66}188 ± 14	^{58}191 ± 14	^{51}208 ± 16	^{68}317 ± 14	^{1164}12255 ± 69	^{1166}12231 ± 72
15	accurascan-003	998397	27018	^{721}1996	^{605}2048 ± 0	^{693}676 ± 1	^{471}677 ± 7	^{455}700 ± 8	^{450}751 ± 16	^{504}950 ± 47	^{164}540 ± 10	^{167}536 ± 10
16	acer-000	109735	88323	-	^{766}2048 ± 0	^{154}222 ± 0	^{99}233 ± 4	^{79}238 ± 4	^{73}262 ± 18	^{90}356 ± 46	^{415}1065 ± 40	^{442}1109 ± 35
17	acer-001	36650	66086	^{130}417	^{140}512 ± 0	^{134}199 ± 0	^{100}237 ± 28	^{75}229 ± 26	^{69}242 ± 37	^{53}259 ± 21	^{764}2453 ± 44	^{769}2461 ± 62
18	acer-002	43922	624858	^{69}192	^{412}2048 ± 0	^{112}184 ± 0	^{63}184 ± 0	^{49}185 ± 0	^{40}185 ± 0	^{28}186 ± 0	^{890}3370 ± 47	^{895}3350 ± 54
19	acisw-003	282029	35664	-	^{1403}18467 ± 8	^{160}232 ± 1	^{114}267 ± 22	^{259}488 ± 28	^{620}990 ± 24	^{1037}2977 ± 129	^{1406}847908 ± 16757	^{1406}851850 ± 17018
20	acisw-006	282029	36107	-	^{1402}18465 ± 8	^{152}219 ± 0	^{97}227 ± 0	^{186}410 ± 1	^{517}838 ± 1	^{1017}2532 ± 10	^{1402}548137 ± 16513	^{1402}549586 ± 9238
21	acisw-007	267619	36111	^{87}287	^{797}2048 ± 0	^{210}283 ± 0	^{134}293 ± 3	^{189}414 ± 0	^{163}404 ± 0	^{167}484 ± 1	^{496}1316 ± 22	^{501}1297 ± 23
22	acisw-008	171703	39359	^{460}1102	^{393}2048 ± 0	^{349}400 ± 1	^{183}362 ± 28	^{154}369 ± 9	^{94}300 ± 2	^{77}336 ± 5	^{498}1327 ± 19	^{509}1337 ± 32
23	adera-001	0	79272	-	^{1123}2560 ± 0	^{40}97 ± 0	-	-	-	-	^{579}1604 ± 71	^{590}1649 ± 56
24	adera-002	0	749797	-	^{1346}5120 ± 0	^{1326}1394 ± 11	^{1017}1381 ± 1	^{1009}1393 ± 1	^{952}1403 ± 1	^{860}1464 ± 2	^{703}2163 ± 32	^{703}2158 ± 28
25	adera-003	0	749778	^{373}917	^{1347}5120 ± 0	^{1312}1381 ± 12	^{1019}1385 ± 1	^{1011}1394 ± 1	^{945}1401 ± 1	^{862}1469 ± 1	^{701}2148 ± 34	^{698}2130 ± 32
26	adera-004	0	959123	^{669}1748	^{1357}6144 ± 0	^{1236}1246 ± 1	^{906}1204 ± 1	^{887}1230 ± 2	^{797}1207 ± 2	^{717}1254 ± 1	^{637}1840 ± 34	^{638}1828 ± 31
27	adera-005	0	959113	^{663}1734	^{1360}6144 ± 0	^{962}914 ± 1	^{641}879 ± 3	^{594}880 ± 2	^{548}886 ± 2	^{481}910 ± 2	^{653}1896 ± 14	^{649}1874 ± 20
28	advance-002	257173	20434	-	^{457}2048 ± 0	^{853}811 ± 2	^{582}803 ± 2	^{450}696 ± 2	^{404}699 ± 4	^{338}718 ± 1	^{383}987 ± 10	^{388}988 ± 45
29	advance-003	258867	78699	^{179}518	^{363}2048 ± 0	^{560}586 ± 0	-	^{335}583 ± 0	^{300}588 ± 0	^{242}591 ± 1	^{636}1813 ± 17	^{629}1788 ± 26
30	advance-004	803133	954494	^{254}681	^{633}2048 ± 0	^{1119}1099 ± 20	^{822}1107 ± 15	^{778}1093 ± 21	^{703}1103 ± 21	^{639}1138 ± 21	^{663}1935 ± 35	^{667}1936 ± 32
31	advance-005	277607	126218	^{226}624	^{825}2048 ± 0	^{539}573 ± 1	^{363}574 ± 2	^{325}573 ± 2	^{286}574 ± 2	^{252}601 ± 2	^{563}1517 ± 16	^{565}1518 ± 26
32	advance-006	472567	136481	^{214}605	^{896}2048 ± 0	^{688}673 ± 0	^{457}670 ± 0	^{429}673 ± 0	^{388}684 ± 0	^{365}745 ± 0	^{333}808 ± 4	^{341}808 ± 1
33	affinsys-ai-000	38016	46159	^{42}142	^{136}512 ± 0	^{14}48 ± 0	^{11}52 ± 0	^{22}106 ± 0	^{19}110 ± 0	^{32}194 ± 0	^{674}2007 ± 25	^{676}2006 ± 28
34	afisbiometrics-000	545886	32882	^{449}1085	^{150}512 ± 0	^{1214}1219 ± 1	^{847}1135 ± 1	^{815}1137 ± 2	^{740}1137 ± 1	^{645}1147 ± 1	^{517}1400 ± 29	^{515}1357 ± 32
35	afrengine-000	151875	382842	^{60}178	^{1195}4096 ± 0	^{50}107 ± 0	^{31}112 ± 0	^{97}284 ± 2	^{403}697 ± 2	^{1047}3299 ± 17	^{1343}54329 ± 140	^{1344}56195 ± 256
36	afrengine-001	410712	391289	^{409}1015	^{1224}4096 ± 0	^{1025}970 ± 0	^{732}982 ± 1	^{675}979 ± 2	^{625}996 ± 0	^{529}990 ± 4	^{1342}54240 ± 169	^{1343}56125 ± 179
37	afrengine-002	579618	239125	^{412}1018	^{471}2048 ± 0	^{900}851 ± 3	^{790}1065 ± 16	^{692}993 ± 7	^{528}855 ± 5	^{449}857 ± 9	^{480}1259 ± 13	^{493}1270 ± 23
38	afrengine-003	579563	239117	^{410}1017	^{637}2048 ± 0	^{1114}1088 ± 1	^{664}911 ± 15	^{762}1067 ± 5	^{510}833 ± 3	^{528}989 ± 2	^{492}1294 ± 48	^{498}1284 ± 29
39	afrengine-004	579587	239117	^{411}1018	^{366}2048 ± 0	^{924}875 ± 2	^{700}951 ± 119	^{715}1018 ± 5	^{555}895 ± 1	^{564}1043 ± 6	^{477}1254 ± 17	^{489}1258 ± 23
40	afrengine-005	694908	239155	^{413}1018	^{736}2048 ± 0	^{880}831 ± 10	^{721}972 ± 52	^{562}834 ± 2	^{552}891 ± 9	^{588}1065 ± 1	^{485}1276 ± 19	^{494}1273 ± 20
41	aifirst-001	224157	808777	^{157}485	^{420}2048 ± 0	^{562}587 ± 2	^{359}568 ± 2	^{337}584 ± 3	^{308}601 ± 6	^{369}755 ± 5	^{430}1099 ± 14	^{435}1087 ± 45
42	aigen-001	256958	595227	^{479}1154	^{356}2048 ± 0	^{1356}1448 ± 9	^{1066}1451 ± 8	^{1091}1759 ± 6	^{1100}2594 ± 4	^{1078}5691 ± 44	^{937}3772 ± 57	^{936}3736 ± 56
43	aigen-002	205300	1316138	^{367}896	^{435}2048 ± 0	^{561}586 ± 24	^{372}582 ± 4	^{623}920 ± 4	^{1047}1758 ± 5	^{1075}5427 ± 17	^{925}3678 ± 44	^{927}3646 ± 48
44	aigroup-000	357973	390046	^{124}398	^{784}2048 ± 0	^{287}351 ± 0	^{162}337 ± 1	^{141}353 ± 1	^{123}356 ± 1	^{108}385 ± 1	^{1127}9603 ± 216	^{1129}9689 ± 373

Notes	
1	The configuration size does not capture static data included in libraries.
2	The library size is the combined total of all files provided in the submission lib folder. These libraries e.g. OpenCV may or may not be installed on any end user's platform natively and would not need to be installed with the algorithm. Some developers put neural network models in their libraries.
3	The memory usage is the peak resident set size reported by the ps system call during template generation.
4	The median template creation times are measured on Intel®Xeon®CPU E5-2630 v4 @ 2.20GHz processors.
5	The comparison durations, in nanoseconds, are estimated using std::chrono::high_resolution_clock which on the machine in (2) counts 1ns clock ticks. Precision is somewhat worse than that however. The ± value is the median absolute deviation times 1.48 for Normal consistency.

Table 22: Summary of algorithms and properties included in this report. The red superscripts give ranking for the quantity in that column.

	ALGORITHM	CONFIG	LIBRARY	TEMPLATE							COMPARISON[4]	
	NAME	DATA	DATA	MEMORY	SIZE	GENERATION TIME (ms)[4]					TIME (ns)[5]	
		(KB)[1]	(KB)[2]	(MB)[3]	(B)	MUGSHOT	480x720	960x1440	1600x2400	3000x4500	GENUINE	IMPOSTOR
45	aigroup-001	298974	390068	^{205}587	^{439}2048 ± 0	^{495}535 ± 0	^{325}531 ± 0	^{297}533 ± 0	^{265}544 ± 5	^{246}595 ± 0	^{1121}9526 ± 170	^{1124}9562 ± 213
46	aigroup-002	271124	396396	^{364}888	^{1092}2078 ± 0	^{197}275 ± 0	^{123}276 ± 0	^{96}283 ± 2	^{102}318 ± 5	^{131}419 ± 0	^{1362}66379 ± 111	^{1362}66387 ± 124
47	ailabs-001	1054663	338989	^{514}1252	^{904}2048 ± 0	^{674}664 ± 4	^{561}774 ± 50	^{824}1145 ± 12	^{1071}1972 ± 74	^{1072}5205 ± 272	^{1389}104034 ± 661	^{1389}103415 ± 7722
48	aimall-001	128820	57257	-	^{223}1024 ± 0	^{261}326 ± 1	-	-	-	-	^{962}4127 ± 72	^{949}3909 ± 166
49	aimall-002	370156	25210	^{623}1576	^{597}2048 ± 0	^{812}776 ± 4	^{683}927 ± 27	^{639}940 ± 21	^{595}955 ± 34	^{542}1003 ± 75	^{1374}72811 ± 7399	^{1370}71216 ± 6286
50	aimall-003	504324	171935	^{705}1913	^{234}1024 ± 0	^{670}662 ± 1	^{534}740 ± 51	^{502}752 ± 62	^{443}741 ± 46	^{411}807 ± 47	^{1301}34565 ± 93	^{1303}34598 ± 118
51	aiseemu-001	0	1005354	^{828}2701	^{1215}4096 ± 0	^{1052}1001 ± 1	^{761}1017 ± 0	^{711}1014 ± 5	^{653}1022 ± 2	^{582}1059 ± 4	^{997}4864 ± 25	^{1001}4855 ± 32
52	aiseemu-002	0	1216980	^{893}3453	^{1256}4096 ± 0	^{1269}1298 ± 5	^{977}1303 ± 4	^{955}1313 ± 2	^{896}1329 ± 0	^{782}1348 ± 2	^{1002}4917 ± 37	^{1003}4916 ± 37
53	aiunionface-000	241642	840295	^{125}402	^{553}2048 ± 0	^{642}637 ± 13	^{548}754 ± 41	^{718}1025 ± 28	^{774}1179 ± 29	^{926}1639 ± 47	^{419}1072 ± 19	^{430}1080 ± 47
54	aize-001	268456	168970	^{609}1546	^{782}2048 ± 0	^{395}437 ± 10	^{253}440 ± 8	^{307}542 ± 17	^{452}756 ± 27	^{913}1583 ± 53	^{665}1937 ± 22	^{658}1919 ± 23
55	aize-002	257106	182517	^{204}586	^{544}2048 ± 0	^{424}467 ± 1	^{283}479 ± 1	^{506}756 ± 1	^{1000}1477 ± 1	^{1065}4617 ± 41	^{191}597 ± 16	^{206}598 ± 14
56	aize-003	257130	33045	^{191}546	^{714}2048 ± 0	^{117}187 ± 0	^{67}188 ± 0	^{47}182 ± 0	^{38}183 ± 0	^{33}195 ± 0	^{218}621 ± 37	^{199}592 ± 1
57	aize-006	276515	27909	^{165}497	^{1080}2060 ± 0	^{461}501 ± 0	^{306}504 ± 0	^{276}505 ± 0	^{237}508 ± 0	^{258}612 ± 0	^{910}3515 ± 35	^{914}3496 ± 40
58	ajou-001	363257	31734	^{141}442	^{559}2048 ± 0	^{486}530 ± 0	^{330}536 ± 0	^{299}535 ± 0	^{272}549 ± 0	^{236}577 ± 0	^{190}597 ± 19	^{203}596 ± 13
59	alchera-000	258450	18848	-	^{839}2048 ± 0	^{563}587 ± 13	^{502}706 ± 48	^{1003}1389 ± 58	^{1103}2722 ± 123	^{1094}9011 ± 455	^{871}3189 ± 32	^{860}3031 ± 142
60	alchera-001	174013	18848	-	^{480}2048 ± 0	^{626}627 ± 11	-	-	-	-	^{887}3342 ± 81	^{886}3243 ± 47
61	alchera-002	405409	22275	-	^{444}2048 ± 0	^{1022}968 ± 1	^{726}976 ± 2	^{676}979 ± 1	^{618}988 ± 1	^{555}1025 ± 2	^{905}3488 ± 63	^{905}3430 ± 63
62	alchera-003	487718	24613	^{564}1376	^{399}2048 ± 0	^{903}854 ± 3	^{625}862 ± 2	^{586}870 ± 1	^{544}882 ± 2	^{486}918 ± 1	^{897}3426 ± 57	^{898}3383 ± 53
63	alchera-004	1001019	388616	^{521}1271	^{577}2048 ± 0	^{1029}975 ± 0	^{704}955 ± 0	^{662}960 ± 0	^{619}989 ± 0	^{647}1152 ± 1	^{913}3529 ± 54	^{920}3530 ± 63
64	alchera-005	1001019	388616	^{522}1272	^{854}2048 ± 0	^{1023}969 ± 1	^{739}987 ± 3	^{682}985 ± 3	^{629}998 ± 0	^{655}1162 ± 2	^{902}3481 ± 59	^{904}3422 ± 57
65	alchera-006	1000967	493456	^{578}1426	^{929}2048 ± 0	^{482}522 ± 2	^{333}540 ± 3	^{309}544 ± 2	^{283}569 ± 3	^{359}739 ± 3	^{718}2233 ± 38	^{724}2253 ± 77
66	alchera-007	1000948	493456	^{583}1430	^{626}2048 ± 0	^{485}530 ± 2	^{348}556 ± 2	^{320}566 ± 2	^{289}581 ± 2	^{374}762 ± 4	^{708}2178 ± 35	^{706}2169 ± 44
67	alchera-008	1002024	493460	^{584}1430	^{380}2048 ± 0	^{567}589 ± 3	^{354}563 ± 4	^{364}614 ± 3	^{318}614 ± 1	^{413}810 ± 3	^{1010}5129 ± 35	^{1150}11226 ± 120
68	alchera-009	2086479	454616	^{842}2763	^{533}2048 ± 0	^{1378}1486 ± 4	^{1086}1507 ± 4	^{1036}1438 ± 9	^{1013}1508 ± 11	^{968}2008 ± 4	^{729}2284 ± 44	^{729}2278 ± 69
69	alfabeta-001	128232	21780	^{17}74	^{134}512 ± 0	^{193}271 ± 0	^{124}276 ± 0	^{233}459 ± 2	^{549}886 ± 2	^{1018}2547 ± 9	^{135}470 ± 25	^{138}458 ± 20
70	alice-000	1741293	19355	^{883}3329	^{1193}4096 ± 0	^{1000}950 ± 2	^{689}933 ± 1	^{649}949 ± 1	^{648}1011 ± 3	^{722}1264 ± 8	^{1192}14975 ± 201	^{1194}14890 ± 229
71	alice-001	1428001	17074	^{260}690	^{831}2048 ± 0	^{1109}1080 ± 1	^{794}1075 ± 0	^{780}1095 ± 1	^{744}1143 ± 1	^{843}1435 ± 1	^{1242}21885 ± 278	^{1247}21921 ± 265
72	alleyes-000	507636	997090	^{348}857	^{390}2048 ± 0	^{820}784 ± 1	^{717}970 ± 61	^{671}974 ± 62	^{586}943 ± 69	^{577}1057 ± 23	^{493}1298 ± 34	^{503}1303 ± 51
73	allgovision-000	172509	155862	^{197}561	^{938}2048 ± 0	^{329}384 ± 8	^{213}395 ± 17	^{188}413 ± 14	^{211}471 ± 14	^{331}710 ± 21	^{1283}29903 ± 406	^{1284}29735 ± 194
74	alphaface-001	259849	81636	^{182}527	^{484}2048 ± 0	^{600}612 ± 1	^{397}613 ± 3	^{359}612 ± 1	^{325}619 ± 1	^{281}640 ± 2	^{391}1008 ± 10	^{398}1002 ± 19
75	alphaface-002	768995	70692	^{585}1434	^{866}2048 ± 0	^{629}628 ± 2	^{537}746 ± 19	^{499}751 ± 18	^{471}779 ± 22	^{422}828 ± 40	^{371}945 ± 25	^{376}935 ± 17
76	alttekglobal-000	649718	3060239	^{250}673	^{771}2048 ± 0	^{1101}1066 ± 2	^{867}1158 ± 2	^{855}1184 ± 1	^{763}1168 ± 1	^{679}1204 ± 2	^{507}1370 ± 23	^{520}1377 ± 26
77	amplifiedgroup-001	0	47053	^{19}81	^{204}866 ± 2	^{37}93 ± 0	-	-	-	-	^{1351}57803 ± 4210	^{1345}56365 ± 1196
78	androvideo-000	174847	585063	^{127}405	^{472}2048 ± 0	^{199}277 ± 0	^{130}285 ± 0	^{114}314 ± 0	^{135}372 ± 1	^{266}620 ± 0	^{830}2860 ± 28	^{829}2847 ± 22
79	anke-000	323402	39031	-	^{1090}2072 ± 0	^{528}566 ± 12	-	-	-	-	^{173}567 ± 20	^{170}545 ± 29
80	anke-001	642061	37364	-	^{1089}2072 ± 0	^{503}541 ± 4	-	-	-	-	^{163}540 ± 16	^{165}530 ± 20
81	anke-002	798686	28364	-	^{1091}2072 ± 0	^{373}419 ± 30	-	-	-	-	^{151}501 ± 17	^{151}492 ± 17
82	anke-003	340160	198638	-	^{1021}2056 ± 0	^{854}811 ± 23	-	-	-	-	^{118}425 ± 28	^{129}437 ± 32
83	anke-004	349388	410776	^{263}706	^{1046}2056 ± 0	^{624}625 ± 1	^{419}627 ± 2	^{394}635 ± 3	^{357}653 ± 2	^{523}982 ± 8	^{232}633 ± 22	^{242}632 ± 34
84	anke-005	328553	429160	^{471}1134	^{1045}2056 ± 0	^{568}590 ± 2	^{383}594 ± 5	^{350}601 ± 3	^{344}638 ± 4	^{419}821 ± 24	^{264}685 ± 19	^{280}687 ± 26
85	antheus-000	119453	41994	^{30}116	^{167}520 ± 0	^{51}109 ± 1	^{65}187 ± 1	^{54}189 ± 1	^{44}195 ± 1	^{45}236 ± 2	^{1074}6901 ± 268	^{1071}6936 ± 103
86	antheus-001	119453	41962	^{31}118	^{171}520 ± 0	^{58}120 ± 1	^{112}265 ± 13	^{242}468 ± 22	^{812}1223 ± 27	^{1020}2660 ± 87	^{1057}6218 ± 47	^{1052}6216 ± 45
87	antheus-002	271192	189635	^{353}875	^{763}2048 ± 0	^{1124}1104 ± 1	^{849}1138 ± 1	^{819}1140 ± 1	^{742}1142 ± 0	^{701}1240 ± 1	^{336}817 ± 5	^{345}824 ± 16
88	anyvision-001	662659	518032	-	^{225}1024 ± 0	^{171}244 ± 0	-	-	-	-	^{1379}74285 ± 212	^{1378}74145 ± 200

Notes	
1	The configuration size does not capture static data included in libraries.
2	The library size is the combined total of all files provided in the submission lib folder. These libraries e.g. OpenCV may or may not be installed on any end user's platform natively and would not need to be installed with the algorithm. Some developers put neural network models in their libraries.
3	The memory usage is the peak resident set size reported by the ps system call during template generation.
4	The median template creation times are measured on Intel®Xeon®CPU E5-2630 v4 @ 2.20GHz processors.
5	The comparison durations, in nanoseconds, are estimated using std::chrono::high_resolution_clock which on the machine in (2) counts 1ns clock ticks. Precision is somewhat worse than that however. The ± value is the median absolute deviation times 1.48 for Normal consistency.

Table 23: Summary of algorithms and properties included in this report. The red superscripts give ranking for the quantity in that column.

	ALGORITHM	CONFIG	LIBRARY	TEMPLATE							COMPARISON[4]	
	NAME	DATA	DATA	MEMORY	SIZE	GENERATION TIME (ms)[4]					TIME (ns)[5]	
		(KB)[1]	(KB)[2]	(MB)[3]	(B)	MUGSHOT	480x720	960x1440	1600x2400	3000x4500	GENUINE	IMPOSTOR
89	anyvision-002	662659	520039	-	^{245}1024 ± 0	^{176}248 ± 0	-	-	-	-	^{1378}74069 ± 188	^{1377}74019 ± 198
90	anyvision-004	401001	630797	^{461}1102	^{241}1024 ± 0	^{291}355 ± 1	-	-	-	-	^{651}1891 ± 51	^{640}1829 ± 85
91	anyvision-005	190979	116595	^{427}1048	^{227}1024 ± 0	^{1039}985 ± 1	^{748}997 ± 1	^{706}1004 ± 1	^{624}995 ± 1	^{534}995 ± 1	^{300}733 ± 14	^{312}733 ± 16
92	aratek-001	254521	15993	^{743}2135	^{822}2048 ± 0	^{179}251 ± 1	^{122}275 ± 0	^{84}252 ± 0	^{81}278 ± 0	^{61}286 ± 0	^{620}1776 ± 20	^{618}1744 ± 38
93	armatura-001	0	374608	^{898}3518	^{767}2048 ± 0	^{716}688 ± 1	^{482}689 ± 1	^{447}693 ± 1	^{413}708 ± 3	^{370}756 ± 13	^{64}270 ± 17	^{73}268 ± 11
94	armatura-002	0	1258644	^{508}1222	^{1358}6144 ± 0	^{1371}1476 ± 3	^{1071}1458 ± 5	^{1076}1535 ± 5	^{1011}1505 ± 12	^{919}1605 ± 26	^{580}1605 ± 26	^{581}1589 ± 25
95	armatura-003	0	836082	^{622}1572	^{1353}6144 ± 0	^{1076}1028 ± 1	^{774}1032 ± 1	^{721}1027 ± 0	^{658}1036 ± 1	^{562}1041 ± 3	^{1340}51850 ± 56	^{1340}51835 ± 48
96	arvis-000	529004	705484	^{355}878	^{252}1024 ± 0	^{142}209 ± 5	^{89}215 ± 1	^{131}342 ± 4	^{359}655 ± 13	^{987}2158 ± 55	^{903}3484 ± 41	^{908}3461 ± 48
97	asr-000	461347	236001	^{388}951	^{1025}2056 ± 0	^{403}450 ± 0	^{274}462 ± 1	^{226}454 ± 0	^{191}453 ± 1	^{170}486 ± 0	^{474}1226 ± 14	^{487}1251 ± 23
98	asr-001	461347	236016	^{387}949	^{1031}2056 ± 0	^{738}701 ± 0	^{503}706 ± 0	^{459}704 ± 0	^{415}709 ± 0	^{407}800 ± 0	^{668}1951 ± 28	^{675}1982 ± 23
99	asusaics-000	257418	245320	^{216}605	^{646}2048 ± 0	^{446}484 ± 13	^{310}506 ± 21	^{573}850 ± 26	^{1052}1789 ± 61	^{1081}6305 ± 188	^{1019}5455 ± 78	^{1020}5422 ± 112
100	asusaics-001	257418	245330	^{210}595	^{1162}4096 ± 0	^{893}842 ± 17	^{755}1008 ± 20	^{998}1377 ± 28	^{1097}2423 ± 90	^{1089}7284 ± 277	^{1114}8618 ± 42	^{1114}8638 ± 136
101	autentika-000	266093	3200425	^{706}1922	^{508}2048 ± 0	^{516}553 ± 1	^{389}605 ± 1	^{356}609 ± 2	^{311}608 ± 1	^{263}618 ± 2	^{1375}72833 ± 577	^{1371}71829 ± 541
102	autentika-001	0	3198534	^{642}1650	^{770}2048 ± 0	^{709}683 ± 2	^{665}912 ± 4	^{612}908 ± 3	^{567}919 ± 3	^{472}893 ± 4	^{1371}71804 ± 600	^{1369}70747 ± 582
103	autentika-002	0	3198136	^{647}1676	^{440}2048 ± 0	^{316}374 ± 1	^{312}511 ± 1	^{295}528 ± 1	^{257}534 ± 1	^{218}546 ± 1	^{1330}46941 ± 1172	^{1326}46351 ± 822
104	autentika-003	0	3198136	^{641}1648	^{678}2048 ± 0	^{394}437 ± 7	^{405}617 ± 14	^{336}584 ± 3	^{315}611 ± 8	^{260}614 ± 2	^{1332}47827 ± 1020	^{1328}46728 ± 916
105	authenmetric-002	449944	91489	-	^{509}2048 ± 0	^{986}942 ± 1	^{699}950 ± 1	^{661}960 ± 1	^{598}960 ± 1	^{530}991 ± 2	^{601}1712 ± 20	^{610}1719 ± 19
106	authenmetric-003	293599	39492	^{351}866	^{383}2048 ± 0	^{1046}992 ± 1	^{753}1006 ± 1	^{704}1003 ± 2	^{634}1002 ± 1	^{560}1036 ± 1	^{616}1757 ± 19	^{619}1755 ± 19
107	authenmetric-004	381165	39492	^{506}1214	^{727}2048 ± 0	^{955}910 ± 1	^{662}909 ± 1	^{616}915 ± 1	^{569}921 ± 2	^{505}950 ± 1	^{606}1724 ± 14	^{599}1691 ± 29
108	authme-001	1015124	37791	^{738}2097	^{1202}4096 ± 0	^{999}949 ± 1	^{716}969 ± 7	^{663}960 ± 6	^{599}961 ± 1	^{513}966 ± 4	^{824}2836 ± 34	^{826}2827 ± 54
109	authme-002	1016682	37819	^{733}2079	^{1177}4096 ± 0	^{1011}959 ± 1	^{711}959 ± 7	^{697}995 ± 5	^{605}966 ± 5	^{526}985 ± 6	^{818}2796 ± 14	^{817}2775 ± 34
110	aware-000	240240	27639	-	^{314}1572 ± 0	^{663}655 ± 26	-	-	-	-	^{957}4030 ± 83	^{853}2984 ± 152
111	aware-001	240240	27639	-	^{316}1572 ± 0	^{667}656 ± 26	-	-	-	-	^{839}2902 ± 51	^{825}2810 ± 111
112	aware-002	271312	36134	-	^{315}1572 ± 0	^{550}582 ± 14	-	-	-	-	^{334}810 ± 32	^{342}812 ± 28
113	aware-003	377729	27975	-	^{1149}3108 ± 0	^{817}783 ± 10	-	-	-	-	^{513}1392 ± 42	^{507}1334 ± 80
114	aware-004	427829	28219	-	^{1101}2084 ± 0	^{946}900 ± 10	^{820}1105 ± 10	^{886}1226 ± 25	^{1029}1585 ± 72	^{1035}2937 ± 166	^{487}1279 ± 50	^{499}1287 ± 100
115	aware-005	300017	26320	^{519}1265	^{313}1572 ± 0	^{938}886 ± 23	^{780}1038 ± 21	^{802}1121 ± 22	^{898}1337 ± 58	^{988}2195 ± 144	^{545}1475 ± 63	^{532}1427 ± 115
116	aware-006	298543	14124	^{382}944	^{76}352 ± 0	^{1156}1148 ± 3	^{859}1146 ± 2	^{856}1190 ± 2	^{874}1306 ± 20	^{942}1754 ± 84	^{789}2598 ± 42	^{788}2559 ± 60
117	aware-007	135312	18711	^{122}388	^{88}480 ± 0	^{753}713 ± 1	^{513}716 ± 1	^{482}731 ± 3	^{478}785 ± 8	^{536}999 ± 30	^{409}1058 ± 23	^{436}1091 ± 37
118	aware-008	135312	18715	^{121}387	^{87}480 ± 0	^{789}751 ± 1	^{529}737 ± 0	^{492}739 ± 3	^{505}825 ± 9	^{545}1007 ± 27	^{440}1120 ± 25	^{461}1152 ± 35
119	awiros-001	15499	87480	^{22}88	^{137}512 ± 0	^{41}97 ± 6	^{24}98 ± 4	^{30}138 ± 6	^{62}225 ± 7	^{225}556 ± 8	^{422}1079 ± 44	^{419}1050 ± 45
120	awiros-002	289016	203723	^{194}556	^{642}2048 ± 0	^{439}479 ± 0	^{302}500 ± 0	^{298}534 ± 0	^{324}618 ± 0	^{502}946 ± 1	^{670}1966 ± 31	^{671}1957 ± 25
121	awiros-003	292302	598824	^{394}976	^{638}2048 ± 0	^{382}428 ± 2	^{255}442 ± 1	^{228}454 ± 2	^{184}442 ± 1	^{145}444 ± 1	^{784}2558 ± 20	^{789}2580 ± 42
122	awiros-004	489913	598874	^{533}1295	^{400}2048 ± 0	^{462}502 ± 0	^{316}517 ± 0	^{288}519 ± 3	^{246}518 ± 1	^{190}512 ± 0	^{778}2527 ± 17	^{783}2537 ± 20
123	aximetria-001	408902	487912	^{803}2539	^{857}2048 ± 0	^{1062}1013 ± 1	^{764}1023 ± 21	^{726}1029 ± 5	^{630}999 ± 2	^{604}1091 ± 5	^{974}4401 ± 94	^{976}4490 ± 80
124	ayftech-001	195423	43580	^{282}731	^{112}512 ± 0	^{361}408 ± 23	^{280}476 ± 52	^{537}814 ± 108	^{1054}1827 ± 384	^{1074}5412 ± 1029	^{214}615 ± 16	^{361}885 ± 44
125	ayftech-003	526164	127257	^{637}1640	^{338}2048 ± 0	^{1054}1003 ± 5	^{760}1017 ± 6	^{708}1006 ± 6	^{646}1009 ± 7	^{585}1063 ± 5	^{495}1301 ± 20	^{502}1300 ± 25
126	ayonix-000	58505	5252	^{14}69	^{270}1036 ± 0	^{2}18 ± 2	-	-	-	-	^{219}621 ± 23	^{231}620 ± 26
127	beethedata-000	227849	1087592	^{195}557	^{411}2048 ± 0	^{420}465 ± 0	^{277}467 ± 0	^{245}468 ± 0	^{209}467 ± 0	^{158}467 ± 0	^{695}2121 ± 34	^{696}2110 ± 38
128	betaface-000	0	1060599	-	^{1107}2116 ± 0	^{887}837 ± 9	-	-	-	-	^{561}1514 ± 28	^{566}1520 ± 66
129	betaface-002	0	1060599	-	^{1108}2116 ± 0	^{914}870 ± 13	-	-	-	-	^{544}1474 ± 50	^{559}1488 ± 41
130	beyneai-000	256958	591433	^{722}1998	^{817}2048 ± 0	^{406}451 ± 8	^{263}449 ± 1	^{512}767 ± 7	^{1032}1603 ± 25	^{1067}4669 ± 124	^{931}3730 ± 57	^{929}3668 ± 54
131	biocube-001	25030	6192987	^{146}457	^{1175}4096 ± 0	^{208}282 ± 22	^{133}292 ± 24	^{290}521 ± 57	^{386}684 ± 59	^{733}1282 ± 68	^{1241}21787 ± 96	^{1245}21812 ± 109
132	biocube-002	69898	10651580	^{152}468	^{1184}4096 ± 0	^{874}826 ± 4	^{610}838 ± 4	^{844}1175 ± 4	^{1106}2933 ± 1074	^{1095}9144 ± 1090	^{1253}23074 ± 94	^{1255}23036 ± 99

Notes	
1	The configuration size does not capture static data included in libraries.
2	The library size is the combined total of all files provided in the submission lib folder. These libraries e.g. OpenCV may or may not be installed on any end user's platform natively and would not need to be installed with the algorithm. Some developers put neural network models in their libraries.
3	The memory usage is the peak resident set size reported by the ps system call during template generation.
4	The median template creation times are measured on Intel®Xeon®CPU E5-2630 v4 @ 2.20GHz processors.
5	The comparison durations, in nanoseconds, are estimated using std::chrono::high_resolution_clock which on the machine in (2) counts 1ns clock ticks. Precision is somewhat worse than that however. The ± value is the median absolute deviation times 1.48 for Normal consistency.

Table 24: Summary of algorithms and properties included in this report. The red superscripts give ranking for the quantity in that column.

	ALGORITHM	CONFIG	LIBRARY	TEMPLATE							COMPARISON[4]	
	NAME	DATA	DATA	MEMORY	SIZE	GENERATION TIME (ms)[4]					TIME (ns)[5]	
		(KB)[1]	(KB)[2]	(MB)[3]	(B)	MUGSHOT	480x720	960x1440	1600x2400	3000x4500	GENUINE	IMPOSTOR
133	bioid-001	361549	144	^{229}629	^{1383}7680 ± 0	^{119}190 ± 1	^{74}192 ± 1	^{99}290 ± 2	^{274}556 ± 7	^{897}1528 ± 25	^{1006}5051 ± 35	^{1010}5042 ± 19
134	bioid-002	364015	149	^{572}1415	^{1382}7680 ± 0	^{116}187 ± 2	^{69}190 ± 3	^{102}295 ± 4	^{278}560 ± 13	^{925}1630 ± 43	^{1008}5052 ± 34	^{1009}5031 ± 23
135	bioid-003	530171	156	^{616}1558	^{1400}15368 ± 0	^{549}582 ± 2	^{378}587 ± 2	^{462}706 ± 3	^{623}994 ± 7	^{981}2123 ± 33	^{1062}6396 ± 25	^{1058}6377 ± 29
136	bioid-004	530301	156	^{620}1568	^{1399}15368 ± 0	^{586}603 ± 1	^{394}611 ± 1	^{401}640 ± 1	^{426}726 ± 2	^{579}1058 ± 3	^{1076}6948 ± 25	^{1072}6948 ± 19
137	bioidtechswiss-000	758466	119955	-	^{26}256 ± 0	^{632}630 ± 2	-	-	-	-	^{1300}34416 ± 137	^{1302}34403 ± 126
138	bioidtechswiss-001	1178769	120811	^{588}1455	^{92}512 ± 0	^{1019}966 ± 4	^{954}1270 ± 270	^{943}1294 ± 96	^{956}1409 ± 157	^{949}1793 ± 79	^{790}2610 ± 25	^{792}2624 ± 32
139	bioidtechswiss-002	744786	114842	^{400}990	^{143}512 ± 0	^{966}917 ± 2	^{685}930 ± 2	^{651}952 ± 2	^{588}947 ± 3	^{578}1058 ± 11	^{707}2177 ± 29	^{707}2170 ± 31
140	bioidtechswiss-003	518317	10378	^{952}4730	^{900}2048 ± 0	^{1107}1075 ± 1	^{852}1139 ± 7	^{1112}2207 ± 9	^{1064}1891 ± 11	^{1070}4787 ± 21	^{1335}50218 ± 204	^{1336}50184 ± 163
141	biometric-vision-000	445487	72132	^{372}915	^{348}2048 ± 0	^{885}836 ± 3	^{603}831 ± 3	^{584}869 ± 5	^{594}955 ± 8	^{795}1370 ± 19	^{1185}14437 ± 161	^{1185}14325 ± 167
142	biometrik-001	23995	68818	^{27}101	^{126}512 ± 0	^{1354}1446 ± 3	^{1064}1448 ± 3	^{1047}1449 ± 3	^{984}1456 ± 3	^{875}1485 ± 3	^{392}1016 ± 5	^{393}999 ± 17
143	biometrik-002	171539	84430	^{110}353	^{344}2048 ± 0	^{1383}1499 ± 3	^{1083}1499 ± 3	^{1069}1501 ± 3	^{1009}1503 ± 3	^{884}1507 ± 2	^{499}1328 ± 19	^{506}1321 ± 19
144	bm-001	287734	38076	^{47}148	^{1}64 ± 0	^{400}444 ± 88	-	-	-	-	^{650}1887 ± 31	^{651}1877 ± 26
145	boetech-001	261376	88710	^{906}3658	^{865}2048 ± 0	^{192}271 ± 1	^{117}268 ± 1	^{88}273 ± 0	^{84}286 ± 1	^{69}318 ± 1	^{1365}68519 ± 1921	^{1364}67648 ± 822
146	boetech-002	294347	88710	^{728}2057	^{757}2048 ± 0	^{238}305 ± 4	^{138}296 ± 1	^{105}302 ± 1	^{99}313 ± 1	^{87}348 ± 2	^{1367}68921 ± 2137	^{1368}69473 ± 2104
147	bresee-000	287880	22872	-	^{614}2048 ± 0	^{1277}1309 ± 1	^{1121}2126 ± 1	^{967}1330 ± 0	^{883}1312 ± 0	^{777}1333 ± 0	^{1323}45317 ± 228	^{1333}48256 ± 425
148	bresee-001	287880	23227	^{509}1223	^{427}2048 ± 0	^{1218}1223 ± 3	^{912}1216 ± 1	^{969}1331 ± 1	^{818}1227 ± 1	^{791}1360 ± 1	^{1309}37240 ± 655	^{1312}37167 ± 584
149	bresee-002	313627	30902	^{713}1951	^{576}2048 ± 0	^{782}743 ± 4	^{855}1143 ± 2	^{825}1146 ± 2	^{748}1148 ± 2	^{666}1176 ± 2	^{622}1778 ± 22	^{624}1775 ± 23
150	btsdigital-001	362015	234409	^{389}955	^{495}2048 ± 0	^{768}728 ± 2	^{512}713 ± 1	^{478}726 ± 4	^{423}716 ± 2	^{355}738 ± 0	^{864}3123 ± 22	^{869}3134 ± 37
151	cakevn-001	271412	587471	^{285}739	^{792}2048 ± 0	^{564}587 ± 0	^{374}584 ± 0	^{338}585 ± 0	^{301}589 ± 0	^{296}664 ± 0	^{1381}78258 ± 72	^{1379}78329 ± 90
152	camvi-001	118759	21678	-	^{215}1024 ± 0	^{108}181 ± 6	-	-	-	-	^{140}481 ± 16	^{149}487 ± 23
153	camvi-002	236278	225285	^{284}737	^{220}1024 ± 0	^{697}677 ± 7	^{520}726 ± 36	^{585}869 ± 28	^{730}1129 ± 43	^{1028}2785 ± 113	^{208}612 ± 26	^{213}603 ± 20
154	camvi-003	285657	225320	-	^{256}1024 ± 0	^{786}750 ± 3	-	-	-	-	^{175}571 ± 23	^{179}565 ± 26
155	camvi-004	280733	615819	^{374}919	^{648}2048 ± 0	^{799}759 ± 10	^{623}861 ± 17	^{683}986 ± 34	^{860}1279 ± 51	^{1034}2891 ± 158	^{372}948 ± 40	^{382}963 ± 31
156	candour-001	150086	97632	^{155}477	^{914}2048 ± 0	^{1330}1400 ± 1	^{1031}1396 ± 1	^{1023}1408 ± 1	^{955}1407 ± 1	^{861}1464 ± 1	^{1143}10725 ± 133	^{1144}10712 ± 127
157	candour-002	149560	65228	^{123}392	^{692}2048 ± 0	^{77}144 ± 0	^{41}143 ± 0	^{33}145 ± 0	^{30}152 ± 1	^{36}206 ± 0	^{1099}7798 ± 56	^{1099}7781 ± 51
158	candour-003	339247	65570	^{330}833	^{1142}3072 ± 0	^{324}380 ± 0	^{211}392 ± 0	^{161}378 ± 0	^{152}393 ± 1	^{148}445 ± 0	^{1299}34039 ± 45	^{1301}34020 ± 44
159	candour-004	1192219	65226	^{798}2490	^{1249}4096 ± 0	^{1409}2243 ± 0	^{1123}2247 ± 0	^{1113}2223 ± 0	^{1090}2270 ± 1	^{1001}2330 ± 0	^{804}2714 ± 20	^{814}2755 ± 23
160	canon-002	446491	130232	-	^{1222}4096 ± 0	^{1276}1308 ± 2	^{987}1315 ± 1	^{964}1326 ± 2	^{901}1345 ± 1	^{856}1452 ± 1	^{1056}6211 ± 25	^{1050}6194 ± 25
161	canon-003	2550850	101378	^{968}5487	^{1363}6180 ± 0	^{1247}1263 ± 3	^{950}1263 ± 1	^{933}1283 ± 1	^{889}1320 ± 1	^{872}1482 ± 2	^{992}4783 ± 17	^{993}4780 ± 19
162	canon-004	2399160	114188	^{990}7037	^{1365}6200 ± 0	^{997}948 ± 4	^{703}955 ± 3	^{660}959 ± 3	^{609}977 ± 3	^{587}1064 ± 2	^{1087}7172 ± 63	^{1084}7169 ± 51
163	canon-005	2521818	80309	^{985}6700	^{1318}4148 ± 0	^{1217}1223 ± 21	^{918}1221 ± 2	^{888}1230 ± 4	^{823}1234 ± 5	^{774}1329 ± 3	^{1052}6142 ± 99	^{1053}6226 ± 146
164	cchonolulu-000	727461	37284	^{129}416	^{135}512 ± 0	^{64}123 ± 13	^{37}126 ± 10	^{29}129 ± 10	^{27}134 ± 10	^{40}223 ± 10	^{607}1726 ± 35	^{600}1697 ± 35
165	cchonolulu-001	733744	37284	^{133}426	^{662}2048 ± 0	^{89}162 ± 21	^{78}197 ± 23	^{280}513 ± 96	^{716}1118 ± 267	^{985}2142 ± 584	^{975}4418 ± 37	^{969}4361 ± 35
166	cdachyd-001	238593	1941345	^{37}135	^{95}512 ± 0	^{1389}1642 ± 2	^{1102}1749 ± 1	^{1125}6467 ± 3	^{1125}17252 ± 10	^{1116}58681 ± 45	^{1153}11594 ± 85	^{1158}11639 ± 130
167	ceiec-001	159618	46136	-	^{226}1024 ± 0	^{246}314 ± 3	-	-	-	-	^{1251}22831 ± 108	^{1254}22813 ± 120
168	ceiec-002	269063	90975	-	^{396}2048 ± 0	^{602}612 ± 17	-	-	-	-	^{709}2188 ± 57	^{735}2301 ± 56
169	ceiec-003	260371	88707	^{137}430	^{833}2048 ± 0	^{862}817 ± 4	^{646}883 ± 57	^{602}897 ± 60	^{557}899 ± 72	^{499}944 ± 72	^{723}2256 ± 38	^{719}2241 ± 54
170	ceiec-004	263476	67011	^{128}408	^{780}2048 ± 0	^{1069}1024 ± 1	^{766}1027 ± 1	^{722}1027 ± 1	^{656}1030 ± 1	^{573}1055 ± 1	^{639}1844 ± 26	^{641}1836 ± 20
171	celloscope-001	38016	59158	^{39}138	^{105}512 ± 0	^{15}49 ± 0	^{10}52 ± 0	^{53}188 ± 0	^{239}509 ± 1	-	^{810}2733 ± 35	^{810}2730 ± 35
172	chosun-000	167093	694	-	^{645}2048 ± 0	^{399}441 ± 1	-	-	-	-	^{381}983 ± 20	^{387}983 ± 29
173	chosun-001	765615	707	^{162}491	^{845}2048 ± 0	^{818}783 ± 2	^{597}826 ± 4	^{1086}1662 ± 13	^{1114}3679 ± 67	^{1109}11694 ± 243	^{387}998 ± 25	^{409}1035 ± 11
174	chosun-002	234001	31875	^{144}451	^{681}2048 ± 0	^{175}248 ± 3	^{119}273 ± 3	^{1067}1495 ± 14	^{1120}7920 ± 90	^{1117}80302 ± 1349	^{221}623 ± 17	^{248}634 ± 13
175	chtface-001	94088	369529	-	^{728}2048 ± 0	^{148}212 ± 10	-	-	-	-	^{722}2256 ± 26	^{723}2252 ± 91
176	chtface-002	363153	369529	-	^{799}2048 ± 0	^{554}584 ± 14	^{510}712 ± 41	^{734}1038 ± 42	^{1058}1861 ± 75	^{1066}4661 ± 232	^{725}2264 ± 26	^{718}2234 ± 103

Notes	
1	The configuration size does not capture static data included in libraries.
2	The library size is the combined total of all files provided in the submission lib folder. These libraries e.g. OpenCV may or may not be installed on any end user's platform natively and would not need to be installed with the algorithm. Some developers put neural network models in their libraries.
3	The memory usage is the peak resident set size reported by the ps system call during template generation.
4	The median template creation times are measured on Intel®Xeon®CPU E5-2630 v4 @ 2.20GHz processors.
5	The comparison durations, in nanoseconds, are estimated using std::chrono::high_resolution_clock which on the machine in (2) counts 1ns clock ticks. Precision is somewhat worse than that however. The ± value is the median absolute deviation times 1.48 for Normal consistency.

Table 25: Summary of algorithms and properties included in this report. The red superscripts give ranking for the quantity in that column.

	ALGORITHM	CONFIG	LIBRARY	TEMPLATE							COMPARISON[4]	
	NAME	DATA	DATA	MEMORY	SIZE	GENERATION TIME (ms)[4]					TIME (ns)[5]	
		(KB)[1]	(KB)[2]	(MB)[3]	(B)	MUGSHOT	480x720	960x1440	1600x2400	3000x4500	GENUINE	IMPOSTOR
177	chtface-003	363153	369529	-	^{901}2048 ± 0	^{577}594 ± 16	^{517}720 ± 33	^{743}1050 ± 41	^{1062}1884 ± 90	^{1076}5606 ± 334	^{693}2110 ± 37	^{714}2219 ± 65
178	chtface-004	409656	311027	^{580}1428	^{640}2048 ± 0	^{268}332 ± 0	^{153}323 ± 1	^{124}329 ± 1	^{114}335 ± 1	^{102}377 ± 1	^{608}1727 ± 17	^{611}1720 ± 16
179	chtface-005	408364	311100	^{571}1415	^{450}2048 ± 0	^{257}322 ± 0	^{146}316 ± 1	^{121}325 ± 2	^{108}324 ± 1	^{127}411 ± 2	^{656}1907 ± 19	^{655}1898 ± 23
180	chtface-006	733645	610439	^{783}2424	^{376}2048 ± 0	^{479}522 ± 1	^{314}514 ± 1	^{300}536 ± 2	^{279}561 ± 1	^{321}693 ± 2	^{679}2034 ± 41	^{686}2049 ± 29
181	chtface-007	733528	610443	^{777}2393	^{683}2048 ± 0	^{218}292 ± 0	^{131}290 ± 0	^{109}307 ± 1	^{111}328 ± 1	^{178}501 ± 1	^{573}1570 ± 53	^{577}1561 ± 34
182	chtface-008	810179	583222	^{1001}8766	^{924}2048 ± 0	^{1088}1043 ± 8	^{763}1019 ± 9	^{717}1022 ± 14	^{662}1039 ± 16	^{589}1066 ± 23	^{560}1513 ± 14	^{572}1535 ± 44
183	chtface-009	810179	342213	^{1005}9371	^{783}2048 ± 0	^{1361}1455 ± 0	^{1073}1468 ± 16	^{1070}1501 ± 26	^{1007}1501 ± 0	^{903}1544 ± 15	^{713}2213 ± 13	^{717}2226 ± 29
184	cib-000	340288	69515	-	^{353}2048 ± 0	^{1048}993 ± 40	-	-	-	-	^{1261}24340 ± 60	^{1272}25972 ± 97
185	cib-001	436253	133766	-	^{404}2048 ± 0	^{655}651 ± 2	^{505}707 ± 13	^{470}716 ± 15	^{430}728 ± 3	^{417}820 ± 5	^{938}3783 ± 38	^{939}3765 ± 37
186	cist-001	0	300551	^{202}582	^{927}2048 ± 0	^{1027}972 ± 0	^{727}977 ± 1	^{679}981 ± 0	^{613}983 ± 0	^{583}1061 ± 0	^{845}2947 ± 20	^{847}2940 ± 22
187	cist-002	0	1186073	^{660}1730	^{1155}3200 ± 0	^{1031}976 ± 0	^{743}992 ± 0	^{769}1085 ± 1	^{859}1279 ± 0	^{977}2101 ± 1	^{1054}6165 ± 22	^{1051}6207 ± 38
188	cist-003	0	1267350	^{829}2706	^{1352}5248 ± 0	^{1266}1291 ± 1	^{976}1300 ± 1	^{983}1352 ± 3	^{867}1287 ± 2	^{760}1313 ± 1	^{1100}7838 ± 63	^{1100}7823 ± 40
189	cist-004	0	1603990	^{808}2563	^{1351}5248 ± 0	^{1234}1243 ± 1	^{955}1271 ± 1	^{917}1264 ± 3	^{835}1252 ± 1	^{736}1287 ± 1	^{876}3216 ± 25	^{882}3220 ± 32
190	clearviewai-000	342491	211852	^{836}2745	^{620}2048 ± 0	^{1332}1402 ± 1	^{1033}1403 ± 1	^{1027}1412 ± 1	^{963}1420 ± 1	^{829}1418 ± 1	^{577}1592 ± 37	^{576}1561 ± 37
191	clearviewai-001	613532	511807	^{553}1353	^{719}2048 ± 0	^{641}635 ± 2	^{436}642 ± 1	^{413}659 ± 1	^{367}664 ± 1	^{305}674 ± 1	^{340}827 ± 10	^{348}829 ± 20
192	clearviewai-002	713008	509504	^{613}1556	^{829}2048 ± 0	^{794}755 ± 2	^{559}773 ± 2	^{510}765 ± 3	^{474}783 ± 2	^{400}790 ± 1	^{348}864 ± 34	^{350}842 ± 29
193	clearviewai-003	712800	540093	^{545}1344	^{809}2048 ± 0	^{1127}1109 ± 0	^{807}1091 ± 0	^{772}1088 ± 0	^{696}1090 ± 0	^{628}1126 ± 0	^{819}2812 ± 45	^{827}2831 ± 50
194	closeli-001	420342	9851	^{300}773	^{1191}4096 ± 0	^{890}839 ± 1	^{613}843 ± 1	^{567}841 ± 1	^{520}845 ± 1	^{454}865 ± 1	^{1018}5404 ± 17	^{1019}5400 ± 25
195	cloudmatrix-000	309939	542141	-	^{849}2048 ± 0	^{792}754 ± 10	^{541}750 ± 2	^{503}754 ± 4	^{459}764 ± 1	^{402}793 ± 2	^{1333}49192 ± 206	^{1334}49275 ± 176
196	cloudmatrix-001	10390	542121	^{12}65	^{340}2048 ± 0	^{54}114 ± 1	^{32}117 ± 0	^{26}118 ± 0	^{23}123 ± 1	^{24}169 ± 1	^{1336}50263 ± 212	^{1337}50243 ± 237
197	cloudmatrix-002	256635	693318	^{424}1036	^{595}2048 ± 0	^{343}395 ± 1	^{219}398 ± 1	^{176}399 ± 1	^{161}402 ± 1	^{139}437 ± 20	^{1334}49578 ± 120	^{1335}49602 ± 180
198	cloudwalk-hr-000	284600	105489	-	^{1071}2057 ± 0	^{580}600 ± 2	-	-	-	-	^{1210}16747 ± 238	^{1212}16627 ± 220
199	cloudwalk-hr-001	346156	104483	-	^{1072}2057 ± 0	^{677}665 ± 3	-	-	-	-	^{1217}17816 ± 260	^{1222}17878 ± 464
200	cloudwalk-hr-002	390059	327494	-	^{1074}2057 ± 0	^{953}908 ± 3	-	-	-	-	^{1249}22530 ± 416	^{1243}21651 ± 533
201	cloudwalk-hr-003	383739	144263	^{397}983	^{1075}2057 ± 0	^{592}606 ± 0	^{379}588 ± 0	^{345}594 ± 0	^{316}612 ± 1	^{219}547 ± 2	^{1078}6982 ± 80	^{1075}6972 ± 84
202	cloudwalk-hr-004	502916	520169	^{568}1399	^{946}2049 ± 0	^{921}873 ± 1	^{639}877 ± 1	^{591}876 ± 1	^{542}879 ± 1	^{479}902 ± 3	^{1156}11652 ± 127	^{1156}11608 ± 123
203	cloudwalk-mt-000	372169	282036	-	^{949}2049 ± 0	^{763}724 ± 12	-	-	-	-	^{593}1678 ± 47	^{583}1614 ± 85
204	cloudwalk-mt-002	290753	145340	-	^{945}2049 ± 0	^{538}573 ± 1	^{514}717 ± 78	^{456}700 ± 66	^{447}749 ± 96	^{387}770 ± 80	^{1088}7205 ± 204	^{1085}7211 ± 244
205	cloudwalk-mt-003	490365	494959	-	^{948}2049 ± 0	^{973}923 ± 1	^{669}918 ± 1	^{632}926 ± 1	^{571}925 ± 1	^{496}936 ± 1	^{1155}11620 ± 179	^{1159}11661 ± 128
206	cloudwalk-mt-004	1384602	512628	-	^{796}2048 ± 0	^{974}923 ± 2	^{672}919 ± 1	^{619}918 ± 0	^{568}919 ± 0	^{491}927 ± 1	^{1157}11744 ± 170	^{1157}11631 ± 126
207	cloudwalk-mt-005	846026	573253	^{902}3615	^{350}2048 ± 0	^{1180}1179 ± 3	^{901}1200 ± 3	^{874}1209 ± 3	^{817}1226 ± 5	^{694}1229 ± 3	^{1172}12525 ± 225	^{1171}12394 ± 152
208	cloudwalk-mt-006	563322	480071	^{896}3499	^{752}2048 ± 0	^{1319}1385 ± 0	^{1025}1392 ± 1	^{1013}1398 ± 1	^{943}1397 ± 4	^{850}1444 ± 2	^{889}3364 ± 96	^{893}3324 ± 83
209	cloudwalk-mt-007	563322	480071	^{897}3499	^{737}2048 ± 0	^{1311}1379 ± 2	^{1050}1425 ± 7	^{1033}1427 ± 6	^{959}1417 ± 2	^{848}1443 ± 7	^{850}3000 ± 68	^{850}2971 ± 74
210	clova-000	198420	6824	-	^{330}2048 ± 0	^{393}437 ± 0	^{240}431 ± 0	^{209}435 ± 0	^{189}452 ± 2	^{188}508 ± 7	^{626}1794 ± 16	^{632}1795 ± 19
211	cmcuni-001	0	604227	^{489}1177	^{545}2048 ± 0	^{1165}1161 ± 1	^{891}1187 ± 1	^{862}1194 ± 5	^{789}1200 ± 1	^{683}1207 ± 1	^{868}3153 ± 22	^{873}3158 ± 26
212	codeline-000	361659	138388	^{501}1194	^{547}2048 ± 0	^{1359}1453 ± 0	^{1070}1456 ± 2	^{1051}1456 ± 0	^{987}1457 ± 0	^{873}1483 ± 1	^{704}2171 ± 69	^{710}2194 ± 84
213	cogent-000	633812	18848	-	^{82}439 ± 0	^{470}511 ± 7	-	-	-	-	^{1122}9541 ± 54	^{1121}9500 ± 51
214	cogent-001	530508	18869	-	^{85}455 ± 0	^{519}557 ± 7	-	-	-	-	^{1140}10477 ± 278	^{1142}10392 ± 75
215	cogent-002	696959	18881	-	^{326}1979 ± 0	^{983}941 ± 0	-	-	-	-	^{1183}14394 ± 134	^{1187}14385 ± 176
216	cogent-003	698290	40430	-	^{214}973 ± 0	^{1007}952 ± 0	-	-	-	-	^{1170}12496 ± 75	^{1161}11822 ± 163
217	cogent-004	722919	389164	-	^{327}1983 ± 0	^{1041}987 ± 50	-	-	-	-	^{1201}15536 ± 75	^{1206}15964 ± 708
218	cogent-005	1876796	75276	-	^{1122}2523 ± 0	^{1216}1221 ± 2	^{929}1236 ± 1	^{935}1289 ± 2	^{964}1420 ± 4	^{918}1602 ± 5	^{1268}24854 ± 69	^{1267}24858 ± 71
219	cogent-006	1078167	58108	^{614}1557	^{278}1062 ± 0	^{806}768 ± 0	^{570}789 ± 1	^{559}831 ± 2	^{574}930 ± 1	^{517}971 ± 1	^{631}1802 ± 17	^{633}1797 ± 23
220	cogent-007	621565	72316	^{702}1888	^{189}550 ± 0	^{1288}1329 ± 2	^{1000}1333 ± 5	^{973}1337 ± 4	^{907}1353 ± 5	^{813}1390 ± 4	^{98}355 ± 8	^{109}367 ± 14

Notes	
1	The configuration size does not capture static data included in libraries.
2	The library size is the combined total of all files provided in the submission lib folder. These libraries e.g. OpenCV may or may not be installed on any end user's platform natively and would not need to be installed with the algorithm. Some developers put neural network models in their libraries.
3	The memory usage is the peak resident set size reported by the ps system call during template generation.
4	The median template creation times are measured on Intel®Xeon®CPU E5-2630 v4 @ 2.20GHz processors.
5	The comparison durations, in nanoseconds, are estimated using std::chrono::high_resolution_clock which on the machine in (2) counts 1ns clock ticks. Precision is somewhat worse than that however. The ± value is the median absolute deviation times 1.48 for Normal consistency.

Table 26: Summary of algorithms and properties included in this report. The red superscripts give ranking for the quantity in that column.

	ALGORITHM	CONFIG	LIBRARY	TEMPLATE							COMPARISON[4]	
	NAME	DATA	DATA	MEMORY	SIZE	GENERATION TIME (ms)[4]					TIME (ns)[5]	
		(KB)[1]	(KB)[2]	(MB)[3]	(B)	MUGSHOT	480x720	960x1440	1600x2400	3000x4500	GENUINE	IMPOSTOR
221	cogent-008	856817	73587	^{750}2176	^{190}550 ± 0	^{1340}1412 ± 1	^{1049}1419 ± 2	^{1032}1426 ± 3	^{976}1437 ± 3	^{869}1476 ± 1	^{121}436 ± 14	^{131}441 ± 23
222	cognitec-000	474759	27371	-	^{1002}2052 ± 0	^{155}224 ± 1	-	-	-	-	^{941}3835 ± 108	^{941}3782 ± 83
223	cognitec-001	476809	27487	-	^{978}2052 ± 0	^{219}293 ± 17	-	-	-	-	^{966}4253 ± 59	^{964}4102 ± 167
224	cognitec-002	394088	62354	-	^{962}2052 ± 0	^{123}192 ± 6	^{90}219 ± 6	^{78}233 ± 8	^{68}241 ± 6	^{67}314 ± 10	^{882}3250 ± 41	^{885}3241 ± 48
225	cognitec-003	471458	62502	^{319}817	^{989}2052 ± 0	^{308}366 ± 9	^{222}403 ± 9	^{185}408 ± 9	^{173}424 ± 9	^{189}509 ± 13	^{896}3417 ± 51	^{906}3433 ± 53
226	cognitec-004	705645	62678	^{200}580	^{990}2052 ± 0	^{418}463 ± 9	^{299}497 ± 9	^{275}504 ± 10	^{248}521 ± 10	^{270}631 ± 12	^{856}3028 ± 197	^{864}3059 ± 238
227	cognitec-005	326804	198231	^{322}819	^{985}2052 ± 0	^{243}311 ± 10	^{185}364 ± 12	^{155}370 ± 10	^{148}390 ± 10	^{177}498 ± 16	^{740}2332 ± 48	^{743}2330 ± 40
228	cognitec-006	368383	40008	^{336}844	^{361}2048 ± 0	^{274}335 ± 7	^{200}381 ± 8	^{172}390 ± 7	^{155}396 ± 8	^{152}455 ± 11	^{738}2316 ± 60	^{721}2252 ± 50
229	cognitec-007	368401	40132	^{337}844	^{379}2048 ± 0	^{413}458 ± 20	^{385}601 ± 17	^{415}660 ± 17	^{494}815 ± 23	^{851}1445 ± 45	^{683}2051 ± 26	^{684}2045 ± 34
230	compal-000	1003818	186200	^{761}2242	^{224}1024 ± 0	^{1242}1255 ± 1	^{969}1293 ± 2	^{944}1294 ± 2	^{871}1300 ± 2	^{765}1322 ± 4	^{1298}33116 ± 349	^{1300}33182 ± 252
231	compal-001	619796	186054	^{887}3395	^{947}2049 ± 0	^{908}861 ± 0	^{633}871 ± 0	^{575}851 ± 0	^{529}857 ± 0	^{468}887 ± 0	^{1394}149573 ± 724	^{1394}149664 ± 582
232	cor-001	1194948	11240	^{513}1249	^{1079}2060 ± 0	^{734}699 ± 3	^{628}863 ± 76	^{582}865 ± 80	^{535}872 ± 89	^{506}952 ± 39	^{1399}270145 ± 2259	^{1399}282686 ± 11788
233	coretech-000	186423	43964	^{97}318	^{107}512 ± 0	^{583}602 ± 15	^{447}659 ± 12	^{817}1139 ± 24	^{749}1149 ± 25	^{659}1165 ± 23	^{87}333 ± 14	^{89}321 ± 13
234	coretech-001	235361	305490	^{600}1523	^{785}2048 ± 0	^{715}688 ± 7	^{488}695 ± 7	^{587}870 ± 17	^{541}879 ± 15	^{462}877 ± 15	^{222}625 ± 25	^{256}641 ± 25
235	coretech-002	339881	296194	^{881}3300	^{838}2048 ± 0	^{416}459 ± 1	^{265}451 ± 1	^{574}851 ± 1	^{538}875 ± 2	^{522}980 ± 2	^{762}2443 ± 17	^{762}2436 ± 13
236	coretech-003	339885	296194	^{696}1861	^{483}2048 ± 0	^{858}815 ± 2	^{611}838 ± 3	^{923}1273 ± 6	^{862}1279 ± 8	^{796}1373 ± 6	^{756}2416 ± 13	^{758}2415 ± 19
237	coretech-004	339885	296194	^{690}1828	^{481}2048 ± 0	^{379}427 ± 1	^{258}443 ± 2	^{570}847 ± 4	^{531}858 ± 2	^{500}945 ± 4	^{758}2436 ± 35	^{760}2432 ± 20
238	corsight-001	1437763	31525	-	^{1085}2064 ± 0	^{1265}1291 ± 3	^{963}1285 ± 1	^{939}1293 ± 1	^{872}1303 ± 2	^{804}1379 ± 3	^{1398}249340 ± 1713	^{1398}248929 ± 1909
239	corsight-002	1474921	32093	^{703}1892	^{1095}2080 ± 0	^{1264}1290 ± 1	^{965}1287 ± 1	^{936}1290 ± 1	^{877}1307 ± 2	^{812}1388 ± 4	^{1269}24953 ± 637	^{1263}24263 ± 578
240	corsight-003	1413063	32198	^{638}1642	^{1098}2080 ± 0	^{1202}1202 ± 2	^{893}1190 ± 5	^{868}1199 ± 3	^{825}1236 ± 3	^{784}1349 ± 7	^{1280}28754 ± 434	^{1283}28279 ± 446
241	csc-001	0	240698	-	^{186}544 ± 0	^{232}302 ± 1	^{142}303 ± 0	^{107}304 ± 0	^{96}309 ± 1	^{83}341 ± 4	^{96}354 ± 8	^{104}344 ± 11
242	csc-002	0	519768	^{4}30	^{185}544 ± 0	^{433}473 ± 0	^{297}494 ± 0	^{251}481 ± 1	^{225}490 ± 1	^{195}514 ± 5	^{102}367 ± 11	^{111}371 ± 10
243	csc-003	0	400435	^{5}31	^{183}544 ± 0	^{456}499 ± 0	^{304}500 ± 1	^{271}502 ± 0	^{238}508 ± 1	^{208}535 ± 4	^{111}393 ± 8	^{121}397 ± 7
244	ctbcbank-000	257208	599238	^{199}570	^{476}2048 ± 0	^{533}568 ± 43	^{391}606 ± 38	^{444}690 ± 53	^{417}711 ± 50	^{427}831 ± 51	^{915}3551 ± 87	^{996}4805 ± 209
245	ctbcbank-001	275511	599238	^{212}603	^{794}2048 ± 0	^{658}652 ± 35	^{567}781 ± 30	^{590}875 ± 43	^{556}898 ± 51	^{557}1030 ± 47	^{946}3926 ± 45	^{950}3924 ± 56
246	ctbcbank-002	550523	253310	^{448}1084	^{130}512 ± 0	^{731}694 ± 0	^{504}707 ± 0	^{480}727 ± 0	^{446}744 ± 0	^{371}758 ± 0	^{987}4656 ± 146	^{1023}5486 ± 179
247	cu-face-002	812008	38655	^{271}723	^{1257}4096 ± 0	^{1092}1054 ± 1	^{788}1059 ± 0	^{753}1060 ± 0	^{674}1063 ± 1	^{591}1070 ± 0	^{1350}57287 ± 1750	^{1349}57027 ± 945
248	cu-face-003	1015124	37791	^{740}2116	^{1240}4096 ± 0	^{994}945 ± 1	^{705}955 ± 3	^{655}957 ± 2	^{591}949 ± 3	^{511}963 ± 2	^{815}2769 ± 19	^{820}2782 ± 41
249	cu-face-004	1016682	37791	^{734}2083	^{1231}4096 ± 0	^{1067}1022 ± 1	^{771}1031 ± 1	^{700}998 ± 3	^{682}1070 ± 1	^{552}1021 ± 2	^{832}2884 ± 38	^{833}2864 ± 48
250	cubox-001	369627	75427	^{240}652	^{859}2048 ± 0	^{948}907 ± 1	^{658}902 ± 1	^{607}903 ± 0	^{566}917 ± 0	^{493}931 ± 0	^{510}1379 ± 37	^{527}1417 ± 38
251	cubox-002	542254	90975	^{716}1966	^{935}2048 ± 0	^{970}921 ± 1	^{675}921 ± 1	^{626}922 ± 1	^{577}933 ± 1	^{543}1003 ± 1	^{675}2008 ± 72	^{673}1969 ± 57
252	cubox-003	1694397	209684	^{895}3491	^{452}2048 ± 0	^{1181}1179 ± 0	^{892}1189 ± 0	^{867}1198 ± 0	^{798}1208 ± 0	^{723}1264 ± 1	^{731}2289 ± 112	^{732}2297 ± 68
253	cubox-004	1304512	209634	^{838}2747	^{538}2048 ± 0	^{1015}963 ± 1	^{736}986 ± 1	^{690}992 ± 0	^{644}1008 ± 0	^{596}1087 ± 0	^{546}1476 ± 62	^{545}1460 ± 42
254	cubox-005	225237	209600	^{565}1387	^{621}2048 ± 0	^{302}362 ± 0	^{193}371 ± 0	^{157}373 ± 0	^{149}390 ± 0	^{150}453 ± 0	^{613}1748 ± 25	^{608}1718 ± 40
255	cudocommunication-001	385258	341277	^{446}1080	^{753}2048 ± 0	^{976}925 ± 1	^{678}923 ± 1	^{636}928 ± 1	^{575}932 ± 0	^{512}964 ± 1	^{779}2534 ± 20	^{784}2537 ± 20
256	cuhkee-001	787853	74917	^{801}2515	^{1003}2052 ± 0	^{1033}977 ± 31	-	-	-	-	^{806}2719 ± 60	^{821}2783 ± 56
257	cybercore-000	86008	55441	-	^{125}512 ± 0	^{665}655 ± 3	^{483}689 ± 71	^{408}649 ± 6	^{352}648 ± 8	^{308}680 ± 6	^{1190}14800 ± 75	^{1205}15757 ± 782
258	cybercore-001	166096	7791	-	^{588}2048 ± 0	^{448}487 ± 0	^{292}486 ± 0	^{258}488 ± 0	^{223}487 ± 0	^{181}502 ± 0	^{1341}52119 ± 111	^{1341}52127 ± 111
259	cybercore-002	166096	7374	^{809}2565	^{921}2048 ± 0	^{450}489 ± 1	^{303}500 ± 4	^{270}500 ± 1	^{231}499 ± 2	^{206}528 ± 1	^{1168}12389 ± 123	^{1170}12352 ± 112
260	cybercore-003	289176	7969	^{936}4311	^{1187}4096 ± 0	^{894}844 ± 2	^{622}855 ± 4	^{580}864 ± 4	^{533}862 ± 4	^{463}878 ± 2	^{1035}5744 ± 41	^{1037}5737 ± 31
261	cyberextruder-001	121211	13629	-	^{27}256 ± 0	^{943}893 ± 25	-	-	-	-	^{424}1083 ± 16	^{429}1079 ± 19
262	cyberextruder-002	168909	13924	-	^{367}2048 ± 0	^{490}532 ± 6	-	-	-	-	^{632}1803 ± 14	^{627}1779 ± 22
263	cyberextruder-003	253300	12354	^{142}444	^{141}512 ± 0	^{338}390 ± 1	^{207}388 ± 1	^{173}393 ± 1	^{158}399 ± 1	^{137}435 ± 1	^{39}198 ± 4	^{38}189 ± 8
264	cyberextruder-004	169301	12354	^{94}302	^{5}128 ± 0	^{139}206 ± 0	^{83}208 ± 0	^{65}209 ± 0	^{64}229 ± 0	^{51}249 ± 1	^{24}145 ± 14	^{26}155 ± 14

Notes	
1	The configuration size does not capture static data included in libraries.
2	The library size is the combined total of all files provided in the submission lib folder. These libraries e.g. OpenCV may or may not be installed on any end user's platform natively and would not need to be installed with the algorithm. Some developers put neural network models in their libraries.
3	The memory usage is the peak resident set size reported by the ps system call during template generation.
4	The median template creation times are measured on Intel®Xeon®CPU E5-2630 v4 @ 2.20GHz processors.
5	The comparison durations, in nanoseconds, are estimated using std::chrono::high_resolution_clock which on the machine in (2) counts 1ns clock ticks. Precision is somewhat worse than that however. The ± value is the median absolute deviation times 1.48 for Normal consistency.

Table 27: Summary of algorithms and properties included in this report. The red superscripts give ranking for the quantity in that column.

	ALGORITHM	CONFIG	LIBRARY	TEMPLATE							COMPARISON[4]	
	NAME	DATA	DATA	MEMORY	SIZE	GENERATION TIME (ms)[4]					TIME (ns)[5]	
		(KB)[1]	(KB)[2]	(MB)[3]	(B)	MUGSHOT	480x720	960x1440	1600x2400	3000x4500	GENUINE	IMPOSTOR
265	cyberextruder-005	269610	45367	^{217}606	^{132}512 ± 0	^{93}168 ± 2	^{51}169 ± 1	^{63}205 ± 3	^{89}295 ± 5	^{437}835 ± 9	^{23}142 ± 8	^{24}144 ± 10
266	cyberextruder-006	184816	45435	^{120}382	^{33}256 ± 0	^{35}91 ± 1	^{20}89 ± 0	^{18}97 ± 0	^{15}95 ± 0	^{18}130 ± 1	^{9}98 ± 7	^{9}101 ± 11
267	cyberlink-000	221801	91440	-	^{980}2052 ± 0	^{277}338 ± 6	-	-	-	-	^{692}2102 ± 40	^{694}2093 ± 32
268	cyberlink-001	222009	91440	-	^{988}2052 ± 0	^{377}425 ± 29	-	-	-	-	^{682}2051 ± 32	^{689}2060 ± 31
269	cyberlink-002	222311	95086	-	^{961}2052 ± 0	^{666}656 ± 22	-	-	-	-	^{726}2264 ± 71	^{797}2649 ± 195
270	cyberlink-003	470949	104369	-	^{995}2052 ± 0	^{375}423 ± 1	-	-	-	-	^{747}2366 ± 38	^{748}2373 ± 45
271	cyberlink-004	340894	104662	-	^{1311}4140 ± 0	^{750}712 ± 1	-	-	-	-	^{930}3693 ± 51	^{947}3898 ± 71
272	cyberlink-005	341680	111358	-	^{1312}4140 ± 0	^{760}721 ± 1	^{545}752 ± 2	^{504}754 ± 2	^{451}755 ± 1	^{401}791 ± 3	^{926}3680 ± 37	^{962}4021 ± 97
273	cyberlink-006	341666	102456	-	^{1367}6212 ± 0	^{722}690 ± 1	^{497}702 ± 0	^{458}703 ± 0	^{418}712 ± 0	^{362}741 ± 0	^{65}270 ± 13	^{74}271 ± 13
274	cyberlink-007	380046	102446	-	^{1369}6212 ± 0	^{764}725 ± 1	^{526}732 ± 1	^{487}734 ± 1	^{440}736 ± 1	^{383}767 ± 1	^{78}304 ± 19	^{82}304 ± 16
275	cyberlink-008	380047	102470	-	^{1371}6212 ± 0	^{769}729 ± 1	^{519}725 ± 0	^{479}727 ± 0	^{437}732 ± 0	^{373}760 ± 0	^{61}263 ± 17	^{66}255 ± 13
276	cyberlink-009	588443	102201	^{653}1707	^{1320}4164 ± 0	^{1317}1384 ± 2	^{1029}1395 ± 2	^{1012}1398 ± 2	^{946}1401 ± 2	^{857}1456 ± 2	^{75}299 ± 17	^{84}304 ± 16
277	cyberlink-010	1590818	102180	^{908}3678	^{1393}8260 ± 0	^{1249}1265 ± 2	^{985}1314 ± 5	^{941}1294 ± 2	^{856}1273 ± 2	^{752}1305 ± 2	^{137}476 ± 23	^{144}472 ± 14
278	cyberlink-011	1397496	102171	^{866}3029	^{1366}6212 ± 0	^{1195}1196 ± 3	^{895}1193 ± 2	^{864}1195 ± 3	^{804}1215 ± 6	^{696}1231 ± 5	^{936}3768 ± 75	^{935}3735 ± 57
279	cyberlink-012	1200318	102281	^{845}2789	^{1370}6212 ± 0	^{582}601 ± 1	^{409}621 ± 5	^{358}610 ± 2	^{319}614 ± 2	^{288}649 ± 5	^{743}2343 ± 26	^{749}2377 ± 34
280	cyberlink-013	893519	102285	^{714}1964	^{1368}6212 ± 0	^{585}603 ± 1	^{386}602 ± 2	^{354}606 ± 2	^{317}613 ± 2	^{284}642 ± 1	^{81}307 ± 7	^{85}306 ± 5
281	cyberlink-014	1190911	102304	^{852}2876	^{1392}8260 ± 0	^{758}720 ± 1	^{527}736 ± 5	^{489}735 ± 10	^{434}731 ± 3	^{375}762 ± 3	^{107}378 ± 8	^{113}377 ± 13
282	cyberlink-015	1190911	102309	^{851}2875	^{1391}8260 ± 0	^{770}730 ± 1	^{535}741 ± 6	^{488}735 ± 12	^{436}732 ± 2	^{394}778 ± 1	^{774}2497 ± 26	^{778}2493 ± 51
283	dahua-000	283642	171917	-	^{803}2048 ± 0	^{304}363 ± 7	-	-	-	-	^{106}373 ± 16	^{107}364 ± 17
284	dahua-001	283642	171917	-	^{482}2048 ± 0	^{303}363 ± 6	-	-	-	-	^{104}367 ± 10	^{106}354 ± 16
285	dahua-002	526452	171518	-	^{558}2048 ± 0	^{628}628 ± 7	-	-	-	-	^{129}461 ± 23	^{135}454 ± 20
286	dahua-003	605337	141332	-	^{735}2048 ± 0	^{497}535 ± 2	-	-	-	-	^{243}648 ± 20	^{241}631 ± 34
287	dahua-004	832455	141070	-	^{806}2048 ± 0	^{775}735 ± 3	-	-	-	-	^{297}730 ± 25	^{294}707 ± 44
288	dahua-005	1586899	169478	-	^{1252}4096 ± 0	^{1341}1418 ± 34	-	-	-	-	^{374}957 ± 23	^{384}969 ± 19
289	dahua-006	831641	119261	^{962}5068	^{581}2048 ± 0	^{1328}1398 ± 2	^{1032}1397 ± 1	^{1019}1404 ± 1	^{949}1402 ± 1	^{817}1402 ± 1	^{57}249 ± 13	^{62}250 ± 11
290	dahua-007	1578737	119418	^{992}7237	^{1208}4096 ± 0	^{1324}1393 ± 2	^{1015}1373 ± 1	^{1000}1378 ± 1	^{928}1378 ± 1	^{803}1379 ± 2	^{103}367 ± 102	^{126}434 ± 108
291	daon-000	280726	2307	^{724}2010	^{1086}2065 ± 0	^{524}562 ± 3	^{370}581 ± 5	^{522}791 ± 9	^{515}838 ± 15	^{572}1055 ± 32	^{1204}16052 ± 88	^{1207}16041 ± 85
292	daon-001	296035	69405	^{207}587	^{526}2048 ± 0	^{704}682 ± 0	^{451}661 ± 0	^{443}688 ± 0	^{385}683 ± 0	^{291}657 ± 0	^{332}803 ± 23	^{343}815 ± 22
293	daon-002	295360	66546	^{278}731	^{755}2048 ± 0	^{801}765 ± 0	^{554}767 ± 1	^{514}768 ± 6	^{468}776 ± 1	^{388}770 ± 0	^{343}840 ± 17	^{354}858 ± 26
294	daon-003	931820	66767	^{675}1776	^{1189}4096 ± 0	^{1407}2048 ± 0	^{1118}2046 ± 0	^{1108}2050 ± 0	^{1077}2069 ± 0	^{973}2047 ± 0	^{710}2194 ± 59	^{712}2203 ± 28
295	datech-000	617605	139575	^{970}5599	^{1201}4096 ± 0	^{537}573 ± 32	^{373}583 ± 44	^{344}593 ± 37	^{1124}14123 ± 9564	^{1112}15514 ± 2343	^{1101}7857 ± 29	^{1101}7852 ± 25
296	datech-001	835404	139615	^{991}7179	^{1173}4096 ± 0	^{1064}1017 ± 83	^{784}1057 ± 65	^{757}1062 ± 88	^{708}1109 ± 81	^{747}1299 ± 92	^{1104}7944 ± 31	^{1105}7981 ± 56
297	datech-002	854184	139615	^{995}7446	^{1198}4096 ± 0	^{1111}1086 ± 115	^{844}1130 ± 119	^{794}1113 ± 123	^{795}1204 ± 107	^{827}1413 ± 145	^{1102}7860 ± 20	^{1102}7857 ± 26
298	decatur-000	350495	171271	^{369}907	^{1284}4100 ± 0	^{1070}1024 ± 2	-	-	-	-	^{1150}11439 ± 80	^{1152}11418 ± 112
299	decatur-001	342866	253734	^{598}1508	^{970}2052 ± 0	^{1123}1103 ± 2	^{789}1064 ± 2	^{758}1063 ± 2	^{677}1067 ± 2	^{595}1084 ± 2	^{205}610 ± 19	^{211}602 ± 8
300	decloakface-001	29693	170719	^{116}368	^{746}2048 ± 0	^{129}196 ± 58	^{79}201 ± 52	^{76}229 ± 53	^{92}298 ± 60	^{207}532 ± 61	^{986}4638 ± 19	^{986}4646 ± 22
301	decloakface-002	1692	143986	^{78}260	^{807}2048 ± 0	^{66}127 ± 0	^{39}135 ± 0	^{39}157 ± 0	^{58}218 ± 0	^{154}458 ± 2	^{972}4380 ± 31	^{973}4383 ± 45
302	deepglint-001	569802	206788	-	^{1214}4096 ± 0	^{761}721 ± 4	-	-	-	-	^{927}3680 ± 35	^{918}3517 ± 182
303	deepglint-002	459642	272878	-	^{1172}4096 ± 0	^{695}677 ± 2	^{596}826 ± 74	^{571}848 ± 42	^{521}849 ± 55	^{467}886 ± 27	^{1177}13633 ± 87	^{1176}12905 ± 440
304	deepglint-003	838065	262081	-	^{1356}6144 ± 0	^{1164}1159 ± 1	^{857}1145 ± 1	^{826}1148 ± 1	^{747}1148 ± 1	^{658}1163 ± 1	^{1213}17227 ± 41	^{1215}17210 ± 51
305	deepglint-004	1073382	261571	^{872}3116	^{442}2048 ± 0	^{1366}1470 ± 1	^{1077}1474 ± 1	^{1064}1485 ± 1	^{997}1474 ± 1	^{879}1492 ± 2	^{1044}5961 ± 34	^{1043}5955 ± 29
306	deepglint-005	960326	213877	^{861}2991	^{658}2048 ± 0	^{1338}1408 ± 1	^{1056}1431 ± 2	^{1031}1424 ± 3	^{967}1424 ± 3	^{853}1446 ± 2	^{1070}6765 ± 38	^{1067}6765 ± 40
307	deepsea-001	147497	336250	^{111}358	^{243}1024 ± 0	^{633}630 ± 7	^{544}752 ± 37	^{497}746 ± 30	^{429}727 ± 32	^{418}820 ± 32	^{519}1401 ± 37	^{548}1467 ± 50
308	deepsense-000	357113	936618	-	^{713}2048 ± 0	^{676}664 ± 3	^{439}645 ± 1	^{416}660 ± 2	^{391}687 ± 2	^{412}808 ± 3	^{138}480 ± 22	^{139}459 ± 34

Notes	
1	The configuration size does not capture static data included in libraries.
2	The library size is the combined total of all files provided in the submission lib folder. These libraries e.g. OpenCV may or may not be installed on any end user's platform natively and would not need to be installed with the algorithm. Some developers put neural network models in their libraries.
3	The memory usage is the peak resident set size reported by the ps system call during template generation.
4	The median template creation times are measured on Intel®Xeon®CPU E5-2630 v4 @ 2.20GHz processors.
5	The comparison durations, in nanoseconds, are estimated using std::chrono::high_resolution_clock which on the machine in (2) counts 1ns clock ticks. Precision is somewhat worse than that however. The ± value is the median absolute deviation times 1.48 for Normal consistency.

Table 28: Summary of algorithms and properties included in this report. The red superscripts give ranking for the quantity in that column.

	ALGORITHM	CONFIG	LIBRARY	TEMPLATE						COMPARISON[4]	
	NAME	DATA	DATA	MEMORY	SIZE	GENERATION TIME (ms)[4]				TIME (ns)[5]	
		(KB)[1]	(KB)[2]	(MB)[3]	(B)	MUGSHOT	480x720	960x1440	1600x2400	3000x4500	GENUINE	IMPOSTOR
309	deepsense-001	73173	1288355	^{964}5314	^{110}512 ± 0	^{1150}1142 ± 2	^{872}1164 ± 3	^{852}1183 ± 3	^{792}1201 ± 3	^{766}1323 ± 2	^{745}2356 ± 35	^{745}2354 ± 42
310	deepsense-002	73173	1266131	^{963}5280	^{206}896 ± 0	^{1296}1350 ± 1	^{975}1299 ± 8	^{961}1324 ± 0	^{904}1348 ± 0	^{868}1474 ± 4	^{906}3505 ± 32	^{917}3515 ± 40
311	deepsense-003	73173	1359497	^{981}6555	^{208}901 ± 0	^{881}832 ± 2	^{693}940 ± 2	^{569}845 ± 4	^{614}983 ± 1	^{521}976 ± 7	^{627}1797 ± 25	^{631}1795 ± 19
312	deepsense-004	560774	1052093	^{994}7310	^{210}916 ± 0	^{1245}1259 ± 2	^{972}1294 ± 9	^{919}1268 ± 7	^{844}1261 ± 8	^{778}1334 ± 7	^{648}1884 ± 19	^{652}1884 ± 25
313	deepsense-005	560774	1052093	^{993}7309	^{209}916 ± 0	^{1345}1430 ± 1	^{951}1264 ± 1	^{900}1246 ± 1	^{838}1254 ± 1	^{787}1353 ± 4	^{660}1920 ± 26	^{665}1932 ± 40
314	deepsense-006	643809	1052098	^{996}7719	^{211}916 ± 0	^{1293}1348 ± 2	^{1004}1347 ± 2	^{854}1184 ± 4	^{922}1369 ± 3	^{866}1473 ± 4	^{643}1860 ± 13	^{645}1853 ± 22
315	deepsense-007	643809	1070446	^{997}7769	^{213}920 ± 0	^{1168}1163 ± 1	^{877}1173 ± 3	^{857}1190 ± 2	^{801}1209 ± 3	^{755}1310 ± 4	^{640}1847 ± 11	^{647}1860 ± 28
316	deepsense-008	643809	1070340	^{998}7770	^{212}920 ± 0	^{1387}1571 ± 1	^{1093}1572 ± 0	^{1085}1610 ± 1	^{1043}1729 ± 1	^{991}2216 ± 1	^{977}4469 ± 109	^{977}4498 ± 68
317	dermalog-001	0	287736	-	^{274}1043 ± 0	^{49}106 ± 1	-	-	-	-	^{1246}22160 ± 166	^{1250}22131 ± 131
318	dermalog-002	0	287738	-	^{273}1043 ± 0	^{29}81 ± 0	-	-	-	-	^{1247}22169 ± 114	^{1249}22105 ± 146
319	dermalog-003	0	309430	-	^{272}1043 ± 0	^{59}121 ± 22	-	-	-	-	^{1252}22957 ± 93	^{1253}22808 ± 131
320	dermalog-004	0	245770	-	^{6}128 ± 0	^{81}149 ± 5	-	-	-	-	^{146}490 ± 26	^{143}471 ± 26
321	dermalog-005	0	317687	-	^{7}128 ± 0	^{68}130 ± 11	-	-	-	-	^{150}499 ± 22	^{153}500 ± 22
322	dermalog-006	0	452387	-	^{11}128 ± 0	^{491}532 ± 12	-	-	-	-	^{153}506 ± 23	^{140}459 ± 23
323	dermalog-007	0	503332	-	^{123}512 ± 0	^{165}239 ± 9	-	-	-	-	^{355}887 ± 23	^{284}690 ± 25
324	dermalog-008	0	937895	-	^{121}512 ± 0	^{354}404 ± 2	^{226}410 ± 3	^{202}424 ± 5	^{176}430 ± 5	^{165}477 ± 5	^{133}468 ± 31	^{95}328 ± 13
325	dermalog-009	0	319363	^{561}1369	^{109}512 ± 0	^{285}349 ± 0	^{174}351 ± 0	^{137}352 ± 0	^{125}357 ± 0	^{111}389 ± 0	^{143}487 ± 34	^{117}385 ± 29
326	dermalog-010	0	525908	^{913}3789	^{146}512 ± 0	^{640}635 ± 0	^{435}640 ± 1	^{399}639 ± 4	^{351}647 ± 3	^{317}691 ± 5	^{125}444 ± 13	^{102}341 ± 26
327	dermalog-011	0	278395	^{269}716	^{9}128 ± 0	^{281}343 ± 0	^{168}345 ± 0	^{134}347 ± 0	^{119}351 ± 0	^{96}363 ± 0	^{76}299 ± 19	^{65}253 ± 14
328	dermalog-012	0	293431	^{272}723	^{4}128 ± 0	^{109}181 ± 0	^{56}179 ± 0	^{46}182 ± 0	^{41}186 ± 0	^{50}242 ± 0	^{26}163 ± 10	^{41}196 ± 16
329	dermalog-013	0	293658	^{934}4263	^{10}128 ± 0	^{111}183 ± 2	^{59}180 ± 2	^{45}181 ± 1	^{39}183 ± 1	^{34}205 ± 1	^{33}186 ± 8	^{50}221 ± 7
330	dermalog-014	0	756422	^{504}1201	^{239}1024 ± 0	^{138}204 ± 0	^{76}197 ± 0	^{60}198 ± 1	^{48}199 ± 0	^{49}241 ± 0	^{116}424 ± 17	^{114}377 ± 17
331	dermalog-015	0	909348	^{792}2452	^{237}1024 ± 0	^{1401}1929 ± 1	^{1111}1891 ± 0	^{1103}1955 ± 1	^{1067}1899 ± 1	^{960}1904 ± 1	^{100}360 ± 25	^{71}267 ± 14
332	dicio-001	61751	119517	^{21}84	^{172}520 ± 0	^{499}538 ± 0	^{355}563 ± 10	^{615}915 ± 3	^{1053}1800 ± 7	^{1073}5286 ± 30	^{821}2818 ± 20	^{823}2807 ± 31
333	dicio-002	571566	85868	^{531}1290	^{1084}2060 ± 0	^{896}846 ± 1	^{552}761 ± 0	^{517}775 ± 1	^{476}784 ± 1	^{428}831 ± 0	^{1058}6242 ± 74	^{1056}6256 ± 80
334	didiglobalface-001	259849	70680	^{181}527	^{801}2048 ± 0	^{604}612 ± 1	^{432}633 ± 3	^{391}634 ± 3	^{354}650 ± 15	^{301}666 ± 4	^{379}973 ± 20	^{389}988 ± 20
335	didiglobalface-002	260054	161508	^{315}812	^{391}2048 ± 0	^{619}622 ± 1	^{431}633 ± 1	^{404}642 ± 2	^{361}659 ± 4	^{347}726 ± 15	^{170}560 ± 10	^{180}567 ± 13
336	didiglobalface-003	1001649	83986	^{523}1274	^{414}2048 ± 0	^{779}740 ± 2	^{531}740 ± 2	^{513}767 ± 5	^{470}779 ± 4	^{446}853 ± 17	^{570}1544 ± 13	^{573}1539 ± 17
337	digidata-000	133370	30249	^{77}259	^{786}2048 ± 0	^{301}361 ± 0	^{179}360 ± 0	^{147}361 ± 0	^{128}363 ± 0	^{104}380 ± 0	^{690}2084 ± 37	^{681}2039 ± 42
338	digidata-001	254564	33036	^{114}367	^{467}2048 ± 0	^{521}559 ± 1	^{352}561 ± 1	^{318}562 ± 1	^{280}564 ± 1	^{254}602 ± 1	^{1138}10308 ± 102	^{1139}10301 ± 121
339	digitalbarriers-000	157794	427472	-	^{1012}2056 ± 0	^{48}104 ± 0	-	-	-	-	^{1174}13232 ± 166	^{1178}13226 ± 146
340	digitalbarriers-001	236915	427537	-	^{1018}2056 ± 0	^{222}294 ± 1	-	-	-	-	^{1167}12311 ± 164	^{1169}12347 ± 197
341	digitalbarriers-002	83002	598577	^{709}1930	^{1043}2056 ± 0	^{141}209 ± 11	^{106}250 ± 19	^{187}411 ± 37	^{489}808 ± 72	^{992}2236 ± 123	^{1175}13409 ± 228	^{1179}13267 ± 206
342	dps-000	0	2211812	^{570}1405	^{1161}4096 ± 0	^{911}868 ± 2	^{653}893 ± 6	^{1043}1445 ± 9	^{1104}2910 ± 38	^{1097}9345 ± 17	^{543}1473 ± 37	^{552}1479 ± 37
343	dralmey-001	571556	82266	^{530}1290	^{1081}2060 ± 0	^{1189}1186 ± 0	^{871}1162 ± 0	^{841}1170 ± 0	^{775}1180 ± 0	^{702}1243 ± 0	^{1181}13996 ± 56	^{1184}13971 ± 60
344	dsk-000	11967	782905	^{75}252	^{99}512 ± 0	^{234}304 ± 47	^{150}317 ± 33	^{702}1001 ± 96	^{1101}2660 ± 170	^{1105}10451 ± 832	^{1086}7152 ± 115	^{1081}7134 ± 111
345	einetworks-000	372608	219883	^{357}880	^{1042}2056 ± 0	^{649}645 ± 3	-	-	-	-	^{999}4876 ± 66	^{1011}5156 ± 77
346	einetworksindia-000	372375	479472	^{543}1322	^{1051}2056 ± 0	^{321}378 ± 1	^{202}382 ± 1	^{168}383 ± 1	^{156}397 ± 0	^{153}456 ± 3	^{1197}15171 ± 41	^{1198}15138 ± 62
347	einetworksindia-001	562398	481792	^{684}1808	^{1057}2056 ± 0	^{440}479 ± 0	^{286}481 ± 1	^{256}485 ± 1	^{229}494 ± 1	^{215}541 ± 1	^{1195}15147 ± 63	^{1197}15134 ± 74
348	einetworksindia-002	1214466	143768	^{796}2462	^{930}2048 ± 0	^{1113}1087 ± 1	^{798}1082 ± 1	^{760}1065 ± 0	^{699}1098 ± 3	^{646}1150 ± 2	^{1178}13785 ± 34	^{1181}13767 ± 56
349	ekin-002	51434	278	^{40}139	^{1143}3072 ± 0	^{1188}1186 ± 13	^{884}1180 ± 12	^{850}1181 ± 11	^{787}1191 ± 11	^{684}1207 ± 8	^{969}4294 ± 80	^{1030}5569 ± 112
350	element-000	721679	24895	^{526}1287	^{524}2048 ± 0	^{346}399 ± 1	^{229}417 ± 1	^{203}428 ± 9	^{218}478 ± 14	^{313}688 ± 45	^{179}583 ± 10	^{189}585 ± 13
351	enface-000	369598	153781	^{249}671	^{250}1024 ± 0	^{517}555 ± 4	^{350}558 ± 4	^{427}669 ± 6	^{617}987 ± 15	^{1003}2349 ± 54	^{1082}7059 ± 62	^{1077}6980 ± 65
352	enface-001	370710	173609	^{248}669	^{240}1024 ± 0	^{514}550 ± 4	^{347}555 ± 3	^{426}668 ± 7	^{611}981 ± 15	^{1012}2416 ± 59	^{1069}6734 ± 68	^{1068}6766 ± 69

Notes	
1	The configuration size does not capture static data included in libraries.
2	The library size is the combined total of all files provided in the submission lib folder. These libraries e.g. OpenCV may or may not be installed on any end user's platform natively and would not need to be installed with the algorithm. Some developers put neural network models in their libraries.
3	The memory usage is the peak resident set size reported by the ps system call during template generation.
4	The median template creation times are measured on Intel®Xeon®CPU E5-2630 v4 @ 2.20GHz processors.
5	The comparison durations, in nanoseconds, are estimated using std::chrono::high_resolution_clock which on the machine in (2) counts 1ns clock ticks. Precision is somewhat worse than that however. The ± value is the median absolute deviation times 1.48 for Normal consistency.

Table 29: Summary of algorithms and properties included in this report. The red superscripts give ranking for the quantity in that column.

	ALGORITHM	CONFIG	LIBRARY	TEMPLATE							COMPARISON[4]	
	NAME	DATA	DATA	MEMORY	SIZE	GENERATION TIME (ms)[4]					TIME (ns)[5]	
		(KB)[1]	(KB)[2]	(MB)[3]	(B)	MUGSHOT	480x720	960x1440	1600x2400	3000x4500	GENUINE	IMPOSTOR
353	enface-002	858356	98741	^{1003}9004	^{253}1024 ± 0	^{1073}1026 ± 1	^{779}1038 ± 3	^{749}1057 ± 7	^{720}1123 ± 4	^{779}1338 ± 8	^{566}1529 ± 23	^{570}1530 ± 35
354	enqura-001	0	6136892	^{516}1263	^{329}2048 ± 0	^{153}221 ± 5	^{91}220 ± 3	^{80}239 ± 3	^{74}262 ± 3	^{62}288 ± 3	^{1}0 ± 0	^{1}0 ± 0
355	eocortex-000	255937	59432	^{71}224	^{616}2048 ± 0	^{237}305 ± 22	^{164}341 ± 25	^{215}440 ± 47	^{207}464 ± 45	^{192}513 ± 44	^{367}923 ± 11	^{374}918 ± 11
356	ercacat-001	811623	58012	^{847}2816	^{1004}2052 ± 0	^{1089}1052 ± 3	-	-	-	-	^{782}2551 ± 62	^{779}2501 ± 81
357	ethiopianlmis-000	309182	549917	^{156}481	^{777}2048 ± 0	^{933}882 ± 2	^{648}887 ± 1	^{549}824 ± 2	^{514}838 ± 2	^{480}903 ± 1	^{754}2400 ± 34	^{756}2407 ± 28
358	euronovate-001	0	1774966	^{547}1346	^{285}1177 ± 0	^{1082}1034 ± 2	^{873}1165 ± 3	^{834}1160 ± 3	^{771}1177 ± 3	^{662}1172 ± 2	^{1383}81294 ± 591	^{1381}81631 ± 931
359	euronovate-002	0	5476674	^{321}818	^{1334}4249 ± 0	^{220}293 ± 0	^{139}296 ± 0	^{104}298 ± 0	^{95}309 ± 0	^{81}339 ± 0	^{1296}32673 ± 391	^{1297}32587 ± 391
360	euronovate-003	0	5637394	^{500}1193	^{1117}2201 ± 0	^{229}300 ± 0	^{141}300 ± 0	^{106}303 ± 0	^{97}310 ± 0	^{82}340 ± 0	^{1311}37908 ± 968	^{1315}38285 ± 938
361	euronovate-004	0	1335993	^{428}1049	^{1118}2201 ± 0	^{215}290 ± 0	^{135}294 ± 0	^{101}294 ± 0	^{90}295 ± 0	^{63}294 ± 0	^{1325}46290 ± 490	^{1325}46199 ± 484
362	everai-000	229700	144802	-	^{764}2048 ± 0	^{411}455 ± 1	-	-	-	-	^{110}385 ± 10	^{116}382 ± 13
363	everai-001	449149	144802	-	^{878}2048 ± 0	^{739}701 ± 1	-	-	-	-	^{112}395 ± 11	^{122}404 ± 23
364	everai-002	561727	281965	-	^{1225}4096 ± 0	^{797}758 ± 0	-	-	-	-	^{241}644 ± 14	^{235}624 ± 35
365	everai-paravision-003	539802	118876	-	^{1260}4096 ± 0	^{690}674 ± 4	-	-	-	-	^{274}699 ± 20	^{300}713 ± 47
366	expasoft-000	15341	240451	-	^{447}2048 ± 0	^{21}68 ± 0	^{14}71 ± 0	^{10}75 ± 0	^{9}71 ± 0	^{8}72 ± 1	^{623}1779 ± 26	^{620}1757 ± 97
367	expasoft-001	39057	983064	^{43}142	^{760}2048 ± 0	^{22}70 ± 0	^{15}74 ± 0	^{11}77 ± 0	^{10}73 ± 0	^{9}74 ± 0	^{591}1660 ± 35	^{595}1676 ± 48
368	expasoft-002	38760	59825	^{57}170	^{864}2048 ± 0	^{8}34 ± 0	^{5}34 ± 0	^{5}34 ± 0	^{4}34 ± 0	^{2}34 ± 0	^{1117}8870 ± 78	^{1118}8838 ± 77
369	f8-001	272977	19668	^{524}1276	^{693}2048 ± 0	^{871}822 ± 39	-	-	-	-	^{1200}15262 ± 139	^{1203}15277 ± 212
370	f8-002	28278	215616	^{20}84	^{550}2048 ± 0	^{11}39 ± 0	^{7}41 ± 0	^{9}75 ± 0	^{47}197 ± 1	^{326}702 ± 1	^{1189}14765 ± 131	^{1192}14790 ± 133
371	facehawk-000	120009	7737	^{36}129	^{201}776 ± 1	^{348}399 ± 0	^{221}402 ± 0	^{190}414 ± 1	^{150}391 ± 2	^{141}440 ± 3	^{1145}10931 ± 155	^{1146}10915 ± 149
372	faceint-001	110744	649612	^{857}2903	^{842}2048 ± 0	^{127}195 ± 0	^{73}191 ± 0	^{59}195 ± 0	^{50}203 ± 3	^{43}232 ± 10	^{529}1434 ± 11	^{533}1431 ± 19
373	facelocate-001	4739	11106	^{789}2449	^{19}168 ± 0	^{7}34 ± 1	^{6}38 ± 0	^{14}84 ± 1	^{20}112 ± 4	^{35}206 ± 13	^{1124}9565 ± 91	^{1128}9629 ± 131
374	facelocate-002	15198	486568	^{82}271	^{142}512 ± 0	^{150}214 ± 1	^{101}239 ± 0	^{196}422 ± 2	^{205}463 ± 5	^{233}571 ± 15	^{207}611 ± 8	^{232}620 ± 17
375	faceonlive-001	0	71529	^{93}300	^{1036}2056 ± 0	^{105}179 ± 0	^{57}179 ± 0	^{56}190 ± 0	^{57}217 ± 0	^{84}343 ± 1	^{414}1064 ± 37	^{408}1033 ± 35
376	faceonlive-002	155220	141019	^{402}997	^{663}2048 ± 0	^{819}783 ± 1	^{577}797 ± 2	^{526}794 ± 2	^{490}809 ± 3	^{477}901 ± 2	^{1179}13798 ± 197	^{1180}13743 ± 127
377	faceonlive-003	518321	560984	^{949}4691	^{229}1024 ± 0	^{1081}1032 ± 4	^{808}1091 ± 3	^{1101}1942 ± 6	^{1041}1723 ± 5	^{1061}4168 ± 3	^{1205}16149 ± 41	^{1208}16135 ± 54
378	facephi-000	148904	5219	^{1011}20248	^{867}2048 ± 0	^{916}871 ± 2	^{642}881 ± 3	^{595}880 ± 4	^{550}888 ± 4	^{503}949 ± 12	^{960}4067 ± 53	^{963}4047 ± 53
379	facephi-001	138133	282874	^{548}1347	^{119}512 ± 0	^{213}285 ± 0	^{118}272 ± 2	^{100}291 ± 5	^{91}296 ± 3	^{172}489 ± 5	^{872}3194 ± 41	^{877}3184 ± 54
380	facephi-002	1031362	112529	^{978}6074	^{397}2048 ± 0	^{1232}1240 ± 5	^{939}1251 ± 5	^{909}1253 ± 21	^{870}1298 ± 5	^{938}1713 ± 19	^{1161}11961 ± 81	^{1164}11970 ± 83
381	facesoft-000	370120	10612	^{308}796	^{834}2048 ± 0	^{692}675 ± 18	^{456}669 ± 3	^{439}686 ± 3	^{378}675 ± 5	^{312}687 ± 2	^{719}2239 ± 28	^{728}2277 ± 96
382	facetag-000	1232331	4022	^{390}965	^{197}684 ± 0	^{290}355 ± 17	^{192}369 ± 8	^{686}989 ± 33	^{1096}2408 ± 91	^{1091}7930 ± 316	^{1372}72003 ± 625	^{1372}71912 ± 612
383	facetag-001	1258247	4022	-	^{1277}4100 ± 0	^{1043}991 ± 3	^{746}995 ± 3	^{714}1018 ± 3	^{681}1069 ± 5	^{735}1284 ± 8	^{885}3323 ± 28	^{891}3287 ± 34
384	facetag-002	819806	4021	^{264}706	^{465}2048 ± 0	^{508}544 ± 1	^{339}544 ± 0	^{306}542 ± 0	^{266}545 ± 0	^{224}554 ± 0	^{609}1730 ± 25	^{615}1733 ± 25
385	facex-001	305074	930372	^{884}3336	^{507}2048 ± 0	^{374}422 ± 4	^{246}434 ± 4	^{289}520 ± 7	^{441}737 ± 13	^{932}1670 ± 27	^{645}1871 ± 23	^{643}1846 ± 29
386	facex-002	305074	928334	^{865}3011	^{590}2048 ± 0	^{378}426 ± 5	^{238}429 ± 4	^{283}516 ± 8	^{433}730 ± 12	^{941}1738 ± 36	^{228}631 ± 25	^{228}614 ± 19
387	facia-001	296496	745403	^{365}889	^{720}2048 ± 0	^{1121}1099 ± 1	^{825}1109 ± 0	^{795}1113 ± 0	^{725}1125 ± 3	^{709}1250 ± 1	^{1358}62245 ± 397	^{1355}62249 ± 496
388	facia-002	585227	694738	^{704}1907	^{984}2052 ± 0	^{1291}1347 ± 4	^{1003}1337 ± 3	^{1073}1509 ± 7	^{1068}1919 ± 11	^{1055}3982 ± 34	^{1243}21963 ± 400	^{1246}21869 ± 318
389	faicetech-000	247687	34022	^{550}1349	^{790}2048 ± 0	^{1183}1179 ± 1	^{900}1199 ± 1	^{859}1193 ± 1	^{794}1202 ± 0	^{699}1240 ± 4	^{185}594 ± 4	^{200}593 ± 1
390	farfaces-001	346494	44581	^{79}262	^{139}512 ± 0	^{1184}1179 ± 1	^{885}1180 ± 1	^{848}1180 ± 0	^{782}1185 ± 1	^{686}1209 ± 2	^{347}855 ± 25	^{355}860 ± 31
391	fastenterprises-000	273365	235899	^{417}1030	^{761}2048 ± 0	^{671}662 ± 1	^{458}671 ± 0	^{423}664 ± 0	^{377}673 ± 3	^{314}688 ± 5	^{939}3806 ± 96	^{1296}32064 ± 185
392	fci-000	1486985	454513	^{873}3123	^{415}2048 ± 0	^{1364}1464 ± 12	^{1082}1494 ± 9	^{1053}1457 ± 10	^{992}1462 ± 11	^{895}1525 ± 5	^{737}2309 ± 8	^{739}2314 ± 14
393	fdu-000	202296	1307	-	^{176}534 ± 0	^{31}84 ± 0	-	-	-	-	^{602}1713 ± 28	^{607}1715 ± 20
394	fdu-001	345583	1329	-	^{319}1808 ± 0	^{69}131 ± 0	-	-	-	-	^{491}1288 ± 26	^{496}1281 ± 22
395	fedu-001	466605	496375	^{615}1557	^{403}2048 ± 0	^{571}592 ± 1	^{411}623 ± 1	^{374}624 ± 0	^{330}623 ± 0	^{285}647 ± 0	^{746}2362 ± 13	^{746}2361 ± 22
396	fiberhome-nanjing-002	207398	596827	-	^{222}1024 ± 0	^{1211}1217 ± 2	^{970}1294 ± 30	^{954}1312 ± 12	^{999}1477 ± 14	^{772}1326 ± 11	^{575}1582 ± 57	^{575}1560 ± 51

Notes	
1	The configuration size does not capture static data included in libraries.
2	The library size is the combined total of all files provided in the submission lib folder. These libraries e.g. OpenCV may or may not be installed on any end user's platform natively and would not need to be installed with the algorithm. Some developers put neural network models in their libraries.
3	The memory usage is the peak resident set size reported by the ps system call during template generation.
4	The median template creation times are measured on Intel®Xeon®CPU E5-2630 v4 @ 2.20GHz processors.
5	The comparison durations, in nanoseconds, are estimated using std::chrono::high_resolution_clock which on the machine in (2) counts 1ns clock ticks. Precision is somewhat worse than that however. The ± value is the median absolute deviation times 1.48 for Normal consistency.

Table 30: Summary of algorithms and properties included in this report. The red superscripts give ranking for the quantity in that column.

	ALGORITHM	CONFIG	LIBRARY	TEMPLATE							COMPARISON[4]	
	NAME	DATA	DATA	MEMORY	SIZE	GENERATION TIME (ms)[4]					TIME (ns)[5]	
		(KB)[1]	(KB)[2]	(MB)[3]	(B)	MUGSHOT	480x720	960x1440	1600x2400	3000x4500	GENUINE	IMPOSTOR
397	fiberhome-nanjing-003	352895	1482309	^{349}859	^{910}2048 ± 0	^{1145}1136 ± 7	^{845}1134 ± 4	^{813}1132 ± 3	^{741}1139 ± 3	^{649}1154 ± 5	^{429}1097 ± 38	^{433}1083 ± 42
398	fiberhome-nanjing-004	443779	1482313	^{444}1077	^{1210}4096 ± 0	^{1283}1321 ± 5	^{979}1304 ± 3	^{951}1307 ± 2	^{878}1308 ± 3	^{771}1326 ± 5	^{486}1276 ± 40	^{491}1265 ± 38
399	fincore-000	256615	19409	^{186}536	^{607}2048 ± 0	^{469}508 ± 3	^{308}505 ± 0	^{277}508 ± 1	^{242}513 ± 2	^{209}535 ± 1	^{617}1765 ± 31	^{622}1763 ± 22
400	firstcreditkz-001	553811	24803	^{465}1113	^{453}2048 ± 0	^{846}808 ± 0	^{747}997 ± 0	^{756}1061 ± 1	^{769}1174 ± 1	^{946}1774 ± 54	^{359}904 ± 20	^{365}903 ± 23
401	firstcreditkz-002	977538	24879	^{712}1951	^{351}2048 ± 0	^{1248}1265 ± 1	^{957}1275 ± 4	^{949}1299 ± 7	^{900}1341 ± 17	^{889}1515 ± 40	^{312}761 ± 28	^{323}774 ± 32
402	firstcreditkz-003	1145884	24907	^{746}2144	^{826}2048 ± 0	^{1191}1188 ± 79	^{1081}1492 ± 77	^{1118}2566 ± 293	^{1117}4939 ± 888	^{1111}14753 ± 3518	^{216}616 ± 10	^{225}613 ± 16
403	firstcreditkz-004	1205746	38973	^{814}2587	^{339}2048 ± 0	^{1097}1060 ± 5	^{928}1236 ± 4	^{976}1343 ± 6	^{1045}1752 ± 15	^{1054}3765 ± 42	^{160}525 ± 16	^{160}521 ± 14
404	foomobi-001	0	219961	^{64}189	^{479}2048 ± 0	^{294}357 ± 0	^{206}388 ± 2	^{816}1138 ± 1	^{1108}2974 ± 10	^{1102}10101 ± 10	^{1331}47409 ± 453	^{1331}47413 ± 421
405	foomobi-002	0	219961	^{63}189	^{445}2048 ± 0	^{228}299 ± 0	^{152}323 ± 0	^{658}957 ± 1	^{1098}2496 ± 2	^{1092}8549 ± 7	^{1286}30257 ± 724	^{1285}30010 ± 320
406	fourthlinecom-001	0	437655	^{778}2410	^{848}2048 ± 0	^{1305}1372 ± 5	^{946}1257 ± 4	^{932}1283 ± 2	^{831}1243 ± 3	^{703}1244 ± 4	^{753}2391 ± 17	^{754}2403 ± 26
407	fpt-000	19013	170633	^{70}219	^{659}2048 ± 0	^{57}118 ± 0	^{34}122 ± 1	^{27}122 ± 0	^{22}120 ± 0	^{27}178 ± 2	^{943}3871 ± 31	^{945}3883 ± 29
408	fpt-001	256529	142347	^{211}600	^{694}2048 ± 0	^{584}602 ± 0	^{390}606 ± 0	^{372}623 ± 1	^{328}621 ± 0	^{278}637 ± 0	^{948}3934 ± 10	^{951}3931 ± 14
409	fpttelecom-000	266955	273536	^{158}485	^{707}2048 ± 0	^{1388}1587 ± 0	^{1096}1589 ± 0	^{1084}1593 ± 0	^{1030}1591 ± 0	^{917}1599 ± 0	^{1103}7881 ± 40	^{1103}7901 ± 48
410	fraudcom-000	354020	561861	^{391}966	^{977}2052 ± 0	^{523}561 ± 2	^{332}539 ± 2	^{303}541 ± 1	^{276}557 ± 5	^{245}594 ± 6	^{724}2258 ± 10	^{725}2256 ± 29
411	frpkauai-001	507771	24807	^{930}4143	^{846}2048 ± 0	^{720}689 ± 1	^{486}691 ± 0	^{451}697 ± 2	^{421}714 ± 6	^{393}775 ± 31	^{306}752 ± 29	^{320}764 ± 23
412	frpkauai-002	519141	24803	^{466}1113	^{776}2048 ± 0	^{841}799 ± 0	^{737}987 ± 0	^{742}1046 ± 1	^{756}1163 ± 2	^{945}1769 ± 4	^{361}907 ± 20	^{362}886 ± 28
413	frpkauai-003	1135621	24939	^{752}2184	^{436}2048 ± 0	^{998}948 ± 3	^{826}1110 ± 2	^{884}1225 ± 5	^{921}1369 ± 16	^{967}2007 ± 34	^{159}524 ± 14	^{164}529 ± 19
414	frpkauai-004	513748	3521	^{512}1248	^{70}296 ± 0	^{254}317 ± 1	^{147}316 ± 3	^{117}317 ± 1	^{106}322 ± 1	^{99}370 ± 9	^{1097}7700 ± 81	^{1096}7659 ± 78
415	fujitsulab-000	0	205894	-	^{94}512 ± 0	^{371}419 ± 1	-	-	-	-	^{921}3613 ± 37	^{925}3621 ± 29
416	fujitsulab-001	0	548917	-	^{1294}4104 ± 0	^{1271}1300 ± 5	^{968}1291 ± 2	^{946}1295 ± 2	^{873}1304 ± 2	^{806}1382 ± 2	^{828}2853 ± 16	^{830}2847 ± 14
417	fujitsulab-002	0	1088887	^{649}1685	^{1299}4104 ± 0	^{1228}1237 ± 2	^{920}1222 ± 2	^{892}1236 ± 1	^{834}1251 ± 2	^{773}1327 ± 2	^{823}2836 ± 25	^{824}2809 ± 44
418	fujitsulab-003	662263	318209	^{984}6691	^{1297}4104 ± 0	^{1004}951 ± 20	^{694}941 ± 19	^{650}952 ± 19	^{607}971 ± 20	^{565}1045 ± 21	^{829}2855 ± 16	^{831}2849 ± 19
419	g42-intellibrain-001	1031335	235521	^{1014}25154	^{63}269 ± 0	^{1032}976 ± 6	^{723}975 ± 1	^{699}997 ± 2	^{679}1068 ± 3	^{793}1362 ± 8	^{1041}5878 ± 96	^{1041}5865 ± 71
420	g42-intellibrain-002	1043920	132389	^{1010}19747	^{64}269 ± 0	^{964}915 ± 2	^{673}920 ± 2	^{646}946 ± 2	^{628}998 ± 4	^{692}1224 ± 8	^{1187}14703 ± 56	^{1191}14658 ± 97
421	geo-000	114483	304983	-	^{516}2048 ± 0	^{899}851 ± 1	-	-	-	-	^{1393}137544 ± 6225	^{1393}137925 ± 6548
422	geo-001	258516	70163	-	^{537}2048 ± 0	^{1108}1079 ± 0	^{795}1076 ± 0	^{765}1076 ± 0	^{691}1078 ± 0	^{608}1102 ± 0	^{870}3163 ± 47	^{874}3158 ± 38
423	geo-002	369903	98667	^{414}1021	^{557}2048 ± 0	^{828}791 ± 1	^{574}793 ± 0	^{525}794 ± 0	^{482}795 ± 1	^{408}803 ± 1	^{893}3407 ± 45	^{903}3422 ± 65
424	geo-003	371712	102175	-	^{855}2048 ± 0	^{1258}1283 ± 1	^{967}1290 ± 1	^{934}1285 ± 1	^{869}1292 ± 1	^{749}1302 ± 1	^{386}997 ± 13	^{397}1001 ± 20
425	geo-004	168980	107714	^{527}1287	^{409}2048 ± 0	^{1250}1268 ± 1	^{959}1279 ± 1	^{926}1274 ± 0	^{842}1259 ± 1	^{744}1296 ± 1	^{396}1023 ± 20	^{406}1028 ± 22
426	gistouch-000	155338	444582	^{190}541	^{758}2048 ± 0	^{260}325 ± 1	^{155}326 ± 1	^{130}337 ± 1	^{121}354 ± 1	^{175}495 ± 1	^{1120}9505 ± 604	^{1119}9443 ± 388
427	gistouch-001	426635	444545	^{643}1651	^{449}2048 ± 0	^{978}930 ± 3	^{671}919 ± 3	^{638}937 ± 4	^{606}966 ± 2	^{616}1113 ± 1	^{1110}8475 ± 133	^{1112}8460 ± 173
428	glory-000	0	98176	-	^{81}418 ± 0	^{91}165 ± 2	-	-	-	-	^{1080}7003 ± 84	^{1076}6978 ± 71
429	glory-001	0	144786	-	^{318}1726 ± 0	^{342}393 ± 2	-	-	-	-	^{1128}9607 ± 128	^{1123}9539 ± 182
430	glory-002	0	385177	-	^{1105}2106 ± 0	^{575}594 ± 3	^{532}740 ± 3	^{648}948 ± 3	^{1084}2168 ± 6	^{30}191 ± 15	^{1071}6787 ± 85	^{1061}6551 ± 249
431	glory-003	0	536910	-	^{1331}4234 ± 0	^{449}489 ± 0	^{356}565 ± 0	^{485}732 ± 0	^{1061}1876 ± 2	^{1093}8941 ± 20	^{1046}6020 ± 90	^{1046}6003 ± 72
432	glory-004	0	999639	^{757}2200	^{1327}4182 ± 0	^{717}688 ± 0	^{549}759 ± 1	^{643}941 ± 1	^{1082}2134 ± 4	^{1098}9360 ± 47	^{1004}4982 ± 66	^{1006}4990 ± 63
433	glory-005	0	999999	^{790}2450	^{1326}4182 ± 0	^{742}703 ± 1	^{571}789 ± 0	^{670}972 ± 1	^{1086}2200 ± 25	^{1100}9679 ± 22	^{1014}5224 ± 93	^{1013}5176 ± 81
434	glory-006	0	1004784	^{786}2438	^{1325}4182 ± 0	^{743}704 ± 1	^{560}774 ± 0	^{667}968 ± 2	^{1092}2286 ± 18	^{1104}10381 ± 151	^{1039}5853 ± 77	^{1040}5819 ± 74
435	glory-007	0	1004846	^{787}2442	^{1324}4182 ± 0	^{333}385 ± 0	^{241}431 ± 0	^{329}575 ± 14	^{993}1464 ± 24	^{1085}6782 ± 62	^{908}3506 ± 51	^{912}3489 ± 66
436	gorilla-000	98290	1122916	-	^{1329}4204 ± 0	^{181}256 ± 14	-	-	-	-	^{945}3875 ± 29	^{944}3872 ± 51
437	gorilla-001	93768	1101838	-	^{1112}2156 ± 0	^{88}160 ± 14	-	-	-	-	^{898}3429 ± 145	^{892}3288 ± 51
438	gorilla-002	93869	1281839	-	^{284}1132 ± 0	^{258}322 ± 14	-	-	-	-	^{805}2715 ± 68	^{790}2585 ± 84
439	gorilla-003	94409	1281823	-	^{283}1132 ± 0	^{273}334 ± 25	-	-	-	-	^{825}2840 ± 42	^{834}2865 ± 87
440	gorilla-004	186952	1274131	-	^{1116}2192 ± 0	^{336}389 ± 3	-	-	-	-	^{814}2768 ± 44	^{813}2745 ± 44

Notes	
1	The configuration size does not capture static data included in libraries.
2	The library size is the combined total of all files provided in the submission lib folder. These libraries e.g. OpenCV may or may not be installed on any end user's platform natively and would not need to be installed with the algorithm. Some developers put neural network models in their libraries.
3	The memory usage is the peak resident set size reported by the ps system call during template generation.
4	The median template creation times are measured on Intel®Xeon®CPU E5-2630 v4 @ 2.20GHz processors.
5	The comparison durations, in nanoseconds, are estimated using std::chrono::high_resolution_clock which on the machine in (2) counts 1ns clock ticks. Precision is somewhat worse than that however. The ± value is the median absolute deviation times 1.48 for Normal consistency.

Table 31: Summary of algorithms and properties included in this report. The red superscripts give ranking for the quantity in that column.

	ALGORITHM	CONFIG	LIBRARY	TEMPLATE							COMPARISON[4]	
	NAME	DATA	DATA	MEMORY	SIZE	GENERATION TIME (ms)[4]					TIME (ns)[5]	
		(KB)[1]	(KB)[2]	(MB)[3]	(B)	MUGSHOT	480x720	960x1440	1600x2400	3000x4500	GENUINE	IMPOSTOR
441	gorilla-005	100684	1297614	-	^{1115}2192 ± 0	^{357}407 ± 3	^{252}437 ± 2	^{220}448 ± 4	^{214}473 ± 4	^{240}589 ± 15	^{798}2678 ± 42	^{816}2770 ± 112
442	gorilla-006	172743	1318812	-	^{1332}4240 ± 0	^{409}454 ± 3	^{290}484 ± 3	^{267}497 ± 5	^{264}543 ± 25	^{492}928 ± 60	^{935}3755 ± 38	^{937}3737 ± 44
443	gorilla-007	441058	708166	^{648}1683	^{1372}6288 ± 0	^{572}592 ± 1	^{381}592 ± 1	^{351}603 ± 1	^{333}625 ± 2	^{343}722 ± 9	^{928}3686 ± 37	^{933}3709 ± 36
444	gorilla-008	450175	707000	^{686}1812	^{1394}8338 ± 0	^{578}595 ± 1	^{380}590 ± 0	^{349}600 ± 1	^{329}621 ± 2	^{341}720 ± 9	^{982}4530 ± 44	^{980}4524 ± 38
445	gorilla-009	329584	297395	^{540}1304	^{1333}4242 ± 0	^{944}899 ± 2	^{677}922 ± 1	^{606}901 ± 3	^{570}924 ± 4	^{558}1032 ± 12	^{733}2294 ± 74	^{736}2301 ± 66
446	gpstechvn-000	108365	345975	^{817}2646	^{375}2048 ± 0	^{225}296 ± 1	^{140}297 ± 1	^{108}304 ± 0	^{100}316 ± 0	^{105}382 ± 0	^{761}2442 ± 11	^{763}2440 ± 16
447	graymatics-001	13095	70406	^{34}128	^{1253}4096 ± 0	^{121}191 ± 1	^{80}203 ± 1	^{343}592 ± 5	^{1037}1698 ± 9	^{1087}7150 ± 34	^{1316}39874 ± 309	^{1318}39762 ± 295
448	griaule-000	0	598214	^{432}1055	^{963}2052 ± 0	^{369}416 ± 6	^{234}425 ± 7	^{516}770 ± 14	^{1044}1749 ± 43	^{1083}6406 ± 189	^{953}3987 ± 42	^{954}3938 ± 38
449	griaule-001	0	412061	^{520}1271	^{987}2052 ± 0	^{1169}1164 ± 1	^{815}1096 ± 5	^{784}1099 ± 4	^{737}1136 ± 2	^{886}1509 ± 2	^{950}3948 ± 23	^{957}3957 ± 32
450	griaule-002	0	1320474	^{698}1870	^{1005}2052 ± 0	^{870}822 ± 1	^{679}924 ± 4	^{611}907 ± 1	^{661}1038 ± 21	^{839}1430 ± 9	^{954}4005 ± 32	^{960}4012 ± 31
451	gtelots-000	252631	59244	^{193}552	^{122}512 ± 0	^{823}785 ± 1	^{575}794 ± 0	^{534}810 ± 0	^{502}823 ± 2	^{461}875 ± 0	^{1244}22029 ± 130	^{1248}21988 ± 93
452	gtelots-001	442881	58709	^{392}966	^{1114}2176 ± 0	^{1075}1027 ± 0	^{768}1028 ± 0	^{733}1037 ± 0	^{680}1069 ± 0	^{660}1167 ± 1	^{148}493 ± 31	^{152}496 ± 38
453	hertasecurity-000	0	780014	-	^{29}256 ± 0	^{43}99 ± 0	^{25}98 ± 0	^{21}100 ± 0	^{18}107 ± 0	^{19}139 ± 0	^{286}710 ± 31	^{268}667 ± 28
454	hertasecurity-001	0	944427	^{495}1188	^{113}512 ± 0	^{283}346 ± 0	^{167}345 ± 0	^{135}349 ± 0	^{122}354 ± 0	^{110}388 ± 0	^{619}1770 ± 45	^{612}1726 ± 48
455	hertasecurity-002	0	944582	^{491}1182	^{111}512 ± 0	^{445}484 ± 7	^{282}478 ± 3	^{250}480 ± 3	^{230}495 ± 3	^{201}520 ± 3	^{732}2289 ± 40	^{727}2267 ± 48
456	hertasecurity-003	0	944583	^{490}1181	^{129}512 ± 0	^{454}495 ± 7	^{285}480 ± 3	^{257}486 ± 3	^{226}491 ± 3	^{202}520 ± 4	^{1095}7619 ± 65	^{1095}7597 ± 94
457	hik-001	667866	9290	^{982}6597	^{295}1408 ± 0	^{656}651 ± 0	^{455}667 ± 8	^{433}677 ± 16	^{390}686 ± 13	^{354}737 ± 12	^{144}488 ± 19	^{146}477 ± 22
458	hisign-001	732412	167488	^{618}1560	^{1099}2080 ± 0	^{1274}1306 ± 1	^{990}1320 ± 1	^{957}1315 ± 1	^{884}1312 ± 1	^{768}1325 ± 1	^{40}201 ± 10	^{36}185 ± 13
459	hisign-002	1014906	102652	^{742}2131	^{1096}2080 ± 0	^{838}797 ± 0	^{579}800 ± 5	^{529}800 ± 0	^{485}801 ± 0	^{409}803 ± 1	^{53}232 ± 11	^{44}207 ± 11
460	hisign-003	2232829	156367	^{630}1599	^{1097}2080 ± 0	^{1086}1040 ± 5	^{799}1083 ± 4	^{770}1085 ± 4	^{695}1088 ± 4	^{605}1093 ± 4	^{27}167 ± 8	^{25}150 ± 10
461	hyperverge-001	260819	88624	-	^{401}2048 ± 0	^{706}682 ± 20	^{489}695 ± 17	^{865}1196 ± 37	^{1095}2400 ± 68	^{1088}7178 ± 204	^{1048}6026 ± 40	^{1045}5984 ± 38
462	hyperverge-002	2951900	198832	^{718}1975	^{249}1024 ± 0	^{982}938 ± 1	^{692}939 ± 1	^{642}941 ± 1	^{587}945 ± 1	^{520}975 ± 1	^{1047}6023 ± 37	^{1044}5966 ± 40
463	hyperverge-003	1167779	282156	^{823}2687	^{216}1024 ± 0	^{1372}1477 ± 2	^{1085}1503 ± 3	^{1075}1520 ± 3	^{1016}1525 ± 4	^{909}1565 ± 3	^{172}566 ± 11	^{176}561 ± 8
464	hyperverge-004	4924393	282156	^{919}3908	^{800}2048 ± 0	^{1368}1471 ± 2	^{1058}1434 ± 1	^{1044}1446 ± 6	^{979}1445 ± 3	^{878}1491 ± 3	^{385}996 ± 10	^{395}1000 ± 19
465	hyperverge-005	3413303	284050	^{822}2686	^{233}1024 ± 0	^{719}689 ± 0	^{484}690 ± 0	^{446}693 ± 0	^{408}702 ± 6	^{367}752 ± 5	^{130}465 ± 2	^{142}464 ± 10
466	hyperverge-006	3901500	284050	^{731}2070	^{255}1024 ± 0	^{805}768 ± 1	^{558}770 ± 2	^{511}766 ± 1	^{466}773 ± 1	^{423}828 ± 6	^{131}466 ± 2	^{141}463 ± 4
467	hyperverge-007	2223041	169168	^{748}2159	^{238}1024 ± 0	^{1286}1327 ± 1	^{973}1296 ± 0	^{931}1280 ± 0	^{866}1286 ± 0	^{783}1348 ± 0	^{251}659 ± 19	^{278}684 ± 26
468	hyundai-roboticslab-000	181134	191546	^{478}1149	^{667}2048 ± 0	^{318}376 ± 3	^{189}368 ± 1	^{153}367 ± 2	^{137}374 ± 0	^{123}408 ± 1	^{820}2815 ± 47	^{822}2790 ± 50
469	hyundai-roboticslab-001	361330	106869	^{324}820	^{922}2048 ± 0	^{297}358 ± 1	^{180}361 ± 1	^{148}362 ± 2	^{138}374 ± 3	^{116}394 ± 0	^{863}3115 ± 34	^{866}3117 ± 45
470	hyundai-roboticslab-002	181140	106752	^{320}817	^{398}2048 ± 0	^{284}347 ± 0	^{175}355 ± 0	^{143}357 ± 0	^{127}362 ± 3	^{109}387 ± 0	^{878}3243 ± 111	^{887}3245 ± 114
471	hyundai-roboticslab-003	484277	106656	^{725}2027	^{934}2048 ± 0	^{1395}1800 ± 0	^{1105}1792 ± 0	^{1095}1802 ± 0	^{1063}1889 ± 0	^{951}1810 ± 0	^{1116}8841 ± 42	^{1117}8819 ± 54
472	hzailu-001	0	372018	-	^{1024}2056 ± 0	^{1140}1126 ± 1	^{841}1128 ± 1	^{811}1130 ± 1	^{734}1132 ± 1	^{652}1159 ± 1	^{357}894 ± 19	^{364}899 ± 22
473	hzailu-002	1515880	74047	^{951}4722	^{1010}2056 ± 0	^{1158}1150 ± 5	^{840}1127 ± 6	^{810}1129 ± 7	^{739}1137 ± 7	^{663}1172 ± 3	^{423}1079 ± 53	^{424}1070 ± 31
474	hzailu-003	1923030	222185	^{957}4858	^{1145}3080 ± 0	^{1321}1389 ± 5	^{998}1331 ± 7	^{970}1334 ± 2	^{905}1349 ± 6	^{835}1424 ± 8	^{549}1483 ± 35	^{547}1464 ± 31
475	hzailu-004	1938475	275639	^{925}4023	^{1148}3080 ± 0	^{1381}1495 ± 8	^{1080}1490 ± 6	^{1066}1493 ± 8	^{1008}1502 ± 8	^{912}1583 ± 17	^{505}1361 ± 32	^{528}1419 ± 44
476	hzailu-005	1573726	275643	^{880}3292	^{1349}5128 ± 0	^{711}684 ± 10	^{466}673 ± 7	^{370}622 ± 1	^{384}682 ± 6	^{335}715 ± 2	^{642}1853 ± 51	^{639}1829 ± 34
477	hzailu-006	2996729	275643	^{977}6070	^{1379}7176 ± 0	^{1382}1498 ± 11	^{1079}1483 ± 15	^{1039}1439 ± 8	^{978}1441 ± 10	^{908}1564 ± 40	^{757}2434 ± 19	^{767}2452 ± 32
478	hzailu-007	2906424	275643	^{972}5897	^{1380}7176 ± 0	^{1347}1430 ± 19	^{1063}1448 ± 10	^{965}1328 ± 3	^{1010}1504 ± 17	^{842}1434 ± 4	^{771}2481 ± 28	^{775}2488 ± 34
479	hzailu-008	2906977	275643	^{973}5898	^{1381}7176 ± 0	^{1358}1452 ± 13	^{1089}1557 ± 10	^{1077}1545 ± 12	^{1022}1561 ± 20	^{899}1533 ± 16	^{773}2492 ± 62	^{776}2489 ± 66
480	i2v-001	276820	26600	^{318}815	^{908}2048 ± 0	^{759}721 ± 0	^{524}729 ± 0	^{483}731 ± 0	^{435}731 ± 0	^{379}764 ± 0	^{1152}11523 ± 176	^{1154}11533 ± 142
481	i2v-002	339732	122488	^{657}1721	^{814}2048 ± 0	^{1352}1438 ± 1	^{1078}1476 ± 1	^{1040}1442 ± 1	^{1002}1480 ± 9	^{898}1533 ± 1	^{250}656 ± 35	^{215}604 ± 28
482	icehouse-000	287028	178880	^{363}887	^{639}2048 ± 0	^{631}629 ± 1	^{407}620 ± 1	^{407}648 ± 1	^{394}690 ± 4	^{510}961 ± 11	^{364}910 ± 11	^{377}938 ± 16
483	icm-002	621586	903	-	^{716}2048 ± 0	^{1080}1031 ± 7	-	-	-	-	^{1260}24052 ± 118	^{1261}24049 ± 124
484	icm-003	1513988	940	^{178}516	^{402}2048 ± 0	^{703}681 ± 6	^{463}672 ± 4	^{468}714 ± 11	^{512}837 ± 41	^{805}1381 ± 131	^{1262}24351 ± 161	^{1262}24227 ± 146

Notes	
1	The configuration size does not capture static data included in libraries.
2	The library size is the combined total of all files provided in the submission lib folder. These libraries e.g. OpenCV may or may not be installed on any end user's platform natively and would not need to be installed with the algorithm. Some developers put neural network models in their libraries.
3	The memory usage is the peak resident set size reported by the ps system call during template generation.
4	The median template creation times are measured on Intel®Xeon®CPU E5-2630 v4 @ 2.20GHz processors.
5	The comparison durations, in nanoseconds, are estimated using std::chrono::high_resolution_clock which on the machine in (2) counts 1ns clock ticks. Precision is somewhat worse than that however. The ± value is the median absolute deviation times 1.48 for Normal consistency.

Table 32: Summary of algorithms and properties included in this report. The red superscripts give ranking for the quantity in that column.

	ALGORITHM	CONFIG	LIBRARY	TEMPLATE							COMPARISON[4]	
	NAME	DATA	DATA	MEMORY	SIZE	GENERATION TIME (ms)[4]					TIME (ns)[5]	
		(KB)[1]	(KB)[2]	(MB)[3]	(B)	MUGSHOT	480x720	960x1440	1600x2400	3000x4500	GENUINE	IMPOSTOR
485	icm-004	2012129	1089	^{431}1052	^{850}2048 ± 0	^{372}419 ± 6	^{224}407 ± 6	^{227}454 ± 15	^{310}603 ± 51	^{896}1527 ± 235	^{1188}14730 ± 154	^{1190}14521 ± 152
486	icm-005	877530	1097	^{467}1116	^{666}2048 ± 0	^{114}185 ± 3	^{62}181 ± 3	^{64}208 ± 9	^{105}321 ± 36	^{550}1014 ± 185	^{1136}10245 ± 65	^{1138}10245 ± 69
487	icomm-000	807818	139431	^{986}6728	^{1178}4096 ± 0	^{589}605 ± 26	^{393}610 ± 30	^{353}605 ± 27	^{312}610 ± 23	^{283}641 ± 32	^{1111}8507 ± 25	^{1113}8516 ± 26
488	icthtc-000	172459	1471004	^{483}1165	^{769}2048 ± 0	^{278}338 ± 11	^{163}338 ± 9	^{211}437 ± 16	^{411}705 ± 24	^{939}1719 ± 44	^{1017}5284 ± 63	^{1018}5290 ± 54
489	id3-001	225574	34433	-	^{168}520 ± 0	^{163}238 ± 19	-	-	-	-	^{408}1058 ± 32	^{418}1049 ± 28
490	id3-002	225574	34433	-	^{170}520 ± 0	^{443}482 ± 34	-	-	-	-	^{431}1100 ± 59	^{416}1048 ± 32
491	id3-003	265951	49731	-	^{56}264 ± 0	^{250}316 ± 19	-	-	-	-	^{500}1330 ± 25	^{513}1354 ± 28
492	id3-004	171526	49725	-	^{61}264 ± 0	^{504}541 ± 11	-	-	-	-	^{443}1135 ± 23	^{465}1156 ± 32
493	id3-005	153439	22125	-	^{58}264 ± 0	^{438}479 ± 1	-	-	-	-	^{1050}6072 ± 35	^{1049}6077 ± 38
494	id3-006	210116	7706	^{398}984	^{169}520 ± 0	^{710}683 ± 0	^{804}1088 ± 1	^{858}1192 ± 1	^{800}1209 ± 1	^{726}1270 ± 1	^{1027}5547 ± 34	^{1029}5563 ± 34
495	id3-007	185030	7728	-	^{57}264 ± 0	^{1063}1016 ± 1	^{853}1139 ± 1	^{1122}3911 ± 2	^{1122}10752 ± 12	^{1118}135182 ± 1912	^{1023}5500 ± 29	^{1022}5486 ± 35
496	id3-008	242416	8151	^{434}1059	^{59}264 ± 0	^{864}819 ± 0	^{910}1209 ± 2	^{948}1297 ± 2	^{895}1329 ± 1	^{841}1433 ± 1	^{1033}5658 ± 44	^{1034}5624 ± 40
497	id3-009	128638	9510	^{430}1051	^{62}264 ± 0	^{477}520 ± 1	^{318}518 ± 1	^{282}515 ± 2	^{247}519 ± 1	^{196}514 ± 2	^{259}682 ± 34	^{270}677 ± 44
498	idemia-003	427244	106432	-	^{77}352 ± 0	^{311}368 ± 6	-	-	-	-	^{1066}6654 ± 75	^{999}4835 ± 90
499	idemia-004	406924	106436	-	^{74}352 ± 0	^{239}306 ± 5	-	-	-	-	^{1030}5592 ± 518	^{1025}5533 ± 426
500	idemia-005	509824	116761	-	^{193}588 ± 0	^{473}514 ± 15	-	-	-	-	^{1067}6657 ± 54	^{1064}6616 ± 53
501	idemia-006	570566	115633	-	^{196}668 ± 0	^{701}679 ± 4	^{682}926 ± 54	^{481}728 ± 7	^{455}760 ± 29	^{425}830 ± 31	^{1013}5223 ± 80	^{1014}5193 ± 72
502	idemia-007	353242	67485	-	^{86}468 ± 0	^{328}384 ± 0	^{208}389 ± 0	^{174}393 ± 1	^{164}405 ± 2	^{142}441 ± 8	^{879}3243 ± 63	^{878}3202 ± 63
503	idemia-008	374017	69922	^{499}1192	^{73}348 ± 0	^{412}457 ± 1	^{272}461 ± 0	^{239}466 ± 1	^{216}476 ± 2	^{193}513 ± 10	^{859}3080 ± 41	^{861}3046 ± 56
504	idemia-009	1066728	70572	^{827}2700	^{195}636 ± 0	^{1204}1207 ± 1	^{915}1218 ± 1	^{882}1222 ± 2	^{811}1222 ± 3	^{731}1280 ± 10	^{1034}5664 ± 84	^{1032}5597 ± 90
505	idemia-010	996690	66244	^{771}2306	^{80}412 ± 0	^{579}596 ± 1	^{429}632 ± 22	^{373}624 ± 18	^{337}633 ± 7	^{339}719 ± 5	^{599}1699 ± 37	^{602}1703 ± 38
506	idemia-011	472694	65098	^{888}3401	^{194}612 ± 0	^{860}816 ± 25	^{618}853 ± 9	^{412}658 ± 2	^{477}785 ± 3	^{350}732 ± 8	^{787}2583 ± 29	^{793}2627 ± 48
507	identy-000	271397	14217	^{153}474	^{546}2048 ± 0	^{718}689 ± 0	^{498}702 ± 0	^{466}712 ± 3	^{454}757 ± 0	^{516}970 ± 1	^{249}655 ± 25	^{251}637 ± 23
508	identy-001	385977	17850	^{494}1187	^{362}2048 ± 0	^{810}772 ± 1	^{612}841 ± 1	^{748}1056 ± 1	^{1024}1567 ± 5	^{1059}4081 ± 9	^{551}1484 ± 16	^{553}1480 ± 17
509	identy-002	1136161	40480	^{779}2414	^{1139}3072 ± 0	^{1385}1548 ± 0	^{1095}1584 ± 0	^{1079}1549 ± 0	^{1046}1757 ± 1	^{994}2246 ± 1	^{853}3020 ± 41	^{858}3007 ± 19
510	idrnd-000	1069136	69522	^{886}3357	^{1295}4104 ± 0	^{850}810 ± 1	^{600}828 ± 11	^{556}830 ± 10	^{540}877 ± 5	^{448}857 ± 9	^{1151}11504 ± 47	^{1153}11494 ± 62
511	idrnd-001	1080396	107151	^{892}3437	^{1301}4104 ± 0	^{576}594 ± 1	^{401}615 ± 6	^{366}615 ± 6	^{322}616 ± 6	^{282}640 ± 8	^{615}1757 ± 8	^{621}1759 ± 16
512	igearx-face-000	665623	298245	^{362}885	^{492}2048 ± 0	^{907}860 ± 1	^{621}855 ± 4	^{568}844 ± 0	^{543}881 ± 0	^{490}924 ± 3	^{585}1628 ± 45	^{592}1657 ± 41
513	iit-000	237317	33898	-	^{231}1024 ± 0	^{130}197 ± 8	-	-	-	-	^{568}1537 ± 81	^{497}1282 ± 20
514	iit-001	269176	52055	-	^{511}2048 ± 0	^{733}699 ± 4	-	-	-	-	^{410}1060 ± 48	^{426}1074 ± 54
515	iit-002	259579	52070	^{280}731	^{600}2048 ± 0	^{472}514 ± 1	^{326}531 ± 2	^{311}547 ± 1	^{292}583 ± 1	^{351}733 ± 2	^{397}1023 ± 7	^{399}1011 ± 66
516	iit-003	261288	53791	^{325}821	^{816}2048 ± 0	^{441}482 ± 0	^{296}493 ± 0	^{278}509 ± 0	^{262}541 ± 0	^{295}661 ± 0	^{86}324 ± 17	^{92}326 ± 8
517	imds-software-001	373399	352623	^{303}785	^{672}2048 ± 0	^{421}465 ± 1	^{709}958 ± 6	^{812}1131 ± 5	^{736}1134 ± 2	^{623}1119 ± 10	^{1159}11885 ± 120	^{1160}11779 ± 174
518	imds-software-002	373632	352627	^{328}833	^{744}2048 ± 0	^{428}469 ± 1	^{702}954 ± 2	^{779}1094 ± 5	^{675}1064 ± 4	^{648}1153 ± 4	^{1147}11100 ± 155	^{1148}11090 ± 145
519	imds-software-003	373648	352628	^{297}769	^{578}2048 ± 0	^{253}317 ± 5	^{444}654 ± 4	^{523}793 ± 6	^{465}770 ± 4	^{443}848 ± 2	^{1065}6624 ± 66	^{1062}6603 ± 77
520	imperial-000	370120	10623	^{309}796	^{684}2048 ± 0	^{680}669 ± 1	^{468}675 ± 3	^{438}683 ± 17	^{379}676 ± 2	^{315}689 ± 2	^{697}2130 ± 32	^{687}2052 ± 100
521	imperial-001	370260	10623	-	^{386}2048 ± 0	^{683}671 ± 0	-	-	-	-	^{691}2090 ± 28	^{690}2062 ± 74
522	imperial-002	472327	16134	^{689}1826	^{615}2048 ± 0	^{534}569 ± 1	^{371}581 ± 15	^{328}575 ± 5	^{287}576 ± 2	^{239}588 ± 3	^{728}2278 ± 90	^{699}2131 ± 44
523	incode-000	23697	18014	-	^{258}1024 ± 0	^{128}196 ± 9	-	-	-	-	^{1011}5175 ± 81	^{1002}4907 ± 77
524	incode-001	155416	18020	-	^{729}2048 ± 0	^{457}499 ± 9	-	-	-	-	^{1053}6154 ± 96	^{1048}6045 ± 182
525	incode-002	73239	32435	-	^{890}2048 ± 0	^{207}281 ± 15	-	-	-	-	^{569}1544 ± 38	^{558}1488 ± 69
526	incode-003	170632	42857	-	^{1255}4096 ± 0	^{330}384 ± 11	-	-	-	-	^{662}1928 ± 44	^{650}1876 ± 81
527	incode-004	260224	51685	-	^{612}2048 ± 0	^{436}479 ± 23	-	-	-	-	^{657}1913 ± 60	^{764}2443 ± 114
528	incode-005	256242	51670	-	^{373}2048 ± 0	^{529}566 ± 1	-	-	-	-	^{598}1695 ± 38	^{593}1663 ± 85

Notes	
1	The configuration size does not capture static data included in libraries.
2	The library size is the combined total of all files provided in the submission lib folder. These libraries e.g. OpenCV may or may not be installed on any end user's platform natively and would not need to be installed with the algorithm. Some developers put neural network models in their libraries.
3	The memory usage is the peak resident set size reported by the ps system call during template generation.
4	The median template creation times are measured on Intel®Xeon®CPU E5-2630 v4 @ 2.20GHz processors.
5	The comparison durations, in nanoseconds, are estimated using std::chrono::high_resolution_clock which on the machine in (2) counts 1ns clock ticks. Precision is somewhat worse than that however. The ± value is the median absolute deviation times 1.48 for Normal consistency.

Table 33: Summary of algorithms and properties included in this report. The red superscripts give ranking for the quantity in that column.

	ALGORITHM	CONFIG	LIBRARY	TEMPLATE							COMPARISON[4]	
	NAME	DATA	DATA	MEMORY	SIZE	GENERATION TIME (ms)[4]					TIME (ns)[5]	
		(KB)[1]	(KB)[2]	(MB)[3]	(B)	MUGSHOT	480x720	960x1440	1600x2400	3000x4500	GENUINE	IMPOSTOR
529	incode-006	266095	63518	-	^{510}2048 ± 0	^{431}472 ± 1	-	-	-	-	^{624}1788 ± 41	^{634}1798 ± 59
530	incode-007	266103	63524	-	^{530}2048 ± 0	^{429}470 ± 1	^{315}516 ± 0	^{284}518 ± 1	^{254}530 ± 2	^{255}603 ± 4	^{629}1799 ± 35	^{630}1789 ± 59
531	incode-008	266103	21014	-	^{377}2048 ± 0	^{459}500 ± 0	^{295}493 ± 0	^{266}496 ± 0	^{236}506 ± 1	^{213}537 ± 0	^{417}1070 ± 28	^{432}1081 ± 34
532	incode-009	266103	21014	-	^{408}2048 ± 0	^{463}503 ± 0	^{294}490 ± 1	^{268}498 ± 0	^{235}505 ± 0	^{211}537 ± 0	^{433}1102 ± 28	^{443}1113 ± 29
533	incode-010	627808	21014	^{805}2543	^{632}2048 ± 0	^{1186}1180 ± 2	^{880}1178 ± 1	^{851}1182 ± 1	^{778}1184 ± 1	^{690}1221 ± 1	^{459}1164 ± 32	^{454}1144 ± 32
534	incode-011	477280	21781	^{594}1483	^{446}2048 ± 0	^{918}872 ± 0	^{637}875 ± 0	^{596}881 ± 1	^{553}892 ± 1	^{497}939 ± 0	^{438}1117 ± 31	^{441}1109 ± 37
535	incode-012	477371	21786	^{592}1479	^{598}2048 ± 0	^{478}521 ± 0	^{311}506 ± 0	^{272}503 ± 0	^{243}514 ± 0	^{234}571 ± 0	^{760}2441 ± 25	^{771}2466 ± 37
536	incode-013	483720	41434	^{640}1647	^{579}2048 ± 0	^{493}535 ± 1	^{344}548 ± 1	^{316}555 ± 4	^{267}545 ± 1	^{264}618 ± 1	^{454}1152 ± 37	^{462}1154 ± 41
537	incode-014	2365157	41516	^{988}6927	^{1388}8196 ± 0	^{1100}1064 ± 4	^{806}1089 ± 2	^{785}1100 ± 5	^{707}1107 ± 7	^{670}1190 ± 3	^{584}1627 ± 42	^{587}1640 ± 59
538	incode-015	1808779	70449	^{980}6430	^{1362}6148 ± 0	^{1095}1056 ± 2	^{887}1182 ± 12	^{768}1081 ± 2	^{693}1084 ± 1	^{669}1187 ± 2	^{509}1373 ± 22	^{511}1352 ± 35
539	infocert-001	1204340	38972	^{596}1490	^{371}2048 ± 0	^{923}874 ± 1	^{650}891 ± 1	^{744}1050 ± 5	^{996}1473 ± 2	^{1043}3174 ± 8	^{1009}5055 ± 108	^{1008}5008 ± 100
540	infocert-002	186823	19501	^{235}641	^{555}2048 ± 0	^{781}742 ± 0	^{530}738 ± 0	^{490}738 ± 0	^{442}738 ± 0	^{358}739 ± 0	^{842}2917 ± 114	^{845}2930 ± 50
541	innefulabs-000	370588	162172	^{139}439	^{821}2048 ± 0	^{1057}1006 ± 3	^{765}1025 ± 3	^{727}1030 ± 4	^{664}1041 ± 2	^{637}1135 ± 3	^{1037}5782 ± 41	^{1038}5741 ± 45
542	innominds-001	102207	777689	^{469}1124	^{906}2048 ± 0	^{272}333 ± 21	^{173}350 ± 19	^{127}335 ± 16	^{117}339 ± 17	^{86}346 ± 18	^{772}2482 ± 23	^{777}2491 ± 29
543	innov8tif-000	170383	2163199	^{597}1494	^{1159}4096 ± 0	^{275}335 ± 23	^{171}348 ± 21	^{613}912 ± 64	^{1102}2661 ± 142	^{1107}10665 ± 528	^{183}591 ± 11	^{188}582 ± 11
544	innov8tif-001	118502	1241515	^{172}508	^{1265}4096 ± 0	^{925}875 ± 83	^{666}915 ± 73	^{1117}2360 ± 185	^{1118}6410 ± 390	^{1113}24097 ± 1477	^{317}775 ± 31	^{324}778 ± 14
545	innovativetechnologyltd-001	177232	335757	^{105}341	^{500}2048 ± 0	^{386}433 ± 7	^{261}446 ± 8	^{213}439 ± 4	^{190}452 ± 4	^{168}485 ± 7	^{647}1877 ± 42	^{661}1924 ± 97
546	innovativetechnologyltd-002	173939	372324	^{370}912	^{498}2048 ± 0	^{668}661 ± 2	^{521}726 ± 4	^{677}981 ± 27	^{627}997 ± 40	^{381}766 ± 3	^{638}1841 ± 50	^{646}1857 ± 59
547	innovatrics-000	0	143500	-	^{15}146 ± 0	^{543}578 ± 5	-	-	-	-	^{1003}4964 ± 63	^{987}4665 ± 262
548	innovatrics-001	0	143500	-	^{65}284 ± 0	^{650}645 ± 5	-	-	-	-	^{1024}5506 ± 131	^{1005}4975 ± 308
549	innovatrics-002	0	249195	-	^{174}530 ± 0	^{82}153 ± 0	-	-	-	-	^{1182}14384 ± 260	^{1189}14497 ± 207
550	innovatrics-003	0	538170	-	^{175}530 ± 0	^{177}250 ± 0	-	-	-	-	^{1203}15709 ± 134	^{1201}15193 ± 292
551	innovatrics-004	0	496988	-	^{280}1076 ± 0	^{340}391 ± 0	-	-	-	-	^{1112}8573 ± 274	^{1104}7929 ± 244
552	innovatrics-005	0	664175	-	^{281}1076 ± 0	^{540}577 ± 1	-	-	-	-	^{1211}16880 ± 194	^{1216}17232 ± 385
553	innovatrics-006	0	466269	-	^{178}538 ± 0	^{866}820 ± 5	^{578}799 ± 4	^{531}805 ± 3	^{483}796 ± 9	^{470}890 ± 15	^{1040}5855 ± 204	^{1016}5266 ± 118
554	innovatrics-007	0	493269	-	^{279}1064 ± 0	^{1377}1485 ± 7	^{1103}1785 ± 184	^{1109}2078 ± 24	^{1081}2123 ± 15	^{989}2210 ± 42	^{1045}5978 ± 88	^{1036}5690 ± 102
555	innovatrics-008	307323	59842	^{581}1429	^{179}538 ± 0	^{813}778 ± 6	^{555}767 ± 3	^{515}770 ± 3	^{486}803 ± 3	^{445}853 ± 10	^{855}3021 ± 66	^{801}2673 ± 88
556	innovatrics-009	624485	105187	^{711}1947	^{1309}4136 ± 0	^{1135}1116 ± 1	^{823}1107 ± 5	^{790}1104 ± 5	^{710}1110 ± 5	^{644}1146 ± 6	^{1007}5051 ± 54	^{990}4733 ± 102
557	innovatrics-010	604731	111234	^{655}1715	^{1310}4136 ± 0	^{596}611 ± 3	^{426}632 ± 2	^{474}723 ± 1	^{432}730 ± 1	^{385}768 ± 6	^{961}4077 ± 42	^{943}3857 ± 65
558	innovatrics-011	643997	50017	^{667}1745	^{1328}4184 ± 0	^{790}754 ± 2	^{556}767 ± 3	^{509}765 ± 3	^{475}783 ± 4	^{456}867 ± 3	^{963}4135 ± 57	^{953}3937 ± 91
559	innovatrics-012	0	680831	^{678}1789	^{1342}4721 ± 0	^{835}797 ± 3	^{608}837 ± 3	^{527}795 ± 1	^{559}904 ± 4	^{540}1001 ± 3	^{1382}80879 ± 981	^{1380}80521 ± 655
560	innovatrics-013	0	1665828	^{923}3931	^{1330}4212 ± 0	^{1194}1195 ± 2	^{926}1230 ± 11	^{883}1223 ± 4	^{820}1233 ± 5	^{775}1329 ± 3	^{1386}85968 ± 990	^{1384}85796 ± 836
561	innovatrics-014	0	2870004	^{979}6138	^{1373}6303 ± 0	^{1066}1022 ± 6	^{772}1031 ± 2	^{745}1051 ± 1	^{668}1052 ± 5	^{657}1163 ± 11	^{1354}60311 ± 644	^{1351}60186 ± 499
562	innovatrics-015	0	5116879	^{1008}15251	^{1375}6327 ± 0	^{1295}1350 ± 5	^{1036}1405 ± 4	^{993}1371 ± 3	^{953}1405 ± 21	^{882}1502 ± 17	^{1361}65175 ± 1027	^{1357}64294 ± 1390
563	innovatrics-016	0	3130540	^{989}6982	^{1374}6303 ± 0	^{1408}2084 ± 0	^{1120}2097 ± 0	^{1110}2103 ± 1	^{1083}2139 ± 0	^{990}2215 ± 0	^{1297}32998 ± 309	^{1299}32967 ± 351
564	insightface-000	806953	16606	-	^{1203}4096 ± 0	^{1059}1009 ± 1	^{762}1019 ± 2	^{713}1017 ± 2	^{651}1020 ± 2	^{559}1032 ± 2	^{621}1778 ± 31	^{623}1773 ± 35
565	insightface-001	776777	16606	^{915}3858	^{730}2048 ± 0	^{1301}1366 ± 2	^{1012}1368 ± 3	^{995}1372 ± 3	^{927}1375 ± 5	^{810}1386 ± 4	^{439}1119 ± 29	^{439}1108 ± 34
566	insightface-002	800572	16606	-	^{791}2048 ± 0	^{1327}1396 ± 2	^{1021}1389 ± 4	^{1017}1403 ± 3	^{950}1402 ± 2	^{826}1413 ± 3	^{460}1169 ± 40	^{446}1118 ± 38
567	insightface-003	1016917	26668	^{612}1550	^{820}2048 ± 0	^{1106}1073 ± 0	^{810}1092 ± 2	^{763}1070 ± 1	^{692}1082 ± 1	^{607}1101 ± 1	^{189}597 ± 16	^{202}595 ± 17
568	insightface-004	928816	26668	^{682}1800	^{725}2048 ± 0	^{1270}1298 ± 1	^{1008}1356 ± 2	^{956}1313 ± 1	^{882}1311 ± 0	^{785}1349 ± 1	^{171}565 ± 7	^{174}559 ± 5
569	inspur-000	364844	91926	^{314}808	^{1213}4096 ± 0	^{1302}1367 ± 1	^{999}1331 ± 2	^{991}1368 ± 2	^{995}1465 ± 1	^{955}1861 ± 3	^{1132}9831 ± 37	^{1132}9860 ± 40
570	inspur-001	364862	91934	^{329}833	^{836}2048 ± 0	^{1318}1385 ± 1	^{1010}1361 ± 4	^{1016}1401 ± 2	^{1006}1495 ± 1	^{959}1891 ± 1	^{1032}5641 ± 42	^{1033}5622 ± 40
571	inspur-002	447948	91934	^{407}1009	^{669}2048 ± 0	^{1094}1056 ± 5	^{783}1056 ± 7	^{782}1096 ± 7	^{1050}1776 ± 23	^{849}1444 ± 12	^{978}4504 ± 32	^{978}4515 ± 35
572	inspur-003	444594	91934	^{420}1033	^{677}2048 ± 0	^{1221}1225 ± 2	^{899}1199 ± 3	^{896}1241 ± 1	^{885}1316 ± 1	^{928}1645 ± 5	^{981}4525 ± 16	^{979}4523 ± 26

Notes	
1	The configuration size does not capture static data included in libraries.
2	The library size is the combined total of all files provided in the submission lib folder. These libraries e.g. OpenCV may or may not be installed on any end user's platform natively and would not need to be installed with the algorithm. Some developers put neural network models in their libraries.
3	The memory usage is the peak resident set size reported by the ps system call during template generation.
4	The median template creation times are measured on Intel®Xeon®CPU E5-2630 v4 @ 2.20GHz processors.
5	The comparison durations, in nanoseconds, are estimated using std::chrono::high_resolution_clock which on the machine in (2) counts 1ns clock ticks. Precision is somewhat worse than that however. The ± value is the median absolute deviation times 1.48 for Normal consistency.

Table 34: Summary of algorithms and properties included in this report. The red superscripts give ranking for the quantity in that column.

	ALGORITHM	CONFIG	LIBRARY	TEMPLATE							COMPARISON[4]	
	NAME	DATA	DATA	MEMORY	SIZE	GENERATION TIME (ms)[4]					TIME (ns)[5]	
		(KB)[1]	(KB)[2]	(MB)[3]	(B)	MUGSHOT	480x720	960x1440	1600x2400	3000x4500	GENUINE	IMPOSTOR
573	intellicloudai-001	220831	868246	^{242}655	^{416}2048 ± 0	^{426}468 ± 2	^{268}456 ± 1	^{240}466 ± 3	^{227}492 ± 1	^{271}632 ± 2	^{407}1056 ± 4	^{420}1051 ± 72
574	intellicloudai-002	259047	58559	^{900}3585	^{1292}4100 ± 0	^{897}847 ± 1	^{615}847 ± 2	^{572}849 ± 1	^{523}853 ± 1	^{464}878 ± 4	^{337}822 ± 28	^{344}818 ± 23
575	intellifusion-001	271872	289387	^{294}762	^{868}2048 ± 0	^{800}764 ± 38	^{562}774 ± 39	^{528}797 ± 42	^{487}803 ± 34	^{410}805 ± 33	^{435}1112 ± 28	^{447}1128 ± 41
576	intellifusion-002	762731	385841	^{381}941	^{1250}4096 ± 0	^{1003}950 ± 2	^{817}1096 ± 42	^{773}1088 ± 33	^{764}1168 ± 31	^{661}1171 ± 10	^{603}1713 ± 57	^{594}1665 ± 87
577	intellivision-001	43692	11649	-	^{1040}2056 ± 0	^{20}62 ± 2	-	-	-	-	^{786}2573 ± 91	^{785}2544 ± 38
578	intellivision-002	43692	14505	-	^{1037}2056 ± 0	^{256}322 ± 1	^{177}355 ± 2	^{156}372 ± 1	^{171}422 ± 2	^{250}600 ± 1	^{1176}13525 ± 134	^{1175}12782 ± 278
579	intellivision-003	64023	133748	^{310}800	^{1054}2056 ± 0	^{359}407 ± 3	^{218}398 ± 2	^{194}418 ± 2	^{188}450 ± 1	^{243}591 ± 4	^{1146}11069 ± 56	^{1147}11066 ± 75
580	intellivision-004	117727	131310	^{177}515	^{1028}2056 ± 0	^{263}330 ± 0	^{158}330 ± 0	^{133}347 ± 0	^{142}382 ± 0	^{194}514 ± 0	^{1148}11197 ± 63	^{1149}11165 ± 72
581	intellivision-005	372608	257259	^{258}686	^{1063}2056 ± 0	^{615}618 ± 0	^{413}623 ± 0	^{392}634 ± 0	^{363}659 ± 0	^{389}771 ± 0	^{1231}19244 ± 68	^{1233}19270 ± 77
582	intellivision-006	287736	262742	^{270}723	^{1061}2056 ± 0	^{149}214 ± 0	^{87}214 ± 0	^{72}221 ± 0	^{79}272 ± 0	^{91}357 ± 1	^{1196}15153 ± 32	^{1199}15142 ± 38
583	intellivision-007	192454	262742	^{131}419	^{1023}2056 ± 0	^{80}148 ± 0	^{46}157 ± 0	^{41}166 ± 0	^{37}180 ± 0	^{56}265 ± 0	^{1193}15100 ± 50	^{1195}15095 ± 45
584	intellivix-001	256654	111858	^{339}846	^{531}2048 ± 0	^{319}378 ± 1	^{197}379 ± 1	^{165}381 ± 1	^{144}384 ± 1	^{132}421 ± 3	^{432}1100 ± 16	^{440}1109 ± 22
585	intellivix-002	361566	116162	^{487}1175	^{644}2048 ± 0	^{1009}956 ± 0	^{698}947 ± 6	^{672}976 ± 0	^{616}984 ± 4	^{600}1089 ± 1	^{1285}30096 ± 128	^{1290}31287 ± 140
586	intellivix-003	234409	116167	^{538}1301	^{506}2048 ± 0	^{949}908 ± 0	^{668}916 ± 1	^{637}930 ± 0	^{600}961 ± 1	^{634}1129 ± 3	^{1284}30025 ± 137	^{1289}31190 ± 131
587	intellivix-004	361668	128097	^{498}1189	^{654}2048 ± 0	^{381}427 ± 0	^{250}437 ± 0	^{217}444 ± 0	^{199}461 ± 0	^{231}565 ± 2	^{557}1498 ± 37	^{551}1478 ± 16
588	intellivix-005	774405	128093	^{909}3692	^{423}2048 ± 0	^{687}673 ± 1	^{438}643 ± 3	^{410}654 ± 3	^{371}666 ± 3	^{386}769 ± 5	^{548}1481 ± 65	^{539}1451 ± 26
589	intellivix-006	792822	128093	^{911}3753	^{723}2048 ± 0	^{678}665 ± 1	^{446}657 ± 2	^{420}662 ± 2	^{381}677 ± 2	^{399}784 ± 1	^{553}1486 ± 13	^{555}1482 ± 16
590	intelresearch-000	388229	307985	-	^{619}2048 ± 0	^{947}902 ± 6	-	-	-	-	^{995}4800 ± 152	^{983}4561 ± 97
591	intelresearch-001	353997	272602	-	^{528}2048 ± 0	^{705}682 ± 4	-	-	-	-	^{916}3553 ± 57	^{909}3462 ± 161
592	intelresearch-002	452850	86454	-	^{591}2048 ± 0	^{745}707 ± 2	^{572}790 ± 33	^{520}788 ± 26	^{509}831 ± 29	^{452}862 ± 22	^{964}4204 ± 91	^{965}4153 ± 93
593	intelresearch-003	401343	85085	^{488}1177	^{749}2048 ± 0	^{1224}1232 ± 3	^{931}1237 ± 2	^{898}1242 ± 2	^{847}1263 ± 2	^{767}1324 ± 3	^{976}4443 ± 75	^{971}4374 ± 77
594	intelresearch-004	646918	85290	^{697}1866	^{571}2048 ± 0	^{1281}1319 ± 2	^{992}1322 ± 3	^{966}1330 ± 3	^{902}1345 ± 3	^{824}1411 ± 5	^{989}4696 ± 63	^{989}4692 ± 66
595	intelresearch-005	398137	85290	^{482}1164	^{844}2048 ± 0	^{1287}1328 ± 1	^{1002}1334 ± 2	^{977}1344 ± 2	^{908}1356 ± 2	^{833}1423 ± 4	^{980}4524 ± 87	^{974}4461 ± 74
596	intelresearch-006	445223	101126	^{441}1069	^{891}2048 ± 0	^{968}918 ± 1	^{643}881 ± 0	^{601}892 ± 0	^{563}913 ± 1	^{547}1008 ± 3	^{1051}6137 ± 410	^{1047}6024 ± 109
597	intelresearch-007	523218	101150	^{503}1197	^{352}2048 ± 0	^{569}590 ± 1	^{375}585 ± 1	^{339}588 ± 1	^{309}603 ± 4	^{302}668 ± 6	^{932}3738 ± 42	^{938}3752 ± 53
598	intelresearch-008	523218	101214	^{502}1196	^{459}2048 ± 0	^{637}634 ± 1	^{421}630 ± 1	^{388}632 ± 1	^{338}635 ± 2	^{333}711 ± 4	^{924}3661 ± 34	^{926}3641 ± 44
599	intelresearch-009	290599	120716	^{606}1535	^{625}2048 ± 0	^{522}560 ± 1	^{452}664 ± 3	^{397}638 ± 3	^{382}678 ± 13	^{319}692 ± 4	^{940}3829 ± 207	^{930}3679 ± 71
600	intelresearch-010	307886	120767	^{644}1655	^{886}2048 ± 0	^{1161}1153 ± 1	^{868}1158 ± 2	^{835}1160 ± 2	^{760}1166 ± 3	^{698}1237 ± 5	^{942}3850 ± 26	^{942}3822 ± 75
601	intelresearch-011	317134	120757	^{671}1758	^{823}2048 ± 0	^{1227}1236 ± 4	^{916}1219 ± 3	^{890}1231 ± 1	^{826}1237 ± 3	^{756}1312 ± 6	^{944}3873 ± 47	^{946}3890 ± 57
602	intelresearch-012	317135	120715	^{670}1758	^{912}2048 ± 0	^{1256}1280 ± 2	^{944}1256 ± 4	^{921}1270 ± 3	^{865}1284 ± 3	^{776}1331 ± 5	^{934}3744 ± 32	^{934}3722 ± 44
603	intema-000	1532392	19488	^{452}1088	^{153}513 ± 0	^{1061}1010 ± 0	^{750}1001 ± 4	^{694}994 ± 0	^{622}993 ± 5	^{574}1056 ± 1	^{365}910 ± 29	^{370}906 ± 32
604	intema-001	1122562	19536	^{589}1458	^{155}513 ± 0	^{1298}1354 ± 1	^{989}1318 ± 5	^{972}1336 ± 4	^{894}1328 ± 2	^{801}1375 ± 0	^{380}977 ± 31	^{386}980 ± 31
605	interlinklabs-001	155897	1013105	^{287}746	^{466}2048 ± 0	^{262}328 ± 3	^{169}346 ± 8	^{132}343 ± 7	^{120}352 ± 3	^{130}418 ± 11	^{533}1441 ± 10	^{538}1450 ± 14
606	interlinklabs-002	286341	1013147	^{559}1364	^{1160}4096 ± 0	^{396}438 ± 1	^{247}435 ± 4	^{208}435 ± 5	^{183}439 ± 0	^{185}505 ± 2	^{800}2699 ± 35	^{803}2678 ± 25
607	interlinklabs-003	528962	951057	^{611}1549	^{1241}4096 ± 0	^{773}734 ± 0	^{542}750 ± 0	^{496}746 ± 0	^{463}769 ± 0	^{494}932 ± 0	^{909}3513 ± 50	^{915}3504 ± 26
608	intozi-001	21863	74210	^{41}140	^{410}2048 ± 0	^{33}85 ± 0	^{19}86 ± 0	^{15}86 ± 0	^{12}87 ± 0	^{10}87 ± 0	^{1125}9579 ± 252	^{1122}9530 ± 167
609	intsysmsu-000	650193	171481	-	^{696}2048 ± 0	^{496}535 ± 20	-	-	-	-	^{204}610 ± 22	^{227}613 ± 31
610	intsysmsu-001	384409	172480	^{306}789	^{569}2048 ± 0	^{606}614 ± 2	^{400}615 ± 2	^{403}642 ± 2	^{448}750 ± 3	^{654}1159 ± 4	^{220}621 ± 8	^{220}611 ± 31
611	intsysmsu-002	765921	172298	^{305}786	^{259}1024 ± 0	^{574}593 ± 1	^{573}793 ± 2	^{550}827 ± 1	^{537}875 ± 104	^{742}1293 ± 3	^{165}549 ± 25	^{171}548 ± 29
612	ionetworks-000	287609	51236	^{109}352	^{365}2048 ± 0	^{384}430 ± 0	^{248}435 ± 0	^{207}433 ± 0	^{177}432 ± 0	^{144}444 ± 0	^{1075}6913 ± 102	^{1082}7150 ± 160
613	ionetworks-001	39860	333205	^{91}298	^{477}2048 ± 0	^{397}439 ± 2	^{244}433 ± 2	^{236}461 ± 2	^{192}454 ± 2	^{171}488 ± 2	^{1060}6335 ± 103	^{1057}6358 ± 91
614	ionetworks-002	337801	73038	^{668}1746	^{670}2048 ± 0	^{721}689 ± 1	^{462}672 ± 5	^{425}665 ± 3	^{374}669 ± 3	^{297}664 ± 6	^{1073}6884 ± 154	^{1069}6808 ± 102
615	ionetworks-003	309918	68642	^{634}1631	^{958}2050 ± 0	^{752}713 ± 0	^{474}681 ± 1	^{424}665 ± 0	^{373}668 ± 0	^{303}671 ± 0	^{1141}10649 ± 225	^{1143}10658 ± 106
616	ionetworks-004	302266	135028	^{688}1813	^{959}2050 ± 0	^{1030}975 ± 0	^{663}910 ± 0	^{624}921 ± 0	^{564}916 ± 0	^{485}917 ± 1	^{1279}27437 ± 130	^{1281}27472 ± 114

Notes	
1	The configuration size does not capture static data included in libraries.
2	The library size is the combined total of all files provided in the submission lib folder. These libraries e.g. OpenCV may or may not be installed on any end user's platform natively and would not need to be installed with the algorithm. Some developers put neural network models in their libraries.
3	The memory usage is the peak resident set size reported by the ps system call during template generation.
4	The median template creation times are measured on Intel®Xeon®CPU E5-2630 v4 @ 2.20GHz processors.
5	The comparison durations, in nanoseconds, are estimated using std::chrono::high_resolution_clock which on the machine in (2) counts 1ns clock ticks. Precision is somewhat worse than that however. The ± value is the median absolute deviation times 1.48 for Normal consistency.

Table 35: Summary of algorithms and properties included in this report. The red superscripts give ranking for the quantity in that column.

	ALGORITHM	CONFIG	LIBRARY	TEMPLATE							COMPARISON[4]	
	NAME	DATA	DATA	MEMORY	SIZE	GENERATION TIME (ms)[4]					TIME (ns)[5]	
		(KB)[1]	(KB)[2]	(MB)[3]	(B)	MUGSHOT	480x720	960x1440	1600x2400	3000x4500	GENUINE	IMPOSTOR
617	iqface-000	268819	596337	^{262}704	^{1343}4750 ± 32	^{498}538 ± 26	^{298}494 ± 2	^{308}543 ± 3	^{438}734 ± 4	^{814}1393 ± 4	^{1405}636433 ± 38446	^{1405}632654 ± 85615
618	iqface-001	1145590	760941	-	^{1344}4752 ± 35	^{587}603 ± 1	-	-	-	-	^{1403}568761 ± 3659	^{1403}570335 ± 5122
619	iqface-003	370803	963398	^{326}821	^{1345}4763 ± 37	^{484}529 ± 1	^{327}532 ± 2	^{347}599 ± 8	^{522}850 ± 2	^{934}1694 ± 2	^{1404}575924 ± 2601	^{1404}576653 ± 2051
620	iqsec-001	172239	41022	^{344}850	^{556}2048 ± 0	^{182}258 ± 6	^{108}254 ± 4	^{249}474 ± 9	^{722}1124 ± 24	^{1060}4155 ± 119	^{1264}24586 ± 143	^{1270}25631 ± 157
621	iqsec-002	172239	41022	^{346}852	^{486}2048 ± 0	^{168}243 ± 6	^{110}259 ± 4	^{273}504 ± 10	^{779}1184 ± 25	^{1058}4081 ± 124	^{1265}24688 ± 149	^{1271}25737 ± 142
622	irex-000	741899	47419	^{736}2090	^{1147}3080 ± 0	^{901}852 ± 2	^{617}850 ± 1	^{589}874 ± 2	^{584}939 ± 1	^{707}1249 ± 5	^{43}201 ± 11	^{45}208 ± 8
623	irisid-001	480885	100974	^{403}1000	^{950}2049 ± 0	^{1020}966 ± 0	^{720}971 ± 0	^{723}1028 ± 0	^{757}1163 ± 0	^{930}1662 ± 1	^{652}1892 ± 13	^{682}2040 ± 17
624	isap-001	99049	204201	^{1}18	^{1228}4096 ± 0	^{1}0 ± 0	-	-	-	-	^{128}459 ± 17	^{137}456 ± 11
625	isap-002	256765	49931	^{88}288	^{503}2048 ± 0	^{807}769 ± 3	^{767}1027 ± 2	^{592}877 ± 2	^{457}761 ± 1	^{482}912 ± 2	^{857}3045 ± 94	^{851}2973 ± 66
626	isityou-000	48010	36621	^{28}110	^{1404}19200 ± 0	^{53}113 ± 5	-	-	-	-	^{1397}237517 ± 1318	^{1397}237374 ± 1279
627	isystems-000	209270	713870	-	^{228}1024 ± 0	^{84}154 ± 4	-	-	-	-	^{113}398 ± 14	^{120}396 ± 16
628	isystems-001	274621	639268	^{457}1091	^{788}2048 ± 0	^{216}291 ± 9	-	-	-	-	^{167}557 ± 16	^{178}564 ± 22
629	isystems-002	358984	803389	^{627}1595	^{835}2048 ± 0	^{869}822 ± 8	-	-	-	-	^{304}749 ± 31	^{244}632 ± 28
630	itmo-001	1923215	62191	-	^{1409}37997 ± 0	^{1012}959 ± 18	-	-	-	-	^{1281}28901 ± 1492	^{1282}27517 ± 186
631	itmo-002	1923215	62191	-	^{1319}4162 ± 0	^{594}611 ± 17	-	-	-	-	^{1092}7423 ± 96	^{1092}7451 ± 94
632	itmo-003	579961	82630	-	^{1106}2114 ± 0	^{28}79 ± 2	-	-	-	-	^{1134}10038 ± 180	^{1135}10030 ± 134
633	itmo-004	487023	79012	-	^{1104}2100 ± 0	^{390}436 ± 0	-	-	-	-	^{1105}8219 ± 100	^{1109}8214 ± 130
634	itmo-005	482155	81168	-	^{1323}4173 ± 0	^{798}759 ± 1	-	-	-	-	^{1173}13214 ± 164	^{1174}12576 ± 257
635	itmo-006	599187	96762	-	^{1111}2121 ± 0	^{856}814 ± 1	^{604}831 ± 26	^{557}830 ± 17	^{508}830 ± 3	^{507}952 ± 38	^{1272}26154 ± 148	^{1273}26217 ± 260
636	itmo-007	415979	245376	^{755}2199	^{739}2048 ± 0	^{780}741 ± 2	-	-	-	-	^{781}2551 ± 50	^{782}2529 ± 80
637	itmo-008	726866	318238	^{563}1376	^{1234}4096 ± 0	^{1098}1060 ± 1	^{785}1058 ± 1	^{751}1059 ± 1	^{685}1072 ± 4	^{611}1104 ± 1	^{918}3578 ± 25	^{924}3580 ± 28
638	ivacognitive-001	256958	62791	^{393}975	^{882}2048 ± 0	^{1267}1292 ± 3	^{966}1289 ± 4	^{938}1292 ± 4	^{868}1292 ± 3	^{763}1321 ± 4	^{965}4228 ± 41	^{966}4226 ± 41
639	iws-000	30875	3063	^{18}77	^{102}512 ± 0	^{200}277 ± 5	^{129}283 ± 1	^{264}494 ± 3	^{615}984 ± 3	^{1038}2987 ± 39	^{388}999 ± 40	^{391}992 ± 22
640	jaakit-001	99024	24754	^{74}251	^{144}512 ± 0	^{25}76 ± 0	^{16}77 ± 0	^{12}79 ± 0	^{11}81 ± 0	^{12}93 ± 0	^{768}2466 ± 57	^{770}2465 ± 66
641	jaakit-002	179256	75037	^{83}277	^{708}2048 ± 0	^{796}758 ± 0	^{551}760 ± 0	^{631}925 ± 0	^{886}1318 ± 1	^{1029}2799 ± 2	^{370}943 ± 7	^{381}963 ± 5
642	kakao-001	107616	285676	-	^{236}1024 ± 0	^{323}379 ± 1	-	-	-	-	^{368}930 ± 22	^{378}948 ± 38
643	kakao-002	479406	412822	-	^{711}2048 ± 0	^{784}747 ± 6	-	-	-	-	^{605}1720 ± 62	^{606}1715 ± 83
644	kakao-003	414379	113944	-	^{587}2048 ± 0	^{928}878 ± 3	-	-	-	-	^{696}2128 ± 34	^{701}2134 ± 60
645	kakao-004	414411	135270	-	^{343}2048 ± 0	^{905}856 ± 1	^{620}855 ± 0	^{578}857 ± 0	^{530}858 ± 0	^{451}860 ± 1	^{669}1957 ± 28	^{670}1953 ± 37
646	kakao-005	414316	152216	-	^{968}2052 ± 0	^{1103}1068 ± 1	^{793}1073 ± 1	^{767}1079 ± 0	^{687}1077 ± 1	^{601}1089 ± 1	^{686}2067 ± 26	^{683}2043 ± 34
647	kakao-007	526993	129545	^{875}3150	^{787}2048 ± 0	^{1008}952 ± 1	^{712}961 ± 1	^{659}958 ± 1	^{601}962 ± 1	^{515}968 ± 1	^{406}1056 ± 16	^{414}1047 ± 28
648	kakao-008	734583	104820	^{918}3879	^{589}2048 ± 0	^{1143}1135 ± 3	^{861}1148 ± 3	^{827}1150 ± 3	^{752}1156 ± 1	^{665}1175 ± 1	^{301}736 ± 23	^{309}727 ± 22
649	kakao-009	766989	104820	^{927}4042	^{461}2048 ± 0	^{573}593 ± 1	^{387}603 ± 4	^{363}613 ± 2	^{323}617 ± 2	^{277}636 ± 4	^{127}457 ± 20	^{132}448 ± 17
650	kakaobank-000	570796	98479	^{824}2690	^{1164}4096 ± 0	^{1225}1234 ± 1	^{941}1254 ± 7	^{903}1248 ± 3	^{936}1389 ± 3	^{952}1843 ± 11	^{994}4790 ± 35	^{995}4803 ± 35
651	kakaobank-001	780621	98829	^{754}2189	^{916}2048 ± 0	^{555}584 ± 0	^{392}608 ± 1	^{355}607 ± 5	^{387}684 ± 1	^{488}922 ± 2	^{1278}27092 ± 174	^{1280}27065 ± 158
652	kakaobank-002	780621	98833	^{795}2459	^{580}2048 ± 0	^{1055}1004 ± 1	^{757}1010 ± 0	^{719}1025 ± 5	^{690}1078 ± 1	^{759}1313 ± 1	^{1276}26972 ± 118	^{1278}27022 ± 139
653	kakaobank-003	1409862	98833	^{932}4186	^{847}2048 ± 0	^{1193}1194 ± 2	^{923}1224 ± 6	^{891}1231 ± 2	^{849}1269 ± 5	^{901}1535 ± 5	^{1277}26986 ± 183	^{1279}27026 ± 151
654	kakaopay-001	397864	179869	^{257}685	^{1262}4096 ± 0	^{402}448 ± 0	^{335}542 ± 0	^{304}542 ± 0	^{263}542 ± 0	^{221}553 ± 0	^{230}633 ± 22	^{238}630 ± 22
655	kasikornlabs-000	256471	61000	^{241}655	^{333}2048 ± 0	^{951}908 ± 36	^{640}878 ± 22	^{668}969 ± 39	^{777}1184 ± 54	^{1008}2382 ± 145	^{1290}31669 ± 188	^{1291}31714 ± 182
656	kasikornlabs-001	256471	61037	^{252}676	^{703}2048 ± 0	^{957}912 ± 38	^{630}868 ± 10	^{707}1005 ± 50	^{770}1176 ± 44	^{1009}2387 ± 147	^{1287}30759 ± 198	^{1287}30867 ± 174
657	kasikornlabs-002	256431	61063	^{221}613	^{741}2048 ± 0	^{967}917 ± 35	^{661}907 ± 13	^{664}963 ± 13	^{888}1320 ± 45	^{1019}2629 ± 178	^{1289}31025 ± 180	^{1288}31054 ± 186
658	kasikornlabs-003	256442	61063	^{290}751	^{905}2048 ± 0	^{659}652 ± 5	^{445}656 ± 5	^{505}755 ± 11	^{642}1007 ± 27	^{993}2240 ± 168	^{1259}24022 ± 121	^{1260}23998 ± 97
659	kasikornlabs-004	466064	61063	^{426}1045	^{474}2048 ± 0	^{1001}950 ± 7	^{719}970 ± 4	^{728}1031 ± 11	^{925}1372 ± 30	^{1005}2368 ± 156	^{1256}23867 ± 56	^{1258}23919 ± 91
660	kasikornlabs-005	466202	61063	^{416}1028	^{657}2048 ± 0	^{981}936 ± 8	^{706}956 ± 14	^{750}1057 ± 14	^{829}1243 ± 28	^{997}2285 ± 145	^{1258}23900 ± 44	^{1259}23923 ± 56

Notes	
1	The configuration size does not capture static data included in libraries.
2	The library size is the combined total of all files provided in the submission lib folder. These libraries e.g. OpenCV may or may not be installed on any end user's platform natively and would not need to be installed with the algorithm. Some developers put neural network models in their libraries.
3	The memory usage is the peak resident set size reported by the ps system call during template generation.
4	The median template creation times are measured on Intel®Xeon®CPU E5-2630 v4 @ 2.20GHz processors.
5	The comparison durations, in nanoseconds, are estimated using std::chrono::high_resolution_clock which on the machine in (2) counts 1ns clock ticks. Precision is somewhat worse than that however. The ± value is the median absolute deviation times 1.48 for Normal consistency.

Table 36: Summary of algorithms and properties included in this report. The red superscripts give ranking for the quantity in that column.

	ALGORITHM	CONFIG	LIBRARY	TEMPLATE							COMPARISON[4]	
	NAME	DATA	DATA	MEMORY	SIZE	GENERATION TIME (ms)[4]					TIME (ns)[5]	
		(KB)[1]	(KB)[2]	(MB)[3]	(B)	MUGSHOT	480x720	960x1440	1600x2400	3000x4500	GENUINE	IMPOSTOR
661	kbyai-000	502373	34357	^{782}2417	^{69}296 ± 0	^{1201}1202 ± 3	^{1122}2167 ± 3	^{1116}2293 ± 9	^{1099}2586 ± 13	^{1053}3689 ± 20	^{1216}17785 ± 51	^{1220}17801 ± 125
662	kedacom-000	245292	37401	^{1013}23574	^{68}292 ± 0	^{466}506 ± 3	^{342}547 ± 10	^{365}614 ± 9	^{298}588 ± 10	^{299}665 ± 24	^{262}684 ± 14	^{275}682 ± 16
663	keyless-000	551302	27472	^{481}1157	^{778}2048 ± 0	^{611}615 ± 0	^{528}736 ± 5	^{1111}2122 ± 2	^{1080}2086 ± 1	^{978}2110 ± 4	^{362}909 ± 8	^{369}905 ± 16
664	kiwitech-000	369711	21375	^{333}841	^{717}2048 ± 0	^{570}591 ± 0	^{382}594 ± 0	^{346}595 ± 1	^{306}596 ± 0	^{257}609 ± 0	^{614}1755 ± 20	^{617}1734 ± 16
665	kloudspot-001	261662	887420	^{359}882	^{525}2048 ± 0	^{264}330 ± 1	^{151}319 ± 6	^{119}325 ± 1	^{101}318 ± 0	^{70}318 ± 0	^{1026}5539 ± 48	^{1028}5555 ± 66
666	kloudspot-002	635738	460698	^{608}1540	^{1243}4096 ± 0	^{1141}1128 ± 1	^{842}1128 ± 2	^{804}1123 ± 0	^{754}1158 ± 2	^{635}1132 ± 0	^{1020}5456 ± 154	^{1021}5460 ± 108
667	kneron-003	58366	1747	^{62}188	^{494}2048 ± 0	^{206}281 ± 3	^{127}280 ± 1	^{115}315 ± 13	^{130}365 ± 7	^{691}1224 ± 30	^{1016}5237 ± 63	^{1017}5274 ± 99
668	kneron-005	375374	13633	^{147}457	^{721}2048 ± 0	^{476}518 ± 2	^{320}522 ± 4	^{317}556 ± 5	^{453}757 ± 19	^{943}1760 ± 25	^{661}1922 ± 11	^{662}1926 ± 20
669	kneron-006	590352	63741	^{569}1402	^{876}2048 ± 0	^{544}579 ± 0	^{369}580 ± 0	^{348}599 ± 0	^{427}726 ± 1	^{730}1278 ± 4	^{720}2247 ± 22	^{722}2252 ± 28
670	knowutech-000	808045	32886	^{541}1312	^{297}1536 ± 0	^{1342}1419 ± 2	^{1014}1372 ± 1	^{999}1377 ± 1	^{929}1382 ± 2	^{809}1386 ± 2	^{933}3743 ± 31	^{931}3693 ± 38
671	kogniza-001	0	394421	^{529}1288	^{298}1536 ± 0	^{1261}1285 ± 2	^{980}1304 ± 4	^{930}1280 ± 2	^{858}1278 ± 2	^{769}1326 ± 2	^{847}2968 ± 37	^{849}2971 ± 20
672	kookmin-001	234001	31875	-	^{432}2048 ± 0	^{55}114 ± 1	^{29}110 ± 1	^{25}116 ± 1	^{25}128 ± 1	^{26}172 ± 1	^{226}629 ± 35	^{230}616 ± 11
673	kookmin-002	371771	30734	^{327}827	^{493}2048 ± 0	^{1084}1038 ± 2	^{781}1047 ± 1	^{739}1045 ± 1	^{673}1061 ± 1	^{619}1116 ± 1	^{239}638 ± 19	^{249}636 ± 20
674	koreaid-001	256261	20152	^{685}1810	^{756}2048 ± 0	^{331}384 ± 2	^{209}390 ± 1	^{218}444 ± 2	^{275}556 ± 6	^{405}795 ± 5	^{235}636 ± 11	^{250}636 ± 10
675	krungthai-002	2360957	15033	^{493}1185	^{359}2048 ± 0	^{240}308 ± 0	^{143}314 ± 5	^{111}309 ± 0	^{104}319 ± 0	^{95}362 ± 0	^{851}3014 ± 20	^{852}2980 ± 22
676	kuke3d-001	403462	68786	^{184}530	^{1217}4096 ± 0	^{857}814 ± 2	^{585}811 ± 2	^{538}814 ± 2	^{492}814 ± 1	^{436}834 ± 1	^{1063}6412 ± 57	^{1059}6413 ± 51
677	kuke3d-002	270544	1227855	^{323}820	^{812}2048 ± 0	^{464}504 ± 3	^{307}504 ± 1	^{279}511 ± 1	^{250}523 ± 2	^{238}585 ± 1	^{844}2943 ± 22	^{848}2966 ± 38
678	lebentech-000	0	10360	^{2}26	^{101}512 ± 0	^{3}22 ± 0	^{1}22 ± 0	^{1}22 ± 0	^{1}23 ± 0	^{1}23 ± 0	^{330}801 ± 42	^{346}825 ± 51
679	lebentech-001	0	144456	^{619}1567	^{837}2048 ± 0	^{99}174 ± 0	^{54}175 ± 0	^{61}200 ± 1	^{63}227 ± 9	^{120}397 ± 20	^{142}485 ± 17	^{145}473 ± 28
680	lemalabs-001	748400	198794	^{837}2745	^{497}2048 ± 0	^{851}810 ± 0	^{587}812 ± 0	^{536}813 ± 0	^{498}819 ± 0	^{441}844 ± 1	^{1160}11930 ± 35	^{1163}11913 ± 37
681	lightvision-000	182569	62181	^{377}930	^{487}2048 ± 0	^{363}411 ± 1	^{201}381 ± 0	^{162}379 ± 1	^{145}386 ± 3	^{118}396 ± 2	^{552}1484 ± 13	^{550}1477 ± 13
682	lightvision-001	266840	62181	^{631}1604	^{705}2048 ± 0	^{487}530 ± 2	^{322}523 ± 2	^{305}542 ± 1	^{270}548 ± 10	^{212}537 ± 1	^{536}1456 ± 10	^{543}1457 ± 14
683	lineclova-000	264443	407003	-	^{406}2048 ± 0	^{559}586 ± 0	^{395}612 ± 0	^{357}609 ± 1	^{314}611 ± 0	^{265}618 ± 1	^{811}2753 ± 19	^{812}2745 ± 23
684	lineclova-001	944355	407058	^{760}2233	^{875}2048 ± 0	^{883}833 ± 10	^{602}830 ± 3	^{553}828 ± 4	^{516}838 ± 8	^{433}833 ± 4	^{799}2696 ± 23	^{802}2677 ± 35
685	lineclova-002	475779	406756	^{551}1352	^{634}2048 ± 0	^{1259}1284 ± 1	^{958}1275 ± 2	^{927}1275 ± 1	^{855}1273 ± 2	^{732}1281 ± 2	^{813}2765 ± 10	^{815}2767 ± 31
686	lineclova-003	585149	410482	^{659}1725	^{793}2048 ± 0	^{1353}1444 ± 1	^{1061}1438 ± 1	^{1038}1439 ± 2	^{977}1440 ± 1	^{852}1446 ± 2	^{834}2890 ± 23	^{839}2899 ± 29
687	lookman-002	138200	25410	^{1009}16518	^{188}548 ± 0	^{96}173 ± 1	-	-	-	-	^{206}610 ± 19	^{223}612 ± 22
688	lookman-004	244775	37401	^{1012}23548	^{187}548 ± 0	^{467}507 ± 5	^{340}545 ± 12	^{362}613 ± 12	^{302}590 ± 11	^{290}656 ± 16	^{349}871 ± 29	^{358}878 ± 29
689	lssytech-000	1316125	197944	^{947}4622	^{1144}3076 ± 0	^{1162}1154 ± 0	^{836}1124 ± 0	^{809}1129 ± 0	^{729}1128 ± 0	^{633}1128 ± 0	^{299}733 ± 17	^{306}722 ± 13
690	luxand-000	0	57908	^{560}1366	^{271}1040 ± 0	^{360}407 ± 23	^{242}433 ± 11	^{219}444 ± 14	^{206}464 ± 14	^{229}562 ± 25	^{341}828 ± 28	^{347}828 ± 32
691	luxand-001	85194	72189	^{232}636	^{871}2048 ± 0	^{385}431 ± 0	^{256}443 ± 0	^{216}443 ± 2	^{186}448 ± 0	^{199}519 ± 0	^{528}1433 ± 16	^{535}1433 ± 16
692	luxand-003	127425	72189	^{342}847	^{722}2048 ± 0	^{744}706 ± 4	^{491}697 ± 1	^{453}698 ± 3	^{400}694 ± 0	^{398}782 ± 3	^{534}1443 ± 17	^{534}1431 ± 17
693	luxand-004	127425	72189	^{343}848	^{470}2048 ± 0	^{696}677 ± 0	^{475}682 ± 0	^{445}691 ± 0	^{410}705 ± 0	^{382}766 ± 0	^{532}1441 ± 10	^{536}1440 ± 11
694	mantra-000	471458	62566	^{288}749	^{966}2052 ± 0	^{365}413 ± 18	^{293}487 ± 19	^{261}494 ± 18	^{240}511 ± 18	^{249}598 ± 19	^{866}3151 ± 51	^{868}3127 ± 63
695	matrixcomsec-000	114103	177320	^{81}264	^{926}2048 ± 0	^{38}94 ± 0	^{22}94 ± 0	^{17}95 ± 0	^{35}173 ± 1	^{20}140 ± 1	^{215}616 ± 22	^{239}630 ± 28
696	matrixcomsec-001	179657	168204	^{474}1141	^{573}2048 ± 0	^{92}166 ± 0	^{50}168 ± 0	^{42}169 ± 0	^{34}171 ± 0	^{29}191 ± 0	^{63}268 ± 53	^{70}261 ± 62
697	maverickresearch-000	256262	20268	^{101}331	^{660}2048 ± 0	^{1049}995 ± 1	^{749}999 ± 1	^{701}999 ± 2	^{626}997 ± 0	^{554}1023 ± 2	^{1237}20268 ± 108	^{1239}20254 ± 121
698	maxvision-000	133114	56426	-	^{100}512 ± 0	^{298}359 ± 0	^{178}356 ± 0	^{146}359 ± 0	^{124}356 ± 0	^{98}370 ± 1	^{766}2461 ± 20	^{766}2452 ± 17
699	maxvision-001	256146	61793	^{867}3037	^{843}2048 ± 0	^{198}275 ± 3	^{121}274 ± 2	^{89}277 ± 4	^{82}280 ± 4	^{71}325 ± 3	^{287}714 ± 13	^{302}717 ± 13
700	maxvision-002	171894	60623	^{672}1765	^{505}2048 ± 0	^{95}172 ± 0	^{53}171 ± 0	^{44}172 ± 0	^{36}174 ± 0	^{39}221 ± 0	^{296}725 ± 5	^{307}725 ± 5
701	maxvision-003	234062	61252	^{791}2452	^{923}2048 ± 0	^{434}474 ± 0	^{278}468 ± 0	^{246}471 ± 0	^{215}475 ± 0	^{200}519 ± 0	^{770}2467 ± 28	^{774}2488 ± 23
702	maxvision-004	394121	61583	^{877}3217	^{623}2048 ± 0	^{648}644 ± 1	^{442}648 ± 0	^{406}647 ± 1	^{343}637 ± 1	^{323}695 ± 1	^{654}1897 ± 10	^{656}1903 ± 14
703	maxvision-005	309326	61739	^{745}2138	^{861}2048 ± 0	^{1058}1007 ± 1	^{936}1245 ± 5	^{712}1017 ± 1	^{663}1040 ± 4	^{746}1299 ± 3	^{667}1950 ± 38	^{669}1948 ± 34
704	maxvision-006	315987	61739	^{876}3172	^{611}2048 ± 0	^{1237}1247 ± 3	^{908}1208 ± 3	^{876}1211 ± 5	^{806}1215 ± 1	^{724}1268 ± 4	^{666}1938 ± 17	^{663}1929 ± 35

Notes	
1	The configuration size does not capture static data included in libraries.
2	The library size is the combined total of all files provided in the submission lib folder. These libraries e.g. OpenCV may or may not be installed on any end user's platform natively and would not need to be installed with the algorithm. Some developers put neural network models in their libraries.
3	The memory usage is the peak resident set size reported by the ps system call during template generation.
4	The median template creation times are measured on Intel®Xeon®CPU E5-2630 v4 @ 2.20GHz processors.
5	The comparison durations, in nanoseconds, are estimated using std::chrono::high_resolution_clock which on the machine in (2) counts 1ns clock ticks. Precision is somewhat worse than that however. The ± value is the median absolute deviation times 1.48 for Normal consistency.

Table 37: Summary of algorithms and properties included in this report. The red superscripts give ranking for the quantity in that column.

	ALGORITHM	CONFIG	LIBRARY	TEMPLATE							COMPARISON[4]	
	NAME	DATA	DATA	MEMORY	SIZE	GENERATION TIME (ms)[4]					TIME (ns)[5]	
		(KB)[1]	(KB)[2]	(MB)[3]	(B)	MUGSHOT	480x720	960x1440	1600x2400	3000x4500	GENUINE	IMPOSTOR
705	mbbankvn-000	472410	139431	^{933}4227	^{765}2048 ± 0	^{423}466 ± 17	^{284}480 ± 26	^{253}481 ± 27	^{219}479 ± 21	^{179}501 ± 29	^{973}4388 ± 14	^{972}4380 ± 17
706	megvii-000	1358915	16014	-	^{523}2048 ± 0	^{821}785 ± 0	-	-	-	-	^{1233}19816 ± 158	^{1235}19805 ± 174
707	megvii-001	1361523	16486	-	^{337}2048 ± 0	^{506}543 ± 0	-	-	-	-	^{1015}5228 ± 32	^{1015}5252 ± 60
708	megvii-002	1809564	16491	-	^{1275}4100 ± 0	^{647}644 ± 0	-	-	-	-	^{1338}50630 ± 183	^{1332}47591 ± 716
709	megvii-003	4430290	42790	-	^{1185}4096 ± 0	^{1205}1210 ± 1	^{921}1223 ± 0	^{987}1356 ± 4	^{1028}1582 ± 7	^{1023}2727 ± 23	^{1395}225342 ± 3574	^{1396}225413 ± 6344
710	megvii-004	3962505	44019	-	^{1268}4097 ± 0	^{1262}1287 ± 1	^{1013}1369 ± 2	^{953}1310 ± 2	^{931}1384 ± 3	^{845}1436 ± 5	^{1328}46801 ± 204	^{1329}46832 ± 207
711	megvii-005	1378009	44038	^{926}4025	^{951}2049 ± 0	^{1282}1319 ± 5	^{938}1247 ± 6	^{895}1240 ± 2	^{832}1245 ± 2	^{745}1298 ± 3	^{1294}32025 ± 121	^{1295}32008 ± 114
712	megvii-006	1554938	44038	^{937}4346	^{956}2049 ± 0	^{1263}1287 ± 3	^{964}1286 ± 0	^{1008}1393 ± 5	^{887}1319 ± 1	^{790}1360 ± 1	^{1292}31845 ± 100	^{1293}31872 ± 118
713	megvii-007	1366028	44035	^{658}1723	^{957}2049 ± 0	^{1157}1148 ± 1	^{862}1153 ± 0	^{842}1172 ± 4	^{767}1172 ± 2	^{738}1288 ± 2	^{1236}20191 ± 1753	^{1237}20191 ± 1620
714	megvii-008	1644071	44035	^{735}2086	^{954}2049 ± 0	^{1279}1313 ± 1	^{1034}1404 ± 4	^{990}1363 ± 2	^{915}1362 ± 3	^{831}1420 ± 2	^{1234}20059 ± 1598	^{1241}20448 ± 1633
715	megvii-009	1644071	44039	^{766}2294	^{953}2049 ± 0	^{1284}1322 ± 1	^{996}1328 ± 1	^{975}1339 ± 3	^{1079}2075 ± 3	^{821}1404 ± 4	^{1235}20081 ± 1621	^{1240}20260 ± 1577
716	meituan-000	259514	333178	-	^{514}2048 ± 0	^{389}436 ± 4	^{254}441 ± 1	^{376}626 ± 5	^{700}1098 ± 15	^{1041}3126 ± 53	^{238}638 ± 17	^{246}633 ± 16
717	meituan-001	615387	333249	^{464}1113	^{852}2048 ± 0	^{1065}1017 ± 4	^{756}1008 ± 3	^{710}1010 ± 2	^{647}1010 ± 3	^{548}1011 ± 4	^{247}654 ± 10	^{265}658 ± 14
718	meituan-002	686111	244091	^{756}2200	^{1230}4096 ± 0	^{1090}1052 ± 0	^{802}1086 ± 1	^{759}1064 ± 2	^{672}1060 ± 5	^{586}1063 ± 1	^{412}1064 ± 10	^{425}1070 ± 16
719	meituan-003	860010	244091	^{844}2772	^{1209}4096 ± 0	^{1379}1487 ± 1	^{1088}1518 ± 0	^{1058}1469 ± 6	^{1001}1478 ± 0	^{864}1471 ± 7	^{434}1112 ± 16	^{437}1097 ± 20
720	meituan-004	850507	244091	^{840}2759	^{1259}4096 ± 0	^{834}796 ± 1	^{593}822 ± 0	^{546}820 ± 11	^{496}815 ± 11	^{420}824 ± 0	^{448}1149 ± 10	^{459}1148 ± 5
721	meiya-001	280055	264913	^{170}507	^{952}2049 ± 0	^{620}622 ± 12	-	-	-	-	^{1107}8356 ± 615	^{1107}8134 ± 97
722	mendaxiatech-000	1941475	45484	^{941}4397	^{1267}4097 ± 0	^{1233}1243 ± 2	^{942}1255 ± 1	^{996}1373 ± 2	^{1031}1598 ± 3	^{1021}2689 ± 8	^{1329}46906 ± 275	^{1330}46872 ± 217
723	metsakuurcompany-001	445177	1091558	^{624}1588	^{1029}2056 ± 0	^{542}578 ± 1	^{377}587 ± 3	^{340}590 ± 1	^{364}659 ± 1	^{447}854 ± 1	^{1113}8600 ± 192	^{1108}8155 ± 298
724	metsakuurcompany-002	0	957558	^{396}980	^{1020}2056 ± 0	^{1036}980 ± 1	^{729}978 ± 1	^{673}976 ± 2	^{638}1005 ± 1	^{610}1103 ± 2	^{1115}8766 ± 326	^{1116}8786 ± 324
725	metsakuurcompany-003	0	957562	^{406}1004	^{1034}2056 ± 0	^{1017}965 ± 2	^{718}970 ± 5	^{752}1060 ± 12	^{640}1005 ± 6	^{625}1121 ± 1	^{1106}8234 ± 145	^{1106}8111 ± 280
726	metsakuurcompany-004	0	1035754	^{433}1056	^{1068}2056 ± 0	^{995}946 ± 10	^{624}861 ± 6	^{593}877 ± 3	^{572}926 ± 4	^{531}991 ± 5	^{1059}6281 ± 160	^{1055}6232 ± 191
727	metsakuurcompany-005	0	305952	^{247}661	^{712}2048 ± 0	^{432}472 ± 0	^{281}477 ± 0	^{262}494 ± 1	^{252}527 ± 1	^{395}778 ± 2	^{892}3376 ± 22	^{899}3383 ± 40
728	miaxis-001	0	215019	^{99}325	^{93}512 ± 0	^{202}279 ± 0	^{126}278 ± 0	^{90}278 ± 1	^{83}285 ± 0	^{64}297 ± 0	^{350}872 ± 14	^{360}881 ± 22
729	miaxis-002	0	216484	^{100}328	^{108}512 ± 0	^{217}292 ± 0	^{132}290 ± 1	^{103}297 ± 0	^{93}298 ± 0	^{93}359 ± 1	^{416}1065 ± 48	^{411}1040 ± 54
730	miaxis-003	0	439726	^{213}604	^{515}2048 ± 0	^{636}634 ± 0	^{415}624 ± 2	^{361}613 ± 0	^{251}524 ± 0	^{298}665 ± 0	^{685}2053 ± 20	^{685}2048 ± 28
731	miaxis-004	729303	89655	^{492}1183	^{955}2049 ± 0	^{1403}1941 ± 0	^{1114}1947 ± 0	^{1100}1940 ± 0	^{1112}3153 ± 0	^{965}1963 ± 0	^{1388}103338 ± 44	^{1388}103361 ± 65
732	microfocus-000	103483	27242	-	^{32}256 ± 0	^{187}263 ± 18	-	-	-	-	^{44}202 ± 5	^{43}203 ± 7
733	microfocus-001	104524	27242	-	^{38}256 ± 0	^{188}264 ± 18	-	-	-	-	^{47}215 ± 8	^{48}217 ± 10
734	microfocus-002	96288	27362	^{59}176	^{24}256 ± 0	^{183}259 ± 18	-	-	-	-	^{89}337 ± 34	^{53}230 ± 25
735	microfocus-003	169603	27689	^{171}507	^{39}256 ± 0	^{451}490 ± 19	^{317}517 ± 30	^{501}752 ± 55	^{726}1126 ± 121	^{1022}2713 ± 345	^{20}121 ± 5	^{19}117 ± 5
736	minivision-000	836697	16597	^{935}4263	^{1239}4096 ± 0	^{1083}1035 ± 1	^{776}1033 ± 2	^{730}1035 ± 1	^{660}1037 ± 1	^{580}1059 ± 2	^{769}2466 ± 26	^{768}2460 ± 25
737	mitek-000	105584	44643	^{84}277	^{230}1024 ± 0	^{180}256 ± 21	^{111}265 ± 10	^{158}375 ± 24	^{268}545 ± 42	^{606}1098 ± 124	^{826}2846 ± 88	^{818}2777 ± 74
738	mitek-001	519928	69522	^{676}1777	^{1059}2056 ± 0	^{314}371 ± 0	^{216}397 ± 0	^{184}407 ± 4	^{154}394 ± 5	^{128}416 ± 2	^{1068}6682 ± 28	^{1066}6694 ± 48
739	mitek-002	534528	68069	^{674}1773	^{1067}2056 ± 0	^{306}365 ± 0	^{194}372 ± 0	^{151}366 ± 2	^{139}377 ± 2	^{115}394 ± 1	^{390}1005 ± 19	^{380}963 ± 23
740	mobai-000	365451	80573	^{304}786	^{1359}6144 ± 0	^{804}766 ± 8	^{631}869 ± 6	^{871}1205 ± 31	^{1059}1867 ± 45	^{1051}3549 ± 190	^{1208}16458 ± 333	^{1211}16423 ± 1473
741	mobai-001	265297	60164	^{185}534	^{565}2048 ± 0	^{601}612 ± 3	^{398}614 ± 3	^{440}687 ± 9	^{547}886 ± 31	^{936}1707 ± 103	^{511}1386 ± 25	^{518}1377 ± 26
742	mobai-002	254811	33242	^{593}1482	^{490}2048 ± 0	^{292}356 ± 0	^{188}366 ± 0	^{145}359 ± 4	^{132}367 ± 2	^{135}428 ± 0	^{1108}8387 ± 126	^{1110}8381 ± 105
743	mobai-003	1046772	427612	^{899}3555	^{1218}4096 ± 0	^{1392}1691 ± 7	^{1101}1698 ± 3	^{1088}1693 ± 1	^{1038}1705 ± 2	^{947}1786 ± 1	^{1390}105417 ± 231	^{1390}105475 ± 169
744	mobbl-000	182052	58727	-	^{903}2048 ± 0	^{184}261 ± 16	^{115}267 ± 22	^{159}375 ± 92	^{358}655 ± 273	^{974}2059 ± 1129	^{1163}12061 ± 142	^{1165}12050 ± 133
745	mobbl-001	231160	58706	^{72}226	^{608}2048 ± 0	^{110}183 ± 32	^{64}184 ± 25	^{142}354 ± 76	^{503}823 ± 396	^{1027}2781 ± 1166	^{1158}11832 ± 109	^{1162}11851 ± 88
746	mobbl-002	242920	60119	-	^{534}2048 ± 0	^{672}663 ± 6	^{448}660 ± 5	^{418}662 ± 5	^{366}663 ± 5	^{306}676 ± 5	^{1154}11616 ± 78	^{1155}11588 ± 97
747	mobbl-003	172248	60960	^{85}282	^{704}2048 ± 0	^{675}664 ± 6	^{450}661 ± 5	^{421}663 ± 5	^{369}665 ± 6	^{318}691 ± 5	^{1171}12506 ± 111	^{1172}12509 ± 100
748	mobbl-004	432204	970955	^{352}872	^{907}2048 ± 0	^{214}288 ± 0	^{128}281 ± 0	^{92}281 ± 1	^{86}288 ± 2	^{65}312 ± 2	^{886}3327 ± 22	^{897}3369 ± 48

Notes	
1	The configuration size does not capture static data included in libraries.
2	The library size is the combined total of all files provided in the submission lib folder. These libraries e.g. OpenCV may or may not be installed on any end user's platform natively and would not need to be installed with the algorithm. Some developers put neural network models in their libraries.
3	The memory usage is the peak resident set size reported by the ps system call during template generation.
4	The median template creation times are measured on Intel®Xeon®CPU E5-2630 v4 @ 2.20GHz processors.
5	The comparison durations, in nanoseconds, are estimated using std::chrono::high_resolution_clock which on the machine in (2) counts 1ns clock ticks. Precision is somewhat worse than that however. The ± value is the median absolute deviation times 1.48 for Normal consistency.

Table 38: Summary of algorithms and properties included in this report. The red superscripts give ranking for the quantity in that column.

	ALGORITHM	CONFIG	LIBRARY	TEMPLATE							COMPARISON[4]	
	NAME	DATA	DATA	MEMORY	SIZE	GENERATION TIME (ms)[4]					TIME (ns)[5]	
		(KB)[1]	(KB)[2]	(MB)[3]	(B)	MUGSHOT	480x720	960x1440	1600x2400	3000x4500	GENUINE	IMPOSTOR
749	mobbl-005	352570	983522	^{395}978	^{832}2048 ± 0	^{1118}1098 ± 1	^{838}1125 ± 2	^{805}1123 ± 2	^{762}1167 ± 2	^{788}1354 ± 1	^{1022}5498 ± 62	^{1024}5492 ± 53
750	mobipintech-000	370514	303291	^{485}1173	^{599}2048 ± 0	^{1235}1245 ± 1	^{927}1234 ± 1	^{916}1264 ± 1	^{913}1360 ± 1	^{937}1707 ± 1	^{1186}14506 ± 214	^{1188}14433 ± 197
751	momovn-001	246938	1013076	^{298}769	^{628}2048 ± 0	^{162}237 ± 1	^{116}268 ± 7	^{110}308 ± 10	^{88}293 ± 5	^{113}390 ± 3	^{531}1438 ± 13	^{537}1443 ± 13
752	momovn-002	320036	1013104	^{289}750	^{468}2048 ± 0	^{170}243 ± 3	^{104}248 ± 0	^{82}245 ± 1	^{72}253 ± 0	^{74}328 ± 2	^{535}1454 ± 8	^{541}1456 ± 16
753	momovn-003	528962	951056	^{610}1548	^{1180}4096 ± 0	^{803}766 ± 1	^{564}777 ± 0	^{519}783 ± 0	^{493}815 ± 1	^{566}1045 ± 1	^{952}3979 ± 23	^{958}3984 ± 29
754	moredian-000	525259	21374	^{423}1035	^{575}2048 ± 0	^{728}694 ± 0	^{492}698 ± 0	^{454}699 ± 0	^{405}700 ± 0	^{334}713 ± 1	^{633}1803 ± 11	^{626}1779 ± 23
755	morpho-000	100806	107129	-	^{3}116 ± 0	^{52}109 ± 1	-	-	-	-	^{384}993 ± 31	^{394}1000 ± 34
756	morpho-001	100806	368573	-	^{2}116 ± 0	^{12}41 ± 1	-	-	-	-	^{398}1030 ± 38	^{412}1042 ± 37
757	morpho-002	383021	110995	-	^{75}352 ± 0	^{364}411 ± 7	-	-	-	-	^{922}3620 ± 94	^{773}2481 ± 65
758	mukh-001	866223	451194	^{639}1647	^{244}1024 ± 0	^{1308}1375 ± 17	^{1022}1390 ± 12	^{1020}1406 ± 8	^{940}1394 ± 10	^{792}1360 ± 11	^{120}433 ± 14	^{128}435 ± 14
759	mukh-002	693809	454936	^{447}1081	^{478}2048 ± 0	^{1021}968 ± 1	^{676}921 ± 12	^{656}957 ± 2	^{593}954 ± 6	^{508}953 ± 5	^{210}612 ± 13	^{221}611 ± 17
760	mukh-003	556405	180996	^{694}1853	^{779}2048 ± 0	^{1399}1896 ± 3	^{1115}1948 ± 1	^{1105}2003 ± 0	^{1072}1981 ± 0	^{970}2016 ± 0	^{188}597 ± 13	^{216}604 ± 16
761	mukh-004	405118	181085	^{552}1353	^{892}2048 ± 0	^{520}558 ± 1	^{358}567 ± 1	^{323}569 ± 1	^{284}569 ± 3	^{244}593 ± 1	^{277}704 ± 1	^{290}703 ± 2
762	mukh-005	555239	264759	^{546}1346	^{881}2048 ± 0	^{391}436 ± 3	^{291}486 ± 6	^{265}495 ± 7	^{253}527 ± 16	^{248}597 ± 25	^{279}705 ± 1	^{292}706 ± 2
763	multimodality-000	0	503924	^{573}1417	^{613}2048 ± 0	^{367}416 ± 0	^{233}420 ± 0	^{198}423 ± 0	^{174}427 ± 0	^{157}463 ± 0	^{346}848 ± 25	^{335}800 ± 28
764	multimodality-001	185719	545045	^{566}1390	^{1192}4096 ± 0	^{1192}1190 ± 2	^{875}1169 ± 2	^{838}1165 ± 2	^{761}1167 ± 2	^{667}1177 ± 2	^{525}1424 ± 35	^{523}1384 ± 42
765	mvision-001	227502	149531	^{273}723	^{131}512 ± 0	^{726}691 ± 21	^{496}702 ± 19	^{452}697 ± 24	^{414}708 ± 29	^{332}710 ± 27	^{441}1123 ± 40	^{464}1154 ± 38
766	nazhiai-000	547484	16141	^{831}2716	^{911}2048 ± 0	^{708}683 ± 3	^{481}687 ± 2	^{563}835 ± 27	^{519}840 ± 31	^{435}834 ± 34	^{716}2230 ± 34	^{700}2133 ± 81
767	ncsgroup-000	95110	345861	^{425}1041	^{384}2048 ± 0	^{86}157 ± 0	^{44}153 ± 0	^{36}151 ± 0	^{31}157 ± 0	^{42}231 ± 0	^{755}2407 ± 16	^{757}2411 ± 22
768	ncssg-001	148743	490151	^{340}847	^{653}2048 ± 0	^{980}936 ± 2	^{697}946 ± 3	^{645}944 ± 2	^{583}938 ± 5	^{518}972 ± 2	^{919}3579 ± 50	^{907}3459 ± 34
769	ncssg-002	148859	415290	^{386}945	^{731}2048 ± 0	^{337}389 ± 1	^{215}397 ± 0	^{177}401 ± 1	^{165}407 ± 0	^{159}469 ± 0	^{1363}66390 ± 246	^{1361}66363 ± 179
770	ncssg-003	148876	414848	^{293}761	^{554}2048 ± 0	^{368}416 ± 1	^{251}437 ± 2	^{210}437 ± 1	^{185}443 ± 2	^{176}497 ± 1	^{1266}24709 ± 68	^{1265}24768 ± 134
771	ncssg-004	521184	483011	^{765}2272	^{360}2048 ± 0	^{714}687 ± 1	^{480}687 ± 0	^{463}706 ± 5	^{398}693 ± 1	^{349}731 ± 21	^{1267}24815 ± 117	^{1266}24799 ± 117
772	neosystems-001	575295	349959	-	^{940}2048 ± 0	^{1146}1137 ± 4	^{818}1098 ± 1	^{1092}1767 ± 4	^{1048}1769 ± 3	^{944}1765 ± 4	^{1223}18557 ± 189	^{1228}18640 ± 192
773	neosystems-002	599441	349942	-	^{443}2048 ± 0	^{1144}1135 ± 2	^{1110}1855 ± 3	^{1114}2258 ± 5	^{1087}2238 ± 3	^{995}2247 ± 3	^{1224}18752 ± 167	^{1227}18610 ± 213
774	neosystems-003	599442	349942	-	^{870}2048 ± 0	^{1151}1143 ± 2	^{1106}1836 ± 7	^{1115}2260 ± 3	^{1091}2273 ± 6	^{996}2273 ± 3	^{1229}19130 ± 223	^{1232}19167 ± 186
775	neosystems-004	243546	352623	^{183}529	^{413}2048 ± 0	^{259}324 ± 0	^{509}711 ± 3	^{552}827 ± 7	^{526}854 ± 2	^{483}916 ± 2	^{1184}14437 ± 176	^{1186}14355 ± 173
776	netbridgetech-001	133108	205875	^{173}508	^{1181}4096 ± 0	^{32}85 ± 1	^{18}83 ± 0	^{13}84 ± 0	^{14}92 ± 0	^{14}113 ± 4	^{1118}9280 ± 74	^{1120}9446 ± 512
777	netbridgetech-002	257687	49931	^{92}299	^{630}2048 ± 0	^{889}838 ± 6	^{609}838 ± 2	^{566}839 ± 1	^{518}839 ± 3	^{450}859 ± 3	^{835}2893 ± 65	^{862}3050 ± 123
778	neurotechnology-000	62129	33905	-	^{1378}7148 ± 0	^{595}611 ± 48	-	-	-	-	^{1380}74288 ± 2194	^{1375}72879 ± 2640
779	neurotechnology-001	280771	35716	-	^{1136}2718 ± 0	^{932}881 ± 46	-	-	-	-	^{1370}69356 ± 684	^{1366}69140 ± 579
780	neurotechnology-002	280771	36036	-	^{1135}2718 ± 0	^{548}581 ± 6	-	-	-	-	^{1366}68738 ± 748	^{1365}68905 ± 993
781	neurotechnology-003	339962	36125	-	^{1350}5214 ± 0	^{547}580 ± 5	-	-	-	-	^{1376}73589 ± 2548	^{1374}72837 ± 1546
782	neurotechnology-004	293384	54399	-	^{35}256 ± 0	^{350}401 ± 0	-	-	-	-	^{49}219 ± 8	^{56}231 ± 13
783	neurotechnology-005	270450	58088	-	^{25}256 ± 0	^{347}399 ± 0	-	-	-	-	^{54}238 ± 10	^{60}237 ± 7
784	neurotechnology-006	525541	54522	-	^{116}512 ± 0	^{698}678 ± 56	-	-	-	-	^{158}513 ± 14	^{166}535 ± 26
785	neurotechnology-008	119718	53462	-	^{34}256 ± 0	^{279}339 ± 0	-	-	-	-	^{132}467 ± 19	^{148}486 ± 26
786	neurotechnology-009	137515	53213	-	^{31}256 ± 0	^{335}388 ± 1	-	-	-	-	^{157}513 ± 10	^{157}512 ± 16
787	neurotechnology-010	362144	50226	-	^{159}514 ± 0	^{833}796 ± 1	^{576}796 ± 1	^{539}815 ± 3	^{525}853 ± 1	^{544}1006 ± 11	^{19}120 ± 8	^{17}115 ± 7
788	neurotechnology-011	364137	51141	-	^{160}514 ± 0	^{839}798 ± 1	^{581}802 ± 1	^{551}827 ± 3	^{536}873 ± 2	^{581}1059 ± 15	^{16}114 ± 11	^{16}114 ± 8
789	neurotechnology-012	147830	51395	-	^{37}256 ± 0	^{332}384 ± 0	^{204}387 ± 0	^{183}404 ± 1	^{180}435 ± 1	^{237}583 ± 7	^{18}119 ± 7	^{18}116 ± 7
790	neurotechnology-013	474749	85552	^{956}4825	^{158}514 ± 0	^{1050}1000 ± 1	^{754}1006 ± 2	^{716}1022 ± 2	^{670}1053 ± 2	^{671}1195 ± 8	^{14}109 ± 4	^{13}110 ± 4
791	neurotechnology-015	474782	86045	^{953}4819	^{161}515 ± 0	^{1077}1028 ± 3	^{775}1033 ± 3	^{747}1055 ± 4	^{698}1097 ± 4	^{751}1304 ± 18	^{21}130 ± 2	^{21}130 ± 4
792	neurotechnology-016	661450	89972	^{929}4074	^{162}515 ± 0	^{1289}1339 ± 3	^{1006}1351 ± 2	^{992}1369 ± 4	^{937}1390 ± 4	^{885}1508 ± 21	^{30}179 ± 20	^{29}171 ± 20

Notes	
1	The configuration size does not capture static data included in libraries.
2	The library size is the combined total of all files provided in the submission lib folder. These libraries e.g. OpenCV may or may not be installed on any end user's platform natively and would not need to be installed with the algorithm. Some developers put neural network models in their libraries.
3	The memory usage is the peak resident set size reported by the ps system call during template generation.
4	The median template creation times are measured on Intel®Xeon®CPU E5-2630 v4 @ 2.20GHz processors.
5	The comparison durations, in nanoseconds, are estimated using std::chrono::high_resolution_clock which on the machine in (2) counts 1ns clock ticks. Precision is somewhat worse than that however. The ± value is the median absolute deviation times 1.48 for Normal consistency.

Table 39: Summary of algorithms and properties included in this report. The red superscripts give ranking for the quantity in that column.

	ALGORITHM	CONFIG	LIBRARY	TEMPLATE							COMPARISON[4]	
	NAME	DATA	DATA	MEMORY	SIZE	GENERATION TIME (ms)[4]					TIME (ns)[5]	
		(KB)[1]	(KB)[2]	(MB)[3]	(B)	MUGSHOT	480x720	960x1440	1600x2400	3000x4500	GENUINE	IMPOSTOR
793	neurotechnology-017	371650	98242	^{776}2385	^{28}256 ± 0	^{468}508 ± 2	^{313}513 ± 0	^{285}519 ± 1	^{256}533 ± 1	^{267}622 ± 15	^{4}80 ± 1	^{4}79 ± 1
794	neurotechnology-018	698669	98271	^{938}4367	^{163}515 ± 0	^{766}725 ± 1	^{539}747 ± 1	^{498}747 ± 4	^{462}769 ± 2	^{434}833 ± 22	^{6}85 ± 2	^{7}87 ± 7
795	neurotechnology-019	365649	103237	^{773}2321	^{30}256 ± 0	^{623}625 ± 1	^{418}625 ± 0	^{389}633 ± 3	^{389}684 ± 2	^{363}742 ± 17	^{2}71 ± 2	^{2}72 ± 4
796	neurotechnology-020	807529	103241	^{961}5010	^{152}513 ± 0	^{1198}1201 ± 4	^{896}1196 ± 5	^{863}1195 ± 8	^{814}1224 ± 7	^{797}1373 ± 22	^{11}102 ± 1	^{8}101 ± 1
797	nextmetalabs-001	361607	4729276	^{228}627	^{535}2048 ± 0	^{959}914 ± 0	^{684}928 ± 0	^{634}928 ± 0	^{589}948 ± 0	^{487}919 ± 0	^{1000}4876 ± 185	^{992}4774 ± 72
798	nextmetalabs-002	571398	5046464	^{468}1123	^{567}2048 ± 0	^{1244}1259 ± 2	^{925}1229 ± 1	^{908}1253 ± 0	^{840}1257 ± 14	^{743}1296 ± 1	^{993}4786 ± 103	^{991}4753 ± 97
799	nextmetalabs-003	1105548	5046426	^{770}2301	^{464}2048 ± 0	^{1212}1218 ± 1	^{913}1217 ± 2	^{885}1225 ± 6	^{796}1207 ± 2	^{715}1253 ± 1	^{998}4874 ± 57	^{998}4833 ± 85
800	nextmetalabs-004	1105548	4174065	^{544}1332	^{651}2048 ± 0	^{1402}1940 ± 1	^{1116}1949 ± 0	^{1099}1919 ± 0	^{1069}1925 ± 1	^{969}2011 ± 2	^{1169}12441 ± 88	^{1173}12539 ± 154
801	nhn-001	336391	817674	-	^{1188}4096 ± 0	^{1074}1027 ± 3	^{770}1029 ± 1	^{725}1029 ± 1	^{665}1044 ± 1	^{602}1090 ± 1	^{1347}56650 ± 260	^{1348}56639 ± 210
802	nhn-002	363471	817674	^{253}679	^{1206}4096 ± 0	^{1148}1141 ± 3	^{850}1138 ± 2	^{820}1141 ± 2	^{750}1151 ± 6	^{677}1203 ± 2	^{1346}56608 ± 579	^{1347}56549 ± 606
803	nhn-003	933665	432730	^{579}1427	^{1246}4096 ± 0	^{1222}1229 ± 2	^{949}1261 ± 1	^{915}1263 ± 3	^{861}1279 ± 2	^{799}1375 ± 3	^{1337}50560 ± 105	^{1338}50592 ± 142
804	nhn-004	931648	432753	^{850}2864	^{1167}4096 ± 0	^{603}612 ± 0	^{427}632 ± 0	^{396}636 ± 0	^{380}676 ± 6	^{416}820 ± 0	^{1214}17323 ± 99	^{1217}17334 ± 133
805	nhn-005	1278729	432776	^{853}2890	^{1182}4096 ± 0	^{852}811 ± 0	^{460}671 ± 13	^{409}652 ± 0	^{428}726 ± 12	^{469}890 ± 3	^{1218}18123 ± 400	^{1223}18214 ± 250
806	noblis-000	713573	253204	-	^{277}1061 ± 0	^{98}174 ± 20	-	-	-	-	^{502}1343 ± 45	^{517}1373 ± 56
807	nodeflux-000	347079	797842	-	^{570}2048 ± 0	^{505}542 ± 1	-	-	-	-	^{884}3283 ± 51	^{890}3285 ± 56
808	nodeflux-001	262553	797842	-	^{880}2048 ± 0	^{174}247 ± 1	-	-	-	-	^{877}3242 ± 81	^{889}3255 ± 93
809	nodeflux-002	774668	690213	^{150}466	^{649}2048 ± 0	^{747}708 ± 4	^{508}709 ± 4	^{469}716 ± 5	^{422}716 ± 7	^{353}736 ± 3	^{901}3475 ± 62	^{902}3408 ± 143
810	nominder-000	547519	102693	^{665}1741	^{44}258 ± 0	^{741}701 ± 0	^{494}701 ± 2	^{473}721 ± 2	^{425}720 ± 3	^{406}796 ± 1	^{82}314 ± 5	^{52}226 ± 45
811	nominder-001	332018	102774	^{484}1172	^{40}258 ± 0	^{115}186 ± 0	^{68}189 ± 1	^{51}188 ± 0	^{49}202 ± 1	^{58}271 ± 1	^{52}226 ± 1	^{31}172 ± 41
812	nominder-002	249049	116931	^{693}1852	^{41}258 ± 0	^{355}405 ± 1	^{235}425 ± 2	^{201}424 ± 1	^{179}434 ± 0	^{183}505 ± 0	^{10}101 ± 11	^{10}102 ± 14
813	nominder-003	249964	116931	^{781}2417	^{46}258 ± 0	^{691}675 ± 2	^{478}683 ± 5	^{432}677 ± 2	^{406}701 ± 3	^{392}775 ± 3	^{7}87 ± 4	^{5}84 ± 4
814	nominder-004	249964	114221	^{780}2416	^{47}258 ± 0	^{793}755 ± 2	^{543}751 ± 4	^{494}740 ± 3	^{461}768 ± 3	^{442}846 ± 1	^{5}81 ± 1	^{6}86 ± 8
815	nominder-005	289014	114221	^{826}2699	^{45}258 ± 0	^{1174}1170 ± 4	^{897}1196 ± 5	^{836}1161 ± 6	^{810}1221 ± 8	^{780}1343 ± 7	^{8}94 ± 14	^{20}117 ± 7
816	nominder-006	304867	114225	^{820}2660	^{42}258 ± 0	^{776}736 ± 2	^{538}746 ± 3	^{507}759 ± 3	^{458}762 ± 2	^{457}869 ± 5	^{13}105 ± 5	^{12}108 ± 10
817	nominder-007	249970	101106	^{378}932	^{43}258 ± 0	^{1110}1085 ± 0	^{792}1071 ± 0	^{783}1099 ± 1	^{714}1117 ± 2	^{697}1235 ± 5	^{28}171 ± 5	^{39}190 ± 7
818	notiontag-000	92753	406791	-	^{192}584 ± 0	^{511}548 ± 64	^{343}548 ± 35	^{1048}1450 ± 99	^{1115}3771 ± 251	^{1110}13146 ± 792	^{1321}44672 ± 269	^{1322}44593 ± 358
819	notiontag-001	92753	427967	^{238}642	^{191}584 ± 0	^{977}929 ± 35	^{809}1092 ± 39	^{1121}3709 ± 81	^{1121}10233 ± 180	^{1115}31181 ± 521	^{1318}43636 ± 286	^{1319}43724 ± 330
820	notiontag-002	271987	967207	^{859}2965	^{1110}2120 ± 0	^{408}453 ± 2	^{266}453 ± 3	^{225}453 ± 3	^{194}458 ± 2	^{160}471 ± 3	^{1238}20278 ± 194	^{1238}20195 ± 186
821	nsensecorp-001	187421	258593	-	^{928}2048 ± 0	^{276}336 ± 0	^{161}335 ± 0	^{128}336 ± 0	^{115}335 ± 0	^{78}337 ± 0	^{1326}46605 ± 93	^{1327}46613 ± 112
822	nsensecorp-002	187421	122407	-	^{434}2048 ± 0	^{269}333 ± 0	^{159}333 ± 0	^{129}337 ± 0	^{116}338 ± 0	^{89}351 ± 0	^{1324}45965 ± 213	^{1324}45988 ± 158
823	nsensecorp-003	199895	117041	^{265}710	^{885}2048 ± 0	^{669}661 ± 0	^{453}664 ± 0	^{419}662 ± 1	^{362}659 ± 1	^{292}659 ± 0	^{1320}44658 ± 51	^{1323}44654 ± 72
824	nsensecorp-004	513276	139178	^{646}1675	^{418}2048 ± 0	^{1349}1433 ± 0	^{1062}1445 ± 7	^{1049}1450 ± 3	^{1005}1487 ± 5	-	^{751}2388 ± 42	^{752}2385 ± 63
825	nsensecorp-005	411845	138437	^{510}1240	^{647}2048 ± 0	^{1360}1455 ± 0	^{1067}1453 ± 0	^{1046}1449 ± 0	^{986}1457 ± 2	^{877}1490 ± 4	^{698}2131 ± 51	^{705}2165 ± 66
826	ntechlab-000	191530	22085	-	^{1137}2906 ± 1	^{201}278 ± 13	-	-	-	-	^{1288}30787 ± 142	^{1286}30846 ± 77
827	ntechlab-001	691296	22848	-	^{1376}6744 ± 1	^{565}587 ± 11	-	-	-	-	^{1364}67692 ± 833	^{1363}67486 ± 244
828	ntechlab-002	894169	25023	-	^{1377}6744 ± 1	^{266}330 ± 11	-	-	-	-	^{1384}82508 ± 213	^{1382}82524 ± 220
829	ntechlab-003	1422738	24649	-	^{1138}2906 ± 1	^{67}128 ± 3	-	-	-	-	^{1303}35327 ± 117	^{1306}35371 ± 123
830	ntechlab-004	3752378	115782	-	^{1157}3482 ± 1	^{863}818 ± 11	-	-	-	-	^{1314}38929 ± 81	^{1317}38916 ± 111
831	ntechlab-005	1726214	116068	-	^{325}1940 ± 0	^{749}712 ± 1	-	-	-	-	^{354}882 ± 42	^{359}880 ± 29
832	ntechlab-006	7901590	43009	-	^{1133}2600 ± 0	^{785}749 ± 1	-	-	-	-	^{405}1055 ± 93	^{352}844 ± 48
833	ntechlab-007	2509686	52474	-	^{1156}3348 ± 0	^{831}792 ± 3	-	-	-	-	^{466}1209 ± 59	^{492}1267 ± 65
834	ntechlab-008	1138002	52483	-	^{292}1300 ± 0	^{518}556 ± 1	-	-	-	-	^{428}1095 ± 45	^{417}1049 ± 51
835	ntechlab-009	1748043	43730	-	^{324}1940 ± 0	^{1134}1115 ± 2	^{829}1114 ± 1	^{800}1119 ± 1	^{731}1130 ± 2	^{675}1202 ± 4	^{212}614 ± 20	^{201}595 ± 28
836	ntechlab-010	698591	217167	-	^{290}1280 ± 0	^{1179}1177 ± 2	^{883}1180 ± 2	^{866}1197 ± 2	^{815}1224 ± 1	^{770}1326 ± 3	^{115}405 ± 13	^{123}416 ± 31

Notes	
1	The configuration size does not capture static data included in libraries.
2	The library size is the combined total of all files provided in the submission lib folder. These libraries e.g. OpenCV may or may not be installed on any end user's platform natively and would not need to be installed with the algorithm. Some developers put neural network models in their libraries.
3	The memory usage is the peak resident set size reported by the ps system call during template generation.
4	The median template creation times are measured on Intel®Xeon®CPU E5-2630 v4 @ 2.20GHz processors.
5	The comparison durations, in nanoseconds, are estimated using std::chrono::high_resolution_clock which on the machine in (2) counts 1ns clock ticks. Precision is somewhat worse than that however. The ± value is the median absolute deviation times 1.48 for Normal consistency.

Table 40: Summary of algorithms and properties included in this report. The red superscripts give ranking for the quantity in that column.

	ALGORITHM	CONFIG	LIBRARY	TEMPLATE							COMPARISON[4]	
	NAME	DATA	DATA	MEMORY	SIZE	GENERATION TIME (ms)[4]					TIME (ns)[5]	
		(KB)[1]	(KB)[2]	(MB)[3]	(B)	MUGSHOT	480x720	960x1440	1600x2400	3000x4500	GENUINE	IMPOSTOR
837	ntechlab-011	786933	209458	^{987}6867	^{286}1280 ± 0	^{1155}1148 ± 2	^{854}1142 ± 1	^{833}1159 ± 1	^{780}1185 ± 1	^{740}1290 ± 3	^{29}179 ± 11	^{32}173 ± 11
838	ntechlab-012	570796	212350	^{966}5450	^{1126}2560 ± 0	^{1278}1309 ± 1	^{994}1323 ± 1	^{968}1331 ± 1	^{914}1360 ± 1	^{859}1460 ± 3	^{46}211 ± 8	^{47}211 ± 7
839	omface-000	45945	844976	^{49}154	^{254}1024 ± 0	^{113}185 ± 1	^{82}206 ± 2	^{62}203 ± 1	^{43}195 ± 1	^{31}193 ± 1	^{139}481 ± 42	^{136}456 ± 20
840	omface-001	146370	1799745	^{46}145	^{246}1024 ± 0	^{126}194 ± 2	^{92}222 ± 2	^{67}209 ± 0	^{55}216 ± 1	^{44}233 ± 1	^{1222}18369 ± 19	^{1225}18366 ± 32
841	omnigarde-000	264057	32882	-	^{248}1024 ± 0	^{991}944 ± 0	^{649}887 ± 0	^{600}888 ± 1	^{554}892 ± 0	^{478}902 ± 0	^{796}2671 ± 35	^{791}2620 ± 29
842	omnigarde-001	200523	32882	^{151}466	^{106}512 ± 0	^{984}941 ± 0	^{645}883 ± 1	^{599}886 ± 1	^{551}891 ± 1	^{475}898 ± 0	^{521}1405 ± 31	^{521}1379 ± 26
843	omnigarde-002	368860	32882	^{292}760	^{242}1024 ± 0	^{1273}1303 ± 1	^{937}1246 ± 1	^{904}1249 ± 1	^{836}1253 ± 1	^{721}1261 ± 1	^{809}2727 ± 34	^{806}2686 ± 32
844	omnigarde-003	427751	35153	^{291}756	^{165}517 ± 0	^{686}673 ± 0	^{425}631 ± 1	^{390}633 ± 1	^{342}637 ± 1	^{286}647 ± 1	^{481}1259 ± 22	^{485}1244 ± 16
845	omnigarde-004	995019	35158	^{699}1873	^{166}517 ± 0	^{1200}1201 ± 1	^{948}1261 ± 1	^{873}1207 ± 1	^{805}1215 ± 0	^{695}1229 ± 0	^{482}1274 ± 22	^{483}1241 ± 26
846	omnigarde-005	1316067	35158	^{806}2545	^{173}525 ± 0	^{1173}1170 ± 1	^{869}1159 ± 0	^{839}1169 ± 7	^{783}1186 ± 1	^{672}1199 ± 1	^{554}1490 ± 40	^{554}1481 ± 38
847	onfido-000	273478	959781	^{371}914	^{369}2048 ± 0	^{415}459 ± 17	^{264}451 ± 15	^{224}451 ± 14	^{201}462 ± 15	^{184}505 ± 18	^{583}1617 ± 50	^{586}1637 ± 53
848	onfido-001	344394	1021960	^{839}2756	^{551}2048 ± 0	^{140}208 ± 4	^{84}208 ± 4	^{69}213 ± 4	^{60}223 ± 3	^{52}250 ± 4	^{353}874 ± 28	^{353}852 ± 20
849	onfido-002	852775	252949	^{405}1003	^{1171}4096 ± 0	^{1197}1199 ± 5	^{903}1202 ± 5	^{869}1203 ± 5	^{802}1213 ± 5	^{708}1250 ± 5	^{793}2625 ± 60	^{794}2628 ± 84
850	onfido-003	852775	252949	^{408}1010	^{1168}4096 ± 0	^{1203}1203 ± 5	^{904}1202 ± 5	^{872}1205 ± 5	^{803}1214 ± 5	^{713}1252 ± 5	^{767}2463 ± 14	^{799}2669 ± 37
851	ooto-001	382081	95138	^{708}1923	^{1140}3072 ± 0	^{992}944 ± 0	^{701}953 ± 1	^{698}997 ± 0	^{596}957 ± 0	^{537}999 ± 0	^{1005}4993 ± 17	^{1007}5004 ± 50
852	openedge-000	447048	272235	^{562}1376	^{1069}2056 ± 0	^{310}367 ± 0	^{223}404 ± 1	^{138}352 ± 1	^{118}350 ± 0	^{107}385 ± 0	^{1194}15122 ± 41	^{1196}15110 ± 48
853	openface-001	0	40111	^{26}100	^{355}2048 ± 0	^{79}148 ± 1	^{45}154 ± 0	^{150}365 ± 3	^{168}409 ± 9	^{261}616 ± 31	^{203}608 ± 14	^{214}604 ± 13
854	ovisionllc-001	192059	252531	^{439}1066	^{251}1024 ± 0	^{101}175 ± 0	^{55}175 ± 0	^{48}183 ± 0	^{46}196 ± 0	^{48}241 ± 0	^{833}2889 ± 38	^{841}2901 ± 47
855	ovisionllc-002	247778	96584	^{591}1478	^{219}1024 ± 0	^{190}266 ± 0	^{109}256 ± 0	^{83}250 ± 0	^{75}263 ± 1	^{66}313 ± 0	^{812}2763 ± 72	^{808}2727 ± 29
856	oz-001	303723	238311	-	^{1307}4125 ± 0	^{1154}1147 ± 3	^{886}1182 ± 3	^{924}1273 ± 4	^{1033}1617 ± 7	^{1033}2890 ± 19	^{1396}228011 ± 5455	^{1395}220746 ± 5572
857	oz-002	716022	170261	-	^{1087}2065 ± 0	^{1099}1064 ± 3	^{876}1171 ± 3	^{1120}2953 ± 6	^{1119}7352 ± 13	^{1114}26658 ± 29	^{1392}131108 ± 1408	^{1392}126758 ± 913
858	oz-003	484147	519652	^{1007}11575	^{1009}2053 ± 0	^{1307}1375 ± 12	^{1020}1388 ± 3	^{1093}1773 ± 16	^{1076}2039 ± 6	^{1044}3209 ± 5	^{1377}73905 ± 456	^{1376}73892 ± 444
859	oz-004	373982	1075452	^{999}7845	^{1008}2053 ± 0	^{882}832 ± 7	^{632}871 ± 6	^{605}899 ± 10	^{689}1078 ± 12	^{920}1608 ± 10	^{1356}61654 ± 418	^{1354}61749 ± 450
860	pa-002	442564	308954	-	^{1401}18436 ± 0	^{70}132 ± 7	-	-	-	-	^{860}3088 ± 32	^{863}3051 ± 28
861	pa-003	714102	1464254	-	^{462}2048 ± 0	^{878}831 ± 31	-	-	-	-	^{376}962 ± 23	^{371}914 ± 38
862	palit-000	428754	144958	^{556}1360	^{1263}4096 ± 0	^{536}570 ± 1	^{367}578 ± 1	^{331}576 ± 3	^{291}583 ± 1	^{259}614 ± 1	^{715}2227 ± 16	^{716}2226 ± 16
863	palit-001	173886	145564	^{206}587	^{631}2048 ± 0	^{156}227 ± 0	^{94}224 ± 1	^{73}224 ± 1	^{65}229 ± 3	^{55}262 ± 2	^{450}1150 ± 16	^{450}1135 ± 23
864	pangiam-000	464252	24512	^{924}3963	^{899}2048 ± 0	^{627}627 ± 5	^{406}618 ± 4	^{367}615 ± 3	^{327}620 ± 3	^{279}639 ± 3	^{17}118 ± 7	^{15}113 ± 7
865	pangiam-001	1015455	37259	^{621}1569	^{617}2048 ± 0	^{1026}972 ± 1	^{733}982 ± 3	^{678}981 ± 2	^{621}990 ± 7	^{570}1052 ± 2	^{22}136 ± 11	^{22}139 ± 13
866	pangiam-002	486035	39834	^{505}1205	^{385}2048 ± 0	^{249}316 ± 0	^{148}316 ± 0	^{116}317 ± 0	^{103}319 ± 1	^{73}326 ± 2	^{15}111 ± 13	^{11}103 ± 2
867	papago-001	669274	52817	^{774}2341	^{652}2048 ± 0	^{1252}1272 ± 6	^{974}1296 ± 7	^{947}1295 ± 6	^{863}1281 ± 3	^{781}1345 ± 3	^{1199}15236 ± 169	^{1200}15184 ± 142
868	papil11-000	1146378	24895	^{753}2184	^{560}2048 ± 0	^{987}942 ± 3	^{824}1108 ± 2	^{870}1204 ± 6	^{923}1369 ± 10	^{971}2033 ± 35	^{209}612 ± 7	^{224}613 ± 11
869	papil11-001	1221825	38957	^{815}2618	^{915}2048 ± 0	^{1006}951 ± 2	^{846}1135 ± 2	^{880}1220 ± 4	^{933}1386 ± 10	^{998}2292 ± 69	^{154}506 ± 22	^{159}519 ± 20
870	papil11-002	1208976	38985	^{804}2543	^{691}2048 ± 0	^{965}916 ± 2	^{812}1094 ± 2	^{837}1163 ± 1	^{875}1307 ± 4	^{984}2140 ± 10	^{169}560 ± 22	^{185}577 ± 22
871	papil11-003	1263123	39005	^{819}2657	^{743}2048 ± 0	^{1085}1038 ± 1	^{919}1222 ± 1	^{940}1293 ± 2	^{972}1431 ± 3	^{999}2298 ± 8	^{155}508 ± 10	^{155}501 ± 10
872	papil11-004	560851	18192	^{462}1104	^{71}296 ± 0	^{481}522 ± 0	^{321}522 ± 0	^{291}524 ± 0	^{255}531 ± 0	^{226}556 ± 2	^{1254}23204 ± 63	^{1256}23224 ± 68
873	papsav1923-001	279210	52652	^{154}474	^{925}2048 ± 0	^{625}626 ± 1	^{420}628 ± 1	^{383}630 ± 1	^{353}648 ± 2	^{364}744 ± 3	^{294}725 ± 25	^{311}731 ± 28
874	papsav1923-002	491185	24727	^{473}1139	^{969}2052 ± 0	^{830}792 ± 1	^{730}978 ± 1	^{736}1042 ± 1	^{753}1158 ± 1	^{927}1641 ± 19	^{467}1209 ± 29	^{477}1206 ± 38
875	papsav1923-003	515576	24803	^{463}1113	^{888}2048 ± 0	^{837}797 ± 0	^{738}987 ± 1	^{738}1043 ± 1	^{773}1178 ± 1	^{950}1809 ± 7	^{358}903 ± 26	^{368}905 ± 34
876	paravision-004	556670	145440	-	^{1245}4096 ± 0	^{876}829 ± 2	^{607}834 ± 6	^{560}832 ± 2	^{511}833 ± 4	^{432}833 ± 2	^{302}737 ± 31	^{303}718 ± 38
877	paravision-006	542423	202234	-	^{1251}4096 ± 0	^{737}700 ± 1	^{500}704 ± 0	^{460}705 ± 0	^{409}704 ± 0	^{328}705 ± 0	^{84}321 ± 16	^{86}315 ± 14
878	paravision-008	542190	204400	^{567}1399	^{1166}4096 ± 0	^{735}699 ± 0	^{493}700 ± 0	^{457}701 ± 0	^{407}702 ± 1	^{327}702 ± 0	^{90}337 ± 17	^{97}330 ± 13
879	paravision-010	688291	205854	^{747}2150	^{1283}4100 ± 0	^{639}634 ± 0	^{434}635 ± 0	^{395}635 ± 0	^{339}635 ± 0	^{275}635 ± 1	^{574}1577 ± 35	^{579}1571 ± 32
880	paravision-011	781138	95589	^{784}2424	^{1290}4100 ± 0	^{902}852 ± 0	^{634}871 ± 1	^{579}858 ± 1	^{527}854 ± 0	^{460}873 ± 1	^{581}1608 ± 35	^{584}1625 ± 32

Notes	
1	The configuration size does not capture static data included in libraries.
2	The library size is the combined total of all files provided in the submission lib folder. These libraries e.g. OpenCV may or may not be installed on any end user's platform natively and would not need to be installed with the algorithm. Some developers put neural network models in their libraries.
3	The memory usage is the peak resident set size reported by the ps system call during template generation.
4	The median template creation times are measured on Intel®Xeon®CPU E5-2630 v4 @ 2.20GHz processors.
5	The comparison durations, in nanoseconds, are estimated using std::chrono::high_resolution_clock which on the machine in (2) counts 1ns clock ticks. Precision is somewhat worse than that however. The ± value is the median absolute deviation times 1.48 for Normal consistency.

Table 41: Summary of algorithms and properties included in this report. The red superscripts give ranking for the quantity in that column.

	ALGORITHM	CONFIG	LIBRARY	TEMPLATE							COMPARISON[4]	
	NAME	DATA	DATA	MEMORY	SIZE	GENERATION TIME (ms)[4]					TIME (ns)[5]	
		(KB)[1]	(KB)[2]	(MB)[3]	(B)	MUGSHOT	480x720	960x1440	1600x2400	3000x4500	GENUINE	IMPOSTOR
881	paravision-013	1537125	95602	^{948}4648	^{1291}4100 ± 0	^{1044}991 ± 9	^{744}993 ± 5	^{691}992 ± 4	^{635}1002 ± 5	^{541}1002 ± 7	^{547}1481 ± 26	^{560}1490 ± 25
882	paravision-015	1584003	164658	^{954}4820	^{1280}4100 ± 0	^{1304}1371 ± 12	^{1094}1577 ± 1	^{1068}1500 ± 4	^{980}1449 ± 1	^{892}1521 ± 7	^{527}1432 ± 11	^{540}1455 ± 32
883	paravision-017	1584003	164639	^{955}4820	^{1279}4100 ± 0	^{1268}1295 ± 11	^{860}1147 ± 4	^{831}1158 ± 8	^{759}1166 ± 7	^{640}1140 ± 12	^{538}1461 ± 10	^{544}1459 ± 16
884	paravision-018	1596372	164639	^{958}4909	^{1293}4100 ± 0	^{1370}1474 ± 11	^{1076}1472 ± 12	^{1062}1475 ± 11	^{989}1459 ± 11	^{893}1523 ± 16	^{567}1532 ± 68	^{567}1520 ± 40
885	paravision-020	1646513	155644	^{894}3487	^{1273}4100 ± 0	^{1406}2043 ± 0	^{1117}2043 ± 0	^{1106}2048 ± 0	^{1075}2038 ± 0	^{976}2100 ± 0	^{694}2110 ± 10	^{695}2110 ± 17
886	pensees-001	1619431	408932	^{707}1922	^{1389}8200 ± 0	^{1126}1108 ± 3	^{1065}1448 ± 17	^{1037}1439 ± 10	^{994}1464 ± 5	^{905}1546 ± 9	^{867}3151 ± 34	^{871}3143 ± 25
887	pentacomp-000	261914	192048	^{244}658	^{426}2048 ± 0	^{407}452 ± 1	^{259}444 ± 0	^{232}458 ± 4	^{193}456 ± 5	^{156}461 ± 3	^{425}1085 ± 25	^{431}1081 ± 38
888	pixelall-002	0	169030	-	^{1125}2560 ± 0	^{120}191 ± 1	-	-	-	-	^{473}1223 ± 56	^{480}1230 ± 47
889	pixelall-003	0	707030	-	^{1129}2560 ± 0	^{736}699 ± 8	-	-	-	-	^{461}1174 ± 28	^{451}1139 ± 68
890	pixelall-004	0	550919	-	^{1128}2560 ± 0	^{405}451 ± 11	^{262}449 ± 3	^{223}451 ± 1	^{196}459 ± 2	^{180}502 ± 4	^{444}1139 ± 65	^{473}1186 ± 31
891	pixelall-005	0	1001355	-	^{1348}5120 ± 0	^{1132}1112 ± 3	^{830}1115 ± 1	^{801}1120 ± 1	^{723}1124 ± 2	^{642}1143 ± 2	^{479}1259 ± 29	^{484}1243 ± 23
892	pixelall-006	0	746305	-	^{1124}2560 ± 0	^{1068}1024 ± 3	^{769}1028 ± 2	^{729}1033 ± 1	^{657}1032 ± 1	^{571}1054 ± 2	^{307}754 ± 14	^{305}722 ± 10
893	pixelall-007	0	444912	-	^{522}2048 ± 0	^{1072}1026 ± 4	^{778}1038 ± 2	^{774}1089 ± 2	^{694}1087 ± 2	^{627}1124 ± 2	^{283}708 ± 14	^{289}701 ± 19
894	pixelall-008	0	992249	^{666}1742	^{1385}8192 ± 0	^{1367}1471 ± 3	^{1037}1405 ± 4	^{1024}1409 ± 4	^{958}1413 ± 3	^{836}1426 ± 4	^{628}1799 ± 50	^{637}1807 ± 48
895	pixelall-009	0	1009114	^{661}1732	^{1386}8192 ± 0	^{1376}1484 ± 3	^{1030}1395 ± 3	^{1015}1400 ± 4	^{938}1391 ± 3	^{840}1433 ± 3	^{641}1848 ± 13	^{642}1842 ± 19
896	pixelall-010	0	1469903	^{825}2693	^{1384}8192 ± 0	^{1160}1153 ± 3	^{800}1084 ± 4	^{788}1103 ± 4	^{697}1093 ± 3	^{622}1118 ± 4	^{655}1906 ± 13	^{654}1898 ± 29
897	pnpsecure-000	9726	146266	^{23}93	^{690}2048 ± 0	^{9}35 ± 0	^{8}42 ± 0	^{34}145 ± 0	^{167}409 ± 1	^{910}1565 ± 5	^{659}1918 ± 11	^{657}1916 ± 16
898	pnpsecure-001	1015928	59243	^{729}2060	^{563}2048 ± 0	^{689}674 ± 0	^{495}701 ± 0	^{597}885 ± 0	^{982}1452 ± 1	^{1046}3286 ± 3	^{792}2621 ± 19	^{796}2649 ± 41
899	privid-001	0	76008	^{45}143	^{1406}30720 ± 0	^{404}450 ± 0	^{267}454 ± 0	^{241}467 ± 1	^{212}472 ± 1	^{182}504 ± 1	^{1212}17041 ± 74	^{1214}17053 ± 100
900	privid-002	0	219733	^{419}1031	^{665}2048 ± 0	^{1246}1261 ± 3	^{864}1156 ± 4	^{829}1155 ± 2	^{755}1162 ± 3	^{750}1302 ± 4	^{265}686 ± 22	^{273}680 ± 20
901	privid-003	0	188341	^{435}1062	^{685}2048 ± 0	^{1346}1430 ± 2	^{1060}1437 ± 6	^{1055}1459 ± 7	^{981}1451 ± 7	^{881}1499 ± 18	^{293}725 ± 7	^{304}720 ± 13
902	privid-004	0	992936	^{539}1304	^{370}2048 ± 0	^{1272}1303 ± 1	^{960}1282 ± 2	^{962}1324 ± 3	^{916}1363 ± 0	^{811}1387 ± 0	^{289}717 ± 29	^{287}699 ± 19
903	psl-000	260619	1537815	-	^{392}2048 ± 0	^{630}629 ± 11	-	-	-	-	^{68}280 ± 17	^{76}280 ± 17
904	psl-001	382035	1461947	-	^{1011}2056 ± 0	^{822}785 ± 16	-	-	-	-	^{74}298 ± 13	^{80}292 ± 14
905	psl-002	804934	1462048	-	^{972}2052 ± 0	^{941}888 ± 9	-	-	-	-	^{576}1590 ± 48	^{449}1133 ± 78
906	psl-003	1159643	1434859	-	^{1109}2120 ± 0	^{910}865 ± 3	-	-	-	-	^{403}1052 ± 14	^{404}1025 ± 51
907	psl-004	771727	1560145	-	^{1153}3144 ± 0	^{891}839 ± 3	-	-	-	-	^{257}680 ± 34	^{269}670 ± 22
908	psl-005	774031	1560153	-	^{1150}3144 ± 0	^{972}922 ± 37	-	-	-	-	^{276}703 ± 32	^{295}708 ± 26
909	psl-006	1211577	524525	-	^{1151}3144 ± 0	^{1351}1438 ± 6	^{1057}1434 ± 4	^{1035}1434 ± 4	^{974}1434 ± 5	^{846}1437 ± 5	^{71}291 ± 34	^{72}268 ± 25
910	psl-007	954351	524521	-	^{1154}3144 ± 0	^{1337}1408 ± 5	^{1046}1417 ± 3	^{1029}1418 ± 3	^{962}1419 ± 2	^{832}1422 ± 3	^{62}265 ± 22	^{68}258 ± 17
911	psl-008	954351	524525	-	^{1152}3144 ± 0	^{1339}1412 ± 4	^{1044}1415 ± 3	^{1028}1416 ± 2	^{960}1418 ± 2	^{830}1418 ± 2	^{60}259 ± 22	^{64}252 ± 22
912	psl-009	411027	411504	-	^{1321}4168 ± 0	^{1313}1382 ± 2	^{1016}1381 ± 1	^{1002}1383 ± 1	^{930}1383 ± 2	^{808}1385 ± 1	^{83}316 ± 14	^{79}289 ± 14
913	psl-010	411027	591157	^{965}5362	^{1322}4168 ± 0	^{1333}1403 ± 9	^{1026}1393 ± 3	^{1007}1392 ± 3	^{941}1395 ± 3	^{816}1396 ± 3	^{97}354 ± 53	^{96}329 ± 29
914	psl-011	814579	606050	^{960}4959	^{1390}8248 ± 0	^{1285}1324 ± 2	^{993}1323 ± 8	^{963}1326 ± 8	^{893}1324 ± 8	^{764}1322 ± 4	^{594}1680 ± 37	^{598}1688 ± 40
915	psl-012	1318147	622004	^{946}4535	^{1315}4144 ± 0	^{1131}1111 ± 2	^{834}1122 ± 2	^{789}1104 ± 2	^{717}1119 ± 1	^{620}1117 ± 1	^{178}583 ± 17	^{194}589 ± 17
916	psl-013	1318151	622036	^{943}4525	^{1313}4144 ± 0	^{1138}1119 ± 1	^{819}1105 ± 1	^{793}1110 ± 1	^{704}1104 ± 1	^{630}1126 ± 1	^{411}1062 ± 62	^{438}1098 ± 51
917	psl-014	915965	622044	^{945}4525	^{1314}4144 ± 0	^{1128}1109 ± 1	^{851}1139 ± 1	^{791}1104 ± 1	^{715}1118 ± 1	^{617}1114 ± 1	^{442}1132 ± 105	^{445}1114 ± 37
918	ptakuratsatu-000	0	585434	^{549}1347	^{177}538 ± 0	^{926}875 ± 3	^{626}863 ± 48	^{635}928 ± 9	^{597}958 ± 17	^{590}1066 ± 26	^{1043}5900 ± 103	^{1035}5687 ± 167
919	pxl-001	110116	78231	^{52}168	^{151}512 ± 0	^{45}101 ± 5	^{28}104 ± 5	^{55}189 ± 12	^{166}408 ± 27	^{863}1470 ± 144	^{1031}5598 ± 45	^{1031}5590 ± 68
920	pyramid-000	372608	219883	^{311}804	^{1048}2056 ± 0	^{552}583 ± 2	-	-	-	-	^{1085}7147 ± 59	^{1094}7586 ± 425
921	pyramid-001	1040862	143739	^{739}2098	^{388}2048 ± 0	^{848}809 ± 0	^{584}806 ± 0	^{540}815 ± 4	^{513}837 ± 0	^{465}881 ± 2	^{1165}12265 ± 48	^{1167}12276 ± 51
922	qazbs-000	362015	805258	^{421}1034	^{808}2048 ± 0	^{1275}1307 ± 1	^{935}1243 ± 0	^{902}1248 ± 9	^{837}1253 ± 1	^{725}1270 ± 0	^{1012}5181 ± 62	^{1012}5167 ± 93
923	qazsmartvisionai-000	560570	99515	^{775}2371	^{145}512 ± 0	^{730}694 ± 1	^{507}708 ± 7	^{471}717 ± 5	^{416}711 ± 5	^{345}723 ± 7	^{326}795 ± 29	^{325}781 ± 34
924	qazsmartvisionai-001	1417181	102251	^{860}2987	^{180}544 ± 0	^{1122}1103 ± 20	^{843}1129 ± 3	^{806}1124 ± 5	^{745}1145 ± 7	^{636}1134 ± 16	^{324}793 ± 29	^{339}804 ± 32

Notes	
1	The configuration size does not capture static data included in libraries.
2	The library size is the combined total of all files provided in the submission lib folder. These libraries e.g. OpenCV may or may not be installed on any end user's platform natively and would not need to be installed with the algorithm. Some developers put neural network models in their libraries.
3	The memory usage is the peak resident set size reported by the ps system call during template generation.
4	The median template creation times are measured on Intel®Xeon®CPU E5-2630 v4 @ 2.20GHz processors.
5	The comparison durations, in nanoseconds, are estimated using std::chrono::high_resolution_clock which on the machine in (2) counts 1ns clock ticks. Precision is somewhat worse than that however. The ± value is the median absolute deviation times 1.48 for Normal consistency.

Table 42: Summary of algorithms and properties included in this report. The red superscripts give ranking for the quantity in that column.

	ALGORITHM	CONFIG	LIBRARY	TEMPLATE							COMPARISON[4]	
	NAME	DATA	DATA	MEMORY	SIZE	GENERATION TIME (ms)[4]					TIME (ns)[5]	
		(KB)[1]	(KB)[2]	(MB)[3]	(B)	MUGSHOT	480x720	960x1440	1600x2400	3000x4500	GENUINE	IMPOSTOR
925	qazsmartvisionai-002	1365926	102252	^{855}2895	^{182}544 ± 0	^{1102}1068 ± 6	^{837}1125 ± 4	^{797}1114 ± 6	^{676}1066 ± 1	^{614}1113 ± 15	^{329}800 ± 31	^{332}798 ± 34
926	qazsmartvisionai-003	1365926	102265	^{854}2894	^{181}544 ± 0	^{1093}1056 ± 5	^{796}1078 ± 12	^{766}1079 ± 10	^{688}1078 ± 10	^{599}1088 ± 18	^{338}822 ± 28	^{338}803 ± 32
927	qazsmartvisionai-004	1564226	102265	^{879}3281	^{184}544 ± 0	^{1257}1280 ± 13	^{982}1310 ± 14	^{974}1338 ± 10	^{891}1323 ± 13	^{618}1115 ± 2	^{308}758 ± 38	^{317}758 ± 31
928	qluevision-001	173605	205230	^{118}376	^{1387}8192 ± 0	^{157}229 ± 1	^{98}230 ± 1	^{77}231 ± 1	^{66}233 ± 1	^{47}239 ± 1	^{891}3374 ± 38	^{896}3365 ± 41
929	qnap-000	186731	15598	-	^{932}2048 ± 0	^{767}726 ± 9	^{269}457 ± 1	^{231}458 ± 0	^{208}464 ± 1	^{166}482 ± 2	^{252}660 ± 25	^{263}654 ± 29
930	qnap-001	196210	13399	^{86}287	^{650}2048 ± 0	^{607}614 ± 1	^{399}615 ± 1	^{380}627 ± 1	^{331}623 ± 1	^{273}634 ± 2	^{245}649 ± 11	^{259}648 ± 14
931	qnap-002	346963	33284	^{358}882	^{596}2048 ± 0	^{867}821 ± 1	^{594}824 ± 1	^{548}824 ± 1	^{507}826 ± 1	^{431}832 ± 1	^{72}293 ± 13	^{77}287 ± 17
932	qnap-003	245476	61427	^{313}807	^{664}2048 ± 0	^{334}387 ± 0	^{212}393 ± 0	^{175}393 ± 0	^{153}393 ± 1	^{121}400 ± 2	^{260}683 ± 20	^{261}651 ± 17
933	qnap-004	371274	61422	^{404}1002	^{802}2048 ± 0	^{305}365 ± 0	^{186}365 ± 1	^{152}367 ± 0	^{134}368 ± 0	^{101}375 ± 3	^{258}681 ± 7	^{274}682 ± 13
934	qnap-005	977818	61429	^{848}2828	^{818}2048 ± 0	^{1024}969 ± 5	^{741}988 ± 8	^{689}992 ± 6	^{633}1000 ± 7	^{546}1008 ± 6	^{231}633 ± 1	^{245}632 ± 13
935	qnap-006	1244083	61533	^{885}3351	^{974}2052 ± 0	^{1071}1025 ± 5	^{782}1051 ± 6	^{735}1041 ± 6	^{671}1055 ± 8	^{576}1057 ± 10	^{268}688 ± 29	^{267}664 ± 10
936	quantasoft-003	370518	211354	^{436}1063	^{342}2048 ± 0	^{634}632 ± 2	^{433}634 ± 0	^{384}632 ± 0	^{335}631 ± 1	^{274}634 ± 0	^{42}201 ± 7	^{42}203 ± 8
937	rankone-000	0	96896	-	^{14}144 ± 0	^{30}82 ± 9	-	-	-	-	^{1317}39932 ± 468	^{1115}8722 ± 171
938	rankone-001	0	97092	-	^{21}208 ± 0	^{17}56 ± 4	-	-	-	-	^{1373}72754 ± 658	^{105}345 ± 29
939	rankone-002	0	98585	-	^{22}224 ± 0	^{24}75 ± 1	-	-	-	-	^{1368}69113 ± 3802	^{110}369 ± 26
940	rankone-003	0	93554	-	^{23}228 ± 0	^{10}37 ± 1	-	-	-	-	^{85}322 ± 20	^{91}324 ± 19
941	rankone-004	0	135727	-	^{13}133 ± 0	^{26}78 ± 1	-	-	-	-	^{92}340 ± 19	^{81}298 ± 17
942	rankone-005	0	104048	-	^{12}133 ± 0	^{23}71 ± 2	-	-	-	-	^{114}403 ± 10	^{99}337 ± 19
943	rankone-006	0	133045	-	^{16}165 ± 0	^{143}210 ± 1	-	-	-	-	^{124}443 ± 26	^{119}395 ± 22
944	rankone-007	0	136942	-	^{18}165 ± 0	^{173}245 ± 5	-	-	-	-	^{267}688 ± 20	^{210}601 ± 16
945	rankone-008	2	141234	-	^{17}165 ± 0	^{195}272 ± 3	-	-	-	-	^{305}750 ± 20	^{226}613 ± 23
946	rankone-009	0	107688	-	^{49}260 ± 0	^{106}179 ± 4	-	-	-	-	^{285}710 ± 32	^{172}552 ± 25
947	rankone-010	0	138435	-	^{50}261 ± 0	^{124}193 ± 1	-	-	-	-	^{69}282 ± 13	^{59}234 ± 16
948	rankone-011	0	179209	-	^{53}261 ± 0	^{531}567 ± 1	^{349}557 ± 1	^{322}567 ± 1	^{295}586 ± 1	^{309}682 ± 3	^{70}283 ± 14	^{49}220 ± 19
949	rankone-012	0	264182	-	^{54}261 ± 0	^{526}564 ± 3	^{346}554 ± 1	^{319}564 ± 1	^{297}586 ± 1	^{322}695 ± 1	^{66}273 ± 17	^{55}231 ± 14
950	rankone-013	0	228729	^{48}150	^{55}261 ± 0	^{723}690 ± 5	^{465}672 ± 1	^{467}712 ± 1	^{472}780 ± 1	^{621}1118 ± 3	^{99}356 ± 23	^{83}304 ± 23
951	rankone-014	0	243130	^{51}164	^{52}261 ± 0	^{740}701 ± 1	^{501}705 ± 0	^{486}732 ± 1	^{484}800 ± 1	^{615}1113 ± 1	^{79}306 ± 16	^{63}251 ± 13
952	rankone-015	0	289078	^{66}190	^{51}261 ± 0	^{510}547 ± 5	^{338}543 ± 6	^{332}578 ± 2	^{334}629 ± 7	^{473}894 ± 9	^{41}201 ± 19	^{30}172 ± 16
953	realnetworks-000	99044	107893	-	^{1287}4100 ± 0	^{78}144 ± 2	-	-	-	-	^{765}2458 ± 26	^{772}2467 ± 35
954	realnetworks-001	99044	107893	-	^{1271}4100 ± 0	^{76}144 ± 2	-	-	-	-	^{775}2500 ± 47	^{759}2420 ± 34
955	realnetworks-002	95328	107088	-	^{321}1848 ± 0	^{178}250 ± 2	^{102}242 ± 4	^{95}282 ± 5	^{141}381 ± 10	^{391}774 ± 15	^{490}1285 ± 17	^{486}1247 ± 42
956	realnetworks-003	95334	104498	-	^{322}1848 ± 0	^{103}177 ± 10	-	-	-	-	^{562}1516 ± 29	^{568}1522 ± 60
957	realnetworks-004	172335	913988	-	^{1070}2056 ± 0	^{265}330 ± 4	^{160}333 ± 3	^{181}402 ± 7	^{294}585 ± 15	^{818}1402 ± 51	^{468}1210 ± 29	^{476}1202 ± 17
958	realnetworks-005	172253	56755	-	^{1022}2056 ± 0	^{145}211 ± 4	^{81}205 ± 3	^{98}290 ± 6	^{244}515 ± 17	^{758}1312 ± 78	^{469}1213 ± 17	^{478}1207 ± 16
959	realnetworks-006	466225	56771	^{629}1596	^{1050}2056 ± 0	^{644}638 ± 4	^{422}630 ± 3	^{428}672 ± 5	^{412}706 ± 5	^{390}774 ± 5	^{134}469 ± 19	^{147}478 ± 25
960	realnetworks-007	570797	101527	^{874}3145	^{1052}2056 ± 0	^{1294}1348 ± 2	^{1009}1358 ± 11	^{989}1363 ± 10	^{932}1386 ± 9	^{890}1517 ± 6	^{168}559 ± 31	^{168}539 ± 35
961	realnetworks-008	73346	75421	^{126}402	^{1060}2056 ± 0	^{226}296 ± 3	^{136}294 ± 3	^{140}353 ± 4	^{126}361 ± 5	^{169}485 ± 5	^{162}539 ± 31	^{169}543 ± 29
962	realsense-001	363245	116558	^{720}1995	^{979}2052 ± 0	^{1398}1867 ± 0	^{1108}1845 ± 0	^{1098}1854 ± 0	^{1060}1875 ± 1	^{963}1952 ± 2	^{1206}16252 ± 121	^{1209}16305 ± 100
963	rebs-000	1375350	62664	^{858}2934	^{1221}4096 ± 0	^{621}623 ± 0	^{430}633 ± 10	^{377}626 ± 10	^{321}616 ± 1	^{262}617 ± 0	^{449}1150 ± 1	^{460}1150 ± 2
964	rebs-001	2038561	62673	^{813}2582	^{1289}4100 ± 0	^{843}802 ± 1	^{586}812 ± 8	^{555}829 ± 1	^{488}807 ± 2	^{414}811 ± 4	^{452}1151 ± 8	^{455}1145 ± 4
965	recognito-000	549308	247223	^{974}5903	^{1131}2564 ± 0	^{1112}1086 ± 2	^{816}1096 ± 1	^{786}1102 ± 2	^{743}1142 ± 3	^{687}1219 ± 7	^{35}193 ± 8	^{40}190 ± 16
966	recognito-001	517547	62334	^{914}3833	^{1130}2564 ± 0	^{1105}1072 ± 1	^{805}1089 ± 1	^{781}1095 ± 4	^{711}1112 ± 2	^{681}1205 ± 4	^{31}183 ± 10	^{34}183 ± 7
967	regula-000	262444	29384	^{219}610	^{805}2048 ± 0	^{1190}1187 ± 1	^{839}1126 ± 1	^{808}1129 ± 0	^{733}1132 ± 1	^{653}1159 ± 1	^{147}491 ± 16	^{154}500 ± 22
968	regula-001	256075	25980	^{399}987	^{686}2048 ± 0	^{1260}1284 ± 1	^{917}1220 ± 1	^{881}1222 ± 1	^{816}1226 ± 1	^{718}1255 ± 1	^{101}361 ± 10	^{103}342 ± 25

Notes	
1	The configuration size does not capture static data included in libraries.
2	The library size is the combined total of all files provided in the submission lib folder. These libraries e.g. OpenCV may or may not be installed on any end user's platform natively and would not need to be installed with the algorithm. Some developers put neural network models in their libraries.
3	The memory usage is the peak resident set size reported by the ps system call during template generation.
4	The median template creation times are measured on Intel®Xeon®CPU E5-2630 v4 @ 2.20GHz processors.
5	The comparison durations, in nanoseconds, are estimated using std::chrono::high_resolution_clock which on the machine in (2) counts 1ns clock ticks. Precision is somewhat worse than that however. The ± value is the median absolute deviation times 1.48 for Normal consistency.

Table 43: Summary of algorithms and properties included in this report. The red superscripts give ranking for the quantity in that column.

	ALGORITHM	CONFIG	LIBRARY	TEMPLATE							COMPARISON[4]	
	NAME	DATA	DATA	MEMORY	SIZE	GENERATION TIME (ms)[4]					TIME (ns)[5]	
		(KB)[1]	(KB)[2]	(MB)[3]	(B)	MUGSHOT	480x720	960x1440	1600x2400	3000x4500	GENUINE	IMPOSTOR
969	regula-002	355812	42119	^{438}1066	^{999}2052 ± 0	^{1013}962 ± 0	^{670}918 ± 0	^{618}917 ± 0	^{576}932 ± 0	^{539}1000 ± 1	^{465}1194 ± 14	^{481}1233 ± 53
970	remarkai-000	240152	868276	-	^{455}2048 ± 0	^{875}829 ± 7	-	-	-	-	^{351}873 ± 4	^{349}835 ± 35
971	remarkai-001	241857	868314	^{276}730	^{994}2052 ± 0	^{879}831 ± 6	^{616}849 ± 18	^{746}1055 ± 25	^{788}1198 ± 34	^{891}1519 ± 38	^{475}1229 ± 20	^{340}805 ± 56
972	remarkai-002	224157	808777	-	^{851}2048 ± 0	^{1002}950 ± 6	^{690}935 ± 4	^{653}953 ± 3	^{604}964 ± 4	^{593}1073 ± 4	^{436}1115 ± 25	^{423}1068 ± 54
973	remarkai-003	280516	58559	^{920}3909	^{1276}4100 ± 0	^{1040}986 ± 1	^{745}993 ± 1	^{688}992 ± 1	^{631}999 ± 3	^{551}1019 ± 2	^{321}787 ± 20	^{330}793 ± 22
974	rendip-000	0	437653	^{283}735	^{676}2048 ± 0	^{419}464 ± 2	^{271}458 ± 0	^{247}473 ± 0	^{221}483 ± 1	^{227}556 ± 4	^{176}576 ± 13	^{183}573 ± 11
975	revealmedia-005	293933	202465	^{296}767	^{1286}4100 ± 0	^{383}428 ± 0	^{237}428 ± 0	^{205}430 ± 0	^{178}433 ± 0	^{143}442 ± 0	^{677}2023 ± 38	^{677}2009 ± 26
976	revealmedia-006	293933	200912	^{286}745	^{965}2052 ± 0	^{325}381 ± 0	^{198}381 ± 0	^{166}382 ± 0	^{143}384 ± 0	^{117}394 ± 0	^{224}626 ± 35	^{209}600 ± 2
977	roc-016	0	674869	^{67}191	^{78}392 ± 0	^{525}562 ± 1	^{337}543 ± 2	^{315}553 ± 2	^{281}564 ± 2	^{268}626 ± 2	^{36}194 ± 8	^{27}161 ± 26
978	roc-017	0	565239	^{89}291	^{79}396 ± 0	^{654}651 ± 2	^{449}660 ± 1	^{430}675 ± 1	^{375}669 ± 2	^{352}736 ± 2	^{38}197 ± 4	^{33}178 ± 7
979	roc-018	0	932665	^{148}459	^{202}792 ± 0	^{1223}1231 ± 3	^{924}1227 ± 4	^{910}1253 ± 2	^{828}1243 ± 4	^{754}1308 ± 3	^{48}217 ± 10	^{87}316 ± 14
980	roc-019	0	944816	^{112}360	^{84}444 ± 0	^{1196}1196 ± 4	^{894}1191 ± 5	^{878}1218 ± 6	^{819}1232 ± 4	^{727}1272 ± 5	^{80}306 ± 7	^{69}259 ± 8
981	roc-020	0	1095173	^{117}375	^{83}444 ± 0	^{1400}1906 ± 0	^{1112}1936 ± 0	^{1104}1985 ± 0	^{1074}2030 ± 1	^{979}2112 ± 1	^{201}602 ± 53	^{177}564 ± 22
982	rokid-000	258612	396624	^{507}1218	^{1030}2056 ± 0	^{509}546 ± 3	^{336}542 ± 2	^{310}545 ± 1	^{249}522 ± 3	^{230}563 ± 4	^{900}3457 ± 62	^{910}3463 ± 77
983	rokid-001	641223	413733	^{442}1071	^{1083}2060 ± 0	^{956}911 ± 2	^{657}901 ± 5	^{604}899 ± 2	^{558}900 ± 3	^{476}901 ± 3	^{888}3345 ± 50	^{894}3346 ± 149
984	s1-001	435491	844340	-	^{1103}2092 ± 0	^{590}605 ± 24	^{412}623 ± 20	^{621}920 ± 39	^{1025}1567 ± 92	-	^{526}1428 ± 34	^{526}1415 ± 85
985	s1-002	520163	95479	-	^{1354}6144 ± 0	^{1243}1257 ± 1	^{947}1260 ± 1	^{912}1261 ± 1	^{846}1262 ± 1	^{729}1273 ± 1	^{979}4513 ± 25	^{975}4479 ± 25
986	s1-003	145509	95446	-	^{1229}4096 ± 0	^{996}947 ± 0	^{710}959 ± 0	^{652}952 ± 0	^{592}952 ± 1	^{509}955 ± 1	^{923}3657 ± 19	^{928}3652 ± 16
987	s1-004	246514	202623	-	^{564}2048 ± 0	^{859}815 ± 0	^{589}818 ± 1	^{544}818 ± 1	^{499}820 ± 1	^{424}828 ± 1	^{880}3245 ± 100	^{875}3161 ± 88
988	s1-005	482369	95685	^{477}1146	^{879}2048 ± 0	^{1051}1001 ± 0	^{752}1002 ± 0	^{705}1004 ± 0	^{643}1008 ± 0	^{556}1029 ± 2	^{223}626 ± 74	^{192}589 ± 14
989	s1-006	482372	95681	^{476}1146	^{527}2048 ± 0	^{1005}951 ± 0	^{707}956 ± 0	^{657}957 ± 0	^{602}962 ± 0	^{524}983 ± 0	^{271}696 ± 23	^{285}696 ± 29
990	s1-007	482385	59657	^{475}1144	^{424}2048 ± 0	^{1042}988 ± 1	^{714}965 ± 0	^{666}966 ± 0	^{608}972 ± 0	^{532}991 ± 0	^{244}648 ± 26	^{264}658 ± 25
991	s1-008	786695	102436	^{810}2573	^{504}2048 ± 0	^{842}800 ± 5	^{588}814 ± 3	^{543}818 ± 10	^{491}809 ± 8	^{439}841 ± 3	^{246}651 ± 32	^{258}647 ± 34
992	s1-009	1457134	102436	^{942}4435	^{429}2048 ± 0	^{1209}1213 ± 9	^{922}1224 ± 13	^{889}1230 ± 4	^{833}1251 ± 3	^{720}1258 ± 11	^{229}632 ± 13	^{233}622 ± 2
993	saffe-001	85973	62488	^{54}168	^{289}1280 ± 0	^{205}281 ± 1	-	-	-	-	^{484}1274 ± 19	^{495}1277 ± 26
994	saffe-002	260622	28285	^{347}855	^{624}2048 ± 0	^{861}817 ± 11	^{583}805 ± 15	^{533}809 ± 19	^{495}815 ± 29	^{415}813 ± 23	^{290}717 ± 7	^{301}714 ± 29
995	samsungsds-000	0	307431	-	^{458}2048 ± 0	^{251}316 ± 0	^{156}326 ± 5	^{123}328 ± 4	^{109}327 ± 1	^{85}343 ± 0	^{1255}23722 ± 295	^{1257}23874 ± 305
996	samsungsds-001	1189592	147444	^{922}3922	^{1204}4096 ± 0	^{1147}1140 ± 3	^{858}1145 ± 4	^{978}1344 ± 5	^{919}1366 ± 5	^{887}1514 ± 7	^{1339}51559 ± 773	^{1339}51721 ± 1003
997	samsungsds-002	1040732	147475	^{882}3321	^{1055}2056 ± 0	^{1137}1118 ± 1	^{879}1175 ± 12	^{994}1372 ± 6	^{892}1324 ± 2	^{876}1489 ± 4	^{1306}35803 ± 266	^{1309}36181 ± 674
998	samtech-000	109774	12807	-	^{1047}2056 ± 0	^{185}262 ± 2	-	-	-	-	^{983}4550 ± 26	^{981}4541 ± 28
999	samtech-001	288082	219883	^{215}605	^{1064}2056 ± 0	^{223}294 ± 3	-	-	-	-	^{1096}7694 ± 59	^{1097}7678 ± 91
1000	samtech-002	192220	474779	^{268}714	^{1049}2056 ± 0	^{147}212 ± 0	^{86}212 ± 0	^{70}215 ± 0	^{61}225 ± 0	^{60}285 ± 1	^{1198}15231 ± 50	^{1202}15215 ± 59
1001	scanovate-001	257083	328532	-	^{451}2048 ± 0	^{541}577 ± 24	^{365}577 ± 21	^{387}632 ± 27	^{464}770 ± 28	^{820}1404 ± 32	^{1162}12054 ± 699	^{1182}13795 ± 705
1002	scanovate-002	256986	457227	^{345}850	^{747}2048 ± 0	^{732}696 ± 32	^{511}713 ± 33	^{491}738 ± 28	^{469}779 ± 32	^{664}1172 ± 53	^{854}3021 ± 38	^{867}3120 ± 163
1003	scanovate-003	135585	89469	^{312}805	^{374}2048 ± 0	^{556}585 ± 1	^{396}613 ± 12	^{341}591 ± 1	^{313}610 ± 2	^{310}684 ± 1	^{843}2926 ± 22	^{843}2925 ± 20
1004	sdc-000	256814	481583	^{302}784	^{860}2048 ± 0	^{958}913 ± 14	^{660}906 ± 9	^{822}1142 ± 19	^{1049}1774 ± 45	^{1068}4719 ± 222	^{1295}32645 ± 93	^{1298}32653 ± 112
1005	seamfix-001	429267	86391	^{98}320	^{566}2048 ± 0	^{756}718 ± 8	^{506}707 ± 25	^{647}947 ± 18	^{1014}1521 ± 55	^{1062}4179 ± 226	^{1042}5897 ± 118	^{1042}5867 ± 123
1006	securifai-001	120291	12456	-	^{1296}4104 ± 0	^{144}211 ± 1	^{85}211 ± 1	^{68}211 ± 1	^{54}211 ± 1	^{38}211 ± 1	^{595}1681 ± 29	^{601}1701 ± 25
1007	securifai-002	198824	13496	-	^{268}1032 ± 0	^{63}123 ± 0	^{35}123 ± 0	^{28}123 ± 0	^{24}123 ± 0	^{17}123 ± 0	^{213}615 ± 22	^{205}597 ± 19
1008	securifai-003	303794	13512	-	^{1298}4104 ± 0	^{512}549 ± 7	^{345}550 ± 7	^{312}549 ± 7	^{269}546 ± 6	^{217}546 ± 6	^{604}1714 ± 26	^{604}1713 ± 37
1009	securifai-004	282177	12027	^{233}636	^{884}2048 ± 0	^{912}869 ± 1	^{629}867 ± 1	^{583}867 ± 1	^{534}867 ± 1	^{455}865 ± 1	^{600}1711 ± 19	^{603}1705 ± 29
1010	securifai-005	252532	81777	^{180}526	^{473}2048 ± 0	^{1309}1377 ± 2	^{1007}1355 ± 1	^{984}1353 ± 0	^{910}1357 ± 0	^{789}1356 ± 0	^{646}1873 ± 25	^{644}1847 ± 35
1011	securifai-006	452474	81856	^{299}771	^{1254}4096 ± 0	^{1115}1090 ± 2	^{803}1086 ± 3	^{776}1093 ± 1	^{705}1104 ± 10	^{603}1090 ± 2	^{893}3376 ± 42	^{901}3399 ± 40
1012	securifai-007	94589	88169	^{203}583	^{687}2048 ± 0	^{460}500 ± 0	^{309}506 ± 0	^{269}499 ± 1	^{232}501 ± 1	^{186}505 ± 1	^{550}1484 ± 11	^{556}1483 ± 13

Notes	
1	The configuration size does not capture static data included in libraries.
2	The library size is the combined total of all files provided in the submission lib folder. These libraries e.g. OpenCV may or may not be installed on any end user's platform natively and would not need to be installed with the algorithm. Some developers put neural network models in their libraries.
3	The memory usage is the peak resident set size reported by the ps system call during template generation.
4	The median template creation times are measured on Intel®Xeon®CPU E5-2630 v4 @ 2.20GHz processors.
5	The comparison durations, in nanoseconds, are estimated using std::chrono::high_resolution_clock which on the machine in (2) counts 1ns clock ticks. Precision is somewhat worse than that however. The ± value is the median absolute deviation times 1.48 for Normal consistency.

Table 44: Summary of algorithms and properties included in this report. The red superscripts give ranking for the quantity in that column.

	ALGORITHM	CONFIG	LIBRARY	TEMPLATE						COMPARISON[4]	
	NAME	DATA	DATA	MEMORY	SIZE	GENERATION TIME (ms)[4]				TIME (ns)[5]	
		(KB)[1]	(KB)[2]	(MB)[3]	(B)	MUGSHOT	480x720	960x1440	1600x2400	3000x4500	GENUINE	IMPOSTOR
1013	securifai-008	111759	84658	^{266}711	^{428}2048 ± 0	^{645}641 ± 4	^{440}647 ± 3	^{422}663 ± 3	^{349}645 ± 3	^{289}649 ± 1	^{558}1498 ± 11	^{557}1487 ± 13
1014	sensetime-001	531783	7203	-	^{996}2052 ± 0	^{765}725 ± 3	-	-	-	-	^{780}2546 ± 102	^{747}2371 ± 45
1015	sensetime-002	531783	7203	-	^{967}2052 ± 0	^{836}797 ± 3	-	-	-	-	^{803}2713 ± 90	^{734}2301 ± 25
1016	sensetime-003	787853	74950	-	^{992}2052 ± 0	^{952}908 ± 4	-	-	-	-	^{777}2527 ± 65	^{857}3004 ± 174
1017	sensetime-004	954663	30733	-	^{260}1028 ± 0	^{1350}1437 ± 15	-	-	-	-	^{476}1239 ± 31	^{470}1171 ± 22
1018	sensetime-005	765353	37673	-	^{264}1028 ± 0	^{1300}1361 ± 27	^{978}1304 ± 1	^{959}1319 ± 1	^{912}1360 ± 1	^{888}1514 ± 1	^{472}1223 ± 28	^{471}1184 ± 29
1019	sensetime-006	765353	37673	^{8}33	^{261}1028 ± 0	^{1297}1352 ± 17	^{983}1311 ± 1	^{960}1323 ± 1	^{909}1357 ± 1	^{894}1523 ± 2	^{462}1179 ± 28	^{467}1157 ± 29
1020	sensetime-007	765353	37533	^{976}5950	^{262}1028 ± 0	^{1320}1386 ± 41	^{995}1323 ± 2	^{980}1347 ± 2	^{920}1366 ± 2	^{916}1593 ± 8	^{537}1460 ± 29	^{531}1425 ± 26
1021	sensetime-008	1176483	60067	^{971}5882	^{266}1028 ± 0	^{1374}1479 ± 31	^{1059}1436 ± 4	^{1063}1482 ± 4	^{1017}1525 ± 5	^{931}1669 ± 2	^{489}1283 ± 51	^{482}1240 ± 47
1022	sensetime-010	1175952	62384	^{983}6671	^{265}1028 ± 0	^{1178}1176 ± 36	^{856}1144 ± 2	^{828}1153 ± 9	^{768}1172 ± 6	^{693}1229 ± 7	^{95}351 ± 1	^{90}324 ± 5
1023	sensetime-011	1176053	63554	^{975}5909	^{276}1060 ± 0	^{1384}1531 ± 1	^{1084}1502 ± 0	^{1078}1547 ± 0	^{1012}1508 ± 0	^{915}1586 ± 0	^{152}501 ± 1	^{156}503 ± 2
1024	serendipity-000	0	346443	^{149}462	^{572}2048 ± 0	^{945}900 ± 8	^{656}901 ± 3	^{625}922 ± 2	^{580}936 ± 1	^{527}987 ± 2	^{200}602 ± 1	^{218}607 ± 10
1025	sertis-000	265572	68770	^{135}427	^{609}2048 ± 0	^{791}754 ± 0	^{550}759 ± 0	^{508}764 ± 0	^{456}760 ± 0	^{378}763 ± 0	^{556}1497 ± 29	^{580}1582 ± 38
1026	sertis-001	292591	68831	-	^{419}2048 ± 0	^{638}634 ± 1	-	-	-	-	^{763}2449 ± 23	^{805}2685 ± 41
1027	sertis-002	460790	68929	^{245}660	^{574}2048 ± 0	^{1187}1181 ± 1	^{881}1178 ± 0	^{853}1183 ± 0	^{785}1187 ± 0	^{689}1221 ± 0	^{426}1086 ± 32	^{427}1076 ± 31
1028	sertis-003	0	451507	^{715}1965	^{552}2048 ± 0	^{398}441 ± 0	^{249}436 ± 2	^{237}461 ± 2	^{204}463 ± 1	^{163}473 ± 4	^{366}915 ± 10	^{373}917 ± 8
1029	seventhsense-000	369850	1561668	-	^{991}2052 ± 0	^{1239}1250 ± 3	^{945}1257 ± 1	^{914}1261 ± 1	^{843}1259 ± 1	^{728}1272 ± 2	^{630}1800 ± 35	^{628}1787 ± 32
1030	seventhsense-001	369850	3183365	^{317}812	^{960}2052 ± 0	^{1241}1255 ± 2	^{971}1294 ± 15	^{928}1277 ± 3	^{857}1275 ± 2	^{739}1288 ± 3	^{664}1936 ± 26	^{668}1943 ± 34
1031	seventhsense-002	452197	1567903	^{384}944	^{971}2052 ± 0	^{1240}1252 ± 1	^{956}1271 ± 1	^{920}1269 ± 1	^{852}1272 ± 1	^{741}1290 ± 1	^{699}2131 ± 45	^{697}2123 ± 45
1032	seventhsense-003	603091	453847	^{455}1090	^{982}2052 ± 0	^{1053}1003 ± 2	^{728}977 ± 0	^{554}828 ± 1	^{497}817 ± 1	^{421}826 ± 2	^{564}1523 ± 25	^{569}1530 ± 22
1033	seventhsense-005	4000865	453775	^{812}2581	^{1270}4100 ± 0	^{1139}1119 ± 1	^{833}1120 ± 1	^{814}1134 ± 4	^{732}1131 ± 2	^{643}1144 ± 1	^{817}2787 ± 28	^{819}2777 ± 22
1034	seventhsense-006	1444389	451757	^{811}2573	^{1285}4100 ± 0	^{1167}1162 ± 1	^{870}1161 ± 2	^{832}1158 ± 2	^{751}1156 ± 0	^{668}1182 ± 2	^{807}2724 ± 16	^{809}2728 ± 16
1035	shaman-000	0	120033	^{169}507	^{1170}4096 ± 0	^{660}653 ± 16	-	-	-	-	^{109}380 ± 25	^{115}379 ± 31
1036	shaman-001	0	174446	^{175}511	^{1190}4096 ± 0	^{221}294 ± 2	-	-	-	-	^{234}635 ± 19	^{130}441 ± 25
1037	shu-001	329513	62157	-	^{475}2048 ± 0	^{599}612 ± 5	-	-	-	-	^{791}2619 ± 19	^{854}2987 ± 143
1038	shu-002	731250	148309	^{366}890	^{1207}4096 ± 0	^{788}751 ± 2	^{557}769 ± 4	^{627}922 ± 4	^{973}1431 ± 9	^{1050}3489 ± 47	^{1410}2930763 ± 47355	^{1410}2929759 ± 39149
1039	shu-003	428774	146940	^{174}511	^{798}2048 ± 0	^{865}820 ± 6	^{601}828 ± 3	^{640}941 ± 9	^{880}1308 ± 15	^{1039}3045 ± 44	^{776}2506 ± 26	^{780}2512 ± 38
1040	shufti-001	442529	2108442	^{710}1941	^{981}2052 ± 0	^{713}687 ± 0	^{487}694 ± 0	^{547}824 ± 1	^{807}1216 ± 4	^{1032}2875 ± 1	^{865}3133 ± 19	^{872}3153 ± 54
1041	siat-002	486842	7738	^{785}2434	^{986}2052 ± 0	^{545}579 ± 0	-	-	-	-	^{315}769 ± 13	^{316}750 ± 13
1042	siat-004	940063	6984	-	^{1272}4100 ± 0	^{681}670 ± 0	^{459}671 ± 7	^{448}693 ± 10	^{444}742 ± 10	^{495}935 ± 17	^{955}4013 ± 45	^{940}3782 ± 173
1043	siat-005	380936	16935	^{536}1299	^{448}2048 ± 0	^{352}403 ± 0	^{220}400 ± 0	^{178}401 ± 0	^{162}403 ± 1	^{134}422 ± 7	^{177}577 ± 13	^{186}580 ± 17
1044	sightropic-000	355144	205017	^{341}847	^{673}2048 ± 0	^{475}515 ± 0	^{323}524 ± 0	^{287}519 ± 0	^{245}516 ± 0	^{216}544 ± 0	^{1135}10207 ± 35	^{1136}10214 ± 59
1045	sightropic-001	765429	490992	^{959}4914	^{1062}2056 ± 0	^{1142}1134 ± 0	^{991}1321 ± 6	^{818}1140 ± 1	^{738}1136 ± 2	^{656}1162 ± 6	^{1239}21280 ± 192	^{1242}21306 ± 176
1046	sjtu-001	347115	148322	-	^{627}2048 ± 0	^{652}650 ± 2	-	-	-	-	^{1409}2243804 ± 12751	^{1409}2249915 ± 19380
1047	sjtu-002	446215	148306	-	^{698}2048 ± 0	^{884}835 ± 2	-	-	-	-	^{1408}2211198 ± 26052	^{1408}2210428 ± 21877
1048	sjtu-003	480795	148243	^{188}539	^{568}2048 ± 0	^{868}821 ± 2	^{590}820 ± 2	^{628}923 ± 3	^{791}1201 ± 3	^{1006}2373 ± 9	^{572}1560 ± 20	^{574}1560 ± 14
1049	sjtu-004	1953267	241108	^{835}2741	^{1330}4608 ± 0	^{1226}1236 ± 2	^{909}1209 ± 2	^{945}1294 ± 4	^{1020}1554 ± 5	^{1029}2738 ± 8	^{858}3057 ± 14	^{865}3070 ± 20
1050	sjtu-005	1953267	241151	^{833}2734	^{1337}4608 ± 0	^{581}601 ± 1	^{404}617 ± 1	^{477}724 ± 2	^{728}1127 ± 3	^{1031}2855 ± 11	^{837}2898 ± 4	^{840}2900 ± 4
1051	sjtu-006	2685387	241394	^{868}3071	^{1340}4608 ± 0	^{657}651 ± 1	^{461}672 ± 4	^{521}788 ± 9	^{610}979 ± 2	^{594}1074 ± 7	^{836}2897 ± 4	^{838}2896 ± 4
1052	sjtu-007	1126310	244296	^{841}2759	^{1338}4608 ± 0	^{960}914 ± 12	^{708}956 ± 12	^{849}1181 ± 37	^{1039}1707 ± 169	^{980}2118 ± 191	^{841}2903 ± 14	^{842}2902 ± 11
1053	sjtu-008	1451928	245324	^{864}2997	^{1339}4608 ± 0	^{1396}1832 ± 1	^{1107}1836 ± 2	^{1096}1835 ± 0	^{1055}1839 ± 1	^{957}1877 ± 1	^{984}4621 ± 10	^{984}4619 ± 25
1054	sjtu-009	894841	245301	^{863}2997	^{1341}4608 ± 0	^{1397}1832 ± 0	^{1109}1845 ± 1	^{1097}1846 ± 1	^{1056}1846 ± 1	^{956}1874 ± 2	^{929}3688 ± 17	^{932}3694 ± 11
1055	sktelecom-000	527132	298496	^{542}1321	^{300}1536 ± 0	^{1130}1110 ± 1	^{828}1113 ± 1	^{796}1114 ± 1	^{718}1120 ± 1	^{650}1155 ± 1	^{1275}26583 ± 128	^{1274}26508 ± 126
1056	smargtech-001	164944	16729	^{255}683	^{699}2048 ± 0	^{1391}1664 ± 6	^{1098}1659 ± 3	^{1089}1717 ± 11	^{1057}1847 ± 31	^{1007}2375 ± 105	^{899}3448 ± 10	^{913}3492 ± 17

Notes	
1	The configuration size does not capture static data included in libraries.
2	The library size is the combined total of all files provided in the submission lib folder. These libraries e.g. OpenCV may or may not be installed on any end user's platform natively and would not need to be installed with the algorithm. Some developers put neural network models in their libraries.
3	The memory usage is the peak resident set size reported by the ps system call during template generation.
4	The median template creation times are measured on Intel®Xeon®CPU E5-2630 v4 @ 2.20GHz processors.
5	The comparison durations, in nanoseconds, are estimated using std::chrono::high_resolution_clock which on the machine in (2) counts 1ns clock ticks. Precision is somewhat worse than that however. The ± value is the median absolute deviation times 1.48 for Normal consistency.

Table 45: Summary of algorithms and properties included in this report. The red superscripts give ranking for the quantity in that column.

	ALGORITHM	CONFIG	LIBRARY	TEMPLATE							COMPARISON[4]	
	NAME	DATA	DATA	MEMORY	SIZE	GENERATION TIME (ms)[4]					TIME (ns)[5]	
		(KB)[1]	(KB)[2]	(MB)[3]	(B)	MUGSHOT	480x720	960x1440	1600x2400	3000x4500	GENUINE	IMPOSTOR
1057	smartbiometrik-001	30875	92620	^{15}72	^{147}512 ± 0	^{618}620 ± 7	^{417}625 ± 7	^{400}640 ± 4	^{431}728 ± 6	^{567}1047 ± 8	^{275}703 ± 31	^{296}710 ± 40
1058	smartengines-000	1711	3025	^{10}50	^{67}288 ± 0	^{94}168 ± 7	^{58}180 ± 1	^{52}188 ± 3	^{56}217 ± 3	^{59}275 ± 1	^{37}197 ± 5	^{28}167 ± 11
1059	smartengines-001	7095	4601	^{9}47	^{66}288 ± 0	^{270}333 ± 89	^{225}408 ± 1	^{199}423 ± 1	^{197}460 ± 2	^{222}553 ± 5	^{25}153 ± 11	^{23}143 ± 13
1060	smartvist-000	5959	134084	^{56}169	^{148}512 ± 0	^{19}59 ± 0	^{13}56 ± 0	^{7}56 ± 0	^{7}58 ± 0	^{11}90 ± 1	^{530}1435 ± 31	^{530}1422 ± 48
1061	smartvist-001	349219	25644	^{368}904	^{368}2048 ± 0	^{313}370 ± 0	^{195}374 ± 0	^{160}377 ± 1	^{170}422 ± 0	^{147}445 ± 0	^{822}2835 ± 99	^{828}2836 ± 80
1062	smilart-001	67339	45737	-	^{114}512 ± 0	^{158}230 ± 11	-	-	-	-	^{508}1371 ± 29	^{514}1356 ± 57
1063	smilart-002	111826	87805	^{80}263	^{217}1024 ± 0	^{102}176 ± 16	-	-	-	-	^{1225}18784 ± 136	^{1229}18795 ± 151
1064	smilart-003	67339	91670	^{68}192	^{103}512 ± 0	^{107}180 ± 12	^{61}181 ± 10	^{113}313 ± 22	^{368}665 ± 49	^{1000}2299 ± 196	^{514}1395 ± 74	^{405}1027 ± 66
1065	sodec-000	836592	13142	^{856}2902	^{1220}4096 ± 0	^{1087}1041 ± 2	^{773}1032 ± 1	^{731}1035 ± 1	^{659}1037 ± 2	^{584}1061 ± 2	^{625}1794 ± 37	^{625}1775 ± 23
1066	sparktek-000	2050067	115114	^{1006}9564	^{1205}4096 ± 0	^{1390}1656 ± 0	^{1099}1661 ± 0	^{1087}1671 ± 0	^{1034}1657 ± 0	^{929}1662 ± 0	^{149}495 ± 11	^{184}577 ± 32
1067	sparsh-001	0	366290	^{944}4525	^{695}2048 ± 0	^{702}680 ± 2	^{441}648 ± 1	^{398}638 ± 0	^{347}642 ± 0	^{336}717 ± 0	^{1126}9600 ± 275	^{1125}9601 ± 290
1068	sqisoft-001	278968	386291	^{259}689	^{1014}2056 ± 0	^{435}477 ± 5	^{1005}1348 ± 18	^{985}1353 ± 26	^{899}1340 ± 14	^{815}1393 ± 28	^{328}797 ± 22	^{327}788 ± 22
1069	sqisoft-002	278039	386291	^{251}675	^{1041}2056 ± 0	^{422}466 ± 8	^{276}466 ± 2	^{243}468 ± 11	^{200}461 ± 6	^{162}472 ± 4	^{309}758 ± 11	^{318}760 ± 23
1070	sqisoft-003	362737	607964	^{316}812	^{1032}2056 ± 0	^{643}638 ± 2	^{467}674 ± 7	^{472}718 ± 17	^{370}665 ± 6	^{340}720 ± 6	^{344}844 ± 11	^{351}844 ± 23
1071	staqu-000	879661	624676	^{437}1064	^{1163}4096 ± 0	^{855}813 ± 25	-	-	-	-	^{848}2979 ± 31	^{859}3007 ± 75
1072	starhybrid-001	100509	289356	^{338}845	^{584}2048 ± 0	^{296}358 ± 82	^{176}355 ± 49	^{164}379 ± 58	^{159}401 ± 79	^{114}393 ± 67	^{421}1075 ± 51	^{428}1078 ± 53
1073	stcon-000	408095	49619	^{472}1137	^{257}1024 ± 0	^{614}617 ± 1	^{428}632 ± 4	^{393}634 ± 1	^{350}645 ± 2	^{307}676 ± 6	^{122}437 ± 10	^{127}434 ± 11
1074	stcon-001	322871	64463	^{350}860	^{235}1024 ± 0	^{1035}980 ± 1	^{742}991 ± 1	^{696}995 ± 5	^{637}1003 ± 6	^{563}1042 ± 4	^{88}336 ± 14	^{98}334 ± 14
1075	stcon-002	1255490	62667	^{737}2095	^{1196}4096 ± 0	^{551}583 ± 0	^{361}570 ± 2	^{327}574 ± 2	^{290}582 ± 1	^{269}630 ± 0	^{445}1143 ± 2	^{452}1142 ± 4
1076	stcon-003	2119710	62673	^{916}3862	^{1282}4100 ± 0	^{872}823 ± 0	^{591}821 ± 1	^{558}831 ± 3	^{501}823 ± 1	^{438}838 ± 2	^{451}1151 ± 5	^{468}1157 ± 5
1077	stcon-004	2831397	64930	^{912}3781	^{1007}2052 ± 0	^{1306}1375 ± 1	^{1018}1384 ± 4	^{981}1348 ± 1	^{917}1365 ± 10	^{800}1375 ± 8	^{182}591 ± 4	^{191}589 ± 1
1078	stcon-005	3126319	50632	^{890}3424	^{1288}4100 ± 0	^{1331}1401 ± 2	^{1045}1415 ± 8	^{1014}1400 ± 10	^{975}1435 ± 1	^{807}1382 ± 1	^{463}1181 ± 31	^{469}1162 ± 5
1079	stcon-006	3126319	50636	^{891}3426	^{1278}4100 ± 0	^{1315}1384 ± 1	^{1051}1426 ± 3	^{1025}1410 ± 1	^{961}1419 ± 21	^{825}1412 ± 7	^{447}1148 ± 1	^{458}1148 ± 1
1080	stcon-007	3126319	50636	^{889}3413	^{1274}4100 ± 0	^{1348}1431 ± 1	^{1052}1427 ± 9	^{1071}1503 ± 8	^{954}1406 ± 7	^{865}1473 ± 1	^{458}1163 ± 10	^{472}1185 ± 32
1081	stcon-008	2124613	56551	^{807}2552	^{1281}4100 ± 0	^{1386}1558 ± 0	^{1091}1564 ± 0	^{1082}1560 ± 0	^{1023}1565 ± 0	^{907}1561 ± 0	^{555}1497 ± 14	^{563}1505 ± 11
1082	stengg-000	361104	34674	^{274}724	^{341}2048 ± 0	^{849}809 ± 1	^{674}921 ± 2	^{703}1002 ± 1	^{481}794 ± 1	^{983}2130 ± 5	^{673}2005 ± 22	^{678}2011 ± 34
1083	sukshi-000	94035	688738	^{119}382	^{1408}32768 ± 0	^{358}407 ± 11	^{227}413 ± 8	^{274}504 ± 8	^{393}689 ± 11	^{911}1574 ± 28	^{1131}9817 ± 50	^{1130}9787 ± 62
1084	sumsub-000	1120840	252	^{443}1074	^{585}2048 ± 0	^{1404}1947 ± 1	^{1113}1947 ± 0	^{1102}1947 ± 1	^{1070}1950 ± 1	^{964}1958 ± 0	^{1369}69114 ± 201	^{1367}69212 ± 246
1085	suprema-000	246761	38507	-	^{346}2048 ± 0	^{808}771 ± 2	^{566}778 ± 1	^{581}864 ± 2	^{709}1109 ± 2	^{986}2150 ± 4	^{597}1690 ± 17	^{597}1688 ± 13
1086	suprema-001	373423	41460	-	^{668}2048 ± 0	^{826}788 ± 1	^{595}826 ± 2	^{614}914 ± 2	^{746}1146 ± 7	^{1014}2443 ± 4	^{874}3212 ± 16	^{883}3220 ± 22
1087	suprema-002	373808	41473	^{662}1733	^{939}2048 ± 0	^{825}787 ± 3	^{606}833 ± 3	^{629}924 ± 4	^{781}1185 ± 6	^{1016}2479 ± 3	^{883}3255 ± 17	^{888}3253 ± 14
1088	suprema-003	498231	116054	^{511}1244	^{819}2048 ± 0	^{1357}1448 ± 1	^{1047}1417 ± 4	^{1030}1418 ± 3	^{965}1421 ± 4	^{855}1451 ± 5	^{711}2201 ± 10	^{711}2198 ± 13
1089	suprema-004	1430475	116085	^{870}3096	^{1236}4096 ± 0	^{1373}1478 ± 2	^{1074}1472 ± 2	^{1059}1469 ± 1	^{998}1476 ± 1	^{880}1496 ± 1	^{873}3201 ± 14	^{879}3202 ± 22
1090	suprema-005	1430177	116089	^{869}3093	^{1165}4096 ± 0	^{832}794 ± 1	^{627}863 ± 1	^{532}808 ± 5	^{545}883 ± 1	^{426}830 ± 5	^{951}3950 ± 7	^{956}3948 ± 4
1091	supremaid-001	258193	23479	^{189}541	^{454}2048 ± 0	^{437}479 ± 1	^{287}481 ± 0	^{252}481 ± 0	^{224}490 ± 0	^{204}522 ± 0	^{278}704 ± 19	^{262}652 ± 19
1092	supremaid-002	256273	23899	^{103}334	^{734}2048 ± 0	^{444}483 ± 0	^{305}501 ± 0	^{260}488 ± 0	^{234}503 ± 0	^{232}565 ± 0	^{672}1990 ± 19	^{660}1923 ± 29
1093	surrey-cvssp-000	158030	70795	^{356}879	^{898}2048 ± 0	^{1149}1141 ± 3	^{866}1157 ± 3	^{830}1158 ± 4	^{758}1163 ± 3	^{705}1245 ± 3	^{1123}9557 ± 143	^{1126}9602 ± 186
1094	surrey-cvssp-001	900280	76392	^{652}1705	^{604}2048 ± 0	^{1215}1221 ± 1	^{933}1238 ± 2	^{894}1240 ± 0	^{830}1243 ± 0	^{719}1257 ± 0	^{1228}18970 ± 161	^{1231}18999 ± 176
1095	surrey-cvssp-002	903493	87776	^{656}1720	^{488}2048 ± 0	^{1208}1213 ± 1	^{911}1211 ± 1	^{929}1279 ± 0	^{864}1282 ± 0	^{748}1300 ± 0	^{1133}9906 ± 120	^{1133}9911 ± 167
1096	surrey-cvssp-003	1013099	109557	^{759}2208	^{405}2048 ± 0	^{827}789 ± 1	^{614}846 ± 1	^{577}854 ± 1	^{822}1234 ± 2	^{1045}3283 ± 3	^{1089}7358 ± 130	^{1087}7336 ± 93
1097	surrey-cvssp-004	1142444	108961	^{758}2203	^{748}2048 ± 0	^{783}747 ± 1	^{1092}1568 ± 2	^{1124}4350 ± 12	^{1123}11245 ± 7	-	^{1098}7794 ± 109	^{1098}7738 ± 118
1098	swsam-001	265887	95072	^{237}642	^{395}2048 ± 0	^{1096}1058 ± 34	^{797}1079 ± 31	^{775}1091 ± 35	^{686}1076 ± 9	^{612}1109 ± 45	^{840}2902 ± 31	^{837}2892 ± 32
1099	synesis-000	340264	76158	-	^{124}512 ± 0	^{56}117 ± 0	-	-	-	-	^{316}775 ± 206	^{181}568 ± 48
1100	synesis-001	340264	78195	-	^{90}512 ± 0	^{61}122 ± 0	-	-	-	-	^{342}828 ± 182	^{286}698 ± 44

Notes	
1	The configuration size does not capture static data included in libraries.
2	The library size is the combined total of all files provided in the submission lib folder. These libraries e.g. OpenCV may or may not be installed on any end user's platform natively and would not need to be installed with the algorithm. Some developers put neural network models in their libraries.
3	The memory usage is the peak resident set size reported by the ps system call during template generation.
4	The median template creation times are measured on Intel®Xeon®CPU E5-2630 v4 @ 2.20GHz processors.
5	The comparison durations, in nanoseconds, are estimated using std::chrono::high_resolution_clock which on the machine in (2) counts 1ns clock ticks. Precision is somewhat worse than that however. The ± value is the median absolute deviation times 1.48 for Normal consistency.

Table 46: Summary of algorithms and properties included in this report. The red superscripts give ranking for the quantity in that column.

	ALGORITHM	CONFIG	LIBRARY	TEMPLATE							COMPARISON[4]	
	NAME	DATA	DATA	MEMORY	SIZE	GENERATION TIME (ms)[4]					TIME (ns)[5]	
		(KB)[1]	(KB)[2]	(MB)[3]	(B)	MUGSHOT	480x720	960x1440	1600x2400	3000x4500	GENUINE	IMPOSTOR
1101	synesis-003	256748	155901	-	^{1194}4096 ± 0	^{34}90 ± 0	-	-	-	-	^{1084}7118 ± 121	^{1083}7162 ± 100
1102	synesis-004	270628	16252	-	^{425}2048 ± 0	^{774}735 ± 15	-	-	-	-	^{117}424 ± 14	^{125}430 ± 22
1103	synesis-005	146509	17726	-	^{697}2048 ± 0	^{146}211 ± 9	-	-	-	-	^{193}599 ± 23	^{187}581 ± 32
1104	synesis-006	731941	21817	^{590}1472	^{1300}4104 ± 0	^{513}549 ± 1	^{341}546 ± 1	^{314}552 ± 1	^{277}558 ± 2	^{280}639 ± 28	^{272}697 ± 32	^{282}688 ± 31
1105	synesis-007	1442961	24145	^{788}2443	^{1146}3080 ± 0	^{1210}1215 ± 5	^{952}1268 ± 30	^{950}1306 ± 67	^{881}1311 ± 58	^{834}1423 ± 52	^{263}684 ± 32	^{279}686 ± 25
1106	synology-000	221021	25809	^{145}453	^{512}2048 ± 0	^{356}407 ± 14	^{228}415 ± 14	^{449}694 ± 31	^{942}1396 ± 58	^{1064}4568 ± 211	^{1232}19720 ± 203	^{1234}19767 ± 379
1107	synology-001	256895	25804	-	^{827}2048 ± 0	^{988}942 ± 21	-	-	-	-	^{520}1402 ± 29	^{614}1730 ± 220
1108	synology-002	256713	25943	^{161}488	^{710}2048 ± 0	^{940}886 ± 4	^{651}892 ± 3	^{622}920 ± 2	^{632}1000 ± 5	^{761}1317 ± 12	^{540}1466 ± 32	^{561}1496 ± 45
1109	syscake-000	50022	12609	^{61}184	^{8}128 ± 0	^{169}243 ± 1	^{103}245 ± 0	^{81}241 ± 1	^{77}269 ± 0	^{92}357 ± 1	^{32}185 ± 1	^{35}185 ± 1
1110	szpu-000	283522	15225	^{821}2660	^{781}2048 ± 0	^{118}190 ± 1	^{75}192 ± 1	^{86}259 ± 6	^{181}438 ± 11	^{680}1204 ± 32	^{956}4026 ± 57	^{961}4021 ± 56
1111	sztu-000	338637	15871	^{535}1298	^{501}2048 ± 0	^{489}531 ± 0	^{328}532 ± 0	^{296}533 ± 0	^{260}537 ± 0	^{220}548 ± 0	^{180}585 ± 11	^{196}592 ± 13
1112	sztu-001	338650	15871	^{537}1299	^{463}2048 ± 0	^{494}535 ± 0	^{331}537 ± 0	^{302}538 ± 0	^{261}540 ± 0	^{223}553 ± 0	^{195}599 ± 10	^{207}598 ± 10
1113	t4isb-000	234227	115237	^{107}345	^{394}2048 ± 0	^{1056}1006 ± 5	^{751}1001 ± 1	^{709}1006 ± 1	^{645}1009 ± 1	^{553}1022 ± 2	^{920}3586 ± 34	^{921}3534 ± 34
1114	tahakom-001	198869	724103	^{201}581	^{894}2048 ± 0	^{231}302 ± 2	^{125}277 ± 3	^{149}364 ± 7	^{133}368 ± 4	^{112}389 ± 4	^{750}2387 ± 28	^{750}2381 ± 22
1115	taiwanmobile-001	170523	1947147	^{198}570	^{1127}2560 ± 0	^{546}579 ± 8	^{563}775 ± 16	^{437}683 ± 4	^{424}718 ± 8	^{396}781 ± 6	^{1312}38086 ± 62	^{1314}38109 ± 66
1116	taiwanmobile-002	170523	1969728	^{90}295	^{754}2048 ± 0	^{85}156 ± 0	^{47}162 ± 0	^{94}281 ± 0	^{271}549 ± 3	^{966}1978 ± 21	^{1344}55746 ± 469	^{1342}55598 ± 410
1117	tcc-000	54057	1188952	^{96}318	^{218}1024 ± 0	^{317}375 ± 93	^{184}363 ± 76	^{630}924 ± 279	^{1093}2339 ± 806	^{1096}9265 ± 3411	^{404}1053 ± 38	^{422}1064 ± 23
1118	tcv-001	171624	816225	^{113}363	^{592}2048 ± 0	^{42}98 ± 0	^{23}98 ± 0	^{20}99 ± 0	^{17}100 ± 0	^{16}122 ± 0	^{418}1070 ± 31	^{413}1045 ± 17
1119	tech5-000	1451185	470097	-	^{247}1024 ± 0	^{455}498 ± 4	-	-	-	-	^{313}763 ± 23	^{321}766 ± 28
1120	tech5-001	636346	470101	-	^{1179}4096 ± 0	^{480}522 ± 5	-	-	-	-	^{427}1087 ± 34	^{333}799 ± 44
1121	tech5-002	1150887	111744	-	^{287}1280 ± 0	^{814}780 ± 10	-	-	-	-	^{523}1406 ± 120	^{415}1048 ± 57
1122	tech5-003	1427464	118901	-	^{299}1536 ± 0	^{936}885 ± 20	-	-	-	-	^{453}1151 ± 37	^{448}1128 ± 32
1123	tech5-004	2410272	118858	-	^{72}321 ± 0	^{920}872 ± 2	^{831}1117 ± 164	^{798}1114 ± 182	^{735}1134 ± 179	^{538}999 ± 44	^{187}597 ± 13	^{197}592 ± 16
1124	tech5-005	1178769	120517	^{577}1426	^{128}512 ± 0	^{1251}1272 ± 109	^{777}1038 ± 63	^{741}1046 ± 39	^{721}1124 ± 38	^{786}1351 ± 44	^{785}2573 ± 37	^{786}2545 ± 32
1125	tech5-007	0	340324	^{818}2647	^{91}512 ± 0	^{1299}1360 ± 0	^{1011}1366 ± 0	^{997}1376 ± 0	^{926}1373 ± 0	^{847}1438 ± 6	^{161}538 ± 19	^{158}516 ± 22
1126	tech5-008	0	365877	^{969}5567	^{830}2048 ± 0	^{664}655 ± 3	^{414}624 ± 11	^{375}625 ± 11	^{336}631 ± 11	^{330}710 ± 12	^{1090}7371 ± 81	^{1088}7367 ± 99
1127	tech5-009	0	361983	^{793}2453	^{635}2048 ± 0	^{1079}1029 ± 25	^{740}988 ± 21	^{724}1028 ± 23	^{641}1006 ± 20	^{613}1111 ± 22	^{1094}7478 ± 131	^{1093}7464 ± 120
1128	techainer-001	198738	703687	^{719}1977	^{853}2048 ± 0	^{326}381 ± 9	^{210}391 ± 5	^{179}402 ± 5	^{151}391 ± 1	^{155}461 ± 5	^{1144}10726 ± 189	^{1145}10714 ± 243
1129	techainer-002	286340	1013105	^{532}1293	^{1183}4096 ± 0	^{380}427 ± 2	^{239}429 ± 4	^{200}424 ± 1	^{182}438 ± 11	^{187}506 ± 6	^{542}1472 ± 10	^{546}1462 ± 16
1130	techbiometricid-001	172553	886937	^{134}427	^{824}2048 ± 0	^{151}218 ± 8	^{96}226 ± 6	^{229}455 ± 19	^{654}1023 ± 36	^{1052}3669 ± 176	^{1353}59682 ± 512	^{1353}61123 ± 662
1131	techbiometricid-002	601291	465337	^{140}439	^{641}2048 ± 0	^{507}543 ± 5	^{334}541 ± 4	^{313}552 ± 5	^{296}586 ± 5	^{380}764 ± 20	^{1207}16395 ± 120	^{1210}16374 ± 124
1132	techsign-000	0	1101622	^{717}1969	^{422}2048 ± 0	^{307}366 ± 1	^{217}398 ± 1	^{843}1172 ± 3	^{1111}3065 ± 18	^{1106}10460 ± 65	^{990}4758 ± 112	^{994}4789 ± 93
1133	techsign-001	0	586983	^{701}1881	^{738}2048 ± 0	^{811}772 ± 35	^{569}788 ± 23	^{530}802 ± 42	^{590}949 ± 10	^{822}1409 ± 26	^{184}592 ± 11	^{198}592 ± 13
1134	telexper-000	266638	74277	^{227}625	^{536}2048 ± 0	^{557}586 ± 1	^{364}576 ± 0	^{342}592 ± 1	^{345}639 ± 0	^{466}886 ± 0	^{1029}5559 ± 54	^{1027}5553 ± 47
1135	tevian-000	455746	16296	-	^{358}2048 ± 0	^{167}242 ± 14	-	-	-	-	^{119}430 ± 38	^{124}427 ± 23
1136	tevian-001	682319	16344	-	^{543}2048 ± 0	^{172}245 ± 13	-	-	-	-	^{94}350 ± 22	^{94}327 ± 13
1137	tevian-002	724437	16352	-	^{943}2049 ± 0	^{227}298 ± 15	-	-	-	-	^{105}369 ± 16	^{118}386 ± 25
1138	tevian-003	791725	16348	-	^{944}2049 ± 0	^{353}404 ± 15	-	-	-	-	^{93}350 ± 11	^{101}338 ± 25
1139	tevian-004	863474	16544	-	^{643}2048 ± 0	^{465}506 ± 30	-	-	-	-	^{136}474 ± 31	^{93}326 ± 20
1140	tevian-005	921043	16556	-	^{936}2048 ± 0	^{635}633 ± 21	^{464}672 ± 25	^{545}818 ± 37	^{713}1117 ± 64	^{1004}2364 ± 121	^{174}568 ± 22	^{219}607 ± 35
1141	tevian-006	692492	19339	-	^{772}2048 ± 0	^{597}611 ± 1	^{454}666 ± 41	^{417}661 ± 32	^{376}672 ± 37	^{346}723 ± 31	^{181}591 ± 19	^{182}573 ± 28
1142	tevian-007	779934	19523	^{654}1712	^{267}1032 ± 0	^{553}583 ± 1	^{368}579 ± 0	^{334}580 ± 0	^{299}588 ± 1	^{276}636 ± 0	^{1001}4894 ± 65	^{1000}4841 ± 83
1143	tevian-008	847177	19519	^{901}3610	^{269}1032 ± 0	^{935}884 ± 2	^{659}903 ± 1	^{608}903 ± 1	^{562}911 ± 1	^{501}946 ± 1	^{996}4828 ± 40	^{997}4811 ± 41
1144	tiger-001	171041	102515	-	^{1395}8632 ± 0	^{244}312 ± 12	-	-	-	-	^{1387}98339 ± 34	^{1387}98327 ± 32

Notes	
1	The configuration size does not capture static data included in libraries.
2	The library size is the combined total of all files provided in the submission lib folder. These libraries e.g. OpenCV may or may not be installed on any end user's platform natively and would not need to be installed with the algorithm. Some developers put neural network models in their libraries.
3	The memory usage is the peak resident set size reported by the ps system call during template generation.
4	The median template creation times are measured on Intel®Xeon®CPU E5-2630 v4 @ 2.20GHz processors.
5	The comparison durations, in nanoseconds, are estimated using std::chrono::high_resolution_clock which on the machine in (2) counts 1ns clock ticks. Precision is somewhat worse than that however. The ± value is the median absolute deviation times 1.48 for Normal consistency.

Table 47: Summary of algorithms and properties included in this report. The red superscripts give ranking for the quantity in that column.

	ALGORITHM	CONFIG	LIBRARY	TEMPLATE						COMPARISON[4]	
	NAME	DATA	DATA	MEMORY	SIZE	GENERATION TIME (ms)[4]				TIME (ns)[5]	
		(KB)[1]	(KB)[2]	(MB)[3]	(B)	MUGSHOT	480x720	960x1440	1600x2400	3000x4500	GENUINE	IMPOSTOR
1145	tiger-002	341638	178194	-	^{1035}2056 ± 0	^{341}393 ± 20	-	-	-	-	^{700}2135 ± 29	^{702}2137 ± 38
1146	tiger-003	426164	560292	-	^{1053}2056 ± 0	^{414}458 ± 21	-	-	-	-	^{678}2031 ± 35	^{680}2029 ± 38
1147	tiger-004	342866	253683	-	^{1006}2052 ± 0	^{840}798 ± 2	-	-	-	-	^{186}595 ± 5	^{208}598 ± 7
1148	tiger-005	342866	253734	^{603}1532	^{1000}2052 ± 0	^{1117}1097 ± 2	^{791}1065 ± 2	^{761}1066 ± 2	^{678}1067 ± 3	^{598}1088 ± 3	^{217}620 ± 19	^{229}615 ± 16
1149	tiger-006	421186	394688	^{267}714	^{976}2052 ± 0	^{1323}1392 ± 16	^{1042}1411 ± 10	^{1041}1444 ± 10	^{1018}1531 ± 11	^{953}1848 ± 10	^{635}1810 ± 20	^{636}1801 ± 13
1150	tiger-007	516470	192057	^{246}661	^{973}2052 ± 0	^{410}455 ± 1	^{275}464 ± 2	^{238}464 ± 3	^{213}472 ± 4	^{210}537 ± 1	^{399}1033 ± 8	^{410}1037 ± 19
1151	tinkoff-001	274660	389272	^{223}616	^{469}2048 ± 0	^{1177}1176 ± 3	^{882}1179 ± 3	^{847}1178 ± 3	^{765}1169 ± 2	^{678}1203 ± 3	^{971}4361 ± 74	^{970}4364 ± 75
1152	tngd-001	73167	519258	^{196}560	^{1001}2052 ± 0	^{100}175 ± 0	^{70}190 ± 0	^{182}404 ± 0	^{198}460 ± 1	^{136}432 ± 0	^{727}2274 ± 29	^{726}2265 ± 20
1153	tngd-002	134027	35925	^{335}843	^{460}2048 ± 0	^{729}694 ± 0	^{522}728 ± 0	^{982}1348 ± 0	^{1107}2974 ± 1	^{1108}10990 ± 7	^{393}1016 ± 4	^{401}1019 ± 4
1154	tnitech-000	234032	13976	^{967}5471	^{889}2048 ± 0	^{366}415 ± 1	^{236}427 ± 1	^{195}419 ± 4	^{175}427 ± 3	^{138}436 ± 2	^{759}2438 ± 14	^{761}2436 ± 19
1155	tongyi-004	947322	138901	-	^{1113}2167 ± 0	^{83}153 ± 0	-	-	-	-	^{1226}18916 ± 120	^{1230}18909 ± 126
1156	tongyi-005	1140701	138919	^{741}2121	^{1102}2089 ± 0	^{90}165 ± 1	-	-	-	-	^{1227}18924 ± 65	^{1236}20158 ± 103
1157	tongyitrans-001	625339	75069	-	^{1076}2058 ± 0	^{242}310 ± 20	-	-	-	-	^{1215}17769 ± 74	^{1218}17750 ± 63
1158	tongyitrans-002	625336	75081	-	^{1077}2058 ± 0	^{293}356 ± 35	-	-	-	-	^{1282}29816 ± 281	^{1219}17799 ± 127
1159	tongyitrans-003	1769974	138883	-	^{1335}4386 ± 0	^{427}468 ± 0	-	-	-	-	^{1357}61793 ± 154	^{1311}37122 ± 155
1160	toppanidgate-000	671181	711850	^{681}1798	^{1197}4096 ± 0	^{963}915 ± 1	^{667}916 ± 1	^{617}916 ± 1	^{565}917 ± 1	^{484}917 ± 1	^{1270}25262 ± 84	^{1268}25264 ± 97
1161	toppansecurity-001	1480690	130296	^{626}1595	^{1304}4113 ± 0	^{1229}1238 ± 3	^{914}1217 ± 0	^{937}1292 ± 0	^{813}1223 ± 0	^{706}1247 ± 1	^{861}3098 ± 28	^{880}3207 ± 38
1162	toshiba-000	3893310	235400	-	^{320}1812 ± 0	^{483}528 ± 3	-	-	-	-	^{721}2255 ± 60	^{720}2251 ± 53
1163	toshiba-001	3893310	235400	-	^{1132}2580 ± 0	^{608}615 ± 3	-	-	-	-	^{838}2900 ± 80	^{836}2881 ± 60
1164	toshiba-002	813606	114260	-	^{311}1560 ± 0	^{502}541 ± 0	-	-	-	-	^{911}3521 ± 369	^{765}2449 ± 124
1165	toshiba-003	984125	114264	-	^{312}1560 ± 0	^{501}540 ± 0	-	-	-	-	^{752}2390 ± 41	^{755}2407 ± 81
1166	toshiba-004	599297	27880	^{628}1596	^{1038}2056 ± 0	^{1355}1447 ± 3	^{1068}1453 ± 2	^{1052}1457 ± 9	^{988}1457 ± 3	^{871}1479 ± 4	^{394}1020 ± 25	^{392}998 ± 32
1167	toshiba-005	599298	61113	-	^{1065}2056 ± 0	^{1362}1456 ± 4	^{1069}1454 ± 2	^{1056}1461 ± 2	^{983}1455 ± 2	^{858}1459 ± 2	^{582}1613 ± 34	^{582}1607 ± 28
1168	toshiba-006	599566	44078	^{625}1588	^{1058}2056 ± 0	^{1375}1481 ± 16	^{1087}1515 ± 7	^{1072}1506 ± 6	^{1015}1521 ± 2	^{904}1546 ± 30	^{395}1022 ± 17	^{403}1022 ± 23
1169	toshiba-007	547545	76675	^{534}1297	^{1027}2056 ± 0	^{762}722 ± 1	^{568}784 ± 0	^{518}777 ± 4	^{460}766 ± 2	^{429}832 ± 15	^{284}709 ± 22	^{298}712 ± 26
1170	toshiba-008	707290	76687	^{679}1791	^{1019}2056 ± 0	^{1034}979 ± 1	^{724}976 ± 0	^{684}986 ± 3	^{639}1005 ± 2	^{575}1056 ± 14	^{253}674 ± 68	^{277}683 ± 71
1171	toshiba-009	651747	76688	^{636}1639	^{1039}2056 ± 0	^{969}921 ± 1	^{688}933 ± 1	^{620}919 ± 2	^{579}935 ± 3	^{535}996 ± 21	^{291}719 ± 48	^{288}700 ± 31
1172	toshiba-010	1091350	76688	^{830}2710	^{1056}2056 ± 0	^{1325}1393 ± 2	^{1097}1638 ± 15	^{1054}1457 ± 1	^{968}1426 ± 14	^{867}1473 ± 19	^{199}601 ± 25	^{217}604 ± 23
1173	toshiba-011	1106463	76900	^{832}2733	^{1017}2056 ± 0	^{1310}1379 ± 1	^{1039}1406 ± 1	^{1021}1407 ± 1	^{924}1370 ± 1	^{854}1448 ± 18	^{282}708 ± 56	^{255}641 ± 37
1174	toshiba-012	1151623	85416	^{763}2253	^{1026}2056 ± 0	^{1405}2020 ± 0	^{1119}2048 ± 0	^{1107}2049 ± 0	^{1078}2073 ± 4	^{982}2125 ± 5	^{488}1281 ± 17	^{505}1315 ± 40
1175	toss-000	993640	94527	^{931}4182	^{858}2048 ± 0	^{1078}1028 ± 0	^{902}1200 ± 3	^{901}1246 ± 7	^{712}1116 ± 2	^{592}1072 ± 0	^{363}909 ± 78	^{372}914 ± 60
1176	touchlessid-000	92561	64467	^{104}341	^{513}2048 ± 0	^{241}309 ± 5	^{143}305 ± 2	^{112}312 ± 5	^{80}277 ± 4	^{88}349 ± 17	^{1293}31935 ± 292	^{1294}31958 ± 243
1177	touchlessid-001	255274	14355	^{187}538	^{671}2048 ± 0	^{282}344 ± 1	^{170}347 ± 1	^{191}414 ± 3	^{305}595 ± 10	^{940}1732 ± 61	^{634}1806 ± 35	^{635}1800 ± 35
1178	touchlessid-002	255586	14284	^{115}367	^{931}2048 ± 0	^{315}371 ± 1	^{196}375 ± 1	^{212}438 ± 3	^{346}640 ± 10	^{906}1548 ± 57	^{658}1915 ± 41	^{648}1871 ± 38
1179	touchlessid-003	271397	14226	^{176}512	^{909}2048 ± 0	^{362}410 ± 0	^{232}419 ± 0	^{204}429 ± 0	^{220}479 ± 1	^{311}685 ± 6	^{202}608 ± 17	^{204}596 ± 1
1180	touchlessid-004	386383	14727	^{236}642	^{702}2048 ± 0	^{904}854 ± 0	^{687}932 ± 2	^{899}1244 ± 6	^{1073}2001 ± 2	^{1071}5013 ± 7	^{565}1527 ± 28	^{562}1501 ± 14
1181	transmitsecurity-001	1786905	2031398	^{558}1363	^{1361}6144 ± 0	^{280}342 ± 13	^{166}344 ± 15	^{126}332 ± 22	^{98}312 ± 15	^{97}370 ± 19	^{1130}9692 ± 23	^{1131}9847 ± 34
1182	trueface-000	255123	796861	-	^{438}2048 ± 0	^{309}367 ± 8	-	-	-	-	^{141}482 ± 13	^{163}528 ± 20
1183	trueface-001	255123	186754	-	^{89}500 ± 0	^{339}390 ± 1	-	-	-	-	^{254}676 ± 26	^{173}558 ± 50
1184	trueface-002	253947	123116	^{160}486	^{328}2000 ± 0	^{300}360 ± 0	^{182}361 ± 0	^{197}423 ± 0	^{303}590 ± 1	-	^{34}192 ± 14	^{37}186 ± 19
1185	trueface-003	346530	24308	^{921}3916	^{529}2048 ± 0	^{1125}1107 ± 22	^{472}677 ± 3	^{484}732 ± 7	^{560}905 ± 5	-	^{12}103 ± 11	^{14}112 ± 29
1186	trueidvng-001	766071	37721	^{677}1781	^{1355}6144 ± 0	^{1028}975 ± 1	^{735}985 ± 1	^{687}989 ± 1	^{650}1016 ± 1	^{632}1128 ± 2	^{1308}37129 ± 216	^{1373}72067 ± 305
1187	truststamp-001	1795742	275073	^{601}1524	^{200}768 ± 0	^{125}194 ± 0	^{72}191 ± 0	^{50}187 ± 0	^{53}210 ± 1	^{79}338 ± 8	^{1109}8415 ± 66	^{1111}8392 ± 71
1188	truststamp-002	1060439	10841	^{730}2066	^{433}2048 ± 0	^{230}300 ± 0	^{157}330 ± 1	^{120}325 ± 0	^{112}335 ± 2	^{149}452 ± 0	^{1149}11281 ± 179	^{1151}11273 ± 203

Notes	
1	The configuration size does not capture static data included in libraries.
2	The library size is the combined total of all files provided in the submission lib folder. These libraries e.g. OpenCV may or may not be installed on any end user's platform natively and would not need to be installed with the algorithm. Some developers put neural network models in their libraries.
3	The memory usage is the peak resident set size reported by the ps system call during template generation.
4	The median template creation times are measured on Intel®Xeon®CPU E5-2630 v4 @ 2.20GHz processors.
5	The comparison durations, in nanoseconds, are estimated using std::chrono::high_resolution_clock which on the machine in (2) counts 1ns clock ticks. Precision is somewhat worse than that however. The ± value is the median absolute deviation times 1.48 for Normal consistency.

Table 48: Summary of algorithms and properties included in this report. The red superscripts give ranking for the quantity in that column.

	ALGORITHM	CONFIG	LIBRARY	TEMPLATE							COMPARISON[4]	
	NAME	DATA	DATA	MEMORY	SIZE	GENERATION TIME (ms)[4]					TIME (ns)[5]	
		(KB)[1]	(KB)[2]	(MB)[3]	(B)	MUGSHOT	480x720	960x1440	1600x2400	3000x4500	GENUINE	IMPOSTOR
1189	truststamp-003	1206119	10474	^{700}1875	^{887}2048 ± 0	^{401}445 ± 0	^{260}445 ± 0	^{221}449 ± 0	^{202}462 ± 1	^{214}539 ± 2	^{1191}14901 ± 619	^{1193}14813 ± 472
1190	ttigroup-000	466606	454674	^{772}2320	^{774}2048 ± 0	^{954}909 ± 2	^{680}925 ± 8	^{603}897 ± 1	^{561}909 ± 3	^{489}923 ± 2	^{748}2382 ± 17	^{753}2387 ± 23
1191	tuputech-000	11476	17185	^{7}33	^{372}2048 ± 0	^{60}122 ± 4	^{33}120 ± 1	^{31}142 ± 2	^{45}196 ± 5	^{125}411 ± 14	^{1257}23893 ± 406	^{1269}25279 ± 406
1192	turingtechvip-001	399874	54535	^{222}615	^{387}2048 ± 0	^{1316}1384 ± 4	^{1024}1391 ± 1	^{1010}1393 ± 1	^{957}1411 ± 1	^{870}1476 ± 2	^{611}1733 ± 19	^{616}1734 ± 20
1193	turingtechvip-002	167556	140995	^{354}877	^{437}2048 ± 0	^{1380}1493 ± 2	^{981}1306 ± 1	^{1001}1382 ± 1	^{897}1337 ± 1	^{837}1426 ± 3	^{1180}13819 ± 103	^{1183}13807 ± 137
1194	turkcell-000	271083	133553	^{234}636	^{489}2048 ± 0	^{1129}1110 ± 1	^{813}1094 ± 0	^{787}1103 ± 0	^{727}1126 ± 1	^{673}1201 ± 1	^{831}2866 ± 23	^{835}2873 ± 40
1195	turkcell-001	287616	133870	^{243}657	^{810}2048 ± 0	^{707}682 ± 0	^{490}695 ± 0	^{442}688 ± 1	^{396}692 ± 0	^{325}702 ± 0	^{970}4342 ± 71	^{968}4310 ± 72
1196	turkcell-002	542178	139150	^{231}633	^{733}2048 ± 0	^{829}791 ± 1	^{351}559 ± 1	^{524}793 ± 3	^{480}793 ± 2	^{235}574 ± 0	^{881}3249 ± 65	^{884}3231 ± 53
1197	twface-000	661735	11782	^{846}2796	^{942}2048 ± 0	^{915}871 ± 1	^{636}873 ± 1	^{588}873 ± 2	^{539}876 ± 2	^{474}898 ± 1	^{559}1504 ± 29	^{564}1510 ± 34
1198	twface-001	671511	11782	^{849}2851	^{750}2048 ± 0	^{975}923 ± 1	^{681}925 ± 2	^{633}926 ± 1	^{573}929 ± 2	^{498}940 ± 2	^{516}1400 ± 32	^{524}1402 ± 37
1199	ulsee-001	370519	57261	-	^{603}2048 ± 0	^{661}654 ± 2	-	-	-	-	^{1049}6065 ± 94	^{1054}6228 ± 77
1200	ultinous-000	90803	503529	-	^{1269}4100 ± 0	^{16}53 ± 0	-	-	-	-	^{968}4263 ± 50	^{967}4262 ± 42
1201	ultinous-001	403572	501651	-	^{1398}12304 ± 0	^{135}200 ± 0	-	-	-	-	^{1307}36357 ± 223	^{1310}36332 ± 210
1202	uluface-002	0	480761	^{453}1088	^{675}2048 ± 0	^{922}873 ± 42	^{619}855 ± 9	^{674}978 ± 24	^{851}1271 ± 40	^{1002}2333 ± 68	^{1230}19207 ± 1114	^{1226}18501 ± 274
1203	uluface-003	97357	529422	^{518}1264	^{1141}3072 ± 0	^{1018}965 ± 11	^{715}968 ± 10	^{771}1087 ± 20	^{934}1387 ± 36	^{1015}2469 ± 86	^{1271}26057 ± 195	^{1277}26865 ± 566
1204	unicc-001	24840	5123261	^{692}1849	^{933}2048 ± 0	^{252}316 ± 4	^{172}349 ± 4	^{564}838 ± 14	^{702}1102 ± 11	^{757}1312 ± 15	^{846}2950 ± 29	^{844}2929 ± 26
1205	unicc-002	277015	1705310	^{645}1673	^{862}2048 ± 0	^{593}609 ± 1	^{408}620 ± 1	^{360}612 ± 0	^{365}660 ± 2	^{377}763 ± 3	^{730}2289 ± 13	^{731}2295 ± 22
1206	unicc-003	361274	1737967	^{683}1806	^{382}2048 ± 0	^{1290}1343 ± 3	^{997}1328 ± 1	^{979}1345 ± 1	^{918}1366 ± 1	^{874}1484 ± 6	^{742}2339 ± 74	^{742}2327 ± 29
1207	unicc-004	361274	1737981	^{680}1793	^{618}2048 ± 0	^{1292}1348 ± 2	^{1001}1334 ± 1	^{986}1355 ± 1	^{944}1397 ± 1	^{921}1613 ± 4	^{736}2306 ± 13	^{737}2304 ± 16
1208	unissey-001	0	1956593	^{379}934	^{1266}4096 ± 0	^{930}880 ± 3	^{652}892 ± 3	^{1050}1452 ± 8	^{1110}3048 ± 12	^{1101}10017 ± 387	^{539}1463 ± 35	^{549}1471 ± 34
1209	unissey-002	0	1443765	^{295}765	^{1219}4096 ± 0	^{777}736 ± 1	^{546}752 ± 1	^{693}994 ± 1	^{969}1426 ± 1	^{1048}3331 ± 2	^{1166}12308 ± 91	^{1168}12302 ± 137
1210	unissey-003	0	814526	^{239}650	^{1226}4096 ± 0	^{757}718 ± 1	^{536}744 ± 0	^{654}956 ± 1	^{951}1403 ± 1	^{1040}3055 ± 2	^{578}1594 ± 20	^{578}1570 ± 44
1211	unissey-004	1	1065839	^{418}1030	^{1248}4096 ± 0	^{289}354 ± 2	^{187}366 ± 0	^{192}416 ± 0	^{169}417 ± 0	^{124}409 ± 0	^{967}4261 ± 124	^{982}4557 ± 480
1212	unissey-005	0	1125043	^{429}1050	^{1199}4096 ± 0	^{288}352 ± 0	^{191}369 ± 0	^{180}402 ± 0	^{157}397 ± 0	^{122}408 ± 0	^{985}4630 ± 97	^{1004}4964 ± 161
1213	unissey-006	0	1315567	^{496}1188	^{1186}4096 ± 0	^{961}914 ± 0	^{686}930 ± 0	^{737}1043 ± 0	^{666}1044 ± 1	^{569}1048 ± 0	^{1055}6189 ± 111	^{1063}6605 ± 186
1214	unissey-007	1	1763338	^{486}1173	^{1238}4096 ± 0	^{1220}1224 ± 22	^{961}1283 ± 17	^{1004}1390 ± 23	^{947}1401 ± 23	^{823}1410 ± 23	^{1263}24488 ± 173	^{1264}24524 ± 185
1215	upc-001	0	89914	^{445}1077	^{275}1052 ± 0	^{515}551 ± 15	^{499}703 ± 56	^{476}724 ± 51	^{449}751 ± 49	^{453}863 ± 33	^{862}3114 ± 44	^{876}3165 ± 97
1216	urielsoft-000	256261	67932	^{950}4700	^{629}2048 ± 0	^{131}197 ± 0	^{95}226 ± 0	^{93}281 ± 2	^{87}289 ± 2	^{205}528 ± 2	^{227}631 ± 10	^{237}630 ± 2
1217	useb-000	1002886	493465	^{587}1437	^{441}2048 ± 0	^{605}613 ± 2	^{388}605 ± 1	^{368}621 ± 2	^{356}653 ± 2	^{444}848 ± 3	^{702}2153 ± 45	^{715}2222 ± 115
1218	useb-001	1000960	493816	^{582}1429	^{548}2048 ± 0	^{685}673 ± 4	^{366}577 ± 4	^{333}579 ± 8	^{307}596 ± 9	^{384}768 ± 2	^{717}2230 ± 65	^{733}2299 ± 90
1219	useb-002	1000967	493456	^{576}1423	^{773}2048 ± 0	^{492}532 ± 2	^{565}778 ± 2	^{411}657 ± 4	^{360}657 ± 2	^{440}843 ± 3	^{741}2336 ± 47	^{740}2323 ± 60
1220	useb-003	1001019	493456	^{595}1484	^{496}2048 ± 0	^{471}512 ± 2	^{319}521 ± 3	^{294}528 ± 12	^{273}550 ± 2	^{344}723 ± 2	^{705}2172 ± 38	^{708}2175 ± 75
1221	useb-004	2086479	454237	^{843}2765	^{381}2048 ± 0	^{1303}1369 ± 2	^{1053}1428 ± 12	^{1034}1428 ± 5	^{1021}1557 ± 10	^{961}1945 ± 4	^{735}2303 ± 54	^{744}2350 ± 94
1222	uxlabs-001	291127	39378	^{261}700	^{1237}4096 ± 0	^{344}395 ± 0	^{205}387 ± 0	^{170}388 ± 0	^{146}390 ± 0	^{119}396 ± 0	^{644}1863 ± 31	^{659}1921 ± 45
1223	uxlabs-003	1051837	37767	^{635}1638	^{1264}4096 ± 0	^{1322}1390 ± 1	^{1041}1410 ± 5	^{1006}1391 ± 3	^{948}1402 ± 6	^{844}1435 ± 1	^{589}1645 ± 10	^{588}1641 ± 37
1224	uzinfocom-000	271124	508385	^{361}885	^{1093}2078 ± 0	^{104}178 ± 0	^{60}180 ± 0	^{57}191 ± 0	^{52}208 ± 12	^{72}325 ± 0	^{413}1064 ± 41	^{421}1055 ± 26
1225	uzinfocom-001	377667	396457	^{456}1091	^{1094}2078 ± 0	^{388}435 ± 0	^{243}433 ± 0	^{222}450 ± 0	^{241}511 ± 0	^{241}589 ± 1	^{1352}59486 ± 145	^{1350}59551 ± 123
1226	vaidio-001	461288	112836	^{440}1068	^{485}2048 ± 0	^{613}616 ± 0	^{410}621 ± 0	^{369}622 ± 0	^{332}623 ± 0	^{316}690 ± 0	^{1345}56447 ± 44	^{1346}56451 ± 63
1227	vcog-002	3229434	118946	^{907}3666	^{1410}61504 ± 5	^{295}357 ± 25	-	-	-	-	^{1400}296154 ± 3077	^{1400}296436 ± 4183
1228	vcortex-001	105305	55240	^{167}502	^{205}896 ± 0	^{136}201 ± 2	^{77}197 ± 0	^{66}209 ± 3	^{70}244 ± 6	^{100}371 ± 19	^{67}279 ± 4	^{75}277 ± 4
1229	vd-000	213686	12962	-	^{263}1028 ± 0	^{72}134 ± 3	-	-	-	-	^{541}1467 ± 19	^{542}1456 ± 16
1230	vd-001	170262	44058	-	^{983}2052 ± 0	^{248}316 ± 6	-	-	-	-	^{478}1258 ± 38	^{456}1148 ± 109
1231	vd-002	254498	34389	^{6}31	^{164}516 ± 0	^{712}684 ± 5	^{473}679 ± 4	^{431}676 ± 5	^{397}693 ± 5	^{368}754 ± 5	^{77}300 ± 14	^{88}319 ± 32
1232	vd-003	254505	44051	^{3}29	^{975}2052 ± 0	^{724}691 ± 5	^{485}690 ± 5	^{436}683 ± 4	^{395}691 ± 5	^{342}722 ± 5	^{389}1003 ± 11	^{396}1001 ± 7

Notes	
1	The configuration size does not capture static data included in libraries.
2	The library size is the combined total of all files provided in the submission lib folder. These libraries e.g. OpenCV may or may not be installed on any end user's platform natively and would not need to be installed with the algorithm. Some developers put neural network models in their libraries.
3	The memory usage is the peak resident set size reported by the ps system call during template generation.
4	The median template creation times are measured on Intel®Xeon®CPU E5-2630 v4 @ 2.20GHz processors.
5	The comparison durations, in nanoseconds, are estimated using std::chrono::high_resolution_clock which on the machine in (2) counts 1ns clock ticks. Precision is somewhat worse than that however. The ± value is the median absolute deviation times 1.48 for Normal consistency.

Table 49: Summary of algorithms and properties included in this report. The red superscripts give ranking for the quantity in that column.

	ALGORITHM	CONFIG	LIBRARY	TEMPLATE							COMPARISON[4]	
	NAME	DATA	DATA	MEMORY	SIZE	GENERATION TIME (ms)[4]					TIME (ns)[5]	
		(KB)[1]	(KB)[2]	(MB)[3]	(B)	MUGSHOT	480x720	960x1440	1600x2400	3000x4500	GENUINE	IMPOSTOR
1233	veridas-001	196540	190018	-	^{541}2048 ± 0	^{682}671 ± 21	-	-	-	-	^{1036}5748 ± 20	^{1080}7111 ± 148
1234	veridas-002	193466	190018	-	^{104}512 ± 0	^{679}669 ± 20	-	-	-	-	^{610}1733 ± 81	^{666}1934 ± 44
1235	veridas-003	293109	141587	-	^{335}2048 ± 0	^{942}890 ± 33	-	-	-	-	^{1021}5484 ± 42	^{1086}7306 ± 410
1236	veridas-004	196585	160684	-	^{602}2048 ± 0	^{699}678 ± 22	^{540}749 ± 27	^{1060}1470 ± 52	^{1113}3228 ± 95	^{1103}10349 ± 273	^{1025}5516 ± 42	^{1090}7425 ± 130
1237	veridas-005	196585	269478	-	^{795}2048 ± 0	^{591}606 ± 12	-	-	-	-	^{1349}56976 ± 200	^{1360}66298 ± 216
1238	veridas-006	355669	896424	-	^{874}2048 ± 0	^{931}880 ± 8	^{647}885 ± 8	^{922}1271 ± 18	^{1089}2242 ± 38	^{1084}6414 ± 156	^{1348}56940 ± 149	^{1359}66077 ± 194
1239	veridas-007	355105	891492	^{802}2522	^{561}2048 ± 0	^{917}872 ± 9	^{638}875 ± 8	^{913}1261 ± 18	^{1088}2238 ± 38	^{1082}6374 ± 147	^{248}655 ± 16	^{266}660 ± 19
1240	veridas-008	1100495	1190915	^{1000}8633	^{354}2048 ± 0	^{990}944 ± 12	^{696}945 ± 11	^{971}1334 ± 27	^{1094}2382 ± 48	^{1086}6959 ± 172	^{292}723 ± 14	^{310}731 ± 16
1241	veridas-009	1100503	625120	^{1004}9163	^{517}2048 ± 0	^{566}589 ± 6	^{357}565 ± 5	^{330}576 ± 5	^{293}583 ± 5	^{300}666 ± 6	^{237}638 ± 5	^{253}638 ± 16
1242	veridas-010	1103722	623326	^{1002}8991	^{700}2048 ± 0	^{754}714 ± 4	^{479}686 ± 4	^{461}705 ± 6	^{392}687 ± 4	^{320}693 ± 5	^{242}644 ± 2	^{257}644 ± 4
1243	veridium-000	0	47198	^{25}98	^{1405}29399 ± 2045	^{27}79 ± 0	^{17}80 ± 0	^{16}89 ± 0	^{13}90 ± 0	^{13}111 ± 0	^{1360}64880 ± 171	^{1358}64697 ± 247
1244	veridium-001	0	40561	^{44}142	^{1120}2489 ± 0	^{13}44 ± 0	^{9}45 ± 0	^{6}48 ± 0	^{6}50 ± 0	^{7}72 ± 0	^{1359}63417 ± 1061	^{1356}63225 ± 2133
1245	veridium-002	0	52482	^{50}161	^{1119}2486 ± 0	^{4}25 ± 0	^{2}25 ± 0	^{3}29 ± 0	^{2}30 ± 0	^{3}51 ± 0	^{1319}43891 ± 177	^{1320}43918 ± 167
1246	veridium-003	0	25975	^{38}136	^{1121}2490 ± 0	^{6}27 ± 0	^{3}25 ± 0	^{2}28 ± 0	^{3}30 ± 0	^{4}53 ± 0	^{1302}34755 ± 140	^{1304}34828 ± 177
1247	verigram-000	256209	7798	^{744}2137	^{532}2048 ± 0	^{844}807 ± 1	^{592}821 ± 1	^{669}972 ± 2	^{911}1358 ± 3	^{1030}2848 ± 13	^{471}1222 ± 17	^{479}1219 ± 17
1248	verigram-001	282155	11773	^{816}2638	^{841}2048 ± 0	^{673}664 ± 2	^{469}675 ± 2	^{561}833 ± 4	^{793}1202 ± 7	^{1024}2733 ± 32	^{592}1664 ± 60	^{589}1648 ± 56
1249	verigram-002	1588249	20691	^{727}2057	^{1232}4096 ± 0	^{1365}1464 ± 3	^{1038}1406 ± 0	^{1065}1486 ± 1	^{971}1431 ± 0	^{914}1586 ± 5	^{1401}453119 ± 13595	^{1401}452140 ± 9654
1250	verigram-003	1590775	20692	^{726}2052	^{1174}4096 ± 0	^{725}691 ± 4	^{470}677 ± 1	^{434}677 ± 1	^{399}694 ± 1	^{366}746 ± 1	^{1313}38843 ± 1140	^{1316}38665 ± 1071
1251	verihubs-inteligensia-000	209562	51877	^{136}430	^{345}2048 ± 0	^{530}567 ± 0	^{1090}1558 ± 8	^{1081}1560 ± 8	^{1026}1568 ± 8	^{923}1621 ± 8	^{1248}22351 ± 91	^{1252}22371 ± 81
1252	verihubs-inteligensia-001	216524	51916	^{138}437	^{937}2048 ± 0	^{527}564 ± 0	^{353}562 ± 0	^{321}566 ± 1	^{282}566 ± 0	^{251}600 ± 0	^{1240}21770 ± 84	^{1244}21735 ± 102
1253	verihubs-inteligensia-002	361105	17045	^{275}727	^{679}2048 ± 0	^{430}471 ± 0	^{270}458 ± 0	^{234}459 ± 0	^{203}463 ± 1	^{161}471 ± 0	^{1219}18131 ± 558	^{1221}17851 ± 197
1254	verijelas-000	254540	10322	^{664}1736	^{364}2048 ± 0	^{255}321 ± 0	^{154}325 ± 1	^{125}329 ± 0	^{113}335 ± 5	^{94}360 ± 0	^{1137}10267 ± 143	^{1137}10218 ± 109
1255	via-000	124422	11151	-	^{917}2048 ± 0	^{746}707 ± 8	^{533}740 ± 5	^{609}906 ± 41	^{585}941 ± 40	^{561}1040 ± 5	^{378}966 ± 28	^{402}1021 ± 44
1256	via-001	370255	11151	^{651}1697	^{872}2048 ± 0	^{1016}964 ± 3	^{758}1011 ± 3	^{720}1026 ± 4	^{667}1045 ± 3	^{638}1137 ± 28	^{382}983 ± 31	^{390}989 ± 40
1257	via-004	530941	93634	^{557}1361	^{724}2048 ± 0	^{312}368 ± 0	^{214}397 ± 1	^{139}352 ± 1	^{129}364 ± 2	^{173}490 ± 1	^{59}255 ± 7	^{67}255 ± 8
1258	via-005	510729	93629	^{764}2257	^{897}2048 ± 0	^{500}538 ± 0	^{324}528 ± 0	^{292}525 ± 1	^{258}535 ± 2	^{253}601 ± 1	^{50}223 ± 2	^{51}222 ± 7
1259	via-006	1087232	93594	^{928}4074	^{789}2048 ± 0	^{919}872 ± 1	^{655}898 ± 1	^{641}941 ± 1	^{581}936 ± 2	^{533}993 ± 1	^{51}224 ± 2	^{54}230 ± 11
1260	viante-000	1244225	19718	^{604}1532	^{1013}2056 ± 0	^{1091}1054 ± 0	^{787}1059 ± 1	^{764}1075 ± 1	^{683}1070 ± 4	^{597}1087 ± 1	^{1064}6461 ± 44	^{1060}6424 ± 32
1261	viante-001	1401078	19722	^{687}1812	^{1033}2056 ± 0	^{1116}1094 ± 1	^{832}1117 ± 5	^{799}1119 ± 6	^{719}1120 ± 3	^{609}1103 ± 1	^{869}3158 ± 45	^{870}3143 ± 53
1262	viante-002	1247402	19718	^{607}1538	^{1015}2056 ± 0	^{1159}1152 ± 1	^{827}1113 ± 3	^{792}1109 ± 1	^{706}1107 ± 2	^{626}1121 ± 2	^{875}3213 ± 90	^{881}3207 ± 90
1263	viante-003	1247402	19705	^{605}1534	^{1016}2056 ± 0	^{1394}1768 ± 2	^{1104}1787 ± 0	^{1094}1775 ± 0	^{1051}1786 ± 8	^{948}1791 ± 0	^{988}4666 ± 111	^{988}4690 ± 83
1264	videmo-000	139643	39470	-	^{334}2048 ± 0	^{74}142 ± 5	^{43}150 ± 4	^{35}150 ± 6	^{29}151 ± 4	^{22}155 ± 8	^{156}513 ± 16	^{161}523 ± 38
1265	videmo-001	212051	95063	^{95}309	^{518}2048 ± 0	^{132}199 ± 0	^{48}164 ± 0	^{40}164 ± 0	^{32}164 ± 0	^{23}165 ± 0	^{73}296 ± 17	^{78}288 ± 16
1266	videmo-002	212053	32963	^{102}333	^{378}2048 ± 0	^{133}199 ± 0	^{52}169 ± 0	^{43}169 ± 0	^{33}170 ± 0	^{25}170 ± 0	^{45}209 ± 7	^{46}208 ± 8
1267	videmo-003	173512	43964	^{143}447	^{97}512 ± 0	^{71}133 ± 0	^{30}111 ± 0	^{24}115 ± 0	^{21}114 ± 0	^{15}115 ± 0	^{3}75 ± 10	^{3}75 ± 16
1268	videonetics-001	30875	5963	^{11}61	^{138}512 ± 0	^{186}262 ± 3	^{120}273 ± 1	^{214}439 ± 3	^{500}820 ± 3	^{1010}2393 ± 43	^{455}1153 ± 38	^{453}1142 ± 65
1269	videonetics-002	121981	6289	^{29}115	^{993}2052 ± 0	^{209}282 ± 5	^{137}295 ± 1	^{281}513 ± 4	^{655}1029 ± 3	^{1042}3151 ± 46	^{470}1219 ± 57	^{490}1262 ± 56
1270	viettelai-000	284612	132031	^{224}619	^{689}2048 ± 0	^{247}315 ± 0	^{149}317 ± 0	^{118}321 ± 0	^{107}322 ± 0	^{76}334 ± 1	^{1245}22074 ± 112	^{1251}22173 ± 163
1271	viettelai-001	528186	132058	^{497}1189	^{583}2048 ± 0	^{755}715 ± 1	-	-	-	-	^{1250}22740 ± 167	^{1385}86287 ± 1073
1272	viettelai-002	528186	132049	^{459}1094	^{920}2048 ± 0	^{751}712 ± 1	^{523}729 ± 0	^{475}724 ± 0	^{439}735 ± 0	^{356}738 ± 5	^{1273}26231 ± 154	^{1386}89838 ± 1111
1273	viettelai-003	528138	130904	^{458}1093	^{502}2048 ± 0	^{748}710 ± 1	^{518}720 ± 0	^{495}743 ± 3	^{473}782 ± 0	^{682}1207 ± 1	^{612}1743 ± 11	^{613}1728 ± 7
1274	viettelai-004	1506350	203627	^{871}3115	^{997}2052 ± 0	^{1410}2910 ± 0	^{1124}2922 ± 1	^{1119}2915 ± 0	^{1105}2917 ± 0	^{1036}2944 ± 0	^{483}1274 ± 17	^{500}1290 ± 32
1275	viettelhightech-000	259471	215557	^{132}421	^{804}2048 ± 0	^{417}461 ± 1	^{273}461 ± 2	^{235}461 ± 1	^{210}467 ± 2	^{174}494 ± 0	^{194}599 ± 11	^{195}591 ± 13
1276	viettelhightech-001	461523	147432	^{454}1088	^{873}2048 ± 0	^{1104}1068 ± 1	^{801}1084 ± 1	^{823}1145 ± 4	^{850}1270 ± 4	^{972}2041 ± 2	^{192}598 ± 14	^{193}589 ± 5

Notes	
1	The configuration size does not capture static data included in libraries.
2	The library size is the combined total of all files provided in the submission lib folder. These libraries e.g. OpenCV may or may not be installed on any end user's platform natively and would not need to be installed with the algorithm. Some developers put neural network models in their libraries.
3	The memory usage is the peak resident set size reported by the ps system call during template generation.
4	The median template creation times are measured on Intel®Xeon®CPU E5-2630 v4 @ 2.20GHz processors.
5	The comparison durations, in nanoseconds, are estimated using std::chrono::high_resolution_clock which on the machine in (2) counts 1ns clock ticks. Precision is somewhat worse than that however. The ± value is the median absolute deviation times 1.48 for Normal consistency.

Table 50: Summary of algorithms and properties included in this report. The red superscripts give ranking for the quantity in that column.

	ALGORITHM	CONFIG	LIBRARY	TEMPLATE							COMPARISON[4]	
	NAME	DATA	DATA	MEMORY	SIZE	GENERATION TIME (ms)[4]					TIME (ns)[5]	
		(KB)[1]	(KB)[2]	(MB)[3]	(B)	MUGSHOT	480x720	960x1440	1600x2400	3000x4500	GENUINE	IMPOSTOR
1277	viettelhightech-002	461606	115515	^{415}1022	^{745}2048 ± 0	^{1393}1700 ± 1	^{1100}1665 ± 0	^{1090}1723 ± 1	^{1065}1893 ± 1	^{1026}2742 ± 1	^{319}778 ± 4	^{326}783 ± 8
1278	vigilantsolutions-000	352218	389974	-	^{1407}31540 ± 0	^{934}884 ± 23	-	-	-	-	^{1220}18201 ± 94	^{1177}13030 ± 83
1279	vigilantsolutions-001	344685	89145	-	^{301}1544 ± 0	^{971}921 ± 2	-	-	-	-	^{240}644 ± 13	^{260}649 ± 16
1280	vigilantsolutions-002	344137	89162	-	^{1082}2060 ± 0	^{895}844 ± 2	-	-	-	-	^{256}679 ± 10	^{272}680 ± 7
1281	vigilantsolutions-003	343048	94301	-	^{302}1548 ± 0	^{873}824 ± 3	-	-	-	-	^{233}634 ± 19	^{254}638 ± 17
1282	vigilantsolutions-004	343048	125719	-	^{306}1548 ± 0	^{886}837 ± 6	-	-	-	-	^{266}686 ± 14	^{281}688 ± 17
1283	vigilantsolutions-005	343048	125719	-	^{308}1548 ± 0	^{888}837 ± 13	-	-	-	-	^{352}874 ± 22	^{252}637 ± 16
1284	vigilantsolutions-006	343048	125719	-	^{305}1548 ± 0	^{892}841 ± 8	-	-	-	-	^{369}939 ± 32	^{297}711 ± 37
1285	vigilantsolutions-007	255600	125715	-	^{307}1548 ± 0	^{452}493 ± 6	-	-	-	-	^{331}803 ± 35	^{336}800 ± 40
1286	vigilantsolutions-008	441835	47824	-	^{310}1548 ± 0	^{651}647 ± 2	-	-	-	-	^{356}889 ± 23	^{366}903 ± 44
1287	vigilantsolutions-009	348798	49973	-	^{309}1548 ± 0	^{612}615 ± 0	^{424}631 ± 0	^{386}632 ± 1	^{340}636 ± 0	^{293}659 ± 0	^{126}452 ± 11	^{133}451 ± 11
1288	vigilantsolutions-010	348798	49973	^{332}841	^{303}1548 ± 0	^{609}615 ± 0	^{423}631 ± 0	^{385}632 ± 0	^{341}636 ± 0	^{294}659 ± 0	^{145}490 ± 13	^{150}488 ± 11
1289	vigilantsolutions-011	255661	49973	^{208}591	^{304}1548 ± 0	^{351}402 ± 0	^{231}418 ± 0	^{193}418 ± 0	^{172}422 ± 0	^{146}445 ± 0	^{91}339 ± 20	^{108}366 ± 37
1290	vinai-000	402391	866522	^{422}1034	^{582}2048 ± 0	^{1120}1099 ± 1	^{814}1095 ± 1	^{777}1093 ± 1	^{701}1099 ± 1	^{629}1126 ± 1	^{849}2996 ± 20	^{856}2993 ± 26
1291	vinbigdata-001	271405	44746	^{209}591	^{540}2048 ± 0	^{1329}1400 ± 5	^{1027}1393 ± 2	^{1005}1391 ± 2	^{939}1393 ± 1	^{819}1404 ± 1	^{503}1351 ± 50	^{504}1310 ± 38
1292	vinbigdata-002	256322	138864	^{218}607	^{655}2048 ± 0	^{535}569 ± 2	^{362}572 ± 1	^{324}571 ± 1	^{285}572 ± 1	^{247}596 ± 1	^{706}2175 ± 44	^{704}2160 ± 53
1293	vinbigdata-003	259968	183557	^{106}342	^{491}2048 ± 0	^{898}849 ± 6	^{984}1312 ± 1	^{576}853 ± 2	^{890}1321 ± 2	^{430}832 ± 2	^{420}1074 ± 37	^{434}1086 ± 40
1294	vinbigdata-004	1570839	333050	^{878}3247	^{1216}4096 ± 0	^{1166}1162 ± 3	^{863}1155 ± 14	^{821}1141 ± 2	^{766}1171 ± 5	^{641}1140 ± 2	^{494}1299 ± 17	^{488}1252 ± 28
1295	vinbigdata-005	1106052	333050	^{767}2294	^{417}2048 ± 0	^{1206}1210 ± 1	^{930}1237 ± 1	^{905}1251 ± 1	^{821}1234 ± 1	^{734}1282 ± 7	^{58}251 ± 17	^{58}234 ± 16
1296	vinbigdata-006	1106052	333624	^{768}2294	^{740}2048 ± 0	^{1207}1210 ± 2	^{907}1205 ± 5	^{845}1175 ± 2	^{772}1178 ± 3	^{674}1202 ± 16	^{55}246 ± 16	^{57}232 ± 16
1297	vinbigdata-007	1106071	335755	^{769}2295	^{813}2048 ± 0	^{1199}1201 ± 10	^{874}1166 ± 3	^{906}1252 ± 6	^{839}1256 ± 15	^{716}1254 ± 20	^{56}249 ± 10	^{61}238 ± 16
1298	vion-000	228219	7533	^{166}498	^{998}2052 ± 0	^{271}333 ± 1	-	-	-	-	^{1315}39839 ± 3561	^{1276}26830 ± 2241
1299	visage-000	49218	70150	^{16}72	^{120}512 ± 0	^{5}27 ± 0	^{4}27 ± 0	^{4}31 ± 0	^{5}38 ± 0	^{6}63 ± 0	^{714}2220 ± 14	^{713}2218 ± 14
1300	visica-001	1	59680	^{13}68	^{221}1024 ± 0	^{75}144 ± 1	^{40}143 ± 1	^{37}151 ± 1	^{42}188 ± 2	^{106}383 ± 11	^{400}1035 ± 41	^{400}1017 ± 56
1301	visica-002	1	63831	^{33}126	^{586}2048 ± 0	^{65}124 ± 1	^{36}125 ± 1	^{38}156 ± 2	^{78}271 ± 4	^{471}892 ± 29	^{991}4759 ± 31	^{985}4630 ± 26
1302	visionbox-000	176501	190645	-	^{913}2048 ± 0	^{235}304 ± 7	-	-	-	-	^{590}1648 ± 57	^{474}1192 ± 42
1303	visionbox-001	256869	190645	-	^{349}2048 ± 0	^{1037}983 ± 7	^{811}1093 ± 46	^{988}1360 ± 68	^{1085}2181 ± 105	^{1079}5955 ± 281	^{457}1161 ± 22	^{463}1154 ± 20
1304	visionbox-002	259063	135281	^{220}613	^{1078}2059 ± 0	^{442}482 ± 1	^{289}482 ± 0	^{255}484 ± 1	^{228}492 ± 1	^{198}517 ± 3	^{671}1969 ± 44	^{664}1931 ± 42
1305	visionbox-003	259542	156891	^{517}1263	^{1088}2068 ± 0	^{700}678 ± 2	^{476}682 ± 1	^{435}682 ± 2	^{401}695 ± 2	^{360}739 ± 5	^{588}1643 ± 56	^{591}1649 ± 66
1306	visionbox-004	309730	154797	^{575}1422	^{1306}4116 ± 0	^{322}378 ± 1	^{190}369 ± 0	^{171}389 ± 5	^{160}402 ± 2	^{140}437 ± 4	^{687}2071 ± 31	^{692}2076 ± 41
1307	visionbox-005	309402	197528	^{673}1771	^{1305}4116 ± 0	^{286}350 ± 1	^{165}343 ± 1	^{136}351 ± 2	^{131}367 ± 5	^{151}454 ± 19	^{688}2074 ± 17	^{691}2067 ± 29
1308	visionbox-006	479723	170096	^{862}2995	^{1302}4107 ± 0	^{979}932 ± 2	^{722}973 ± 4	^{695}994 ± 6	^{636}1003 ± 11	^{624}1120 ± 20	^{680}2038 ± 74	^{679}2022 ± 31
1309	visionbox-007	479723	364416	^{794}2456	^{1303}4107 ± 0	^{616}619 ± 1	^{402}616 ± 0	^{382}629 ± 2	^{372}666 ± 7	^{404}794 ± 32	^{912}3524 ± 29	^{919}3527 ± 40
1310	visionlabs-001	343661	127922	-	^{20}204 ± 0	^{989}943 ± 8	-	-	-	-	^{515}1395 ± 45	^{457}1148 ± 53
1311	visionlabs-002	591936	46855	-	^{60}264 ± 0	^{189}265 ± 8	-	-	-	-	^{327}796 ± 35	^{334}799 ± 31
1312	visionlabs-003	639849	15246	-	^{48}260 ± 0	^{159}231 ± 5	-	-	-	-	^{123}439 ± 23	^{134}454 ± 20
1313	visionlabs-004	313016	90858	-	^{36}256 ± 0	^{236}304 ± 0	-	-	-	-	^{339}827 ± 26	^{356}865 ± 32
1314	visionlabs-005	369602	16523	-	^{96}512 ± 0	^{245}313 ± 0	-	-	-	-	^{345}848 ± 26	^{363}889 ± 37
1315	visionlabs-006	353044	16655	-	^{127}512 ± 0	^{191}270 ± 0	-	-	-	-	^{273}698 ± 19	^{313}734 ± 28
1316	visionlabs-007	357204	16643	-	^{149}512 ± 0	^{194}272 ± 0	-	-	-	-	^{377}965 ± 41	^{385}972 ± 31
1317	visionlabs-008	706099	19705	-	^{118}512 ± 0	^{425}467 ± 1	-	-	-	-	^{373}955 ± 23	^{379}962 ± 25
1318	visionlabs-009	706099	19862	-	^{154}513 ± 0	^{474}515 ± 41	^{279}472 ± 1	^{248}474 ± 1	^{217}476 ± 1	^{203}521 ± 1	^{375}957 ± 28	^{383}965 ± 32
1319	visionlabs-010	1067280	19357	^{360}883	^{157}513 ± 0	^{771}730 ± 0	^{516}717 ± 1	^{464}709 ± 0	^{419}713 ± 1	^{357}739 ± 0	^{197}600 ± 41	^{236}626 ± 35
1320	visionlabs-011	1067280	19353	^{376}923	^{156}513 ± 0	^{772}731 ± 1	^{515}717 ± 1	^{465}710 ± 1	^{420}714 ± 1	^{361}741 ± 1	^{166}556 ± 26	^{175}559 ± 25

Notes	
1	The configuration size does not capture static data included in libraries.
2	The library size is the combined total of all files provided in the submission lib folder. These libraries e.g. OpenCV may or may not be installed on any end user's platform natively and would not need to be installed with the algorithm. Some developers put neural network models in their libraries.
3	The memory usage is the peak resident set size reported by the ps system call during template generation.
4	The median template creation times are measured on Intel®Xeon®CPU E5-2630 v4 @ 2.20GHz processors.
5	The comparison durations, in nanoseconds, are estimated using std::chrono::high_resolution_clock which on the machine in (2) counts 1ns clock ticks. Precision is somewhat worse than that however. The ± value is the median absolute deviation times 1.48 for Normal consistency.

Table 51: Summary of algorithms and properties included in this report. The red superscripts give ranking for the quantity in that column.

	ALGORITHM	CONFIG	LIBRARY	TEMPLATE							COMPARISON[4]	
	NAME	DATA	DATA	MEMORY	SIZE	GENERATION TIME (ms)[4]					TIME (ns)[5]	
		(KB)[1]	(KB)[2]	(MB)[3]	(B)	MUGSHOT	480x720	960x1440	1600x2400	3000x4500	GENUINE	IMPOSTOR
1321	visteam-000	32729	17740	-	^{296}1536 ± 0	^{39}96 ± 7	^{27}102 ± 8	^{144}358 ± 19	^{652}1022 ± 50	^{1056}3987 ± 211	^{1061}6361 ± 87	^{1065}6668 ± 277
1322	visteam-001	186440	30878	-	^{1223}4096 ± 0	^{913}869 ± 7	^{635}872 ± 6	^{803}1121 ± 15	^{1040}1719 ± 38	^{1063}4375 ± 157	^{1081}7054 ± 108	^{1078}7025 ± 109
1323	visteam-002	186440	30888	-	^{1258}4096 ± 0	^{877}829 ± 5	^{605}832 ± 6	^{565}839 ± 7	^{524}853 ± 6	^{549}1013 ± 14	^{1077}6952 ± 118	^{1074}6970 ± 120
1324	visteam-003	215359	33730	^{163}493	^{1242}4096 ± 0	^{1238}1249 ± 4	^{940}1251 ± 4	^{918}1266 ± 5	^{854}1272 ± 5	^{794}1370 ± 9	^{1072}6816 ± 111	^{1070}6816 ± 105
1325	visteam-004	61594	35369	^{53}168	^{762}2048 ± 0	^{233}303 ± 5	^{144}313 ± 6	^{91}278 ± 4	^{85}288 ± 4	^{103}377 ± 7	^{949}3936 ± 72	^{955}3938 ± 79
1326	visteam-005	288140	35427	^{108}347	^{347}2048 ± 0	^{1136}1117 ± 6	^{821}1106 ± 6	^{754}1060 ± 4	^{684}1071 ± 4	^{651}1156 ± 8	^{947}3932 ± 97	^{952}3932 ± 71
1327	visteam-006	339353	47921	^{164}493	^{421}2048 ± 0	^{1060}1009 ± 1	^{759}1015 ± 1	^{732}1035 ± 2	^{649}1014 ± 1	^{568}1047 ± 2	^{802}2711 ± 32	^{807}2704 ± 41
1328	visteam-007	331673	264832	^{159}485	^{709}2048 ± 0	^{598}611 ± 1	^{416}625 ± 1	^{379}626 ± 1	^{320}615 ± 1	^{287}647 ± 0	^{801}2704 ± 38	^{811}2732 ± 54
1329	visteam-008	582800	264832	^{277}731	^{828}2048 ± 0	^{1182}1179 ± 1	^{878}1173 ± 1	^{875}1210 ± 1	^{786}1190 ± 3	^{685}1208 ± 1	^{794}2632 ± 28	^{795}2647 ± 42
1330	visteam-009	582793	48090	^{279}731	^{656}2048 ± 0	^{1176}1174 ± 1	^{889}1184 ± 1	^{879}1218 ± 2	^{808}1219 ± 2	^{714}1253 ± 2	^{795}2668 ± 34	^{800}2671 ± 38
1331	visteam-010	582793	48090	^{281}731	^{539}2048 ± 0	^{1175}1174 ± 1	^{905}1203 ± 2	^{877}1215 ± 1	^{809}1221 ± 1	^{712}1252 ± 1	^{797}2675 ± 51	^{804}2681 ± 57
1332	vivotek-001	15240	247926	^{35}128	^{332}2048 ± 0	^{44}100 ± 0	^{26}101 ± 0	^{23}106 ± 0	^{26}134 ± 0	^{46}238 ± 1	^{1274}26504 ± 57	^{1275}26520 ± 69
1333	vivotek-002	12769	247949	^{32}124	^{593}2048 ± 0	^{36}93 ± 0	^{21}93 ± 0	^{19}98 ± 0	^{16}95 ± 0	^{21}150 ± 0	^{749}2384 ± 19	^{751}2385 ± 20
1334	vixvizion-000	183453	599571	-	^{918}2048 ± 0	^{376}425 ± 24	-	-	-	-	^{446}1145 ± 25	^{609}1718 ± 63
1335	vixvizion-001	282680	256875	-	^{357}2048 ± 0	^{845}807 ± 29	-	-	-	-	^{402}1045 ± 22	^{375}934 ± 45
1336	vixvizion-002	227766	318409	-	^{688}2048 ± 0	^{824}786 ± 1	^{553}766 ± 2	^{598}885 ± 3	^{970}1430 ± 3	^{1057}4080 ± 10	^{255}676 ± 16	^{240}630 ± 20
1337	vixvizion-003	254860	378019	-	^{431}2048 ± 0	^{909}865 ± 2	^{691}938 ± 1	^{1083}1577 ± 1	^{1109}3002 ± 3	^{1099}9521 ± 16	^{303}738 ± 26	^{276}683 ± 25
1338	vixvizion-004	254405	380049	-	^{715}2048 ± 0	^{622}624 ± 1	^{376}587 ± 10	^{378}626 ± 3	^{304}592 ± 3	^{337}717 ± 6	^{310}760 ± 22	^{291}703 ± 28
1339	vixvizion-005	38886	534579	^{301}776	^{336}2048 ± 0	^{387}433 ± 4	^{199}381 ± 3	^{167}383 ± 3	^{136}373 ± 1	^{126}411 ± 1	^{298}731 ± 63	^{243}632 ± 32
1340	vixvizion-006	594053	396294	^{555}1359	^{732}2048 ± 0	^{927}876 ± 9	^{598}828 ± 3	^{542}817 ± 1	^{504}825 ± 2	^{459}871 ± 1	^{196}600 ± 23	^{222}611 ± 25
1341	vixvizion-007	594053	470119	^{586}1435	^{840}2048 ± 0	^{937}885 ± 35	^{599}828 ± 1	^{541}816 ± 1	^{506}825 ± 1	^{458}870 ± 1	^{198}600 ± 28	^{212}602 ± 34
1342	vnis-000	285395	1404886	^{192}546	^{519}2048 ± 0	^{392}437 ± 1	^{257}443 ± 1	^{230}456 ± 2	^{195}458 ± 2	^{164}477 ± 2	^{512}1386 ± 10	^{522}1382 ± 16
1343	vnpay-000	258919	1404844	^{168}504	^{562}2048 ± 0	^{164}239 ± 1	^{105}248 ± 0	^{85}252 ± 0	^{71}249 ± 0	^{54}260 ± 0	^{504}1353 ± 11	^{512}1353 ± 23
1344	vnpay-001	1044099	3060240	^{380}937	^{877}2048 ± 0	^{1163}1156 ± 1	^{943}1255 ± 1	^{907}1252 ± 2	^{845}1261 ± 2	^{737}1288 ± 10	^{524}1421 ± 32	^{529}1421 ± 26
1345	vnpt-001	266499	535529	-	^{706}2048 ± 0	^{458}499 ± 2	^{301}499 ± 2	^{263}494 ± 3	^{233}502 ± 3	^{191}512 ± 2	^{681}2049 ± 29	^{100}337 ± 121
1346	vnpt-002	271649	3203296	-	^{499}2048 ± 0	^{778}739 ± 2	^{525}731 ± 2	^{493}740 ± 1	^{445}742 ± 2	^{376}763 ± 2	^{314}766 ± 13	^{319}762 ± 13
1347	vnpt-003	369956	297799	-	^{1235}4096 ± 0	^{1280}1315 ± 4	^{986}1315 ± 4	^{958}1318 ± 2	^{906}1350 ± 3	^{838}1428 ± 3	^{1091}7397 ± 31	^{1089}7384 ± 29
1348	vnpt-004	370110	240841	^{401}992	^{895}2048 ± 0	^{1231}1238 ± 1	^{934}1241 ± 1	^{897}1242 ± 2	^{876}1307 ± 2	^{883}1505 ± 2	^{959}4047 ± 48	^{959}4008 ± 108
1349	vnpt-005	560630	240888	^{480}1157	^{869}2048 ± 0	^{1334}1403 ± 0	^{1035}1404 ± 6	^{1018}1403 ± 6	^{985}1456 ± 0	^{924}1630 ± 10	^{917}3562 ± 23	^{923}3554 ± 29
1350	vnpt-006	1114807	360198	^{762}2245	^{594}2048 ± 0	^{1254}1277 ± 2	^{1023}1390 ± 19	^{1026}1410 ± 14	^{1003}1481 ± 30	^{935}1703 ± 69	^{894}3400 ± 20	^{900}3393 ± 22
1351	vnpt-007	2113252	360190	^{903}3622	^{701}2048 ± 0	^{1152}1143 ± 1	^{865}1157 ± 4	^{840}1170 ± 2	^{776}1183 ± 3	^{688}1219 ± 3	^{904}3486 ± 41	^{911}3485 ± 35
1352	vnpt-008	1114270	360190	^{905}3641	^{661}2048 ± 0	^{1170}1165 ± 1	^{890}1186 ± 2	^{846}1177 ± 9	^{790}1201 ± 2	^{704}1244 ± 2	^{907}3506 ± 16	^{916}3510 ± 23
1353	vnpt-009	1114270	360190	^{904}3641	^{456}2048 ± 0	^{1171}1166 ± 1	^{898}1197 ± 6	^{860}1193 ± 6	^{799}1209 ± 3	^{711}1251 ± 4	^{914}3539 ± 17	^{922}3551 ± 31
1354	vocalize-001	0	38841	^{24}96	^{98}512 ± 0	^{18}57 ± 0	^{12}55 ± 0	^{8}56 ± 0	^{8}60 ± 0	^{5}62 ± 0	^{518}1400 ± 59	^{516}1365 ± 26
1355	vocord-001	616989	109135	-	^{1364}6194 ± 0	^{950}908 ± 16	-	-	-	-	^{1407}1094730 ± 64282	^{1407}1107193 ± 66523
1356	vocord-002	918292	648259	-	^{293}1330 ± 0	^{816}782 ± 36	-	-	-	-	^{1385}83063 ± 517	^{1383}83072 ± 714
1357	vocord-003	900909	1140643	-	^{203}817 ± 0	^{224}296 ± 3	-	-	-	-	^{1327}46683 ± 378	^{1308}36007 ± 292
1358	vocord-004	1754886	129419	-	^{207}896 ± 0	^{617}619 ± 1	-	-	-	-	^{649}1885 ± 66	^{653}1889 ± 71
1359	vocord-005	1060445	189974	-	^{198}768 ± 0	^{809}771 ± 1	-	-	-	-	^{618}1768 ± 48	^{605}1713 ± 77
1360	vocord-006	559457	189913	-	^{199}768 ± 0	^{939}886 ± 1	-	-	-	-	^{676}2020 ± 72	^{674}1969 ± 62
1361	vocord-007	587489	344995	-	^{317}1664 ± 0	^{815}780 ± 2	-	-	-	-	^{788}2593 ± 83	^{781}2526 ± 59
1362	vocord-008	603867	345047	-	^{1134}2688 ± 0	^{1014}962 ± 2	^{725}976 ± 2	^{755}1061 ± 3	^{824}1236 ± 23	^{954}1851 ± 9	^{852}3015 ± 50	^{855}2988 ± 62
1363	vocord-009	1380132	201560	^{940}4372	^{323}1920 ± 0	^{1369}1472 ± 2	^{1075}1472 ± 1	^{1080}1549 ± 1	^{1035}1667 ± 2	^{975}2064 ± 2	^{684}2052 ± 50	^{688}2056 ± 39
1364	vocord-010	902552	206873	^{917}3866	^{282}1088 ± 0	^{1363}1459 ± 2	^{1072}1459 ± 1	^{1057}1463 ± 2	^{1004}1484 ± 1	^{900}1535 ± 3	^{808}2724 ± 31	^{798}2653 ± 45

Notes	
1	The configuration size does not capture static data included in libraries.
2	The library size is the combined total of all files provided in the submission lib folder. These libraries e.g. OpenCV may or may not be installed on any end user's platform natively and would not need to be installed with the algorithm. Some developers put neural network models in their libraries.
3	The memory usage is the peak resident set size reported by the ps system call during template generation.
4	The median template creation times are measured on Intel®Xeon®CPU E5-2630 v4 @ 2.20GHz processors.
5	The comparison durations, in nanoseconds, are estimated using std::chrono::high_resolution_clock which on the machine in (2) counts 1ns clock ticks. Precision is somewhat worse than that however. The ± value is the median absolute deviation times 1.48 for Normal consistency.

Table 52: Summary of algorithms and properties included in this report. The red superscripts give ranking for the quantity in that column.

	ALGORITHM	CONFIG	LIBRARY	TEMPLATE							COMPARISON[4]	
	NAME	DATA	DATA	MEMORY	SIZE	GENERATION TIME (ms)[4]					TIME (ns)[5]	
		(KB)[1]	(KB)[2]	(MB)[3]	(B)	MUGSHOT	480x720	960x1440	1600x2400	3000x4500	GENUINE	IMPOSTOR
1365	vsoft-001	10202	61965	^{58}175	^{622}2048 ± 0	^{62}123 ± 8	^{38}131 ± 7	^{244}468 ± 19	^{966}1422 ± 48	^{1077}5622 ± 229	^{783}2553 ± 48	^{787}2559 ± 44
1366	vsoft-002	10202	62518	^{55}169	^{542}2048 ± 0	^{87}160 ± 10	^{49}164 ± 11	^{301}537 ± 21	^{1027}1581 ± 53	^{1080}6279 ± 228	^{958}4030 ± 260	^{948}3902 ± 137
1367	vsoft-003	10202	62894	^{76}258	^{1073}2057 ± 0	^{122}191 ± 14	^{71}191 ± 14	^{381}628 ± 27	^{1066}1895 ± 66	^{1090}7545 ± 376	^{1209}16609 ± 97	^{1213}16649 ± 154
1368	vts-000	256589	169760	^{650}1697	^{636}2048 ± 0	^{447}486 ± 1	^{288}481 ± 0	^{254}484 ± 0	^{222}485 ± 1	^{197}517 ± 0	^{1391}124209 ± 352	^{1391}123652 ± 358
1369	vts-001	293000	475743	^{225}622	^{682}2048 ± 0	^{694}676 ± 1	^{477}683 ± 6	^{441}687 ± 3	^{402}695 ± 2	^{329}709 ± 2	^{1129}9620 ± 44	^{1127}9618 ± 54
1370	vts-002	361977	904603	^{331}840	^{742}2048 ± 0	^{370}416 ± 5	^{245}434 ± 3	^{206}432 ± 3	^{187}449 ± 3	^{228}556 ± 4	^{1093}7447 ± 34	^{1091}7450 ± 54
1371	wicket-000	826392	641802	^{732}2071	^{674}2048 ± 0	^{1343}1419 ± 2	^{1054}1429 ± 3	^{1042}1444 ± 4	^{990}1460 ± 3	^{902}1537 ± 6	^{1355}60976 ± 232	^{1352}61096 ± 323
1372	winsense-000	270819	32034	-	^{291}1280 ± 0	^{211}283 ± 1	-	-	-	-	^{571}1551 ± 31	^{571}1532 ± 42
1373	winsense-001	264428	32035	^{375}922	^{288}1280 ± 0	^{802}766 ± 7	^{786}1058 ± 47	^{680}983 ± 97	^{669}1053 ± 119	^{762}1320 ± 84	^{586}1631 ± 28	^{672}1964 ± 171
1374	winsense-002	281379	25780	^{695}1855	^{606}2048 ± 0	^{453}494 ± 2	^{300}498 ± 1	^{286}519 ± 1	^{259}537 ± 1	^{272}634 ± 1	^{596}1683 ± 8	^{596}1685 ± 7
1375	wiseai-001	189467	60781	^{73}245	^{759}2048 ± 0	^{166}240 ± 0	^{107}251 ± 0	^{122}328 ± 1	^{110}327 ± 0	^{75}332 ± 0	^{827}2850 ± 29	^{832}2852 ± 31
1376	wuhantianyu-001	465118	66457	^{451}1086	^{610}2048 ± 0	^{646}642 ± 1	^{437}642 ± 1	^{405}644 ± 0	^{355}652 ± 0	^{324}697 ± 0	^{1119}9502 ± 151	^{1134}9920 ± 253
1377	x-laboratory-000	520020	197310	^{602}1524	^{1066}2056 ± 0	^{847}808 ± 7	^{654}897 ± 113	^{610}907 ± 103	^{546}886 ± 103	^{304}673 ± 39	^{295}725 ± 19	^{315}749 ± 34
1378	x-laboratory-001	625140	398792	^{691}1844	^{1044}2056 ± 0	^{558}586 ± 2	^{384}596 ± 5	^{352}603 ± 6	^{326}620 ± 7	^{403}793 ± 14	^{335}813 ± 28	^{357}872 ± 32
1379	xforwardai-000	242457	175556	-	^{407}2048 ± 0	^{795}757 ± 6	-	-	-	-	^{464}1185 ± 44	^{466}1157 ± 44
1380	xforwardai-001	340100	51163	^{751}2176	^{521}2048 ± 0	^{1185}1180 ± 2	^{888}1182 ± 1	^{861}1194 ± 1	^{784}1186 ± 2	^{676}1203 ± 1	^{320}779 ± 17	^{331}797 ± 13
1381	xforwardai-002	707715	51163	^{723}2003	^{1211}4096 ± 0	^{993}944 ± 1	^{695}942 ± 1	^{644}943 ± 4	^{578}935 ± 1	^{514}967 ± 1	^{522}1406 ± 8	^{525}1405 ± 13
1382	xm-000	578041	148920	^{256}684	^{964}2052 ± 0	^{929}878 ± 2	^{644}882 ± 1	^{685}988 ± 2	^{841}1258 ± 3	^{1013}2434 ± 7	^{587}1634 ± 17	^{585}1632 ± 20
1383	yisheng-000	122704	41760	-	^{815}2048 ± 0	^{47}103 ± 1	-	-	-	-	^{322}790 ± 23	^{328}789 ± 20
1384	yisheng-001	120112	41760	-	^{549}2048 ± 0	^{46}103 ± 1	-	-	-	-	^{360}906 ± 31	^{367}905 ± 25
1385	yisheng-002	604097	42014	-	^{294}1348 ± 0	^{267}332 ± 1	-	-	-	-	^{211}613 ± 40	^{190}588 ± 26
1386	yisheng-004	486351	38653	^{525}1279	^{1158}3704 ± 0	^{320}378 ± 12	-	-	-	-	^{270}693 ± 137	^{162}526 ± 34
1387	yitu-000	2211068	76146	-	^{1308}4130 ± 0	^{684}672 ± 2	-	-	-	-	^{1304}35352 ± 114	^{1313}37848 ± 1773
1388	yitu-001	2069440	138901	-	^{1316}4146 ± 0	^{787}751 ± 0	-	-	-	-	^{1310}37810 ± 127	^{1307}35486 ± 203
1389	yitu-002	1726673	138901	-	^{1317}4147 ± 0	^{727}691 ± 0	-	-	-	-	^{1305}35435 ± 111	^{1305}35325 ± 131
1390	yitu-003	1525719	138919	^{910}3737	^{1100}2082 ± 0	^{906}860 ± 0	-	-	-	-	^{1221}18305 ± 71	^{1224}18286 ± 62
1391	yoonik-000	290414	206059	-	^{718}2048 ± 0	^{985}941 ± 3	^{713}965 ± 13	^{665}964 ± 10	^{603}964 ± 9	^{519}974 ± 23	^{437}1116 ± 34	^{444}1113 ± 54
1392	yoonik-001	346629	265353	-	^{919}2048 ± 0	^{1219}1223 ± 3	^{932}1238 ± 1	^{893}1238 ± 1	^{827}1240 ± 1	^{700}1240 ± 1	^{280}706 ± 29	^{283}690 ± 26
1393	yoonik-002	453720	265415	^{834}2737	^{768}2048 ± 0	^{1153}1145 ± 4	^{835}1123 ± 2	^{807}1124 ± 2	^{724}1125 ± 2	^{631}1126 ± 3	^{311}761 ± 32	^{314}736 ± 32
1394	yoonik-003	346691	265415	^{749}2161	^{751}2048 ± 0	^{1045}991 ± 3	^{731}980 ± 1	^{681}984 ± 4	^{612}982 ± 1	^{525}983 ± 1	^{261}684 ± 45	^{271}678 ± 41
1395	yoonik-004	469597	88673	^{307}792	^{430}2048 ± 0	^{1213}1219 ± 1	^{962}1284 ± 1	^{911}1255 ± 1	^{848}1266 ± 0	^{710}1251 ± 1	^{401}1039 ± 42	^{407}1030 ± 40
1396	yoti-001	267246	470114	^{470}1125	^{902}2048 ± 0	^{1230}1238 ± 4	^{988}1316 ± 17	^{1123}4099 ± 13	^{1116}4160 ± 45	^{1069}4774 ± 95	^{1139}10352 ± 247	^{1141}10364 ± 246
1397	yoti-002	164043	470114	^{450}1086	^{389}2048 ± 0	^{588}604 ± 1	^{580}802 ± 3	^{535}812 ± 4	^{582}938 ± 15	^{798}1373 ± 4	^{1142}10662 ± 805	^{1140}10320 ± 265
1398	ytu-000	1477360	44032	^{797}2484	^{775}2048 ± 0	^{488}530 ± 0	^{329}533 ± 0	^{402}640 ± 0	^{532}861 ± 2	^{962}1949 ± 8	^{1291}31797 ± 131	^{1292}31794 ± 133
1399	yuan-000	370472	331437	-	^{680}2048 ± 0	^{1133}1112 ± 6	-	-	-	-	^{816}2777 ± 44	^{846}2937 ± 87
1400	yuan-001	370473	189558	-	^{883}2048 ± 0	^{1314}1383 ± 3	^{1028}1394 ± 3	^{1022}1408 ± 3	^{991}1461 ± 4	^{922}1615 ± 4	^{744}2344 ± 25	^{741}2325 ± 42
1401	yuan-002	370472	165662	-	^{331}2048 ± 0	^{1344}1420 ± 3	^{1055}1429 ± 4	^{1074}1511 ± 4	^{1036}1695 ± 4	^{1011}2408 ± 5	^{734}2297 ± 23	^{738}2310 ± 31
1402	yuan-003	370419	147783	-	^{941}2048 ± 0	^{1335}1405 ± 2	^{1043}1413 ± 3	^{1045}1446 ± 3	^{1019}1547 ± 5	^{958}1878 ± 5	^{739}2320 ± 32	^{730}2287 ± 34
1403	yuan-004	428665	50011	^{554}1356	^{1227}4096 ± 0	^{532}567 ± 0	^{360}569 ± 0	^{326}573 ± 0	^{288}579 ± 0	^{256}607 ± 0	^{1038}5816 ± 35	^{1039}5800 ± 31
1404	yuan-005	258312	145564	^{334}843	^{726}2048 ± 0	^{327}381 ± 0	^{203}386 ± 0	^{169}387 ± 2	^{147}390 ± 4	^{133}421 ± 3	^{456}1156 ± 8	^{475}1196 ± 26
1405	yuan-006	1622733	145572	^{939}4371	^{1176}4096 ± 0	^{1255}1280 ± 2	^{953}1268 ± 1	^{925}1273 ± 0	^{853}1272 ± 2	^{753}1306 ± 3	^{712}2202 ± 19	^{709}2190 ± 20
1406	yuan-007	258312	145568	^{632}1614	^{856}2048 ± 0	^{299}359 ± 0	^{181}361 ± 1	^{163}379 ± 4	^{140}380 ± 0	^{129}417 ± 0	^{288}715 ± 4	^{308}726 ± 16
1407	yuan-008	620369	167833	^{633}1626	^{1244}4096 ± 0	^{1172}1169 ± 0	^{547}752 ± 0	^{500}752 ± 3	^{467}775 ± 4	^{397}782 ± 0	^{506}1362 ± 16	^{519}1377 ± 19
1408	yuan-009	1161457	167833	^{800}2507	^{1200}4096 ± 0	^{1336}1408 ± 2	^{1048}1418 ± 2	^{1061}1471 ± 1	^{935}1387 ± 8	^{828}1414 ± 12	^{497}1326 ± 11	^{508}1336 ± 29

Notes	
1	The configuration size does not capture static data included in libraries.
2	The library size is the combined total of all files provided in the submission lib folder. These libraries e.g. OpenCV may or may not be installed on any end user's platform natively and would not need to be installed with the algorithm. Some developers put neural network models in their libraries.
3	The memory usage is the peak resident set size reported by the ps system call during template generation.
4	The median template creation times are measured on Intel®Xeon®CPU E5-2630 v4 @ 2.20GHz processors.
5	The comparison durations, in nanoseconds, are estimated using std::chrono::high_resolution_clock which on the machine in (2) counts 1ns clock ticks. Precision is somewhat worse than that however. The ± value is the median absolute deviation times 1.48 for Normal consistency.

Table 53: Summary of algorithms and properties included in this report. The red superscripts give ranking for the quantity in that column.

	ALGORITHM	CONFIG	LIBRARY	TEMPLATE							COMPARISON[4]	
	NAME	DATA	DATA	MEMORY	SIZE	GENERATION TIME (ms)[4]					TIME (ns)[5]	
		(KB)[1]	(KB)[2]	(MB)[3]	(B)	MUGSHOT	480x720	960x1440	1600x2400	3000x4500	GENUINE	IMPOSTOR
1409	yuan-010	1054332	167833	^{799}2499	^{1212}4096 ± 0	^{1253}1276 ± 1	^{1040}1406 ± 8	^{942}1294 ± 1	^{879}1308 ± 2	^{802}1375 ± 2	^{501}1331 ± 22	^{510}1349 ± 47
1410	yuanli-001	136632	47927	^{65}190	^{232}1024 ± 0	^{73}142 ± 0	^{42}143 ± 0	^{32}145 ± 0	^{28}150 ± 0	^{37}210 ± 1	^{689}2080 ± 16	^{693}2083 ± 22

Notes	
1	The configuration size does not capture static data included in libraries.
2	The library size is the combined total of all files provided in the submission lib folder. These libraries e.g. OpenCV may or may not be installed on any end user's platform natively and would not need to be installed with the algorithm. Some developers put neural network models in their libraries.
3	The memory usage is the peak resident set size reported by the ps system call during template generation.
4	The median template creation times are measured on Intel®Xeon®CPU E5-2630 v4 @ 2.20GHz processors.
5	The comparison durations, in nanoseconds, are estimated using std::chrono::high_resolution_clock which on the machine in (2) counts 1ns clock ticks. Precision is somewhat worse than that however. The ± value is the median absolute deviation times 1.48 for Normal consistency.

Table 54: Summary of algorithms and properties included in this report. The red superscripts give ranking for the quantity in that column.

		FALSE NON-MATCH RATE (FNMR)															
	Algorithm	CONSTRAINED, COOPERATIVE														LESS CONSTRAINED, NON-COOP.	
	Name	VISAMC		VISA		MUGSHOT		MUGSHOT12+YRS		VISABORDER		BORDER		BORDER		KIOSKBORDER	
	FMR	0.0001		1E-06		1E-05		1E-05		1E-06		1E-06		1E-05		1E-06	
1	2060io-001	-		-		0.9149	1281	0.9720	1277	0.9773	1236	0.9768	1092	0.8672	1123	0.9993	737
2	2060io-002	-		-		0.8904	1279	0.9587	1275	0.9020	1222	1.0000	1230	1.0000	1251	1.0000	831
3	20face-000	0.1268	936	0.1828	928	0.1748	1180	0.2768	1180	0.1765	1103	0.1864	808	0.0927	886	0.5943	541
4	20face-001	0.0521	859	0.0732	852	0.1414	1173	0.2549	1176	0.0769	1051	0.1354	783	0.0419	796	0.8953	633
5	3divi-000	-		0.1335	901	-		-		-		-		-		-	
6	3divi-001	0.0777	898	0.1540	914	-		-		-		-		-		-	
7	3divi-002	0.0788	900	0.1539	912	-		-		-		-		-		-	
8	3divi-003	0.0318	821	0.0588	831	0.0389	1085	0.0639	1079	0.0619	1036	0.0928	738	0.0555	836	-	
9	3divi-004	0.0095	550	0.0153	563	0.0097	845	0.0145	835	0.0175	824	0.0330	578	0.0242	699	-	
10	3divi-005	0.0094	546	0.0151	558	0.0078	768	0.0121	767	0.0135	748	0.0231	503	0.0156	578	-	
11	3divi-006	0.0064	430	0.0094	430	0.0047	586	0.0066	590	0.0091	622	0.0191	456	0.0113	471	0.2854	463
12	3divi-007	0.0024	139	0.0038	150	0.0028	289	0.0034	290	0.0046	400	0.0101	290	0.0082	359	0.2515	444
13	accurascan-001	0.3670	1002	0.4777	1008	0.5313	1231	0.6155	1224	0.5583	1170	0.6120	960	0.2569	982	0.8833	624
14	accurascan-002	0.4209	1012	0.5213	1018	0.5826	1239	0.6642	1228	0.6295	1174	0.6937	978	0.3116	1004	0.9162	640
15	accurascan-003	0.0017	83	0.0028	91	0.0024	133	0.0024	103	0.0029	192	0.0057	107	0.0048	142	0.0629	110
16	acer-000	0.1393	941	0.9075	1068	0.9981	1294	1.0000	1301	1.0000	1258	1.0000	1205	0.9998	1224	-	
17	acer-001	0.0294	806	0.0504	811	0.0240	1037	0.0463	1042	0.0436	995	0.0622	697	0.0360	776	-	
18	acer-002	0.0169	708	0.0262	708	0.0103	862	0.0167	883	0.0182	834	0.0281	541	0.0159	581	0.1555	369
19	acisw-003	0.9682	1067	0.9971	1078	0.7892	1272	0.8738	1266	0.8752	1216	0.8275	1025	0.6698	1081	-	
20	acisw-006	0.2945	990	0.9788	1074	0.6044	1241	0.7588	1239	0.9900	1240	1.0000	1209	0.9999	1231	-	
21	acisw-007	0.4276	1014	0.5493	1025	0.8425	1275	0.9185	1273	0.8424	1207	0.9976	1147	0.9930	1188	0.9999	769
22	acisw-008	0.0100	566	0.0147	551	0.0094	831	0.0126	777	0.1740	1102	0.6651	973	0.4545	1041	0.9302	646
23	adera-001	0.1021	918	0.1757	921	0.1823	1181	0.2967	1183	0.1714	1101	0.6357	964	0.1127	903	-	
24	adera-002	0.0052	352	0.0071	340	0.0047	579	0.0064	582	0.0087	604	0.0159	403	0.0136	533	-	
25	adera-003	0.0043	294	0.0059	287	0.0036	459	0.0043	415	0.0076	561	0.0151	387	0.0128	512	0.1526	368
26	adera-004	0.0014	53	0.0022	54	0.0035	448	0.0050	475	0.0023	81	0.0212	476	0.0058	214	0.1469	359
27	adera-005	0.0017	76	0.0026	74	0.0027	262	0.0030	220	0.0024	93	0.0134	355	0.0049	146	0.1246	320
28	advance-002	0.0089	527	0.0137	533	0.0073	747	0.0115	755	0.0400	982	0.0722	719	0.0593	845	-	
29	advance-003	0.0060	412	0.0087	406	0.0052	623	0.0067	593	0.0389	979	0.4914	926	0.1291	916	0.7998	595
30	advance-004	0.0083	513	0.0101	464	0.0037	484	0.0054	510	0.0051	436	0.3555	890	0.1088	899	0.8285	601
31	advance-005	0.0059	404	0.0084	398	0.0043	548	0.0060	552	0.0065	518	0.9998	1192	0.9993	1212	1.0000	844
32	advance-006	-		-		0.0032	398	0.0042	404	0.0034	277	0.9982	1153	0.5024	1050	1.0000	837
33	affinsys-ai-000	-		-		0.1154	1162	0.1788	1155	0.1886	1110	0.2159	827	0.1383	924	0.6126	546
34	afisbiometrics-000	0.0051	347	0.0073	349	0.0030	347	0.0050	480	0.0044	376	0.0077	190	0.0057	211	0.0796	196
35	afrengine-000	0.6244	1045	0.7336	1052	0.8318	1274	0.9083	1270	0.8122	1199	0.9980	1151	0.9895	1183	1.0000	773
36	afrengine-001	0.0071	462	0.0129	521	0.0094	836	0.0201	921	0.0097	653	0.9737	1090	0.8179	1114	0.9999	754
37	afrengine-002	0.0052	357	0.0071	338	0.0032	387	0.0043	420	0.0194	857	0.2125	825	0.0450	807	0.2330	436
38	afrengine-003	-		-		0.0028	303	0.0031	253	0.0116	708	0.0224	493	0.0208	666	0.0860	216
39	afrengine-004	-		-		0.0027	277	0.0028	192	0.1475	1091	0.2477	847	0.2470	978	0.2062	421
40	afrengine-005	-		-		0.0028	306	0.0031	238	0.0035	286	0.0078	195	0.0059	229	0.0768	183
41	aifirst-001	0.0119	620	0.0170	595	0.0084	798	0.0127	787	0.0131	738	0.0212	475	0.0138	538	-	
42	aigen-001	0.0124	632	0.0219	662	0.0143	956	0.0217	933	0.0236	899	0.8960	1045	0.3255	1010	-	
43	aigen-002	0.0192	736	0.0343	752	0.0256	1041	0.0402	1020	0.0389	978	0.9196	1054	0.3876	1026	0.9994	742
44	aigroup-000	-		-		0.0683	1132	0.0774	1097	0.0612	1032	0.9816	1099	0.9069	1139	1.0000	1158

Table 55: FNMR is the proportion of mated comparisons below a threshold set to achieve the FMR given in the header on the fourth row. FMR is the proportion of impostor comparisons at or above that threshold. The light grey values give rank over all algorithms in that column. The pink columns use only same-sex impostors; others are selected regardless of demographics. The exception, in the green column, uses "matched-covariates" i.e. impostors of the same sex, age group, and country of birth. The second pink column includes effects of extended ageing. Missing entries for border, visa, mugshot and wild images generally mean the algorithm did not run to completion. The VISA *columns compare images described in section 2.1. The* MUGSHOT *columns compare images described in section 2.5. The* VISA-BORDER *column compare images described in section 2.2 with those of section 2.4. The* BORDER *column compares images described in section 2.4. The* KIOSK-BORDER *columns compare images described in section 2.6 with those of section 2.4.*

	Algorithm	FALSE NON-MATCH RATE (FNMR)													
		CONSTRAINED, COOPERATIVE												LESS CONSTRAINED, NON-COOP.	
	Name	VISAMC		VISA		MUGSHOT		MUGSHOT12+YRS		VISABORDER		BORDER		BORDER		KIOSKBORDER	
	FMR	0.0001		1E-06		1E-05		1E-05		1E-06		1E-06		1E-05		1E-06	
45	aigroup-001	-		-		0.0114	903	0.0192	912	0.0179	827	0.9998	1194	0.9986	1209	1.0000	1064
46	aigroup-002	-		-		0.0034	427	0.0049	473	0.0041	349	0.9104	1050	0.7156	1095	0.9949	708
47	ailabs-001	0.0158	695	0.0276	716	0.0192	998	0.0317	994	0.0352	963	0.0608	693	0.0434	801	-	
48	aimall-001	0.0176	719	0.0324	741	0.0225	1026	0.0407	1024	-		-		-		-	
49	aimall-002	0.0119	619	0.0167	589	0.0224	1023	0.0411	1025	0.0233	891	0.0373	619	0.0235	692	-	
50	aimall-003	0.0033	218	0.0041	174	0.0033	419	0.0035	321	0.0056	469	0.0109	312	0.0087	379	-	
51	aiseemu-001	0.0021	111	0.0029	97	0.0027	259	0.0033	277	0.0038	318	0.0339	591	0.0057	212	0.4819	514
52	aiseemu-002	0.0023	128	0.0032	113	0.0026	218	0.0027	161	0.0036	293	0.0439	637	0.0057	207	0.4259	502
53	aiunionface-000	0.0104	577	0.0154	564	0.0082	790	0.0122	770	0.0141	759	0.0243	510	0.0169	599	-	
54	aize-001	0.0223	762	0.0344	754	0.0199	1004	0.0313	990	0.0367	970	0.0522	670	0.0359	774	0.2506	443
55	aize-002	0.0210	752	0.0327	742	0.0280	1051	0.0489	1053	0.0504	1012	0.0692	714	0.0434	800	0.2657	455
56	aize-003	0.0086	520	0.0125	517	0.0072	739	0.0126	781	0.0516	1016	0.6137	961	0.1038	895	0.9911	698
57	aize-006	-		-		0.0081	785	0.0160	866	0.0133	743	0.9925	1125	0.9473	1153	1.0000	779
58	ajou-001	0.0093	544	0.0147	550	0.0071	738	0.0126	778	0.0173	821	0.0274	535	0.0186	632	-	
59	alchera-000	0.0165	705	0.0243	687	0.0125	925	0.0186	905	0.0204	866	0.0349	598	0.0243	701	-	
60	alchera-001	0.0183	728	0.0299	727	0.0142	951	0.0234	948	0.0239	906	0.0388	626	0.0267	723	-	
61	alchera-002	0.0107	588	0.0157	574	0.0104	866	0.0229	944	0.0144	767	0.0246	514	0.0198	653	-	
62	alchera-003	0.0044	299	0.0055	269	0.0031	363	0.0039	368	0.0042	357	0.0077	192	0.0065	250	0.0777	187
63	alchera-004	0.0035	242	0.0052	256	0.0028	310	0.0039	369	0.0029	196	0.0075	180	0.0044	120	0.0742	164
64	alchera-005	0.0027	165	0.0040	165	0.0026	209	0.0030	215	0.0025	127	0.0055	103	0.0040	94	0.0642	121
65	alchera-006	0.0028	177	0.0039	161	0.0026	217	0.0031	244	0.0025	120	0.0090	247	0.0042	103	0.0867	217
66	alchera-007	0.0034	235	0.0049	239	0.0026	216	0.0031	246	0.0026	148	0.0096	273	0.0044	115	0.0834	212
67	alchera-008	-		-		0.0026	203	0.0030	222	0.0024	113	0.0099	281	0.0043	109	0.0951	259
68	alchera-009	-		-		0.0026	238	0.0029	205	0.0022	66	0.5197	936	0.2232	973	0.8470	606
69	alfabeta-001	0.4867	1030	0.5831	1033	0.6855	1251	0.8156	1252	0.8253	1205	0.7765	1003	0.6416	1079	0.9627	660
70	alice-000	0.0119	621	0.0192	631	0.0106	873	0.0170	886	0.0167	808	0.0265	529	0.0150	568	0.1824	399
71	alice-001	0.0034	236	0.0046	219	0.0032	385	0.0037	347	0.0030	221	0.3164	875	0.1088	900	0.8336	602
72	alleyes-000	0.0058	393	0.0090	419	0.0055	646	0.0087	687	0.0068	526	0.0105	302	0.0076	330	-	
73	allgovision-000	0.0346	830	0.0527	818	0.0232	1031	0.0339	997	0.0372	974	0.0620	696	0.0443	806	-	
74	alphaface-001	0.0065	436	0.0097	445	0.0039	505	0.0063	578	0.0083	589	-		-		-	
75	alphaface-002	0.0052	358	0.0075	360	0.0030	333	0.0044	429	1.0000	1268	0.0115	330	0.0084	370	-	
76	alttekglobal-000	-		-		0.0031	353	0.0046	438	0.0051	435	0.0097	279	0.0075	318	0.0927	252
77	amplifiedgroup-001	0.5034	1032	0.5848	1034	0.6973	1255	0.8316	1253	0.7807	1194	0.7724	1000	0.6354	1074	-	
78	androvideo-000	0.0243	774	0.0438	789	0.0239	1035	0.0365	1012	0.0483	1006	0.1870	809	0.0635	850	-	
79	anke-000	0.0194	739	0.0260	705	-		-		-		-		-		-	
80	anke-001	0.0186	731	0.0238	684	-		-		-		-		-		-	
81	anke-002	0.0402	840	0.0759	858	0.0271	1049	0.0484	1051	-		-		-		-	
82	anke-003	0.0131	648	0.0213	655	0.0094	833	0.0175	888	0.0134	745	0.9951	1133	0.0150	567	-	
83	anke-004	0.0080	502	0.0154	565	0.0073	746	0.0112	749	0.0102	671	0.0178	437	0.0118	486	-	
84	anke-005	0.0070	454	0.0109	481	0.0059	675	0.0094	701	0.0105	677	0.0142	366	0.0102	435	-	
85	antheus-000	0.2564	982	0.3776	990	0.7240	1259	0.8699	1263	0.8899	1219	0.9872	1108	0.9483	1154	-	
86	antheus-001	0.1311	937	0.2306	948	0.5113	1229	0.6797	1230	0.8748	1215	0.9908	1118	0.9649	1165	-	
87	antheus-002	-		-		0.0119	913	0.0157	856	0.0104	676	0.9974	1145	0.9791	1173	1.0000	803
88	anyvision-001	0.0716	891	0.0859	869	-		-		-		-		-		-	

Table 56: FNMR is the proportion of mated comparisons below a threshold set to achieve the FMR given in the header on the fourth row. FMR is the proportion of impostor comparisons at or above that threshold. The light grey values give rank over all algorithms in that column. The pink columns use only same-sex impostors; others are selected regardless of demographics. The exception, in the green column, uses "matched-covariates" i.e. impostors of the same sex, age group, and country of birth. The second pink column includes effects of extended ageing. Missing entries for border, visa, mugshot and wild images generally mean the algorithm did not run to completion. The VISA *columns compare images described in section 2.1. The* MUGSHOT *columns compare images described in section 2.5. The* VISA-BORDER *column compare images described in section 2.2 with those of section 2.4. The* BORDER *column compares images described in section 2.4. The* KIOSK-BORDER *columns compare images described in section 2.6 with those of section 2.4.*

		FALSE NON-MATCH RATE (FNMR)															
	Algorithm	CONSTRAINED, COOPERATIVE														LESS CONSTRAINED, NON-COOP.	
	Name	VISAMC		VISA		MUGSHOT		MUGSHOT12+YRS		VISABORDER		BORDER		BORDER		KIOSKBORDER	
	FMR	0.0001		1E-06		1E-05		1E-05		1E-06		1E-06		1E-05		1E-06	
89	anyvision-002	0.0660	886	0.0898	875	0.0928	1149	0.1512	1144	0.0899	1065	0.1191	769	0.0801	869	-	
90	anyvision-004	0.0267	792	0.0385	772	0.0258	1043	0.0487	1052	0.0234	896	0.0301	553	0.0191	639	-	
91	anyvision-005	0.0023	132	0.0037	147	0.0027	284	0.0035	311	0.0049	423	0.0084	226	0.0069	276	-	
92	aratek-001	0.0033	224	0.0045	212	0.0028	299	0.0031	254	0.0043	362	0.0092	256	0.0069	279	0.0897	232
93	armatura-001	0.0033	214	0.0042	182	0.0031	362	0.0037	341	0.0056	468	0.0110	313	0.0092	399	0.4625	510
94	armatura-002	0.0041	281	0.0052	254	0.0034	428	0.0044	422	0.0040	335	0.8502	1031	0.0275	728	0.9970	721
95	armatura-003	0.0020	106	0.0029	96	0.0026	231	0.0028	172	0.0025	132	0.0049	82	0.0043	110	0.0608	98
96	arvis-000	-		-		0.3652	1212	0.4777	1207	1.0000	1397	1.0000	1396	1.0000	1356	1.0000	903
97	asr-000	-		-		0.5523	1233	0.7662	1240	0.8807	1217	1.0000	1236	1.0000	1237	1.0000	832
98	asr-001	-		-		0.0030	331	0.0039	366	0.0027	167	0.3390	881	0.1327	921	0.7167	572
99	asusaics-000	0.0125	636	0.0209	650	0.0085	800	0.0134	803	0.0143	765	0.7189	984	0.0285	735	-	
100	asusaics-001	0.0125	637	0.0210	652	0.0085	802	0.0134	804	0.0143	766	0.7437	990	0.0289	740	-	
101	autentika-000	0.1415	943	0.1916	932	0.4130	1219	0.5521	1216	0.4217	1159	0.9998	1190	0.9954	1195	1.0000	846
102	autentika-001	0.0444	850	0.0688	847	0.0987	1151	0.1531	1145	0.1547	1094	1.0000	1206	0.9997	1223	1.0000	823
103	autentika-002	0.0536	863	0.0866	871	0.0657	1129	0.1084	1123	0.1548	1095	0.9993	1170	0.9939	1191	1.0000	826
104	autentika-003	-		-		0.0203	1006	0.0314	991	0.0404	984	0.9791	1095	0.9294	1147	0.9994	741
105	authenmetric-002	0.0092	539	0.0134	527	0.0095	837	0.0177	890	0.0192	850	0.0463	650	0.0236	694	-	
106	authenmetric-003	0.0036	251	0.0053	262	0.0039	513	0.0051	485	0.0095	644	0.9930	1126	0.5932	1066	1.0000	795
107	authenmetric-004	0.0027	170	0.0042	183	0.0033	410	0.0036	337	0.0083	592	0.9879	1111	0.4058	1033	1.0000	784
108	authme-001	0.0036	243	0.0049	235	0.0037	486	0.0040	377	0.0030	218	0.3075	869	0.1310	919	0.7046	567
109	authme-002	-		-		0.0032	393	0.0035	314	0.0026	156	0.4284	914	0.2115	970	0.7861	591
110	aware-000	0.1965	965	0.3090	972	-		-		-		-		-		-	
111	aware-001	0.1965	964	0.3092	973	-		-		-		-		-		-	
112	aware-002	0.1951	963	0.3202	976	-		-		-		-		-		-	
113	aware-003	0.0793	901	0.1161	895	0.1028	1153	0.1708	1151	0.1698	1100	0.2333	838	0.1174	909	-	
114	aware-004	0.0690	889	0.0949	881	0.0837	1144	0.1436	1142	0.1171	1079	0.8137	1016	0.1056	896	-	
115	aware-005	0.0457	853	0.0643	837	0.0603	1122	0.1094	1127	0.0613	1033	0.1075	758	0.0491	819	-	
116	aware-006	0.0487	856	0.0819	865	0.0529	1114	0.1090	1125	0.1011	1075	0.1058	753	0.0502	823	0.5309	523
117	aware-007	0.0101	571	0.0198	642	0.0060	686	0.0133	800	0.0224	882	0.5813	951	0.1673	952	0.8871	628
118	aware-008	-		-		0.0062	694	0.0143	832	0.0135	747	0.0332	581	0.0133	521	0.3622	481
119	awiros-001	0.4044	1008	0.4622	1005	0.5530	1234	0.6518	1226	0.2008	1113	0.1994	815	0.1386	926	-	
120	awiros-002	0.1990	968	0.2561	955	0.3319	1209	0.4411	1204	0.3821	1152	0.9938	1128	0.2634	988	-	
121	awiros-003	-		-		0.0128	932	0.0158	861	0.9978	1244	1.0000	1228	1.0000	1243	1.0000	841
122	awiros-004	-		-		0.0158	981	0.0255	958	0.9981	1247	1.0000	1231	1.0000	1248	1.0000	800
123	aximetria-001	0.0111	598	0.0186	622	0.0110	883	0.0148	843	0.0170	814	0.3928	904	0.2090	968	0.7924	592
124	ayftech-001	0.0946	913	0.1941	934	0.2438	1195	0.3625	1193	0.1558	1096	0.1589	797	0.0936	888	-	
125	ayftech-003	0.0023	136	0.0037	144	0.0026	239	0.0030	235	0.0072	546	0.5411	942	0.2515	979	0.8902	629
126	ayonix-000	0.4351	1017	0.4872	1011	0.6150	1243	0.7510	1238	0.6557	1180	0.6361	965	0.4981	1048	-	
127	beethedata-000	0.0127	642	0.0195	634	0.0092	821	0.0157	857	0.0171	817	0.0306	557	0.0204	659	0.1617	381
128	betaface-000	0.8804	1060	0.8998	1064	-		-		-		-		-		-	
129	betaface-002	0.8813	1061	0.8998	1065	-		-		-		-		-		-	
130	beyneai-000	0.0071	464	0.0107	478	0.0104	867	0.0131	796	0.0170	815	0.9837	1102	0.6171	1070	1.0000	771
131	biocube-001	0.5596	1040	0.6834	1046	0.7700	1270	0.8712	1264	0.8446	1208	0.9661	1085	0.7922	1110	0.9846	687
132	biocube-002	0.0612	875	0.0856	868	0.2330	1193	0.2972	1184	0.2365	1130	0.9327	1067	0.6947	1085	0.9989	732

Table 57: FNMR is the proportion of mated comparisons below a threshold set to achieve the FMR given in the header on the fourth row. FMR is the proportion of impostor comparisons at or above that threshold. The light grey values give rank over all algorithms in that column. The pink columns use only same-sex impostors; others are selected regardless of demographics. The exception, in the green column, uses "matched-covariates" i.e. impostors of the same sex, age group, and country of birth. The second pink column includes effects of extended ageing. Missing entries for border, visa, mugshot and wild images generally mean the algorithm did not run to completion. The VISA *columns compare images described in section 2.1. The* MUGSHOT *columns compare images described in section 2.5. The* VISA-BORDER *column compare images described in section 2.2 with those of section 2.4. The* BORDER *column compares images described in section 2.4. The* KIOSK-BORDER *columns compare images described in section 2.6 with those of section 2.4.*

	Algorithm	FALSE NON-MATCH RATE (FNMR)															
		CONSTRAINED, COOPERATIVE														LESS CONSTRAINED, NON-COOP.	
	Name	VISAMC		VISA		MUGSHOT		MUGSHOT12+YRS		VISABORDER		BORDER		BORDER		KIOSKBORDER	
	FMR	0.0001		1E-06		1E-05		1E-05		1E-06		1E-06		1E-05		1E-06	
133	bioid-001	-		-		0.0121	917	0.0197	919	0.0148	772	0.9883	1112	0.7807	1107	0.9997	748
134	bioid-002	-		-		0.0127	930	0.0205	924	0.0158	788	0.7684	999	0.0224	681	0.9859	689
135	bioid-003	-		-		0.0083	794	0.0137	812	0.0112	699	0.1141	763	0.0135	526	0.3783	489
136	bioid-004	-		-		0.0083	797	0.0136	809	0.0109	691	0.1377	787	0.0139	542	0.5446	527
137	bioidtechswiss-000	0.0066	442	0.0082	393	0.0113	899	0.0225	939	0.0078	570	0.0139	362	0.0092	394	-	
138	bioidtechswiss-001	0.0054	367	0.0072	342	0.0069	728	0.0124	773	0.0060	490	0.0094	266	0.0065	258	-	
139	bioidtechswiss-002	0.0049	326	0.0067	321	0.0064	702	0.0116	757	0.0067	523	0.0117	335	0.0086	376	-	
140	bioidtechswiss-003	-		-		0.0045	564	0.0050	478	0.0193	854	0.0360	606	0.0356	770	0.1320	328
141	biometric-vision-000	0.0023	131	0.0036	136	0.0028	302	0.0034	304	0.0028	188	0.3109	872	0.1504	935	0.6849	562
142	biometrik-001	-		-		0.7415	1263	0.8509	1256	0.9980	1246	1.0000	1369	0.9877	1181	1.0000	1003
143	biometrik-002	-		-		0.0641	1126	0.0984	1117	0.0419	989	0.3401	882	0.0292	744	0.9219	645
144	bm-001	0.7431	1052	0.9494	1072	0.9586	1286	0.9843	1282	0.9049	1223	0.9021	1049	0.8395	1118	-	
145	boetech-001	0.0662	887	0.0802	863	0.0493	1107	0.0791	1099	0.0682	1044	0.1074	757	0.0758	863	0.9951	709
146	boetech-002	0.0535	862	0.0565	827	0.0114	901	0.0136	808	0.0403	983	0.0650	700	0.0606	846	0.3470	479
147	bresee-000	0.8467	1058	0.9472	1070	0.9819	1287	0.9903	1283	0.9940	1242	0.9919	1121	0.9760	1171	-	
148	bresee-001	0.0085	517	0.0143	542	0.0086	808	0.0153	850	0.0108	686	0.0168	422	0.0115	478	-	
149	bresee-002	0.0079	500	0.0101	461	0.0065	711	0.0079	655	0.0129	730	0.0263	527	0.0224	682	0.2137	427
150	btsdigital-001	-		-		0.0046	574	0.0072	620	0.0077	564	0.0141	364	0.0092	397	0.1256	323
151	cakevn-001	-		-		0.0311	1067	0.0677	1084	0.0212	873	0.1427	789	0.0185	629	0.9170	642
152	camvi-001	0.3822	1006	0.5375	1022	-		-		-		-		-		-	
153	camvi-002	0.0125	638	0.0221	665	0.0089	815	0.0145	837	0.0142	762	0.2650	853	0.0166	597	-	
154	camvi-003	0.0184	730	0.0320	739	0.0134	941	0.0255	959	-		-		-		-	
155	camvi-004	0.0171	712	0.0316	738	0.0042	540	0.0049	469	0.0097	655	0.6636	972	0.0141	546	-	
156	candour-001	0.1048	921	0.3189	975	0.0130	936	0.0182	897	0.3879	1154	0.9216	1056	0.7071	1090	0.9836	682
157	candour-002	-		-		0.0036	465	0.0061	566	0.1489	1093	0.4137	911	0.2751	992	0.8795	620
158	candour-003	-		-		0.0040	523	0.0068	599	0.0041	350	0.1321	779	0.0225	684	0.6090	545
159	candour-004	-		-		0.0027	274	0.0039	374	0.0030	211	0.1049	752	0.0121	497	0.5691	533
160	canon-002	0.0034	230	0.0050	243	0.0026	240	0.0033	271	0.0043	370	0.0182	441	0.0065	256	-	
161	canon-003	0.0041	283	0.0059	282	0.0030	332	0.0040	379	0.0040	330	0.0073	174	0.0059	222	0.0735	161
162	canon-004	0.0052	356	0.0091	422	0.0033	417	0.0058	538	0.0037	302	0.0770	726	0.0494	820	0.3192	474
163	canon-005	0.0024	140	0.0035	133	0.0025	184	0.0033	287	0.0052	446	0.0096	276	0.0090	387	0.0542	64
164	cchonolulu-000	0.7910	1056	0.8611	1060	0.9824	1288	0.9926	1285	0.9940	1241	0.9861	1103	0.9534	1156	1.0000	774
165	cchonolulu-001	0.4202	1011	0.4853	1010	0.6298	1244	0.7694	1241	0.7402	1187	0.9720	1089	0.8870	1133	0.9951	710
166	cdachyd-001	-		-		0.7397	1262	0.8335	1254	0.7630	1189	0.7410	988	0.5756	1064	0.9588	657
167	ceiec-001	0.0328	826	0.0475	802	0.0295	1064	0.0478	1049	0.0621	1037	0.1059	754	0.0932	887	-	
168	ceiec-002	0.0161	701	0.0193	632	0.0122	920	0.0164	879	0.0270	923	0.0555	677	0.0472	816	-	
169	ceiec-003	0.0071	465	0.0107	476	0.0061	690	0.0079	660	0.0160	793	0.0316	564	0.0260	716	-	
170	ceiec-004	0.0038	264	0.0051	249	0.0045	571	0.0053	499	0.0062	507	0.3939	906	0.0104	445	-	
171	celloscope-001	-		-		0.1245	1166	0.1840	1156	0.1886	1109	0.2636	852	0.1485	934	0.7055	569
172	chosun-000	0.8481	1059	1.0000	1120	1.0000	1363	0.9999	1299	1.0000	1285	1.0000	1267	1.0000	1321	-	
173	chosun-001	0.0525	860	0.0936	879	0.0742	1136	0.1263	1136	0.0978	1072	1.0000	1233	0.9354	1148	-	
174	chosun-002	0.0390	839	0.0646	838	0.0339	1074	0.0576	1070	0.0455	1002	0.6904	976	0.1746	953	-	
175	chtface-001	0.9993	1071	0.9994	1079	0.9999	1301	0.9996	1292	1.0000	1257	1.0000	1210	0.9999	1232	-	
176	chtface-002	0.0150	683	0.0268	710	0.0096	844	0.0140	823	0.0186	839	0.0320	570	0.0194	647	-	

Table 58: FNMR is the proportion of mated comparisons below a threshold set to achieve the FMR given in the header on the fourth row. FMR is the proportion of impostor comparisons at or above that threshold. The light grey values give rank over all algorithms in that column. The pink columns use only same-sex impostors; others are selected regardless of demographics. The exception, in the green column, uses "matched-covariates" i.e. impostors of the same sex, age group, and country of birth. The second pink column includes effects of extended ageing. Missing entries for border, visa, mugshot and wild images generally mean the algorithm did not run to completion. The VISA *columns compare images described in section 2.1. The* MUGSHOT *columns compare images described in section 2.5. The* VISA-BORDER *column compare images described in section 2.2 with those of section 2.4. The* BORDER *column compares images described in section 2.4. The* KIOSK-BORDER *columns compare images described in section 2.6 with those of section 2.4.*

	Algorithm	FALSE NON-MATCH RATE (FNMR)													
		CONSTRAINED, COOPERATIVE												LESS CONSTRAINED, NON-COOP.	
	Name	VISAMC		VISA		MUGSHOT		MUGSHOT12+YRS		VISABORDER		BORDER		BORDER		KIOSKBORDER	
	FMR	0.0001		1E-06		1E-05		1E-05		1E-06		1E-06		1E-05		1E-06	
177	chtface-003	0.0091	533	0.0146	548	0.0083	795	0.0128	789	0.0132	739	0.0220	488	0.0149	565	-	
178	chtface-004	0.0046	317	0.0062	308	0.0052	622	0.0080	662	0.0088	615	0.0152	388	0.0106	450	0.1152	301
179	chtface-005	0.0033	215	0.0049	230	0.0029	317	0.0041	393	0.0044	375	0.0317	567	0.0066	261	0.1952	414
180	chtface-006	0.0029	185	0.0043	190	0.0026	246	0.0034	305	0.0040	336	0.2701	857	0.0065	254	0.4464	506
181	chtface-007	-		-		0.0025	183	0.0032	261	0.0040	332	0.2018	817	0.0064	249	0.4751	513
182	chtface-008	-		-		0.0022	57	0.0026	131	0.0025	128	0.1246	773	0.0400	788	0.4384	505
183	chtface-009	-		-		0.0023	81	0.0027	152	0.0024	106	0.3659	895	0.1226	914	0.7714	583
184	canon-000	0.0084	514	0.0156	571	0.0049	601	0.0051	487	0.0275	931	0.1371	785	0.0138	540	-	
185	canon-001	0.0041	279	0.0061	293	0.0030	351	0.0041	391	0.0048	415	0.0578	682	0.0069	278	-	
186	cist-001	0.0046	310	0.0065	315	0.0042	544	0.0063	576	0.9675	1235	0.9997	1185	0.9994	1214	1.0000	786
187	cist-002	0.0073	474	0.0096	443	0.0085	803	0.0090	694	0.9990	1249	0.9997	1184	0.9996	1221	0.9998	750
188	cist-003	0.0065	438	0.0087	412	0.0046	577	0.0068	598	0.9993	1252	0.9994	1174	0.9993	1213	0.9995	744
189	cist-004	0.0043	296	0.0062	302	0.0031	360	0.0041	398	0.0031	227	0.0363	612	0.0069	281	0.2732	457
190	clearviewai-000	0.0010	27	0.0019	43	0.0024	115	0.0028	178	0.0030	206	0.0058	110	0.0050	151	0.0604	95
191	clearviewai-001	0.0015	60	0.0021	48	0.0024	120	0.0030	224	0.0022	74	0.0745	721	0.0194	646	0.2740	458
192	clearviewai-002	-		-		0.0024	117	0.0031	252	0.0022	72	0.0042	47	0.0037	63	0.0531	54
193	clearviewai-003	-		-		0.0023	65	0.0025	111	0.0022	69	0.0042	49	0.0038	66	0.0533	55
194	closeli-001	0.0136	655	0.0163	580	0.0039	510	0.0054	508	0.0072	544	1.0000	1211	0.0094	407	1.0000	836
195	cloudmatrix-000	0.0192	737	0.0340	750	0.0133	940	0.0220	935	0.9837	1238	1.0000	1217	0.0281	729	-	
196	cloudmatrix-001	0.0668	888	0.1141	894	0.0539	1115	0.0905	1113	0.3509	1148	0.9819	1100	0.9010	1137	0.9999	755
197	cloudmatrix-002	0.0075	481	0.0113	495	0.0084	799	0.0120	761	0.9248	1228	0.9997	1183	0.9985	1208	1.0000	848
198	cloudwalk-hr-000	0.0265	791	0.0434	787	0.0340	1075	0.0646	1081	-		-		-		-	
199	cloudwalk-hr-001	0.0044	298	0.0072	346	0.0073	749	0.0108	743	0.0125	723	0.0228	500	0.0145	557	-	
200	cloudwalk-hr-002	0.0043	293	0.0059	283	0.0054	638	0.0076	638	0.0076	562	0.5932	956	0.0093	402	-	
201	cloudwalk-hr-003	0.0026	160	0.0041	171	0.0040	520	0.0058	537	0.0060	499	0.9992	1167	0.0094	403	-	
202	cloudwalk-hr-004	0.0009	17	0.0018	37	0.0034	422	0.0028	188	0.0052	441	0.9992	1168	0.0093	401	-	
203	cloudwalk-mt-000	0.0100	564	0.0170	594	0.0074	754	0.0118	759	0.0127	726	0.0197	462	0.0129	514	-	
204	cloudwalk-mt-002	0.0064	434	0.0085	402	0.0054	641	0.0098	720	0.0070	536	0.0108	309	0.0076	329	-	
205	cloudwalk-mt-003	0.0013	49	0.0022	53	0.0026	206	0.0027	160	0.0039	322	0.0076	181	0.0067	264	-	
206	cloudwalk-mt-004	0.0009	21	0.0013	15	0.0024	130	0.0021	26	0.0028	178	0.0054	99	0.0050	152	0.0572	79
207	cloudwalk-mt-005	0.0006	9	0.0009	9	0.0025	179	0.0022	50	0.0017	24	0.9286	1062	0.5956	1067	0.9948	707
208	cloudwalk-mt-006	0.0006	11	0.0006	1	0.0023	78	0.0019	1	0.0016	13	0.0032	12	0.0030	25	0.0427	14
209	cloudwalk-mt-007	0.0006	10	0.0007	3	0.0023	84	0.0019	2	0.0016	11	0.0032	10	0.0030	23	0.0419	11
210	clova-000	0.0099	560	0.0150	554	0.0094	834	0.0147	841	0.0136	750	0.0213	479	0.0152	572	-	
211	cmcuni-001	0.0025	153	0.0038	149	0.0025	172	0.0025	126	0.0022	70	0.0052	92	0.0034	42	0.0660	135
212	codeline-000	0.0057	384	0.0079	378	0.0037	478	0.0053	506	0.2721	1135	1.0000	1214	0.9763	1172	1.0000	845
213	cogent-000	0.0435	848	0.0835	867	-		-		-		-		-		-	
214	cogent-001	0.0176	721	0.0385	773	-		-		-		-		-		-	
215	cogent-002	0.0148	678	0.0321	740	0.0095	839	0.0127	784	-		-		-		-	
216	cogent-003	0.0091	534	0.0188	624	0.0098	847	0.0132	797	0.0187	840	0.0319	568	0.0224	683	-	
217	cogent-004	0.0064	435	0.0116	497	0.0096	842	0.0134	805	0.0157	785	0.0325	574	0.0204	658	-	
218	cogent-005	0.0060	408	0.0112	491	0.0064	706	0.0070	609	0.0095	642	0.0184	445	0.0135	527	-	
219	cogent-006	0.0046	318	0.0059	289	0.0036	450	0.0047	444	0.0058	486	0.0113	325	0.0091	390	0.1522	367
220	cogent-007	0.0022	124	0.0038	154	0.0028	307	0.0031	236	0.0040	338	0.0082	214	0.0067	263	0.1395	342

Table 59: FNMR is the proportion of mated comparisons below a threshold set to achieve the FMR given in the header on the fourth row. FMR is the proportion of impostor comparisons at or above that threshold. The light grey values give rank over all algorithms in that column. The pink columns use only same-sex impostors; others are selected regardless of demographics. The exception, in the green column, uses "matched-covariates" i.e. impostors of the same sex, age group, and country of birth. The second pink column includes effects of extended ageing. Missing entries for border, visa, mugshot and wild images generally mean the algorithm did not run to completion. The VISA *columns compare images described in section 2.1. The* MUGSHOT *columns compare images described in section 2.5. The* VISA-BORDER *column compare images described in section 2.2 with those of section 2.4. The* BORDER *column compares images described in section 2.4. The* KIOSK-BORDER *columns compare images described in section 2.6 with those of section 2.4.*

	Algorithm	FALSE NON-MATCH RATE (FNMR)															
		CONSTRAINED, COOPERATIVE														LESS CONSTRAINED, NON-COOP.	
	Name	VISAMC		VISA		MUGSHOT		MUGSHOT12+YRS		VISABORDER		BORDER		BORDER		KIOSKBORDER	
	FMR	0.0001		1E-06		1E-05		1E-05		1E-06		1E-06		1E-05		1E-06	
221	cogent-008	0.0015	63	0.0027	86	0.0023	86	0.0025	117	0.0033	261	0.0063	138	0.0055	194	0.0884	225
222	cognitec-000	0.0116	609	0.0177	608	0.0118	912	0.0167	882	0.0285	935	0.9924	1124	0.0435	802	-	
223	cognitec-001	0.0126	640	0.0185	620	0.0120	916	0.0168	884	0.0270	921	0.0554	675	0.0357	771	-	
224	cognitec-002	0.0066	439	0.0101	459	0.0079	771	0.0108	741	0.0181	831	0.0317	566	0.0237	695	-	
225	cognitec-003	0.0038	259	0.0052	251	0.0054	643	0.0057	532	0.0225	883	0.0416	635	0.0388	783	0.1397	343
226	cognitec-004	0.0036	245	0.0053	259	0.0053	629	0.0056	523	0.0098	657	0.0202	469	0.0154	573	0.3436	478
227	cognitec-005	0.0022	120	0.0030	105	0.0035	445	0.0041	385	0.0079	571	0.0480	656	0.0233	690	0.2134	425
228	cognitec-006	-		-		0.0034	433	0.0039	373	0.0069	529	0.0160	404	0.0108	456	0.1197	312
229	cognitec-007	-		-		0.0035	449	0.0042	407	0.0069	532	0.0114	328	0.0091	389	0.1112	294
230	compal-000	-		-		0.0028	314	0.0033	288	0.0039	326	0.0064	143	0.0051	164	0.0736	162
231	compal-001	-		-		0.0073	745	0.0053	501	0.0092	628	0.1965	814	0.0165	594	0.2610	453
232	cor-001	0.0075	483	0.0113	493	0.0055	651	0.0084	675	0.0091	624	0.0148	379	0.0092	398	-	
233	coretech-000	0.7699	1055	1.0000	1107	1.0000	1360	0.9999	1300	1.0000	1290	1.0000	1258	1.0000	1329	1.0000	1356
234	coretech-001	0.0052	350	0.0067	324	0.0083	796	0.0092	698	0.0346	960	0.1363	784	0.0252	708	0.6210	551
235	coretech-002	0.0020	104	0.0036	137	0.0064	708	0.0064	581	0.0118	710	0.0157	401	0.0110	461	0.3091	469
236	coretech-003	-		-		0.0045	569	0.0051	484	0.1155	1078	0.1539	794	0.1515	936	0.1180	306
237	coretech-004	-		-		0.0044	557	0.0048	454	0.0051	439	0.0093	261	0.0070	286	0.0893	229
238	corsight-001	0.0040	272	0.0057	278	0.0033	418	0.0047	443	0.0045	391	0.0095	269	0.0063	241	-	
239	corsight-002	0.0053	360	0.0068	330	0.0030	341	0.0041	397	0.0039	327	0.0079	199	0.0054	187	0.0747	169
240	corsight-003	0.0026	161	0.0040	167	0.0028	290	0.0045	434	0.0035	290	0.0059	122	0.0046	127	0.0637	118
241	csc-001	0.9158	1063	0.9346	1069	0.9899	1289	0.9993	1290	0.9999	1254	0.9959	1135	0.9906	1185	-	
242	csc-002	0.0099	563	0.0132	523	0.0077	762	0.0142	831	0.0126	724	0.0195	461	0.0146	560	-	
243	csc-003	0.0053	361	0.0065	313	0.0037	480	0.0047	447	0.0074	555	0.0124	345	0.0112	469	0.0928	253
244	ctbcbank-000	0.0168	707	0.0250	697	0.0146	961	0.0224	937	0.0211	872	0.8964	1047	0.3779	1023	-	
245	ctbcbank-001	0.0155	688	0.0235	682	0.0148	968	0.0243	953	0.0207	867	0.9279	1061	0.3469	1015	-	
246	ctbcbank-002	-		-		0.0031	352	0.0049	465	0.0037	305	0.7785	1004	0.4878	1046	0.9727	667
247	cu-face-002	0.0105	584	0.0116	498	0.0650	1127	0.0568	1067	0.0271	925	0.0139	361	0.0076	325	0.1122	295
248	cu-face-003	0.0036	246	0.0049	238	0.0031	373	0.0037	346	0.0030	214	0.3075	868	0.1310	920	0.7046	566
249	cu-face-004	-		-		0.0032	392	0.0035	315	0.0026	157	0.4284	915	0.2115	969	0.7861	590
250	cubox-001	0.0064	431	0.0080	380	0.0037	473	0.0055	516	0.0060	491	0.0111	318	0.0077	335	-	
251	cubox-002	0.0034	234	0.0041	170	0.0025	165	0.0025	128	0.0033	260	0.0064	141	0.0058	216	0.0519	49
252	cubox-003	0.0021	108	0.0028	92	0.0024	152	0.0026	142	0.0025	130	0.0046	62	0.0037	64	0.0495	40
253	cubox-004	-		-		0.0025	189	0.0027	165	0.0023	88	0.0044	59	0.0038	67	0.0490	37
254	cubox-005	-		-		0.0026	223	0.0030	231	0.0025	122	0.0047	72	0.0039	79	0.0515	48
255	cudocommunication-001	0.4777	1026	1.0000	1090	0.4373	1221	0.5360	1213	1.0000	1279	1.0000	1247	1.0000	1339	1.0000	1401
256	cuhkee-001	0.0036	253	0.0045	209	0.0031	375	0.0046	439	0.0051	440	0.0095	270	0.0079	341	-	
257	cybercore-000	0.0728	893	0.1110	890	0.1521	1176	0.2375	1170	0.1874	1106	0.1907	811	0.1178	911	-	
258	cybercore-001	0.3759	1004	0.5677	1029	0.6928	1254	0.7926	1245	0.8118	1198	0.9291	1065	0.7080	1091	0.9782	674
259	cybercore-002	0.0092	540	0.0119	504	0.0049	599	0.0072	617	0.9105	1226	1.0000	1229	1.0000	1239	1.0000	849
260	cybercore-003	0.0155	687	0.0164	583	0.0032	397	0.0033	285	0.0024	97	0.9719	1088	0.8213	1116	0.9993	738
261	cyberextruder-001	0.1972	966	0.2547	954	0.4686	1227	0.6387	1225	0.3807	1151	0.3806	901	0.2582	983	-	
262	cyberextruder-002	0.0811	906	0.1336	902	0.1465	1174	0.2266	1169	0.2086	1119	1.0000	1322	1.0000	1267	-	
263	cyberextruder-003	0.0109	593	0.0169	593	0.0071	736	0.0112	751	0.0165	804	0.0410	633	0.0272	727	0.2308	433
264	cyberextruder-004	0.0118	617	0.0181	613	0.0081	782	0.0133	799	0.0191	849	0.0329	577	0.0268	725	0.1904	406

Table 60: FNMR is the proportion of mated comparisons below a threshold set to achieve the FMR given in the header on the fourth row. FMR is the proportion of impostor comparisons at or above that threshold. The light grey values give rank over all algorithms in that column. The pink columns use only same-sex impostors; others are selected regardless of demographics. The exception, in the green column, uses "matched-covariates" i.e. impostors of the same sex, age group, and country of birth. The second pink column includes effects of extended ageing. Missing entries for border, visa, mugshot and wild images generally mean the algorithm did not run to completion. The VISA *columns compare images described in section 2.1. The* MUGSHOT *columns compare images described in section 2.5. The* VISA-BORDER *column compare images described in section 2.2 with those of section 2.4. The* BORDER *column compares images described in section 2.4. The* KIOSK-BORDER *columns compare images described in section 2.6 with those of section 2.4.*

		FALSE NON-MATCH RATE (FNMR)													
	Algorithm	CONSTRAINED, COOPERATIVE												LESS CONSTRAINED, NON-COOP.	
	Name	VISAMC		VISA		MUGSHOT		MUGSHOT12+YRS		VISABORDER		BORDER		BORDER		KIOSKBORDER	
	FMR	0.0001		1E-06		1E-05		1E-05		1E-06		1E-06		1E-05		1E-06	
265	cyberextruder-005	-		-		0.0049	598	0.0063	574	0.0055	456	0.0105	300	0.0079	345	0.0806	201
266	cyberextruder-006	-		-		0.0083	791	0.0138	815	0.0100	665	0.0180	439	0.0114	476	0.1276	325
267	cyberlink-000	0.0181	726	0.0274	713	0.0125	927	0.0180	895	-		-		-		-	
268	cyberlink-001	0.0131	647	0.0210	651	0.0439	1098	0.0517	1059	0.0173	822	0.0333	585	0.0209	667	-	
269	cyberlink-002	0.0114	605	0.0195	633	0.0101	857	0.0163	875	0.0160	794	0.0302	554	0.0192	642	-	
270	cyberlink-003	0.0118	614	0.0192	629	0.0098	850	0.0161	869	0.0153	778	0.0288	547	0.0159	583	-	
271	cyberlink-004	0.0074	477	0.0105	471	0.0068	724	0.0089	690	0.0094	638	0.0176	435	0.0117	483	-	
272	cyberlink-005	0.0060	405	0.0092	427	0.0058	670	0.0067	595	0.0074	551	0.0146	376	0.0105	449	-	
273	cyberlink-006	0.0042	290	0.0054	268	0.0043	547	0.0049	462	0.0052	445	0.0097	278	0.0077	336	-	
274	cyberlink-007	0.0032	212	0.0053	260	0.0041	529	0.0043	413	0.0052	444	0.0243	509	0.0084	371	0.3366	476
275	cyberlink-008	0.0042	288	0.0056	277	0.0038	502	0.0048	455	0.0053	448	0.0099	284	0.0074	313	0.1354	339
276	cyberlink-009	0.0018	88	0.0027	82	0.0047	578	0.0046	436	0.0040	342	0.0086	240	0.0062	238	0.1104	288
277	cyberlink-010	0.0011	38	0.0019	44	0.0041	526	0.0041	386	0.0039	321	0.1829	807	0.0054	188	0.8629	611
278	cyberlink-011	0.0010	29	0.0017	31	0.0035	444	0.0034	293	0.0045	383	0.0080	202	0.0070	289	0.0877	222
279	cyberlink-012	0.0010	26	0.0016	29	0.0036	454	0.0035	319	0.0047	411	0.0099	283	0.0074	314	0.1350	337
280	cyberlink-013	0.0011	37	0.0017	33	0.0037	475	0.0036	330	0.0045	385	0.0090	248	0.0080	349	0.0924	250
281	cyberlink-014	-		-		0.0026	243	0.0027	150	0.0030	204	0.0065	147	0.0052	171	0.0869	219
282	cyberlink-015	-		-		0.0025	174	0.0026	136	0.0028	180	0.0063	137	0.0050	155	0.0835	214
283	dahua-000	0.0249	778	0.0477	804	-		-		-		-		-		-	
284	dahua-001	0.0250	782	0.0466	799	0.0228	1029	0.0379	1015	-		-		-		-	
285	dahua-002	0.0129	643	0.0157	573	0.0116	907	0.0153	851	0.0134	744	0.0222	491	0.0170	602	-	
286	dahua-003	0.0052	354	0.0068	327	0.0056	654	0.0062	569	0.0113	702	0.0207	473	0.0185	631	-	
287	dahua-004	0.0045	307	0.0058	281	0.0036	460	0.0048	453	0.0051	437	0.0086	236	0.0070	290	-	
288	dahua-005	0.0031	201	0.0046	216	0.0035	447	0.0049	470	0.0046	395	0.0076	183	0.0062	237	-	
289	dahua-006	0.0027	166	0.0039	158	0.0031	368	0.0039	371	0.0039	325	0.0067	158	0.0058	213	-	
290	dahua-007	0.0017	78	0.0023	59	0.0026	229	0.0032	258	0.0033	253	0.0060	126	0.0054	186	0.0678	141
291	daon-000	0.0095	553	0.0117	500	0.0068	720	0.0077	647	0.0092	632	0.0174	431	0.0137	536	0.1430	352
292	daon-001	-		-		0.0036	455	0.0058	536	0.0050	429	0.0084	222	0.0057	208	0.0805	199
293	daon-002	-		-		0.0030	344	0.0042	403	0.0039	320	0.0146	377	0.0055	196	0.7444	577
294	daon-003	-		-		0.0024	150	0.0029	199	0.0030	212	0.0059	124	0.0048	143	0.0639	120
295	datech-000	0.0020	107	0.0031	111	0.0031	365	0.0041	394	0.0033	259	0.1646	799	0.0667	854	0.4898	517
296	datech-001	-		-		0.0028	294	0.0034	299	0.0026	162	0.2308	836	0.0818	873	0.5505	528
297	datech-002	-		-		0.0028	293	0.0034	301	0.0026	142	0.3779	899	0.1654	951	0.7940	593
298	decatur-000	0.0714	890	0.1115	892	0.0608	1123	0.1106	1128	0.0866	1061	1.0000	1224	0.0714	860	-	
299	decatur-001	0.0424	844	0.0711	849	0.0237	1032	0.0458	1038	0.0447	1000	1.0000	1202	0.9969	1201	1.0000	858
300	decloakface-001	0.0795	902	0.1131	893	0.3127	1205	0.4259	1200	0.2118	1122	0.7926	1008	0.6088	1069	0.9589	658
301	decloakface-002	-		-		0.0048	588	0.0077	646	1.0000	1266	0.9998	1191	0.9997	1222	1.0000	838
302	deepglint-001	0.0040	271	0.0062	298	0.0047	584	0.0067	594	0.0069	530	1.0000	1226	1.0000	1238	-	
303	deepglint-002	0.0016	68	0.0027	81	0.0032	383	0.0033	286	0.0043	369	0.0084	227	0.0077	333	-	
304	deepglint-003	0.0027	169	0.0038	148	0.0030	340	0.0032	256	0.0043	360	0.0082	215	0.0076	326	-	
305	deepglint-004	0.0025	150	0.0034	123	0.0039	511	0.0061	565	0.0050	431	0.0091	252	0.0082	358	0.1003	266
306	deepglint-005	0.0052	351	0.0059	290	0.0030	334	0.0031	237	0.0033	265	0.7620	997	0.1535	937	0.9912	699
307	deepsea-001	0.0136	657	0.0215	658	0.0142	953	0.0214	930	0.0163	798	0.0250	516	0.0192	643	-	
308	deepsense-000	0.0145	673	0.0265	709	0.0113	896	0.0196	917	0.0151	775	0.0215	482	0.0129	515	-	

Table 61: FNMR is the proportion of mated comparisons below a threshold set to achieve the FMR given in the header on the fourth row. FMR is the proportion of impostor comparisons at or above that threshold. The light grey values give rank over all algorithms in that column. The pink columns use only same-sex impostors; others are selected regardless of demographics. The exception, in the green column, uses "matched-covariates" i.e. impostors of the same sex, age group, and country of birth. The second pink column includes effects of extended ageing. Missing entries for border, visa, mugshot and wild images generally mean the algorithm did not run to completion. The VISA *columns compare images described in section 2.1. The* MUGSHOT *columns compare images described in section 2.5. The* VISA-BORDER *column compare images described in section 2.2 with those of section 2.4. The* BORDER *column compares images described in section 2.4. The* KIOSK-BORDER *columns compare images described in section 2.6 with those of section 2.4.*

	Algorithm	FALSE NON-MATCH RATE (FNMR)															
		CONSTRAINED, COOPERATIVE														LESS CONSTRAINED, NON-COOP.	
	Name	VISAMC		VISA		MUGSHOT		MUGSHOT12+YRS		VISABORDER		BORDER		BORDER		KIOSKBORDER	
	FMR	0.0001		1E-06		1E-05		1E-05		1E-06		1E-06		1E-05		1E-06	
309	deepsense-001	0.0013	47	0.0019	42	0.0024	141	0.0025	119	0.0027	171	0.0115	331	0.0053	177	0.1394	341
310	deepsense-002	0.0010	28	0.0016	30	0.0024	104	0.0023	72	0.0026	147	0.0052	93	0.0043	111	0.0781	188
311	deepsense-003	0.0009	19	0.0015	24	0.0025	185	0.0024	82	0.0023	86	0.0457	647	0.0097	417	0.2547	447
312	deepsense-004	-		-		0.0023	62	0.0021	31	0.0020	50	0.0111	317	0.0040	97	0.1195	310
313	deepsense-005	-		-		0.0023	60	0.0021	37	0.0019	39	0.0081	210	0.0035	51	0.0922	249
314	deepsense-006	-		-		0.0022	43	0.0022	56	0.0018	31	0.0336	588	0.0059	221	0.2813	462
315	deepsense-007	-		-		0.0022	45	0.0022	55	0.0018	30	0.0035	25	0.0030	26	0.0440	20
316	deepsense-008	-		-		0.0022	47	0.0022	58	0.0018	28	0.0034	24	0.0030	24	0.0434	16
317	dermalog-001	-		0.3049	971	-		-		-		-		-		-	
318	dermalog-002	-		0.3154	974	-		-		-		-		-		-	
319	dermalog-003	0.2355	976	0.2795	964	-		-		-		-		-		-	
320	dermalog-004	0.1810	959	0.2399	951	-		-		-		-		-		-	
321	dermalog-005	0.1526	947	0.1823	926	0.2580	1196	0.4018	1197	-		0.2651	854	0.1585	942	-	
322	dermalog-006	0.0253	784	0.0369	768	0.0171	989	0.0283	978	0.0217	878	0.0358	603	0.0230	686	-	
323	dermalog-007	0.0564	872	0.0798	862	0.1351	1170	0.2471	1172	0.2343	1129	0.2223	829	0.1397	927	-	
324	dermalog-008	0.0096	556	0.0166	588	0.0086	805	0.0133	798	0.0165	803	0.0586	687	0.0226	685	-	
325	dermalog-009	0.0067	444	0.0094	429	0.0051	618	0.0069	602	0.0116	709	0.0312	559	0.0177	618	0.3747	488
326	dermalog-010	0.0030	194	0.0041	175	0.0034	431	0.0037	350	0.0075	556	0.5181	934	0.2530	980	0.8853	626
327	dermalog-011	0.0045	308	0.0062	306	0.0035	446	0.0059	547	0.0057	479	0.2242	831	0.0407	791	0.6329	552
328	dermalog-012	0.0080	503	0.0101	463	0.0037	483	0.0057	533	0.0055	461	0.0095	271	0.0068	272	0.0834	213
329	dermalog-013	-		-		0.0036	462	0.0057	530	0.0058	482	0.0103	292	0.0073	304	0.0894	230
330	dermalog-014	-		-		0.0029	323	0.0039	372	0.0037	307	0.0069	164	0.0057	206	0.0646	124
331	dermalog-015	-		-		0.0025	178	0.0025	107	0.0033	251	0.0064	144	0.0054	189	0.0587	89
332	dicio-001	0.5486	1038	0.6442	1039	0.7516	1265	0.8607	1259	0.8678	1214	0.8268	1023	0.7034	1088	0.9752	672
333	dicio-002	-		-		0.0057	662	0.0095	708	0.0097	656	0.9998	1188	0.9989	1211	1.0000	805
334	didiglobalface-001	0.0055	373	0.0092	426	0.0030	338	0.0045	433	0.0088	608	0.0119	339	0.0085	374	-	
335	didiglobalface-002	0.0033	226	0.0051	247	0.0026	230	0.0034	307	0.0033	258	0.0085	229	0.0047	135	0.1135	298
336	didiglobalface-003	-		-		0.0023	70	0.0025	127	0.0027	169	0.1115	761	0.0052	174	0.5374	525
337	digidata-000	0.0967	914	0.1410	909	0.2596	1197	0.3462	1191	0.0293	941	0.0363	611	0.0212	669	0.1849	404
338	digidata-001	0.0224	763	0.0352	757	0.0330	1070	0.0570	1069	0.0109	692	0.0481	657	0.0123	502	0.3055	468
339	digitalbarriers-000	0.3683	1003	0.4630	1006	-		-		-		-		-		-	
340	digitalbarriers-001	0.4683	1024	0.5024	1015	-		-		-		-		-		-	
341	digitalbarriers-002	0.3360	998	0.3690	988	0.0877	1146	0.1557	1146	0.0971	1071	0.0951	744	0.0497	821	-	
342	dps-000	0.0115	607	0.0176	605	0.0149	971	0.0185	904	0.0173	820	0.0275	537	0.0180	622	0.1757	394
343	dralmey-001	-		-		0.0036	458	0.0052	497	0.0057	474	0.9985	1159	0.9872	1180	1.0000	802
344	dsk-000	0.1526	946	0.2169	942	0.3787	1214	0.5426	1215	0.3115	1142	0.3089	870	0.1994	964	-	
345	einetworks-000	0.0099	562	0.0180	611	0.0088	813	0.0140	825	0.0130	733	0.0225	496	0.0147	562	-	
346	einetworksindia-000	0.0058	392	0.0074	355	0.0051	616	0.0061	567	0.0074	552	0.0193	459	0.0102	436	0.1819	398
347	einetworksindia-001	0.0042	289	0.0062	300	0.0048	587	0.0064	579	0.0057	477	0.0473	654	0.0092	395	0.3984	498
348	einetworksindia-002	-		-		0.0024	129	0.0027	151	0.0023	79	0.1534	793	0.0513	825	0.4614	509
349	ekin-002	0.1168	929	0.2042	938	0.1530	1177	0.2524	1175	0.1777	1105	0.2773	859	0.1347	922	0.8954	634
350	element-000	0.0023	134	0.0035	132	0.0024	140	0.0026	133	0.0029	195	0.0060	129	0.0048	139	0.0631	114
351	enface-000	0.0028	178	0.0049	237	0.0043	552	0.0072	615	0.0058	487	0.0150	384	0.0090	388	0.7851	589
352	enface-001	0.0072	472	0.0107	477	0.0071	732	0.0138	816	0.0068	527	0.0515	667	0.0094	408	0.9942	705

Table 62: FNMR is the proportion of mated comparisons below a threshold set to achieve the FMR given in the header on the fourth row. FMR is the proportion of impostor comparisons at or above that threshold. The light grey values give rank over all algorithms in that column. The pink columns use only same-sex impostors; others are selected regardless of demographics. The exception, in the green column, uses "matched-covariates" i.e. impostors of the same sex, age group, and country of birth. The second pink column includes effects of extended ageing. Missing entries for border, visa, mugshot and wild images generally mean the algorithm did not run to completion. The VISA *columns compare images described in section 2.1. The* MUGSHOT *columns compare images described in section 2.5. The* VISA-BORDER *column compare images described in section 2.2 with those of section 2.4. The* BORDER *column compares images described in section 2.4. The* KIOSK-BORDER *columns compare images described in section 2.6 with those of section 2.4.*

	Algorithm	FALSE NON-MATCH RATE (FNMR)															
		CONSTRAINED, COOPERATIVE														LESS CONSTRAINED, NON-COOP.	
	Name	VISAMC		VISA		MUGSHOT		MUGSHOT12+YRS		VISABORDER		BORDER		BORDER		KIOSKBORDER	
	FMR	0.0001		1E-06		1E-05		1E-05		1E-06		1E-06		1E-05		1E-06	
353	enface-002	0.0033	223	0.0052	255	0.0038	498	0.0073	623	0.0026	161	0.9998	1193	0.9995	1218	1.0000	842
354	enqura-001	-		-		0.0155	977	0.0144	834	0.0312	951	0.0597	689	0.0485	818	0.2970	466
355	eocortex-000	0.3485	1000	0.6943	1048	0.1122	1159	0.1574	1147	0.2155	1123	0.2257	835	0.1606	947	-	
356	ercacat-001	0.0036	249	0.0044	202	0.0033	409	0.0047	448	0.0106	680	0.0202	468	0.0184	627	-	
357	ethiopianlmis-000	-		-		0.2967	1201	0.4098	1198	0.9992	1251	1.0000	1207	0.9999	1229	1.0000	857
358	euronovate-001	0.2786	985	0.3608	987	0.4489	1223	0.6105	1223	0.5010	1164	0.5392	941	0.3769	1022	0.8802	622
359	euronovate-002	0.0256	787	0.0436	788	0.0226	1027	0.0425	1031	0.0301	946	0.0691	713	0.0319	753	0.3687	484
360	euronovate-003	0.0061	415	0.0088	414	0.0040	524	0.0060	554	0.0065	519	0.7815	1006	0.5034	1051	0.9823	678
361	euronovate-004	0.0082	508	0.0110	483	0.0050	611	0.0077	645	0.0074	553	0.6949	980	0.3354	1013	0.9791	676
362	everai-000	0.0122	626	0.0225	670	-		-		-		-		-		-	
363	everai-001	0.0085	518	0.0156	570	0.0072	742	0.0114	754	-		-		-		-	
364	everai-002	0.0104	581	0.0159	575	0.0063	700	0.0112	750	0.0182	833	0.0353	600	0.0264	722	-	
365	paravision-003	0.0034	231	0.0050	244	0.0036	467	0.0052	496	0.0092	631	0.0193	458	0.0156	577	-	
366	expasoft-000	0.0427	845	0.0655	842	0.0239	1034	0.0393	1017	0.0673	1043	0.8963	1046	0.3832	1025	-	
367	expasoft-001	0.0328	825	0.0488	808	0.0211	1015	0.0342	999	0.0629	1038	0.6483	968	0.2816	994	-	
368	expasoft-002	0.0170	710	0.0274	714	0.0787	1140	0.0768	1096	0.1629	1097	0.9996	1181	0.9631	1164	1.0000	809
369	f8-001	0.0249	781	0.0336	747	0.0178	992	0.0232	946	0.0303	947	0.0615	695	0.0408	792	-	
370	f8-002	0.0340	828	0.0591	833	0.0213	1017	0.0374	1013	0.0452	1001	0.0760	722	0.0502	824	0.2708	456
371	facehawk-000	1.0000	1398	1.0000	1289	1.0000	1320	1.0000	1383	1.0000	1361	1.0000	1352	1.0000	1394	1.0000	1058
372	faceint-001	-		-		0.0105	871	0.0124	774	0.0313	952	0.3318	878	0.0557	838	0.9851	688
373	facelocate-001	-		-		0.0664	1130	0.1171	1131	0.0950	1068	0.9219	1057	0.7041	1089	0.9985	727
374	facelocate-002	-		-		0.0335	1071	0.0634	1076	0.0393	980	0.9988	1165	0.8977	1136	1.0000	787
375	faceonlive-001	0.0269	794	0.0359	763	0.0387	1084	0.0721	1091	0.0246	911	0.0349	597	0.0220	676	0.2408	438
376	faceonlive-002	0.0121	622	0.0135	530	0.0033	413	0.0041	389	0.0037	309	0.9427	1070	0.7927	1111	0.9993	736
377	faceonlive-003	-		-		0.0045	565	0.0050	479	0.0193	855	0.0360	607	0.0356	769	0.1320	327
378	facephi-000	0.0044	301	0.0059	284	0.0047	580	0.0057	534	0.0088	614	1.0000	1242	1.0000	1245	1.0000	851
379	facephi-001	-		-		0.0031	370	0.0037	345	0.0058	485	0.0111	315	0.0098	422	0.1048	277
380	facephi-002	-		-		0.0024	105	0.0022	52	0.0036	296	0.0093	260	0.0070	283	0.1136	299
381	facesoft-000	0.0085	516	0.0112	489	0.0064	704	0.0107	738	0.0091	623	0.0171	427	0.0107	452	-	
382	facetag-000	0.2836	986	0.4081	997	0.2933	1200	0.4303	1201	0.3448	1146	0.6312	963	0.3530	1016	0.9753	673
383	facetag-001	0.2920	988	0.4538	1003	0.3220	1207	0.4371	1202	1.0000	1303	1.0000	1276	0.3254	1009	1.0000	1292
384	facetag-002	0.0098	559	0.0147	552	0.0064	709	0.0110	746	0.0116	707	0.0190	455	0.0119	492	0.1334	333
385	facex-001	1.0000	1313	1.0000	1357	1.0000	1302	1.0000	1303	1.0000	1393	1.0000	1383	1.0000	1255	-	
386	facex-002	0.0803	904	0.1404	907	0.1283	1167	0.1979	1163	0.1440	1090	0.1952	813	0.1299	918	0.7427	575
387	facia-001	0.0083	512	0.0124	509	0.0064	707	0.0097	713	0.0098	658	0.9983	1155	0.9849	1177	1.0000	833
388	facia-002	-		-		0.0072	741	0.0109	744	0.0122	717	0.0460	648	0.0135	528	0.4464	507
389	faicetech-000	-		-		0.0026	244	0.0031	242	0.0023	89	0.0116	333	0.0037	62	0.0904	237
390	farfaces-001	0.4890	1031	0.5860	1035	0.5650	1235	0.7268	1235	0.8015	1197	0.7511	993	0.5892	1065	0.9536	653
391	fastenterprises-000	0.0093	543	0.0151	559	0.0098	848	0.0140	826	0.0209	869	0.2991	864	0.1608	948	0.6727	559
392	fci-000	-		-		0.0027	258	0.0027	159	0.0028	181	0.1269	776	0.0563	839	0.3886	493
393	fdu-000	0.0386	838	0.0576	829	-		-		-		-		-		-	
394	fdu-001	0.0347	831	0.0439	791	-		-		-		-		-		-	
395	fedu-001	-		-		0.0033	403	0.0047	442	0.0128	727	0.9816	1098	0.9216	1144	0.9999	760
396	fiberhome-nanjing-002	0.0217	757	0.0381	771	0.0874	1145	0.1770	1154	0.0271	924	0.0351	599	0.0188	635	-	

Table 63: FNMR is the proportion of mated comparisons below a threshold set to achieve the FMR given in the header on the fourth row. FMR is the proportion of impostor comparisons at or above that threshold. The light grey values give rank over all algorithms in that column. The pink columns use only same-sex impostors; others are selected regardless of demographics. The exception, in the green column, uses "matched-covariates" i.e. impostors of the same sex, age group, and country of birth. The second pink column includes effects of extended ageing. Missing entries for border, visa, mugshot and wild images generally mean the algorithm did not run to completion. The VISA *columns compare images described in section 2.1. The* MUGSHOT *columns compare images described in section 2.5. The* VISA-BORDER *column compare images described in section 2.2 with those of section 2.4. The* BORDER *column compares images described in section 2.4. The* KIOSK-BORDER *columns compare images described in section 2.6 with those of section 2.4.*

	Algorithm	FALSE NON-MATCH RATE (FNMR)															
		CONSTRAINED, COOPERATIVE														LESS CONSTRAINED, NON-COOP.	
	Name	VISAMC		VISA		MUGSHOT		MUGSHOT12+YRS		VISABORDER		BORDER		BORDER		KIOSKBORDER	
	FMR	0.0001		1E-06		1E-05		1E-05		1E-06		1E-06		1E-05		1E-06	
397	fiberhome-nanjing-003	0.0090	528	0.0139	537	0.0082	788	0.0144	833	0.0110	694	0.0174	429	0.0107	454	-	
398	fiberhome-nanjing-004	0.0037	257	0.0056	276	0.0031	364	0.0043	414	0.0043	371	0.0083	221	0.0061	234	-	
399	fincore-000	0.0309	815	0.0502	810	0.0281	1052	0.0510	1057	0.0521	1018	0.0815	729	0.0522	827	0.3100	470
400	firstcreditkz-001	0.0024	145	0.0034	122	0.0024	147	0.0024	104	0.0034	266	1.0000	1365	1.0000	1381	1.0000	1017
401	firstcreditkz-002	0.0018	87	0.0026	73	0.0024	132	0.0024	92	0.0029	202	0.0056	105	0.0049	147	0.0624	107
402	firstcreditkz-003	-		-		0.0023	91	0.0024	97	0.0026	152	0.0104	298	0.0047	132	0.0910	242
403	firstcreditkz-004	-		-		0.0023	77	0.0024	84	0.0024	99	0.0360	608	0.0061	233	0.2315	434
404	foomobi-001	0.4827	1029	0.5795	1030	0.6823	1249	0.8132	1248	0.8217	1202	1.0000	1364	1.0000	1382	1.0000	1016
405	foomobi-002	0.4827	1028	0.5795	1031	0.6823	1250	0.8132	1249	0.8217	1203	1.0000	1403	1.0000	1349	1.0000	889
406	fourthlinecom-001	-		-		0.0442	1099	0.0696	1087	0.0609	1031	0.8783	1038	0.7523	1102	0.9917	700
407	fpt-000	-		-		0.0213	1018	0.0375	1014	0.0364	969	0.9528	1074	0.8729	1126	0.9993	739
408	fpt-001	-		-		0.0099	851	0.0148	842	0.8158	1200	0.9986	1160	0.9934	1189	1.0000	854
409	fpttelecom-000	-		-		0.0586	1120	0.0761	1095	0.2308	1128	0.9988	1164	0.9937	1190	1.0000	816
410	fraudcom-000	0.0110	596	0.0173	597	0.0083	792	0.0139	821	0.0166	805	0.0258	526	0.0177	615	0.1488	363
411	frpkauai-001	0.0023	130	0.0035	131	0.0026	204	0.0030	230	0.0040	340	0.0080	206	0.0072	299	0.0706	150
412	frpkauai-002	0.0024	146	0.0035	130	0.0024	144	0.0024	100	0.0033	263	0.0065	150	0.0058	217	0.0599	92
413	frpkauai-003	-		-		0.0023	85	0.0023	77	0.0024	92	0.0075	179	0.0039	80	0.0762	178
414	frpkauai-004	-		-		0.0037	472	0.0036	338	0.0069	531	0.0226	497	0.0138	537	0.1354	338
415	fujitsulab-000	0.0123	628	0.0212	654	0.0091	819	0.0133	801	0.0251	913	0.4200	913	0.0360	775	-	
416	fujitsulab-001	0.0059	400	0.0082	389	0.0132	938	0.0258	961	0.0140	758	0.0246	513	0.0142	549	-	
417	fujitsulab-002	0.0091	537	0.0124	512	0.0105	868	0.0156	854	0.0169	813	0.0345	595	0.0146	561	-	
418	fujitsulab-003	0.0045	306	0.0065	314	0.0057	665	0.0083	671	0.0080	579	0.0154	394	0.0101	428	0.5564	530
419	g42-intellibrain-001	0.0006	8	0.0009	10	0.0037	477	0.0044	423	0.0030	222	0.0059	120	0.0053	183	0.0750	175
420	g42-intellibrain-002	0.0006	7	0.0011	11	0.0029	315	0.0037	348	0.0028	177	0.0212	477	0.0091	391	0.1398	345
421	geo-000	0.0543	866	0.0814	864	0.1042	1155	0.1592	1148	0.1637	1098	0.8533	1032	0.1800	956	-	
422	geo-001	0.0180	725	0.0198	641	0.0037	476	0.0055	514	0.0070	534	0.0129	352	0.0094	404	-	
423	geo-002	0.0171	713	0.0187	623	0.0035	439	0.0051	489	0.0064	511	0.0117	336	0.0083	367	0.0938	255
424	geo-003	0.0180	724	0.0313	735	0.0239	1036	0.0552	1061	0.0319	955	0.0487	660	0.0222	679	0.1962	416
425	geo-004	0.0030	188	0.0041	172	0.0025	186	0.0030	212	0.0035	289	0.0065	148	0.0053	182	0.0648	126
426	gistouch-000	0.0296	808	0.0518	815	0.0342	1076	0.0609	1073	0.0493	1010	1.0000	1241	1.0000	1254	1.0000	861
427	gistouch-001	0.0176	720	0.0312	734	0.8931	1280	0.9735	1278	0.8625	1210	1.0000	1284	1.0000	1305	1.0000	1273
428	glory-000	0.1094	925	0.1286	898	0.2179	1190	0.2656	1178	-		-		-		-	
429	glory-001	0.0902	910	0.1082	888	0.1642	1179	0.2065	1168	0.2186	1124	0.2669	855	0.2089	967	-	
430	glory-002	0.0241	769	0.0311	733	0.0116	908	0.0151	849	0.0157	787	0.0264	528	0.0188	637	-	
431	glory-003	0.0076	486	0.0125	514	0.0077	765	0.0103	732	0.0130	732	0.0205	470	0.0143	552	-	
432	glory-004	0.0077	489	0.0123	508	0.0074	755	0.0098	721	0.0122	720	0.0193	457	0.0134	525	0.1520	366
433	glory-005	0.0056	376	0.0076	364	0.0054	644	0.0072	618	0.0075	557	0.9237	1059	0.7853	1108	0.9974	723
434	glory-006	0.0050	333	0.0068	326	0.0051	619	0.0070	608	0.0069	533	0.7869	1007	0.5076	1052	0.9719	666
435	glory-007	0.0050	338	0.0068	331	0.0050	609	0.0069	604	0.0068	524	0.0126	350	0.0083	366	0.1066	279
436	gorilla-000	0.0802	903	0.1409	908	-		-		-		-		-		-	
437	gorilla-001	0.0488	857	0.0756	855	0.1218	1165	0.2034	1165	-		-		-		-	
438	gorilla-002	0.0256	788	0.0413	779	0.0478	1104	0.0912	1114	-		-		-		-	
439	gorilla-003	0.0165	704	0.0291	720	0.0205	1012	0.0437	1032	0.0297	944	0.9658	1084	0.0262	717	-	
440	gorilla-004	0.0138	661	0.0239	686	0.0243	1038	0.0444	1034	0.0275	930	0.0369	614	0.0204	661	-	

Table 64: FNMR is the proportion of mated comparisons below a threshold set to achieve the FMR given in the header on the fourth row. FMR is the proportion of impostor comparisons at or above that threshold. The light grey values give rank over all algorithms in that column. The pink columns use only same-sex impostors; others are selected regardless of demographics. The exception, in the green column, uses "matched-covariates" i.e. impostors of the same sex, age group, and country of birth. The second pink column includes effects of extended ageing. Missing entries for border, visa, mugshot and wild images generally mean the algorithm did not run to completion. The VISA *columns compare images described in section 2.1. The* MUGSHOT *columns compare images described in section 2.5. The* VISA-BORDER *column compare images described in section 2.2 with those of section 2.4. The* BORDER *column compares images described in section 2.4. The* KIOSK-BORDER *columns compare images described in section 2.6 with those of section 2.4.*

		FALSE NON-MATCH RATE (FNMR)															
	Algorithm	CONSTRAINED, COOPERATIVE														LESS CONSTRAINED, NON-COOP.	
	Name	VISAMC		VISA		MUGSHOT		MUGSHOT12+YRS		VISABORDER		BORDER		BORDER		KIOSKBORDER	
	FMR	0.0001		1E-06		1E-05		1E-05		1E-06		1E-06		1E-05		1E-06	
441	gorilla-005	-		-		0.0142	954	0.0267	971	0.0228	887	0.0358	602	0.0195	648	-	
442	gorilla-006	0.0105	587	0.0152	561	0.0106	872	0.0203	923	0.0155	780	0.0218	486	0.0136	530	-	
443	gorilla-007	0.0074	479	0.0111	487	0.0065	712	0.0126	779	0.0100	668	0.0151	386	0.0102	432	0.1450	356
444	gorilla-008	0.0058	389	0.0091	420	0.0049	597	0.0079	659	0.0079	576	0.0126	349	0.0091	392	0.1217	317
445	gorilla-009	0.0049	327	0.0072	343	0.0038	492	0.0056	524	0.0065	515	0.0104	294	0.0070	284	0.1103	287
446	gpstechvn-000	0.0202	747	0.0355	760	0.0142	952	0.0248	955	0.0208	868	0.0495	662	0.0207	664	0.5098	521
447	graymatics-001	0.1039	919	0.1620	918	0.1344	1169	0.1917	1159	0.1648	1099	0.5160	932	0.2689	989	0.9194	643
448	griaule-000	0.0071	467	0.0099	453	0.0050	604	0.0072	614	0.0160	791	0.0304	555	0.0267	724	0.1480	361
449	griaule-001	0.0057	381	0.0078	373	0.0045	570	0.0065	585	0.0070	537	0.7515	994	0.5106	1053	0.9747	670
450	griaule-002	0.0021	114	0.0032	112	0.0025	198	0.0027	166	0.0034	278	0.0996	750	0.0201	655	0.3978	496
451	gtelots-000	-		-		0.0059	672	0.0098	717	0.0090	620	0.9995	1178	0.9975	1202	1.0000	815
452	gtelots-001	-		-		0.0053	631	0.0102	731	0.0071	538	0.0111	319	0.0070	282	0.1173	304
453	hertasecurity-000	0.0630	880	0.0780	861	0.0503	1110	0.0898	1109	0.0738	1047	0.0693	716	0.0420	797	-	
454	hertasecurity-001	0.0249	780	0.0309	732	0.0105	869	0.0161	868	0.0245	909	0.0447	642	0.0359	773	0.1850	405
455	hertasecurity-002	0.0206	750	0.0315	736	0.0060	679	0.0078	653	0.0253	916	0.0696	717	0.0457	808	0.4565	508
456	hertasecurity-003	0.0079	501	0.0104	470	0.0060	681	0.0078	649	0.0255	917	0.0732	720	0.0460	809	0.4731	511
457	hik-001	0.0096	555	0.0125	513	0.0093	828	0.0164	878	0.0108	687	0.0937	740	0.0127	509	-	
458	hisign-001	0.0036	248	0.0050	241	0.0034	420	0.0046	437	0.0079	575	0.0153	393	0.0133	522	0.1080	281
459	hisign-002	0.0029	183	0.0044	199	0.0027	280	0.0032	270	0.0028	187	0.0409	632	0.0132	520	0.2016	420
460	hisign-003	-		-		0.0030	336	0.0036	328	0.0036	299	0.0582	685	0.0201	656	0.2584	449
461	hyperverge-001	1.0000	1241	1.0000	1105	1.0000	1361	1.0000	1319	1.0000	1289	1.0000	1257	1.0000	1330	-	
462	hyperverge-002	0.0050	335	0.0066	320	0.0035	438	0.0051	483	0.0062	505	0.0107	305	0.0074	315	0.0921	248
463	hyperverge-003	0.0019	99	0.0030	100	0.0025	168	0.0029	201	0.0027	164	0.0049	88	0.0042	107	0.0576	81
464	hyperverge-004	0.0072	473	0.0116	499	0.0040	518	0.0071	613	0.0058	484	0.0080	204	0.0057	209	0.0621	105
465	hyperverge-005	0.0026	162	0.0039	162	0.0027	253	0.0031	251	0.0036	301	0.0066	152	0.0055	193	0.0658	133
466	hyperverge-006	-		-		0.0025	194	0.0030	217	0.0033	257	0.0060	128	0.0051	166	0.0601	93
467	hyperverge-007	-		-		0.0026	212	0.0030	226	0.0034	275	0.0061	131	0.0052	169	0.0605	96
468	hyundai-roboticslab-000	-		-		0.0037	474	0.0052	493	0.0063	509	1.0000	1329	0.0872	880	1.0000	1135
469	hyundai-roboticslab-001	-		-		0.0048	595	0.0066	591	0.0193	853	0.8620	1033	0.6861	1083	0.9861	690
470	hyundai-roboticslab-002	-		-		0.0039	516	0.0054	509	0.0086	603	0.9589	1077	0.8817	1131	0.9986	729
471	hyundai-roboticslab-003	-		-		0.0024	109	0.0028	174	0.0027	172	0.6384	966	0.2934	998	0.8692	614
472	hzailu-001	0.0122	624	0.0164	584	0.0095	838	0.0196	915	0.0079	573	0.0118	337	0.0090	386	0.1173	305
473	hzailu-002	0.0051	344	0.0072	341	0.0038	504	0.0055	519	0.0040	337	0.0077	184	0.0062	239	0.0928	254
474	hzailu-003	0.0178	722	0.0291	719	0.0031	379	0.0042	410	0.0035	280	0.0061	134	0.0052	168	0.0799	197
475	hzailu-004	0.0175	717	0.0197	640	0.0031	381	0.0042	406	0.0034	274	0.0060	130	0.0051	158	0.0775	186
476	hzailu-005	0.0172	715	0.0197	638	0.0028	304	0.0036	333	0.0032	248	0.0058	111	0.0048	140	0.0751	176
477	hzailu-006	0.0161	700	0.0174	599	0.0024	137	0.0027	146	0.0026	153	0.0049	87	0.0044	121	0.0654	130
478	hzailu-007	-		-		0.0025	162	0.0027	162	0.0026	143	0.0048	78	0.0044	118	0.0653	129
479	hzailu-008	-		-		0.0024	155	0.0026	145	0.0025	137	0.0048	76	0.0044	116	0.0652	128
480	i2v-001	-		-		0.0946	1150	0.1369	1138	0.3989	1156	0.9998	1189	0.9966	1198	1.0000	812
481	i2v-002	-		-		0.0035	442	0.0044	427	0.0037	304	0.9355	1068	0.4823	1044	0.9960	713
482	icehouse-000	-		-		0.0027	254	0.0036	336	0.0047	405	0.0088	245	0.0072	295	0.0726	156
483	icm-002	0.0143	670	0.0249	695	0.0144	959	0.0256	960	0.0236	901	0.0386	625	0.0263	721	-	
484	icm-003	0.0138	662	0.0222	669	0.0149	969	0.0282	977	0.0227	886	0.0384	623	0.0257	712	0.1938	411

Table 65: FNMR is the proportion of mated comparisons below a threshold set to achieve the FMR given in the header on the fourth row. FMR is the proportion of impostor comparisons at or above that threshold. The light grey values give rank over all algorithms in that column. The pink columns use only same-sex impostors; others are selected regardless of demographics. The exception, in the green column, uses "matched-covariates" i.e. impostors of the same sex, age group, and country of birth. The second pink column includes effects of extended ageing. Missing entries for border, visa, mugshot and wild images generally mean the algorithm did not run to completion. The VISA *columns compare images described in section 2.1. The* MUGSHOT *columns compare images described in section 2.5. The* VISA-BORDER *column compare images described in section 2.2 with those of section 2.4. The* BORDER *column compares images described in section 2.4. The* KIOSK-BORDER *columns compare images described in section 2.6 with those of section 2.4.*

		FALSE NON-MATCH RATE (FNMR)															
	Algorithm	CONSTRAINED, COOPERATIVE														LESS CONSTRAINED, NON-COOP.	
	Name	VISAMC		VISA		MUGSHOT		MUGSHOT12+YRS		VISABORDER		BORDER		BORDER		KIOSKBORDER	
	FMR	0.0001		1E-06		1E-05		1E-05		1E-06		1E-06		1E-05		1E-06	
485	icm-004	0.0079	498	0.0120	505	0.0074	752	0.0107	737	0.0091	625	0.0281	542	0.0128	513	0.2778	460
486	icm-005	0.0100	565	0.0140	539	0.0091	816	0.0108	739	0.0169	812	0.0319	569	0.0290	741	0.1775	397
487	icomm-000	0.0019	97	0.0033	118	0.0033	412	0.0044	424	0.0031	238	0.1350	782	0.0552	835	0.4196	501
488	icthtc-000	0.0260	790	0.0396	777	0.0207	1013	0.0339	998	0.0291	940	0.0474	655	0.0346	764	-	
489	id3-001	0.1698	953	0.2499	953	-		-		-		-		-		-	
490	id3-002	0.1615	952	0.2393	950	-		-		-		-		-		-	
491	id3-003	0.0361	835	0.0757	857	0.0292	1058	0.0476	1046	0.0447	999	0.0674	708	0.0396	786	-	
492	id3-004	0.0198	744	0.0344	753	0.0238	1033	0.0423	1030	0.0289	939	0.0416	634	0.0257	711	-	
493	id3-005	0.0104	579	0.0169	592	0.0080	780	0.0133	802	0.0194	856	0.0334	586	0.0262	718	-	
494	id3-006	0.0072	471	0.0103	466	0.0049	600	0.0074	628	0.0095	640	0.0165	416	0.0119	491	-	
495	id3-007	0.0056	377	0.0078	370	0.0060	684	0.0072	622	0.0275	928	0.1374	786	0.0519	826	-	
496	id3-008	0.0039	265	0.0055	271	0.0032	395	0.0042	402	0.0081	584	0.0155	396	0.0134	523	0.1186	308
497	id3-009	-		-		0.0035	443	0.0049	471	0.0046	394	0.4689	923	0.0214	673	0.9377	648
498	idemia-003	0.0222	760	0.0316	737	0.0188	995	0.0325	995	0.0548	1023	-		-		-	
499	idemia-004	0.0160	698	0.0244	691	0.0199	1005	0.0354	1004	0.0268	919	0.1489	792	0.0263	720	-	
500	idemia-005	0.0132	650	0.0216	660	0.0121	918	0.0218	934	0.0215	875	0.0323	573	0.0188	636	-	
501	idemia-006	0.0046	315	0.0062	305	0.0047	582	0.0066	587	0.0073	548	0.2882	861	0.0094	409	-	
502	idemia-007	0.0024	138	0.0039	163	0.0032	401	0.0038	360	0.0046	397	0.0092	257	0.0070	291	-	
503	idemia-008	0.0023	129	0.0032	114	0.0023	95	0.0028	169	0.0034	279	0.0067	157	0.0056	204	0.0765	180
504	idemia-009	0.0022	122	0.0030	102	0.0022	51	0.0023	79	0.0023	78	0.0046	63	0.0039	75	0.0533	56
505	idemia-010	0.0015	59	0.0026	70	0.0022	56	0.0020	7	0.0020	48	0.0040	39	0.0033	36	0.0465	28
506	idemia-011	-		-		0.0021	24	0.0021	32	0.0018	34	0.0077	189	0.0038	68	0.0782	191
507	identy-000	0.0073	475	0.0095	438	0.0050	605	0.0067	592	0.0071	541	0.8257	1022	0.4310	1036	0.9839	684
508	identy-001	-		-		0.0029	322	0.0034	289	0.0037	310	0.0066	153	0.0055	195	0.0748	174
509	identy-002	-		-		0.0027	263	0.0029	211	0.0030	205	0.0058	112	0.0051	161	0.0691	145
510	idrnd-000	-		-		0.0041	536	0.0053	505	0.0050	426	0.0094	263	0.0075	316	0.1026	271
511	idrnd-001	-		-		0.0025	197	0.0033	281	0.0032	244	0.0528	672	0.0173	610	0.2243	429
512	igearx-face-000	0.0091	532	0.0146	549	0.0163	984	0.0362	1009	0.0399	981	0.6436	967	0.3305	1011	0.7832	588
513	iit-000	0.1516	945	0.1981	935	0.0828	1143	0.1442	1143	0.2214	1125	0.2943	862	0.1877	959	-	
514	iit-001	0.0104	576	0.0179	610	0.0099	854	0.0142	830	0.1222	1080	0.2677	856	0.2171	972	-	
515	iit-002	0.0111	599	0.0177	609	0.0085	801	0.0140	824	0.0193	852	0.0332	583	0.0260	714	-	
516	iit-003	0.0082	511	0.0151	560	0.0053	632	0.0084	676	0.0122	719	0.0199	466	0.0137	535	-	
517	imds-software-001	0.0126	639	0.0228	673	0.0130	934	0.0221	936	0.0231	889	0.0469	653	0.0199	654	0.4260	503
518	imds-software-002	0.0048	323	0.0072	348	0.0036	457	0.0052	498	0.0047	409	0.9981	1152	0.0078	339	1.0000	814
519	imds-software-003	0.0032	206	0.0047	223	0.0028	287	0.0036	335	0.0036	300	0.9987	1161	0.0063	242	1.0000	808
520	imperial-000	0.0067	446	0.0108	480	0.0080	778	0.0134	806	0.0087	605	0.0581	684	0.0102	437	-	
521	imperial-001	0.0094	549	0.0154	566	0.0072	740	0.0120	763	0.0103	672	0.0190	453	0.0120	495	-	
522	imperial-002	0.0058	390	0.0081	387	0.0055	649	0.0085	679	0.0083	590	0.0157	398	0.0103	438	-	
523	incode-000	0.0766	896	0.1029	887	-		-		-		-		-		-	
524	incode-001	0.0550	869	0.0773	859	-		-		-		-		-		-	
525	incode-002	0.0293	804	0.0548	825	0.0436	1097	0.0785	1098	-		-		-		-	
526	incode-003	0.0142	668	0.0249	696	0.0448	1100	0.0869	1105	0.0354	964	0.0661	703	0.0320	754	-	
527	incode-004	0.0077	491	0.0132	525	0.0096	843	0.0160	864	0.0171	816	0.0281	540	0.0179	620	-	
528	incode-005	0.0111	601	0.0189	625	0.0156	979	0.0304	986	0.0195	859	0.0307	558	0.0172	606	-	

Table 66: FNMR is the proportion of mated comparisons below a threshold set to achieve the FMR given in the header on the fourth row. FMR is the proportion of impostor comparisons at or above that threshold. The light grey values give rank over all algorithms in that column. The pink columns use only same-sex impostors; others are selected regardless of demographics. The exception, in the green column, uses "matched-covariates" i.e. impostors of the same sex, age group, and country of birth. The second pink column includes effects of extended ageing. Missing entries for border, visa, mugshot and wild images generally mean the algorithm did not run to completion. The VISA *columns compare images described in section 2.1. The* MUGSHOT *columns compare images described in section 2.5. The* VISA-BORDER *column compare images described in section 2.2 with those of section 2.4. The* BORDER *column compares images described in section 2.4. The* KIOSK-BORDER *columns compare images described in section 2.6 with those of section 2.4.*

		FALSE NON-MATCH RATE (FNMR)															
	Algorithm	CONSTRAINED, COOPERATIVE														LESS CONSTRAINED, NON-COOP.	
	Name	VISAMC		VISA		MUGSHOT		MUGSHOT12+YRS		VISABORDER		BORDER		BORDER		KIOSKBORDER	
	FMR	0.0001		1E-06		1E-05		1E-05		1E-06		1E-06		1E-05		1E-06	
529	incode-006	0.0156	689	0.0273	712	0.0117	909	0.0238	951	0.0202	864	0.0339	592	0.0164	592	-	
530	incode-007	0.0109	592	0.0155	568	0.0056	658	0.0099	722	0.0107	682	0.0168	421	0.0102	433	-	
531	incode-008	0.0063	427	0.0101	460	0.0046	575	0.0086	685	0.0057	475	0.0104	295	0.0074	309	-	
532	incode-009	0.0044	300	0.0067	325	0.0034	426	0.0051	482	0.0049	424	0.0091	251	0.0067	266	0.0892	228
533	incode-010	0.0041	280	0.0063	309	0.0028	308	0.0043	412	0.0047	413	0.0077	191	0.0061	232	0.0770	184
534	incode-011	0.0032	205	0.0044	198	0.0026	236	0.0034	302	0.0032	239	0.0359	604	0.0140	544	0.1840	403
535	incode-012	0.0027	167	0.0043	191	0.0025	171	0.0035	316	0.0034	271	0.0966	748	0.0385	781	0.3387	477
536	incode-013	0.0035	239	0.0049	231	0.0032	386	0.0039	370	0.0051	433	0.0094	264	0.0081	356	0.0768	182
537	incode-014	-		-		0.0022	53	0.0023	73	0.0034	270	0.0066	155	0.0062	240	0.0569	77
538	incode-015	-		-		0.0021	10	0.0022	57	0.0020	51	0.0040	41	0.0037	60	0.0537	60
539	infocert-001	0.0105	586	0.0172	596	0.0078	767	0.0125	776	0.0159	789	0.1573	796	0.0565	840	0.5716	534
540	infocert-002	-		-		1.0000	1354	0.9993	1289	1.0000	1297	1.0000	1269	1.0000	1319	1.0000	1329
541	innefulabs-000	0.0122	625	0.0199	643	0.0112	893	0.0197	918	0.0222	881	0.0372	618	0.0271	726	-	
542	innominds-001	0.5569	1039	0.6541	1042	0.7642	1269	0.8665	1262	0.7629	1188	0.8200	1018	0.6359	1075	0.9841	686
543	innov8tif-000	-		-		0.1842	1182	0.3028	1188	0.2056	1117	0.2348	840	0.1449	930	0.6142	547
544	innov8tif-001	-		-		0.1865	1184	0.2951	1182	0.1976	1112	0.2564	850	0.1593	943	0.6665	556
545	innovativetechnologyltd-001	0.0578	873	0.0938	880	0.0501	1109	0.0981	1116	0.0592	1030	0.0779	727	0.0422	798	-	
546	innovativetechnologyltd-002	0.0451	851	0.0716	851	0.0541	1116	0.1009	1121	0.0506	1013	0.0682	710	0.0371	778	-	
547	innovatrics-000	0.1105	926	0.1905	931	-		-		-		-		-		-	
548	innovatrics-001	0.1077	924	0.1828	927	-		-		-		-		-		-	
549	innovatrics-002	0.4049	1009	0.6142	1036	-		-		-		-		-		-	
550	innovatrics-003	0.0349	832	0.0483	806	-		-		-		-		-		-	
551	innovatrics-004	0.0194	740	0.0292	721	0.0344	1077	0.0617	1074	0.0562	1025	0.0762	723	0.0412	793	-	
552	innovatrics-005	0.0230	766	0.0353	758	0.0398	1088	0.0721	1092	-		-		-		-	
553	innovatrics-006	0.0058	397	0.0089	417	0.0061	691	0.0096	711	0.0096	650	0.0165	417	0.0103	439	-	
554	innovatrics-007	0.0040	276	0.0054	266	0.0057	660	0.0078	648	0.0079	574	0.0123	342	0.0088	382	-	
555	innovatrics-008	0.0047	321	0.0064	312	0.0038	500	0.0052	495	0.0053	449	0.0088	242	0.0069	280	0.0899	234
556	innovatrics-009	0.0022	119	0.0031	109	0.0028	286	0.0032	267	0.0034	269	0.1165	766	0.0326	755	0.3866	492
557	innovatrics-010	0.0017	81	0.0031	110	0.0027	276	0.0028	173	0.0041	345	0.0078	193	0.0066	262	0.0744	167
558	innovatrics-011	-		-		0.0026	237	0.0027	149	0.0032	246	0.0060	125	0.0044	117	0.0615	103
559	innovatrics-012	-		-		0.0025	175	0.0026	130	0.0034	273	0.9309	1066	0.4977	1047	0.9960	712
560	innovatrics-013	-		-		0.0022	35	0.0021	34	0.0026	144	0.9984	1156	0.3780	1024	1.0000	806
561	innovatrics-014	-		-		0.0021	19	0.0020	5	0.0017	22	0.0033	17	0.0029	14	0.0417	10
562	innovatrics-015	-		-		0.0021	9	0.0020	16	0.0019	42	0.0036	28	0.0031	28	0.0468	29
563	innovatrics-016	-		-		0.0021	13	0.0020	17	0.0018	27	0.0034	22	0.0029	18	0.0451	23
564	insightface-000	0.0018	92	0.0027	85	0.0029	316	0.0030	233	0.0038	316	0.0077	188	0.0068	270	0.0765	179
565	insightface-001	0.0009	18	0.0014	19	0.0027	257	0.0024	102	0.0035	288	0.0070	166	0.0065	252	0.0692	146
566	insightface-002	0.0011	36	0.0019	41	0.0027	275	0.0026	135	0.0036	298	0.0069	162	0.0065	251	0.0694	147
567	insightface-003	0.0015	64	0.0021	51	0.0045	568	0.0034	306	0.1298	1082	1.0000	1351	0.9407	1150	1.0000	1070
568	insightface-004	0.0015	58	0.0023	58	0.0052	625	0.0036	334	0.1403	1088	0.9923	1123	0.9128	1140	0.9989	731
569	inspur-000	0.0060	410	0.0078	369	0.7415	1264	0.9093	1271	0.2838	1138	0.9996	1179	0.9976	1203	1.0000	850
570	inspur-001	0.0035	238	0.0049	232	0.0025	173	0.0030	221	0.0029	200	0.9951	1132	0.9592	1161	1.0000	791
571	inspur-002	0.0025	148	0.0039	157	0.0024	107	0.0027	148	0.0031	226	0.0062	136	0.0047	133	0.1112	291
572	inspur-003	-		-		0.0023	82	0.0026	139	0.0031	228	0.0060	127	0.0046	128	0.0812	206

Table 67: FNMR is the proportion of mated comparisons below a threshold set to achieve the FMR given in the header on the fourth row. FMR is the proportion of impostor comparisons at or above that threshold. The light grey values give rank over all algorithms in that column. The pink columns use only same-sex impostors; others are selected regardless of demographics. The exception, in the green column, uses "matched-covariates" i.e. impostors of the same sex, age group, and country of birth. The second pink column includes effects of extended ageing. Missing entries for border, visa, mugshot and wild images generally mean the algorithm did not run to completion. The VISA *columns compare images described in section 2.1. The* MUGSHOT *columns compare images described in section 2.5. The* VISA-BORDER *column compare images described in section 2.2 with those of section 2.4. The* BORDER *column compares images described in section 2.4. The* KIOSK-BORDER *columns compare images described in section 2.6 with those of section 2.4.*

		FALSE NON-MATCH RATE (FNMR)															
	Algorithm	CONSTRAINED, COOPERATIVE														LESS CONSTRAINED, NON-COOP.	
	Name	VISAMC		VISA		MUGSHOT		MUGSHOT12+YRS		VISABORDER		BORDER		BORDER		KIOSKBORDER	
	FMR	0.0001		1E-06		1E-05		1E-05		1E-06		1E-06		1E-05		1E-06	
573	intellicloudai-001	0.0142	669	0.0234	680	0.0092	823	0.0145	836	0.0162	796	0.0371	617	0.0171	605	-	
574	intellicloudai-002	0.0059	403	0.0085	401	0.0060	682	0.0069	605	0.0108	685	0.2477	848	0.0171	604	-	
575	intellifusion-001	0.0072	469	0.0094	433	0.0056	659	0.0085	680	0.0111	698	0.0212	478	0.0143	551	-	
576	intellifusion-002	0.0059	398	0.0077	366	0.0040	519	0.0074	627	0.0085	599	0.5352	940	0.0104	446	-	
577	intellivision-001	0.1335	938	0.2205	945	0.1090	1157	0.1670	1150	0.1385	1085	0.1676	801	0.1170	908	-	
578	intellivision-002	0.1000	915	0.1775	922	0.0610	1124	0.1009	1120	0.0805	1056	0.1074	756	0.0682	855	-	
579	intellivision-003	0.1177	931	0.2006	937	0.0760	1137	0.1244	1135	0.1069	1076	0.1431	790	0.0839	874	0.4940	519
580	intellivision-004	0.0271	796	0.0559	826	0.0294	1062	0.0503	1056	0.0327	956	0.0461	649	0.0293	746	0.2860	464
581	intellivision-005	0.0105	583	0.0182	616	0.0093	829	0.0141	827	0.0146	770	0.0252	518	0.0172	608	0.1763	396
582	intellivision-006	0.0111	600	0.0174	600	0.0110	885	0.0162	870	0.0181	829	0.0313	560	0.0191	640	0.2416	440
583	intellivision-007	0.0086	519	0.0128	520	0.0098	849	0.0159	862	0.0133	740	0.0218	487	0.0154	574	0.1751	393
584	intellivix-001	0.0064	433	0.0087	410	0.0046	573	0.0063	577	0.0072	542	0.9233	1058	0.7856	1109	0.9977	725
585	intellivix-002	0.0062	420	0.0085	400	0.0039	508	0.0056	522	0.0060	497	0.3464	885	0.0857	878	0.8759	617
586	intellivix-003	0.0075	482	0.0125	516	0.0052	624	0.0091	697	0.0066	521	0.0297	550	0.0096	416	0.1907	408
587	intellivix-004	0.0032	209	0.0045	211	0.0025	191	0.0031	250	0.0040	334	0.0074	176	0.0063	243	0.0662	136
588	intellivix-005	0.0034	232	0.0048	226	0.0024	116	0.0027	164	0.0035	287	0.0067	156	0.0059	230	0.0609	99
589	intellivix-006	-		-		0.0024	154	0.0030	228	0.0026	145	0.0085	228	0.0040	88	0.0918	245
590	intelresearch-000	0.0307	814	0.0578	830	0.0385	1082	0.0751	1094	0.0409	986	0.9870	1107	0.5380	1058	-	
591	intelresearch-001	0.0242	771	0.0595	834	0.0129	933	0.0292	982	0.0351	962	0.9993	1169	0.1854	958	-	
592	intelresearch-002	0.0058	396	0.0082	391	0.0050	613	0.0086	682	0.0136	749	0.0434	636	0.0216	674	-	
593	intelresearch-003	0.0046	319	0.0062	303	0.0038	496	0.0060	555	0.0088	610	0.0168	423	0.0136	531	-	
594	intelresearch-004	0.0025	147	0.0035	128	0.0032	389	0.0038	355	0.0049	425	0.0094	262	0.0072	297	-	
595	intelresearch-005	0.0016	67	0.0023	57	0.0028	285	0.0034	296	0.0042	359	0.0084	223	0.0066	260	0.1433	353
596	intelresearch-006	0.0010	30	0.0015	25	0.0026	251	0.0028	183	0.0032	245	0.8123	1015	0.4742	1042	0.9907	696
597	intelresearch-007	0.0009	25	0.0013	16	0.0025	169	0.0025	108	0.0035	284	0.0069	163	0.0057	205	0.0746	168
598	intelresearch-008	0.0009	24	0.0013	17	0.0025	170	0.0025	109	0.0028	184	0.0304	556	0.0048	141	0.2375	437
599	intelresearch-009	-		-		0.0024	156	0.0025	114	0.0028	186	0.0058	115	0.0046	129	0.0665	137
600	intelresearch-010	-		-		0.0023	88	0.0024	86	0.0029	201	0.0058	116	0.0050	153	0.0683	144
601	intelresearch-011	-		-		0.0023	63	0.0023	60	0.0025	126	0.0049	85	0.0040	95	0.0549	66
602	intelresearch-012	-		-		0.0023	76	0.0023	66	0.0025	118	0.0048	79	0.0040	93	0.0549	65
603	intema-000	0.0012	41	0.0017	35	0.0023	58	0.0022	53	0.0022	71	0.0172	428	0.0061	231	0.0996	265
604	intema-001	0.0010	33	0.0014	22	0.0021	17	0.0020	18	0.0019	44	0.0037	30	0.0030	27	0.0457	26
605	interlinklabs-001	-		-		0.0102	860	0.0205	925	0.0195	858	0.0237	505	0.0115	480	0.1579	371
606	interlinklabs-002	-		-		0.0033	414	0.0049	466	0.0040	331	0.9968	1142	0.9807	1174	1.0000	777
607	interlinklabs-003	-		-		0.0029	326	0.0034	309	0.0046	398	0.0083	219	0.0074	308	0.0620	104
608	intozi-001	0.9982	1070	0.9998	1081	0.9998	1299	1.0000	1304	1.0000	1262	1.0000	1234	1.0000	1247	1.0000	1296
609	intsysmsu-000	0.0135	653	0.0204	644	0.0112	892	0.0161	867	0.0148	773	0.0244	511	0.0172	607	-	
610	intsysmsu-001	0.9543	1066	0.9888	1075	0.9923	1290	0.9948	1286	0.9977	1243	0.9955	1134	0.9892	1182	-	
611	intsysmsu-002	0.0130	645	0.0254	699	0.0137	946	0.0267	972	0.0160	792	0.0267	531	0.0145	558	-	
612	ionetworks-000	0.0060	411	0.0087	408	0.0044	554	0.0058	542	0.0080	583	0.0144	372	0.0112	467	0.1149	300
613	ionetworks-001	0.0254	785	0.0388	774	0.0435	1094	0.0662	1082	0.0426	992	0.8936	1044	0.7391	1099	0.9964	716
614	ionetworks-002	0.0045	303	0.0066	316	0.0033	408	0.0047	449	0.0544	1021	0.9648	1082	0.8765	1128	0.9994	740
615	ionetworks-003	-		-		0.0034	432	0.0049	474	0.0043	367	0.0079	198	0.0056	201	0.0812	205
616	ionetworks-004	-		-		0.0034	436	0.0050	477	0.0043	363	0.0079	197	0.0056	199	0.0808	203

Table 68: FNMR is the proportion of mated comparisons below a threshold set to achieve the FMR given in the header on the fourth row. FMR is the proportion of impostor comparisons at or above that threshold. The light grey values give rank over all algorithms in that column. The pink columns use only same-sex impostors; others are selected regardless of demographics. The exception, in the green column, uses "matched-covariates" i.e. impostors of the same sex, age group, and country of birth. The second pink column includes effects of extended ageing. Missing entries for border, visa, mugshot and wild images generally mean the algorithm did not run to completion. The VISA *columns compare images described in section 2.1. The* MUGSHOT *columns compare images described in section 2.5. The* VISA-BORDER *column compare images described in section 2.2 with those of section 2.4. The* BORDER *column compares images described in section 2.4. The* KIOSK-BORDER *columns compare images described in section 2.6 with those of section 2.4.*

	Algorithm	FALSE NON-MATCH RATE (FNMR)															
		CONSTRAINED, COOPERATIVE														LESS CONSTRAINED, NON-COOP.	
	Name	VISAMC		VISA		MUGSHOT		MUGSHOT12+YRS		VISABORDER		BORDER		BORDER		KIOSKBORDER	
	FMR	0.0001		1E-06		1E-05		1E-05		1E-06		1E-06		1E-05		1E-06	
617	iqface-000	0.0091	536	0.0143	540	0.0075	756	0.0110	747	0.0171	818	0.2234	830	0.0359	772	-	
618	iqface-001	0.0088	525	0.0117	501	0.0177	990	0.0230	945	0.0165	802	0.5514	943	0.0286	736	-	
619	iqface-003	0.0058	394	0.0079	379	0.0051	617	0.0058	543	0.0104	675	0.0200	467	0.0193	644	-	
620	iqsec-001	-		-		0.7050	1257	0.8569	1258	0.7728	1190	0.9962	1140	0.9840	1175	1.0000	793
621	iqsec-002	-		-		0.7050	1256	0.8569	1257	0.7728	1191	0.9962	1139	0.9841	1176	1.0000	792
622	irex-000	0.0052	353	0.0099	450	0.0056	657	0.0083	673	0.0137	754	0.0163	413	0.0078	338	-	
623	irisid-001	-		-		0.0034	429	0.0048	452	0.0058	483	0.0108	310	0.0079	342	0.1024	270
624	isap-001	0.5092	1033	0.6588	1043	0.6899	1253	0.7978	1246	0.7200	1184	0.7253	985	0.5373	1057	-	
625	isap-002	0.0114	606	0.0186	621	0.0087	810	0.0151	848	0.0156	784	0.5134	931	0.0333	759	-	
626	isityou-000	0.5682	1041	0.7033	1050	1.0000	1341	0.9999	1298	1.0000	1395	1.0000	1386	1.0000	1364	-	
627	isystems-000	0.1267	935	0.1795	924	-		-		-		-		-		-	
628	isystems-001	0.0149	682	0.0245	692	0.0138	949	0.0210	928	0.0209	871	0.0332	582	0.0223	680	-	
629	isystems-002	0.0118	615	0.0182	615	0.0111	888	0.0162	873	0.0166	807	0.0284	544	0.0195	649	-	
630	itmo-001	-		0.4408	1001	-		-		-		-		-		-	
631	itmo-002	0.1607	950	0.2866	967	-		-		-		-		-		-	
632	itmo-003	0.0749	895	0.1398	906	-		-		-		-		-		-	
633	itmo-004	0.0255	786	0.0543	823	-		-		-		-		-		-	
634	itmo-005	0.0182	727	0.0345	755	0.0181	993	0.0348	1003	0.0225	884	0.0378	621	0.0230	687	-	
635	itmo-006	0.0125	635	0.0220	664	0.0149	970	0.0266	968	0.0233	892	0.0383	622	0.0285	734	-	
636	itmo-007	0.0080	504	0.0125	515	0.0107	874	0.0185	902	0.0167	809	0.0222	492	0.0144	555	-	
637	itmo-008	0.0090	530	0.0150	556	0.0058	668	0.0059	550	0.0187	841	0.0355	601	0.0339	760	0.1758	395
638	ivacognitive-001	0.0189	734	0.0351	756	0.0123	921	0.0235	949	0.0198	861	0.0274	536	0.0155	575	-	
639	iws-000	0.4824	1027	0.5801	1032	0.6859	1252	0.8155	1251	0.8251	1204	0.7756	1002	0.6400	1078	-	
640	jaakit-001	0.5830	1042	0.7146	1051	0.8173	1273	0.8893	1268	0.8950	1220	0.8387	1029	0.7091	1092	0.9733	669
641	jaakit-002	-		-		0.5729	1237	0.6951	1232	0.6495	1178	0.9894	1116	0.9721	1169	0.9999	762
642	kakao-001	0.4553	1022	0.5532	1027	0.6580	1247	0.8150	1250	0.4831	1163	1.0000	1277	1.0000	1312	-	
643	kakao-002	0.0625	879	0.1779	923	0.0791	1141	0.1381	1140	0.0636	1039	1.0000	1373	1.0000	1374	-	
644	kakao-003	0.0130	646	0.0185	619	0.0261	1045	0.0464	1043	0.0252	915	0.2380	842	0.0284	733	-	
645	kakao-004	0.0078	492	0.0103	467	0.0059	677	0.0102	728	0.0155	781	0.1182	768	0.0230	688	-	
646	kakao-005	0.0040	270	0.0059	285	0.0036	466	0.0057	531	0.0085	597	0.0239	507	0.0125	505	-	
647	kakao-007	0.0019	96	0.0028	88	0.0024	114	0.0026	137	0.0033	256	0.0061	132	0.0053	178	0.0580	82
648	kakao-008	0.0011	35	0.0018	39	0.0023	68	0.0023	69	0.0021	62	0.0041	45	0.0035	49	0.0475	33
649	kakao-009	0.0009	23	0.0013	14	0.0023	74	0.0023	71	0.0020	52	0.0039	36	0.0034	41	0.0468	30
650	kakaobank-000	0.0041	284	0.0058	280	0.0041	528	0.0058	545	0.0060	498	0.9988	1163	0.3243	1008	1.0000	804
651	kakaobank-001	0.0030	193	0.0046	213	0.0032	399	0.0039	361	0.0049	422	0.9998	1195	0.9994	1215	1.0000	860
652	kakaobank-002	-		-		0.0026	226	0.0036	326	0.0038	313	0.3184	876	0.1174	910	0.6931	564
653	kakaobank-003	-		-		0.0023	92	0.0025	125	0.0029	197	0.0065	145	0.0052	173	0.0733	159
654	kakaopay-001	0.0152	686	0.0252	698	0.0145	960	0.0270	973	0.0232	890	0.0344	594	0.0194	645	0.2005	419
655	kasikornlabs-000	0.0112	602	0.0184	618	0.0086	806	0.0137	814	0.0130	735	0.0225	495	0.0148	564	0.1660	386
656	kasikornlabs-001	0.0138	660	0.0206	646	0.0087	809	0.0139	822	0.0142	760	0.0236	504	0.0171	603	0.1684	389
657	kasikornlabs-002	0.0069	453	0.0091	421	0.0048	590	0.0063	572	0.0076	560	0.0144	371	0.0110	463	0.1249	321
658	kasikornlabs-003	0.0057	378	0.0076	362	0.0042	543	0.0056	525	0.0059	488	0.0123	341	0.0098	418	0.1212	316
659	kasikornlabs-004	-		-		0.0041	534	0.0054	511	0.0057	471	0.0112	322	0.0095	410	0.1101	285
660	kasikornlabs-005	-		-		0.0037	469	0.0043	417	0.0054	451	0.0107	306	0.0093	400	0.1069	280

Table 69: FNMR is the proportion of mated comparisons below a threshold set to achieve the FMR given in the header on the fourth row. FMR is the proportion of impostor comparisons at or above that threshold. The light grey values give rank over all algorithms in that column. The pink columns use only same-sex impostors; others are selected regardless of demographics. The exception, in the green column, uses "matched-covariates" i.e. impostors of the same sex, age group, and country of birth. The second pink column includes effects of extended ageing. Missing entries for border, visa, mugshot and wild images generally mean the algorithm did not run to completion. The VISA *columns compare images described in section 2.1. The* MUGSHOT *columns compare images described in section 2.5. The* VISA-BORDER *column compare images described in section 2.2 with those of section 2.4. The* BORDER *column compares images described in section 2.4. The* KIOSK-BORDER *columns compare images described in section 2.6 with those of section 2.4.*

	Algorithm	FALSE NON-MATCH RATE (FNMR)															
		CONSTRAINED, COOPERATIVE														LESS CONSTRAINED, NON-COOP.	
	Name	VISAMC		VISA		MUGSHOT		MUGSHOT12+YRS		VISABORDER		BORDER		BORDER		KIOSKBORDER	
	FMR	0.0001		1E-06		1E-05		1E-05		1E-06		1E-06		1E-05		1E-06	
661	kbyai-000	-		-		0.0027	271	0.0032	265	0.0031	235	0.0079	200	0.0049	148	0.0655	131
662	kedacom-000	0.0055	370	0.0081	385	0.0111	891	0.0120	762	0.0415	987	0.0966	747	0.0686	856	-	
663	keyless-000	-		-		0.0025	187	0.0034	294	0.0031	234	0.1874	810	0.0568	841	0.5543	529
664	kiwitech-000	0.0076	487	0.0105	472	0.0081	783	0.0128	791	0.0096	646	0.0163	412	0.0101	430	-	
665	kloudspot-001	-		-		0.0140	950	0.0259	962	0.9999	1256	1.0000	1240	1.0000	1252	1.0000	817
666	kloudspot-002	-		-		0.0255	1040	0.0423	1029	0.0192	851	0.8748	1036	0.7143	1094	0.9929	701
667	kneron-003	0.0542	865	0.0902	876	0.0346	1078	0.0562	1065	0.0919	1066	0.1251	774	0.0973	890	-	
668	kneron-005	0.0157	691	0.0259	703	0.0126	929	0.0212	929	0.0406	985	0.0693	715	0.0542	832	-	
669	kneron-006	-		-		0.0094	832	0.0125	775	0.1305	1083	0.9751	1091	0.9033	1138	0.9987	730
670	knowutech-000	0.0039	267	0.0055	270	0.0028	313	0.0042	400	0.0042	352	0.0077	186	0.0059	224	0.0820	208
671	kogniza-001	-		-		0.0028	312	0.0031	255	0.0025	125	0.0048	75	0.0042	101	0.0557	68
672	kookmin-001	0.0462	855	0.0750	853	0.0489	1106	0.0842	1102	0.0659	1041	0.8380	1028	0.3212	1007	-	
673	kookmin-002	0.0054	369	0.0077	367	0.0043	549	0.0065	584	0.0123	721	0.7591	996	0.0198	652	-	
674	koreaid-001	0.0031	199	0.0045	206	0.0026	227	0.0032	262	0.0043	366	0.0083	216	0.0068	274	0.0743	165
675	krungthai-002	0.0105	582	0.0161	578	0.0091	820	0.0141	828	0.7350	1186	0.9889	1114	0.9605	1162	0.9999	759
676	kuke3d-001	0.0058	385	0.0104	469	0.0083	793	0.0093	700	0.0270	922	0.9901	1117	0.8341	1117	1.0000	794
677	kuke3d-002	0.0077	488	0.0135	529	0.0069	727	0.0098	718	0.0111	697	1.0000	1239	1.0000	1246	1.0000	821
678	lebentech-000	0.5940	1043	0.7032	1049	0.8854	1278	0.9511	1274	0.9089	1225	0.9970	1143	0.9861	1179	0.9999	766
679	lebentech-001	0.0304	812	0.9032	1066	0.9998	1300	1.0000	1302	1.0000	1263	1.0000	1222	0.9999	1236	1.0000	853
680	lemalabs-001	0.0111	597	0.0175	603	0.0088	811	0.0142	829	0.0143	763	0.0228	499	0.0140	543	0.1646	383
681	lightvision-000	-		-		0.0146	964	0.0232	947	0.0237	902	0.9638	1081	0.7768	1106	0.9986	728
682	lightvision-001	-		-		0.0068	722	0.0096	710	0.0084	595	0.9948	1131	0.9288	1146	1.0000	781
683	lineclova-000	0.0172	714	0.0236	683	0.0109	880	0.0194	914	0.0183	835	0.0291	549	0.0204	660	0.1936	410
684	lineclova-001	0.0025	149	0.0040	166	0.0026	250	0.0034	308	0.0045	393	0.4127	910	0.0080	347	0.9824	679
685	lineclova-002	0.0021	109	0.0035	126	0.0025	161	0.0027	156	0.0041	343	0.0086	234	0.0072	298	0.1595	375
686	lineclova-003	0.0018	90	0.0030	101	0.0028	309	0.0031	239	0.0041	344	0.0083	220	0.0075	323	0.1014	269
687	lookman-002	0.0297	809	0.0547	824	0.0339	1073	0.0562	1064	0.0614	1034	0.0960	746	0.0790	866	-	
688	lookman-004	0.0074	480	0.0099	451	0.0124	924	0.0149	844	0.0430	994	0.0866	735	0.0694	857	-	
689	lssytech-000	-		-		0.0023	69	0.0023	74	0.0021	63	0.0040	43	0.0036	57	0.0574	80
690	luxand-000	0.2056	970	0.2814	965	0.4053	1216	0.5365	1214	0.3497	1147	0.3743	898	0.2605	986	-	
691	luxand-001	0.0116	608	0.0925	877	0.0144	958	0.0267	969	1.0000	1333	1.0000	1302	1.0000	1287	1.0000	1227
692	luxand-003	-		-		0.9938	1292	0.9999	1295	0.2905	1139	0.2256	834	0.0849	877	0.4876	515
693	luxand-004	-		-		0.0031	376	0.0042	401	0.0110	693	0.9994	1175	0.9969	1200	1.0000	867
694	mantra-000	0.0037	256	0.0052	257	0.0054	640	0.0056	527	0.0097	654	0.0181	440	0.0151	569	-	
695	matrixcomsec-000	-		-		0.1032	1154	0.0895	1108	1.0000	1298	1.0000	1271	1.0000	1317	1.0000	1319
696	matrixcomsec-001	-		-		0.0070	729	0.0136	807	0.8826	1218	1.0000	1279	1.0000	1310	1.0000	1287
697	maverickresearch-000	-		-		0.0143	955	0.0192	910	0.0216	876	0.0362	610	0.0250	706	0.2293	430
698	maxvision-000	0.0078	496	0.0106	474	0.0110	884	0.0147	839	0.0368	972	1.0000	1394	0.1545	938	1.0000	914
699	maxvision-001	0.0305	813	0.0528	819	0.1028	1152	0.1921	1160	0.0650	1040	0.3001	865	0.1553	940	0.6188	550
700	maxvision-002	0.0070	459	0.0107	475	0.0061	689	0.0093	699	0.0080	580	0.5726	948	0.2943	999	0.9160	639
701	maxvision-003	0.0056	374	0.0083	396	0.0038	501	0.0060	557	0.0061	501	0.2614	851	0.0650	851	0.5812	536
702	maxvision-004	0.0024	143	0.0038	155	0.0025	202	0.0029	204	0.0029	193	0.4732	924	0.1965	961	0.8141	598
703	maxvision-005	0.0014	52	0.0026	76	0.0024	123	0.0024	85	0.0025	115	0.1216	770	0.0332	757	0.3922	495
704	maxvision-006	0.0016	72	0.0026	72	0.0024	128	0.0024	89	0.0024	111	0.4012	908	0.1799	955	0.7634	578

Table 70: FNMR is the proportion of mated comparisons below a threshold set to achieve the FMR given in the header on the fourth row. FMR is the proportion of impostor comparisons at or above that threshold. The light grey values give rank over all algorithms in that column. The pink columns use only same-sex impostors; others are selected regardless of demographics. The exception, in the green column, uses "matched-covariates" i.e. impostors of the same sex, age group, and country of birth. The second pink column includes effects of extended ageing. Missing entries for border, visa, mugshot and wild images generally mean the algorithm did not run to completion. The VISA *columns compare images described in section 2.1. The* MUGSHOT *columns compare images described in section 2.5. The* VISA-BORDER *column compare images described in section 2.2 with those of section 2.4. The* BORDER *column compares images described in section 2.4. The* KIOSK-BORDER *columns compare images described in section 2.6 with those of section 2.4.*

	Algorithm	FALSE NON-MATCH RATE (FNMR)													
		CONSTRAINED, COOPERATIVE												LESS CONSTRAINED, NON-COOP.	
	Name	VISAMC		VISA		MUGSHOT		MUGSHOT12+YRS		VISABORDER		BORDER		BORDER		KIOSKBORDER	
	FMR	0.0001		1E-06		1E-05		1E-05		1E-06		1E-06		1E-05		1E-06	
705	mbbankvn-000	-		-		0.0030	335	0.0035	310	0.0026	141	0.3822	902	0.1130	904	0.7052	568
706	megvii-000	0.0159	696	0.0246	694	-		-		-		-		-		-	
707	megvii-001	0.0157	692	0.0244	689	0.0392	1087	0.0671	1083	0.0168	811	0.0455	646	0.0164	591	-	
708	megvii-002	0.0104	578	0.0145	544	0.0225	1024	0.0345	1001	0.0099	664	0.0286	545	0.0240	698	-	
709	megvii-003	0.0064	428	0.0094	431	0.0136	945	0.0260	964	0.0050	427	0.0080	205	0.0059	226	-	
710	megvii-004	0.0020	100	0.0033	119	0.0028	301	0.0035	322	0.0037	312	0.0074	177	0.0068	275	0.0736	163
711	megvii-005	0.0010	32	0.0015	23	0.0026	219	0.0031	245	0.0019	40	0.0500	663	0.0057	210	0.1991	417
712	megvii-006	0.0011	34	0.0016	28	0.0026	245	0.0033	282	0.0025	123	0.0050	89	0.0048	137	0.0588	91
713	megvii-007	0.0006	12	0.0016	26	0.0025	188	0.0028	175	0.0024	107	0.0048	80	0.0047	134	0.0586	85
714	megvii-008	0.0003	2	0.0008	7	0.0023	94	0.0021	39	0.0024	112	0.0049	83	0.0047	136	0.0541	62
715	megvii-009	0.0003	3	0.0008	6	0.0023	96	0.0021	40	0.0018	25	0.0149	382	0.0036	53	0.1096	284
716	meituan-000	0.0197	741	0.0424	785	0.0078	769	0.0074	626	0.0103	673	0.0193	460	0.0164	590	0.1133	297
717	meituan-001	0.0164	703	0.1886	930	0.0025	177	0.0026	132	0.0030	210	0.0074	175	0.0051	162	0.0791	193
718	meituan-002	0.0017	77	0.0025	65	0.0024	127	0.0023	67	0.0024	109	0.0067	159	0.0044	123	0.0773	185
719	meituan-003	0.0017	74	0.0021	49	0.0024	119	0.0023	80	0.0024	104	0.0084	224	0.0046	126	0.0883	224
720	meituan-004	0.0014	51	0.0021	47	0.0024	121	0.0024	98	0.0023	90	0.0070	165	0.0044	119	0.0813	207
721	meiya-001	0.0171	711	0.0275	715	0.0159	983	0.0261	967	0.0311	949	0.2250	833	0.0245	703	-	
722	mendaxiatech-000	0.0027	168	0.0036	134	0.0029	318	0.0036	339	0.0031	231	0.0057	109	0.0051	163	-	
723	metsakuurcompany-001	0.0068	452	0.0087	411	0.0068	725	0.0078	651	0.0095	641	0.8972	1048	0.5635	1061	0.9970	720
724	metsakuurcompany-002	0.0048	324	0.0071	339	0.0030	345	0.0043	419	0.0032	247	0.2059	822	0.0665	853	0.5374	524
725	metsakuurcompany-003	0.0034	227	0.0051	246	0.0026	224	0.0036	324	0.0028	179	0.2418	843	0.1001	892	0.5866	540
726	metsakuurcompany-004	-		-		0.0026	248	0.0032	257	0.0032	240	0.4488	920	0.2015	965	0.8129	597
727	metsakuurcompany-005	-		-		0.0030	346	0.0041	390	0.0039	323	0.1725	803	0.0054	191	0.8274	600
728	miaxis-001	0.0068	449	0.0099	454	0.0059	676	0.0097	715	0.0096	649	0.0231	502	0.0109	460	0.1592	372
729	miaxis-002	0.0745	894	0.0774	860	0.3215	1206	0.4000	1196	0.1485	1092	0.2087	823	0.2058	966	0.3846	491
730	miaxis-003	0.0045	304	0.0067	322	0.0037	485	0.0050	476	0.0061	503	0.0139	360	0.0088	380	0.1322	329
731	miaxis-004	-		-		0.0037	468	0.0046	440	0.0057	476	0.0107	307	0.0084	372	0.1261	324
732	microfocus-000	0.4656	1023	0.5624	1028	-		-		-		-		-		-	
733	microfocus-001	0.4482	1020	0.5524	1026	0.7256	1260	0.8416	1255	0.7301	1185	0.6926	977	0.5180	1054	-	
734	microfocus-002	0.3605	1001	0.5057	1016	0.5783	1238	0.7223	1234	0.5909	1171	0.5963	958	0.4160	1034	-	
735	microfocus-003	0.0416	842	0.0607	836	0.0652	1128	0.1025	1122	0.0793	1053	0.2248	832	0.0923	885	0.6153	548
736	minivision-000	0.0033	217	0.0048	227	0.0038	497	0.0049	461	0.0055	458	0.0094	268	0.0079	344	-	
737	mitek-000	0.6882	1050	0.8192	1058	0.9568	1285	0.9788	1281	0.9545	1233	0.9437	1071	0.8494	1120	0.9931	703
738	mitek-001	-		-		0.0050	608	0.0068	597	0.0053	447	0.0096	275	0.0077	334	0.1130	296
739	mitek-002	-		-		0.0039	514	0.0054	507	0.0044	378	0.0085	231	0.0065	255	0.1112	292
740	mobai-000	0.0360	834	0.0439	792	0.0372	1081	0.0700	1088	0.0367	971	0.0939	741	0.0795	868	-	
741	mobai-001	0.0199	745	0.0219	661	0.0047	581	0.0061	562	0.0093	637	0.0174	430	0.0138	539	-	
742	mobai-002	-		-		0.0048	591	0.0070	607	0.0088	616	0.5904	954	0.3167	1006	0.8952	632
743	mobai-003	-		-		0.0053	635	0.0090	693	0.0689	1045	0.9994	1173	0.9982	1205	1.0000	825
744	mobbl-000	0.2938	989	0.3861	993	0.5391	1232	0.6888	1231	0.6545	1179	0.8027	1011	0.6207	1071	-	
745	mobbl-001	0.3208	993	0.4375	1000	0.5680	1236	0.7193	1233	0.6282	1173	0.5783	949	0.3984	1029	0.8864	627
746	mobbl-002	0.9914	1069	0.9970	1077	0.9355	1282	0.9923	1284	1.0000	1261	1.0000	1212	0.9999	1230	1.0000	827
747	mobbl-003	0.0087	522	0.0134	528	0.0062	693	0.0087	686	0.0099	660	0.0197	463	0.0122	501	0.1618	382
748	mobbl-004	-		-		0.0031	374	0.0043	416	0.0088	611	1.0000	1219	1.0000	1240	1.0000	828

Table 71: FNMR is the proportion of mated comparisons below a threshold set to achieve the FMR given in the header on the fourth row. FMR is the proportion of impostor comparisons at or above that threshold. The light grey values give rank over all algorithms in that column. The pink columns use only same-sex impostors; others are selected regardless of demographics. The exception, in the green column, uses "matched-covariates" i.e. impostors of the same sex, age group, and country of birth. The second pink column includes effects of extended ageing. Missing entries for border, visa, mugshot and wild images generally mean the algorithm did not run to completion. The VISA *columns compare images described in section 2.1. The* MUGSHOT *columns compare images described in section 2.5. The* VISA-BORDER *column compare images described in section 2.2 with those of section 2.4. The* BORDER *column compares images described in section 2.4. The* KIOSK-BORDER *columns compare images described in section 2.6 with those of section 2.4.*

	Algorithm	FALSE NON-MATCH RATE (FNMR)															
		CONSTRAINED, COOPERATIVE														LESS CONSTRAINED, NON-COOP.	
	Name	VISAMC		VISA		MUGSHOT		MUGSHOT12+YRS		VISABORDER		BORDER		BORDER		KIOSKBORDER	
	FMR	0.0001		1E-06		1E-05		1E-05		1E-06		1E-06		1E-05		1E-06	
749	mobbl-005	-		-		0.0031	366	0.0044	430	0.0045	381	0.4420	918	0.1465	931	0.7973	594
750	mobipintech-000	0.0090	529	0.0149	553	0.0039	517	0.0057	528	0.0115	706	0.0465	651	0.0182	624	0.6443	553
751	momovn-001	0.1044	920	0.1694	920	0.3253	1208	0.5244	1211	0.3861	1153	0.9995	1177	0.9985	1206	1.0000	835
752	momovn-002	-		-		0.0042	541	0.0060	559	0.0062	506	0.7672	998	0.5456	1059	0.9731	668
753	momovn-003	-		-		0.0029	320	0.0033	275	0.0056	466	0.0093	258	0.0076	327	0.0612	101
754	moredian-000	0.3874	1007	0.4912	1012	0.9988	1297	0.9999	1297	0.9990	1250	0.9999	1199	0.9998	1228	-	
755	morpho-000	0.1020	917	0.1343	903	-		-		-		-		-		-	
756	morpho-001	-		0.2772	962	-		-		-		-		-		-	
757	morpho-002	0.0377	836	0.0680	846	0.0368	1080	0.0716	1090	-		-		-		-	
758	mukh-001	0.0170	709	0.0285	717	0.0225	1025	0.0405	1023	0.0272	926	0.0950	743	0.0291	743	0.5846	539
759	mukh-002	0.0269	795	0.0357	761	0.0435	1096	0.0799	1100	0.0143	764	0.0213	480	0.0122	500	0.1908	409
760	mukh-003	0.0077	490	0.0113	494	0.0111	889	0.0224	938	0.0061	502	0.7813	1005	0.4504	1039	0.9899	695
761	mukh-004	0.0050	337	0.0069	335	0.0051	615	0.0099	724	0.0045	384	0.0083	218	0.0059	227	0.1030	273
762	mukh-005	-		-		0.0023	66	0.0024	105	0.0056	465	0.0161	407	0.0067	265	0.1398	344
763	multimodality-000	0.0034	228	0.0047	220	0.0036	463	0.0044	428	0.0077	566	0.9976	1148	0.4456	1038	1.0000	819
764	multimodality-001	0.0029	182	0.0042	179	0.0031	358	0.0035	313	0.0038	314	0.0071	169	0.0059	223	0.0732	157
765	mvision-001	0.0191	735	0.0233	677	0.0204	1009	0.0356	1005	0.0198	862	0.0337	589	0.0242	700	-	
766	nazhiai-000	0.0040	273	0.0059	291	0.0036	451	0.0048	458	0.0057	478	0.0125	346	0.0083	365	-	
767	ncsgroup-000	-		-		0.0126	928	0.0226	940	0.0179	826	0.1715	802	0.0287	738	0.6160	549
768	ncssg-001	0.0207	751	0.1540	913	0.0045	562	0.0067	596	0.0056	470	0.1180	767	0.0301	747	0.3908	494
769	ncssg-002	-		-		0.0032	394	0.0038	357	0.0033	252	0.3144	873	0.1061	897	0.7441	576
770	ncssg-003	-		-		0.0033	411	0.0040	381	0.0033	264	0.2511	849	0.0959	889	0.6553	555
771	ncssg-004	-		-		0.0033	406	0.0041	399	0.0029	203	0.2454	845	0.0860	879	0.6010	542
772	neosystems-001	1.0000	1243	1.0000	1118	0.2987	1203	0.4382	1203	0.5173	1166	0.6570	970	0.4043	1032	-	
773	neosystems-002	0.2905	987	0.4077	996	0.2028	1188	0.3252	1189	0.4088	1158	0.5519	944	0.3331	1012	0.9561	655
774	neosystems-003	0.2429	978	0.3349	981	0.1844	1183	0.2999	1186	0.5942	1172	0.3936	905	0.2292	975	0.8482	607
775	neosystems-004	0.0279	799	0.0495	809	0.0289	1056	0.0585	1072	0.0439	997	0.9621	1079	0.1296	917	0.9996	746
776	netbridgetech-001	0.4749	1025	0.6599	1044	0.4438	1222	0.5676	1217	0.4491	1161	1.0000	1204	0.9541	1157	-	
777	netbridgetech-002	0.0101	568	0.0166	587	0.0077	764	0.0127	786	0.0133	742	0.8215	1020	0.0523	828	-	
778	neurotechnology-000	-		0.2371	949	-		-		-		-		-		-	
779	neurotechnology-001	0.1393	940	0.2218	946	-		-		-		-		-		-	
780	neurotechnology-002	0.1115	927	0.1663	919	-		-		-		-		-		-	
781	neurotechnology-003	0.0617	876	0.0880	872	-		-		-		-		-		-	
782	neurotechnology-004	0.0146	674	0.0297	725	0.0107	876	0.0164	877	-		-		-		-	
783	neurotechnology-005	0.0141	667	0.0300	728	0.0108	879	0.0163	876	0.0204	865	0.0875	736	0.0246	705	-	
784	neurotechnology-006	0.0098	558	0.0136	532	0.0105	870	0.0182	896	0.0164	800	0.0843	732	0.0214	670	-	
785	neurotechnology-008	0.0091	538	0.0184	617	0.0076	760	0.0116	756	0.0157	786	0.9973	1144	0.1803	957	-	
786	neurotechnology-009	0.0049	331	0.0087	413	0.0057	664	0.0094	702	0.0079	578	1.0000	1208	0.0101	429	-	
787	neurotechnology-010	0.0048	325	0.0085	403	0.0056	656	0.0090	692	0.0077	569	1.0000	1213	0.0113	470	-	
788	neurotechnology-011	0.0050	339	0.0087	405	0.0061	692	0.0097	714	0.0077	568	0.0404	631	0.0092	396	-	
789	neurotechnology-012	0.0051	349	0.0070	337	0.0038	489	0.0056	526	0.0066	520	0.0112	323	0.0075	320	0.1009	268
790	neurotechnology-013	0.0032	213	0.0045	208	0.0026	249	0.0036	325	0.0037	303	0.0068	160	0.0052	176	0.0747	170
791	neurotechnology-015	0.0022	123	0.0036	138	0.0024	113	0.0028	181	0.0030	207	0.0052	94	0.0041	100	0.0646	125
792	neurotechnology-016	0.0022	126	0.0032	115	0.0023	83	0.0027	157	0.0027	163	0.0049	84	0.0039	86	0.0613	102

Table 72: FNMR is the proportion of mated comparisons below a threshold set to achieve the FMR given in the header on the fourth row. FMR is the proportion of impostor comparisons at or above that threshold. The light grey values give rank over all algorithms in that column. The pink columns use only same-sex impostors; others are selected regardless of demographics. The exception, in the green column, uses "matched-covariates" i.e. impostors of the same sex, age group, and country of birth. The second pink column includes effects of extended ageing. Missing entries for border, visa, mugshot and wild images generally mean the algorithm did not run to completion. The VISA *columns compare images described in section 2.1. The* MUGSHOT *columns compare images described in section 2.5. The* VISA-BORDER *column compare images described in section 2.2 with those of section 2.4. The* BORDER *column compares images described in section 2.4. The* KIOSK-BORDER *columns compare images described in section 2.6 with those of section 2.4.*

	Algorithm	FALSE NON-MATCH RATE (FNMR)															
		CONSTRAINED, COOPERATIVE														LESS CONSTRAINED, NON-COOP.	
	Name	VISAMC		VISA		MUGSHOT		MUGSHOT12+YRS		VISABORDER		BORDER		BORDER		KIOSKBORDER	
	FMR	0.0001		1E-06		1E-05		1E-05		1E-06		1E-06		1E-05		1E-06	
793	neurotechnology-017	0.0017	82	0.0031	106	0.0023	64	0.0025	120	0.0025	131	0.0047	73	0.0038	72	0.0612	100
794	neurotechnology-018	0.0020	103	0.0029	94	0.0022	46	0.0024	93	0.0024	108	0.0046	64	0.0037	61	0.0586	86
795	neurotechnology-019	-		-		0.0022	44	0.0024	81	0.0022	68	0.0042	48	0.0034	38	0.0526	51
796	neurotechnology-020	-		-		0.0023	93	0.0028	197	0.0024	94	0.0043	55	0.0035	47	0.0562	72
797	nextmetalabs-001	-		-		0.1126	1160	0.1962	1162	0.1137	1077	1.0000	1218	0.9998	1225	1.0000	840
798	nextmetalabs-002	-		-		0.0066	716	0.0081	669	0.0097	652	0.9946	1130	0.9565	1159	1.0000	788
799	nextmetalabs-003	-		-		0.0023	102	0.0028	191	0.0028	174	0.9681	1086	0.8769	1129	0.9995	745
800	nextmetalabs-004	-		-		0.0023	103	0.0028	190	0.0029	191	0.0055	102	0.0048	138	0.0716	153
801	nhn-001	0.0066	443	0.0098	446	0.0053	633	0.0079	661	0.0093	633	0.0156	397	0.0109	458	-	
802	nhn-002	0.0068	450	0.0096	439	0.0057	666	0.0087	688	0.0136	753	0.0253	520	0.0186	634	0.1464	357
803	nhn-003	0.0033	216	0.0048	225	0.0027	270	0.0038	354	0.0036	295	0.0198	464	0.0071	293	0.1280	326
804	nhn-004	0.0030	186	0.0044	205	0.0025	190	0.0029	208	0.0030	223	0.0331	579	0.0113	473	0.1598	377
805	nhn-005	0.0028	173	0.0043	192	0.0023	87	0.0027	147	0.0025	116	0.0047	67	0.0038	71	0.0554	67
806	noblis-000	0.4424	1019	0.5415	1024	-		-		-		-		-		-	
807	nodeflux-000	1.0000	1258	1.0000	1372	1.0000	1337	-		0.9079	1224	-		-		-	
808	nodeflux-001	1.0000	1288	1.0000	1401	1.0000	1334	0.9998	1294	0.5169	1165	1.0000	1408	0.5654	1062	-	
809	nodeflux-002	0.0186	732	0.0340	748	0.0261	1044	0.0451	1036	0.0548	1022	1.0000	1227	1.0000	1244	-	
810	nominder-000	0.0025	152	0.0036	142	0.0029	325	0.0033	280	0.0026	155	0.9919	1122	0.8877	1134	1.0000	798
811	nominder-001	0.0029	184	0.0042	184	0.0031	378	0.0038	356	0.0031	230	0.9975	1146	0.9180	1142	0.9999	768
812	nominder-002	0.0025	154	0.0037	143	0.0033	405	0.0037	344	0.0026	160	0.5785	950	0.1435	929	0.8381	603
813	nominder-003	-		-		0.0031	355	0.0034	298	0.0026	146	0.7010	981	0.2159	971	0.8909	630
814	nominder-004	-		-		0.0028	305	0.0033	276	0.0024	95	0.0316	565	0.0045	124	0.1348	335
815	nominder-005	-		-		0.0025	176	0.0029	203	0.0024	103	0.0046	65	0.0037	65	0.0537	61
816	nominder-006	-		-		0.0027	272	0.0032	260	0.0030	220	0.0059	118	0.0052	170	0.0644	123
817	nominder-007	-		-		0.0027	256	0.0031	241	0.0023	87	0.0072	172	0.0036	52	0.0946	257
818	notiontag-000	0.6669	1048	0.7885	1056	0.3715	1213	0.4978	1210	0.8571	1209	0.8102	1014	0.6460	1080	-	
819	notiontag-001	0.6846	1049	0.8006	1057	0.3955	1215	0.5247	1212	0.8669	1212	0.8313	1026	0.6362	1077	-	
820	notiontag-002	0.0066	441	0.0089	416	0.0045	561	0.0061	563	0.0077	567	0.0137	359	0.0104	443	0.1106	289
821	nsensecorp-001	0.9909	1068	0.9994	1080	0.9987	1296	0.9999	1296	1.0000	1264	1.0000	1237	1.0000	1249	-	
822	nsensecorp-002	0.4277	1015	0.5375	1021	0.6734	1248	0.7924	1244	0.7194	1183	0.6937	979	0.5617	1060	0.9392	649
823	nsensecorp-003	0.0251	783	0.0295	724	0.0212	1016	0.0305	988	0.0131	737	0.2139	826	0.0141	547	0.9968	719
824	nsensecorp-004	0.1370	939	0.1397	905	0.0066	715	0.0094	703	1.0000	1399	1.0000	1399	1.0000	1353	1.0000	905
825	nsensecorp-005	0.0055	372	0.0080	384	0.0039	509	0.0058	544	0.2723	1136	0.9999	1198	0.9949	1192	1.0000	843
826	ntechlab-000	-		0.0862	870	-		-		-		-		-		-	
827	ntechlab-001	-		0.0825	866	-		-		-		-		-		-	
828	ntechlab-002	0.0558	871	0.0649	839	-		-		-		-		-		-	
829	ntechlab-003	0.0286	803	0.0390	775	-		-		-		-		-		-	
830	ntechlab-004	0.0090	531	0.0132	524	-		-		-		-		-		-	
831	ntechlab-005	0.0093	542	0.0145	545	0.0131	937	0.0275	975	-		-		-		-	
832	ntechlab-006	0.0078	495	0.0111	485	0.0112	895	0.0227	943	0.0108	684	0.0149	383	0.0098	420	-	
833	ntechlab-007	0.0056	375	0.0076	361	0.0073	750	0.0128	790	0.0079	577	0.0144	370	0.0102	431	-	
834	ntechlab-008	0.0041	286	0.0061	297	0.0056	653	0.0108	740	0.0042	358	0.0080	203	0.0063	246	-	
835	ntechlab-009	0.0039	266	0.0054	265	0.0042	545	0.0063	573	0.0275	929	0.0674	707	0.0532	829	-	
836	ntechlab-010	0.0013	50	0.0017	32	0.0024	146	0.0029	206	0.0031	232	0.0058	117	0.0050	154	0.0656	132

Table 73: FNMR is the proportion of mated comparisons below a threshold set to achieve the FMR given in the header on the fourth row. FMR is the proportion of impostor comparisons at or above that threshold. The light grey values give rank over all algorithms in that column. The pink columns use only same-sex impostors; others are selected regardless of demographics. The exception, in the green column, uses "matched-covariates" i.e. impostors of the same sex, age group, and country of birth. The second pink column includes effects of extended ageing. Missing entries for border, visa, mugshot and wild images generally mean the algorithm did not run to completion. The VISA *columns compare images described in section 2.1. The* MUGSHOT *columns compare images described in section 2.5. The* VISA-BORDER *column compare images described in section 2.2 with those of section 2.4. The* BORDER *column compares images described in section 2.4. The* KIOSK-BORDER *columns compare images described in section 2.6 with those of section 2.4.*

		FALSE NON-MATCH RATE (FNMR)															
	Algorithm	CONSTRAINED, COOPERATIVE														LESS CONSTRAINED, NON-COOP.	
	Name	VISAMC		VISA		MUGSHOT		MUGSHOT12+YRS		VISABORDER		BORDER		BORDER		KIOSKBORDER	
	FMR	0.0001		1E-06		1E-05		1E-05		1E-06		1E-06		1E-05		1E-06	
837	ntechlab-011	0.0012	43	0.0019	40	0.0024	138	0.0028	194	0.0029	199	0.0055	100	0.0047	131	0.0630	112
838	ntechlab-012	0.0011	39	0.0016	27	0.0023	99	0.0030	219	0.0026	149	0.0050	91	0.0043	108	0.0587	88
839	omface-000	0.2573	983	0.3835	992	0.3590	1211	0.4903	1208	0.3956	1155	0.5003	927	0.2595	985	0.9137	638
840	omface-001	0.0137	659	0.0212	653	0.0114	905	0.0187	906	0.0174	823	1.0000	1377	0.0214	672	1.0000	976
841	omnigarde-000	0.0633	881	0.1002	885	0.1109	1158	0.2042	1166	0.1288	1081	0.5113	930	0.1227	915	0.9604	659
842	omnigarde-001	0.0168	706	0.0260	704	0.0203	1007	0.0402	1019	0.0243	907	0.0327	575	0.0177	616	0.2164	428
843	omnigarde-002	0.0033	221	0.0046	217	0.0027	283	0.0039	363	0.0041	346	0.0076	182	0.0059	228	0.0806	202
844	omnigarde-003	0.0024	141	0.0038	152	0.0024	153	0.0029	198	0.0032	249	0.0059	121	0.0049	150	0.0706	151
845	omnigarde-004	-		-		0.0022	41	0.0024	83	0.0023	80	0.0044	58	0.0038	73	0.0559	70
846	omnigarde-005	-		-		0.0022	52	0.0024	91	0.0024	100	0.0045	61	0.0039	84	0.0582	83
847	onfido-000	0.1472	944	0.2881	968	0.0335	1072	0.0731	1093	0.0515	1015	0.9915	1120	0.9579	1160	1.0000	772
848	onfido-001	-		-		0.0146	962	0.0294	983	0.0190	846	0.0702	718	0.0352	767	0.3117	471
849	onfido-002	-		-		0.0067	717	0.0098	719	0.0062	508	0.0167	420	0.0091	393	0.1228	319
850	onfido-003	-		-		0.0045	566	0.0070	606	0.0043	364	0.0164	415	0.0076	328	0.1153	302
851	ooto-001	-		-		0.0193	1000	0.0290	981	0.0529	1020	0.0272	533	0.0255	709	0.1956	415
852	openedge-000	0.0045	309	0.0062	307	0.0049	596	0.0069	603	0.0049	421	0.9889	1115	0.7991	1113	0.9999	764
853	openface-001	0.1804	958	0.2921	970	0.2878	1199	0.3906	1195	0.2054	1116	0.2338	839	0.1549	939	0.6531	554
854	ovisionllc-001	-		-		0.0058	671	0.0081	663	0.8171	1201	1.0000	1238	1.0000	1241	1.0000	813
855	ovisionllc-002	-		-		0.1963	1185	0.2522	1174	1.0000	1267	1.0000	1243	1.0000	1253	1.0000	820
856	oz-001	0.0133	651	0.0215	659	0.0109	881	0.0160	865	0.0235	898	1.0000	1361	1.0000	1385	-	
857	oz-002	0.0071	468	0.0099	457	0.0099	855	0.0100	725	0.0139	756	0.0502	665	0.0202	657	-	
858	oz-003	0.0095	554	0.0143	541	0.0054	642	0.0077	644	0.0096	648	0.0175	434	0.0118	487	0.1404	346
859	oz-004	0.0033	222	0.0049	233	0.0038	503	0.0055	515	0.0081	586	0.0163	414	0.0142	550	-	
860	pa-002	0.1847	960	0.2859	966	-		-		-		-		-		-	
861	pa-003	0.0453	852	0.0679	845	-		-		-		-		-		-	
862	palit-000	0.0062	416	0.0084	397	0.0039	507	0.0055	512	0.0055	460	0.4610	921	0.2468	977	0.8695	615
863	palit-001	0.0050	332	0.0068	328	0.0032	400	0.0047	450	0.0045	388	0.0110	314	0.0058	220	0.1446	354
864	pangiam-000	0.0031	202	0.0043	196	0.0026	208	0.0030	234	0.0038	315	0.0071	171	0.0061	236	0.0667	139
865	pangiam-001	0.0031	198	0.0044	203	0.0029	319	0.0040	384	0.0028	185	0.0362	609	0.0056	203	0.1711	391
866	pangiam-002	0.0030	190	0.0042	181	0.0026	241	0.0031	247	0.0030	217	0.1772	804	0.0385	780	0.6076	544
867	papago-001	0.0067	448	0.0096	442	0.0051	621	0.0077	642	0.0071	539	0.0126	347	0.0086	377	0.1033	275
868	papil11-000	0.0021	115	0.0030	103	0.0024	106	0.0024	101	0.0025	134	0.0047	70	0.0040	91	0.0536	58
869	papil11-001	-		-		0.0023	100	0.0024	99	0.0023	77	0.0185	447	0.0040	98	0.1449	355
870	papil11-002	-		-		0.0023	97	0.0024	94	0.0023	76	0.0130	353	0.0039	81	0.1112	293
871	papil11-003	-		-		0.0023	89	0.0024	95	0.0023	85	0.0042	50	0.0035	48	0.0529	53
872	papil11-004	-		-		0.0027	266	0.0029	209	0.0025	136	0.0153	391	0.0058	219	0.0972	261
873	papsav1923-001	0.0078	494	0.0130	522	0.0068	723	0.0105	734	0.0119	712	0.0221	490	0.0136	532	-	
874	papsav1923-002	0.0021	116	0.0034	121	0.0026	210	0.0030	232	0.0048	417	0.0093	259	0.0086	375	0.0630	111
875	papsav1923-003	0.0025	151	0.0035	124	0.0024	149	0.0025	110	0.0034	267	0.0066	151	0.0058	218	0.0603	94
876	paravision-004	0.0030	191	0.0046	215	0.0030	339	0.0036	329	0.0091	627	0.0188	451	0.0173	609	-	
877	paravision-006	0.0016	71	0.0025	68	0.0026	221	0.0026	144	0.0075	558	0.9933	1127	0.0142	548	-	
878	paravision-008	0.0018	86	0.0025	67	0.0024	126	0.0025	118	0.0036	294	0.0070	167	0.0063	245	0.0747	171
879	paravision-010	0.0012	40	0.0021	46	0.0022	40	0.0021	33	0.0027	170	0.0055	101	0.0050	156	0.0534	57
880	paravision-011	0.0008	14	0.0020	45	0.0021	26	0.0020	15	0.0026	150	0.0053	95	0.0049	149	0.0498	41

Table 74: FNMR is the proportion of mated comparisons below a threshold set to achieve the FMR given in the header on the fourth row. FMR is the proportion of impostor comparisons at or above that threshold. The light grey values give rank over all algorithms in that column. The pink columns use only same-sex impostors; others are selected regardless of demographics. The exception, in the green column, uses "matched-covariates" i.e. impostors of the same sex, age group, and country of birth. The second pink column includes effects of extended ageing. Missing entries for border, visa, mugshot and wild images generally mean the algorithm did not run to completion. The VISA *columns compare images described in section 2.1. The* MUGSHOT *columns compare images described in section 2.5. The* VISA-BORDER *column compare images described in section 2.2 with those of section 2.4. The* BORDER *column compares images described in section 2.4. The* KIOSK-BORDER *columns compare images described in section 2.6 with those of section 2.4.*

		FALSE NON-MATCH RATE (FNMR)															
	Algorithm	CONSTRAINED, COOPERATIVE														LESS CONSTRAINED, NON-COOP.	
	Name	VISAMC		VISA		MUGSHOT		MUGSHOT12+YRS		VISABORDER		BORDER		BORDER		KIOSKBORDER	
	FMR	0.0001		1E-06		1E-05		1E-05		1E-06		1E-06		1E-05		1E-06	
881	paravision-013	0.0010	31	0.0018	38	0.0021	18	0.0019	3	0.0019	46	0.0041	46	0.0036	55	0.0442	22
882	paravision-015	-		-		0.0021	23	0.0021	38	0.0021	54	0.0043	52	0.0039	77	0.0528	52
883	paravision-017	-		-		0.0021	15	0.0021	23	0.0019	36	0.0038	33	0.0035	44	0.0458	27
884	paravision-018	-		-		0.0020	5	0.0020	13	0.0016	12	0.0034	20	0.0029	19	0.0414	9
885	paravision-020	-		-		0.0020	1	0.0020	10	0.0015	8	0.0033	14	0.0028	12	0.0410	8
886	pensees-001	0.0087	523	0.0133	526	0.0071	734	0.0122	772	0.0145	768	0.0252	519	0.0195	650	-	
887	pentacomp-000	-		-		0.0041	535	0.0061	561	0.0047	407	0.3501	887	0.1211	913	0.7162	571
888	pixelall-002	0.0193	738	0.0340	749	0.0127	931	0.0209	926	0.0234	897	0.9182	1053	0.2728	991	-	
889	pixelall-003	0.0074	478	0.0118	502	0.0057	661	0.0079	656	0.0121	716	0.0390	627	0.0170	601	-	
890	pixelall-004	0.0040	278	0.0061	296	0.0055	648	0.0069	601	0.0100	666	0.5663	947	0.0371	777	-	
891	pixelall-005	0.0038	260	0.0052	253	0.0043	550	0.0051	486	0.0077	565	0.0839	731	0.0136	534	-	
892	pixelall-006	0.0032	207	0.0042	180	0.0032	388	0.0039	365	0.0063	510	0.9960	1137	0.0723	861	1.0000	801
893	pixelall-007	0.0036	252	0.0049	234	0.0039	506	0.0044	421	0.0068	525	0.9873	1109	0.0217	675	1.0000	780
894	pixelall-008	0.0015	57	0.0023	60	0.0034	434	0.0049	460	0.0031	229	0.0057	108	0.0052	167	0.0682	143
895	pixelall-009	0.0018	85	0.0025	66	0.0024	143	0.0026	138	0.0031	237	0.3475	886	0.0053	181	0.9006	635
896	pixelall-010	0.0020	102	0.0030	104	0.0025	182	0.0028	196	0.0031	233	0.3512	888	0.0054	185	0.8813	623
897	pnpsecure-000	-		-		0.0190	997	0.0274	974	0.9980	1245	0.9997	1186	0.9996	1220	0.9997	749
898	pnpsecure-001	-		-		0.0050	610	0.0040	380	0.0037	311	0.0166	419	0.0075	319	0.1059	278
899	privid-001	0.3350	997	0.5013	1014	0.4327	1220	0.5880	1218	0.9790	1237	1.0000	1220	0.9998	1226	1.0000	855
900	privid-002	0.0460	854	0.0652	841	0.0524	1113	0.0882	1107	0.0671	1042	0.9769	1093	0.8960	1135	0.9999	758
901	privid-003	-		-		0.0030	342	0.0039	362	0.0045	390	0.9996	1182	0.9985	1207	1.0000	811
902	privid-004	-		-		0.0026	242	0.0028	179	0.0034	268	0.9939	1129	0.9657	1166	1.0000	790
903	psl-000	0.0216	755	0.0333	745	-		-		-		-		-		-	
904	psl-001	0.0549	868	0.0927	878	0.0096	841	0.0149	845	-		-		-		-	
905	psl-002	0.0107	589	0.0180	612	0.0089	814	0.0120	765	0.0790	1052	0.0270	532	0.0192	641	-	
906	psl-003	0.0065	437	0.0099	452	0.0055	645	0.0075	634	1.0000	1265	0.0188	452	0.0129	516	-	
907	psl-004	0.0064	432	0.0094	437	0.0035	440	0.0050	481	0.0084	593	0.0145	375	0.0106	451	-	
908	psl-005	0.0060	409	0.0094	432	0.0034	435	0.0048	456	0.0081	585	0.0140	363	0.0103	440	-	
909	psl-006	0.0025	156	0.0039	164	0.0028	300	0.0030	227	0.0160	790	0.0482	658	0.0310	749	-	
910	psl-007	0.0026	163	0.0040	169	0.0027	260	0.0030	223	0.0054	450	0.0101	291	0.0081	354	-	
911	psl-008	0.0026	158	0.0040	168	0.0024	136	0.0028	189	0.0041	348	0.0077	185	0.0055	192	0.0719	154
912	psl-009	0.0161	699	0.0294	723	0.0023	79	0.0025	112	0.0036	297	0.0065	149	0.0048	144	0.0659	134
913	psl-010	0.0017	80	0.0035	125	0.0023	72	0.0025	106	0.0035	285	0.0104	296	0.0052	175	0.0994	264
914	psl-011	0.0013	48	0.0026	77	0.0021	7	0.0021	29	0.0024	98	0.0047	69	0.0035	50	0.0565	75
915	psl-012	0.0017	73	0.0027	83	0.0021	29	0.0023	61	0.0021	55	0.0039	35	0.0032	32	0.0494	39
916	psl-013	-		-		0.0022	34	0.0023	64	0.0021	61	0.0039	38	0.0033	34	0.0499	44
917	psl-014	-		-		0.0021	28	0.0023	62	0.0021	59	0.0039	37	0.0033	33	0.0498	42
918	ptakuratsatu-000	0.0060	406	0.0089	418	0.0070	731	0.0104	733	0.0096	651	0.0152	390	0.0100	426	-	
919	pxl-001	0.0488	858	0.0752	854	0.0586	1121	0.1087	1124	0.0946	1067	0.1065	755	0.0625	849	-	
920	pyramid-000	0.0136	656	0.0233	679	0.0117	910	0.0192	911	0.0185	838	0.0322	572	0.0206	663	-	
921	pyramid-001	-		-		0.0025	163	0.0030	229	0.0025	124	0.0099	282	0.0044	114	0.1031	274
922	qazbs-000	0.0058	388	0.0083	395	0.0046	576	0.0072	616	0.0130	734	0.0244	512	0.0196	651	0.7784	585
923	qazsmartvisionai-000	0.0008	16	0.0011	12	0.0021	8	0.0022	43	0.0018	32	0.0035	26	0.0030	22	0.0441	21
924	qazsmartvisionai-001	0.0003	4	0.0008	8	0.0020	6	0.0020	20	0.0015	7	0.0031	7	0.0027	7	0.0394	6

Table 75: FNMR is the proportion of mated comparisons below a threshold set to achieve the FMR given in the header on the fourth row. FMR is the proportion of impostor comparisons at or above that threshold. The light grey values give rank over all algorithms in that column. The pink columns use only same-sex impostors; others are selected regardless of demographics. The exception, in the green column, uses "matched-covariates" i.e. impostors of the same sex, age group, and country of birth. The second pink column includes effects of extended ageing. Missing entries for border, visa, mugshot and wild images generally mean the algorithm did not run to completion. The VISA *columns compare images described in section 2.1. The* MUGSHOT *columns compare images described in section 2.5. The* VISA-BORDER *column compare images described in section 2.2 with those of section 2.4. The* BORDER *column compares images described in section 2.4. The* KIOSK-BORDER *columns compare images described in section 2.6 with those of section 2.4.*

		FALSE NON-MATCH RATE (FNMR)															
	Algorithm	CONSTRAINED, COOPERATIVE														LESS CONSTRAINED, NON-COOP.	
	Name	VISAMC		VISA		MUGSHOT		MUGSHOT12+YRS		VISABORDER		BORDER		BORDER		KIOSKBORDER	
	FMR	0.0001		1E-06		1E-05		1E-05		1E-06		1E-06		1E-05		1E-06	
925	qazsmartvisionai-002	-		-		0.0020	2	0.0020	8	0.0014	2	0.0028	2	0.0025	2	0.0380	2
926	qazsmartvisionai-003	-		-		0.0020	3	0.0020	9	0.0015	3	0.0029	4	0.0025	3	0.0381	3
927	qazsmartvisionai-004	-		-		0.0020	4	0.0020	12	0.0014	1	0.0028	1	0.0025	1	0.0377	1
928	qluevision-001	0.0223	761	0.0419	781	0.0205	1011	0.0343	1000	0.0327	957	0.8762	1037	0.7413	1100	0.9908	697
929	qnap-000	0.0149	679	0.0228	672	0.0155	976	0.0267	970	0.0238	905	0.8329	1027	0.0396	785	0.9992	735
930	qnap-001	0.0148	677	0.0215	657	0.0103	863	0.0162	872	0.0183	837	0.0301	552	0.0186	633	0.1995	418
931	qnap-002	0.0122	623	0.0191	627	0.0075	759	0.0095	707	0.0146	769	0.0281	543	0.0184	626	0.1829	401
932	qnap-003	0.0637	882	0.0657	843	0.0058	669	0.0078	650	0.0082	588	0.9985	1158	0.9658	1167	1.0000	818
933	qnap-004	0.0046	314	0.0061	295	0.0038	493	0.0059	551	0.0042	356	0.9960	1136	0.9442	1151	1.0000	785
934	qnap-005	0.0033	220	0.0047	222	0.0068	721	0.0071	612	0.0096	647	0.0184	446	0.0163	588	0.0948	258
935	qnap-006	-		-		0.0030	348	0.0041	395	0.0044	377	0.0088	244	0.0065	257	0.0799	198
936	quantasoft-003	0.0081	507	0.0113	492	0.0056	655	0.0076	637	0.0091	626	0.0161	409	0.0107	455	0.1193	309
937	rankone-000	-		0.2760	960	-		-		-		-		-		-	
938	rankone-001	-		0.4198	998	-		-		-		-		-		-	
939	rankone-002	0.1547	948	0.2170	943	-		-		-		-		-		-	
940	rankone-003	0.1175	930	0.1838	929	-		-		-		-		-		-	
941	rankone-004	0.0548	867	0.1015	886	-		-		-		-		-		-	
942	rankone-005	0.0405	841	0.0757	856	0.0170	988	0.0299	985	-		-		-		-	
943	rankone-006	0.0242	770	0.0460	797	0.0119	914	0.0188	908	0.0315	953	0.0539	674	0.0385	782	-	
944	rankone-007	0.0197	743	0.0366	766	0.0113	898	0.0177	891	0.0286	936	0.0454	645	0.0333	758	-	
945	rankone-008	0.0124	629	0.0232	676	0.0082	787	0.0107	736	0.0188	843	0.0320	571	0.0244	702	-	
946	rankone-009	0.0087	521	0.0119	503	0.0065	710	0.0086	684	0.0088	612	0.0161	406	0.0121	498	-	
947	rankone-010	0.0079	499	0.0112	490	0.0061	687	0.0081	667	0.0088	609	0.0149	380	0.0117	485	-	
948	rankone-011	0.0049	329	0.0075	358	0.0038	488	0.0048	457	0.0060	496	0.0143	369	0.0080	350	0.1839	402
949	rankone-012	0.0043	295	0.0058	279	0.0031	382	0.0038	352	0.0047	406	0.0081	209	0.0065	253	0.0842	215
950	rankone-013	0.0028	174	0.0041	173	0.0026	213	0.0033	278	0.0028	189	0.0055	104	0.0040	90	0.0725	155
951	rankone-014	0.0016	69	0.0021	50	0.0024	110	0.0027	155	0.0022	73	0.0047	71	0.0035	46	0.0666	138
952	rankone-015	0.0009	20	0.0014	21	0.0024	118	0.0026	134	0.0024	110	0.0044	60	0.0037	58	0.0635	117
953	realnetworks-000	0.0325	823	0.0463	798	-		-		-		-		-		-	
954	realnetworks-001	0.0315	820	0.0455	795	0.0920	1148	0.1938	1161	-		-		-		-	
955	realnetworks-002	0.0248	776	0.0358	762	0.0513	1111	0.1127	1130	0.0371	973	0.0614	694	0.0316	752	-	
956	realnetworks-003	0.0259	789	0.0372	769	0.0541	1117	0.1208	1134	0.0378	976	0.0578	683	0.0306	748	-	
957	realnetworks-004	0.0075	484	0.0101	458	0.0066	713	0.0097	716	0.0108	690	0.0187	449	0.0131	518	0.1430	351
958	realnetworks-005	0.0070	455	0.0093	428	0.0063	698	0.0089	691	0.0092	630	0.0161	410	0.0104	444	0.1249	322
959	realnetworks-006	0.0040	274	0.0056	274	0.8657	1277	0.9705	1276	0.0059	489	0.0112	320	0.0085	373	0.0911	243
960	realnetworks-007	0.0031	203	0.0051	250	0.0028	297	0.0035	317	0.0048	418	0.0091	250	0.0074	311	0.0945	256
961	realnetworks-008	0.0022	121	0.0039	160	0.0038	490	0.0045	431	0.0055	455	0.0100	289	0.0080	353	0.0889	226
962	realsense-001	-		-		0.0023	71	0.0025	122	0.0023	91	0.0046	66	0.0039	76	0.0537	59
963	rebs-000	0.0030	189	0.0043	194	0.0024	124	0.0032	259	0.0024	96	0.3069	867	0.1170	907	0.7667	580
964	rebs-001	0.0037	255	0.0049	236	0.0024	148	0.0033	274	0.0025	117	0.0257	525	0.0096	415	0.1487	362
965	recognito-000	0.0004	5	0.0006	2	0.0021	25	0.0022	54	0.0016	15	0.0555	676	0.0207	665	0.1943	412
966	recognito-001	0.0003	1	0.0007	5	0.0021	16	0.0022	47	0.0016	9	0.0663	704	0.0257	710	0.1825	400
967	regula-000	0.0184	729	0.0376	770	0.0103	864	0.0185	901	0.0120	714	0.9983	1154	0.0231	689	1.0000	824
968	regula-001	0.0072	470	0.0107	479	0.0102	861	0.0179	893	0.0123	722	0.0333	584	0.0174	611	0.3711	487

Table 76: FNMR is the proportion of mated comparisons below a threshold set to achieve the FMR given in the header on the fourth row. FMR is the proportion of impostor comparisons at or above that threshold. The light grey values give rank over all algorithms in that column. The pink columns use only same-sex impostors; others are selected regardless of demographics. The exception, in the green column, uses "matched-covariates" i.e. impostors of the same sex, age group, and country of birth. The second pink column includes effects of extended ageing. Missing entries for border, visa, mugshot and wild images generally mean the algorithm did not run to completion. The VISA *columns compare images described in section 2.1. The* MUGSHOT *columns compare images described in section 2.5. The* VISA-BORDER *column compare images described in section 2.2 with those of section 2.4. The* BORDER *column compares images described in section 2.4. The* KIOSK-BORDER *columns compare images described in section 2.6 with those of section 2.4.*

	Algorithm	FALSE NON-MATCH RATE (FNMR)															
		CONSTRAINED, COOPERATIVE														LESS CONSTRAINED, NON-COOP.	
	Name	VISAMC		VISA		MUGSHOT		MUGSHOT12+YRS		VISABORDER		BORDER		BORDER		KIOSKBORDER	
	FMR	0.0001		1E-06		1E-05		1E-05		1E-06		1E-06		1E-05		1E-06	
969	regula-002	-		-		0.0053	628	0.0058	541	0.0044	380	0.9999	1197	0.9995	1216	1.0000	822
970	remarkai-000	0.0147	676	0.0257	702	0.0102	858	0.0158	860	0.0163	799	0.0577	681	0.0185	628	-	
971	remarkai-001	0.0144	671	0.0256	700	0.0102	859	0.0159	863	0.0162	797	0.0582	686	0.0185	630	-	
972	remarkai-002	0.0151	684	0.0197	639	0.0075	757	0.0108	742	0.0119	713	0.0187	450	0.0127	508	-	
973	remarkai-003	0.0047	322	0.0063	310	0.0033	416	0.0049	464	0.0054	452	0.0100	288	0.0072	300	0.0908	240
974	rendip-000	0.0055	371	0.0077	368	0.0048	593	0.0060	558	0.0080	581	0.0142	368	0.0110	464	0.1027	272
975	revealmedia-005	0.0050	336	0.0074	354	0.0050	606	0.0068	600	0.0075	559	0.0124	343	0.0104	447	0.0895	231
976	revealmedia-006	0.0040	275	0.0067	323	0.0041	531	0.0056	521	0.0056	463	0.0085	233	0.0068	269	0.0872	221
977	roc-016	0.0009	22	0.0014	20	0.0023	75	0.0024	87	0.0024	101	0.0042	51	0.0035	45	0.0558	69
978	roc-017	-		-		0.0023	67	0.0025	124	0.0021	60	0.0039	34	0.0032	29	0.0542	63
979	roc-018	0.0007	13	0.0012	13	0.0022	42	0.0022	49	0.0018	33	0.0034	23	0.0029	16	0.0493	38
980	roc-019	-		-		0.0021	31	0.0021	28	0.0016	16	0.0032	9	0.0027	9	0.0439	19
981	roc-020	-		-		0.0021	11	0.0021	21	0.0016	14	0.0032	11	0.0027	8	0.0452	24
982	rokid-000	0.0093	545	0.0145	546	0.0073	748	0.0102	730	0.0164	801	0.0280	539	0.0214	671	-	
983	rokid-001	0.0105	585	0.0162	579	0.0094	835	0.0163	874	0.0181	830	0.0276	538	0.0165	595	-	
984	s1-001	0.0314	819	0.0651	840	0.0252	1039	0.0357	1006	0.0444	998	0.0653	701	0.0429	799	-	
985	s1-002	0.0095	552	0.0144	543	0.0112	894	0.0196	916	0.0234	895	0.0371	616	0.0282	732	-	
986	s1-003	0.0051	346	0.0073	350	0.0044	555	0.0063	575	0.0052	443	0.0096	274	0.0070	285	0.0870	220
987	s1-004	0.0053	362	0.0080	383	0.0038	491	0.0059	549	0.0057	473	0.0103	293	0.0073	306	0.0899	235
988	s1-005	0.0024	142	0.0036	139	0.0025	196	0.0029	207	0.0026	158	0.0048	81	0.0038	69	0.0638	119
989	s1-006	0.0029	181	0.0044	201	0.0028	288	0.0033	272	0.0035	282	0.0073	173	0.0044	122	0.7160	570
990	s1-007	0.0023	135	0.0056	275	0.0024	111	0.0028	170	0.0025	129	0.0048	77	0.0039	78	0.0608	97
991	s1-008	-		-		0.0093	827	0.0137	811	0.0179	828	0.9118	1051	0.0286	737	0.9999	761
992	s1-009	-		-		0.0023	101	0.0023	76	0.0022	67	0.0043	53	0.0037	59	0.0504	47
993	saffe-001	0.4339	1016	0.5261	1019	0.7539	1267	0.8736	1265	0.7977	1196	0.9810	1097	0.7435	1101	-	
994	saffe-002	0.0119	618	0.0206	645	0.0107	878	0.0177	889	0.0244	908	0.9998	1187	0.2785	993	-	
995	samsungsds-000	0.0046	316	0.0069	332	0.0132	939	0.0081	664	0.0099	661	0.0179	438	0.0162	587	0.1101	286
996	samsungsds-001	0.0015	61	0.0026	78	0.0023	80	0.0023	75	0.0024	102	0.1660	800	0.0536	830	0.4995	520
997	samsungsds-002	0.0017	84	0.0027	80	0.0023	73	0.0022	44	0.0021	57	0.0043	54	0.0036	56	0.0586	87
998	samtech-000	0.3418	999	0.4425	1002	-		-		-		-		-		-	
999	samtech-001	0.0197	742	0.0365	764	0.0146	966	0.0241	952	0.0238	904	0.0394	628	0.0251	707	-	
1000	samtech-002	0.0084	515	0.0127	519	0.0093	825	0.0158	858	0.0113	703	0.0442	639	0.0132	519	0.4110	500
1001	scanovate-001	0.0175	718	0.0331	744	0.0163	986	0.0248	954	0.2476	1131	0.3801	900	0.3740	1021	-	
1002	scanovate-002	0.0175	716	0.0355	759	0.0146	963	0.0286	979	0.0269	920	0.0301	551	0.0178	619	-	
1003	scanovate-003	0.0054	365	0.0080	382	0.0054	636	0.0072	621	0.0312	950	0.0599	690	0.0568	842	-	
1004	sdc-000	0.0303	811	0.0526	817	0.0572	1119	0.1094	1126	0.0867	1062	0.6230	962	0.3682	1020	0.8797	621
1005	seamfix-001	-		-		0.1973	1186	0.2878	1181	0.2613	1134	0.3156	874	0.1976	963	0.8176	599
1006	securifai-001	0.4538	1021	0.6142	1037	0.5844	1240	0.7428	1236	0.7051	1182	0.9961	1138	0.9558	1158	-	
1007	securifai-002	0.7557	1054	0.8574	1059	0.4550	1224	0.5953	1219	0.9860	1239	0.9796	1096	0.9158	1141	-	
1008	securifai-003	0.4086	1010	0.7577	1054	0.7233	1258	0.8070	1247	0.7787	1193	1.0000	1232	0.9988	1210	1.0000	839
1009	securifai-004	0.0136	654	0.0192	630	0.0064	703	0.0099	723	0.0115	705	0.0272	534	0.0127	510	0.4881	516
1010	securifai-005	0.0125	633	0.0190	626	0.0080	779	0.0126	780	0.0134	746	0.9861	1104	0.9205	1143	1.0000	778
1011	securifai-006	0.0140	666	0.0196	637	0.0067	719	0.0102	727	0.0113	701	0.9888	1113	0.9239	1145	1.0000	782
1012	securifai-007	0.0124	631	0.0175	604	0.0064	705	0.0105	735	0.0108	683	0.9999	1196	0.9966	1199	1.0000	834

Table 77: FNMR is the proportion of mated comparisons below a threshold set to achieve the FMR given in the header on the fourth row. FMR is the proportion of impostor comparisons at or above that threshold. The light grey values give rank over all algorithms in that column. The pink columns use only same-sex impostors; others are selected regardless of demographics. The exception, in the green column, uses "matched-covariates" i.e. impostors of the same sex, age group, and country of birth. The second pink column includes effects of extended ageing. Missing entries for border, visa, mugshot and wild images generally mean the algorithm did not run to completion. The VISA *columns compare images described in section 2.1. The* MUGSHOT *columns compare images described in section 2.5. The* VISA-BORDER *column compare images described in section 2.2 with those of section 2.4. The* BORDER *column compares images described in section 2.4. The* KIOSK-BORDER *columns compare images described in section 2.6 with those of section 2.4.*

		FALSE NON-MATCH RATE (FNMR)															
	Algorithm	CONSTRAINED, COOPERATIVE														LESS CONSTRAINED, NON-COOP.	
	Name	VISAMC		VISA		MUGSHOT		MUGSHOT12+YRS		VISABORDER		BORDER		BORDER		KIOSKBORDER	
	FMR	0.0001		1E-06		1E-05		1E-05		1E-06		1E-06		1E-05		1E-06	
1013	securifai-008	-		-		0.0060	685	0.0102	729	0.2096	1120	0.9649	1083	0.8757	1127	0.9990	733
1014	sensetime-001	0.0063	425	0.0092	423	0.0130	935	-		0.0252	914	0.0886	737	0.0886	883	-	
1015	sensetime-002	0.0068	451	0.0098	447	0.0143	957	1.0000	1306	0.0278	933	0.0502	664	0.0502	822	-	
1016	sensetime-003	0.0021	117	0.0027	84	0.0027	252	0.0027	163	0.0051	438	0.0100	287	0.0089	384	-	
1017	sensetime-004	0.0026	164	0.0038	151	0.0022	48	0.0023	68	0.0042	353	0.0082	213	0.0078	337	-	
1018	sensetime-005	0.0019	95	0.0029	93	0.0022	38	0.0021	30	0.0023	83	0.0044	56	0.0039	74	0.0564	73
1019	sensetime-006	0.0014	55	0.0024	62	0.0021	27	0.0020	11	0.0021	53	0.0040	42	0.0036	54	0.0525	50
1020	sensetime-007	0.0012	46	0.0022	52	0.0021	30	0.0020	14	0.0018	29	0.0034	18	0.0029	21	0.0479	36
1021	sensetime-008	0.0008	15	0.0014	18	0.0021	12	0.0020	6	0.0018	35	0.0036	27	0.0033	35	0.0504	46
1022	sensetime-010	-		-		0.0022	33	0.0021	27	0.0018	26	0.0034	21	0.0029	20	0.0437	17
1023	sensetime-011	-		-		0.0022	32	0.0020	19	0.0017	21	0.0033	16	0.0029	15	0.0438	18
1024	serendipity-000	0.0046	311	0.0069	334	0.0042	546	0.0056	520	0.0073	549	0.9129	1052	0.7189	1097	0.9952	711
1025	sertis-000	0.0118	616	0.0208	648	0.0080	775	0.0127	783	0.0110	696	0.0176	436	0.0114	474	-	
1026	sertis-001	0.0113	603	0.0182	614	0.0204	1010	0.0403	1022	0.0216	877	0.0763	725	0.0282	731	-	
1027	sertis-002	0.0049	328	0.0061	292	0.0039	515	0.0061	568	0.0055	457	0.0099	285	0.0070	287	0.0921	247
1028	sertis-003	0.0049	330	0.0059	288	0.0037	479	0.0058	540	0.0055	462	0.0100	286	0.0072	301	0.0881	223
1029	seventhsense-000	0.0067	447	0.0099	456	0.0045	559	0.0065	586	0.0093	634	0.0169	426	0.0124	504	0.1325	331
1030	seventhsense-001	0.0034	237	0.0047	224	0.0025	195	0.0031	243	0.0029	198	0.0338	590	0.0109	459	0.2135	426
1031	seventhsense-002	0.0036	250	0.0050	242	0.0028	296	0.0036	327	0.0035	283	0.0811	728	0.0183	625	0.5444	526
1032	seventhsense-003	0.0035	240	0.0046	214	0.0026	235	0.0033	273	0.0062	504	0.0448	643	0.0175	613	0.2594	450
1033	seventhsense-005	0.0031	200	0.0045	207	0.0028	291	0.0030	213	0.0028	183	0.0466	652	0.0165	596	0.1949	413
1034	seventhsense-006	-		-		0.0029	321	0.0034	303	0.0035	291	0.2052	821	0.0802	870	0.4742	512
1035	shaman-000	0.9297	1065	0.9774	1073	0.9990	1298	0.9997	1293	0.9999	1255	1.0000	1215	0.9999	1234	-	
1036	shaman-001	0.3346	996	0.4616	1004	0.2368	1194	0.3723	1194	0.3574	1149	0.3527	889	0.2304	976	-	
1037	shu-001	0.0103	575	0.0140	538	0.0293	1061	0.0688	1086	0.0172	819	0.0182	442	0.0120	494	-	
1038	shu-002	-		0.0079	377	0.0146	965	0.0308	989	1.0000	1260	0.0183	443	0.0115	477	-	
1039	shu-003	0.0028	171	0.0041	178	0.0050	603	0.0088	689	0.0081	587	0.0133	354	0.0094	405	-	
1040	shufti-001	-		-		0.0053	627	0.0083	672	0.0085	598	1.0000	1255	0.0098	421	1.0000	1364
1041	siat-002	0.0091	535	0.0126	518	0.0109	882	0.0190	909	0.0276	932	0.0516	668	0.0464	814	-	
1042	siat-004	0.0067	445	0.0099	449	0.0152	974	1.0000	1305	0.0275	927	0.4823	925	0.4823	1043	-	
1043	siat-005	0.0021	113	0.0038	153	0.0059	674	0.0049	467	0.0742	1048	0.9623	1080	0.6801	1082	0.9833	681
1044	sightropic-000	-		-		0.0028	311	0.0038	359	0.0029	194	0.2207	828	0.0810	872	0.5137	522
1045	sightropic-001	-		-		0.0052	626	0.0049	468	0.0050	430	0.0094	265	0.0081	357	0.0672	140
1046	sjtu-001	0.0051	345	0.0080	381	0.0211	1014	0.0446	1035	0.0131	736	0.0175	432	0.0110	462	-	
1047	sjtu-002	0.0053	364	0.0078	374	0.0138	947	0.0296	984	0.0084	594	0.0136	357	0.0095	411	-	
1048	sjtu-003	0.0017	75	0.0033	116	0.0030	343	0.0037	342	0.0058	480	0.0104	297	0.0081	355	-	
1049	sjtu-004	0.0014	54	0.0025	64	0.0027	261	0.0028	195	0.0046	396	0.0086	237	0.0073	305	0.0906	238
1050	sjtu-005	0.0029	179	0.0036	140	0.0025	200	0.0027	158	0.0044	373	0.0120	340	0.0072	296	0.1325	330
1051	sjtu-006	-		-		0.0027	268	0.0028	176	0.0044	379	0.0081	212	0.0071	294	0.0715	152
1052	sjtu-007	-		-		0.0023	98	0.0023	59	0.0040	333	0.0251	517	0.0126	507	0.1694	390
1053	sjtu-008	-		-		0.0022	37	0.0023	63	0.0029	190	0.0078	196	0.0055	197	0.0748	172
1054	sjtu-009	-		-		0.0022	39	0.0021	41	0.0028	176	0.5621	945	0.0397	787	0.6795	561
1055	sktelecom-000	0.0038	262	0.0054	267	0.0031	354	0.0051	488	0.0042	351	0.3418	883	0.0061	235	0.9499	652
1056	smargtech-001	-		-		0.4604	1226	0.6005	1221	0.5247	1167	0.5858	952	0.3098	1003	0.9826	680

Table 78: FNMR is the proportion of mated comparisons below a threshold set to achieve the FMR given in the header on the fourth row. FMR is the proportion of impostor comparisons at or above that threshold. The light grey values give rank over all algorithms in that column. The pink columns use only same-sex impostors; others are selected regardless of demographics. The exception, in the green column, uses "matched-covariates" i.e. impostors of the same sex, age group, and country of birth. The second pink column includes effects of extended ageing. Missing entries for border, visa, mugshot and wild images generally mean the algorithm did not run to completion. The VISA *columns compare images described in section 2.1. The* MUGSHOT *columns compare images described in section 2.5. The* VISA-BORDER *column compare images described in section 2.2 with those of section 2.4. The* BORDER *column compares images described in section 2.4. The* KIOSK-BORDER *columns compare images described in section 2.6 with those of section 2.4.*

	Algorithm	FALSE NON-MATCH RATE (FNMR)															
		CONSTRAINED, COOPERATIVE														LESS CONSTRAINED, NON-COOP.	
	Name	VISAMC		VISA		MUGSHOT		MUGSHOT12+YRS		VISABORDER		BORDER		BORDER		KIOSKBORDER	
	FMR	0.0001		1E-06		1E-05		1E-05		1E-06		1E-06		1E-05		1E-06	
1057	smartbiometrik-001	0.5485	1037	0.6442	1040	0.7550	1268	0.8611	1261	0.8677	1213	0.8270	1024	0.7030	1087	0.9752	671
1058	smartengines-000	0.6240	1044	0.7562	1053	0.9552	1284	0.9784	1280	0.9515	1232	0.9288	1064	0.8200	1115	0.9930	702
1059	smartengines-001	0.6434	1046	0.7666	1055	0.9446	1283	0.9750	1279	0.9387	1230	0.9556	1075	0.8647	1122	0.9972	722
1060	smartvist-000	0.0912	911	0.1587	915	0.1163	1163	0.1841	1157	0.1397	1087	0.9372	1069	0.7107	1093	0.9990	734
1061	smartvist-001	0.0137	658	0.0244	688	0.0099	853	0.0158	859	0.0151	776	0.1349	781	0.0419	795	0.5589	532
1062	smilart-001	0.6476	1047	0.8779	1061	-		-		-		-		-		-	
1063	smilart-002	0.2440	979	0.3532	986	-		-		0.3785	1150	0.4145	912	0.2611	987	-	
1064	smilart-003	0.6944	1051	0.8836	1062	0.0695	1133	0.1193	1132	0.0894	1064	0.1221	771	0.0737	862	-	
1065	sodec-000	0.0033	225	0.0044	204	0.0040	521	0.0053	503	0.0054	453	0.0096	272	0.0080	346	0.0915	244
1066	sparktek-000	-		-		0.0025	157	0.0025	116	0.0031	236	0.0058	114	0.0053	179	0.0643	122
1067	sparsh-001	0.0018	91	0.0029	99	0.0026	222	0.0028	186	0.0027	165	0.8806	1039	0.6313	1073	0.9963	714
1068	sqisoft-001	0.1220	933	0.2088	939	0.1978	1187	0.3386	1190	0.2111	1121	0.2798	860	0.1474	933	0.7820	587
1069	sqisoft-002	0.0082	510	0.0124	511	0.0051	614	0.0086	683	0.0102	670	0.0183	444	0.0122	499	0.1498	364
1070	sqisoft-003	0.0041	285	0.0055	272	0.0026	207	0.0032	269	0.0039	328	1.0000	1401	1.0000	1351	1.0000	888
1071	staqu-000	0.0139	663	0.0208	649	0.0104	865	0.0145	838	0.0156	782	0.8063	1012	0.1408	928	-	
1072	starhybrid-001	0.0108	590	0.0138	534	0.0081	781	0.0113	752	0.0152	777	0.0265	530	0.0189	638	-	
1073	stcon-000	0.0040	277	0.0056	273	0.0031	369	0.0047	445	0.0048	419	0.9863	1105	0.3562	1018	0.9999	763
1074	stcon-001	0.0040	269	0.0053	263	0.0030	349	0.0045	432	0.0047	404	0.8632	1035	0.1788	954	0.9892	693
1075	stcon-002	0.0031	196	0.0043	186	0.0025	167	0.0034	297	0.0030	216	0.9988	1162	0.9855	1178	1.0000	796
1076	stcon-003	0.0038	261	0.0050	245	0.0024	112	0.0032	266	0.0023	82	0.1082	759	0.0350	766	0.3982	497
1077	stcon-004	-		-		0.0022	50	0.0025	123	0.0020	49	0.0519	669	0.0145	556	0.2564	448
1078	stcon-005	-		-		0.0021	21	0.0021	24	0.0017	19	0.0336	587	0.0115	479	0.1725	392
1079	stcon-006	-		-		0.0021	22	0.0021	25	0.0017	18	0.0034	19	0.0028	11	0.0425	13
1080	stcon-007	-		-		0.0021	20	0.0021	22	0.0017	17	0.0033	15	0.0028	10	0.0424	12
1081	stcon-008	-		-		0.0021	14	0.0020	4	0.0015	4	0.0029	6	0.0026	4	0.0390	5
1082	stengg-000	0.0059	401	0.0082	388	0.0037	482	0.0060	556	0.0050	428	0.5065	929	0.0792	867	0.9348	647
1083	sukshi-000	0.5409	1035	0.6612	1045	0.4556	1225	0.6567	1227	0.9296	1229	0.8898	1043	0.7384	1098	0.9899	694
1084	sumsub-000	-		-		0.0041	532	0.0043	418	0.0038	317	0.5301	939	0.2536	981	0.9068	636
1085	suprema-000	0.0064	429	0.0092	424	0.0081	784	0.0096	712	0.0139	757	0.0254	523	0.0220	677	-	
1086	suprema-001	0.0041	282	0.0053	258	0.0038	499	0.0047	446	0.0060	493	0.0111	316	0.0095	414	0.0907	239
1087	suprema-002	0.0030	192	0.0041	176	0.0034	423	0.0040	376	0.0045	382	0.0085	230	0.0072	302	0.0781	190
1088	suprema-003	0.0028	176	0.0041	177	0.0034	421	0.0039	364	0.0030	219	0.3095	871	0.0580	844	0.6672	557
1089	suprema-004	0.0024	137	0.0035	127	0.0032	391	0.0036	331	0.0028	173	0.0053	96	0.0045	125	0.0625	108
1090	suprema-005	0.0022	118	0.0036	135	0.0034	437	0.0031	249	0.0026	159	0.0050	90	0.0044	113	0.0588	90
1091	supremaid-001	0.0053	363	0.0073	351	0.0045	560	0.0066	589	0.0099	663	0.0186	448	0.0148	563	0.1040	276
1092	supremaid-002	0.0063	424	0.0094	434	0.0044	553	0.0062	570	0.0072	547	0.0229	501	0.0095	413	0.2986	467
1093	surrey-cvssp-000	0.9084	1062	0.9909	1076	0.9923	1291	0.9950	1287	0.9981	1248	0.9994	1172	0.9979	1204	0.9998	753
1094	surrey-cvssp-001	1.0000	1179	1.0000	1122	0.0077	766	0.0079	658	0.0266	918	0.3822	903	0.0551	834	0.7285	573
1095	surrey-cvssp-002	0.0019	94	0.0028	87	0.0027	279	0.0028	177	0.0024	105	0.5978	959	0.1206	912	0.8488	608
1096	surrey-cvssp-003	0.0016	70	0.0028	89	0.0022	49	0.0024	88	0.0022	75	0.3048	866	0.0539	831	0.5830	538
1097	surrey-cvssp-004	-		-		0.0029	328	0.0025	129	0.0025	135	0.0690	712	0.0076	331	0.2741	459
1098	swsam-001	0.0268	793	0.0476	803	0.0271	1048	0.0460	1039	0.0584	1029	0.7745	1001	0.5013	1049	0.9642	661
1099	synesis-000	0.1752	955	0.3241	979	-		-		-		-		-		-	
1100	synesis-001	0.1777	956	1.0000	1321	1.0000	1305	-		-		-		-		-	

Table 79: FNMR is the proportion of mated comparisons below a threshold set to achieve the FMR given in the header on the fourth row. FMR is the proportion of impostor comparisons at or above that threshold. The light grey values give rank over all algorithms in that column. The pink columns use only same-sex impostors; others are selected regardless of demographics. The exception, in the green column, uses "matched-covariates" i.e. impostors of the same sex, age group, and country of birth. The second pink column includes effects of extended ageing. Missing entries for border, visa, mugshot and wild images generally mean the algorithm did not run to completion. The VISA *columns compare images described in section 2.1. The* MUGSHOT *columns compare images described in section 2.5. The* VISA-BORDER *column compare images described in section 2.2 with those of section 2.4. The* BORDER *column compares images described in section 2.4. The* KIOSK-BORDER *columns compare images described in section 2.6 with those of section 2.4.*

		FALSE NON-MATCH RATE (FNMR)															
	Algorithm	CONSTRAINED, COOPERATIVE														LESS CONSTRAINED, NON-COOP.	
	Name	VISAMC		VISA		MUGSHOT		MUGSHOT12+YRS		VISABORDER		BORDER		BORDER		KIOSKBORDER	
	FMR	0.0001		1E-06		1E-05		1E-05		1E-06		1E-06		1E-05		1E-06	
1101	synesis-003	0.8375	1057	0.8857	1063	0.8548	1276	0.9178	1272	-		-		-		-	
1102	synesis-004	0.0310	816	0.0480	805	0.0476	1103	0.0443	1033	0.0764	1050	-		-		-	
1103	synesis-005	0.0147	675	0.0226	671	0.0153	975	0.0226	941	0.0213	874	0.0375	620	0.0262	719	-	
1104	synesis-006	0.0070	458	0.0096	440	0.0107	875	0.0166	881	-		0.0128	351	0.0089	383	-	
1105	synesis-007	0.0050	340	0.0073	353	0.0062	697	0.0076	636	-		0.0105	299	0.0080	351	-	
1106	synology-000	0.0149	681	0.0238	685	0.0148	967	0.0261	965	0.0221	880	0.0331	580	0.0209	668	-	
1107	synology-001	0.0214	753	0.0307	730	0.0266	1047	0.0513	1058	0.0283	934	0.8884	1041	0.2589	984	-	
1108	synology-002	0.0104	580	0.0153	562	0.0107	877	0.0184	898	0.0189	845	0.2032	819	0.0180	621	-	
1109	syscake-000	-		-		0.0091	817	0.0155	853	0.0142	761	0.0287	546	0.0145	559	0.1682	388
1110	szpu-000	-		-		0.0034	424	0.0037	343	0.0039	324	0.8444	1030	0.3886	1027	0.8849	625
1111	sztu-000	0.0092	541	0.0139	536	0.0091	818	0.0201	922	0.0136	751	0.0685	711	0.0118	489	-	
1112	sztu-001	0.0031	197	0.0043	195	0.0025	180	0.0028	187	0.0051	432	0.0113	326	0.0089	385	0.9963	715
1113	t4isb-000	0.0058	387	0.0087	407	0.0041	539	0.0064	583	0.0083	591	0.0157	399	0.0103	441	0.1196	311
1114	tahakom-001	-		-		0.0223	1022	0.0364	1010	0.0361	968	1.0000	1216	0.9998	1227	1.0000	829
1115	taiwanmobile-001	-		-		0.2136	1189	0.3014	1187	0.3408	1145	0.9439	1072	0.7559	1103	0.9966	718
1116	taiwanmobile-002	-		-		0.0088	812	0.0114	753	0.0108	688	0.9776	1094	0.8683	1124	0.9998	752
1117	tcc-000	-		-		0.1374	1171	0.2052	1167	0.6334	1175	0.9985	1157	0.9897	1184	0.9999	757
1118	tcv-001	-		-		0.0301	1065	0.0556	1062	0.0570	1027	0.1222	772	0.0786	864	0.3172	473
1119	tech5-000	0.0114	604	0.0160	576	-		-		-		-		-		-	
1120	tech5-001	0.0130	644	0.0176	607	0.0218	1020	0.0419	1027	0.0156	783	-		-		-	
1121	tech5-002	0.0046	313	0.0063	311	0.0113	900	0.0216	932	0.0233	893	0.9609	1078	0.7704	1105	-	
1122	tech5-003	0.0053	359	0.0070	336	0.0099	852	0.0185	900	0.0095	643	0.6670	974	0.1024	894	-	
1123	tech5-004	0.0123	627	0.0234	681	0.0086	807	0.0162	871	0.0065	517	0.0112	321	0.0082	361	-	
1124	tech5-005	0.0054	368	0.0072	345	0.0069	726	0.0122	771	0.0060	492	0.0094	267	0.0066	259	-	
1125	tech5-007	0.0020	101	0.0029	95	0.0024	125	0.0028	171	0.0034	276	0.8622	1034	0.5335	1056	0.9867	691
1126	tech5-008	0.0020	105	0.0031	107	0.0026	220	0.0028	182	0.0026	151	0.9238	1060	0.7170	1096	0.9984	726
1127	tech5-009	-		-		0.0041	533	0.0040	375	0.0045	386	0.0087	241	0.0080	348	0.0821	209
1128	techainer-001	0.0061	414	0.0092	425	0.0046	572	0.0073	624	0.0060	494	0.9575	1076	0.8567	1121	0.9995	743
1129	techainer-002	-		-		0.0058	667	0.0121	768	0.0136	752	0.0853	734	0.0313	750	0.1610	379
1130	techbiometricid-001	-		-		0.0877	1147	0.1663	1149	0.1000	1074	0.5946	957	0.3065	1001	0.9792	677
1131	techbiometricid-002	-		-		0.0060	680	0.0091	695	0.8984	1221	1.0000	1235	1.0000	1250	1.0000	852
1132	techsign-000	0.0325	822	0.0511	813	0.0435	1095	0.0710	1089	0.0746	1049	0.1104	760	0.0841	875	0.4288	504
1133	techsign-001	0.0110	594	0.0196	636	0.0067	718	0.0120	764	0.0087	607	0.2475	846	0.0883	882	0.6767	560
1134	telexper-000	-		-		0.0056	652	0.0077	641	0.0104	674	0.9976	1149	0.8691	1125	0.9999	765
1135	tevian-000	0.0871	908	0.1289	900	-		-		-		-		-		-	
1136	tevian-001	0.0813	907	0.1266	897	-		-		-		-		-		-	
1137	tevian-002	0.0279	800	0.0392	776	-		-		-		-		-		-	
1138	tevian-003	0.0217	756	0.0298	726	0.0230	1030	0.0484	1050	-		-		-		-	
1139	tevian-004	0.0228	765	0.0304	729	0.0226	1028	0.0478	1047	0.0128	729	0.0228	498	0.0138	541	-	
1140	tevian-005	0.0043	297	0.0062	301	0.0057	663	0.0085	681	0.0070	535	0.0135	356	0.0119	490	-	
1141	tevian-006	0.0045	305	0.0061	294	0.0045	567	0.0066	588	0.0046	402	0.0091	249	0.0075	322	-	
1142	tevian-007	0.0019	98	0.0027	79	0.0032	396	0.0041	388	0.0045	387	0.0086	235	0.0078	340	0.0925	251
1143	tevian-008	0.0012	45	0.0017	36	0.0033	402	0.0042	409	0.0042	354	0.0081	208	0.0068	271	0.0909	241
1144	tiger-001	0.3120	992	0.3974	994	-		-		-		-		-		-	

Table 80: FNMR is the proportion of mated comparisons below a threshold set to achieve the FMR given in the header on the fourth row. FMR is the proportion of impostor comparisons at or above that threshold. The light grey values give rank over all algorithms in that column. The pink columns use only same-sex impostors; others are selected regardless of demographics. The exception, in the green column, uses "matched-covariates" i.e. impostors of the same sex, age group, and country of birth. The second pink column includes effects of extended ageing. Missing entries for border, visa, mugshot and wild images generally mean the algorithm did not run to completion. The VISA *columns compare images described in section 2.1. The* MUGSHOT *columns compare images described in section 2.5. The* VISA-BORDER *column compare images described in section 2.2 with those of section 2.4. The* BORDER *column compares images described in section 2.4. The* KIOSK-BORDER *columns compare images described in section 2.6 with those of section 2.4.*

		FALSE NON-MATCH RATE (FNMR)															
	Algorithm	CONSTRAINED, COOPERATIVE														LESS CONSTRAINED, NON-COOP.	
	Name	VISAMC		VISA		MUGSHOT		MUGSHOT12+YRS		VISABORDER		BORDER		BORDER		KIOSKBORDER	
	FMR	0.0001		1E-06		1E-05		1E-05		1E-06		1E-06		1E-05		1E-06	
1145	tiger-002	0.0658	884	0.0889	874	0.1083	1156	0.1766	1153	0.0952	1069	0.1568	795	0.0661	852	-	
1146	tiger-003	0.0313	818	0.0602	835	0.0188	996	0.0359	1008	0.0344	959	-		-		-	
1147	tiger-004	0.0779	899	0.1393	904	0.0488	1105	0.0905	1112	0.0800	1054	0.1640	798	0.0617	847	-	
1148	tiger-005	0.0624	878	0.2450	952	0.0292	1059	0.0556	1063	0.0430	993	1.0000	1201	0.9964	1196	1.0000	797
1149	tiger-006	0.0066	440	0.0101	462	0.0050	612	0.0075	635	0.0089	618	0.0158	402	0.0117	484	0.1466	358
1150	tiger-007	-		-		0.0041	538	0.0063	571	0.0088	613	0.7340	987	0.3935	1028	0.9464	651
1151	tinkoff-001	0.0145	672	0.0244	690	0.0318	1068	0.0636	1077	0.0236	900	1.0000	1264	0.0339	761	1.0000	1333
1152	tngd-001	-		-		0.0827	1142	0.1404	1141	0.0981	1073	0.1409	788	0.0808	871	0.7653	579
1153	tngd-002	-		-		0.1471	1175	0.2504	1173	0.1879	1108	0.7463	991	0.6359	1076	0.9555	654
1154	tnitech-000	0.0025	157	0.0037	145	0.0033	407	0.0035	318	0.0025	121	0.8893	1042	0.6283	1072	0.9883	692
1155	tongyi-004	0.0428	846	0.0540	820	-		-		-		-		-		-	
1156	tongyi-005	0.0073	476	0.0146	547	0.0187	994	0.0421	1028	0.0161	795	0.0215	481	0.0149	566	-	
1157	tongyitrans-001	0.0617	877	0.0715	850	-		-		-		-		-		-	
1158	tongyitrans-002	0.0437	849	0.0657	844	-		-		-		-		-		-	
1159	tongyitrans-003	0.0249	779	0.0474	801	-		-		-		-		-		-	
1160	toppanidgate-000	0.0021	112	0.0033	117	0.0026	215	0.0028	180	0.0039	329	0.0075	178	0.0068	267	0.0631	113
1161	toppansecurity-001	-		-		0.0025	164	0.0027	168	0.0032	241	0.0059	123	0.0051	160	0.0499	43
1162	toshiba-000	0.1906	962	0.2896	969	-		-		-		-		-		-	
1163	toshiba-001	0.1063	923	0.1926	933	-		-		-		-		-		-	
1164	toshiba-002	0.0134	652	0.0222	667	0.0097	846	0.0154	852	-		0.0327	576	0.0158	580	-	
1165	toshiba-003	0.0125	634	0.0214	656	0.0085	804	0.0131	795	-		0.0241	508	0.0151	571	-	
1166	toshiba-004	0.0030	187	0.0042	185	0.0025	181	0.0027	167	0.0034	272	0.0063	140	0.0053	184	0.0700	149
1167	toshiba-005	0.0023	133	0.0037	146	0.0024	131	0.0026	140	0.0072	545	0.0141	365	0.0130	517	0.0918	246
1168	toshiba-006	0.0022	125	0.0035	129	0.0024	142	0.0025	121	0.0027	166	0.7425	989	0.3070	1002	0.9691	664
1169	toshiba-007	0.0016	65	0.0023	61	0.0024	151	0.0023	65	0.0021	56	0.0629	698	0.0056	200	0.2301	431
1170	toshiba-008	0.0012	42	0.0017	34	0.0024	135	0.0022	51	0.0019	43	0.0108	308	0.0039	85	0.0899	233
1171	toshiba-009	-		-		0.0024	122	0.0021	42	0.0019	41	0.0256	524	0.0055	198	0.1500	365
1172	toshiba-010	-		-		0.0024	108	0.0021	35	0.0017	23	0.0316	563	0.0053	180	0.1331	332
1173	toshiba-011	-		-		0.0024	134	0.0022	46	0.0019	38	0.0037	32	0.0033	37	0.0453	25
1174	toshiba-012	-		-		0.0022	55	0.0022	45	0.0019	37	0.0040	40	0.0034	39	0.0503	45
1175	toss-000	-		-		0.0023	59	0.0022	48	0.0021	58	0.0041	44	0.0035	43	0.0474	31
1176	touchlessid-000	0.3296	995	0.4804	1009	0.4111	1218	0.6026	1222	0.5324	1169	0.9996	1180	0.9964	1197	1.0000	810
1177	touchlessid-001	0.0076	485	0.0104	468	0.0680	1131	0.0842	1103	0.1358	1084	1.0000	1203	0.9995	1217	1.0000	859
1178	touchlessid-002	0.0070	457	0.0096	444	0.0407	1090	0.0469	1044	0.4234	1160	0.9991	1166	0.9953	1194	1.0000	799
1179	touchlessid-003	0.0061	413	0.0081	386	0.0040	525	0.0053	504	0.0056	467	0.0155	395	0.0082	360	0.1370	340
1180	touchlessid-004	-		-		0.0035	441	0.0049	459	0.0043	368	0.0077	187	0.0058	215	0.0793	195
1181	transmitsecurity-001	-		-		0.0051	620	0.0078	652	0.0089	619	0.0151	385	0.0111	466	0.1181	307
1182	trueface-000	0.0249	777	0.4321	999	0.0119	915	0.0180	894	0.0297	945	0.7467	992	0.1602	946	-	
1183	trueface-001	0.0204	749	0.0438	790	0.0095	840	0.0138	819	0.0154	779	0.0253	521	0.0169	600	-	
1184	trueface-002	0.0060	407	0.0096	441	0.0048	592	0.0061	564	0.0112	700	0.0198	465	0.0155	576	-	
1185	trueface-003	0.0070	460	0.0094	436	0.0053	630	0.0081	668	0.0122	718	0.0217	485	0.0159	582	0.1204	314
1186	trueidvng-001	0.0063	422	0.0077	365	0.0033	415	0.0044	425	0.0046	399	0.0086	238	0.0069	277	0.0809	204
1187	truststamp-001	0.0242	772	0.0484	807	0.0194	1001	0.0359	1007	0.0381	977	0.8808	1040	0.6898	1084	0.9948	706
1188	truststamp-002	-		-		0.0080	774	0.0138	820	0.0128	728	0.9718	1087	0.8779	1130	0.9998	751

Table 81: FNMR is the proportion of mated comparisons below a threshold set to achieve the FMR given in the header on the fourth row. FMR is the proportion of impostor comparisons at or above that threshold. The light grey values give rank over all algorithms in that column. The pink columns use only same-sex impostors; others are selected regardless of demographics. The exception, in the green column, uses "matched-covariates" i.e. impostors of the same sex, age group, and country of birth. The second pink column includes effects of extended ageing. Missing entries for border, visa, mugshot and wild images generally mean the algorithm did not run to completion. The VISA *columns compare images described in section 2.1. The* MUGSHOT *columns compare images described in section 2.5. The* VISA-BORDER *column compare images described in section 2.2 with those of section 2.4. The* BORDER *column compares images described in section 2.4. The* KIOSK-BORDER *columns compare images described in section 2.6 with those of section 2.4.*

		FALSE NON-MATCH RATE (FNMR)															
	Algorithm	CONSTRAINED, COOPERATIVE														LESS CONSTRAINED, NON-COOP.	
	Name	VISAMC		VISA		MUGSHOT		MUGSHOT12+YRS		VISABORDER		BORDER		BORDER		KIOSKBORDER	
	FMR	0.0001		1E-06		1E-05		1E-05		1E-06		1E-06		1E-05		1E-06	
1189	truststamp-003	-		-		0.0047	585	0.0070	610	0.0073	550	0.7132	983	0.4538	1040	0.9578	656
1190	ttigroup-000	-		-		0.0028	298	0.0034	292	0.0043	372	0.9208	1055	0.7608	1104	0.9975	724
1191	tuputech-000	0.3218	994	0.3696	989	-		-		0.3237	1143	0.4304	916	0.2973	1000	-	
1192	turingtechvip-001	0.0330	827	0.0540	821	0.0458	1102	0.1007	1118	0.4715	1162	0.9286	1063	0.8448	1119	0.9964	717
1193	turingtechvip-002	0.0126	641	0.0163	581	0.0092	824	0.0118	758	0.2264	1127	1.0000	1387	0.9925	1187	0.9999	767
1194	turkcell-000	0.1134	928	0.1288	899	0.0770	1139	0.1112	1129	0.2570	1132	1.0000	1200	0.9999	1233	1.0000	830
1195	turkcell-001	0.0043	292	0.0066	317	0.0037	487	0.0055	518	0.0043	361	0.0440	638	0.0082	362	0.3148	472
1196	turkcell-002	-		-		0.0036	456	0.0053	502	0.0044	374	0.0371	615	0.0075	317	0.2871	465
1197	twface-000	0.0051	343	0.0072	347	0.0041	530	0.0058	535	0.0071	540	0.0153	392	0.0100	423	0.1595	374
1198	twface-001	0.0036	247	0.0051	248	0.0031	371	0.0038	351	0.0049	420	0.0091	254	0.0075	321	0.0831	211
1199	ulsee-001	0.0151	685	0.0246	693	0.0113	897	0.0185	903	0.0187	842	0.6766	975	0.0181	623	-	
1200	ultinous-000	0.2343	975	0.3484	984	-		-		-		-		-		-	
1201	ultinous-001	0.2485	980	0.4003	995	-		-		-		-		-		-	
1202	uluface-002	0.0081	506	0.0123	507	0.0071	733	0.0095	709	0.0107	681	1.0000	1381	0.0140	545	-	
1203	uluface-003	0.0100	567	0.0150	555	0.0079	770	0.0128	788	-		-		-		-	
1204	unicc-001	0.5101	1034	0.6167	1038	0.6577	1246	0.7894	1243	0.9208	1227	0.9866	1106	0.9386	1149	0.9999	770
1205	unicc-002	0.2153	972	0.2190	944	0.0417	1092	0.0526	1060	0.0891	1063	0.1321	780	0.1125	902	0.3813	490
1206	unicc-003	0.0217	758	0.0260	706	0.0093	830	0.0136	810	0.0129	731	0.0216	483	0.0143	553	0.2091	422
1207	unicc-004	-		-		0.0055	647	0.0077	643	0.0076	563	0.0147	378	0.0102	434	0.1421	350
1208	unissey-001	0.0095	551	0.0160	577	0.0134	942	0.0150	846	0.0147	771	0.0253	522	0.0163	589	0.1651	385
1209	unissey-002	0.0094	547	0.0151	557	0.0079	772	0.0110	745	0.0114	704	0.4424	919	0.1914	960	0.8051	596
1210	unissey-003	0.0057	379	0.0082	392	0.0047	583	0.0082	670	0.0067	522	0.5179	933	0.2863	996	0.8684	613
1211	unissey-004	0.0043	291	0.0066	319	0.0037	471	0.0052	491	0.0048	416	0.5272	938	0.2903	997	0.8777	619
1212	unissey-005	-		-		0.0037	470	0.0052	492	0.0086	602	0.0161	408	0.0134	524	0.1006	267
1213	unissey-006	-		-		0.0073	743	0.0121	769	0.0288	937	0.0529	673	0.0464	813	0.2808	461
1214	unissey-007	-		-		0.3124	1204	0.4571	1205	0.6912	1181	0.9823	1101	0.8827	1132	1.0000	783
1215	upc-001	0.0234	767	0.0519	816	0.0291	1057	0.0490	1054	0.0294	942	0.2316	837	0.0389	784	-	
1216	urielsoft-000	-		-		0.0026	228	0.0032	263	0.0043	365	0.0083	217	0.0068	273	0.0744	166
1217	useb-000	0.0158	693	0.0222	666	0.0123	923	0.0168	885	0.0182	832	0.0289	548	0.0167	598	0.1614	380
1218	useb-001	0.0035	241	0.0053	261	0.0027	269	0.0033	284	0.0027	168	0.0085	232	0.0044	112	0.0806	200
1219	useb-002	0.0028	175	0.0039	159	0.0027	267	0.0031	248	0.0025	119	0.0090	246	0.0042	102	0.0867	218
1220	useb-003	-		-		0.0026	205	0.0030	214	0.0025	114	0.0091	253	0.0042	104	0.0901	236
1221	useb-004	-		-		0.0025	193	0.0028	193	0.0022	65	0.5197	937	0.2232	974	0.8470	605
1222	uxlabs-001	0.0534	861	0.0570	828	0.0118	911	0.0131	794	0.0237	903	0.0399	630	0.0288	739	0.2097	424
1223	uxlabs-003	0.2133	971	0.2143	940	0.0386	1083	0.0457	1037	0.0374	975	0.3343	879	0.1554	941	0.6941	565
1224	uzinfocom-000	-		-		0.0070	730	0.0120	766	0.0086	601	0.9874	1110	0.9469	1152	0.9999	756
1225	uzinfocom-001	-		-		0.0029	327	0.0038	353	0.0041	347	0.9963	1141	0.9725	1170	1.0000	789
1226	vaidio-001	-		-		0.0135	943	0.0166	880	0.0079	572	0.6587	971	0.4279	1035	0.9123	637
1227	vcog-002	0.7522	1053	0.9033	1067	-		-		-		-		-		-	
1228	vcortex-001	0.0131	649	0.0207	647	0.0192	999	0.0315	992	0.2238	1126	0.3586	892	0.3536	1017	0.3569	480
1229	vd-000	0.3790	1005	0.4973	1013	-		-		-		-		-		-	
1230	vd-001	0.0243	773	0.0452	794	0.0271	1050	0.0402	1021	0.0424	991	-		-		-	
1231	vd-002	0.0429	847	0.0704	848	0.0569	1118	0.0844	1104	0.0801	1055	0.0937	739	0.0577	843	-	
1232	vd-003	0.0199	746	0.0222	668	0.0115	906	0.0130	793	0.0138	755	0.0239	506	0.0177	617	0.1647	384

Table 82: FNMR is the proportion of mated comparisons below a threshold set to achieve the FMR given in the header on the fourth row. FMR is the proportion of impostor comparisons at or above that threshold. The light grey values give rank over all algorithms in that column. The pink columns use only same-sex impostors; others are selected regardless of demographics. The exception, in the green column, uses "matched-covariates" i.e. impostors of the same sex, age group, and country of birth. The second pink column includes effects of extended ageing. Missing entries for border, visa, mugshot and wild images generally mean the algorithm did not run to completion. The VISA *columns compare images described in section 2.1. The* MUGSHOT *columns compare images described in section 2.5. The* VISA-BORDER *column compare images described in section 2.2 with those of section 2.4. The* BORDER *column compares images described in section 2.4. The* KIOSK-BORDER *columns compare images described in section 2.6 with those of section 2.4.*

	Algorithm	FALSE NON-MATCH RATE (FNMR)															
		CONSTRAINED, COOPERATIVE														LESS CONSTRAINED, NON-COOP.	
	Name	VISAMC		VISA		MUGSHOT		MUGSHOT12+YRS		VISABORDER		BORDER		BORDER		KIOSKBORDER	
	FMR	0.0001		1E-06		1E-05		1E-05		1E-06		1E-06		1E-05		1E-06	
1233	veridas-001	0.1998	969	0.2724	959	0.2987	1202	0.4587	1206	0.2599	1133	0.2454	844	0.1357	923	-	
1234	veridas-002	0.1733	954	0.2257	947	0.2617	1198	0.4147	1199	0.2073	1118	0.2028	818	0.1112	901	-	
1235	veridas-003	0.0557	870	0.0983	883	0.0734	1135	0.1267	1137	0.0694	1046	0.0951	745	0.0480	817	-	
1236	veridas-004	0.0281	801	0.0467	800	0.0353	1079	0.0643	1080	0.0424	990	0.0644	699	0.0342	762	-	
1237	veridas-005	0.0599	874	0.1110	891	0.0294	1063	0.0639	1078	0.0811	1058	0.1130	762	0.0548	833	-	
1238	veridas-006	0.0098	557	0.0167	590	0.0079	773	0.0127	782	0.0127	725	0.0217	484	0.0151	570	0.1573	370
1239	veridas-007	0.0063	426	0.0083	394	0.0044	556	0.0058	539	0.0080	582	0.0152	389	0.0120	496	0.1199	313
1240	veridas-008	0.0032	210	0.0045	210	0.0030	337	0.0033	279	0.0085	600	0.0206	471	0.0143	554	0.1228	318
1241	veridas-009	0.0031	195	0.0043	188	0.0030	350	0.0035	312	0.0055	454	0.0106	303	0.0100	424	0.0959	260
1242	veridas-010	-		-		0.0027	278	0.0033	283	0.0042	355	0.0080	207	0.0073	303	0.0649	127
1243	veridium-000	0.0726	892	0.1248	896	0.5226	1230	0.6652	1229	0.6425	1177	0.8150	1017	0.7989	1112	0.8772	618
1244	veridium-001	0.0274	797	0.0368	767	0.0292	1060	0.0475	1045	0.0488	1007	0.0673	706	0.0463	811	0.3691	486
1245	veridium-002	0.0343	829	0.0427	786	0.0283	1054	0.0460	1040	0.0489	1008	0.0673	705	0.0464	812	0.3658	482
1246	veridium-003	-		-		0.0286	1055	0.0462	1041	0.0492	1009	0.0679	709	0.0470	815	0.3672	483
1247	verigram-000	0.0032	204	0.0043	189	0.0031	357	0.0034	295	0.0093	636	0.0175	433	0.0164	593	0.1158	303
1248	verigram-001	0.0032	211	0.0044	200	0.0027	264	0.0032	264	0.0030	208	0.9995	1176	0.9953	1193	1.0000	856
1249	verigram-002	0.0079	497	0.0089	415	0.0038	494	0.0040	378	0.0060	495	0.0113	327	0.0107	453	0.0634	115
1250	verigram-003	0.0101	569	0.0109	482	0.0034	425	0.0039	367	0.0037	306	0.0070	168	0.0063	244	0.0559	71
1251	verihubs-inteligensia-000	0.0070	461	0.0098	448	0.0048	594	0.0076	640	0.0092	629	0.0160	405	0.0117	482	0.1348	336
1252	verihubs-inteligensia-001	0.0071	463	0.0114	496	0.0050	607	0.0076	639	0.0096	645	0.0165	418	0.0114	475	0.1409	348
1253	verihubs-inteligensia-002	0.0028	172	0.0043	193	0.0025	201	0.0030	216	0.0047	408	0.0092	255	0.0083	368	0.0983	263
1254	verijelas-000	0.2488	981	0.3431	982	0.4861	1228	0.6004	1220	0.0811	1057	0.1148	764	0.0440	803	0.4077	499
1255	via-000	0.0216	754	0.0365	765	0.0177	991	0.0287	980	0.0296	943	0.0572	679	0.0290	742	-	
1256	via-001	0.0149	680	0.0229	675	0.0114	904	0.0177	892	0.0183	836	0.4056	909	0.0176	614	-	
1257	via-004	0.0099	561	0.0135	531	0.0031	377	0.0044	426	0.0055	459	0.4009	907	0.0080	352	0.9840	685
1258	via-005	0.0063	421	0.0082	390	0.0031	359	0.0037	349	0.0032	242	0.3659	894	0.0068	268	0.8709	616
1259	via-006	-		-		0.0025	158	0.0027	153	0.0025	138	0.5904	955	0.0315	751	0.9455	650
1260	viante-000	0.0004	6	0.0007	4	0.0026	233	0.0026	143	0.0017	20	0.0033	13	0.0029	17	0.0475	34
1261	viante-001	-		-		0.0025	199	0.0025	113	0.0016	10	0.0031	8	0.0028	13	0.0432	15
1262	viante-002	-		-		0.0025	166	0.0024	90	0.0015	6	0.0029	5	0.0027	6	0.0399	7
1263	viante-003	-		-		0.0025	160	0.0023	70	0.0015	5	0.0029	3	0.0026	5	0.0388	4
1264	videmo-000	0.0298	810	0.0423	783	0.0155	978	0.0260	963	0.0246	910	0.0397	629	0.0239	697	-	
1265	videmo-001	0.0295	807	0.0417	780	0.0164	987	0.0261	966	0.0355	965	0.0603	692	0.0442	805	0.2428	441
1266	videmo-002	0.0158	694	0.0288	718	0.0149	972	0.0249	956	0.0230	888	0.3429	884	0.1468	932	0.8393	604
1267	videmo-003	-		-		0.0082	789	0.0138	818	0.0133	741	0.0220	489	0.0119	493	0.1596	376
1268	videonetics-001	0.5483	1036	0.6446	1041	0.7517	1266	0.8607	1260	0.8664	1211	0.8255	1021	0.6956	1086	-	
1269	videonetics-002	0.4274	1013	0.5329	1020	0.6081	1242	0.7438	1237	0.7775	1192	0.7297	986	0.5756	1063	-	
1270	viettelai-000	0.0051	348	0.0068	329	0.0054	637	0.0064	580	0.9451	1231	1.0000	1356	1.0000	1390	1.0000	1046
1271	viettelai-001	0.0054	366	0.0076	363	0.0049	602	0.0079	657	0.0064	513	0.0225	494	0.0083	364	1.0000	1302
1272	viettelai-002	-		-		0.0029	324	0.0041	392	0.0069	528	0.0126	348	0.0074	312	0.1095	283
1273	viettelai-003	-		-		0.0034	430	0.0041	396	0.2038	1114	0.3193	877	0.1067	898	0.8681	612
1274	viettelai-004	-		-		0.0023	90	0.0028	185	0.0023	84	0.0044	57	0.0034	40	0.0566	76
1275	viettelhightech-000	0.0117	612	0.0166	586	0.0110	886	0.0198	920	0.0167	810	0.0249	515	0.0158	579	0.1604	378
1276	viettelhightech-001	-		-		0.0031	372	0.0040	383	0.0032	250	0.0063	139	0.0051	159	0.0781	189

Table 83: FNMR is the proportion of mated comparisons below a threshold set to achieve the FMR given in the header on the fourth row. FMR is the proportion of impostor comparisons at or above that threshold. The light grey values give rank over all algorithms in that column. The pink columns use only same-sex impostors; others are selected regardless of demographics. The exception, in the green column, uses "matched-covariates" i.e. impostors of the same sex, age group, and country of birth. The second pink column includes effects of extended ageing. Missing entries for border, visa, mugshot and wild images generally mean the algorithm did not run to completion. The VISA *columns compare images described in section 2.1. The* MUGSHOT *columns compare images described in section 2.5. The* VISA-BORDER *column compare images described in section 2.2 with those of section 2.4. The* BORDER *column compares images described in section 2.4. The* KIOSK-BORDER *columns compare images described in section 2.6 with those of section 2.4.*

		FALSE NON-MATCH RATE (FNMR)															
	Algorithm	CONSTRAINED, COOPERATIVE														LESS CONSTRAINED, NON-COOP.	
	Name	VISAMC		VISA		MUGSHOT		MUGSHOT12+YRS		VISABORDER		BORDER		BORDER		KIOSKBORDER	
	FMR	0.0001		1E-06		1E-05		1E-05		1E-06		1E-06		1E-05		1E-06	
1277	viettelhightech-002	-		-		0.0031	356	0.0042	411	0.0033	254	0.0061	135	0.0051	157	0.0758	177
1278	vigilantsolutions-000	-		0.6881	1047	-		-		-		-		-		-	
1279	vigilantsolutions-001	-		0.3475	983	-		-		-		-		-		-	
1280	vigilantsolutions-002	0.2290	974	0.3214	977	-		-		-		-		-		-	
1281	vigilantsolutions-003	0.1878	961	0.2673	958	-		-		-		-		-		-	
1282	vigilantsolutions-004	0.1780	957	0.2598	956	-		-		-		-		-		-	
1283	vigilantsolutions-005	0.1613	951	0.4702	1007	0.0163	985	0.0279	976	-		-		-		-	
1284	vigilantsolutions-006	0.1264	934	0.3221	978	0.0150	973	0.0254	957	0.0493	1011	0.2991	863	0.0403	790	-	
1285	vigilantsolutions-007	0.0202	748	0.0307	731	0.0136	944	0.0227	942	0.0356	967	1.0000	1331	1.0000	1259	-	
1286	vigilantsolutions-008	0.0156	690	0.0233	678	0.0101	856	0.0147	840	0.0355	966	0.0492	661	0.0293	745	-	
1287	vigilantsolutions-009	0.0117	613	0.0165	585	0.0075	758	0.0101	726	0.0219	879	0.0385	624	0.0238	696	-	
1288	vigilantsolutions-010	0.0109	591	0.0164	582	0.0074	753	0.0095	706	0.0209	870	0.0365	613	0.0233	691	0.2465	442
1289	vigilantsolutions-011	0.0124	630	0.0176	606	0.0073	744	0.0095	705	0.0196	860	0.0360	605	0.0221	678	0.2633	454
1290	vinai-000	0.0081	505	0.0124	510	0.0045	558	0.0072	619	0.0089	617	0.1814	806	0.0112	468	-	
1291	vinbigdata-001	0.2576	984	0.2763	961	0.1404	1172	0.1988	1164	0.1407	1089	0.1150	765	0.0703	859	0.3688	485
1292	vinbigdata-002	0.0102	573	0.0175	602	0.0071	737	0.0084	677	0.0090	621	0.8017	1010	0.3134	1005	0.9936	704
1293	vinbigdata-003	0.0771	897	0.0992	884	0.1202	1164	0.1756	1152	0.2762	1137	0.2369	841	0.0100	425	0.8914	631
1294	vinbigdata-004	-		-		0.0031	361	0.0046	435	0.0037	308	0.1476	791	0.0063	247	0.4917	518
1295	vinbigdata-005	-		-		0.0023	61	0.0024	96	0.0022	64	0.0068	161	0.0038	70	0.0699	148
1296	vinbigdata-006	-		-		0.0022	54	0.0023	78	0.0019	47	0.0037	31	0.0032	30	0.0479	35
1297	vinbigdata-007	-		-		0.0022	36	0.0021	36	0.0019	45	0.0036	29	0.0032	31	0.0475	32
1298	vion-000	0.0419	843	0.0590	832	0.0422	1093	0.0478	1048	0.0581	1028	0.0968	749	0.0847	876	-	
1299	visage-000	0.0933	912	0.1441	911	0.1316	1168	0.2416	1171	0.1395	1086	0.1920	812	0.1001	891	-	
1300	visica-001	-		-		0.2293	1192	0.3588	1192	0.2936	1140	0.3564	891	0.1967	962	0.7795	586
1301	visica-002	-		-		0.0520	1112	0.0898	1110	0.2960	1141	0.8202	1019	0.5956	1068	0.9838	683
1302	visionbox-000	0.0293	805	0.0541	822	0.0197	1003	0.0339	996	0.0349	961	0.0593	688	0.0329	756	-	
1303	visionbox-001	0.0159	697	0.0270	711	0.0111	890	0.0173	887	0.0190	847	0.0315	561	0.0205	662	-	
1304	visionbox-002	0.0058	386	0.0079	375	0.0060	678	0.0074	625	0.0084	596	0.0149	381	0.0113	472	0.0979	262
1305	visionbox-003	0.0057	383	0.0075	357	0.0062	695	0.0083	674	0.0100	667	0.9915	1119	0.9625	1163	1.0000	776
1306	visionbox-004	0.0046	320	0.0075	359	0.0060	683	0.0075	633	0.0056	464	0.0316	562	0.0070	288	0.2528	445
1307	visionbox-005	-		-		0.0041	527	0.0057	529	0.0046	403	0.0109	311	0.0088	381	0.0767	181
1308	visionbox-006	-		-		0.0063	699	0.0075	630	0.0048	414	0.0116	332	0.0094	406	0.0789	192
1309	visionbox-007	-		-		0.0063	701	0.0075	629	0.0047	412	0.0116	334	0.0095	412	0.0793	194
1310	visionlabs-001	0.1049	922	0.1803	925	-		-		-		-		-		-	
1311	visionlabs-002	0.0326	824	0.0507	812	-		-		-		-		-		-	
1312	visionlabs-003	0.0178	723	0.0293	722	-		-		-		-		-		-	
1313	visionlabs-004	0.0219	759	0.0457	796	-		-		-		-		-		-	
1314	visionlabs-005	0.0088	524	0.0156	572	0.0048	589	0.0070	611	-		-		-		-	
1315	visionlabs-006	0.0037	254	0.0066	318	0.0041	537	0.0060	553	0.0061	500	0.0106	304	0.0076	332	-	
1316	visionlabs-007	0.0038	263	0.0048	229	0.0036	461	0.0048	451	0.0057	472	0.0097	277	0.0071	292	-	
1317	visionlabs-008	0.0026	159	0.0036	141	0.0031	380	0.0040	382	0.0045	389	0.0079	201	0.0064	248	-	
1318	visionlabs-009	0.0018	89	0.0025	69	0.0026	214	0.0029	210	0.0035	281	0.0064	142	0.0054	190	-	
1319	visionlabs-010	0.0017	79	0.0024	63	0.0026	232	0.0030	225	0.0033	262	0.0061	133	0.0052	172	-	
1320	visionlabs-011	0.0012	44	0.0022	55	0.0024	145	0.0026	141	0.0028	175	0.0053	97	0.0046	130	0.0635	116

Table 84: FNMR is the proportion of mated comparisons below a threshold set to achieve the FMR given in the header on the fourth row. FMR is the proportion of impostor comparisons at or above that threshold. The light grey values give rank over all algorithms in that column. The pink columns use only same-sex impostors; others are selected regardless of demographics. The exception, in the green column, uses "matched-covariates" i.e. impostors of the same sex, age group, and country of birth. The second pink column includes effects of extended ageing. Missing entries for border, visa, mugshot and wild images generally mean the algorithm did not run to completion. The VISA *columns compare images described in section 2.1. The* MUGSHOT *columns compare images described in section 2.5. The* VISA-BORDER *column compare images described in section 2.2 with those of section 2.4. The* BORDER *column compares images described in section 2.4. The* KIOSK-BORDER *columns compare images described in section 2.6 with those of section 2.4.*

		FALSE NON-MATCH RATE (FNMR)															
	Algorithm	CONSTRAINED, COOPERATIVE														LESS CONSTRAINED, NON-COOP.	
	Name	VISAMC		VISA		MUGSHOT		MUGSHOT12+YRS		VISABORDER		BORDER		BORDER		KIOSKBORDER	
	FMR	0.0001		1E-06		1E-05		1E-05		1E-06		1E-06		1E-05		1E-06	
1321	visteam-000	0.9200	1064	0.9489	1071	0.9959	1293	0.9984	1288	0.9994	1253	0.9978	1150	0.9914	1186	-	
1322	visteam-001	0.4417	1018	0.5385	1023	0.6410	1245	0.7788	1242	0.6386	1176	0.5904	953	0.4023	1031	-	
1323	visteam-002	0.1564	949	0.2789	963	0.1581	1178	0.2567	1177	0.1776	1104	0.2090	824	0.1021	893	0.5820	537
1324	visteam-003	0.0804	905	0.2166	941	0.0613	1125	0.1204	1133	0.0963	1070	0.1269	777	0.0441	804	0.6049	543
1325	visteam-004	0.0541	864	0.5202	1017	0.0406	1089	0.0827	1101	0.1879	1107	0.1795	805	0.0347	765	0.9673	663
1326	visteam-005	0.0235	768	0.0333	746	0.0265	1046	0.0583	1071	0.0341	958	0.0524	671	0.0259	713	0.2413	439
1327	visteam-006	0.0188	733	0.0256	701	0.0158	982	0.0365	1011	0.0198	863	0.0340	593	0.0174	612	0.1904	407
1328	visteam-007	0.0312	817	0.0448	793	0.0416	1091	0.1008	1119	0.0466	1003	0.0602	691	0.0281	730	0.2601	451
1329	visteam-008	0.0378	837	0.0515	814	0.0391	1086	0.0937	1115	0.0437	996	0.0567	678	0.0260	715	0.2533	446
1330	visteam-009	-		-		0.0138	948	0.0304	987	0.0166	806	0.9993	1171	0.9719	1168	0.9997	747
1331	visteam-010	-		-		0.0156	980	0.0347	1002	0.0189	844	1.0000	1221	0.9996	1219	1.0000	775
1332	vivotek-001	-		-		0.9982	1295	0.9994	1291	1.0000	1259	1.0000	1223	0.9999	1235	1.0000	807
1333	vivotek-002	-		-		0.0761	1138	0.1380	1139	0.9587	1234	1.0000	1225	1.0000	1242	1.0000	847
1334	vixvizion-000	0.0642	883	0.0882	873	0.0497	1108	0.0905	1111	0.0848	1060	0.1026	751	0.0618	848	-	
1335	vixvizion-001	0.0245	775	0.0407	778	0.0257	1042	0.0497	1055	0.0514	1014	0.0656	702	0.0400	789	-	
1336	vixvizion-002	0.0062	419	0.0086	404	0.0053	634	0.0075	631	0.0121	715	0.0207	472	0.0161	585	-	
1337	vixvizion-003	0.0059	402	0.0084	399	0.0059	673	0.0081	665	0.0119	711	0.0209	474	0.0162	586	-	
1338	vixvizion-004	0.0063	423	0.0094	435	0.0055	650	0.0081	666	0.0098	659	0.0157	400	0.0111	465	0.1417	349
1339	vixvizion-005	0.0276	798	0.0420	782	0.0302	1066	0.0629	1075	0.0288	938	0.0447	641	0.0235	693	0.2304	432
1340	vixvizion-006	0.0082	509	0.0122	506	0.0093	826	0.0194	913	0.0099	662	0.0169	425	0.0108	457	0.1338	334
1341	vixvizion-007	0.0110	595	0.0191	628	0.0080	777	0.0157	855	0.0101	669	0.0190	454	0.0118	488	0.1407	347
1342	vnis-000	0.1397	942	0.1608	917	0.2184	1191	0.2976	1185	0.5277	1168	0.3603	893	0.2714	990	0.6929	563
1343	vnpay-000	0.2380	977	0.2614	957	0.4054	1217	0.4968	1209	0.3993	1157	0.4389	917	0.4006	1030	0.7693	582
1344	vnpay-001	-		-		0.0026	234	0.0030	218	0.0065	516	0.0124	344	0.0116	481	0.0826	210
1345	vnpt-001	0.3117	991	0.3523	985	0.3474	1210	0.2747	1179	0.3405	1144	0.5015	928	0.4827	1045	-	
1346	vnpt-002	0.0351	833	0.0424	784	0.0220	1021	0.0316	993	0.0471	1004	0.0817	730	0.0698	858	0.2610	452
1347	vnpt-003	0.0117	611	0.0138	535	0.0040	522	0.0058	546	0.0087	606	0.0161	411	0.0126	506	0.1110	290
1348	vnpt-004	0.0058	391	0.0078	372	0.0037	481	0.0053	500	0.0051	434	0.4640	922	0.1384	925	0.7753	584
1349	vnpt-005	0.0036	244	0.0052	252	0.0027	265	0.0031	240	0.0036	292	0.0066	154	0.0056	202	0.0621	106
1350	vnpt-006	0.0034	233	0.0050	240	0.0027	255	0.0035	323	0.0026	154	0.0049	86	0.0040	96	0.0585	84
1351	vnpt-007	-		-		0.0025	192	0.0029	202	0.0025	133	0.0047	68	0.0039	83	0.0564	74
1352	vnpt-008	-		-		0.0026	211	0.0029	200	0.0025	139	0.0047	74	0.0040	87	0.0570	78
1353	vnpt-009	-		-		0.0030	330	0.0042	405	0.0030	215	0.0053	98	0.0042	105	0.0628	109
1354	vocalize-001	-		-		0.7356	1261	0.8750	1267	0.7830	1195	0.7067	982	0.5268	1055	0.9164	641
1355	vocord-001	-		0.1415	910	-		-		-		-		-		-	
1356	vocord-002	0.0228	764	0.0341	751	-		-		-		-		-		-	
1357	vocord-003	0.1003	916	0.1092	889	-		-		-		-		-		-	
1358	vocord-004	0.0101	570	0.0174	601	0.0196	1002	0.0384	1016	-		-		-		-	
1359	vocord-005	0.0089	526	0.0155	569	0.0216	1019	0.0414	1026	-		-		-		-	
1360	vocord-006	0.0062	418	0.0102	465	0.0082	786	0.0151	847	0.0475	1005	0.0852	733	0.0788	865	-	
1361	vocord-007	0.0039	268	0.0053	264	0.0061	688	0.0094	704	0.0520	1017	0.0939	742	0.0910	884	-	
1362	vocord-008	0.0029	180	0.0038	156	0.0042	542	0.0055	513	0.0045	392	0.0086	239	0.0073	307	-	
1363	vocord-009	0.0022	127	0.0029	98	0.0036	452	0.0046	441	0.0052	442	0.0098	280	0.0086	378	-	
1364	vocord-010	0.0024	144	0.0031	108	0.0036	453	0.0049	472	0.0025	140	0.0065	146	0.0040	89	0.0679	142

Table 85: FNMR is the proportion of mated comparisons below a threshold set to achieve the FMR given in the header on the fourth row. FMR is the proportion of impostor comparisons at or above that threshold. The light grey values give rank over all algorithms in that column. The pink columns use only same-sex impostors; others are selected regardless of demographics. The exception, in the green column, uses "matched-covariates" i.e. impostors of the same sex, age group, and country of birth. The second pink column includes effects of extended ageing. Missing entries for border, visa, mugshot and wild images generally mean the algorithm did not run to completion. The VISA *columns compare images described in section 2.1. The* MUGSHOT *columns compare images described in section 2.5. The* VISA-BORDER *column compare images described in section 2.2 with those of section 2.4. The* BORDER *column compares images described in section 2.4. The* KIOSK-BORDER *columns compare images described in section 2.6 with those of section 2.4.*

		FALSE NON-MATCH RATE (FNMR)															
	Algorithm	CONSTRAINED, COOPERATIVE														LESS CONSTRAINED, NON-COOP.	
	Name	VISAMC		VISA		MUGSHOT		MUGSHOT12+YRS		VISABORDER		BORDER		BORDER		KIOSKBORDER	
	FMR	0.0001		1E-06		1E-05		1E-05		1E-06		1E-06		1E-05		1E-06	
1365	vsoft-001	-		-		0.0707	1134	0.0877	1106	0.8390	1206	0.9519	1073	0.9506	1155	0.9655	662
1366	vsoft-002	-		-		0.0451	1101	0.0679	1085	0.0550	1024	0.3671	896	0.1633	949	0.8586	609
1367	vsoft-003	-		-		0.0326	1069	0.0563	1066	0.0526	1019	0.3671	897	0.1633	950	0.8586	610
1368	vts-000	0.0103	574	0.0174	598	0.0080	776	0.0129	792	0.0250	912	0.0450	644	0.0372	779	-	
1369	vts-001	0.0033	219	0.0048	228	0.0027	273	0.0036	332	0.0032	243	0.6519	969	0.3563	1019	0.9218	644
1370	vts-002	-		-		0.0025	159	0.0032	268	0.0030	209	0.0113	324	0.0042	106	0.1593	373
1371	wicket-000	0.0018	93	0.0028	90	0.0024	139	0.0027	154	0.0031	225	0.7968	1009	0.4340	1037	0.9788	675
1372	winsense-000	0.0140	665	0.0228	674	0.0125	926	0.0215	931	0.0226	885	0.8091	1013	0.0461	810	-	
1373	winsense-001	0.0062	417	0.0099	455	0.0092	822	0.0210	927	0.0093	635	0.0144	374	0.0098	419	-	
1374	winsense-002	0.0050	342	0.0073	352	0.0038	495	0.0059	548	0.0064	512	0.0118	338	0.0084	369	-	
1375	wiseai-001	0.0658	885	0.0964	882	0.7743	1271	0.8956	1269	0.1967	1111	0.7526	995	0.3419	1014	0.9695	665
1376	wuhantianyu-001	0.0163	702	0.0262	707	0.0281	1053	0.0569	1068	0.0316	954	0.0486	659	0.0344	763	0.2097	423
1377	x-laboratory-000	0.0071	466	0.0106	473	0.0123	922	0.0138	817	0.0419	988	0.5629	946	0.2852	995	-	
1378	x-laboratory-001	0.0059	399	0.0110	484	0.0054	639	0.0078	654	0.0094	639	0.0142	367	0.0100	427	-	
1379	xforwardai-000	0.0050	341	0.0072	344	0.0036	464	0.0051	490	0.0074	554	0.0136	358	0.0105	448	-	
1380	xforwardai-001	0.0021	110	0.0034	120	0.0027	281	0.0028	184	0.0046	401	0.0088	243	0.0079	343	-	
1381	xforwardai-002	0.0016	66	0.0023	56	0.0026	247	0.0025	115	0.0040	339	0.0081	211	0.0074	310	-	
1382	xm-000	0.0015	56	0.0026	75	0.0031	367	0.0038	358	0.0058	481	0.0105	301	0.0082	363	-	
1383	yisheng-000	0.1215	932	0.1990	936	-		-		-		-		-		-	
1384	yisheng-001	0.0892	909	0.1600	916	-		-		-		-		-		-	
1385	yisheng-002	0.2241	973	0.3795	991	-		-		-		-		-		-	
1386	yisheng-004	0.1988	967	0.3329	980	0.1147	1161	0.1849	1158	0.2044	1115	-		-		-	
1387	yitu-000	0.0284	802	0.0330	743	-		-		-		-		-		-	
1388	yitu-001	0.0050	334	0.0074	356	-		-		-		-		-		-	
1389	yitu-002	0.0025	155	0.0043	197	-		-		-		-		-		-	
1390	yitu-003	0.0015	62	0.0026	71	0.0066	714	0.0085	678	0.0064	514	0.0114	329	0.0103	442	-	
1391	yoonik-000	0.0070	456	0.0112	488	0.0074	751	0.0118	760	0.0564	1026	0.2013	816	0.1160	905	-	
1392	yoonik-001	0.0057	380	0.0079	376	0.0043	551	0.0061	560	0.0307	948	0.0762	724	0.0556	837	-	
1393	yoonik-002	0.0052	355	0.0062	304	0.0029	329	0.0034	300	0.0615	1035	0.1279	778	0.1166	906	0.2329	435
1394	yoonik-003	0.0034	229	0.0047	221	0.0032	390	0.0037	340	0.0816	1059	0.2033	820	0.1601	945	0.3210	475
1395	yoonik-004	0.0041	287	0.0059	286	0.0033	404	0.0052	494	0.0040	341	0.0071	170	0.0051	165	0.0732	158
1396	yoti-001	0.0139	664	0.0195	635	0.0110	887	0.0187	907	0.0191	848	0.1255	775	0.0415	794	0.5578	531
1397	yoti-002	-		-		0.0076	761	0.0137	813	0.0106	678	0.3375	880	0.1599	944	0.7672	581
1398	ytu-000	0.0057	382	0.0087	409	0.0121	919	0.0238	950	0.0047	410	0.0078	194	0.0059	225	-	
1399	yuan-000	0.0101	572	0.0168	591	0.0077	763	0.0127	785	0.0178	825	0.5189	935	0.0245	704	-	
1400	yuan-001	0.0116	610	0.0220	663	0.0114	902	0.0184	899	0.0149	774	0.0574	680	0.0160	584	-	
1401	yuan-002	0.0094	548	0.0154	567	0.0071	735	0.0110	748	0.0108	689	0.0348	596	0.0127	511	0.5738	535
1402	yuan-003	0.0078	493	0.0111	486	0.0062	696	0.0091	696	0.0106	679	0.0511	666	0.0123	503	0.7337	574
1403	yuan-004	0.0058	395	0.0078	371	0.0039	512	0.0055	517	0.0234	894	0.0442	640	0.0353	768	0.1673	387
1404	yuan-005	0.0037	258	0.0046	218	0.0027	282	0.0035	320	0.0033	255	0.2706	858	0.0876	881	0.6695	558
1405	yuan-006	0.0045	302	0.0062	299	0.0032	384	0.0049	463	0.0038	319	0.0084	225	0.0049	145	0.1211	315
1406	yuan-007	0.0046	312	0.0069	333	0.0045	563	0.0075	632	0.0072	543	0.0144	373	0.0076	324	0.1081	282
1407	yuan-008	0.0032	208	0.0043	187	0.0026	225	0.0034	291	0.0028	182	0.0059	119	0.0039	82	0.0891	227
1408	yuan-009	-		-		0.0028	295	0.0042	408	0.0030	213	0.0057	106	0.0040	92	0.0733	160

Table 86: FNMR is the proportion of mated comparisons below a threshold set to achieve the FMR given in the header on the fourth row. FMR is the proportion of impostor comparisons at or above that threshold. The light grey values give rank over all algorithms in that column. The pink columns use only same-sex impostors; others are selected regardless of demographics. The exception, in the green column, uses "matched-covariates" i.e. impostors of the same sex, age group, and country of birth. The second pink column includes effects of extended ageing. Missing entries for border, visa, mugshot and wild images generally mean the algorithm did not run to completion. The VISA *columns compare images described in section 2.1. The* MUGSHOT *columns compare images described in section 2.5. The* VISA-BORDER *column compare images described in section 2.2 with those of section 2.4. The* BORDER *column compares images described in section 2.4. The* KIOSK-BORDER *columns compare images described in section 2.6 with those of section 2.4.*

		FALSE NON-MATCH RATE (FNMR)															
	Algorithm	CONSTRAINED, COOPERATIVE														LESS CONSTRAINED, NON-COOP.	
	Name	VISAMC		VISA		MUGSHOT		MUGSHOT12+YRS		VISABORDER		BORDER		BORDER		KIOSKBORDER	
	FMR	0.0001		1E-06		1E-05		1E-05		1E-06		1E-06		1E-05		1E-06	
1409	yuan-010	-		-		0.0028	292	0.0041	387	0.0030	224	0.0058	113	0.0041	99	0.0748	173
1410	yuanli-001	-		-		0.0203	1008	0.0399	1018	0.0110	695	0.0168	424	0.0135	529	0.1476	360

Table 87: FNMR is the proportion of mated comparisons below a threshold set to achieve the FMR given in the header on the fourth row. FMR is the proportion of impostor comparisons at or above that threshold. The light grey values give rank over all algorithms in that column. The pink columns use only same-sex impostors; others are selected regardless of demographics. The exception, in the green column, uses "matched-covariates" i.e. impostors of the same sex, age group, and country of birth. The second pink column includes effects of extended ageing. Missing entries for border, visa, mugshot and wild images generally mean the algorithm did not run to completion. The VISA *columns compare images described in section 2.1. The* MUGSHOT *columns compare images described in section 2.5. The* VISA-BORDER *column compare images described in section 2.2 with those of section 2.4. The* BORDER *column compares images described in section 2.4. The* KIOSK-BORDER *columns compare images described in section 2.6 with those of section 2.4.*

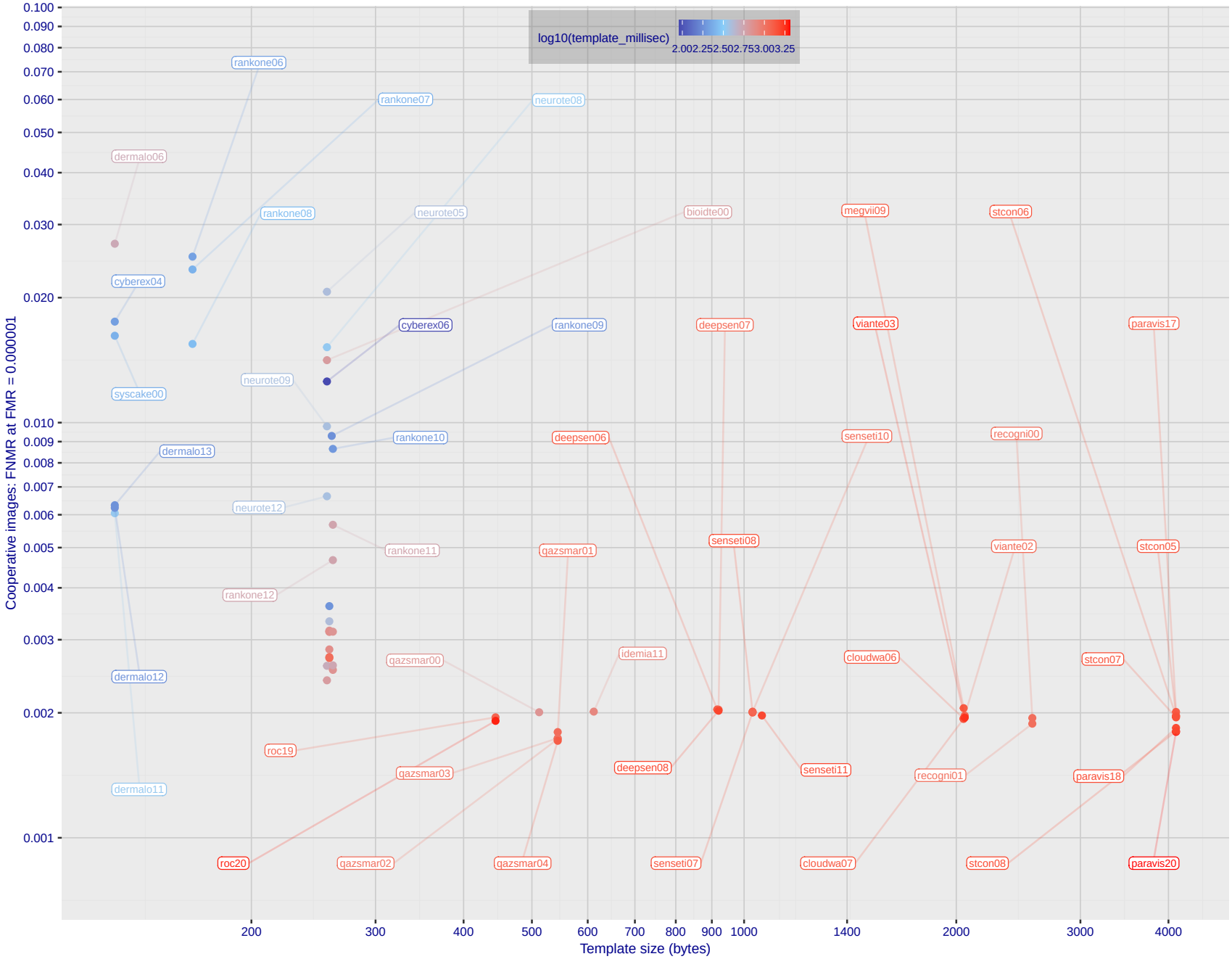

Figure 1: The points show false non-match rates (FNMR) versus the size of the encoded template. FNMR is the geometric mean of FNMR values for visa-border and mugshot images (from Figs. 218 and 284) at the false match rate (FMR) given in the y-axis label. The color of the points encodes template generation time - which spans at least one order of magnitude. Durations are measured on a single core of a c. 2016 Intel Xeon CPU E5-2630 v4 running at 2.20GHz. Algorithms with poor FNMR are omitted.

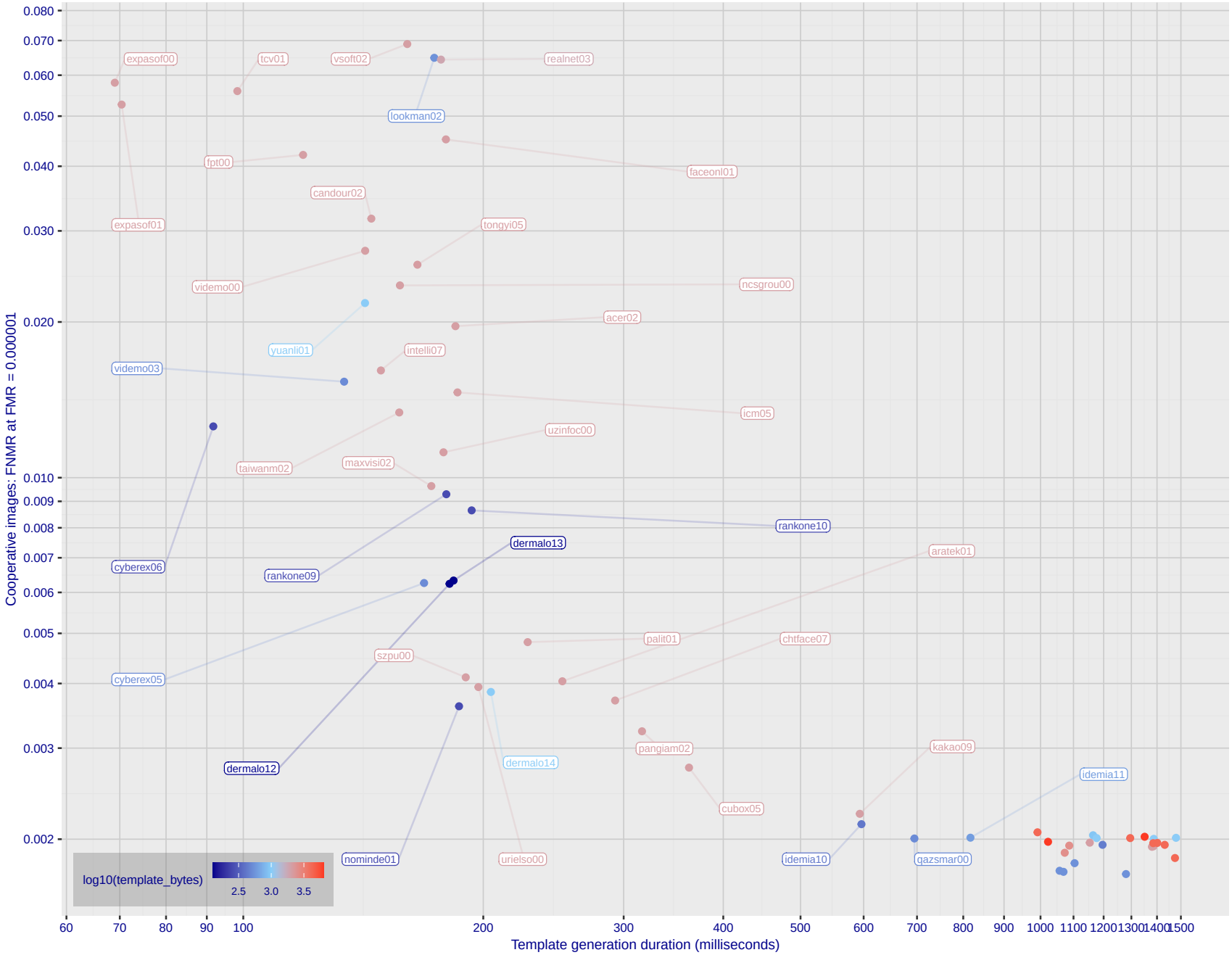

Figure 2: The points show false non-match rates (FNMR) versus the duration of the template generation operation. FNMR is the geometric mean of FNMR values for visa-border and mugshot images (from Figs. 218 and 284) at a false match rate (FMR) given in the y-axis label. Template generation time is a median estimated over 640 x 480 pixel portraits. It is measured on a single core of a c. 2016 Intel Xeon CPU E5-2630 v4 running at 2.20GHz. The color of the points encodes template size - which spans two orders of magnitude. Algorithms with poor FNMR are omitted.

1 Metrics

1.1 Core accuracy

Given a vector of N genuine scores, u, the false non-match rate (FNMR) is computed as the proportion below some threshold, T:

$$\text{FNMR}(T) = 1 - \frac{1}{N}\sum_{i=1}^{N} H(u_i - T) \tag{1}$$

where $H(x)$ is the unit step function, and $H(0)$ taken to be 1.

Similarly, given a vector of N impostor scores, v, the false match rate (FMR) is computed as the proportion above T:

$$\text{FMR}(T) = \frac{1}{N}\sum_{i=1}^{N} H(v_i - T) \tag{2}$$

The threshold, T, can take on any value. We typically generate a set of thresholds from quantiles of the observed impostor scores, v, as follows. Given some interesting false match rate range, $[\text{FMR}_L, \text{FMR}_U]$, we form a vector of K thresholds corresponding to FMR measurements evenly spaced on a logarithmic scale

$$T_k = Q_v(1 - \text{FMR}_k) \tag{3}$$

where Q is the quantile function, and FMR_k comes from

$$\log_{10}\text{FMR}_k = \log_{10}\text{FMR}_L + \frac{k}{K}\,[\log_{10}\text{FMR}_U - \log_{10}\text{FMR}_L] \tag{4}$$

Error tradeoff characteristics are plots of FNMR(T) vs. FMR(T). These are plotted with $\text{FMR}_U \to 1$ and FMR_L as low as is sustained by the number of impostor comparisons, N. This is somewhat higher than the "rule of three" limit $3/N$ because samples are not independent, due to re-use of images.

1.2 Multi-template scoring methodology

There are some scenarios when one or more people exist and are detected in an image, and some of the proposed test images include K $>$ 1 persons for some images and situations where the subject of interest may or may not be the foreground face (largest face in the image). The NIST FRTE 1:1 API supports this by allowing generation of multiple templates representing each person detected in an image. When this occurs, NIST will match all templates generated from the enrollment image with all templates generated from the verification image and use the **maximum** similarity score across all template comparisons. This scoring approach will be used in our calculation of FMR and FNMR (this applies to both genuine and imposter comparisons).

2 Datasets

2.1 Visa images

- The number of images is on the order of 10^5.
- The number of subjects is on the order of 10^5.
- The number of subjects with two images is on the order of 10^4.
- The images have geometry in reasonable conformance with the ISO/IEC 19794-5 Full Frontal image type. Pose is generally excellent.
- The images are of size 252x300 pixels. The mean interocular distance (IOD) is 69 pixels.
- The images are of subjects from greater than 100 countries, with significant imbalance due to visa issuance patterns.
- The images are of subjects of all ages, including children, again with imbalance due to visa issuance demand.
- Many of the images are live capture. A substantial number of the images are photographs of paper photographs.
- When these images are input to the algorithm, they are labelled as being of type "ISO" - see Table 4 of the FRTE API.

2.2 Application images

- The number of images is on the order of 10^6.
- The number of subjects is on the order of 10^6.
- The number of subjects with two images is on the order of 10^6.
- The images have geometry in good conformance with the ISO/IEC 19794-5 Full Frontal image type. Pose is generally excellent.
- The images are of size 300x300 pixels. The mean interocular distance (IOD) is 61 pixels.
- The images are of subjects from greater than 100 countries, with significant imbalance due to population and immigration patterns.
- The images are of subjects of adults.
- All of the images are live capture.
- When these images are input to the algorithm, they are labelled as being of type "ISO" - see Table 4 of the FRTE API.

2.3 Application images with head yaw

- The number of images is on the order of 10^5.
- The number of subjects is on the order of 10^5.
- The number of subjects with two images is on the order of 10^5.
- The images have geometry in good conformance with the ISO/IEC 19794-5 Full Frontal image type *except* the yaw angle is between 25 and 85 degrees. Our pose estimates are approximate, with an angular error that increases with yaw. The angular estimates will be improved over time.
- The images are of size 300x300 pixels. The mean interocular distance (IOD), if frontal, would be about pixels, but reduces with cosine of yaw.
- The images are of subjects from greater than 100 countries, with significant imbalance due to population and immigration patterns.

- ▷ The images are of subjects of adults.
- ▷ All of the images are live capture.
- ▷ When these images are input to the algorithm, they are labelled as being of type "WILD" - see Table 4 of the FRTE API.

2.4 Border crossing images

- ▷ The number of images is on the order of 10^6.
- ▷ The number of subjects is on the order of 10^6.
- ▷ The number of subjects with two images is on the order of 10^6.
- ▷ The images are taken with at camera oriented by an attendant toward a cooperating subject. This is done under time constraints so there are role, pitch and yaw angle variations. Also background illumination is sometimes strong, so the face is under-exposed. There is some perspective distortion due to close range images. Some faces are partially cropped.
- ▷ The images have mean IOD of 38 pixels.
- ▷ The images are of subjects of adults and childen aged 12 or above.
- ▷ The images are of subjects from greater than 100 countries, with significant imbalance due to population and immigration patterns.
- ▷ The images are all live capture.
- ▷ When these images are input to the algorithm, they are labelled as being of type "WILD" - see Table 4 of the FRTE API.

2.5 Mugshot images

- ▷ The number of images is on the order of 10^6.
- ▷ The number of subjects is on the order of 10^6.
- ▷ The number of subjects with two images is on the order of 10^6.
- ▷ The images have geometry in reasonable conformance with the ISO/IEC 19794-5 Full Frontal image type.
- ▷ The images are of variable sizes. The median IOD is 105 pixels. The mean IOD is 113 pixels. The 1-st, 5-th, 10-th, 25-th, 75-th, 90-th and 99-th percentiles are 34, 58, 70, 87, 121, 161 and 297 pixels.
- ▷ The images are of subjects from the United States.
- ▷ The images are of adults.
- ▷ The images are all live capture.
- ▷ When these images are input to the algorithm, they are labelled as being of type "mugshot" - see Table 4 of the FRTE API.

2.6 Kiosk images

- ▷ The number of images is on the order of 10^6.
- ▷ The number of subjects is on the order of 10^5.
- ▷ The number of subjects with multiple images is the order of 10^5.

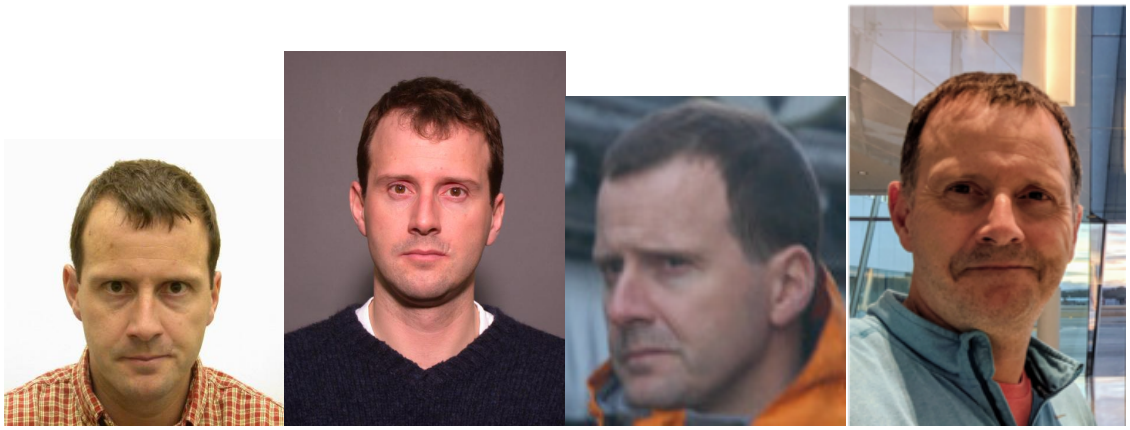

(a) Visa (b) Mugshot (c) Wild (d) Border

Figure 3: The figure gives simulated samples of image types used in this report.

- The images are taken at kiosk equipped with a camera intended to capture a centered face. However the images have specific quality defects arising from the camera triggering before the subject looks at it. These are downward pitch of the face relative to the optical axis; cropping of the forehead; and cropping of left or right part of the face. Partial cropping affects perhaps 10% of the images. Resolution does not vary widely.
- The images are of adults.
- The images have mean IOD of 44 pixels, with maximum below 75, and minimum when both eyes are present above 25 pixels.
- All of the images are live capture, none are scanned.
- When these images are input to the algorithm, they are labelled as being of type "WILD" - see Table 4 of the FRTE API.

2.7 Wild images

- The number of images is on the order of 10^5.
- The number of subjects is on the order of 10^4.
- The number of subjects with two images on the order of 10^4.
- The images include many photojournalism-style images. Images are given to the algorithm using a variable but generally tight crop of the head. Resolution varies very widely. The images are very unconstrained, with wide yaw and pitch pose variation. Faces can be occluded, including hair and hands.
- The images are of adults.
- All of the images are live capture, none are scanned.
- When these images are input to the algorithm, they are labelled as being of type "WILD" - see Table 4 of the FRTE API.

3 Results

3.1 Test goals

- To state absolute accuracy for different kinds of images, including those with and without subject cooperation.

FNMR(T) "False non-match rate"
FMR(T) "False match rate"

- To state comparative accuracy, across algorithms.

3.2 Test design

Method: For visa images:

- The comparisons are of visa photos against visa photos.
- The number of genuine comparisons is on the order of 10^4.
- The number of impostor comparisons is on the order of 10^{10}.
- The comparisons are fully zero-effort, meaning impostors are paired without attention to sex, age or other covariates. However, later analysis is conducted on subsets.
- The number of persons is on the order of 10^5.
- The number of images used to make a template is one.
- The number of templates used to make each comparison score is two corresponding to simple one-to-one verification.

Method: For mugshot images:

- The comparisons are of mugshot photos against mugshot photos.
- The number of genuine comparisons is on the order of 10^6.
- The number of impostor comparisons is on the order of 10^8.
- The impostors are paired by sex, but not by age or other covariates.
- The number of persons is on the order of 10^6.
- The number of images used to make a template is one.
- The number of templates used to make each comparison score is two, corresponding to simple one-to-one verification.

Method: For visa-border comparisons:

- The comparisons are of visa-like frontals against border crossing webcam photos.
- The number of genuine comparisons is on the order of 10^6.
- The number of impostor comparisons is on the order of 10^8.
- The impostors are paired by sex, but not by age or other covariates.
- The number of persons is on the order of 10^6.
- The number of images used to make a template is one.
- The number of templates used to make each comparison score is two, corresponding to simple one-to-one verification.

Method: For visa-border non-frontal yaw comparisons:

- The comparisons are of visa-like images with yaw 25 to 85 degrees against border crossing webcam photos.
- The number of genuine comparisons is on the order of 10^5.
- The number of impostor comparisons is on the order of 10^8.
- The impostors are paired by sex, but not by age or other covariates.

FNMR(T) "False non-match rate"
FMR(T) "False match rate"

- ▷ The number of persons is on the order of 10^5.
- ▷ The number of images used to make a template is one.
- ▷ The number of templates used to make each comparison score is two, corresponding to simple one-to-one verification.

Method: For kiosk-border comparisons:

- ▷ The comparisons are of visa-like frontals against kiosk-style photos.
- ▷ The number of genuine comparisons is on the order of 10^6.
- ▷ The number of impostor comparisons is on the order of 10^8.
- ▷ The impostors are paired by sex, but not by age or other covariates.
- ▷ The number of persons is on the order of 10^5.
- ▷ The number of images used to make a template is one.
- ▷ The number of templates used to make each comparison score is two, corresponding to simple one-to-one verification.

Method: For border-border comparisons:

- ▷ The comparisons are of border crossing webcam photos.
- ▷ The number of genuine comparisons is on the order of 10^6.
- ▷ The number of impostor comparisons is on the order of 10^8.
- ▷ The impostors are paired by sex, but not by age or other covariates.
- ▷ The number of persons is on the order of 10^6.
- ▷ The number of images used to make a template is one.
- ▷ The number of templates used to make each comparison score is two corresponding to simple one-to-one verification.

Method: For wild images:

- ▷ The comparisons are of wild photos against wild photos.
- ▷ The number of genuine comparisons is on the order of 10^6.
- ▷ The number of impostor comparisons is on the order of 10^8.
- ▷ The comparisons are fully zero-effort, meaning impostors are paired without attention to sex, age or other covariates.
- ▷ The number of persons is on the order of 10^4.
- ▷ The number of images used to make a template is one.
- ▷ The number of templates used to make each comparison score is two corresponding to simple one-to-one verification.

Method: For child exploitation images:

- ▷ The comparisons are of unconstrained child exploitation photos against others of the same type.
- ▷ The number of genuine comparisons is on the order of 10^4.
- ▷ The number of impostor comparisons is on the order of 10^7.

- ▷ The comparisons are fully zero-effort, meaning impostors are paired without attention to sex, age or other covariates.
- ▷ The number of persons is on the order of 10^3.
- ▷ The number of images used to make 1 template is 1.
- ▷ The number of templates used to make each comparison score is two corresponding to simple one-to-one verification.
- ▷ We produce two performance statements. First, is a DET as used for visa and mugshot images. The second is a cumulative match characteristic (CMC) summarizing a simulated one-to-many search process. This is done as follows.
  - We regard M enrollment templates as items in a gallery.
  - These M templates come from $M > N$ individuals, because multiple images of a subject are present in the gallery under separate identifiers.
  - We regard the verification templates as search templates.
  - For each search we compute the rank of the highest scoring mate.
  - This process should properly be conducted with a 1:N algorithm, such as those tested in NIST IR 8009. We use the 1:1 algorithms in a simulated 1:N mode here to a) better reflect what a child exploitation analyst does, and b) to show algorithm efficacy is better than that revealed in the verification DETs.

FNMR(T) "False non-match rate"
FMR(T) "False match rate"

3.3 Failure to enroll

FNMR(T) "False non-match rate"
FMR(T) "False match rate"

	Algorithm	Failure to Enrol Rate[1]									
	Name	APPLICATION		BORDER		KIOSK		MUGSHOT		VISA	
	Name	SEC. 2.2		SEC. 2.4		SEC. 2.6		SEC. 2.5		SEC. 2.1	
1	2060io-001	0.0160	1247	0.0998	1247	0.4698	890	0.0193	1307	-	1247
2	2060io-002	0.0000	977	0.0015	893	0.0238	588	0.0028	1264	-	1301
3	20face-000	0.0000	685	0.0008	647	0.0217	539	0.0000	340	0.0004	614
4	20face-001	0.0000	807	0.0008	648	0.0000	69	0.0000	343	0.0004	615
5	3divi-000	-	1293	-	1306	-	1312	-	1401	0.0008	933
6	3divi-001	-	1303	-	1287	-	1354	-	1396	0.0007	923
7	3divi-002	-	1344	-	1330	-	987	-	1324	0.0010	952
8	3divi-003	0.0001	1160	0.0059	1147	-	1349	0.0007	1148	0.0006	892
9	3divi-004	0.0001	1161	0.0059	1148	-	1388	0.0008	1163	0.0006	899
10	3divi-005	0.0000	845	0.0008	618	-	1214	0.0000	476	0.0002	272
11	3divi-006	0.0000	651	0.0007	567	0.0214	535	0.0001	677	0.0002	277
12	3divi-007	0.0000	806	0.0007	568	0.0214	536	0.0001	679	0.0002	278
13	accurascan-001	0.0001	1150	0.0060	1151	0.0838	852	0.0006	1137	0.0022	1030
14	accurascan-002	0.0001	1151	0.0060	1152	0.0838	851	0.0006	1136	0.0022	1031
15	accurascan-003	0.0000	615	0.0009	732	0.0226	557	0.0000	480	0.0003	395
16	acer-000	0.0000	1009	0.0024	1006	-	1209	0.0002	861	0.0004	732
17	acer-001	0.0000	494	0.0011	803	-	1178	0.0001	600	0.0004	640
18	acer-002	0.0000	1065	0.0008	631	0.0191	477	0.0003	950	0.0004	646
19	acisw-003	0.0000	336	0.0000	132	-	993	0.0000	37	0.0000	124
20	acisw-006	0.0000	159	0.0000	95	-	1324	0.0000	276	0.0000	91
21	acisw-007	0.0000	103	0.0000	15	0.0000	114	0.0000	176	0.0000	18
22	acisw-008	0.0000	741	0.0009	711	0.0173	423	0.0004	1046	0.0004	438
23	adera-001	0.0000	1011	0.0034	1077	-	1358	0.0003	970	0.0005	858
24	adera-002	0.0000	1013	0.0034	1079	-	1008	0.0003	968	0.0005	859
25	adera-003	0.0000	1012	0.0034	1078	0.0403	758	0.0003	969	0.0005	857
26	adera-004	0.0000	636	0.0008	628	0.0202	495	0.0003	1001	0.0004	559
27	adera-005	0.0000	527	0.0008	627	0.0202	494	0.0003	1000	0.0004	558
28	advance-002	0.0000	541	0.0013	867	-	1245	0.0000	561	0.0004	638
29	advance-003	0.0000	985	0.0012	827	0.0247	601	0.0001	740	0.0004	745
30	advance-004	0.0001	1157	0.0010	777	0.0157	393	0.0008	1173	0.0006	901
31	advance-005	0.0000	790	0.0003	305	0.0074	221	0.0002	851	0.0003	290
32	advance-006	0.0001	1153	0.0012	840	0.0202	493	0.0008	1170	-	1226
33	affinsys-ai-000	0.0000	1072	0.0068	1155	0.0641	812	0.0016	1229	-	1111
34	afisbiometrics-000	0.0000	618	0.0008	605	0.0213	533	0.0000	354	0.0004	641
35	afrengine-000	0.0000	546	0.0015	897	0.0254	621	0.0008	1171	0.0004	501
36	afrengine-001	0.0000	683	0.0007	587	0.0183	446	0.0005	1080	0.0004	744
37	afrengine-002	0.0000	551	0.0007	585	0.0183	447	0.0005	1082	0.0004	740
38	afrengine-003	0.0000	515	0.0099	1181	0.0384	742	0.0005	1083	-	1158
39	afrengine-004	0.0000	817	0.1602	1251	0.0528	788	0.0005	1081	-	1334
40	afrengine-005	0.0000	681	0.0012	837	0.0232	580	0.0006	1121	-	1302
41	aifirst-001	0.0000	71	0.0000	5	-	1230	0.0000	160	0.0000	6
42	aigen-001	0.0000	394	0.0000	215	-	1063	0.0000	115	0.0000	216
43	aigen-002	0.0000	60	0.0000	51	0.0000	103	0.0000	204	0.0000	52
44	aigroup-000	0.0000	67	0.0005	403	0.0103	275	0.0000	158	-	1099
45	aigroup-001	0.0000	863	0.0005	418	0.0104	278	0.0001	795	-	1221
46	aigroup-002	0.0000	229	0.0003	333	0.0083	249	0.0001	681	-	1282
47	ailabs-001	0.0000	496	0.0090	1178	-	1181	0.0007	1161	0.0005	797
48	aimall-001	0.0000	83	0.0000	10	-	1248	0.0000	151	0.0000	12
49	aimall-002	0.0000	1015	0.0043	1112	-	1215	0.0012	1205	0.0005	848
50	aimall-003	0.0000	938	0.0012	841	-	1385	0.0004	1023	0.0005	780
51	aiseemu-001	0.0000	366	0.0000	136	0.0000	47	0.0000	20	0.0000	126
52	aiseemu-002	0.0000	204	0.0000	67	0.0000	141	0.0000	240	0.0000	66
53	aiunionface-000	0.0000	467	0.0000	195	-	1135	0.0000	110	0.0000	192
54	aize-001	0.0001	1159	0.0040	1095	0.0652	814	0.0026	1260	0.0022	1029
55	aize-002	0.0000	74	0.0014	885	0.0230	575	0.0005	1119	0.0004	604
56	aize-003	0.0000	156	0.0000	248	0.0001	150	0.0000	274	0.0000	241
57	aize-006	0.0000	642	0.0004	351	0.0090	264	0.0001	793	-	1209
58	ajou-001	0.0000	764	0.0020	972	-	1062	0.0001	683	0.0004	753

Table 88: FTE is the proportion of failed template generation attempts. Failures can occur because the software throws an exception, or because the software electively refuses to process the input image. This would typically occur if a face is not detected. FTE is measured as the number of function calls that give EITHER a non-zero error code OR that give a "small" template. This is defined as one whose size is less than 0.3 times the median template size for that algorithm. This second rule is needed because some algorithms incorrectly fail to return a non-zero error code when template generation fails.
A hyphen "-" indicates the dataset was not produced. [1]The effects of FTE are included in the accuracy results of this report by regarding any template comparison involving a failed template to produce a low similarity score. Thus higher FTE results in higher FNMR and lower FMR.

FNMR(T) "False non-match rate"
FMR(T) "False match rate"

	Algorithm	Failure to Enrol Rate[1]									
	Name	APPLICATION		BORDER		KIOSK		MUGSHOT		VISA	
	Name	SEC. 2.2		SEC. 2.4		SEC. 2.6		SEC. 2.5		SEC. 2.1	
59	alchera-000	0.0000	1118	0.0041	1107	-	1279	0.0004	1044	0.0014	1006
60	alchera-001	0.0000	1119	0.0041	1108	-	1328	0.0004	1045	0.0014	1007
61	alchera-002	0.0000	697	0.0008	658	-	950	0.0001	758	0.0004	493
62	alchera-003	0.0001	1180	0.0013	863	0.0317	677	0.0002	888	0.0004	660
63	alchera-004	0.0000	613	0.0009	704	0.0228	567	0.0001	767	0.0004	507
64	alchera-005	0.0000	630	0.0009	705	0.0228	568	0.0001	766	0.0004	508
65	alchera-006	0.0000	834	0.0009	708	0.0228	564	0.0001	759	0.0004	522
66	alchera-007	0.0000	543	0.0009	702	0.0228	566	0.0001	763	0.0004	502
67	alchera-008	0.0000	695	0.0009	707	0.0228	561	0.0001	757	-	1315
68	alchera-009	0.0000	492	0.0004	387	0.0112	304	0.0002	869	-	1138
69	alfabeta-001	0.0005	1204	0.0650	1237	0.2142	881	0.0024	1253	0.0018	1020
70	alice-000	0.0000	276	0.0006	469	0.0133	337	0.0000	413	0.0004	494
71	alice-001	0.0000	348	0.0006	468	0.0133	338	0.0000	409	0.0004	490
72	alleyes-000	0.0000	735	0.0010	753	-	1003	0.0002	796	0.0004	692
73	allgovision-000	0.0007	1212	0.0062	1153	-	1199	0.0026	1258	0.0052	1069
74	alphaface-001	0.0000	553	0.0012	815	-	1261	0.0000	571	0.0004	686
75	alphaface-002	0.0000	666	0.0012	816	-	910	0.0000	565	0.0004	694
76	alttekglobal-000	0.0000	498	0.0020	964	0.0471	772	0.0000	575	-	1147
77	amplifiedgroup-001	0.0114	1243	0.1023	1248	-	1235	0.0189	1306	0.0279	1084
78	androvideo-000	0.0000	235	0.0000	142	-	900	0.0000	52	0.0000	135
79	anke-000	-	1340	-	1321	-	972	-	1315	0.0021	1025
80	anke-001	-	1356	-	1340	-	1019	-	1319	0.0047	1068
81	anke-002	-	1269	-	1281	-	1218	0.0004	1029	0.0009	939
82	anke-003	-	1312	-	1289	-	1375	0.0001	707	0.0004	578
83	anke-004	0.0000	787	0.0011	798	-	1082	0.0001	709	0.0004	718
84	anke-005	0.0000	711	0.0012	823	-	973	0.0001	746	0.0004	735
85	antheus-000	0.0000	102	0.0000	11	-	1268	0.0000	170	0.0000	22
86	antheus-001	0.0000	169	0.0000	102	-	1336	0.0000	268	0.0000	97
87	antheus-002	0.0000	1105	0.0015	895	0.0213	527	0.0044	1281	-	1311
88	anyvision-001	-	1372	-	1399	-	1066	-	1360	0.0091	1077
89	anyvision-002	0.0060	1233	0.0230	1208	-	1386	0.0070	1294	0.0090	1076
90	anyvision-004	0.0000	981	0.0017	931	-	1001	0.0001	747	0.0004	629
91	anyvision-005	0.0000	753	0.0013	850	-	1048	0.0000	486	0.0004	499
92	aratek-001	0.0000	35	0.0000	39	0.0000	95	0.0000	180	0.0000	37
93	armatura-001	0.0000	1039	0.0021	983	0.0257	627	0.0005	1103	0.0005	819
94	armatura-002	0.0000	973	0.0018	937	0.0206	505	0.0003	1002	0.0004	741
95	armatura-003	0.0000	586	0.0012	828	0.0333	705	0.0004	1038	0.0004	586
96	arvis-000	0.0008	1216	0.0014	878	0.0195	485	0.0083	1296	-	1404
97	asr-000	0.0000	873	0.0007	570	0.0152	376	0.0002	914	-	1185
98	asr-001	0.0000	854	0.0006	509	0.0138	344	0.0002	932	-	1126
99	asusaics-000	0.0000	175	0.0000	99	-	1347	0.0000	266	0.0000	94
100	asusaics-001	0.0000	45	0.0000	48	-	1201	0.0000	209	0.0000	46
101	autentika-000	0.0000	358	0.0000	139	0.0000	44	0.0000	27	0.0000	131
102	autentika-001	0.0000	15	0.0000	27	0.0000	88	0.0000	194	0.0000	30
103	autentika-002	0.0000	365	0.0000	137	0.0000	46	0.0000	21	0.0000	127
104	autentika-003	0.0000	225	0.0000	151	0.0000	5	0.0000	55	-	1287
105	authenmetric-002	0.0000	441	0.0000	176	-	1109	0.0000	89	0.0000	173
106	authenmetric-003	0.0000	386	0.0000	220	0.0000	53	0.0000	122	0.0000	219
107	authenmetric-004	0.0000	176	0.0000	57	0.0000	134	0.0000	225	0.0000	56
108	authme-001	0.0000	1073	0.0009	725	0.0245	598	0.0003	991	0.0005	781
109	authme-002	0.0000	875	0.0007	593	0.0179	436	0.0001	742	-	1176
110	aware-000	-	1371	-	1398	-	1059	-	1361	0.0005	803
111	aware-001	-	1383	-	1366	-	1103	-	1345	0.0002	261
112	aware-002	-	1280	-	1271	-	1263	-	1382	0.0006	872
113	aware-003	-	1382	-	1365	-	1102	0.0016	1227	0.0013	996
114	aware-004	0.0000	923	0.0023	996	-	1143	0.0002	826	0.0005	784
115	aware-005	0.0000	892	0.0020	968	-	938	0.0001	790	0.0004	715
116	aware-006	0.0000	493	0.0009	691	0.0249	606	0.0000	500	0.0004	619

Table 89: FTE is the proportion of failed template generation attempts. Failures can occur because the software throws an exception, or because the software electively refuses to process the input image. This would typically occur if a face is not detected. FTE is measured as the number of function calls that give EITHER a non-zero error code OR that give a "small" template. This is defined as one whose size is less than 0.3 times the median template size for that algorithm. This second rule is needed because some algorithms incorrectly fail to return a non-zero error code when template generation fails.
A hyphen "-" indicates the dataset was not produced. [1]The effects of FTE are included in the accuracy results of this report by regarding any template comparison involving a failed template to produce a low similarity score. Thus higher FTE results in higher FNMR and lower FMR.

	Algorithm	Failure to Enrol Rate[1]									
	Name	APPLICATION		BORDER		KIOSK		MUGSHOT		VISA	
	Name	SEC. 2.2		SEC. 2.4		SEC. 2.6		SEC. 2.5		SEC. 2.1	
117	aware-007	0.0000	621	0.0012	829	0.0325	691	0.0000	514	0.0004	659
118	aware-008	0.0000	822	0.0012	835	0.0327	693	0.0000	506	-	1330
119	awiros-001	0.0039	1225	0.0369	1225	-	1306	0.0386	1310	0.0872	1089
120	awiros-002	0.0000	1070	0.0038	1091	-	1399	0.0007	1157	0.0012	995
121	awiros-003	0.0000	37	0.0000	45	0.0000	97	0.0000	212	-	1164
122	awiros-004	0.0000	64	0.0000	53	0.0000	104	0.0000	200	-	1167
123	aximetria-001	0.0000	882	0.0010	782	0.0217	540	0.0001	792	0.0004	609
124	ayftech-001	0.0002	1188	0.0046	1119	-	952	0.0043	1280	0.0011	960
125	ayftech-003	0.0000	281	0.0006	523	0.0123	320	0.0000	69	0.0000	169
126	ayonix-000	0.0053	1230	0.0341	1221	-	1187	0.0113	1301	0.0137	1079
127	beethedata-000	0.0005	1201	0.0042	1110	0.0366	727	0.0002	833	0.0010	948
128	betaface-000	-	1393	-	1377	-	1131	-	1359	0.0011	965
129	betaface-002	-	1261	-	1277	-	1185	-	1386	0.0010	950
130	beyneai-000	0.0000	44	0.0000	49	0.0000	99	0.0000	210	0.0000	47
131	biocube-001	0.0006	1207	0.0391	1226	0.1207	862	0.0015	1221	0.0020	1024
132	biocube-002	0.0000	678	0.0046	1122	0.0721	840	0.0008	1169	0.0012	985
133	bioid-001	0.0005	1203	0.0019	960	0.0324	690	0.0005	1093	-	1397
134	bioid-002	0.0000	16	0.0000	28	0.0000	89	0.0000	188	-	1130
135	bioid-003	0.0000	415	0.0000	224	0.0000	59	0.0000	139	-	1392
136	bioid-004	0.0000	371	0.0000	211	0.0000	49	0.0000	129	-	1372
137	bioidtechswiss-000	0.0000	530	0.0008	611	-	1223	0.0003	961	0.0004	746
138	bioidtechswiss-001	0.0000	625	0.0007	559	-	1364	0.0000	453	0.0004	677
139	bioidtechswiss-002	0.0000	596	0.0007	566	-	1325	0.0000	470	0.0004	662
140	bioidtechswiss-003	0.0000	937	0.0202	1203	0.0980	858	0.0005	1096	-	1181
141	biometric-vision-000	0.0000	547	0.0005	415	0.0107	293	0.0002	917	0.0004	530
142	biometrik-001	0.0000	25	0.0000	42	0.0000	93	0.0000	184	-	1142
143	biometrik-002	0.0000	333	0.0000	130	0.0000	37	0.0000	38	-	1269
144	bm-001	0.0000	425	0.0000	229	-	1093	0.0000	292	0.0000	228
145	boetech-001	0.0087	1240	0.0272	1213	0.2117	878	0.0032	1268	0.0160	1081
146	boetech-002	0.0087	1239	0.0272	1212	0.2117	879	0.0032	1269	0.0160	1080
147	bresee-000	0.0000	514	0.0010	768	-	1200	0.0002	835	0.0003	354
148	bresee-001	0.0000	614	0.0010	769	-	1352	0.0002	836	0.0003	356
149	bresee-002	0.0000	995	0.0020	976	0.0219	547	0.0008	1162	0.0004	581
150	btsdigital-001	0.0000	40	0.0009	688	0.0265	637	0.0000	404	-	1163
151	cakevn-001	0.0000	144	0.0007	575	0.0130	332	0.0000	248	-	1227
152	camvi-001	-	1301	-	1314	-	1340	-	1408	0.0010	956
153	camvi-002	0.0000	251	0.0000	156	-	920	0.0000	39	0.0000	146
154	camvi-003	-	1302	-	1315	-	1345	0.0000	264	0.0000	95
155	camvi-004	0.0000	145	0.0000	244	-	1308	0.0000	246	0.0000	86
156	candour-001	0.0000	418	0.0000	226	0.0000	61	0.0000	142	0.0000	221
157	candour-002	0.0000	59	0.0000	50	0.0000	102	0.0000	203	-	1170
158	candour-003	0.0000	458	0.0000	185	0.0000	73	0.0000	83	-	1331
159	candour-004	0.0000	436	0.0000	180	0.0000	67	0.0000	91	-	1329
160	canon-002	0.0000	26	0.0000	43	-	1188	0.0000	185	0.0000	41
161	canon-003	0.0000	791	0.0008	607	0.0234	583	0.0000	549	0.0004	657
162	canon-004	0.0000	766	0.0008	606	0.0234	582	0.0000	548	0.0004	655
163	canon-005	0.0000	298	0.0044	1114	0.0269	642	0.0000	435	0.0004	537
164	cchonolulu-000	0.0054	1231	0.0395	1228	0.2802	886	0.0036	1272	0.0012	983
165	cchonolulu-001	0.0056	1232	0.0414	1229	0.2894	888	0.0038	1277	0.0012	987
166	cdachyd-001	0.0005	1202	0.0639	1233	0.2112	877	0.0023	1248	-	1361
167	ceiec-001	-	1337	-	1319	-	964	0.0029	1266	0.0023	1035
168	ceiec-002	0.0002	1187	0.0056	1144	-	1392	0.0036	1273	0.0031	1051
169	ceiec-003	0.0000	311	0.0013	871	-	967	0.0001	621	0.0004	681
170	ceiec-004	0.0000	335	0.0008	644	-	990	0.0000	473	0.0004	513
171	celloscope-001	0.0000	1060	0.0056	1143	0.0540	790	0.0022	1245	-	1357
172	chosun-000	0.0000	250	0.0000	157	-	919	0.0000	40	0.0000	147
173	chosun-001	0.0000	487	0.0000	200	-	1167	0.0000	96	0.0000	198
174	chosun-002	0.0000	399	0.0000	217	-	1067	0.0000	117	0.0000	213

Table 90: FTE is the proportion of failed template generation attempts. Failures can occur because the software throws an exception, or because the software electively refuses to process the input image. This would typically occur if a face is not detected. FTE is measured as the number of function calls that give EITHER a non-zero error code OR that give a "small" template. This is defined as one whose size is less than 0.3 times the median template size for that algorithm. This second rule is needed because some algorithms incorrectly fail to return a non-zero error code when template generation fails.
A hyphen "-" indicates the dataset was not produced. [1]The effects of FTE are included in the accuracy results of this report by regarding any template comparison involving a failed template to produce a low similarity score. Thus higher FTE results in higher FNMR and lower FMR.

	Algorithm	Failure to Enrol Rate[1]									
	Name	APPLICATION		BORDER		KIOSK		MUGSHOT		VISA	
	Name	SEC. 2.2		SEC. 2.4		SEC. 2.6		SEC. 2.5		SEC. 2.1	
175	chtface-001	0.0000	485	0.0000	199	-	1162	0.0000	100	0.0000	199
176	chtface-002	0.0000	1061	0.0021	985	-	1275	0.0002	942	0.0007	915
177	chtface-003	0.0000	1004	0.0018	942	-	1041	0.0001	641	0.0006	873
178	chtface-004	0.0000	385	0.0017	925	0.0320	682	0.0000	519	0.0004	701
179	chtface-005	0.0000	379	0.0017	924	0.0320	681	0.0000	520	0.0004	699
180	chtface-006	0.0000	162	0.0017	922	0.0320	683	0.0000	525	0.0004	689
181	chtface-007	0.0000	226	0.0017	923	0.0320	680	0.0000	517	-	1285
182	chtface-008	0.0000	562	0.0009	674	0.0221	550	0.0000	464	-	1112
183	chtface-009	0.0000	712	0.0009	675	0.0221	549	0.0000	455	-	1261
184	cib-000	0.0000	346	0.0000	128	-	1004	0.0001	769	0.0000	117
185	cib-001	0.0000	456	0.0000	184	-	1124	0.0000	82	0.0000	181
186	cist-001	0.0000	259	0.0005	452	0.0087	259	0.0000	78	0.0000	160
187	cist-002	0.0000	108	0.0048	1124	0.0128	326	0.0000	169	0.0000	13
188	cist-003	0.0000	135	0.0011	795	0.0343	716	0.0000	255	0.0000	73
189	cist-004	0.0000	462	0.0005	420	0.0108	295	0.0000	113	0.0000	194
190	clearviewai-000	0.0000	819	0.0003	312	0.0081	238	0.0000	528	0.0003	316
191	clearviewai-001	0.0000	510	0.0006	487	0.0174	425	0.0001	581	0.0004	451
192	clearviewai-002	0.0000	908	0.0009	731	0.0244	593	0.0001	607	-	1378
193	clearviewai-003	0.0000	861	0.0009	729	0.0244	594	0.0001	615	-	1217
194	closeli-001	0.0000	196	0.0000	62	0.0000	140	0.0000	218	0.0000	57
195	cloudmatrix-000	0.0000	903	0.0012	830	-	1049	0.0001	608	0.0004	476
196	cloudmatrix-001	0.0000	849	0.0028	1025	0.0225	554	0.0001	610	0.0004	446
197	cloudmatrix-002	0.0000	916	0.0028	1026	0.0225	553	0.0001	605	0.0004	474
198	cloudwalk-hr-000	-	1324	-	1349	-	908	0.0003	984	0.0008	930
199	cloudwalk-hr-001	0.0000	659	0.0007	583	-	903	0.0001	586	0.0004	564
200	cloudwalk-hr-002	0.0000	532	0.0007	580	-	1226	0.0002	873	0.0004	706
201	cloudwalk-hr-003	0.0000	506	0.0008	649	-	1192	0.0001	639	0.0004	478
202	cloudwalk-hr-004	0.0000	702	0.0011	812	-	956	0.0004	1032	0.0003	411
203	cloudwalk-mt-000	0.0000	703	0.0008	620	-	959	0.0002	876	0.0004	711
204	cloudwalk-mt-002	0.0000	503	0.0003	304	-	1190	0.0001	589	0.0004	452
205	cloudwalk-mt-003	0.0000	534	0.0007	546	-	1231	0.0002	864	0.0004	704
206	cloudwalk-mt-004	0.0000	664	0.0009	664	0.0191	475	0.0002	890	0.0004	743
207	cloudwalk-mt-005	0.0000	772	0.0005	431	0.0130	333	0.0003	944	0.0004	716
208	cloudwalk-mt-006	0.0000	589	0.0006	474	0.0158	394	0.0002	866	0.0004	709
209	cloudwalk-mt-007	0.0000	649	0.0006	473	0.0158	395	0.0002	865	0.0004	708
210	clova-000	0.0000	1043	0.0022	992	-	1158	0.0006	1134	0.0005	789
211	cmcuni-001	0.0000	19	0.0005	437	0.0119	316	0.0000	190	0.0000	27
212	codeline-000	0.0000	118	0.0000	79	0.0000	121	0.0000	260	0.0000	81
213	cogent-000	-	1299	-	1316	-	1333	-	1410	0.0005	834
214	cogent-001	-	1275	-	1265	-	1246	-	1375	0.0004	756
215	cogent-002	-	1266	-	1283	-	1210	0.0002	806	0.0004	759
216	cogent-003	0.0000	1000	0.0018	943	-	1382	0.0001	642	0.0004	606
217	cogent-004	0.0000	219	0.0000	72	-	1407	0.0000	228	0.0000	71
218	cogent-005	0.0000	149	0.0000	84	-	1313	0.0000	245	0.0000	84
219	cogent-006	0.0000	213	0.0000	74	0.0000	143	0.0000	234	0.0000	72
220	cogent-007	0.0000	991	0.0000	241	0.0000	145	0.0000	488	0.0000	246
221	cogent-008	0.0000	48	0.0010	783	0.0304	668	0.0000	544	0.0004	433
222	cognitec-000	0.0005	1198	0.0112	1188	-	1094	0.0007	1153	0.0007	922
223	cognitec-001	0.0003	1194	0.0110	1187	-	924	0.0008	1172	0.0010	944
224	cognitec-002	0.0001	1137	0.0069	1157	-	1243	0.0003	997	0.0005	799
225	cognitec-003	0.0001	1138	0.0194	1202	0.0820	849	0.0003	987	0.0005	806
226	cognitec-004	0.0001	1139	0.0037	1089	0.0580	797	0.0003	988	0.0005	809
227	cognitec-005	0.0000	1055	0.0026	1011	0.0550	792	0.0002	817	0.0005	794
228	cognitec-006	0.0000	1048	0.0016	914	0.0511	778	0.0002	797	-	1094
229	cognitec-007	0.0000	1130	0.0025	1010	0.0736	842	0.0002	839	-	1278
230	compal-000	0.0000	355	0.0000	138	0.0000	43	0.0000	26	-	1274
231	compal-001	0.0000	959	0.0060	1150	0.0320	684	0.0012	1203	-	1384
232	cor-001	0.0000	805	0.0006	491	-	1114	0.0002	919	0.0004	633

Table 91: FTE is the proportion of failed template generation attempts. Failures can occur because the software throws an exception, or because the software electively refuses to process the input image. This would typically occur if a face is not detected. FTE is measured as the number of function calls that give EITHER a non-zero error code OR that give a "small" template. This is defined as one whose size is less than 0.3 times the median template size for that algorithm. This second rule is needed because some algorithms incorrectly fail to return a non-zero error code when template generation fails.
A hyphen "-" indicates the dataset was not produced. [1]The effects of FTE are included in the accuracy results of this report by regarding any template comparison involving a failed template to produce a low similarity score. Thus higher FTE results in higher FNMR and lower FMR.

FNMR(T) "False non-match rate"
FMR(T) "False match rate"

	Algorithm	Failure to Enrol Rate[1]									
	Name	APPLICATION		BORDER		KIOSK		MUGSHOT		VISA	
	Name	SEC. 2.2		SEC. 2.4		SEC. 2.6		SEC. 2.5		SEC. 2.1	
233	coretech-000	0.0000	33	0.0000	36	0.0000	94	0.0000	182	0.0000	39
234	coretech-001	0.0000	1112	0.0033	1072	0.0677	823	0.0005	1115	0.0011	975
235	coretech-002	0.0000	470	0.0013	874	0.0301	663	0.0000	345	0.0004	652
236	coretech-003	0.0000	411	0.0012	842	0.0282	646	0.0000	461	-	1396
237	coretech-004	0.0000	356	0.0013	873	0.0301	662	0.0000	337	-	1273
238	corsight-001	0.0000	646	0.0006	510	-	1404	0.0001	777	0.0004	579
239	corsight-002	0.0000	758	0.0005	458	0.0152	377	0.0001	715	0.0004	600
240	corsight-003	0.0000	811	0.0006	512	0.0175	428	0.0001	692	0.0004	617
241	csc-001	0.0000	1089	0.0030	1050	-	947	0.0002	822	0.0005	787
242	csc-002	0.0015	1220	0.0033	1064	-	1342	0.0006	1142	0.0006	905
243	csc-003	0.0015	1221	0.0033	1065	0.0445	770	0.0006	1141	0.0006	906
244	ctbcbank-000	0.0001	1144	0.0051	1132	-	1356	0.0011	1193	0.0019	1021
245	ctbcbank-001	0.0000	1068	0.0036	1087	-	1253	0.0005	1107	0.0010	945
246	ctbcbank-002	0.0000	283	0.0006	461	0.0150	371	0.0000	383	-	1319
247	cu-face-002	0.0000	286	0.0000	169	0.0000	22	0.0000	63	0.0000	165
248	cu-face-003	0.0000	999	0.0009	723	0.0245	599	0.0003	953	0.0004	707
249	cu-face-004	0.0000	874	0.0007	594	0.0179	435	0.0001	743	-	1184
250	cubox-001	0.0000	3	0.0000	31	-	1176	0.0000	198	0.0000	35
251	cubox-002	0.0000	910	0.0006	500	0.0159	398	0.0002	920	0.0005	856
252	cubox-003	0.0000	7	0.0010	775	0.0210	520	0.0002	820	0.0004	673
253	cubox-004	0.0000	968	0.0009	722	0.0193	480	0.0003	1009	-	1153
254	cubox-005	0.0000	976	0.0009	724	0.0193	481	0.0003	1012	-	1208
255	cudocommunication-001	0.0000	332	0.0000	113	0.0000	36	0.0000	2	0.0000	108
256	cuhkee-001	0.0000	760	0.0011	808	-	1058	0.0000	347	0.0004	599
257	cybercore-000	0.0000	783	0.0073	1161	-	1079	0.0001	671	0.0005	804
258	cybercore-001	0.0000	1023	0.0001	261	0.0014	159	0.0002	814	0.0002	264
259	cybercore-002	0.0000	1030	0.0001	262	0.0014	158	0.0002	809	0.0002	270
260	cybercore-003	0.0000	797	0.0003	315	0.0060	191	0.0005	1117	0.0003	327
261	cyberextruder-001	0.0029	1224	0.0293	1214	-	1256	0.0024	1251	0.0029	1048
262	cyberextruder-002	0.0013	1217	0.0840	1245	-	963	0.0027	1261	0.0028	1044
263	cyberextruder-003	0.0000	1028	0.0077	1165	0.0887	854	0.0001	779	0.0006	893
264	cyberextruder-004	0.0000	1010	0.0097	1180	0.1025	860	0.0001	755	0.0007	907
265	cyberextruder-005	0.0000	249	0.0000	154	0.0000	14	0.0000	43	-	1289
266	cyberextruder-006	0.0000	320	0.0000	120	0.0000	29	0.0000	10	-	1257
267	cyberlink-000	-	1389	-	1371	-	1120	0.0006	1138	0.0008	927
268	cyberlink-001	-	1298	-	1312	-	1331	0.0073	1295	0.0005	790
269	cyberlink-002	-	1391	-	1368	-	1127	0.0004	1018	0.0004	774
270	cyberlink-003	0.0000	402	0.0007	574	-	1068	0.0001	598	0.0004	527
271	cyberlink-004	0.0000	550	0.0010	791	-	1255	0.0004	1022	0.0003	407
272	cyberlink-005	0.0000	592	0.0009	690	-	1318	0.0003	1004	0.0003	409
273	cyberlink-006	0.0000	306	0.0005	406	-	954	0.0000	303	0.0003	360
274	cyberlink-007	0.0000	139	0.0003	283	0.0067	209	0.0000	330	0.0003	358
275	cyberlink-008	0.0000	491	0.0004	384	0.0106	287	0.0000	316	0.0003	368
276	cyberlink-009	0.0000	481	0.0004	385	0.0106	286	0.0000	318	0.0003	369
277	cyberlink-010	0.0000	307	0.0004	381	0.0106	285	0.0000	302	0.0003	361
278	cyberlink-011	0.0000	57	0.0004	379	0.0106	288	0.0000	325	0.0003	355
279	cyberlink-012	0.0000	299	0.0004	382	0.0106	284	0.0000	304	0.0003	362
280	cyberlink-013	0.0000	290	0.0004	383	0.0106	283	0.0000	311	0.0003	365
281	cyberlink-014	0.0000	184	0.0004	380	0.0106	290	0.0000	328	-	1180
282	cyberlink-015	0.0000	61	0.0004	378	0.0106	289	0.0000	324	-	1168
283	dahua-000	-	1262	-	1278	-	1186	-	1385	0.0000	42
284	dahua-001	-	1273	-	1257	-	1236	0.0000	155	0.0000	4
285	dahua-002	-	1399	-	1374	-	1148	0.0024	1254	0.0022	1032
286	dahua-003	0.0000	80	0.0019	949	-	1240	0.0002	877	0.0003	309
287	dahua-004	0.0000	96	0.0009	727	-	1264	0.0001	741	0.0003	287
288	dahua-005	0.0000	172	0.0000	236	-	1341	0.0000	491	0.0003	359
289	dahua-006	0.0000	380	0.0000	239	-	1042	0.0000	539	0.0003	416
290	dahua-007	0.0000	297	0.0000	237	0.0000	146	0.0000	536	0.0003	412

Table 92: FTE is the proportion of failed template generation attempts. Failures can occur because the software throws an exception, or because the software electively refuses to process the input image. This would typically occur if a face is not detected. FTE is measured as the number of function calls that give EITHER a non-zero error code OR that give a "small" template. This is defined as one whose size is less than 0.3 times the median template size for that algorithm. This second rule is needed because some algorithms incorrectly fail to return a non-zero error code when template generation fails.
A hyphen "-" indicates the dataset was not produced. [1]The effects of FTE are included in the accuracy results of this report by regarding any template comparison involving a failed template to produce a low similarity score. Thus higher FTE results in higher FNMR and lower FMR.

	Algorithm	Failure to Enrol Rate[1]									
	Name	APPLICATION		BORDER		KIOSK		MUGSHOT		VISA	
	Name	SEC. 2.2		SEC. 2.4		SEC. 2.6		SEC. 2.5		SEC. 2.1	
291	daon-000	0.0000	1079	0.0028	1034	0.0577	796	0.0014	1215	0.0015	1010
292	daon-001	0.0000	427	0.0009	673	0.0206	504	0.0000	459	-	1405
293	daon-002	0.0000	210	0.0004	396	0.0094	267	0.0000	232	-	1213
294	daon-003	0.0000	20	0.0008	623	0.0174	426	0.0000	370	-	1148
295	datech-000	0.0000	627	0.0004	339	0.0089	263	0.0000	490	0.0003	295
296	datech-001	0.0000	524	0.0004	338	0.0089	261	0.0000	489	-	1172
297	datech-002	0.0000	545	0.0004	337	0.0089	262	0.0000	487	-	1102
298	decatur-000	0.0000	919	0.0020	967	-	1132	0.0004	1062	0.0005	785
299	decatur-001	0.0000	696	0.0009	717	0.0194	482	0.0001	647	0.0004	568
300	decloakface-001	0.0000	567	0.0016	913	0.0392	748	0.0001	699	0.0005	863
301	decloakface-002	0.0000	483	0.0011	799	0.0218	544	0.0001	588	-	1362
302	deepglint-001	0.0000	328	0.0000	112	-	979	0.0000	1	0.0000	109
303	deepglint-002	0.0000	518	0.0004	377	-	1204	0.0002	892	0.0004	533
304	deepglint-003	0.0000	542	0.0004	376	-	1247	0.0002	891	0.0004	531
305	deepglint-004	0.0000	779	0.0005	409	0.0130	328	0.0002	912	0.0004	524
306	deepglint-005	0.0000	951	0.0019	952	0.0438	768	0.0006	1132	0.0006	902
307	deepsea-001	0.0000	361	0.0000	134	-	1023	0.0000	23	0.0000	129
308	deepsense-000	0.0000	266	0.0006	514	-	927	0.0000	395	0.0004	427
309	deepsense-001	0.0000	90	0.0006	521	0.0191	471	0.0000	422	0.0004	432
310	deepsense-002	0.0000	271	0.0006	522	0.0191	470	0.0000	414	0.0004	439
311	deepsense-003	0.0000	318	0.0004	367	0.0110	297	0.0000	334	0.0003	326
312	deepsense-004	0.0000	598	0.0007	561	0.0179	437	0.0001	661	-	1235
313	deepsense-005	0.0000	85	0.0005	456	0.0144	359	0.0001	623	-	1105
314	deepsense-006	0.0000	426	0.0005	410	0.0113	306	0.0000	421	-	1406
315	deepsense-007	0.0000	98	0.0005	407	0.0113	307	0.0000	424	-	1119
316	deepsense-008	0.0000	237	0.0005	408	0.0113	305	0.0000	412	-	1281
317	dermalog-001	-	1314	-	1297	-	1383	-	1400	0.0013	997
318	dermalog-002	-	1367	-	1393	-	1044	-	1364	0.0013	998
319	dermalog-003	-	1387	-	1361	-	1117	-	1343	0.0025	1038
320	dermalog-004	-	1321	-	1347	-	904	-	1329	0.0090	1075
321	dermalog-005	-	1290	0.0031	1054	-	1303	0.0013	1212	0.0041	1062
322	dermalog-006	0.0005	1200	0.0031	1058	-	1045	0.0013	1209	0.0041	1063
323	dermalog-007	0.0000	622	0.0006	472	-	1361	0.0000	522	0.0002	274
324	dermalog-008	0.0000	1051	0.0031	1055	-	1401	0.0006	1124	0.0003	298
325	dermalog-009	0.0000	1059	0.0031	1057	0.0148	366	0.0006	1122	0.0003	302
326	dermalog-010	0.0000	1050	0.0031	1056	0.0148	365	0.0006	1125	0.0003	300
327	dermalog-011	0.0000	1101	0.0005	411	0.0116	311	0.0001	601	0.0003	315
328	dermalog-012	0.0000	714	0.0003	324	0.0068	212	0.0003	956	0.0005	868
329	dermalog-013	0.0000	663	0.0002	280	0.0051	179	0.0002	803	-	1293
330	dermalog-014	0.0000	809	0.0003	325	0.0068	213	0.0003	957	-	1323
331	dermalog-015	0.0000	544	0.0003	323	0.0068	214	0.0003	958	-	1103
332	dicio-001	0.0005	1206	0.0649	1234	0.2136	880	0.0024	1250	0.0012	984
333	dicio-002	0.0000	87	0.0007	552	0.0185	455	0.0000	400	-	1101
334	didiglobalface-001	0.0000	786	0.0012	819	-	1081	0.0000	568	0.0004	703
335	didiglobalface-002	0.0000	802	0.0012	817	0.0247	603	0.0000	566	0.0004	697
336	didiglobalface-003	0.0000	770	0.0012	821	0.0247	604	0.0000	569	-	1401
337	digidata-000	0.0000	556	0.0023	997	0.0375	736	0.0004	1072	0.0006	887
338	digidata-001	0.0000	647	0.0023	999	0.0375	738	0.0004	1074	0.0006	889
339	digitalbarriers-000	-	1385	-	1359	-	1115	-	1341	0.0019	1022
340	digitalbarriers-001	-	1336	-	1356	-	946	-	1333	0.0018	1019
341	digitalbarriers-002	0.0001	1169	0.0045	1116	-	1016	0.0028	1263	0.0027	1041
342	dps-000	0.0000	349	0.0000	129	0.0000	42	0.0000	31	0.0000	116
343	dralmey-001	0.0000	540	0.0007	548	0.0185	454	0.0000	401	-	1108
344	dsk-000	0.0000	244	0.0000	160	-	914	0.0000	45	0.0000	151
345	einetworks-000	0.0000	1067	0.0017	929	-	1220	0.0002	874	0.0005	839
346	einetworksindia-000	0.0000	1032	0.0018	940	0.0516	780	0.0002	937	0.0005	846
347	einetworksindia-001	0.0000	1035	0.0018	941	0.0516	782	0.0002	938	0.0005	847
348	einetworksindia-002	0.0000	601	0.0006	477	0.0159	400	0.0000	577	-	1243

Table 93: FTE is the proportion of failed template generation attempts. Failures can occur because the software throws an exception, or because the software electively refuses to process the input image. This would typically occur if a face is not detected. FTE is measured as the number of function calls that give EITHER a non-zero error code OR that give a "small" template. This is defined as one whose size is less than 0.3 times the median template size for that algorithm. This second rule is needed because some algorithms incorrectly fail to return a non-zero error code when template generation fails.
A hyphen "-" indicates the dataset was not produced. [1]The effects of FTE are included in the accuracy results of this report by regarding any template comparison involving a failed template to produce a low similarity score. Thus higher FTE results in higher FNMR and lower FMR.

	Algorithm	Failure to Enrol Rate[1]									
	Name	APPLICATION		BORDER		KIOSK		MUGSHOT		VISA	
	Name	SEC. 2.2		SEC. 2.4		SEC. 2.6		SEC. 2.5		SEC. 2.1	
349	ekin-002	0.0000	158	0.0000	245	0.0004	154	0.0000	333	0.0000	240
350	element-000	0.0000	788	0.0008	656	0.0192	478	0.0000	475	0.0003	375
351	enface-000	0.0000	303	0.0012	838	0.0305	670	0.0000	505	0.0004	611
352	enface-001	0.0000	404	0.0012	836	0.0304	669	0.0000	446	0.0004	601
353	enface-002	0.0000	803	0.0004	352	0.0084	252	0.0000	384	0.0004	441
354	enqura-001	0.0003	1189	0.0203	1205	0.1737	873	0.0023	1247	-	1129
355	eocortex-000	0.0095	1241	0.0602	1232	-	1046	0.0094	1298	0.0059	1070
356	ercacat-001	0.0000	445	0.0005	442	-	1111	0.0000	507	0.0003	373
357	ethiopianlmis-000	0.0001	1141	0.0019	958	0.0159	402	0.0009	1179	-	1156
358	euronovate-001	0.0255	1254	0.0102	1184	0.0517	783	0.0021	1241	0.0004	758
359	euronovate-002	0.0000	675	0.0010	740	0.0265	635	0.0000	415	0.0004	696
360	euronovate-003	0.0000	602	0.0006	482	0.0159	397	0.0002	870	0.0004	691
361	euronovate-004	0.0000	1041	0.0016	907	0.0236	584	0.0015	1222	0.0006	891
362	everai-000	-	1402	-	1386	-	1154	-	1353	0.0004	475
363	everai-001	-	1322	-	1346	-	905	0.0004	1049	0.0004	762
364	everai-002	-	1354	-	1336	-	1015	0.0002	881	0.0004	469
365	everai-paravision-003	0.0000	848	0.0008	657	-	1241	0.0002	815	0.0004	500
366	expasoft-000	0.0000	397	0.0000	218	-	1065	0.0000	118	0.0000	212
367	expasoft-001	0.0000	227	0.0000	150	-	894	0.0000	54	0.0000	140
368	expasoft-002	0.0000	107	0.0000	16	0.0000	115	0.0000	167	0.0000	15
369	f8-001	0.0003	1192	0.0059	1146	-	1036	0.0035	1271	0.0030	1050
370	f8-002	0.0000	1122	0.0150	1196	0.0685	827	0.0005	1076	0.0013	1002
371	facehawk-000	0.0000	994	0.0357	1222	0.0720	839	0.0021	1242	0.0009	938
372	faceint-001	0.0001	1158	0.0190	1200	0.0898	855	0.0014	1220	-	1203
373	facelocate-001	0.0000	12	0.0019	955	0.0329	697	0.0000	531	-	1135
374	facelocate-002	0.0000	655	0.0025	1008	0.0387	746	0.0001	587	-	1286
375	faceonlive-001	0.0000	1095	0.0029	1040	0.0481	775	0.0013	1213	0.0011	961
376	faceonlive-002	0.0002	1185	0.0009	719	0.0075	227	0.0008	1166	0.0008	935
377	faceonlive-003	0.0000	956	0.0202	1204	0.0980	857	0.0005	1095	-	1272
378	facephi-000	0.0000	110	0.0004	340	0.0090	265	0.0001	717	0.0004	450
379	facephi-001	0.0000	867	0.0034	1076	0.0499	777	0.0003	972	-	1233
380	facephi-002	0.0000	692	0.0016	911	0.0286	652	0.0002	887	-	1317
381	facesoft-000	0.0000	202	0.0000	66	-	1389	0.0000	238	0.0000	67
382	facetag-000	0.0000	460	0.0000	187	0.0000	75	0.0000	80	0.0000	179
383	facetag-001	0.0000	222	0.0000	146	0.0000	2	0.0000	56	0.0000	143
384	facetag-002	0.0000	146	0.0000	88	0.0000	125	0.0000	250	0.0000	85
385	facex-001	0.0001	1179	0.0360	1224	-	1061	0.0047	1283	0.0027	1043
386	facex-002	0.0001	1178	0.0360	1223	0.2663	884	0.0047	1284	0.0027	1042
387	facia-001	0.0000	131	0.0005	405	0.0122	319	0.0001	583	0.0004	487
388	facia-002	0.0000	946	0.0017	927	0.0185	453	0.0002	924	-	1309
389	faicetech-000	0.0000	773	0.0007	564	0.0130	331	0.0002	926	-	1399
390	farfaces-001	0.0000	1064	0.0007	562	0.0061	193	0.0003	979	0.0003	337
391	fastenterprises-000	0.0000	824	0.0082	1173	0.0169	419	0.0001	773	0.0003	367
392	fci-000	0.0000	94	0.0000	18	0.0000	111	0.0000	177	-	1120
393	fdu-000	-	1338	-	1318	-	962	-	1316	0.0011	977
394	fdu-001	-	1410	-	1385	-	1169	-	1349	0.0009	943
395	fedu-001	0.0000	160	0.0000	96	0.0000	129	0.0000	277	-	1236
396	fiberhome-nanjing-002	0.0000	844	0.0006	517	-	1207	0.0001	664	0.0004	505
397	fiberhome-nanjing-003	0.0000	294	0.0004	360	-	949	0.0000	60	0.0003	303
398	fiberhome-nanjing-004	0.0000	282	0.0004	361	-	940	0.0000	65	0.0003	304
399	fincore-000	0.0000	733	0.0008	653	0.0185	457	0.0001	584	0.0004	682
400	firstcreditkz-001	0.0000	936	0.0019	961	0.0321	687	0.0000	563	0.0004	588
401	firstcreditkz-002	0.0000	776	0.0010	785	0.0232	581	0.0000	510	0.0004	525
402	firstcreditkz-003	0.0000	1075	0.0010	776	0.0219	545	0.0000	495	-	1379
403	firstcreditkz-004	0.0000	609	0.0004	372	0.0124	321	0.0000	332	-	1239
404	foomobi-001	0.0007	1209	0.0000	152	0.0000	12	0.0020	1238	0.0011	964
405	foomobi-002	0.0007	1208	0.0000	76	0.0000	123	0.0020	1240	0.0011	962
406	fourthlinecom-001	0.0000	852	0.0004	370	0.0078	232	0.0005	1090	-	1113

Table 94: FTE is the proportion of failed template generation attempts. Failures can occur because the software throws an exception, or because the software electively refuses to process the input image. This would typically occur if a face is not detected. FTE is measured as the number of function calls that give EITHER a non-zero error code OR that give a "small" template. This is defined as one whose size is less than 0.3 times the median template size for that algorithm. This second rule is needed because some algorithms incorrectly fail to return a non-zero error code when template generation fails.
A hyphen "-" indicates the dataset was not produced. [1]The effects of FTE are included in the accuracy results of this report by regarding any template comparison involving a failed template to produce a low similarity score. Thus higher FTE results in higher FNMR and lower FMR.

	Algorithm	Failure to Enrol Rate[1]									
	Name	APPLICATION		BORDER		KIOSK		MUGSHOT		VISA	
	Name	SEC. 2.2		SEC. 2.4		SEC. 2.6		SEC. 2.5		SEC. 2.1	
407	fpt-000	0.0001	1147	0.0007	571	0.0076	228	0.0006	1144	-	1223
408	fpt-001	0.0001	1148	0.0005	446	0.0067	210	0.0006	1127	-	1155
409	fpttelecom-000	0.0000	327	0.0000	110	0.0000	33	0.0000	6	-	1253
410	fraudcom-000	0.0000	894	0.0055	1141	0.0308	674	0.0002	882	0.0004	684
411	frpkauai-001	0.0000	931	0.0024	1007	0.0360	725	0.0001	612	0.0004	719
412	frpkauai-002	0.0000	955	0.0019	963	0.0321	686	0.0000	556	0.0004	591
413	frpkauai-003	0.0000	684	0.0006	493	0.0145	362	0.0000	456	-	1298
414	frpkauai-004	0.0001	1168	0.0051	1130	0.0730	841	0.0011	1194	-	1365
415	fujitsulab-000	0.0000	1109	0.0033	1069	-	921	0.0005	1094	0.0002	263
416	fujitsulab-001	0.0000	128	0.0014	883	-	1294	0.0002	899	0.0003	398
417	fujitsulab-002	0.0000	377	0.0009	682	-	1035	0.0001	739	0.0003	305
418	fujitsulab-003	0.0000	34	0.0008	625	0.0166	413	0.0001	706	0.0001	257
419	g42-intellibrain-001	0.0000	255	0.0000	164	0.0000	16	0.0000	76	0.0000	161
420	g42-intellibrain-002	0.0000	342	0.0000	125	0.0000	41	0.0000	33	0.0000	121
421	geo-000	0.0000	309	0.0000	104	-	957	0.0000	17	0.0000	105
422	geo-001	0.0000	836	0.0011	797	-	1166	0.0000	558	0.0004	596
423	geo-002	0.0000	571	0.0015	894	0.0332	703	0.0001	580	0.0004	731
424	geo-003	0.0000	821	0.0010	756	0.0244	595	0.0000	362	0.0004	727
425	geo-004	0.0000	671	0.0005	455	0.0138	345	0.0001	676	0.0004	540
426	gistouch-000	0.0000	1120	0.0188	1199	0.1345	865	0.0018	1233	0.0007	908
427	gistouch-001	0.0000	373	0.0002	265	0.0027	166	0.0001	669	0.0003	317
428	glory-000	-	1335	-	1357	-	945	0.0053	1289	0.0013	1000
429	glory-001	0.0160	1246	0.0314	1218	-	991	0.0051	1288	0.0010	949
430	glory-002	0.0003	1190	0.0045	1115	-	1350	0.0015	1223	0.0011	976
431	glory-003	0.0000	953	0.0027	1024	-	988	0.0004	1031	0.0005	795
432	glory-004	0.0000	896	0.0020	974	0.0345	717	0.0001	718	0.0004	724
433	glory-005	0.0000	905	0.0020	975	0.0345	718	0.0001	722	0.0004	728
434	glory-006	0.0000	864	0.0020	973	0.0345	719	0.0001	733	0.0004	723
435	glory-007	0.0000	934	0.0020	981	0.0403	759	0.0002	893	0.0005	777
436	gorilla-000	-	1348	-	1325	-	1000	-	1321	0.0004	770
437	gorilla-001	-	1376	-	1410	-	1080	0.0003	1007	0.0004	776
438	gorilla-002	-	1265	-	1279	-	1198	0.0003	1010	0.0004	767
439	gorilla-003	-	1384	-	1367	-	1106	0.0003	1006	0.0004	773
440	gorilla-004	0.0000	455	0.0008	637	-	1125	0.0000	441	0.0003	342
441	gorilla-005	0.0000	429	0.0008	645	-	1097	0.0000	442	0.0003	341
442	gorilla-006	0.0000	197	0.0006	531	-	1380	0.0000	405	0.0003	338
443	gorilla-007	0.0000	708	0.0009	734	0.0252	617	0.0001	645	0.0004	663
444	gorilla-008	0.0000	516	0.0009	733	0.0259	628	0.0001	650	0.0004	676
445	gorilla-009	0.0000	672	0.0010	763	0.0276	645	0.0001	604	0.0004	650
446	gpstechvn-000	0.0000	468	0.0000	198	0.0000	79	0.0000	112	0.0000	191
447	graymatics-001	0.0000	97	0.0010	738	0.0210	516	0.0001	774	0.0004	555
448	griaule-000	0.0000	1087	0.0026	1022	0.0531	789	0.0004	1071	0.0010	946
449	griaule-001	0.0000	242	0.0012	839	0.0366	730	0.0000	394	0.0004	667
450	griaule-002	0.0000	130	0.0007	573	0.0209	508	0.0000	554	0.0004	580
451	gtelots-000	0.0000	964	0.0003	331	0.0081	245	0.0004	1028	-	1350
452	gtelots-001	0.0000	978	0.0009	695	0.0177	431	0.0004	1042	-	1318
453	hertasecurity-000	0.0133	1245	0.0077	1166	-	969	0.0025	1257	0.0243	1082
454	hertasecurity-001	0.0000	51	0.0000	247	0.0000	148	0.0000	372	0.0001	248
455	hertasecurity-002	0.0000	288	0.0000	168	0.0000	23	0.0000	361	0.0000	237
456	hertasecurity-003	0.0000	240	0.0000	145	0.0000	9	0.0000	309	0.0000	235
457	hik-001	0.0000	270	0.0000	250	-	931	0.0000	71	0.0000	154
458	hisign-001	0.0000	36	0.0000	38	0.0000	96	0.0000	179	0.0000	36
459	hisign-002	0.0000	856	0.0006	502	0.0150	372	0.0001	734	0.0003	393
460	hisign-003	0.0000	868	0.0008	652	0.0237	586	0.0001	735	-	1231
461	hyperverge-001	0.0000	1117	0.0072	1158	-	1260	0.0015	1225	0.0014	1005
462	hyperverge-002	0.0000	347	0.0008	621	0.0210	521	0.0002	923	0.0004	563
463	hyperverge-003	0.0000	217	0.0008	616	0.0210	519	0.0002	930	0.0004	560
464	hyperverge-004	0.0000	823	0.0008	650	0.0218	541	0.0002	879	0.0004	593

Table 95: FTE is the proportion of failed template generation attempts. Failures can occur because the software throws an exception, or because the software electively refuses to process the input image. This would typically occur if a face is not detected. FTE is measured as the number of function calls that give EITHER a non-zero error code OR that give a "small" template. This is defined as one whose size is less than 0.3 times the median template size for that algorithm. This second rule is needed because some algorithms incorrectly fail to return a non-zero error code when template generation fails.
A hyphen "-" indicates the dataset was not produced. [1]The effects of FTE are included in the accuracy results of this report by regarding any template comparison involving a failed template to produce a low similarity score. Thus higher FTE results in higher FNMR and lower FMR.

	Algorithm	Failure to Enrol Rate[1]									
	Name	APPLICATION		BORDER		KIOSK		MUGSHOT		VISA	
	Name	SEC. 2.2		SEC. 2.4		SEC. 2.6		SEC. 2.5		SEC. 2.1	
465	hyperverge-005	0.0000	104	0.0008	615	0.0210	518	0.0002	928	0.0004	554
466	hyperverge-006	0.0000	401	0.0008	617	0.0210	517	0.0002	927	-	1402
467	hyperverge-007	0.0000	369	0.0008	622	0.0210	522	0.0002	925	-	1375
468	hyundai-roboticslab-000	0.0000	273	0.0011	810	0.0246	600	0.0001	705	-	1295
469	hyundai-roboticslab-001	0.0000	364	0.0105	1186	0.1972	874	0.0007	1156	-	1270
470	hyundai-roboticslab-002	0.0000	262	0.0020	980	0.0299	661	0.0002	908	-	1305
471	hyundai-roboticslab-003	0.0000	463	0.0005	412	0.0136	341	0.0000	346	-	1354
472	hzailu-001	0.0000	1036	0.0016	912	0.0449	771	0.0003	999	0.0005	851
473	hzailu-002	0.0000	1037	0.0015	901	0.0424	761	0.0003	998	0.0005	850
474	hzailu-003	0.0000	789	0.0004	347	0.0081	243	0.0002	810	0.0003	391
475	hzailu-004	0.0000	778	0.0004	345	0.0081	242	0.0002	811	0.0003	389
476	hzailu-005	0.0000	808	0.0004	344	0.0081	244	0.0002	808	0.0003	387
477	hzailu-006	0.0000	769	0.0004	346	0.0081	241	0.0002	812	0.0003	390
478	hzailu-007	0.0000	889	0.0004	343	0.0081	239	0.0003	965	-	1306
479	hzailu-008	0.0000	901	0.0004	342	0.0081	240	0.0003	964	-	1271
480	i2v-001	0.0000	1038	0.0018	946	0.0341	715	0.0001	672	-	1400
481	i2v-002	0.0000	932	0.0012	814	0.0244	596	0.0000	503	-	1157
482	icehouse-000	0.0000	330	0.0000	115	0.0000	35	0.0000	3	-	1251
483	icm-002	0.0000	354	0.0001	255	-	1013	0.0000	29	0.0000	232
484	icm-003	0.0000	189	0.0001	254	0.0023	161	0.0000	222	0.0000	231
485	icm-004	0.0000	1080	0.0033	1075	0.0698	831	0.0006	1140	0.0010	957
486	icm-005	0.0002	1184	0.0117	1191	0.1223	863	0.0018	1236	0.0014	1009
487	icomm-000	0.0000	606	0.0004	364	0.0098	274	0.0000	534	0.0003	340
488	icthtc-000	0.0001	1176	0.0047	1123	-	1138	0.0028	1265	0.0029	1045
489	id3-001	-	1313	-	1293	-	1377	-	1392	0.0043	1066
490	id3-002	-	1342	-	1323	-	980	-	1313	0.0032	1052
491	id3-003	0.0001	1140	0.0052	1135	-	1405	0.0016	1228	0.0011	974
492	id3-004	0.0000	1131	0.0052	1133	-	1217	0.0015	1226	0.0011	973
493	id3-005	0.0000	537	0.0074	1163	-	1237	0.0002	832	0.0005	793
494	id3-006	0.0000	957	0.0009	728	-	1032	0.0004	1047	0.0005	835
495	id3-007	0.0000	576	0.0041	1101	-	1286	0.0001	711	0.0004	627
496	id3-008	0.0000	38	0.0006	508	0.0184	450	0.0001	770	0.0004	434
497	id3-009	0.0000	857	0.0003	332	0.0088	260	0.0001	726	-	1121
498	idemia-003	-	1292	-	1309	-	1311	0.0000	431	0.0004	460
499	idemia-004	0.0000	582	0.0006	488	-	1301	0.0000	469	0.0004	485
500	idemia-005	0.0000	206	0.0004	391	-	1394	0.0000	376	0.0003	381
501	idemia-006	0.0000	132	0.0004	392	-	1298	0.0000	378	0.0003	382
502	idemia-007	0.0000	1	0.0004	388	-	1173	0.0000	371	0.0003	378
503	idemia-008	0.0000	92	0.0004	386	0.0078	235	0.0000	369	0.0003	376
504	idemia-009	0.0000	253	0.0004	373	0.0077	230	0.0000	360	0.0003	385
505	idemia-010	0.0000	148	0.0004	336	0.0074	222	0.0000	244	0.0003	339
506	idemia-011	0.0000	112	0.0003	286	0.0055	184	0.0000	163	-	1123
507	identy-000	0.0000	1121	0.0020	977	0.0152	375	0.0012	1200	0.0004	720
508	identy-001	0.0000	1126	0.0013	870	0.0398	754	0.0002	918	-	1151
509	identy-002	0.0000	1128	0.0013	868	0.0401	755	0.0002	913	-	1095
510	idrnd-000	0.0000	877	0.0020	966	0.0566	794	0.0003	1011	-	1190
511	idrnd-001	0.0000	126	0.0006	492	0.0182	441	0.0000	407	-	1218
512	igearx-face-000	0.0000	730	0.0006	467	0.0153	380	0.0004	1039	0.0004	665
513	iit-000	-	1277	-	1263	-	1252	0.0007	1146	0.0011	966
514	iit-001	0.0000	939	0.0806	1244	-	1390	0.0001	789	0.0004	643
515	iit-002	0.0000	1078	0.0021	982	-	995	0.0009	1181	0.0005	860
516	iit-003	0.0000	617	0.0008	651	-	1357	0.0000	479	0.0004	453
517	imds-software-001	0.0000	161	0.0000	89	0.0000	131	0.0000	271	0.0000	90
518	imds-software-002	0.0000	428	0.0000	231	0.0000	64	0.0000	134	0.0000	227
519	imds-software-003	0.0000	375	0.0000	208	0.0000	50	0.0000	126	0.0000	209
520	imperial-000	0.0000	192	0.0000	63	-	1370	0.0000	219	0.0000	61
521	imperial-001	-	1274	-	1258	-	1244	0.0000	154	0.0000	1
522	imperial-002	0.0000	265	0.0000	167	-	926	0.0000	74	0.0000	157

Table 96: FTE is the proportion of failed template generation attempts. Failures can occur because the software throws an exception, or because the software electively refuses to process the input image. This would typically occur if a face is not detected. FTE is measured as the number of function calls that give EITHER a non-zero error code OR that give a "small" template. This is defined as one whose size is less than 0.3 times the median template size for that algorithm. This second rule is needed because some algorithms incorrectly fail to return a non-zero error code when template generation fails.
A hyphen "-" indicates the dataset was not produced. [1]The effects of FTE are included in the accuracy results of this report by regarding any template comparison involving a failed template to produce a low similarity score. Thus higher FTE results in higher FNMR and lower FMR.

	Algorithm	Failure to Enrol Rate[1]									
	Name	APPLICATION		BORDER		KIOSK		MUGSHOT		VISA	
	Name	SEC. 2.2		SEC. 2.4		SEC. 2.6		SEC. 2.5		SEC. 2.1	
523	incode-000	-	1330	-	1354	-	923	-	1338	0.0035	1054
524	incode-001	-	1380	-	1364	-	1099	-	1346	0.0035	1055
525	incode-002	-	1374	-	1403	-	1070	0.0004	1068	0.0007	911
526	incode-003	-	1352	-	1335	-	1012	0.0004	1065	0.0007	910
527	incode-004	-	1351	-	1326	-	1011	0.0004	1066	0.0007	909
528	incode-005	0.0000	236	0.0008	614	-	901	0.0001	653	0.0004	647
529	incode-006	0.0000	721	0.0005	423	-	985	0.0001	753	0.0004	425
530	incode-007	0.0000	921	0.0009	698	-	1136	0.0002	842	0.0004	545
531	incode-008	0.0000	913	0.0009	701	-	1085	0.0002	844	0.0004	552
532	incode-009	0.0000	883	0.0009	696	0.0255	625	0.0002	846	0.0004	534
533	incode-010	0.0000	902	0.0009	697	0.0255	622	0.0002	838	0.0004	539
534	incode-011	0.0000	909	0.0009	700	0.0255	623	0.0002	843	0.0004	548
535	incode-012	0.0000	930	0.0009	699	0.0255	624	0.0002	840	0.0004	546
536	incode-013	0.0001	1181	0.0012	831	0.0254	620	0.0005	1102	0.0004	749
537	incode-014	0.0000	277	0.0006	520	0.0166	412	0.0001	782	-	1322
538	incode-015	0.0000	317	0.0007	590	0.0195	484	0.0000	408	-	1259
539	infocert-001	0.0000	979	0.0059	1149	0.0424	762	0.0001	652	0.0006	878
540	infocert-002	0.0084	1238	0.0041	1109	0.0084	253	0.0085	1297	-	1128
541	innefulabs-000	0.0000	633	0.0024	1005	-	1378	0.0003	978	0.0005	829
542	innominds-001	0.0000	1027	0.0030	1049	0.0637	811	0.0010	1190	0.0008	932
543	innov8tif-000	0.0000	1071	0.0029	1046	0.0657	815	0.0004	1058	-	1353
544	innov8tif-001	0.0000	1069	0.0029	1045	0.0657	816	0.0004	1060	-	1222
545	innovativetechnologyltd-001	0.0001	1173	0.0050	1129	-	1304	0.0024	1256	0.0025	1037
546	innovativetechnologyltd-002	0.0000	965	0.0046	1118	-	1145	0.0057	1291	0.0005	833
547	innovatrics-000	-	1306	-	1295	-	1366	-	1395	0.0004	733
548	innovatrics-001	-	1326	-	1351	-	912	-	1328	0.0004	736
549	innovatrics-002	-	1291	-	1310	-	1310	-	1404	0.0004	461
550	innovatrics-003	-	1360	-	1395	-	1028	-	1368	0.0005	786
551	innovatrics-004	0.0000	840	0.0017	928	-	1195	0.0000	562	0.0004	674
552	innovatrics-005	-	1373	-	1404	-	1069	0.0000	560	0.0004	672
553	innovatrics-006	0.0000	572	0.0009	721	-	1282	0.0000	498	0.0004	449
554	innovatrics-007	0.0000	520	0.0007	582	-	1206	0.0001	582	0.0003	336
555	innovatrics-008	0.0000	577	0.0009	713	0.0204	496	0.0000	504	0.0004	423
556	innovatrics-009	0.0000	216	0.0005	402	0.0142	354	0.0000	230	0.0000	239
557	innovatrics-010	0.0000	701	0.0019	954	0.0393	749	0.0001	646	0.0004	437
558	innovatrics-011	0.0000	584	0.0001	256	0.0017	160	0.0000	331	-	1215
559	innovatrics-012	0.0000	660	0.0004	399	0.0118	312	0.0000	485	-	1280
560	innovatrics-013	0.0000	509	0.0001	259	0.0027	165	0.0000	297	-	1140
561	innovatrics-014	0.0000	749	0.0007	553	0.0165	409	0.0000	420	-	1371
562	innovatrics-015	0.0000	528	0.0008	641	0.0236	585	0.0000	403	-	1169
563	innovatrics-016	0.0000	826	0.0006	470	0.0177	433	0.0000	290	-	1349
564	insightface-000	0.0000	182	0.0000	60	0.0000	137	0.0000	224	0.0000	54
565	insightface-001	0.0000	221	0.0000	147	0.0000	1	0.0000	57	0.0000	144
566	insightface-002	0.0000	119	0.0000	78	0.0000	120	0.0000	261	0.0000	80
567	insightface-003	0.0000	389	0.0000	222	0.0000	54	0.0000	121	0.0000	218
568	insightface-004	0.0000	11	0.0000	25	0.0000	87	0.0000	192	0.0000	32
569	inspur-000	0.0000	69	0.0000	3	0.0000	105	0.0000	156	0.0000	7
570	inspur-001	0.0000	153	0.0000	92	0.0000	127	0.0000	278	0.0000	93
571	inspur-002	0.0000	179	0.0000	58	0.0000	135	0.0000	227	0.0000	55
572	inspur-003	0.0000	22	0.0000	41	0.0000	91	0.0000	187	-	1149
573	intellicloudai-001	0.0000	396	0.0000	219	-	1064	0.0000	120	0.0000	214
574	intellicloudai-002	0.0000	469	0.0008	635	-	1139	0.0000	474	0.0004	442
575	intellifusion-001	0.0000	645	0.0005	448	-	1403	0.0001	635	0.0003	397
576	intellifusion-002	0.0000	475	0.0000	246	-	1152	0.0000	289	0.0000	186
577	intellivision-001	0.0042	1228	0.0296	1215	-	1280	0.0048	1285	0.0042	1064
578	intellivision-002	0.0000	1125	0.0046	1117	-	1007	0.0012	1202	0.0005	869
579	intellivision-003	0.0000	718	0.0012	826	0.0308	672	0.0003	963	0.0004	769
580	intellivision-004	0.0000	573	0.0011	800	0.0266	639	0.0002	934	0.0004	757

Table 97: FTE is the proportion of failed template generation attempts. Failures can occur because the software throws an exception, or because the software electively refuses to process the input image. This would typically occur if a face is not detected. FTE is measured as the number of function calls that give EITHER a non-zero error code OR that give a "small" template. This is defined as one whose size is less than 0.3 times the median template size for that algorithm. This second rule is needed because some algorithms incorrectly fail to return a non-zero error code when template generation fails.
A hyphen "-" indicates the dataset was not produced. [1]The effects of FTE are included in the accuracy results of this report by regarding any template comparison involving a failed template to produce a low similarity score. Thus higher FTE results in higher FNMR and lower FMR.

	Algorithm	Failure to Enrol Rate[1]									
	Name	APPLICATION		BORDER		KIOSK		MUGSHOT		VISA	
	Name	SEC. 2.2		SEC. 2.4		SEC. 2.6		SEC. 2.5		SEC. 2.1	
581	intellivision-005	0.0001	1165	0.0041	1105	0.0528	786	0.0005	1099	0.0007	921
582	intellivision-006	0.0001	1167	0.0041	1103	0.0528	787	0.0005	1097	0.0007	919
583	intellivision-007	0.0001	1164	0.0041	1104	0.0528	785	0.0005	1100	0.0007	920
584	intellivix-001	0.0000	368	0.0000	210	0.0000	48	0.0000	133	0.0000	211
585	intellivix-002	0.0000	136	0.0009	720	0.0184	451	0.0000	254	0.0000	74
586	intellivix-003	0.0000	248	0.0000	155	0.0000	13	0.0000	44	0.0000	148
587	intellivix-004	0.0000	63	0.0022	988	0.0333	707	0.0000	201	0.0000	50
588	intellivix-005	0.0000	378	0.0022	989	0.0333	706	0.0000	128	0.0000	208
589	intellivix-006	0.0000	68	0.0007	555	0.0180	438	0.0000	157	-	1098
590	intelresearch-000	0.0000	705	0.0006	460	-	966	0.0000	526	0.0003	401
591	intelresearch-001	0.0000	1100	0.0082	1172	-	1208	0.0005	1109	0.0010	947
592	intelresearch-002	0.0000	694	0.0022	986	-	948	0.0000	527	0.0004	428
593	intelresearch-003	0.0000	658	0.0006	480	-	902	0.0000	411	0.0004	515
594	intelresearch-004	0.0000	519	0.0006	484	-	1203	0.0000	429	0.0004	506
595	intelresearch-005	0.0000	729	0.0006	485	0.0144	361	0.0000	410	0.0004	512
596	intelresearch-006	0.0000	263	0.0000	242	0.0004	155	0.0000	313	0.0004	518
597	intelresearch-007	0.0000	351	0.0007	539	0.0168	416	0.0000	305	0.0004	514
598	intelresearch-008	0.0000	260	0.0006	532	0.0169	420	0.0000	314	0.0004	543
599	intelresearch-009	0.0000	211	0.0007	595	0.0232	579	0.0000	329	-	1210
600	intelresearch-010	0.0000	713	0.0010	784	0.0335	709	0.0000	482	-	1260
601	intelresearch-011	0.0000	523	0.0006	525	0.0175	427	0.0000	468	-	1174
602	intelresearch-012	0.0000	679	0.0007	563	0.0191	476	0.0000	457	-	1303
603	intema-000	0.0000	177	0.0005	421	0.0126	323	0.0000	545	0.0004	454
604	intema-001	0.0000	512	0.0004	371	0.0106	291	0.0000	326	0.0003	408
605	interlinklabs-001	0.0000	1084	0.0004	395	0.0085	255	0.0005	1086	-	1356
606	interlinklabs-002	0.0000	1082	0.0004	390	0.0085	257	0.0005	1088	-	1200
607	interlinklabs-003	0.0000	879	0.0031	1061	0.0249	608	0.0003	981	-	1188
608	intozi-001	0.0000	508	0.0005	454	0.0126	322	0.0001	791	0.0004	422
609	intsysmsu-000	-	1309	-	1291	-	1372	0.0004	1041	0.0012	981
610	intsysmsu-001	0.0000	405	0.0010	767	-	1071	0.0001	684	0.0004	635
611	intsysmsu-002	0.0000	188	0.0010	764	-	1365	0.0001	685	0.0004	622
612	ionetworks-000	0.0000	166	0.0016	919	0.0387	745	0.0004	1014	0.0005	798
613	ionetworks-001	0.0000	268	0.0081	1169	0.0666	817	0.0000	72	0.0000	156
614	ionetworks-002	0.0000	46	0.0003	297	0.0048	176	0.0000	211	0.0000	45
615	ionetworks-003	0.0000	422	0.0004	353	0.0079	237	0.0000	137	-	1410
616	ionetworks-004	0.0000	147	0.0004	341	0.0086	258	0.0000	249	-	1225
617	iqface-000	0.0000	451	0.0000	188	-	1122	0.0000	86	0.0000	185
618	iqface-001	0.0000	284	0.0000	175	-	942	0.0000	286	0.0000	167
619	iqface-003	0.0000	1074	0.0076	1164	-	1033	0.0006	1123	0.0005	867
620	iqsec-001	0.0000	41	0.0763	1242	0.1617	870	0.0000	214	-	1160
621	iqsec-002	0.0000	370	0.0763	1243	0.1617	869	0.0000	130	-	1374
622	irex-000	0.0000	987	0.0009	718	-	1101	0.0000	529	0.0005	783
623	irisid-001	0.0000	560	0.0016	909	0.0441	769	0.0000	574	-	1115
624	isap-001	0.0000	174	0.0000	98	-	1346	0.0000	263	0.0000	96
625	isap-002	0.0000	477	0.0000	205	-	1153	0.0000	104	0.0000	203
626	isityou-000	0.0068	1236	0.0316	1219	-	1285	0.0023	1246	0.0010	953
627	isystems-000	-	1294	-	1308	-	1314	-	1403	0.0010	954
628	isystems-001	0.0000	1091	0.0035	1083	-	1174	0.0010	1188	0.0007	916
629	isystems-002	0.0000	1092	0.0035	1084	-	996	0.0010	1187	0.0007	917
630	itmo-001	-	1358	-	1333	-	1022	-	1317	0.0047	1067
631	itmo-002	-	1267	-	1285	-	1213	-	1391	0.0029	1049
632	itmo-003	-	1307	-	1296	-	1369	-	1394	0.0008	925
633	itmo-004	-	1378	-	1406	-	1092	-	1372	0.0004	765
634	itmo-005	-	1343	-	1324	-	982	0.0005	1084	0.0002	267
635	itmo-006	0.0000	121	0.0015	900	-	1289	0.0004	1069	0.0004	626
636	itmo-007	0.0000	452	0.0009	677	-	1123	0.0003	1003	0.0000	183
637	itmo-008	0.0000	86	0.0135	1193	0.1239	864	0.0024	1255	0.0000	11
638	ivacognitive-001	0.0000	912	0.0011	802	-	1084	0.0001	609	0.0004	738

Table 98: FTE is the proportion of failed template generation attempts. Failures can occur because the software throws an exception, or because the software electively refuses to process the input image. This would typically occur if a face is not detected. FTE is measured as the number of function calls that give EITHER a non-zero error code OR that give a "small" template. This is defined as one whose size is less than 0.3 times the median template size for that algorithm. This second rule is needed because some algorithms incorrectly fail to return a non-zero error code when template generation fails.
A hyphen "-" indicates the dataset was not produced. [1]The effects of FTE are included in the accuracy results of this report by regarding any template comparison involving a failed template to produce a low similarity score. Thus higher FTE results in higher FNMR and lower FMR.

FNMR(T) "False non-match rate"
FMR(T) "False match rate"

	Algorithm	Failure to Enrol Rate[1]									
	Name	APPLICATION		BORDER		KIOSK		MUGSHOT		VISA	
	Name	SEC. 2.2		SEC. 2.4		SEC. 2.6		SEC. 2.5		SEC. 2.1	
639	iws-000	0.0005	1205	0.0650	1236	-	1391	0.0024	1252	0.0012	986
640	jaakit-001	0.0008	1214	0.0858	1246	0.2713	885	0.0042	1278	0.0021	1028
641	jaakit-002	0.0000	178	0.0000	59	0.0000	136	0.0000	226	-	1187
642	kakao-001	-	1264	-	1276	-	1196	0.0002	898	0.0005	807
643	kakao-002	0.0000	961	0.0057	1145	-	1091	0.0002	897	0.0005	818
644	kakao-003	0.0000	31	0.0000	37	-	1193	0.0000	183	0.0000	38
645	kakao-004	0.0000	56	0.0000	55	-	1212	0.0000	206	0.0000	53
646	kakao-005	0.0000	205	0.0000	235	-	1393	0.0000	235	0.0000	243
647	kakao-007	0.0000	245	0.0007	537	0.0165	410	0.0001	667	0.0004	516
648	kakao-008	0.0000	10	0.0009	685	0.0209	513	0.0001	673	0.0004	503
649	kakao-009	0.0000	464	0.0009	687	0.0209	512	0.0001	668	0.0004	521
650	kakaobank-000	0.0000	4	0.0000	33	0.0000	84	0.0000	196	0.0000	34
651	kakaobank-001	0.0000	359	0.0006	483	0.0176	429	0.0000	358	0.0004	468
652	kakaobank-002	0.0000	497	0.0010	792	0.0303	667	0.0000	450	-	1127
653	kakaobank-003	0.0000	568	0.0013	869	0.0397	751	0.0000	423	-	1125
654	kakaopay-001	0.0000	897	0.0013	865	0.0322	688	0.0001	619	0.0004	742
655	kasikornlabs-000	0.0000	1107	0.0035	1082	0.0713	837	0.0004	1063	0.0012	993
656	kasikornlabs-001	0.0001	1175	0.0050	1128	0.0885	853	0.0006	1143	0.0035	1057
657	kasikornlabs-002	0.0000	1102	0.0033	1066	0.0698	835	0.0004	1056	0.0012	979
658	kasikornlabs-003	0.0000	1099	0.0033	1067	0.0698	834	0.0004	1057	0.0012	980
659	kasikornlabs-004	0.0000	1103	0.0033	1068	0.0698	832	0.0004	1051	-	1255
660	kasikornlabs-005	0.0000	1104	0.0033	1070	0.0698	833	0.0004	1055	-	1344
661	kbyai-000	0.0000	561	0.0013	849	0.0265	638	0.0001	599	-	1114
662	kedacom-000	0.0000	99	0.0000	12	-	1266	0.0000	171	0.0000	20
663	keyless-000	0.0000	656	0.0010	760	0.0308	673	0.0000	438	-	1284
664	kiwitech-000	0.0000	691	0.0009	671	-	944	0.0004	1052	0.0005	791
665	kloudspot-001	0.0000	949	0.0010	759	0.0211	523	0.0001	744	-	1245
666	kloudspot-002	0.0000	66	0.0006	526	0.0159	401	0.0002	884	-	1166
667	kneron-003	0.0239	1252	0.0306	1216	-	1351	0.0044	1282	0.0016	1017
668	kneron-005	0.0000	1096	0.0226	1207	-	1337	0.0006	1120	0.0005	821
669	kneron-006	0.0000	1063	0.1109	1249	0.0686	828	0.0012	1201	-	1192
670	knowutech-000	0.0000	837	0.0008	608	0.0215	537	0.0000	494	0.0004	654
671	kogniza-001	0.0000	717	0.0012	844	0.0337	714	0.0003	992	-	1254
672	kookmin-001	0.0000	360	0.0000	133	-	1021	0.0000	22	0.0000	130
673	kookmin-002	0.0000	207	0.0000	70	-	1395	0.0000	237	0.0000	64
674	koreaid-001	0.0000	191	0.0023	1000	0.0371	734	0.0000	550	0.0005	779
675	krungthai-002	0.0000	608	0.0005	432	0.0111	300	0.0002	875	0.0003	410
676	kuke3d-001	0.0000	488	0.0000	203	0.0000	83	0.0000	99	0.0000	197
677	kuke3d-002	0.0000	393	0.0000	213	0.0000	56	0.0000	114	0.0000	217
678	lebentech-000	0.0042	1226	0.0029	1047	0.0252	616	0.0051	1287	0.0066	1072
679	lebentech-001	0.0000	1132	0.0012	843	0.0317	678	0.0004	1064	0.0005	840
680	lemalabs-001	0.0000	300	0.0005	451	0.0141	352	0.0002	862	0.0004	465
681	lightvision-000	0.0000	465	0.0000	196	0.0000	77	0.0000	111	-	1352
682	lightvision-001	0.0000	43	0.0000	46	0.0000	98	0.0000	213	-	1161
683	lineclova-000	0.0000	95	0.0000	19	0.0000	112	0.0000	178	0.0000	23
684	lineclova-001	0.0000	254	0.0000	158	0.0000	15	0.0000	41	0.0000	145
685	lineclova-002	0.0000	100	0.0007	538	0.0181	440	0.0000	173	0.0000	19
686	lineclova-003	0.0000	1044	0.0023	994	0.0700	836	0.0002	935	0.0005	778
687	lookman-002	0.0000	308	0.0000	103	-	958	0.0000	16	0.0000	106
688	lookman-004	0.0000	168	0.0000	101	-	1334	0.0000	267	0.0000	99
689	lssytech-000	0.0000	838	0.0006	515	0.0177	430	0.0000	508	-	1355
690	luxand-000	0.0000	120	0.0000	80	-	1290	0.0000	259	0.0000	79
691	luxand-001	0.0000	970	0.0016	916	0.0366	728	0.0006	1130	0.0005	837
692	luxand-003	0.0000	974	0.0016	917	0.0366	729	0.0006	1131	-	1193
693	luxand-004	0.0000	619	0.0003	318	0.0061	195	0.0003	946	-	1178
694	mantra-000	0.0001	1142	0.0041	1106	0.0680	826	0.0003	974	0.0004	763
695	matrixcomsec-000	0.0002	1182	1.0000	1298	1.0000	1384	0.0336	1309	-	1201
696	matrixcomsec-001	0.0000	215	0.0009	681	0.0252	615	0.0000	231	-	1204

Table 99: FTE is the proportion of failed template generation attempts. Failures can occur because the software throws an exception, or because the software electively refuses to process the input image. This would typically occur if a face is not detected. FTE is measured as the number of function calls that give EITHER a non-zero error code OR that give a "small" template. This is defined as one whose size is less than 0.3 times the median template size for that algorithm. This second rule is needed because some algorithms incorrectly fail to return a non-zero error code when template generation fails.
A hyphen "-" indicates the dataset was not produced. [1]The effects of FTE are included in the accuracy results of this report by regarding any template comparison involving a failed template to produce a low similarity score. Thus higher FTE results in higher FNMR and lower FMR.

	Algorithm	Failure to Enrol Rate[1]									
	Name	APPLICATION		BORDER		KIOSK		MUGSHOT		VISA	
	Name	SEC. 2.2		SEC. 2.4		SEC. 2.6		SEC. 2.5		SEC. 2.1	
697	maverickresearch-000	0.0000	947	0.0096	1179	0.0574	795	0.0013	1211	-	1297
698	maxvision-000	0.0000	453	0.0000	238	0.0000	71	0.0000	84	0.0000	182
699	maxvision-001	0.0000	163	0.0000	90	0.0000	130	0.0000	273	0.0000	89
700	maxvision-002	0.0000	820	0.0009	667	0.0229	571	0.0002	799	0.0004	594
701	maxvision-003	0.0000	768	0.0009	668	0.0229	570	0.0002	800	0.0004	602
702	maxvision-004	0.0000	548	0.0009	665	0.0229	572	0.0002	805	0.0004	583
703	maxvision-005	0.0000	594	0.0009	666	0.0229	573	0.0002	807	0.0004	587
704	maxvision-006	0.0000	706	0.0007	599	0.0226	556	0.0002	824	0.0004	589
705	mbbankvn-000	0.0000	748	0.0004	365	0.0098	273	0.0000	530	-	1376
706	megvii-000	-	1397	-	1372	-	1140	-	1357	0.0003	311
707	megvii-001	0.0000	233	0.0006	490	-	899	0.0007	1154	0.0004	492
708	megvii-002	0.0000	340	0.0006	489	-	997	0.0054	1290	0.0004	491
709	megvii-003	0.0000	792	0.0010	787	-	1086	0.0002	911	0.0004	717
710	megvii-004	0.0000	771	0.0010	761	-	1072	0.0002	845	0.0004	656
711	megvii-005	0.0000	799	0.0010	747	0.0206	502	0.0002	905	0.0004	698
712	megvii-006	0.0000	774	0.0010	748	0.0206	501	0.0002	906	0.0004	702
713	megvii-007	0.0000	686	0.0010	746	0.0206	499	0.0002	904	0.0004	695
714	megvii-008	0.0000	738	0.0010	744	0.0206	500	0.0002	903	0.0004	693
715	megvii-009	0.0000	522	0.0010	742	0.0206	503	0.0002	907	0.0004	688
716	meituan-000	0.0000	423	0.0001	260	0.0013	157	0.0000	367	0.0002	275
717	meituan-001	0.0000	727	0.0014	886	0.0295	657	0.0001	688	0.0004	666
718	meituan-002	0.0000	648	0.0013	859	0.0251	613	0.0001	693	0.0004	644
719	meituan-003	0.0000	673	0.0013	861	0.0251	612	0.0001	690	0.0004	649
720	meituan-004	0.0000	653	0.0013	860	0.0251	611	0.0001	691	0.0004	648
721	meiya-001	0.0000	1086	0.0028	1035	-	1362	0.0004	1070	0.0010	955
722	mendaxiatech-000	0.0000	604	0.0010	743	0.0206	498	0.0002	915	0.0004	690
723	metsakuurcompany-001	0.0000	400	0.0011	794	0.0208	507	0.0002	901	0.0004	526
724	metsakuurcompany-002	0.0000	473	0.0000	190	0.0000	80	0.0000	107	0.0000	189
725	metsakuurcompany-003	0.0000	408	0.0000	223	0.0000	58	0.0000	145	0.0000	225
726	metsakuurcompany-004	0.0000	321	0.0000	119	0.0000	30	0.0000	9	-	1258
727	metsakuurcompany-005	0.0000	291	0.0000	171	0.0000	24	0.0000	61	-	1314
728	miaxis-001	0.0000	555	0.0013	855	0.0262	632	0.0001	775	0.0003	323
729	miaxis-002	0.0448	1257	0.1162	1250	0.2565	883	0.2128	1312	0.0347	1086
730	miaxis-003	0.0000	628	0.0013	856	0.0262	633	0.0001	776	0.0003	324
731	miaxis-004	0.0000	185	0.0000	56	0.0000	138	0.0000	223	-	1179
732	microfocus-000	-	1407	-	1381	-	1165	-	1350	0.0016	1015
733	microfocus-001	0.0001	1170	0.0053	1138	-	1262	0.0008	1168	0.0016	1013
734	microfocus-002	0.0001	1172	0.0053	1139	-	1010	0.0008	1167	0.0016	1014
735	microfocus-003	0.0001	1163	0.0049	1127	0.0819	848	0.0007	1158	0.0015	1012
736	minivision-000	0.0000	125	0.0000	83	-	1291	0.0000	257	0.0000	76
737	mitek-000	0.0000	969	0.0029	1039	0.0521	784	0.0002	868	0.0003	345
738	mitek-001	0.0000	839	0.0020	965	0.0566	793	0.0003	1008	-	1134
739	mitek-002	0.0000	419	0.0012	833	0.0373	735	0.0000	521	-	1391
740	mobai-000	0.0000	1007	0.0114	1189	-	1108	0.0003	985	0.0012	989
741	mobai-001	0.0000	907	0.0040	1094	-	1057	0.0001	714	0.0012	988
742	mobai-002	0.0000	846	0.0008	610	0.0149	367	0.0002	813	-	1165
743	mobai-003	0.0000	398	0.0000	240	0.0001	149	0.0000	119	-	1377
744	mobbl-000	0.0116	1244	0.0720	1241	-	930	0.0119	1302	0.0063	1071
745	mobbl-001	0.0000	1076	0.0052	1134	0.0678	824	0.0002	821	0.0005	843
746	mobbl-002	0.0000	1097	0.0029	1041	0.0633	810	0.0002	889	0.0009	940
747	mobbl-003	0.0000	1098	0.0029	1042	0.0633	809	0.0002	886	0.0009	941
748	mobbl-004	0.0000	326	0.0012	832	0.0312	676	0.0000	434	-	1252
749	mobbl-005	0.0000	747	0.0009	678	0.0217	538	0.0000	419	-	1373
750	mobipintech-000	0.0000	224	0.0000	148	0.0000	4	0.0000	58	0.0000	142
751	momovn-001	0.0015	1219	0.0010	736	0.0103	277	0.0011	1196	0.0008	928
752	momovn-002	0.0015	1218	0.0010	737	0.0103	276	0.0011	1197	-	1229
753	momovn-003	0.0000	847	0.0031	1060	0.0249	607	0.0003	980	-	1097
754	moredian-000	0.0000	687	0.0009	672	-	936	0.0004	1053	0.0005	792

Table 100: FTE is the proportion of failed template generation attempts. Failures can occur because the software throws an exception, or because the software electively refuses to process the input image. This would typically occur if a face is not detected. FTE is measured as the number of function calls that give EITHER a non-zero error code OR that give a "small" template. This is defined as one whose size is less than 0.3 times the median template size for that algorithm. This second rule is needed because some algorithms incorrectly fail to return a non-zero error code when template generation fails.
A hyphen "-" indicates the dataset was not produced. [1]The effects of FTE are included in the accuracy results of this report by regarding any template comparison involving a failed template to produce a low similarity score. Thus higher FTE results in higher FNMR and lower FMR.

	Algorithm	Failure to Enrol Rate[1]									
	Name	APPLICATION		BORDER		KIOSK		MUGSHOT		VISA	
	Name	SEC. 2.2		SEC. 2.4		SEC. 2.6		SEC. 2.5		SEC. 2.1	
755	morpho-000	-	1327	-	1350	-	913	-	1327	0.0000	150
756	morpho-001	-	1405	-	1389	-	1160	-	1352	0.0000	201
757	morpho-002	-	1370	-	1402	-	1055	0.0000	518	0.0004	498
758	mukh-001	0.0000	305	0.0010	765	0.0154	388	0.0001	704	0.0003	292
759	mukh-002	0.0000	5	0.0022	993	0.0513	779	0.0002	816	0.0004	575
760	mukh-003	0.0000	635	0.0003	292	0.0060	192	0.0001	794	0.0003	396
761	mukh-004	0.0000	750	0.0013	864	0.0327	692	0.0000	540	0.0004	430
762	mukh-005	0.0000	736	0.0009	730	0.0245	597	0.0000	471	-	1262
763	multimodality-000	0.0000	230	0.0000	141	0.0000	6	0.0000	51	0.0000	139
764	multimodality-001	0.0000	105	0.0009	662	0.0259	629	0.0000	175	0.0000	17
765	mvision-001	0.0000	256	0.0000	163	-	922	0.0000	75	0.0000	162
766	nazhiai-000	0.0000	208	0.0000	69	-	1396	0.0000	236	0.0000	63
767	ncsgroup-000	0.0000	457	0.0000	183	0.0000	72	0.0000	81	-	1333
768	ncssg-001	0.0000	234	0.0000	143	0.0000	7	0.0000	53	0.0000	136
769	ncssg-002	0.0000	164	0.0000	91	0.0000	132	0.0000	270	-	1232
770	ncssg-003	0.0000	661	0.0006	504	0.0149	368	0.0003	954	-	1277
771	ncssg-004	0.0000	680	0.0006	506	0.0149	369	0.0003	955	-	1304
772	neosystems-001	0.0000	194	0.0000	234	-	1373	0.0013	1210	0.9994	1093
773	neosystems-002	0.0000	450	0.0000	189	0.0000	70	0.0000	87	0.0000	184
774	neosystems-003	0.0000	72	0.0000	4	0.0000	106	0.0000	159	0.0000	5
775	neosystems-004	0.0000	337	0.0000	131	0.0000	38	0.0000	36	0.0000	123
776	netbridgetech-001	0.0000	313	0.0000	108	-	971	0.0000	15	0.0000	101
777	netbridgetech-002	0.0000	88	0.0000	7	-	1251	0.0000	148	0.0000	10
778	neurotechnology-000	-	1271	-	1259	-	1227	-	1376	0.0000	8
779	neurotechnology-001	-	1300	-	1317	-	1335	-	1409	0.0000	98
780	neurotechnology-002	-	1317	-	1300	-	1408	-	1398	0.0000	69
781	neurotechnology-003	-	1369	-	1401	-	1054	-	1362	0.0005	796
782	neurotechnology-004	-	1279	-	1264	-	1257	0.0000	399	0.0001	258
783	neurotechnology-005	-	1394	-	1379	-	1133	0.0004	1026	0.0004	569
784	neurotechnology-006	0.0000	971	0.0006	501	-	1281	0.0004	1027	0.0004	556
785	neurotechnology-008	0.0000	944	0.0006	499	-	911	0.0004	1024	0.0004	541
786	neurotechnology-009	0.0000	917	0.0008	613	-	1129	0.0002	829	0.0004	496
787	neurotechnology-010	0.0000	600	0.0001	257	-	1330	0.0000	535	0.0002	266
788	neurotechnology-011	0.0000	850	0.0013	846	-	1249	0.0002	825	0.0003	392
789	neurotechnology-012	0.0000	1045	0.0010	793	0.0242	592	0.0001	745	0.0004	621
790	neurotechnology-013	0.0000	362	0.0008	655	0.0185	456	0.0000	336	0.0001	249
791	neurotechnology-015	0.0000	238	0.0004	350	0.0082	246	0.0000	48	0.0000	236
792	neurotechnology-016	0.0000	143	0.0003	303	0.0069	216	0.0000	247	0.0000	233
793	neurotechnology-017	0.0000	407	0.0003	327	0.0065	206	0.0000	144	0.0000	238
794	neurotechnology-018	0.0000	835	0.0003	334	0.0074	223	0.0000	416	0.0004	443
795	neurotechnology-019	0.0000	688	0.0004	368	0.0115	309	0.0000	312	-	1320
796	neurotechnology-020	0.0000	629	0.0004	366	0.0115	310	0.0000	327	-	1191
797	nextmetalabs-001	0.0000	476	0.0000	193	0.0000	81	0.0000	106	-	1345
798	nextmetalabs-002	0.0000	155	0.0000	93	0.0000	128	0.0000	279	-	1237
799	nextmetalabs-003	0.0000	643	0.0006	533	0.0184	452	0.0000	374	-	1205
800	nextmetalabs-004	0.0000	777	0.0008	661	0.0255	626	0.0000	368	-	1394
801	nhn-001	0.0000	801	0.0019	948	-	1104	0.0001	648	0.0004	751
802	nhn-002	0.0000	75	0.0004	397	0.0091	266	0.0000	463	0.0003	313
803	nhn-003	0.0000	963	0.0000	197	0.0000	76	0.0001	786	0.0004	671
804	nhn-004	0.0000	945	0.0000	162	0.0000	17	0.0001	784	0.0004	668
805	nhn-005	0.0000	715	0.0000	118	0.0000	28	0.0000	497	0.0004	489
806	noblis-000	-	1365	-	1390	-	1039	-	1366	0.0000	207
807	nodeflux-000	-	1329	-	1344	-	918	0.0001	713	0.0002	284
808	nodeflux-001	0.0000	367	0.0016	910	-	1027	0.0001	716	0.0002	286
809	nodeflux-002	0.0000	638	0.0261	1211	-	1387	0.0008	1165	0.0005	832
810	nominder-000	0.0000	716	0.0003	281	0.0053	181	0.0000	433	0.0003	383
811	nominder-001	0.0000	800	0.0003	282	0.0053	182	0.0000	443	0.0003	388
812	nominder-002	0.0000	599	0.0006	475	0.0119	313	0.0002	885	0.0003	400

Table 101: FTE is the proportion of failed template generation attempts. Failures can occur because the software throws an exception, or because the software electively refuses to process the input image. This would typically occur if a face is not detected. FTE is measured as the number of function calls that give EITHER a non-zero error code OR that give a "small" template. This is defined as one whose size is less than 0.3 times the median template size for that algorithm. This second rule is needed because some algorithms incorrectly fail to return a non-zero error code when template generation fails.
A hyphen "-" indicates the dataset was not produced. [1]The effects of FTE are included in the accuracy results of this report by regarding any template comparison involving a failed template to produce a low similarity score. Thus higher FTE results in higher FNMR and lower FMR.

	Algorithm	Failure to Enrol Rate[1]									
	Name	APPLICATION		BORDER		KIOSK		MUGSHOT		VISA	
	Name	SEC. 2.2		SEC. 2.4		SEC. 2.6		SEC. 2.5		SEC. 2.1	
813	nominder-003	0.0000	637	0.0005	439	0.0095	271	0.0002	830	-	1198
814	nominder-004	0.0000	526	0.0007	565	0.0130	330	0.0002	929	-	1171
815	nominder-005	0.0000	413	0.0009	680	0.0206	497	0.0000	460	-	1393
816	nominder-006	0.0000	866	0.0017	920	0.0379	741	0.0003	995	-	1234
817	nominder-007	0.0000	922	0.0006	529	0.0119	314	0.0003	993	-	1348
818	notiontag-000	0.0000	200	0.0000	71	-	1381	0.0000	241	0.0000	68
819	notiontag-001	0.0000	392	0.0000	216	-	1060	0.0027	1262	0.0000	215
820	notiontag-002	0.0000	203	0.0000	68	0.0000	142	0.0000	239	0.0000	65
821	nsensecorp-001	0.0000	1116	0.0024	1003	-	1017	0.0014	1219	0.0101	1078
822	nsensecorp-002	0.0000	574	0.0009	676	0.0219	546	0.0003	951	0.0011	958
823	nsensecorp-003	0.0000	471	0.0000	253	0.0002	151	0.0000	417	0.0007	924
824	nsensecorp-004	0.0406	1256	0.0035	1081	0.0181	439	0.0016	1230	0.0760	1087
825	nsensecorp-005	0.0000	363	0.0000	135	0.0000	45	0.0000	24	0.0000	128
826	ntechlab-000	-	1259	-	1274	-	1175	-	1388	0.0016	1016
827	ntechlab-001	-	1295	-	1307	-	1315	-	1402	0.0005	801
828	ntechlab-002	-	1404	-	1387	-	1156	-	1354	0.0005	802
829	ntechlab-003	-	1375	-	1409	-	1077	-	1373	0.0005	805
830	ntechlab-004	-	1350	-	1327	-	1009	-	1322	0.0004	510
831	ntechlab-005	-	1316	-	1302	-	1400	0.0000	390	0.0004	484
832	ntechlab-006	-	1403	-	1388	-	1155	0.0000	319	0.0004	444
833	ntechlab-007	0.0000	869	0.0019	950	-	1332	0.0001	617	0.0004	464
834	ntechlab-008	0.0000	860	0.0005	404	-	1299	0.0001	626	0.0004	457
835	ntechlab-009	0.0000	984	0.0009	692	-	1076	0.0001	748	0.0004	431
836	ntechlab-010	0.0000	632	0.0005	447	0.0107	294	0.0001	703	0.0004	455
837	ntechlab-011	0.0000	73	0.0003	285	0.0057	188	0.0000	541	0.0004	418
838	ntechlab-012	0.0000	269	0.0003	287	0.0057	187	0.0000	537	0.0004	426
839	omface-000	0.0000	264	0.0000	166	0.0000	19	0.0000	73	0.0000	158
840	omface-001	0.0000	437	0.0000	243	0.0000	147	0.0000	90	0.0000	176
841	omnigarde-000	0.0000	725	0.0008	603	0.0213	530	0.0000	437	0.0004	631
842	omnigarde-001	0.0000	507	0.0008	601	0.0213	532	0.0000	449	0.0004	620
843	omnigarde-002	0.0000	732	0.0008	602	0.0213	531	0.0000	436	0.0004	630
844	omnigarde-003	0.0000	243	0.0007	598	0.0212	526	0.0000	306	0.0004	517
845	omnigarde-004	0.0000	201	0.0007	597	0.0213	529	0.0000	355	-	1199
846	omnigarde-005	0.0000	24	0.0007	596	0.0213	528	0.0000	351	-	1144
847	onfido-000	0.0000	1090	0.0040	1093	0.0804	847	0.0004	1015	0.0012	982
848	onfido-001	0.0000	785	0.0006	530	0.0183	444	0.0000	293	-	1409
849	onfido-002	0.0000	810	0.0006	528	0.0183	445	0.0000	288	-	1341
850	onfido-003	0.0000	652	0.0006	527	0.0183	443	0.0000	283	-	1288
851	ooto-001	0.0000	84	0.0000	9	0.0000	108	0.0000	150	-	1104
852	openedge-000	0.0000	612	0.0014	875	0.0212	524	0.0003	971	0.0004	680
853	openface-001	0.0000	1031	0.0104	1185	0.0668	818	0.0004	1040	0.0006	903
854	ovisionllc-001	0.0000	382	0.0000	209	0.0000	51	0.0000	125	-	1368
855	ovisionllc-002	0.0000	123	0.0000	77	0.0000	122	0.0000	258	-	1219
856	oz-001	0.0000	986	0.0011	811	-	1083	0.0006	1135	0.0004	572
857	oz-002	0.0000	432	0.0003	288	-	1098	0.0000	396	0.0003	350
858	oz-003	0.0000	381	0.0002	267	0.0042	171	0.0000	322	0.0003	289
859	oz-004	0.0000	1040	0.0003	300	0.0041	170	0.0000	348	0.0002	262
860	pa-002	-	1345	-	1329	-	986	-	1325	0.0000	125
861	pa-003	-	1332	-	1352	-	933	-	1335	0.0000	153
862	palit-000	0.0000	831	0.0005	443	0.0134	340	0.0002	850	0.0004	520
863	palit-001	0.0000	780	0.0007	600	0.0201	490	0.0002	852	0.0004	529
864	pangiam-000	0.0000	430	0.0021	984	0.0364	726	0.0001	578	0.0005	788
865	pangiam-001	0.0000	252	0.0005	449	0.0128	325	0.0002	941	0.0003	414
866	pangiam-002	0.0000	134	0.0003	319	0.0072	218	0.0000	432	0.0003	347
867	papago-001	0.0000	872	0.0008	619	0.0159	399	0.0002	939	0.0004	582
868	papil11-000	0.0000	724	0.0008	654	0.0192	479	0.0000	484	0.0003	413
869	papil11-001	0.0000	793	0.0005	417	0.0133	336	0.0000	398	-	1407
870	papil11-002	0.0000	521	0.0004	349	0.0115	308	0.0000	352	-	1150

Table 102: FTE is the proportion of failed template generation attempts. Failures can occur because the software throws an exception, or because the software electively refuses to process the input image. This would typically occur if a face is not detected. FTE is measured as the number of function calls that give EITHER a non-zero error code OR that give a "small" template. This is defined as one whose size is less than 0.3 times the median template size for that algorithm. This second rule is needed because some algorithms incorrectly fail to return a non-zero error code when template generation fails.
A hyphen "-" indicates the dataset was not produced. [1]The effects of FTE are included in the accuracy results of this report by regarding any template comparison involving a failed template to produce a low similarity score. Thus higher FTE results in higher FNMR and lower FMR.

	Algorithm	Failure to Enrol Rate[1]									
	Name	APPLICATION		BORDER		KIOSK		MUGSHOT		VISA	
	Name	SEC. 2.2		SEC. 2.4		SEC. 2.6		SEC. 2.5		SEC. 2.1	
871	papil11-003	0.0000	448	0.0003	328	0.0077	231	0.0000	315	-	1324
872	papil11-004	0.0000	812	0.0008	612	0.0227	560	0.0003	977	-	1340
873	papsav1923-001	0.0000	816	0.0007	569	-	1128	0.0001	678	0.0002	279
874	papsav1923-002	0.0000	626	0.0018	944	0.0268	641	0.0000	512	0.0004	642
875	papsav1923-003	0.0000	948	0.0019	962	0.0321	685	0.0000	555	0.0004	590
876	paravision-004	0.0000	989	0.0007	588	-	1164	0.0002	863	0.0004	597
877	paravision-006	0.0000	372	0.0000	212	-	1031	0.0000	131	0.0000	210
878	paravision-008	0.0000	170	0.0010	752	0.0201	489	0.0001	660	0.0004	436
879	paravision-010	0.0000	154	0.0010	751	0.0201	488	0.0001	662	0.0004	435
880	paravision-011	0.0000	287	0.0010	755	0.0201	486	0.0001	654	0.0004	440
881	paravision-013	0.0000	403	0.0010	757	0.0201	487	0.0001	656	0.0004	445
882	paravision-015	0.0000	279	0.0009	714	0.0266	640	0.0000	557	-	1321
883	paravision-017	0.0000	634	0.0009	669	0.0220	548	0.0001	640	-	1189
884	paravision-018	0.0000	444	0.0005	457	0.0142	358	0.0000	344	-	1326
885	paravision-020	0.0000	449	0.0004	356	0.0107	292	0.0000	341	-	1337
886	pensees-001	0.0000	557	0.0000	13	-	1267	0.0000	172	0.0000	21
887	pentacomp-000	0.0001	1152	0.0010	735	0.0206	506	0.0004	1030	-	1216
888	pixelall-002	0.0000	17	0.0000	30	-	1184	0.0000	191	0.0000	29
889	pixelall-003	0.0000	79	0.0000	1	-	1238	0.0000	153	0.0000	3
890	pixelall-004	0.0000	138	0.0000	87	-	1307	0.0000	252	0.0000	87
891	pixelall-005	0.0000	231	0.0000	140	-	898	0.0000	49	0.0000	138
892	pixelall-006	0.0000	18	0.0000	29	0.0000	90	0.0000	189	0.0000	28
893	pixelall-007	0.0000	312	0.0000	107	0.0000	26	0.0000	14	0.0000	102
894	pixelall-008	0.0000	357	0.0008	639	0.0247	602	0.0000	25	0.0000	133
895	pixelall-009	0.0000	78	0.0000	2	0.0000	107	0.0000	152	0.0000	2
896	pixelall-010	0.0000	261	0.0000	165	0.0000	18	0.0000	77	0.0000	159
897	pnpsecure-000	0.0000	81	0.0030	1048	0.0390	747	0.0003	945	-	1106
898	pnpsecure-001	0.0000	274	0.0023	995	0.0328	694	0.0002	828	-	1294
899	privid-001	0.0001	1177	0.0176	1198	0.0598	804	0.0021	1243	0.0021	1027
900	privid-002	0.0198	1249	0.0040	1097	0.0386	744	0.0014	1216	0.0011	967
901	privid-003	0.0000	966	0.0002	271	0.0030	167	0.0001	760	-	1363
902	privid-004	0.0000	827	0.0001	264	0.0025	163	0.0001	632	-	1346
903	psl-000	-	1284	-	1269	-	1274	-	1379	0.0000	14
904	psl-001	-	1310	-	1290	-	1374	0.0000	216	0.0000	59
905	psl-002	-	1341	-	1322	-	978	0.0000	7	0.0000	110
906	psl-003	0.0000	644	0.0007	542	-	1402	0.0000	533	0.0004	608
907	psl-004	0.0000	531	0.0007	541	-	1225	0.0000	532	0.0004	605
908	psl-005	0.0000	539	0.0007	534	-	1242	0.0000	447	0.0004	553
909	psl-006	0.0000	745	0.0002	268	-	1026	0.0000	132	0.0003	288
910	psl-007	0.0000	579	0.0007	545	-	1295	0.0000	546	0.0003	357
911	psl-008	0.0000	517	0.0003	294	0.0068	211	0.0000	353	0.0003	346
912	psl-009	0.0000	569	0.0004	359	0.0095	270	0.0000	295	0.0004	421
913	psl-010	0.0000	549	0.0004	358	0.0095	269	0.0000	294	0.0004	419
914	psl-011	0.0000	641	0.0003	291	0.0063	198	0.0000	299	0.0003	380
915	psl-012	0.0000	737	0.0003	298	0.0067	208	0.0000	281	0.0003	384
916	psl-013	0.0000	620	0.0003	290	0.0063	197	0.0000	523	-	1177
917	psl-014	0.0000	495	0.0003	289	0.0063	196	0.0000	298	-	1132
918	ptakuratsatu-000	0.0000	782	0.0007	584	-	1078	0.0001	579	0.0003	344
919	pxl-001	0.0000	1136	0.0044	1113	-	925	0.0005	1101	0.0022	1033
920	pyramid-000	0.0001	1166	0.0041	1102	-	983	0.0005	1098	0.0007	918
921	pyramid-001	0.0000	796	0.0008	624	0.0231	576	0.0001	749	-	1403
922	qazbs-000	0.0000	390	0.0009	689	0.0265	636	0.0000	397	0.0004	570
923	qazsmartvisionai-000	0.0000	662	0.0003	330	0.0083	250	0.0000	308	0.0003	349
924	qazsmartvisionai-001	0.0000	825	0.0003	309	0.0064	202	0.0000	321	0.0003	328
925	qazsmartvisionai-002	0.0000	775	0.0003	310	0.0064	201	0.0000	323	-	1398
926	qazsmartvisionai-003	0.0000	828	0.0003	308	0.0064	203	0.0000	320	-	1347
927	qazsmartvisionai-004	0.0000	669	0.0003	307	0.0064	200	0.0000	307	-	1291
928	qluevision-001	0.0000	980	0.0008	630	0.0153	379	0.0008	1164	0.0004	771

Table 103: FTE is the proportion of failed template generation attempts. Failures can occur because the software throws an exception, or because the software electively refuses to process the input image. This would typically occur if a face is not detected. FTE is measured as the number of function calls that give EITHER a non-zero error code OR that give a "small" template. This is defined as one whose size is less than 0.3 times the median template size for that algorithm. This second rule is needed because some algorithms incorrectly fail to return a non-zero error code when template generation fails.
A hyphen "-" indicates the dataset was not produced. [1]The effects of FTE are included in the accuracy results of this report by regarding any template comparison involving a failed template to produce a low similarity score. Thus higher FTE results in higher FNMR and lower FMR.

FNMR(T) "False non-match rate"
FMR(T) "False match rate"

	Algorithm	Failure to Enrol Rate[1]									
	Name	APPLICATION		BORDER		KIOSK		MUGSHOT		VISA	
	Name	SEC. 2.2		SEC. 2.4		SEC. 2.6		SEC. 2.5		SEC. 2.1	
929	qnap-000	0.0000	316	0.0007	586	0.0174	424	0.0002	837	0.0002	259
930	qnap-001	0.0000	731	0.0000	249	0.0002	152	0.0000	516	0.0001	252
931	qnap-002	0.0000	1077	0.0033	1063	0.0761	844	0.0004	1025	0.0002	260
932	qnap-003	0.0000	183	0.0016	905	0.0402	757	0.0000	553	0.0001	250
933	qnap-004	0.0000	409	0.0016	906	0.0402	756	0.0000	551	0.0001	251
934	qnap-005	0.0001	1149	0.0078	1167	0.0581	798	0.0010	1189	0.0005	866
935	qnap-006	0.0000	862	0.0018	936	0.0427	764	0.0002	878	-	1228
936	quantasoft-003	0.0000	996	0.0015	903	0.0355	722	0.0005	1092	0.0006	890
937	rankone-000	-	1331	-	1355	-	928	-	1337	0.0003	364
938	rankone-001	-	1406	-	1382	-	1163	-	1351	0.0000	247
939	rankone-002	-	1286	-	1268	-	1276	-	1378	0.0000	242
940	rankone-003	-	1366	-	1394	-	1040	-	1365	0.0000	244
941	rankone-004	-	1368	-	1400	-	1051	-	1363	0.0000	245
942	rankone-005	-	1363	-	1391	-	1038	0.0000	127	0.0000	206
943	rankone-006	-	1297	-	1311	-	1329	0.0000	272	0.0000	88
944	rankone-007	0.0000	1135	0.0048	1125	-	895	0.0003	976	0.0004	726
945	rankone-008	0.0000	1115	0.0049	1126	-	1272	0.0003	943	0.0004	420
946	rankone-009	0.0000	314	0.0000	117	-	974	0.0000	12	0.0000	115
947	rankone-010	0.0000	440	0.0000	181	-	1107	0.0000	92	0.0000	174
948	rankone-011	0.0000	246	0.0000	153	0.0000	11	0.0000	42	0.0000	149
949	rankone-012	0.0000	137	0.0000	75	0.0000	124	0.0000	253	0.0000	75
950	rankone-013	0.0000	344	0.0005	422	0.0126	324	0.0000	381	0.0003	301
951	rankone-014	0.0000	353	0.0005	413	0.0129	327	0.0000	380	0.0002	268
952	rankone-015	0.0000	341	0.0000	126	0.0000	40	0.0000	34	0.0000	119
953	realnetworks-000	-	1272	-	1260	-	1232	-	1377	0.0003	318
954	realnetworks-001	-	1278	-	1262	-	1254	0.0004	1019	0.0003	319
955	realnetworks-002	0.0000	943	0.0003	322	-	906	0.0004	1017	0.0003	321
956	realnetworks-003	0.0000	950	0.0003	321	-	961	0.0004	1016	0.0003	320
957	realnetworks-004	0.0000	502	0.0003	284	0.0052	180	0.0000	296	0.0002	281
958	realnetworks-005	0.0000	593	0.0002	275	0.0045	175	0.0000	301	0.0002	283
959	realnetworks-006	0.0000	767	0.0002	277	0.0045	173	0.0000	291	0.0002	282
960	realnetworks-007	0.0000	833	0.0013	866	0.0425	763	0.0000	317	0.0004	598
961	realnetworks-008	0.0000	814	0.0002	276	0.0045	174	0.0000	287	0.0002	285
962	realsense-001	0.0000	757	0.0006	524	0.0177	432	0.0000	445	-	1386
963	rebs-000	0.0000	30	0.0005	414	0.0130	329	0.0000	426	0.0004	480
964	rebs-001	0.0000	42	0.0005	429	0.0144	360	0.0000	477	0.0004	576
965	recognito-000	0.0000	563	0.0003	295	0.0056	186	0.0000	496	0.0003	377
966	recognito-001	0.0000	665	0.0003	296	0.0056	185	0.0000	492	0.0003	386
967	regula-000	0.0000	241	0.0000	159	0.0000	10	0.0000	46	0.0000	152
968	regula-001	0.0000	478	0.0000	204	0.0000	82	0.0000	103	0.0000	204
969	regula-002	0.0000	387	0.0009	726	0.0283	647	0.0000	123	-	1387
970	remarkai-000	-	1357	-	1339	-	1020	0.0000	28	0.0000	132
971	remarkai-001	0.0000	474	0.0000	192	-	1149	0.0000	105	0.0000	188
972	remarkai-002	0.0000	127	0.0000	82	-	1293	0.0000	256	0.0000	77
973	remarkai-003	0.0000	616	0.0007	560	0.0187	459	0.0000	524	0.0004	483
974	rendip-000	0.0000	935	0.0016	915	0.0293	656	0.0002	848	0.0004	761
975	revealmedia-005	0.0000	975	0.0007	576	0.0189	464	0.0009	1180	0.0004	768
976	revealmedia-006	0.0000	275	0.0009	715	0.0238	587	0.0001	696	0.0004	685
977	roc-016	0.0000	141	0.0000	251	0.0006	156	0.0000	251	0.0000	234
978	roc-017	0.0000	388	0.0003	335	0.0073	220	0.0000	386	-	1385
979	roc-018	0.0000	689	0.0006	516	0.0160	404	0.0000	440	0.0004	473
980	roc-019	0.0000	726	0.0007	558	0.0187	458	0.0000	472	-	1266
981	roc-020	0.0000	657	0.0006	497	0.0157	392	0.0000	310	-	1283
982	rokid-000	0.0000	322	0.0072	1159	-	976	0.0001	666	0.0005	822
983	rokid-001	0.0000	232	0.0013	858	-	897	0.0000	50	0.0000	137
984	s1-001	0.0000	1133	0.0073	1162	-	1326	0.0013	1206	0.0007	912
985	s1-002	0.0000	876	0.0089	1177	-	1367	0.0001	736	0.0005	830
986	s1-003	0.0000	151	0.0002	270	0.0040	169	0.0007	1152	0.0003	308

Table 104: FTE is the proportion of failed template generation attempts. Failures can occur because the software throws an exception, or because the software electively refuses to process the input image. This would typically occur if a face is not detected. FTE is measured as the number of function calls that give EITHER a non-zero error code OR that give a "small" template. This is defined as one whose size is less than 0.3 times the median template size for that algorithm. This second rule is needed because some algorithms incorrectly fail to return a non-zero error code when template generation fails.
A hyphen "-" indicates the dataset was not produced. [1]The effects of FTE are included in the accuracy results of this report by regarding any template comparison involving a failed template to produce a low similarity score. Thus higher FTE results in higher FNMR and lower FMR.

	Algorithm	Failure to Enrol Rate[1]									
	Name	APPLICATION		BORDER		KIOSK		MUGSHOT		VISA	
	Name	SEC. 2.2		SEC. 2.4		SEC. 2.6		SEC. 2.5		SEC. 2.1	
987	s1-004	0.0000	301	0.0000	252	0.0003	153	0.0000	564	0.0001	256
988	s1-005	0.0000	220	0.0004	362	0.0120	317	0.0001	613	0.0002	265
989	s1-006	0.0000	47	0.0003	293	0.0074	225	0.0001	602	0.0002	271
990	s1-007	0.0000	431	0.0006	478	0.0110	298	0.0001	606	0.0002	269
991	s1-008	0.0000	674	0.0018	947	0.0252	618	0.0005	1118	-	1307
992	s1-009	0.0000	165	0.0006	476	0.0110	299	0.0001	618	-	1230
993	saffe-001	0.0000	414	0.0000	225	-	1074	0.0000	141	0.0000	224
994	saffe-002	0.0000	14	0.0000	26	-	1182	0.0000	193	0.0000	31
995	samsungsds-000	0.0000	942	0.0055	1142	0.0646	813	0.0038	1275	0.0005	823
996	samsungsds-001	0.0000	142	0.0005	445	0.0146	363	0.0001	659	0.0003	399
997	samsungsds-002	0.0000	391	0.0004	369	0.0119	315	0.0001	655	0.0003	374
998	samtech-000	-	1325	-	1348	-	909	-	1330	0.0042	1065
999	samtech-001	0.0001	1162	0.0032	1062	-	1113	0.0004	1054	0.0008	926
1000	samtech-002	0.0000	1033	0.0018	939	0.0516	781	0.0002	936	0.0005	845
1001	scanovate-001	0.0208	1250	0.2388	1253	-	1397	0.0024	1249	0.0014	1004
1002	scanovate-002	0.0000	906	0.0018	938	-	1056	0.0000	567	0.0004	754
1003	scanovate-003	0.0000	918	0.0233	1209	0.3371	889	0.0006	1126	0.0004	775
1004	sdc-000	0.0000	1111	0.0035	1080	0.0678	825	0.0005	1114	0.0011	969
1005	seamfix-001	0.0000	91	0.0000	8	0.0000	110	0.0000	147	-	1100
1006	securifai-001	0.0000	319	0.0000	121	-	975	0.0000	280	0.0000	114
1007	securifai-002	0.0000	39	0.0000	47	-	1197	0.0000	215	0.0000	48
1008	securifai-003	0.0000	89	0.0000	6	0.0000	109	0.0000	149	0.0000	9
1009	securifai-004	0.0000	406	0.0000	228	0.0000	57	0.0000	146	0.0000	226
1010	securifai-005	0.0000	325	0.0000	111	0.0000	32	0.0000	8	0.0000	111
1011	securifai-006	0.0000	167	0.0000	100	0.0000	133	0.0000	269	0.0000	100
1012	securifai-007	0.0000	339	0.0000	123	0.0000	39	0.0000	32	0.0000	122
1013	securifai-008	0.0000	6	0.0000	32	0.0000	85	0.0000	195	-	1136
1014	sensetime-001	-	1285	-	1270	-	1273	0.0000	465	0.0004	573
1015	sensetime-002	0.0004	1197	0.0082	1171	-	917	0.0011	1199	0.0005	861
1016	sensetime-003	0.0000	722	0.0011	807	-	984	0.0000	282	0.0004	592
1017	sensetime-004	0.0000	591	0.0011	806	-	1316	0.0000	300	0.0004	585
1018	sensetime-005	0.0000	93	0.0004	355	0.0106	282	0.0000	466	0.0003	335
1019	sensetime-006	0.0000	374	0.0004	357	0.0106	280	0.0000	458	0.0003	343
1020	sensetime-007	0.0000	82	0.0004	354	0.0106	281	0.0000	462	0.0003	334
1021	sensetime-008	0.0000	295	0.0007	581	0.0250	609	0.0000	285	0.0003	415
1022	sensetime-010	0.0000	376	0.0005	444	0.0111	301	0.0000	509	-	1370
1023	sensetime-011	0.0000	214	0.0005	440	0.0111	302	0.0000	515	-	1206
1024	serendipity-000	0.0000	700	0.0008	626	0.0202	492	0.0001	781	0.0004	612
1025	sertis-000	0.0000	267	0.0007	572	-	929	0.0000	572	0.0004	542
1026	sertis-001	0.0000	442	0.0004	400	-	1110	0.0002	883	0.0005	870
1027	sertis-002	0.0000	412	0.0007	554	0.0152	374	0.0000	559	0.0004	551
1028	sertis-003	0.0000	740	0.0008	638	0.0183	442	0.0000	483	0.0004	613
1029	seventhsense-000	0.0000	587	0.0006	519	0.0184	449	0.0001	592	0.0004	628
1030	seventhsense-001	0.0000	583	0.0006	518	0.0184	448	0.0001	593	0.0004	624
1031	seventhsense-002	0.0000	433	0.0003	329	0.0076	229	0.0000	573	0.0004	429
1032	seventhsense-003	0.0000	762	0.0003	317	0.0083	251	0.0000	385	0.0002	280
1033	seventhsense-005	0.0000	565	0.0002	278	0.0065	205	0.0000	402	0.0003	307
1034	seventhsense-006	0.0000	709	0.0002	279	0.0065	204	0.0000	392	-	1244
1035	shaman-000	0.0000	447	0.0000	177	-	1112	0.0000	88	0.0000	172
1036	shaman-001	0.0000	272	0.0000	161	-	932	0.0000	70	0.0000	155
1037	shu-001	0.0000	1085	0.0022	991	-	1202	0.0010	1186	0.0006	886
1038	shu-002	0.0000	911	0.0010	771	-	1073	0.0005	1077	0.0004	729
1039	shu-003	0.0000	13	0.0007	549	-	1180	0.0001	596	0.0003	330
1040	shufti-001	0.0000	639	0.0005	453	0.0131	334	0.0001	788	-	1197
1041	siat-002	0.0000	781	0.0012	834	-	1075	0.0000	502	0.0004	603
1042	siat-004	0.0000	529	0.0011	804	-	1222	0.0000	467	0.0004	577
1043	siat-005	0.0000	195	0.0000	61	0.0000	144	0.0000	217	0.0000	58
1044	sightropic-000	0.0000	899	0.0006	511	0.0138	343	0.0002	931	-	1265

Table 105: FTE is the proportion of failed template generation attempts. Failures can occur because the software throws an exception, or because the software electively refuses to process the input image. This would typically occur if a face is not detected. FTE is measured as the number of function calls that give EITHER a non-zero error code OR that give a "small" template. This is defined as one whose size is less than 0.3 times the median template size for that algorithm. This second rule is needed because some algorithms incorrectly fail to return a non-zero error code when template generation fails.
A hyphen "-" indicates the dataset was not produced. [1]The effects of FTE are included in the accuracy results of this report by regarding any template comparison involving a failed template to produce a low similarity score. Thus higher FTE results in higher FNMR and lower FMR.

FNMR(T) "False non-match rate"
FMR(T) "False match rate"

	Algorithm	Failure to Enrol Rate[1]									
	Name	APPLICATION		BORDER		KIOSK		MUGSHOT		VISA	
	Name	SEC. 2.2		SEC. 2.4		SEC. 2.6		SEC. 2.5		SEC. 2.1	
1045	sightropic-001	0.0000	881	0.0037	1088	0.0261	631	0.0007	1160	-	1212
1046	sjtu-001	0.0000	904	0.0010	790	-	1052	0.0005	1091	0.0004	755
1047	sjtu-002	0.0000	878	0.0010	770	-	1379	0.0005	1078	0.0004	721
1048	sjtu-003	0.0000	62	0.0005	459	-	1221	0.0000	543	0.0003	314
1049	sjtu-004	0.0000	315	0.0000	116	0.0000	27	0.0000	13	0.0003	310
1050	sjtu-005	0.0000	1123	0.0000	233	0.0000	63	0.0000	136	0.0006	885
1051	sjtu-006	0.0000	558	0.0026	1012	0.0298	658	0.0002	819	-	1117
1052	sjtu-007	0.0000	292	0.0002	274	0.0054	183	0.0000	284	-	1313
1053	sjtu-008	0.0000	173	0.0003	301	0.0074	226	0.0000	265	-	1238
1054	sjtu-009	0.0000	454	0.0003	302	0.0074	224	0.0000	85	-	1335
1055	sktelecom-000	0.0000	829	0.0008	640	0.0190	468	0.0000	538	0.0004	651
1056	smargtech-001	0.0000	101	0.0000	14	0.0000	113	0.0000	174	-	1116
1057	smartbiometrik-001	0.0005	1199	0.0649	1235	0.2147	882	0.0017	1232	0.0008	934
1058	smartengines-000	0.0066	1235	0.0150	1195	0.1656	871	0.0022	1244	0.0013	1001
1059	smartengines-001	0.0003	1193	0.0073	1160	0.0714	838	0.0007	1150	0.0005	836
1060	smartvist-000	0.0000	117	0.0026	1021	0.0357	724	0.0002	798	0.0011	970
1061	smartvist-001	0.0000	654	0.0005	419	0.0069	215	0.0001	756	0.0003	363
1062	smilart-001	-	1328	-	1343	-	916	-	1326	0.0273	1083
1063	smilart-002	0.0000	1106	0.0036	1085	-	1305	-	1405	0.0011	968
1064	smilart-003	0.0003	1191	0.0100	1182	-	1002	0.0014	1214	0.0013	1003
1065	sodec-000	0.0000	278	0.0000	174	0.0000	20	0.0000	68	0.0000	171
1066	sparktek-000	0.0000	1022	0.0016	908	0.0356	723	0.0001	651	-	1186
1067	sparsh-001	0.0000	133	0.0007	536	0.0168	415	0.0000	356	0.0004	486
1068	sqisoft-001	0.0000	461	0.0003	316	0.0078	233	0.0000	363	0.0003	402
1069	sqisoft-002	0.0000	77	0.0003	311	0.0078	234	0.0000	388	0.0003	406
1070	sqisoft-003	0.0000	410	0.0003	320	0.0078	236	0.0000	387	0.0003	352
1071	staqu-000	0.0000	218	0.0000	73	-	1406	0.0000	229	0.0000	70
1072	starhybrid-001	0.0001	1171	0.0033	1074	-	1277	0.0009	1178	0.0023	1036
1073	stcon-000	0.0000	559	0.0017	933	0.0301	666	0.0000	448	0.0003	370
1074	stcon-001	0.0000	525	0.0017	934	0.0301	665	0.0000	451	0.0003	372
1075	stcon-002	0.0000	755	0.0011	796	0.0226	558	0.0000	418	0.0003	322
1076	stcon-003	0.0000	55	0.0005	425	0.0142	356	0.0000	428	0.0004	482
1077	stcon-004	0.0000	29	0.0005	424	0.0142	355	0.0000	425	-	1141
1078	stcon-005	0.0000	181	0.0005	426	0.0142	357	0.0000	430	-	1182
1079	stcon-006	0.0000	479	0.0007	544	0.0191	473	0.0000	444	-	1366
1080	stcon-007	0.0000	293	0.0007	543	0.0191	472	0.0000	439	-	1312
1081	stcon-008	0.0000	49	0.0007	540	0.0191	474	0.0000	452	-	1154
1082	stengg-000	0.0000	198	0.0013	862	0.0350	720	0.0000	481	0.0004	607
1083	sukshi-000	0.0000	384	0.0000	221	0.0000	52	0.0000	124	0.0000	220
1084	sumsub-000	0.0000	1006	0.0018	945	0.0189	463	0.0011	1198	-	1408
1085	suprema-000	0.0000	843	0.0017	926	-	1205	0.0002	880	0.0004	658
1086	suprema-001	0.0000	940	0.0027	1023	0.0471	773	0.0003	959	0.0004	747
1087	suprema-002	0.0000	898	0.0010	780	0.0271	644	0.0002	831	0.0004	538
1088	suprema-003	0.0000	580	0.0008	646	0.0231	577	0.0000	379	0.0004	535
1089	suprema-004	0.0000	590	0.0014	880	0.0299	660	0.0000	377	0.0004	536
1090	suprema-005	0.0000	858	0.0014	879	0.0299	659	0.0005	1089	0.0004	661
1091	supremaid-001	0.0000	605	0.0020	970	0.0330	699	0.0001	687	0.0004	748
1092	supremaid-002	0.0000	798	0.0020	971	0.0330	698	0.0001	682	0.0004	752
1093	surrey-cvssp-000	0.0000	280	0.0000	173	0.0000	21	0.0000	67	0.0000	170
1094	surrey-cvssp-001	0.0173	1248	0.0007	556	0.0179	434	0.0011	1195	0.0015	1011
1095	surrey-cvssp-002	0.0000	1049	0.0006	486	0.0156	389	0.0001	649	0.0004	574
1096	surrey-cvssp-003	0.0000	58	0.0009	679	0.0165	411	0.0000	202	0.0001	253
1097	surrey-cvssp-004	0.0000	728	0.0015	899	0.0311	675	0.0004	1021	-	1264
1098	swsam-001	0.0000	285	0.0012	845	0.0263	634	0.0000	66	0.0000	166
1099	synesis-000	-	1386	-	1362	-	1116	-	1344	0.0007	914
1100	synesis-001	-	1323	-	1345	-	907	0.0035	1270	0.0021	1026
1101	synesis-003	-	1346	-	1331	-	992	0.0102	1299	0.1184	1091
1102	synesis-004	-	1359	-	1334	-	1024	0.0164	1304	0.0035	1056

Table 106: FTE is the proportion of failed template generation attempts. Failures can occur because the software throws an exception, or because the software electively refuses to process the input image. This would typically occur if a face is not detected. FTE is measured as the number of function calls that give EITHER a non-zero error code OR that give a "small" template. This is defined as one whose size is less than 0.3 times the median template size for that algorithm. This second rule is needed because some algorithms incorrectly fail to return a non-zero error code when template generation fails.
A hyphen "-" indicates the dataset was not produced. [1]The effects of FTE are included in the accuracy results of this report by regarding any template comparison involving a failed template to produce a low similarity score. Thus higher FTE results in higher FNMR and lower FMR.

	Algorithm	Failure to Enrol Rate[1]									
	Name	APPLICATION		BORDER		KIOSK		MUGSHOT		VISA	
	Name	SEC. 2.2		SEC. 2.4		SEC. 2.6		SEC. 2.5		SEC. 2.1	
1103	synesis-005	0.0000	723	0.0019	951	-	989	0.0001	663	0.0005	782
1104	synesis-006	0.0000	70	0.0003	326	-	1229	0.0000	542	0.0003	296
1105	synesis-007	0.0000	830	0.0013	857	-	1147	0.0002	900	0.0004	595
1106	synology-000	0.0000	27	0.0000	35	-	1189	0.0000	181	0.0000	40
1107	synology-001	0.0000	122	0.0000	81	-	1288	0.0000	262	0.0000	78
1108	synology-002	0.0000	472	0.0000	191	-	1142	0.0000	108	0.0000	190
1109	syscake-000	0.0008	1215	0.0017	932	0.0287	653	0.0007	1147	-	1107
1110	szpu-000	0.0000	199	0.0014	890	0.0330	700	0.0001	614	-	1202
1111	sztu-000	0.0000	490	0.0000	201	-	1172	0.0000	97	0.0000	196
1112	sztu-001	0.0000	439	0.0000	182	0.0000	68	0.0000	93	0.0000	175
1113	t4isb-000	0.0000	9	0.0000	34	0.0000	86	0.0000	197	0.0000	33
1114	tahakom-001	0.0025	1222	0.0020	979	0.0139	346	0.0020	1237	-	1364
1115	taiwanmobile-001	0.0000	967	0.0023	1002	0.0331	702	0.0006	1128	-	1162
1116	taiwanmobile-002	0.0000	982	0.0015	892	0.0238	589	0.0004	1061	-	1263
1117	tcc-000	0.0000	693	0.0699	1240	0.0478	774	0.0000	339	-	1316
1118	tcv-001	0.0000	607	0.0013	847	0.0152	378	0.0001	778	-	1240
1119	tech5-000	-	1268	-	1280	-	1216	-	1390	0.0003	394
1120	tech5-001	-	1281	-	1272	-	1265	0.0004	1043	0.0003	353
1121	tech5-002	-	1381	-	1363	-	1100	0.0001	636	0.0003	293
1122	tech5-003	0.0000	851	0.0005	430	-	1258	0.0001	637	0.0003	306
1123	tech5-004	0.0000	536	0.0008	609	-	1234	0.0003	960	0.0004	739
1124	tech5-005	0.0000	588	0.0007	592	-	1309	0.0000	454	0.0004	679
1125	tech5-007	0.0000	734	0.0014	887	0.0305	671	0.0000	393	0.0004	511
1126	tech5-008	0.0000	115	0.0007	535	0.0168	414	0.0000	349	0.0004	477
1127	tech5-009	0.0000	960	0.0030	1052	0.0542	791	0.0002	871	-	1381
1128	techainer-001	0.0000	1083	0.0004	393	0.0085	254	0.0005	1085	0.0004	664
1129	techainer-002	0.0000	1081	0.0004	389	0.0085	256	0.0005	1087	-	1173
1130	techbiometricid-001	0.0000	54	0.0000	54	0.0000	101	0.0000	205	-	1175
1131	techbiometricid-002	0.0000	111	0.0000	20	0.0000	117	0.0000	164	-	1124
1132	techsign-000	0.0007	1210	0.0334	1220	0.2093	876	0.0020	1239	0.0011	963
1133	techsign-001	0.0000	744	0.0008	660	0.0253	619	0.0002	855	0.0004	618
1134	telexper-000	0.0000	920	0.0006	513	0.0147	364	0.0003	994	-	1351
1135	tevian-000	-	1289	-	1303	-	1302	-	1406	0.0012	994
1136	tevian-001	-	1282	-	1267	-	1269	-	1381	0.0012	991
1137	tevian-002	-	1260	-	1273	-	1179	-	1387	0.0005	864
1138	tevian-003	-	1311	-	1288	-	1376	0.0003	962	0.0005	865
1139	tevian-004	0.0000	998	0.0024	1004	-	1353	0.0002	827	0.0005	852
1140	tevian-005	0.0001	1174	0.0041	1100	-	1319	0.0006	1129	0.0006	904
1141	tevian-006	0.0000	186	0.0012	824	-	1359	0.0003	973	0.0005	828
1142	tevian-007	0.0000	538	0.0015	904	0.0429	765	0.0002	872	0.0004	636
1143	tevian-008	0.0000	499	0.0006	471	0.0109	296	0.0000	427	0.0003	331
1144	tiger-001	-	1379	-	1408	-	1096	-	1370	0.0006	894
1145	tiger-002	0.0000	505	0.0010	758	-	1191	0.0001	727	0.0004	557
1146	tiger-003	0.0000	794	-	1407	-	1089	0.0001	725	0.0004	571
1147	tiger-004	0.0000	1129	0.0022	990	-	1050	0.0001	723	0.0004	737
1148	tiger-005	0.0000	707	0.0009	716	0.0194	483	0.0001	644	0.0004	562
1149	tiger-006	0.0000	855	0.0011	805	0.0396	750	0.0001	764	0.0004	766
1150	tiger-007	0.0000	870	0.0051	1131	0.0201	491	0.0002	847	-	1242
1151	tinkoff-001	0.0000	888	0.0008	636	0.0171	421	0.0001	738	0.0004	566
1152	tngd-001	0.0000	624	0.0009	663	0.0218	542	0.0000	513	-	1194
1153	tngd-002	0.0000	395	0.0000	214	0.0000	55	0.0000	116	-	1380
1154	tnitech-000	0.0000	719	0.0003	314	0.0060	190	0.0005	1116	0.0003	325
1155	tongyi-004	-	1392	-	1370	-	1130	-	1339	0.0006	897
1156	tongyi-005	0.0000	424	0.0000	230	-	1090	0.0000	135	0.0000	229
1157	tongyitrans-001	-	1353	-	1337	-	1014	-	1320	0.0040	1061
1158	tongyitrans-002	-	1315	-	1301	-	1398	-	1399	0.0040	1060
1159	tongyitrans-003	-	1396	-	1380	-	1137	-	1358	0.0006	898
1160	toppanidgate-000	0.0000	640	0.0008	629	0.0232	578	0.0004	1020	0.0004	623

Table 107: FTE is the proportion of failed template generation attempts. Failures can occur because the software throws an exception, or because the software electively refuses to process the input image. This would typically occur if a face is not detected. FTE is measured as the number of function calls that give EITHER a non-zero error code OR that give a "small" template. This is defined as one whose size is less than 0.3 times the median template size for that algorithm. This second rule is needed because some algorithms incorrectly fail to return a non-zero error code when template generation fails.
A hyphen "-" indicates the dataset was not produced. [1]The effects of FTE are included in the accuracy results of this report by regarding any template comparison involving a failed template to produce a low similarity score. Thus higher FTE results in higher FNMR and lower FMR.

	Algorithm	Failure to Enrol Rate[1]									
	Name	APPLICATION		BORDER		KIOSK		MUGSHOT		VISA	
	Name	SEC. 2.2		SEC. 2.4		SEC. 2.6		SEC. 2.5		SEC. 2.1	
1161	toppansecurity-001	0.0000	853	0.0020	969	0.0161	408	0.0001	643	-	1110
1162	toshiba-000	-	1398	-	1375	-	1146	-	1355	0.0000	187
1163	toshiba-001	-	1334	-	1358	-	937	-	1334	0.0000	168
1164	toshiba-002	0.0000	157	0.0000	94	-	1321	0.0000	275	0.0000	92
1165	toshiba-003	0.0000	304	0.0001	258	-	953	0.0001	720	0.0001	255
1166	toshiba-004	0.0000	324	0.0000	109	0.0000	31	0.0000	5	0.0000	112
1167	toshiba-005	0.0000	699	0.0004	375	0.0050	177	0.0001	750	0.0003	333
1168	toshiba-006	0.0000	552	0.0004	374	0.0050	178	0.0001	752	0.0003	329
1169	toshiba-007	0.0000	914	0.0005	428	0.0082	247	0.0002	921	0.0004	616
1170	toshiba-008	0.0000	865	0.0005	427	0.0082	248	0.0002	922	0.0004	610
1171	toshiba-009	0.0000	761	0.0004	398	0.0070	217	0.0002	909	-	1382
1172	toshiba-010	0.0000	886	0.0004	363	0.0064	199	0.0002	896	-	1279
1173	toshiba-011	0.0000	813	0.0006	481	0.0137	342	0.0002	894	-	1338
1174	toshiba-012	0.0000	535	0.0004	401	0.0120	318	0.0000	570	-	1096
1175	toss-000	0.0000	52	0.0009	686	0.0209	514	0.0001	674	-	1152
1176	touchlessid-000	0.0042	1227	0.0133	1192	0.2009	875	0.0018	1235	0.0032	1053
1177	touchlessid-001	0.0000	53	0.0036	1086	0.0923	856	0.0000	208	0.0000	43
1178	touchlessid-002	0.0000	416	0.0043	1111	0.1087	861	0.0000	140	0.0000	223
1179	touchlessid-003	0.0000	611	0.0010	762	0.0287	654	0.0002	802	0.0004	734
1180	touchlessid-004	0.0000	1127	0.0013	872	0.0398	753	0.0002	916	-	1300
1181	transmitsecurity-001	0.0000	554	0.0009	683	0.0226	559	0.0000	499	-	1118
1182	trueface-000	0.0000	704	0.0000	105	-	965	0.0000	18	0.0000	103
1183	trueface-001	0.0000	915	0.0038	1092	-	1119	0.0007	1159	0.0005	831
1184	trueface-002	0.0000	871	0.0046	1121	-	1339	0.0003	949	0.0005	854
1185	trueface-003	0.0000	884	0.0046	1120	0.0397	752	0.0003	948	0.0005	853
1186	trueidvng-001	0.0000	926	0.0020	978	0.0385	743	0.0002	859	0.0005	824
1187	truststamp-001	0.0000	504	0.0010	749	0.0189	466	0.0000	389	0.0003	371
1188	truststamp-002	0.0000	668	0.0010	754	0.0189	465	0.0000	382	-	1292
1189	truststamp-003	0.0000	575	0.0010	750	0.0189	467	0.0000	391	-	1220
1190	ttigroup-000	0.0000	113	0.0000	21	0.0000	118	0.0000	165	-	1122
1191	tuputech-000	0.0003	1195	0.0116	1190	-	1259	-	1383	0.0081	1074
1192	turingtechvip-001	0.0001	1154	0.0007	578	0.0061	194	0.0007	1151	0.0006	881
1193	turingtechvip-002	0.0001	1155	0.0017	930	0.0097	272	0.0007	1149	0.0006	882
1194	turkcell-000	0.0110	1242	0.0234	1210	0.0350	721	0.0103	1300	0.0306	1085
1195	turkcell-001	0.0000	140	0.0002	273	0.0034	168	0.0001	665	0.0003	291
1196	turkcell-002	0.0000	486	0.0002	266	0.0026	164	0.0001	591	-	1359
1197	twface-000	0.0000	114	0.0000	23	0.0000	119	0.0000	162	0.0000	25
1198	twface-001	0.0000	150	0.0000	85	0.0000	126	0.0000	242	0.0000	83
1199	ulsee-001	0.0000	482	0.0000	206	-	1157	0.0000	101	0.0000	202
1200	ultinous-000	-	1401	-	1376	-	1151	-	1356	0.0003	351
1201	ultinous-001	-	1355	-	1338	-	1018	-	1318	0.0003	348
1202	uluface-002	0.0000	106	0.0000	17	-	1271	0.0000	168	0.0000	16
1203	uluface-003	0.0000	383	0.0001	263	-	1047	0.0002	804	0.0002	273
1204	unicc-001	0.0000	228	0.0012	822	0.0230	574	0.0004	1067	0.0004	565
1205	unicc-002	0.0316	1255	0.0082	1170	0.0188	460	0.0226	1308	0.0936	1090
1206	unicc-003	0.0007	1211	0.0022	987	0.0094	268	0.0026	1259	0.0029	1046
1207	unicc-004	0.0000	1124	0.0012	820	0.0066	207	0.0012	1204	-	1299
1208	unissey-001	0.0000	109	0.0000	24	0.0000	116	0.0000	166	0.0000	26
1209	unissey-002	0.0000	466	0.0000	194	0.0000	78	0.0000	109	0.0000	193
1210	unissey-003	0.0000	8	0.0008	604	0.0191	469	0.0001	658	0.0004	504
1211	unissey-004	0.0000	28	0.0009	694	0.0240	591	0.0001	701	0.0004	584
1212	unissey-005	0.0000	2	0.0009	693	0.0240	590	0.0001	702	-	1137
1213	unissey-006	0.0000	676	0.0220	1206	0.0583	799	0.0003	983	-	1308
1214	unissey-007	0.0000	585	0.0101	1183	0.0376	739	0.0004	1013	-	1214
1215	upc-001	0.0000	1034	0.0003	306	-	1348	0.0003	952	0.0003	379
1216	urielsoft-000	0.0000	257	0.0023	1001	0.0371	733	0.0000	547	-	1310
1217	useb-000	0.0000	751	0.0009	709	0.0228	562	0.0001	761	0.0004	523
1218	useb-001	0.0000	784	0.0009	710	0.0228	563	0.0001	762	0.0004	528

Table 108: FTE is the proportion of failed template generation attempts. Failures can occur because the software throws an exception, or because the software electively refuses to process the input image. This would typically occur if a face is not detected. FTE is measured as the number of function calls that give EITHER a non-zero error code OR that give a "small" template. This is defined as one whose size is less than 0.3 times the median template size for that algorithm. This second rule is needed because some algorithms incorrectly fail to return a non-zero error code when template generation fails.
A hyphen "-" indicates the dataset was not produced. [1]The effects of FTE are included in the accuracy results of this report by regarding any template comparison involving a failed template to produce a low similarity score. Thus higher FTE results in higher FNMR and lower FMR.

FNMR(T) "False non-match rate"
FMR(T) "False match rate"

	Algorithm	Failure to Enrol Rate[1]									
	Name	APPLICATION		BORDER		KIOSK		MUGSHOT		VISA	
	Name	SEC. 2.2		SEC. 2.4		SEC. 2.6		SEC. 2.5		SEC. 2.1	
1219	useb-002	0.0000	650	0.0009	706	0.0228	569	0.0001	768	0.0004	509
1220	useb-003	0.0000	511	0.0009	703	0.0228	565	0.0001	765	-	1139
1221	useb-004	0.0000	739	0.0004	394	0.0112	303	0.0002	867	-	1275
1222	uxlabs-001	0.0000	421	0.0000	232	0.0000	62	0.0000	138	0.0000	230
1223	uxlabs-003	0.0000	223	0.0000	149	0.0000	3	0.0000	59	0.0000	141
1224	uzinfocom-000	0.0000	171	0.0005	416	0.0132	335	0.0001	712	-	1241
1225	uzinfocom-001	0.0000	438	0.0002	272	0.0044	172	0.0001	630	-	1328
1226	vaidio-001	0.0000	564	0.0006	503	0.0157	391	0.0043	1279	-	1109
1227	vcog-002	-	1390	-	1369	-	1126	-	1340	0.0019	1023
1228	vcortex-001	0.0000	1066	0.2295	1252	0.0802	846	0.0017	1231	0.0006	880
1229	vd-000	-	1270	-	1282	-	1219	-	1389	0.0000	51
1230	vd-001	0.0000	1094	0.0030	1053	-	1177	0.0004	1048	0.0009	937
1231	vd-002	0.0000	116	0.0000	22	1.0000	1284	0.0000	161	0.0000	24
1232	vd-003	0.0001	1156	0.0041	1099	0.0676	822	0.0030	1267	0.0029	1047
1233	veridas-001	-	1305	-	1294	-	1363	0.0001	729	0.0005	810
1234	veridas-002	0.0000	1026	0.0026	1020	-	951	0.0001	721	0.0005	815
1235	veridas-003	0.0000	1019	0.0026	1015	-	1322	0.0001	731	0.0005	812
1236	veridas-004	0.0000	1021	0.0026	1019	-	1343	0.0001	730	0.0005	814
1237	veridas-005	0.0000	1018	0.0026	1014	-	1320	0.0001	732	0.0005	813
1238	veridas-006	0.0000	1029	0.0026	1017	0.0595	801	0.0001	724	0.0005	817
1239	veridas-007	0.0000	1014	0.0026	1013	0.0595	802	0.0001	728	0.0005	808
1240	veridas-008	0.0000	1025	0.0026	1016	0.0595	800	0.0001	719	0.0005	816
1241	veridas-009	0.0000	1017	0.0026	1018	0.0597	803	0.0001	657	0.0005	820
1242	veridas-010	0.0000	880	0.0011	809	0.0212	525	0.0004	1059	-	1196
1243	veridium-000	0.0061	1234	0.5956	1255	0.2889	887	0.0050	1286	0.0009	936
1244	veridium-001	0.0001	1146	0.0087	1176	0.1615	867	0.0014	1217	0.0006	874
1245	veridium-002	0.0000	1134	0.0083	1174	0.1591	866	0.0010	1183	0.0005	849
1246	veridium-003	0.0001	1145	0.0087	1175	0.1615	868	0.0014	1218	-	1224
1247	verigram-000	0.0000	954	0.0068	1154	0.0822	850	0.0003	1005	0.0005	842
1248	verigram-001	0.0000	927	0.0003	313	0.0060	189	0.0002	895	0.0003	404
1249	verigram-002	0.0000	1062	0.0052	1137	0.0378	740	0.0010	1185	0.0006	900
1250	verigram-003	0.0000	1108	0.0025	1009	0.0288	655	0.0009	1182	0.0008	929
1251	verihubs-inteligensia-000	0.0000	578	0.0029	1037	0.0669	821	0.0001	616	0.0004	678
1252	verihubs-inteligensia-001	0.0000	501	0.0029	1036	0.0669	820	0.0001	611	0.0004	675
1253	verihubs-inteligensia-002	0.0000	742	0.0029	1038	0.0669	819	0.0001	603	0.0004	683
1254	verijelas-000	0.0000	631	0.0023	998	0.0375	737	0.0004	1073	0.0006	888
1255	via-000	0.0000	489	0.0000	202	-	1171	0.0000	98	0.0000	195
1256	via-001	0.0000	310	0.0000	106	-	960	0.0000	19	0.0000	104
1257	via-004	0.0000	417	0.0000	227	0.0000	60	0.0000	143	0.0000	222
1258	via-005	0.0000	459	0.0000	186	0.0000	74	0.0000	79	0.0000	180
1259	via-006	0.0000	23	0.0000	40	0.0000	92	0.0000	186	-	1146
1260	viante-000	0.0000	887	0.0008	642	0.0168	417	0.0001	695	0.0004	772
1261	viante-001	0.0000	925	0.0008	643	0.0168	418	0.0001	697	-	1343
1262	viante-002	0.0000	752	0.0007	591	0.0154	382	0.0001	698	-	1369
1263	viante-003	0.0000	720	0.0007	589	0.0154	381	0.0001	694	-	1250
1264	videmo-000	0.0000	895	0.0019	956	-	955	0.0003	982	0.0012	992
1265	videmo-001	0.0000	1005	0.0170	1197	0.0332	704	0.0010	1192	0.0011	978
1266	videmo-002	0.0000	443	0.0006	507	0.0189	461	0.0001	680	0.0004	495
1267	videmo-003	0.0000	247	0.0006	505	0.0189	462	0.0001	675	-	1290
1268	videonetics-001	0.0004	1196	0.0309	1217	-	1183	0.0015	1224	0.0010	951
1269	videonetics-002	0.0000	958	0.0459	1230	-	1043	0.0006	1133	0.0005	862
1270	viettelai-000	0.0000	331	0.0000	114	0.0000	34	0.0000	4	0.0000	107
1271	viettelai-001	0.0000	841	0.0010	741	0.0161	407	0.0000	552	0.0004	481
1272	viettelai-002	0.0000	952	0.0019	953	0.0334	708	0.0002	902	-	1256
1273	viettelai-003	0.0000	890	0.0011	813	0.0218	543	0.0001	594	-	1296
1274	viettelai-004	0.0000	623	0.0005	438	0.0139	347	0.0000	478	-	1195
1275	viettelhightech-000	0.0000	1053	0.0019	959	0.0368	731	0.0007	1155	0.0005	855
1276	viettelhightech-001	0.0000	818	0.0014	876	0.0434	767	0.0001	785	-	1332

Table 109: FTE is the proportion of failed template generation attempts. Failures can occur because the software throws an exception, or because the software electively refuses to process the input image. This would typically occur if a face is not detected. FTE is measured as the number of function calls that give EITHER a non-zero error code OR that give a "small" template. This is defined as one whose size is less than 0.3 times the median template size for that algorithm. This second rule is needed because some algorithms incorrectly fail to return a non-zero error code when template generation fails.
A hyphen "-" indicates the dataset was not produced. [1]The effects of FTE are included in the accuracy results of this report by regarding any template comparison involving a failed template to produce a low similarity score. Thus higher FTE results in higher FNMR and lower FMR.

	Algorithm	Failure to Enrol Rate[1]									
	Name	APPLICATION		BORDER		KIOSK		MUGSHOT		VISA	
	Name	SEC. 2.2		SEC. 2.4		SEC. 2.6		SEC. 2.5		SEC. 2.1	
1277	viettelhightech-002	0.0000	756	0.0014	877	0.0434	766	0.0001	787	-	1388
1278	vigilantsolutions-000	-	1377	-	1405	-	1087	-	1371	0.0007	913
1279	vigilantsolutions-001	-	1361	-	1396	-	1030	-	1369	0.0004	700
1280	vigilantsolutions-002	-	1263	-	1275	-	1194	-	1384	0.0004	687
1281	vigilantsolutions-003	-	1320	-	1341	-	896	-	1331	0.0004	470
1282	vigilantsolutions-004	-	1319	-	1342	-	892	-	1332	0.0004	471
1283	vigilantsolutions-005	-	1287	-	1305	-	1297	0.0001	628	0.0004	458
1284	vigilantsolutions-006	0.0000	1001	0.0028	1028	-	1409	0.0001	625	0.0004	456
1285	vigilantsolutions-007	0.0000	997	0.0028	1030	-	1344	0.0001	629	0.0004	462
1286	vigilantsolutions-008	0.0000	993	0.0028	1029	-	1292	0.0001	627	0.0004	459
1287	vigilantsolutions-009	0.0000	992	0.0028	1027	-	1283	0.0001	624	0.0004	447
1288	vigilantsolutions-010	0.0000	1002	0.0028	1031	0.0609	805	0.0001	620	0.0004	466
1289	vigilantsolutions-011	0.0000	1003	0.0028	1032	0.0609	806	0.0001	622	0.0004	467
1290	vinai-000	0.0000	323	0.0000	122	-	977	0.0000	11	0.0000	113
1291	vinbigdata-001	0.0000	50	0.0000	44	0.0000	100	0.0000	207	0.0000	44
1292	vinbigdata-002	0.0000	258	0.0015	898	0.0250	610	0.0000	493	0.0004	714
1293	vinbigdata-003	0.0000	603	0.0007	551	0.0151	373	0.0000	576	0.0004	488
1294	vinbigdata-004	0.0000	754	0.0005	436	0.0141	348	0.0000	366	-	1389
1295	vinbigdata-005	0.0000	513	0.0005	433	0.0141	351	0.0000	373	-	1159
1296	vinbigdata-006	0.0000	832	0.0005	435	0.0141	350	0.0000	365	-	1342
1297	vinbigdata-007	0.0000	804	0.0005	434	0.0141	349	0.0000	364	-	1325
1298	vion-000	0.0050	1229	0.0392	1227	-	1121	0.0130	1303	0.0078	1073
1299	visage-000	0.0000	1058	0.0054	1140	-	1088	0.0009	1176	0.0006	883
1300	visica-001	0.0000	1093	0.0068	1156	0.0692	829	0.0010	1184	-	1383
1301	visica-002	0.0000	929	0.0080	1168	0.1006	859	0.0004	1050	-	1358
1302	visionbox-000	0.0000	1113	0.0033	1071	-	1300	0.0005	1113	0.0011	971
1303	visionbox-001	0.0000	1114	0.0033	1073	-	1159	0.0005	1112	0.0011	972
1304	visionbox-002	0.0000	124	0.0017	921	0.0270	643	0.0000	501	0.0004	760
1305	visionbox-003	0.0000	941	0.0010	739	0.0209	515	0.0001	686	0.0004	645
1306	visionbox-004	0.0000	885	0.0013	848	0.0248	605	0.0001	751	0.0004	725
1307	visionbox-005	0.0000	1008	0.0037	1090	0.0301	664	0.0005	1075	-	1360
1308	visionbox-006	0.0000	1046	0.0040	1096	0.0331	701	0.0007	1145	-	1145
1309	visionbox-007	0.0000	1042	0.0041	1098	0.0324	689	0.0006	1139	-	1327
1310	visionlabs-001	-	1347	-	1332	-	994	-	1323	0.0014	1008
1311	visionlabs-002	-	1283	-	1266	-	1270	-	1380	0.0026	1040
1312	visionlabs-003	-	1409	-	1384	-	1170	-	1348	0.0025	1039
1313	visionlabs-004	-	1308	-	1292	-	1371	-	1393	0.0008	931
1314	visionlabs-005	-	1349	-	1328	-	1006	0.0002	940	0.0023	1034
1315	visionlabs-006	-	1296	-	1313	-	1323	0.0003	989	0.0005	811
1316	visionlabs-007	0.0000	859	0.0014	884	-	1287	0.0003	986	0.0005	800
1317	visionlabs-008	0.0000	759	0.0015	896	-	1053	0.0002	933	0.0004	764
1318	visionlabs-009	0.0000	670	0.0010	745	-	915	0.0001	585	0.0004	632
1319	visionlabs-010	0.0000	983	0.0009	684	-	1029	0.0001	754	0.0004	634
1320	visionlabs-011	0.0000	32	0.0006	498	0.0156	390	0.0001	634	0.0004	479
1321	visteam-000	0.0000	1110	0.0031	1059	-	941	0.0005	1105	0.0011	959
1322	visteam-001	0.0000	988	0.0014	881	-	1141	0.0002	841	0.0004	653
1323	visteam-002	0.0000	972	0.0014	882	0.0285	651	0.0002	834	0.0004	639
1324	visteam-003	0.0000	765	0.0010	774	0.0225	555	0.0001	595	0.0004	549
1325	visteam-004	0.0000	746	0.0010	773	0.0225	552	0.0001	700	0.0004	547
1326	visteam-005	0.0000	763	0.0010	772	0.0224	551	0.0001	633	0.0004	550
1327	visteam-006	0.0000	610	0.0008	633	0.0209	511	0.0000	357	0.0004	463
1328	visteam-007	0.0000	667	0.0008	634	0.0209	509	0.0000	338	0.0004	472
1329	visteam-008	0.0000	570	0.0008	632	0.0209	510	0.0000	350	0.0004	448
1330	visteam-009	0.0000	698	0.0010	788	0.0328	695	0.0000	335	-	1249
1331	visteam-010	0.0000	815	0.0010	789	0.0328	696	0.0000	342	-	1336
1332	vivotek-001	0.0000	338	0.0006	495	0.0161	405	0.0000	35	-	1267
1333	vivotek-002	0.0000	209	0.0006	494	0.0161	406	0.0000	233	-	1211
1334	vixvizion-000	0.0002	1183	0.0028	1033	-	1239	0.0010	1191	0.0012	990

Table 110: FTE is the proportion of failed template generation attempts. Failures can occur because the software throws an exception, or because the software electively refuses to process the input image. This would typically occur if a face is not detected. FTE is measured as the number of function calls that give EITHER a non-zero error code OR that give a "small" template. This is defined as one whose size is less than 0.3 times the median template size for that algorithm. This second rule is needed because some algorithms incorrectly fail to return a non-zero error code when template generation fails.
A hyphen "-" indicates the dataset was not produced. [1]The effects of FTE are included in the accuracy results of this report by regarding any template comparison involving a failed template to produce a low similarity score. Thus higher FTE results in higher FNMR and lower FMR.

FNMR(T) "False non-match rate"
FMR(T) "False match rate"

	Algorithm	Failure to Enrol Rate[1]									
	Name	APPLICATION		BORDER		KIOSK		MUGSHOT		VISA	
	Name	SEC. 2.2		SEC. 2.4		SEC. 2.6		SEC. 2.5		SEC. 2.1	
1335	vixvizion-001	0.0000	891	0.0030	1051	-	935	0.0001	708	0.0004	669
1336	vixvizion-002	0.0000	933	0.0018	935	-	1233	0.0000	511	0.0004	637
1337	vixvizion-003	0.0000	65	0.0000	52	-	1224	0.0000	199	0.0000	49
1338	vixvizion-004	0.0000	435	0.0000	179	0.0000	66	0.0000	95	0.0000	177
1339	vixvizion-005	0.0000	296	0.0000	172	0.0000	25	0.0000	62	0.0000	163
1340	vixvizion-006	0.0000	193	0.0000	65	0.0000	139	0.0000	221	0.0000	60
1341	vixvizion-007	0.0000	239	0.0000	144	0.0000	8	0.0000	47	0.0000	134
1342	vnis-000	0.0007	1213	0.0695	1239	0.0756	843	0.0038	1276	0.0009	942
1343	vnpay-000	0.0000	990	0.0657	1238	0.0693	830	0.0037	1274	0.0006	875
1344	vnpay-001	0.0000	500	0.0052	1136	0.0497	776	0.0001	710	-	1143
1345	vnpt-001	0.0652	1258	0.2829	1254	-	1144	0.2116	1311	0.1598	1092
1346	vnpt-002	0.0000	595	0.0002	269	0.0024	162	0.0003	990	0.0003	299
1347	vnpt-003	0.0000	76	0.0004	348	0.0105	279	0.0002	801	0.0004	417
1348	vnpt-004	0.0000	682	0.0006	479	0.0160	403	0.0002	823	0.0004	567
1349	vnpt-005	0.0000	446	0.0006	465	0.0154	385	0.0002	854	0.0004	544
1350	vnpt-006	0.0000	21	0.0006	462	0.0154	386	0.0002	857	0.0004	532
1351	vnpt-007	0.0000	302	0.0006	464	0.0154	383	0.0002	853	-	1248
1352	vnpt-008	0.0000	180	0.0006	463	0.0154	387	0.0002	858	-	1183
1353	vnpt-009	0.0000	420	0.0006	466	0.0154	384	0.0002	856	-	1390
1354	vocalize-001	0.0216	1251	0.0193	1201	0.1691	872	0.0068	1293	-	1339
1355	vocord-001	-	1339	-	1320	-	968	-	1314	0.0038	1059
1356	vocord-002	-	1333	-	1353	-	934	-	1336	0.0037	1058
1357	vocord-003	-	1408	-	1383	-	1168	-	1347	0.0776	1088
1358	vocord-004	-	1395	-	1378	-	1134	0.0005	1104	0.0003	312
1359	vocord-005	-	1362	-	1397	-	1034	0.0013	1208	0.0003	405
1360	vocord-006	-	1400	-	1373	-	1150	0.0003	975	0.0003	366
1361	vocord-007	0.0000	900	0.0535	1231	-	998	0.0001	772	0.0004	424
1362	vocord-008	0.0000	690	0.0015	902	-	939	0.0003	996	0.0001	254
1363	vocord-009	0.0000	566	0.0006	496	-	1278	0.0001	780	0.0003	297
1364	vocord-010	0.0000	928	0.0005	450	0.0141	353	0.0002	860	0.0003	403
1365	vsoft-001	0.0069	1237	0.8292	1256	0.8200	891	0.0173	1305	-	1131
1366	vsoft-002	0.0026	1223	0.0029	1044	0.0613	807	0.0059	1292	-	1395
1367	vsoft-003	0.0000	1088	0.0029	1043	0.0613	808	0.0005	1079	-	1133
1368	vts-000	0.0000	962	0.0011	801	-	1105	0.0001	783	0.0004	750
1369	vts-001	0.0000	352	0.0003	299	0.0073	219	0.0000	359	0.0003	294
1370	vts-002	0.0000	212	0.0008	659	0.0150	370	0.0000	375	-	1207
1371	wicket-000	0.0000	581	0.0009	670	0.0260	630	0.0000	406	0.0004	561
1372	winsense-000	0.0000	345	0.0000	127	-	1005	0.0000	30	0.0000	118
1373	winsense-001	0.0000	484	0.0000	207	-	1161	0.0000	102	0.0000	200
1374	winsense-002	0.0000	152	0.0000	86	-	1317	0.0000	243	0.0000	82
1375	wiseai-001	0.0001	1143	0.0137	1194	0.0768	845	0.0018	1234	0.0018	1018
1376	wuhantianyu-001	0.0000	129	0.0007	557	0.0159	396	0.0001	590	0.0004	625
1377	x-laboratory-000	0.0247	1253	0.0000	97	-	1338	0.0005	1111	0.0002	276
1378	x-laboratory-001	0.0000	597	0.0012	825	-	1327	0.0001	737	0.0004	722
1379	xforwardai-000	0.0000	190	0.0000	64	-	1368	0.0000	220	0.0000	62
1380	xforwardai-001	0.0000	710	0.0007	579	-	970	0.0003	966	0.0004	710
1381	xforwardai-002	0.0000	533	0.0007	577	-	1228	0.0003	967	0.0004	705
1382	xm-000	0.0000	187	0.0007	550	-	1360	0.0001	597	0.0003	332
1383	yisheng-000	-	1288	-	1304	-	1296	-	1407	0.0006	877
1384	yisheng-001	-	1276	-	1261	-	1250	-	1374	0.0006	876
1385	yisheng-002	-	1388	-	1360	-	1118	-	1342	0.0006	879
1386	yisheng-004	0.0002	1186	-	1284	-	1211	0.0013	1207	0.0006	895
1387	yitu-000	-	1318	-	1299	-	1410	-	1397	0.0013	999
1388	yitu-001	-	1304	-	1286	-	1355	0.0009	1177	0.0006	896
1389	yitu-002	-	1364	-	1392	-	1037	-	1367	0.0000	205
1390	yitu-003	0.0000	343	0.0000	124	-	999	0.0009	1175	0.0000	120
1391	yoonik-000	0.0000	795	0.0019	957	-	1095	0.0001	670	0.0004	730
1392	yoonik-001	0.0000	329	0.0014	888	-	981	0.0001	771	0.0004	712

Table 111: FTE is the proportion of failed template generation attempts. Failures can occur because the software throws an exception, or because the software electively refuses to process the input image. This would typically occur if a face is not detected. FTE is measured as the number of function calls that give EITHER a non-zero error code OR that give a "small" template. This is defined as one whose size is less than 0.3 times the median template size for that algorithm. This second rule is needed because some algorithms incorrectly fail to return a non-zero error code when template generation fails.
A hyphen "-" indicates the dataset was not produced. [1]The effects of FTE are included in the accuracy results of this report by regarding any template comparison involving a failed template to produce a low similarity score. Thus higher FTE results in higher FNMR and lower FMR.

	Algorithm	Failure to Enrol Rate[1]									
	Name	APPLICATION		BORDER		KIOSK		MUGSHOT		VISA	
	Name	SEC. 2.2		SEC. 2.4		SEC. 2.6		SEC. 2.5		SEC. 2.1	
1393	yoonik-002	0.0000	893	0.0010	766	0.0284	650	0.0003	947	0.0006	871
1394	yoonik-003	0.0000	924	0.0009	712	0.0214	534	0.0002	818	0.0004	670
1395	yoonik-004	0.0000	480	0.0012	818	0.0251	614	0.0001	631	0.0004	497
1396	yoti-001	0.0000	842	0.0014	889	0.0418	760	0.0008	1174	0.0006	884
1397	yoti-002	0.0000	334	0.0007	547	0.0171	422	0.0001	689	-	1268
1398	ytu-000	0.0000	743	0.0010	786	-	1025	0.0002	910	0.0004	713
1399	yuan-000	0.0000	289	0.0000	170	-	943	0.0000	64	0.0000	164
1400	yuan-001	0.0000	1024	0.0010	781	-	893	0.0005	1106	0.0005	827
1401	yuan-002	0.0000	1016	0.0010	778	0.0284	648	0.0005	1108	0.0005	825
1402	yuan-003	0.0000	1020	0.0010	779	0.0284	649	0.0005	1110	0.0005	826
1403	yuan-004	0.0000	434	0.0000	178	0.0000	65	0.0000	94	0.0000	178
1404	yuan-005	0.0000	677	0.0005	441	0.0134	339	0.0002	849	0.0004	519
1405	yuan-006	0.0000	1052	0.0014	891	0.0369	732	0.0004	1037	0.0005	841
1406	yuan-007	0.0000	1057	0.0013	854	0.0336	712	0.0004	1035	0.0005	844
1407	yuan-008	0.0000	1047	0.0013	851	0.0336	713	0.0004	1036	0.0005	838
1408	yuan-009	0.0000	1054	0.0013	852	0.0336	710	0.0004	1033	-	1246
1409	yuan-010	0.0000	1056	0.0013	853	0.0336	711	0.0004	1034	-	1367
1410	yuanli-001	0.0000	350	0.0016	918	0.0318	679	0.0001	638	-	1276

Table 112: FTE is the proportion of failed template generation attempts. Failures can occur because the software throws an exception, or because the software electively refuses to process the input image. This would typically occur if a face is not detected. FTE is measured as the number of function calls that give EITHER a non-zero error code OR that give a "small" template. This is defined as one whose size is less than 0.3 times the median template size for that algorithm. This second rule is needed because some algorithms incorrectly fail to return a non-zero error code when template generation fails.
A hyphen "-" indicates the dataset was not produced. [1]The effects of FTE are included in the accuracy results of this report by regarding any template comparison involving a failed template to produce a low similarity score. Thus higher FTE results in higher FNMR and lower FMR.

FNMR(T) "False non-match rate"
FMR(T) "False match rate"

3.4 Recognition accuracy

Core algorithm accuracy is stated via:

- ▷ **Cooperative subjects**
  - The summary table of Figure 87;
  - The visa image DETs of Figure 218;
  - The mugshot DETs of Figure 284;
  - The mugshot ageing profiles of Figure 781;
  - The human-difficult pairs of Figure 108
- ▷ **Non-cooperative subjects**
  - The photojournalism DET of Figure 320

Figure 609 shows dependence of false match rate on algorithm score threshold. This allows a deployer to set a threshold to target a particular false match rate appropriate to the security objectives of the application.

Figure 608 likewise shows FMR(T) but for mugshots, and specially four subsets of the population.

Note that in both the mugshot and visa sets false match rates vary with the ethnicity, age, and sex, of the enrollee and impostor. For example figure 386 summarizes FMR for impostors paired from four groups black females, black males, white females, white males.

FNMR(T) "False non-match rate"
FMR(T) "False match rate"

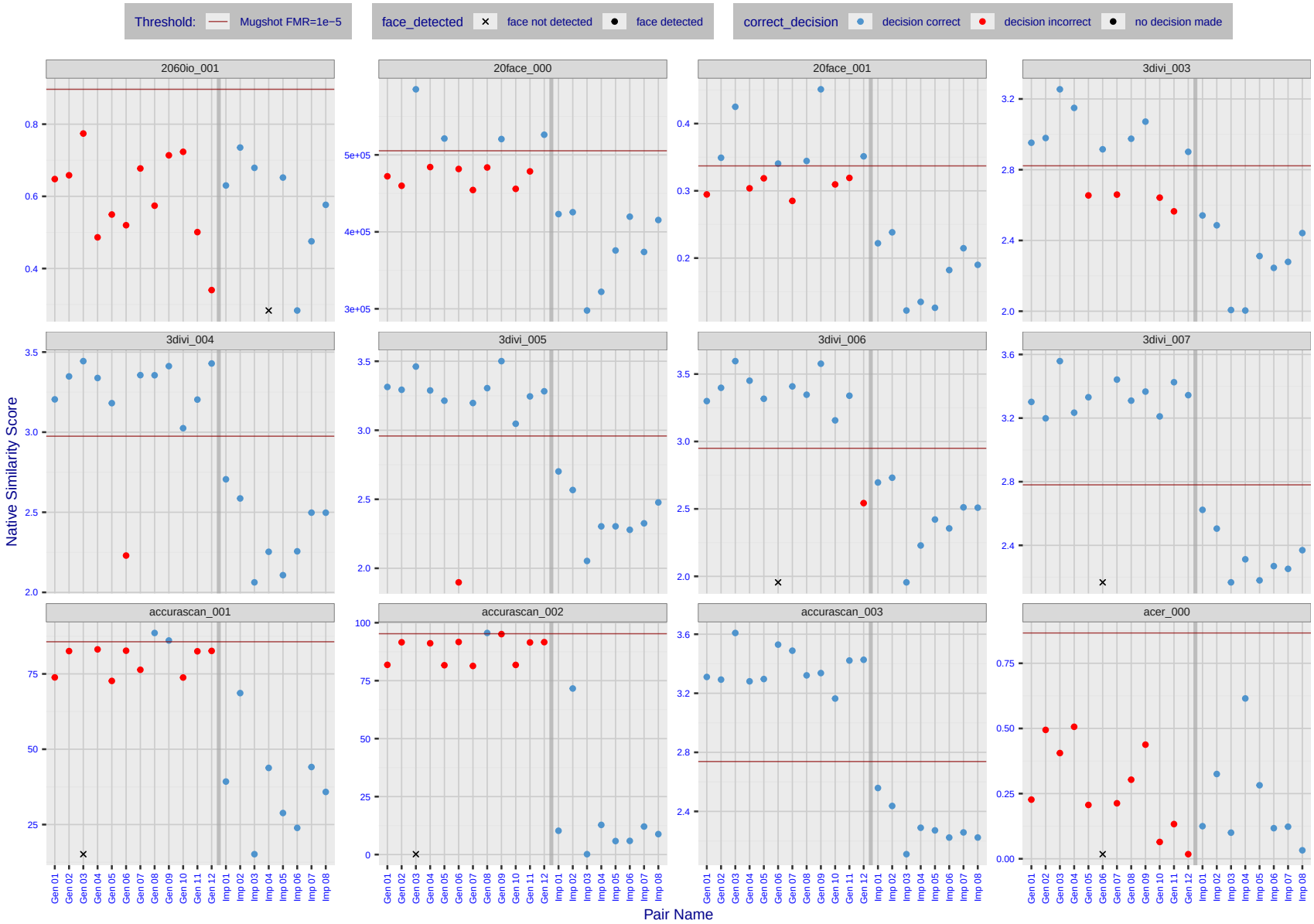

Figure 4: The figure shows algorithms' similarity scores for 12 genuine and 8 impostor image pairs used in a May 2018 paper by Phillips et al. ([1]). The threshold (red horizontal line) is a value calibrated to give FMR = 0.0001 on mugshot images. Points above the threshold correspond to pairs determined to be genuine, and points below the threshold correspond to pairs determined to be impostors. If the determined class (genuine or impostor) matches the real class, points will be blue; if not, red. An X represents face detection failure in either of the images in the pair. Note that the sample size (n=20) is small, and the figure may change substantially if larger or different sets are used. The images can be viewed on p. 13 of the Appendix, where Gen 01 corresponds to Same-Identity Pair 1, Gen 02 corresponds to Same-Identity Pair 2, and so on.

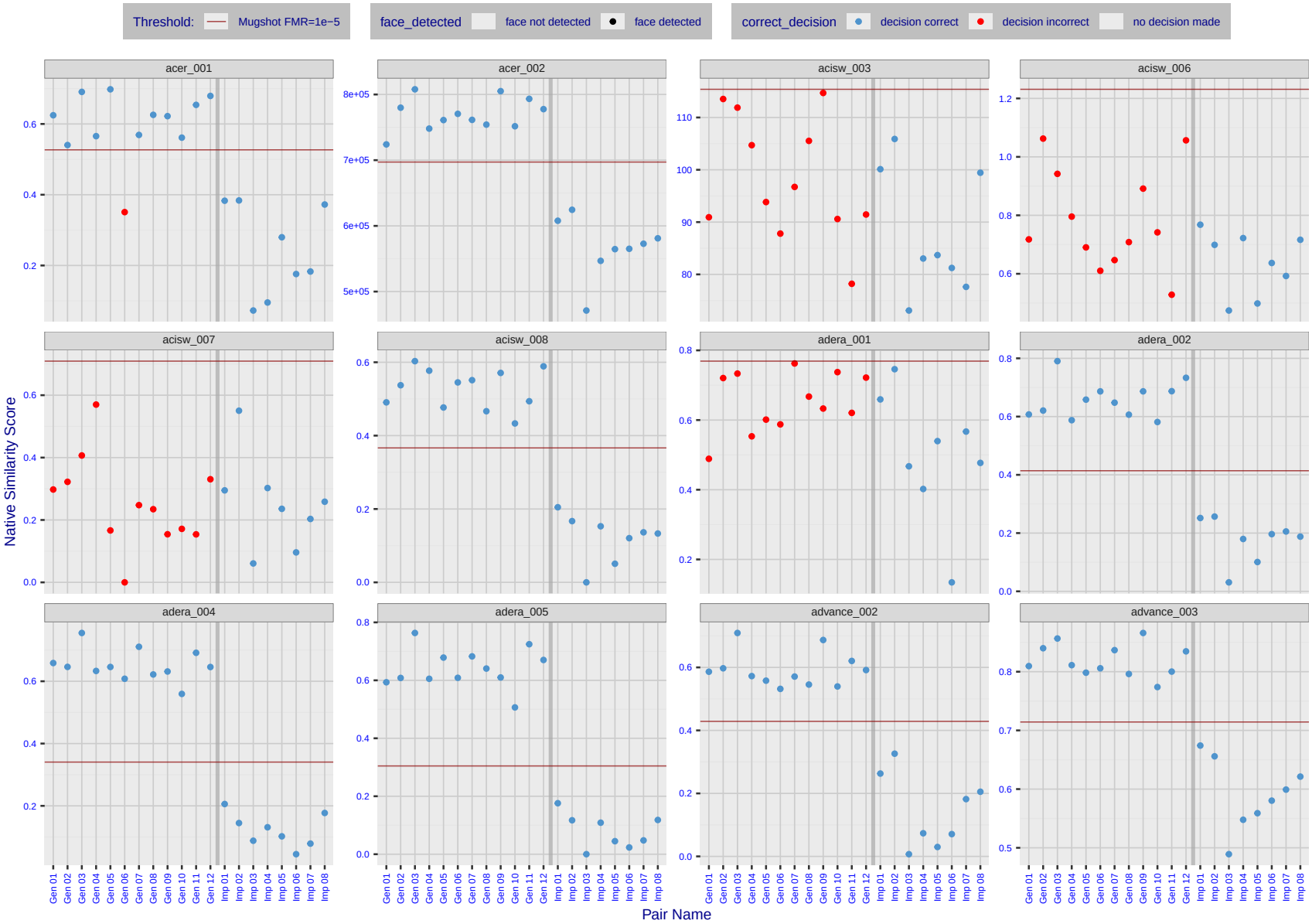

Figure 5: The figure shows algorithms' similarity scores for 12 genuine and 8 impostor image pairs used in a May 2018 paper by Phillips et al. ([1]). The threshold (red horizontal line) is a value calibrated to give FMR = 0.0001 on mugshot images. Points above the threshold correspond to pairs determined to be genuine, and points below the threshold correspond to pairs determined to be impostors. If the determined class (genuine or impostor) matches the real class, points will be blue; if not, red. An X represents face detection failure in either of the images in the pair. Note that the sample size (n=20) is small, and the figure may change substantially if larger or different sets are used. The images can be viewed on p. 13 of the Appendix, where Gen 01 corresponds to Same-Identity Pair 1, Gen 02 corresponds to Same-Identity Pair 2, and so on.

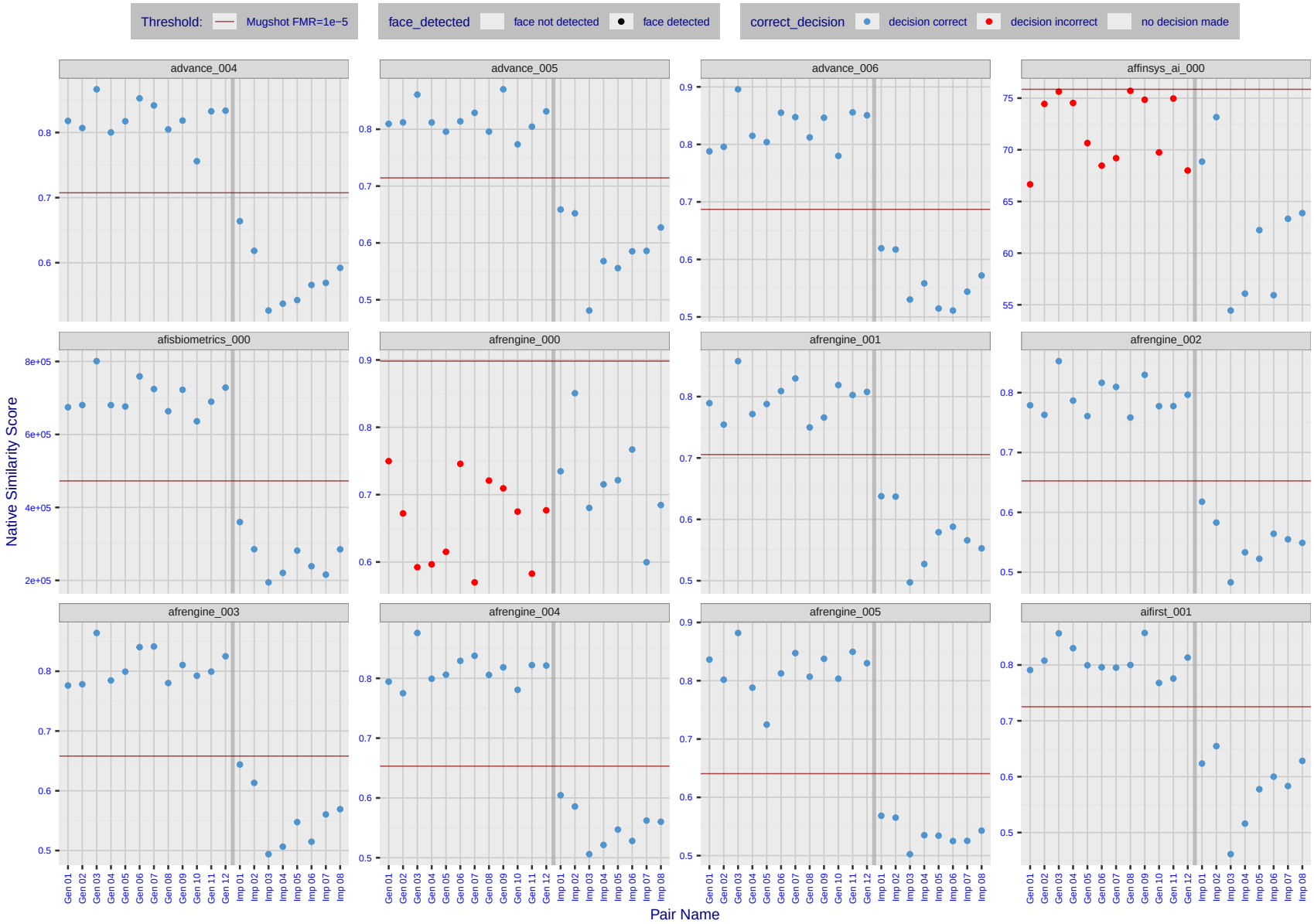

Figure 6: The figure shows algorithms' similarity scores for 12 genuine and 8 impostor image pairs used in a May 2018 paper by Phillips et al. ([1]). The threshold (red horizontal line) is a value calibrated to give FMR = 0.0001 on mugshot images. Points above the threshold correspond to pairs determined to be genuine, and points below the threshold correspond to pairs determined to be impostors. If the determined class (genuine or impostor) matches the real class, points will be blue; if not, red. An X represents face detection failure in either of the images in the pair. Note that the sample size (n=20) is small, and the figure may change substantially if larger or different sets are used. The images can be viewed on p. 13 of the Appendix, where Gen 01 corresponds to Same-Identity Pair 1, Gen 02 corresponds to Same-Identity Pair 2, and so on.

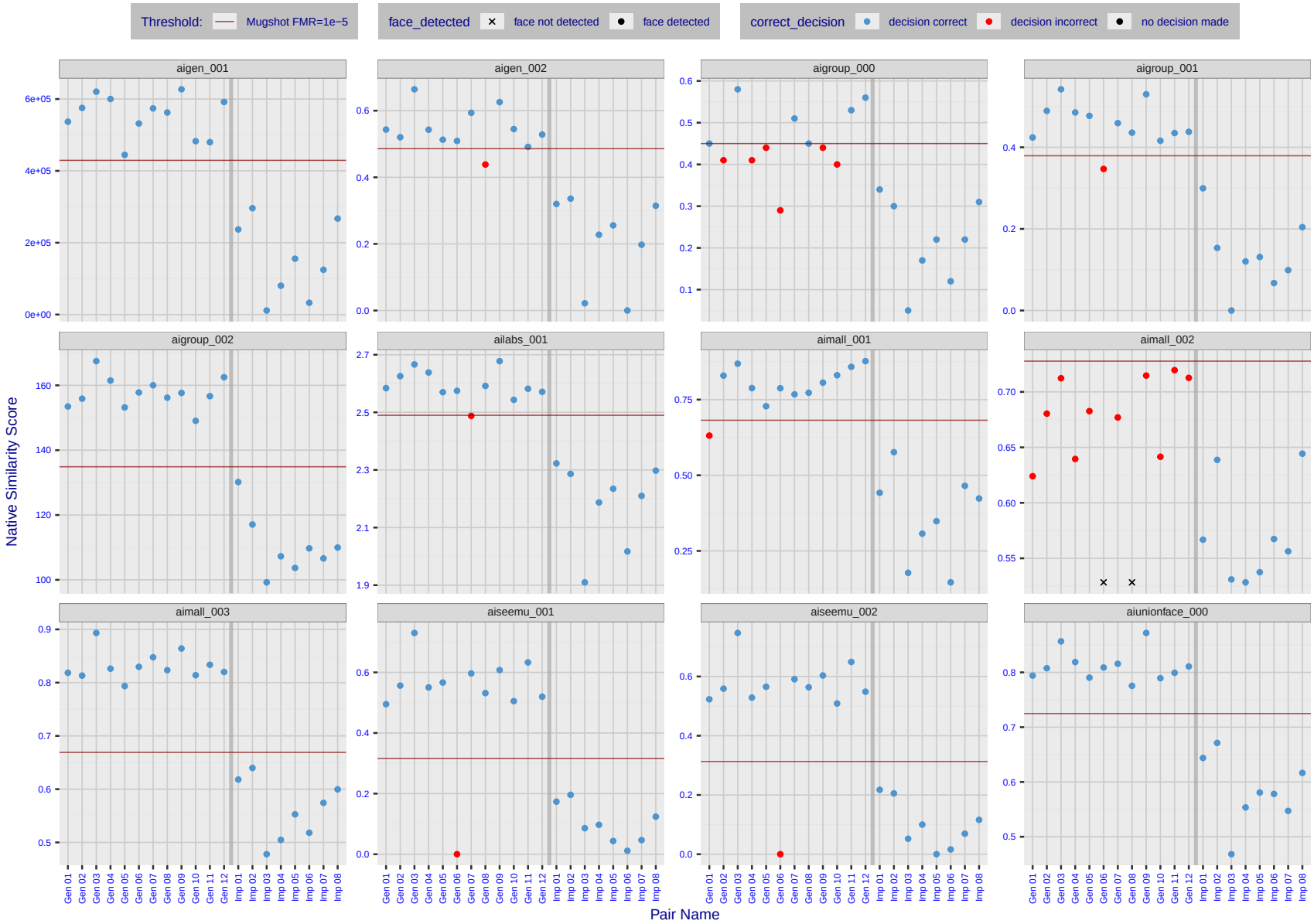

Figure 7: The figure shows algorithms' similarity scores for 12 genuine and 8 impostor image pairs used in a May 2018 paper by Phillips et al. ([1]). The threshold (red horizontal line) is a value calibrated to give FMR = 0.0001 on mugshot images. Points above the threshold correspond to pairs determined to be genuine, and points below the threshold correspond to pairs determined to be impostors. If the determined class (genuine or impostor) matches the real class, points will be blue; if not, red. An X represents face detection failure in either of the images in the pair. Note that the sample size (n=20) is small, and the figure may change substantially if larger or different sets are used. The images can be viewed on p. 13 of the Appendix, where Gen 01 corresponds to Same-Identity Pair 1, Gen 02 corresponds to Same-Identity Pair 2, and so on.

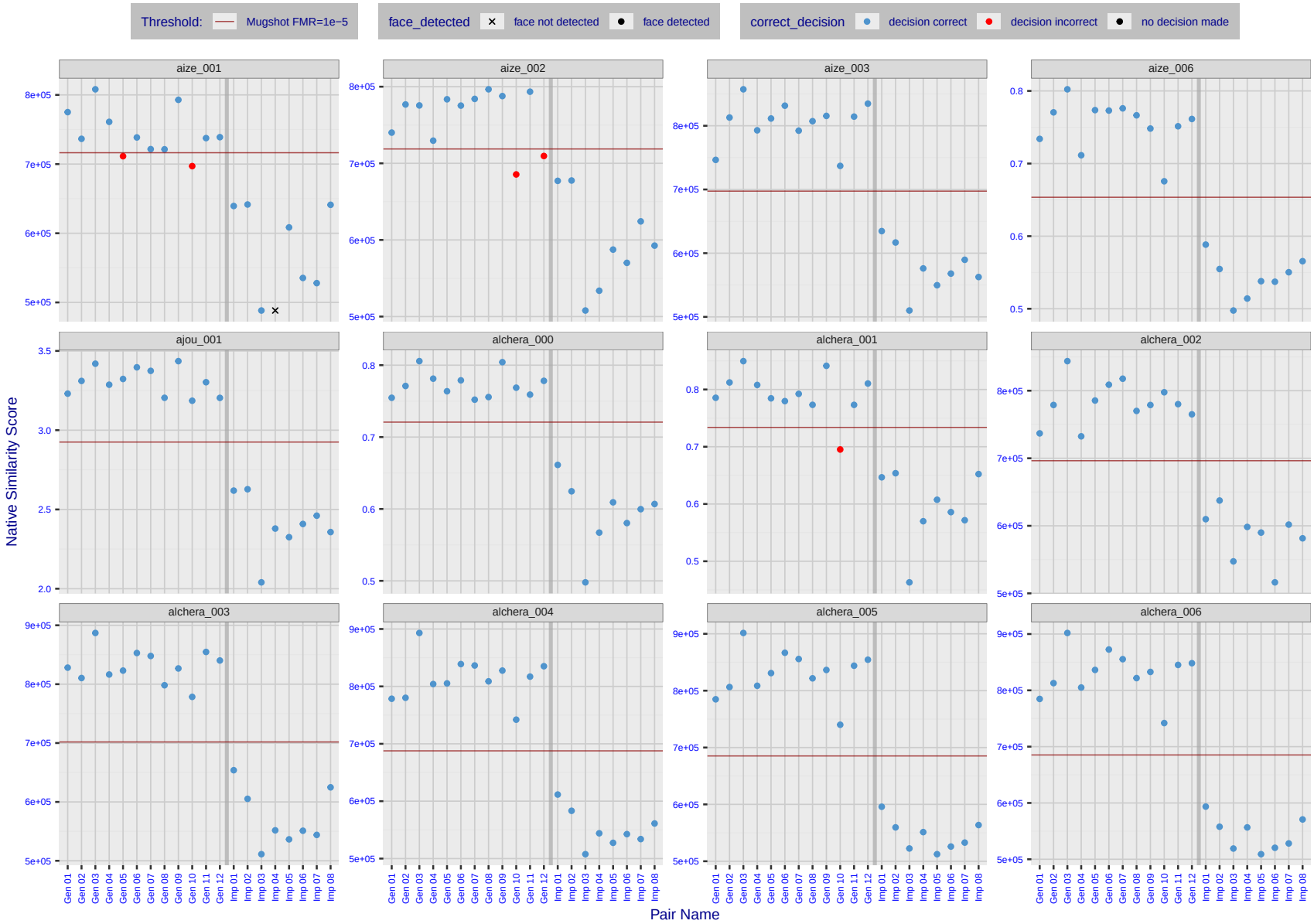

Figure 8: The figure shows algorithms' similarity scores for 12 genuine and 8 impostor image pairs used in a May 2018 paper by Phillips et al. ([1]). The threshold (red horizontal line) is a value calibrated to give FMR = 0.0001 on mugshot images. Points above the threshold correspond to pairs determined to be genuine, and points below the threshold correspond to pairs determined to be impostors. If the determined class (genuine or impostor) matches the real class, points will be blue; if not, red. An X represents face detection failure in either of the images in the pair. Note that the sample size (n=20) is small, and the figure may change substantially if larger or different sets are used. The images can be viewed on p. 13 of the Appendix, where Gen 01 corresponds to Same-Identity Pair 1, Gen 02 corresponds to Same-Identity Pair 2, and so on.

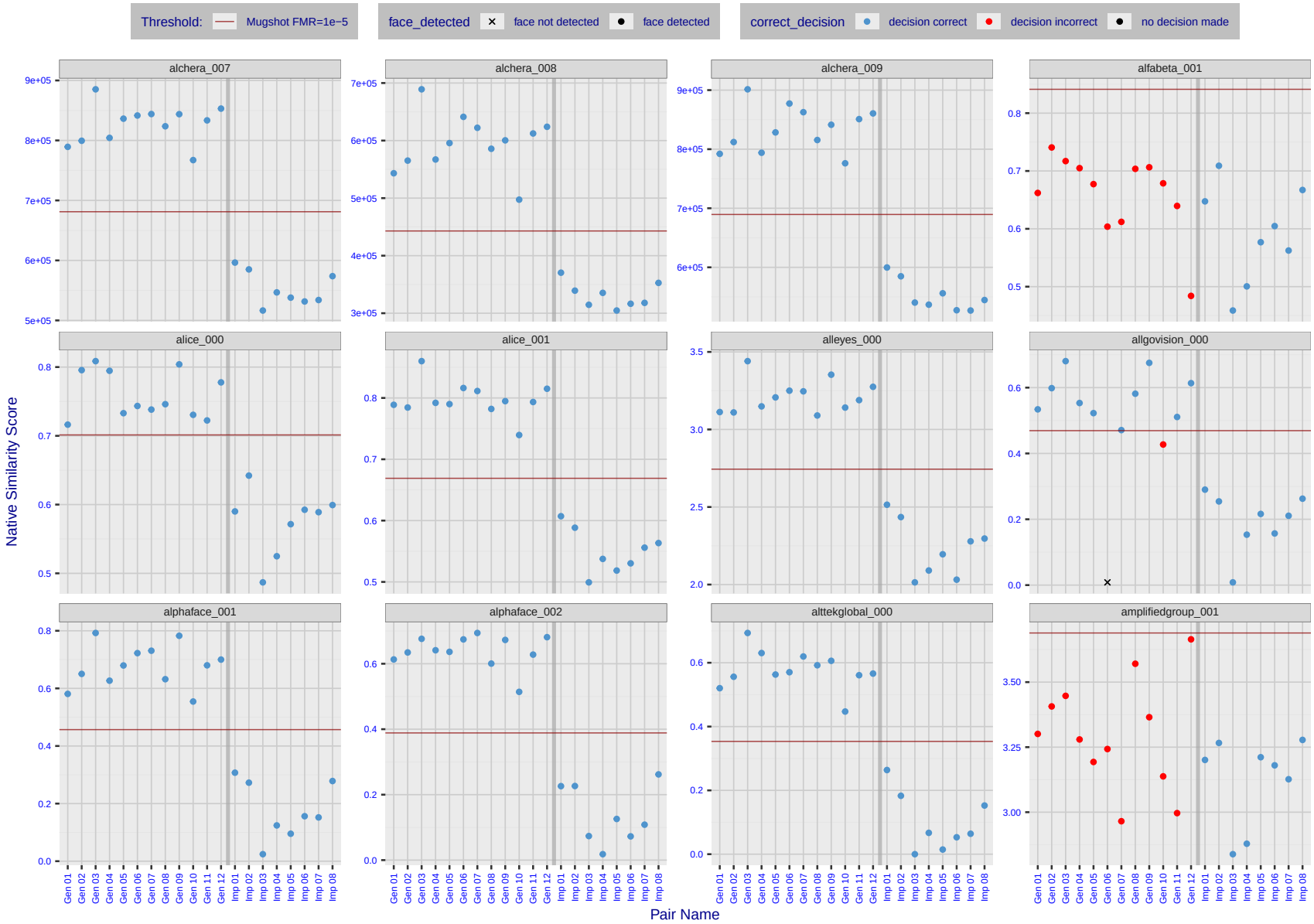

Figure 9: The figure shows algorithms' similarity scores for 12 genuine and 8 impostor image pairs used in a May 2018 paper by Phillips et al. ([1]). The threshold (red horizontal line) is a value calibrated to give FMR = 0.0001 on mugshot images. Points above the threshold correspond to pairs determined to be genuine, and points below the threshold correspond to pairs determined to be impostors. If the determined class (genuine or impostor) matches the real class, points will be blue; if not, red. An X represents face detection failure in either of the images in the pair. Note that the sample size (n=20) is small, and the figure may change substantially if larger or different sets are used. The images can be viewed on p. 13 of the Appendix, where Gen 01 corresponds to Same-Identity Pair 1, Gen 02 corresponds to Same-Identity Pair 2, and so on.

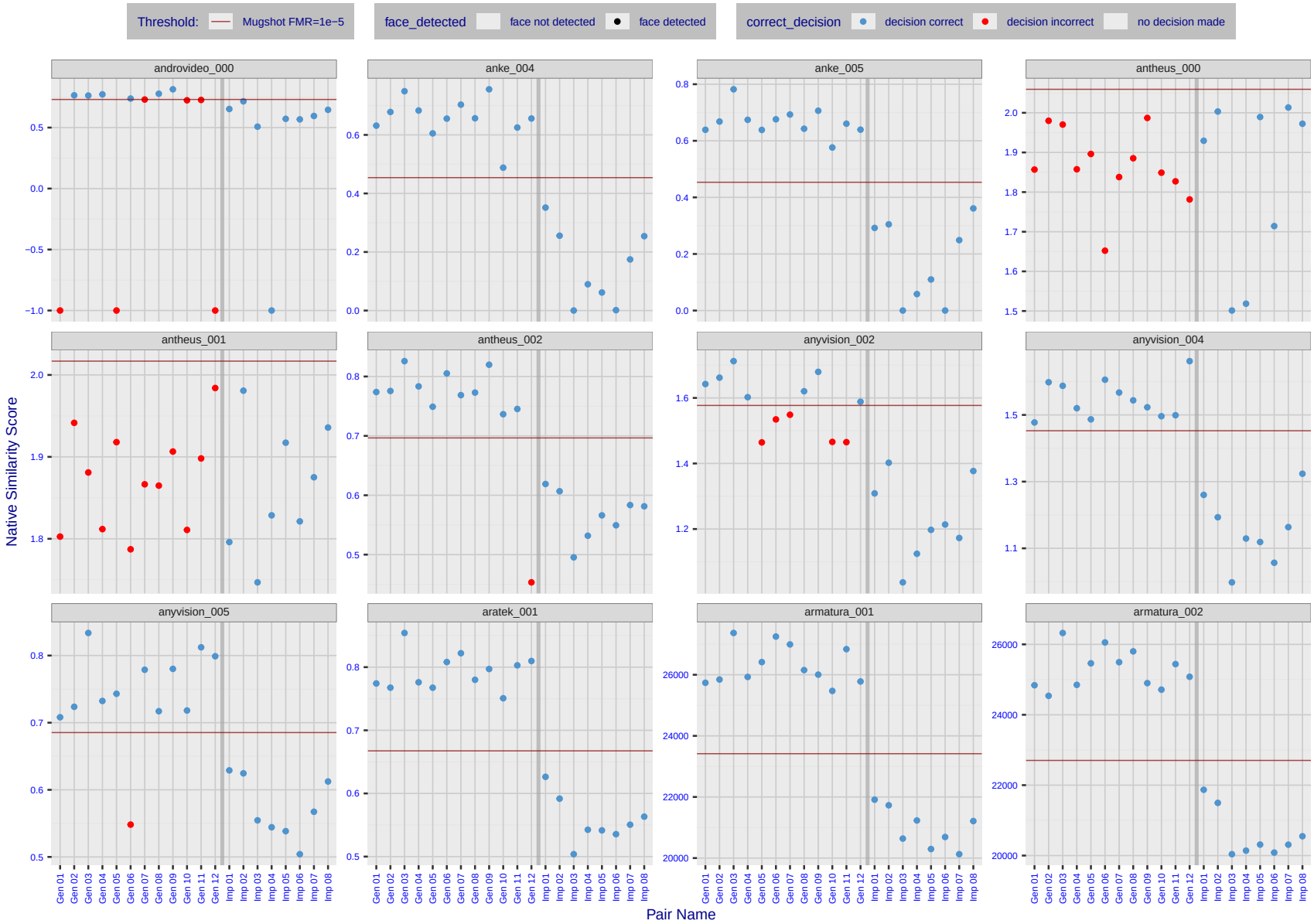

Figure 10: The figure shows algorithms' similarity scores for 12 genuine and 8 impostor image pairs used in a May 2018 paper by Phillips et al. ([1]). The threshold (red horizontal line) is a value calibrated to give FMR = 0.0001 on mugshot images. Points above the threshold correspond to pairs determined to be genuine, and points below the threshold correspond to pairs determined to be impostors. If the determined class (genuine or impostor) matches the real class, points will be blue; if not, red. An X represents face detection failure in either of the images in the pair. Note that the sample size (n=20) is small, and the figure may change substantially if larger or different sets are used. The images can be viewed on p. 13 of the Appendix, where Gen 01 corresponds to Same-Identity Pair 1, Gen 02 corresponds to Same-Identity Pair 2, and so on.

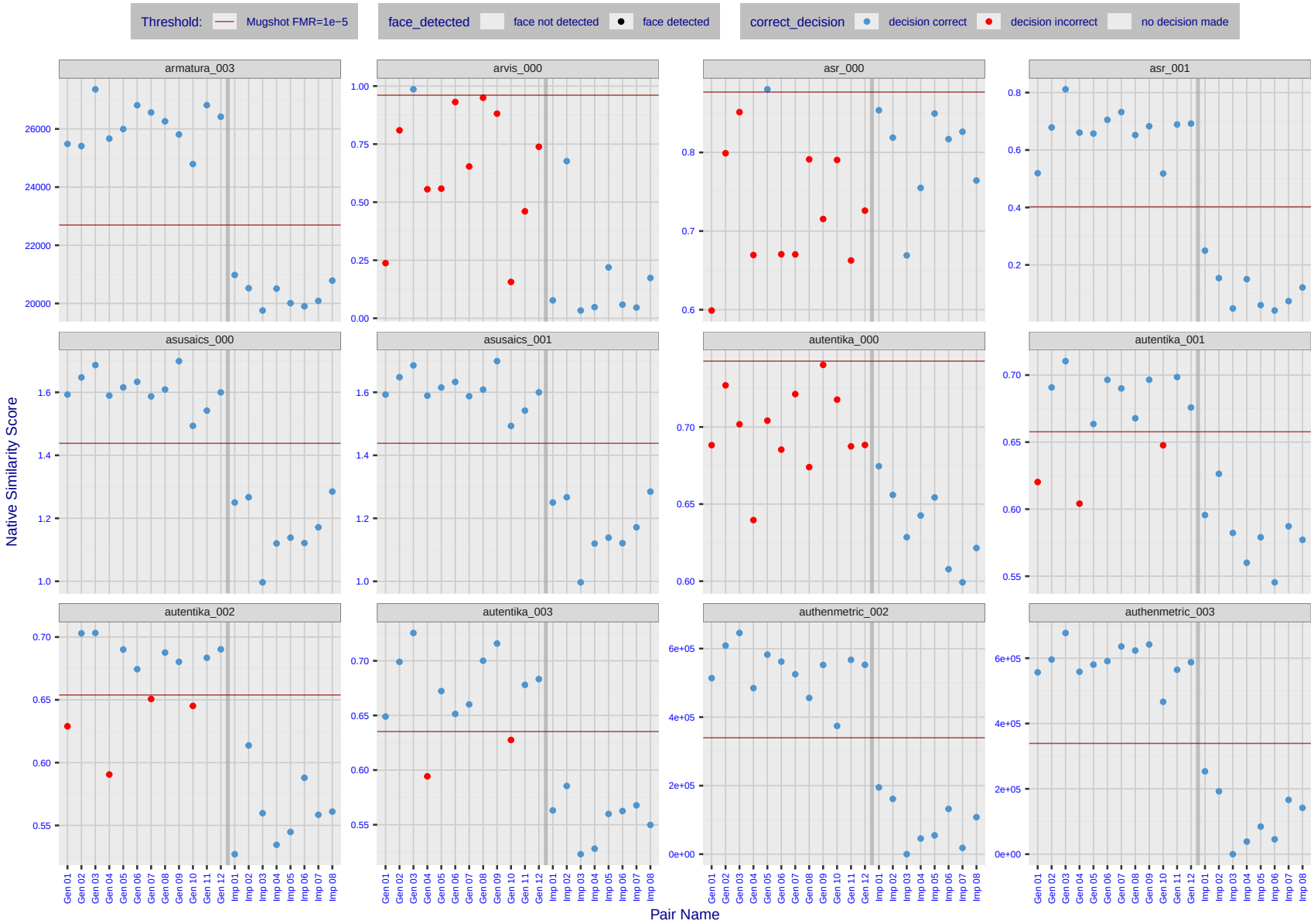

Figure 11: The figure shows algorithms' similarity scores for 12 genuine and 8 impostor image pairs used in a May 2018 paper by Phillips et al. ([1]). The threshold (red horizontal line) is a value calibrated to give FMR = 0.0001 on mugshot images. Points above the threshold correspond to pairs determined to be genuine, and points below the threshold correspond to pairs determined to be impostors. If the determined class (genuine or impostor) matches the real class, points will be blue; if not, red. An X represents face detection failure in either of the images in the pair. Note that the sample size (n=20) is small, and the figure may change substantially if larger or different sets are used. The images can be viewed on p. 13 of the Appendix, where Gen 01 corresponds to Same-Identity Pair 1, Gen 02 corresponds to Same-Identity Pair 2, and so on.

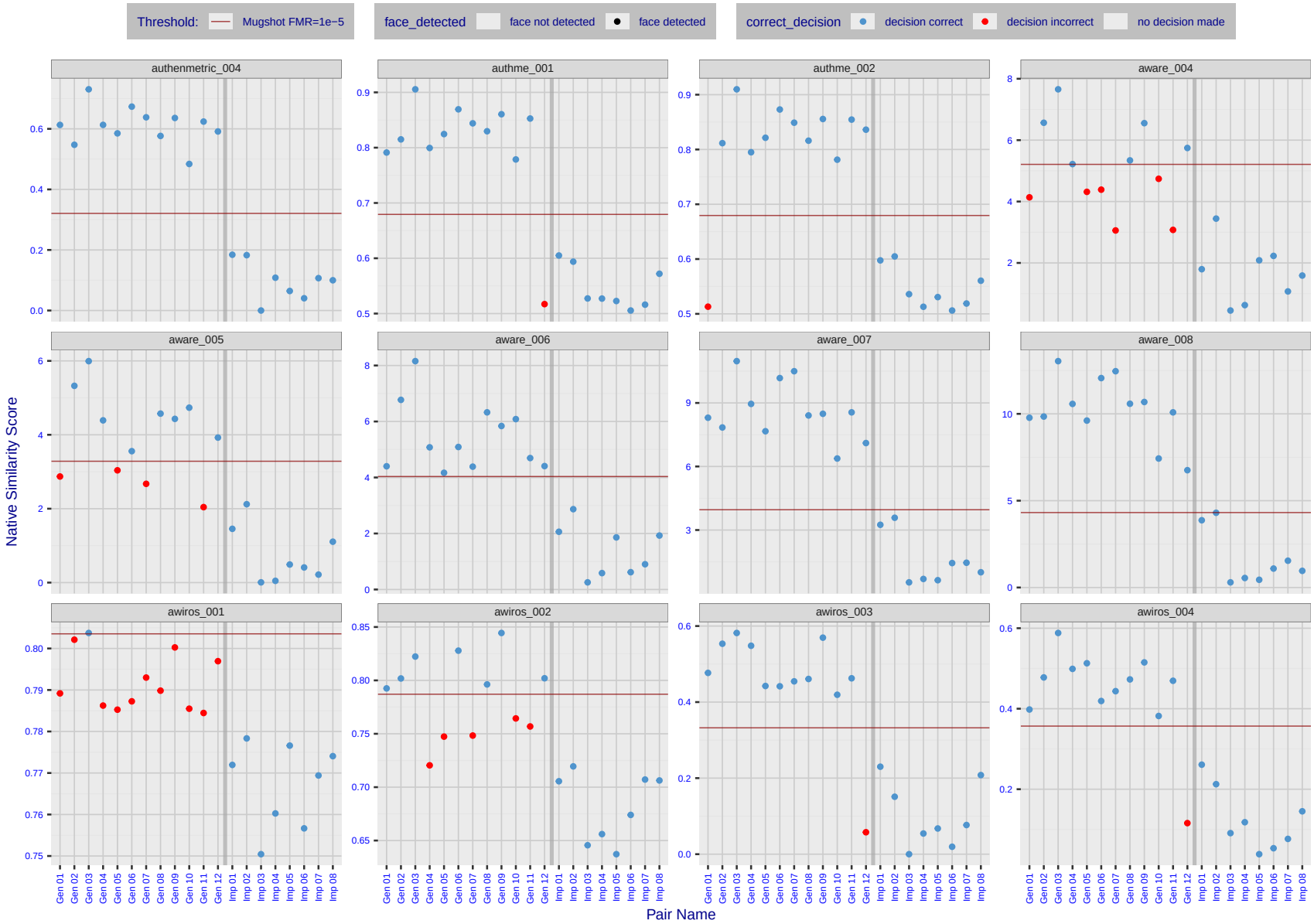

Figure 12: The figure shows algorithms' similarity scores for 12 genuine and 8 impostor image pairs used in a May 2018 paper by Phillips et al. ([1]). The threshold (red horizontal line) is a value calibrated to give FMR = 0.0001 on mugshot images. Points above the threshold correspond to pairs determined to be genuine, and points below the threshold correspond to pairs determined to be impostors. If the determined class (genuine or impostor) matches the real class, points will be blue; if not, red. An X represents face detection failure in either of the images in the pair. Note that the sample size (n=20) is small, and the figure may change substantially if larger or different sets are used. The images can be viewed on p. 13 of the Appendix, where Gen 01 corresponds to Same-Identity Pair 1, Gen 02 corresponds to Same-Identity Pair 2, and so on.

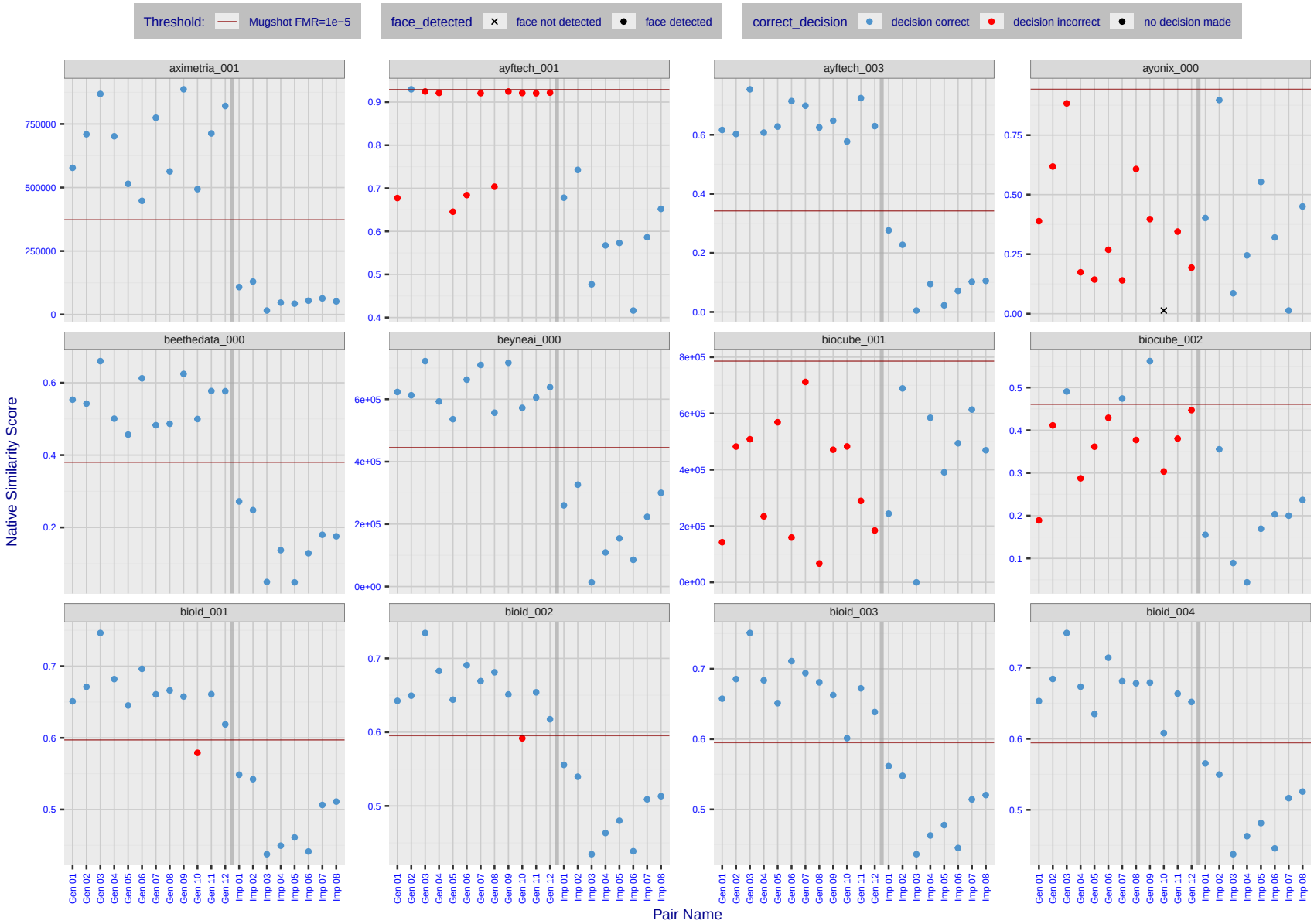

Figure 13: The figure shows algorithms' similarity scores for 12 genuine and 8 impostor image pairs used in a May 2018 paper by Phillips et al. ([1]). The threshold (red horizontal line) is a value calibrated to give FMR = 0.0001 on mugshot images. Points above the threshold correspond to pairs determined to be genuine, and points below the threshold correspond to pairs determined to be impostors. If the determined class (genuine or impostor) matches the real class, points will be blue; if not, red. An X represents face detection failure in either of the images in the pair. Note that the sample size (n=20) is small, and the figure may change substantially if larger or different sets are used. The images can be viewed on p. 13 of the Appendix, where Gen 01 corresponds to Same-Identity Pair 1, Gen 02 corresponds to Same-Identity Pair 2, and so on.

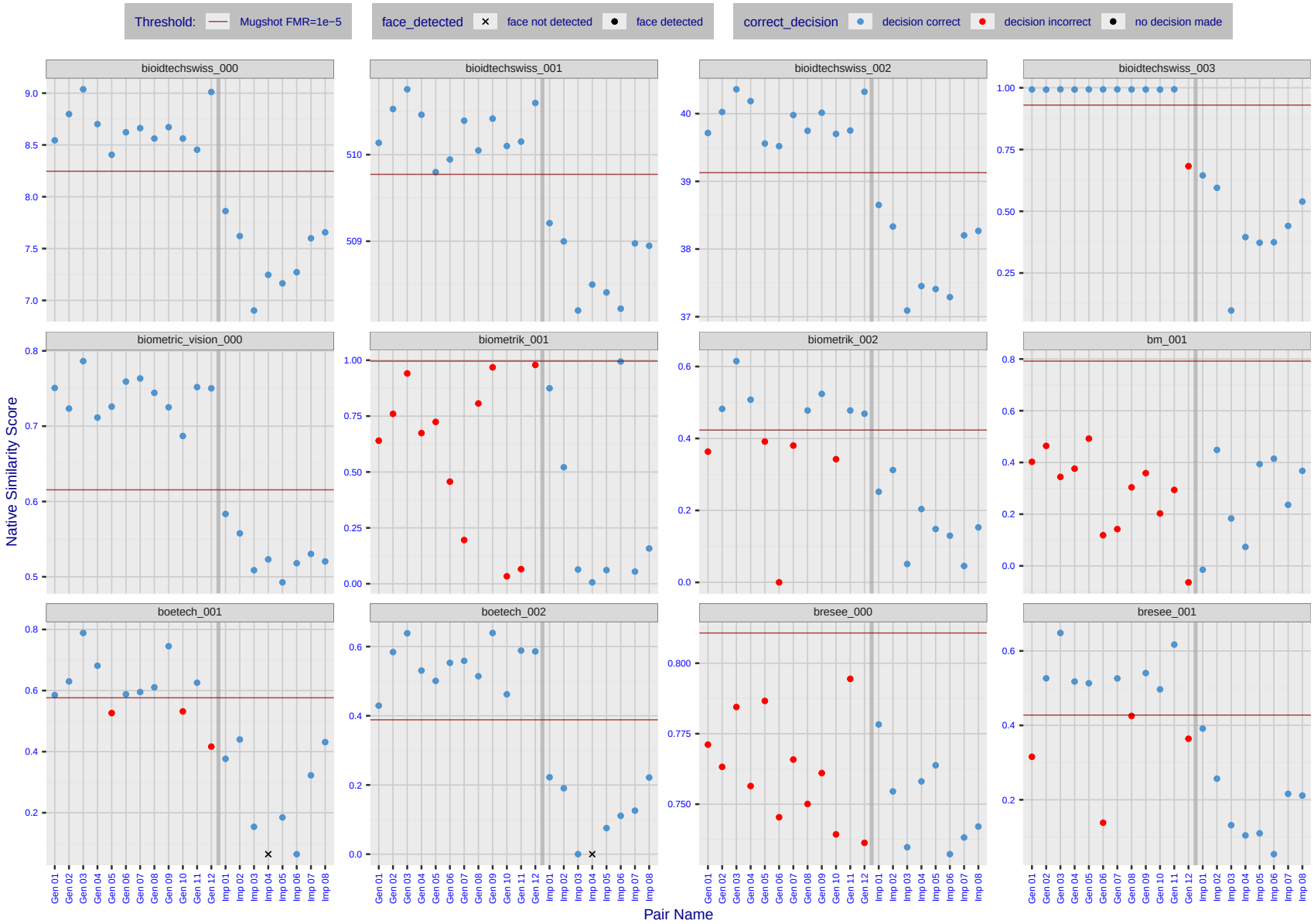

Figure 14: The figure shows algorithms' similarity scores for 12 genuine and 8 impostor image pairs used in a May 2018 paper by Phillips et al. ([1]). The threshold (red horizontal line) is a value calibrated to give FMR = 0.0001 on mugshot images. Points above the threshold correspond to pairs determined to be genuine, and points below the threshold correspond to pairs determined to be impostors. If the determined class (genuine or impostor) matches the real class, points will be blue; if not, red. An X represents face detection failure in either of the images in the pair. Note that the sample size (n=20) is small, and the figure may change substantially if larger or different sets are used. The images can be viewed on p. 13 of the Appendix, where Gen 01 corresponds to Same-Identity Pair 1, Gen 02 corresponds to Same-Identity Pair 2, and so on.

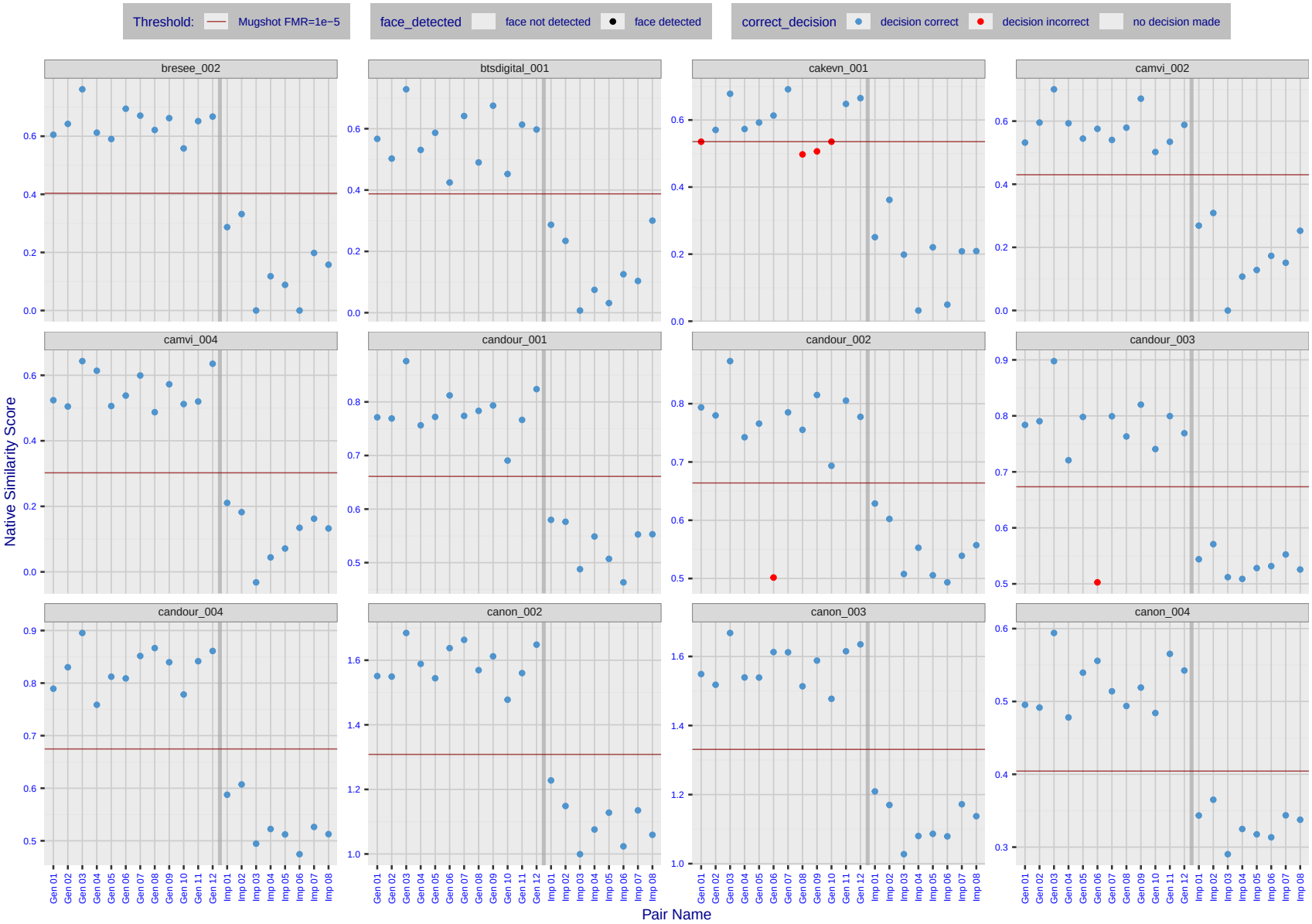

Figure 15: The figure shows algorithms' similarity scores for 12 genuine and 8 impostor image pairs used in a May 2018 paper by Phillips et al. ([1]). The threshold (red horizontal line) is a value calibrated to give FMR = 0.0001 on mugshot images. Points above the threshold correspond to pairs determined to be genuine, and points below the threshold correspond to pairs determined to be impostors. If the determined class (genuine or impostor) matches the real class, points will be blue; if not, red. An X represents face detection failure in either of the images in the pair. Note that the sample size (n=20) is small, and the figure may change substantially if larger or different sets are used. The images can be viewed on p. 13 of the Appendix, where Gen 01 corresponds to Same-Identity Pair 1, Gen 02 corresponds to Same-Identity Pair 2, and so on.

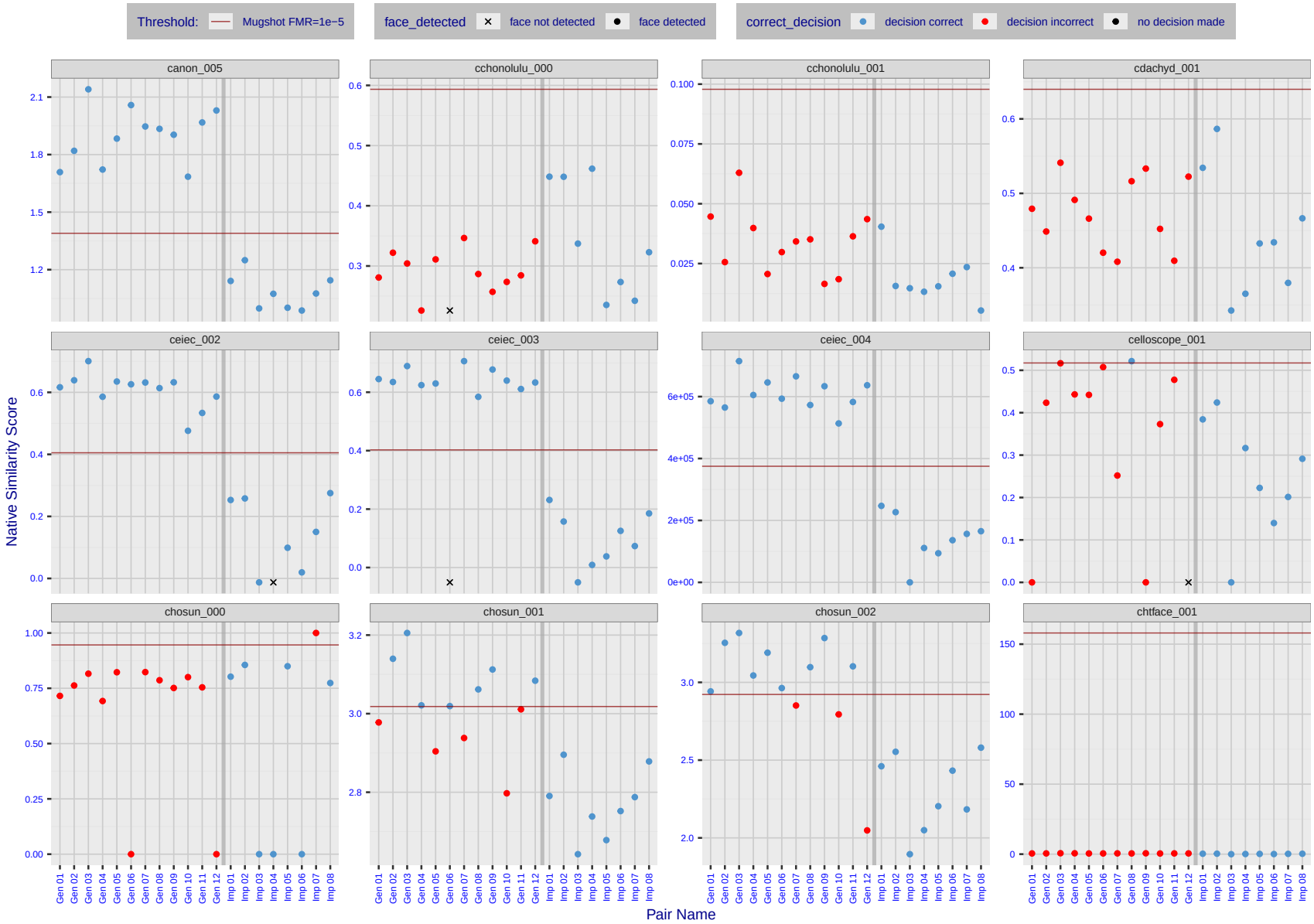

Figure 16: The figure shows algorithms' similarity scores for 12 genuine and 8 impostor image pairs used in a May 2018 paper by Phillips et al. ([1]). The threshold (red horizontal line) is a value calibrated to give FMR = 0.0001 on mugshot images. Points above the threshold correspond to pairs determined to be genuine, and points below the threshold correspond to pairs determined to be impostors. If the determined class (genuine or impostor) matches the real class, points will be blue; if not, red. An X represents face detection failure in either of the images in the pair. Note that the sample size (n=20) is small, and the figure may change substantially if larger or different sets are used. The images can be viewed on p. 13 of the Appendix, where Gen 01 corresponds to Same-Identity Pair 1, Gen 02 corresponds to Same-Identity Pair 2, and so on.

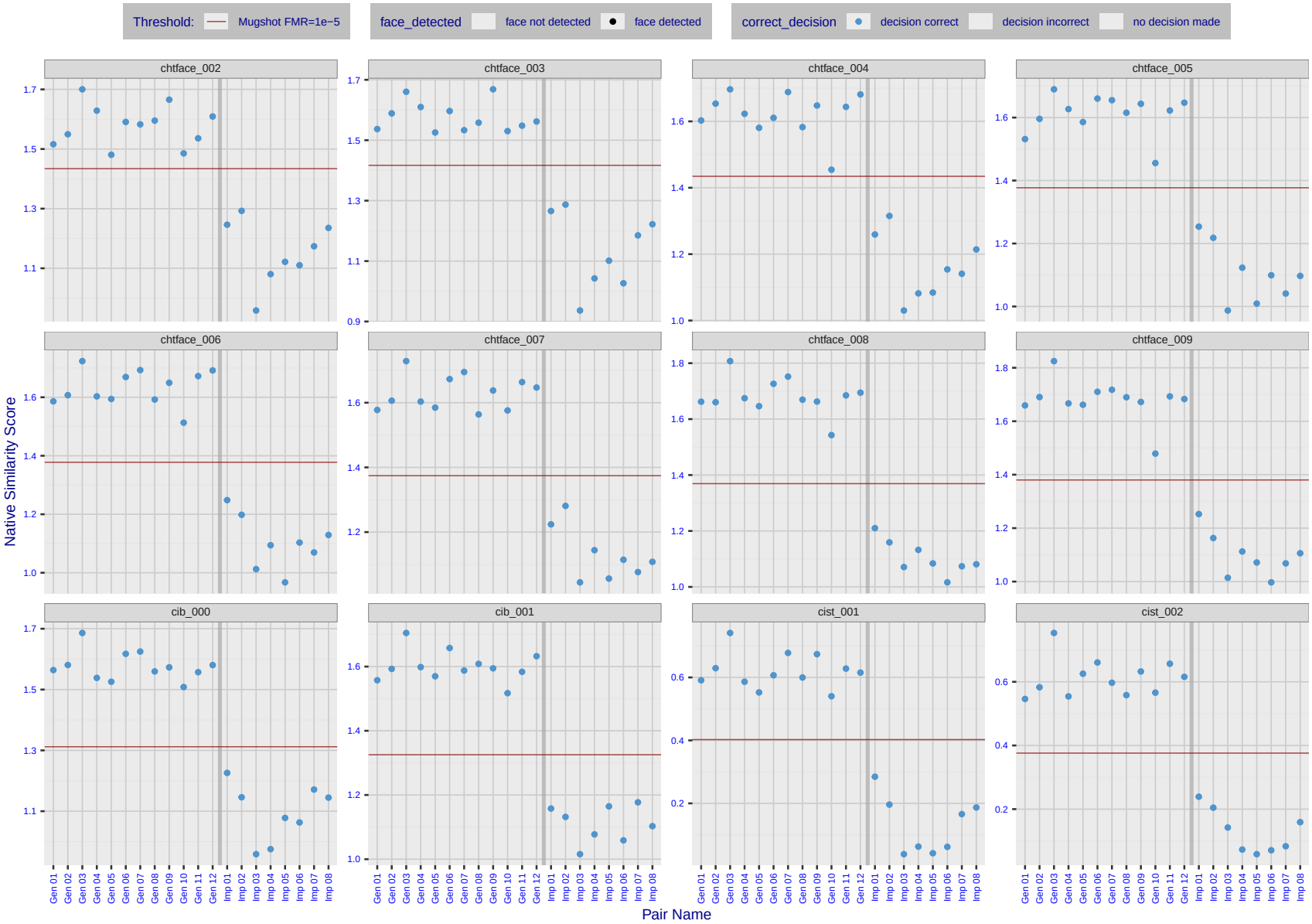

Figure 17: The figure shows algorithms' similarity scores for 12 genuine and 8 impostor image pairs used in a May 2018 paper by Phillips et al. ([1]). The threshold (red horizontal line) is a value calibrated to give FMR = 0.0001 on mugshot images. Points above the threshold correspond to pairs determined to be genuine, and points below the threshold correspond to pairs determined to be impostors. If the determined class (genuine or impostor) matches the real class, points will be blue; if not, red. An X represents face detection failure in either of the images in the pair. Note that the sample size (n=20) is small, and the figure may change substantially if larger or different sets are used. The images can be viewed on p. 13 of the Appendix, where Gen 01 corresponds to Same-Identity Pair 1, Gen 02 corresponds to Same-Identity Pair 2, and so on.

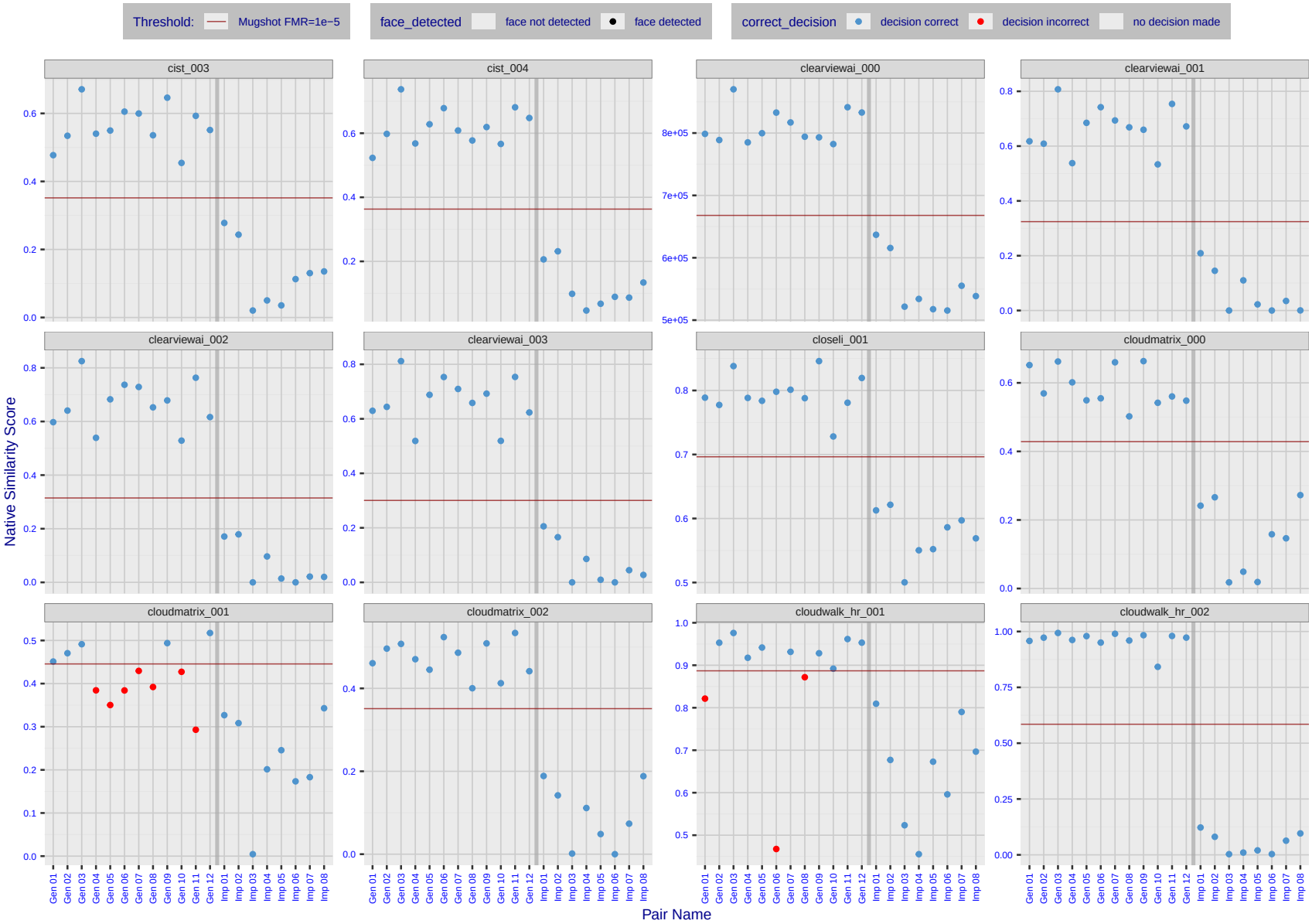

Figure 18: The figure shows algorithms' similarity scores for 12 genuine and 8 impostor image pairs used in a May 2018 paper by Phillips et al. ([1]). The threshold (red horizontal line) is a value calibrated to give FMR = 0.0001 on mugshot images. Points above the threshold correspond to pairs determined to be genuine, and points below the threshold correspond to pairs determined to be impostors. If the determined class (genuine or impostor) matches the real class, points will be blue; if not, red. An X represents face detection failure in either of the images in the pair. Note that the sample size (n=20) is small, and the figure may change substantially if larger or different sets are used. The images can be viewed on p. 13 of the Appendix, where Gen 01 corresponds to Same-Identity Pair 1, Gen 02 corresponds to Same-Identity Pair 2, and so on.

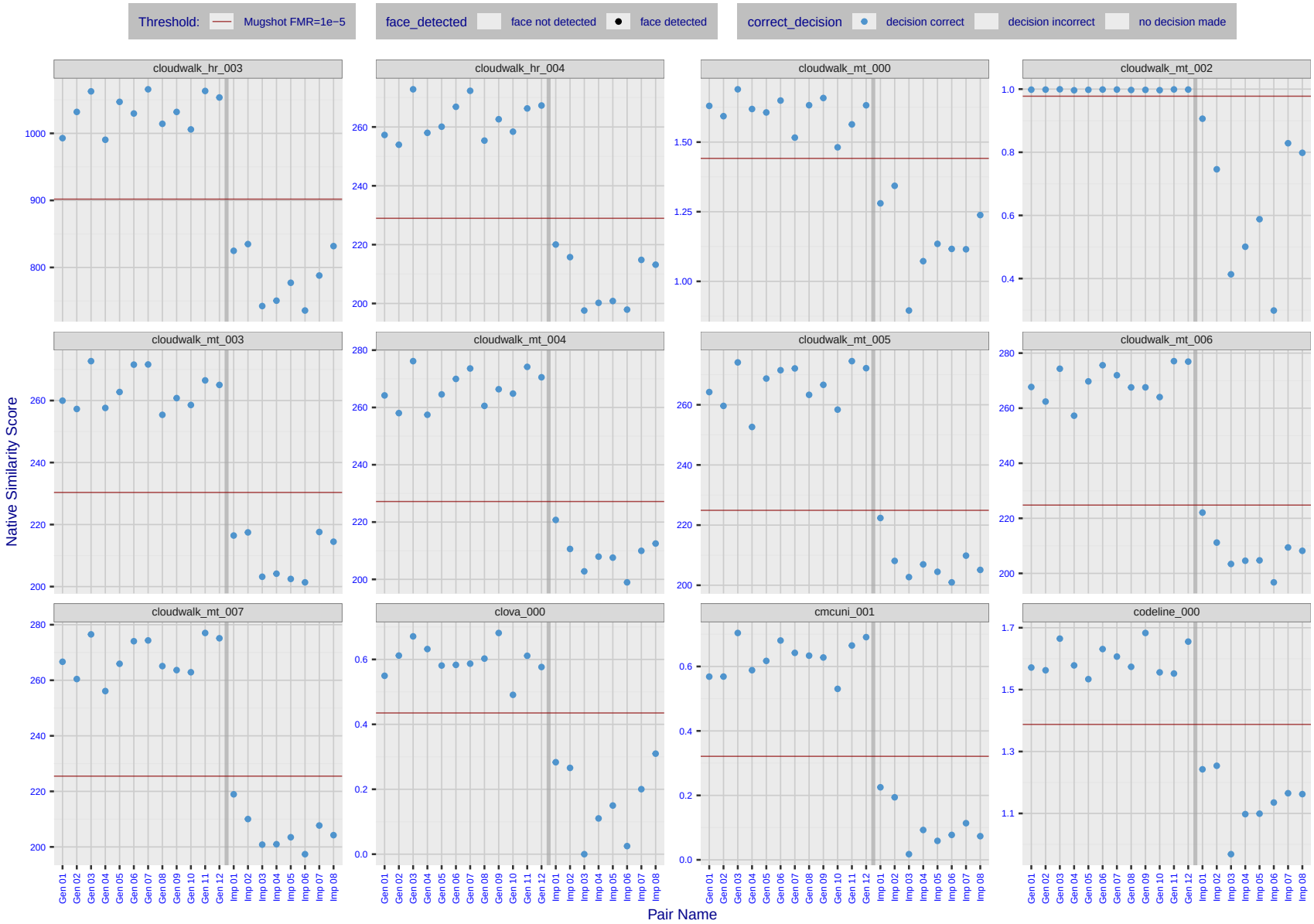

Figure 19: The figure shows algorithms' similarity scores for 12 genuine and 8 impostor image pairs used in a May 2018 paper by Phillips et al. ([1]). The threshold (red horizontal line) is a value calibrated to give FMR = 0.0001 on mugshot images. Points above the threshold correspond to pairs determined to be genuine, and points below the threshold correspond to pairs determined to be impostors. If the determined class (genuine or impostor) matches the real class, points will be blue; if not, red. An X represents face detection failure in either of the images in the pair. Note that the sample size (n=20) is small, and the figure may change substantially if larger or different sets are used. The images can be viewed on p. 13 of the Appendix, where Gen 01 corresponds to Same-Identity Pair 1, Gen 02 corresponds to Same-Identity Pair 2, and so on.

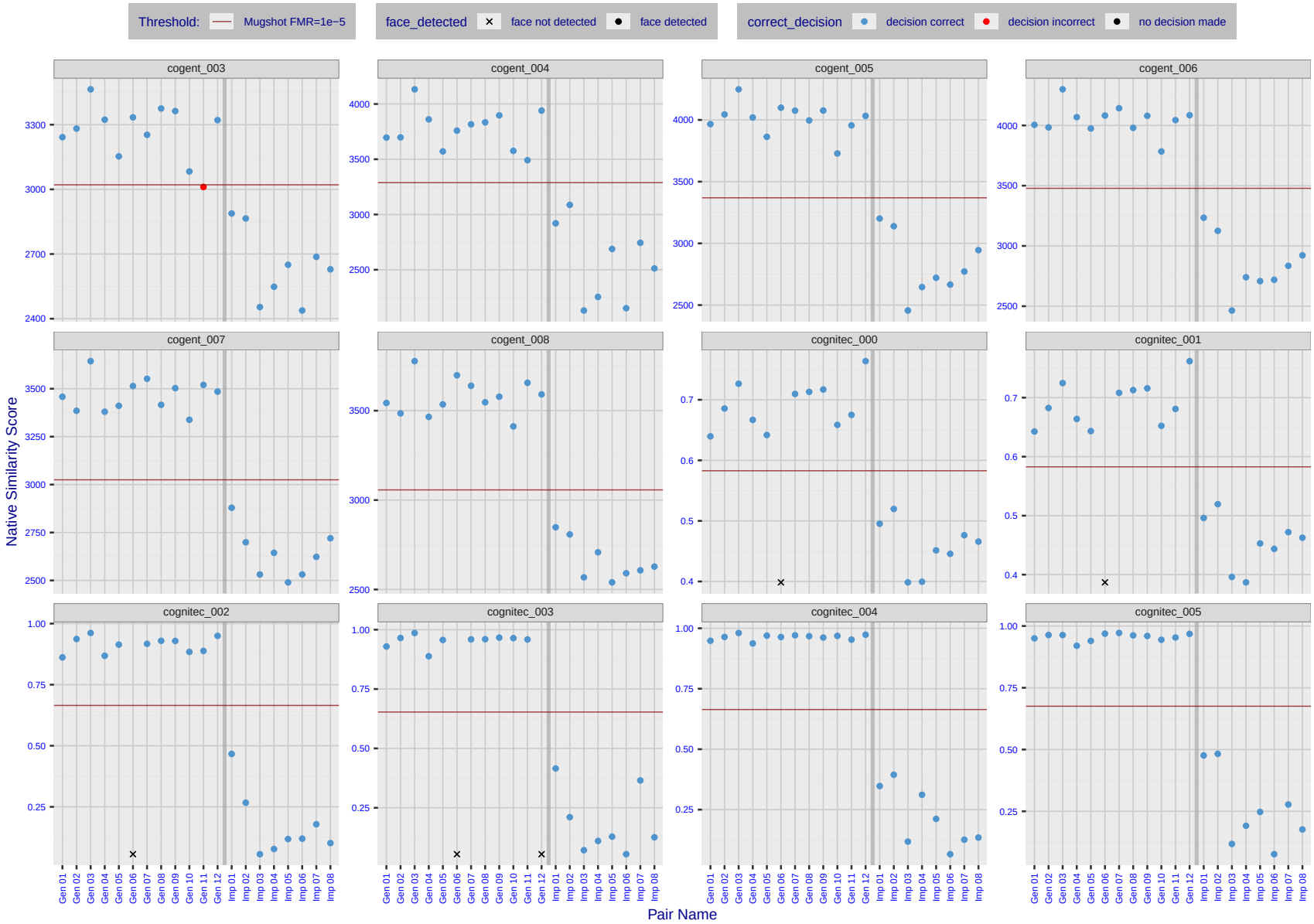

Figure 20: The figure shows algorithms' similarity scores for 12 genuine and 8 impostor image pairs used in a May 2018 paper by Phillips et al. ([1]). The threshold (red horizontal line) is a value calibrated to give FMR = 0.0001 on mugshot images. Points above the threshold correspond to pairs determined to be genuine, and points below the threshold correspond to pairs determined to be impostors. If the determined class (genuine or impostor) matches the real class, points will be blue; if not, red. An X represents face detection failure in either of the images in the pair. Note that the sample size (n=20) is small, and the figure may change substantially if larger or different sets are used. The images can be viewed on p. 13 of the Appendix, where Gen 01 corresponds to Same-Identity Pair 1, Gen 02 corresponds to Same-Identity Pair 2, and so on.

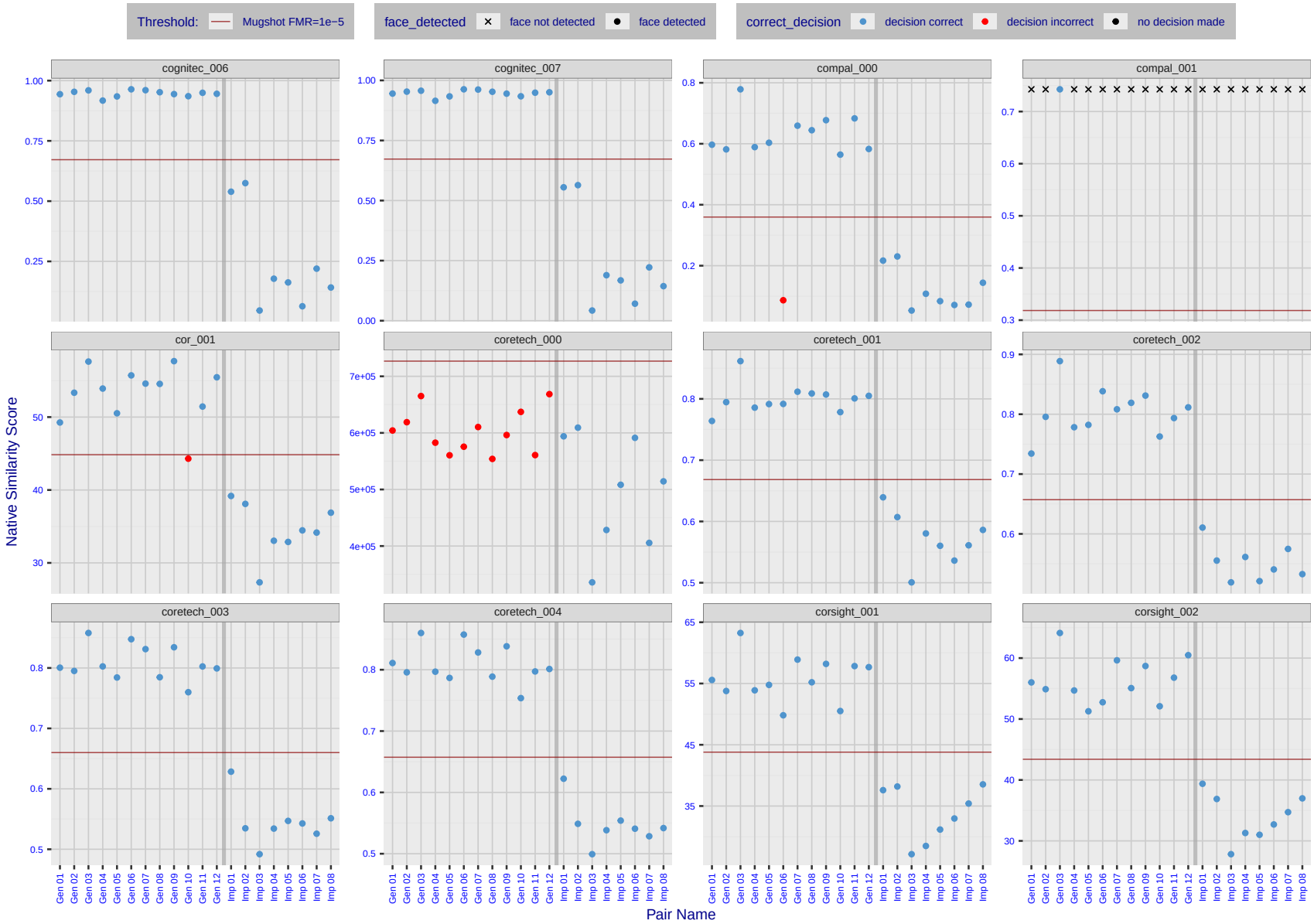

Figure 21: The figure shows algorithms' similarity scores for 12 genuine and 8 impostor image pairs used in a May 2018 paper by Phillips et al. ([1]). The threshold (red horizontal line) is a value calibrated to give FMR = 0.0001 on mugshot images. Points above the threshold correspond to pairs determined to be genuine, and points below the threshold correspond to pairs determined to be impostors. If the determined class (genuine or impostor) matches the real class, points will be blue; if not, red. An X represents face detection failure in either of the images in the pair. Note that the sample size (n=20) is small, and the figure may change substantially if larger or different sets are used. The images can be viewed on p. 13 of the Appendix, where Gen 01 corresponds to Same-Identity Pair 1, Gen 02 corresponds to Same-Identity Pair 2, and so on.

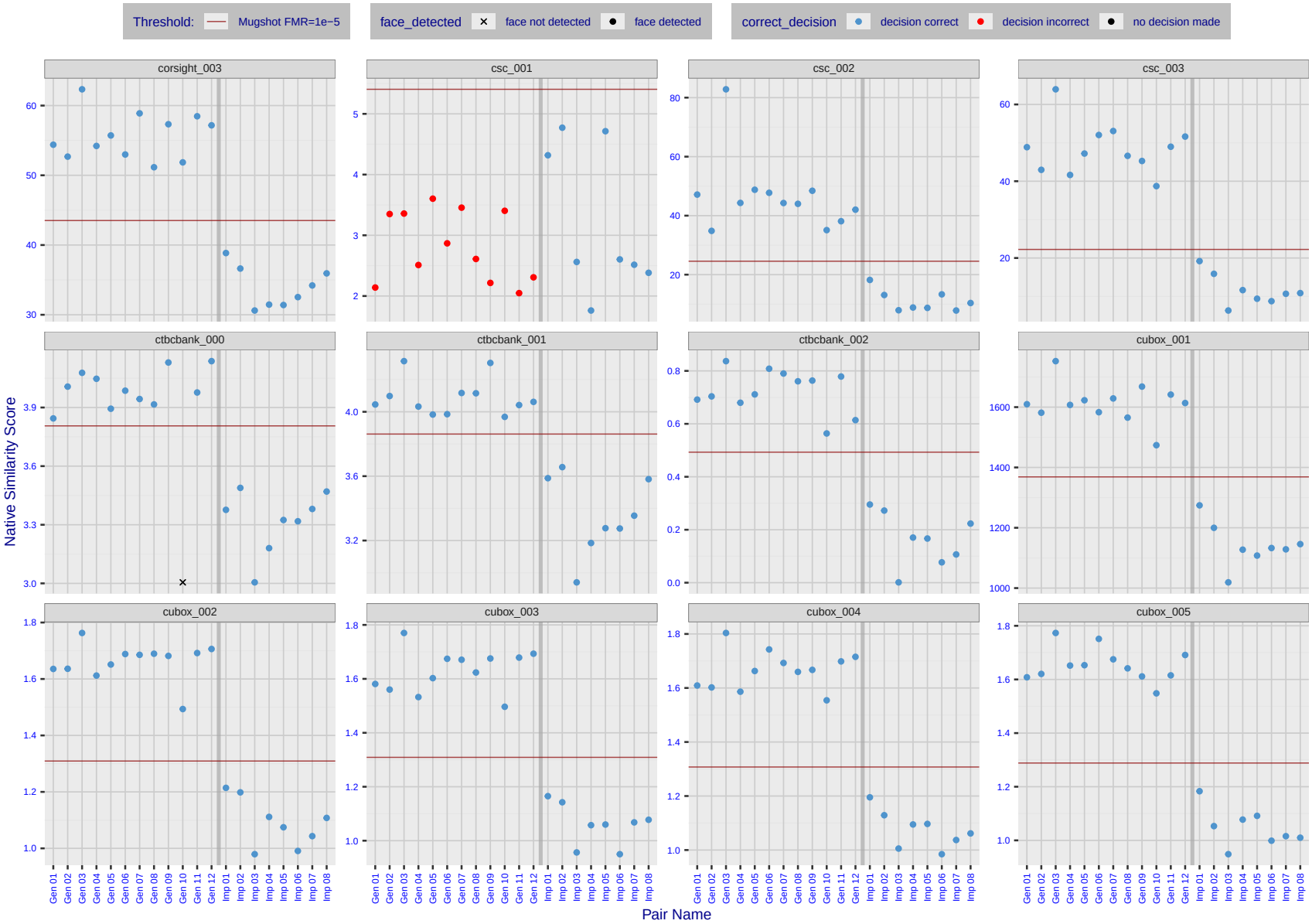

Figure 22: The figure shows algorithms' similarity scores for 12 genuine and 8 impostor image pairs used in a May 2018 paper by Phillips et al. ([1]). The threshold (red horizontal line) is a value calibrated to give FMR = 0.0001 on mugshot images. Points above the threshold correspond to pairs determined to be genuine, and points below the threshold correspond to pairs determined to be impostors. If the determined class (genuine or impostor) matches the real class, points will be blue; if not, red. An X represents face detection failure in either of the images in the pair. Note that the sample size (n=20) is small, and the figure may change substantially if larger or different sets are used. The images can be viewed on p. 13 of the Appendix, where Gen 01 corresponds to Same-Identity Pair 1, Gen 02 corresponds to Same-Identity Pair 2, and so on.

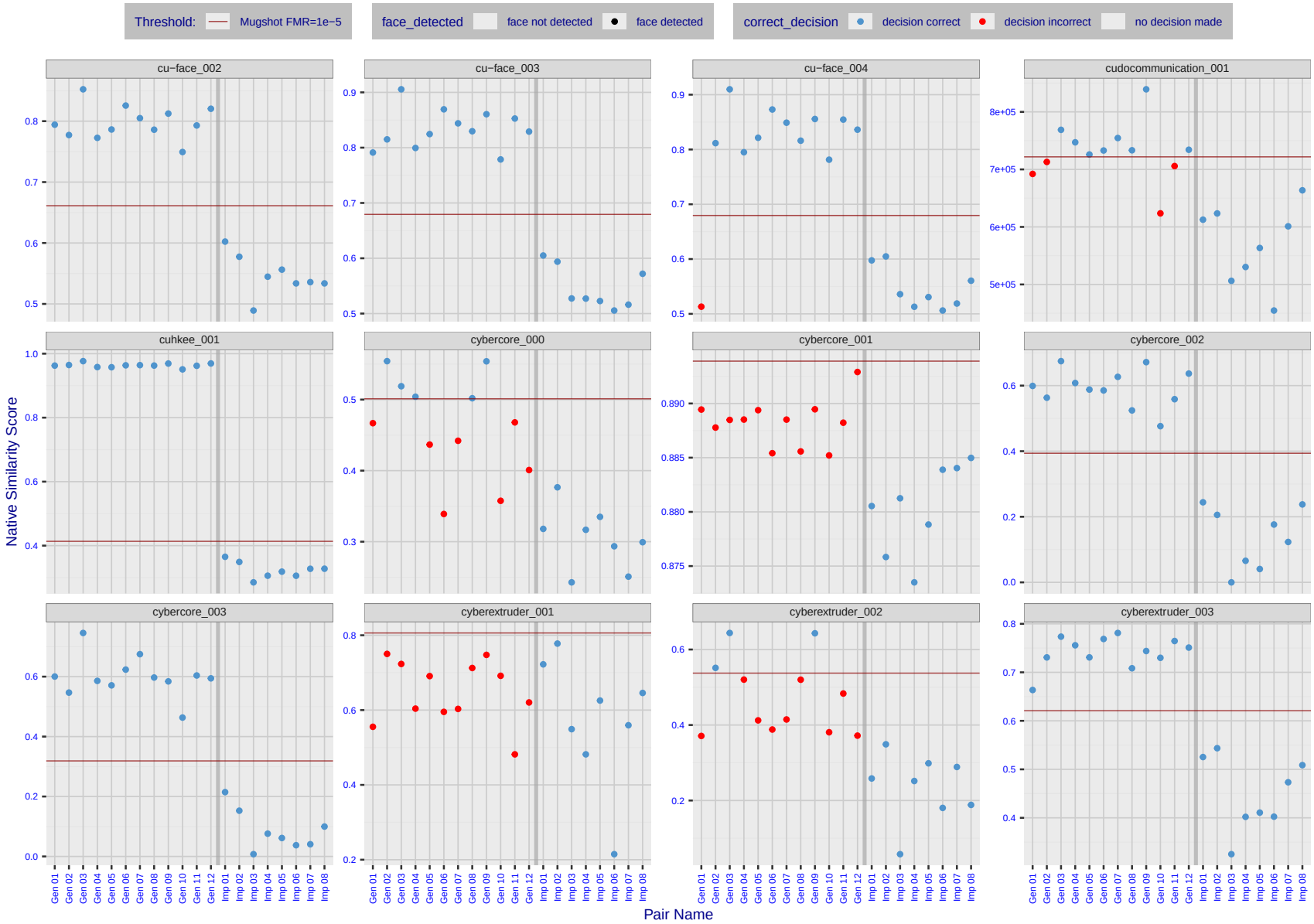

Figure 23: The figure shows algorithms' similarity scores for 12 genuine and 8 impostor image pairs used in a May 2018 paper by Phillips et al. ([1]). The threshold (red horizontal line) is a value calibrated to give FMR = 0.0001 on mugshot images. Points above the threshold correspond to pairs determined to be genuine, and points below the threshold correspond to pairs determined to be impostors. If the determined class (genuine or impostor) matches the real class, points will be blue; if not, red. An X represents face detection failure in either of the images in the pair. Note that the sample size (n=20) is small, and the figure may change substantially if larger or different sets are used. The images can be viewed on p. 13 of the Appendix, where Gen 01 corresponds to Same-Identity Pair 1, Gen 02 corresponds to Same-Identity Pair 2, and so on.

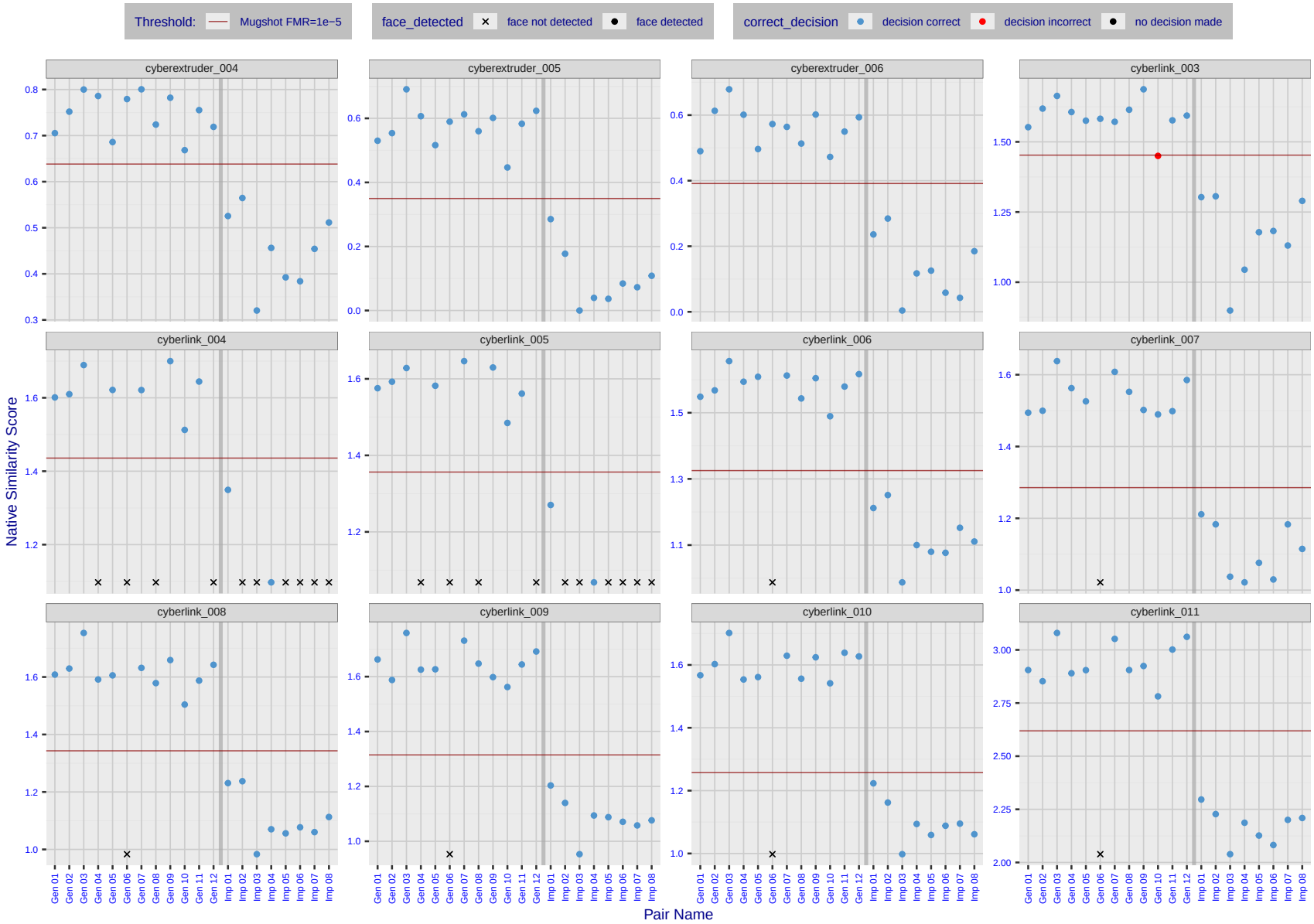

Figure 24: The figure shows algorithms' similarity scores for 12 genuine and 8 impostor image pairs used in a May 2018 paper by Phillips et al. ([1]). The threshold (red horizontal line) is a value calibrated to give FMR = 0.0001 on mugshot images. Points above the threshold correspond to pairs determined to be genuine, and points below the threshold correspond to pairs determined to be impostors. If the determined class (genuine or impostor) matches the real class, points will be blue; if not, red. An X represents face detection failure in either of the images in the pair. Note that the sample size (n=20) is small, and the figure may change substantially if larger or different sets are used. The images can be viewed on p. 13 of the Appendix, where Gen 01 corresponds to Same-Identity Pair 1, Gen 02 corresponds to Same-Identity Pair 2, and so on.

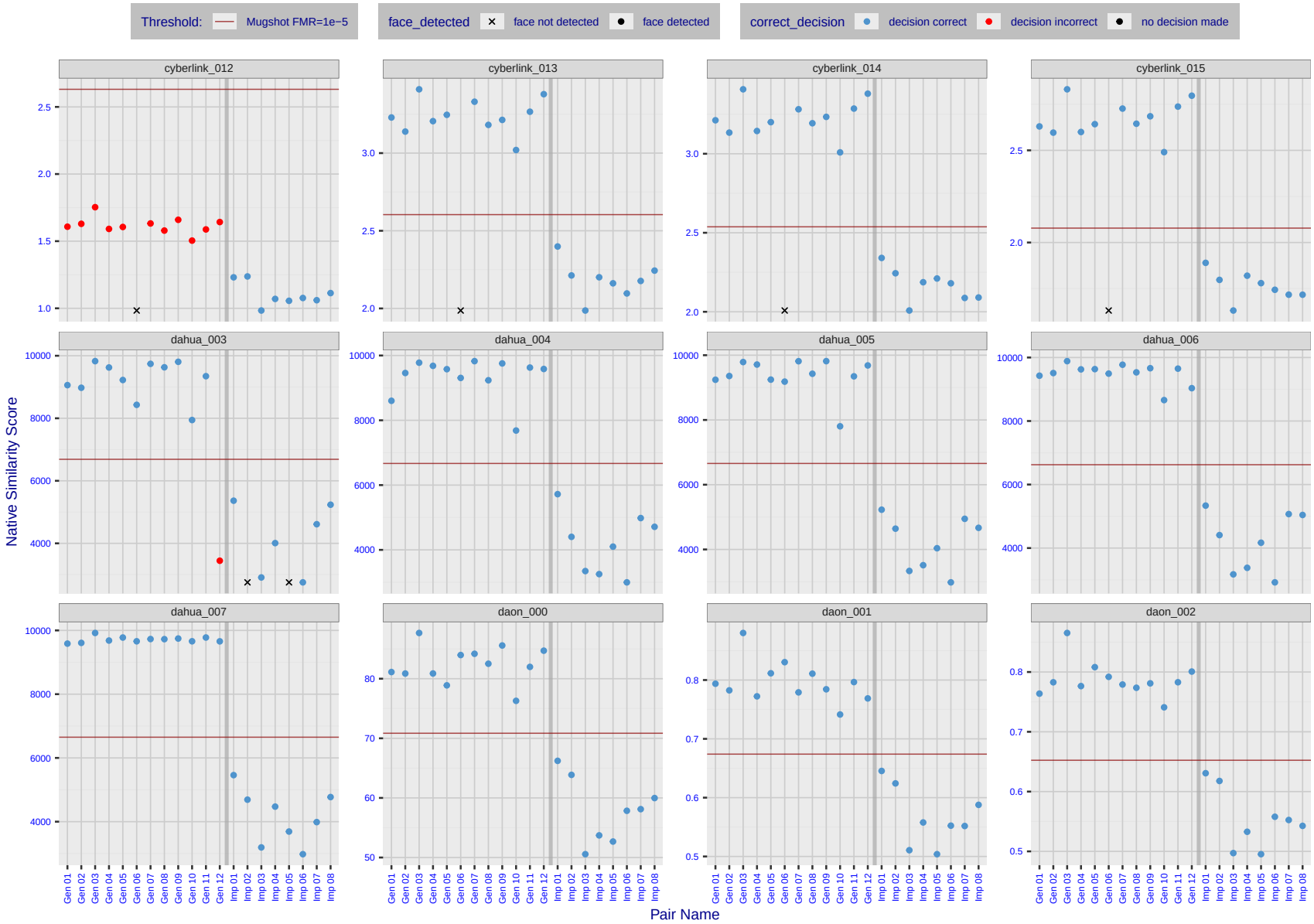

Figure 25: The figure shows algorithms' similarity scores for 12 genuine and 8 impostor image pairs used in a May 2018 paper by Phillips et al. ([1]). The threshold (red horizontal line) is a value calibrated to give FMR = 0.0001 on mugshot images. Points above the threshold correspond to pairs determined to be genuine, and points below the threshold correspond to pairs determined to be impostors. If the determined class (genuine or impostor) matches the real class, points will be blue; if not, red. An X represents face detection failure in either of the images in the pair. Note that the sample size (n=20) is small, and the figure may change substantially if larger or different sets are used. The images can be viewed on p. 13 of the Appendix, where Gen 01 corresponds to Same-Identity Pair 1, Gen 02 corresponds to Same-Identity Pair 2, and so on.

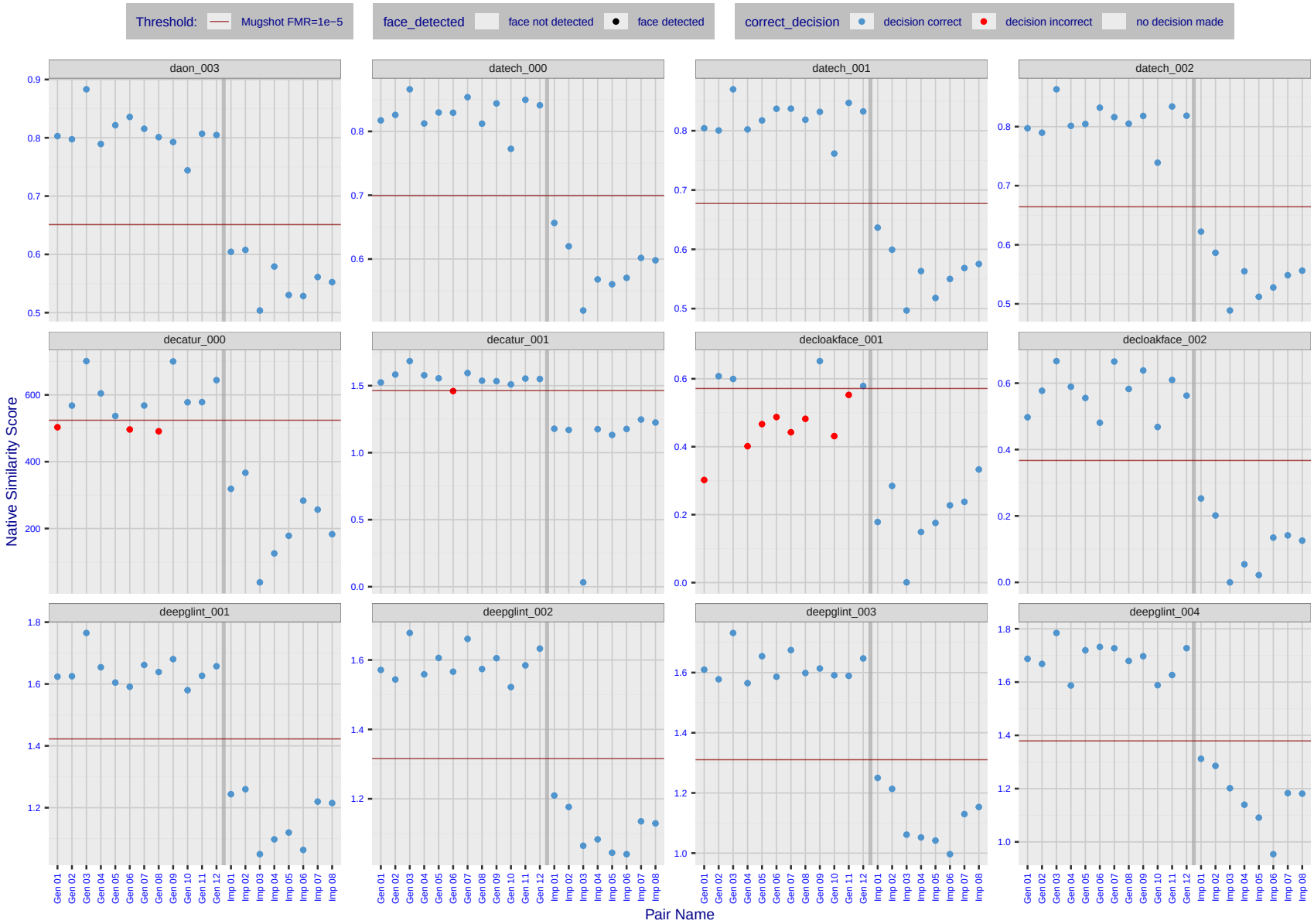

Figure 26: The figure shows algorithms' similarity scores for 12 genuine and 8 impostor image pairs used in a May 2018 paper by Phillips et al. ([1]). The threshold (red horizontal line) is a value calibrated to give FMR = 0.0001 on mugshot images. Points above the threshold correspond to pairs determined to be genuine, and points below the threshold correspond to pairs determined to be impostors. If the determined class (genuine or impostor) matches the real class, points will be blue; if not, red. An X represents face detection failure in either of the images in the pair. Note that the sample size (n=20) is small, and the figure may change substantially if larger or different sets are used. The images can be viewed on p. 13 of the Appendix, where Gen 01 corresponds to Same-Identity Pair 1, Gen 02 corresponds to Same-Identity Pair 2, and so on.

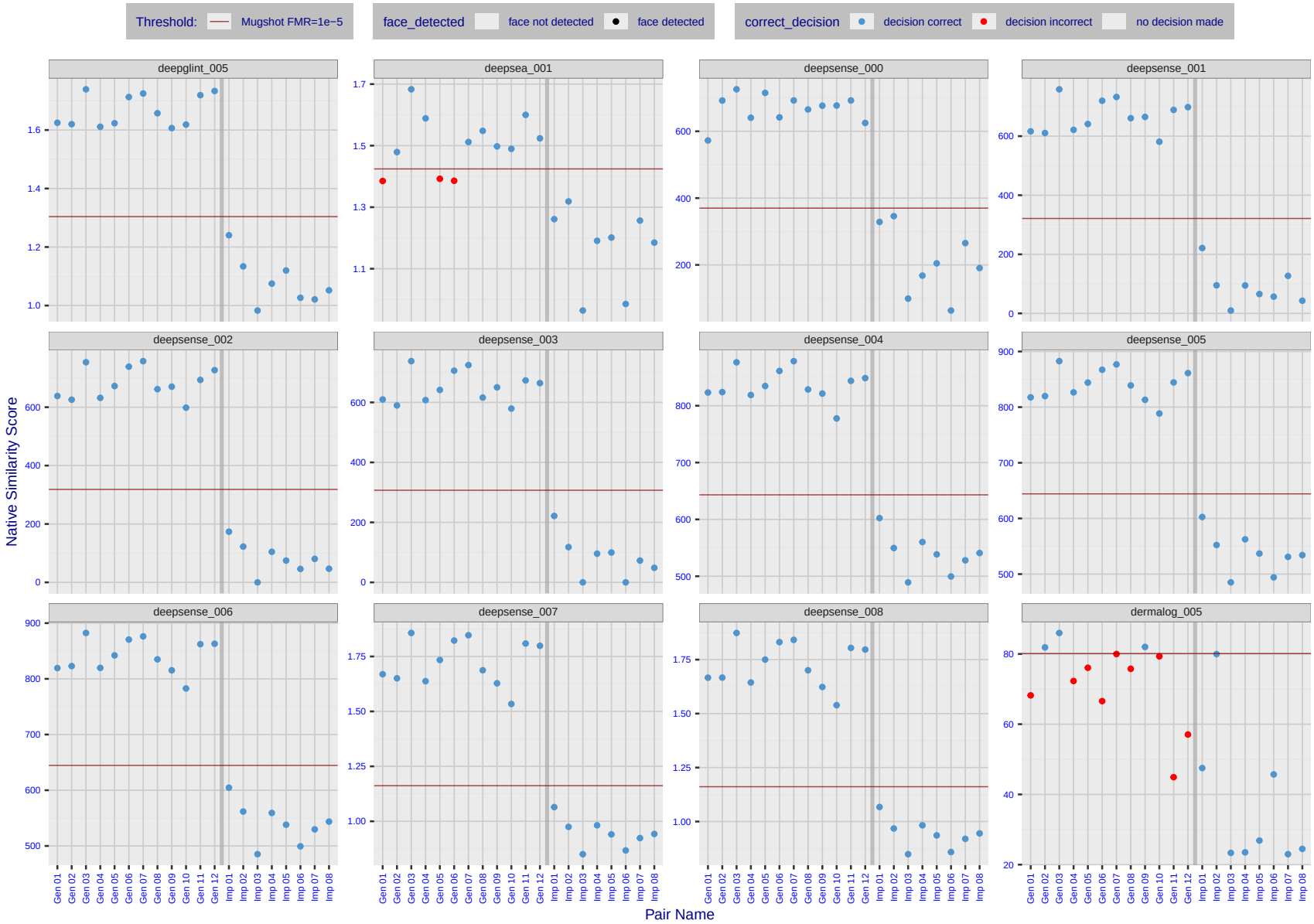

Figure 27: The figure shows algorithms' similarity scores for 12 genuine and 8 impostor image pairs used in a May 2018 paper by Phillips et al. ([1]). The threshold (red horizontal line) is a value calibrated to give FMR = 0.0001 on mugshot images. Points above the threshold correspond to pairs determined to be genuine, and points below the threshold correspond to pairs determined to be impostors. If the determined class (genuine or impostor) matches the real class, points will be blue; if not, red. An X represents face detection failure in either of the images in the pair. Note that the sample size (n=20) is small, and the figure may change substantially if larger or different sets are used. The images can be viewed on p. 13 of the Appendix, where Gen 01 corresponds to Same-Identity Pair 1, Gen 02 corresponds to Same-Identity Pair 2, and so on.

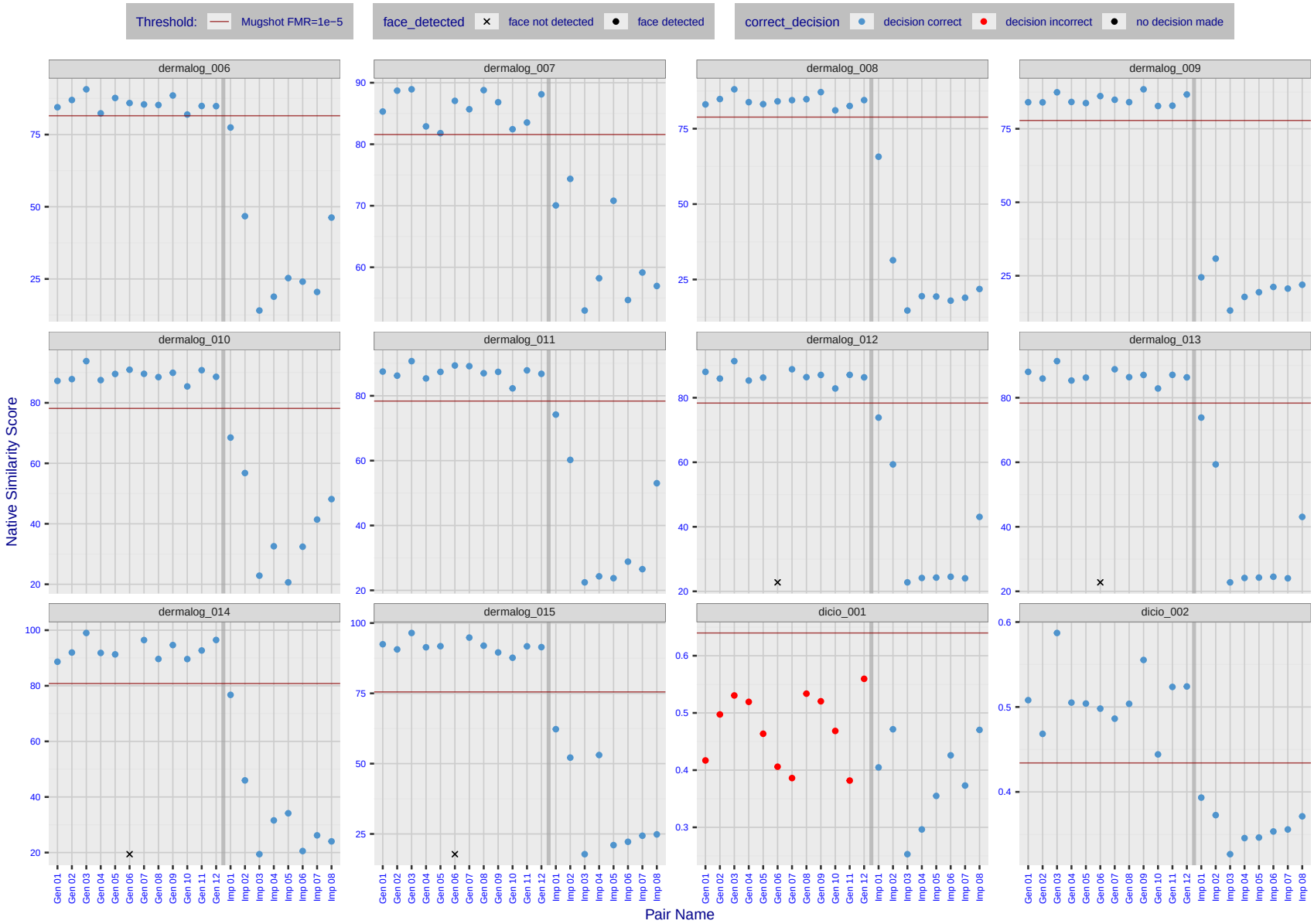

Figure 28: The figure shows algorithms' similarity scores for 12 genuine and 8 impostor image pairs used in a May 2018 paper by Phillips et al. ([1]). The threshold (red horizontal line) is a value calibrated to give FMR = 0.0001 on mugshot images. Points above the threshold correspond to pairs determined to be genuine, and points below the threshold correspond to pairs determined to be impostors. If the determined class (genuine or impostor) matches the real class, points will be blue; if not, red. An X represents face detection failure in either of the images in the pair. Note that the sample size (n=20) is small, and the figure may change substantially if larger or different sets are used. The images can be viewed on p. 13 of the Appendix, where Gen 01 corresponds to Same-Identity Pair 1, Gen 02 corresponds to Same-Identity Pair 2, and so on.

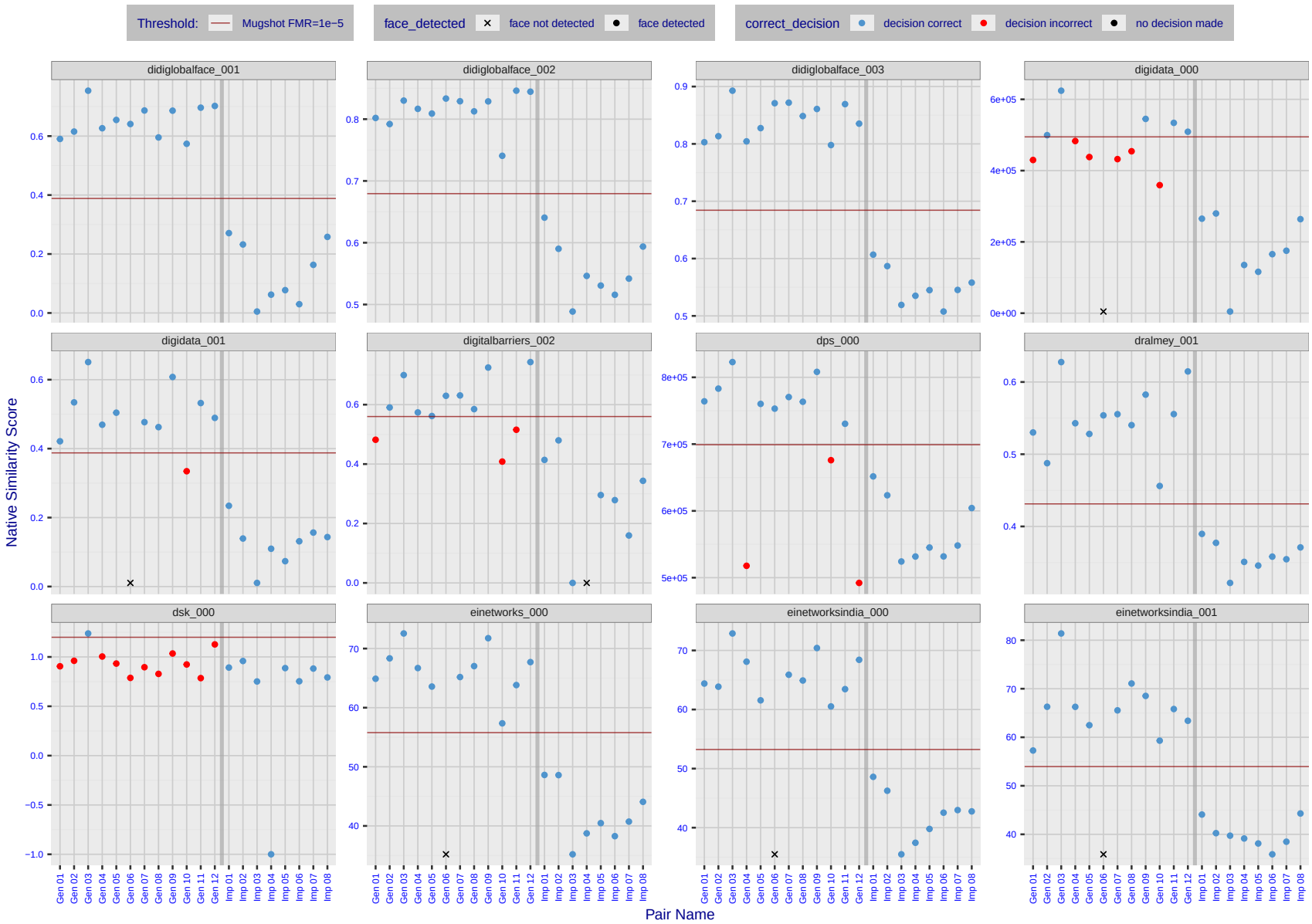

Figure 29: The figure shows algorithms' similarity scores for 12 genuine and 8 impostor image pairs used in a May 2018 paper by Phillips et al. ([1]). The threshold (red horizontal line) is a value calibrated to give FMR = 0.0001 on mugshot images. Points above the threshold correspond to pairs determined to be genuine, and points below the threshold correspond to pairs determined to be impostors. If the determined class (genuine or impostor) matches the real class, points will be blue; if not, red. An X represents face detection failure in either of the images in the pair. Note that the sample size (n=20) is small, and the figure may change substantially if larger or different sets are used. The images can be viewed on p. 13 of the Appendix, where Gen 01 corresponds to Same-Identity Pair 1, Gen 02 corresponds to Same-Identity Pair 2, and so on.

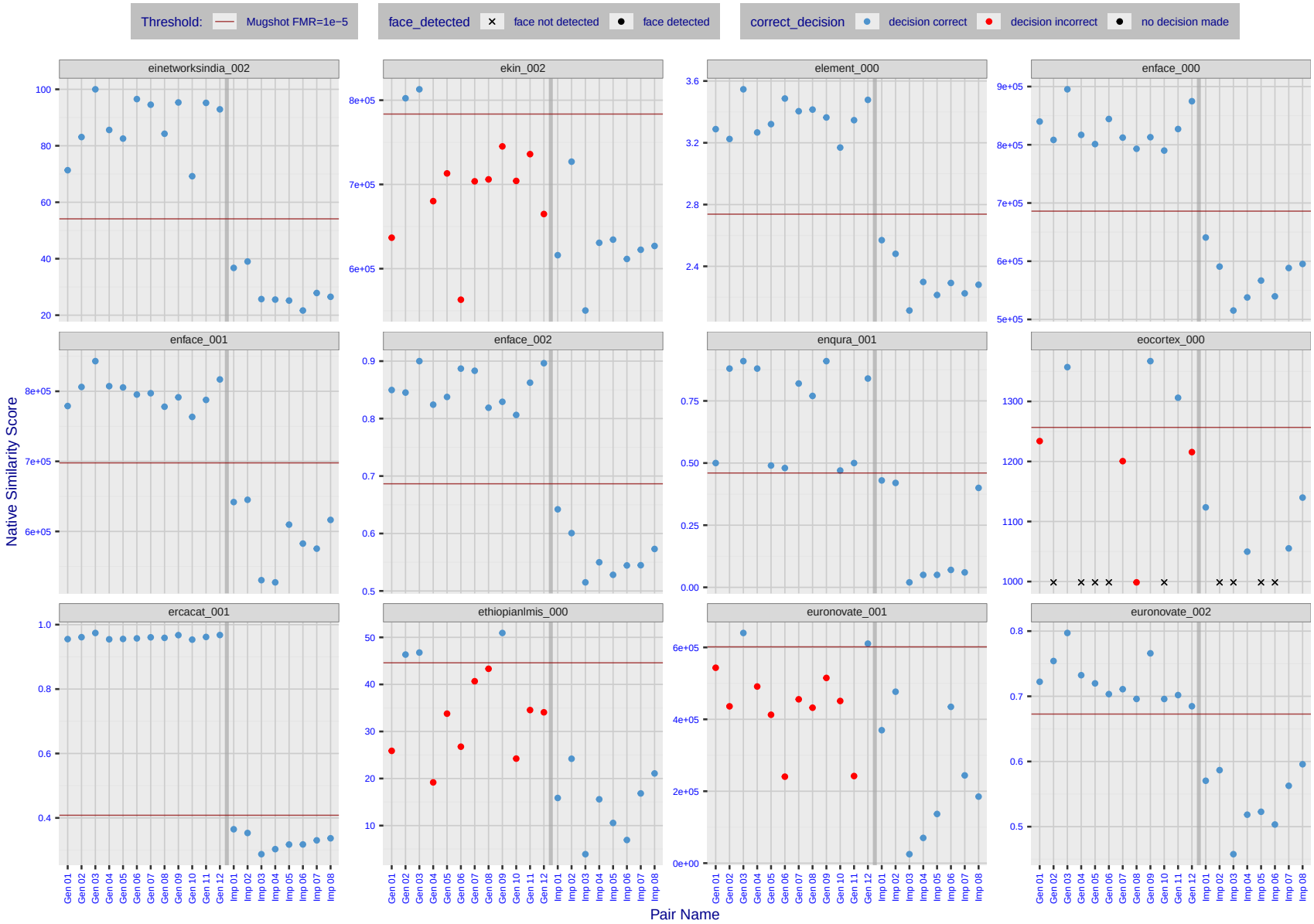

Figure 30: The figure shows algorithms' similarity scores for 12 genuine and 8 impostor image pairs used in a May 2018 paper by Phillips et al. ([1]). The threshold (red horizontal line) is a value calibrated to give FMR = 0.0001 on mugshot images. Points above the threshold correspond to pairs determined to be genuine, and points below the threshold correspond to pairs determined to be impostors. If the determined class (genuine or impostor) matches the real class, points will be blue; if not, red. An X represents face detection failure in either of the images in the pair. Note that the sample size (n=20) is small, and the figure may change substantially if larger or different sets are used. The images can be viewed on p. 13 of the Appendix, where Gen 01 corresponds to Same-Identity Pair 1, Gen 02 corresponds to Same-Identity Pair 2, and so on.

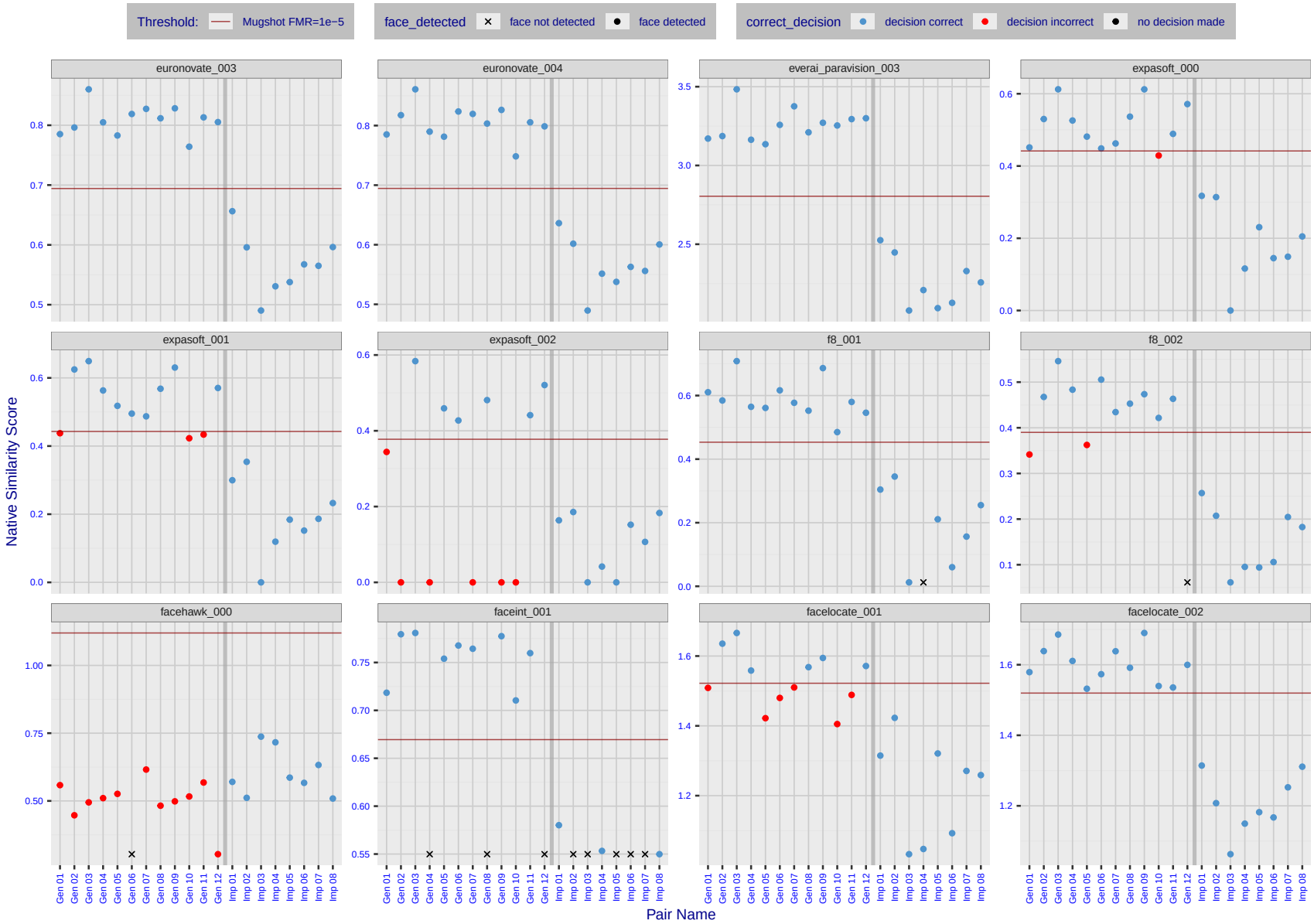

Figure 31: The figure shows algorithms' similarity scores for 12 genuine and 8 impostor image pairs used in a May 2018 paper by Phillips et al. ([1]). The threshold (red horizontal line) is a value calibrated to give FMR = 0.0001 on mugshot images. Points above the threshold correspond to pairs determined to be genuine, and points below the threshold correspond to pairs determined to be impostors. If the determined class (genuine or impostor) matches the real class, points will be blue; if not, red. An X represents face detection failure in either of the images in the pair. Note that the sample size (n=20) is small, and the figure may change substantially if larger or different sets are used. The images can be viewed on p. 13 of the Appendix, where Gen 01 corresponds to Same-Identity Pair 1, Gen 02 corresponds to Same-Identity Pair 2, and so on.

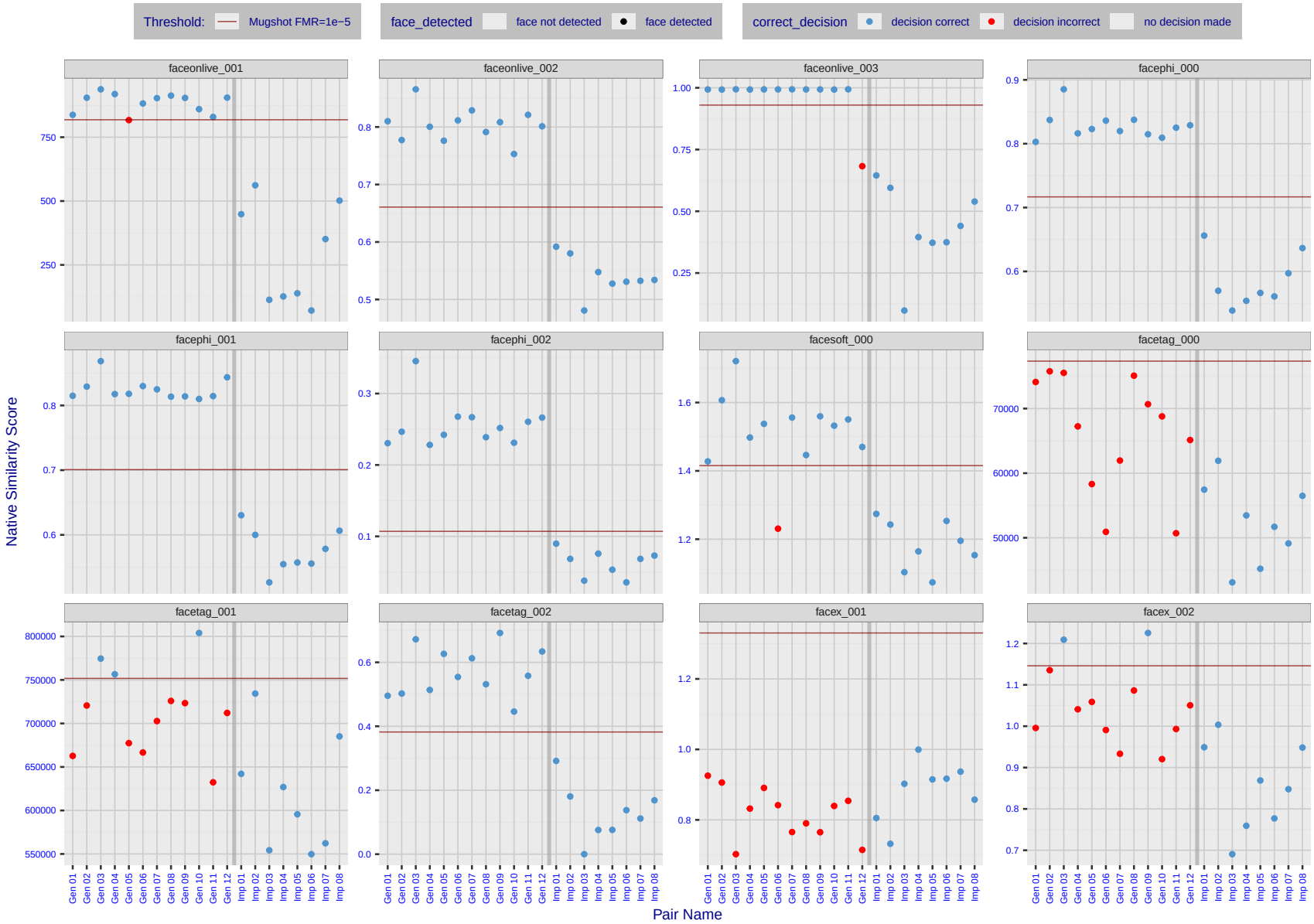

Figure 32: The figure shows algorithms' similarity scores for 12 genuine and 8 impostor image pairs used in a May 2018 paper by Phillips et al. ([1]). The threshold (red horizontal line) is a value calibrated to give FMR = 0.0001 on mugshot images. Points above the threshold correspond to pairs determined to be genuine, and points below the threshold correspond to pairs determined to be impostors. If the determined class (genuine or impostor) matches the real class, points will be blue; if not, red. An X represents face detection failure in either of the images in the pair. Note that the sample size (n=20) is small, and the figure may change substantially if larger or different sets are used. The images can be viewed on p. 13 of the Appendix, where Gen 01 corresponds to Same-Identity Pair 1, Gen 02 corresponds to Same-Identity Pair 2, and so on.

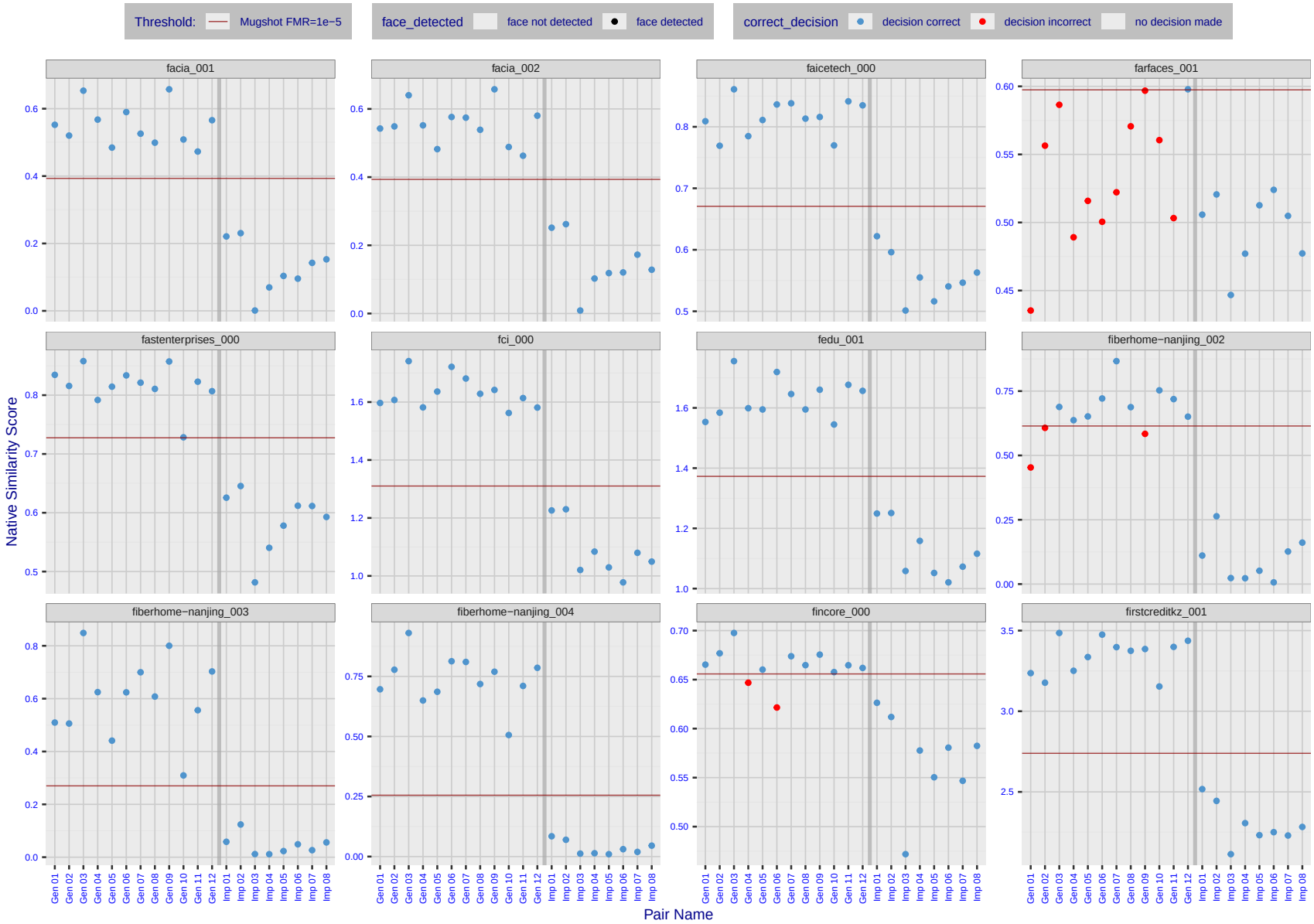

Figure 33: The figure shows algorithms' similarity scores for 12 genuine and 8 impostor image pairs used in a May 2018 paper by Phillips et al. ([1]). The threshold (red horizontal line) is a value calibrated to give FMR = 0.0001 on mugshot images. Points above the threshold correspond to pairs determined to be genuine, and points below the threshold correspond to pairs determined to be impostors. If the determined class (genuine or impostor) matches the real class, points will be blue; if not, red. An X represents face detection failure in either of the images in the pair. Note that the sample size (n=20) is small, and the figure may change substantially if larger or different sets are used. The images can be viewed on p. 13 of the Appendix, where Gen 01 corresponds to Same-Identity Pair 1, Gen 02 corresponds to Same-Identity Pair 2, and so on.

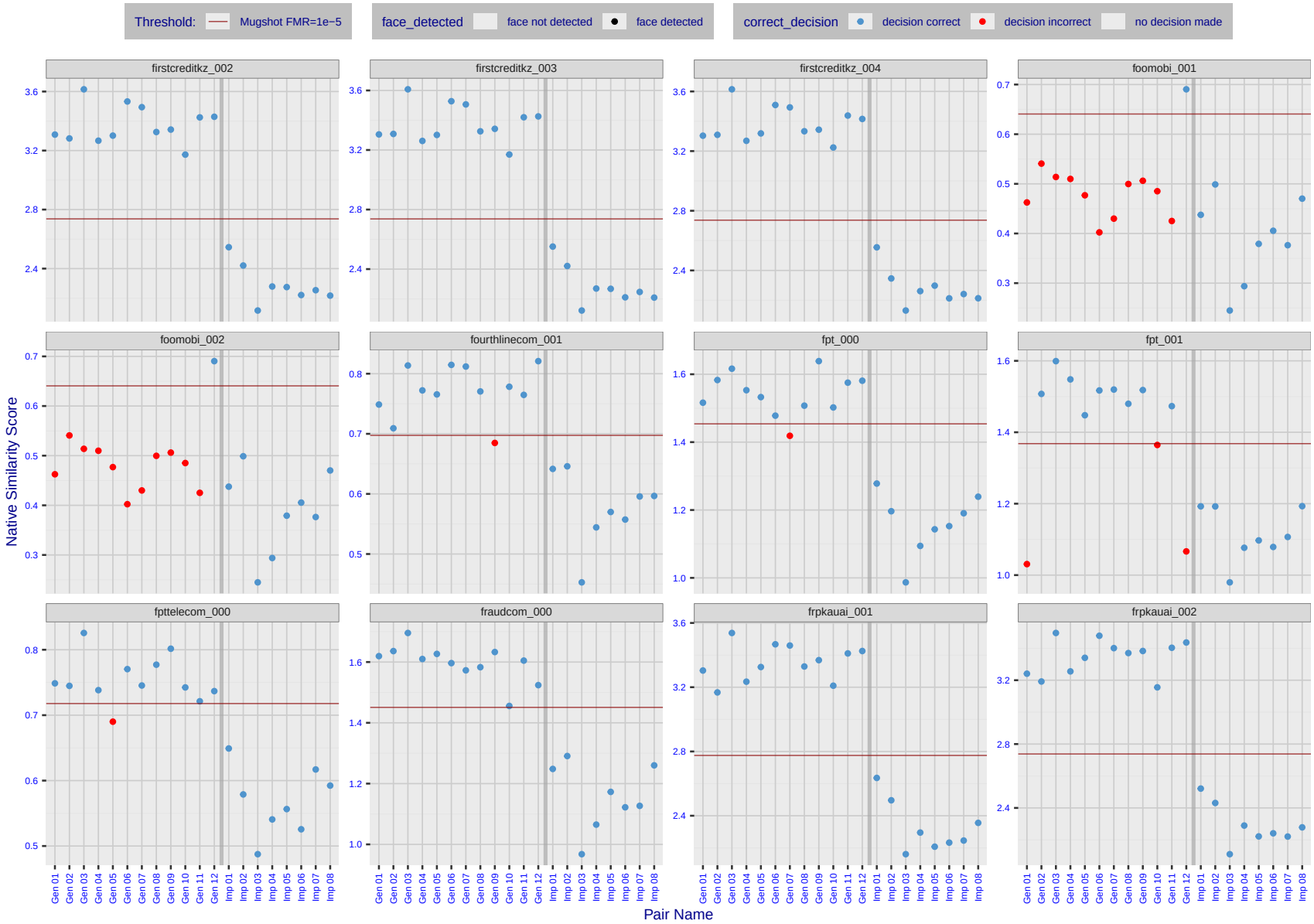

Figure 34: The figure shows algorithms' similarity scores for 12 genuine and 8 impostor image pairs used in a May 2018 paper by Phillips et al. ([1]). The threshold (red horizontal line) is a value calibrated to give FMR = 0.0001 on mugshot images. Points above the threshold correspond to pairs determined to be genuine, and points below the threshold correspond to pairs determined to be impostors. If the determined class (genuine or impostor) matches the real class, points will be blue; if not, red. An X represents face detection failure in either of the images in the pair. Note that the sample size (n=20) is small, and the figure may change substantially if larger or different sets are used. The images can be viewed on p. 13 of the Appendix, where Gen 01 corresponds to Same-Identity Pair 1, Gen 02 corresponds to Same-Identity Pair 2, and so on.

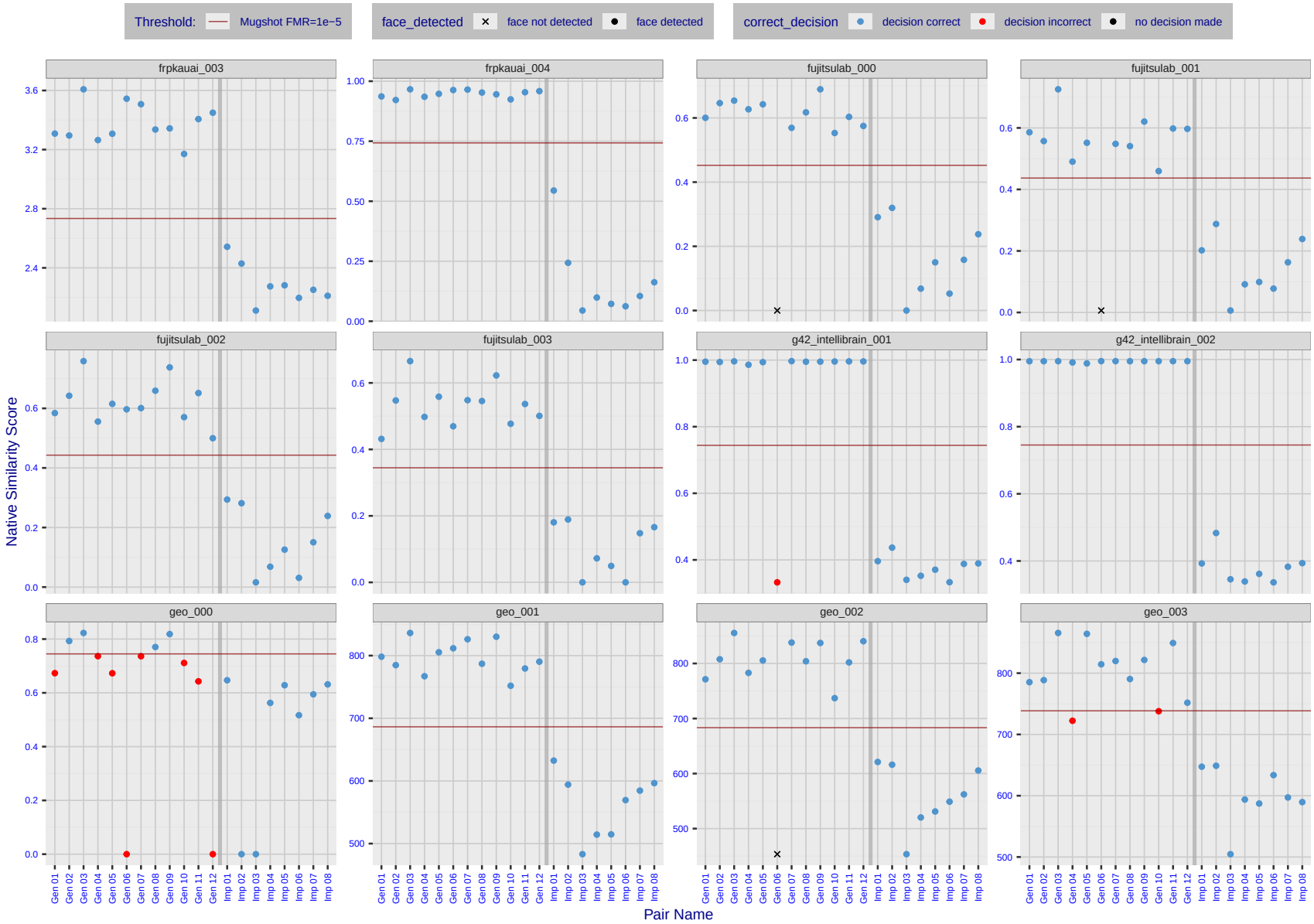

Figure 35: The figure shows algorithms' similarity scores for 12 genuine and 8 impostor image pairs used in a May 2018 paper by Phillips et al. ([1]). The threshold (red horizontal line) is a value calibrated to give FMR = 0.0001 on mugshot images. Points above the threshold correspond to pairs determined to be genuine, and points below the threshold correspond to pairs determined to be impostors. If the determined class (genuine or impostor) matches the real class, points will be blue; if not, red. An X represents face detection failure in either of the images in the pair. Note that the sample size (n=20) is small, and the figure may change substantially if larger or different sets are used. The images can be viewed on p. 13 of the Appendix, where Gen 01 corresponds to Same-Identity Pair 1, Gen 02 corresponds to Same-Identity Pair 2, and so on.

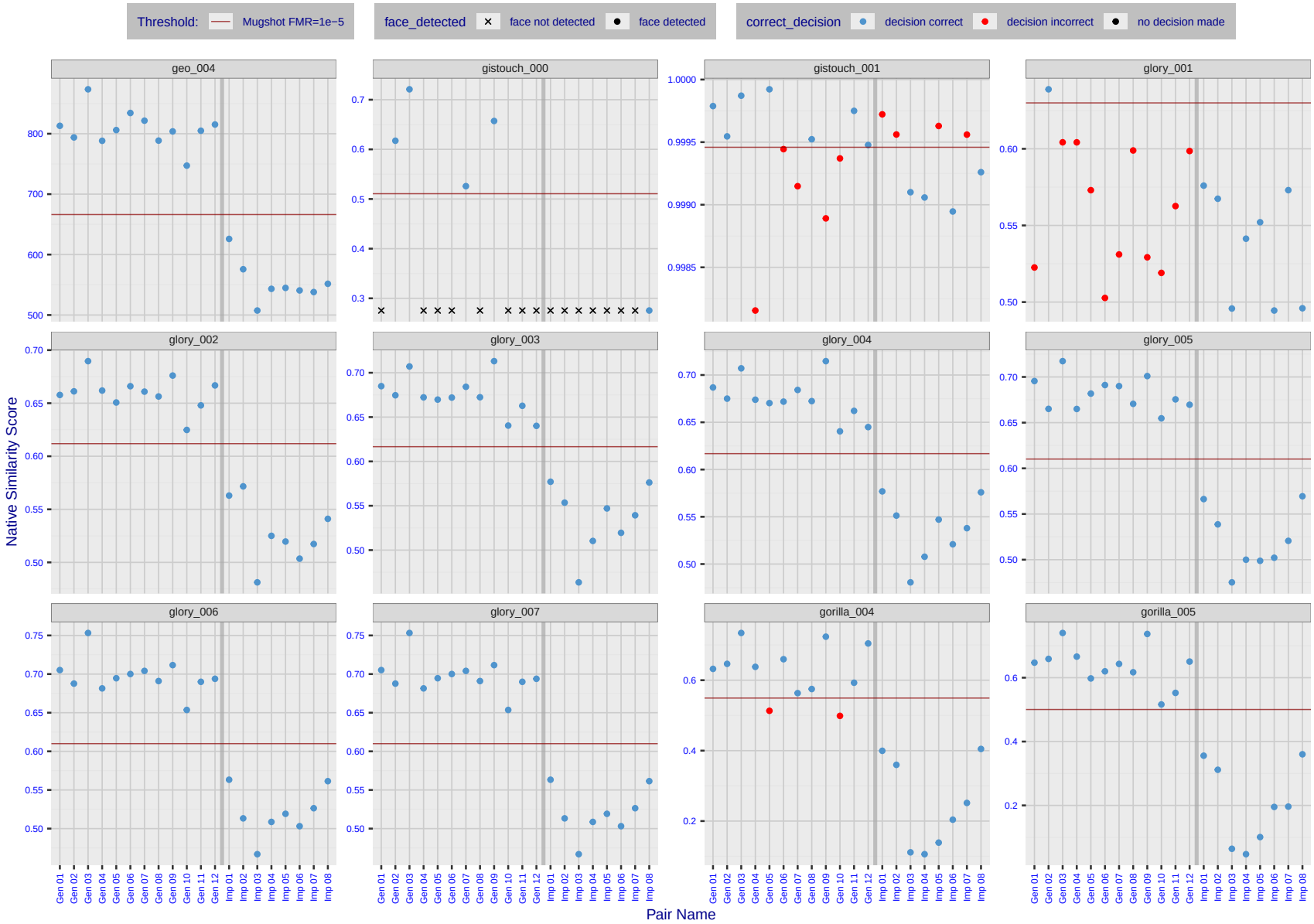

Figure 36: The figure shows algorithms' similarity scores for 12 genuine and 8 impostor image pairs used in a May 2018 paper by Phillips et al. ([1]). The threshold (red horizontal line) is a value calibrated to give FMR = 0.0001 on mugshot images. Points above the threshold correspond to pairs determined to be genuine, and points below the threshold correspond to pairs determined to be impostors. If the determined class (genuine or impostor) matches the real class, points will be blue; if not, red. An X represents face detection failure in either of the images in the pair. Note that the sample size (n=20) is small, and the figure may change substantially if larger or different sets are used. The images can be viewed on p. 13 of the Appendix, where Gen 01 corresponds to Same-Identity Pair 1, Gen 02 corresponds to Same-Identity Pair 2, and so on.

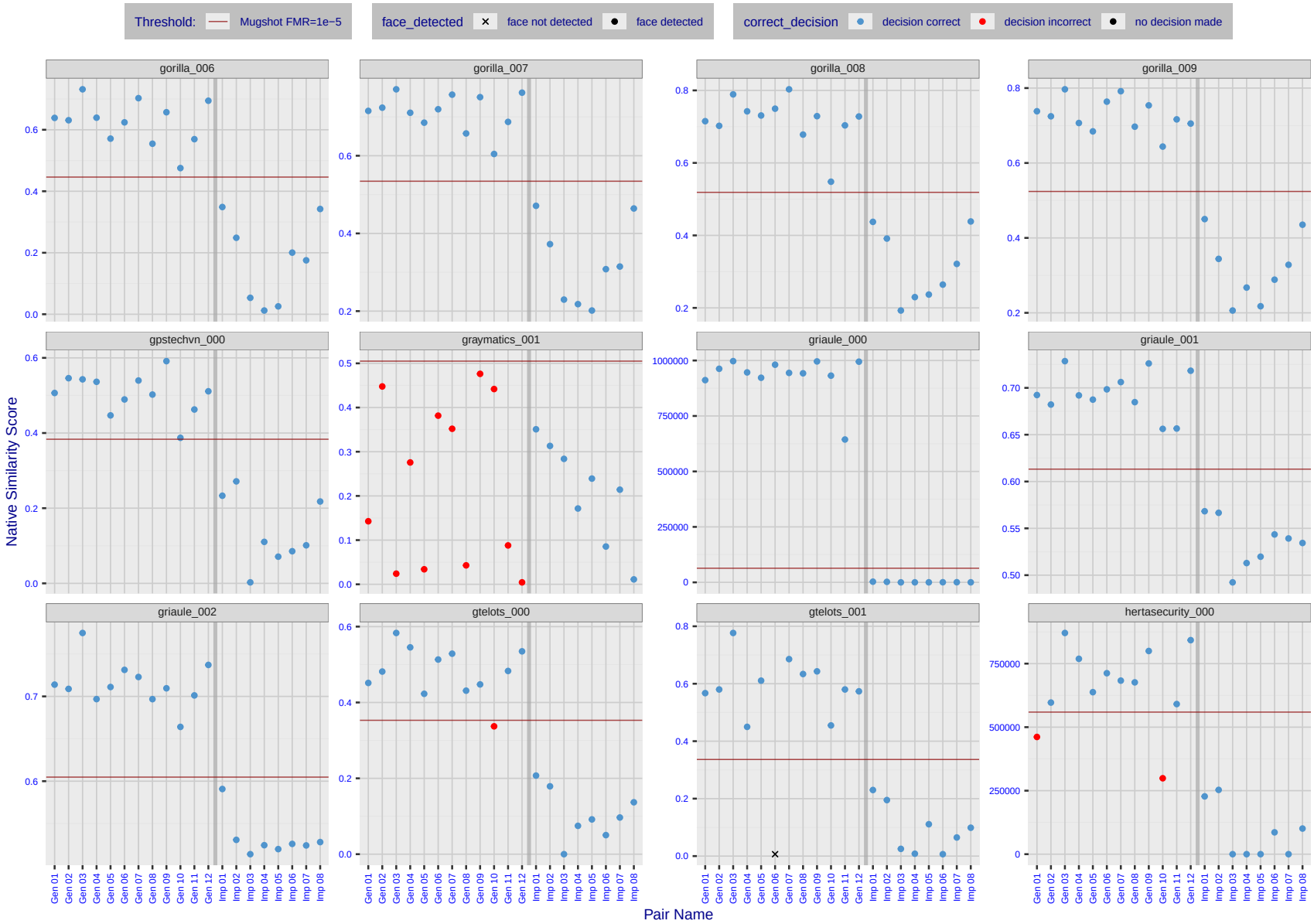

Figure 37: The figure shows algorithms' similarity scores for 12 genuine and 8 impostor image pairs used in a May 2018 paper by Phillips et al. ([1]). The threshold (red horizontal line) is a value calibrated to give FMR = 0.0001 on mugshot images. Points above the threshold correspond to pairs determined to be genuine, and points below the threshold correspond to pairs determined to be impostors. If the determined class (genuine or impostor) matches the real class, points will be blue; if not, red. An X represents face detection failure in either of the images in the pair. Note that the sample size (n=20) is small, and the figure may change substantially if larger or different sets are used. The images can be viewed on p. 13 of the Appendix, where Gen 01 corresponds to Same-Identity Pair 1, Gen 02 corresponds to Same-Identity Pair 2, and so on.

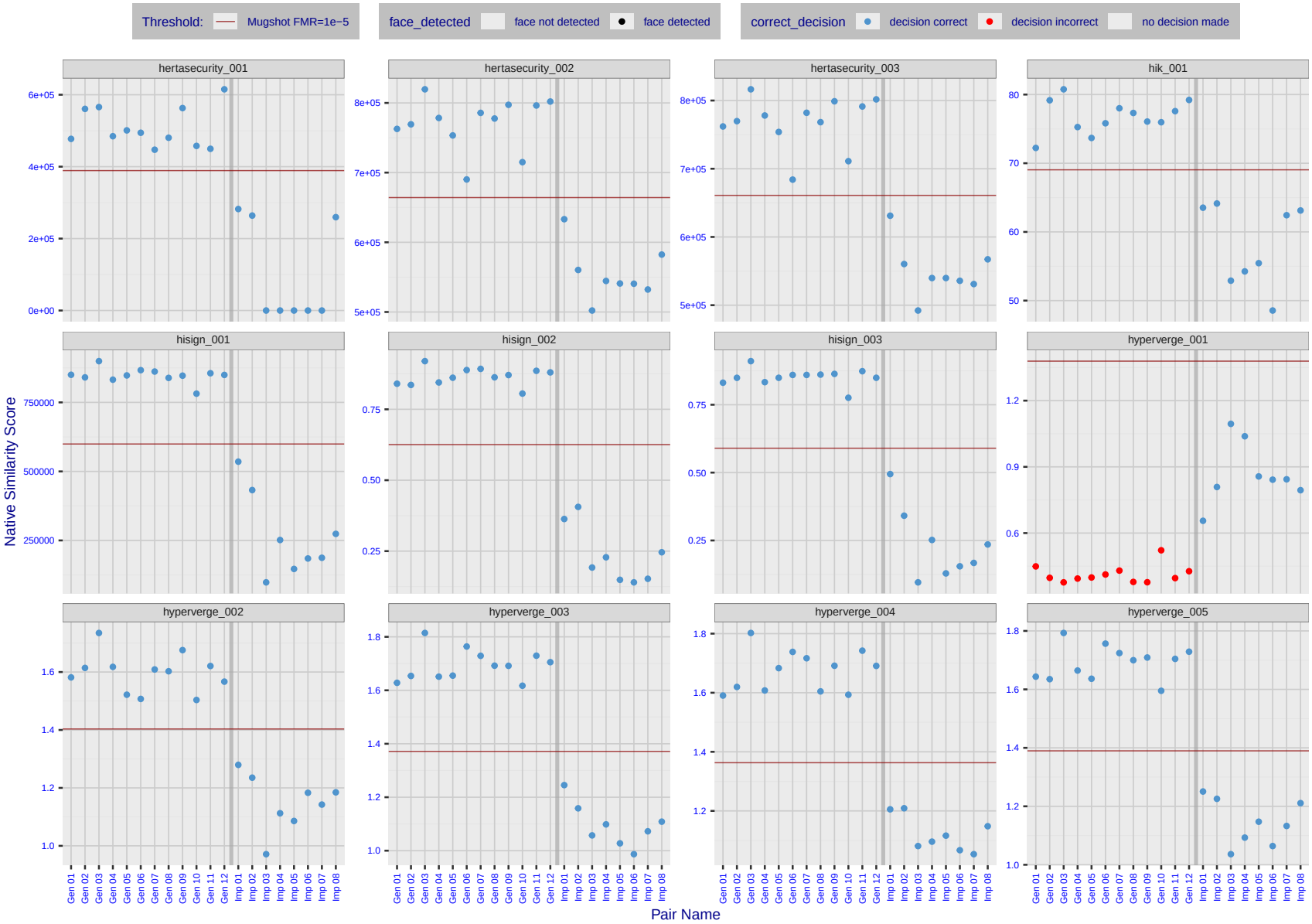

Figure 38: The figure shows algorithms' similarity scores for 12 genuine and 8 impostor image pairs used in a May 2018 paper by Phillips et al. ([1]). The threshold (red horizontal line) is a value calibrated to give FMR = 0.0001 on mugshot images. Points above the threshold correspond to pairs determined to be genuine, and points below the threshold correspond to pairs determined to be impostors. If the determined class (genuine or impostor) matches the real class, points will be blue; if not, red. An X represents face detection failure in either of the images in the pair. Note that the sample size (n=20) is small, and the figure may change substantially if larger or different sets are used. The images can be viewed on p. 13 of the Appendix, where Gen 01 corresponds to Same-Identity Pair 1, Gen 02 corresponds to Same-Identity Pair 2, and so on.

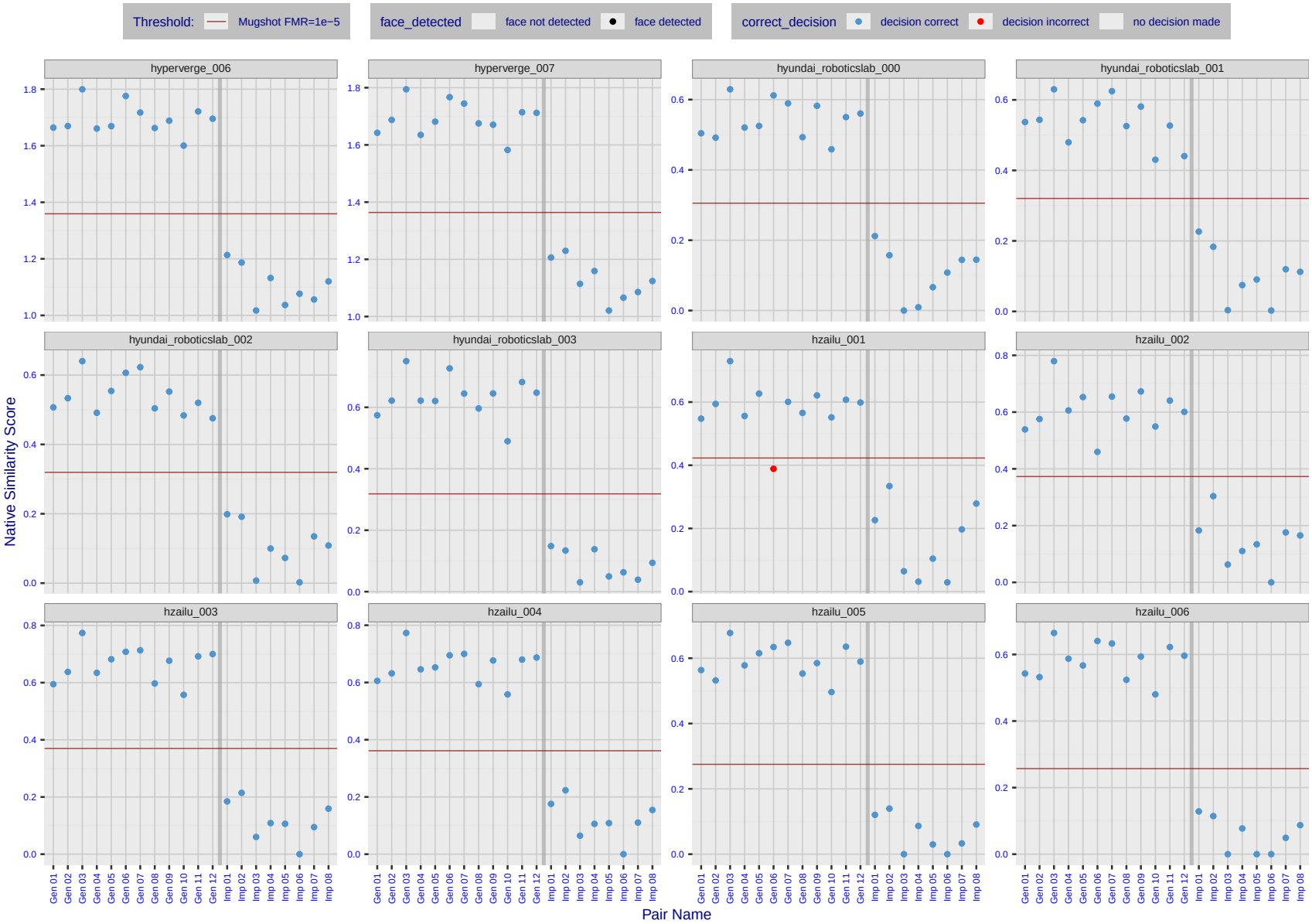

Figure 39: The figure shows algorithms' similarity scores for 12 genuine and 8 impostor image pairs used in a May 2018 paper by Phillips et al. ([1]). The threshold (red horizontal line) is a value calibrated to give FMR = 0.0001 on mugshot images. Points above the threshold correspond to pairs determined to be genuine, and points below the threshold correspond to pairs determined to be impostors. If the determined class (genuine or impostor) matches the real class, points will be blue; if not, red. An X represents face detection failure in either of the images in the pair. Note that the sample size (n=20) is small, and the figure may change substantially if larger or different sets are used. The images can be viewed on p. 13 of the Appendix, where Gen 01 corresponds to Same-Identity Pair 1, Gen 02 corresponds to Same-Identity Pair 2, and so on.

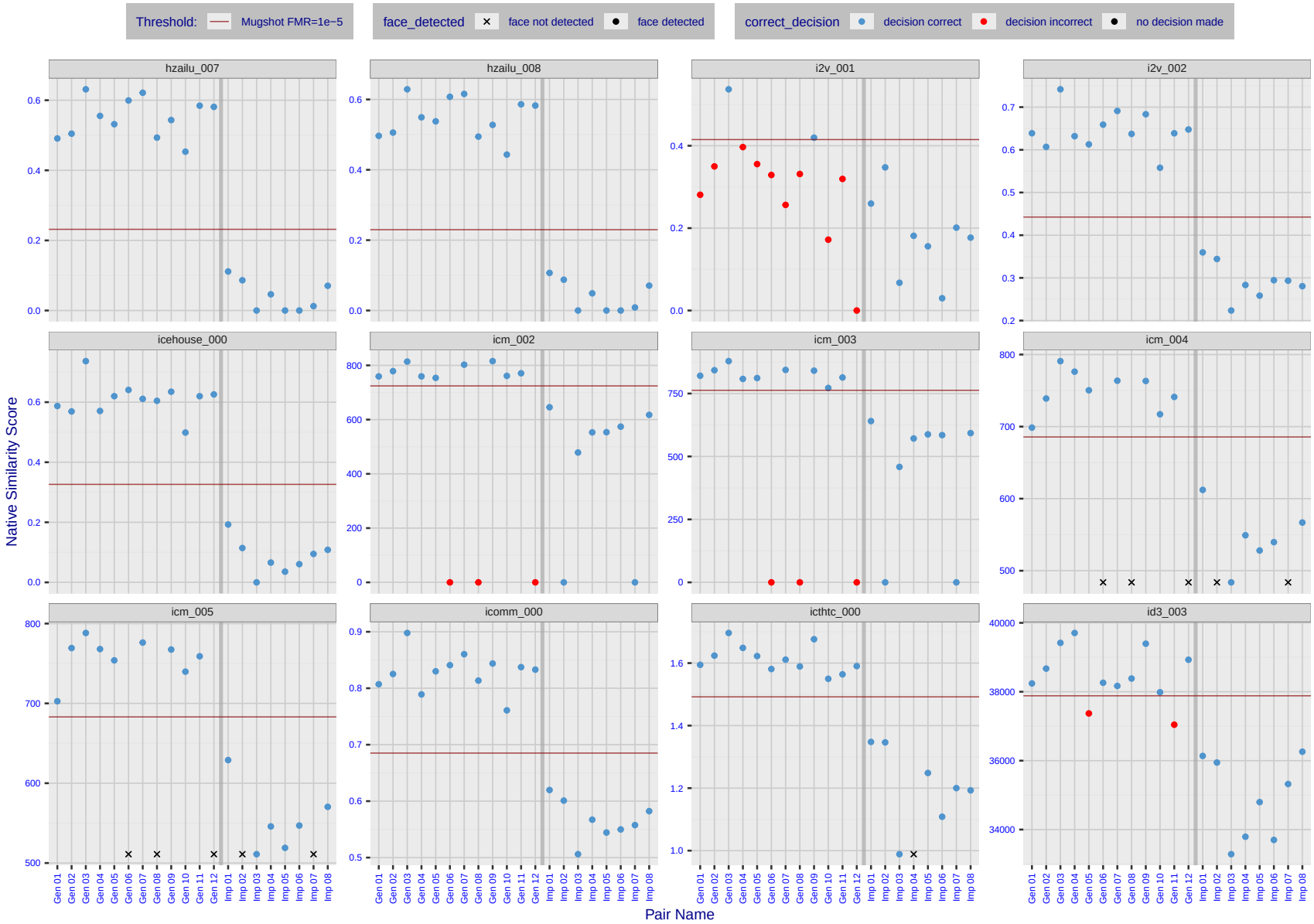

Figure 40: The figure shows algorithms' similarity scores for 12 genuine and 8 impostor image pairs used in a May 2018 paper by Phillips et al. ([1]). The threshold (red horizontal line) is a value calibrated to give FMR = 0.0001 on mugshot images. Points above the threshold correspond to pairs determined to be genuine, and points below the threshold correspond to pairs determined to be impostors. If the determined class (genuine or impostor) matches the real class, points will be blue; if not, red. An X represents face detection failure in either of the images in the pair. Note that the sample size (n=20) is small, and the figure may change substantially if larger or different sets are used. The images can be viewed on p. 13 of the Appendix, where Gen 01 corresponds to Same-Identity Pair 1, Gen 02 corresponds to Same-Identity Pair 2, and so on.

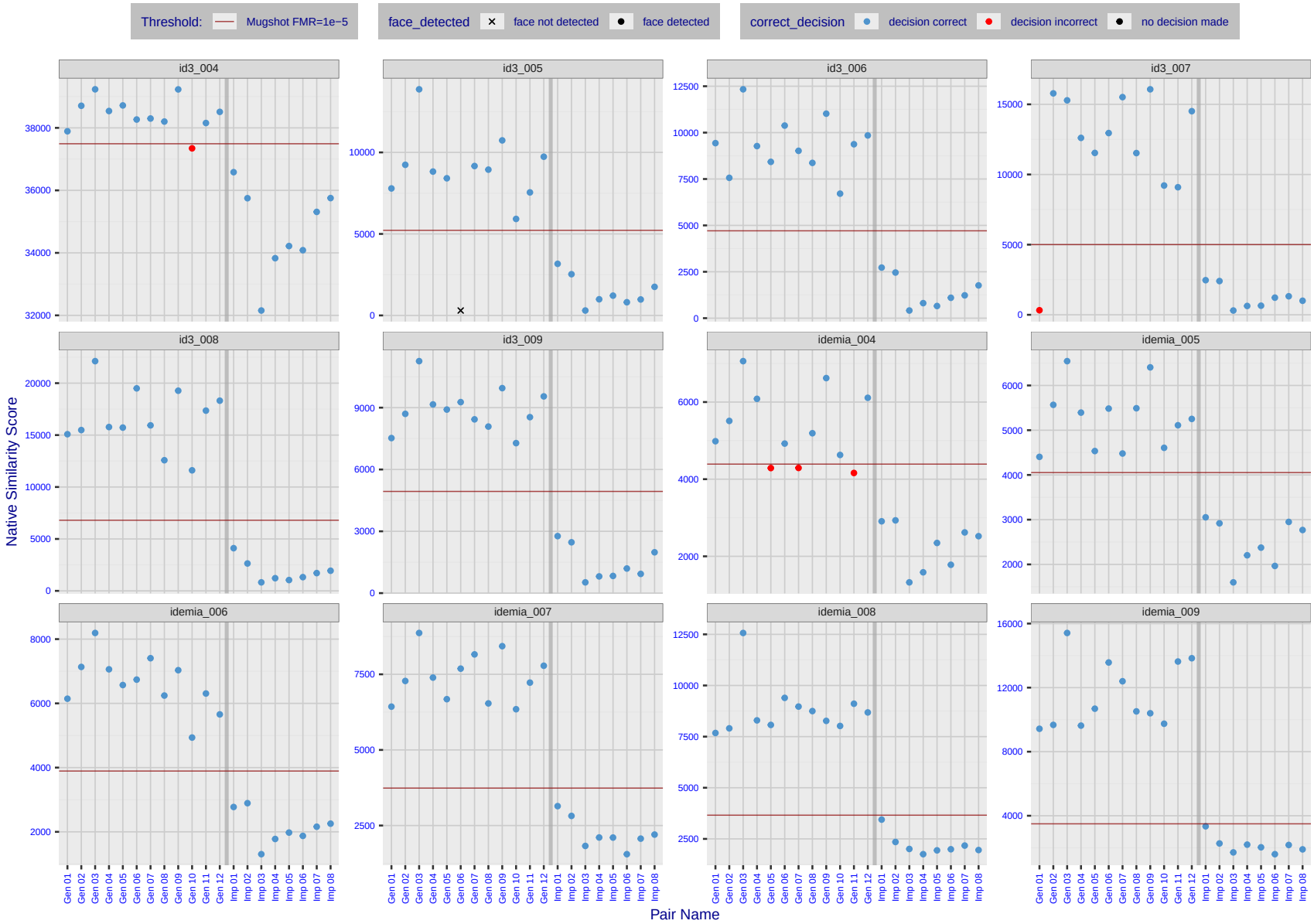

Figure 41: The figure shows algorithms' similarity scores for 12 genuine and 8 impostor image pairs used in a May 2018 paper by Phillips et al. ([1]). The threshold (red horizontal line) is a value calibrated to give FMR = 0.0001 on mugshot images. Points above the threshold correspond to pairs determined to be genuine, and points below the threshold correspond to pairs determined to be impostors. If the determined class (genuine or impostor) matches the real class, points will be blue; if not, red. An X represents face detection failure in either of the images in the pair. Note that the sample size (n=20) is small, and the figure may change substantially if larger or different sets are used. The images can be viewed on p. 13 of the Appendix, where Gen 01 corresponds to Same-Identity Pair 1, Gen 02 corresponds to Same-Identity Pair 2, and so on.

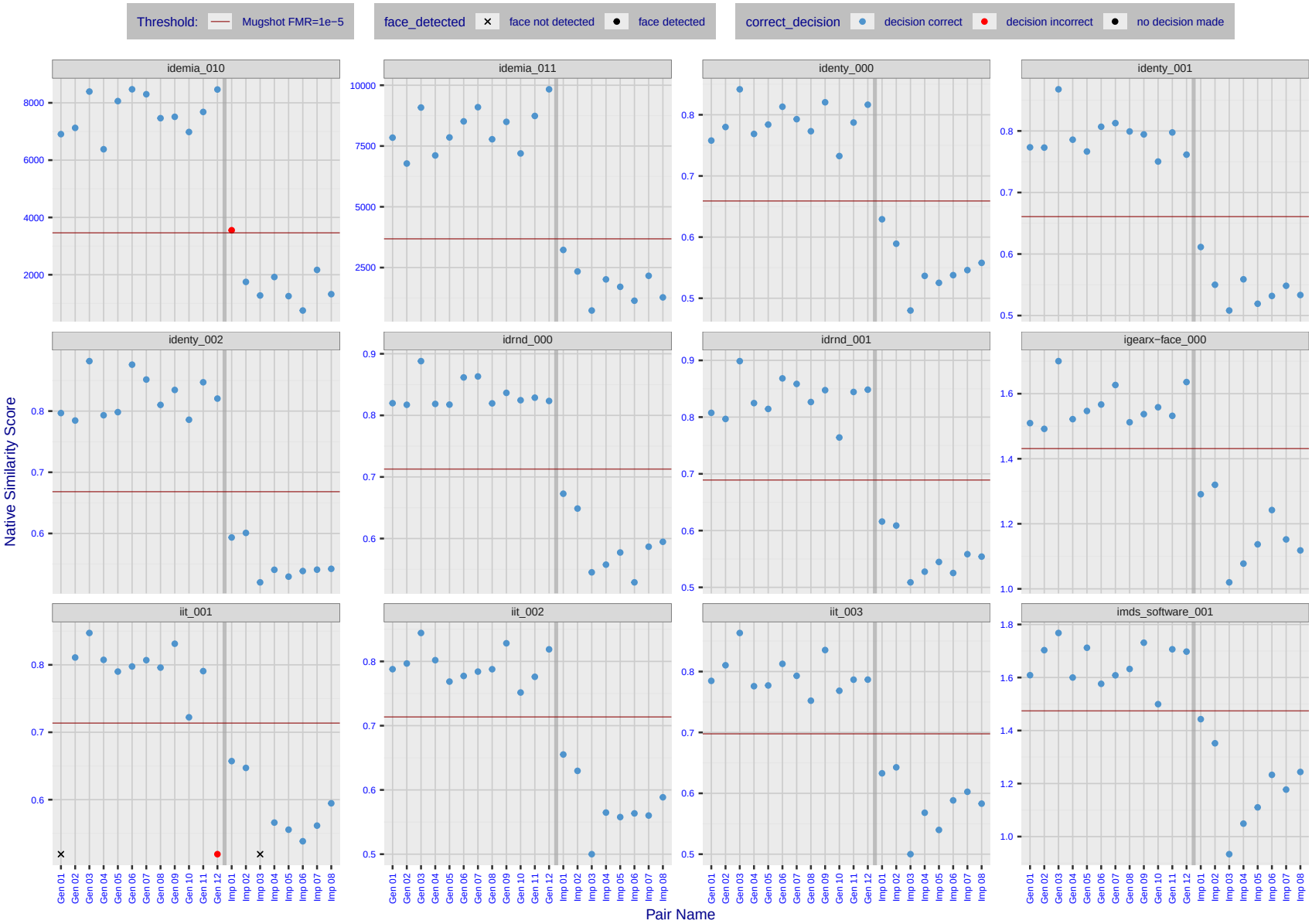

Figure 42: The figure shows algorithms' similarity scores for 12 genuine and 8 impostor image pairs used in a May 2018 paper by Phillips et al. ([1]). The threshold (red horizontal line) is a value calibrated to give FMR = 0.0001 on mugshot images. Points above the threshold correspond to pairs determined to be genuine, and points below the threshold correspond to pairs determined to be impostors. If the determined class (genuine or impostor) matches the real class, points will be blue; if not, red. An X represents face detection failure in either of the images in the pair. Note that the sample size (n=20) is small, and the figure may change substantially if larger or different sets are used. The images can be viewed on p. 13 of the Appendix, where Gen 01 corresponds to Same-Identity Pair 1, Gen 02 corresponds to Same-Identity Pair 2, and so on.

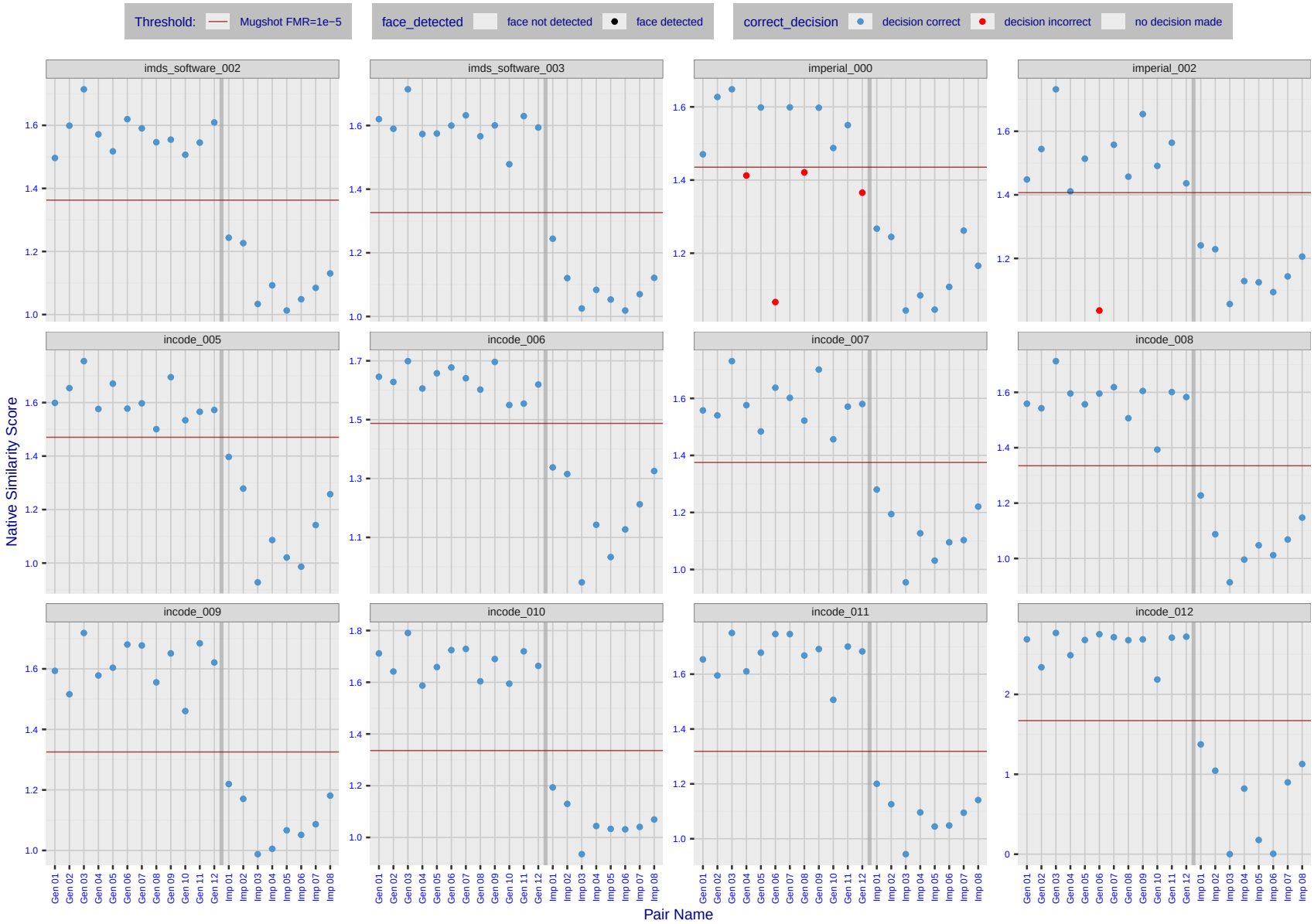

Figure 43: The figure shows algorithms' similarity scores for 12 genuine and 8 impostor image pairs used in a May 2018 paper by Phillips et al. ([1]). The threshold (red horizontal line) is a value calibrated to give FMR = 0.0001 on mugshot images. Points above the threshold correspond to pairs determined to be genuine, and points below the threshold correspond to pairs determined to be impostors. If the determined class (genuine or impostor) matches the real class, points will be blue; if not, red. An X represents face detection failure in either of the images in the pair. Note that the sample size (n=20) is small, and the figure may change substantially if larger or different sets are used. The images can be viewed on p. 13 of the Appendix, where Gen 01 corresponds to Same-Identity Pair 1, Gen 02 corresponds to Same-Identity Pair 2, and so on.

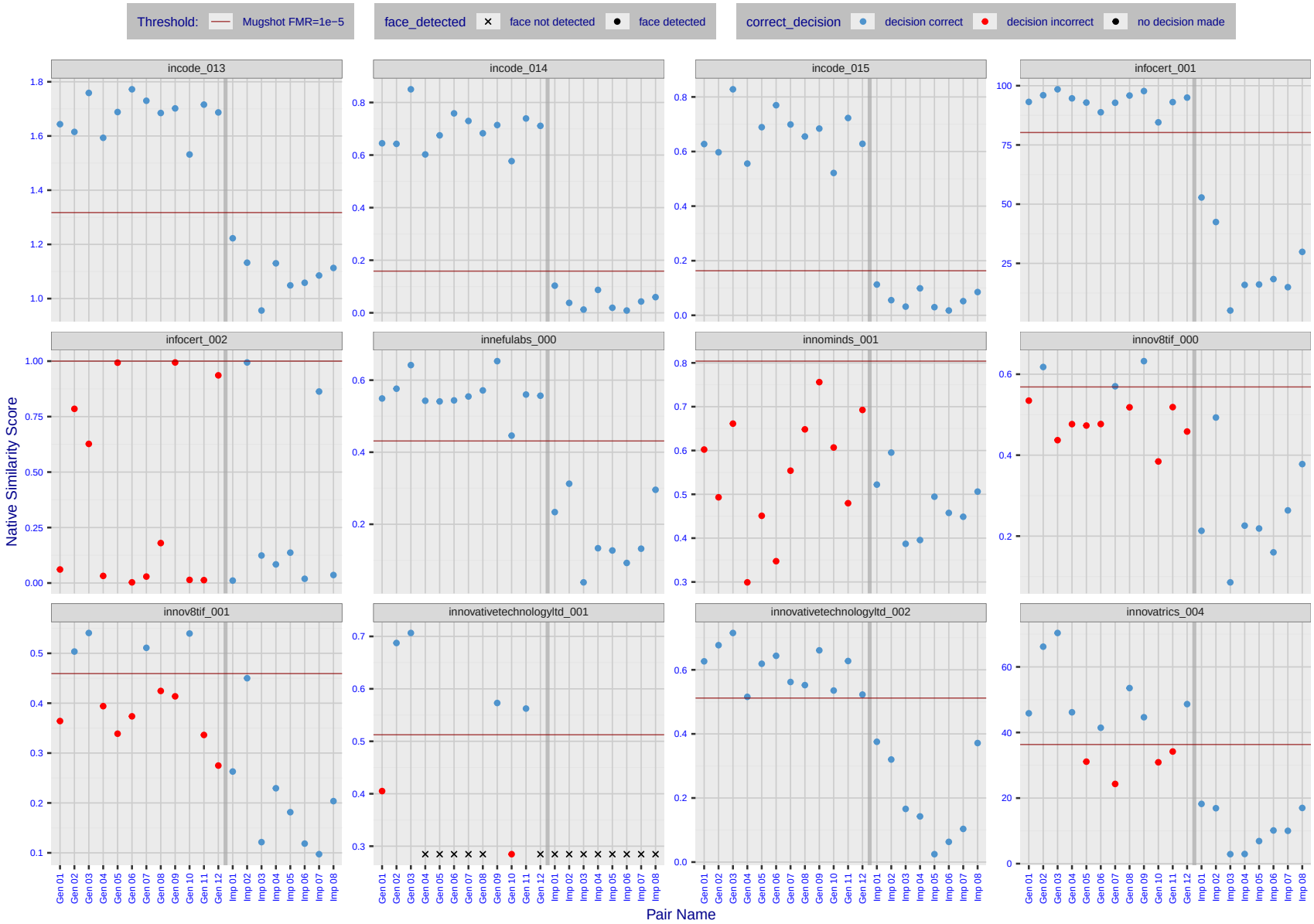

Figure 44: The figure shows algorithms' similarity scores for 12 genuine and 8 impostor image pairs used in a May 2018 paper by Phillips et al. ([1]). The threshold (red horizontal line) is a value calibrated to give FMR = 0.0001 on mugshot images. Points above the threshold correspond to pairs determined to be genuine, and points below the threshold correspond to pairs determined to be impostors. If the determined class (genuine or impostor) matches the real class, points will be blue; if not, red. An X represents face detection failure in either of the images in the pair. Note that the sample size (n=20) is small, and the figure may change substantially if larger or different sets are used. The images can be viewed on p. 13 of the Appendix, where Gen 01 corresponds to Same-Identity Pair 1, Gen 02 corresponds to Same-Identity Pair 2, and so on.

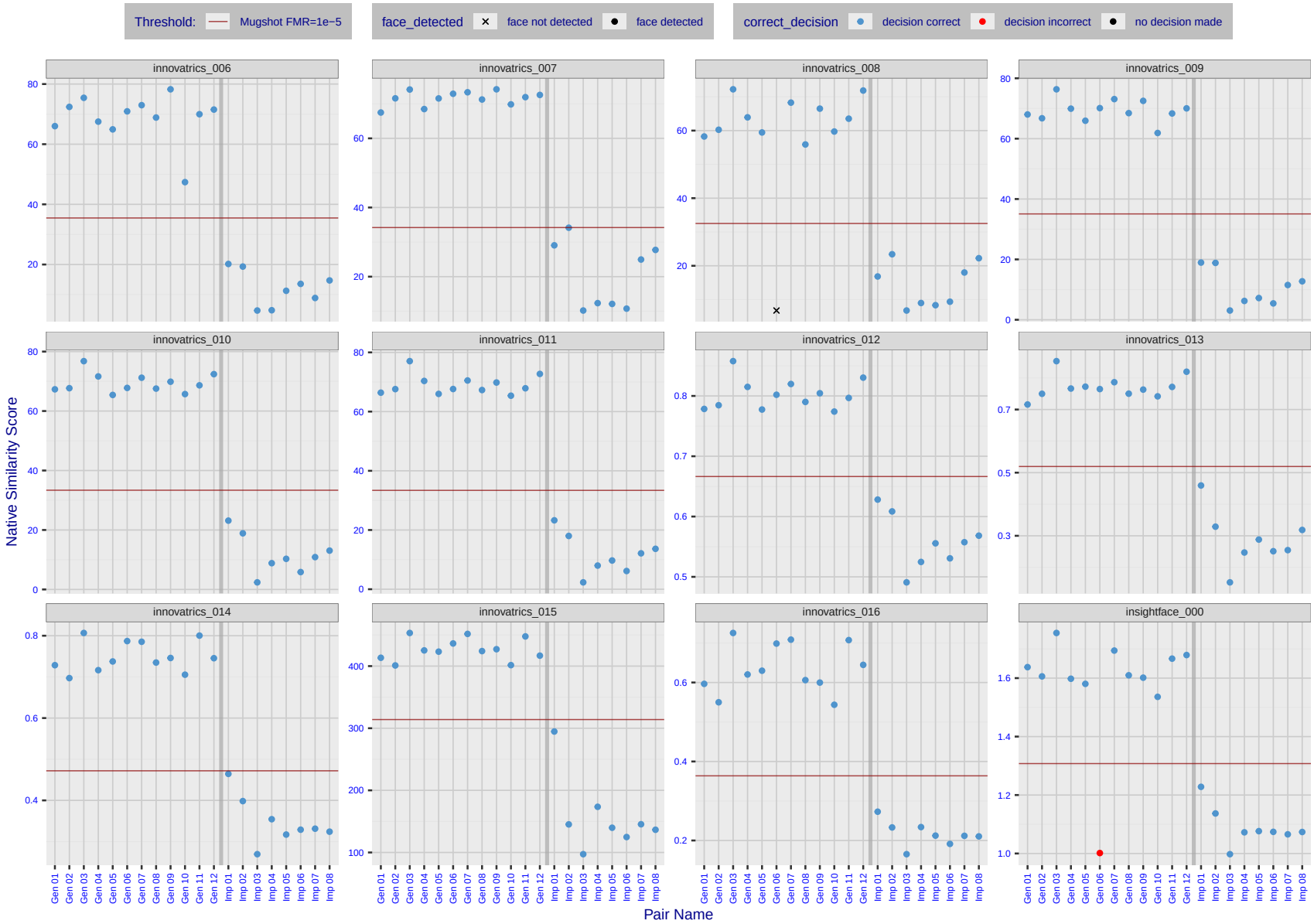

Figure 45: The figure shows algorithms' similarity scores for 12 genuine and 8 impostor image pairs used in a May 2018 paper by Phillips et al. ([1]). The threshold (red horizontal line) is a value calibrated to give FMR = 0.0001 on mugshot images. Points above the threshold correspond to pairs determined to be genuine, and points below the threshold correspond to pairs determined to be impostors. If the determined class (genuine or impostor) matches the real class, points will be blue; if not, red. An X represents face detection failure in either of the images in the pair. Note that the sample size (n=20) is small, and the figure may change substantially if larger or different sets are used. The images can be viewed on p. 13 of the Appendix, where Gen 01 corresponds to Same-Identity Pair 1, Gen 02 corresponds to Same-Identity Pair 2, and so on.

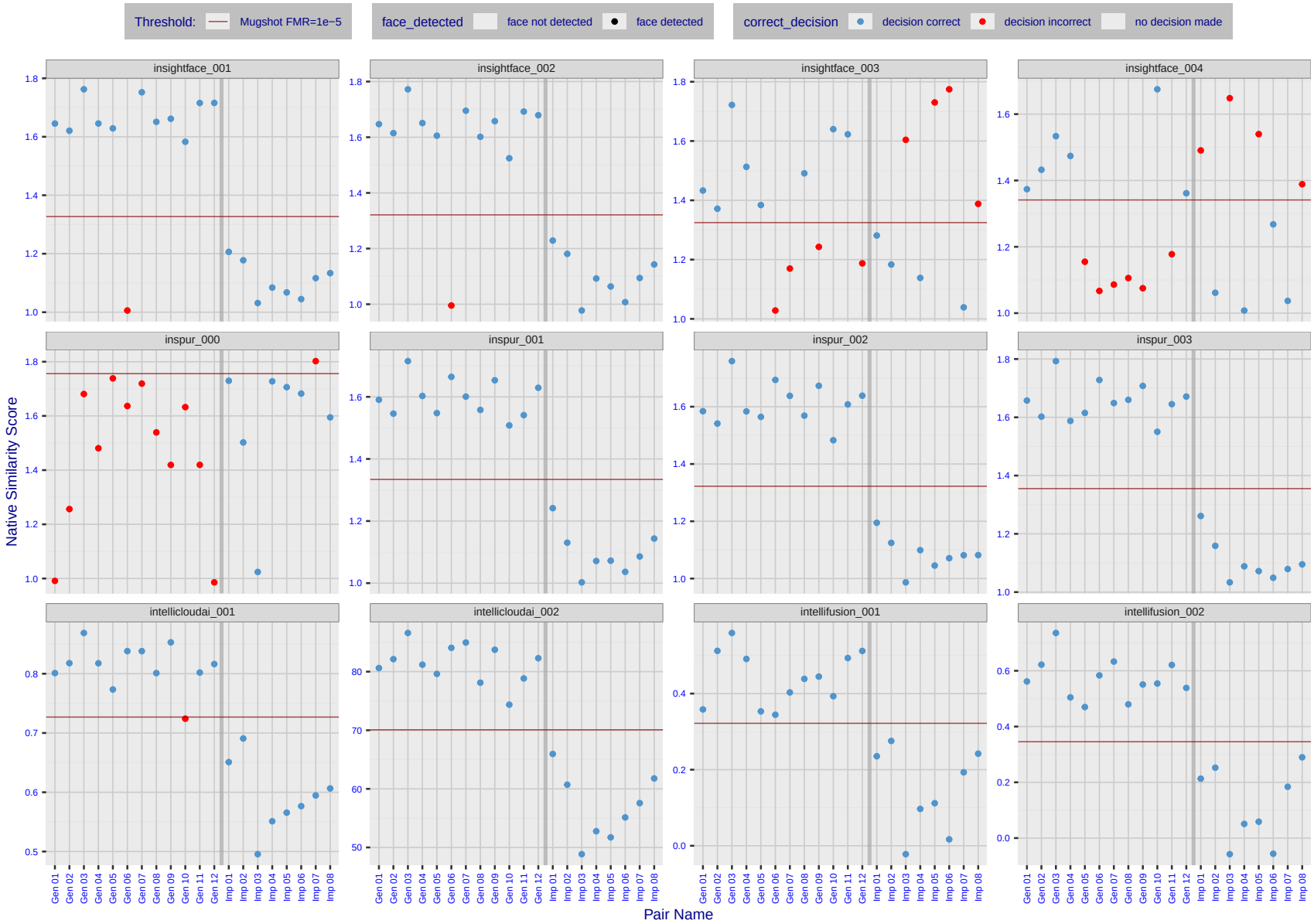

Figure 46: The figure shows algorithms' similarity scores for 12 genuine and 8 impostor image pairs used in a May 2018 paper by Phillips et al. ([1]). The threshold (red horizontal line) is a value calibrated to give FMR = 0.0001 on mugshot images. Points above the threshold correspond to pairs determined to be genuine, and points below the threshold correspond to pairs determined to be impostors. If the determined class (genuine or impostor) matches the real class, points will be blue; if not, red. An X represents face detection failure in either of the images in the pair. Note that the sample size (n=20) is small, and the figure may change substantially if larger or different sets are used. The images can be viewed on p. 13 of the Appendix, where Gen 01 corresponds to Same-Identity Pair 1, Gen 02 corresponds to Same-Identity Pair 2, and so on.

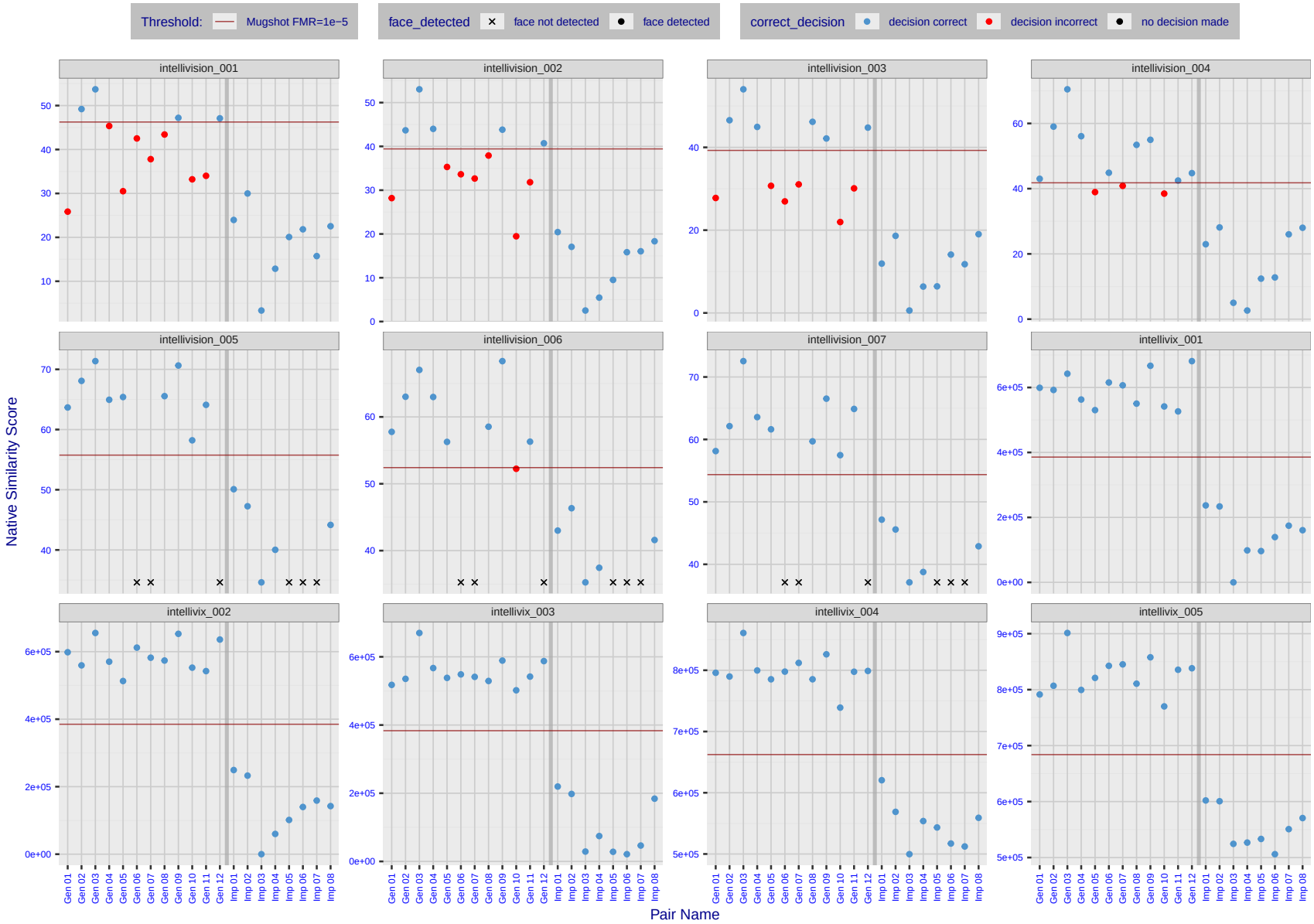

Figure 47: The figure shows algorithms' similarity scores for 12 genuine and 8 impostor image pairs used in a May 2018 paper by Phillips et al. ([1]). The threshold (red horizontal line) is a value calibrated to give FMR = 0.0001 on mugshot images. Points above the threshold correspond to pairs determined to be genuine, and points below the threshold correspond to pairs determined to be impostors. If the determined class (genuine or impostor) matches the real class, points will be blue; if not, red. An X represents face detection failure in either of the images in the pair. Note that the sample size (n=20) is small, and the figure may change substantially if larger or different sets are used. The images can be viewed on p. 13 of the Appendix, where Gen 01 corresponds to Same-Identity Pair 1, Gen 02 corresponds to Same-Identity Pair 2, and so on.

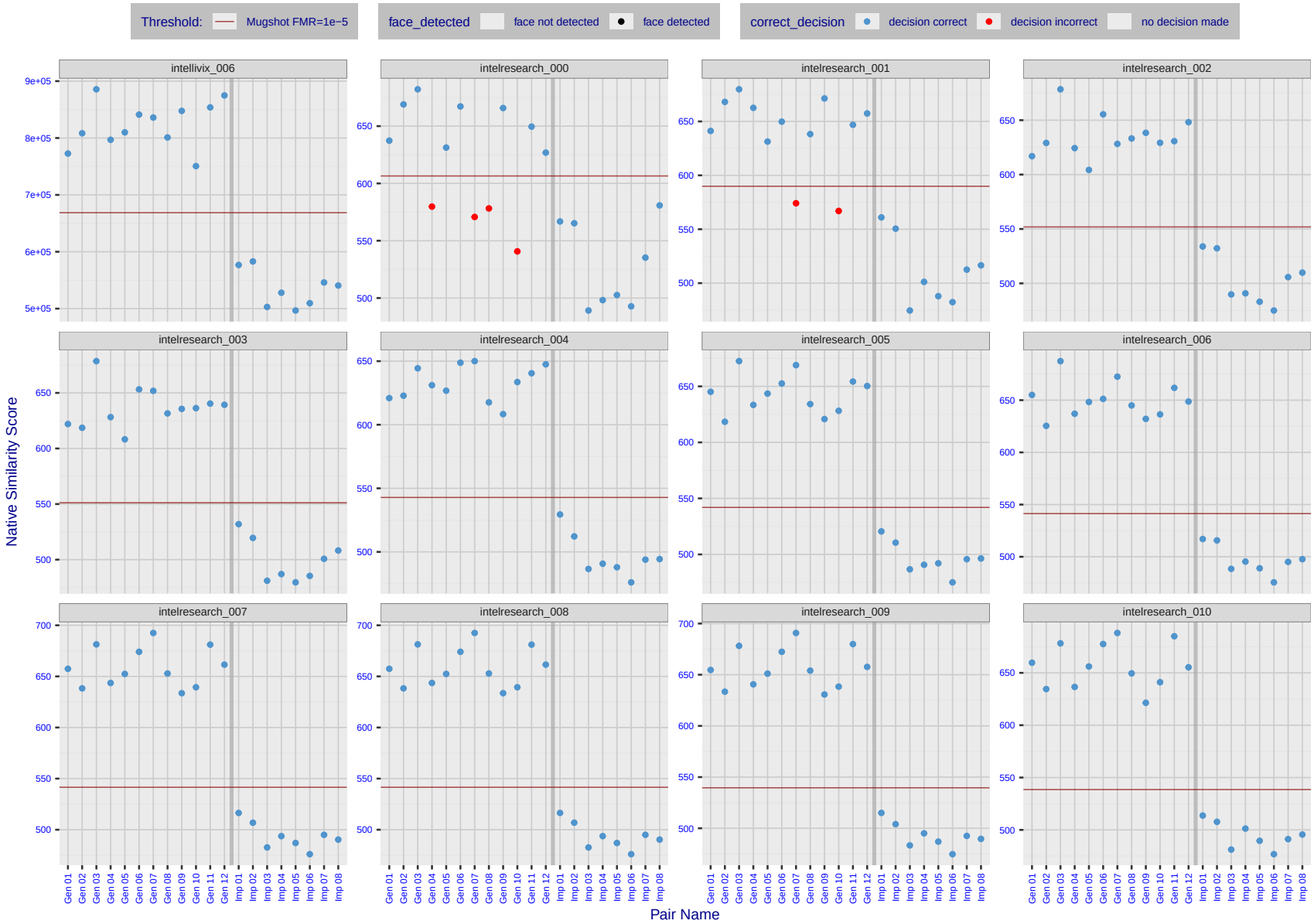

Figure 48: The figure shows algorithms' similarity scores for 12 genuine and 8 impostor image pairs used in a May 2018 paper by Phillips et al. ([1]). The threshold (red horizontal line) is a value calibrated to give FMR = 0.0001 on mugshot images. Points above the threshold correspond to pairs determined to be genuine, and points below the threshold correspond to pairs determined to be impostors. If the determined class (genuine or impostor) matches the real class, points will be blue; if not, red. An X represents face detection failure in either of the images in the pair. Note that the sample size (n=20) is small, and the figure may change substantially if larger or different sets are used. The images can be viewed on p. 13 of the Appendix, where Gen 01 corresponds to Same-Identity Pair 1, Gen 02 corresponds to Same-Identity Pair 2, and so on.

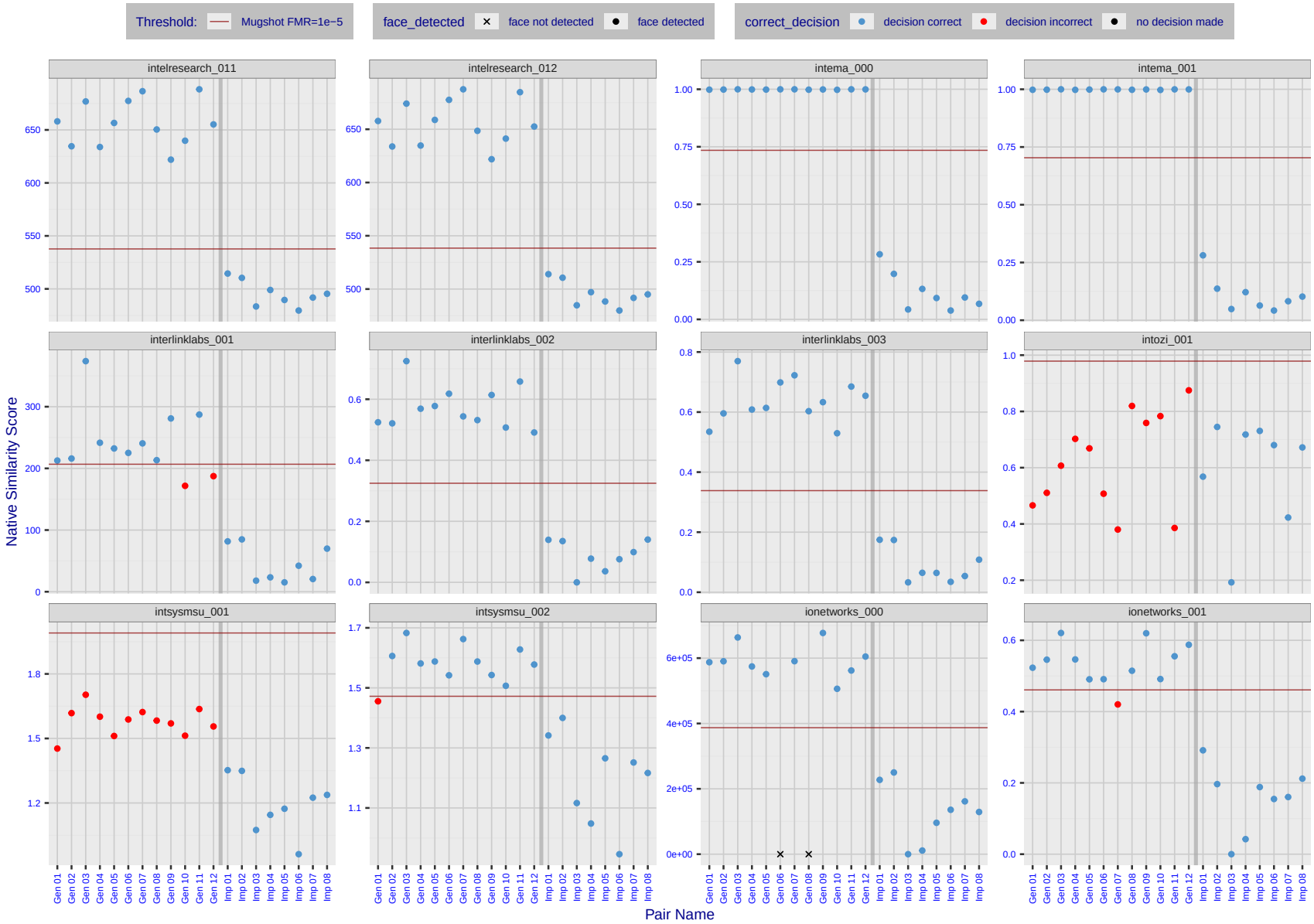

Figure 49: The figure shows algorithms' similarity scores for 12 genuine and 8 impostor image pairs used in a May 2018 paper by Phillips et al. ([1]). The threshold (red horizontal line) is a value calibrated to give FMR = 0.0001 on mugshot images. Points above the threshold correspond to pairs determined to be genuine, and points below the threshold correspond to pairs determined to be impostors. If the determined class (genuine or impostor) matches the real class, points will be blue; if not, red. An X represents face detection failure in either of the images in the pair. Note that the sample size (n=20) is small, and the figure may change substantially if larger or different sets are used. The images can be viewed on p. 13 of the Appendix, where Gen 01 corresponds to Same-Identity Pair 1, Gen 02 corresponds to Same-Identity Pair 2, and so on.

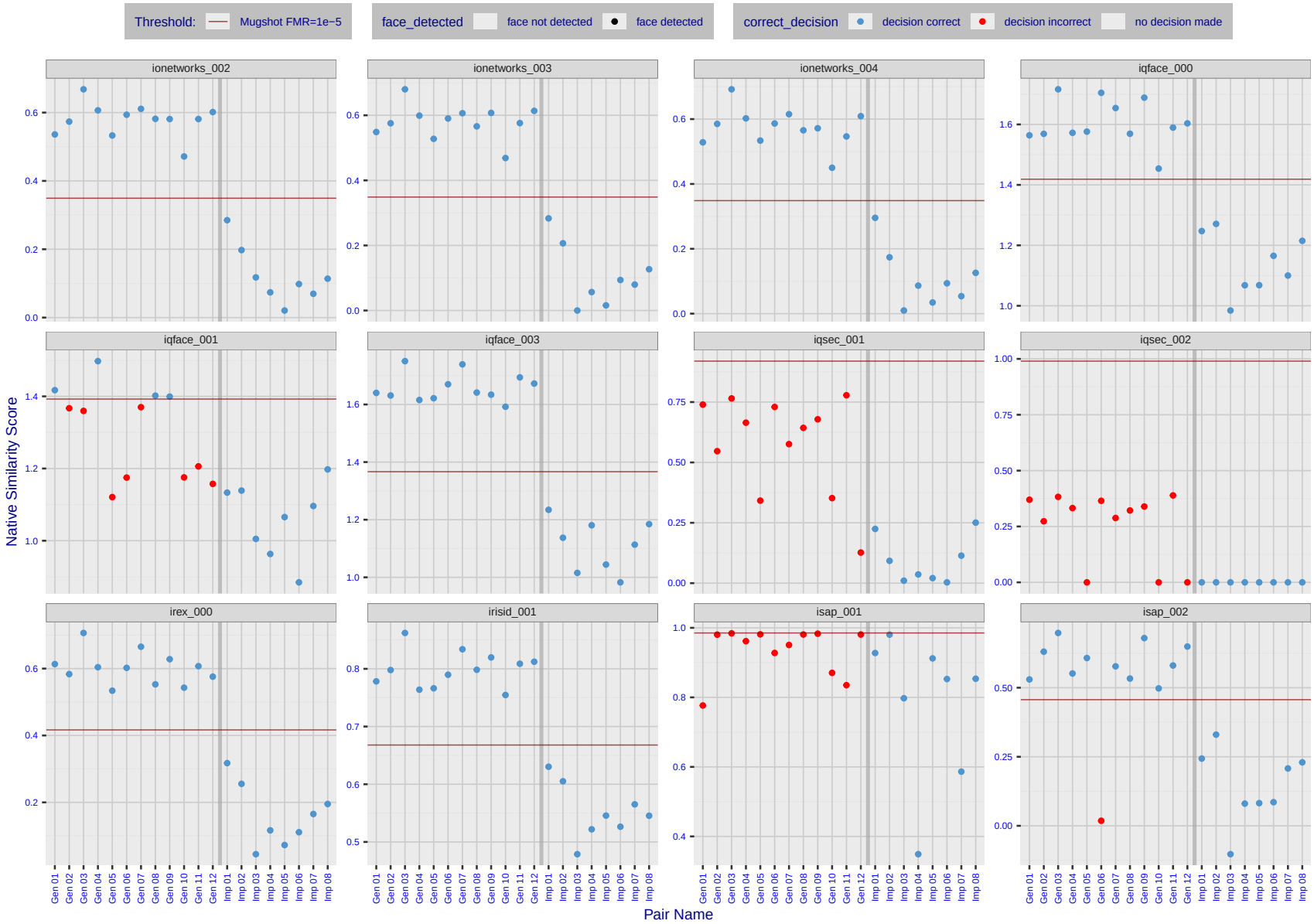

Figure 50: The figure shows algorithms' similarity scores for 12 genuine and 8 impostor image pairs used in a May 2018 paper by Phillips et al. ([1]). The threshold (red horizontal line) is a value calibrated to give FMR = 0.0001 on mugshot images. Points above the threshold correspond to pairs determined to be genuine, and points below the threshold correspond to pairs determined to be impostors. If the determined class (genuine or impostor) matches the real class, points will be blue; if not, red. An X represents face detection failure in either of the images in the pair. Note that the sample size (n=20) is small, and the figure may change substantially if larger or different sets are used. The images can be viewed on p. 13 of the Appendix, where Gen 01 corresponds to Same-Identity Pair 1, Gen 02 corresponds to Same-Identity Pair 2, and so on.

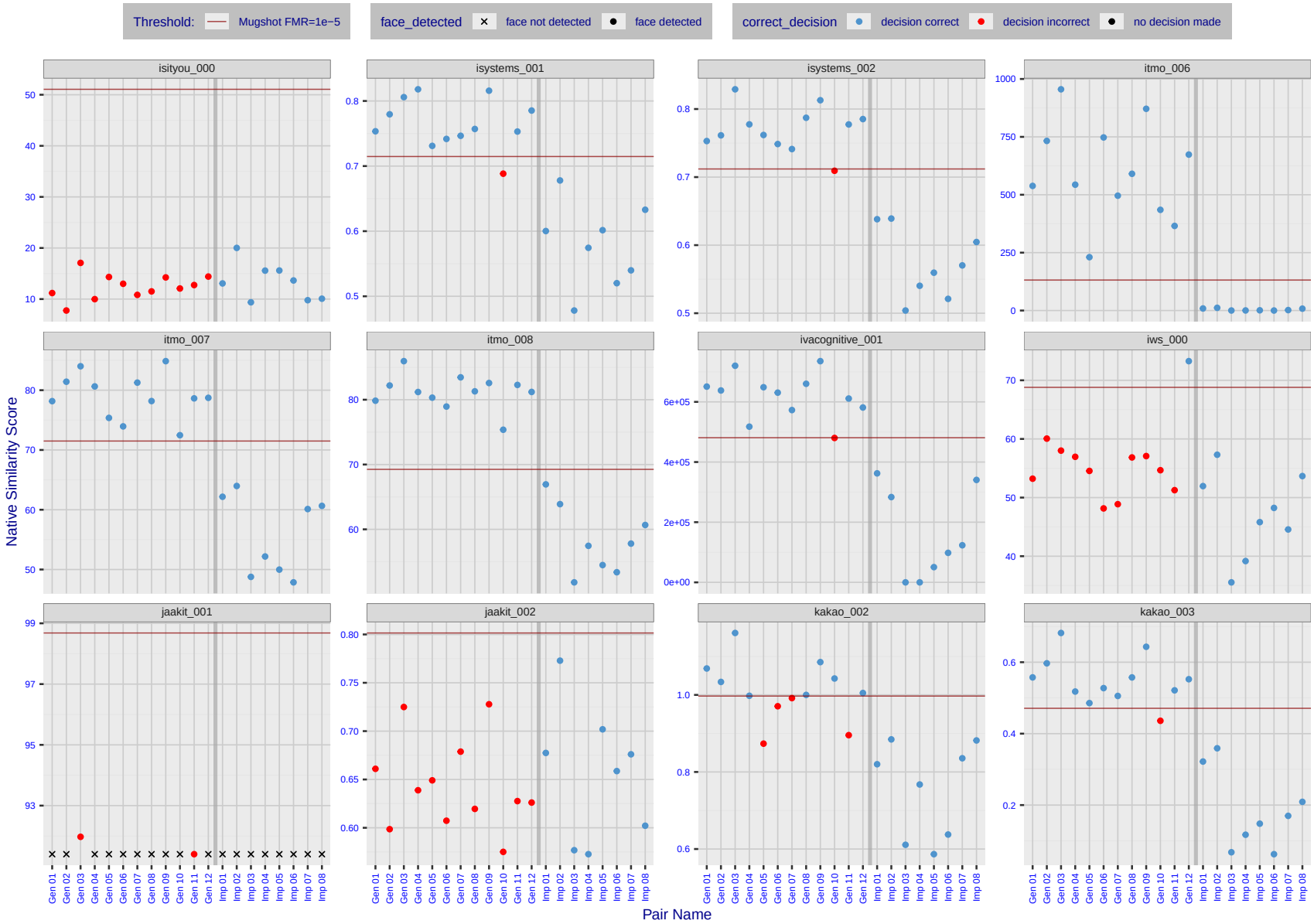

Figure 51: The figure shows algorithms' similarity scores for 12 genuine and 8 impostor image pairs used in a May 2018 paper by Phillips et al. ([1]). The threshold (red horizontal line) is a value calibrated to give FMR = 0.0001 on mugshot images. Points above the threshold correspond to pairs determined to be genuine, and points below the threshold correspond to pairs determined to be impostors. If the determined class (genuine or impostor) matches the real class, points will be blue; if not, red. An X represents face detection failure in either of the images in the pair. Note that the sample size (n=20) is small, and the figure may change substantially if larger or different sets are used. The images can be viewed on p. 13 of the Appendix, where Gen 01 corresponds to Same-Identity Pair 1, Gen 02 corresponds to Same-Identity Pair 2, and so on.

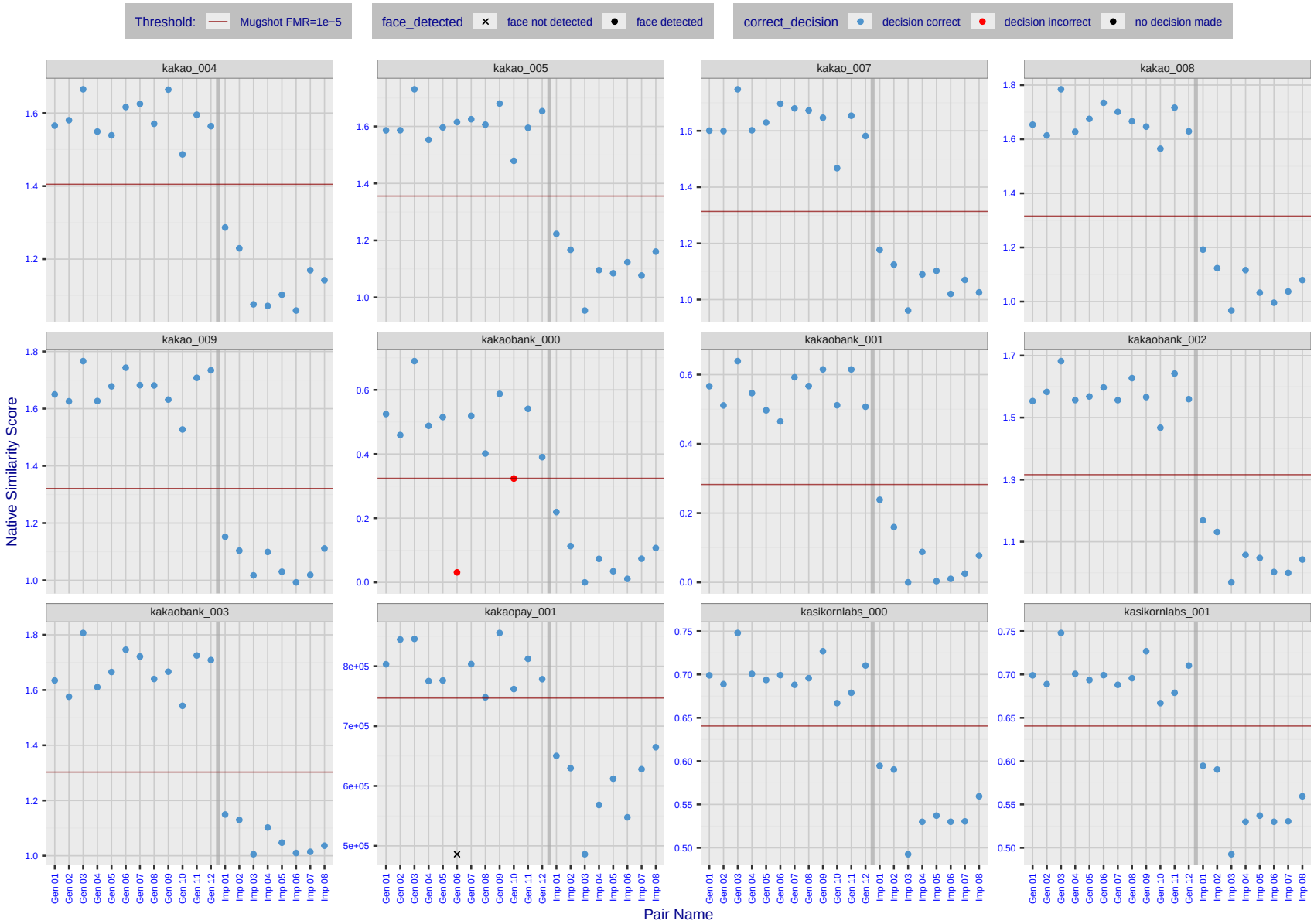

Figure 52: The figure shows algorithms' similarity scores for 12 genuine and 8 impostor image pairs used in a May 2018 paper by Phillips et al. ([1]). The threshold (red horizontal line) is a value calibrated to give FMR = 0.0001 on mugshot images. Points above the threshold correspond to pairs determined to be genuine, and points below the threshold correspond to pairs determined to be impostors. If the determined class (genuine or impostor) matches the real class, points will be blue; if not, red. An X represents face detection failure in either of the images in the pair. Note that the sample size (n=20) is small, and the figure may change substantially if larger or different sets are used. The images can be viewed on p. 13 of the Appendix, where Gen 01 corresponds to Same-Identity Pair 1, Gen 02 corresponds to Same-Identity Pair 2, and so on.

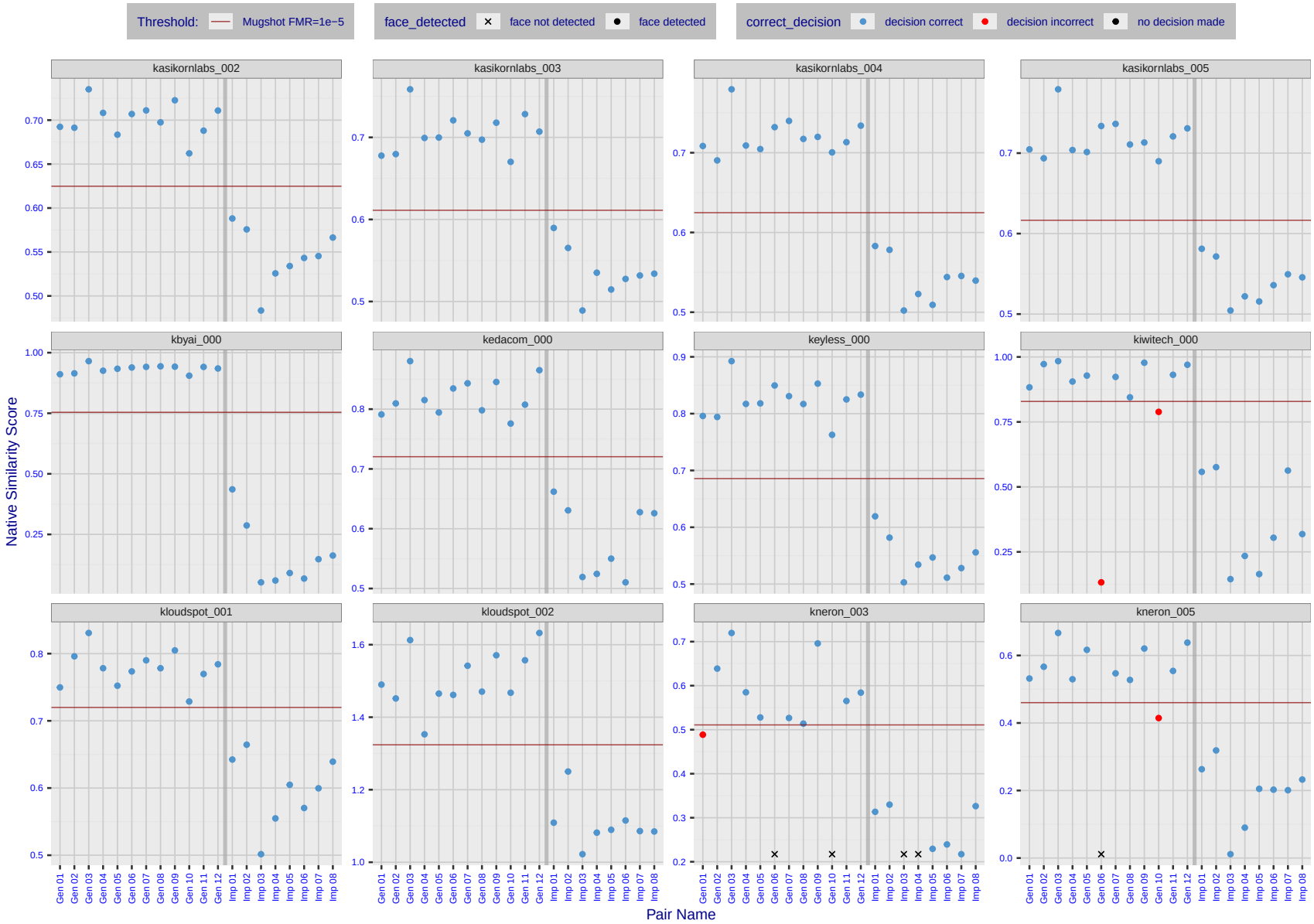

Figure 53: The figure shows algorithms' similarity scores for 12 genuine and 8 impostor image pairs used in a May 2018 paper by Phillips et al. ([1]). The threshold (red horizontal line) is a value calibrated to give FMR = 0.0001 on mugshot images. Points above the threshold correspond to pairs determined to be genuine, and points below the threshold correspond to pairs determined to be impostors. If the determined class (genuine or impostor) matches the real class, points will be blue; if not, red. An X represents face detection failure in either of the images in the pair. Note that the sample size (n=20) is small, and the figure may change substantially if larger or different sets are used. The images can be viewed on p. 13 of the Appendix, where Gen 01 corresponds to Same-Identity Pair 1, Gen 02 corresponds to Same-Identity Pair 2, and so on.

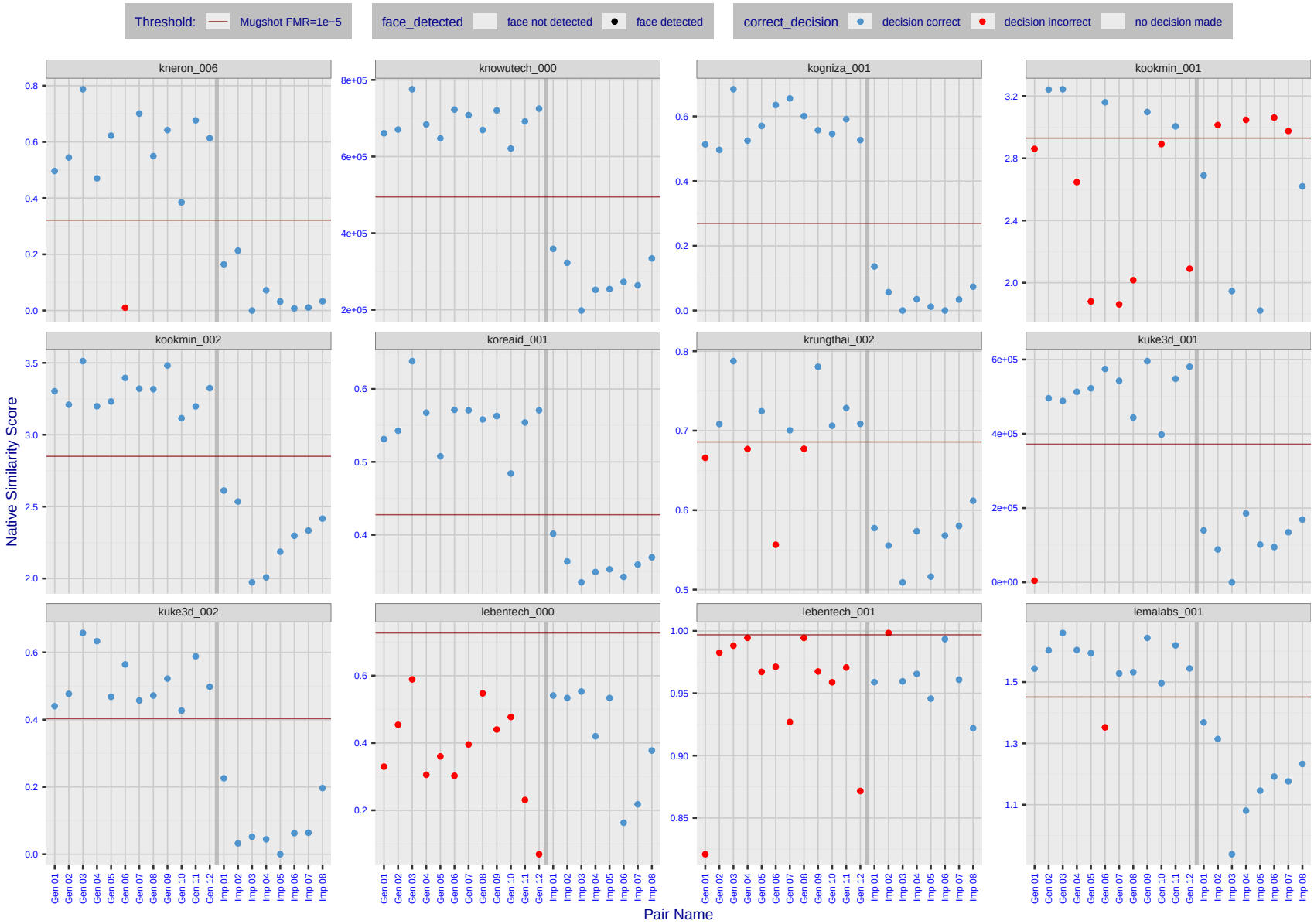

Figure 54: The figure shows algorithms' similarity scores for 12 genuine and 8 impostor image pairs used in a May 2018 paper by Phillips et al. ([1]). The threshold (red horizontal line) is a value calibrated to give FMR = 0.0001 on mugshot images. Points above the threshold correspond to pairs determined to be genuine, and points below the threshold correspond to pairs determined to be impostors. If the determined class (genuine or impostor) matches the real class, points will be blue; if not, red. An X represents face detection failure in either of the images in the pair. Note that the sample size (n=20) is small, and the figure may change substantially if larger or different sets are used. The images can be viewed on p. 13 of the Appendix, where Gen 01 corresponds to Same-Identity Pair 1, Gen 02 corresponds to Same-Identity Pair 2, and so on.

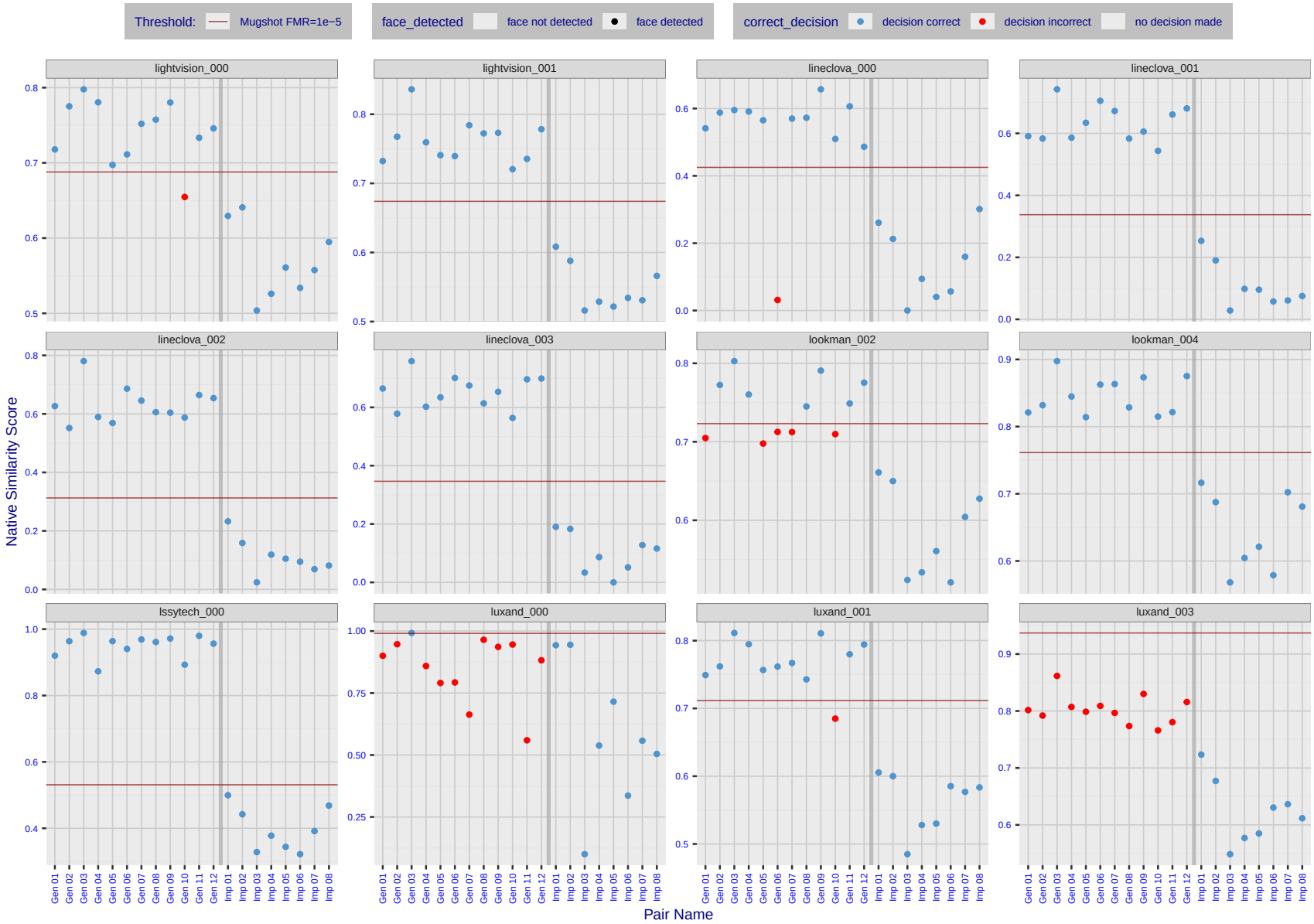

Figure 55: The figure shows algorithms' similarity scores for 12 genuine and 8 impostor image pairs used in a May 2018 paper by Phillips et al. ([1]). The threshold (red horizontal line) is a value calibrated to give FMR = 0.0001 on mugshot images. Points above the threshold correspond to pairs determined to be genuine, and points below the threshold correspond to pairs determined to be impostors. If the determined class (genuine or impostor) matches the real class, points will be blue; if not, red. An X represents face detection failure in either of the images in the pair. Note that the sample size (n=20) is small, and the figure may change substantially if larger or different sets are used. The images can be viewed on p. 13 of the Appendix, where Gen 01 corresponds to Same-Identity Pair 1, Gen 02 corresponds to Same-Identity Pair 2, and so on.

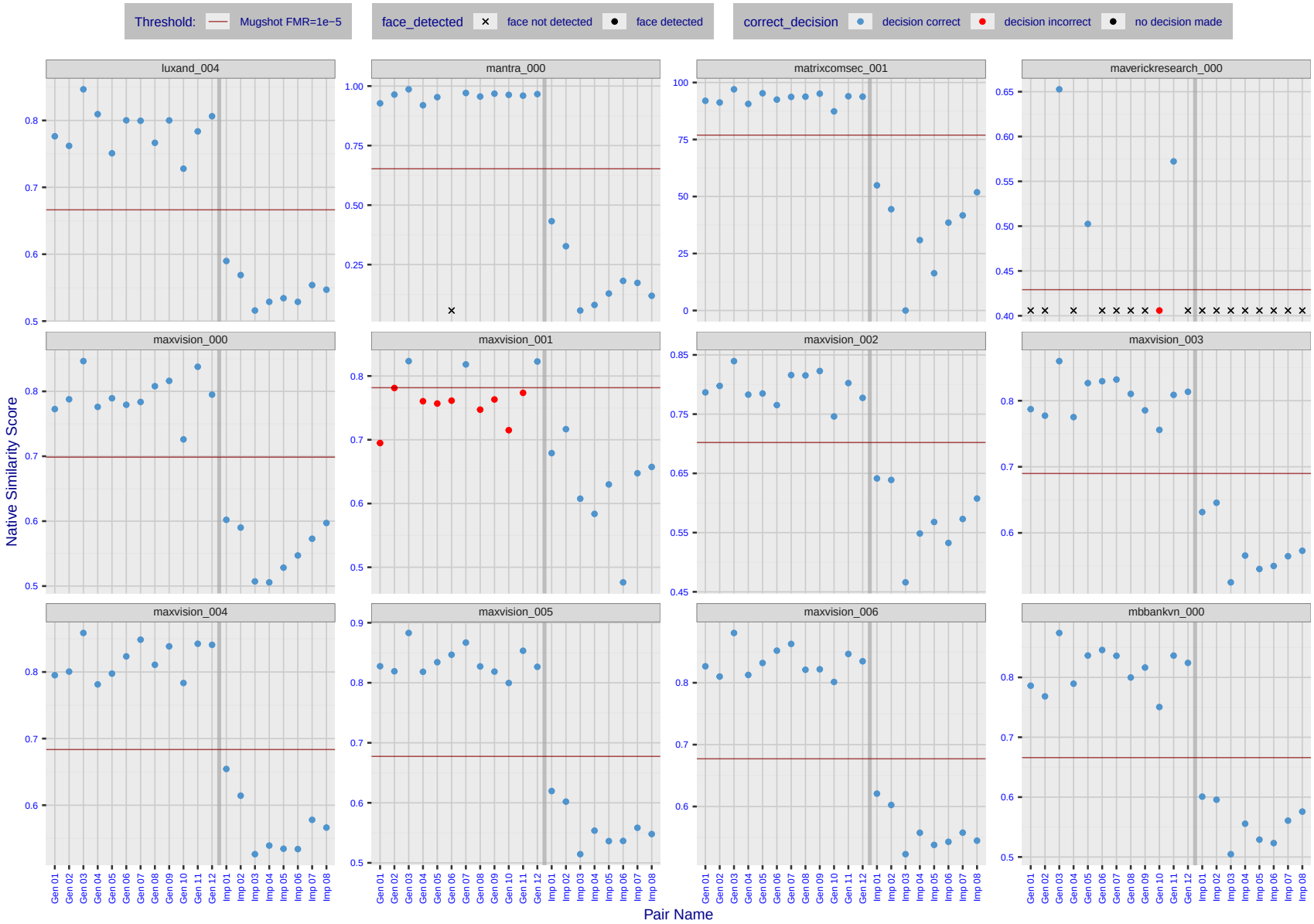

Figure 56: The figure shows algorithms' similarity scores for 12 genuine and 8 impostor image pairs used in a May 2018 paper by Phillips et al. ([1]). The threshold (red horizontal line) is a value calibrated to give FMR = 0.0001 on mugshot images. Points above the threshold correspond to pairs determined to be genuine, and points below the threshold correspond to pairs determined to be impostors. If the determined class (genuine or impostor) matches the real class, points will be blue; if not, red. An X represents face detection failure in either of the images in the pair. Note that the sample size (n=20) is small, and the figure may change substantially if larger or different sets are used. The images can be viewed on p. 13 of the Appendix, where Gen 01 corresponds to Same-Identity Pair 1, Gen 02 corresponds to Same-Identity Pair 2, and so on.

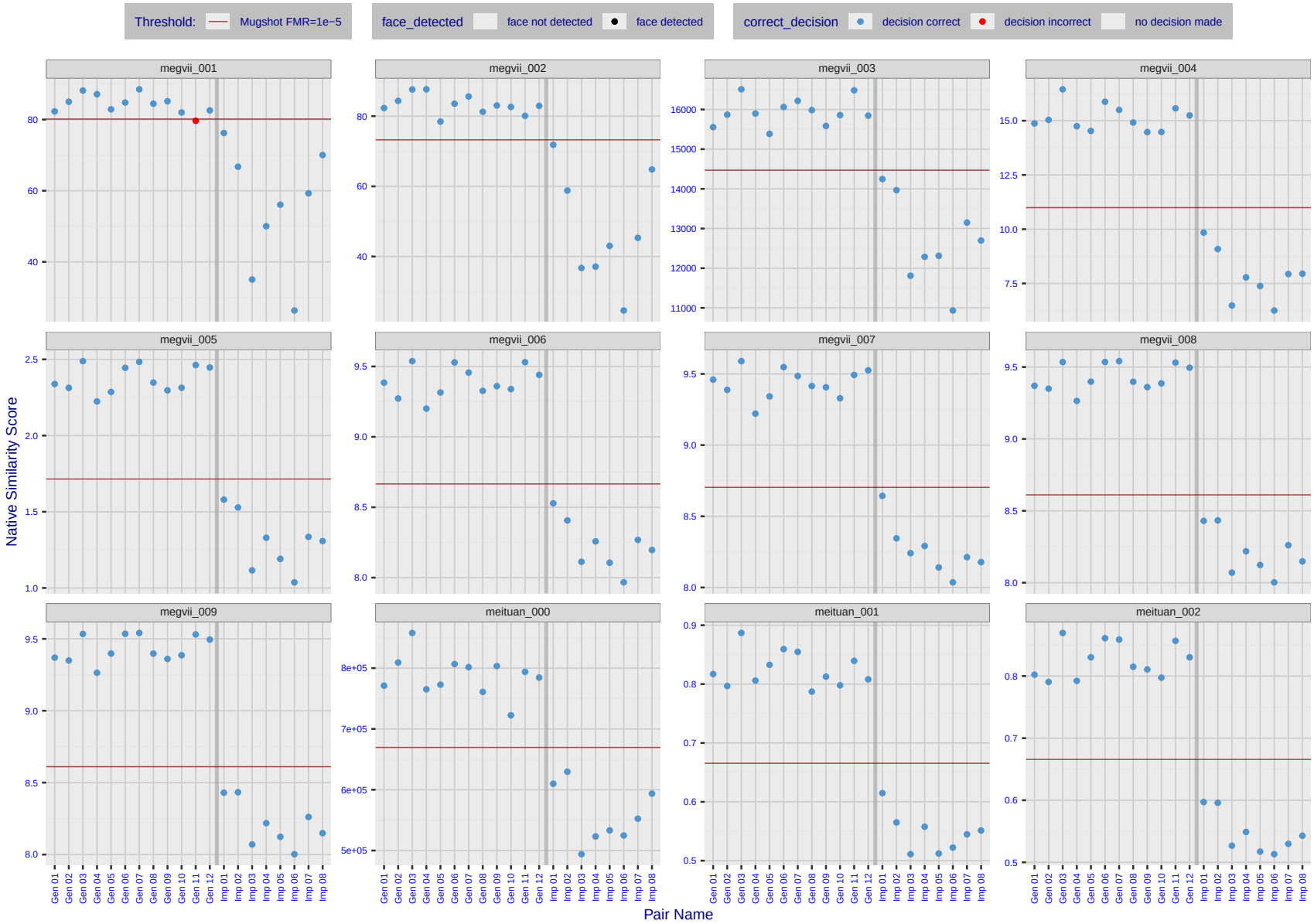

Figure 57: The figure shows algorithms' similarity scores for 12 genuine and 8 impostor image pairs used in a May 2018 paper by Phillips et al. ([1]). The threshold (red horizontal line) is a value calibrated to give FMR = 0.0001 on mugshot images. Points above the threshold correspond to pairs determined to be genuine, and points below the threshold correspond to pairs determined to be impostors. If the determined class (genuine or impostor) matches the real class, points will be blue; if not, red. An X represents face detection failure in either of the images in the pair. Note that the sample size (n=20) is small, and the figure may change substantially if larger or different sets are used. The images can be viewed on p. 13 of the Appendix, where Gen 01 corresponds to Same-Identity Pair 1, Gen 02 corresponds to Same-Identity Pair 2, and so on.

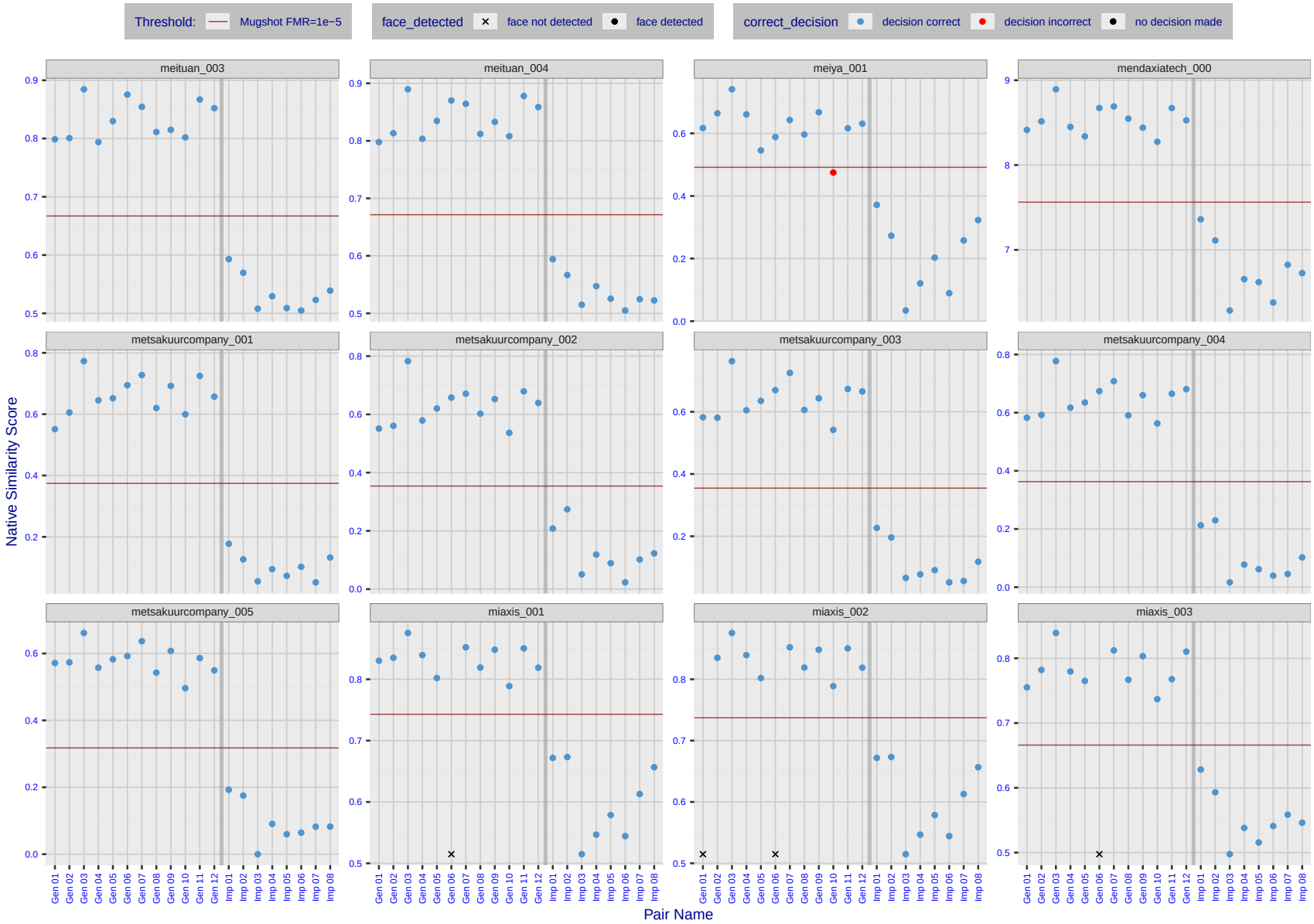

Figure 58: The figure shows algorithms' similarity scores for 12 genuine and 8 impostor image pairs used in a May 2018 paper by Phillips et al. ([1]). The threshold (red horizontal line) is a value calibrated to give FMR = 0.0001 on mugshot images. Points above the threshold correspond to pairs determined to be genuine, and points below the threshold correspond to pairs determined to be impostors. If the determined class (genuine or impostor) matches the real class, points will be blue; if not, red. An X represents face detection failure in either of the images in the pair. Note that the sample size (n=20) is small, and the figure may change substantially if larger or different sets are used. The images can be viewed on p. 13 of the Appendix, where Gen 01 corresponds to Same-Identity Pair 1, Gen 02 corresponds to Same-Identity Pair 2, and so on.

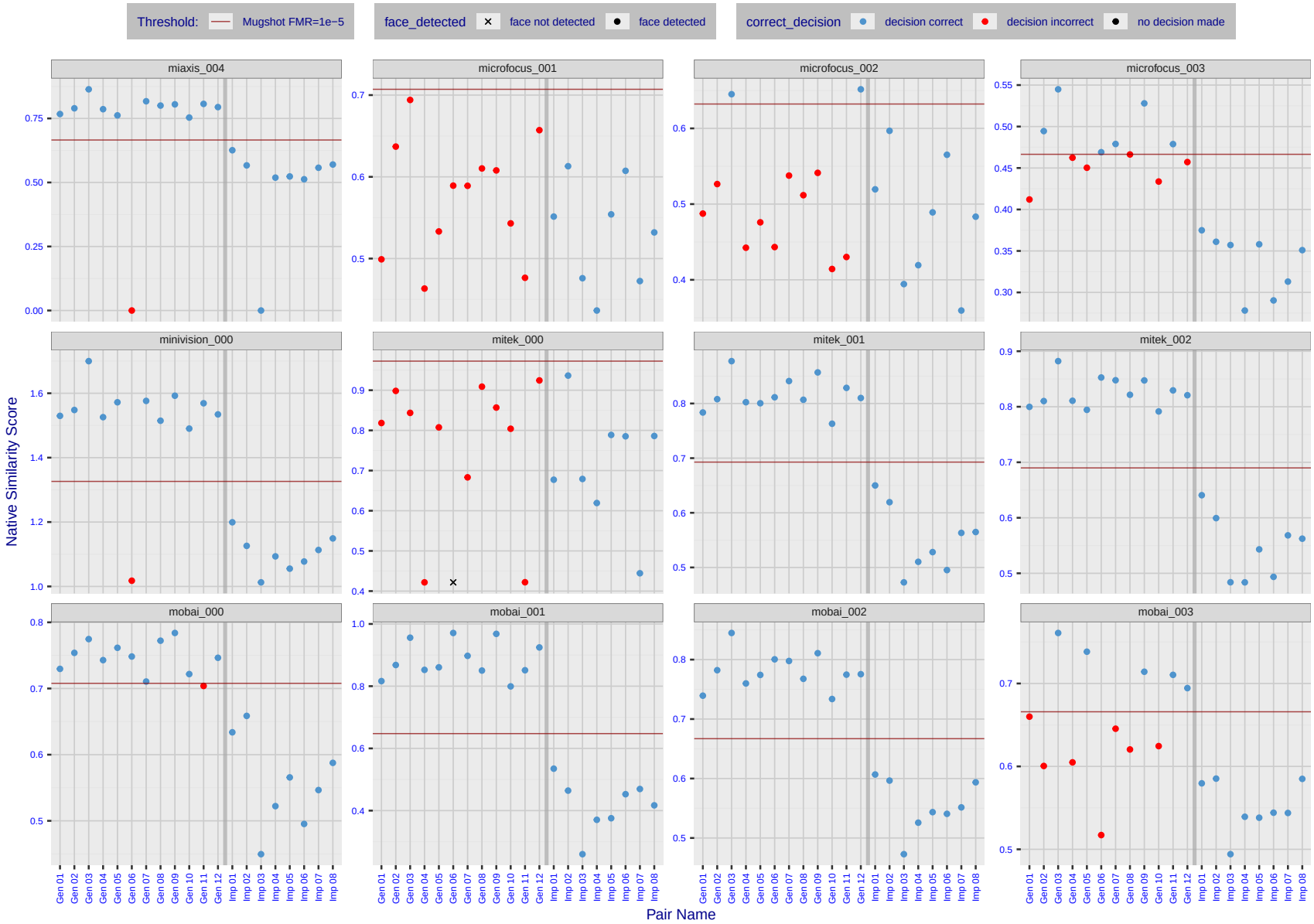

Figure 59: The figure shows algorithms' similarity scores for 12 genuine and 8 impostor image pairs used in a May 2018 paper by Phillips et al. ([1]). The threshold (red horizontal line) is a value calibrated to give FMR = 0.0001 on mugshot images. Points above the threshold correspond to pairs determined to be genuine, and points below the threshold correspond to pairs determined to be impostors. If the determined class (genuine or impostor) matches the real class, points will be blue; if not, red. An X represents face detection failure in either of the images in the pair. Note that the sample size (n=20) is small, and the figure may change substantially if larger or different sets are used. The images can be viewed on p. 13 of the Appendix, where Gen 01 corresponds to Same-Identity Pair 1, Gen 02 corresponds to Same-Identity Pair 2, and so on.

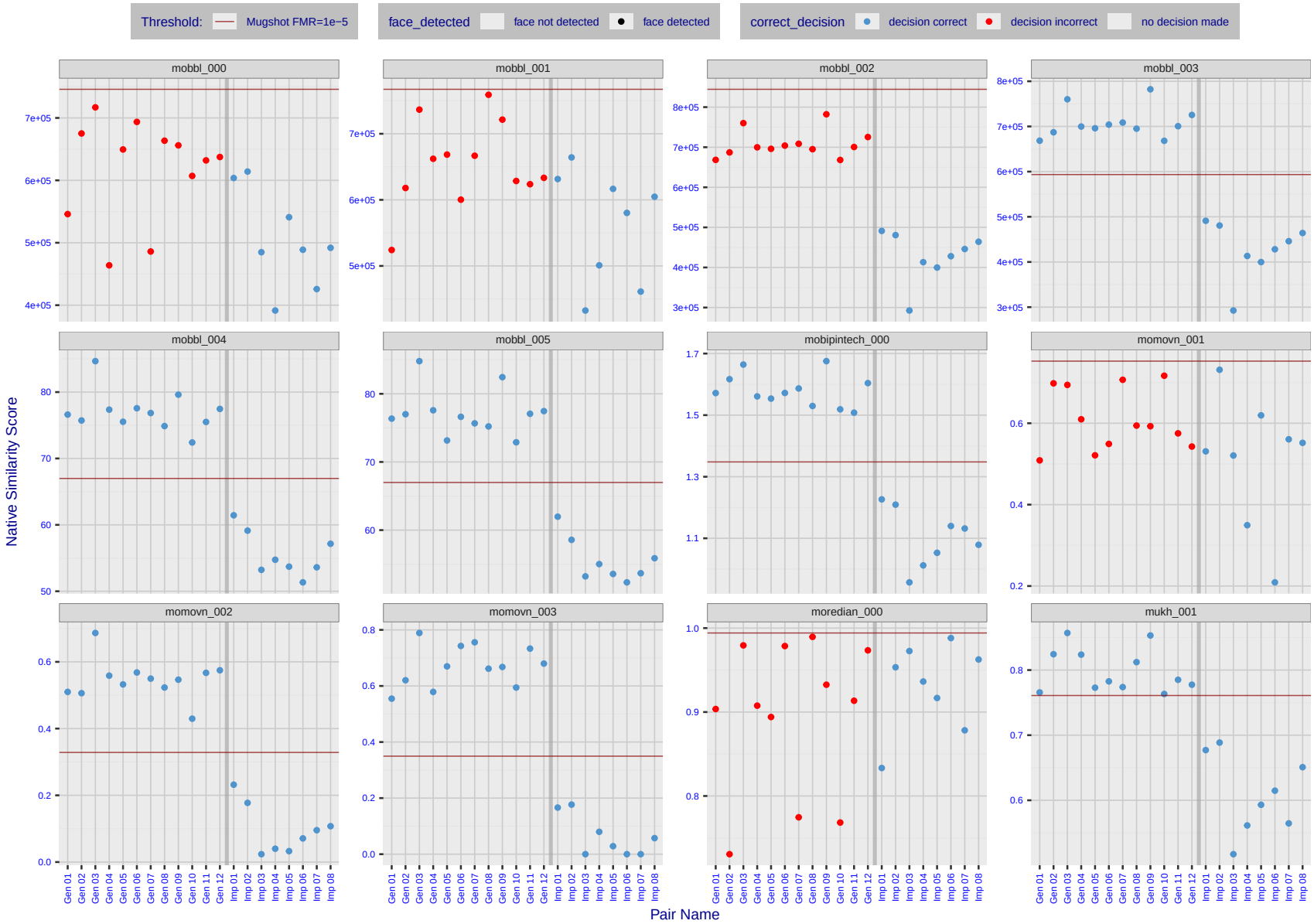

Figure 60: The figure shows algorithms' similarity scores for 12 genuine and 8 impostor image pairs used in a May 2018 paper by Phillips et al. ([1]). The threshold (red horizontal line) is a value calibrated to give FMR = 0.0001 on mugshot images. Points above the threshold correspond to pairs determined to be genuine, and points below the threshold correspond to pairs determined to be impostors. If the determined class (genuine or impostor) matches the real class, points will be blue; if not, red. An X represents face detection failure in either of the images in the pair. Note that the sample size (n=20) is small, and the figure may change substantially if larger or different sets are used. The images can be viewed on p. 13 of the Appendix, where Gen 01 corresponds to Same-Identity Pair 1, Gen 02 corresponds to Same-Identity Pair 2, and so on.

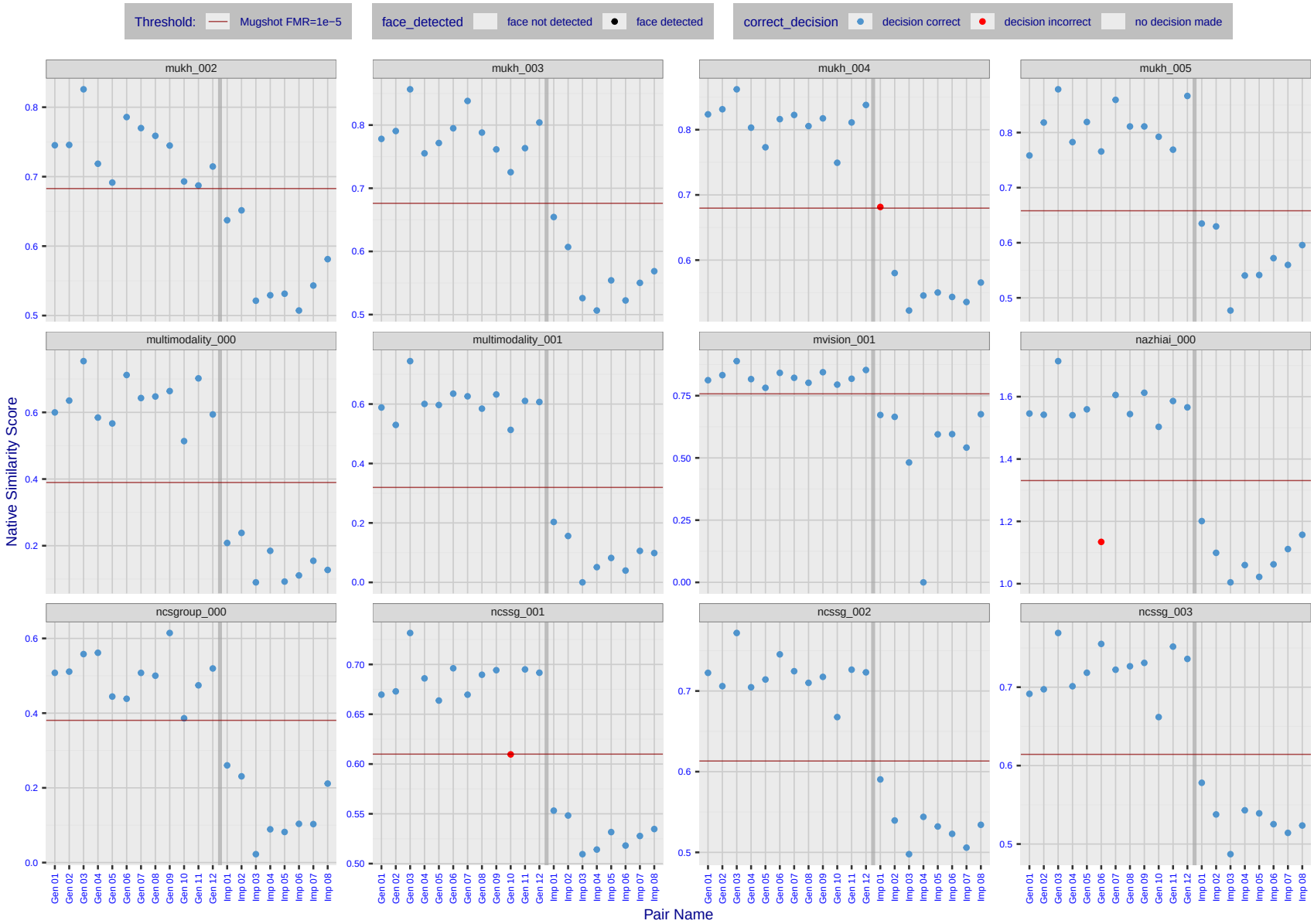

Figure 61: The figure shows algorithms' similarity scores for 12 genuine and 8 impostor image pairs used in a May 2018 paper by Phillips et al. ([1]). The threshold (red horizontal line) is a value calibrated to give FMR = 0.0001 on mugshot images. Points above the threshold correspond to pairs determined to be genuine, and points below the threshold correspond to pairs determined to be impostors. If the determined class (genuine or impostor) matches the real class, points will be blue; if not, red. An X represents face detection failure in either of the images in the pair. Note that the sample size (n=20) is small, and the figure may change substantially if larger or different sets are used. The images can be viewed on p. 13 of the Appendix, where Gen 01 corresponds to Same-Identity Pair 1, Gen 02 corresponds to Same-Identity Pair 2, and so on.

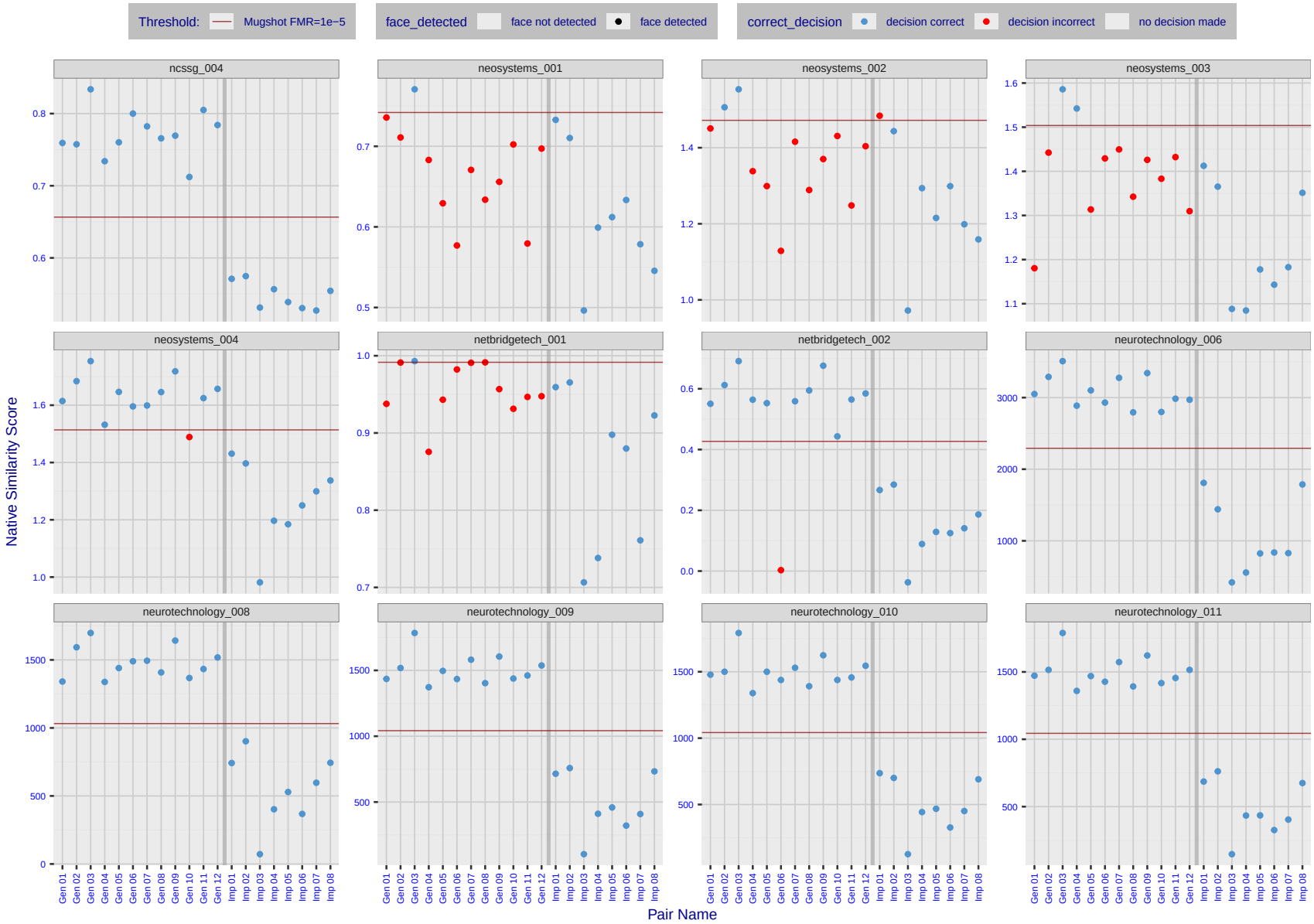

Figure 62: The figure shows algorithms' similarity scores for 12 genuine and 8 impostor image pairs used in a May 2018 paper by Phillips et al. ([1]). The threshold (red horizontal line) is a value calibrated to give FMR = 0.0001 on mugshot images. Points above the threshold correspond to pairs determined to be genuine, and points below the threshold correspond to pairs determined to be impostors. If the determined class (genuine or impostor) matches the real class, points will be blue; if not, red. An X represents face detection failure in either of the images in the pair. Note that the sample size (n=20) is small, and the figure may change substantially if larger or different sets are used. The images can be viewed on p. 13 of the Appendix, where Gen 01 corresponds to Same-Identity Pair 1, Gen 02 corresponds to Same-Identity Pair 2, and so on.

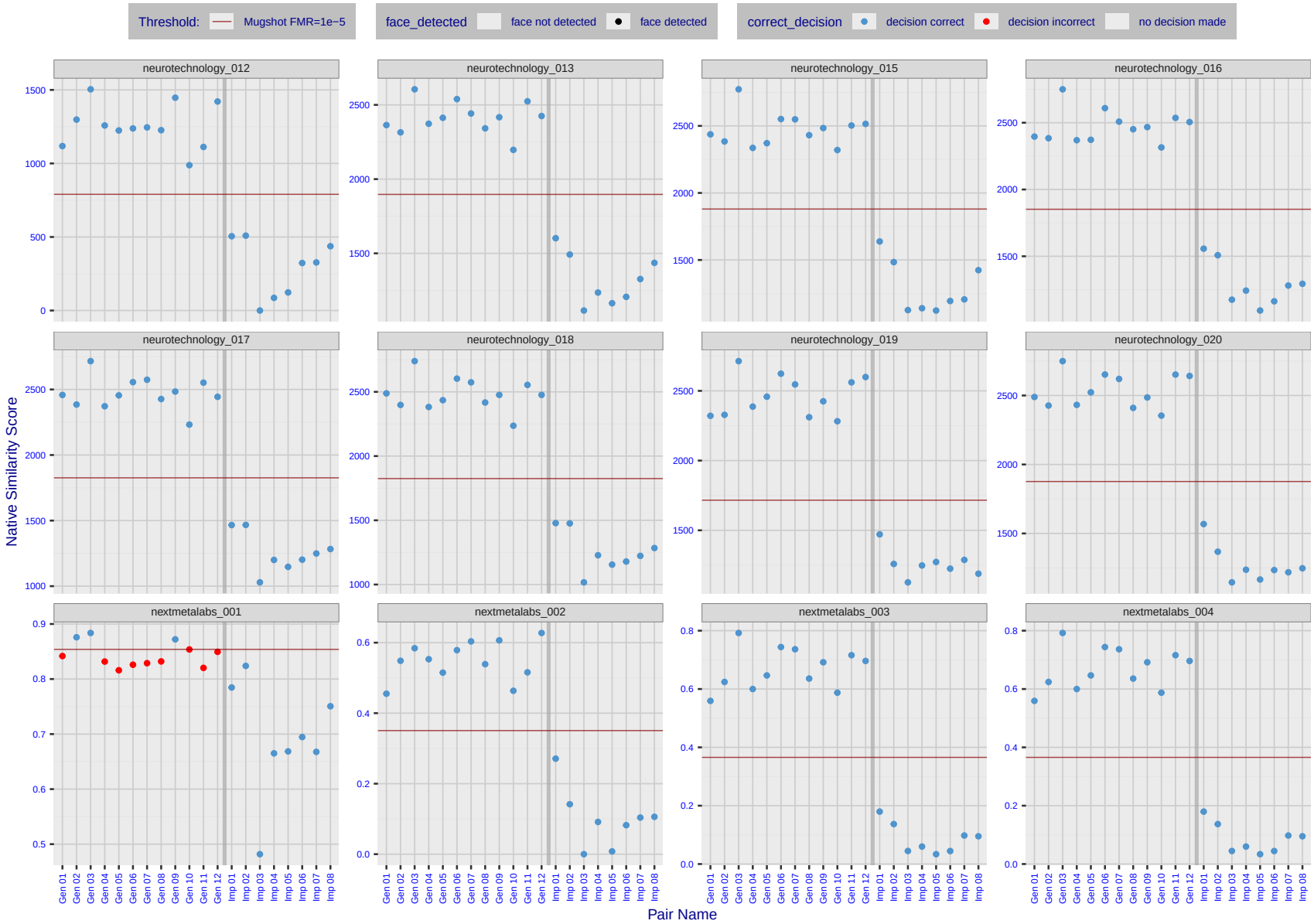

Figure 63: The figure shows algorithms' similarity scores for 12 genuine and 8 impostor image pairs used in a May 2018 paper by Phillips et al. ([1]). The threshold (red horizontal line) is a value calibrated to give FMR = 0.0001 on mugshot images. Points above the threshold correspond to pairs determined to be genuine, and points below the threshold correspond to pairs determined to be impostors. If the determined class (genuine or impostor) matches the real class, points will be blue; if not, red. An X represents face detection failure in either of the images in the pair. Note that the sample size (n=20) is small, and the figure may change substantially if larger or different sets are used. The images can be viewed on p. 13 of the Appendix, where Gen 01 corresponds to Same-Identity Pair 1, Gen 02 corresponds to Same-Identity Pair 2, and so on.

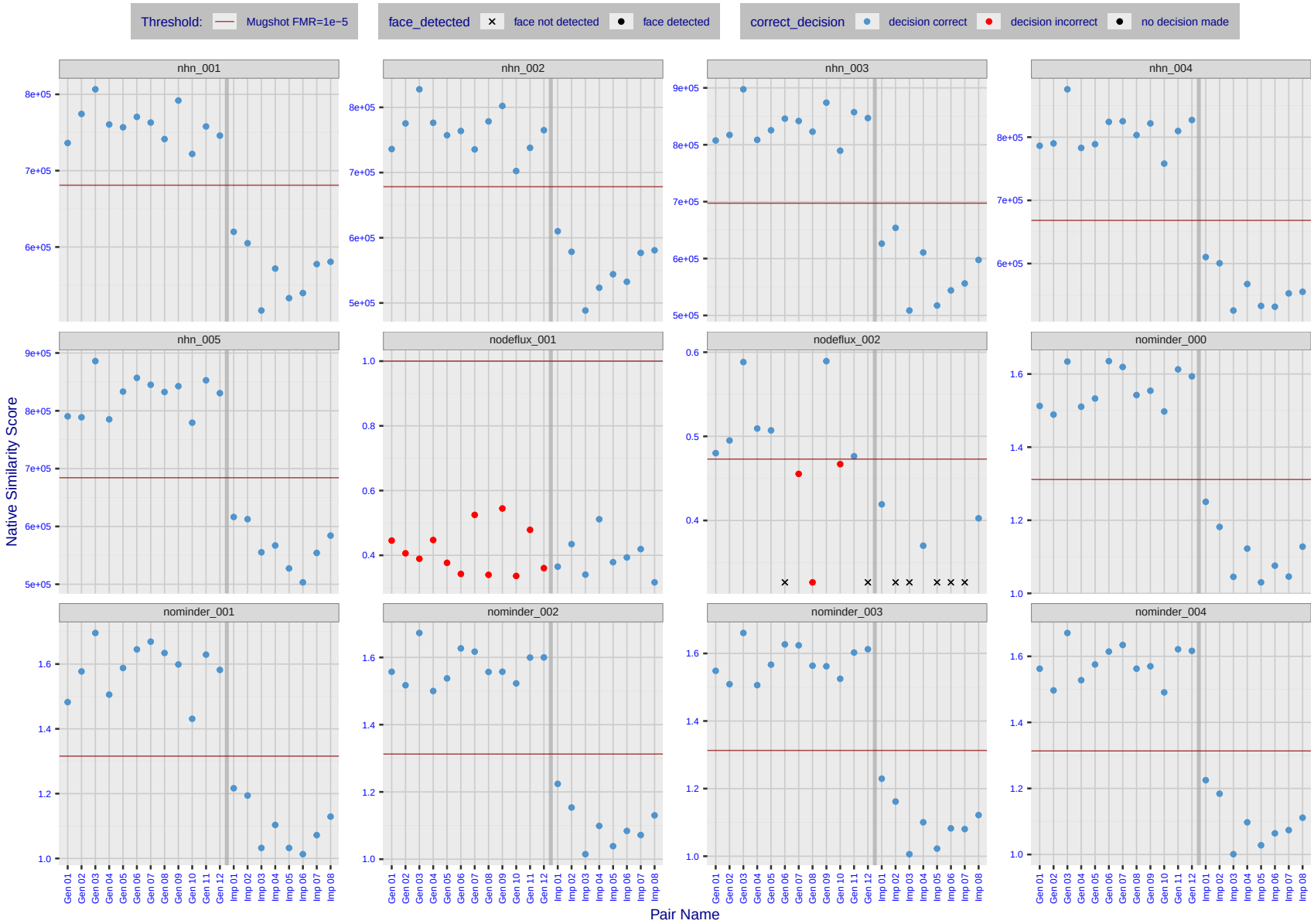

Figure 64: The figure shows algorithms' similarity scores for 12 genuine and 8 impostor image pairs used in a May 2018 paper by Phillips et al. ([1]). The threshold (red horizontal line) is a value calibrated to give FMR = 0.0001 on mugshot images. Points above the threshold correspond to pairs determined to be genuine, and points below the threshold correspond to pairs determined to be impostors. If the determined class (genuine or impostor) matches the real class, points will be blue; if not, red. An X represents face detection failure in either of the images in the pair. Note that the sample size (n=20) is small, and the figure may change substantially if larger or different sets are used. The images can be viewed on p. 13 of the Appendix, where Gen 01 corresponds to Same-Identity Pair 1, Gen 02 corresponds to Same-Identity Pair 2, and so on.

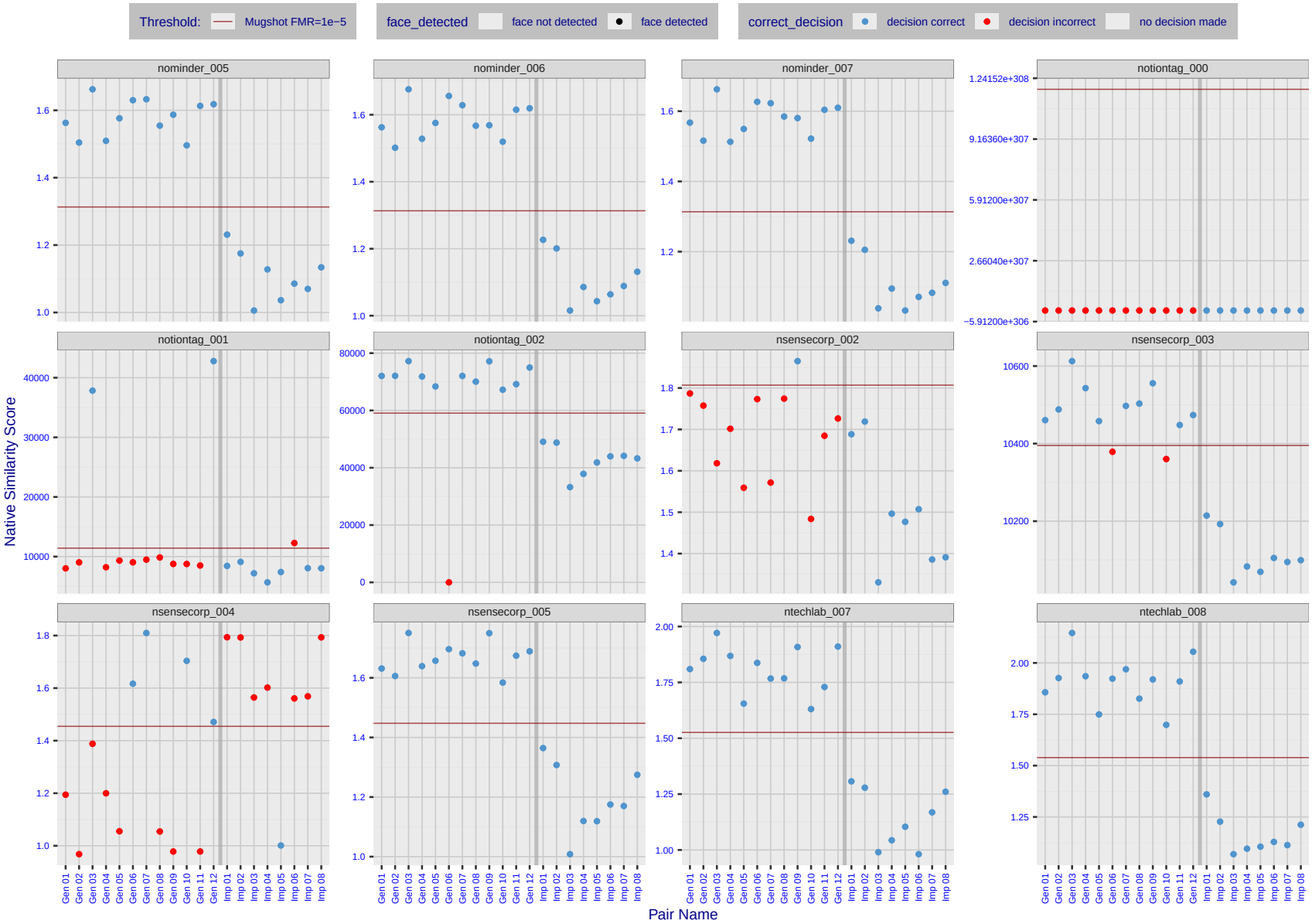

Figure 65: The figure shows algorithms' similarity scores for 12 genuine and 8 impostor image pairs used in a May 2018 paper by Phillips et al. ([1]). The threshold (red horizontal line) is a value calibrated to give FMR = 0.0001 on mugshot images. Points above the threshold correspond to pairs determined to be genuine, and points below the threshold correspond to pairs determined to be impostors. If the determined class (genuine or impostor) matches the real class, points will be blue; if not, red. An X represents face detection failure in either of the images in the pair. Note that the sample size (n=20) is small, and the figure may change substantially if larger or different sets are used. The images can be viewed on p. 13 of the Appendix, where Gen 01 corresponds to Same-Identity Pair 1, Gen 02 corresponds to Same-Identity Pair 2, and so on.

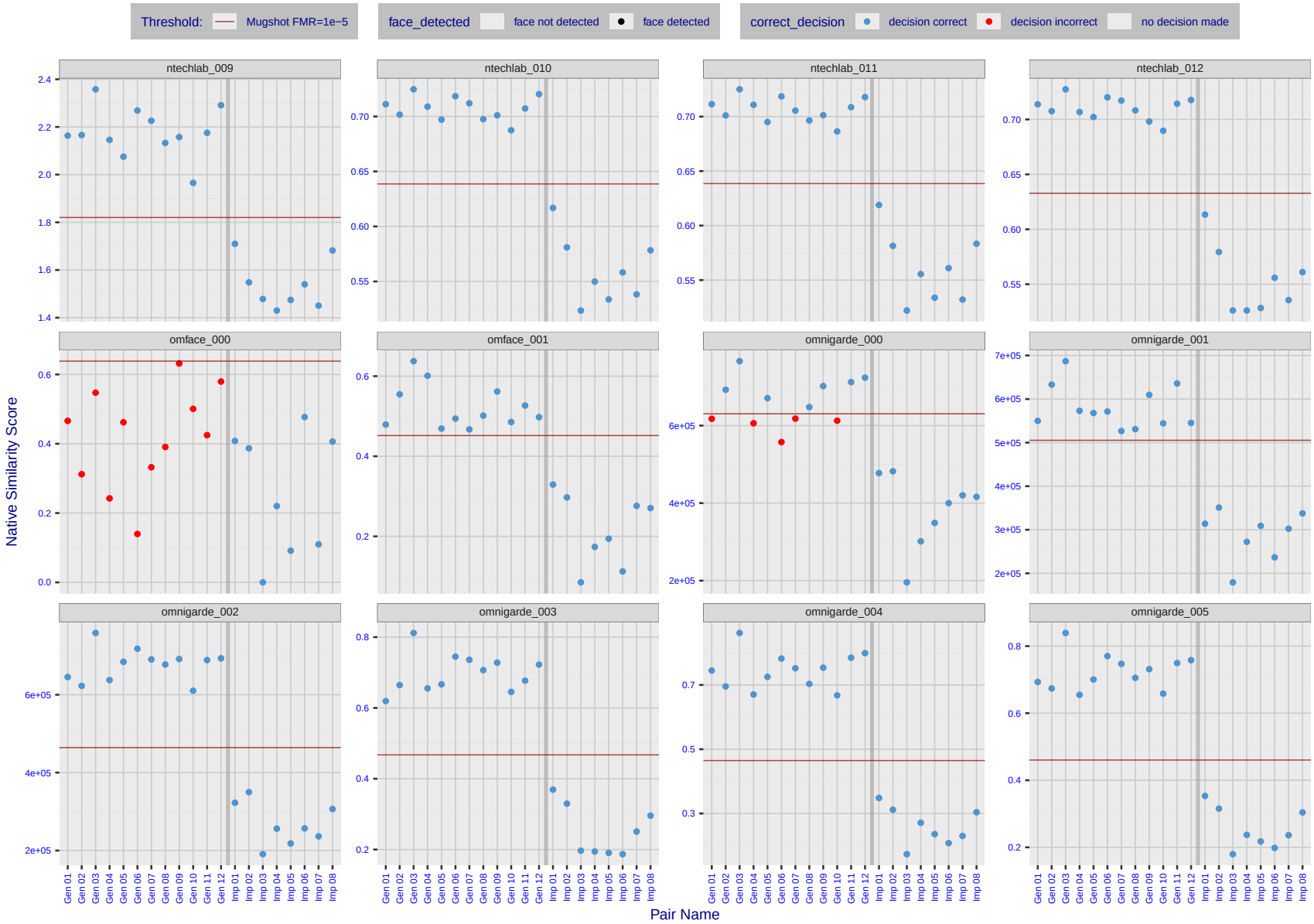

Figure 66: The figure shows algorithms' similarity scores for 12 genuine and 8 impostor image pairs used in a May 2018 paper by Phillips et al. ([1]). The threshold (red horizontal line) is a value calibrated to give FMR = 0.0001 on mugshot images. Points above the threshold correspond to pairs determined to be genuine, and points below the threshold correspond to pairs determined to be impostors. If the determined class (genuine or impostor) matches the real class, points will be blue; if not, red. An X represents face detection failure in either of the images in the pair. Note that the sample size (n=20) is small, and the figure may change substantially if larger or different sets are used. The images can be viewed on p. 13 of the Appendix, where Gen 01 corresponds to Same-Identity Pair 1, Gen 02 corresponds to Same-Identity Pair 2, and so on.

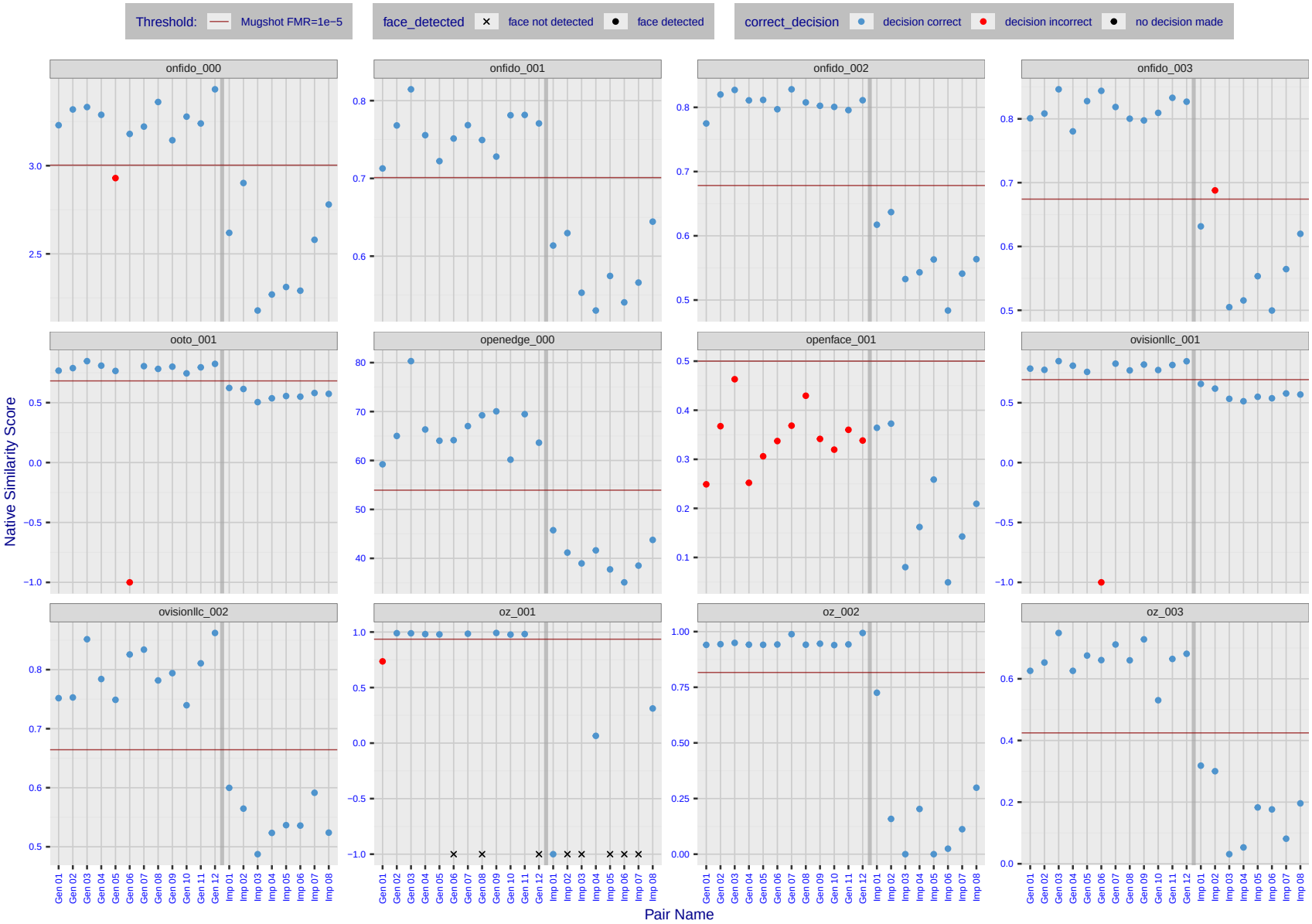

Figure 67: The figure shows algorithms' similarity scores for 12 genuine and 8 impostor image pairs used in a May 2018 paper by Phillips et al. ([1]). The threshold (red horizontal line) is a value calibrated to give FMR = 0.0001 on mugshot images. Points above the threshold correspond to pairs determined to be genuine, and points below the threshold correspond to pairs determined to be impostors. If the determined class (genuine or impostor) matches the real class, points will be blue; if not, red. An X represents face detection failure in either of the images in the pair. Note that the sample size (n=20) is small, and the figure may change substantially if larger or different sets are used. The images can be viewed on p. 13 of the Appendix, where Gen 01 corresponds to Same-Identity Pair 1, Gen 02 corresponds to Same-Identity Pair 2, and so on.

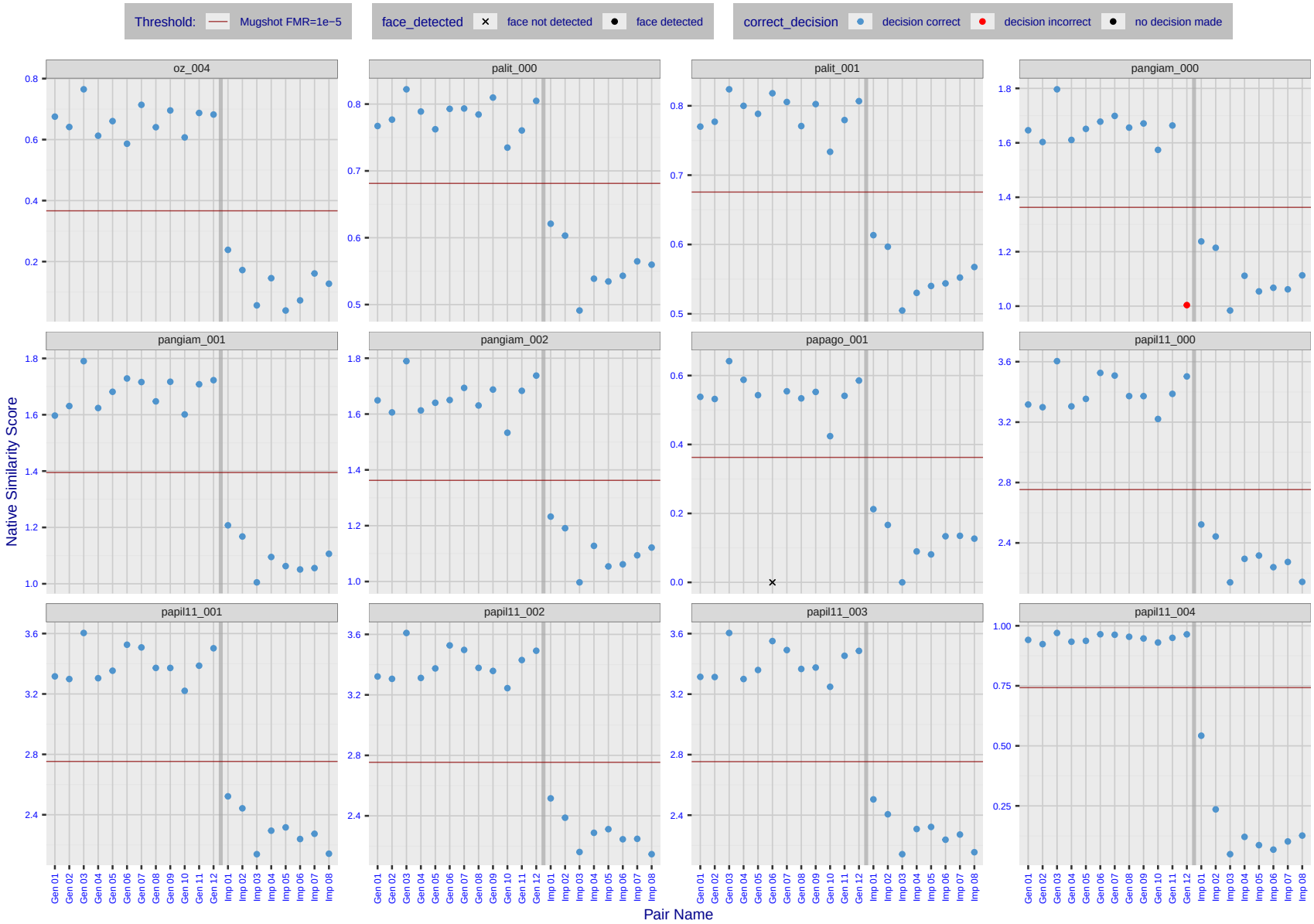

Figure 68: The figure shows algorithms' similarity scores for 12 genuine and 8 impostor image pairs used in a May 2018 paper by Phillips et al. ([1]). The threshold (red horizontal line) is a value calibrated to give FMR = 0.0001 on mugshot images. Points above the threshold correspond to pairs determined to be genuine, and points below the threshold correspond to pairs determined to be impostors. If the determined class (genuine or impostor) matches the real class, points will be blue; if not, red. An X represents face detection failure in either of the images in the pair. Note that the sample size (n=20) is small, and the figure may change substantially if larger or different sets are used. The images can be viewed on p. 13 of the Appendix, where Gen 01 corresponds to Same-Identity Pair 1, Gen 02 corresponds to Same-Identity Pair 2, and so on.

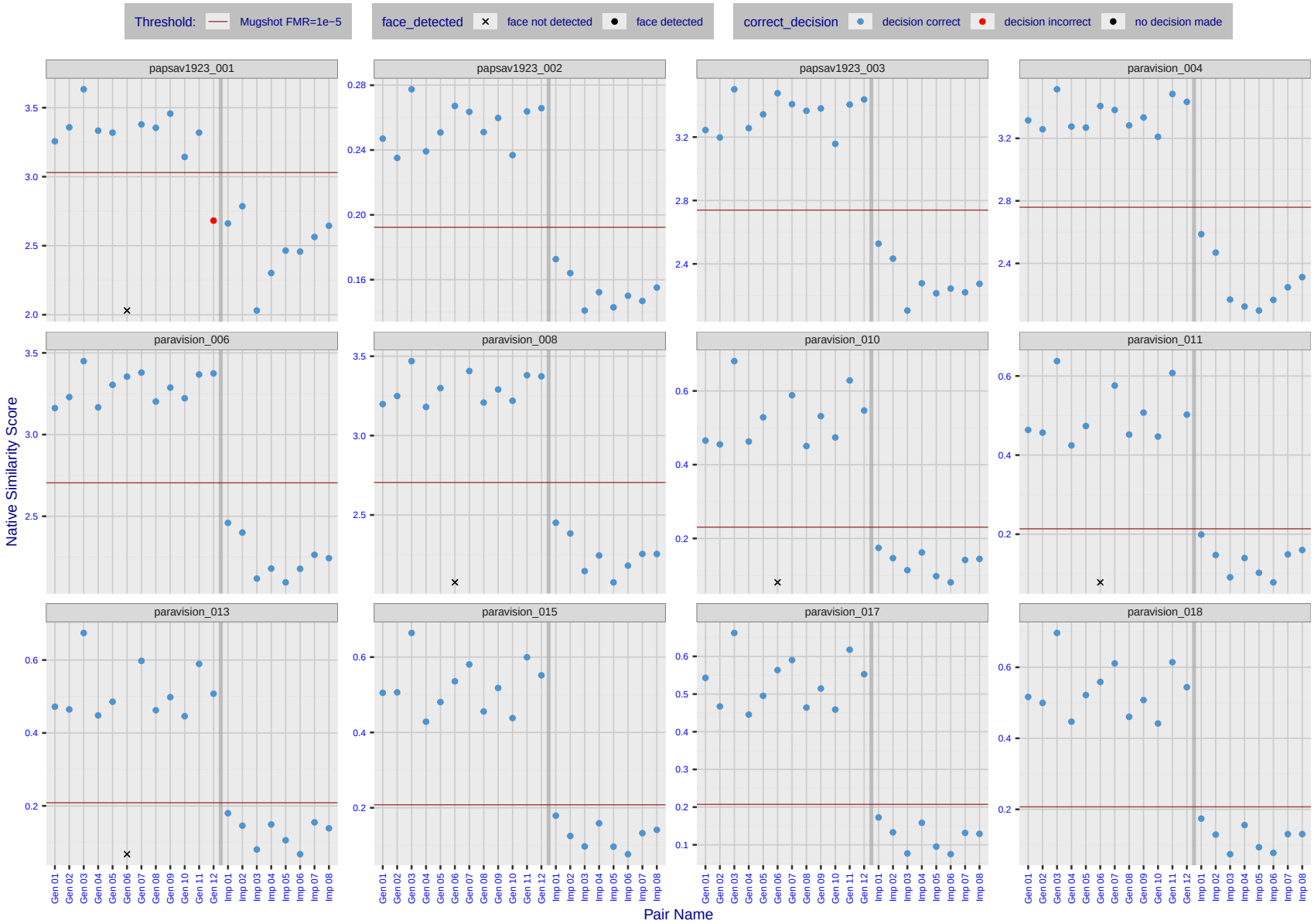

Figure 69: The figure shows algorithms' similarity scores for 12 genuine and 8 impostor image pairs used in a May 2018 paper by Phillips et al. ([1]). The threshold (red horizontal line) is a value calibrated to give FMR = 0.0001 on mugshot images. Points above the threshold correspond to pairs determined to be genuine, and points below the threshold correspond to pairs determined to be impostors. If the determined class (genuine or impostor) matches the real class, points will be blue; if not, red. An X represents face detection failure in either of the images in the pair. Note that the sample size (n=20) is small, and the figure may change substantially if larger or different sets are used. The images can be viewed on p. 13 of the Appendix, where Gen 01 corresponds to Same-Identity Pair 1, Gen 02 corresponds to Same-Identity Pair 2, and so on.

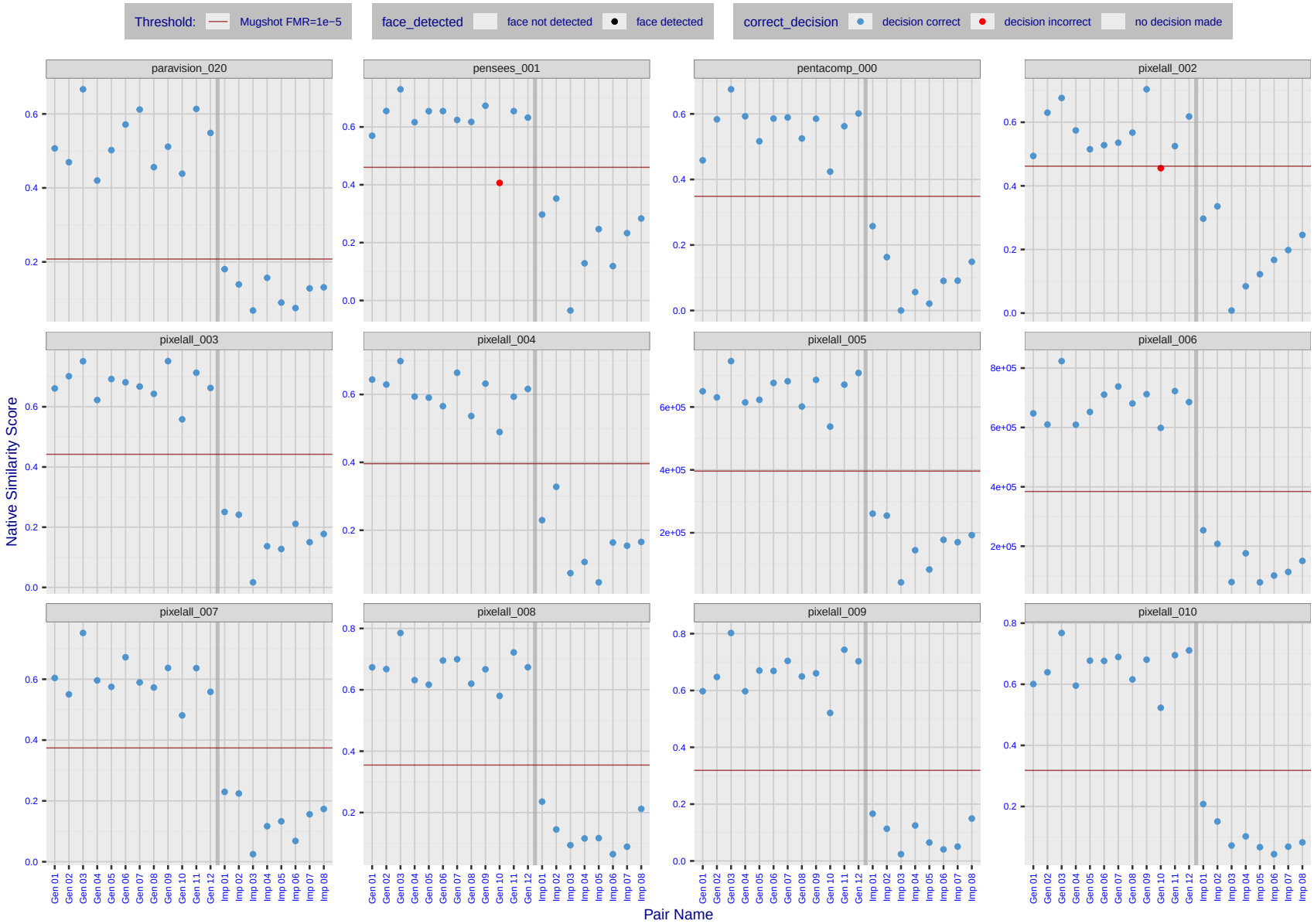

Figure 70: The figure shows algorithms' similarity scores for 12 genuine and 8 impostor image pairs used in a May 2018 paper by Phillips et al. ([1]). The threshold (red horizontal line) is a value calibrated to give FMR = 0.0001 on mugshot images. Points above the threshold correspond to pairs determined to be genuine, and points below the threshold correspond to pairs determined to be impostors. If the determined class (genuine or impostor) matches the real class, points will be blue; if not, red. An X represents face detection failure in either of the images in the pair. Note that the sample size (n=20) is small, and the figure may change substantially if larger or different sets are used. The images can be viewed on p. 13 of the Appendix, where Gen 01 corresponds to Same-Identity Pair 1, Gen 02 corresponds to Same-Identity Pair 2, and so on.

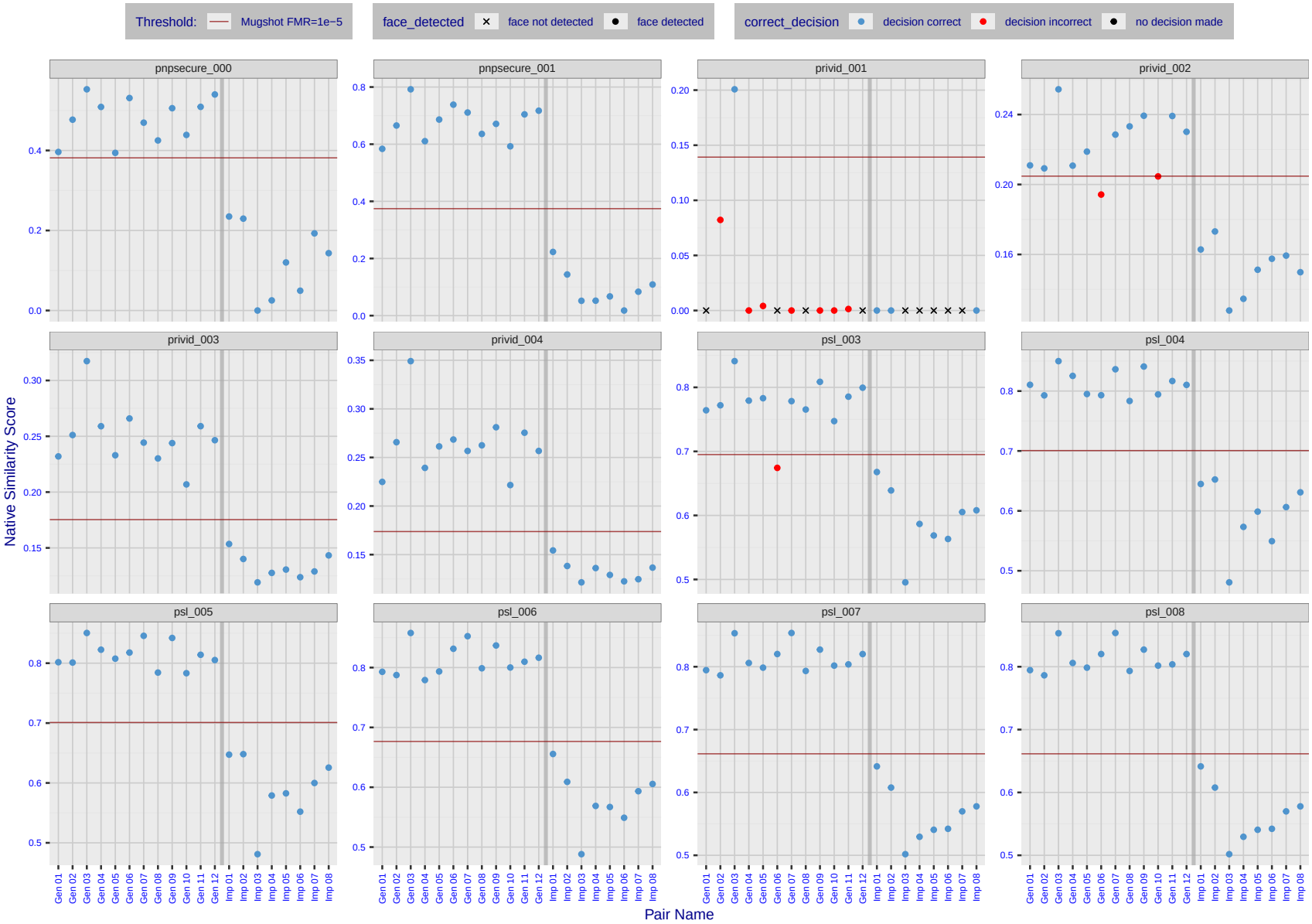

Figure 71: The figure shows algorithms' similarity scores for 12 genuine and 8 impostor image pairs used in a May 2018 paper by Phillips et al. ([1]). The threshold (red horizontal line) is a value calibrated to give FMR = 0.0001 on mugshot images. Points above the threshold correspond to pairs determined to be genuine, and points below the threshold correspond to pairs determined to be impostors. If the determined class (genuine or impostor) matches the real class, points will be blue; if not, red. An X represents face detection failure in either of the images in the pair. Note that the sample size (n=20) is small, and the figure may change substantially if larger or different sets are used. The images can be viewed on p. 13 of the Appendix, where Gen 01 corresponds to Same-Identity Pair 1, Gen 02 corresponds to Same-Identity Pair 2, and so on.

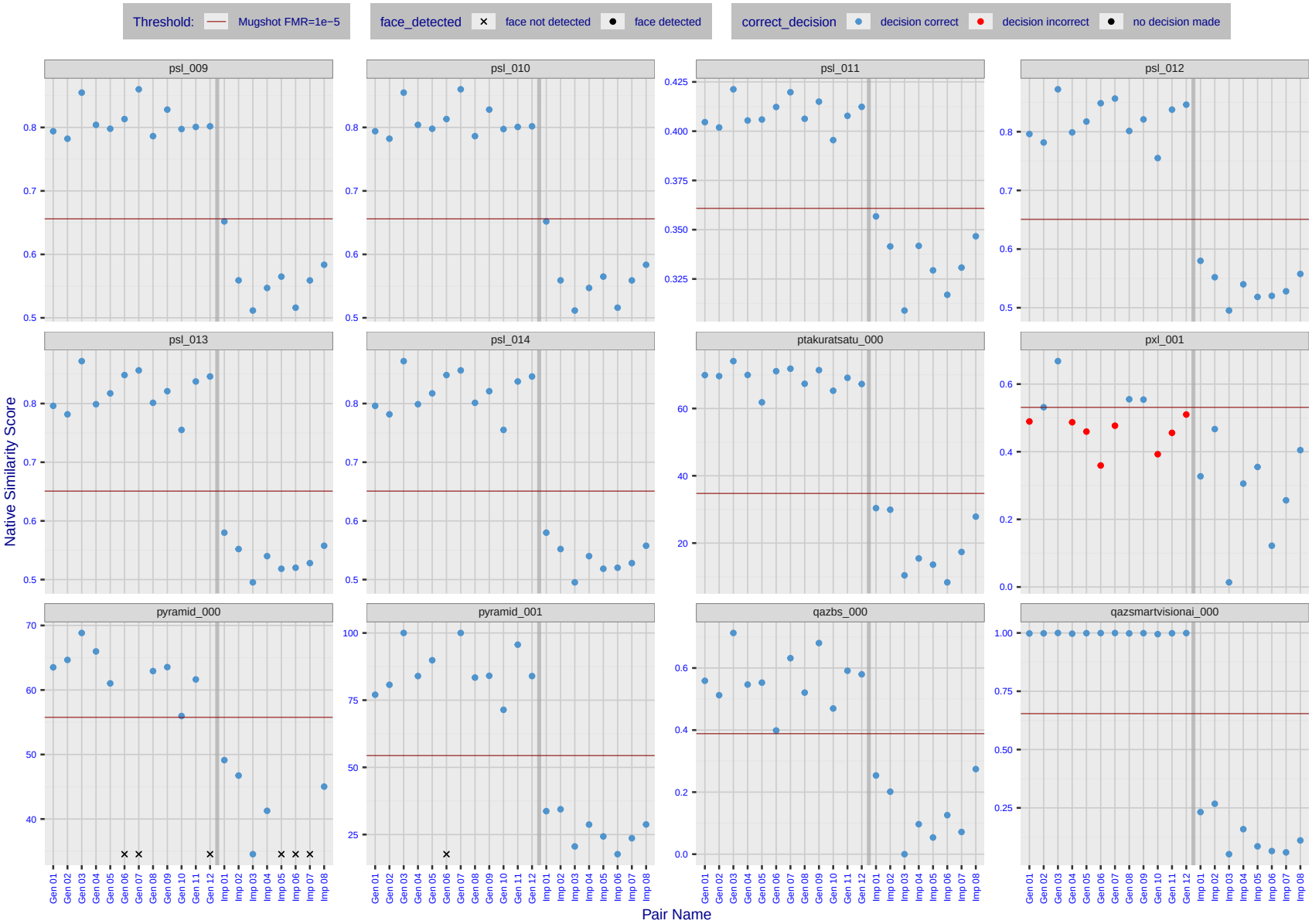

Figure 72: The figure shows algorithms' similarity scores for 12 genuine and 8 impostor image pairs used in a May 2018 paper by Phillips et al. ([1]). The threshold (red horizontal line) is a value calibrated to give FMR = 0.0001 on mugshot images. Points above the threshold correspond to pairs determined to be genuine, and points below the threshold correspond to pairs determined to be impostors. If the determined class (genuine or impostor) matches the real class, points will be blue; if not, red. An X represents face detection failure in either of the images in the pair. Note that the sample size (n=20) is small, and the figure may change substantially if larger or different sets are used. The images can be viewed on p. 13 of the Appendix, where Gen 01 corresponds to Same-Identity Pair 1, Gen 02 corresponds to Same-Identity Pair 2, and so on.

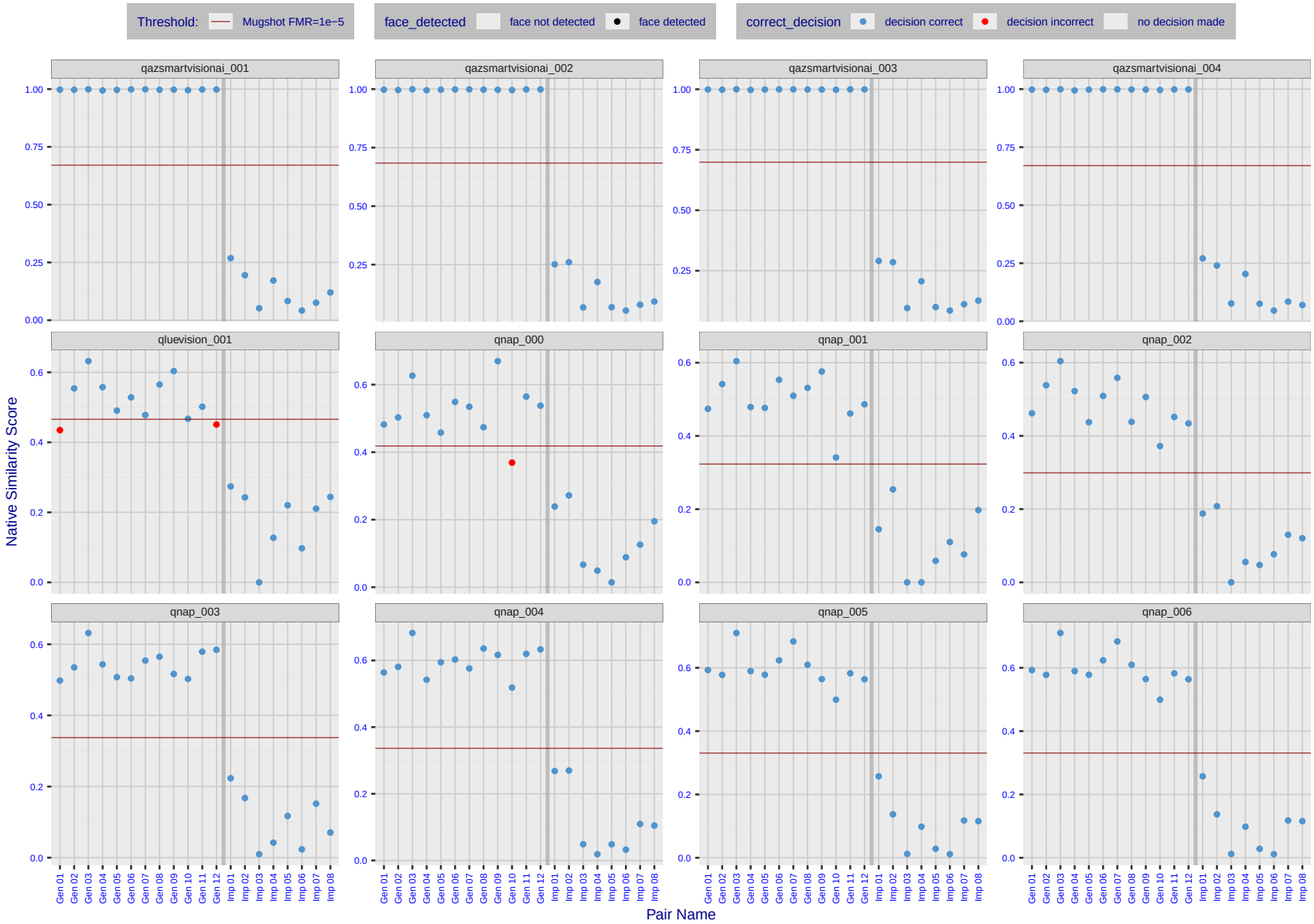

Figure 73: The figure shows algorithms' similarity scores for 12 genuine and 8 impostor image pairs used in a May 2018 paper by Phillips et al. ([1]). The threshold (red horizontal line) is a value calibrated to give FMR = 0.0001 on mugshot images. Points above the threshold correspond to pairs determined to be genuine, and points below the threshold correspond to pairs determined to be impostors. If the determined class (genuine or impostor) matches the real class, points will be blue; if not, red. An X represents face detection failure in either of the images in the pair. Note that the sample size (n=20) is small, and the figure may change substantially if larger or different sets are used. The images can be viewed on p. 13 of the Appendix, where Gen 01 corresponds to Same-Identity Pair 1, Gen 02 corresponds to Same-Identity Pair 2, and so on.

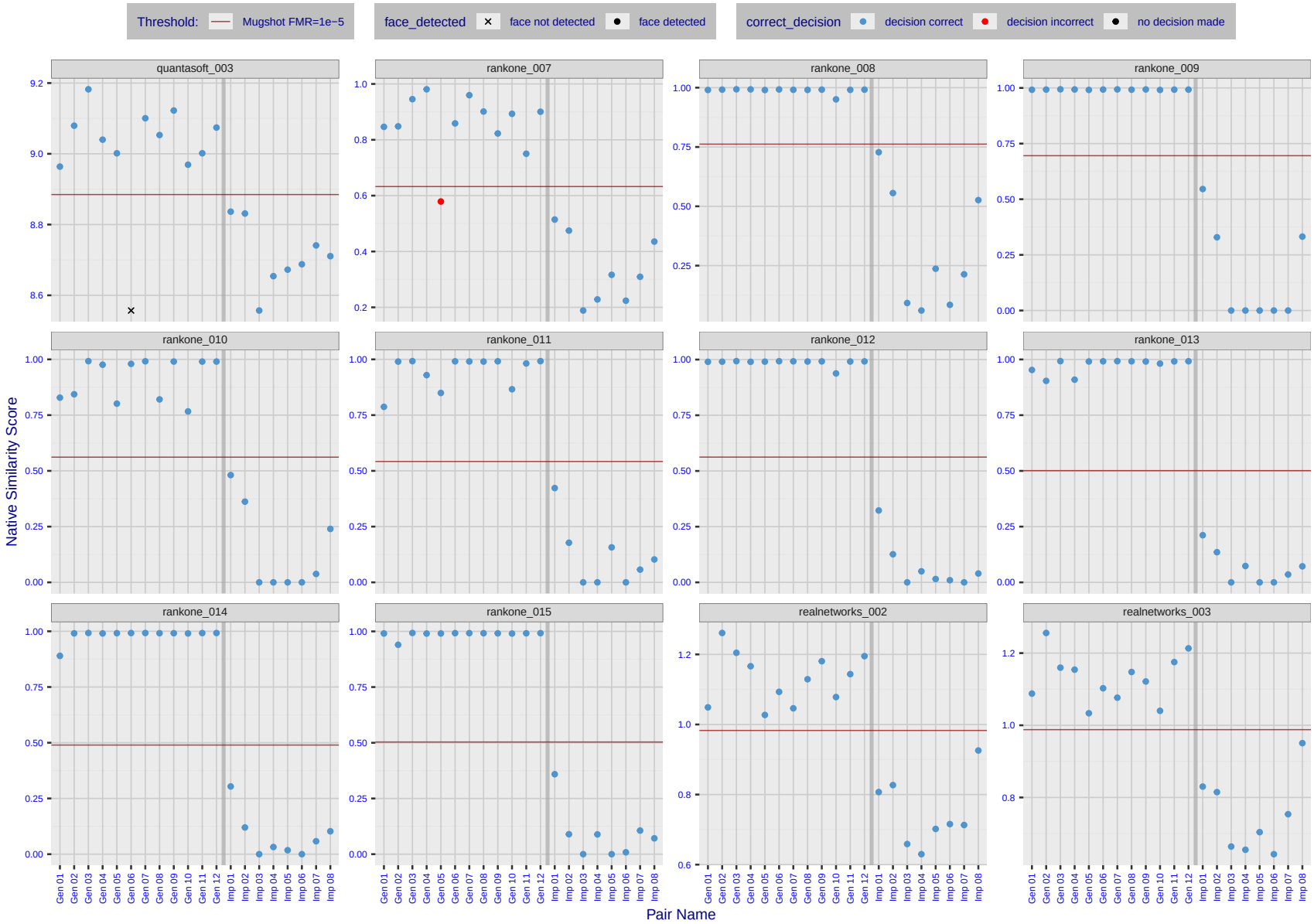

Figure 74: The figure shows algorithms' similarity scores for 12 genuine and 8 impostor image pairs used in a May 2018 paper by Phillips et al. ([1]). The threshold (red horizontal line) is a value calibrated to give FMR = 0.0001 on mugshot images. Points above the threshold correspond to pairs determined to be genuine, and points below the threshold correspond to pairs determined to be impostors. If the determined class (genuine or impostor) matches the real class, points will be blue; if not, red. An X represents face detection failure in either of the images in the pair. Note that the sample size (n=20) is small, and the figure may change substantially if larger or different sets are used. The images can be viewed on p. 13 of the Appendix, where Gen 01 corresponds to Same-Identity Pair 1, Gen 02 corresponds to Same-Identity Pair 2, and so on.

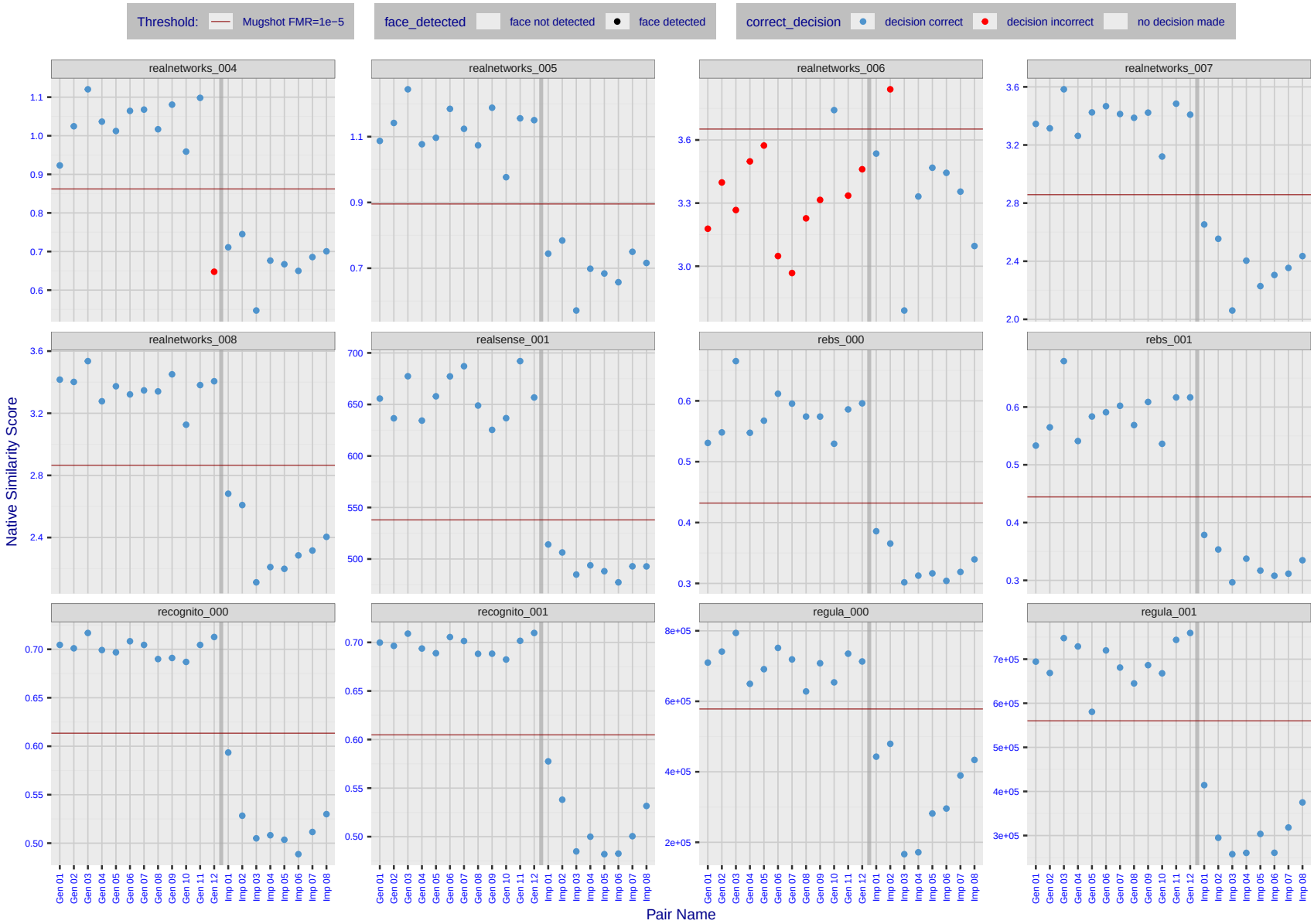

Figure 75: The figure shows algorithms' similarity scores for 12 genuine and 8 impostor image pairs used in a May 2018 paper by Phillips et al. ([1]). The threshold (red horizontal line) is a value calibrated to give FMR = 0.0001 on mugshot images. Points above the threshold correspond to pairs determined to be genuine, and points below the threshold correspond to pairs determined to be impostors. If the determined class (genuine or impostor) matches the real class, points will be blue; if not, red. An X represents face detection failure in either of the images in the pair. Note that the sample size (n=20) is small, and the figure may change substantially if larger or different sets are used. The images can be viewed on p. 13 of the Appendix, where Gen 01 corresponds to Same-Identity Pair 1, Gen 02 corresponds to Same-Identity Pair 2, and so on.

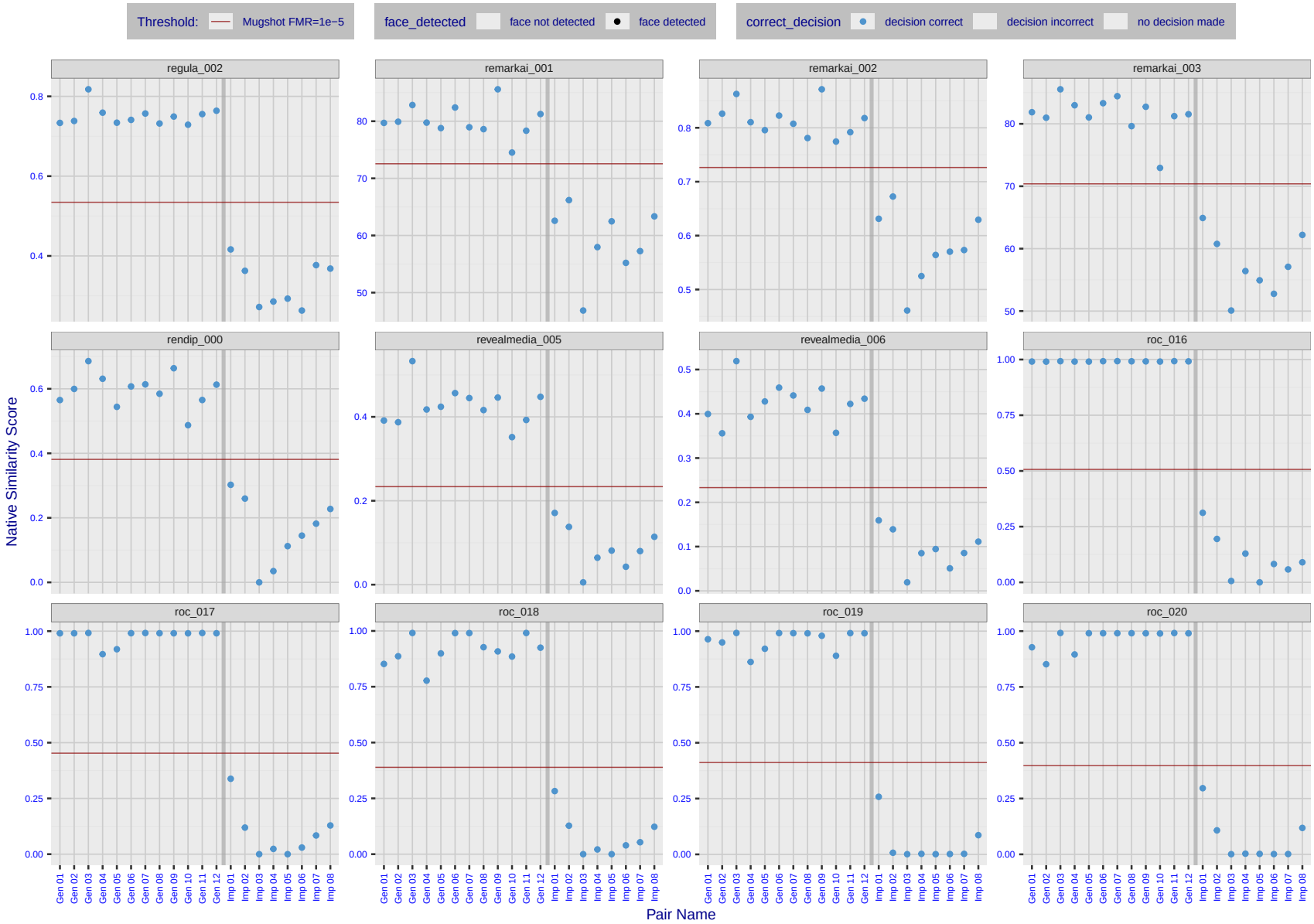

Figure 76: The figure shows algorithms' similarity scores for 12 genuine and 8 impostor image pairs used in a May 2018 paper by Phillips et al. ([1]). The threshold (red horizontal line) is a value calibrated to give FMR = 0.0001 on mugshot images. Points above the threshold correspond to pairs determined to be genuine, and points below the threshold correspond to pairs determined to be impostors. If the determined class (genuine or impostor) matches the real class, points will be blue; if not, red. An X represents face detection failure in either of the images in the pair. Note that the sample size (n=20) is small, and the figure may change substantially if larger or different sets are used. The images can be viewed on p. 13 of the Appendix, where Gen 01 corresponds to Same-Identity Pair 1, Gen 02 corresponds to Same-Identity Pair 2, and so on.

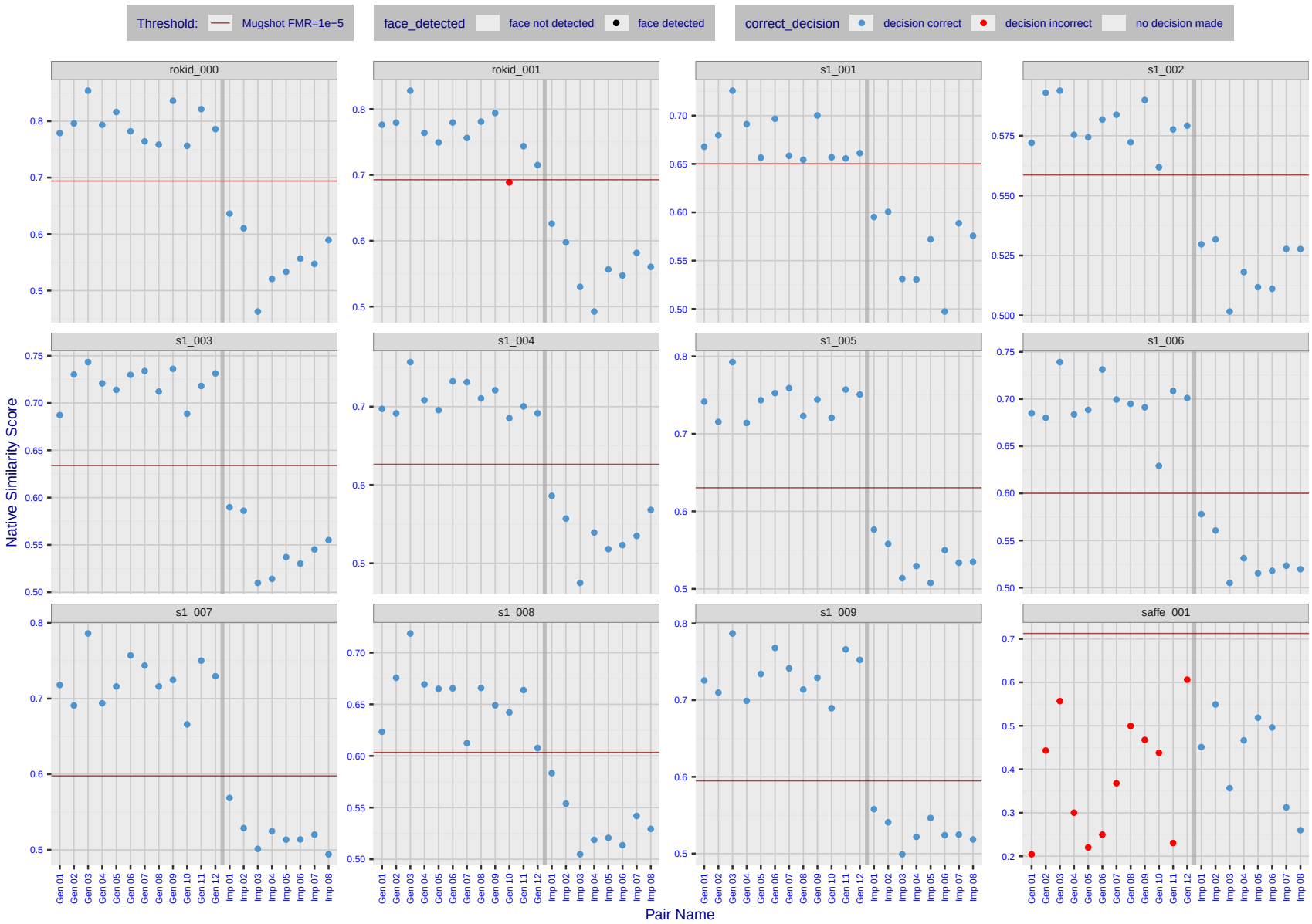

Figure 77: The figure shows algorithms' similarity scores for 12 genuine and 8 impostor image pairs used in a May 2018 paper by Phillips et al. ([1]). The threshold (red horizontal line) is a value calibrated to give FMR = 0.0001 on mugshot images. Points above the threshold correspond to pairs determined to be genuine, and points below the threshold correspond to pairs determined to be impostors. If the determined class (genuine or impostor) matches the real class, points will be blue; if not, red. An X represents face detection failure in either of the images in the pair. Note that the sample size (n=20) is small, and the figure may change substantially if larger or different sets are used. The images can be viewed on p. 13 of the Appendix, where Gen 01 corresponds to Same-Identity Pair 1, Gen 02 corresponds to Same-Identity Pair 2, and so on.

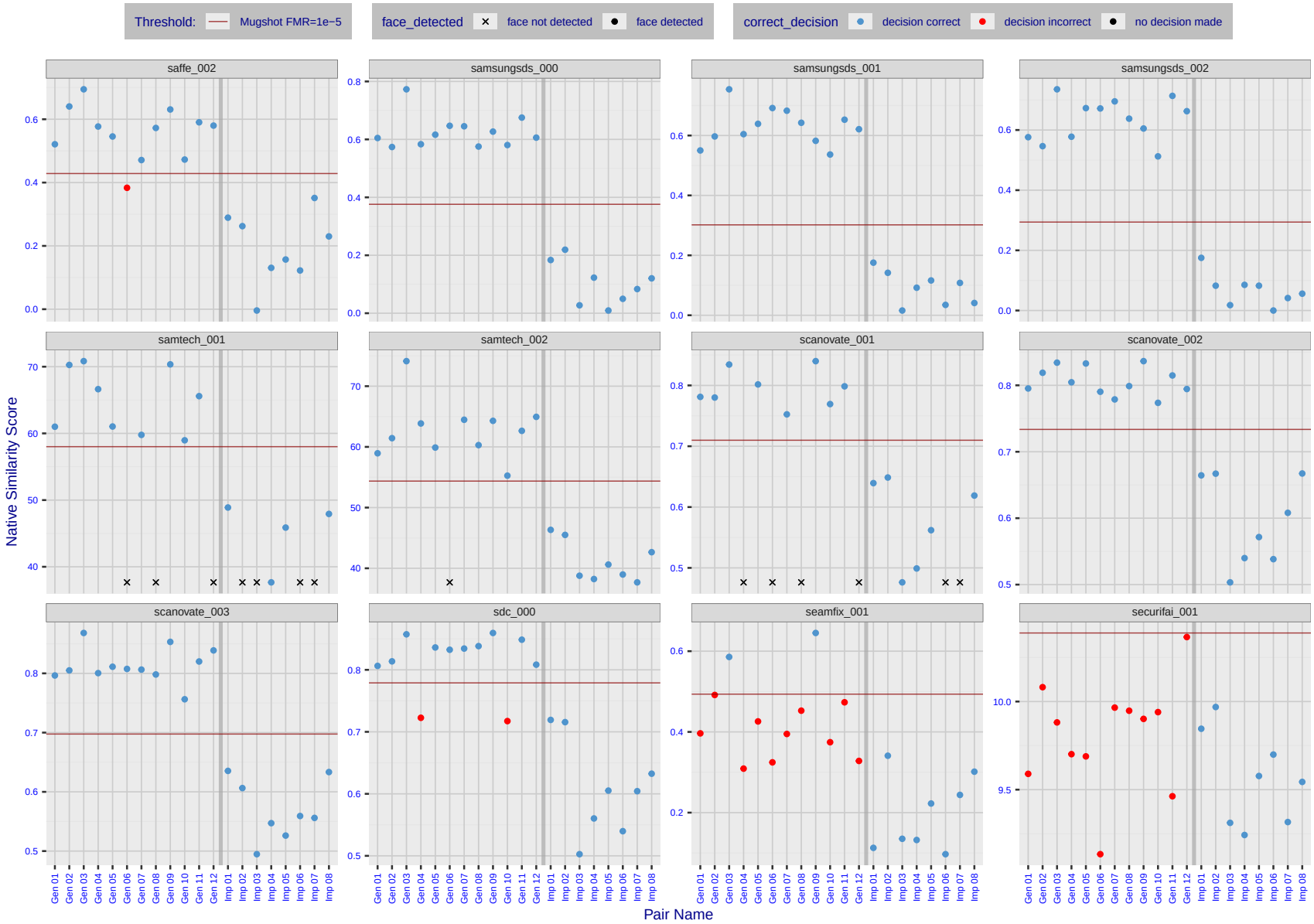

Figure 78: The figure shows algorithms' similarity scores for 12 genuine and 8 impostor image pairs used in a May 2018 paper by Phillips et al. ([1]). The threshold (red horizontal line) is a value calibrated to give FMR = 0.0001 on mugshot images. Points above the threshold correspond to pairs determined to be genuine, and points below the threshold correspond to pairs determined to be impostors. If the determined class (genuine or impostor) matches the real class, points will be blue; if not, red. An X represents face detection failure in either of the images in the pair. Note that the sample size (n=20) is small, and the figure may change substantially if larger or different sets are used. The images can be viewed on p. 13 of the Appendix, where Gen 01 corresponds to Same-Identity Pair 1, Gen 02 corresponds to Same-Identity Pair 2, and so on.

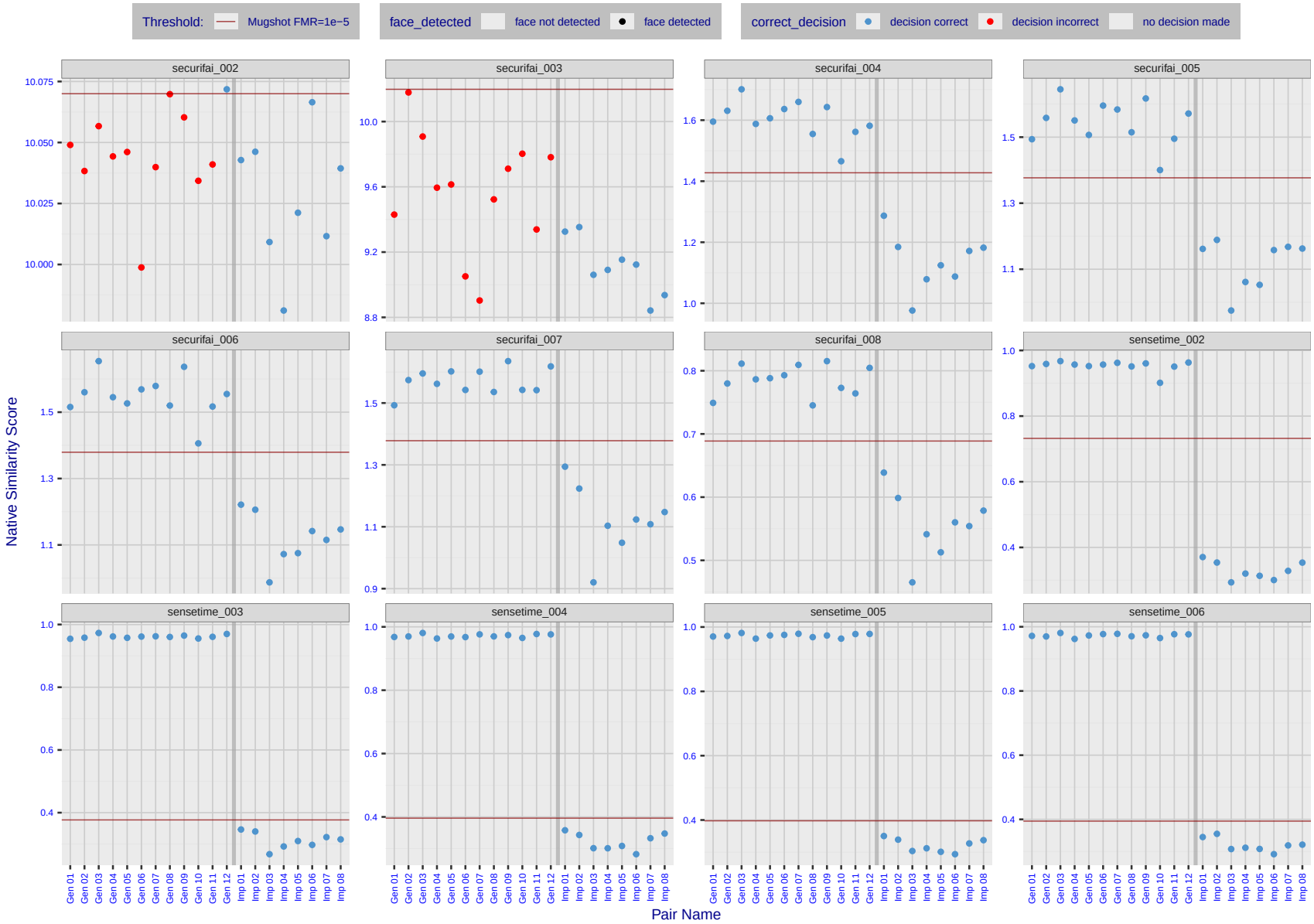

Figure 79: The figure shows algorithms' similarity scores for 12 genuine and 8 impostor image pairs used in a May 2018 paper by Phillips et al. ([1]). The threshold (red horizontal line) is a value calibrated to give FMR = 0.0001 on mugshot images. Points above the threshold correspond to pairs determined to be genuine, and points below the threshold correspond to pairs determined to be impostors. If the determined class (genuine or impostor) matches the real class, points will be blue; if not, red. An X represents face detection failure in either of the images in the pair. Note that the sample size (n=20) is small, and the figure may change substantially if larger or different sets are used. The images can be viewed on p. 13 of the Appendix, where Gen 01 corresponds to Same-Identity Pair 1, Gen 02 corresponds to Same-Identity Pair 2, and so on.

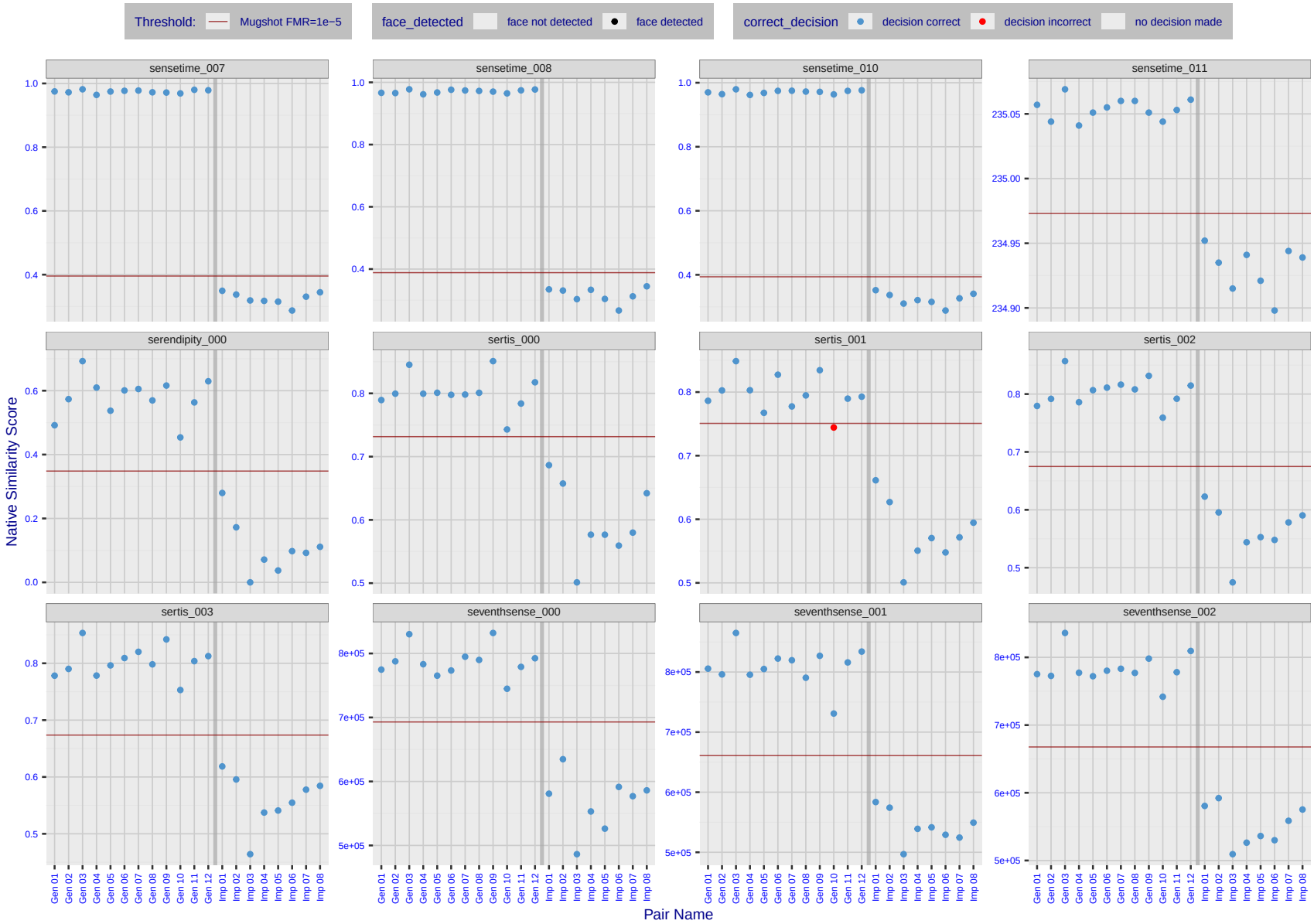

Figure 80: The figure shows algorithms' similarity scores for 12 genuine and 8 impostor image pairs used in a May 2018 paper by Phillips et al. ([1]). The threshold (red horizontal line) is a value calibrated to give FMR = 0.0001 on mugshot images. Points above the threshold correspond to pairs determined to be genuine, and points below the threshold correspond to pairs determined to be impostors. If the determined class (genuine or impostor) matches the real class, points will be blue; if not, red. An X represents face detection failure in either of the images in the pair. Note that the sample size (n=20) is small, and the figure may change substantially if larger or different sets are used. The images can be viewed on p. 13 of the Appendix, where Gen 01 corresponds to Same-Identity Pair 1, Gen 02 corresponds to Same-Identity Pair 2, and so on.

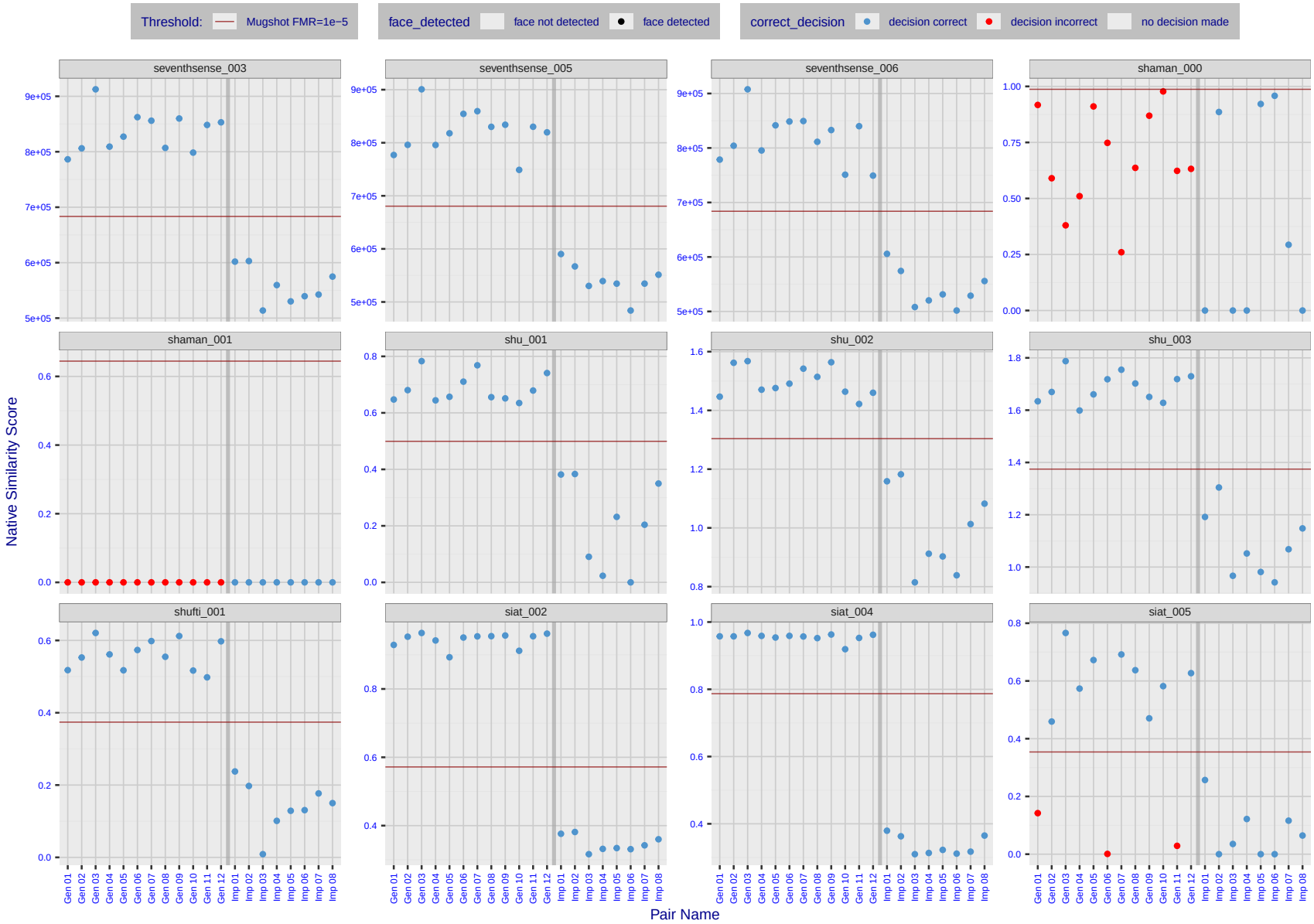

Figure 81: The figure shows algorithms' similarity scores for 12 genuine and 8 impostor image pairs used in a May 2018 paper by Phillips et al. ([1]). The threshold (red horizontal line) is a value calibrated to give FMR = 0.0001 on mugshot images. Points above the threshold correspond to pairs determined to be genuine, and points below the threshold correspond to pairs determined to be impostors. If the determined class (genuine or impostor) matches the real class, points will be blue; if not, red. An X represents face detection failure in either of the images in the pair. Note that the sample size (n=20) is small, and the figure may change substantially if larger or different sets are used. The images can be viewed on p. 13 of the Appendix, where Gen 01 corresponds to Same-Identity Pair 1, Gen 02 corresponds to Same-Identity Pair 2, and so on.

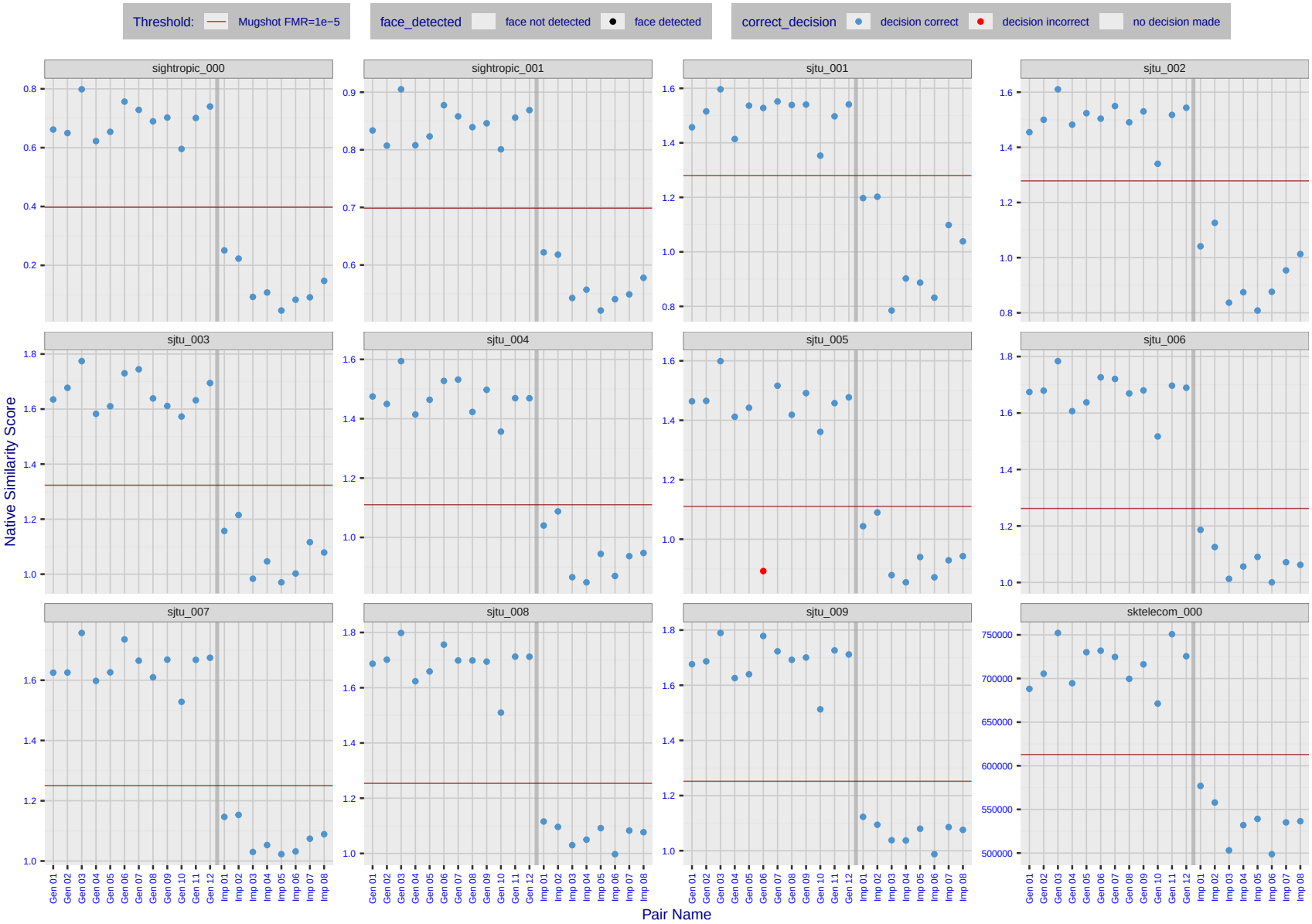

Figure 82: The figure shows algorithms' similarity scores for 12 genuine and 8 impostor image pairs used in a May 2018 paper by Phillips et al. ([1]). The threshold (red horizontal line) is a value calibrated to give FMR = 0.0001 on mugshot images. Points above the threshold correspond to pairs determined to be genuine, and points below the threshold correspond to pairs determined to be impostors. If the determined class (genuine or impostor) matches the real class, points will be blue; if not, red. An X represents face detection failure in either of the images in the pair. Note that the sample size (n=20) is small, and the figure may change substantially if larger or different sets are used. The images can be viewed on p. 13 of the Appendix, where Gen 01 corresponds to Same-Identity Pair 1, Gen 02 corresponds to Same-Identity Pair 2, and so on.

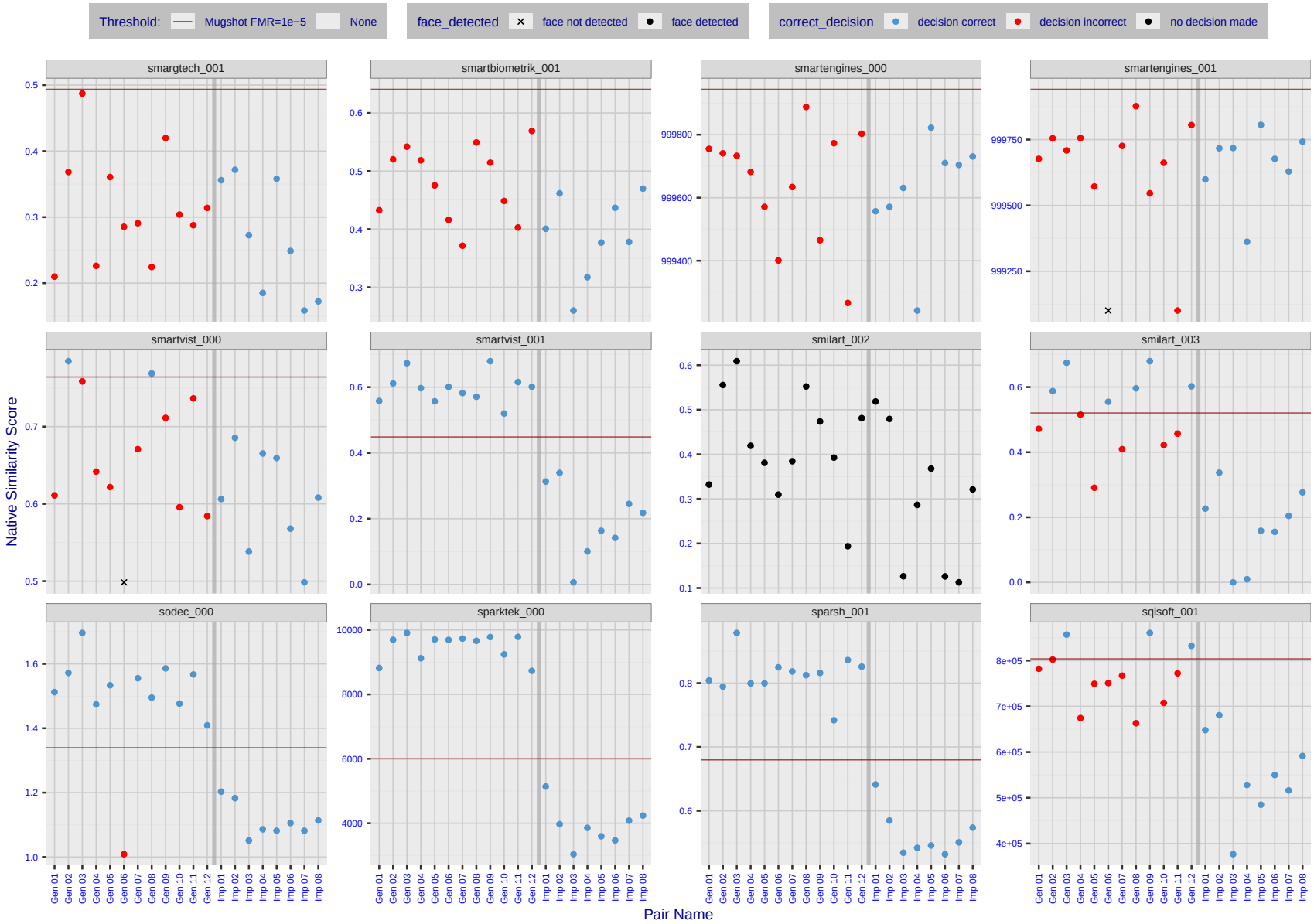

Figure 83: The figure shows algorithms' similarity scores for 12 genuine and 8 impostor image pairs used in a May 2018 paper by Phillips et al. ([1]). The threshold (red horizontal line) is a value calibrated to give FMR = 0.0001 on mugshot images. Points above the threshold correspond to pairs determined to be genuine, and points below the threshold correspond to pairs determined to be impostors. If the determined class (genuine or impostor) matches the real class, points will be blue; if not, red. An X represents face detection failure in either of the images in the pair. Note that the sample size (n=20) is small, and the figure may change substantially if larger or different sets are used. The images can be viewed on p. 13 of the Appendix, where Gen 01 corresponds to Same-Identity Pair 1, Gen 02 corresponds to Same-Identity Pair 2, and so on.

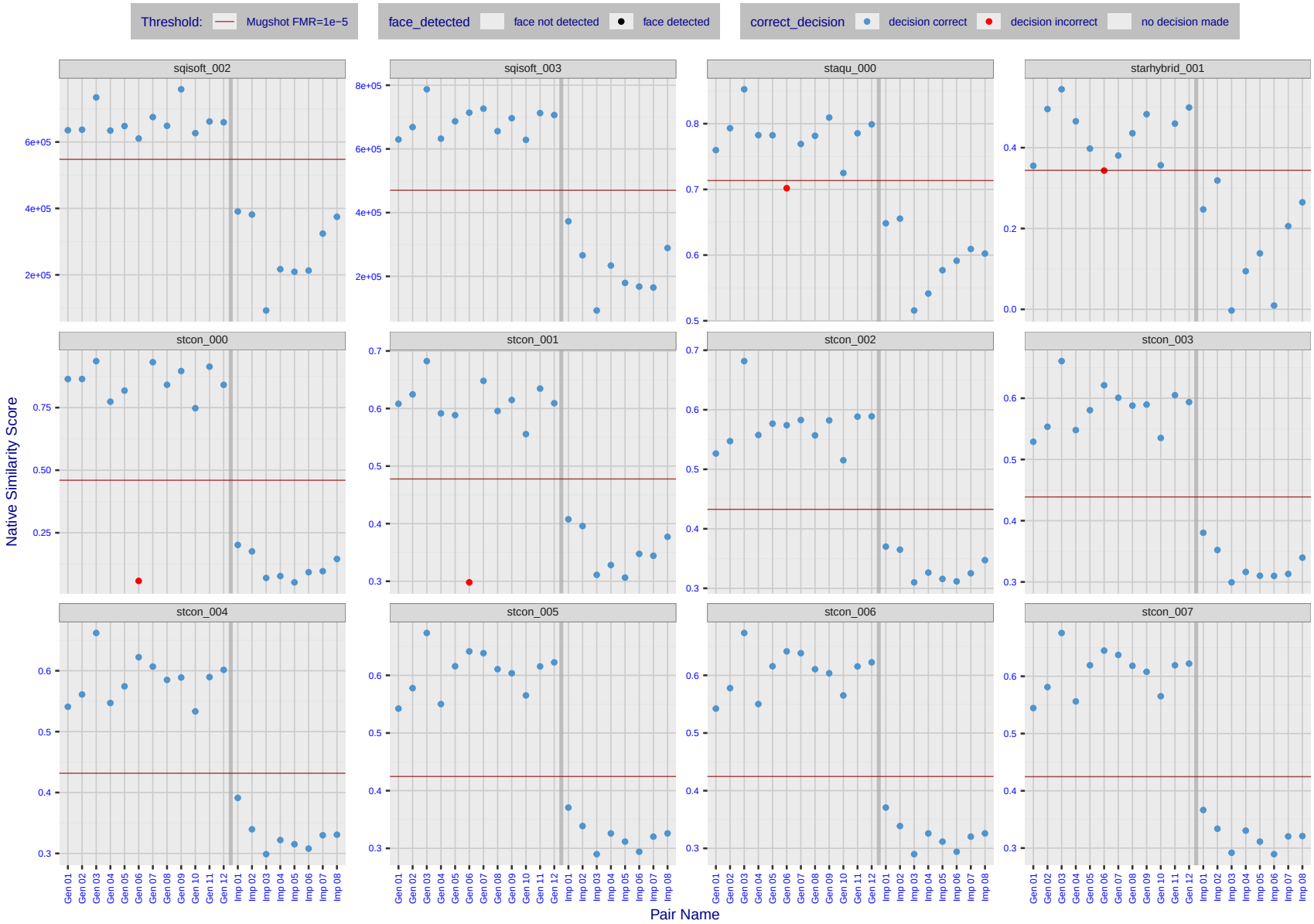

Figure 84: The figure shows algorithms' similarity scores for 12 genuine and 8 impostor image pairs used in a May 2018 paper by Phillips et al. ([1]). The threshold (red horizontal line) is a value calibrated to give FMR = 0.0001 on mugshot images. Points above the threshold correspond to pairs determined to be genuine, and points below the threshold correspond to pairs determined to be impostors. If the determined class (genuine or impostor) matches the real class, points will be blue; if not, red. An X represents face detection failure in either of the images in the pair. Note that the sample size (n=20) is small, and the figure may change substantially if larger or different sets are used. The images can be viewed on p. 13 of the Appendix, where Gen 01 corresponds to Same-Identity Pair 1, Gen 02 corresponds to Same-Identity Pair 2, and so on.

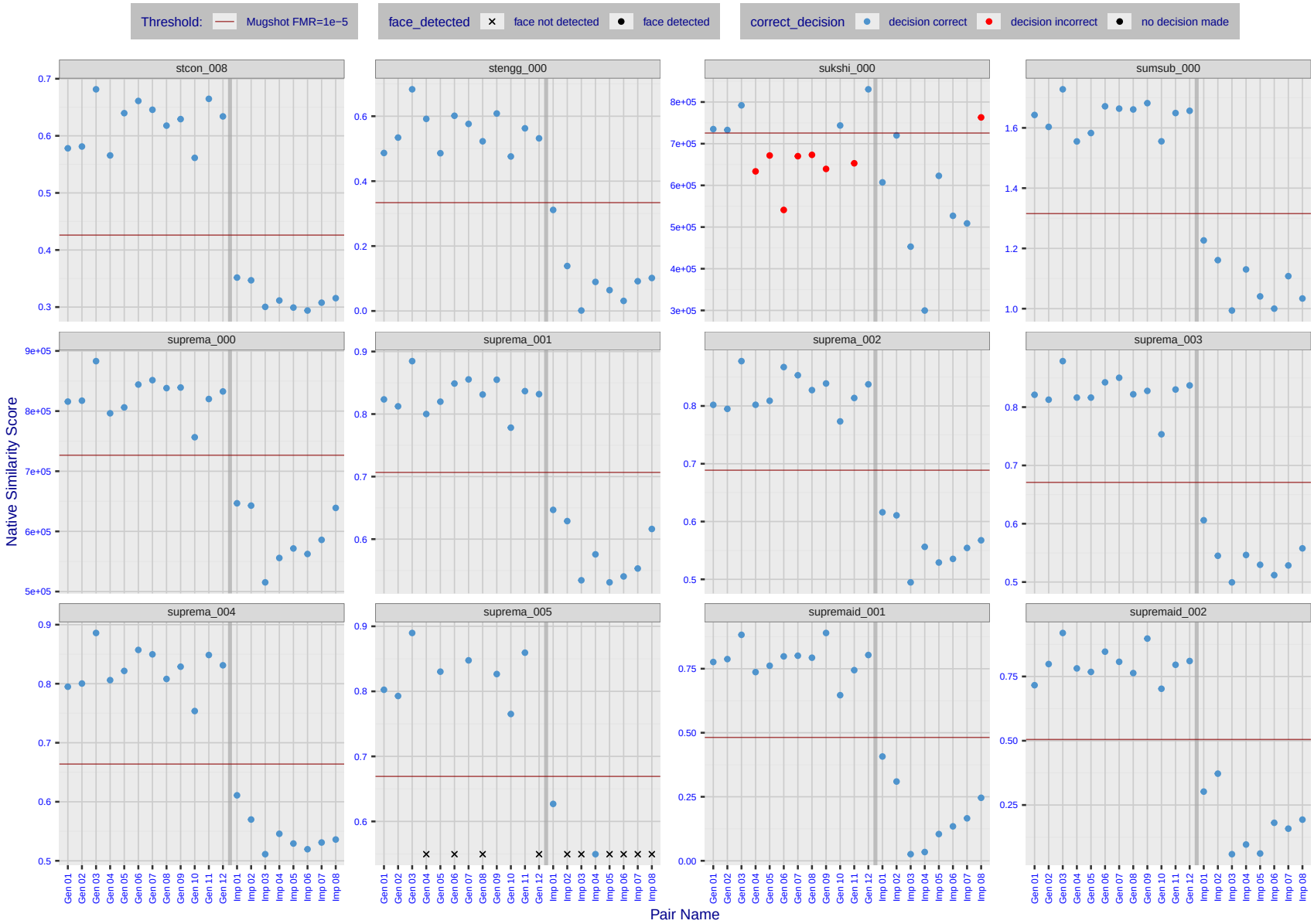

Figure 85: The figure shows algorithms' similarity scores for 12 genuine and 8 impostor image pairs used in a May 2018 paper by Phillips et al. ([1]). The threshold (red horizontal line) is a value calibrated to give FMR = 0.0001 on mugshot images. Points above the threshold correspond to pairs determined to be genuine, and points below the threshold correspond to pairs determined to be impostors. If the determined class (genuine or impostor) matches the real class, points will be blue; if not, red. An X represents face detection failure in either of the images in the pair. Note that the sample size (n=20) is small, and the figure may change substantially if larger or different sets are used. The images can be viewed on p. 13 of the Appendix, where Gen 01 corresponds to Same-Identity Pair 1, Gen 02 corresponds to Same-Identity Pair 2, and so on.

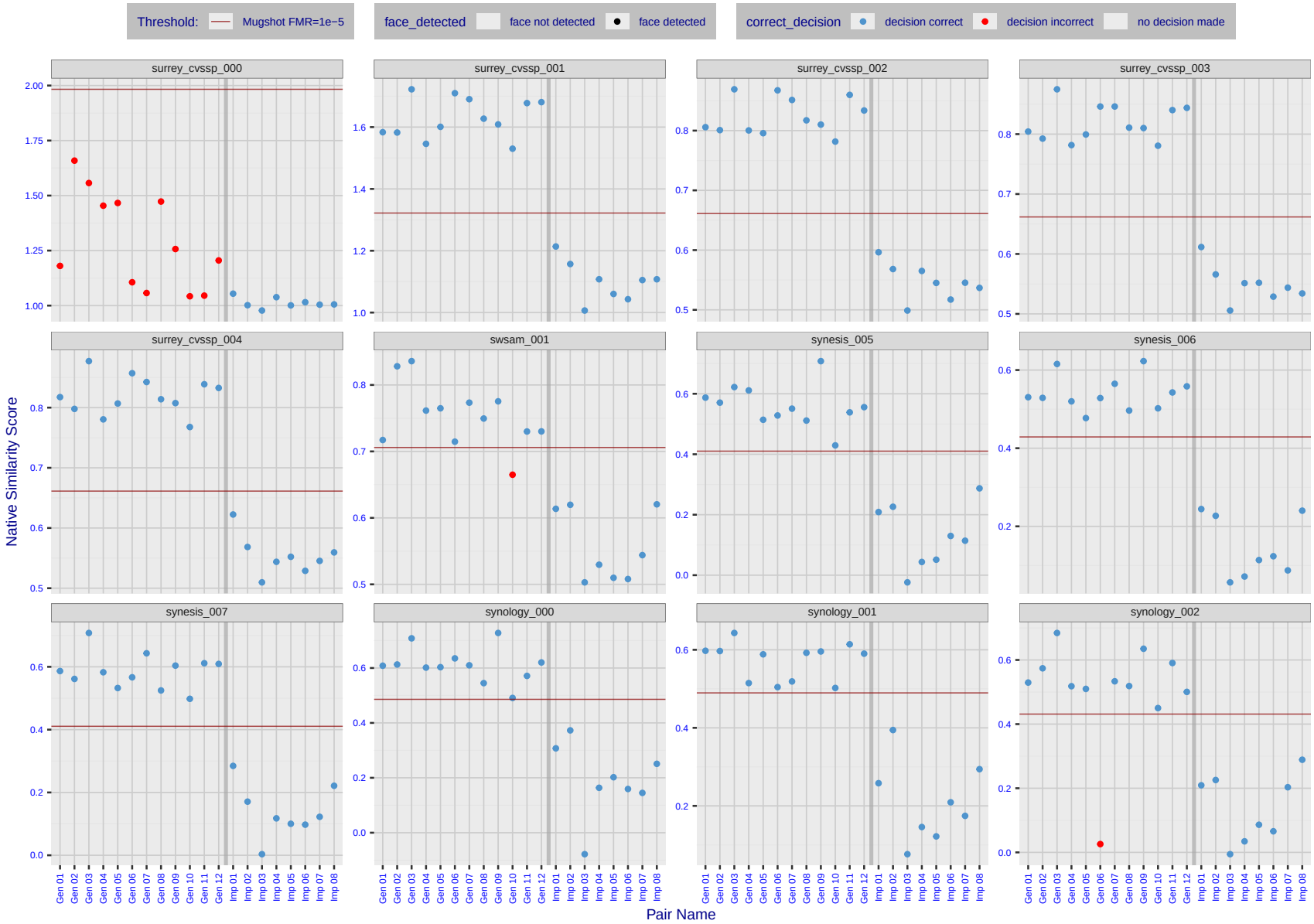

Figure 86: The figure shows algorithms' similarity scores for 12 genuine and 8 impostor image pairs used in a May 2018 paper by Phillips et al. ([1]). The threshold (red horizontal line) is a value calibrated to give FMR = 0.0001 on mugshot images. Points above the threshold correspond to pairs determined to be genuine, and points below the threshold correspond to pairs determined to be impostors. If the determined class (genuine or impostor) matches the real class, points will be blue; if not, red. An X represents face detection failure in either of the images in the pair. Note that the sample size (n=20) is small, and the figure may change substantially if larger or different sets are used. The images can be viewed on p. 13 of the Appendix, where Gen 01 corresponds to Same-Identity Pair 1, Gen 02 corresponds to Same-Identity Pair 2, and so on.

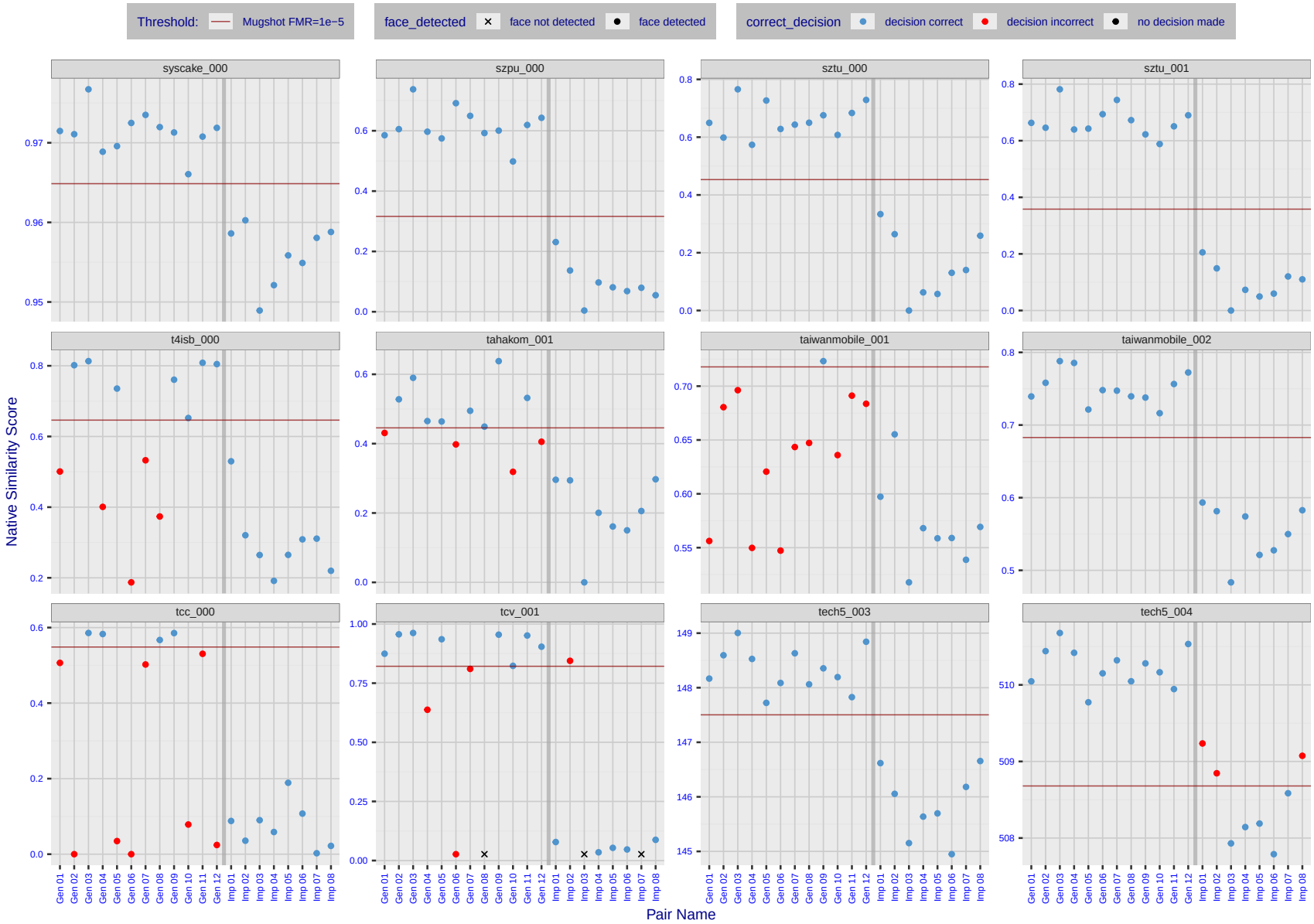

Figure 87: The figure shows algorithms' similarity scores for 12 genuine and 8 impostor image pairs used in a May 2018 paper by Phillips et al. ([1]). The threshold (red horizontal line) is a value calibrated to give FMR = 0.0001 on mugshot images. Points above the threshold correspond to pairs determined to be genuine, and points below the threshold correspond to pairs determined to be impostors. If the determined class (genuine or impostor) matches the real class, points will be blue; if not, red. An X represents face detection failure in either of the images in the pair. Note that the sample size (n=20) is small, and the figure may change substantially if larger or different sets are used. The images can be viewed on p. 13 of the Appendix, where Gen 01 corresponds to Same-Identity Pair 1, Gen 02 corresponds to Same-Identity Pair 2, and so on.

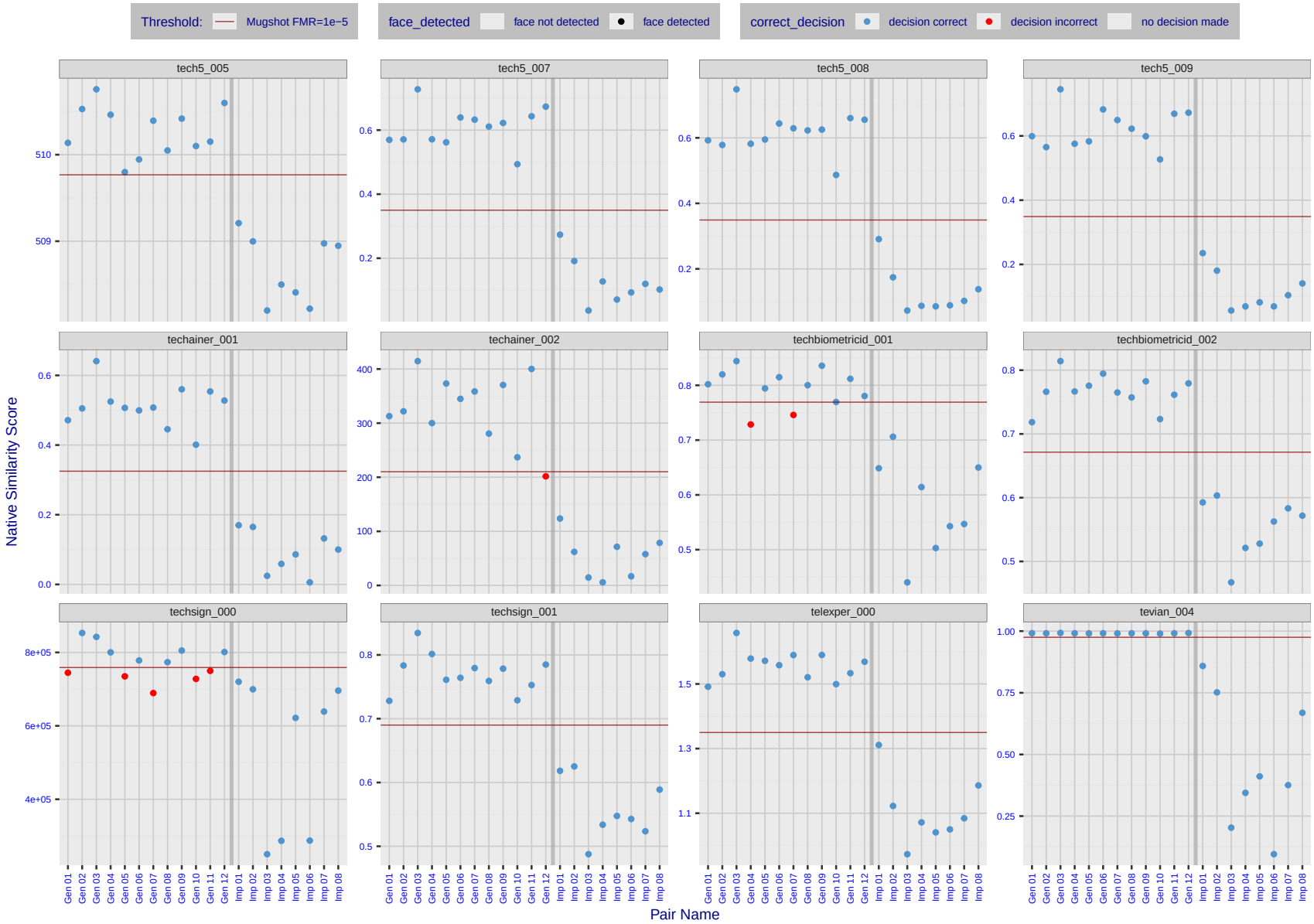

Figure 88: The figure shows algorithms' similarity scores for 12 genuine and 8 impostor image pairs used in a May 2018 paper by Phillips et al. ([1]). The threshold (red horizontal line) is a value calibrated to give FMR = 0.0001 on mugshot images. Points above the threshold correspond to pairs determined to be genuine, and points below the threshold correspond to pairs determined to be impostors. If the determined class (genuine or impostor) matches the real class, points will be blue; if not, red. An X represents face detection failure in either of the images in the pair. Note that the sample size (n=20) is small, and the figure may change substantially if larger or different sets are used. The images can be viewed on p. 13 of the Appendix, where Gen 01 corresponds to Same-Identity Pair 1, Gen 02 corresponds to Same-Identity Pair 2, and so on.

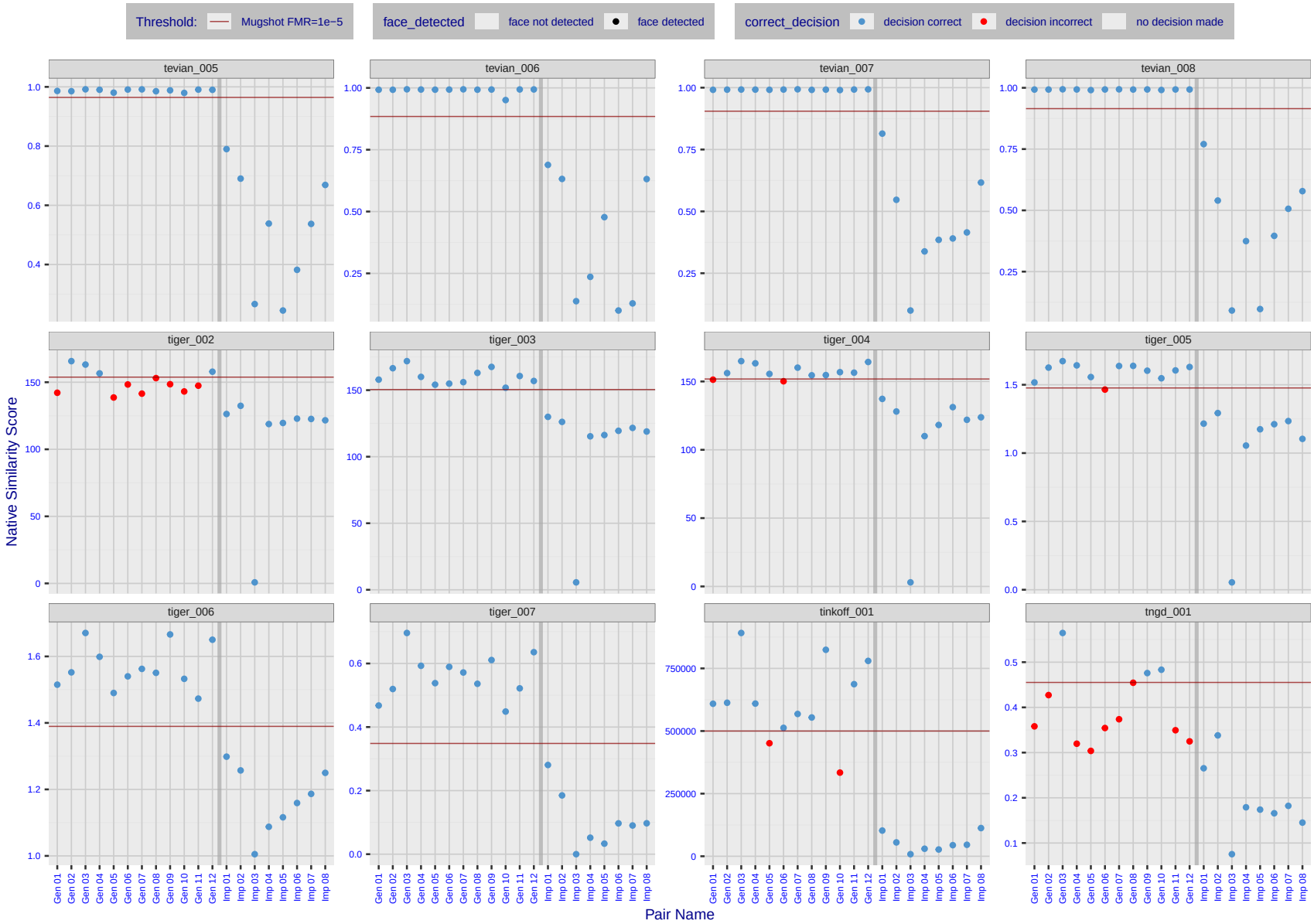

Figure 89: The figure shows algorithms' similarity scores for 12 genuine and 8 impostor image pairs used in a May 2018 paper by Phillips et al. ([1]). The threshold (red horizontal line) is a value calibrated to give FMR = 0.0001 on mugshot images. Points above the threshold correspond to pairs determined to be genuine, and points below the threshold correspond to pairs determined to be impostors. If the determined class (genuine or impostor) matches the real class, points will be blue; if not, red. An X represents face detection failure in either of the images in the pair. Note that the sample size (n=20) is small, and the figure may change substantially if larger or different sets are used. The images can be viewed on p. 13 of the Appendix, where Gen 01 corresponds to Same-Identity Pair 1, Gen 02 corresponds to Same-Identity Pair 2, and so on.

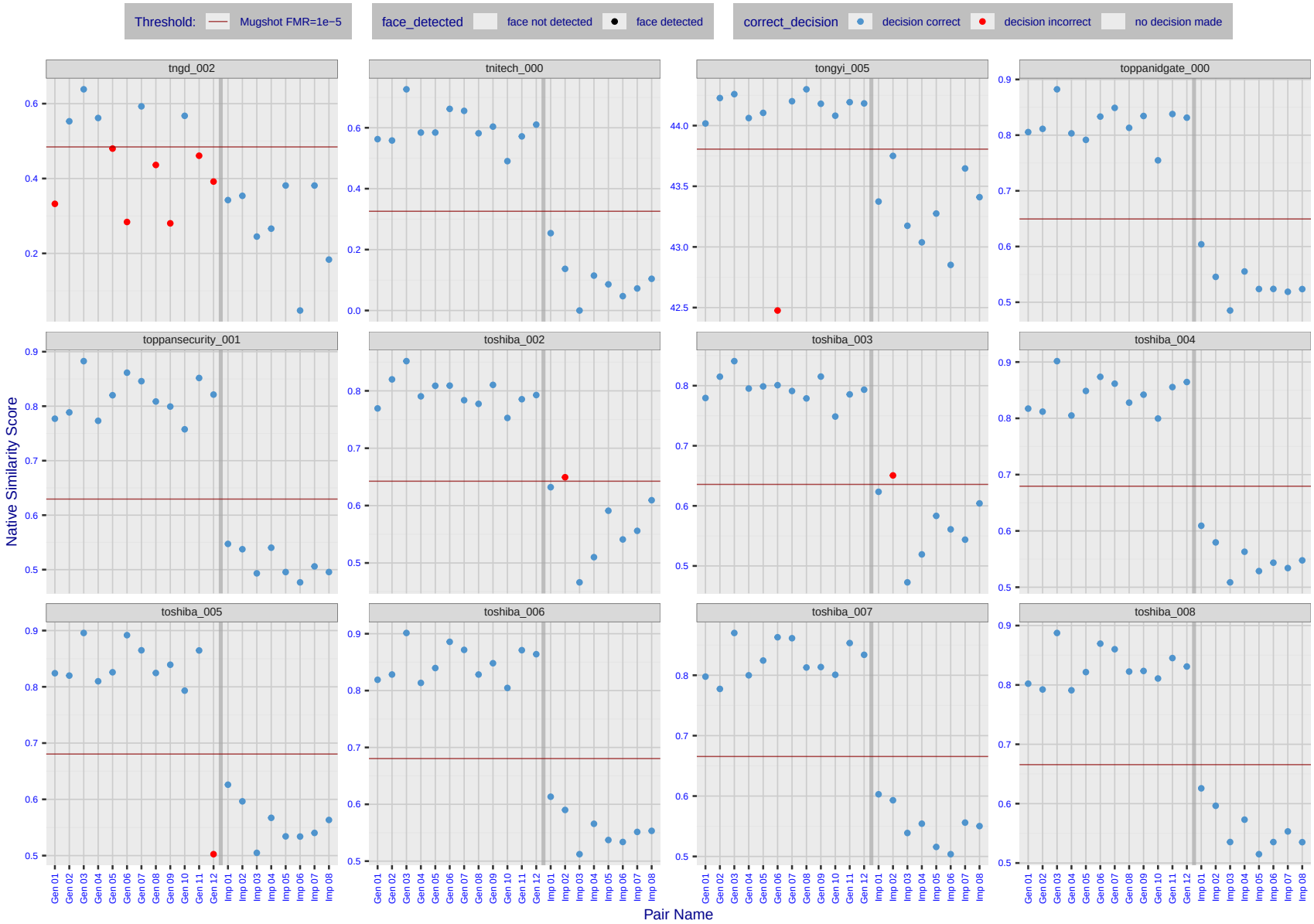

Figure 90: The figure shows algorithms' similarity scores for 12 genuine and 8 impostor image pairs used in a May 2018 paper by Phillips et al. ([1]). The threshold (red horizontal line) is a value calibrated to give FMR = 0.0001 on mugshot images. Points above the threshold correspond to pairs determined to be genuine, and points below the threshold correspond to pairs determined to be impostors. If the determined class (genuine or impostor) matches the real class, points will be blue; if not, red. An X represents face detection failure in either of the images in the pair. Note that the sample size (n=20) is small, and the figure may change substantially if larger or different sets are used. The images can be viewed on p. 13 of the Appendix, where Gen 01 corresponds to Same-Identity Pair 1, Gen 02 corresponds to Same-Identity Pair 2, and so on.

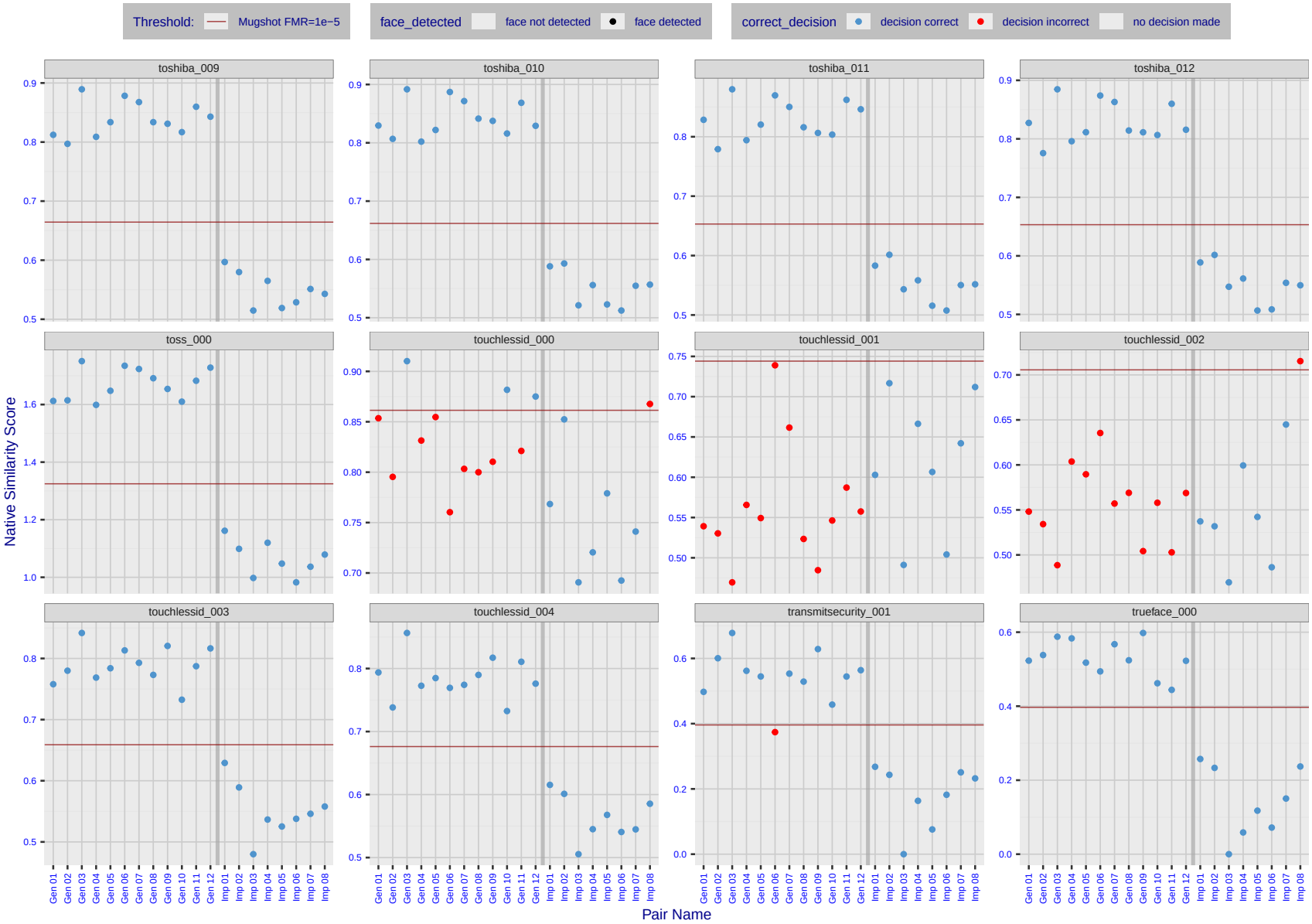

Figure 91: The figure shows algorithms' similarity scores for 12 genuine and 8 impostor image pairs used in a May 2018 paper by Phillips et al. ([1]). The threshold (red horizontal line) is a value calibrated to give FMR = 0.0001 on mugshot images. Points above the threshold correspond to pairs determined to be genuine, and points below the threshold correspond to pairs determined to be impostors. If the determined class (genuine or impostor) matches the real class, points will be blue; if not, red. An X represents face detection failure in either of the images in the pair. Note that the sample size (n=20) is small, and the figure may change substantially if larger or different sets are used. The images can be viewed on p. 13 of the Appendix, where Gen 01 corresponds to Same-Identity Pair 1, Gen 02 corresponds to Same-Identity Pair 2, and so on.

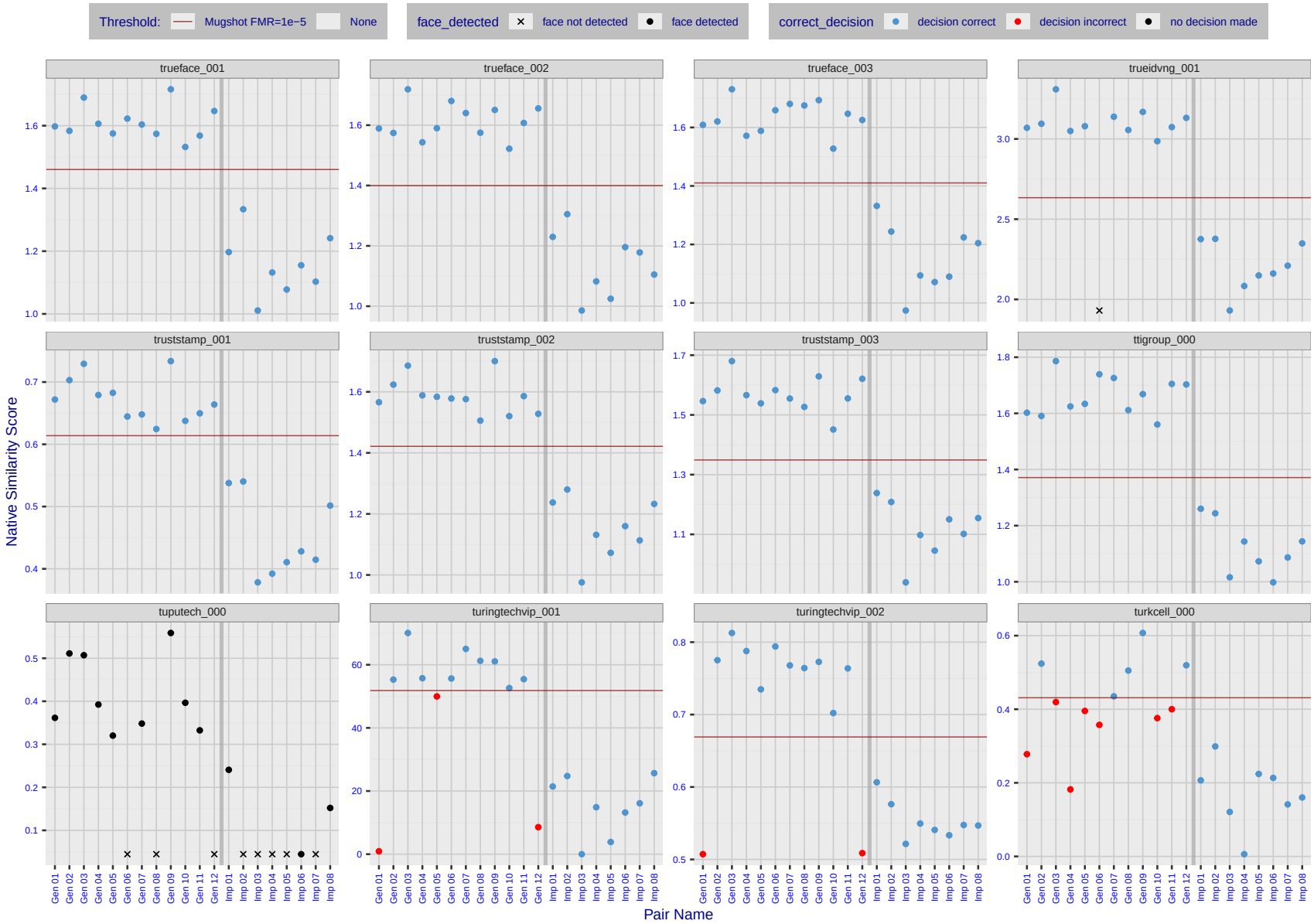

Figure 92: The figure shows algorithms' similarity scores for 12 genuine and 8 impostor image pairs used in a May 2018 paper by Phillips et al. ([1]). The threshold (red horizontal line) is a value calibrated to give FMR = 0.0001 on mugshot images. Points above the threshold correspond to pairs determined to be genuine, and points below the threshold correspond to pairs determined to be impostors. If the determined class (genuine or impostor) matches the real class, points will be blue; if not, red. An X represents face detection failure in either of the images in the pair. Note that the sample size (n=20) is small, and the figure may change substantially if larger or different sets are used. The images can be viewed on p. 13 of the Appendix, where Gen 01 corresponds to Same-Identity Pair 1, Gen 02 corresponds to Same-Identity Pair 2, and so on.

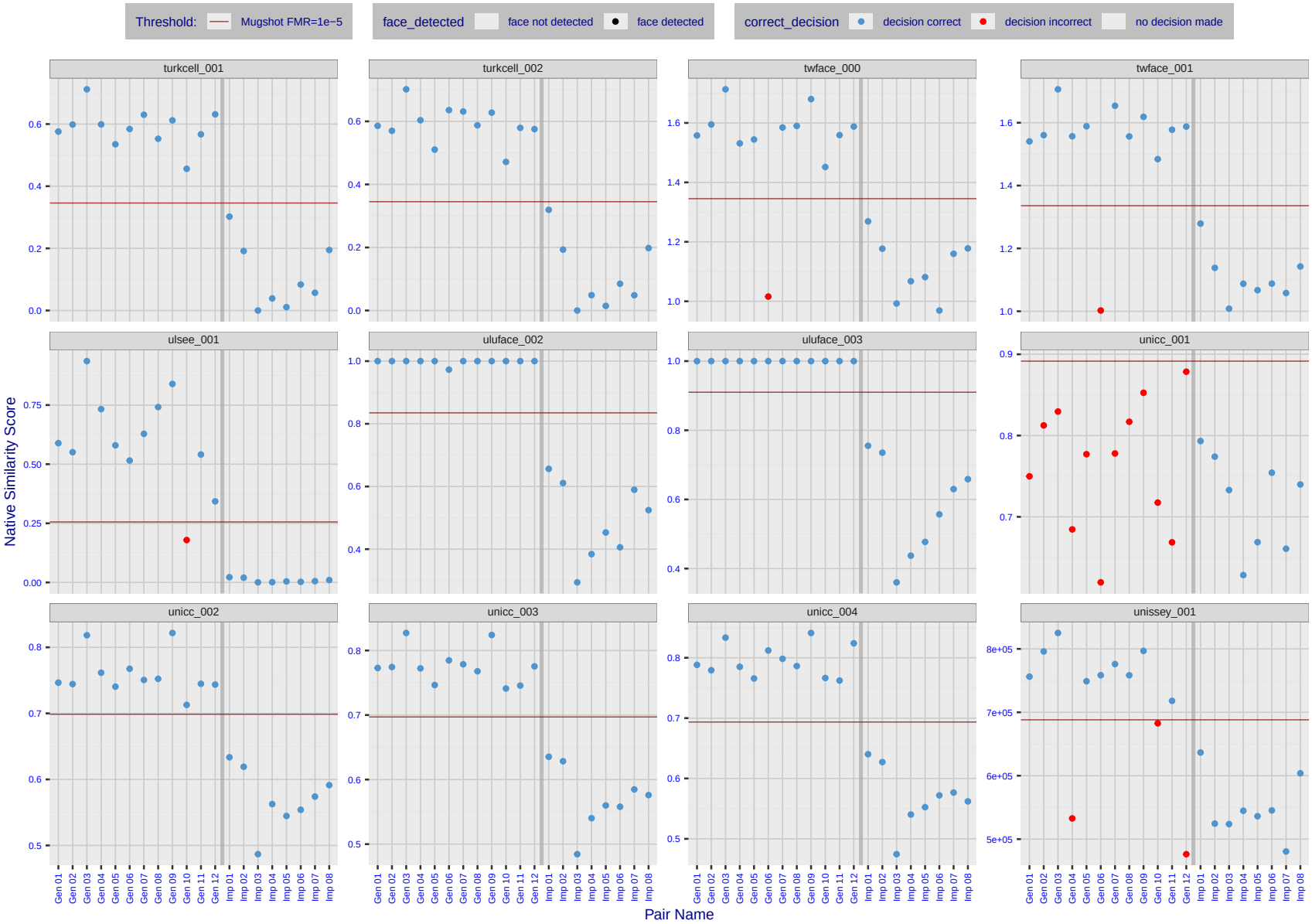

Figure 93: The figure shows algorithms' similarity scores for 12 genuine and 8 impostor image pairs used in a May 2018 paper by Phillips et al. ([1]). The threshold (red horizontal line) is a value calibrated to give FMR = 0.0001 on mugshot images. Points above the threshold correspond to pairs determined to be genuine, and points below the threshold correspond to pairs determined to be impostors. If the determined class (genuine or impostor) matches the real class, points will be blue; if not, red. An X represents face detection failure in either of the images in the pair. Note that the sample size (n=20) is small, and the figure may change substantially if larger or different sets are used. The images can be viewed on p. 13 of the Appendix, where Gen 01 corresponds to Same-Identity Pair 1, Gen 02 corresponds to Same-Identity Pair 2, and so on.

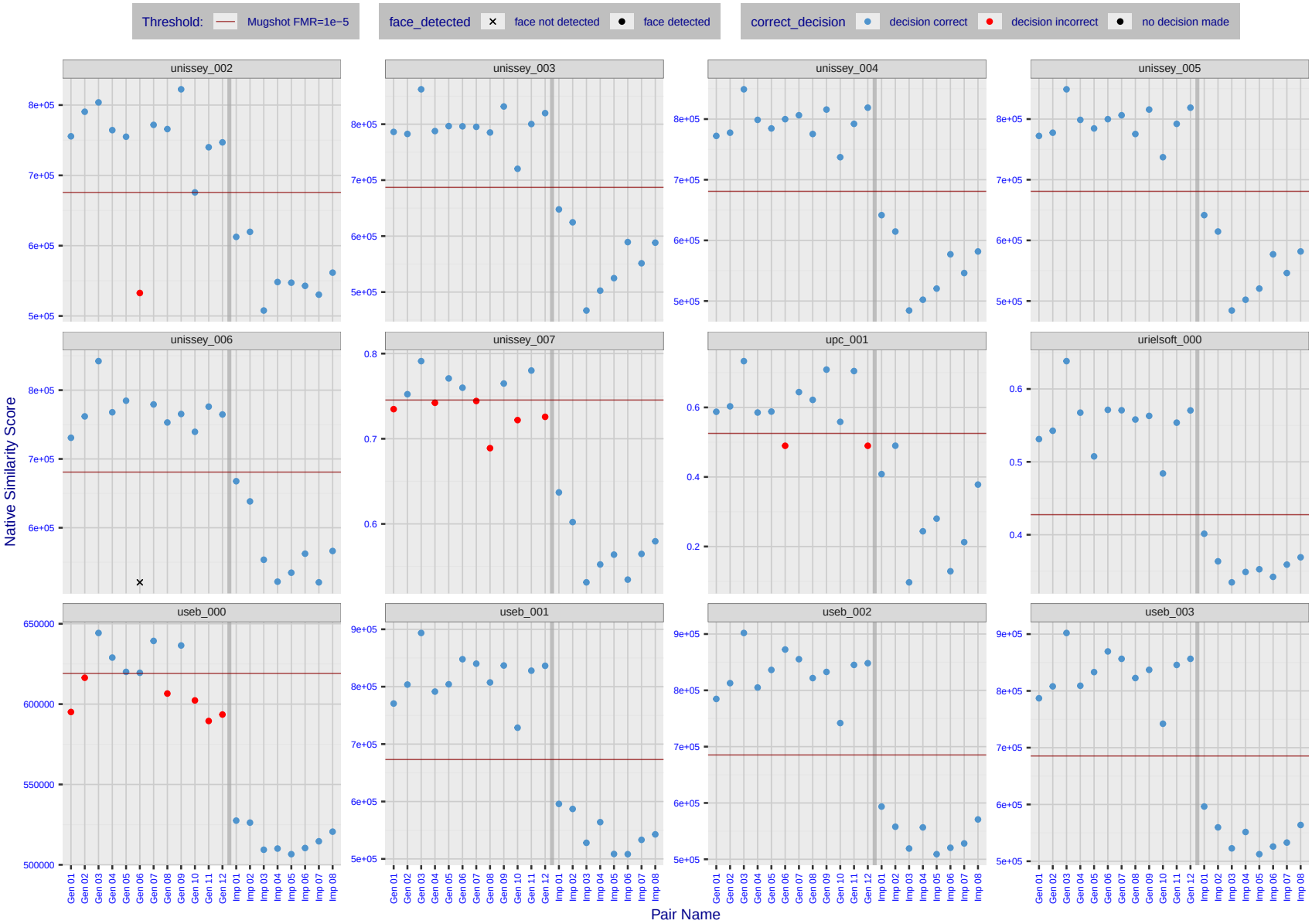

Figure 94: The figure shows algorithms' similarity scores for 12 genuine and 8 impostor image pairs used in a May 2018 paper by Phillips et al. ([1]). The threshold (red horizontal line) is a value calibrated to give FMR = 0.0001 on mugshot images. Points above the threshold correspond to pairs determined to be genuine, and points below the threshold correspond to pairs determined to be impostors. If the determined class (genuine or impostor) matches the real class, points will be blue; if not, red. An X represents face detection failure in either of the images in the pair. Note that the sample size (n=20) is small, and the figure may change substantially if larger or different sets are used. The images can be viewed on p. 13 of the Appendix, where Gen 01 corresponds to Same-Identity Pair 1, Gen 02 corresponds to Same-Identity Pair 2, and so on.

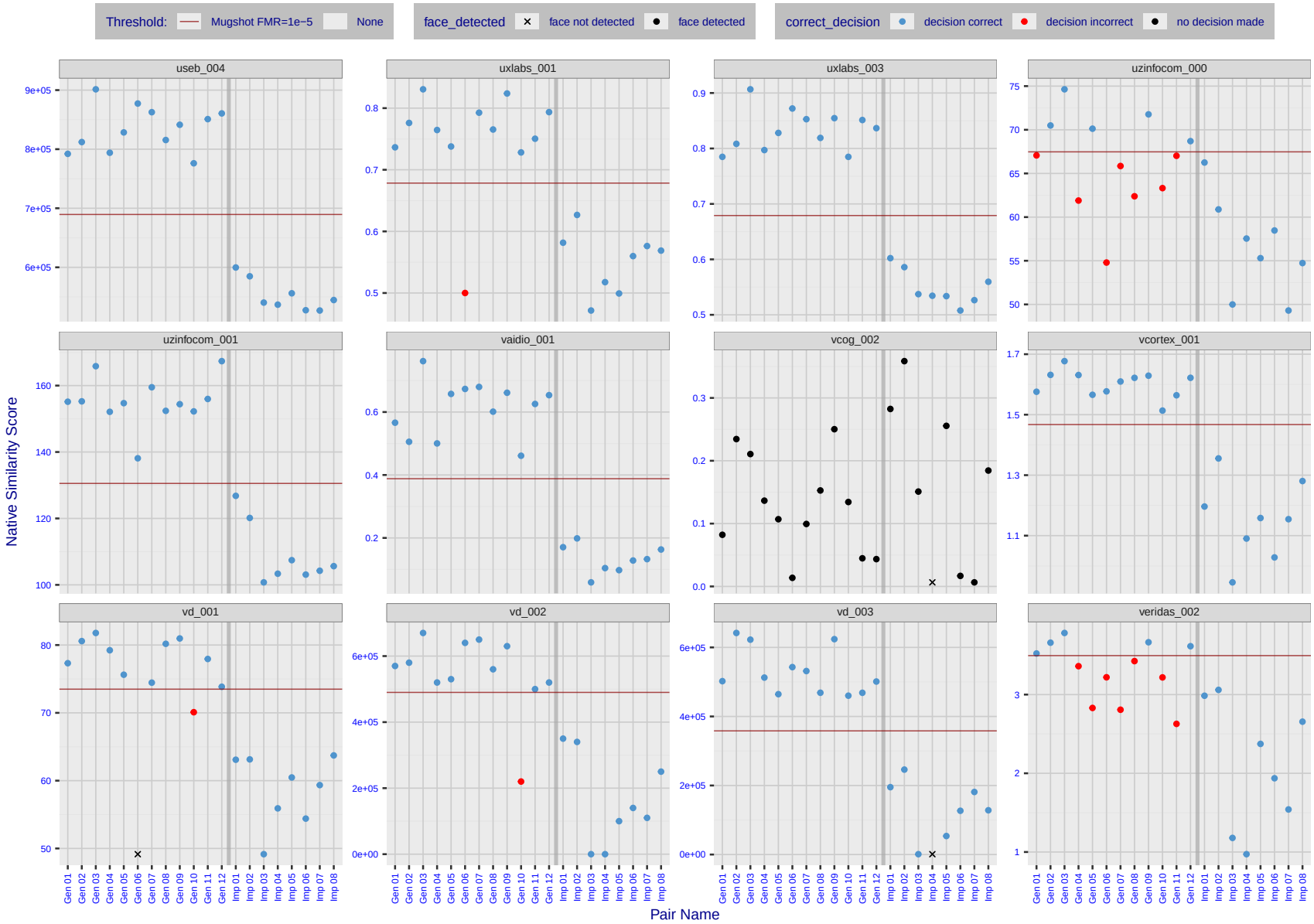

Figure 95: The figure shows algorithms' similarity scores for 12 genuine and 8 impostor image pairs used in a May 2018 paper by Phillips et al. ([1]). The threshold (red horizontal line) is a value calibrated to give FMR = 0.0001 on mugshot images. Points above the threshold correspond to pairs determined to be genuine, and points below the threshold correspond to pairs determined to be impostors. If the determined class (genuine or impostor) matches the real class, points will be blue; if not, red. An X represents face detection failure in either of the images in the pair. Note that the sample size (n=20) is small, and the figure may change substantially if larger or different sets are used. The images can be viewed on p. 13 of the Appendix, where Gen 01 corresponds to Same-Identity Pair 1, Gen 02 corresponds to Same-Identity Pair 2, and so on.

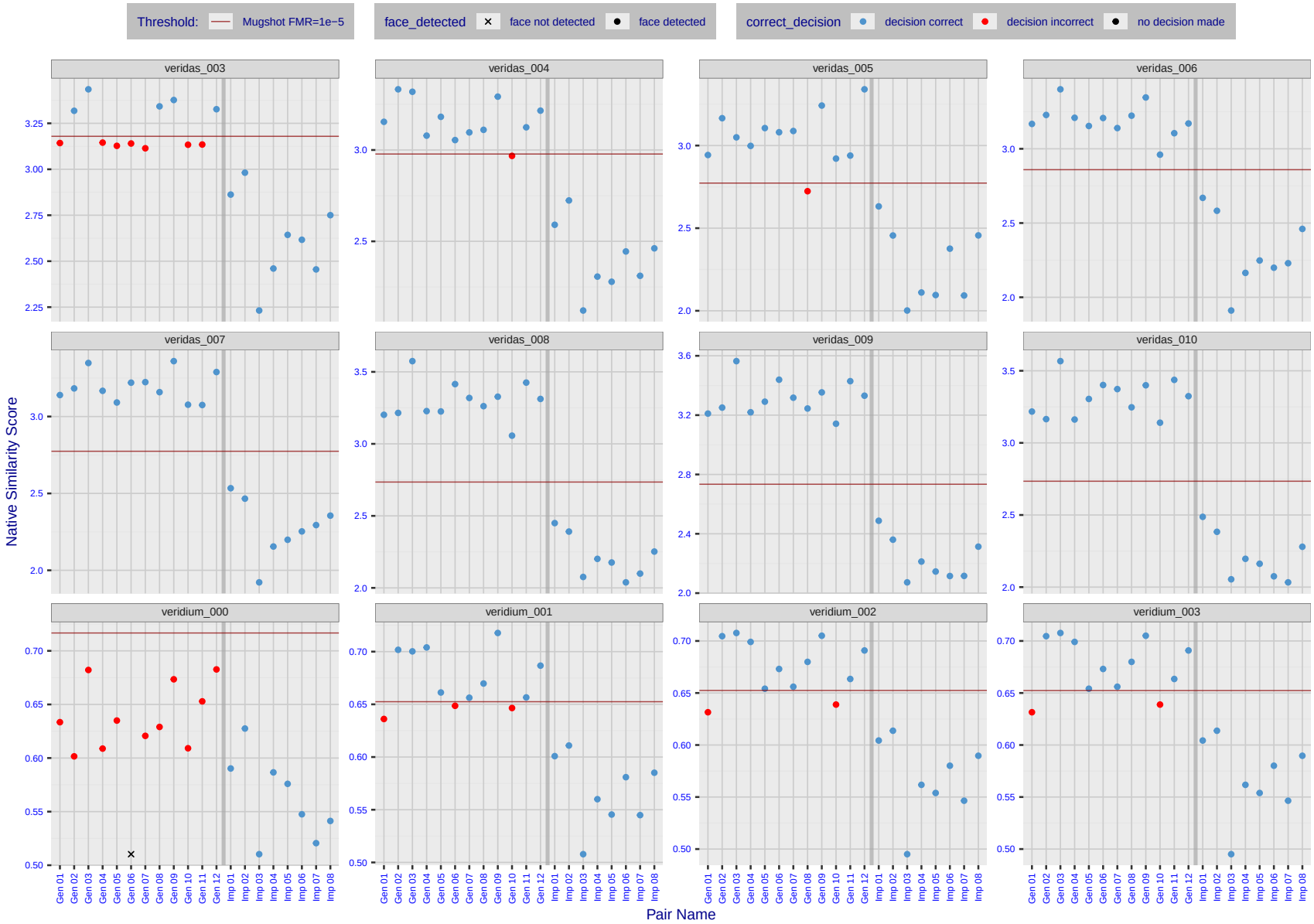

Figure 96: The figure shows algorithms' similarity scores for 12 genuine and 8 impostor image pairs used in a May 2018 paper by Phillips et al. ([1]). The threshold (red horizontal line) is a value calibrated to give FMR = 0.0001 on mugshot images. Points above the threshold correspond to pairs determined to be genuine, and points below the threshold correspond to pairs determined to be impostors. If the determined class (genuine or impostor) matches the real class, points will be blue; if not, red. An X represents face detection failure in either of the images in the pair. Note that the sample size (n=20) is small, and the figure may change substantially if larger or different sets are used. The images can be viewed on p. 13 of the Appendix, where Gen 01 corresponds to Same-Identity Pair 1, Gen 02 corresponds to Same-Identity Pair 2, and so on.

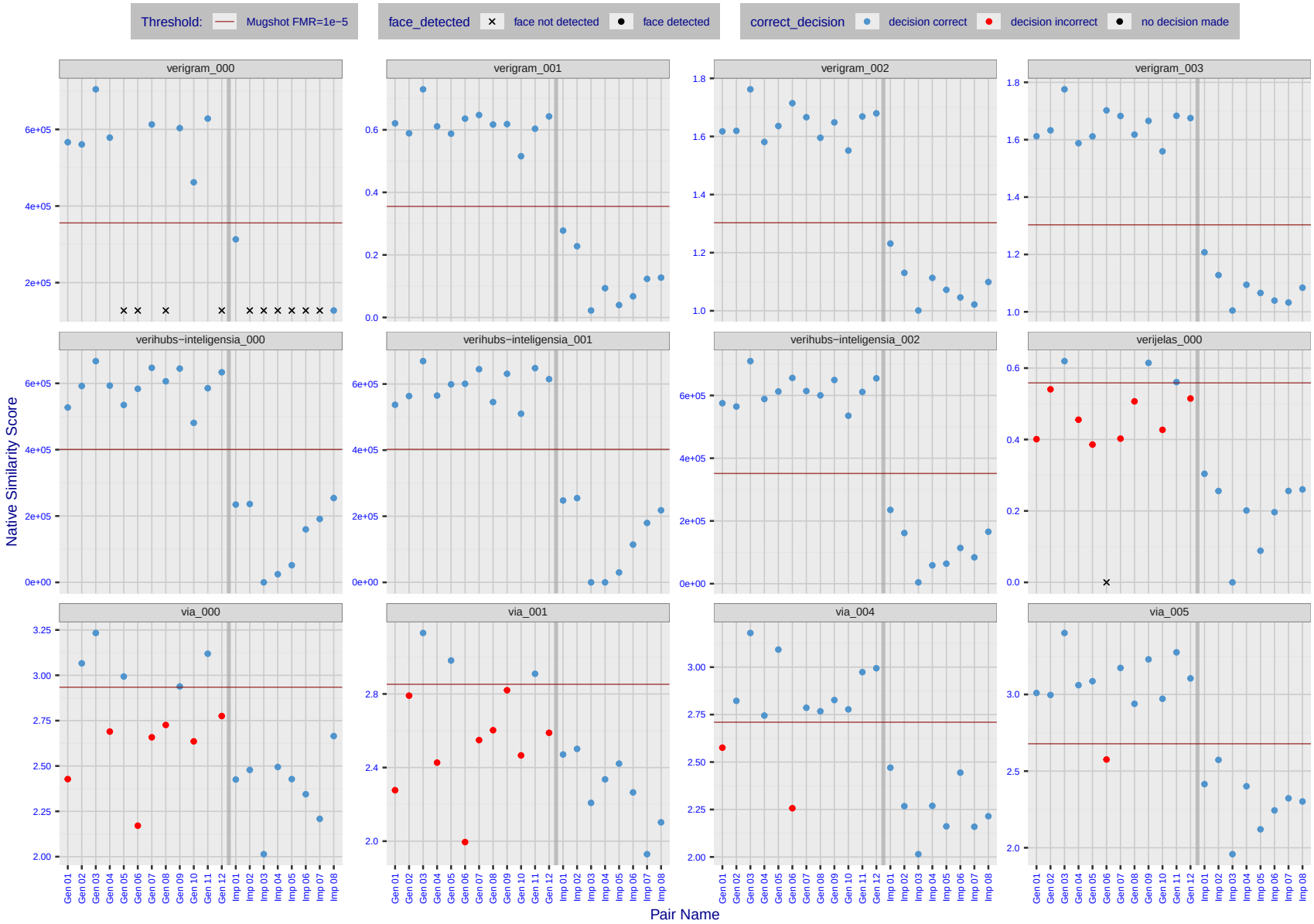

Figure 97: The figure shows algorithms' similarity scores for 12 genuine and 8 impostor image pairs used in a May 2018 paper by Phillips et al. ([1]). The threshold (red horizontal line) is a value calibrated to give FMR = 0.0001 on mugshot images. Points above the threshold correspond to pairs determined to be genuine, and points below the threshold correspond to pairs determined to be impostors. If the determined class (genuine or impostor) matches the real class, points will be blue; if not, red. An X represents face detection failure in either of the images in the pair. Note that the sample size (n=20) is small, and the figure may change substantially if larger or different sets are used. The images can be viewed on p. 13 of the Appendix, where Gen 01 corresponds to Same-Identity Pair 1, Gen 02 corresponds to Same-Identity Pair 2, and so on.

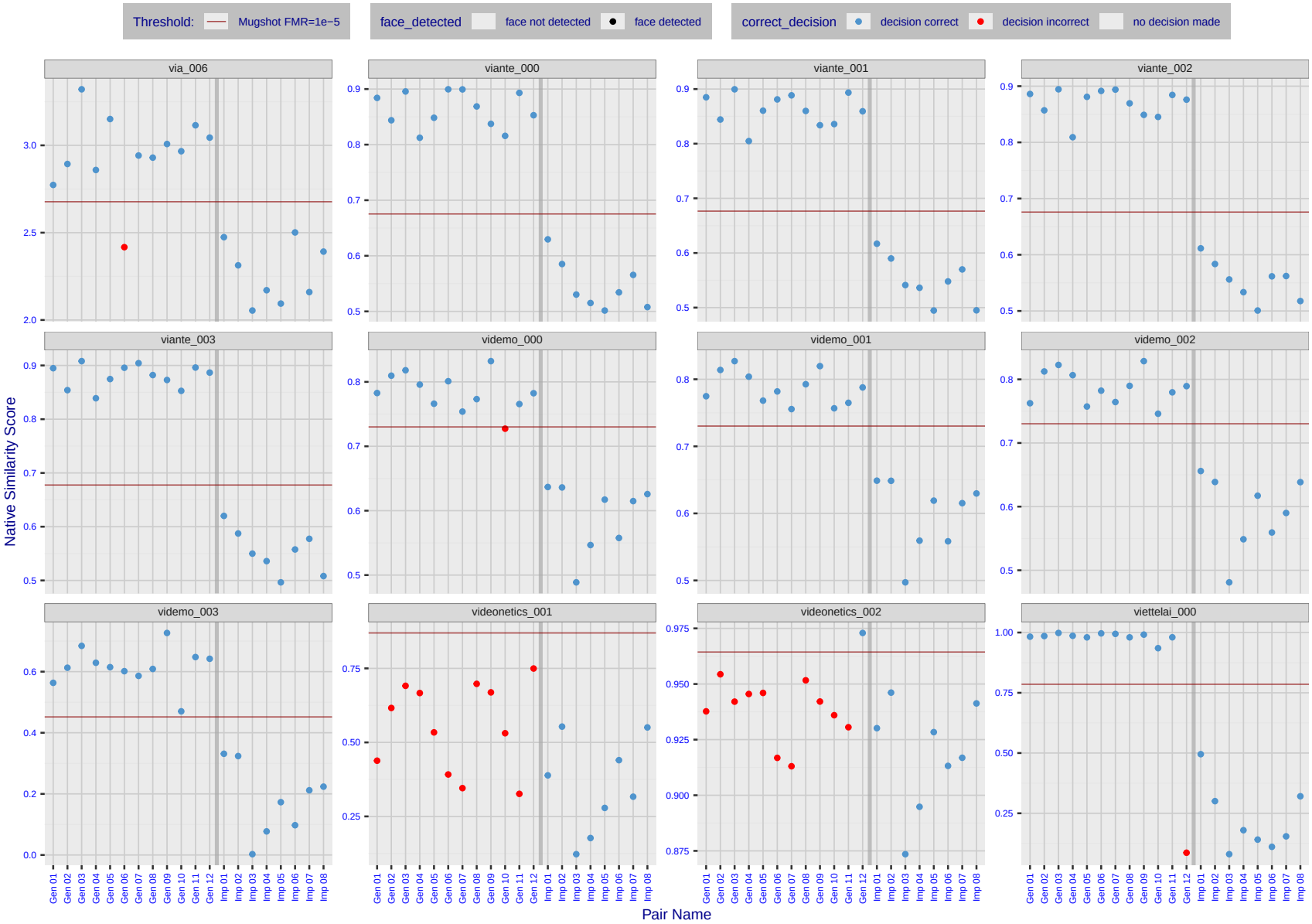

Figure 98: The figure shows algorithms' similarity scores for 12 genuine and 8 impostor image pairs used in a May 2018 paper by Phillips et al. ([1]). The threshold (red horizontal line) is a value calibrated to give FMR = 0.0001 on mugshot images. Points above the threshold correspond to pairs determined to be genuine, and points below the threshold correspond to pairs determined to be impostors. If the determined class (genuine or impostor) matches the real class, points will be blue; if not, red. An X represents face detection failure in either of the images in the pair. Note that the sample size (n=20) is small, and the figure may change substantially if larger or different sets are used. The images can be viewed on p. 13 of the Appendix, where Gen 01 corresponds to Same-Identity Pair 1, Gen 02 corresponds to Same-Identity Pair 2, and so on.

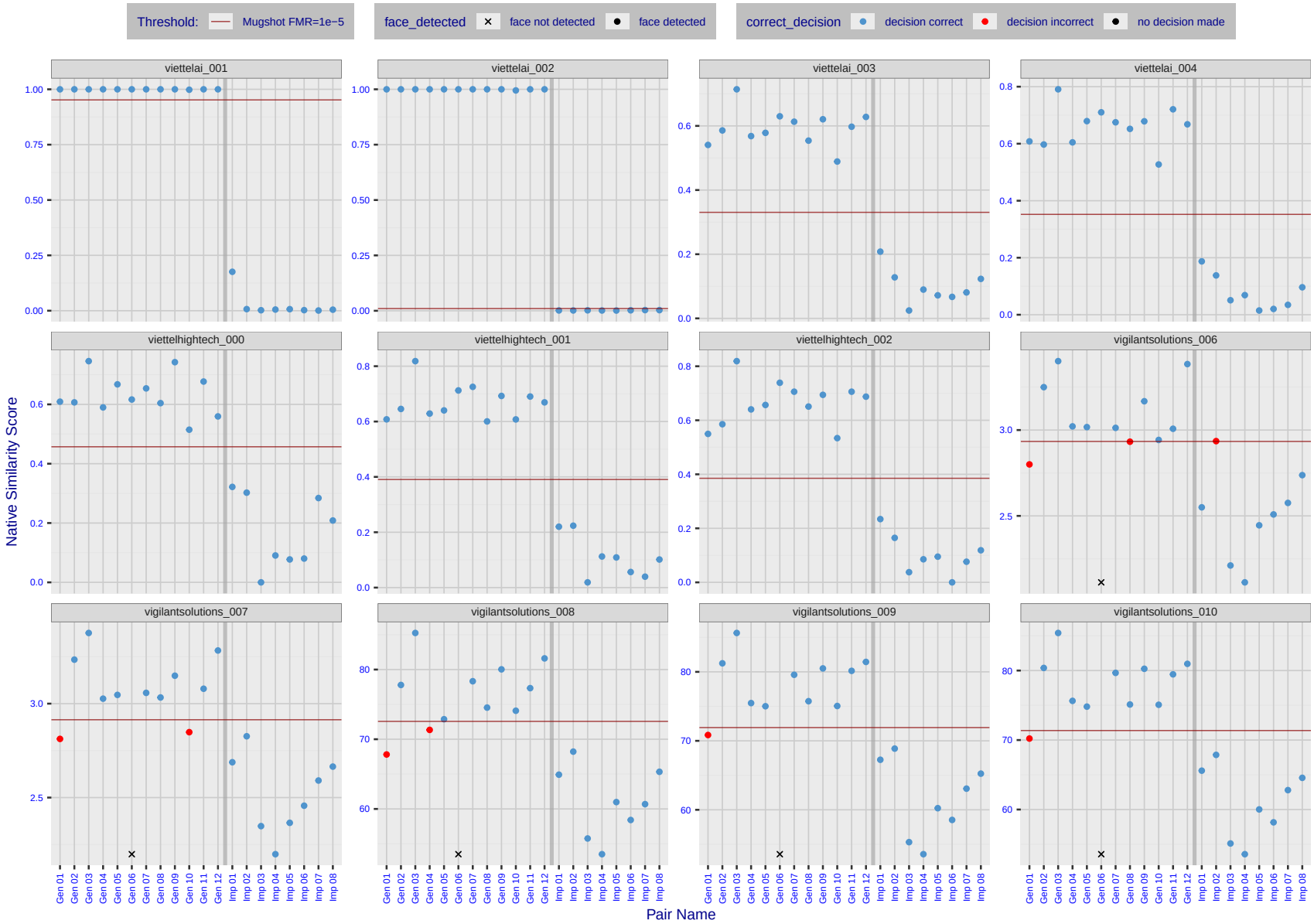

Figure 99: The figure shows algorithms' similarity scores for 12 genuine and 8 impostor image pairs used in a May 2018 paper by Phillips et al. ([1]). The threshold (red horizontal line) is a value calibrated to give FMR = 0.0001 on mugshot images. Points above the threshold correspond to pairs determined to be genuine, and points below the threshold correspond to pairs determined to be impostors. If the determined class (genuine or impostor) matches the real class, points will be blue; if not, red. An X represents face detection failure in either of the images in the pair. Note that the sample size (n=20) is small, and the figure may change substantially if larger or different sets are used. The images can be viewed on p. 13 of the Appendix, where Gen 01 corresponds to Same-Identity Pair 1, Gen 02 corresponds to Same-Identity Pair 2, and so on.

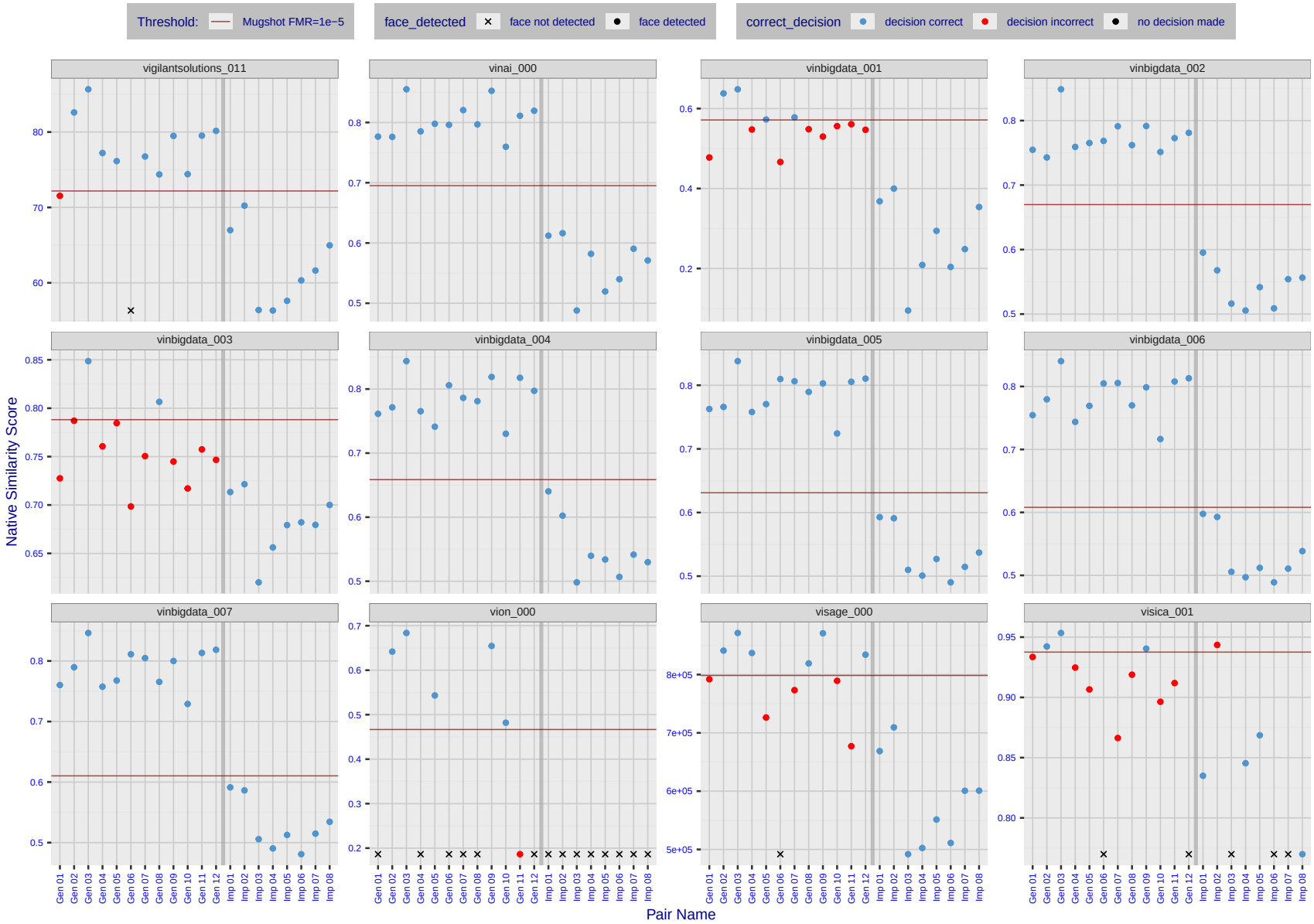

Figure 100: The figure shows algorithms' similarity scores for 12 genuine and 8 impostor image pairs used in a May 2018 paper by Phillips et al. ([1]). The threshold (red horizontal line) is a value calibrated to give FMR = 0.0001 on mugshot images. Points above the threshold correspond to pairs determined to be genuine, and points below the threshold correspond to pairs determined to be impostors. If the determined class (genuine or impostor) matches the real class, points will be blue; if not, red. An X represents face detection failure in either of the images in the pair. Note that the sample size (n=20) is small, and the figure may change substantially if larger or different sets are used. The images can be viewed on p. 13 of the Appendix, where Gen 01 corresponds to Same-Identity Pair 1, Gen 02 corresponds to Same-Identity Pair 2, and so on.

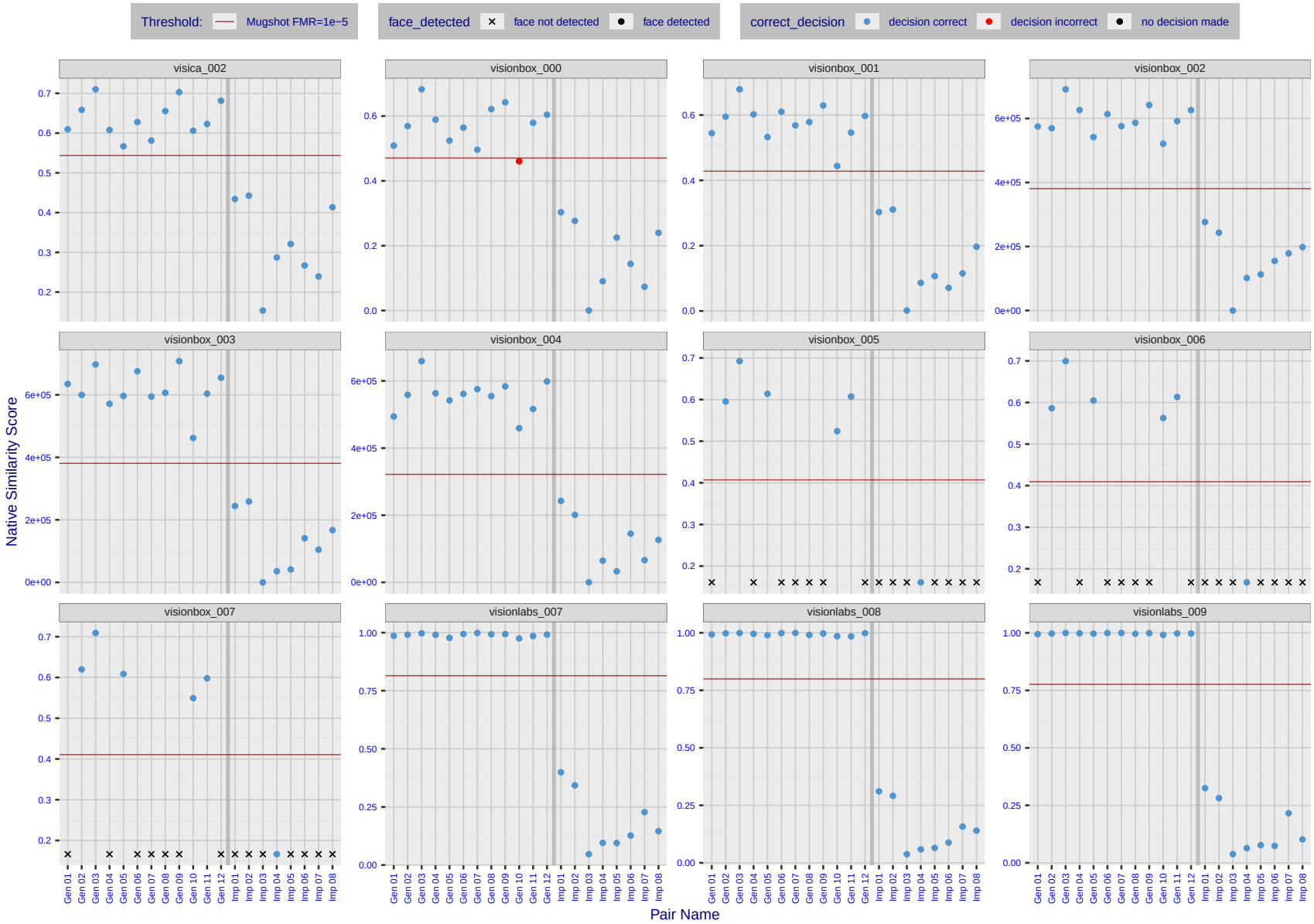

Figure 101: The figure shows algorithms' similarity scores for 12 genuine and 8 impostor image pairs used in a May 2018 paper by Phillips et al. ([1]). The threshold (red horizontal line) is a value calibrated to give FMR = 0.0001 on mugshot images. Points above the threshold correspond to pairs determined to be genuine, and points below the threshold correspond to pairs determined to be impostors. If the determined class (genuine or impostor) matches the real class, points will be blue; if not, red. An X represents face detection failure in either of the images in the pair. Note that the sample size (n=20) is small, and the figure may change substantially if larger or different sets are used. The images can be viewed on p. 13 of the Appendix, where Gen 01 corresponds to Same-Identity Pair 1, Gen 02 corresponds to Same-Identity Pair 2, and so on.

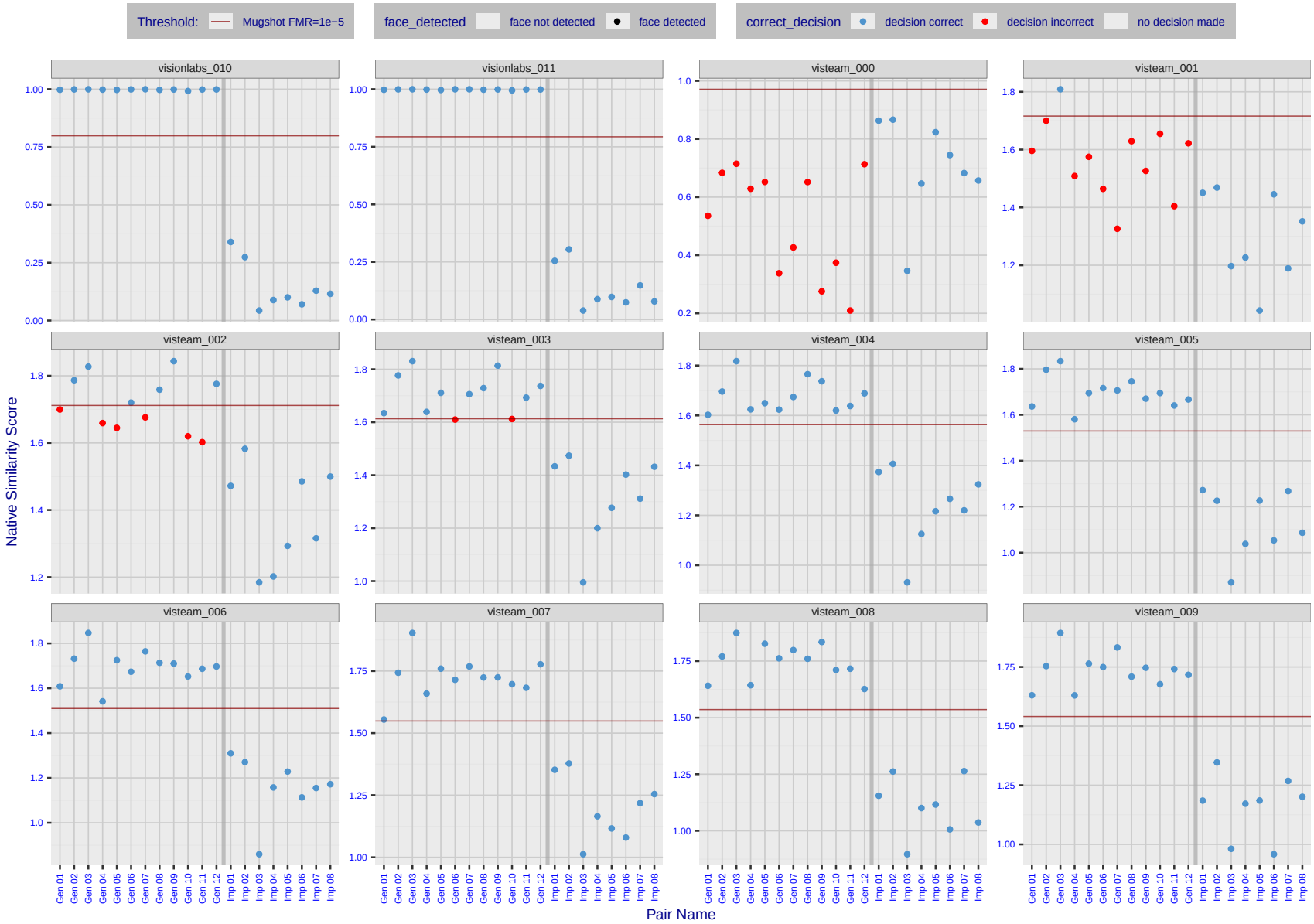

Figure 102: The figure shows algorithms' similarity scores for 12 genuine and 8 impostor image pairs used in a May 2018 paper by Phillips et al. ([1]). The threshold (red horizontal line) is a value calibrated to give FMR = 0.0001 on mugshot images. Points above the threshold correspond to pairs determined to be genuine, and points below the threshold correspond to pairs determined to be impostors. If the determined class (genuine or impostor) matches the real class, points will be blue; if not, red. An X represents face detection failure in either of the images in the pair. Note that the sample size (n=20) is small, and the figure may change substantially if larger or different sets are used. The images can be viewed on p. 13 of the Appendix, where Gen 01 corresponds to Same-Identity Pair 1, Gen 02 corresponds to Same-Identity Pair 2, and so on.

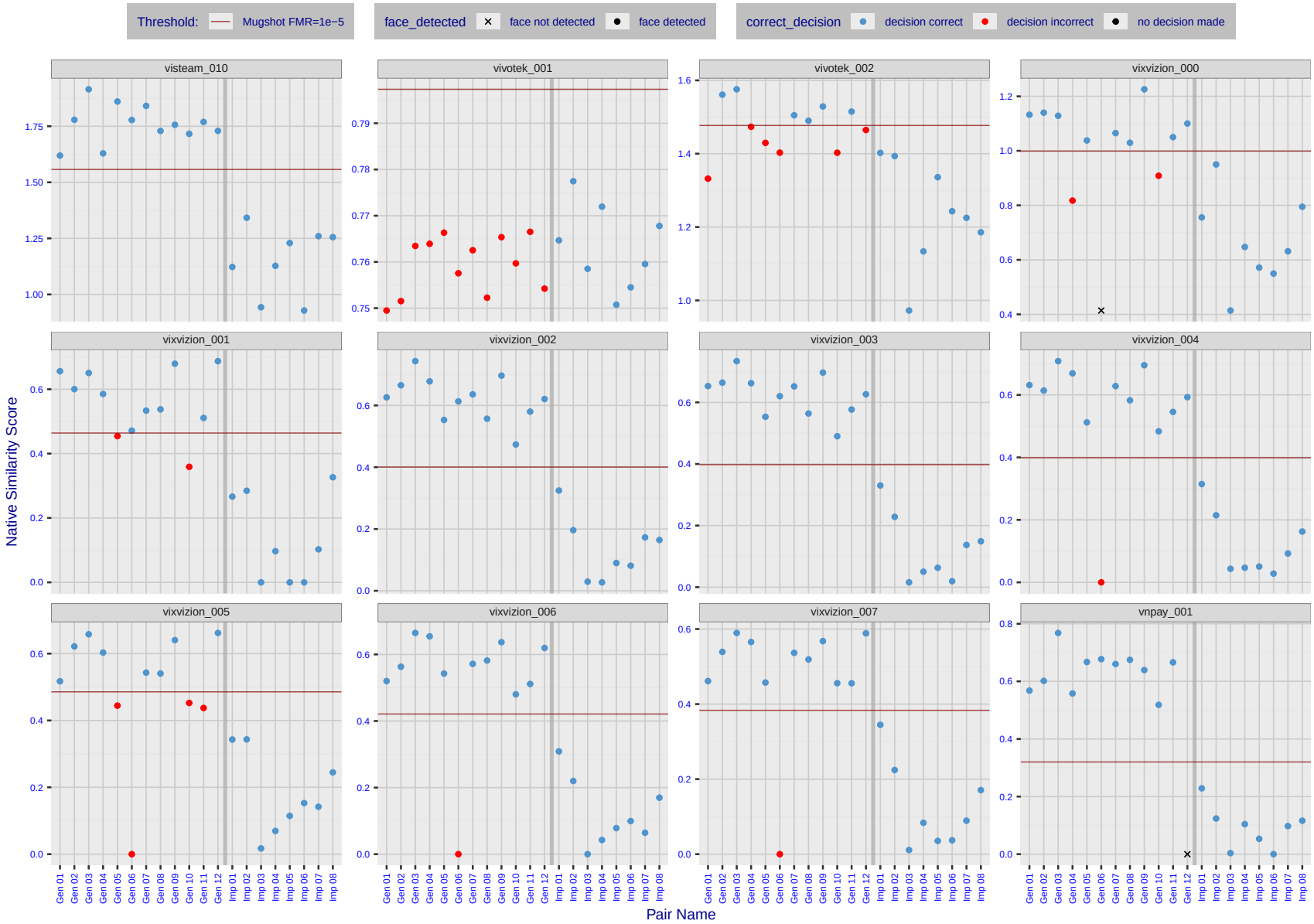

Figure 103: The figure shows algorithms' similarity scores for 12 genuine and 8 impostor image pairs used in a May 2018 paper by Phillips et al. ([1]). The threshold (red horizontal line) is a value calibrated to give FMR = 0.0001 on mugshot images. Points above the threshold correspond to pairs determined to be genuine, and points below the threshold correspond to pairs determined to be impostors. If the determined class (genuine or impostor) matches the real class, points will be blue; if not, red. An X represents face detection failure in either of the images in the pair. Note that the sample size (n=20) is small, and the figure may change substantially if larger or different sets are used. The images can be viewed on p. 13 of the Appendix, where Gen 01 corresponds to Same-Identity Pair 1, Gen 02 corresponds to Same-Identity Pair 2, and so on.

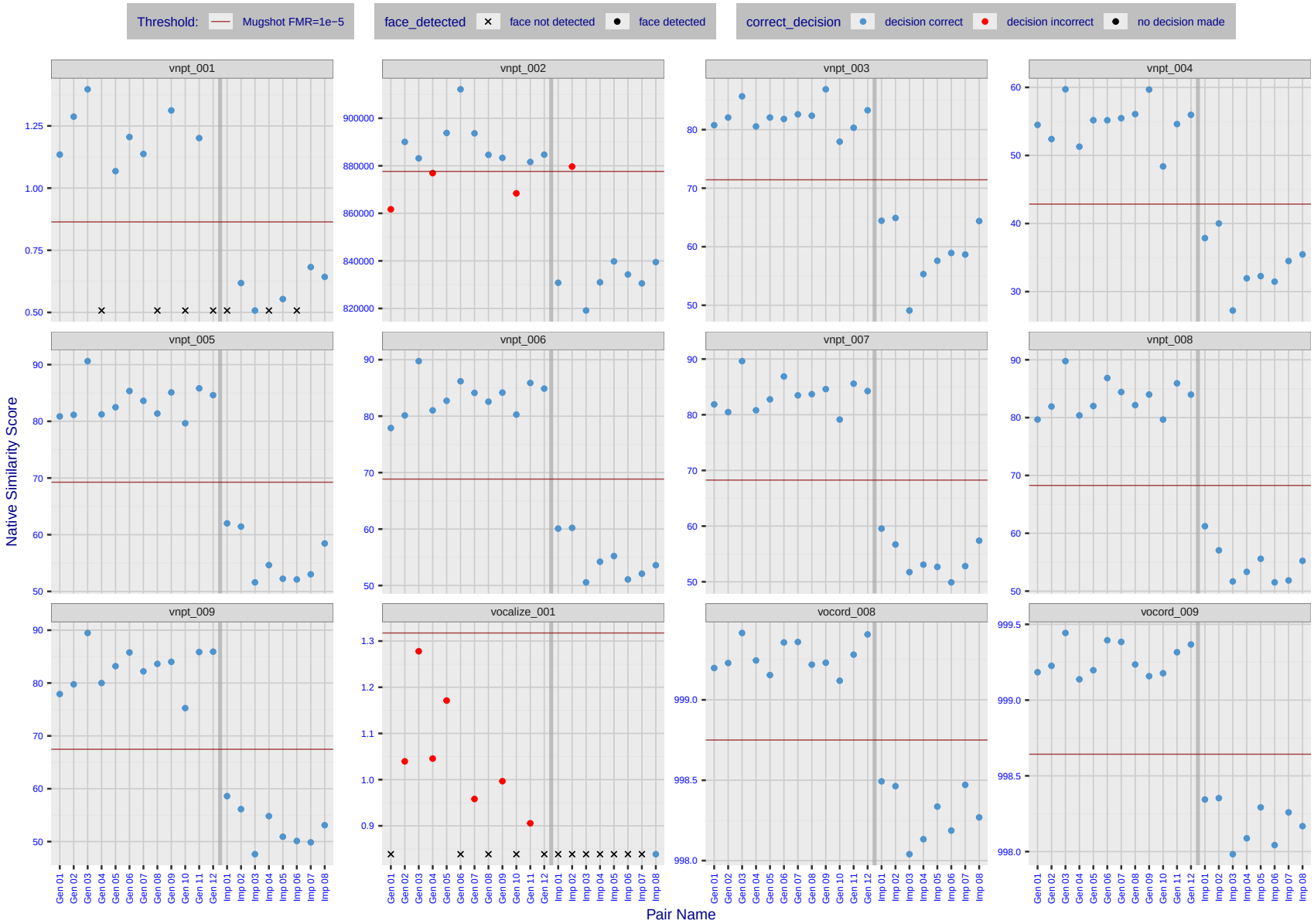

Figure 104: The figure shows algorithms' similarity scores for 12 genuine and 8 impostor image pairs used in a May 2018 paper by Phillips et al. ([1]). The threshold (red horizontal line) is a value calibrated to give FMR = 0.0001 on mugshot images. Points above the threshold correspond to pairs determined to be genuine, and points below the threshold correspond to pairs determined to be impostors. If the determined class (genuine or impostor) matches the real class, points will be blue; if not, red. An X represents face detection failure in either of the images in the pair. Note that the sample size (n=20) is small, and the figure may change substantially if larger or different sets are used. The images can be viewed on p. 13 of the Appendix, where Gen 01 corresponds to Same-Identity Pair 1, Gen 02 corresponds to Same-Identity Pair 2, and so on.

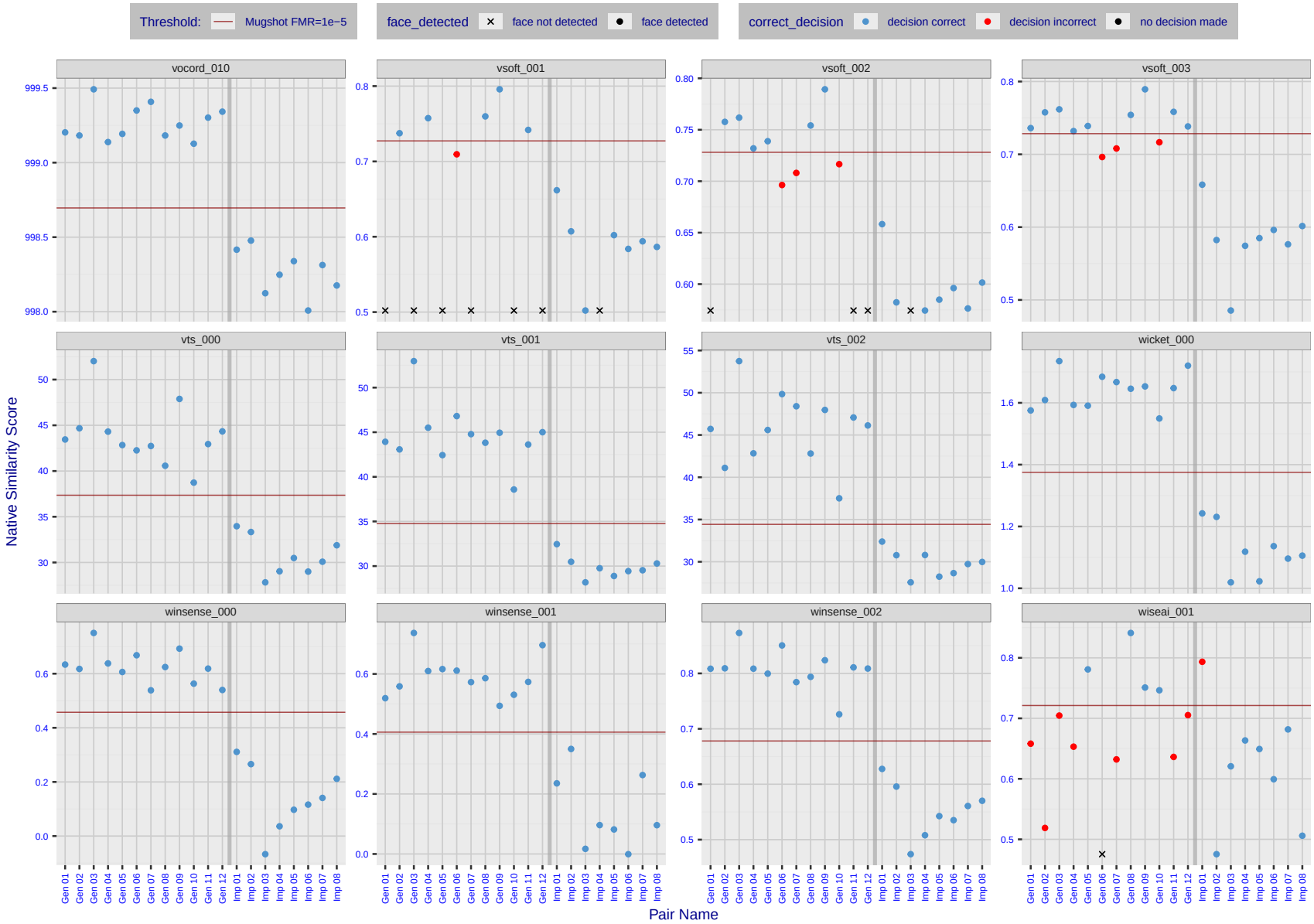

Figure 105: The figure shows algorithms' similarity scores for 12 genuine and 8 impostor image pairs used in a May 2018 paper by Phillips et al. ([1]). The threshold (red horizontal line) is a value calibrated to give FMR = 0.0001 on mugshot images. Points above the threshold correspond to pairs determined to be genuine, and points below the threshold correspond to pairs determined to be impostors. If the determined class (genuine or impostor) matches the real class, points will be blue; if not, red. An X represents face detection failure in either of the images in the pair. Note that the sample size (n=20) is small, and the figure may change substantially if larger or different sets are used. The images can be viewed on p. 13 of the Appendix, where Gen 01 corresponds to Same-Identity Pair 1, Gen 02 corresponds to Same-Identity Pair 2, and so on.

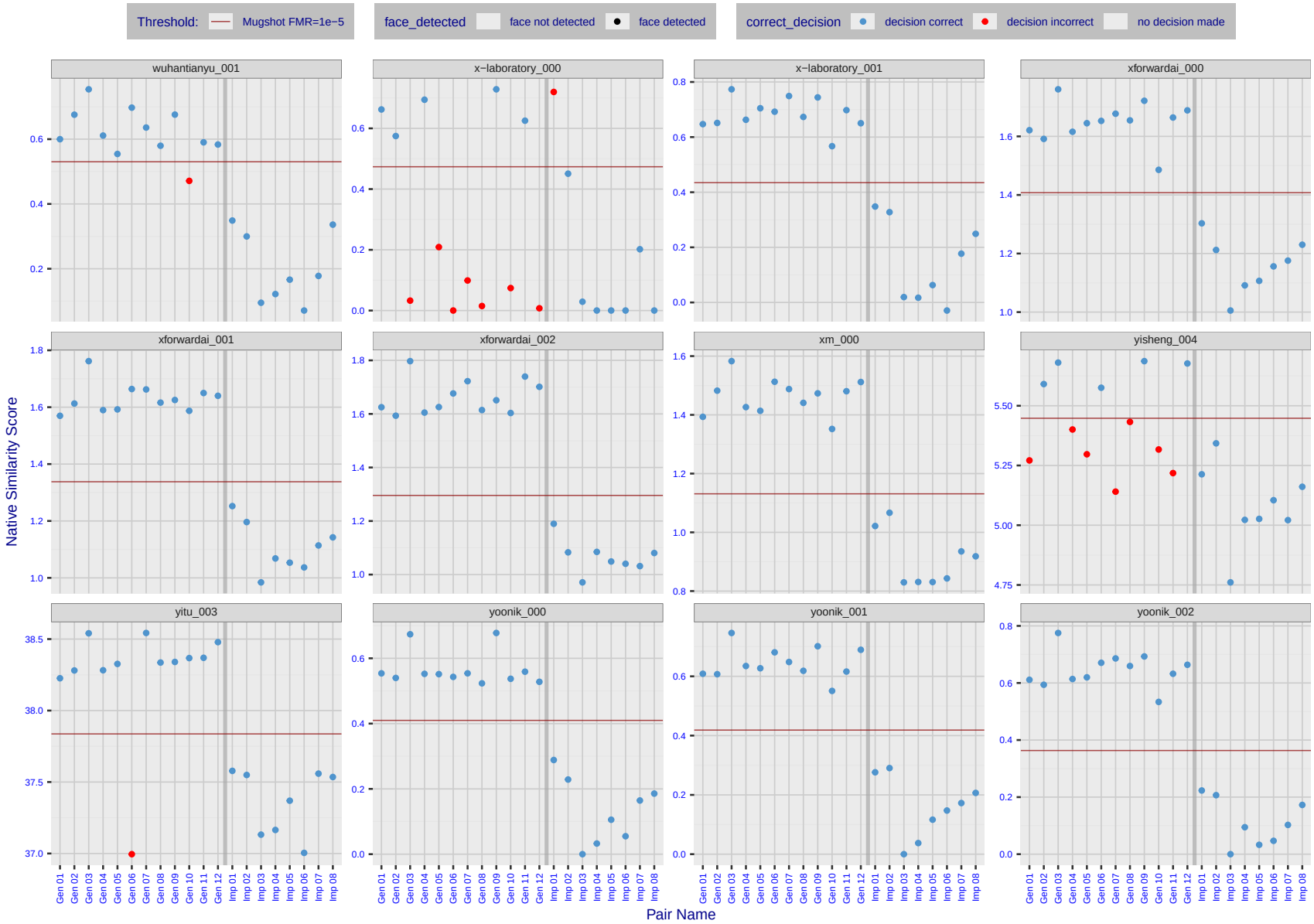

Figure 106: The figure shows algorithms' similarity scores for 12 genuine and 8 impostor image pairs used in a May 2018 paper by Phillips et al. ([1]). The threshold (red horizontal line) is a value calibrated to give FMR = 0.0001 on mugshot images. Points above the threshold correspond to pairs determined to be genuine, and points below the threshold correspond to pairs determined to be impostors. If the determined class (genuine or impostor) matches the real class, points will be blue; if not, red. An X represents face detection failure in either of the images in the pair. Note that the sample size (n=20) is small, and the figure may change substantially if larger or different sets are used. The images can be viewed on p. 13 of the Appendix, where Gen 01 corresponds to Same-Identity Pair 1, Gen 02 corresponds to Same-Identity Pair 2, and so on.

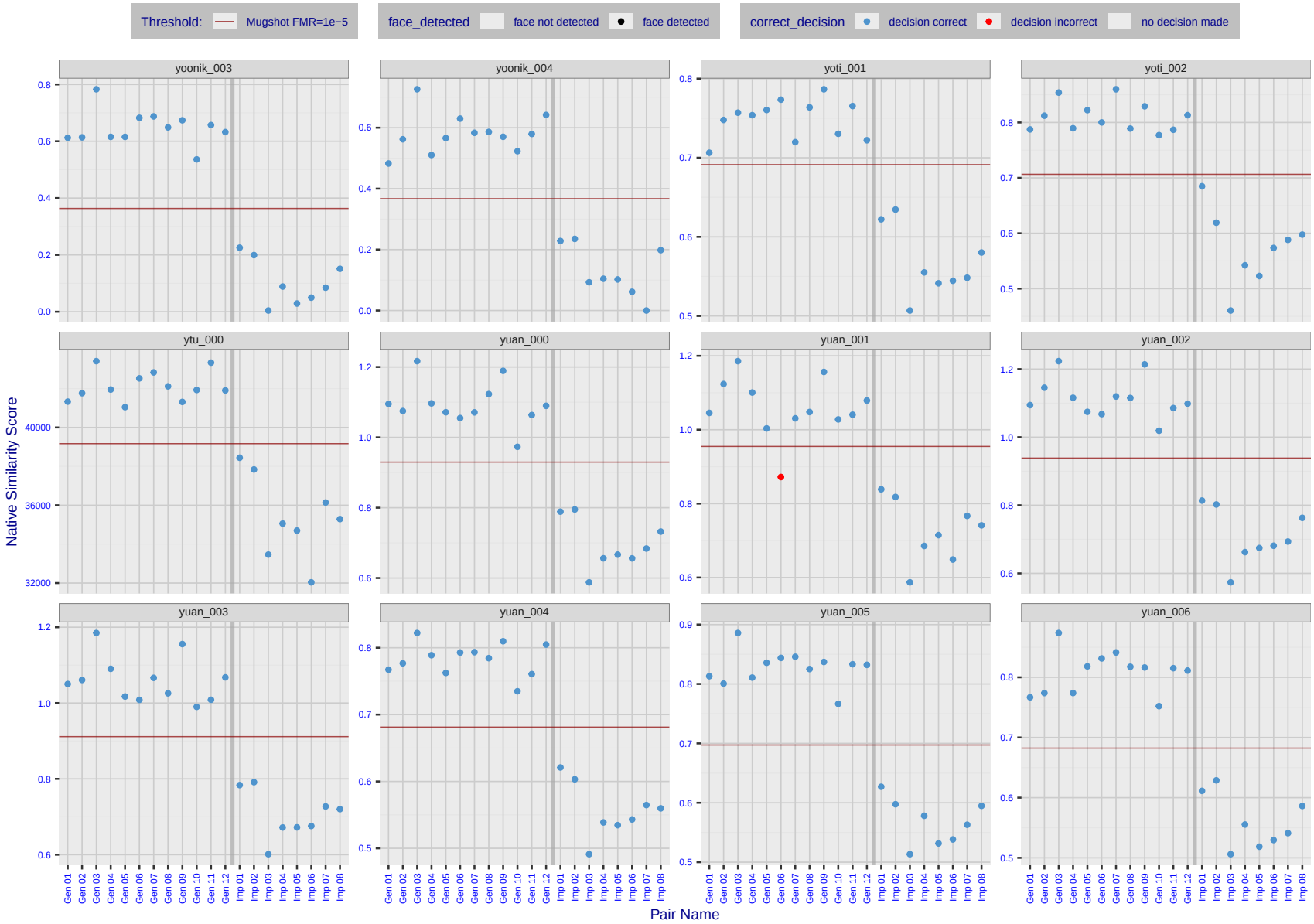

Figure 107: The figure shows algorithms' similarity scores for 12 genuine and 8 impostor image pairs used in a May 2018 paper by Phillips et al. ([1]). The threshold (red horizontal line) is a value calibrated to give FMR = 0.0001 on mugshot images. Points above the threshold correspond to pairs determined to be genuine, and points below the threshold correspond to pairs determined to be impostors. If the determined class (genuine or impostor) matches the real class, points will be blue; if not, red. An X represents face detection failure in either of the images in the pair. Note that the sample size (n=20) is small, and the figure may change substantially if larger or different sets are used. The images can be viewed on p. 13 of the Appendix, where Gen 01 corresponds to Same-Identity Pair 1, Gen 02 corresponds to Same-Identity Pair 2, and so on.

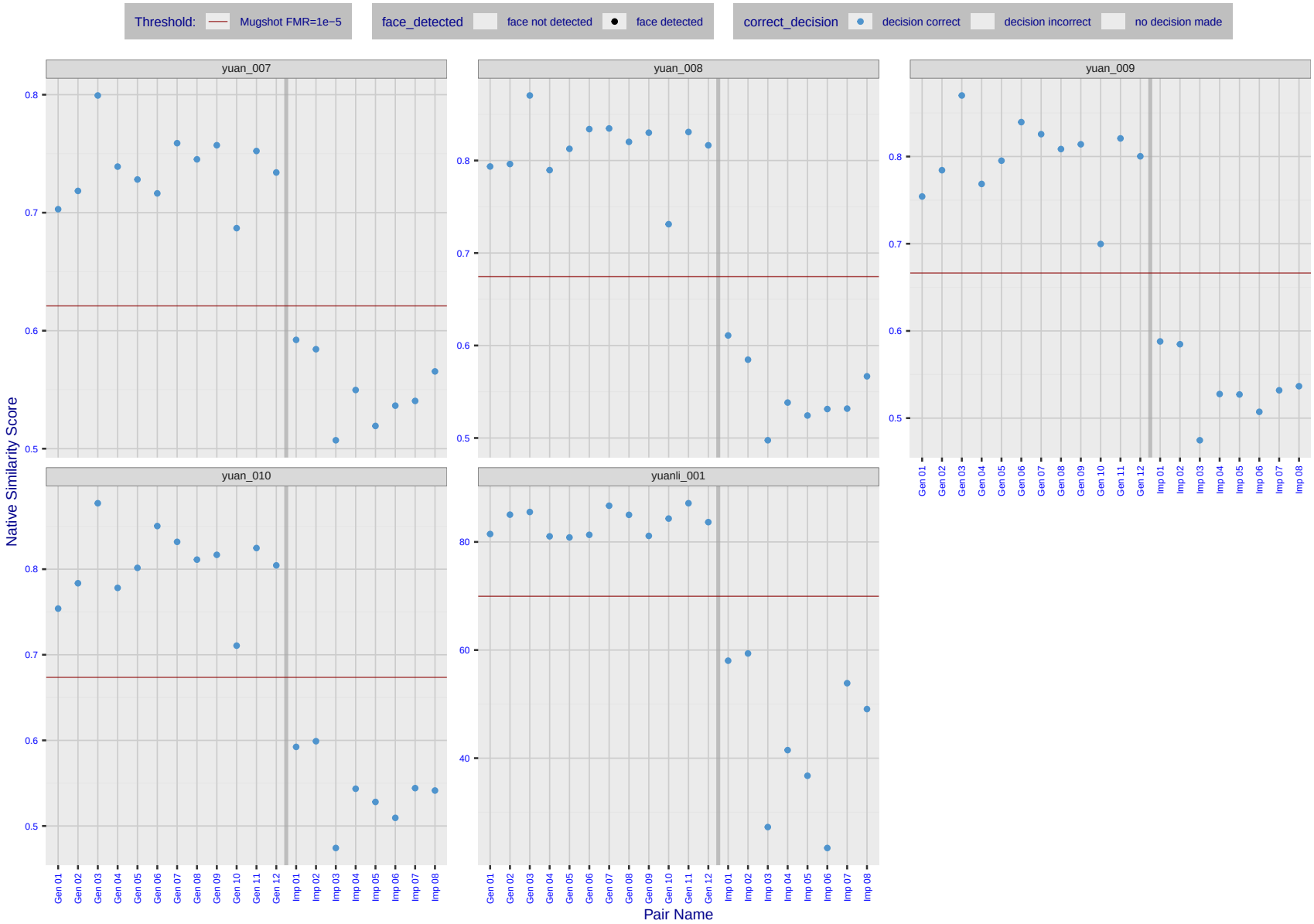

Figure 108: The figure shows algorithms' similarity scores for 12 genuine and 8 impostor image pairs used in a May 2018 paper by Phillips et al. ([1]). The threshold (red horizontal line) is a value calibrated to give FMR = 0.0001 on mugshot images. Points above the threshold correspond to pairs determined to be genuine, and points below the threshold correspond to pairs determined to be impostors. If the determined class (genuine or impostor) matches the real class, points will be blue; if not, red. An X represents face detection failure in either of the images in the pair. Note that the sample size (n=20) is small, and the figure may change substantially if larger or different sets are used. The images can be viewed on p. 13 of the Appendix, where Gen 01 corresponds to Same-Identity Pair 1, Gen 02 corresponds to Same-Identity Pair 2, and so on.

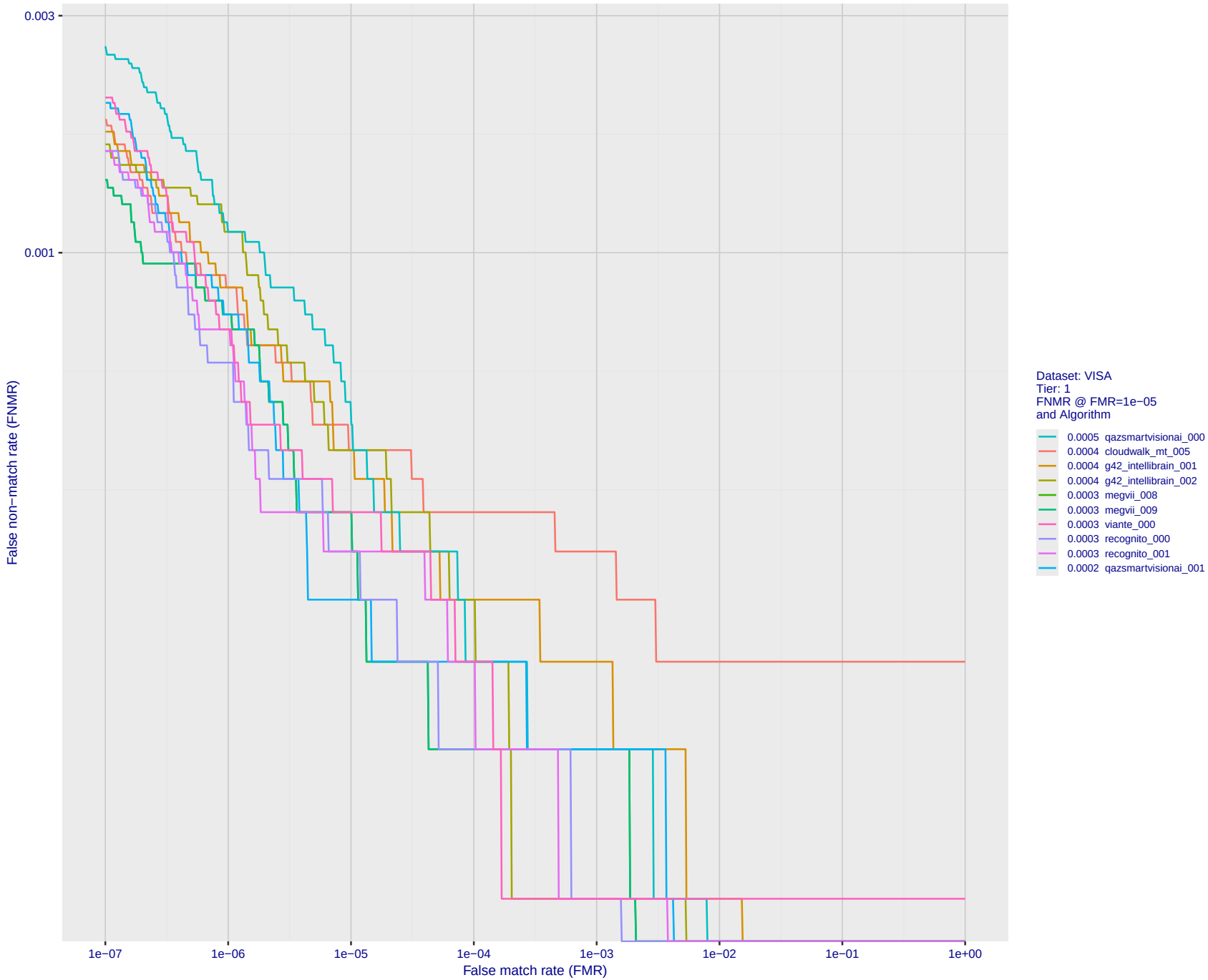

Figure 109: For the visa images, detection error tradeoff (DET) characteristics showing false non-match rate vs. false match rate plotted parametrically on threshold, T. The scales are logarithmic in order to show many decades of FMR.

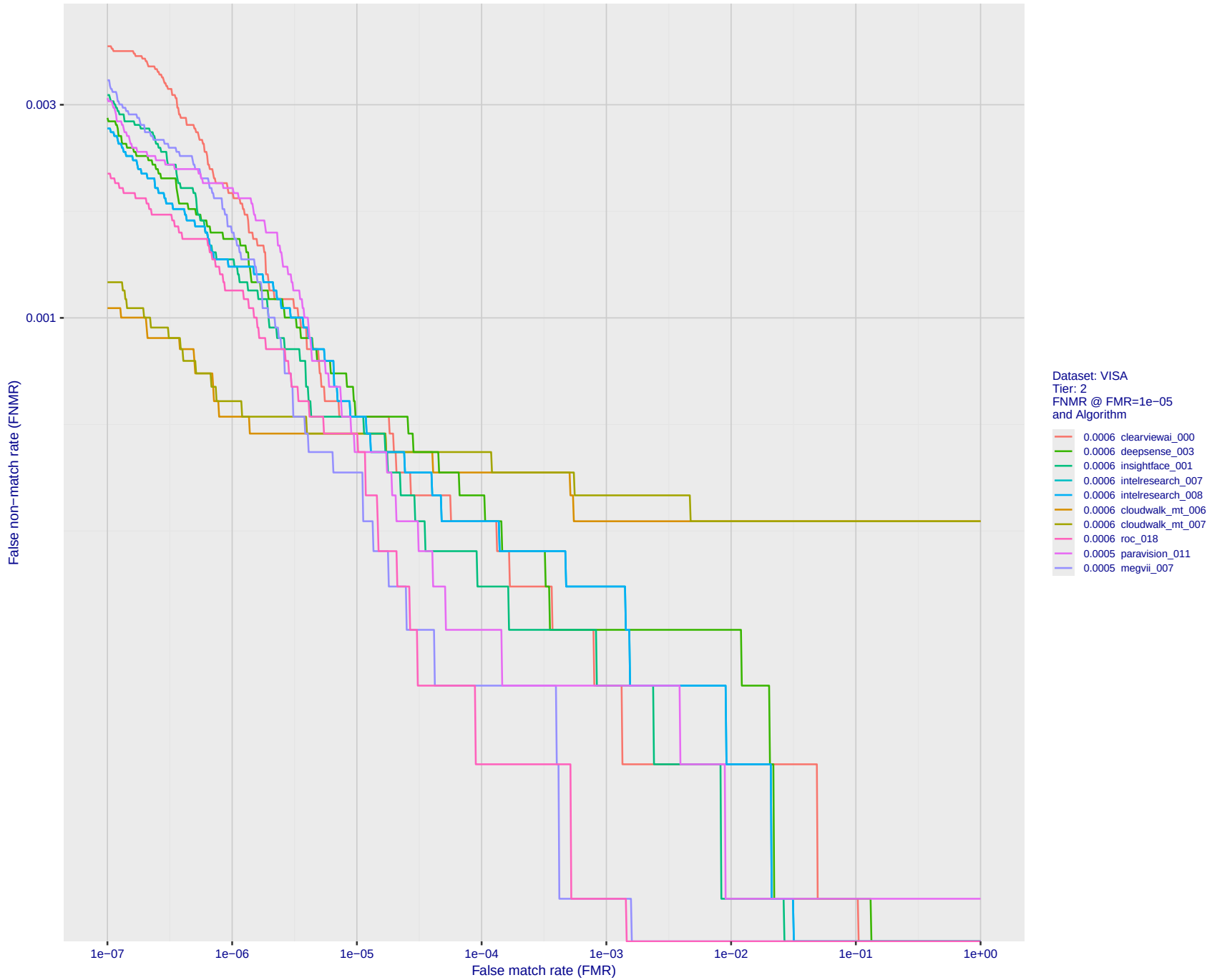

Figure 110: For the visa images, detection error tradeoff (DET) characteristics showing false non-match rate vs. false match rate plotted parametrically on threshold, T. The scales are logarithmic in order to show many decades of FMR.

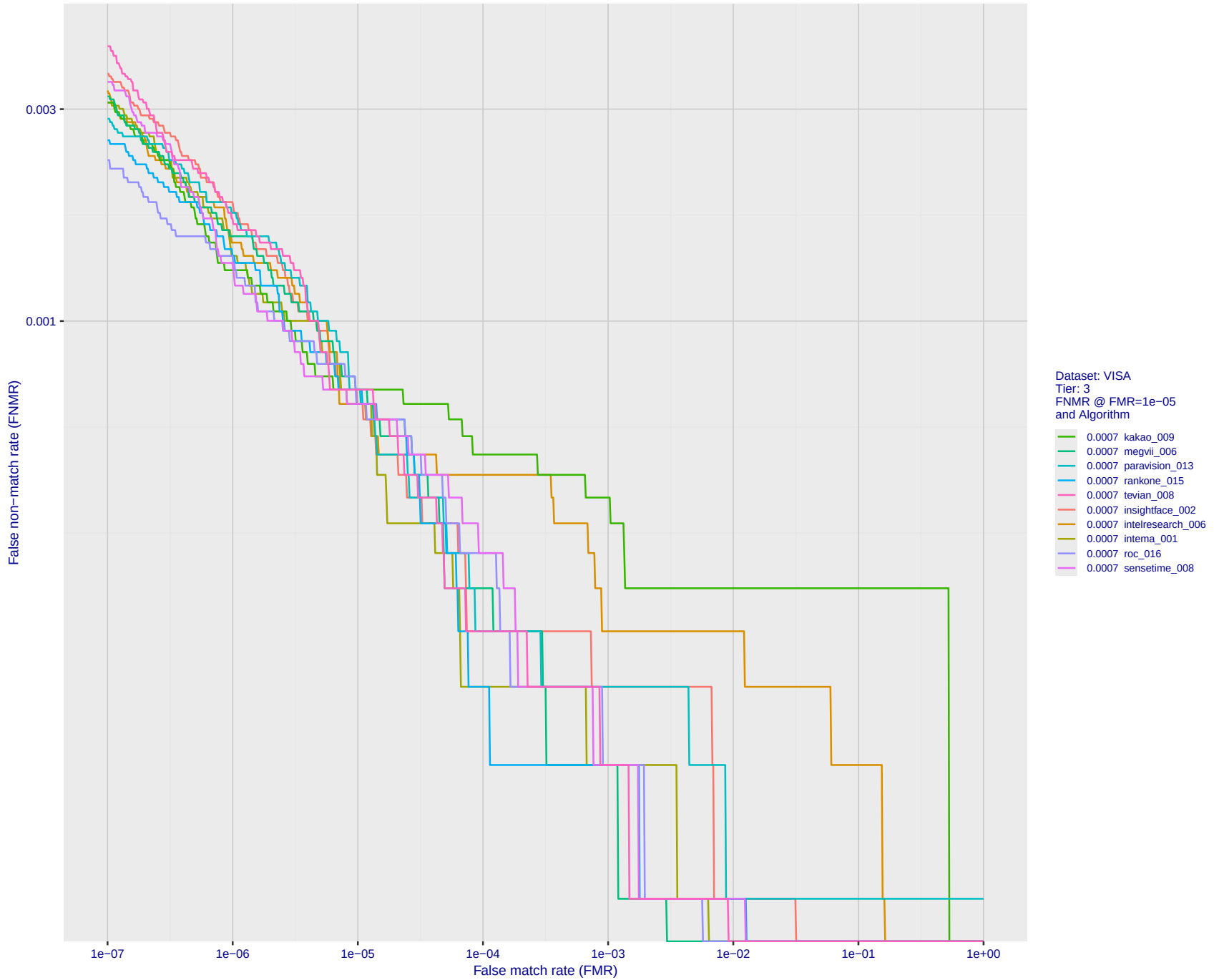

Figure 111: For the visa images, detection error tradeoff (DET) characteristics showing false non-match rate vs. false match rate plotted parametrically on threshold, T. The scales are logarithmic in order to show many decades of FMR.

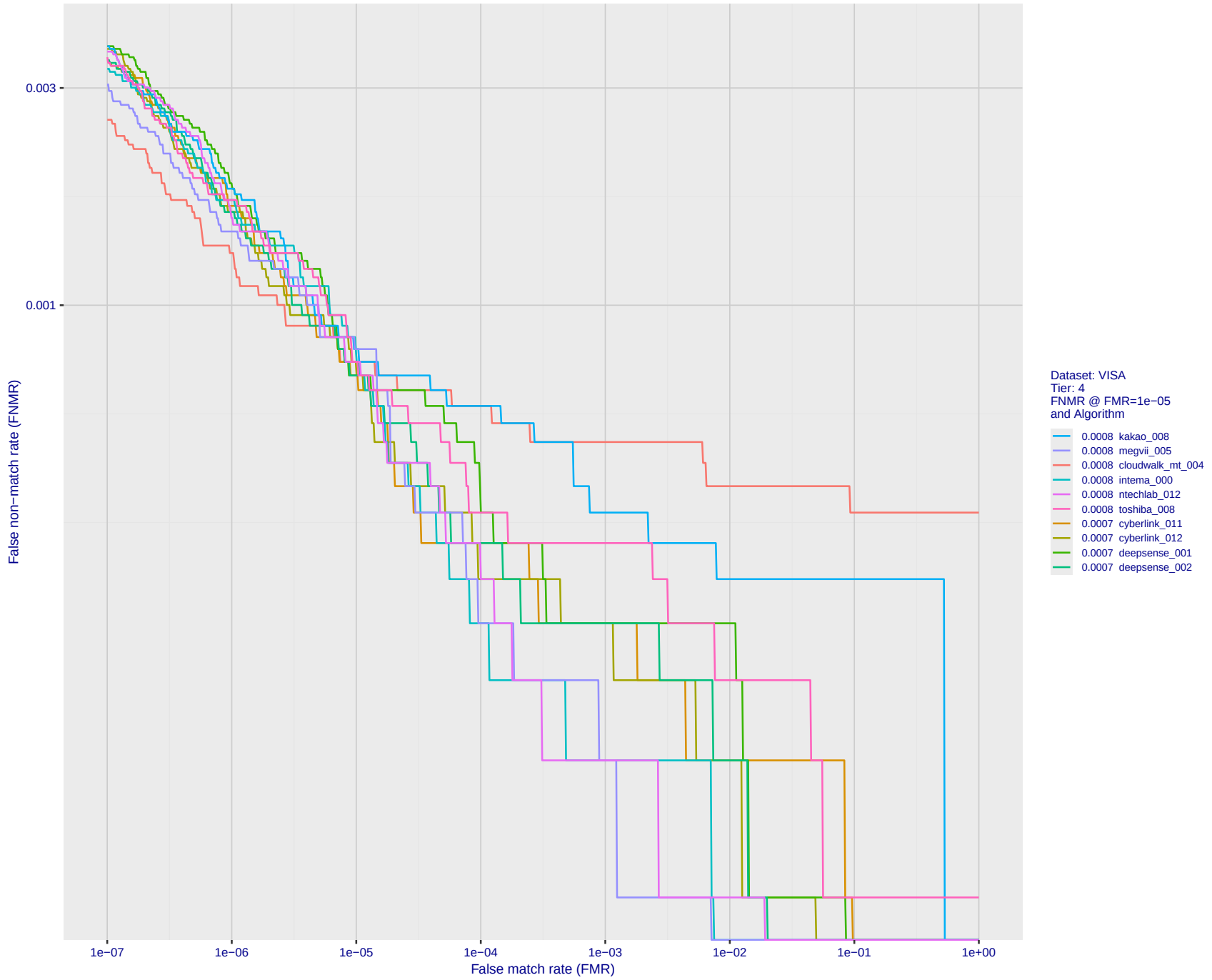

Figure 112: For the visa images, detection error tradeoff (DET) characteristics showing false non-match rate vs. false match rate plotted parametrically on threshold, T. The scales are logarithmic in order to show many decades of FMR.

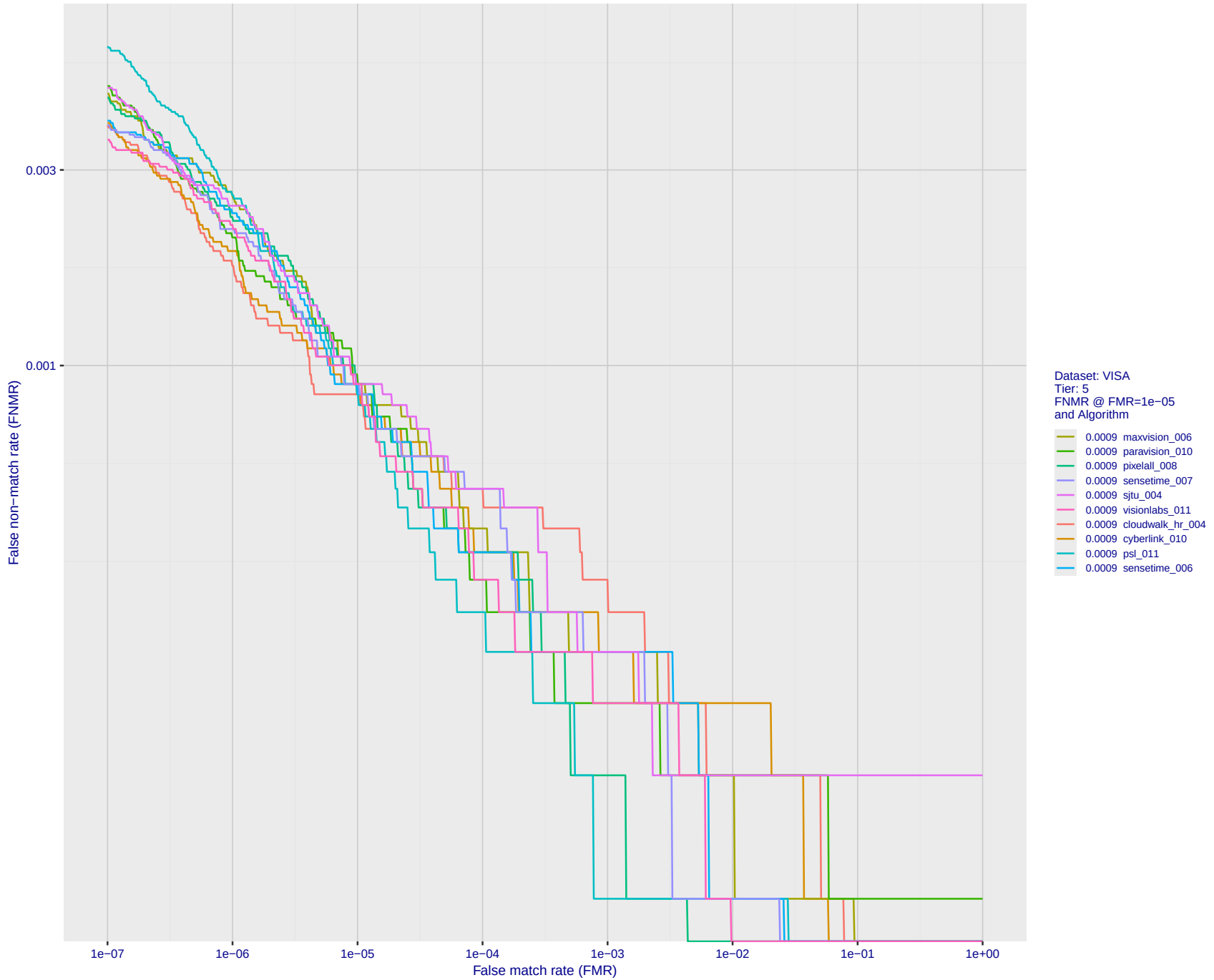

Figure 113: For the visa images, detection error tradeoff (DET) characteristics showing false non-match rate vs. false match rate plotted parametrically on threshold, T. The scales are logarithmic in order to show many decades of FMR.

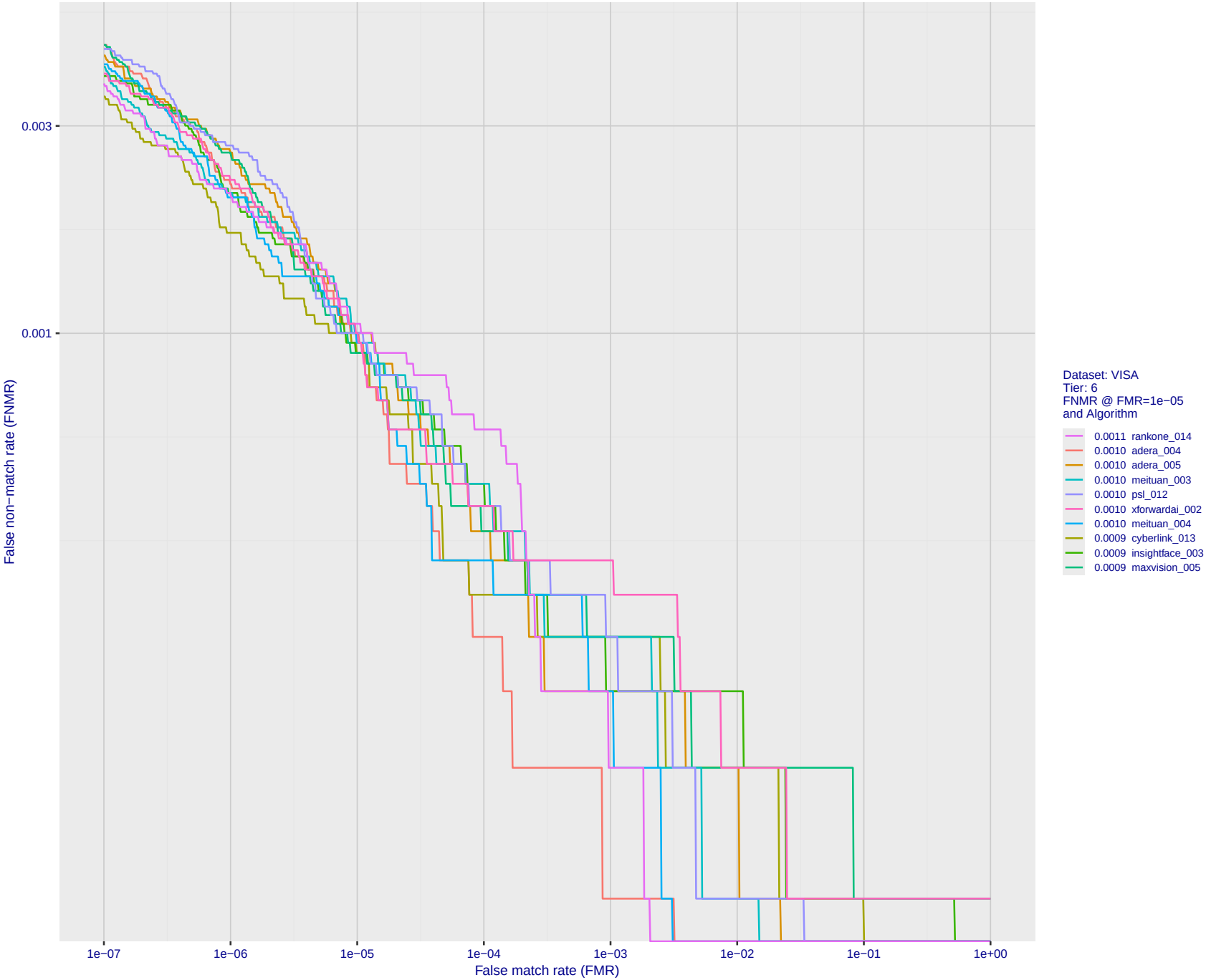

Figure 114: For the visa images, detection error tradeoff (DET) characteristics showing false non-match rate vs. false match rate plotted parametrically on threshold, T. The scales are logarithmic in order to show many decades of FMR.

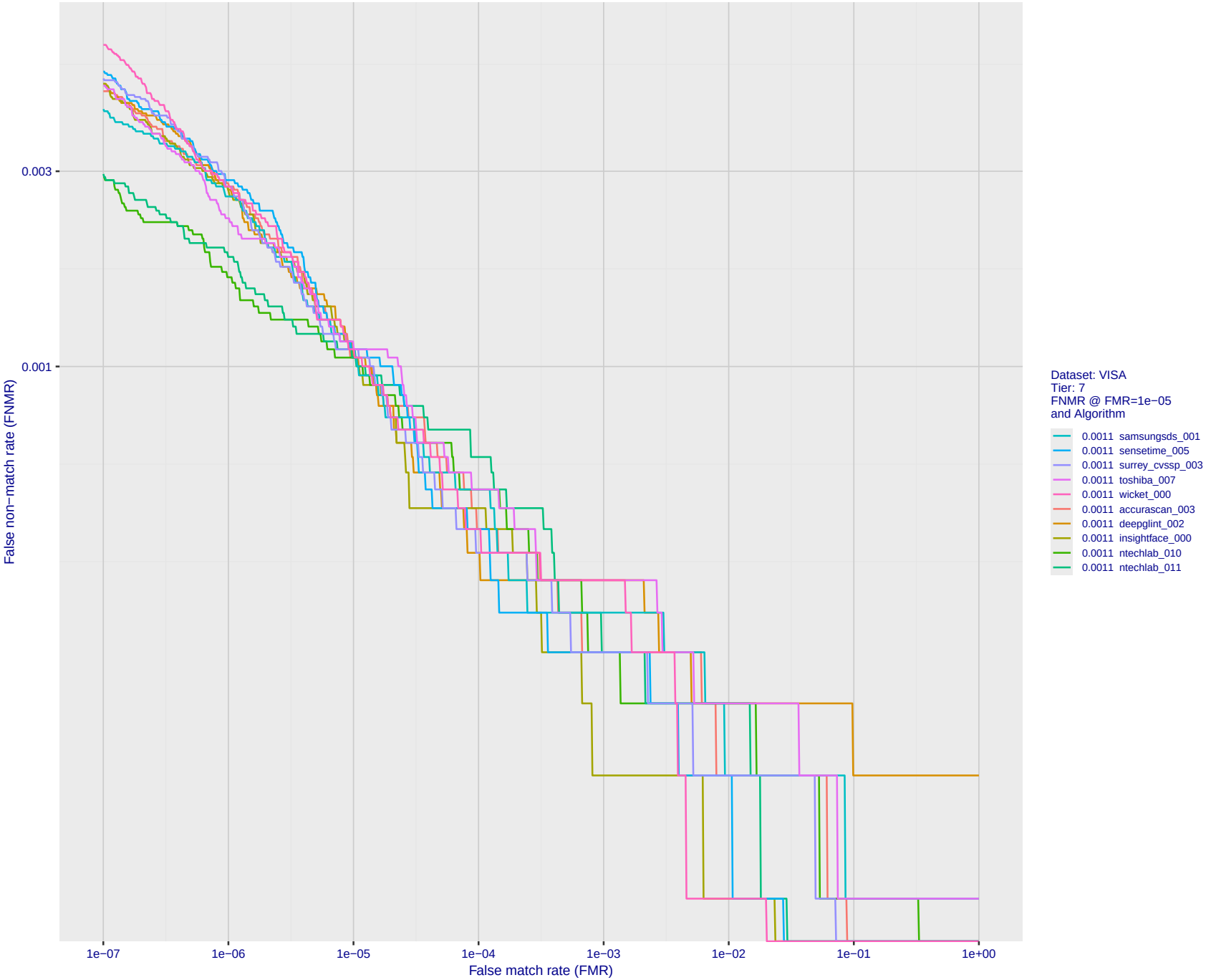

Figure 115: For the visa images, detection error tradeoff (DET) characteristics showing false non-match rate vs. false match rate plotted parametrically on threshold, T. The scales are logarithmic in order to show many decades of FMR.

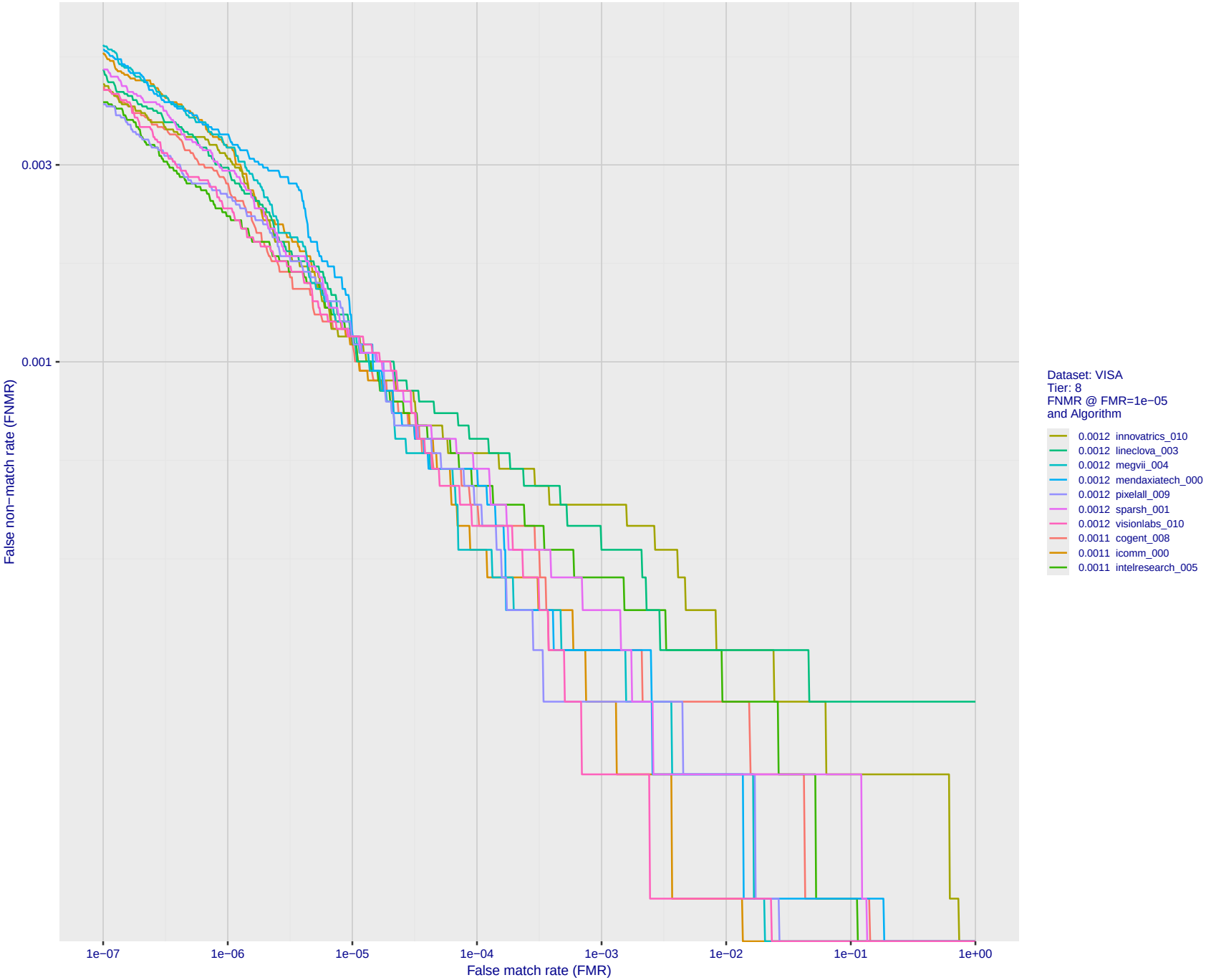

Figure 116: For the visa images, detection error tradeoff (DET) characteristics showing false non-match rate vs. false match rate plotted parametrically on threshold, T. The scales are logarithmic in order to show many decades of FMR.

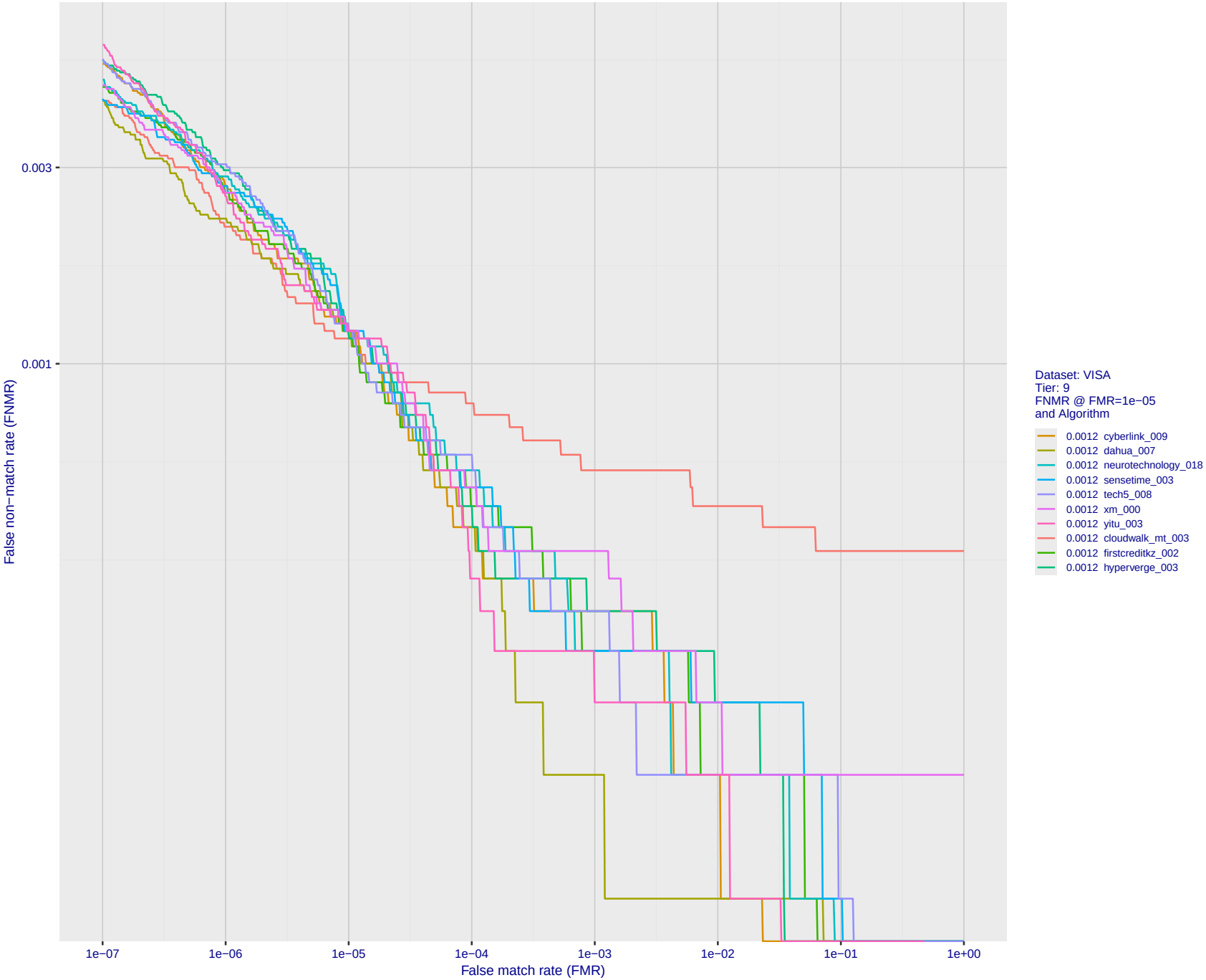

Figure 117: For the visa images, detection error tradeoff (DET) characteristics showing false non-match rate vs. false match rate plotted parametrically on threshold, T. The scales are logarithmic in order to show many decades of FMR.

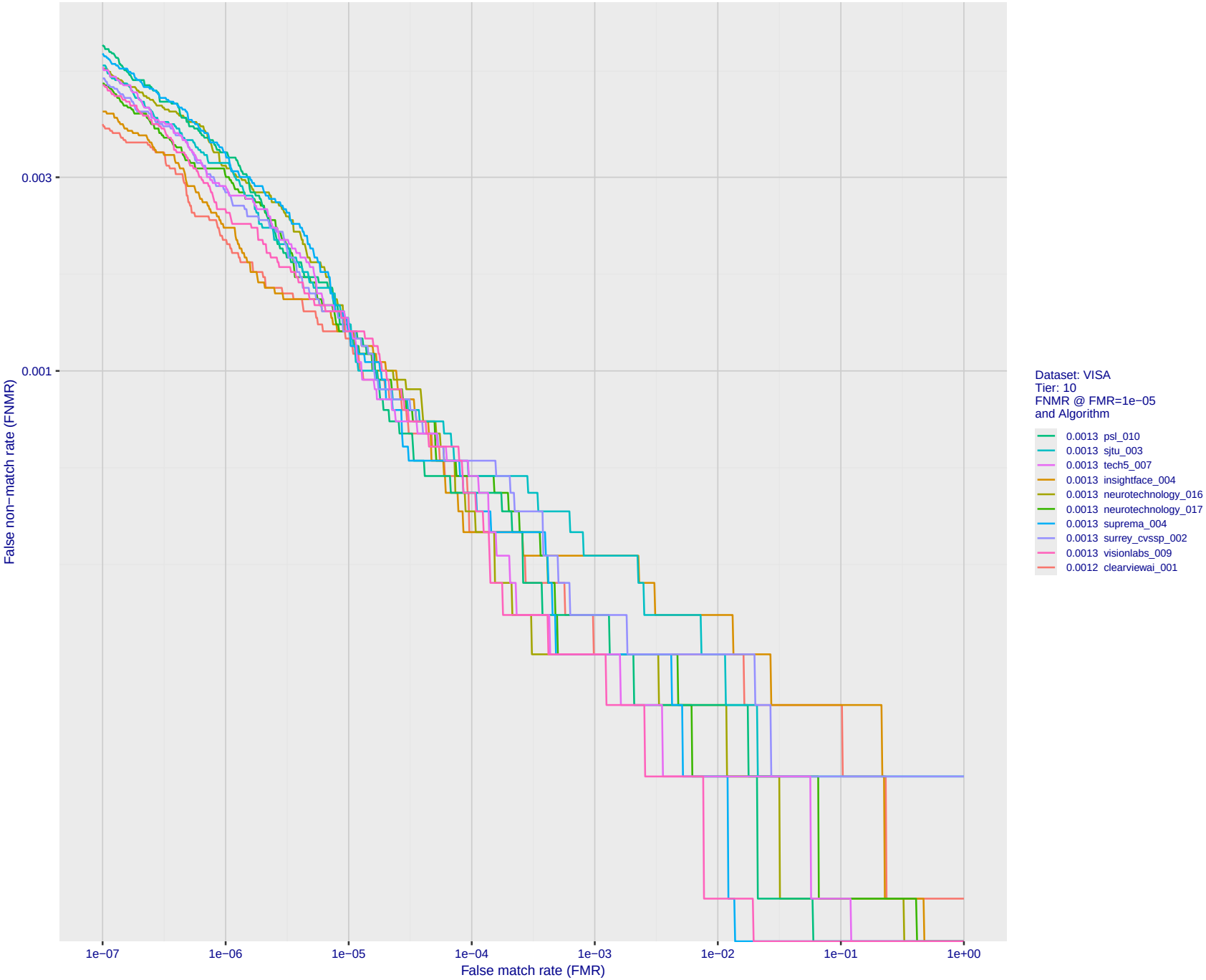

Figure 118: For the visa images, detection error tradeoff (DET) characteristics showing false non-match rate vs. false match rate plotted parametrically on threshold, T. The scales are logarithmic in order to show many decades of FMR.

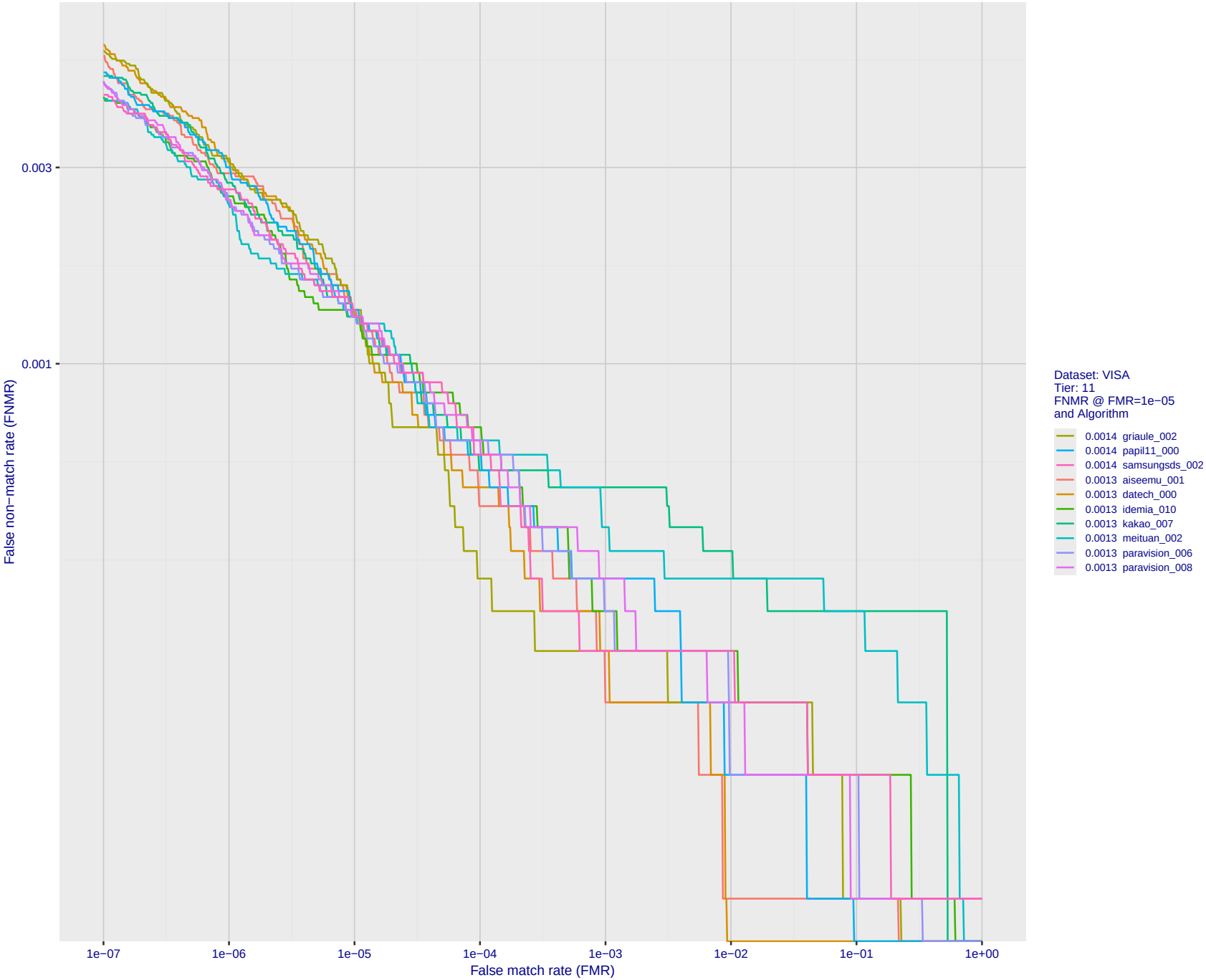

Figure 119: For the visa images, detection error tradeoff (DET) characteristics showing false non-match rate vs. false match rate plotted parametrically on threshold, T. The scales are logarithmic in order to show many decades of FMR.

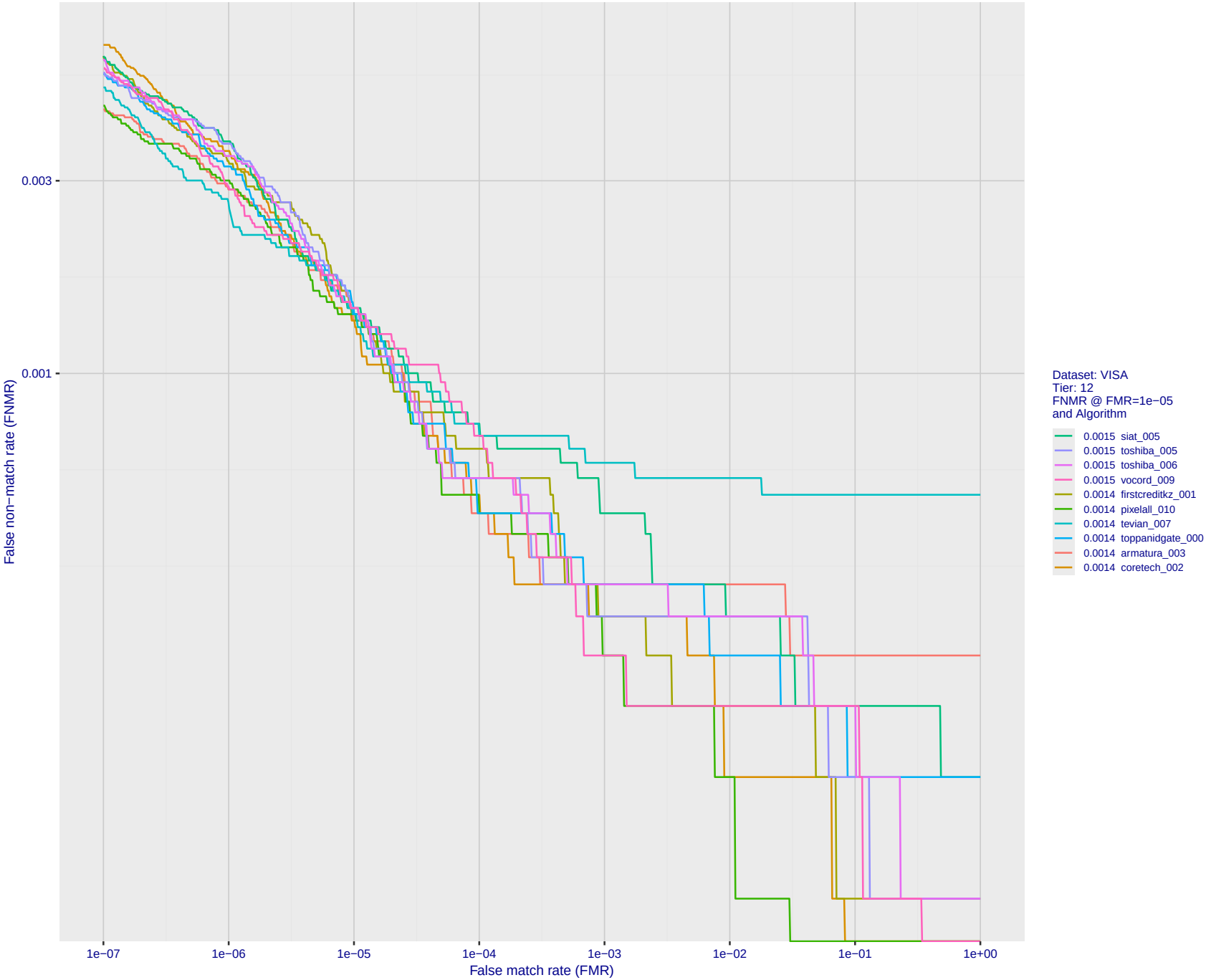

Figure 120: For the visa images, detection error tradeoff (DET) characteristics showing false non-match rate vs. false match rate plotted parametrically on threshold, T. The scales are logarithmic in order to show many decades of FMR.

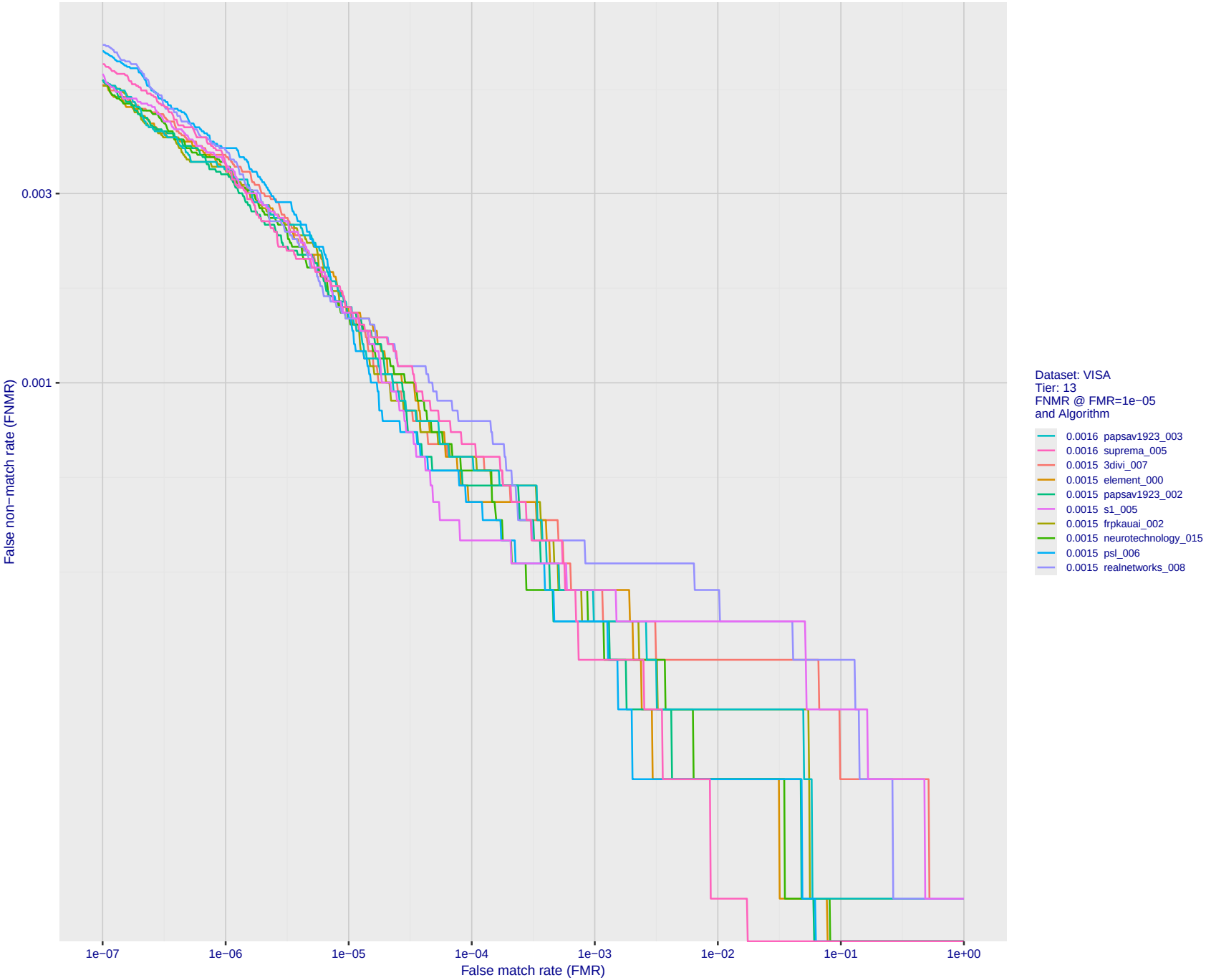

Figure 121: For the visa images, detection error tradeoff (DET) characteristics showing false non-match rate vs. false match rate plotted parametrically on threshold, T. The scales are logarithmic in order to show many decades of FMR.

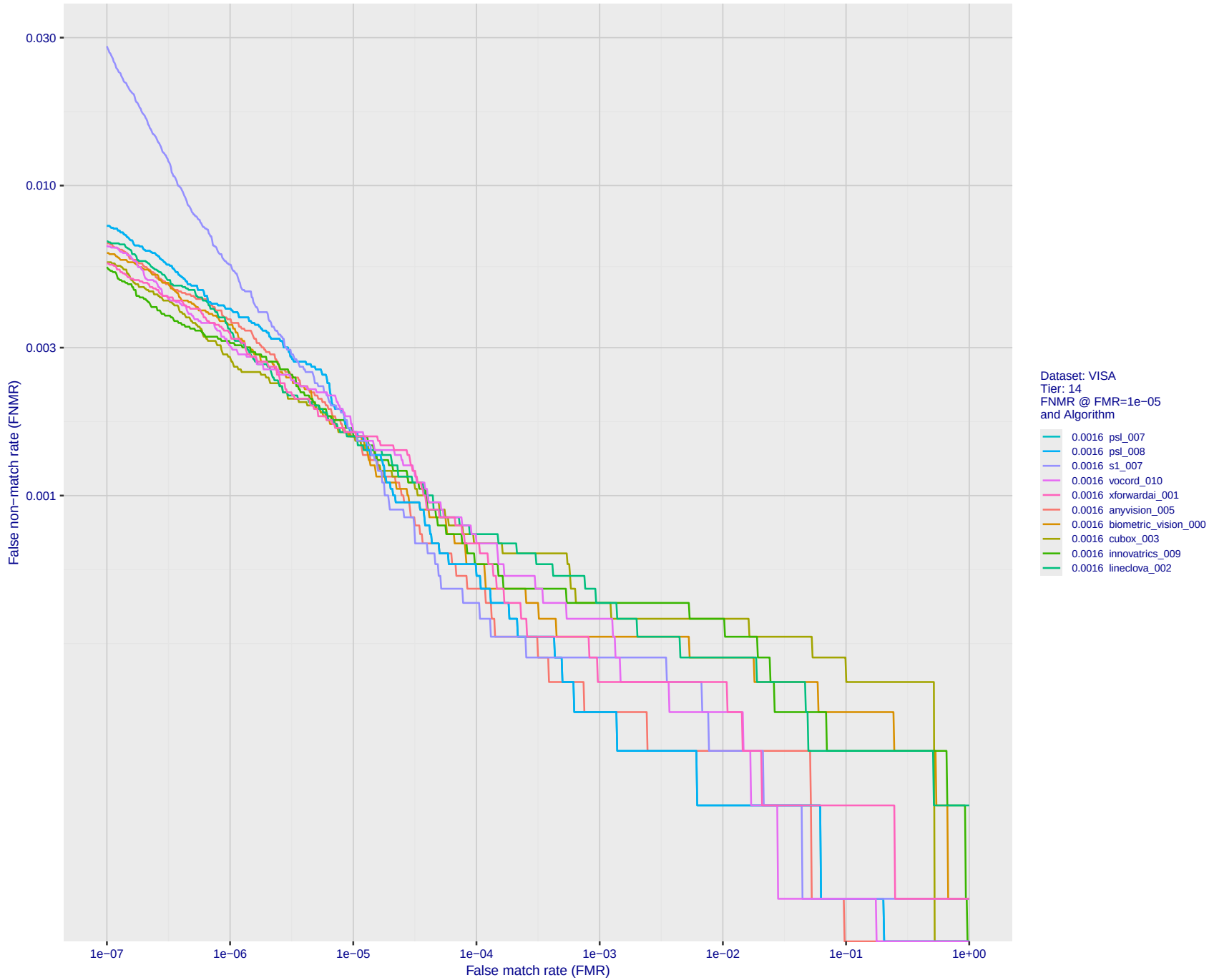

Figure 122: For the visa images, detection error tradeoff (DET) characteristics showing false non-match rate vs. false match rate plotted parametrically on threshold, T. The scales are logarithmic in order to show many decades of FMR.

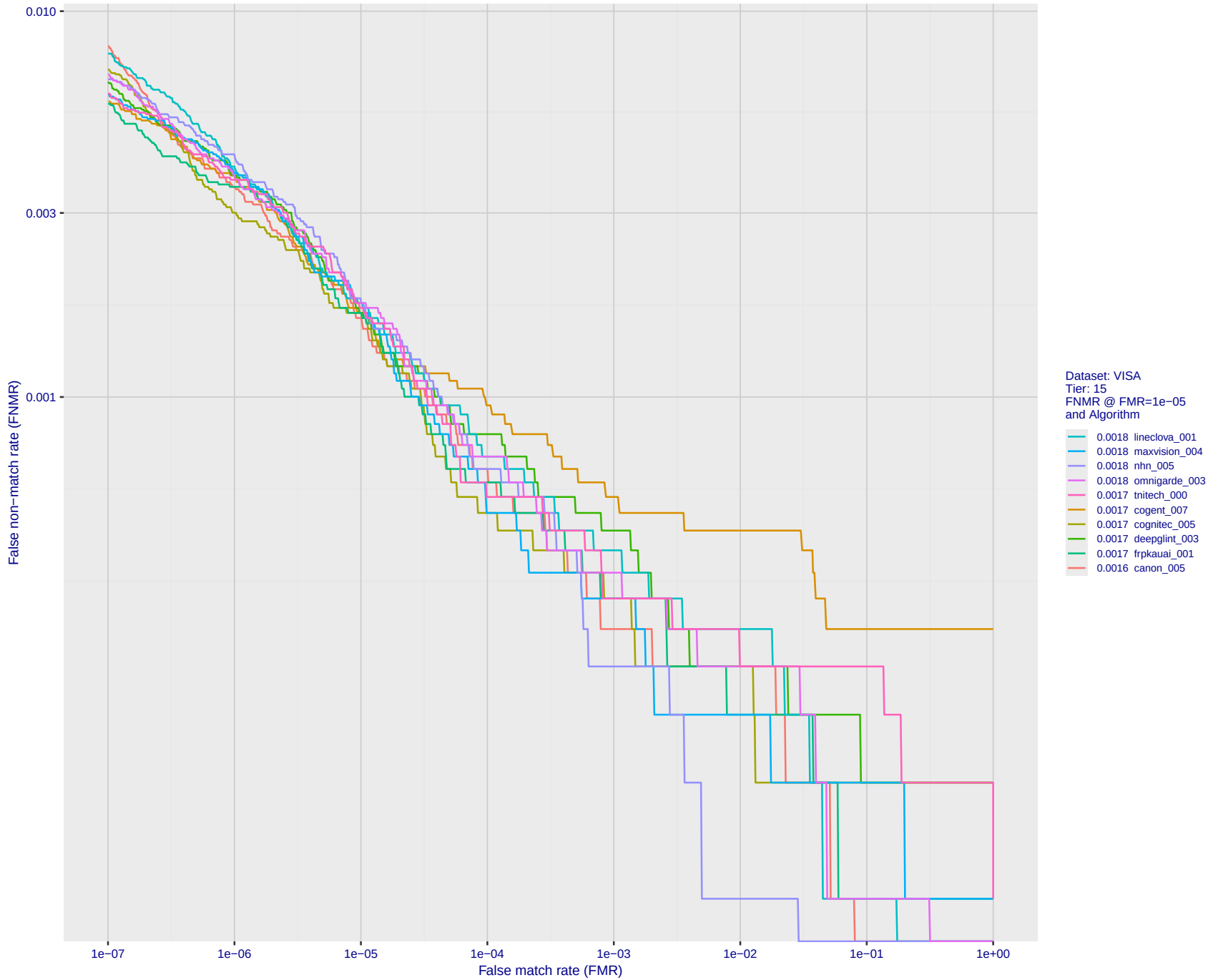

Figure 123: For the visa images, detection error tradeoff (DET) characteristics showing false non-match rate vs. false match rate plotted parametrically on threshold, T. The scales are logarithmic in order to show many decades of FMR.

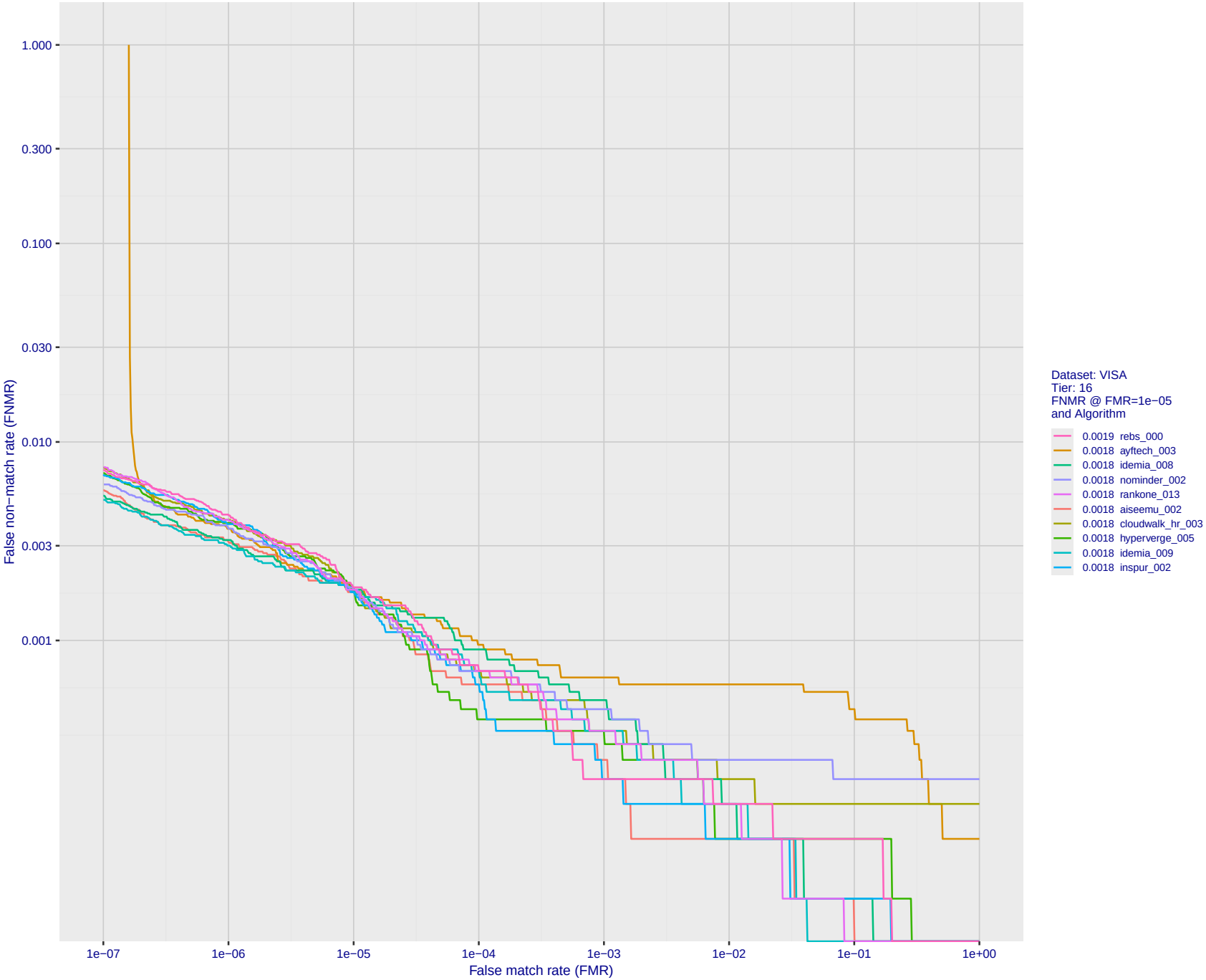

Figure 124: For the visa images, detection error tradeoff (DET) characteristics showing false non-match rate vs. false match rate plotted parametrically on threshold, T. The scales are logarithmic in order to show many decades of FMR.

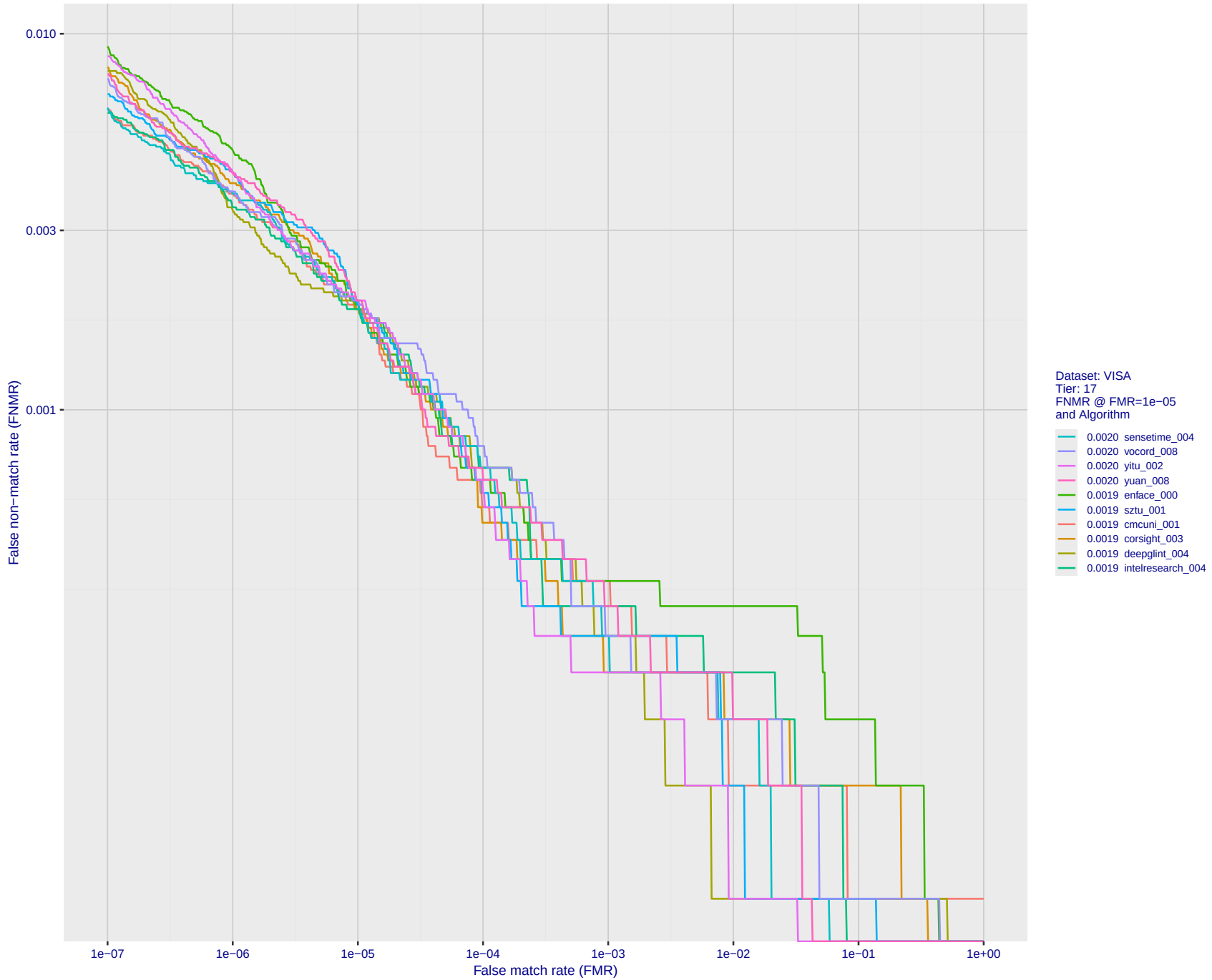

Figure 125: For the visa images, detection error tradeoff (DET) characteristics showing false non-match rate vs. false match rate plotted parametrically on threshold, T. The scales are logarithmic in order to show many decades of FMR.

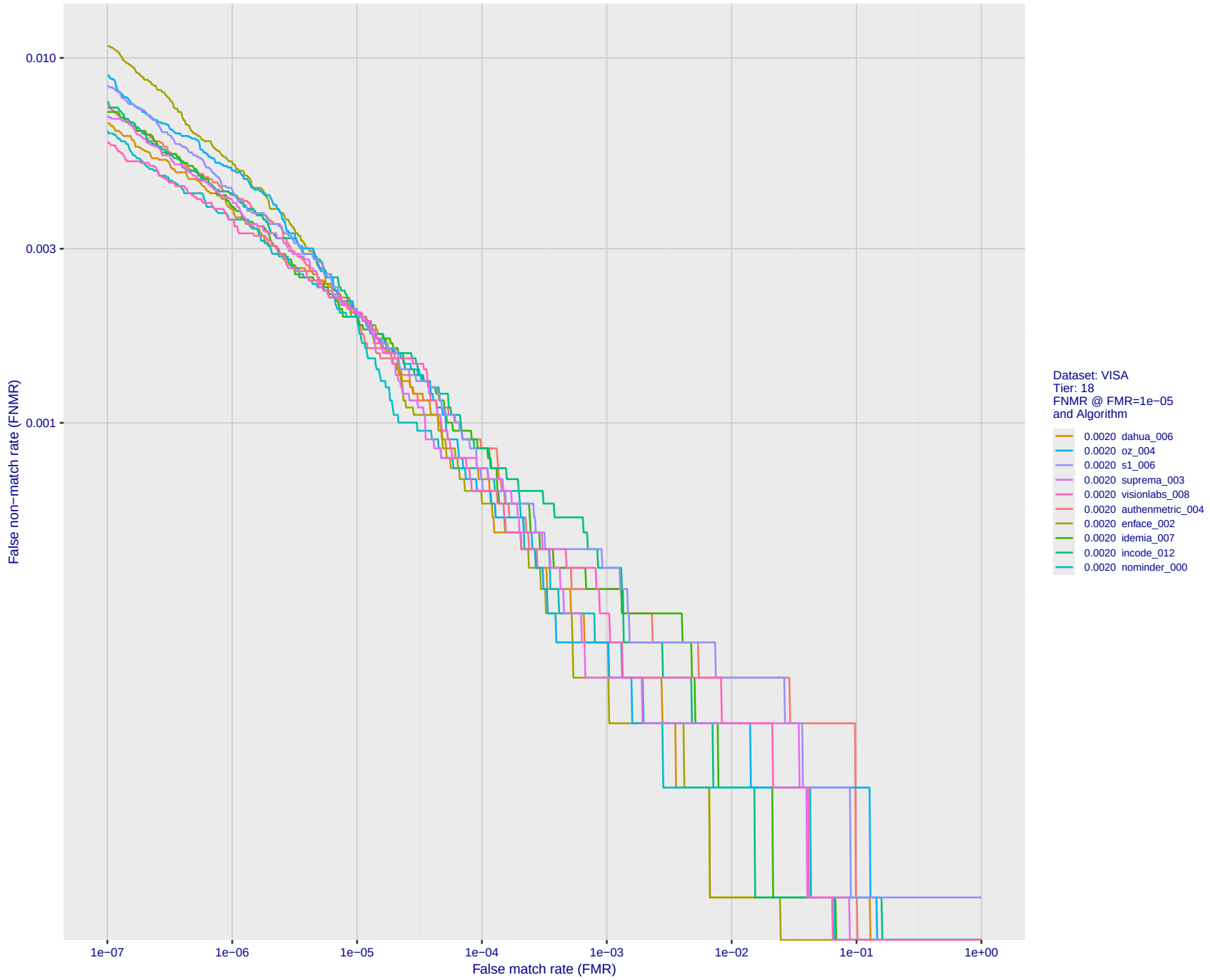

Figure 126: For the visa images, detection error tradeoff (DET) characteristics showing false non-match rate vs. false match rate plotted parametrically on threshold, T. The scales are logarithmic in order to show many decades of FMR.

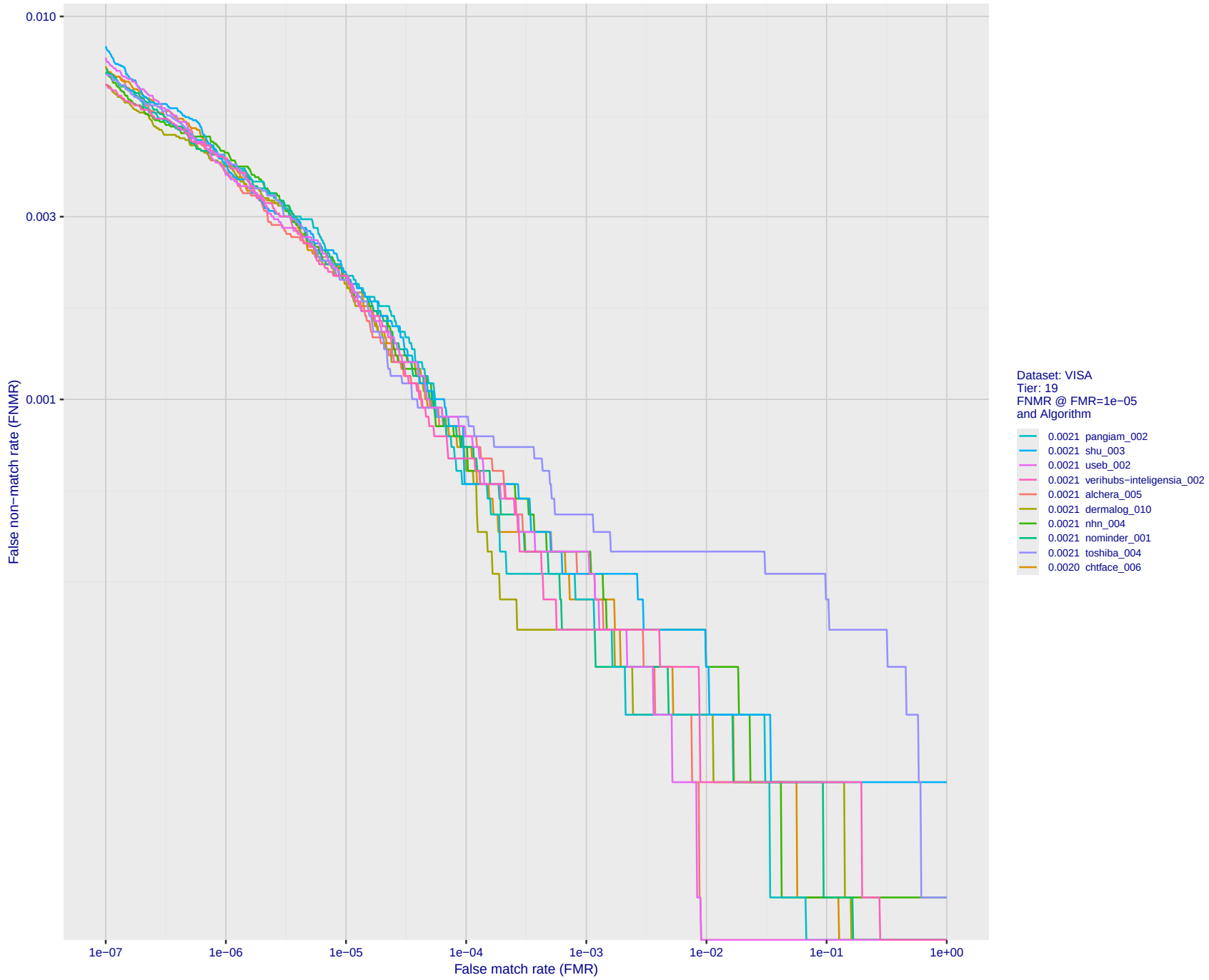

Figure 127: For the visa images, detection error tradeoff (DET) characteristics showing false non-match rate vs. false match rate plotted parametrically on threshold, T. The scales are logarithmic in order to show many decades of FMR.

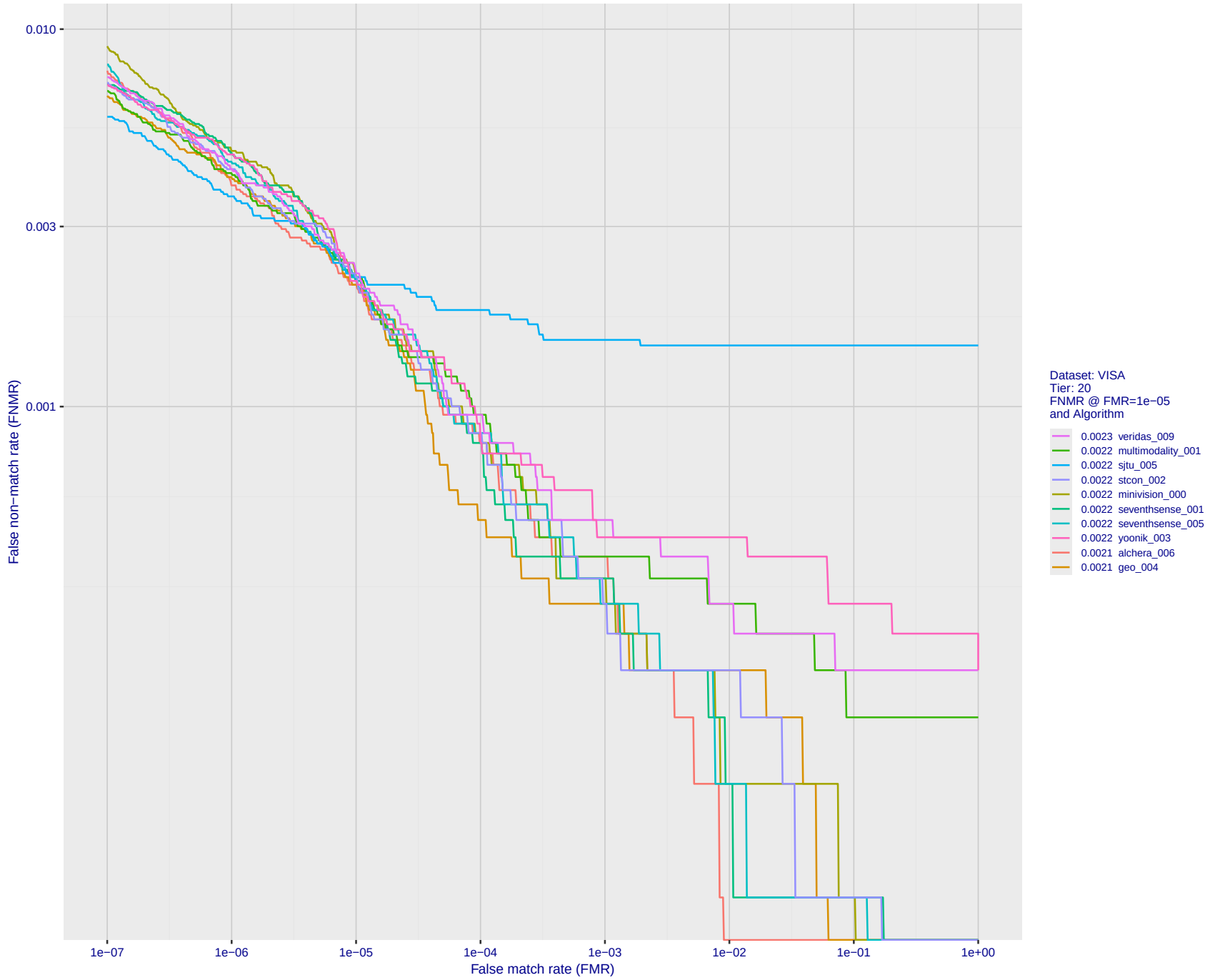

Figure 128: For the visa images, detection error tradeoff (DET) characteristics showing false non-match rate vs. false match rate plotted parametrically on threshold, T. The scales are logarithmic in order to show many decades of FMR.

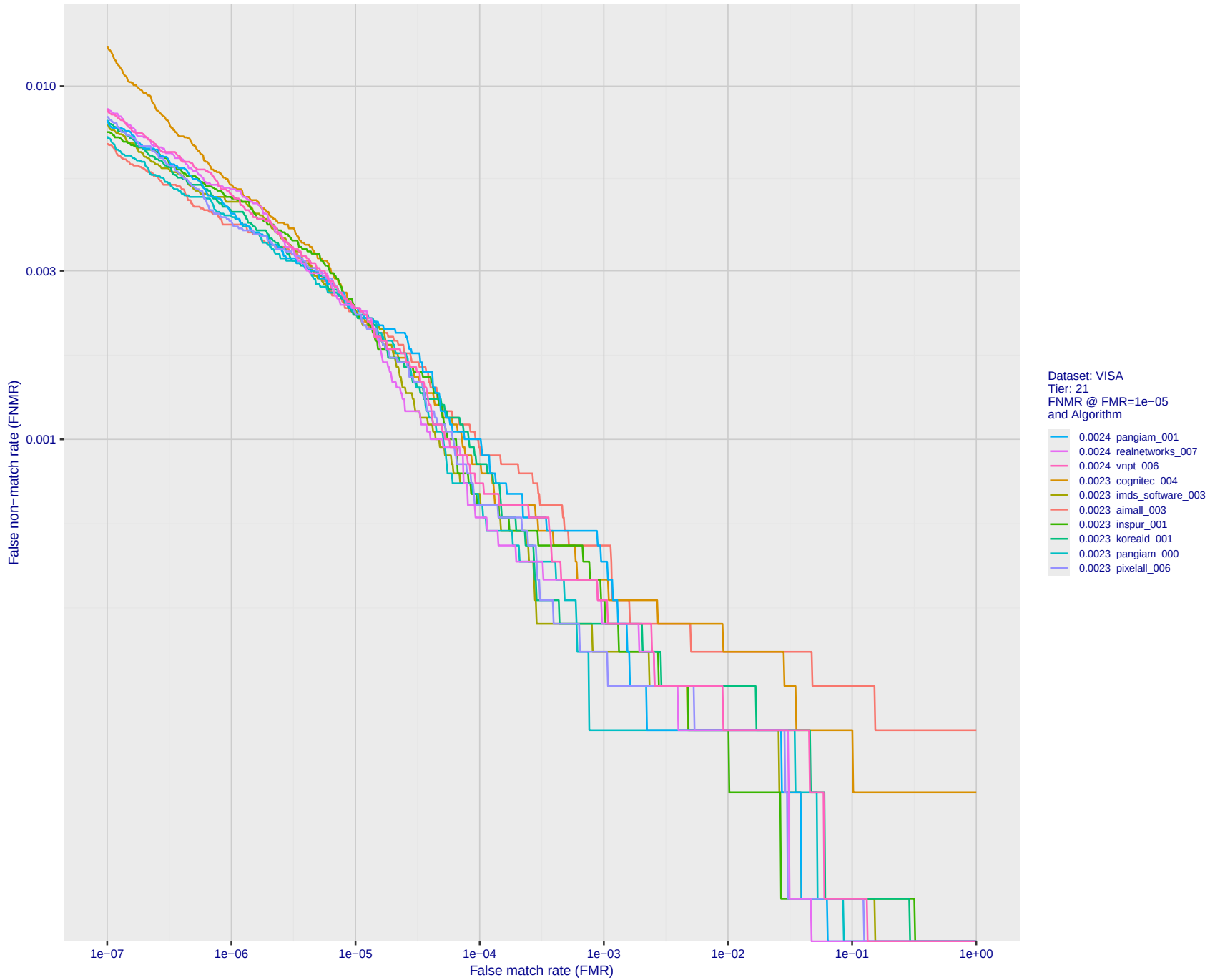

Figure 129: For the visa images, detection error tradeoff (DET) characteristics showing false non-match rate vs. false match rate plotted parametrically on threshold, T. The scales are logarithmic in order to show many decades of FMR.

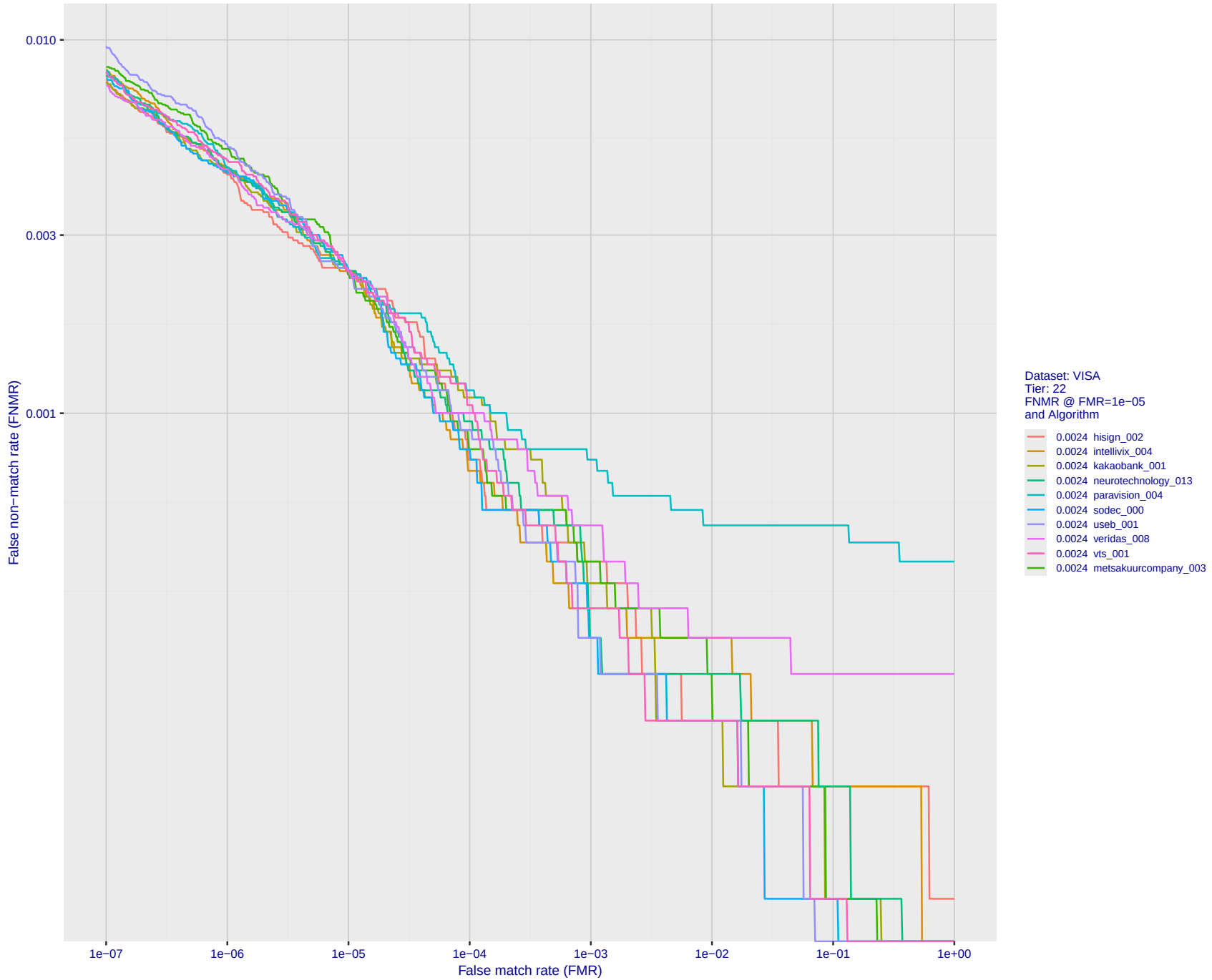

Figure 130: For the visa images, detection error tradeoff (DET) characteristics showing false non-match rate vs. false match rate plotted parametrically on threshold, T. The scales are logarithmic in order to show many decades of FMR.

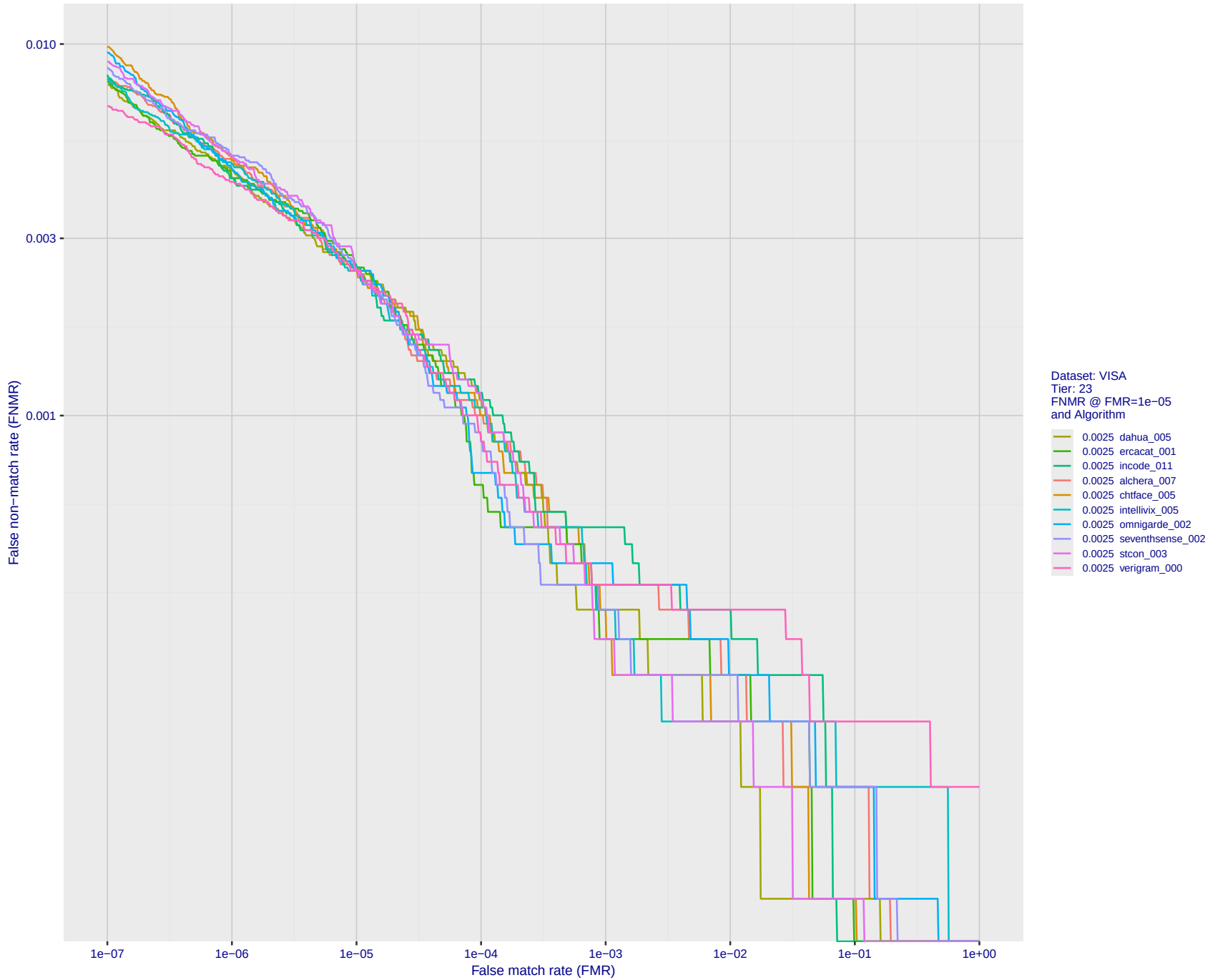

Figure 131: For the visa images, detection error tradeoff (DET) characteristics showing false non-match rate vs. false match rate plotted parametrically on threshold, T. The scales are logarithmic in order to show many decades of FMR.

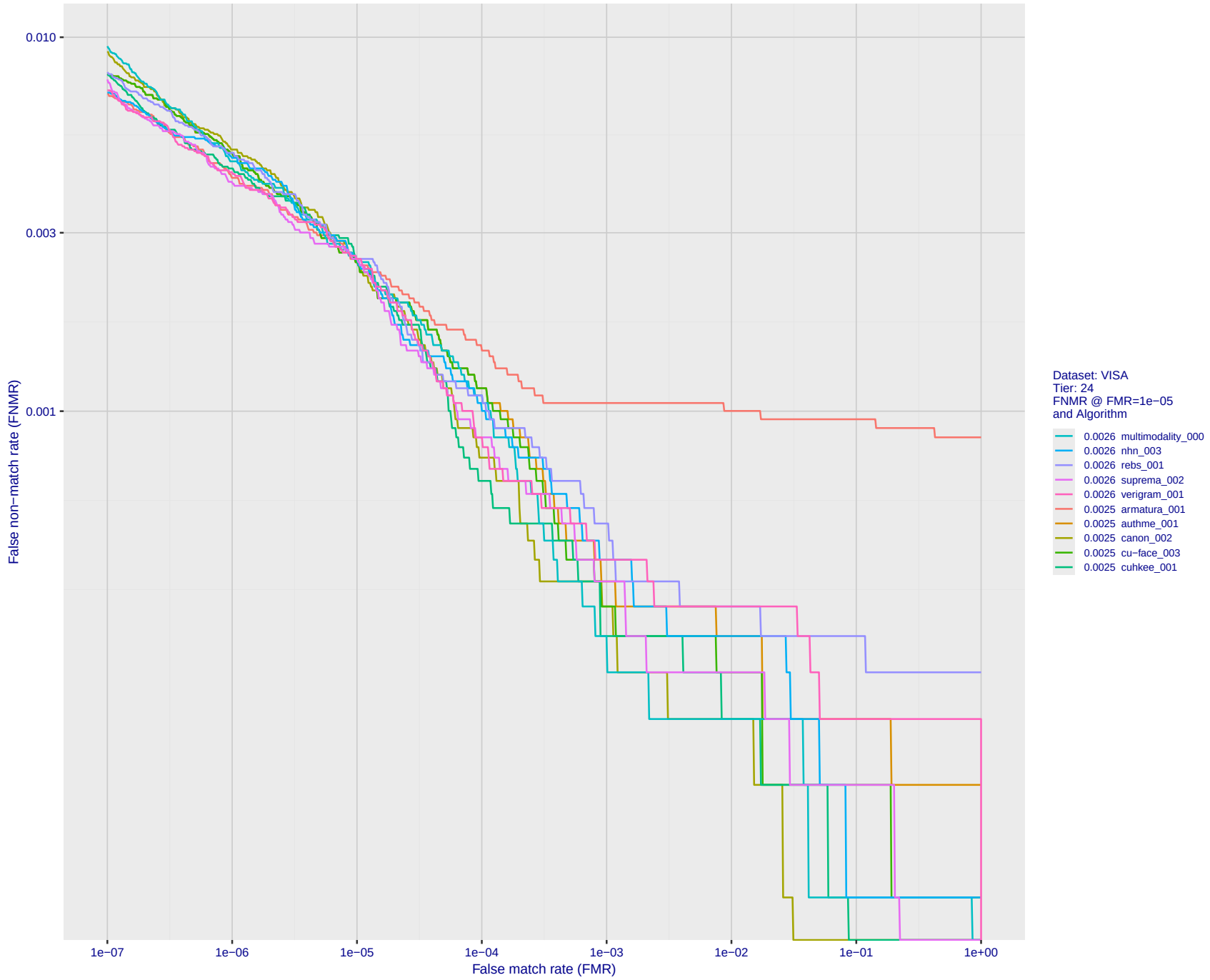

Figure 132: For the visa images, detection error tradeoff (DET) characteristics showing false non-match rate vs. false match rate plotted parametrically on threshold, T. The scales are logarithmic in order to show many decades of FMR.

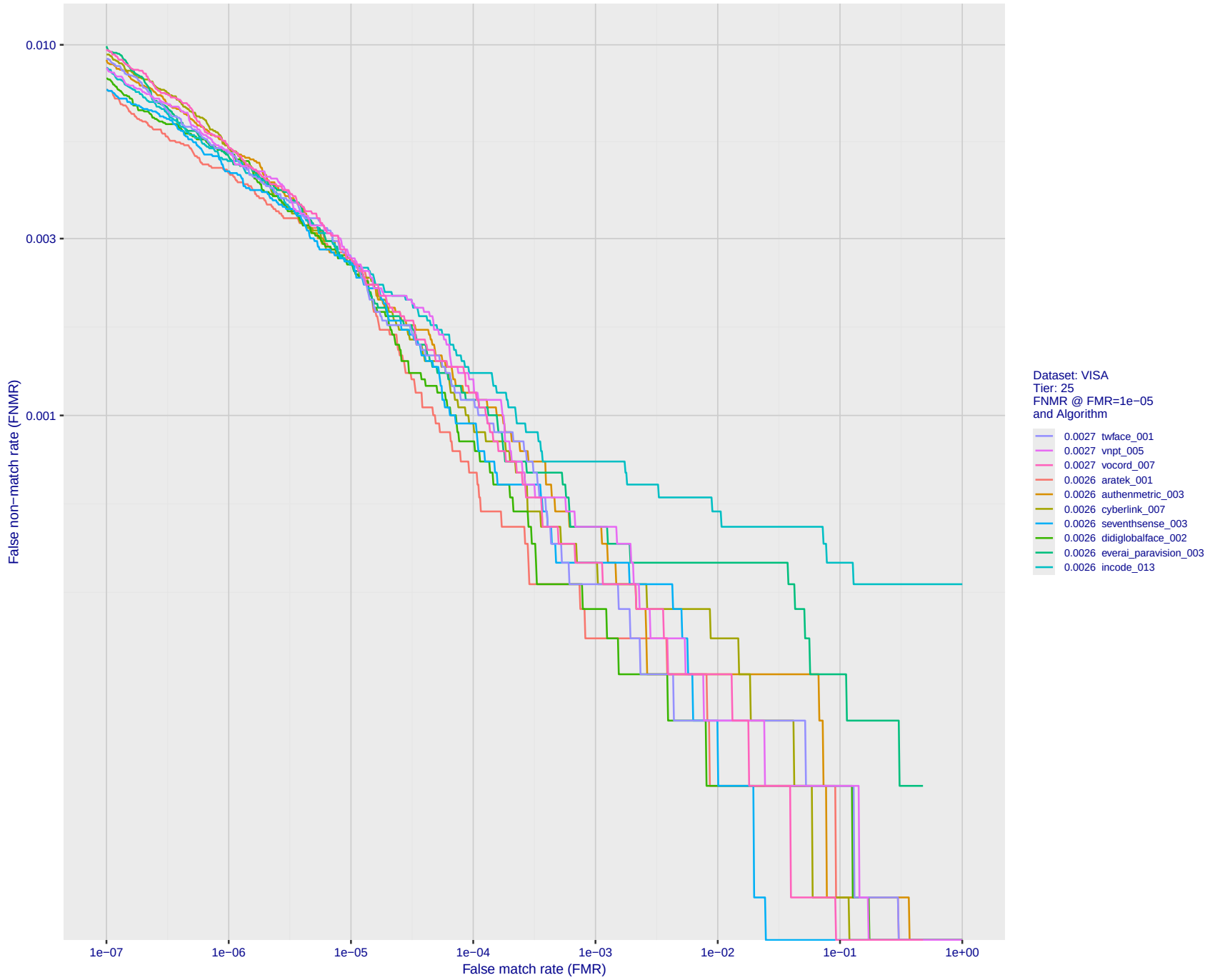

Figure 133: For the visa images, detection error tradeoff (DET) characteristics showing false non-match rate vs. false match rate plotted parametrically on threshold, T. The scales are logarithmic in order to show many decades of FMR.

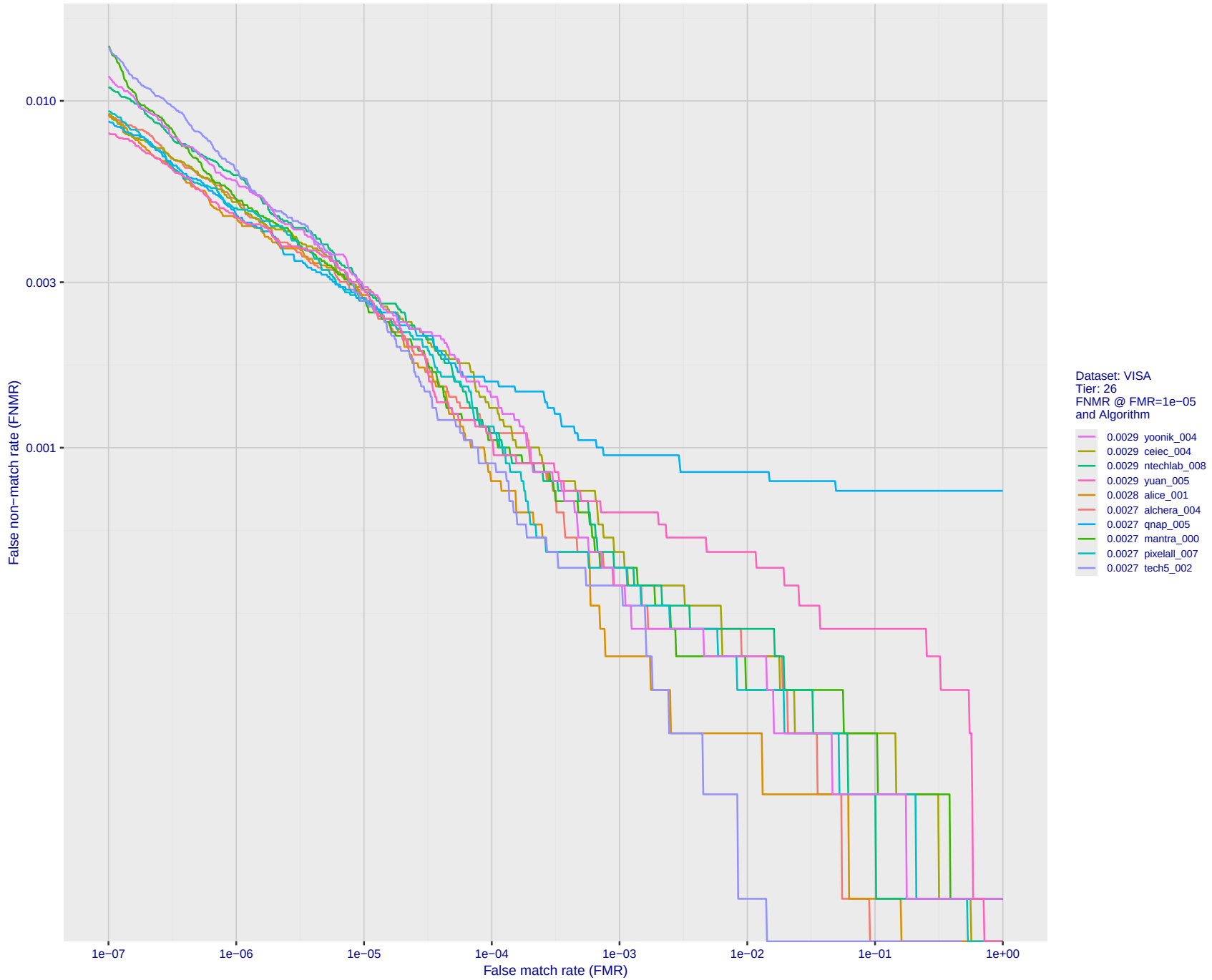

Figure 134: For the visa images, detection error tradeoff (DET) characteristics showing false non-match rate vs. false match rate plotted parametrically on threshold, T. The scales are logarithmic in order to show many decades of FMR.

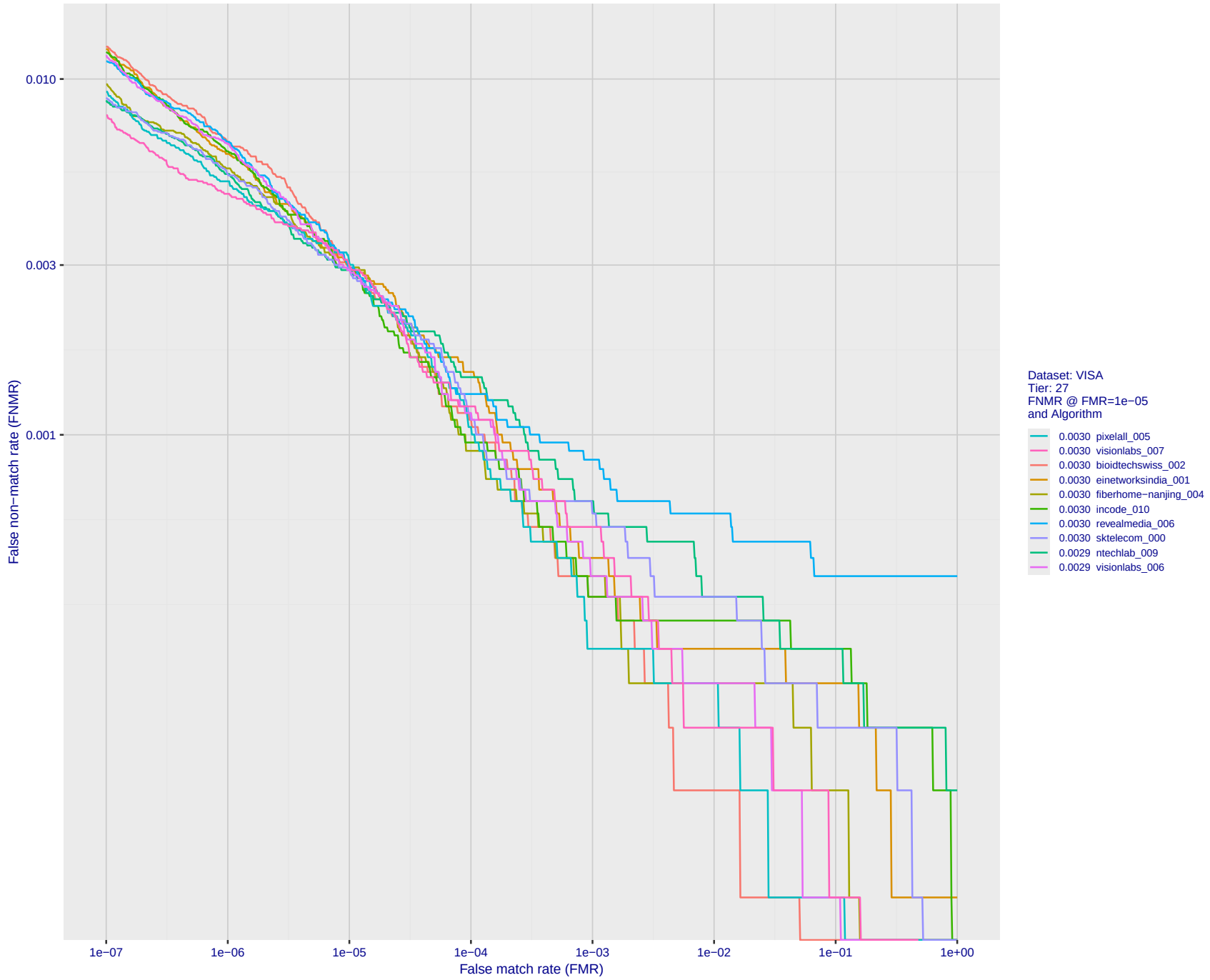

Figure 135: For the visa images, detection error tradeoff (DET) characteristics showing false non-match rate vs. false match rate plotted parametrically on threshold, T. The scales are logarithmic in order to show many decades of FMR.

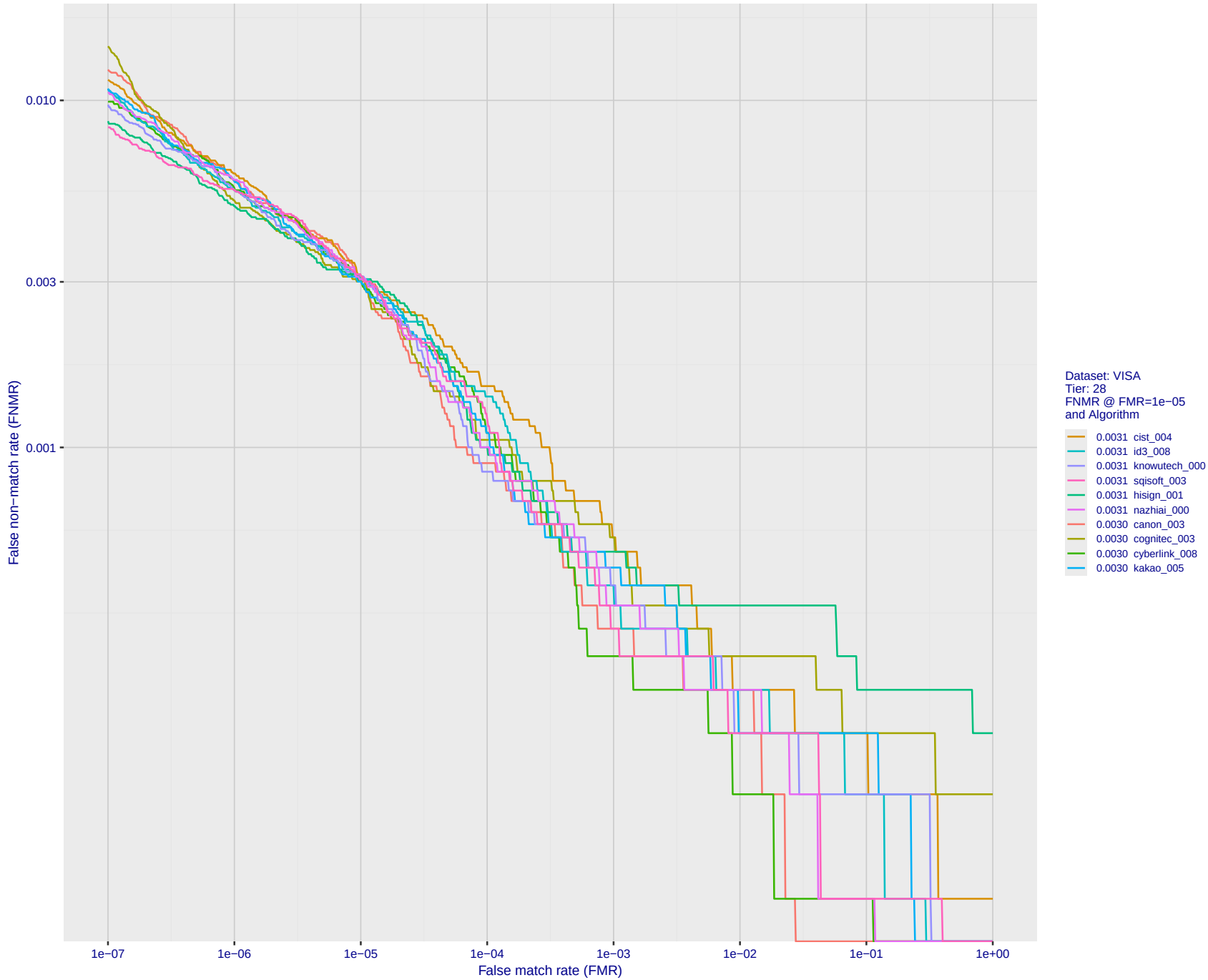

Figure 136: For the visa images, detection error tradeoff (DET) characteristics showing false non-match rate vs. false match rate plotted parametrically on threshold, T. The scales are logarithmic in order to show many decades of FMR.

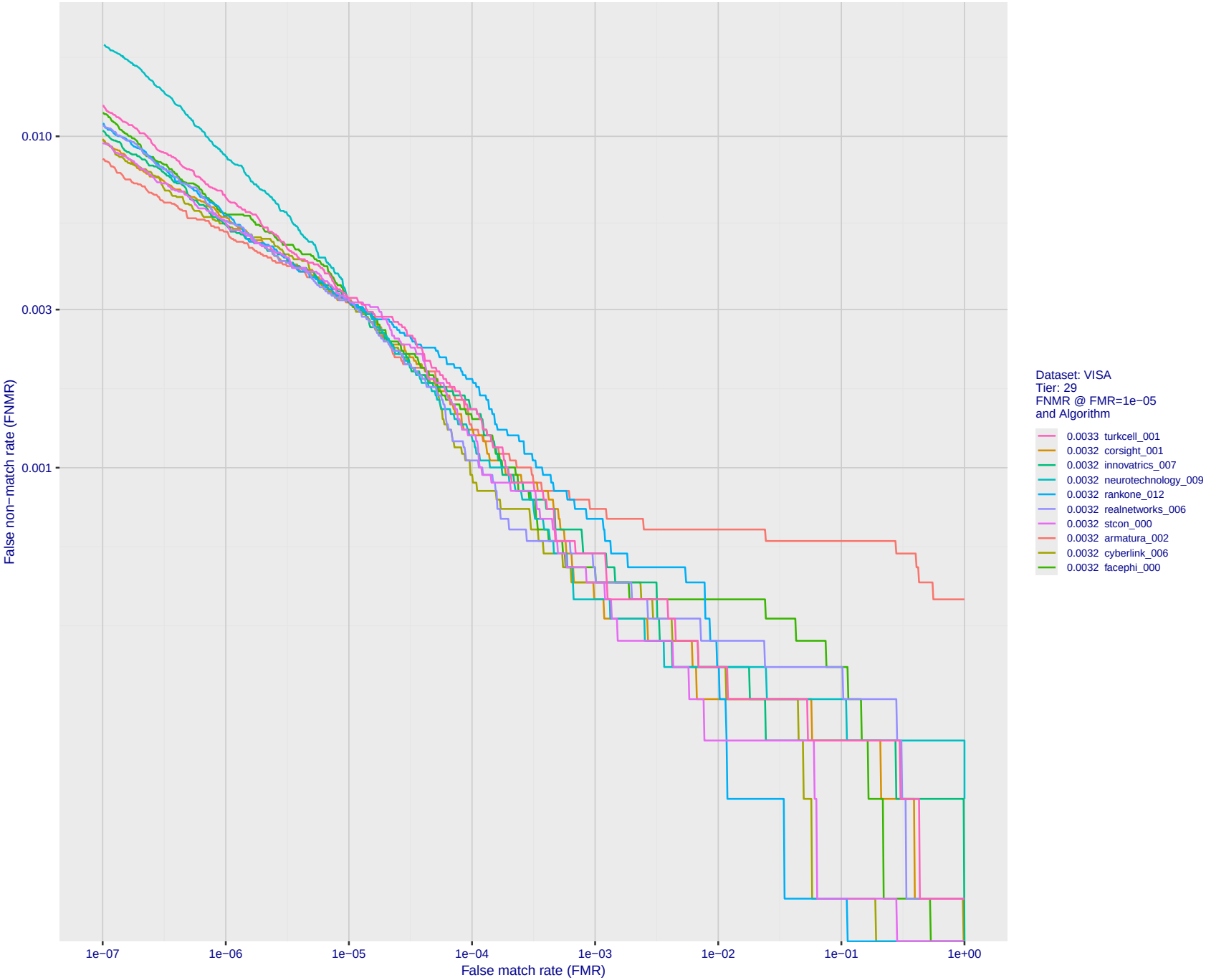

Figure 137: For the visa images, detection error tradeoff (DET) characteristics showing false non-match rate vs. false match rate plotted parametrically on threshold, T. The scales are logarithmic in order to show many decades of FMR.

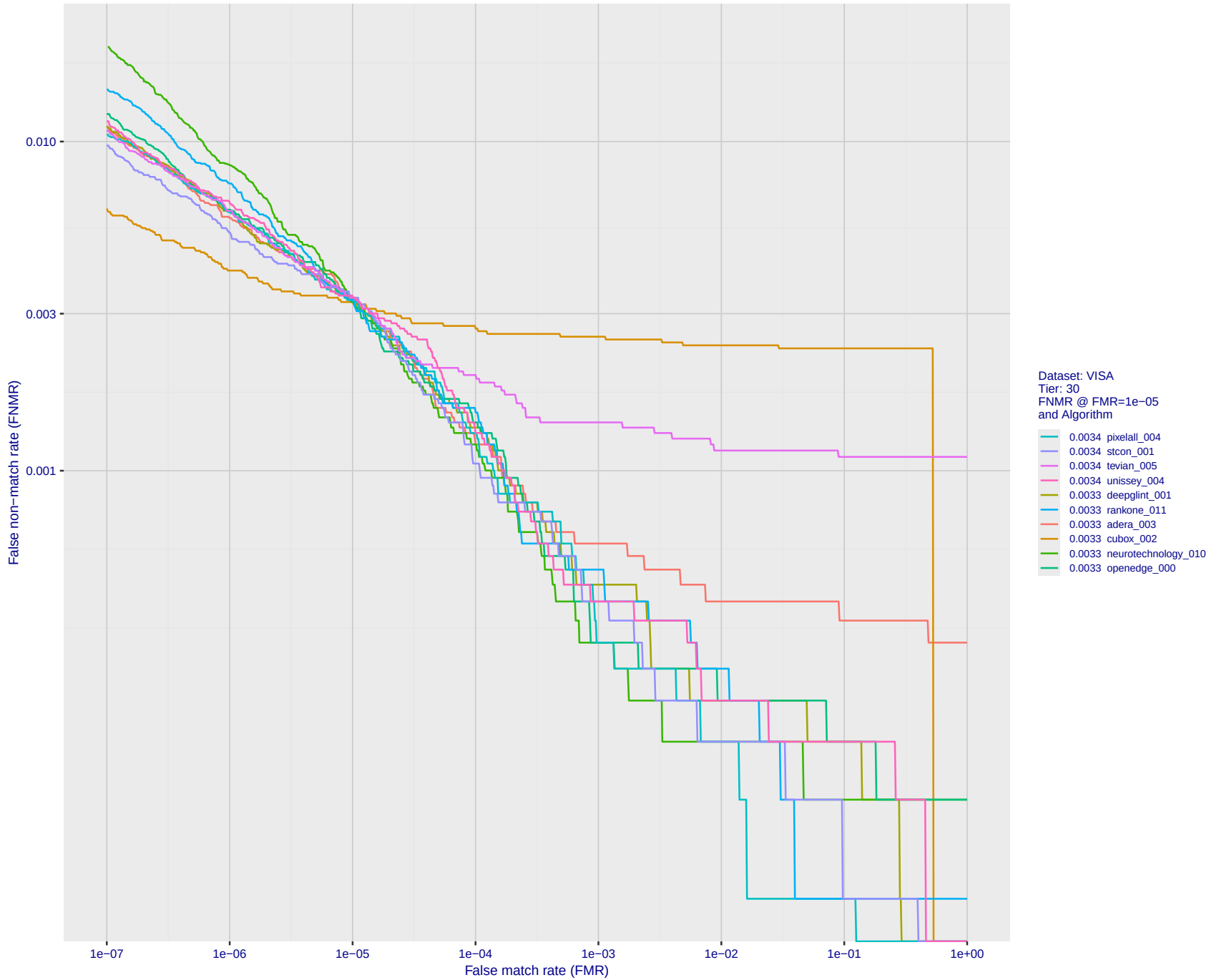

Figure 138: For the visa images, detection error tradeoff (DET) characteristics showing false non-match rate vs. false match rate plotted parametrically on threshold, T. The scales are logarithmic in order to show many decades of FMR.

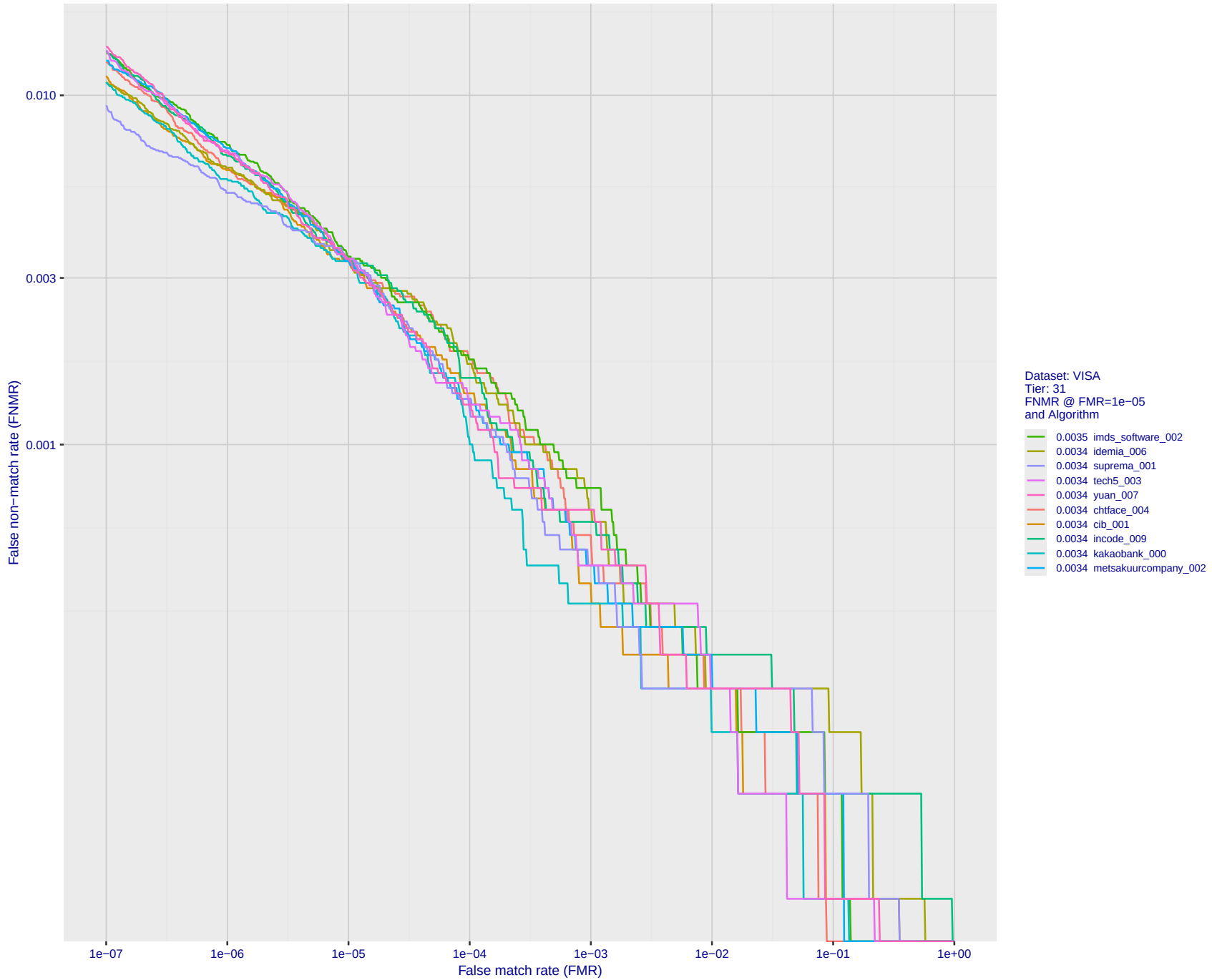

Figure 139: For the visa images, detection error tradeoff (DET) characteristics showing false non-match rate vs. false match rate plotted parametrically on threshold, T. The scales are logarithmic in order to show many decades of FMR.

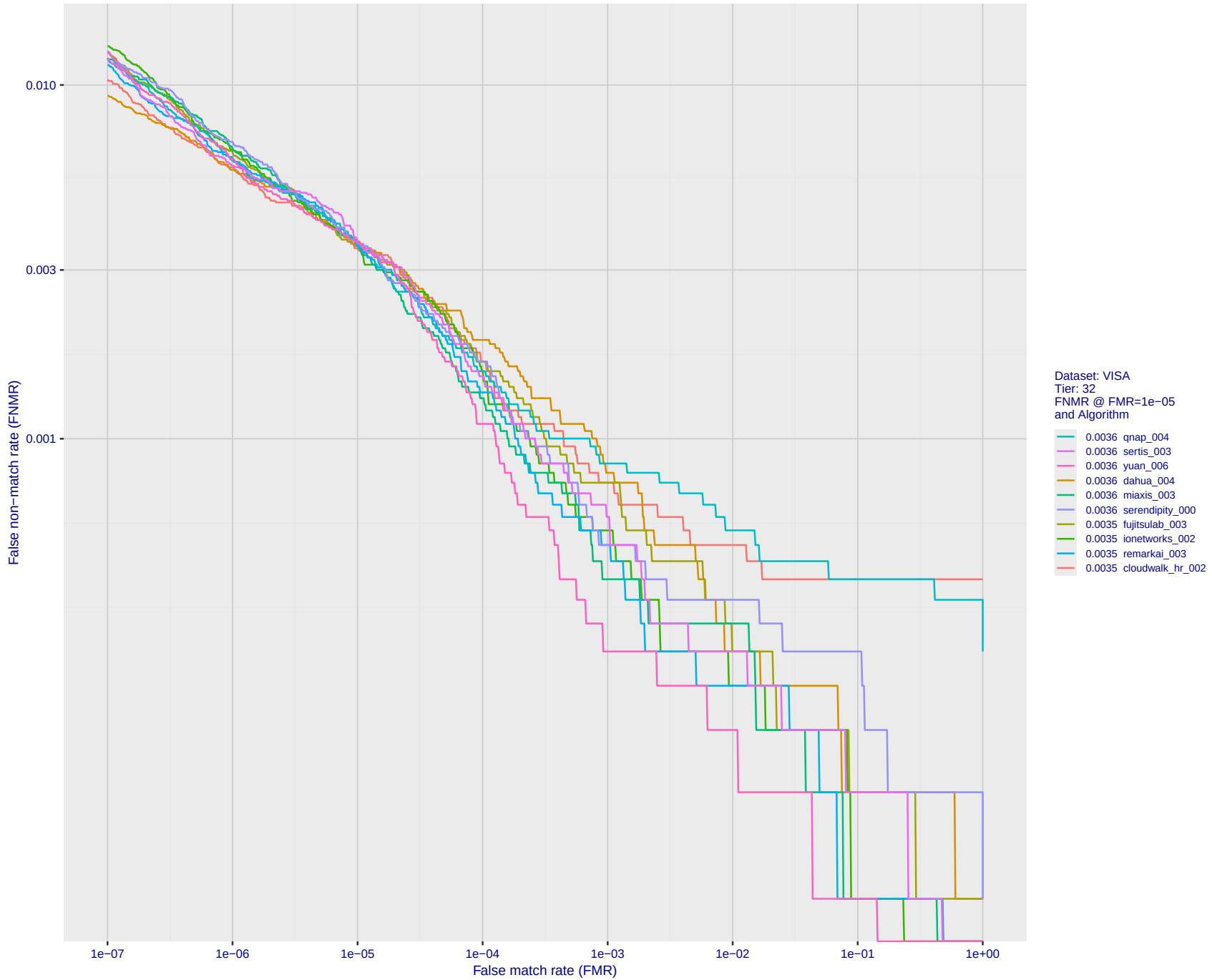

Figure 140: For the visa images, detection error tradeoff (DET) characteristics showing false non-match rate vs. false match rate plotted parametrically on threshold, T. The scales are logarithmic in order to show many decades of FMR.

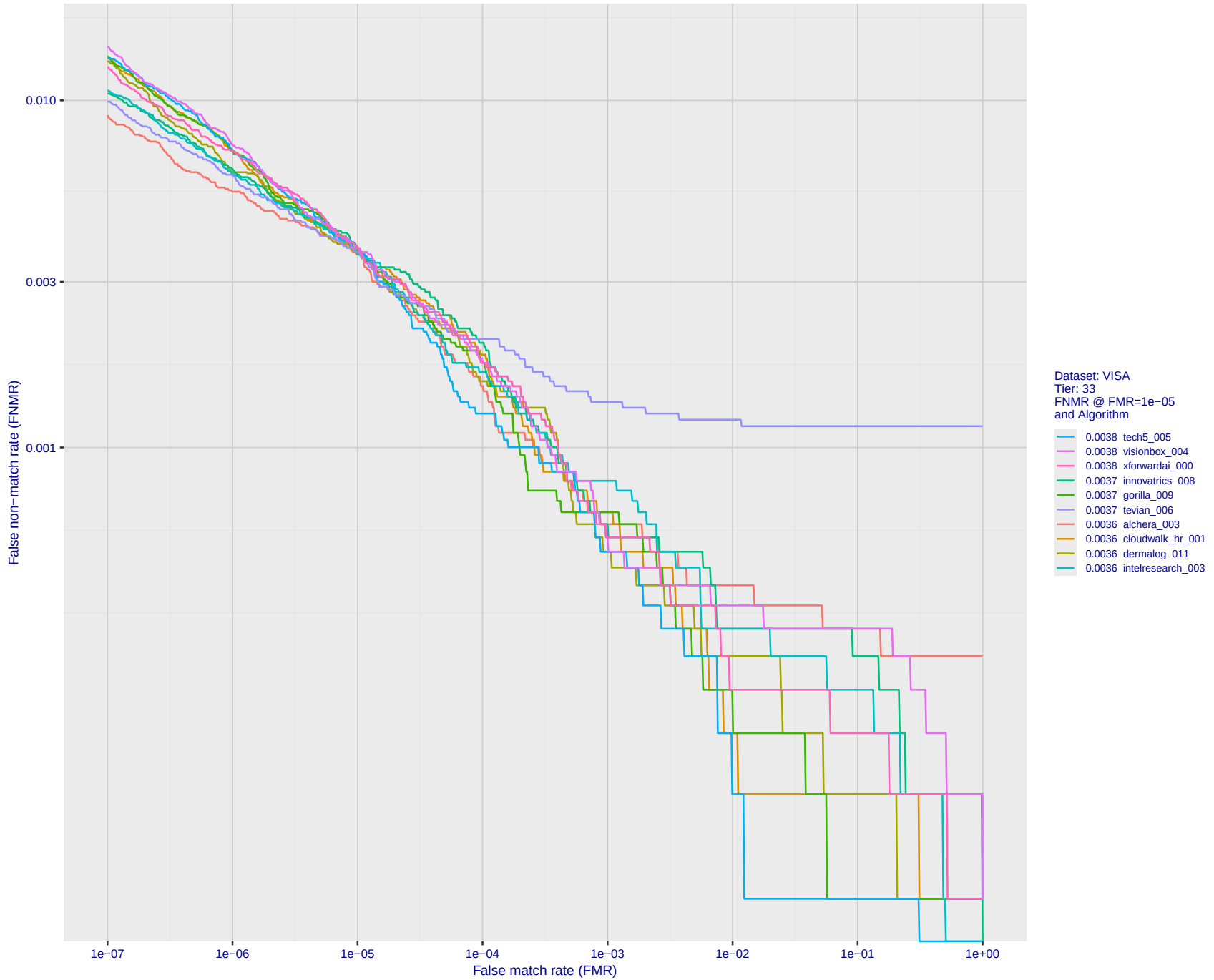

Figure 141: For the visa images, detection error tradeoff (DET) characteristics showing false non-match rate vs. false match rate plotted parametrically on threshold, T. The scales are logarithmic in order to show many decades of FMR.

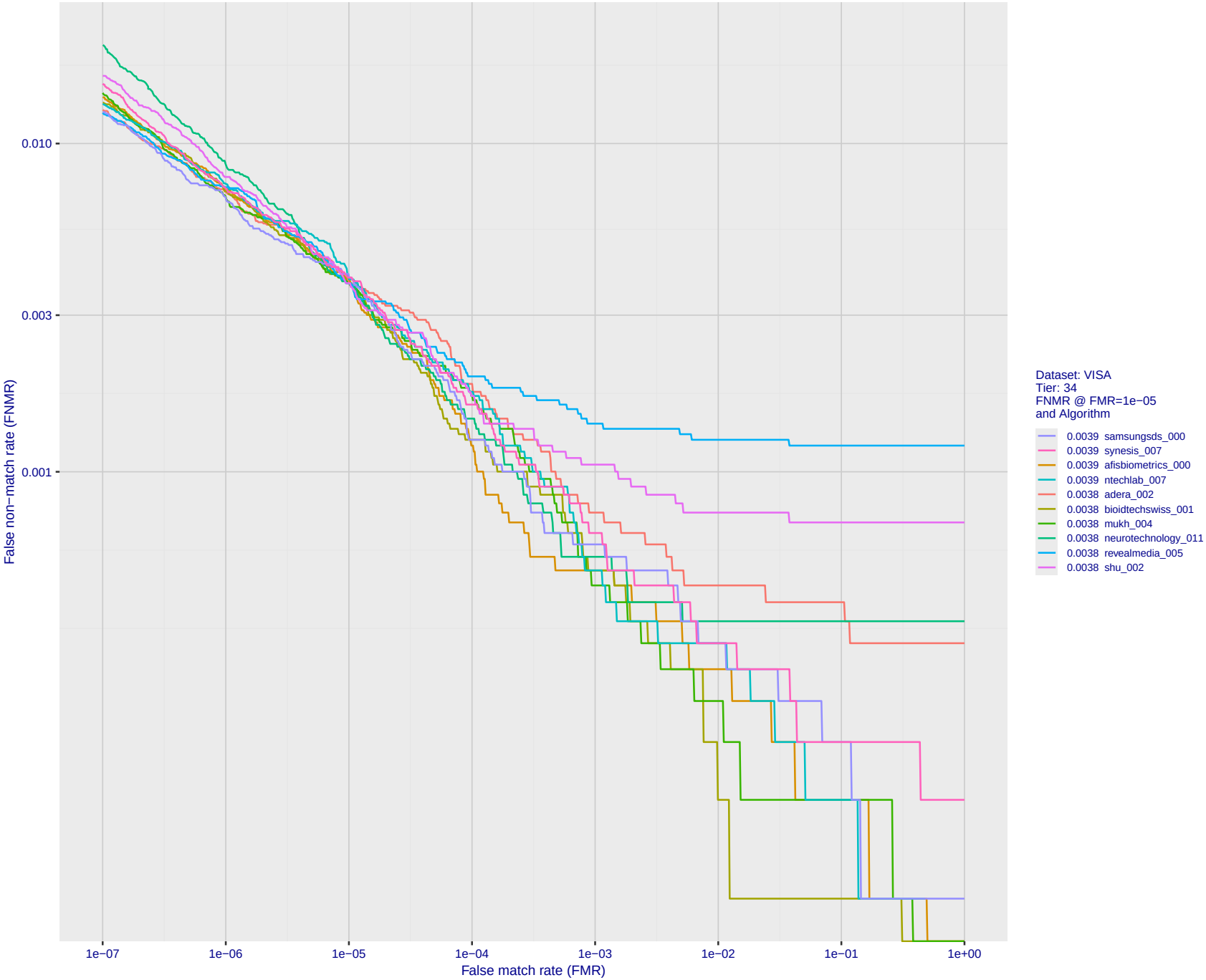

Figure 142: For the visa images, detection error tradeoff (DET) characteristics showing false non-match rate vs. false match rate plotted parametrically on threshold, T. The scales are logarithmic in order to show many decades of FMR.

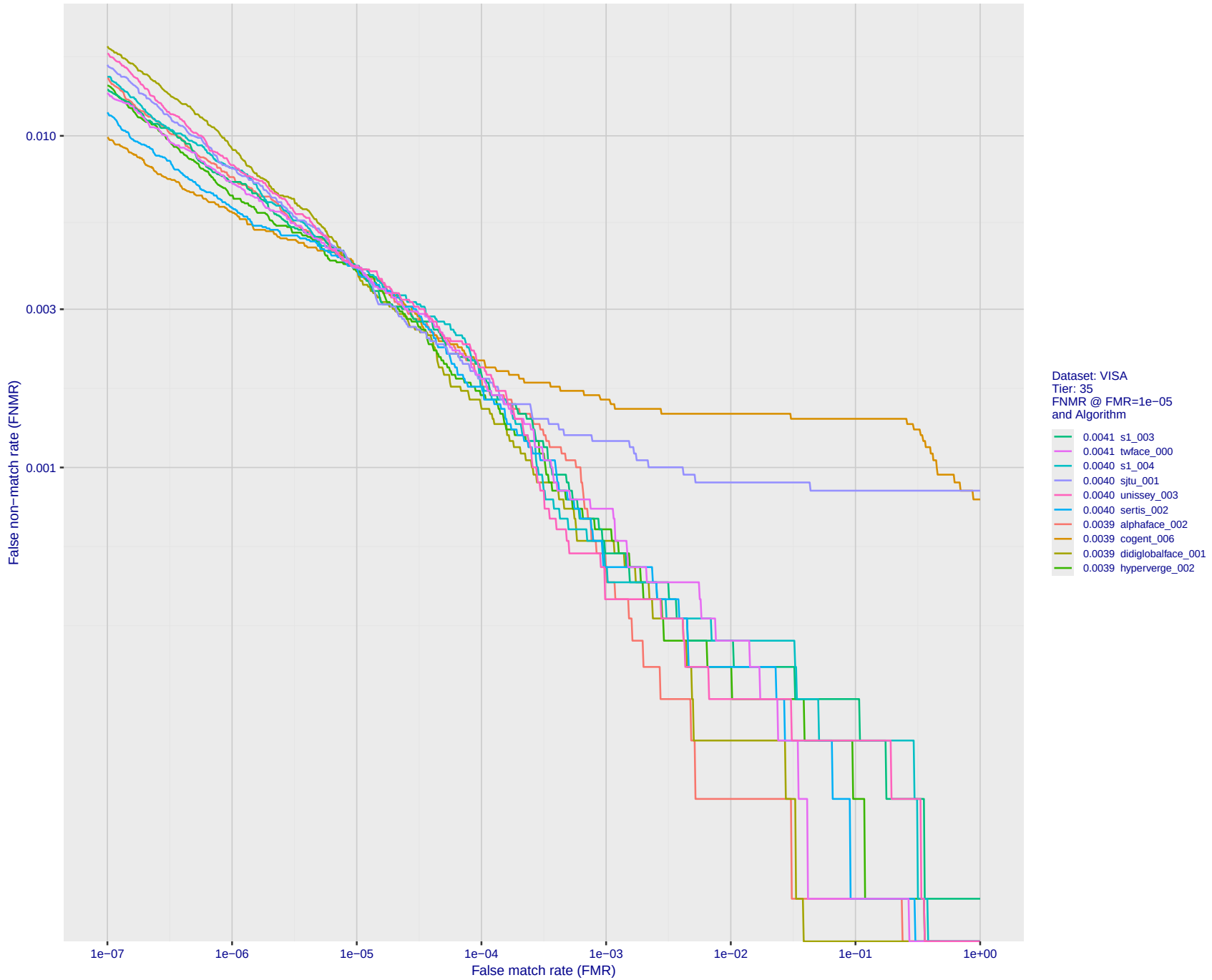

Figure 143: For the visa images, detection error tradeoff (DET) characteristics showing false non-match rate vs. false match rate plotted parametrically on threshold, T. The scales are logarithmic in order to show many decades of FMR.

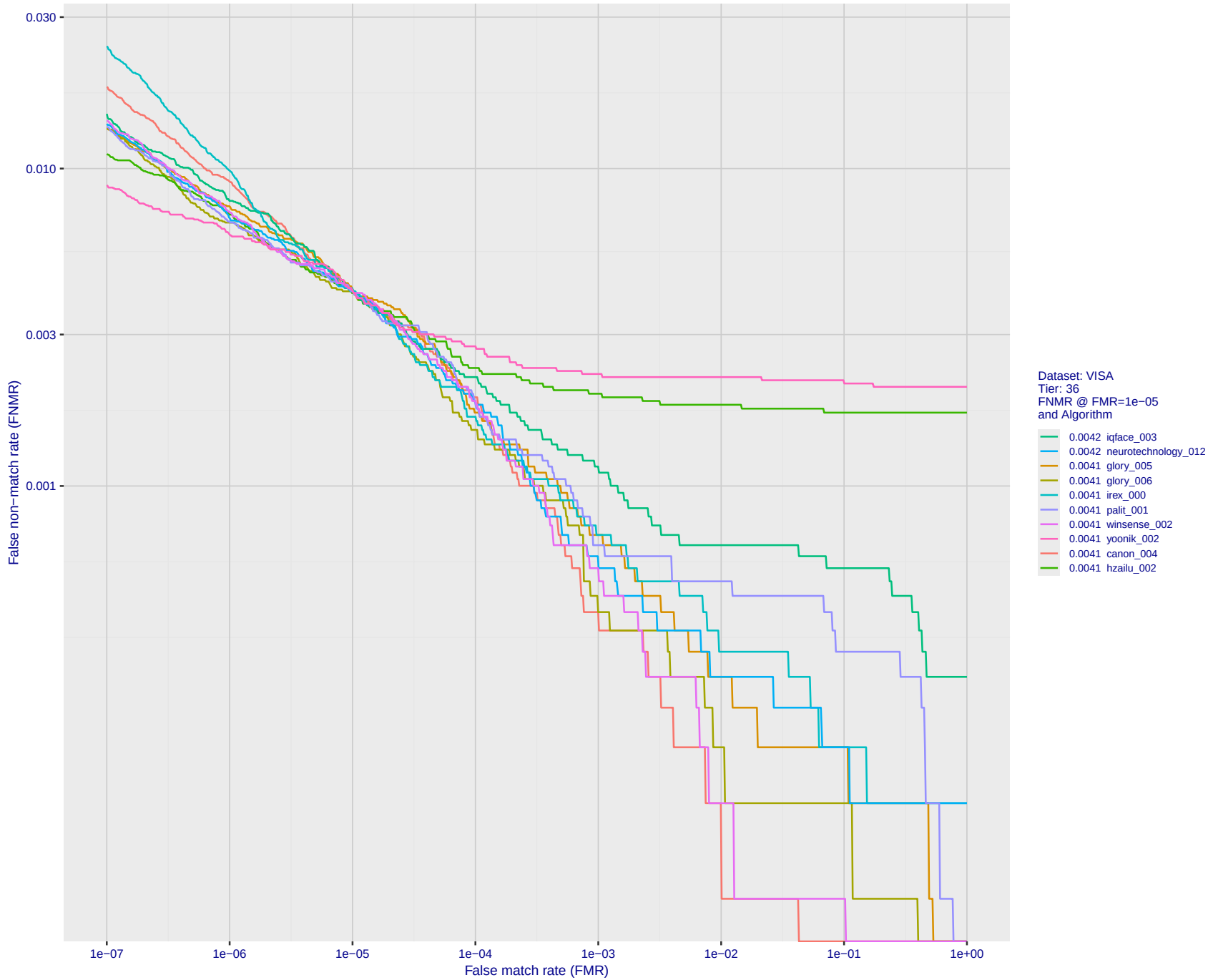

Figure 144: For the visa images, detection error tradeoff (DET) characteristics showing false non-match rate vs. false match rate plotted parametrically on threshold, T. The scales are logarithmic in order to show many decades of FMR.

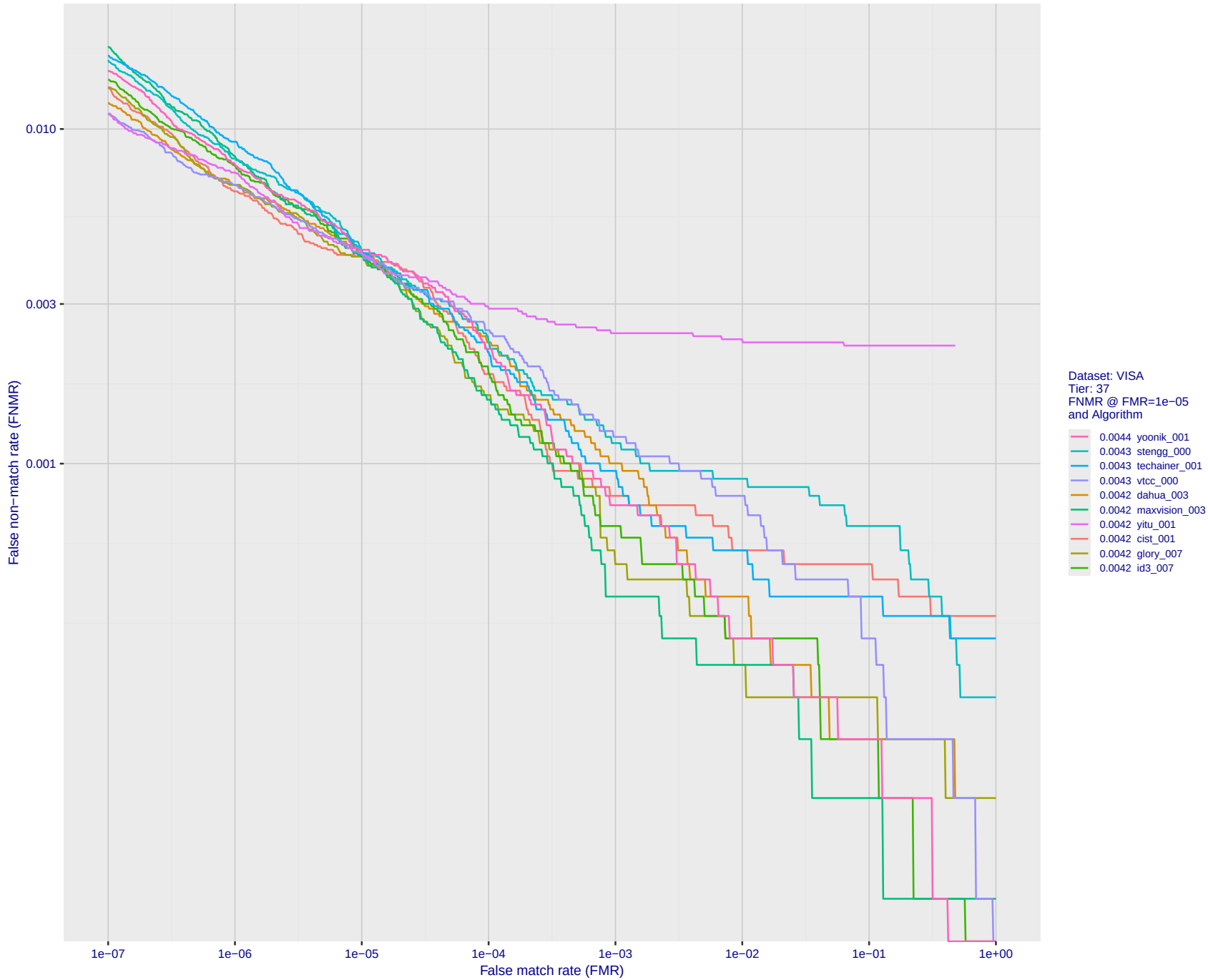

Figure 145: For the visa images, detection error tradeoff (DET) characteristics showing false non-match rate vs. false match rate plotted parametrically on threshold, T. The scales are logarithmic in order to show many decades of FMR.

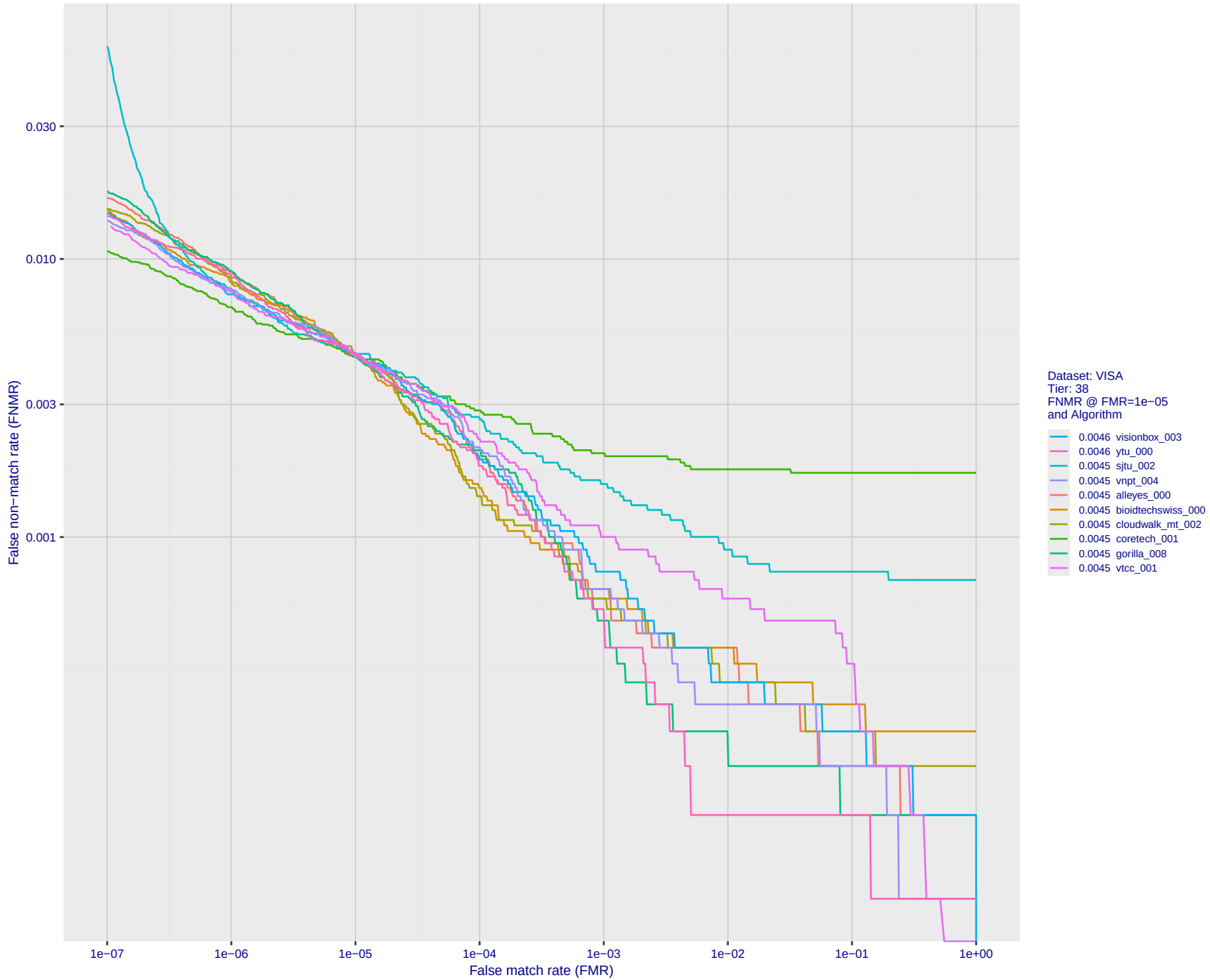

Figure 146: For the visa images, detection error tradeoff (DET) characteristics showing false non-match rate vs. false match rate plotted parametrically on threshold, T. The scales are logarithmic in order to show many decades of FMR.

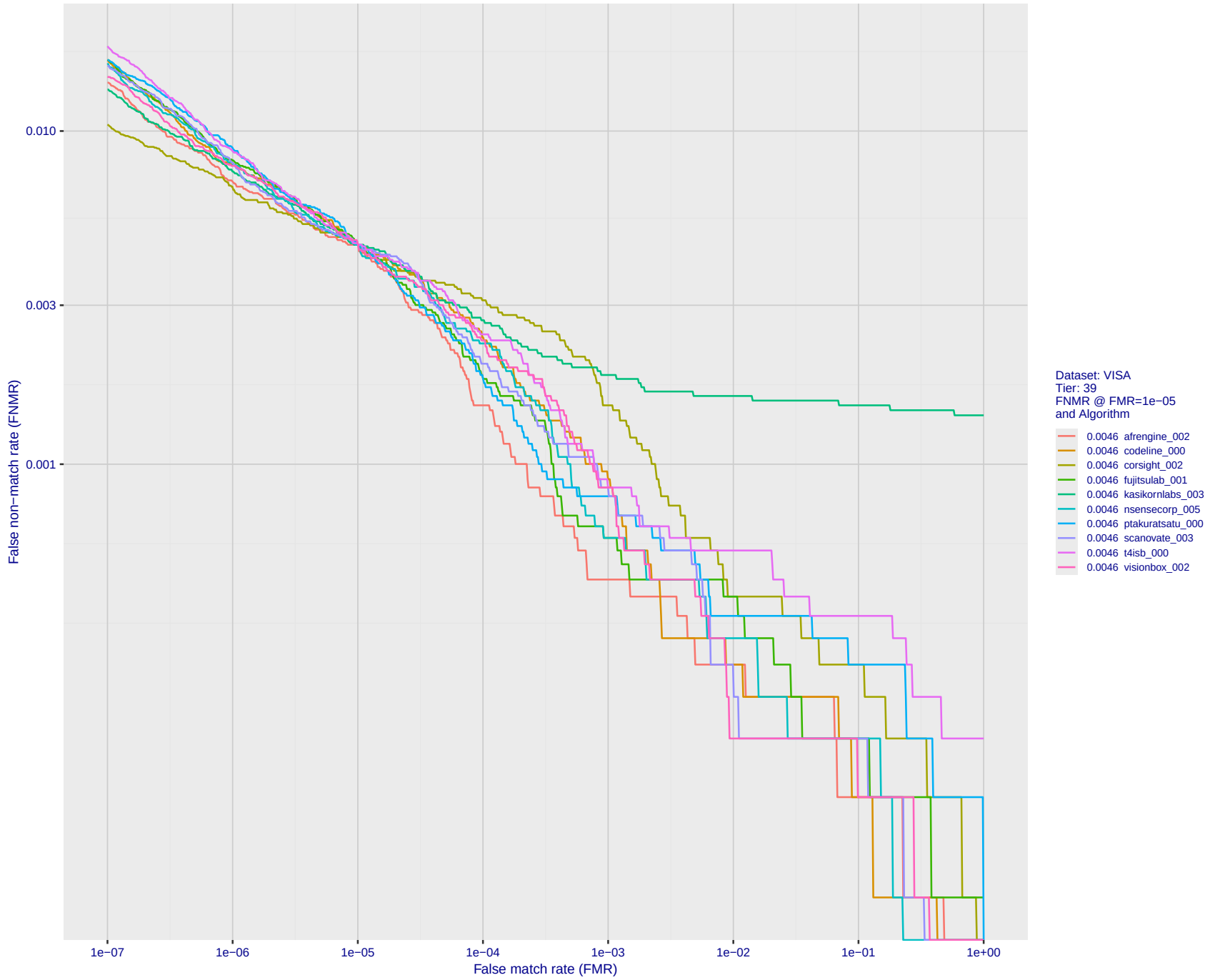

Figure 147: For the visa images, detection error tradeoff (DET) characteristics showing false non-match rate vs. false match rate plotted parametrically on threshold, T. The scales are logarithmic in order to show many decades of FMR.

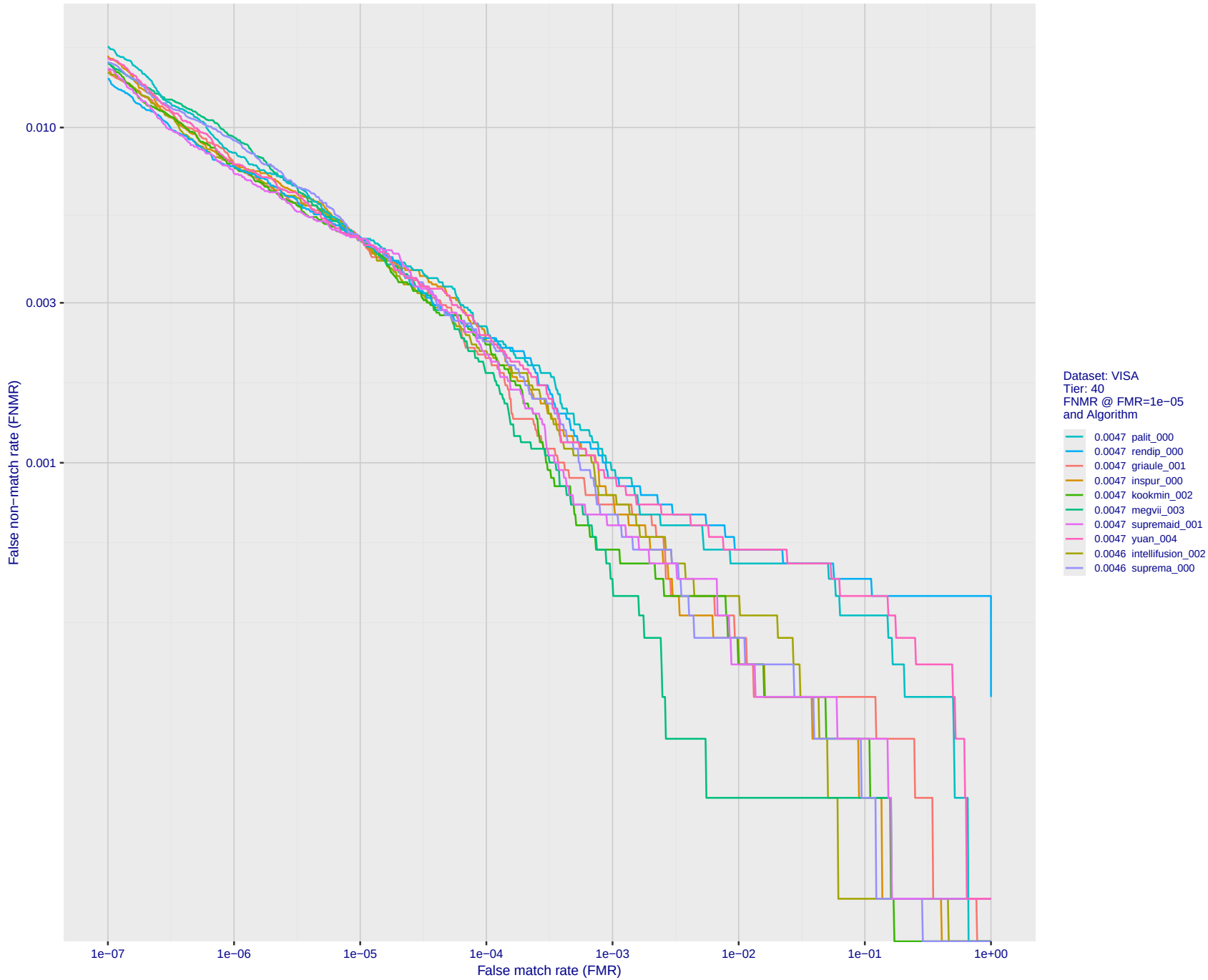

Figure 148: For the visa images, detection error tradeoff (DET) characteristics showing false non-match rate vs. false match rate plotted parametrically on threshold, T. The scales are logarithmic in order to show many decades of FMR.

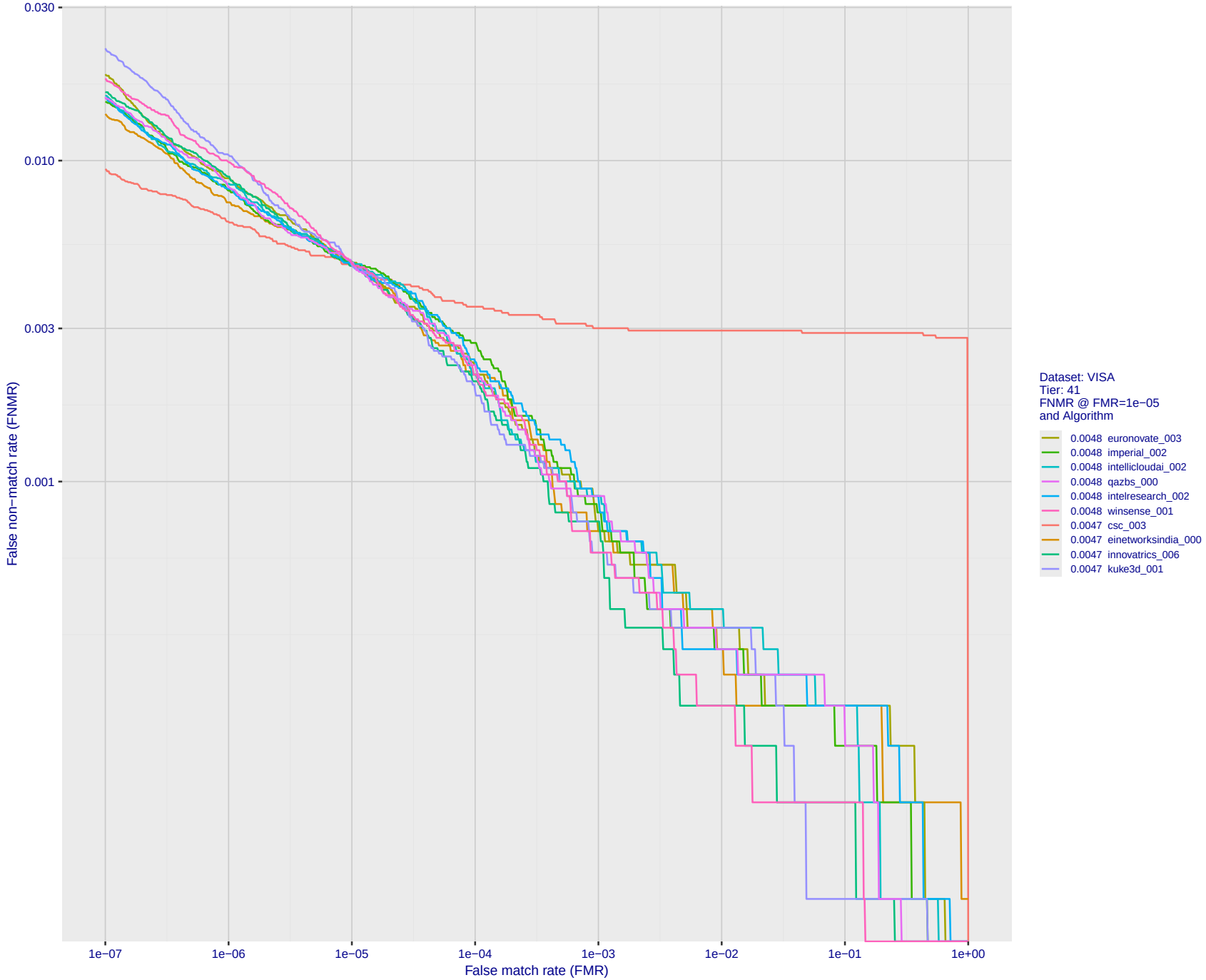

Figure 149: For the visa images, detection error tradeoff (DET) characteristics showing false non-match rate vs. false match rate plotted parametrically on threshold, T. The scales are logarithmic in order to show many decades of FMR.

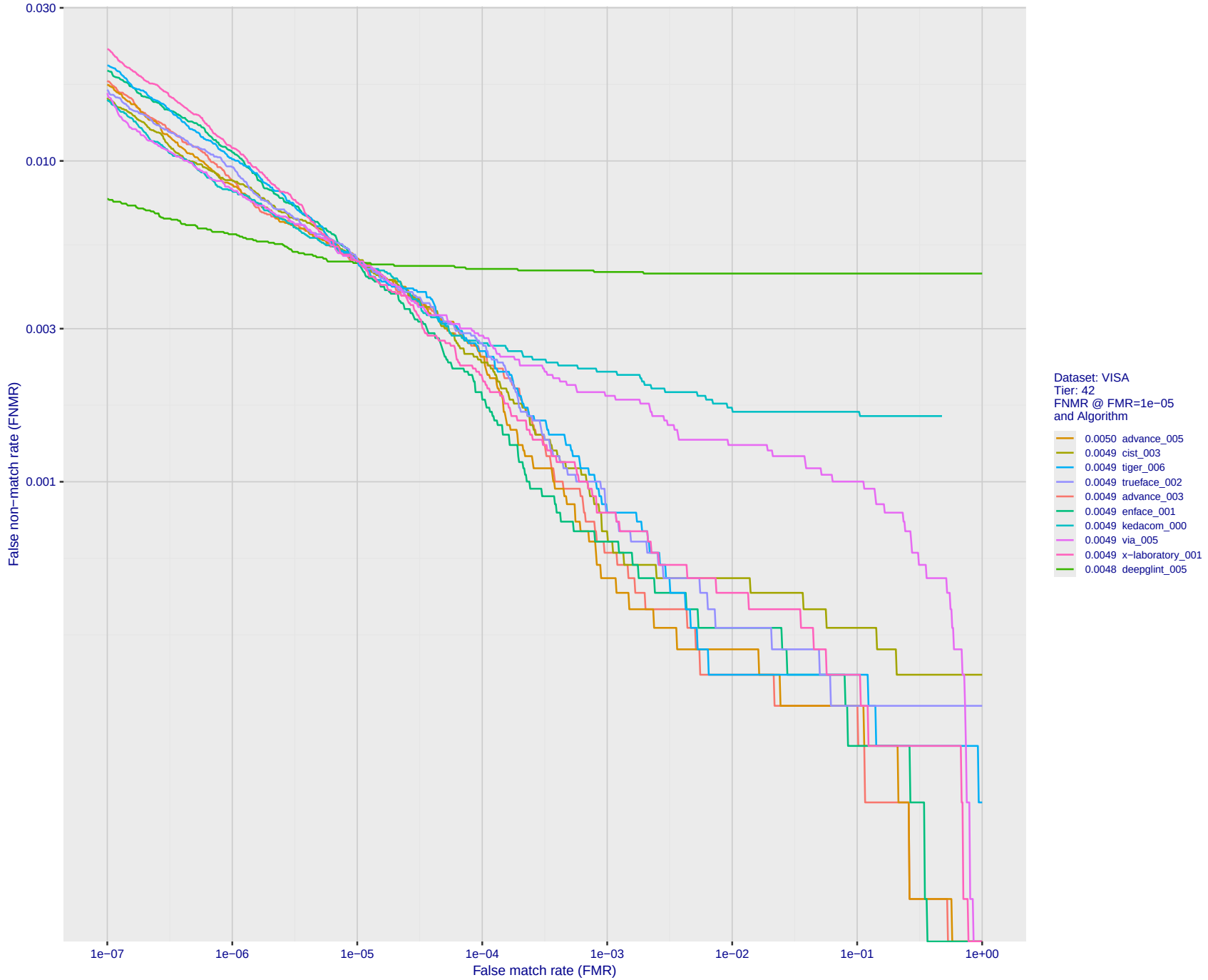

Figure 150: For the visa images, detection error tradeoff (DET) characteristics showing false non-match rate vs. false match rate plotted parametrically on threshold, T. The scales are logarithmic in order to show many decades of FMR.

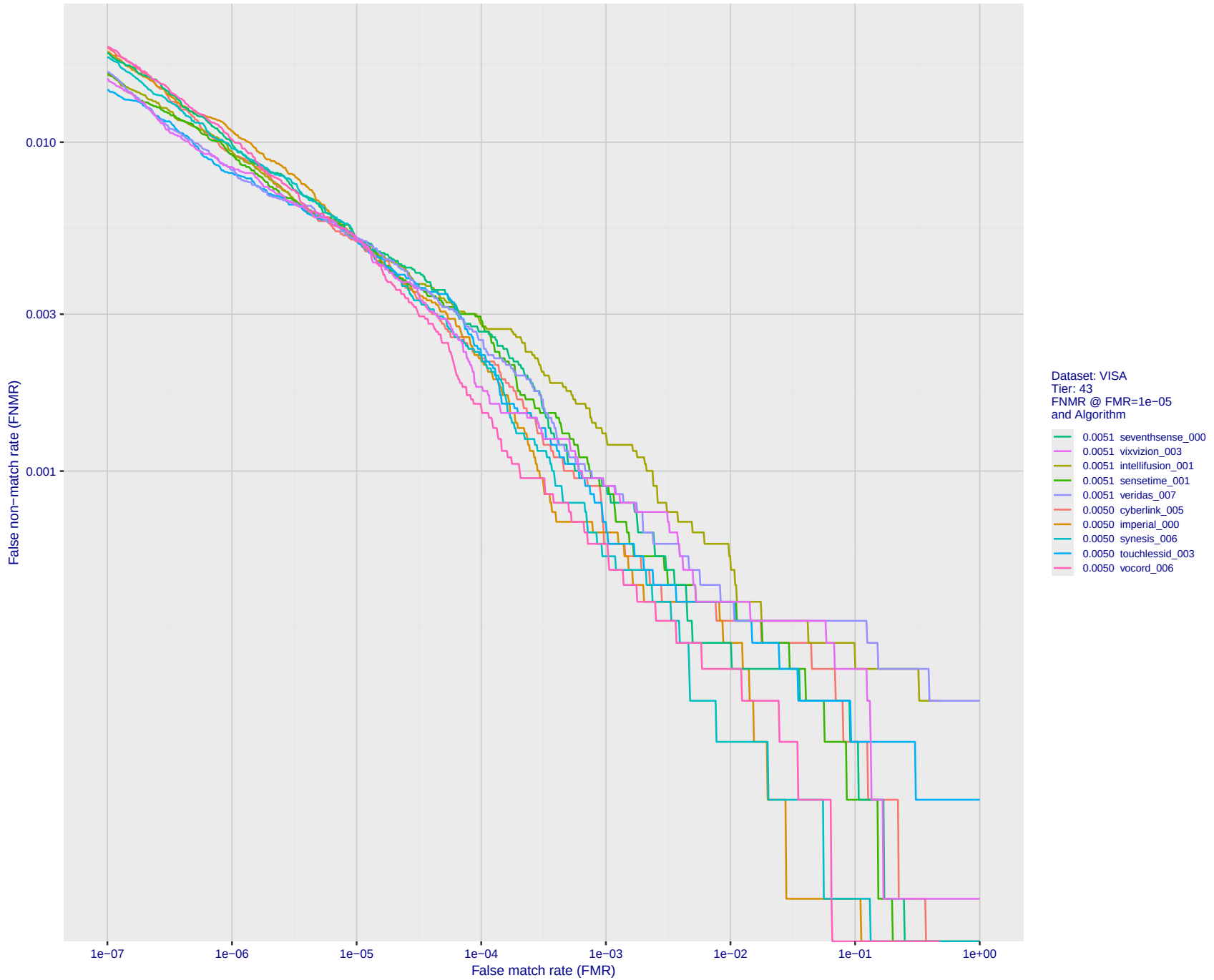

Figure 151: For the visa images, detection error tradeoff (DET) characteristics showing false non-match rate vs. false match rate plotted parametrically on threshold, T. The scales are logarithmic in order to show many decades of FMR.

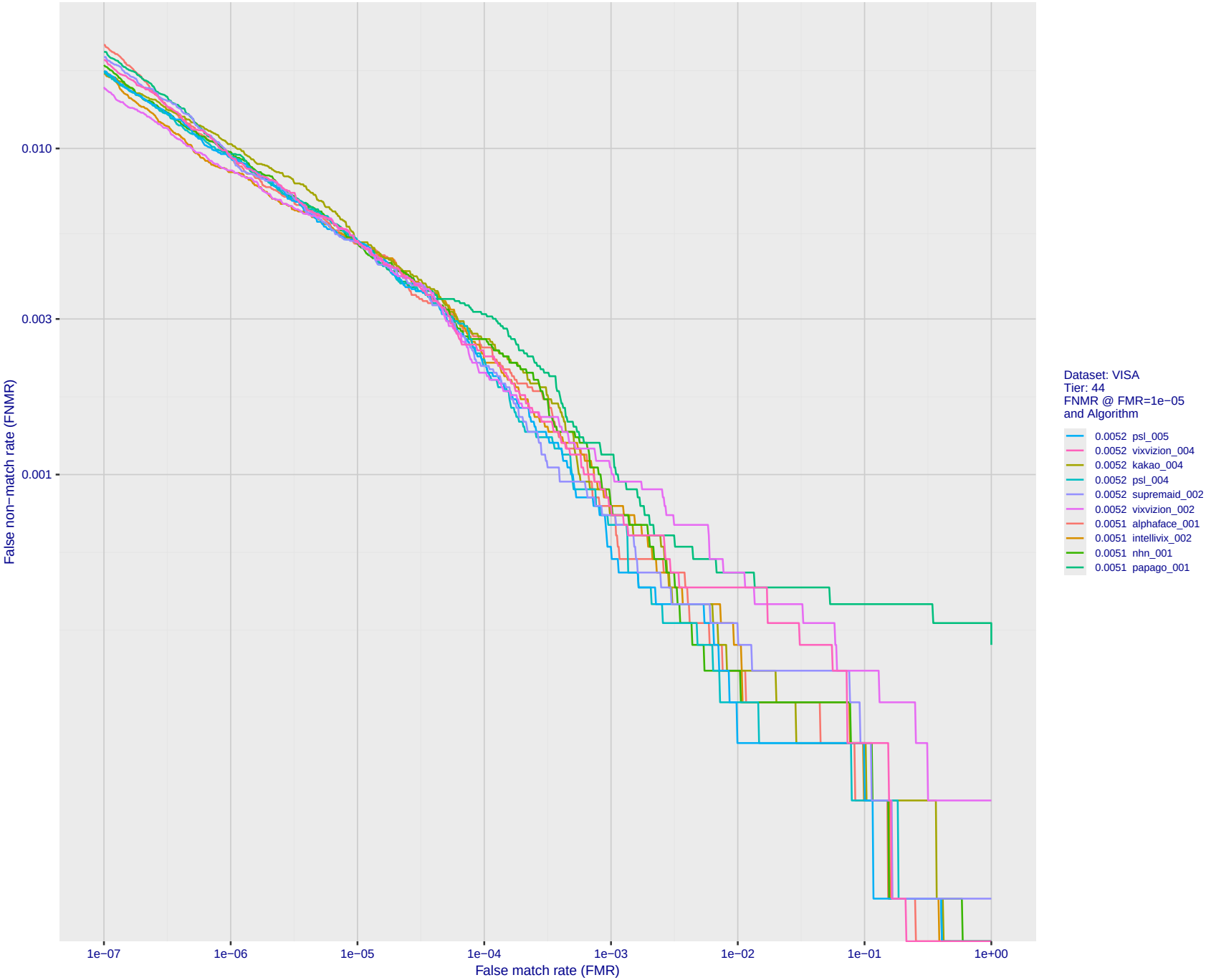

Figure 152: For the visa images, detection error tradeoff (DET) characteristics showing false non-match rate vs. false match rate plotted parametrically on threshold, T. The scales are logarithmic in order to show many decades of FMR.

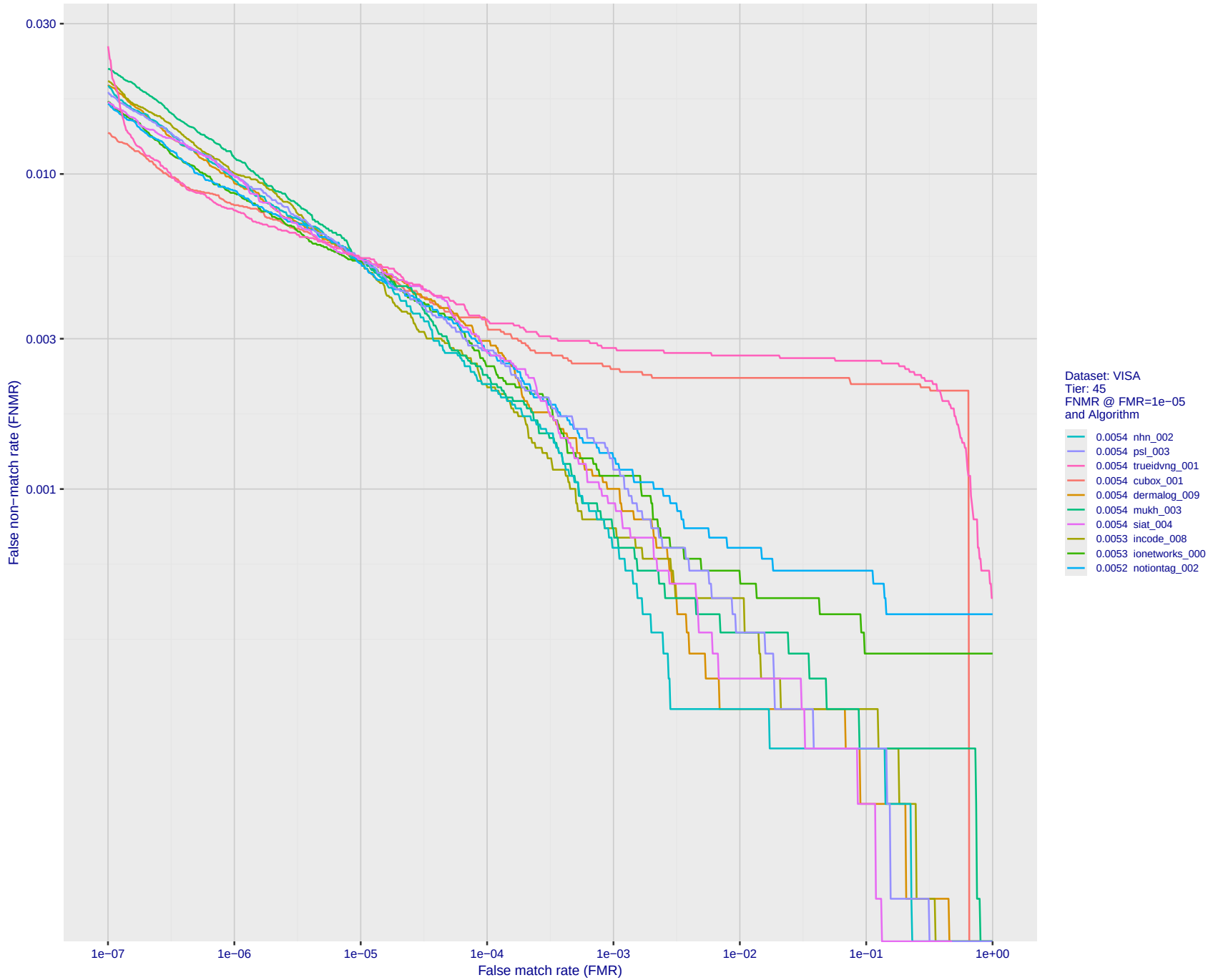

Figure 153: For the visa images, detection error tradeoff (DET) characteristics showing false non-match rate vs. false match rate plotted parametrically on threshold, T. The scales are logarithmic in order to show many decades of FMR.

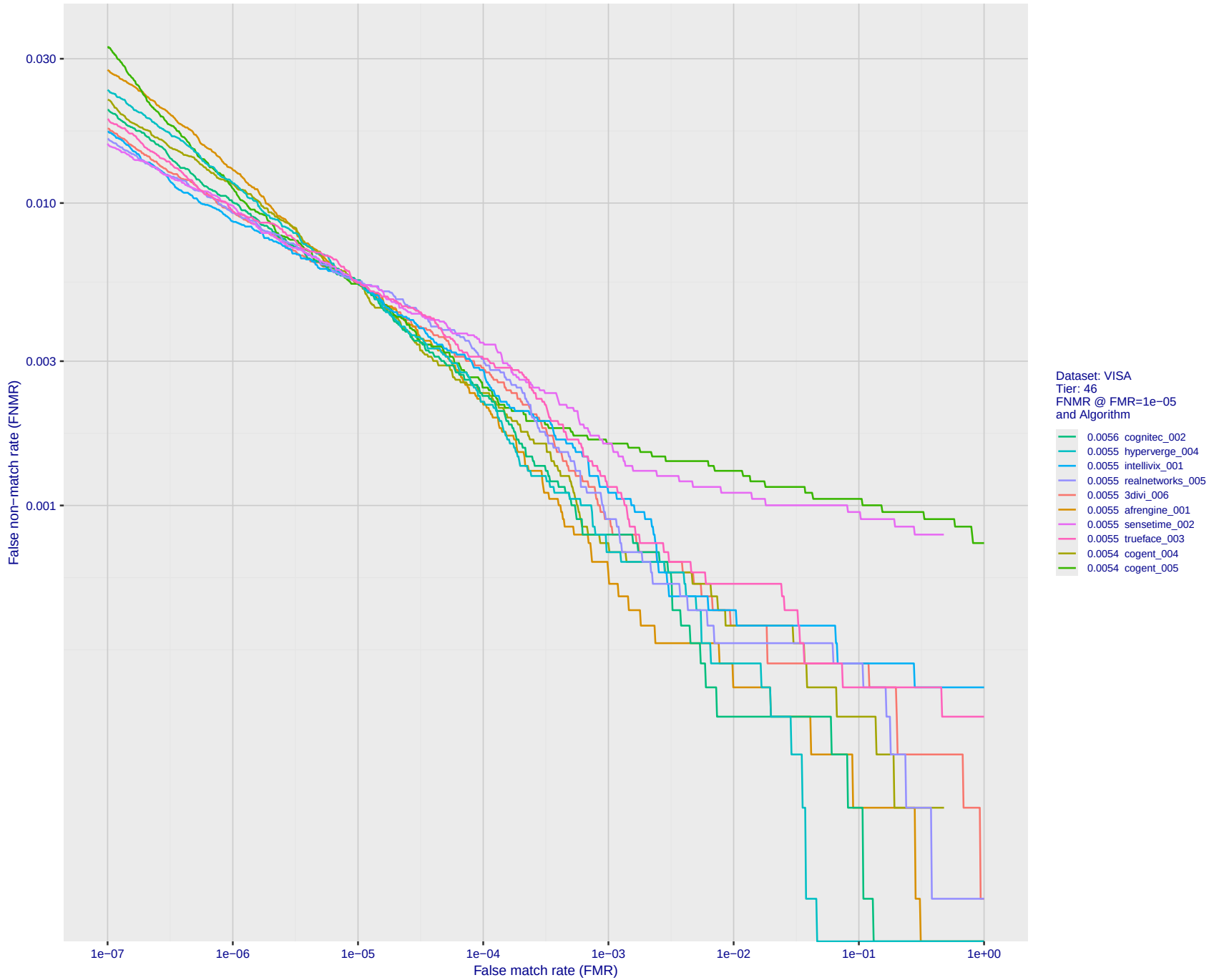

Figure 154: For the visa images, detection error tradeoff (DET) characteristics showing false non-match rate vs. false match rate plotted parametrically on threshold, T. The scales are logarithmic in order to show many decades of FMR.

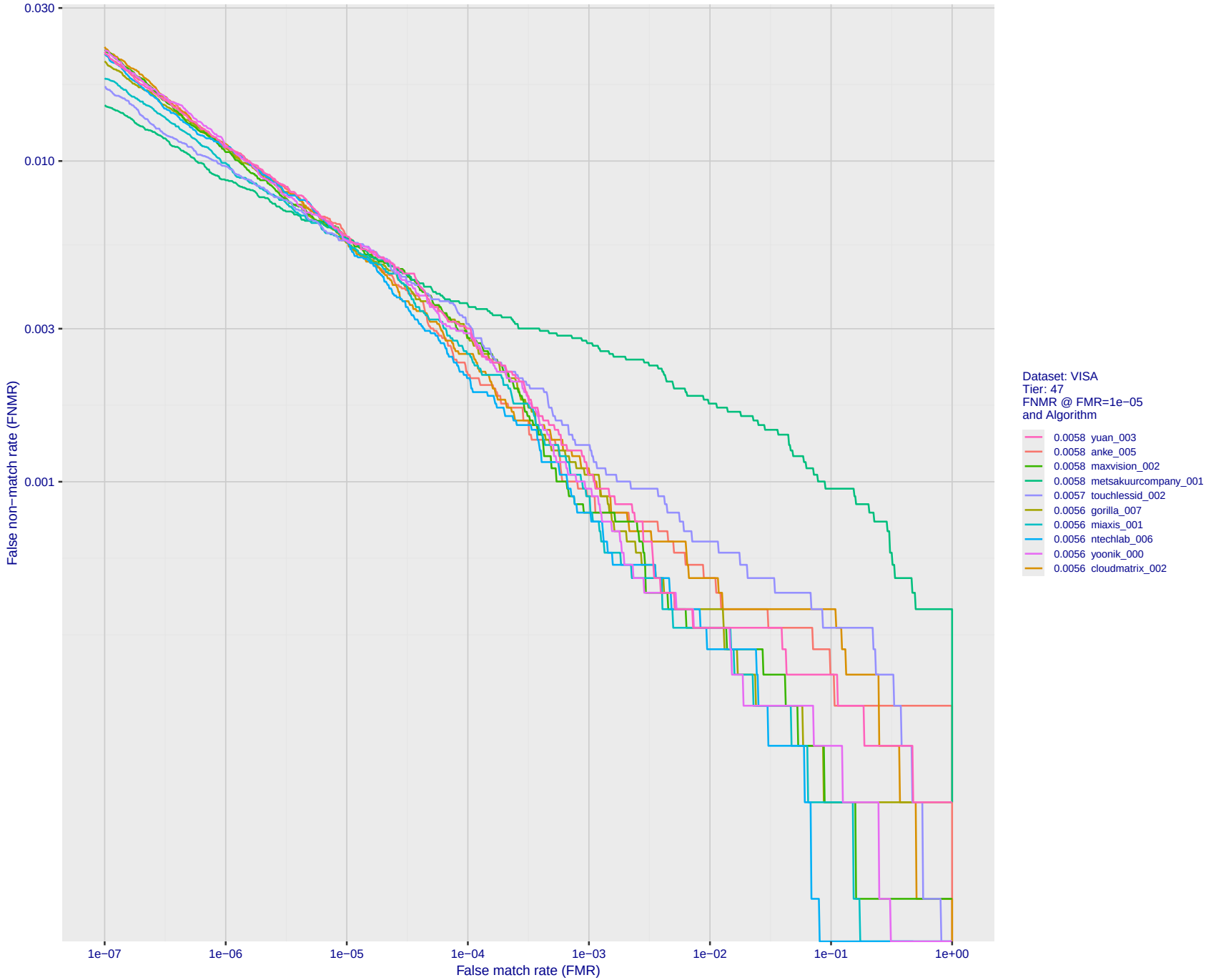

Figure 155: For the visa images, detection error tradeoff (DET) characteristics showing false non-match rate vs. false match rate plotted parametrically on threshold, T. The scales are logarithmic in order to show many decades of FMR.

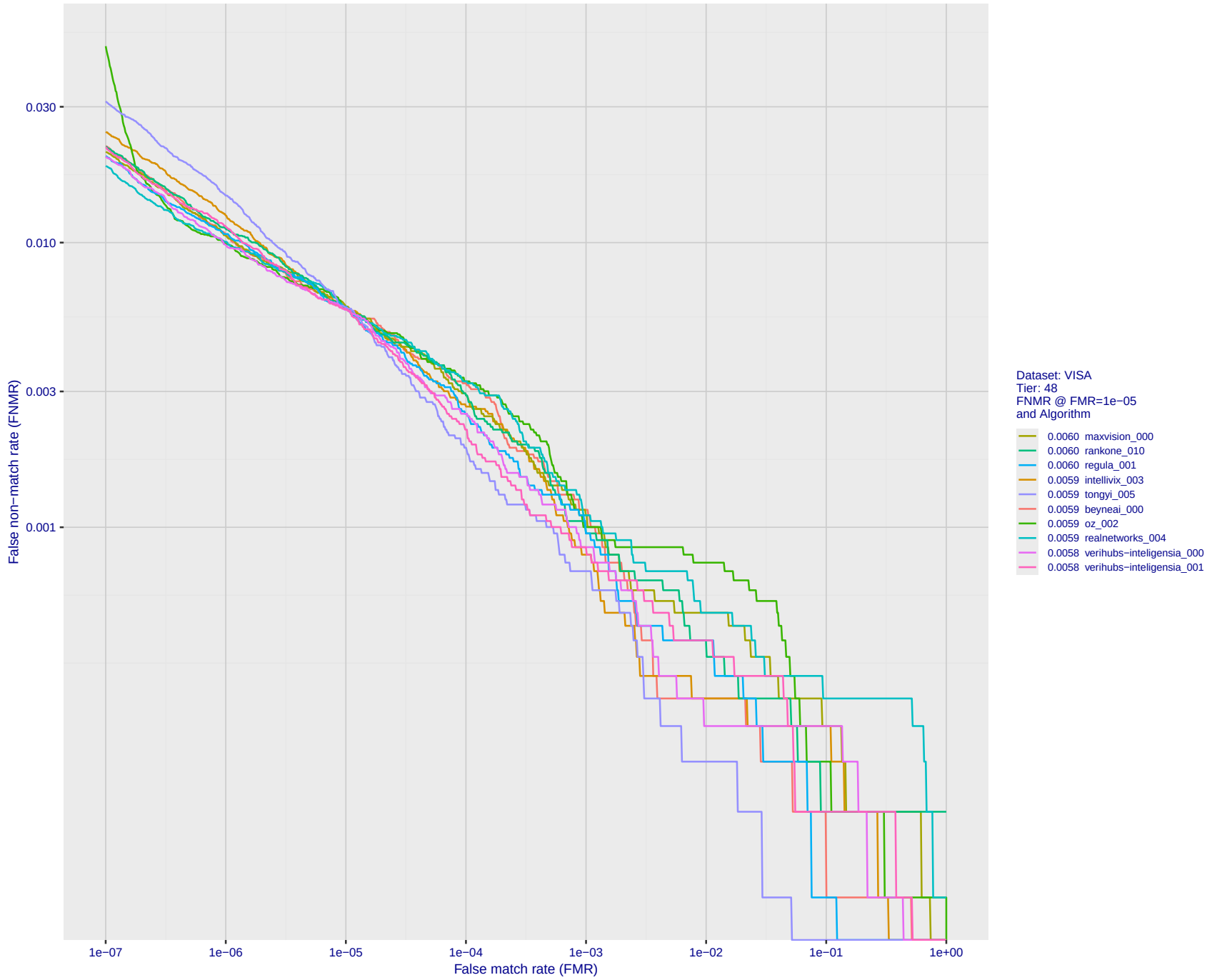

Figure 156: For the visa images, detection error tradeoff (DET) characteristics showing false non-match rate vs. false match rate plotted parametrically on threshold, T. The scales are logarithmic in order to show many decades of FMR.

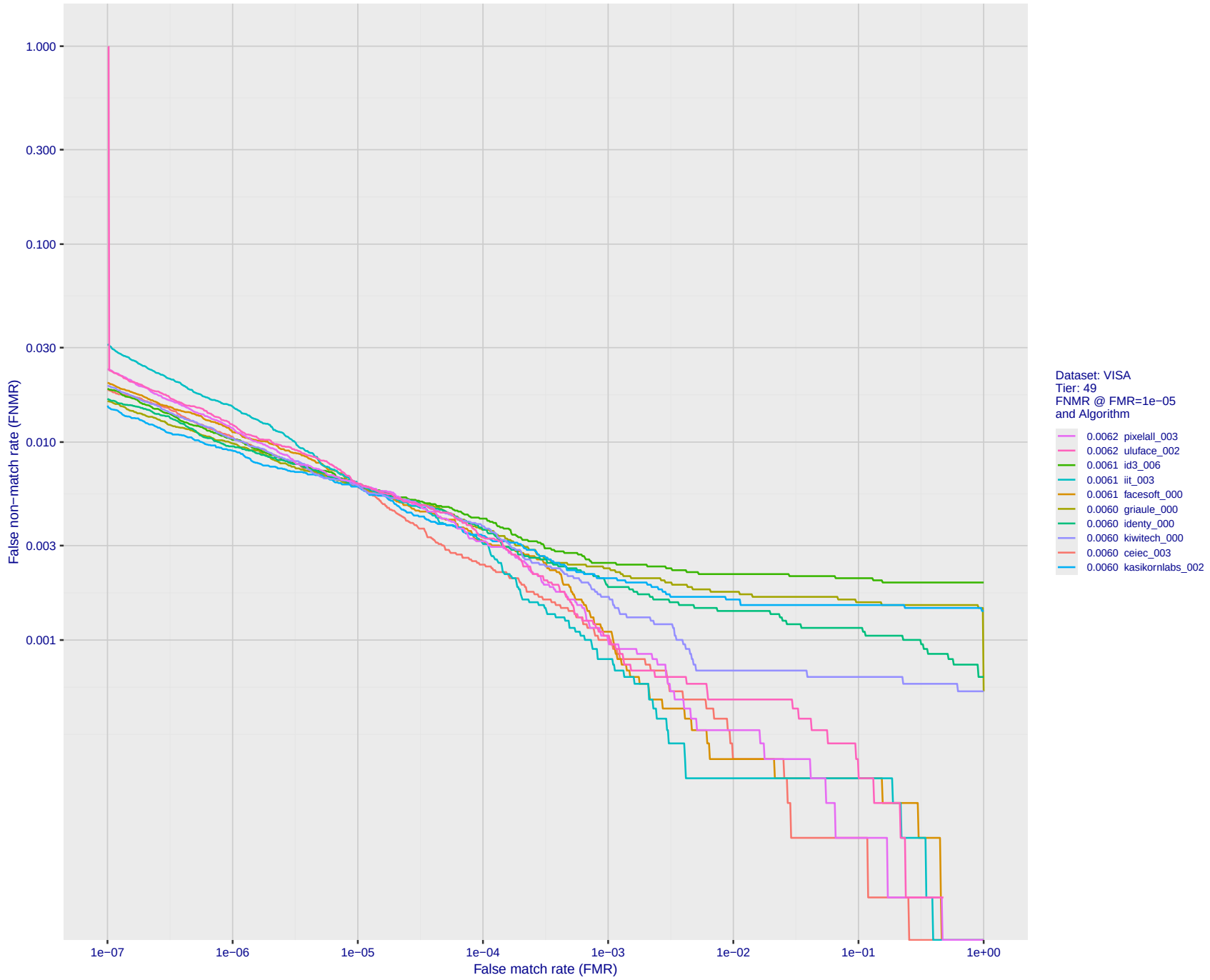

Figure 157: For the visa images, detection error tradeoff (DET) characteristics showing false non-match rate vs. false match rate plotted parametrically on threshold, T. The scales are logarithmic in order to show many decades of FMR.

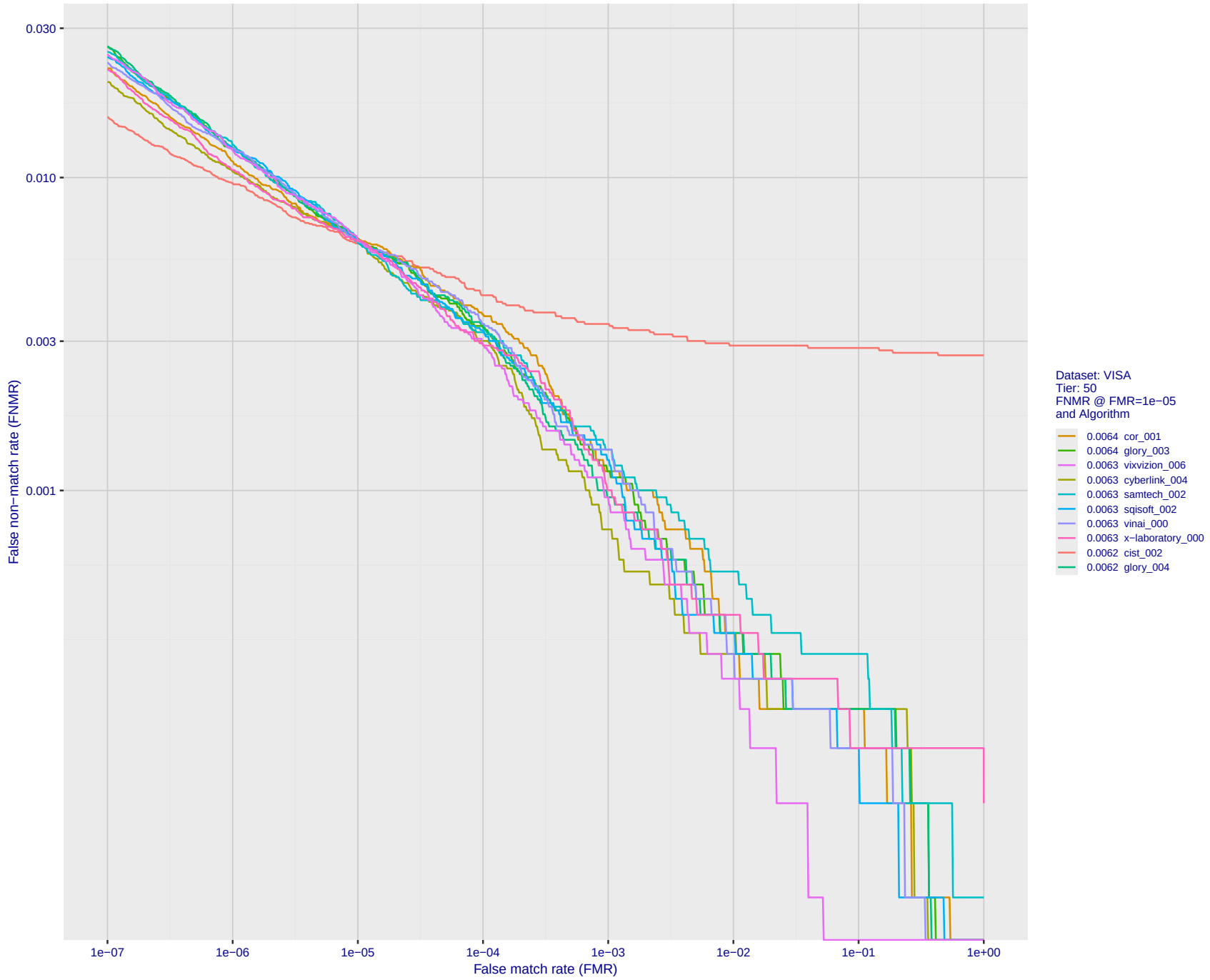

Figure 158: For the visa images, detection error tradeoff (DET) characteristics showing false non-match rate vs. false match rate plotted parametrically on threshold, T. The scales are logarithmic in order to show many decades of FMR.

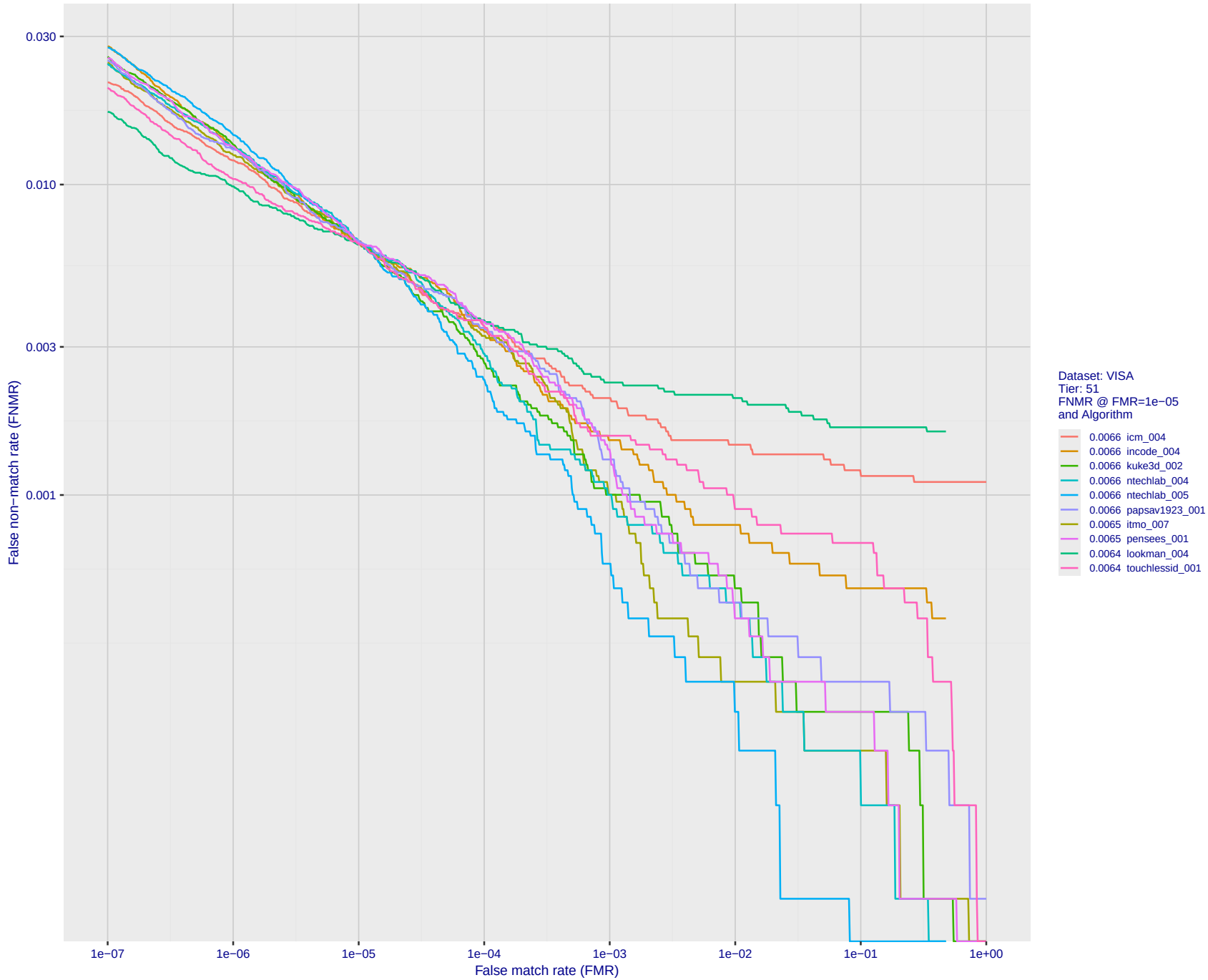

Figure 159: For the visa images, detection error tradeoff (DET) characteristics showing false non-match rate vs. false match rate plotted parametrically on threshold, T. The scales are logarithmic in order to show many decades of FMR.

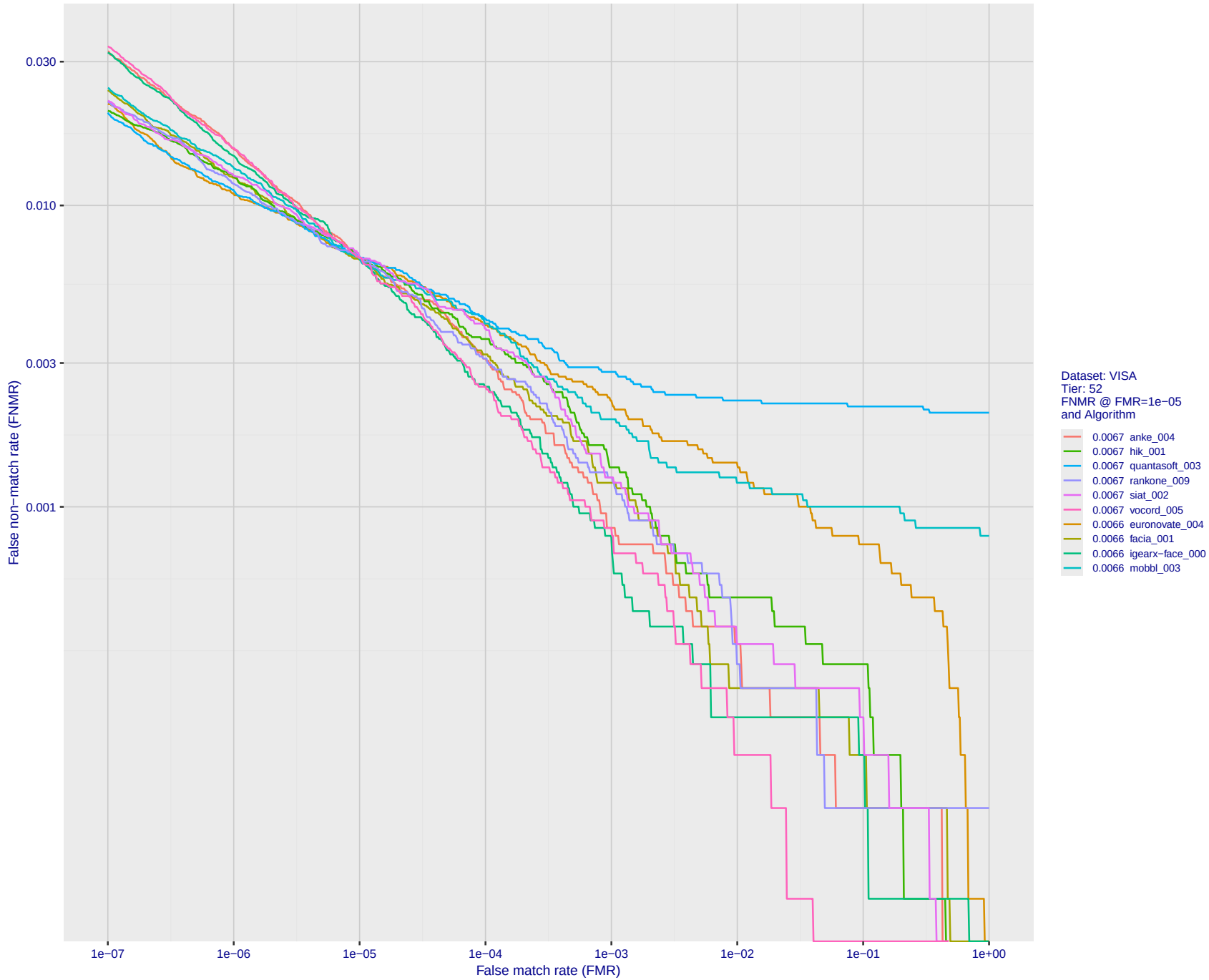

Figure 160: For the visa images, detection error tradeoff (DET) characteristics showing false non-match rate vs. false match rate plotted parametrically on threshold, T. The scales are logarithmic in order to show many decades of FMR.

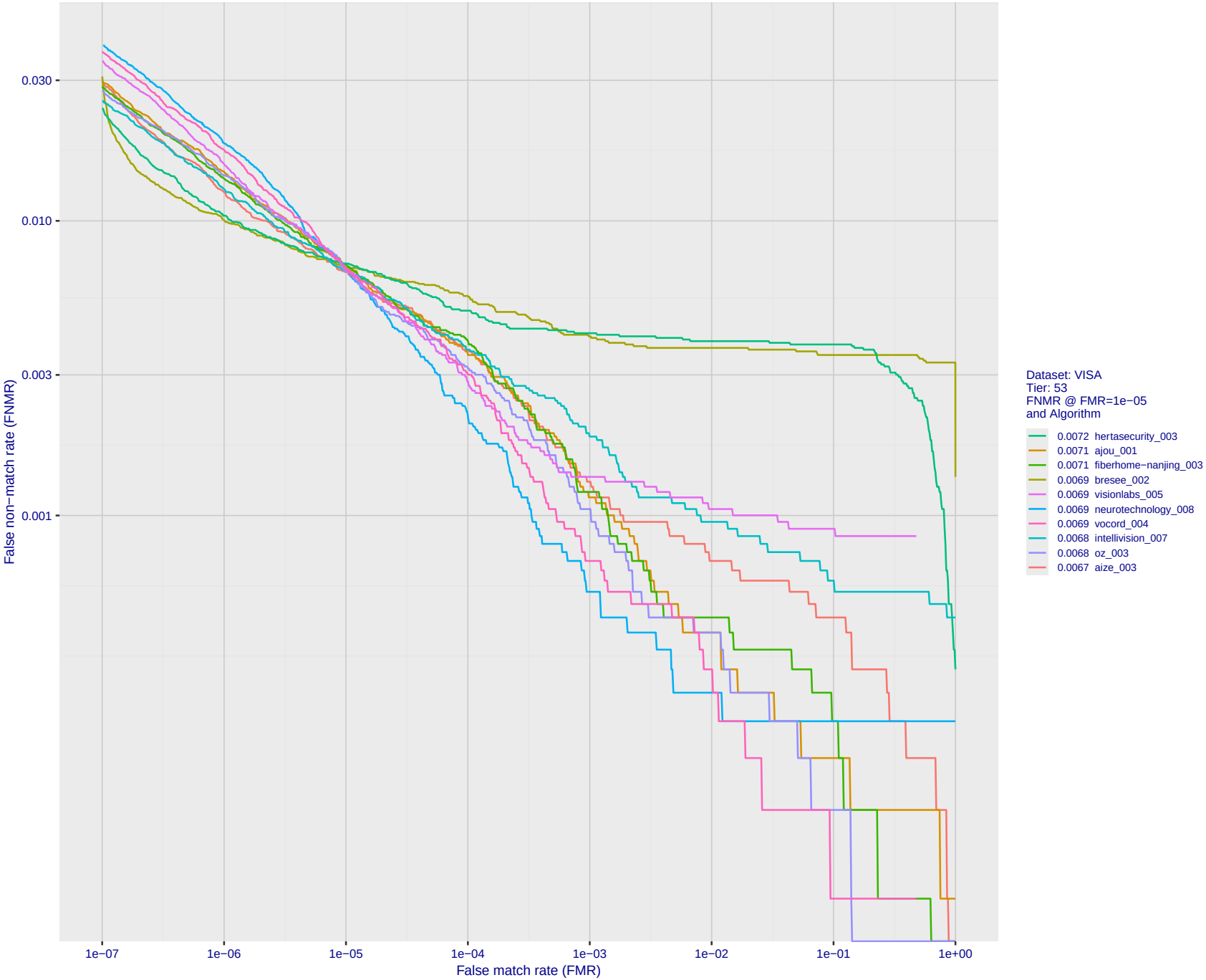

Figure 161: For the visa images, detection error tradeoff (DET) characteristics showing false non-match rate vs. false match rate plotted parametrically on threshold, T. The scales are logarithmic in order to show many decades of FMR.

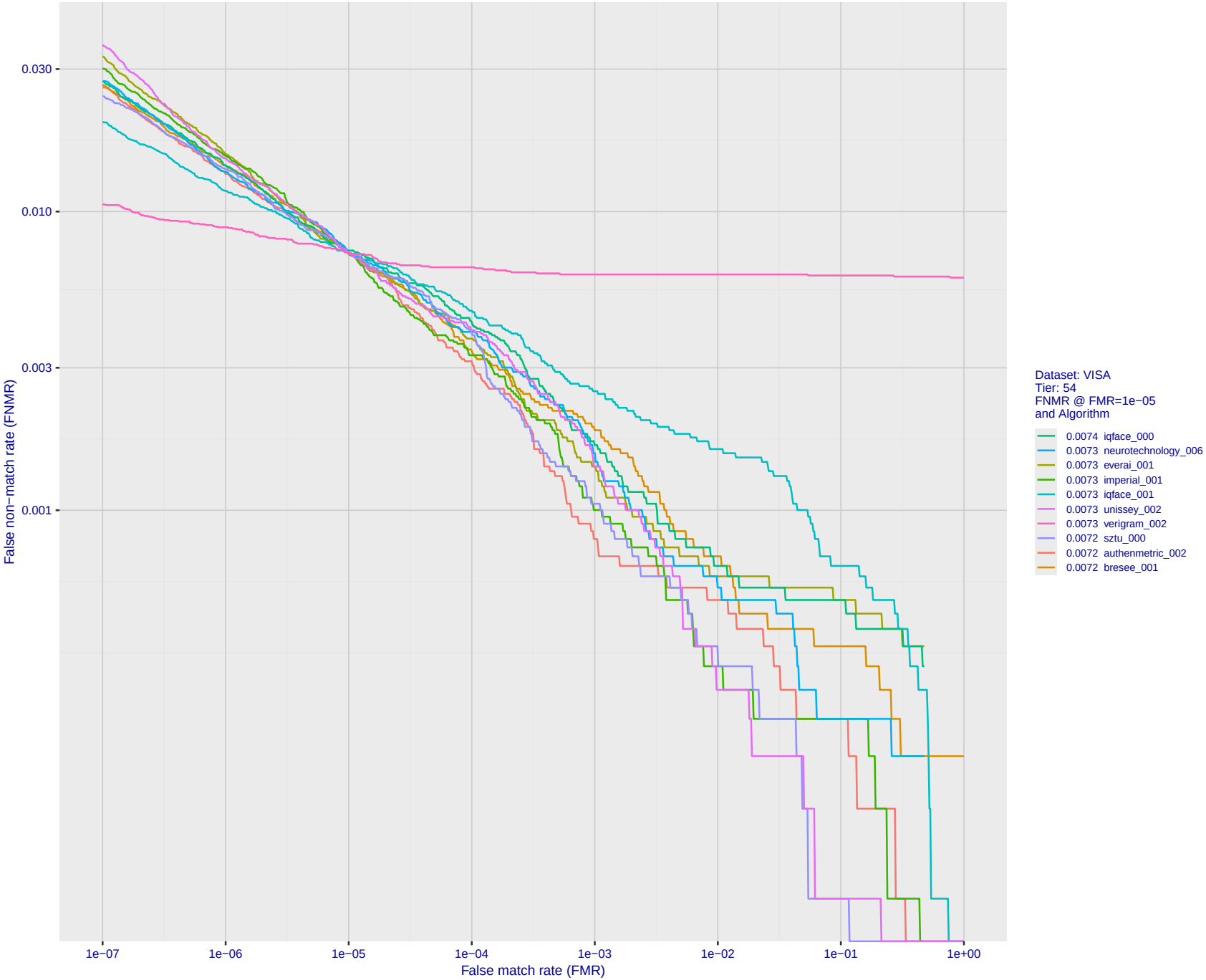

Figure 162: For the visa images, detection error tradeoff (DET) characteristics showing false non-match rate vs. false match rate plotted parametrically on threshold, T. The scales are logarithmic in order to show many decades of FMR.

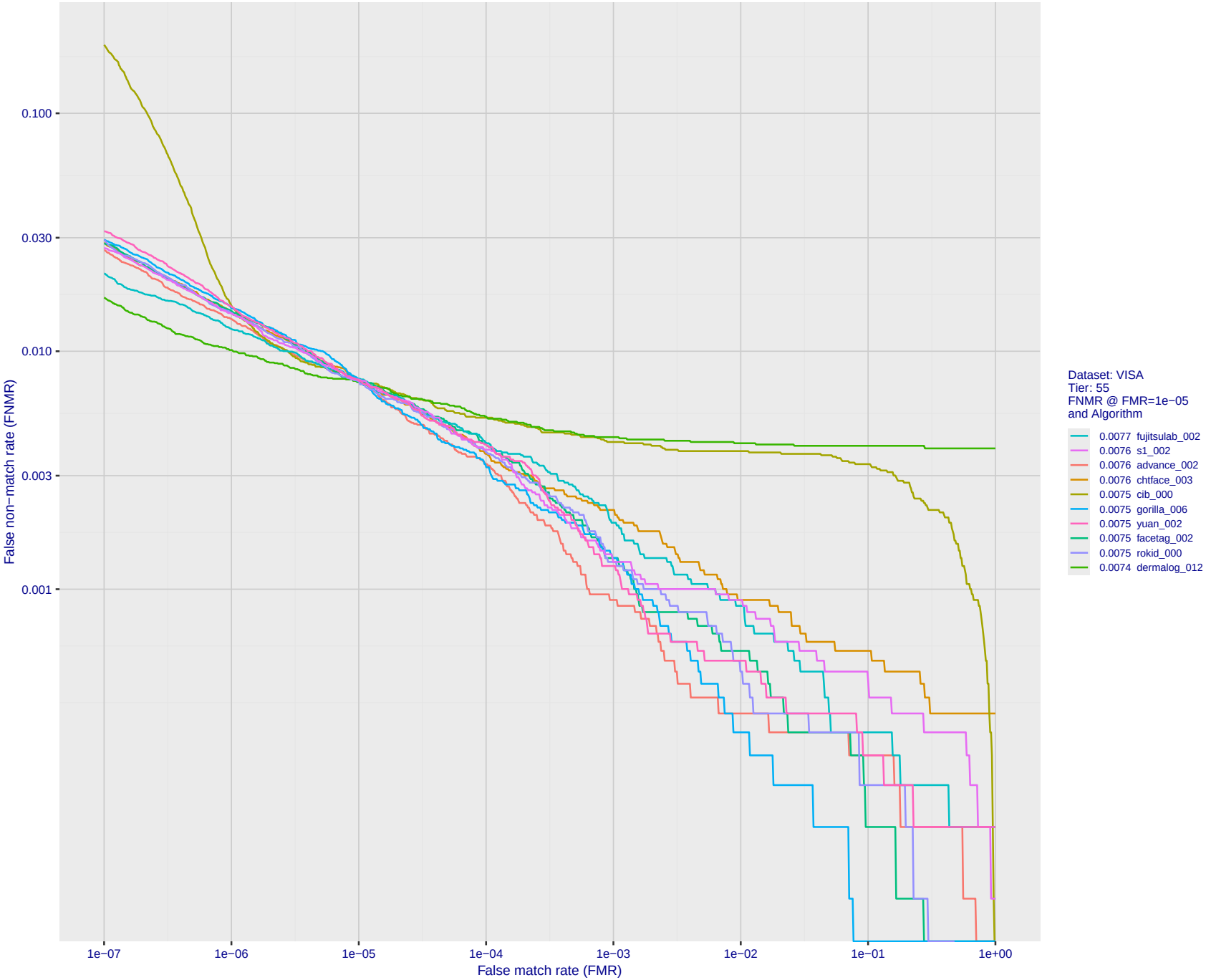

Figure 163: For the visa images, detection error tradeoff (DET) characteristics showing false non-match rate vs. false match rate plotted parametrically on threshold, T. The scales are logarithmic in order to show many decades of FMR.

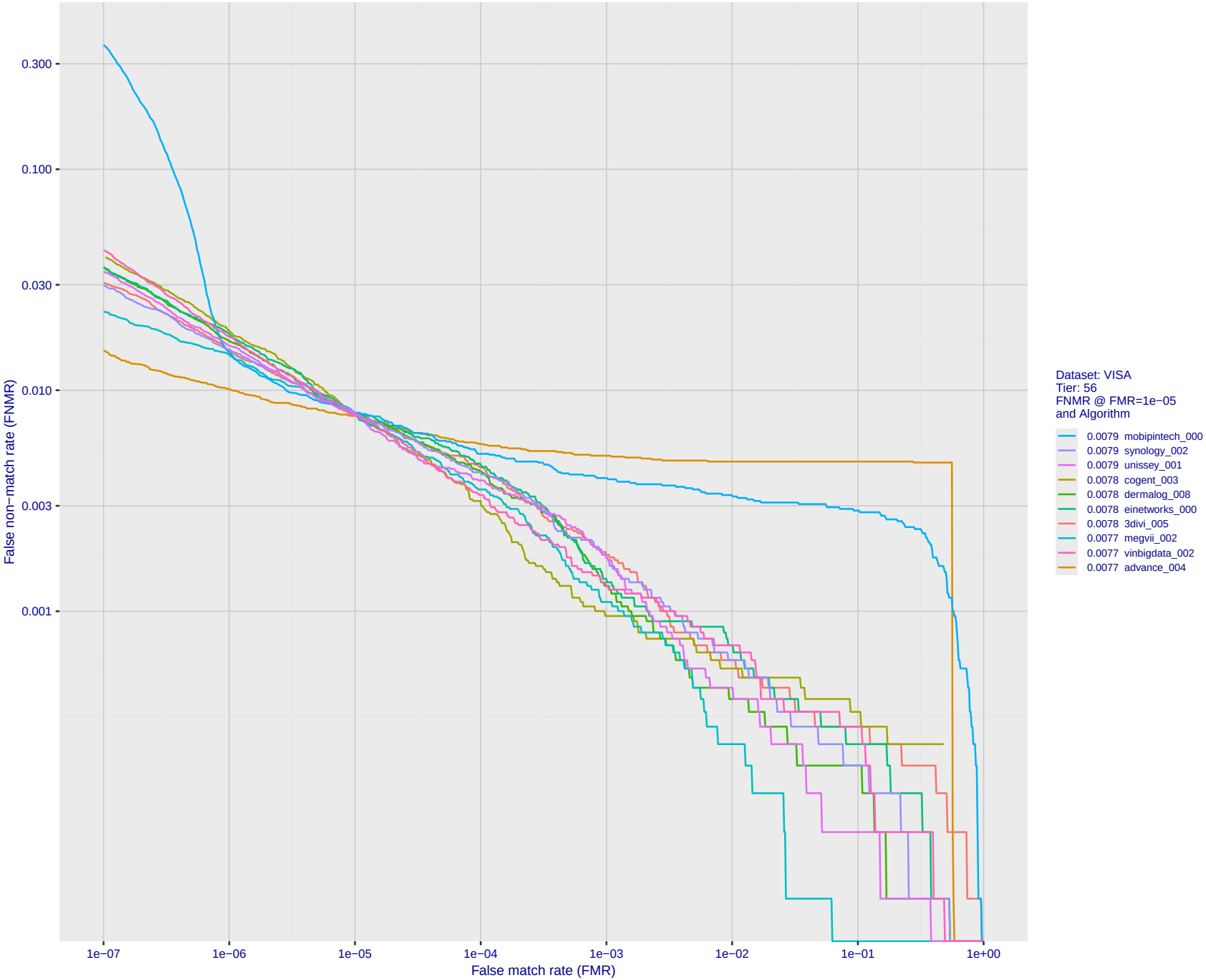

Figure 164: For the visa images, detection error tradeoff (DET) characteristics showing false non-match rate vs. false match rate plotted parametrically on threshold, T. The scales are logarithmic in order to show many decades of FMR.

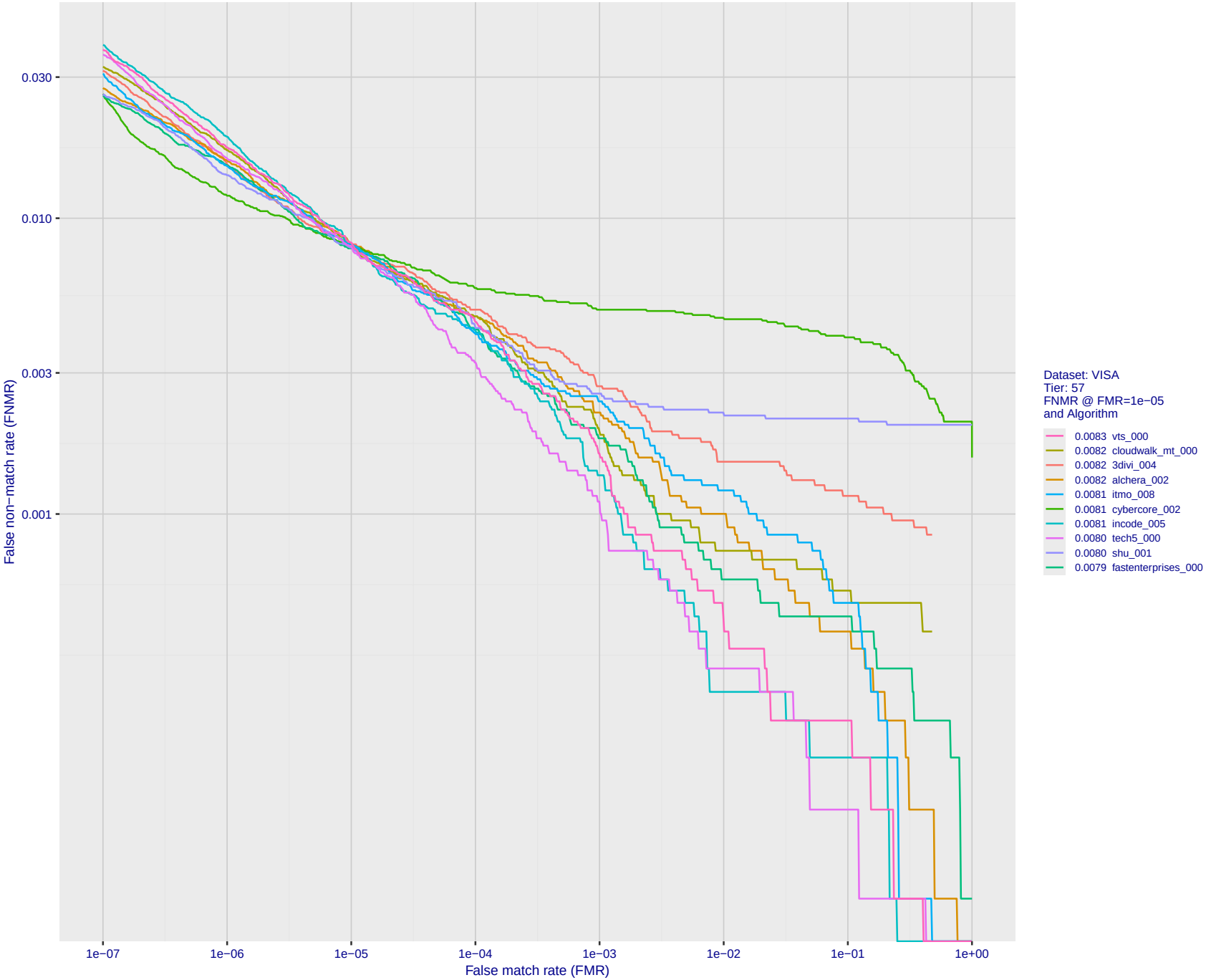

Figure 165: For the visa images, detection error tradeoff (DET) characteristics showing false non-match rate vs. false match rate plotted parametrically on threshold, T. The scales are logarithmic in order to show many decades of FMR.

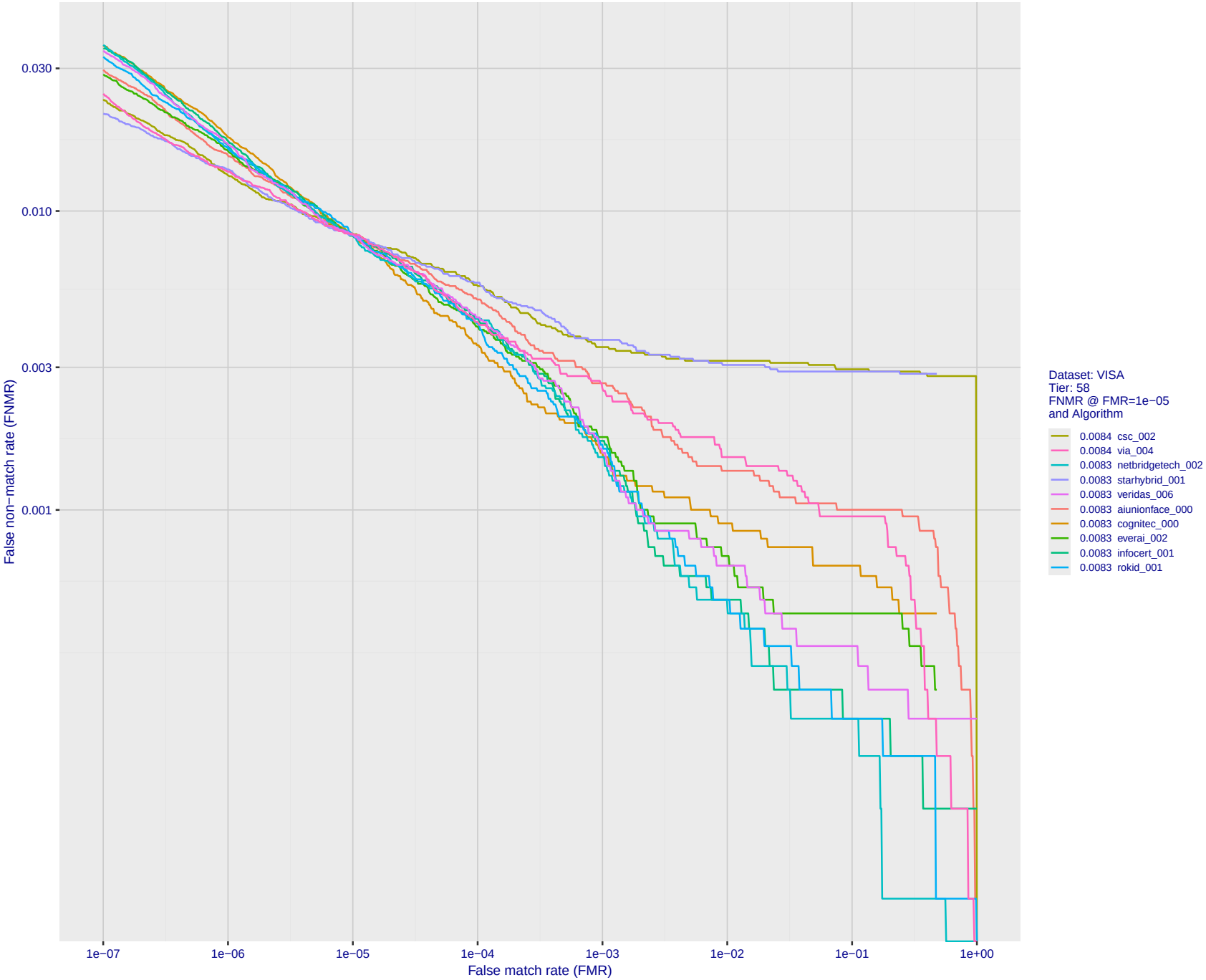

Figure 166: For the visa images, detection error tradeoff (DET) characteristics showing false non-match rate vs. false match rate plotted parametrically on threshold, T. The scales are logarithmic in order to show many decades of FMR.

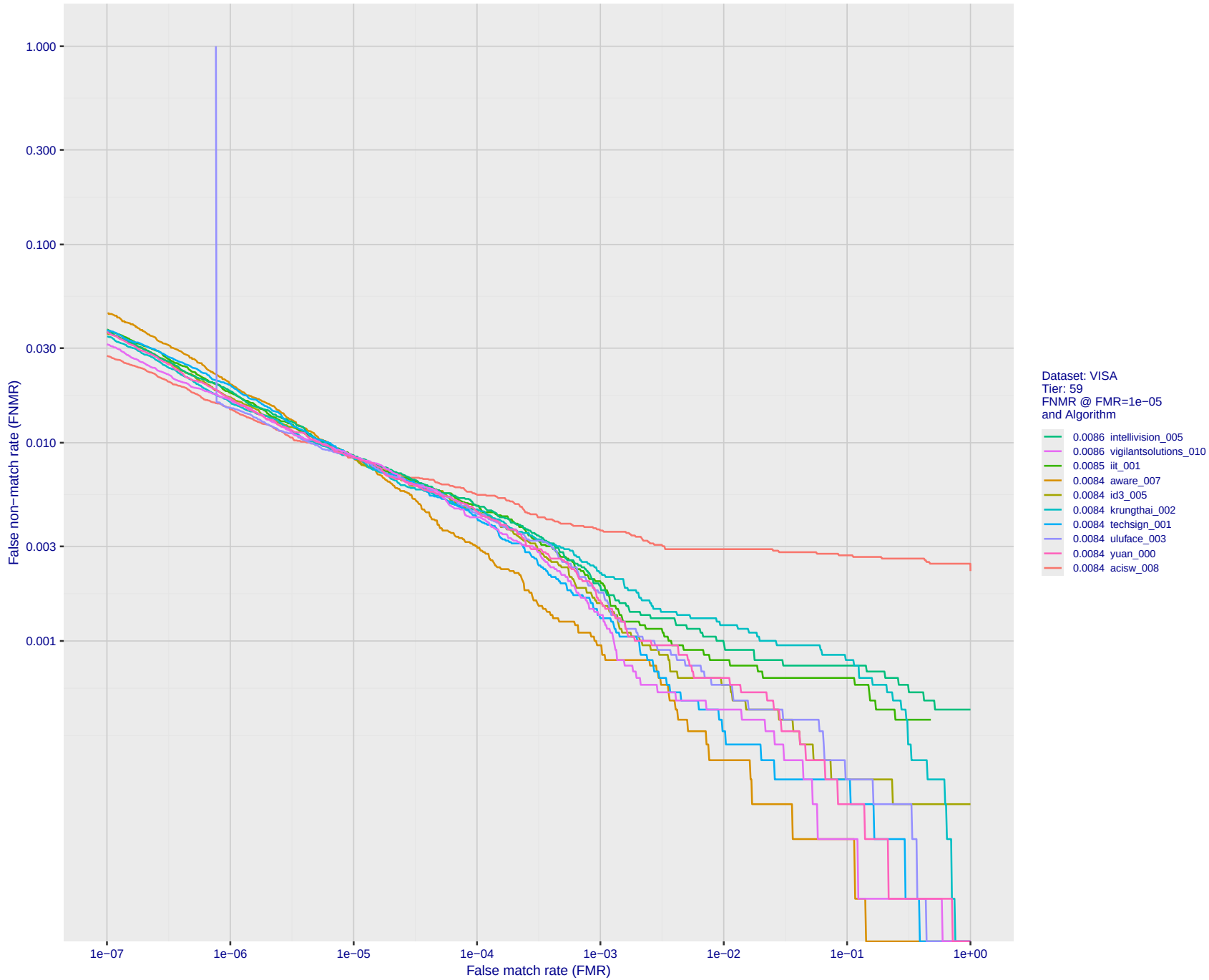

Figure 167: For the visa images, detection error tradeoff (DET) characteristics showing false non-match rate vs. false match rate plotted parametrically on threshold, T. The scales are logarithmic in order to show many decades of FMR.

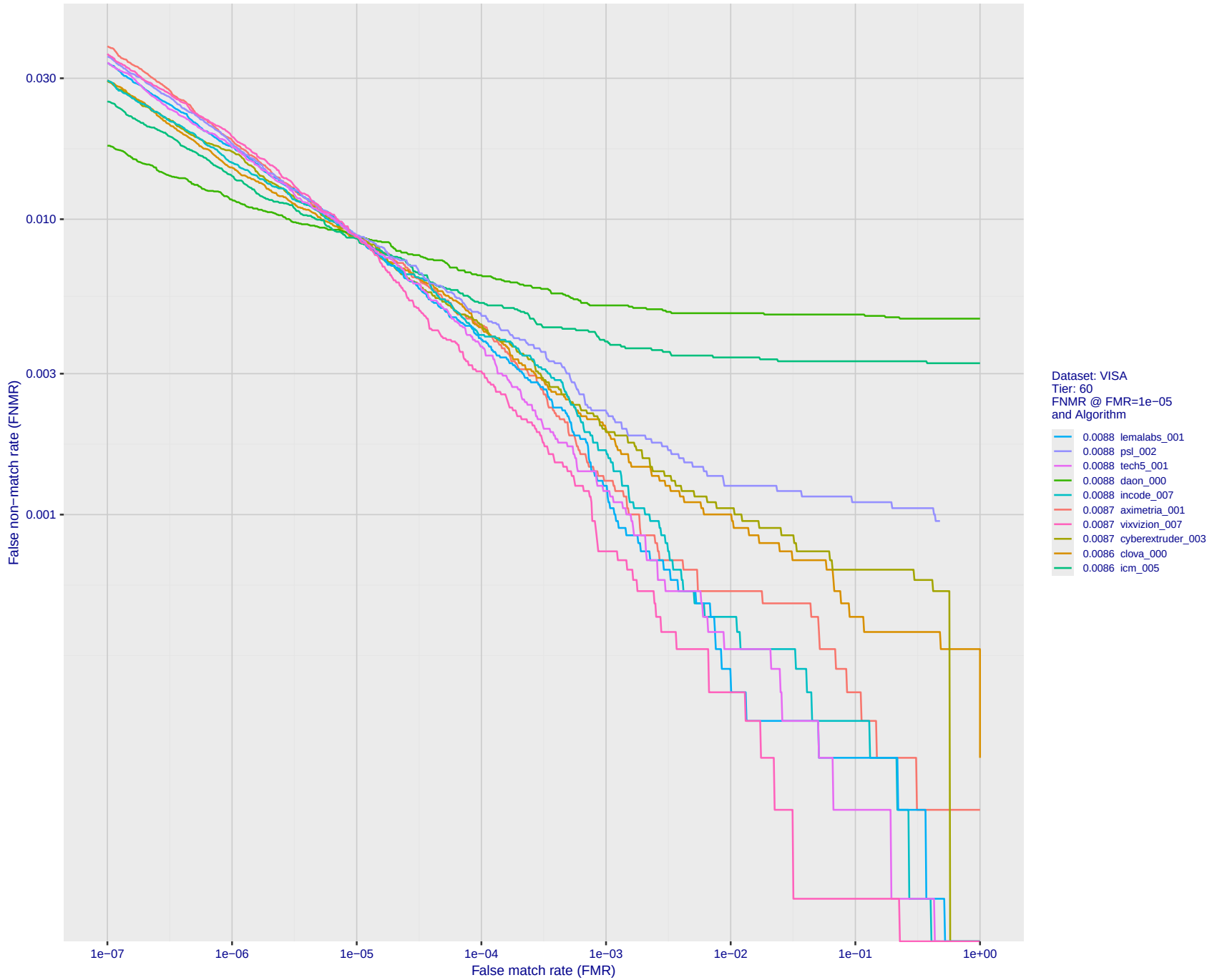

Figure 168: For the visa images, detection error tradeoff (DET) characteristics showing false non-match rate vs. false match rate plotted parametrically on threshold, T. The scales are logarithmic in order to show many decades of FMR.

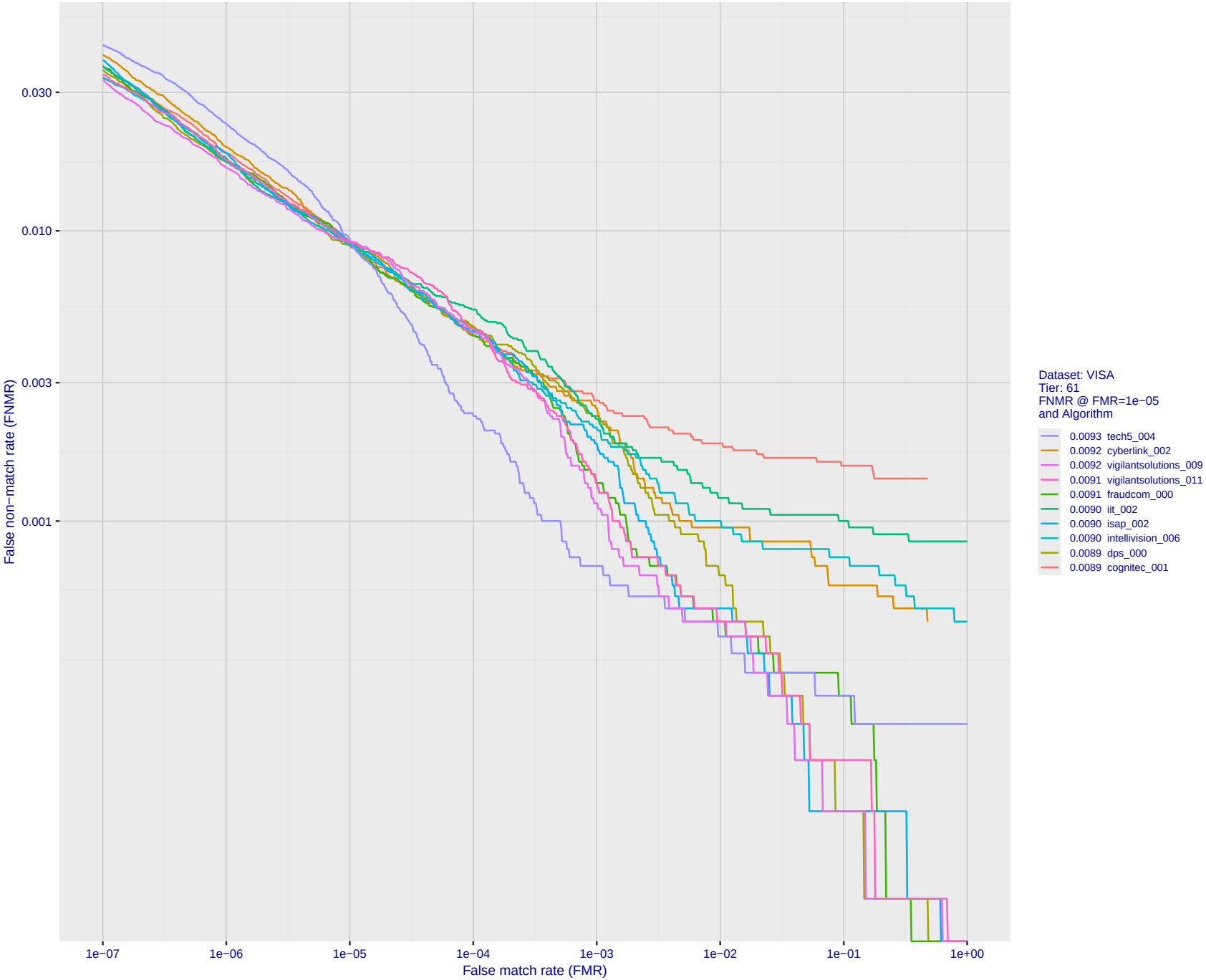

Figure 169: For the visa images, detection error tradeoff (DET) characteristics showing false non-match rate vs. false match rate plotted parametrically on threshold, T. The scales are logarithmic in order to show many decades of FMR.

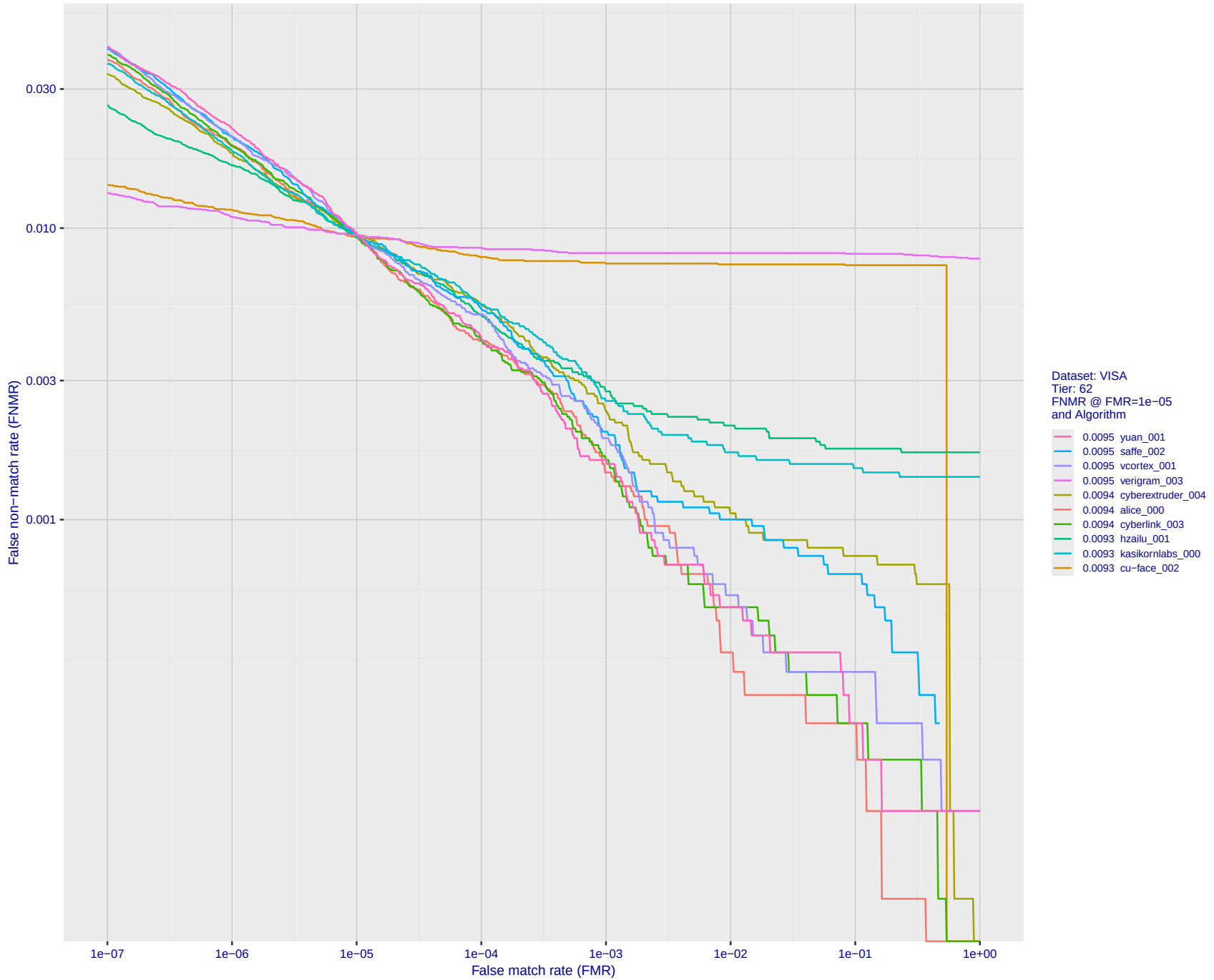

Figure 170: For the visa images, detection error tradeoff (DET) characteristics showing false non-match rate vs. false match rate plotted parametrically on threshold, T. The scales are logarithmic in order to show many decades of FMR.

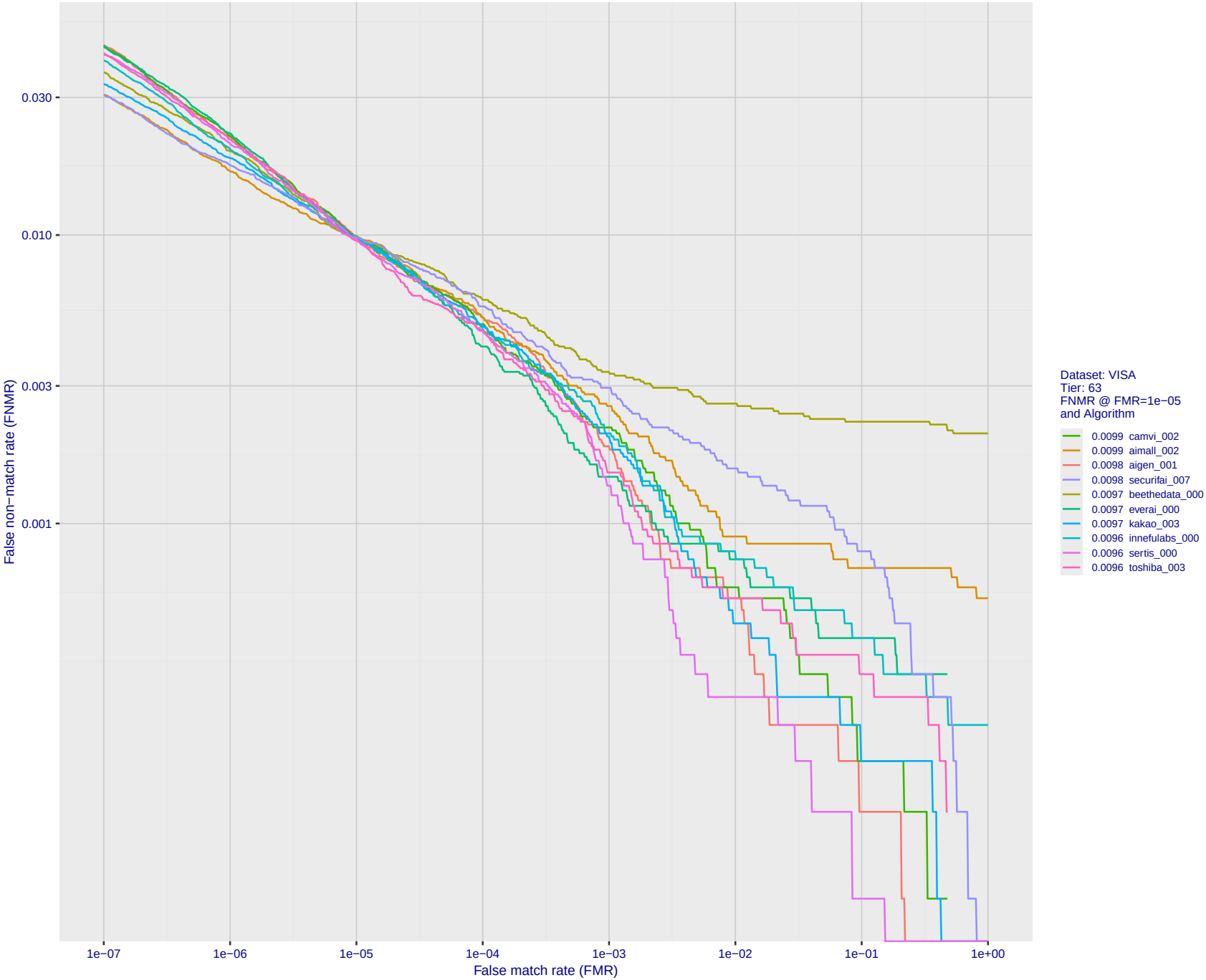

Figure 171: For the visa images, detection error tradeoff (DET) characteristics showing false non-match rate vs. false match rate plotted parametrically on threshold, T. The scales are logarithmic in order to show many decades of FMR.

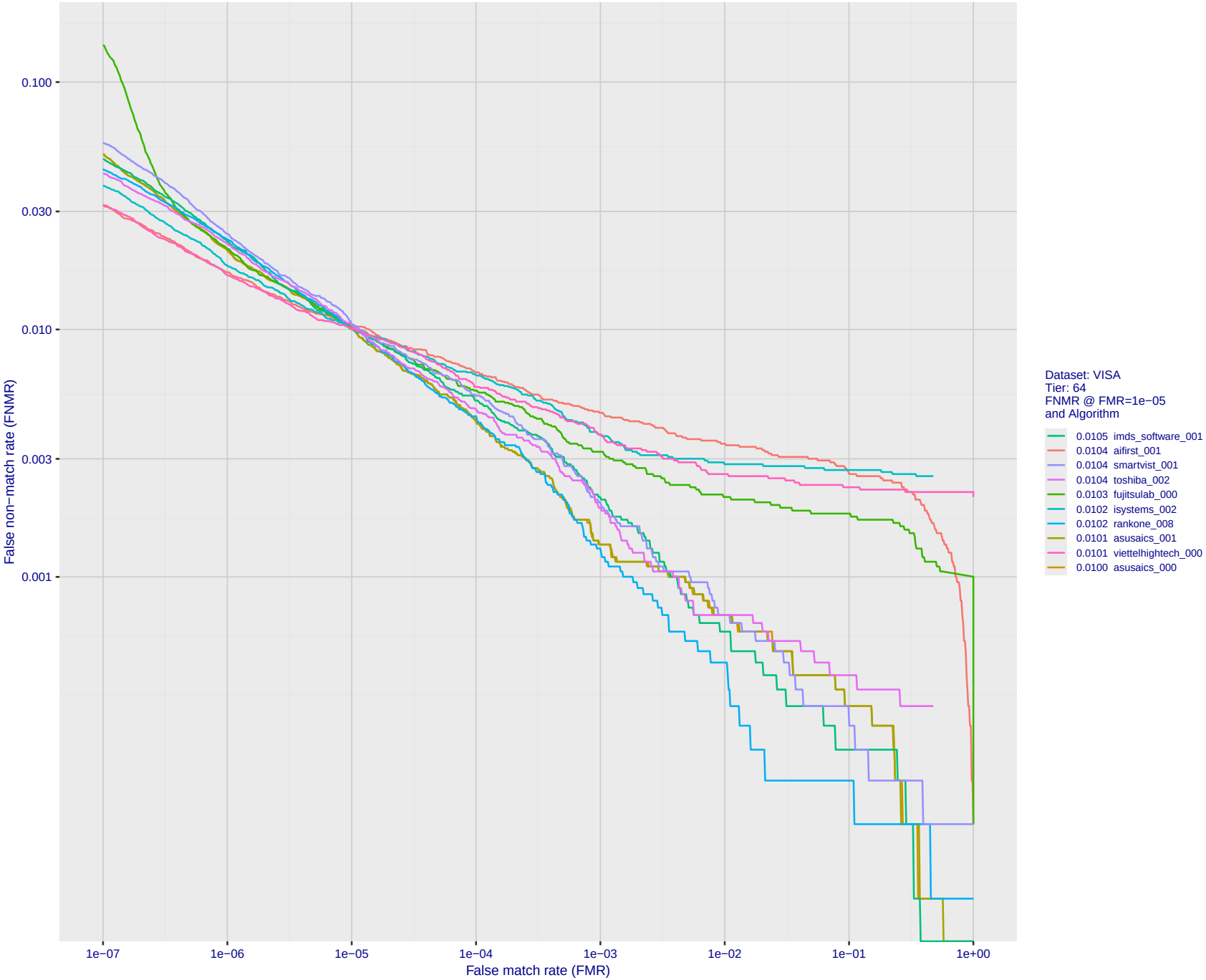

Figure 172: For the visa images, detection error tradeoff (DET) characteristics showing false non-match rate vs. false match rate plotted parametrically on threshold, T. The scales are logarithmic in order to show many decades of FMR.

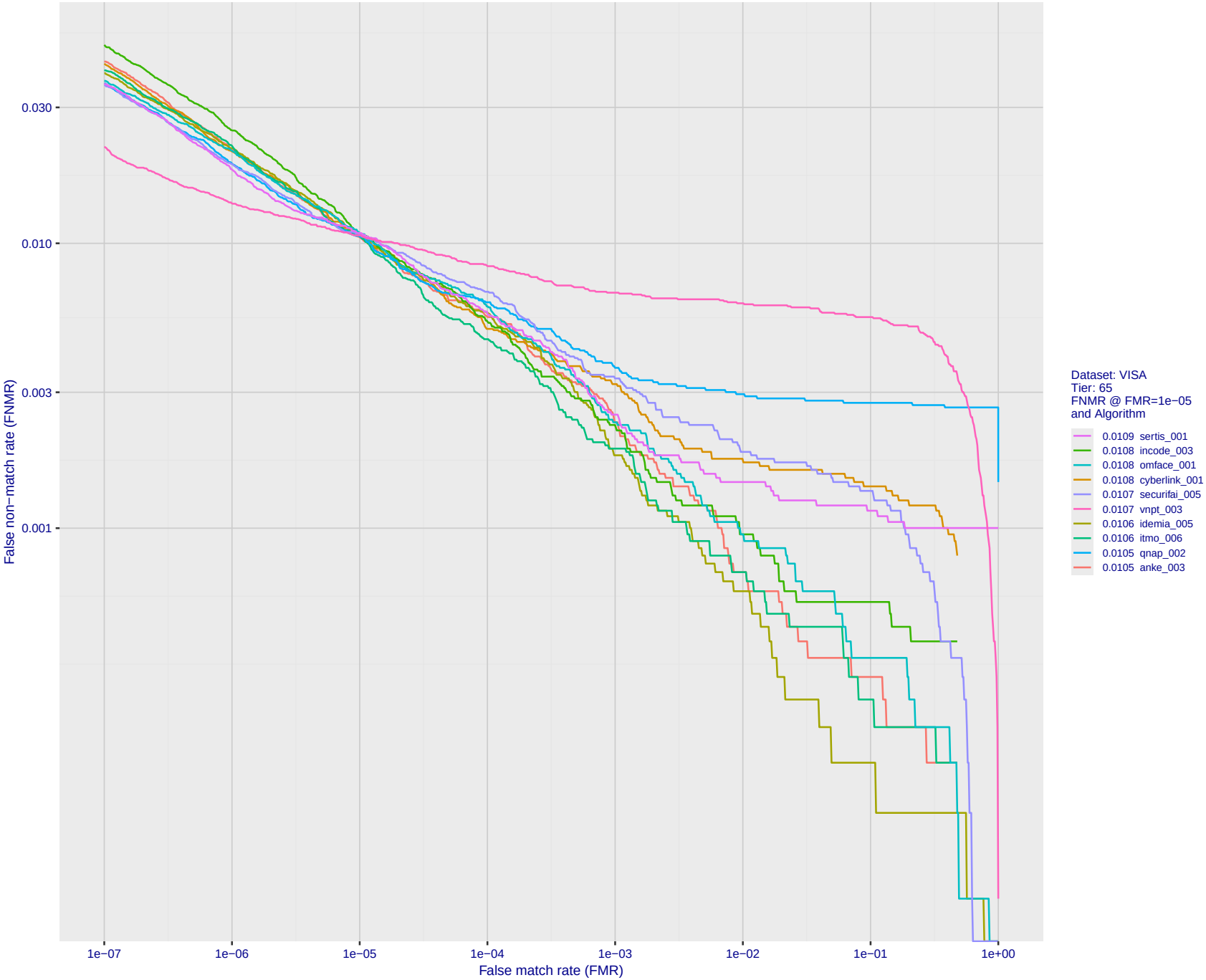

Figure 173: For the visa images, detection error tradeoff (DET) characteristics showing false non-match rate vs. false match rate plotted parametrically on threshold, T. The scales are logarithmic in order to show many decades of FMR.

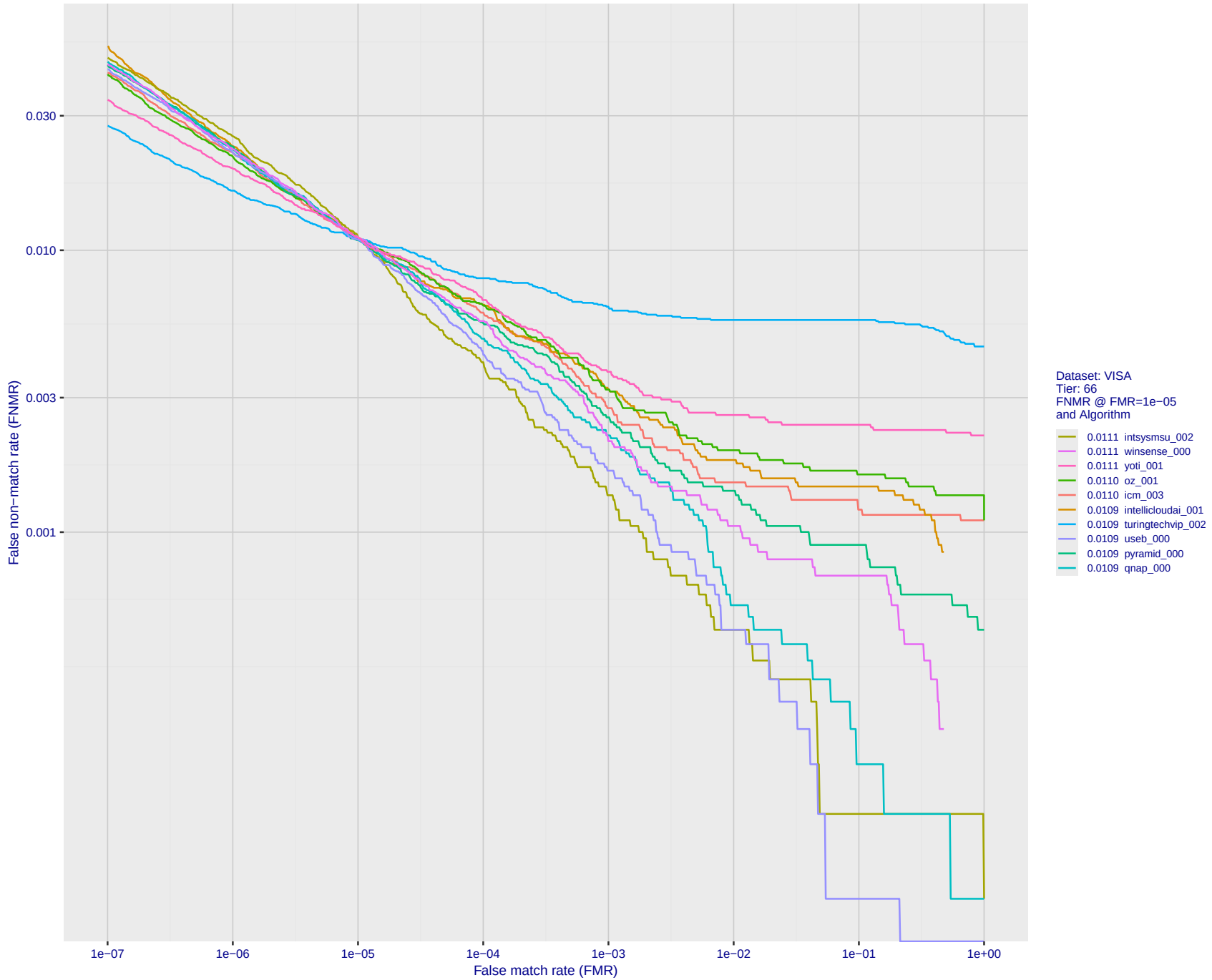

Figure 174: For the visa images, detection error tradeoff (DET) characteristics showing false non-match rate vs. false match rate plotted parametrically on threshold, T. The scales are logarithmic in order to show many decades of FMR.

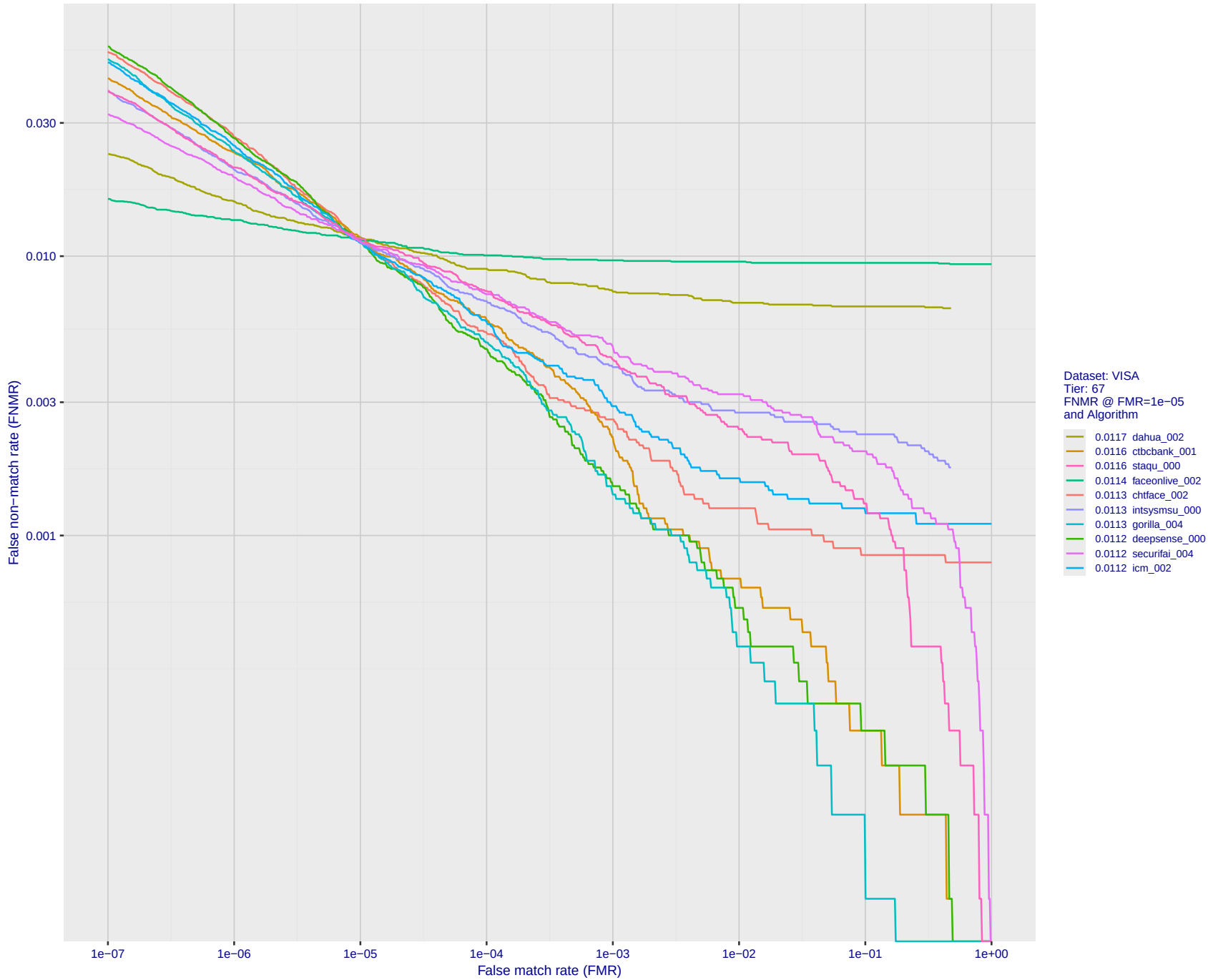

Figure 175: For the visa images, detection error tradeoff (DET) characteristics showing false non-match rate vs. false match rate plotted parametrically on threshold, T. The scales are logarithmic in order to show many decades of FMR.

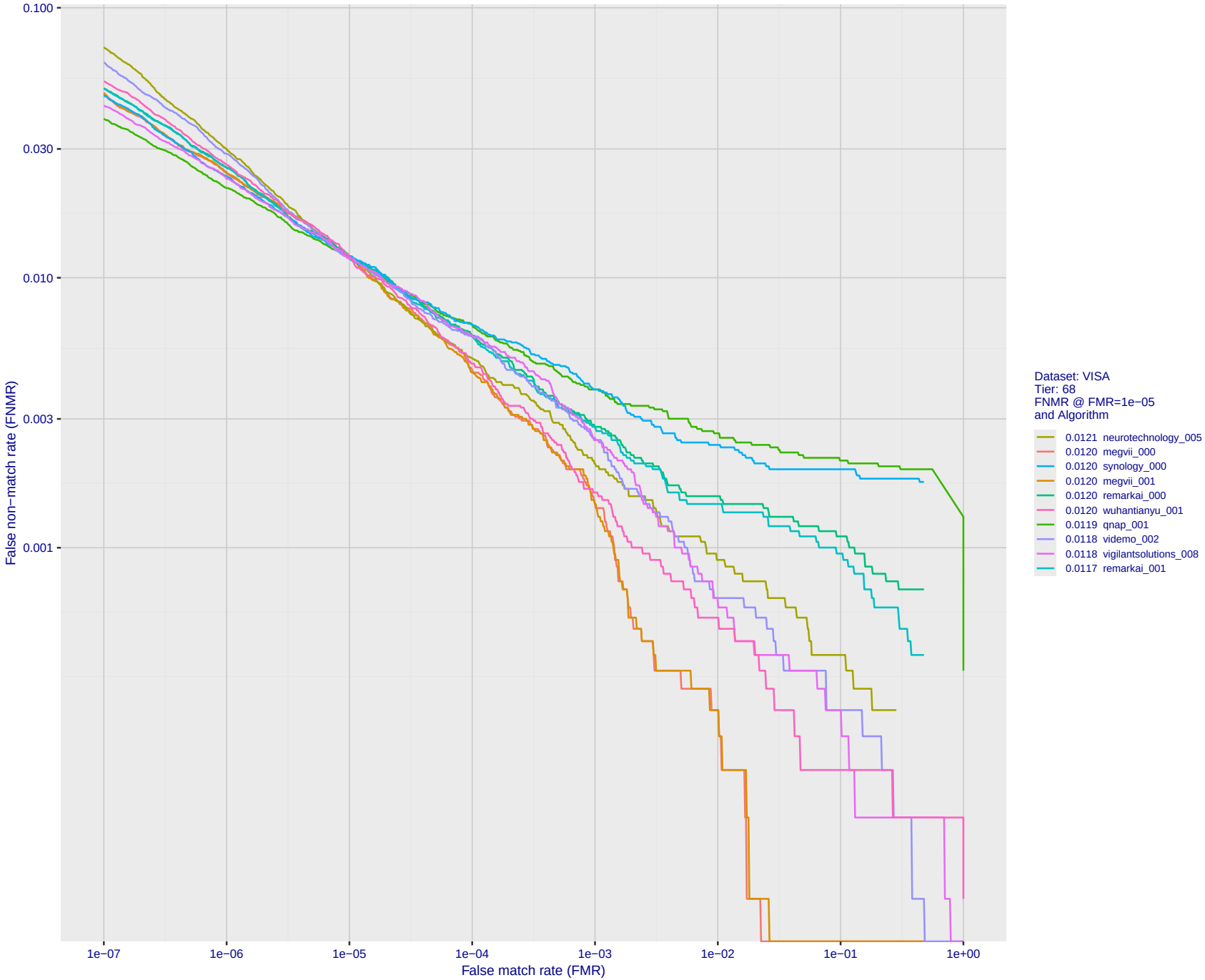

Figure 176: For the visa images, detection error tradeoff (DET) characteristics showing false non-match rate vs. false match rate plotted parametrically on threshold, T. The scales are logarithmic in order to show many decades of FMR.

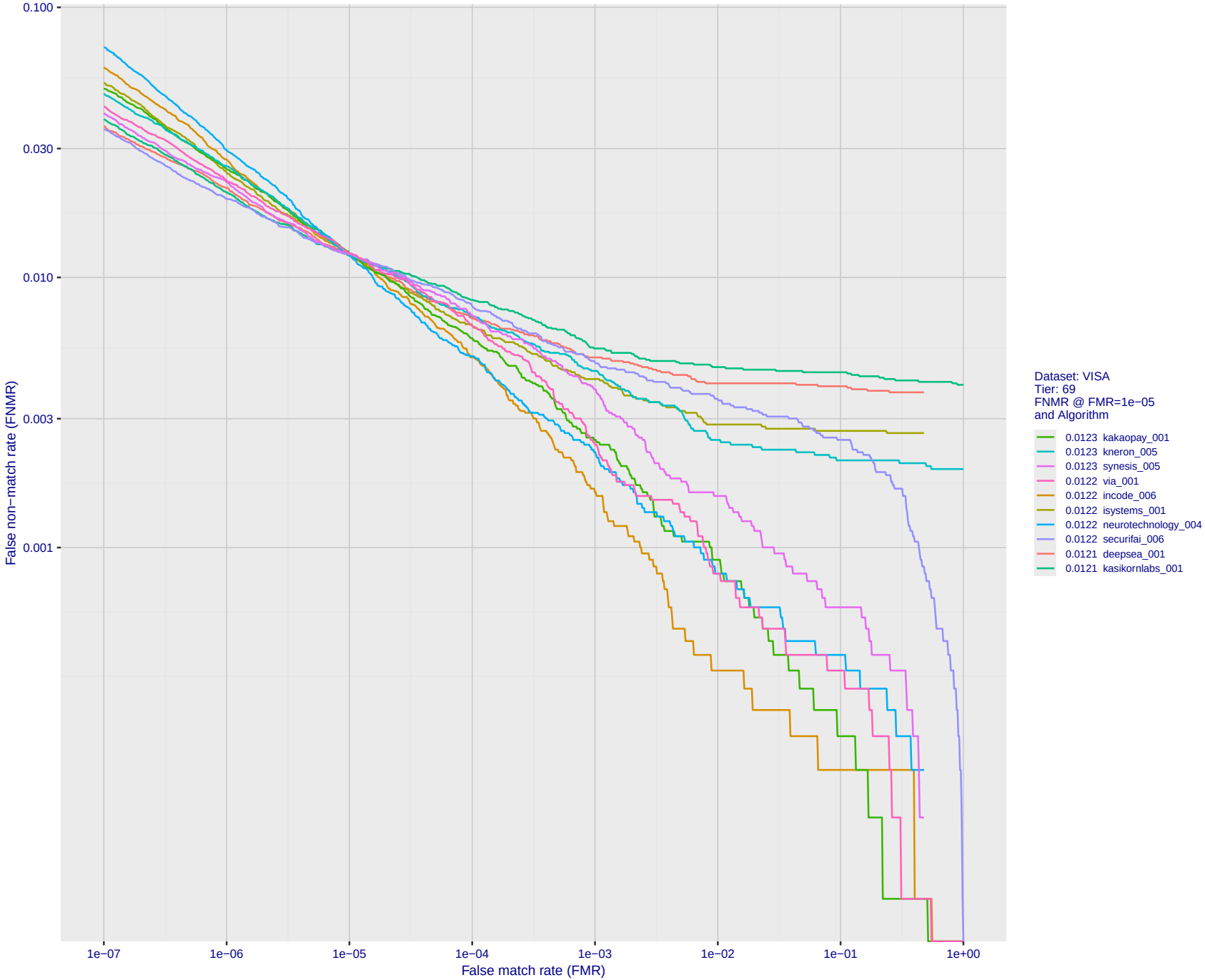

Figure 177: For the visa images, detection error tradeoff (DET) characteristics showing false non-match rate vs. false match rate plotted parametrically on threshold, T. The scales are logarithmic in order to show many decades of FMR.

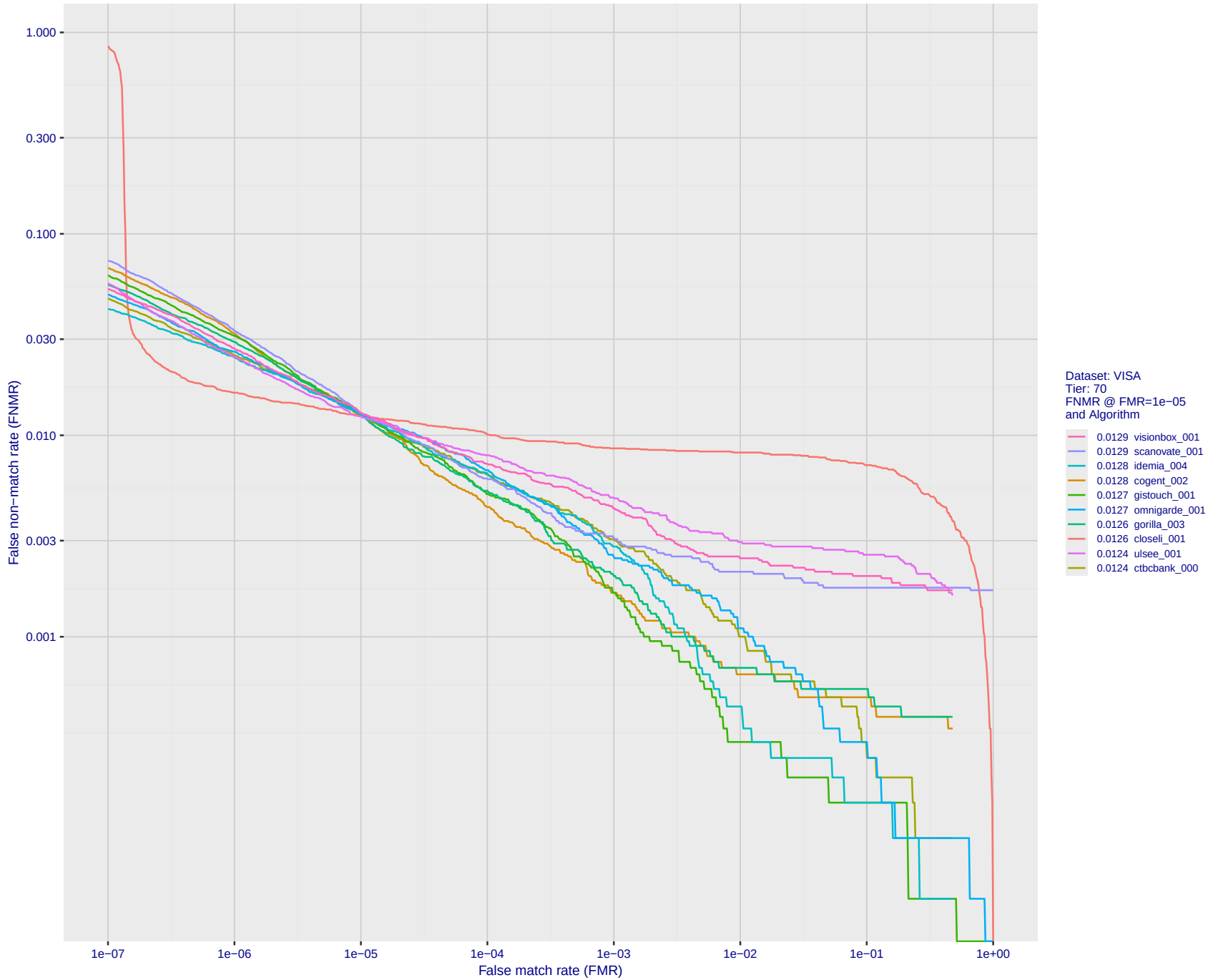

Figure 178: For the visa images, detection error tradeoff (DET) characteristics showing false non-match rate vs. false match rate plotted parametrically on threshold, T. The scales are logarithmic in order to show many decades of FMR.

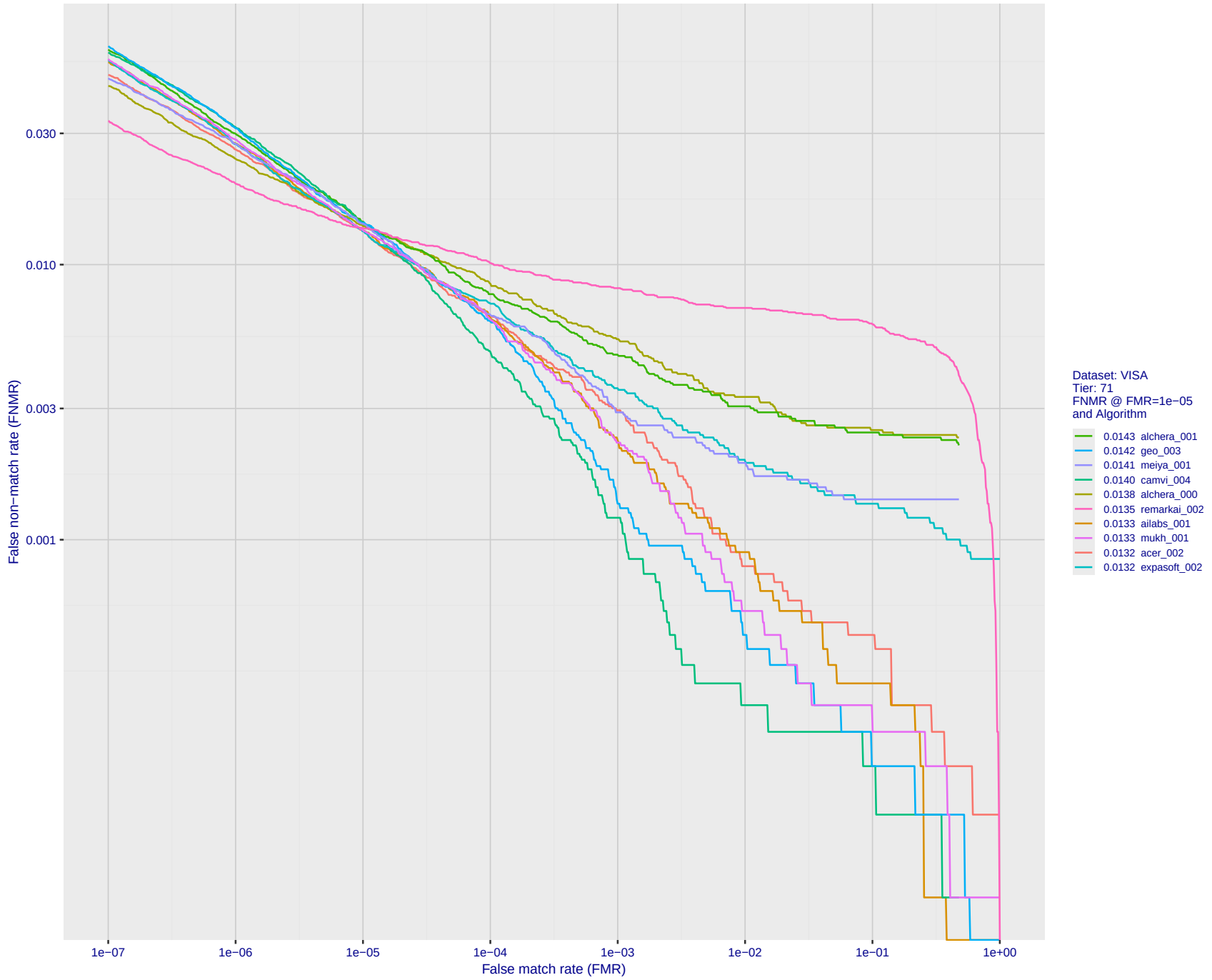

Figure 179: For the visa images, detection error tradeoff (DET) characteristics showing false non-match rate vs. false match rate plotted parametrically on threshold, T. The scales are logarithmic in order to show many decades of FMR.

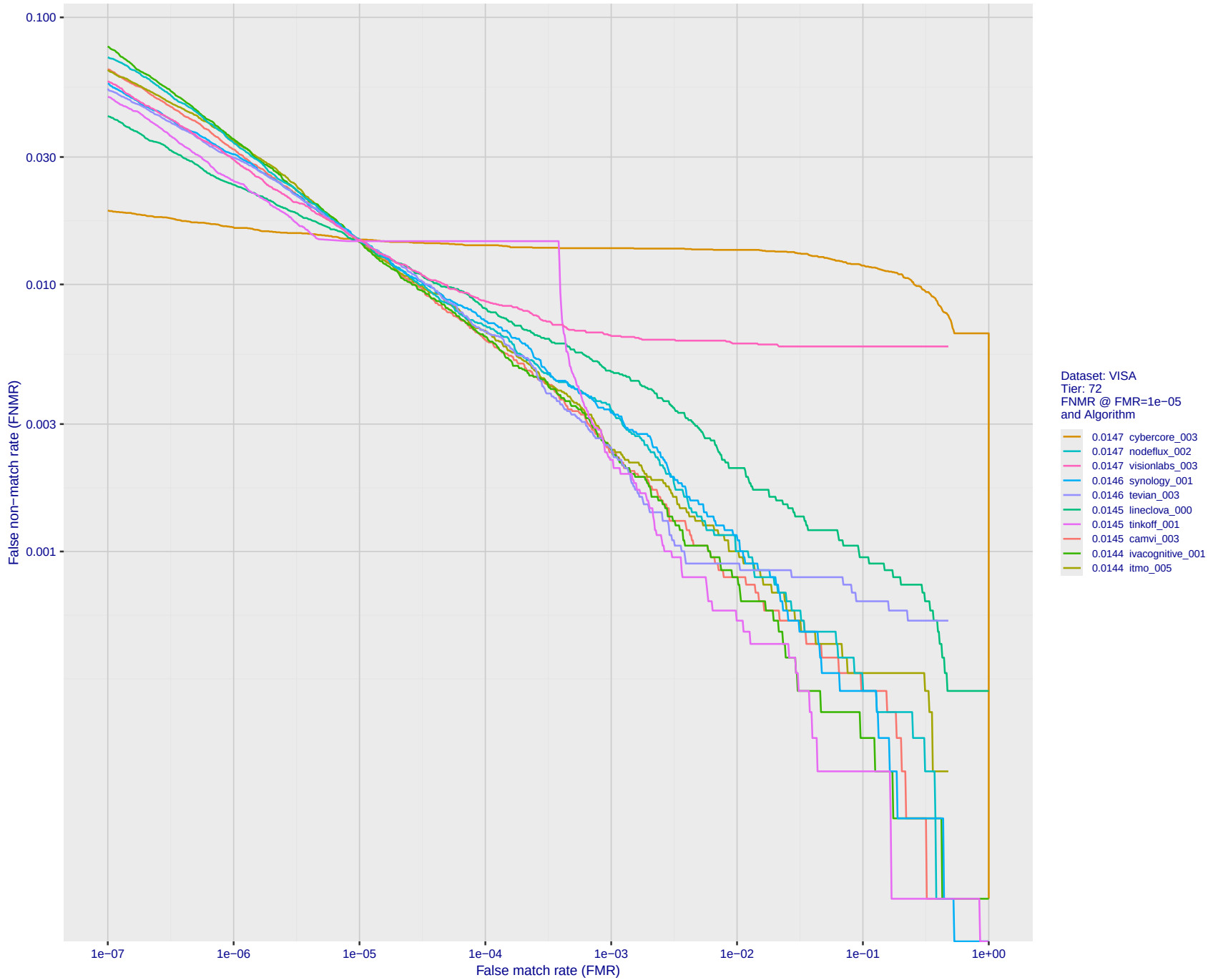

Figure 180: For the visa images, detection error tradeoff (DET) characteristics showing false non-match rate vs. false match rate plotted parametrically on threshold, T. The scales are logarithmic in order to show many decades of FMR.

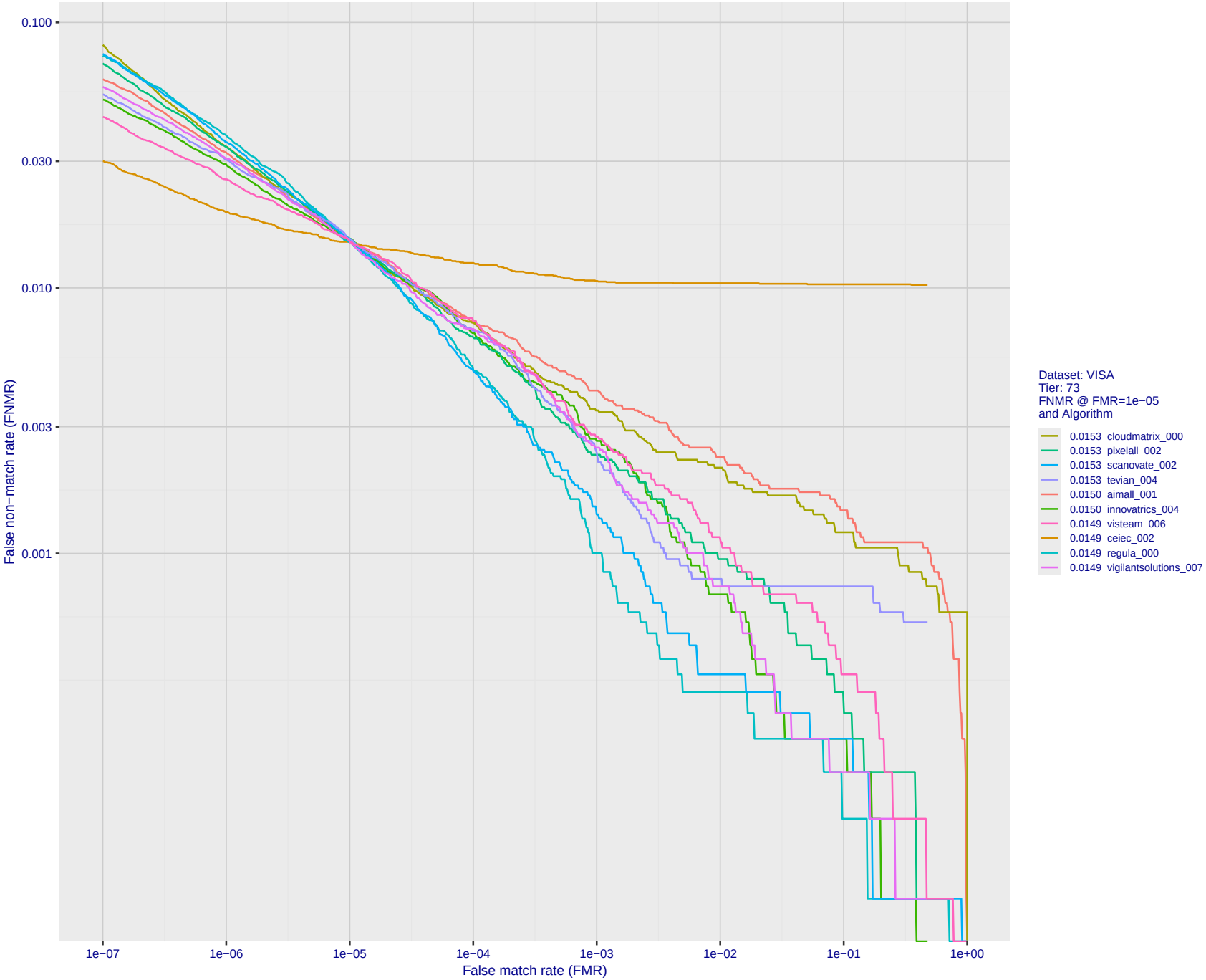

Figure 181: For the visa images, detection error tradeoff (DET) characteristics showing false non-match rate vs. false match rate plotted parametrically on threshold, T. The scales are logarithmic in order to show many decades of FMR.

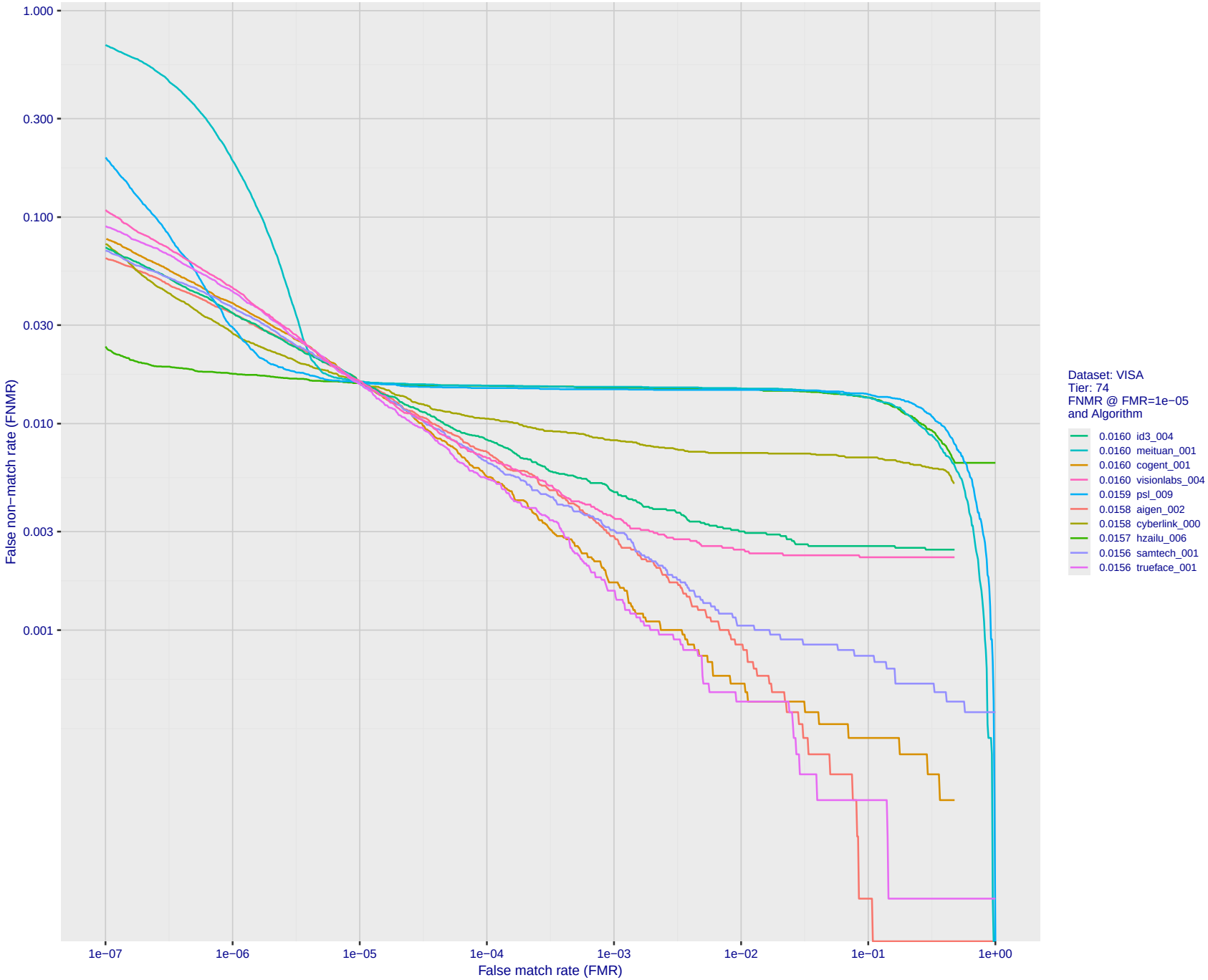

Figure 182: For the visa images, detection error tradeoff (DET) characteristics showing false non-match rate vs. false match rate plotted parametrically on threshold, T. The scales are logarithmic in order to show many decades of FMR.

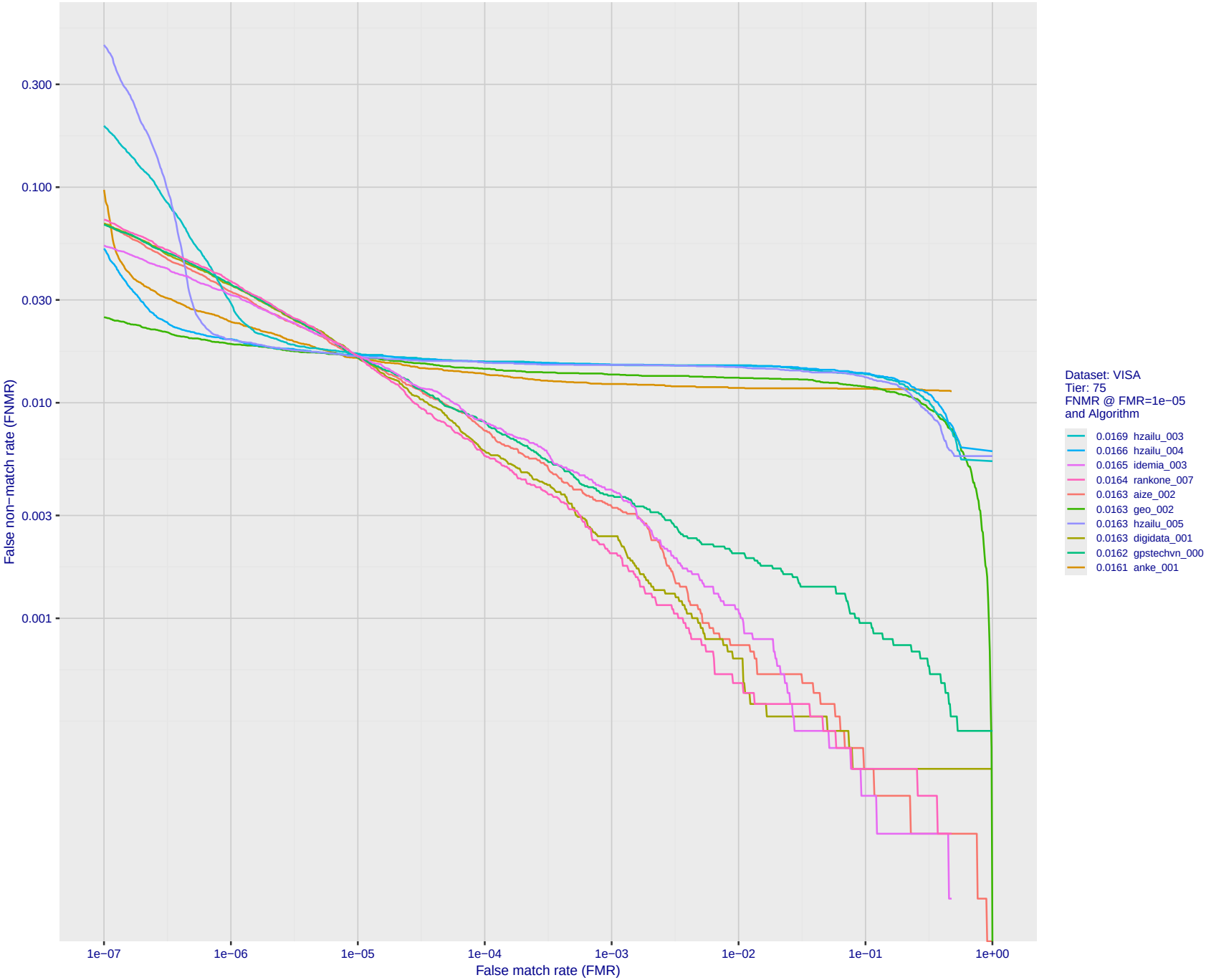

Figure 183: For the visa images, detection error tradeoff (DET) characteristics showing false non-match rate vs. false match rate plotted parametrically on threshold, T. The scales are logarithmic in order to show many decades of FMR.

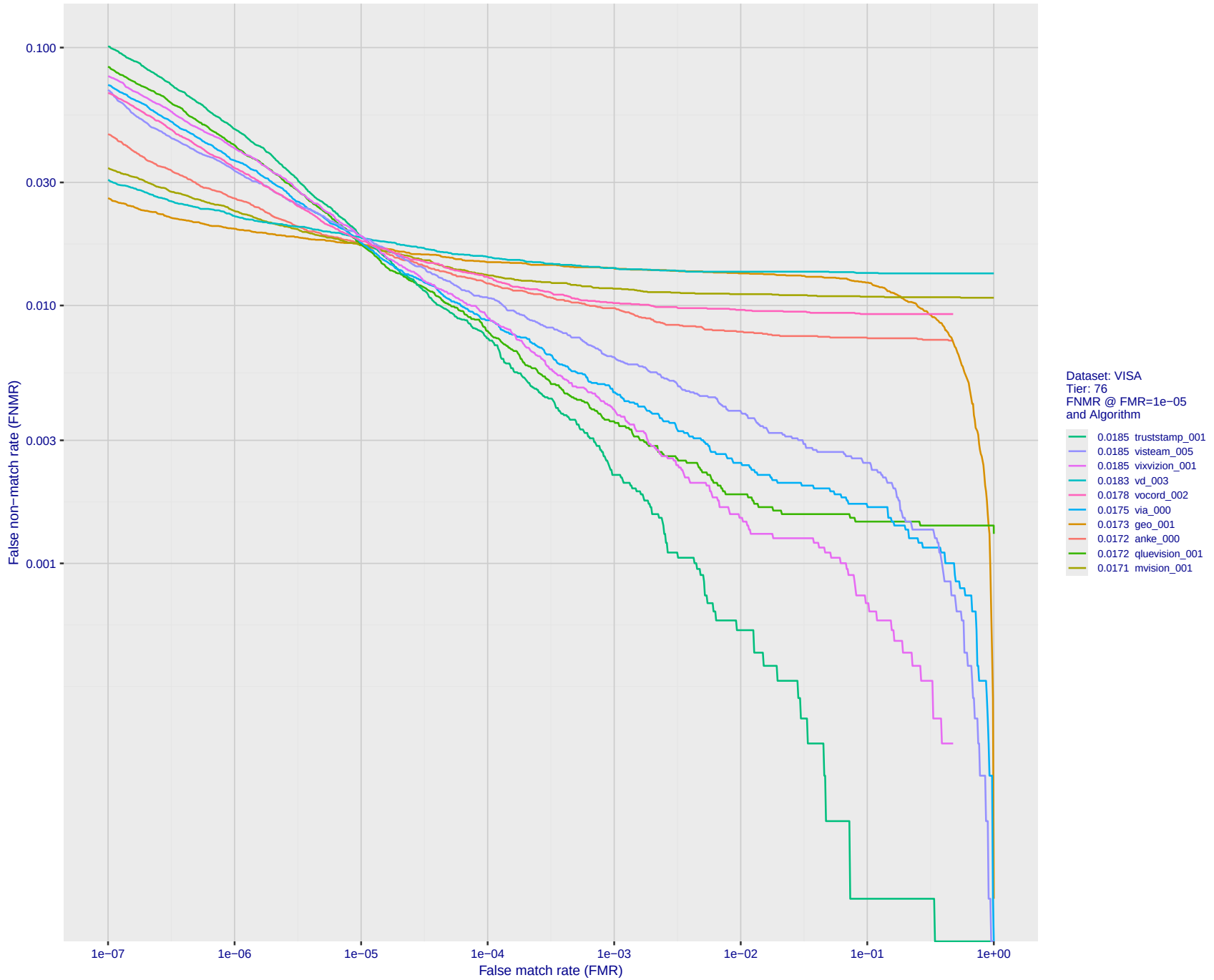

Figure 184: For the visa images, detection error tradeoff (DET) characteristics showing false non-match rate vs. false match rate plotted parametrically on threshold, T. The scales are logarithmic in order to show many decades of FMR.

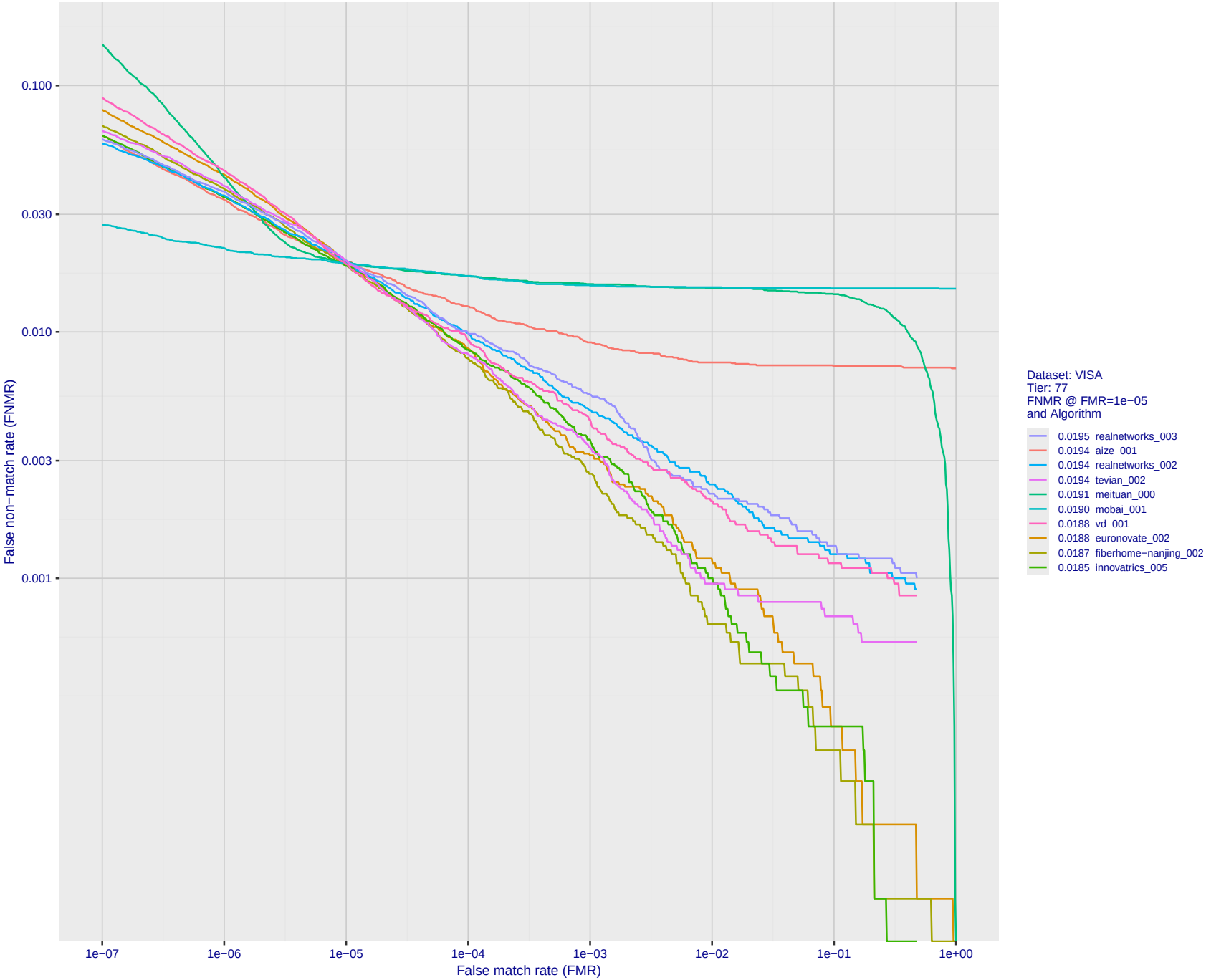

Figure 185: For the visa images, detection error tradeoff (DET) characteristics showing false non-match rate vs. false match rate plotted parametrically on threshold, T. The scales are logarithmic in order to show many decades of FMR.

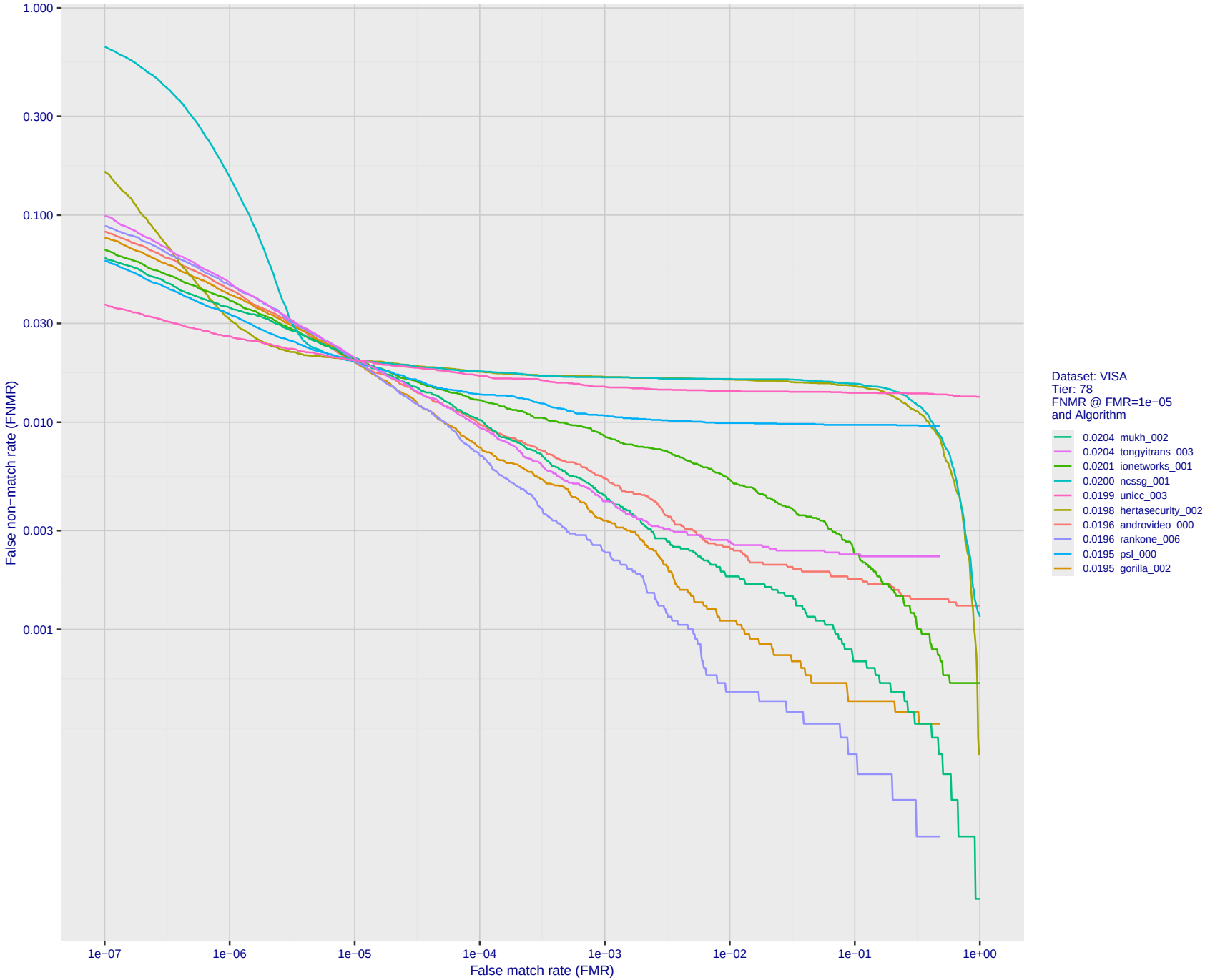

Figure 186: For the visa images, detection error tradeoff (DET) characteristics showing false non-match rate vs. false match rate plotted parametrically on threshold, T. The scales are logarithmic in order to show many decades of FMR.

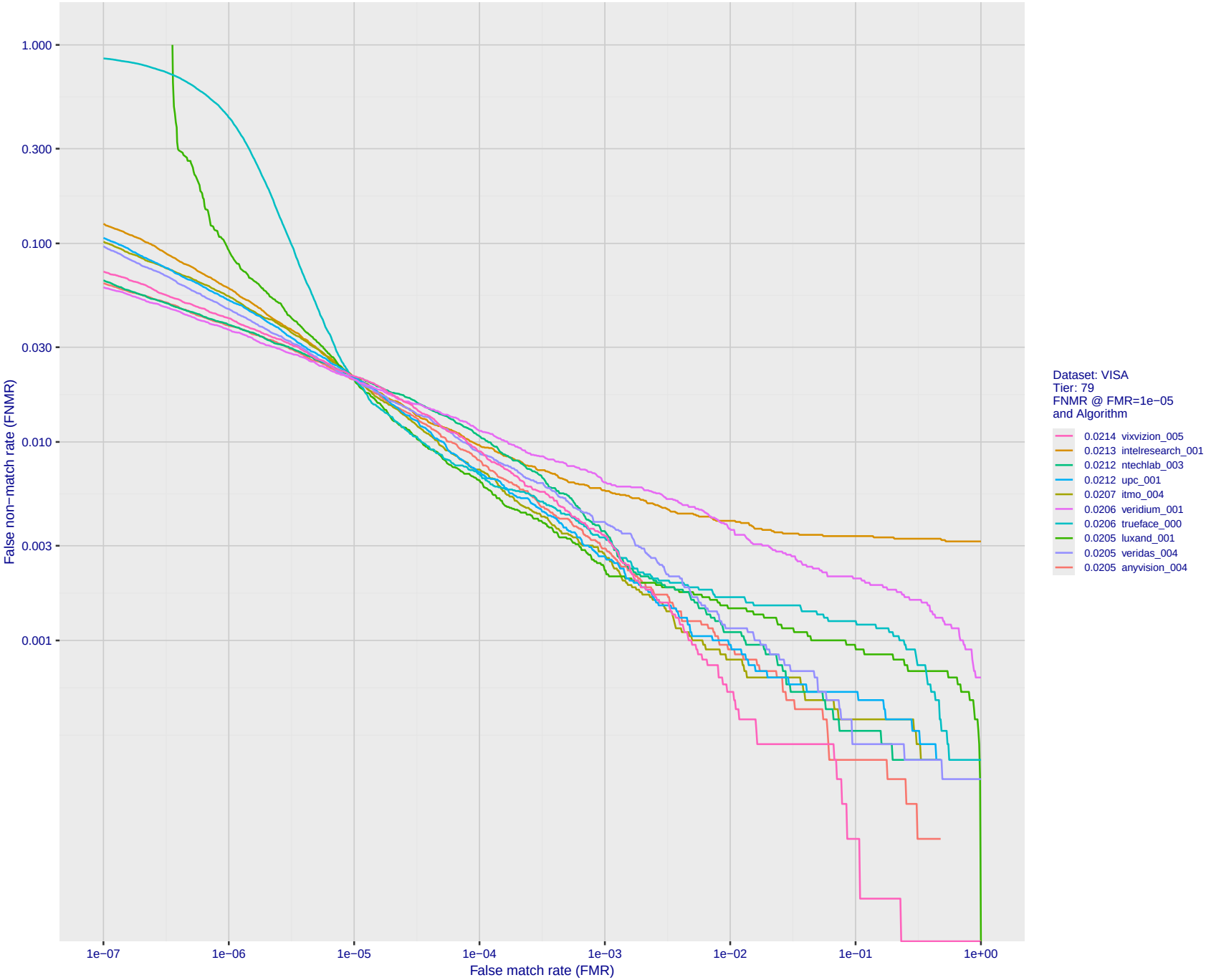

Figure 187: For the visa images, detection error tradeoff (DET) characteristics showing false non-match rate vs. false match rate plotted parametrically on threshold, T. The scales are logarithmic in order to show many decades of FMR.

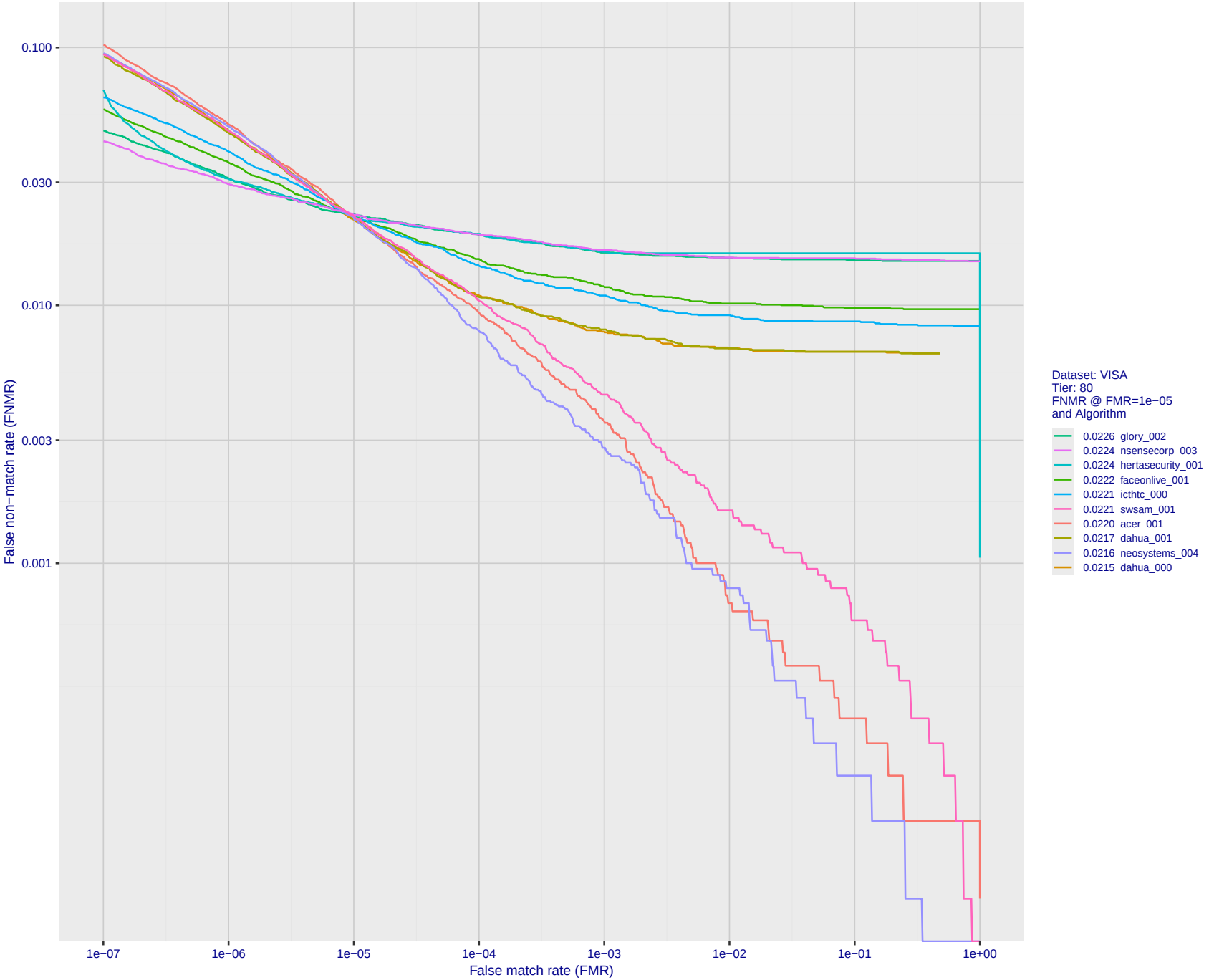

Figure 188: For the visa images, detection error tradeoff (DET) characteristics showing false non-match rate vs. false match rate plotted parametrically on threshold, T. The scales are logarithmic in order to show many decades of FMR.

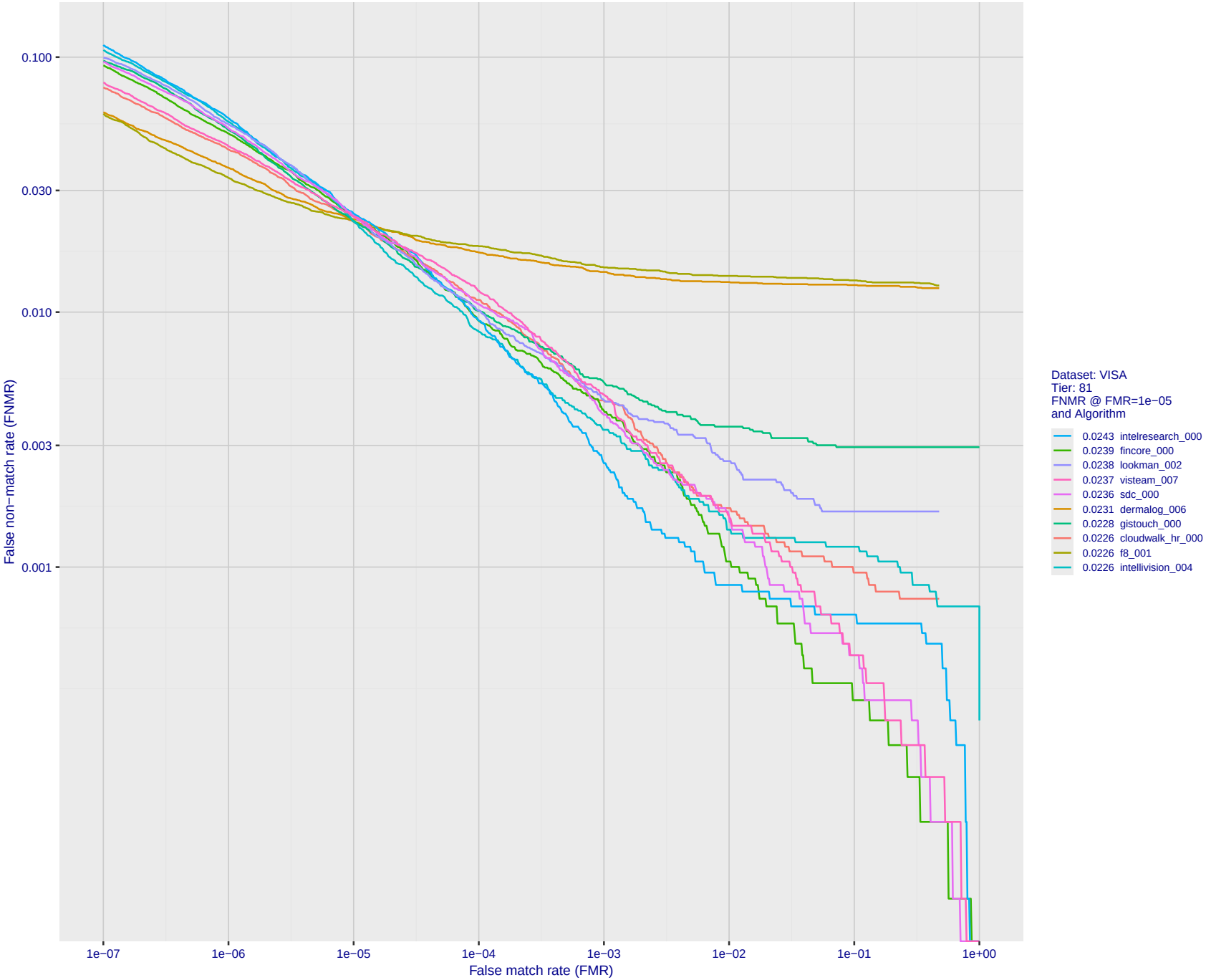

Figure 189: For the visa images, detection error tradeoff (DET) characteristics showing false non-match rate vs. false match rate plotted parametrically on threshold, T. The scales are logarithmic in order to show many decades of FMR.

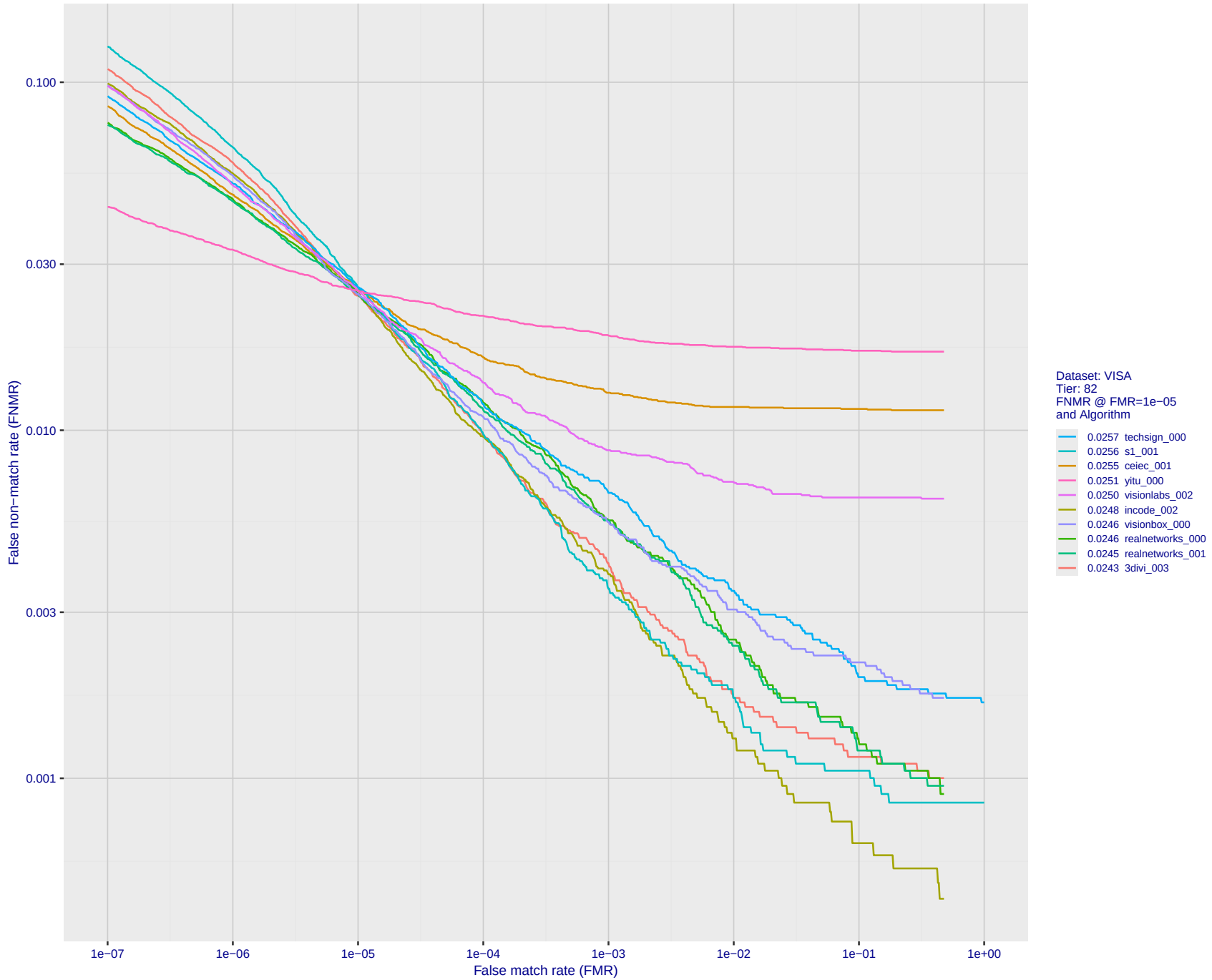

Figure 190: For the visa images, detection error tradeoff (DET) characteristics showing false non-match rate vs. false match rate plotted parametrically on threshold, T. The scales are logarithmic in order to show many decades of FMR.

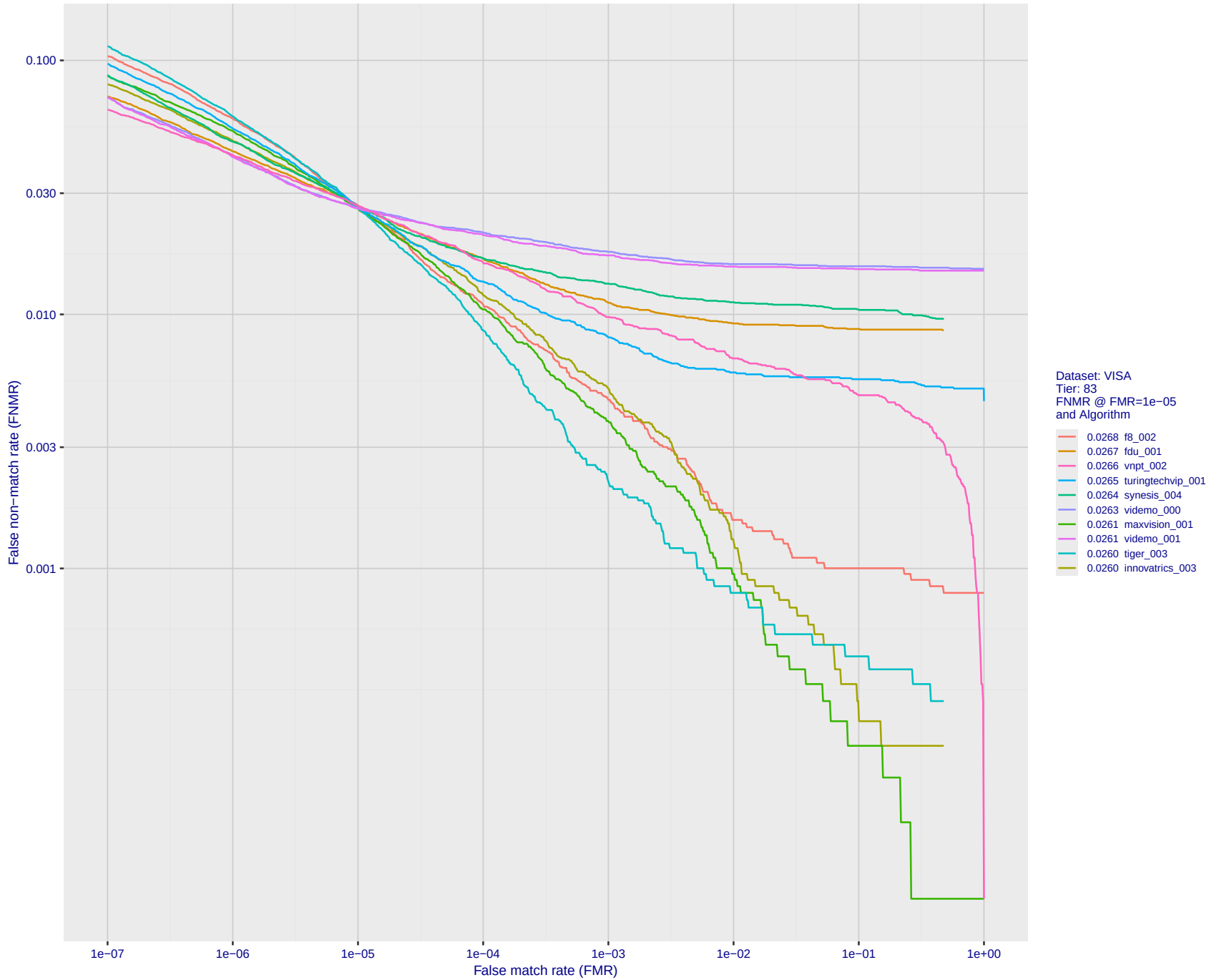

Figure 191: For the visa images, detection error tradeoff (DET) characteristics showing false non-match rate vs. false match rate plotted parametrically on threshold, T. The scales are logarithmic in order to show many decades of FMR.

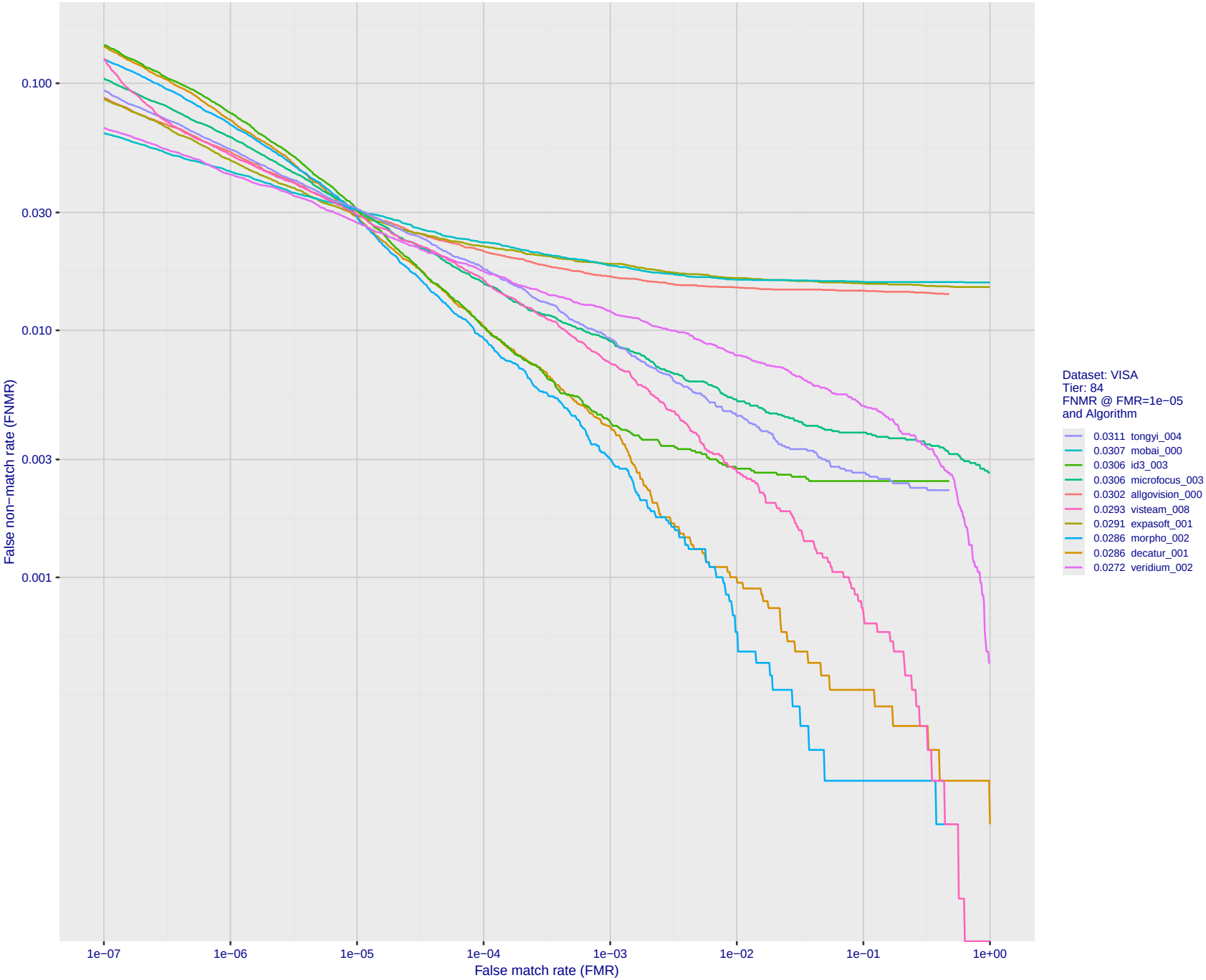

Figure 192: For the visa images, detection error tradeoff (DET) characteristics showing false non-match rate vs. false match rate plotted parametrically on threshold, T. The scales are logarithmic in order to show many decades of FMR.

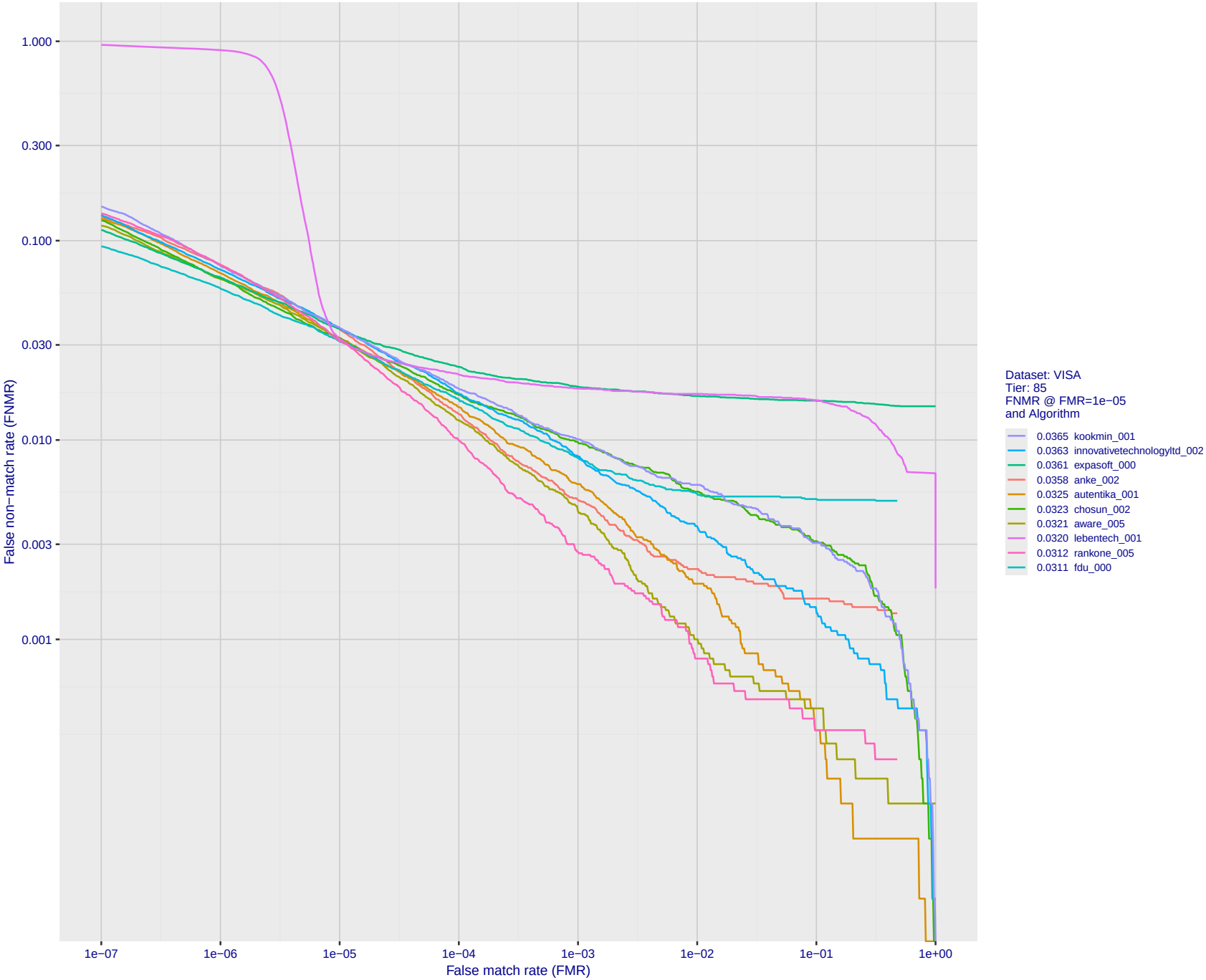

Figure 193: For the visa images, detection error tradeoff (DET) characteristics showing false non-match rate vs. false match rate plotted parametrically on threshold, T. The scales are logarithmic in order to show many decades of FMR.

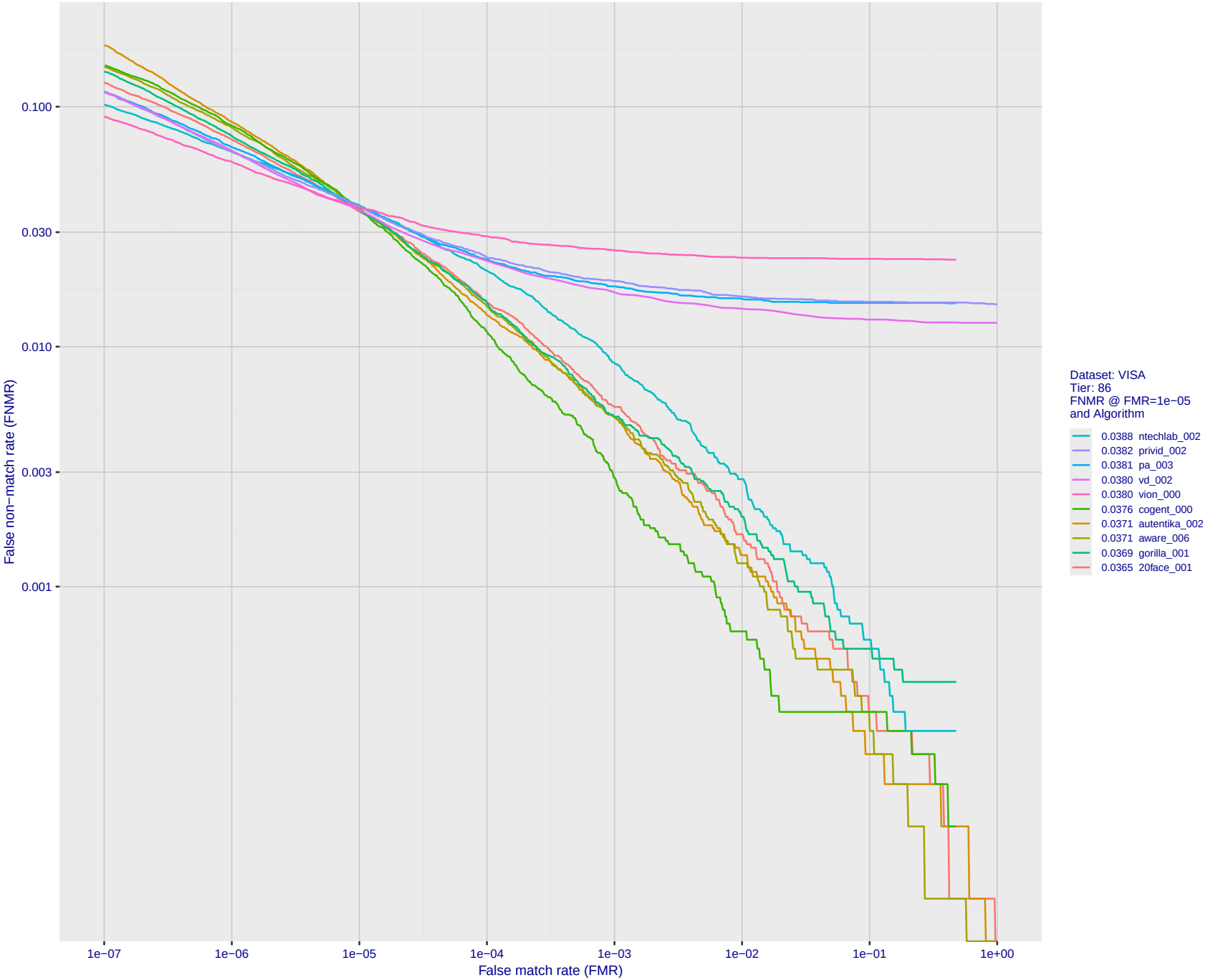

Figure 194: For the visa images, detection error tradeoff (DET) characteristics showing false non-match rate vs. false match rate plotted parametrically on threshold, T. The scales are logarithmic in order to show many decades of FMR.

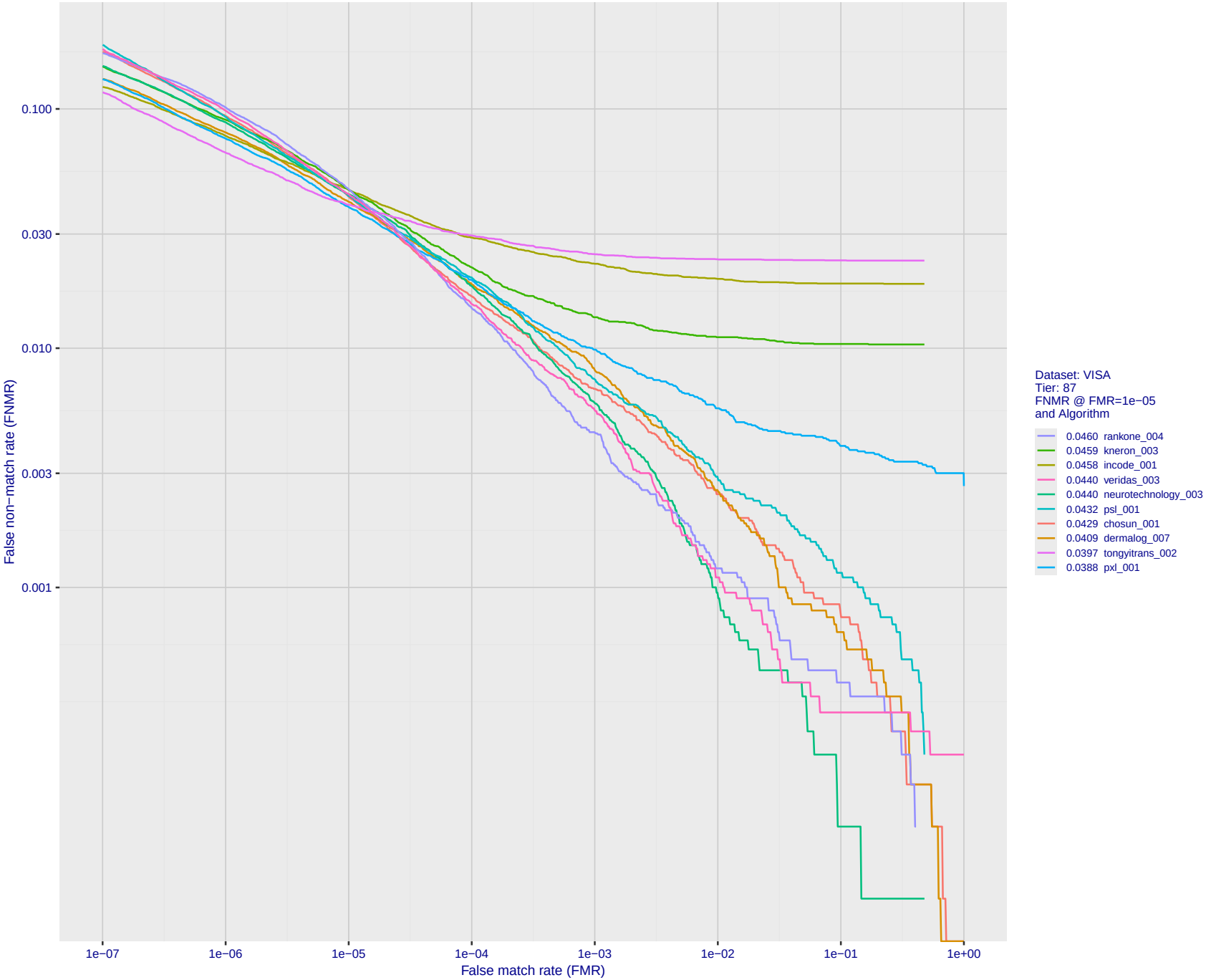

Figure 195: For the visa images, detection error tradeoff (DET) characteristics showing false non-match rate vs. false match rate plotted parametrically on threshold, T. The scales are logarithmic in order to show many decades of FMR.

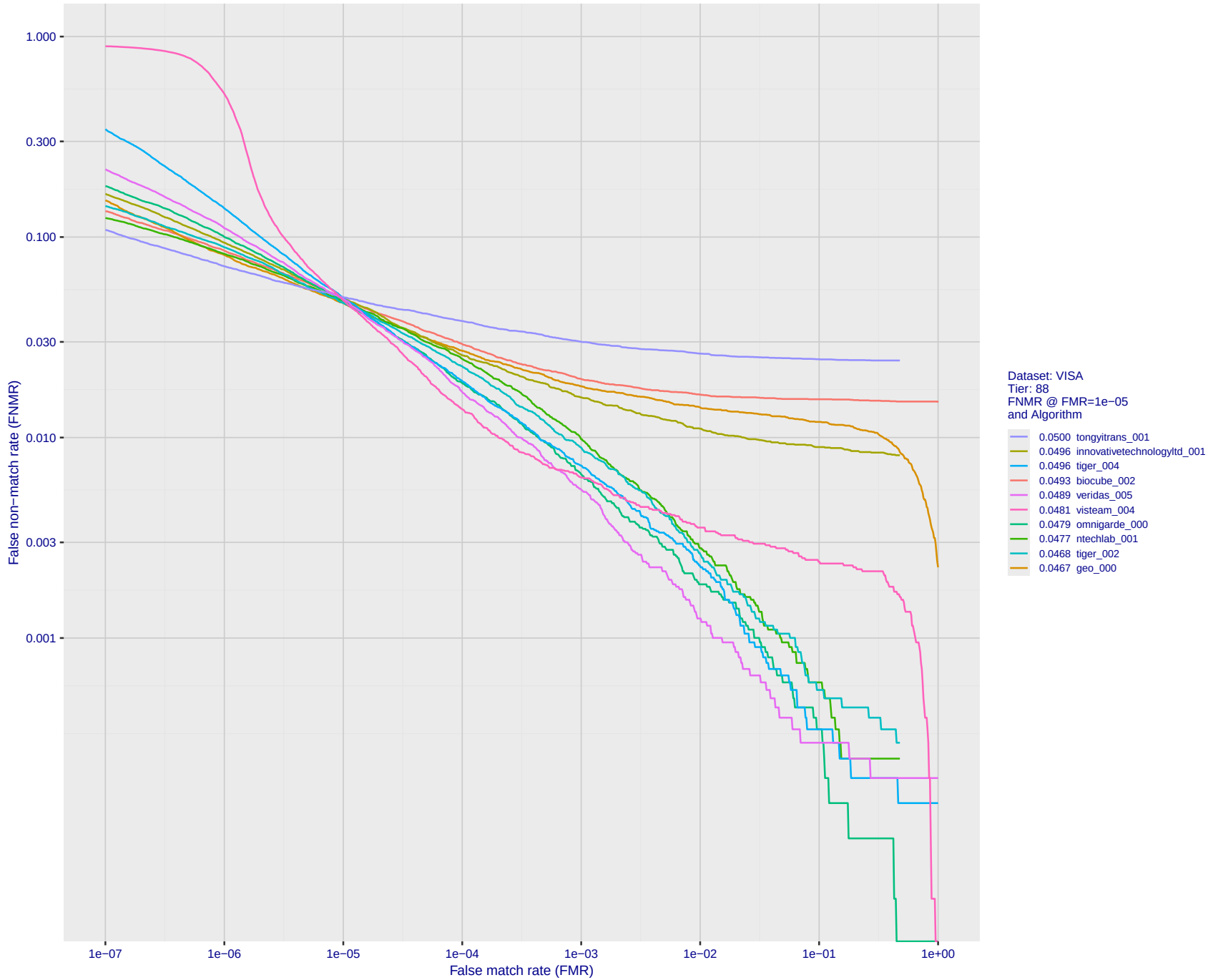

Figure 196: For the visa images, detection error tradeoff (DET) characteristics showing false non-match rate vs. false match rate plotted parametrically on threshold, T. The scales are logarithmic in order to show many decades of FMR.

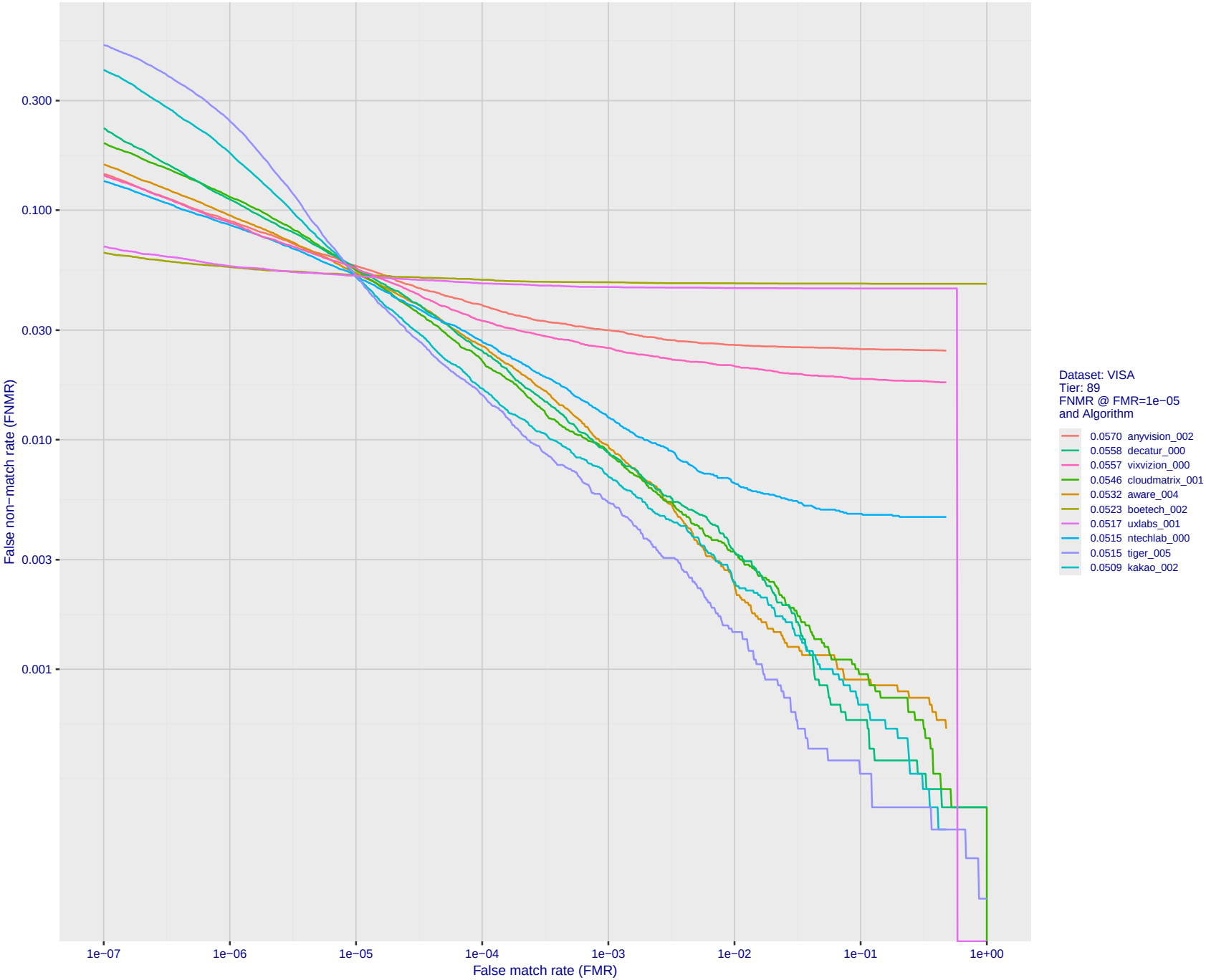

Figure 197: For the visa images, detection error tradeoff (DET) characteristics showing false non-match rate vs. false match rate plotted parametrically on threshold, T. The scales are logarithmic in order to show many decades of FMR.

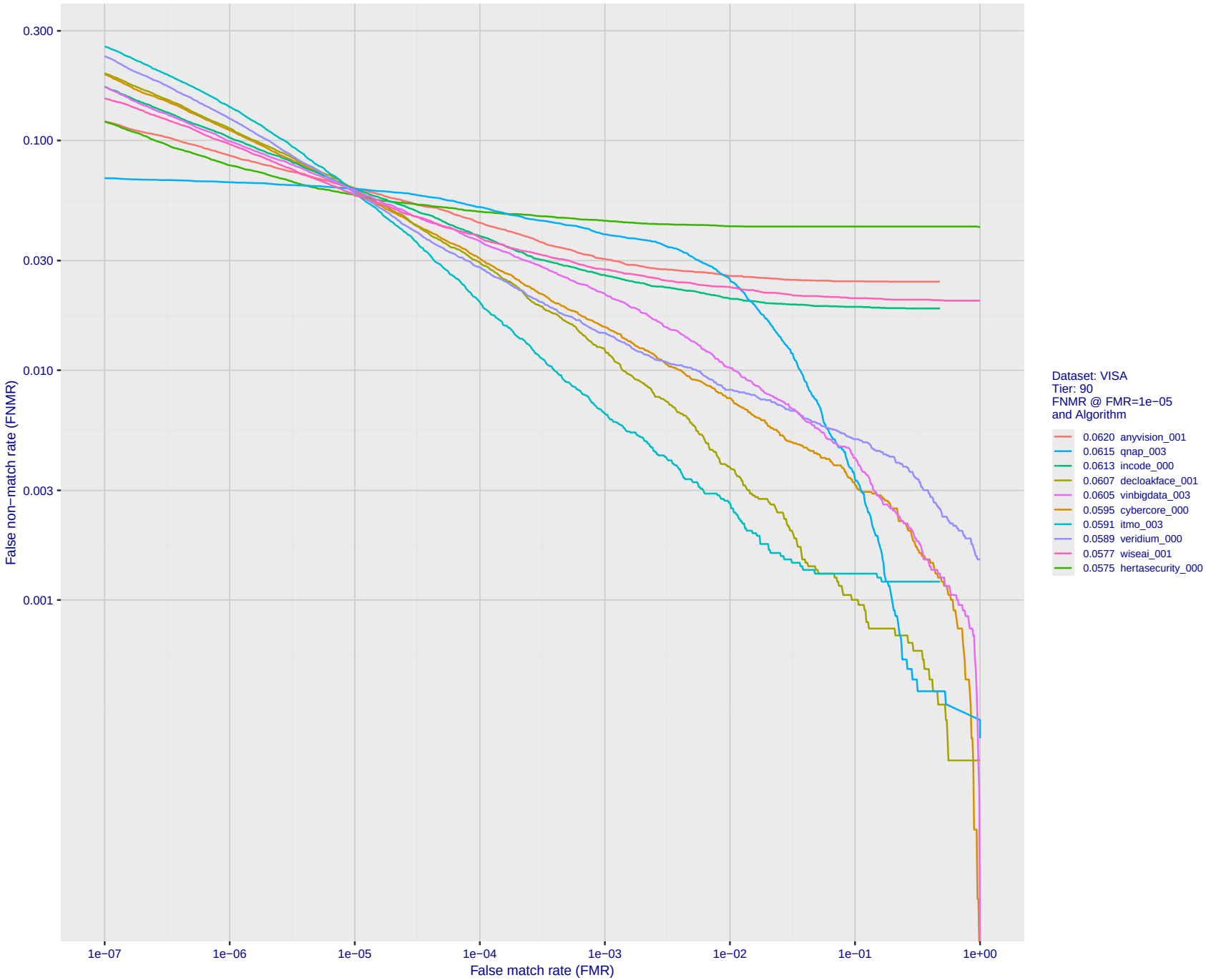

Figure 198: For the visa images, detection error tradeoff (DET) characteristics showing false non-match rate vs. false match rate plotted parametrically on threshold, T. The scales are logarithmic in order to show many decades of FMR.

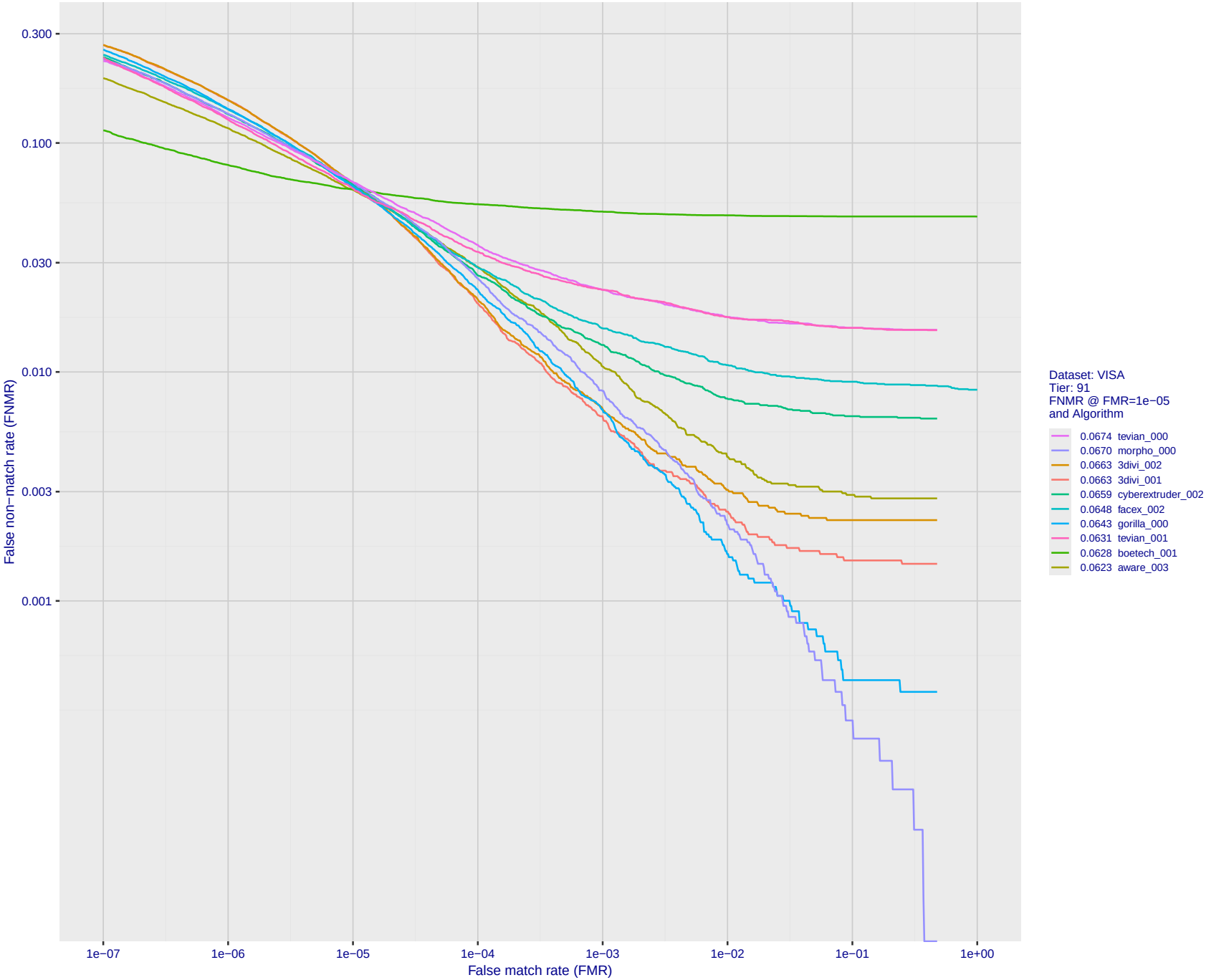

Figure 199: For the visa images, detection error tradeoff (DET) characteristics showing false non-match rate vs. false match rate plotted parametrically on threshold, T. The scales are logarithmic in order to show many decades of FMR.

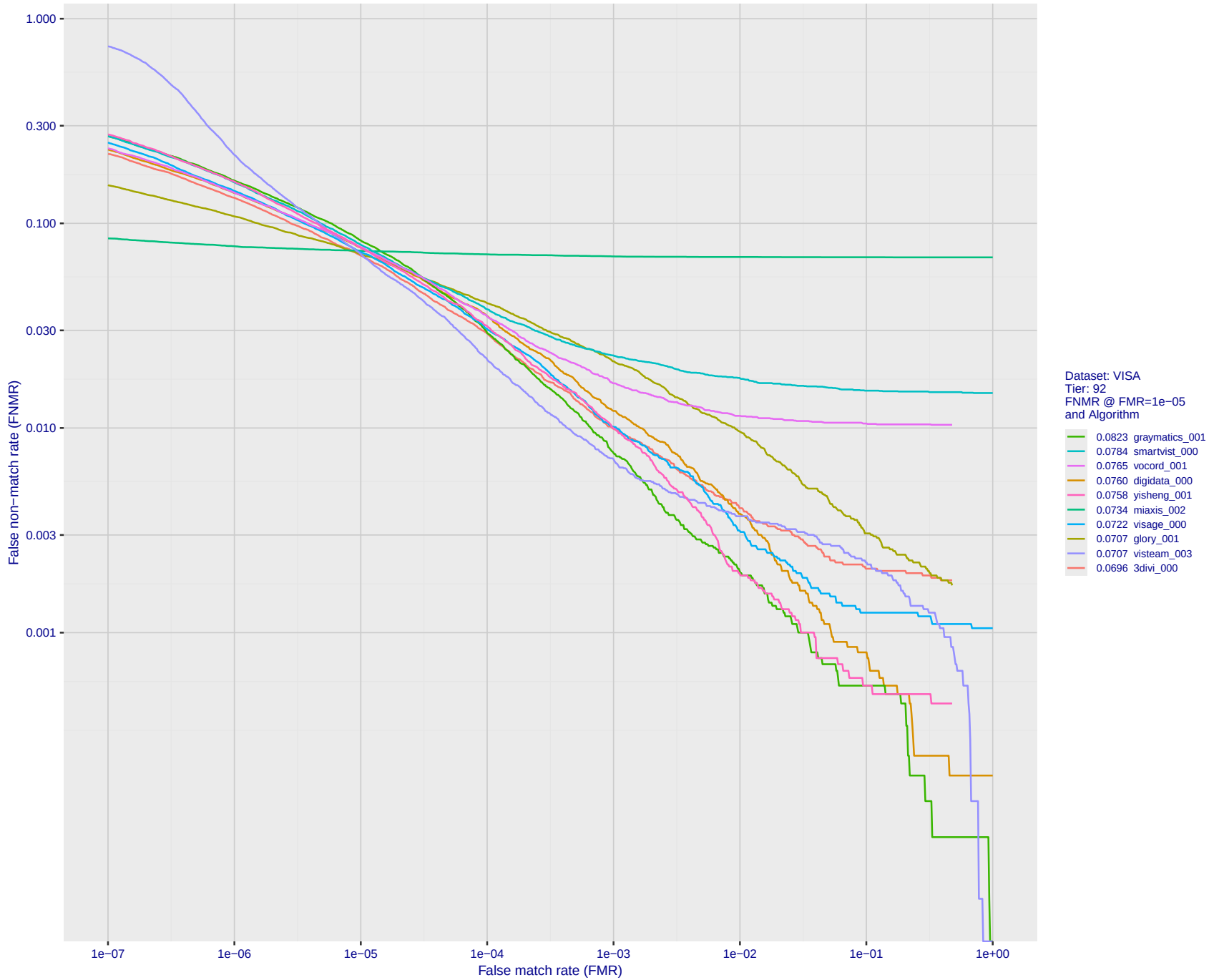

Figure 200: For the visa images, detection error tradeoff (DET) characteristics showing false non-match rate vs. false match rate plotted parametrically on threshold, T. The scales are logarithmic in order to show many decades of FMR.

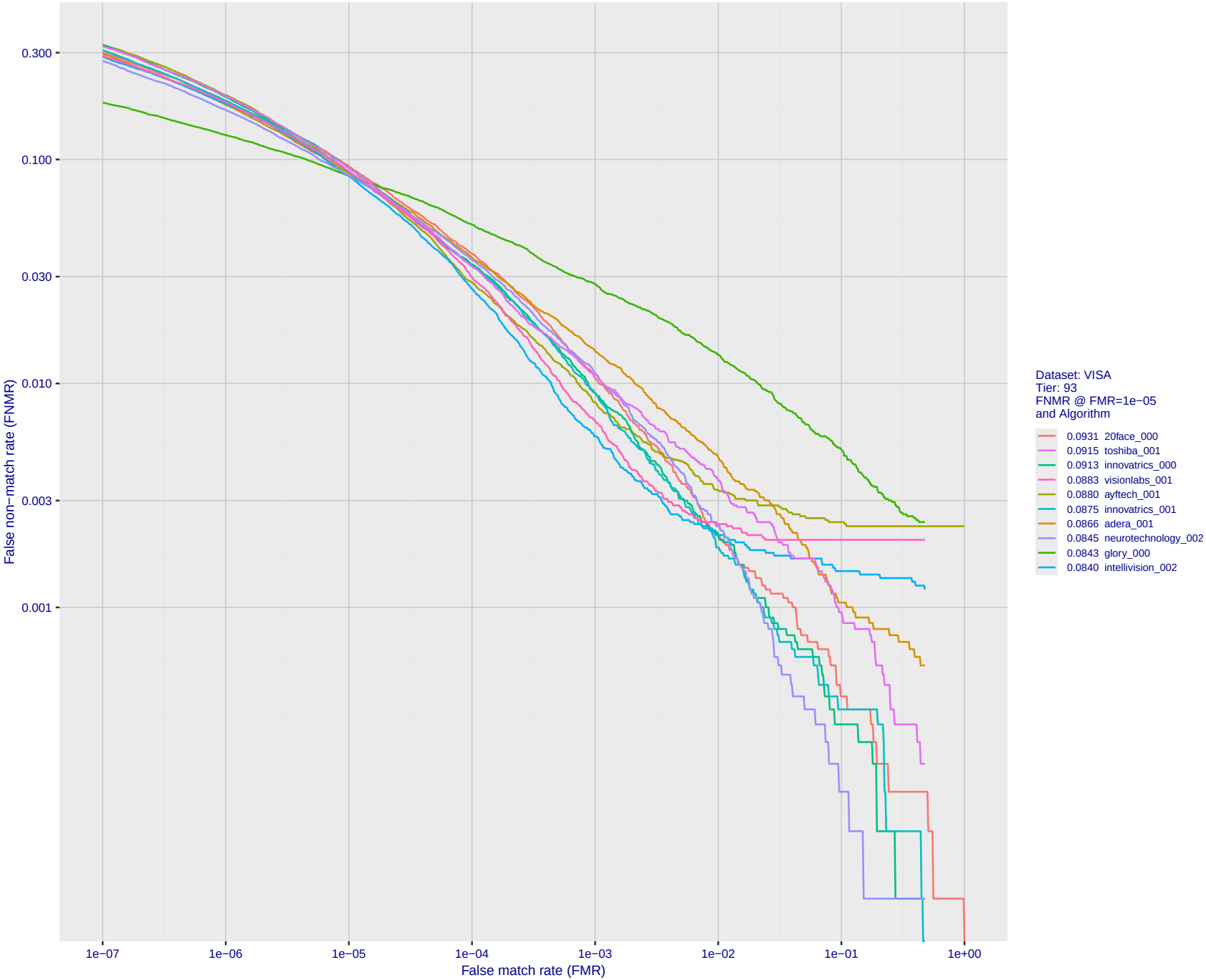

Figure 201: For the visa images, detection error tradeoff (DET) characteristics showing false non-match rate vs. false match rate plotted parametrically on threshold, T. The scales are logarithmic in order to show many decades of FMR.

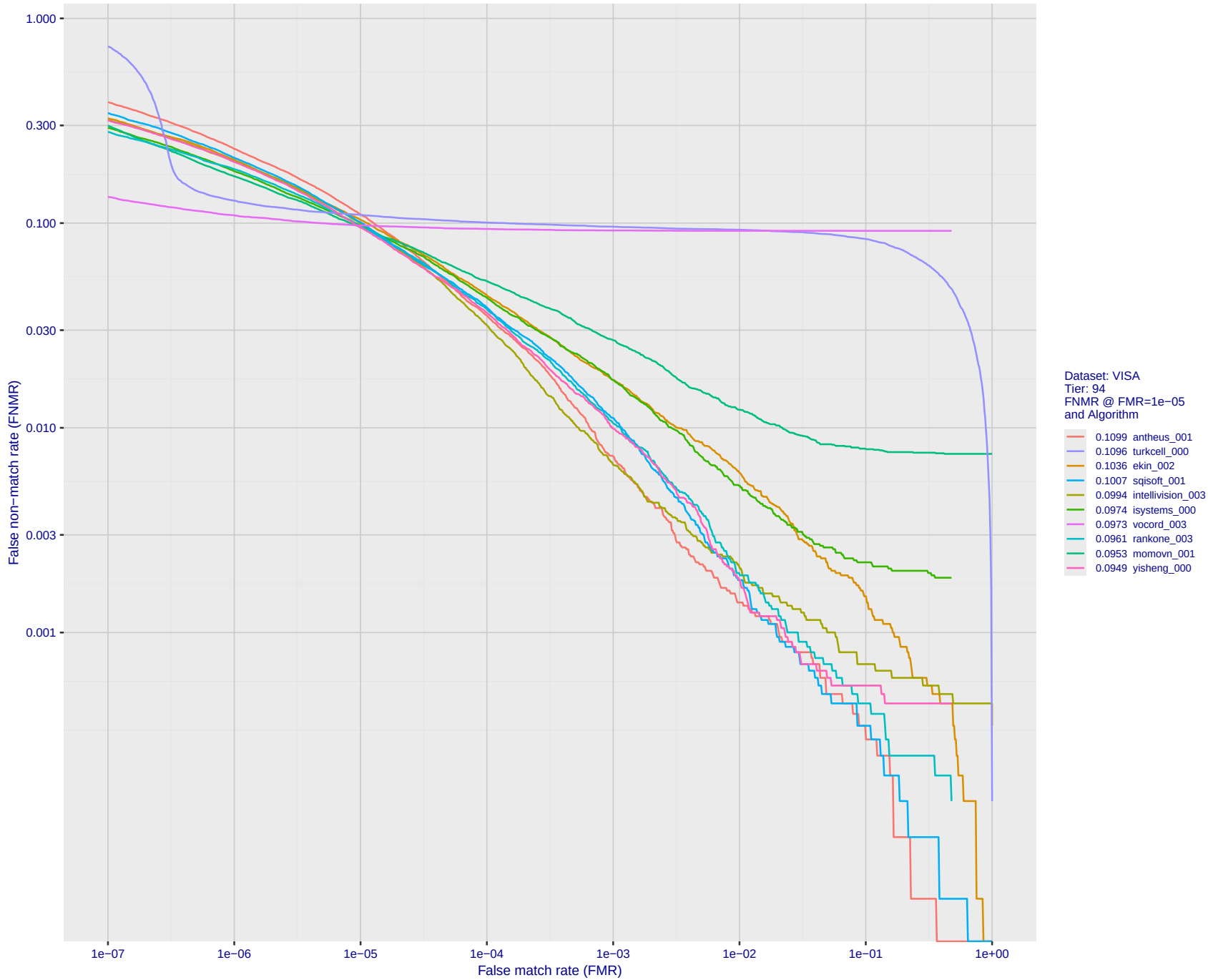

Figure 202: For the visa images, detection error tradeoff (DET) characteristics showing false non-match rate vs. false match rate plotted parametrically on threshold, T. The scales are logarithmic in order to show many decades of FMR.

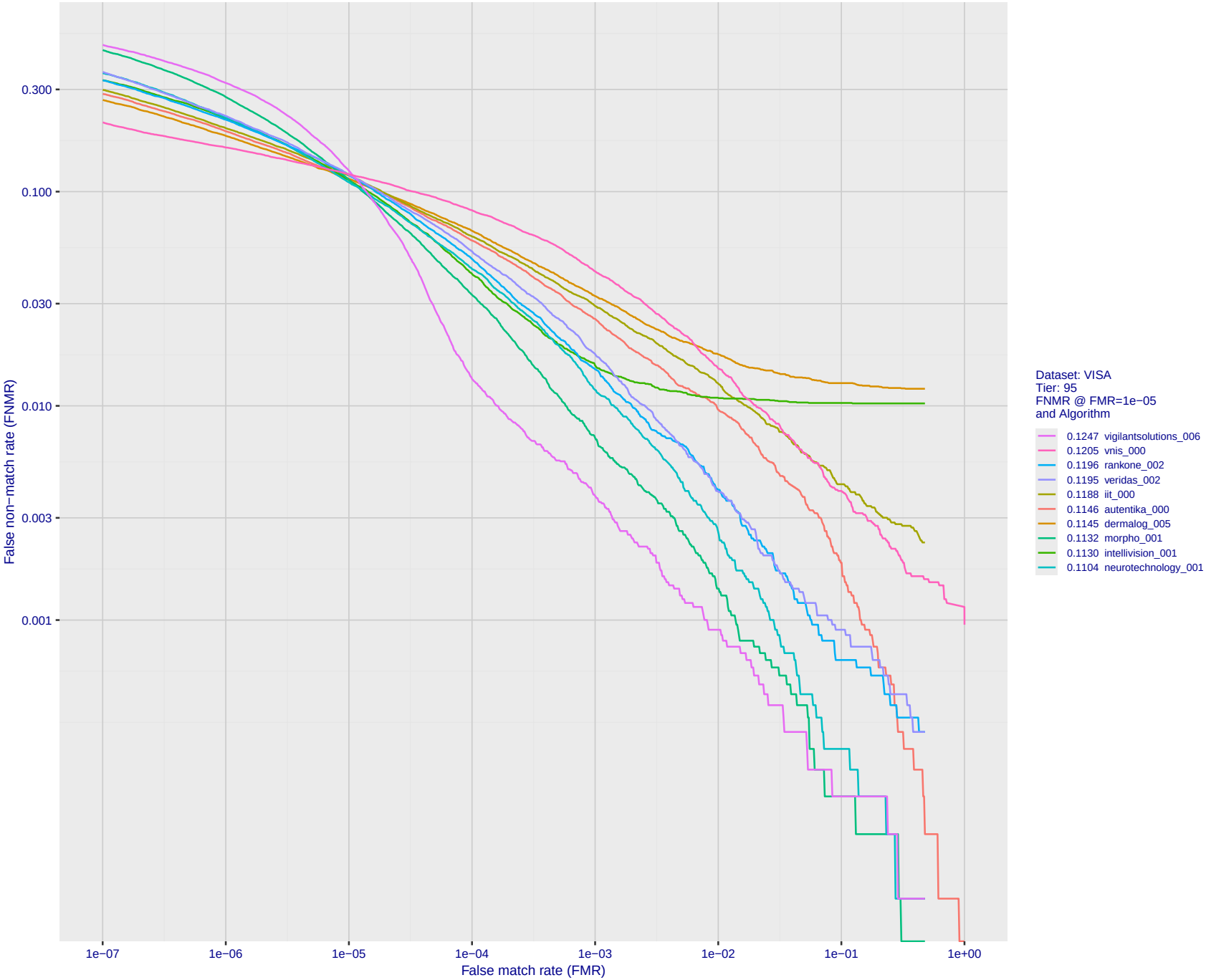

Figure 203: For the visa images, detection error tradeoff (DET) characteristics showing false non-match rate vs. false match rate plotted parametrically on threshold, T. The scales are logarithmic in order to show many decades of FMR.

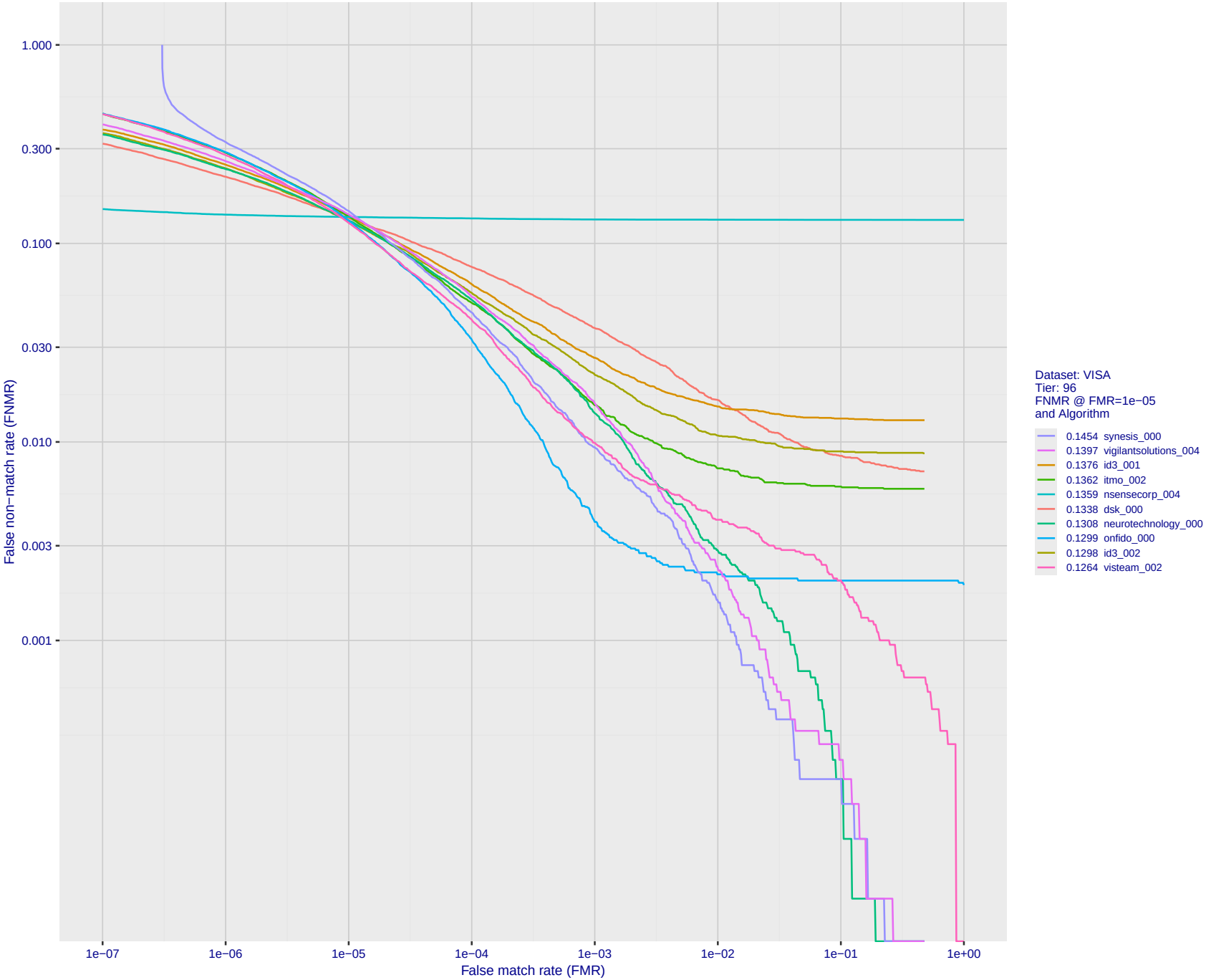

Figure 204: For the visa images, detection error tradeoff (DET) characteristics showing false non-match rate vs. false match rate plotted parametrically on threshold, T. The scales are logarithmic in order to show many decades of FMR.

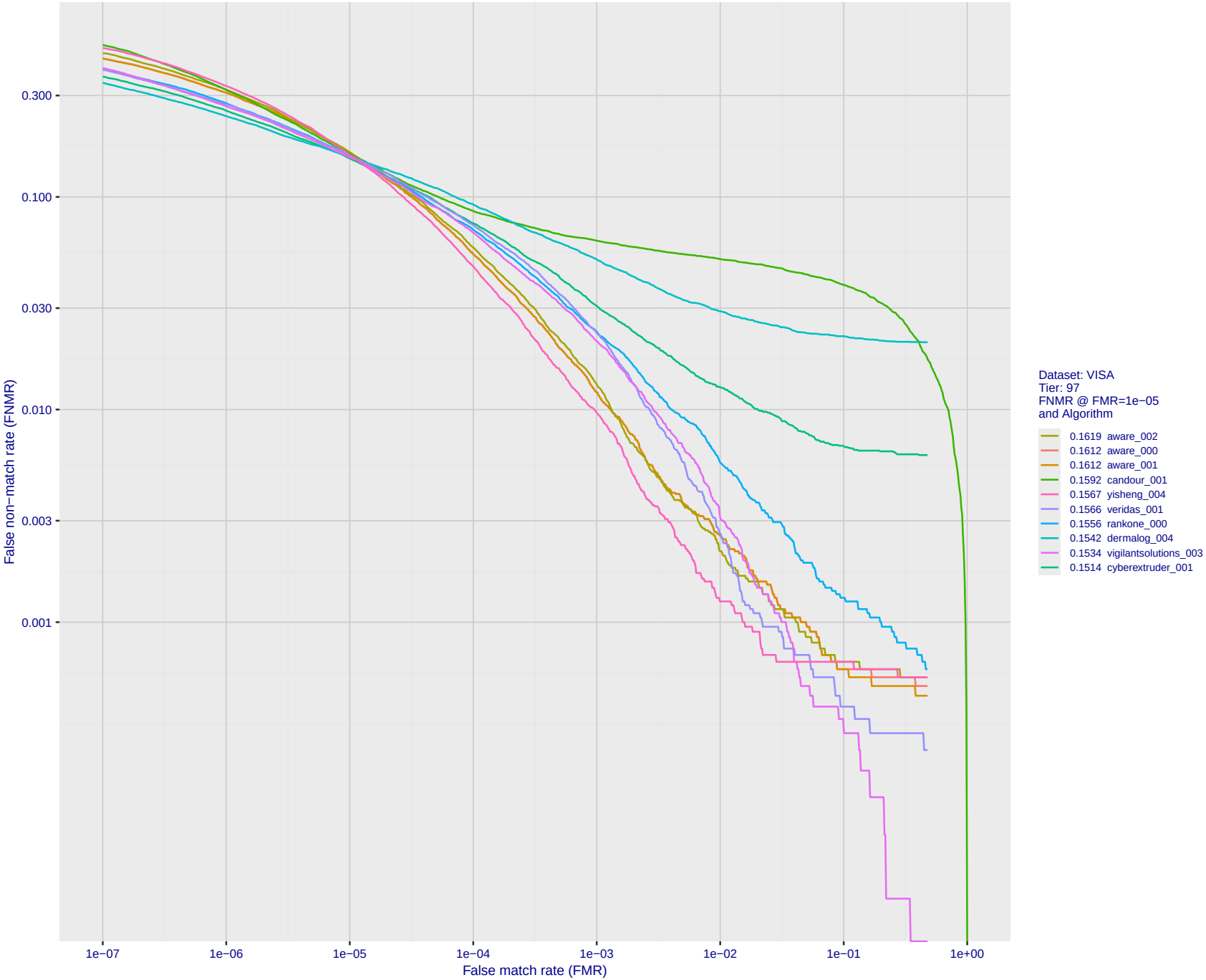

Figure 205: For the visa images, detection error tradeoff (DET) characteristics showing false non-match rate vs. false match rate plotted parametrically on threshold, T. The scales are logarithmic in order to show many decades of FMR.

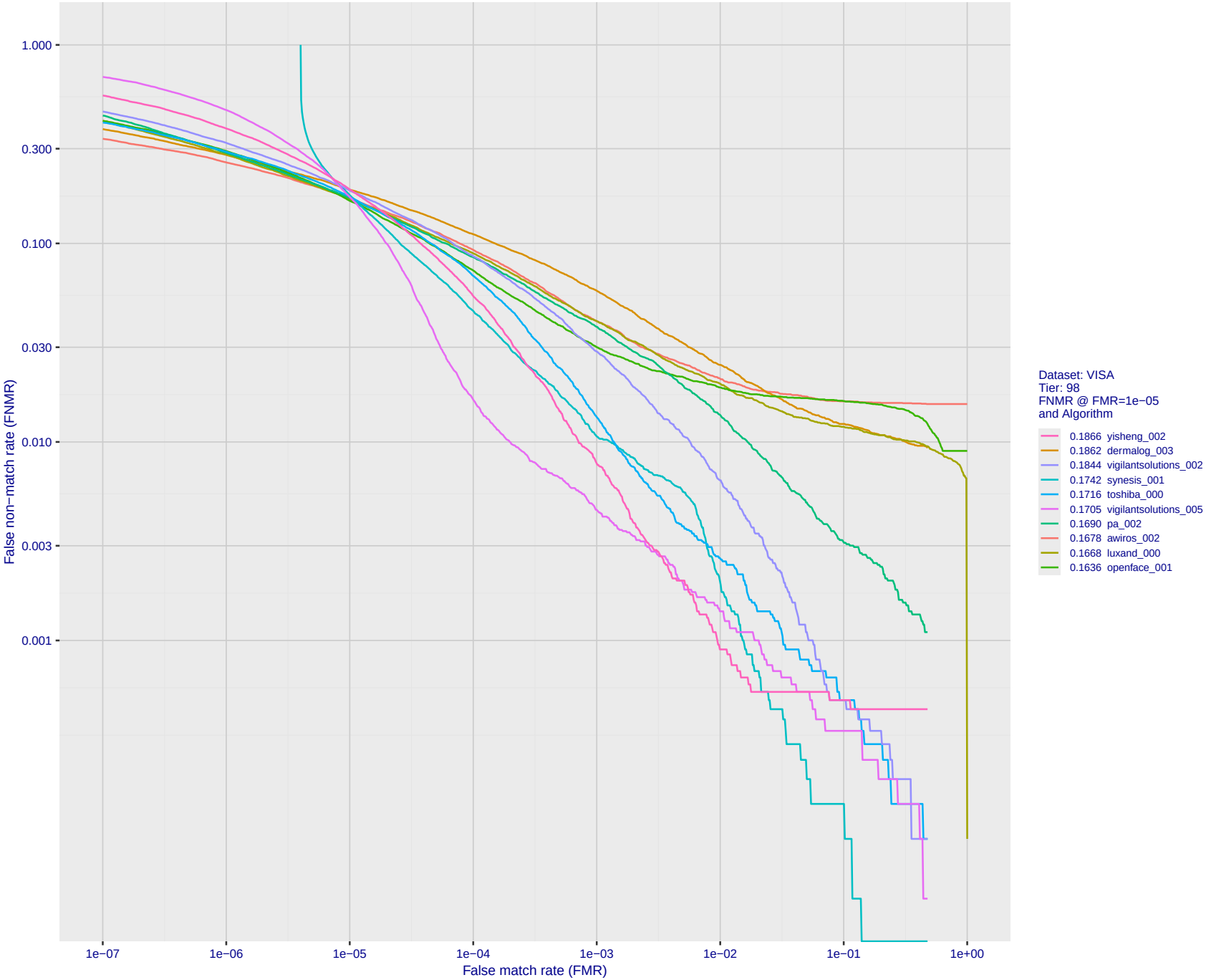

Figure 206: For the visa images, detection error tradeoff (DET) characteristics showing false non-match rate vs. false match rate plotted parametrically on threshold, T. The scales are logarithmic in order to show many decades of FMR.

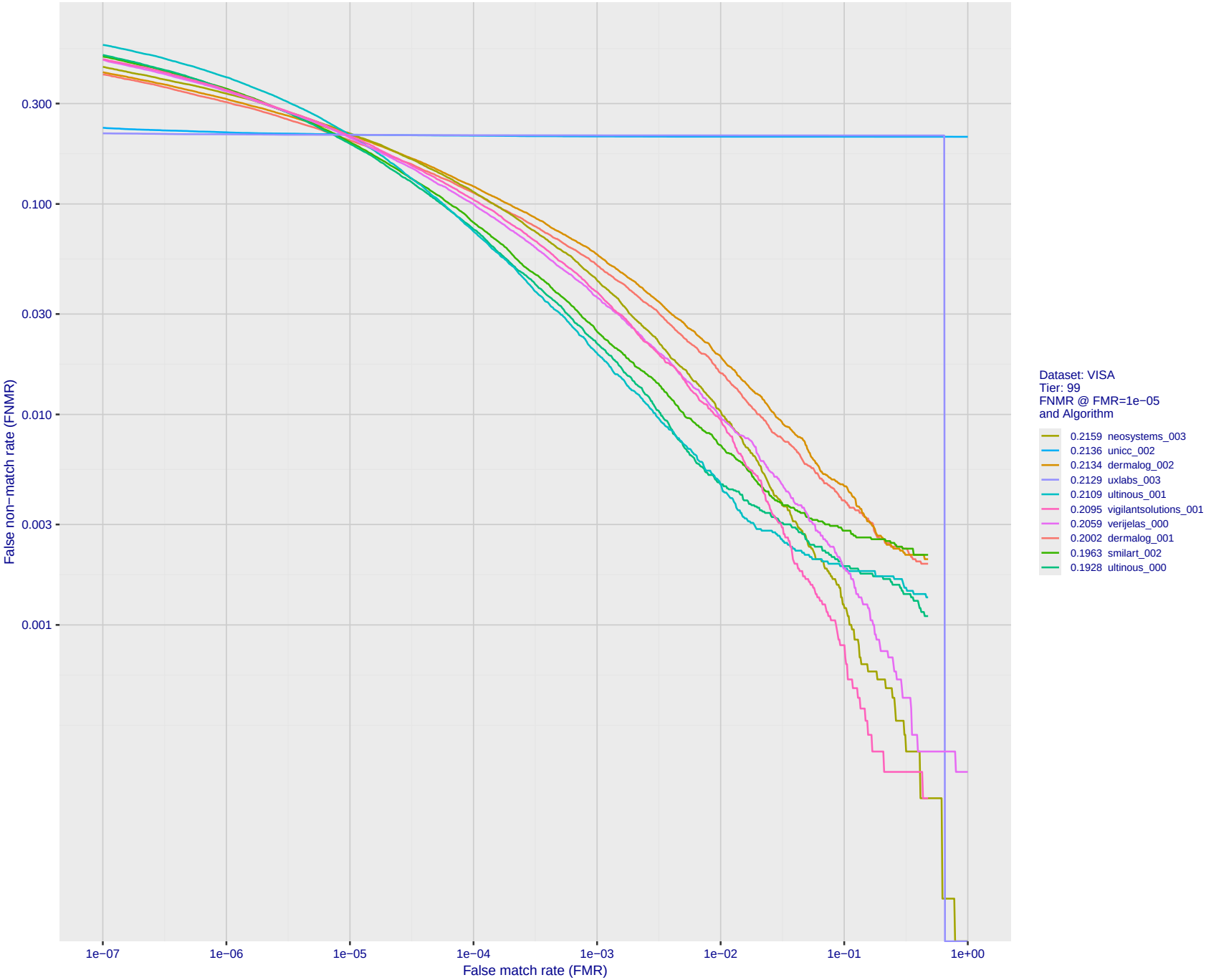

Figure 207: For the visa images, detection error tradeoff (DET) characteristics showing false non-match rate vs. false match rate plotted parametrically on threshold, T. The scales are logarithmic in order to show many decades of FMR.

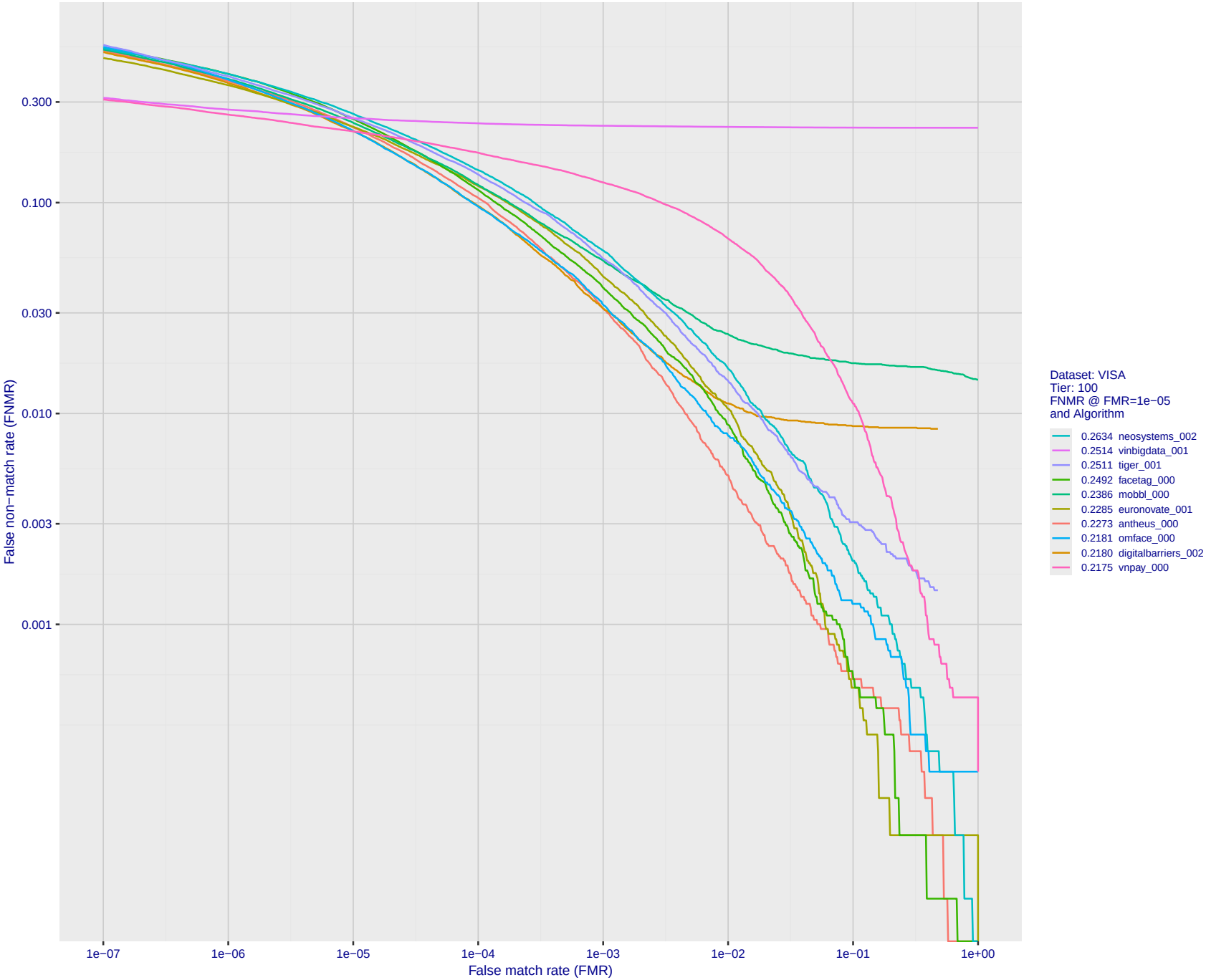

Figure 208: For the visa images, detection error tradeoff (DET) characteristics showing false non-match rate vs. false match rate plotted parametrically on threshold, T. The scales are logarithmic in order to show many decades of FMR.

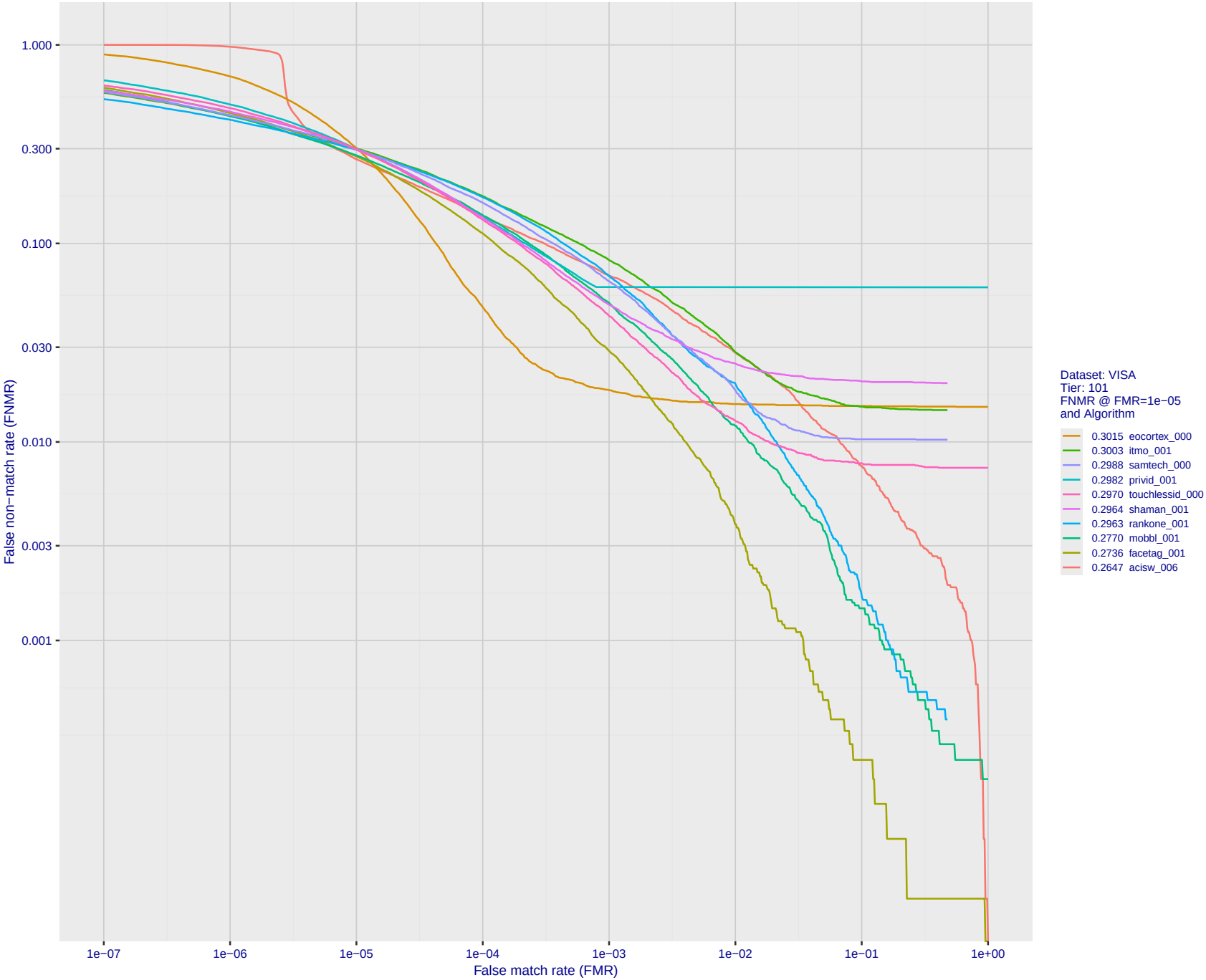

Figure 209: For the visa images, detection error tradeoff (DET) characteristics showing false non-match rate vs. false match rate plotted parametrically on threshold, T. The scales are logarithmic in order to show many decades of FMR.

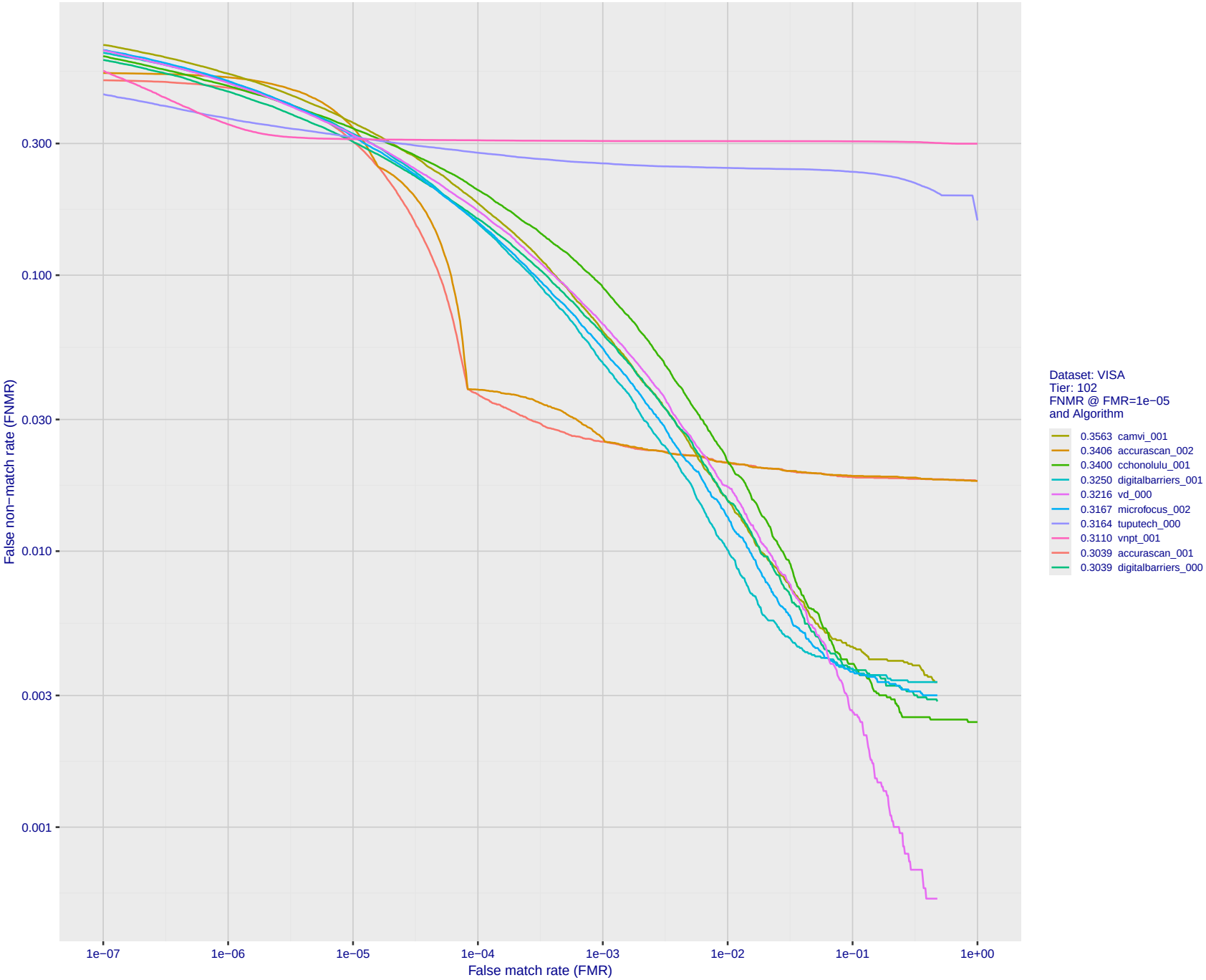

Figure 210: For the visa images, detection error tradeoff (DET) characteristics showing false non-match rate vs. false match rate plotted parametrically on threshold, T. The scales are logarithmic in order to show many decades of FMR.

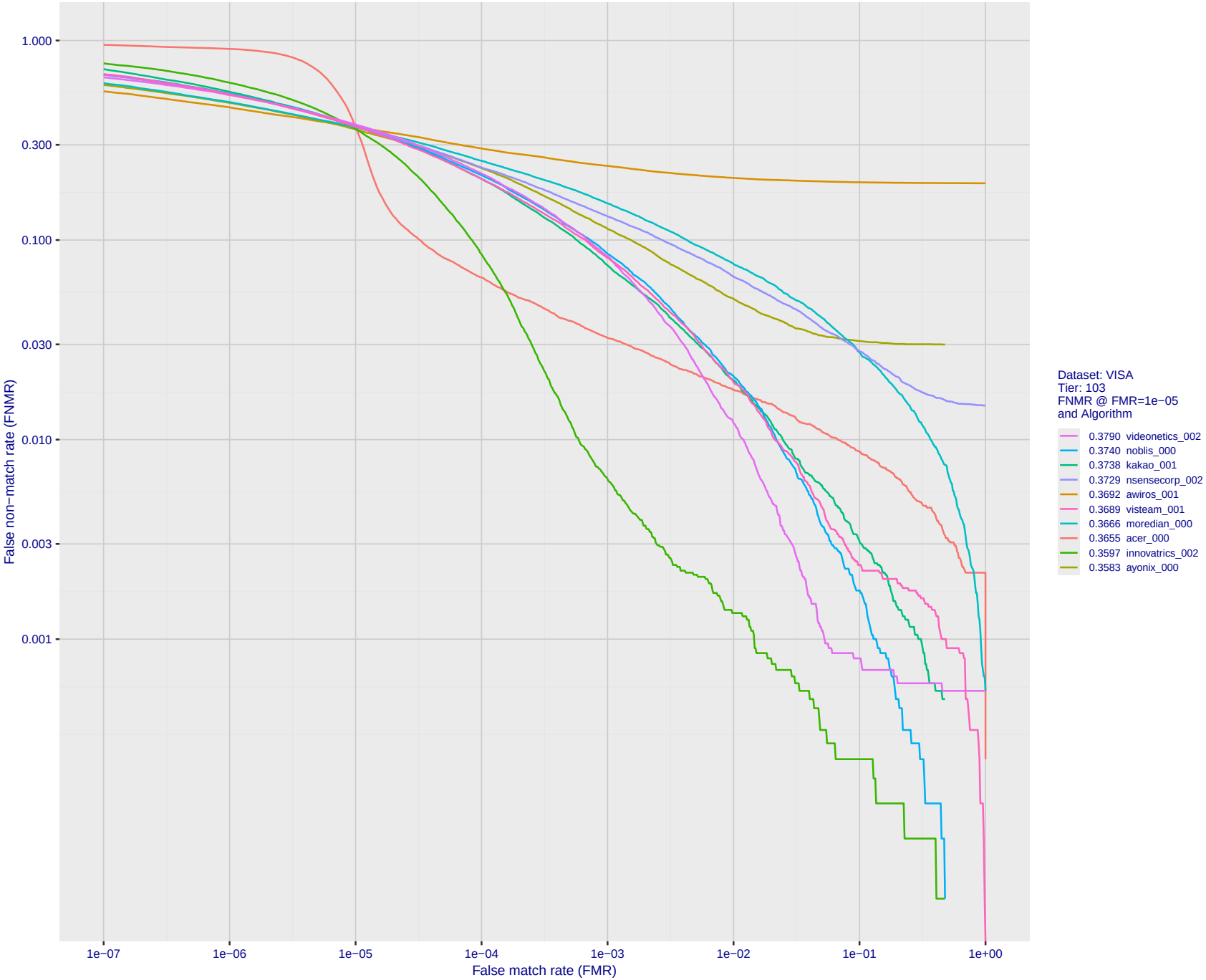

Figure 211: For the visa images, detection error tradeoff (DET) characteristics showing false non-match rate vs. false match rate plotted parametrically on threshold, T. The scales are logarithmic in order to show many decades of FMR.

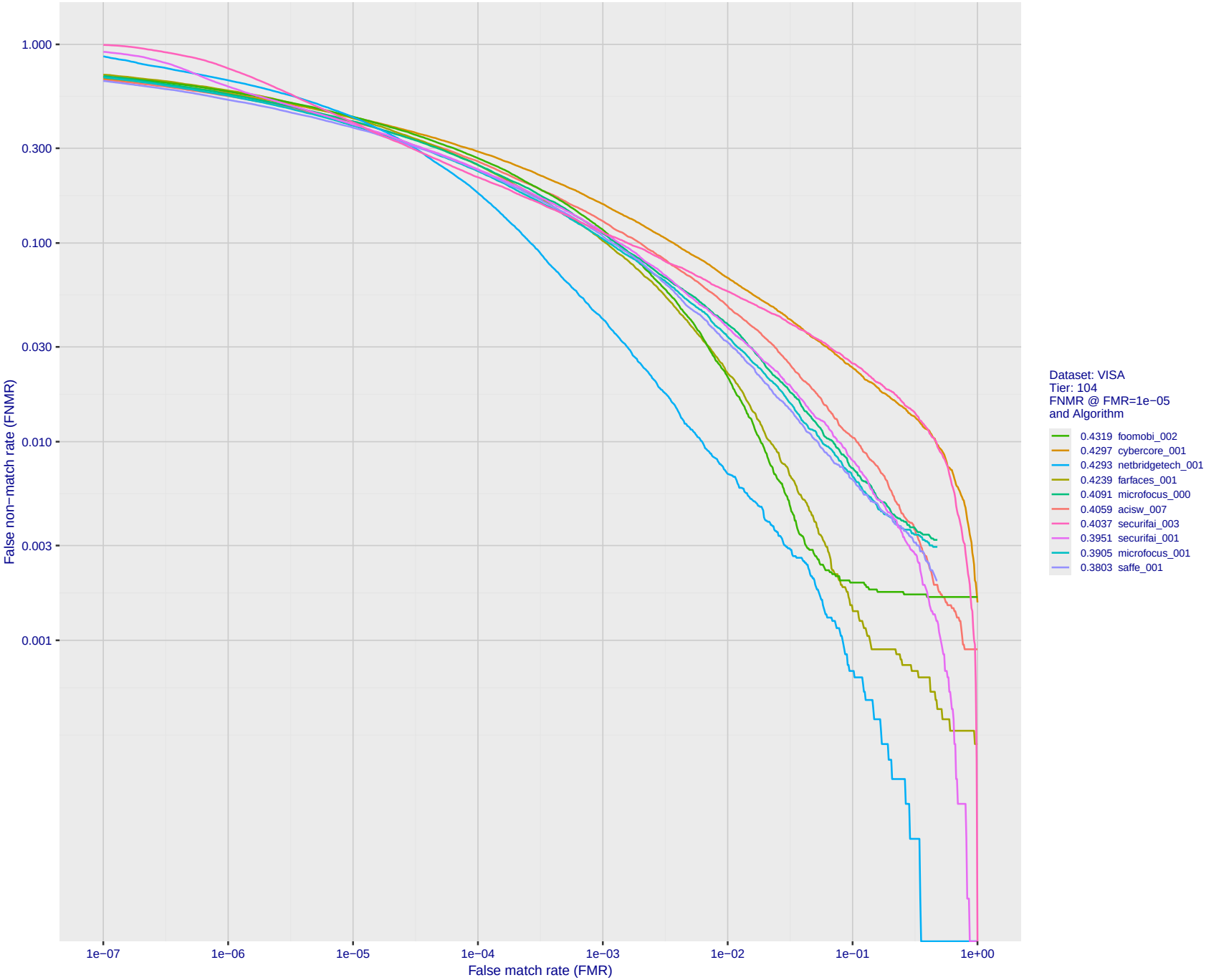

Figure 212: For the visa images, detection error tradeoff (DET) characteristics showing false non-match rate vs. false match rate plotted parametrically on threshold, T. The scales are logarithmic in order to show many decades of FMR.

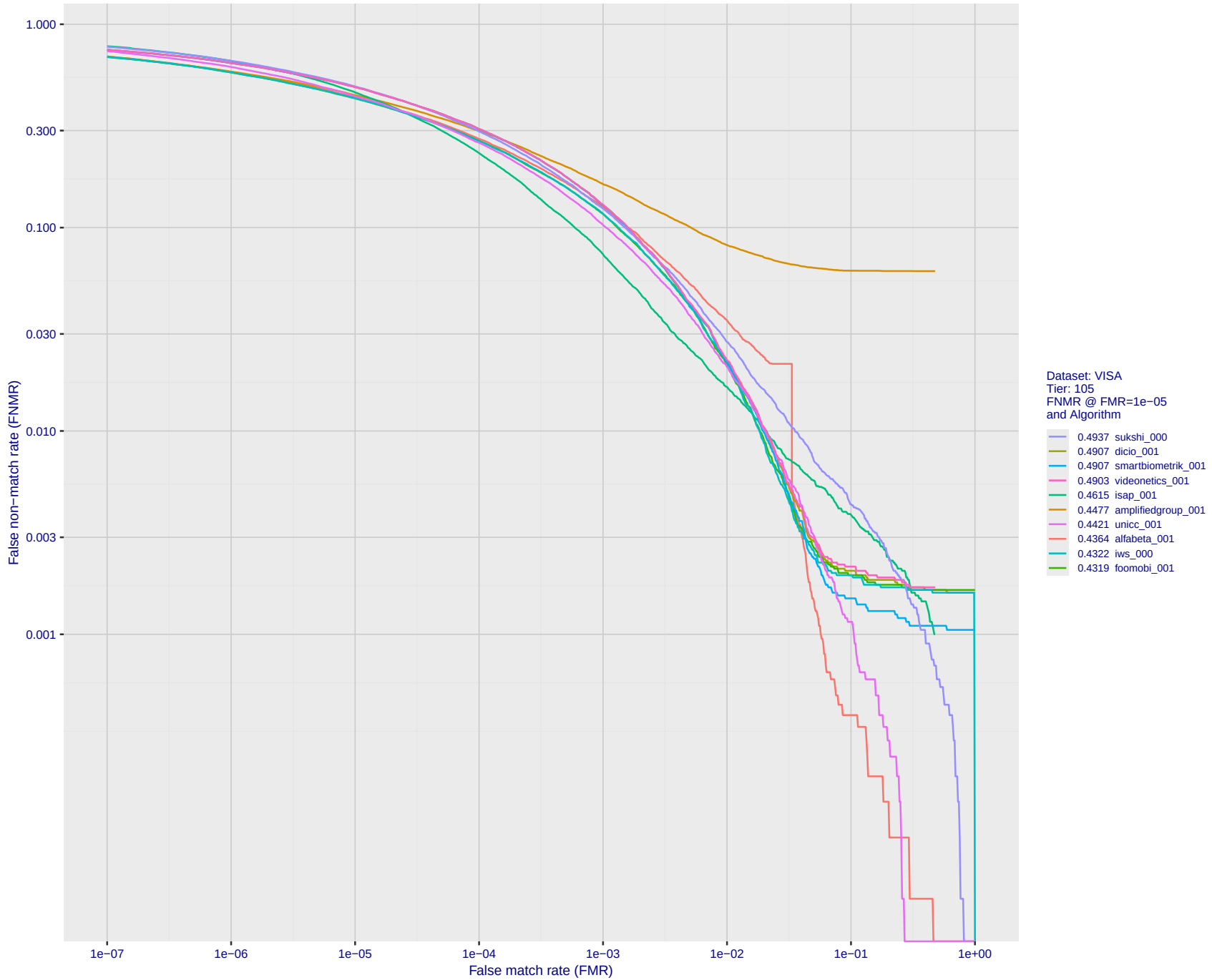

Figure 213: For the visa images, detection error tradeoff (DET) characteristics showing false non-match rate vs. false match rate plotted parametrically on threshold, T. The scales are logarithmic in order to show many decades of FMR.

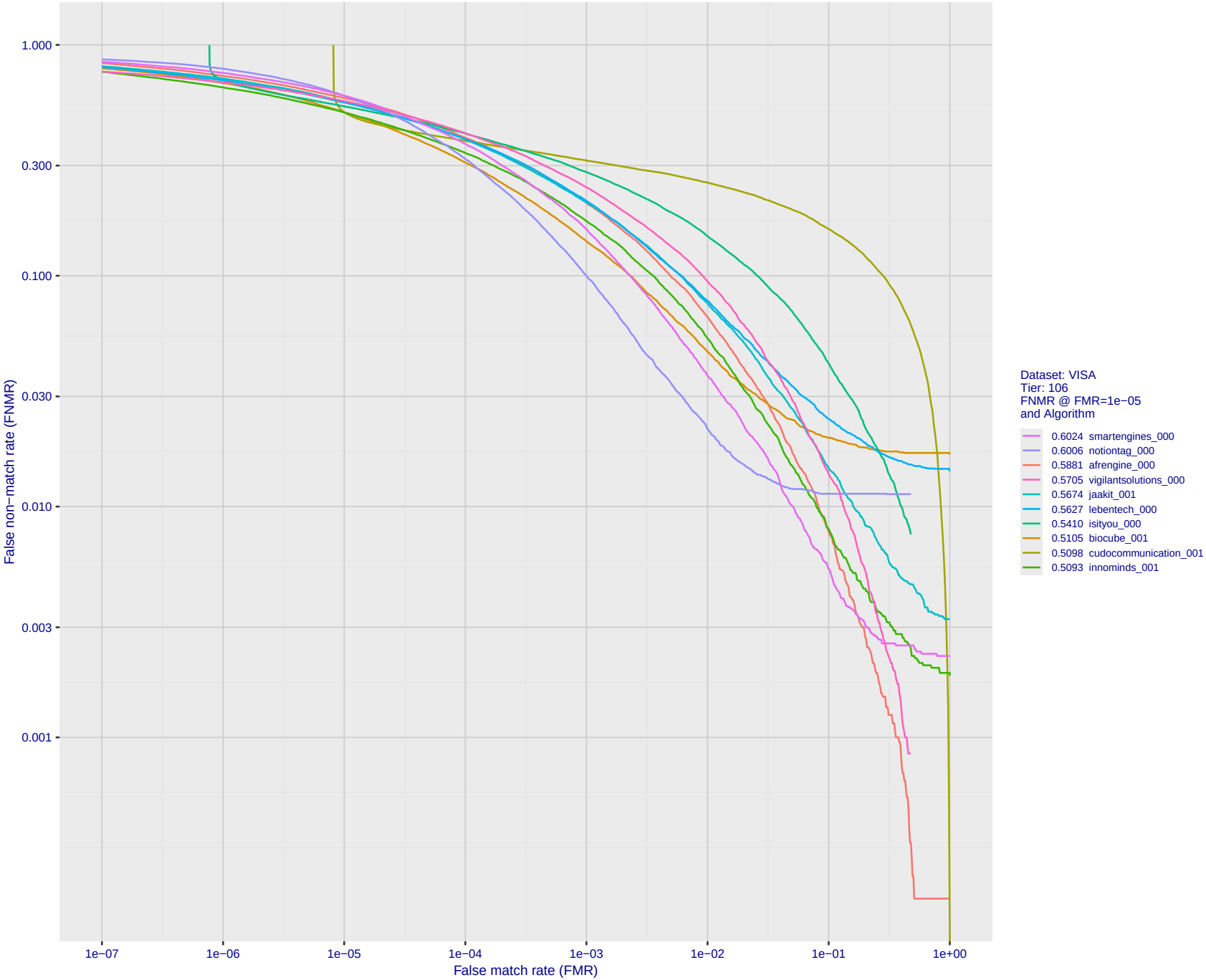

Figure 214: For the visa images, detection error tradeoff (DET) characteristics showing false non-match rate vs. false match rate plotted parametrically on threshold, T. The scales are logarithmic in order to show many decades of FMR.

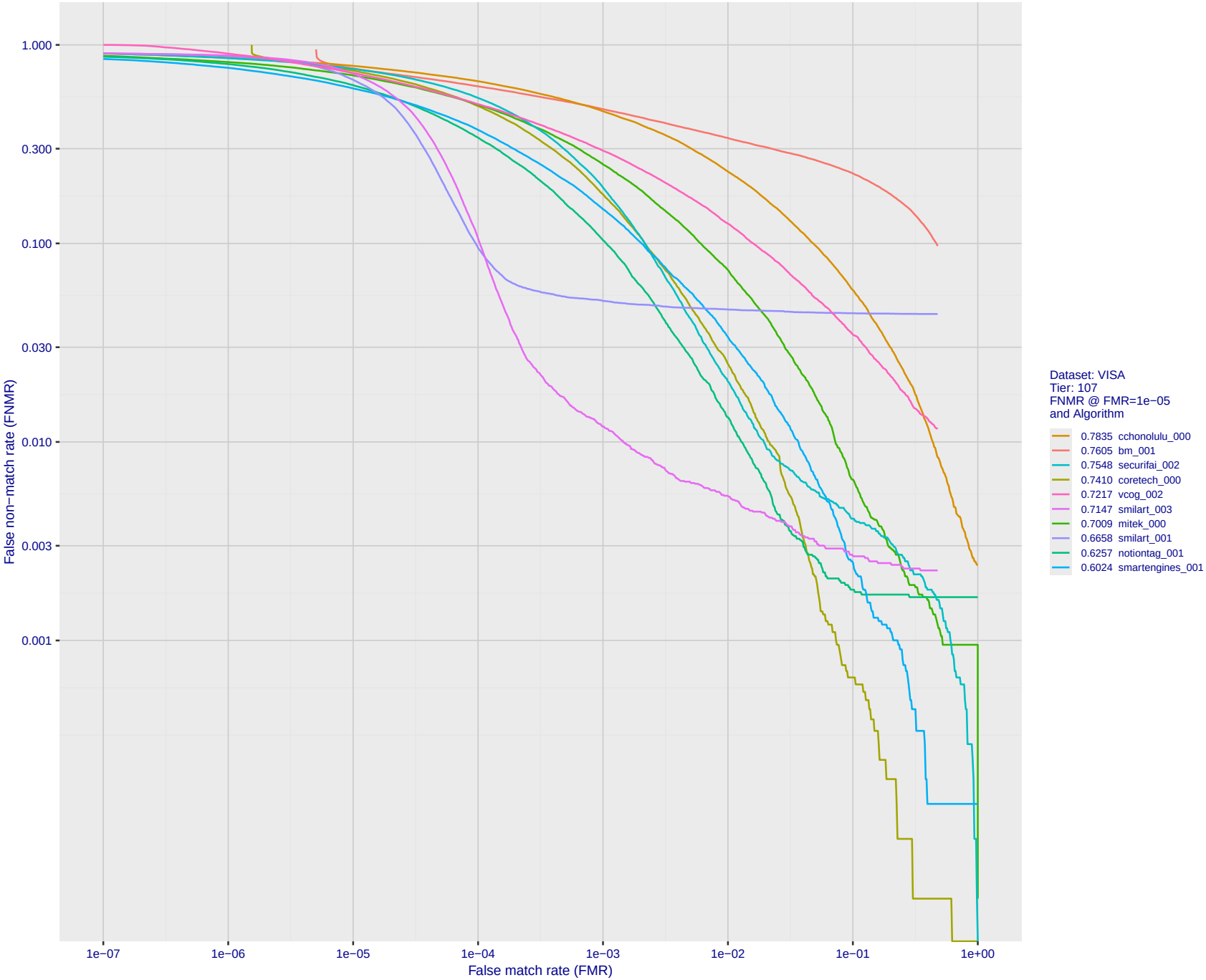

Figure 215: For the visa images, detection error tradeoff (DET) characteristics showing false non-match rate vs. false match rate plotted parametrically on threshold, T. The scales are logarithmic in order to show many decades of FMR.

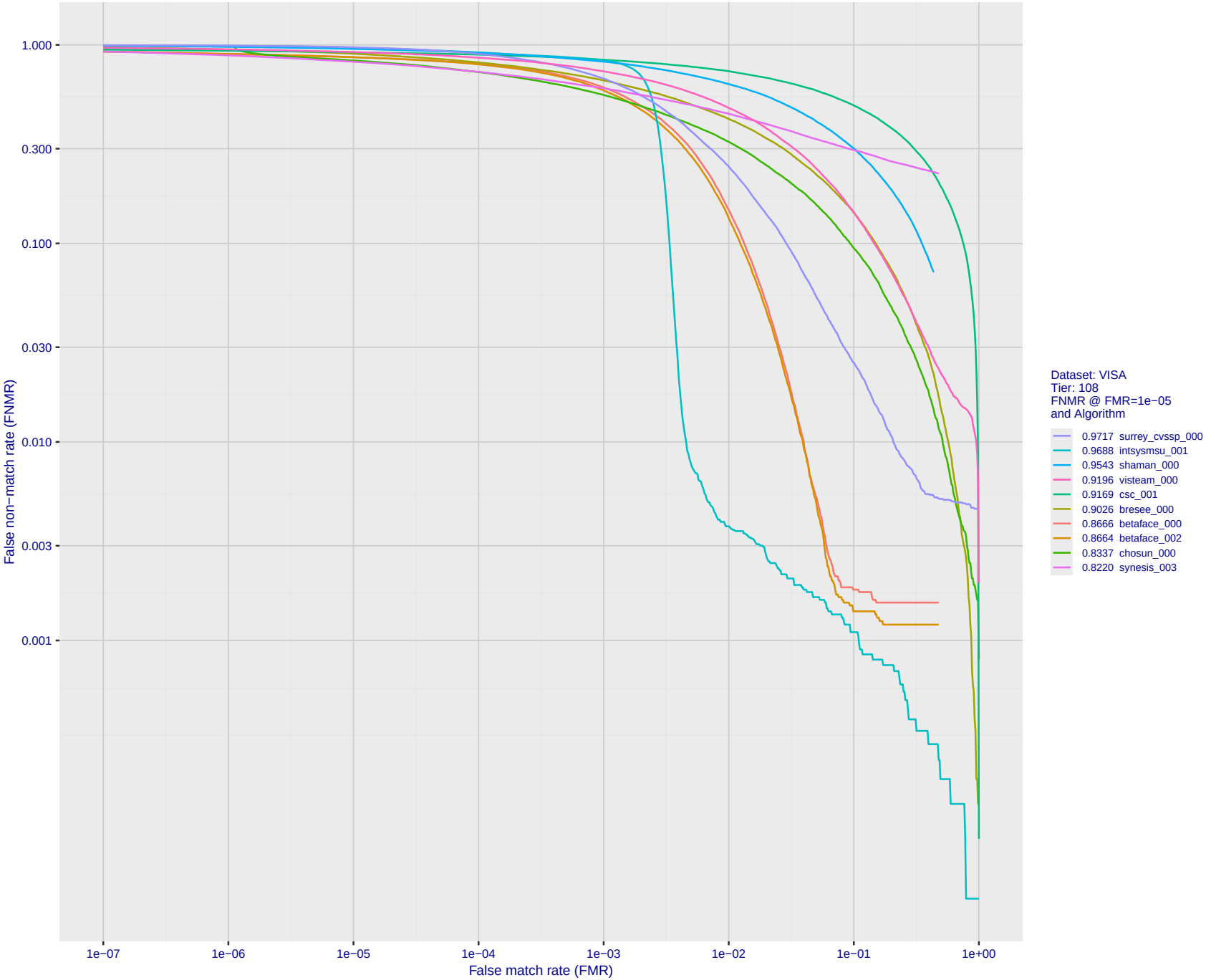

Figure 216: For the visa images, detection error tradeoff (DET) characteristics showing false non-match rate vs. false match rate plotted parametrically on threshold, T. The scales are logarithmic in order to show many decades of FMR.

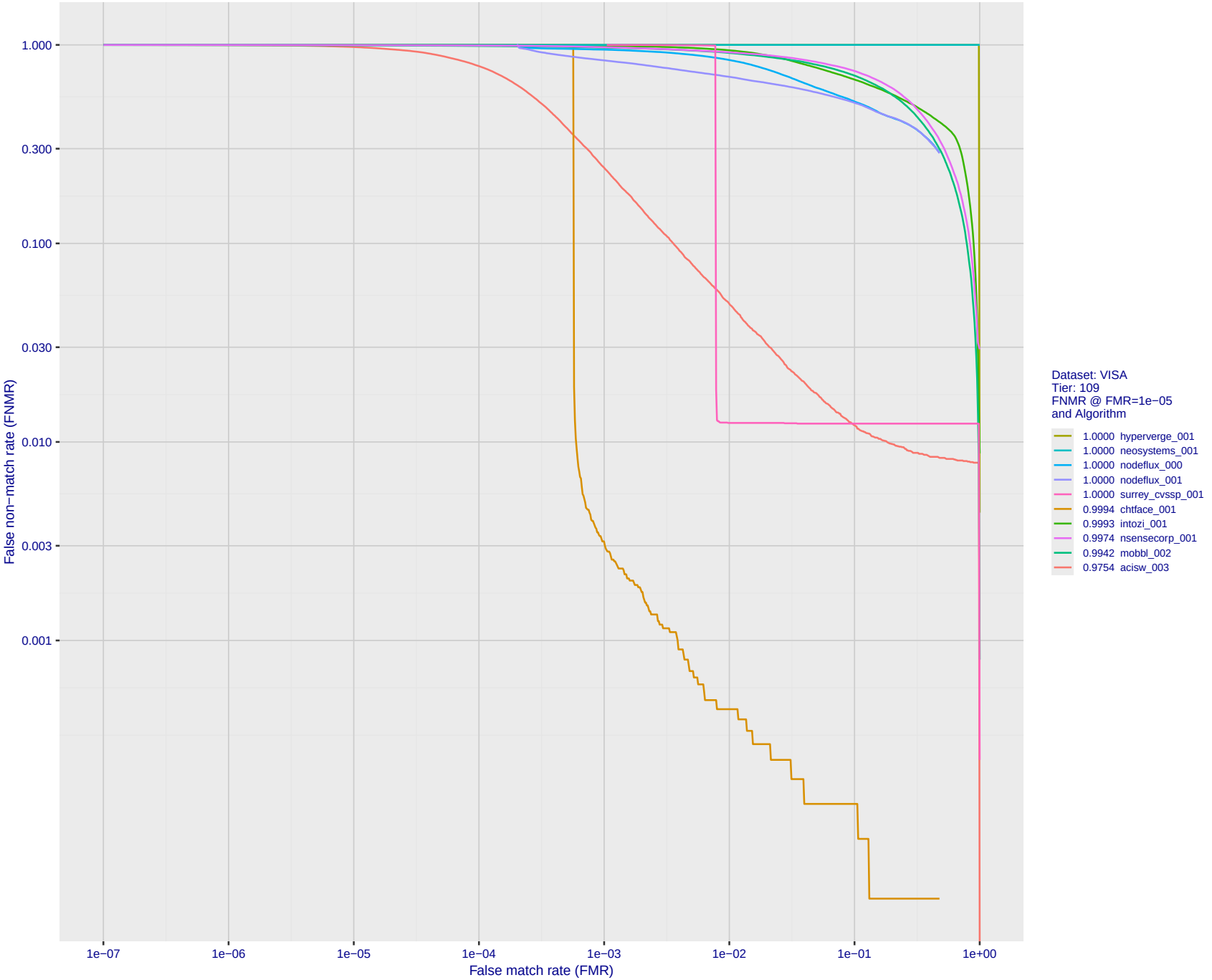

Figure 217: For the visa images, detection error tradeoff (DET) characteristics showing false non-match rate vs. false match rate plotted parametrically on threshold, T. The scales are logarithmic in order to show many decades of FMR.

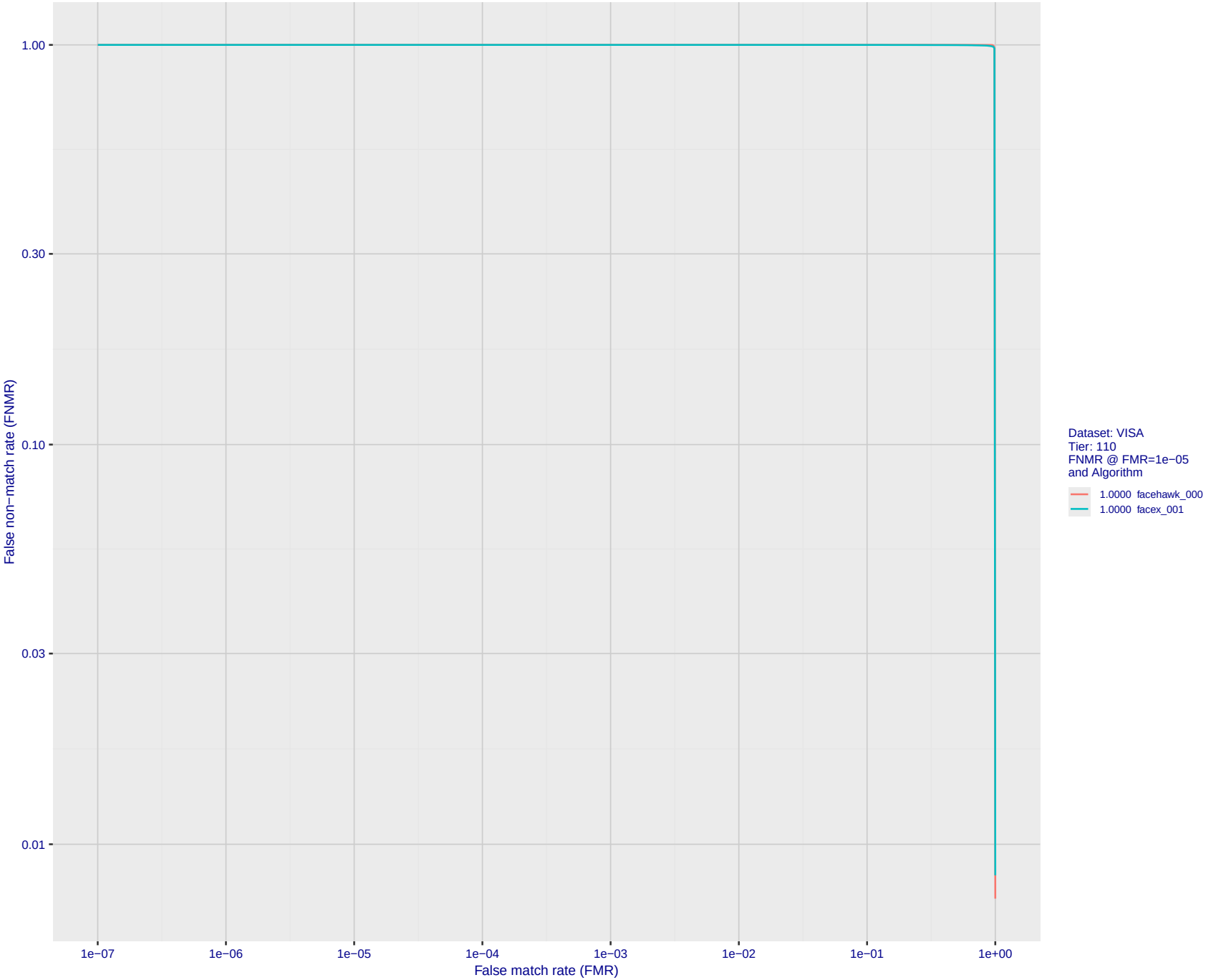

Figure 218: For the visa images, detection error tradeoff (DET) characteristics showing false non-match rate vs. false match rate plotted parametrically on threshold, T. The scales are logarithmic in order to show many decades of FMR.

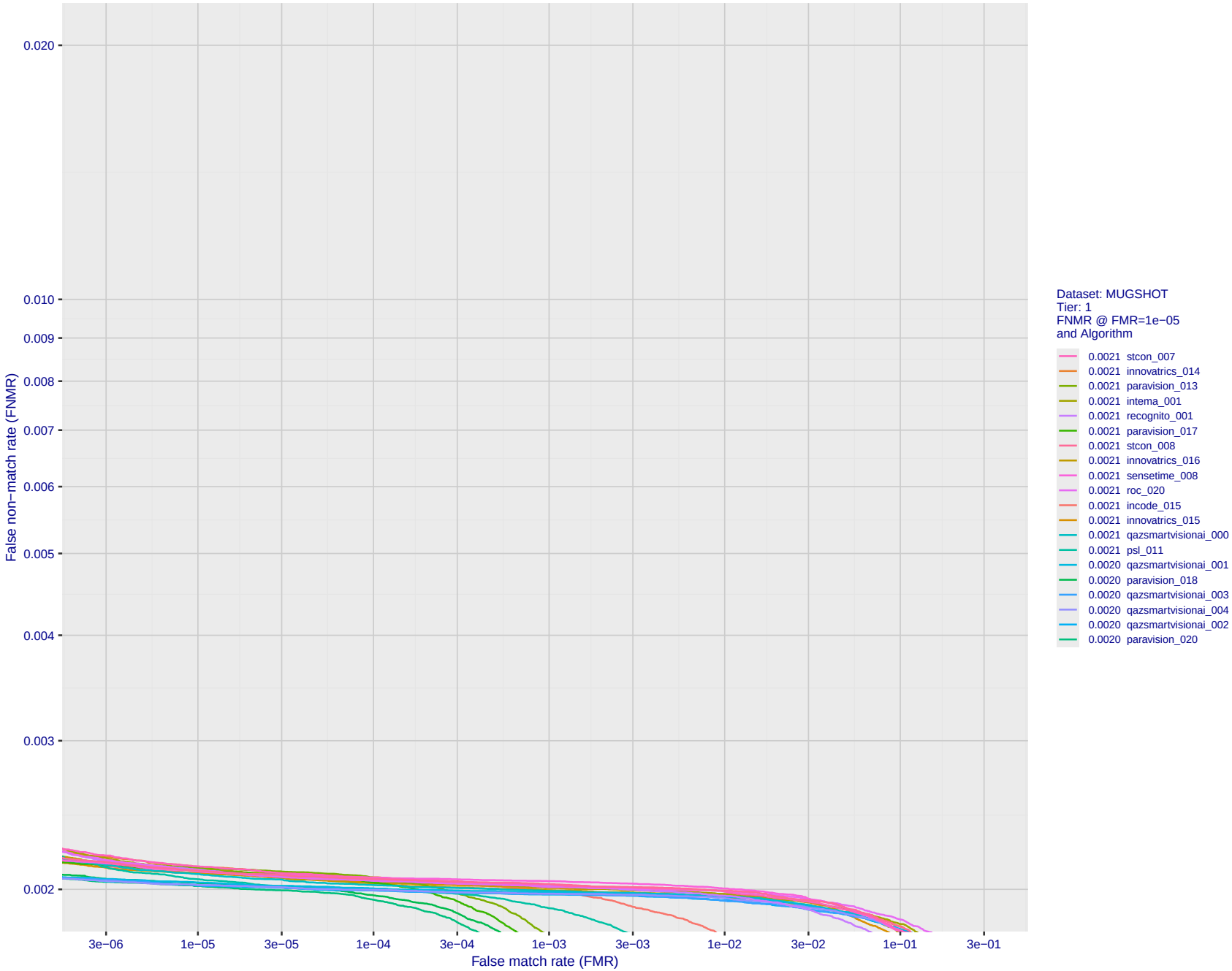

Figure 219: For the mugshot images, detection error tradeoff (DET) characteristics showing false non-match rate vs. false match rate plotted parametrically on threshold, T. The scales are logarithmic in order to show decades of FMR.

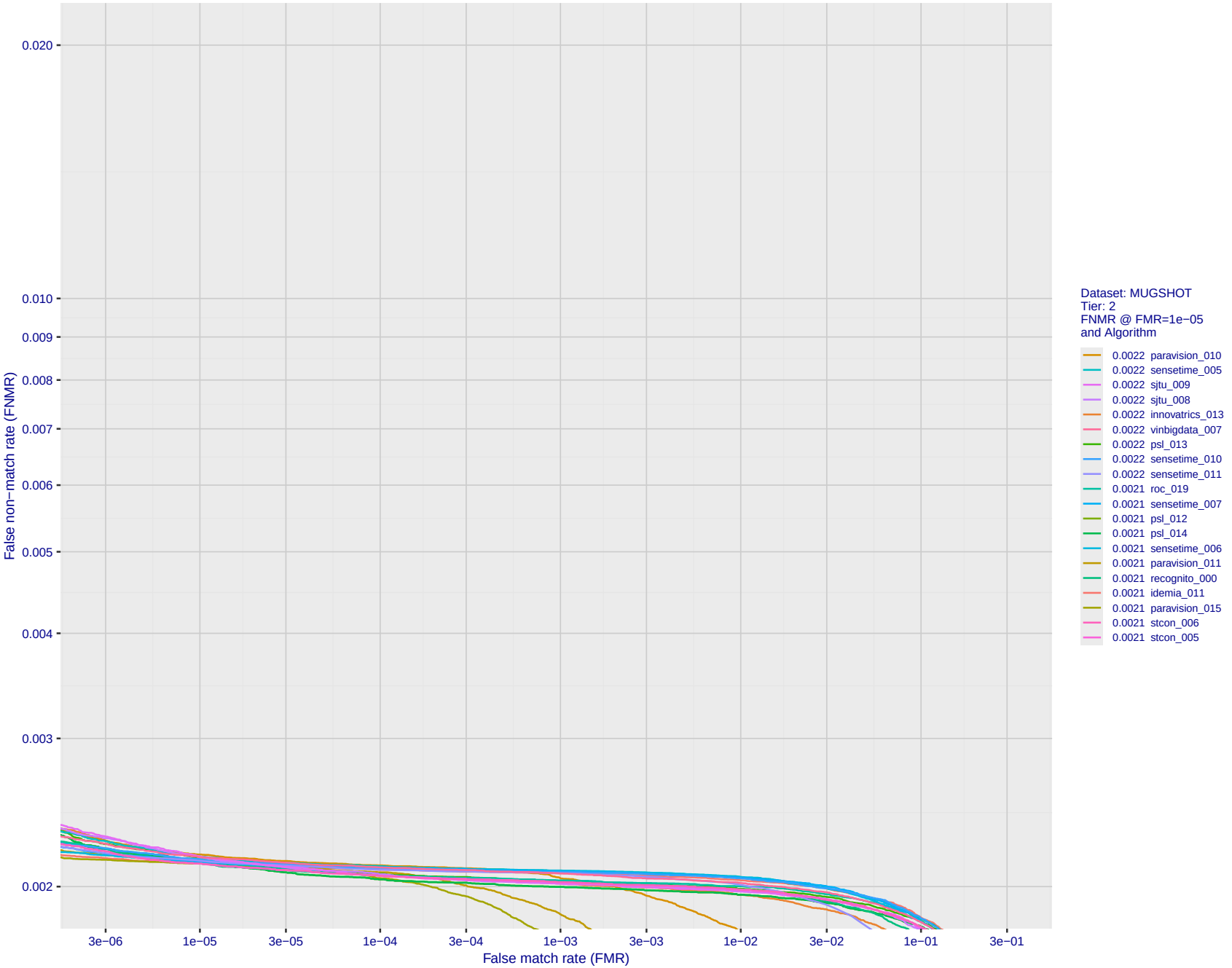

Figure 220: For the mugshot images, detection error tradeoff (DET) characteristics showing false non-match rate vs. false match rate plotted parametrically on threshold, T. The scales are logarithmic in order to show decades of FMR.

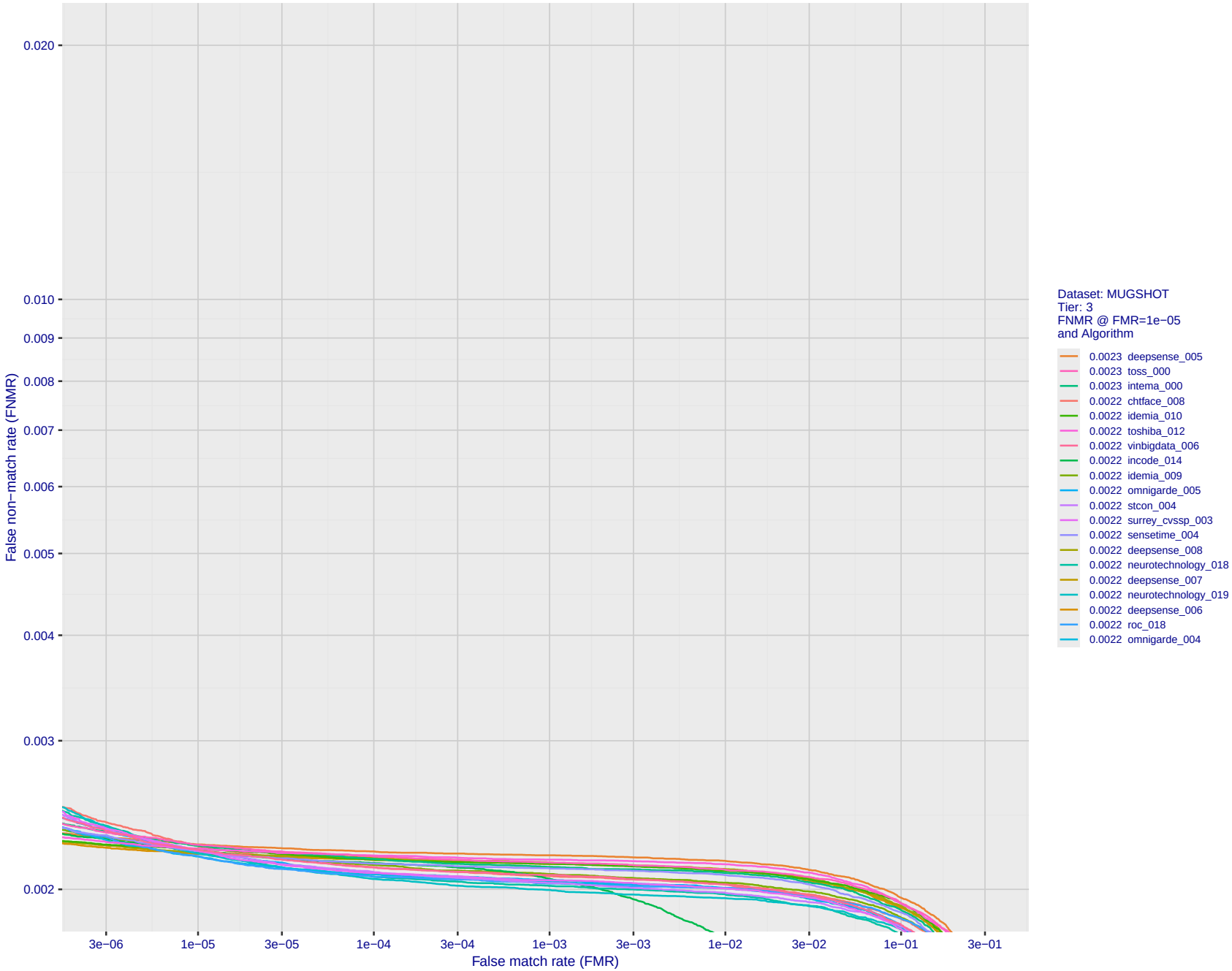

Figure 221: For the mugshot images, detection error tradeoff (DET) characteristics showing false non-match rate vs. false match rate plotted parametrically on threshold, T. The scales are logarithmic in order to show decades of FMR.

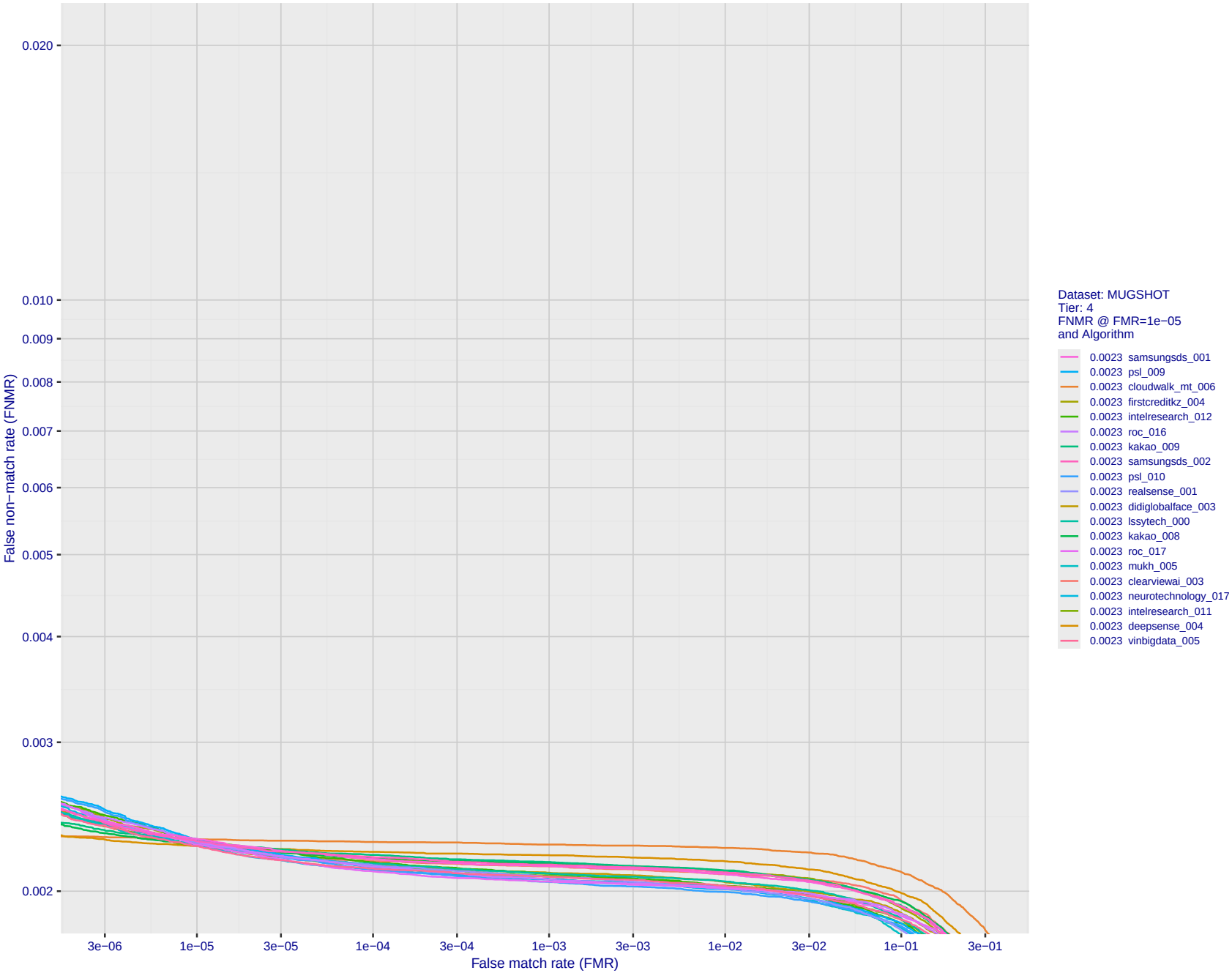

Figure 222: For the mugshot images, detection error tradeoff (DET) characteristics showing false non-match rate vs. false match rate plotted parametrically on threshold, T. The scales are logarithmic in order to show decades of FMR.

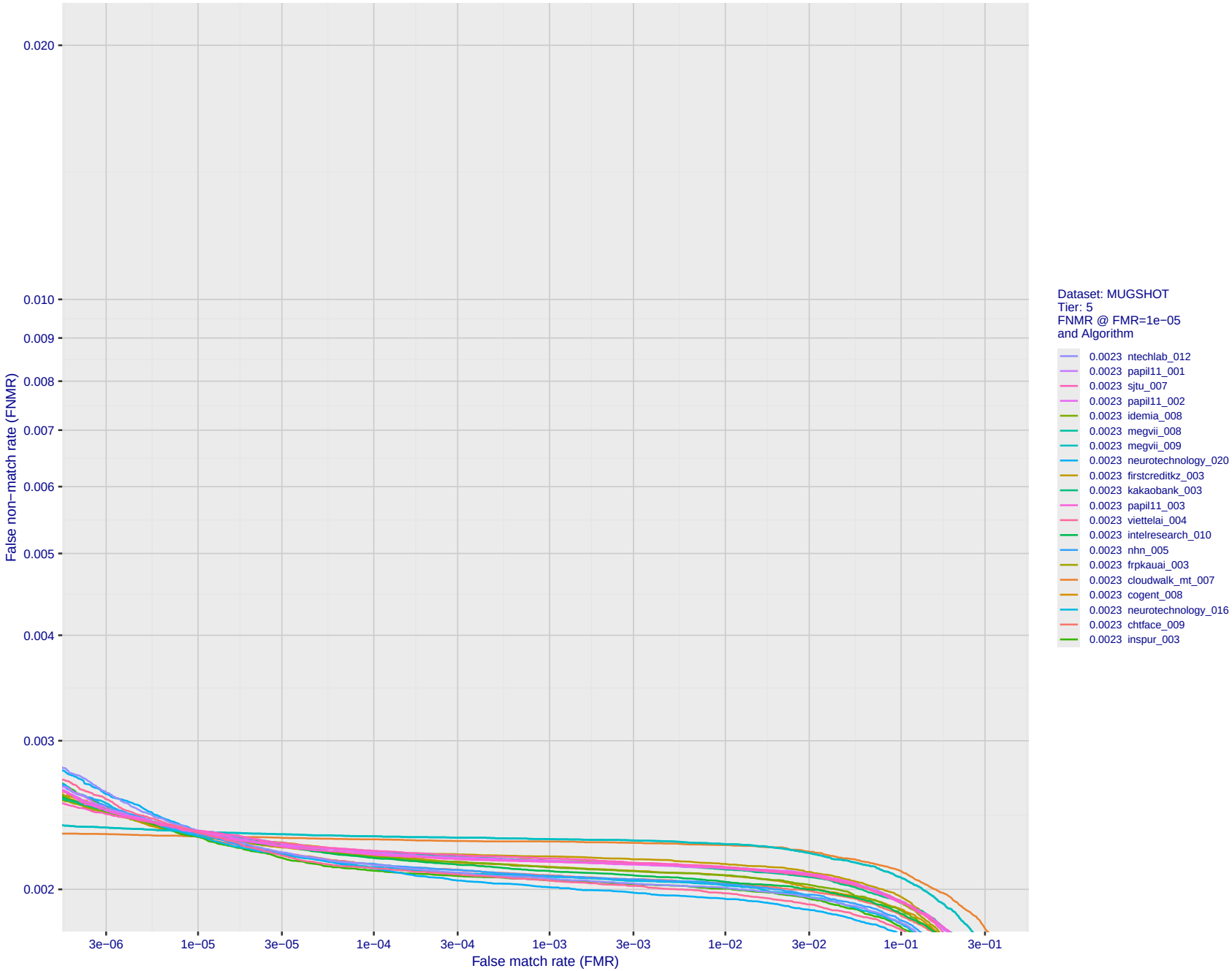

Figure 223: For the mugshot images, detection error tradeoff (DET) characteristics showing false non-match rate vs. false match rate plotted parametrically on threshold, T. The scales are logarithmic in order to show decades of FMR.

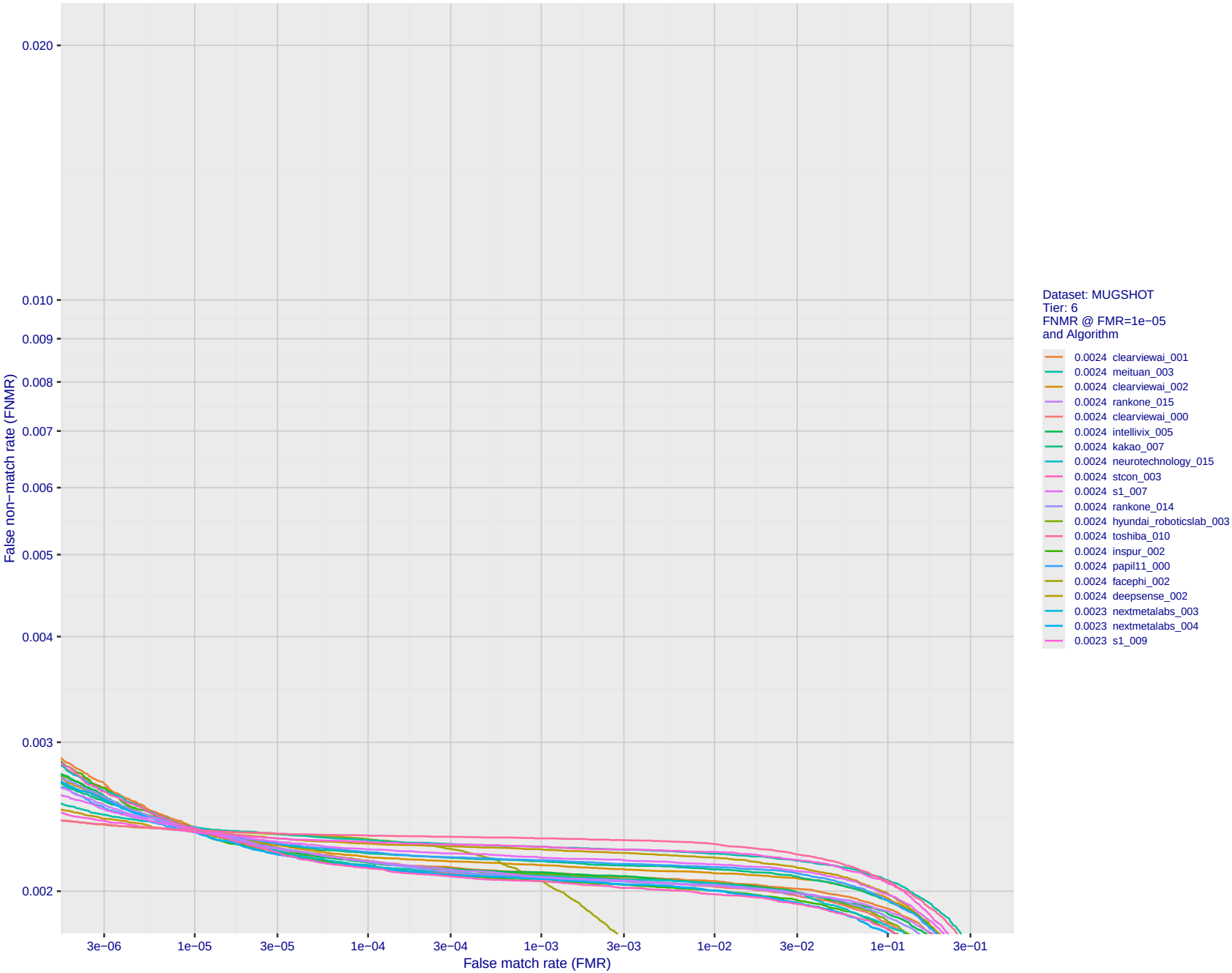

Figure 224: For the mugshot images, detection error tradeoff (DET) characteristics showing false non-match rate vs. false match rate plotted parametrically on threshold, T. The scales are logarithmic in order to show decades of FMR.

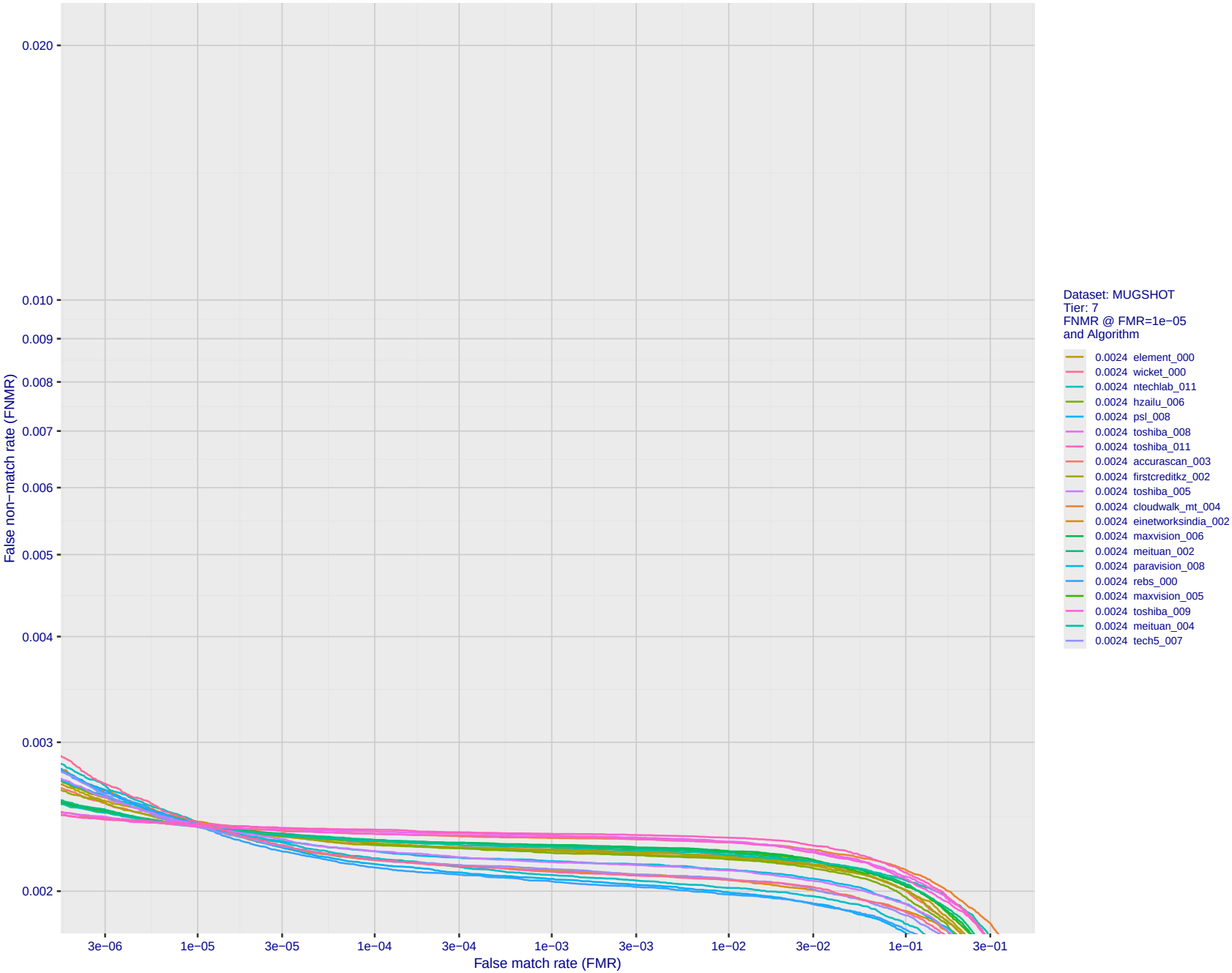

Figure 225: For the mugshot images, detection error tradeoff (DET) characteristics showing false non-match rate vs. false match rate plotted parametrically on threshold, T. The scales are logarithmic in order to show decades of FMR.

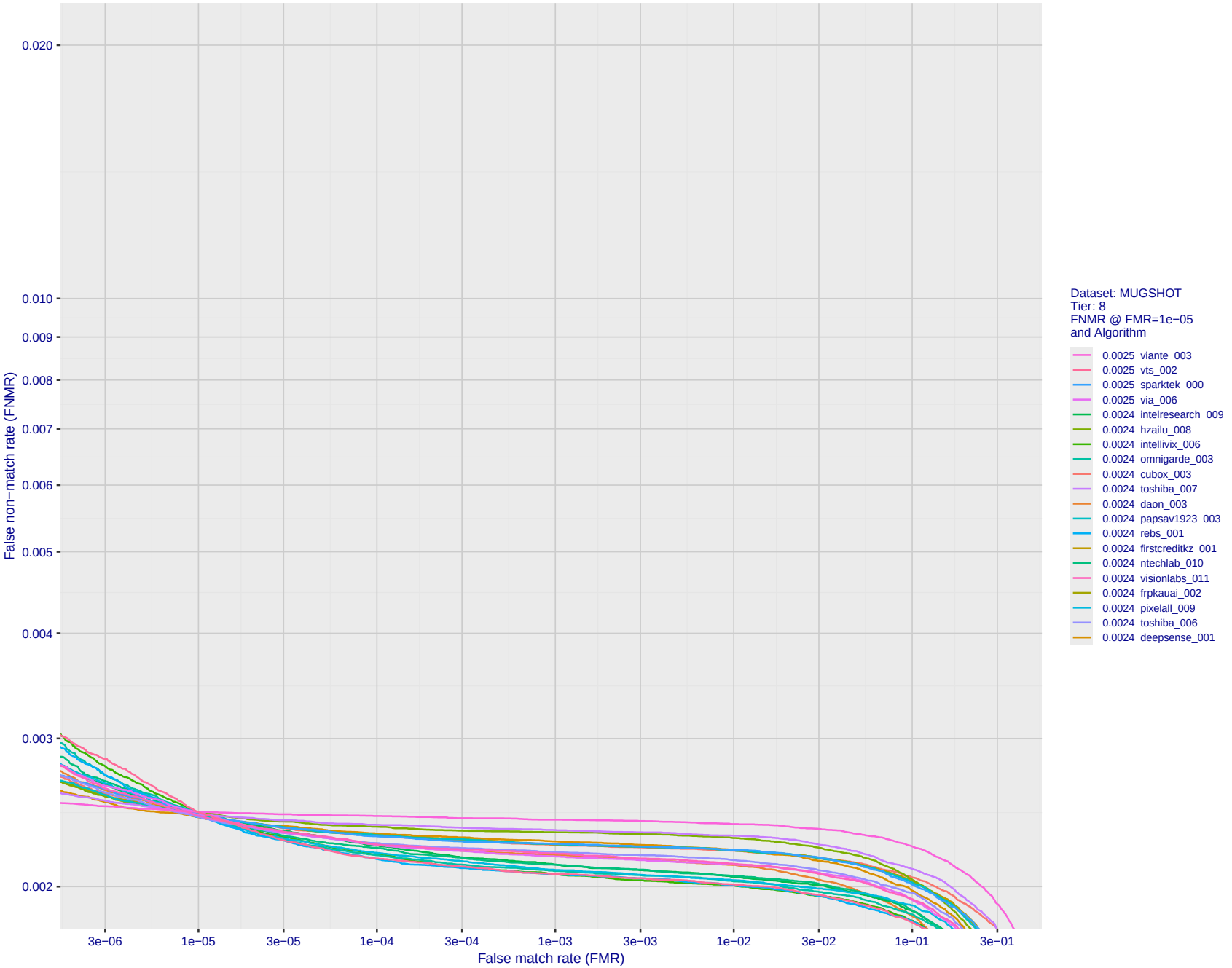

Figure 226: For the mugshot images, detection error tradeoff (DET) characteristics showing false non-match rate vs. false match rate plotted parametrically on threshold, T. The scales are logarithmic in order to show decades of FMR.

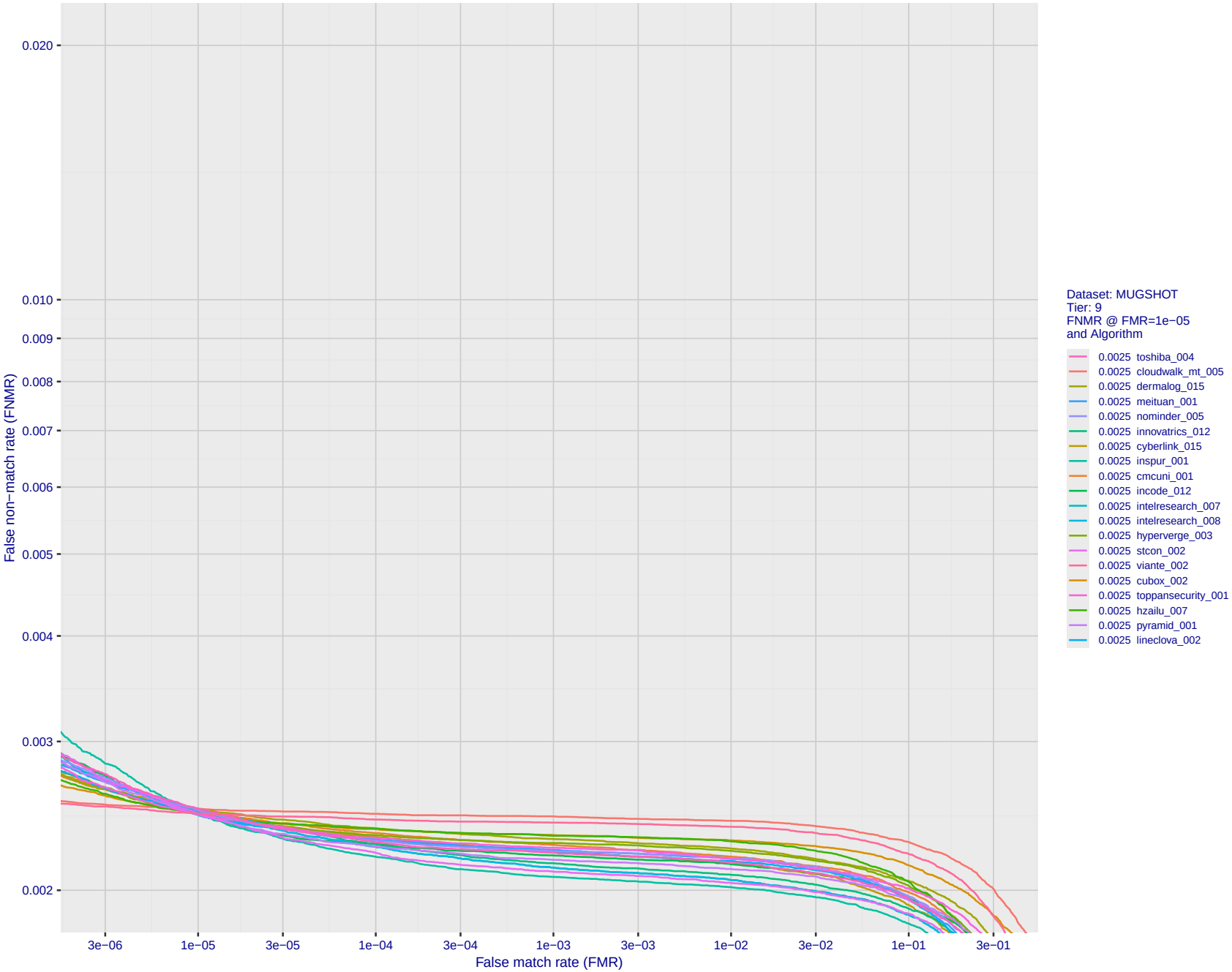

Figure 227: For the mugshot images, detection error tradeoff (DET) characteristics showing false non-match rate vs. false match rate plotted parametrically on threshold, T. The scales are logarithmic in order to show decades of FMR.

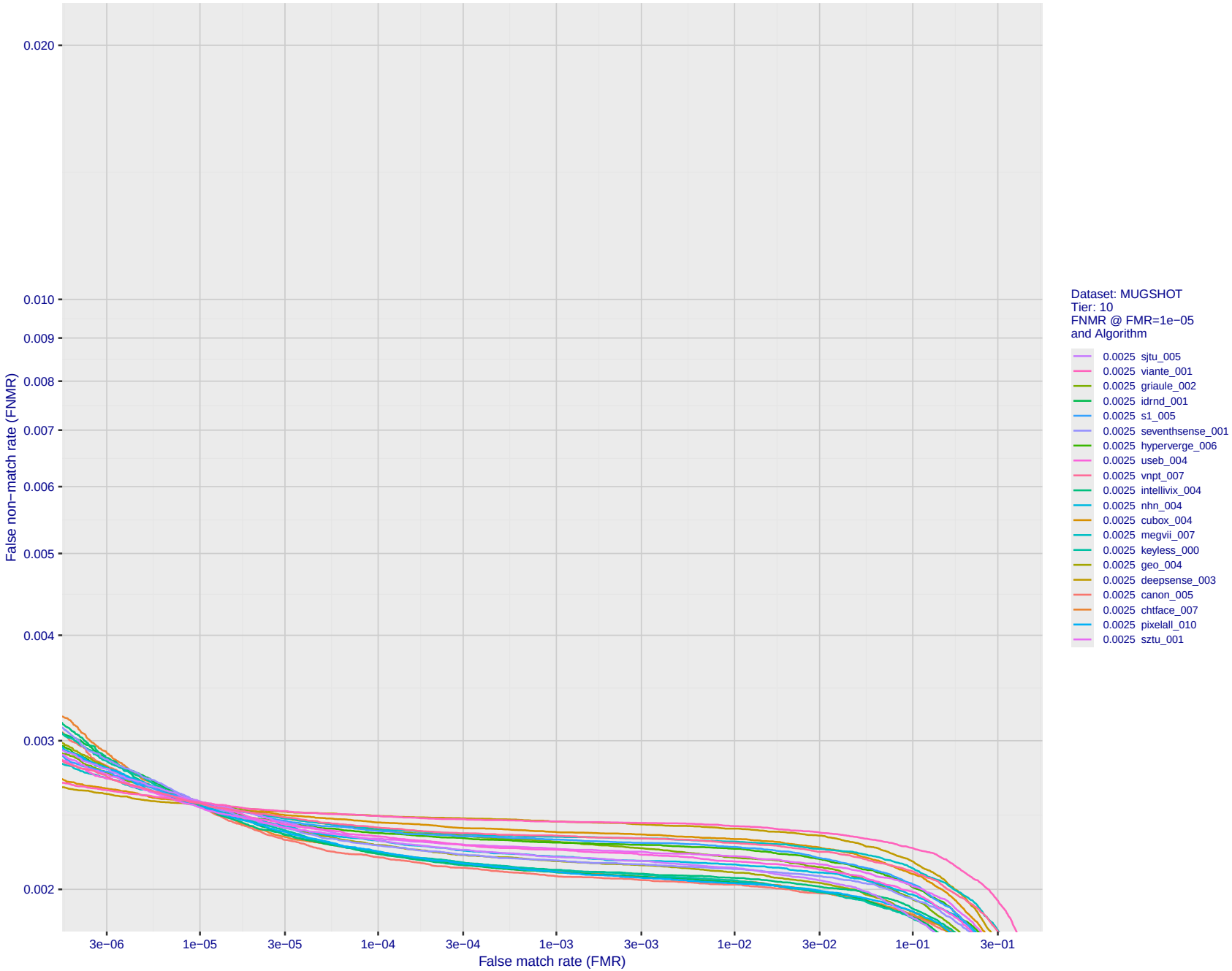

Figure 228: For the mugshot images, detection error tradeoff (DET) characteristics showing false non-match rate vs. false match rate plotted parametrically on threshold, T. The scales are logarithmic in order to show decades of FMR.

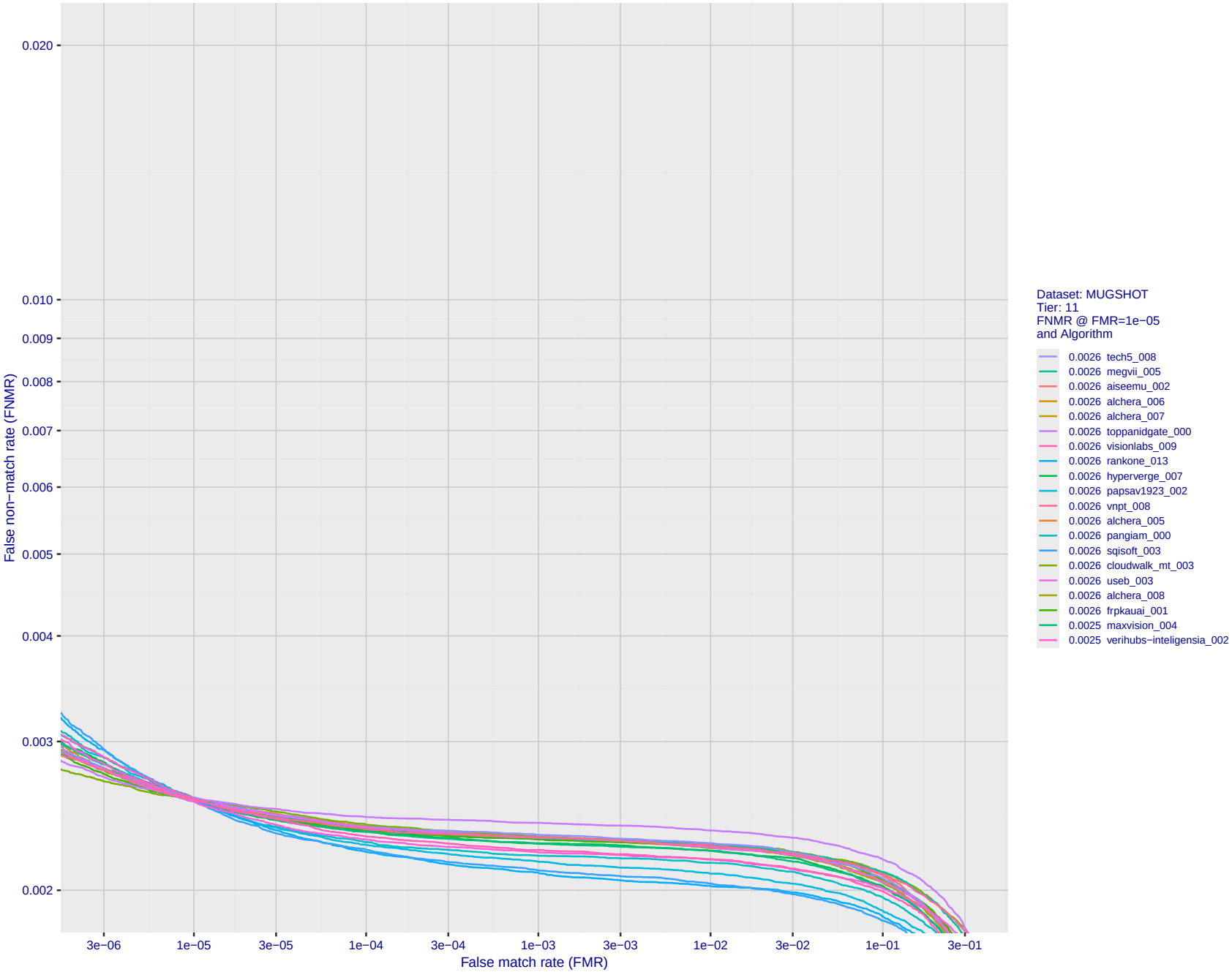

Figure 229: For the mugshot images, detection error tradeoff (DET) characteristics showing false non-match rate vs. false match rate plotted parametrically on threshold, T. The scales are logarithmic in order to show decades of FMR.

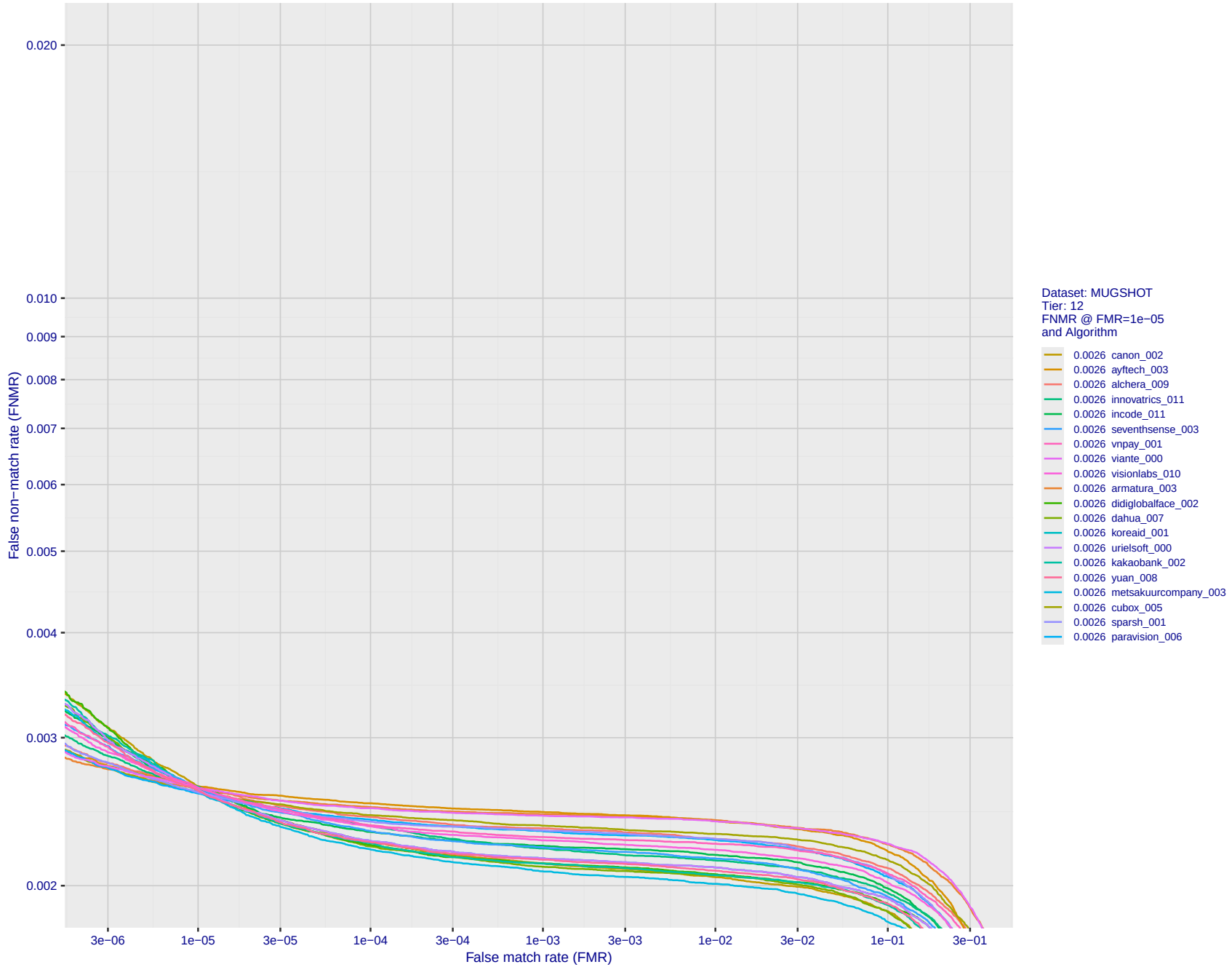

Figure 230: For the mugshot images, detection error tradeoff (DET) characteristics showing false non-match rate vs. false match rate plotted parametrically on threshold, T. The scales are logarithmic in order to show decades of FMR.

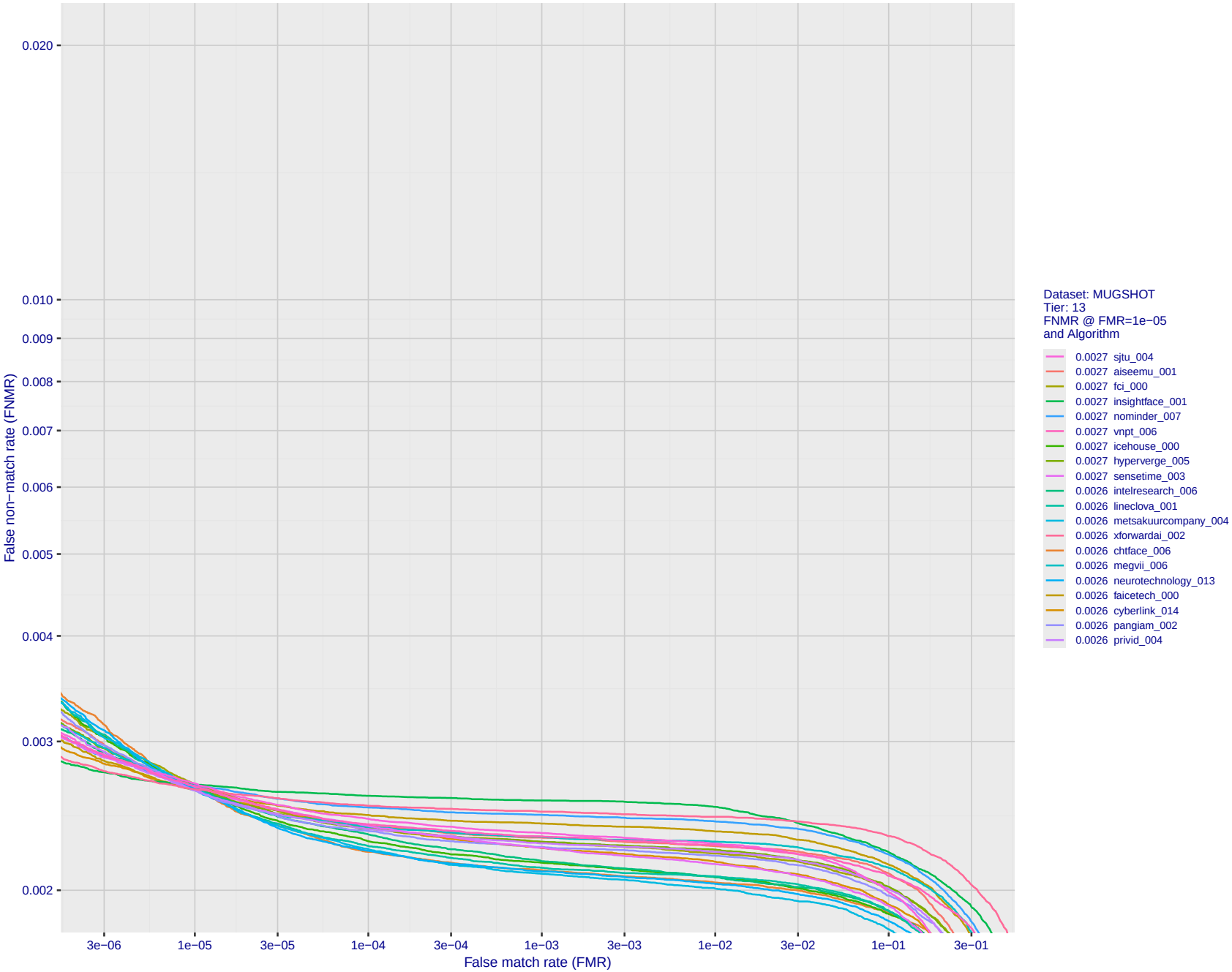

Figure 231: For the mugshot images, detection error tradeoff (DET) characteristics showing false non-match rate vs. false match rate plotted parametrically on threshold, T. The scales are logarithmic in order to show decades of FMR.

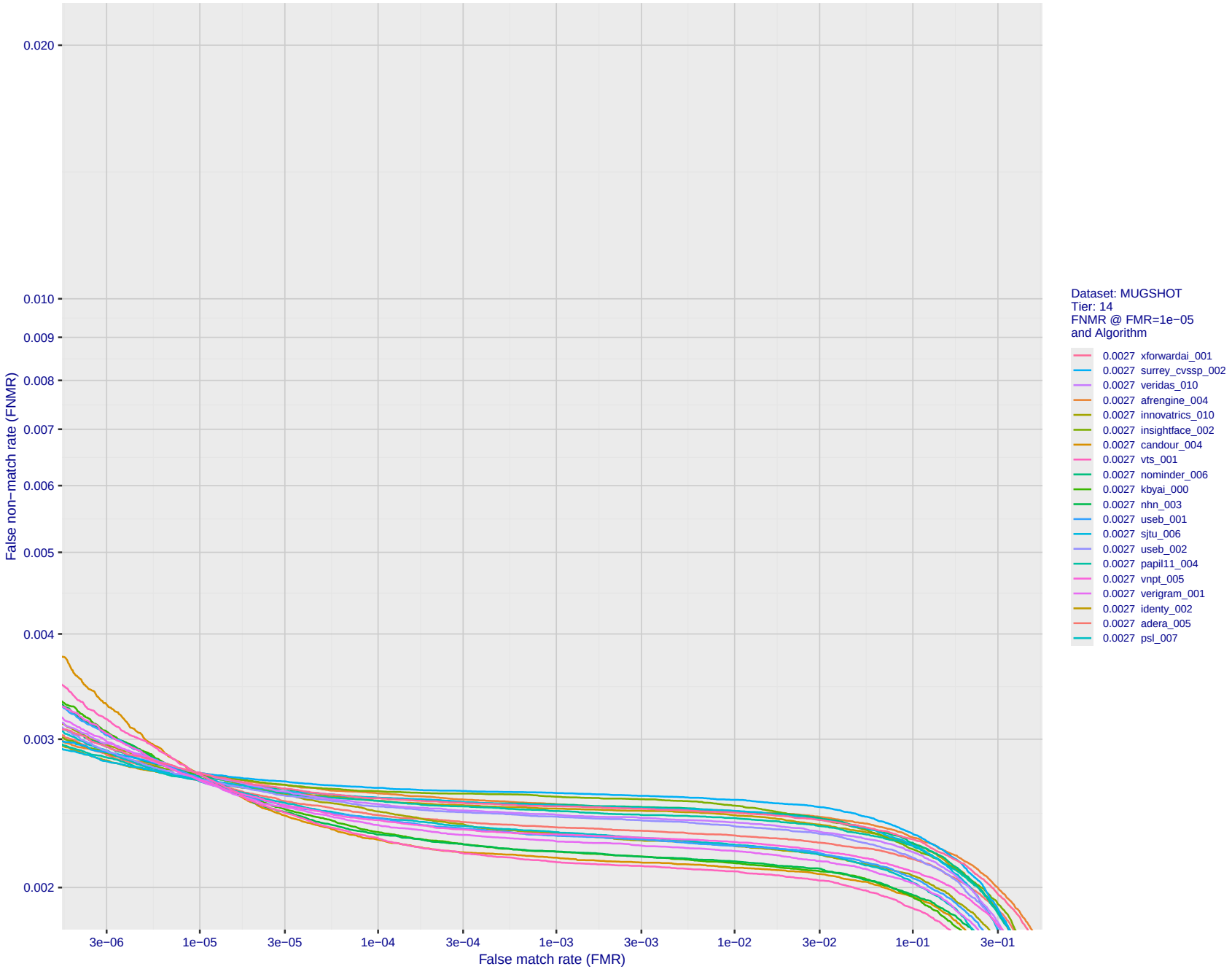

Figure 232: For the mugshot images, detection error tradeoff (DET) characteristics showing false non-match rate vs. false match rate plotted parametrically on threshold, T. The scales are logarithmic in order to show decades of FMR.

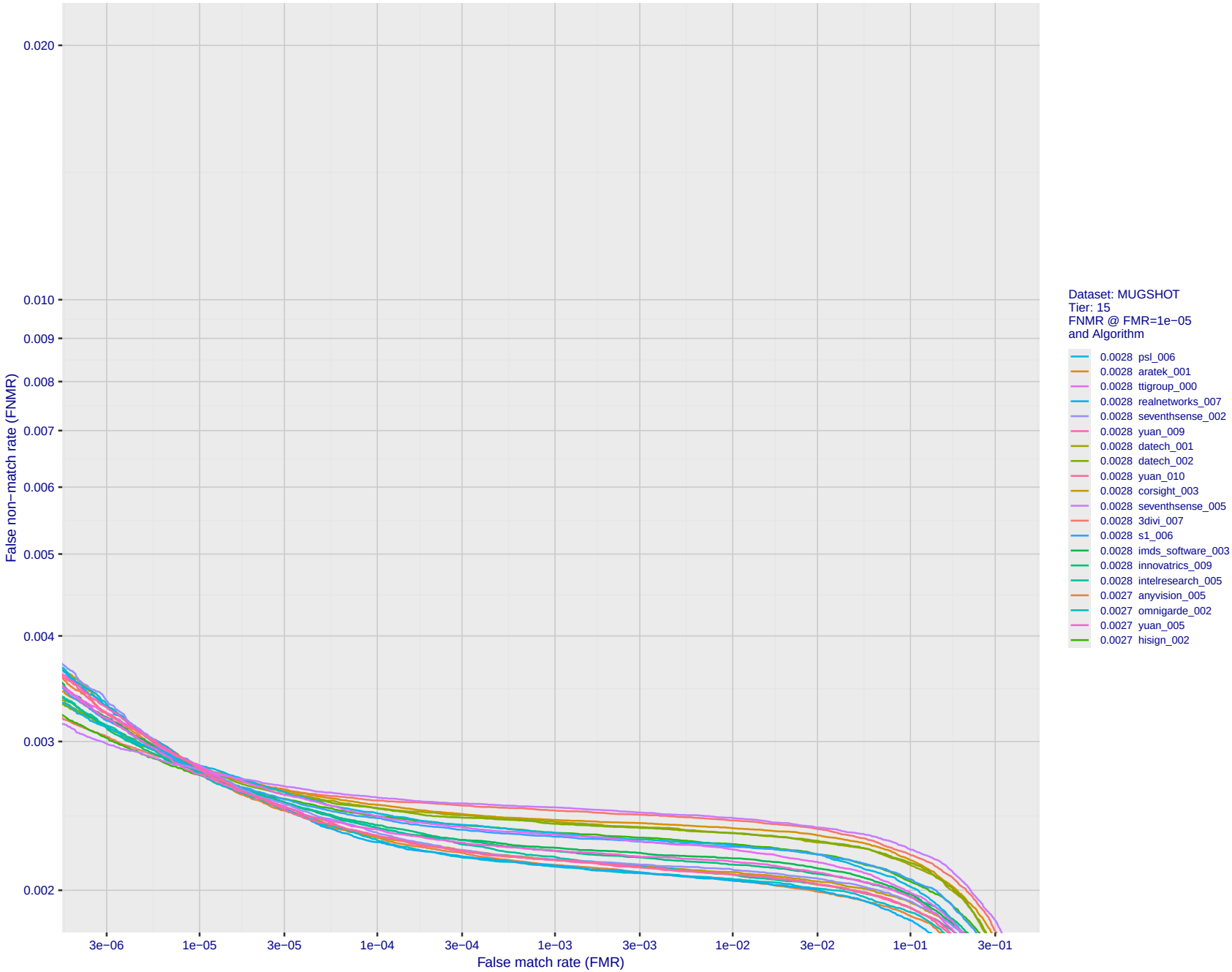

Figure 233: For the mugshot images, detection error tradeoff (DET) characteristics showing false non-match rate vs. false match rate plotted parametrically on threshold, T. The scales are logarithmic in order to show decades of FMR.

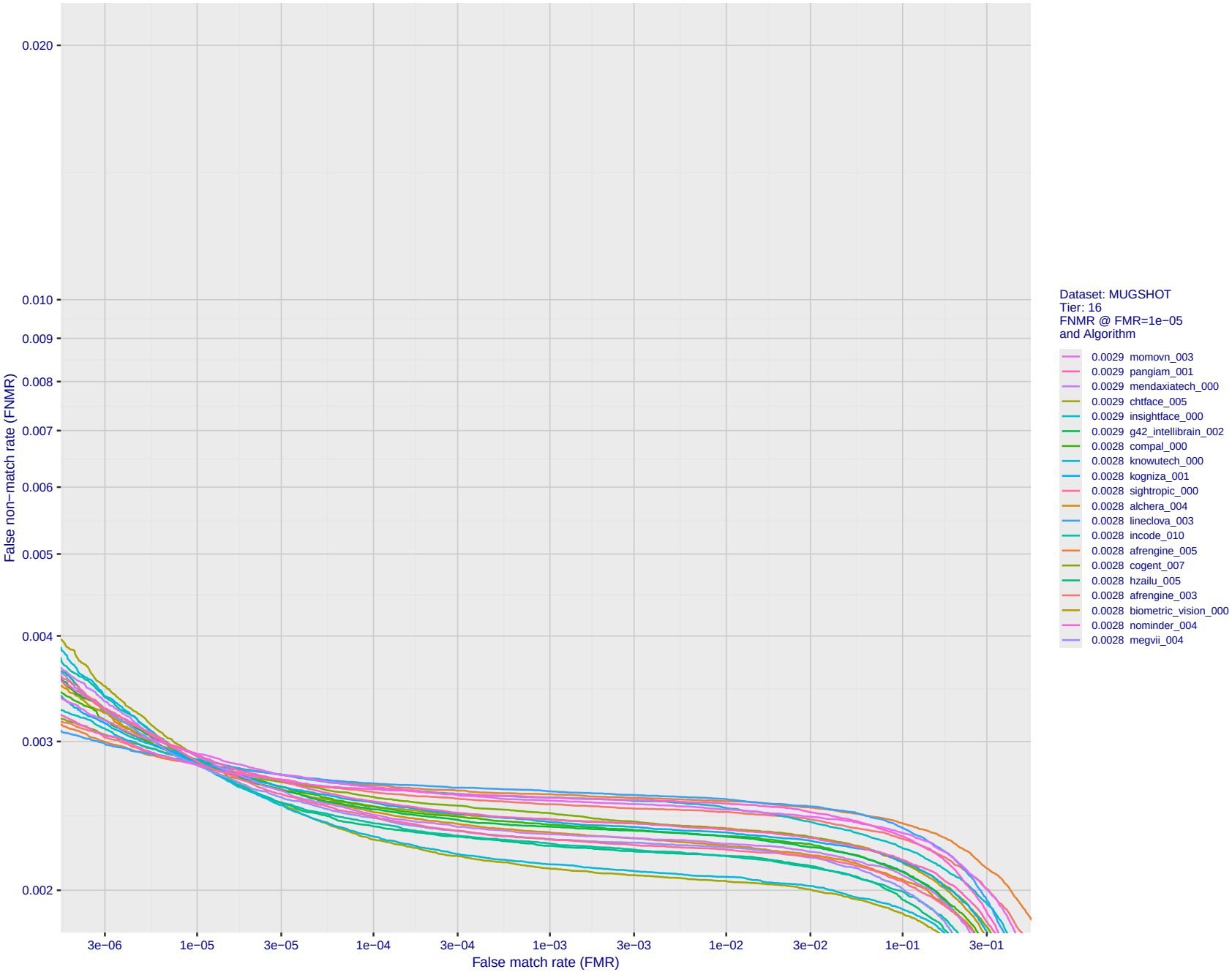

Figure 234: For the mugshot images, detection error tradeoff (DET) characteristics showing false non-match rate vs. false match rate plotted parametrically on threshold, T. The scales are logarithmic in order to show decades of FMR.

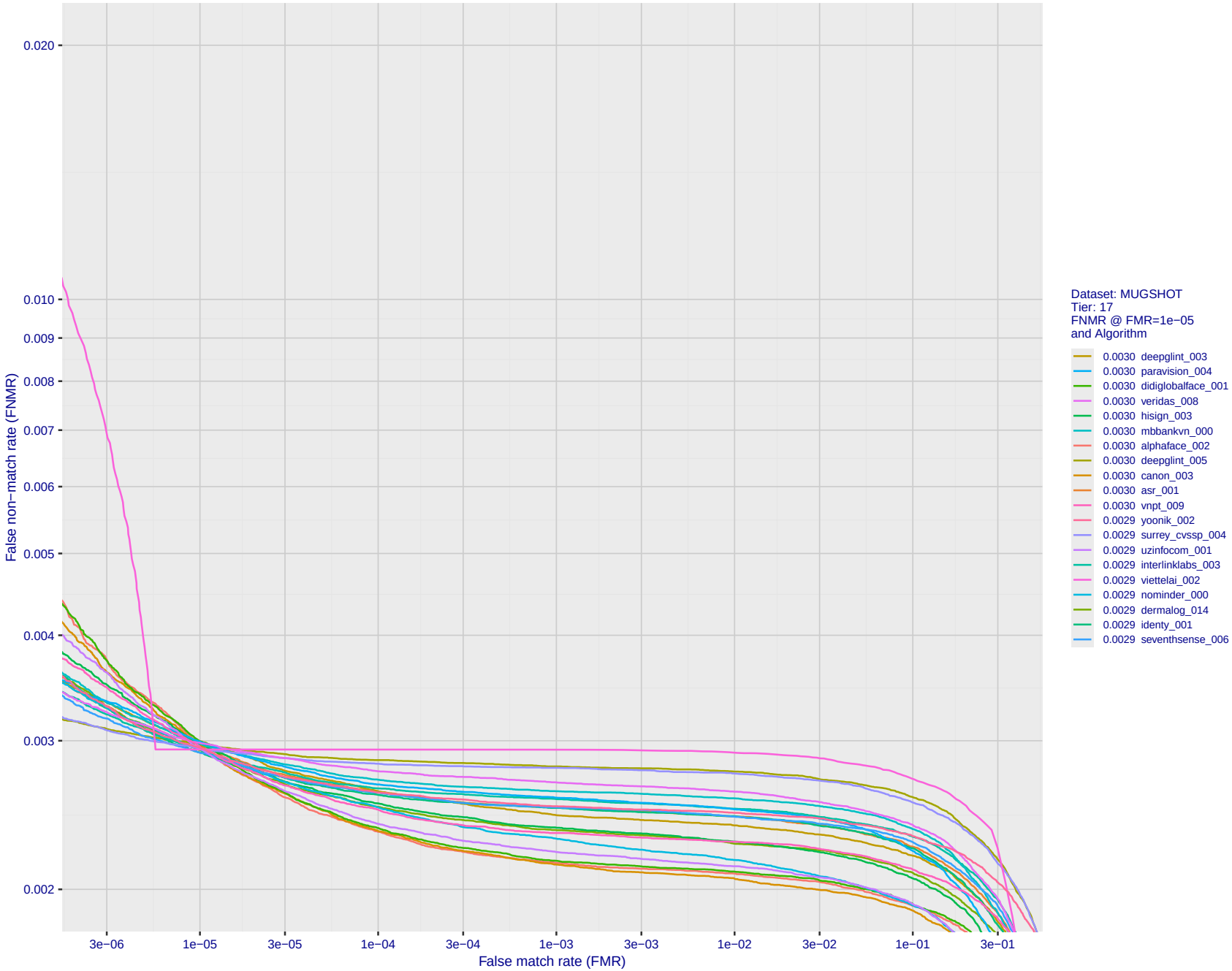

Figure 235: For the mugshot images, detection error tradeoff (DET) characteristics showing false non-match rate vs. false match rate plotted parametrically on threshold, T. The scales are logarithmic in order to show decades of FMR.

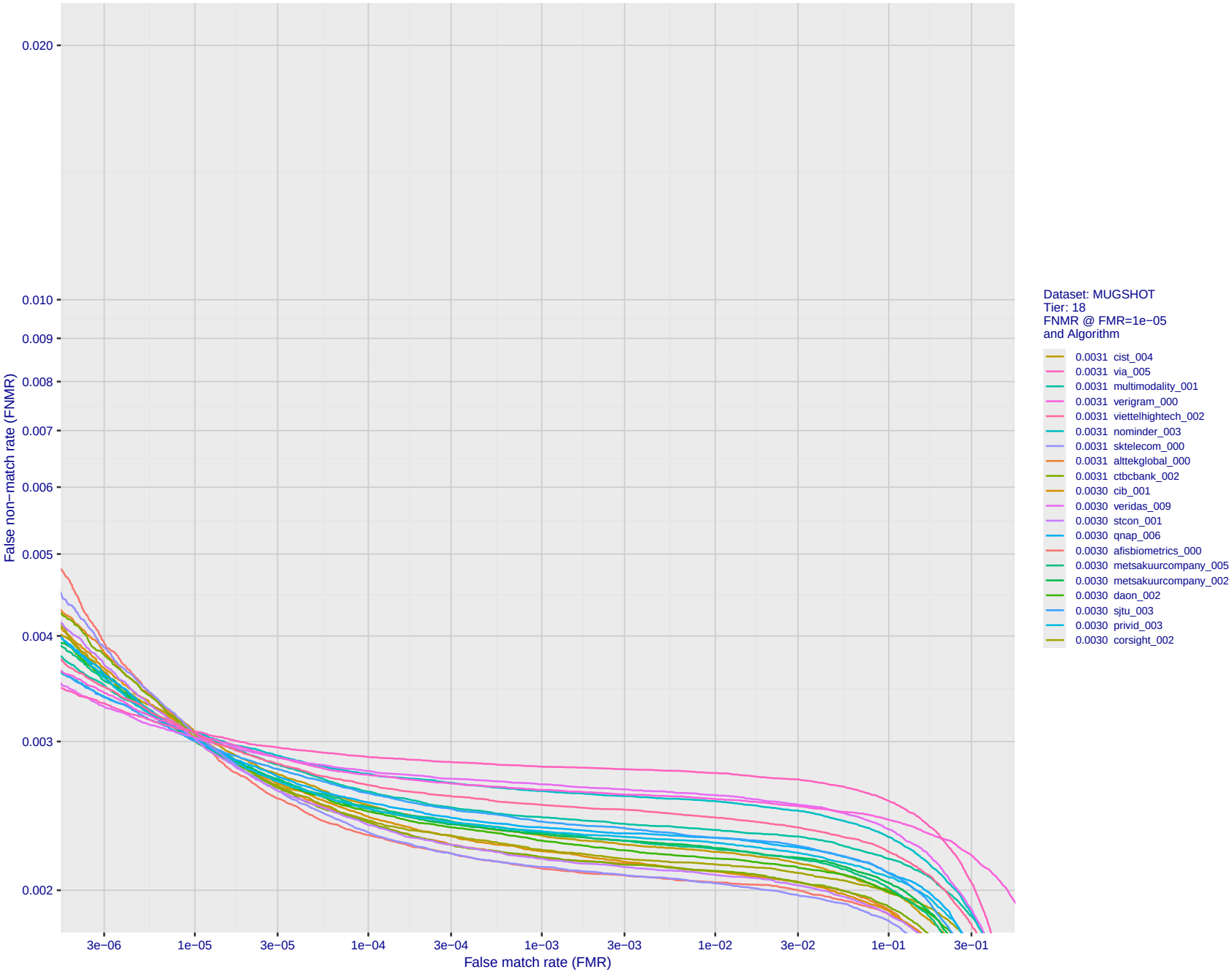

Figure 236: For the mugshot images, detection error tradeoff (DET) characteristics showing false non-match rate vs. false match rate plotted parametrically on threshold, T. The scales are logarithmic in order to show decades of FMR.

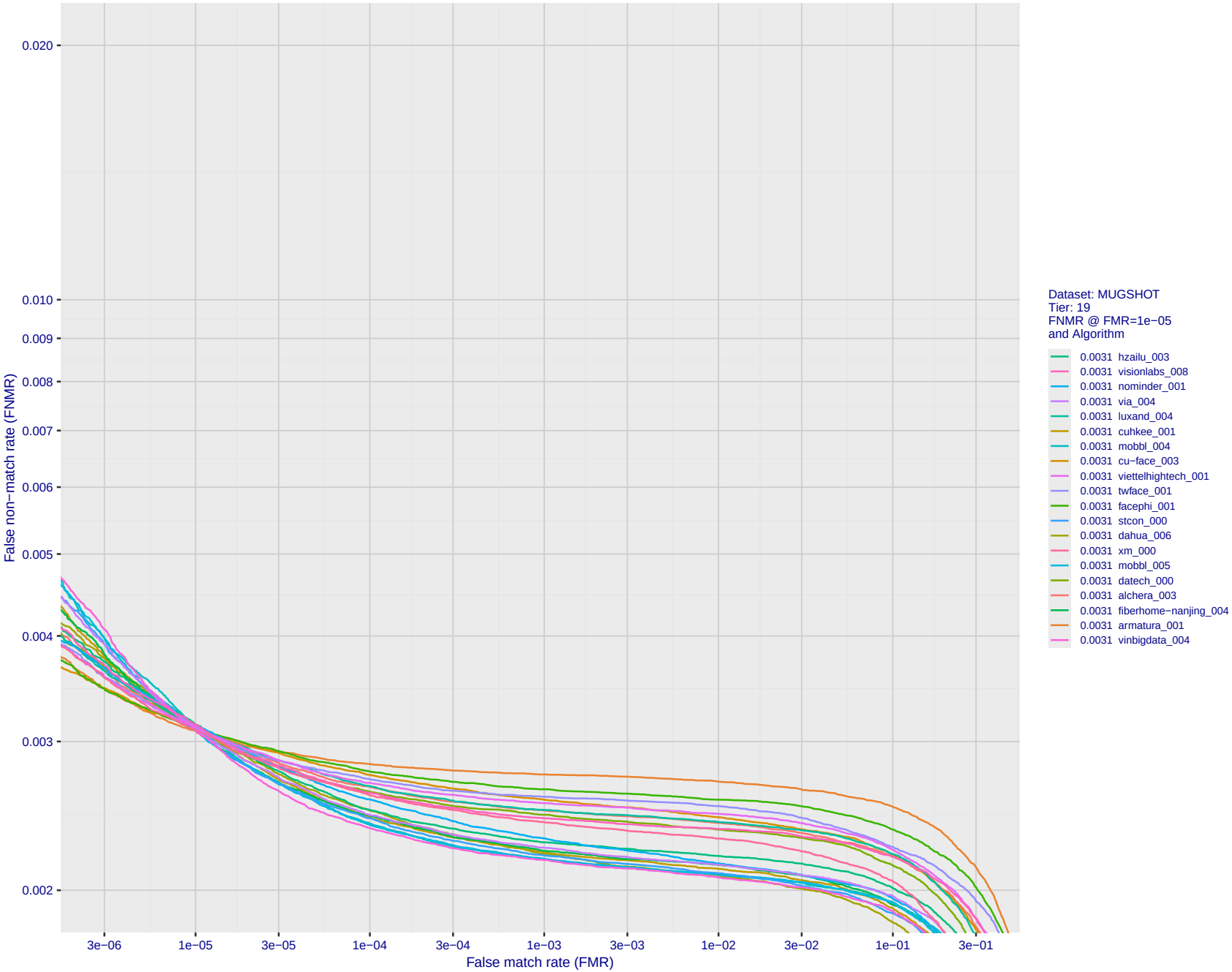

Figure 237: For the mugshot images, detection error tradeoff (DET) characteristics showing false non-match rate vs. false match rate plotted parametrically on threshold, T. The scales are logarithmic in order to show decades of FMR.

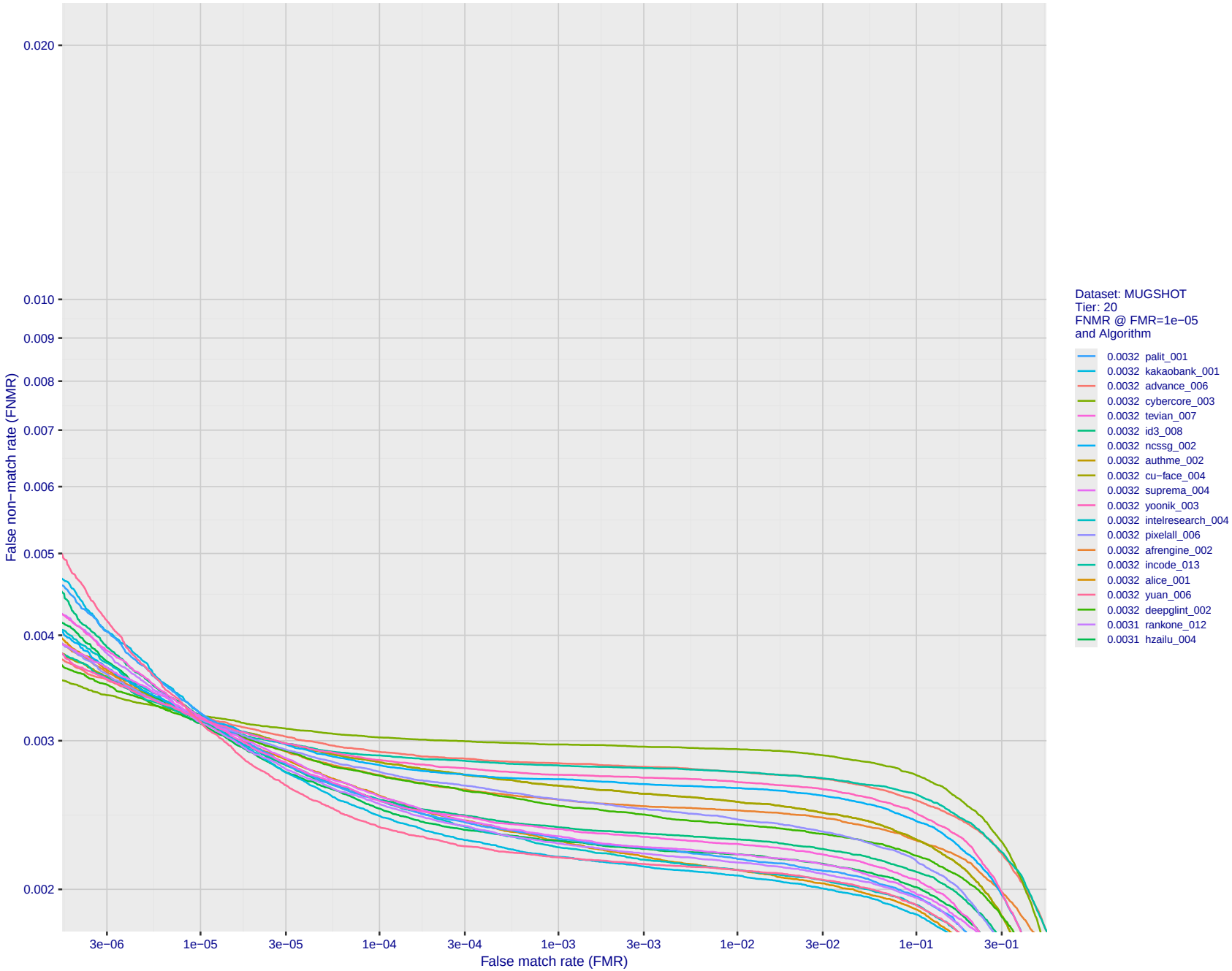

Figure 238: For the mugshot images, detection error tradeoff (DET) characteristics showing false non-match rate vs. false match rate plotted parametrically on threshold, T. The scales are logarithmic in order to show decades of FMR.

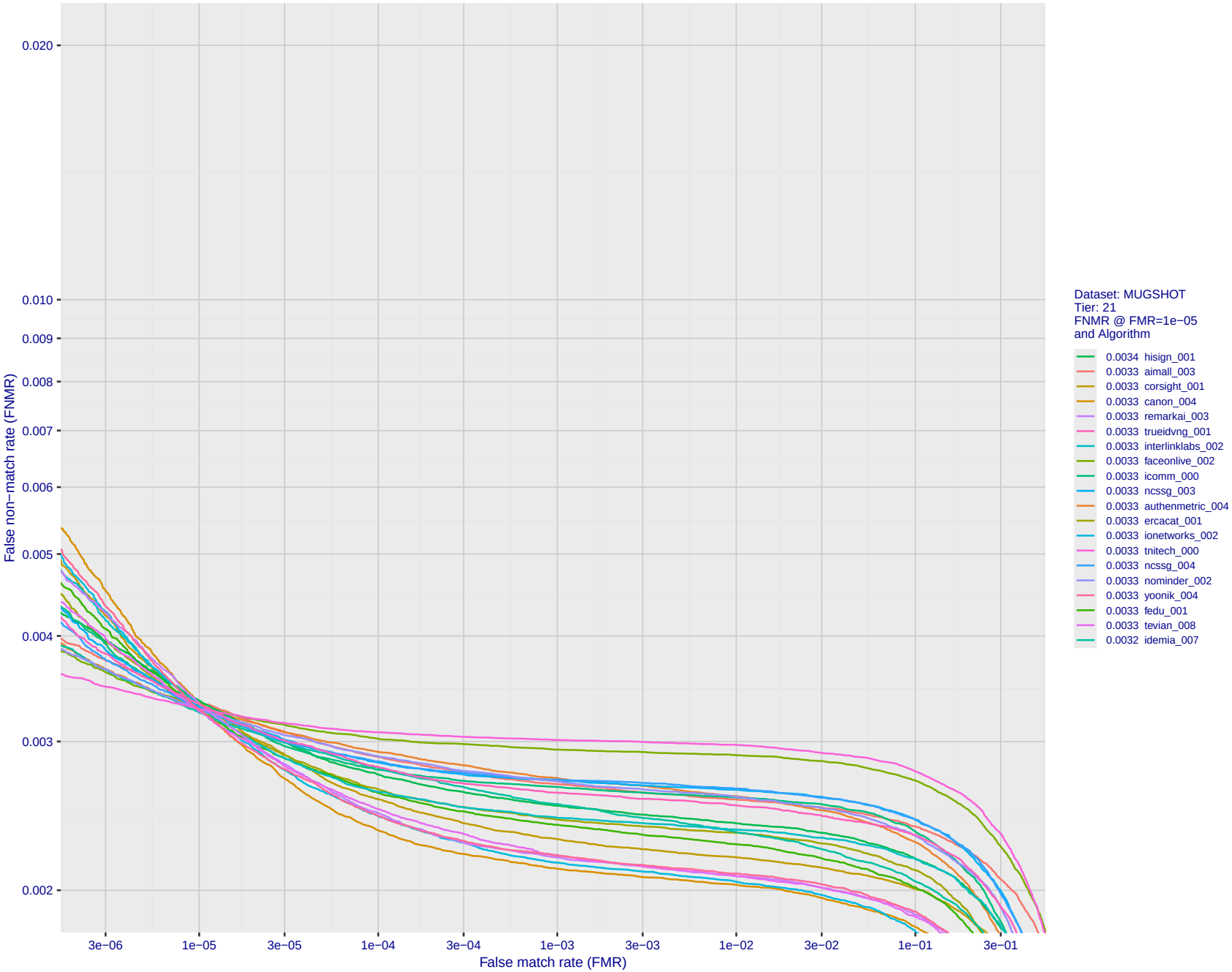

Figure 239: For the mugshot images, detection error tradeoff (DET) characteristics showing false non-match rate vs. false match rate plotted parametrically on threshold, T. The scales are logarithmic in order to show decades of FMR.

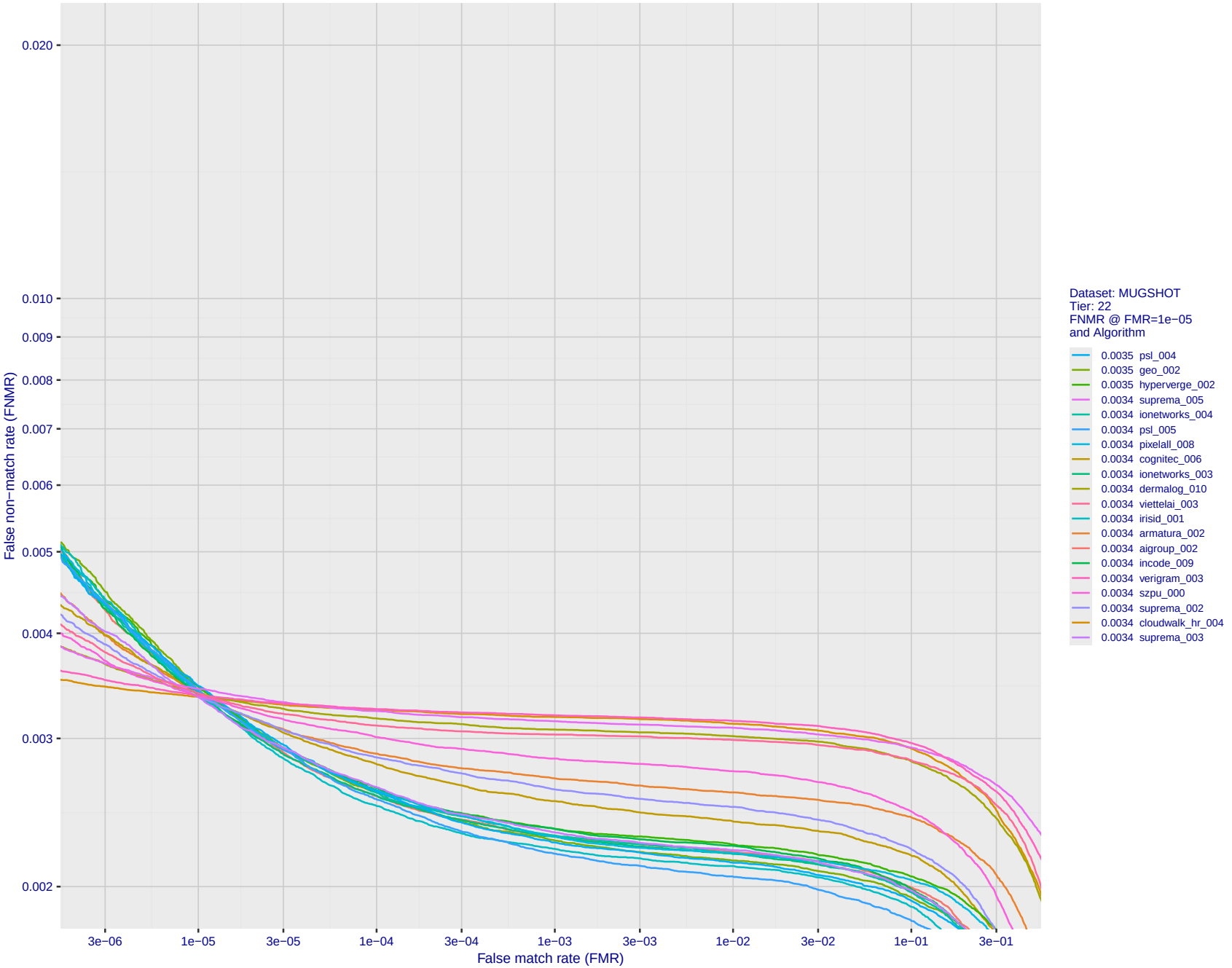

Figure 240: For the mugshot images, detection error tradeoff (DET) characteristics showing false non-match rate vs. false match rate plotted parametrically on threshold, T. The scales are logarithmic in order to show decades of FMR.

FNMR(T) "False non-match rate"
FMR(T) "False match rate"

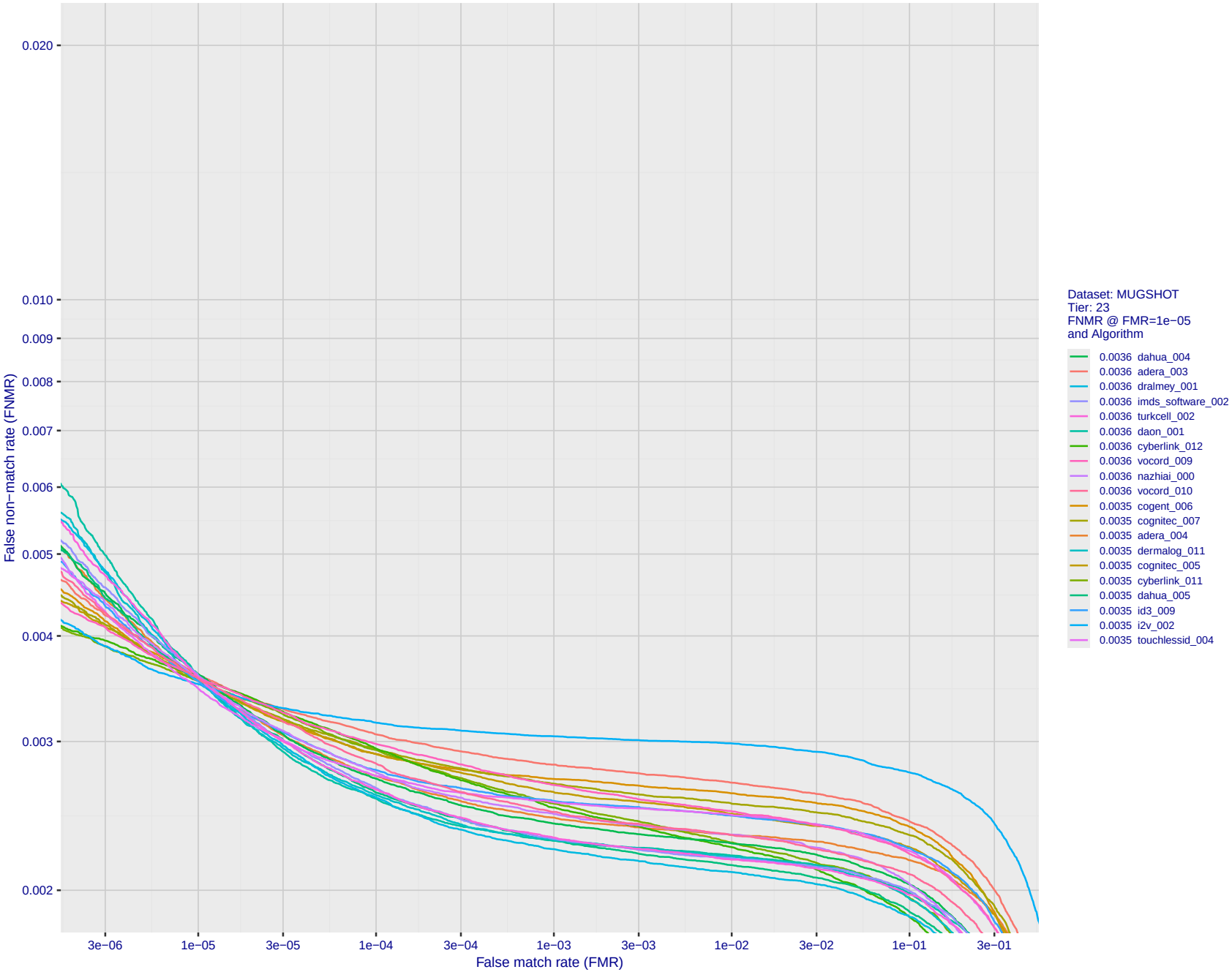

Figure 241: For the mugshot images, detection error tradeoff (DET) characteristics showing false non-match rate vs. false match rate plotted parametrically on threshold, T. The scales are logarithmic in order to show decades of FMR.

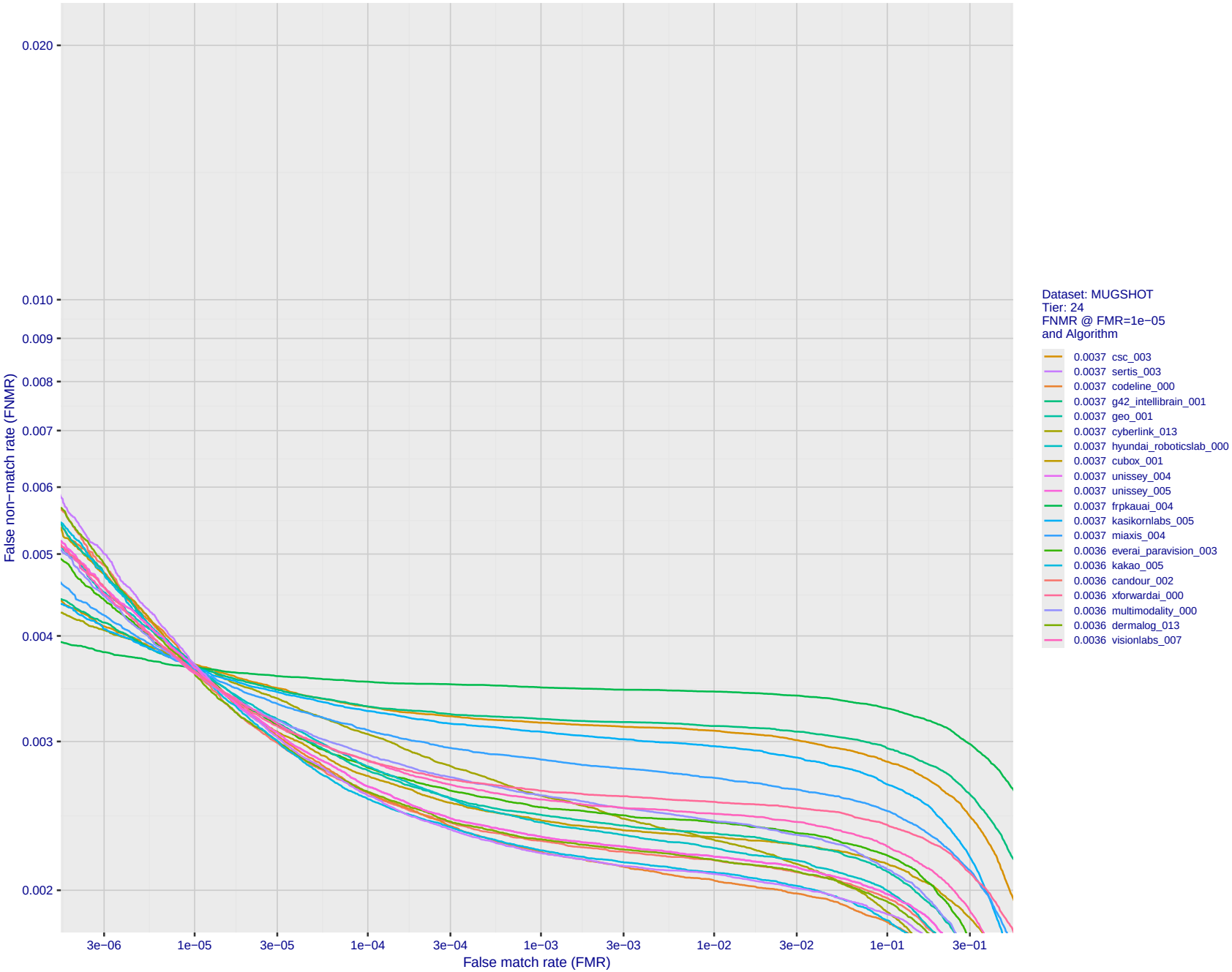

Figure 242: For the mugshot images, detection error tradeoff (DET) characteristics showing false non-match rate vs. false match rate plotted parametrically on threshold, T. The scales are logarithmic in order to show decades of FMR.

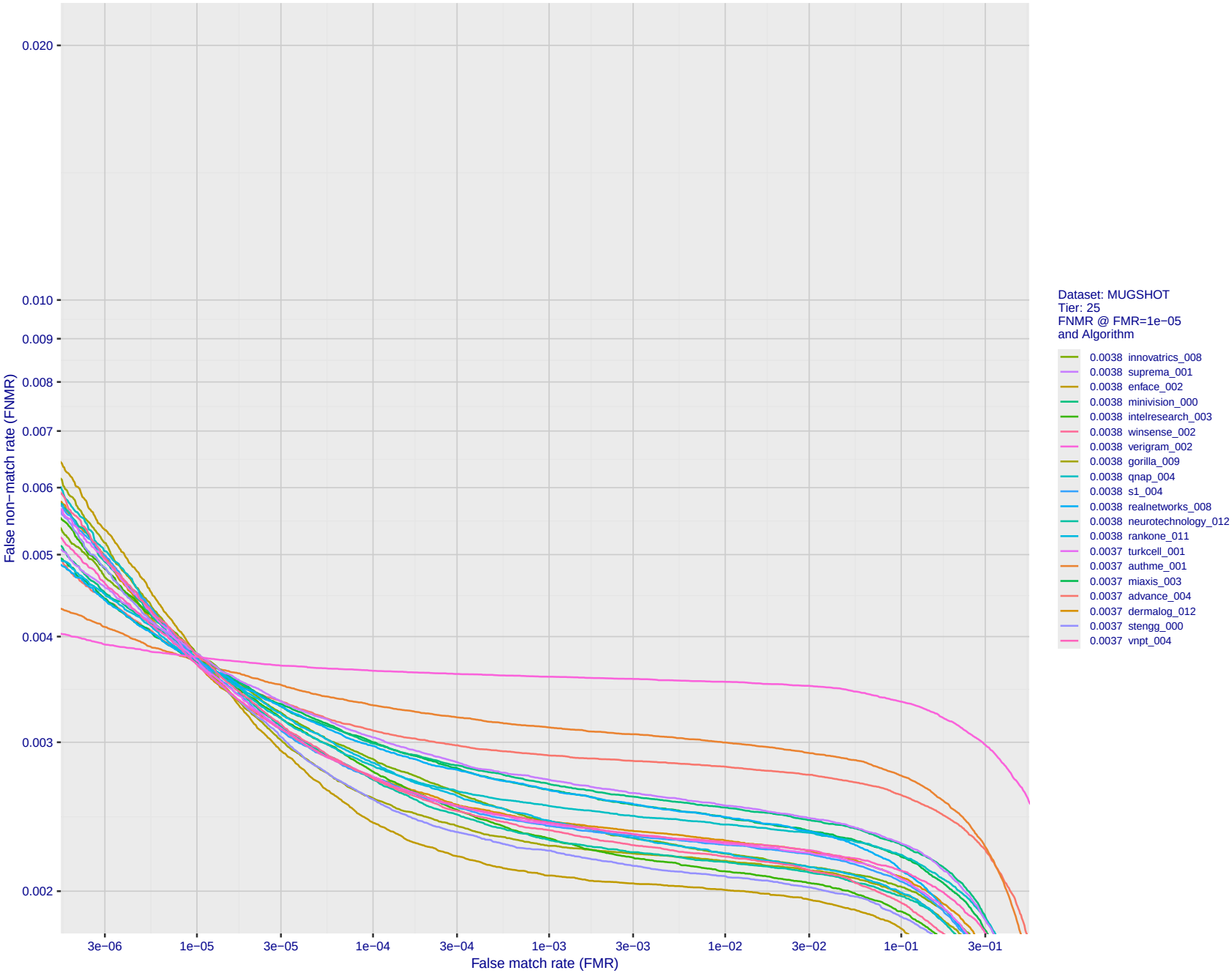

Figure 243: For the mugshot images, detection error tradeoff (DET) characteristics showing false non-match rate vs. false match rate plotted parametrically on threshold, T. The scales are logarithmic in order to show decades of FMR.

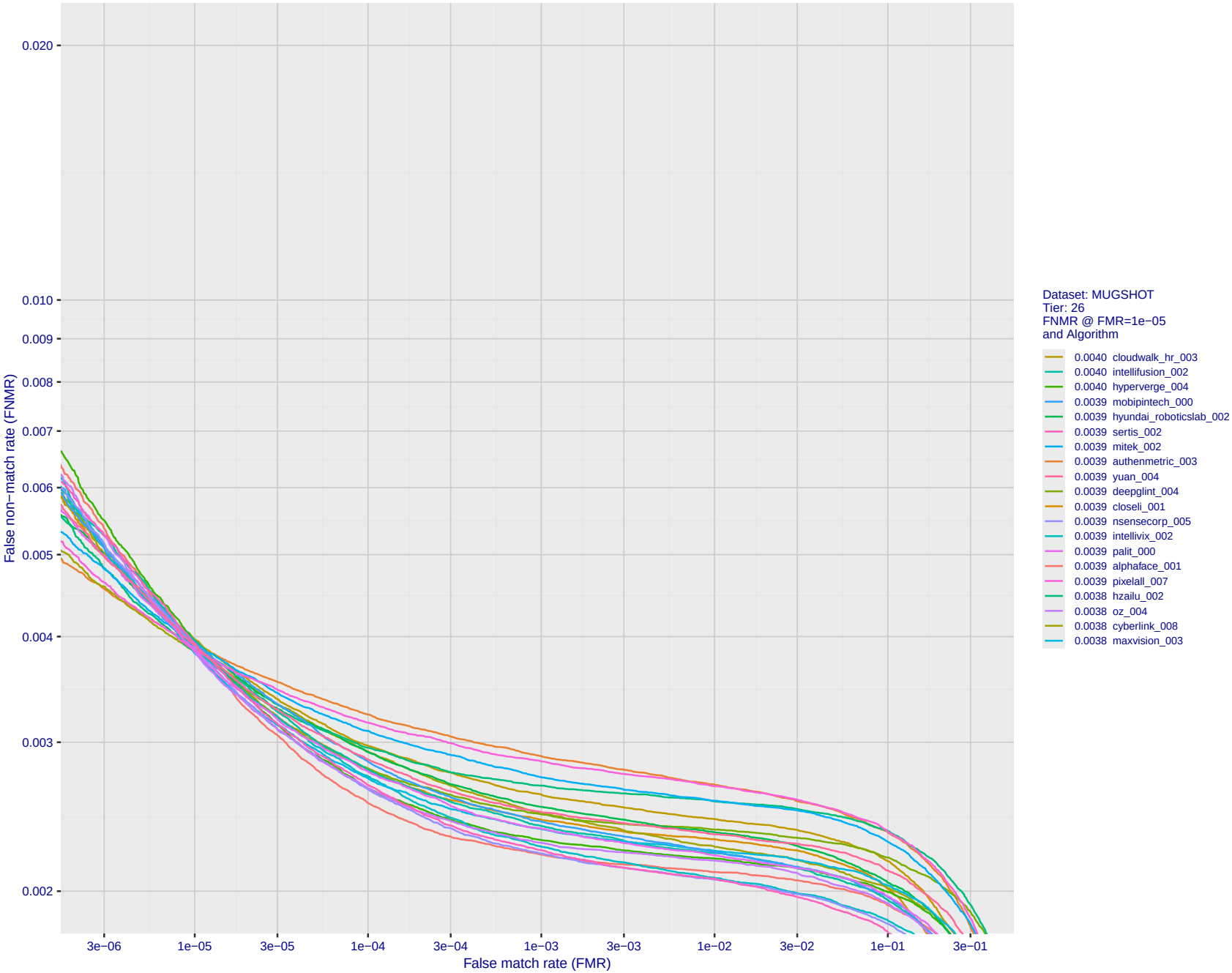

Figure 244: For the mugshot images, detection error tradeoff (DET) characteristics showing false non-match rate vs. false match rate plotted parametrically on threshold, T. The scales are logarithmic in order to show decades of FMR.

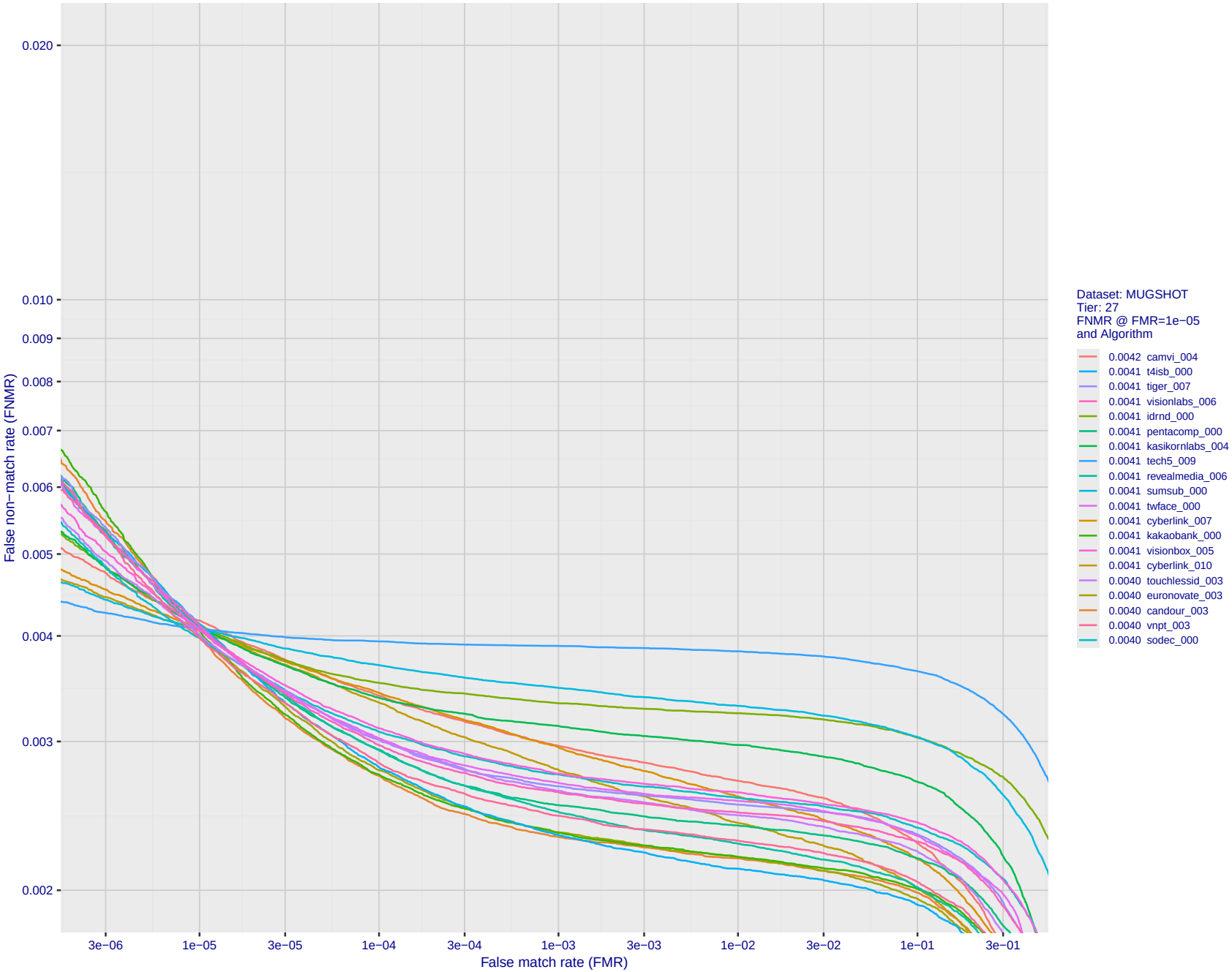

Figure 245: For the mugshot images, detection error tradeoff (DET) characteristics showing false non-match rate vs. false match rate plotted parametrically on threshold, T. The scales are logarithmic in order to show decades of FMR.

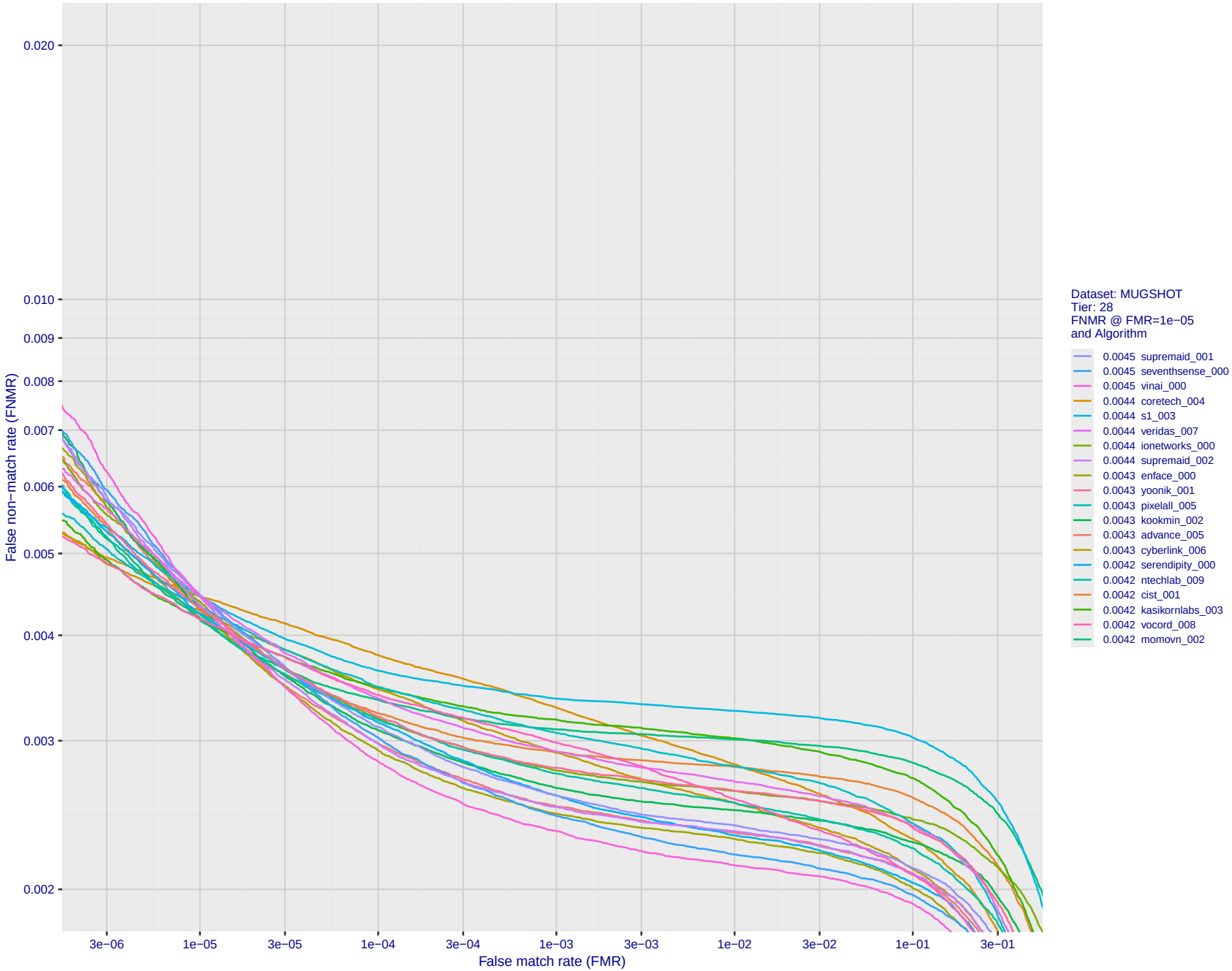

Figure 246: For the mugshot images, detection error tradeoff (DET) characteristics showing false non-match rate vs. false match rate plotted parametrically on threshold, T. The scales are logarithmic in order to show decades of FMR.

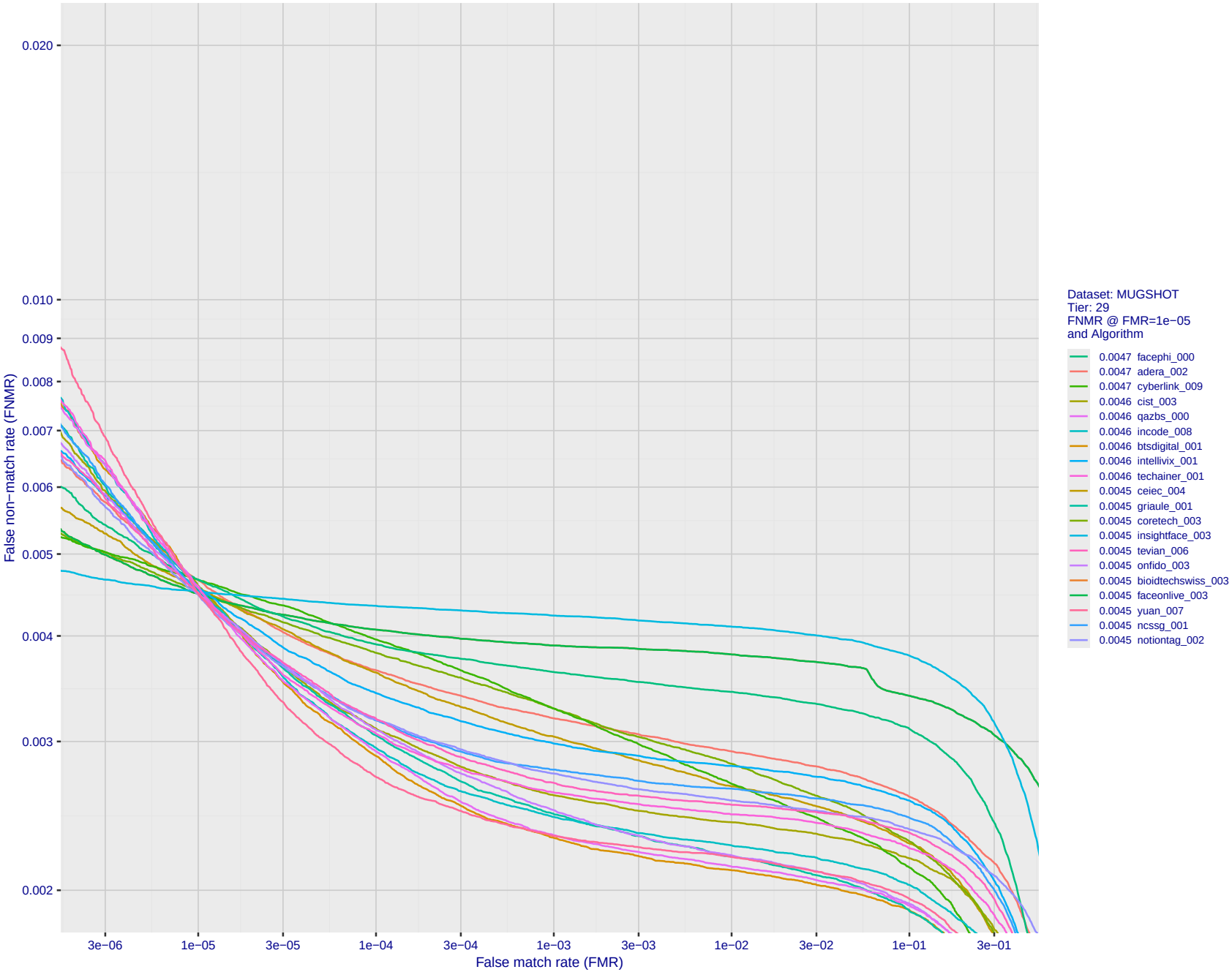

Figure 247: For the mugshot images, detection error tradeoff (DET) characteristics showing false non-match rate vs. false match rate plotted parametrically on threshold, T. The scales are logarithmic in order to show decades of FMR.

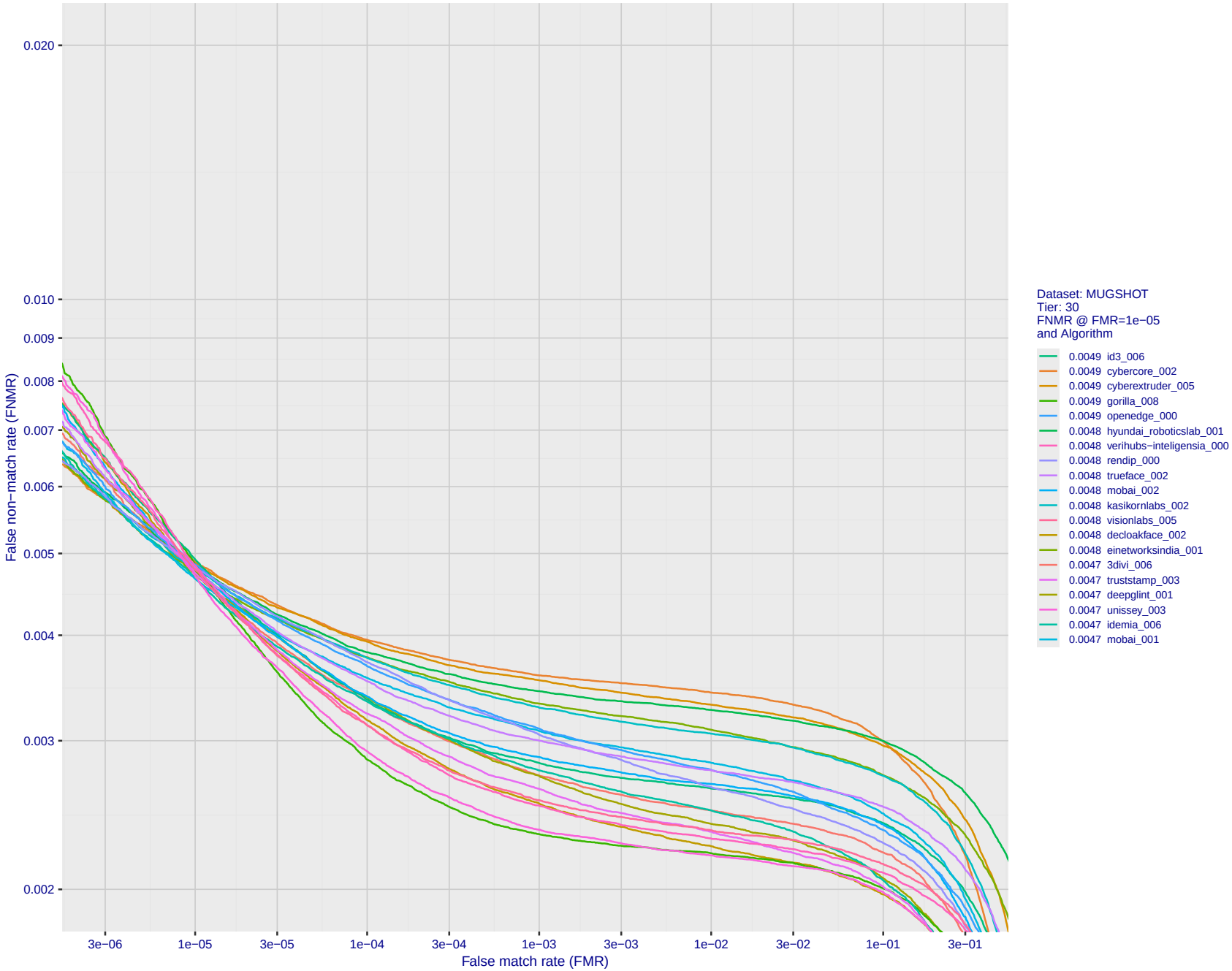

Figure 248: For the mugshot images, detection error tradeoff (DET) characteristics showing false non-match rate vs. false match rate plotted parametrically on threshold, T. The scales are logarithmic in order to show decades of FMR.

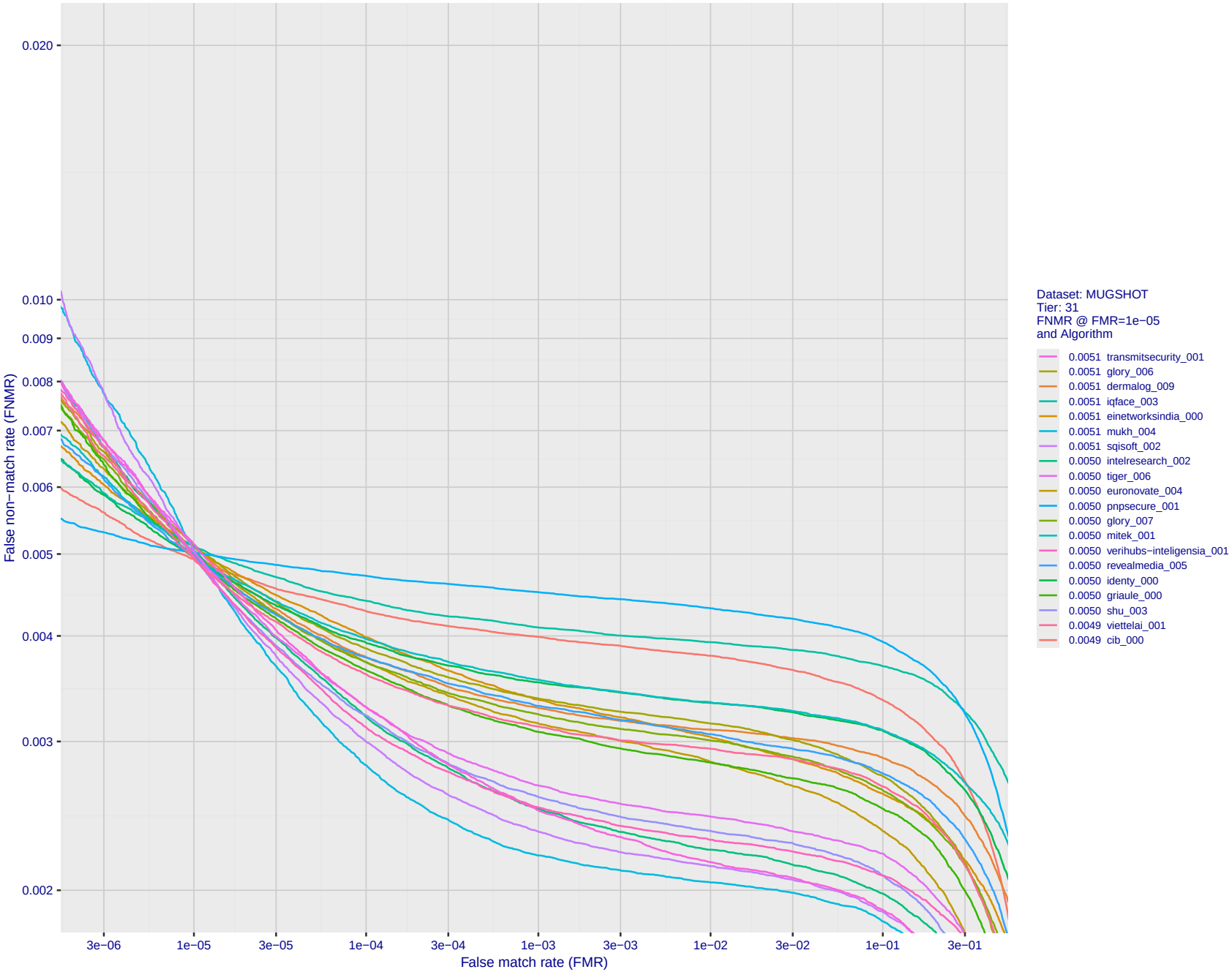

Figure 249: For the mugshot images, detection error tradeoff (DET) characteristics showing false non-match rate vs. false match rate plotted parametrically on threshold, T. The scales are logarithmic in order to show decades of FMR.

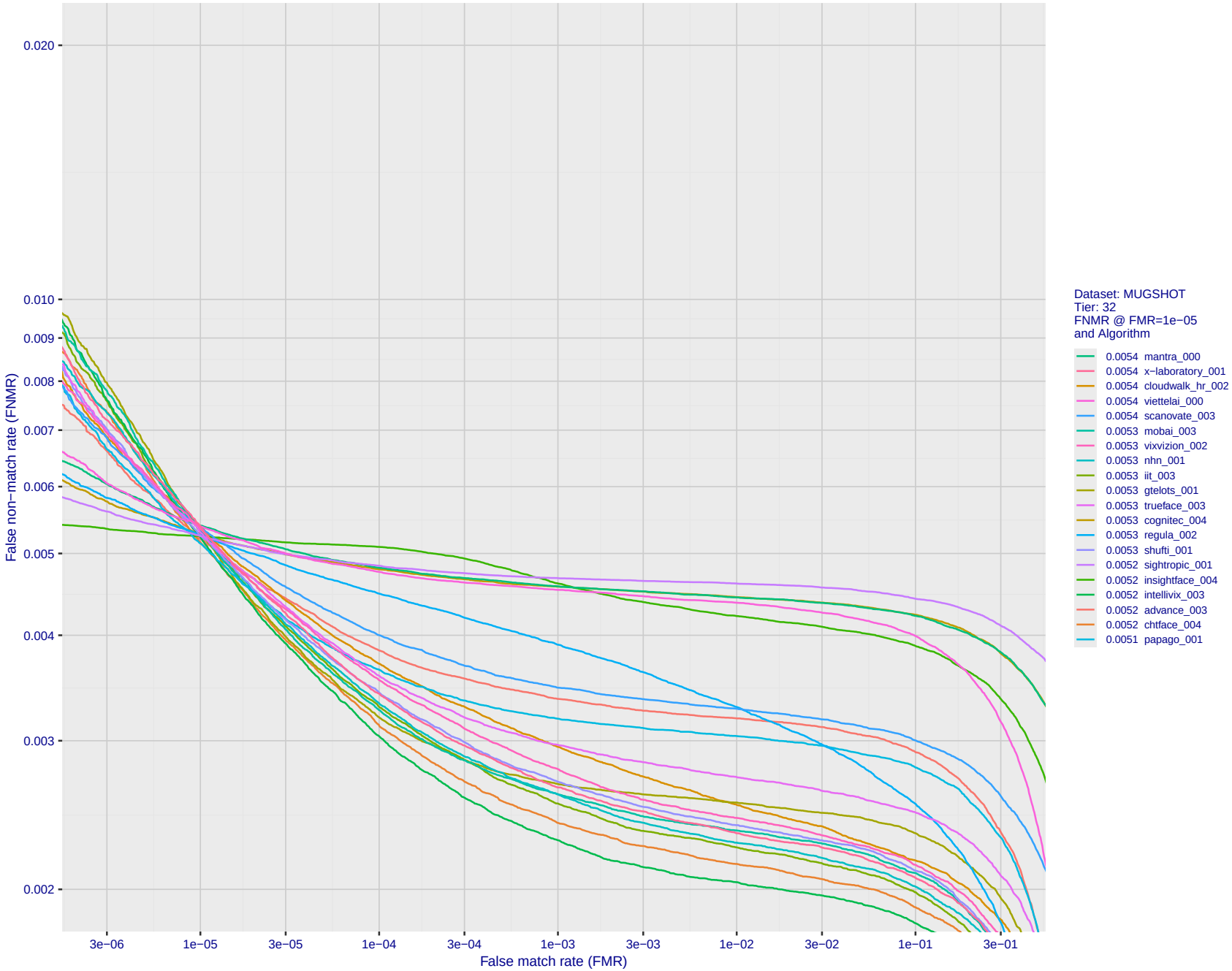

Figure 250: For the mugshot images, detection error tradeoff (DET) characteristics showing false non-match rate vs. false match rate plotted parametrically on threshold, T. The scales are logarithmic in order to show decades of FMR.

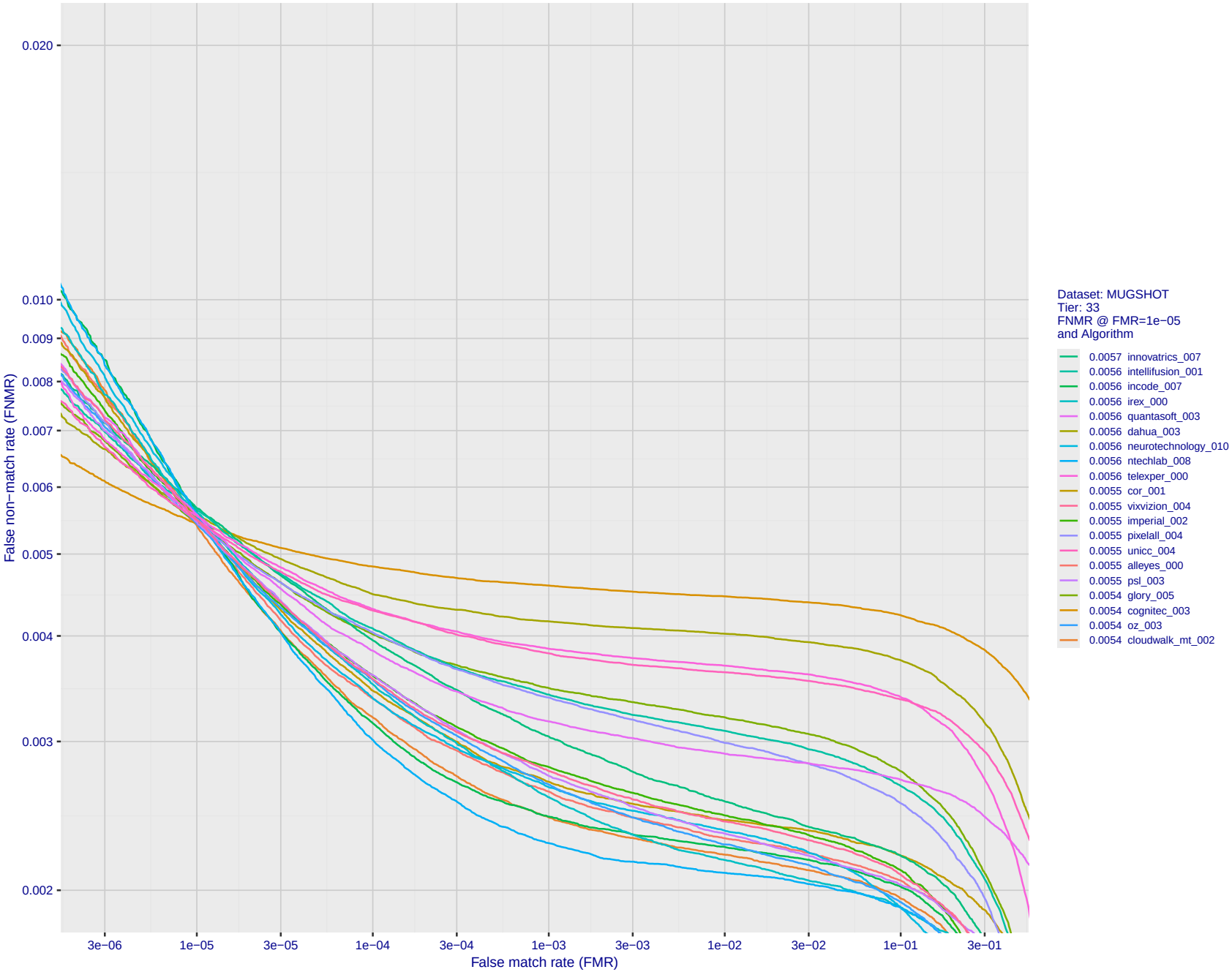

Figure 251: For the mugshot images, detection error tradeoff (DET) characteristics showing false non-match rate vs. false match rate plotted parametrically on threshold, T. The scales are logarithmic in order to show decades of FMR.

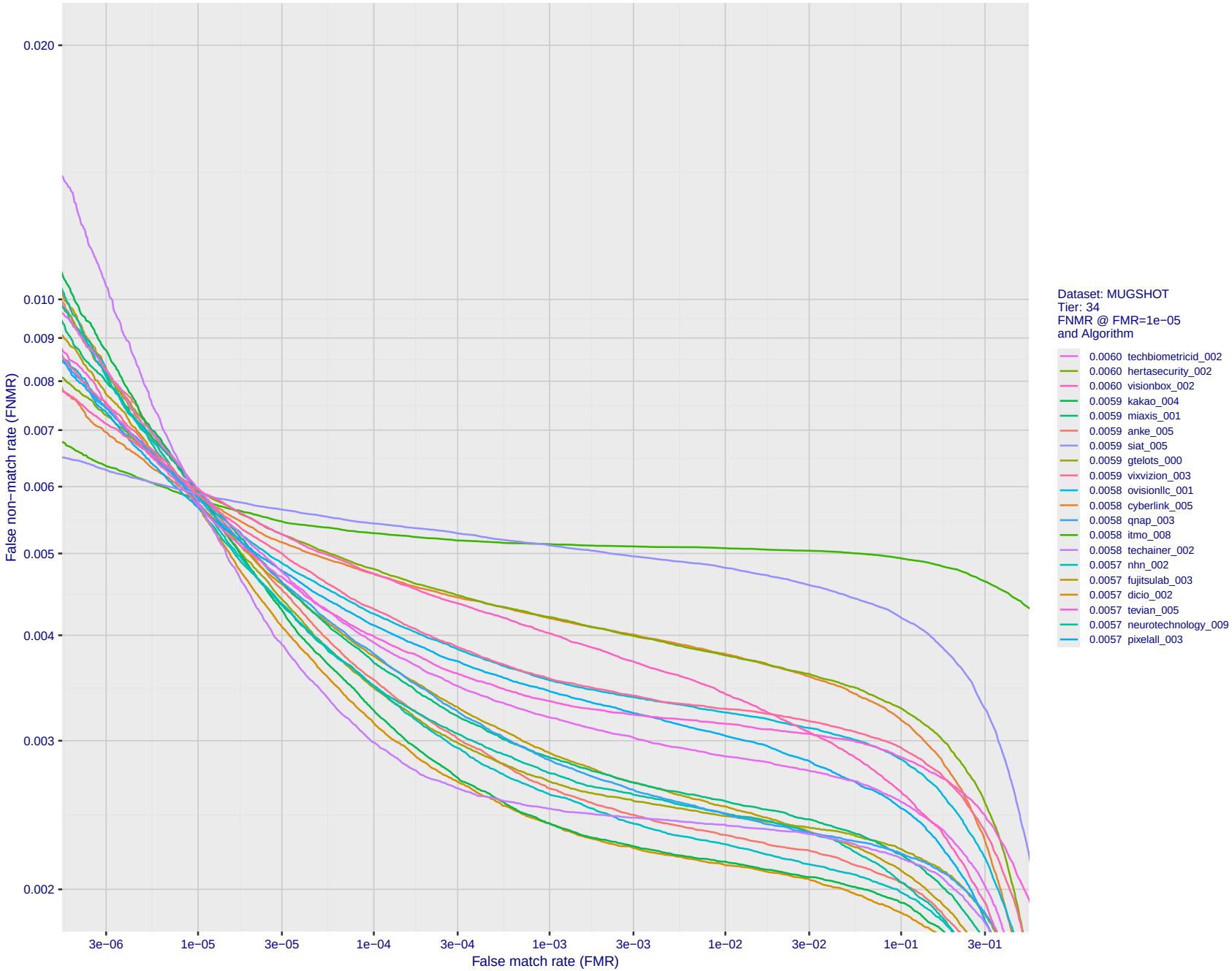

Figure 252: For the mugshot images, detection error tradeoff (DET) characteristics showing false non-match rate vs. false match rate plotted parametrically on threshold, T. The scales are logarithmic in order to show decades of FMR.

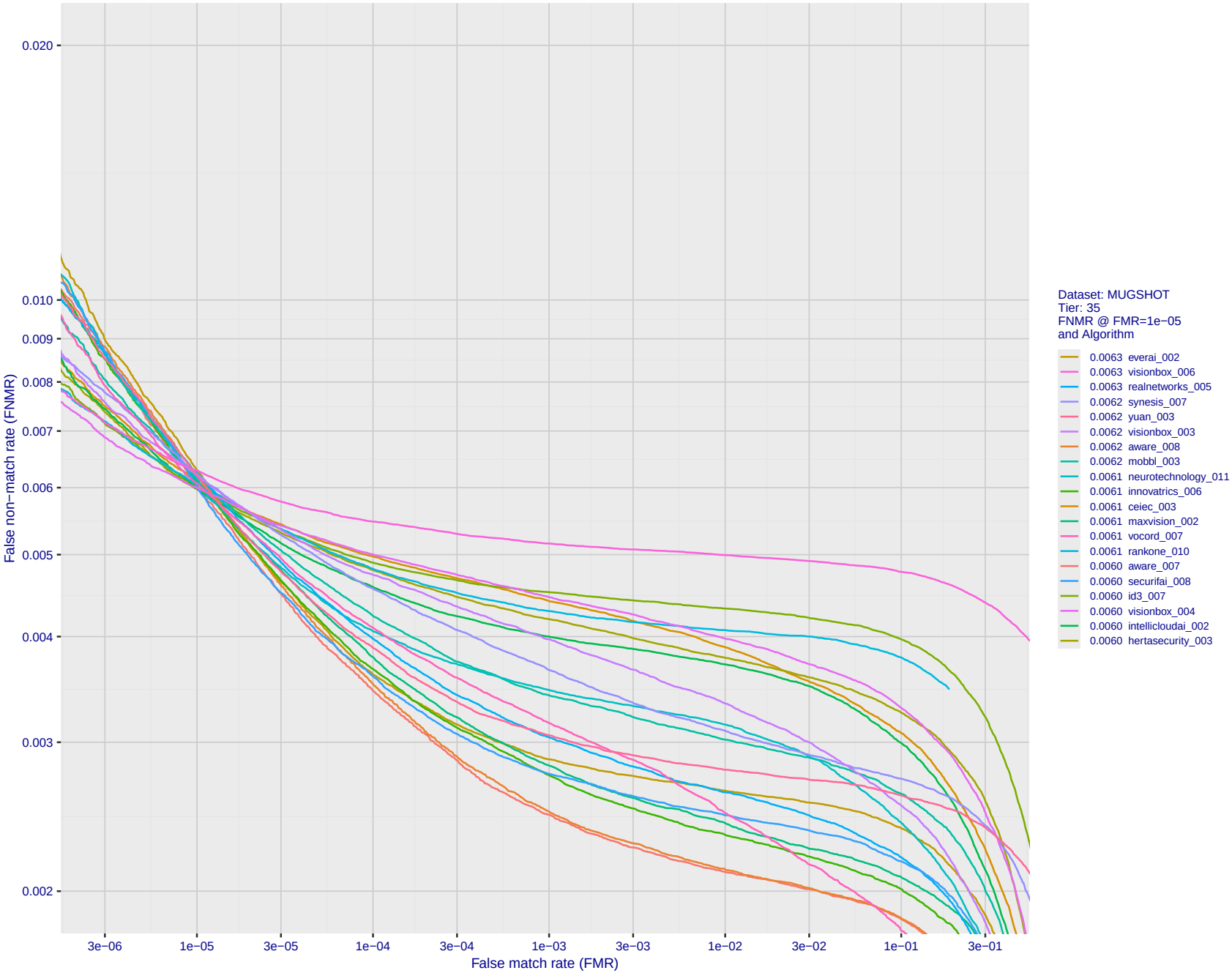

Figure 253: For the mugshot images, detection error tradeoff (DET) characteristics showing false non-match rate vs. false match rate plotted parametrically on threshold, T. The scales are logarithmic in order to show decades of FMR.

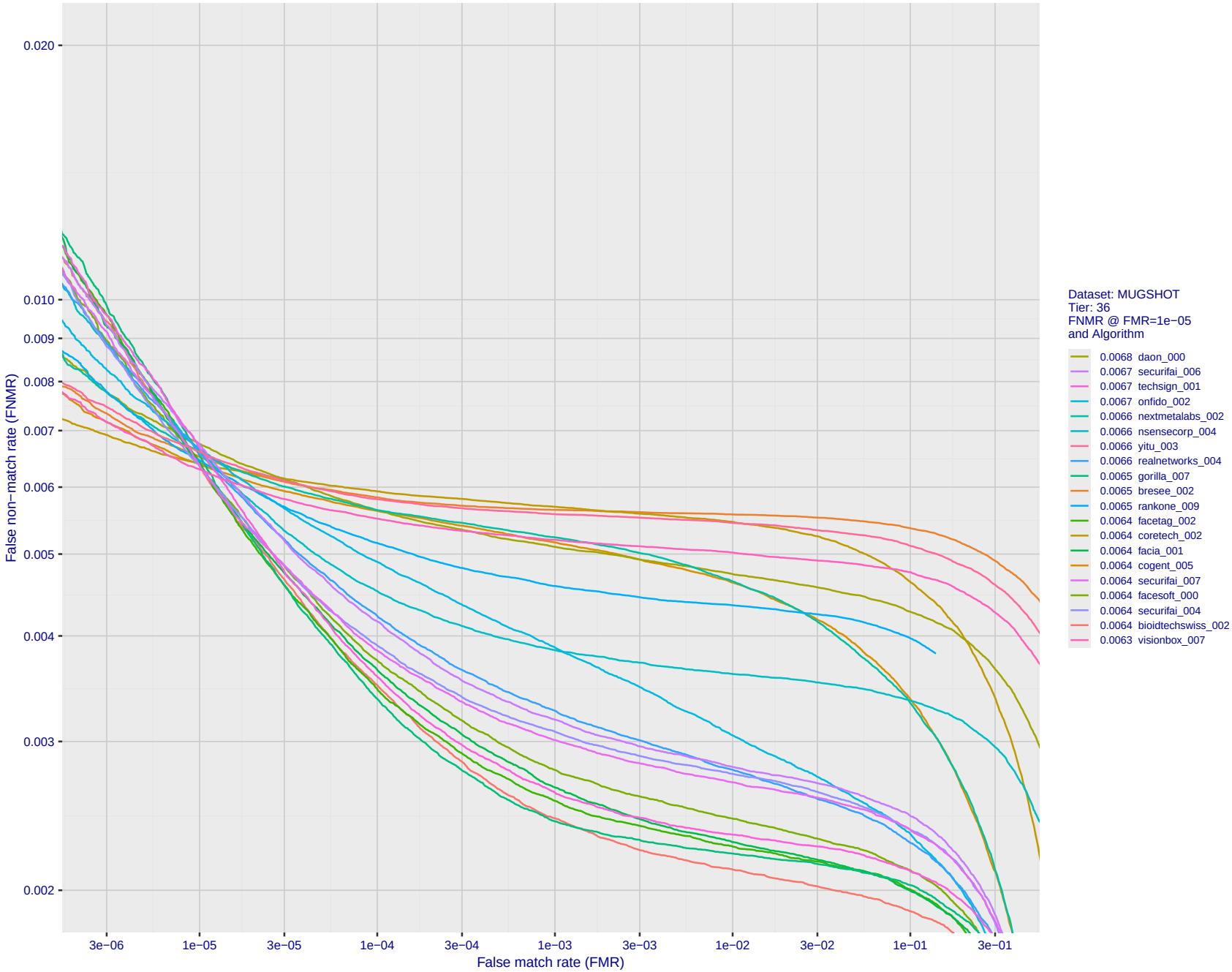

Figure 254: For the mugshot images, detection error tradeoff (DET) characteristics showing false non-match rate vs. false match rate plotted parametrically on threshold, T. The scales are logarithmic in order to show decades of FMR.

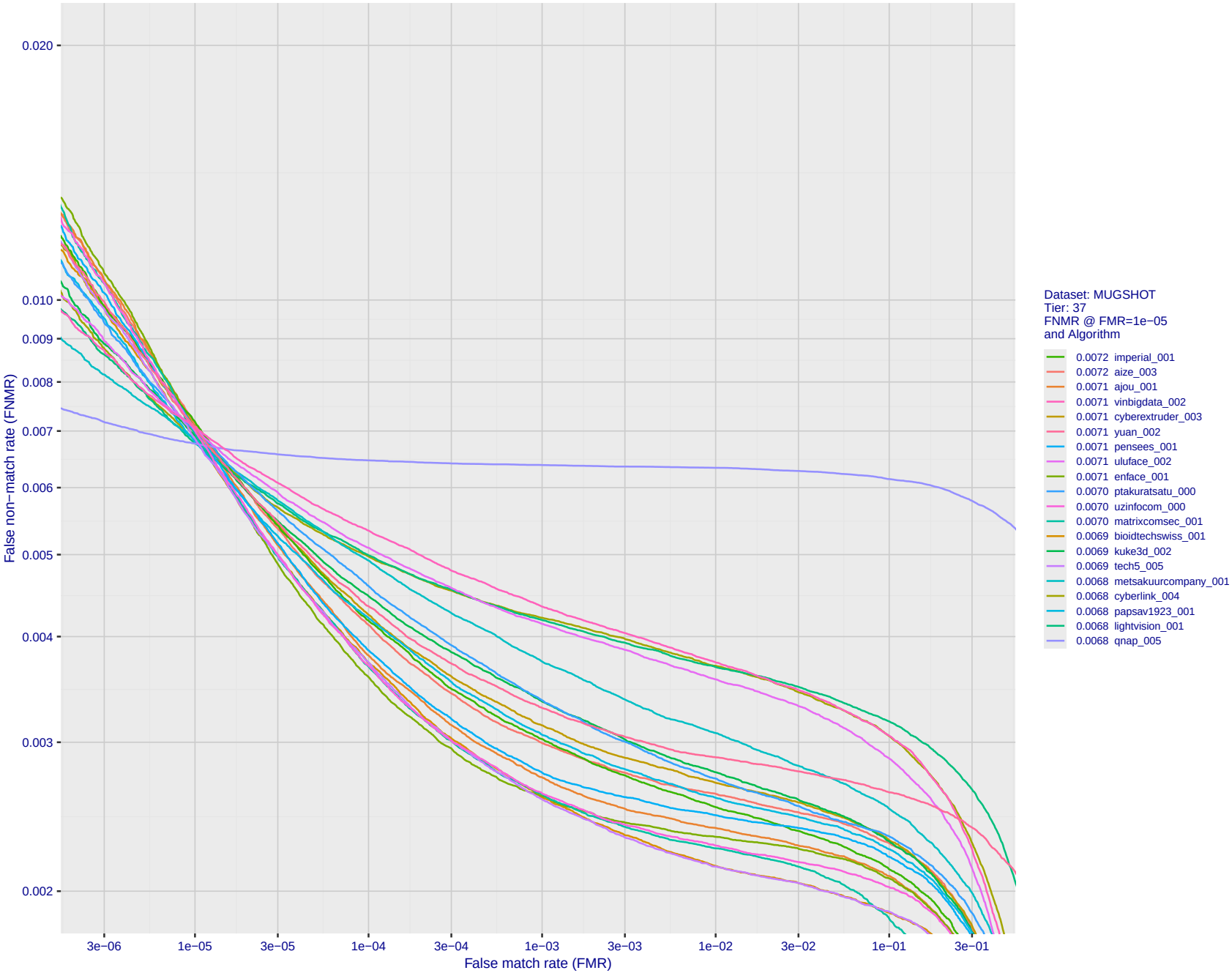

Figure 255: For the mugshot images, detection error tradeoff (DET) characteristics showing false non-match rate vs. false match rate plotted parametrically on threshold, T. The scales are logarithmic in order to show decades of FMR.

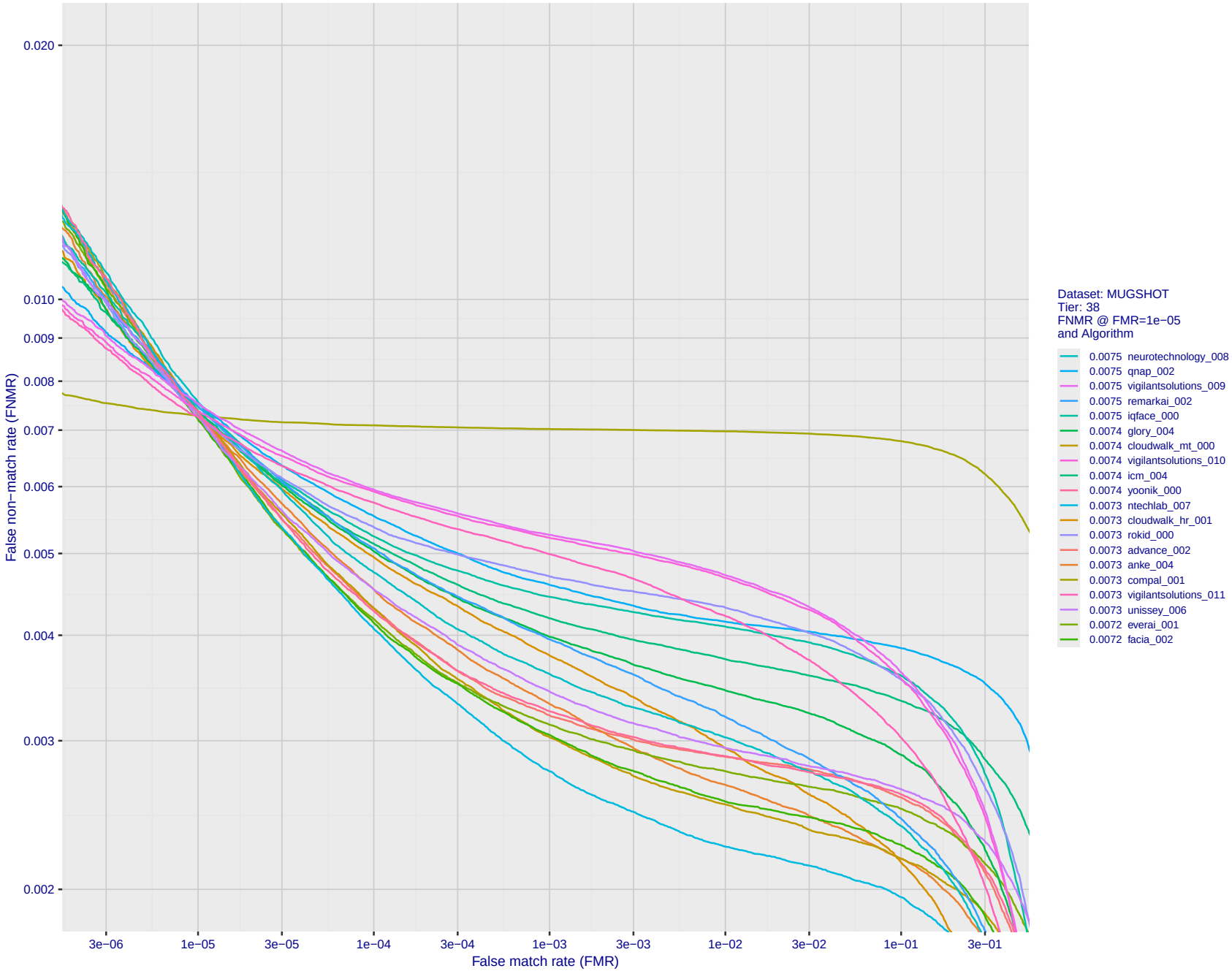

Figure 256: For the mugshot images, detection error tradeoff (DET) characteristics showing false non-match rate vs. false match rate plotted parametrically on threshold, T. The scales are logarithmic in order to show decades of FMR.

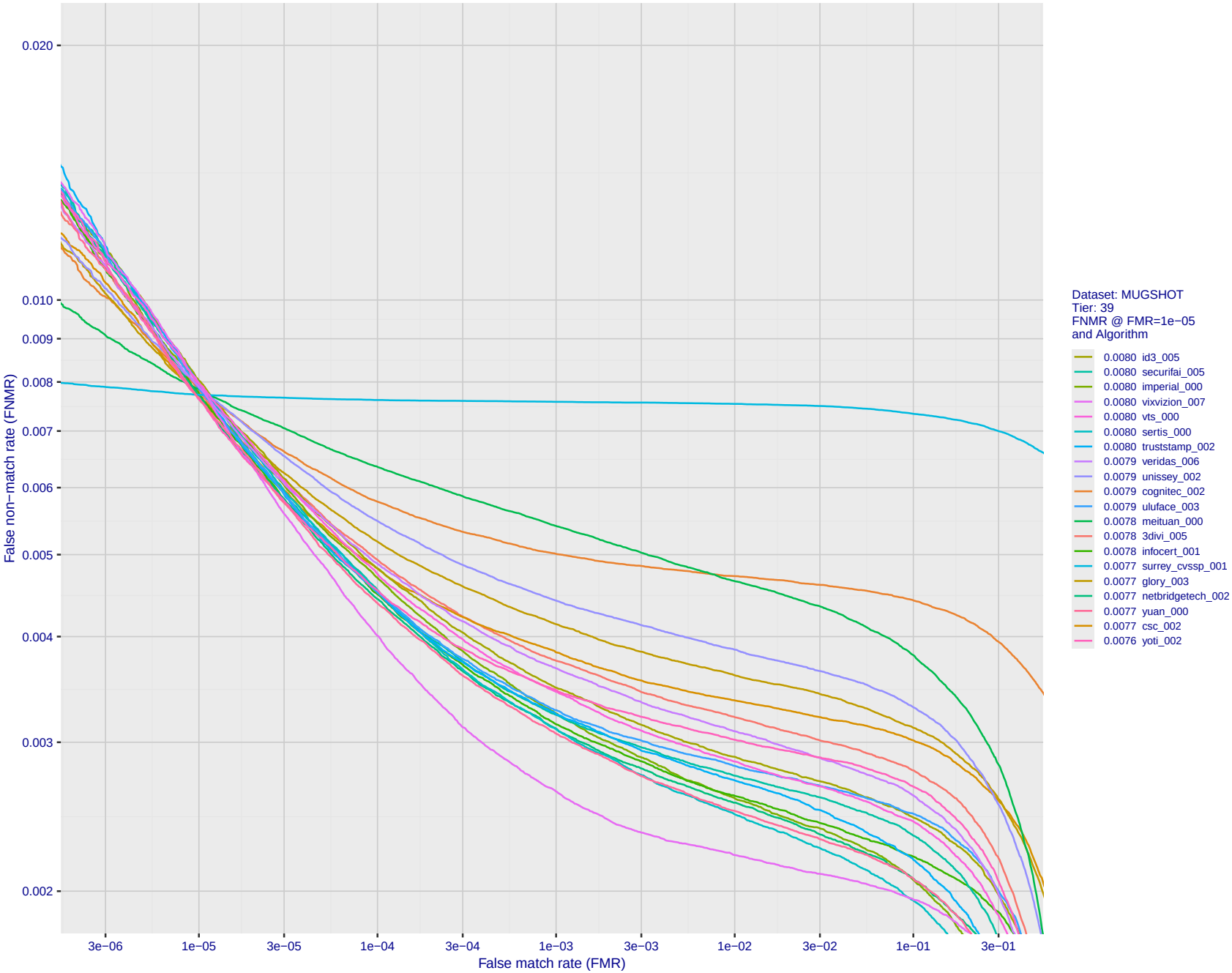

Figure 257: For the mugshot images, detection error tradeoff (DET) characteristics showing false non-match rate vs. false match rate plotted parametrically on threshold, T. The scales are logarithmic in order to show decades of FMR.

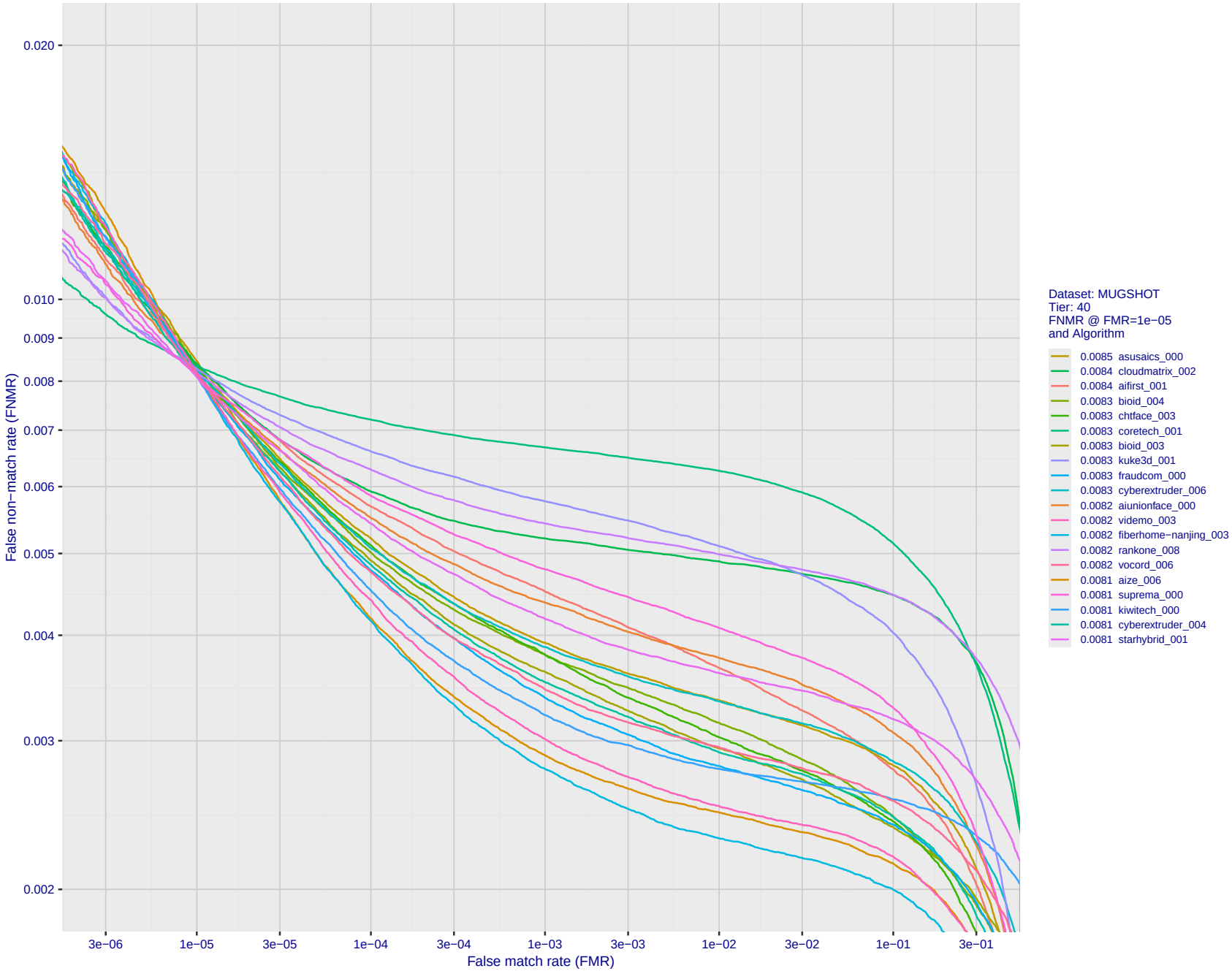

Figure 258: For the mugshot images, detection error tradeoff (DET) characteristics showing false non-match rate vs. false match rate plotted parametrically on threshold, T. The scales are logarithmic in order to show decades of FMR.

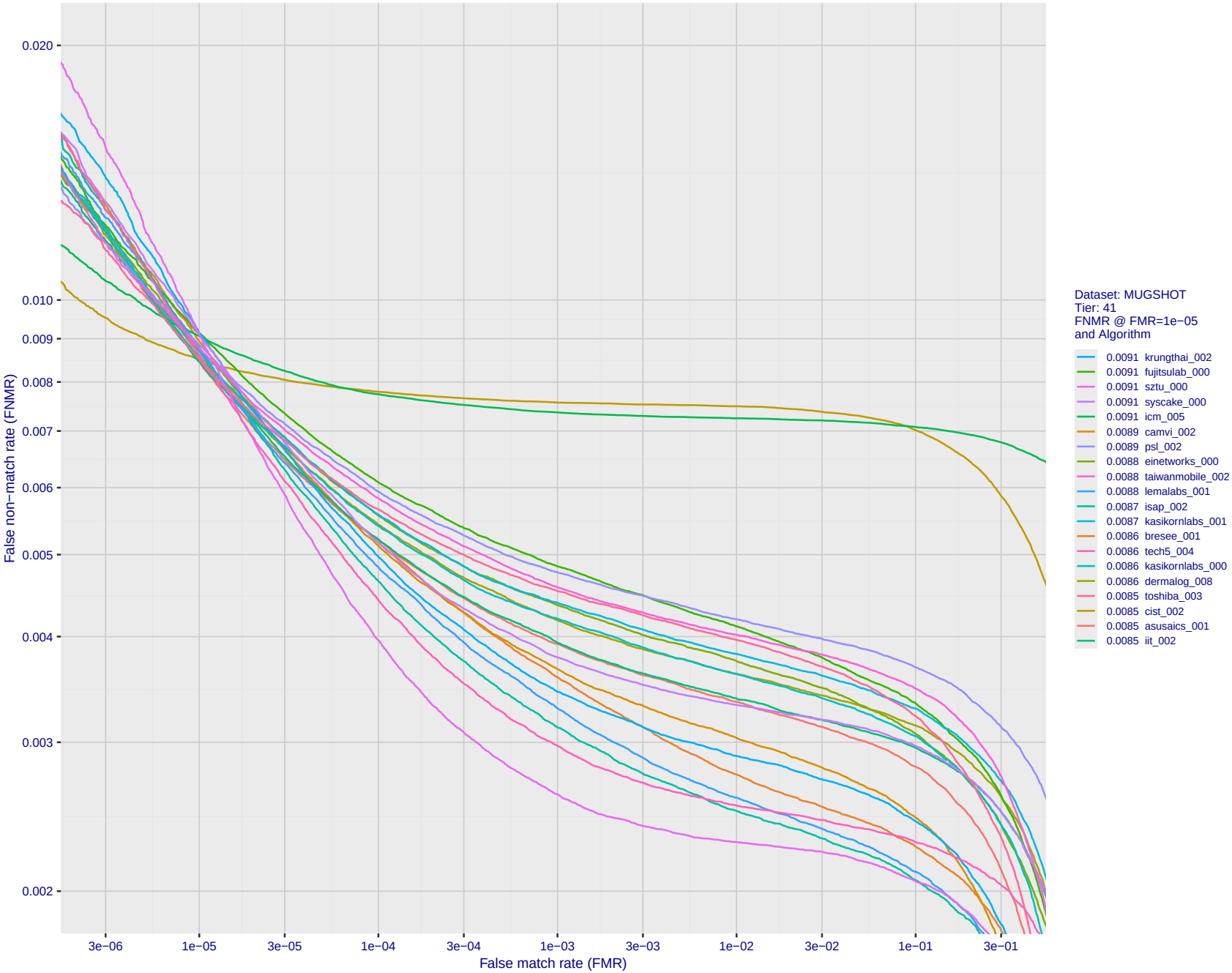

Figure 259: For the mugshot images, detection error tradeoff (DET) characteristics showing false non-match rate vs. false match rate plotted parametrically on threshold, T. The scales are logarithmic in order to show decades of FMR.

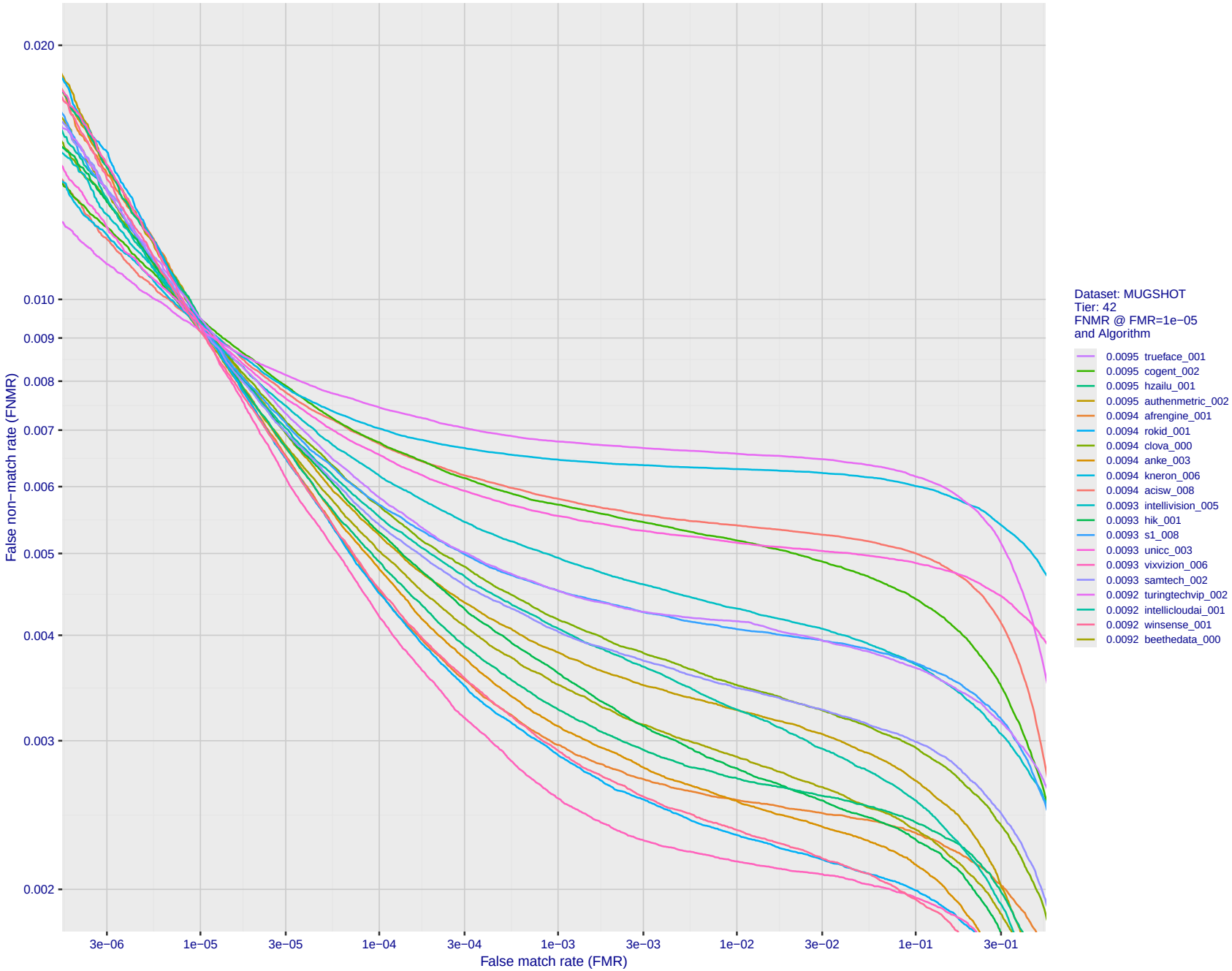

Figure 260: For the mugshot images, detection error tradeoff (DET) characteristics showing false non-match rate vs. false match rate plotted parametrically on threshold, T. The scales are logarithmic in order to show decades of FMR.

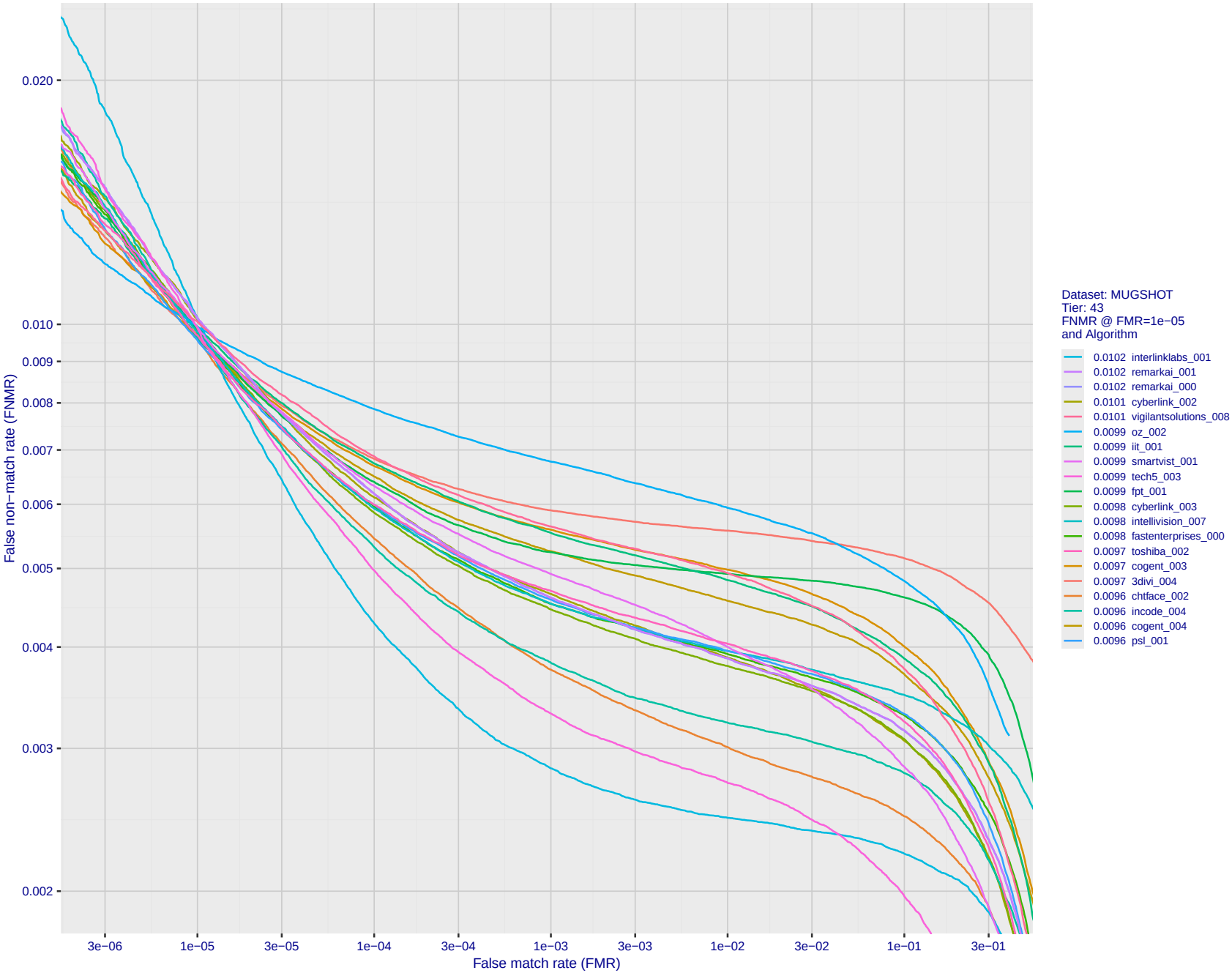

Figure 261: For the mugshot images, detection error tradeoff (DET) characteristics showing false non-match rate vs. false match rate plotted parametrically on threshold, T. The scales are logarithmic in order to show decades of FMR.

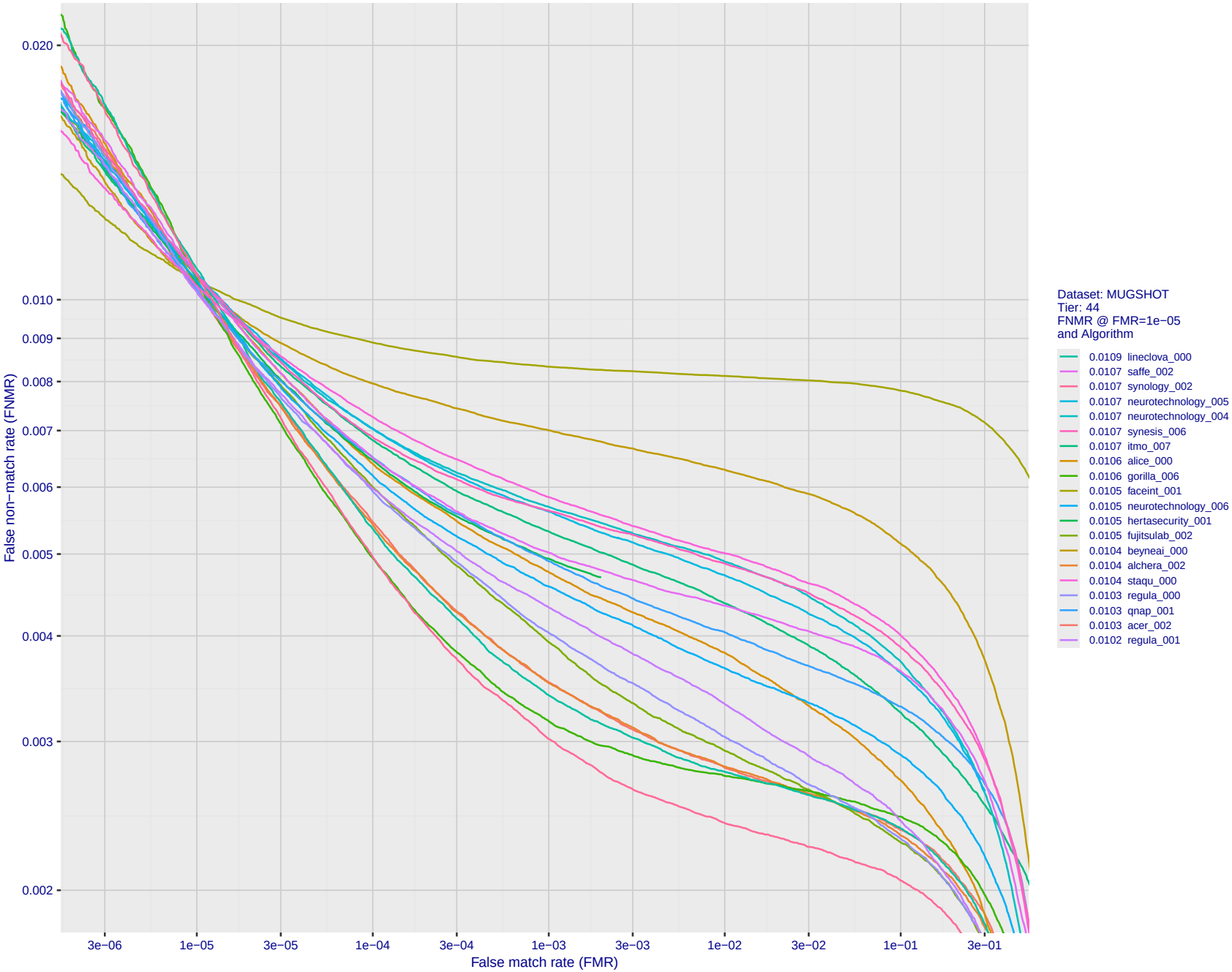

Figure 262: For the mugshot images, detection error tradeoff (DET) characteristics showing false non-match rate vs. false match rate plotted parametrically on threshold, T. The scales are logarithmic in order to show decades of FMR.

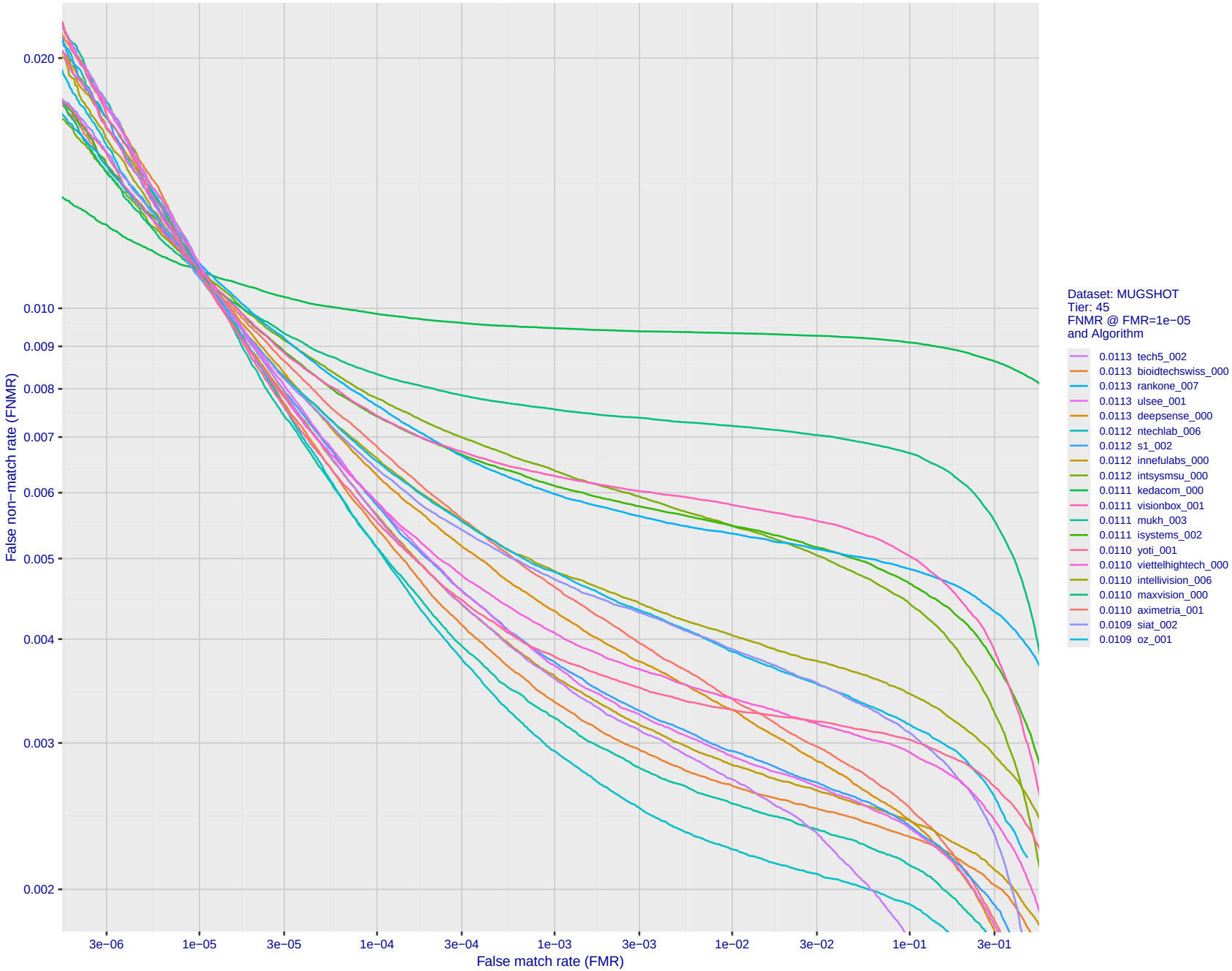

Figure 263: For the mugshot images, detection error tradeoff (DET) characteristics showing false non-match rate vs. false match rate plotted parametrically on threshold, T. The scales are logarithmic in order to show decades of FMR.

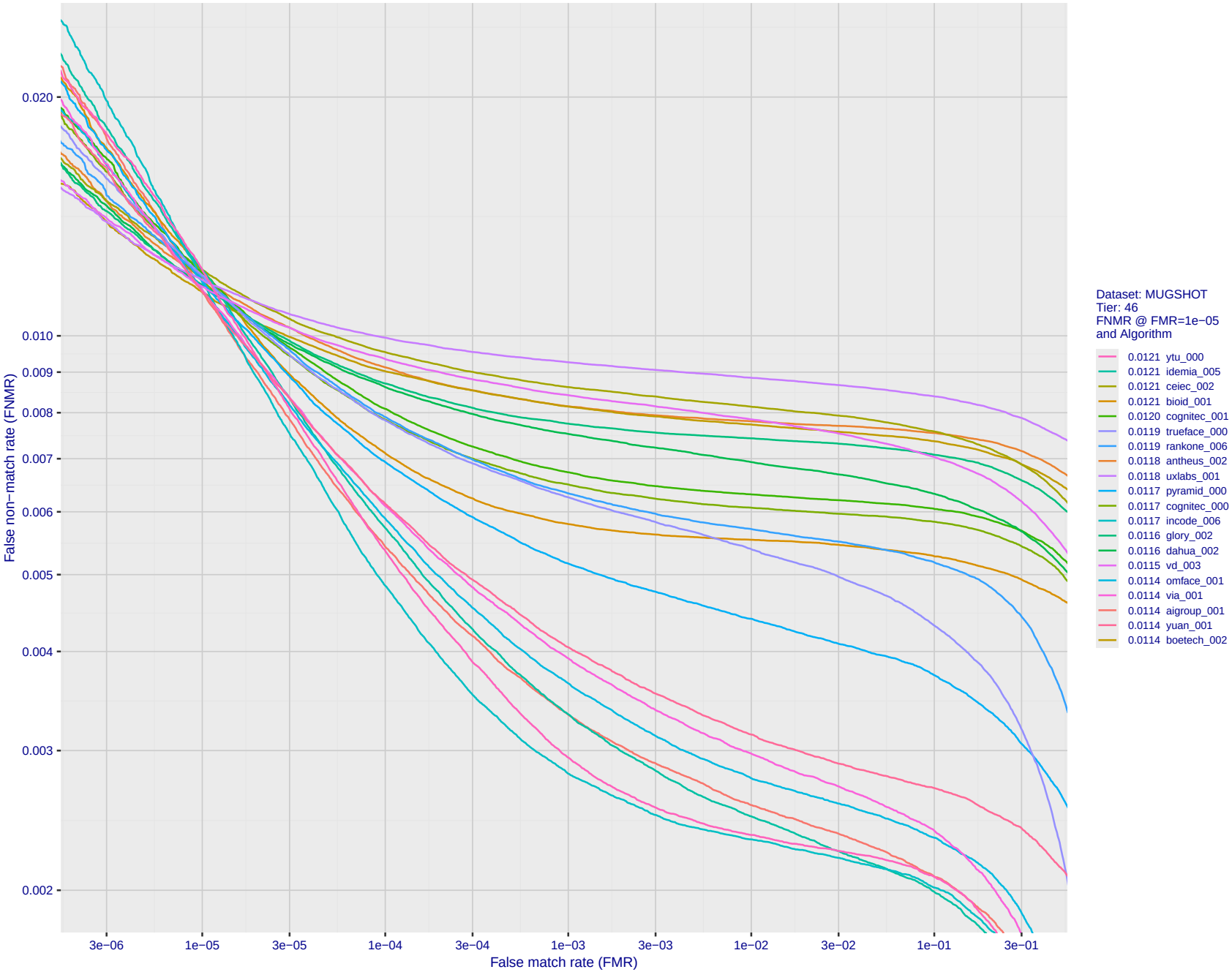

Figure 264: For the mugshot images, detection error tradeoff (DET) characteristics showing false non-match rate vs. false match rate plotted parametrically on threshold, T. The scales are logarithmic in order to show decades of FMR.

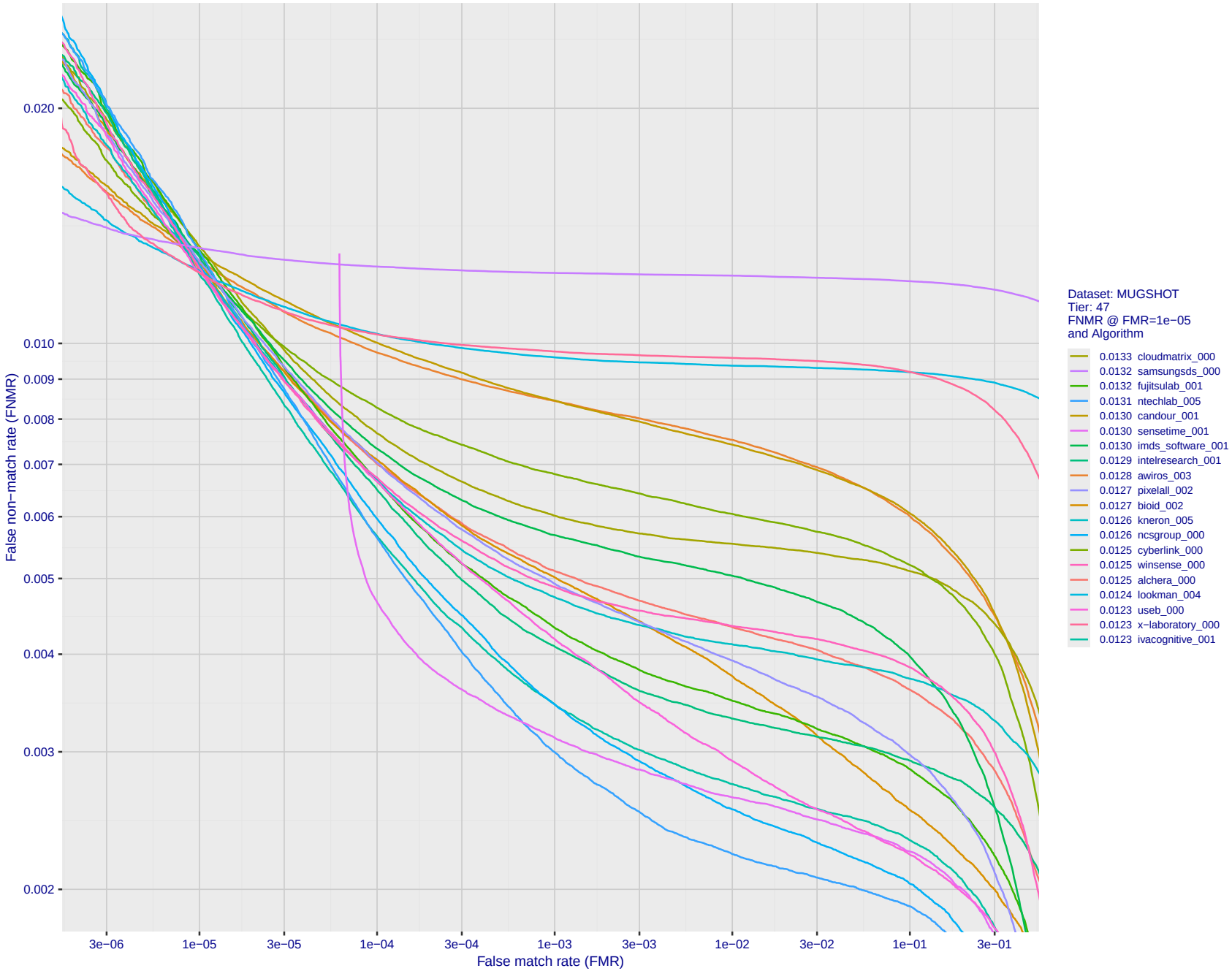

Figure 265: For the mugshot images, detection error tradeoff (DET) characteristics showing false non-match rate vs. false match rate plotted parametrically on threshold, T. The scales are logarithmic in order to show decades of FMR.

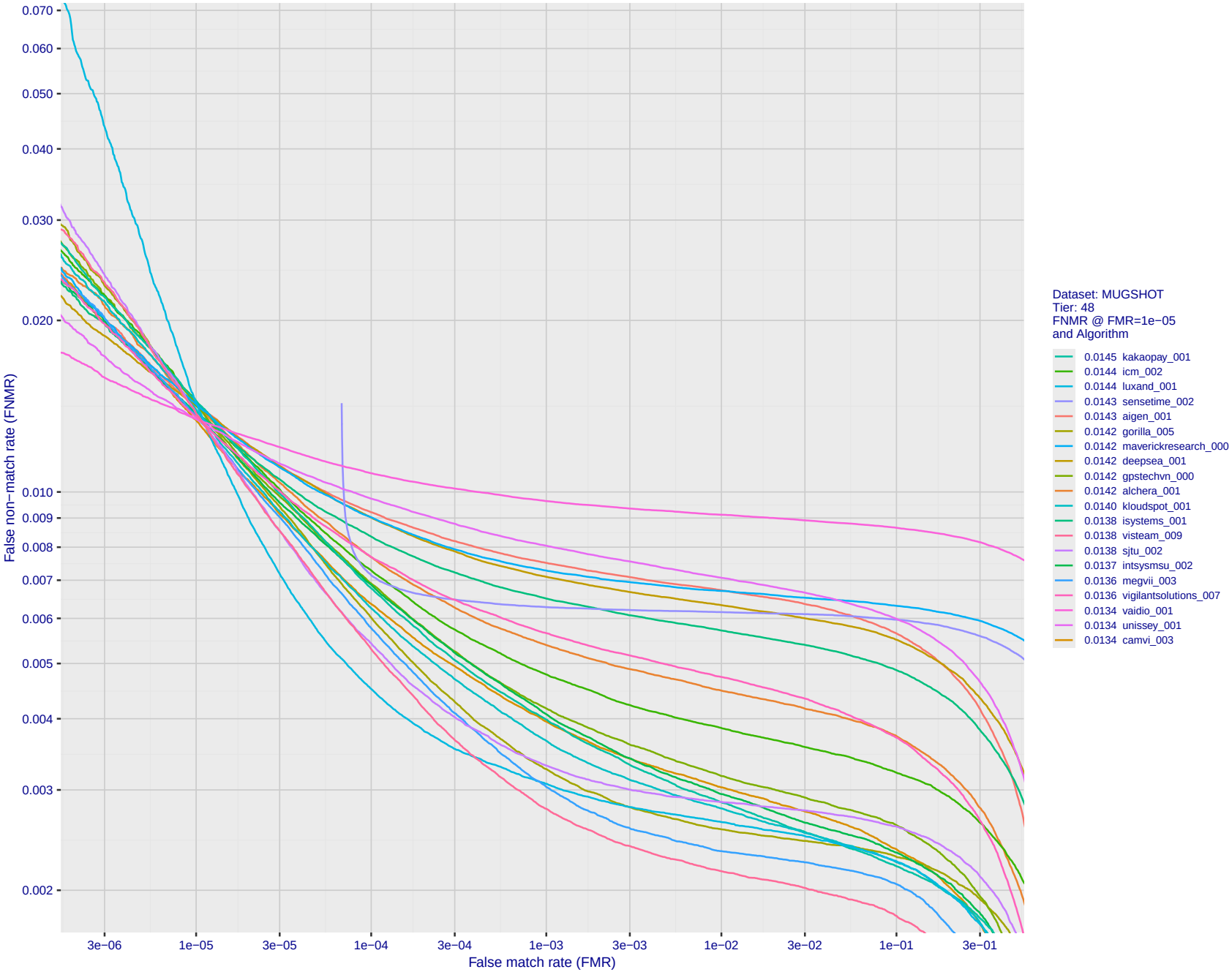

Figure 266: For the mugshot images, detection error tradeoff (DET) characteristics showing false non-match rate vs. false match rate plotted parametrically on threshold, T. The scales are logarithmic in order to show decades of FMR.

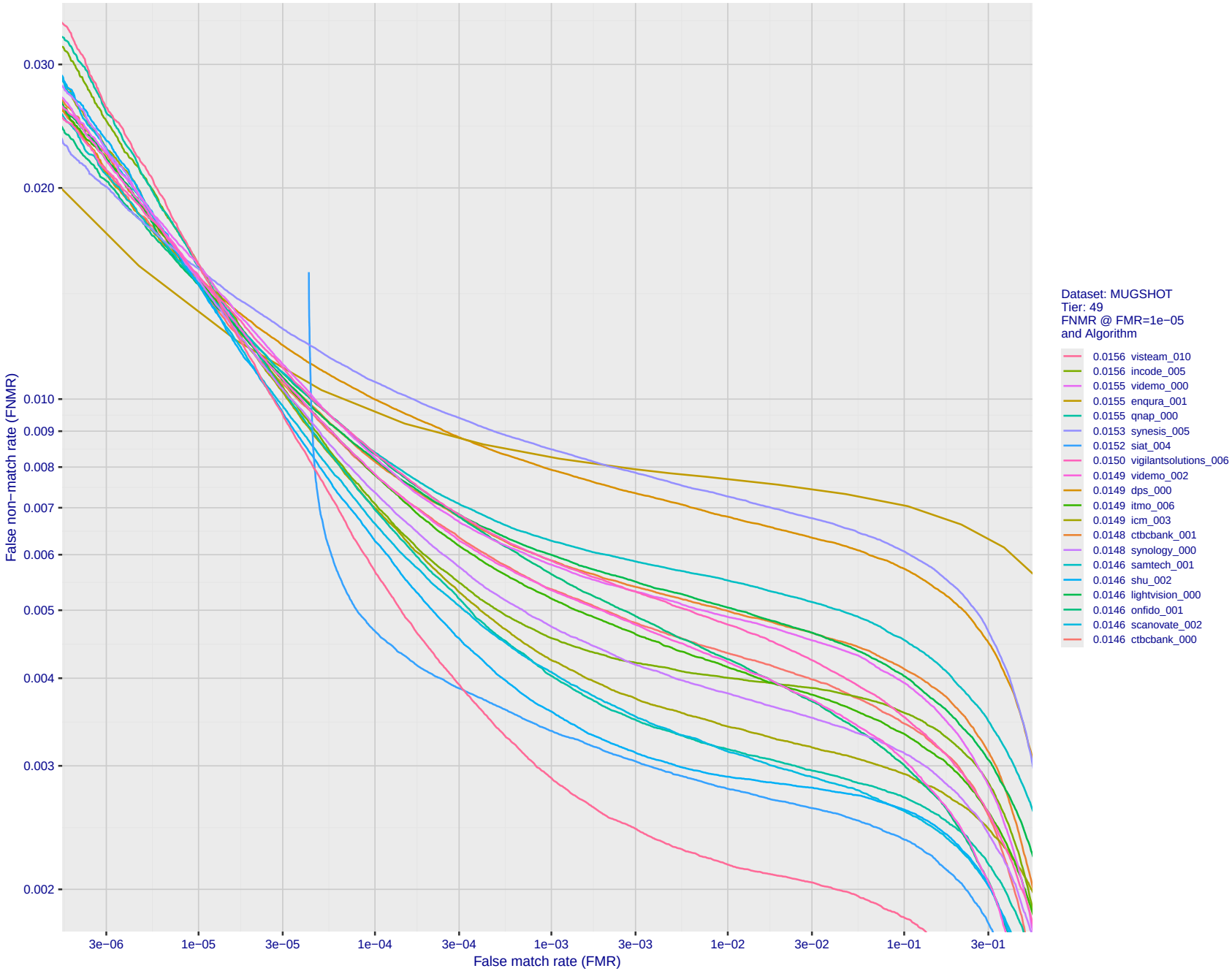

Figure 267: For the mugshot images, detection error tradeoff (DET) characteristics showing false non-match rate vs. false match rate plotted parametrically on threshold, T. The scales are logarithmic in order to show decades of FMR.

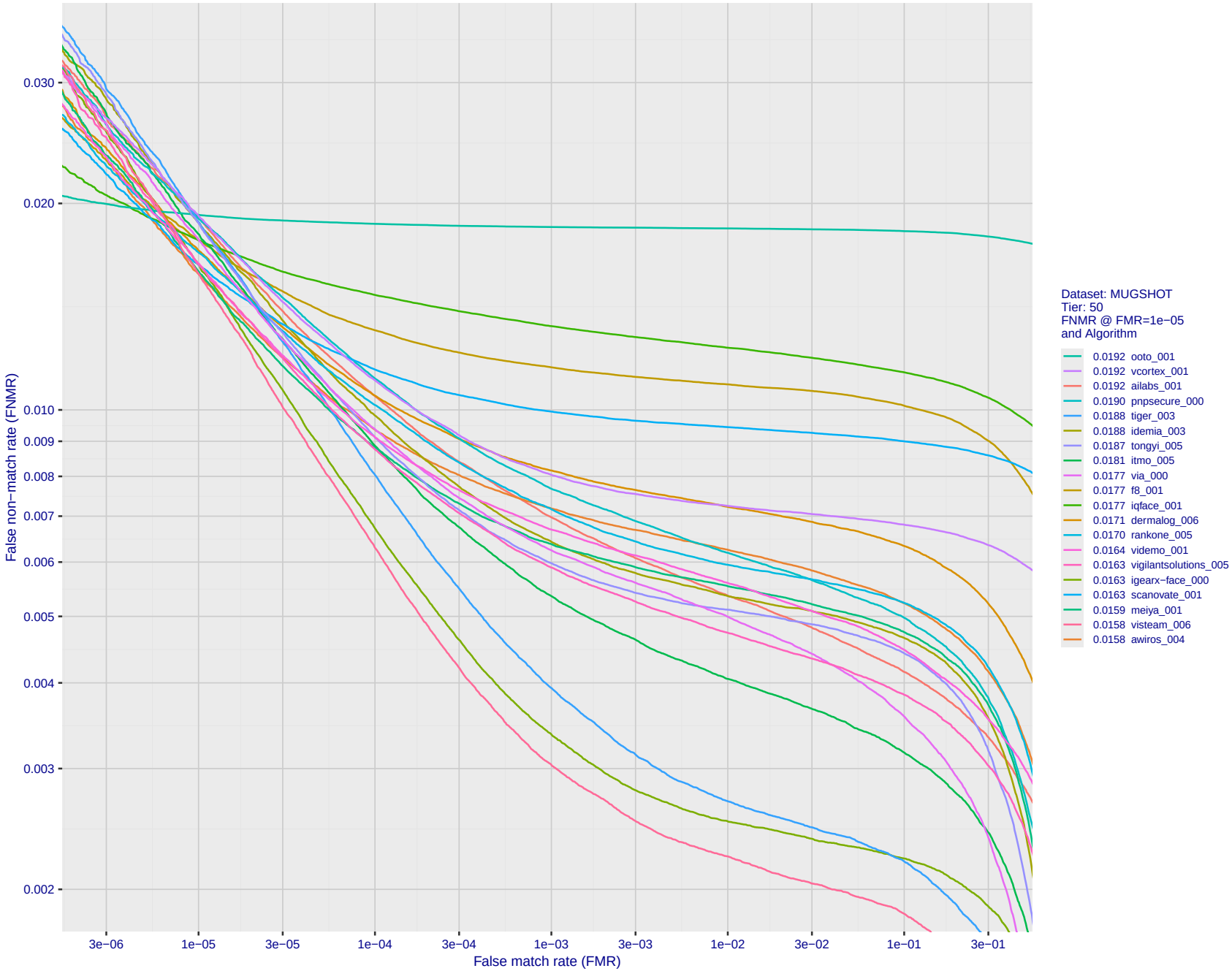

Figure 268: For the mugshot images, detection error tradeoff (DET) characteristics showing false non-match rate vs. false match rate plotted parametrically on threshold, T. The scales are logarithmic in order to show decades of FMR.

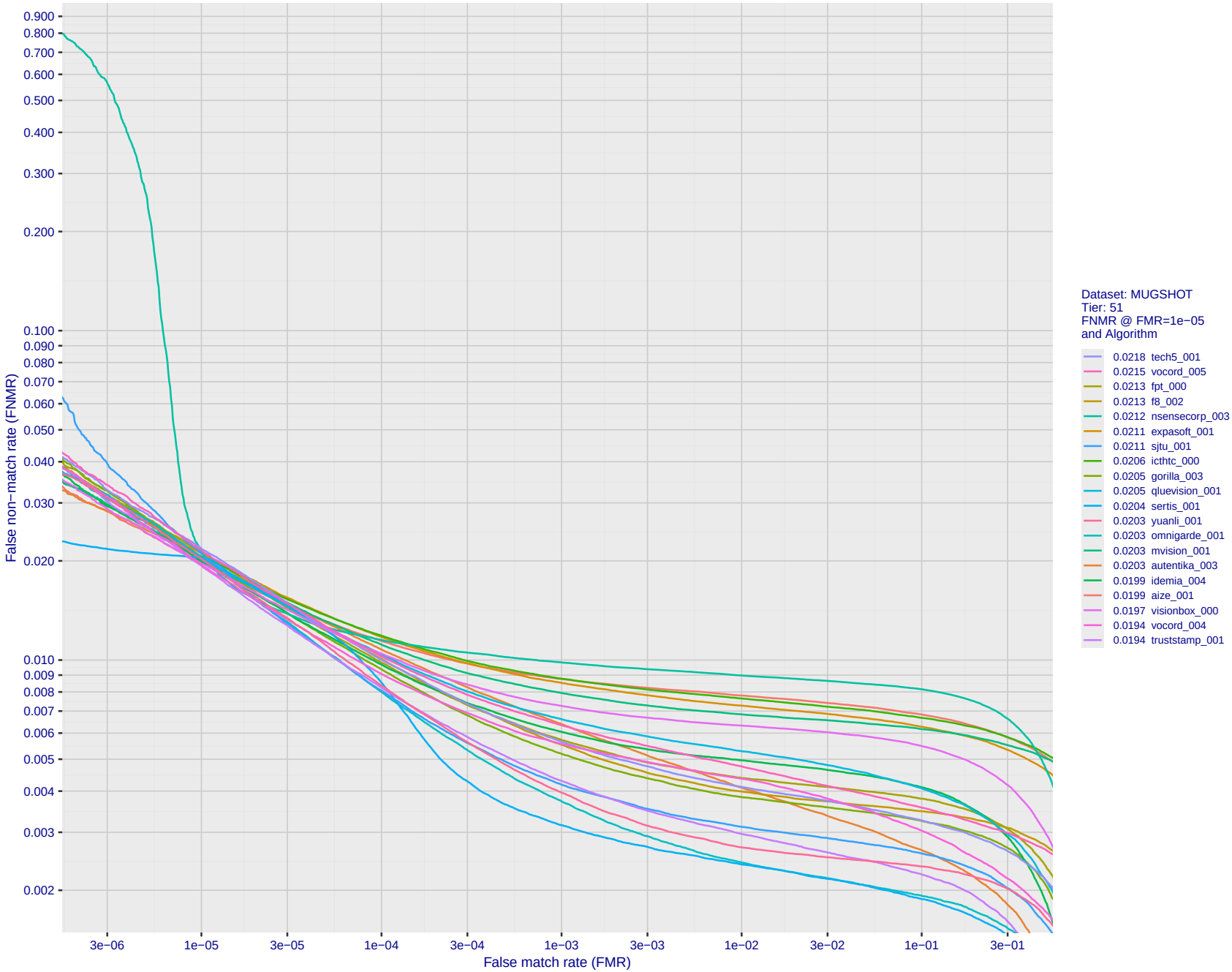

Figure 269: For the mugshot images, detection error tradeoff (DET) characteristics showing false non-match rate vs. false match rate plotted parametrically on threshold, T. The scales are logarithmic in order to show decades of FMR.

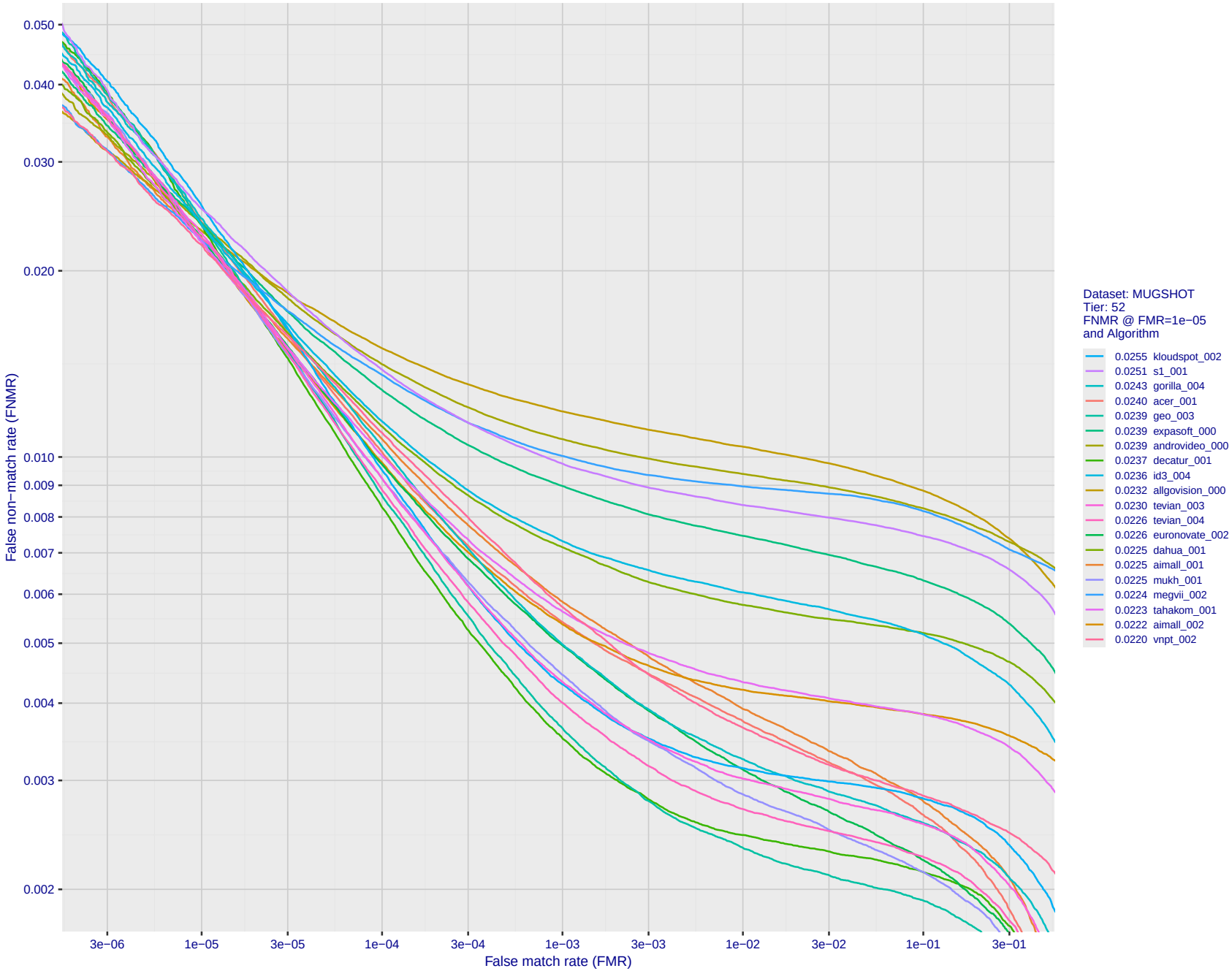

Figure 270: For the mugshot images, detection error tradeoff (DET) characteristics showing false non-match rate vs. false match rate plotted parametrically on threshold, T. The scales are logarithmic in order to show decades of FMR.

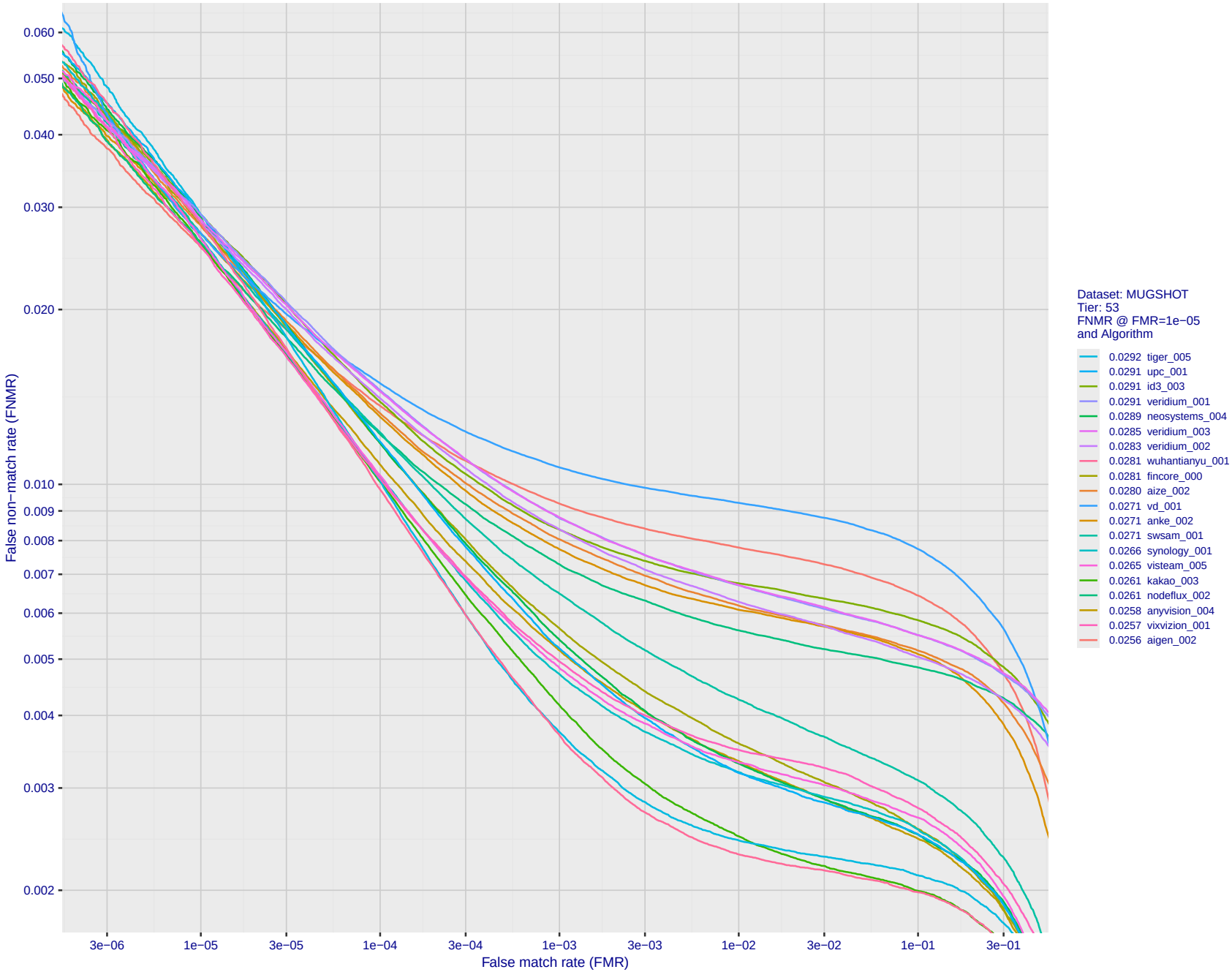

Figure 271: For the mugshot images, detection error tradeoff (DET) characteristics showing false non-match rate vs. false match rate plotted parametrically on threshold, T. The scales are logarithmic in order to show decades of FMR.

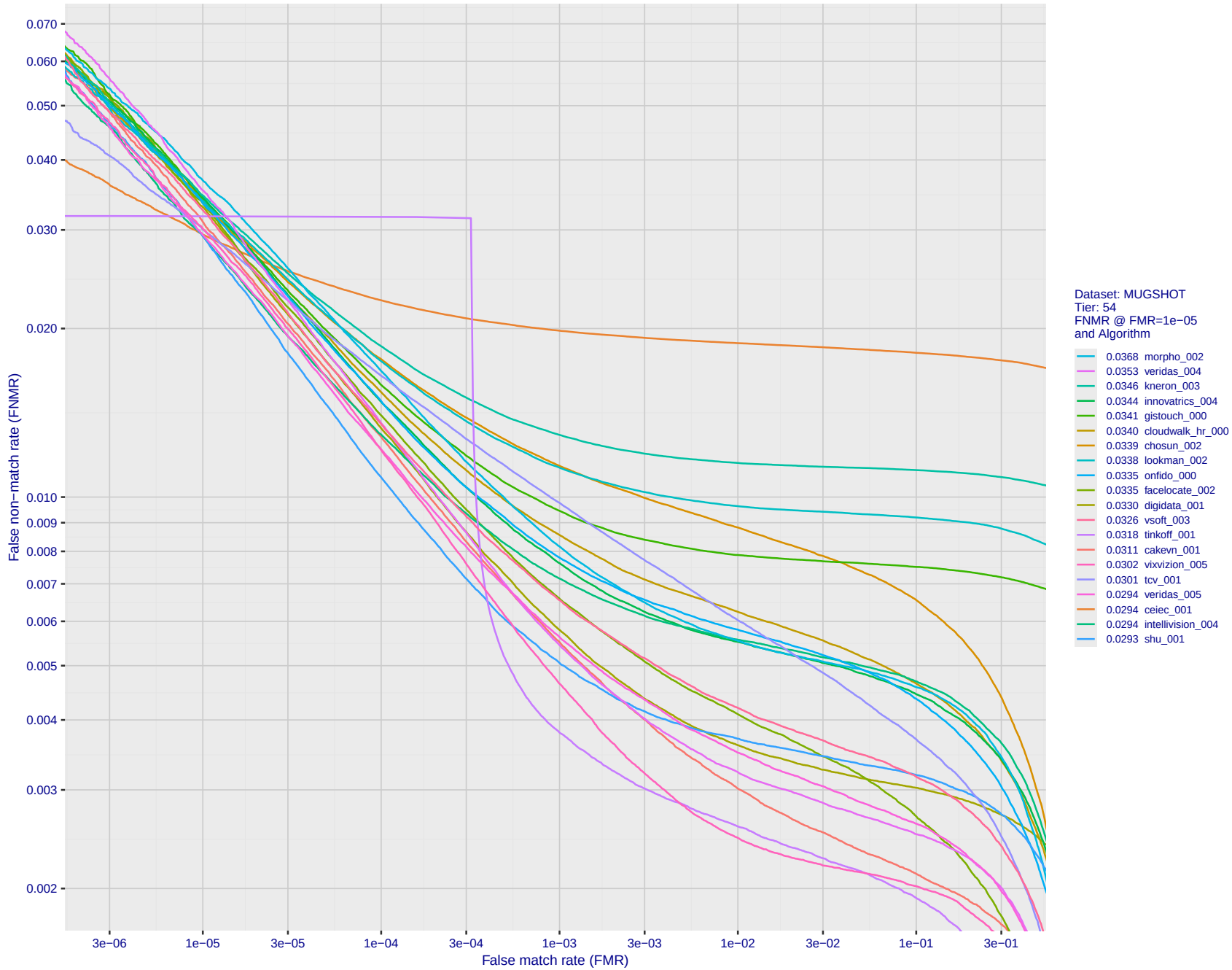

Figure 272: For the mugshot images, detection error tradeoff (DET) characteristics showing false non-match rate vs. false match rate plotted parametrically on threshold, T. The scales are logarithmic in order to show decades of FMR.

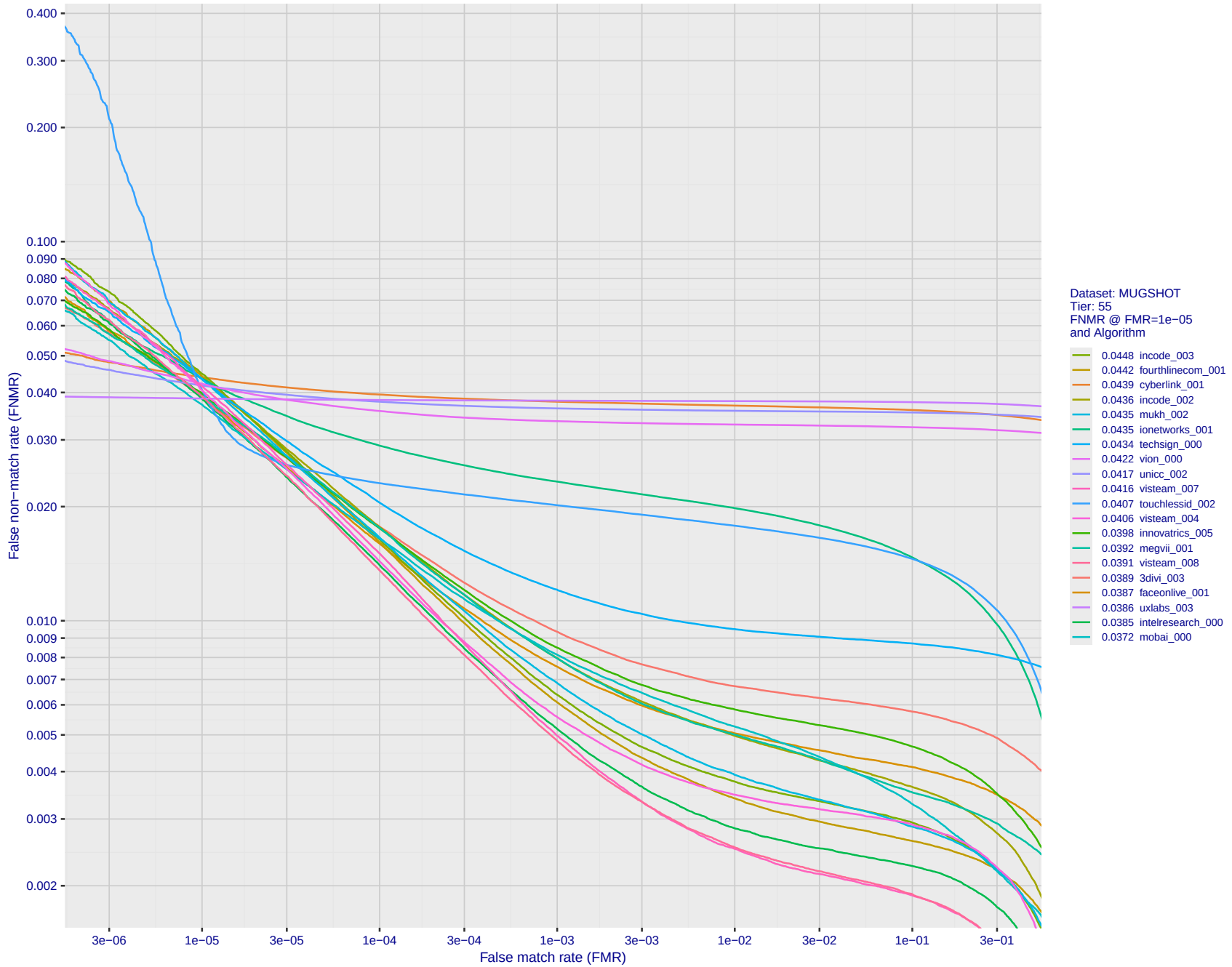

Figure 273: For the mugshot images, detection error tradeoff (DET) characteristics showing false non-match rate vs. false match rate plotted parametrically on threshold, T. The scales are logarithmic in order to show decades of FMR.

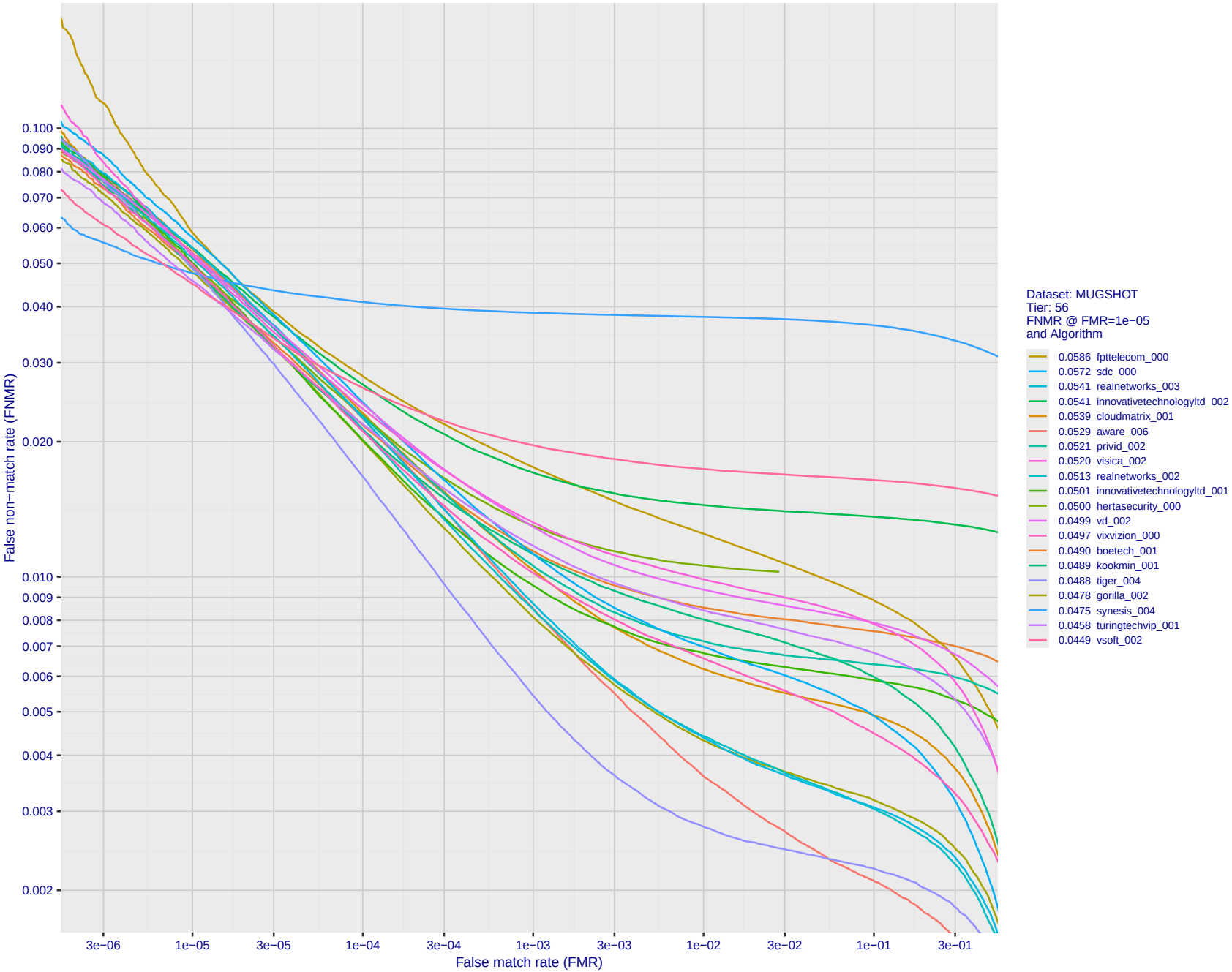

Figure 274: For the mugshot images, detection error tradeoff (DET) characteristics showing false non-match rate vs. false match rate plotted parametrically on threshold, T. The scales are logarithmic in order to show decades of FMR.

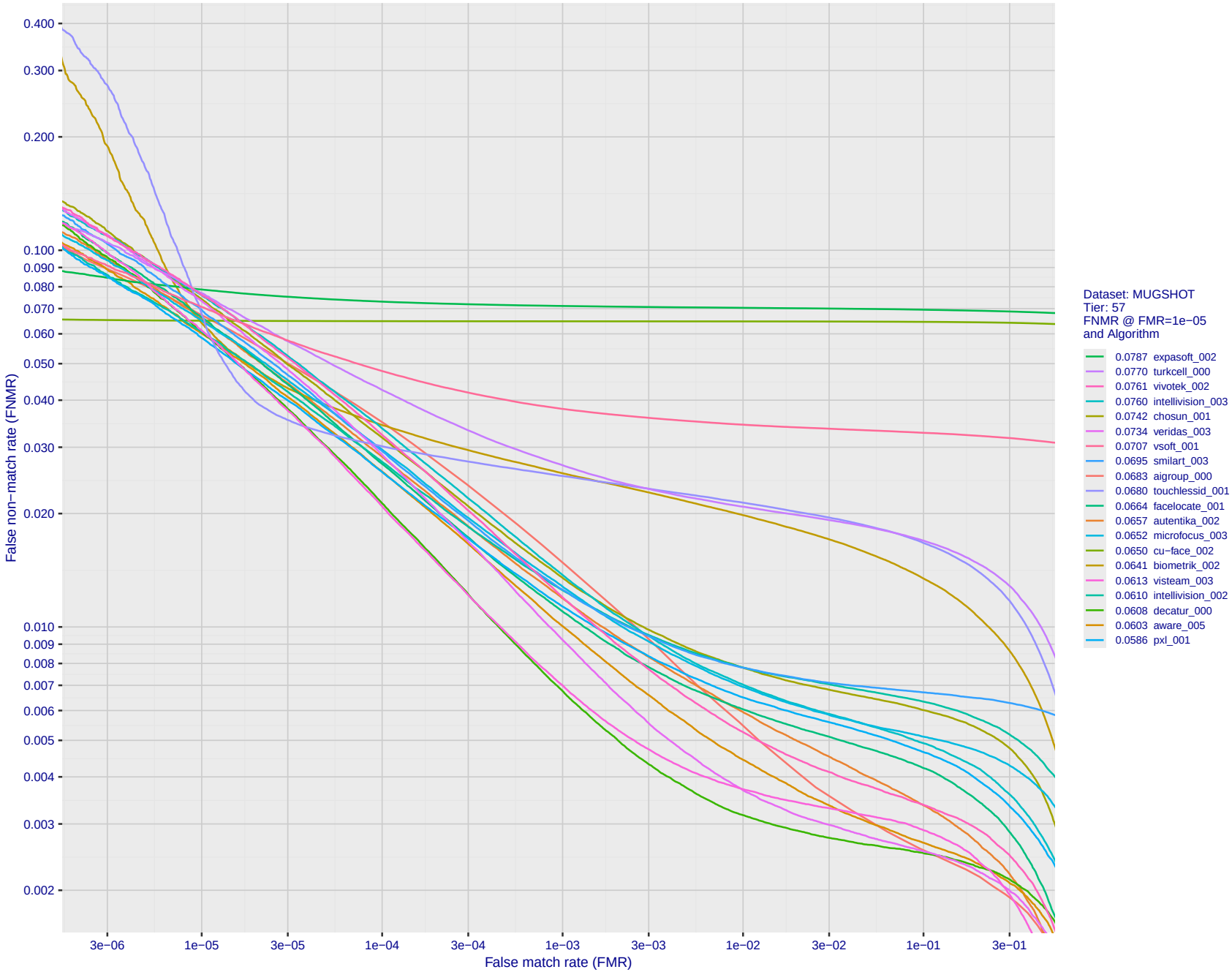

Figure 275: For the mugshot images, detection error tradeoff (DET) characteristics showing false non-match rate vs. false match rate plotted parametrically on threshold, T. The scales are logarithmic in order to show decades of FMR.

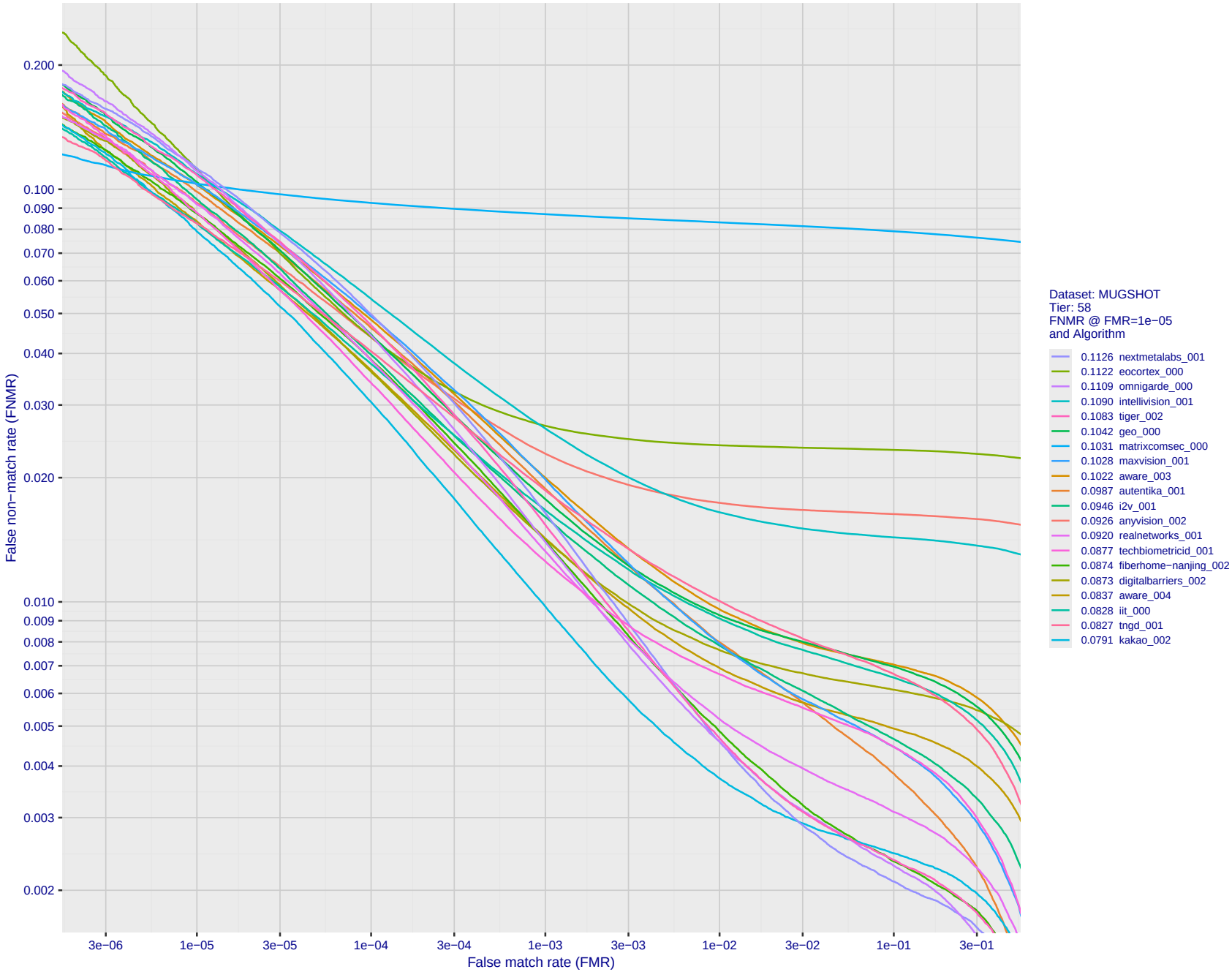

Figure 276: For the mugshot images, detection error tradeoff (DET) characteristics showing false non-match rate vs. false match rate plotted parametrically on threshold, T. The scales are logarithmic in order to show decades of FMR.

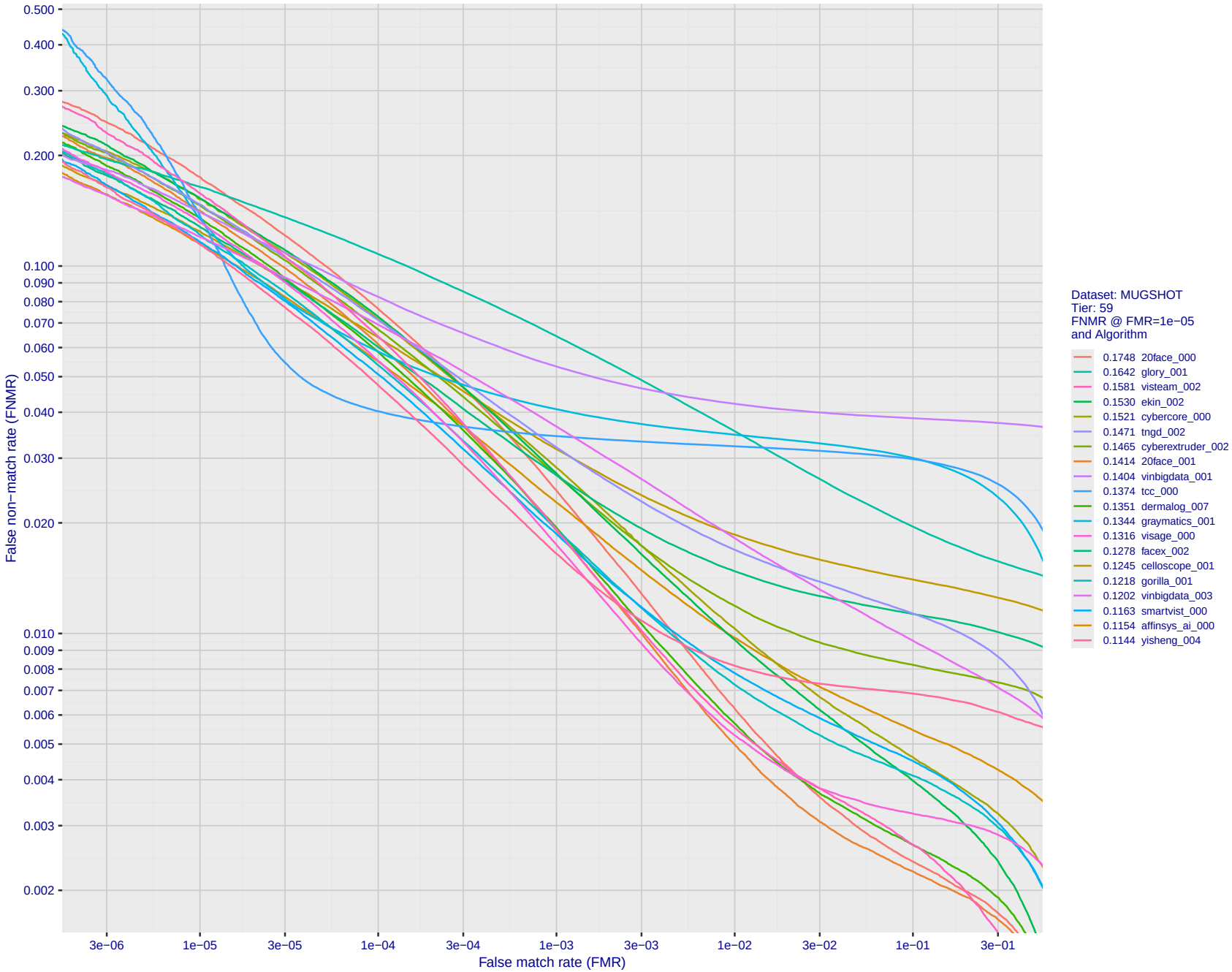

Figure 277: For the mugshot images, detection error tradeoff (DET) characteristics showing false non-match rate vs. false match rate plotted parametrically on threshold, T. The scales are logarithmic in order to show decades of FMR.

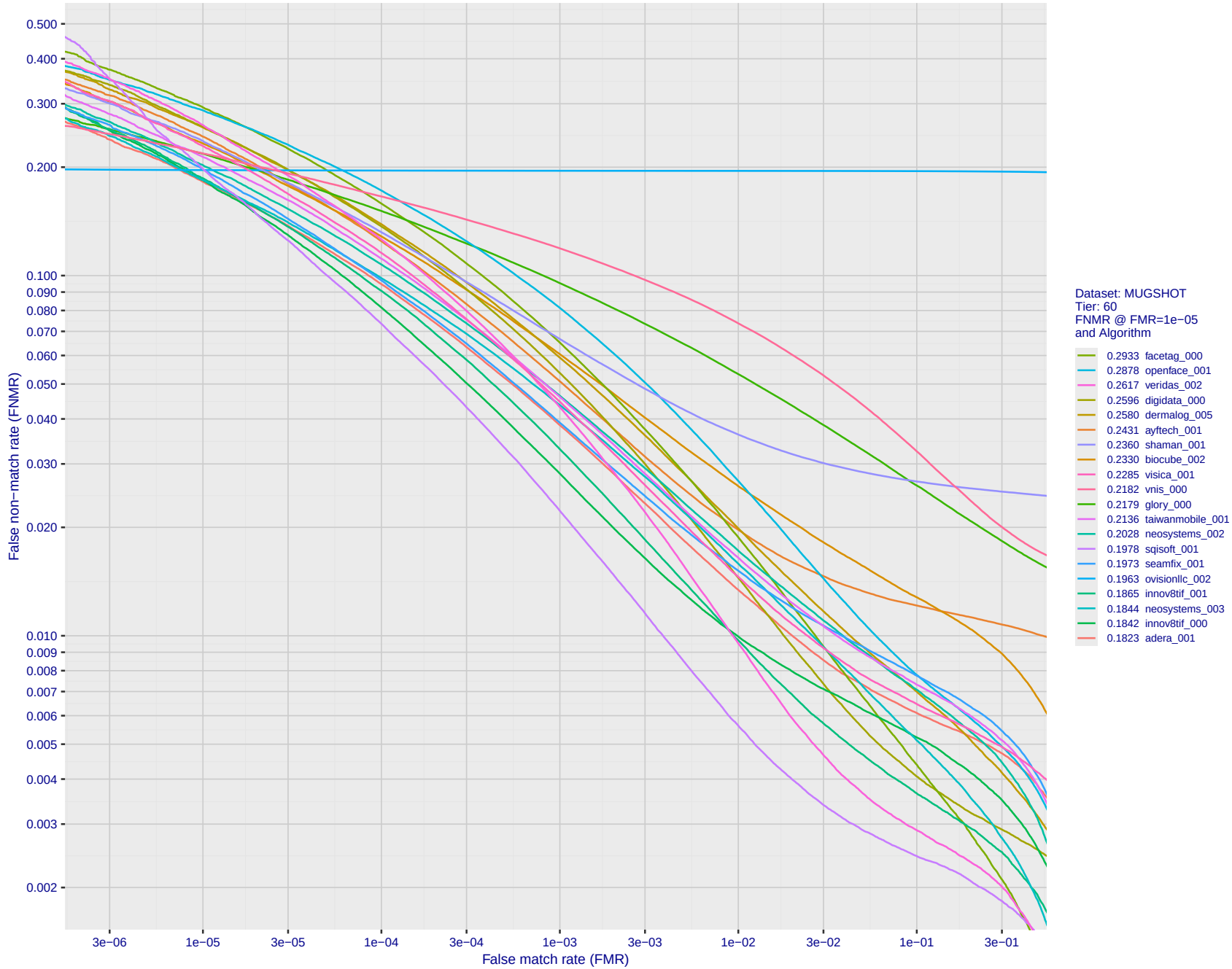

Figure 278: For the mugshot images, detection error tradeoff (DET) characteristics showing false non-match rate vs. false match rate plotted parametrically on threshold, T. The scales are logarithmic in order to show decades of FMR.

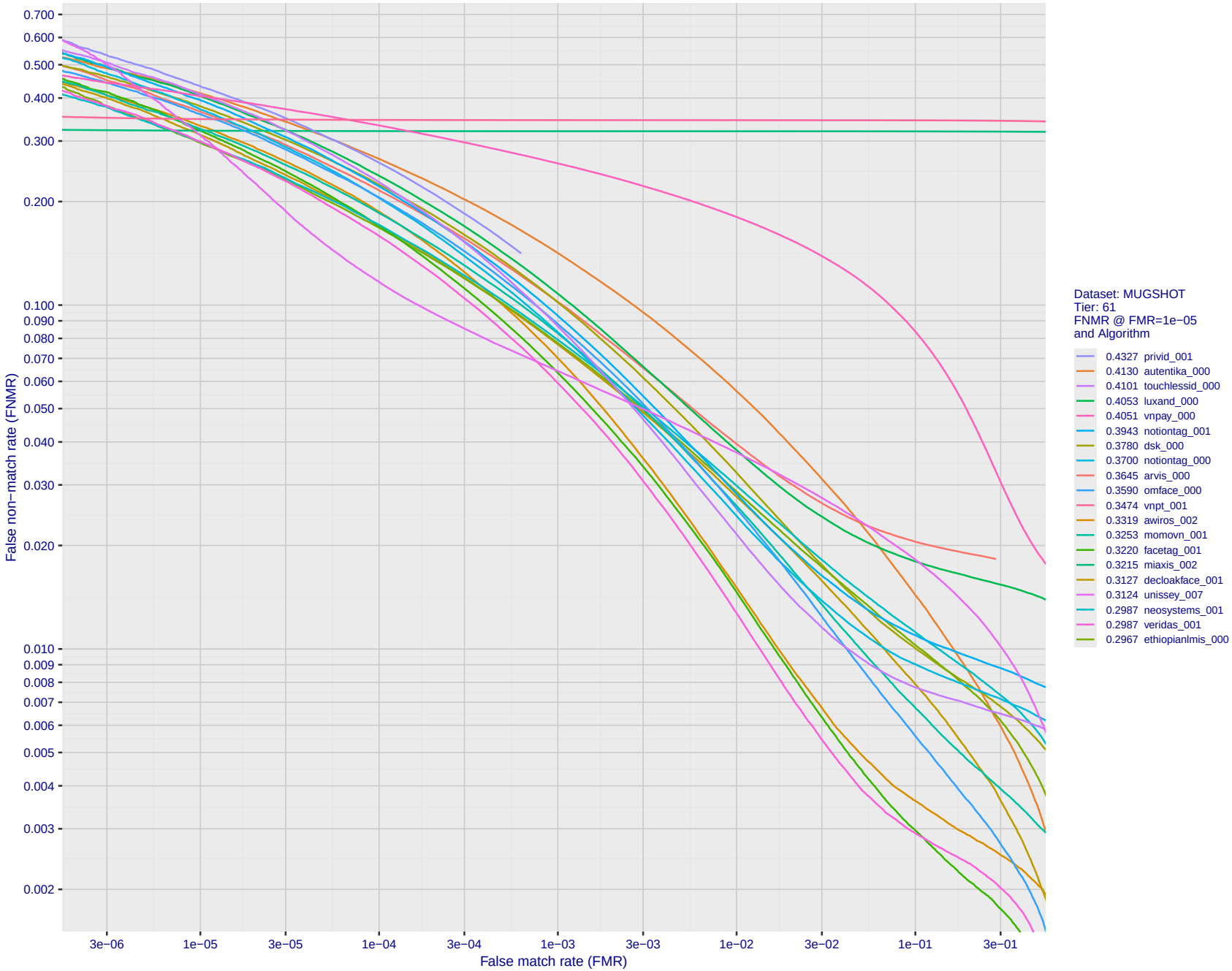

Figure 279: For the mugshot images, detection error tradeoff (DET) characteristics showing false non-match rate vs. false match rate plotted parametrically on threshold, T. The scales are logarithmic in order to show decades of FMR.

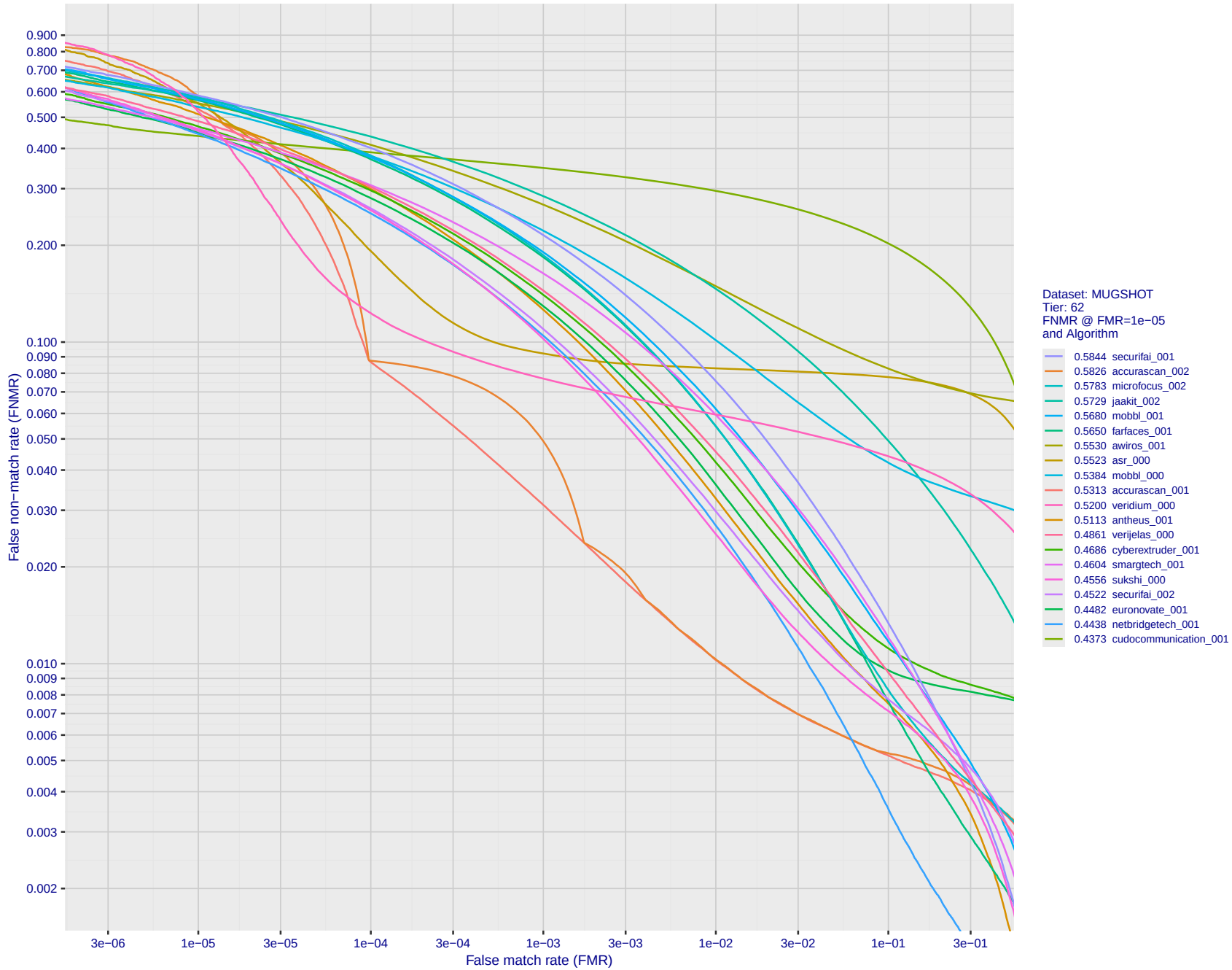

Figure 280: For the mugshot images, detection error tradeoff (DET) characteristics showing false non-match rate vs. false match rate plotted parametrically on threshold, T. The scales are logarithmic in order to show decades of FMR.

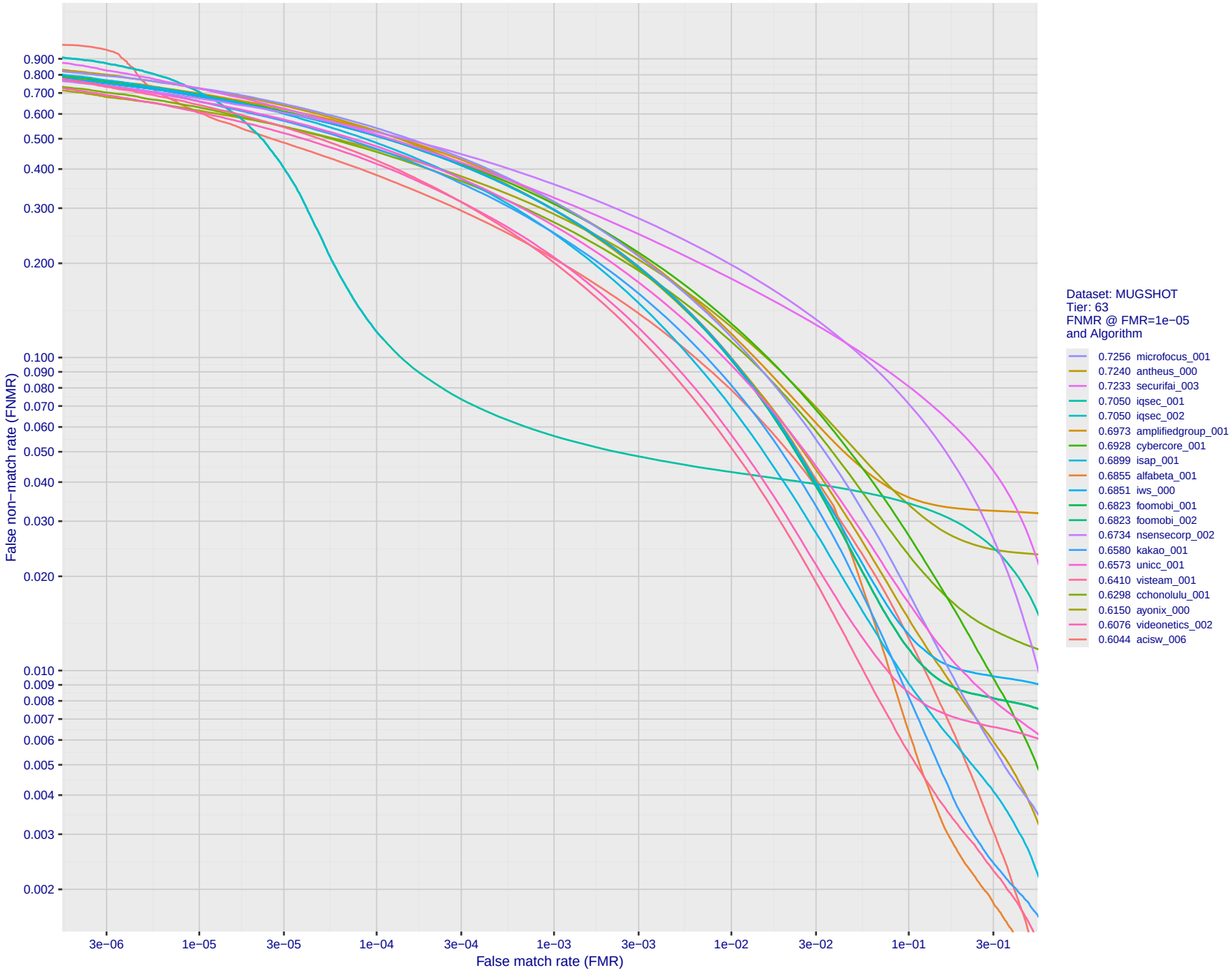

Figure 281: For the mugshot images, detection error tradeoff (DET) characteristics showing false non-match rate vs. false match rate plotted parametrically on threshold, T. The scales are logarithmic in order to show decades of FMR.

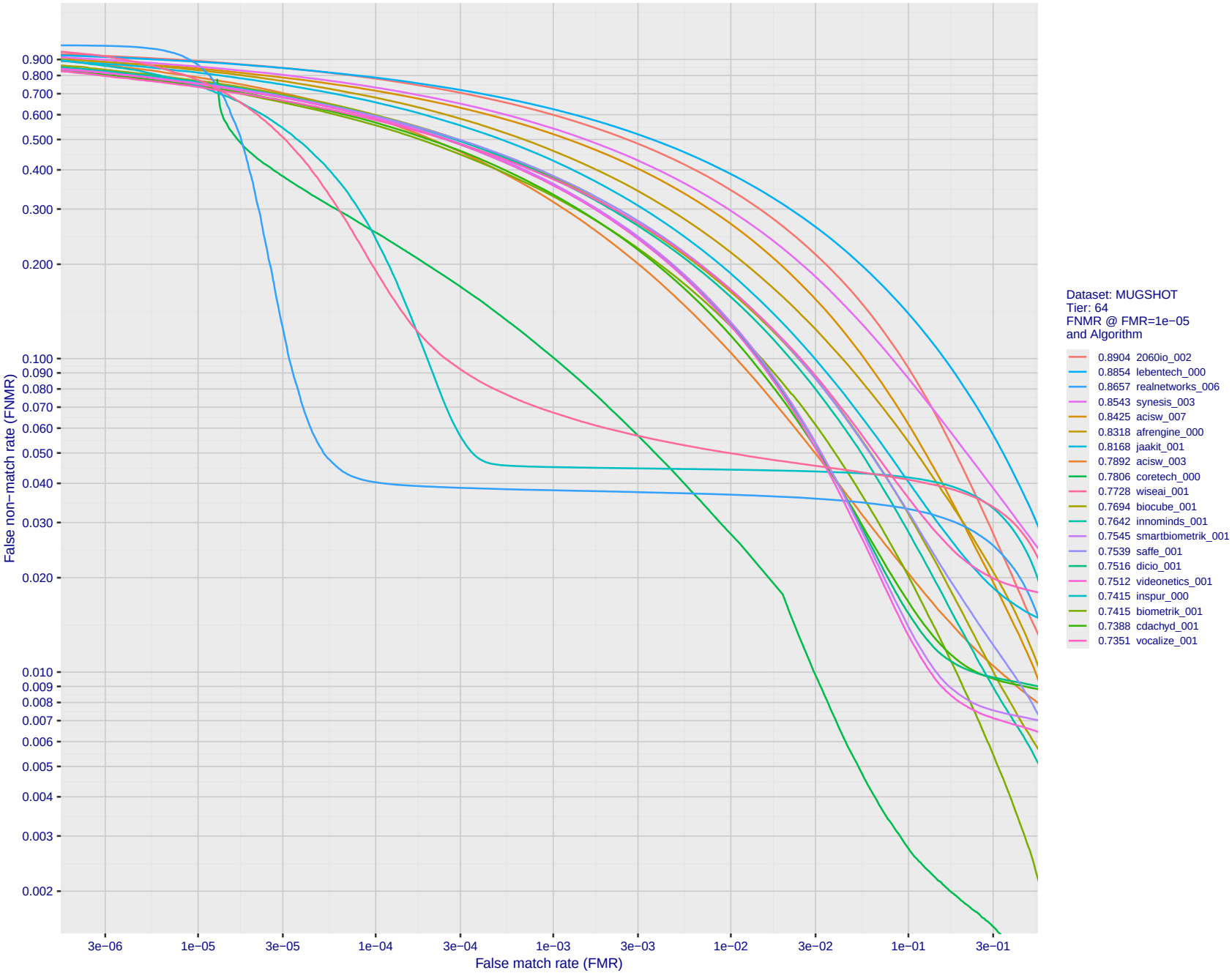

Figure 282: For the mugshot images, detection error tradeoff (DET) characteristics showing false non-match rate vs. false match rate plotted parametrically on threshold, T. The scales are logarithmic in order to show decades of FMR.

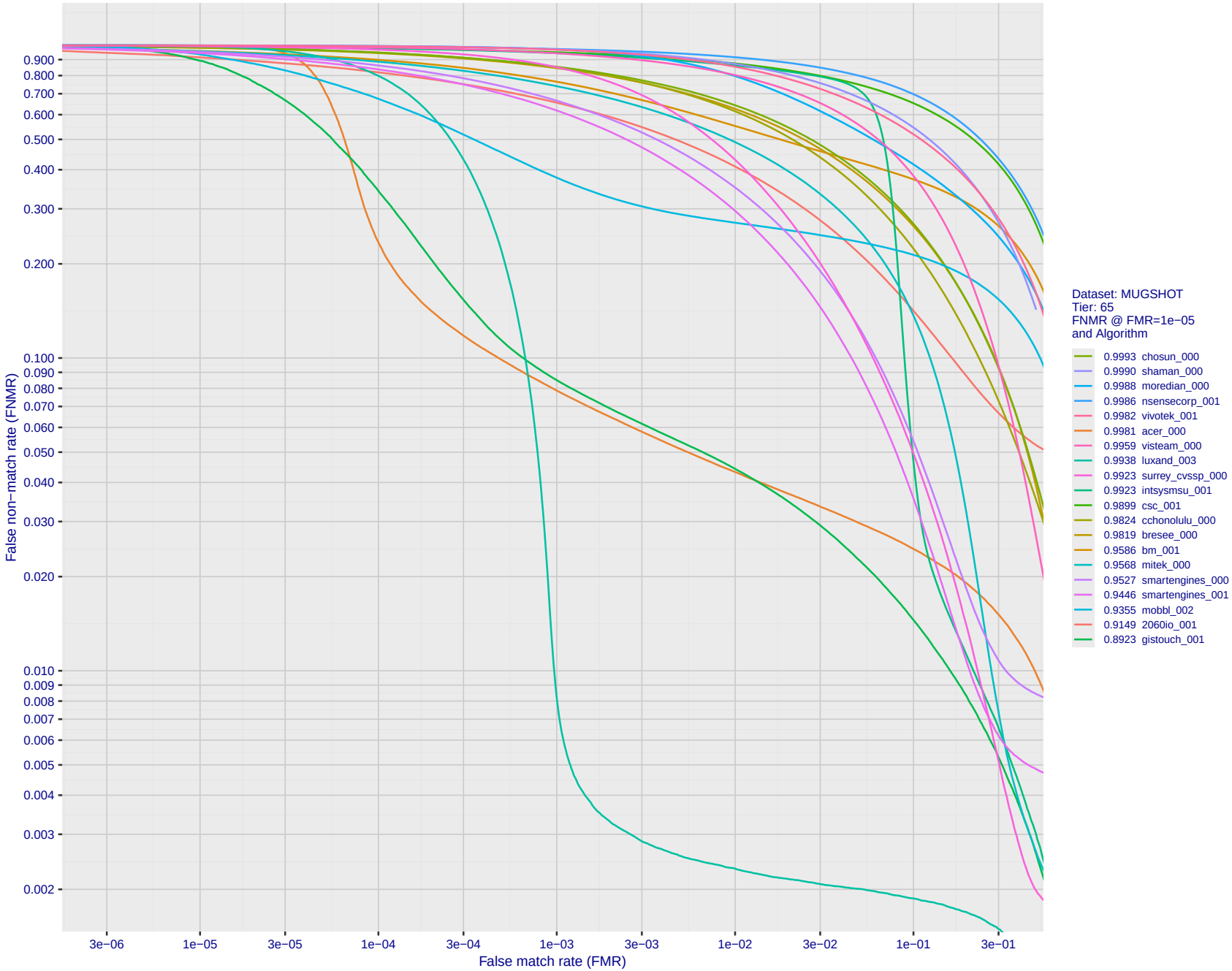

Figure 283: For the mugshot images, detection error tradeoff (DET) characteristics showing false non-match rate vs. false match rate plotted parametrically on threshold, T. The scales are logarithmic in order to show decades of FMR.

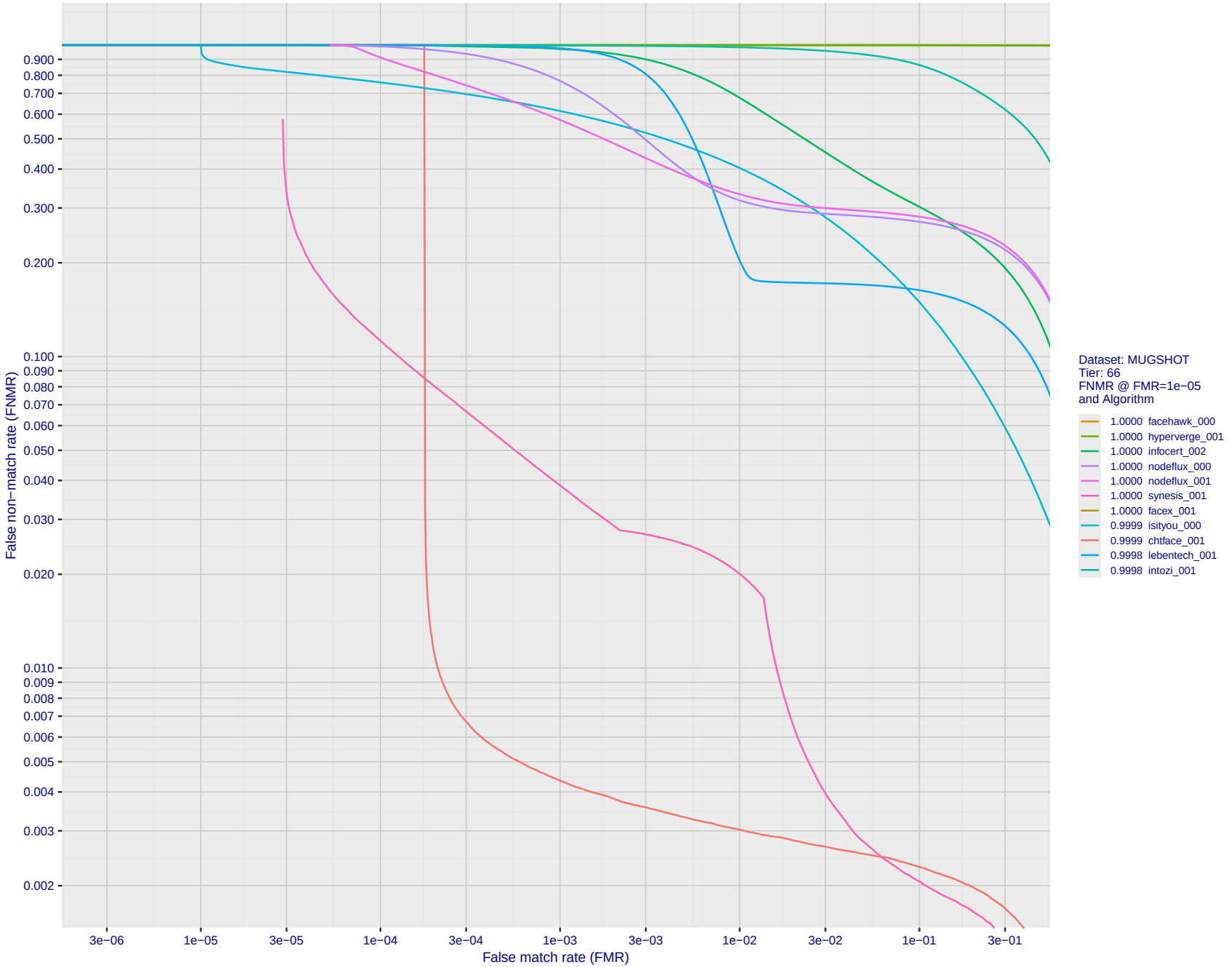

Figure 284: For the mugshot images, detection error tradeoff (DET) characteristics showing false non-match rate vs. false match rate plotted parametrically on threshold, T. The scales are logarithmic in order to show decades of FMR.

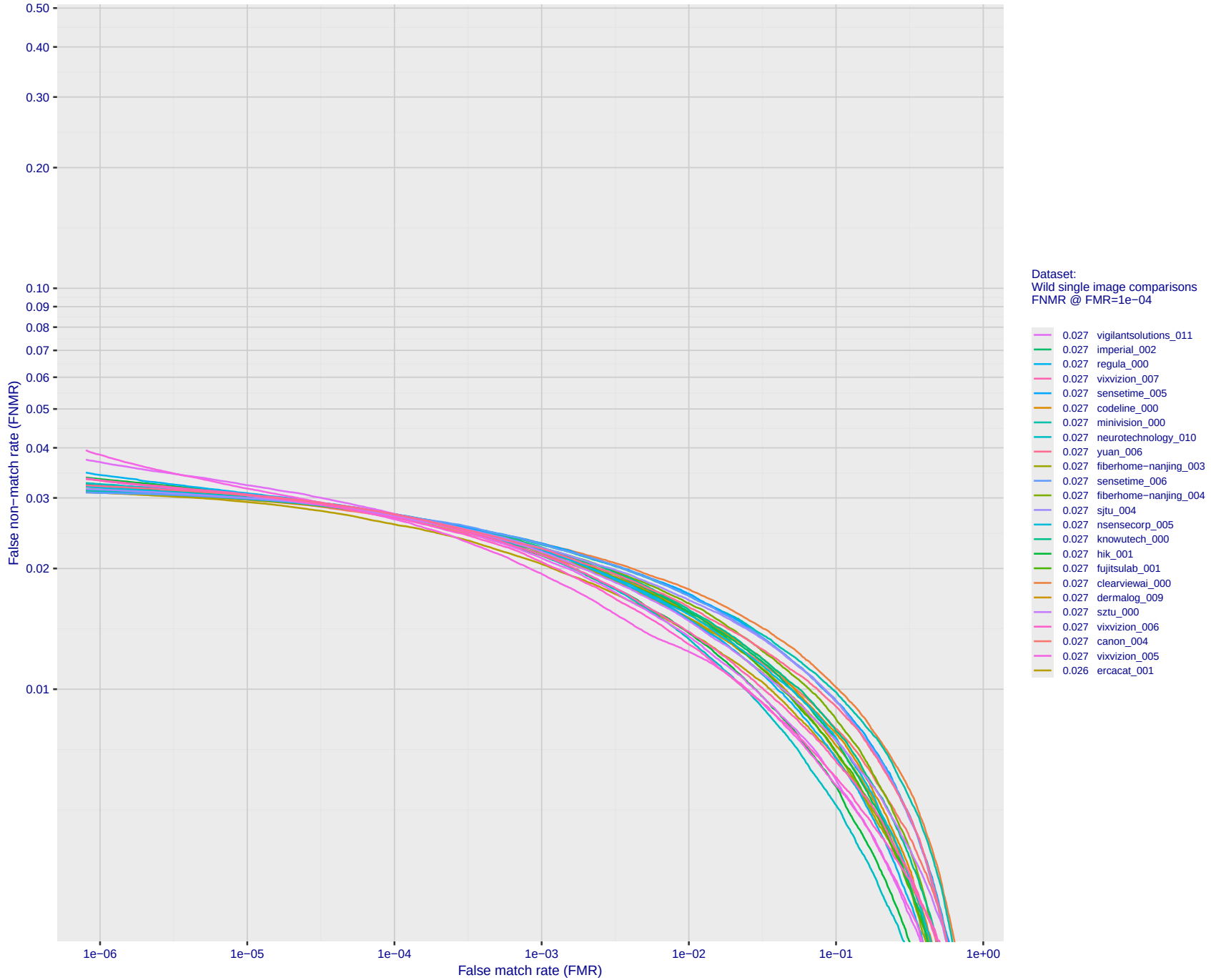

Figure 285: For the 2018 wild image comparisons, detection error tradeoff (DET) characteristics showing false non-match rate vs. false match rate plotted parametrically on threshold, T. The scales are logarithmic in order to show several decades of FMR.

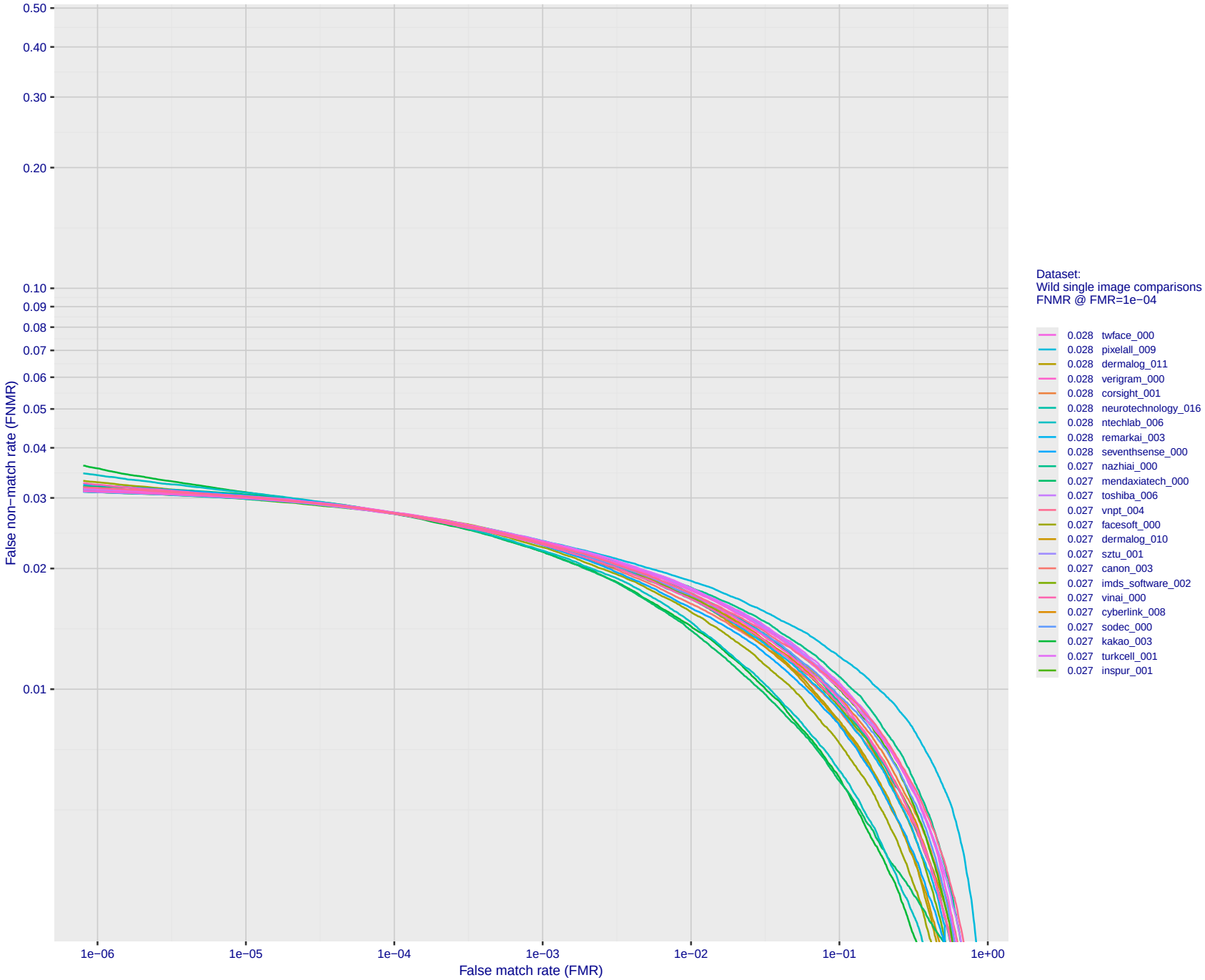

Figure 286: For the 2018 wild image comparisons, detection error tradeoff (DET) characteristics showing false non-match rate vs. false match rate plotted parametrically on threshold, T. The scales are logarithmic in order to show several decades of FMR.

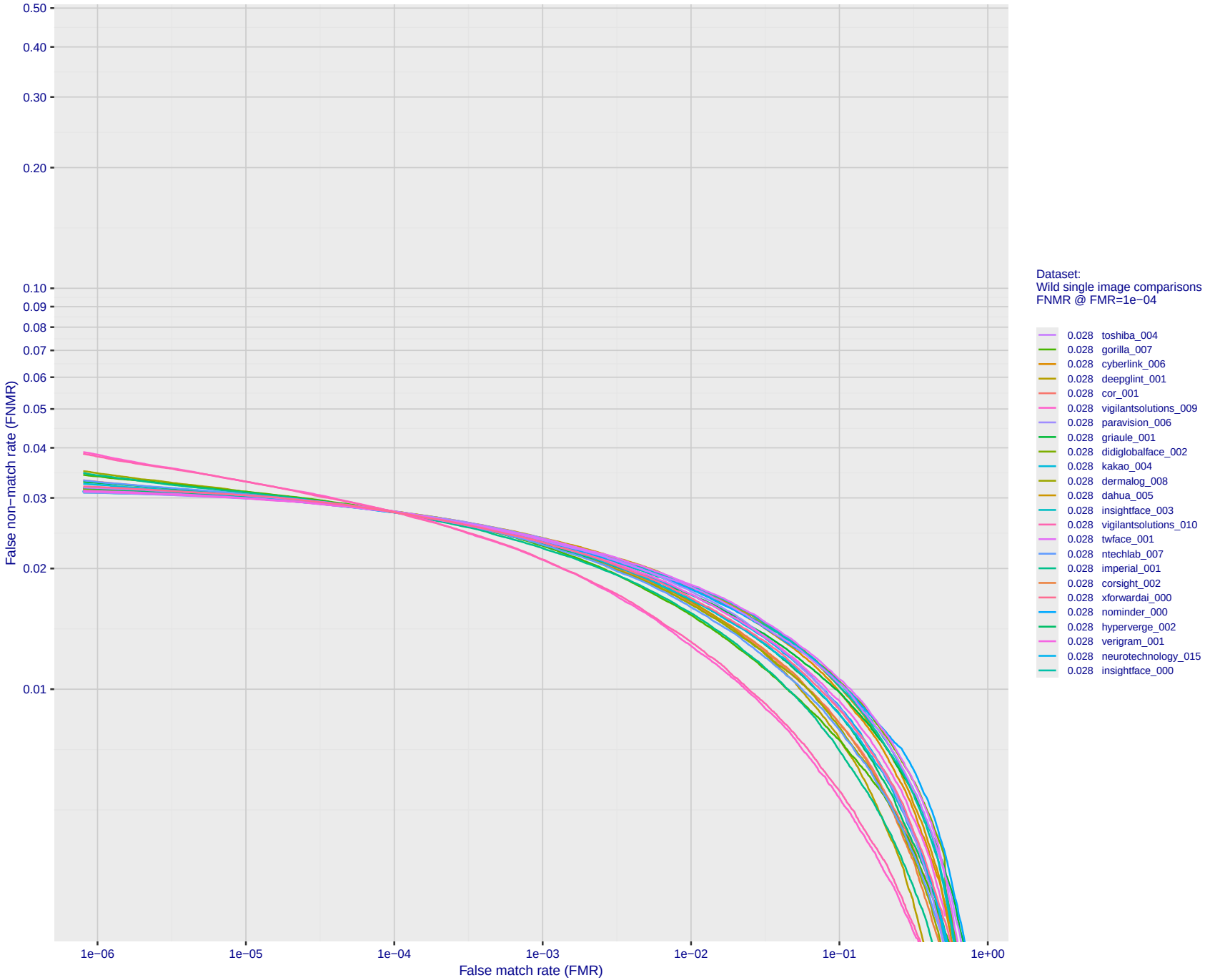

Figure 287: For the 2018 wild image comparisons, detection error tradeoff (DET) characteristics showing false non-match rate vs. false match rate plotted parametrically on threshold, T. The scales are logarithmic in order to show several decades of FMR.

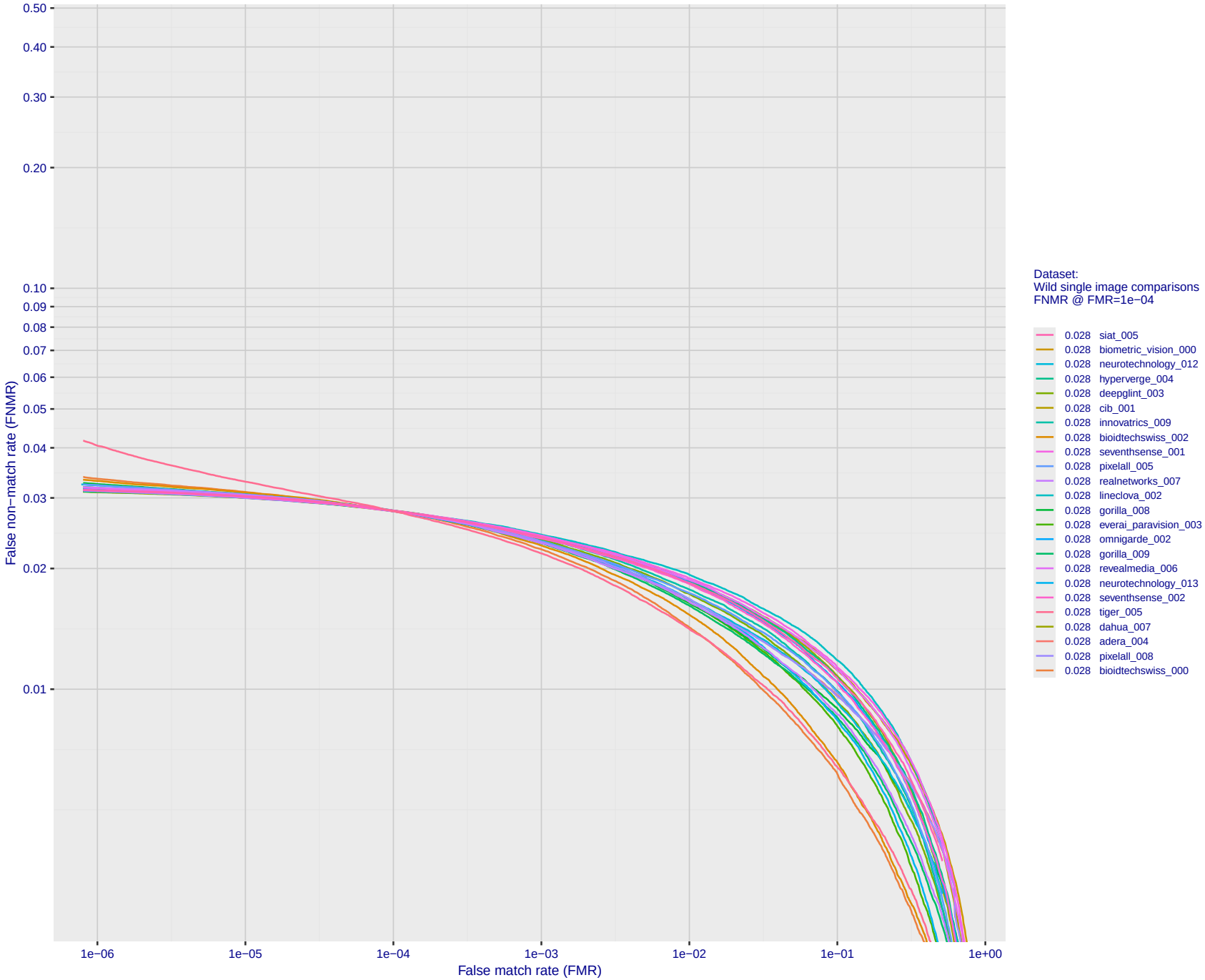

Figure 288: For the 2018 wild image comparisons, detection error tradeoff (DET) characteristics showing false non-match rate vs. false match rate plotted parametrically on threshold, T. The scales are logarithmic in order to show several decades of FMR.

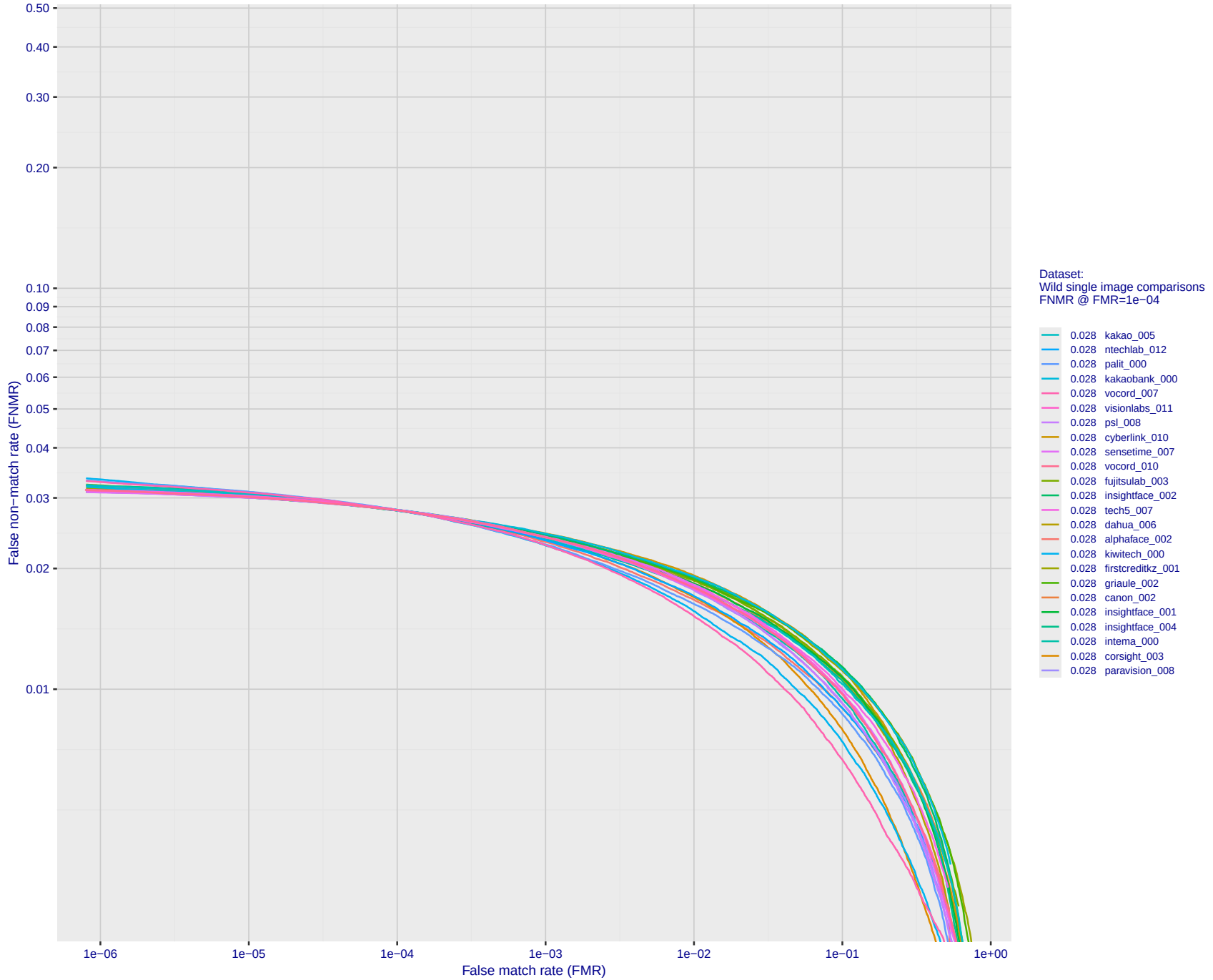

Figure 289: For the 2018 wild image comparisons, detection error tradeoff (DET) characteristics showing false non-match rate vs. false match rate plotted parametrically on threshold, T. The scales are logarithmic in order to show several decades of FMR.

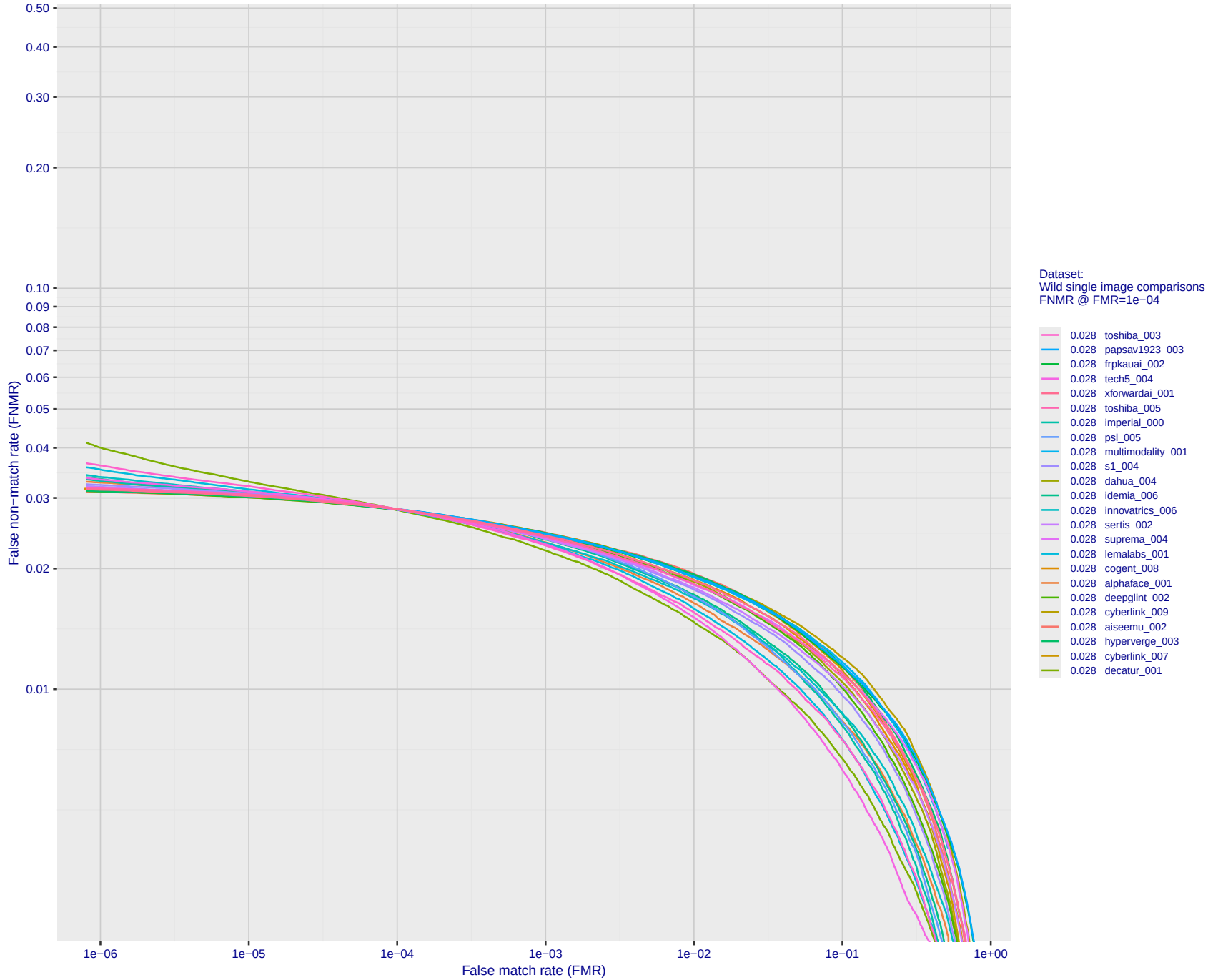

Figure 290: For the 2018 wild image comparisons, detection error tradeoff (DET) characteristics showing false non-match rate vs. false match rate plotted parametrically on threshold, T. The scales are logarithmic in order to show several decades of FMR.

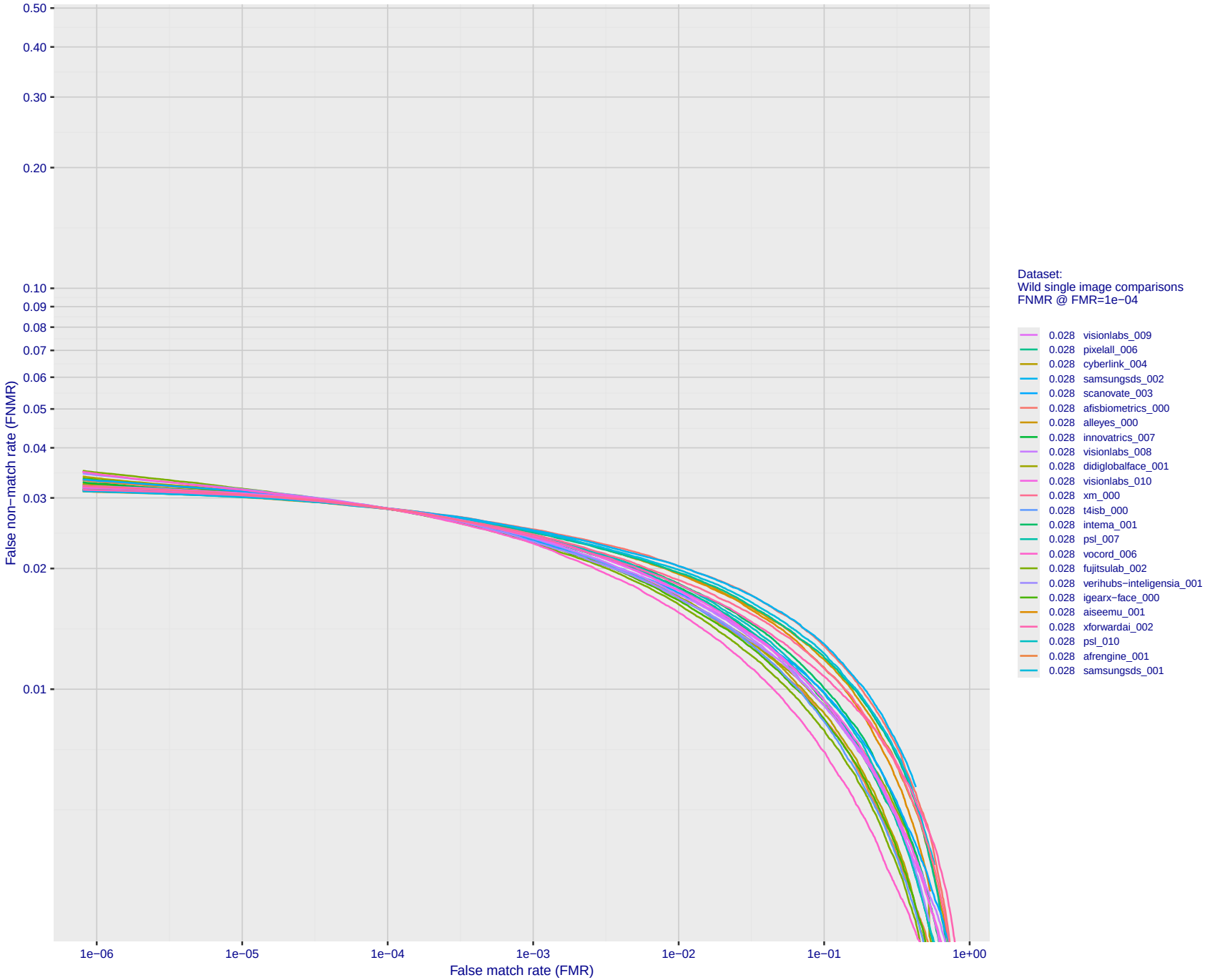

Figure 291: For the 2018 wild image comparisons, detection error tradeoff (DET) characteristics showing false non-match rate vs. false match rate plotted parametrically on threshold, T. The scales are logarithmic in order to show several decades of FMR.

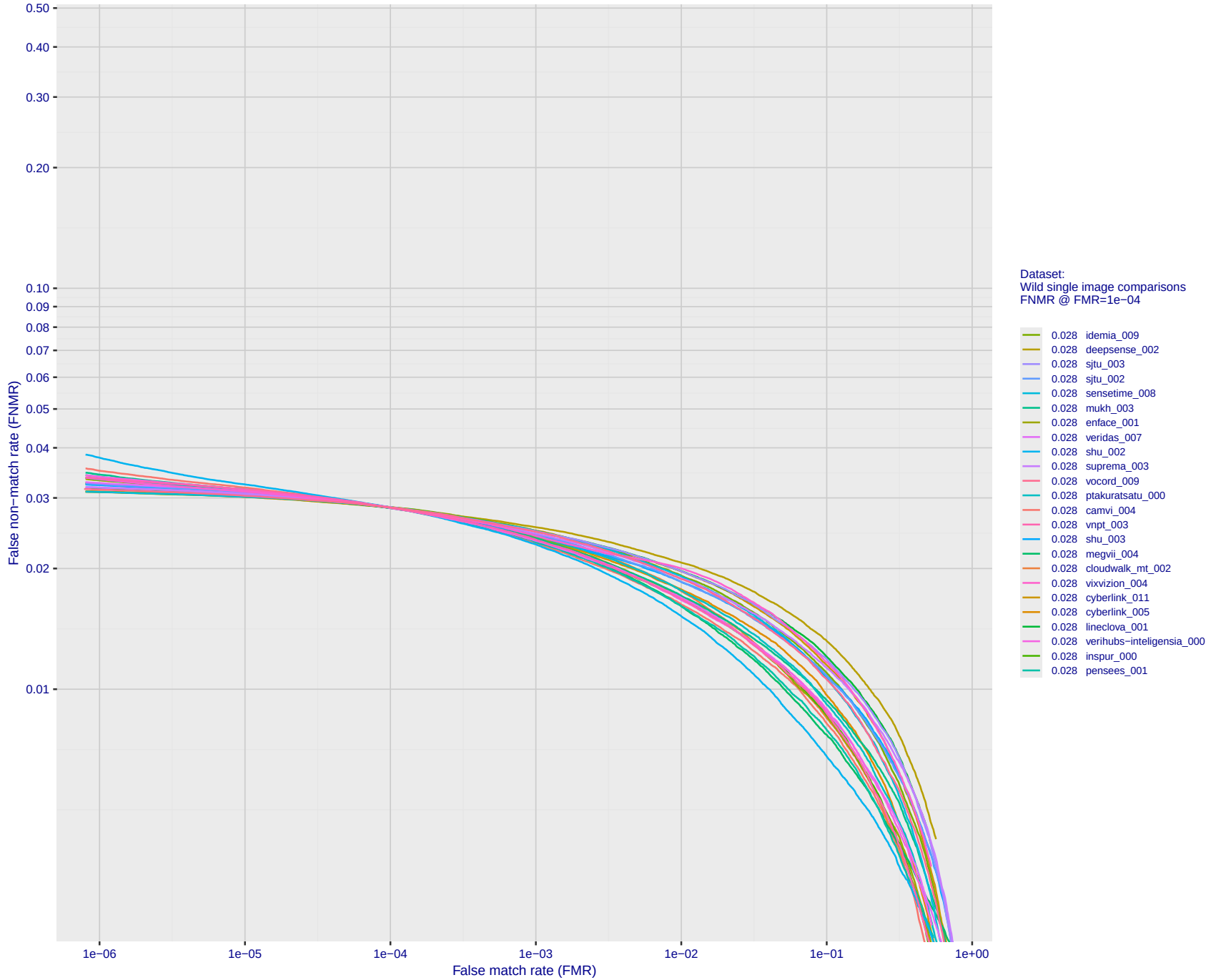

Figure 292: For the 2018 wild image comparisons, detection error tradeoff (DET) characteristics showing false non-match rate vs. false match rate plotted parametrically on threshold, T. The scales are logarithmic in order to show several decades of FMR.

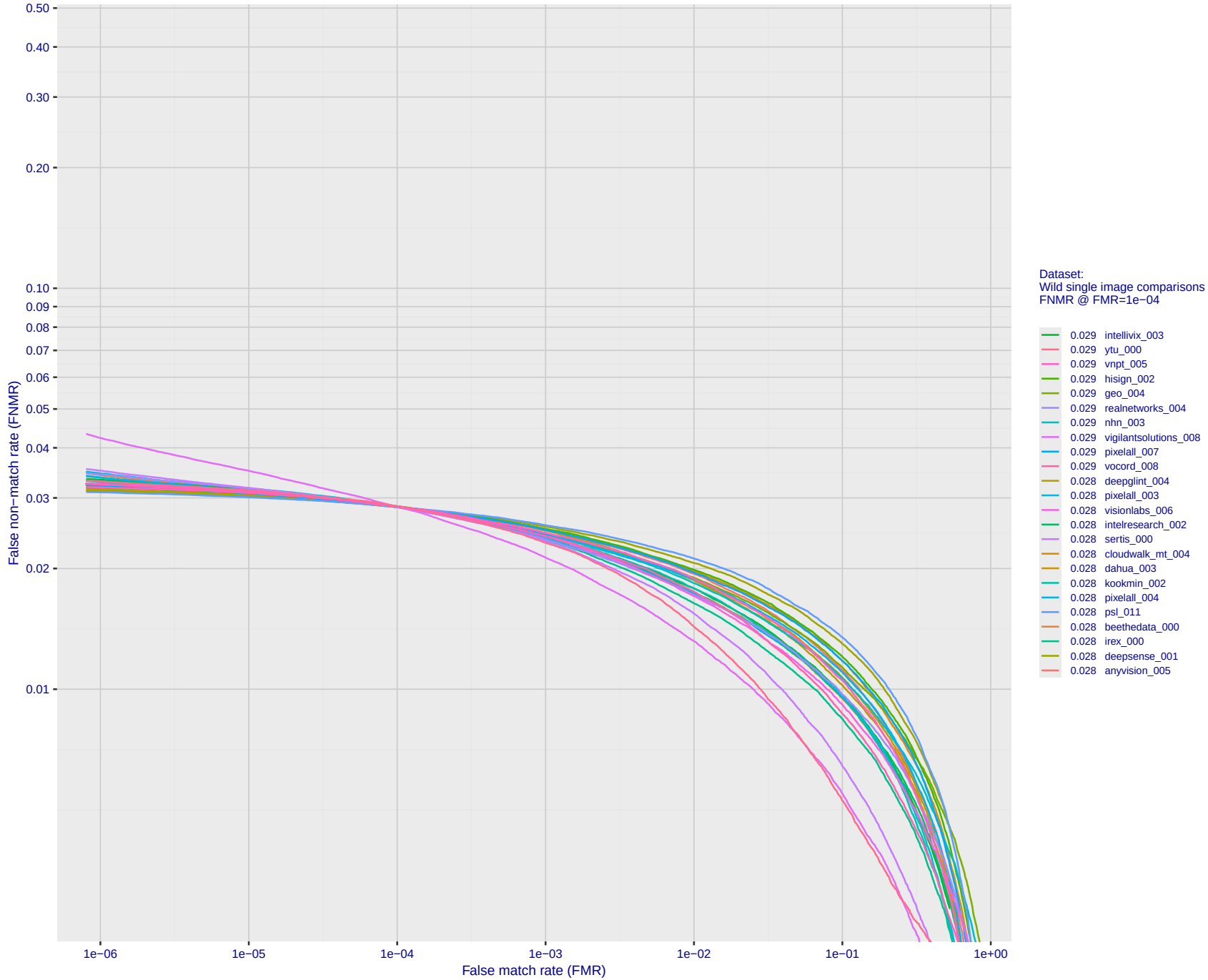

Figure 293: For the 2018 wild image comparisons, detection error tradeoff (DET) characteristics showing false non-match rate vs. false match rate plotted parametrically on threshold, T. The scales are logarithmic in order to show several decades of FMR.

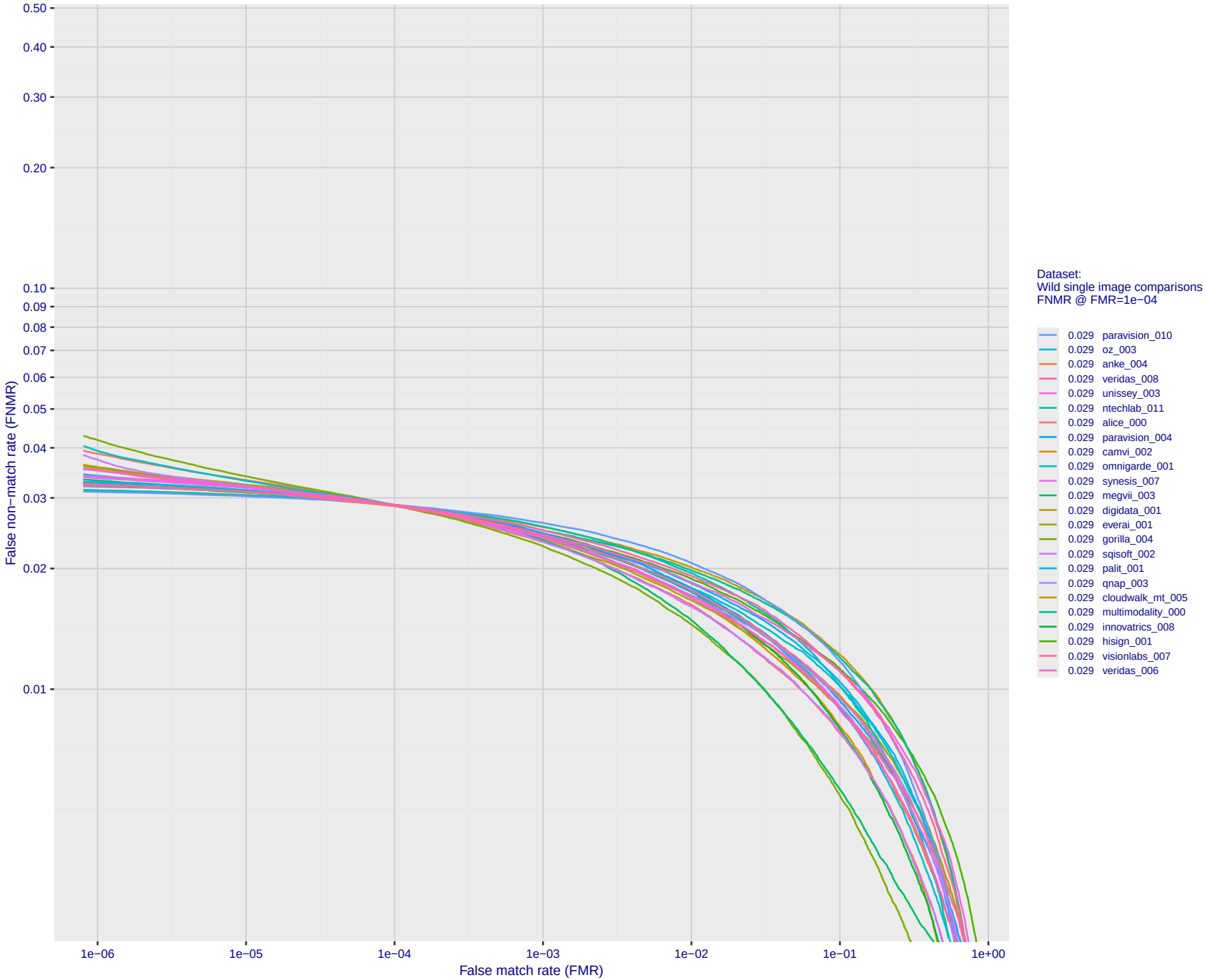

Figure 294: For the 2018 wild image comparisons, detection error tradeoff (DET) characteristics showing false non-match rate vs. false match rate plotted parametrically on threshold, T. The scales are logarithmic in order to show several decades of FMR.

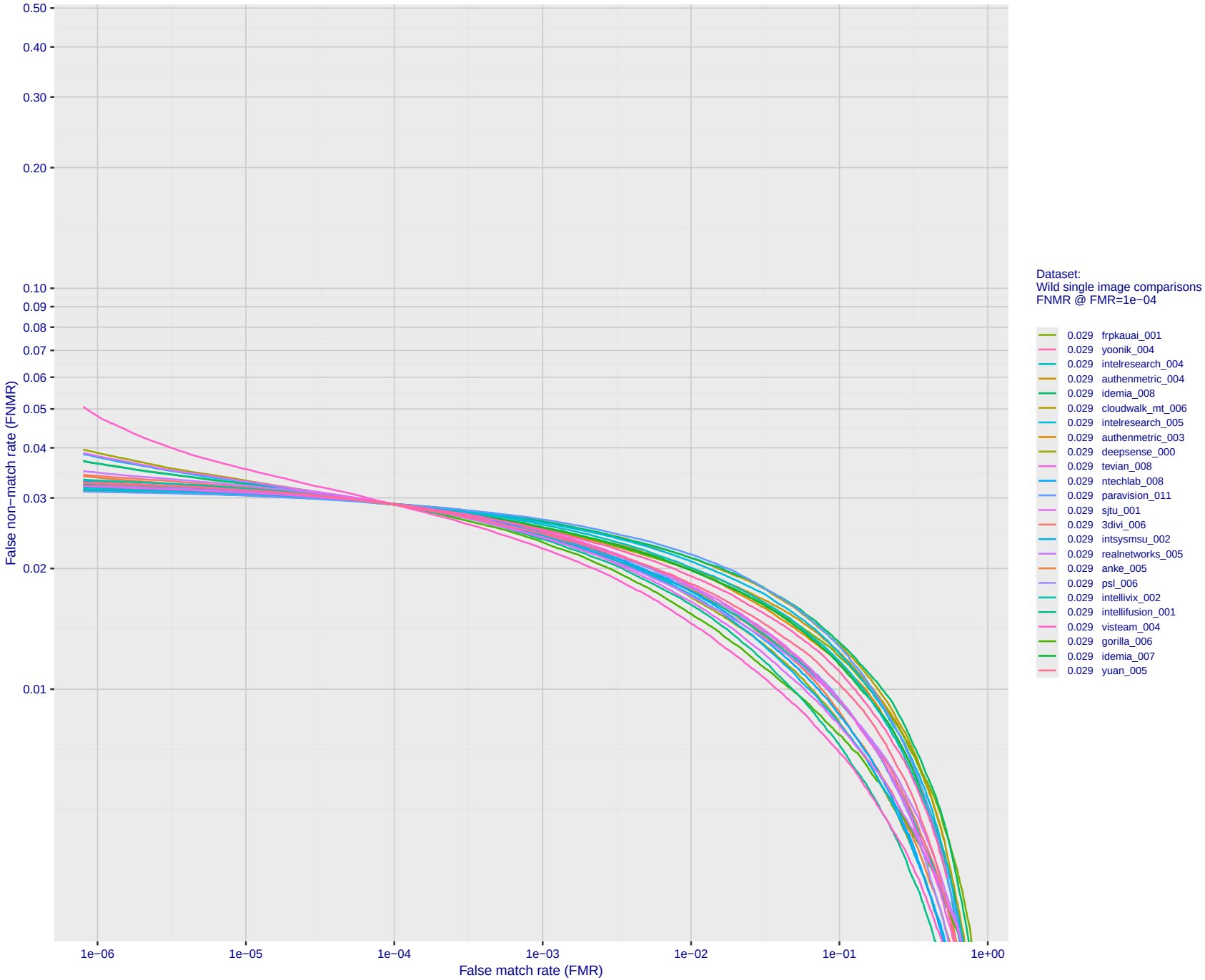

Figure 295: For the 2018 wild image comparisons, detection error tradeoff (DET) characteristics showing false non-match rate vs. false match rate plotted parametrically on threshold, T. The scales are logarithmic in order to show several decades of FMR.

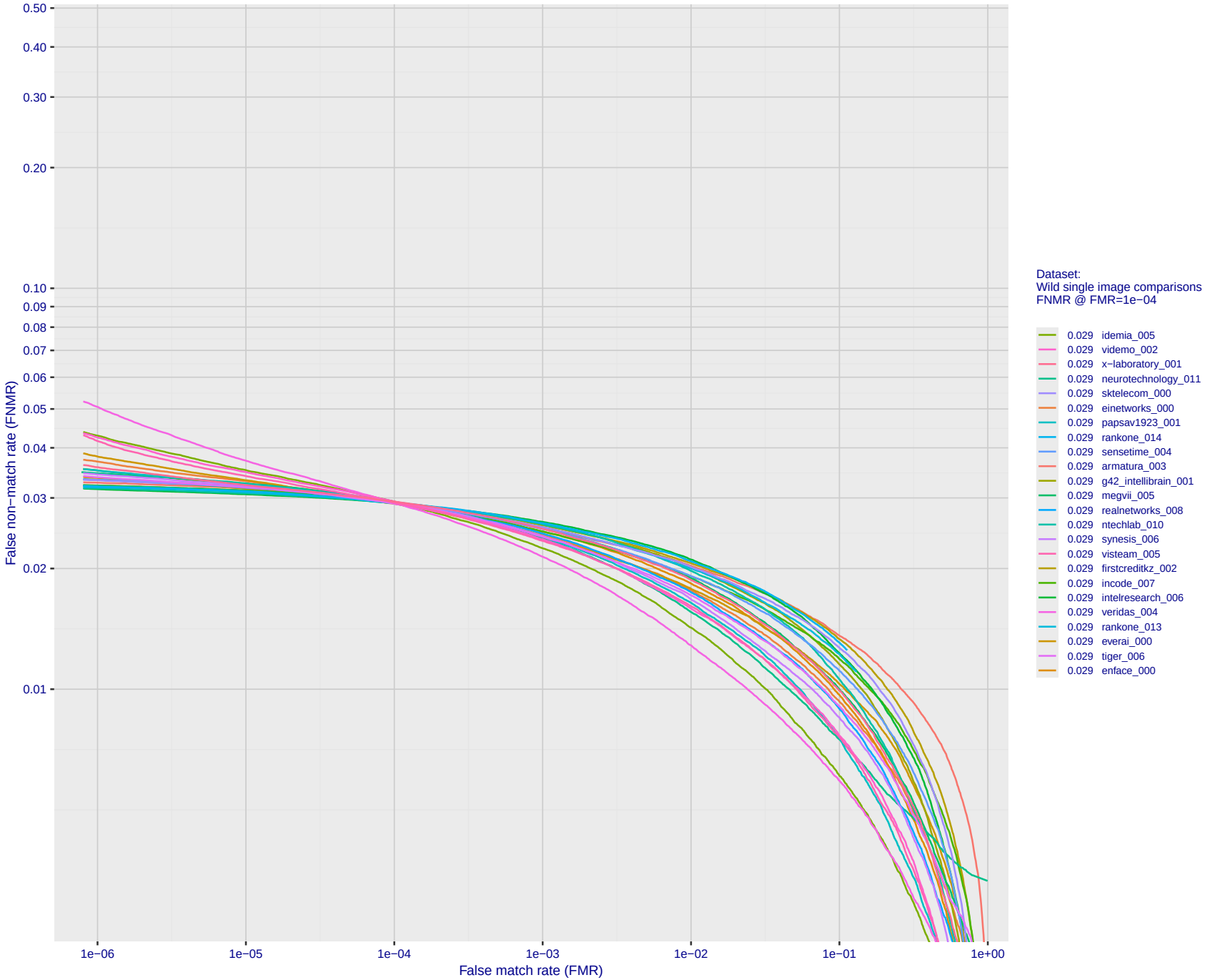

Figure 296: For the 2018 wild image comparisons, detection error tradeoff (DET) characteristics showing false non-match rate vs. false match rate plotted parametrically on threshold, T. The scales are logarithmic in order to show several decades of FMR.

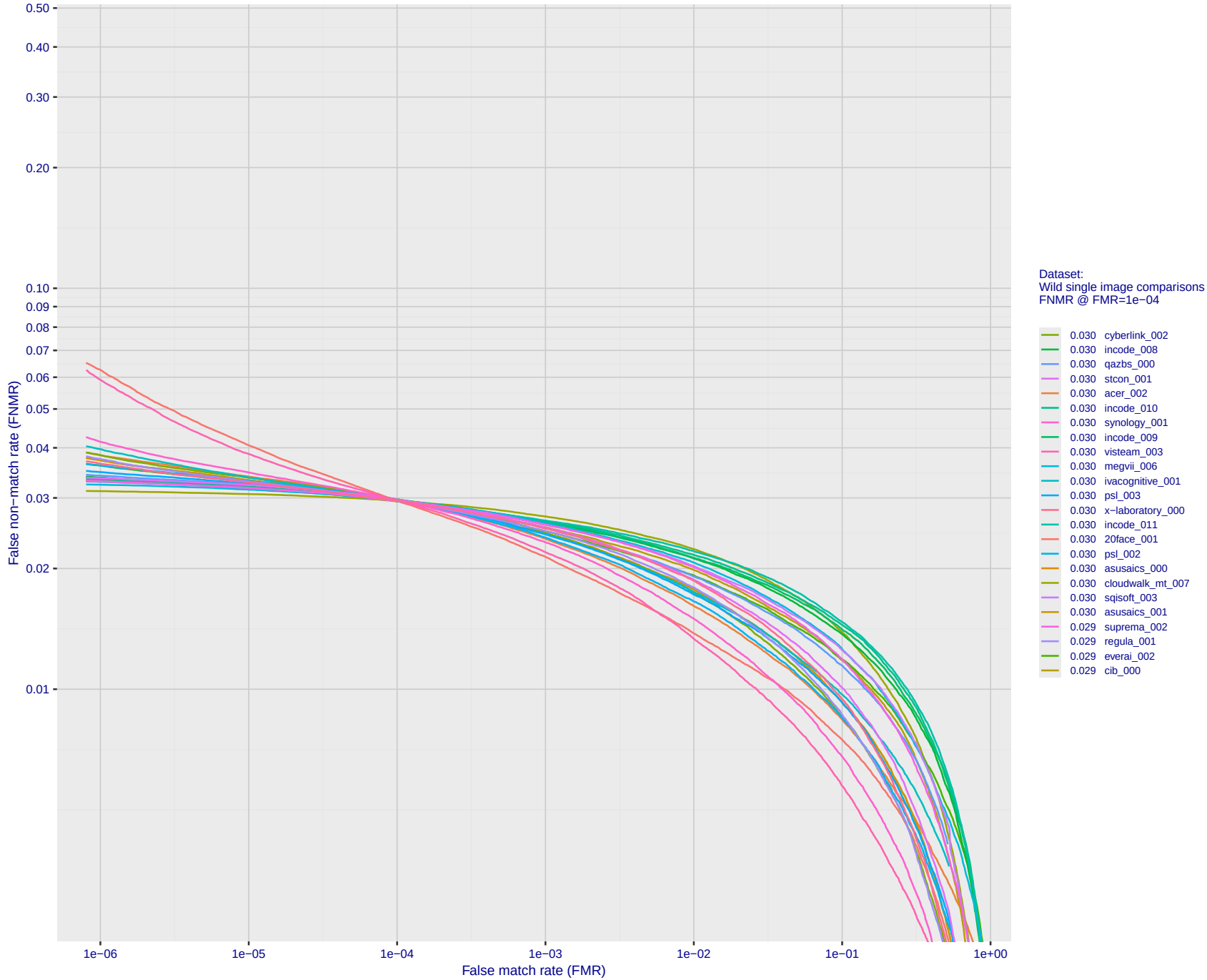

Figure 297: For the 2018 wild image comparisons, detection error tradeoff (DET) characteristics showing false non-match rate vs. false match rate plotted parametrically on threshold, T. The scales are logarithmic in order to show several decades of FMR.

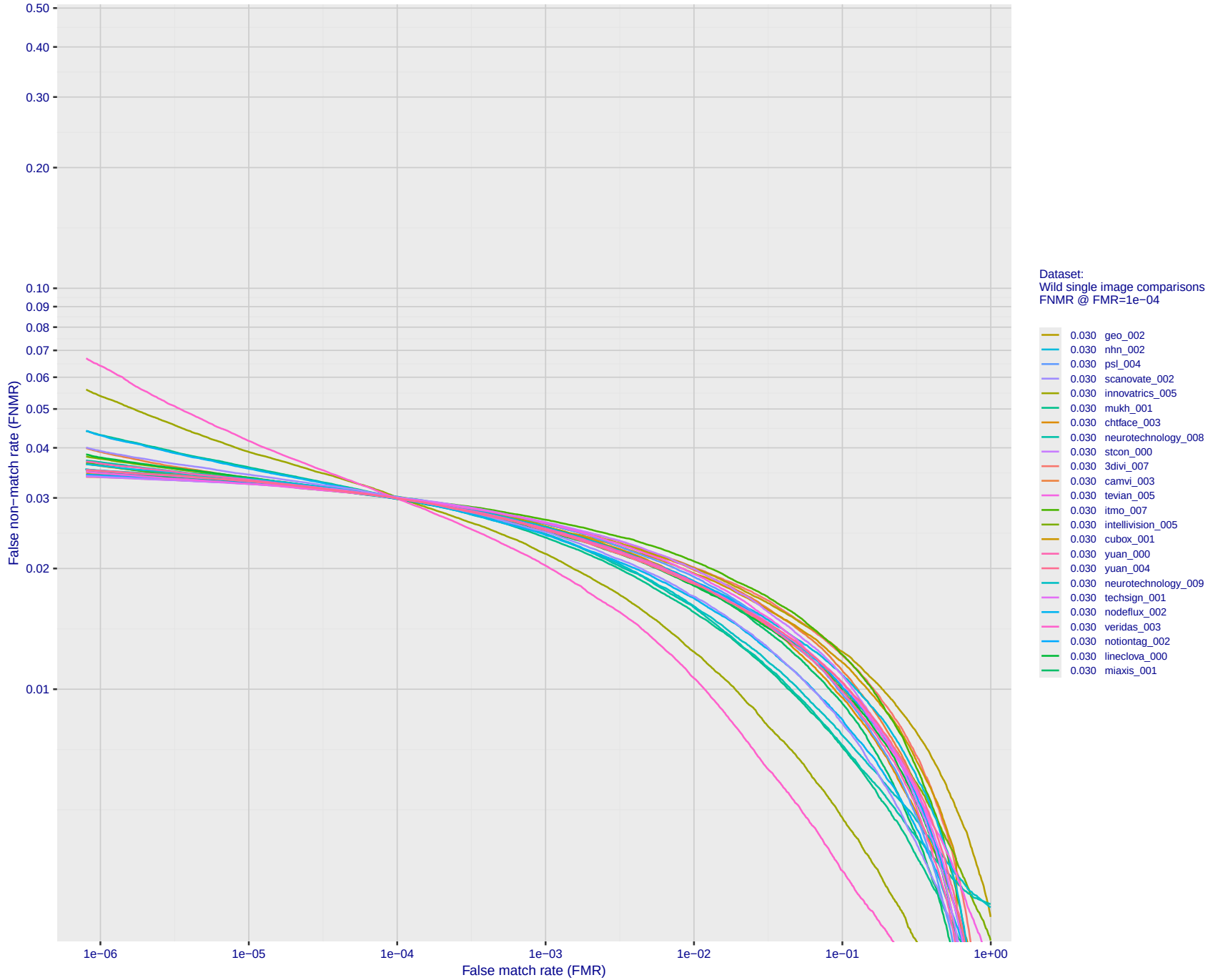

Figure 298: For the 2018 wild image comparisons, detection error tradeoff (DET) characteristics showing false non-match rate vs. false match rate plotted parametrically on threshold, T. The scales are logarithmic in order to show several decades of FMR.

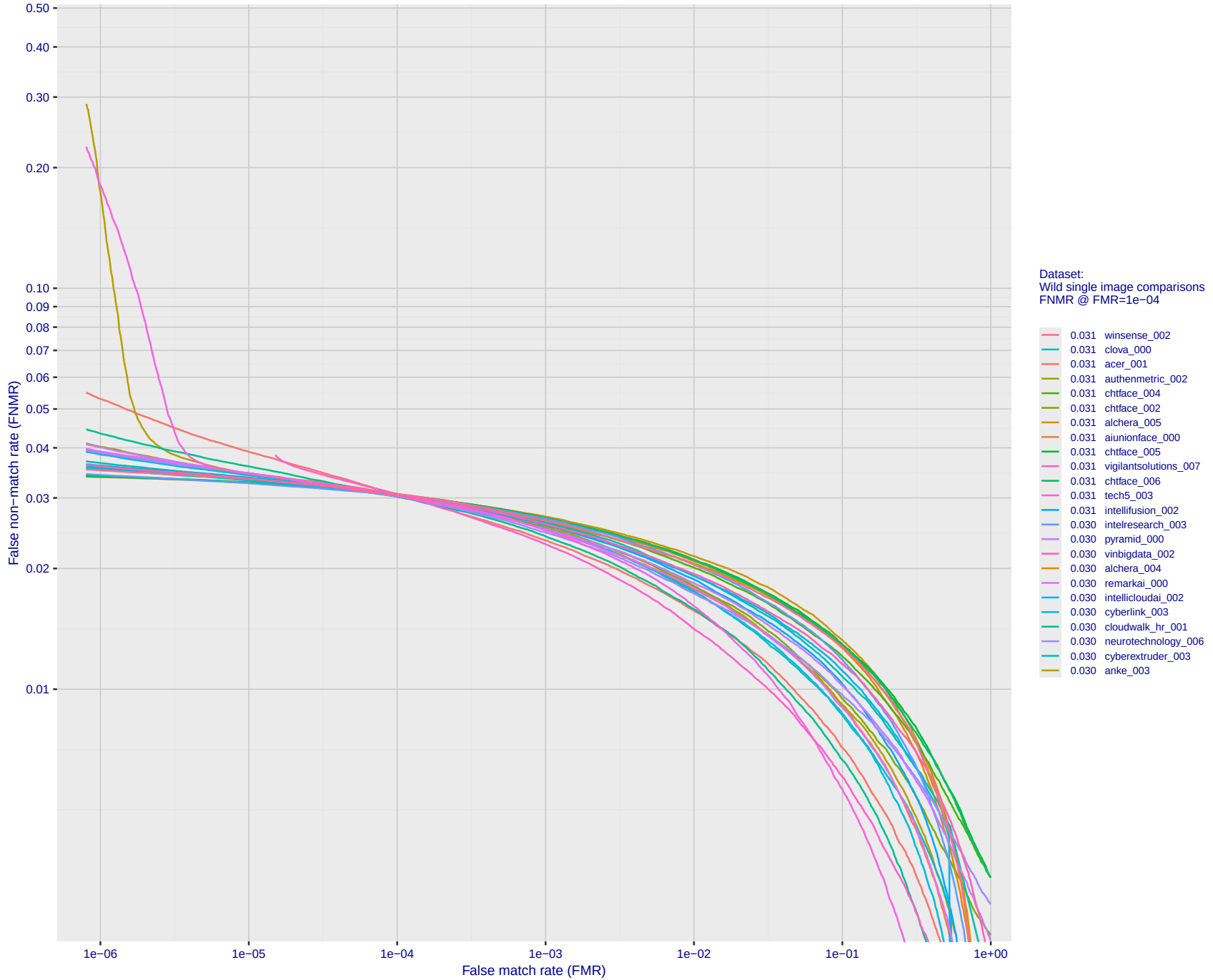

Figure 299: For the 2018 wild image comparisons, detection error tradeoff (DET) characteristics showing false non-match rate vs. false match rate plotted parametrically on threshold, T. The scales are logarithmic in order to show several decades of FMR.

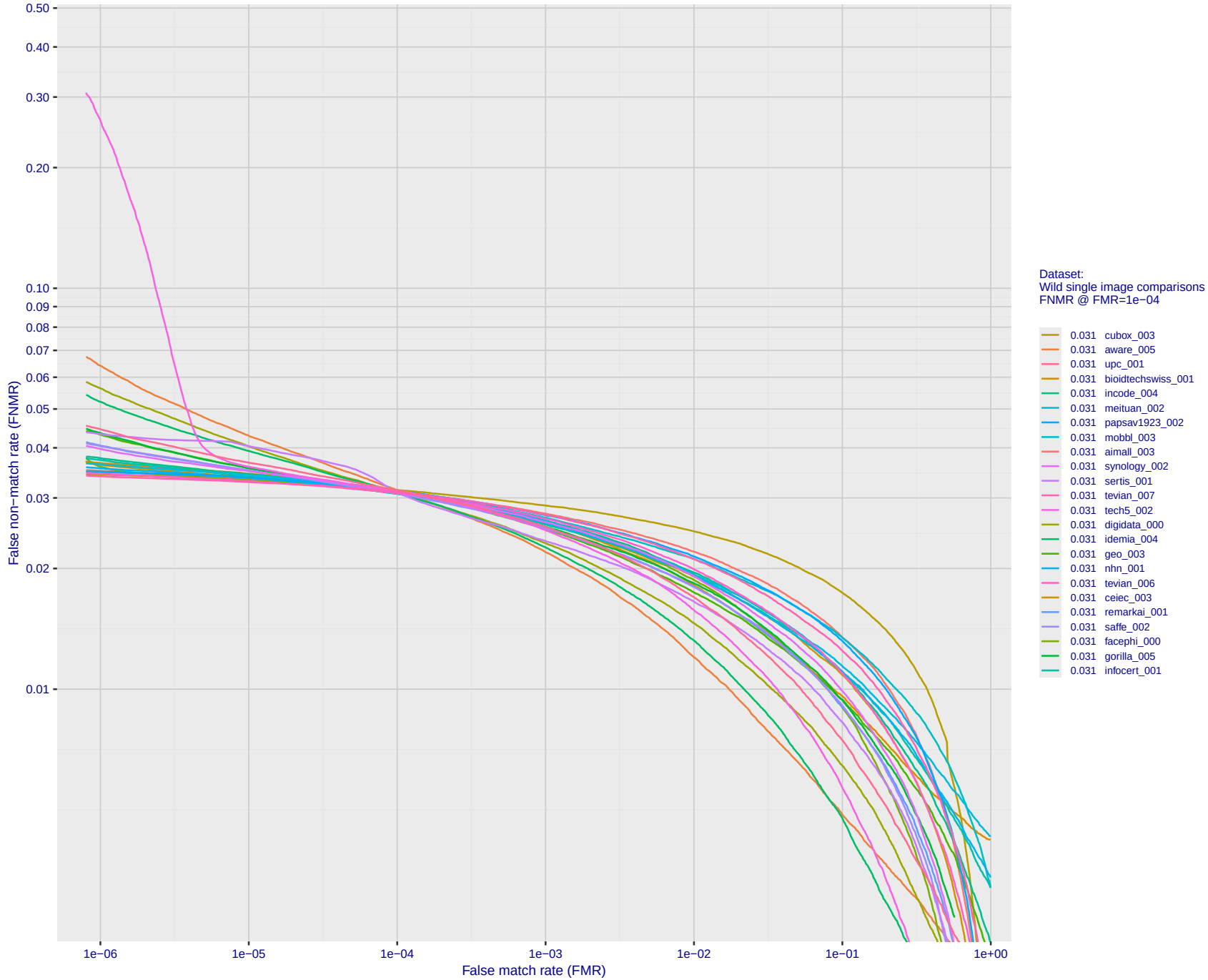

Figure 300: For the 2018 wild image comparisons, detection error tradeoff (DET) characteristics showing false non-match rate vs. false match rate plotted parametrically on threshold, T. The scales are logarithmic in order to show several decades of FMR.

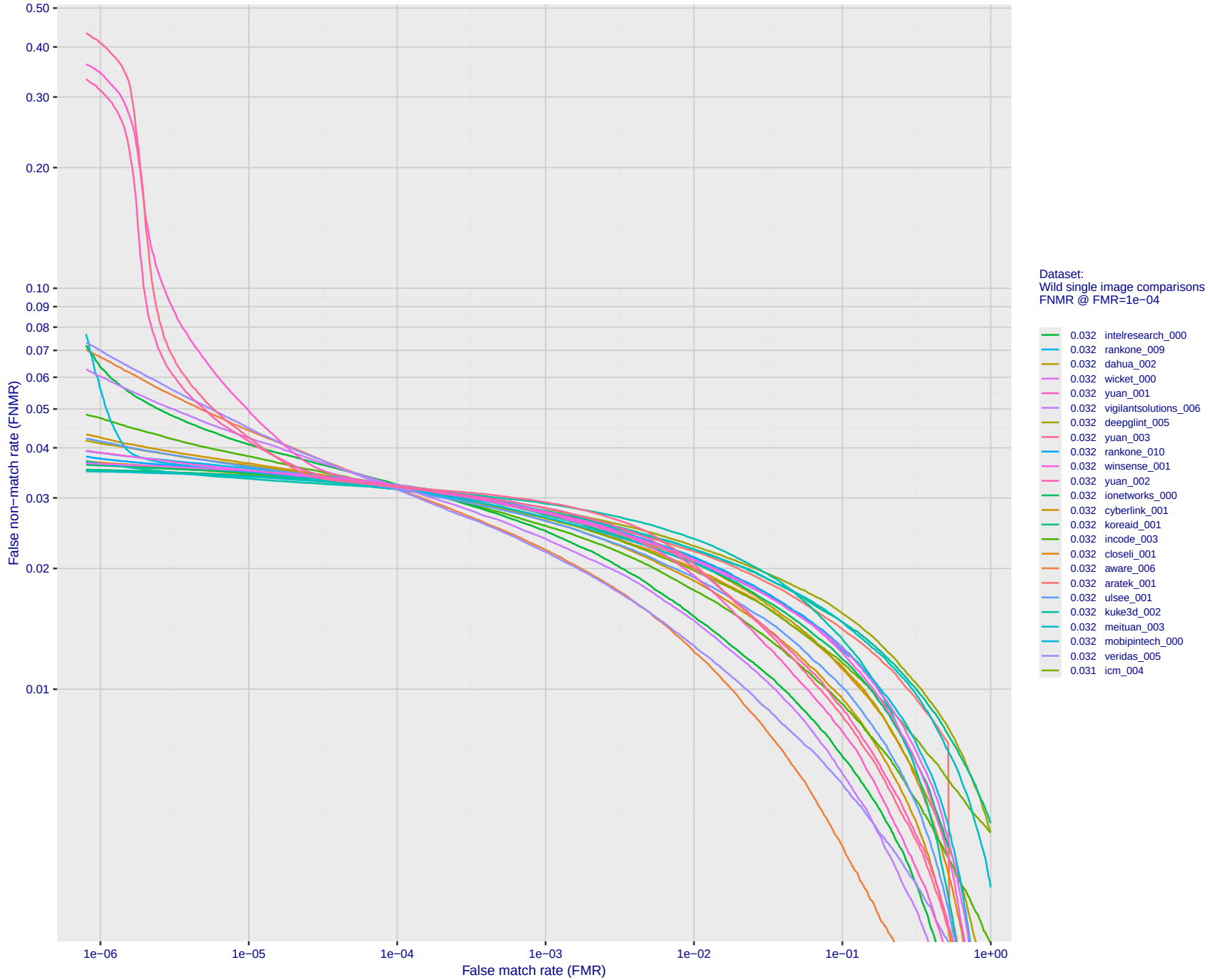

Figure 301: For the 2018 wild image comparisons, detection error tradeoff (DET) characteristics showing false non-match rate vs. false match rate plotted parametrically on threshold, T. The scales are logarithmic in order to show several decades of FMR.

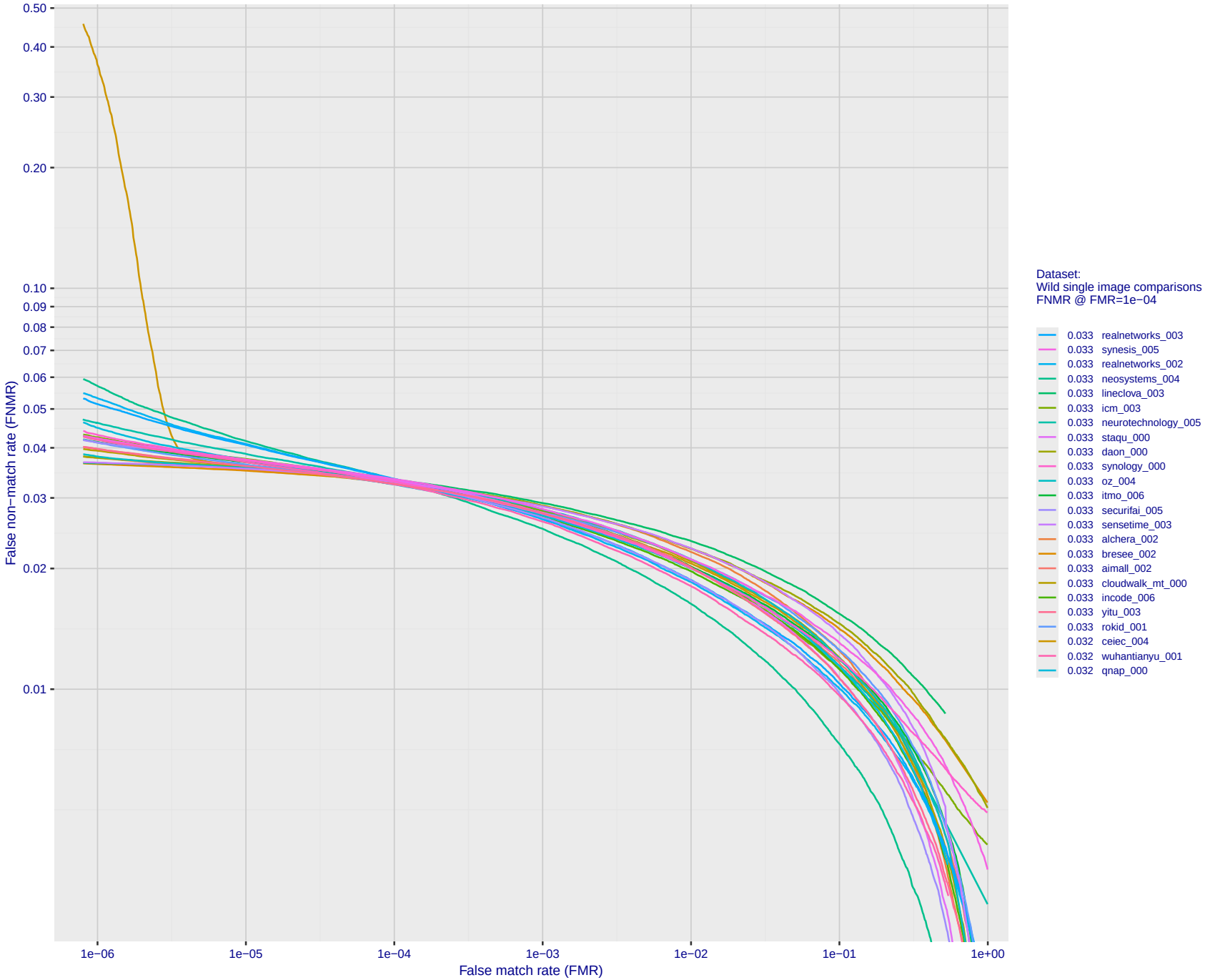

Figure 302: For the 2018 wild image comparisons, detection error tradeoff (DET) characteristics showing false non-match rate vs. false match rate plotted parametrically on threshold, T. The scales are logarithmic in order to show several decades of FMR.

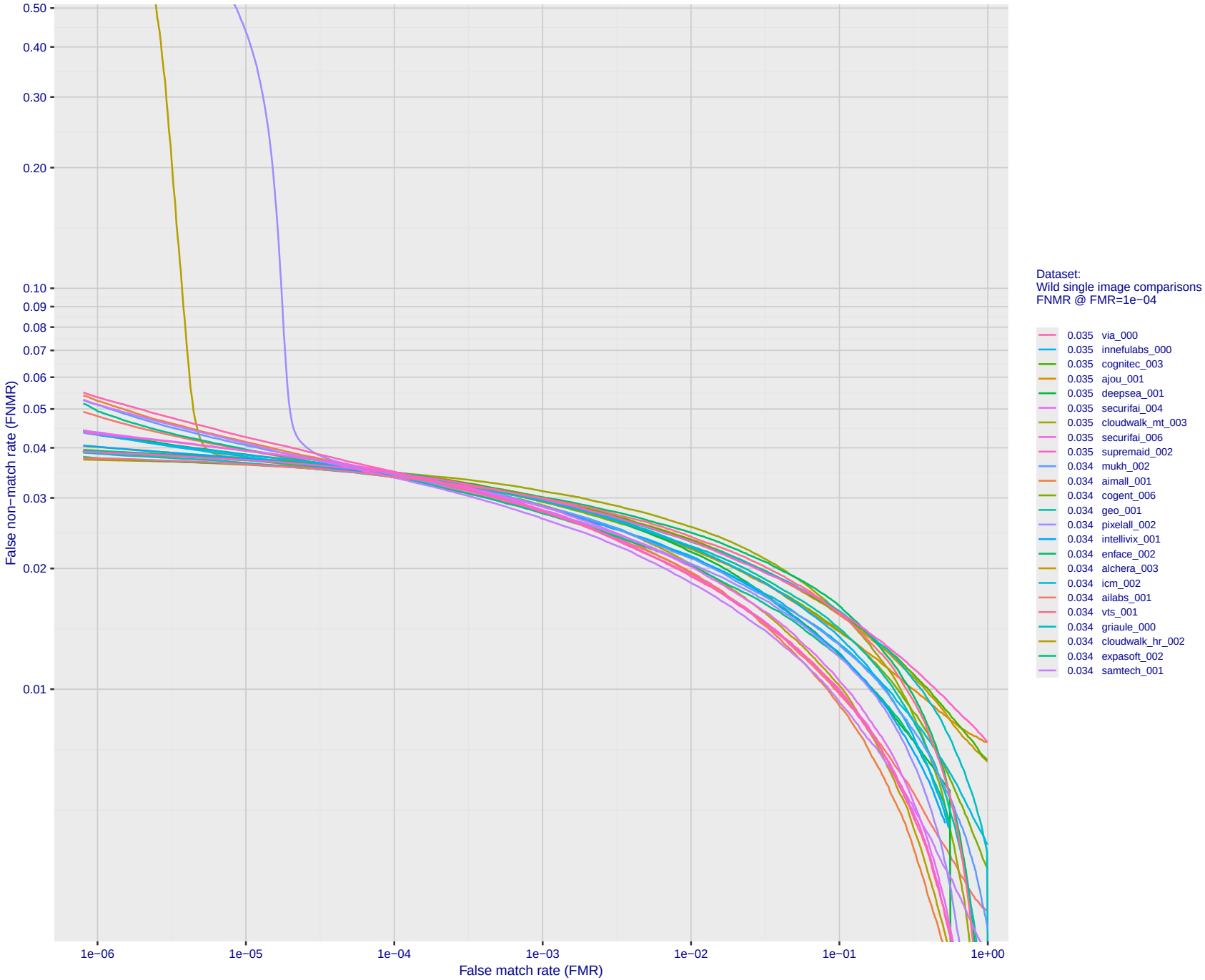

Figure 303: For the 2018 wild image comparisons, detection error tradeoff (DET) characteristics showing false non-match rate vs. false match rate plotted parametrically on threshold, T. The scales are logarithmic in order to show several decades of FMR.

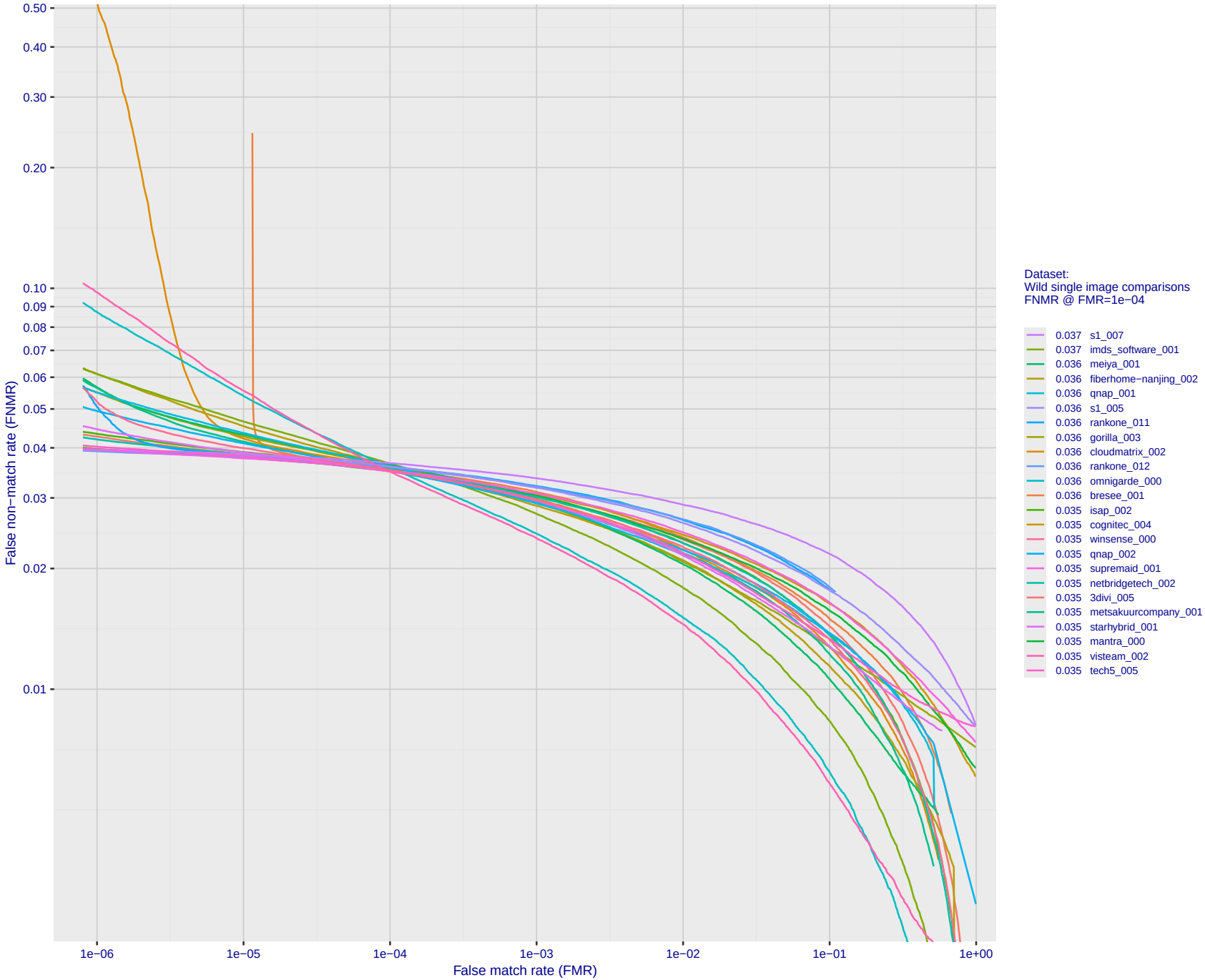

Figure 304: For the 2018 wild image comparisons, detection error tradeoff (DET) characteristics showing false non-match rate vs. false match rate plotted parametrically on threshold, T. The scales are logarithmic in order to show several decades of FMR.

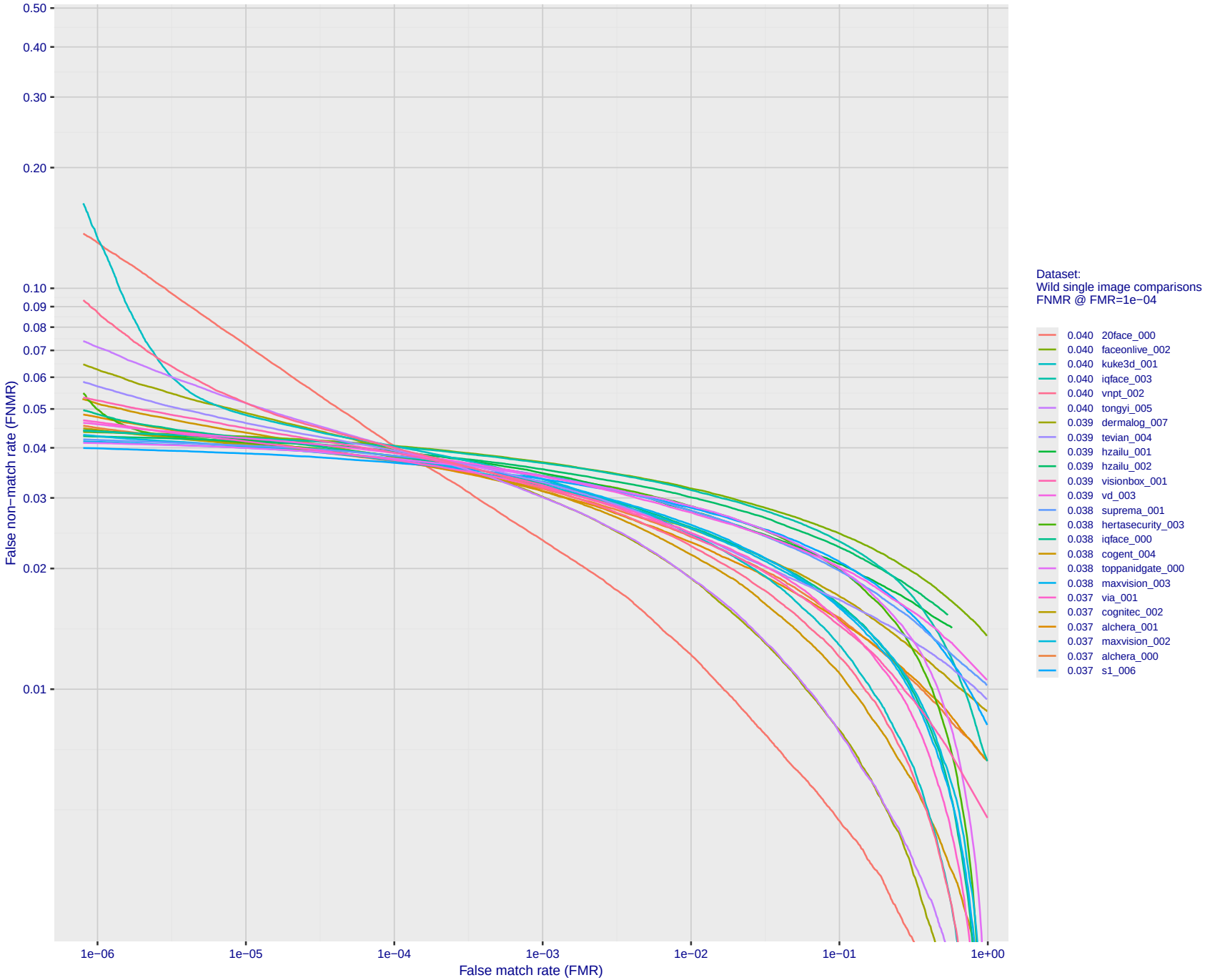

Figure 305: For the 2018 wild image comparisons, detection error tradeoff (DET) characteristics showing false non-match rate vs. false match rate plotted parametrically on threshold, T. The scales are logarithmic in order to show several decades of FMR.

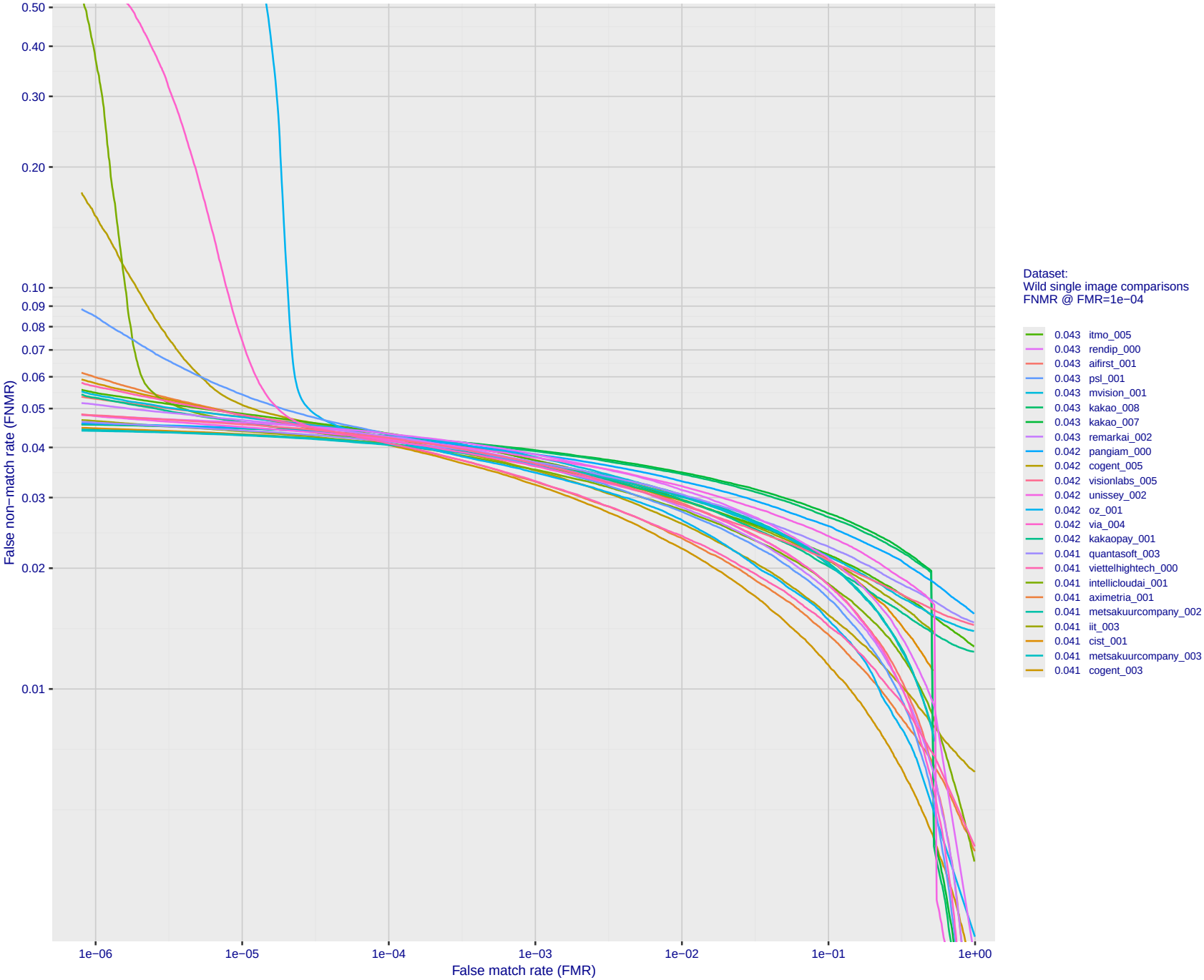

Figure 306: For the 2018 wild image comparisons, detection error tradeoff (DET) characteristics showing false non-match rate vs. false match rate plotted parametrically on threshold, T. The scales are logarithmic in order to show several decades of FMR.

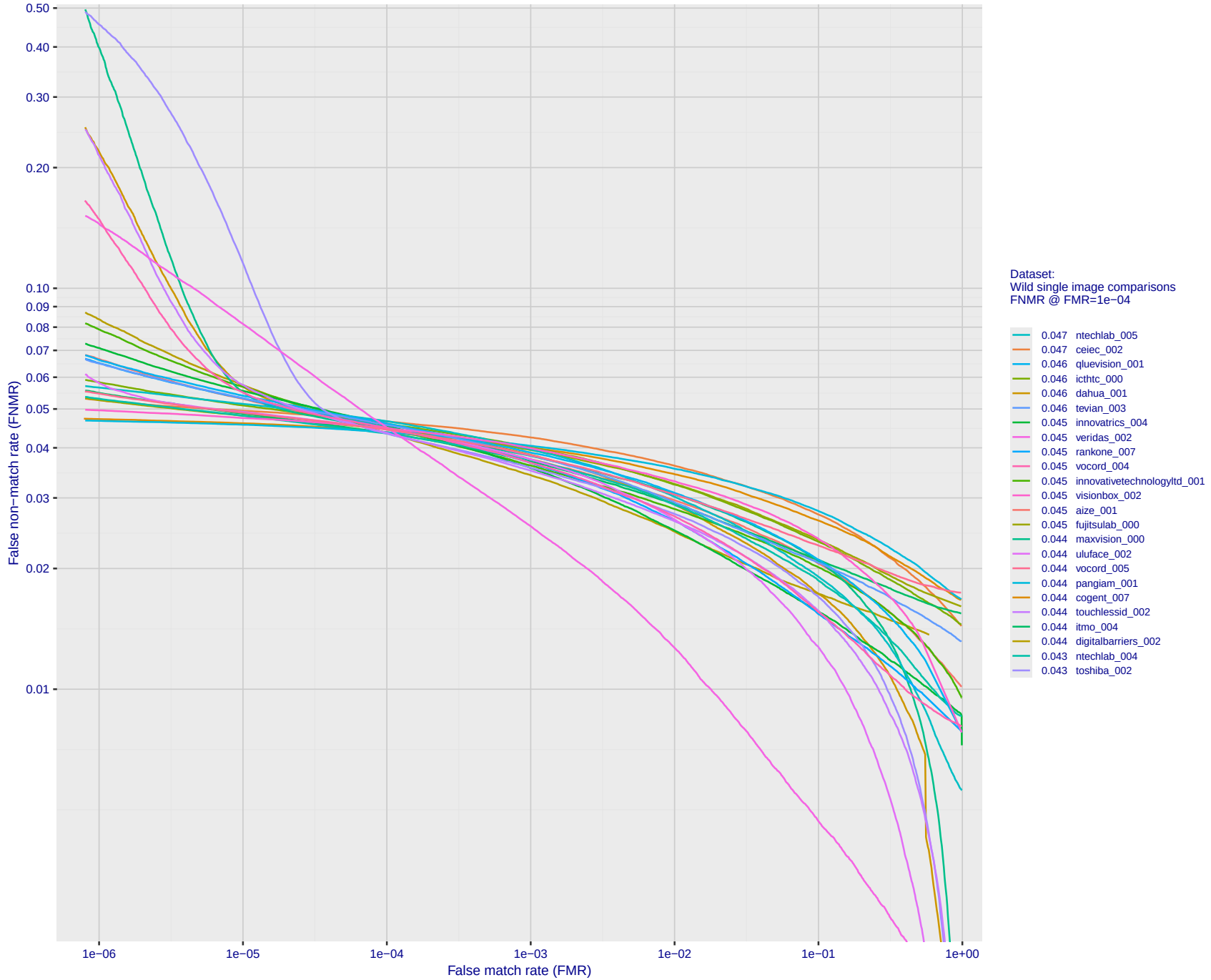

Figure 307: For the 2018 wild image comparisons, detection error tradeoff (DET) characteristics showing false non-match rate vs. false match rate plotted parametrically on threshold, T. The scales are logarithmic in order to show several decades of FMR.

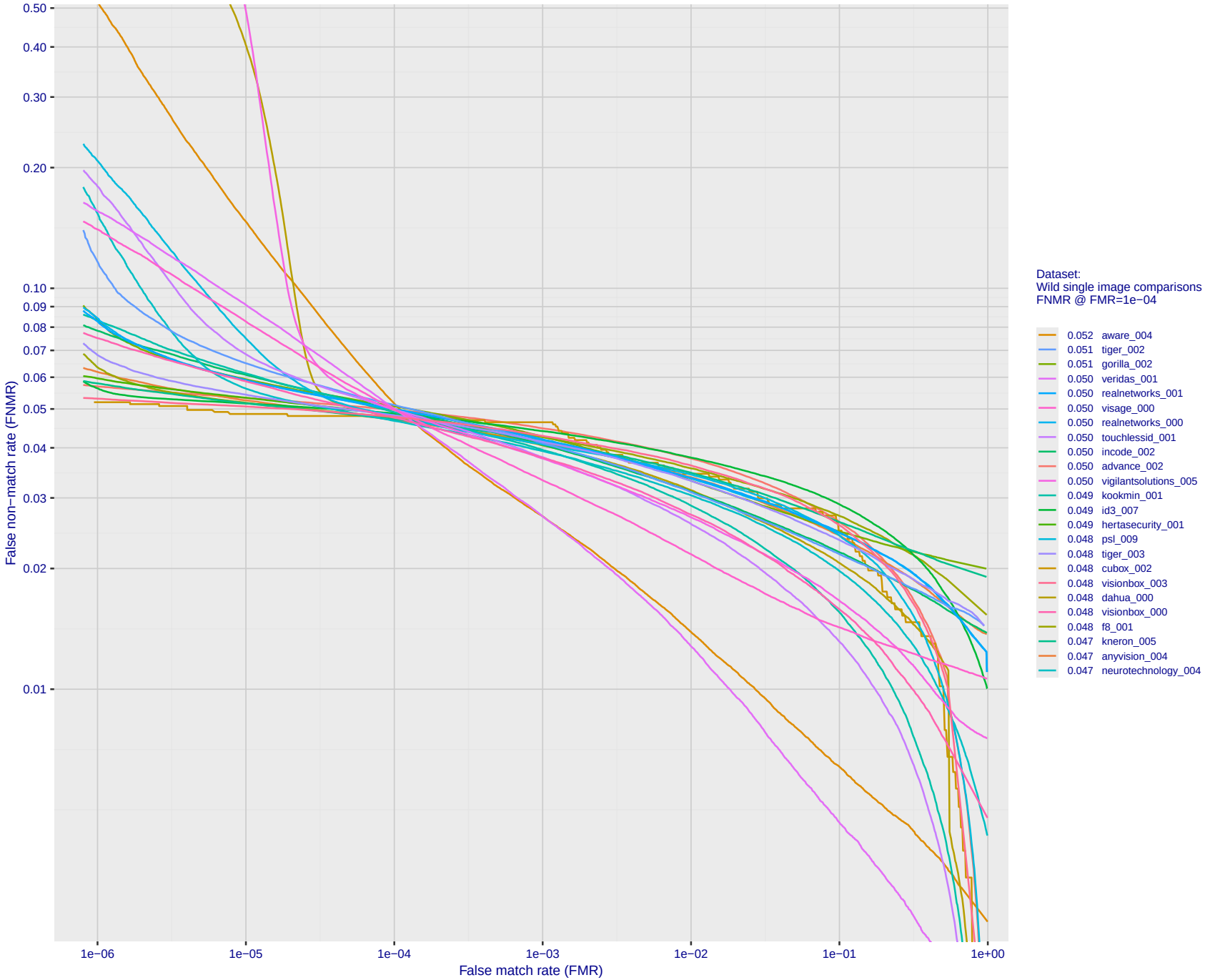

Figure 308: For the 2018 wild image comparisons, detection error tradeoff (DET) characteristics showing false non-match rate vs. false match rate plotted parametrically on threshold, T. The scales are logarithmic in order to show several decades of FMR.

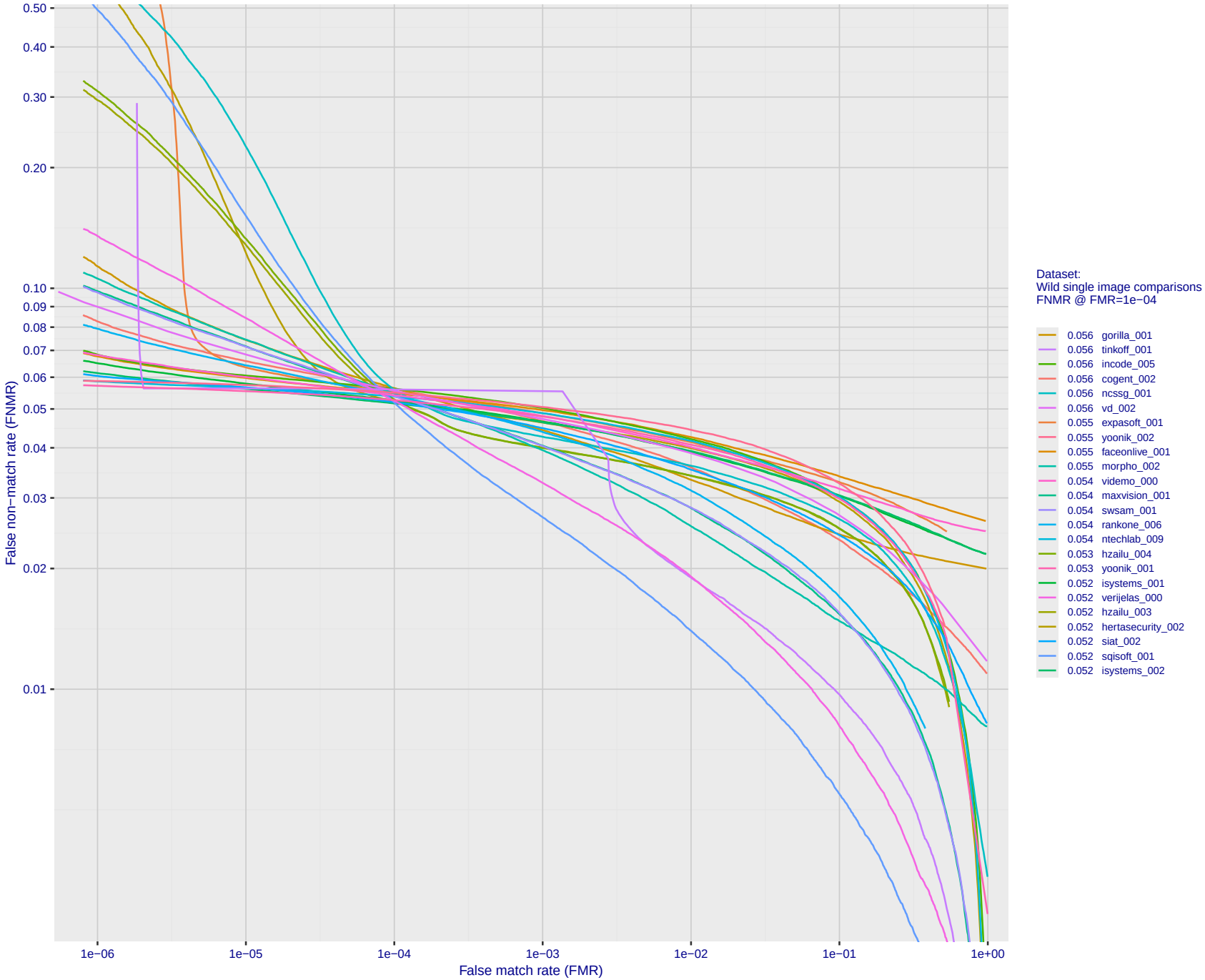

Figure 309: For the 2018 wild image comparisons, detection error tradeoff (DET) characteristics showing false non-match rate vs. false match rate plotted parametrically on threshold, T. The scales are logarithmic in order to show several decades of FMR.

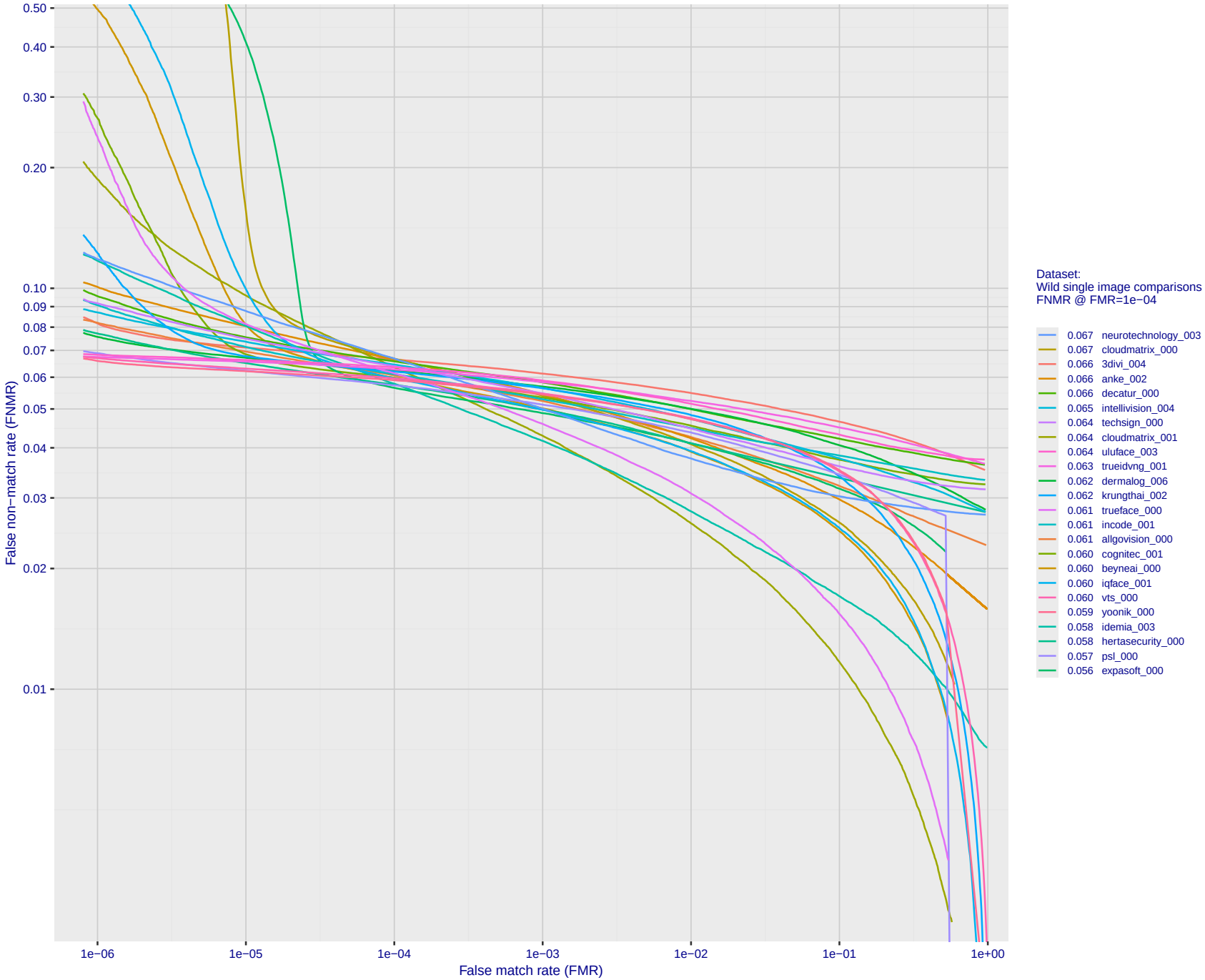

Figure 310: For the 2018 wild image comparisons, detection error tradeoff (DET) characteristics showing false non-match rate vs. false match rate plotted parametrically on threshold, T. The scales are logarithmic in order to show several decades of FMR.

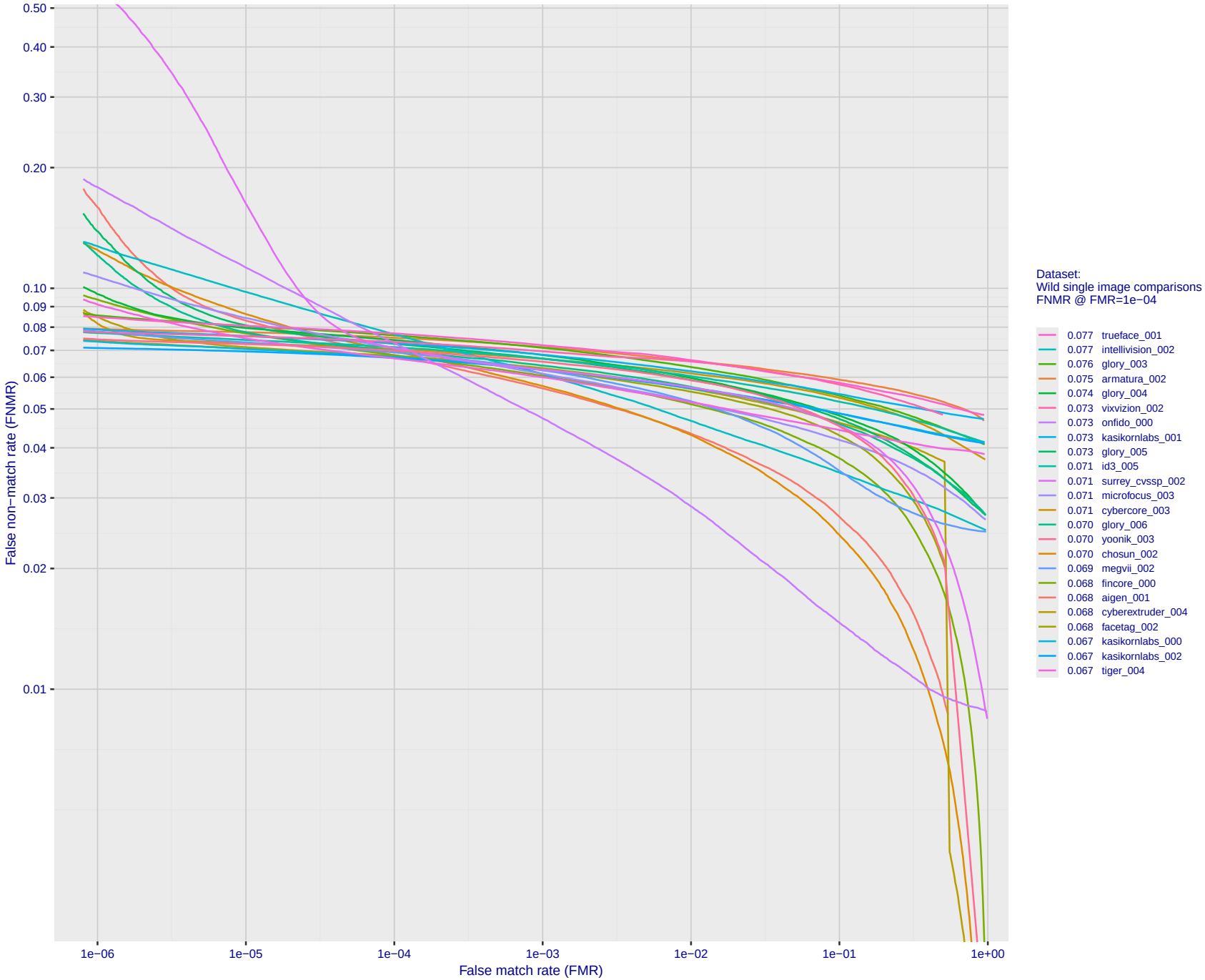

Figure 311: For the 2018 wild image comparisons, detection error tradeoff (DET) characteristics showing false non-match rate vs. false match rate plotted parametrically on threshold, T. The scales are logarithmic in order to show several decades of FMR.

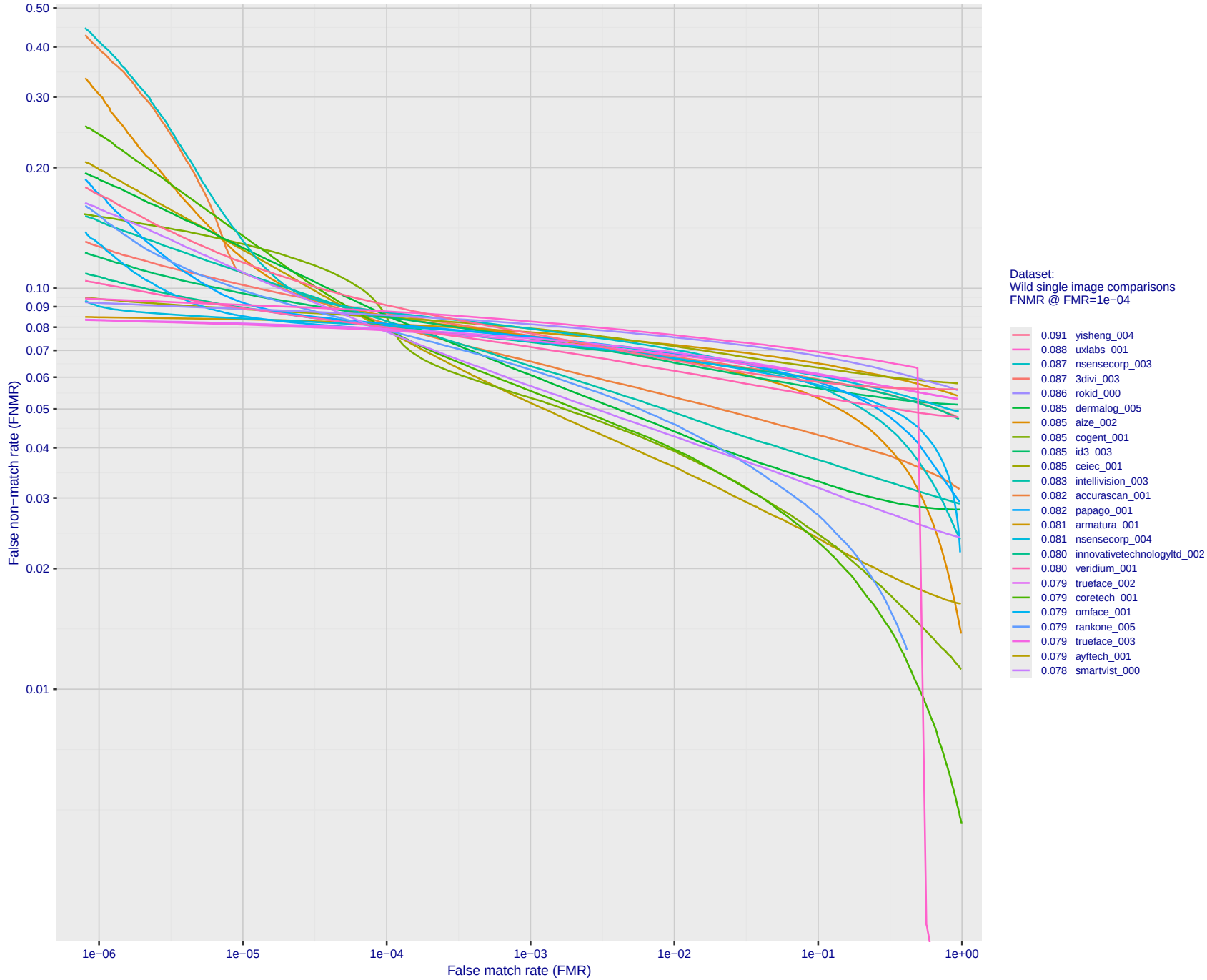

Figure 312: For the 2018 wild image comparisons, detection error tradeoff (DET) characteristics showing false non-match rate vs. false match rate plotted parametrically on threshold, T. The scales are logarithmic in order to show several decades of FMR.

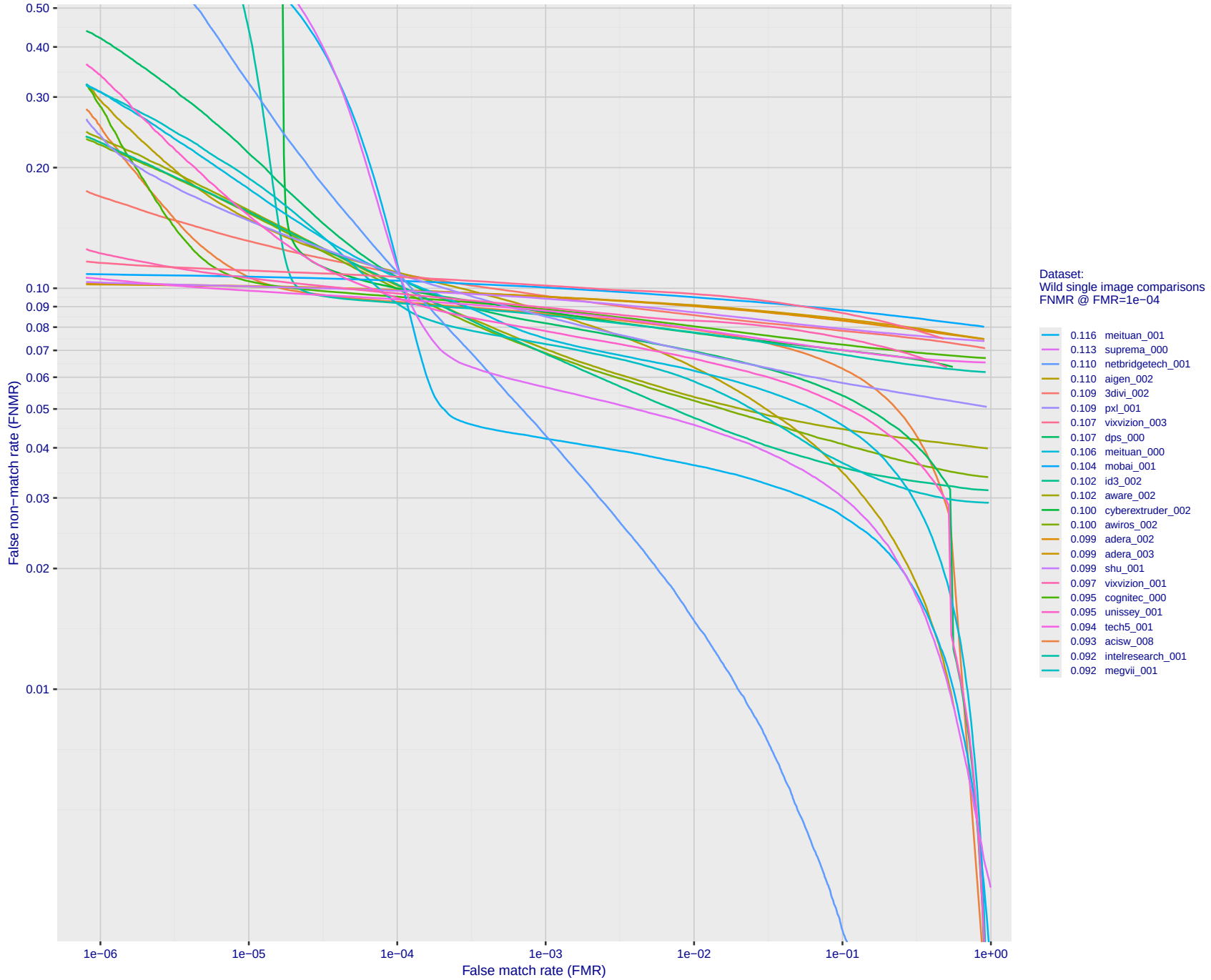

Figure 313: For the 2018 wild image comparisons, detection error tradeoff (DET) characteristics showing false non-match rate vs. false match rate plotted parametrically on threshold, T. The scales are logarithmic in order to show several decades of FMR.

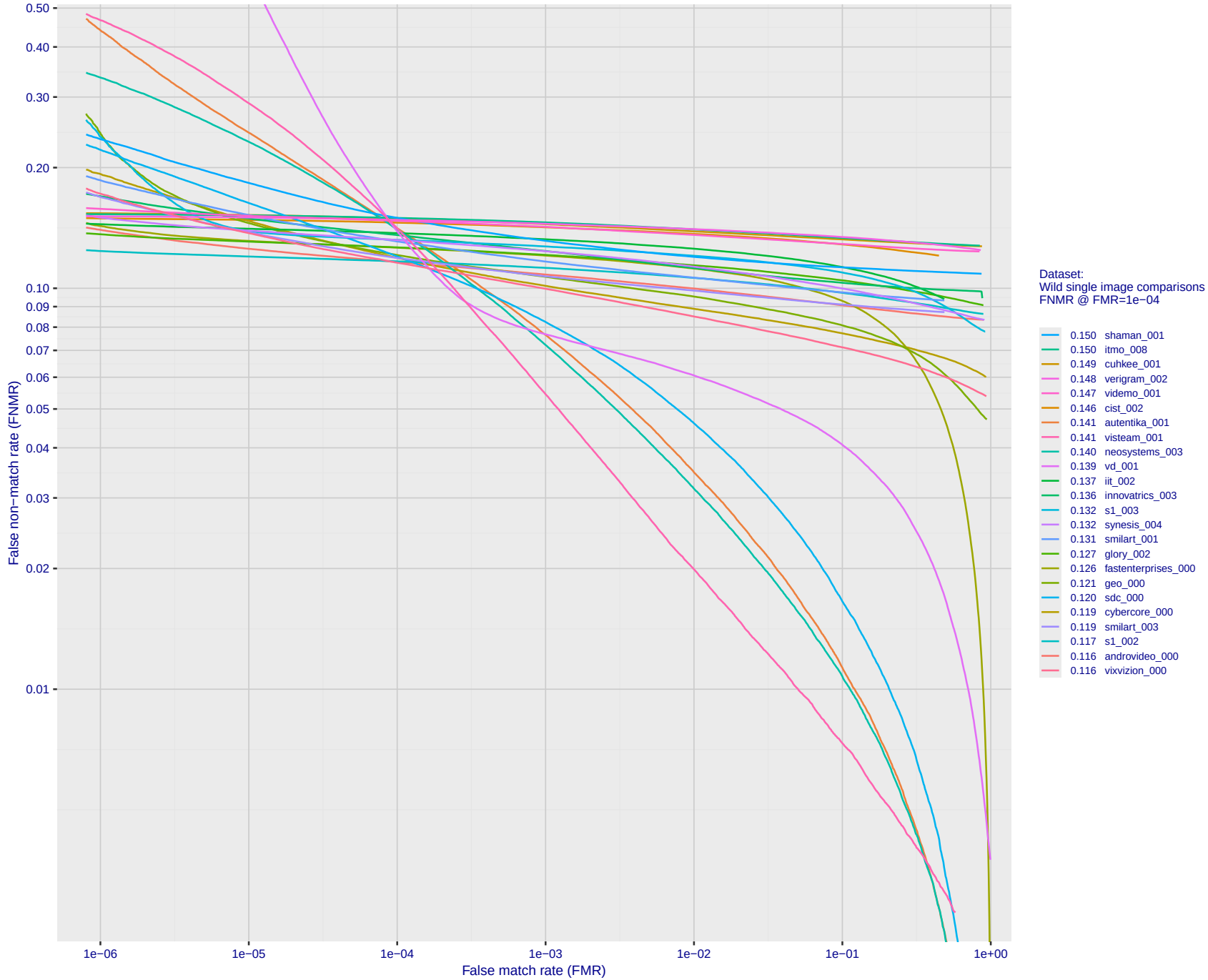

Figure 314: For the 2018 wild image comparisons, detection error tradeoff (DET) characteristics showing false non-match rate vs. false match rate plotted parametrically on threshold, T. The scales are logarithmic in order to show several decades of FMR.

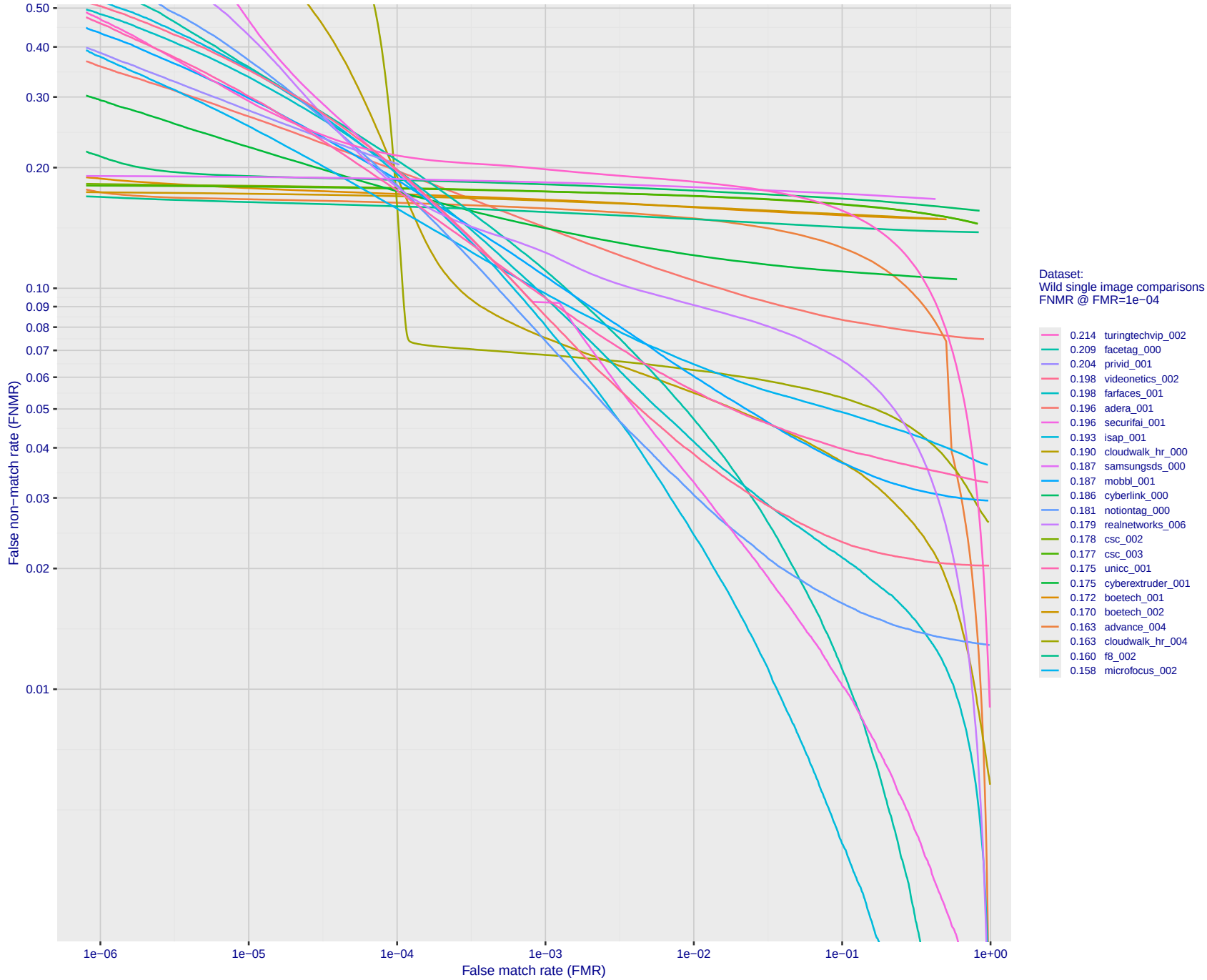

Figure 315: For the 2018 wild image comparisons, detection error tradeoff (DET) characteristics showing false non-match rate vs. false match rate plotted parametrically on threshold, T. The scales are logarithmic in order to show several decades of FMR.

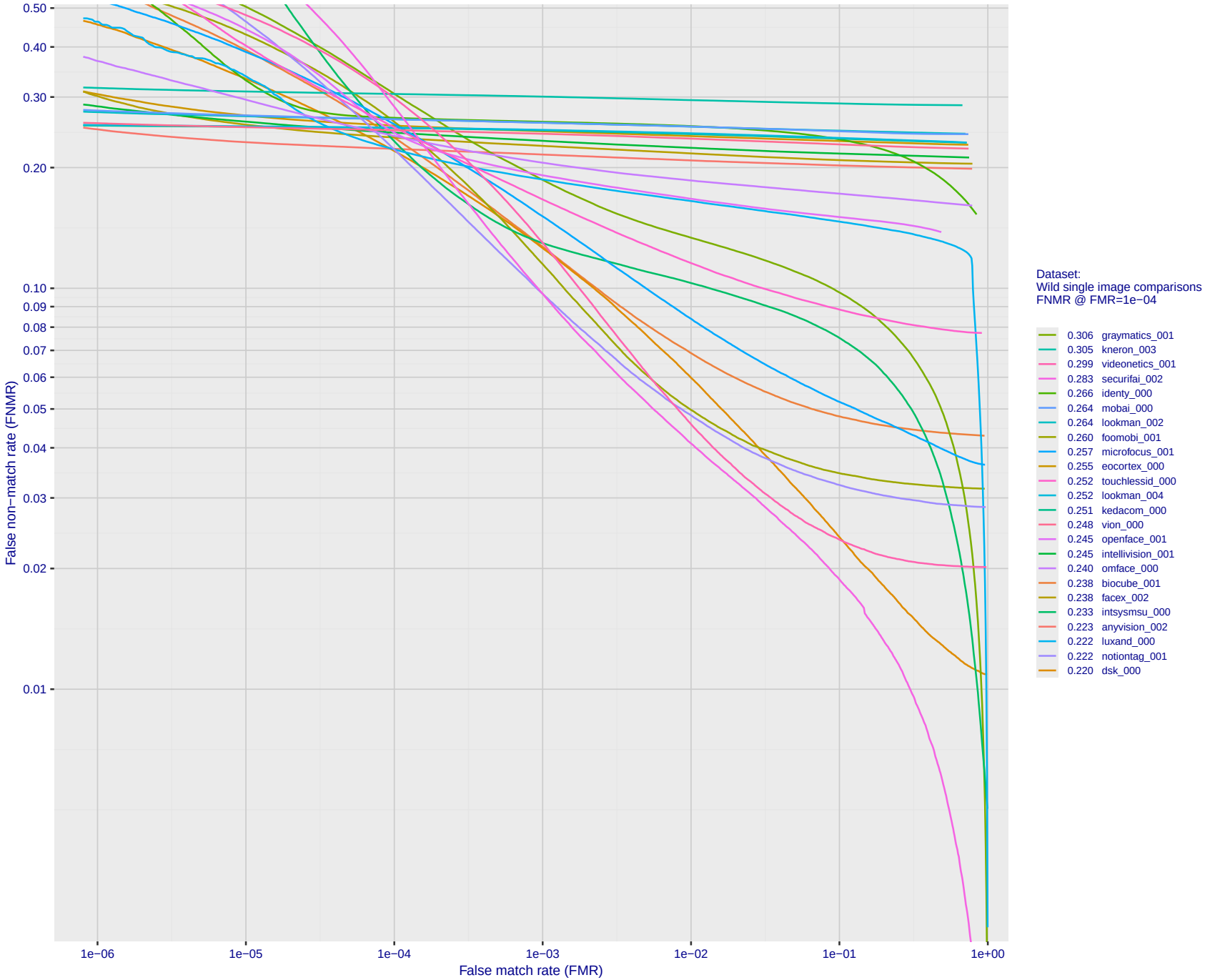

Figure 316: For the 2018 wild image comparisons, detection error tradeoff (DET) characteristics showing false non-match rate vs. false match rate plotted parametrically on threshold, T. The scales are logarithmic in order to show several decades of FMR.

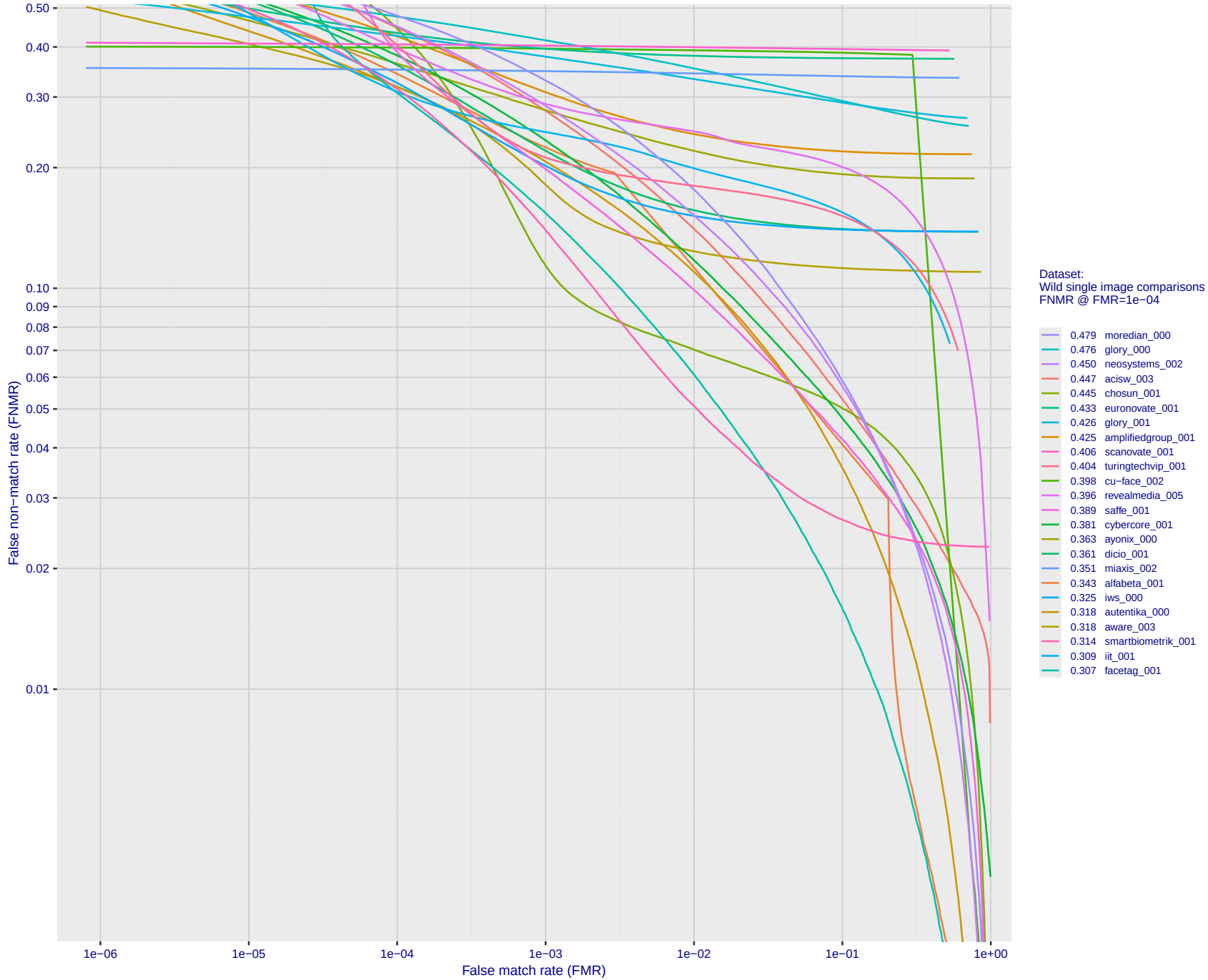

Figure 317: For the 2018 wild image comparisons, detection error tradeoff (DET) characteristics showing false non-match rate vs. false match rate plotted parametrically on threshold, T. The scales are logarithmic in order to show several decades of FMR.

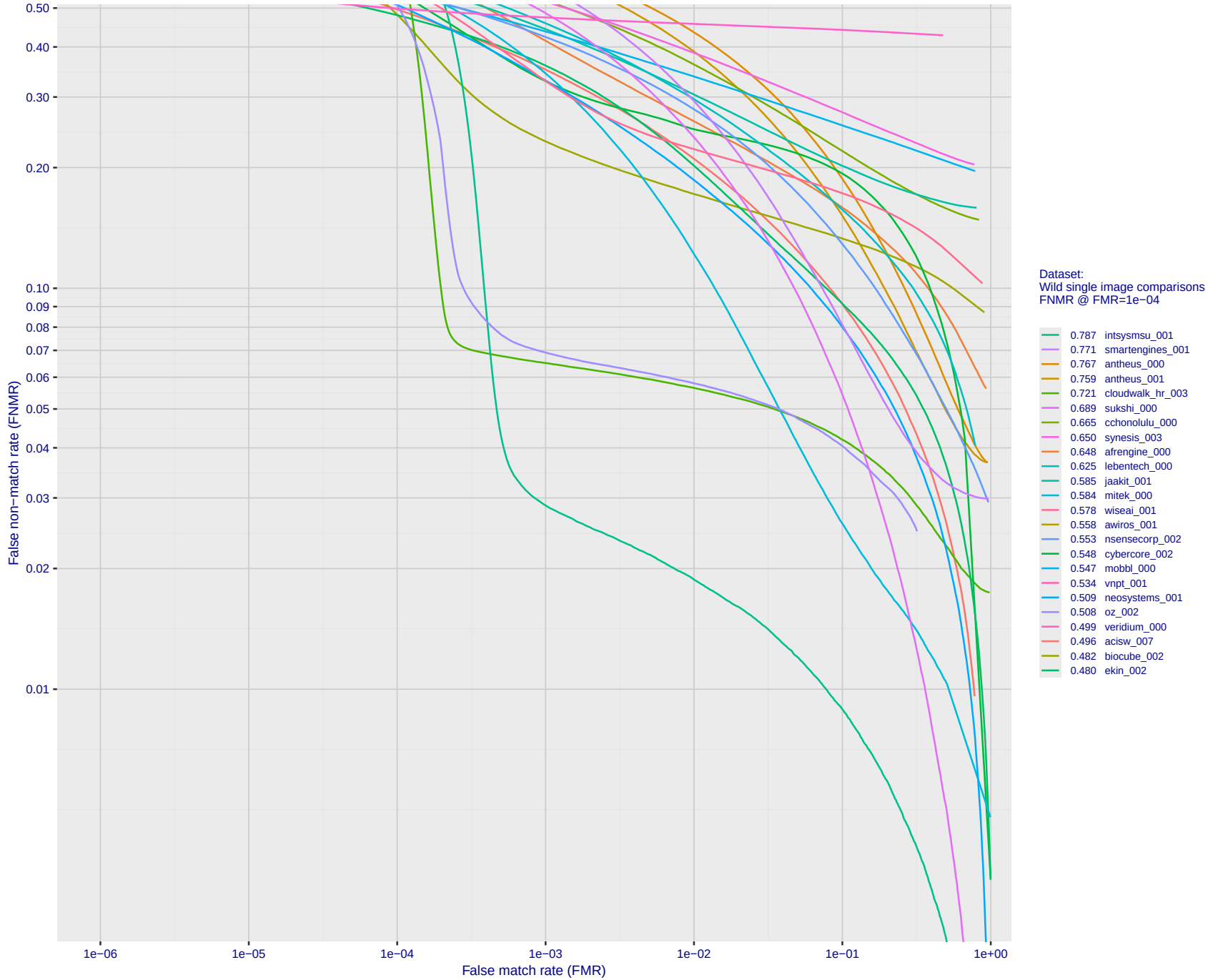

Figure 318: For the 2018 wild image comparisons, detection error tradeoff (DET) characteristics showing false non-match rate vs. false match rate plotted parametrically on threshold, T. The scales are logarithmic in order to show several decades of FMR.

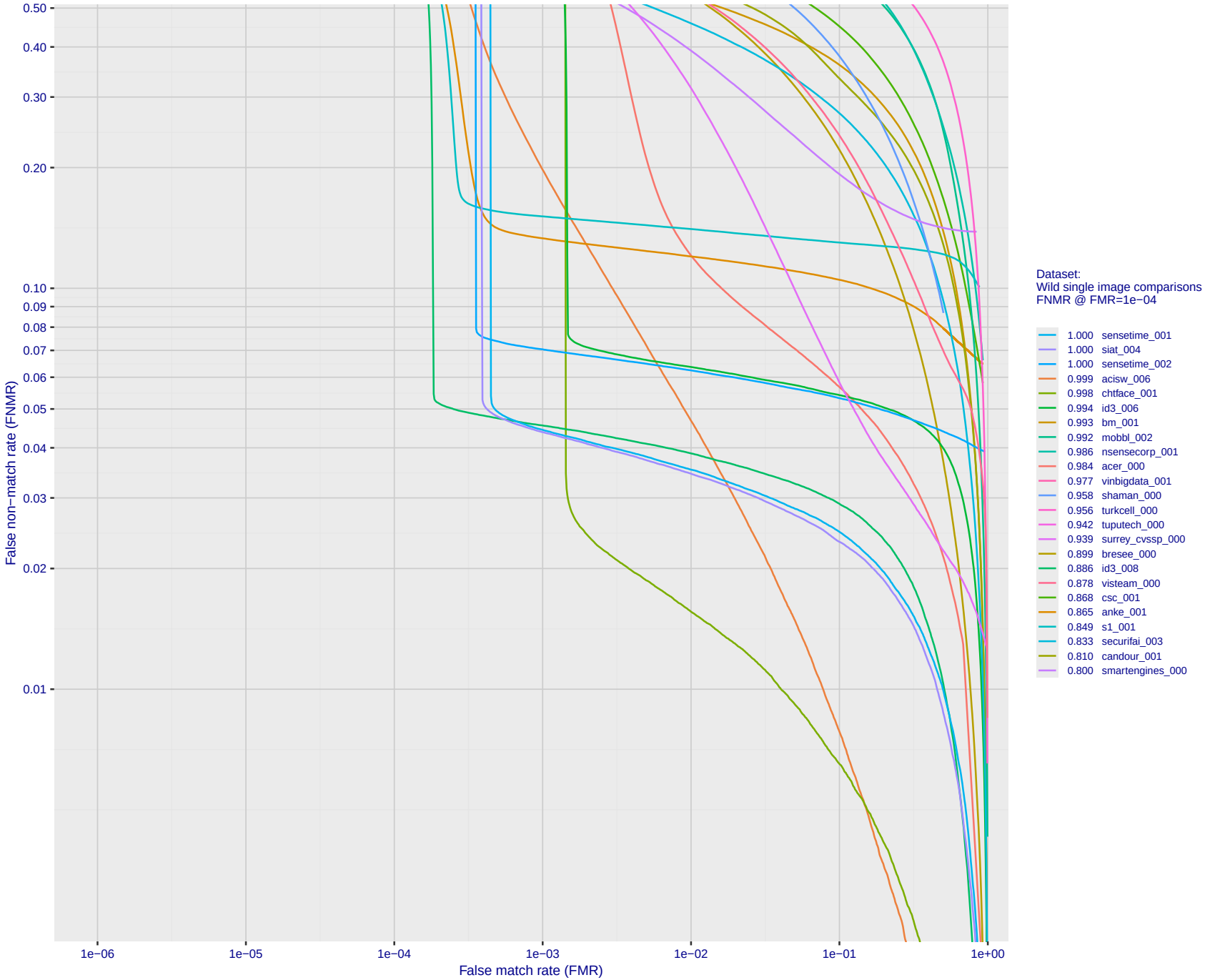

Figure 319: For the 2018 wild image comparisons, detection error tradeoff (DET) characteristics showing false non-match rate vs. false match rate plotted parametrically on threshold, T. The scales are logarithmic in order to show several decades of FMR.

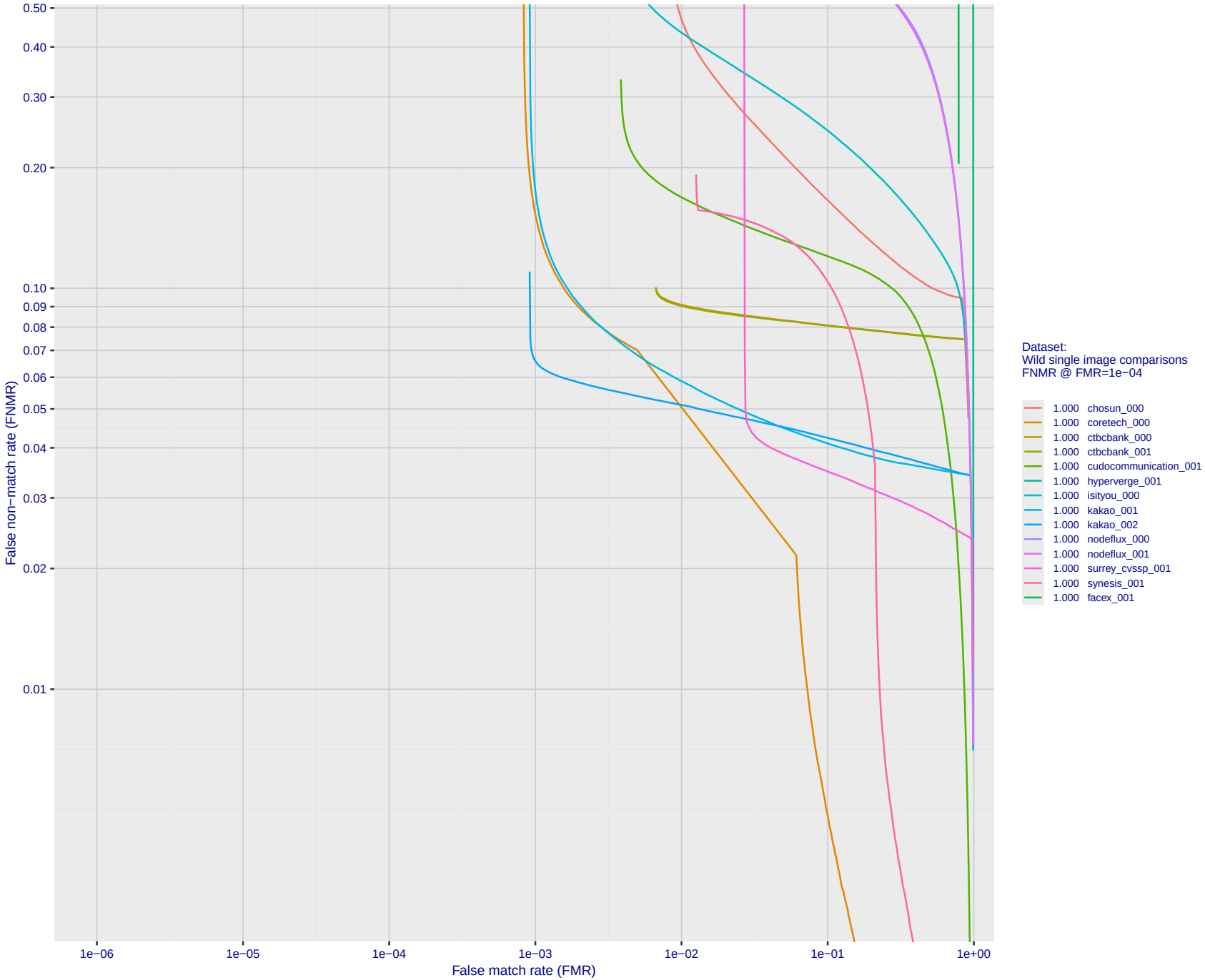

Figure 320: For the 2018 wild image comparisons, detection error tradeoff (DET) characteristics showing false non-match rate vs. false match rate plotted parametrically on threshold, T. The scales are logarithmic in order to show several decades of FMR.

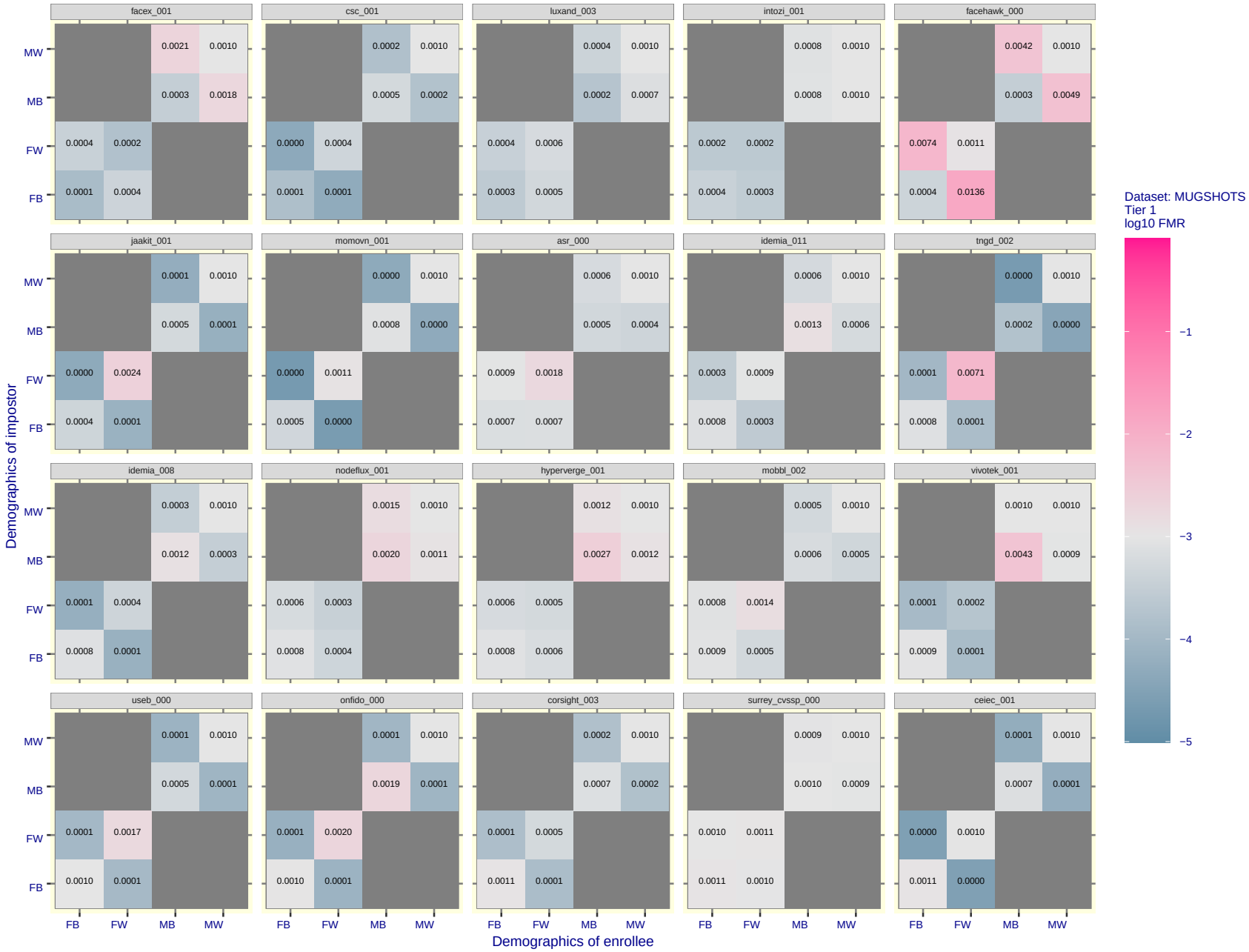

Figure 321: For the mugshot images, FMR *for same-sex impostor pairs of images annotated with codes for black female, black male, white female, white male. The threshold is set for each algorithm to give* FMR *= 0.001 for white males which is the demographic that usually gives the lowest* FMR*. This means the top right box is the same color in all panels. The panels are sorted over multiple pages in order of* FMR *on black females, which is the demographc that usually gives the highest* FMR*.*

Figure 322: For the mugshot images, FMR *for same-sex impostor pairs of images annotated with codes for black female, black male, white female, white male. The threshold is set for each algorithm to give* FMR *= 0.001 for white males which is the demographic that usually gives the lowest* FMR*. This means the top right box is the same color in all panels. The panels are sorted over multiple pages in order of* FMR *on black females, which is the demographc that usually gives the highest* FMR*.*

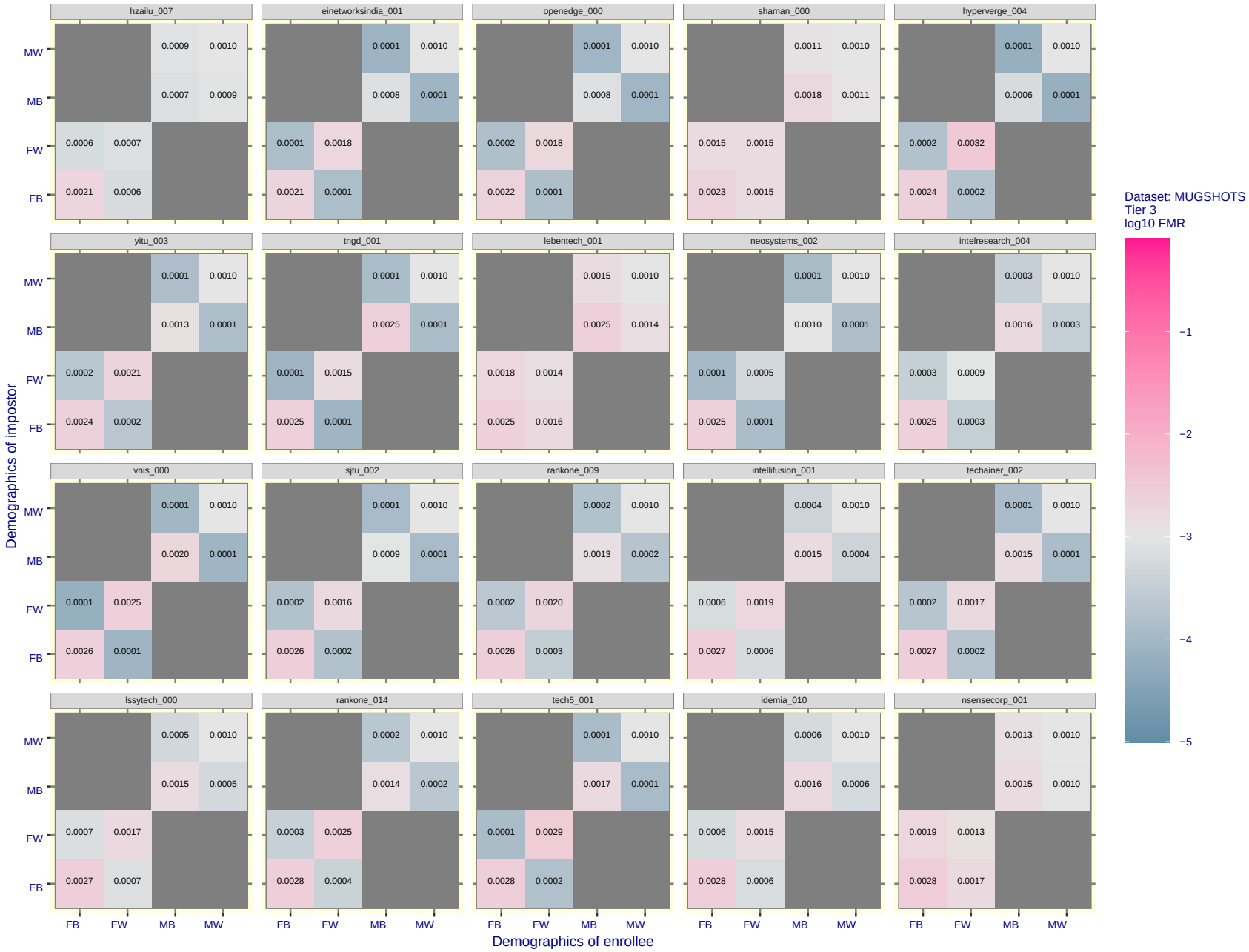

Figure 323: For the mugshot images, FMR *for same-sex impostor pairs of images annotated with codes for black female, black male, white female, white male. The threshold is set for each algorithm to give* FMR *= 0.001 for white males which is the demographic that usually gives the lowest* FMR*. This means the top right box is the same color in all panels. The panels are sorted over multiple pages in order of* FMR *on black females, which is the demographc that usually gives the highest* FMR*.*

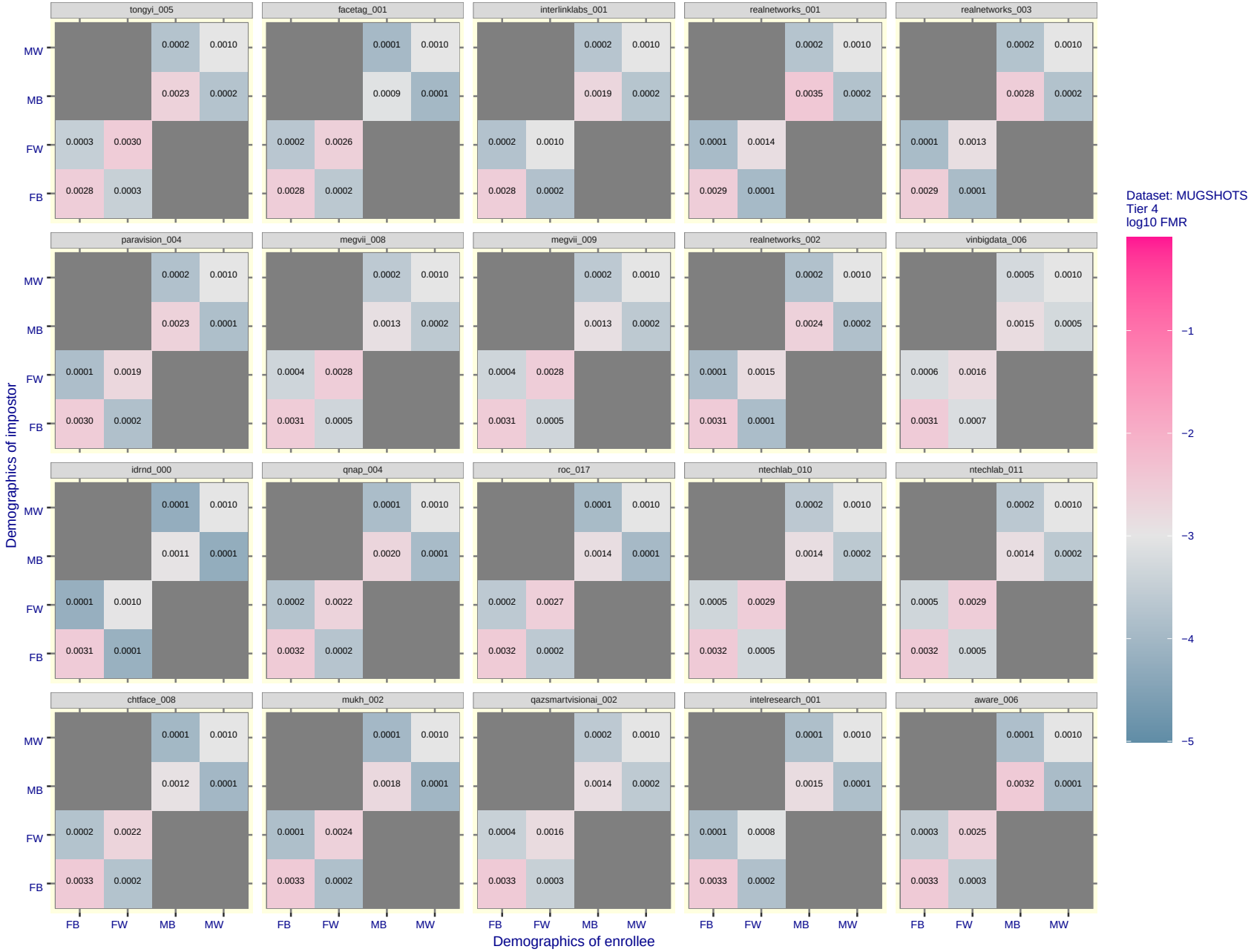

Figure 324: For the mugshot images, FMR *for same-sex impostor pairs of images annotated with codes for black female, black male, white female, white male. The threshold is set for each algorithm to give* FMR *= 0.001 for white males which is the demographic that usually gives the lowest* FMR*. This means the top right box is the same color in all panels. The panels are sorted over multiple pages in order of* FMR *on black females, which is the demographc that usually gives the highest* FMR*.*

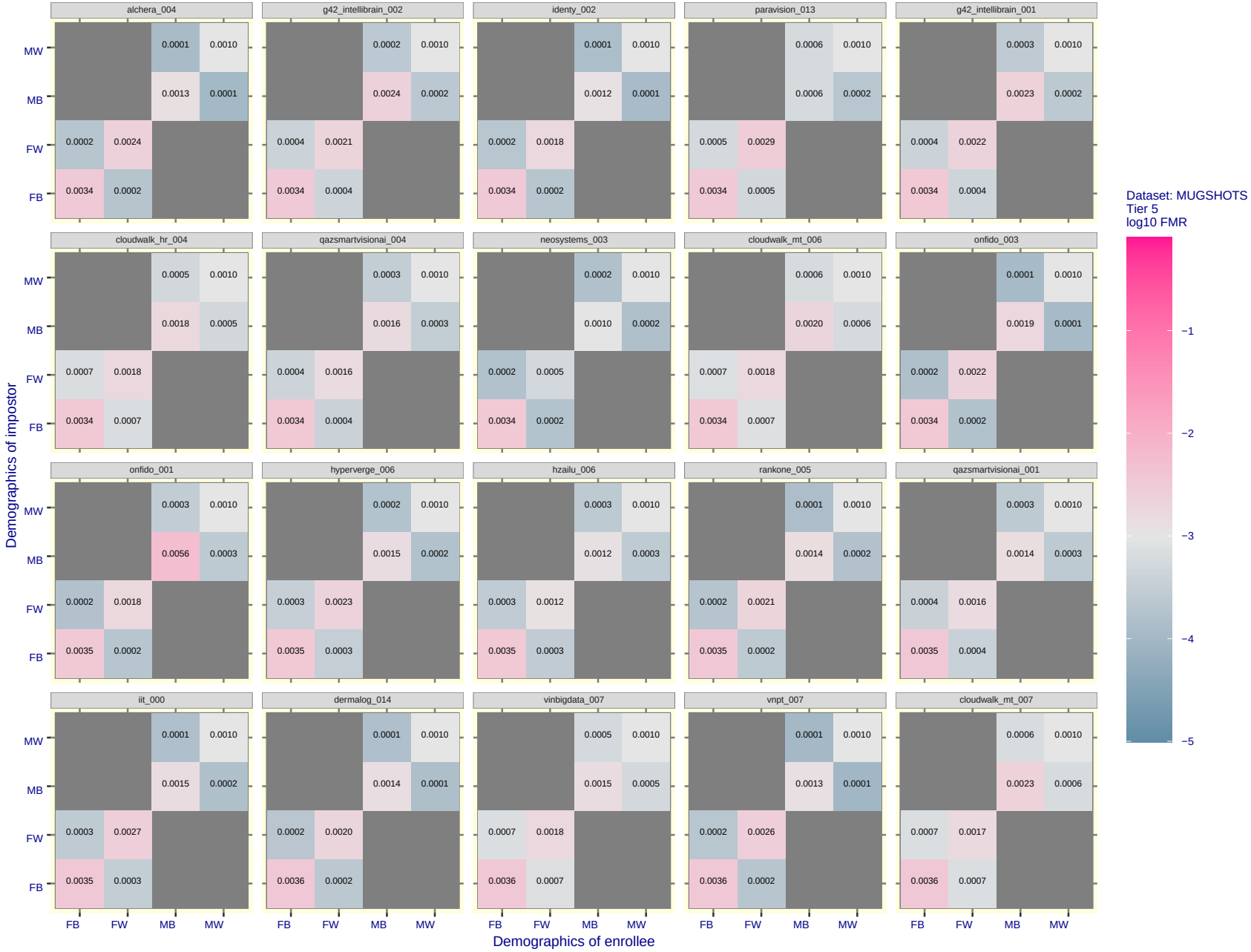

Figure 325: For the mugshot images, FMR *for same-sex impostor pairs of images annotated with codes for black female, black male, white female, white male. The threshold is set for each algorithm to give* FMR *= 0.001 for white males which is the demographic that usually gives the lowest* FMR*. This means the top right box is the same color in all panels. The panels are sorted over multiple pages in order of* FMR *on black females, which is the demographc that usually gives the highest* FMR*.*

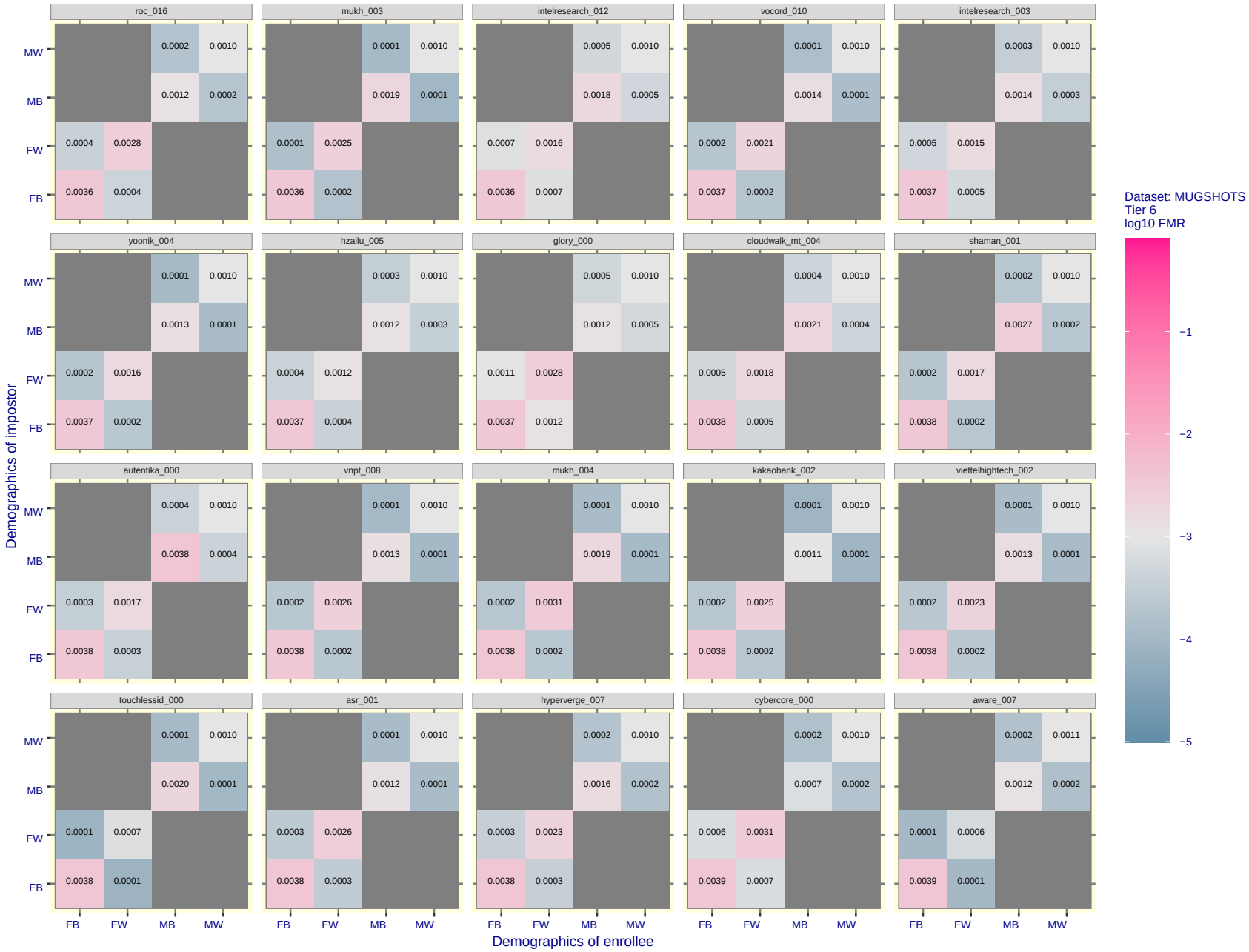

Figure 326: For the mugshot images, FMR *for same-sex impostor pairs of images annotated with codes for black female, black male, white female, white male. The threshold is set for each algorithm to give* FMR *= 0.001 for white males which is the demographic that usually gives the lowest* FMR*. This means the top right box is the same color in all panels. The panels are sorted over multiple pages in order of* FMR *on black females, which is the demographc that usually gives the highest* FMR*.*

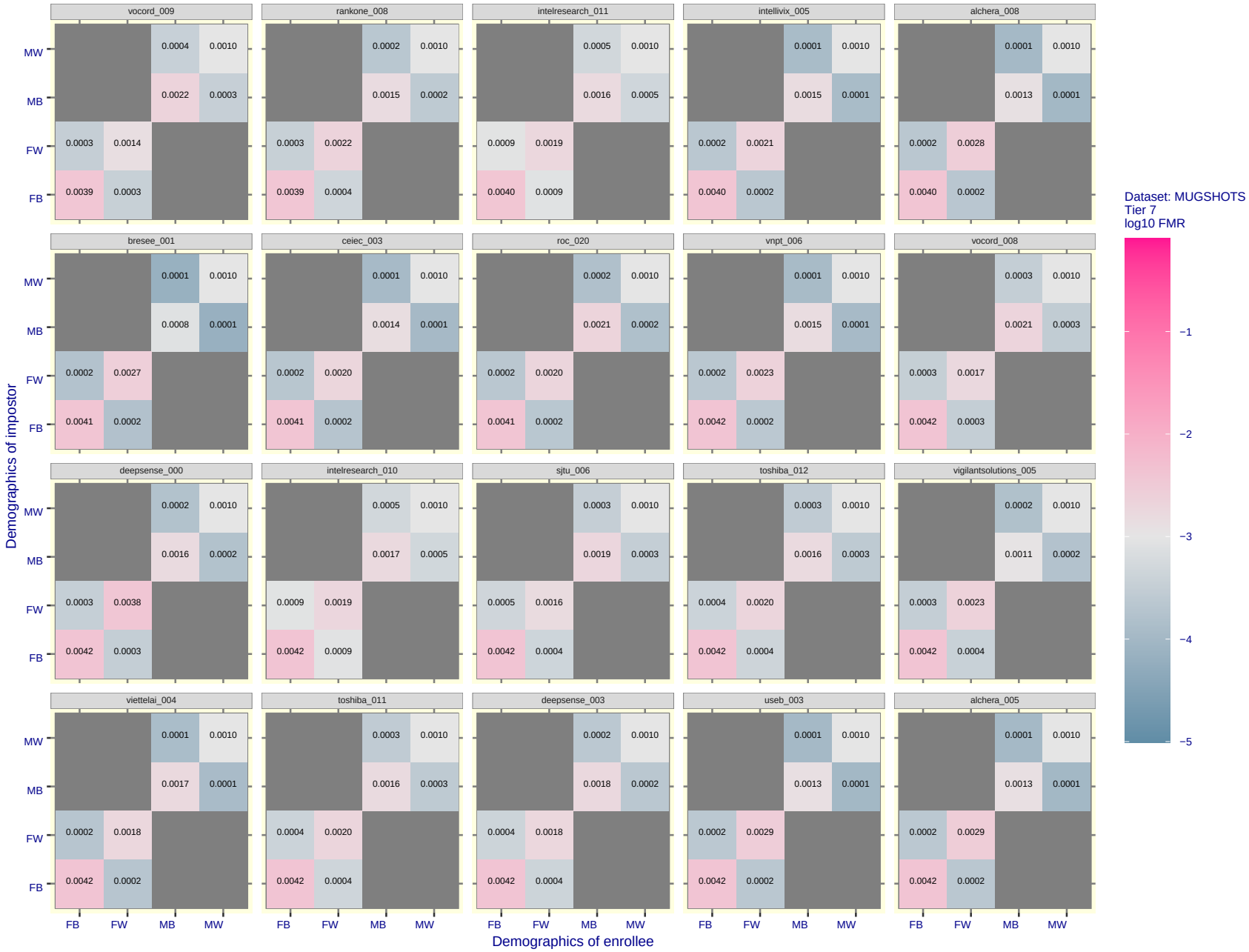

Figure 327: For the mugshot images, FMR *for same-sex impostor pairs of images annotated with codes for black female, black male, white female, white male. The threshold is set for each algorithm to give* FMR *= 0.001 for white males which is the demographic that usually gives the lowest* FMR*. This means the top right box is the same color in all panels. The panels are sorted over multiple pages in order of* FMR *on black females, which is the demographc that usually gives the highest* FMR*.*

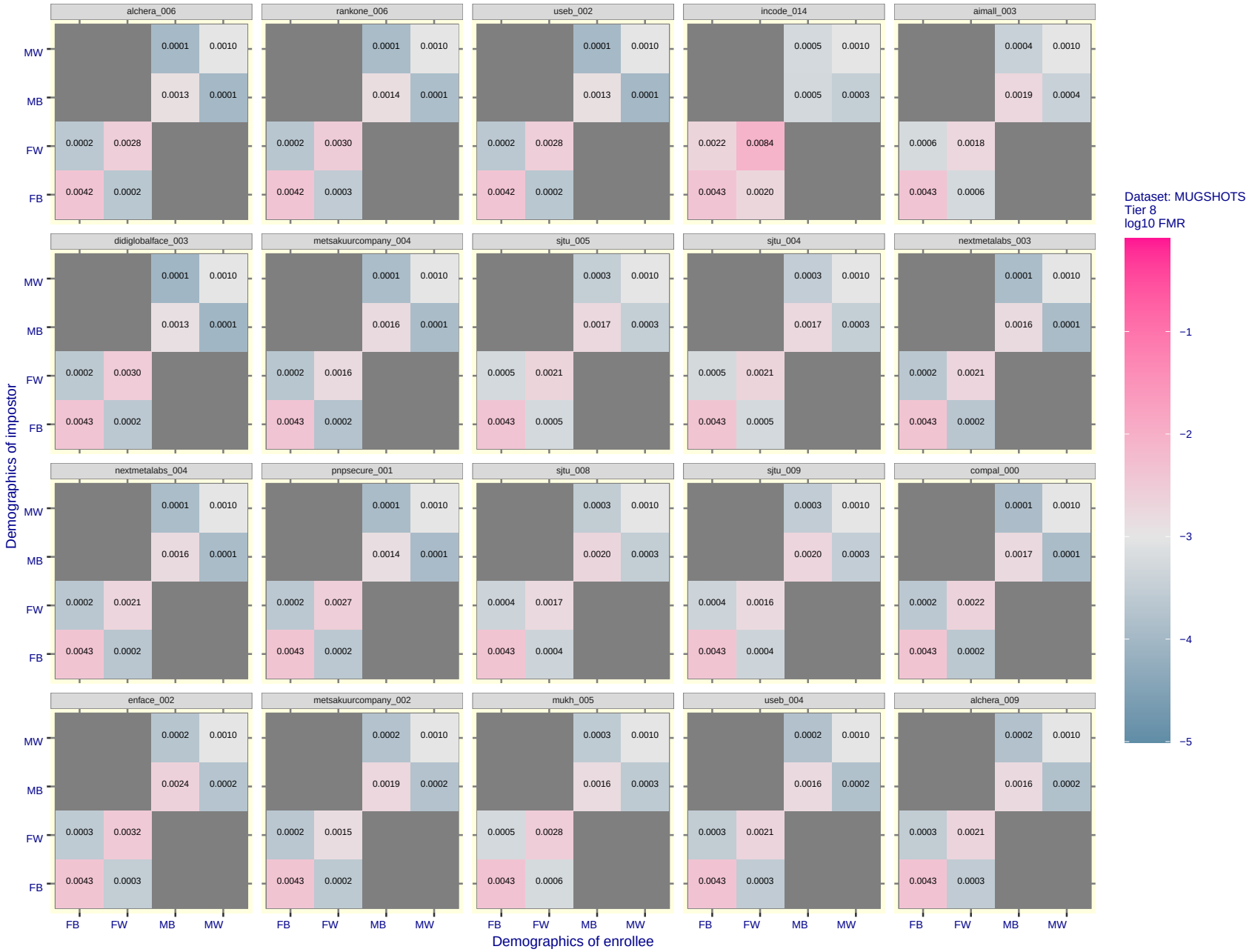

Figure 328: For the mugshot images, FMR *for same-sex impostor pairs of images annotated with codes for black female, black male, white female, white male. The threshold is set for each algorithm to give* FMR *= 0.001 for white males which is the demographic that usually gives the lowest* FMR*. This means the top right box is the same color in all panels. The panels are sorted over multiple pages in order of* FMR *on black females, which is the demographc that usually gives the highest* FMR*.*

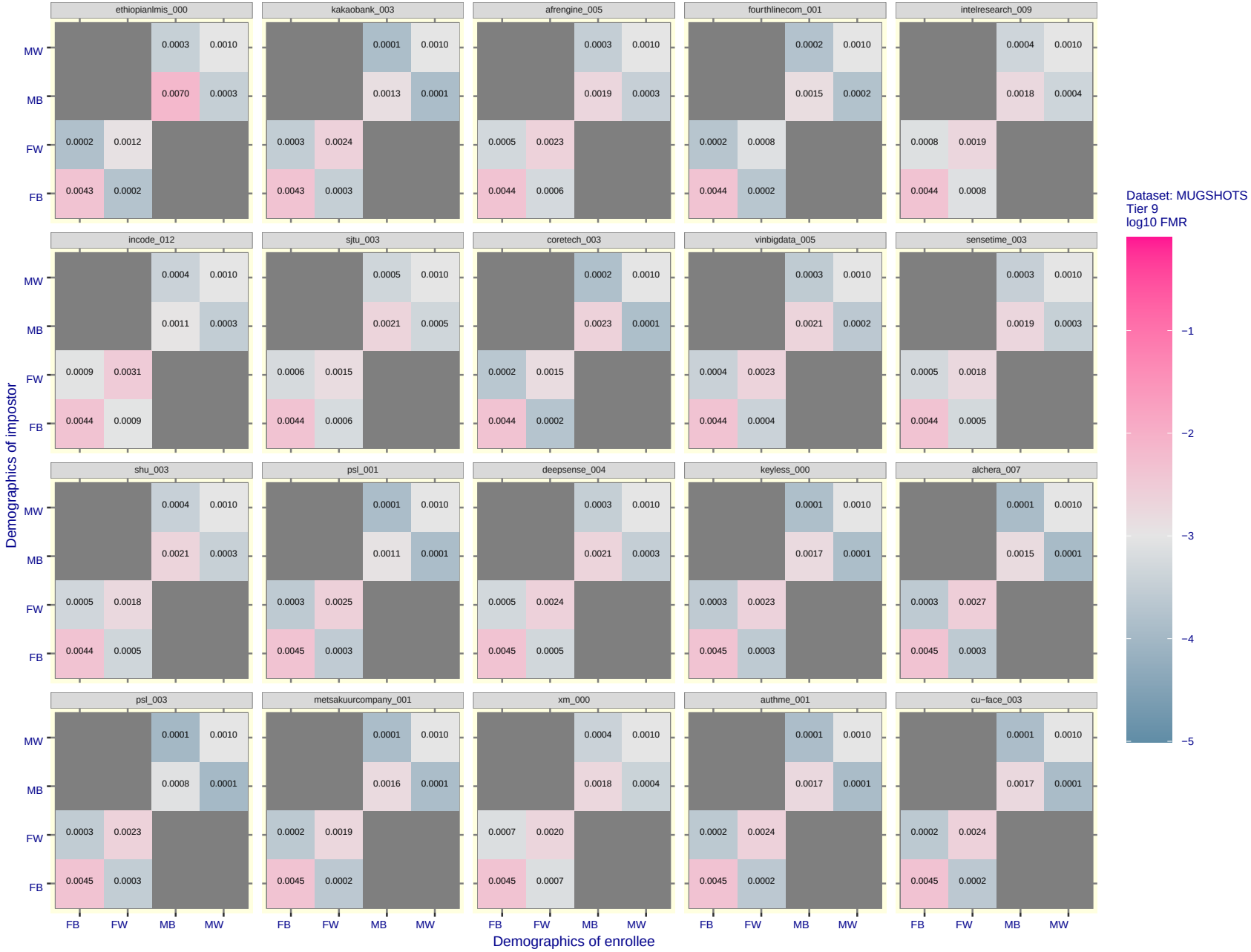

Figure 329: For the mugshot images, FMR *for same-sex impostor pairs of images annotated with codes for black female, black male, white female, white male. The threshold is set for each algorithm to give* FMR *= 0.001 for white males which is the demographic that usually gives the lowest* FMR*. This means the top right box is the same color in all panels. The panels are sorted over multiple pages in order of* FMR *on black females, which is the demographc that usually gives the highest* FMR*.*

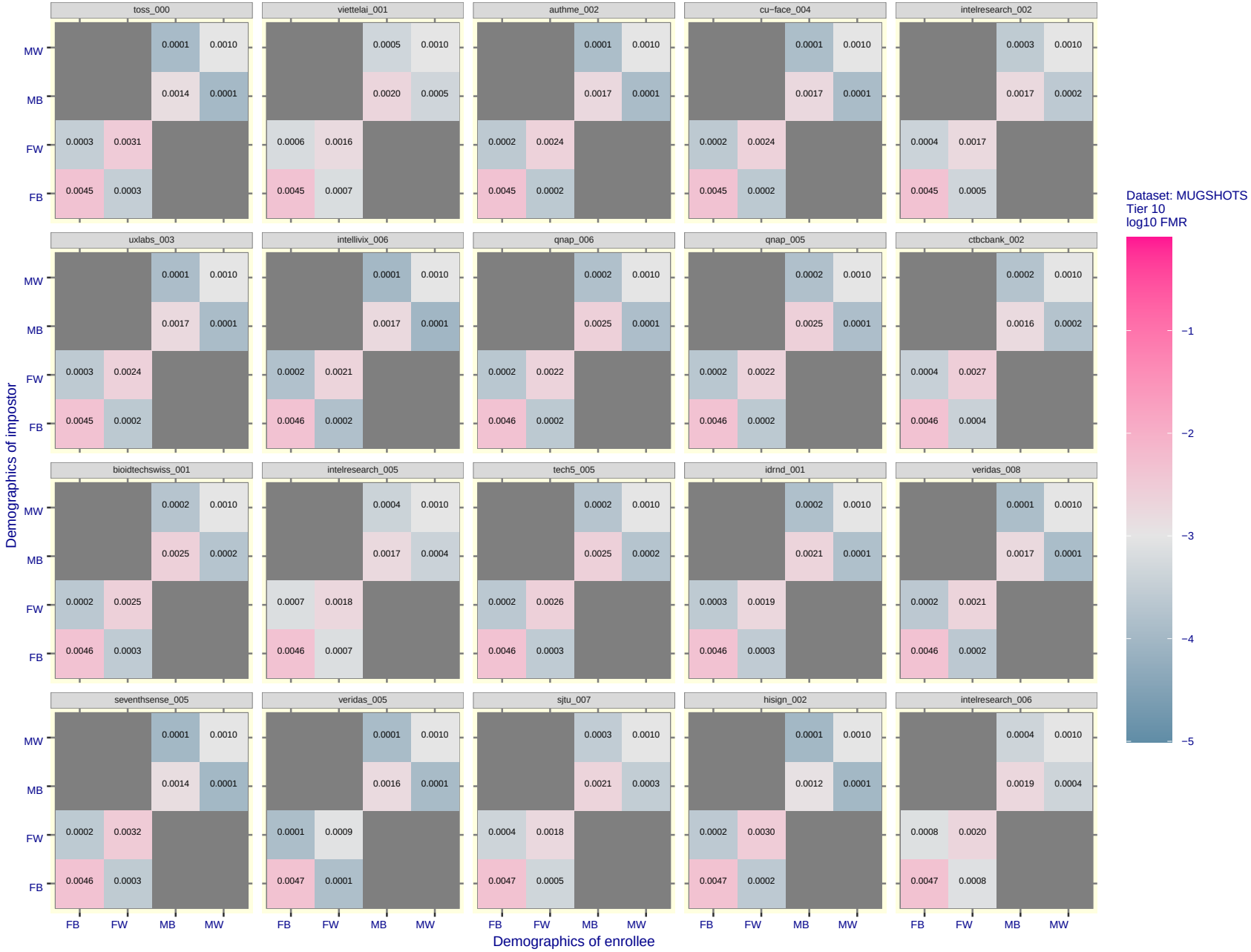

Figure 330: For the mugshot images, FMR *for same-sex impostor pairs of images annotated with codes for black female, black male, white female, white male. The threshold is set for each algorithm to give* FMR *= 0.001 for white males which is the demographic that usually gives the lowest* FMR*. This means the top right box is the same color in all panels. The panels are sorted over multiple pages in order of* FMR *on black females, which is the demographc that usually gives the highest* FMR*.*

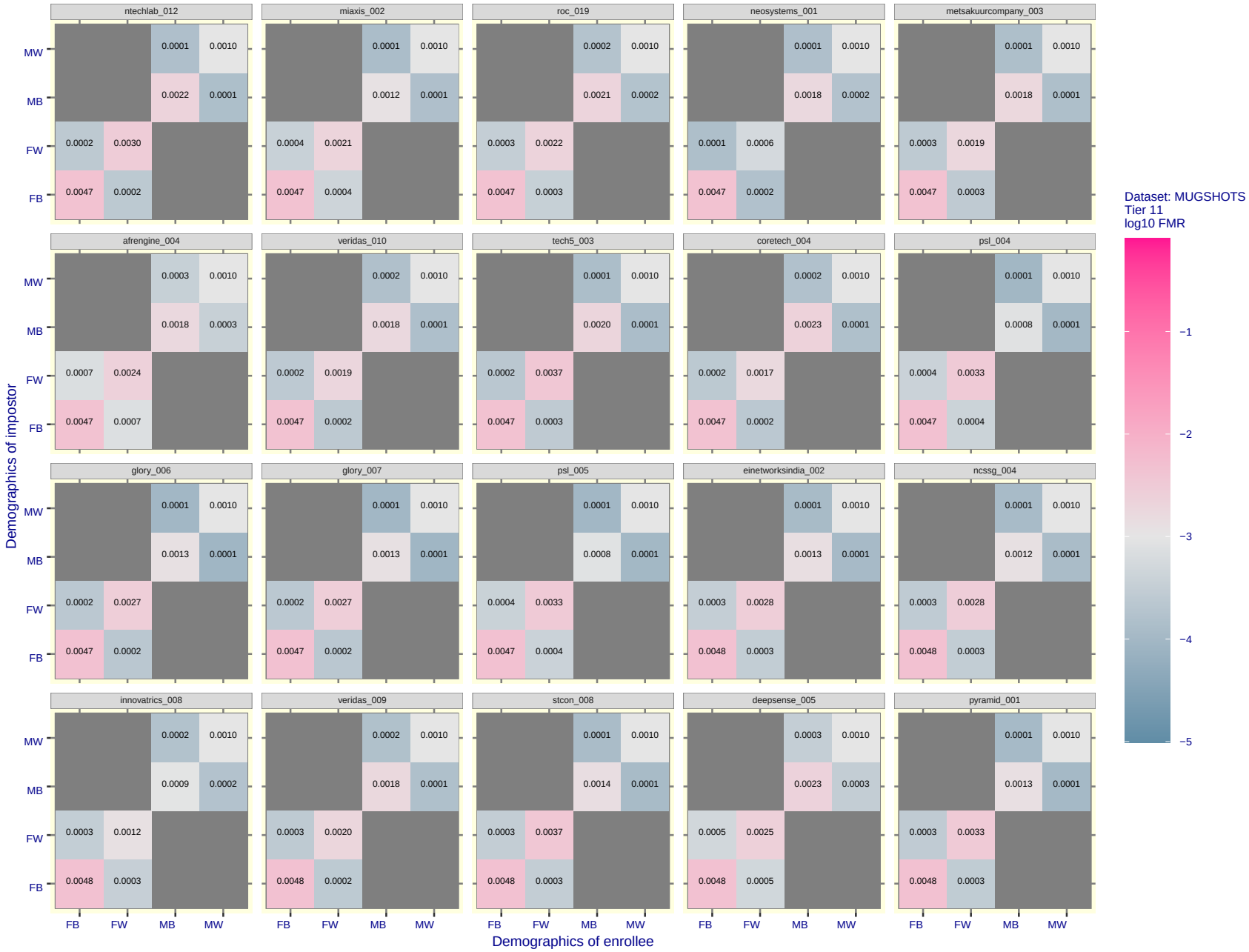

Figure 331: For the mugshot images, FMR *for same-sex impostor pairs of images annotated with codes for black female, black male, white female, white male. The threshold is set for each algorithm to give* FMR *= 0.001 for white males which is the demographic that usually gives the lowest* FMR*. This means the top right box is the same color in all panels. The panels are sorted over multiple pages in order of* FMR *on black females, which is the demographc that usually gives the highest* FMR*.*

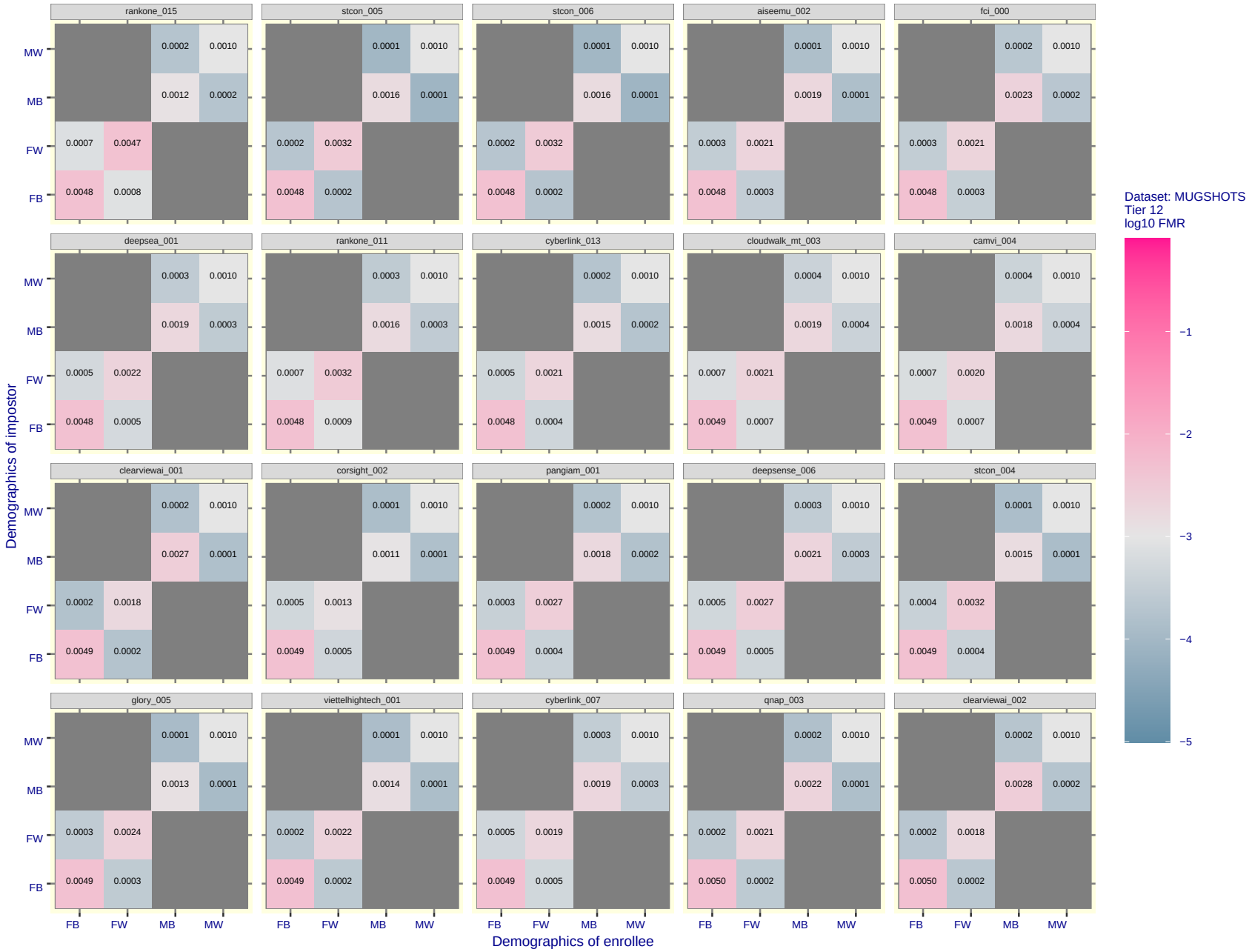

Figure 332: For the mugshot images, FMR *for same-sex impostor pairs of images annotated with codes for black female, black male, white female, white male. The threshold is set for each algorithm to give* FMR *= 0.001 for white males which is the demographic that usually gives the lowest* FMR*. This means the top right box is the same color in all panels. The panels are sorted over multiple pages in order of* FMR *on black females, which is the demographc that usually gives the highest* FMR*.*

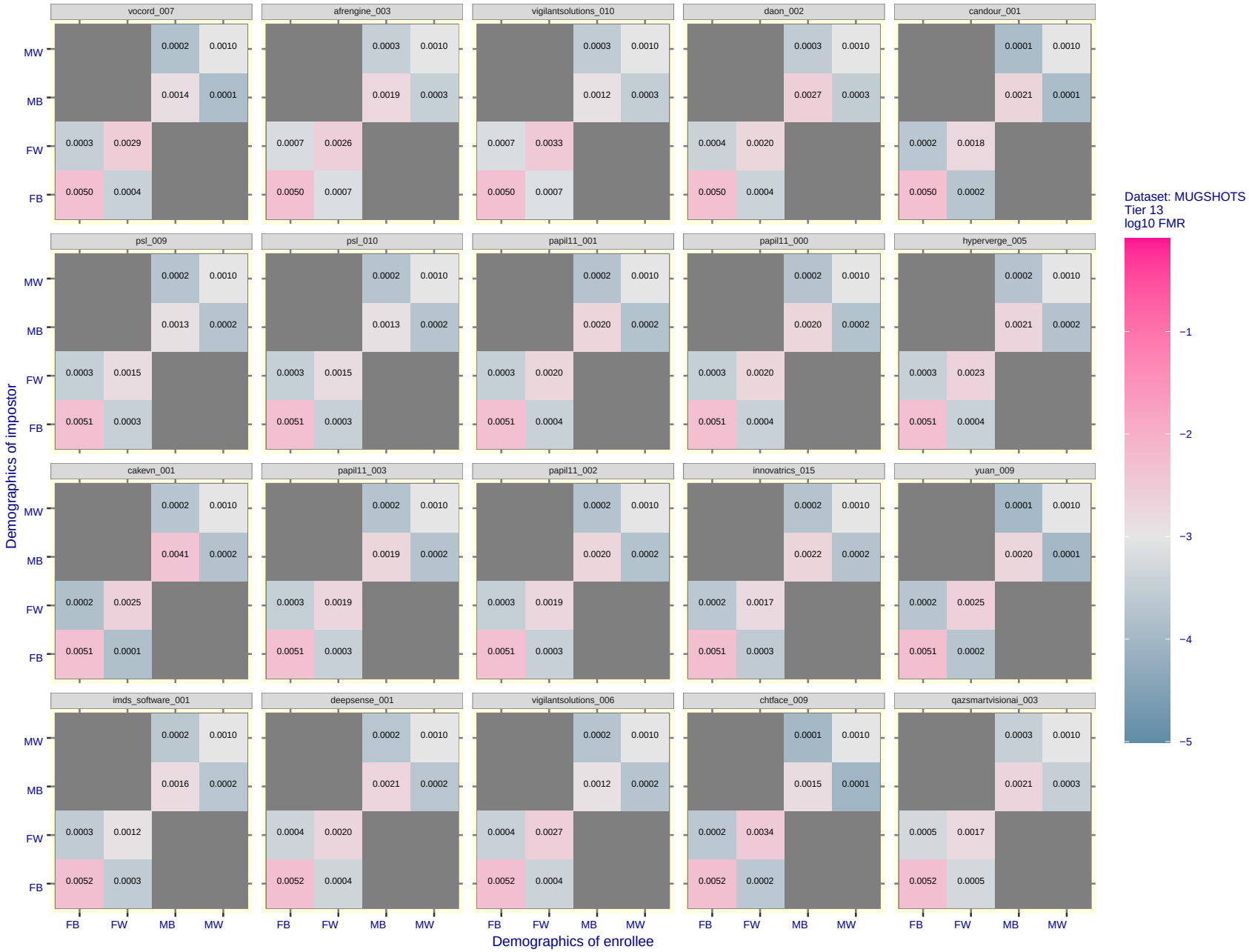

Figure 333: For the mugshot images, FMR *for same-sex impostor pairs of images annotated with codes for black female, black male, white female, white male. The threshold is set for each algorithm to give* FMR *= 0.001 for white males which is the demographic that usually gives the lowest* FMR*. This means the top right box is the same color in all panels. The panels are sorted over multiple pages in order of* FMR *on black females, which is the demographc that usually gives the highest* FMR*.*

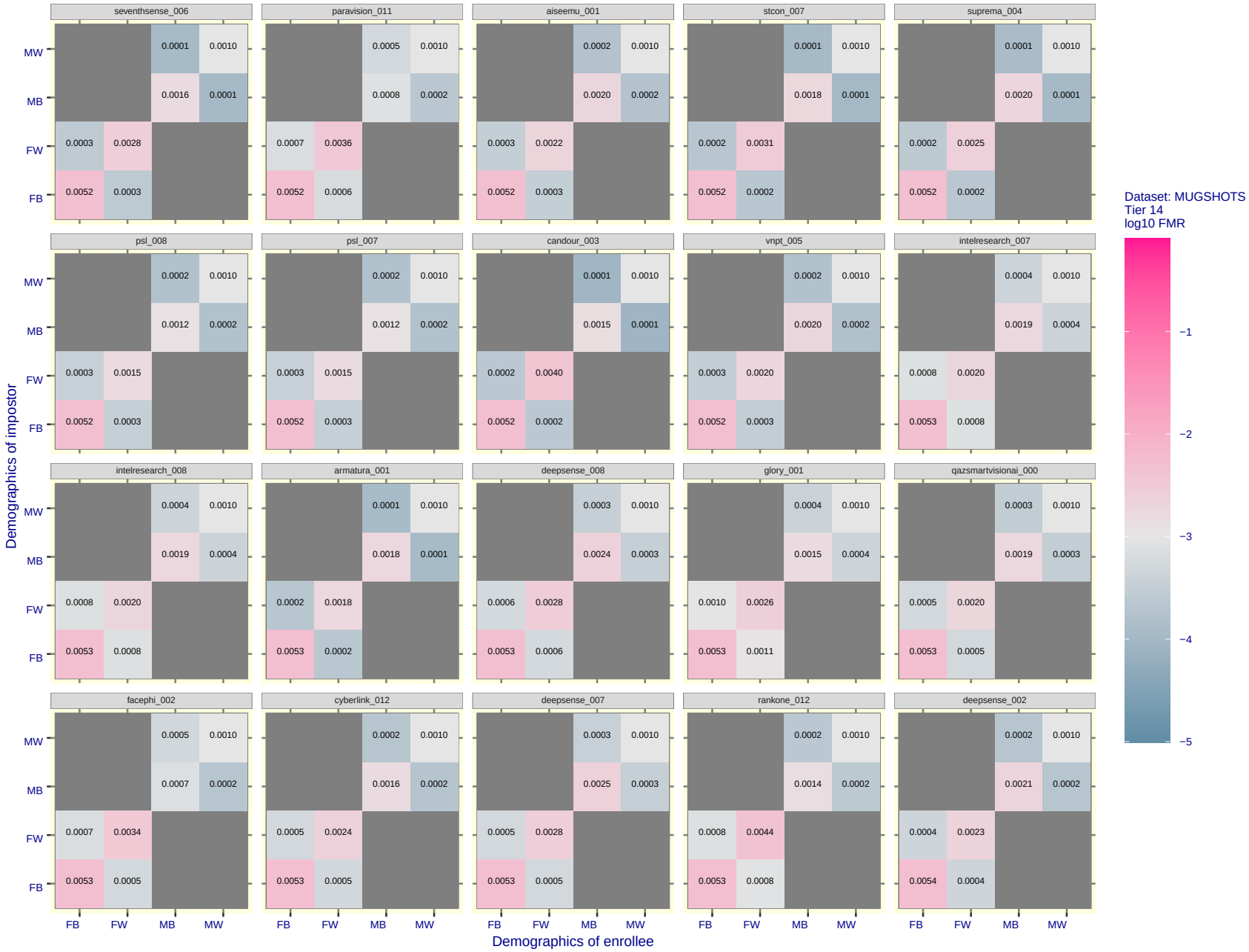

Figure 334: For the mugshot images, FMR *for same-sex impostor pairs of images annotated with codes for black female, black male, white female, white male. The threshold is set for each algorithm to give* FMR *= 0.001 for white males which is the demographic that usually gives the lowest* FMR*. This means the top right box is the same color in all panels. The panels are sorted over multiple pages in order of* FMR *on black females, which is the demographc that usually gives the highest* FMR*.*

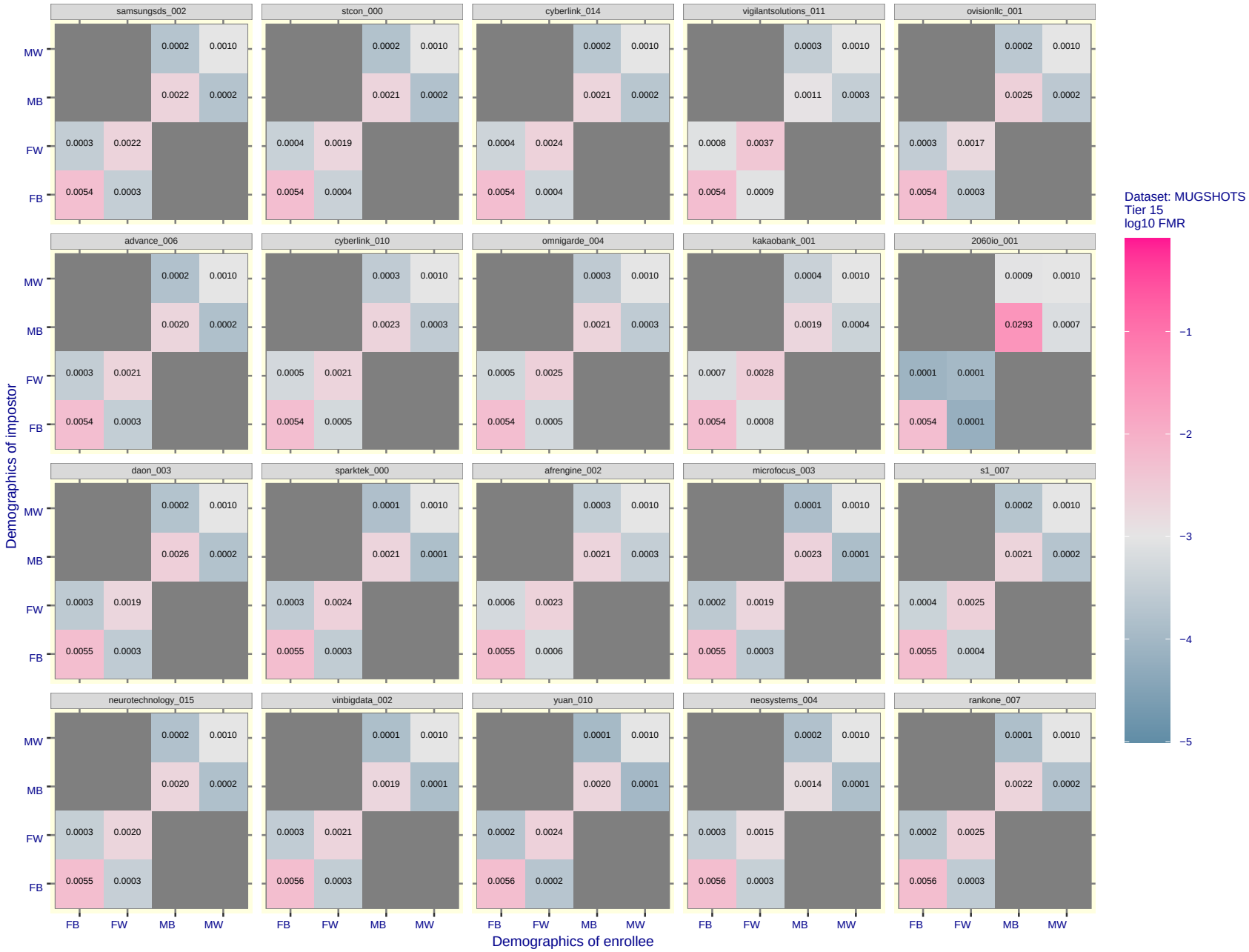

Figure 335: For the mugshot images, FMR *for same-sex impostor pairs of images annotated with codes for black female, black male, white female, white male. The threshold is set for each algorithm to give* FMR *= 0.001 for white males which is the demographic that usually gives the lowest* FMR*. This means the top right box is the same color in all panels. The panels are sorted over multiple pages in order of* FMR *on black females, which is the demographc that usually gives the highest* FMR*.*

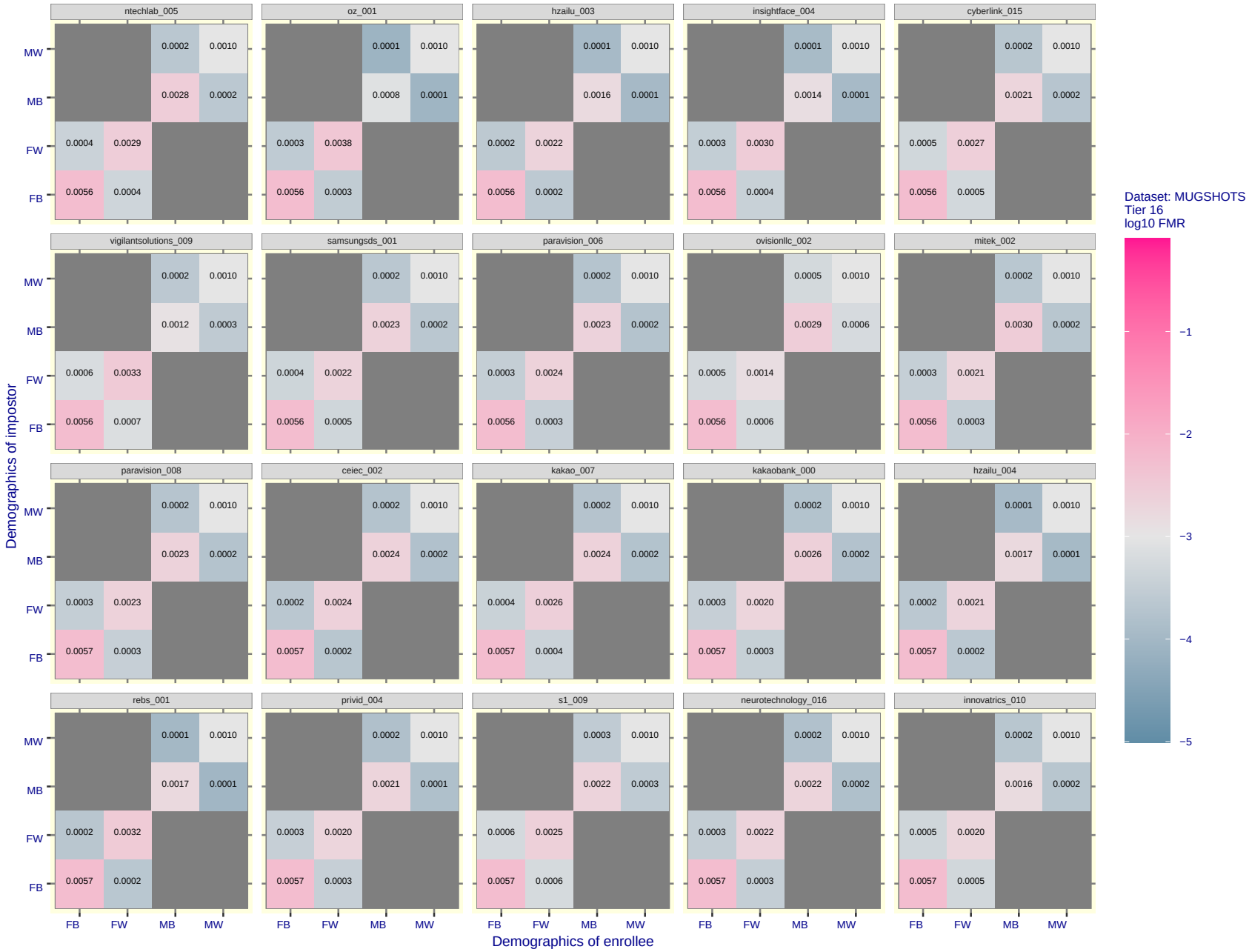

Figure 336: For the mugshot images, FMR *for same-sex impostor pairs of images annotated with codes for black female, black male, white female, white male. The threshold is set for each algorithm to give* FMR *= 0.001 for white males which is the demographic that usually gives the lowest* FMR*. This means the top right box is the same color in all panels. The panels are sorted over multiple pages in order of* FMR *on black females, which is the demographc that usually gives the highest* FMR*.*

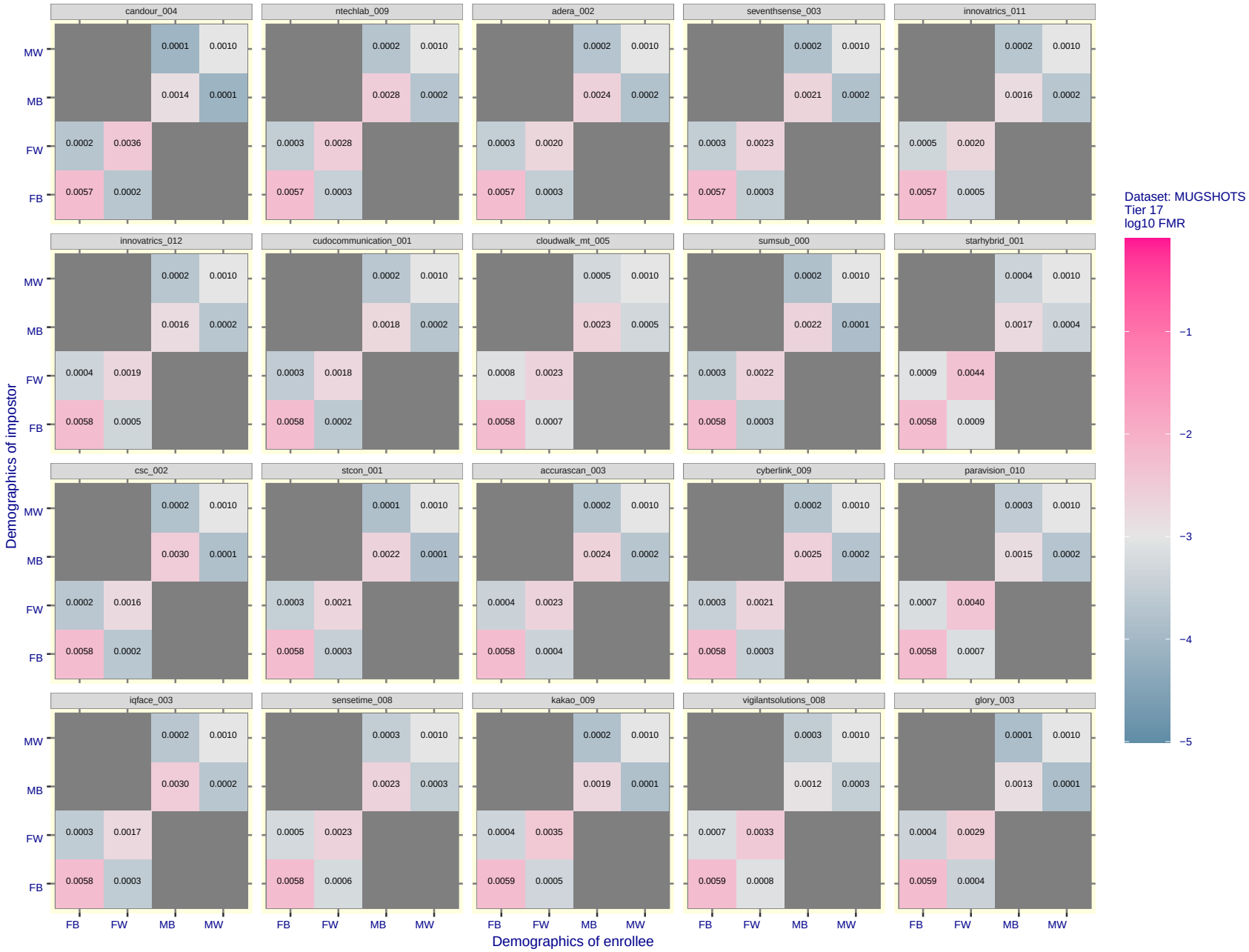

Figure 337: For the mugshot images, FMR *for same-sex impostor pairs of images annotated with codes for black female, black male, white female, white male. The threshold is set for each algorithm to give* FMR *= 0.001 for white males which is the demographic that usually gives the lowest* FMR*. This means the top right box is the same color in all panels. The panels are sorted over multiple pages in order of* FMR *on black females, which is the demographc that usually gives the highest* FMR*.*

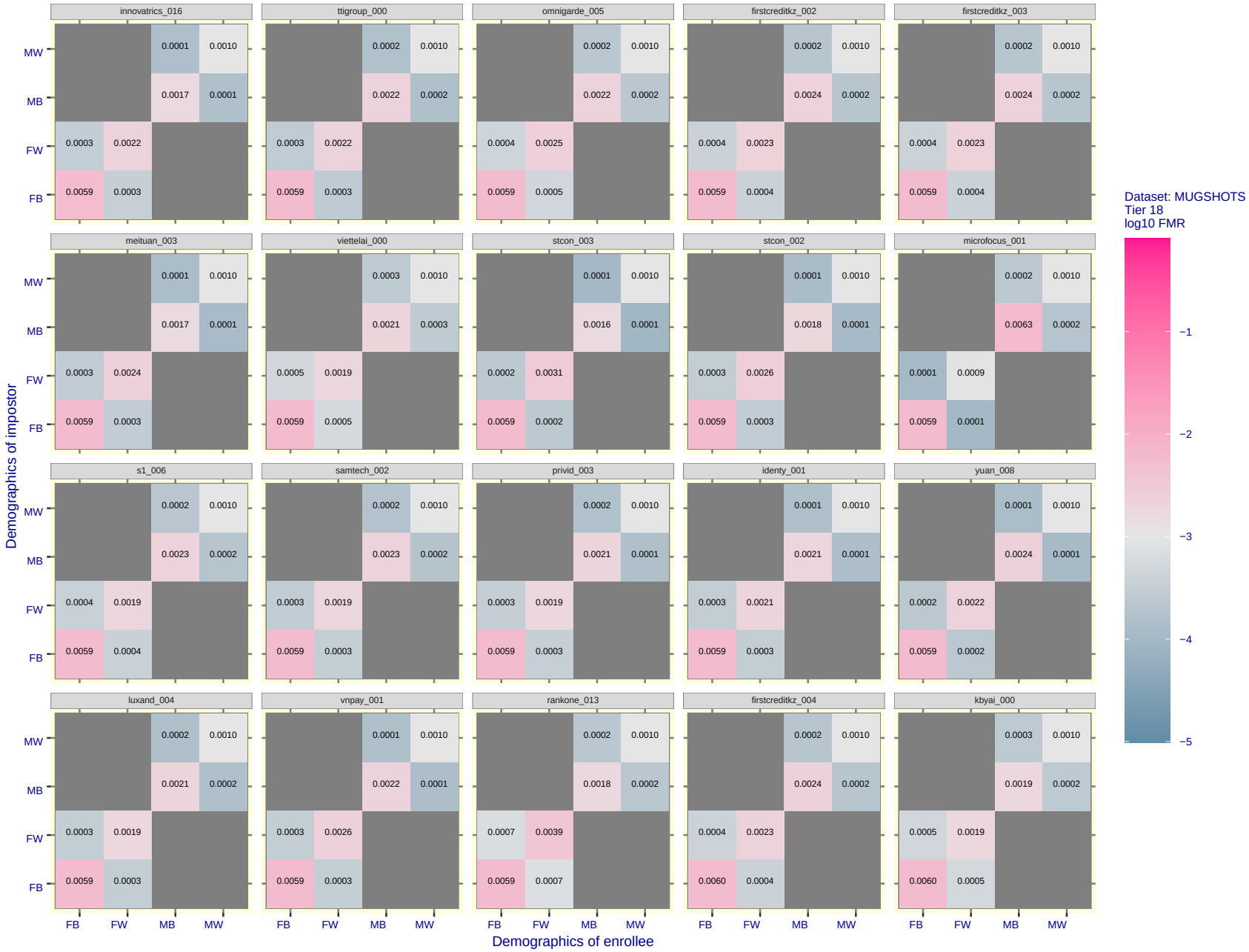

Figure 338: For the mugshot images, FMR *for same-sex impostor pairs of images annotated with codes for black female, black male, white female, white male. The threshold is set for each algorithm to give* FMR *= 0.001 for white males which is the demographic that usually gives the lowest* FMR*. This means the top right box is the same color in all panels. The panels are sorted over multiple pages in order of* FMR *on black females, which is the demographc that usually gives the highest* FMR*.*

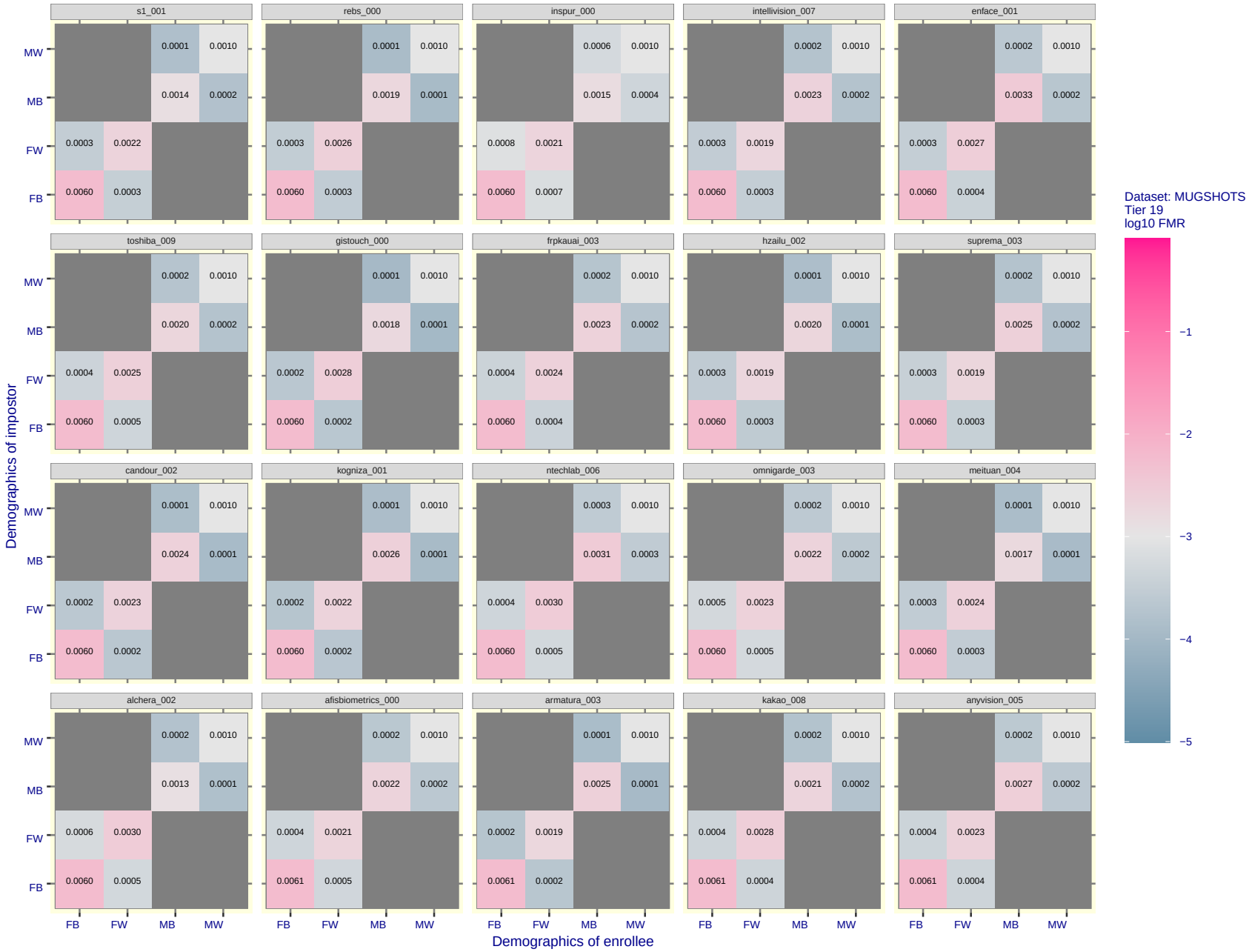

Figure 339: For the mugshot images, FMR *for same-sex impostor pairs of images annotated with codes for black female, black male, white female, white male. The threshold is set for each algorithm to give* FMR *= 0.001 for white males which is the demographic that usually gives the lowest* FMR*. This means the top right box is the same color in all panels. The panels are sorted over multiple pages in order of* FMR *on black females, which is the demographc that usually gives the highest* FMR*.*

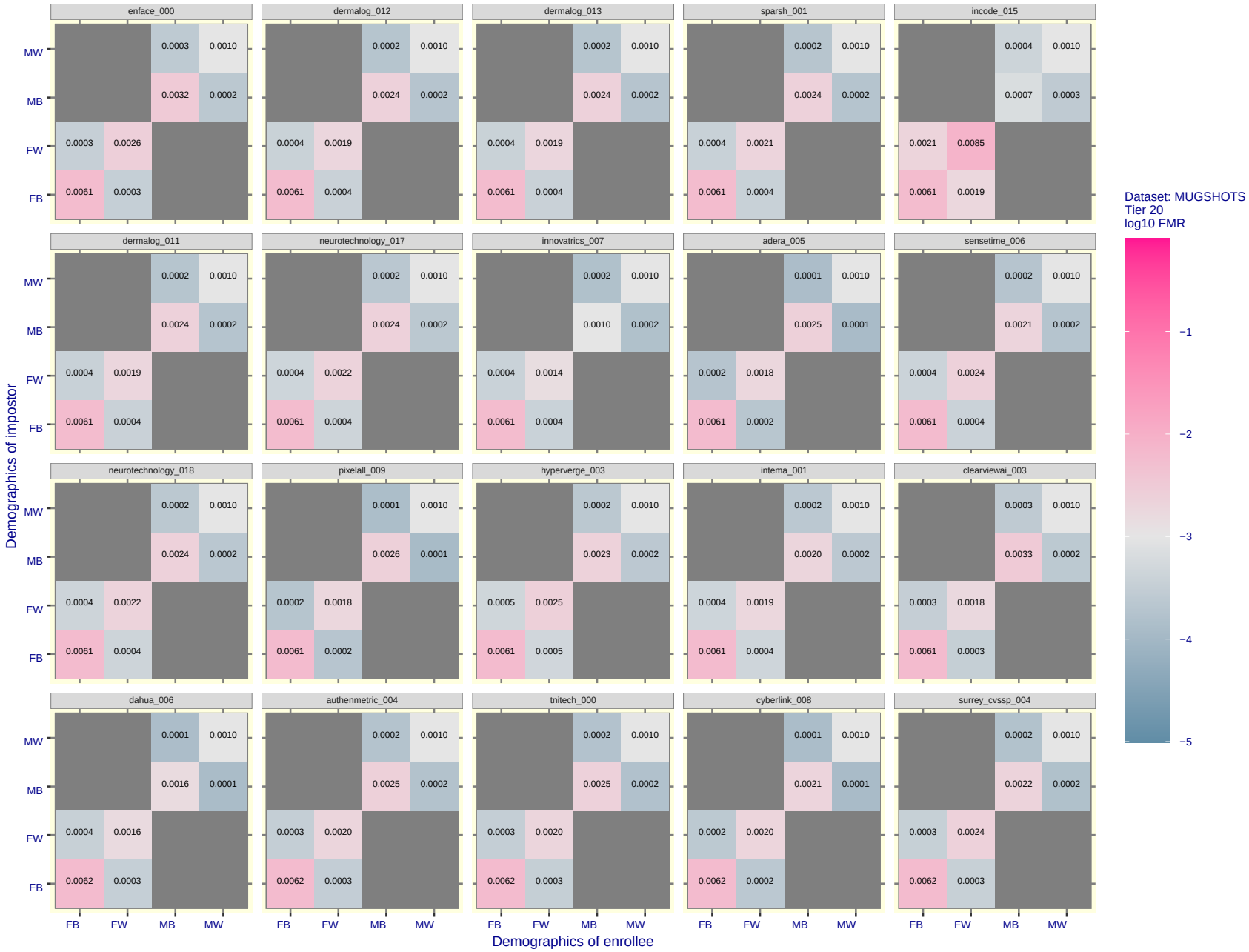

Figure 340: For the mugshot images, FMR *for same-sex impostor pairs of images annotated with codes for black female, black male, white female, white male. The threshold is set for each algorithm to give* FMR *= 0.001 for white males which is the demographic that usually gives the lowest* FMR*. This means the top right box is the same color in all panels. The panels are sorted over multiple pages in order of* FMR *on black females, which is the demographc that usually gives the highest* FMR*.*

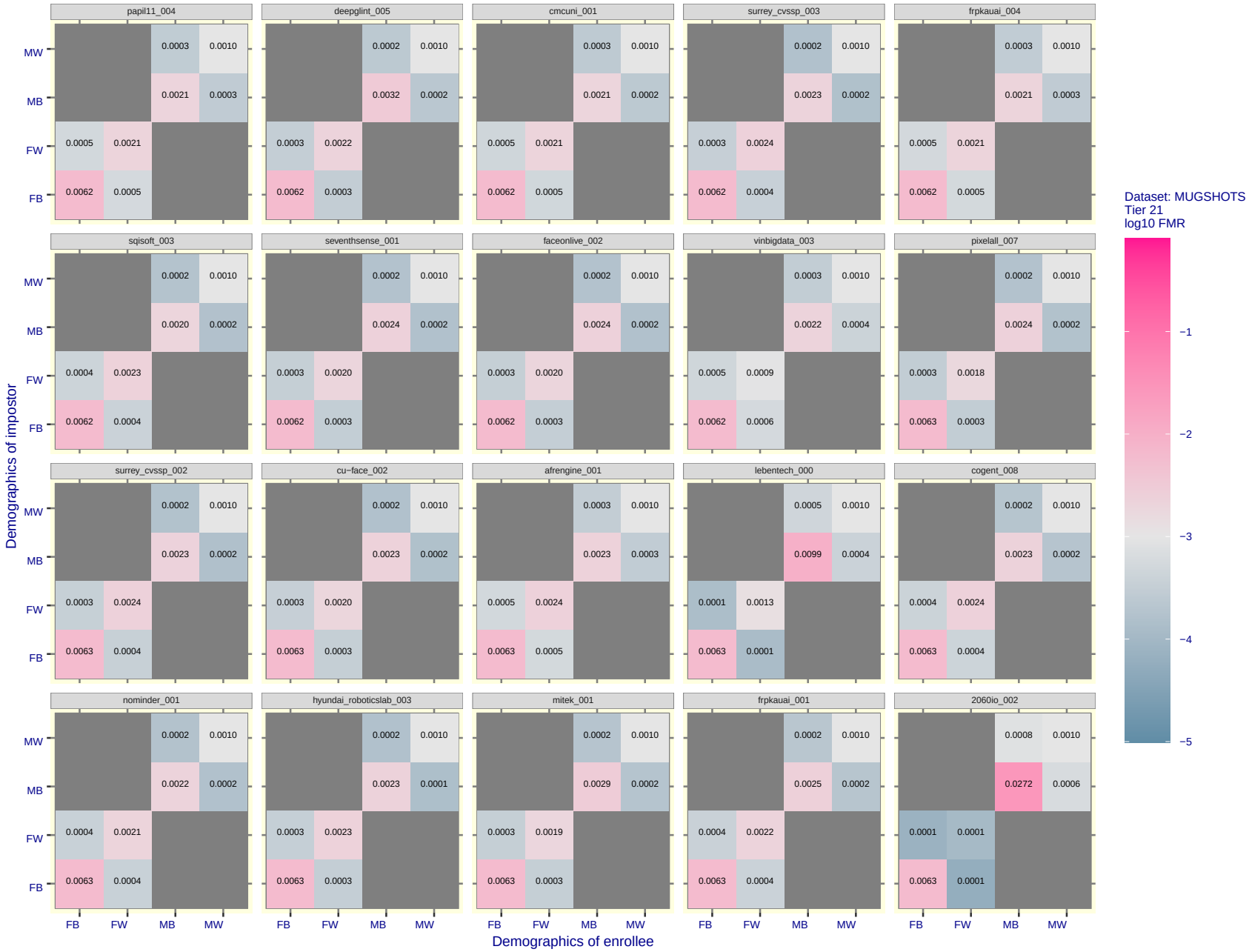

Figure 341: For the mugshot images, FMR *for same-sex impostor pairs of images annotated with codes for black female, black male, white female, white male. The threshold is set for each algorithm to give* FMR *= 0.001 for white males which is the demographic that usually gives the lowest* FMR*. This means the top right box is the same color in all panels. The panels are sorted over multiple pages in order of* FMR *on black females, which is the demographc that usually gives the highest* FMR*.*

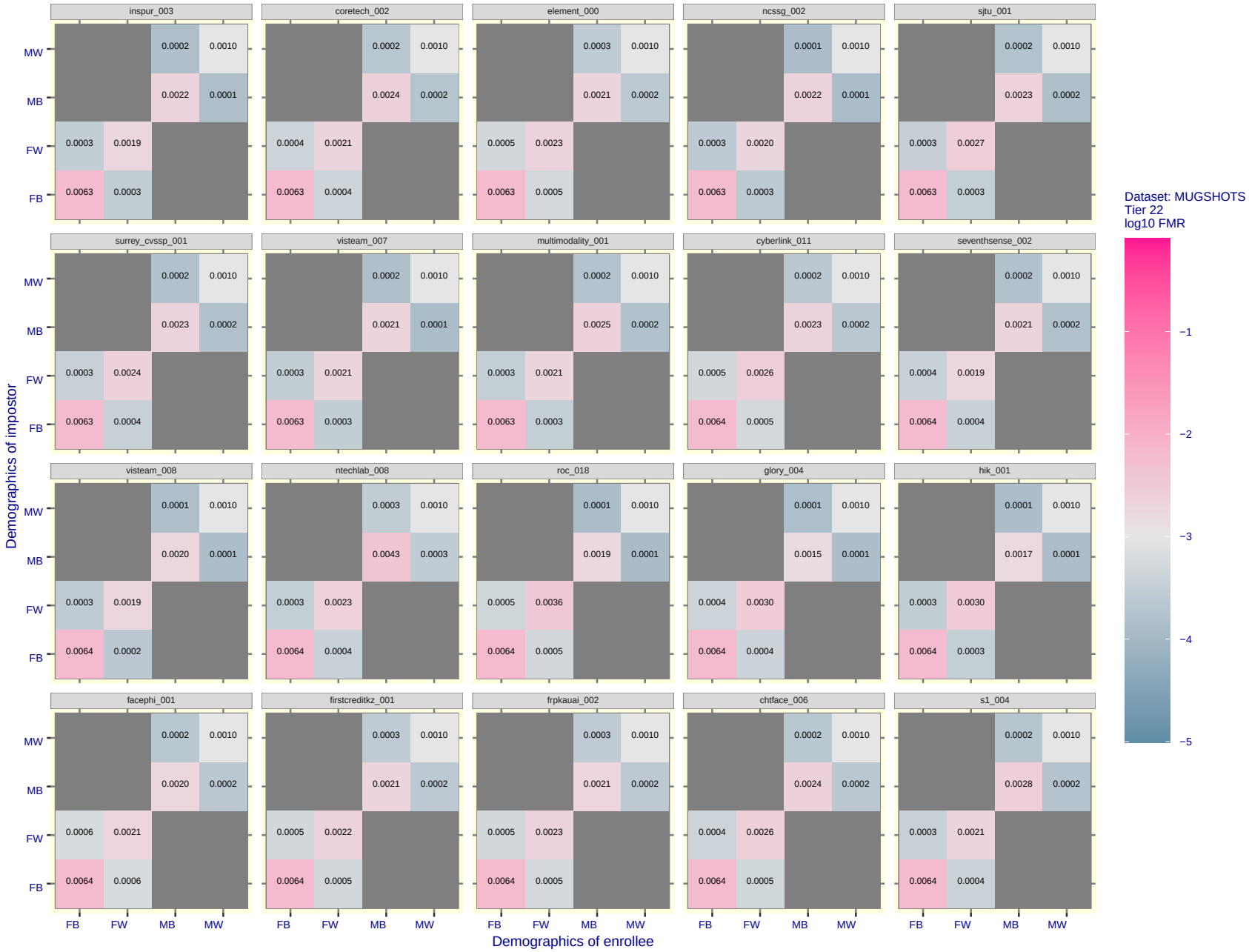

Figure 342: For the mugshot images, FMR *for same-sex impostor pairs of images annotated with codes for black female, black male, white female, white male. The threshold is set for each algorithm to give* FMR *= 0.001 for white males which is the demographic that usually gives the lowest* FMR*. This means the top right box is the same color in all panels. The panels are sorted over multiple pages in order of* FMR *on black females, which is the demographc that usually gives the highest* FMR*.*

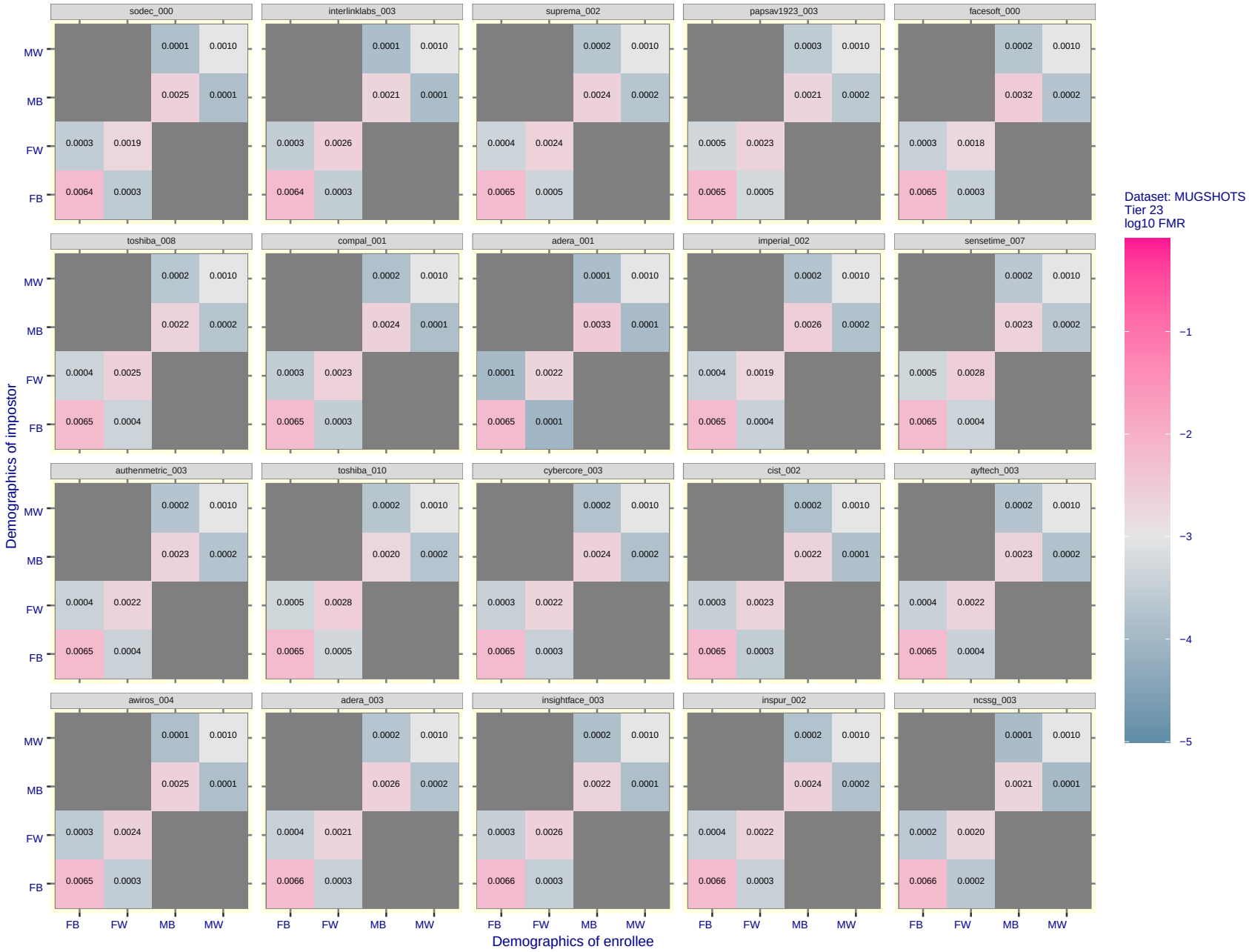

Figure 343: For the mugshot images, FMR *for same-sex impostor pairs of images annotated with codes for black female, black male, white female, white male. The threshold is set for each algorithm to give* FMR *= 0.001 for white males which is the demographic that usually gives the lowest* FMR*. This means the top right box is the same color in all panels. The panels are sorted over multiple pages in order of* FMR *on black females, which is the demographc that usually gives the highest* FMR*.*

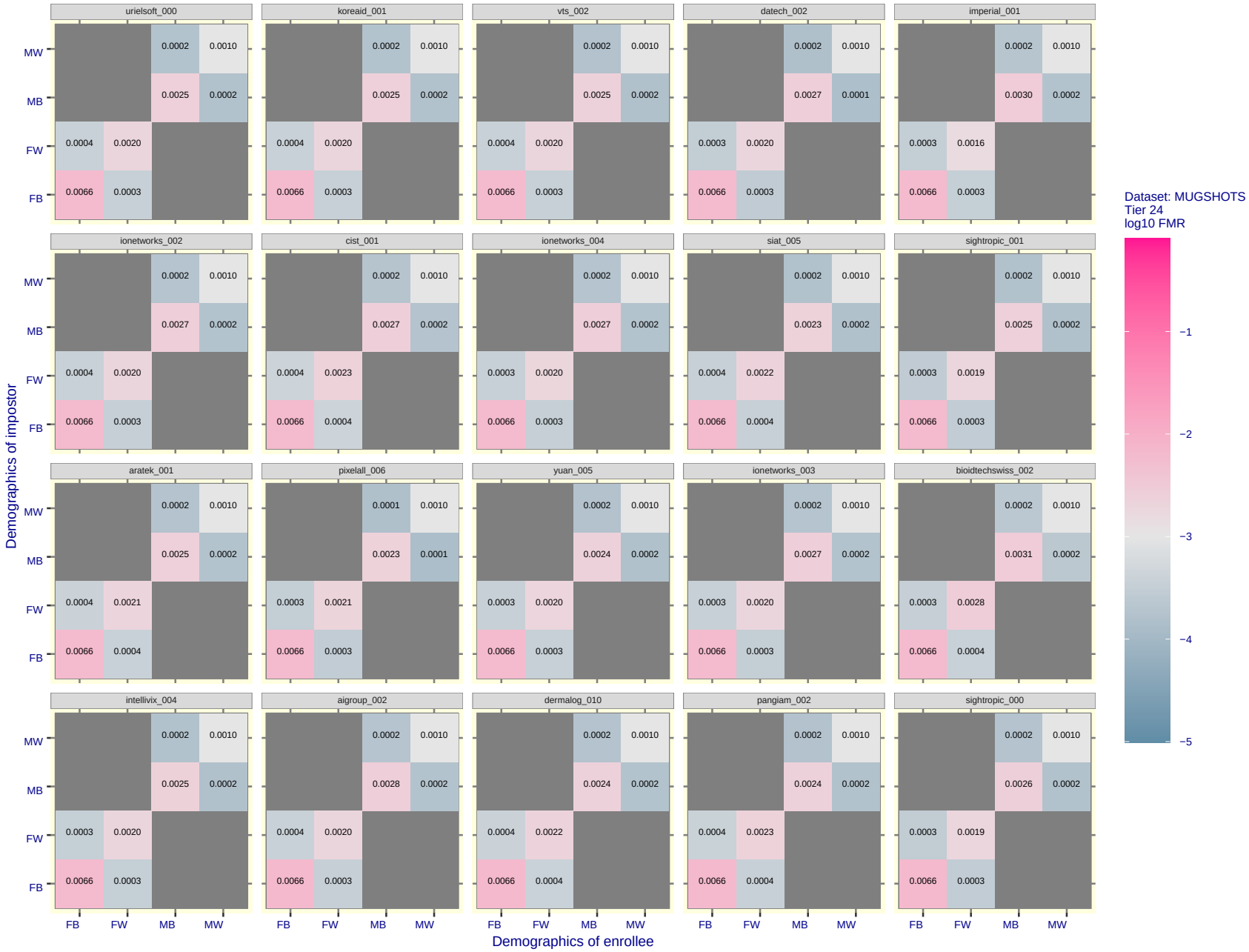

Figure 344: For the mugshot images, FMR *for same-sex impostor pairs of images annotated with codes for black female, black male, white female, white male. The threshold is set for each algorithm to give* FMR *= 0.001 for white males which is the demographic that usually gives the lowest* FMR*. This means the top right box is the same color in all panels. The panels are sorted over multiple pages in order of* FMR *on black females, which is the demographc that usually gives the highest* FMR*.*

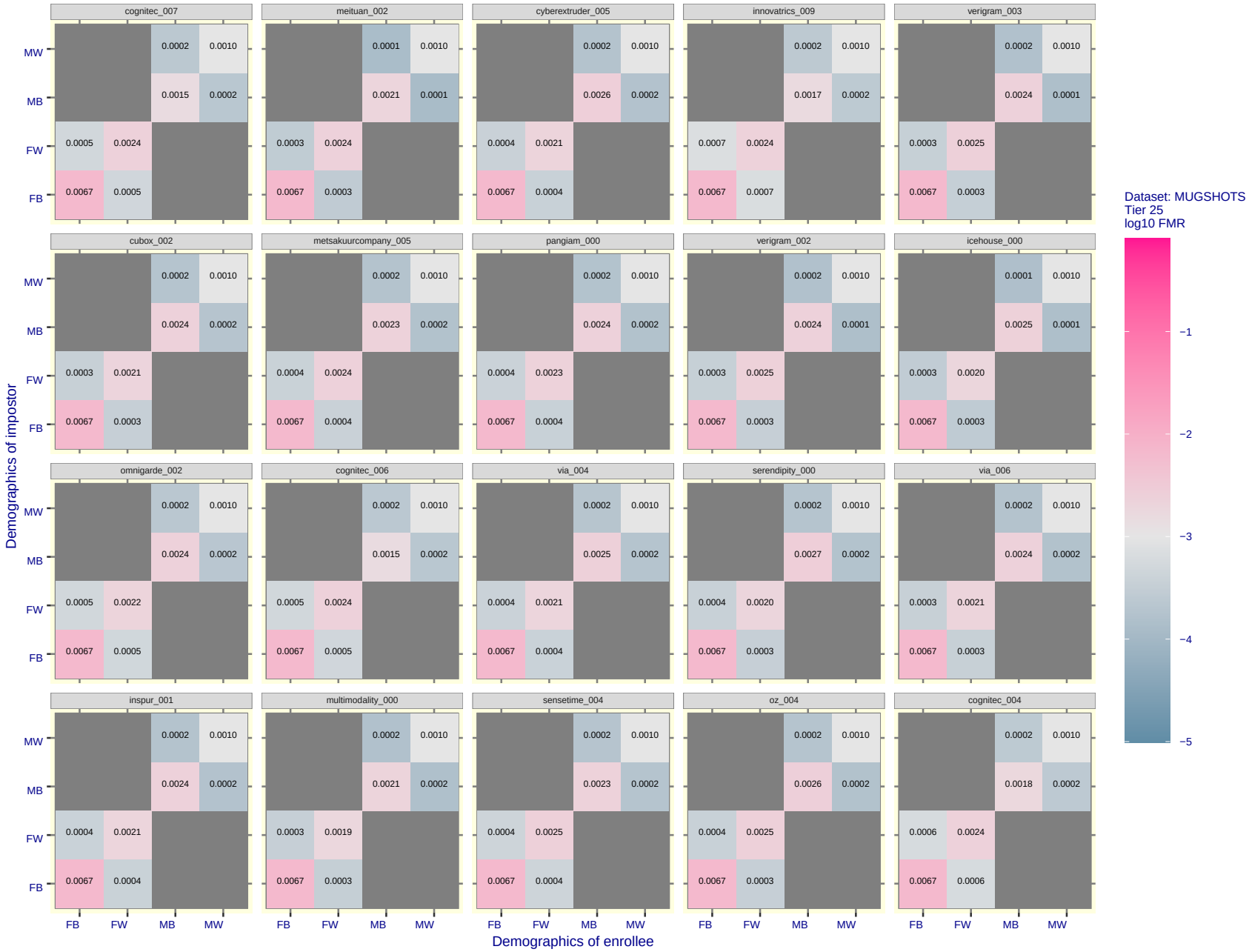

Figure 345: For the mugshot images, FMR *for same-sex impostor pairs of images annotated with codes for black female, black male, white female, white male. The threshold is set for each algorithm to give* FMR *= 0.001 for white males which is the demographic that usually gives the lowest* FMR*. This means the top right box is the same color in all panels. The panels are sorted over multiple pages in order of* FMR *on black females, which is the demographc that usually gives the highest* FMR*.*

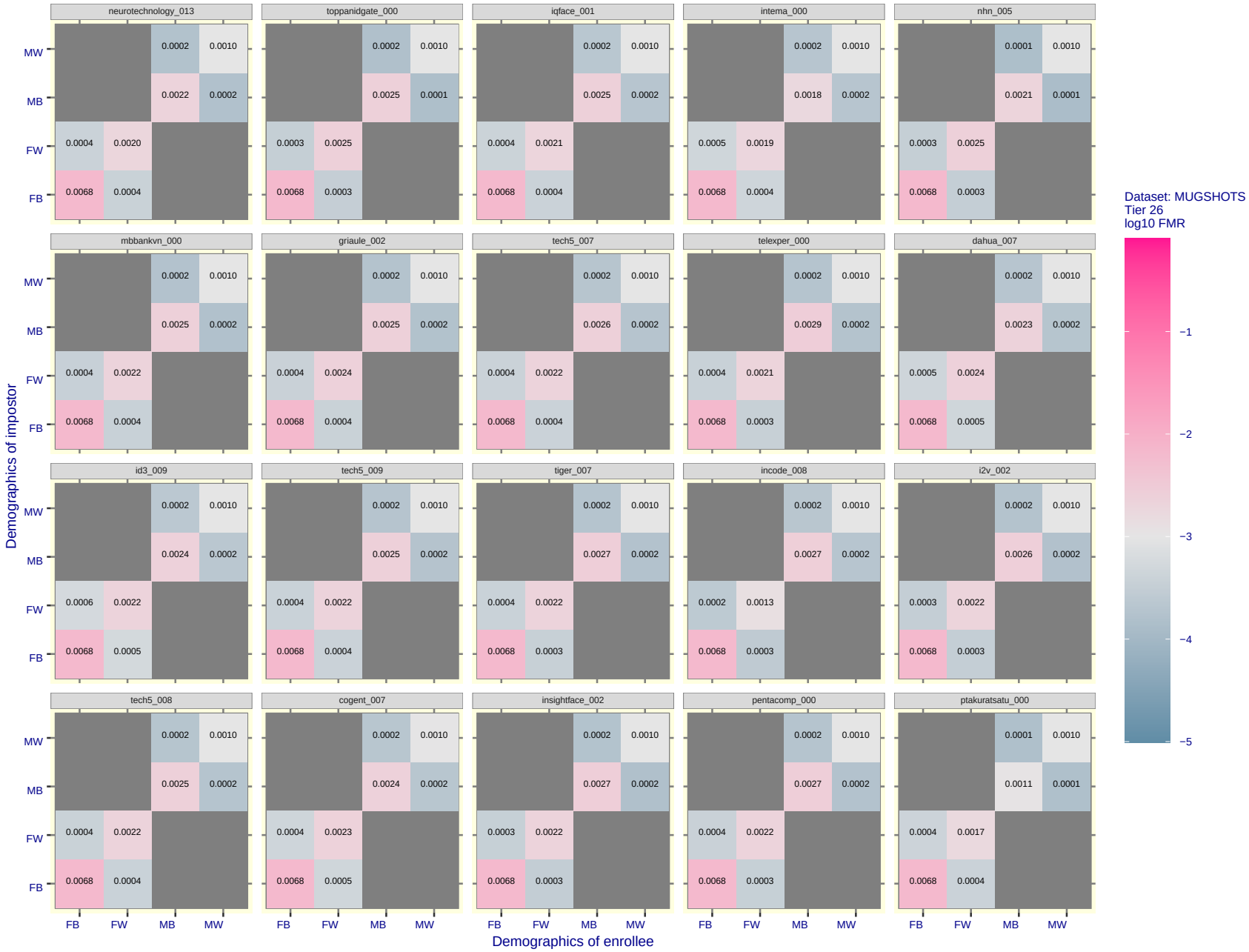

Figure 346: For the mugshot images, FMR *for same-sex impostor pairs of images annotated with codes for black female, black male, white female, white male. The threshold is set for each algorithm to give* FMR *= 0.001 for white males which is the demographic that usually gives the lowest* FMR*. This means the top right box is the same color in all panels. The panels are sorted over multiple pages in order of* FMR *on black females, which is the demographc that usually gives the highest* FMR*.*

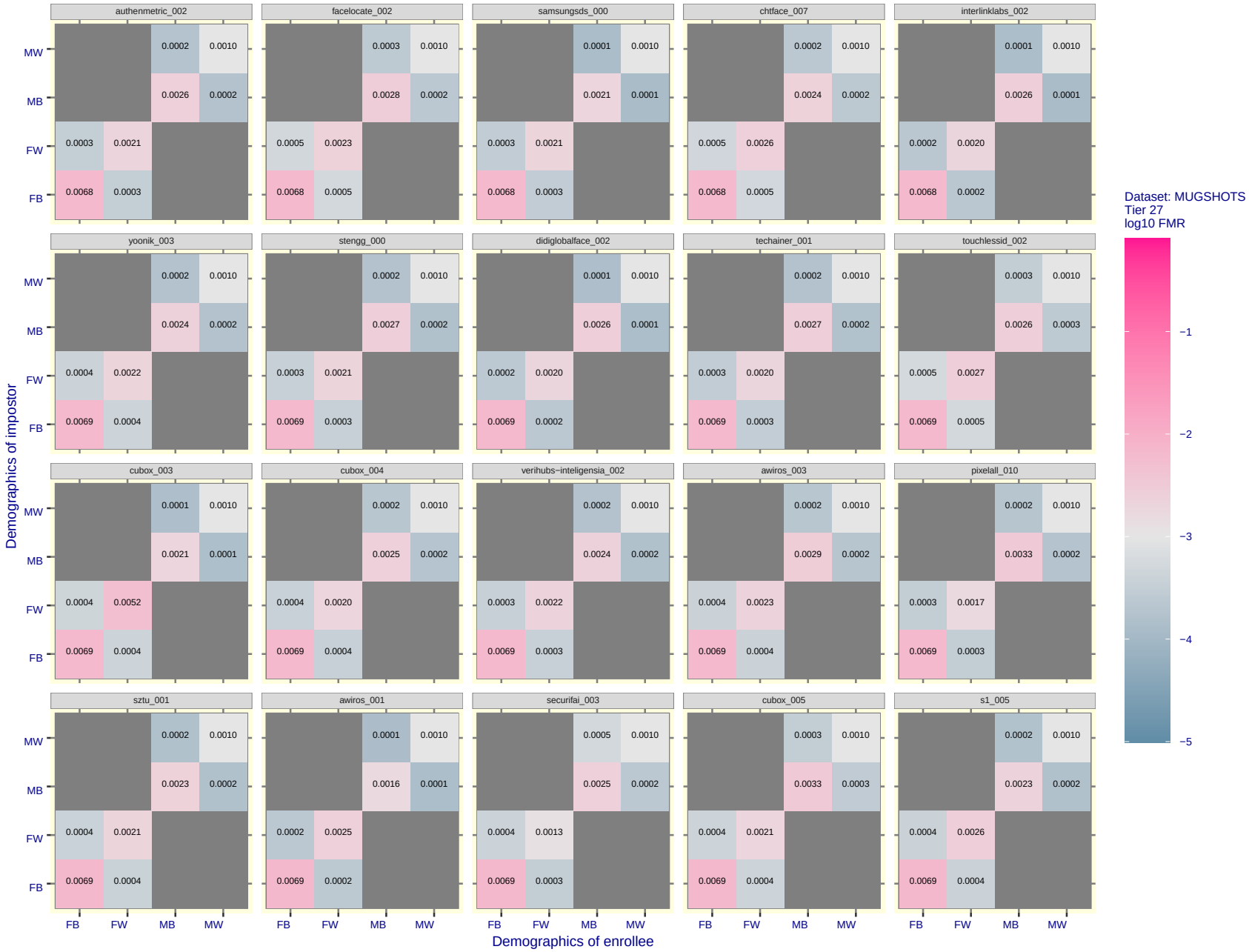

Figure 347: For the mugshot images, FMR *for same-sex impostor pairs of images annotated with codes for black female, black male, white female, white male. The threshold is set for each algorithm to give* FMR *= 0.001 for white males which is the demographic that usually gives the lowest* FMR*. This means the top right box is the same color in all panels. The panels are sorted over multiple pages in order of* FMR *on black females, which is the demographc that usually gives the highest* FMR*.*

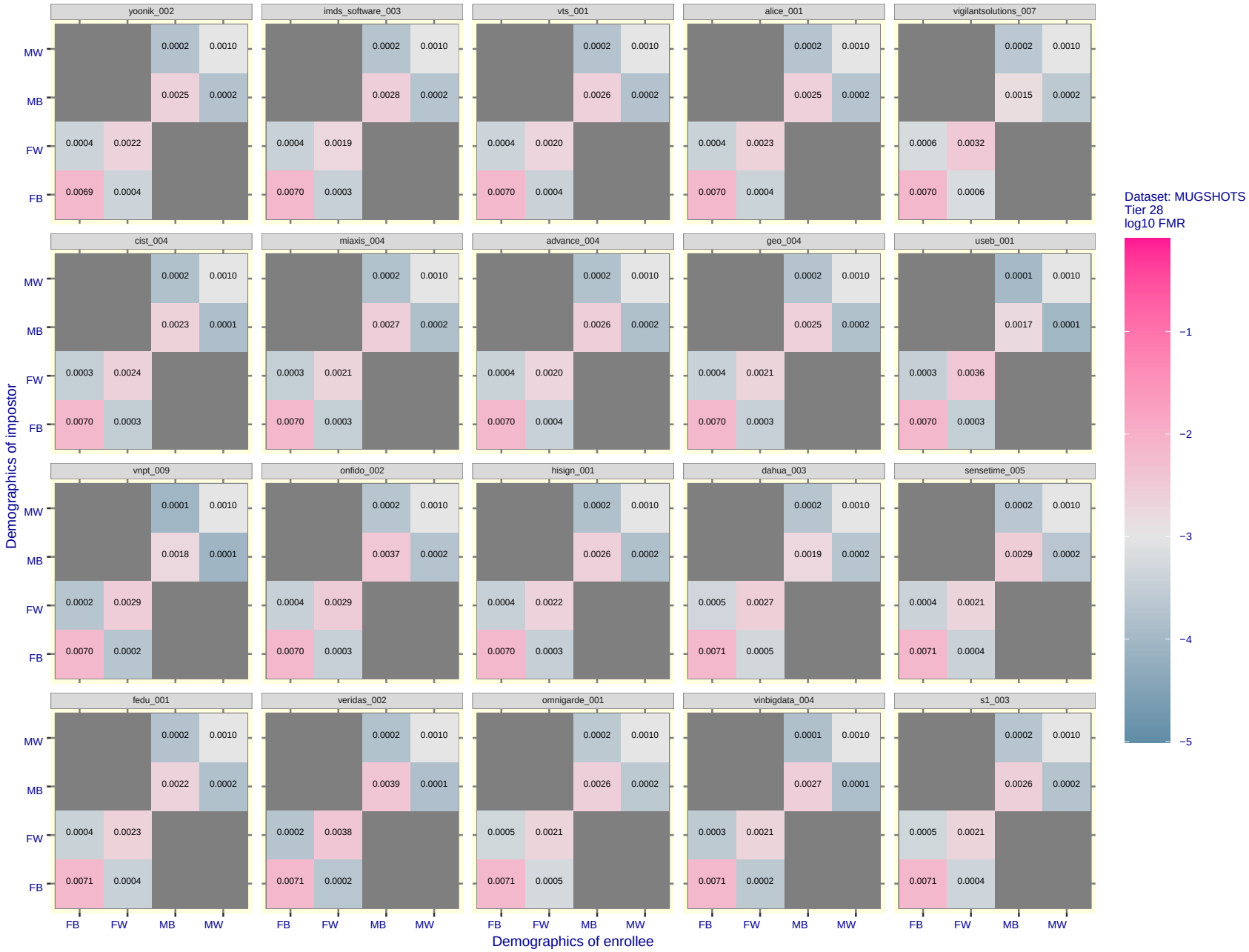

Figure 348: For the mugshot images, FMR *for same-sex impostor pairs of images annotated with codes for black female, black male, white female, white male. The threshold is set for each algorithm to give* FMR *= 0.001 for white males which is the demographic that usually gives the lowest* FMR*. This means the top right box is the same color in all panels. The panels are sorted over multiple pages in order of* FMR *on black females, which is the demographc that usually gives the highest* FMR*.*

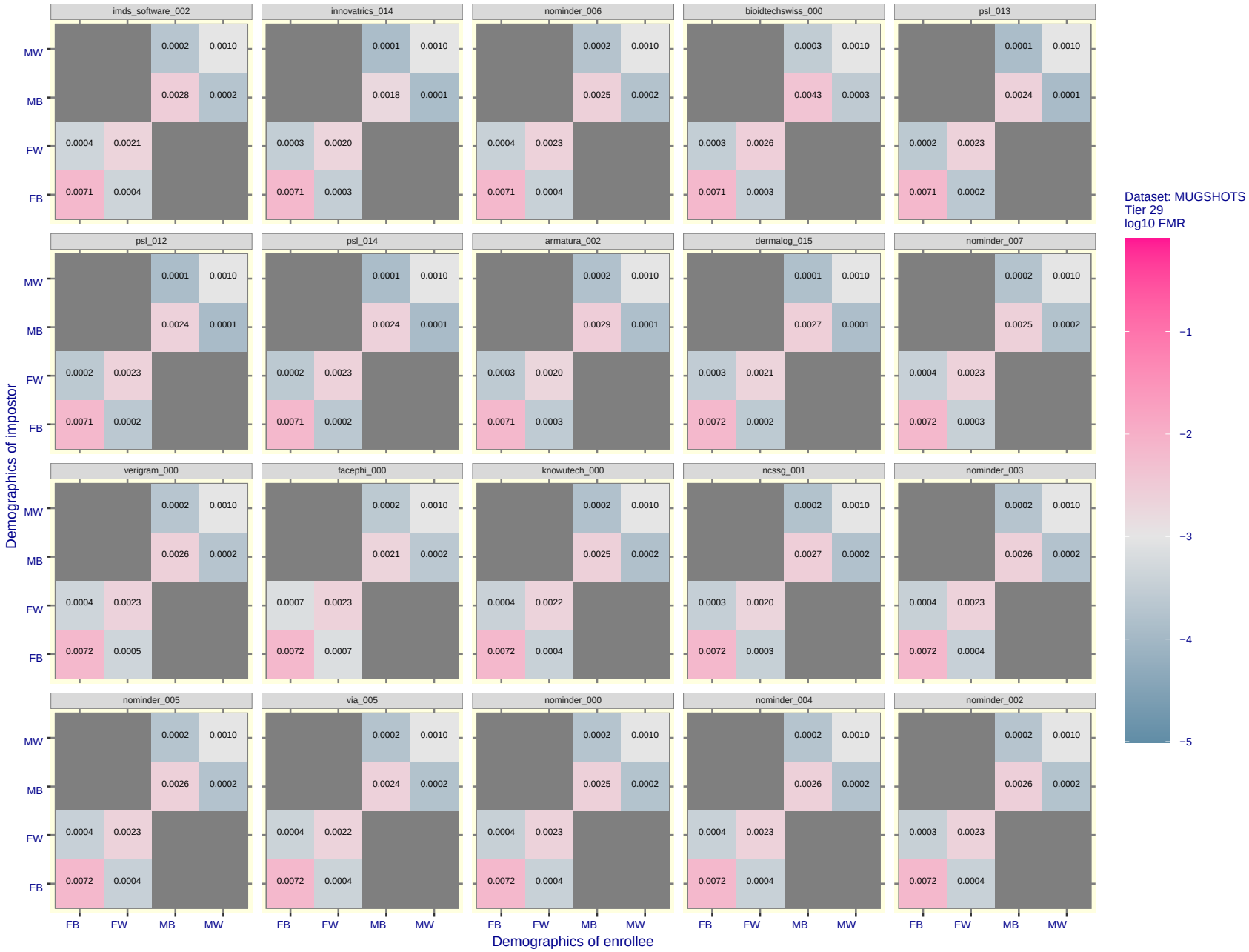

Figure 349: For the mugshot images, FMR *for same-sex impostor pairs of images annotated with codes for black female, black male, white female, white male. The threshold is set for each algorithm to give* FMR *= 0.001 for white males which is the demographic that usually gives the lowest* FMR*. This means the top right box is the same color in all panels. The panels are sorted over multiple pages in order of* FMR *on black females, which is the demographc that usually gives the highest* FMR*.*

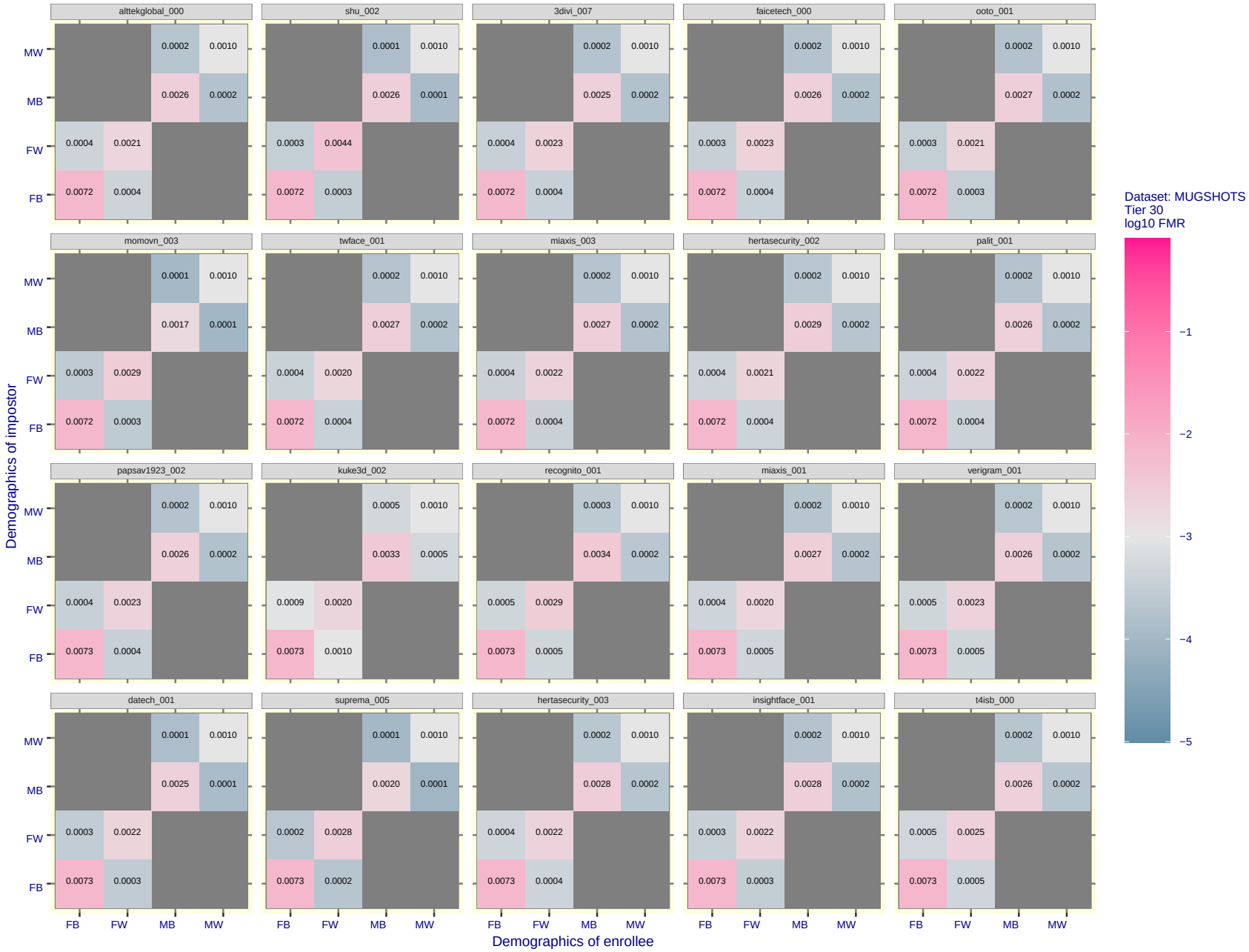

Figure 350: For the mugshot images, FMR *for same-sex impostor pairs of images annotated with codes for black female, black male, white female, white male. The threshold is set for each algorithm to give* FMR *= 0.001 for white males which is the demographic that usually gives the lowest* FMR*. This means the top right box is the same color in all panels. The panels are sorted over multiple pages in order of* FMR *on black females, which is the demographc that usually gives the highest* FMR*.*

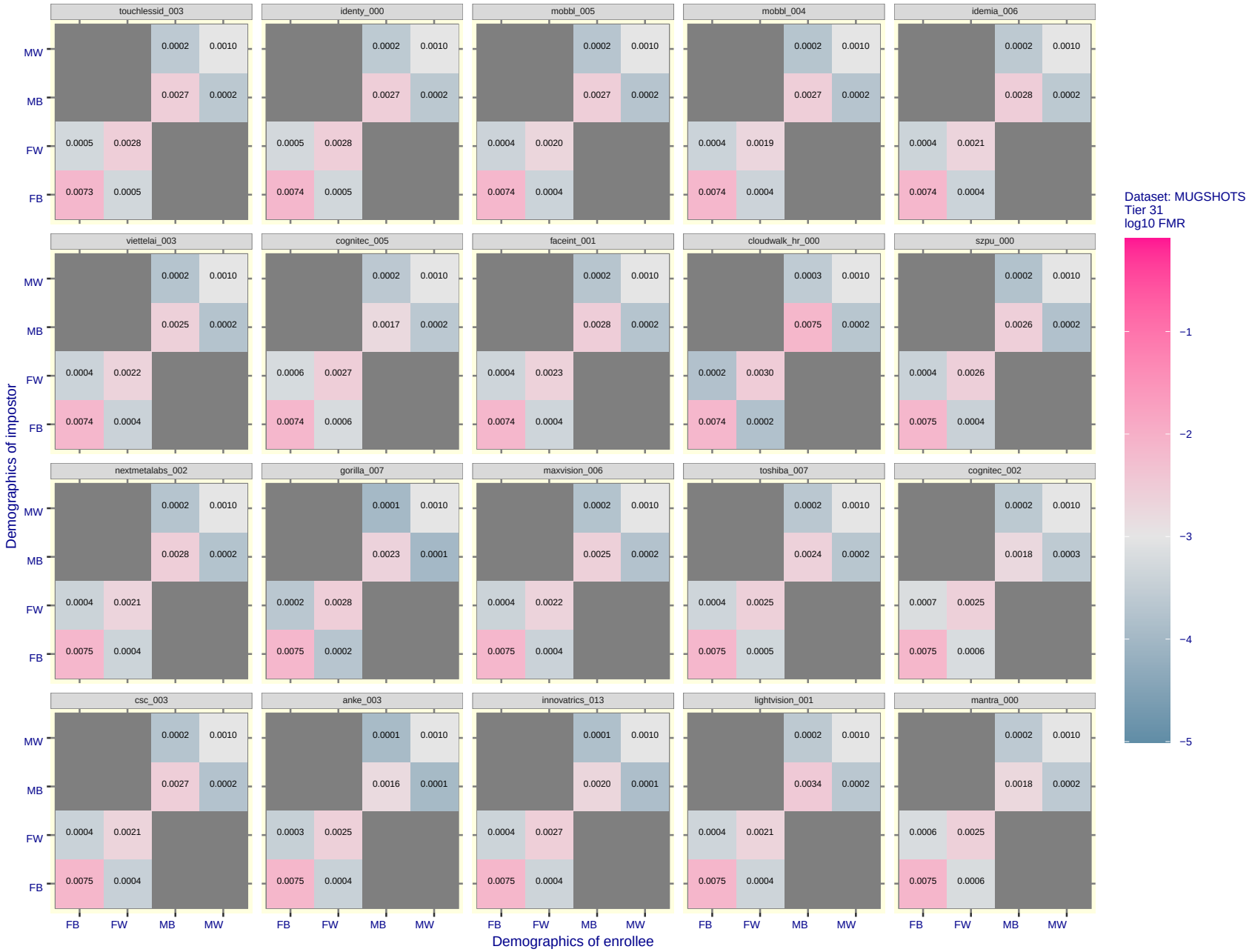

Figure 351: For the mugshot images, FMR *for same-sex impostor pairs of images annotated with codes for black female, black male, white female, white male. The threshold is set for each algorithm to give* FMR *= 0.001 for white males which is the demographic that usually gives the lowest* FMR*. This means the top right box is the same color in all panels. The panels are sorted over multiple pages in order of* FMR *on black females, which is the demographc that usually gives the highest* FMR*.*

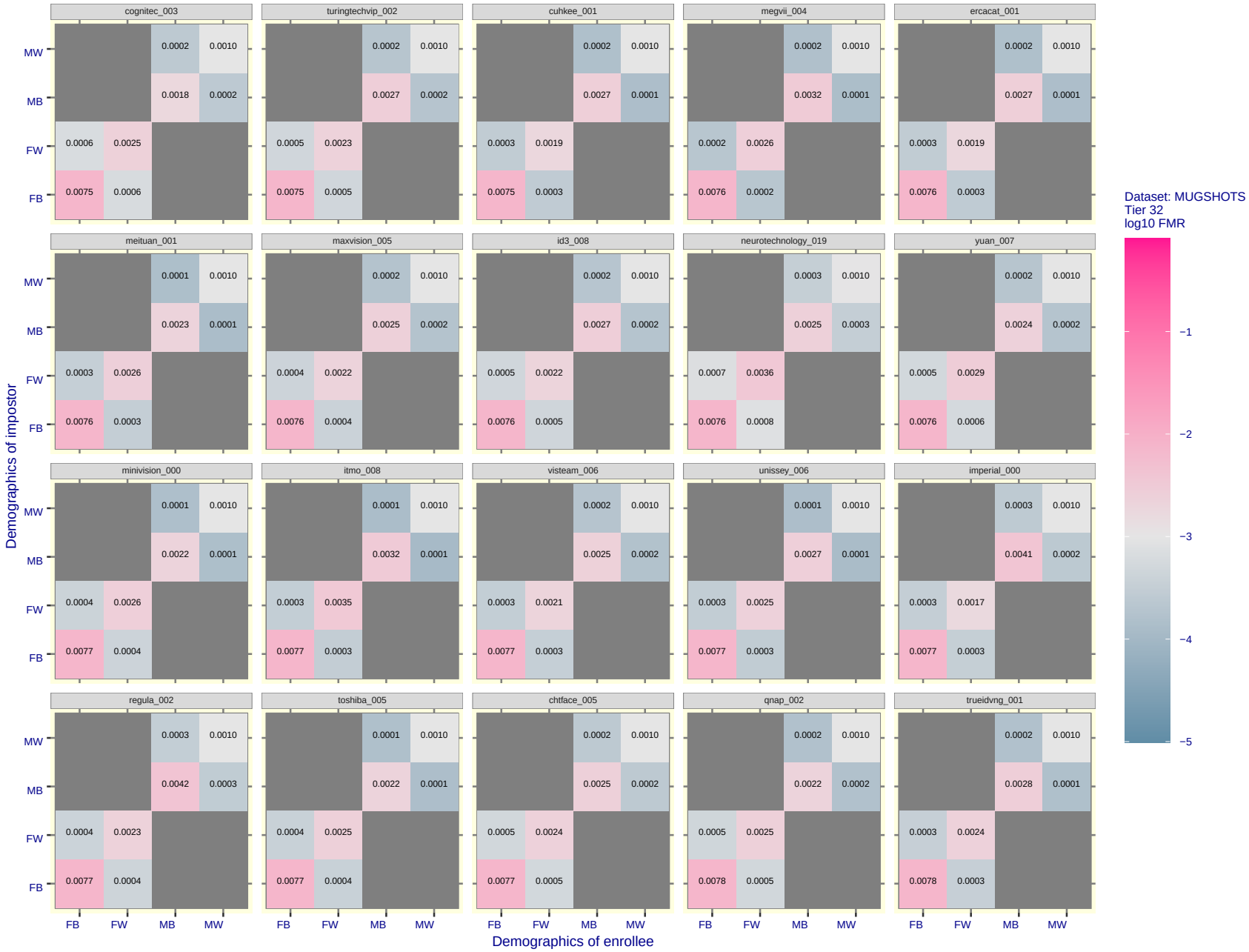

Figure 352: For the mugshot images, FMR *for same-sex impostor pairs of images annotated with codes for black female, black male, white female, white male. The threshold is set for each algorithm to give* FMR *= 0.001 for white males which is the demographic that usually gives the lowest* FMR*. This means the top right box is the same color in all panels. The panels are sorted over multiple pages in order of* FMR *on black females, which is the demographc that usually gives the highest* FMR*.*

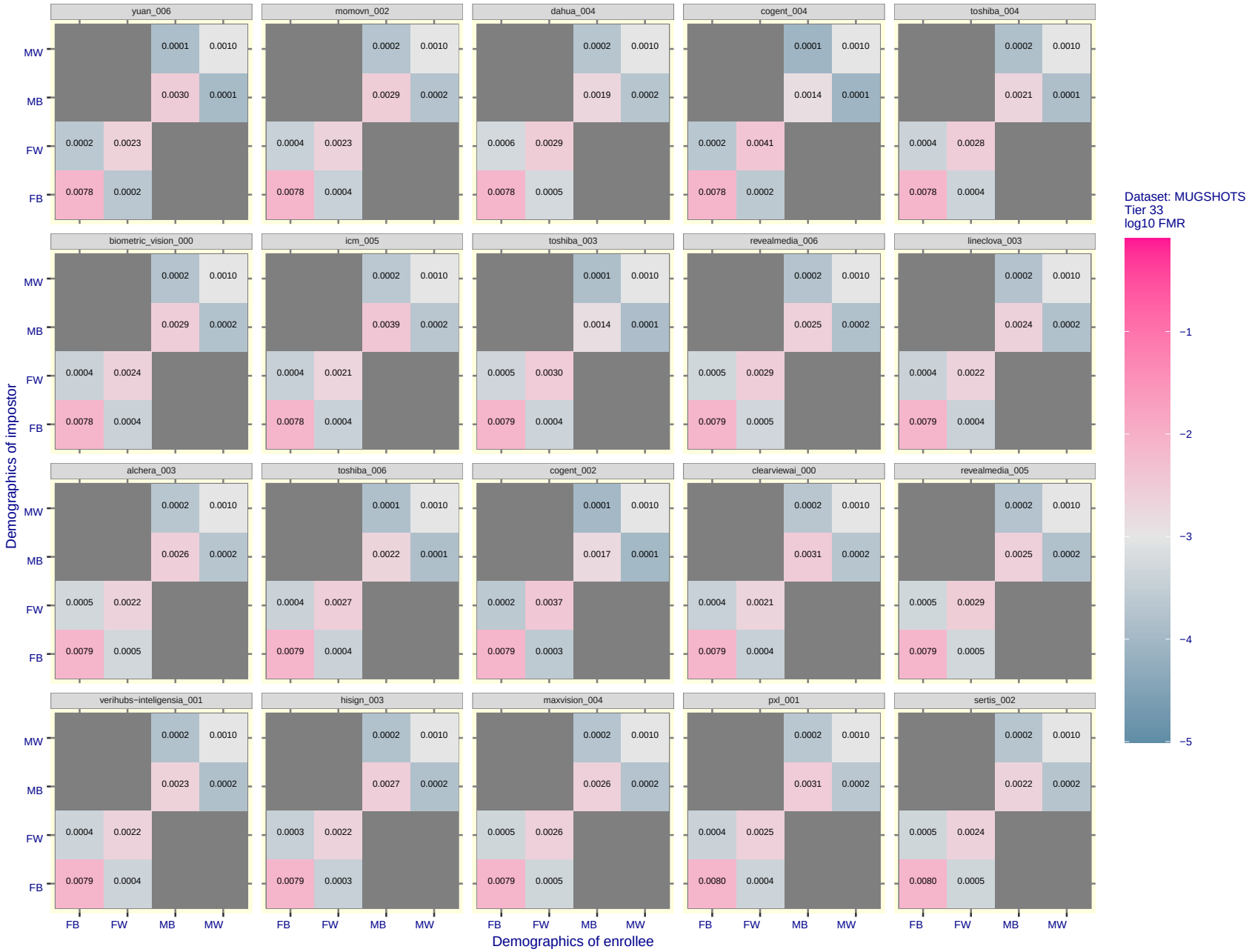

Figure 353: For the mugshot images, FMR *for same-sex impostor pairs of images annotated with codes for black female, black male, white female, white male. The threshold is set for each algorithm to give* FMR *= 0.001 for white males which is the demographic that usually gives the lowest* FMR*. This means the top right box is the same color in all panels. The panels are sorted over multiple pages in order of* FMR *on black females, which is the demographc that usually gives the highest* FMR*.*

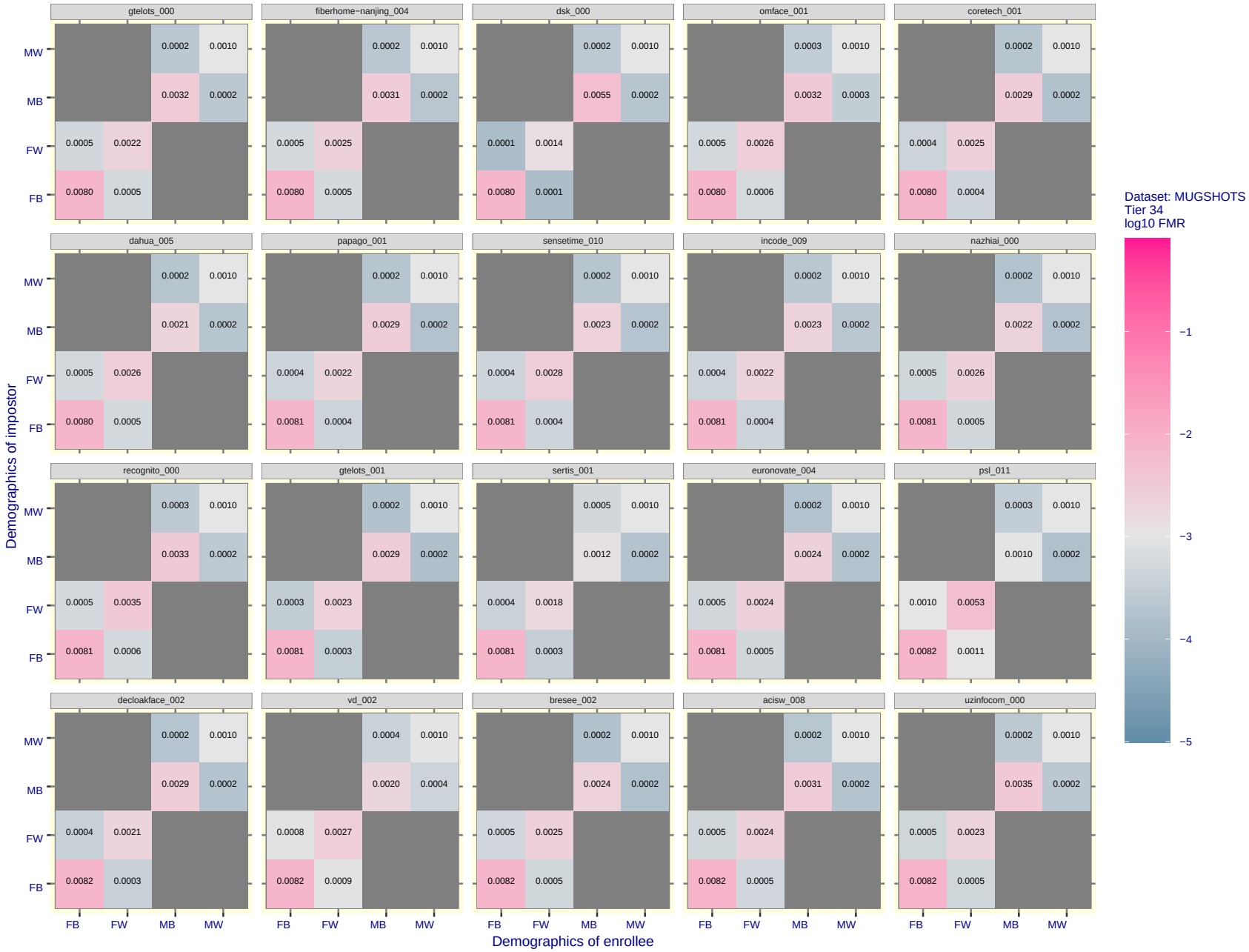

Figure 354: For the mugshot images, FMR *for same-sex impostor pairs of images annotated with codes for black female, black male, white female, white male. The threshold is set for each algorithm to give* FMR *= 0.001 for white males which is the demographic that usually gives the lowest* FMR*. This means the top right box is the same color in all panels. The panels are sorted over multiple pages in order of* FMR *on black females, which is the demographc that usually gives the highest* FMR*.*

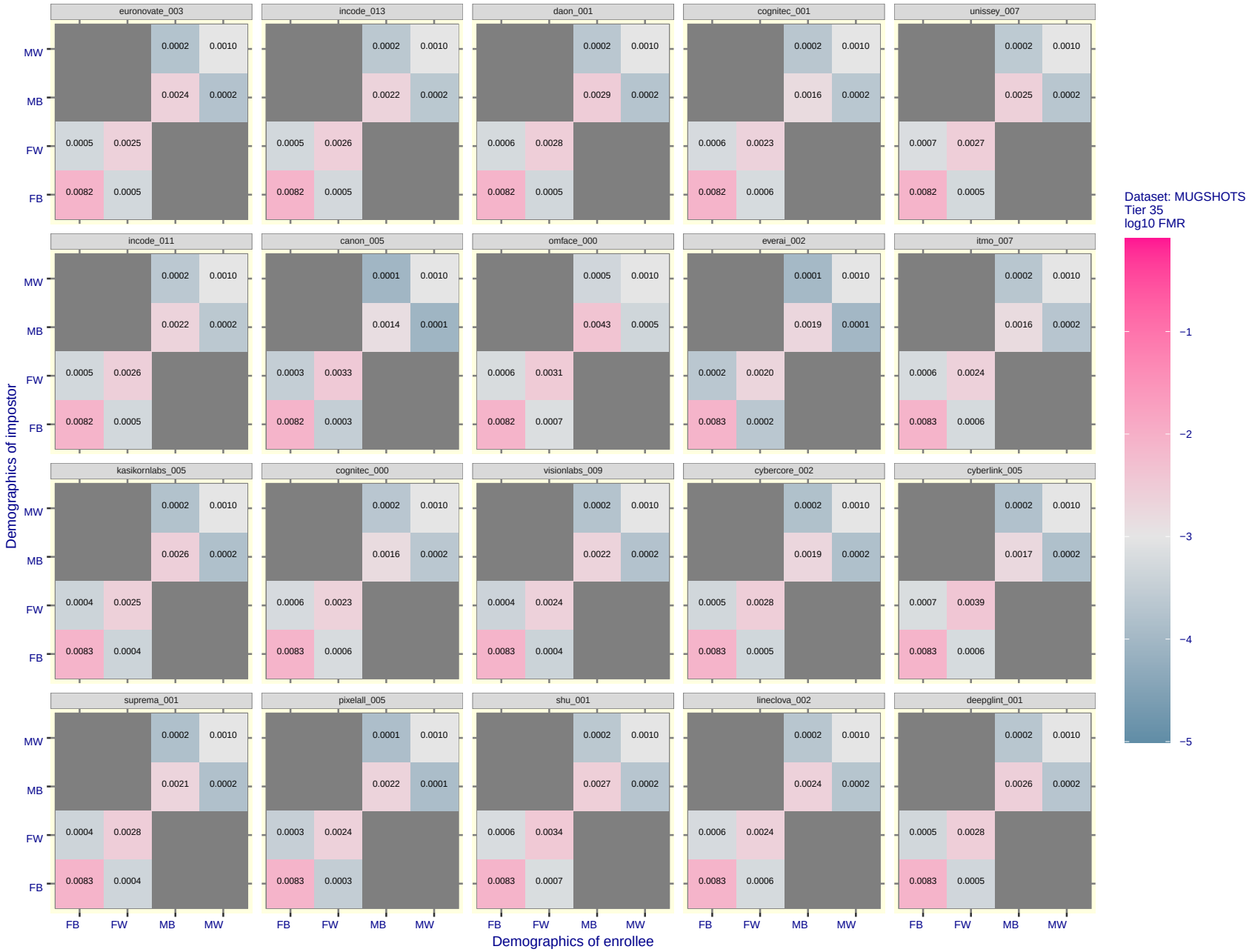

Figure 355: For the mugshot images, FMR *for same-sex impostor pairs of images annotated with codes for black female, black male, white female, white male. The threshold is set for each algorithm to give* FMR *= 0.001 for white males which is the demographic that usually gives the lowest* FMR*. This means the top right box is the same color in all panels. The panels are sorted over multiple pages in order of* FMR *on black females, which is the demographc that usually gives the highest* FMR*.*

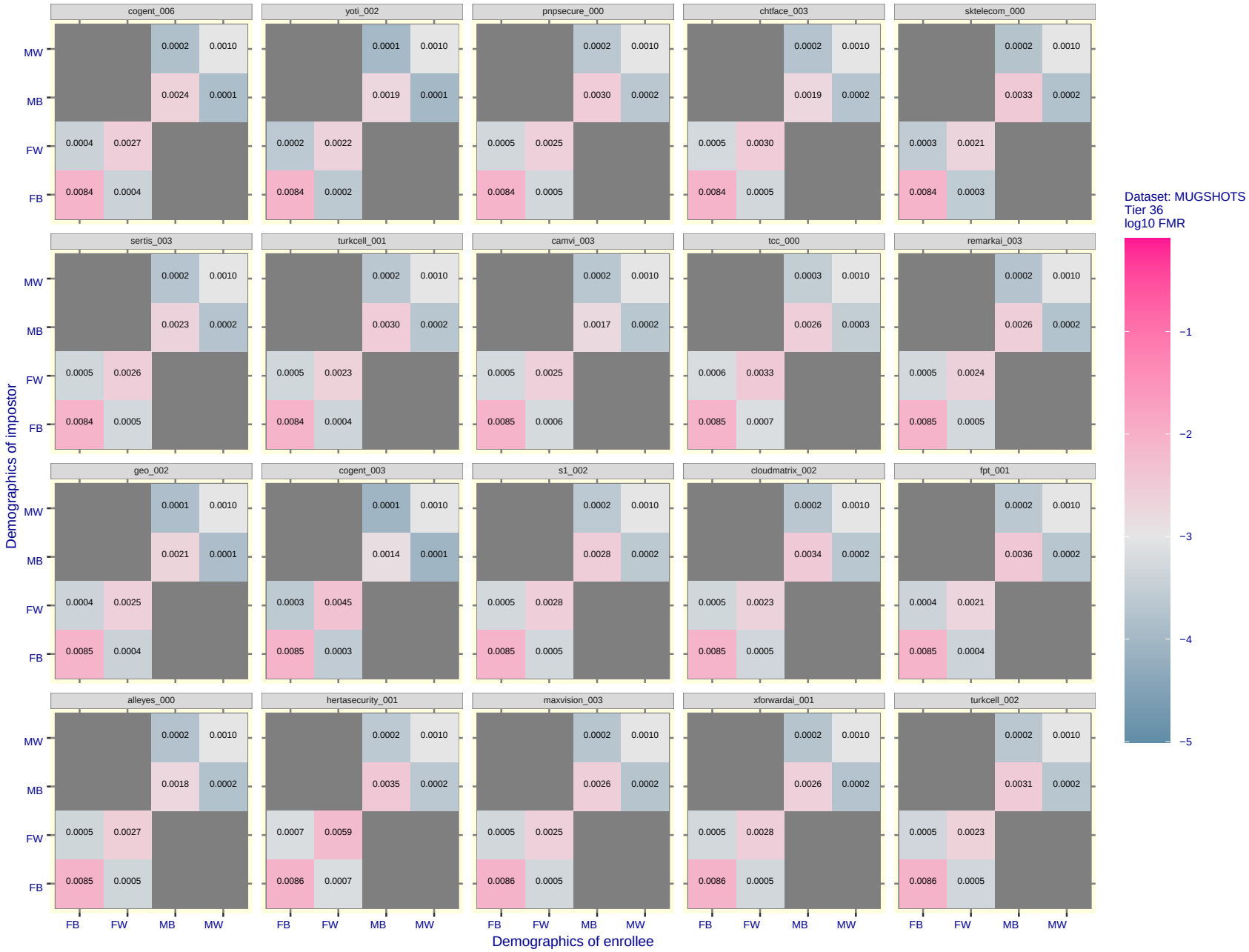

Figure 356: For the mugshot images, FMR *for same-sex impostor pairs of images annotated with codes for black female, black male, white female, white male. The threshold is set for each algorithm to give* FMR *= 0.001 for white males which is the demographic that usually gives the lowest* FMR*. This means the top right box is the same color in all panels. The panels are sorted over multiple pages in order of* FMR *on black females, which is the demographc that usually gives the highest* FMR*.*

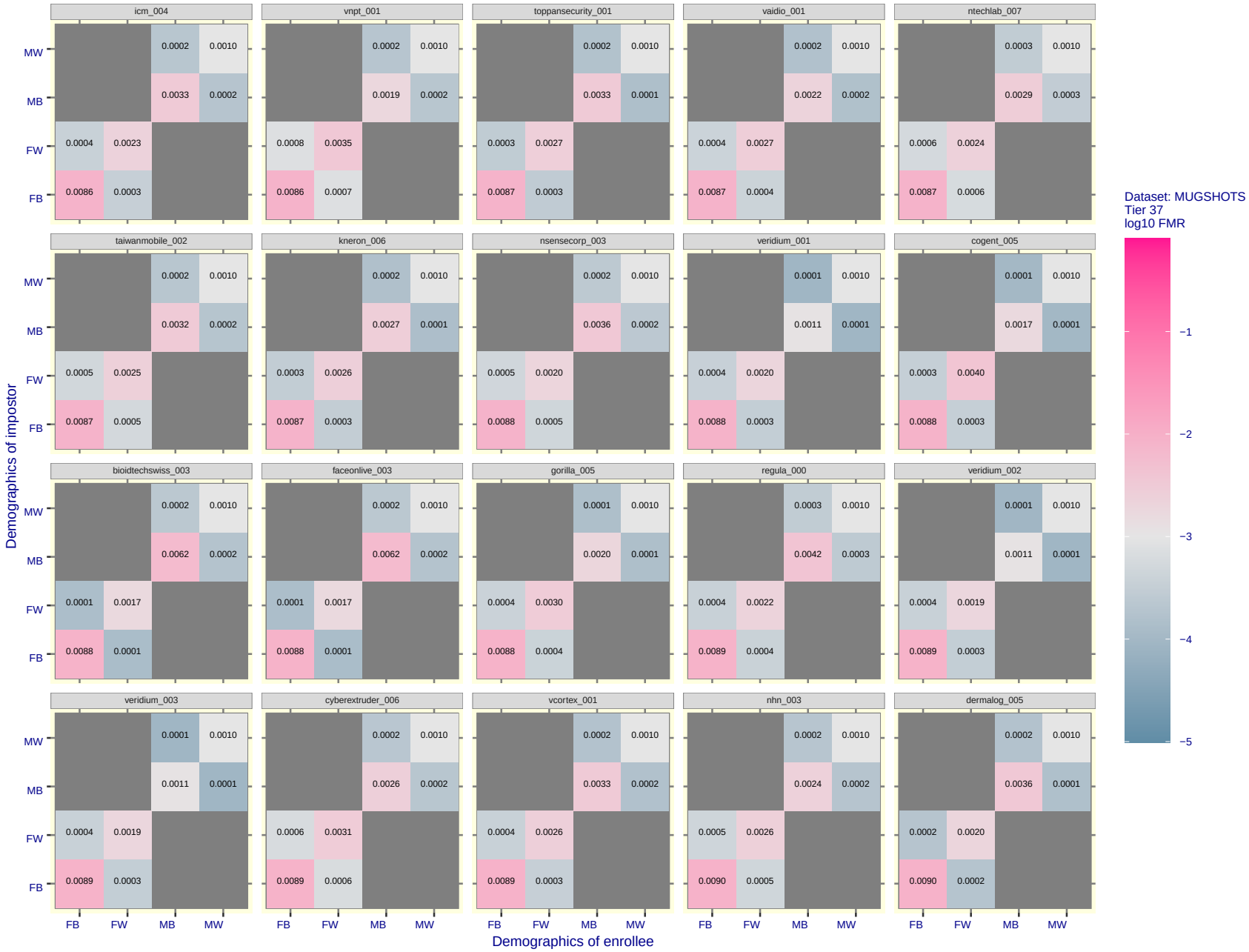

Figure 357: For the mugshot images, FMR *for same-sex impostor pairs of images annotated with codes for black female, black male, white female, white male. The threshold is set for each algorithm to give* FMR *= 0.001 for white males which is the demographic that usually gives the lowest* FMR*. This means the top right box is the same color in all panels. The panels are sorted over multiple pages in order of* FMR *on black females, which is the demographc that usually gives the highest* FMR*.*

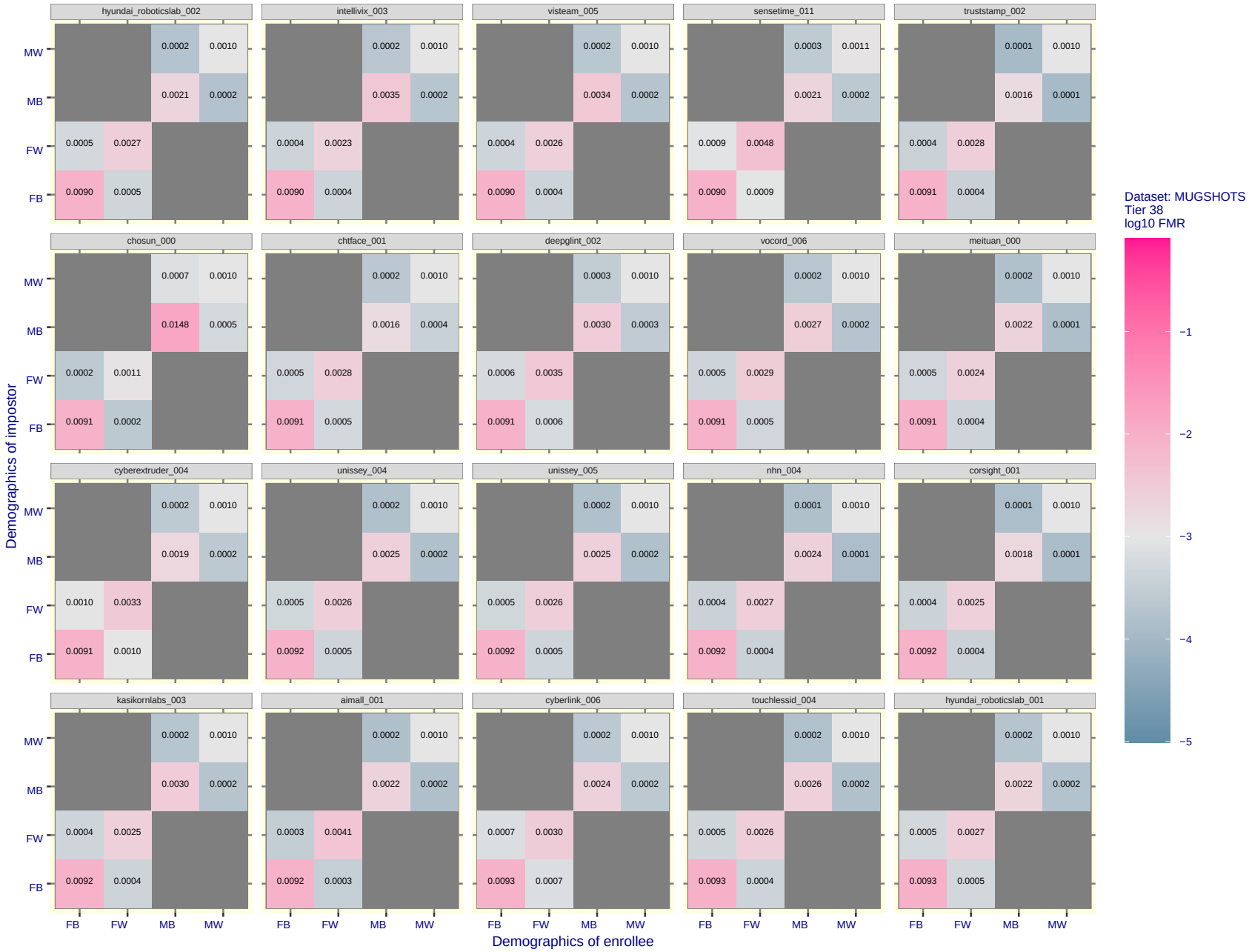

Figure 358: For the mugshot images, FMR *for same-sex impostor pairs of images annotated with codes for black female, black male, white female, white male. The threshold is set for each algorithm to give* FMR *= 0.001 for white males which is the demographic that usually gives the lowest* FMR*. This means the top right box is the same color in all panels. The panels are sorted over multiple pages in order of* FMR *on black females, which is the demographc that usually gives the highest* FMR*.*

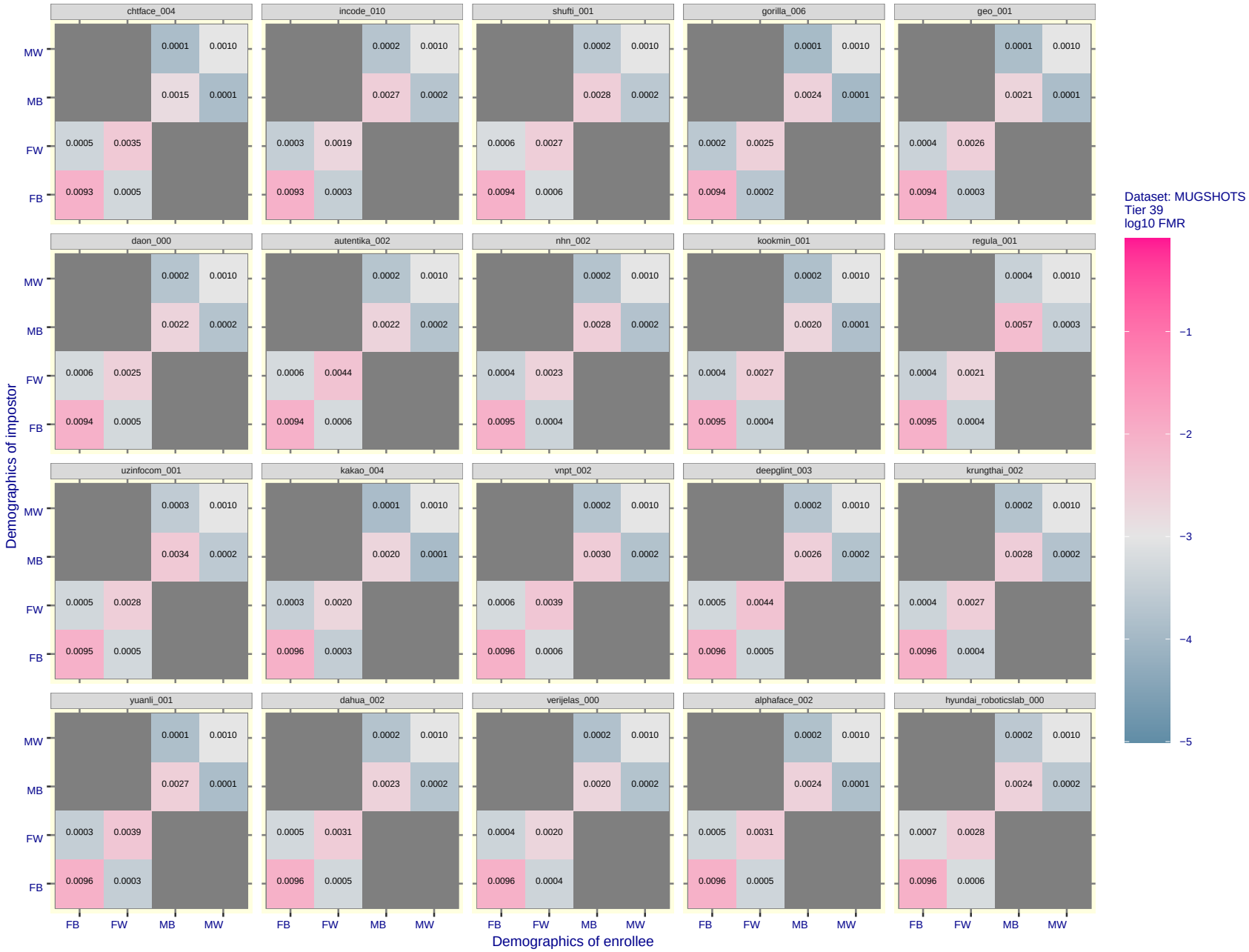

Figure 359: For the mugshot images, FMR *for same-sex impostor pairs of images annotated with codes for black female, black male, white female, white male. The threshold is set for each algorithm to give* FMR *= 0.001 for white males which is the demographic that usually gives the lowest* FMR*. This means the top right box is the same color in all panels. The panels are sorted over multiple pages in order of* FMR *on black females, which is the demographc that usually gives the highest* FMR*.*

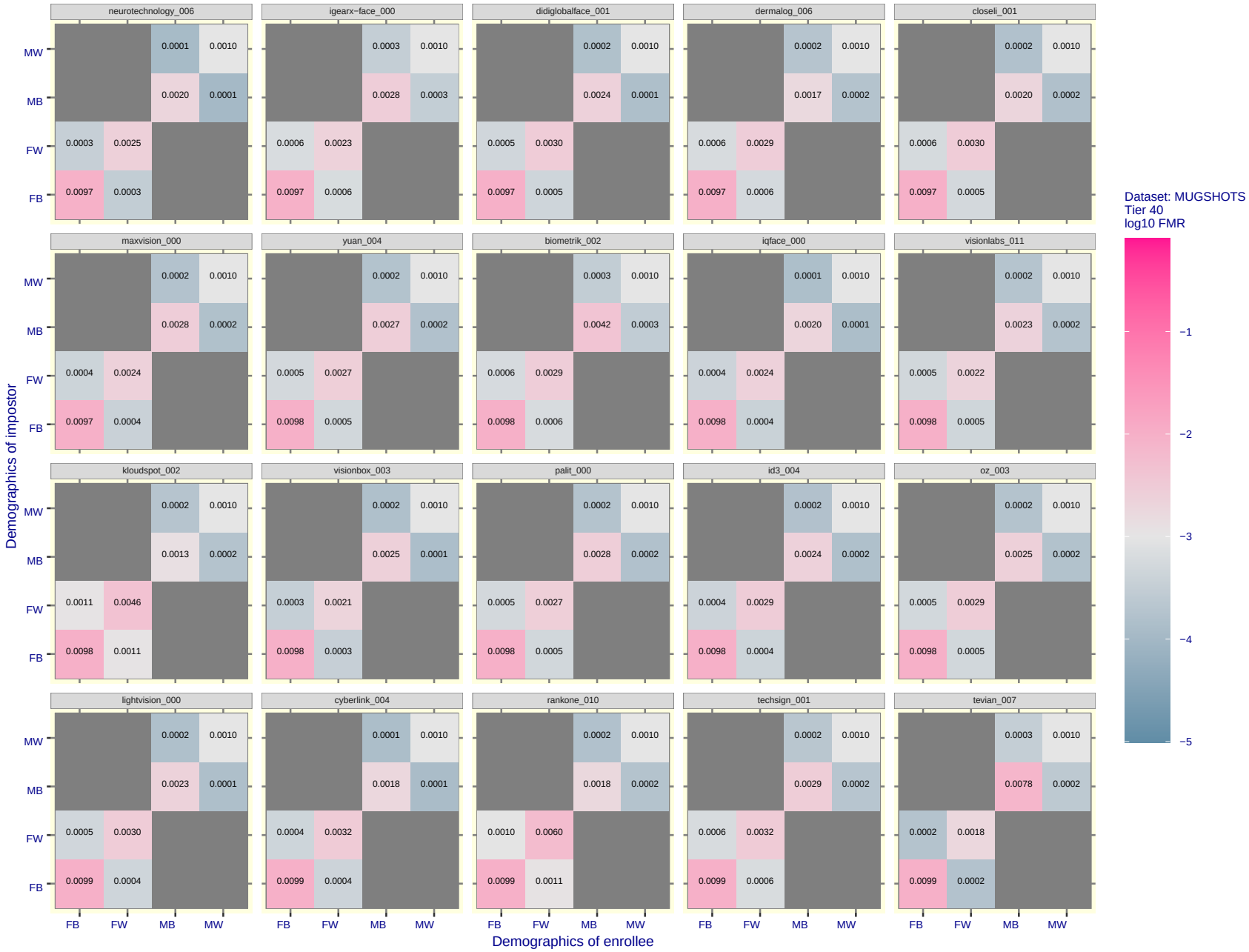

Figure 360: For the mugshot images, FMR *for same-sex impostor pairs of images annotated with codes for black female, black male, white female, white male. The threshold is set for each algorithm to give* FMR *= 0.001 for white males which is the demographic that usually gives the lowest* FMR*. This means the top right box is the same color in all panels. The panels are sorted over multiple pages in order of* FMR *on black females, which is the demographc that usually gives the highest* FMR*.*

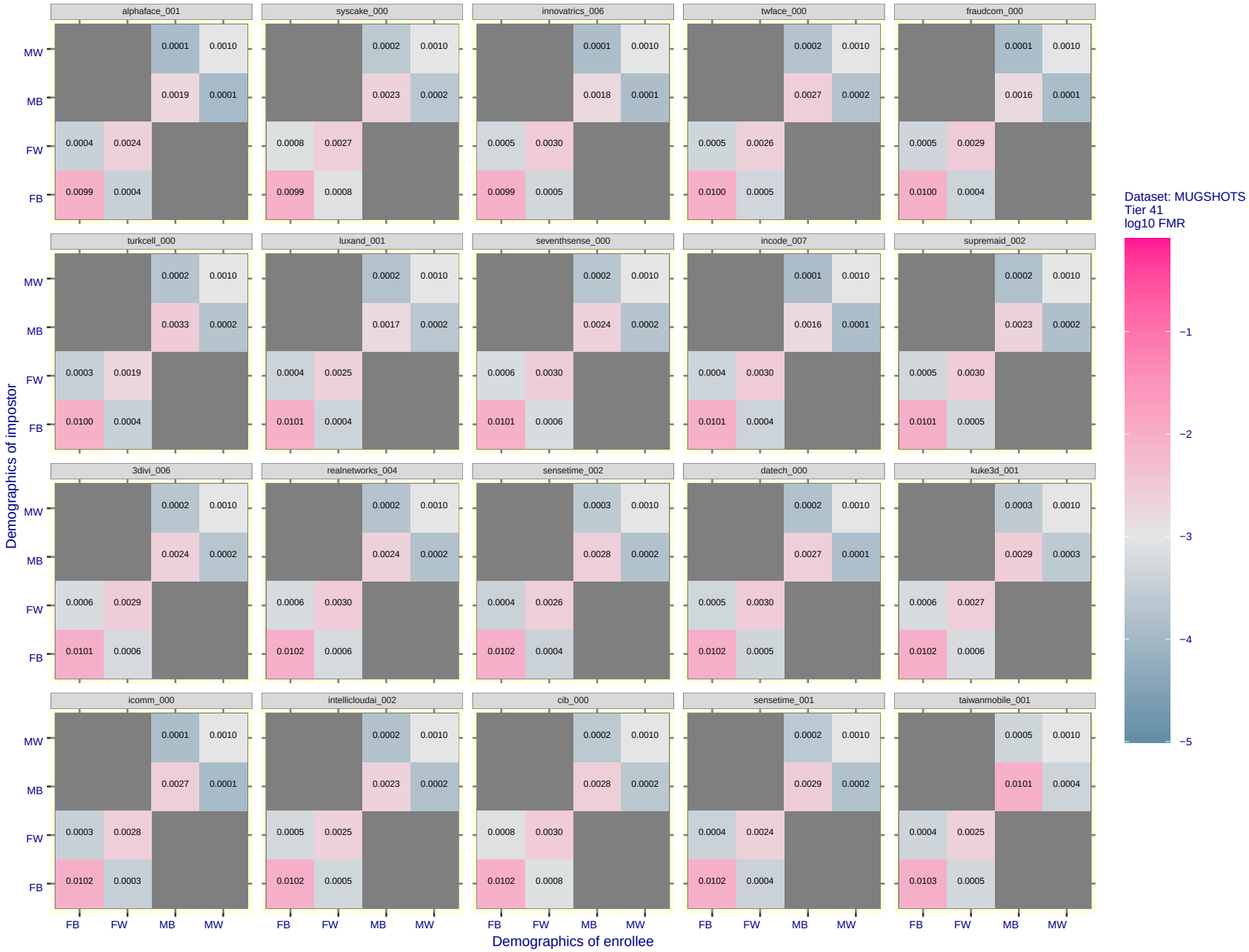

Figure 361: For the mugshot images, FMR *for same-sex impostor pairs of images annotated with codes for black female, black male, white female, white male. The threshold is set for each algorithm to give* FMR *= 0.001 for white males which is the demographic that usually gives the lowest* FMR*. This means the top right box is the same color in all panels. The panels are sorted over multiple pages in order of* FMR *on black females, which is the demographc that usually gives the highest* FMR*.*

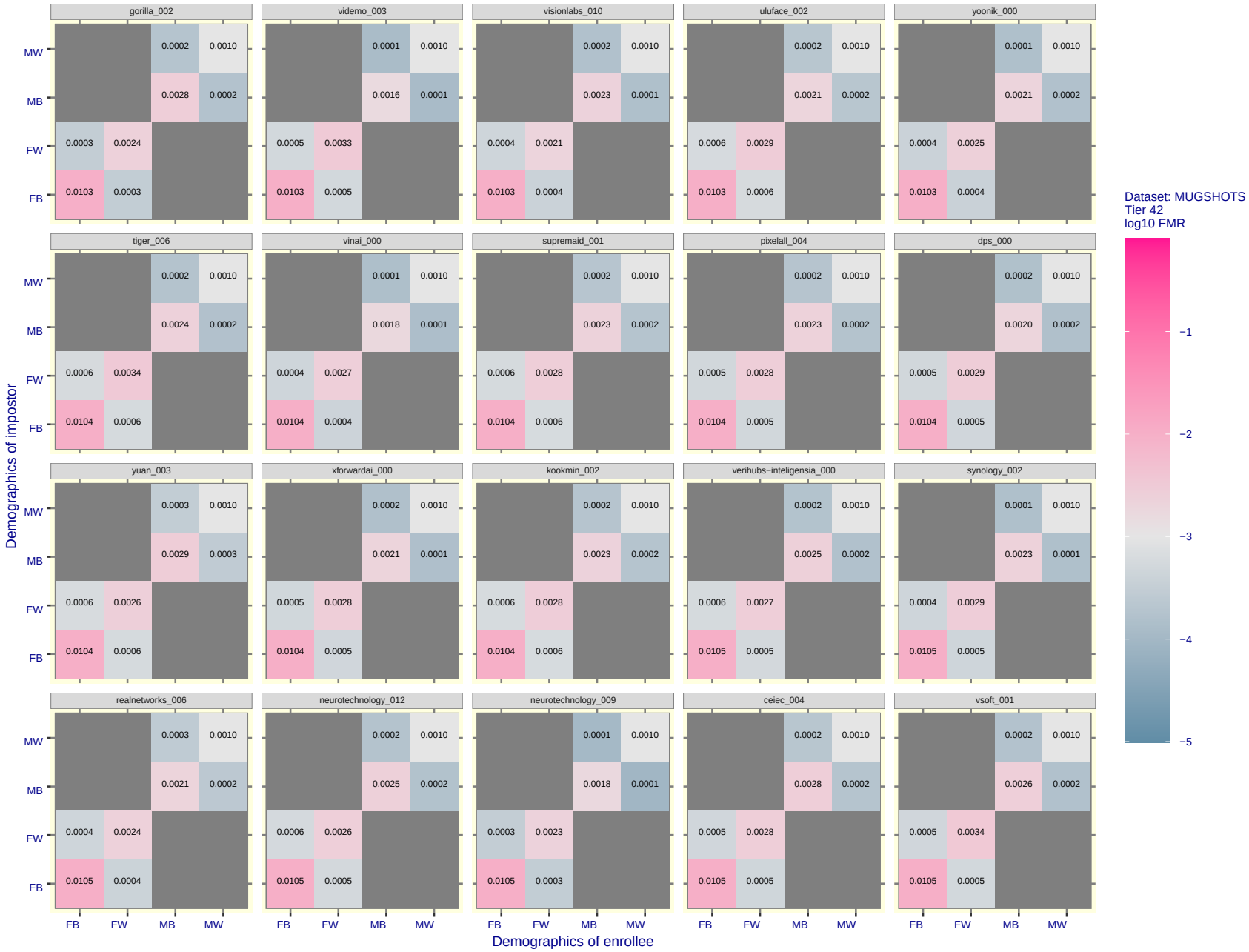

Figure 362: For the mugshot images, FMR *for same-sex impostor pairs of images annotated with codes for black female, black male, white female, white male. The threshold is set for each algorithm to give* FMR *= 0.001 for white males which is the demographic that usually gives the lowest* FMR*. This means the top right box is the same color in all panels. The panels are sorted over multiple pages in order of* FMR *on black females, which is the demographc that usually gives the highest* FMR*.*

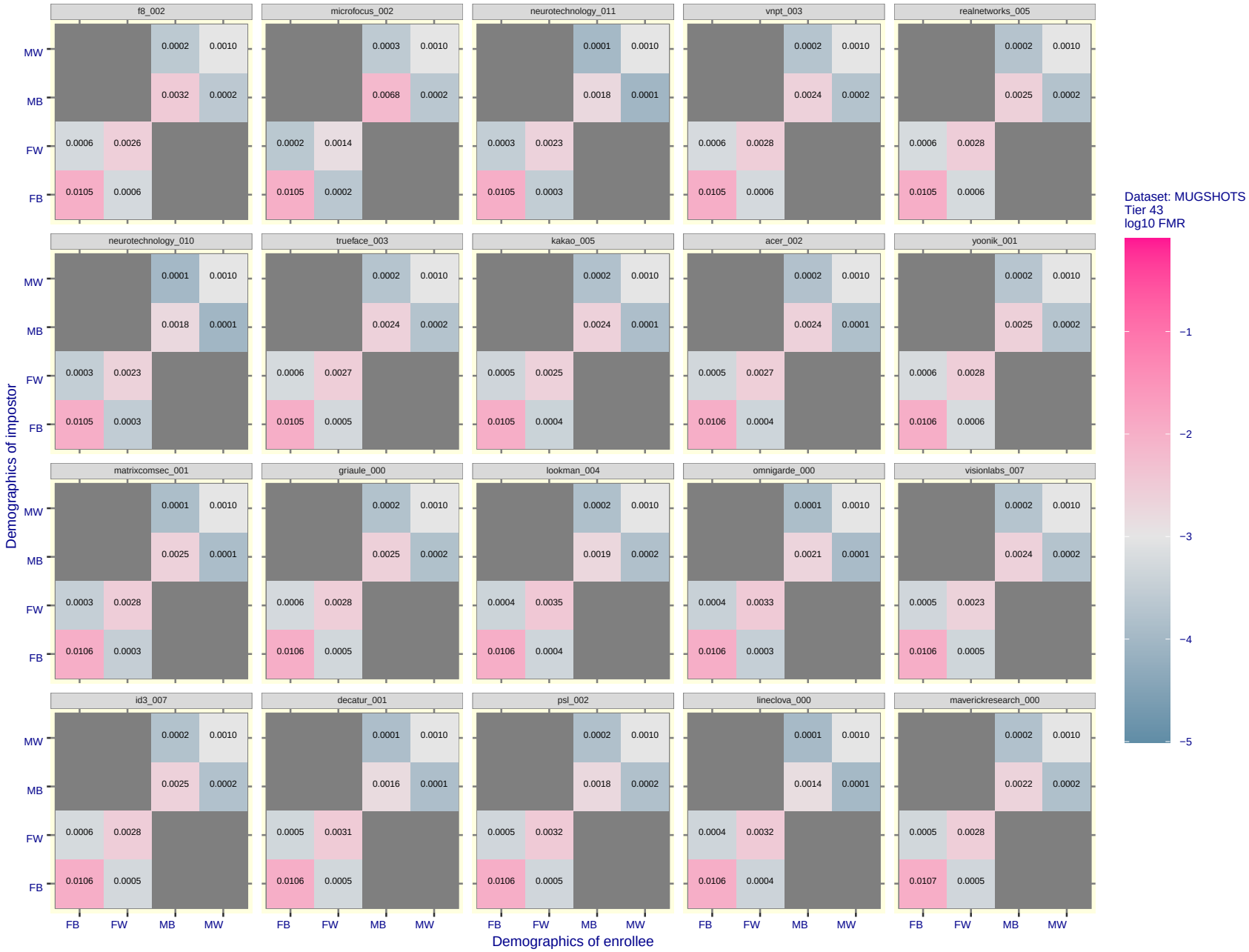

Figure 363: For the mugshot images, FMR *for same-sex impostor pairs of images annotated with codes for black female, black male, white female, white male. The threshold is set for each algorithm to give* FMR *= 0.001 for white males which is the demographic that usually gives the lowest* FMR*. This means the top right box is the same color in all panels. The panels are sorted over multiple pages in order of* FMR *on black females, which is the demographc that usually gives the highest* FMR*.*

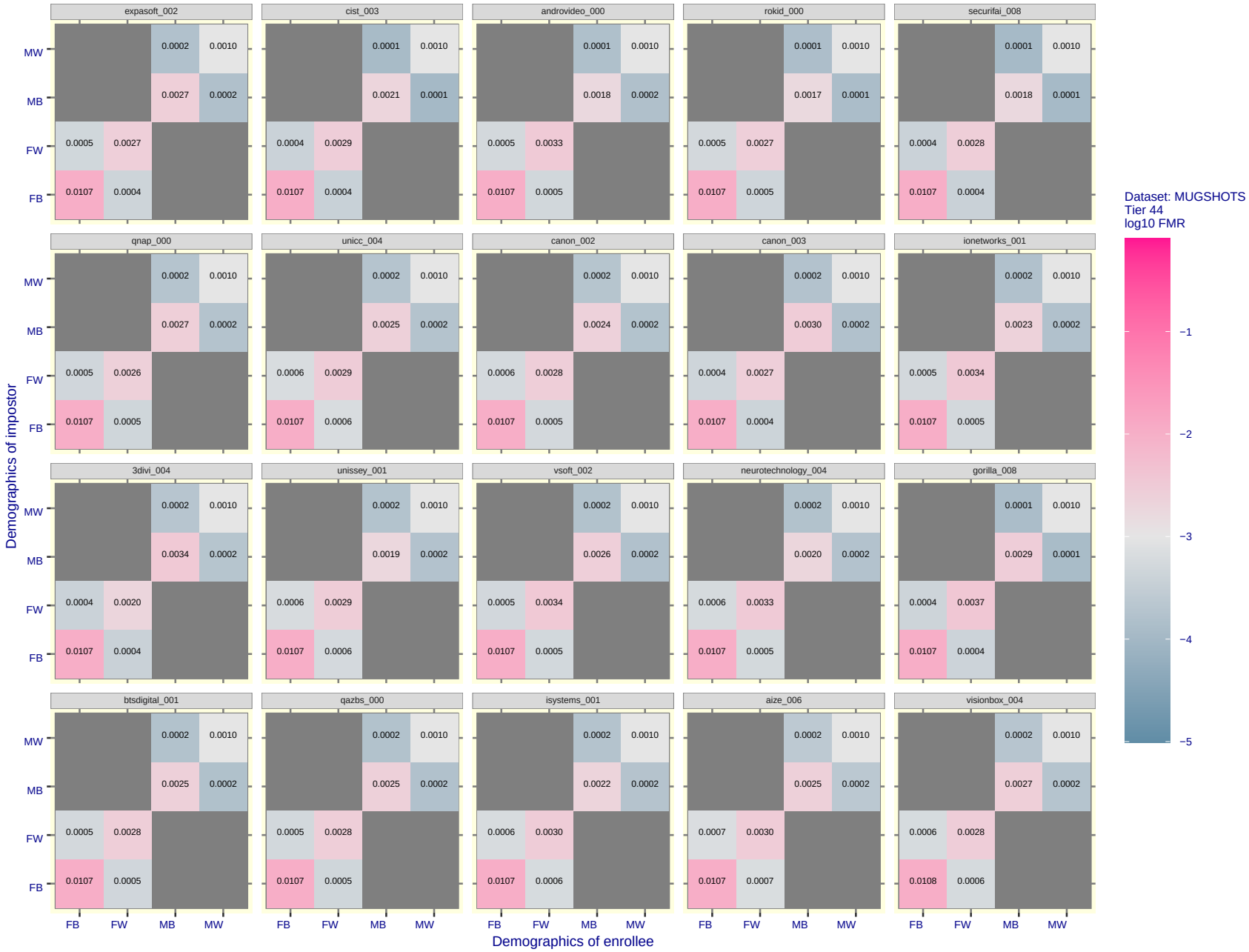

Figure 364: For the mugshot images, FMR *for same-sex impostor pairs of images annotated with codes for black female, black male, white female, white male. The threshold is set for each algorithm to give* FMR *= 0.001 for white males which is the demographic that usually gives the lowest* FMR*. This means the top right box is the same color in all panels. The panels are sorted over multiple pages in order of* FMR *on black females, which is the demographc that usually gives the highest* FMR*.*

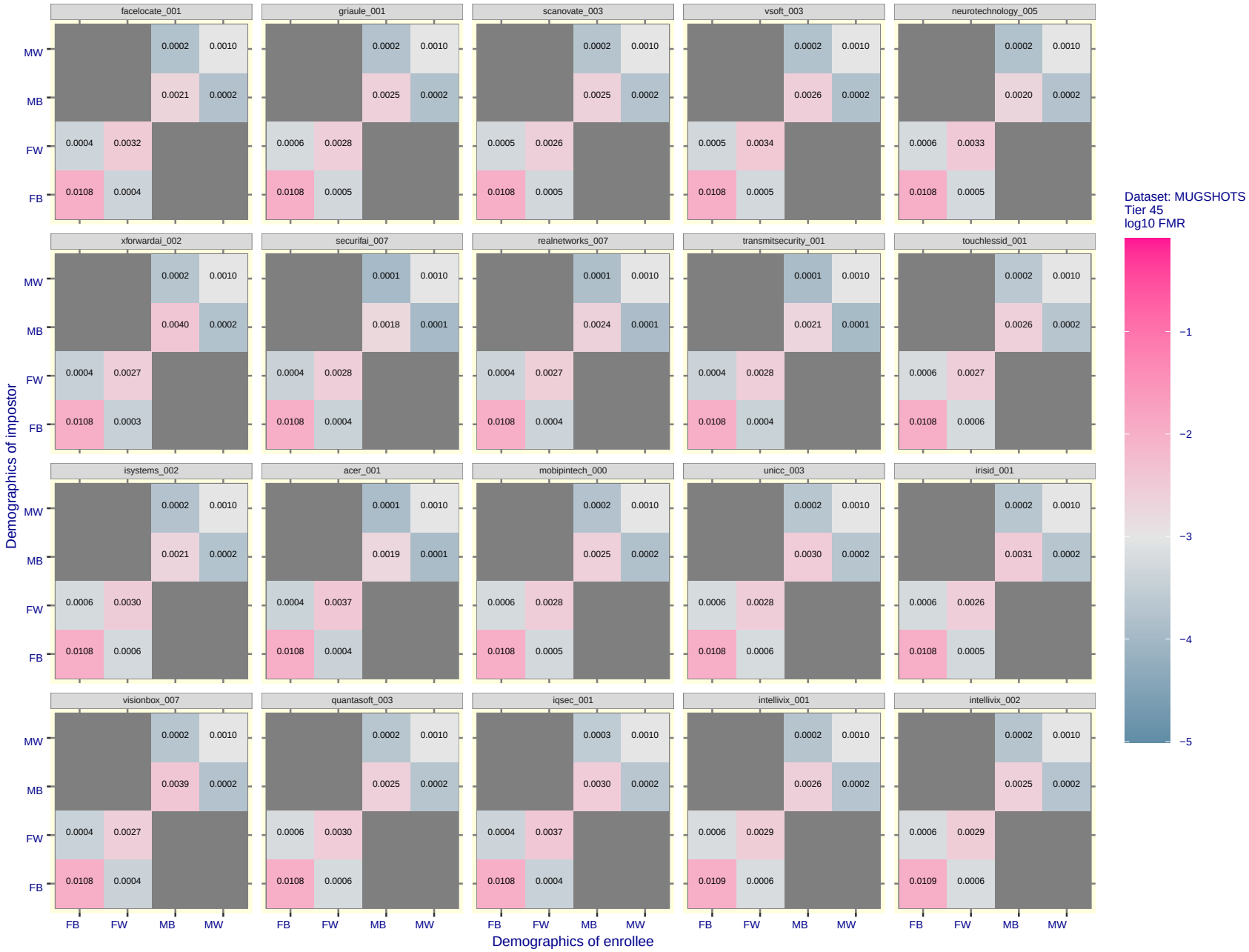

Figure 365: For the mugshot images, FMR *for same-sex impostor pairs of images annotated with codes for black female, black male, white female, white male. The threshold is set for each algorithm to give* FMR *= 0.001 for white males which is the demographic that usually gives the lowest* FMR*. This means the top right box is the same color in all panels. The panels are sorted over multiple pages in order of* FMR *on black females, which is the demographc that usually gives the highest* FMR*.*

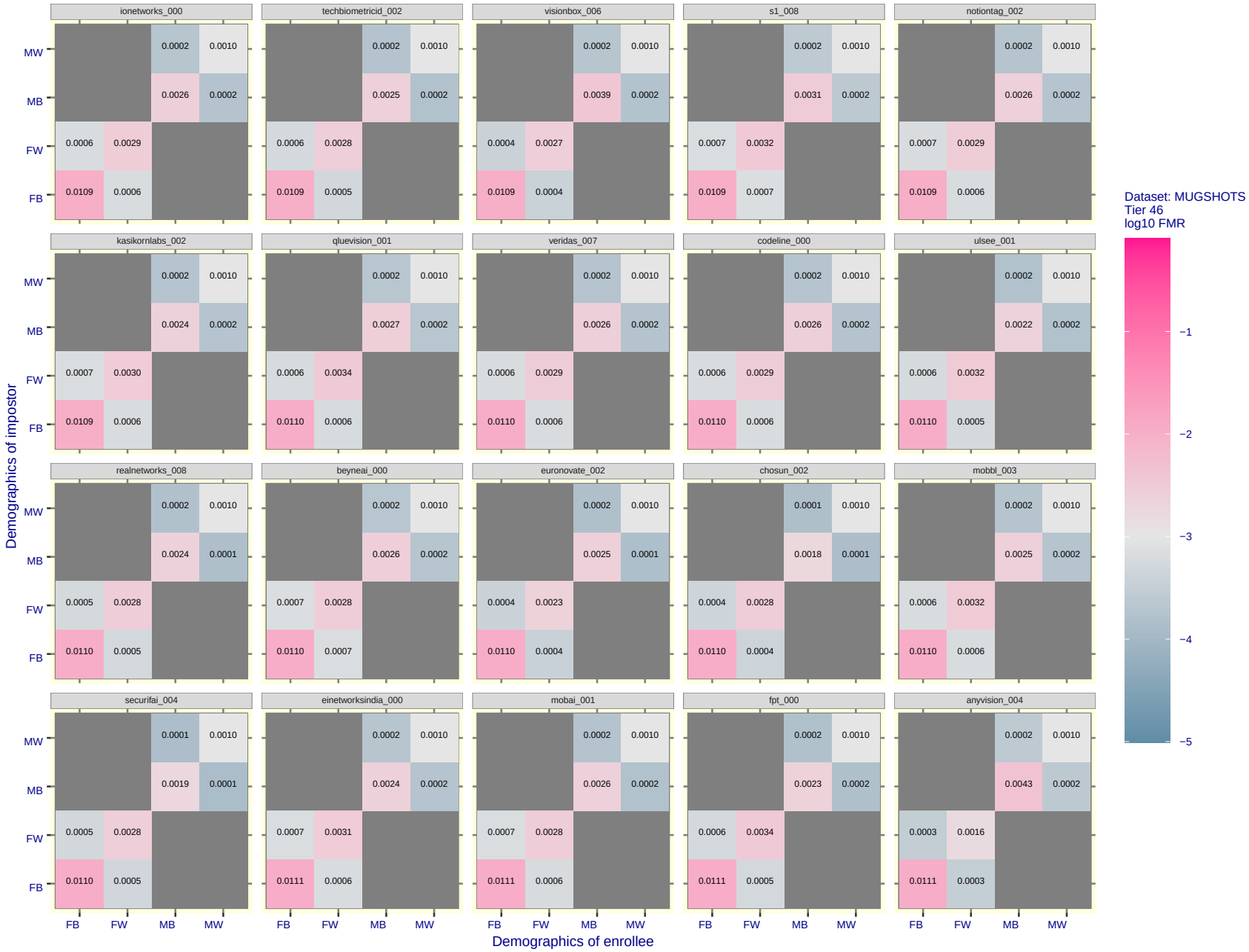

Figure 366: For the mugshot images, FMR *for same-sex impostor pairs of images annotated with codes for black female, black male, white female, white male. The threshold is set for each algorithm to give* FMR *= 0.001 for white males which is the demographic that usually gives the lowest* FMR*. This means the top right box is the same color in all panels. The panels are sorted over multiple pages in order of* FMR *on black females, which is the demographc that usually gives the highest* FMR*.*

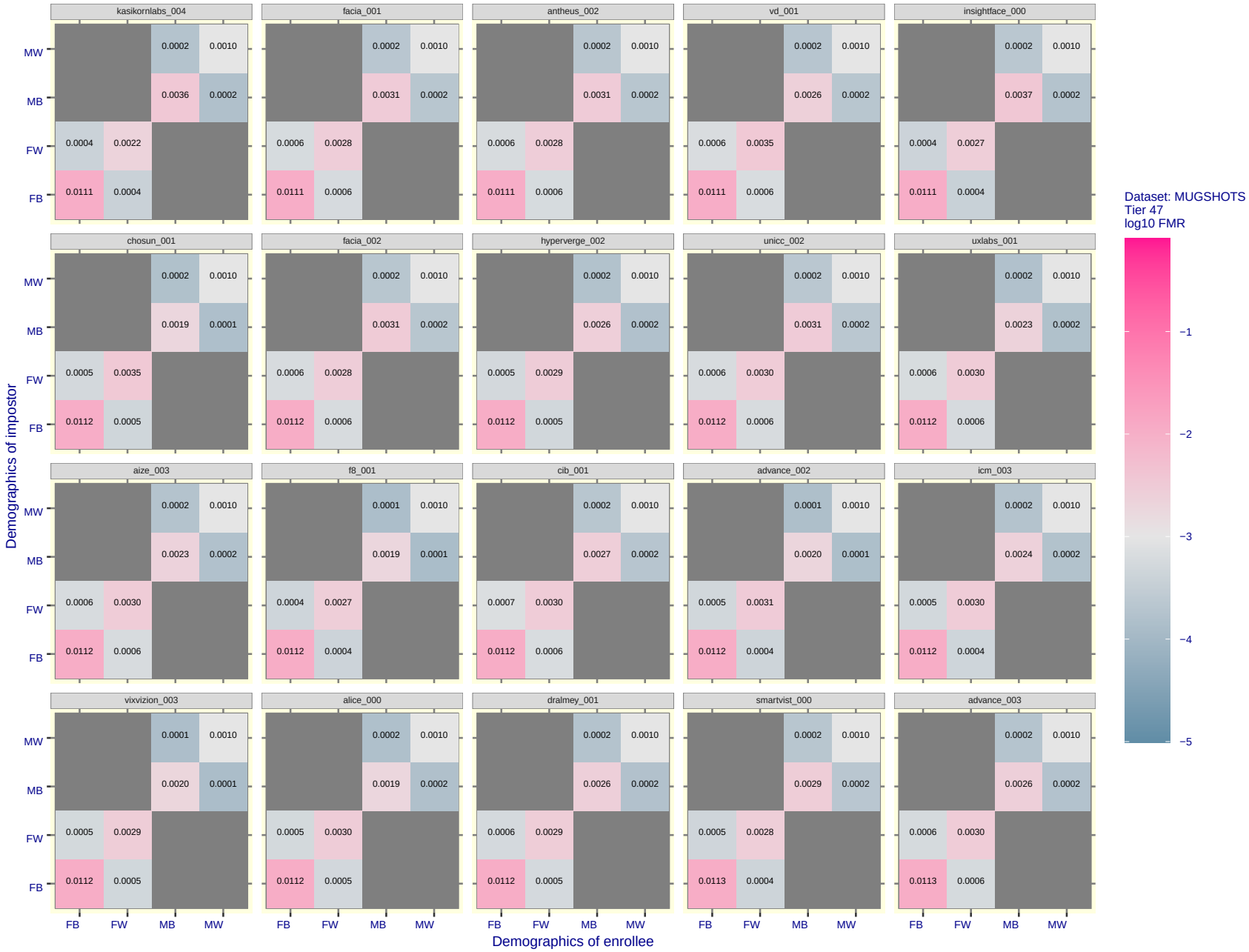

Figure 367: For the mugshot images, FMR *for same-sex impostor pairs of images annotated with codes for black female, black male, white female, white male. The threshold is set for each algorithm to give* FMR *= 0.001 for white males which is the demographic that usually gives the lowest* FMR*. This means the top right box is the same color in all panels. The panels are sorted over multiple pages in order of* FMR *on black females, which is the demographc that usually gives the highest* FMR*.*

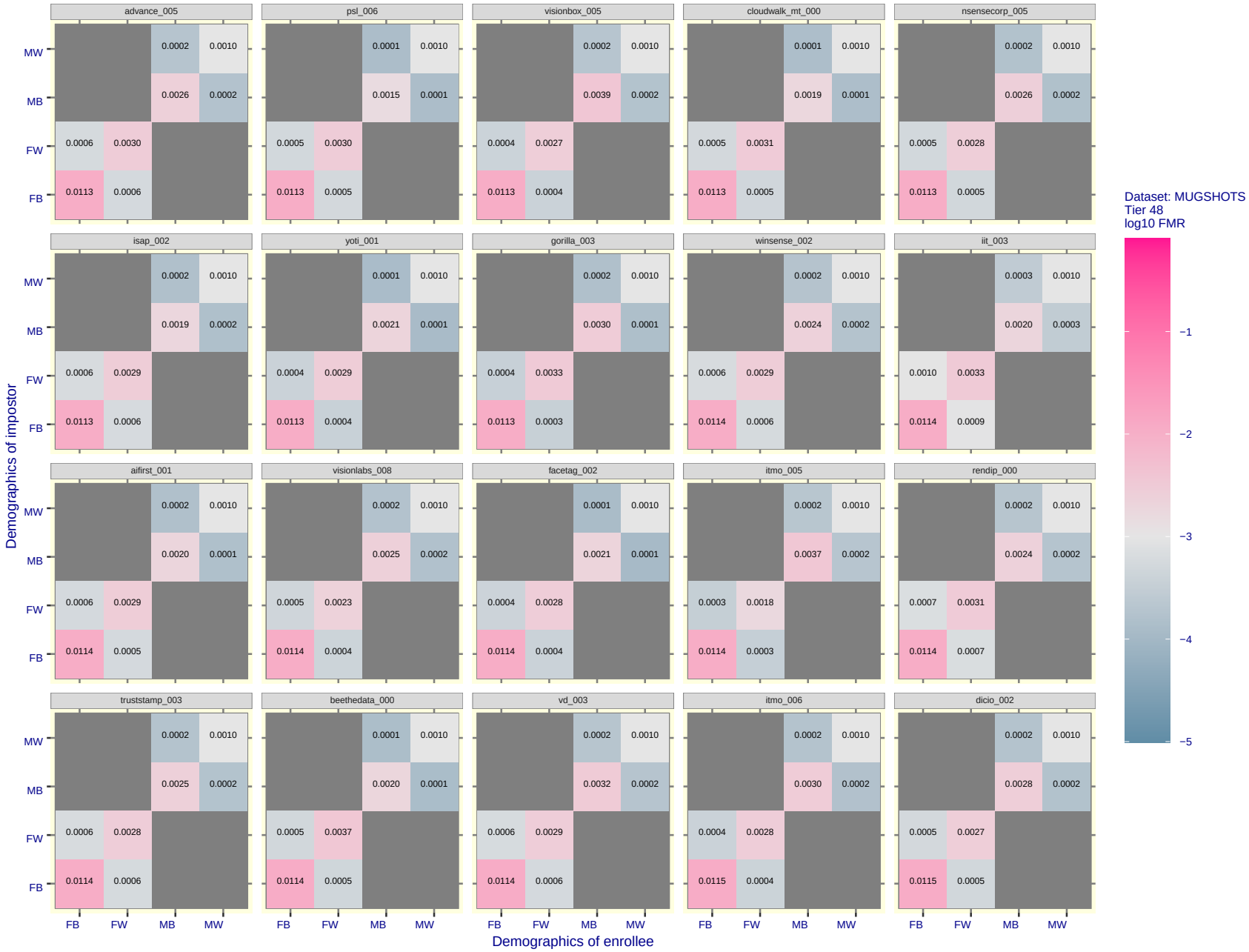

Figure 368: For the mugshot images, FMR *for same-sex impostor pairs of images annotated with codes for black female, black male, white female, white male. The threshold is set for each algorithm to give* FMR *= 0.001 for white males which is the demographic that usually gives the lowest* FMR*. This means the top right box is the same color in all panels. The panels are sorted over multiple pages in order of* FMR *on black females, which is the demographc that usually gives the highest* FMR*.*

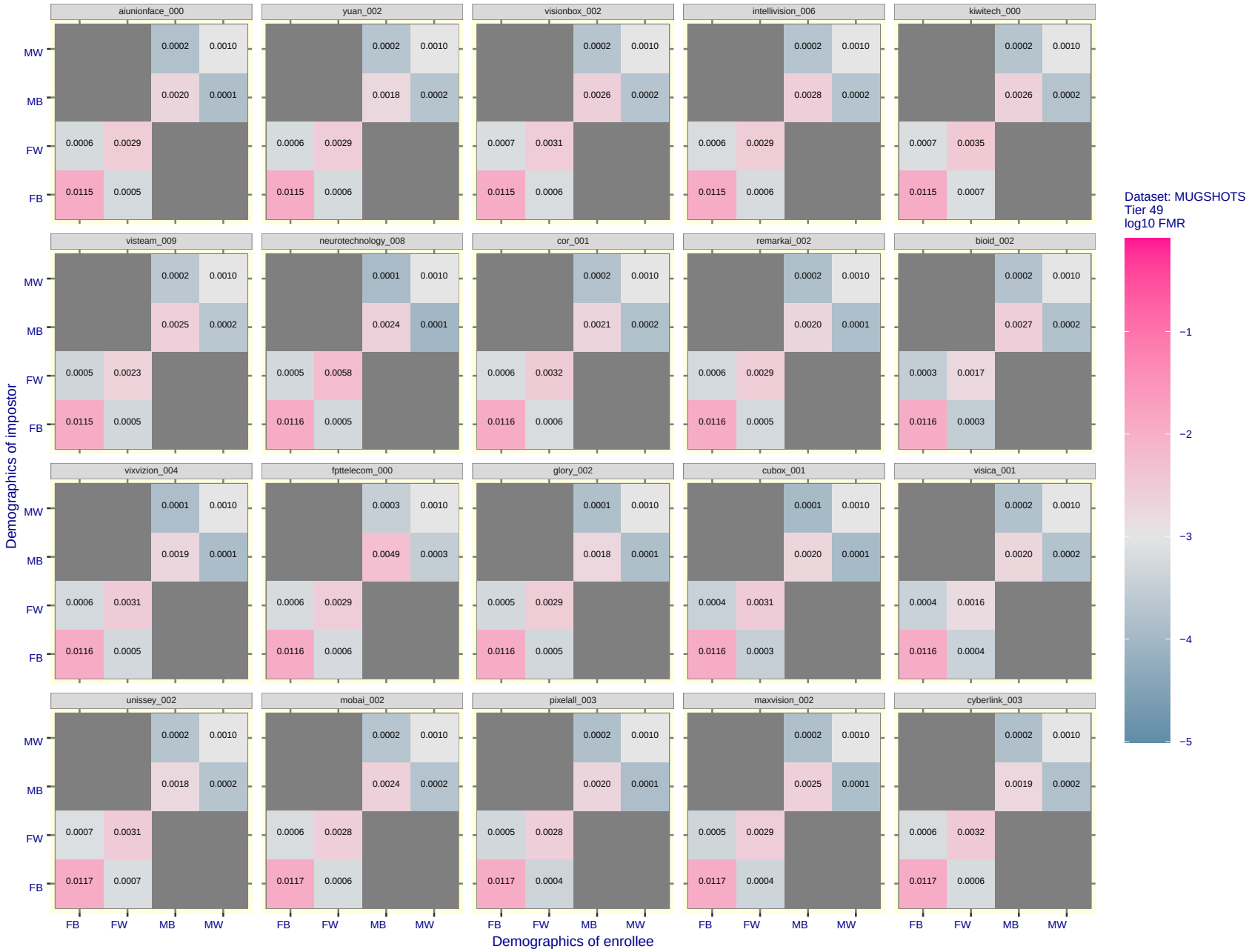

Figure 369: For the mugshot images, FMR *for same-sex impostor pairs of images annotated with codes for black female, black male, white female, white male. The threshold is set for each algorithm to give* FMR *= 0.001 for white males which is the demographic that usually gives the lowest* FMR*. This means the top right box is the same color in all panels. The panels are sorted over multiple pages in order of* FMR *on black females, which is the demographc that usually gives the highest* FMR*.*

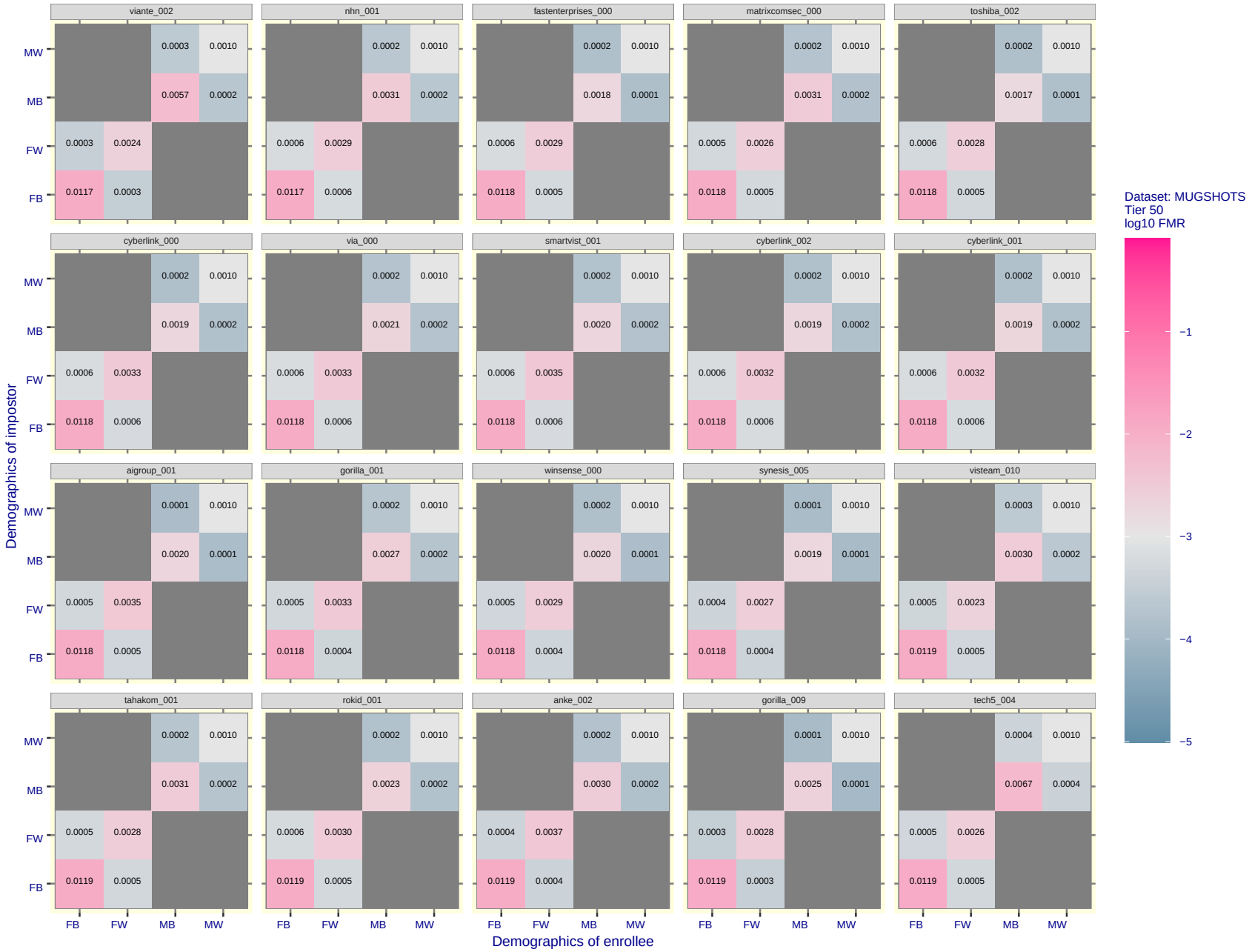

Figure 370: For the mugshot images, FMR *for same-sex impostor pairs of images annotated with codes for black female, black male, white female, white male. The threshold is set for each algorithm to give* FMR *= 0.001 for white males which is the demographic that usually gives the lowest* FMR*. This means the top right box is the same color in all panels. The panels are sorted over multiple pages in order of* FMR *on black females, which is the demographc that usually gives the highest* FMR*.*

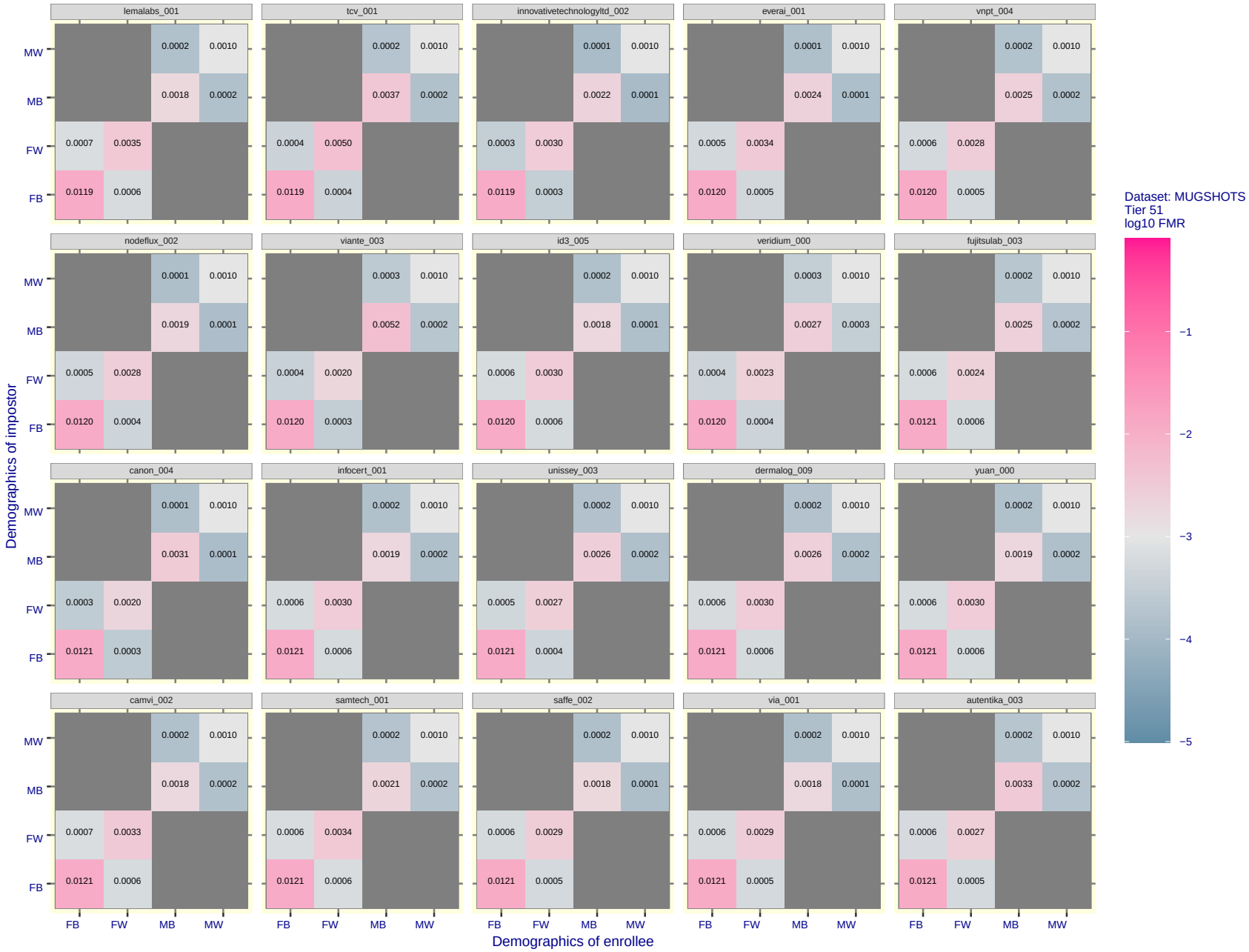

Figure 371: For the mugshot images, FMR *for same-sex impostor pairs of images annotated with codes for black female, black male, white female, white male. The threshold is set for each algorithm to give* FMR *= 0.001 for white males which is the demographic that usually gives the lowest* FMR*. This means the top right box is the same color in all panels. The panels are sorted over multiple pages in order of* FMR *on black females, which is the demographc that usually gives the highest* FMR*.*

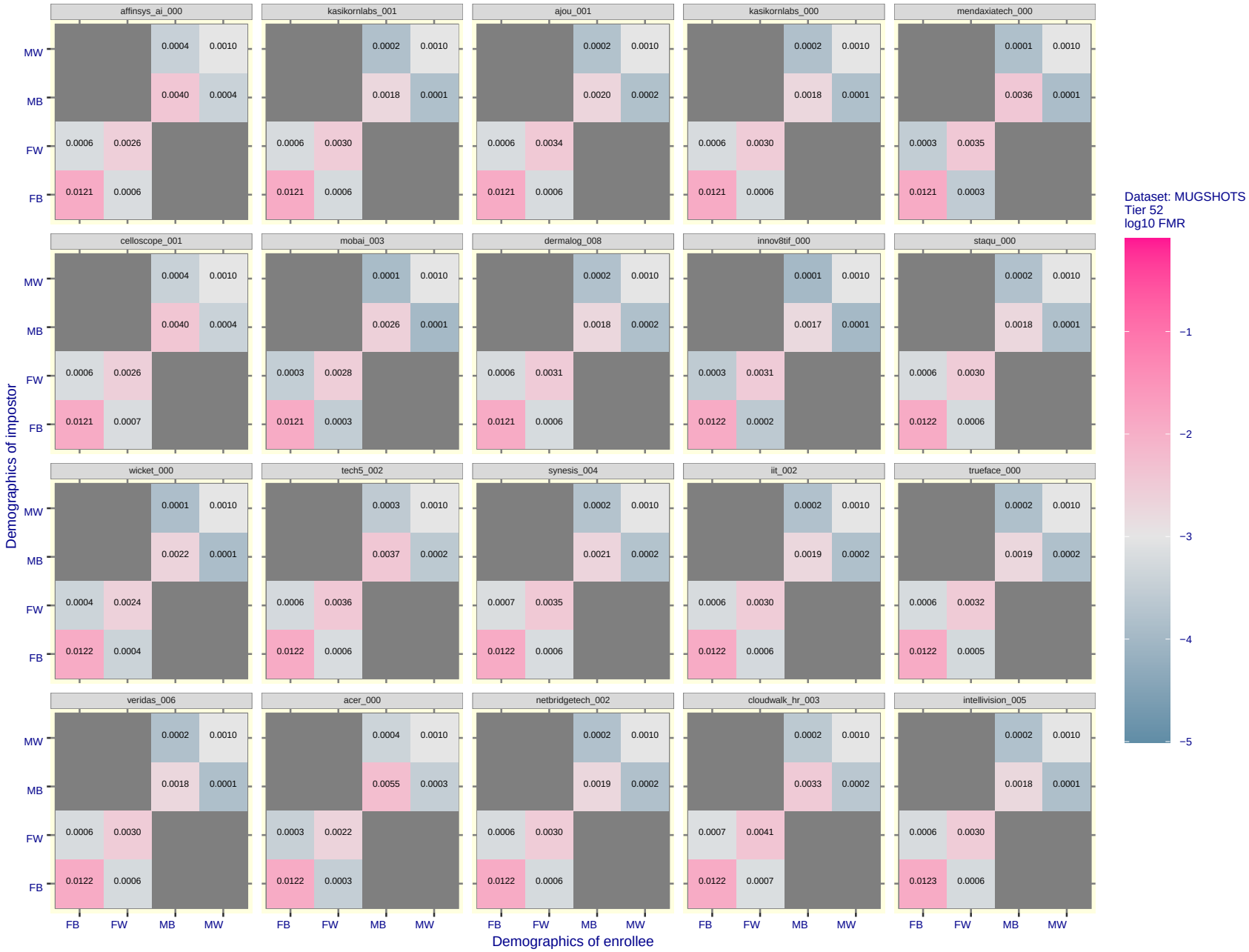

Figure 372: For the mugshot images, FMR *for same-sex impostor pairs of images annotated with codes for black female, black male, white female, white male. The threshold is set for each algorithm to give* FMR *= 0.001 for white males which is the demographic that usually gives the lowest* FMR*. This means the top right box is the same color in all panels. The panels are sorted over multiple pages in order of* FMR *on black females, which is the demographc that usually gives the highest* FMR*.*

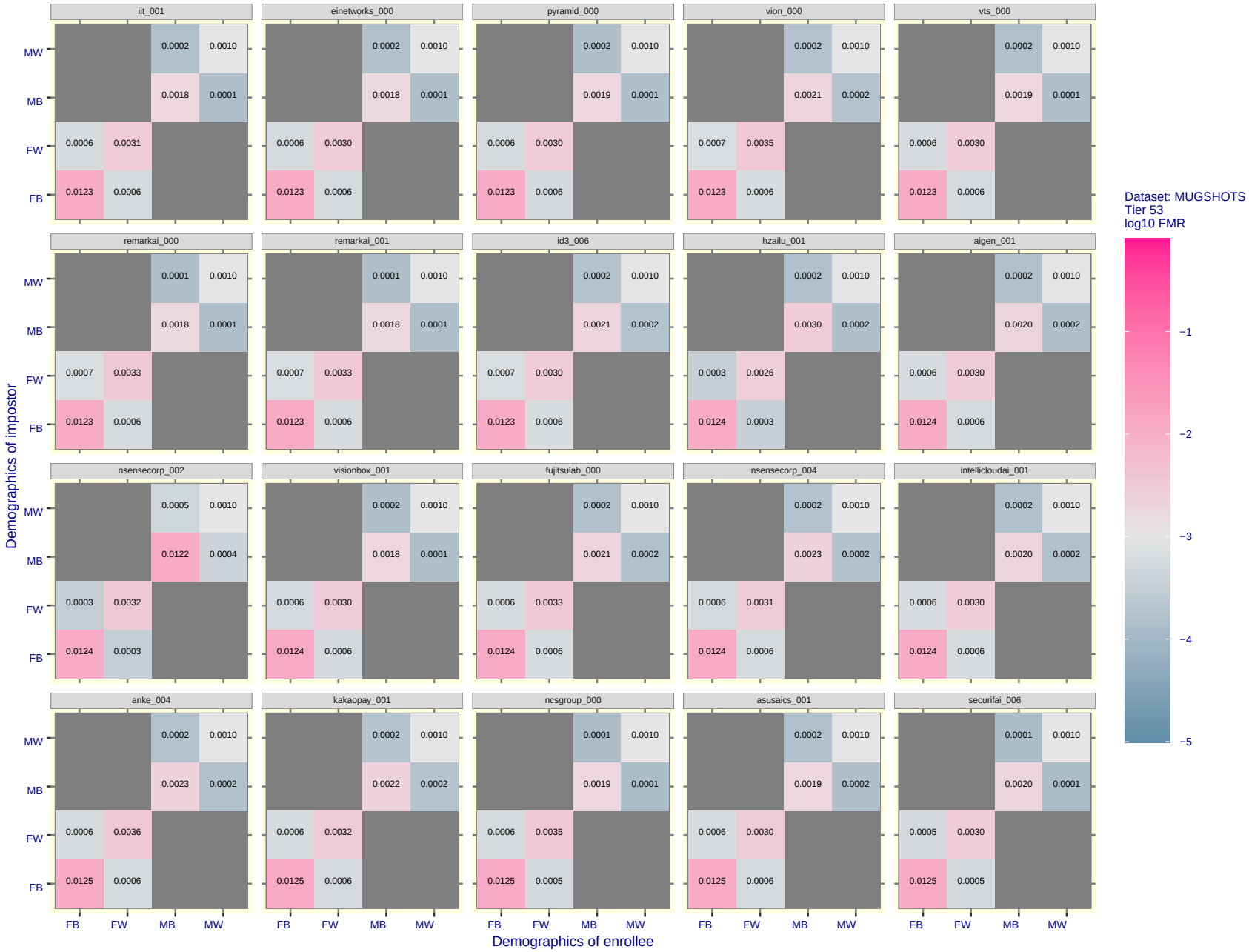

Figure 373: For the mugshot images, FMR *for same-sex impostor pairs of images annotated with codes for black female, black male, white female, white male. The threshold is set for each algorithm to give* FMR *= 0.001 for white males which is the demographic that usually gives the lowest* FMR*. This means the top right box is the same color in all panels. The panels are sorted over multiple pages in order of* FMR *on black females, which is the demographc that usually gives the highest* FMR*.*

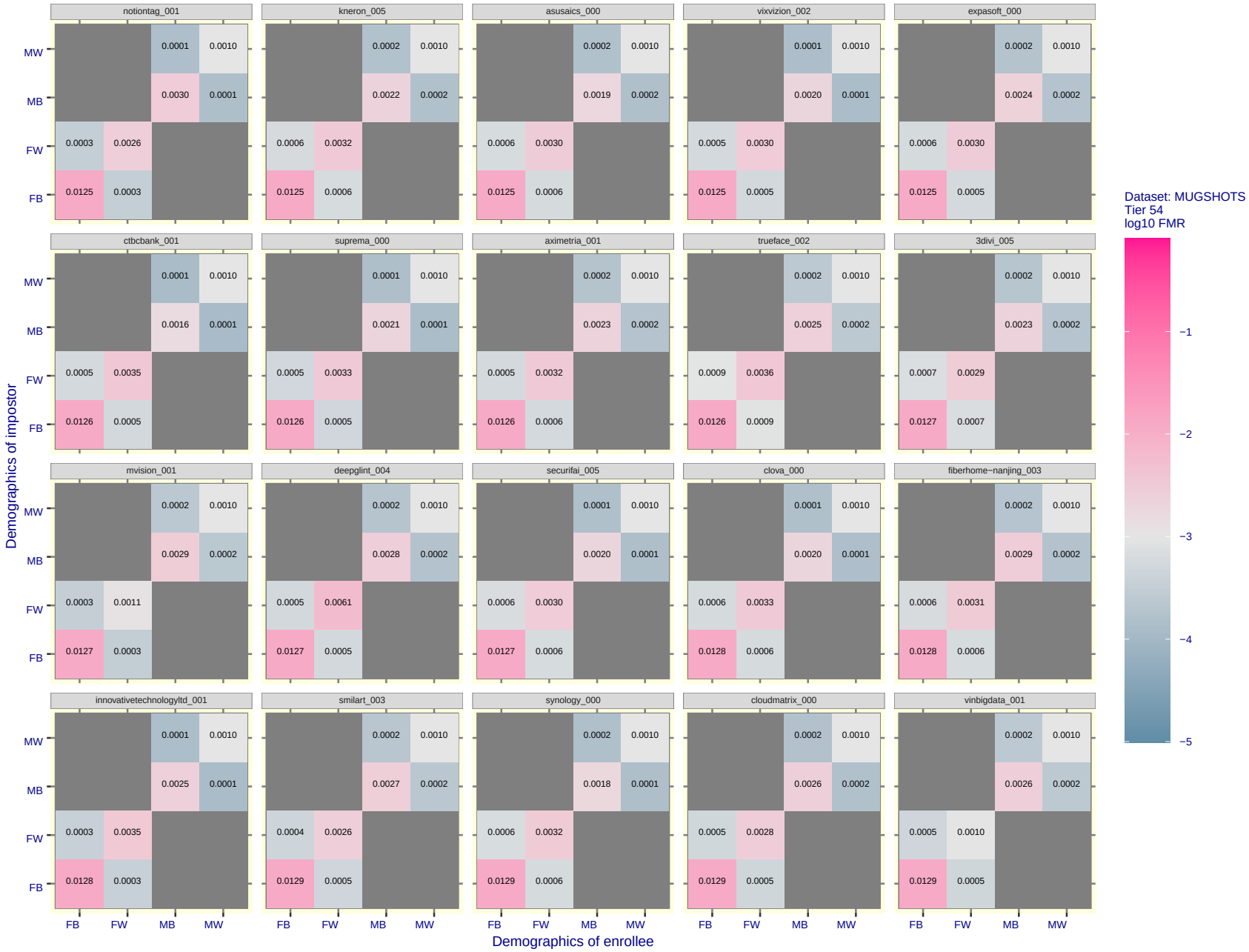

Figure 374: For the mugshot images, FMR *for same-sex impostor pairs of images annotated with codes for black female, black male, white female, white male. The threshold is set for each algorithm to give* FMR *= 0.001 for white males which is the demographic that usually gives the lowest* FMR*. This means the top right box is the same color in all panels. The panels are sorted over multiple pages in order of* FMR *on black females, which is the demographc that usually gives the highest* FMR*.*

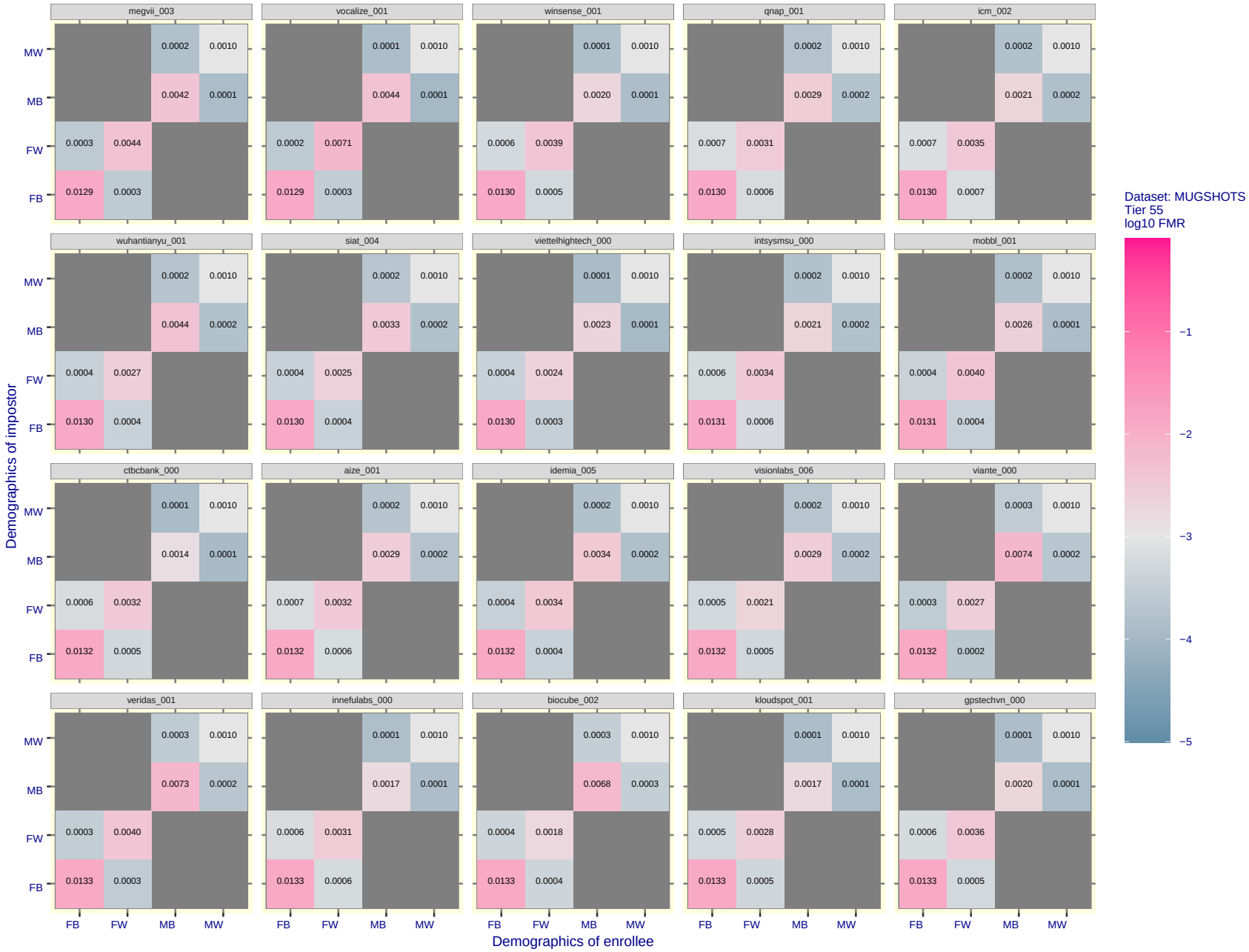

Figure 375: For the mugshot images, FMR *for same-sex impostor pairs of images annotated with codes for black female, black male, white female, white male. The threshold is set for each algorithm to give* FMR *= 0.001 for white males which is the demographic that usually gives the lowest* FMR*. This means the top right box is the same color in all panels. The panels are sorted over multiple pages in order of* FMR *on black females, which is the demographc that usually gives the highest* FMR*.*

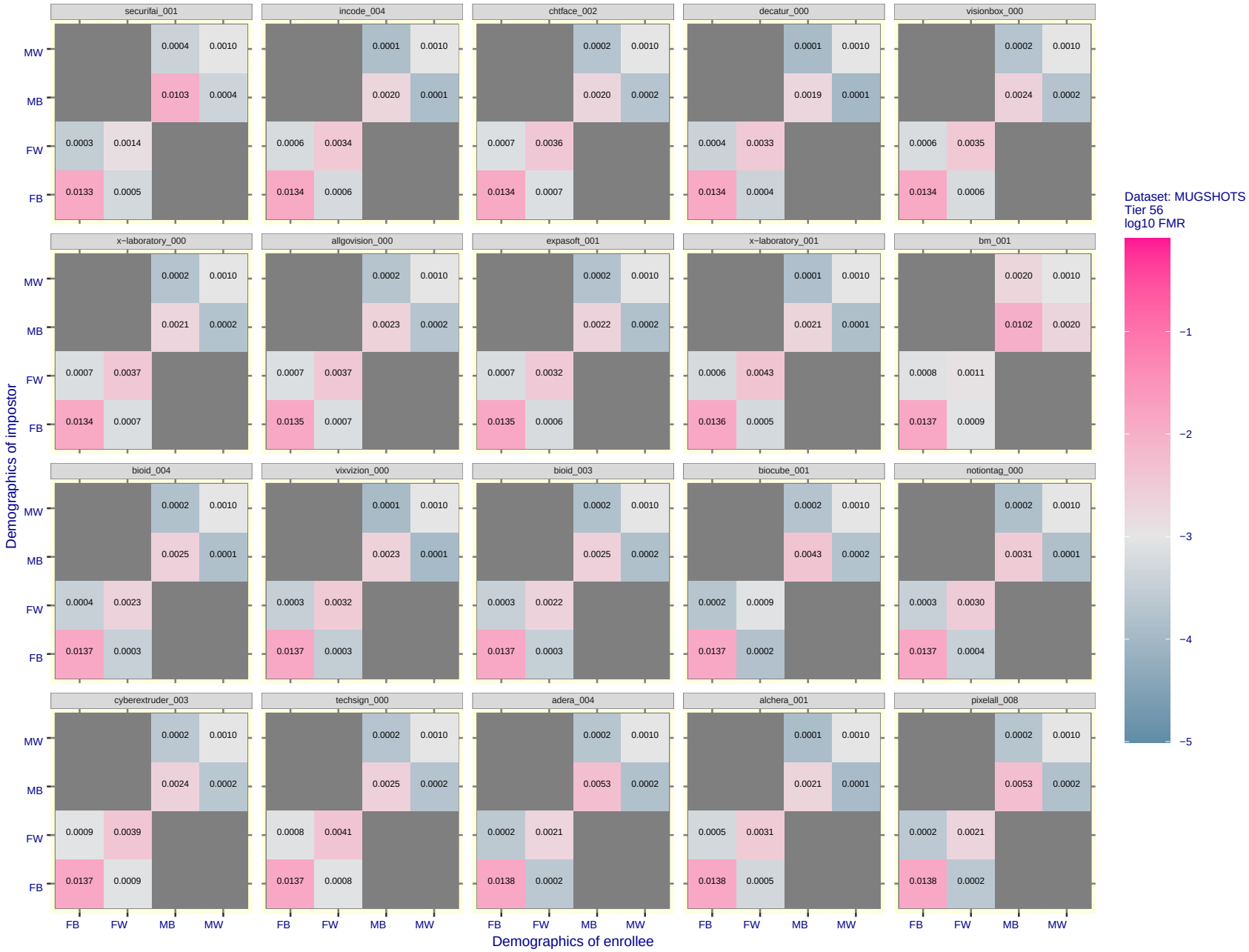

Figure 376: For the mugshot images, FMR *for same-sex impostor pairs of images annotated with codes for black female, black male, white female, white male. The threshold is set for each algorithm to give* FMR *= 0.001 for white males which is the demographic that usually gives the lowest* FMR*. This means the top right box is the same color in all panels. The panels are sorted over multiple pages in order of* FMR *on black females, which is the demographc that usually gives the highest* FMR*.*

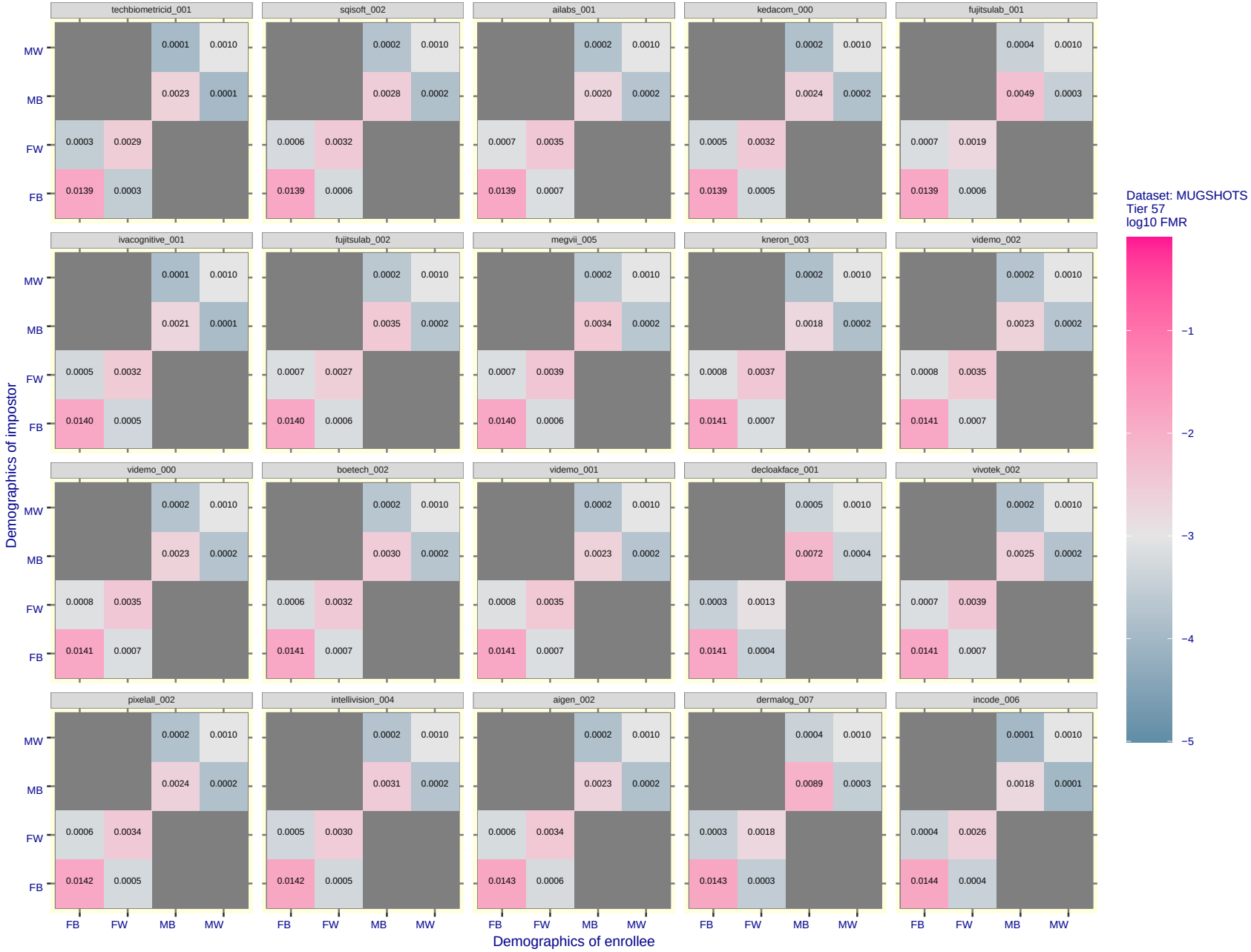

Figure 377: For the mugshot images, FMR *for same-sex impostor pairs of images annotated with codes for black female, black male, white female, white male. The threshold is set for each algorithm to give* FMR *= 0.001 for white males which is the demographic that usually gives the lowest* FMR*. This means the top right box is the same color in all panels. The panels are sorted over multiple pages in order of* FMR *on black females, which is the demographc that usually gives the highest* FMR*.*

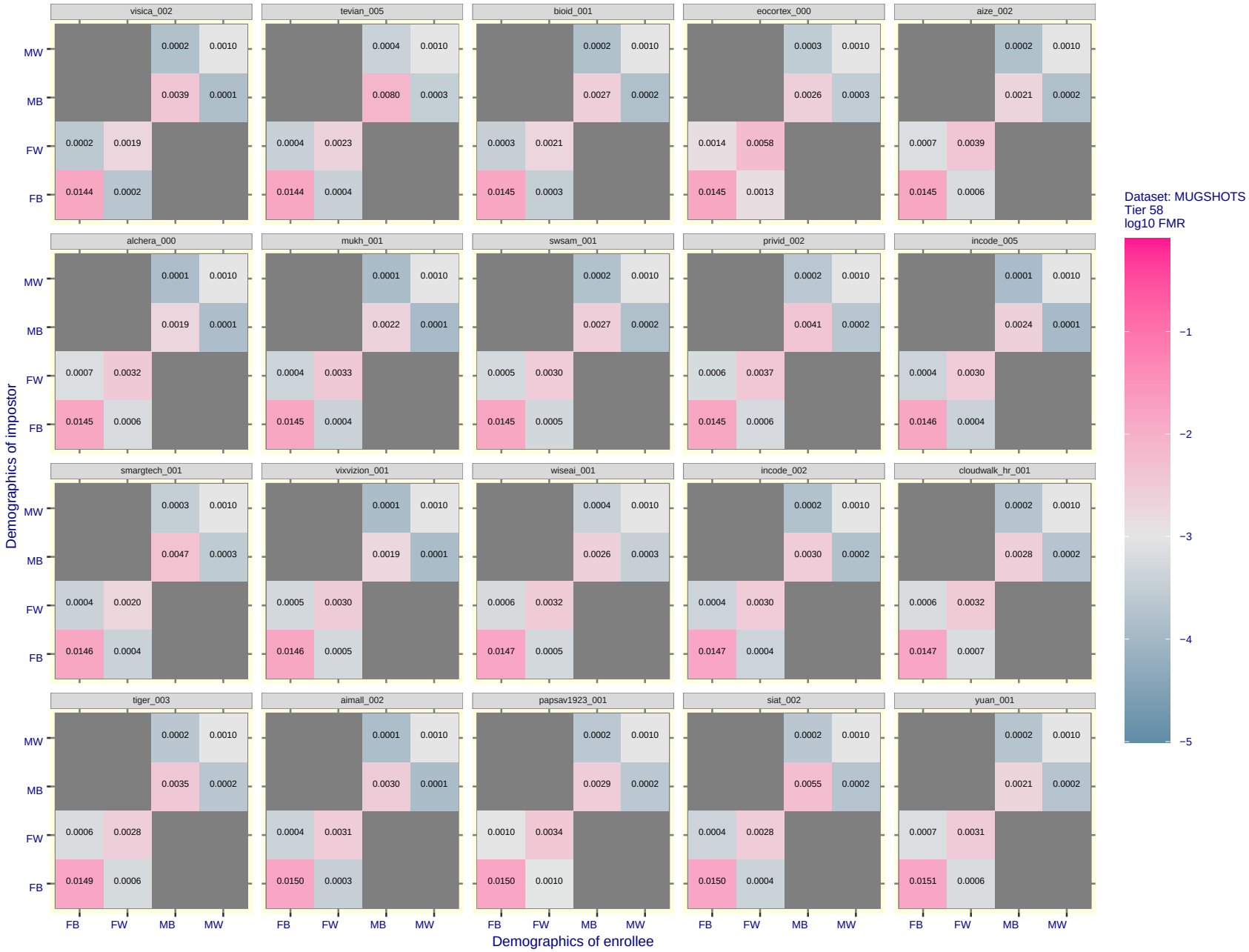

Figure 378: For the mugshot images, FMR *for same-sex impostor pairs of images annotated with codes for black female, black male, white female, white male. The threshold is set for each algorithm to give* FMR *= 0.001 for white males which is the demographic that usually gives the lowest* FMR*. This means the top right box is the same color in all panels. The panels are sorted over multiple pages in order of* FMR *on black females, which is the demographc that usually gives the highest* FMR*.*

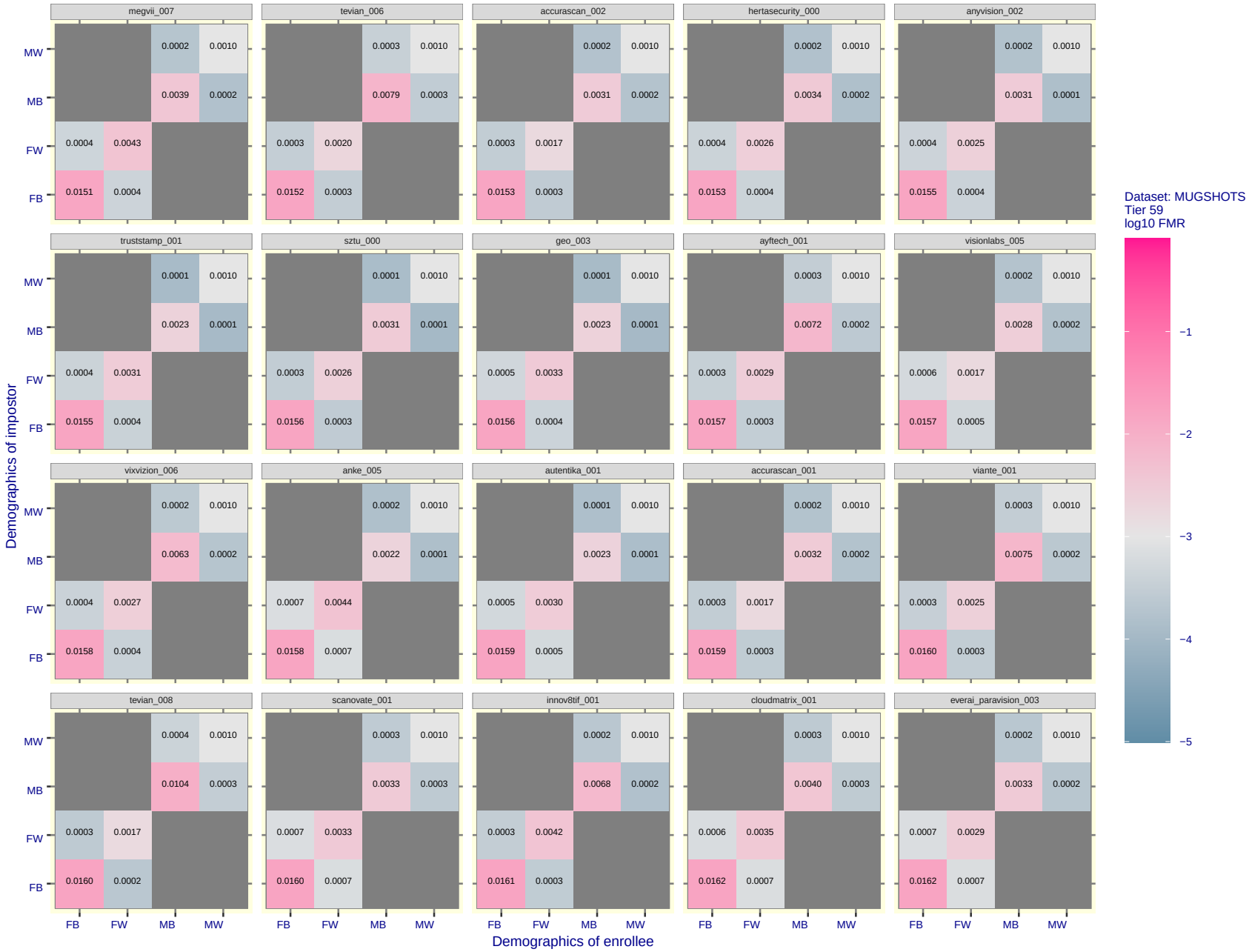

Figure 379: For the mugshot images, FMR *for same-sex impostor pairs of images annotated with codes for black female, black male, white female, white male. The threshold is set for each algorithm to give* FMR *= 0.001 for white males which is the demographic that usually gives the lowest* FMR*. This means the top right box is the same color in all panels. The panels are sorted over multiple pages in order of* FMR *on black females, which is the demographc that usually gives the highest* FMR*.*

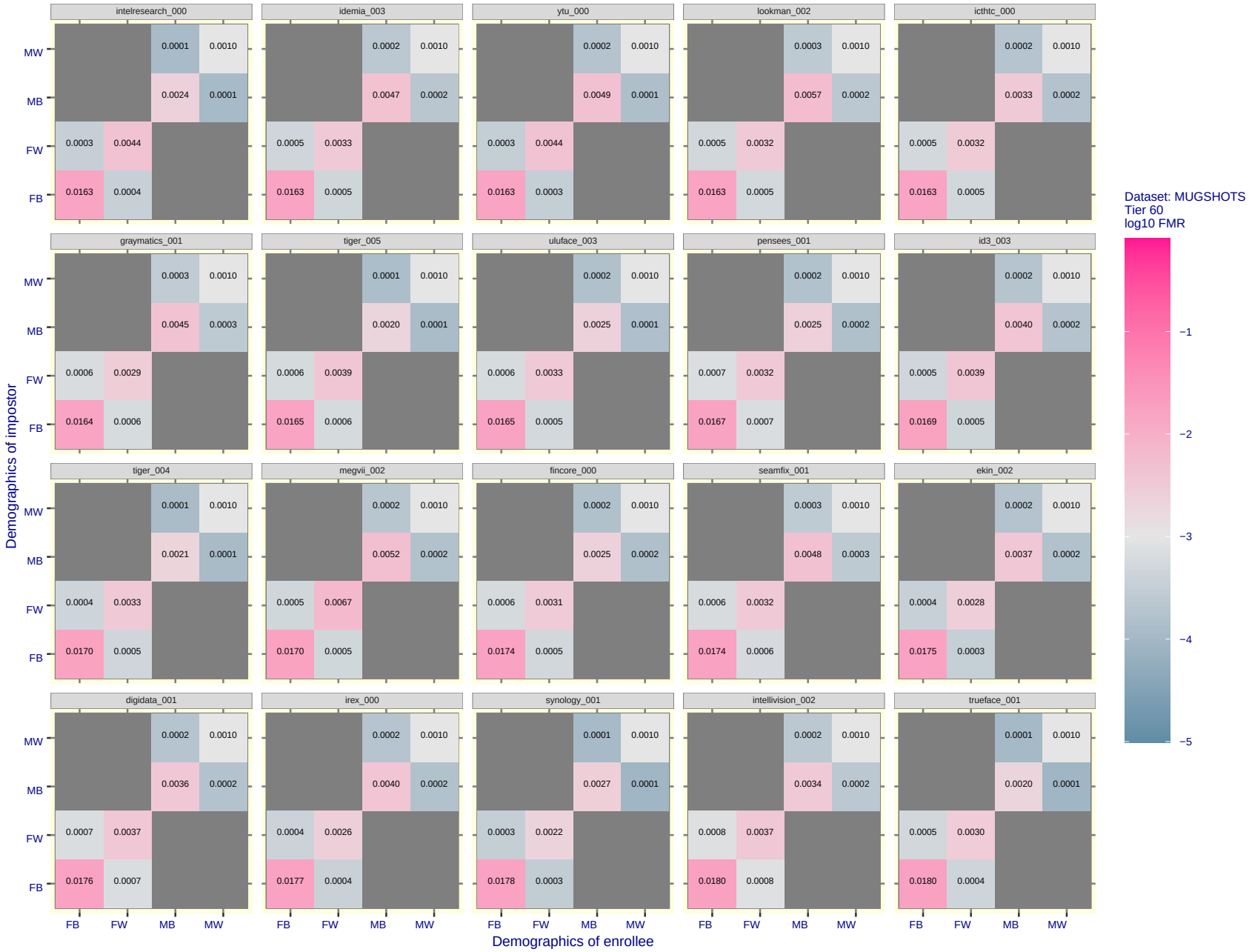

Figure 380: For the mugshot images, FMR *for same-sex impostor pairs of images annotated with codes for black female, black male, white female, white male. The threshold is set for each algorithm to give* FMR *= 0.001 for white males which is the demographic that usually gives the lowest* FMR*. This means the top right box is the same color in all panels. The panels are sorted over multiple pages in order of* FMR *on black females, which is the demographc that usually gives the highest* FMR*.*

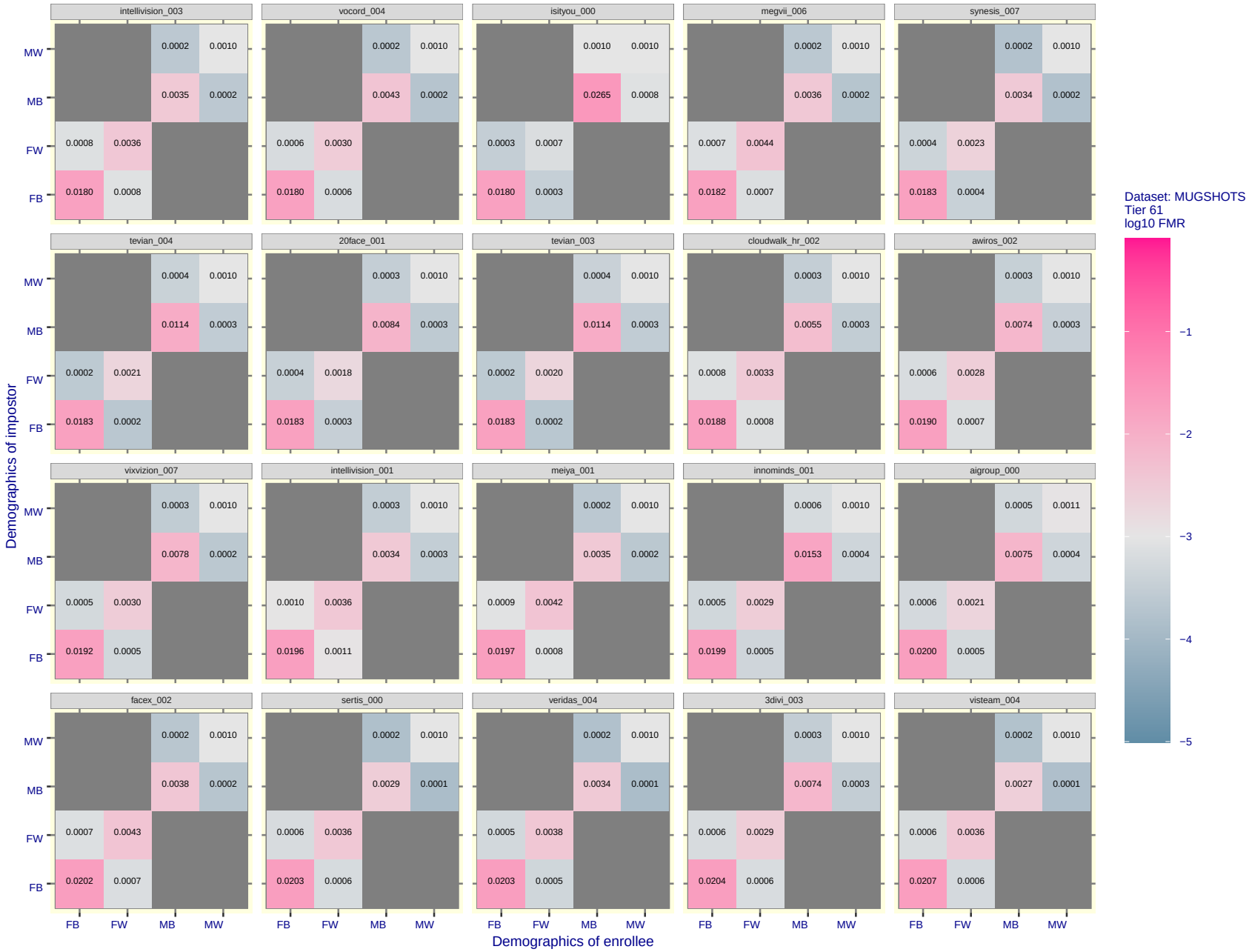

Figure 381: For the mugshot images, FMR *for same-sex impostor pairs of images annotated with codes for black female, black male, white female, white male. The threshold is set for each algorithm to give* FMR *= 0.001 for white males which is the demographic that usually gives the lowest* FMR*. This means the top right box is the same color in all panels. The panels are sorted over multiple pages in order of* FMR *on black females, which is the demographc that usually gives the highest* FMR*.*

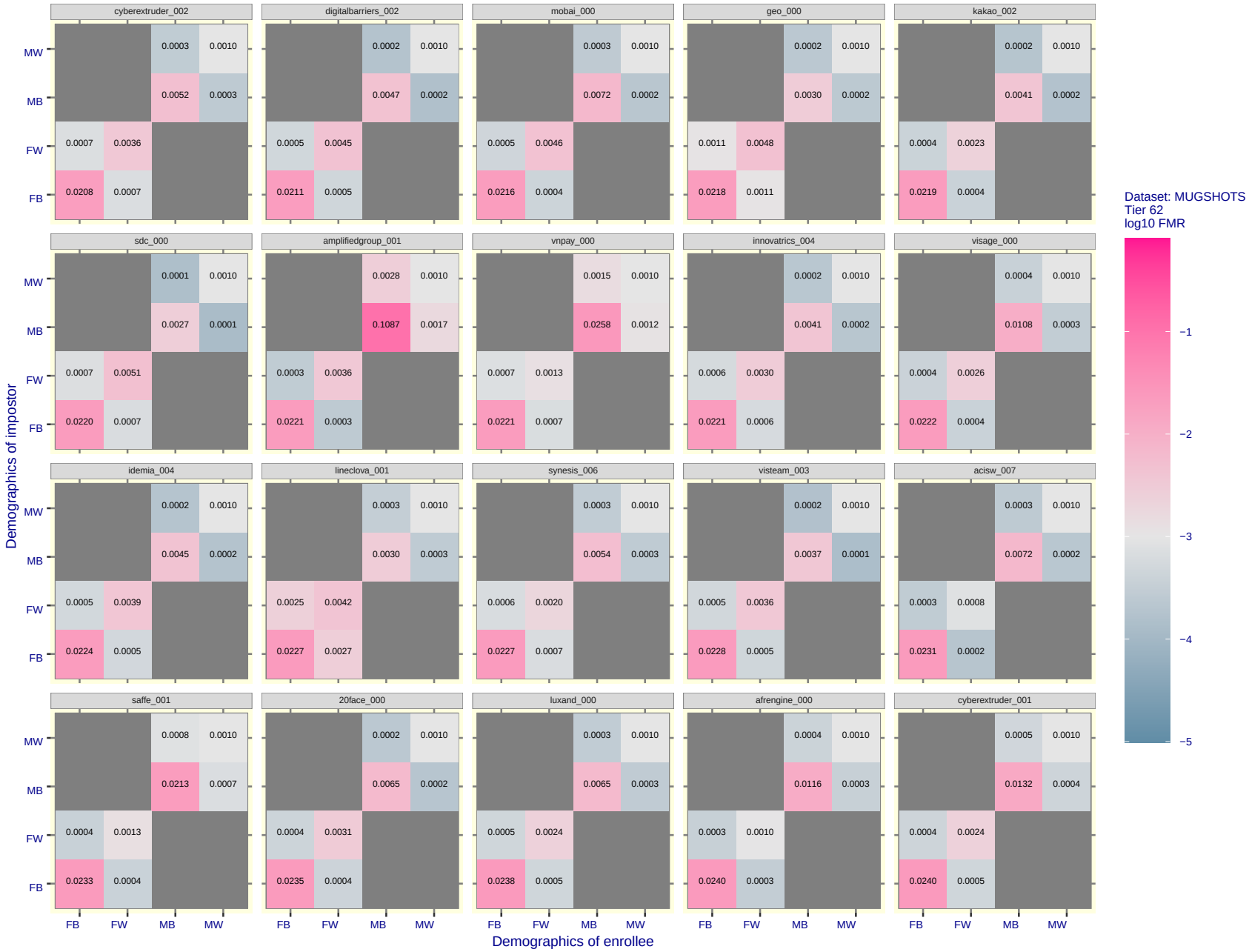

Figure 382: For the mugshot images, FMR *for same-sex impostor pairs of images annotated with codes for black female, black male, white female, white male. The threshold is set for each algorithm to give* FMR *= 0.001 for white males which is the demographic that usually gives the lowest* FMR*. This means the top right box is the same color in all panels. The panels are sorted over multiple pages in order of* FMR *on black females, which is the demographc that usually gives the highest* FMR*.*

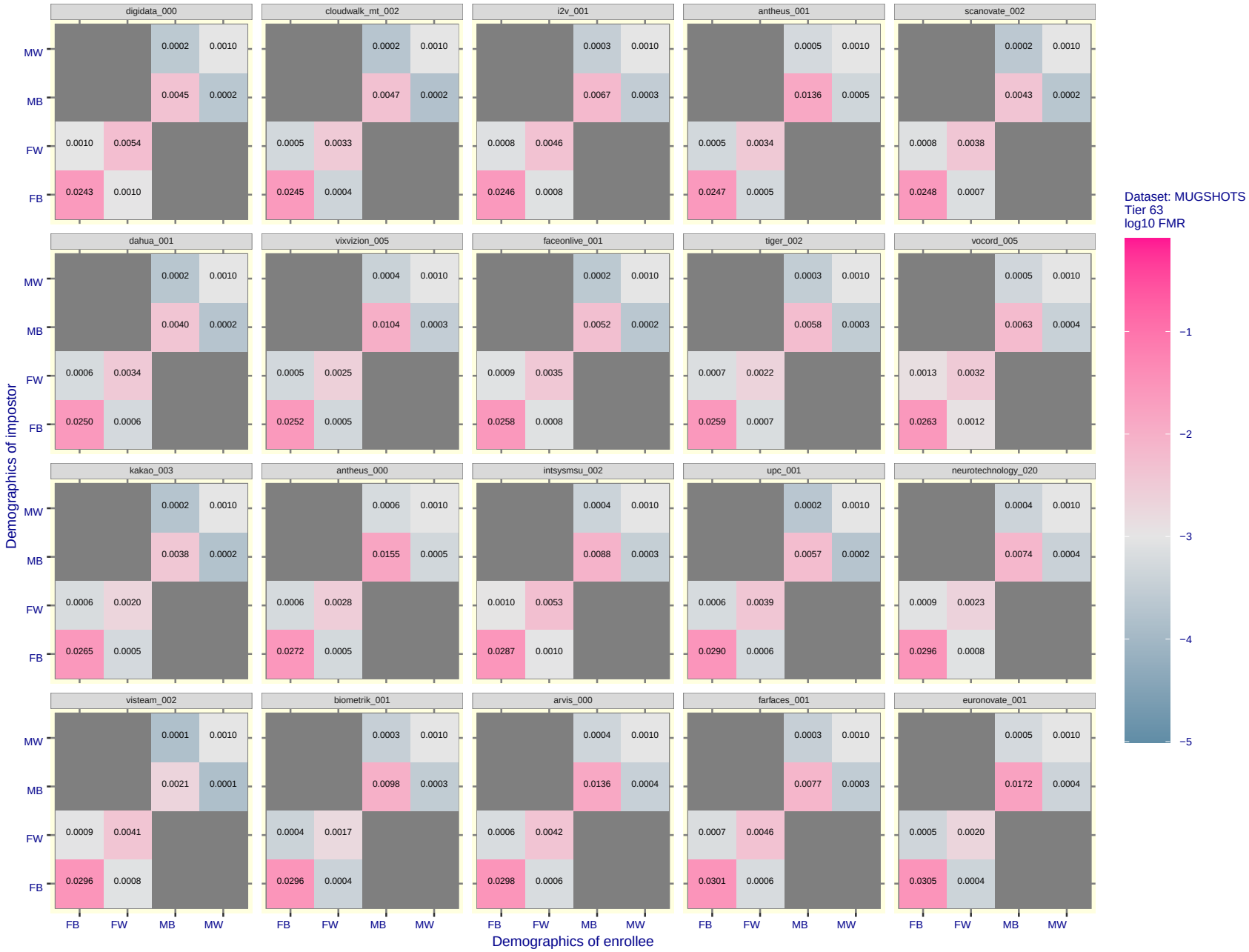

Figure 383: For the mugshot images, FMR *for same-sex impostor pairs of images annotated with codes for black female, black male, white female, white male. The threshold is set for each algorithm to give* FMR *= 0.001 for white males which is the demographic that usually gives the lowest* FMR*. This means the top right box is the same color in all panels. The panels are sorted over multiple pages in order of* FMR *on black females, which is the demographc that usually gives the highest* FMR*.*

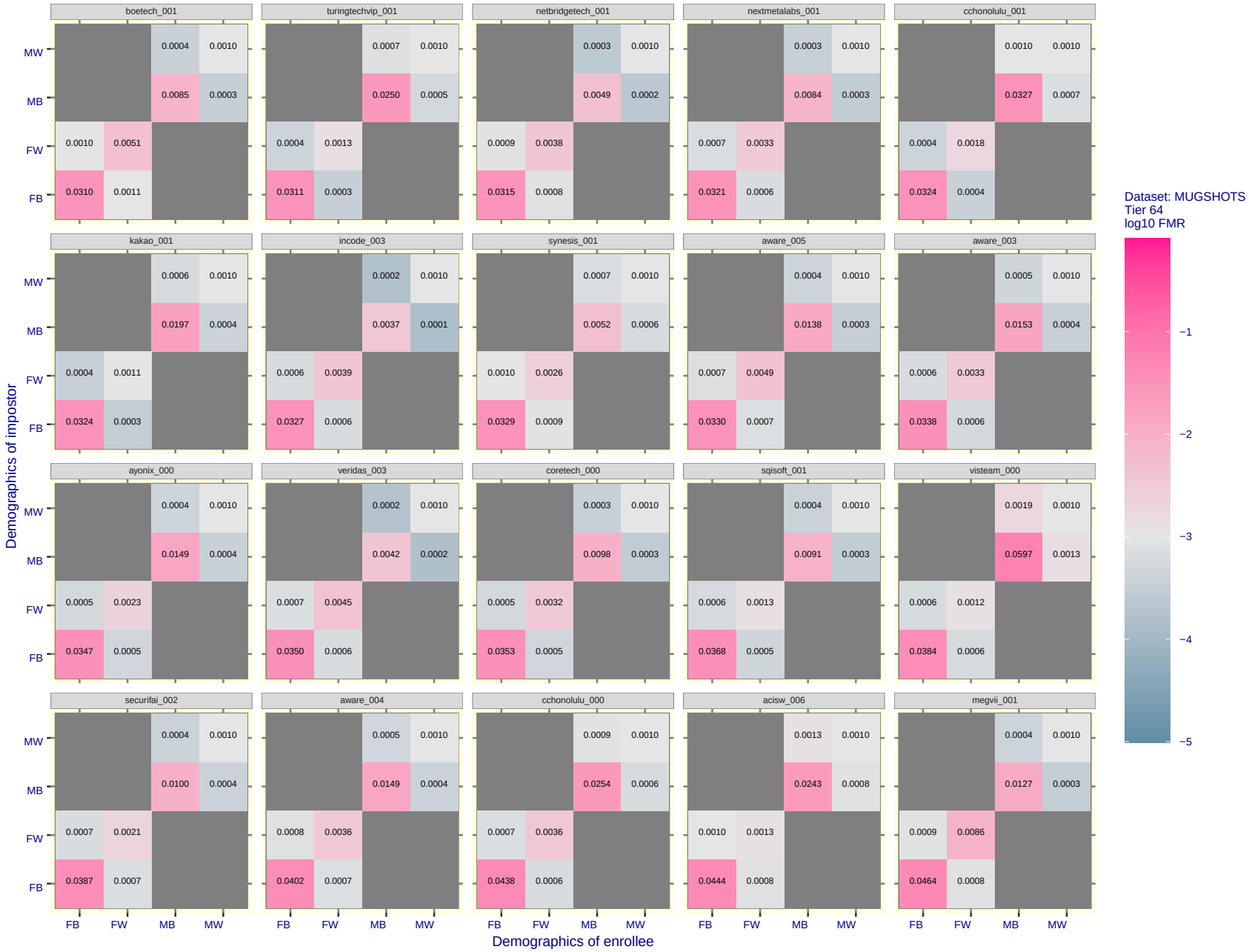

Figure 384: For the mugshot images, FMR *for same-sex impostor pairs of images annotated with codes for black female, black male, white female, white male. The threshold is set for each algorithm to give* FMR *= 0.001 for white males which is the demographic that usually gives the lowest* FMR*. This means the top right box is the same color in all panels. The panels are sorted over multiple pages in order of* FMR *on black females, which is the demographc that usually gives the highest* FMR*.*

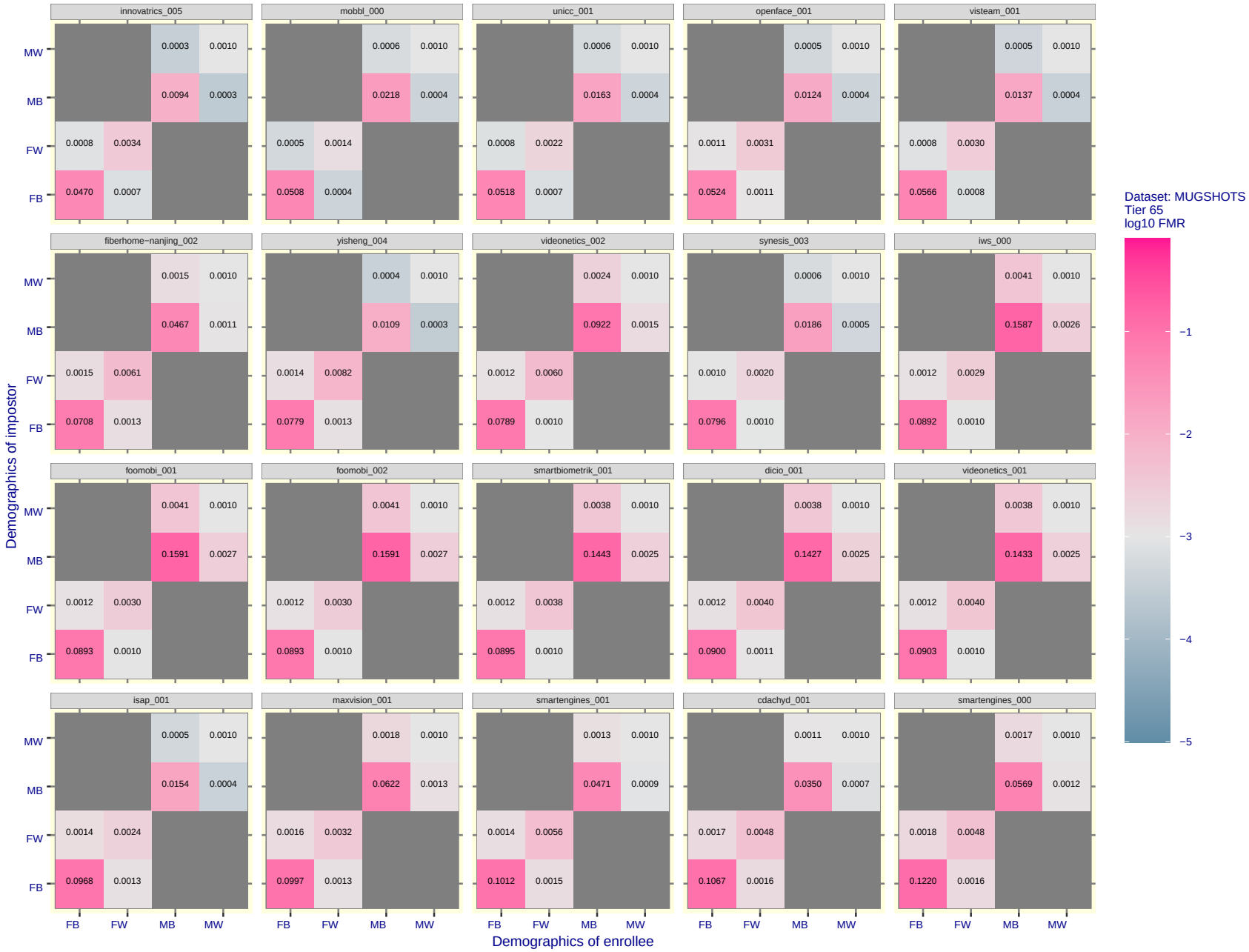

Figure 385: For the mugshot images, FMR *for same-sex impostor pairs of images annotated with codes for black female, black male, white female, white male. The threshold is set for each algorithm to give* FMR *= 0.001 for white males which is the demographic that usually gives the lowest* FMR*. This means the top right box is the same color in all panels. The panels are sorted over multiple pages in order of* FMR *on black females, which is the demographc that usually gives the highest* FMR*.*

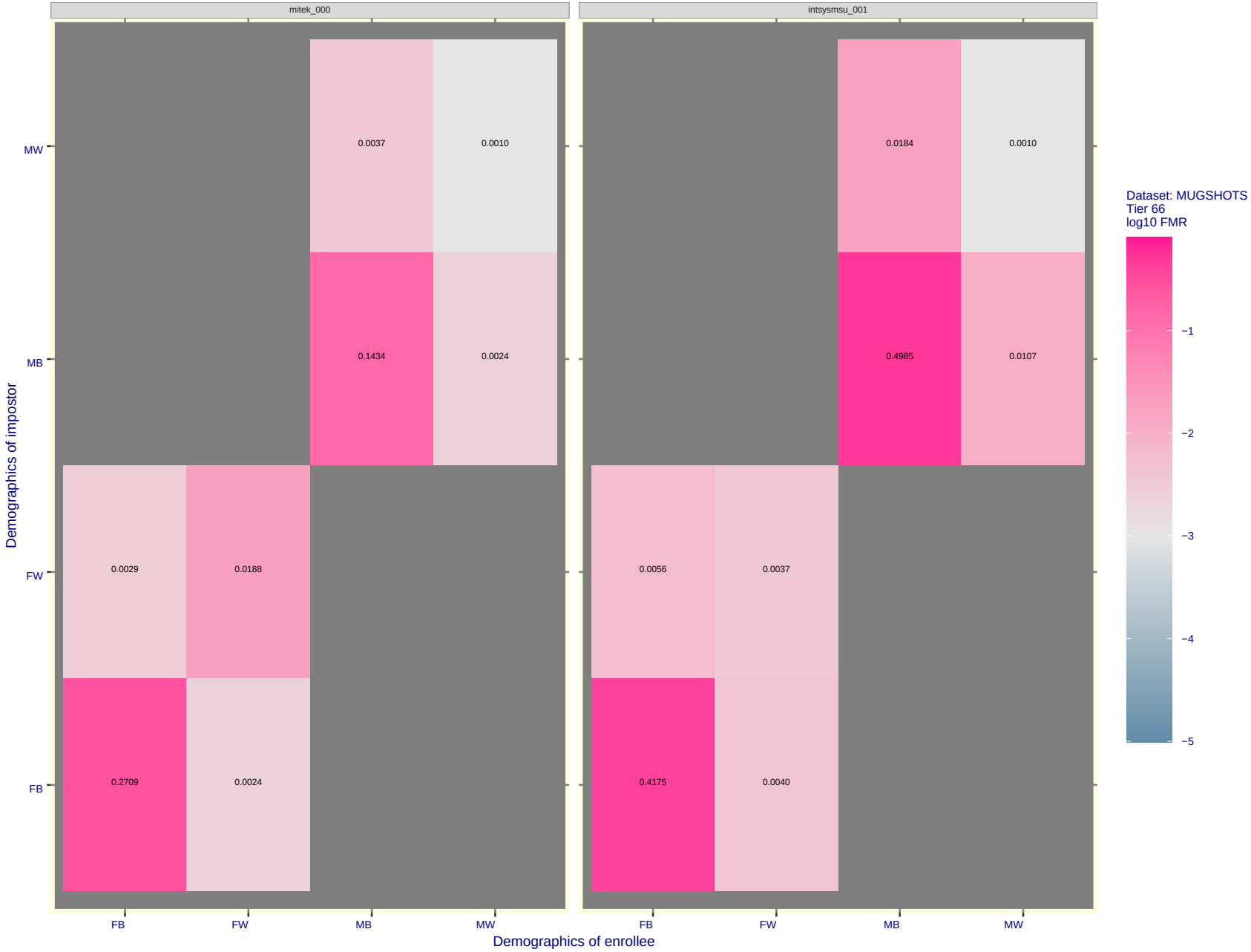

Figure 386: For the mugshot images, FMR *for same-sex impostor pairs of images annotated with codes for black female, black male, white female, white male. The threshold is set for each algorithm to give* FMR *= 0.001 for white males which is the demographic that usually gives the lowest* FMR*. This means the top right box is the same color in all panels. The panels are sorted over multiple pages in order of* FMR *on black females, which is the demographc that usually gives the highest* FMR*.*

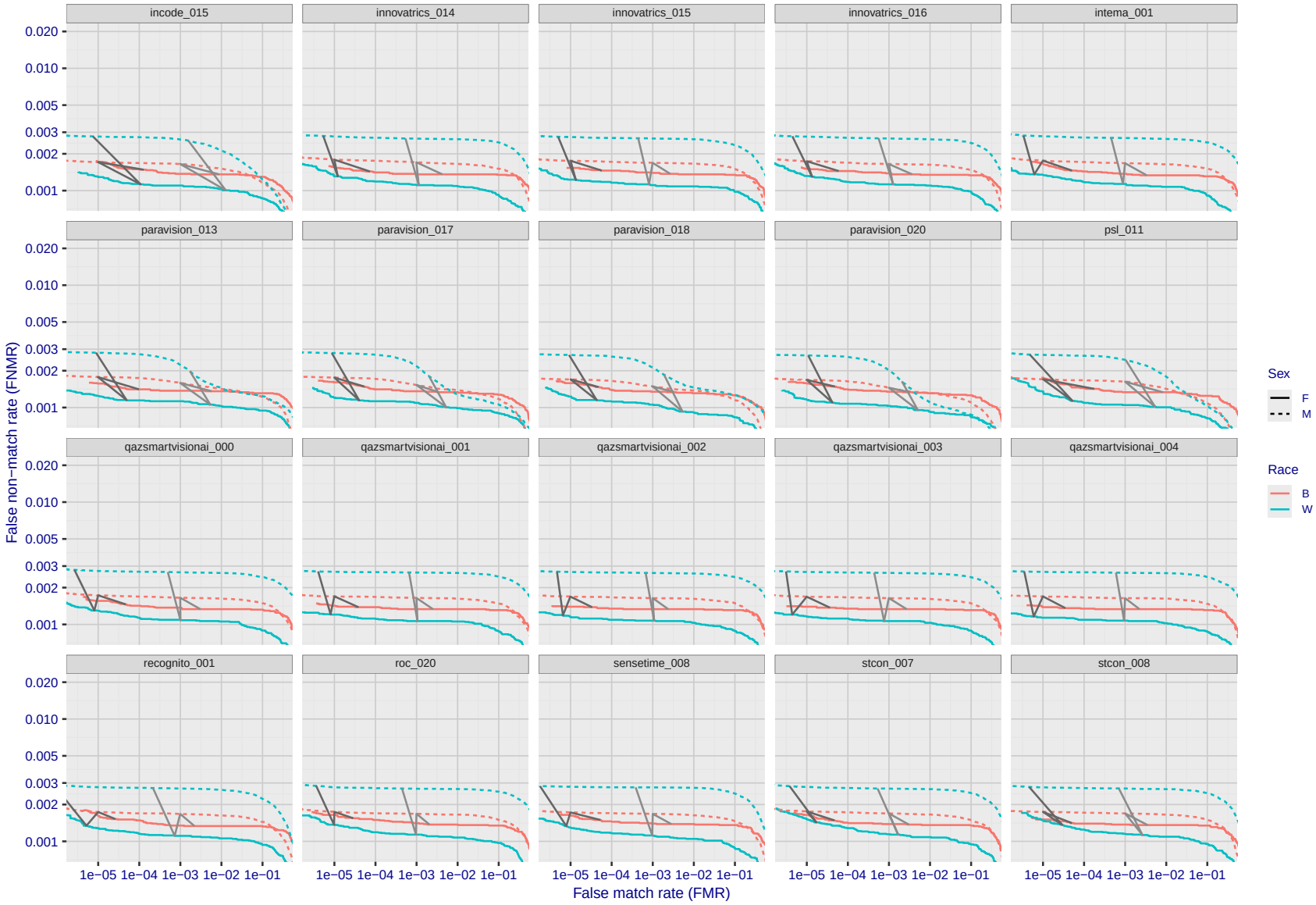

Figure 387: For the mugshot images, error tradeoff characteristics for white females, black females, black males and white males. The Z-shaped grey lines correspond to fixed thresholds, showing both *FNMR and FMR vary at one T value. Note: Many of the plots will naively be read as saying women gives worse error rates than men because the solid traces lie above the dotted ones. However, this is misleading and incomplete: The grey lines show the traces reveal horizontal shifts. Thus for the cogent-003 algorithm FNMR for men is* higher *than for women* at a fixed threshold *but, at the same time, FMR is higher for women - see Figure 608. As access control systems almost always operate at a fixed threshold, the naive interpretation is incorrect.*

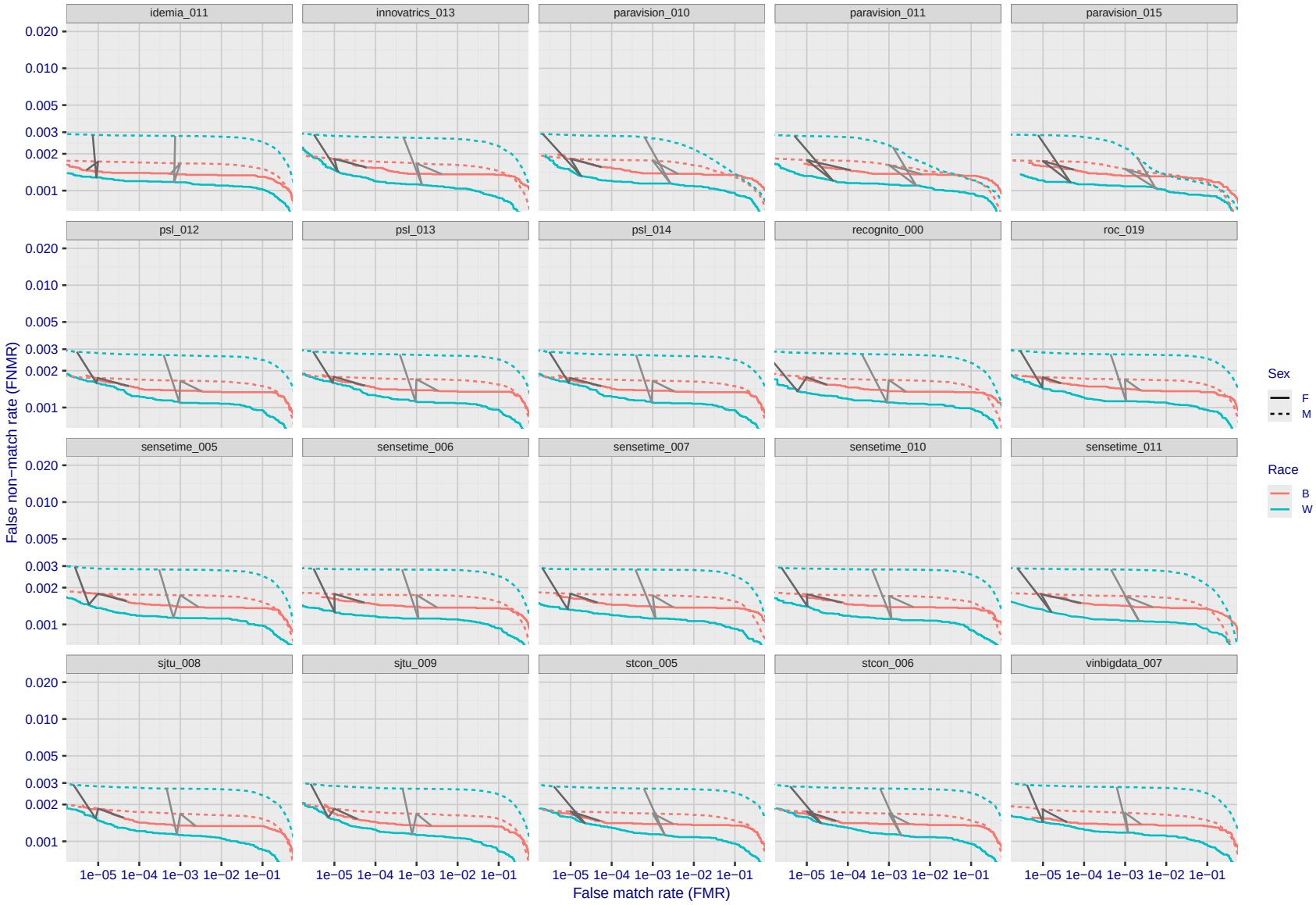

Figure 388: For the mugshot images, error tradeoff characteristics for white females, black females, black males and white males. The Z-shaped grey lines correspond to fixed thresholds, showing both *FNMR and FMR vary at one T value. Note: Many of the plots will naively be read as saying women gives worse error rates than men because the solid traces lie above the dotted ones. However, this is misleading and incomplete: The grey lines show the traces reveal horizontal shifts. Thus for the cogent-003 algorithm FNMR for men is* higher *than for women* at a fixed threshold *but, at the same time, FMR is higher for women - see Figure 608. As access control systems almost always operate at a fixed threshold, the naive interpretation is incorrect.*

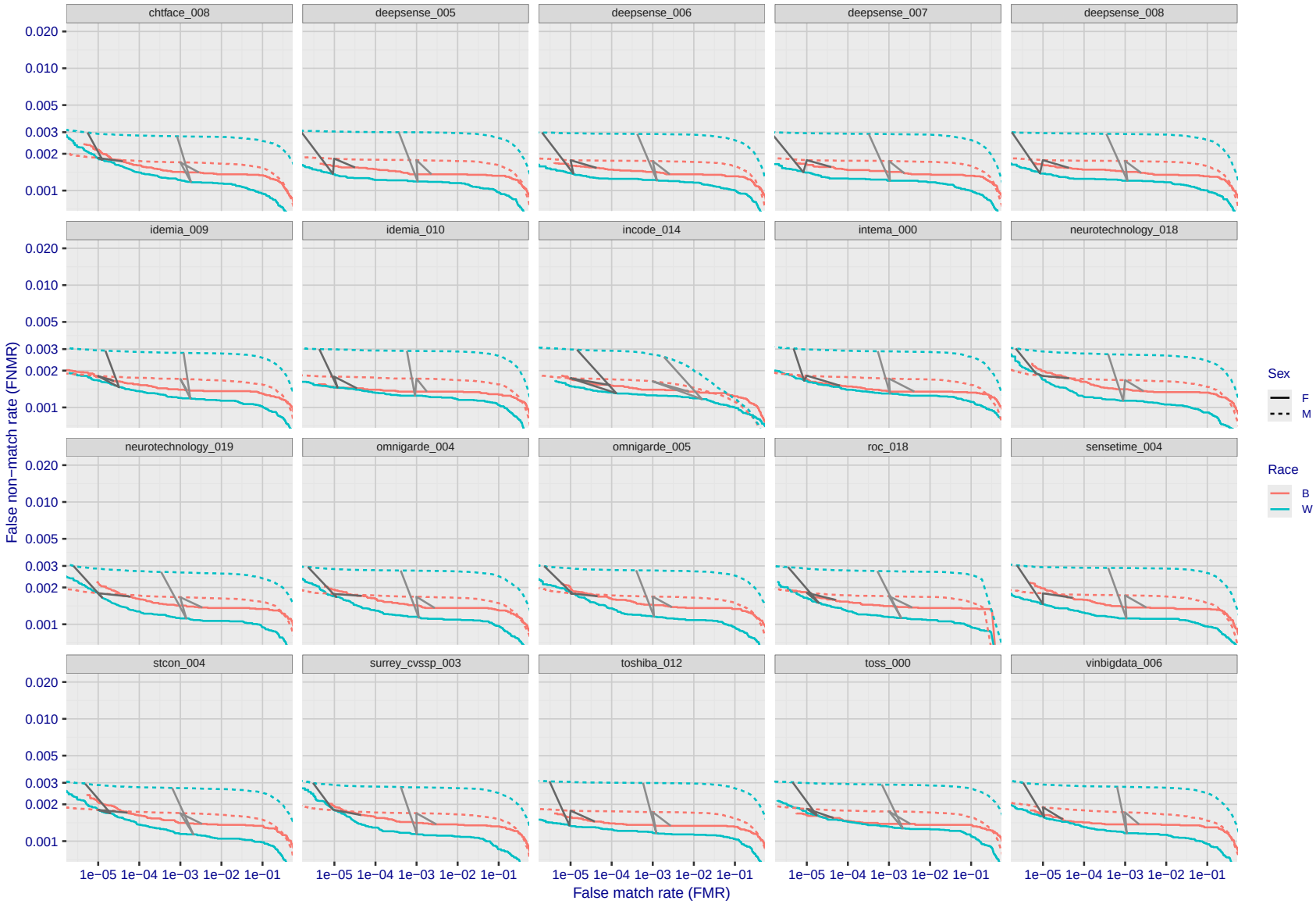

Figure 389: For the mugshot images, error tradeoff characteristics for white females, black females, black males and white males. The Z-shaped grey lines correspond to fixed thresholds, showing both *FNMR and FMR vary at one T value. Note: Many of the plots will naively be read as saying women gives worse error rates than men because the solid traces lie above the dotted ones. However, this is misleading and incomplete: The grey lines show the traces reveal horizontal shifts. Thus for the cogent-003 algorithm FNMR for men is* higher *than for women* at a fixed threshold *but, at the same time, FMR is higher for women - see Figure 608. As access control systems almost always operate at a fixed threshold, the naive interpretation is incorrect.*

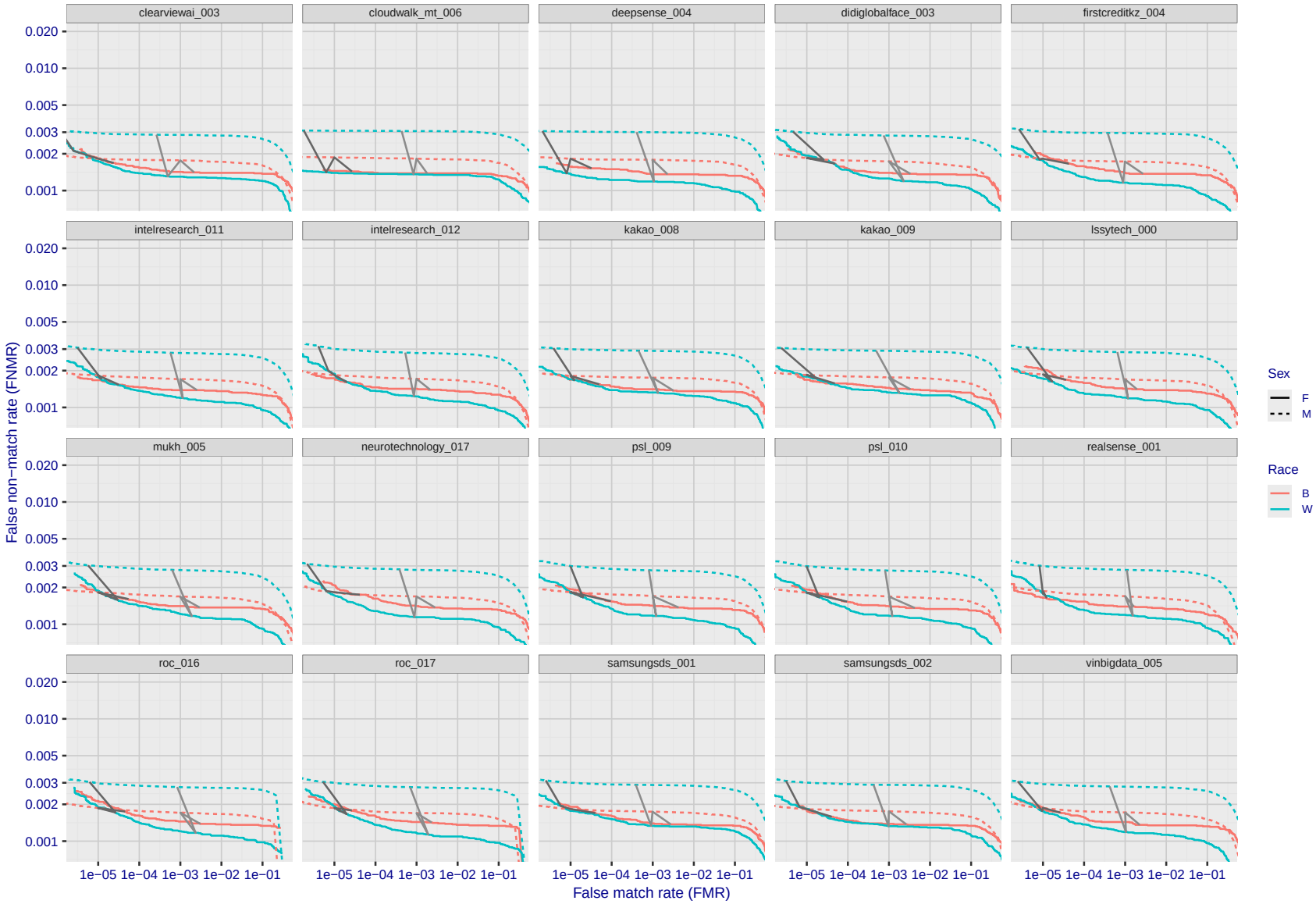

Figure 390: For the mugshot images, error tradeoff characteristics for white females, black females, black males and white males. The Z-shaped grey lines correspond to fixed thresholds, showing both *FNMR and FMR vary at one T value. Note: Many of the plots will naively be read as saying women gives worse error rates than men because the solid traces lie above the dotted ones. However, this is misleading and incomplete: The grey lines show the traces reveal horizontal shifts. Thus for the cogent-003 algorithm FNMR for men is* higher *than for women* at a fixed threshold *but, at the same time, FMR is higher for women - see Figure 608. As access control systems almost always operate at a fixed threshold, the naive interpretation is incorrect.*

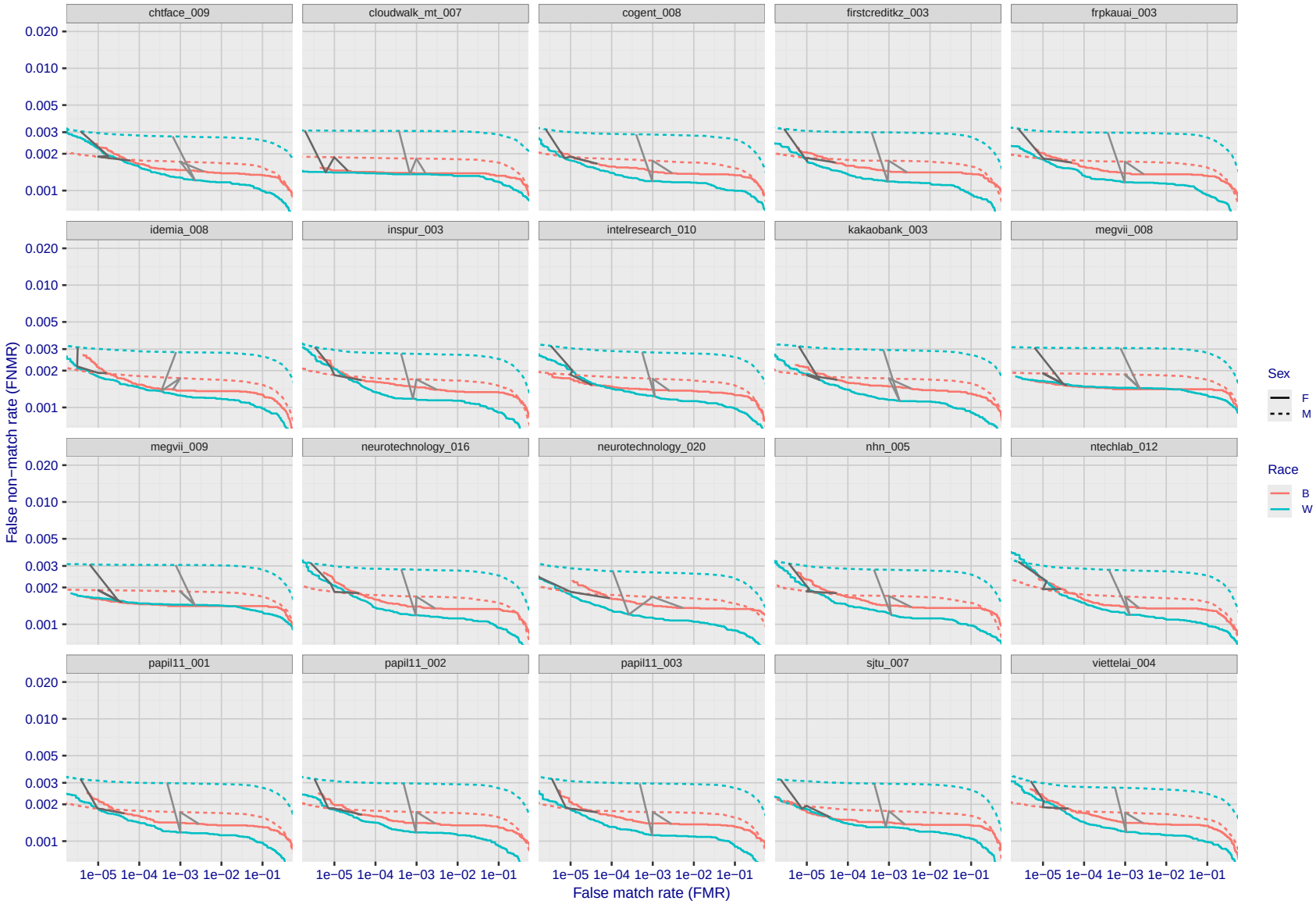

Figure 391: For the mugshot images, error tradeoff characteristics for white females, black females, black males and white males. The Z-shaped grey lines correspond to fixed thresholds, showing both *FNMR and FMR vary at one T value. Note: Many of the plots will naively be read as saying women gives worse error rates than men because the solid traces lie above the dotted ones. However, this is misleading and incomplete: The grey lines show the traces reveal horizontal shifts. Thus for the cogent-003 algorithm FNMR for men is* higher *than for women* at a fixed threshold *but, at the same time, FMR is higher for women - see Figure 608. As access control systems almost always operate at a fixed threshold, the naive interpretation is incorrect.*

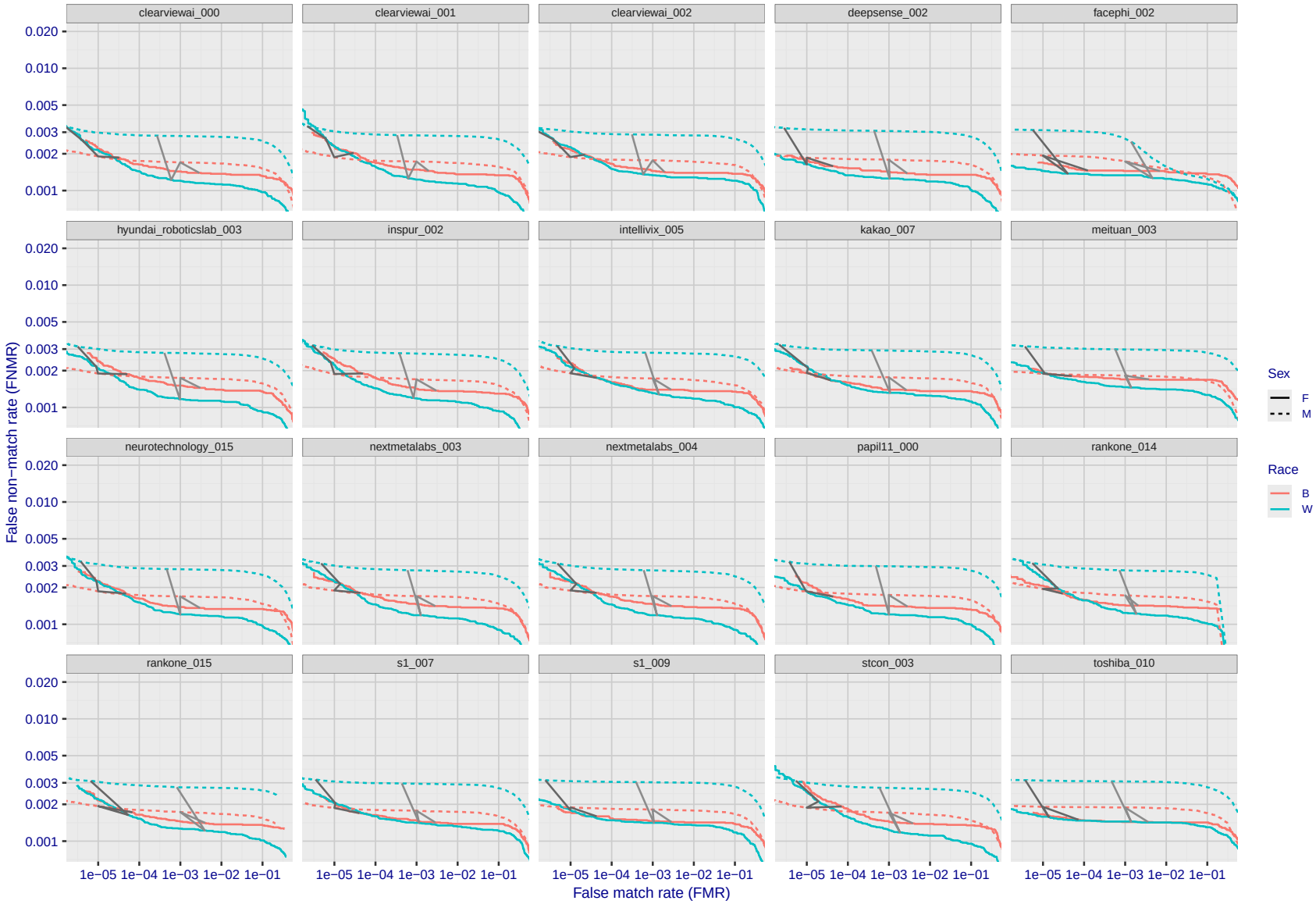

Figure 392: For the mugshot images, error tradeoff characteristics for white females, black females, black males and white males. The Z-shaped grey lines correspond to fixed thresholds, showing both *FNMR and FMR vary at one T value. Note: Many of the plots will naively be read as saying women gives worse error rates than men because the solid traces lie above the dotted ones. However, this is misleading and incomplete: The grey lines show the traces reveal horizontal shifts. Thus for the cogent-003 algorithm FNMR for men is* higher *than for women* at a fixed threshold *but, at the same time, FMR is higher for women - see Figure 608. As access control systems almost always operate at a fixed threshold, the naive interpretation is incorrect.*

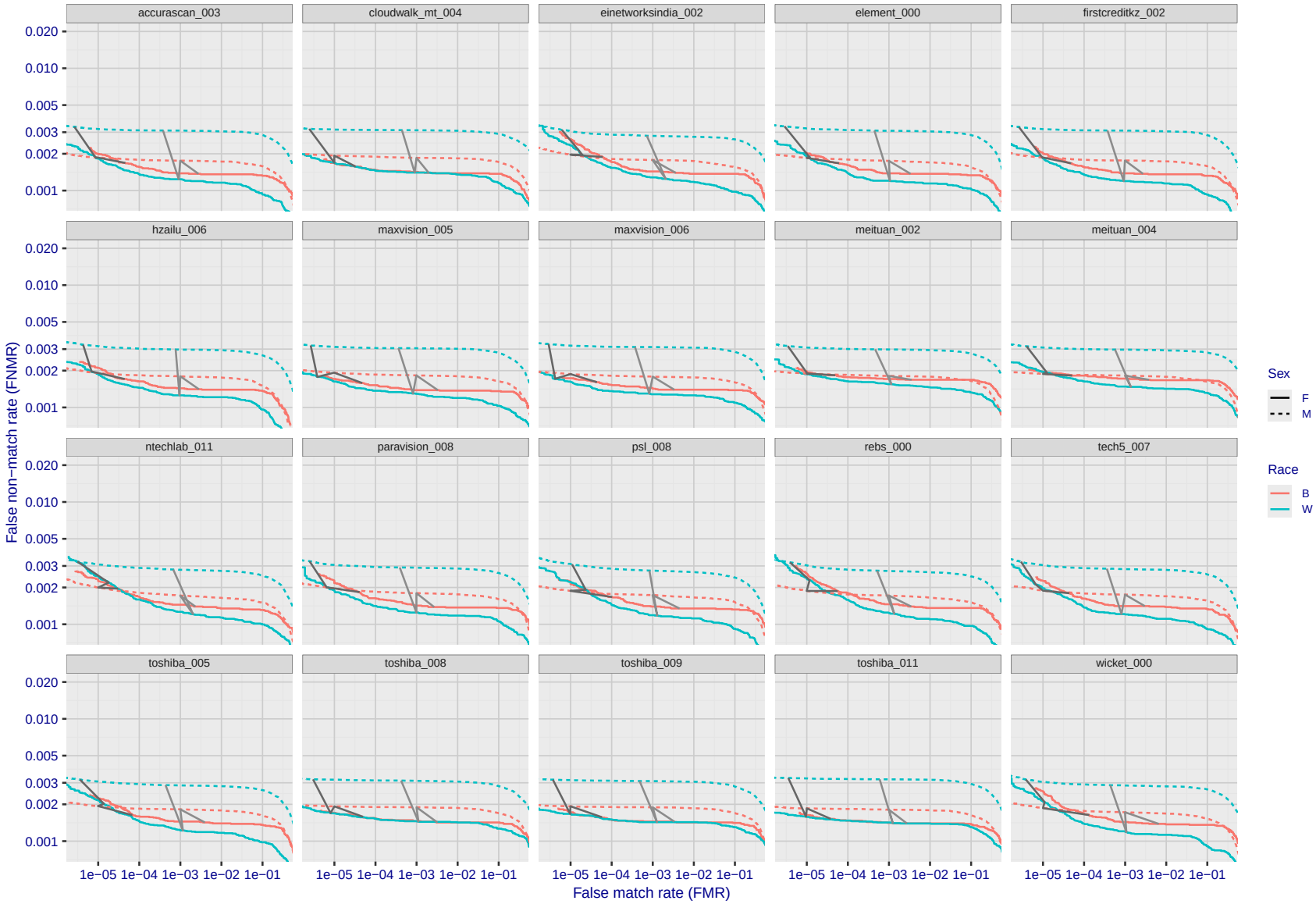

Figure 393: For the mugshot images, error tradeoff characteristics for white females, black females, black males and white males. The Z-shaped grey lines correspond to fixed thresholds, showing both *FNMR and FMR vary at one T value. Note: Many of the plots will naively be read as saying women gives worse error rates than men because the solid traces lie above the dotted ones. However, this is misleading and incomplete: The grey lines show the traces reveal horizontal shifts. Thus for the cogent-003 algorithm FNMR for men is* higher *than for women* at a fixed threshold *but, at the same time, FMR is higher for women - see Figure 608. As access control systems almost always operate at a fixed threshold, the naive interpretation is incorrect.*

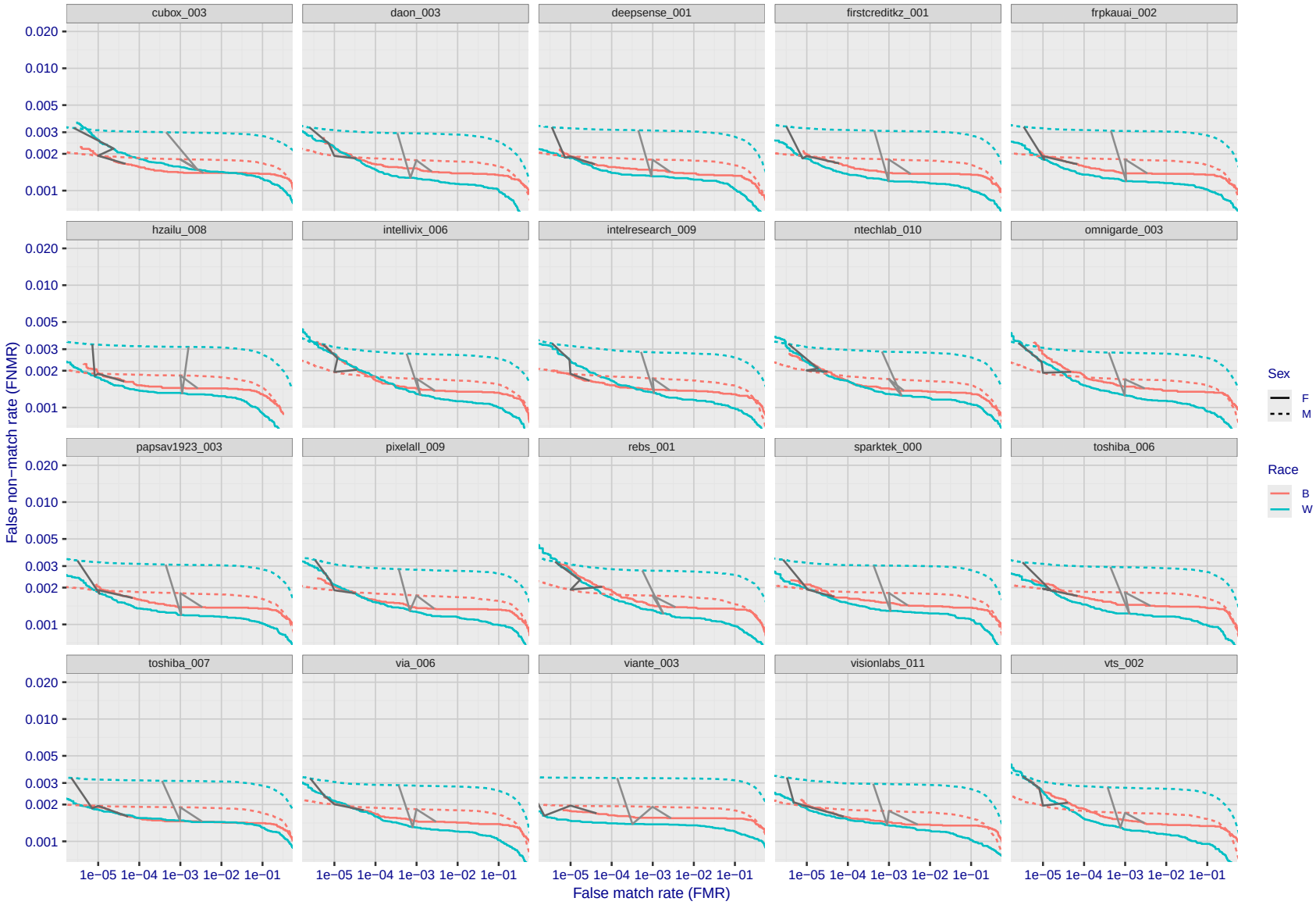

Figure 394: For the mugshot images, error tradeoff characteristics for white females, black females, black males and white males. The Z-shaped grey lines correspond to fixed thresholds, showing both *FNMR and FMR vary at one T value. Note: Many of the plots will naively be read as saying women gives worse error rates than men because the solid traces lie above the dotted ones. However, this is misleading and incomplete: The grey lines show the traces reveal horizontal shifts. Thus for the cogent-003 algorithm FNMR for men is* higher *than for women* at a fixed threshold *but, at the same time, FMR is higher for women - see Figure 608. As access control systems almost always operate at a fixed threshold, the naive interpretation is incorrect.*

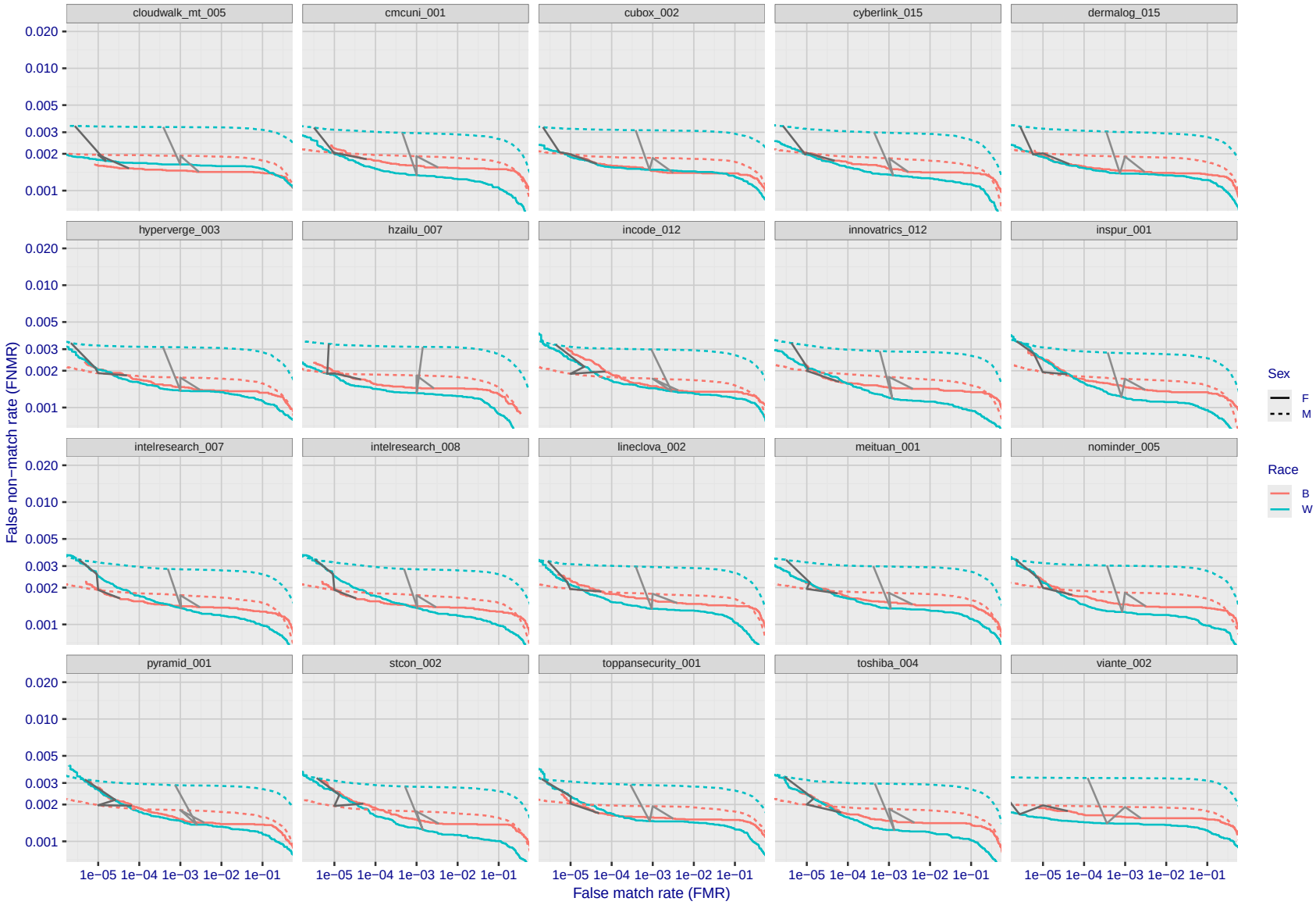

Figure 395: For the mugshot images, error tradeoff characteristics for white females, black females, black males and white males. The Z-shaped grey lines correspond to fixed thresholds, showing both *FNMR and FMR vary at one T value. Note: Many of the plots will naively be read as saying women gives worse error rates than men because the solid traces lie above the dotted ones. However, this is misleading and incomplete: The grey lines show the traces reveal horizontal shifts. Thus for the cogent-003 algorithm FNMR for men is* higher *than for women* at a fixed threshold *but, at the same time, FMR is higher for women - see Figure 608. As access control systems almost always operate at a fixed threshold, the naive interpretation is incorrect.*

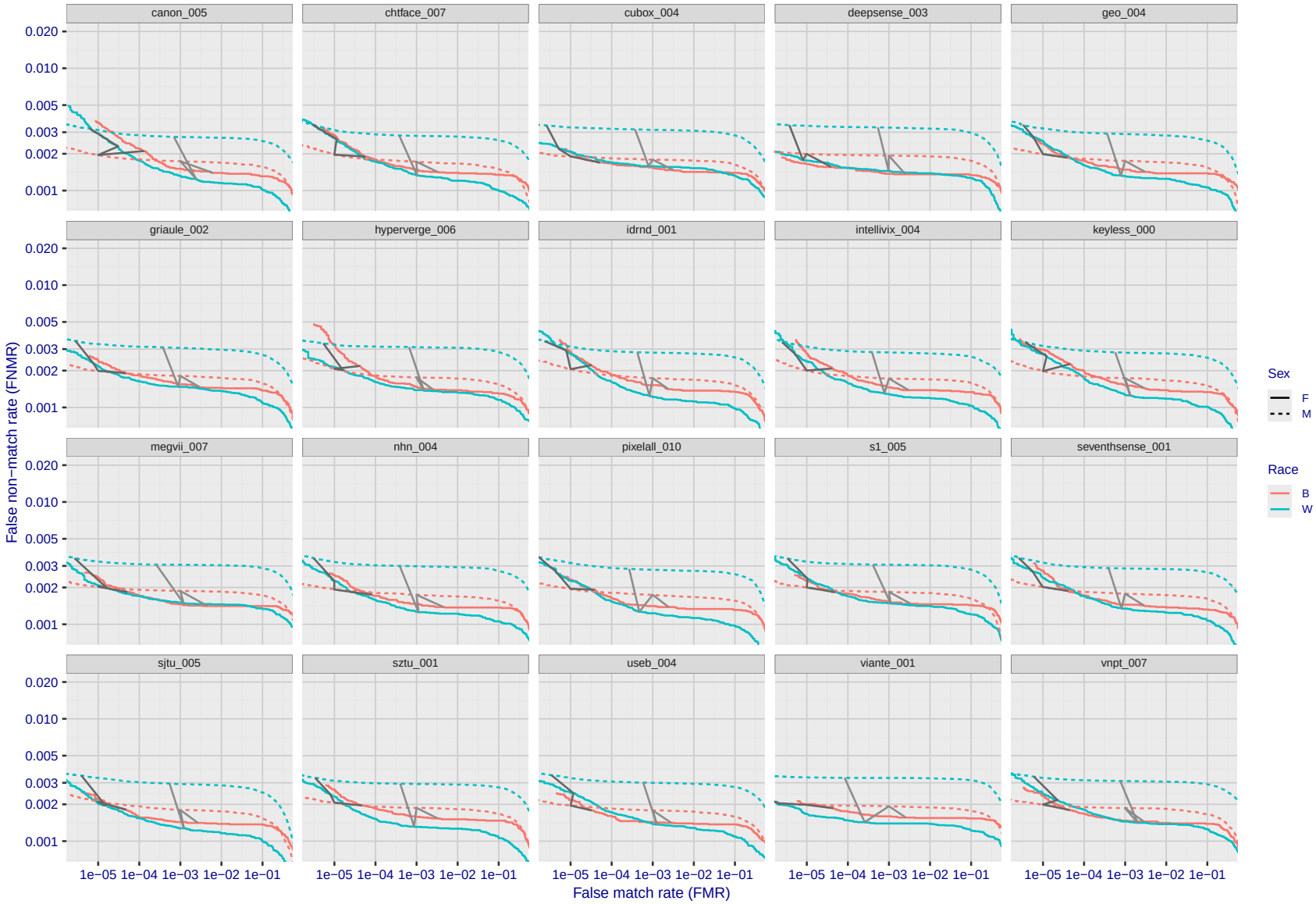

Figure 396: For the mugshot images, error tradeoff characteristics for white females, black females, black males and white males. The Z-shaped grey lines correspond to fixed thresholds, showing both *FNMR and FMR vary at one T value. Note: Many of the plots will naively be read as saying women gives worse error rates than men because the solid traces lie above the dotted ones. However, this is misleading and incomplete: The grey lines show the traces reveal horizontal shifts. Thus for the cogent-003 algorithm FNMR for men is* higher *than for women* at a fixed threshold *but, at the same time, FMR is higher for women - see Figure 608. As access control systems almost always operate at a fixed threshold, the naive interpretation is incorrect.*

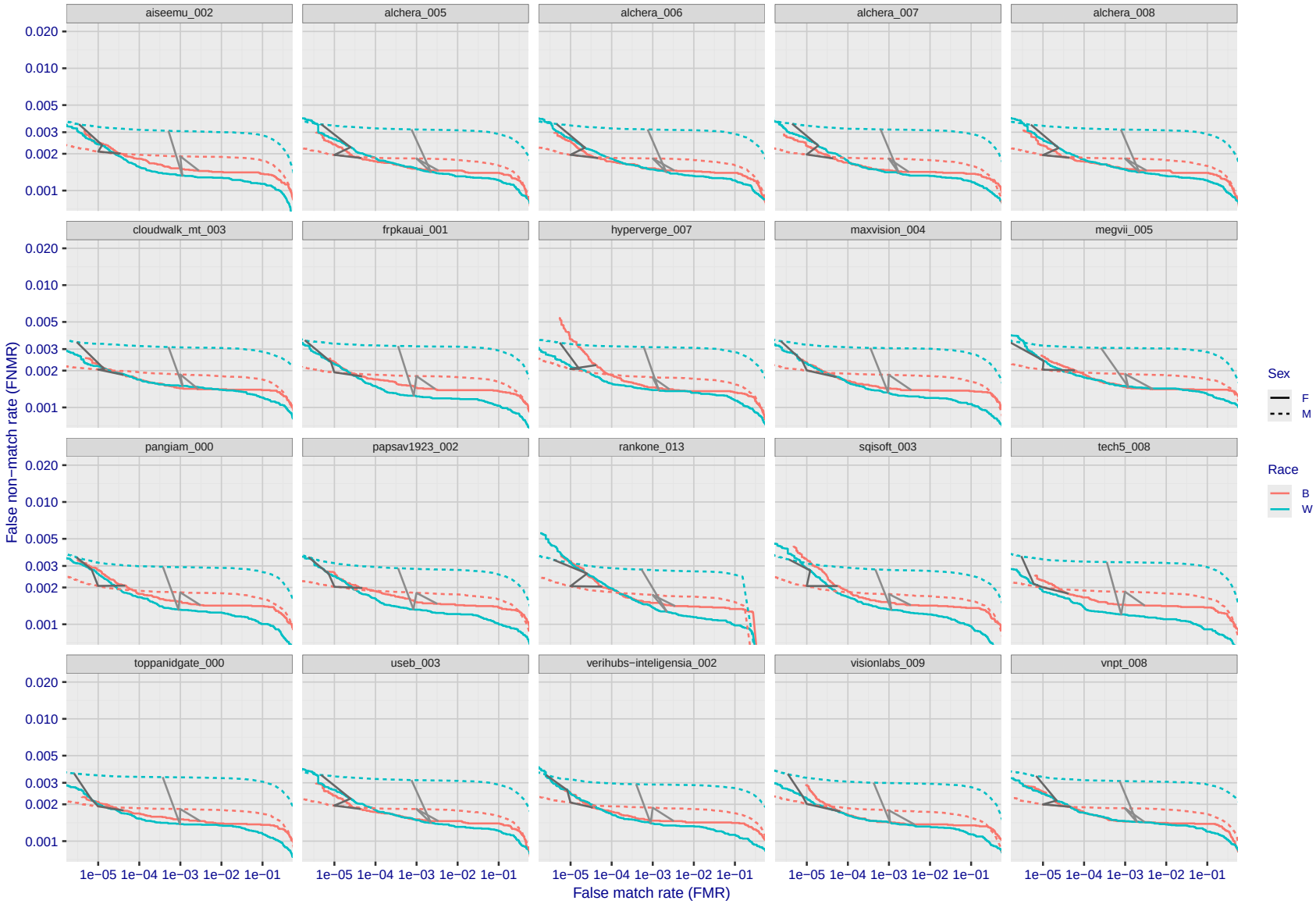

Figure 397: For the mugshot images, error tradeoff characteristics for white females, black females, black males and white males. The Z-shaped grey lines correspond to fixed thresholds, showing both *FNMR and FMR vary at one T value. Note: Many of the plots will naively be read as saying women gives worse error rates than men because the solid traces lie above the dotted ones. However, this is misleading and incomplete: The grey lines show the traces reveal horizontal shifts. Thus for the cogent-003 algorithm FNMR for men is* higher *than for women* at a fixed threshold *but, at the same time, FMR is higher for women - see Figure 608. As access control systems almost always operate at a fixed threshold, the naive interpretation is incorrect.*

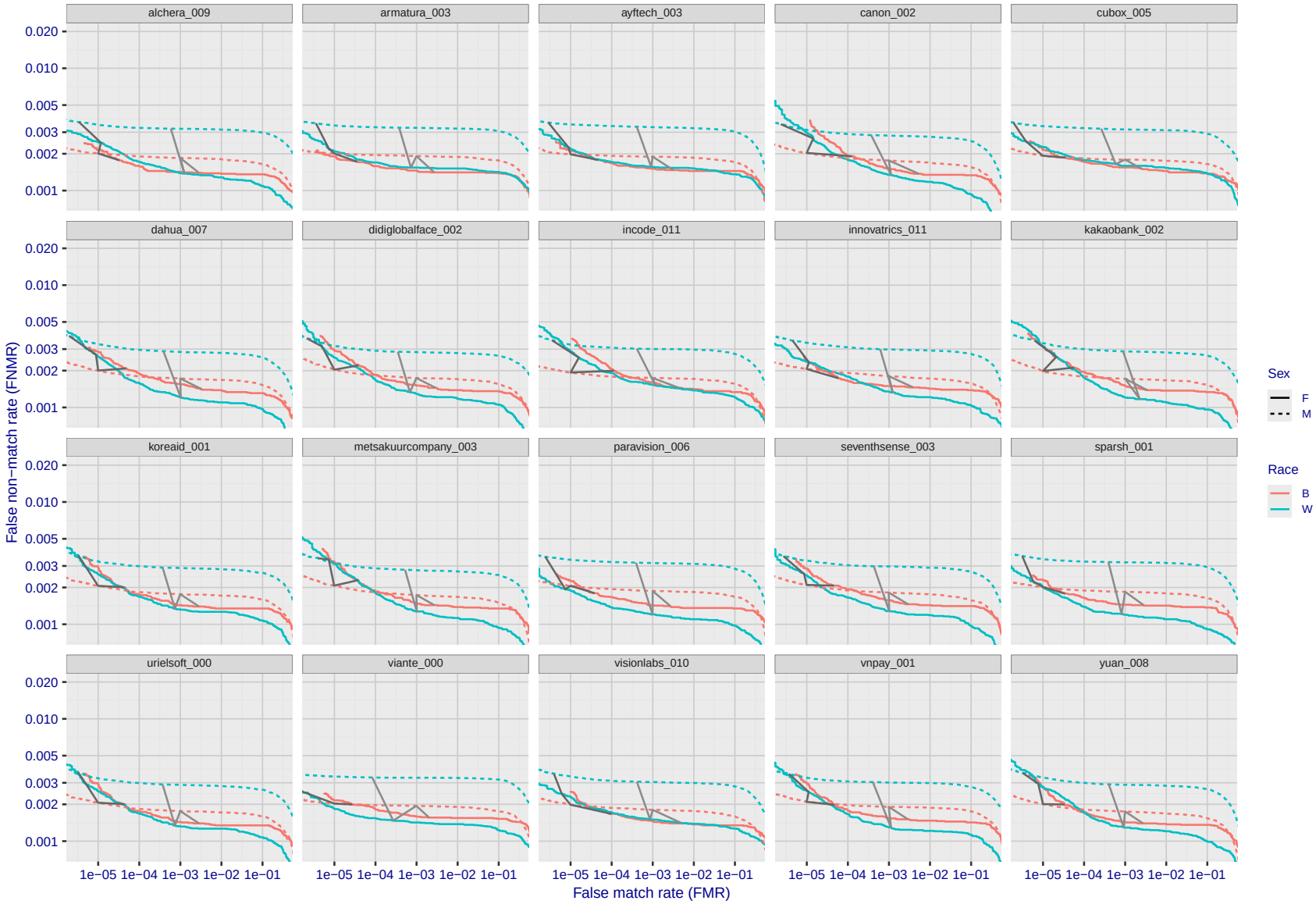

Figure 398: For the mugshot images, error tradeoff characteristics for white females, black females, black males and white males. The Z-shaped grey lines correspond to fixed thresholds, showing both *FNMR and FMR vary at one T value. Note: Many of the plots will naively be read as saying women gives worse error rates than men because the solid traces lie above the dotted ones. However, this is misleading and incomplete: The grey lines show the traces reveal horizontal shifts. Thus for the cogent-003 algorithm FNMR for men is* higher *than for women* at a fixed threshold *but, at the same time, FMR is higher for women - see Figure 608. As access control systems almost always operate at a fixed threshold, the naive interpretation is incorrect.*

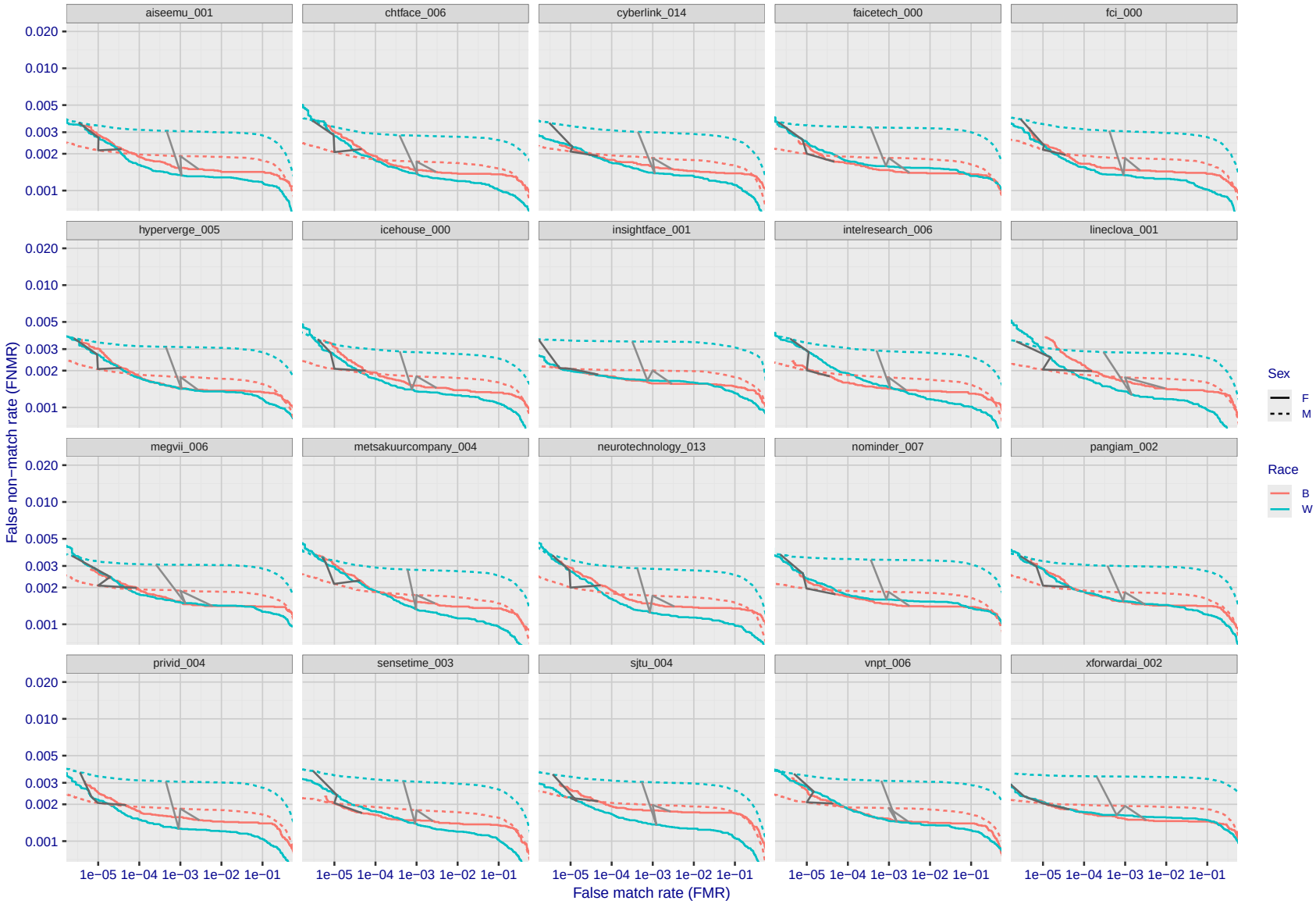

Figure 399: For the mugshot images, error tradeoff characteristics for white females, black females, black males and white males. The Z-shaped grey lines correspond to fixed thresholds, showing both *FNMR and FMR vary at one T value. Note: Many of the plots will naively be read as saying women gives worse error rates than men because the solid traces lie above the dotted ones. However, this is misleading and incomplete: The grey lines show the traces reveal horizontal shifts. Thus for the cogent-003 algorithm FNMR for men is* higher *than for women* at a fixed threshold *but, at the same time, FMR is higher for women - see Figure 608. As access control systems almost always operate at a fixed threshold, the naive interpretation is incorrect.*

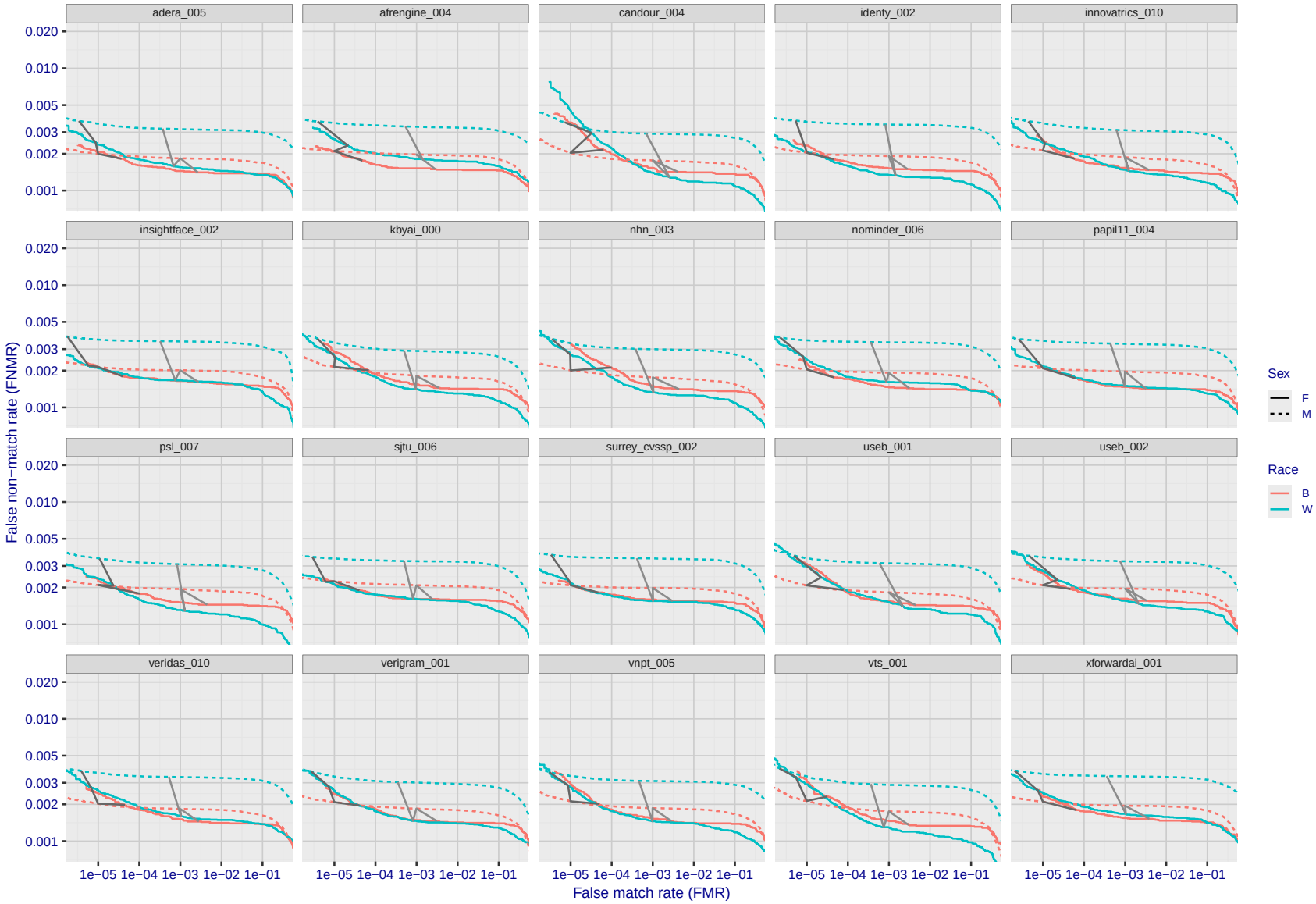

Figure 400: For the mugshot images, error tradeoff characteristics for white females, black females, black males and white males. The Z-shaped grey lines correspond to fixed thresholds, showing both *FNMR and FMR vary at one T value. Note: Many of the plots will naively be read as saying women gives worse error rates than men because the solid traces lie above the dotted ones. However, this is misleading and incomplete: The grey lines show the traces reveal horizontal shifts. Thus for the cogent-003 algorithm FNMR for men is* higher *than for women* at a fixed threshold *but, at the same time, FMR is higher for women - see Figure 608. As access control systems almost always operate at a fixed threshold, the naive interpretation is incorrect.*

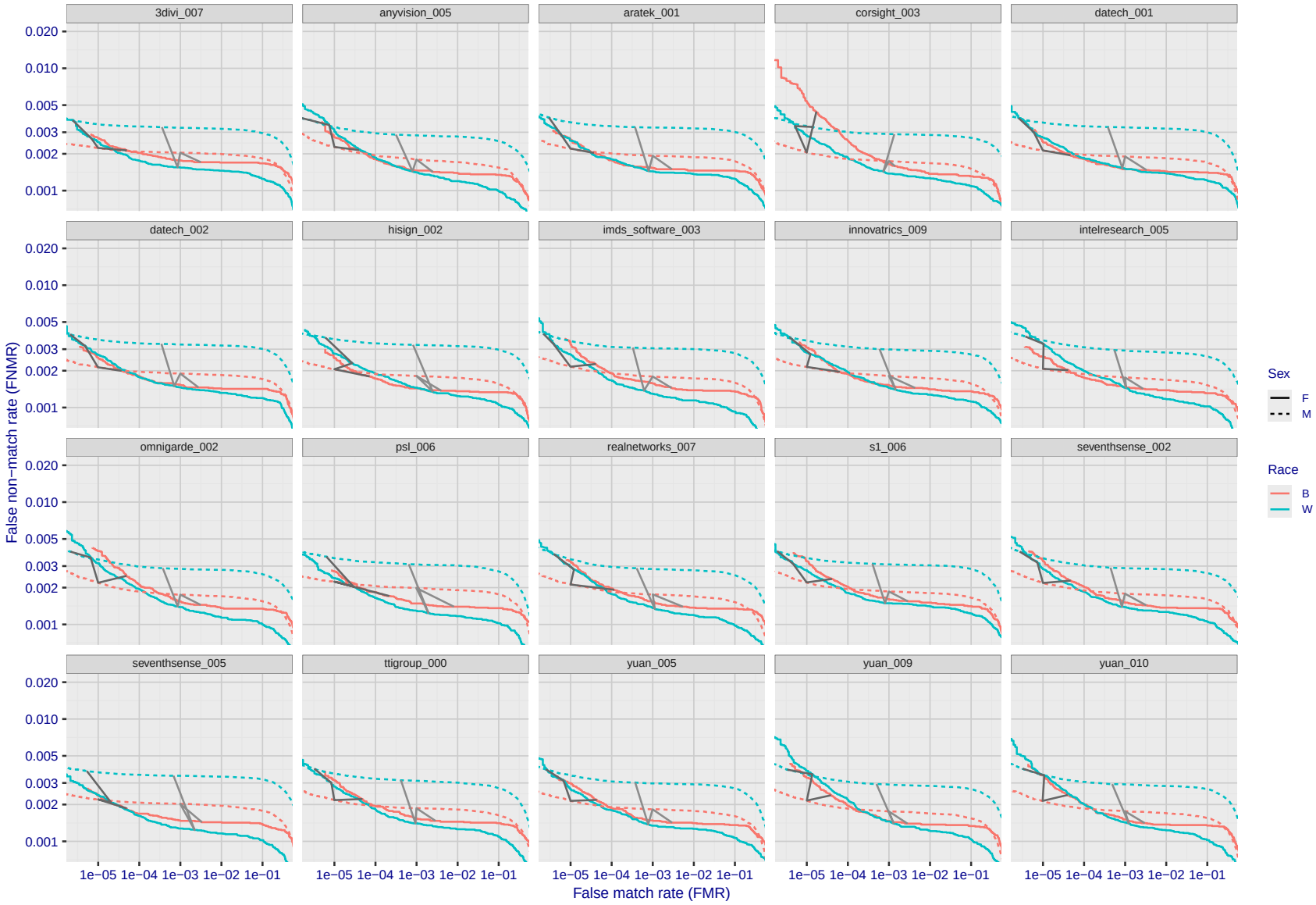

Figure 401: For the mugshot images, error tradeoff characteristics for white females, black females, black males and white males. The Z-shaped grey lines correspond to fixed thresholds, showing both *FNMR and FMR vary at one T value. Note: Many of the plots will naively be read as saying women gives worse error rates than men because the solid traces lie above the dotted ones. However, this is misleading and incomplete: The grey lines show the traces reveal horizontal shifts. Thus for the cogent-003 algorithm FNMR for men is* higher *than for women* at a fixed threshold *but, at the same time, FMR is higher for women - see Figure 608. As access control systems almost always operate at a fixed threshold, the naive interpretation is incorrect.*

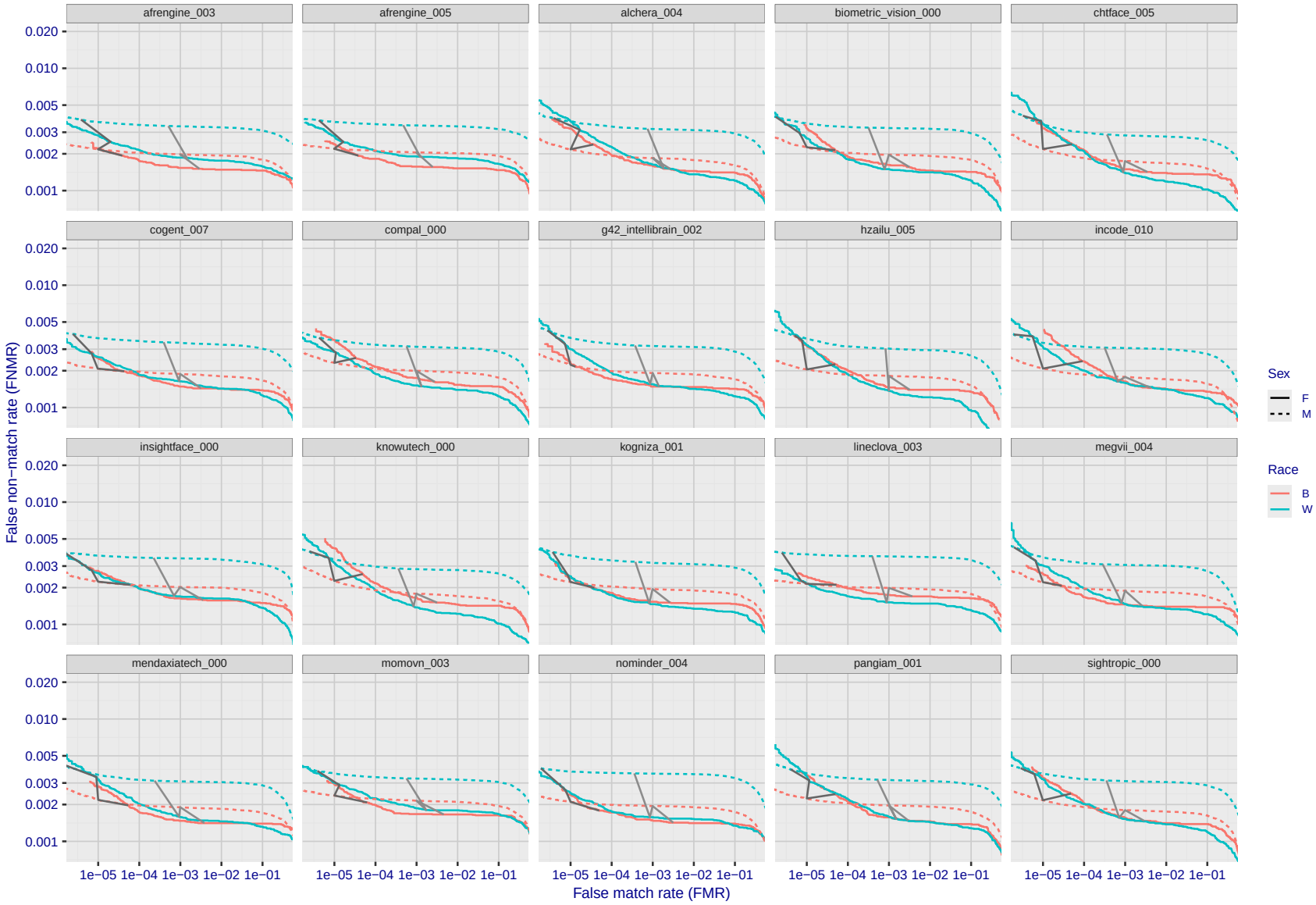

Figure 402: For the mugshot images, error tradeoff characteristics for white females, black females, black males and white males. The Z-shaped grey lines correspond to fixed thresholds, showing both *FNMR and FMR vary at one T value. Note: Many of the plots will naively be read as saying women gives worse error rates than men because the solid traces lie above the dotted ones. However, this is misleading and incomplete: The grey lines show the traces reveal horizontal shifts. Thus for the cogent-003 algorithm FNMR for men is* higher *than for women* at a fixed threshold *but, at the same time, FMR is higher for women - see Figure 608. As access control systems almost always operate at a fixed threshold, the naive interpretation is incorrect.*

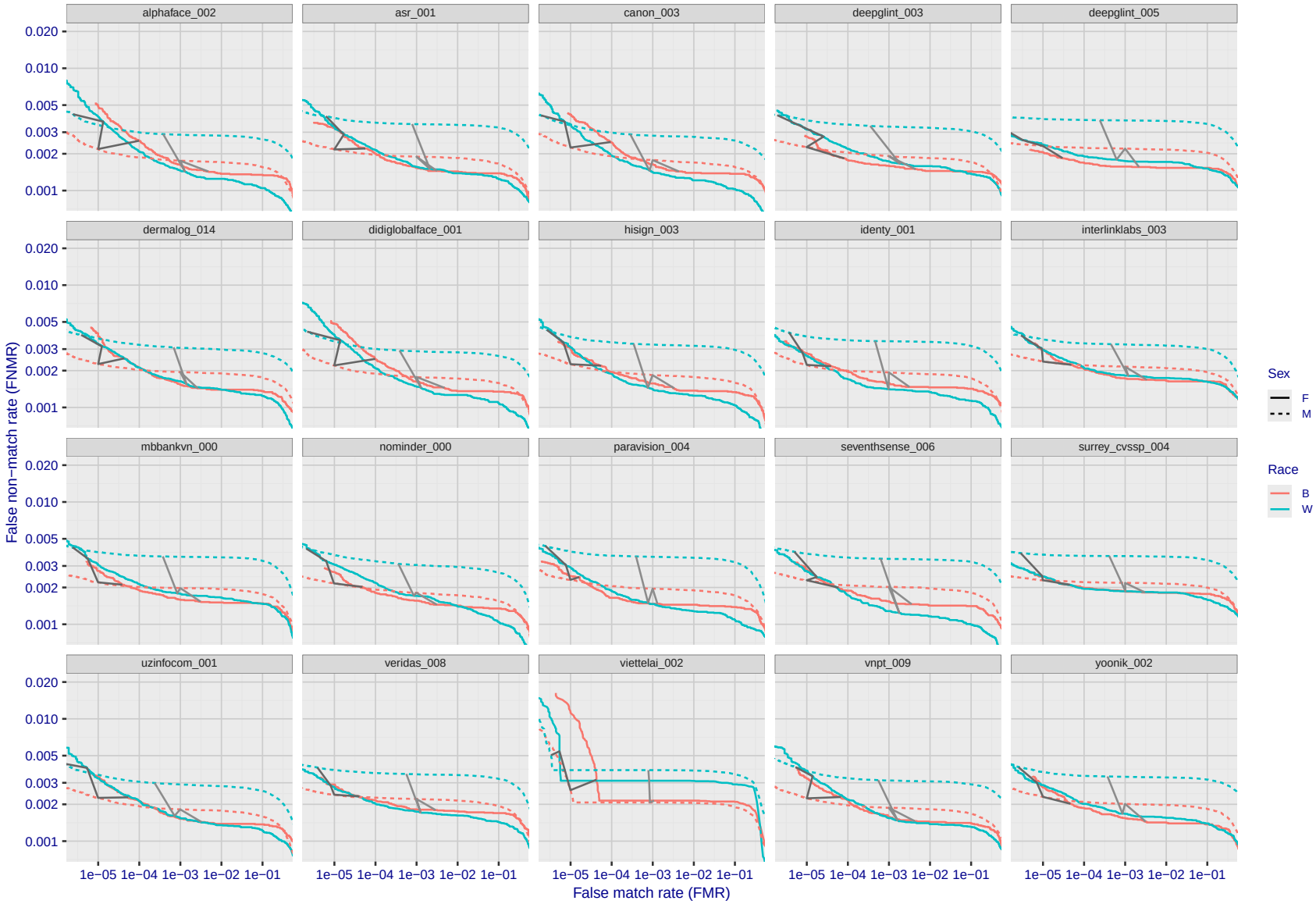

Figure 403: For the mugshot images, error tradeoff characteristics for white females, black females, black males and white males. The Z-shaped grey lines correspond to fixed thresholds, showing both *FNMR and FMR vary at one T value. Note: Many of the plots will naively be read as saying women gives worse error rates than men because the solid traces lie above the dotted ones. However, this is misleading and incomplete: The grey lines show the traces reveal horizontal shifts. Thus for the cogent-003 algorithm FNMR for men is* higher *than for women* at a fixed threshold *but, at the same time, FMR is higher for women - see Figure 608. As access control systems almost always operate at a fixed threshold, the naive interpretation is incorrect.*

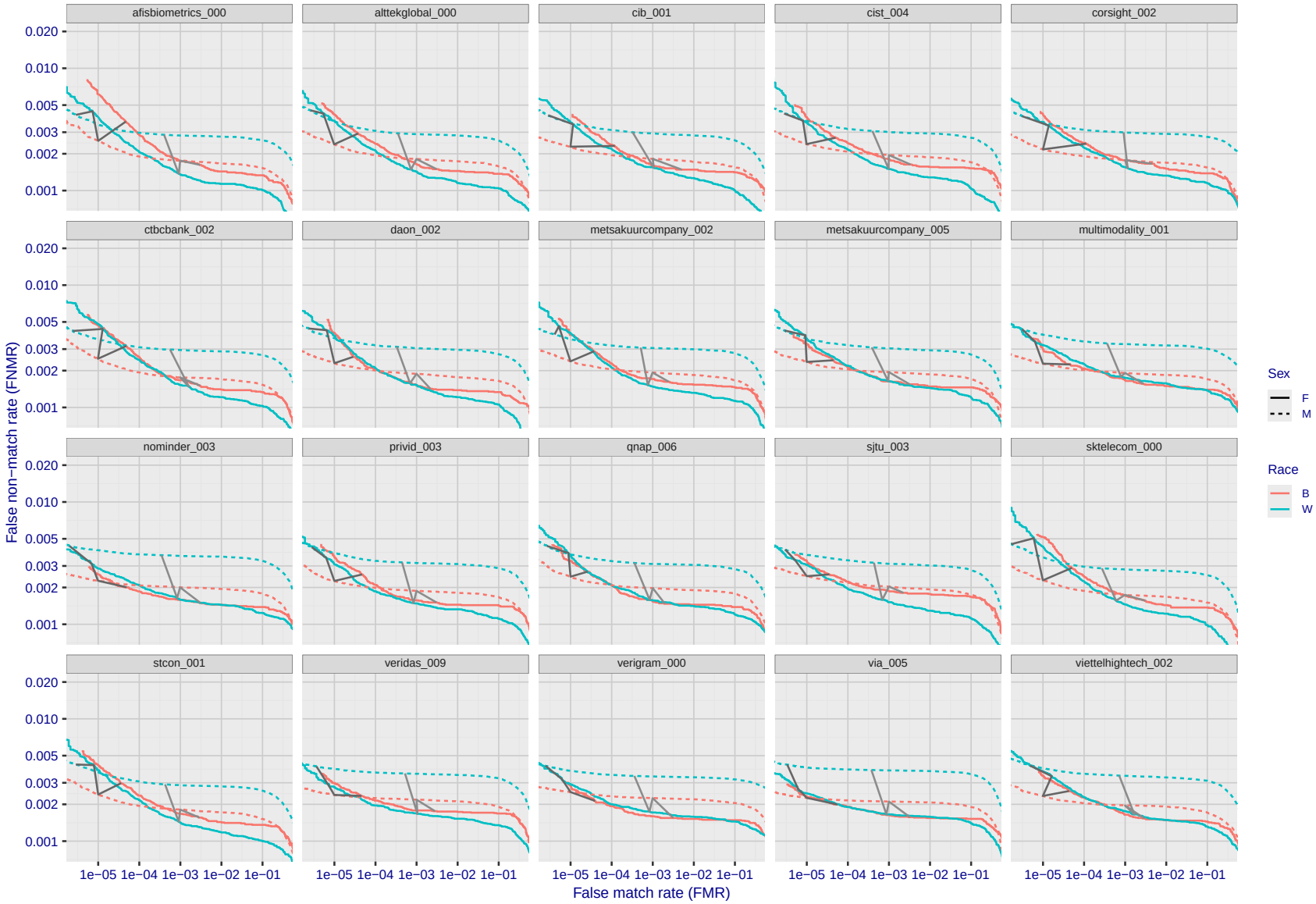

Figure 404: For the mugshot images, error tradeoff characteristics for white females, black females, black males and white males. The Z-shaped grey lines correspond to fixed thresholds, showing both *FNMR and FMR vary at one T value. Note: Many of the plots will naively be read as saying women gives worse error rates than men because the solid traces lie above the dotted ones. However, this is misleading and incomplete: The grey lines show the traces reveal horizontal shifts. Thus for the cogent-003 algorithm FNMR for men is* higher *than for women* at a fixed threshold *but, at the same time, FMR is higher for women - see Figure 608. As access control systems almost always operate at a fixed threshold, the naive interpretation is incorrect.*

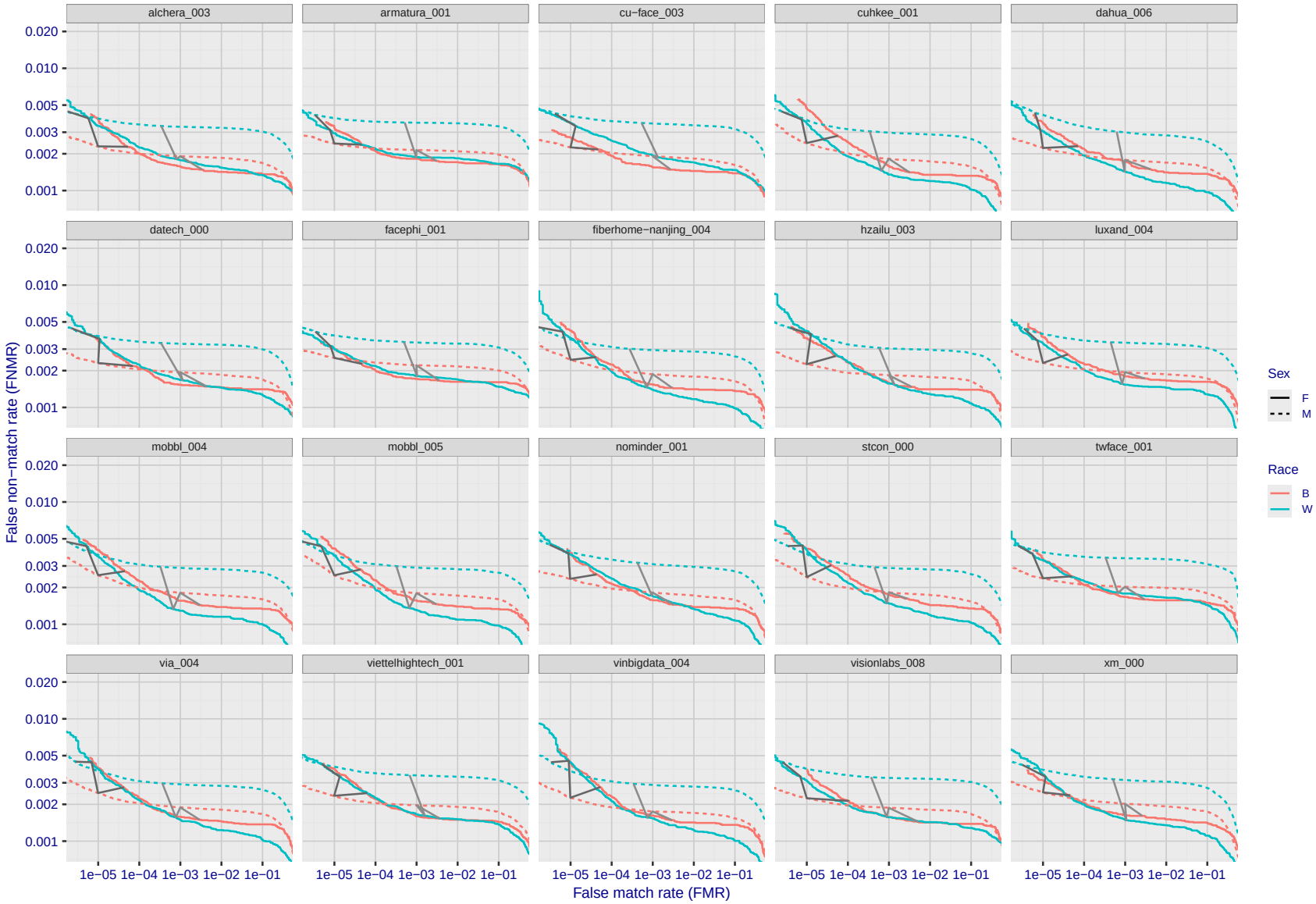

Figure 405: For the mugshot images, error tradeoff characteristics for white females, black females, black males and white males. The Z-shaped grey lines correspond to fixed thresholds, showing both *FNMR and FMR vary at one T value. Note: Many of the plots will naively be read as saying women gives worse error rates than men because the solid traces lie above the dotted ones. However, this is misleading and incomplete: The grey lines show the traces reveal horizontal shifts. Thus for the cogent-003 algorithm FNMR for men is* higher *than for women* at a fixed threshold *but, at the same time, FMR is higher for women - see Figure 608. As access control systems almost always operate at a fixed threshold, the naive interpretation is incorrect.*

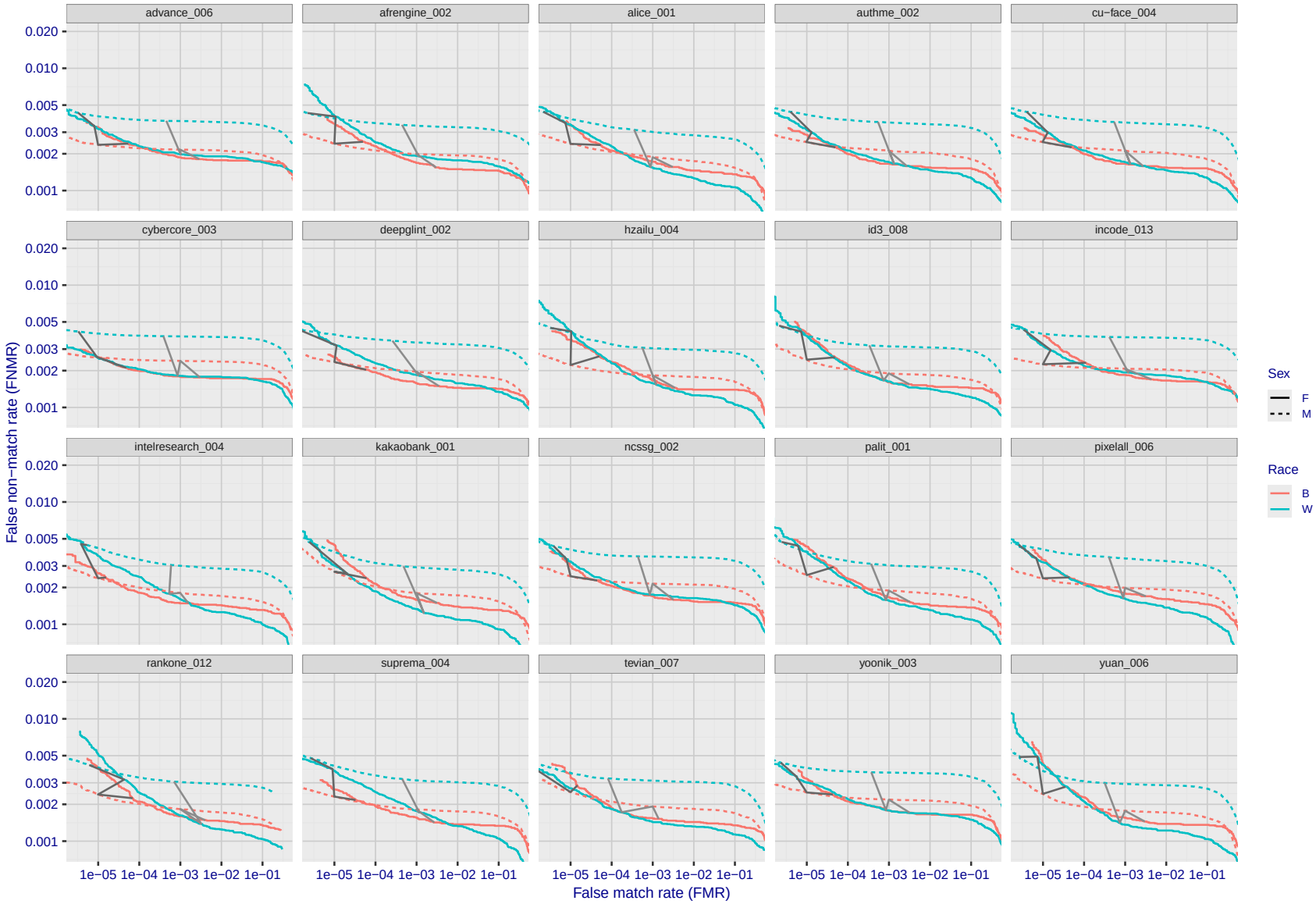

Figure 406: For the mugshot images, error tradeoff characteristics for white females, black females, black males and white males. The Z-shaped grey lines correspond to fixed thresholds, showing both *FNMR and FMR vary at one T value. Note: Many of the plots will naively be read as saying women gives worse error rates than men because the solid traces lie above the dotted ones. However, this is misleading and incomplete: The grey lines show the traces reveal horizontal shifts. Thus for the cogent-003 algorithm FNMR for men is* higher *than for women* at a fixed threshold *but, at the same time, FMR is higher for women - see Figure 608. As access control systems almost always operate at a fixed threshold, the naive interpretation is incorrect.*

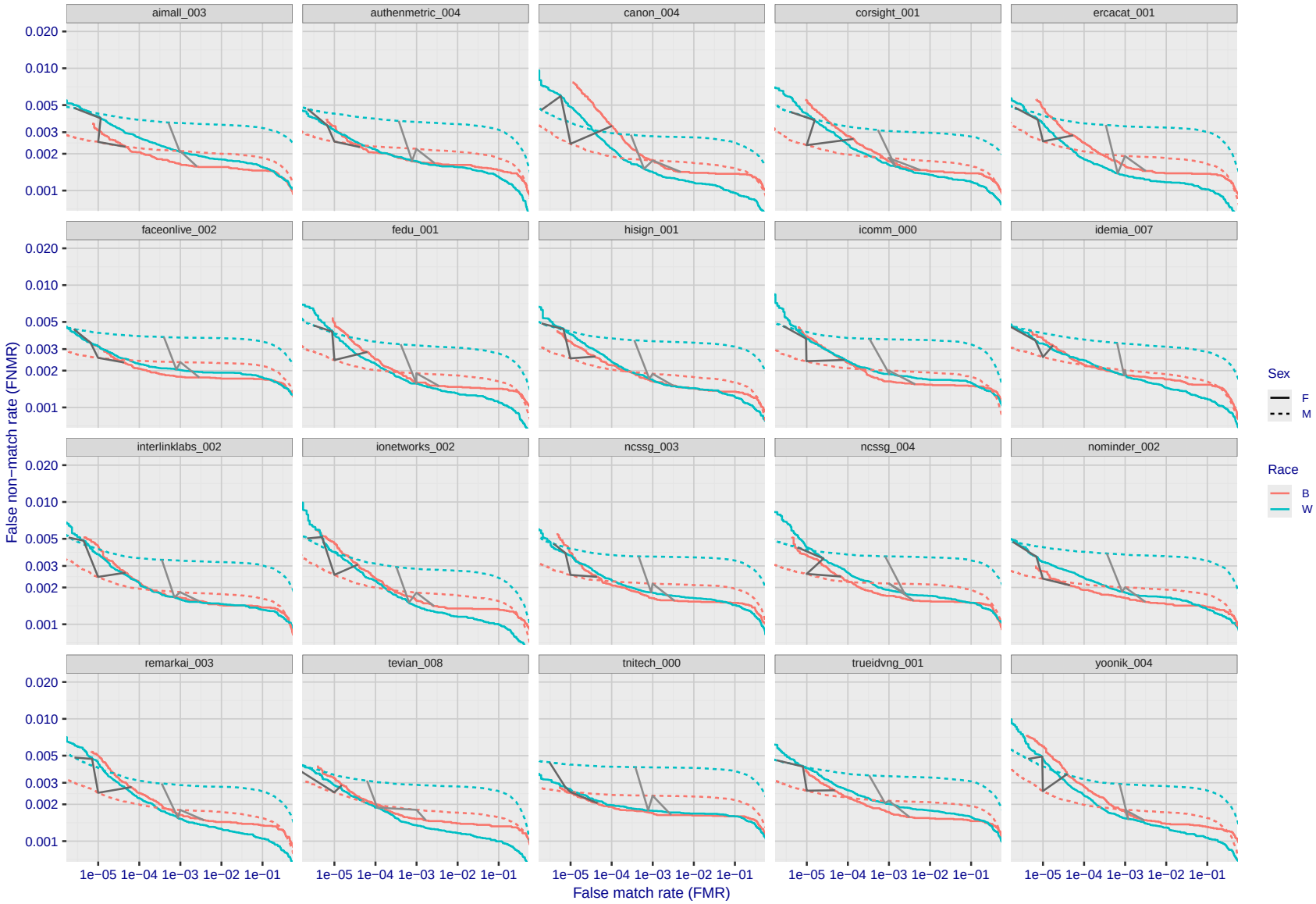

Figure 407: For the mugshot images, error tradeoff characteristics for white females, black females, black males and white males. The Z-shaped grey lines correspond to fixed thresholds, showing both *FNMR and FMR vary at one T value. Note: Many of the plots will naively be read as saying women gives worse error rates than men because the solid traces lie above the dotted ones. However, this is misleading and incomplete: The grey lines show the traces reveal horizontal shifts. Thus for the cogent-003 algorithm FNMR for men is* higher *than for women* at a fixed threshold *but, at the same time, FMR is higher for women - see Figure 608. As access control systems almost always operate at a fixed threshold, the naive interpretation is incorrect.*

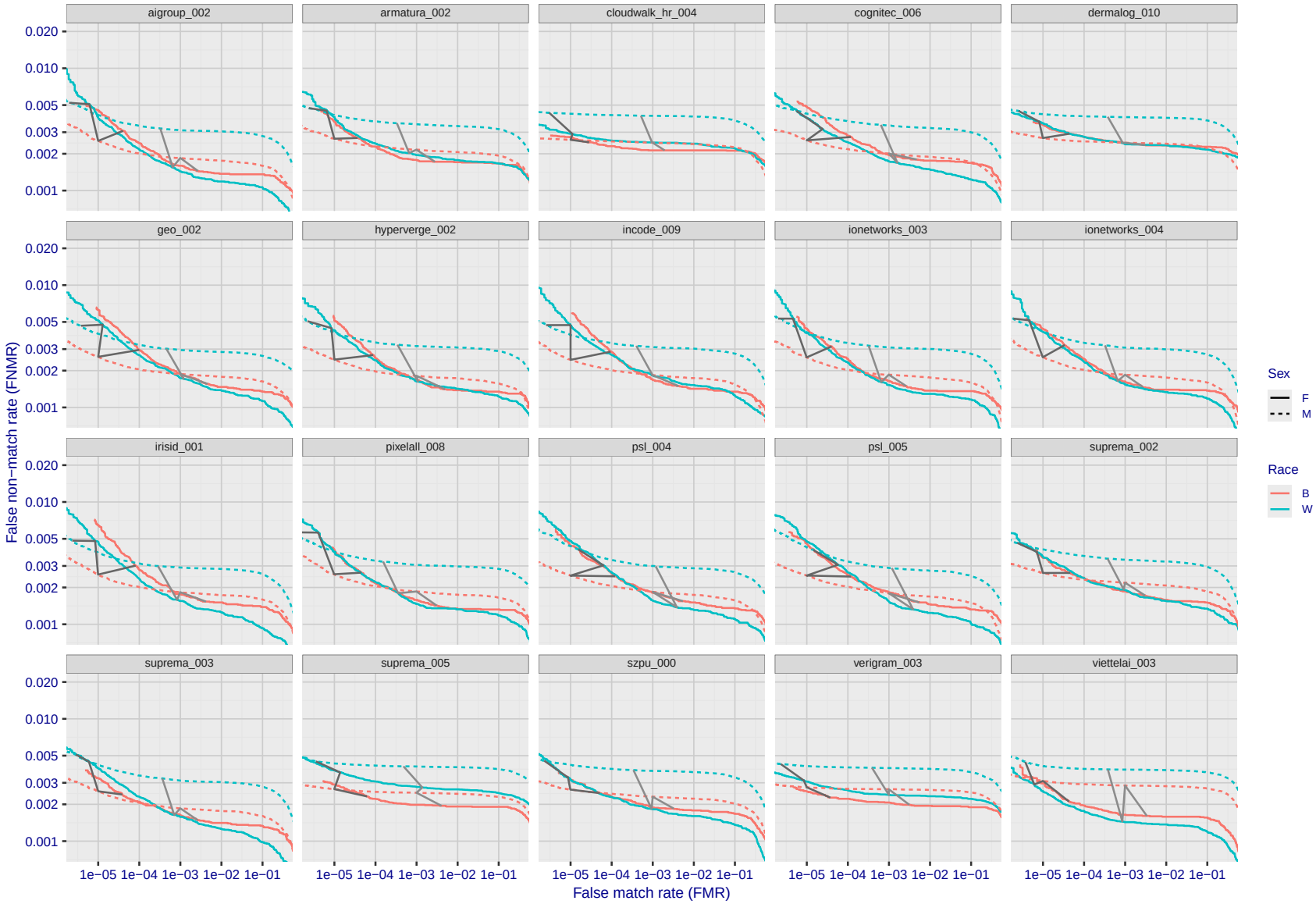

Figure 408: For the mugshot images, error tradeoff characteristics for white females, black females, black males and white males. The Z-shaped grey lines correspond to fixed thresholds, showing both *FNMR and FMR vary at one T value. Note: Many of the plots will naively be read as saying women gives worse error rates than men because the solid traces lie above the dotted ones. However, this is misleading and incomplete: The grey lines show the traces reveal horizontal shifts. Thus for the cogent-003 algorithm FNMR for men is* higher *than for women* at a fixed threshold *but, at the same time, FMR is higher for women - see Figure 608. As access control systems almost always operate at a fixed threshold, the naive interpretation is incorrect.*

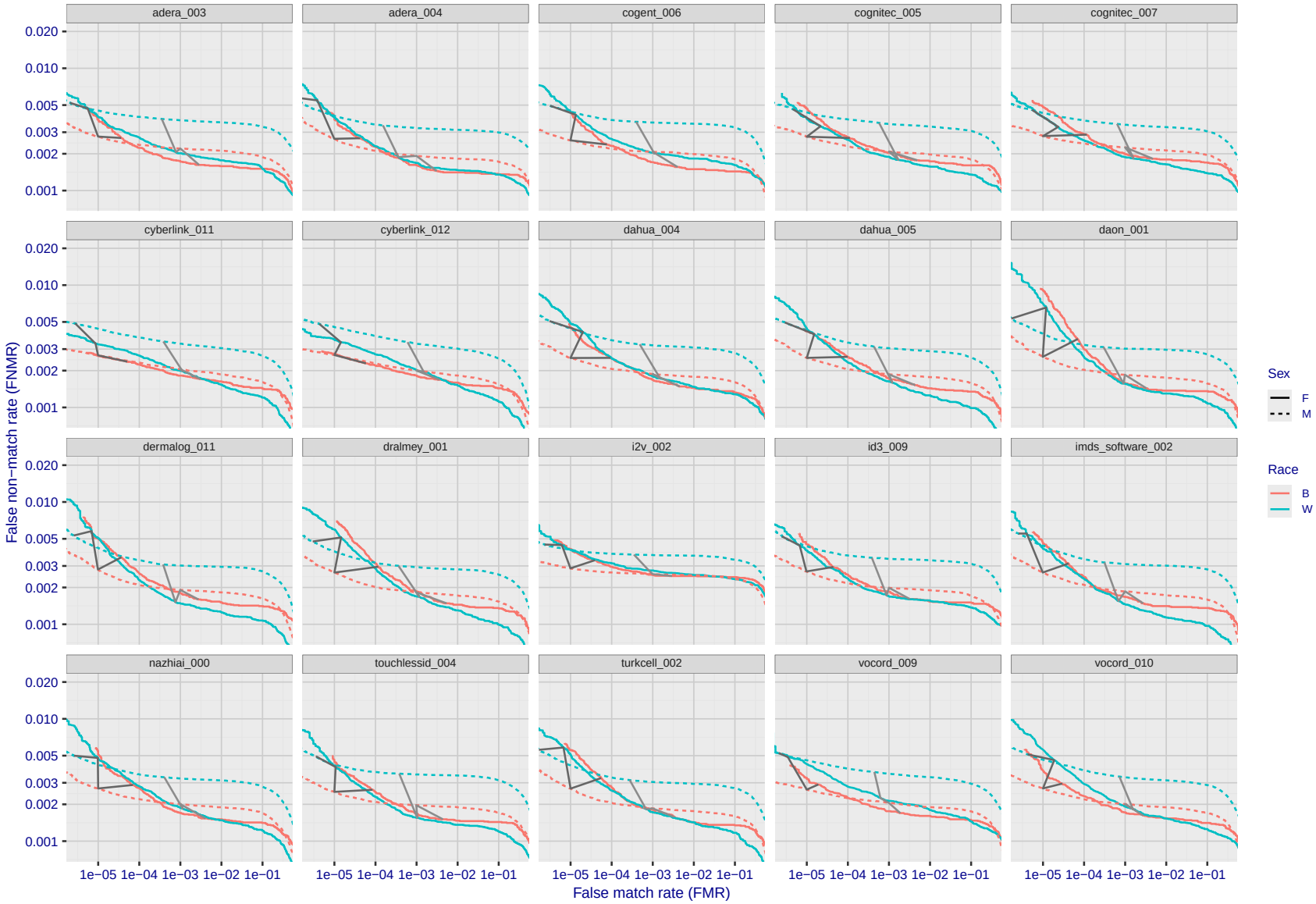

Figure 409: For the mugshot images, error tradeoff characteristics for white females, black females, black males and white males. The Z-shaped grey lines correspond to fixed thresholds, showing both *FNMR and FMR vary at one T value. Note: Many of the plots will naively be read as saying women gives worse error rates than men because the solid traces lie above the dotted ones. However, this is misleading and incomplete: The grey lines show the traces reveal horizontal shifts. Thus for the cogent-003 algorithm FNMR for men is* higher *than for women* at a fixed threshold *but, at the same time, FMR is higher for women - see Figure 608. As access control systems almost always operate at a fixed threshold, the naive interpretation is incorrect.*

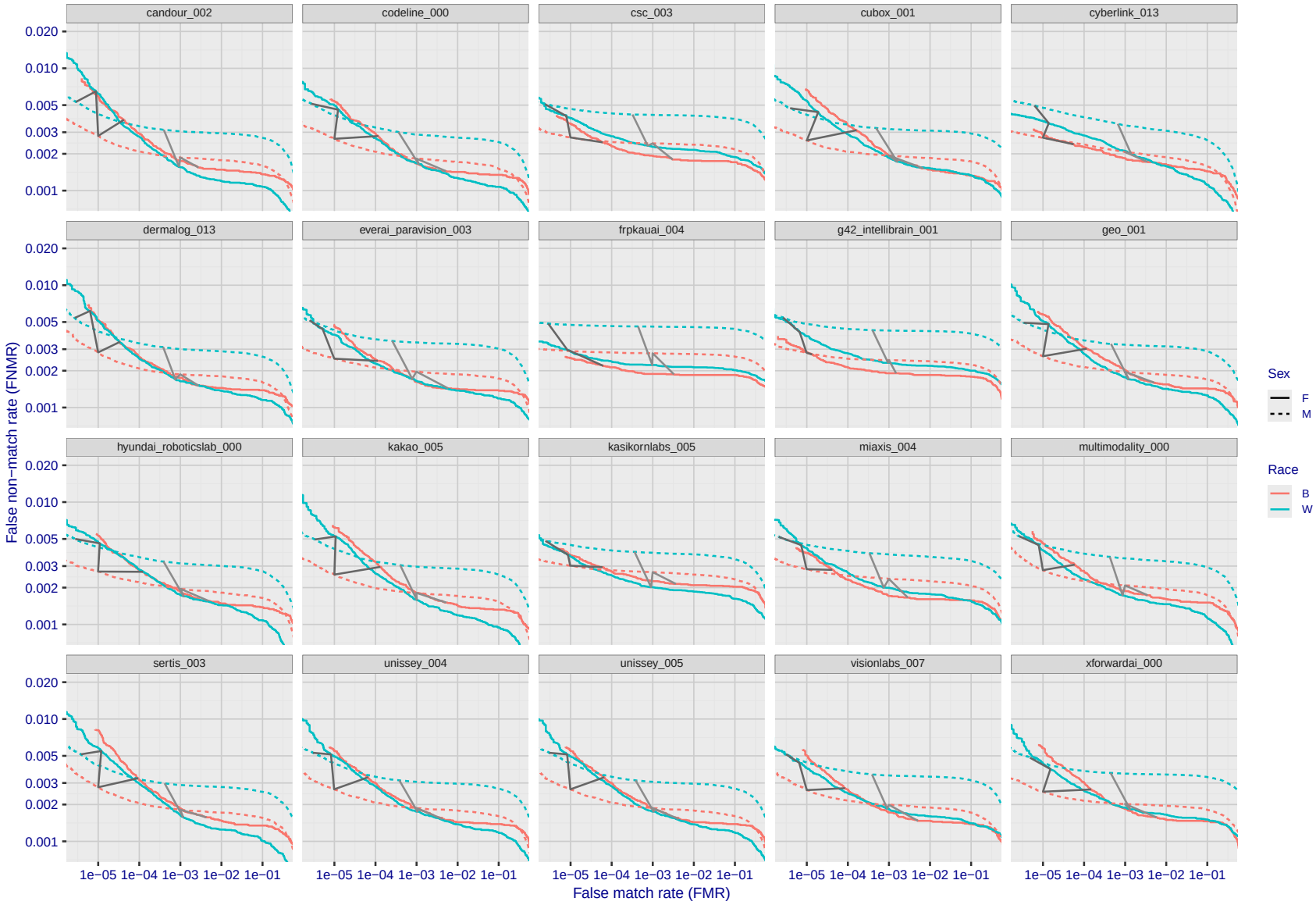

Figure 410: For the mugshot images, error tradeoff characteristics for white females, black females, black males and white males. The Z-shaped grey lines correspond to fixed thresholds, showing both *FNMR and FMR vary at one T value. Note: Many of the plots will naively be read as saying women gives worse error rates than men because the solid traces lie above the dotted ones. However, this is misleading and incomplete: The grey lines show the traces reveal horizontal shifts. Thus for the cogent-003 algorithm FNMR for men is* higher *than for women* at a fixed threshold *but, at the same time, FMR is higher for women - see Figure 608. As access control systems almost always operate at a fixed threshold, the naive interpretation is incorrect.*

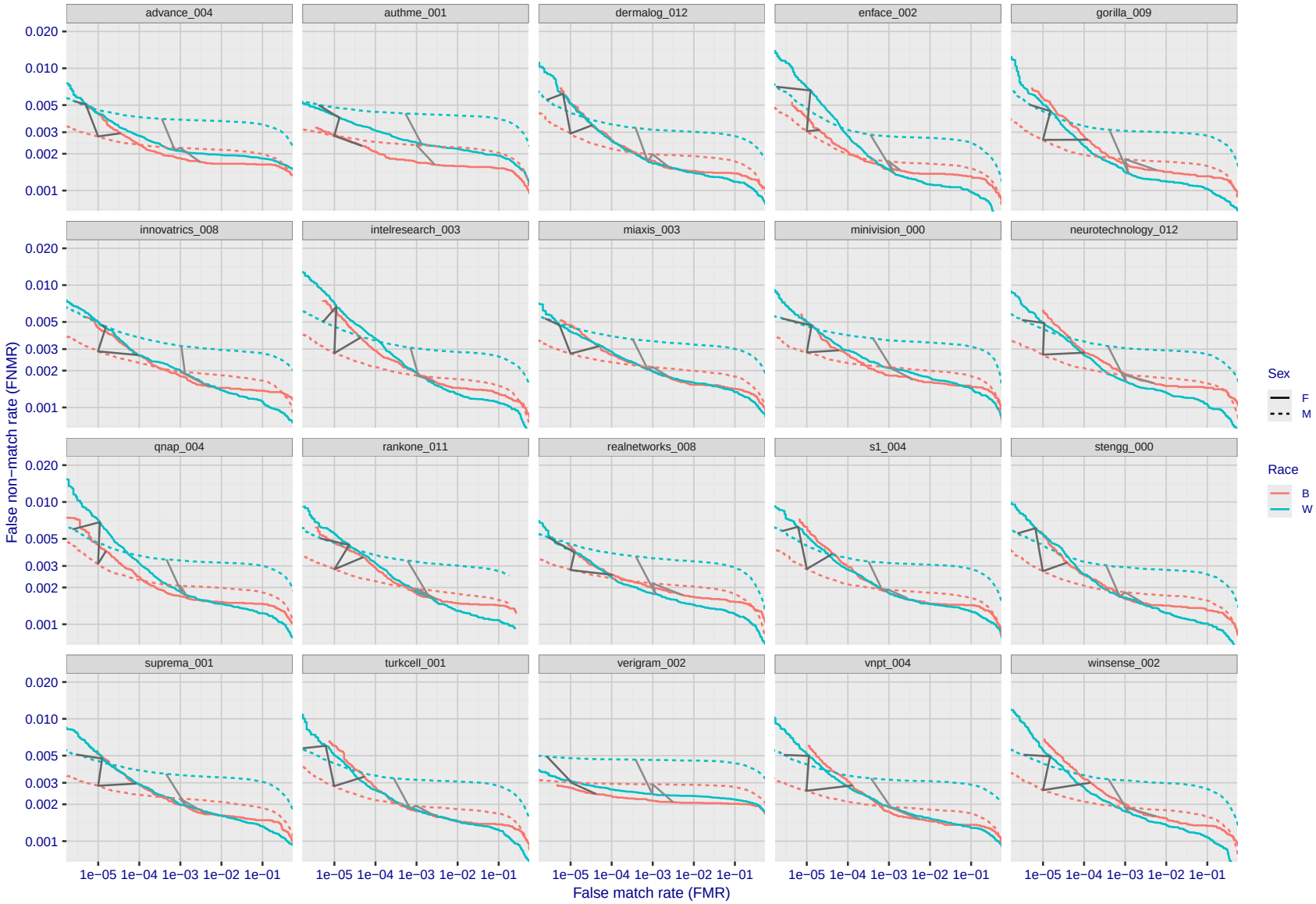

Figure 411: For the mugshot images, error tradeoff characteristics for white females, black females, black males and white males. The Z-shaped grey lines correspond to fixed thresholds, showing both *FNMR and FMR vary at one T value. Note: Many of the plots will naively be read as saying women gives worse error rates than men because the solid traces lie above the dotted ones. However, this is misleading and incomplete: The grey lines show the traces reveal horizontal shifts. Thus for the cogent-003 algorithm FNMR for men is* higher *than for women* at a fixed threshold *but, at the same time, FMR is higher for women - see Figure 608. As access control systems almost always operate at a fixed threshold, the naive interpretation is incorrect.*

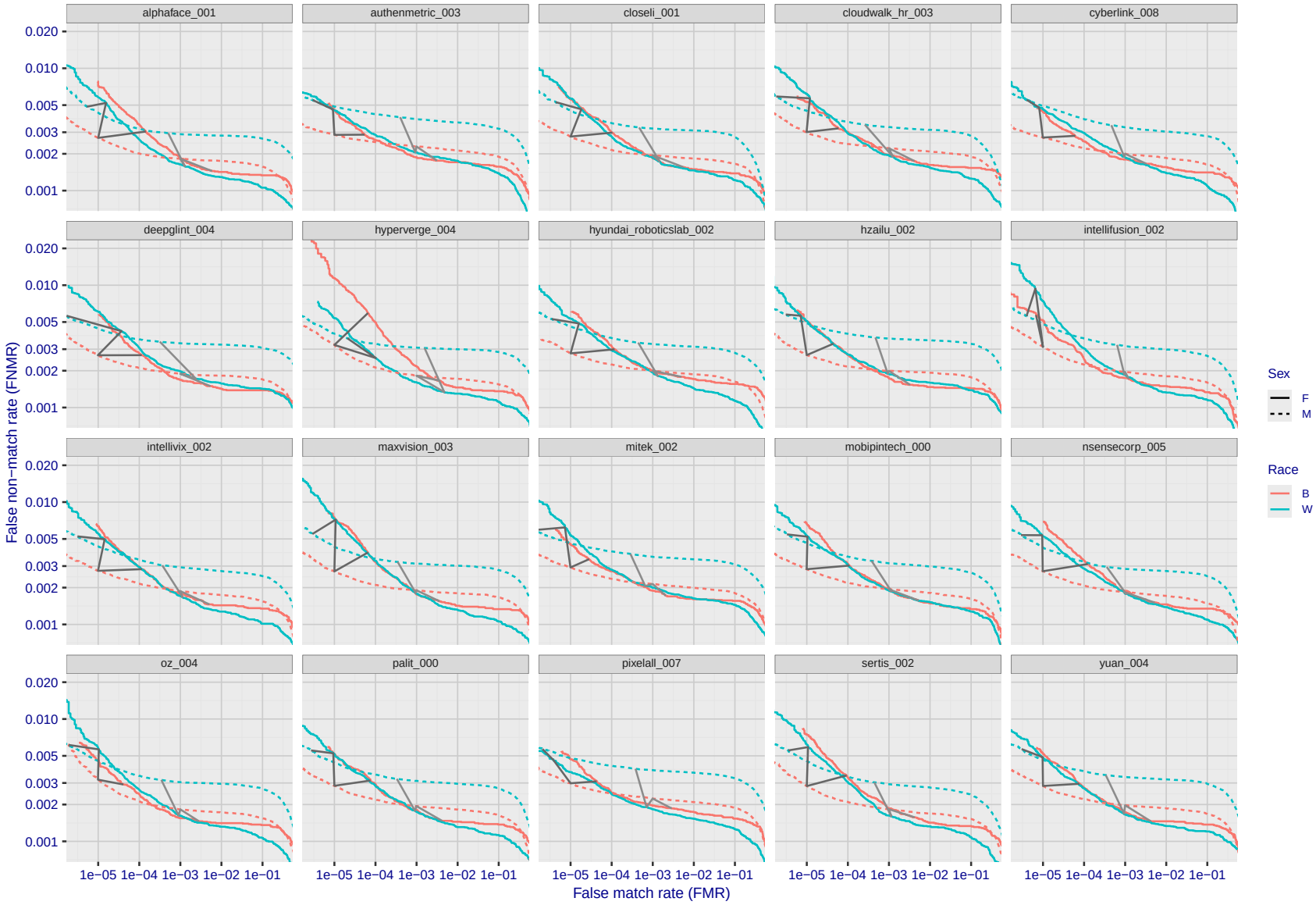

Figure 412: For the mugshot images, error tradeoff characteristics for white females, black females, black males and white males. The Z-shaped grey lines correspond to fixed thresholds, showing both *FNMR and FMR vary at one T value. Note: Many of the plots will naively be read as saying women gives worse error rates than men because the solid traces lie above the dotted ones. However, this is misleading and incomplete: The grey lines show the traces reveal horizontal shifts. Thus for the cogent-003 algorithm FNMR for men is* higher *than for women* at a fixed threshold *but, at the same time, FMR is higher for women - see Figure 608. As access control systems almost always operate at a fixed threshold, the naive interpretation is incorrect.*

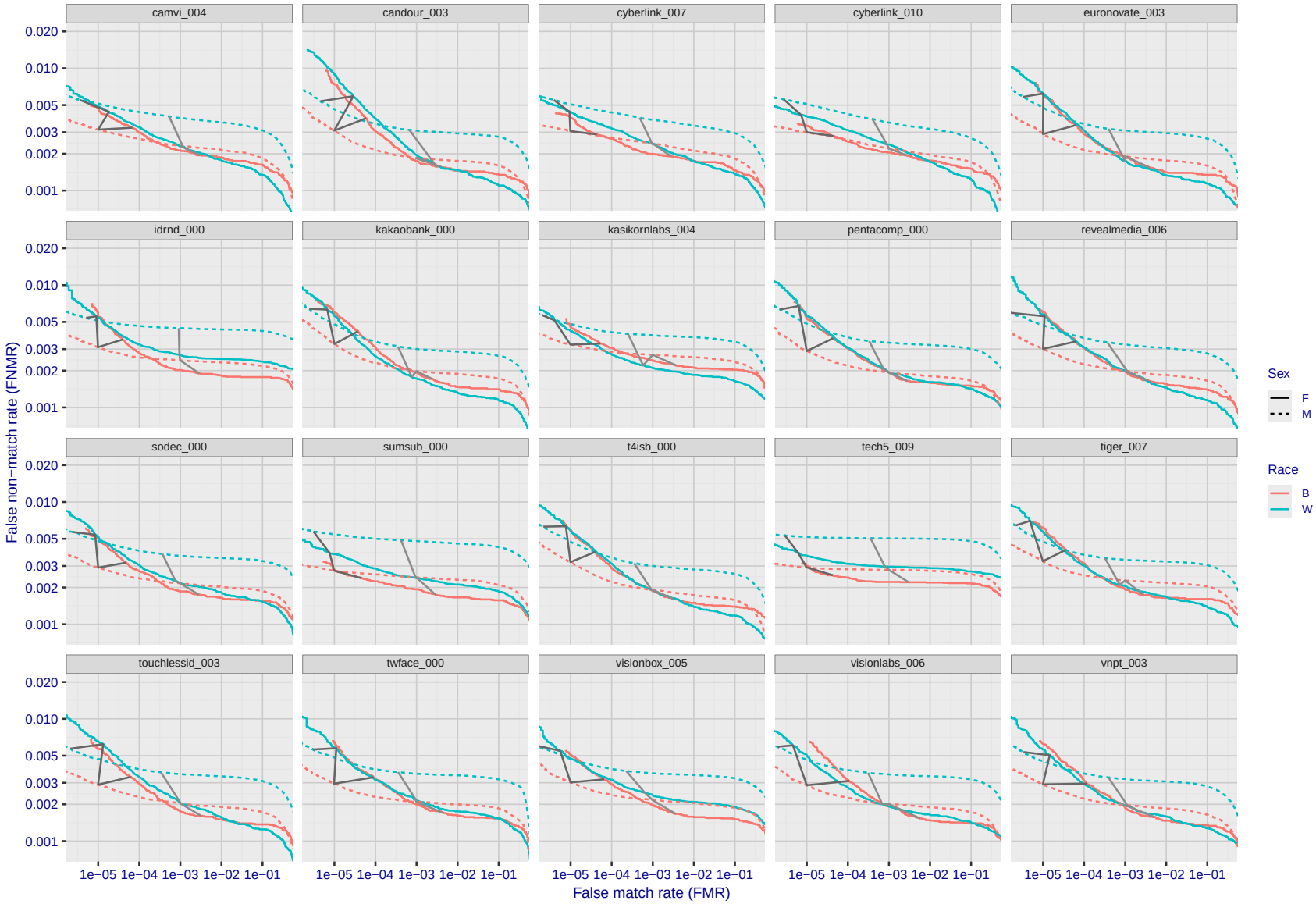

Figure 413: For the mugshot images, error tradeoff characteristics for white females, black females, black males and white males. The Z-shaped grey lines correspond to fixed thresholds, showing both *FNMR and FMR vary at one T value. Note: Many of the plots will naively be read as saying women gives worse error rates than men because the solid traces lie above the dotted ones. However, this is misleading and incomplete: The grey lines show the traces reveal horizontal shifts. Thus for the cogent-003 algorithm FNMR for men is* higher *than for women* at a fixed threshold *but, at the same time, FMR is higher for women - see Figure 608. As access control systems almost always operate at a fixed threshold, the naive interpretation is incorrect.*

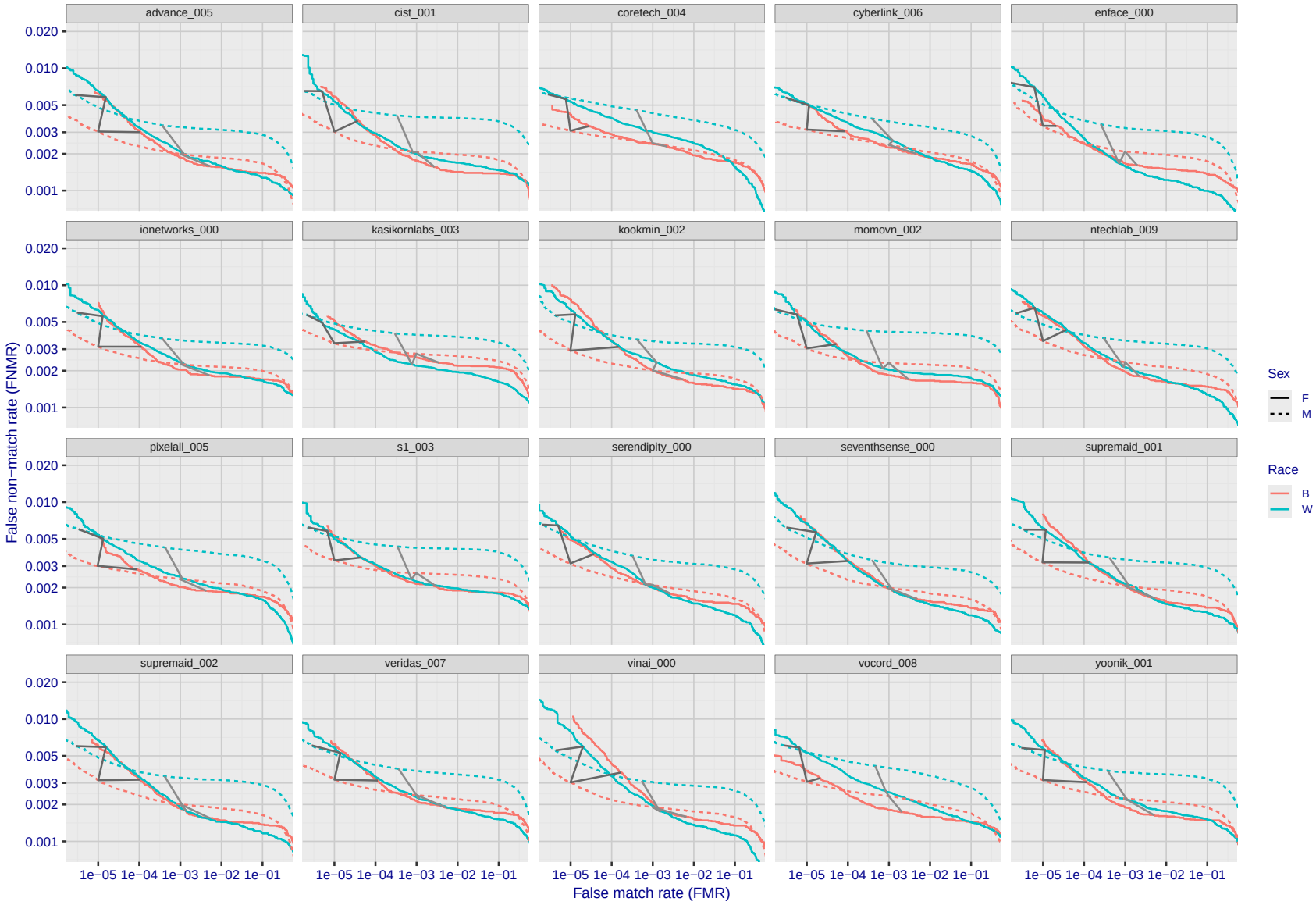

Figure 414: For the mugshot images, error tradeoff characteristics for white females, black females, black males and white males. The Z-shaped grey lines correspond to fixed thresholds, showing both *FNMR and FMR vary at one T value. Note: Many of the plots will naively be read as saying women gives worse error rates than men because the solid traces lie above the dotted ones. However, this is misleading and incomplete: The grey lines show the traces reveal horizontal shifts. Thus for the cogent-003 algorithm FNMR for men is* higher *than for women* at a fixed threshold *but, at the same time, FMR is higher for women - see Figure 608. As access control systems almost always operate at a fixed threshold, the naive interpretation is incorrect.*

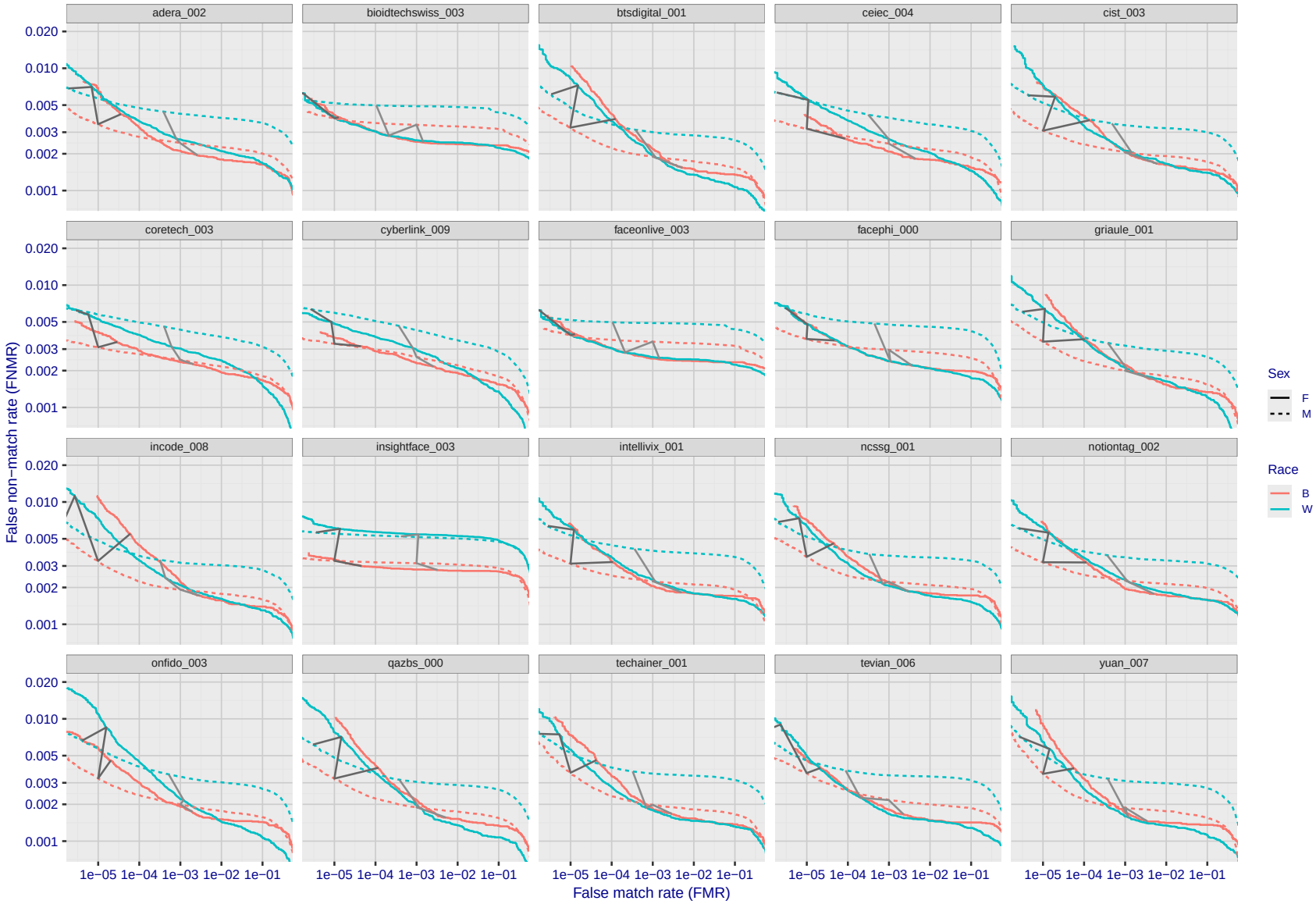

Figure 415: For the mugshot images, error tradeoff characteristics for white females, black females, black males and white males. The Z-shaped grey lines correspond to fixed thresholds, showing both *FNMR and FMR vary at one T value. Note: Many of the plots will naively be read as saying women gives worse error rates than men because the solid traces lie above the dotted ones. However, this is misleading and incomplete: The grey lines show the traces reveal horizontal shifts. Thus for the cogent-003 algorithm FNMR for men is* higher *than for women* at a fixed threshold *but, at the same time, FMR is higher for women - see Figure 608. As access control systems almost always operate at a fixed threshold, the naive interpretation is incorrect.*

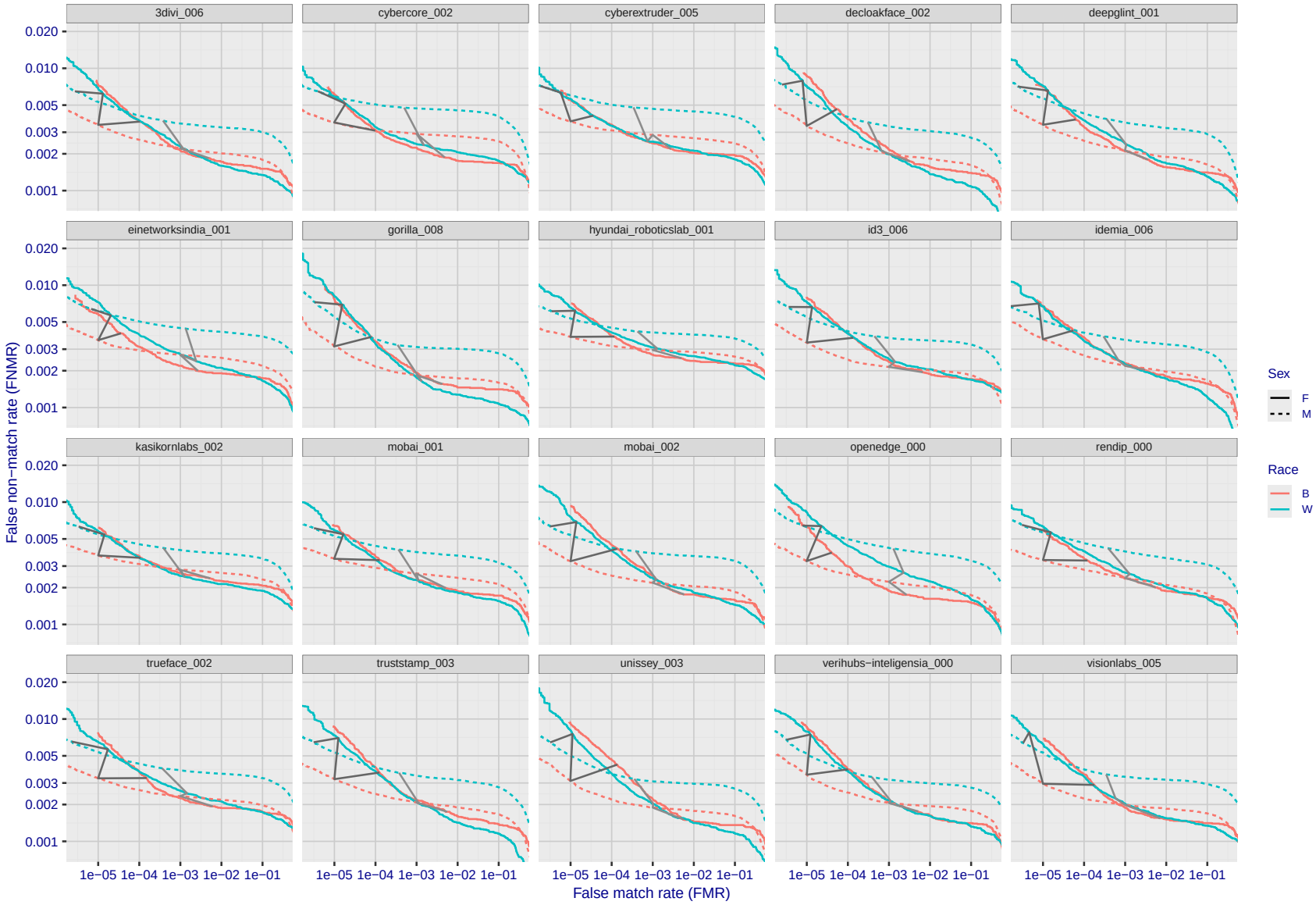

Figure 416: For the mugshot images, error tradeoff characteristics for white females, black females, black males and white males. The Z-shaped grey lines correspond to fixed thresholds, showing both *FNMR and FMR vary at one T value. Note: Many of the plots will naively be read as saying women gives worse error rates than men because the solid traces lie above the dotted ones. However, this is misleading and incomplete: The grey lines show the traces reveal horizontal shifts. Thus for the cogent-003 algorithm FNMR for men is* higher *than for women* at a fixed threshold *but, at the same time, FMR is higher for women - see Figure 608. As access control systems almost always operate at a fixed threshold, the naive interpretation is incorrect.*

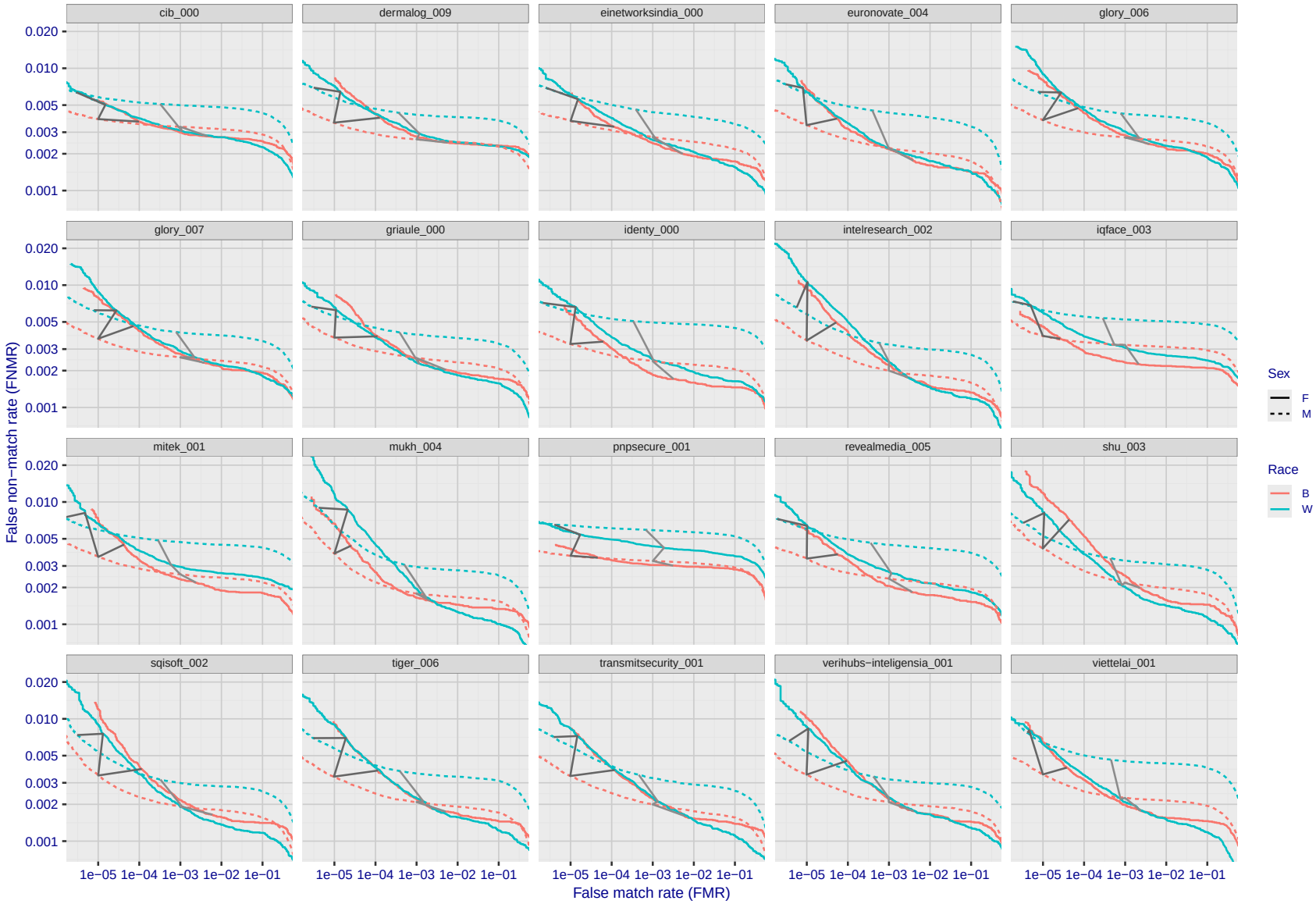

Figure 417: For the mugshot images, error tradeoff characteristics for white females, black females, black males and white males. The Z-shaped grey lines correspond to fixed thresholds, showing both *FNMR and FMR vary at one T value. Note: Many of the plots will naively be read as saying women gives worse error rates than men because the solid traces lie above the dotted ones. However, this is misleading and incomplete: The grey lines show the traces reveal horizontal shifts. Thus for the cogent-003 algorithm FNMR for men is* higher *than for women* at a fixed threshold *but, at the same time, FMR is higher for women - see Figure 608. As access control systems almost always operate at a fixed threshold, the naive interpretation is incorrect.*

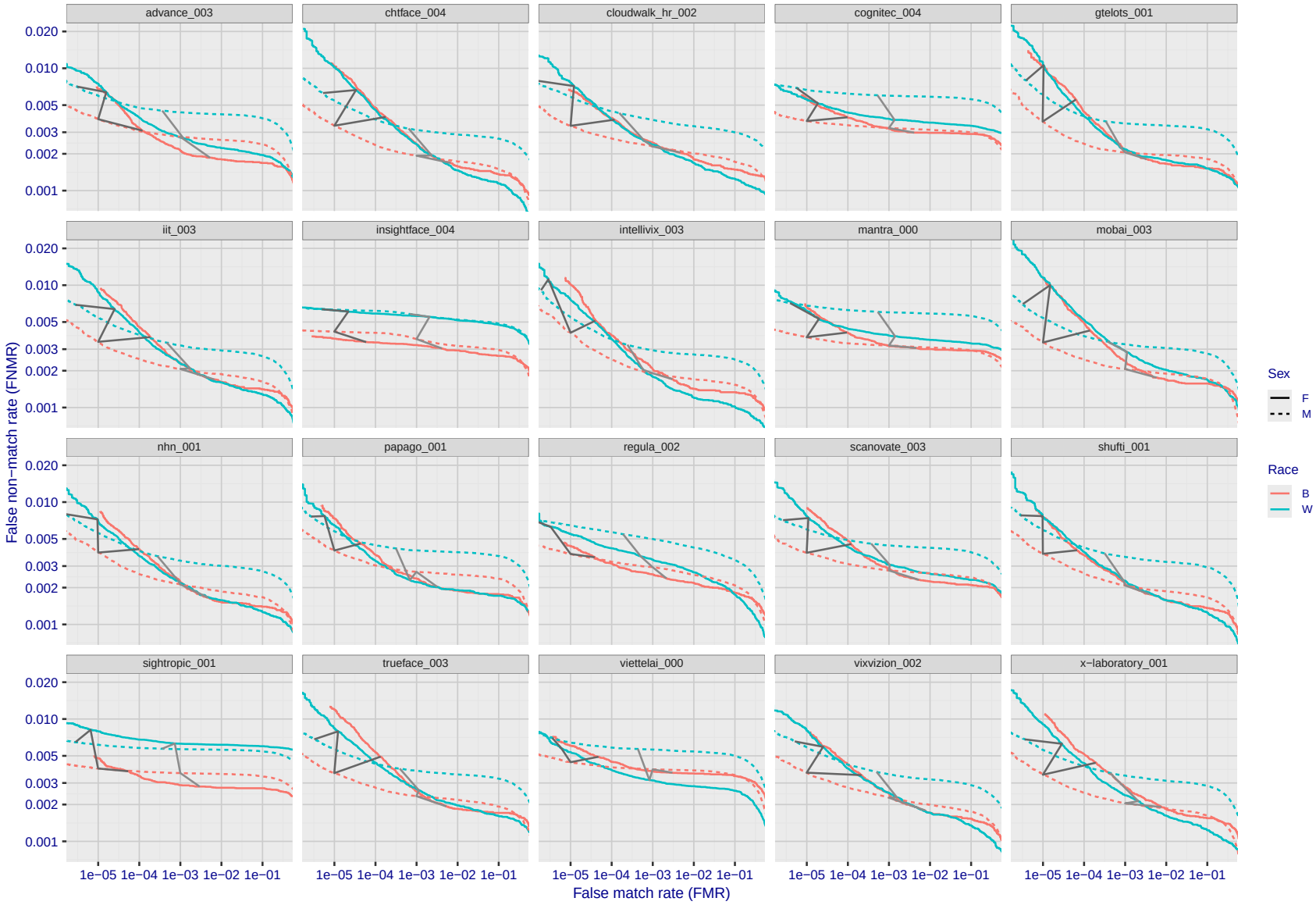

Figure 418: For the mugshot images, error tradeoff characteristics for white females, black females, black males and white males. The Z-shaped grey lines correspond to fixed thresholds, showing both *FNMR and FMR vary at one T value. Note: Many of the plots will naively be read as saying women gives worse error rates than men because the solid traces lie above the dotted ones. However, this is misleading and incomplete: The grey lines show the traces reveal horizontal shifts. Thus for the cogent-003 algorithm FNMR for men is* higher *than for women* at a fixed threshold *but, at the same time, FMR is higher for women - see Figure 608. As access control systems almost always operate at a fixed threshold, the naive interpretation is incorrect.*

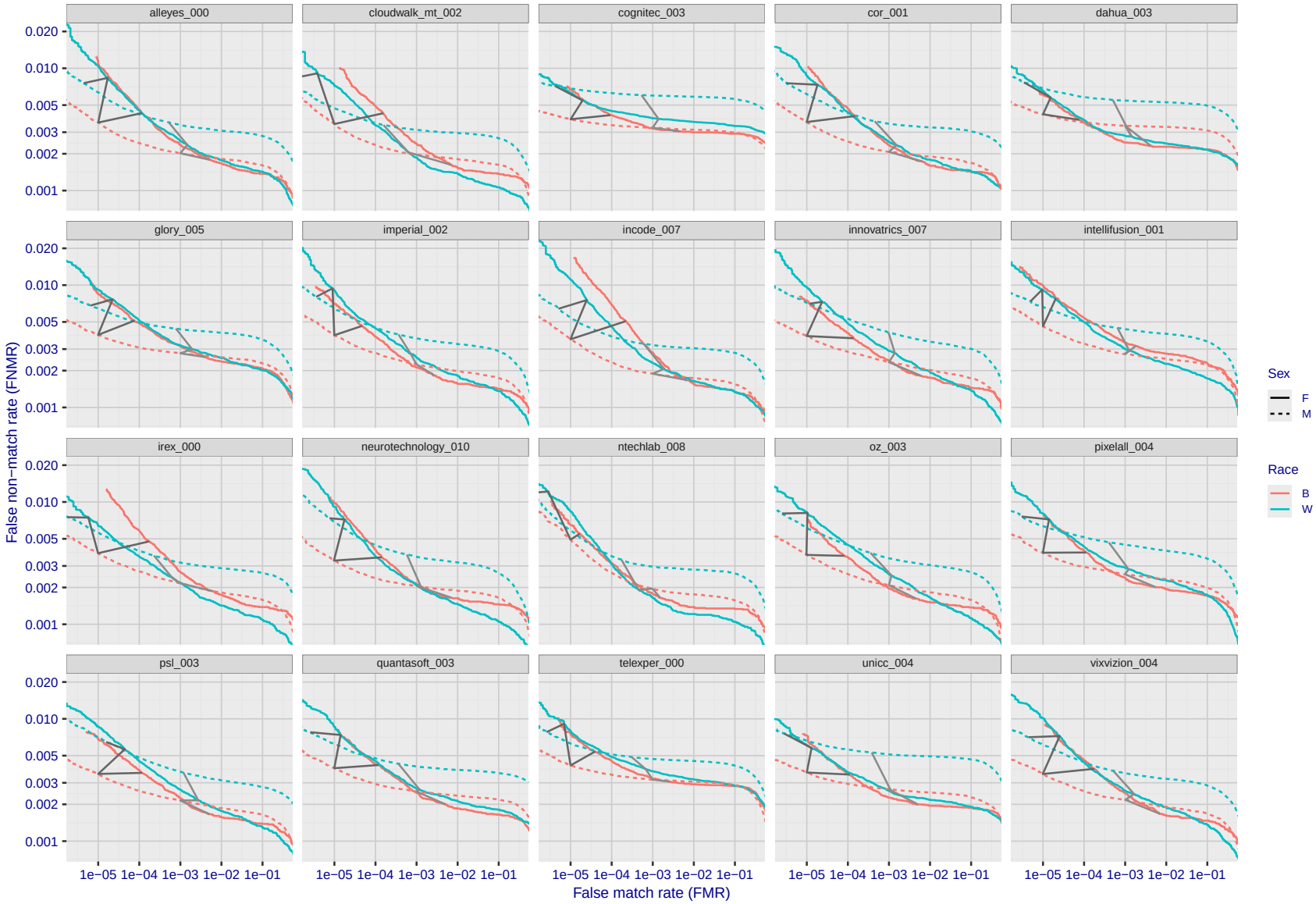

Figure 419: For the mugshot images, error tradeoff characteristics for white females, black females, black males and white males. The Z-shaped grey lines correspond to fixed thresholds, showing both *FNMR and FMR vary at one T value. Note: Many of the plots will naively be read as saying women gives worse error rates than men because the solid traces lie above the dotted ones. However, this is misleading and incomplete: The grey lines show the traces reveal horizontal shifts. Thus for the cogent-003 algorithm FNMR for men is* higher *than for women* at a fixed threshold *but, at the same time, FMR is higher for women - see Figure 608. As access control systems almost always operate at a fixed threshold, the naive interpretation is incorrect.*

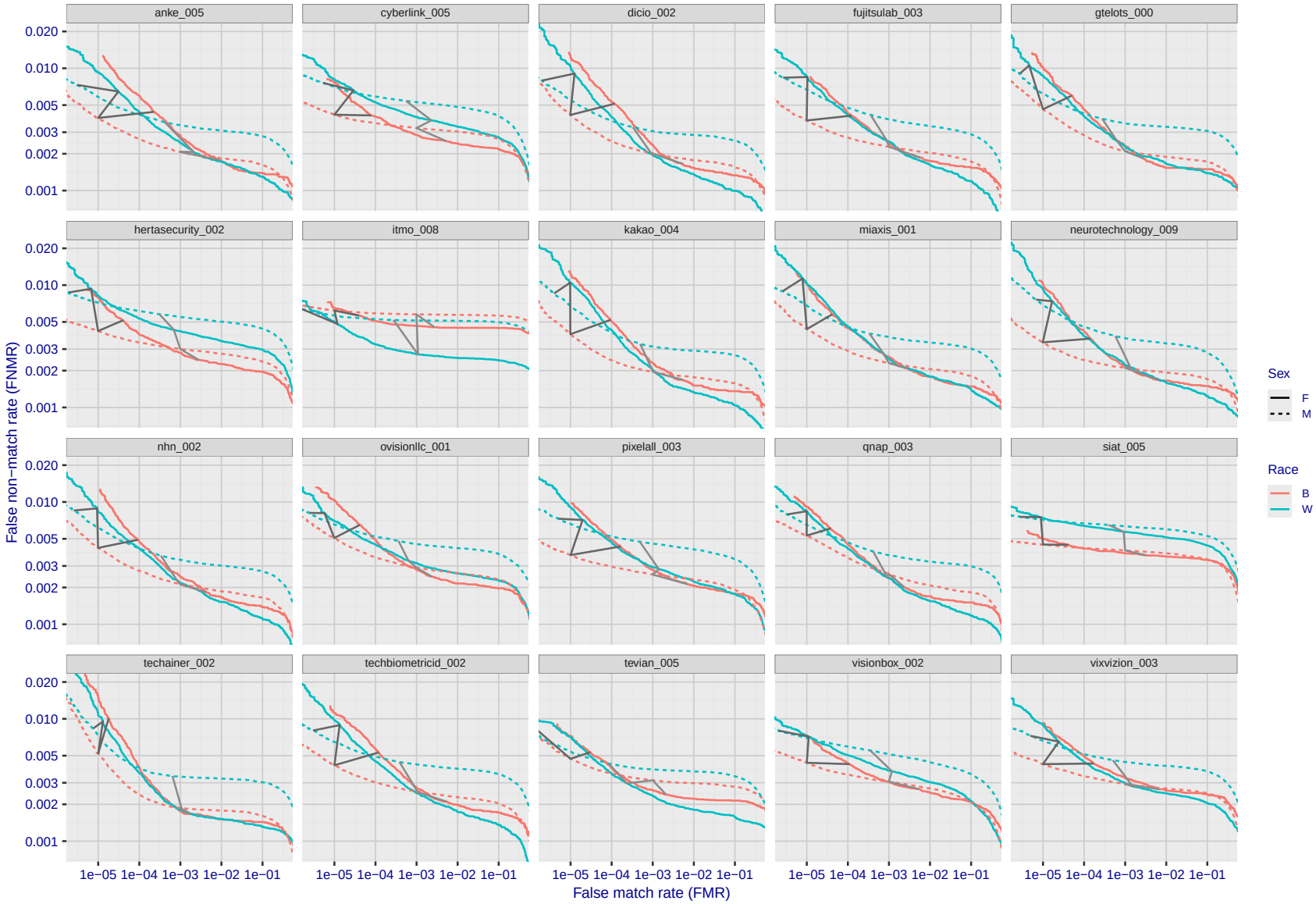

Figure 420: For the mugshot images, error tradeoff characteristics for white females, black females, black males and white males. The Z-shaped grey lines correspond to fixed thresholds, showing both *FNMR and FMR vary at one T value. Note: Many of the plots will naively be read as saying women gives worse error rates than men because the solid traces lie above the dotted ones. However, this is misleading and incomplete: The grey lines show the traces reveal horizontal shifts. Thus for the cogent-003 algorithm FNMR for men is* higher *than for women* at a fixed threshold *but, at the same time, FMR is higher for women - see Figure 608. As access control systems almost always operate at a fixed threshold, the naive interpretation is incorrect.*

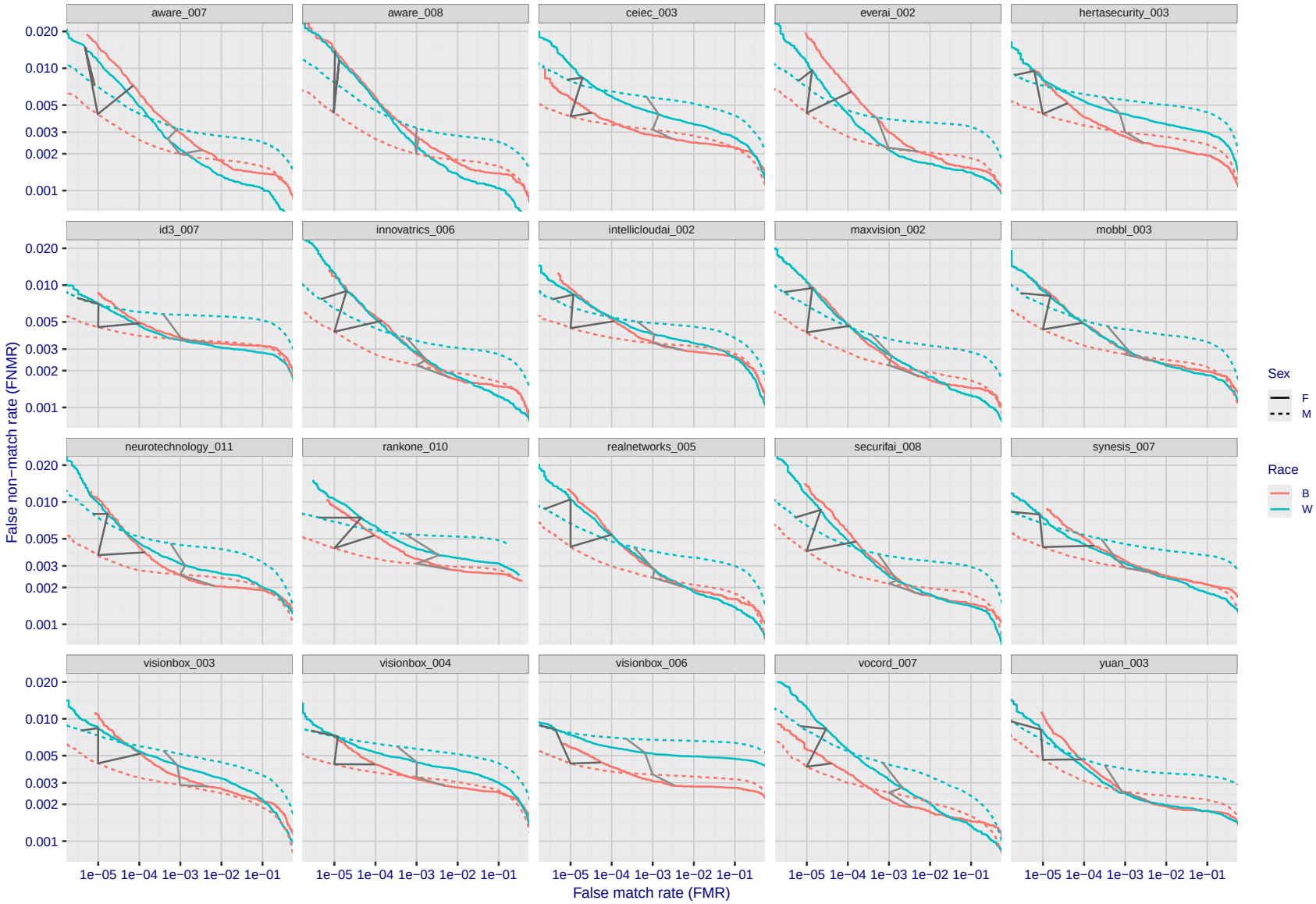

Figure 421: For the mugshot images, error tradeoff characteristics for white females, black females, black males and white males. The Z-shaped grey lines correspond to fixed thresholds, showing both *FNMR and FMR vary at one T value. Note: Many of the plots will naively be read as saying women gives worse error rates than men because the solid traces lie above the dotted ones. However, this is misleading and incomplete: The grey lines show the traces reveal horizontal shifts. Thus for the cogent-003 algorithm FNMR for men is* higher *than for women* at a fixed threshold *but, at the same time, FMR is higher for women - see Figure 608. As access control systems almost always operate at a fixed threshold, the naive interpretation is incorrect.*

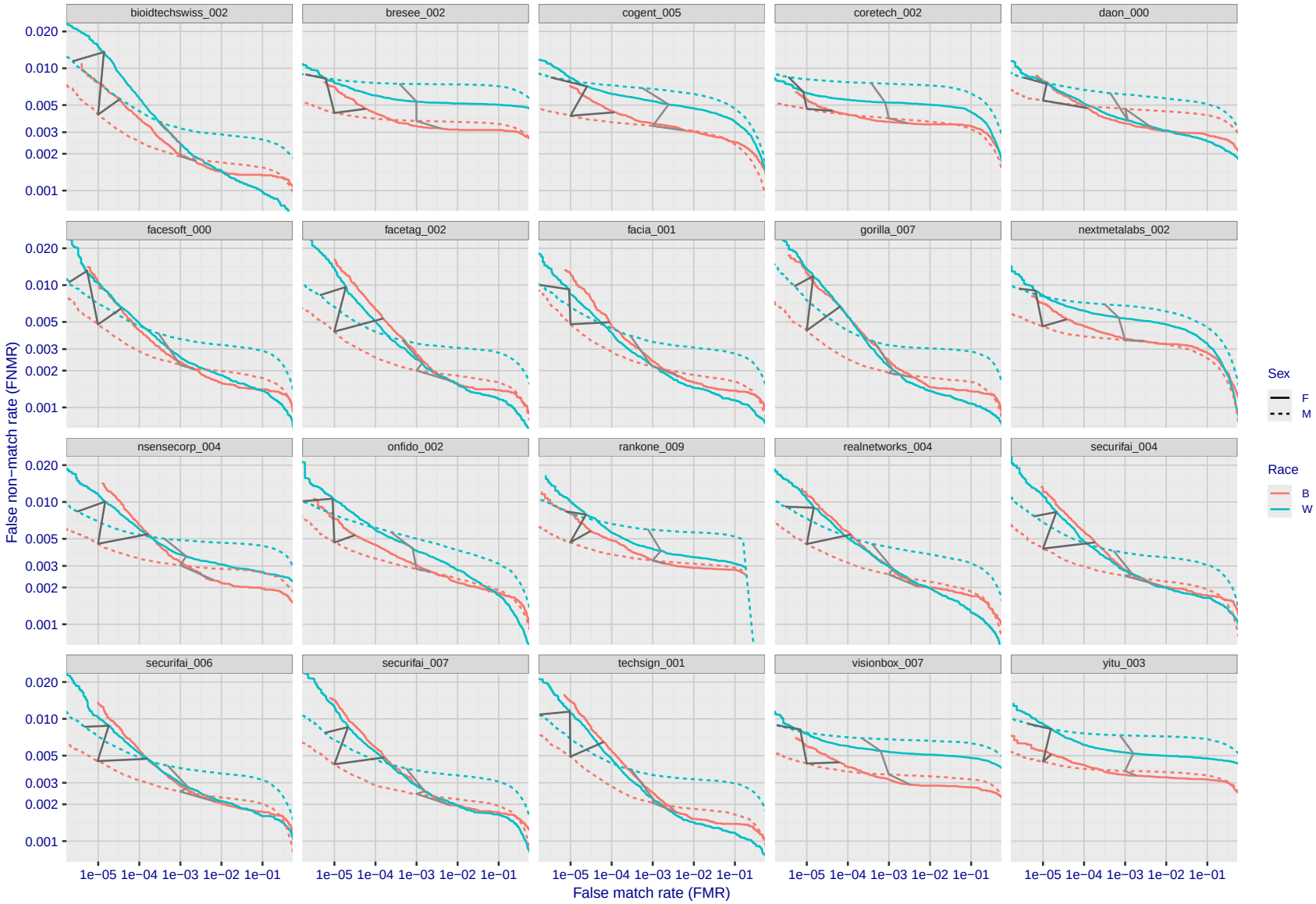

Figure 422: For the mugshot images, error tradeoff characteristics for white females, black females, black males and white males. The Z-shaped grey lines correspond to fixed thresholds, showing both *FNMR and FMR vary at one T value. Note: Many of the plots will naively be read as saying women gives worse error rates than men because the solid traces lie above the dotted ones. However, this is misleading and incomplete: The grey lines show the traces reveal horizontal shifts. Thus for the cogent-003 algorithm FNMR for men is* higher *than for women* at a fixed threshold *but, at the same time, FMR is higher for women - see Figure 608. As access control systems almost always operate at a fixed threshold, the naive interpretation is incorrect.*

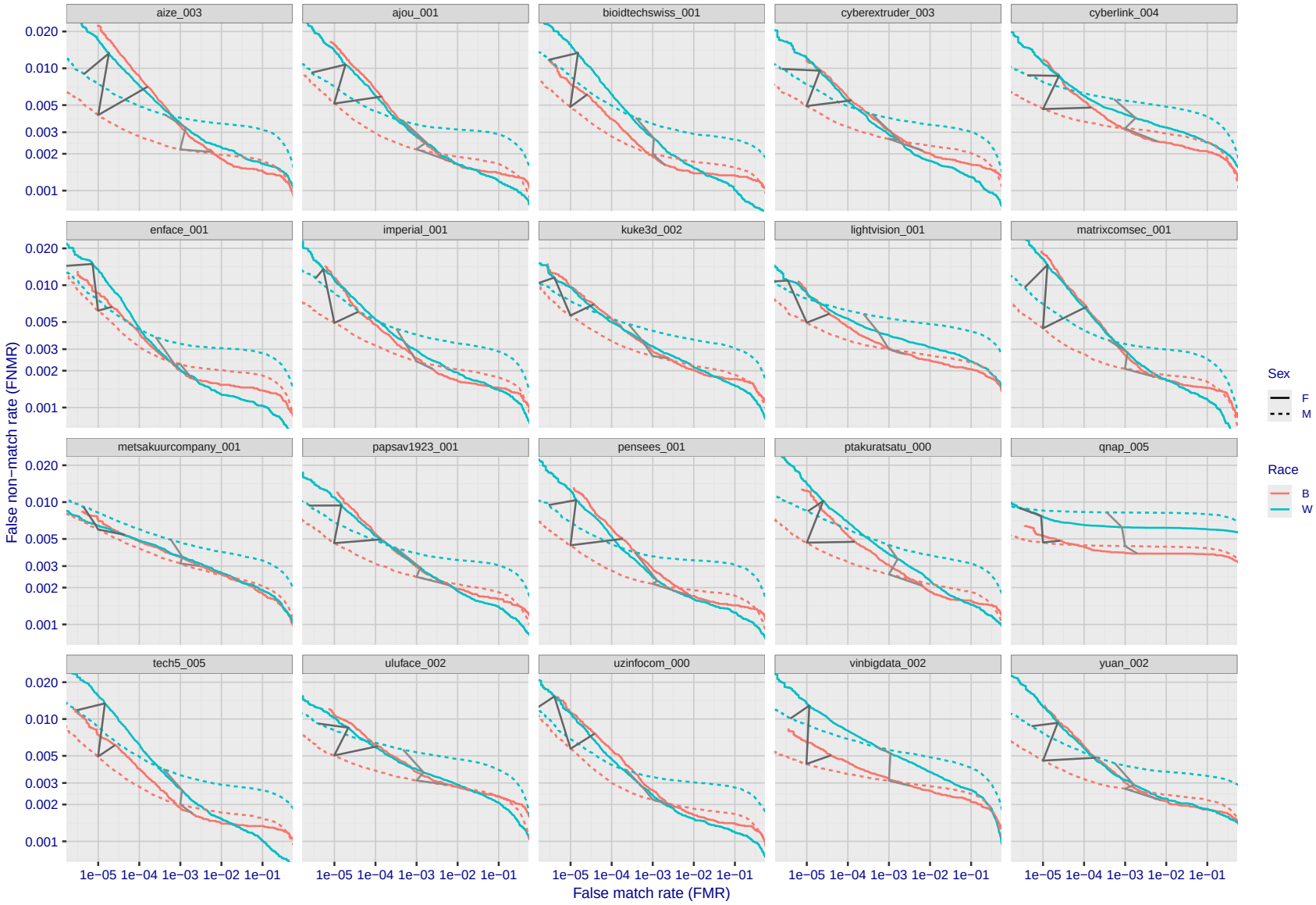

Figure 423: For the mugshot images, error tradeoff characteristics for white females, black females, black males and white males. The Z-shaped grey lines correspond to fixed thresholds, showing both *FNMR and FMR vary at one T value. Note: Many of the plots will naively be read as saying women gives worse error rates than men because the solid traces lie above the dotted ones. However, this is misleading and incomplete: The grey lines show the traces reveal horizontal shifts. Thus for the cogent-003 algorithm FNMR for men is* higher *than for women* at a fixed threshold *but, at the same time, FMR is higher for women - see Figure 608. As access control systems almost always operate at a fixed threshold, the naive interpretation is incorrect.*

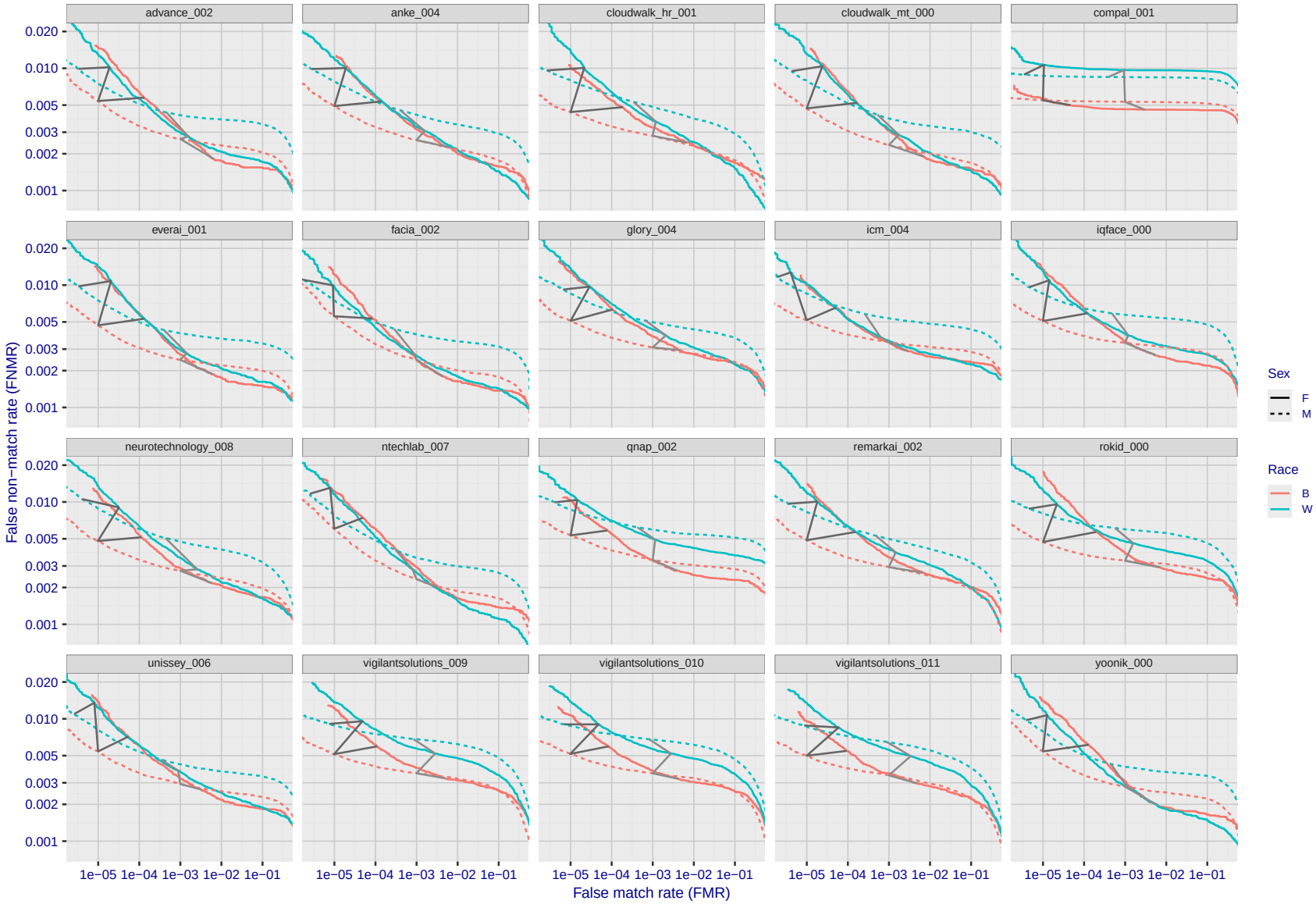

Figure 424: For the mugshot images, error tradeoff characteristics for white females, black females, black males and white males. The Z-shaped grey lines correspond to fixed thresholds, showing both *FNMR and FMR vary at one T value. Note: Many of the plots will naively be read as saying women gives worse error rates than men because the solid traces lie above the dotted ones. However, this is misleading and incomplete: The grey lines show the traces reveal horizontal shifts. Thus for the cogent-003 algorithm FNMR for men is* higher *than for women* at a fixed threshold *but, at the same time, FMR is higher for women - see Figure 608. As access control systems almost always operate at a fixed threshold, the naive interpretation is incorrect.*

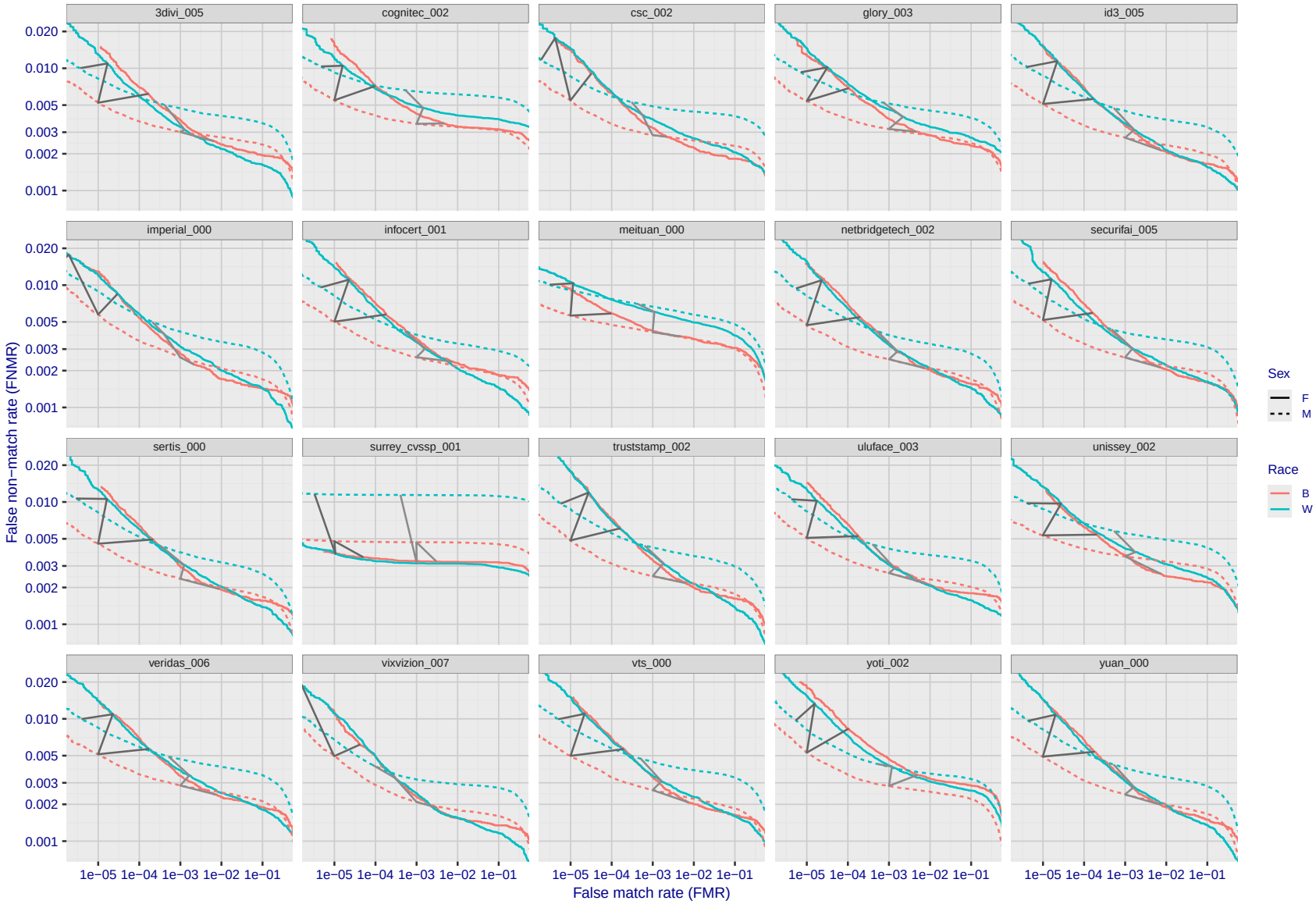

Figure 425: For the mugshot images, error tradeoff characteristics for white females, black females, black males and white males. The Z-shaped grey lines correspond to fixed thresholds, showing both *FNMR and FMR vary at one T value. Note: Many of the plots will naively be read as saying women gives worse error rates than men because the solid traces lie above the dotted ones. However, this is misleading and incomplete: The grey lines show the traces reveal horizontal shifts. Thus for the cogent-003 algorithm FNMR for men is* higher *than for women* at a fixed threshold *but, at the same time, FMR is higher for women - see Figure 608. As access control systems almost always operate at a fixed threshold, the naive interpretation is incorrect.*

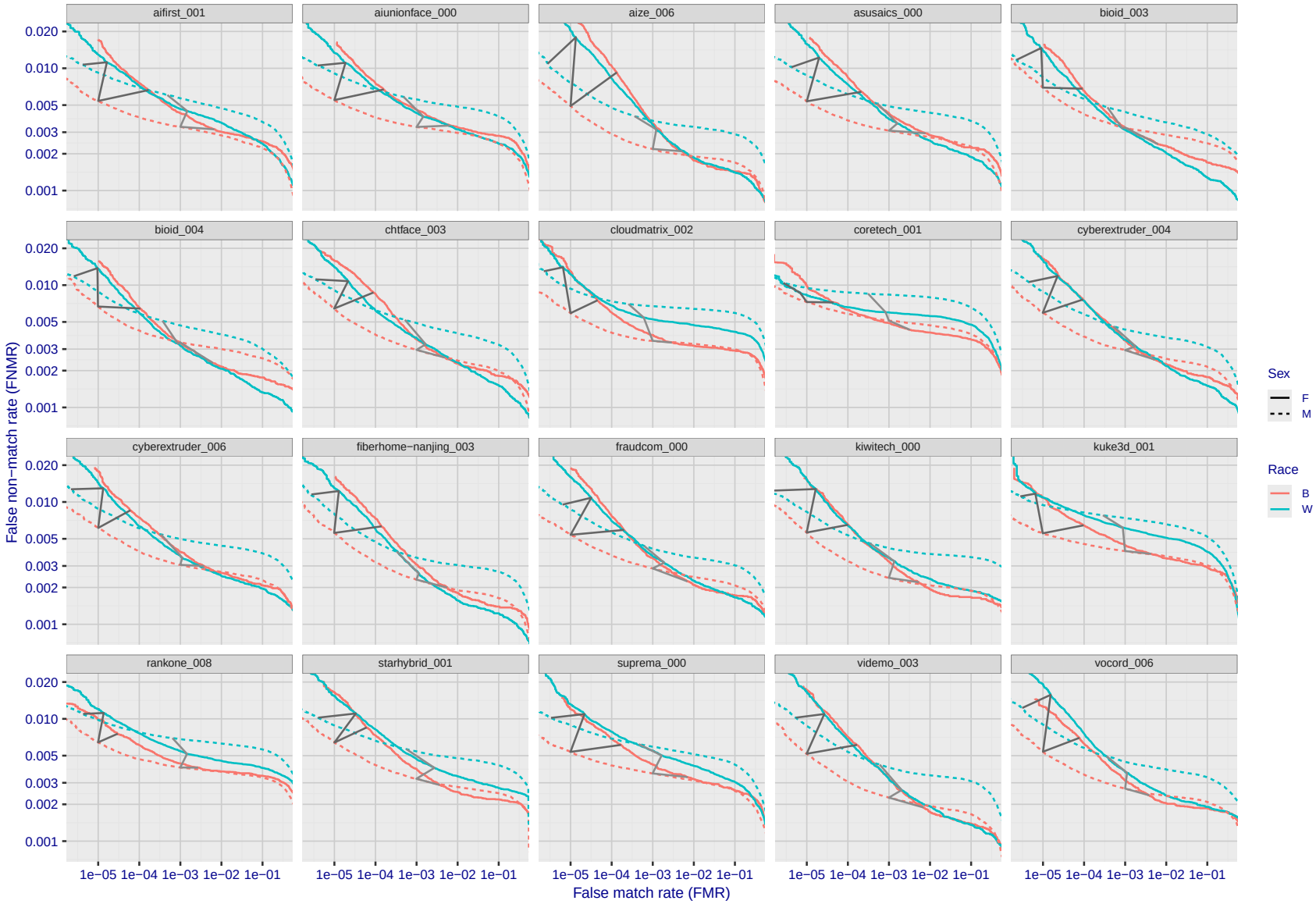

Figure 426: For the mugshot images, error tradeoff characteristics for white females, black females, black males and white males. The Z-shaped grey lines correspond to fixed thresholds, showing both *FNMR and FMR vary at one T value. Note: Many of the plots will naively be read as saying women gives worse error rates than men because the solid traces lie above the dotted ones. However, this is misleading and incomplete: The grey lines show the traces reveal horizontal shifts. Thus for the cogent-003 algorithm FNMR for men is* higher *than for women* at a fixed threshold *but, at the same time, FMR is higher for women - see Figure 608. As access control systems almost always operate at a fixed threshold, the naive interpretation is incorrect.*

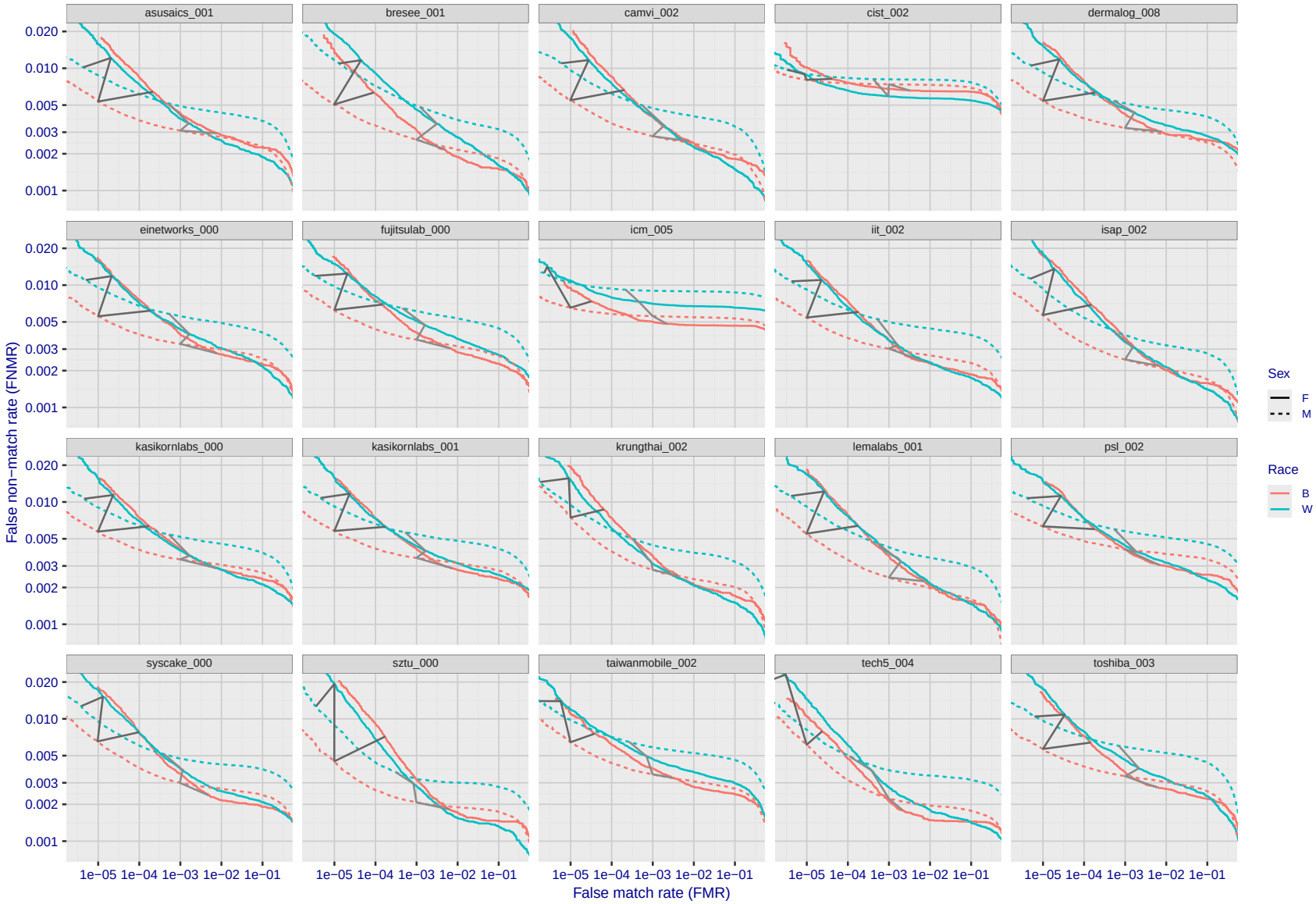

Figure 427: For the mugshot images, error tradeoff characteristics for white females, black females, black males and white males. The Z-shaped grey lines correspond to fixed thresholds, showing both *FNMR and FMR vary at one T value. Note: Many of the plots will naively be read as saying women gives worse error rates than men because the solid traces lie above the dotted ones. However, this is misleading and incomplete: The grey lines show the traces reveal horizontal shifts. Thus for the cogent-003 algorithm FNMR for men is* higher *than for women* at a fixed threshold *but, at the same time, FMR is higher for women - see Figure 608. As access control systems almost always operate at a fixed threshold, the naive interpretation is incorrect.*

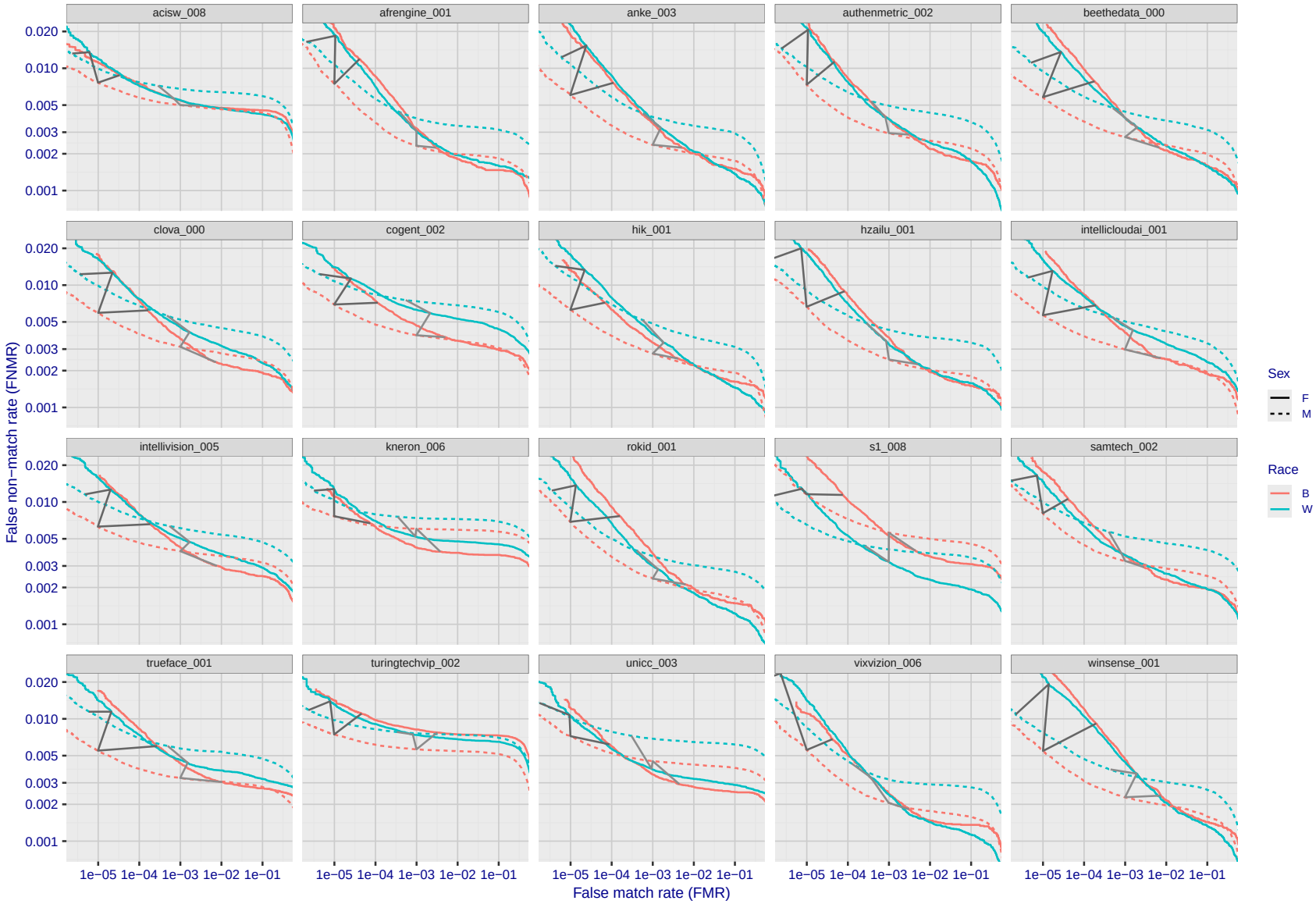

Figure 428: For the mugshot images, error tradeoff characteristics for white females, black females, black males and white males. The Z-shaped grey lines correspond to fixed thresholds, showing both *FNMR and FMR vary at one T value. Note: Many of the plots will naively be read as saying women gives worse error rates than men because the solid traces lie above the dotted ones. However, this is misleading and incomplete: The grey lines show the traces reveal horizontal shifts. Thus for the cogent-003 algorithm FNMR for men is* higher *than for women* at a fixed threshold *but, at the same time, FMR is higher for women - see Figure 608. As access control systems almost always operate at a fixed threshold, the naive interpretation is incorrect.*

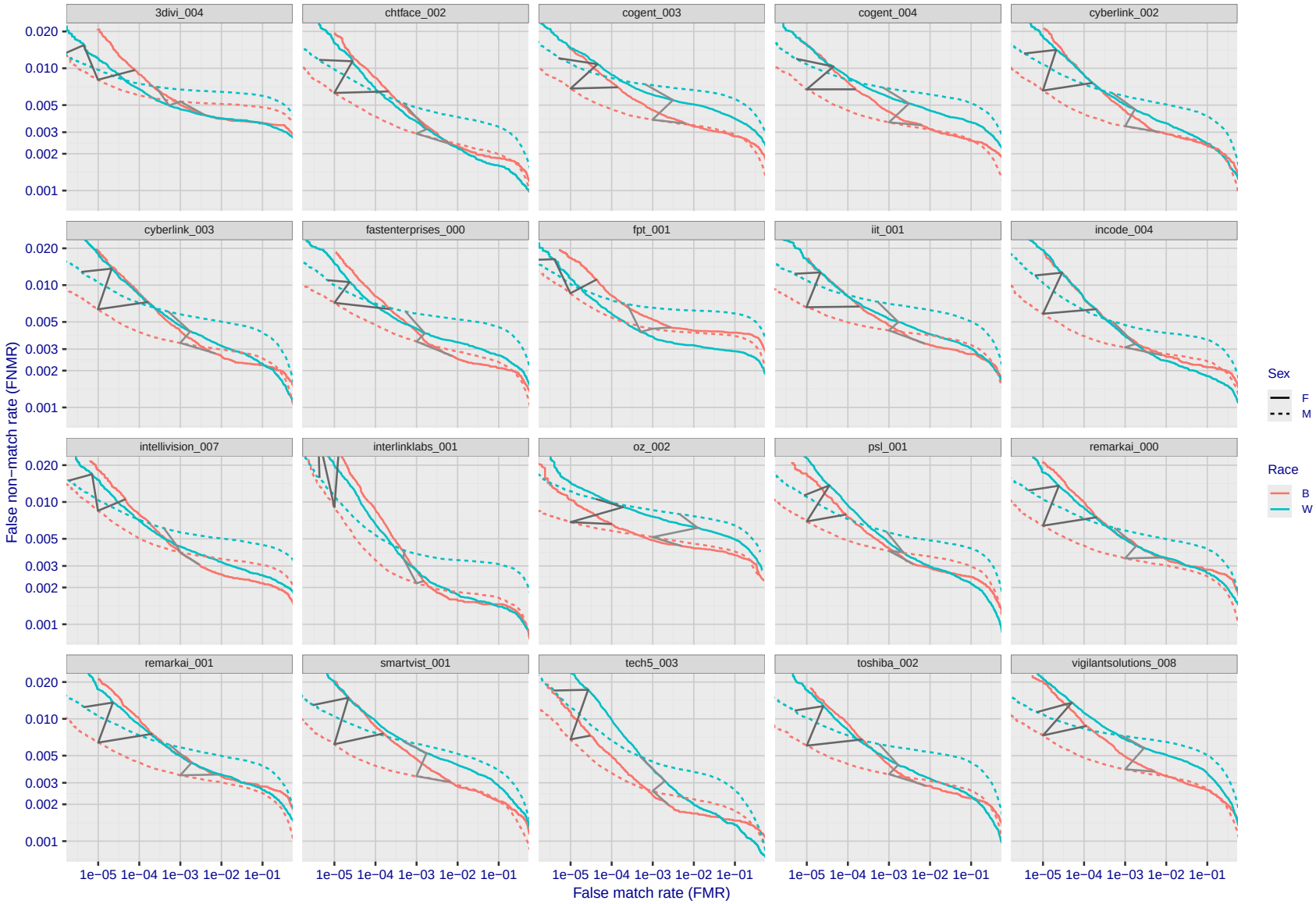

Figure 429: For the mugshot images, error tradeoff characteristics for white females, black females, black males and white males. The Z-shaped grey lines correspond to fixed thresholds, showing both *FNMR and FMR vary at one T value. Note: Many of the plots will naively be read as saying women gives worse error rates than men because the solid traces lie above the dotted ones. However, this is misleading and incomplete: The grey lines show the traces reveal horizontal shifts. Thus for the cogent-003 algorithm FNMR for men is* higher *than for women* at a fixed threshold *but, at the same time, FMR is higher for women - see Figure 608. As access control systems almost always operate at a fixed threshold, the naive interpretation is incorrect.*

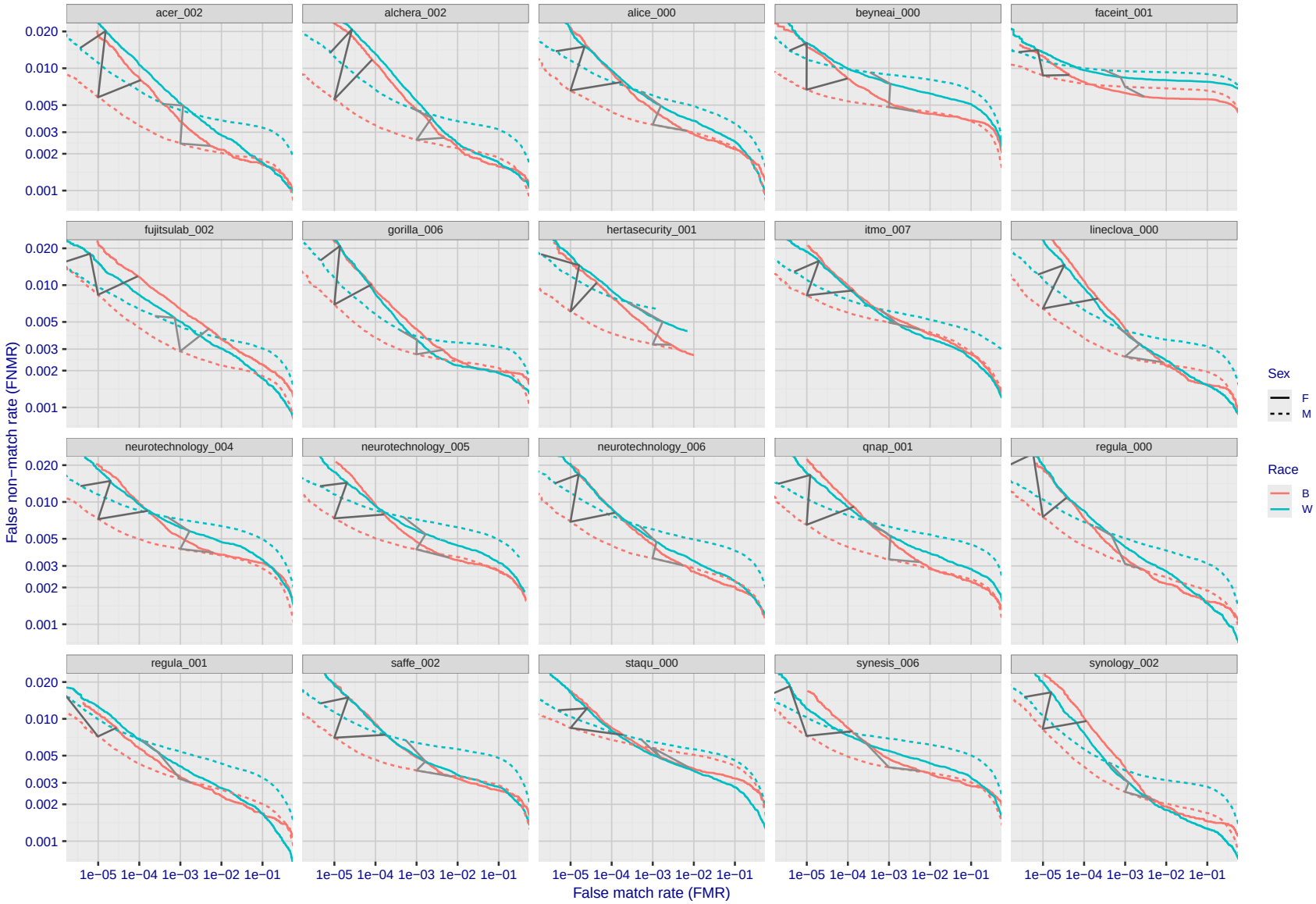

Figure 430: For the mugshot images, error tradeoff characteristics for white females, black females, black males and white males. The Z-shaped grey lines correspond to fixed thresholds, showing both *FNMR and FMR vary at one T value. Note: Many of the plots will naively be read as saying women gives worse error rates than men because the solid traces lie above the dotted ones. However, this is misleading and incomplete: The grey lines show the traces reveal horizontal shifts. Thus for the cogent-003 algorithm FNMR for men is* higher *than for women* at a fixed threshold *but, at the same time, FMR is higher for women - see Figure 608. As access control systems almost always operate at a fixed threshold, the naive interpretation is incorrect.*

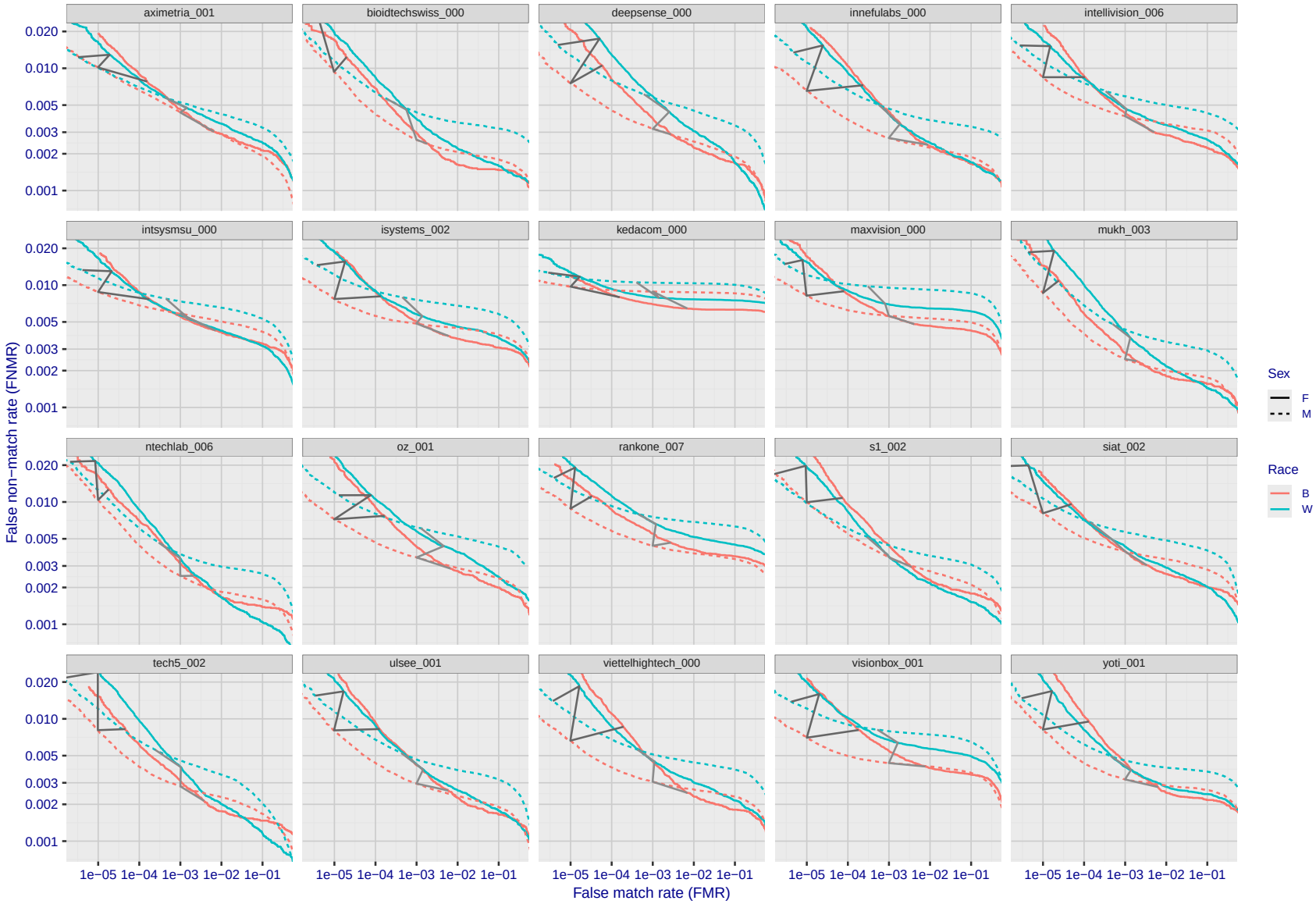

Figure 431: For the mugshot images, error tradeoff characteristics for white females, black females, black males and white males. The Z-shaped grey lines correspond to fixed thresholds, showing both *FNMR and FMR vary at one T value. Note: Many of the plots will naively be read as saying women gives worse error rates than men because the solid traces lie above the dotted ones. However, this is misleading and incomplete: The grey lines show the traces reveal horizontal shifts. Thus for the cogent-003 algorithm FNMR for men is* higher *than for women* at a fixed threshold *but, at the same time, FMR is higher for women - see Figure 608. As access control systems almost always operate at a fixed threshold, the naive interpretation is incorrect.*

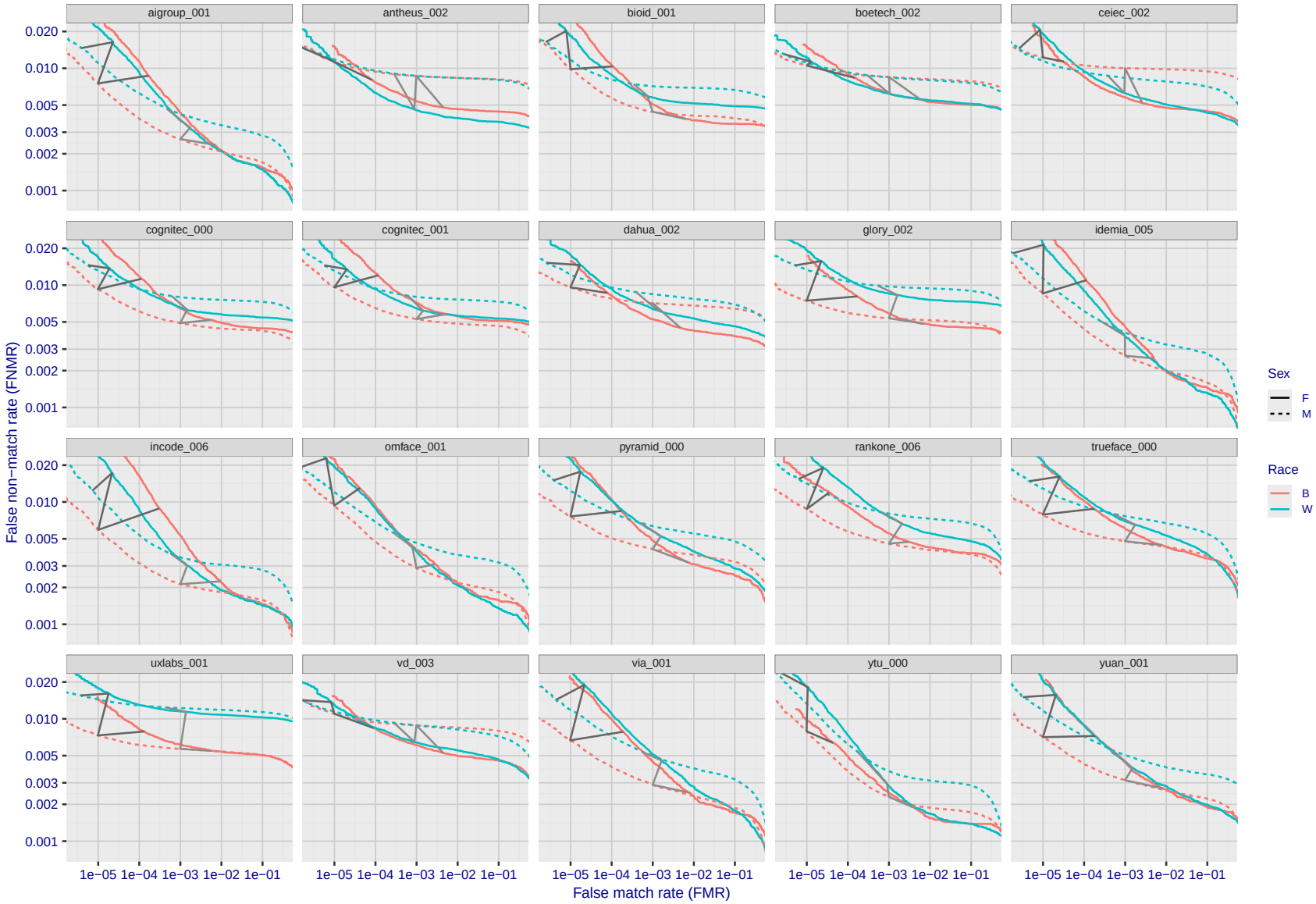

Figure 432: For the mugshot images, error tradeoff characteristics for white females, black females, black males and white males. The Z-shaped grey lines correspond to fixed thresholds, showing both *FNMR and FMR vary at one T value. Note: Many of the plots will naively be read as saying women gives worse error rates than men because the solid traces lie above the dotted ones. However, this is misleading and incomplete: The grey lines show the traces reveal horizontal shifts. Thus for the cogent-003 algorithm FNMR for men is* higher *than for women* at a fixed threshold *but, at the same time, FMR is higher for women - see Figure 608. As access control systems almost always operate at a fixed threshold, the naive interpretation is incorrect.*

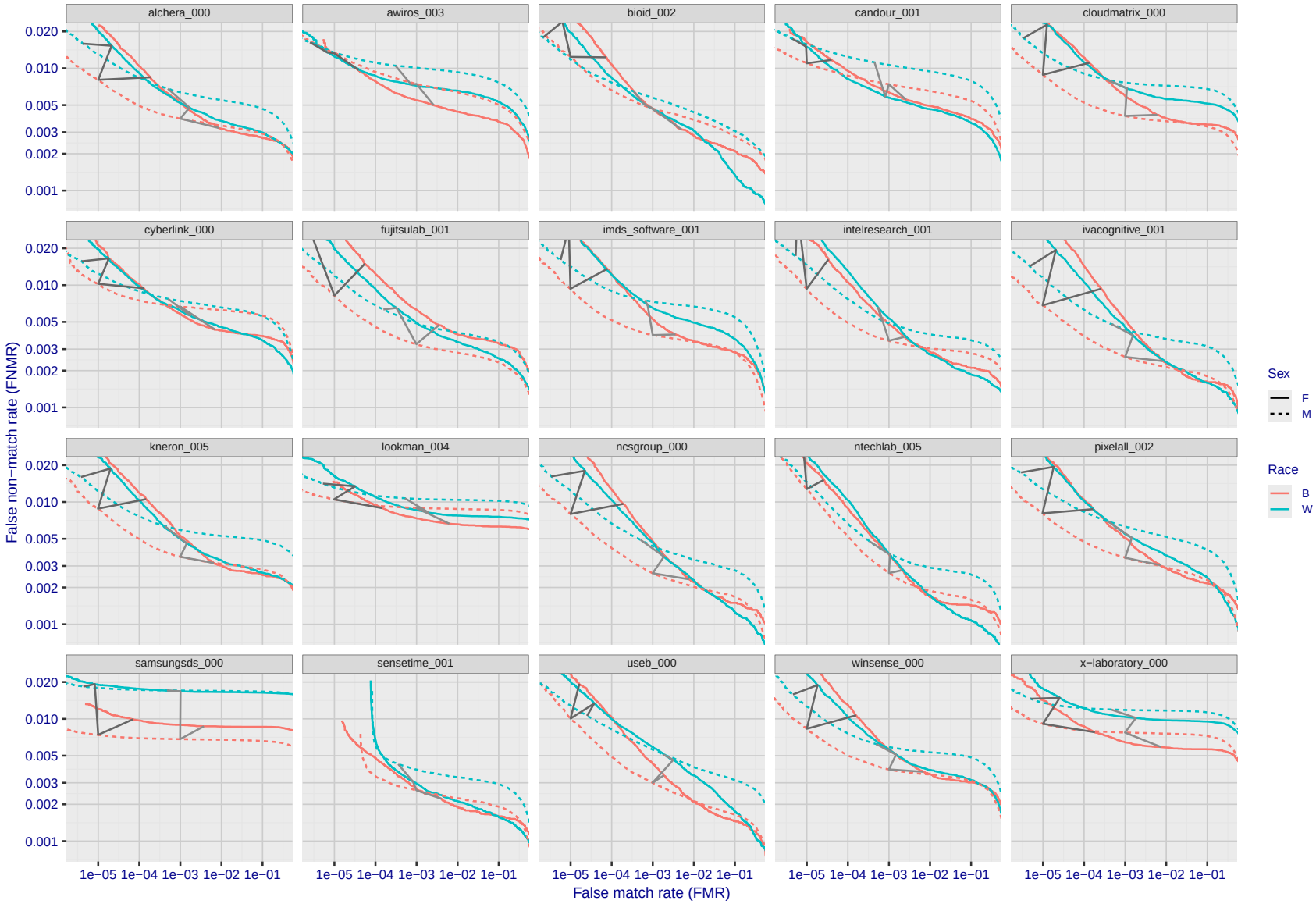

Figure 433: For the mugshot images, error tradeoff characteristics for white females, black females, black males and white males. The Z-shaped grey lines correspond to fixed thresholds, showing both *FNMR and FMR vary at one T value. Note: Many of the plots will naively be read as saying women gives worse error rates than men because the solid traces lie above the dotted ones. However, this is misleading and incomplete: The grey lines show the traces reveal horizontal shifts. Thus for the cogent-003 algorithm FNMR for men is* higher *than for women* at a fixed threshold *but, at the same time, FMR is higher for women - see Figure 608. As access control systems almost always operate at a fixed threshold, the naive interpretation is incorrect.*

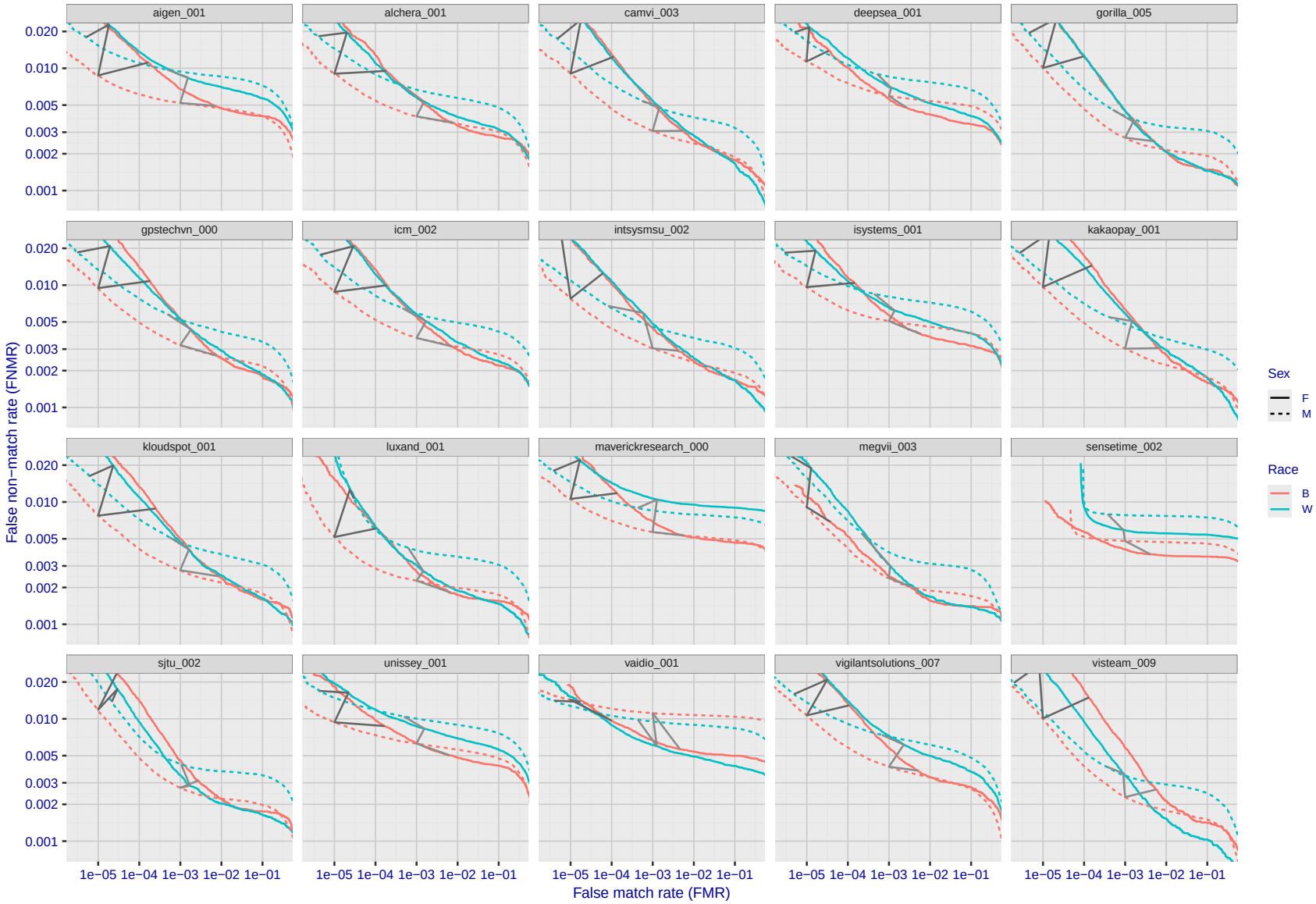

Figure 434: For the mugshot images, error tradeoff characteristics for white females, black females, black males and white males. The Z-shaped grey lines correspond to fixed thresholds, showing both *FNMR and FMR vary at one T value. Note: Many of the plots will naively be read as saying women gives worse error rates than men because the solid traces lie above the dotted ones. However, this is misleading and incomplete: The grey lines show the traces reveal horizontal shifts. Thus for the cogent-003 algorithm FNMR for men is* higher *than for women* at a fixed threshold *but, at the same time, FMR is higher for women - see Figure 608. As access control systems almost always operate at a fixed threshold, the naive interpretation is incorrect.*

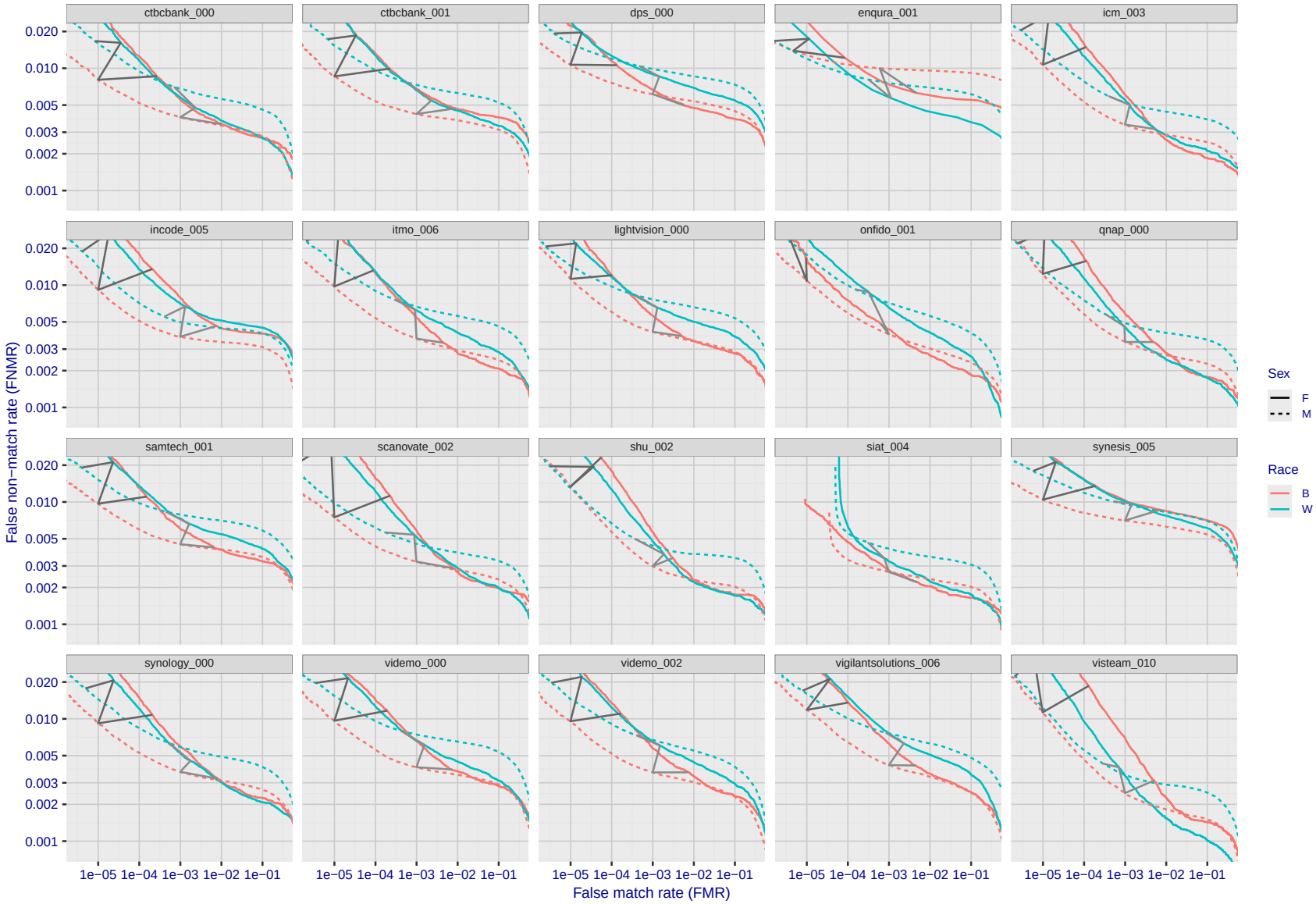

Figure 435: For the mugshot images, error tradeoff characteristics for white females, black females, black males and white males. The Z-shaped grey lines correspond to fixed thresholds, showing both *FNMR and FMR vary at one T value. Note: Many of the plots will naively be read as saying women gives worse error rates than men because the solid traces lie above the dotted ones. However, this is misleading and incomplete: The grey lines show the traces reveal horizontal shifts. Thus for the cogent-003 algorithm FNMR for men is* higher *than for women* at a fixed threshold *but, at the same time, FMR is higher for women - see Figure 608. As access control systems almost always operate at a fixed threshold, the naive interpretation is incorrect.*

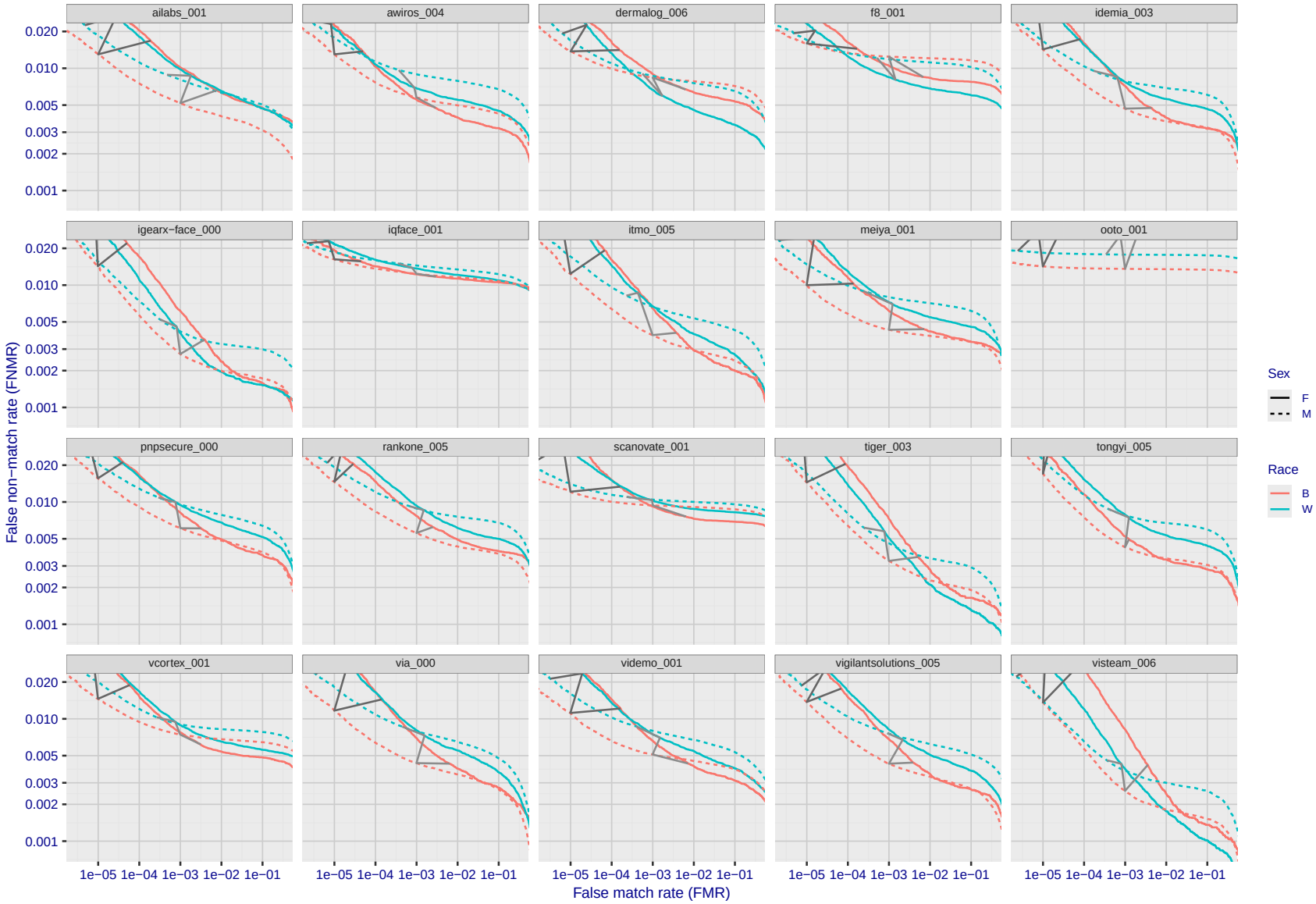

Figure 436: For the mugshot images, error tradeoff characteristics for white females, black females, black males and white males. The Z-shaped grey lines correspond to fixed thresholds, showing both *FNMR and FMR vary at one T value. Note: Many of the plots will naively be read as saying women gives worse error rates than men because the solid traces lie above the dotted ones. However, this is misleading and incomplete: The grey lines show the traces reveal horizontal shifts. Thus for the cogent-003 algorithm FNMR for men is* higher *than for women* at a fixed threshold *but, at the same time, FMR is higher for women - see Figure 608. As access control systems almost always operate at a fixed threshold, the naive interpretation is incorrect.*

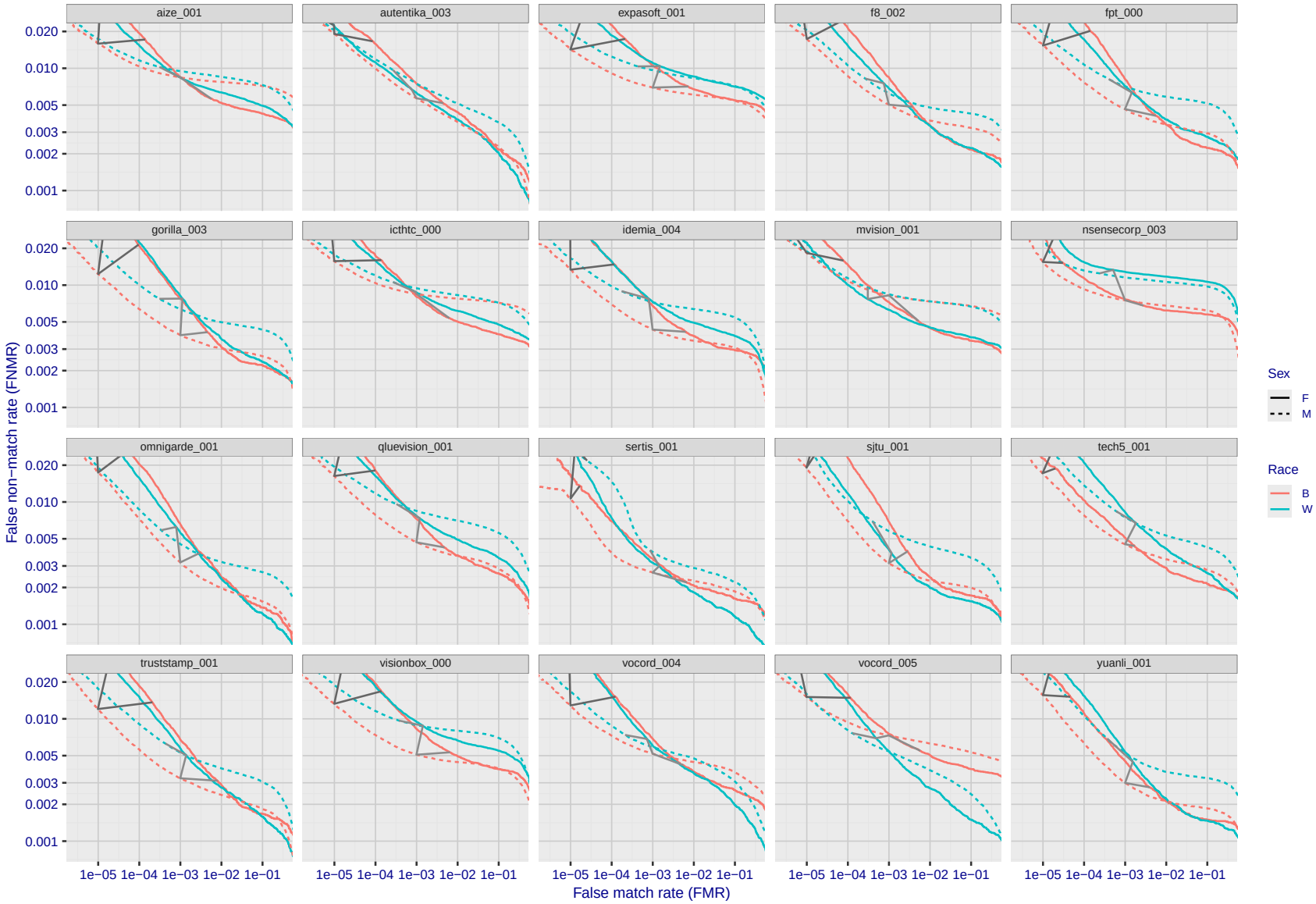

Figure 437: For the mugshot images, error tradeoff characteristics for white females, black females, black males and white males. The Z-shaped grey lines correspond to fixed thresholds, showing both *FNMR and FMR vary at one T value. Note: Many of the plots will naively be read as saying women gives worse error rates than men because the solid traces lie above the dotted ones. However, this is misleading and incomplete: The grey lines show the traces reveal horizontal shifts. Thus for the cogent-003 algorithm FNMR for men is* higher *than for women* at a fixed threshold *but, at the same time, FMR is higher for women - see Figure 608. As access control systems almost always operate at a fixed threshold, the naive interpretation is incorrect.*

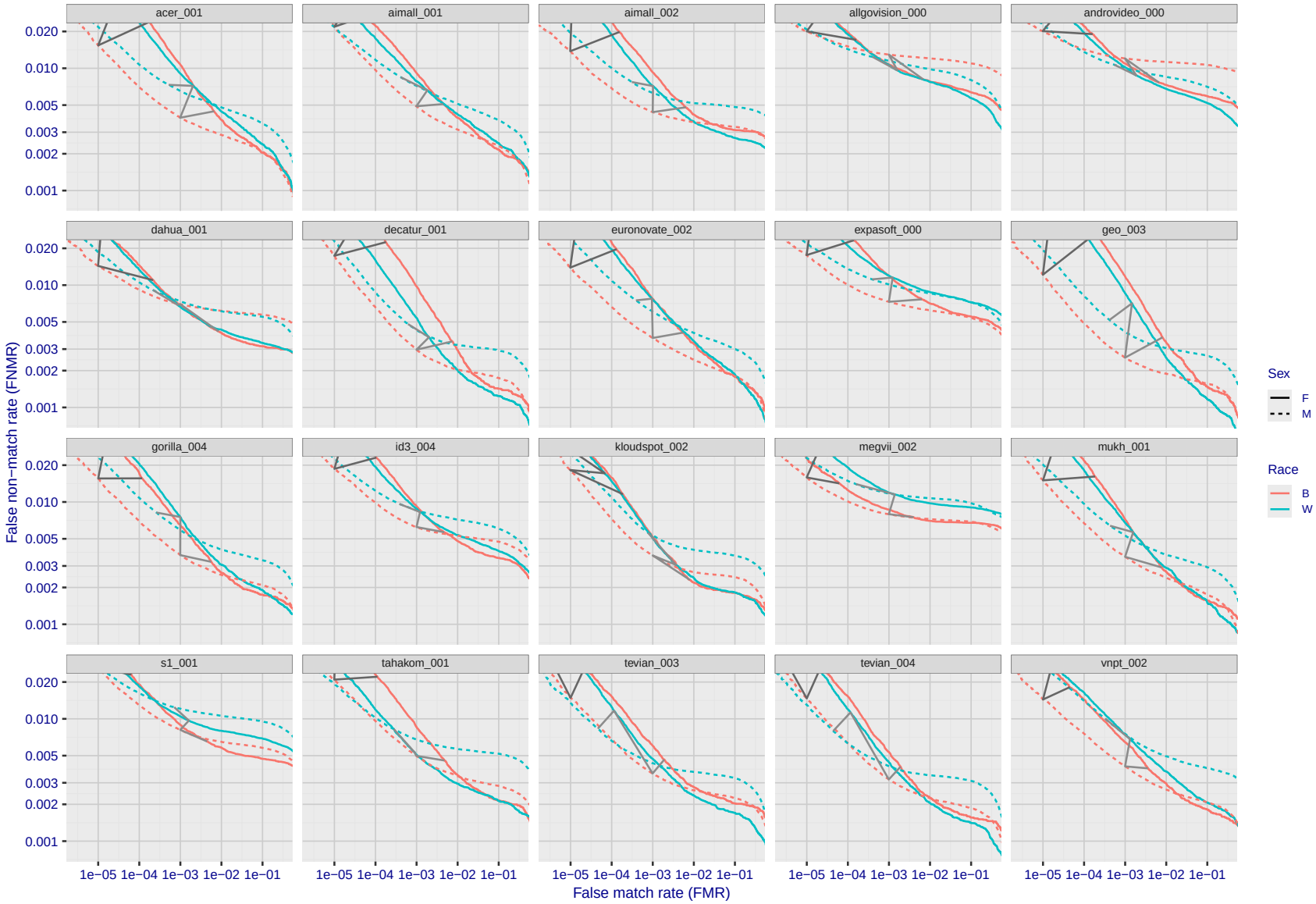

Figure 438: For the mugshot images, error tradeoff characteristics for white females, black females, black males and white males. The Z-shaped grey lines correspond to fixed thresholds, showing both *FNMR and FMR vary at one T value. Note: Many of the plots will naively be read as saying women gives worse error rates than men because the solid traces lie above the dotted ones. However, this is misleading and incomplete: The grey lines show the traces reveal horizontal shifts. Thus for the cogent-003 algorithm FNMR for men is* higher *than for women* at a fixed threshold *but, at the same time, FMR is higher for women - see Figure 608. As access control systems almost always operate at a fixed threshold, the naive interpretation is incorrect.*

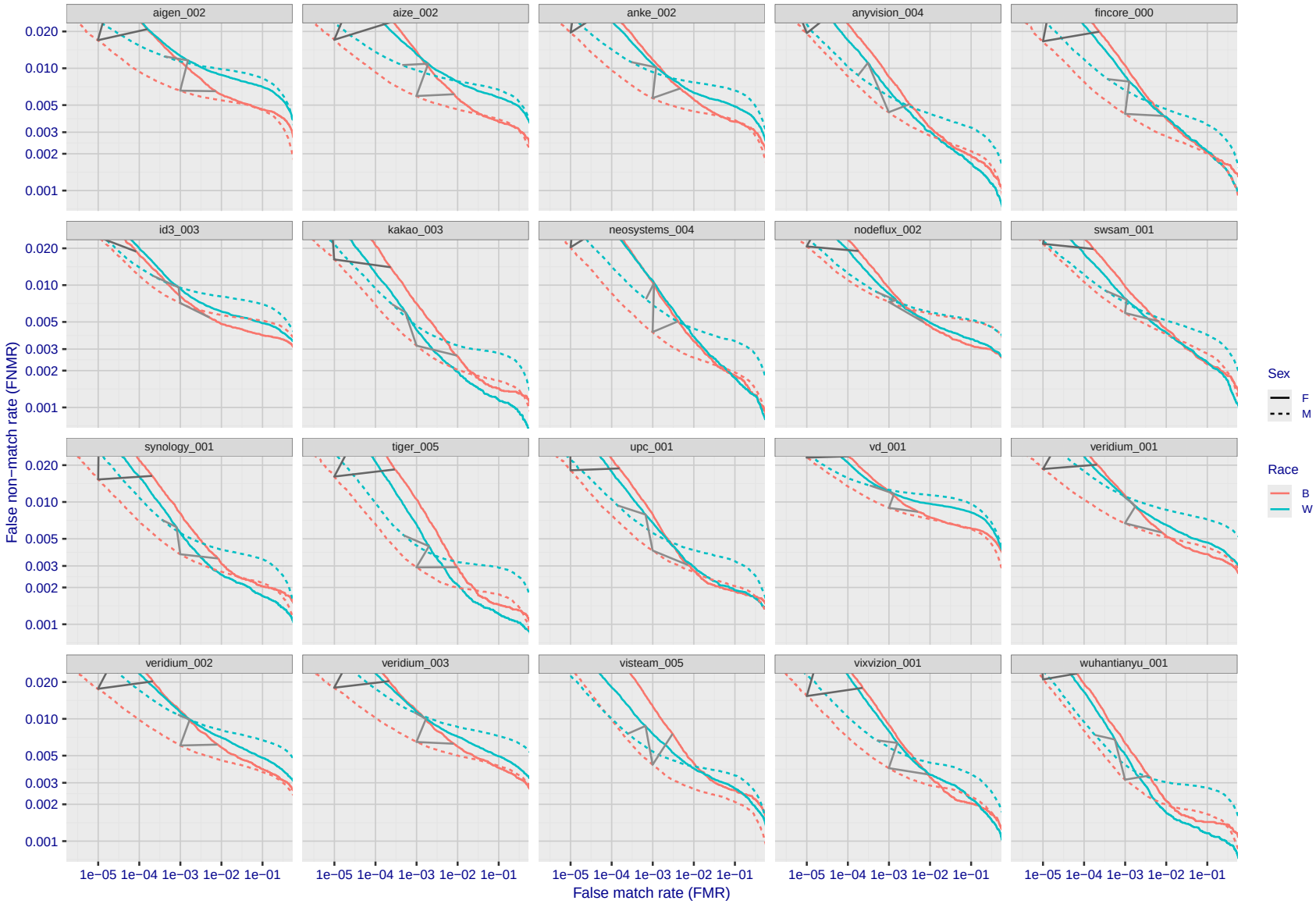

Figure 439: For the mugshot images, error tradeoff characteristics for white females, black females, black males and white males. The Z-shaped grey lines correspond to fixed thresholds, showing both *FNMR and FMR vary at one T value. Note: Many of the plots will naively be read as saying women gives worse error rates than men because the solid traces lie above the dotted ones. However, this is misleading and incomplete: The grey lines show the traces reveal horizontal shifts. Thus for the cogent-003 algorithm FNMR for men is* higher *than for women* at a fixed threshold *but, at the same time, FMR is higher for women - see Figure 608. As access control systems almost always operate at a fixed threshold, the naive interpretation is incorrect.*

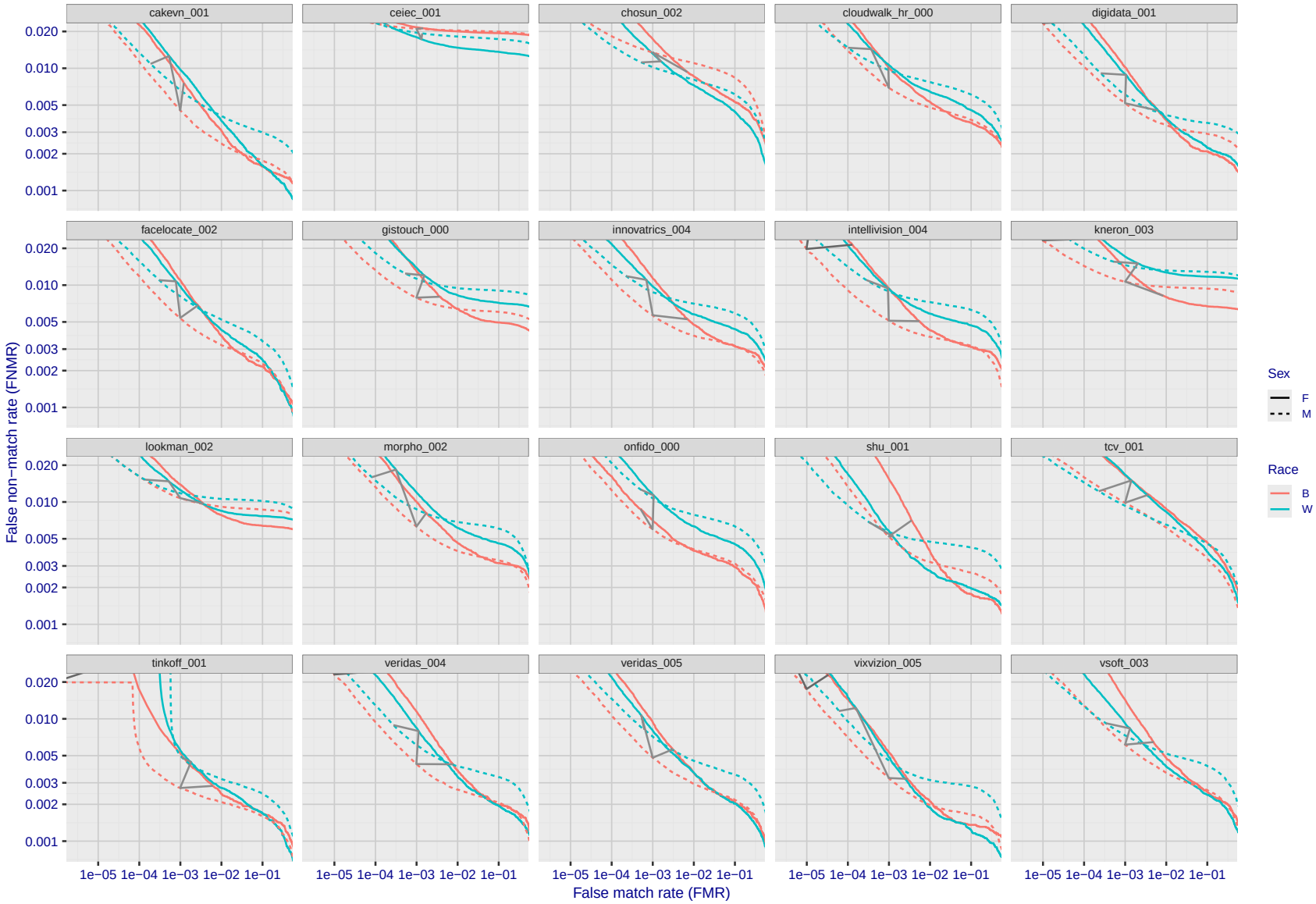

Figure 440: For the mugshot images, error tradeoff characteristics for white females, black females, black males and white males. The Z-shaped grey lines correspond to fixed thresholds, showing both *FNMR and FMR vary at one T value. Note: Many of the plots will naively be read as saying women gives worse error rates than men because the solid traces lie above the dotted ones. However, this is misleading and incomplete: The grey lines show the traces reveal horizontal shifts. Thus for the cogent-003 algorithm FNMR for men is* higher *than for women* at a fixed threshold *but, at the same time, FMR is higher for women - see Figure 608. As access control systems almost always operate at a fixed threshold, the naive interpretation is incorrect.*

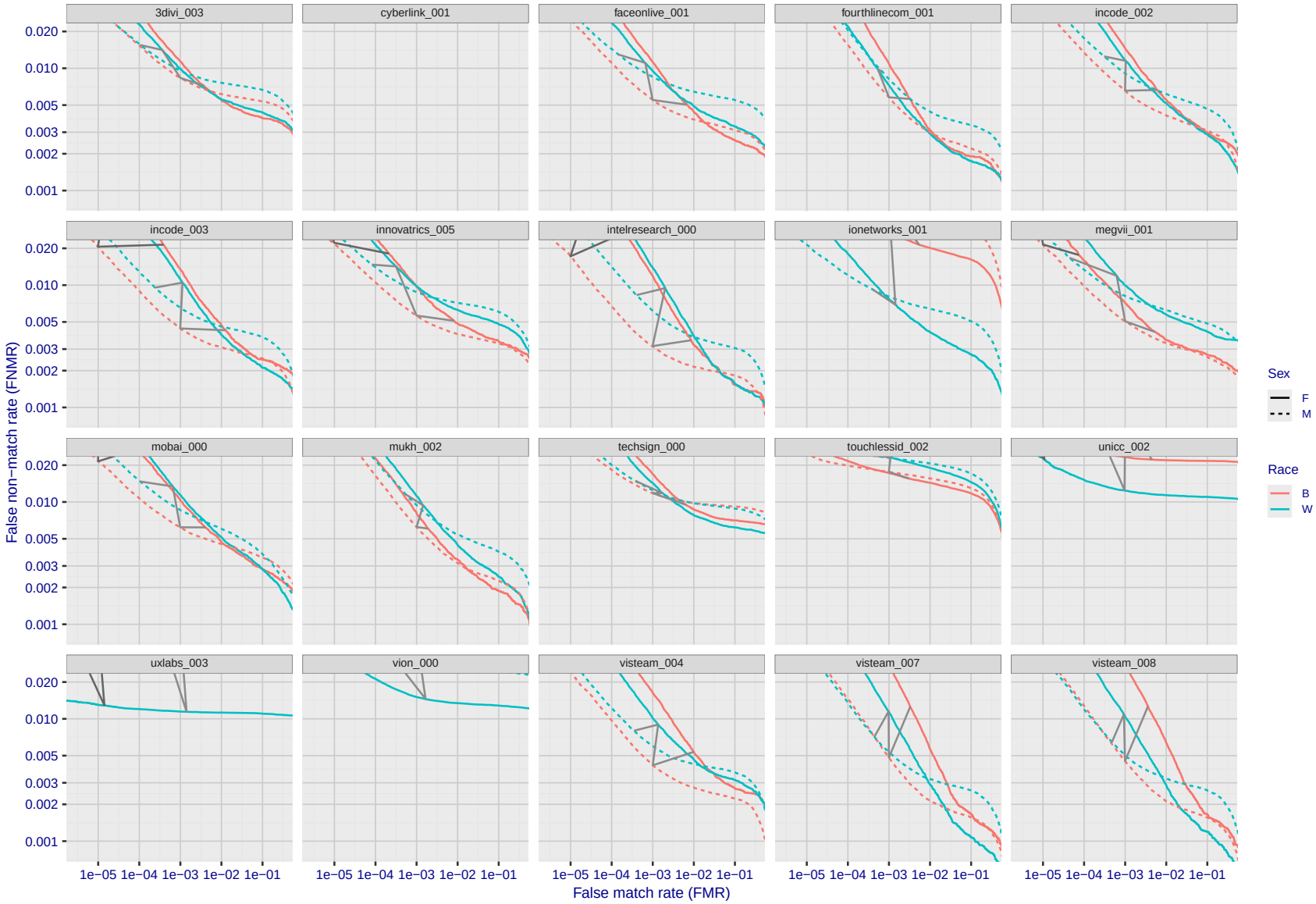

Figure 441: For the mugshot images, error tradeoff characteristics for white females, black females, black males and white males. The Z-shaped grey lines correspond to fixed thresholds, showing both *FNMR and FMR vary at one T value. Note: Many of the plots will naively be read as saying women gives worse error rates than men because the solid traces lie above the dotted ones. However, this is misleading and incomplete: The grey lines show the traces reveal horizontal shifts. Thus for the cogent-003 algorithm FNMR for men is* higher *than for women* at a fixed threshold *but, at the same time, FMR is higher for women - see Figure 608. As access control systems almost always operate at a fixed threshold, the naive interpretation is incorrect.*

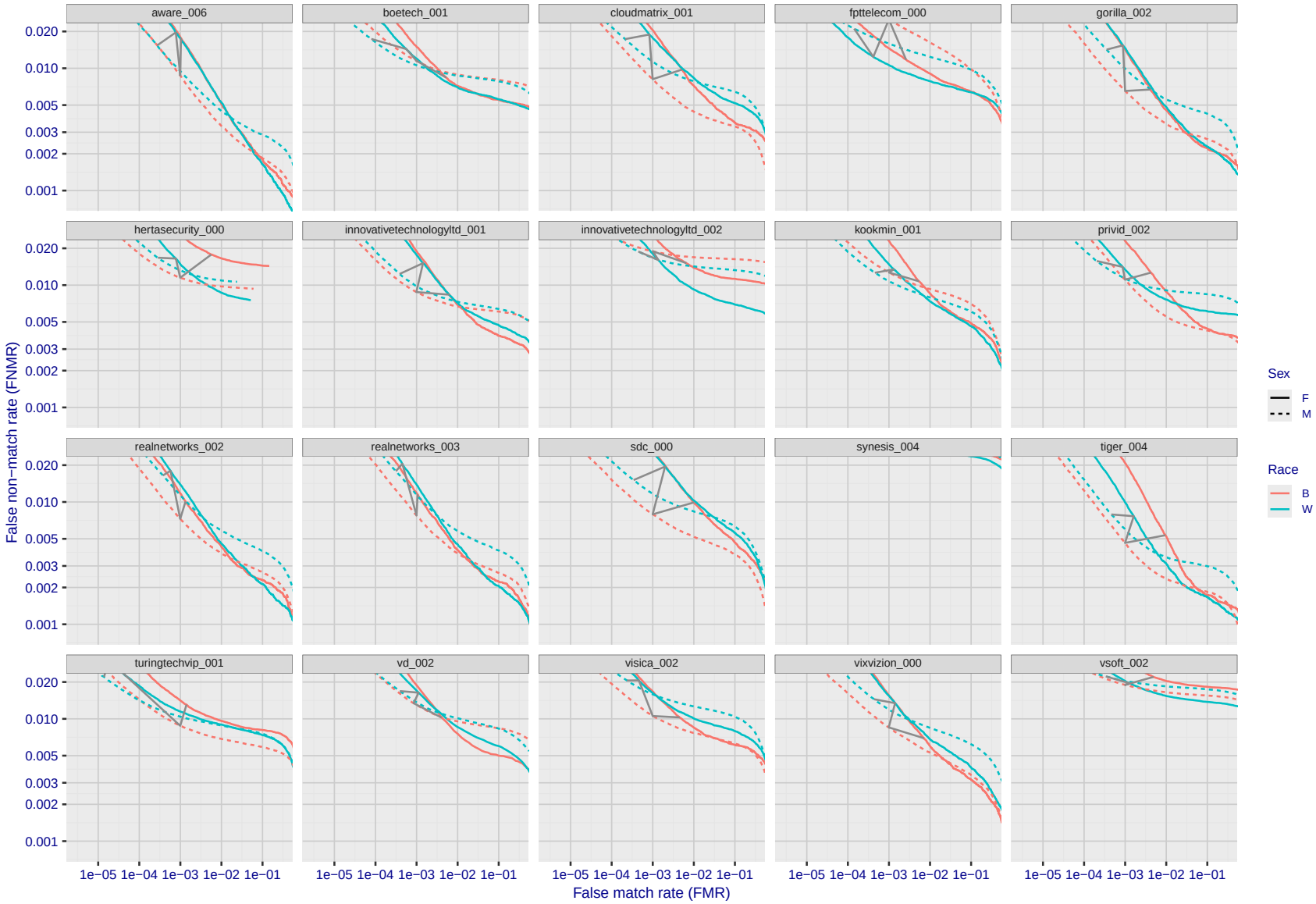

Figure 442: For the mugshot images, error tradeoff characteristics for white females, black females, black males and white males. The Z-shaped grey lines correspond to fixed thresholds, showing both *FNMR and FMR vary at one T value. Note: Many of the plots will naively be read as saying women gives worse error rates than men because the solid traces lie above the dotted ones. However, this is misleading and incomplete: The grey lines show the traces reveal horizontal shifts. Thus for the cogent-003 algorithm FNMR for men is* higher *than for women* at a fixed threshold *but, at the same time, FMR is higher for women - see Figure 608. As access control systems almost always operate at a fixed threshold, the naive interpretation is incorrect.*

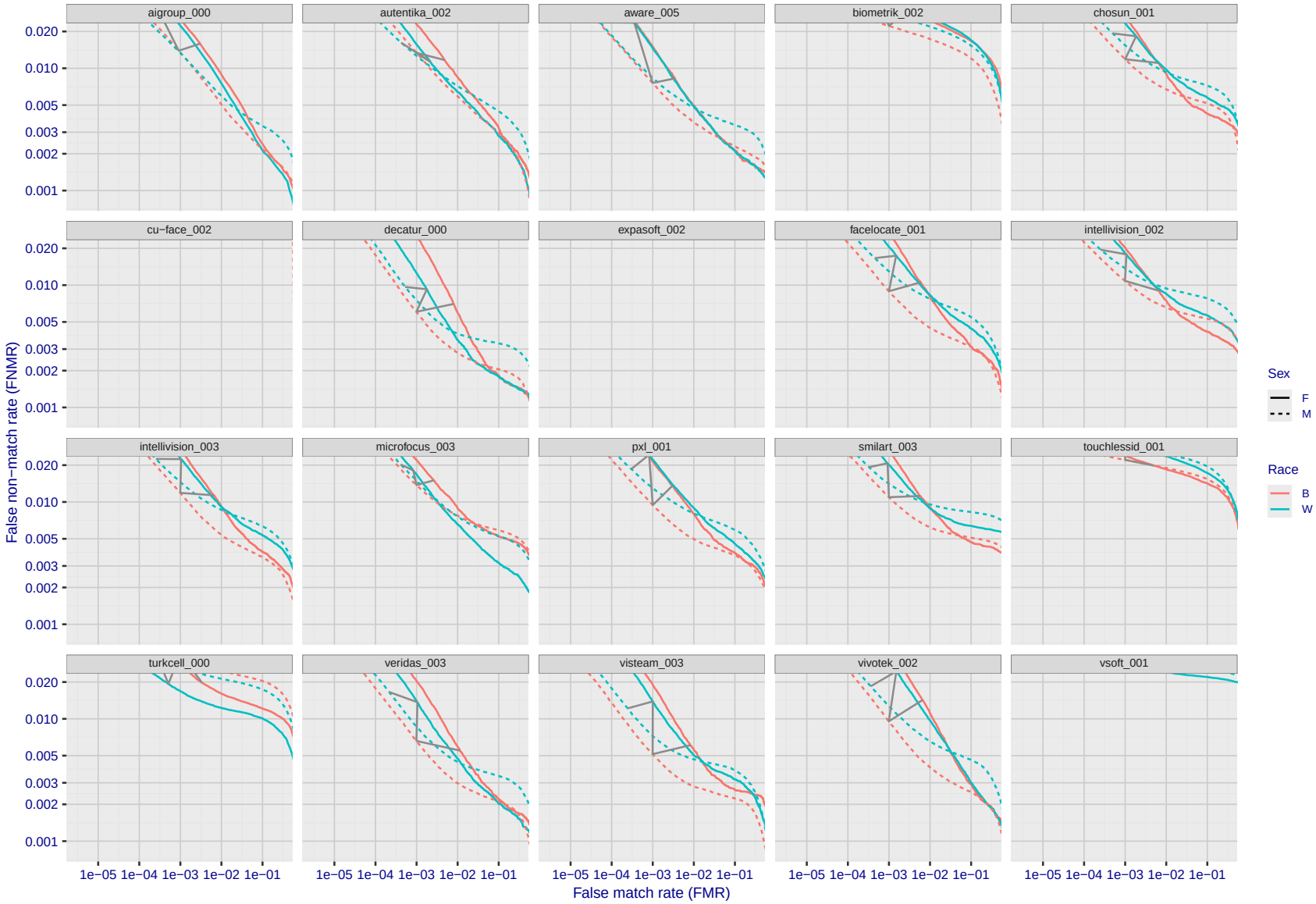

Figure 443: For the mugshot images, error tradeoff characteristics for white females, black females, black males and white males. The Z-shaped grey lines correspond to fixed thresholds, showing both *FNMR and FMR vary at one T value. Note: Many of the plots will naively be read as saying women gives worse error rates than men because the solid traces lie above the dotted ones. However, this is misleading and incomplete: The grey lines show the traces reveal horizontal shifts. Thus for the cogent-003 algorithm FNMR for men is* higher *than for women* at a fixed threshold *but, at the same time, FMR is higher for women - see Figure 608. As access control systems almost always operate at a fixed threshold, the naive interpretation is incorrect.*

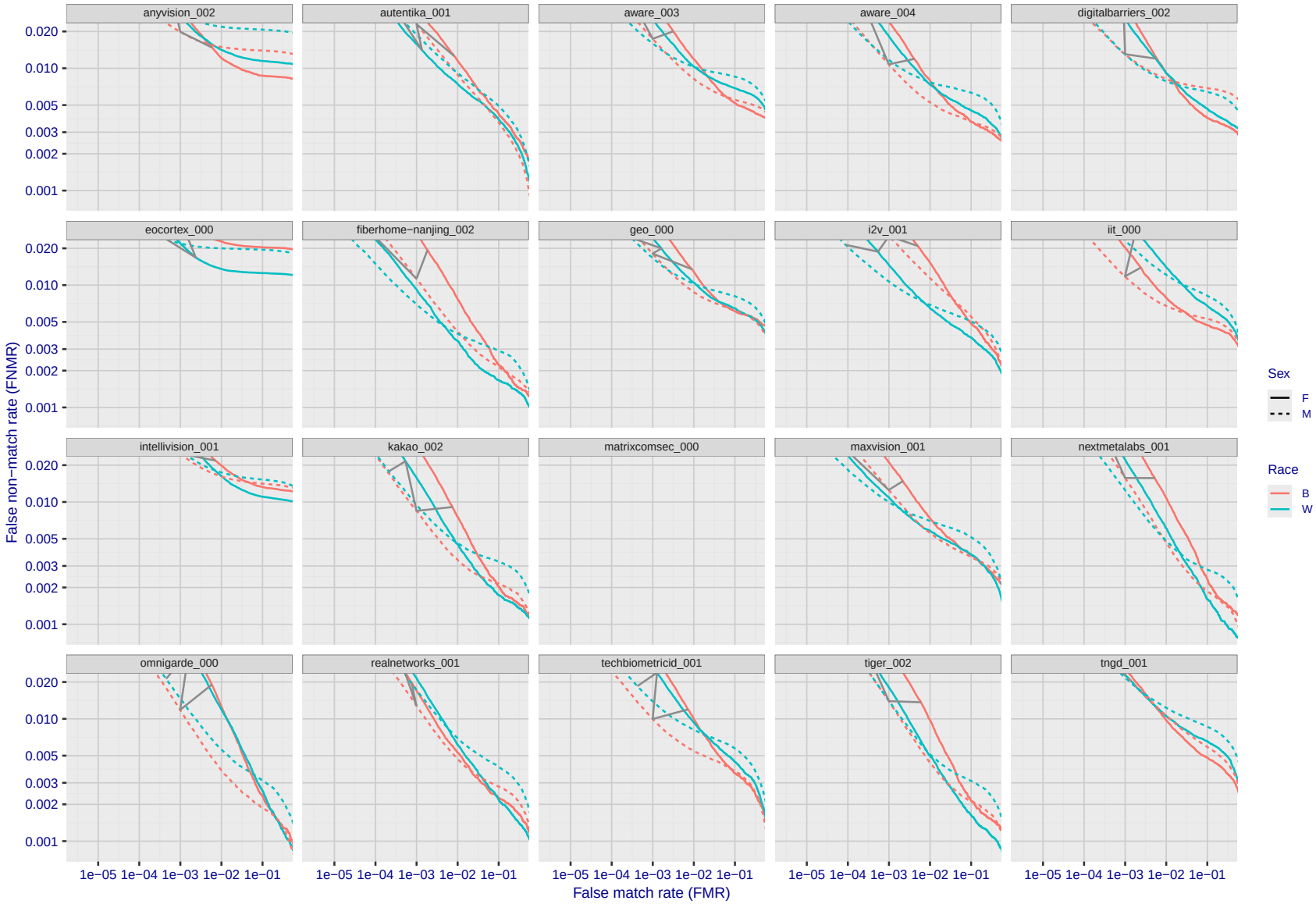

Figure 444: For the mugshot images, error tradeoff characteristics for white females, black females, black males and white males. The Z-shaped grey lines correspond to fixed thresholds, showing both *FNMR and FMR vary at one T value. Note: Many of the plots will naively be read as saying women gives worse error rates than men because the solid traces lie above the dotted ones. However, this is misleading and incomplete: The grey lines show the traces reveal horizontal shifts. Thus for the cogent-003 algorithm FNMR for men is* higher *than for women* at a fixed threshold *but, at the same time, FMR is higher for women - see Figure 608. As access control systems almost always operate at a fixed threshold, the naive interpretation is incorrect.*

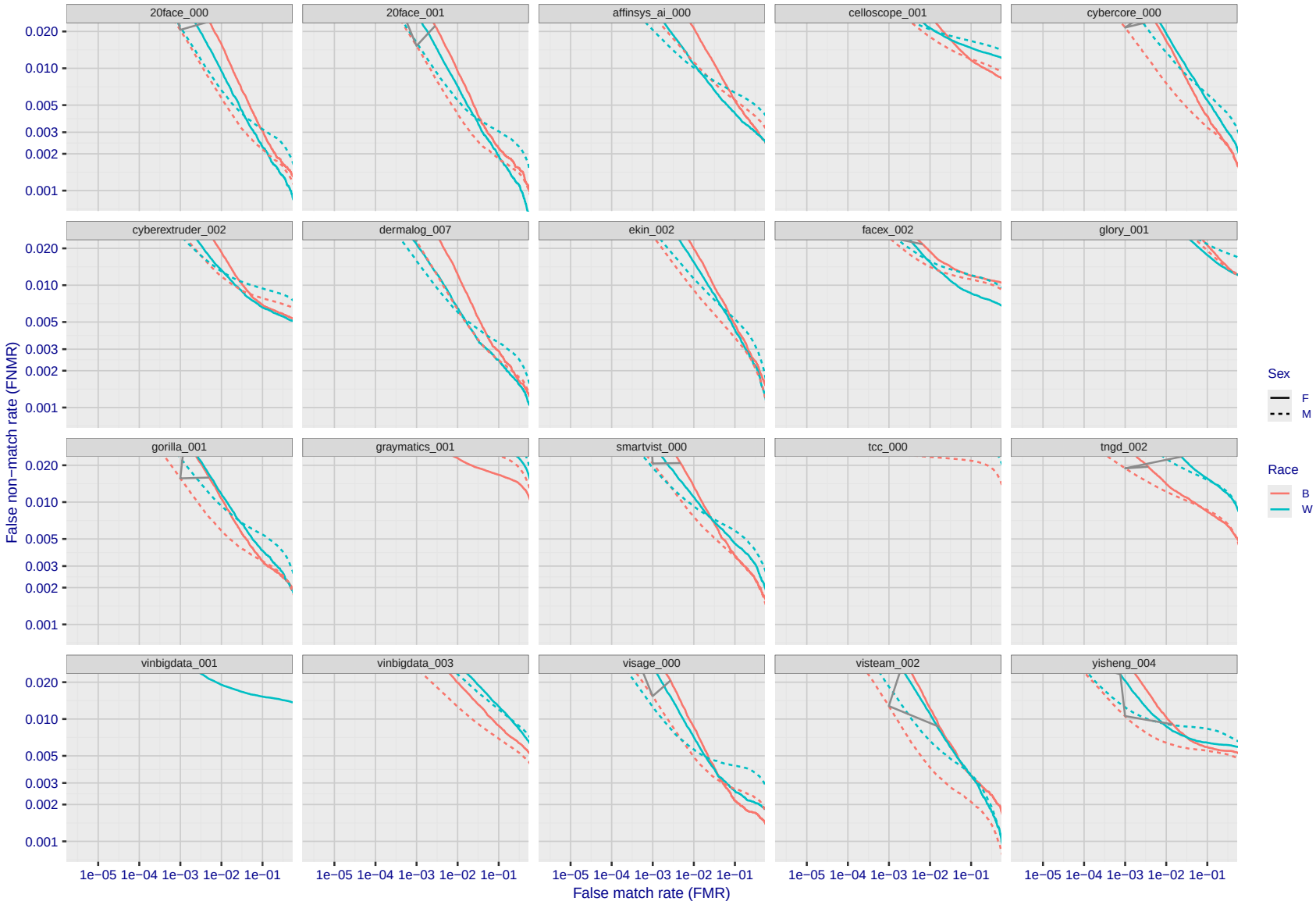

Figure 445: For the mugshot images, error tradeoff characteristics for white females, black females, black males and white males. The Z-shaped grey lines correspond to fixed thresholds, showing both *FNMR and FMR vary at one T value. Note: Many of the plots will naively be read as saying women gives worse error rates than men because the solid traces lie above the dotted ones. However, this is misleading and incomplete: The grey lines show the traces reveal horizontal shifts. Thus for the cogent-003 algorithm FNMR for men is* higher *than for women* at a fixed threshold *but, at the same time, FMR is higher for women - see Figure 608. As access control systems almost always operate at a fixed threshold, the naive interpretation is incorrect.*

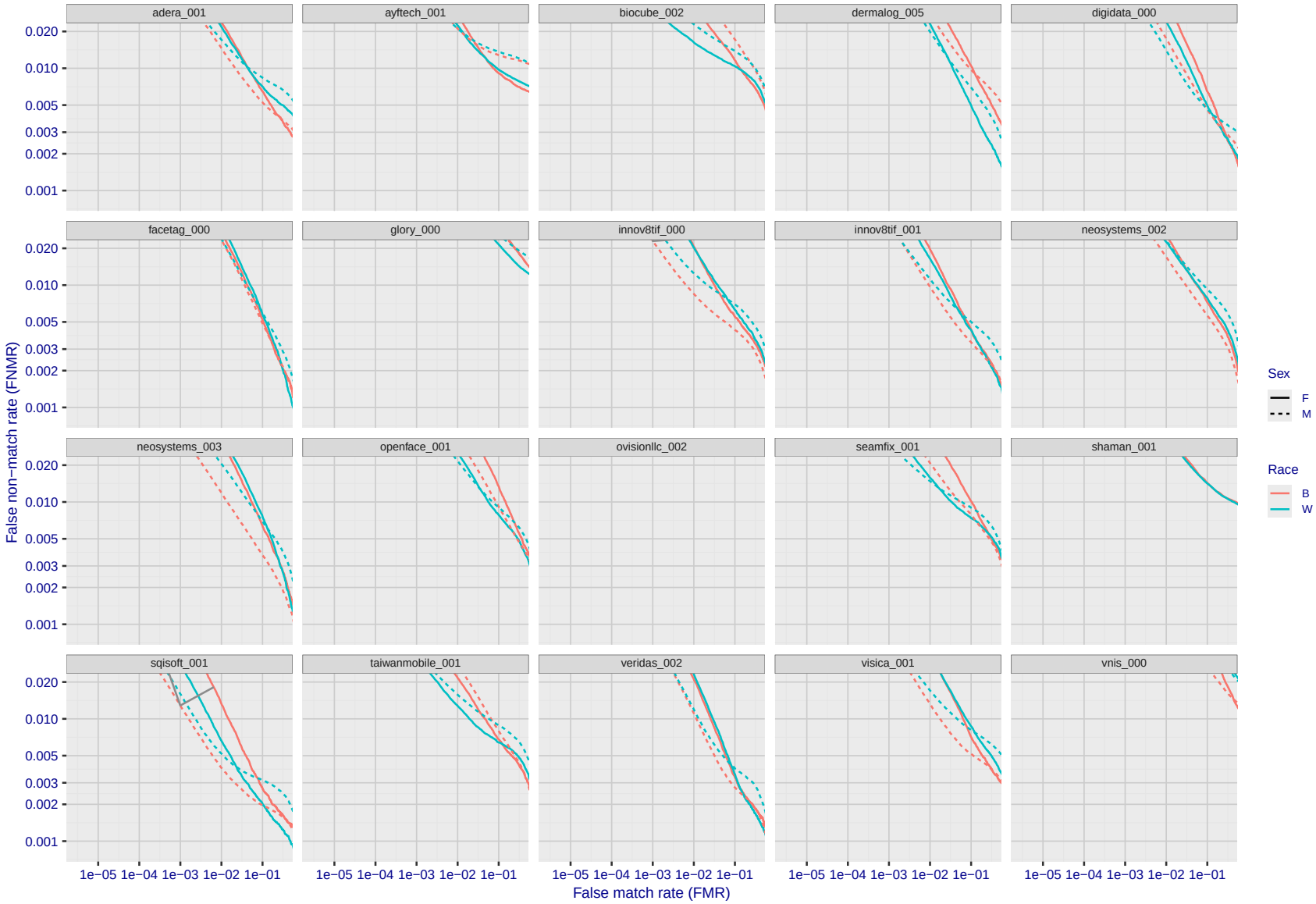

Figure 446: For the mugshot images, error tradeoff characteristics for white females, black females, black males and white males. The Z-shaped grey lines correspond to fixed thresholds, showing both *FNMR and FMR vary at one T value. Note: Many of the plots will naively be read as saying women gives worse error rates than men because the solid traces lie above the dotted ones. However, this is misleading and incomplete: The grey lines show the traces reveal horizontal shifts. Thus for the cogent-003 algorithm FNMR for men is* higher *than for women* at a fixed threshold *but, at the same time, FMR is higher for women - see Figure 608. As access control systems almost always operate at a fixed threshold, the naive interpretation is incorrect.*

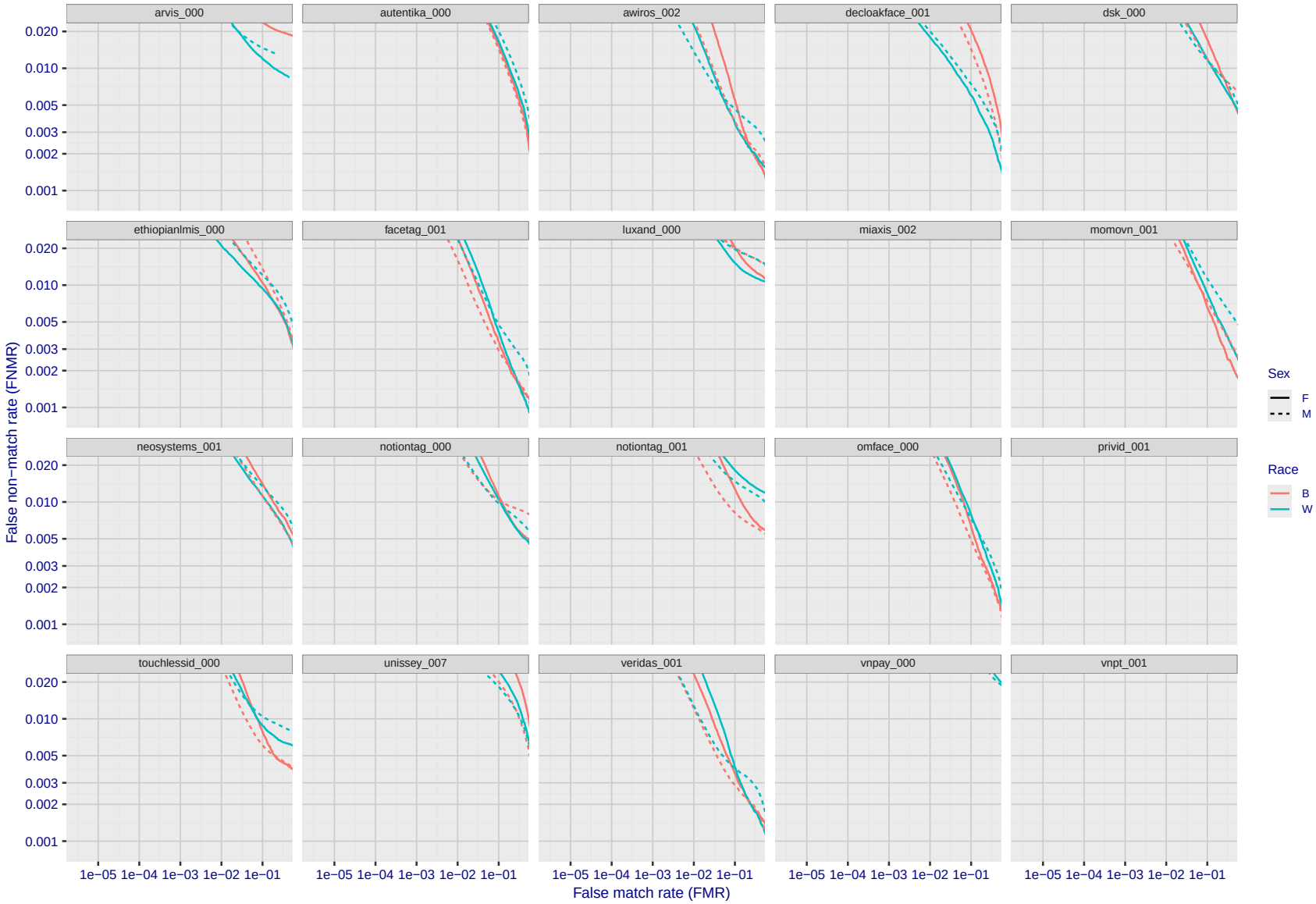

Figure 447: For the mugshot images, error tradeoff characteristics for white females, black females, black males and white males. The Z-shaped grey lines correspond to fixed thresholds, showing both *FNMR and FMR vary at one T value. Note: Many of the plots will naively be read as saying women gives worse error rates than men because the solid traces lie above the dotted ones. However, this is misleading and incomplete: The grey lines show the traces reveal horizontal shifts. Thus for the cogent-003 algorithm FNMR for men is* higher *than for women* at a fixed threshold *but, at the same time, FMR is higher for women - see Figure 608. As access control systems almost always operate at a fixed threshold, the naive interpretation is incorrect.*

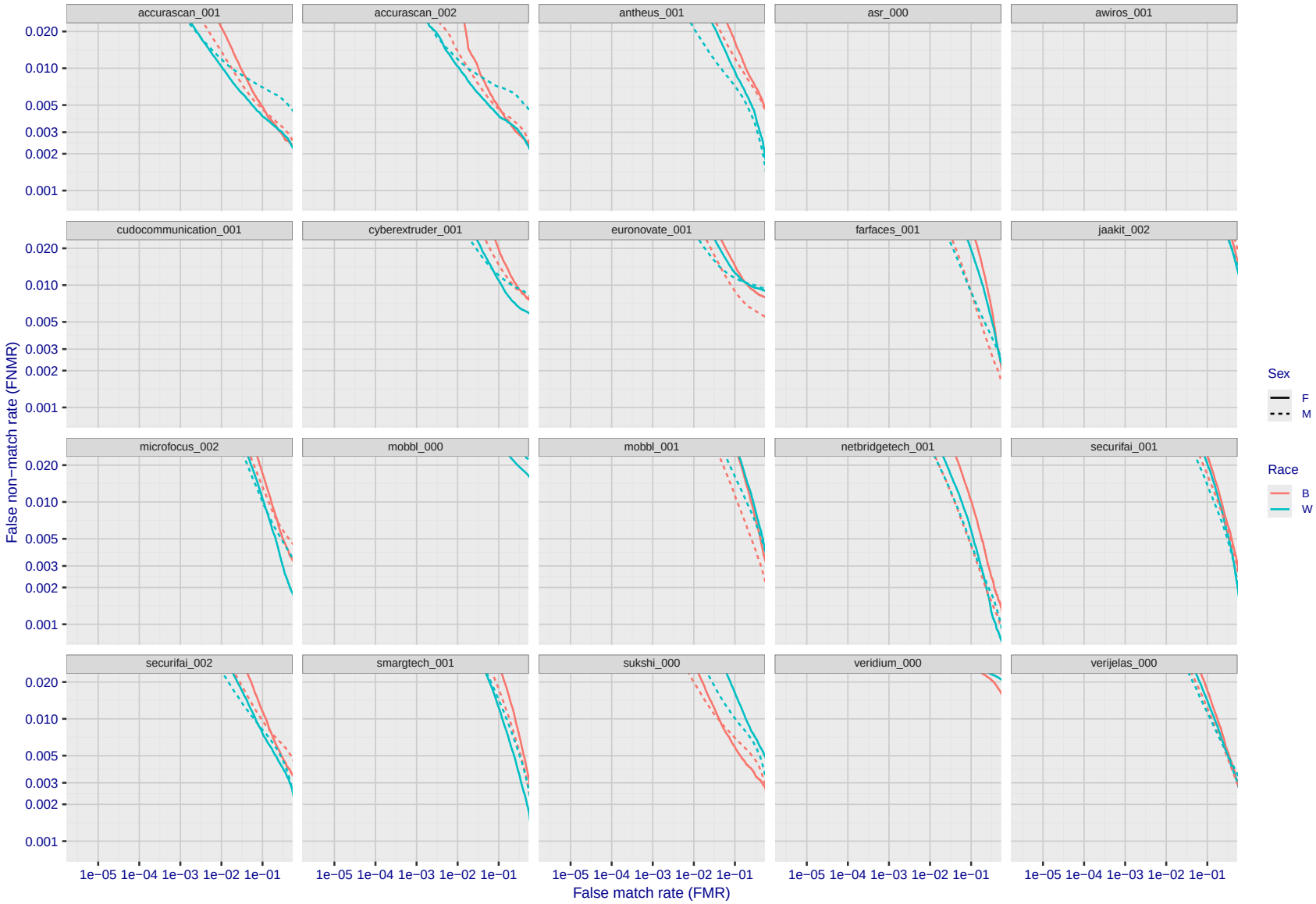

Figure 448: For the mugshot images, error tradeoff characteristics for white females, black females, black males and white males. The Z-shaped grey lines correspond to fixed thresholds, showing both *FNMR and FMR vary at one T value. Note: Many of the plots will naively be read as saying women gives worse error rates than men because the solid traces lie above the dotted ones. However, this is misleading and incomplete: The grey lines show the traces reveal horizontal shifts. Thus for the cogent-003 algorithm FNMR for men is* higher *than for women* at a fixed threshold *but, at the same time, FMR is higher for women - see Figure 608. As access control systems almost always operate at a fixed threshold, the naive interpretation is incorrect.*

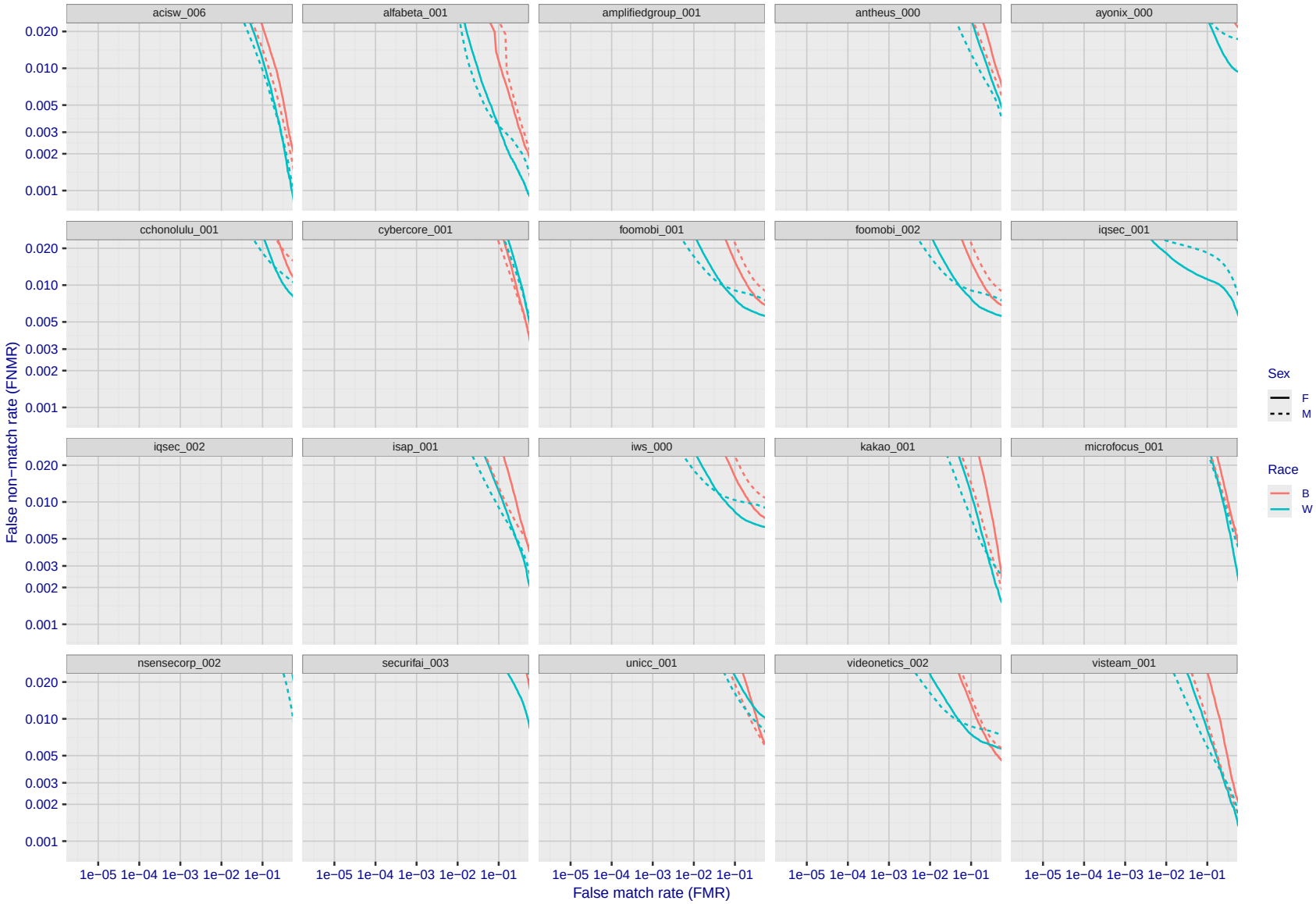

Figure 449: For the mugshot images, error tradeoff characteristics for white females, black females, black males and white males. The Z-shaped grey lines correspond to fixed thresholds, showing both *FNMR and FMR vary at one T value. Note: Many of the plots will naively be read as saying women gives worse error rates than men because the solid traces lie above the dotted ones. However, this is misleading and incomplete: The grey lines show the traces reveal horizontal shifts. Thus for the cogent-003 algorithm FNMR for men is* higher *than for women* at a fixed threshold *but, at the same time, FMR is higher for women - see Figure 608. As access control systems almost always operate at a fixed threshold, the naive interpretation is incorrect.*

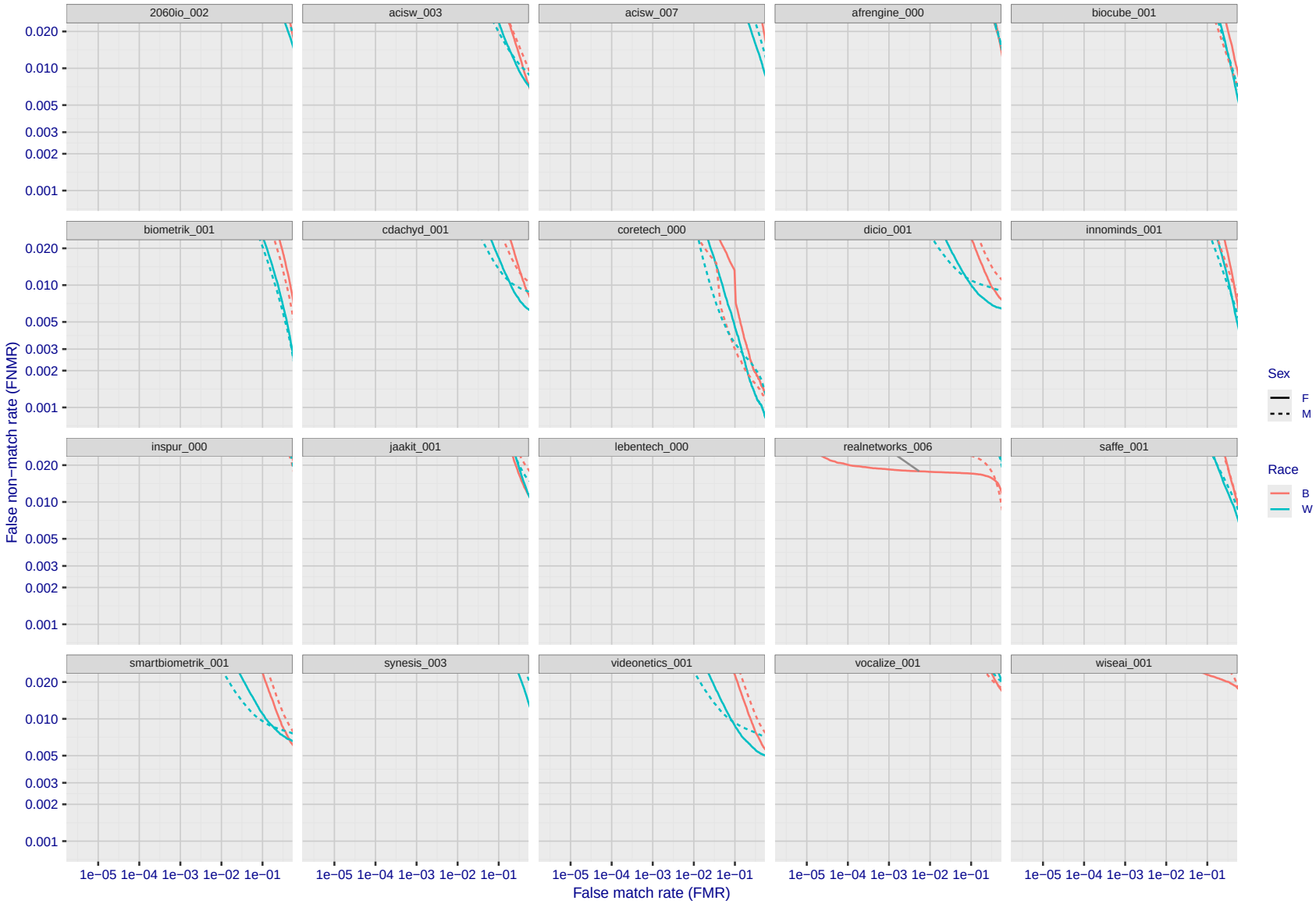

Figure 450: For the mugshot images, error tradeoff characteristics for white females, black females, black males and white males. The Z-shaped grey lines correspond to fixed thresholds, showing both *FNMR and FMR vary at one T value. Note: Many of the plots will naively be read as saying women gives worse error rates than men because the solid traces lie above the dotted ones. However, this is misleading and incomplete: The grey lines show the traces reveal horizontal shifts. Thus for the cogent-003 algorithm FNMR for men is* higher *than for women* at a fixed threshold *but, at the same time, FMR is higher for women - see Figure 608. As access control systems almost always operate at a fixed threshold, the naive interpretation is incorrect.*

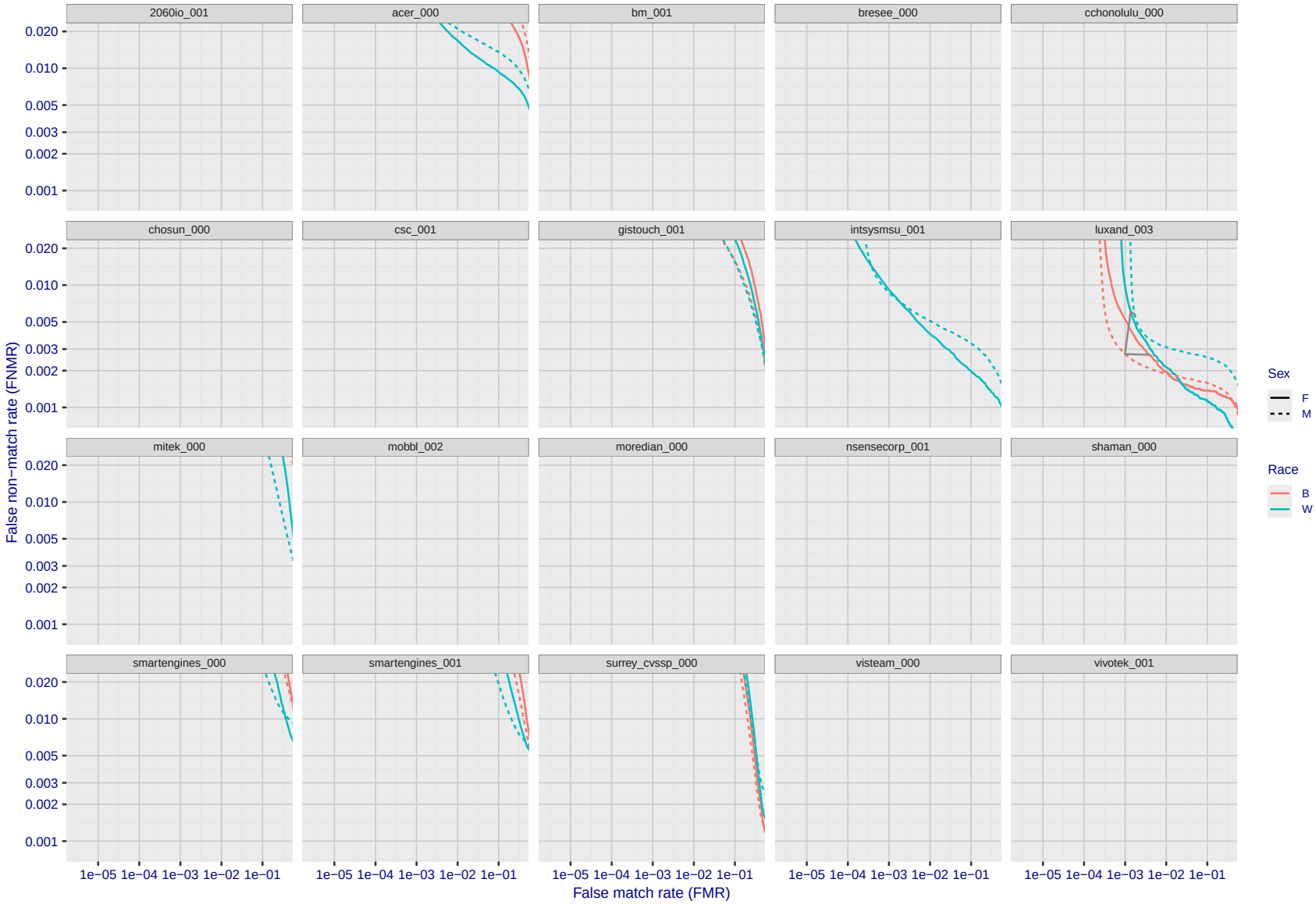

Figure 451: For the mugshot images, error tradeoff characteristics for white females, black females, black males and white males. The Z-shaped grey lines correspond to fixed thresholds, showing both *FNMR and FMR vary at one T value. Note: Many of the plots will naively be read as saying women gives worse error rates than men because the solid traces lie above the dotted ones. However, this is misleading and incomplete: The grey lines show the traces reveal horizontal shifts. Thus for the cogent-003 algorithm FNMR for men is* higher *than for women* at a fixed threshold *but, at the same time, FMR is higher for women - see Figure 608. As access control systems almost always operate at a fixed threshold, the naive interpretation is incorrect.*

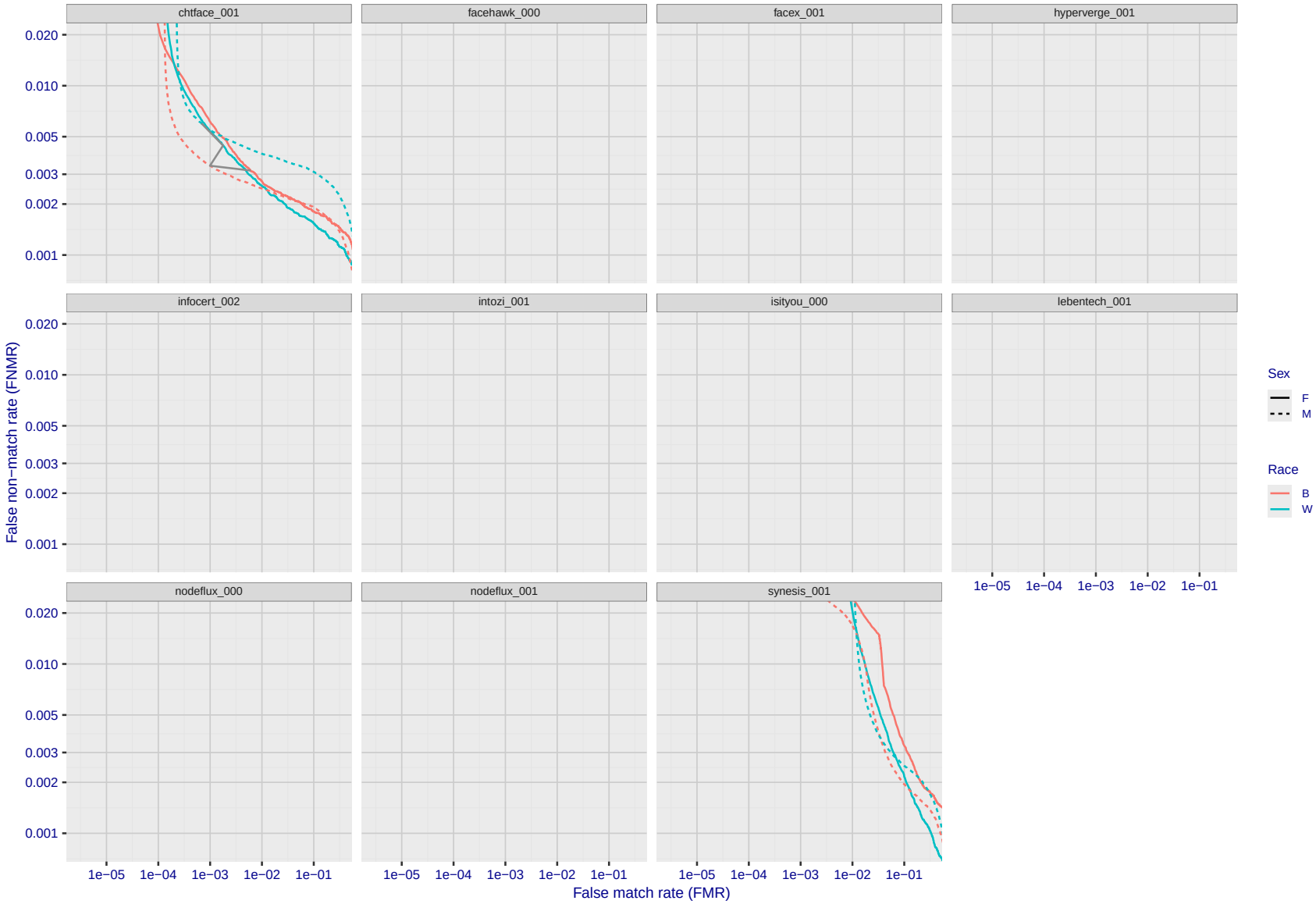

Figure 452: For the mugshot images, error tradeoff characteristics for white females, black females, black males and white males. The Z-shaped grey lines correspond to fixed thresholds, showing both *FNMR and FMR vary at one T value. Note: Many of the plots will naively be read as saying women gives worse error rates than men because the solid traces lie above the dotted ones. However, this is misleading and incomplete: The grey lines show the traces reveal horizontal shifts. Thus for the cogent-003 algorithm FNMR for men is* higher *than for women* at a fixed threshold *but, at the same time, FMR is higher for women - see Figure 608. As access control systems almost always operate at a fixed threshold, the naive interpretation is incorrect.*

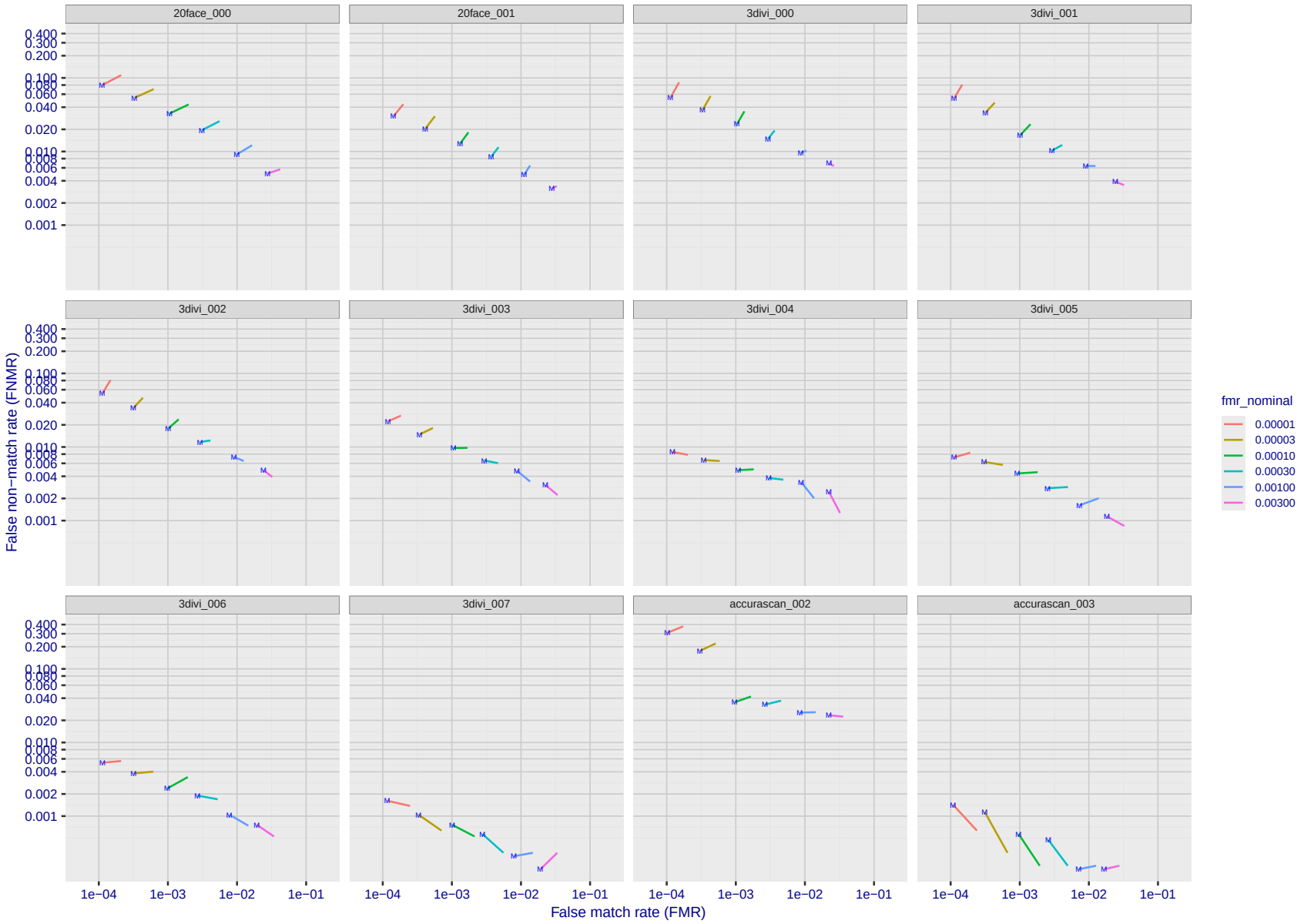

Figure 453: For the visa images, FNMR and FMR at six operating points along the DET characteristic. At each point a line is drawn between (FMR,FNMR)$_{\text{MALE}}$ and (FMR,FNMR)$_{\text{FEMALE}}$ showing how which sex has lower FMR and/or FNMR. The "M" label denotes male, the other end of the line corresponds to female. The six operating thresholds are selected to give the nominal false match rates given in the legend, and are computed over all impostor pairs regardless of age, sex, and place of birth. The plotted FMR values are broadly an order of magnitude larger than the nominal rates because FMR is computed over demographically-matched impostor pairs i.e individuals of the same sex, from the same geographic region (see section 3.6.1), and the same age group (see section 3.6.2).

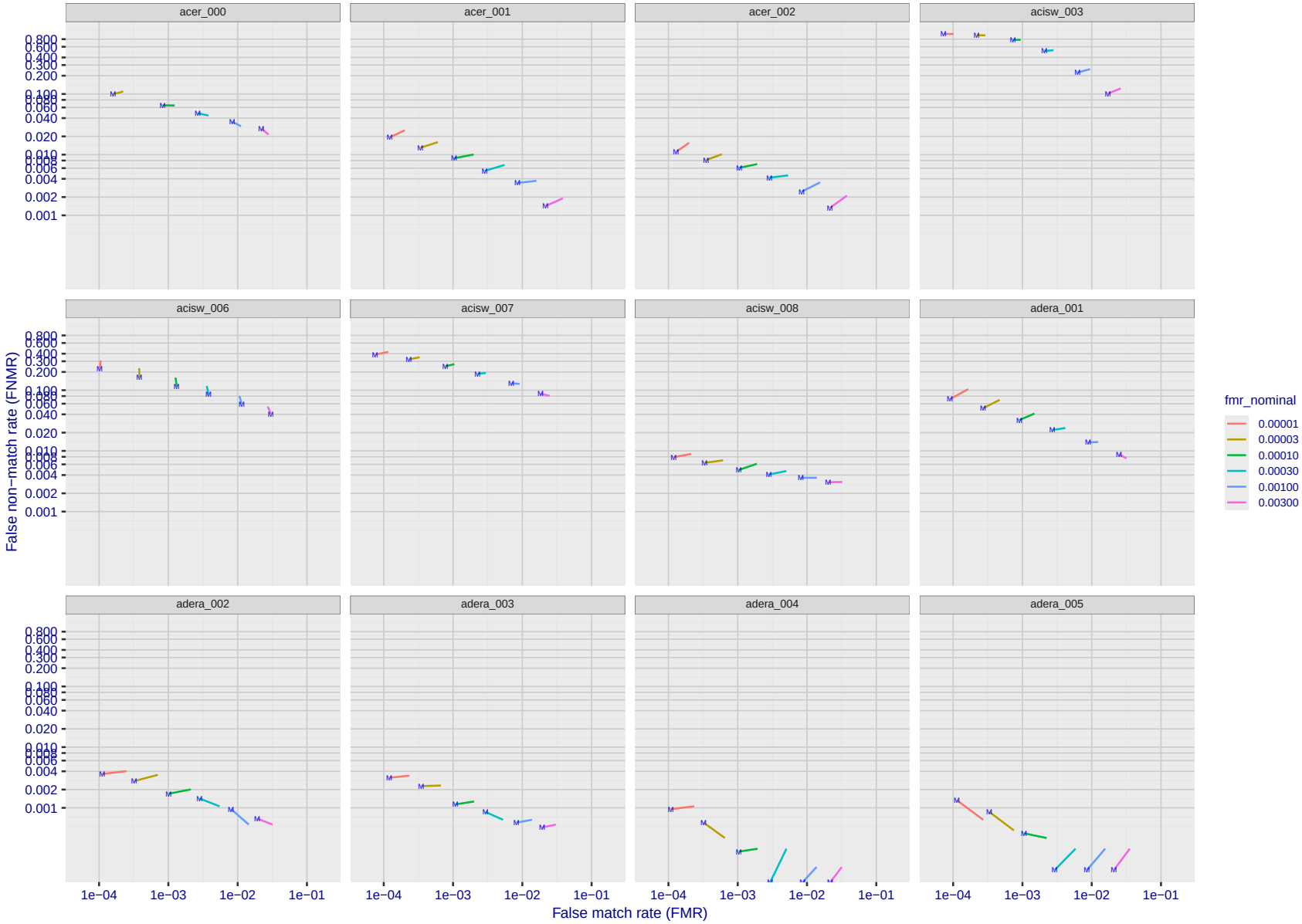

Figure 454: For the visa images, FNMR and FMR at six operating points along the DET characteristic. At each point a line is drawn between (FMR,FNMR)$_{\text{MALE}}$ and (FMR,FNMR)$_{\text{FEMALE}}$ showing how which sex has lower FMR and/or FNMR. The "M" label denotes male, the other end of the line corresponds to female. The six operating thresholds are selected to give the nominal false match rates given in the legend, and are computed over all impostor pairs regardless of age, sex, and place of birth. The plotted FMR values are broadly an order of magnitude larger than the nominal rates because FMR is computed over demographically-matched impostor pairs i.e individuals of the same sex, from the same geographic region (see section 3.6.1), and the same age group (see section 3.6.2).

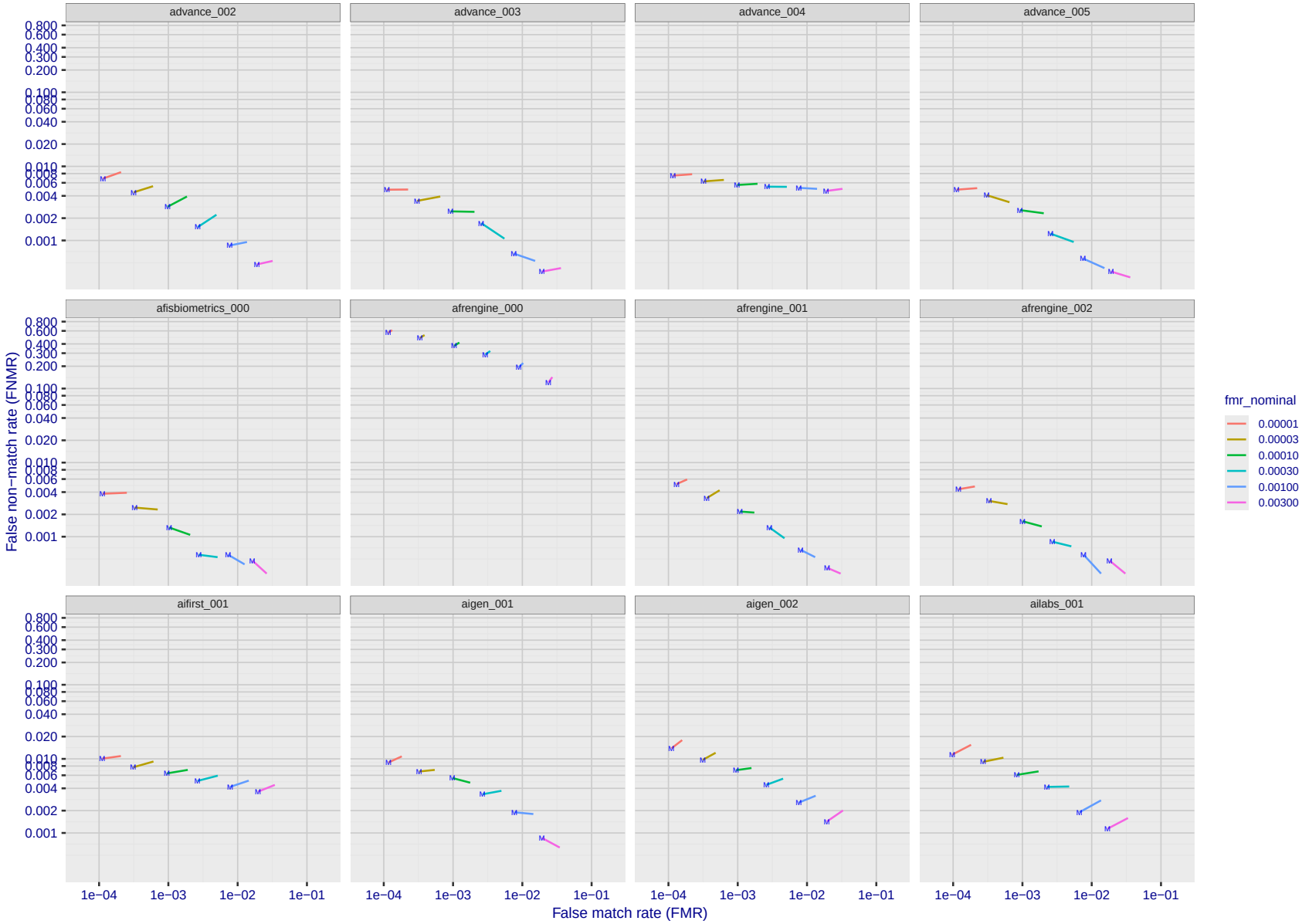

Figure 455: For the visa images, FNMR and FMR at six operating points along the DET characteristic. At each point a line is drawn between (FMR,FNMR)$_{\text{MALE}}$ and (FMR,FNMR)$_{\text{FEMALE}}$ showing how which sex has lower FMR and/or FNMR. The "M" label denotes male, the other end of the line corresponds to female. The six operating thresholds are selected to give the nominal false match rates given in the legend, and are computed over all impostor pairs regardless of age, sex, and place of birth. The plotted FMR values are broadly an order of magnitude larger than the nominal rates because FMR is computed over demographically-matched impostor pairs i.e individuals of the same sex, from the same geographic region (see section 3.6.1), and the same age group (see section 3.6.2).

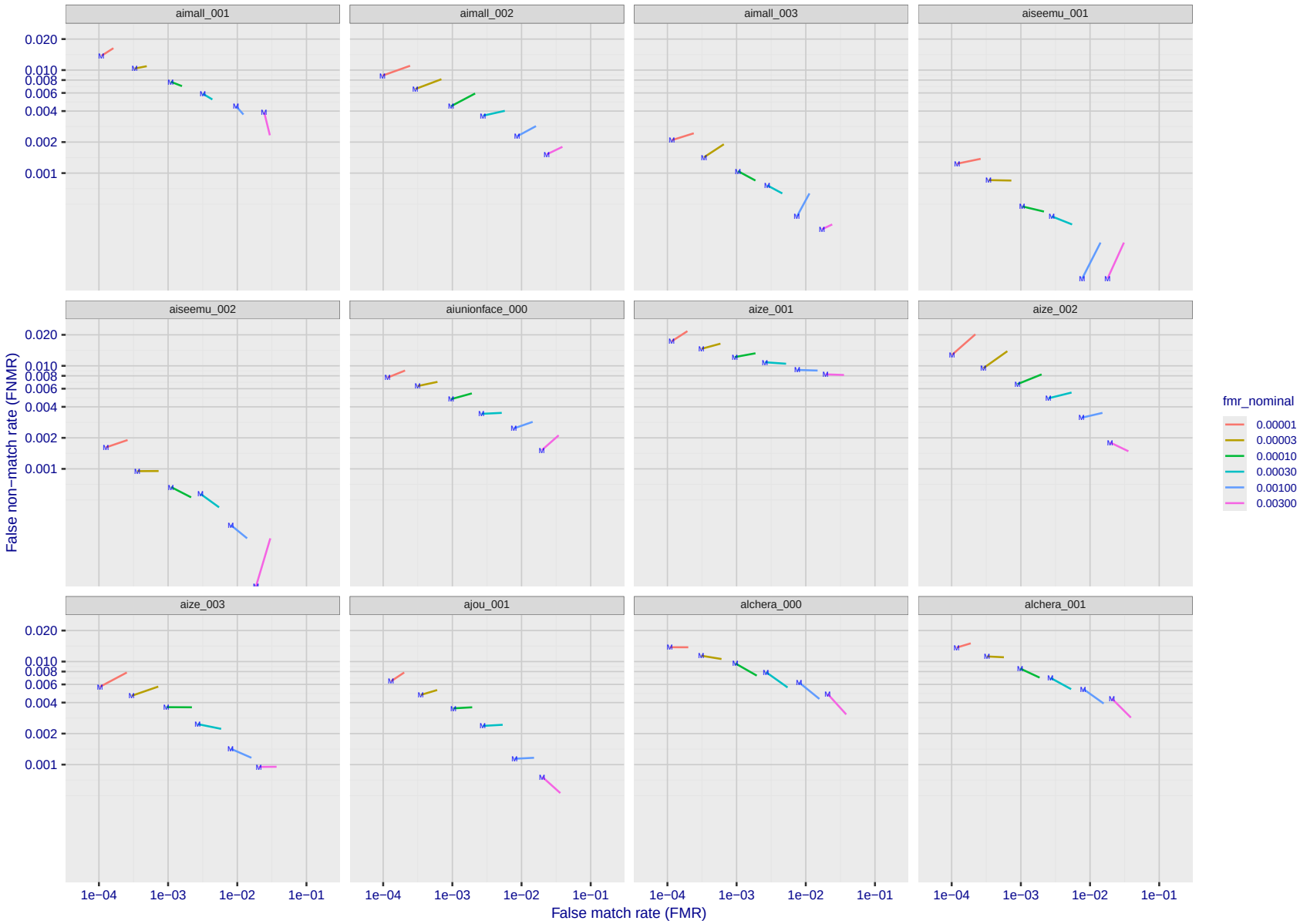

Figure 456: For the visa images, FNMR and FMR at six operating points along the DET characteristic. At each point a line is drawn between (FMR,FNMR)$_{\text{MALE}}$ and (FMR,FNMR)$_{\text{FEMALE}}$ showing how which sex has lower FMR and/or FNMR. The "M" label denotes male, the other end of the line corresponds to female. The six operating thresholds are selected to give the nominal false match rates given in the legend, and are computed over all impostor pairs regardless of age, sex, and place of birth. The plotted FMR values are broadly an order of magnitude larger than the nominal rates because FMR is computed over demographically-matched impostor pairs i.e individuals of the same sex, from the same geographic region (see section 3.6.1), and the same age group (see section 3.6.2).

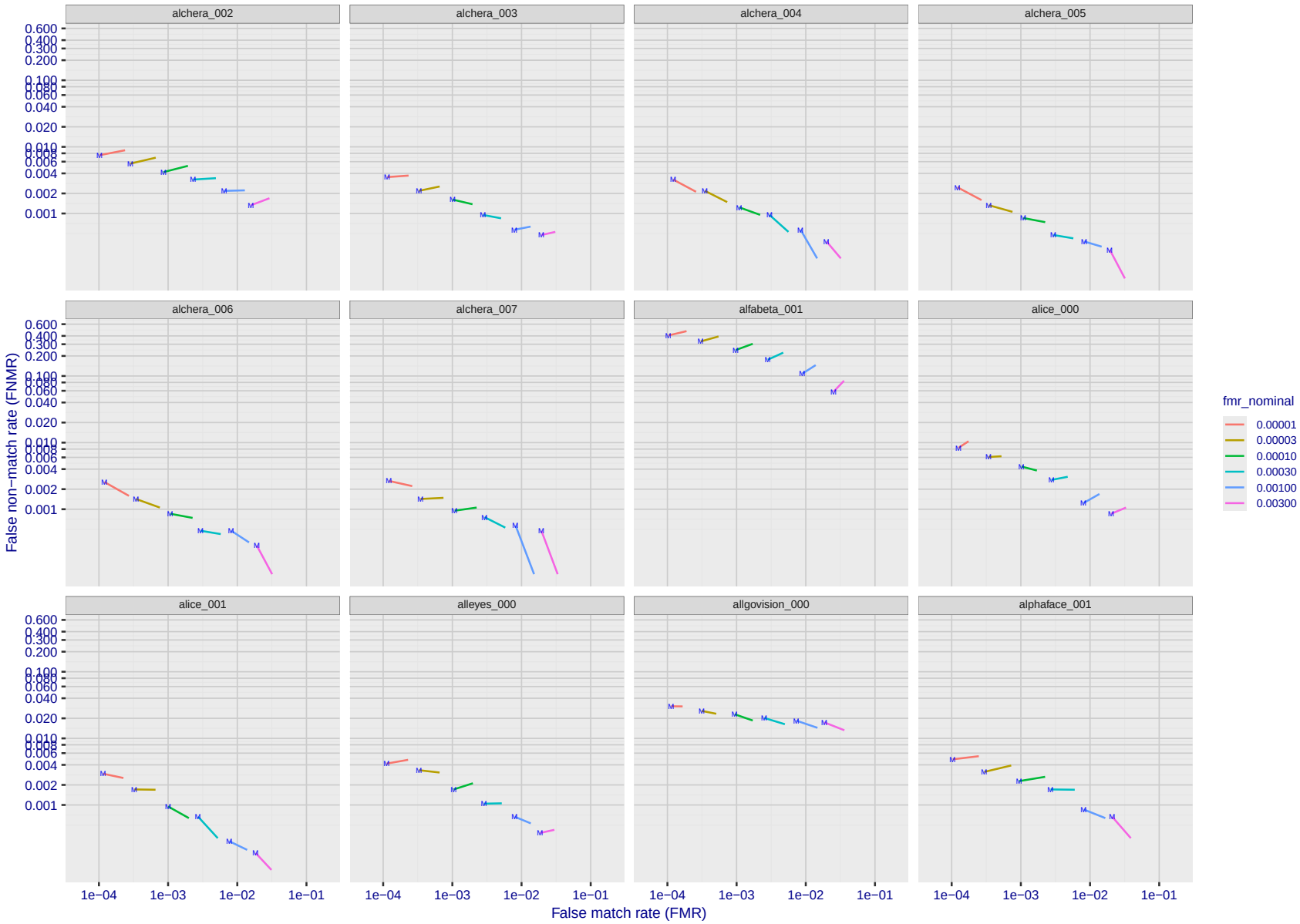

Figure 457: For the visa images, FNMR and FMR at six operating points along the DET characteristic. At each point a line is drawn between (FMR,FNMR)$_{\text{MALE}}$ and (FMR,FNMR)$_{\text{FEMALE}}$ showing how which sex has lower FMR and/or FNMR. The "M" label denotes male, the other end of the line corresponds to female. The six operating thresholds are selected to give the nominal false match rates given in the legend, and are computed over all impostor pairs regardless of age, sex, and place of birth. The plotted FMR values are broadly an order of magnitude larger than the nominal rates because FMR is computed over demographically-matched impostor pairs i.e individuals of the same sex, from the same geographic region (see section 3.6.1), and the same age group (see section 3.6.2).

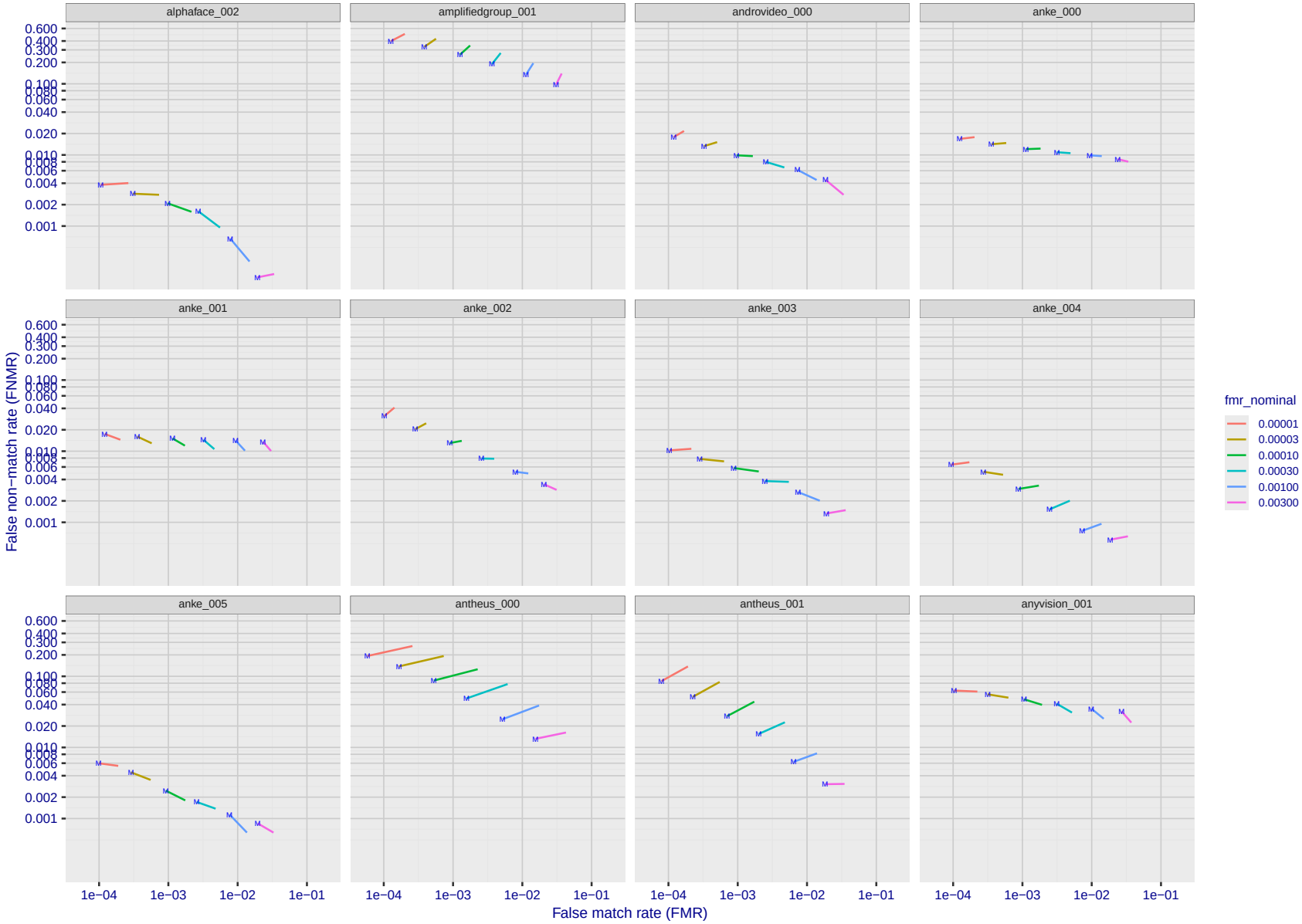

Figure 458: For the visa images, FNMR and FMR at six operating points along the DET characteristic. At each point a line is drawn between (FMR,FNMR)$_{\text{MALE}}$ and (FMR,FNMR)$_{\text{FEMALE}}$ showing how which sex has lower FMR and/or FNMR. The "M" label denotes male, the other end of the line corresponds to female. The six operating thresholds are selected to give the nominal false match rates given in the legend, and are computed over all impostor pairs regardless of age, sex, and place of birth. The plotted FMR values are broadly an order of magnitude larger than the nominal rates because FMR is computed over demographically-matched impostor pairs i.e individuals of the same sex, from the same geographic region (see section 3.6.1), and the same age group (see section 3.6.2).

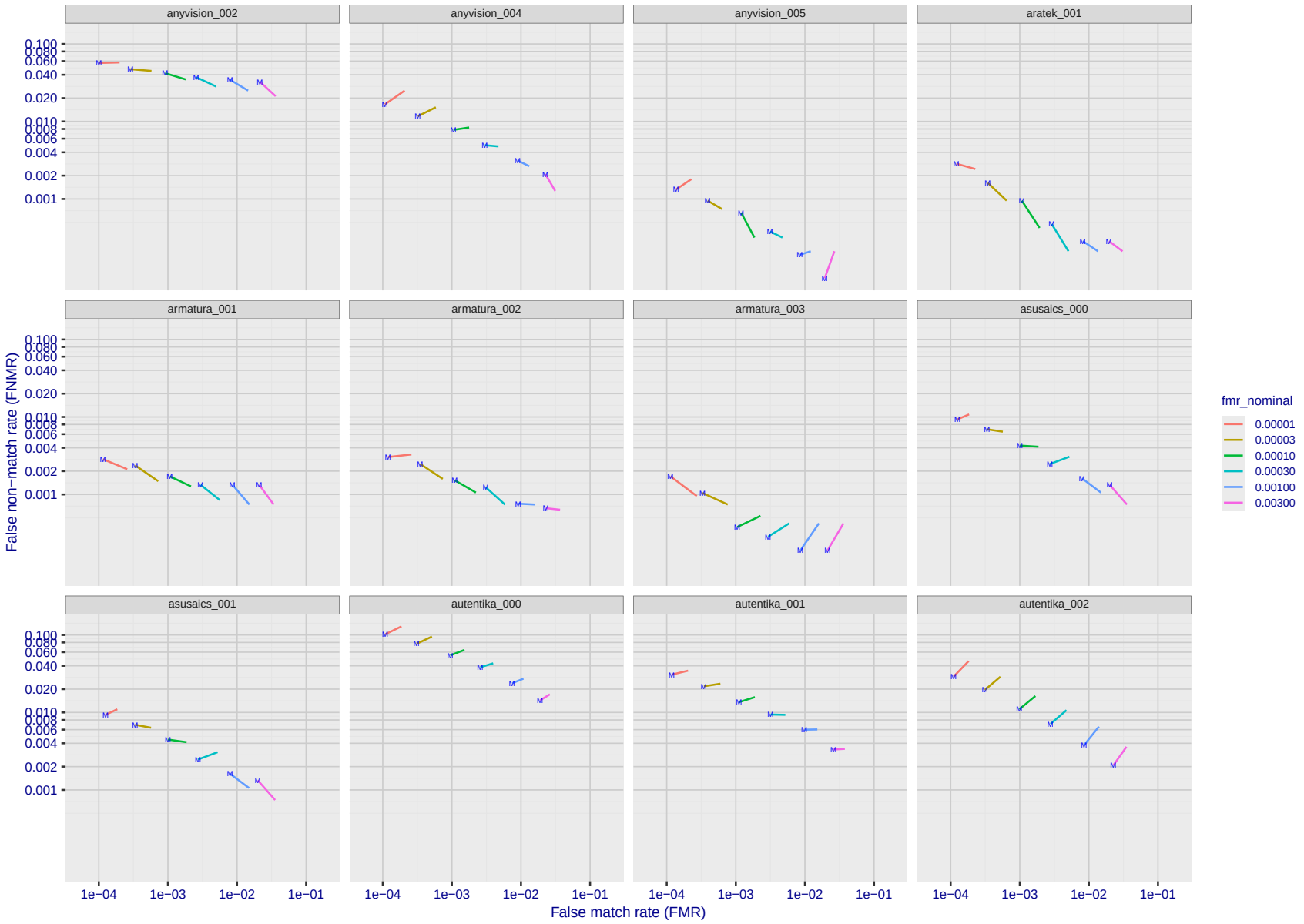

Figure 459: For the visa images, FNMR and FMR at six operating points along the DET characteristic. At each point a line is drawn between (FMR,FNMR)$_{\text{MALE}}$ and (FMR,FNMR)$_{\text{FEMALE}}$ showing how which sex has lower FMR and/or FNMR. The "M" label denotes male, the other end of the line corresponds to female. The six operating thresholds are selected to give the nominal false match rates given in the legend, and are computed over all impostor pairs regardless of age, sex, and place of birth. The plotted FMR values are broadly an order of magnitude larger than the nominal rates because FMR is computed over demographically-matched impostor pairs i.e individuals of the same sex, from the same geographic region (see section 3.6.1), and the same age group (see section 3.6.2).

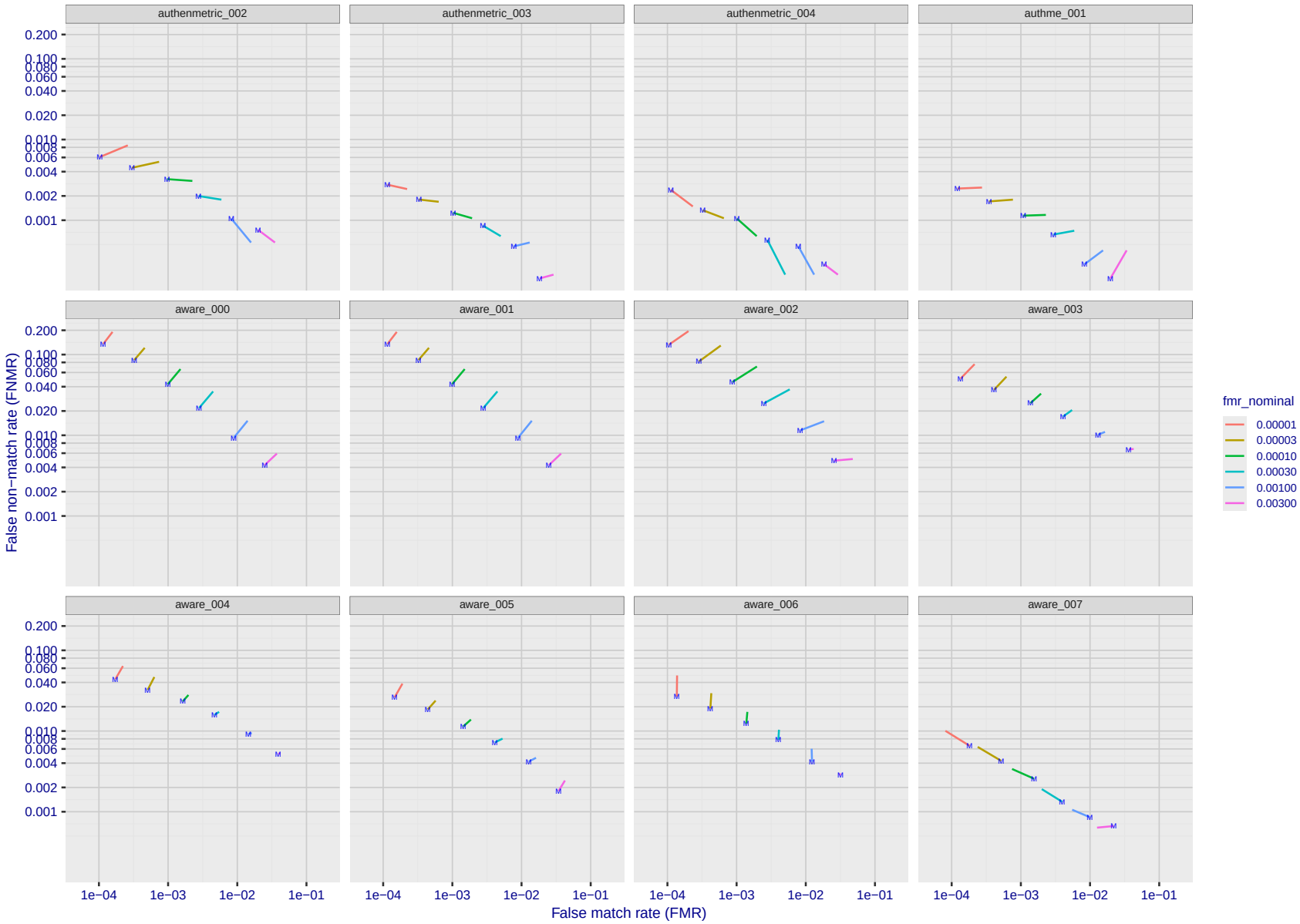

Figure 460: For the visa images, FNMR and FMR at six operating points along the DET characteristic. At each point a line is drawn between (FMR,FNMR)$_{\text{MALE}}$ and (FMR,FNMR)$_{\text{FEMALE}}$ showing how which sex has lower FMR and/or FNMR. The "M" label denotes male, the other end of the line corresponds to female. The six operating thresholds are selected to give the nominal false match rates given in the legend, and are computed over all impostor pairs regardless of age, sex, and place of birth. The plotted FMR values are broadly an order of magnitude larger than the nominal rates because FMR is computed over demographically-matched impostor pairs i.e individuals of the same sex, from the same geographic region (see section 3.6.1), and the same age group (see section 3.6.2).

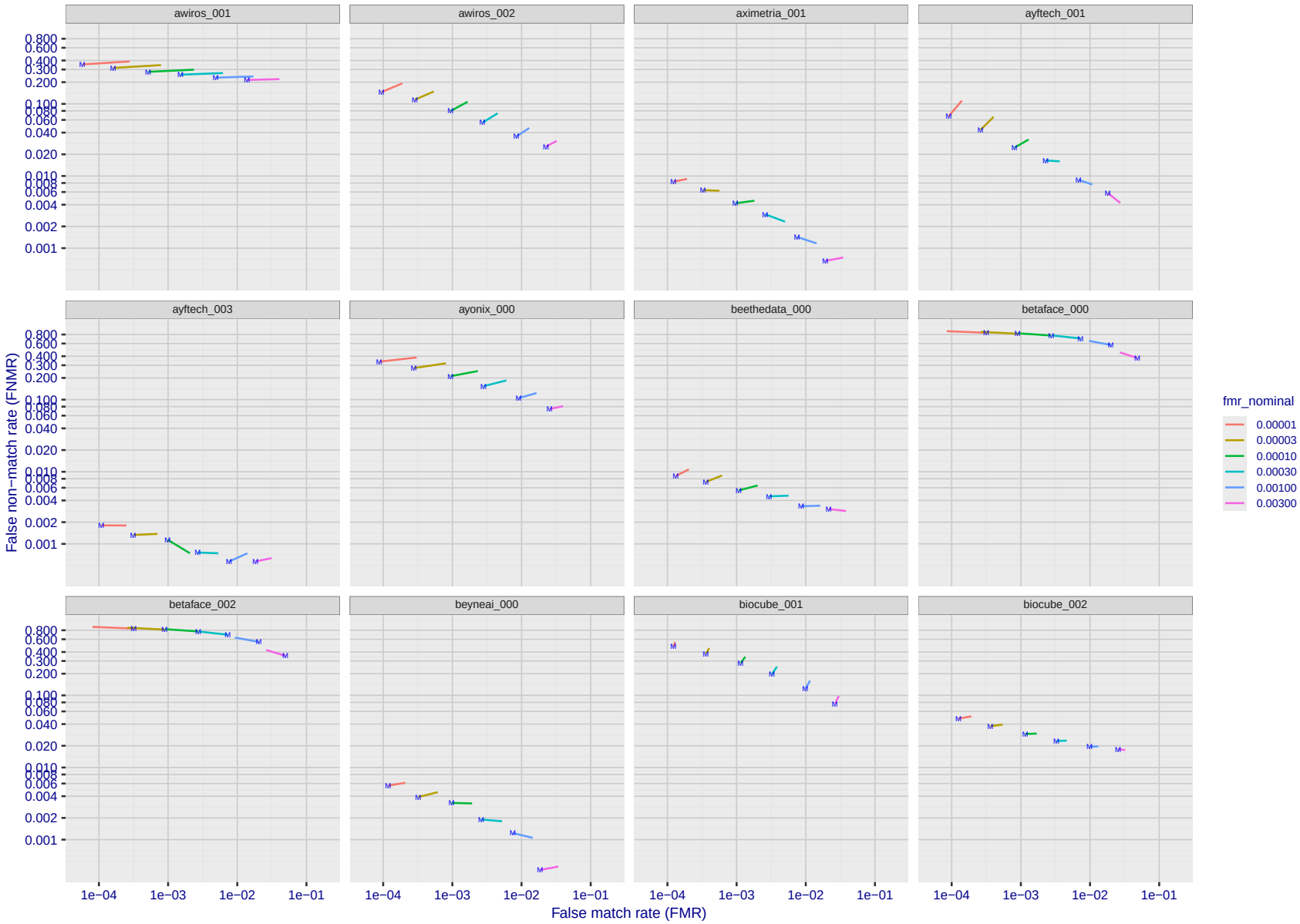

Figure 461: For the visa images, FNMR and FMR at six operating points along the DET characteristic. At each point a line is drawn between (FMR,FNMR)$_{\text{MALE}}$ and (FMR,FNMR)$_{\text{FEMALE}}$ showing how which sex has lower FMR and/or FNMR. The "M" label denotes male, the other end of the line corresponds to female. The six operating thresholds are selected to give the nominal false match rates given in the legend, and are computed over all impostor pairs regardless of age, sex, and place of birth. The plotted FMR values are broadly an order of magnitude larger than the nominal rates because FMR is computed over demographically-matched impostor pairs i.e individuals of the same sex, from the same geographic region (see section 3.6.1), and the same age group (see section 3.6.2).

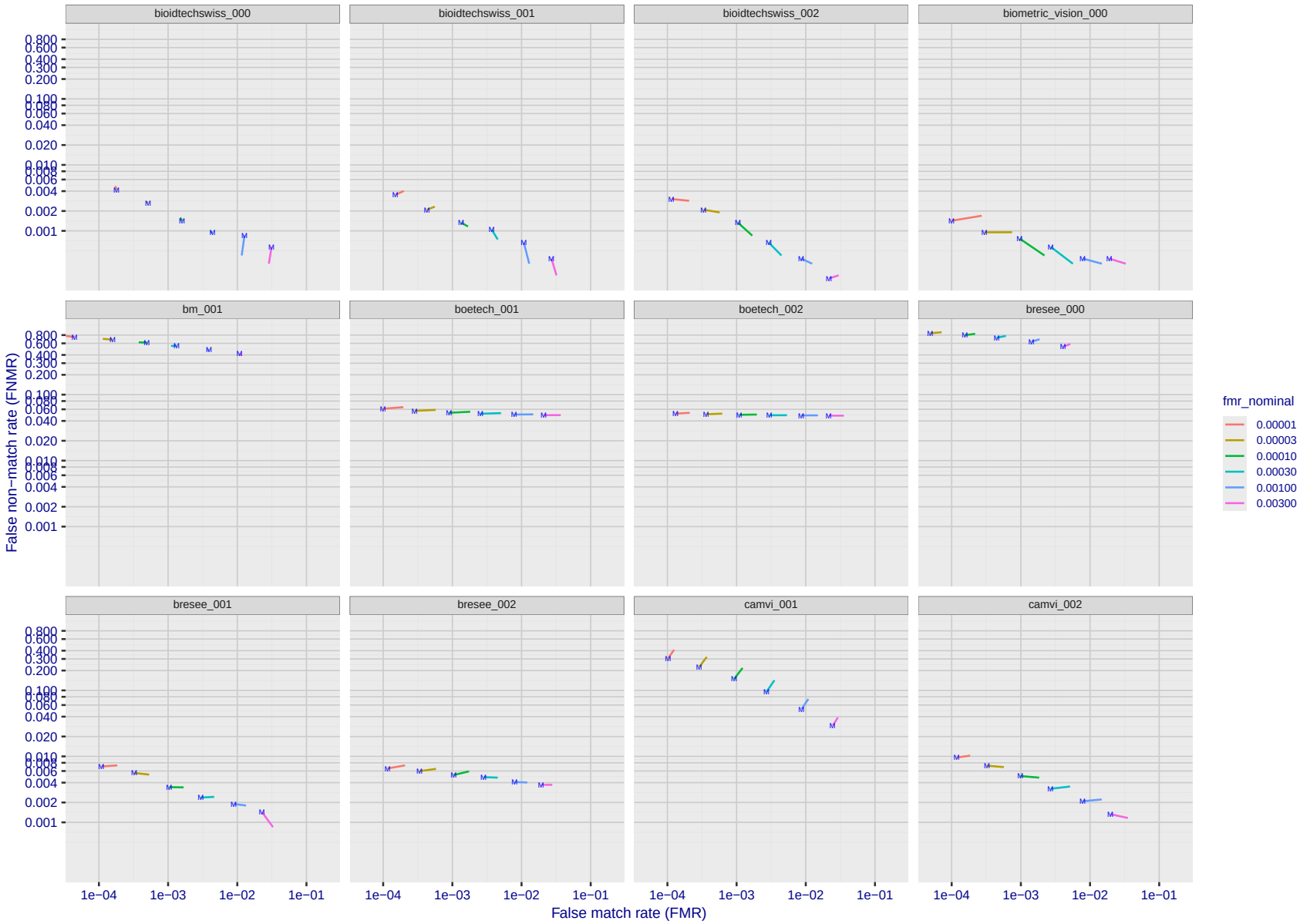

Figure 462: For the visa images, FNMR and FMR at six operating points along the DET characteristic. At each point a line is drawn between (FMR,FNMR)$_{\text{MALE}}$ and (FMR,FNMR)$_{\text{FEMALE}}$ showing how which sex has lower FMR and/or FNMR. The "M" label denotes male, the other end of the line corresponds to female. The six operating thresholds are selected to give the nominal false match rates given in the legend, and are computed over all impostor pairs regardless of age, sex, and place of birth. The plotted FMR values are broadly an order of magnitude larger than the nominal rates because FMR is computed over demographically-matched impostor pairs i.e individuals of the same sex, from the same geographic region (see section 3.6.1), and the same age group (see section 3.6.2).

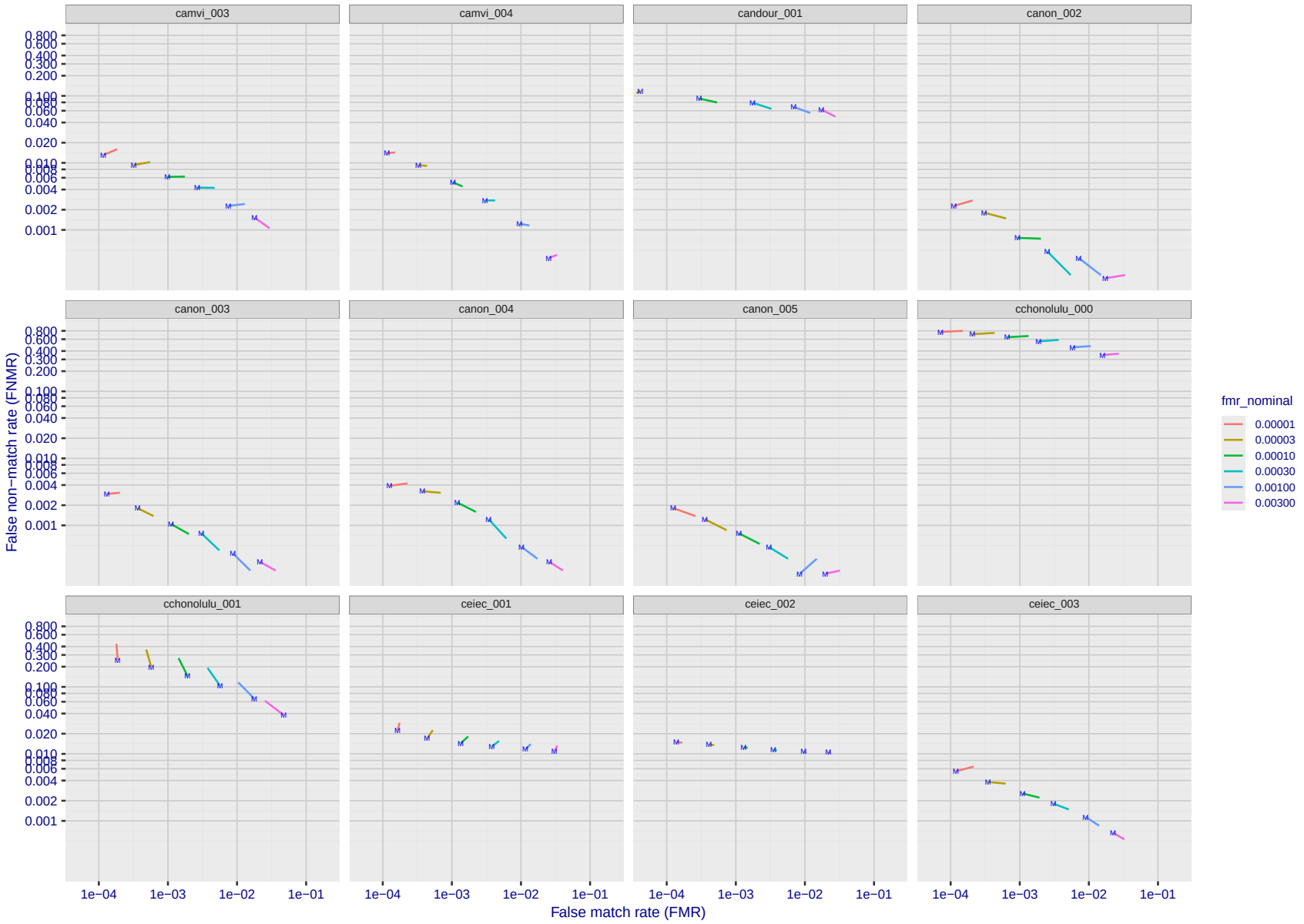

Figure 463: For the visa images, FNMR and FMR at six operating points along the DET characteristic. At each point a line is drawn between (FMR,FNMR)$_{\text{MALE}}$ and (FMR,FNMR)$_{\text{FEMALE}}$ showing how which sex has lower FMR and/or FNMR. The "M" label denotes male, the other end of the line corresponds to female. The six operating thresholds are selected to give the nominal false match rates given in the legend, and are computed over all impostor pairs regardless of age, sex, and place of birth. The plotted FMR values are broadly an order of magnitude larger than the nominal rates because FMR is computed over demographically-matched impostor pairs i.e individuals of the same sex, from the same geographic region (see section 3.6.1), and the same age group (see section 3.6.2).

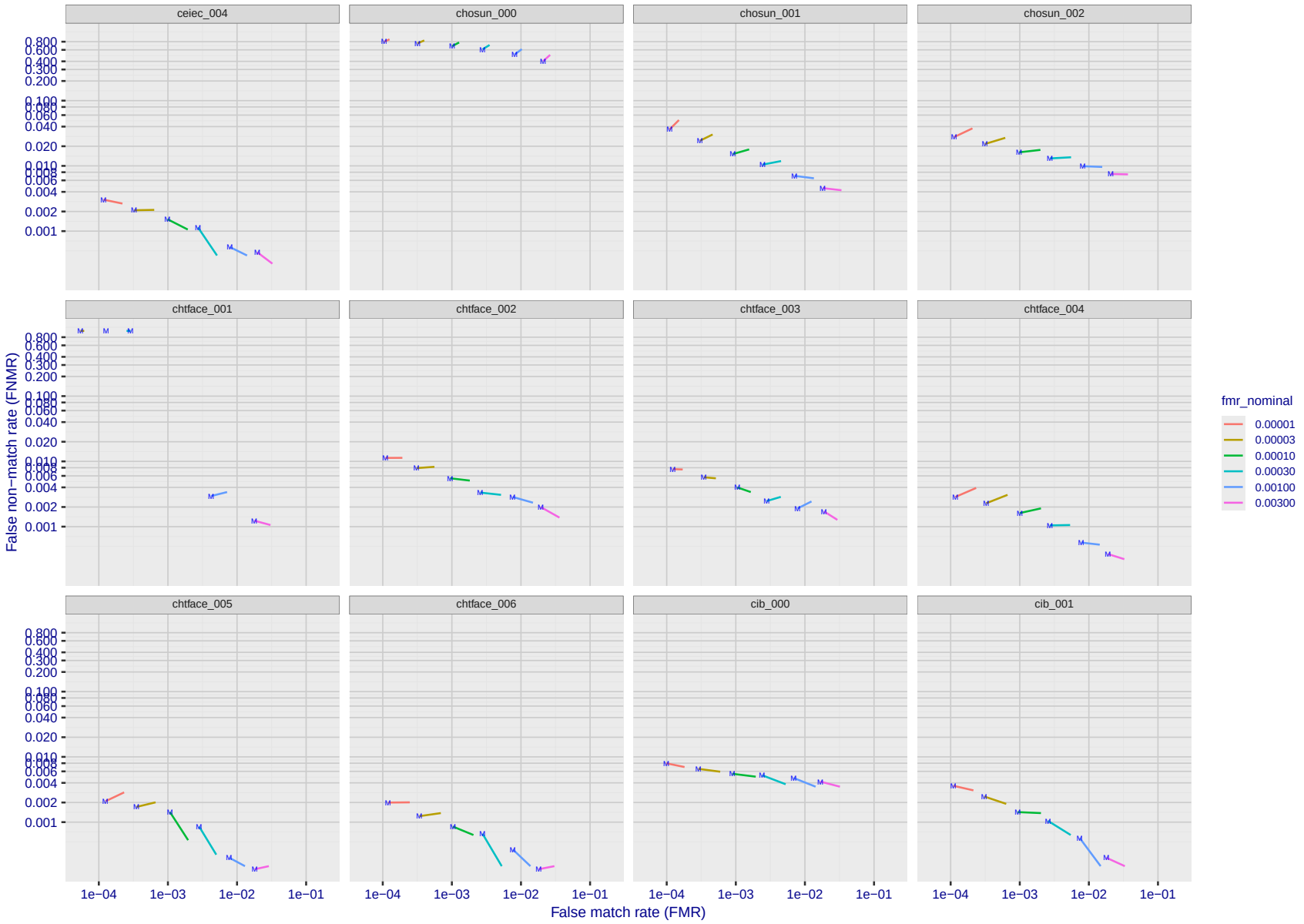

Figure 464: For the visa images, FNMR and FMR at six operating points along the DET characteristic. At each point a line is drawn between (FMR,FNMR)$_{\text{MALE}}$ and (FMR,FNMR)$_{\text{FEMALE}}$ showing how which sex has lower FMR and/or FNMR. The "M" label denotes male, the other end of the line corresponds to female. The six operating thresholds are selected to give the nominal false match rates given in the legend, and are computed over all impostor pairs regardless of age, sex, and place of birth. The plotted FMR values are broadly an order of magnitude larger than the nominal rates because FMR is computed over demographically-matched impostor pairs i.e individuals of the same sex, from the same geographic region (see section 3.6.1), and the same age group (see section 3.6.2).

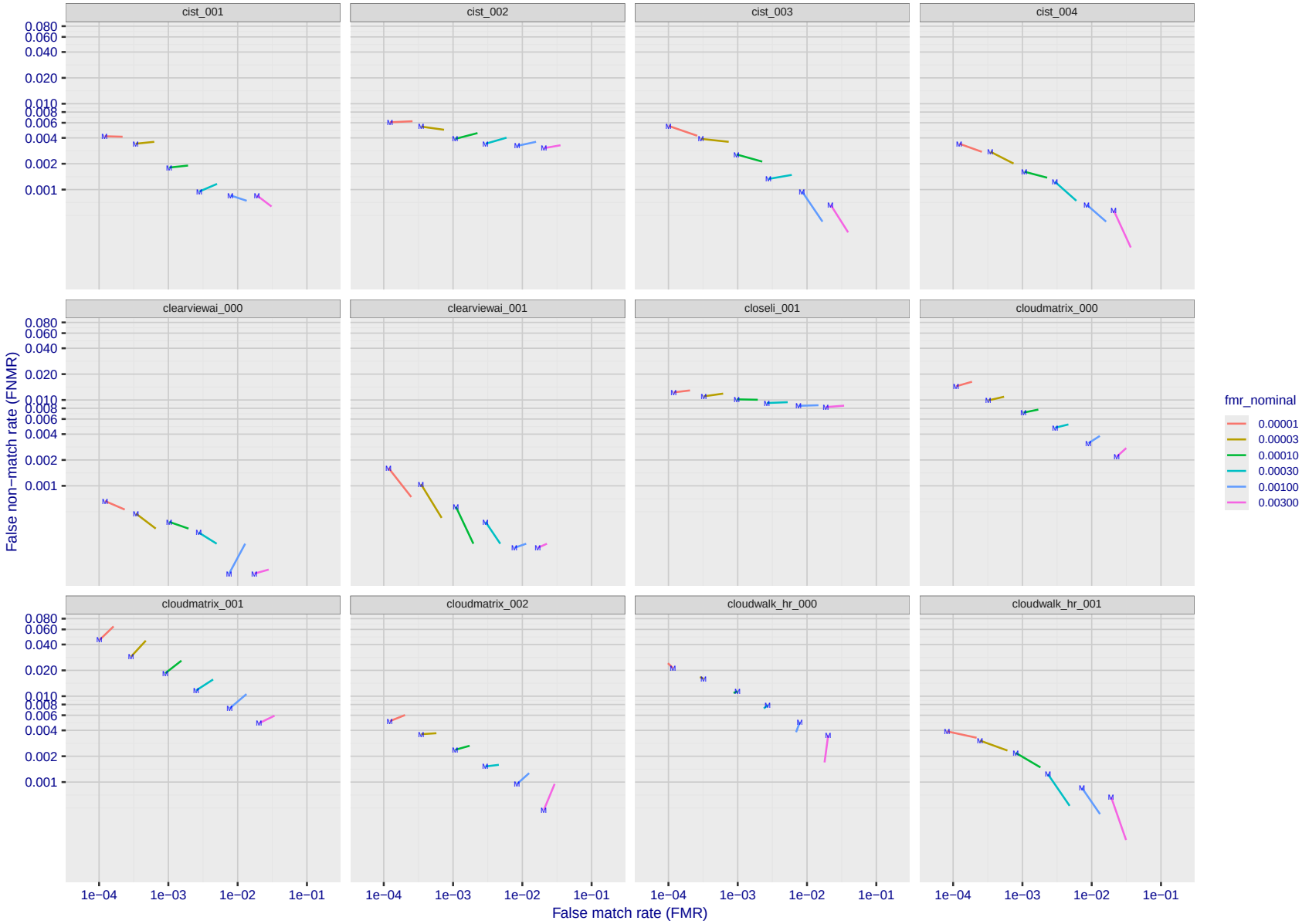

Figure 465: For the visa images, FNMR and FMR at six operating points along the DET characteristic. At each point a line is drawn between (FMR,FNMR)$_{\text{MALE}}$ and (FMR,FNMR)$_{\text{FEMALE}}$ showing how which sex has lower FMR and/or FNMR. The "M" label denotes male, the other end of the line corresponds to female. The six operating thresholds are selected to give the nominal false match rates given in the legend, and are computed over all impostor pairs regardless of age, sex, and place of birth. The plotted FMR values are broadly an order of magnitude larger than the nominal rates because FMR is computed over demographically-matched impostor pairs i.e individuals of the same sex, from the same geographic region (see section 3.6.1), and the same age group (see section 3.6.2).

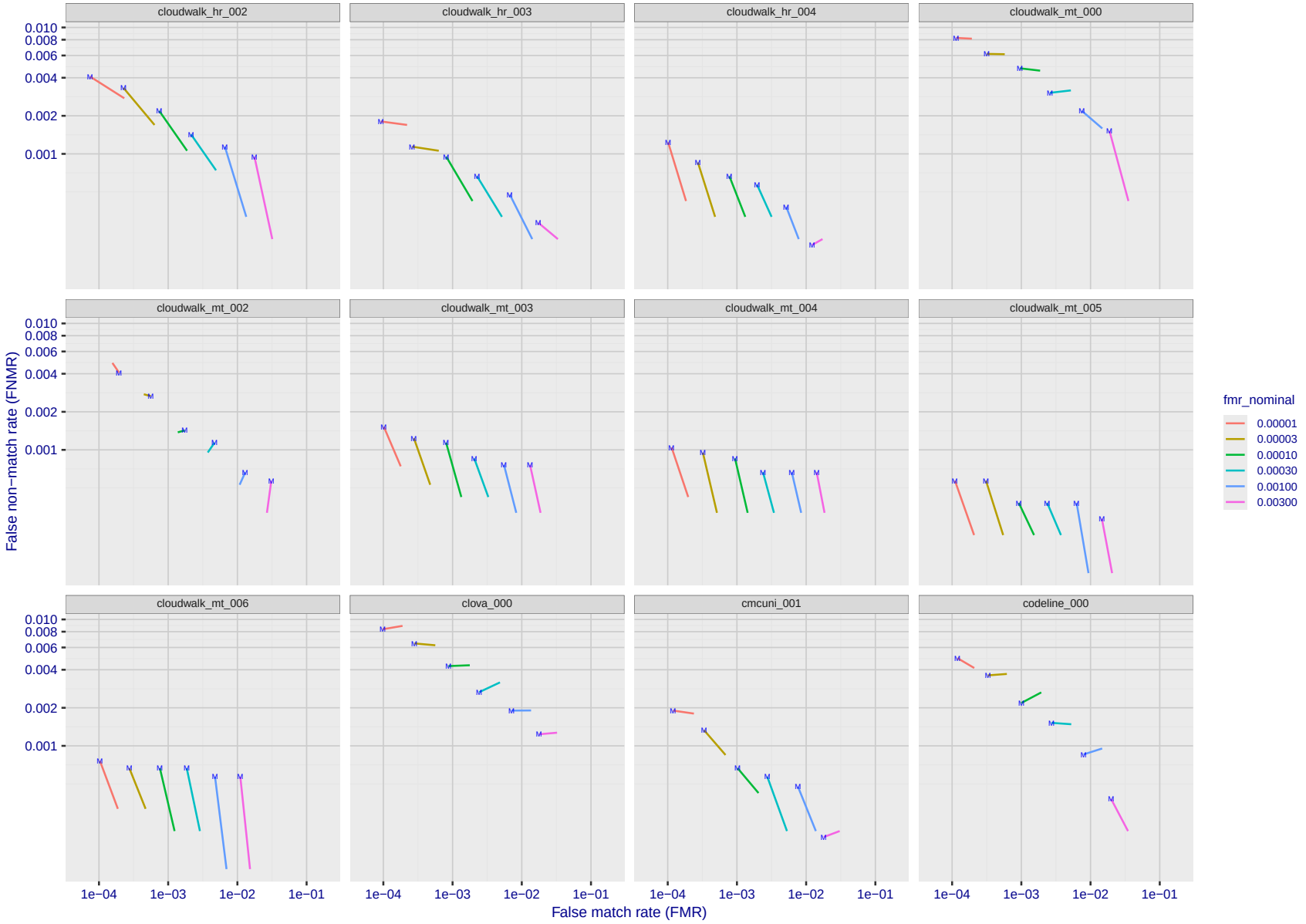

Figure 466: For the visa images, FNMR and FMR at six operating points along the DET characteristic. At each point a line is drawn between (FMR,FNMR)$_{\text{MALE}}$ and (FMR,FNMR)$_{\text{FEMALE}}$ showing how which sex has lower FMR and/or FNMR. The "M" label denotes male, the other end of the line corresponds to female. The six operating thresholds are selected to give the nominal false match rates given in the legend, and are computed over all impostor pairs regardless of age, sex, and place of birth. The plotted FMR values are broadly an order of magnitude larger than the nominal rates because FMR is computed over demographically-matched impostor pairs i.e individuals of the same sex, from the same geographic region (see section 3.6.1), and the same age group (see section 3.6.2).

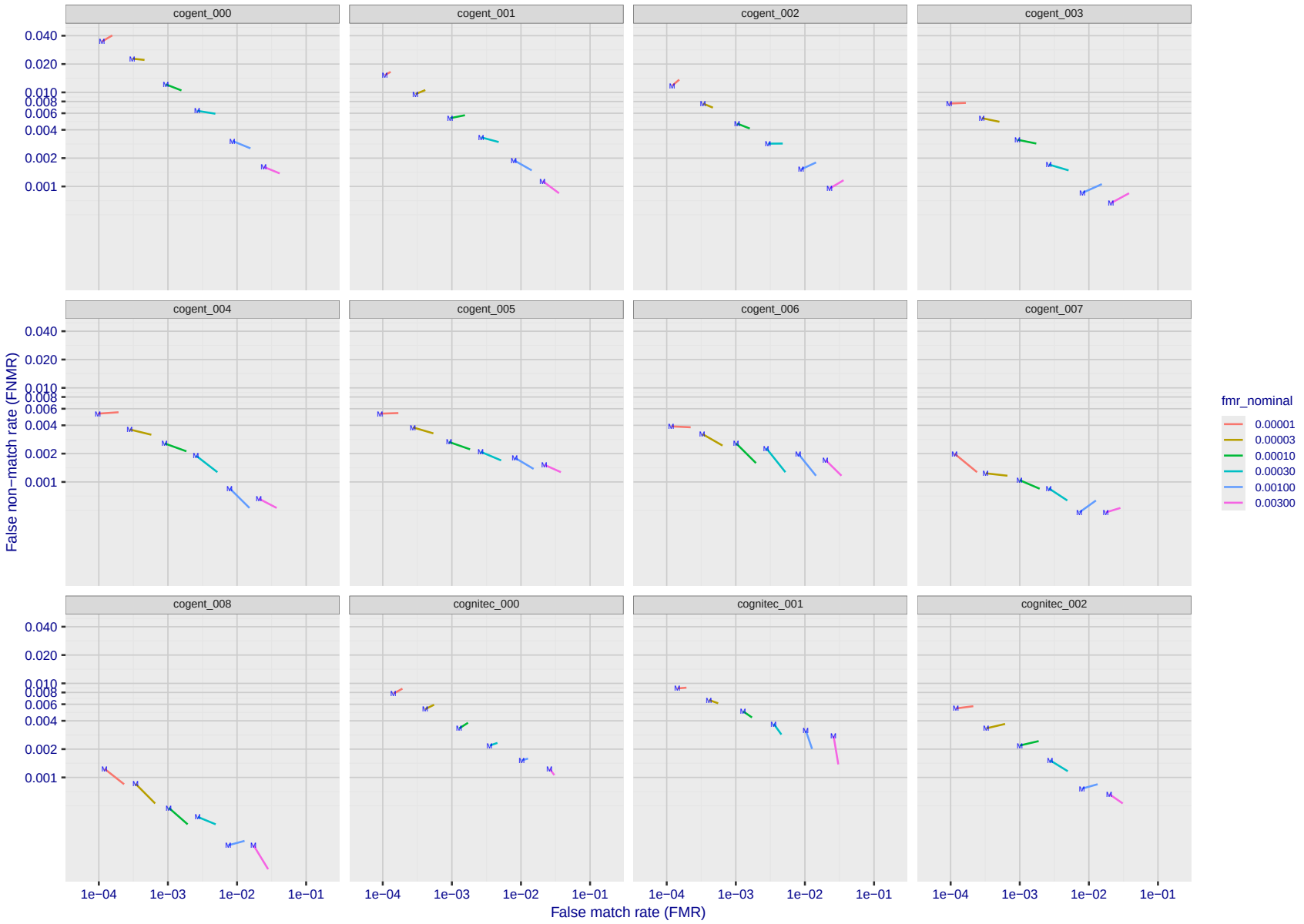

Figure 467: For the visa images, FNMR and FMR at six operating points along the DET characteristic. At each point a line is drawn between (FMR,FNMR)$_{\text{MALE}}$ and (FMR,FNMR)$_{\text{FEMALE}}$ showing how which sex has lower FMR and/or FNMR. The "M" label denotes male, the other end of the line corresponds to female. The six operating thresholds are selected to give the nominal false match rates given in the legend, and are computed over all impostor pairs regardless of age, sex, and place of birth. The plotted FMR values are broadly an order of magnitude larger than the nominal rates because FMR is computed over demographically-matched impostor pairs i.e individuals of the same sex, from the same geographic region (see section 3.6.1), and the same age group (see section 3.6.2).

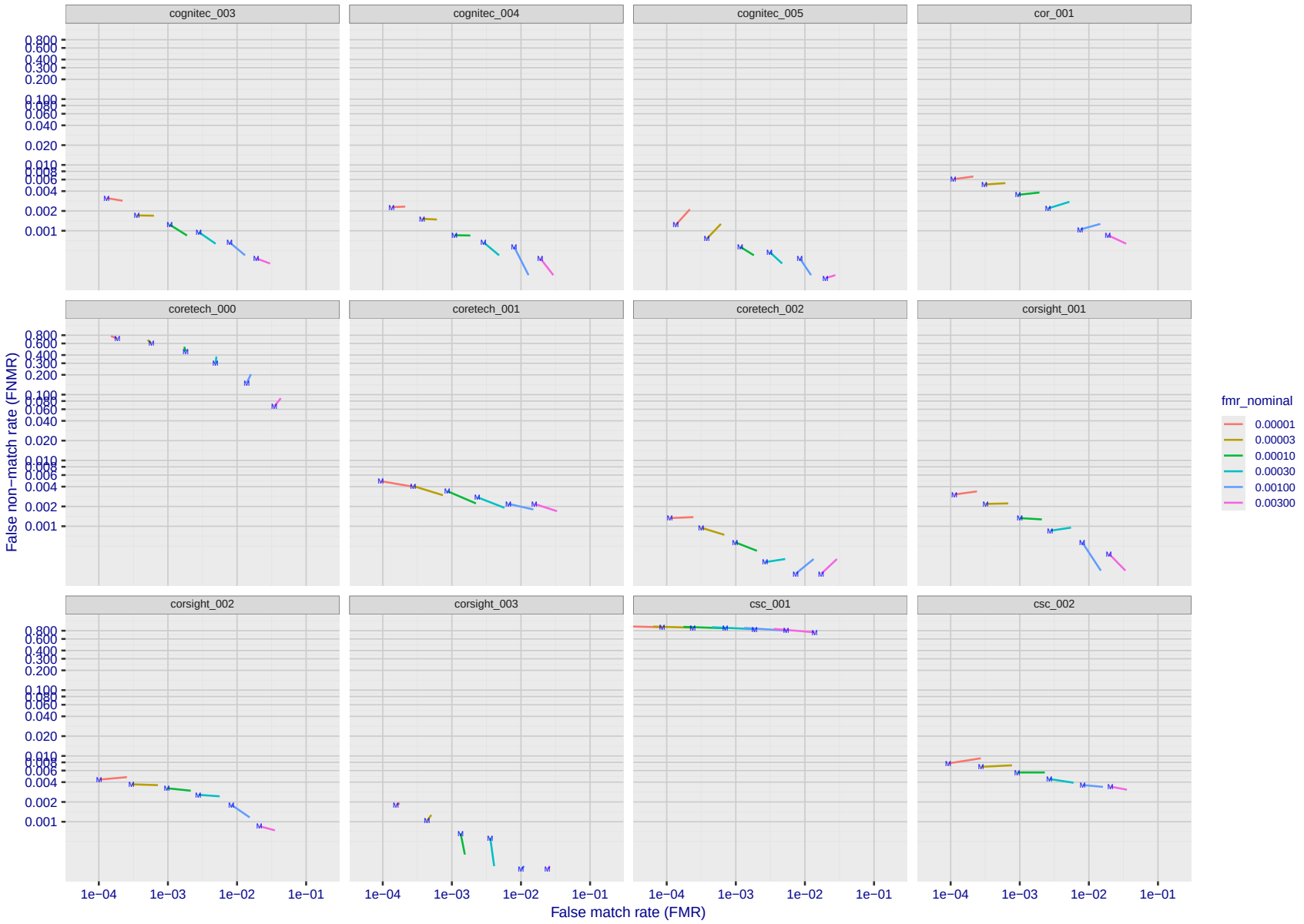

Figure 468: For the visa images, FNMR and FMR at six operating points along the DET characteristic. At each point a line is drawn between (FMR,FNMR)$_{\text{MALE}}$ and (FMR,FNMR)$_{\text{FEMALE}}$ showing how which sex has lower FMR and/or FNMR. The "M" label denotes male, the other end of the line corresponds to female. The six operating thresholds are selected to give the nominal false match rates given in the legend, and are computed over all impostor pairs regardless of age, sex, and place of birth. The plotted FMR values are broadly an order of magnitude larger than the nominal rates because FMR is computed over demographically-matched impostor pairs i.e individuals of the same sex, from the same geographic region (see section 3.6.1), and the same age group (see section 3.6.2).

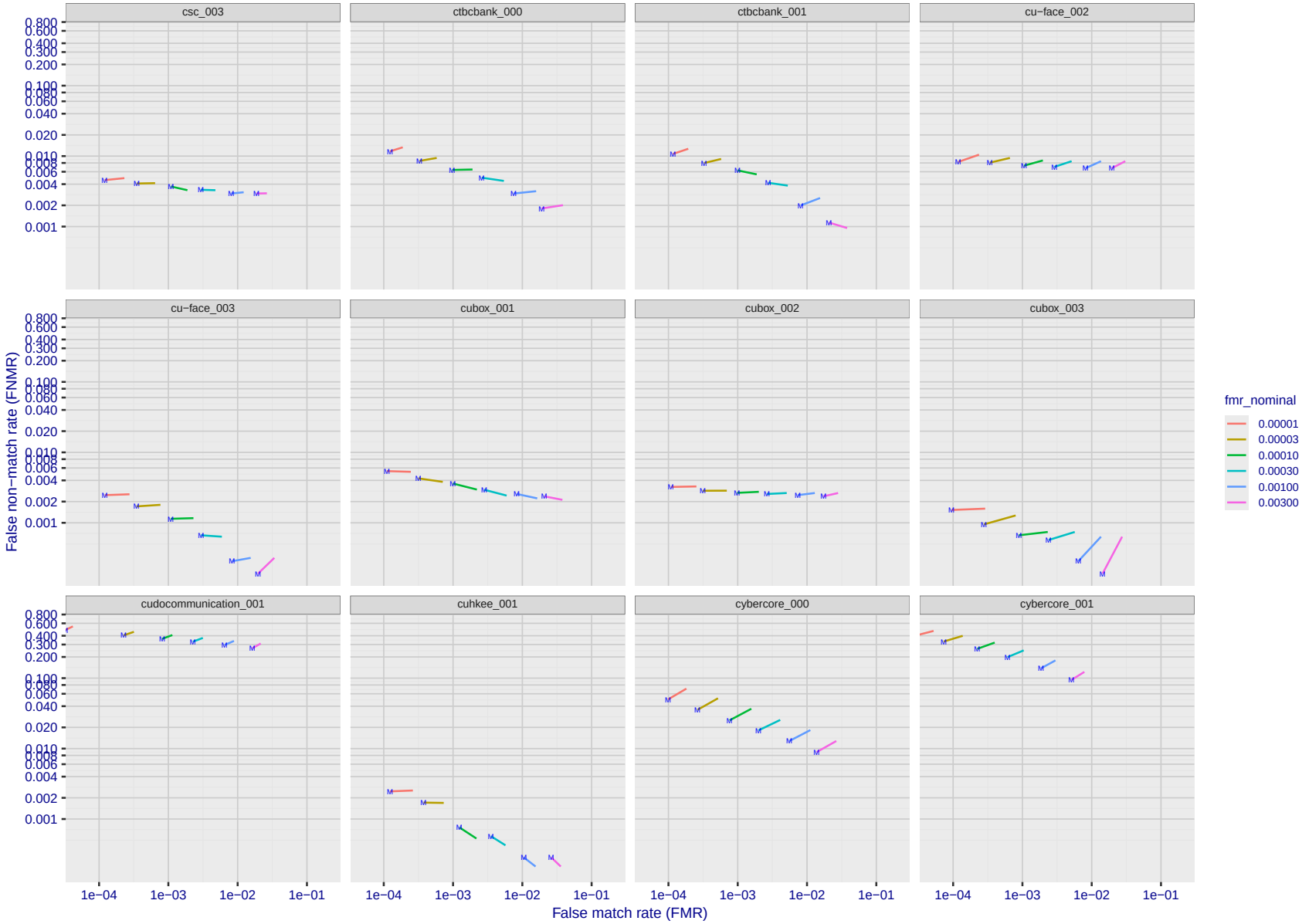

Figure 469: For the visa images, FNMR and FMR at six operating points along the DET characteristic. At each point a line is drawn between (FMR,FNMR)$_{\text{MALE}}$ and (FMR,FNMR)$_{\text{FEMALE}}$ showing how which sex has lower FMR and/or FNMR. The "M" label denotes male, the other end of the line corresponds to female. The six operating thresholds are selected to give the nominal false match rates given in the legend, and are computed over all impostor pairs regardless of age, sex, and place of birth. The plotted FMR values are broadly an order of magnitude larger than the nominal rates because FMR is computed over demographically-matched impostor pairs i.e individuals of the same sex, from the same geographic region (see section 3.6.1), and the same age group (see section 3.6.2).

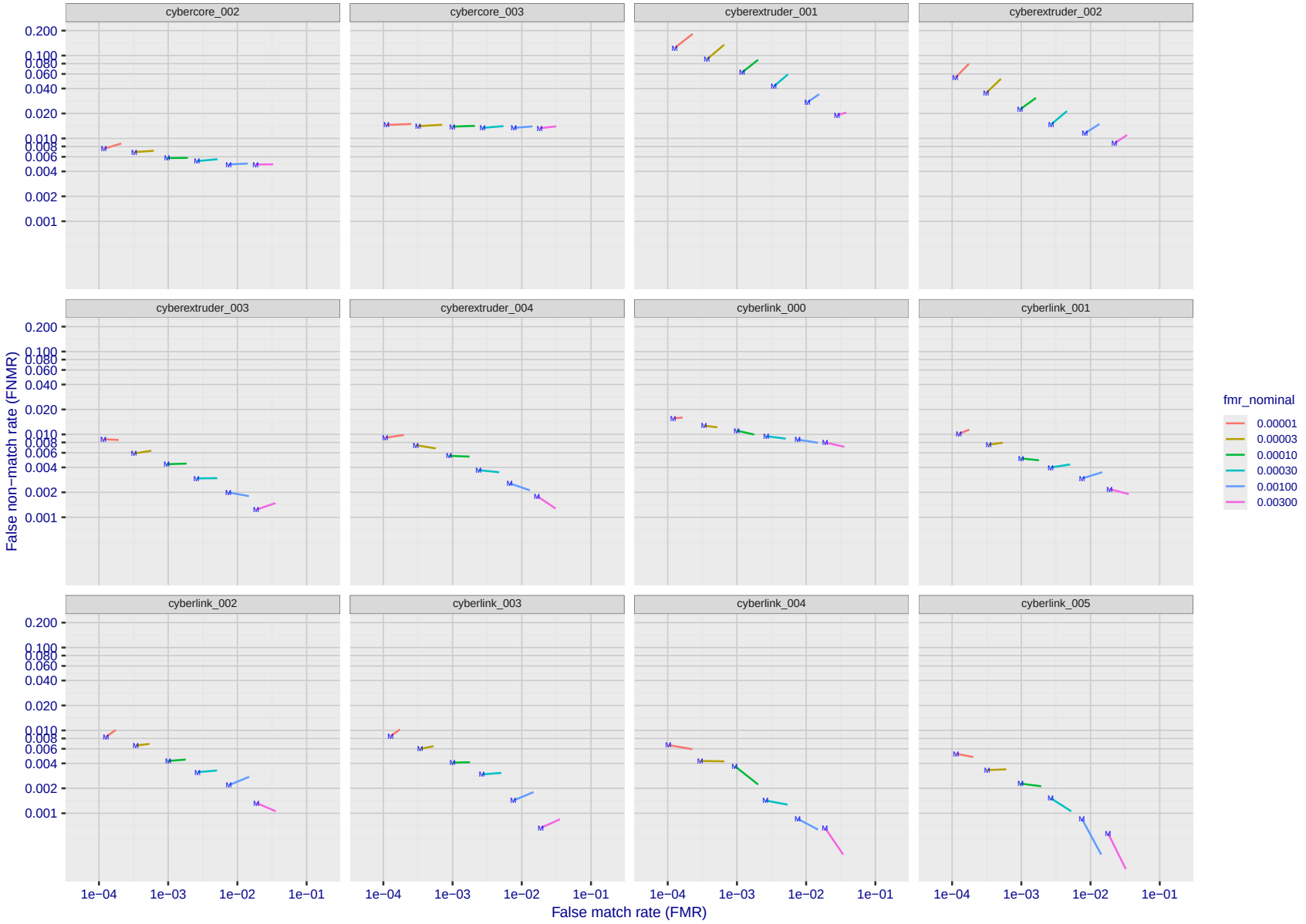

Figure 470: For the visa images, FNMR and FMR at six operating points along the DET characteristic. At each point a line is drawn between (FMR,FNMR)$_{\text{MALE}}$ and (FMR,FNMR)$_{\text{FEMALE}}$ showing how which sex has lower FMR and/or FNMR. The "M" label denotes male, the other end of the line corresponds to female. The six operating thresholds are selected to give the nominal false match rates given in the legend, and are computed over all impostor pairs regardless of age, sex, and place of birth. The plotted FMR values are broadly an order of magnitude larger than the nominal rates because FMR is computed over demographically-matched impostor pairs i.e individuals of the same sex, from the same geographic region (see section 3.6.1), and the same age group (see section 3.6.2).

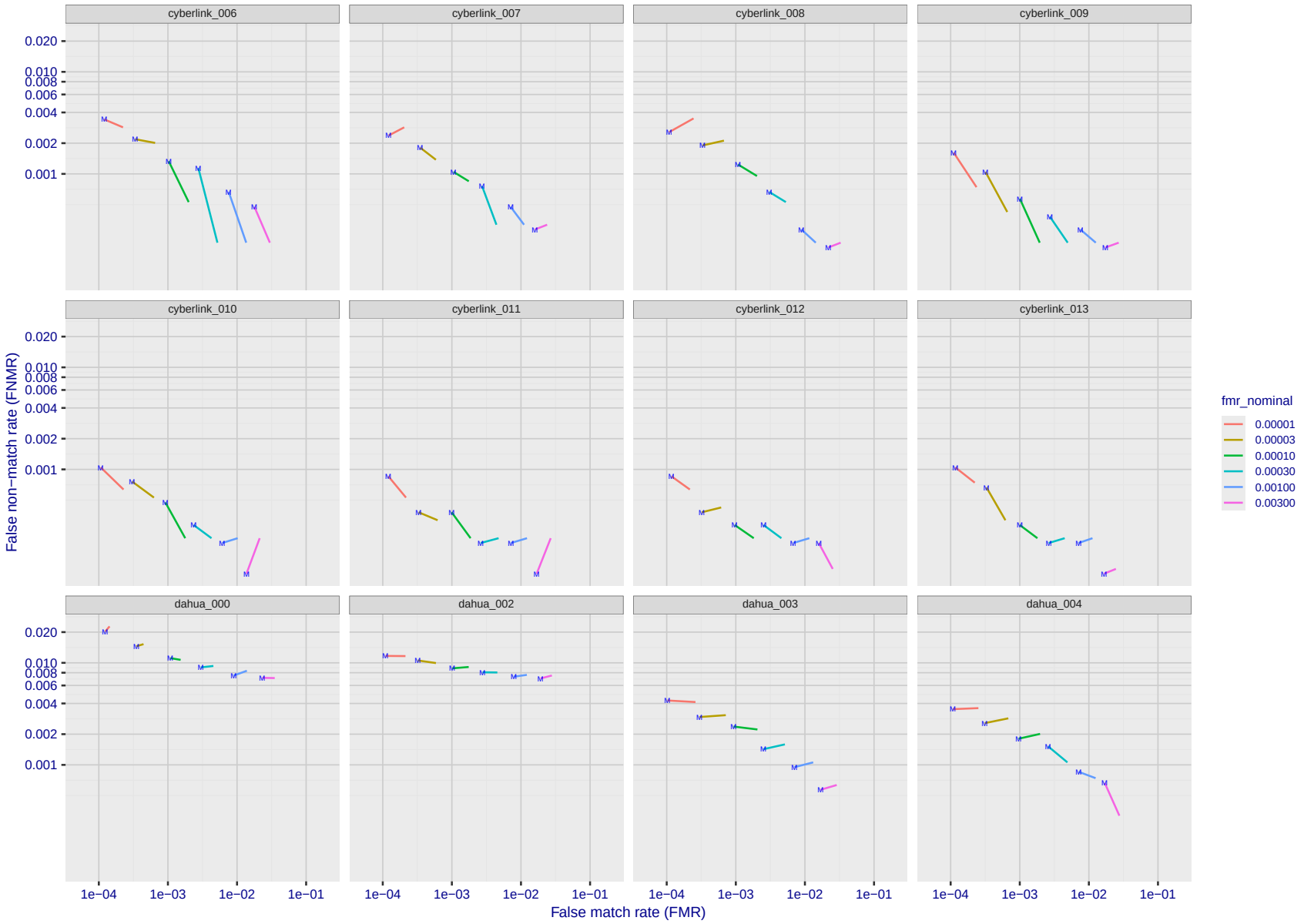

Figure 471: For the visa images, FNMR and FMR at six operating points along the DET characteristic. At each point a line is drawn between (FMR,FNMR)$_{\text{MALE}}$ and (FMR,FNMR)$_{\text{FEMALE}}$ showing how which sex has lower FMR and/or FNMR. The "M" label denotes male, the other end of the line corresponds to female. The six operating thresholds are selected to give the nominal false match rates given in the legend, and are computed over all impostor pairs regardless of age, sex, and place of birth. The plotted FMR values are broadly an order of magnitude larger than the nominal rates because FMR is computed over demographically-matched impostor pairs i.e individuals of the same sex, from the same geographic region (see section 3.6.1), and the same age group (see section 3.6.2).

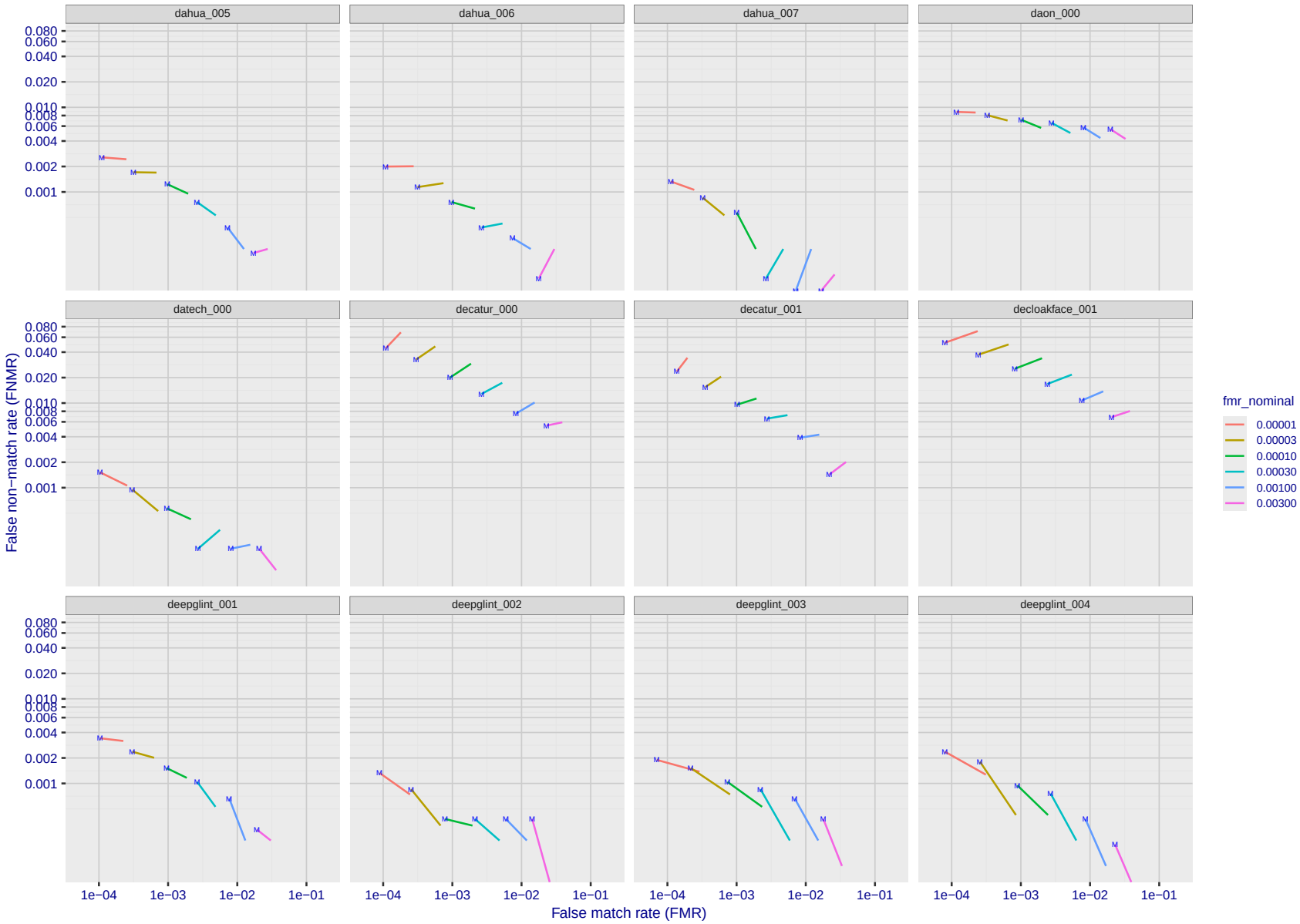

Figure 472: For the visa images, FNMR and FMR at six operating points along the DET characteristic. At each point a line is drawn between (FMR,FNMR)$_{\text{MALE}}$ and (FMR,FNMR)$_{\text{FEMALE}}$ showing how which sex has lower FMR and/or FNMR. The "M" label denotes male, the other end of the line corresponds to female. The six operating thresholds are selected to give the nominal false match rates given in the legend, and are computed over all impostor pairs regardless of age, sex, and place of birth. The plotted FMR values are broadly an order of magnitude larger than the nominal rates because FMR is computed over demographically-matched impostor pairs i.e individuals of the same sex, from the same geographic region (see section 3.6.1), and the same age group (see section 3.6.2).

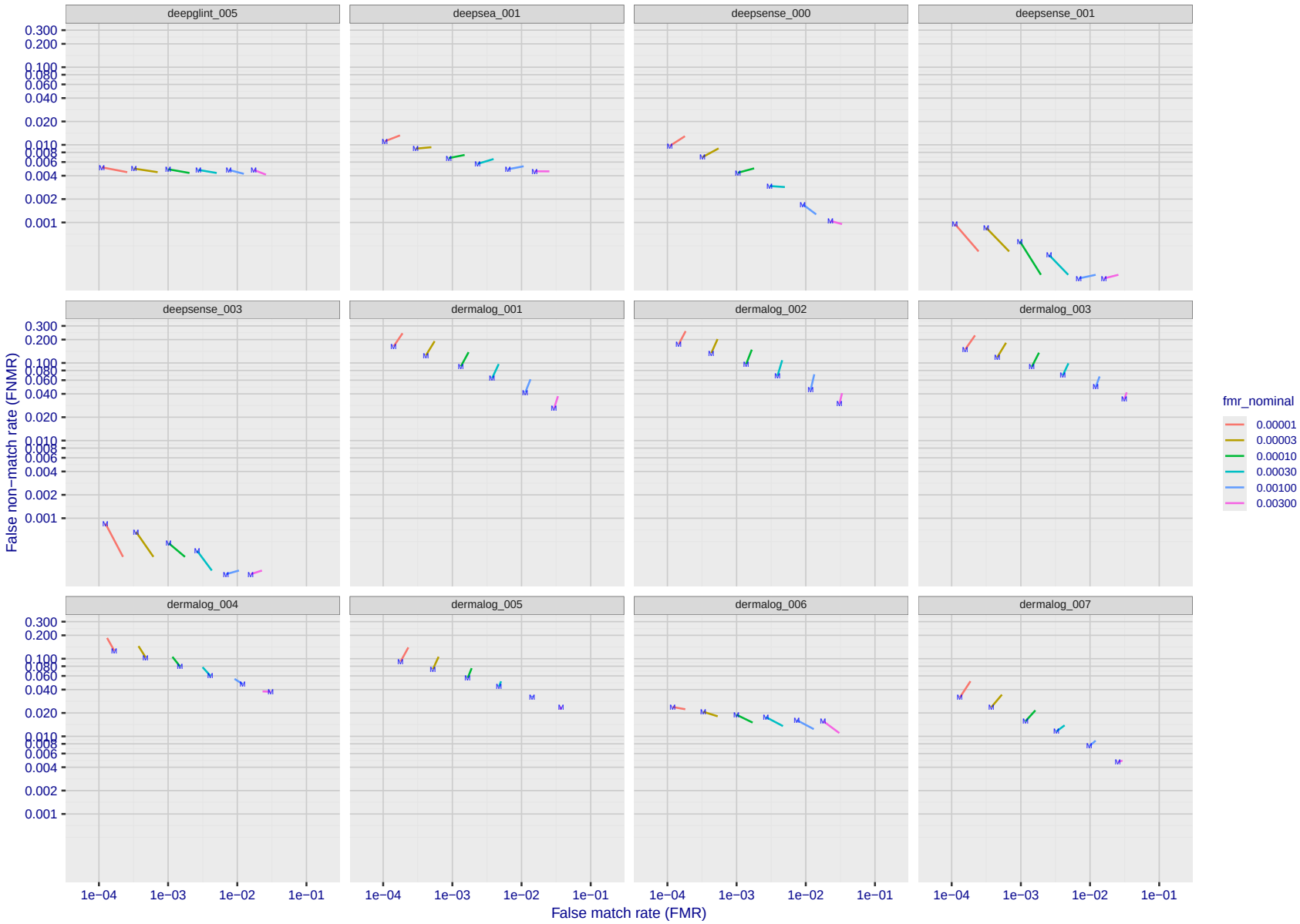

Figure 473: For the visa images, FNMR and FMR at six operating points along the DET characteristic. At each point a line is drawn between (FMR,FNMR)$_{\text{MALE}}$ and (FMR,FNMR)$_{\text{FEMALE}}$ showing how which sex has lower FMR and/or FNMR. The "M" label denotes male, the other end of the line corresponds to female. The six operating thresholds are selected to give the nominal false match rates given in the legend, and are computed over all impostor pairs regardless of age, sex, and place of birth. The plotted FMR values are broadly an order of magnitude larger than the nominal rates because FMR is computed over demographically-matched impostor pairs i.e individuals of the same sex, from the same geographic region (see section 3.6.1), and the same age group (see section 3.6.2).

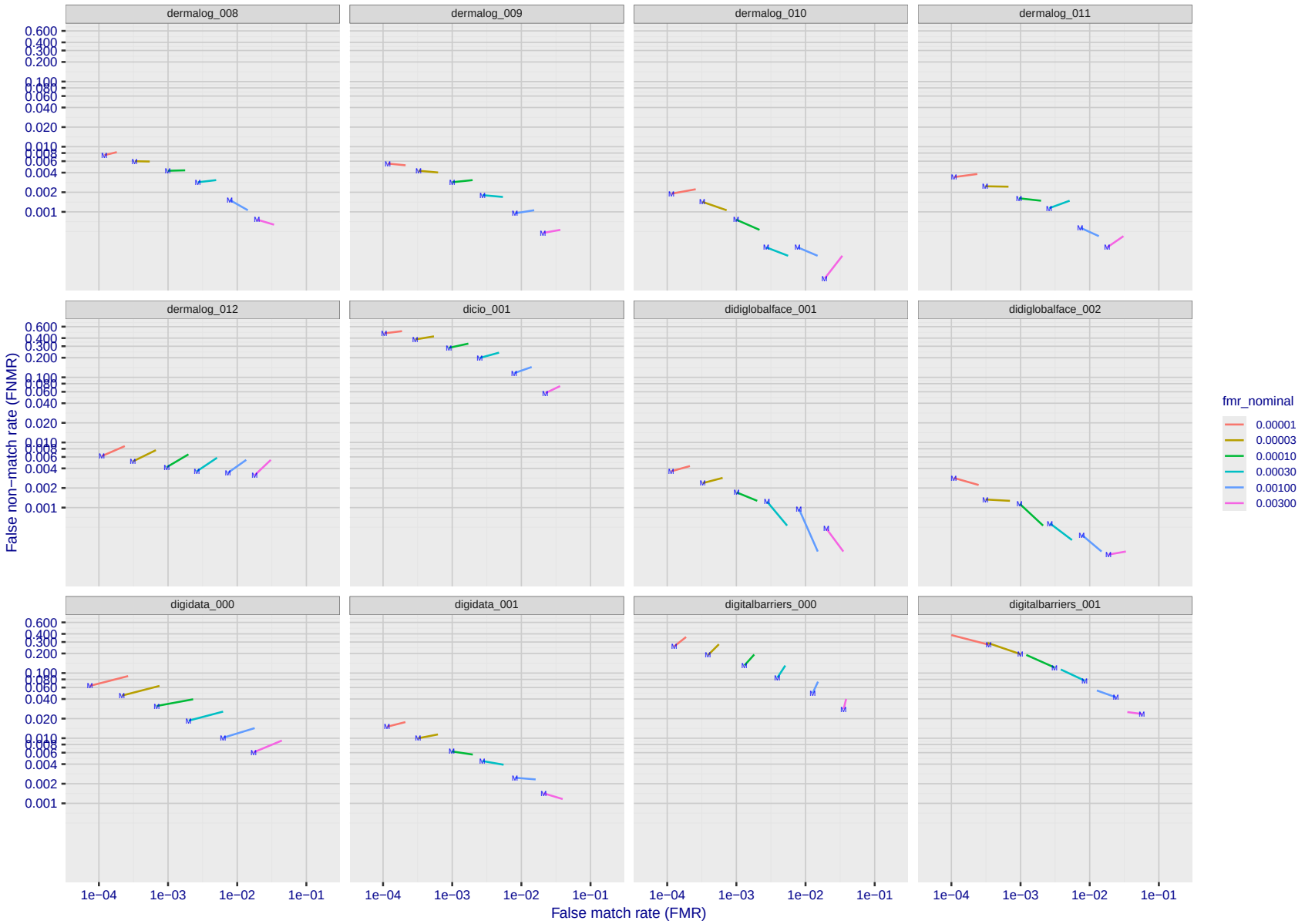

Figure 474: For the visa images, FNMR and FMR at six operating points along the DET characteristic. At each point a line is drawn between (FMR,FNMR)$_{\text{MALE}}$ and (FMR,FNMR)$_{\text{FEMALE}}$ showing how which sex has lower FMR and/or FNMR. The "M" label denotes male, the other end of the line corresponds to female. The six operating thresholds are selected to give the nominal false match rates given in the legend, and are computed over all impostor pairs regardless of age, sex, and place of birth. The plotted FMR values are broadly an order of magnitude larger than the nominal rates because FMR is computed over demographically-matched impostor pairs i.e individuals of the same sex, from the same geographic region (see section 3.6.1), and the same age group (see section 3.6.2).

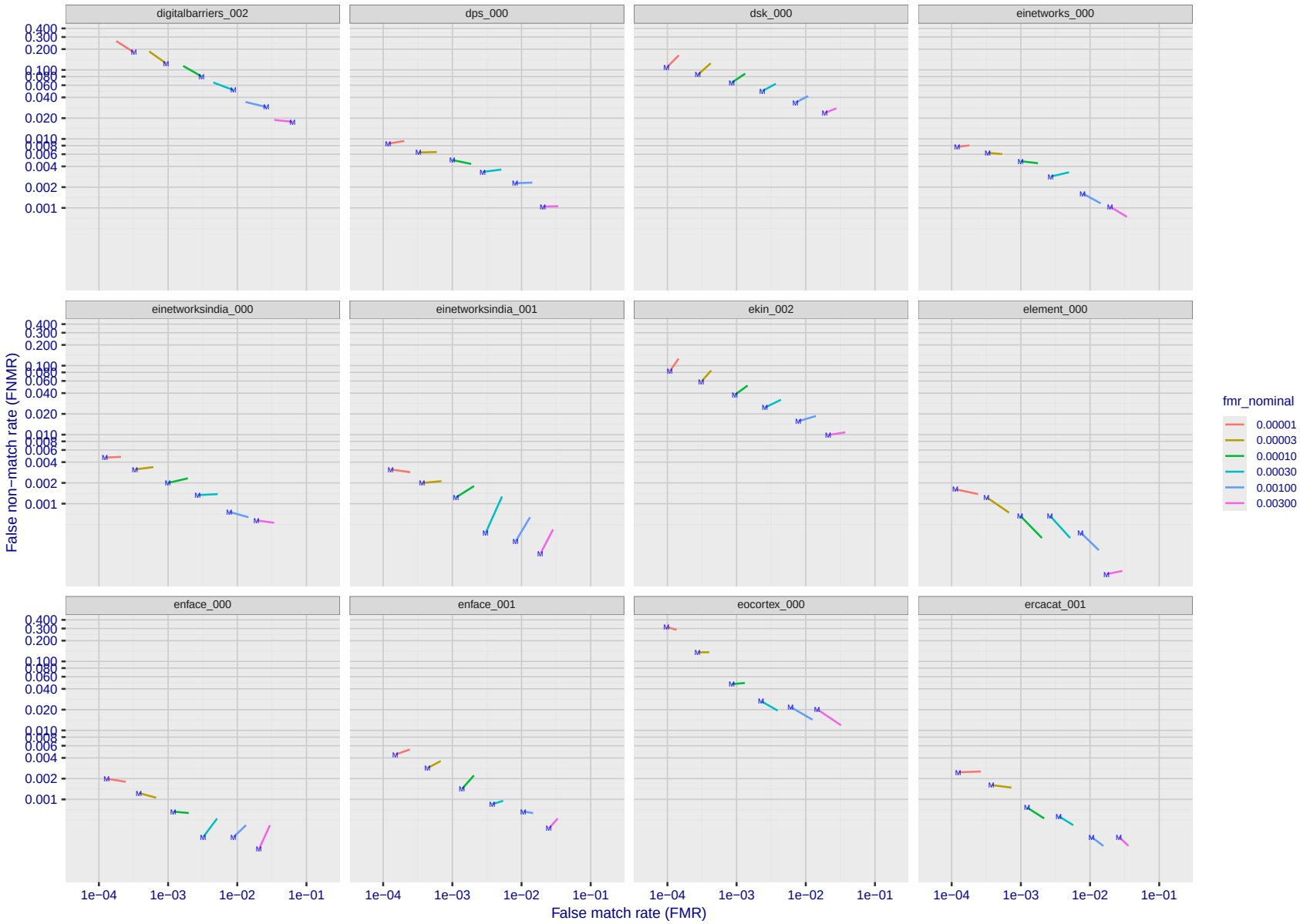

Figure 475: For the visa images, FNMR and FMR at six operating points along the DET characteristic. At each point a line is drawn between (FMR,FNMR)$_{\text{MALE}}$ and (FMR,FNMR)$_{\text{FEMALE}}$ showing how which sex has lower FMR and/or FNMR. The "M" label denotes male, the other end of the line corresponds to female. The six operating thresholds are selected to give the nominal false match rates given in the legend, and are computed over all impostor pairs regardless of age, sex, and place of birth. The plotted FMR values are broadly an order of magnitude larger than the nominal rates because FMR is computed over demographically-matched impostor pairs i.e individuals of the same sex, from the same geographic region (see section 3.6.1), and the same age group (see section 3.6.2).

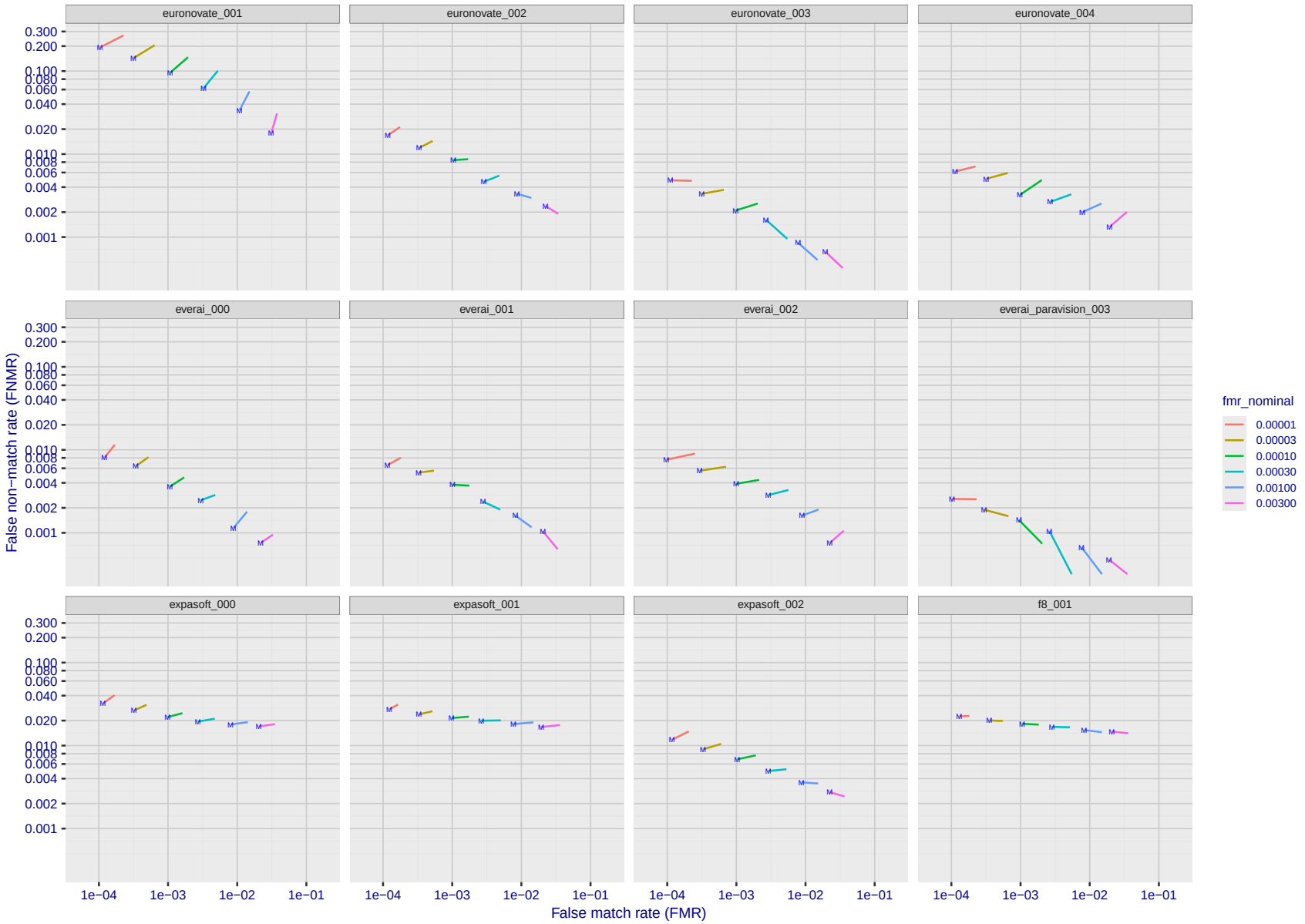

Figure 476: For the visa images, FNMR and FMR at six operating points along the DET characteristic. At each point a line is drawn between (FMR,FNMR)$_{\text{MALE}}$ and (FMR,FNMR)$_{\text{FEMALE}}$ showing how which sex has lower FMR and/or FNMR. The "M" label denotes male, the other end of the line corresponds to female. The six operating thresholds are selected to give the nominal false match rates given in the legend, and are computed over all impostor pairs regardless of age, sex, and place of birth. The plotted FMR values are broadly an order of magnitude larger than the nominal rates because FMR is computed over demographically-matched impostor pairs i.e individuals of the same sex, from the same geographic region (see section 3.6.1), and the same age group (see section 3.6.2).

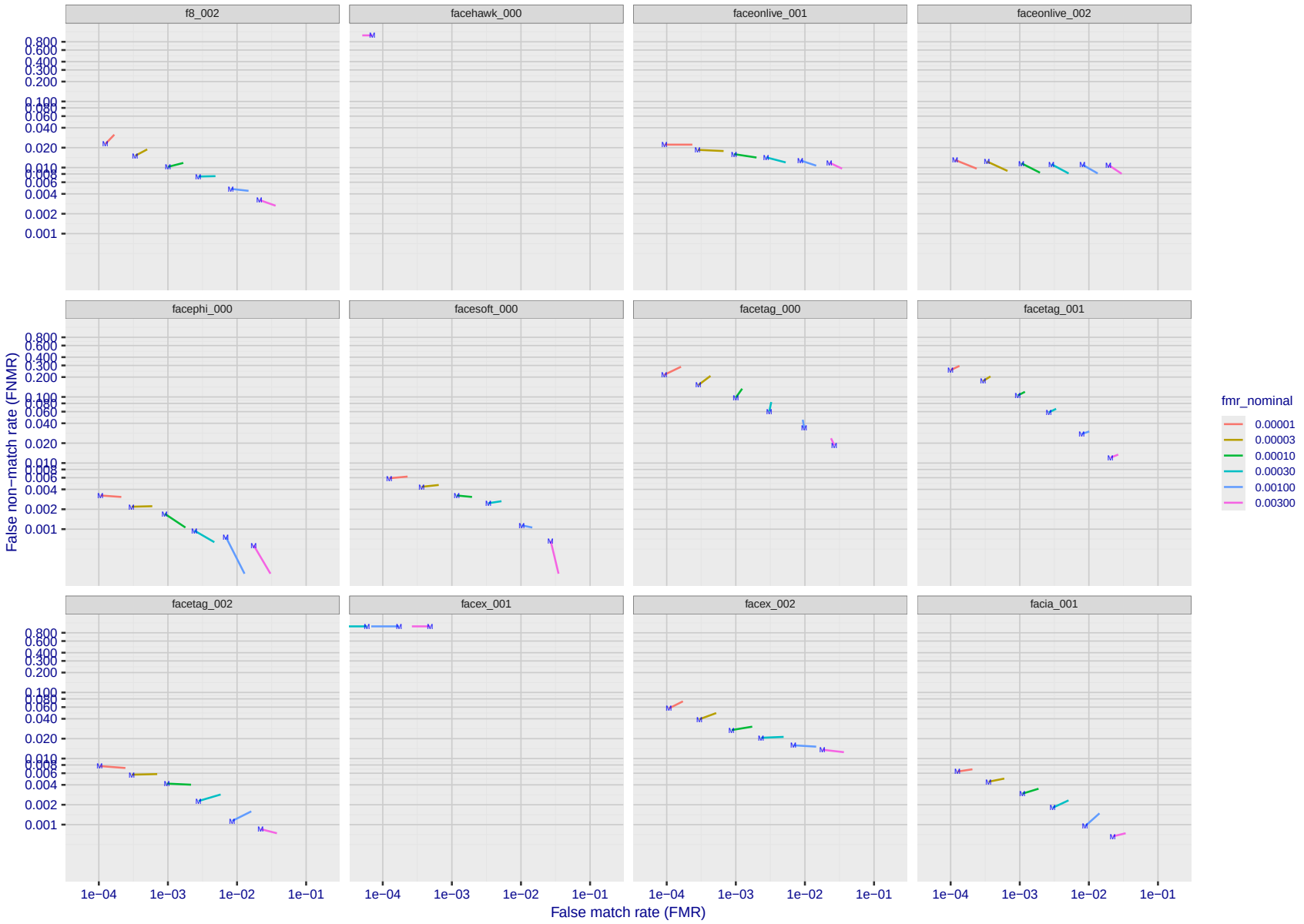

Figure 477: For the visa images, FNMR and FMR at six operating points along the DET characteristic. At each point a line is drawn between (FMR,FNMR)$_{\text{MALE}}$ and (FMR,FNMR)$_{\text{FEMALE}}$ showing how which sex has lower FMR and/or FNMR. The "M" label denotes male, the other end of the line corresponds to female. The six operating thresholds are selected to give the nominal false match rates given in the legend, and are computed over all impostor pairs regardless of age, sex, and place of birth. The plotted FMR values are broadly an order of magnitude larger than the nominal rates because FMR is computed over demographically-matched impostor pairs i.e individuals of the same sex, from the same geographic region (see section 3.6.1), and the same age group (see section 3.6.2).

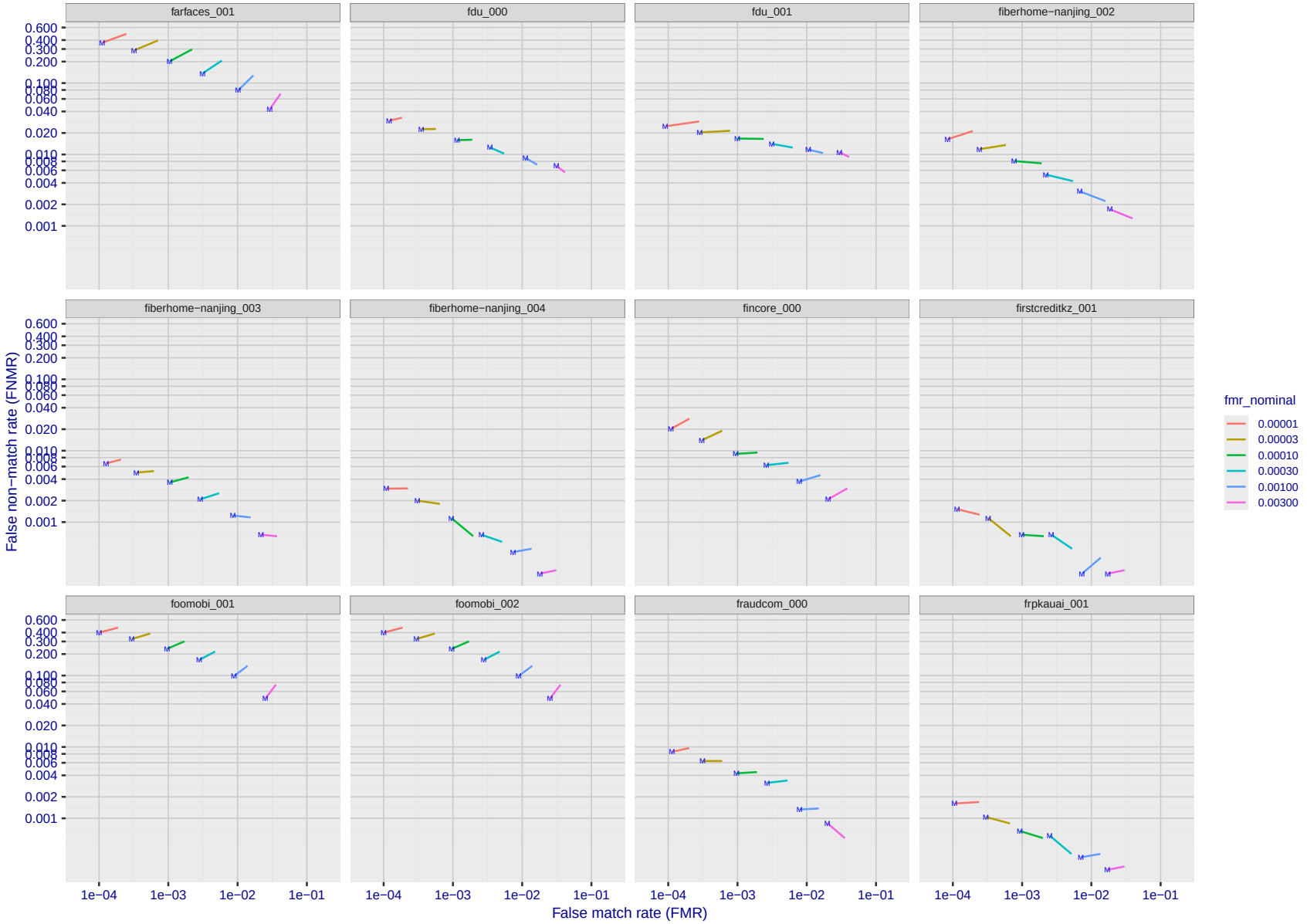

Figure 478: For the visa images, FNMR and FMR at six operating points along the DET characteristic. At each point a line is drawn between (FMR,FNMR)$_{\text{MALE}}$ and (FMR,FNMR)$_{\text{FEMALE}}$ showing how which sex has lower FMR and/or FNMR. The "M" label denotes male, the other end of the line corresponds to female. The six operating thresholds are selected to give the nominal false match rates given in the legend, and are computed over all impostor pairs regardless of age, sex, and place of birth. The plotted FMR values are broadly an order of magnitude larger than the nominal rates because FMR is computed over demographically-matched impostor pairs i.e individuals of the same sex, from the same geographic region (see section 3.6.1), and the same age group (see section 3.6.2).

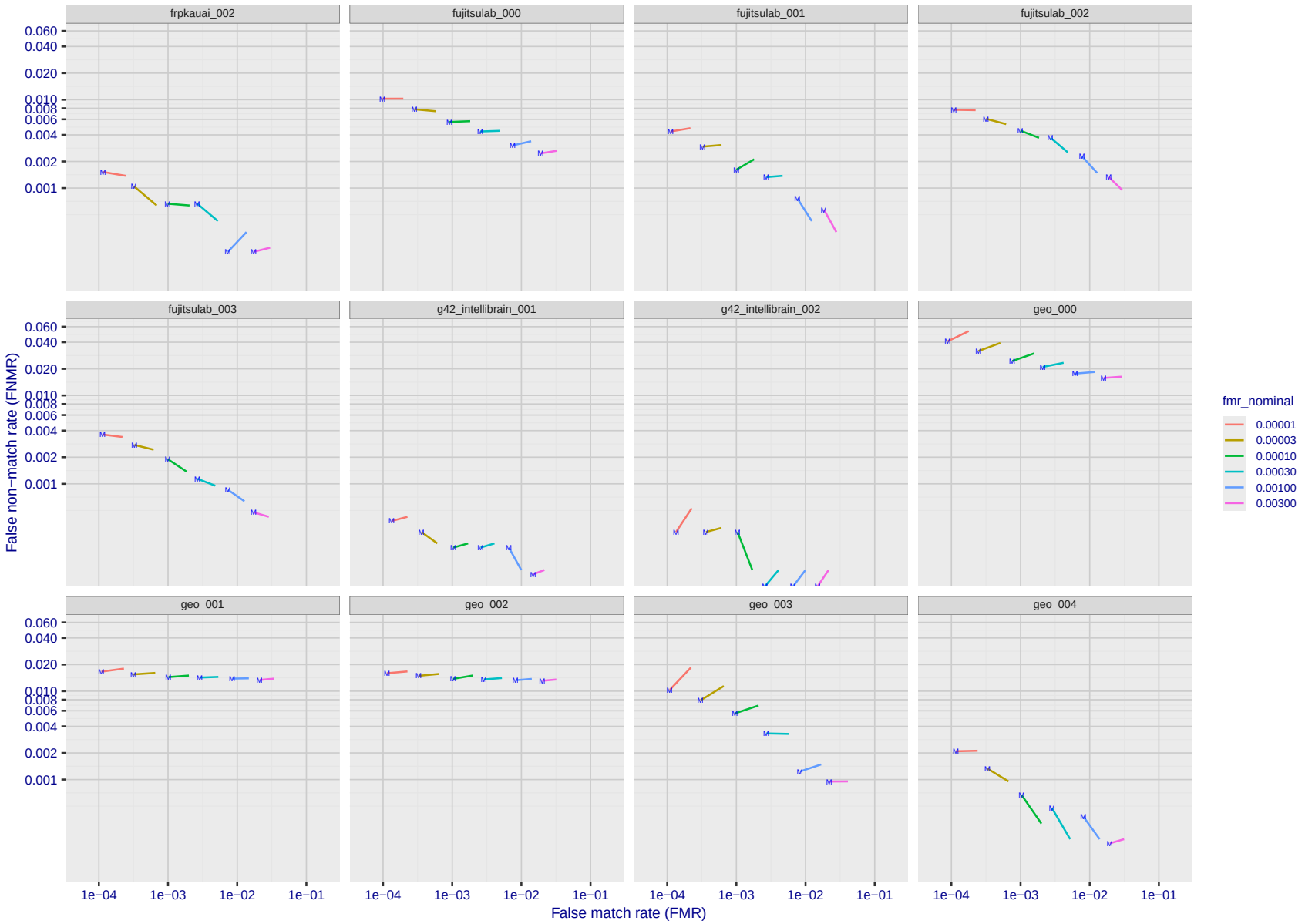

Figure 479: For the visa images, FNMR and FMR at six operating points along the DET characteristic. At each point a line is drawn between (FMR,FNMR)$_{\text{MALE}}$ and (FMR,FNMR)$_{\text{FEMALE}}$ showing how which sex has lower FMR and/or FNMR. The "M" label denotes male, the other end of the line corresponds to female. The six operating thresholds are selected to give the nominal false match rates given in the legend, and are computed over all impostor pairs regardless of age, sex, and place of birth. The plotted FMR values are broadly an order of magnitude larger than the nominal rates because FMR is computed over demographically-matched impostor pairs i.e individuals of the same sex, from the same geographic region (see section 3.6.1), and the same age group (see section 3.6.2).

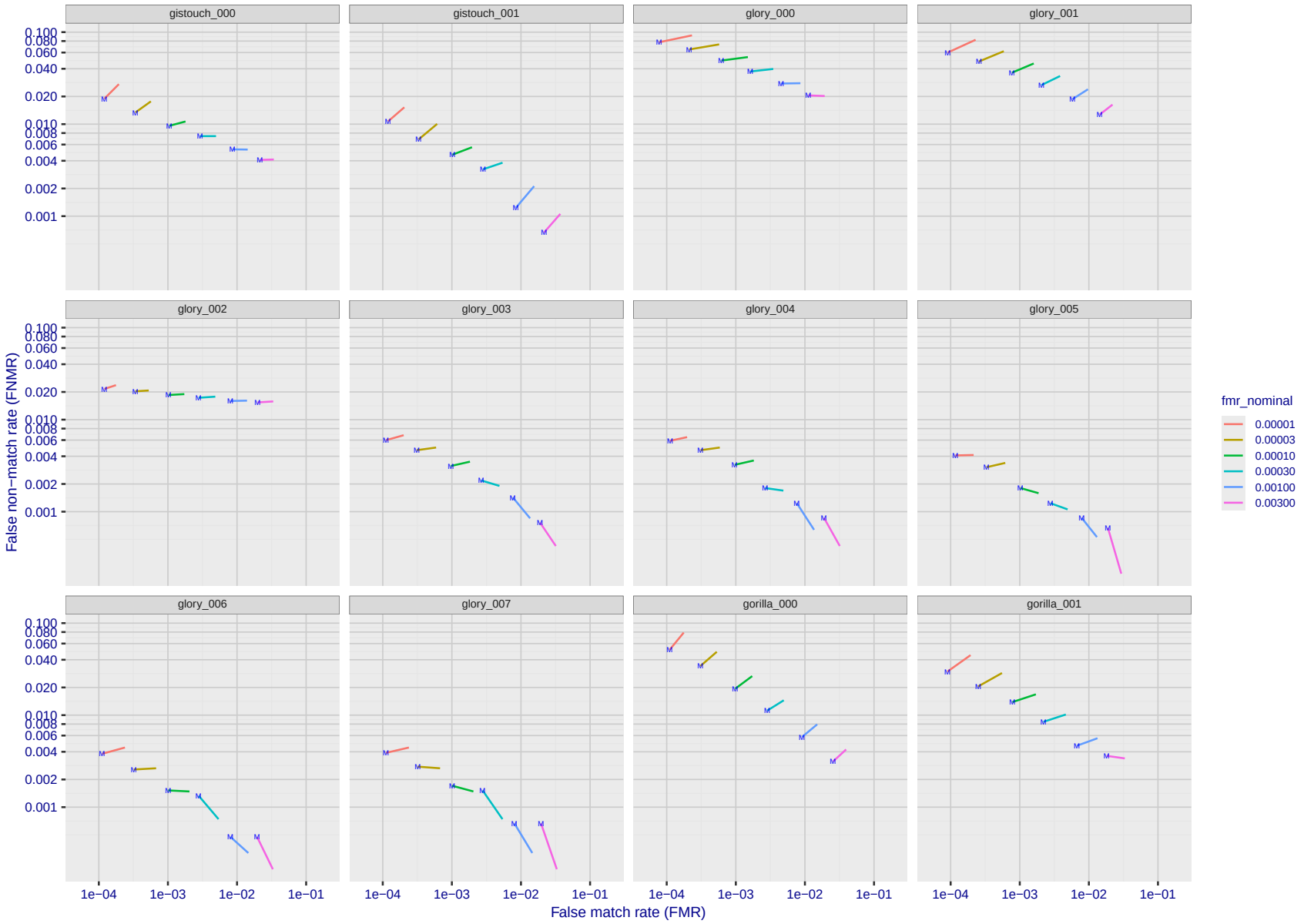

Figure 480: For the visa images, FNMR and FMR at six operating points along the DET characteristic. At each point a line is drawn between (FMR,FNMR)$_{\text{MALE}}$ and (FMR,FNMR)$_{\text{FEMALE}}$ showing how which sex has lower FMR and/or FNMR. The "M" label denotes male, the other end of the line corresponds to female. The six operating thresholds are selected to give the nominal false match rates given in the legend, and are computed over all impostor pairs regardless of age, sex, and place of birth. The plotted FMR values are broadly an order of magnitude larger than the nominal rates because FMR is computed over demographically-matched impostor pairs i.e individuals of the same sex, from the same geographic region (see section 3.6.1), and the same age group (see section 3.6.2).

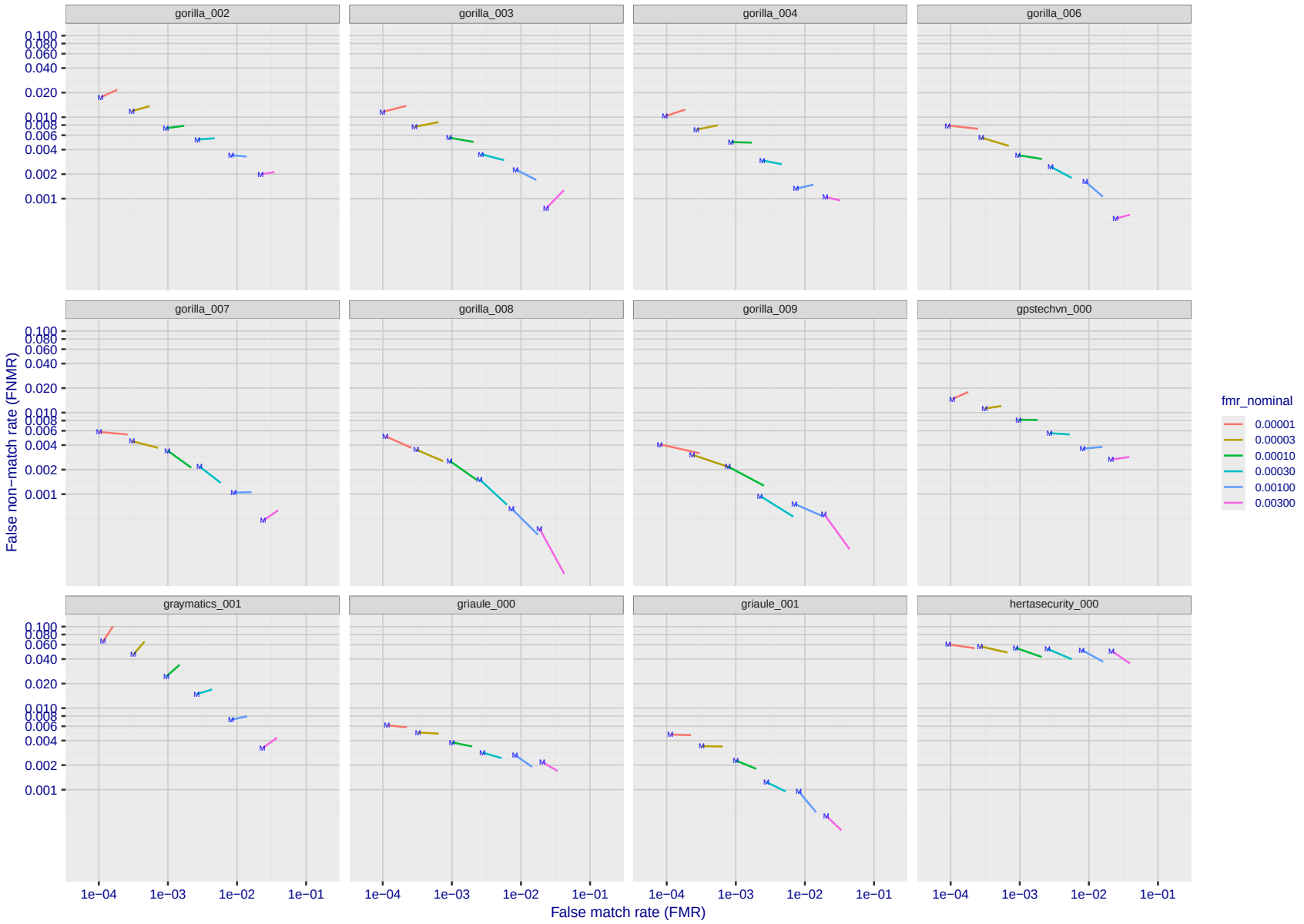

Figure 481: For the visa images, FNMR and FMR at six operating points along the DET characteristic. At each point a line is drawn between (FMR,FNMR)$_{\text{MALE}}$ and (FMR,FNMR)$_{\text{FEMALE}}$ showing how which sex has lower FMR and/or FNMR. The "M" label denotes male, the other end of the line corresponds to female. The six operating thresholds are selected to give the nominal false match rates given in the legend, and are computed over all impostor pairs regardless of age, sex, and place of birth. The plotted FMR values are broadly an order of magnitude larger than the nominal rates because FMR is computed over demographically-matched impostor pairs i.e individuals of the same sex, from the same geographic region (see section 3.6.1), and the same age group (see section 3.6.2).

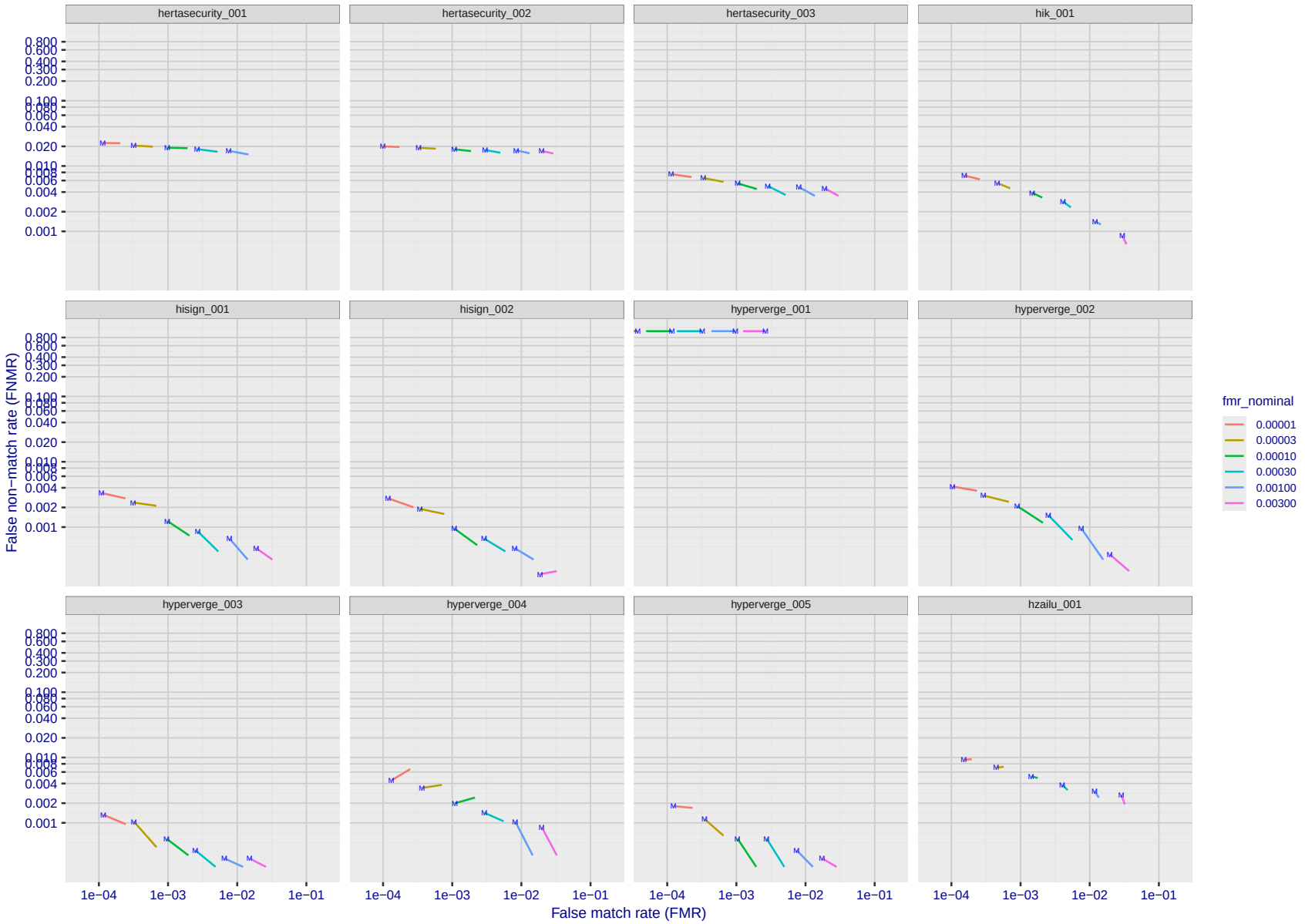

Figure 482: For the visa images, FNMR and FMR at six operating points along the DET characteristic. At each point a line is drawn between (FMR,FNMR)$_{\text{MALE}}$ and (FMR,FNMR)$_{\text{FEMALE}}$ showing how which sex has lower FMR and/or FNMR. The "M" label denotes male, the other end of the line corresponds to female. The six operating thresholds are selected to give the nominal false match rates given in the legend, and are computed over all impostor pairs regardless of age, sex, and place of birth. The plotted FMR values are broadly an order of magnitude larger than the nominal rates because FMR is computed over demographically-matched impostor pairs i.e individuals of the same sex, from the same geographic region (see section 3.6.1), and the same age group (see section 3.6.2).

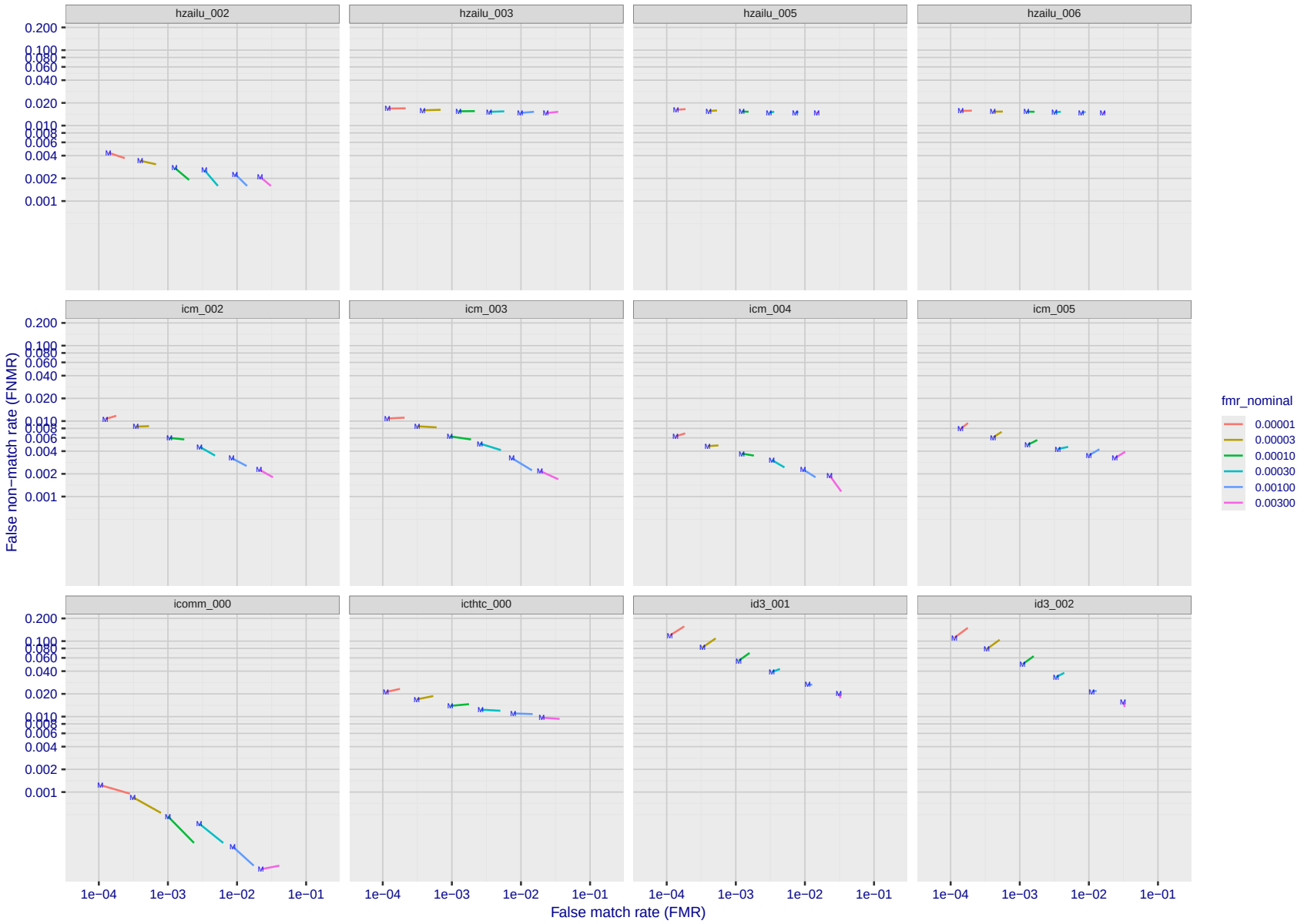

Figure 483: For the visa images, FNMR and FMR at six operating points along the DET characteristic. At each point a line is drawn between (FMR,FNMR)$_{\text{MALE}}$ and (FMR,FNMR)$_{\text{FEMALE}}$ showing how which sex has lower FMR and/or FNMR. The "M" label denotes male, the other end of the line corresponds to female. The six operating thresholds are selected to give the nominal false match rates given in the legend, and are computed over all impostor pairs regardless of age, sex, and place of birth. The plotted FMR values are broadly an order of magnitude larger than the nominal rates because FMR is computed over demographically-matched impostor pairs i.e individuals of the same sex, from the same geographic region (see section 3.6.1), and the same age group (see section 3.6.2).

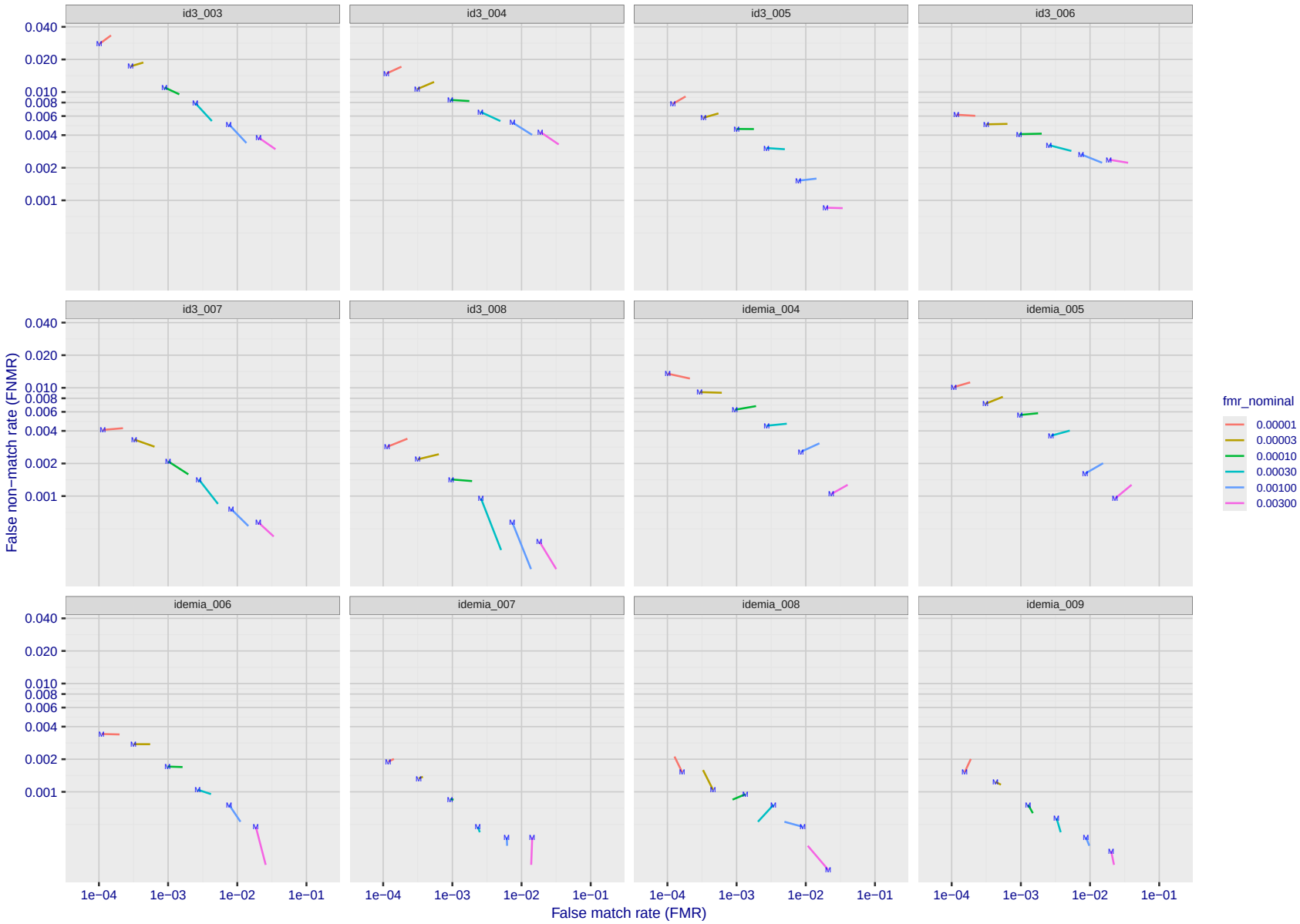

Figure 484: For the visa images, FNMR and FMR at six operating points along the DET characteristic. At each point a line is drawn between (FMR,FNMR)$_{\text{MALE}}$ and (FMR,FNMR)$_{\text{FEMALE}}$ showing how which sex has lower FMR and/or FNMR. The "M" label denotes male, the other end of the line corresponds to female. The six operating thresholds are selected to give the nominal false match rates given in the legend, and are computed over all impostor pairs regardless of age, sex, and place of birth. The plotted FMR values are broadly an order of magnitude larger than the nominal rates because FMR is computed over demographically-matched impostor pairs i.e individuals of the same sex, from the same geographic region (see section 3.6.1), and the same age group (see section 3.6.2).

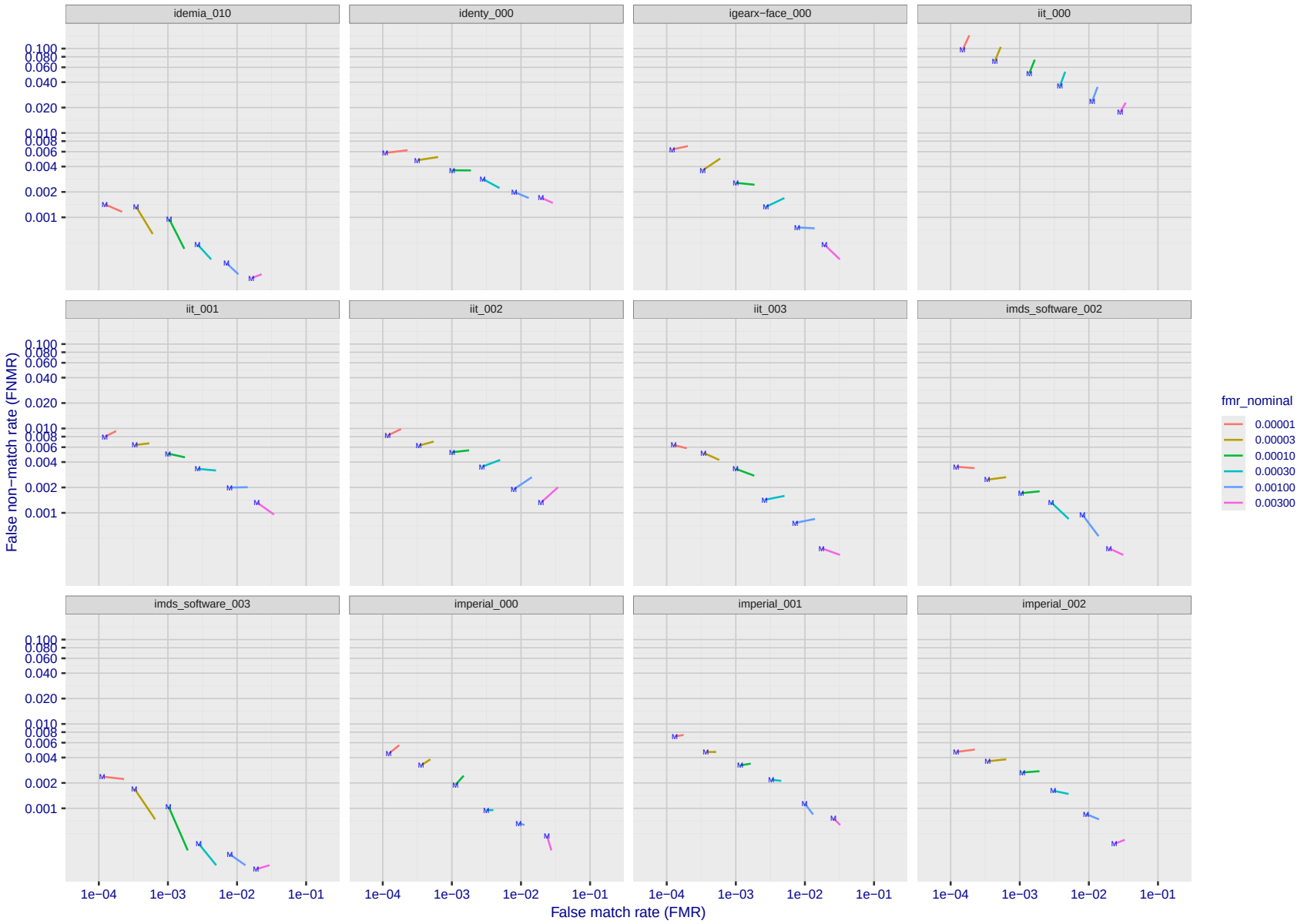

Figure 485: For the visa images, FNMR and FMR at six operating points along the DET characteristic. At each point a line is drawn between (FMR,FNMR)$_{\text{MALE}}$ and (FMR,FNMR)$_{\text{FEMALE}}$ showing how which sex has lower FMR and/or FNMR. The "M" label denotes male, the other end of the line corresponds to female. The six operating thresholds are selected to give the nominal false match rates given in the legend, and are computed over all impostor pairs regardless of age, sex, and place of birth. The plotted FMR values are broadly an order of magnitude larger than the nominal rates because FMR is computed over demographically-matched impostor pairs i.e individuals of the same sex, from the same geographic region (see section 3.6.1), and the same age group (see section 3.6.2).

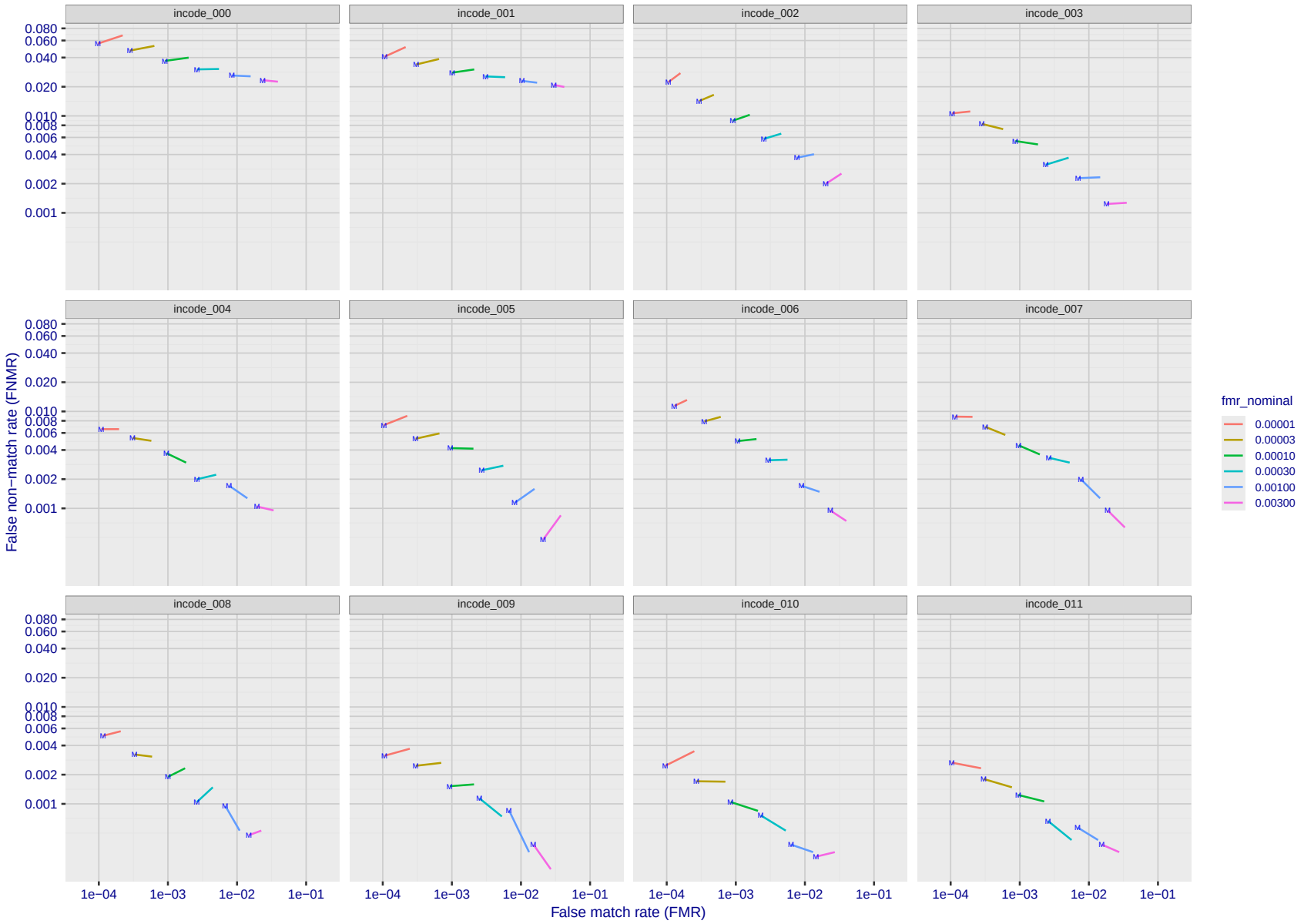

Figure 486: For the visa images, FNMR and FMR at six operating points along the DET characteristic. At each point a line is drawn between (FMR,FNMR)$_{\text{MALE}}$ and (FMR,FNMR)$_{\text{FEMALE}}$ showing how which sex has lower FMR and/or FNMR. The "M" label denotes male, the other end of the line corresponds to female. The six operating thresholds are selected to give the nominal false match rates given in the legend, and are computed over all impostor pairs regardless of age, sex, and place of birth. The plotted FMR values are broadly an order of magnitude larger than the nominal rates because FMR is computed over demographically-matched impostor pairs i.e individuals of the same sex, from the same geographic region (see section 3.6.1), and the same age group (see section 3.6.2).

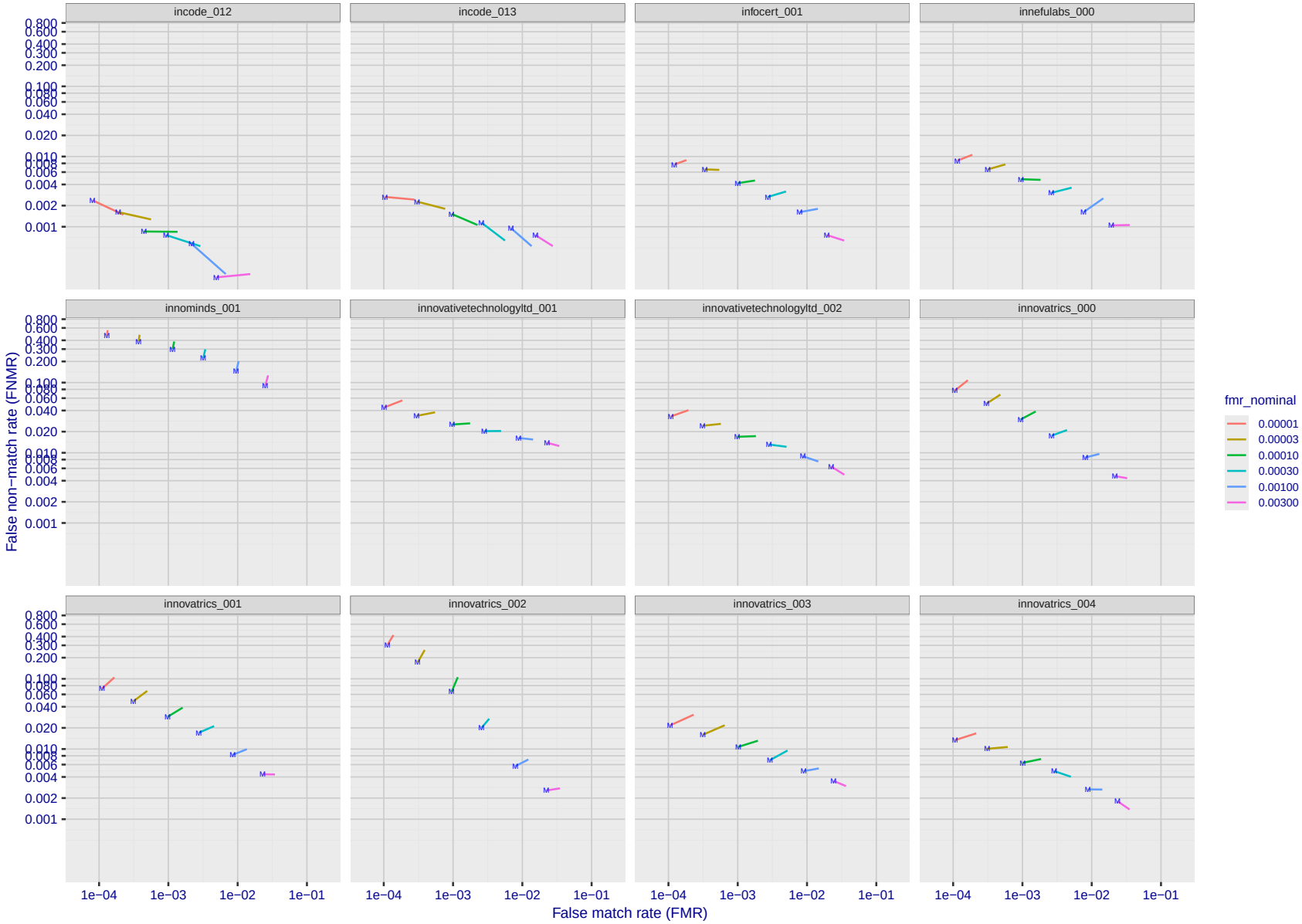

Figure 487: For the visa images, FNMR and FMR at six operating points along the DET characteristic. At each point a line is drawn between (FMR,FNMR)$_{\text{MALE}}$ and (FMR,FNMR)$_{\text{FEMALE}}$ showing how which sex has lower FMR and/or FNMR. The "M" label denotes male, the other end of the line corresponds to female. The six operating thresholds are selected to give the nominal false match rates given in the legend, and are computed over all impostor pairs regardless of age, sex, and place of birth. The plotted FMR values are broadly an order of magnitude larger than the nominal rates because FMR is computed over demographically-matched impostor pairs i.e individuals of the same sex, from the same geographic region (see section 3.6.1), and the same age group (see section 3.6.2).

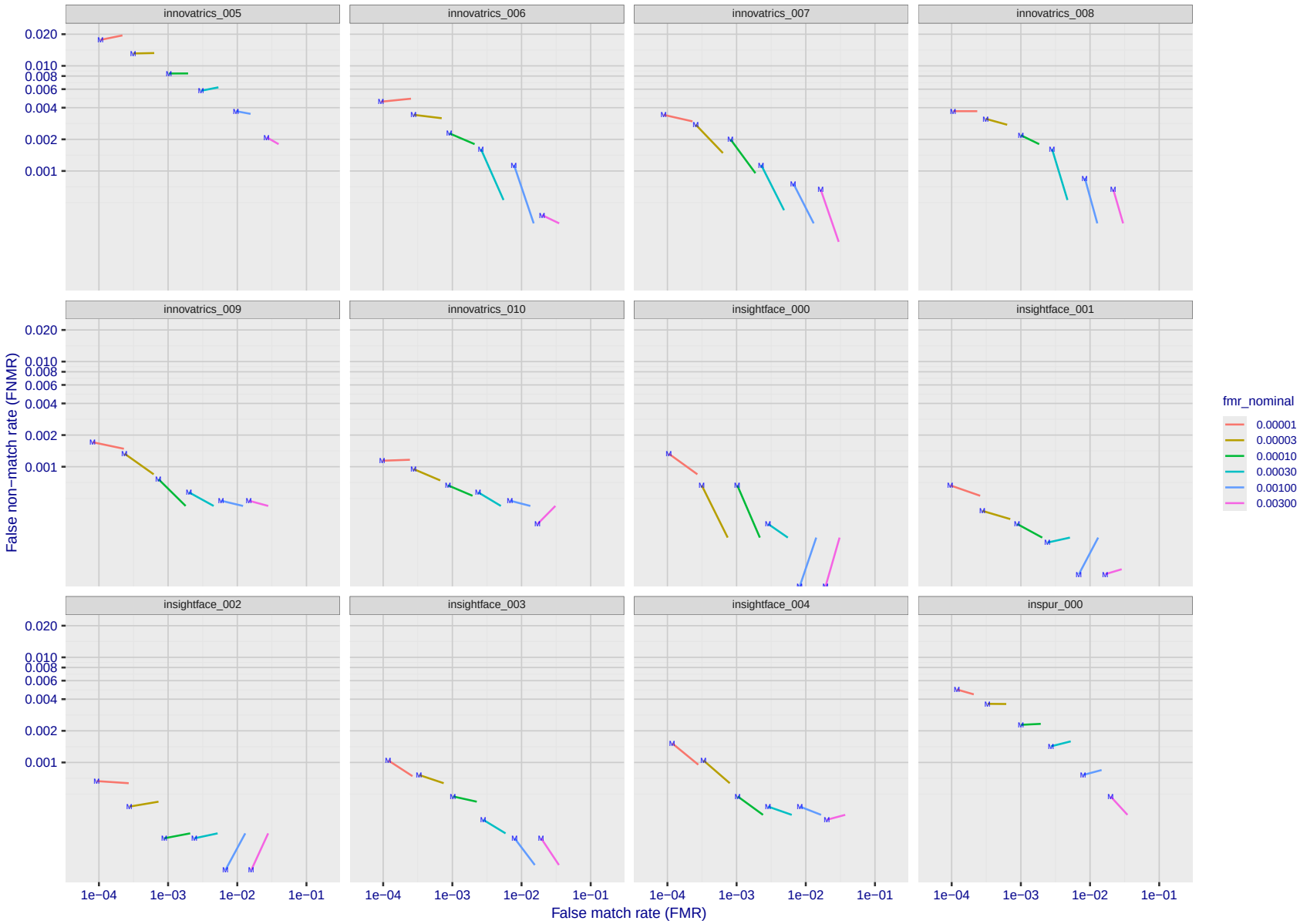

Figure 488: For the visa images, FNMR and FMR at six operating points along the DET characteristic. At each point a line is drawn between (FMR,FNMR)$_{\text{MALE}}$ and (FMR,FNMR)$_{\text{FEMALE}}$ showing how which sex has lower FMR and/or FNMR. The "M" label denotes male, the other end of the line corresponds to female. The six operating thresholds are selected to give the nominal false match rates given in the legend, and are computed over all impostor pairs regardless of age, sex, and place of birth. The plotted FMR values are broadly an order of magnitude larger than the nominal rates because FMR is computed over demographically-matched impostor pairs i.e individuals of the same sex, from the same geographic region (see section 3.6.1), and the same age group (see section 3.6.2).

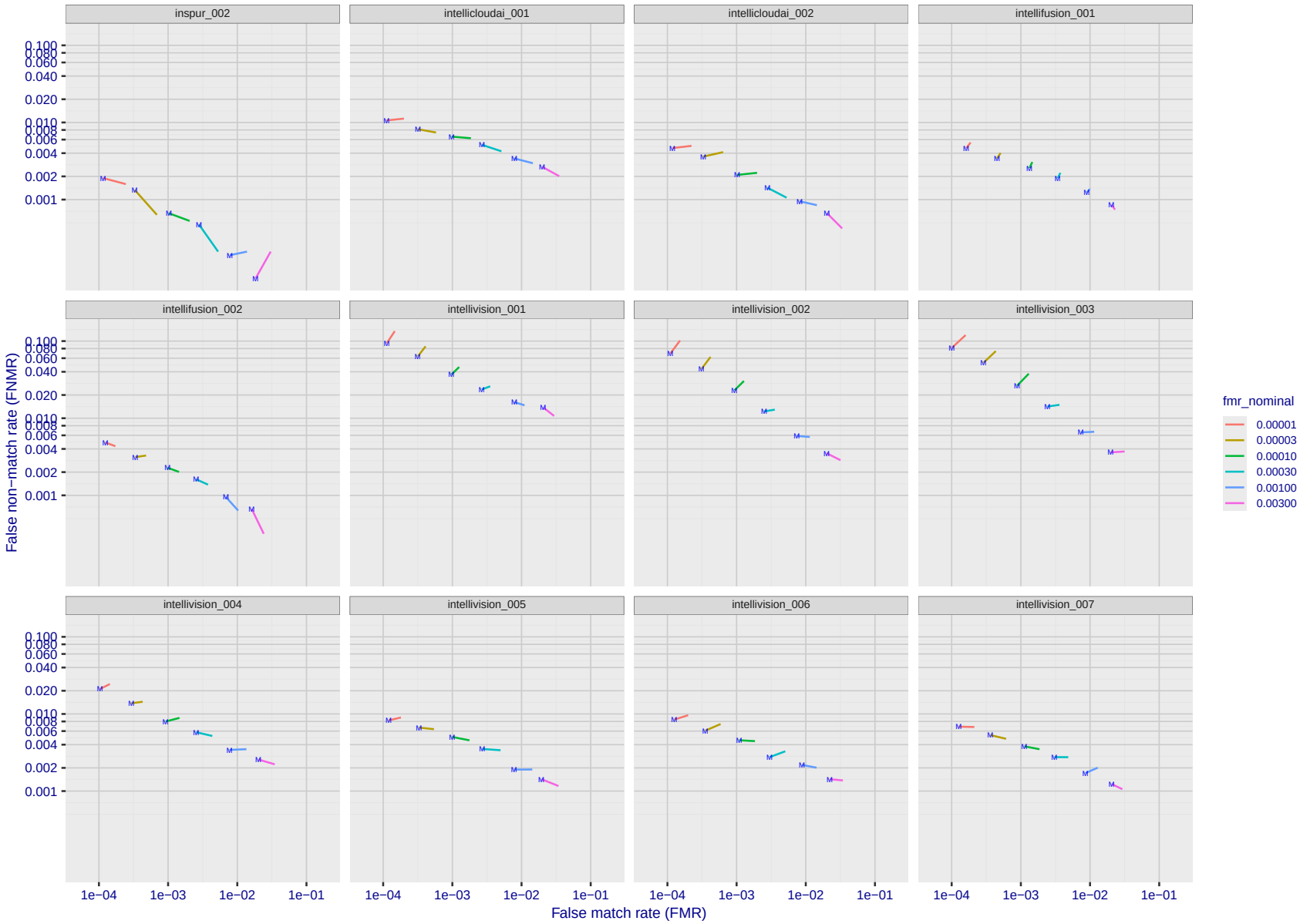

Figure 489: For the visa images, FNMR and FMR at six operating points along the DET characteristic. At each point a line is drawn between (FMR,FNMR)$_{\text{MALE}}$ and (FMR,FNMR)$_{\text{FEMALE}}$ showing how which sex has lower FMR and/or FNMR. The "M" label denotes male, the other end of the line corresponds to female. The six operating thresholds are selected to give the nominal false match rates given in the legend, and are computed over all impostor pairs regardless of age, sex, and place of birth. The plotted FMR values are broadly an order of magnitude larger than the nominal rates because FMR is computed over demographically-matched impostor pairs i.e individuals of the same sex, from the same geographic region (see section 3.6.1), and the same age group (see section 3.6.2).

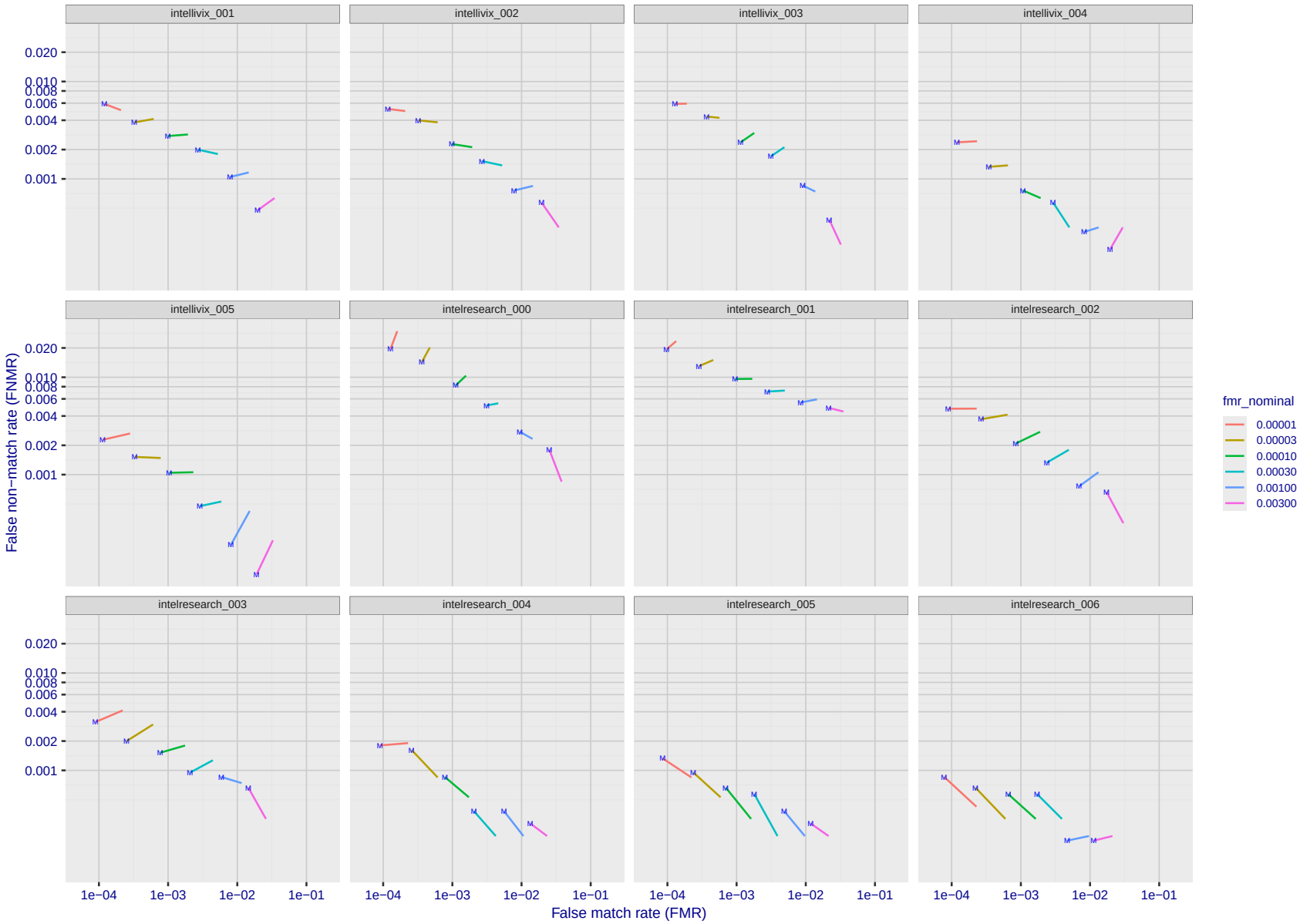

Figure 490: For the visa images, FNMR and FMR at six operating points along the DET characteristic. At each point a line is drawn between (FMR,FNMR)$_{\text{MALE}}$ and (FMR,FNMR)$_{\text{FEMALE}}$ showing how which sex has lower FMR and/or FNMR. The "M" label denotes male, the other end of the line corresponds to female. The six operating thresholds are selected to give the nominal false match rates given in the legend, and are computed over all impostor pairs regardless of age, sex, and place of birth. The plotted FMR values are broadly an order of magnitude larger than the nominal rates because FMR is computed over demographically-matched impostor pairs i.e individuals of the same sex, from the same geographic region (see section 3.6.1), and the same age group (see section 3.6.2).

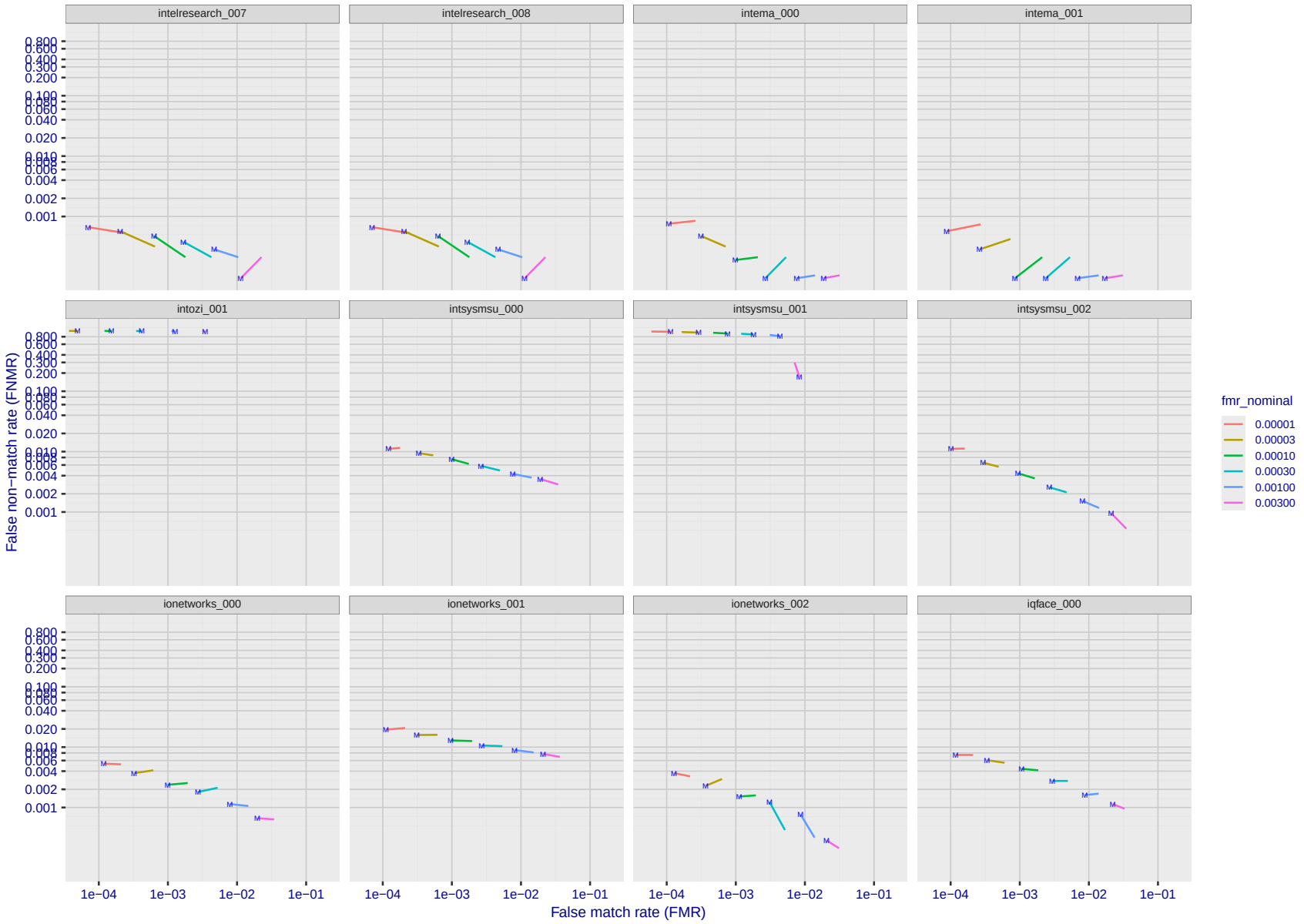

Figure 491: For the visa images, FNMR and FMR at six operating points along the DET characteristic. At each point a line is drawn between (FMR,FNMR)$_{\text{MALE}}$ and (FMR,FNMR)$_{\text{FEMALE}}$ showing how which sex has lower FMR and/or FNMR. The "M" label denotes male, the other end of the line corresponds to female. The six operating thresholds are selected to give the nominal false match rates given in the legend, and are computed over all impostor pairs regardless of age, sex, and place of birth. The plotted FMR values are broadly an order of magnitude larger than the nominal rates because FMR is computed over demographically-matched impostor pairs i.e individuals of the same sex, from the same geographic region (see section 3.6.1), and the same age group (see section 3.6.2).

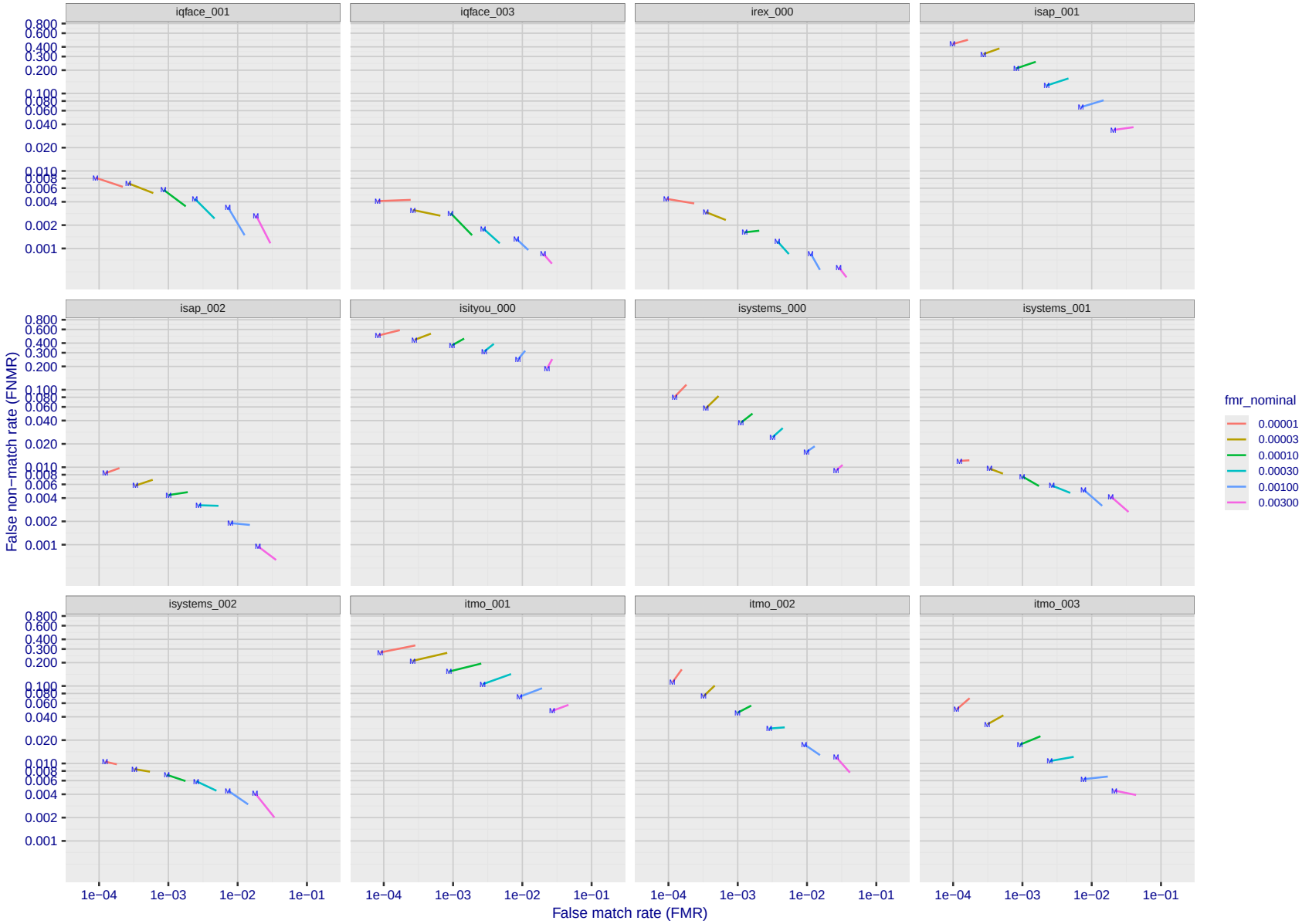

Figure 492: For the visa images, FNMR and FMR at six operating points along the DET characteristic. At each point a line is drawn between (FMR,FNMR)$_{\text{MALE}}$ and (FMR,FNMR)$_{\text{FEMALE}}$ showing how which sex has lower FMR and/or FNMR. The "M" label denotes male, the other end of the line corresponds to female. The six operating thresholds are selected to give the nominal false match rates given in the legend, and are computed over all impostor pairs regardless of age, sex, and place of birth. The plotted FMR values are broadly an order of magnitude larger than the nominal rates because FMR is computed over demographically-matched impostor pairs i.e individuals of the same sex, from the same geographic region (see section 3.6.1), and the same age group (see section 3.6.2).

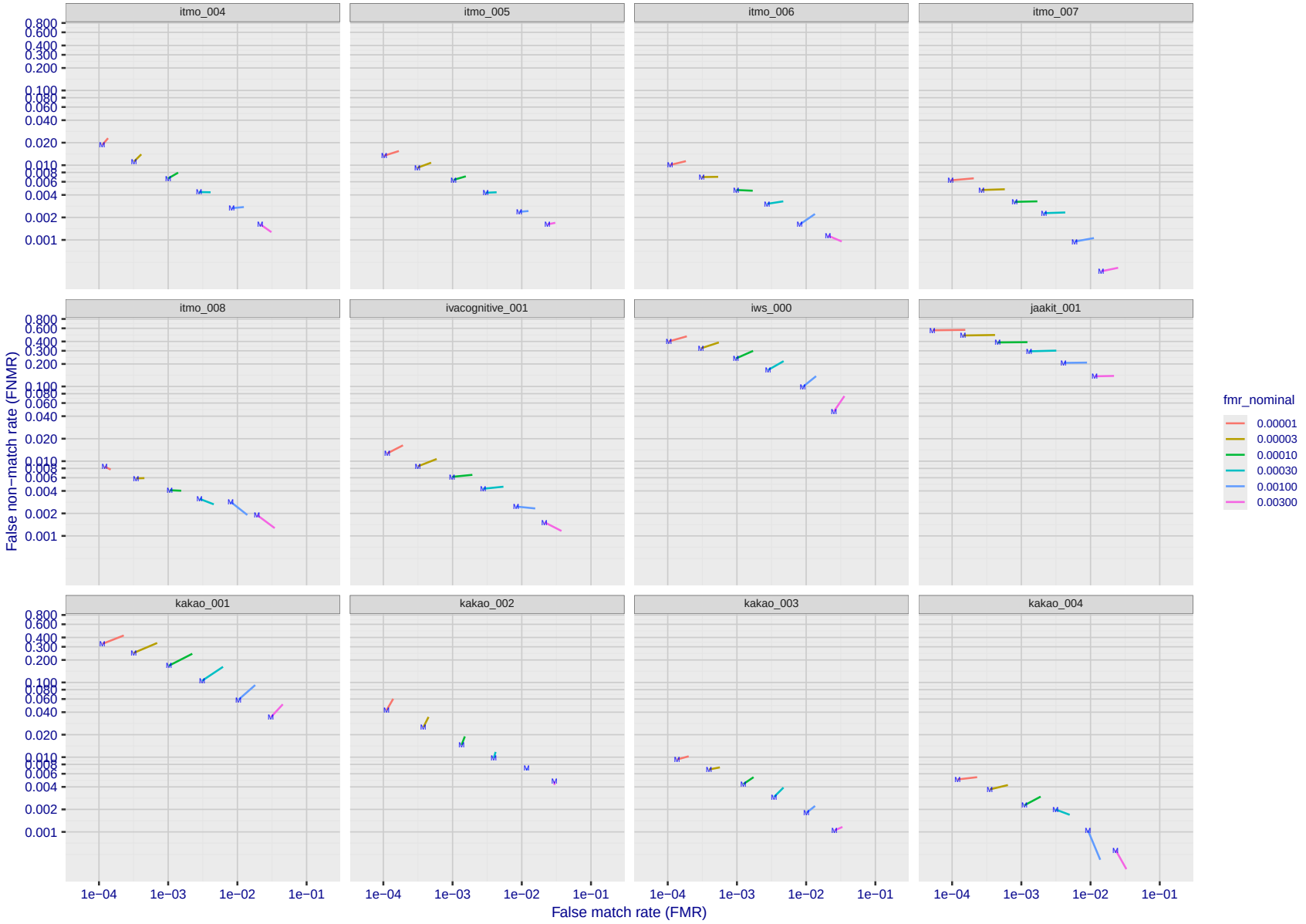

Figure 493: For the visa images, FNMR and FMR at six operating points along the DET characteristic. At each point a line is drawn between (FMR,FNMR)$_{\text{MALE}}$ and (FMR,FNMR)$_{\text{FEMALE}}$ showing how which sex has lower FMR and/or FNMR. The "M" label denotes male, the other end of the line corresponds to female. The six operating thresholds are selected to give the nominal false match rates given in the legend, and are computed over all impostor pairs regardless of age, sex, and place of birth. The plotted FMR values are broadly an order of magnitude larger than the nominal rates because FMR is computed over demographically-matched impostor pairs i.e individuals of the same sex, from the same geographic region (see section 3.6.1), and the same age group (see section 3.6.2).

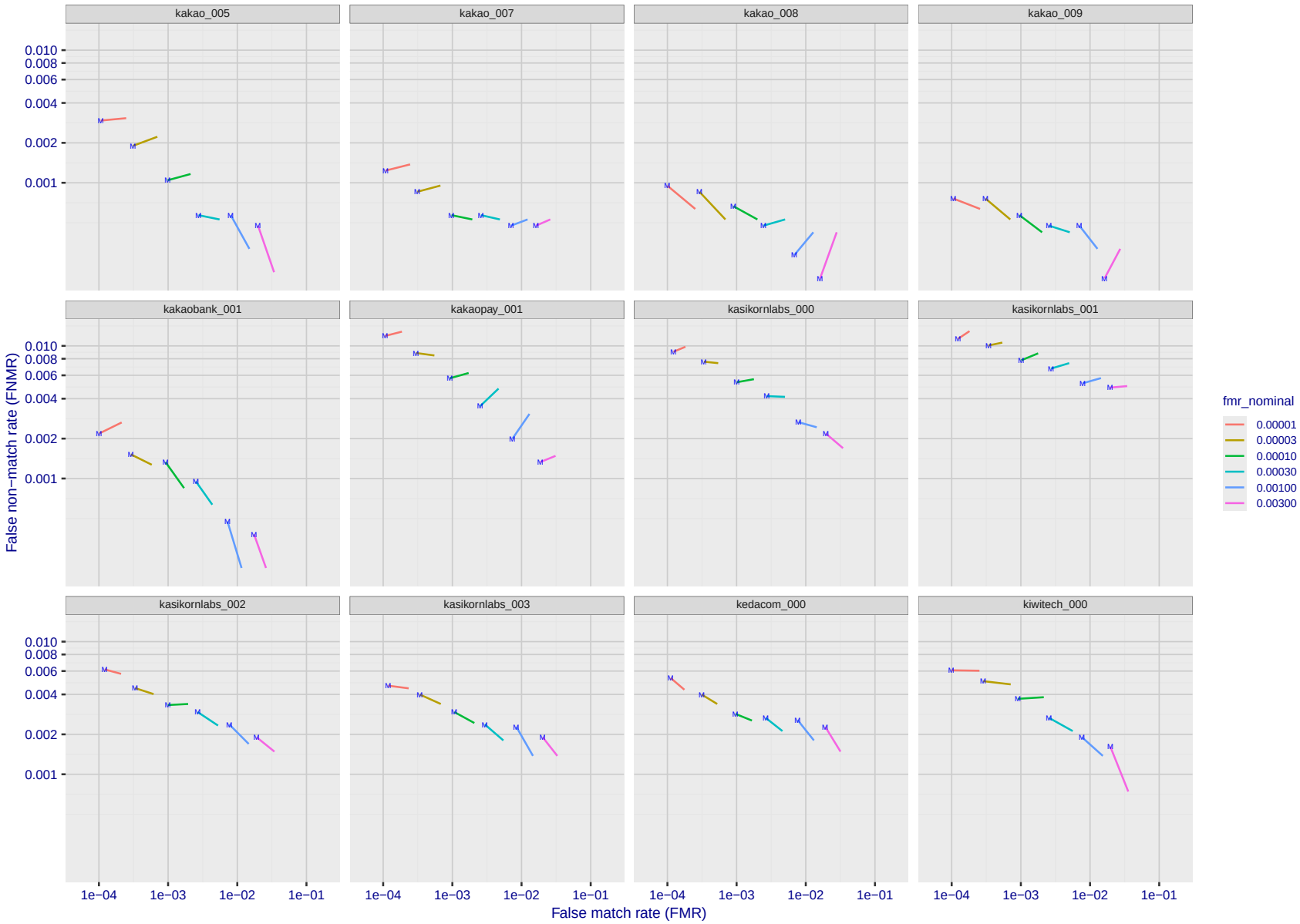

Figure 494: For the visa images, FNMR and FMR at six operating points along the DET characteristic. At each point a line is drawn between (FMR,FNMR)$_{\text{MALE}}$ and (FMR,FNMR)$_{\text{FEMALE}}$ showing how which sex has lower FMR and/or FNMR. The "M" label denotes male, the other end of the line corresponds to female. The six operating thresholds are selected to give the nominal false match rates given in the legend, and are computed over all impostor pairs regardless of age, sex, and place of birth. The plotted FMR values are broadly an order of magnitude larger than the nominal rates because FMR is computed over demographically-matched impostor pairs i.e individuals of the same sex, from the same geographic region (see section 3.6.1), and the same age group (see section 3.6.2).

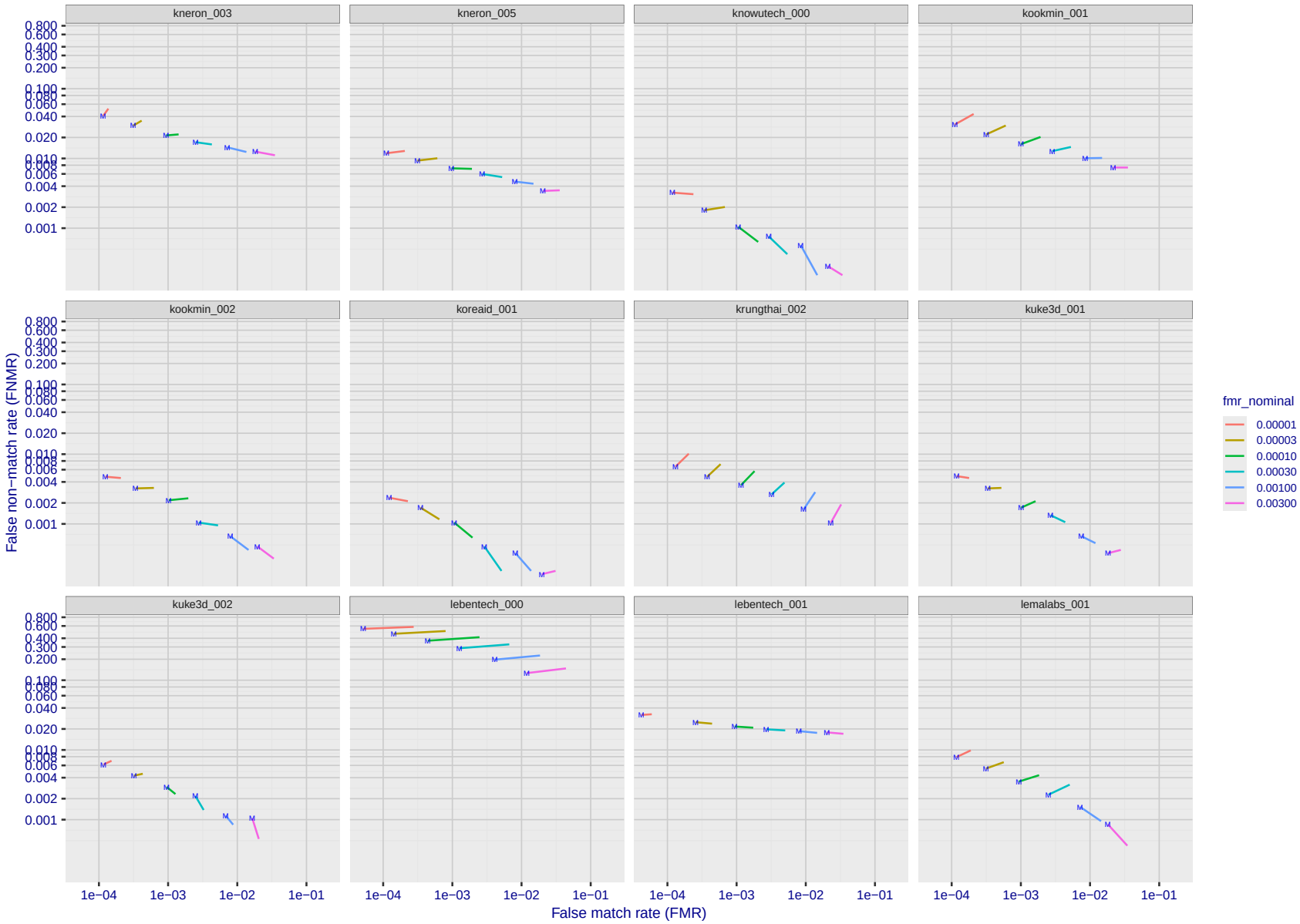

Figure 495: For the visa images, FNMR and FMR at six operating points along the DET characteristic. At each point a line is drawn between (FMR,FNMR)$_{\text{MALE}}$ and (FMR,FNMR)$_{\text{FEMALE}}$ showing how which sex has lower FMR and/or FNMR. The "M" label denotes male, the other end of the line corresponds to female. The six operating thresholds are selected to give the nominal false match rates given in the legend, and are computed over all impostor pairs regardless of age, sex, and place of birth. The plotted FMR values are broadly an order of magnitude larger than the nominal rates because FMR is computed over demographically-matched impostor pairs i.e individuals of the same sex, from the same geographic region (see section 3.6.1), and the same age group (see section 3.6.2).

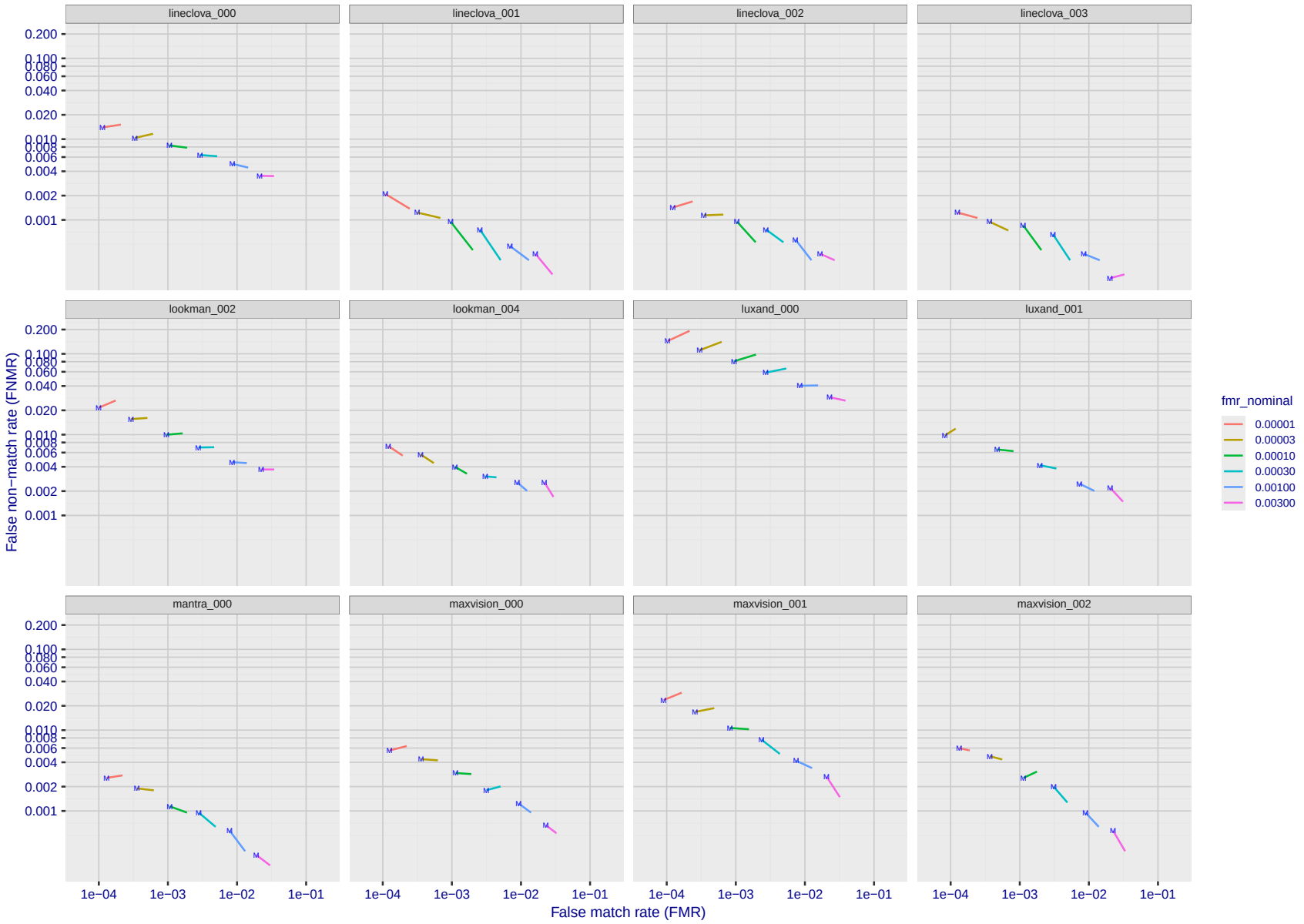

Figure 496: For the visa images, FNMR and FMR at six operating points along the DET characteristic. At each point a line is drawn between (FMR,FNMR)$_{\text{MALE}}$ and (FMR,FNMR)$_{\text{FEMALE}}$ showing how which sex has lower FMR and/or FNMR. The "M" label denotes male, the other end of the line corresponds to female. The six operating thresholds are selected to give the nominal false match rates given in the legend, and are computed over all impostor pairs regardless of age, sex, and place of birth. The plotted FMR values are broadly an order of magnitude larger than the nominal rates because FMR is computed over demographically-matched impostor pairs i.e individuals of the same sex, from the same geographic region (see section 3.6.1), and the same age group (see section 3.6.2).

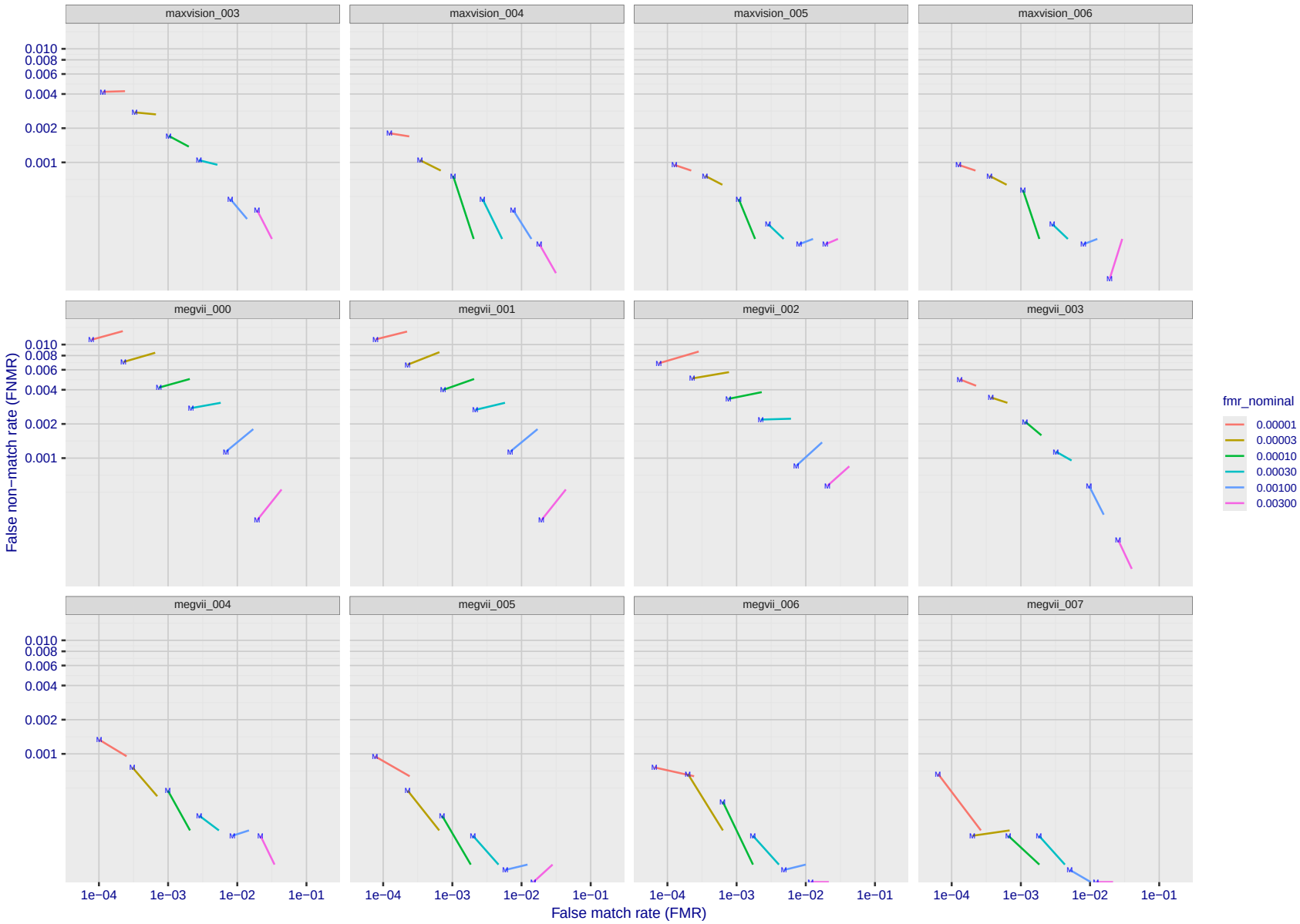

Figure 497: For the visa images, FNMR and FMR at six operating points along the DET characteristic. At each point a line is drawn between (FMR,FNMR)$_{\text{MALE}}$ and (FMR,FNMR)$_{\text{FEMALE}}$ showing how which sex has lower FMR and/or FNMR. The "M" label denotes male, the other end of the line corresponds to female. The six operating thresholds are selected to give the nominal false match rates given in the legend, and are computed over all impostor pairs regardless of age, sex, and place of birth. The plotted FMR values are broadly an order of magnitude larger than the nominal rates because FMR is computed over demographically-matched impostor pairs i.e individuals of the same sex, from the same geographic region (see section 3.6.1), and the same age group (see section 3.6.2).

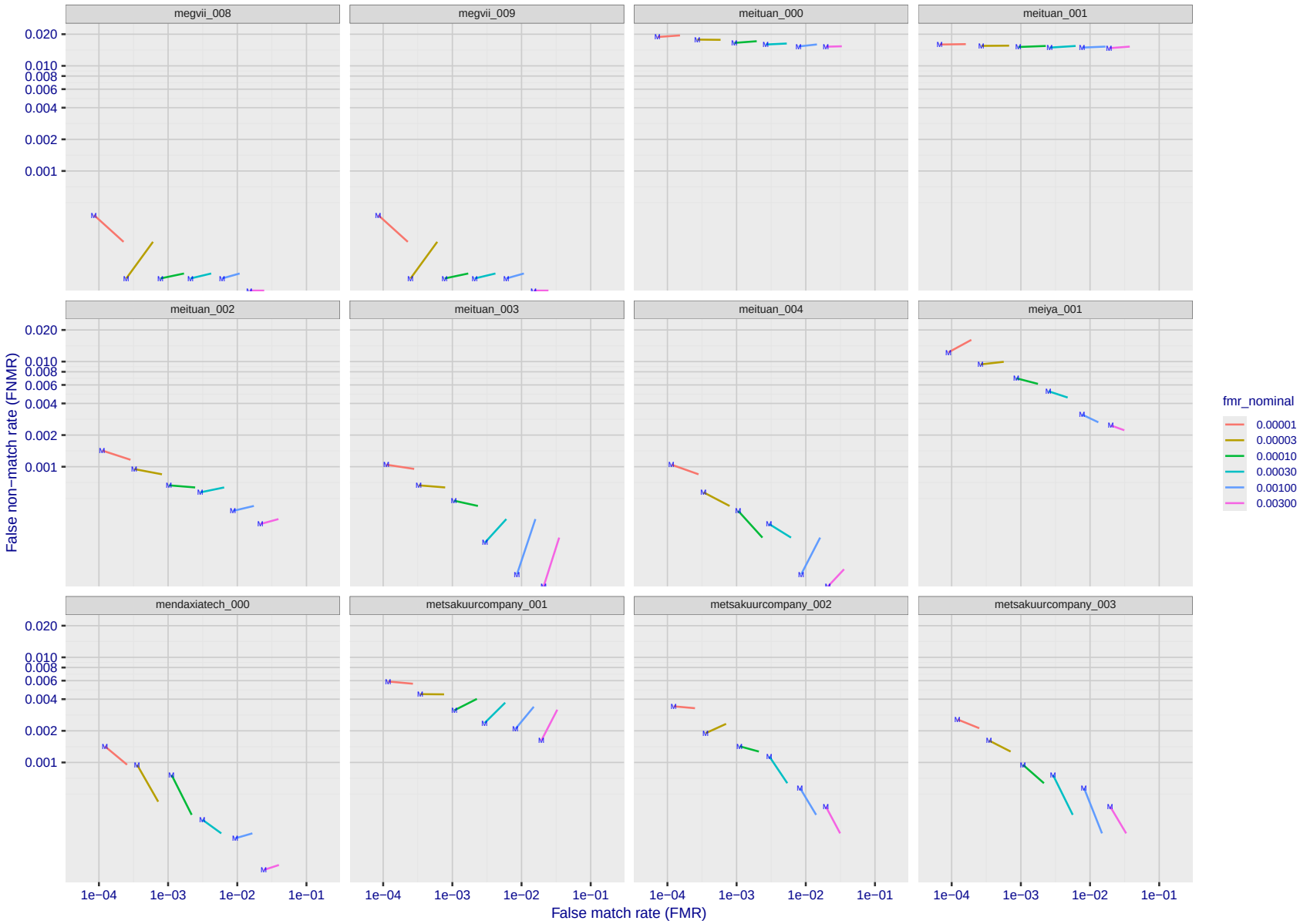

Figure 498: For the visa images, FNMR and FMR at six operating points along the DET characteristic. At each point a line is drawn between (FMR,FNMR)$_{\text{MALE}}$ and (FMR,FNMR)$_{\text{FEMALE}}$ showing how which sex has lower FMR and/or FNMR. The "M" label denotes male, the other end of the line corresponds to female. The six operating thresholds are selected to give the nominal false match rates given in the legend, and are computed over all impostor pairs regardless of age, sex, and place of birth. The plotted FMR values are broadly an order of magnitude larger than the nominal rates because FMR is computed over demographically-matched impostor pairs i.e individuals of the same sex, from the same geographic region (see section 3.6.1), and the same age group (see section 3.6.2).

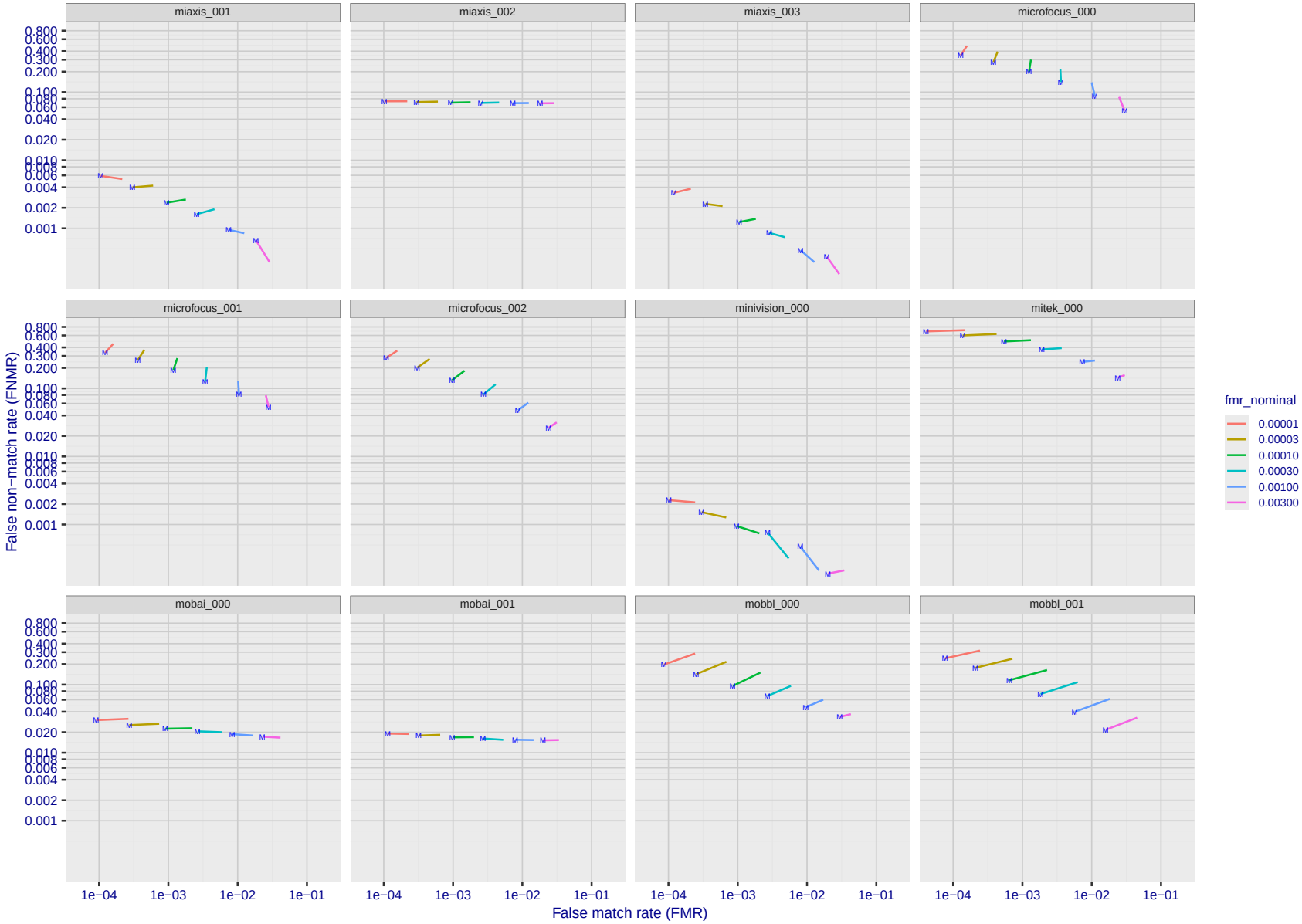

Figure 499: For the visa images, FNMR and FMR at six operating points along the DET characteristic. At each point a line is drawn between (FMR,FNMR)$_{\text{MALE}}$ and (FMR,FNMR)$_{\text{FEMALE}}$ showing how which sex has lower FMR and/or FNMR. The "M" label denotes male, the other end of the line corresponds to female. The six operating thresholds are selected to give the nominal false match rates given in the legend, and are computed over all impostor pairs regardless of age, sex, and place of birth. The plotted FMR values are broadly an order of magnitude larger than the nominal rates because FMR is computed over demographically-matched impostor pairs i.e individuals of the same sex, from the same geographic region (see section 3.6.1), and the same age group (see section 3.6.2).

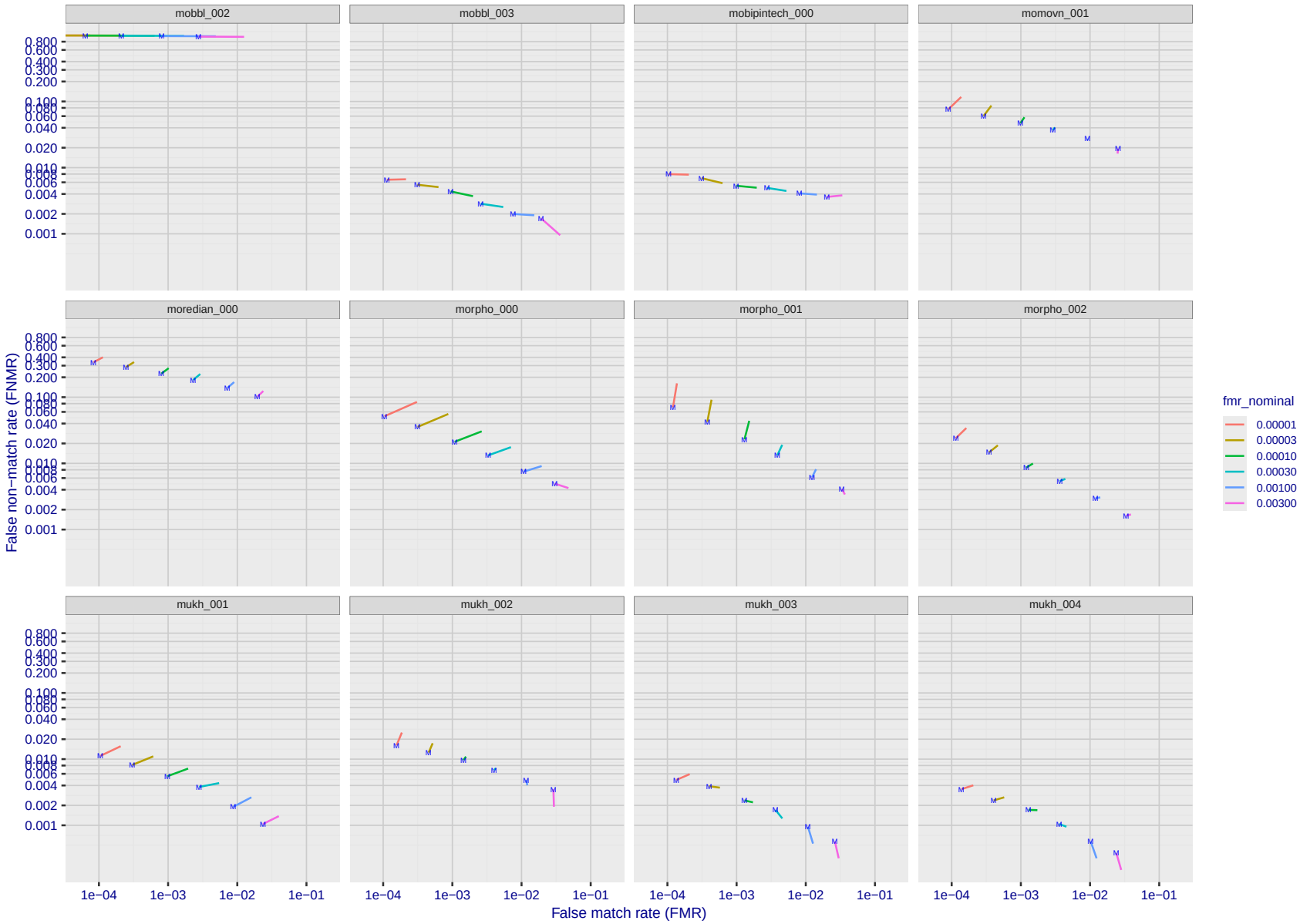

Figure 500: For the visa images, FNMR and FMR at six operating points along the DET characteristic. At each point a line is drawn between (FMR,FNMR)$_{\text{MALE}}$ and (FMR,FNMR)$_{\text{FEMALE}}$ showing how which sex has lower FMR and/or FNMR. The "M" label denotes male, the other end of the line corresponds to female. The six operating thresholds are selected to give the nominal false match rates given in the legend, and are computed over all impostor pairs regardless of age, sex, and place of birth. The plotted FMR values are broadly an order of magnitude larger than the nominal rates because FMR is computed over demographically-matched impostor pairs i.e individuals of the same sex, from the same geographic region (see section 3.6.1), and the same age group (see section 3.6.2).

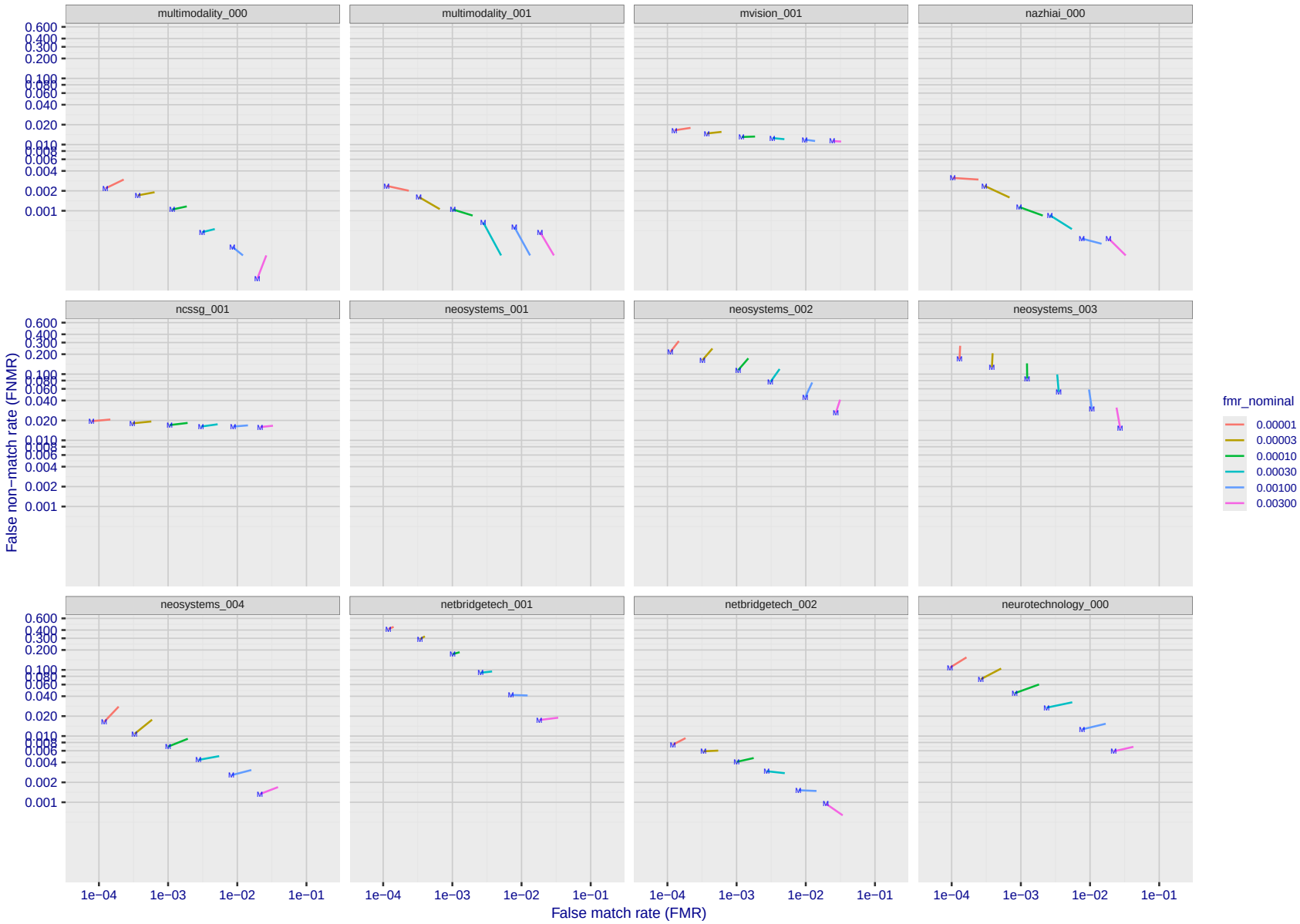

Figure 501: For the visa images, FNMR and FMR at six operating points along the DET characteristic. At each point a line is drawn between (FMR,FNMR)$_{\text{MALE}}$ and (FMR,FNMR)$_{\text{FEMALE}}$ showing how which sex has lower FMR and/or FNMR. The "M" label denotes male, the other end of the line corresponds to female. The six operating thresholds are selected to give the nominal false match rates given in the legend, and are computed over all impostor pairs regardless of age, sex, and place of birth. The plotted FMR values are broadly an order of magnitude larger than the nominal rates because FMR is computed over demographically-matched impostor pairs i.e individuals of the same sex, from the same geographic region (see section 3.6.1), and the same age group (see section 3.6.2).

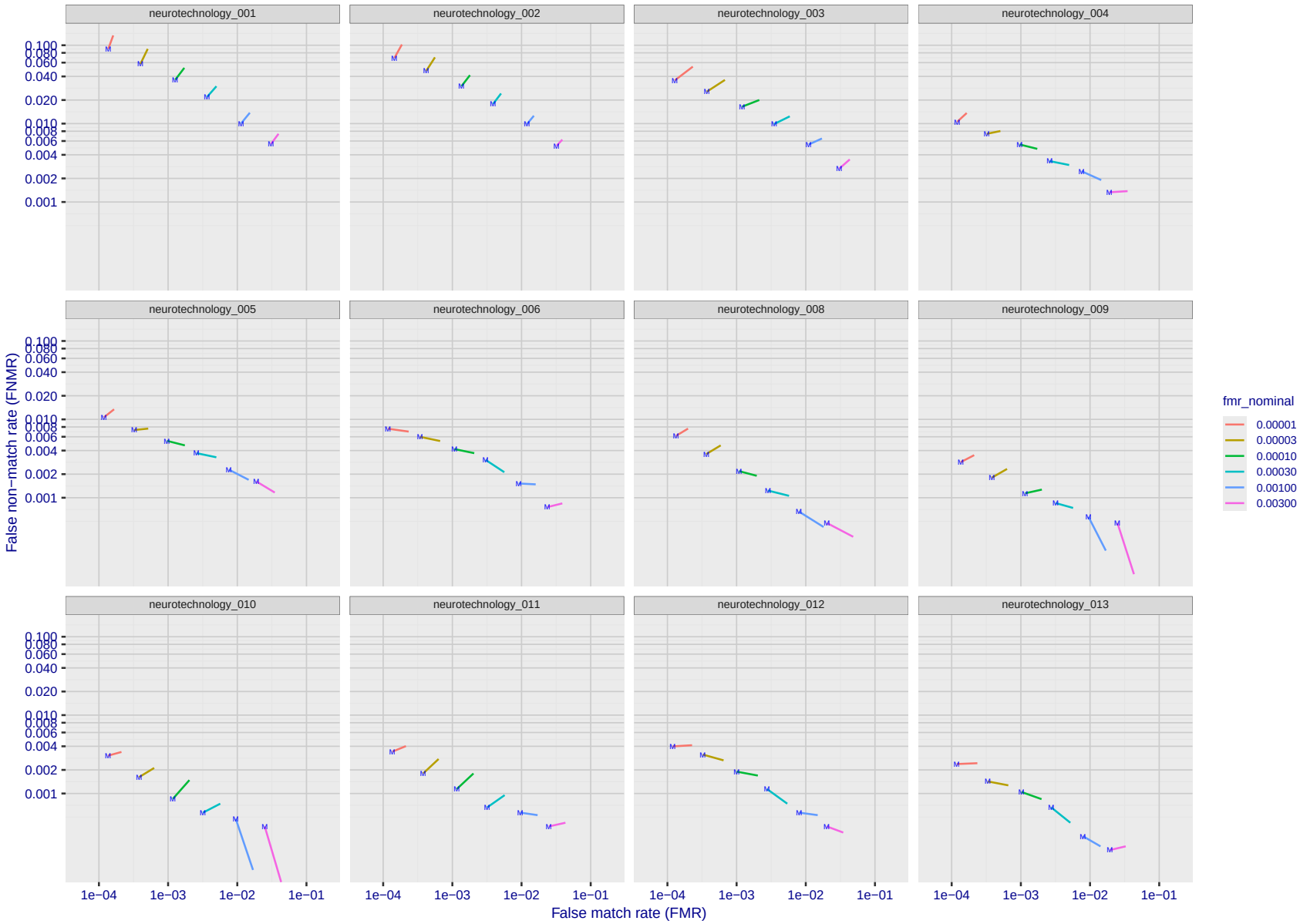

Figure 502: For the visa images, FNMR and FMR at six operating points along the DET characteristic. At each point a line is drawn between (FMR,FNMR)$_{\text{MALE}}$ and (FMR,FNMR)$_{\text{FEMALE}}$ showing how which sex has lower FMR and/or FNMR. The "M" label denotes male, the other end of the line corresponds to female. The six operating thresholds are selected to give the nominal false match rates given in the legend, and are computed over all impostor pairs regardless of age, sex, and place of birth. The plotted FMR values are broadly an order of magnitude larger than the nominal rates because FMR is computed over demographically-matched impostor pairs i.e individuals of the same sex, from the same geographic region (see section 3.6.1), and the same age group (see section 3.6.2).

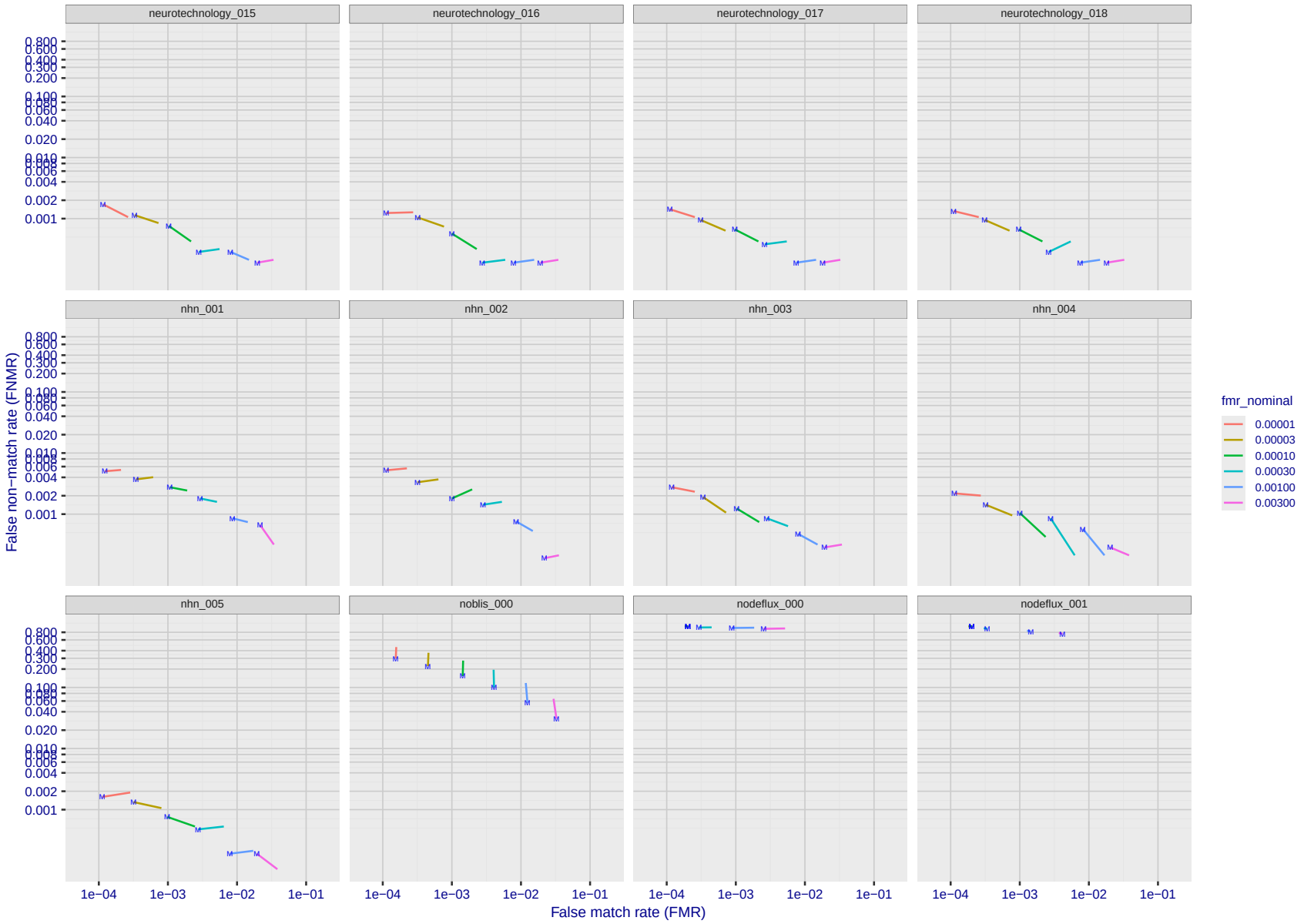

Figure 503: For the visa images, FNMR and FMR at six operating points along the DET characteristic. At each point a line is drawn between (FMR,FNMR)$_{\text{MALE}}$ and (FMR,FNMR)$_{\text{FEMALE}}$ showing how which sex has lower FMR and/or FNMR. The "M" label denotes male, the other end of the line corresponds to female. The six operating thresholds are selected to give the nominal false match rates given in the legend, and are computed over all impostor pairs regardless of age, sex, and place of birth. The plotted FMR values are broadly an order of magnitude larger than the nominal rates because FMR is computed over demographically-matched impostor pairs i.e individuals of the same sex, from the same geographic region (see section 3.6.1), and the same age group (see section 3.6.2).

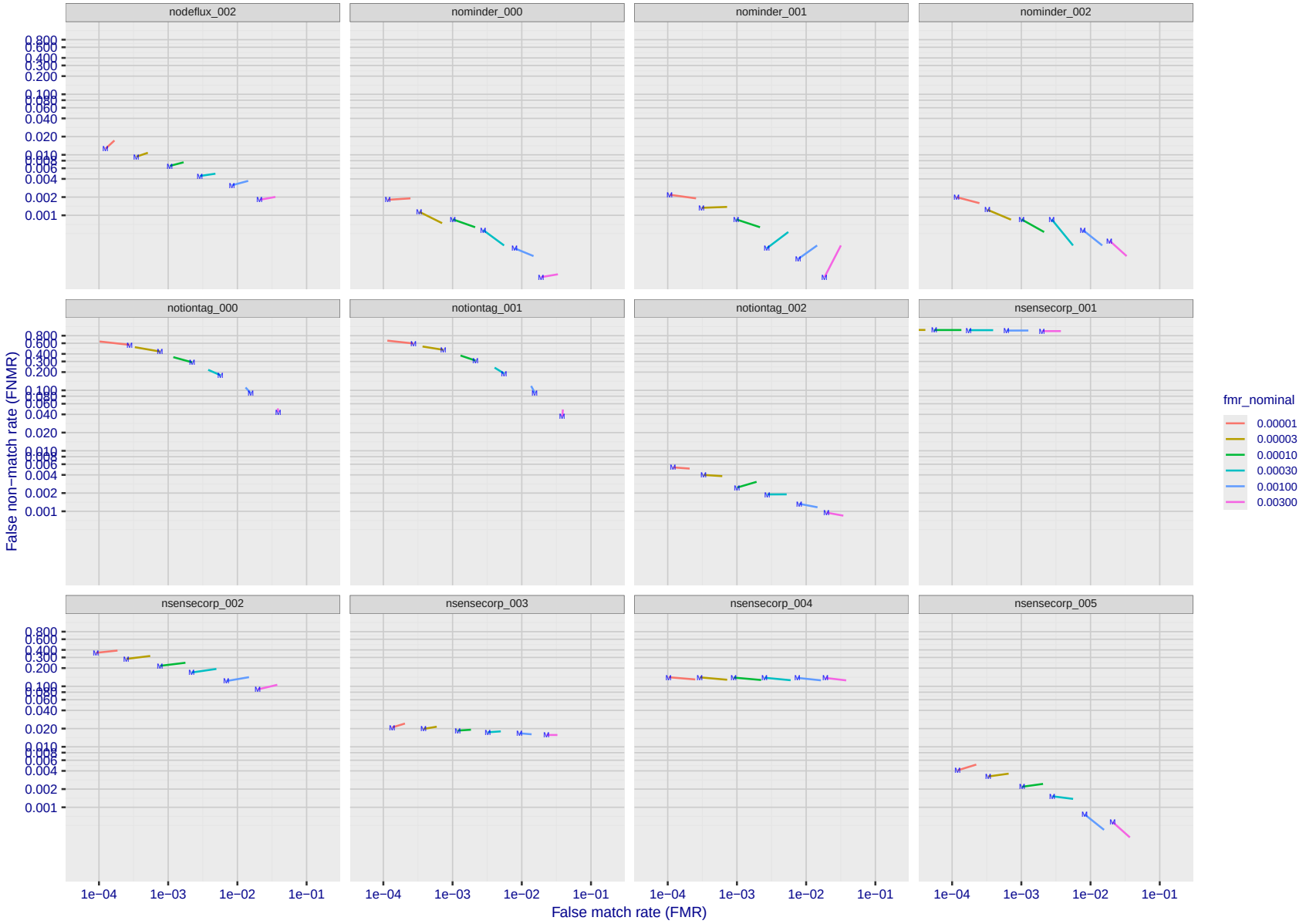

Figure 504: For the visa images, FNMR and FMR at six operating points along the DET characteristic. At each point a line is drawn between (FMR,FNMR)$_{\text{MALE}}$ and (FMR,FNMR)$_{\text{FEMALE}}$ showing how which sex has lower FMR and/or FNMR. The "M" label denotes male, the other end of the line corresponds to female. The six operating thresholds are selected to give the nominal false match rates given in the legend, and are computed over all impostor pairs regardless of age, sex, and place of birth. The plotted FMR values are broadly an order of magnitude larger than the nominal rates because FMR is computed over demographically-matched impostor pairs i.e individuals of the same sex, from the same geographic region (see section 3.6.1), and the same age group (see section 3.6.2).

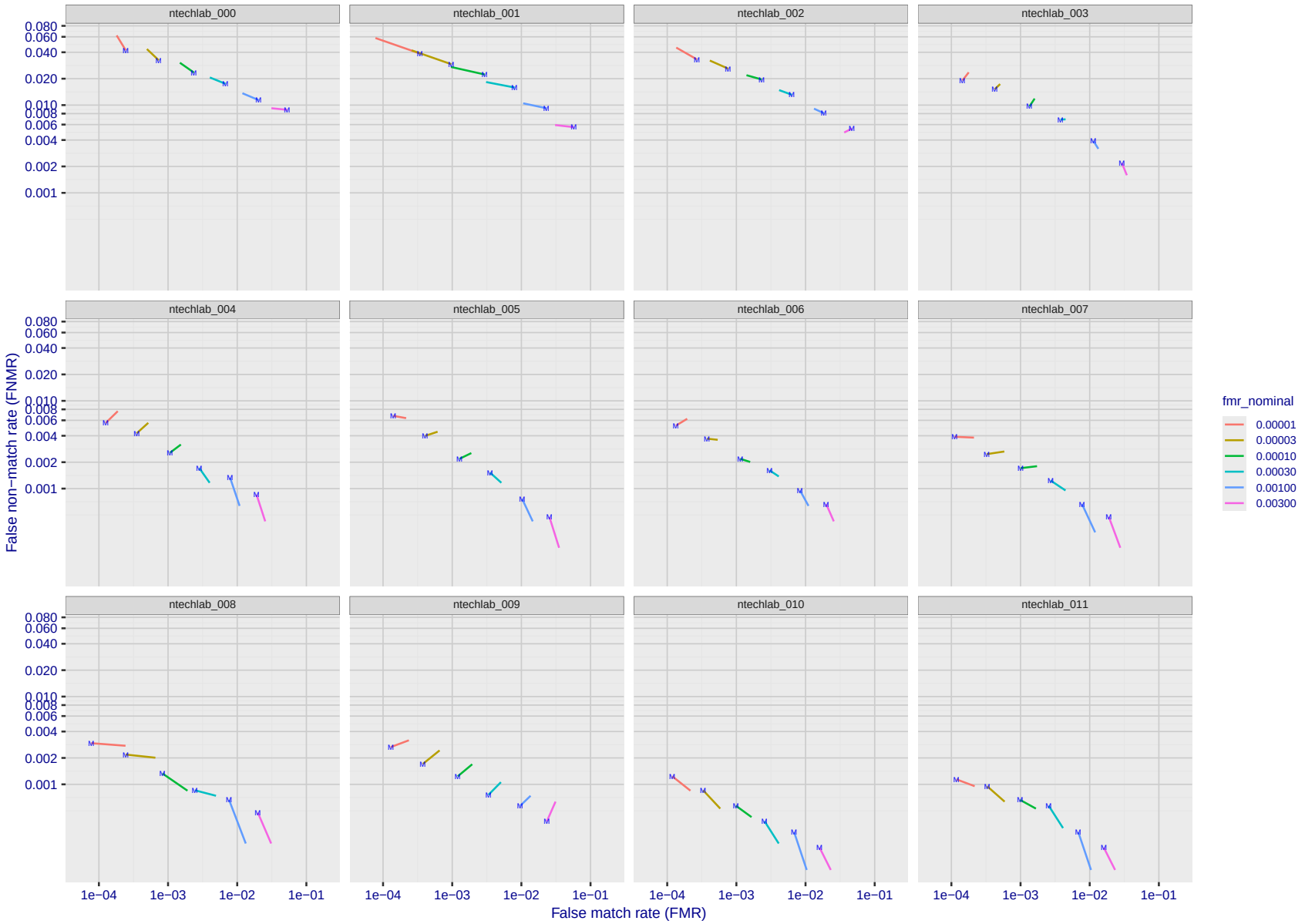

Figure 505: For the visa images, FNMR and FMR at six operating points along the DET characteristic. At each point a line is drawn between (FMR,FNMR)$_{\text{MALE}}$ and (FMR,FNMR)$_{\text{FEMALE}}$ showing how which sex has lower FMR and/or FNMR. The "M" label denotes male, the other end of the line corresponds to female. The six operating thresholds are selected to give the nominal false match rates given in the legend, and are computed over all impostor pairs regardless of age, sex, and place of birth. The plotted FMR values are broadly an order of magnitude larger than the nominal rates because FMR is computed over demographically-matched impostor pairs i.e individuals of the same sex, from the same geographic region (see section 3.6.1), and the same age group (see section 3.6.2).

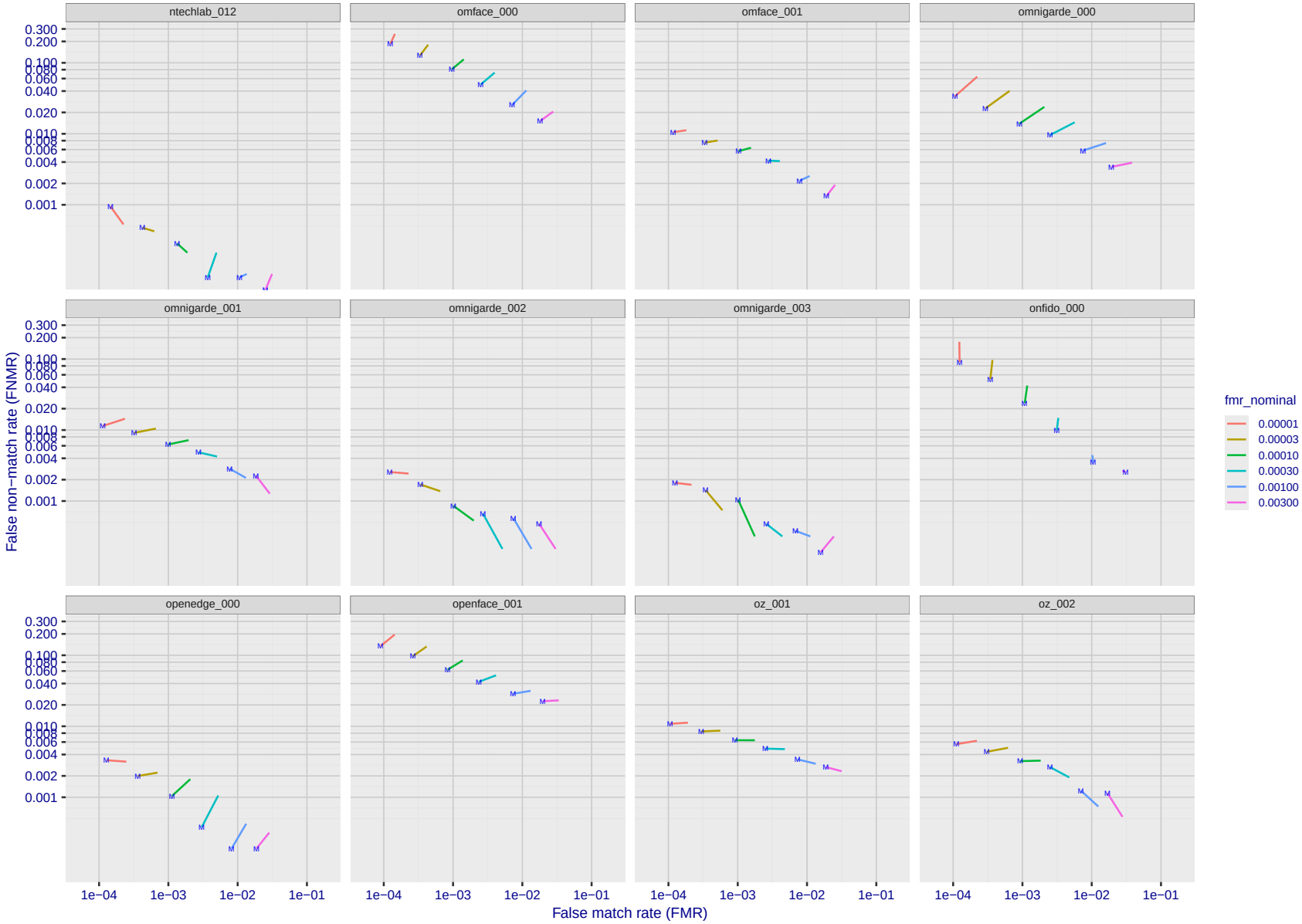

Figure 506: For the visa images, FNMR and FMR at six operating points along the DET characteristic. At each point a line is drawn between (FMR,FNMR)$_{\text{MALE}}$ and (FMR,FNMR)$_{\text{FEMALE}}$ showing how which sex has lower FMR and/or FNMR. The "M" label denotes male, the other end of the line corresponds to female. The six operating thresholds are selected to give the nominal false match rates given in the legend, and are computed over all impostor pairs regardless of age, sex, and place of birth. The plotted FMR values are broadly an order of magnitude larger than the nominal rates because FMR is computed over demographically-matched impostor pairs i.e individuals of the same sex, from the same geographic region (see section 3.6.1), and the same age group (see section 3.6.2).

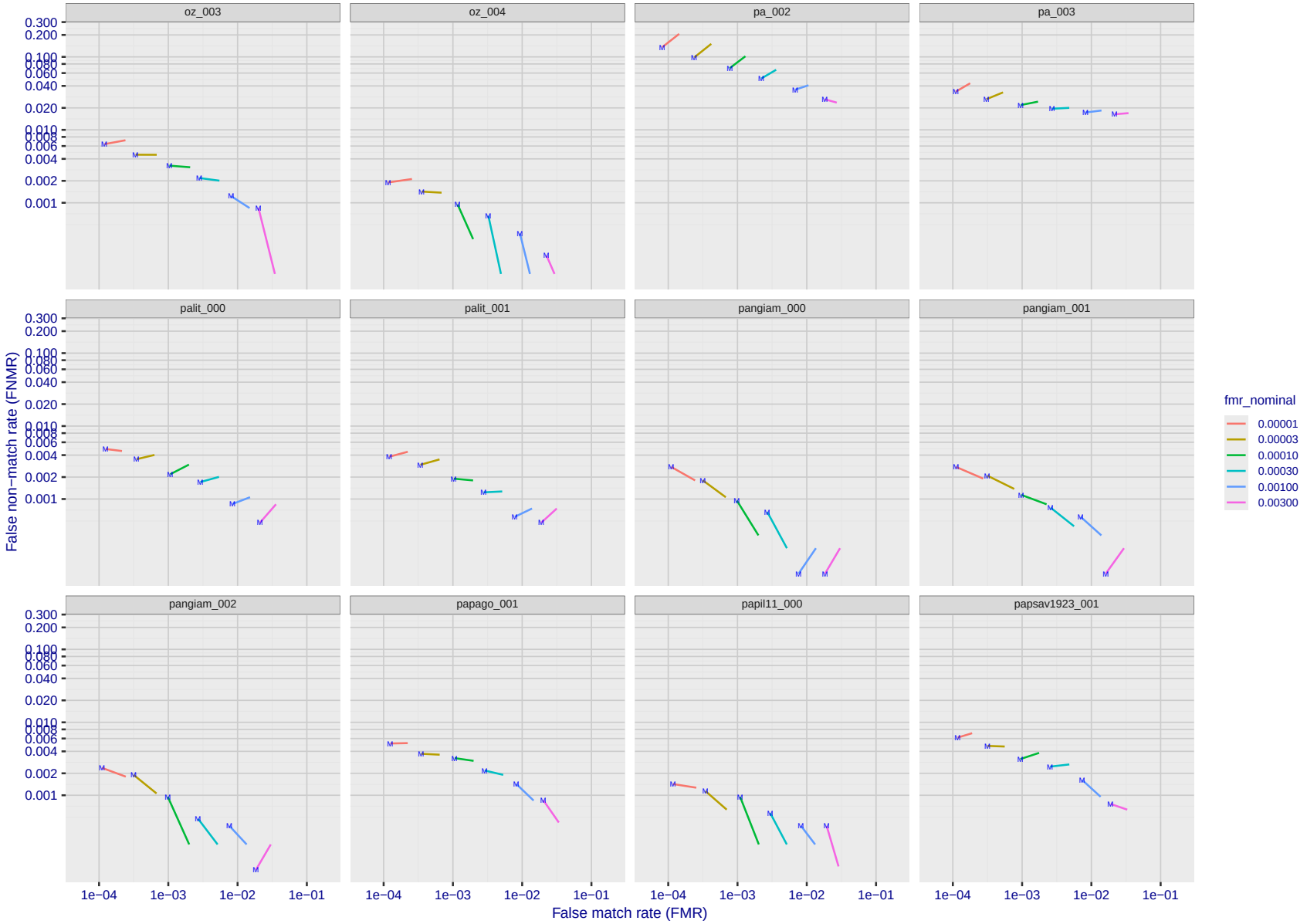

Figure 507: For the visa images, FNMR and FMR at six operating points along the DET characteristic. At each point a line is drawn between (FMR,FNMR)$_{\text{MALE}}$ and (FMR,FNMR)$_{\text{FEMALE}}$ showing how which sex has lower FMR and/or FNMR. The "M" label denotes male, the other end of the line corresponds to female. The six operating thresholds are selected to give the nominal false match rates given in the legend, and are computed over all impostor pairs regardless of age, sex, and place of birth. The plotted FMR values are broadly an order of magnitude larger than the nominal rates because FMR is computed over demographically-matched impostor pairs i.e individuals of the same sex, from the same geographic region (see section 3.6.1), and the same age group (see section 3.6.2).

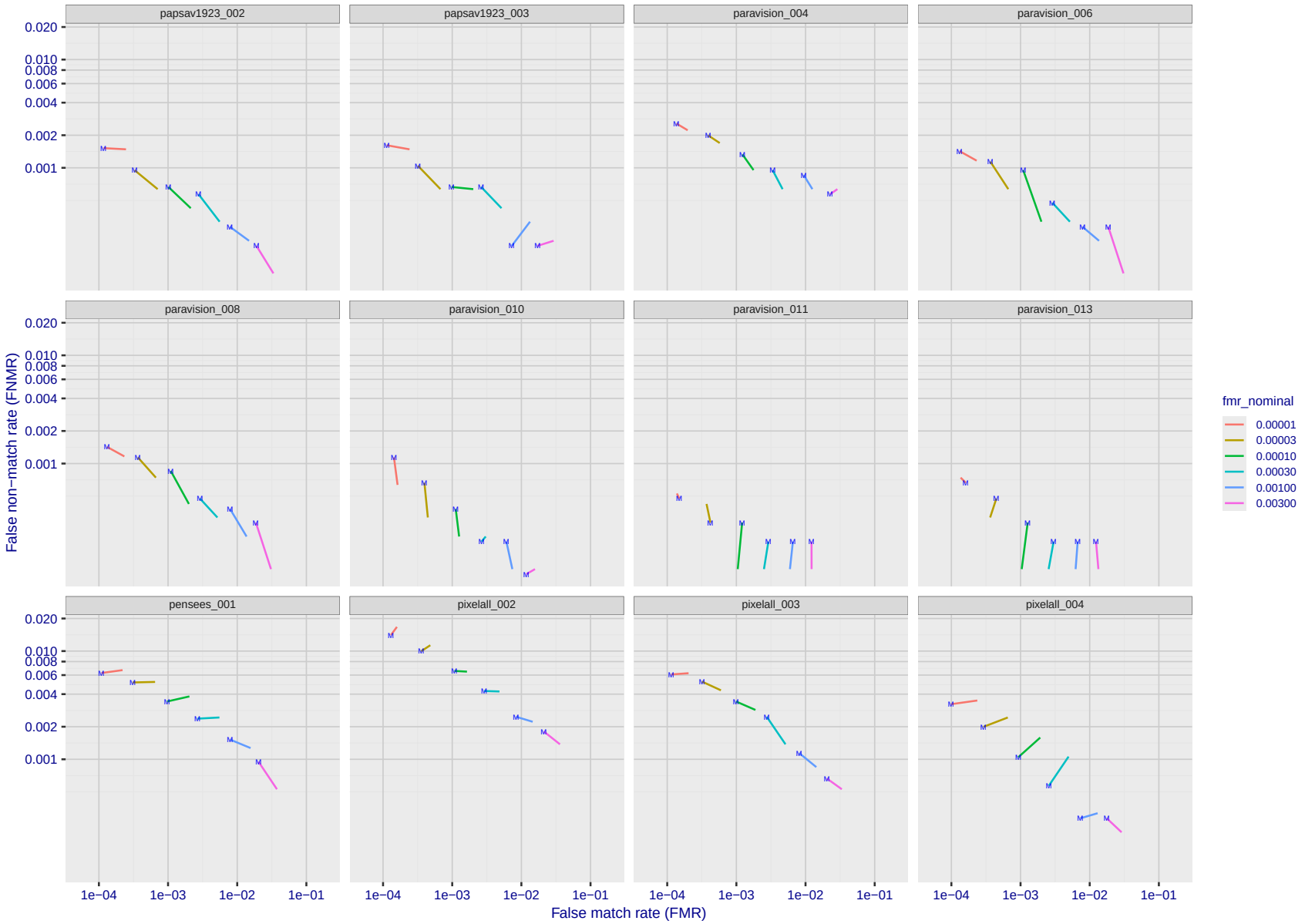

Figure 508: For the visa images, FNMR and FMR at six operating points along the DET characteristic. At each point a line is drawn between (FMR,FNMR)$_{\text{MALE}}$ and (FMR,FNMR)$_{\text{FEMALE}}$ showing how which sex has lower FMR and/or FNMR. The "M" label denotes male, the other end of the line corresponds to female. The six operating thresholds are selected to give the nominal false match rates given in the legend, and are computed over all impostor pairs regardless of age, sex, and place of birth. The plotted FMR values are broadly an order of magnitude larger than the nominal rates because FMR is computed over demographically-matched impostor pairs i.e individuals of the same sex, from the same geographic region (see section 3.6.1), and the same age group (see section 3.6.2).

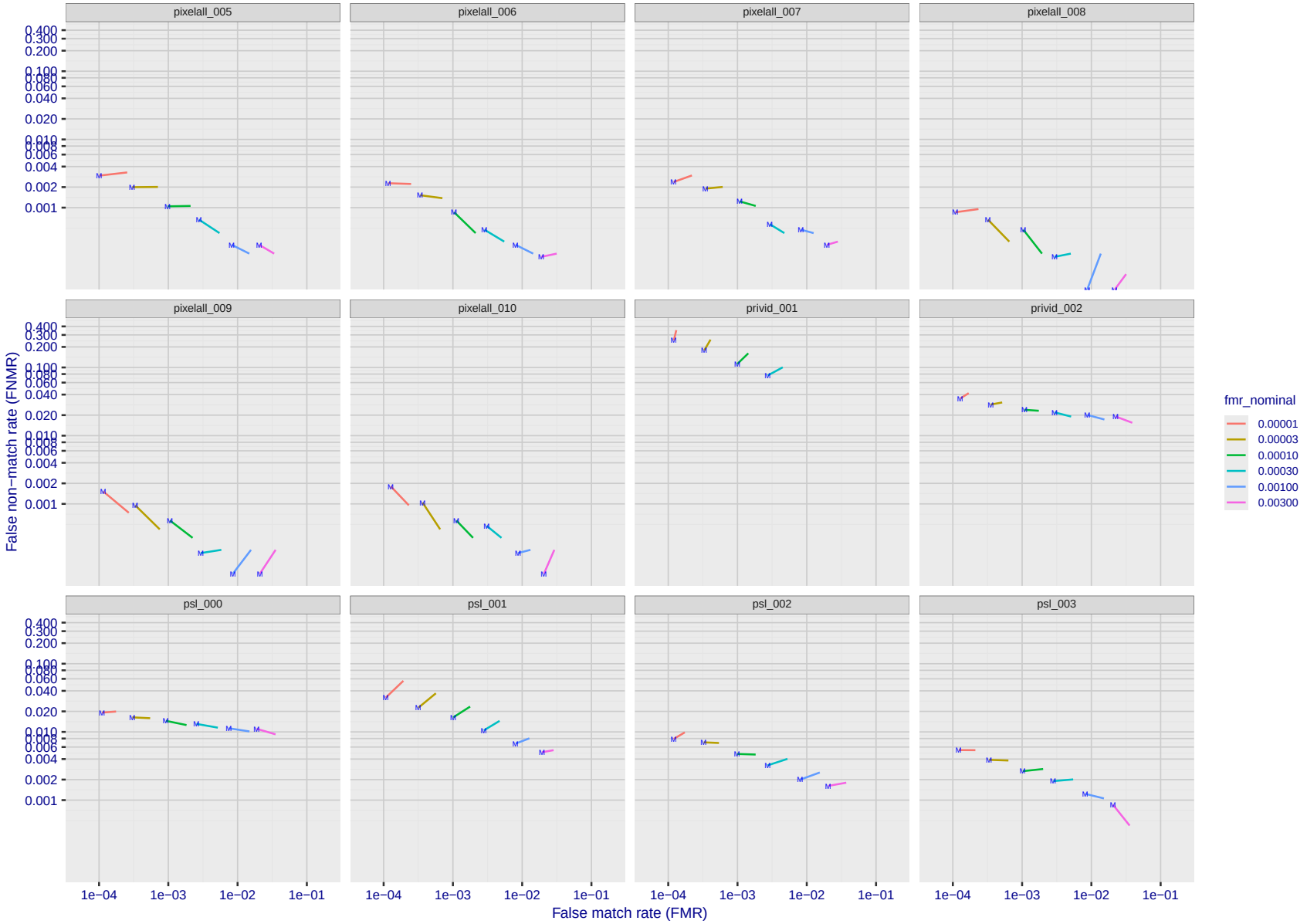

Figure 509: For the visa images, FNMR and FMR at six operating points along the DET characteristic. At each point a line is drawn between (FMR,FNMR)$_{\text{MALE}}$ and (FMR,FNMR)$_{\text{FEMALE}}$ showing how which sex has lower FMR and/or FNMR. The "M" label denotes male, the other end of the line corresponds to female. The six operating thresholds are selected to give the nominal false match rates given in the legend, and are computed over all impostor pairs regardless of age, sex, and place of birth. The plotted FMR values are broadly an order of magnitude larger than the nominal rates because FMR is computed over demographically-matched impostor pairs i.e individuals of the same sex, from the same geographic region (see section 3.6.1), and the same age group (see section 3.6.2).

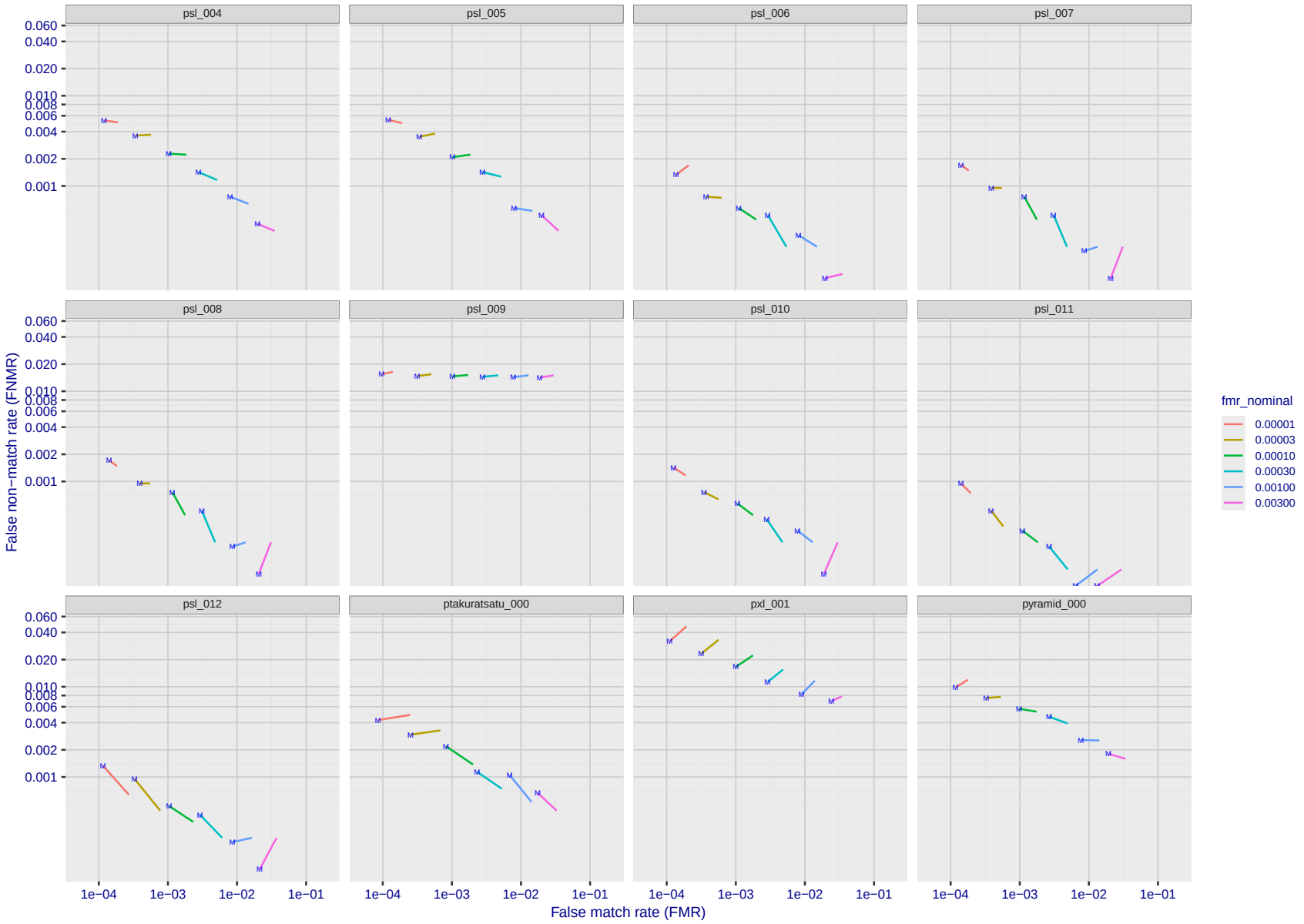

Figure 510: For the visa images, FNMR and FMR at six operating points along the DET characteristic. At each point a line is drawn between (FMR,FNMR)$_{\text{MALE}}$ and (FMR,FNMR)$_{\text{FEMALE}}$ showing how which sex has lower FMR and/or FNMR. The "M" label denotes male, the other end of the line corresponds to female. The six operating thresholds are selected to give the nominal false match rates given in the legend, and are computed over all impostor pairs regardless of age, sex, and place of birth. The plotted FMR values are broadly an order of magnitude larger than the nominal rates because FMR is computed over demographically-matched impostor pairs i.e individuals of the same sex, from the same geographic region (see section 3.6.1), and the same age group (see section 3.6.2).

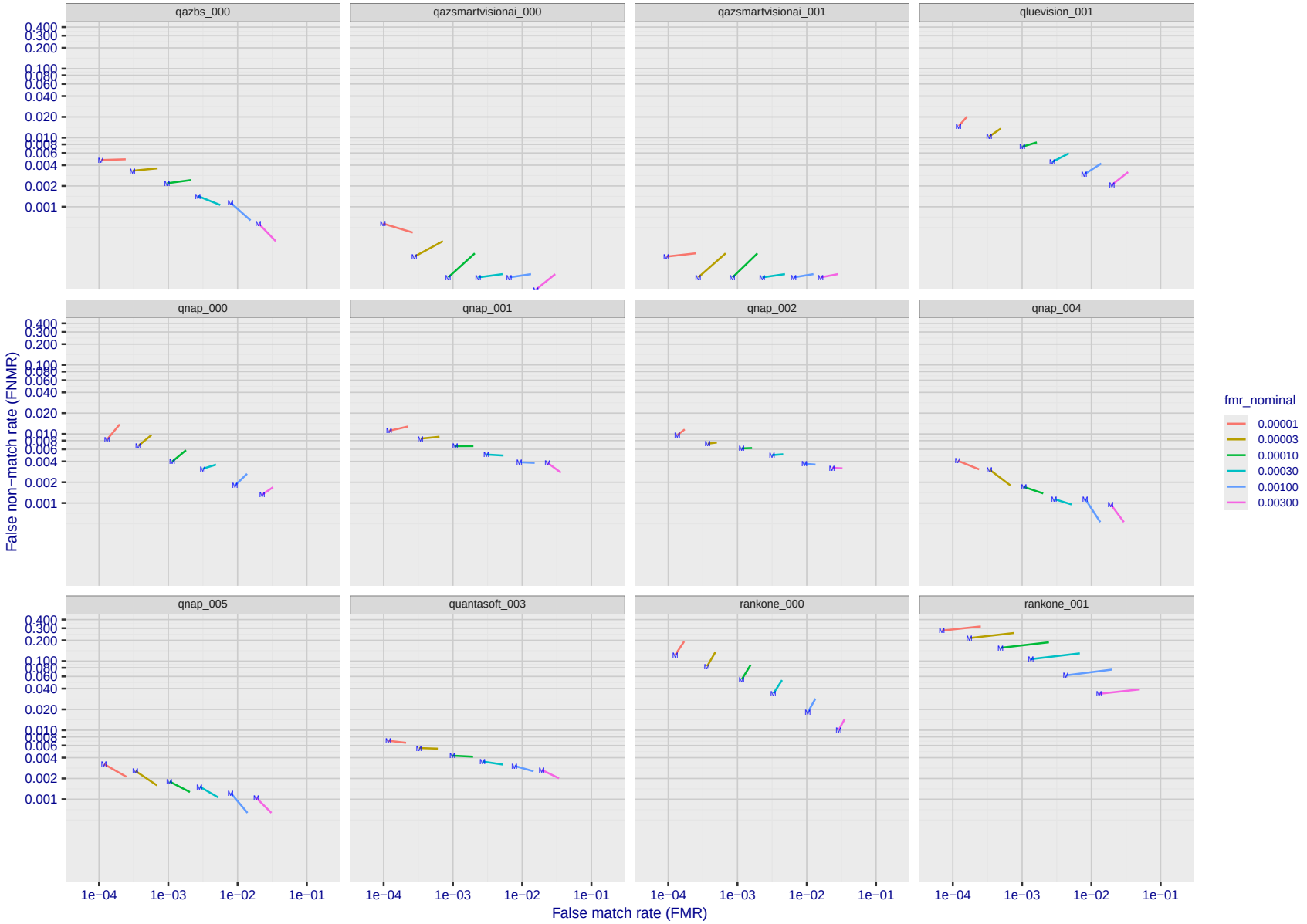

Figure 511: For the visa images, FNMR and FMR at six operating points along the DET characteristic. At each point a line is drawn between (FMR,FNMR)$_{\text{MALE}}$ and (FMR,FNMR)$_{\text{FEMALE}}$ showing how which sex has lower FMR and/or FNMR. The "M" label denotes male, the other end of the line corresponds to female. The six operating thresholds are selected to give the nominal false match rates given in the legend, and are computed over all impostor pairs regardless of age, sex, and place of birth. The plotted FMR values are broadly an order of magnitude larger than the nominal rates because FMR is computed over demographically-matched impostor pairs i.e individuals of the same sex, from the same geographic region (see section 3.6.1), and the same age group (see section 3.6.2).

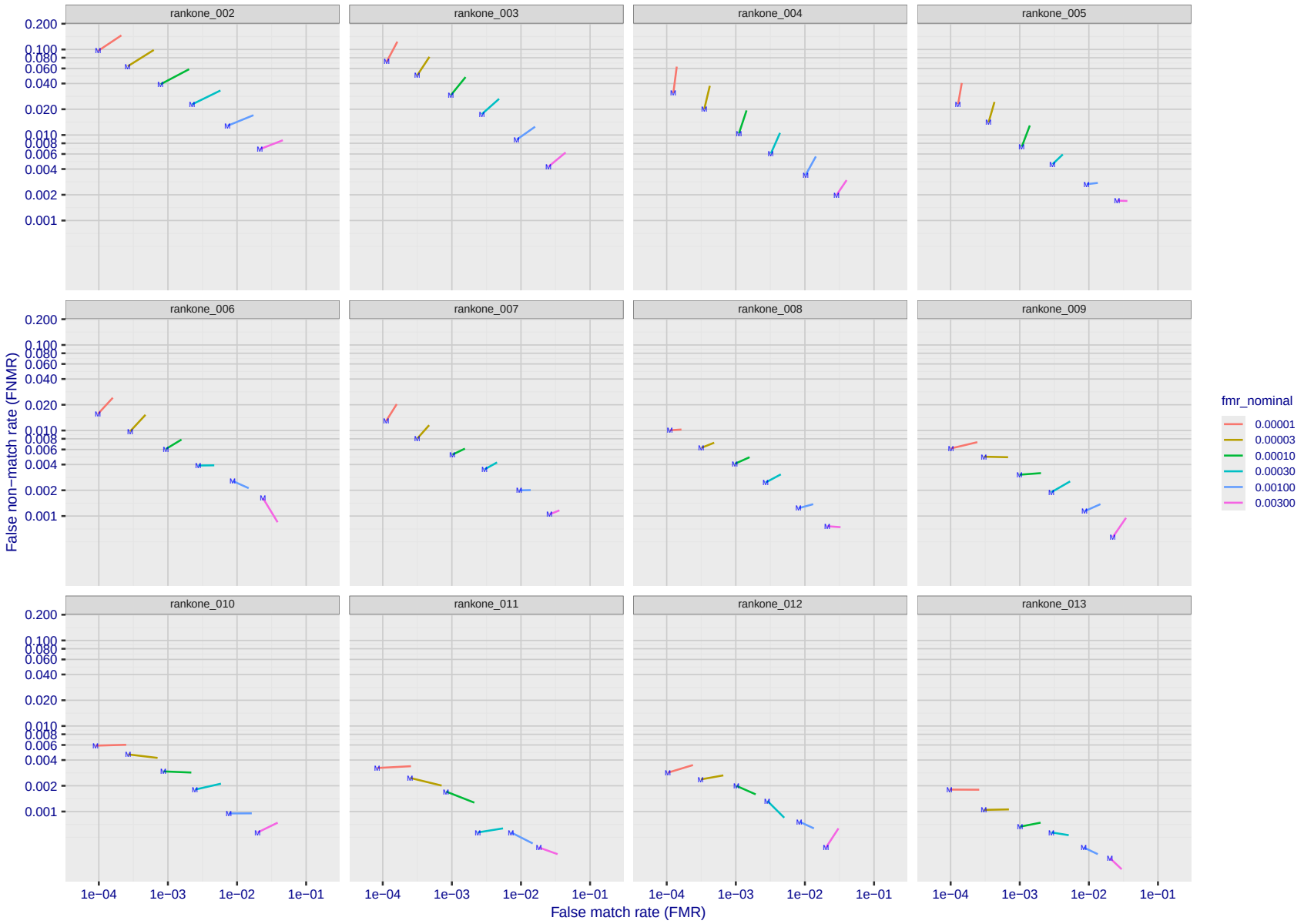

Figure 512: For the visa images, FNMR and FMR at six operating points along the DET characteristic. At each point a line is drawn between (FMR,FNMR)$_{\text{MALE}}$ and (FMR,FNMR)$_{\text{FEMALE}}$ showing how which sex has lower FMR and/or FNMR. The "M" label denotes male, the other end of the line corresponds to female. The six operating thresholds are selected to give the nominal false match rates given in the legend, and are computed over all impostor pairs regardless of age, sex, and place of birth. The plotted FMR values are broadly an order of magnitude larger than the nominal rates because FMR is computed over demographically-matched impostor pairs i.e individuals of the same sex, from the same geographic region (see section 3.6.1), and the same age group (see section 3.6.2).

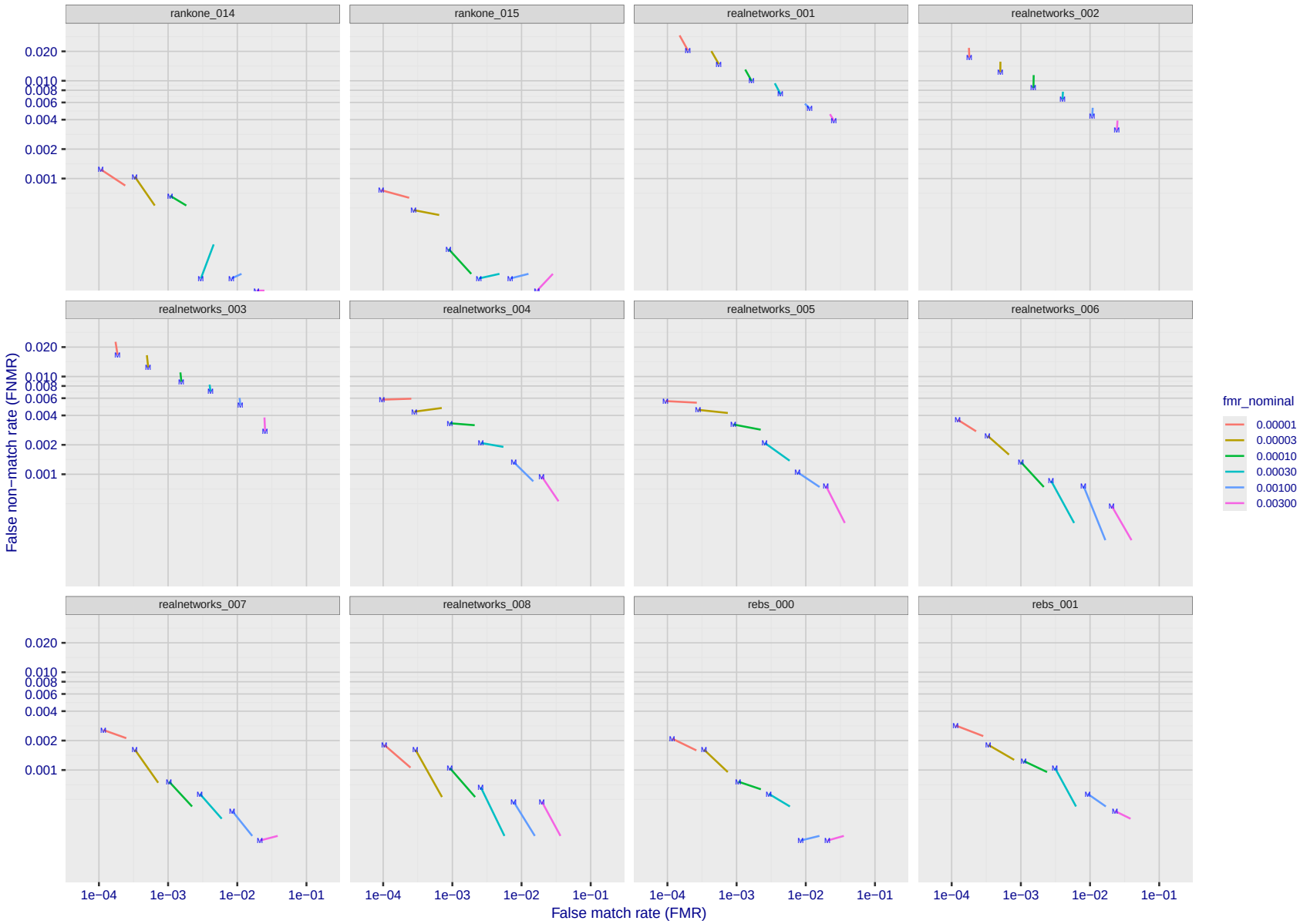

Figure 513: For the visa images, FNMR and FMR at six operating points along the DET characteristic. At each point a line is drawn between (FMR,FNMR)$_{\text{MALE}}$ and (FMR,FNMR)$_{\text{FEMALE}}$ showing how which sex has lower FMR and/or FNMR. The "M" label denotes male, the other end of the line corresponds to female. The six operating thresholds are selected to give the nominal false match rates given in the legend, and are computed over all impostor pairs regardless of age, sex, and place of birth. The plotted FMR values are broadly an order of magnitude larger than the nominal rates because FMR is computed over demographically-matched impostor pairs i.e individuals of the same sex, from the same geographic region (see section 3.6.1), and the same age group (see section 3.6.2).

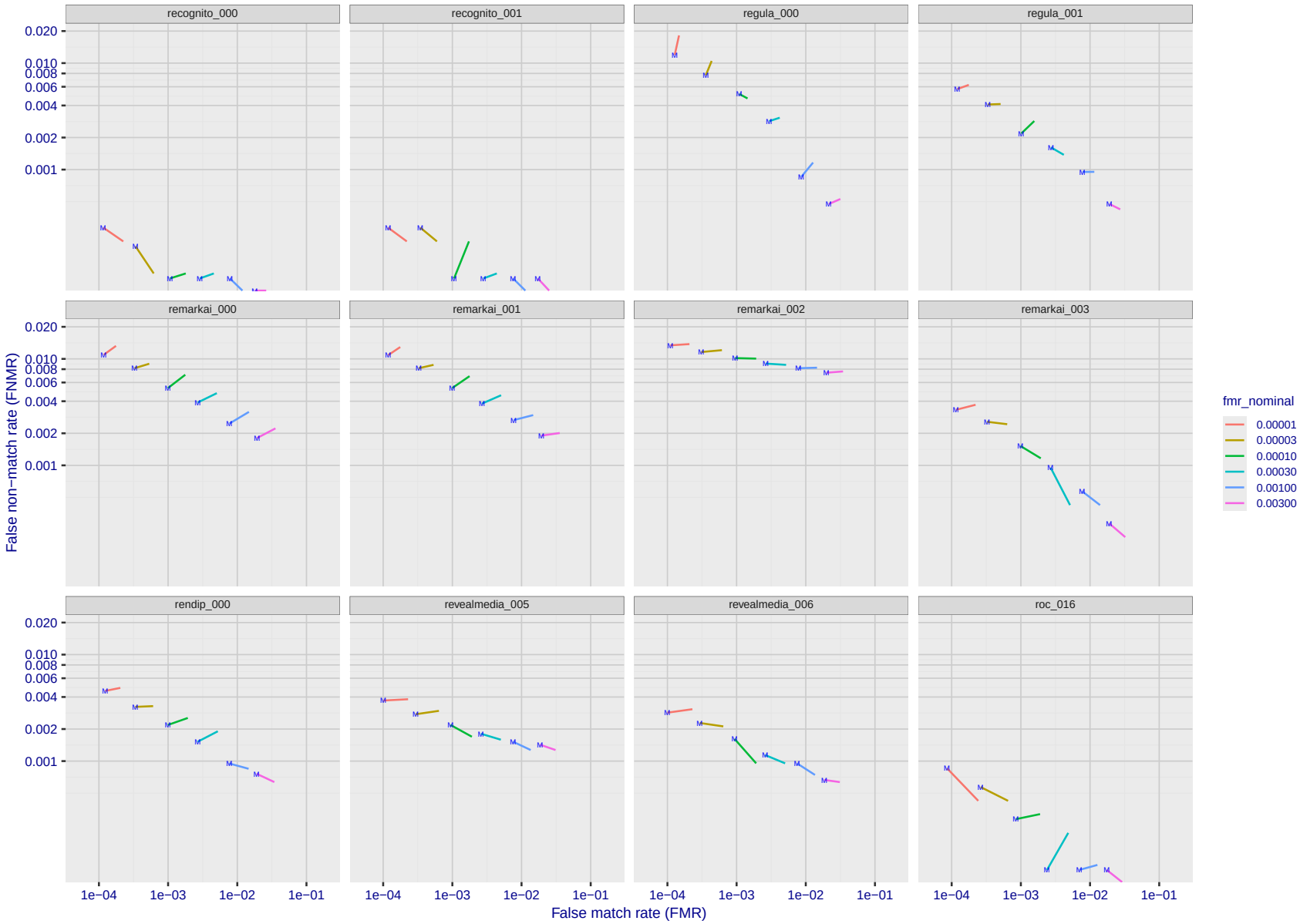

Figure 514: For the visa images, FNMR and FMR at six operating points along the DET characteristic. At each point a line is drawn between (FMR,FNMR)$_{\text{MALE}}$ and (FMR,FNMR)$_{\text{FEMALE}}$ showing how which sex has lower FMR and/or FNMR. The "M" label denotes male, the other end of the line corresponds to female. The six operating thresholds are selected to give the nominal false match rates given in the legend, and are computed over all impostor pairs regardless of age, sex, and place of birth. The plotted FMR values are broadly an order of magnitude larger than the nominal rates because FMR is computed over demographically-matched impostor pairs i.e individuals of the same sex, from the same geographic region (see section 3.6.1), and the same age group (see section 3.6.2).

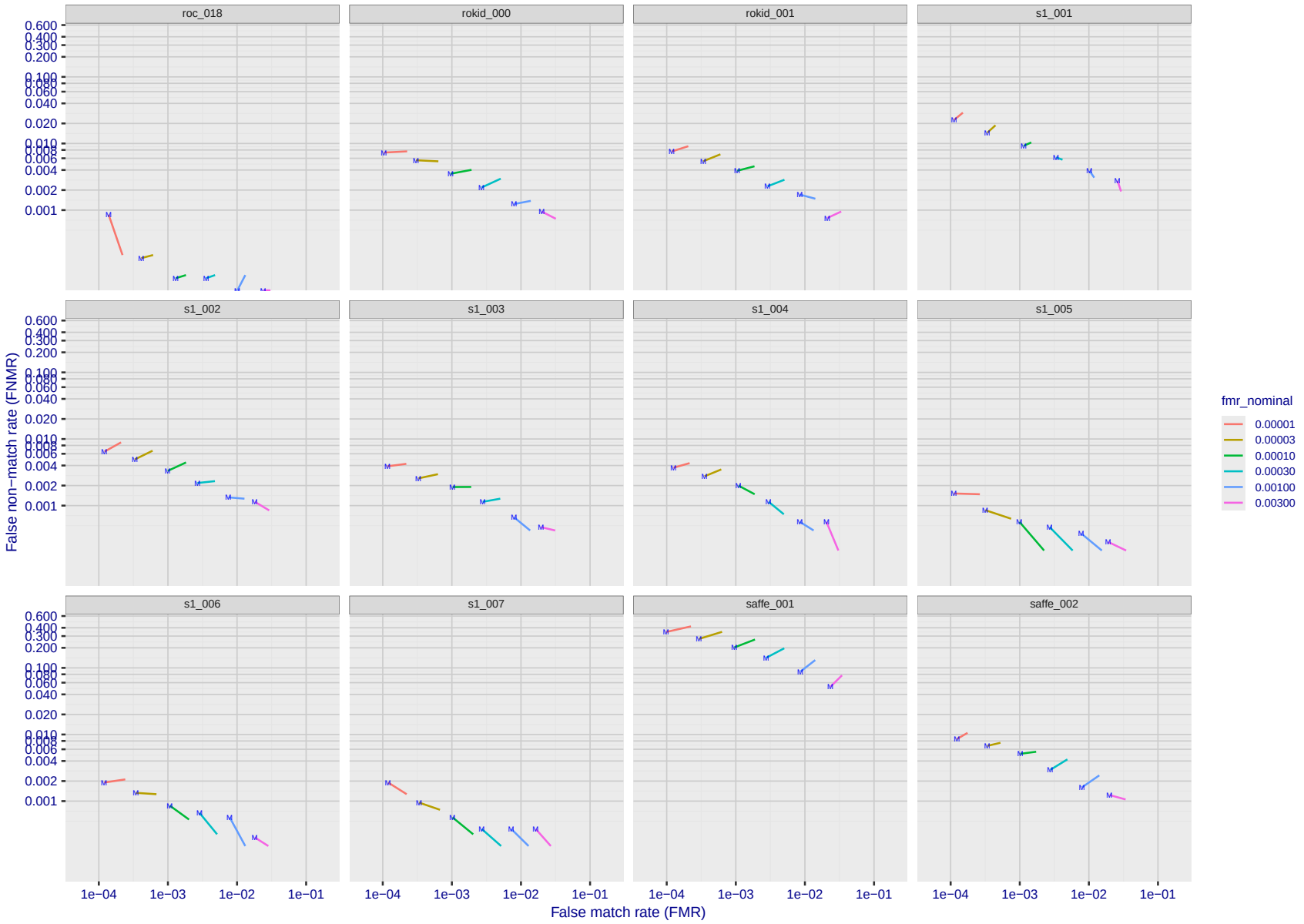

Figure 515: For the visa images, FNMR and FMR at six operating points along the DET characteristic. At each point a line is drawn between (FMR,FNMR)$_{\text{MALE}}$ and (FMR,FNMR)$_{\text{FEMALE}}$ showing how which sex has lower FMR and/or FNMR. The "M" label denotes male, the other end of the line corresponds to female. The six operating thresholds are selected to give the nominal false match rates given in the legend, and are computed over all impostor pairs regardless of age, sex, and place of birth. The plotted FMR values are broadly an order of magnitude larger than the nominal rates because FMR is computed over demographically-matched impostor pairs i.e individuals of the same sex, from the same geographic region (see section 3.6.1), and the same age group (see section 3.6.2).

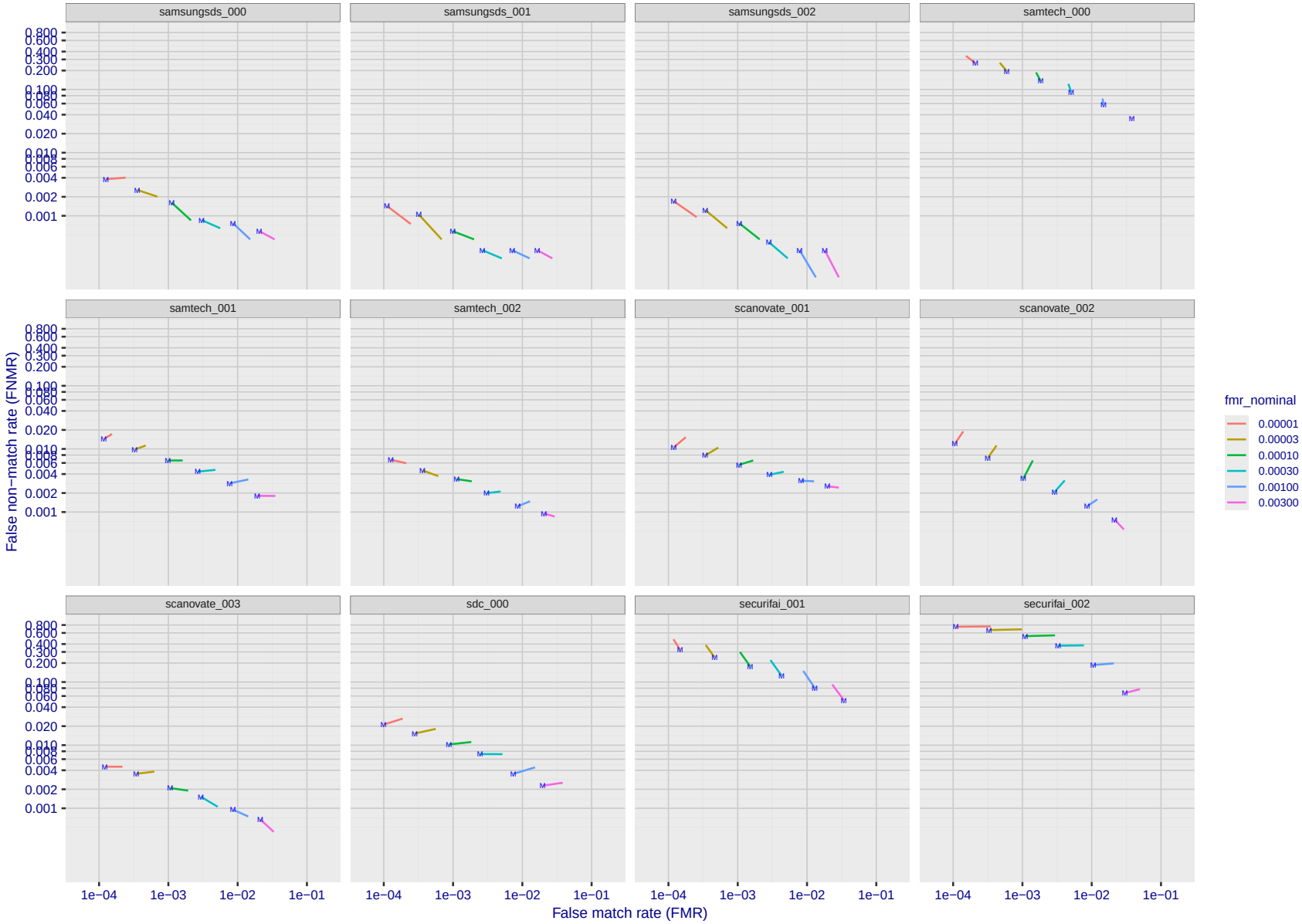

Figure 516: For the visa images, FNMR and FMR at six operating points along the DET characteristic. At each point a line is drawn between (FMR,FNMR)$_{\text{MALE}}$ and (FMR,FNMR)$_{\text{FEMALE}}$ showing how which sex has lower FMR and/or FNMR. The "M" label denotes male, the other end of the line corresponds to female. The six operating thresholds are selected to give the nominal false match rates given in the legend, and are computed over all impostor pairs regardless of age, sex, and place of birth. The plotted FMR values are broadly an order of magnitude larger than the nominal rates because FMR is computed over demographically-matched impostor pairs i.e individuals of the same sex, from the same geographic region (see section 3.6.1), and the same age group (see section 3.6.2).

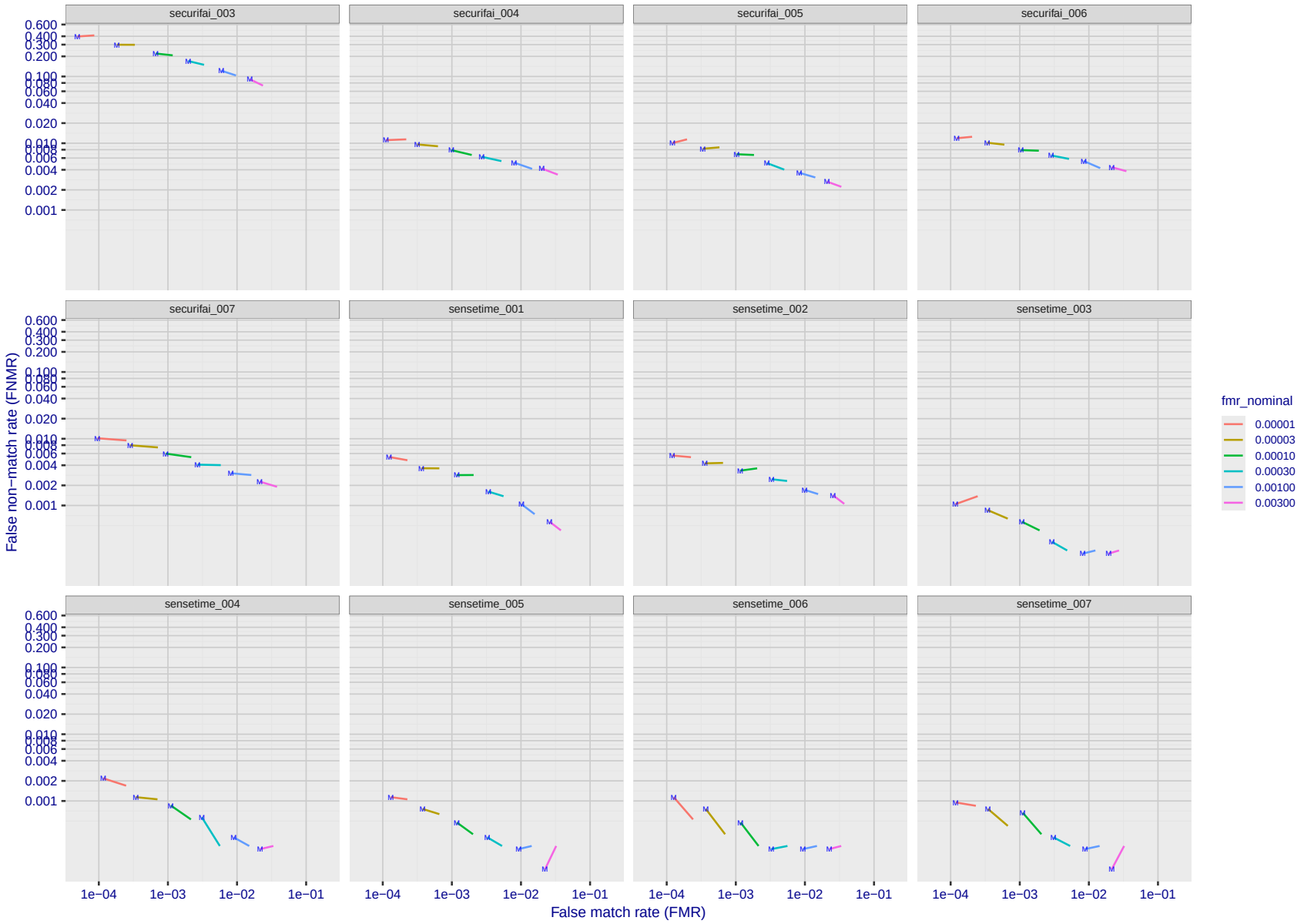

Figure 517: For the visa images, FNMR and FMR at six operating points along the DET characteristic. At each point a line is drawn between (FMR,FNMR)$_{\text{MALE}}$ and (FMR,FNMR)$_{\text{FEMALE}}$ showing how which sex has lower FMR and/or FNMR. The "M" label denotes male, the other end of the line corresponds to female. The six operating thresholds are selected to give the nominal false match rates given in the legend, and are computed over all impostor pairs regardless of age, sex, and place of birth. The plotted FMR values are broadly an order of magnitude larger than the nominal rates because FMR is computed over demographically-matched impostor pairs i.e individuals of the same sex, from the same geographic region (see section 3.6.1), and the same age group (see section 3.6.2).

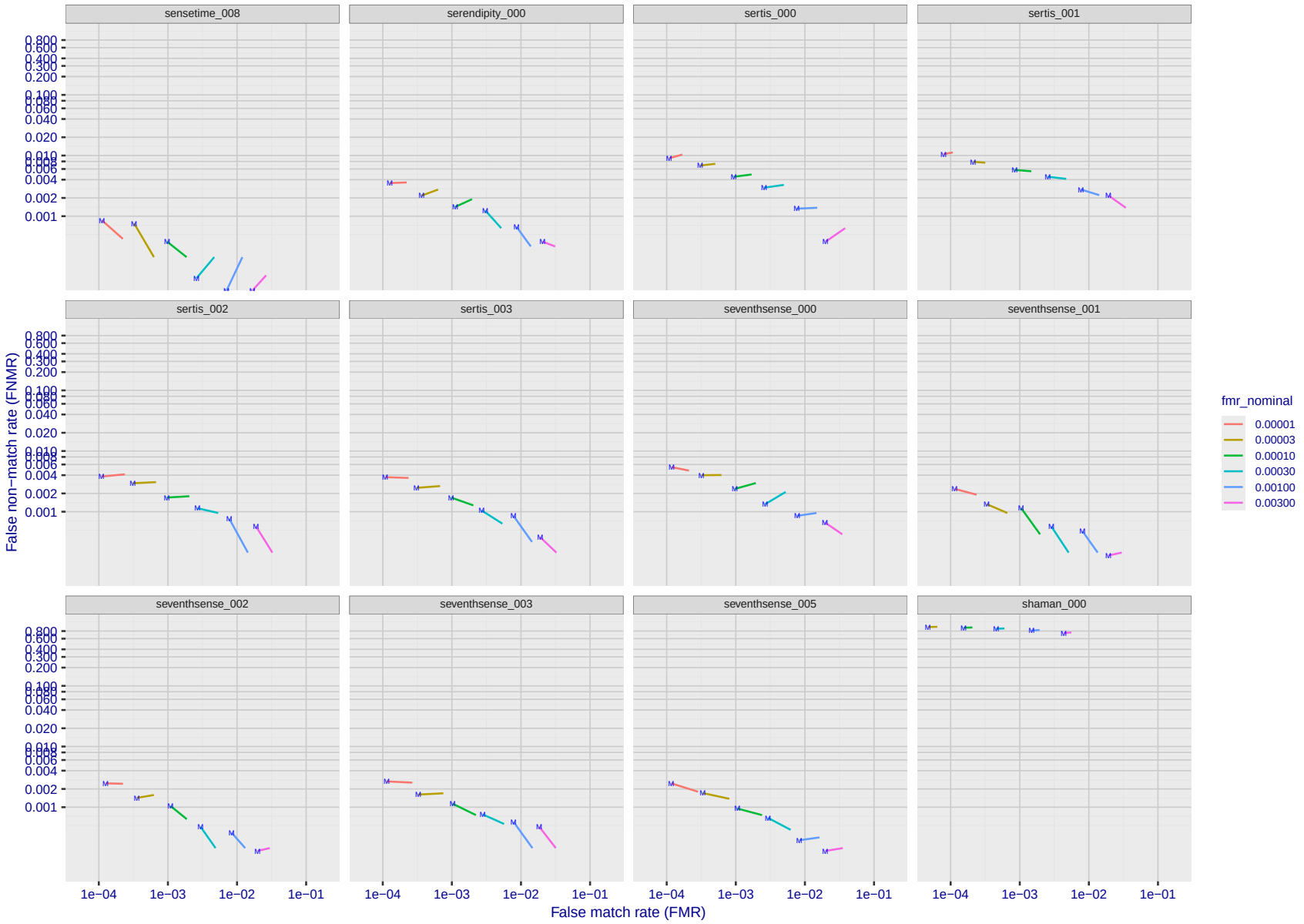

Figure 518: For the visa images, FNMR and FMR at six operating points along the DET characteristic. At each point a line is drawn between (FMR,FNMR)$_{\text{MALE}}$ and (FMR,FNMR)$_{\text{FEMALE}}$ showing how which sex has lower FMR and/or FNMR. The "M" label denotes male, the other end of the line corresponds to female. The six operating thresholds are selected to give the nominal false match rates given in the legend, and are computed over all impostor pairs regardless of age, sex, and place of birth. The plotted FMR values are broadly an order of magnitude larger than the nominal rates because FMR is computed over demographically-matched impostor pairs i.e individuals of the same sex, from the same geographic region (see section 3.6.1), and the same age group (see section 3.6.2).

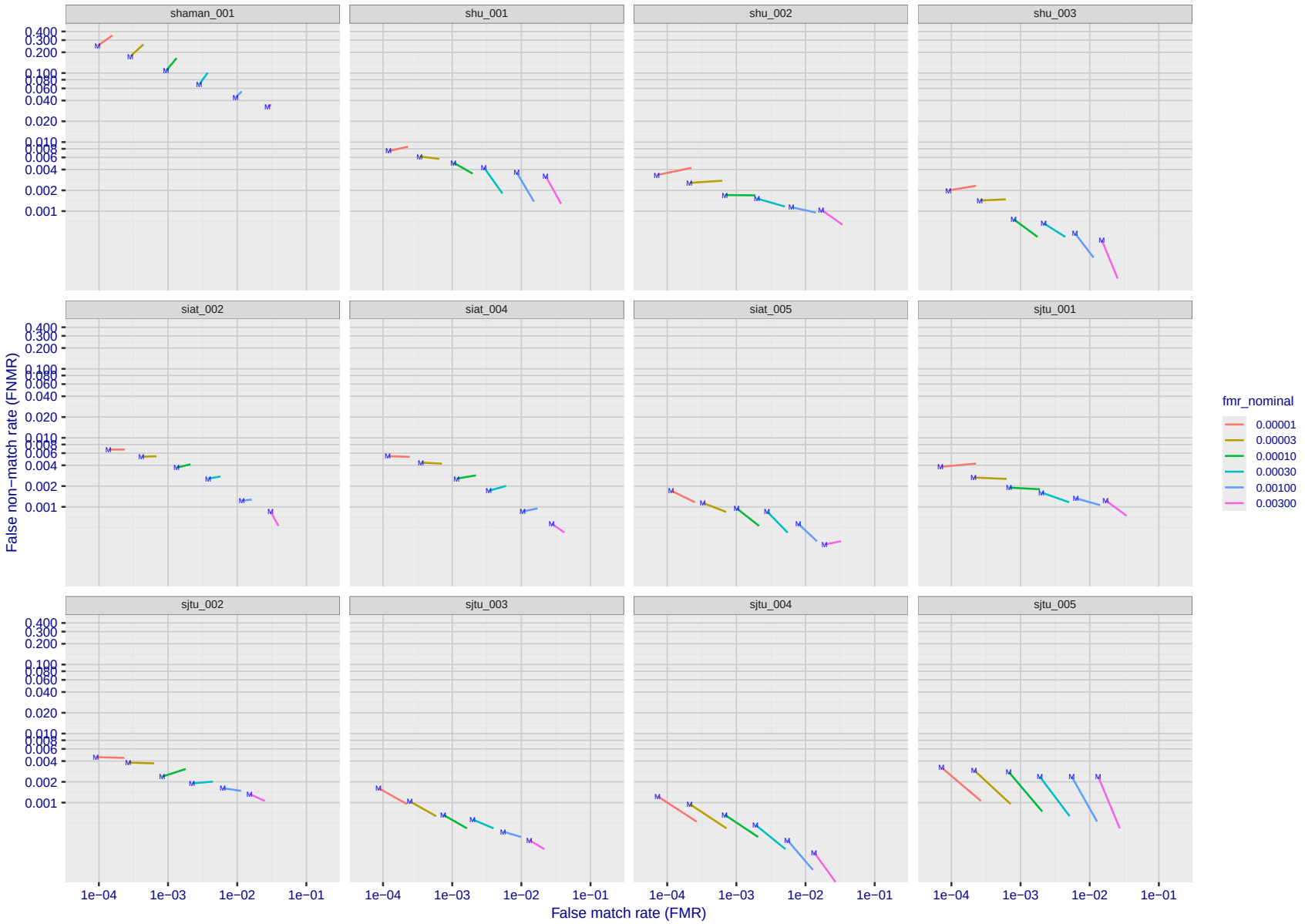

Figure 519: For the visa images, FNMR and FMR at six operating points along the DET characteristic. At each point a line is drawn between (FMR,FNMR)$_{\text{MALE}}$ and (FMR,FNMR)$_{\text{FEMALE}}$ showing how which sex has lower FMR and/or FNMR. The "M" label denotes male, the other end of the line corresponds to female. The six operating thresholds are selected to give the nominal false match rates given in the legend, and are computed over all impostor pairs regardless of age, sex, and place of birth. The plotted FMR values are broadly an order of magnitude larger than the nominal rates because FMR is computed over demographically-matched impostor pairs i.e individuals of the same sex, from the same geographic region (see section 3.6.1), and the same age group (see section 3.6.2).

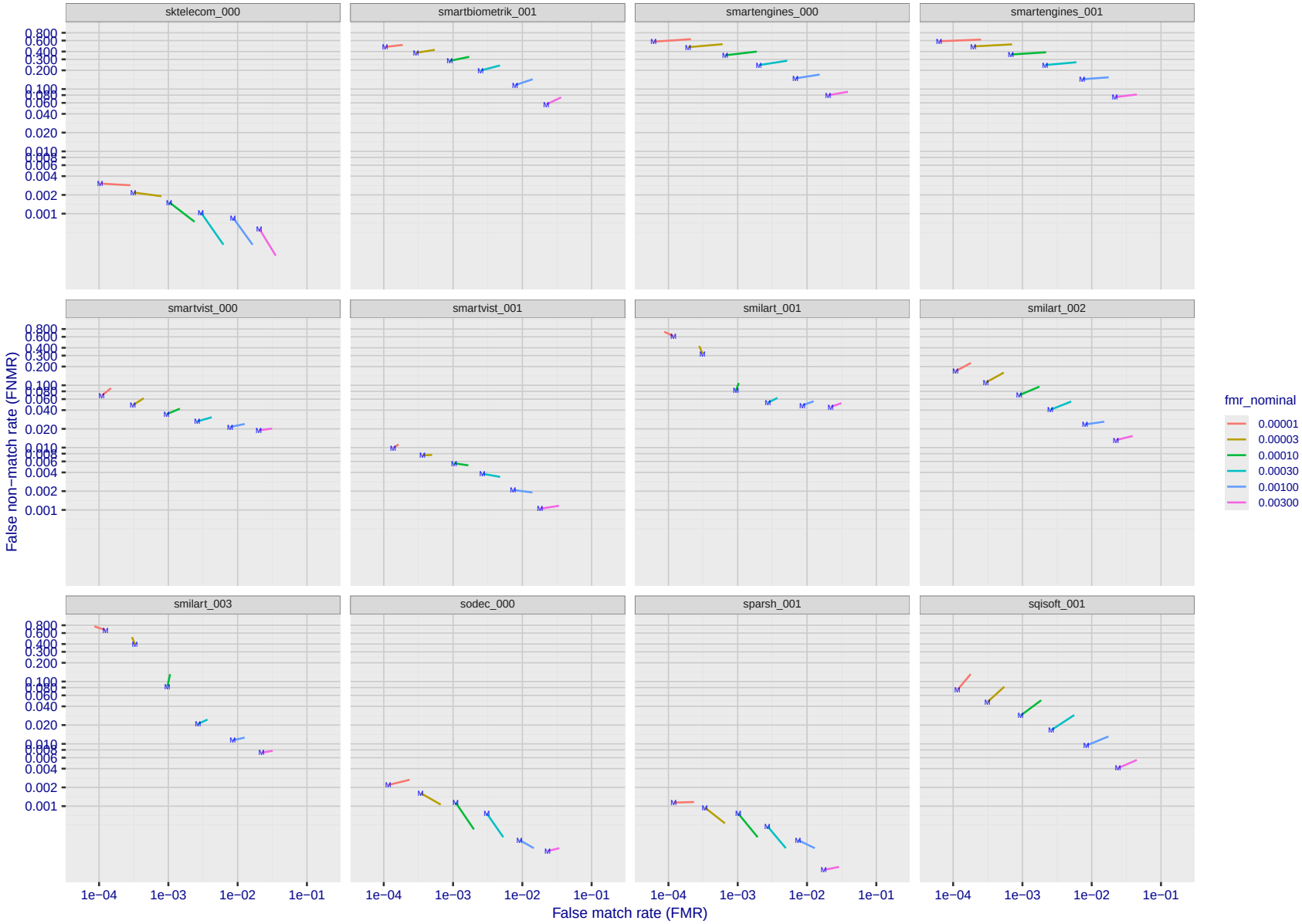

Figure 520: For the visa images, FNMR and FMR at six operating points along the DET characteristic. At each point a line is drawn between (FMR,FNMR)$_{\text{MALE}}$ and (FMR,FNMR)$_{\text{FEMALE}}$ showing how which sex has lower FMR and/or FNMR. The "M" label denotes male, the other end of the line corresponds to female. The six operating thresholds are selected to give the nominal false match rates given in the legend, and are computed over all impostor pairs regardless of age, sex, and place of birth. The plotted FMR values are broadly an order of magnitude larger than the nominal rates because FMR is computed over demographically-matched impostor pairs i.e individuals of the same sex, from the same geographic region (see section 3.6.1), and the same age group (see section 3.6.2).

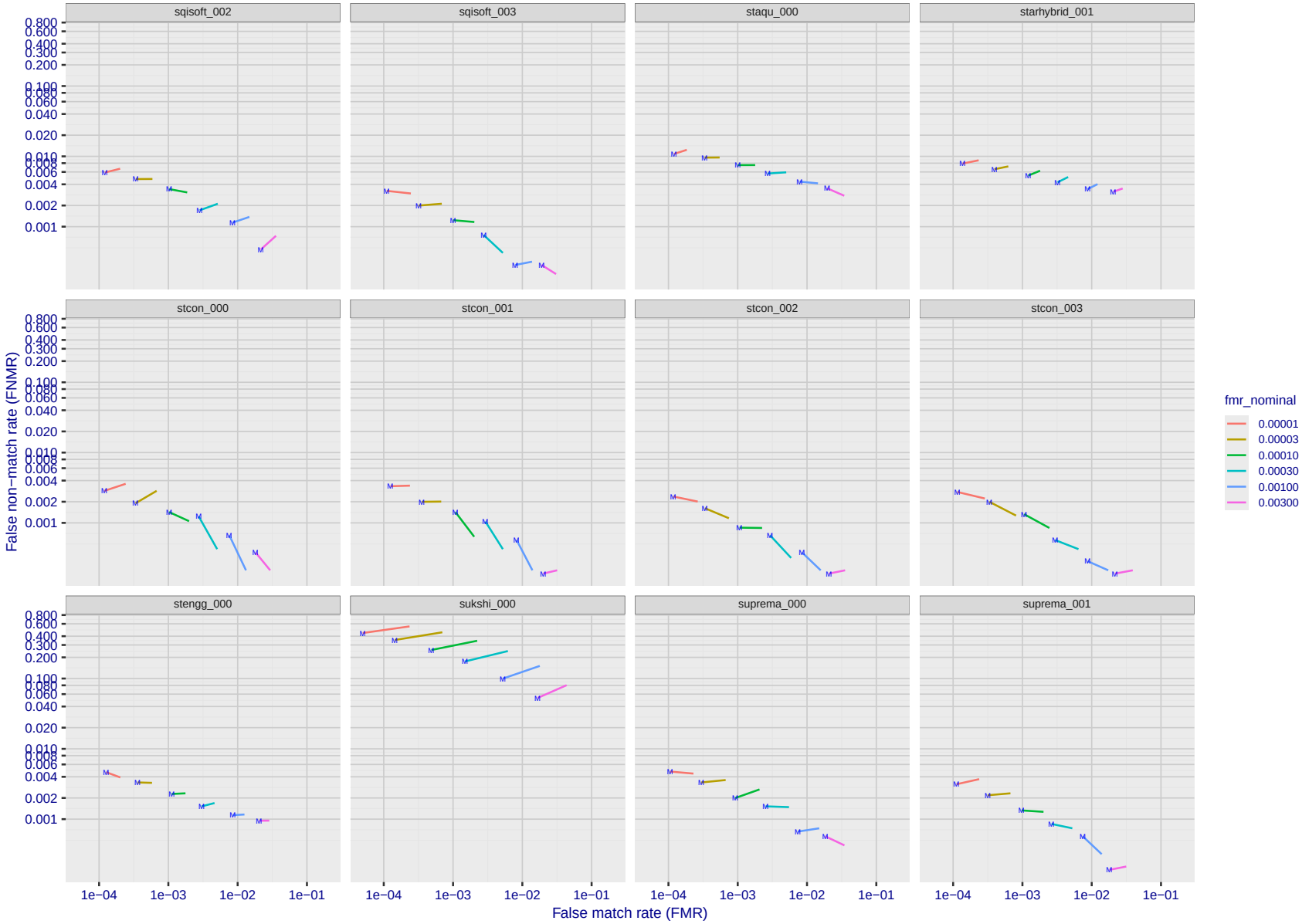

Figure 521: For the visa images, FNMR and FMR at six operating points along the DET characteristic. At each point a line is drawn between (FMR,FNMR)$_{\text{MALE}}$ and (FMR,FNMR)$_{\text{FEMALE}}$ showing how which sex has lower FMR and/or FNMR. The "M" label denotes male, the other end of the line corresponds to female. The six operating thresholds are selected to give the nominal false match rates given in the legend, and are computed over all impostor pairs regardless of age, sex, and place of birth. The plotted FMR values are broadly an order of magnitude larger than the nominal rates because FMR is computed over demographically-matched impostor pairs i.e individuals of the same sex, from the same geographic region (see section 3.6.1), and the same age group (see section 3.6.2).

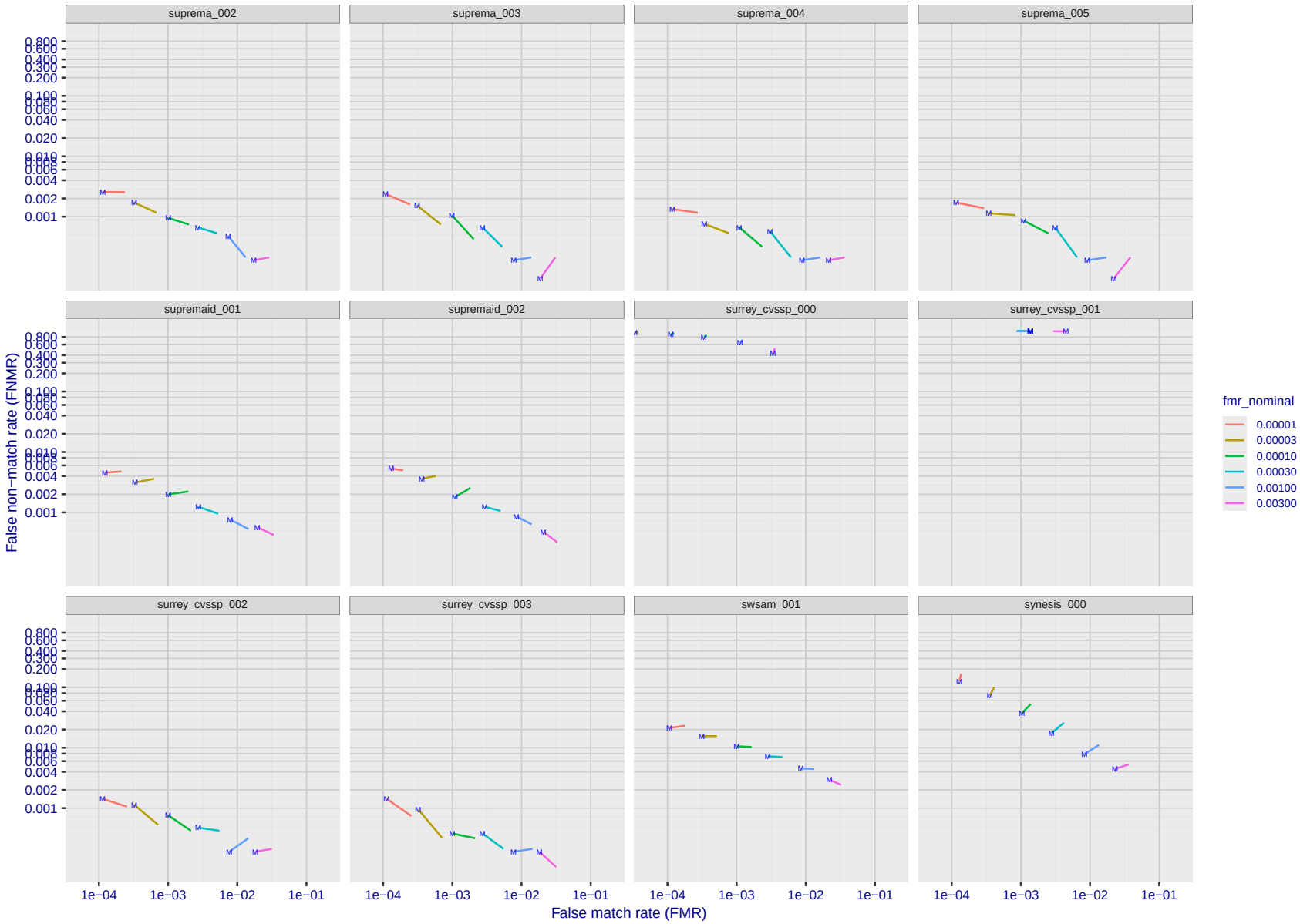

Figure 522: For the visa images, FNMR and FMR at six operating points along the DET characteristic. At each point a line is drawn between (FMR,FNMR)$_{\text{MALE}}$ and (FMR,FNMR)$_{\text{FEMALE}}$ showing how which sex has lower FMR and/or FNMR. The "M" label denotes male, the other end of the line corresponds to female. The six operating thresholds are selected to give the nominal false match rates given in the legend, and are computed over all impostor pairs regardless of age, sex, and place of birth. The plotted FMR values are broadly an order of magnitude larger than the nominal rates because FMR is computed over demographically-matched impostor pairs i.e individuals of the same sex, from the same geographic region (see section 3.6.1), and the same age group (see section 3.6.2).

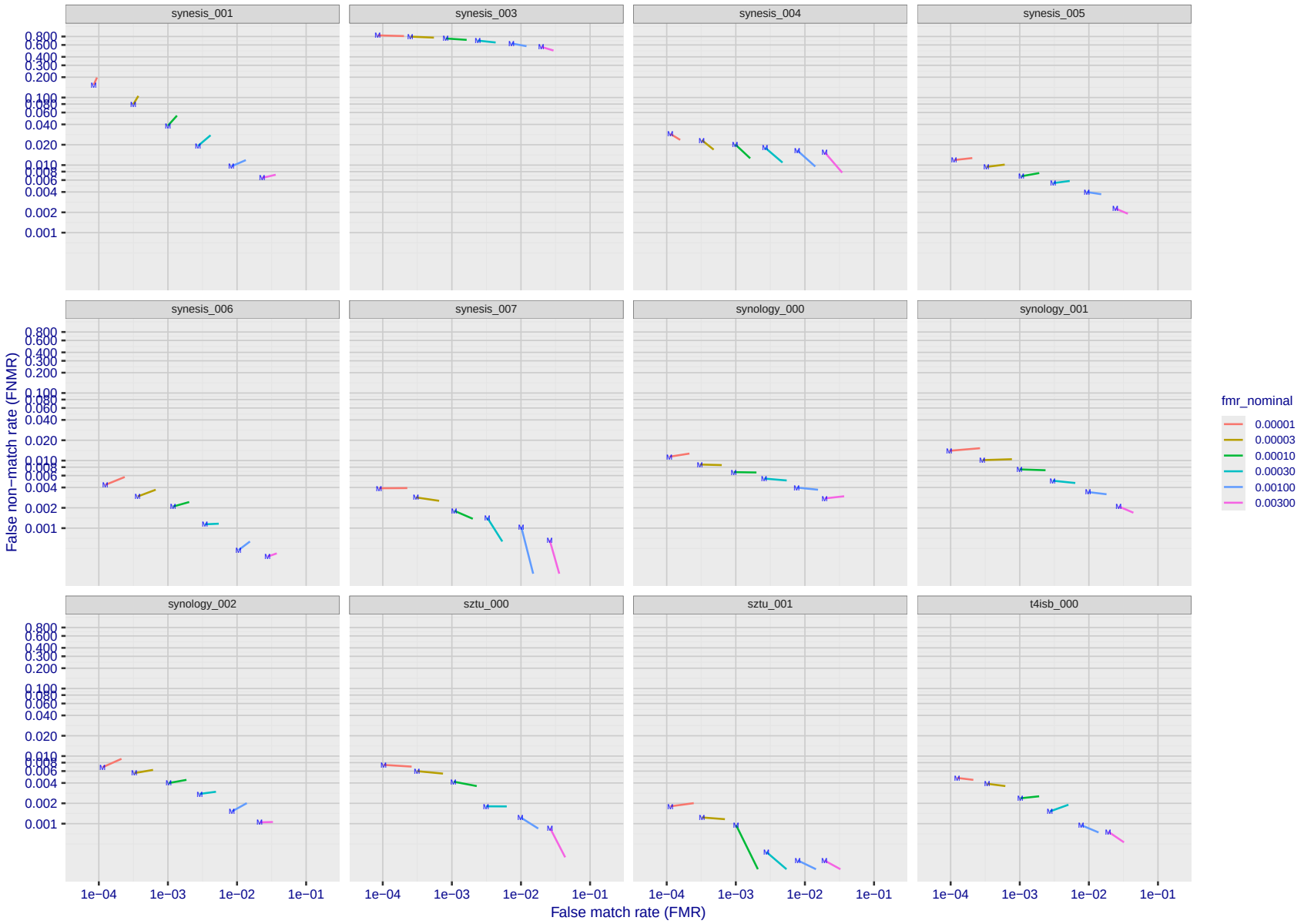

Figure 523: For the visa images, FNMR and FMR at six operating points along the DET characteristic. At each point a line is drawn between (FMR,FNMR)$_{\text{MALE}}$ and (FMR,FNMR)$_{\text{FEMALE}}$ showing how which sex has lower FMR and/or FNMR. The "M" label denotes male, the other end of the line corresponds to female. The six operating thresholds are selected to give the nominal false match rates given in the legend, and are computed over all impostor pairs regardless of age, sex, and place of birth. The plotted FMR values are broadly an order of magnitude larger than the nominal rates because FMR is computed over demographically-matched impostor pairs i.e individuals of the same sex, from the same geographic region (see section 3.6.1), and the same age group (see section 3.6.2).

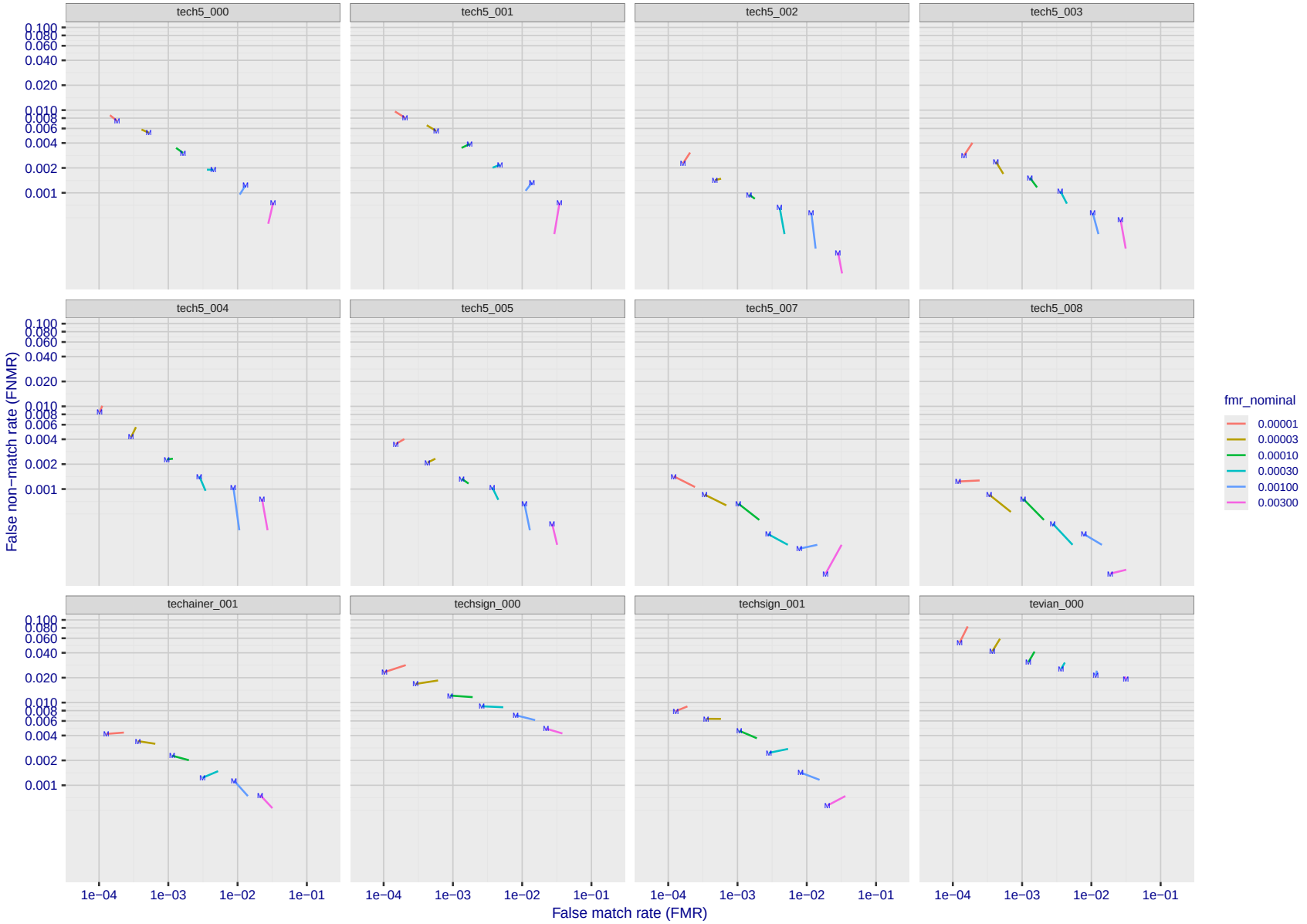

Figure 524: For the visa images, FNMR and FMR at six operating points along the DET characteristic. At each point a line is drawn between (FMR,FNMR)$_{\text{MALE}}$ and (FMR,FNMR)$_{\text{FEMALE}}$ showing how which sex has lower FMR and/or FNMR. The "M" label denotes male, the other end of the line corresponds to female. The six operating thresholds are selected to give the nominal false match rates given in the legend, and are computed over all impostor pairs regardless of age, sex, and place of birth. The plotted FMR values are broadly an order of magnitude larger than the nominal rates because FMR is computed over demographically-matched impostor pairs i.e individuals of the same sex, from the same geographic region (see section 3.6.1), and the same age group (see section 3.6.2).

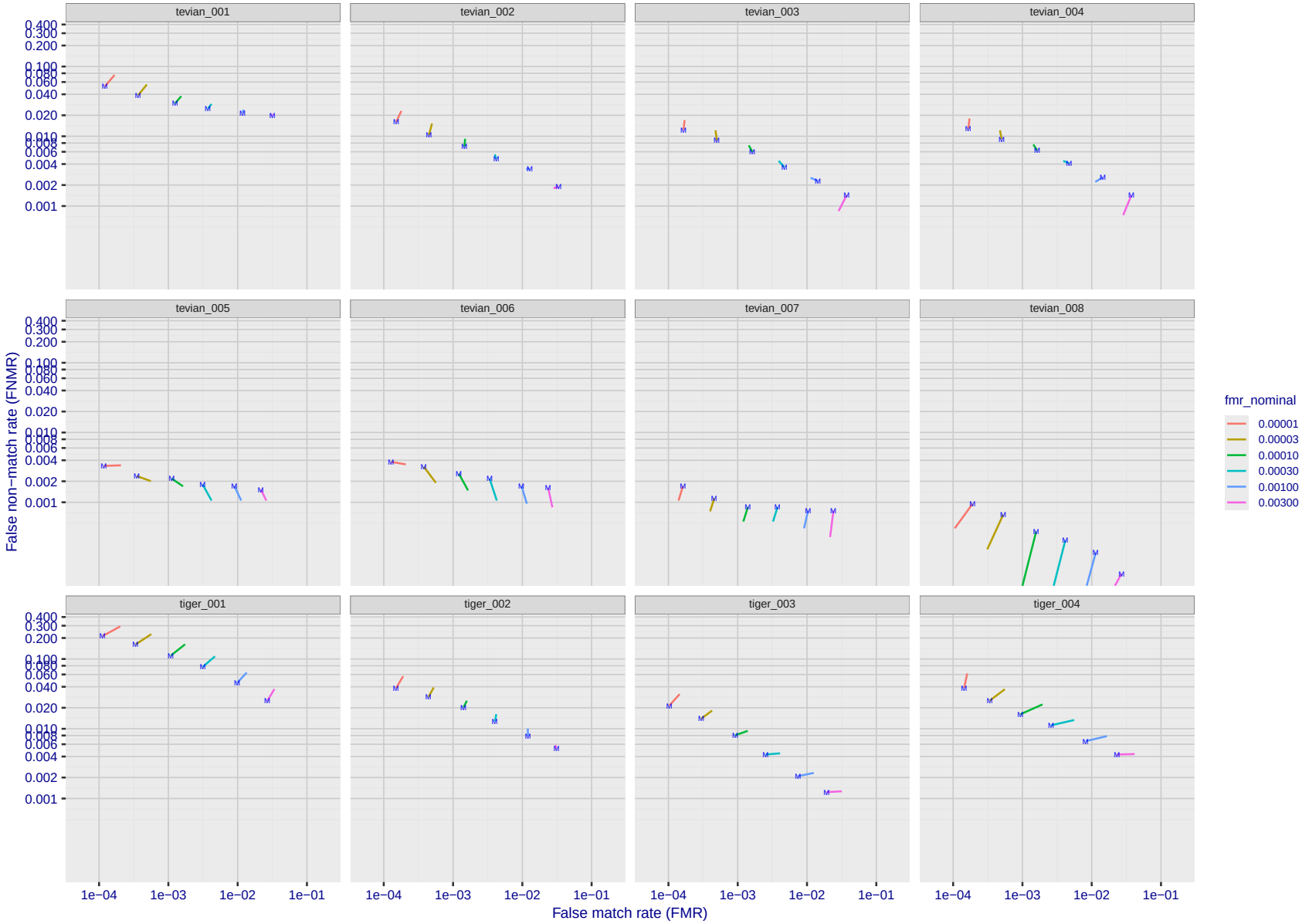

Figure 525: For the visa images, FNMR and FMR at six operating points along the DET characteristic. At each point a line is drawn between (FMR,FNMR)$_{\text{MALE}}$ and (FMR,FNMR)$_{\text{FEMALE}}$ showing how which sex has lower FMR and/or FNMR. The "M" label denotes male, the other end of the line corresponds to female. The six operating thresholds are selected to give the nominal false match rates given in the legend, and are computed over all impostor pairs regardless of age, sex, and place of birth. The plotted FMR values are broadly an order of magnitude larger than the nominal rates because FMR is computed over demographically-matched impostor pairs i.e individuals of the same sex, from the same geographic region (see section 3.6.1), and the same age group (see section 3.6.2).

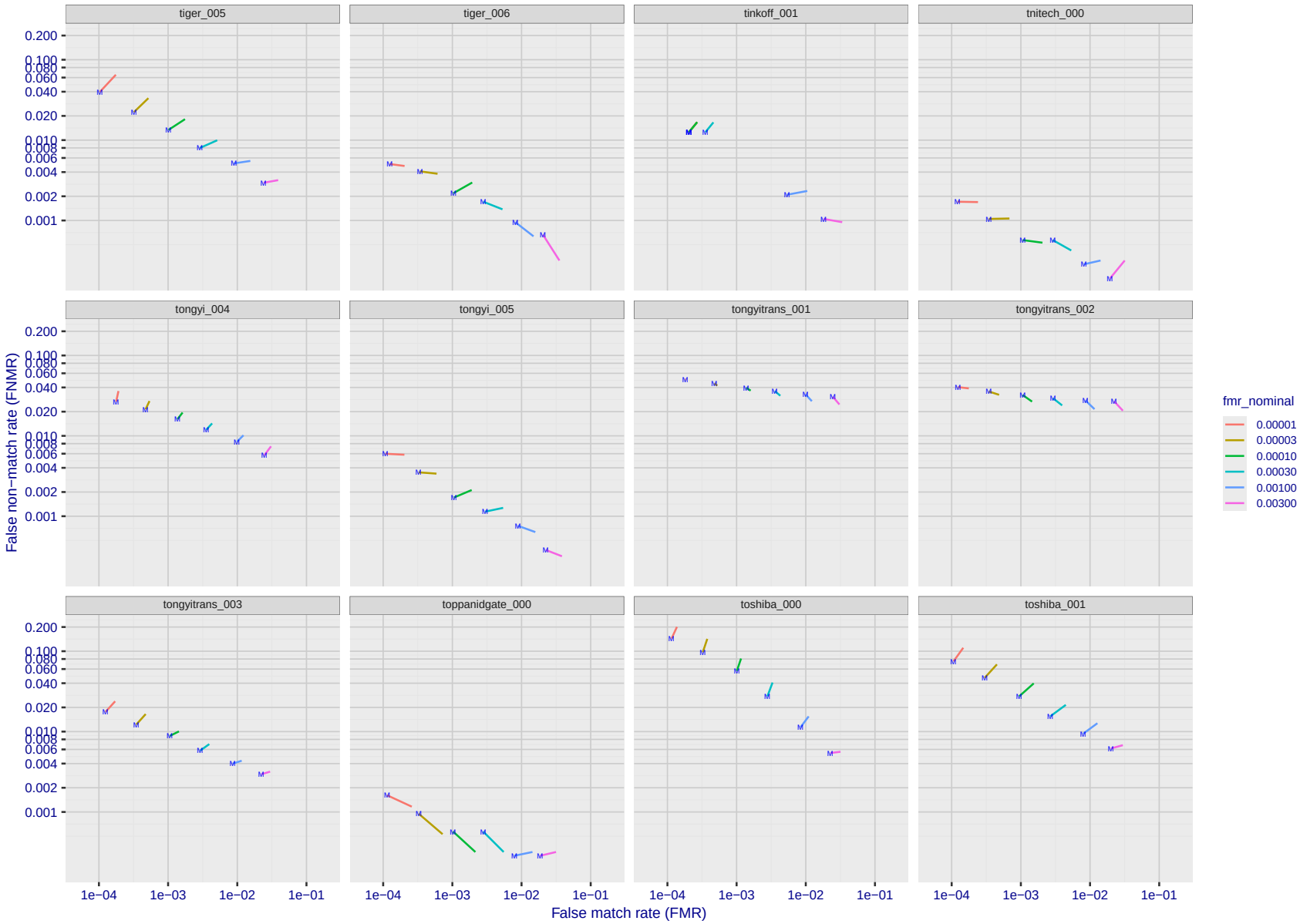

Figure 526: For the visa images, FNMR and FMR at six operating points along the DET characteristic. At each point a line is drawn between (FMR,FNMR)$_{\text{MALE}}$ and (FMR,FNMR)$_{\text{FEMALE}}$ showing how which sex has lower FMR and/or FNMR. The "M" label denotes male, the other end of the line corresponds to female. The six operating thresholds are selected to give the nominal false match rates given in the legend, and are computed over all impostor pairs regardless of age, sex, and place of birth. The plotted FMR values are broadly an order of magnitude larger than the nominal rates because FMR is computed over demographically-matched impostor pairs i.e individuals of the same sex, from the same geographic region (see section 3.6.1), and the same age group (see section 3.6.2).

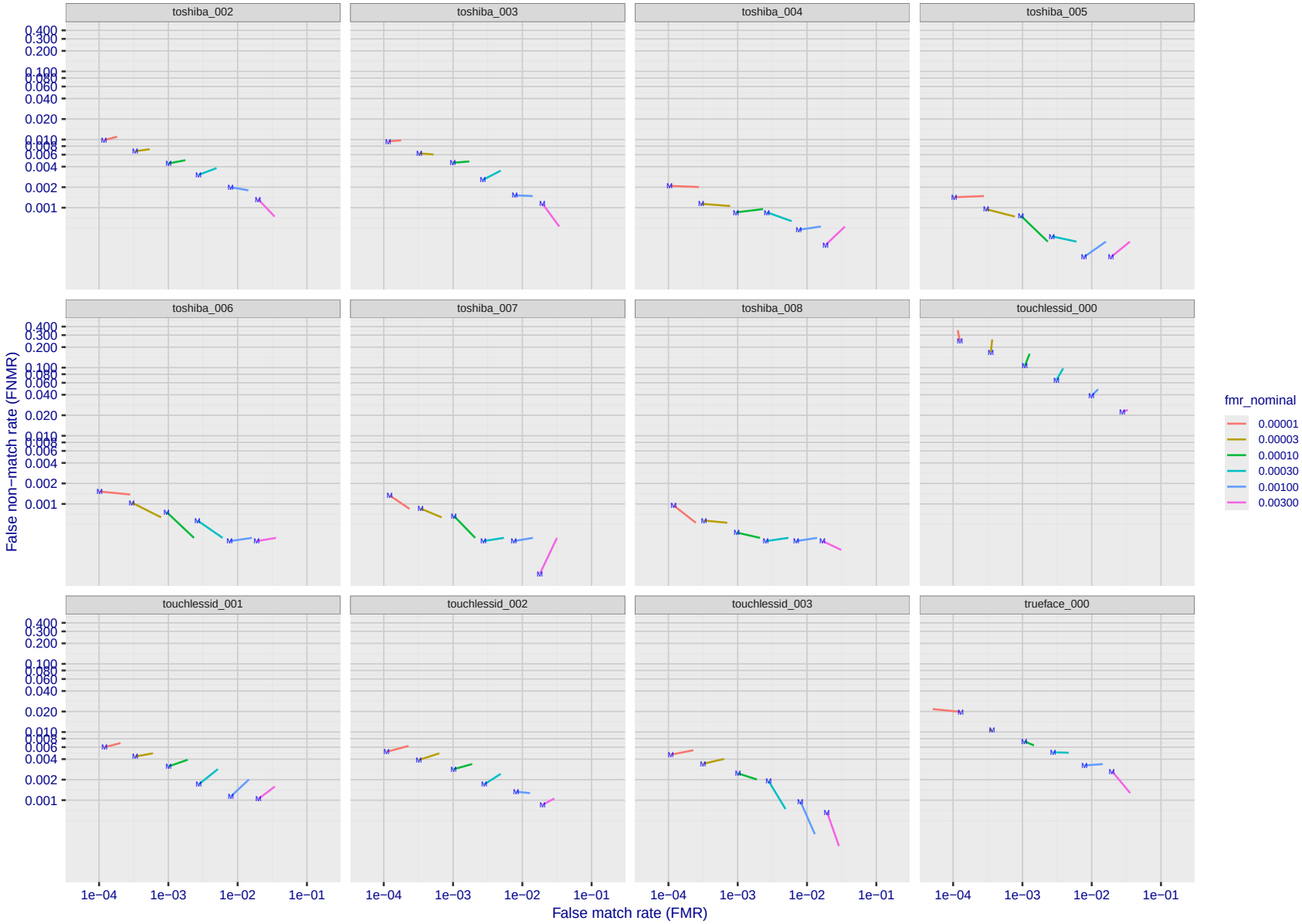

Figure 527: For the visa images, FNMR and FMR at six operating points along the DET characteristic. At each point a line is drawn between (FMR,FNMR)$_{\text{MALE}}$ and (FMR,FNMR)$_{\text{FEMALE}}$ showing how which sex has lower FMR and/or FNMR. The "M" label denotes male, the other end of the line corresponds to female. The six operating thresholds are selected to give the nominal false match rates given in the legend, and are computed over all impostor pairs regardless of age, sex, and place of birth. The plotted FMR values are broadly an order of magnitude larger than the nominal rates because FMR is computed over demographically-matched impostor pairs i.e individuals of the same sex, from the same geographic region (see section 3.6.1), and the same age group (see section 3.6.2).

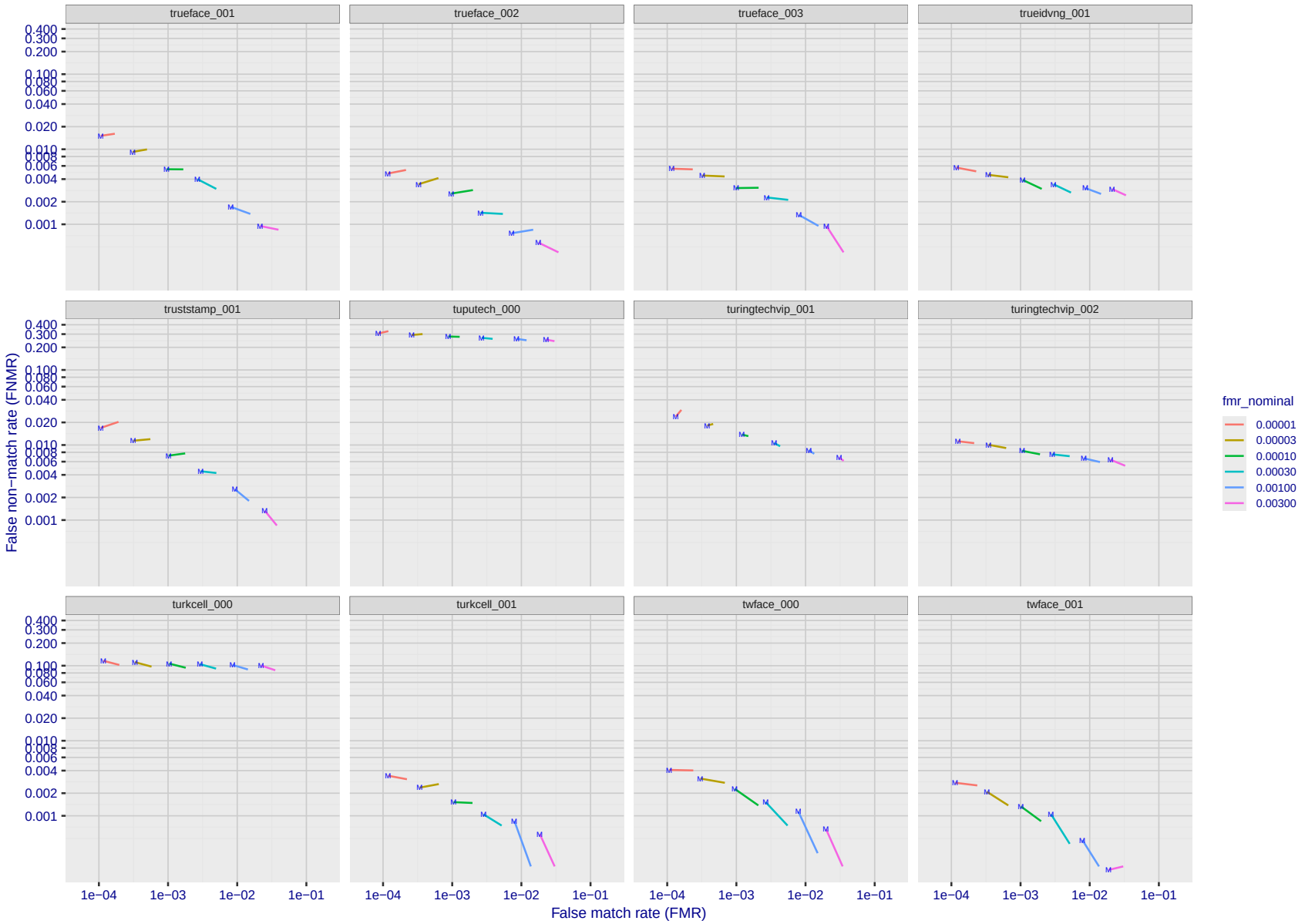

Figure 528: For the visa images, FNMR and FMR at six operating points along the DET characteristic. At each point a line is drawn between (FMR,FNMR)$_{\text{MALE}}$ and (FMR,FNMR)$_{\text{FEMALE}}$ showing how which sex has lower FMR and/or FNMR. The "M" label denotes male, the other end of the line corresponds to female. The six operating thresholds are selected to give the nominal false match rates given in the legend, and are computed over all impostor pairs regardless of age, sex, and place of birth. The plotted FMR values are broadly an order of magnitude larger than the nominal rates because FMR is computed over demographically-matched impostor pairs i.e individuals of the same sex, from the same geographic region (see section 3.6.1), and the same age group (see section 3.6.2).

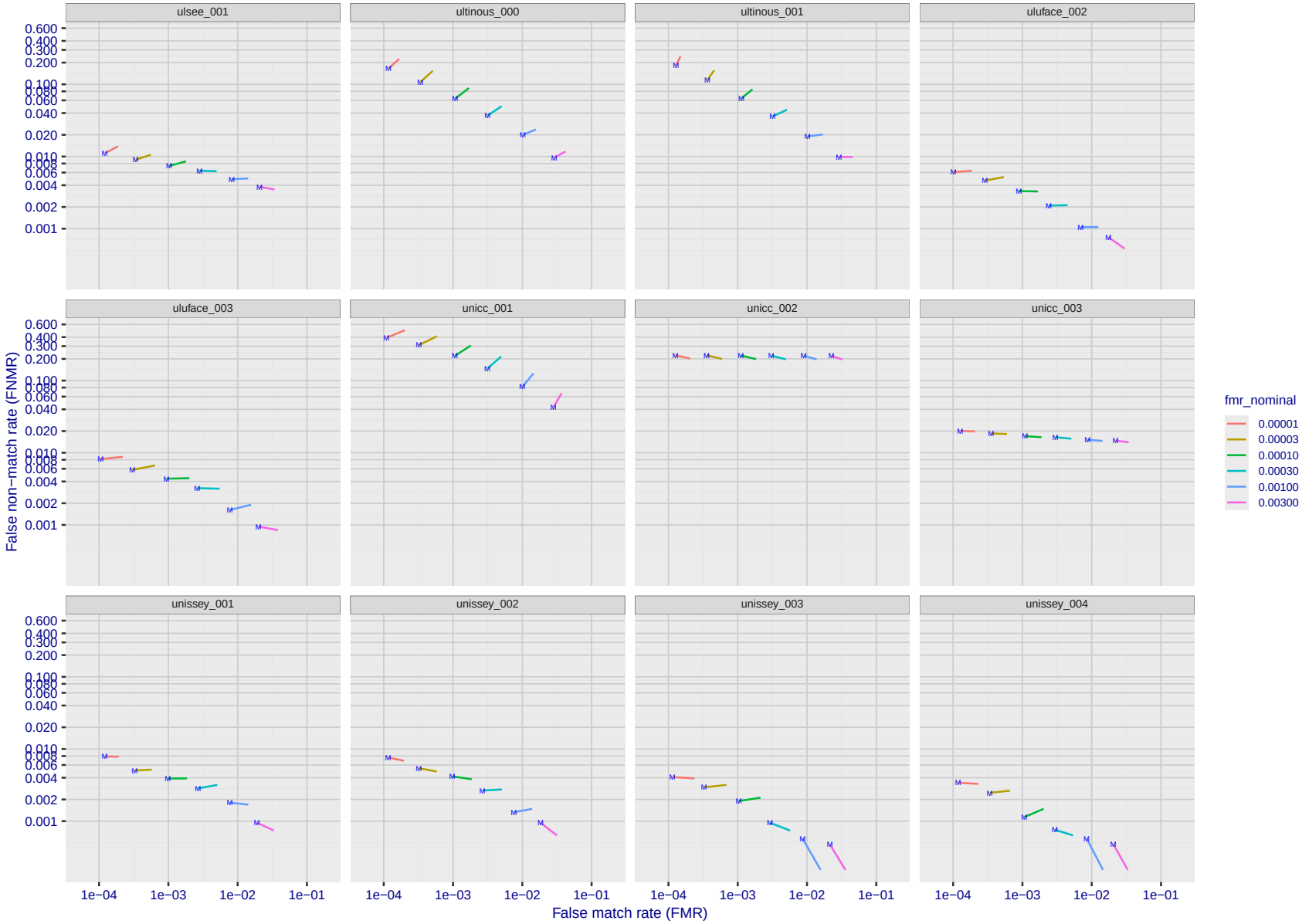

Figure 529: For the visa images, FNMR and FMR at six operating points along the DET characteristic. At each point a line is drawn between (FMR,FNMR)$_{\text{MALE}}$ and (FMR,FNMR)$_{\text{FEMALE}}$ showing how which sex has lower FMR and/or FNMR. The "M" label denotes male, the other end of the line corresponds to female. The six operating thresholds are selected to give the nominal false match rates given in the legend, and are computed over all impostor pairs regardless of age, sex, and place of birth. The plotted FMR values are broadly an order of magnitude larger than the nominal rates because FMR is computed over demographically-matched impostor pairs i.e individuals of the same sex, from the same geographic region (see section 3.6.1), and the same age group (see section 3.6.2).

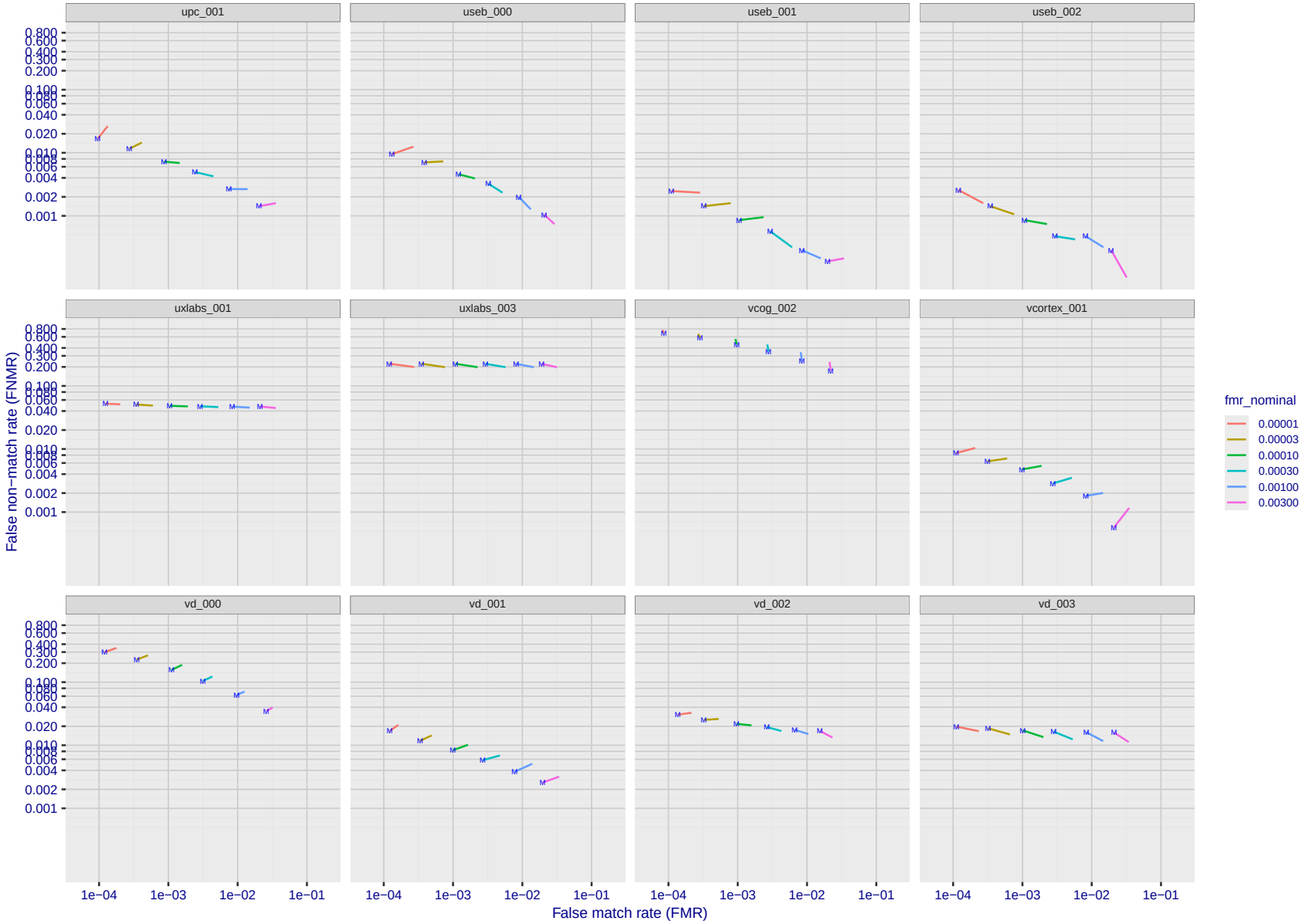

Figure 530: For the visa images, FNMR and FMR at six operating points along the DET characteristic. At each point a line is drawn between (FMR,FNMR)$_{\text{MALE}}$ and (FMR,FNMR)$_{\text{FEMALE}}$ showing how which sex has lower FMR and/or FNMR. The "M" label denotes male, the other end of the line corresponds to female. The six operating thresholds are selected to give the nominal false match rates given in the legend, and are computed over all impostor pairs regardless of age, sex, and place of birth. The plotted FMR values are broadly an order of magnitude larger than the nominal rates because FMR is computed over demographically-matched impostor pairs i.e individuals of the same sex, from the same geographic region (see section 3.6.1), and the same age group (see section 3.6.2).

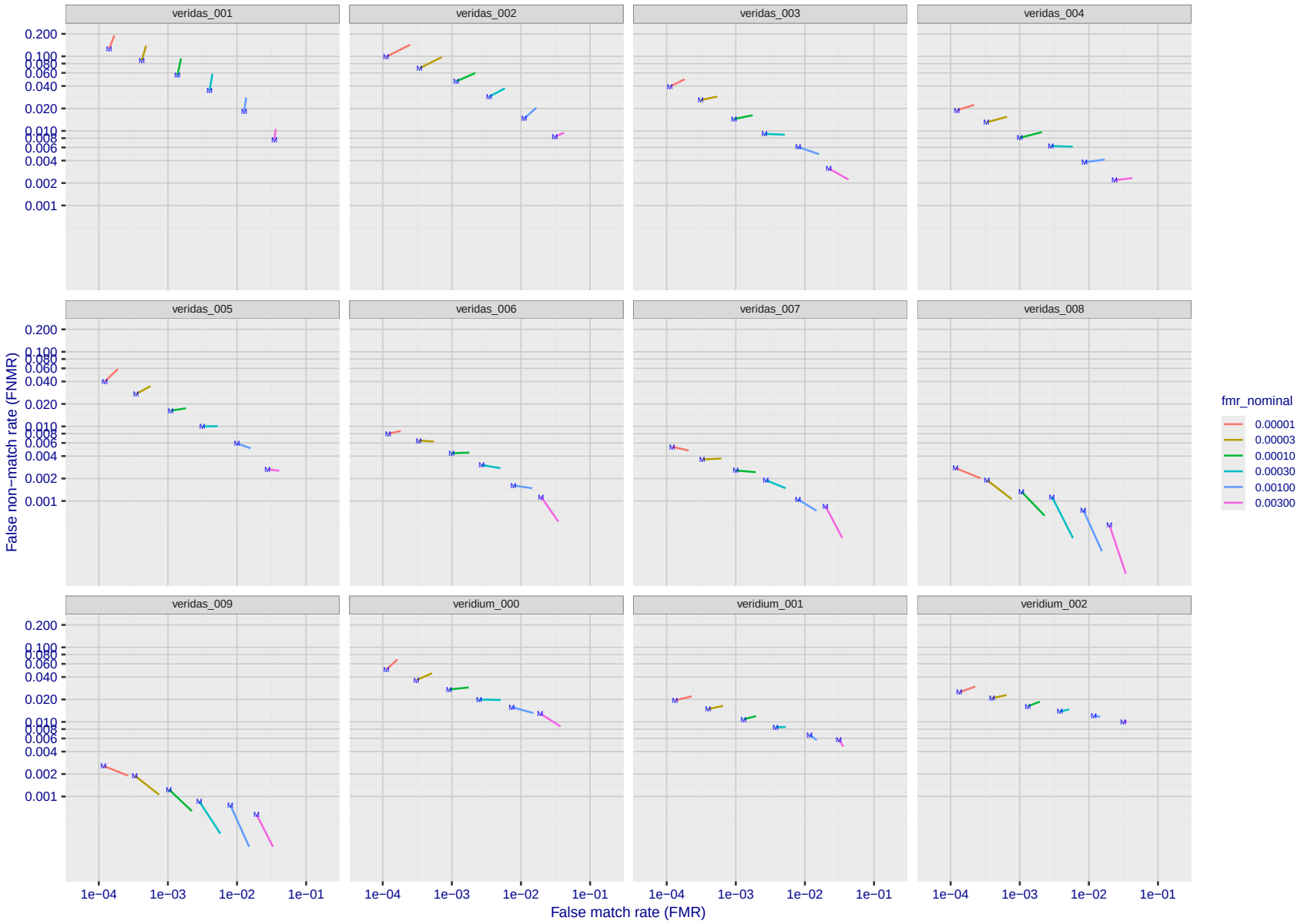

Figure 531: For the visa images, FNMR and FMR at six operating points along the DET characteristic. At each point a line is drawn between (FMR,FNMR)$_{\text{MALE}}$ and (FMR,FNMR)$_{\text{FEMALE}}$ showing how which sex has lower FMR and/or FNMR. The "M" label denotes male, the other end of the line corresponds to female. The six operating thresholds are selected to give the nominal false match rates given in the legend, and are computed over all impostor pairs regardless of age, sex, and place of birth. The plotted FMR values are broadly an order of magnitude larger than the nominal rates because FMR is computed over demographically-matched impostor pairs i.e individuals of the same sex, from the same geographic region (see section 3.6.1), and the same age group (see section 3.6.2).

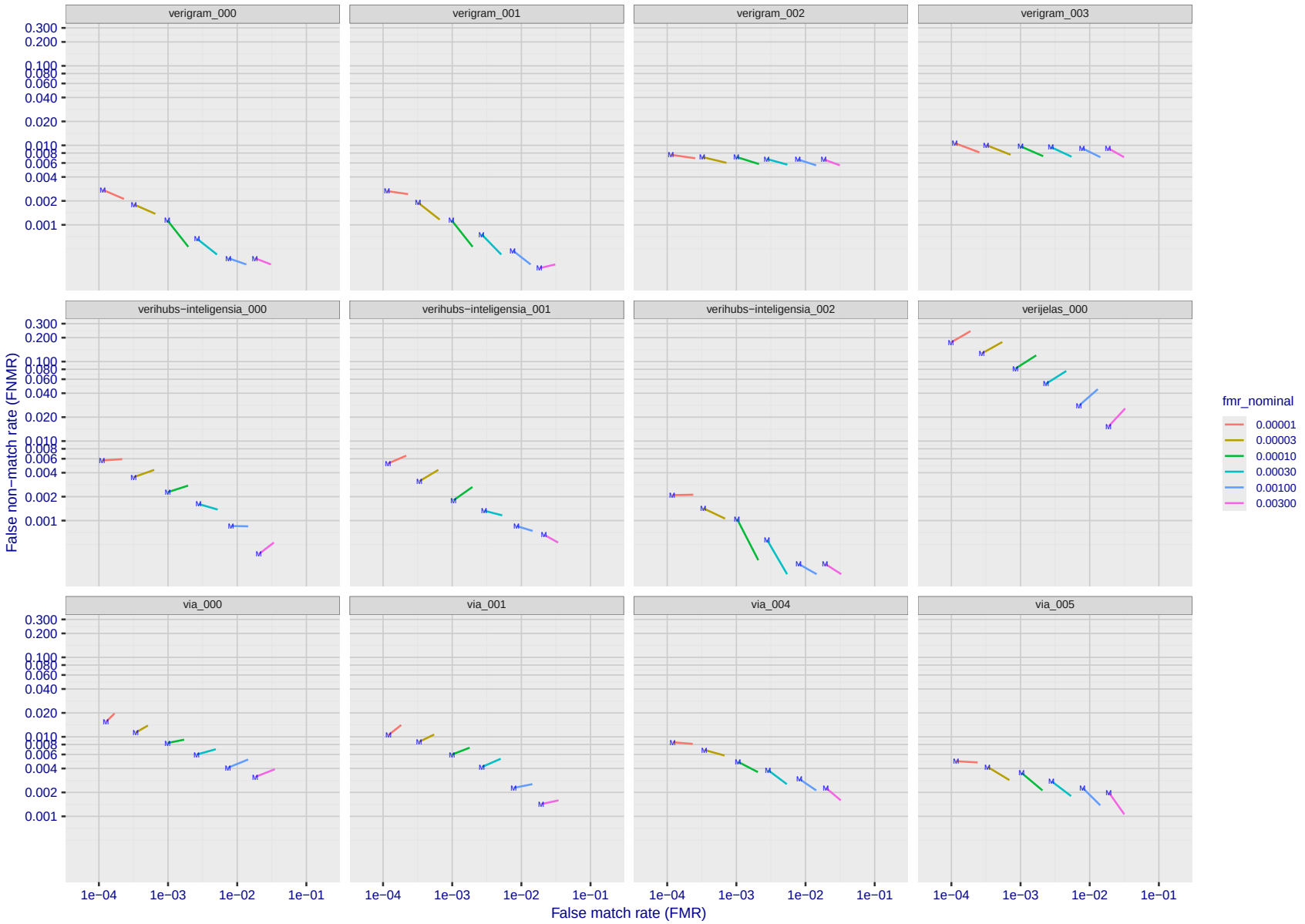

Figure 532: For the visa images, FNMR and FMR at six operating points along the DET characteristic. At each point a line is drawn between (FMR,FNMR)$_{\text{MALE}}$ and (FMR,FNMR)$_{\text{FEMALE}}$ showing how which sex has lower FMR and/or FNMR. The "M" label denotes male, the other end of the line corresponds to female. The six operating thresholds are selected to give the nominal false match rates given in the legend, and are computed over all impostor pairs regardless of age, sex, and place of birth. The plotted FMR values are broadly an order of magnitude larger than the nominal rates because FMR is computed over demographically-matched impostor pairs i.e individuals of the same sex, from the same geographic region (see section 3.6.1), and the same age group (see section 3.6.2).

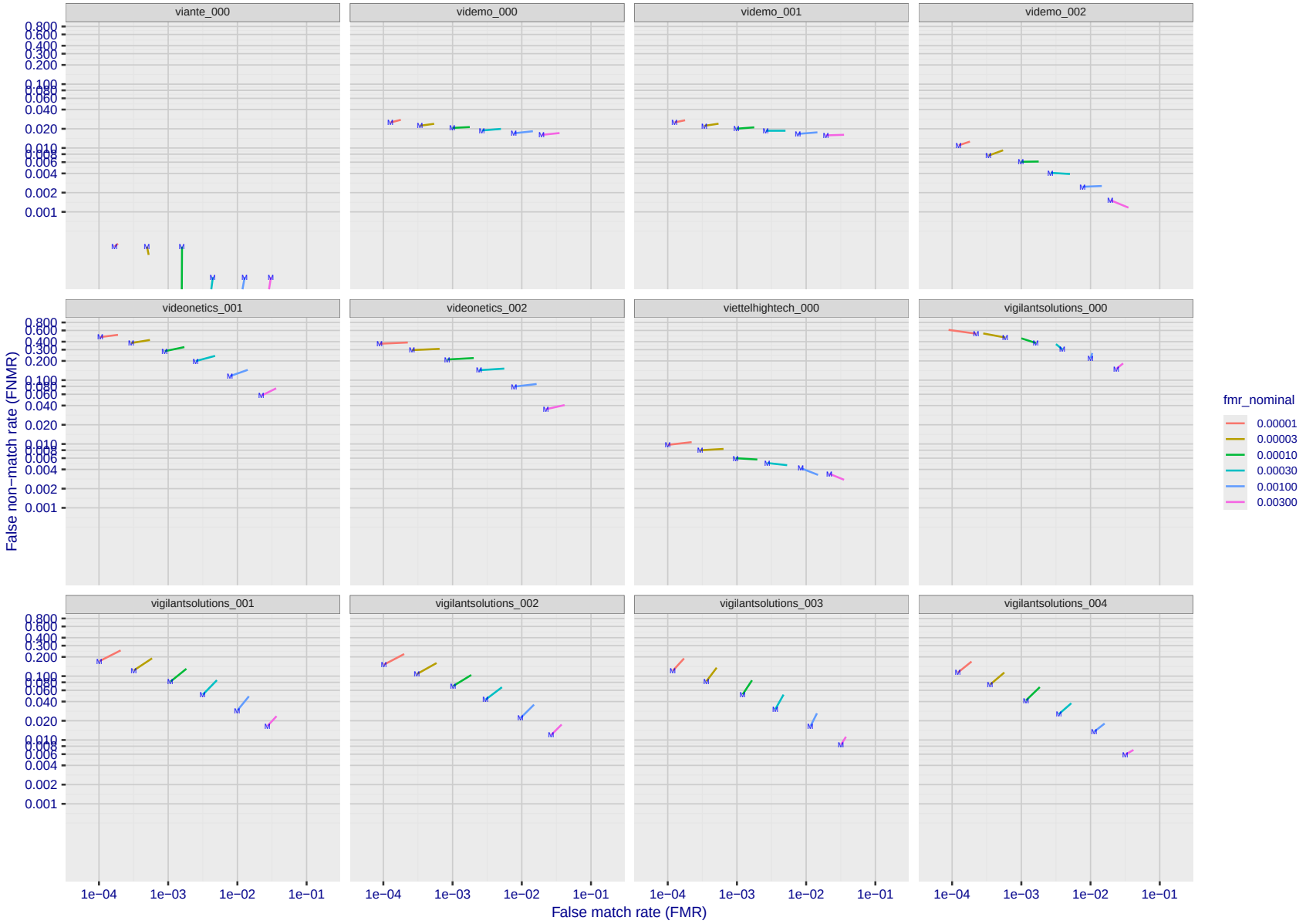

Figure 533: For the visa images, FNMR and FMR at six operating points along the DET characteristic. At each point a line is drawn between (FMR,FNMR)$_{\text{MALE}}$ and (FMR,FNMR)$_{\text{FEMALE}}$ showing how which sex has lower FMR and/or FNMR. The "M" label denotes male, the other end of the line corresponds to female. The six operating thresholds are selected to give the nominal false match rates given in the legend, and are computed over all impostor pairs regardless of age, sex, and place of birth. The plotted FMR values are broadly an order of magnitude larger than the nominal rates because FMR is computed over demographically-matched impostor pairs i.e individuals of the same sex, from the same geographic region (see section 3.6.1), and the same age group (see section 3.6.2).

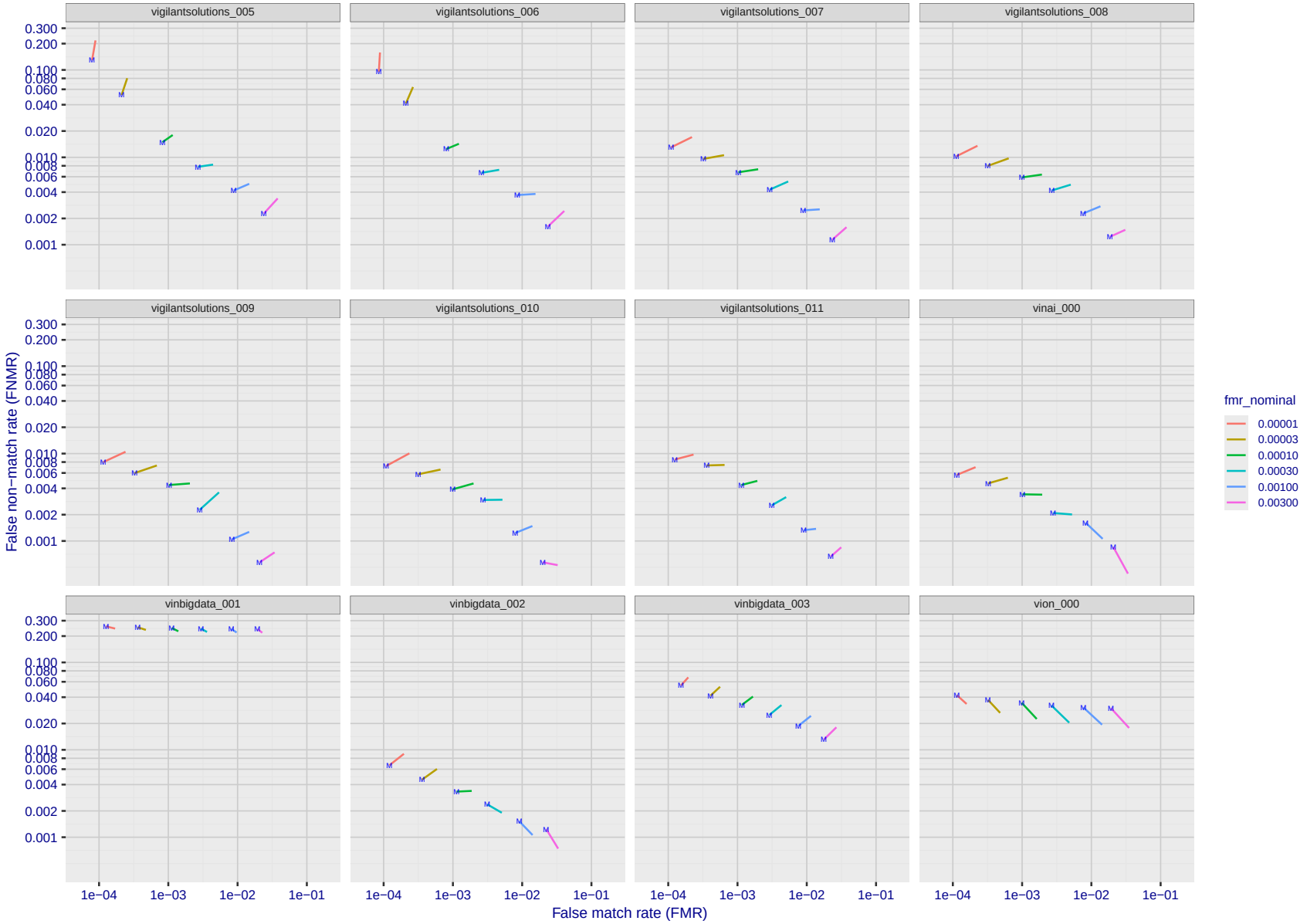

Figure 534: For the visa images, FNMR and FMR at six operating points along the DET characteristic. At each point a line is drawn between (FMR,FNMR)$_{\text{MALE}}$ and (FMR,FNMR)$_{\text{FEMALE}}$ showing how which sex has lower FMR and/or FNMR. The "M" label denotes male, the other end of the line corresponds to female. The six operating thresholds are selected to give the nominal false match rates given in the legend, and are computed over all impostor pairs regardless of age, sex, and place of birth. The plotted FMR values are broadly an order of magnitude larger than the nominal rates because FMR is computed over demographically-matched impostor pairs i.e individuals of the same sex, from the same geographic region (see section 3.6.1), and the same age group (see section 3.6.2).

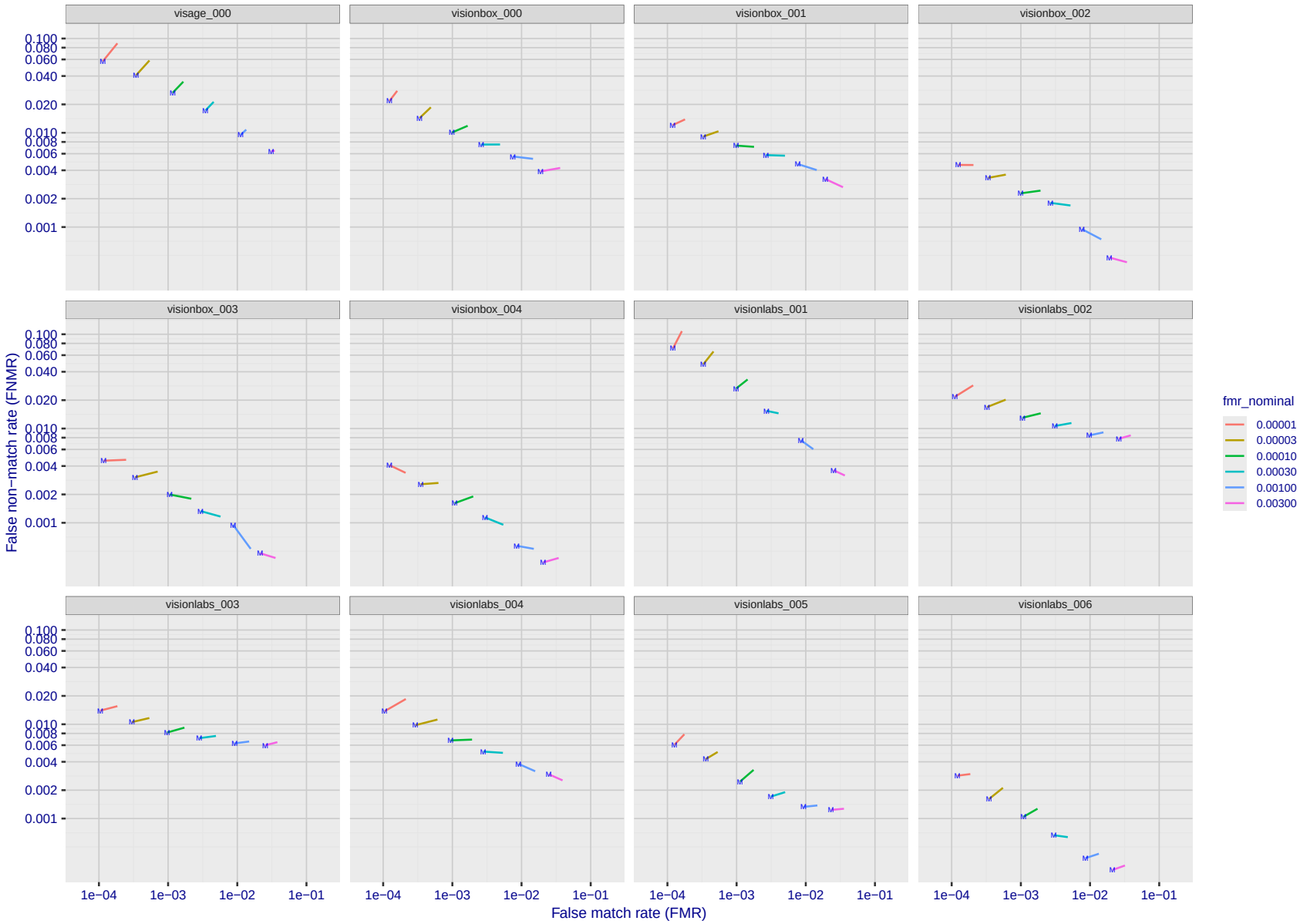

Figure 535: For the visa images, FNMR and FMR at six operating points along the DET characteristic. At each point a line is drawn between (FMR,FNMR)$_{\text{MALE}}$ and (FMR,FNMR)$_{\text{FEMALE}}$ showing how which sex has lower FMR and/or FNMR. The "M" label denotes male, the other end of the line corresponds to female. The six operating thresholds are selected to give the nominal false match rates given in the legend, and are computed over all impostor pairs regardless of age, sex, and place of birth. The plotted FMR values are broadly an order of magnitude larger than the nominal rates because FMR is computed over demographically-matched impostor pairs i.e individuals of the same sex, from the same geographic region (see section 3.6.1), and the same age group (see section 3.6.2).

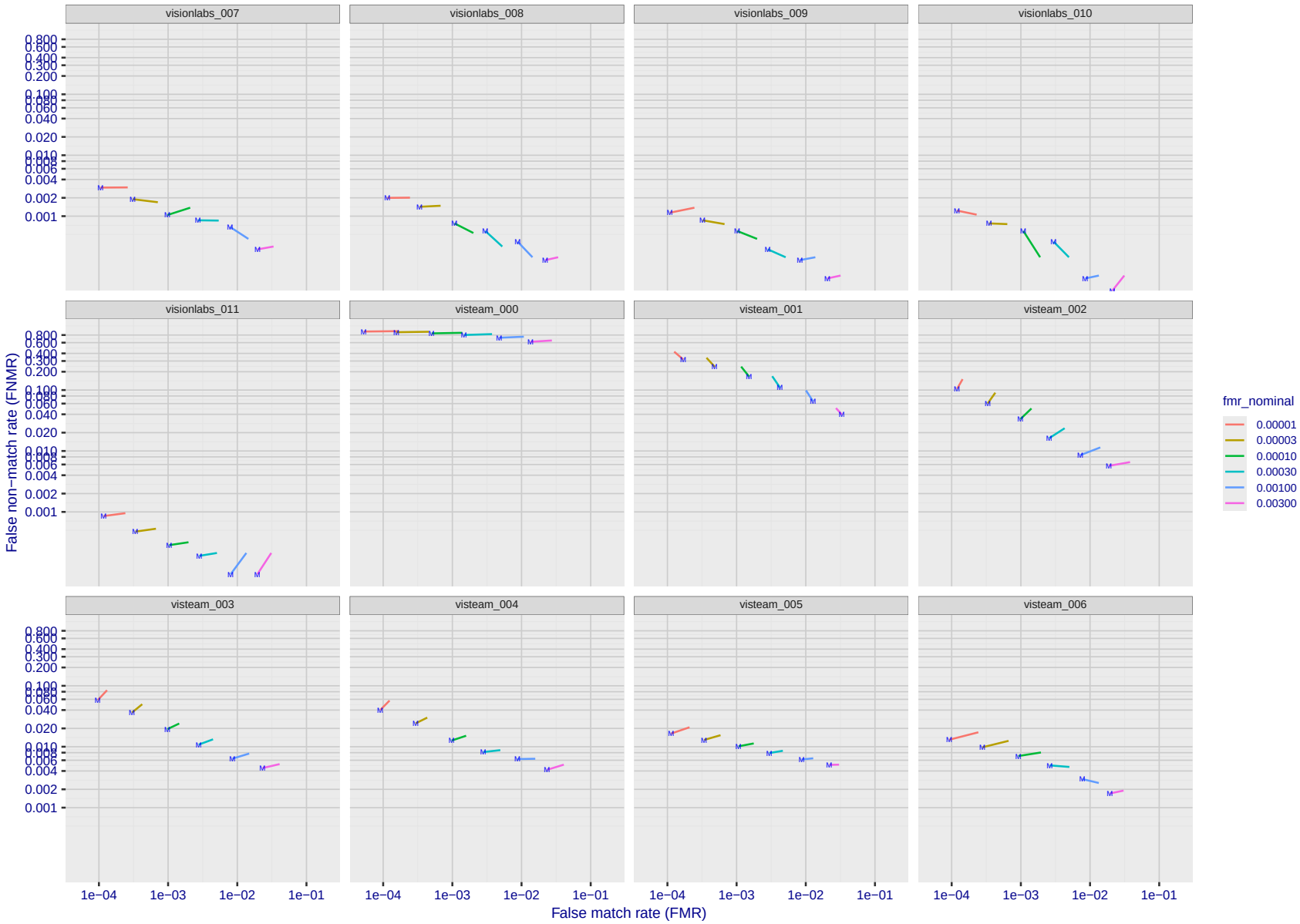

Figure 536: For the visa images, FNMR and FMR at six operating points along the DET characteristic. At each point a line is drawn between (FMR,FNMR)$_{\text{MALE}}$ and (FMR,FNMR)$_{\text{FEMALE}}$ showing how which sex has lower FMR and/or FNMR. The "M" label denotes male, the other end of the line corresponds to female. The six operating thresholds are selected to give the nominal false match rates given in the legend, and are computed over all impostor pairs regardless of age, sex, and place of birth. The plotted FMR values are broadly an order of magnitude larger than the nominal rates because FMR is computed over demographically-matched impostor pairs i.e individuals of the same sex, from the same geographic region (see section 3.6.1), and the same age group (see section 3.6.2).

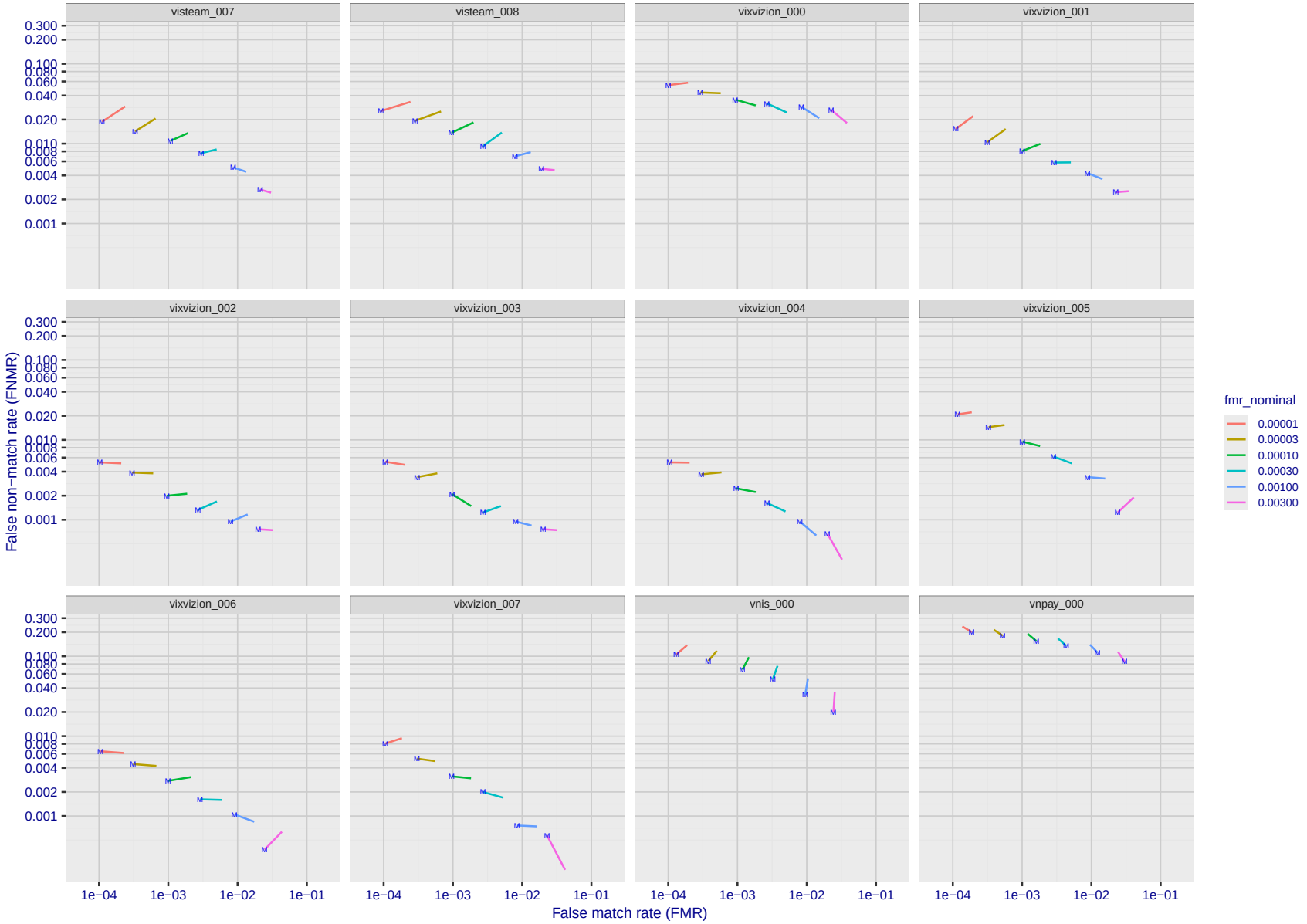

Figure 537: For the visa images, FNMR and FMR at six operating points along the DET characteristic. At each point a line is drawn between (FMR,FNMR)$_{\text{MALE}}$ and (FMR,FNMR)$_{\text{FEMALE}}$ showing how which sex has lower FMR and/or FNMR. The "M" label denotes male, the other end of the line corresponds to female. The six operating thresholds are selected to give the nominal false match rates given in the legend, and are computed over all impostor pairs regardless of age, sex, and place of birth. The plotted FMR values are broadly an order of magnitude larger than the nominal rates because FMR is computed over demographically-matched impostor pairs i.e individuals of the same sex, from the same geographic region (see section 3.6.1), and the same age group (see section 3.6.2).

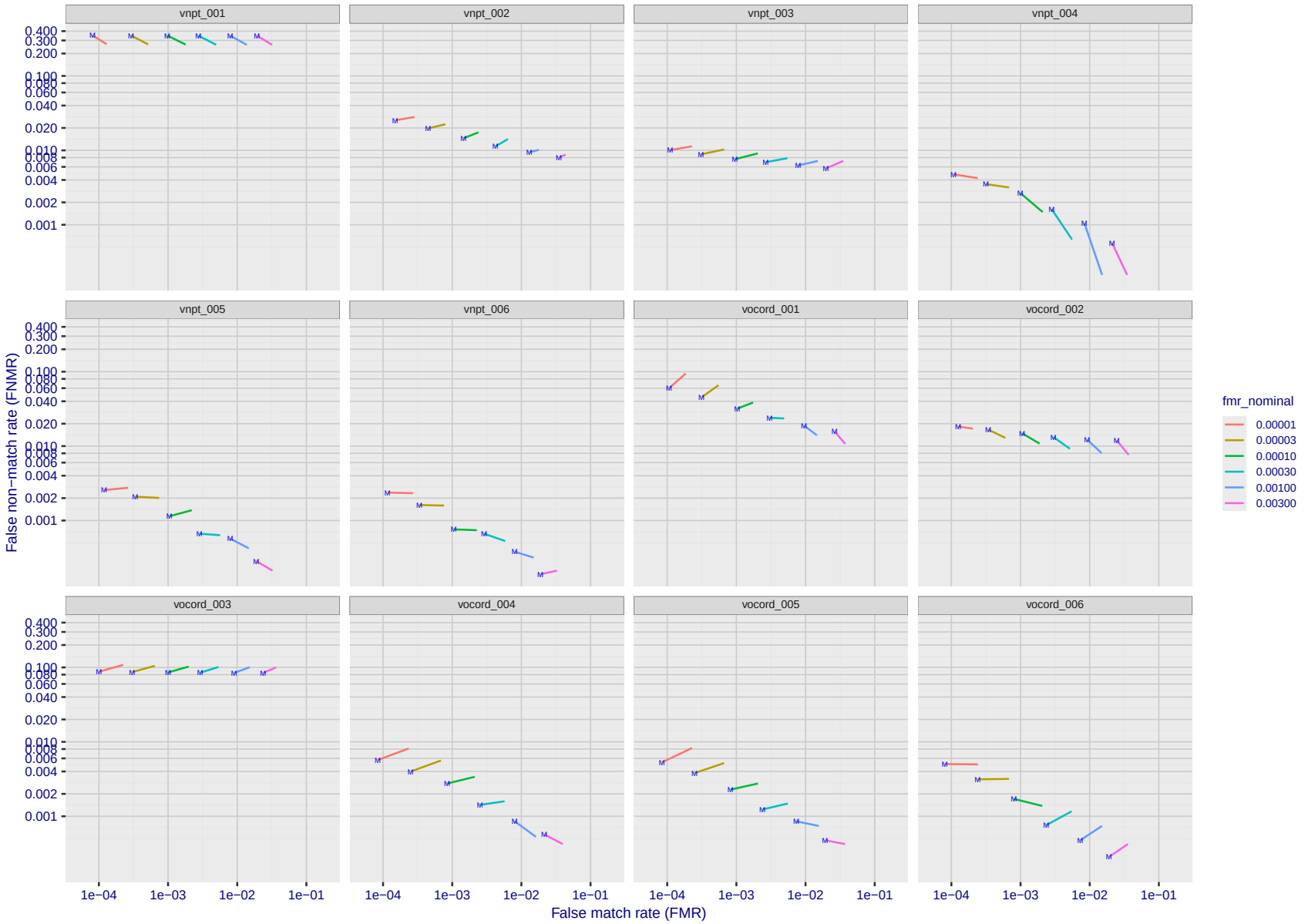

Figure 538: For the visa images, FNMR and FMR at six operating points along the DET characteristic. At each point a line is drawn between (FMR,FNMR)$_{\text{MALE}}$ and (FMR,FNMR)$_{\text{FEMALE}}$ showing how which sex has lower FMR and/or FNMR. The "M" label denotes male, the other end of the line corresponds to female. The six operating thresholds are selected to give the nominal false match rates given in the legend, and are computed over all impostor pairs regardless of age, sex, and place of birth. The plotted FMR values are broadly an order of magnitude larger than the nominal rates because FMR is computed over demographically-matched impostor pairs i.e individuals of the same sex, from the same geographic region (see section 3.6.1), and the same age group (see section 3.6.2).

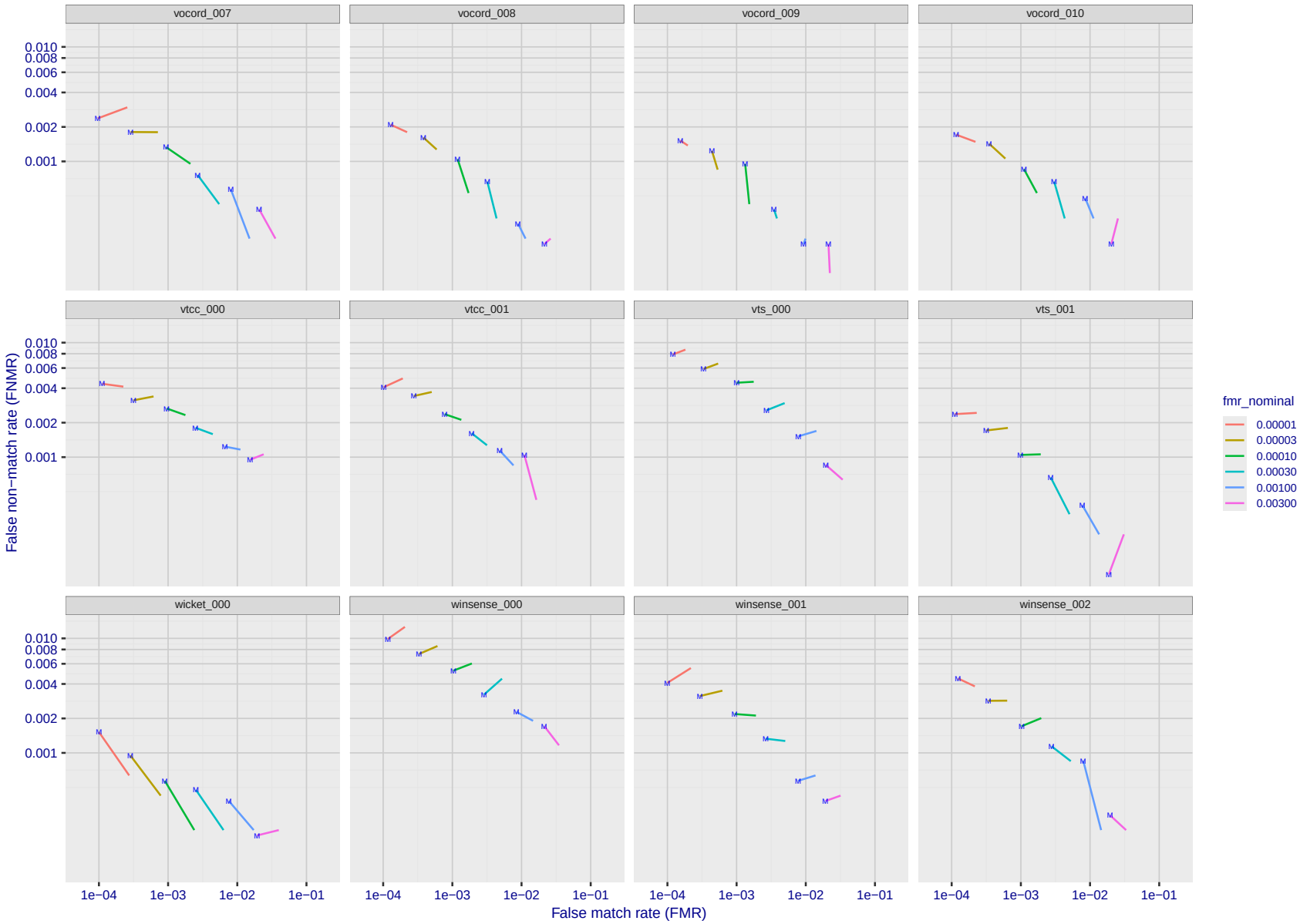

Figure 539: For the visa images, FNMR and FMR at six operating points along the DET characteristic. At each point a line is drawn between (FMR,FNMR)$_{\text{MALE}}$ and (FMR,FNMR)$_{\text{FEMALE}}$ showing how which sex has lower FMR and/or FNMR. The "M" label denotes male, the other end of the line corresponds to female. The six operating thresholds are selected to give the nominal false match rates given in the legend, and are computed over all impostor pairs regardless of age, sex, and place of birth. The plotted FMR values are broadly an order of magnitude larger than the nominal rates because FMR is computed over demographically-matched impostor pairs i.e individuals of the same sex, from the same geographic region (see section 3.6.1), and the same age group (see section 3.6.2).

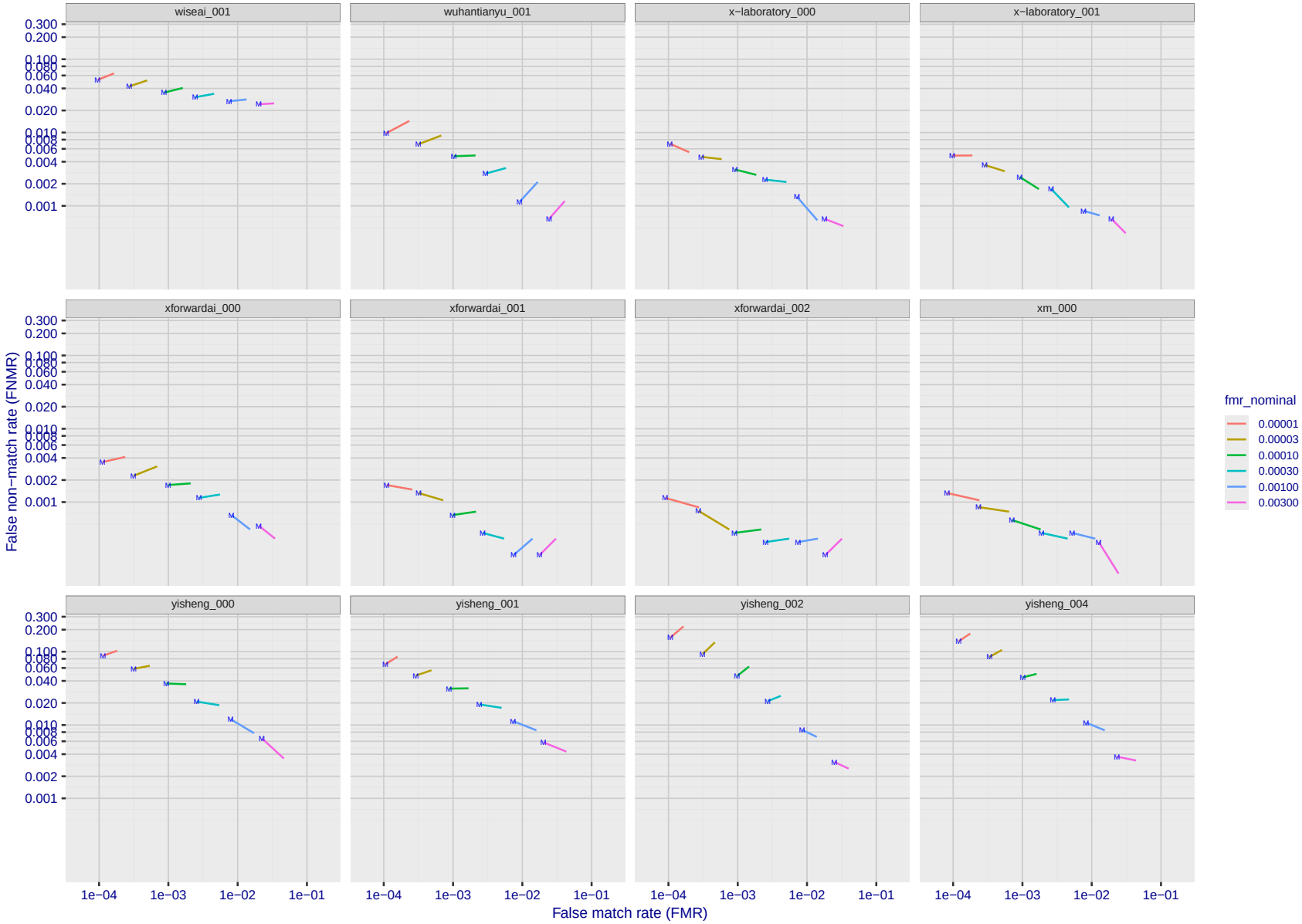

Figure 540: For the visa images, FNMR and FMR at six operating points along the DET characteristic. At each point a line is drawn between (FMR,FNMR)$_{\text{MALE}}$ and (FMR,FNMR)$_{\text{FEMALE}}$ showing how which sex has lower FMR and/or FNMR. The "M" label denotes male, the other end of the line corresponds to female. The six operating thresholds are selected to give the nominal false match rates given in the legend, and are computed over all impostor pairs regardless of age, sex, and place of birth. The plotted FMR values are broadly an order of magnitude larger than the nominal rates because FMR is computed over demographically-matched impostor pairs i.e individuals of the same sex, from the same geographic region (see section 3.6.1), and the same age group (see section 3.6.2).

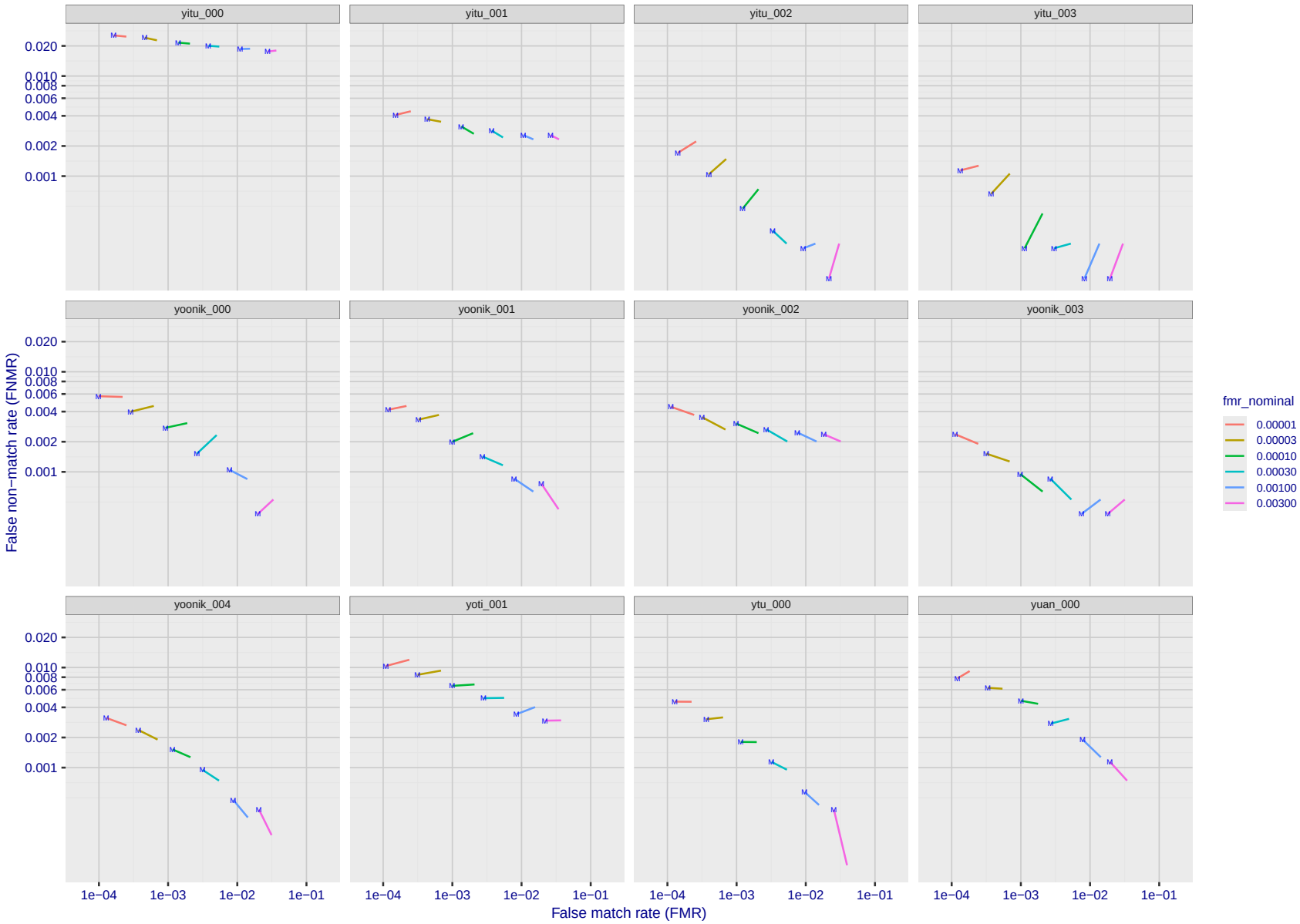

Figure 541: For the visa images, FNMR and FMR at six operating points along the DET characteristic. At each point a line is drawn between (FMR,FNMR)$_{\text{MALE}}$ and (FMR,FNMR)$_{\text{FEMALE}}$ showing how which sex has lower FMR and/or FNMR. The "M" label denotes male, the other end of the line corresponds to female. The six operating thresholds are selected to give the nominal false match rates given in the legend, and are computed over all impostor pairs regardless of age, sex, and place of birth. The plotted FMR values are broadly an order of magnitude larger than the nominal rates because FMR is computed over demographically-matched impostor pairs i.e individuals of the same sex, from the same geographic region (see section 3.6.1), and the same age group (see section 3.6.2).

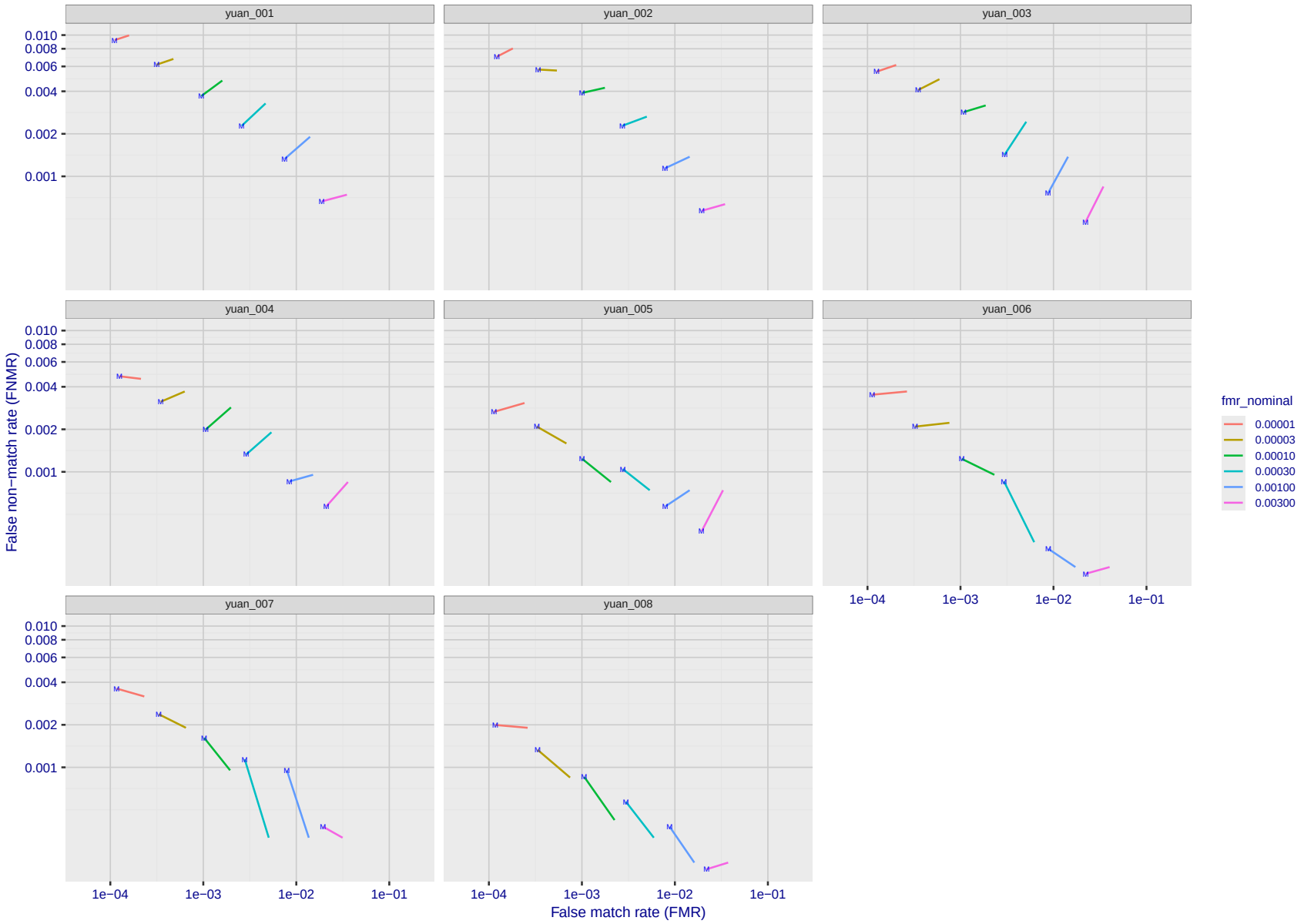

Figure 542: For the visa images, FNMR and FMR at six operating points along the DET characteristic. At each point a line is drawn between (FMR,FNMR)$_{\text{MALE}}$ and (FMR,FNMR)$_{\text{FEMALE}}$ showing how which sex has lower FMR and/or FNMR. The "M" label denotes male, the other end of the line corresponds to female. The six operating thresholds are selected to give the nominal false match rates given in the legend, and are computed over all impostor pairs regardless of age, sex, and place of birth. The plotted FMR values are broadly an order of magnitude larger than the nominal rates because FMR is computed over demographically-matched impostor pairs i.e individuals of the same sex, from the same geographic region (see section 3.6.1), and the same age group (see section 3.6.2).

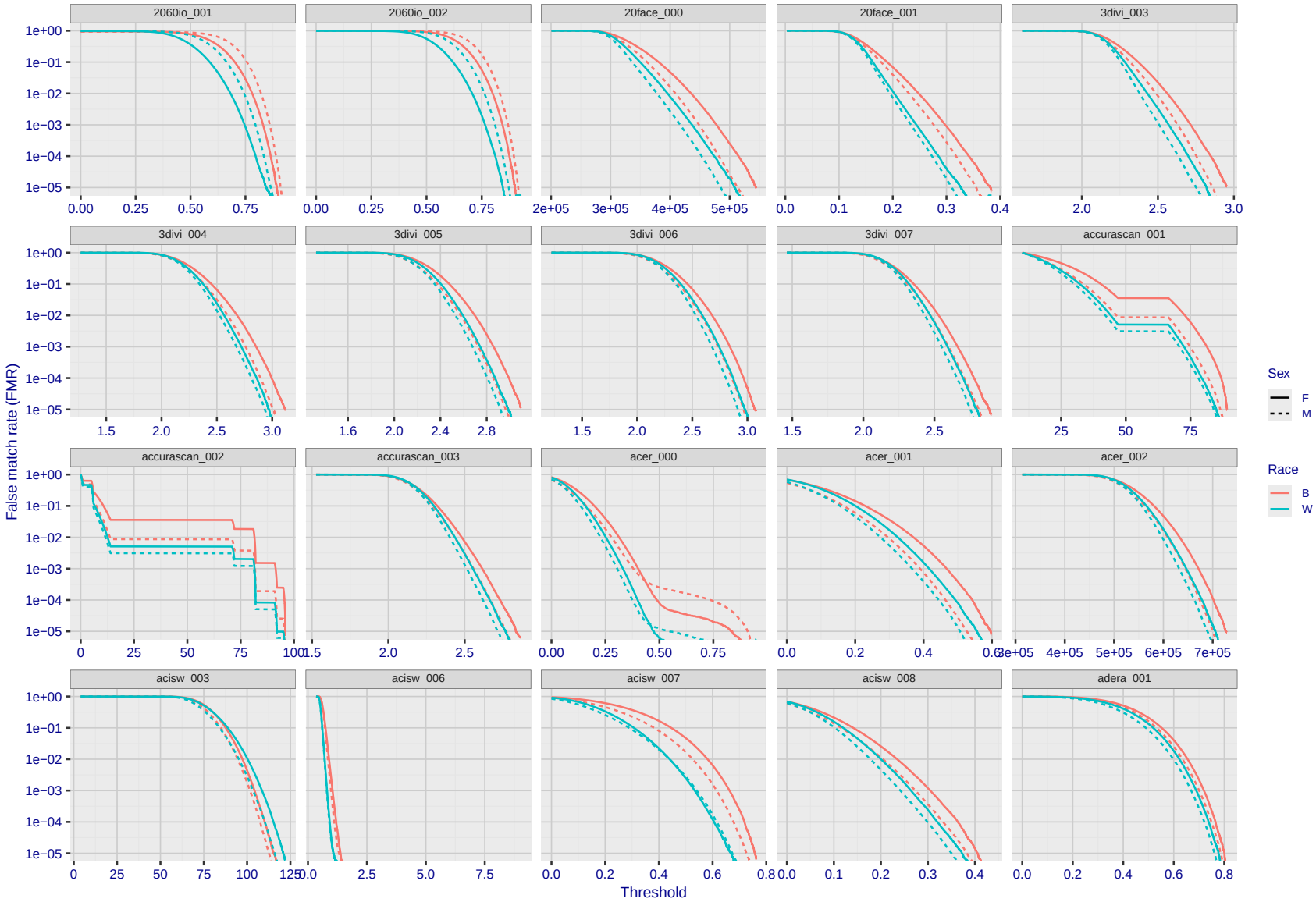

Figure 543: For the mugshot images, the false match calibration curves show false match rate vs. threshold. Separate curves appear for white females, black females, black males and white males.

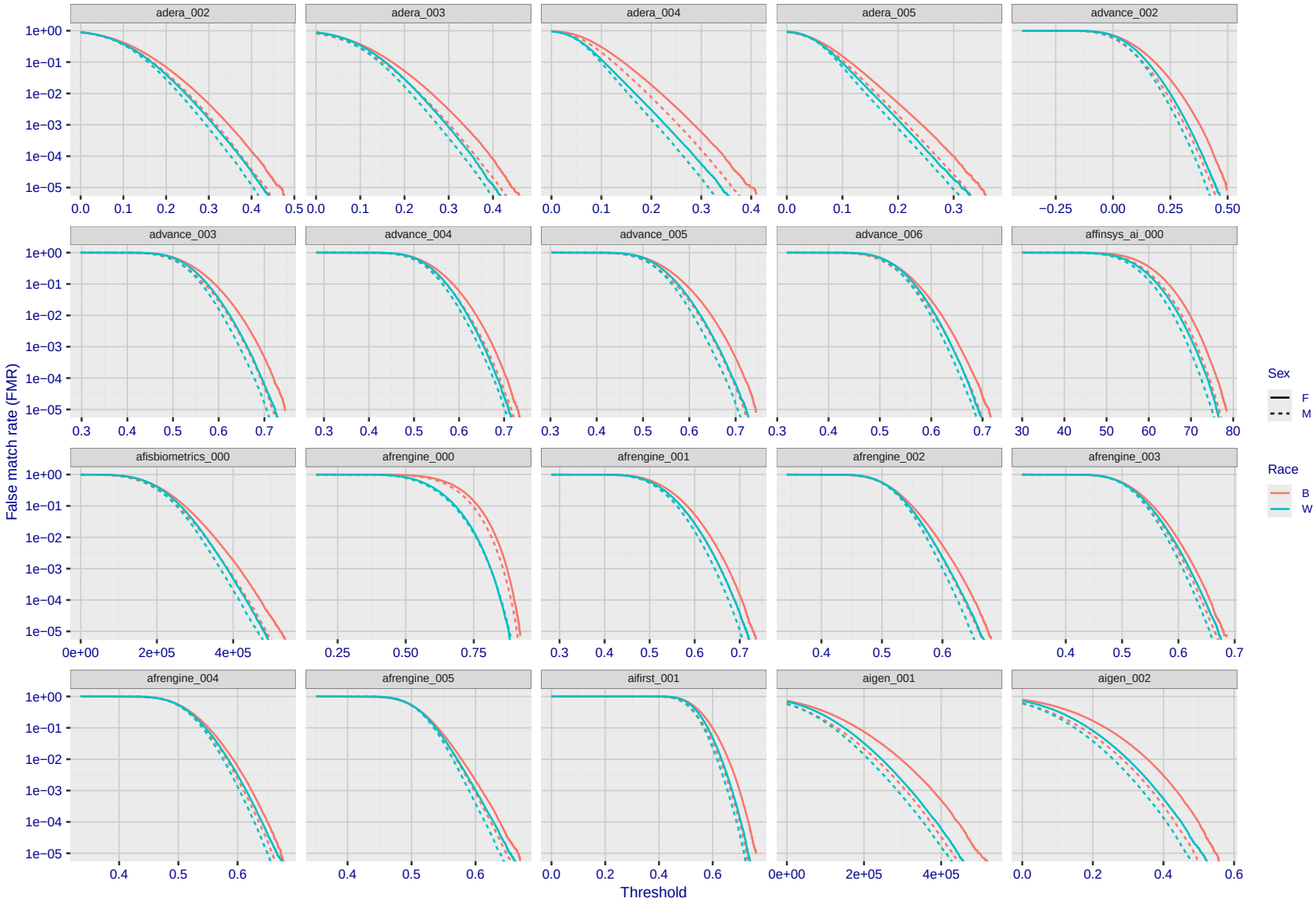

Figure 544: For the mugshot images, the false match calibration curves show false match rate vs. threshold. Separate curves appear for white females, black females, black males and white males.

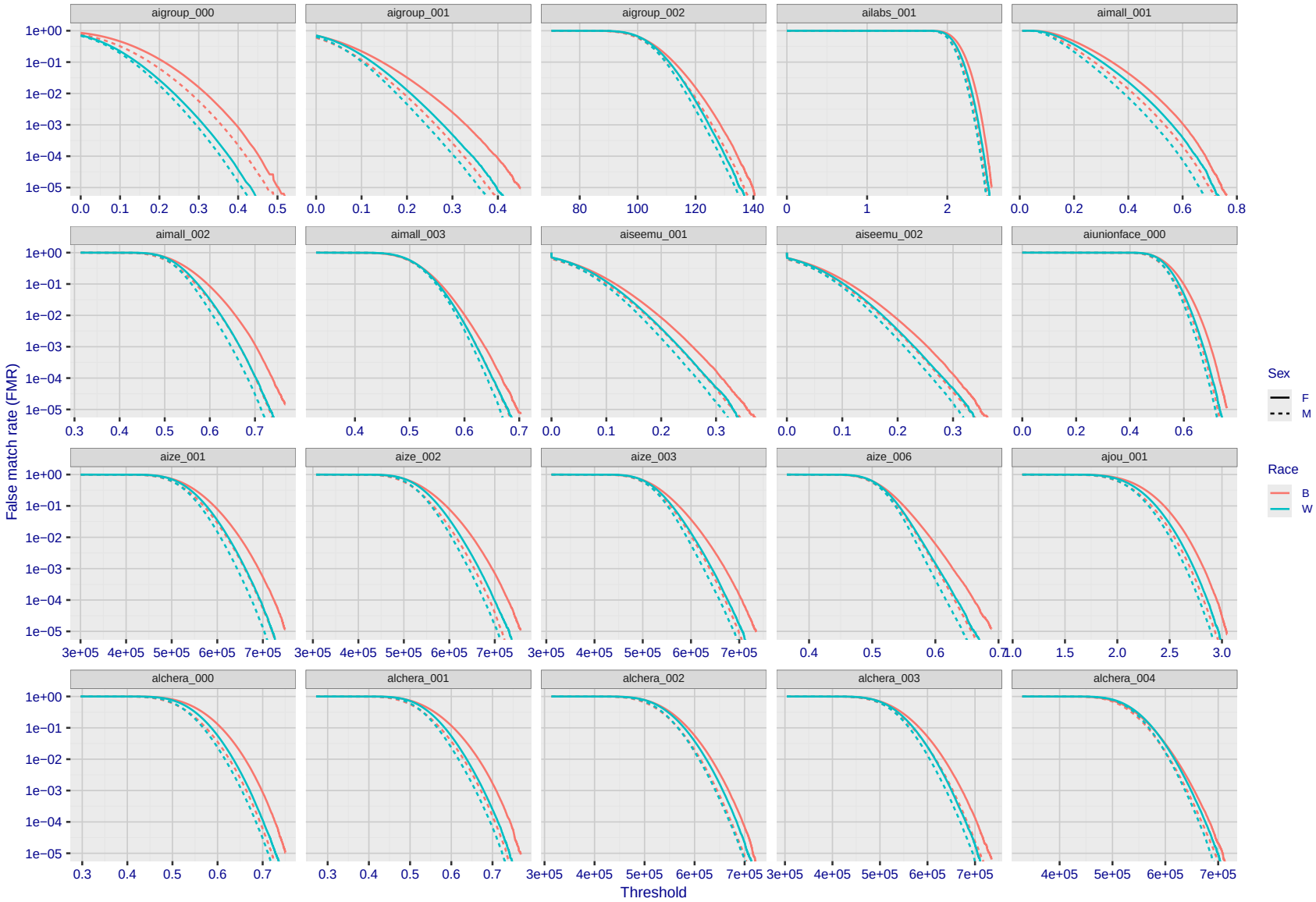

Figure 545: For the mugshot images, the false match calibration curves show false match rate vs. threshold. Separate curves appear for white females, black females, black males and white males.

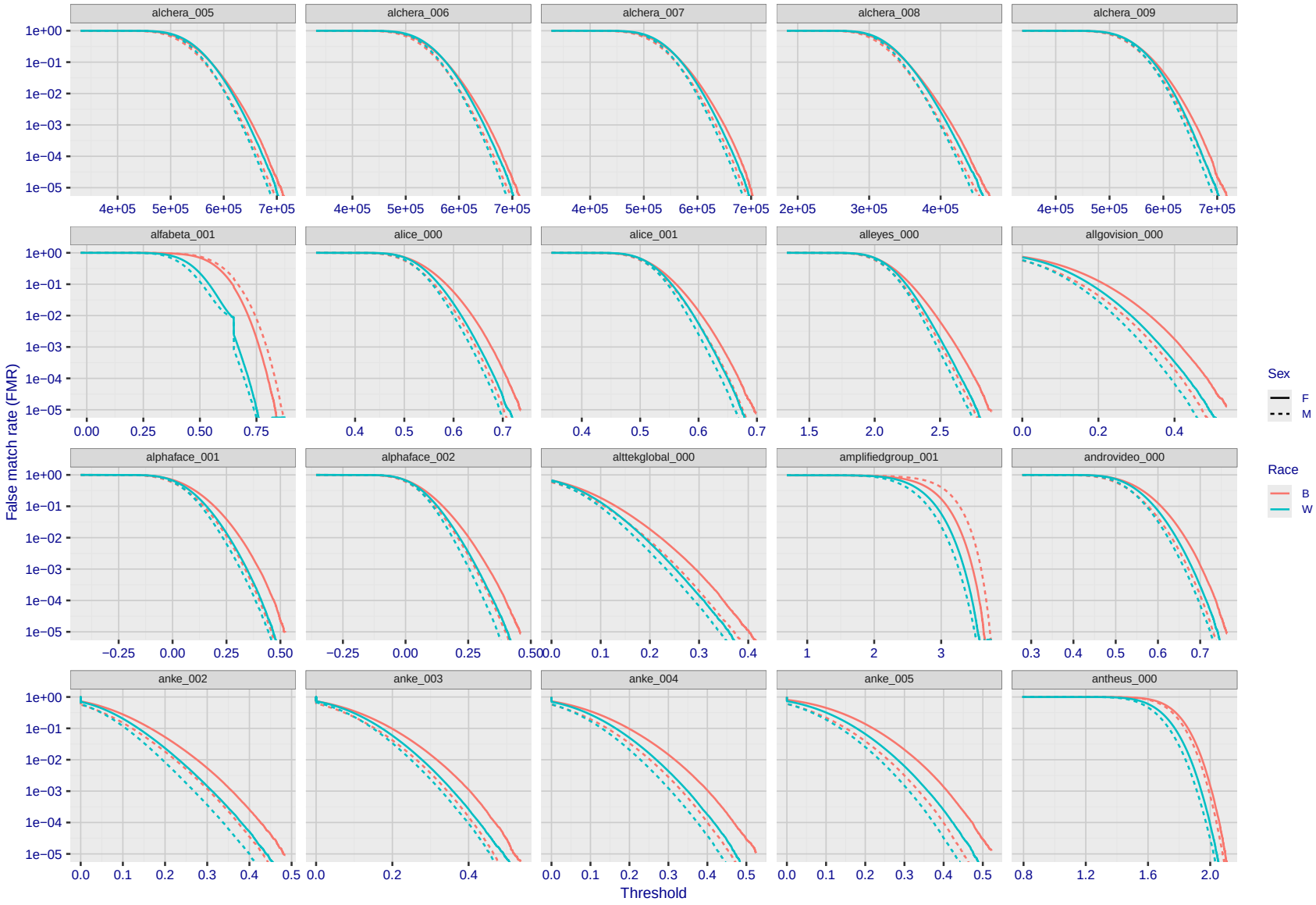

Figure 546: For the mugshot images, the false match calibration curves show false match rate vs. threshold. Separate curves appear for white females, black females, black males and white males.

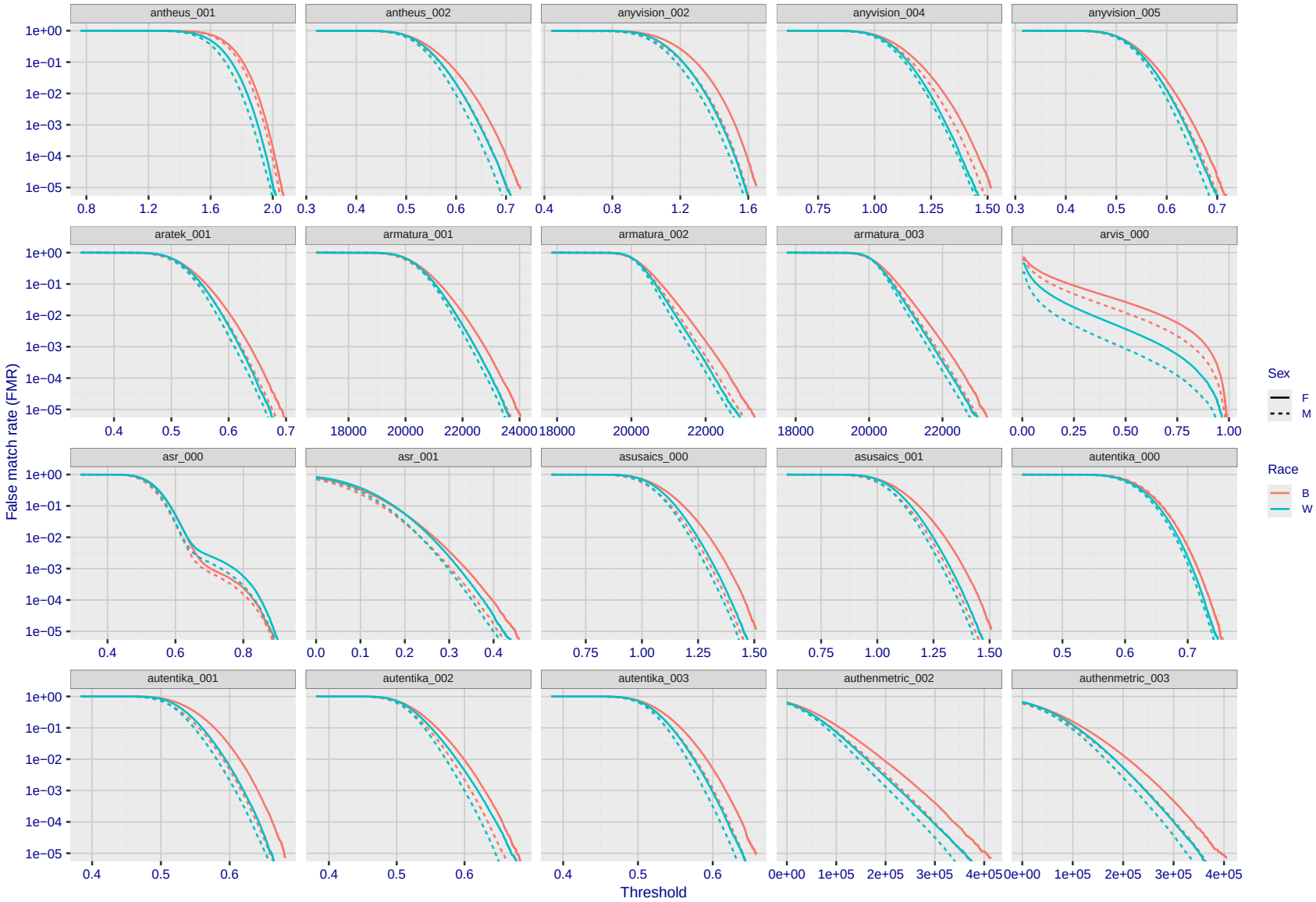

Figure 547: For the mugshot images, the false match calibration curves show false match rate vs. threshold. Separate curves appear for white females, black females, black males and white males.

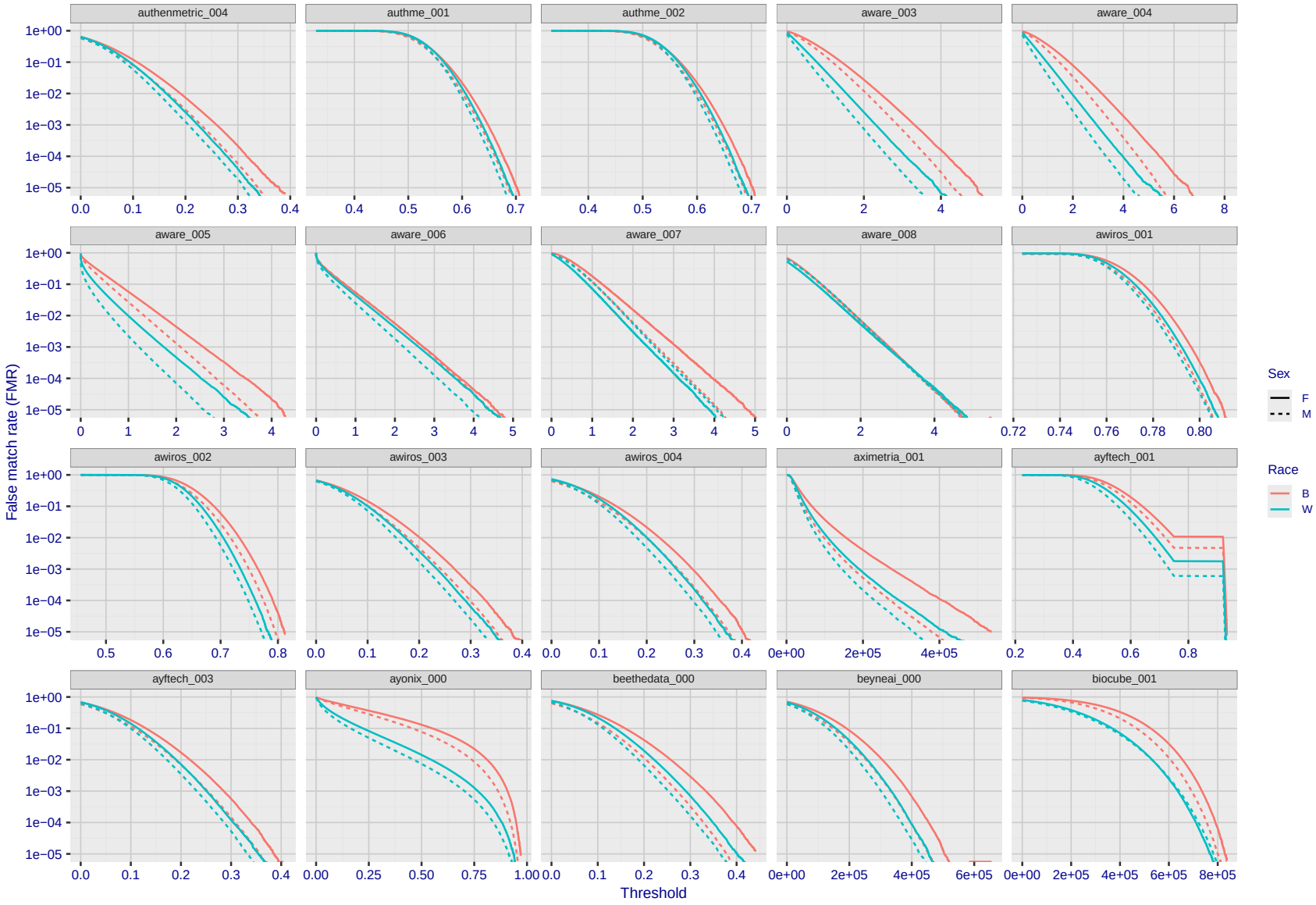

Figure 548: For the mugshot images, the false match calibration curves show false match rate vs. threshold. Separate curves appear for white females, black females, black males and white males.

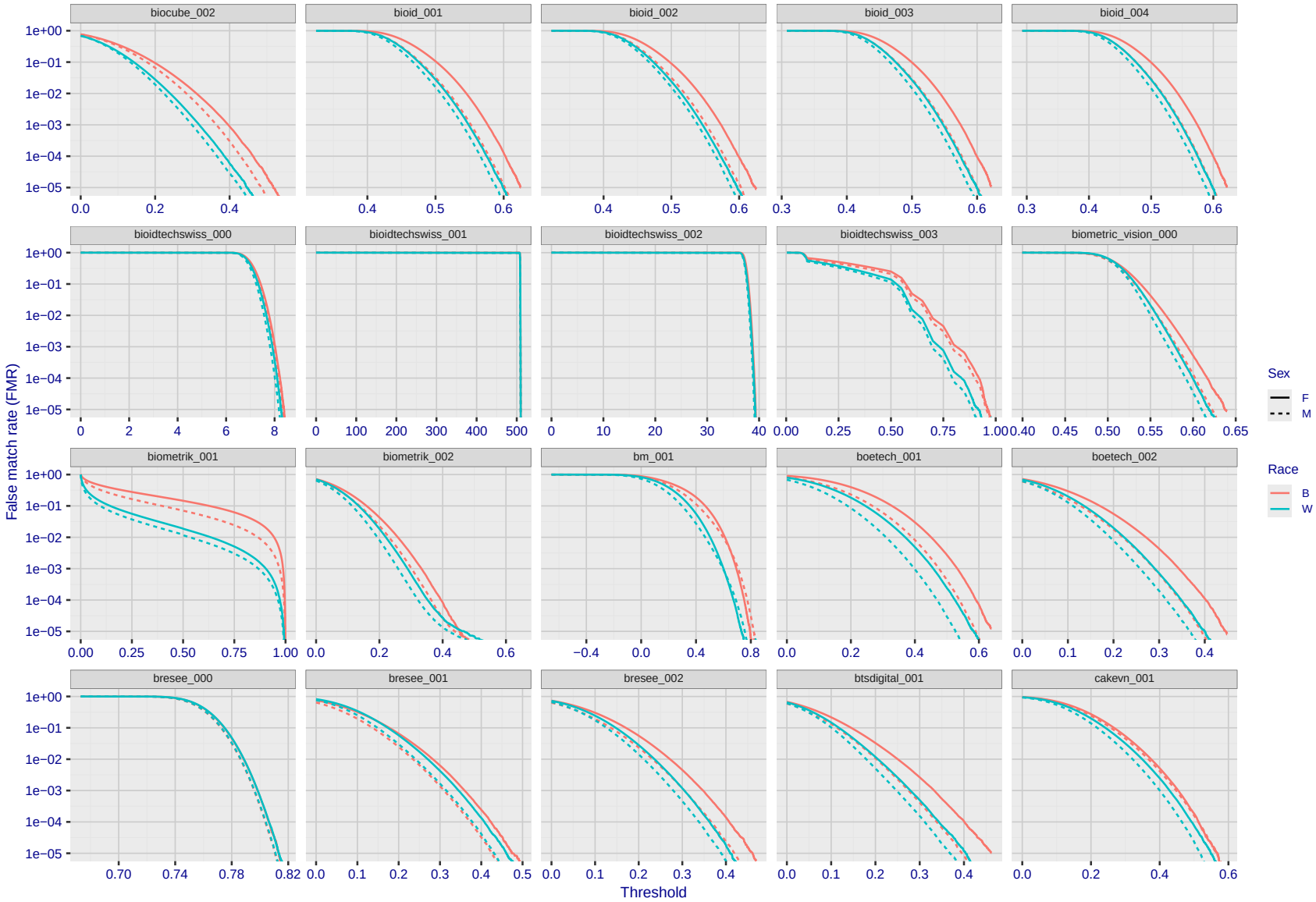

Figure 549: For the mugshot images, the false match calibration curves show false match rate vs. threshold. Separate curves appear for white females, black females, black males and white males.

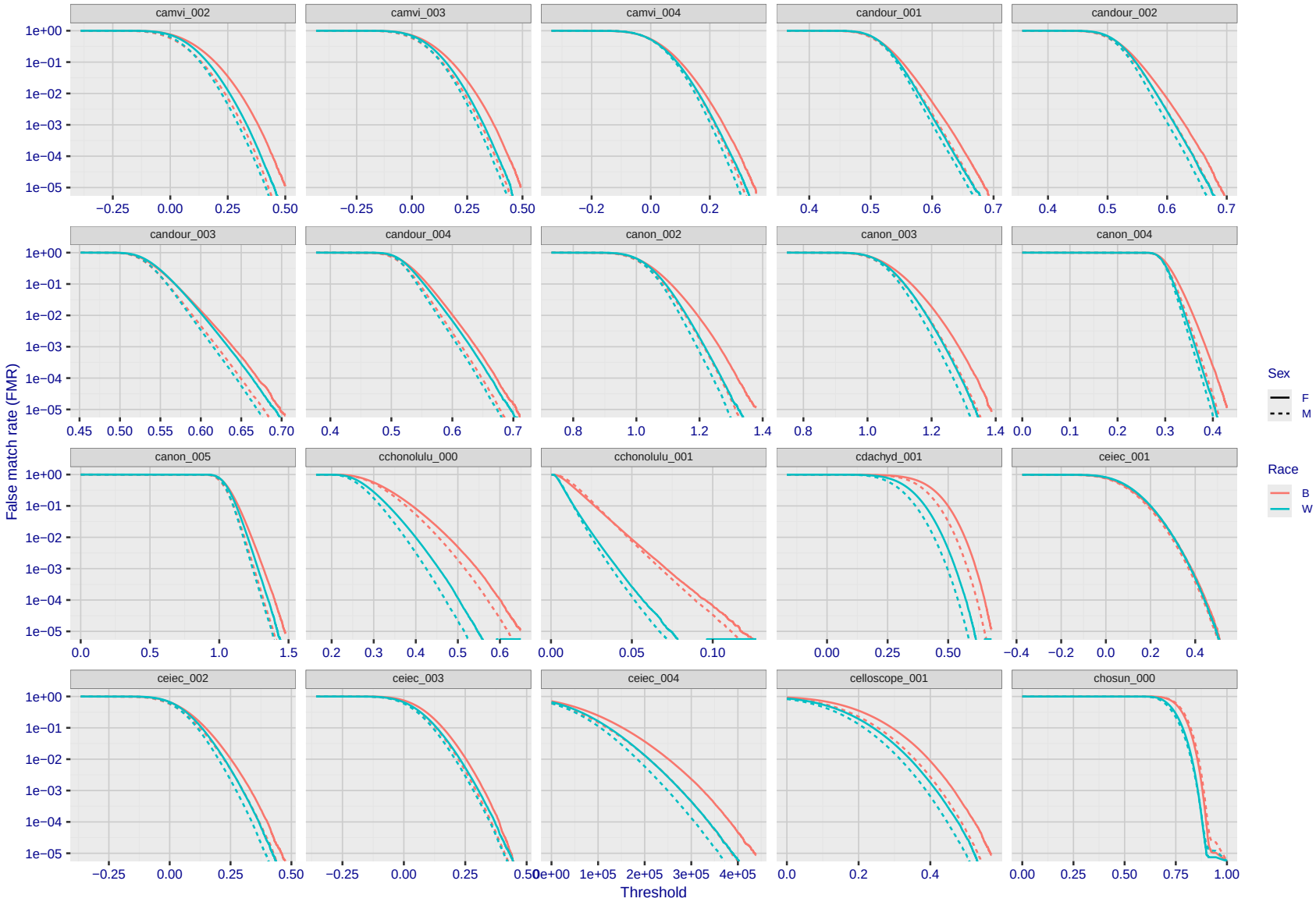

Figure 550: For the mugshot images, the false match calibration curves show false match rate vs. threshold. Separate curves appear for white females, black females, black males and white males.

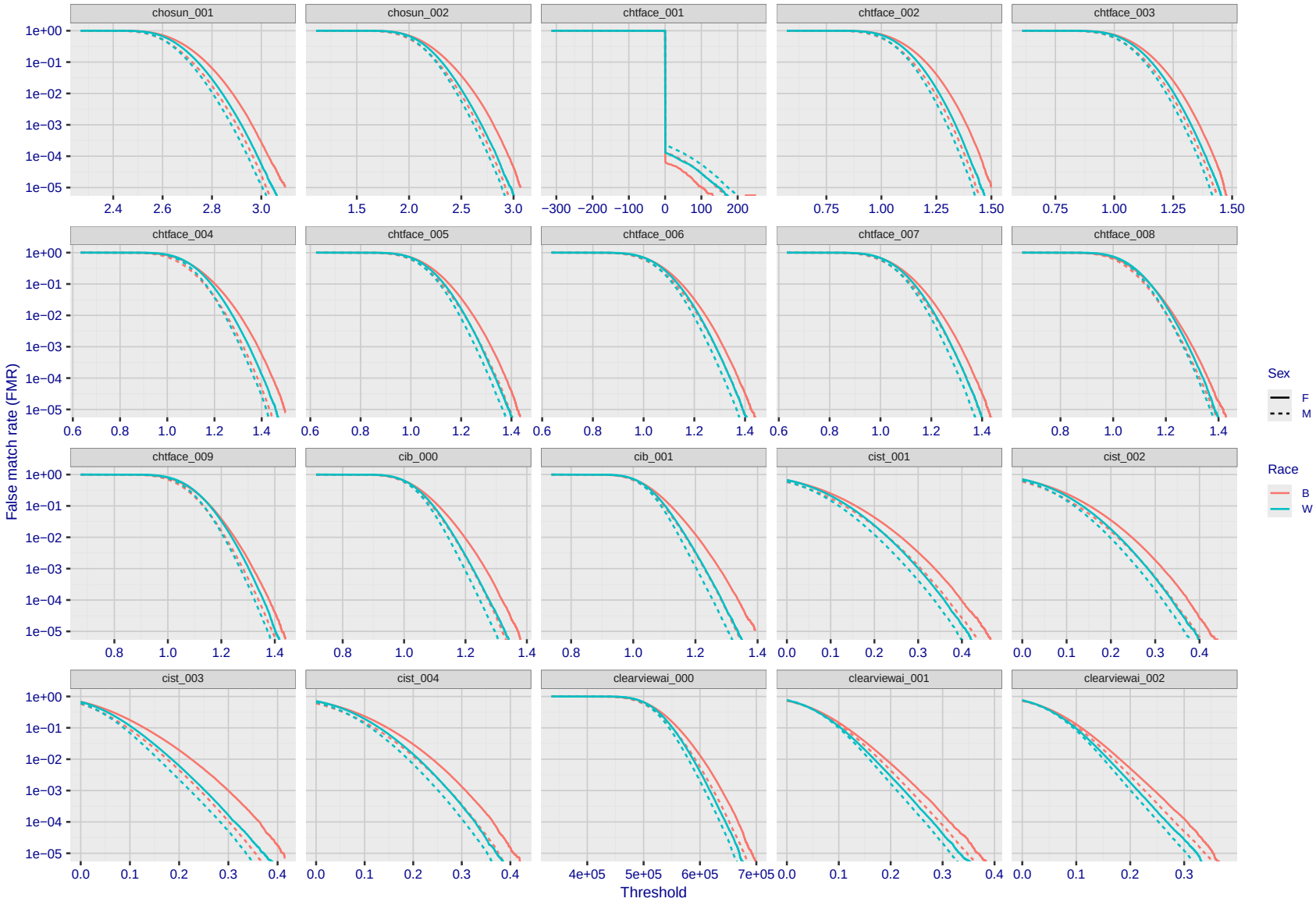

Figure 551: For the mugshot images, the false match calibration curves show false match rate vs. threshold. Separate curves appear for white females, black females, black males and white males.

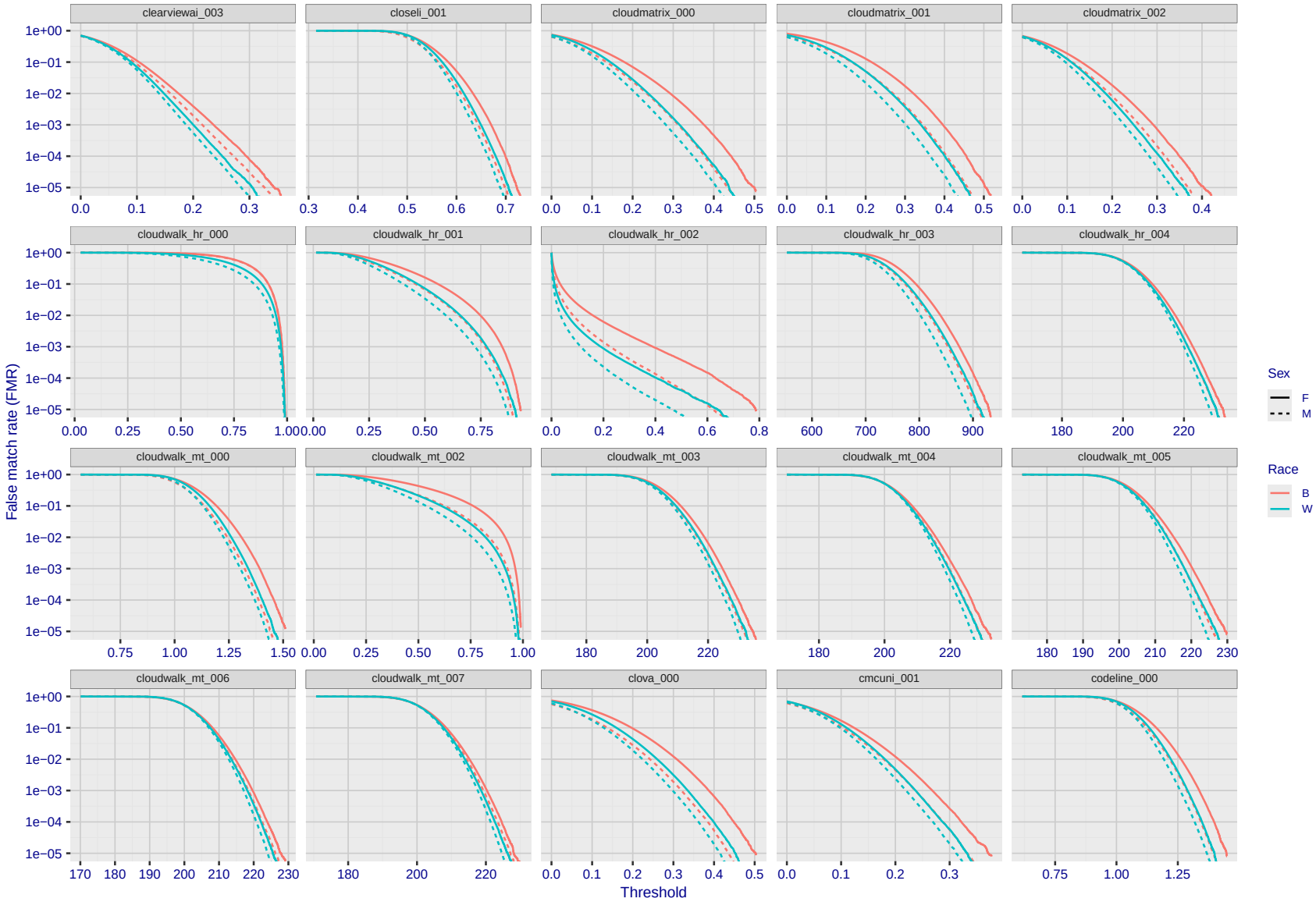

Figure 552: For the mugshot images, the false match calibration curves show false match rate vs. threshold. Separate curves appear for white females, black females, black males and white males.

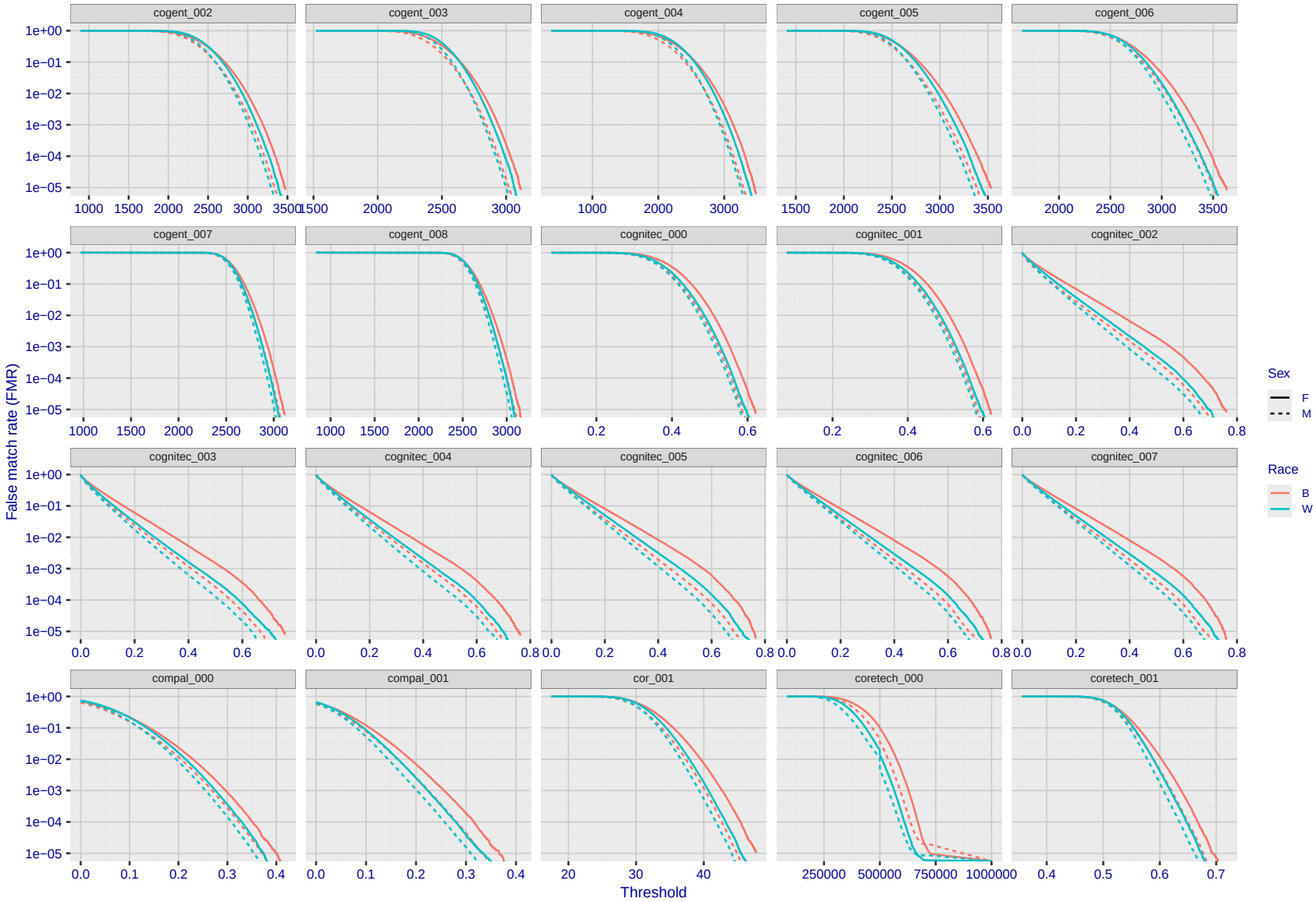

Figure 553: For the mugshot images, the false match calibration curves show false match rate vs. threshold. Separate curves appear for white females, black females, black males and white males.

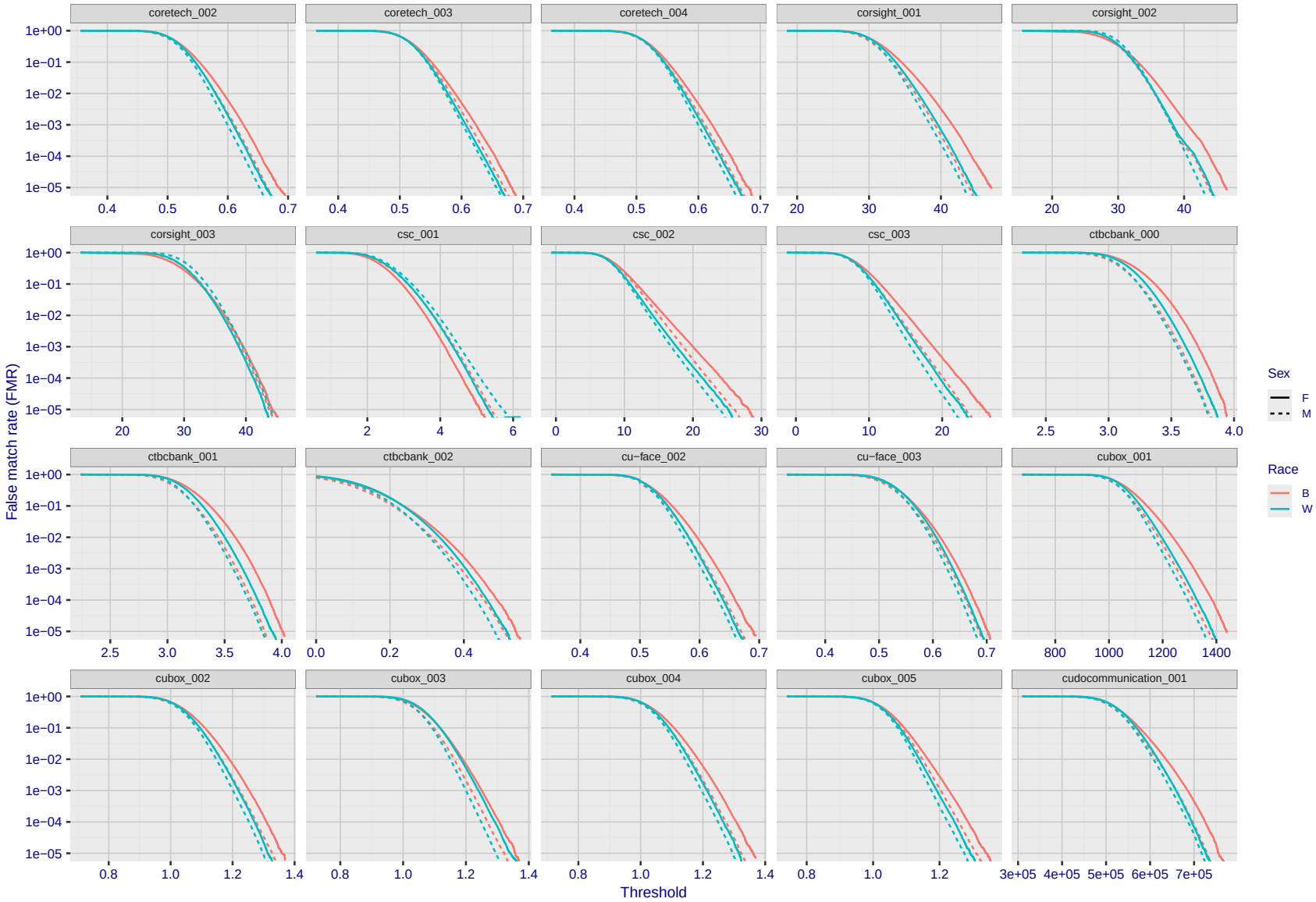

Figure 554: For the mugshot images, the false match calibration curves show false match rate vs. threshold. Separate curves appear for white females, black females, black males and white males.

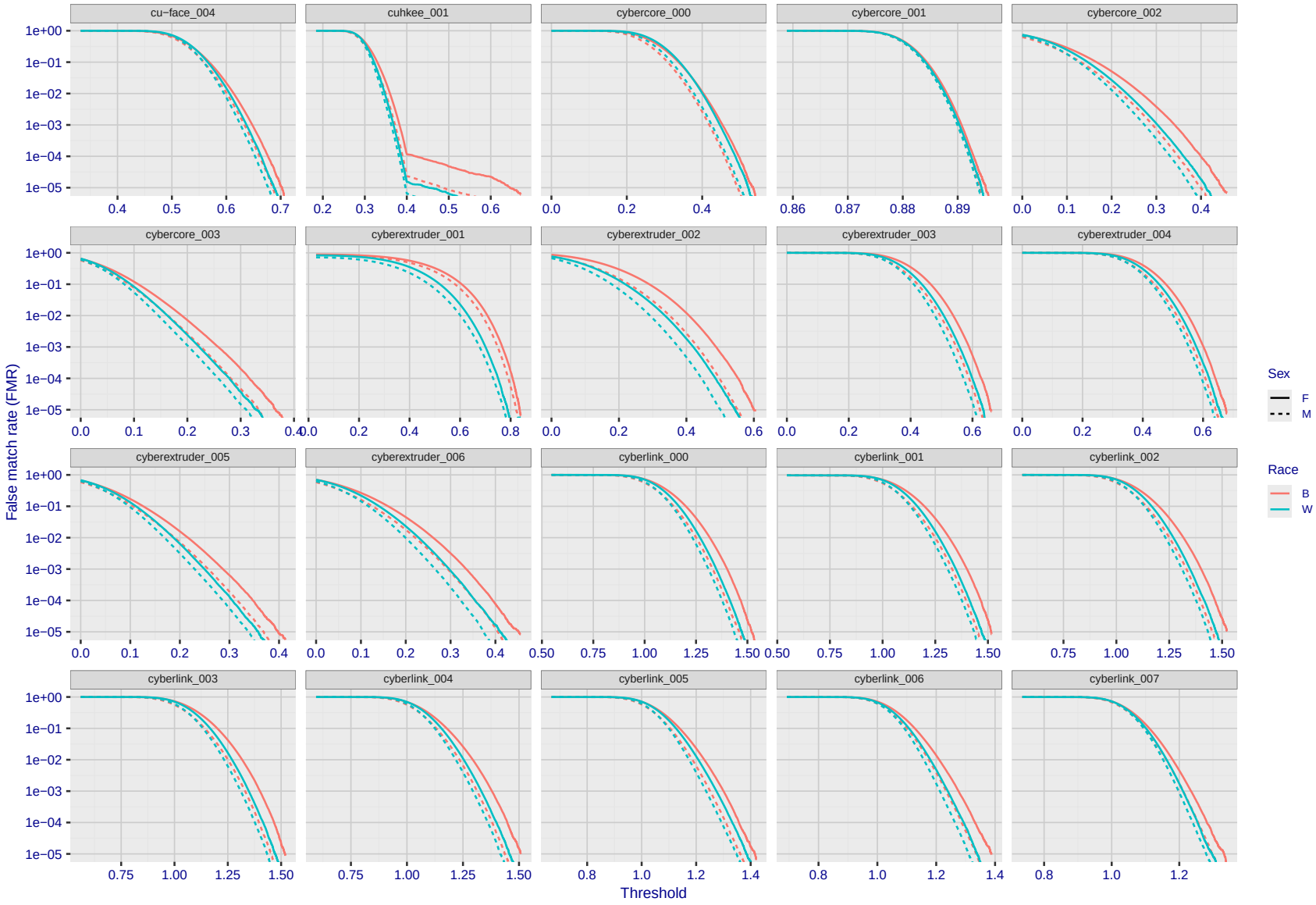

Figure 555: For the mugshot images, the false match calibration curves show false match rate vs. threshold. Separate curves appear for white females, black females, black males and white males.

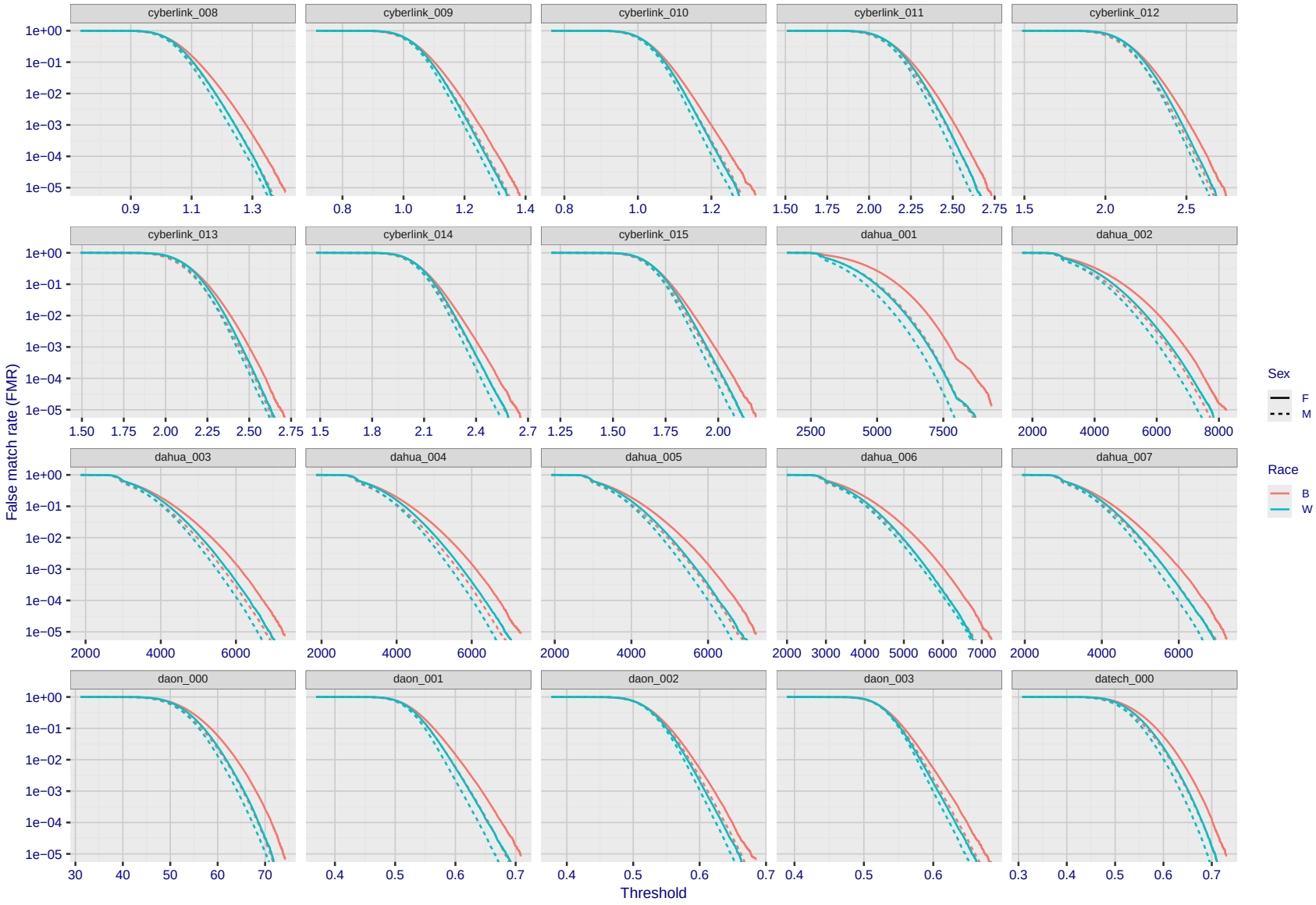

Figure 556: For the mugshot images, the false match calibration curves show false match rate vs. threshold. Separate curves appear for white females, black females, black males and white males.

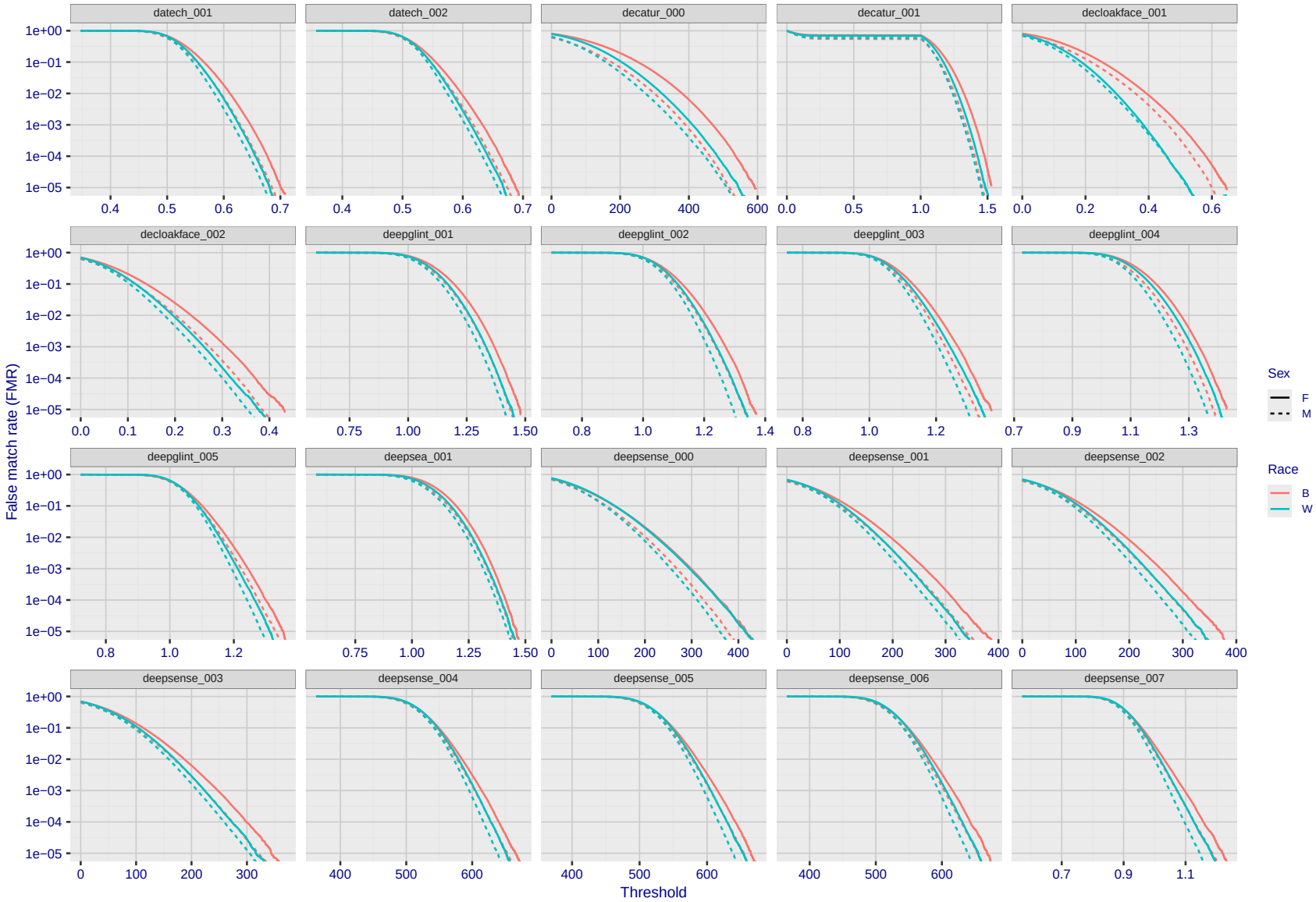

Figure 557: For the mugshot images, the false match calibration curves show false match rate vs. threshold. Separate curves appear for white females, black females, black males and white males.

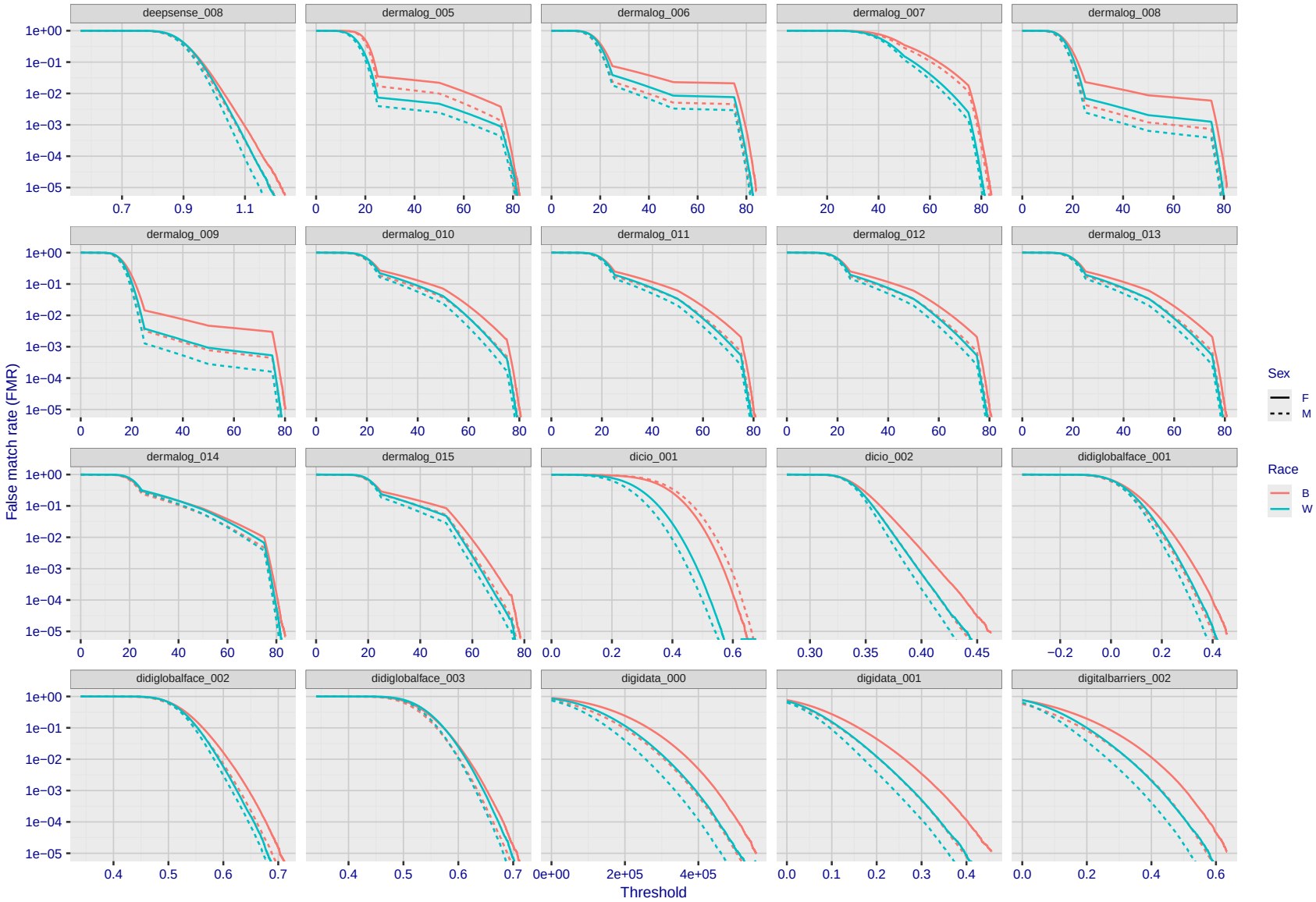

Figure 558: For the mugshot images, the false match calibration curves show false match rate vs. threshold. Separate curves appear for white females, black females, black males and white males.

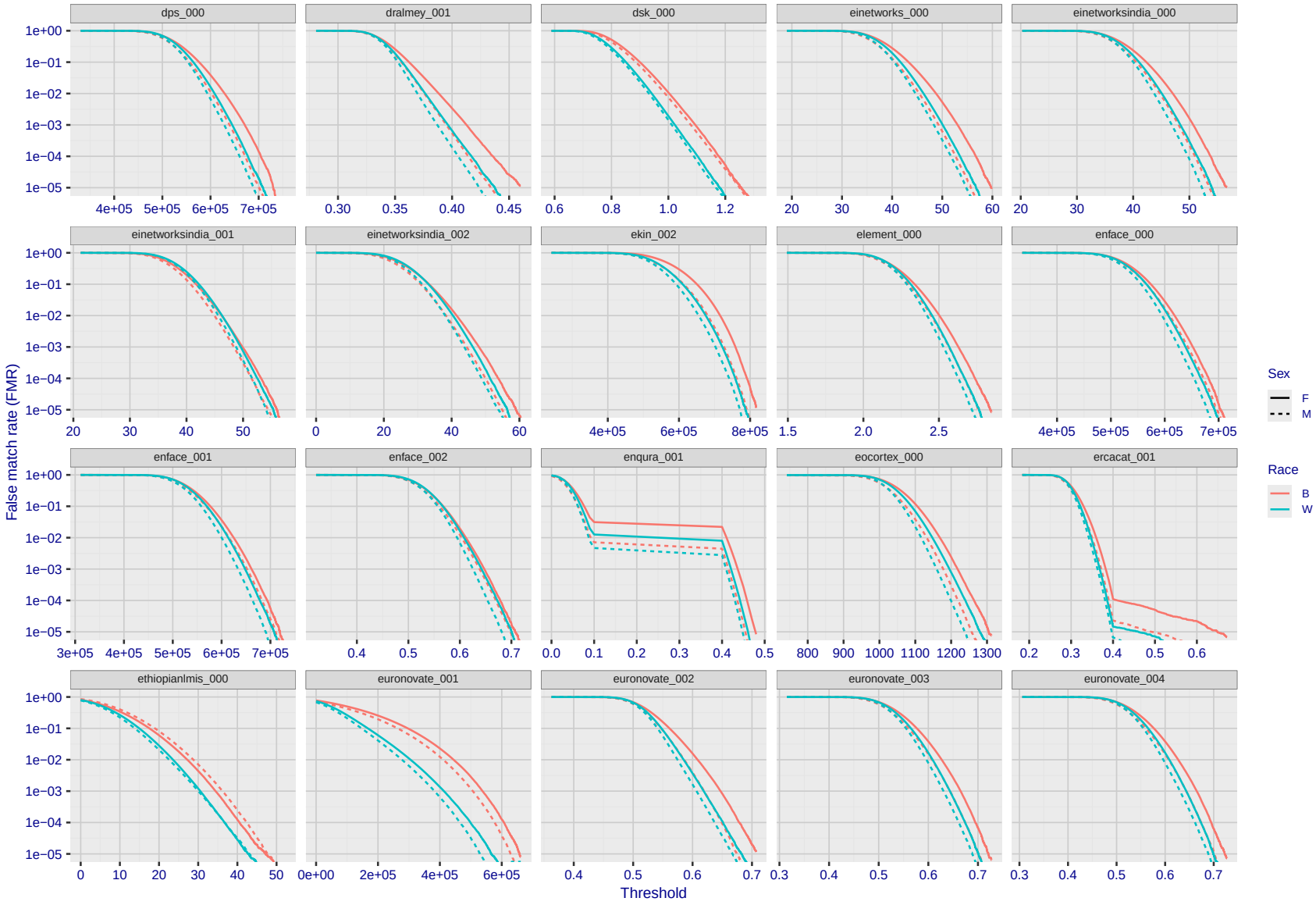

Figure 559: For the mugshot images, the false match calibration curves show false match rate vs. threshold. Separate curves appear for white females, black females, black males and white males.

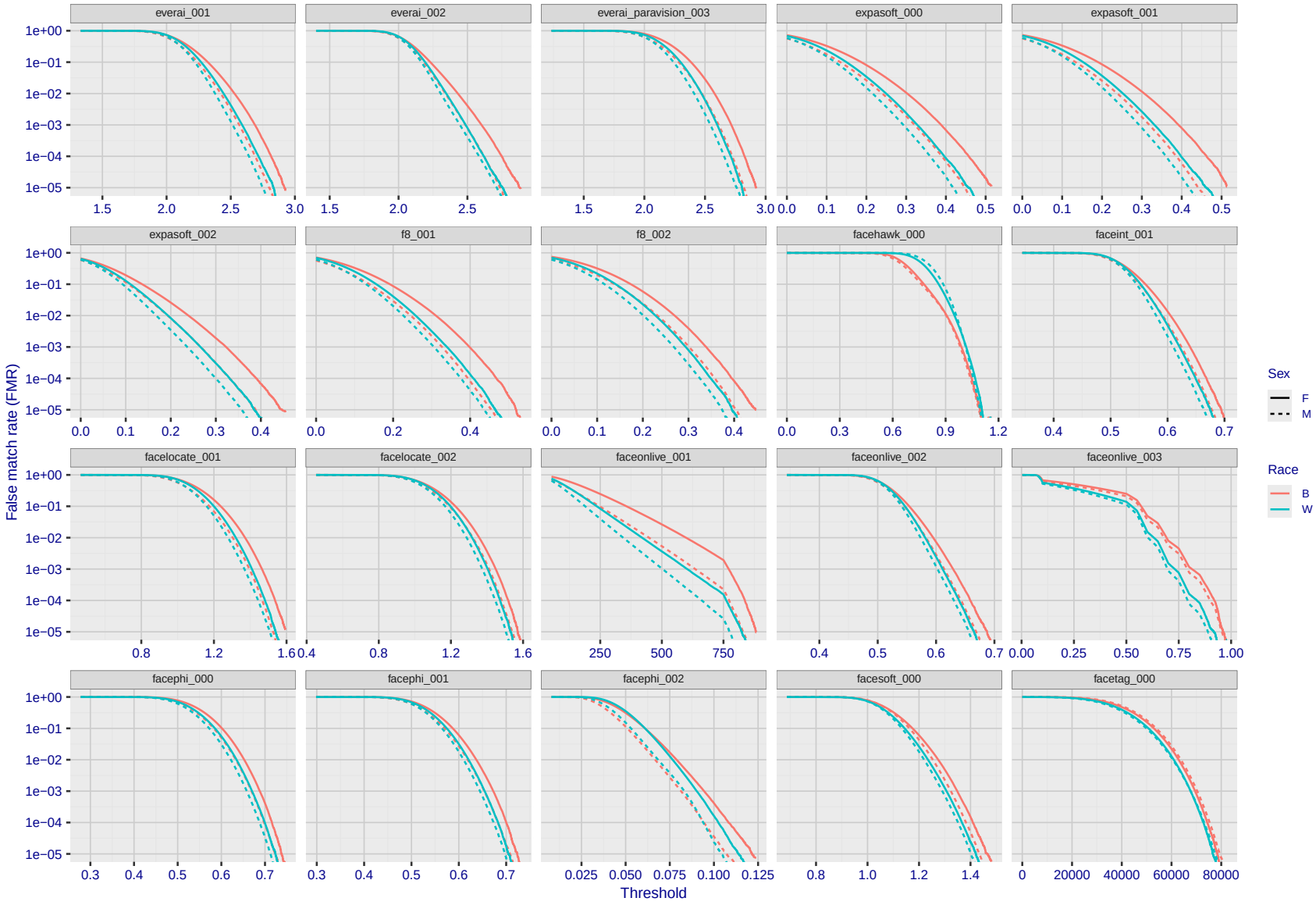

Figure 560: For the mugshot images, the false match calibration curves show false match rate vs. threshold. Separate curves appear for white females, black females, black males and white males.

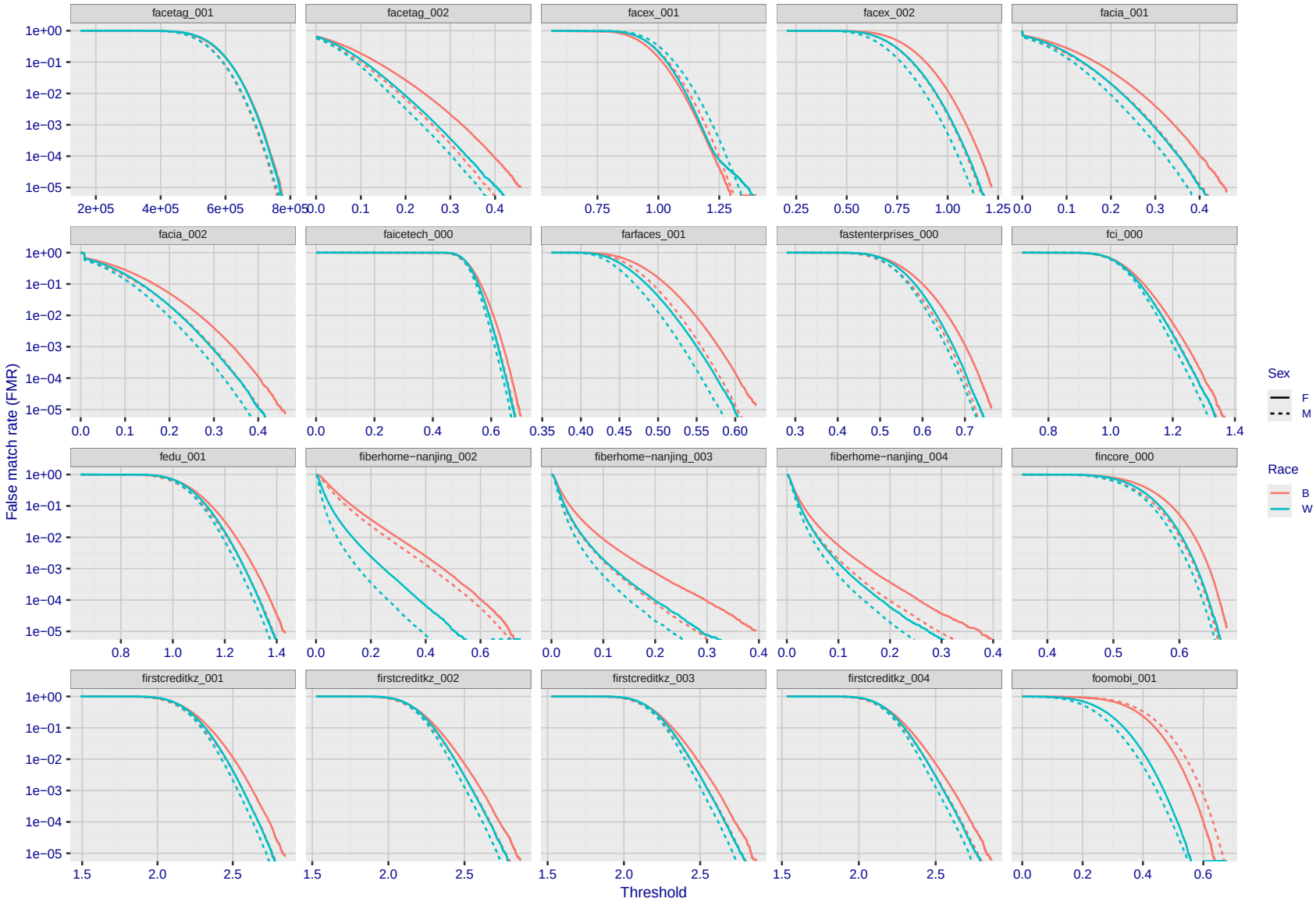

Figure 561: For the mugshot images, the false match calibration curves show false match rate vs. threshold. Separate curves appear for white females, black females, black males and white males.

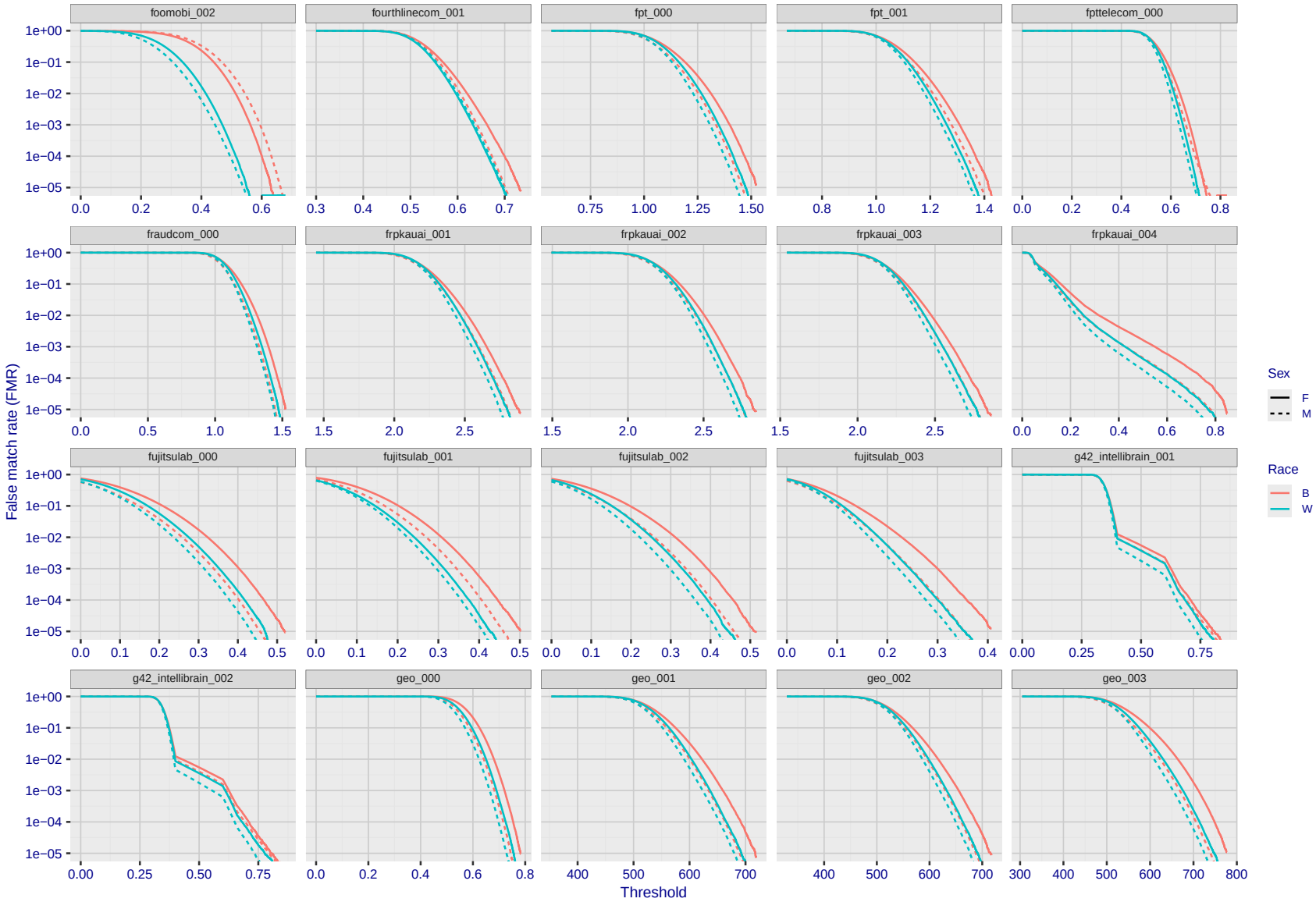

Figure 562: For the mugshot images, the false match calibration curves show false match rate vs. threshold. Separate curves appear for white females, black females, black males and white males.

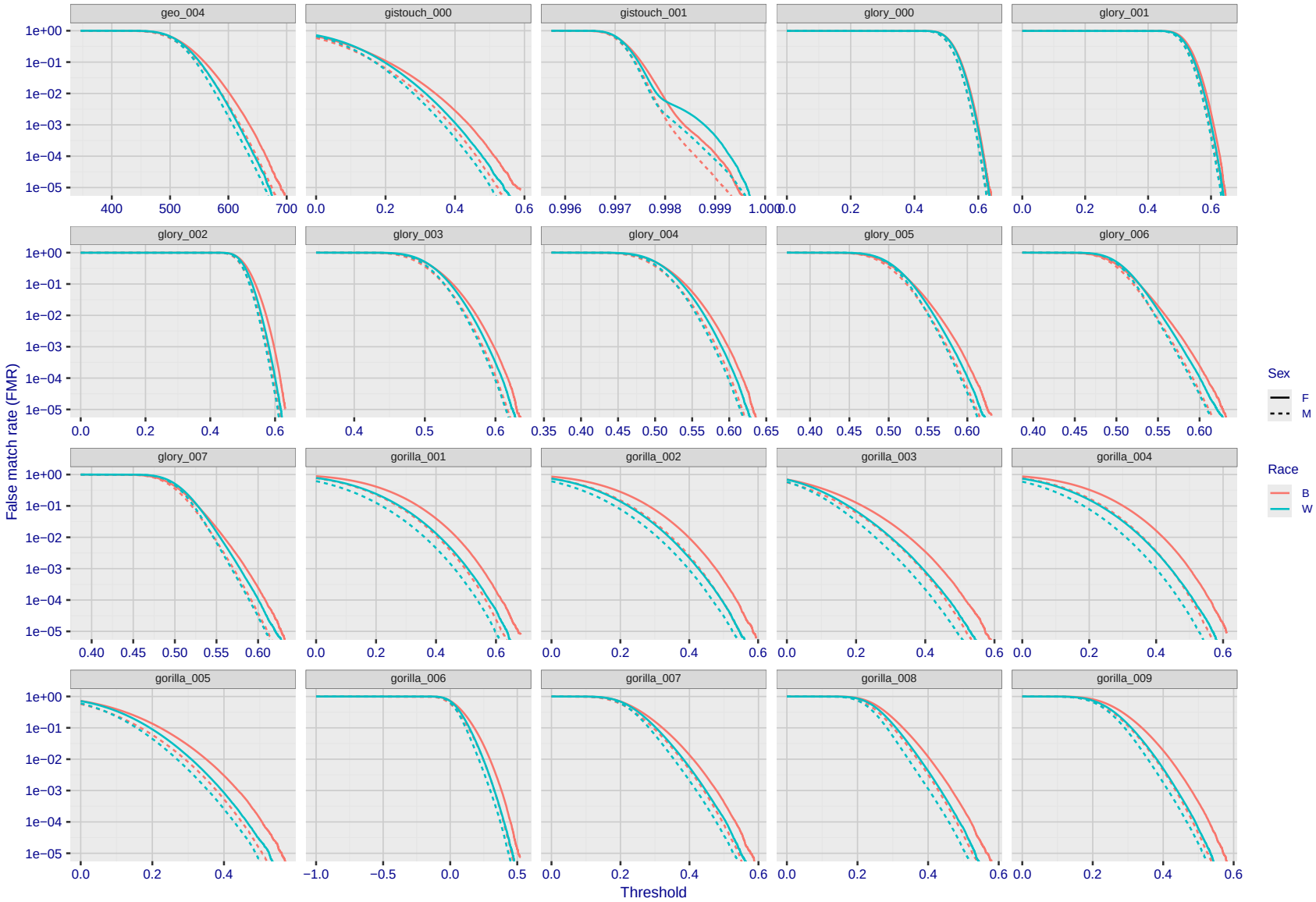

Figure 563: For the mugshot images, the false match calibration curves show false match rate vs. threshold. Separate curves appear for white females, black females, black males and white males.

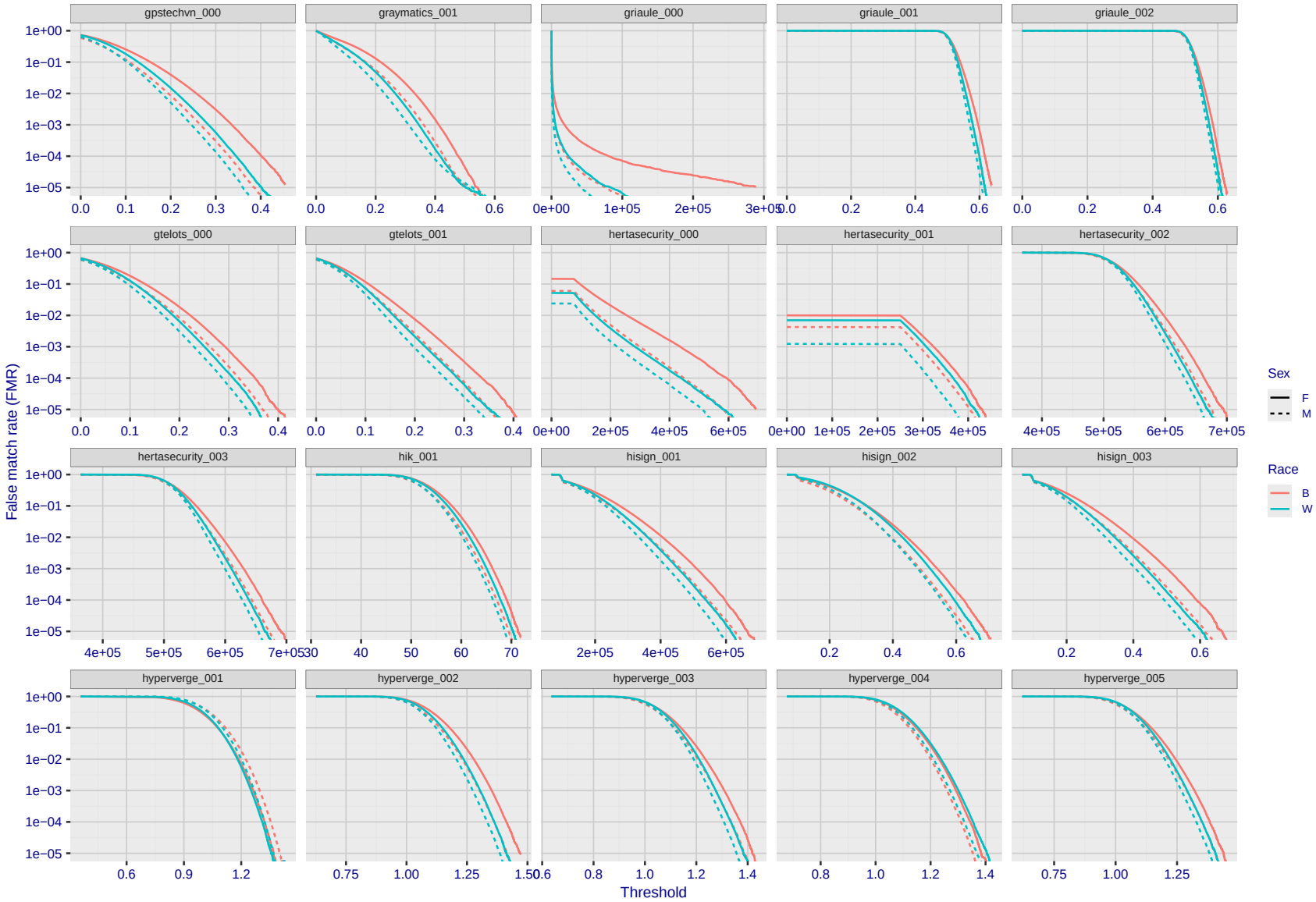

Figure 564: For the mugshot images, the false match calibration curves show false match rate vs. threshold. Separate curves appear for white females, black females, black males and white males.

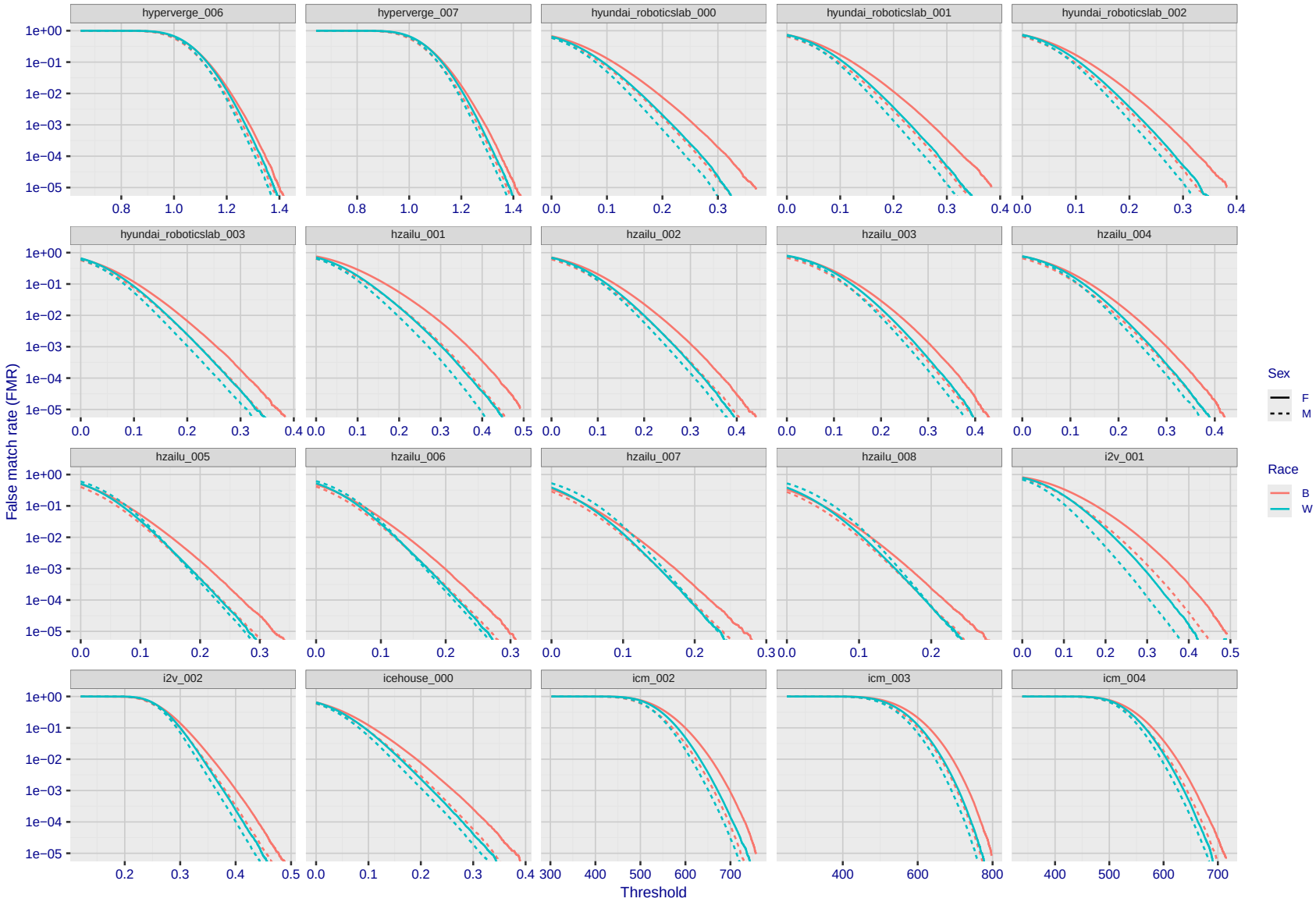

Figure 565: For the mugshot images, the false match calibration curves show false match rate vs. threshold. Separate curves appear for white females, black females, black males and white males.

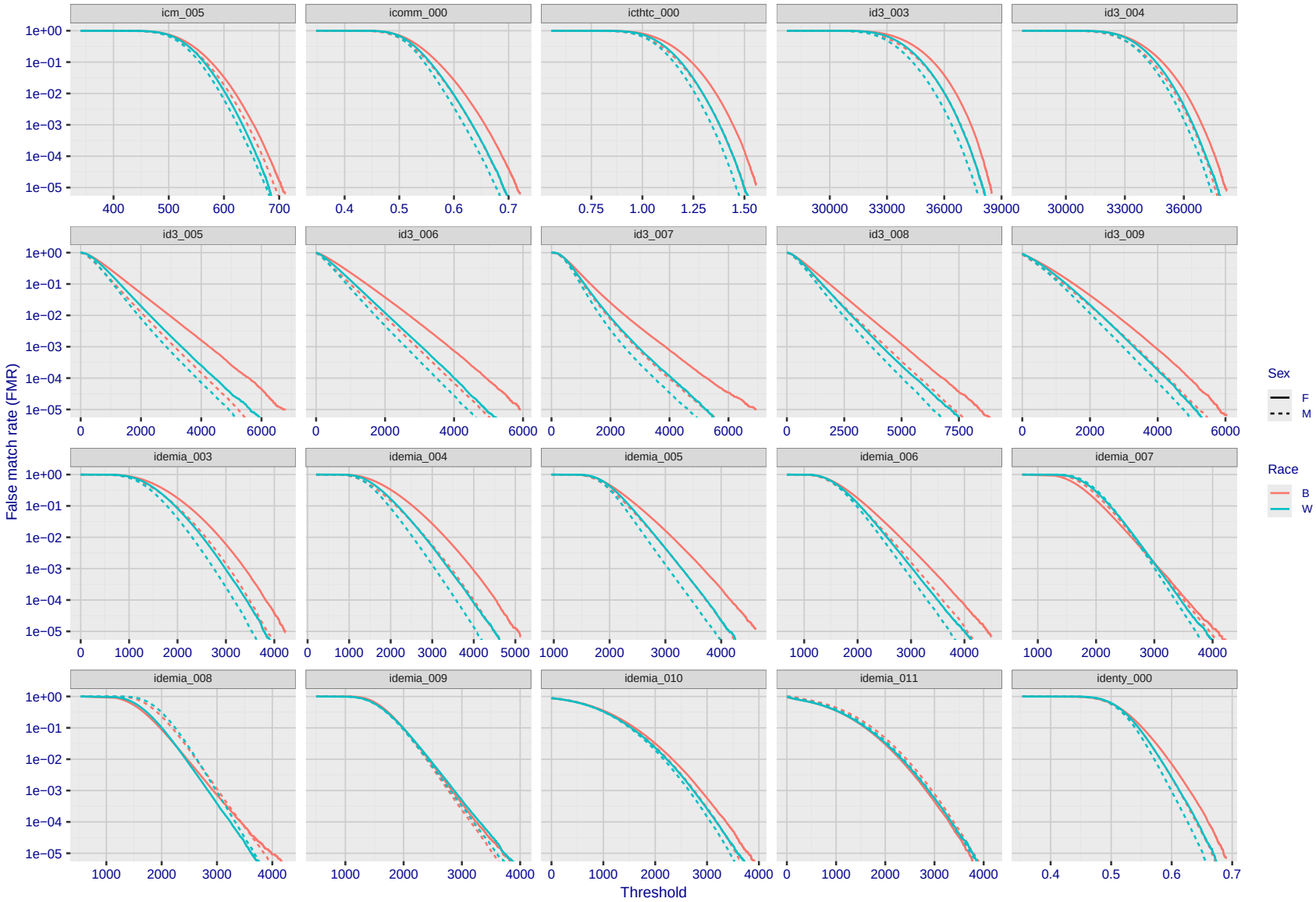

Figure 566: For the mugshot images, the false match calibration curves show false match rate vs. threshold. Separate curves appear for white females, black females, black males and white males.

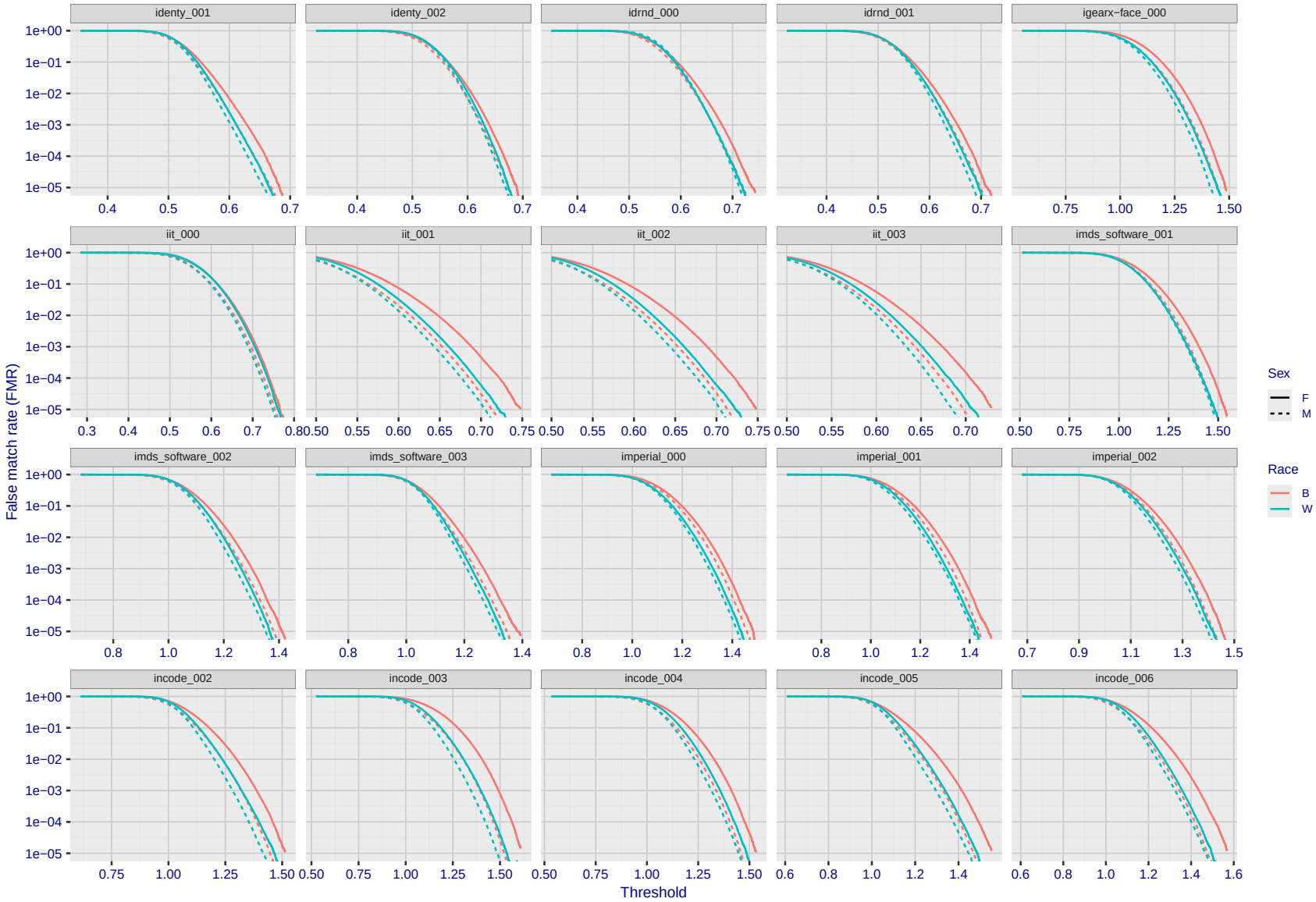

Figure 567: For the mugshot images, the false match calibration curves show false match rate vs. threshold. Separate curves appear for white females, black females, black males and white males.

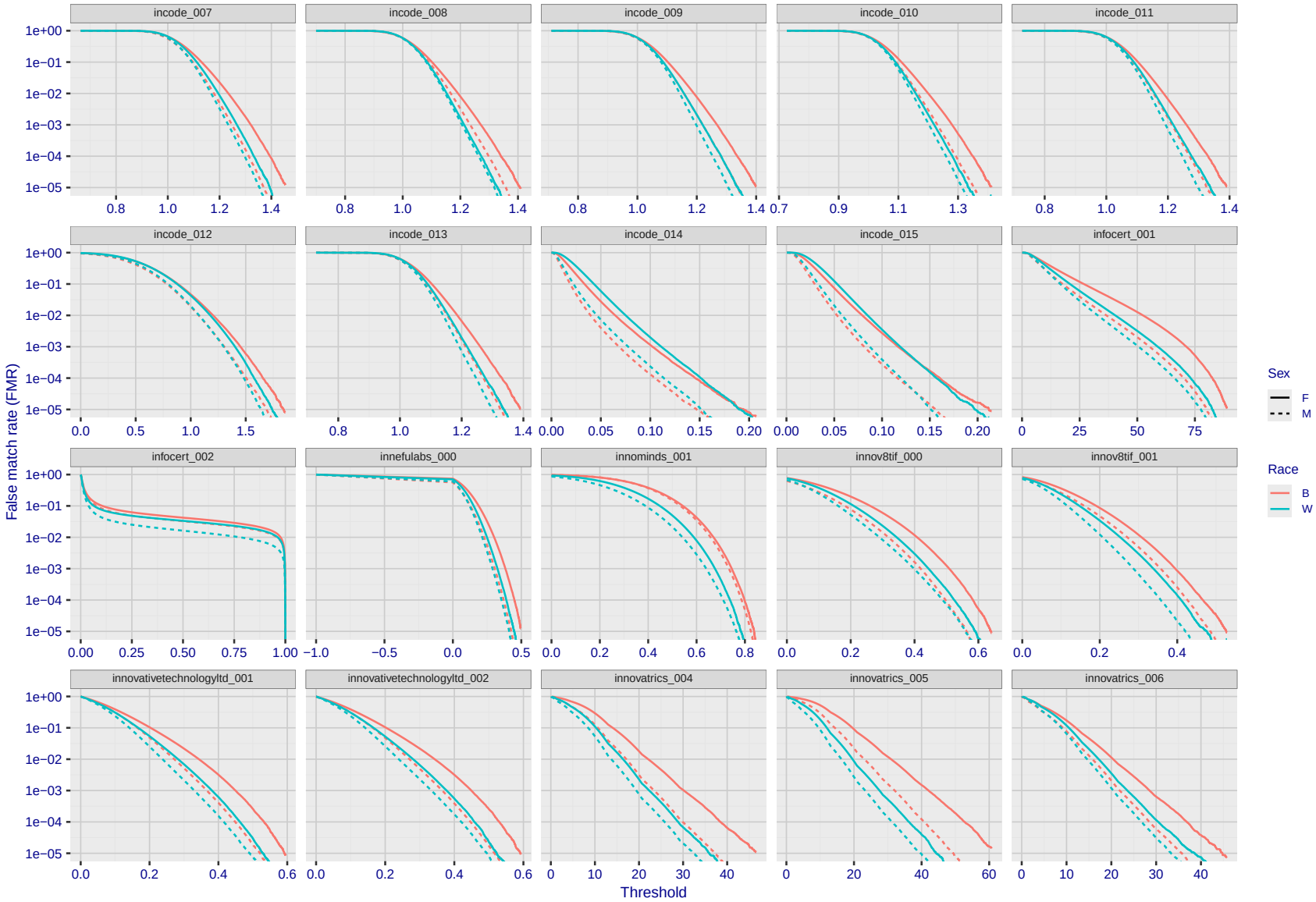

Figure 568: For the mugshot images, the false match calibration curves show false match rate vs. threshold. Separate curves appear for white females, black females, black males and white males.

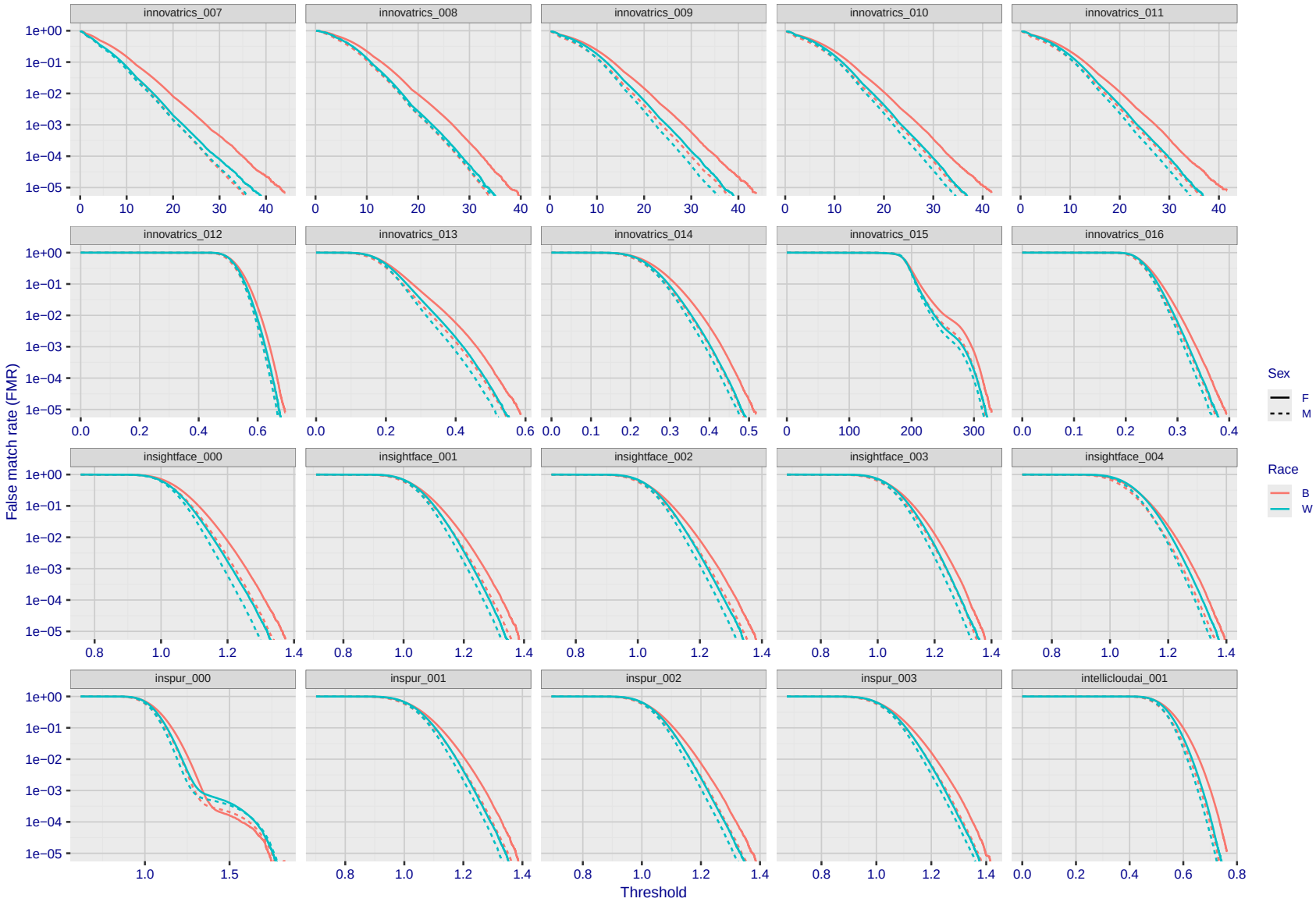

Figure 569: For the mugshot images, the false match calibration curves show false match rate vs. threshold. Separate curves appear for white females, black females, black males and white males.

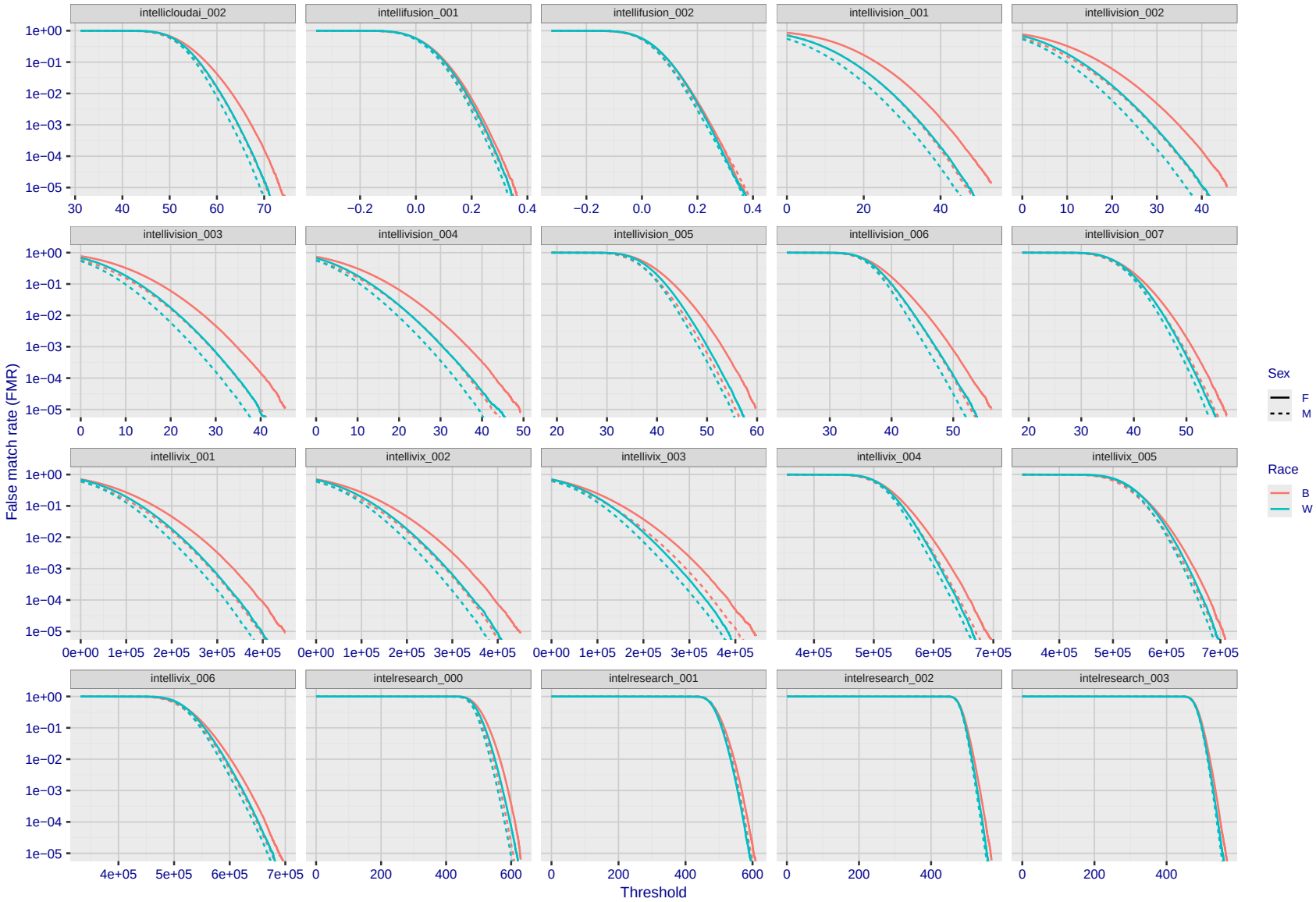

Figure 570: For the mugshot images, the false match calibration curves show false match rate vs. threshold. Separate curves appear for white females, black females, black males and white males.

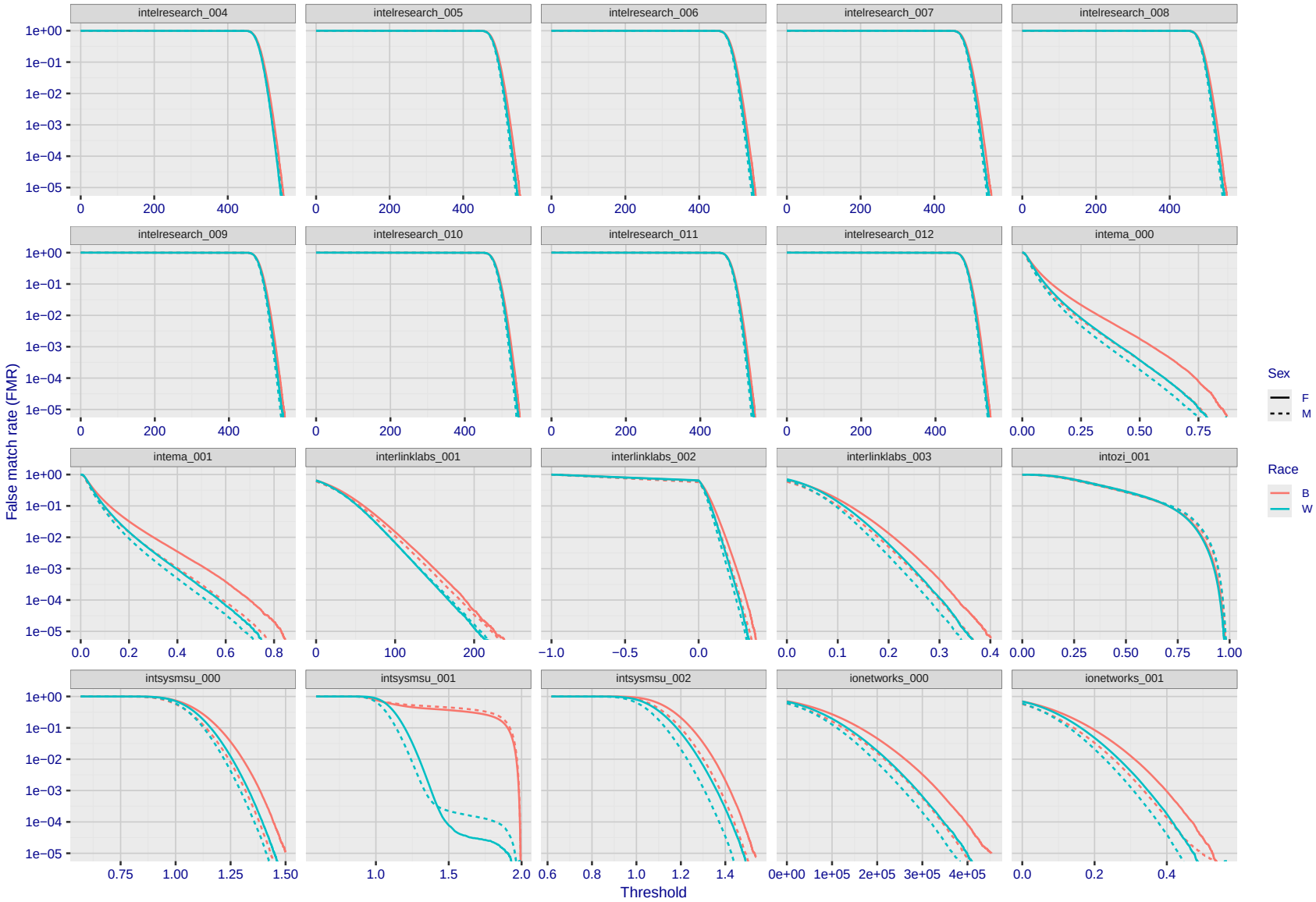

Figure 571: For the mugshot images, the false match calibration curves show false match rate vs. threshold. Separate curves appear for white females, black females, black males and white males.

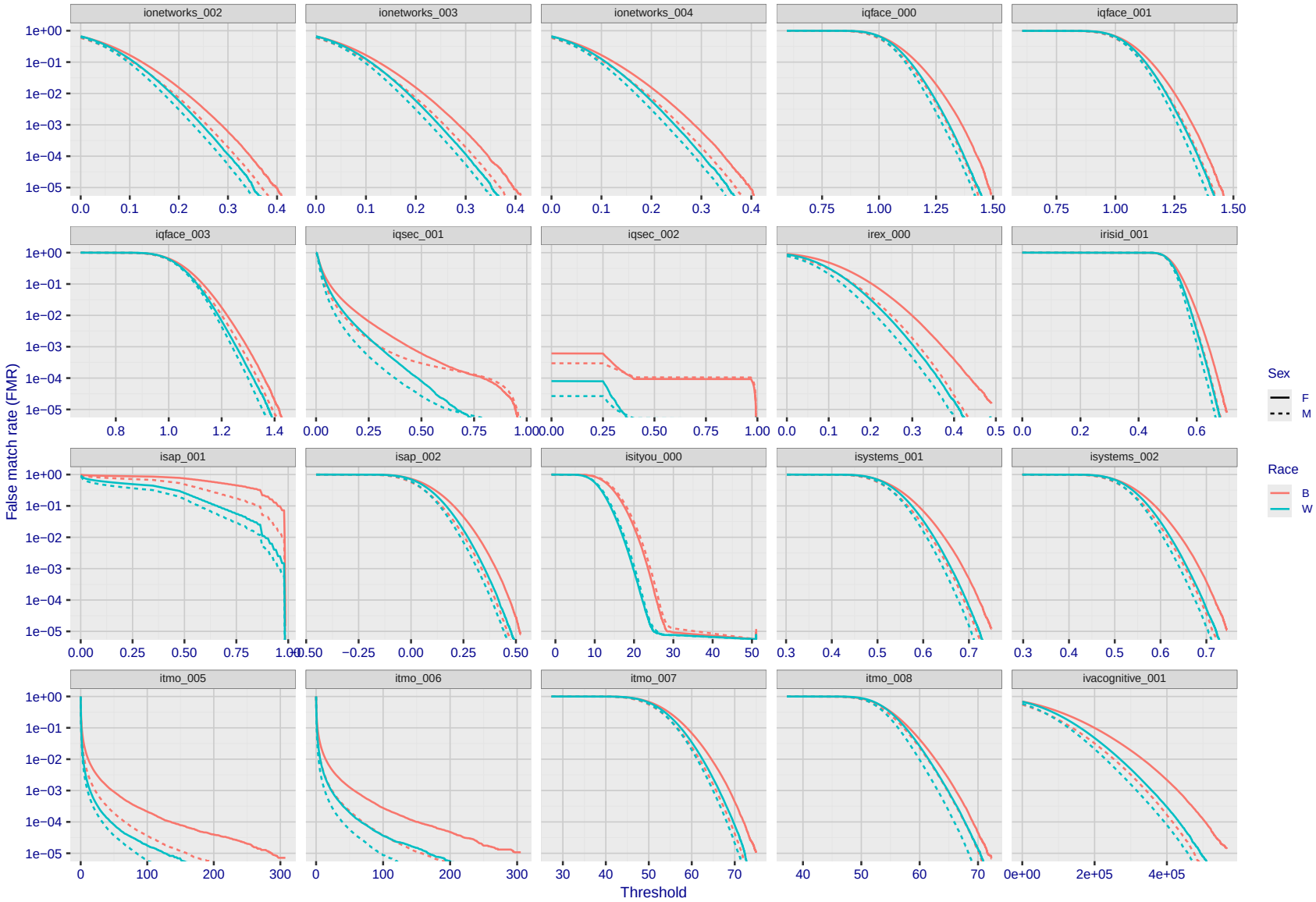

Figure 572: For the mugshot images, the false match calibration curves show false match rate vs. threshold. Separate curves appear for white females, black females, black males and white males.

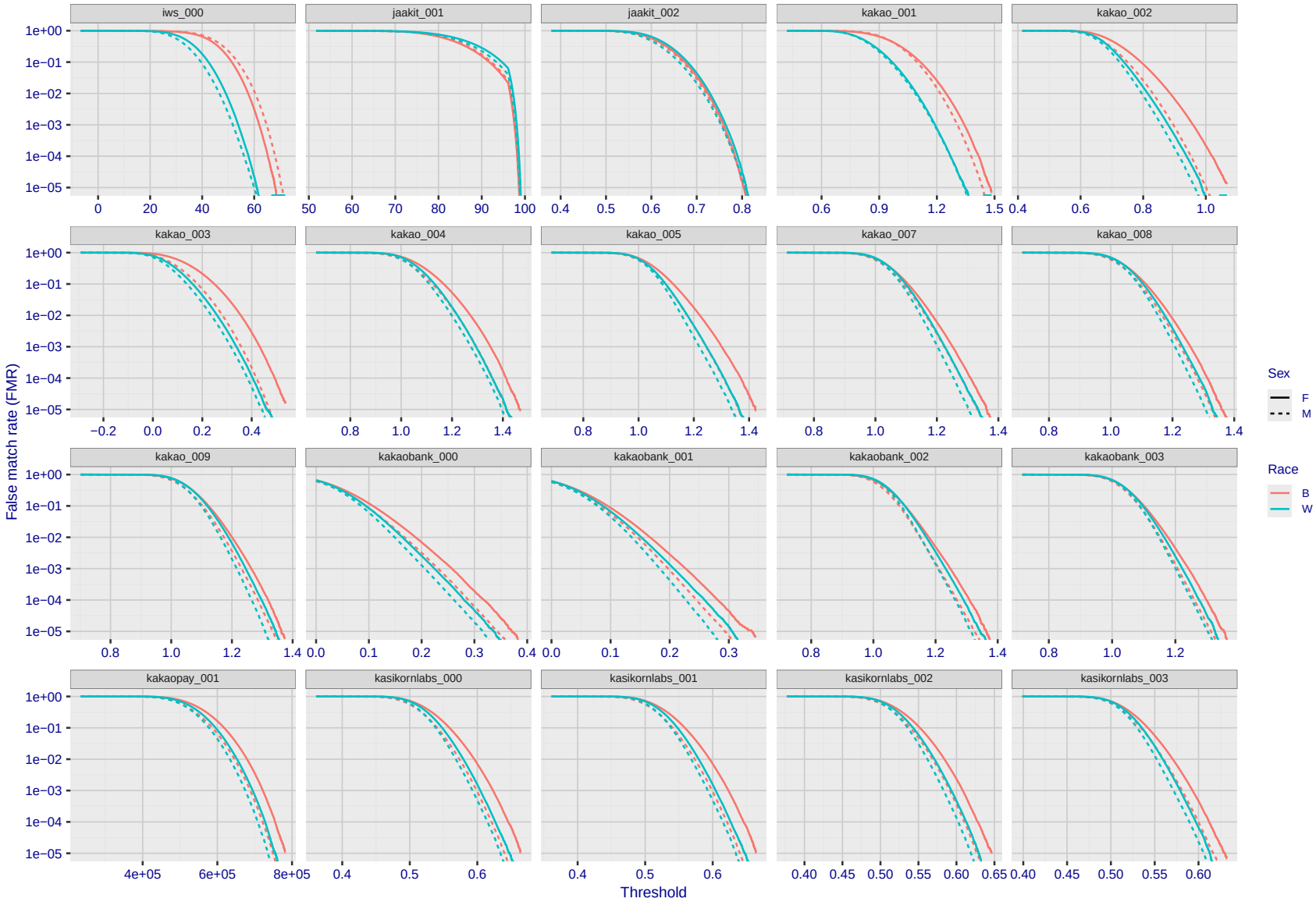

Figure 573: For the mugshot images, the false match calibration curves show false match rate vs. threshold. Separate curves appear for white females, black females, black males and white males.

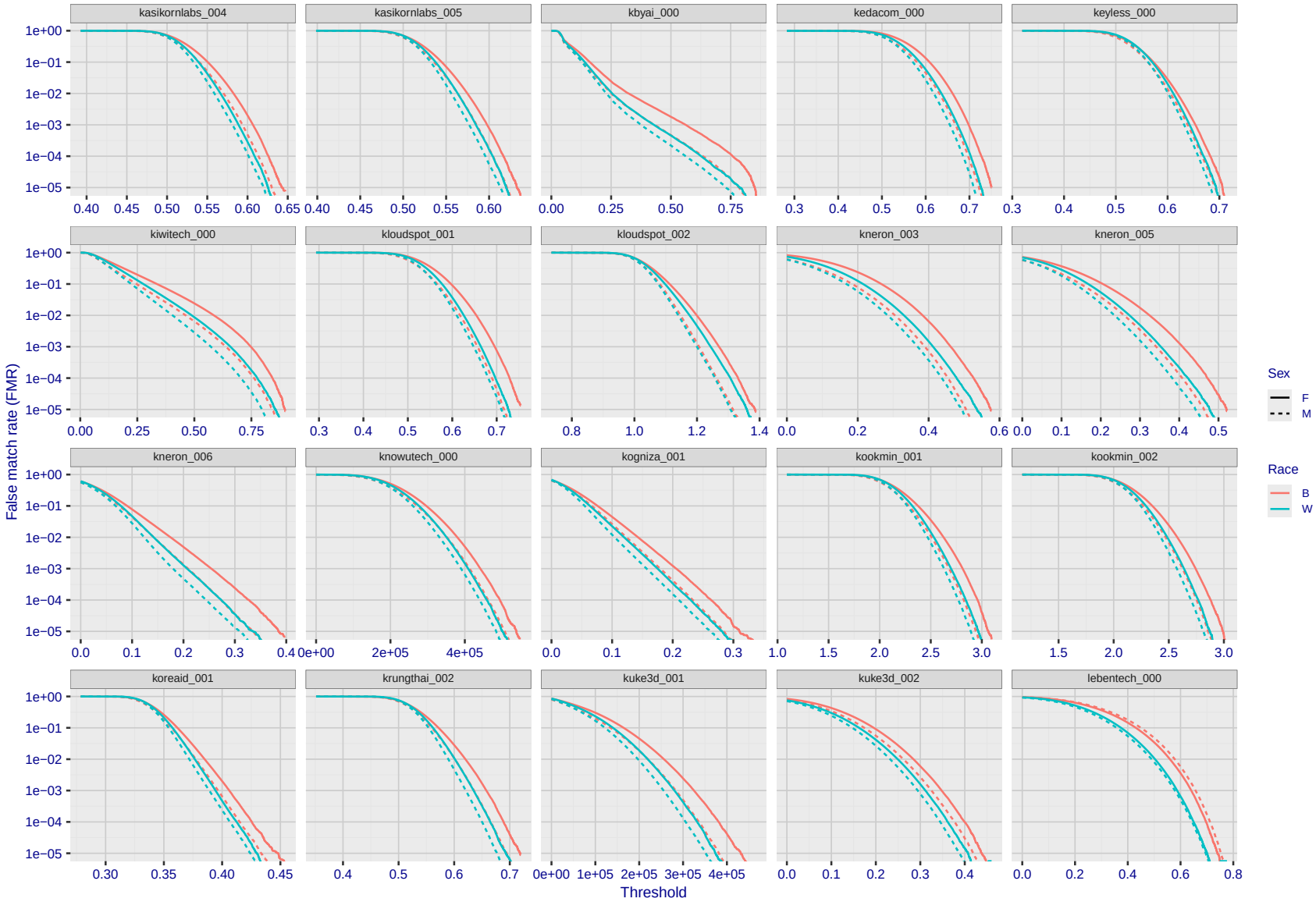

Figure 574: For the mugshot images, the false match calibration curves show false match rate vs. threshold. Separate curves appear for white females, black females, black males and white males.

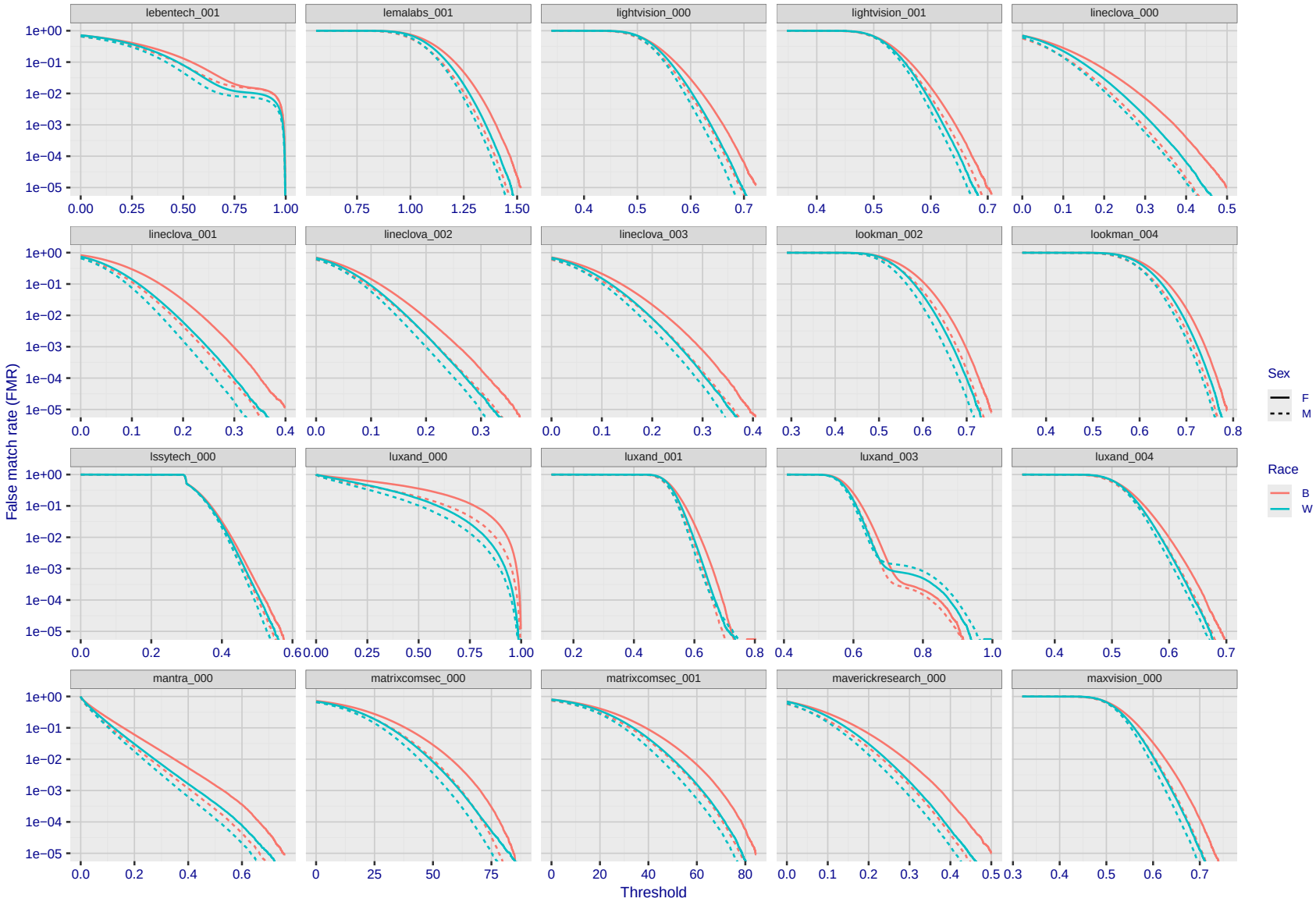

Figure 575: For the mugshot images, the false match calibration curves show false match rate vs. threshold. Separate curves appear for white females, black females, black males and white males.

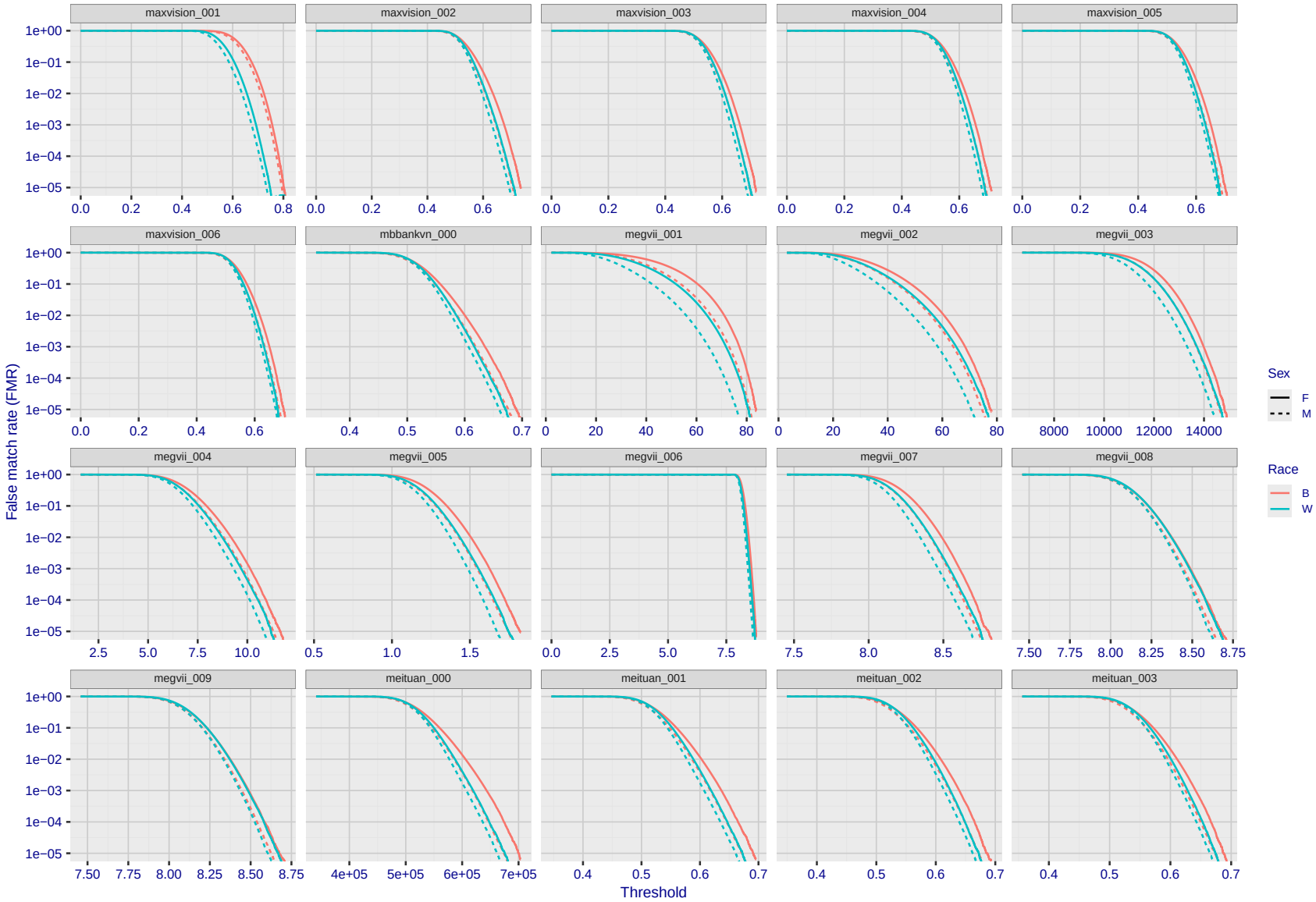

Figure 576: For the mugshot images, the false match calibration curves show false match rate vs. threshold. Separate curves appear for white females, black females, black males and white males.

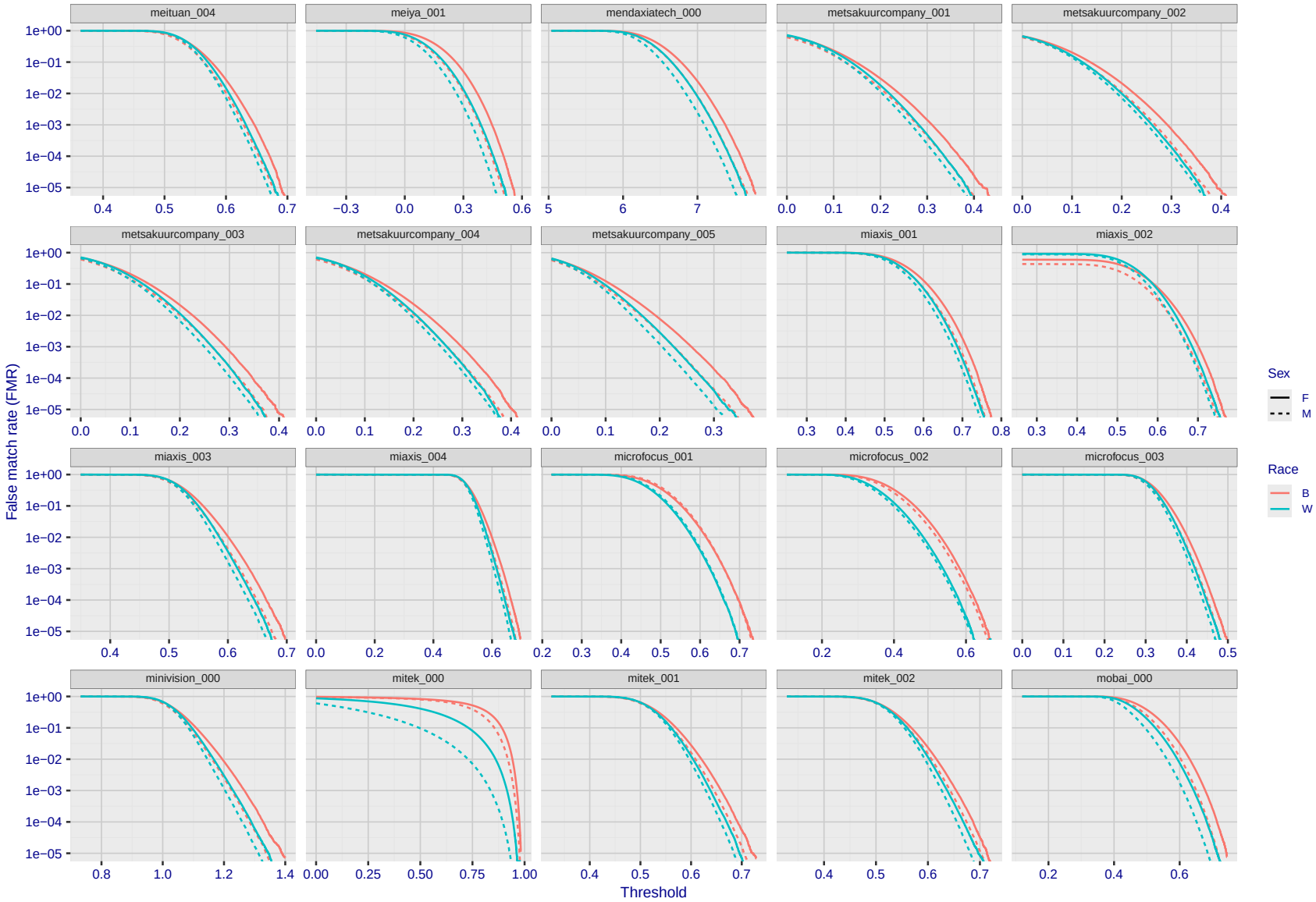

Figure 577: For the mugshot images, the false match calibration curves show false match rate vs. threshold. Separate curves appear for white females, black females, black males and white males.

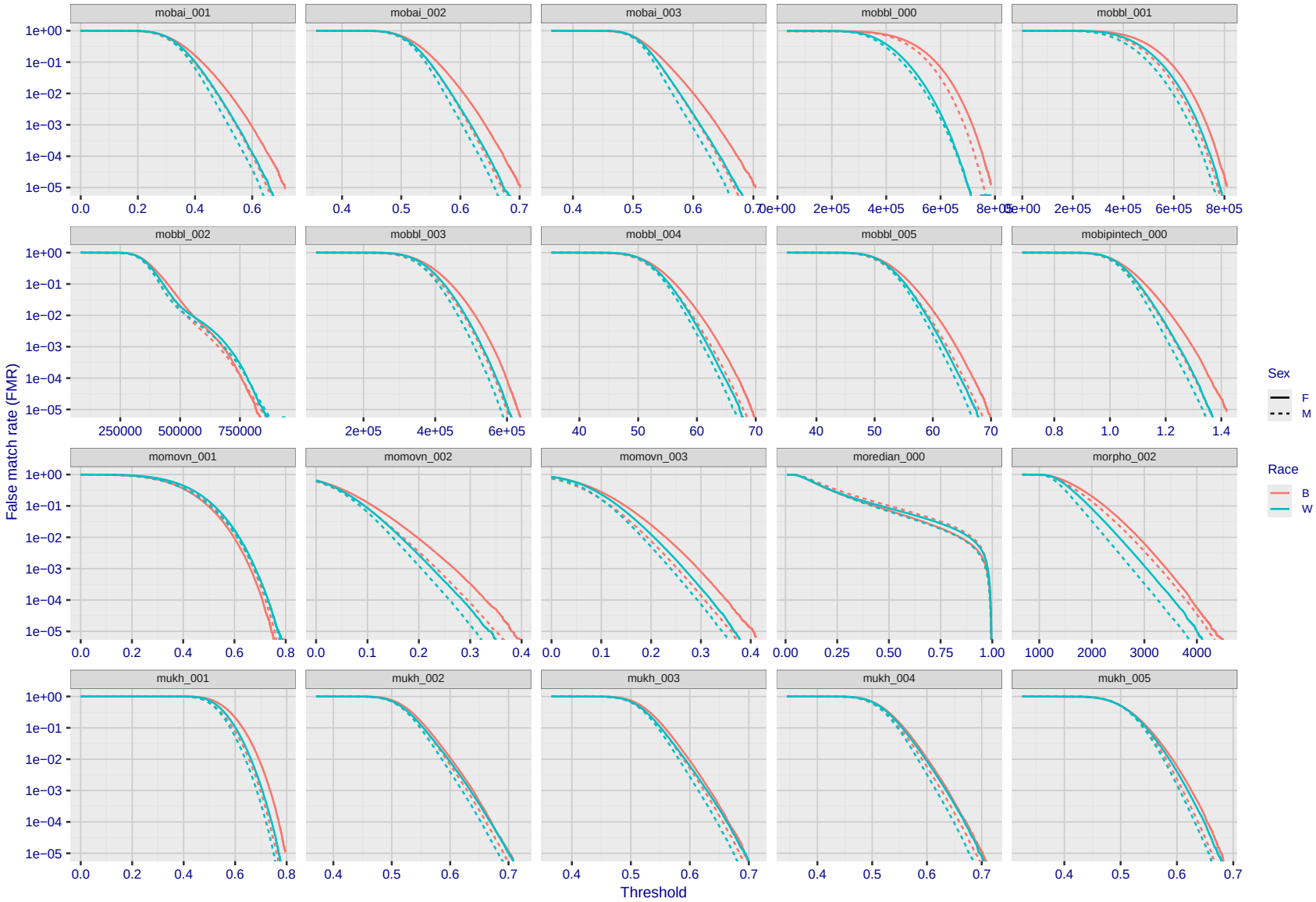

Figure 578: For the mugshot images, the false match calibration curves show false match rate vs. threshold. Separate curves appear for white females, black females, black males and white males.

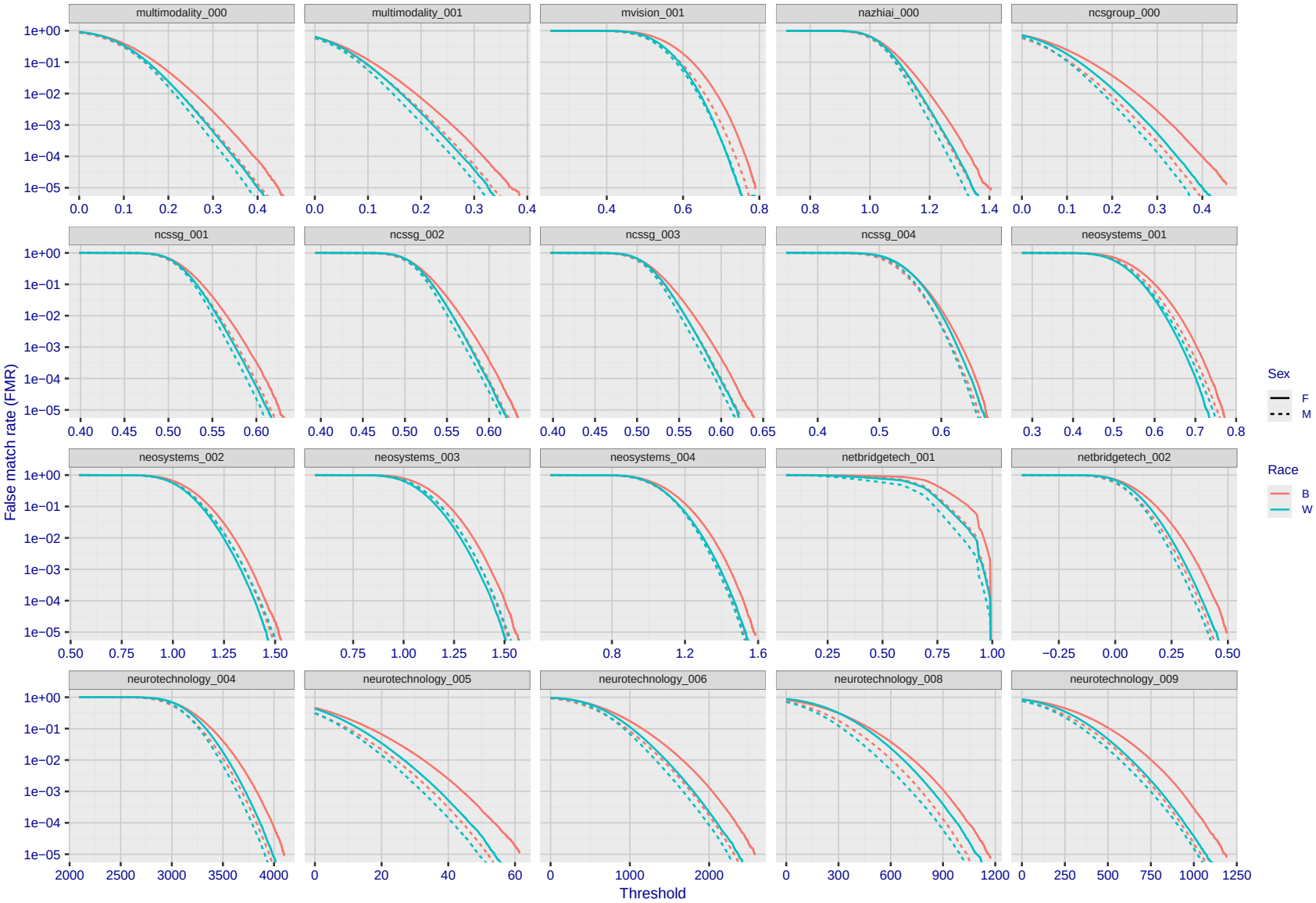

Figure 579: For the mugshot images, the false match calibration curves show false match rate vs. threshold. Separate curves appear for white females, black females, black males and white males.

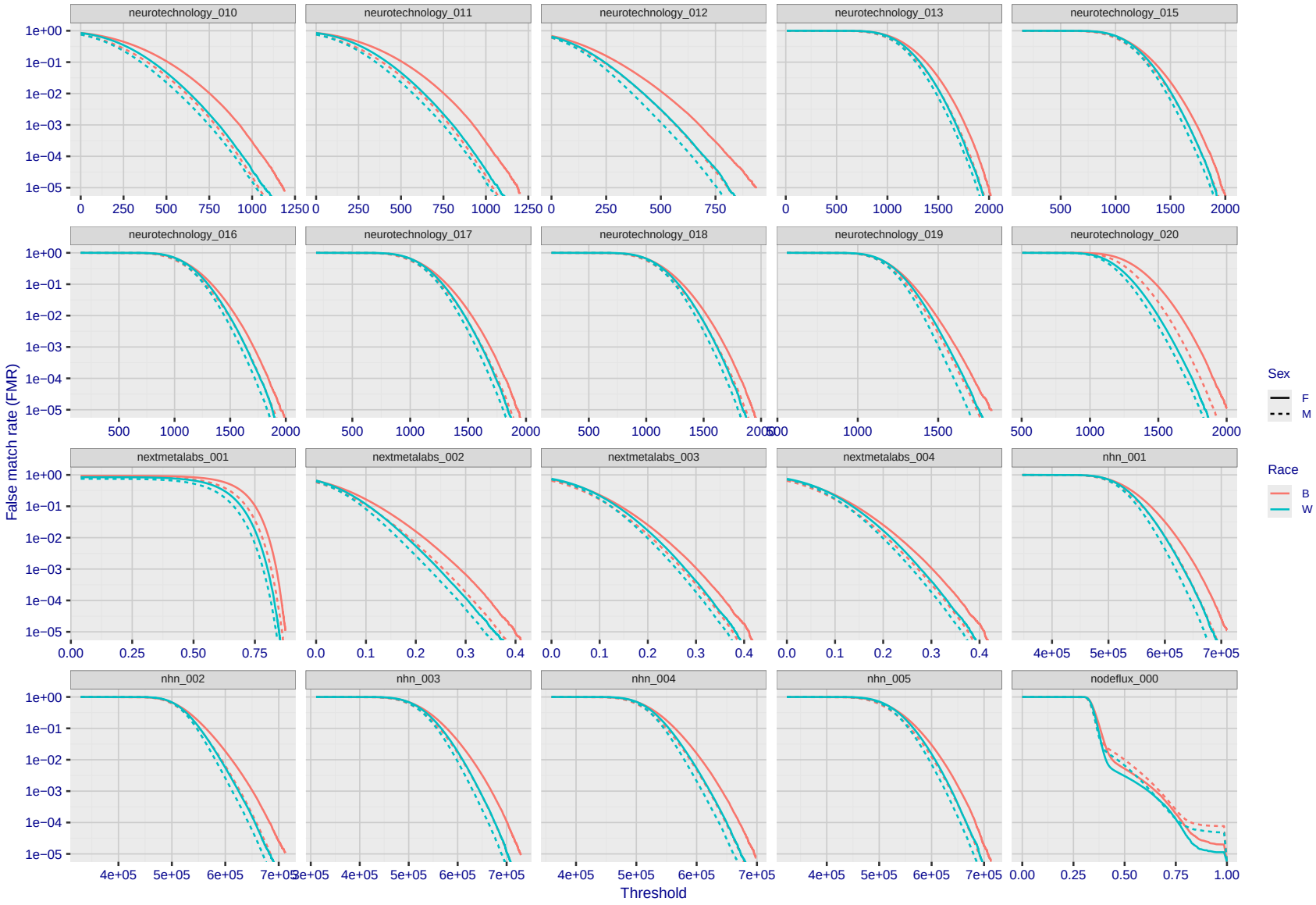

Figure 580: For the mugshot images, the false match calibration curves show false match rate vs. threshold. Separate curves appear for white females, black females, black males and white males.

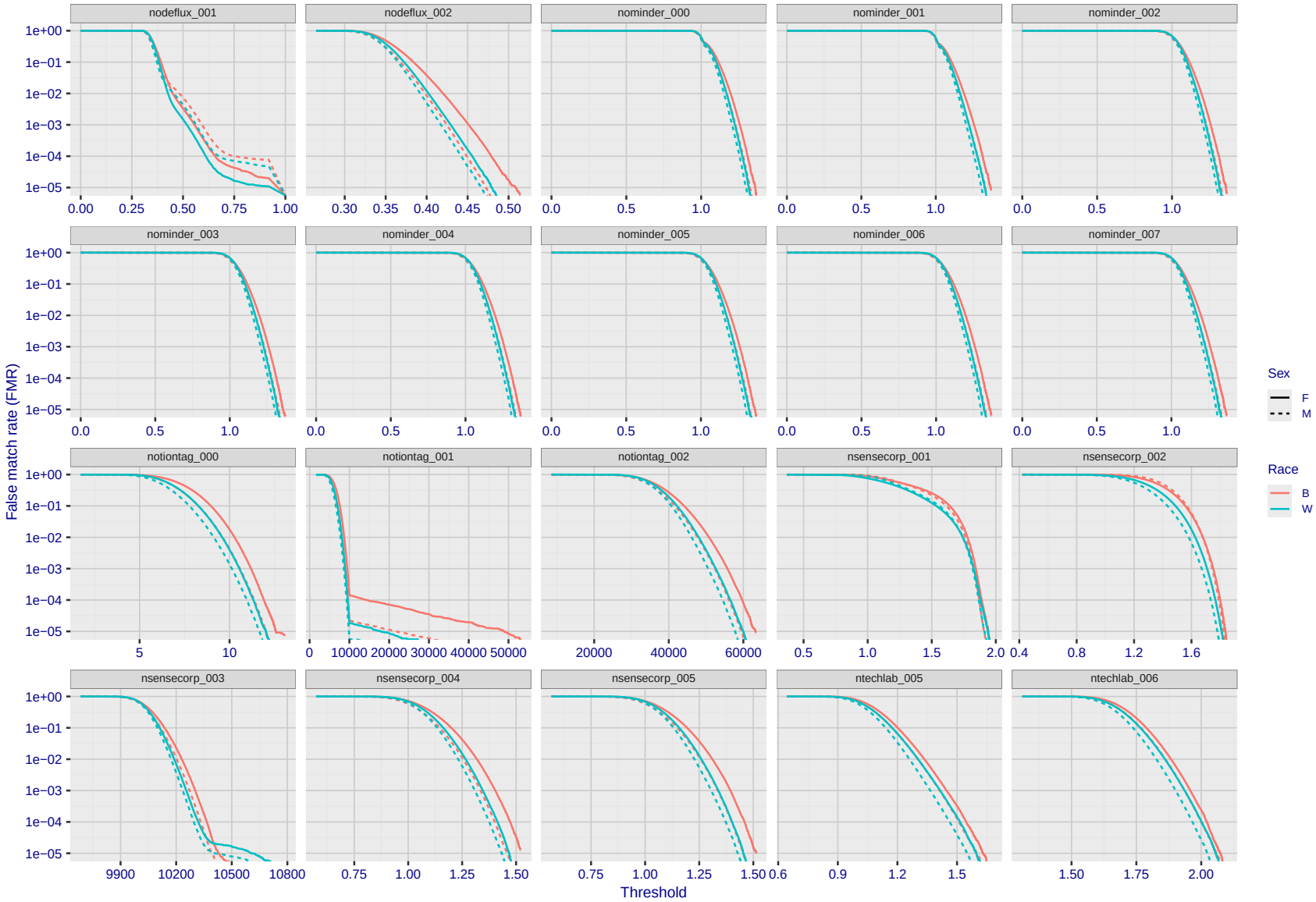

Figure 581: For the mugshot images, the false match calibration curves show false match rate vs. threshold. Separate curves appear for white females, black females, black males and white males.

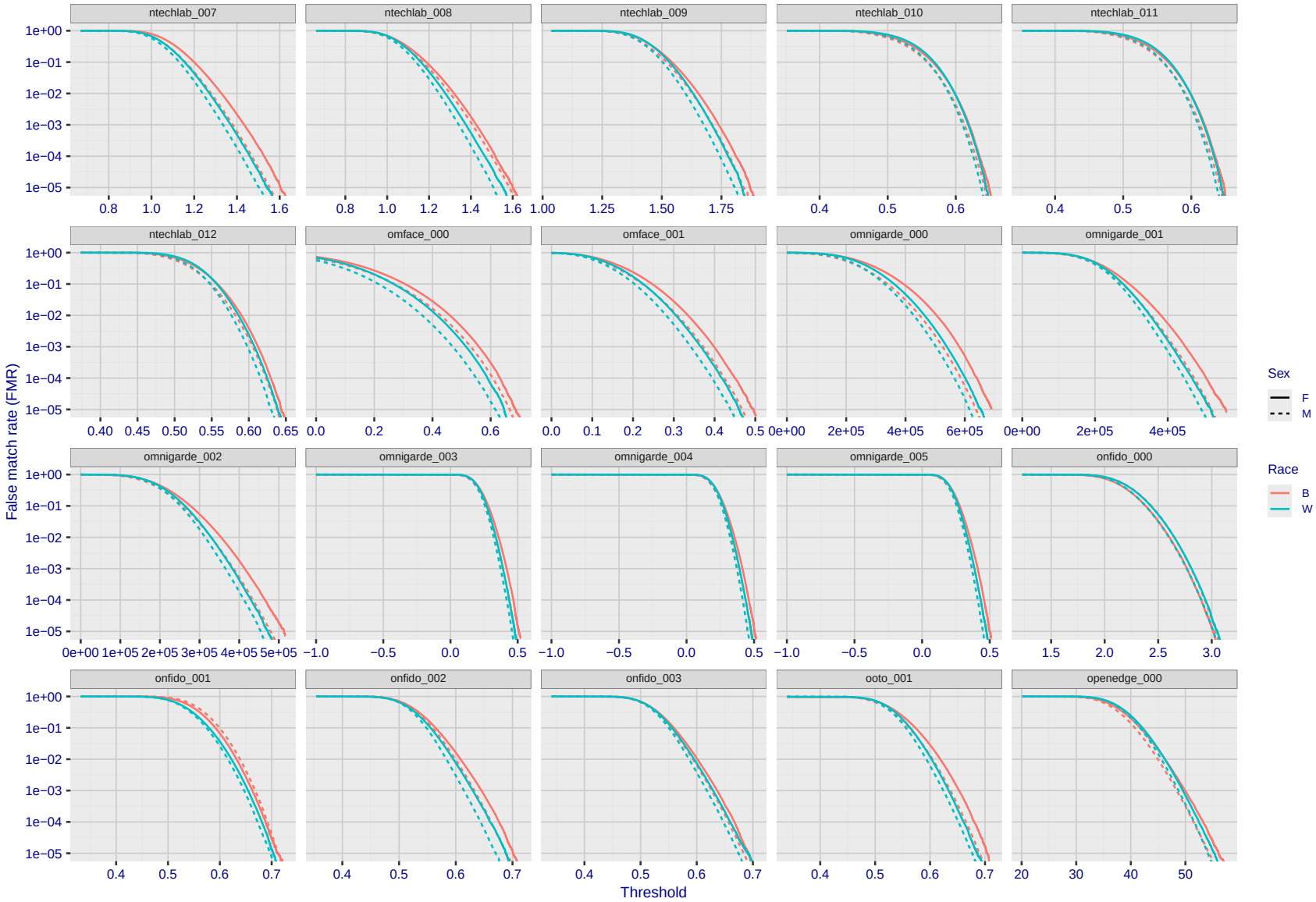

Figure 582: For the mugshot images, the false match calibration curves show false match rate vs. threshold. Separate curves appear for white females, black females, black males and white males.

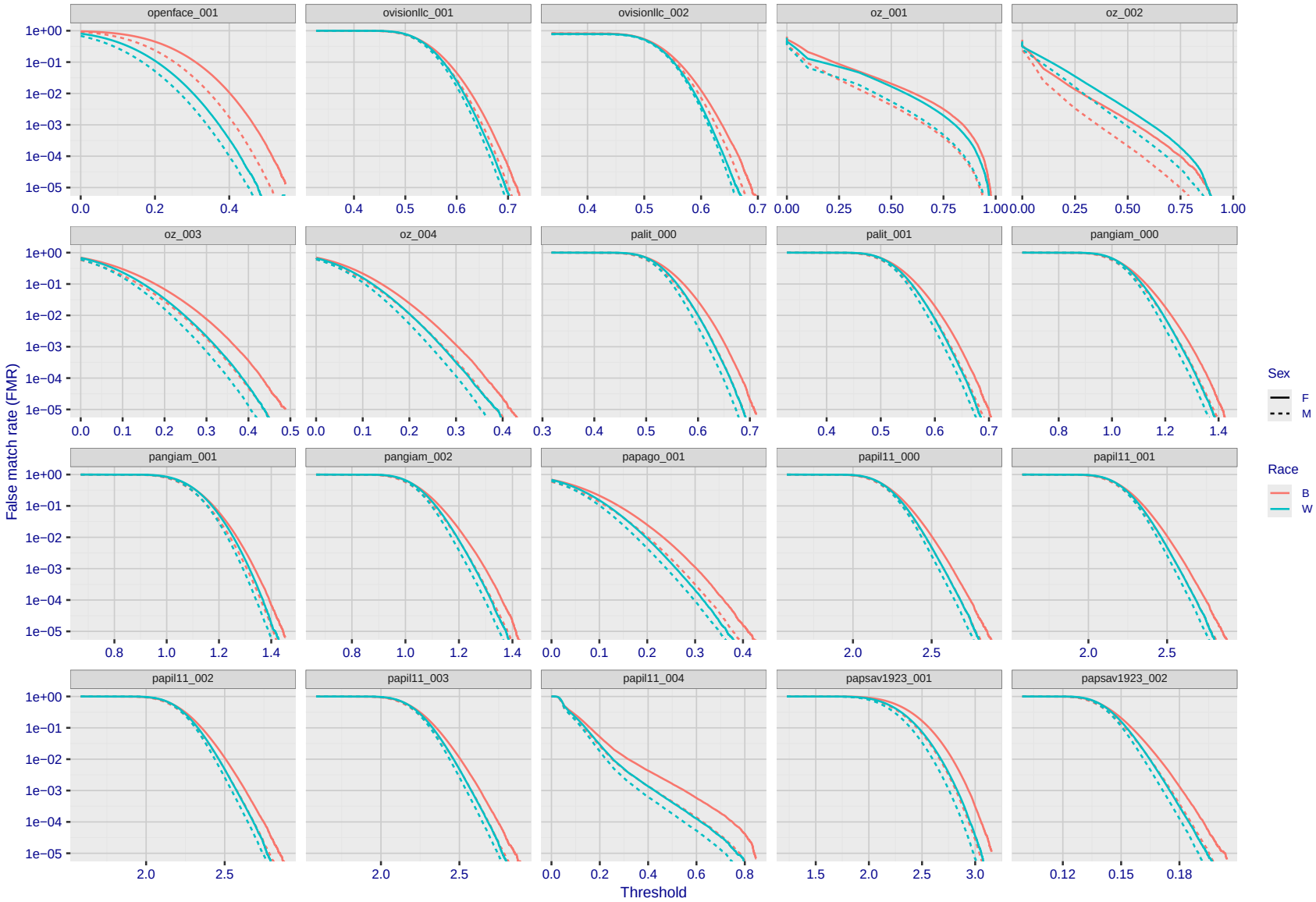

Figure 583: For the mugshot images, the false match calibration curves show false match rate vs. threshold. Separate curves appear for white females, black females, black males and white males.

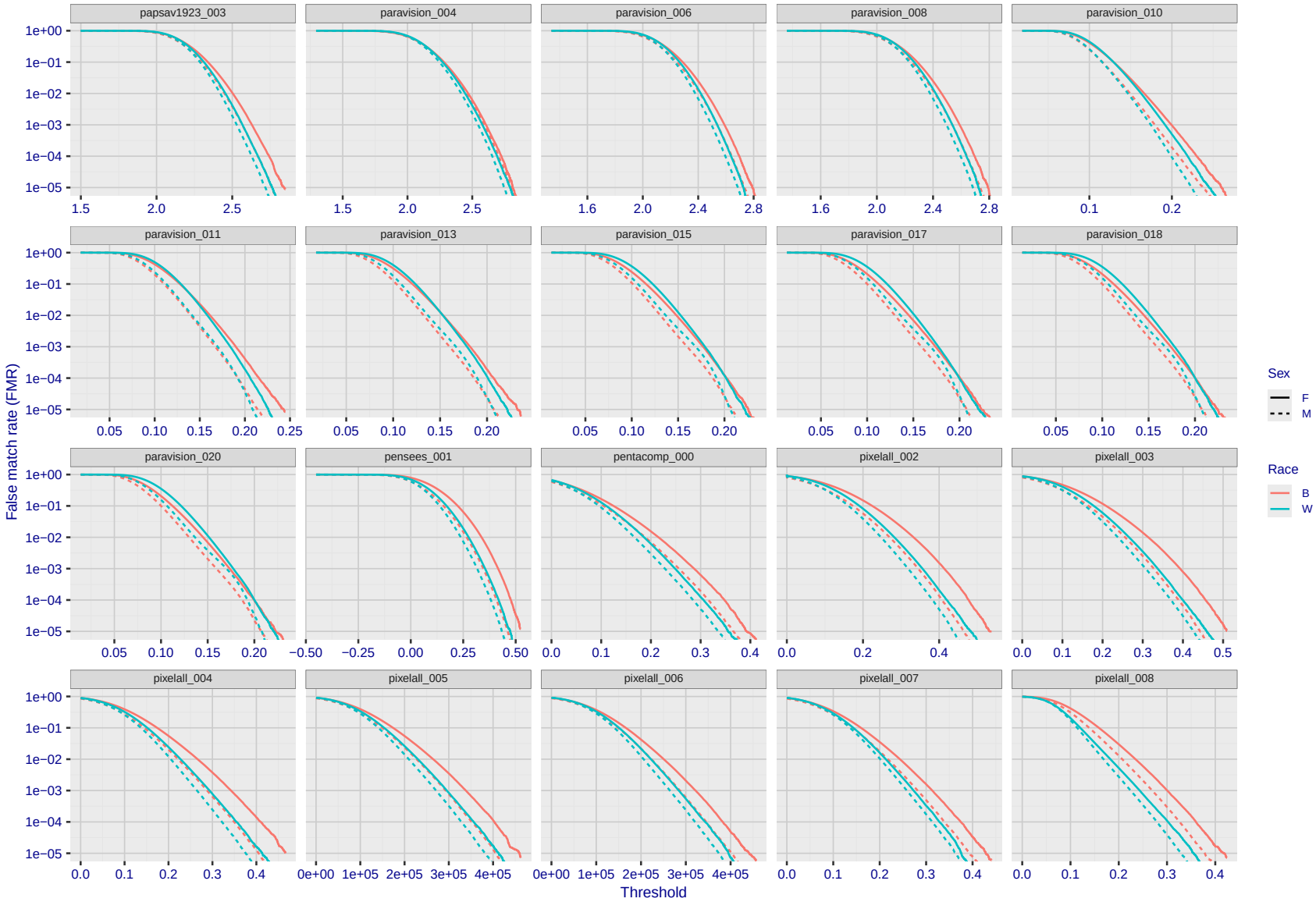

Figure 584: For the mugshot images, the false match calibration curves show false match rate vs. threshold. Separate curves appear for white females, black females, black males and white males.

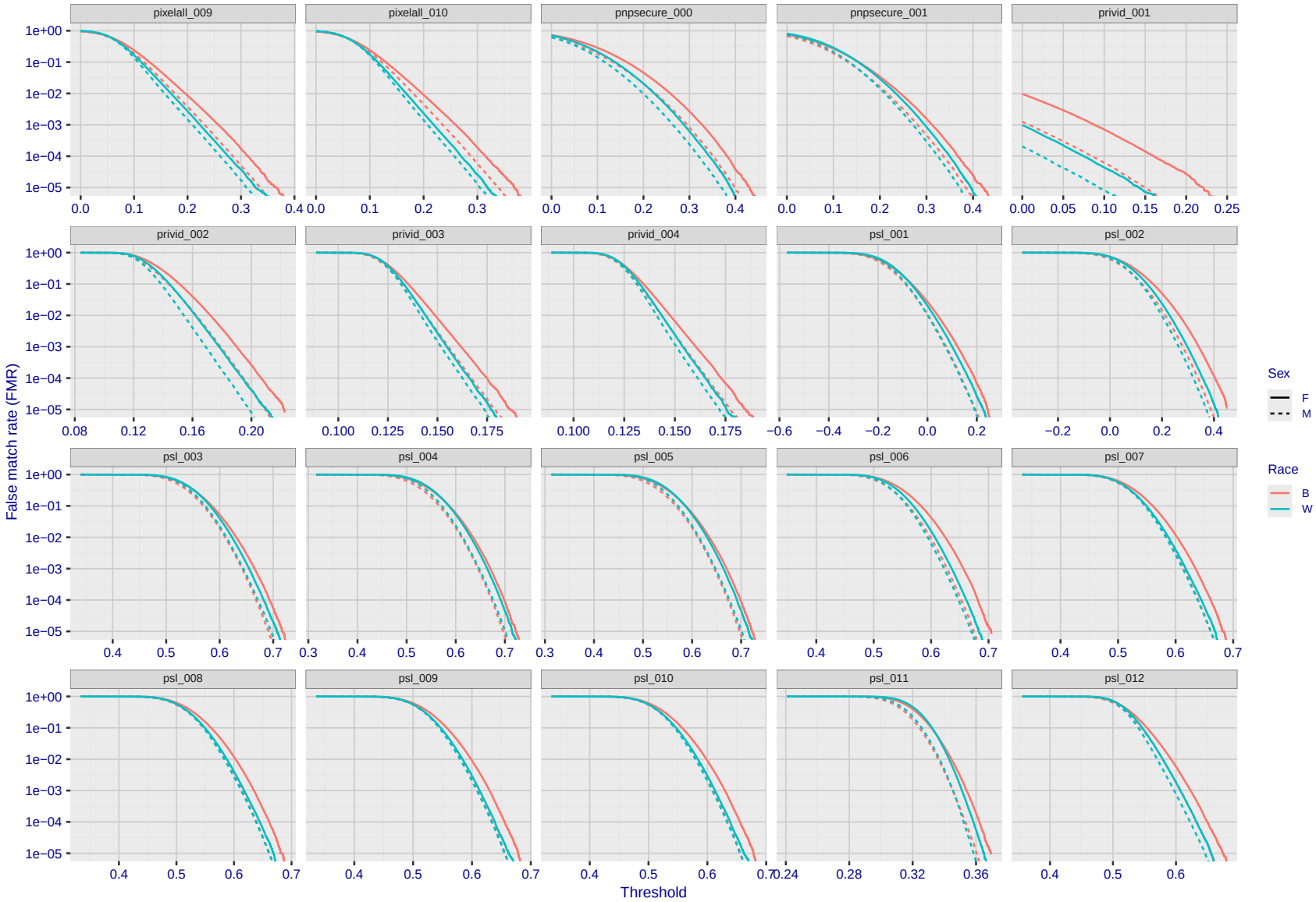

Figure 585: For the mugshot images, the false match calibration curves show false match rate vs. threshold. Separate curves appear for white females, black females, black males and white males.

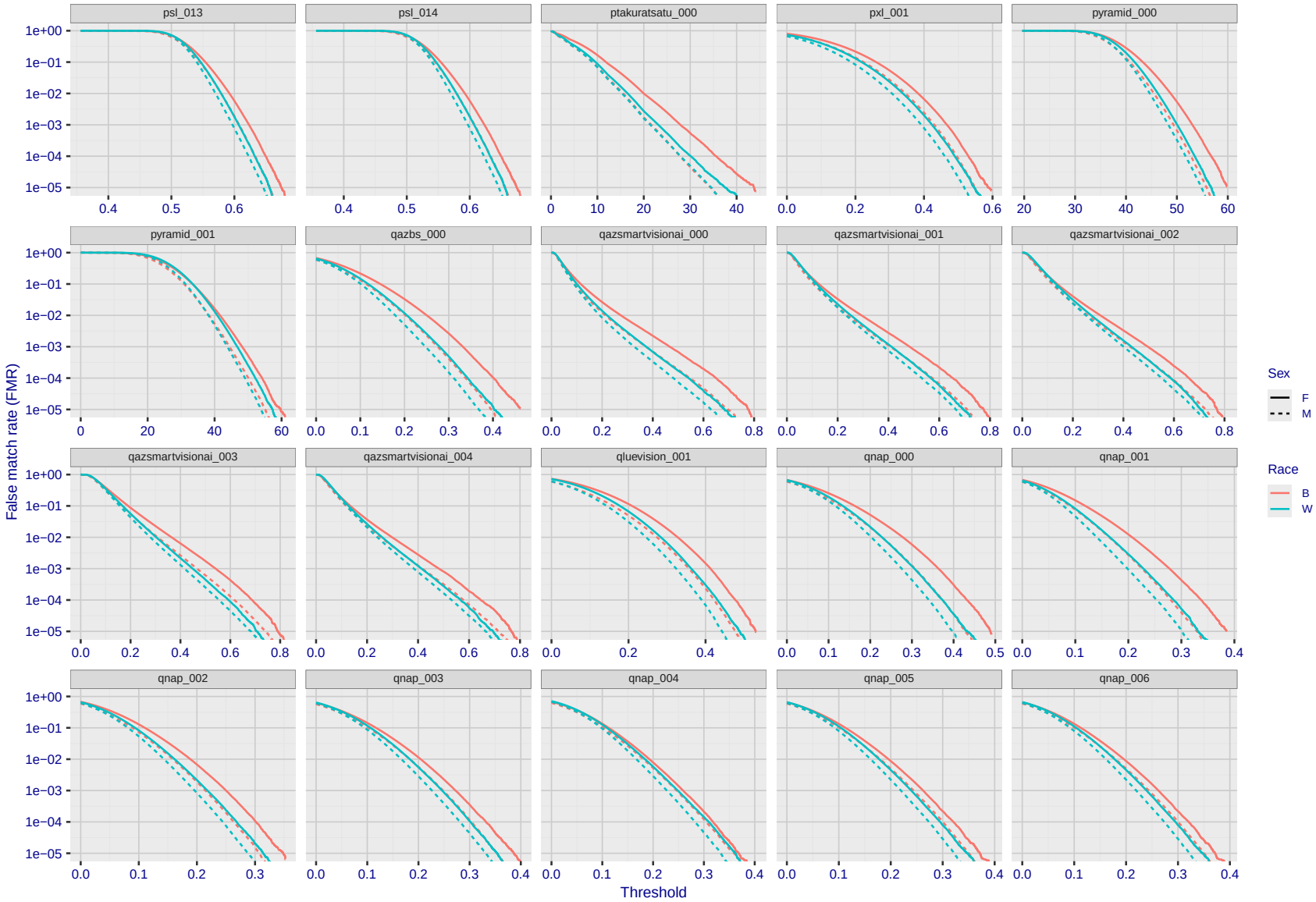

Figure 586: For the mugshot images, the false match calibration curves show false match rate vs. threshold. Separate curves appear for white females, black females, black males and white males.

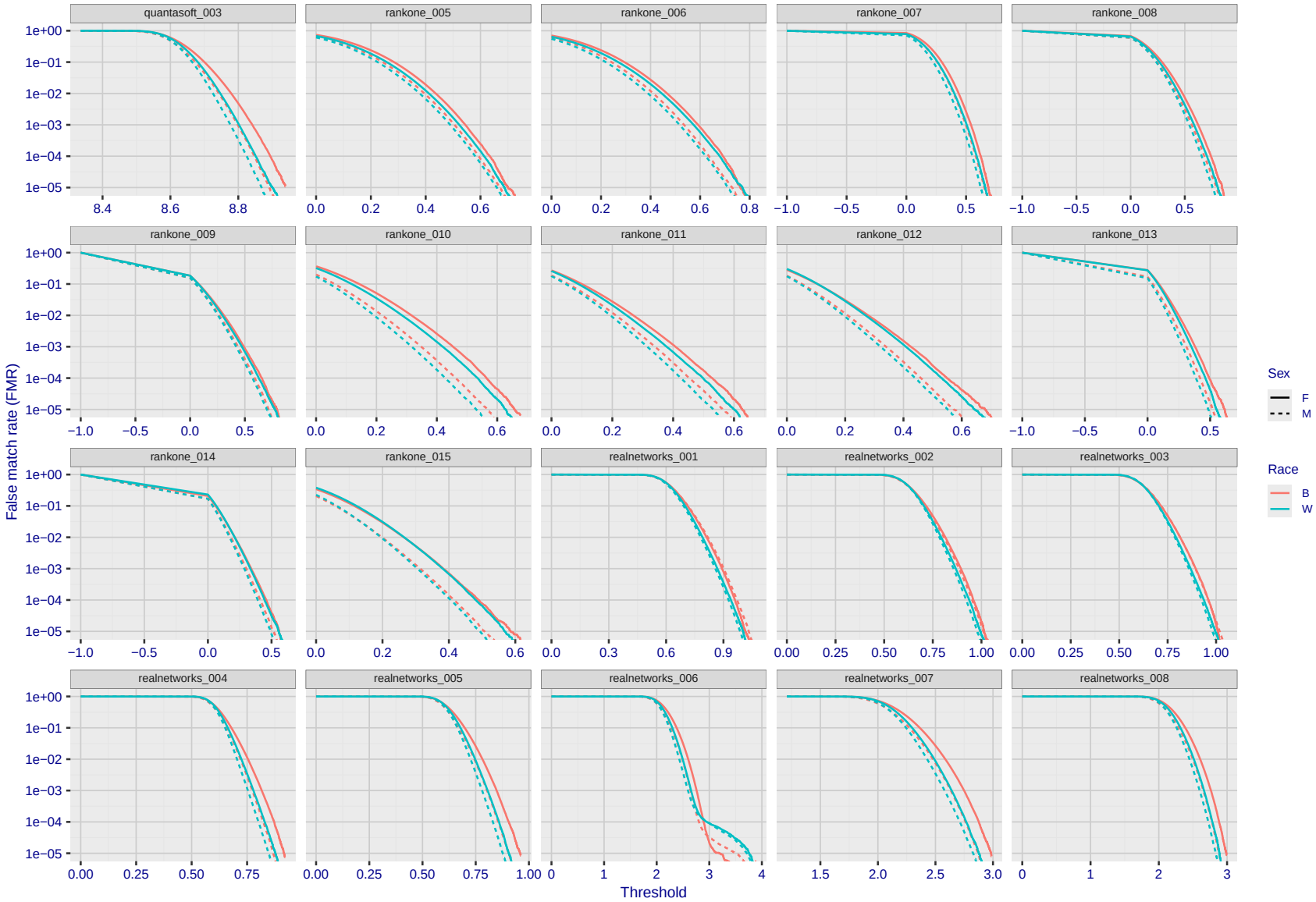

Figure 587: For the mugshot images, the false match calibration curves show false match rate vs. threshold. Separate curves appear for white females, black females, black males and white males.

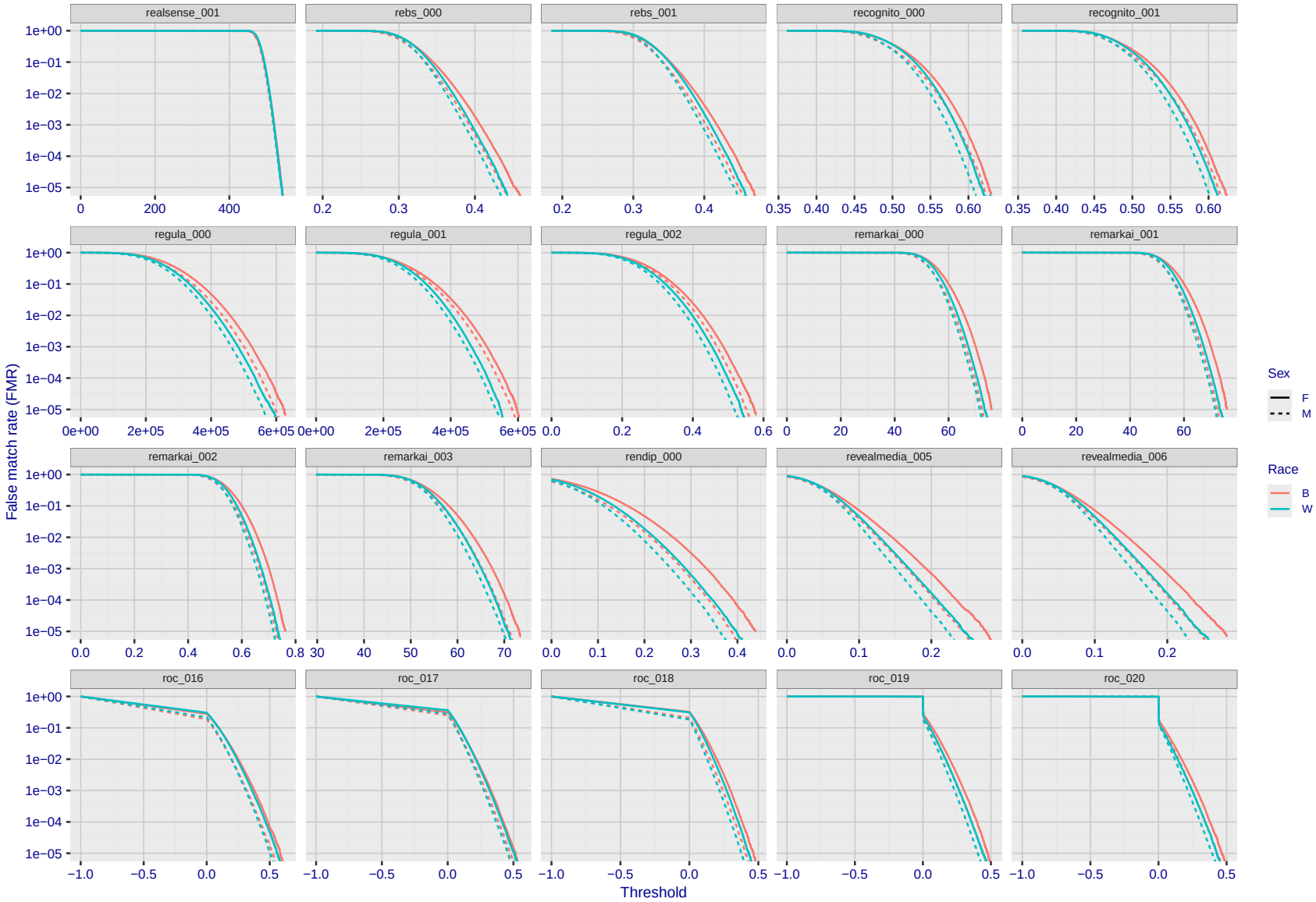

Figure 588: For the mugshot images, the false match calibration curves show false match rate vs. threshold. Separate curves appear for white females, black females, black males and white males.

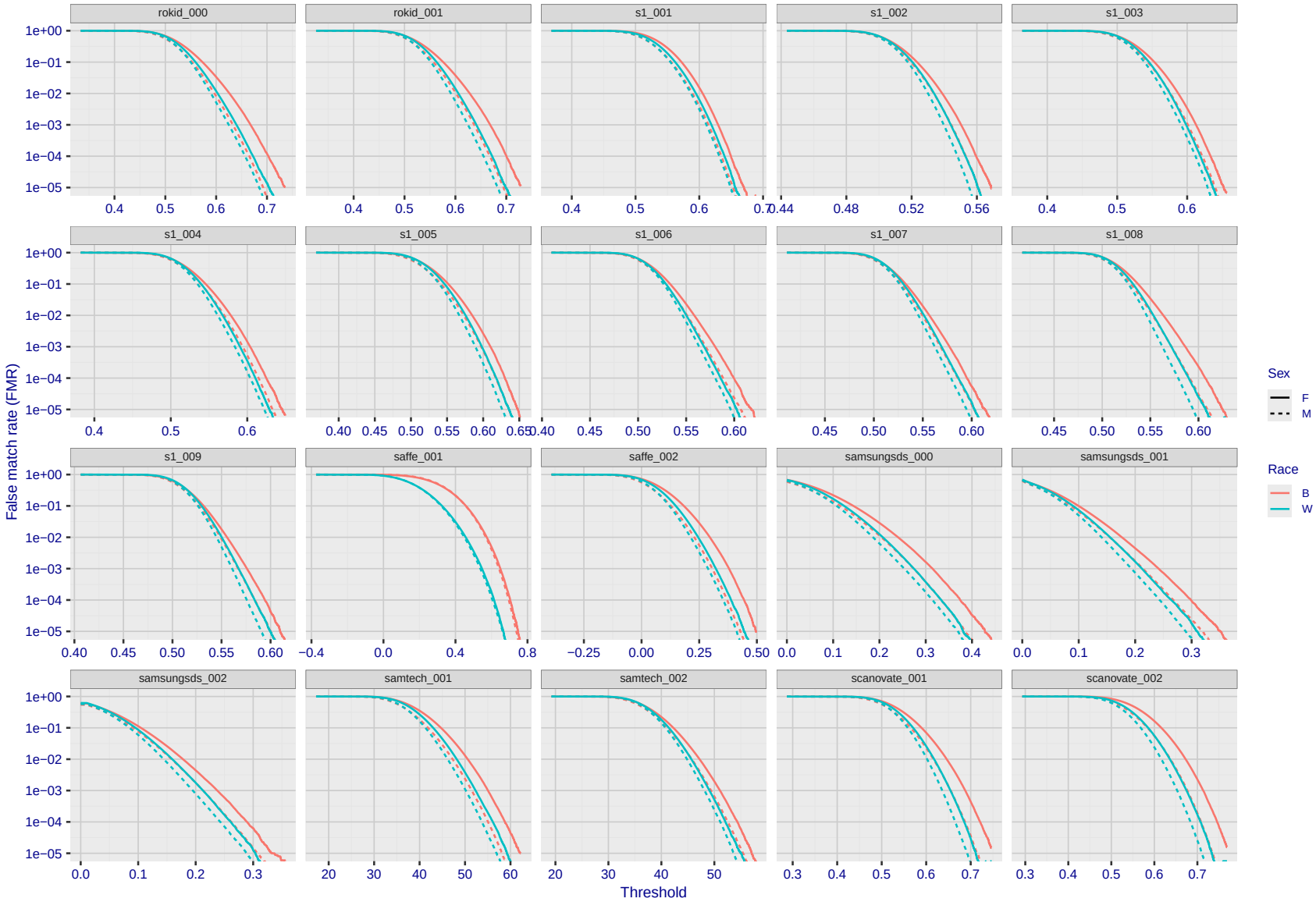

Figure 589: For the mugshot images, the false match calibration curves show false match rate vs. threshold. Separate curves appear for white females, black females, black males and white males.

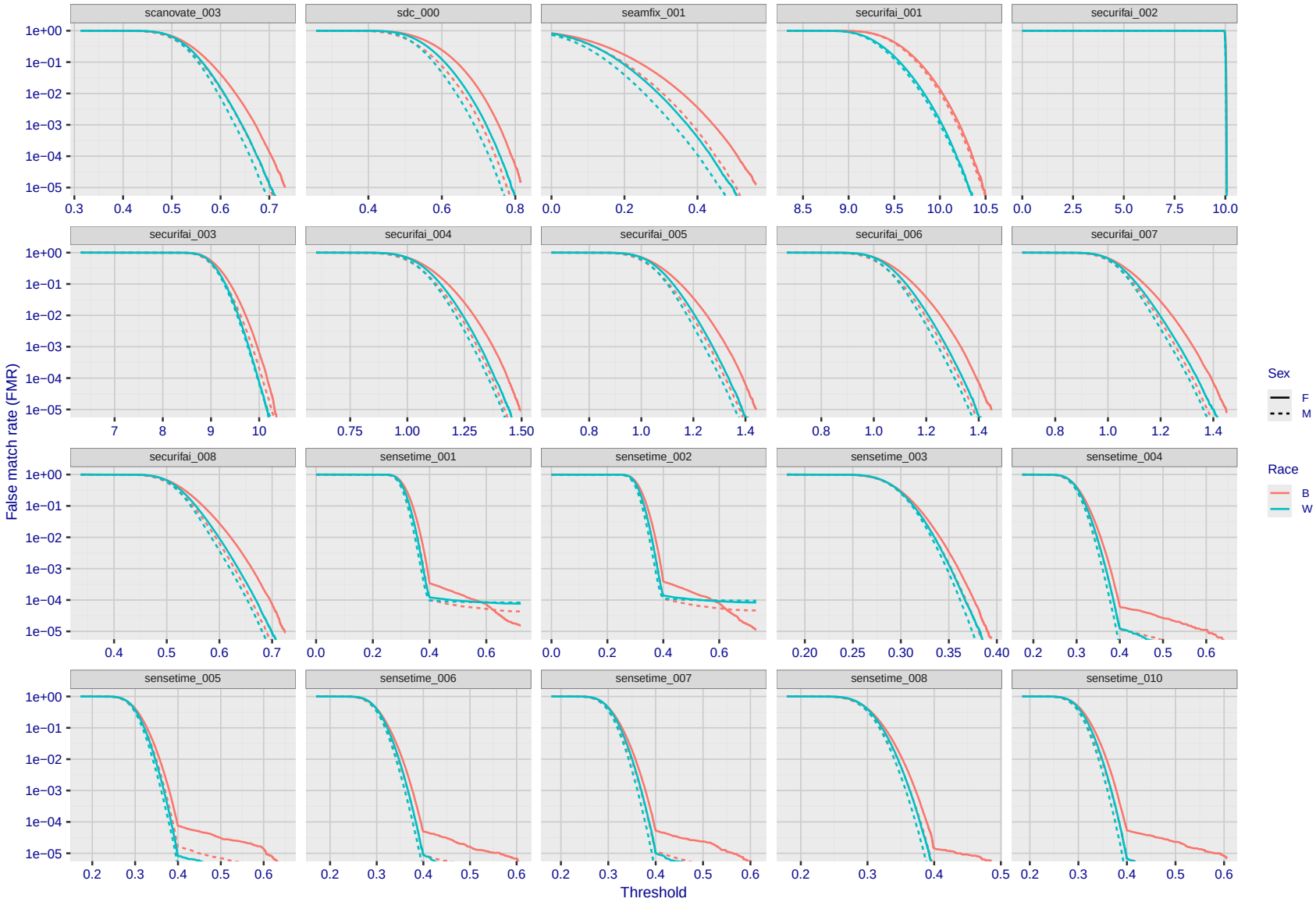

Figure 590: For the mugshot images, the false match calibration curves show false match rate vs. threshold. Separate curves appear for white females, black females, black males and white males.

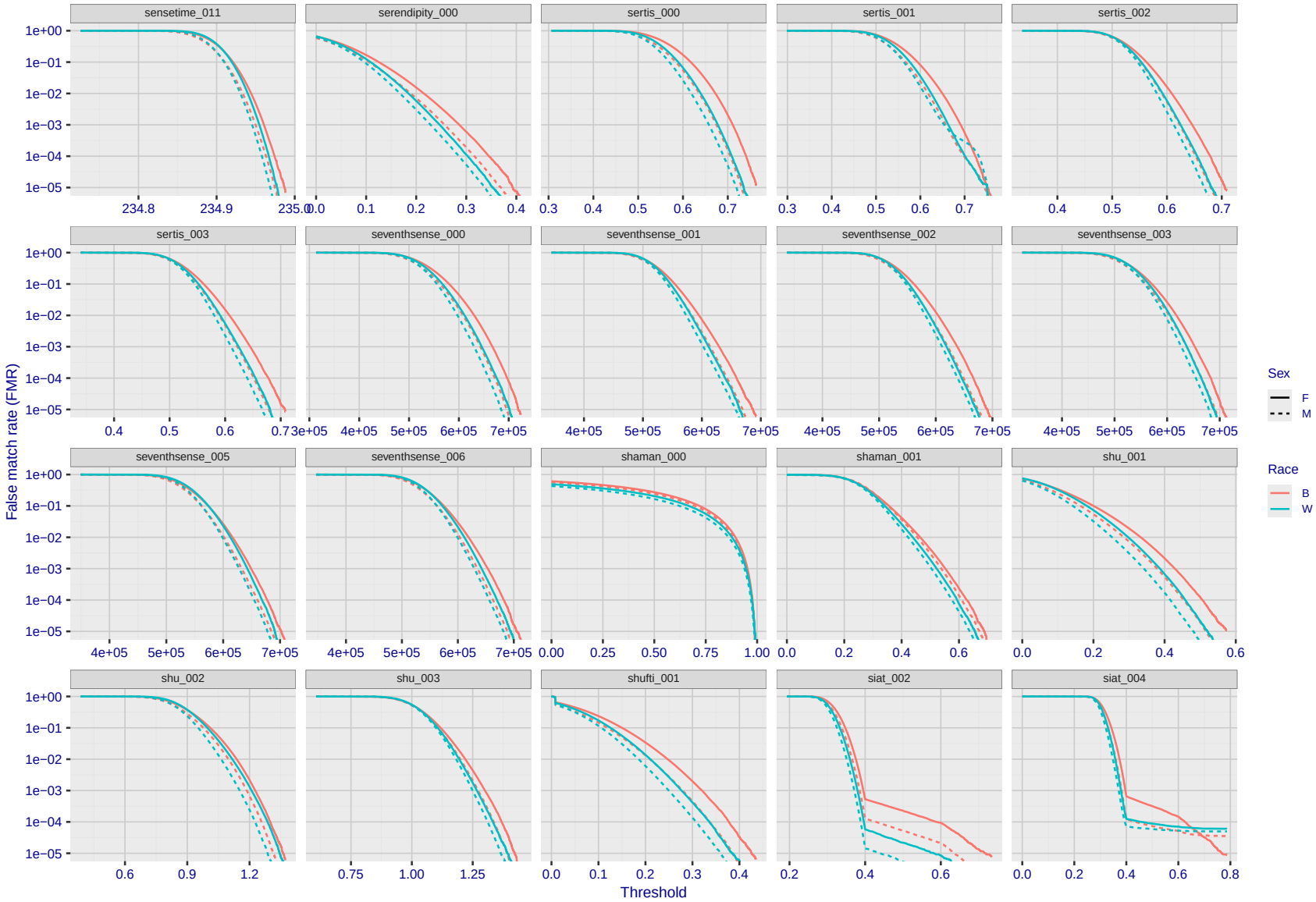

Figure 591: For the mugshot images, the false match calibration curves show false match rate vs. threshold. Separate curves appear for white females, black females, black males and white males.

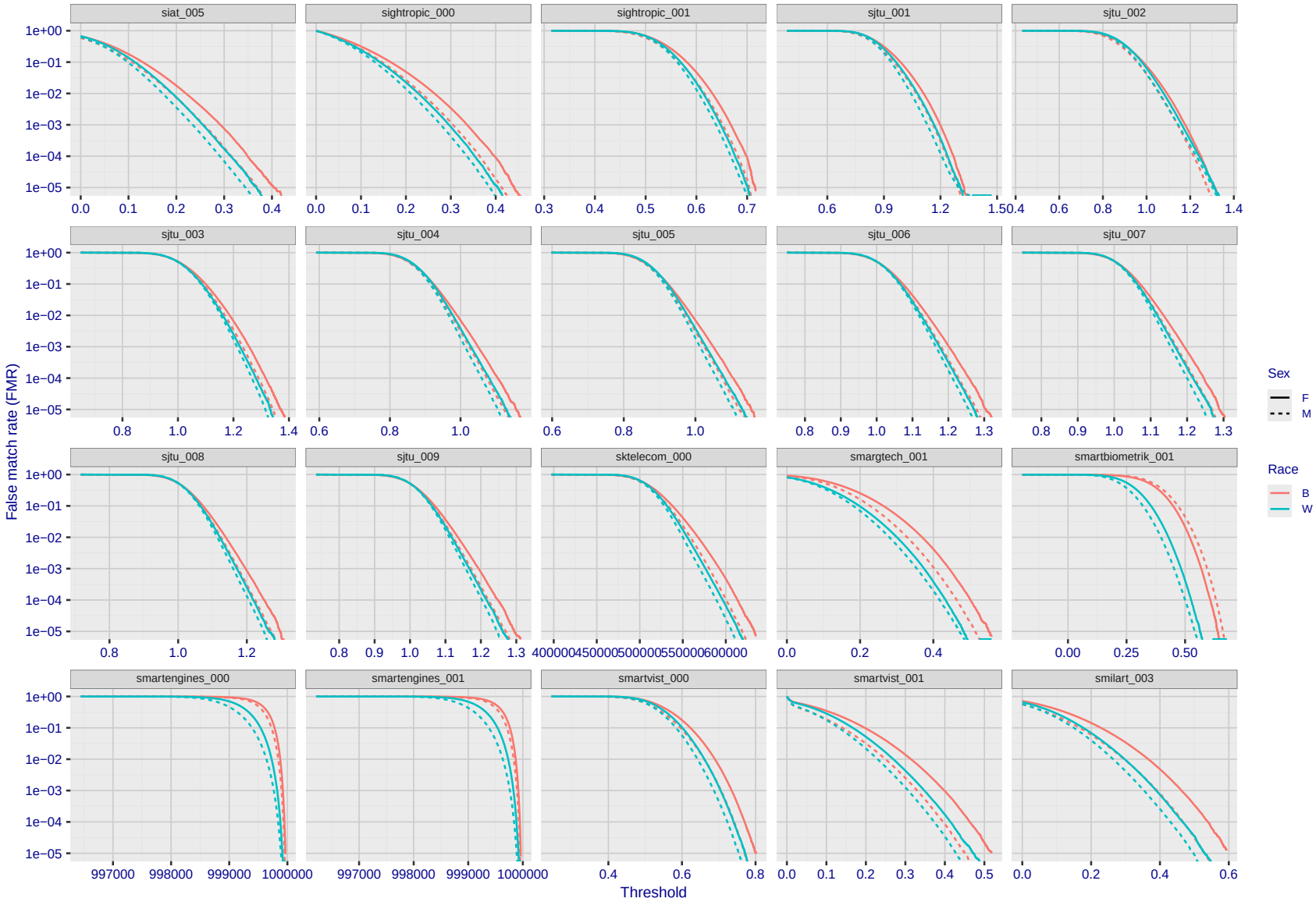

Figure 592: For the mugshot images, the false match calibration curves show false match rate vs. threshold. Separate curves appear for white females, black females, black males and white males.

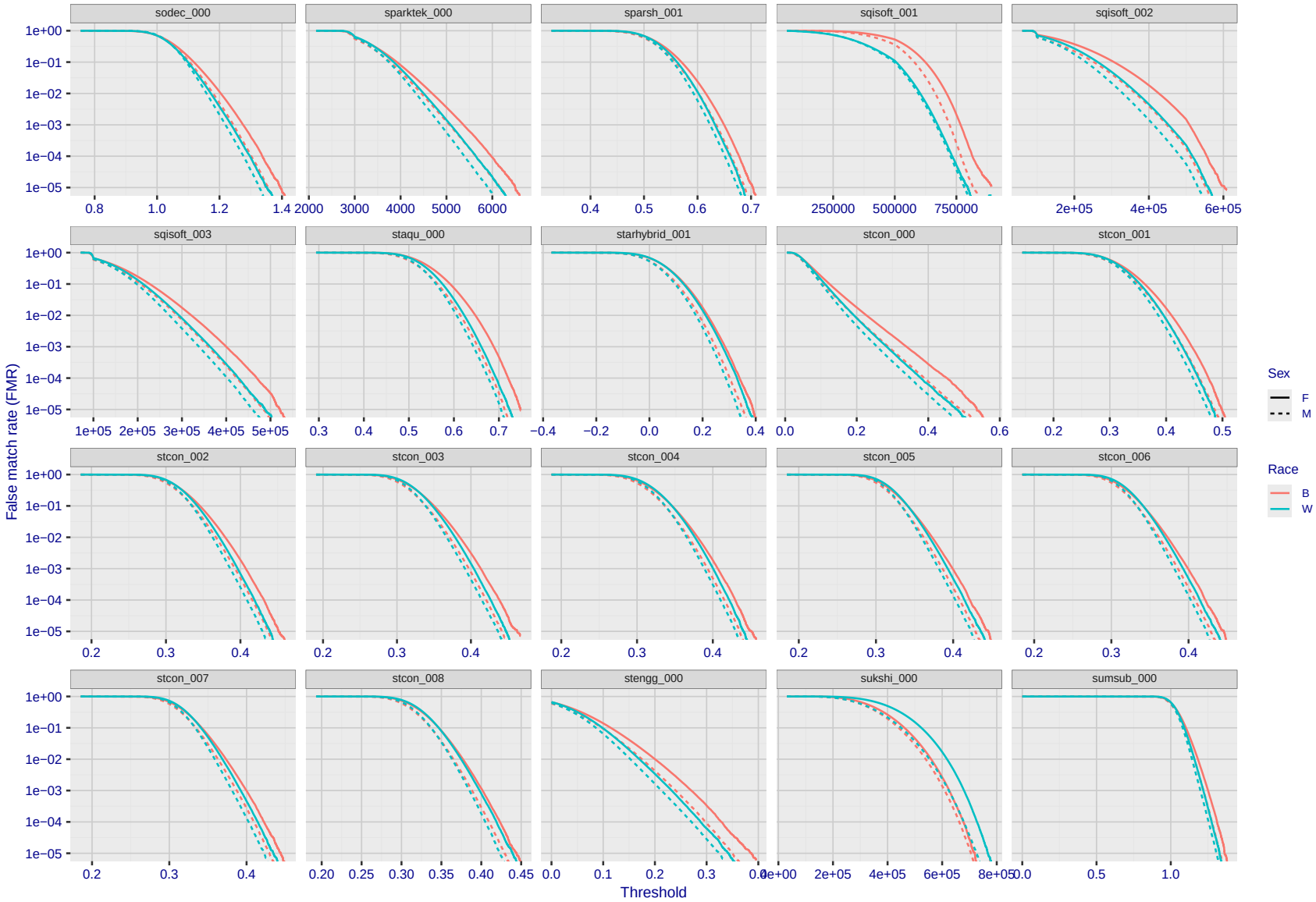

Figure 593: For the mugshot images, the false match calibration curves show false match rate vs. threshold. Separate curves appear for white females, black females, black males and white males.

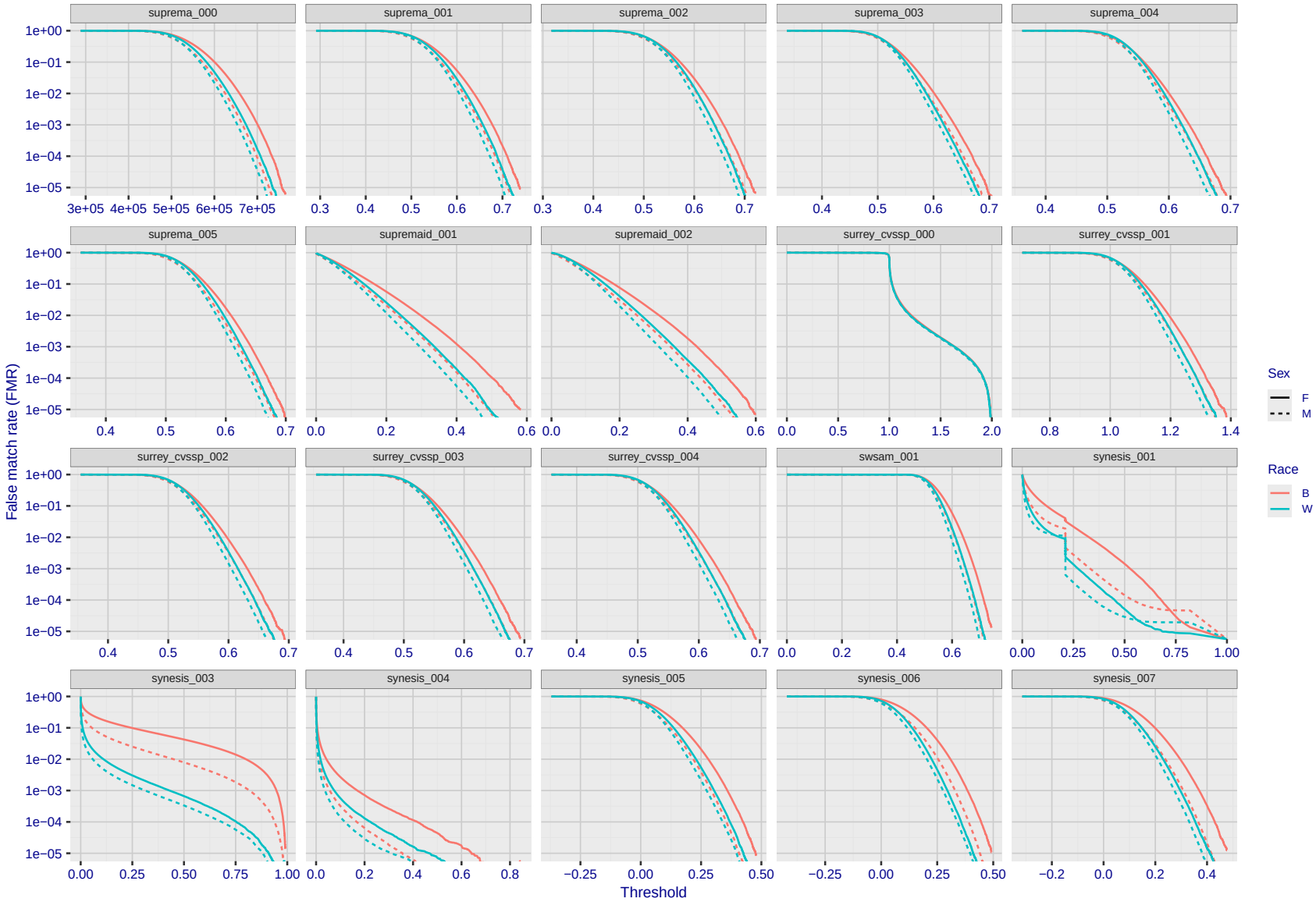

Figure 594: For the mugshot images, the false match calibration curves show false match rate vs. threshold. Separate curves appear for white females, black females, black males and white males.

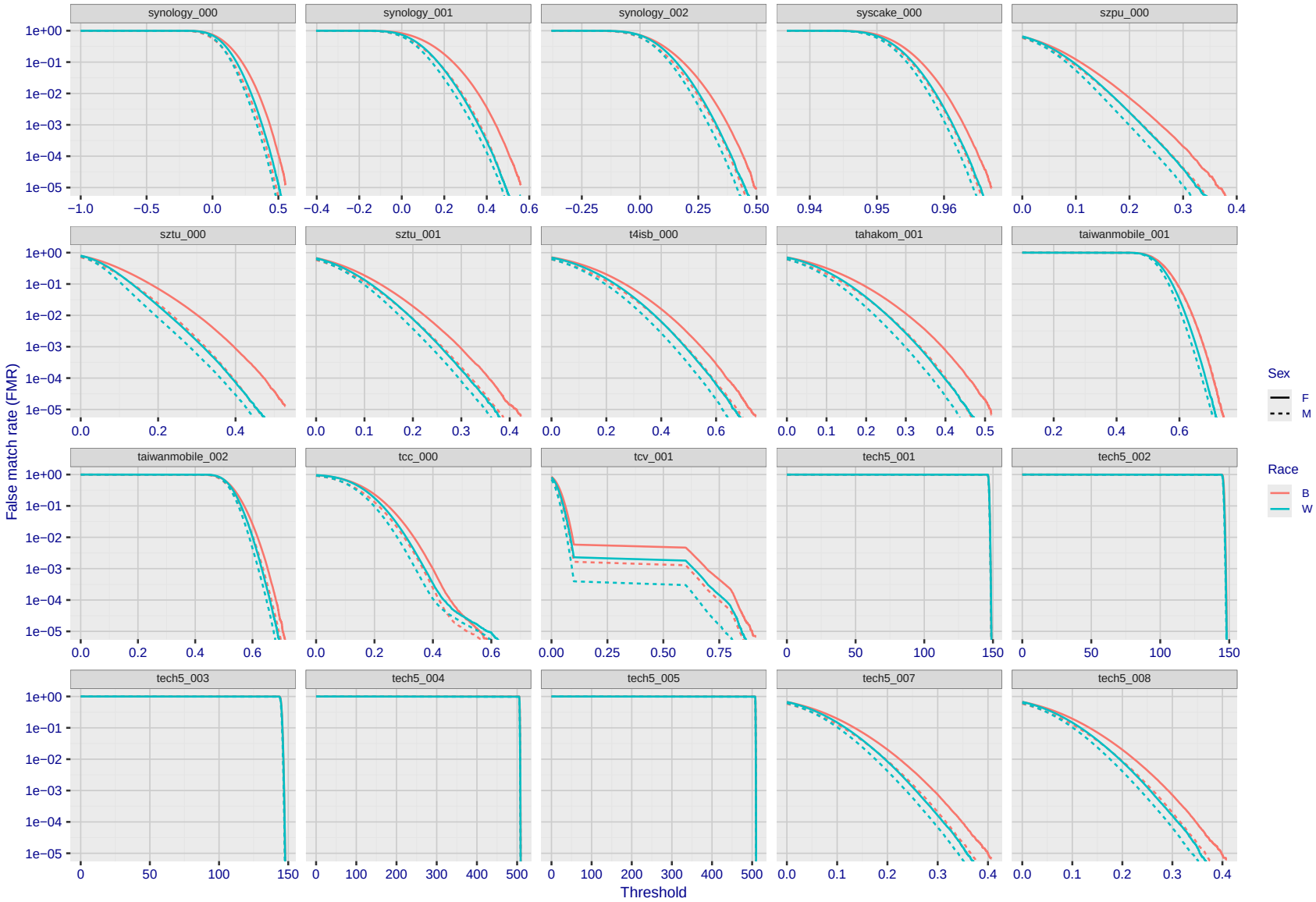

Figure 595: For the mugshot images, the false match calibration curves show false match rate vs. threshold. Separate curves appear for white females, black females, black males and white males.

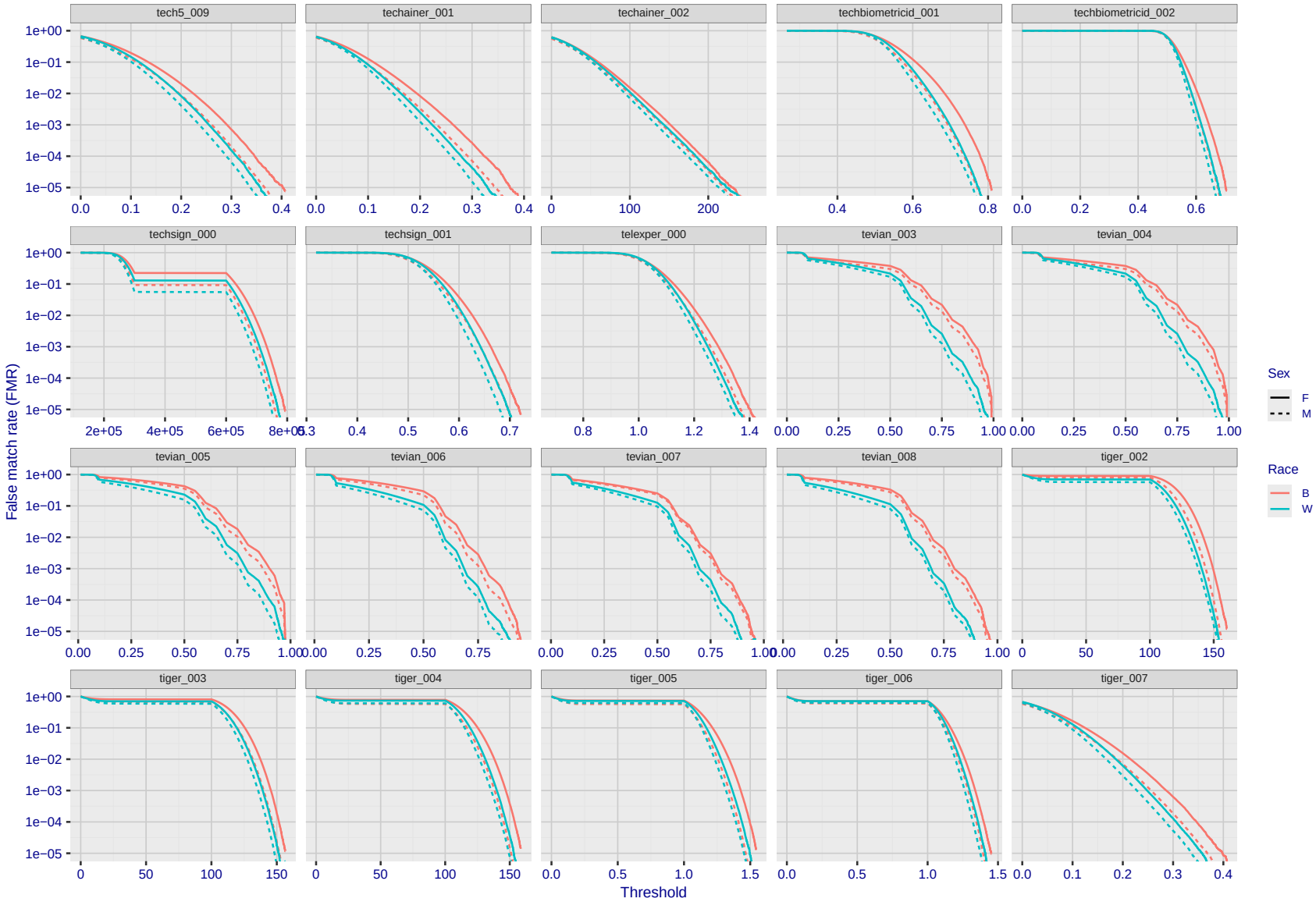

Figure 596: For the mugshot images, the false match calibration curves show false match rate vs. threshold. Separate curves appear for white females, black females, black males and white males.

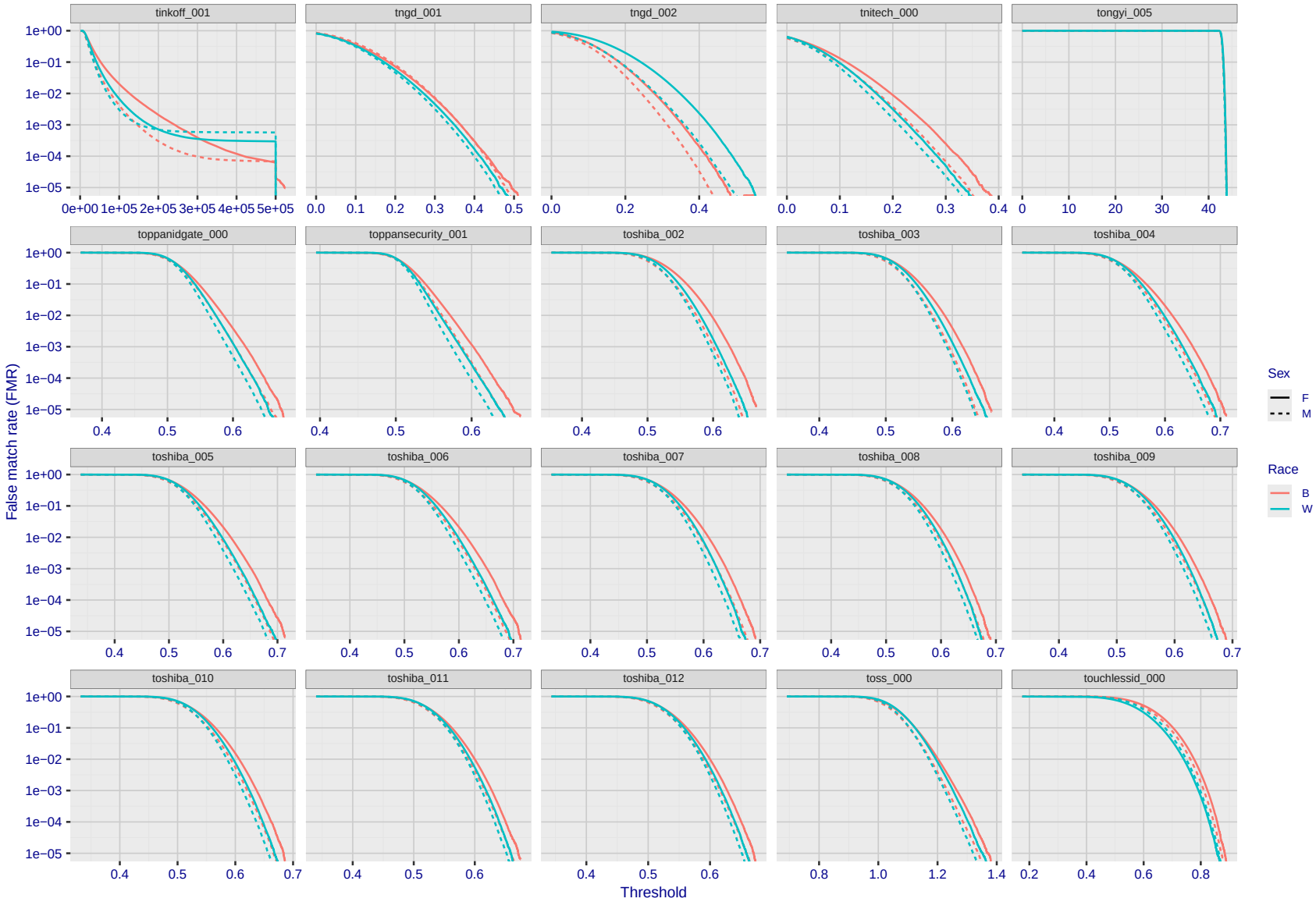

Figure 597: For the mugshot images, the false match calibration curves show false match rate vs. threshold. Separate curves appear for white females, black females, black males and white males.

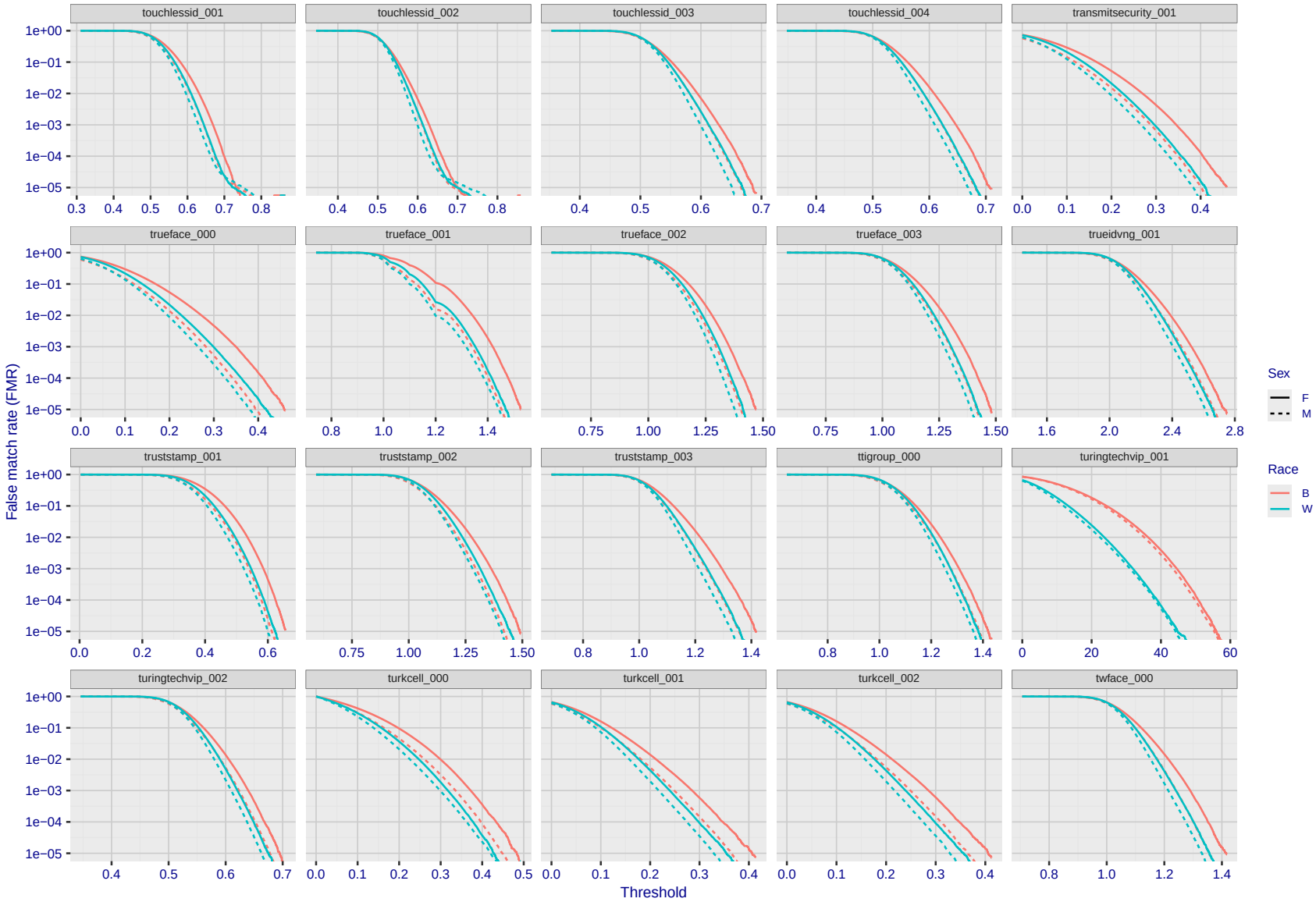

Figure 598: For the mugshot images, the false match calibration curves show false match rate vs. threshold. Separate curves appear for white females, black females, black males and white males.

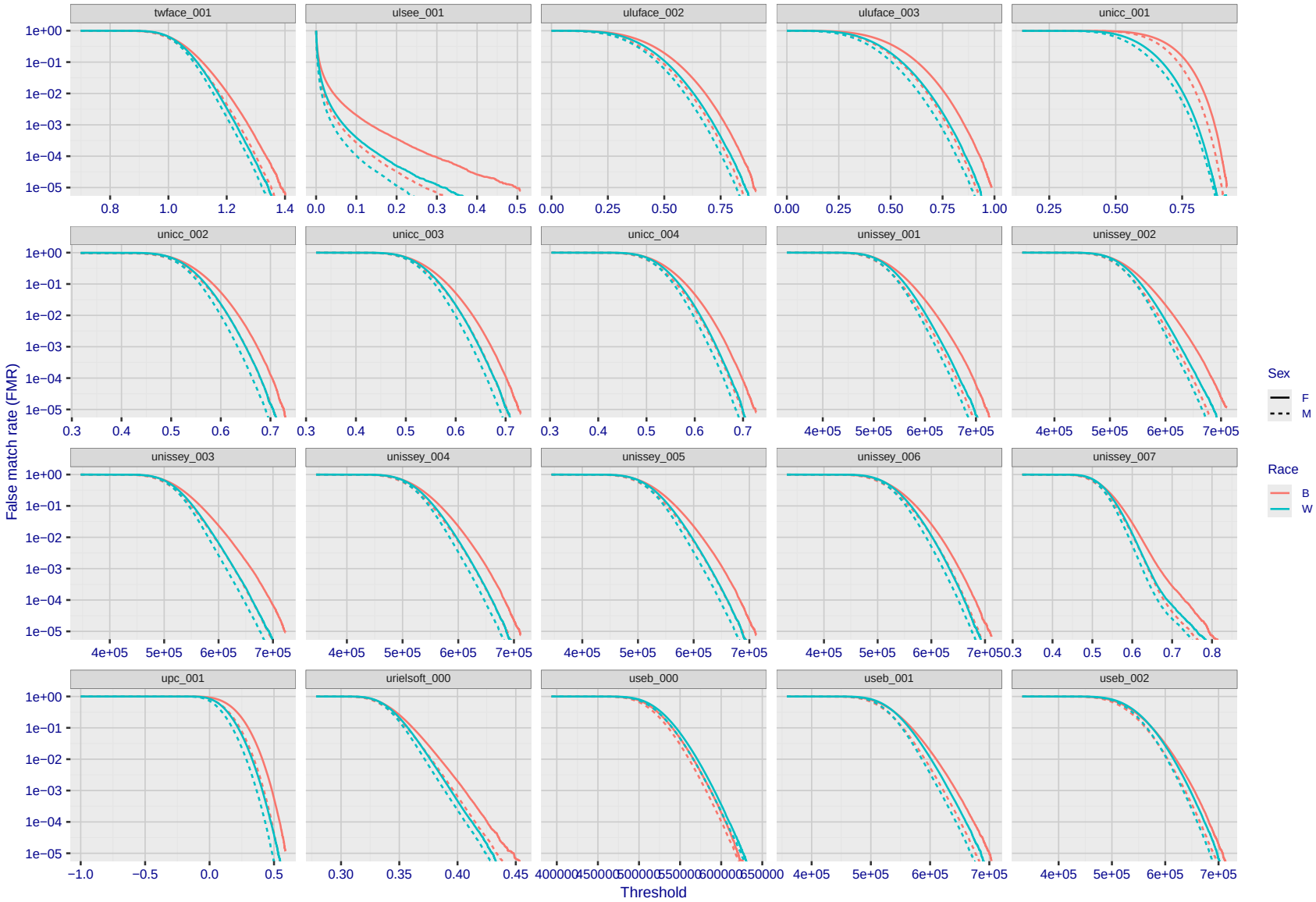

Figure 599: For the mugshot images, the false match calibration curves show false match rate vs. threshold. Separate curves appear for white females, black females, black males and white males.

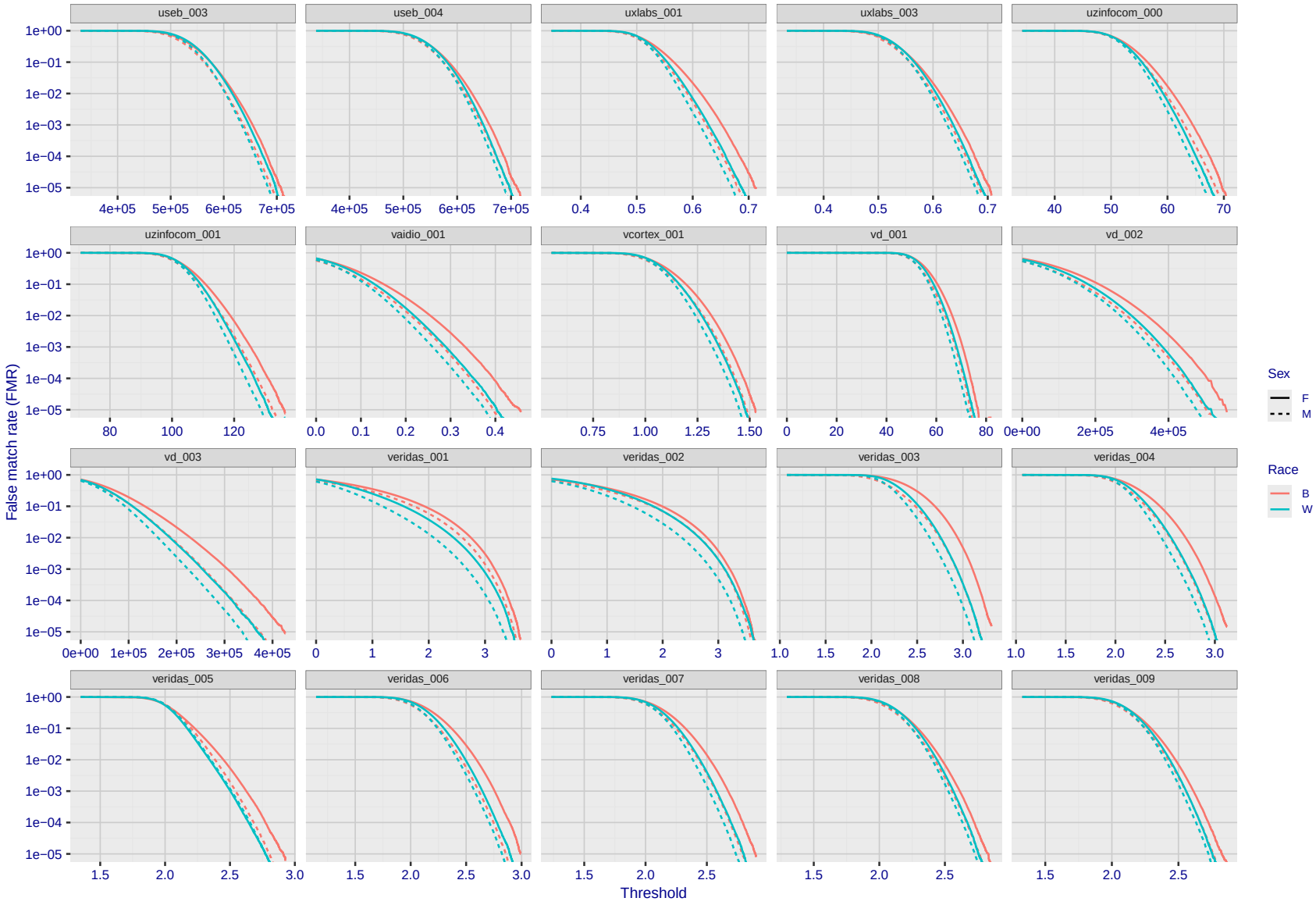

Figure 600: For the mugshot images, the false match calibration curves show false match rate vs. threshold. Separate curves appear for white females, black females, black males and white males.

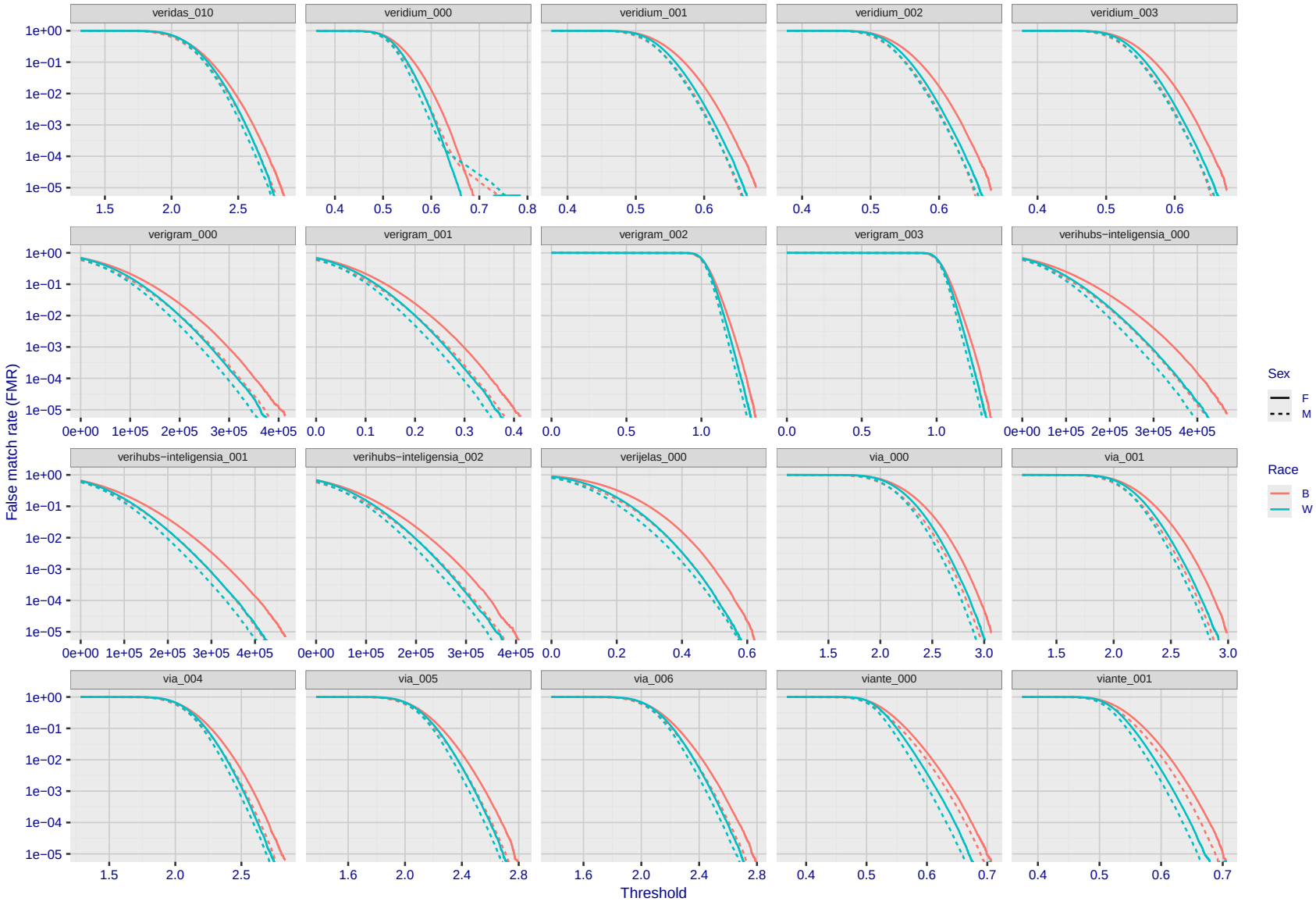

Figure 601: For the mugshot images, the false match calibration curves show false match rate vs. threshold. Separate curves appear for white females, black females, black males and white males.

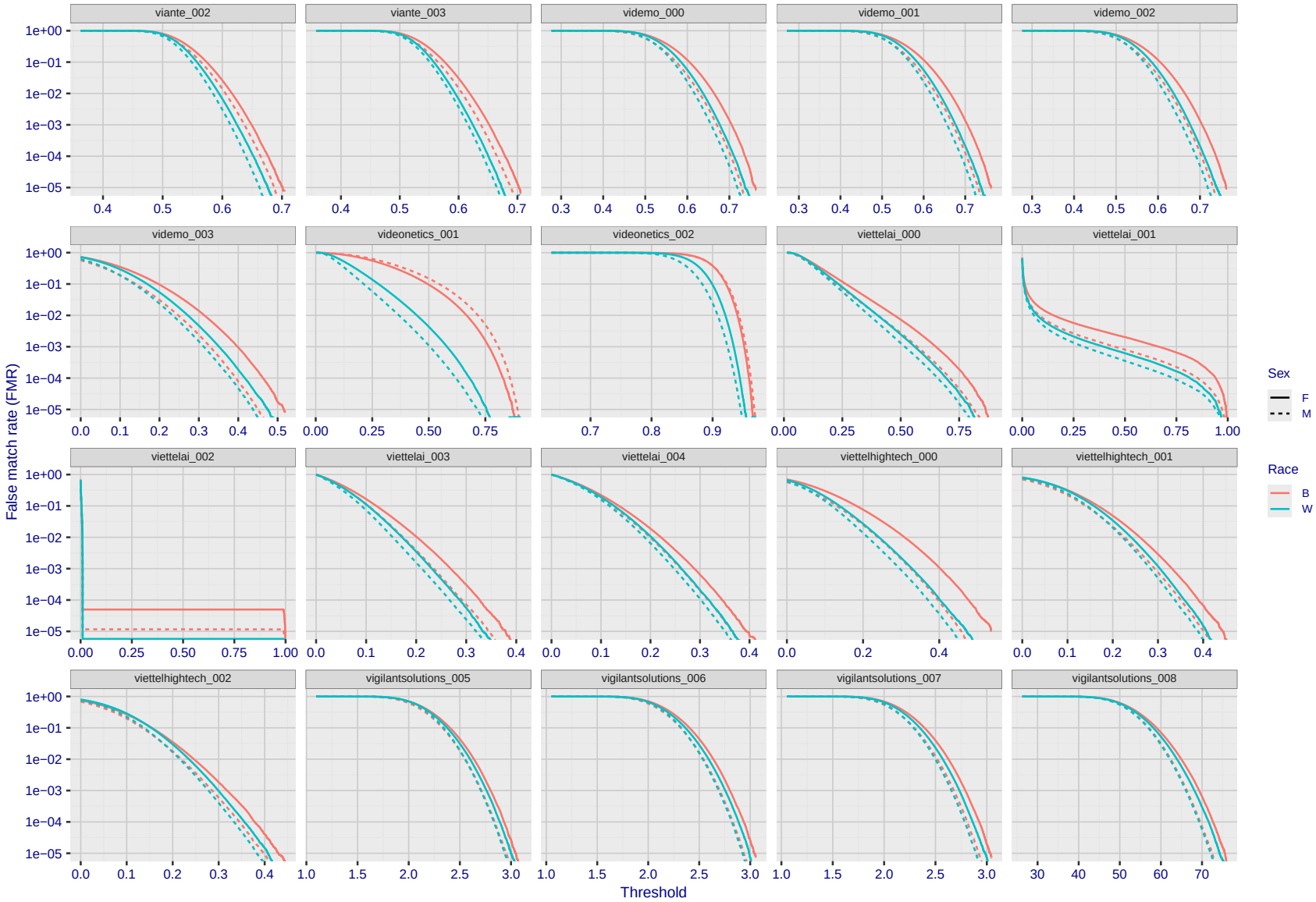

Figure 602: For the mugshot images, the false match calibration curves show false match rate vs. threshold. Separate curves appear for white females, black females, black males and white males.

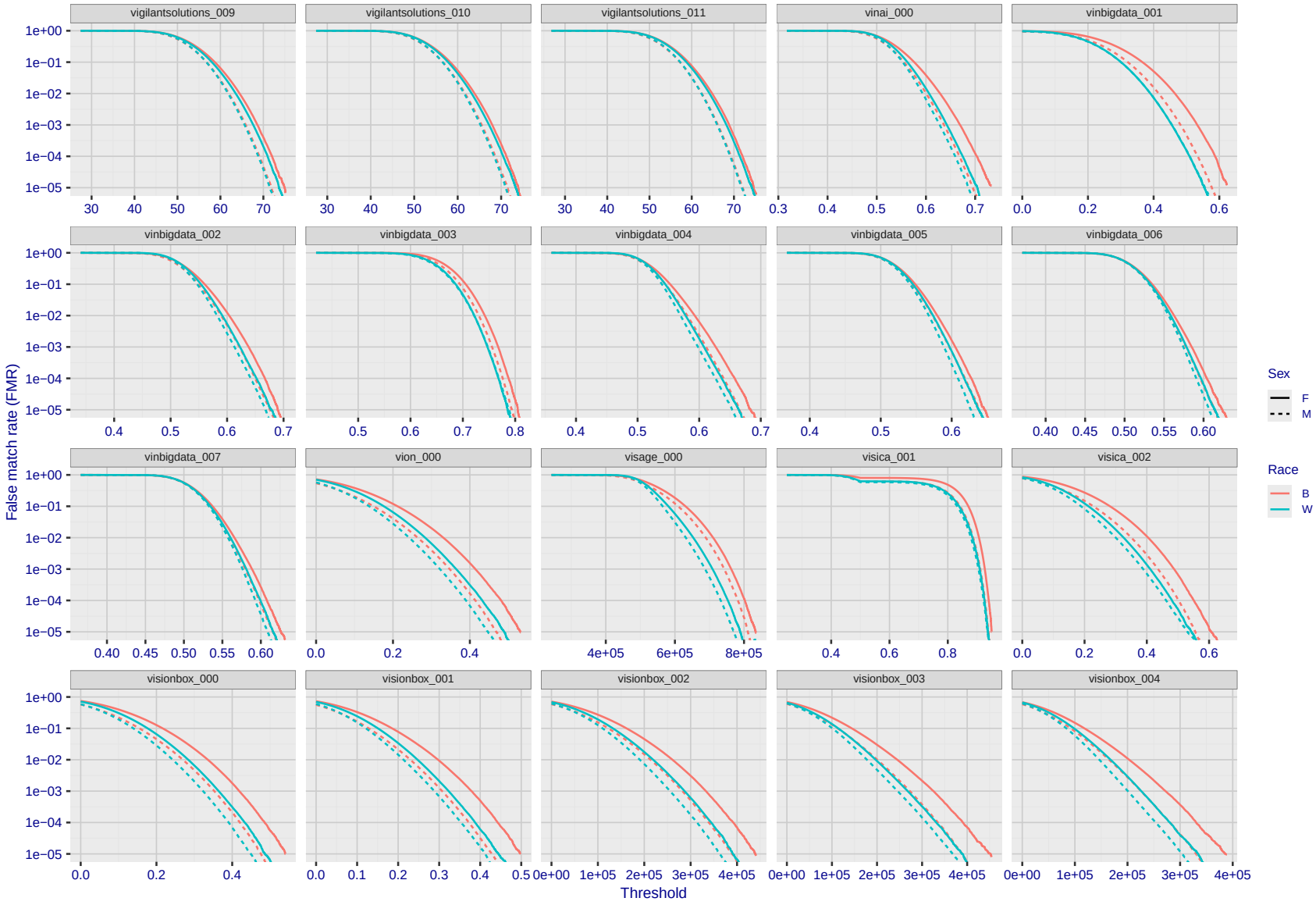

Figure 603: For the mugshot images, the false match calibration curves show false match rate vs. threshold. Separate curves appear for white females, black females, black males and white males.

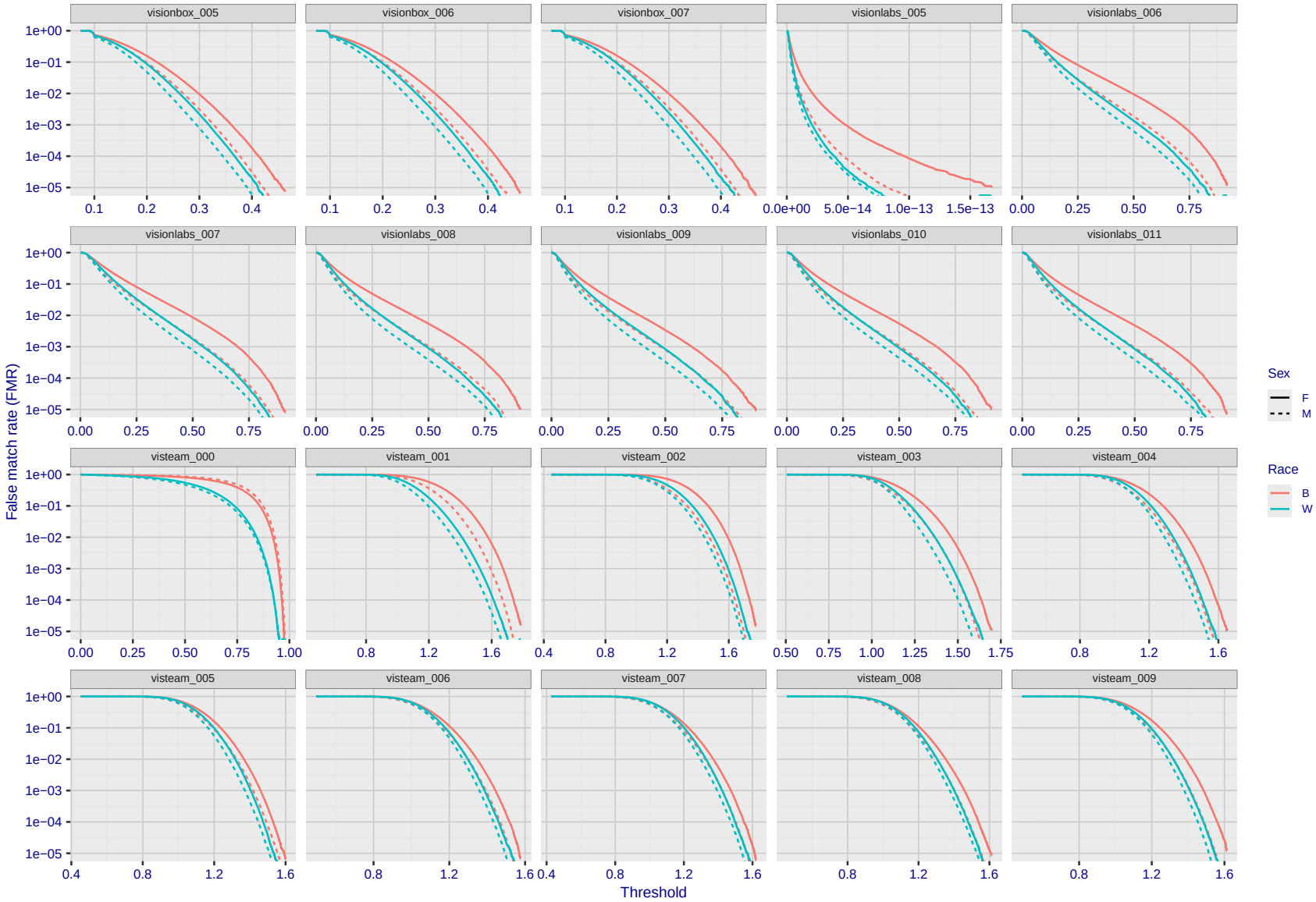

Figure 604: For the mugshot images, the false match calibration curves show false match rate vs. threshold. Separate curves appear for white females, black females, black males and white males.

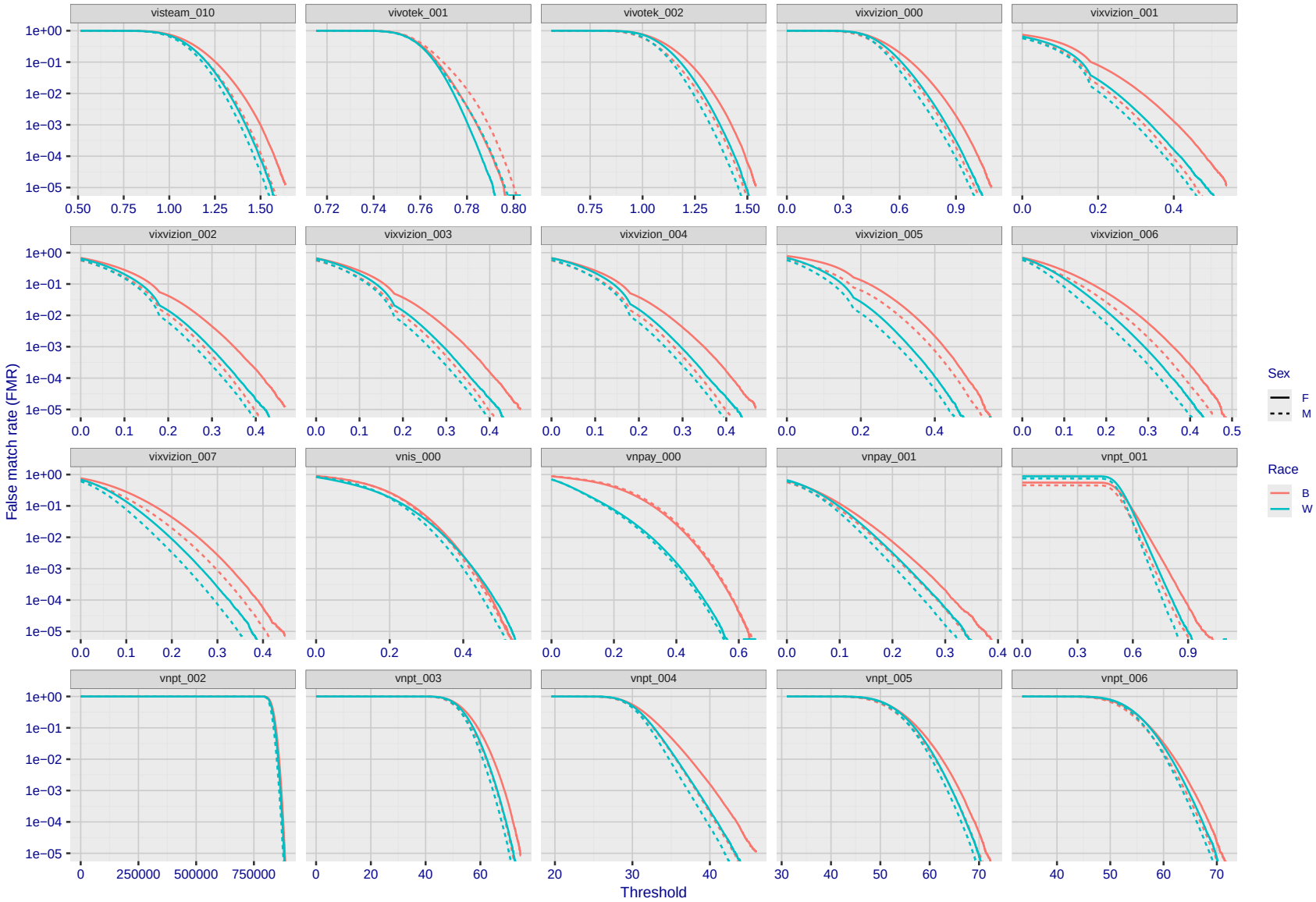

Figure 605: For the mugshot images, the false match calibration curves show false match rate vs. threshold. Separate curves appear for white females, black females, black males and white males.

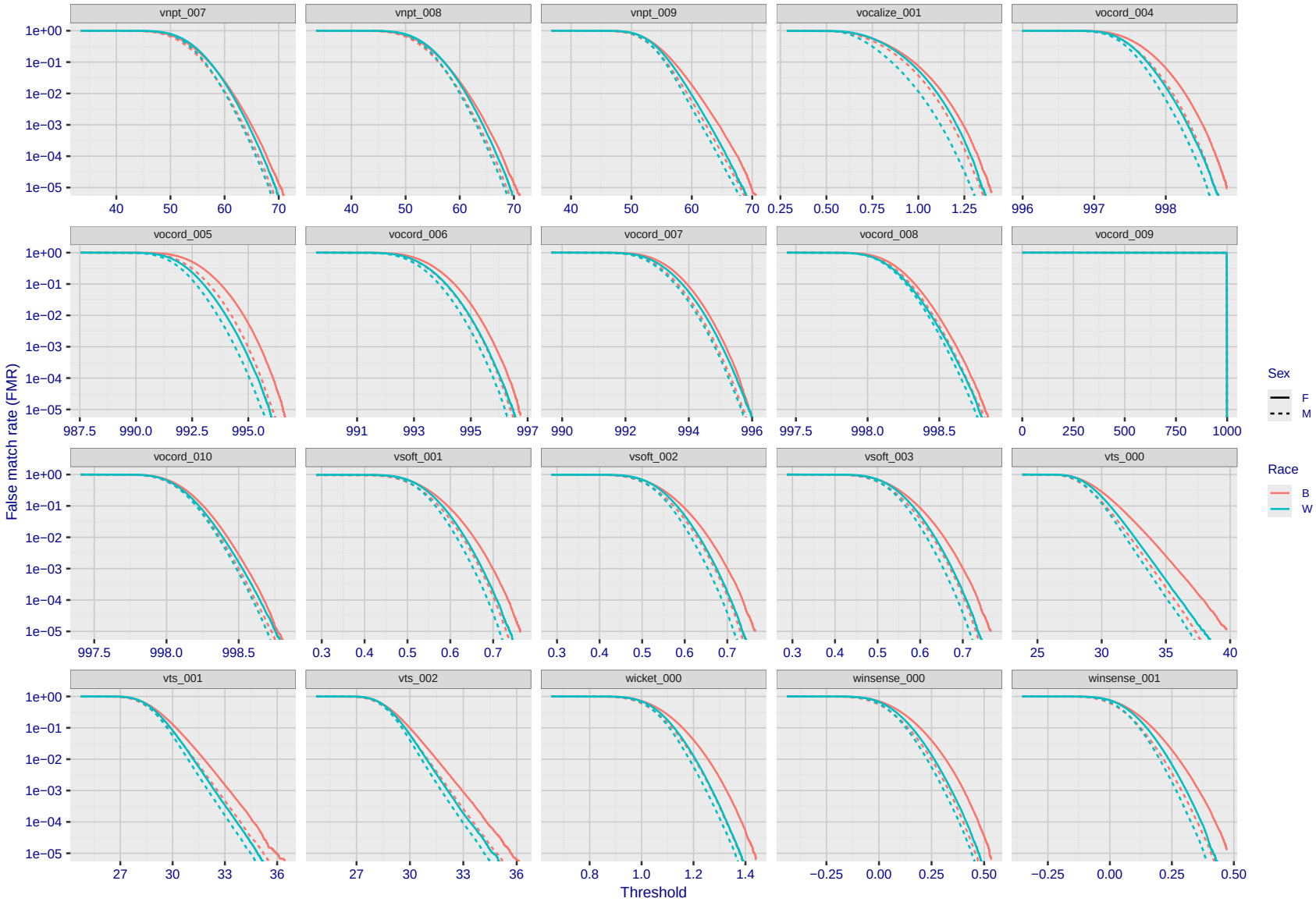

Figure 606: For the mugshot images, the false match calibration curves show false match rate vs. threshold. Separate curves appear for white females, black females, black males and white males.

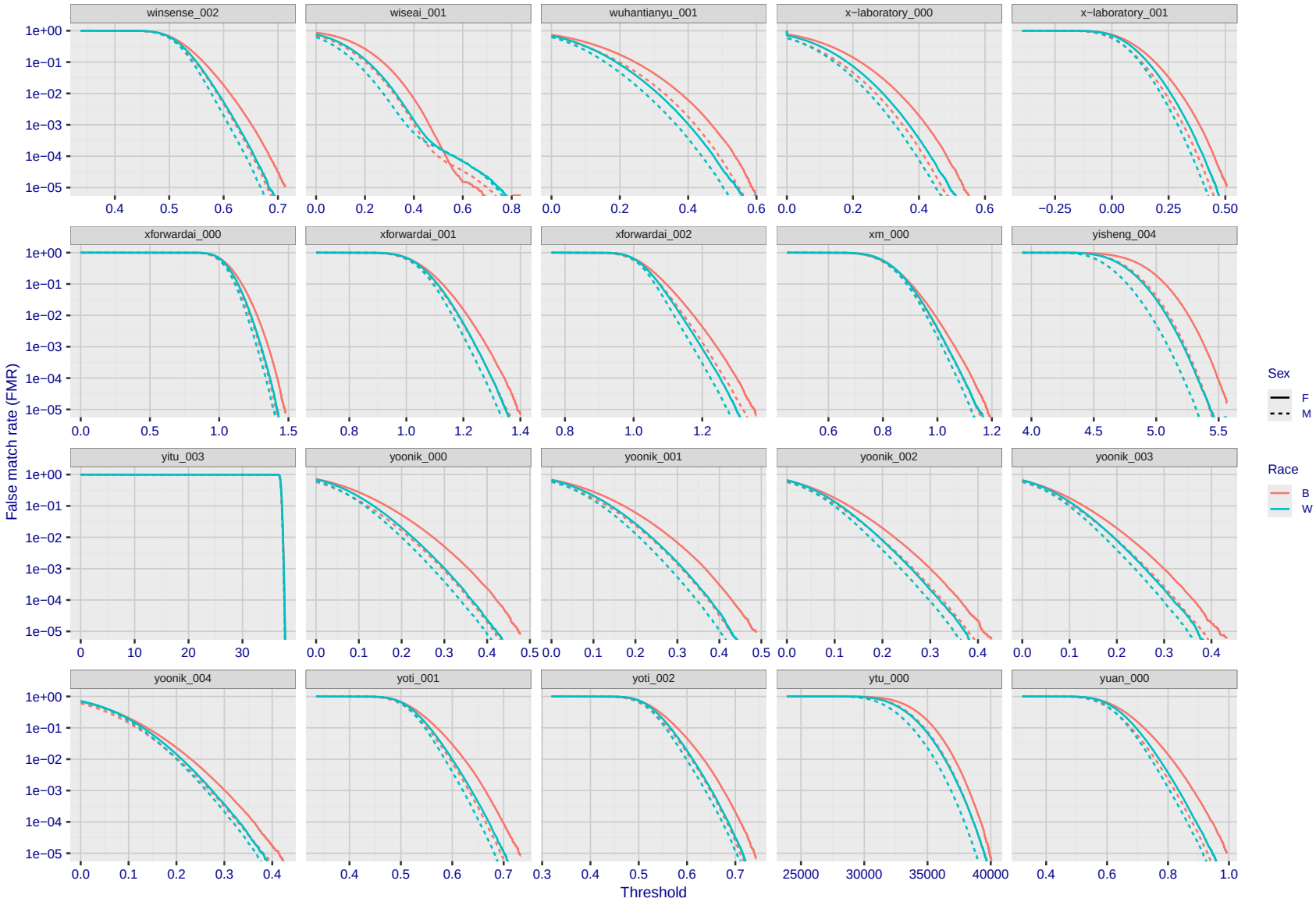

Figure 607: For the mugshot images, the false match calibration curves show false match rate vs. threshold. Separate curves appear for white females, black females, black males and white males.

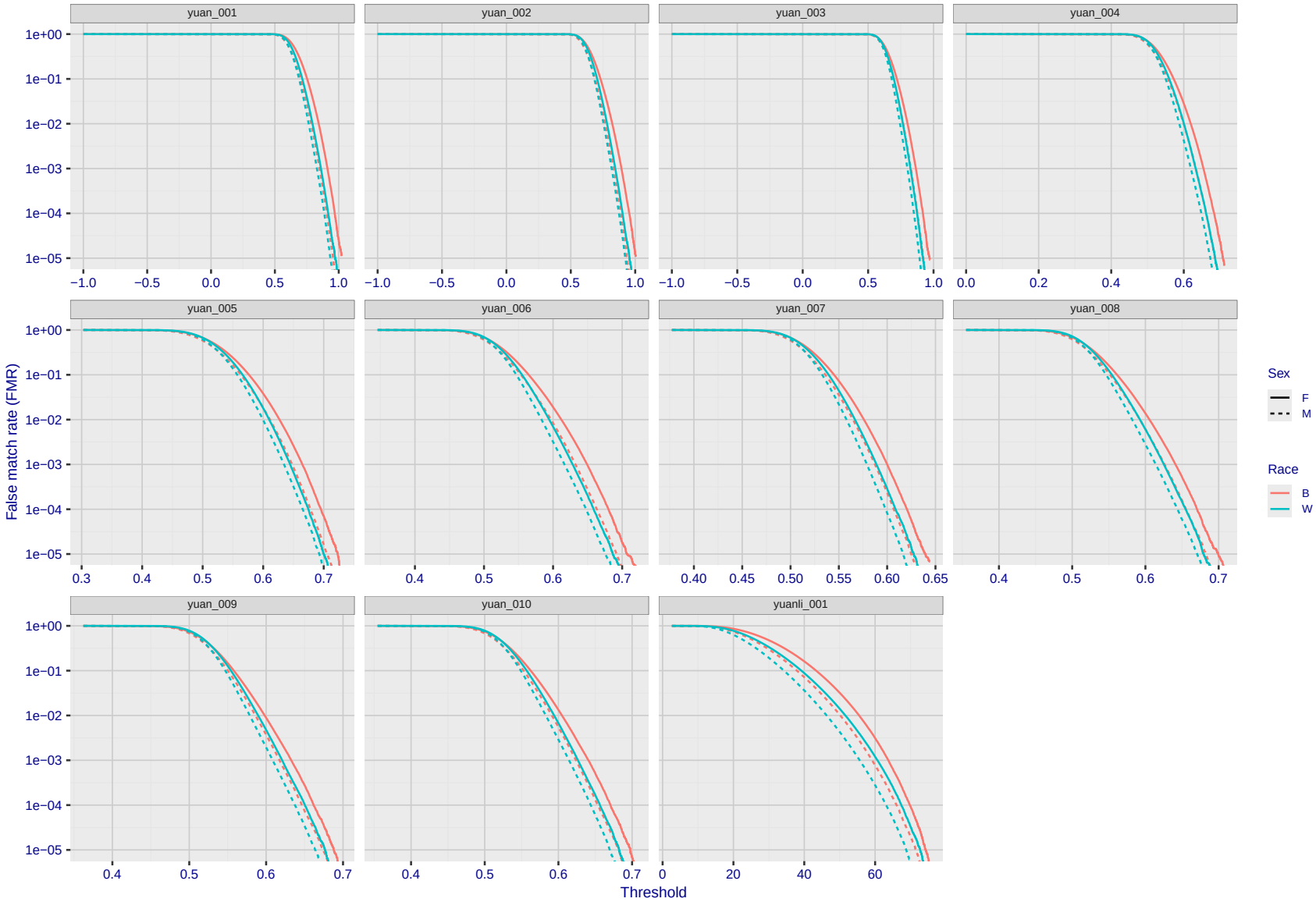

Figure 608: For the mugshot images, the false match calibration curves show false match rate vs. threshold. Separate curves appear for white females, black females, black males and white males.

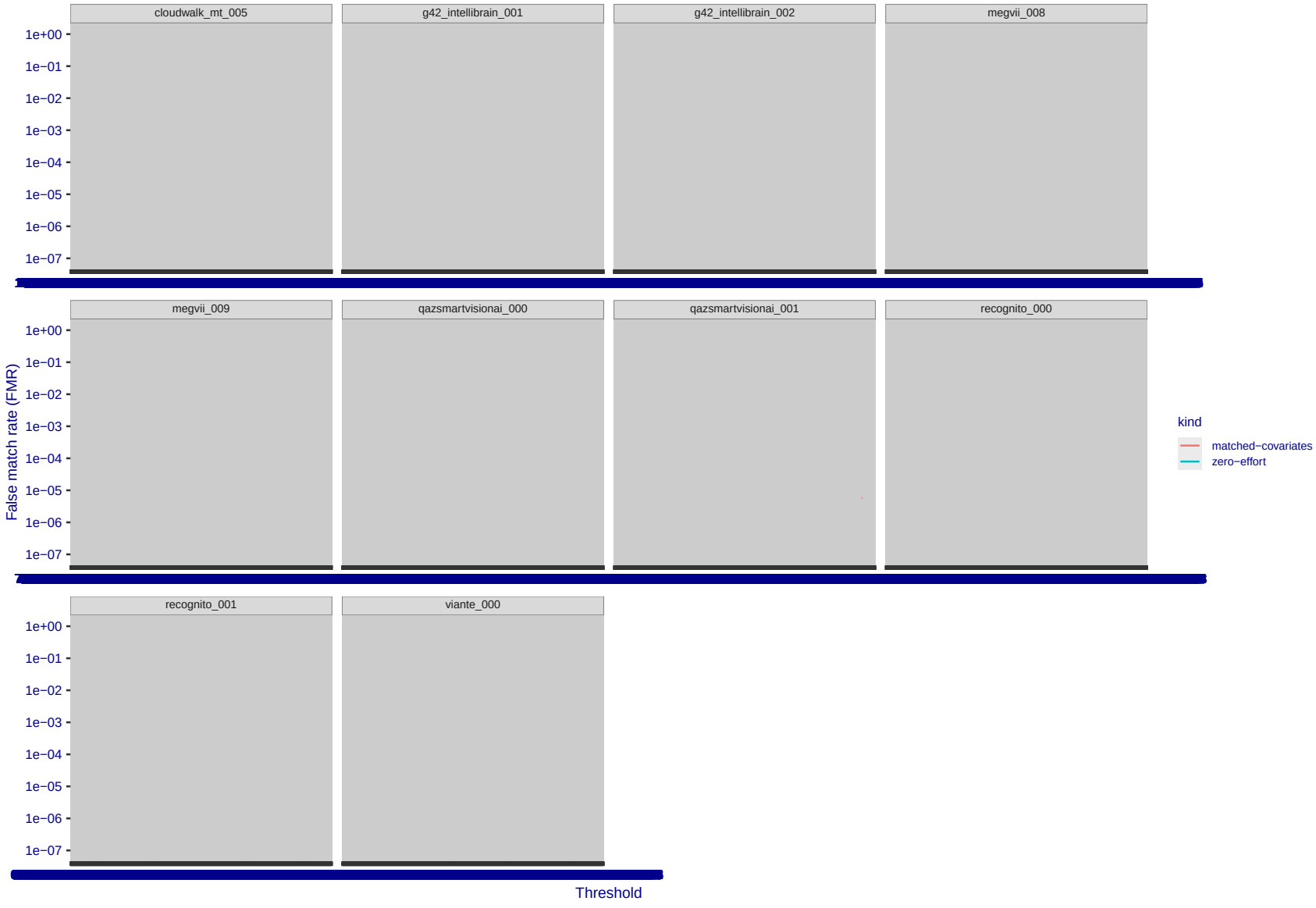

Figure 609: For the visa images, the false match calibration curves show FMR vs. threshold, T. The blue (lower) curves are for zero-effort impostors (i.e. comparing all images against all). The red (upper) curves are for persons of the same-sex, same-age, and same national-origin. This shows that FMR is underestimated (by a factor of 10 or more) by using a zero-effort impostor calculation to calibrate T. As shown later (sec. 3.6), FMR is higher for demographic-matched impostors.

3.5 Genuine distribution stability

3.5.1 Effect of birth place on the genuine distribution

Background: Both skin tone and bone structure vary geographically. Prior studies have reported variations in FNMR and FMR.

Goal: To measure false non-match rate (FNMR) variation with country of birth.

Methods: Thresholds are determined that give FMR = $\{0.001, 0.0001\}$ over the entire impostor set. Then FNMR is measured over 1000 bootstrap replications of the genuine scores. Only those countries with at least 140 individuals are included in the analysis.

Results: Figure 699 shows FNMR by country of birth for the two thresholds.

FNMR(T) "False non-match rate"
FMR(T) "False match rate"

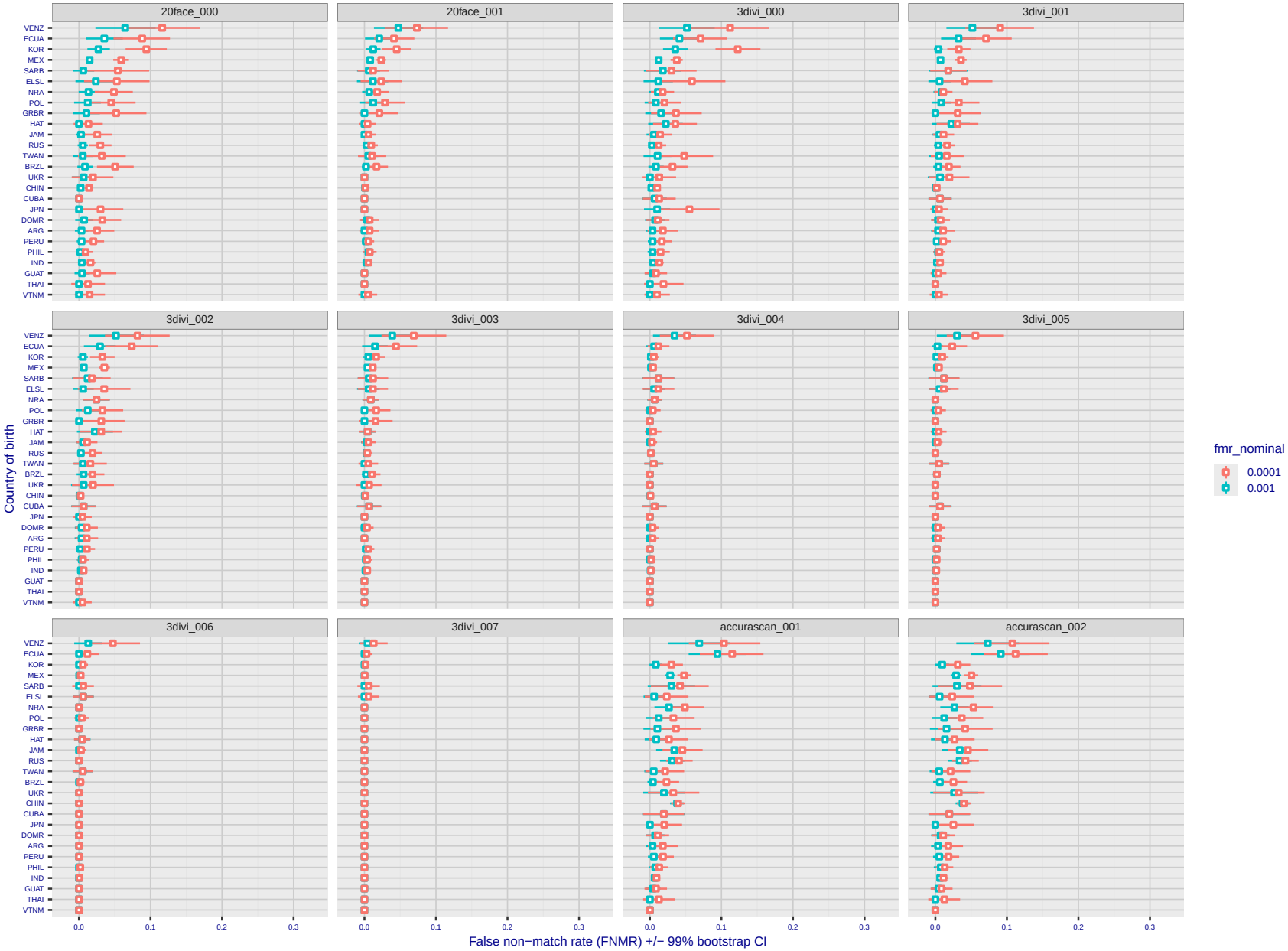

Figure 610: For the visa images, the dots show FNMR by country of birth for two globally set operating thresholds corresponding to FMR = $\{0.001, 0.0001\}$ computed over all on the order of 10^{10} impostor scores. The FMR in each bin will vary also - see subsequent impostor heatmaps in sec. 3.6.1. The figures shows an order of magnitude variation in FNMR across country of birth; these effects are likely due quality variations, then demographics like age and race. The error rates in some cases are zero, and in others the DET is flat so the error rates at the two thresholds are identical. The lines span 1% and 99% of boostrap replicated FNMR estimates.

Figure 611: For the visa images, the dots show FNMR by country of birth for two globally set operating thresholds corresponding to FMR = $\{0.001, 0.0001\}$ computed over all on the order of 10^{10} impostor scores. The FMR in each bin will vary also - see subsequent impostor heatmaps in sec. 3.6.1. The figures shows an order of magnitude variation in FNMR across country of birth; these effects are likely due quality variations, then demographics like age and race. The error rates in some cases are zero, and in others the DET is flat so the error rates at the two thresholds are identical. The lines span 1% and 99% of boostrap replicated FNMR estimates.

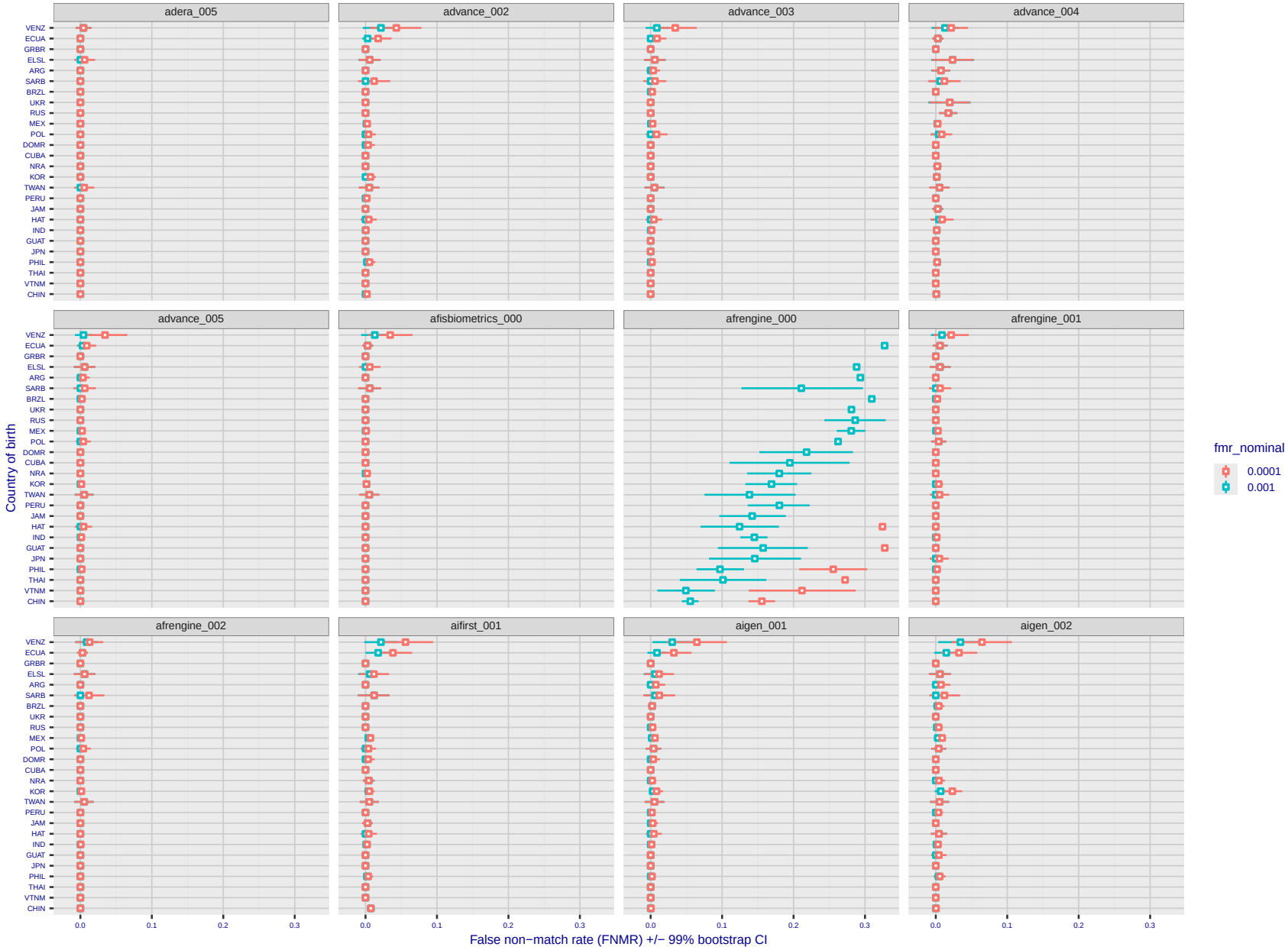

Figure 612: For the visa images, the dots show FNMR by country of birth for two globally set operating thresholds corresponding to FMR = $\{0.001, 0.0001\}$ computed over all on the order of 10^{10} impostor scores. The FMR in each bin will vary also - see subsequent impostor heatmaps in sec. 3.6.1. The figures shows an order of magnitude variation in FNMR across country of birth; these effects are likely due quality variations, then demographics like age and race. The error rates in some cases are zero, and in others the DET is flat so the error rates at the two thresholds are identical. The lines span 1% and 99% of boostrap replicated FNMR estimates.

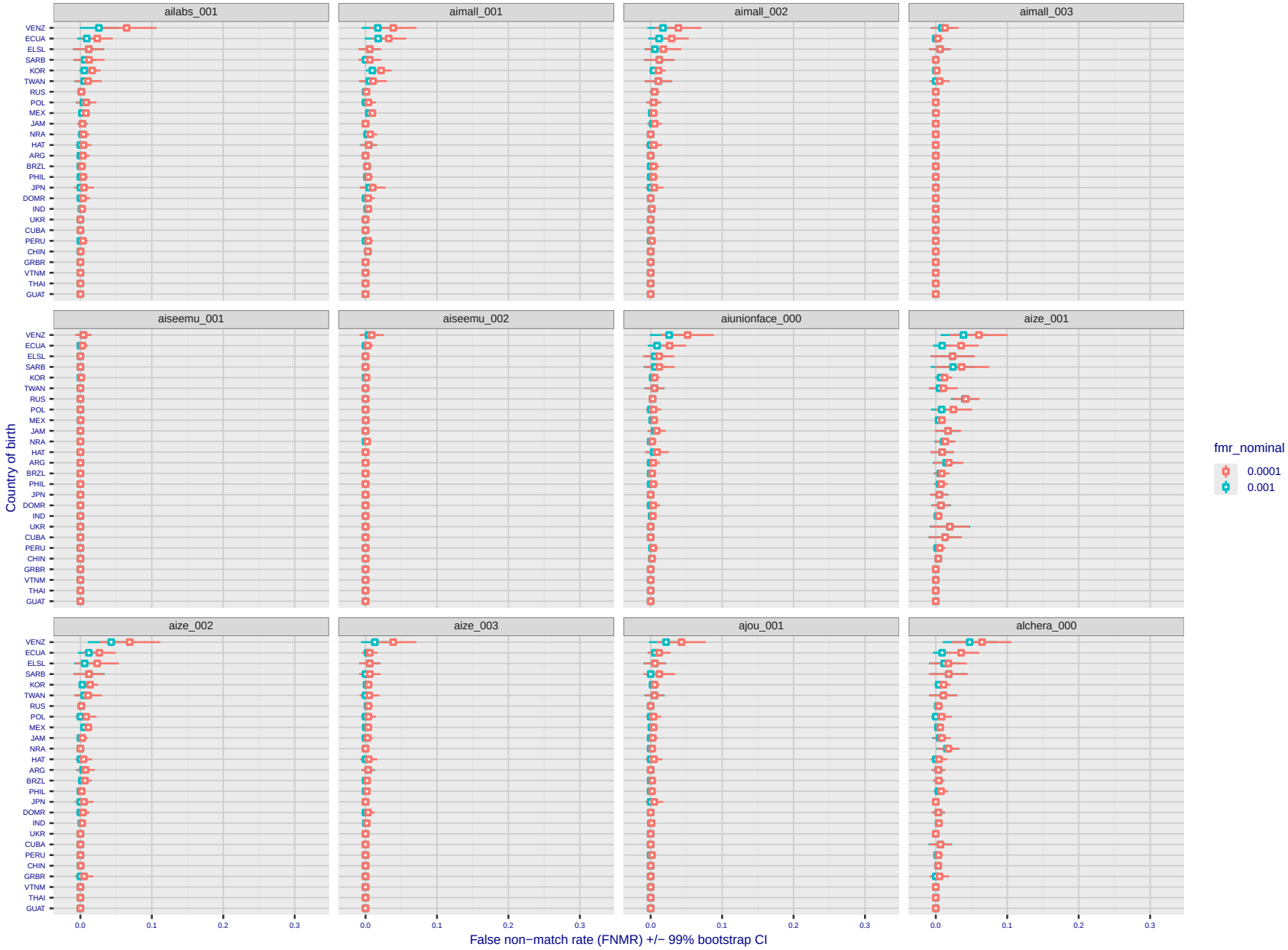

Figure 613: For the visa images, the dots show FNMR by country of birth for two globally set operating thresholds corresponding to FMR = $\{0.001, 0.0001\}$ computed over all on the order of 10^{10} impostor scores. The FMR in each bin will vary also - see subsequent impostor heatmaps in sec. 3.6.1. The figures shows an order of magnitude variation in FNMR across country of birth; these effects are likely due quality variations, then demographics like age and race. The error rates in some cases are zero, and in others the DET is flat so the error rates at the two thresholds are identical. The lines span 1% and 99% of boostrap replicated FNMR estimates.

Figure 614: For the visa images, the dots show FNMR by country of birth for two globally set operating thresholds corresponding to FMR = $\{0.001, 0.0001\}$ computed over all on the order of 10^{10} impostor scores. The FMR in each bin will vary also - see subsequent impostor heatmaps in sec. 3.6.1. The figures shows an order of magnitude variation in FNMR across country of birth; these effects are likely due quality variations, then demographics like age and race. The error rates in some cases are zero, and in others the DET is flat so the error rates at the two thresholds are identical. The lines span 1% and 99% of boostrap replicated FNMR estimates.

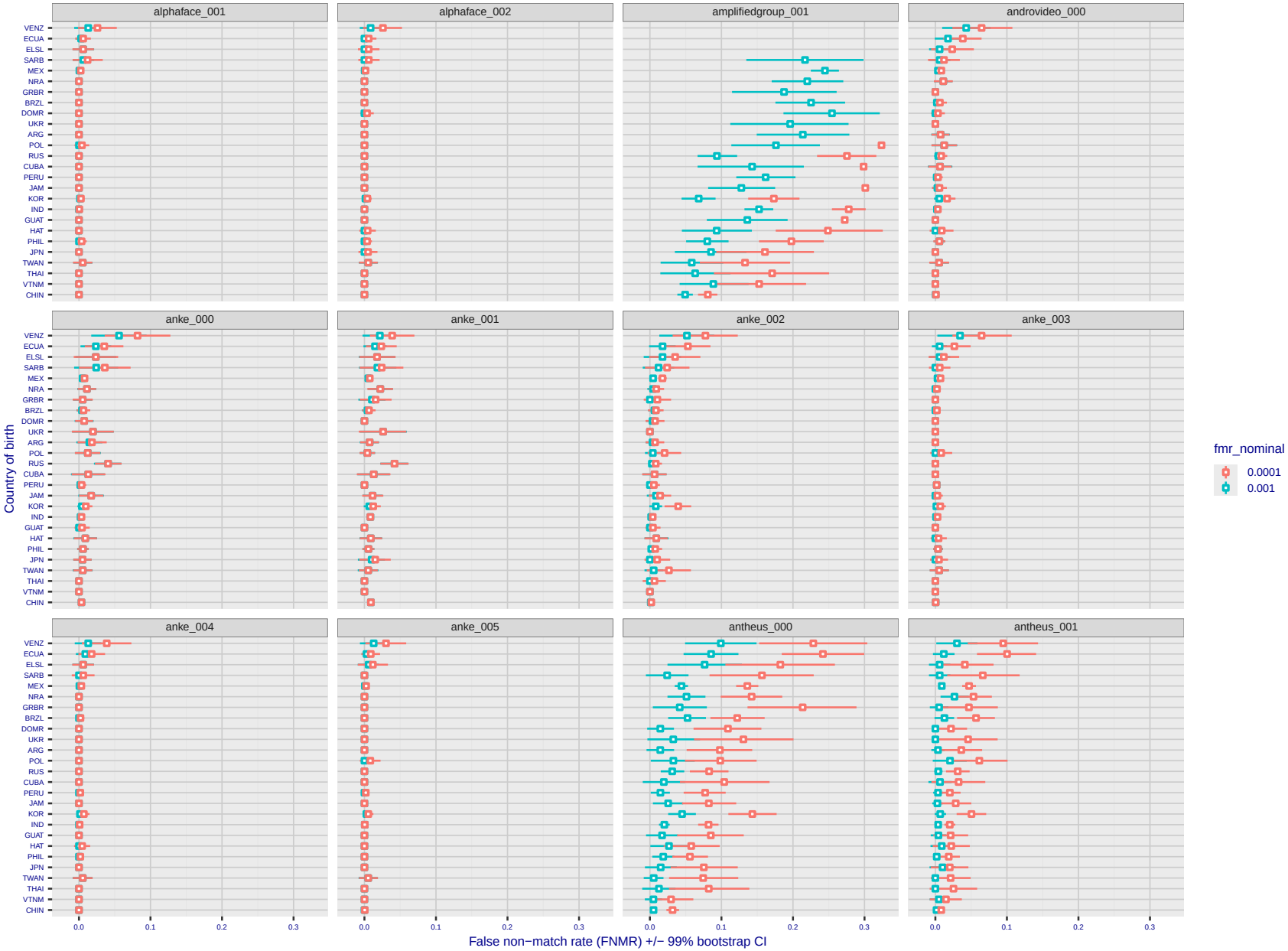

Figure 615: For the visa images, the dots show FNMR by country of birth for two globally set operating thresholds corresponding to FMR = $\{0.001, 0.0001\}$ computed over all on the order of 10^{10} impostor scores. The FMR in each bin will vary also - see subsequent impostor heatmaps in sec. 3.6.1. The figures shows an order of magnitude variation in FNMR across country of birth; these effects are likely due quality variations, then demographics like age and race. The error rates in some cases are zero, and in others the DET is flat so the error rates at the two thresholds are identical. The lines span 1% and 99% of boostrap replicated FNMR estimates.

Figure 616: For the visa images, the dots show FNMR by country of birth for two globally set operating thresholds corresponding to FMR = $\{0.001, 0.0001\}$ computed over all on the order of 10^{10} impostor scores. The FMR in each bin will vary also - see subsequent impostor heatmaps in sec. 3.6.1. The figures shows an order of magnitude variation in FNMR across country of birth; these effects are likely due quality variations, then demographics like age and race. The error rates in some cases are zero, and in others the DET is flat so the error rates at the two thresholds are identical. The lines span 1% and 99% of boostrap replicated FNMR estimates.

Figure 617: For the visa images, the dots show FNMR by country of birth for two globally set operating thresholds corresponding to FMR = $\{0.001, 0.0001\}$ computed over all on the order of 10^{10} impostor scores. The FMR in each bin will vary also - see subsequent impostor heatmaps in sec. 3.6.1. The figures shows an order of magnitude variation in FNMR across country of birth; these effects are likely due quality variations, then demographics like age and race. The error rates in some cases are zero, and in others the DET is flat so the error rates at the two thresholds are identical. The lines span 1% and 99% of boostrap replicated FNMR estimates.

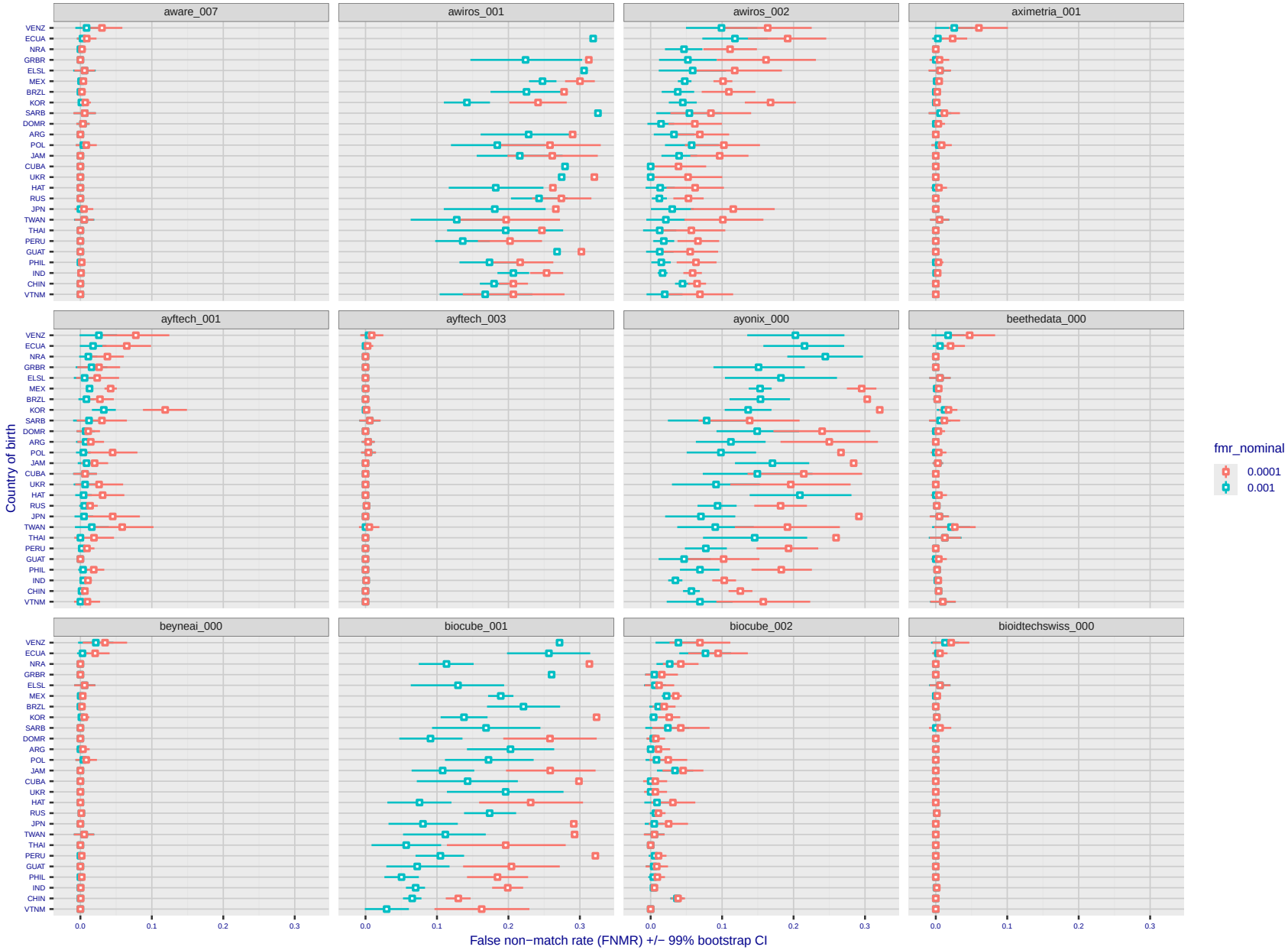

Figure 618: For the visa images, the dots show FNMR by country of birth for two globally set operating thresholds corresponding to FMR = $\{0.001, 0.0001\}$ computed over all on the order of 10^{10} impostor scores. The FMR in each bin will vary also - see subsequent impostor heatmaps in sec. 3.6.1. The figures shows an order of magnitude variation in FNMR across country of birth; these effects are likely due quality variations, then demographics like age and race. The error rates in some cases are zero, and in others the DET is flat so the error rates at the two thresholds are identical. The lines span 1% and 99% of boostrap replicated FNMR estimates.

Figure 619: For the visa images, the dots show FNMR by country of birth for two globally set operating thresholds corresponding to FMR = $\{0.001, 0.0001\}$ computed over all on the order of 10^{10} impostor scores. The FMR in each bin will vary also - see subsequent impostor heatmaps in sec. 3.6.1. The figures shows an order of magnitude variation in FNMR across country of birth; these effects are likely due quality variations, then demographics like age and race. The error rates in some cases are zero, and in others the DET is flat so the error rates at the two thresholds are identical. The lines span 1% and 99% of boostrap replicated FNMR estimates.

Figure 620: For the visa images, the dots show FNMR by country of birth for two globally set operating thresholds corresponding to FMR = $\{0.001, 0.0001\}$ computed over all on the order of 10^{10} impostor scores. The FMR in each bin will vary also - see subsequent impostor heatmaps in sec. 3.6.1. The figures shows an order of magnitude variation in FNMR across country of birth; these effects are likely due quality variations, then demographics like age and race. The error rates in some cases are zero, and in others the DET is flat so the error rates at the two thresholds are identical. The lines span 1% and 99% of boostrap replicated FNMR estimates.

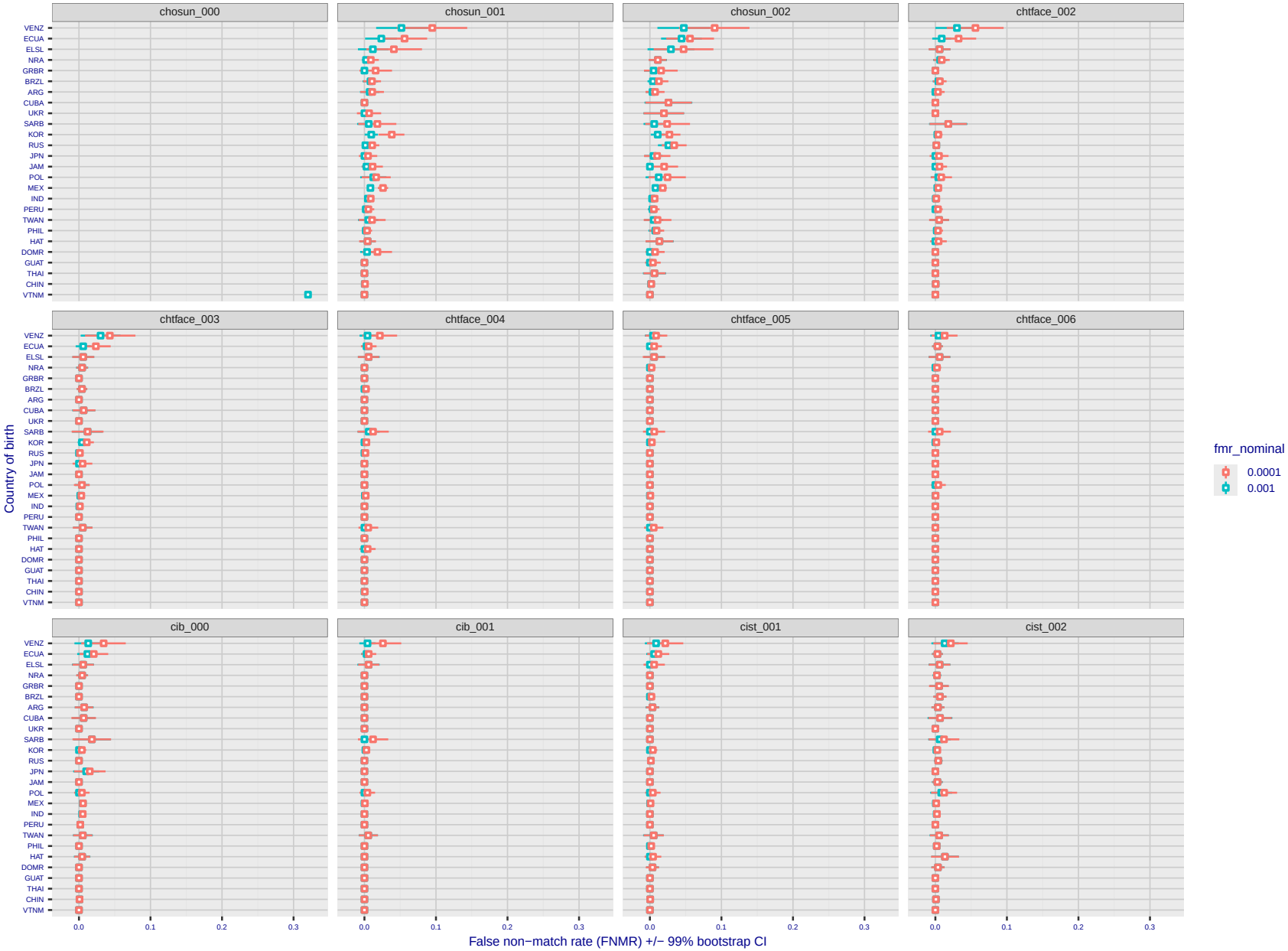

Figure 621: For the visa images, the dots show FNMR by country of birth for two globally set operating thresholds corresponding to FMR = $\{0.001, 0.0001\}$ computed over all on the order of 10^{10} impostor scores. The FMR in each bin will vary also - see subsequent impostor heatmaps in sec. 3.6.1. The figures shows an order of magnitude variation in FNMR across country of birth; these effects are likely due quality variations, then demographics like age and race. The error rates in some cases are zero, and in others the DET is flat so the error rates at the two thresholds are identical. The lines span 1% and 99% of boostrap replicated FNMR estimates.

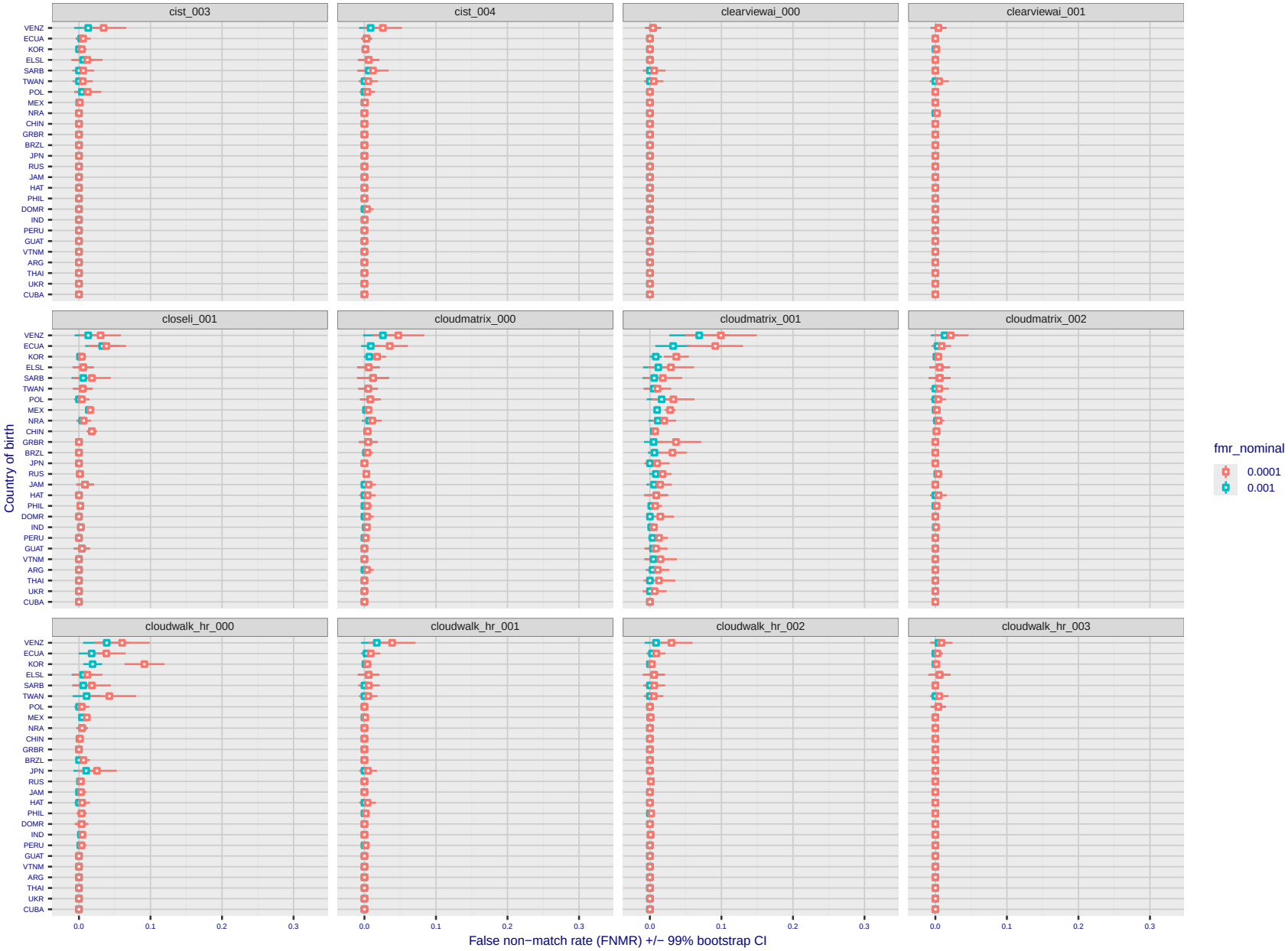

Figure 622: For the visa images, the dots show FNMR by country of birth for two globally set operating thresholds corresponding to FMR = $\{0.001, 0.0001\}$ computed over all on the order of 10^{10} impostor scores. The FMR in each bin will vary also - see subsequent impostor heatmaps in sec. 3.6.1. The figures shows an order of magnitude variation in FNMR across country of birth; these effects are likely due quality variations, then demographics like age and race. The error rates in some cases are zero, and in others the DET is flat so the error rates at the two thresholds are identical. The lines span 1% and 99% of boostrap replicated FNMR estimates.

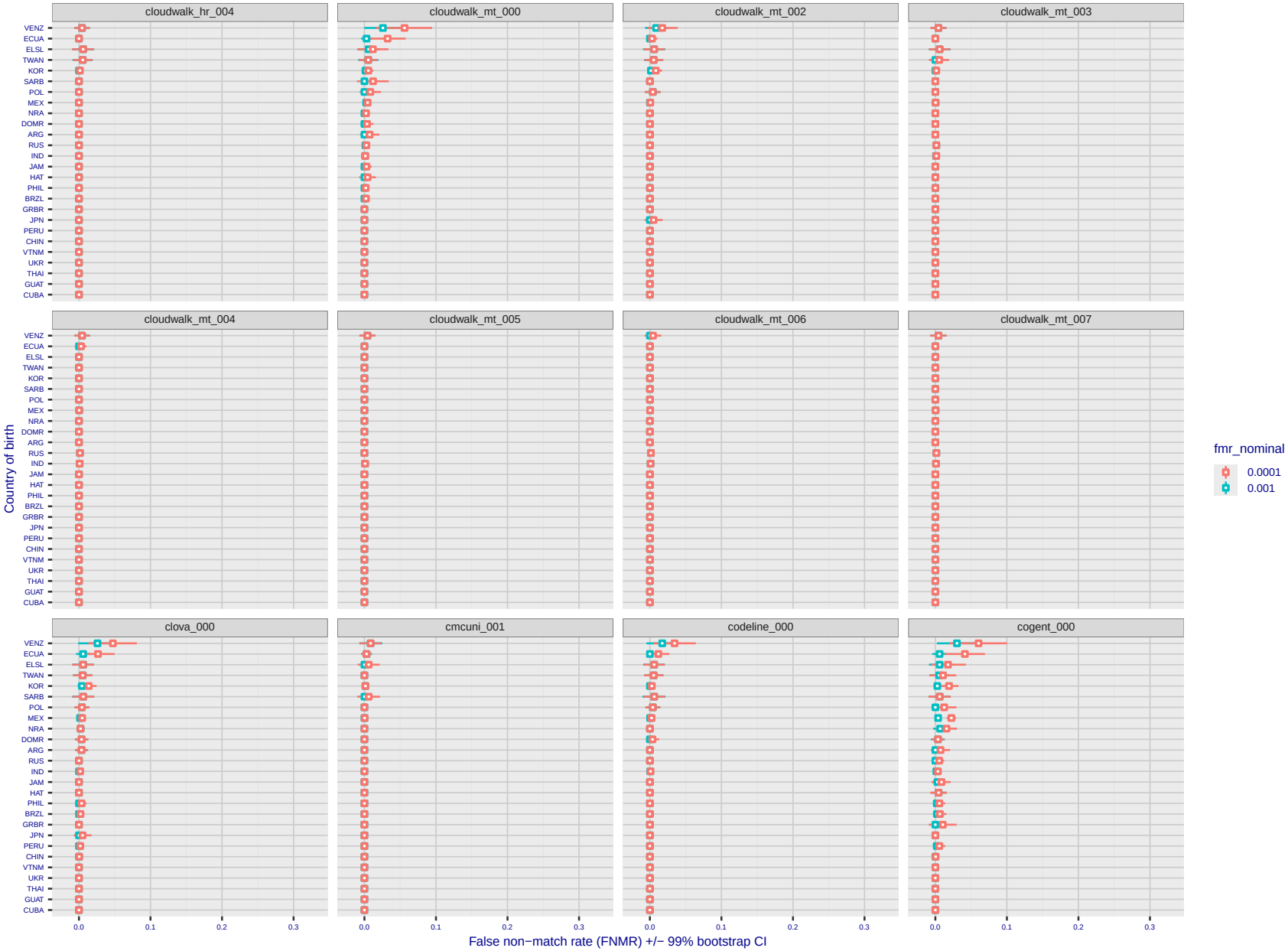

Figure 623: For the visa images, the dots show FNMR by country of birth for two globally set operating thresholds corresponding to FMR = $\{0.001, 0.0001\}$ computed over all on the order of 10^{10} impostor scores. The FMR in each bin will vary also - see subsequent impostor heatmaps in sec. 3.6.1. The figures shows an order of magnitude variation in FNMR across country of birth; these effects are likely due quality variations, then demographics like age and race. The error rates in some cases are zero, and in others the DET is flat so the error rates at the two thresholds are identical. The lines span 1% and 99% of boostrap replicated FNMR estimates.

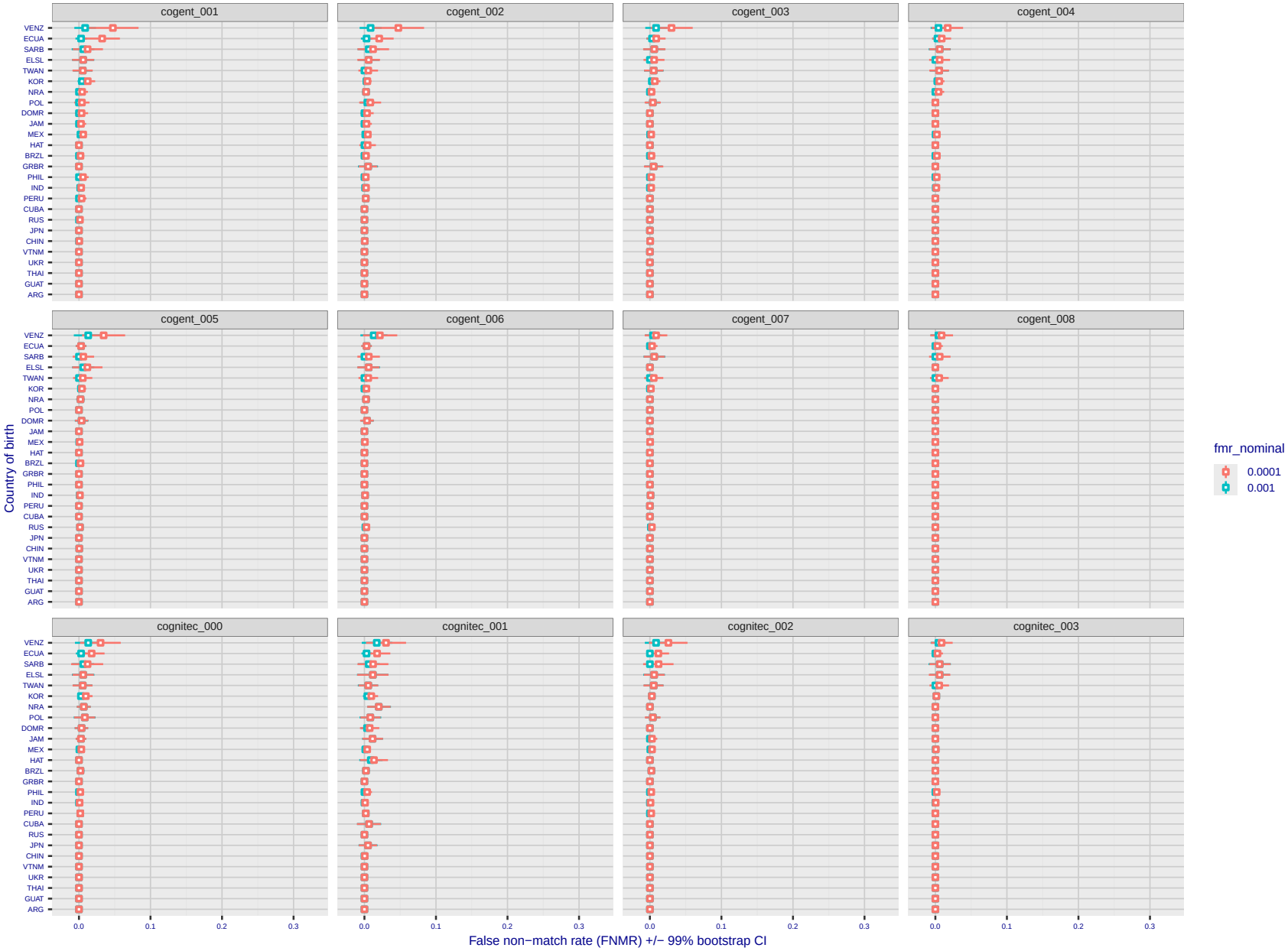

Figure 624: For the visa images, the dots show FNMR by country of birth for two globally set operating thresholds corresponding to FMR = $\{0.001, 0.0001\}$ computed over all on the order of 10^{10} impostor scores. The FMR in each bin will vary also - see subsequent impostor heatmaps in sec. 3.6.1. The figures shows an order of magnitude variation in FNMR across country of birth; these effects are likely due quality variations, then demographics like age and race. The error rates in some cases are zero, and in others the DET is flat so the error rates at the two thresholds are identical. The lines span 1% and 99% of boostrap replicated FNMR estimates.

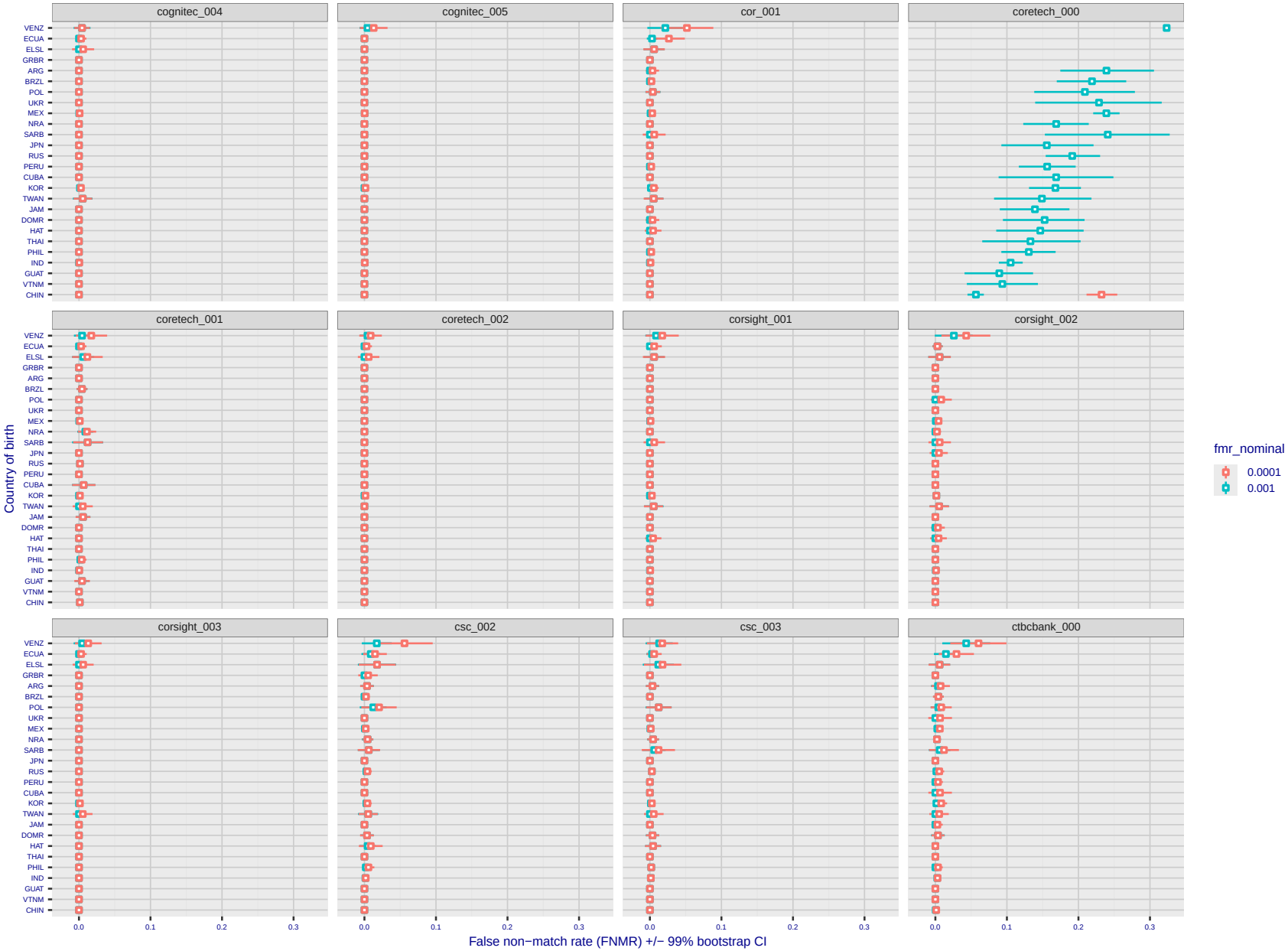

Figure 625: For the visa images, the dots show FNMR by country of birth for two globally set operating thresholds corresponding to FMR = $\{0.001, 0.0001\}$ computed over all on the order of 10^{10} impostor scores. The FMR in each bin will vary also - see subsequent impostor heatmaps in sec. 3.6.1. The figures shows an order of magnitude variation in FNMR across country of birth; these effects are likely due quality variations, then demographics like age and race. The error rates in some cases are zero, and in others the DET is flat so the error rates at the two thresholds are identical. The lines span 1% and 99% of boostrap replicated FNMR estimates.

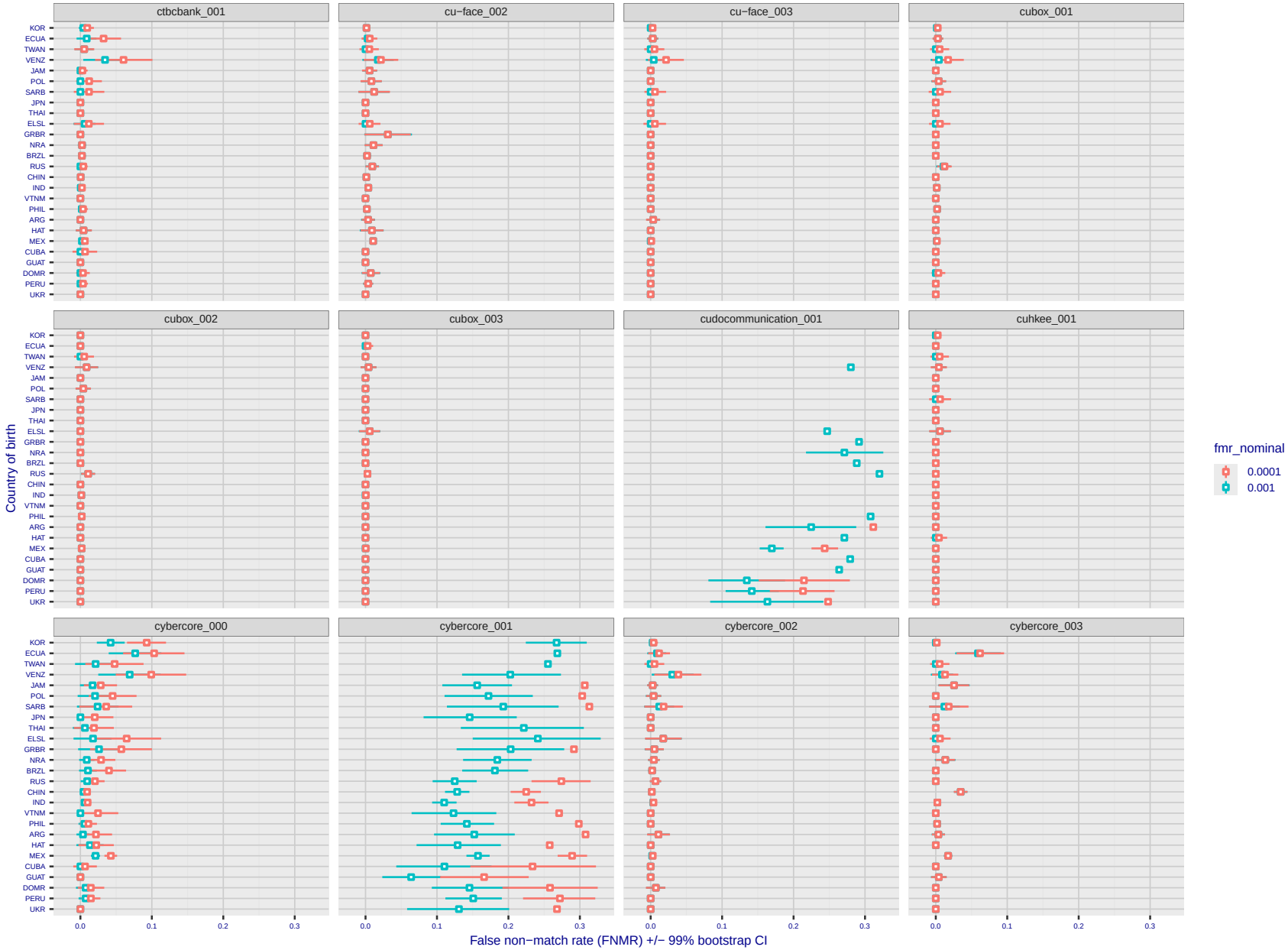

Figure 626: For the visa images, the dots show FNMR by country of birth for two globally set operating thresholds corresponding to FMR = $\{0.001, 0.0001\}$ computed over all on the order of 10^{10} impostor scores. The FMR in each bin will vary also - see subsequent impostor heatmaps in sec. 3.6.1. The figures shows an order of magnitude variation in FNMR across country of birth; these effects are likely due quality variations, then demographics like age and race. The error rates in some cases are zero, and in others the DET is flat so the error rates at the two thresholds are identical. The lines span 1% and 99% of boostrap replicated FNMR estimates.

Figure 627: For the visa images, the dots show FNMR by country of birth for two globally set operating thresholds corresponding to FMR = $\{0.001, 0.0001\}$ computed over all on the order of 10^{10} impostor scores. The FMR in each bin will vary also - see subsequent impostor heatmaps in sec. 3.6.1. The figures shows an order of magnitude variation in FNMR across country of birth; these effects are likely due quality variations, then demographics like age and race. The error rates in some cases are zero, and in others the DET is flat so the error rates at the two thresholds are identical. The lines span 1% and 99% of boostrap replicated FNMR estimates.

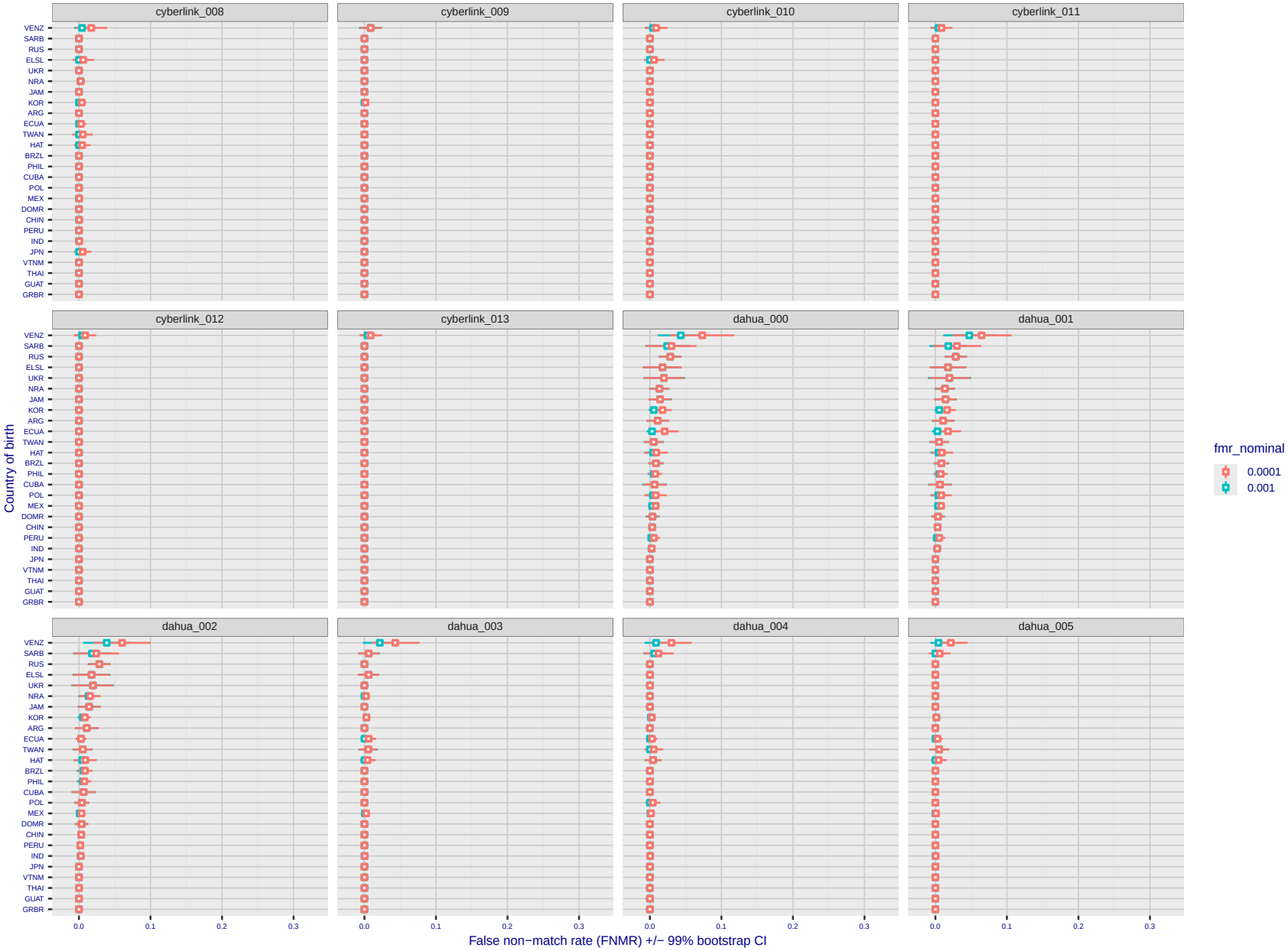

Figure 628: For the visa images, the dots show FNMR by country of birth for two globally set operating thresholds corresponding to FMR = $\{0.001, 0.0001\}$ computed over all on the order of 10^{10} impostor scores. The FMR in each bin will vary also - see subsequent impostor heatmaps in sec. 3.6.1. The figures shows an order of magnitude variation in FNMR across country of birth; these effects are likely due quality variations, then demographics like age and race. The error rates in some cases are zero, and in others the DET is flat so the error rates at the two thresholds are identical. The lines span 1% and 99% of boostrap replicated FNMR estimates.

Figure 629: For the visa images, the dots show FNMR by country of birth for two globally set operating thresholds corresponding to FMR = $\{0.001, 0.0001\}$ computed over all on the order of 10^{10} impostor scores. The FMR in each bin will vary also - see subsequent impostor heatmaps in sec. 3.6.1. The figures shows an order of magnitude variation in FNMR across country of birth; these effects are likely due quality variations, then demographics like age and race. The error rates in some cases are zero, and in others the DET is flat so the error rates at the two thresholds are identical. The lines span 1% and 99% of boostrap replicated FNMR estimates.

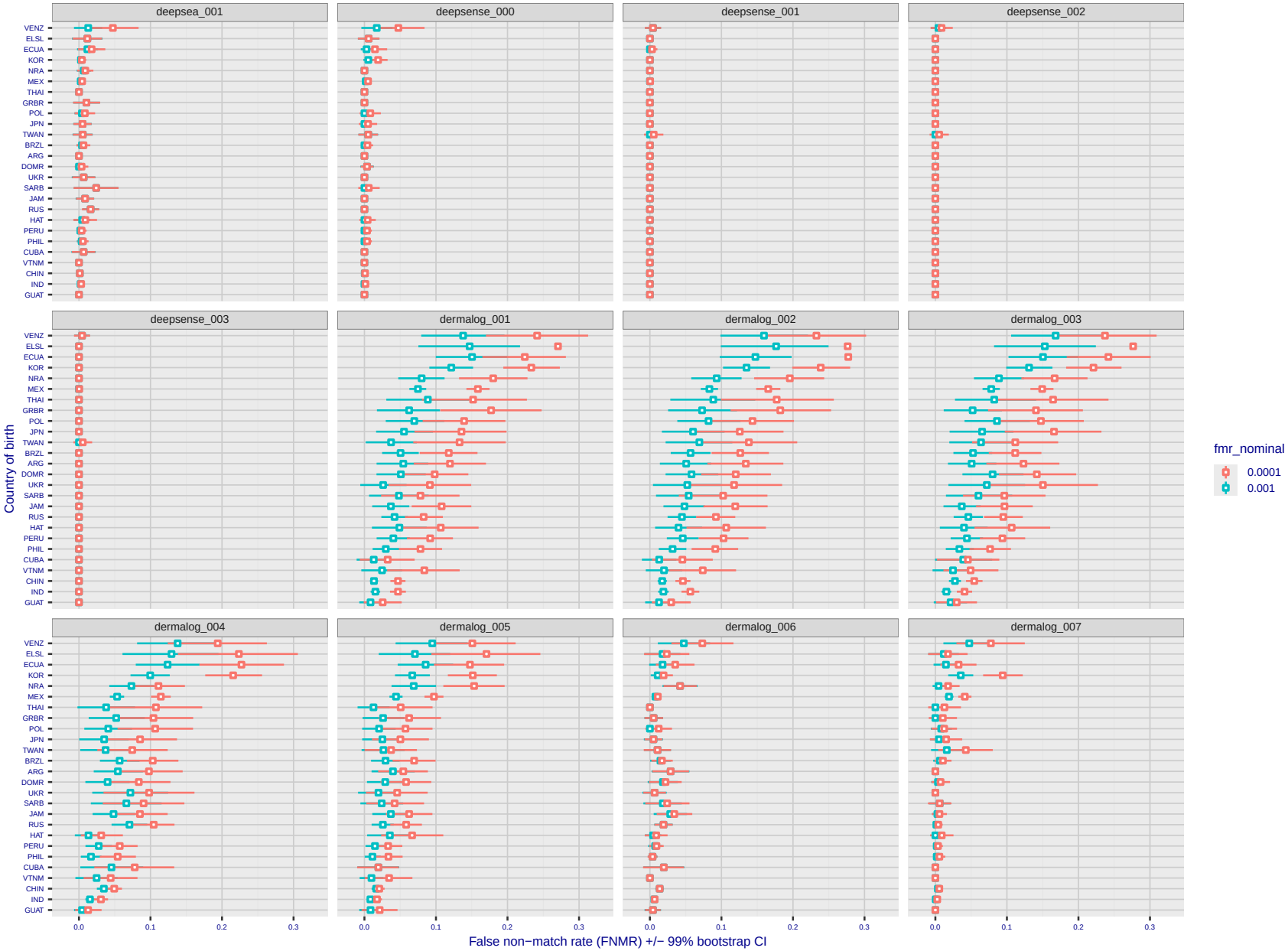

Figure 630: For the visa images, the dots show FNMR by country of birth for two globally set operating thresholds corresponding to FMR = $\{0.001, 0.0001\}$ computed over all on the order of 10^{10} impostor scores. The FMR in each bin will vary also - see subsequent impostor heatmaps in sec. 3.6.1. The figures shows an order of magnitude variation in FNMR across country of birth; these effects are likely due quality variations, then demographics like age and race. The error rates in some cases are zero, and in others the DET is flat so the error rates at the two thresholds are identical. The lines span 1% and 99% of boostrap replicated FNMR estimates.

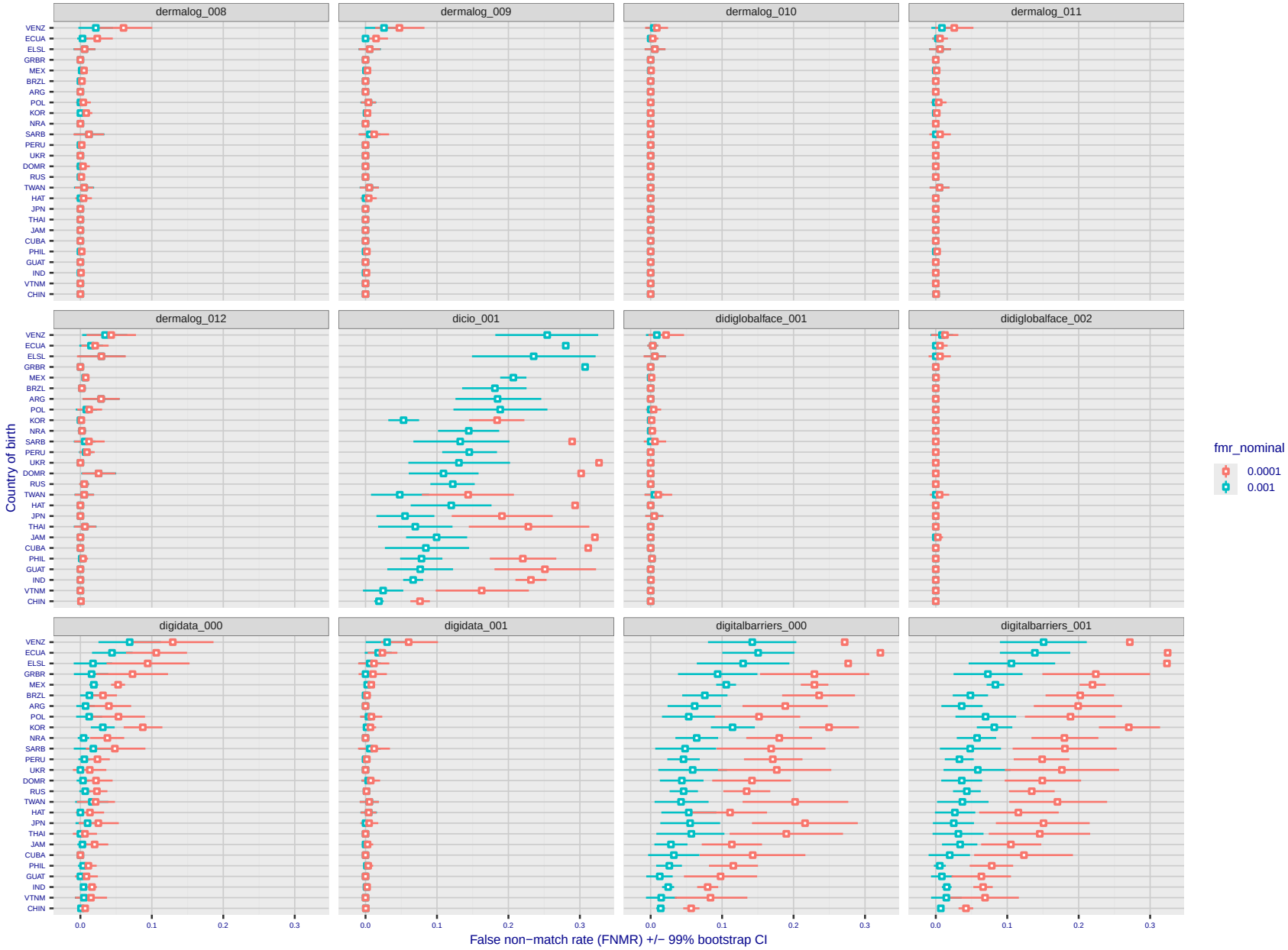

Figure 631: For the visa images, the dots show FNMR by country of birth for two globally set operating thresholds corresponding to FMR = $\{0.001, 0.0001\}$ computed over all on the order of 10^{10} impostor scores. The FMR in each bin will vary also - see subsequent impostor heatmaps in sec. 3.6.1. The figures shows an order of magnitude variation in FNMR across country of birth; these effects are likely due quality variations, then demographics like age and race. The error rates in some cases are zero, and in others the DET is flat so the error rates at the two thresholds are identical. The lines span 1% and 99% of boostrap replicated FNMR estimates.

Figure 632: For the visa images, the dots show FNMR by country of birth for two globally set operating thresholds corresponding to FMR = $\{0.001, 0.0001\}$ computed over all on the order of 10^{10} impostor scores. The FMR in each bin will vary also - see subsequent impostor heatmaps in sec. 3.6.1. The figures shows an order of magnitude variation in FNMR across country of birth; these effects are likely due quality variations, then demographics like age and race. The error rates in some cases are zero, and in others the DET is flat so the error rates at the two thresholds are identical. The lines span 1% and 99% of boostrap replicated FNMR estimates.

Figure 633: For the visa images, the dots show FNMR by country of birth for two globally set operating thresholds corresponding to FMR = $\{0.001, 0.0001\}$ computed over all on the order of 10^{10} impostor scores. The FMR in each bin will vary also - see subsequent impostor heatmaps in sec. 3.6.1. The figures shows an order of magnitude variation in FNMR across country of birth; these effects are likely due quality variations, then demographics like age and race. The error rates in some cases are zero, and in others the DET is flat so the error rates at the two thresholds are identical. The lines span 1% and 99% of boostrap replicated FNMR estimates.

Figure 634: For the visa images, the dots show FNMR by country of birth for two globally set operating thresholds corresponding to FMR = $\{0.001, 0.0001\}$ computed over all on the order of 10^{10} impostor scores. The FMR in each bin will vary also - see subsequent impostor heatmaps in sec. 3.6.1. The figures shows an order of magnitude variation in FNMR across country of birth; these effects are likely due quality variations, then demographics like age and race. The error rates in some cases are zero, and in others the DET is flat so the error rates at the two thresholds are identical. The lines span 1% and 99% of boostrap replicated FNMR estimates.

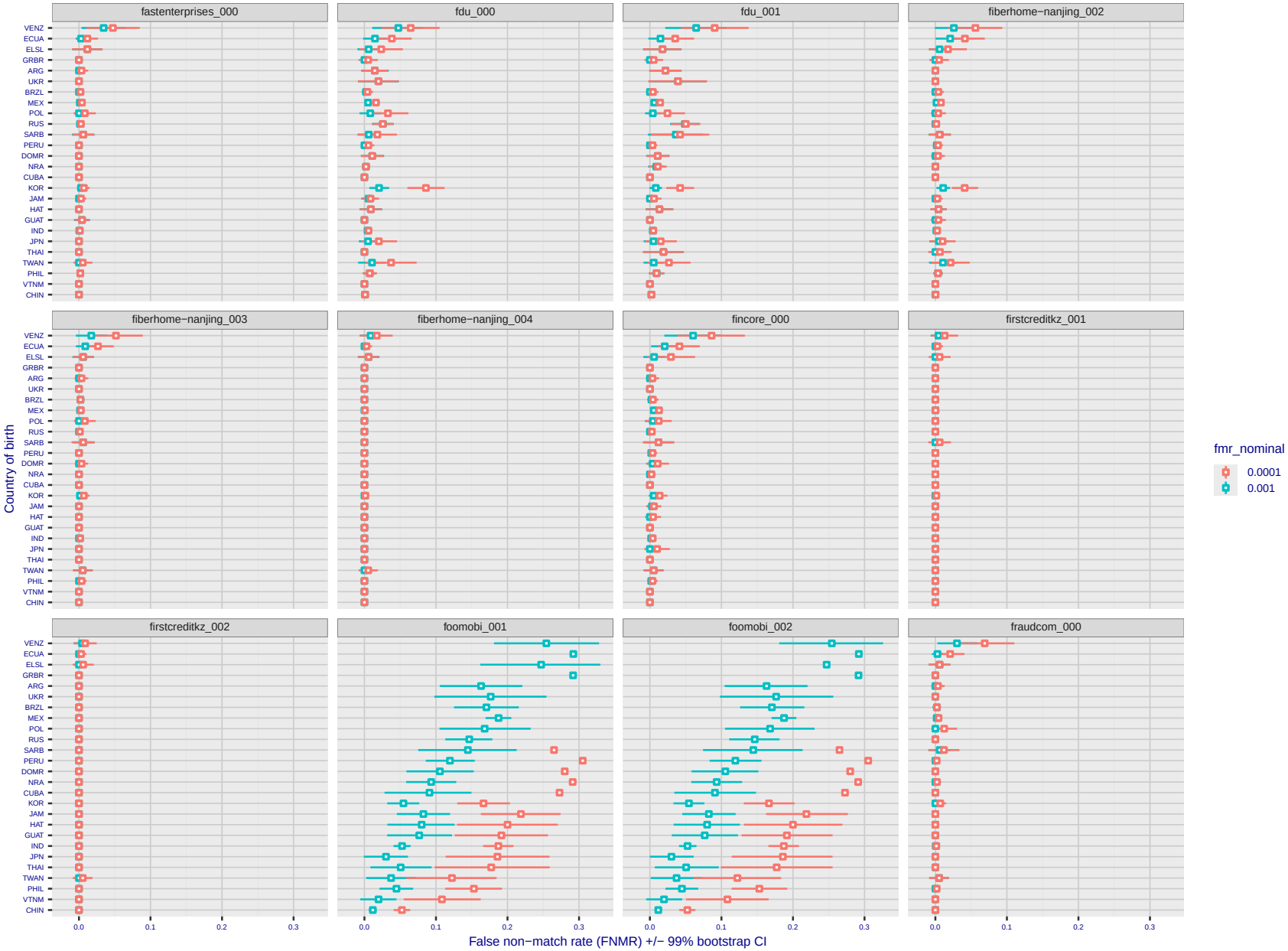

Figure 635: For the visa images, the dots show FNMR by country of birth for two globally set operating thresholds corresponding to FMR = $\{0.001, 0.0001\}$ computed over all on the order of 10^{10} impostor scores. The FMR in each bin will vary also - see subsequent impostor heatmaps in sec. 3.6.1. The figures shows an order of magnitude variation in FNMR across country of birth; these effects are likely due quality variations, then demographics like age and race. The error rates in some cases are zero, and in others the DET is flat so the error rates at the two thresholds are identical. The lines span 1% and 99% of boostrap replicated FNMR estimates.

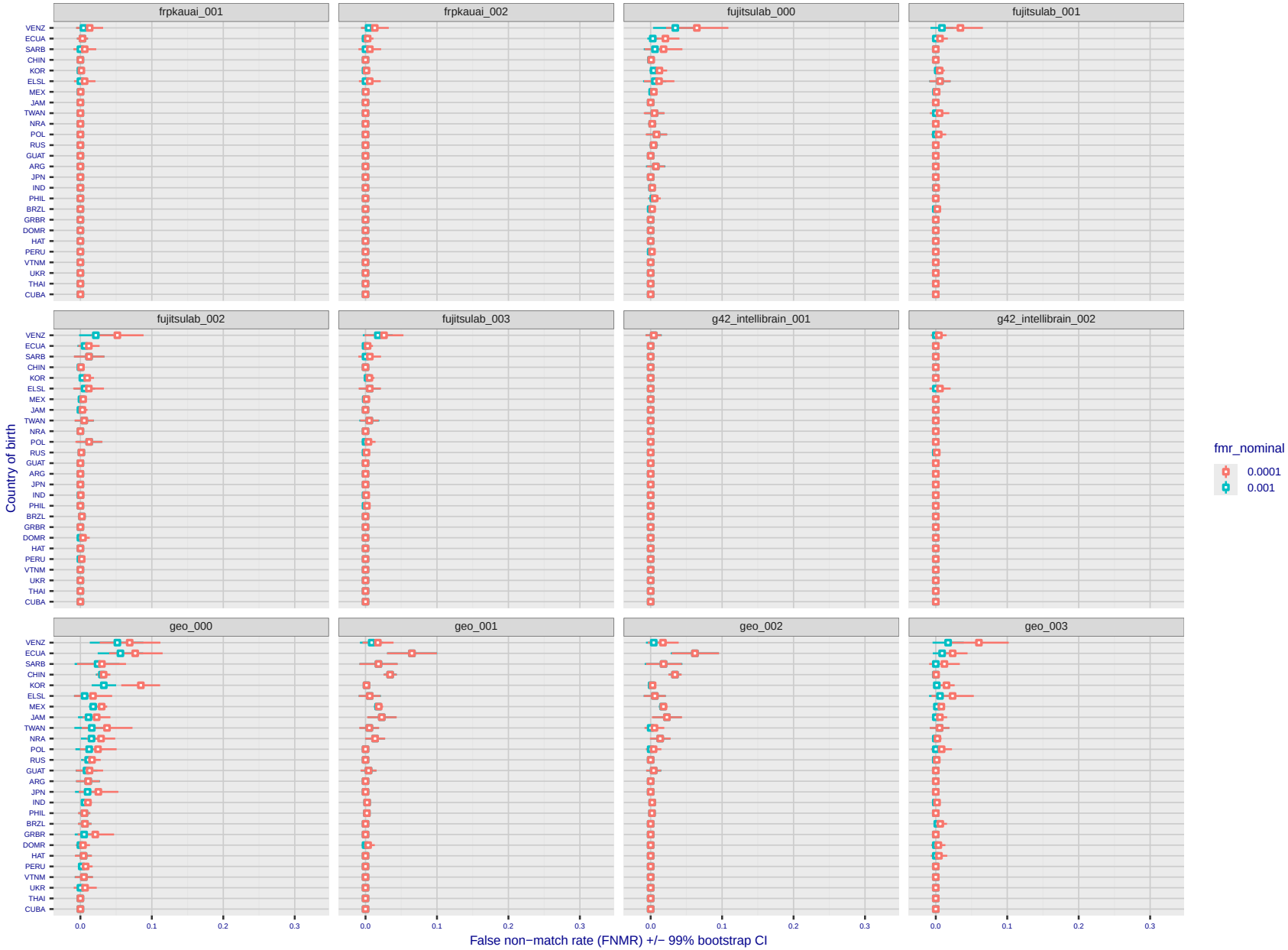

Figure 636: For the visa images, the dots show FNMR by country of birth for two globally set operating thresholds corresponding to FMR = $\{0.001, 0.0001\}$ computed over all on the order of 10^{10} impostor scores. The FMR in each bin will vary also - see subsequent impostor heatmaps in sec. 3.6.1. The figures shows an order of magnitude variation in FNMR across country of birth; these effects are likely due quality variations, then demographics like age and race. The error rates in some cases are zero, and in others the DET is flat so the error rates at the two thresholds are identical. The lines span 1% and 99% of boostrap replicated FNMR estimates.

Figure 637: For the visa images, the dots show FNMR by country of birth for two globally set operating thresholds corresponding to FMR = $\{0.001, 0.0001\}$ computed over all on the order of 10^{10} impostor scores. The FMR in each bin will vary also - see subsequent impostor heatmaps in sec. 3.6.1. The figures shows an order of magnitude variation in FNMR across country of birth; these effects are likely due quality variations, then demographics like age and race. The error rates in some cases are zero, and in others the DET is flat so the error rates at the two thresholds are identical. The lines span 1% and 99% of boostrap replicated FNMR estimates.

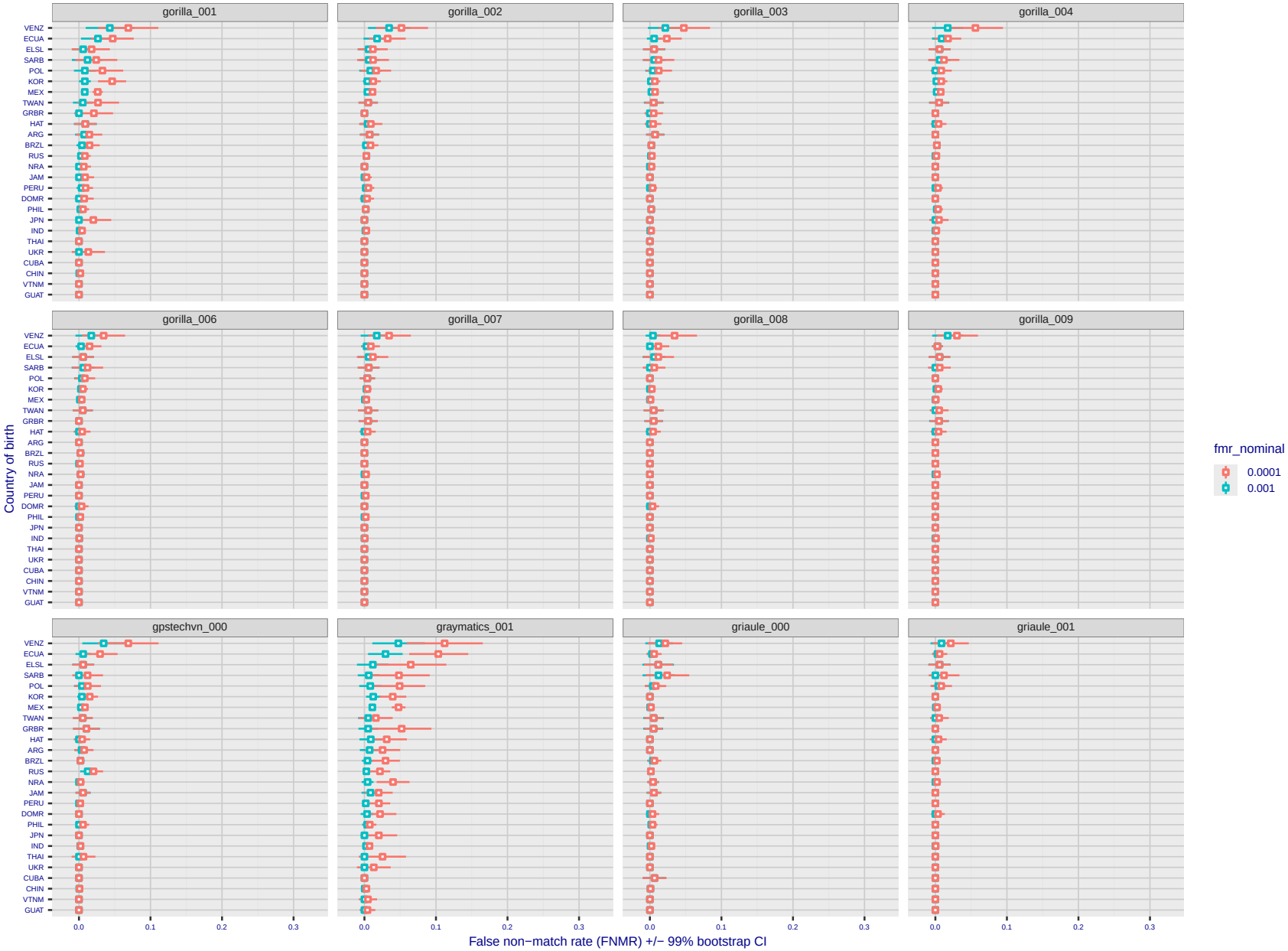

Figure 638: For the visa images, the dots show FNMR by country of birth for two globally set operating thresholds corresponding to FMR = $\{0.001, 0.0001\}$ computed over all on the order of 10^{10} impostor scores. The FMR in each bin will vary also - see subsequent impostor heatmaps in sec. 3.6.1. The figures shows an order of magnitude variation in FNMR across country of birth; these effects are likely due quality variations, then demographics like age and race. The error rates in some cases are zero, and in others the DET is flat so the error rates at the two thresholds are identical. The lines span 1% and 99% of boostrap replicated FNMR estimates.

Figure 639: For the visa images, the dots show FNMR by country of birth for two globally set operating thresholds corresponding to FMR = $\{0.001, 0.0001\}$ computed over all on the order of 10^{10} impostor scores. The FMR in each bin will vary also - see subsequent impostor heatmaps in sec. 3.6.1. The figures shows an order of magnitude variation in FNMR across country of birth; these effects are likely due quality variations, then demographics like age and race. The error rates in some cases are zero, and in others the DET is flat so the error rates at the two thresholds are identical. The lines span 1% and 99% of boostrap replicated FNMR estimates.

Figure 640: For the visa images, the dots show FNMR by country of birth for two globally set operating thresholds corresponding to FMR = $\{0.001, 0.0001\}$ computed over all on the order of 10^{10} impostor scores. The FMR in each bin will vary also - see subsequent impostor heatmaps in sec. 3.6.1. The figures shows an order of magnitude variation in FNMR across country of birth; these effects are likely due quality variations, then demographics like age and race. The error rates in some cases are zero, and in others the DET is flat so the error rates at the two thresholds are identical. The lines span 1% and 99% of boostrap replicated FNMR estimates.

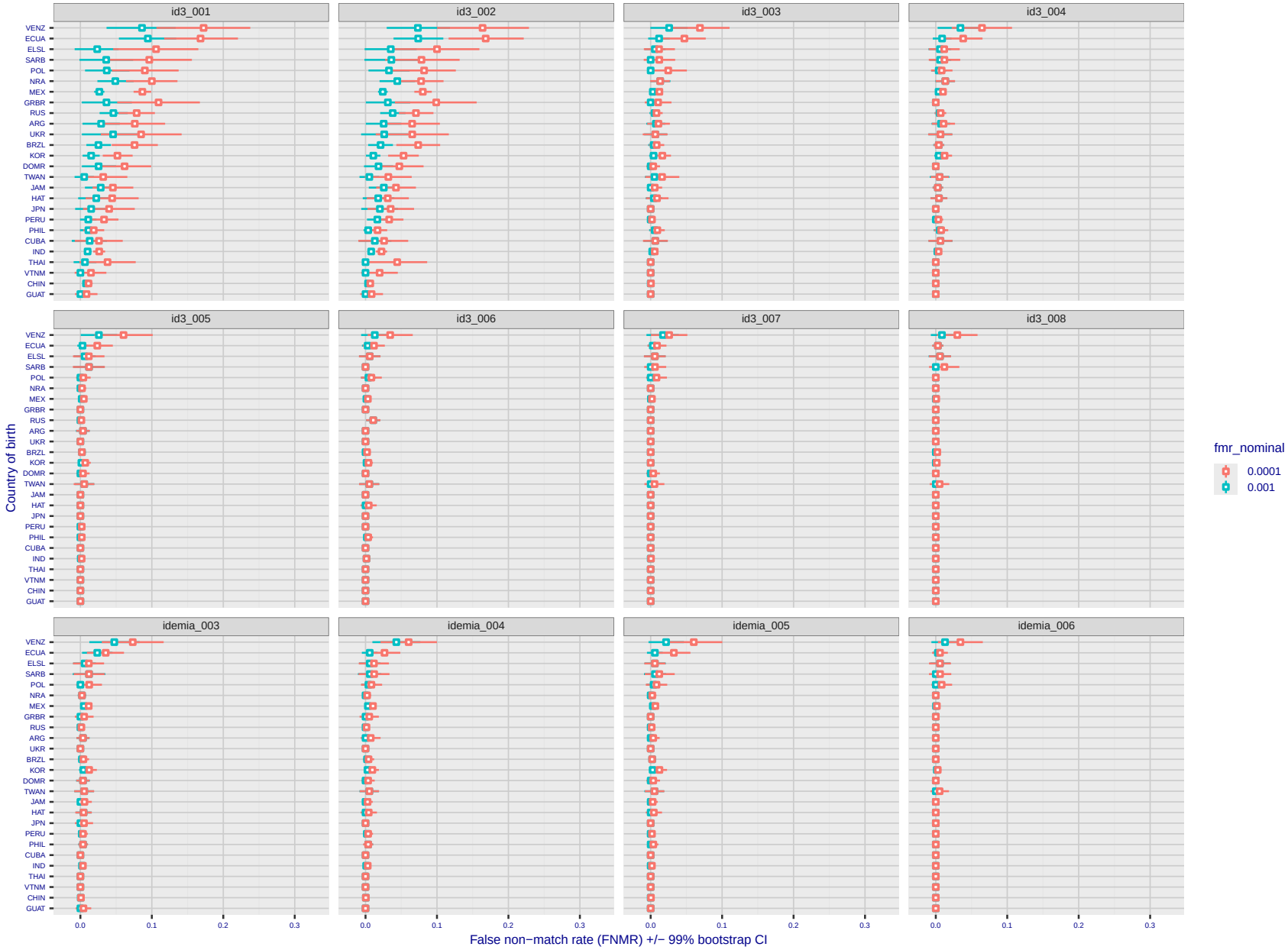

Figure 641: For the visa images, the dots show FNMR by country of birth for two globally set operating thresholds corresponding to FMR = $\{0.001, 0.0001\}$ computed over all on the order of 10^{10} impostor scores. The FMR in each bin will vary also - see subsequent impostor heatmaps in sec. 3.6.1. The figures shows an order of magnitude variation in FNMR across country of birth; these effects are likely due quality variations, then demographics like age and race. The error rates in some cases are zero, and in others the DET is flat so the error rates at the two thresholds are identical. The lines span 1% and 99% of boostrap replicated FNMR estimates.

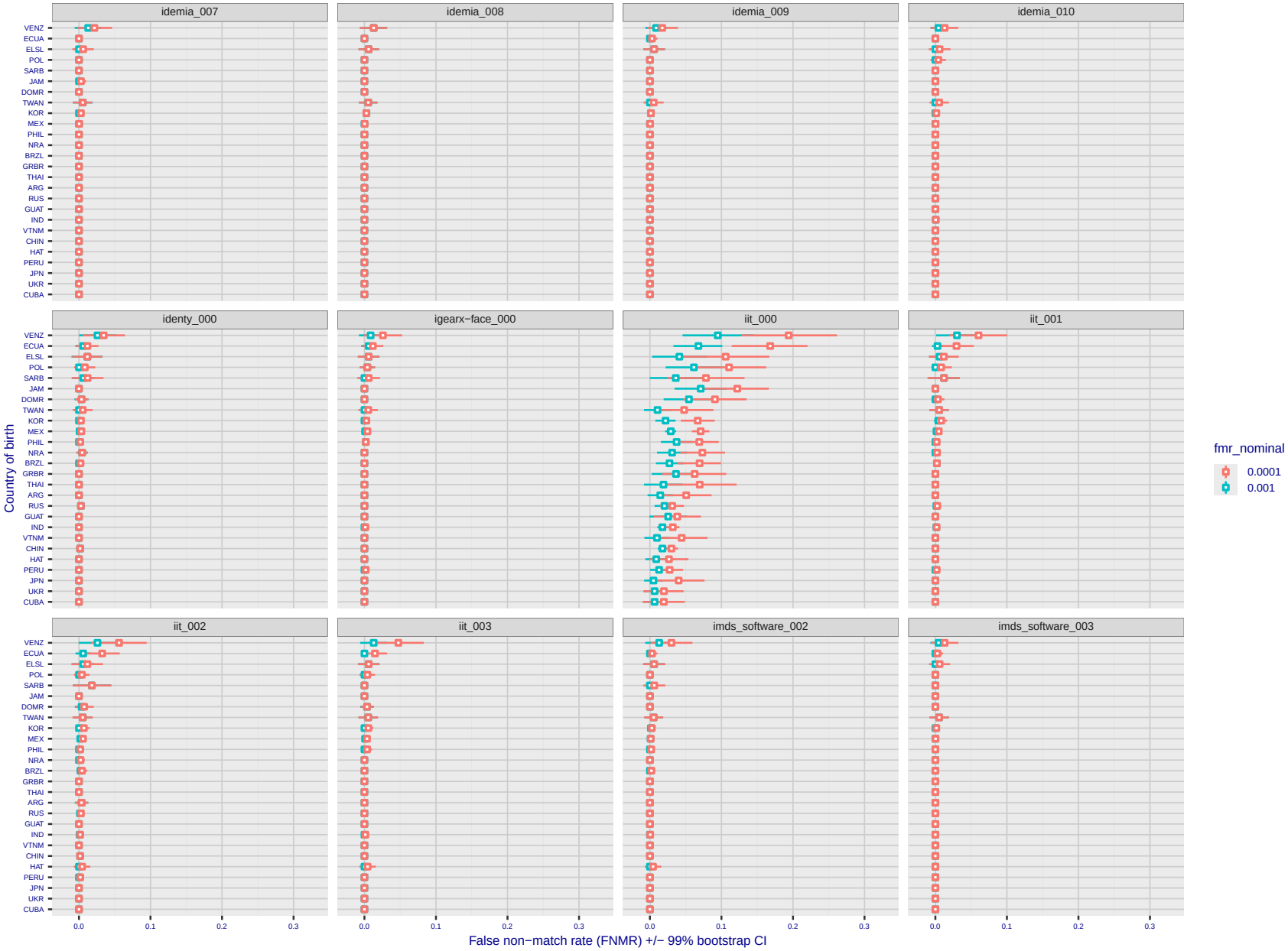

Figure 642: For the visa images, the dots show FNMR by country of birth for two globally set operating thresholds corresponding to FMR = $\{0.001, 0.0001\}$ computed over all on the order of 10^{10} impostor scores. The FMR in each bin will vary also - see subsequent impostor heatmaps in sec. 3.6.1. The figures shows an order of magnitude variation in FNMR across country of birth; these effects are likely due quality variations, then demographics like age and race. The error rates in some cases are zero, and in others the DET is flat so the error rates at the two thresholds are identical. The lines span 1% and 99% of boostrap replicated FNMR estimates.

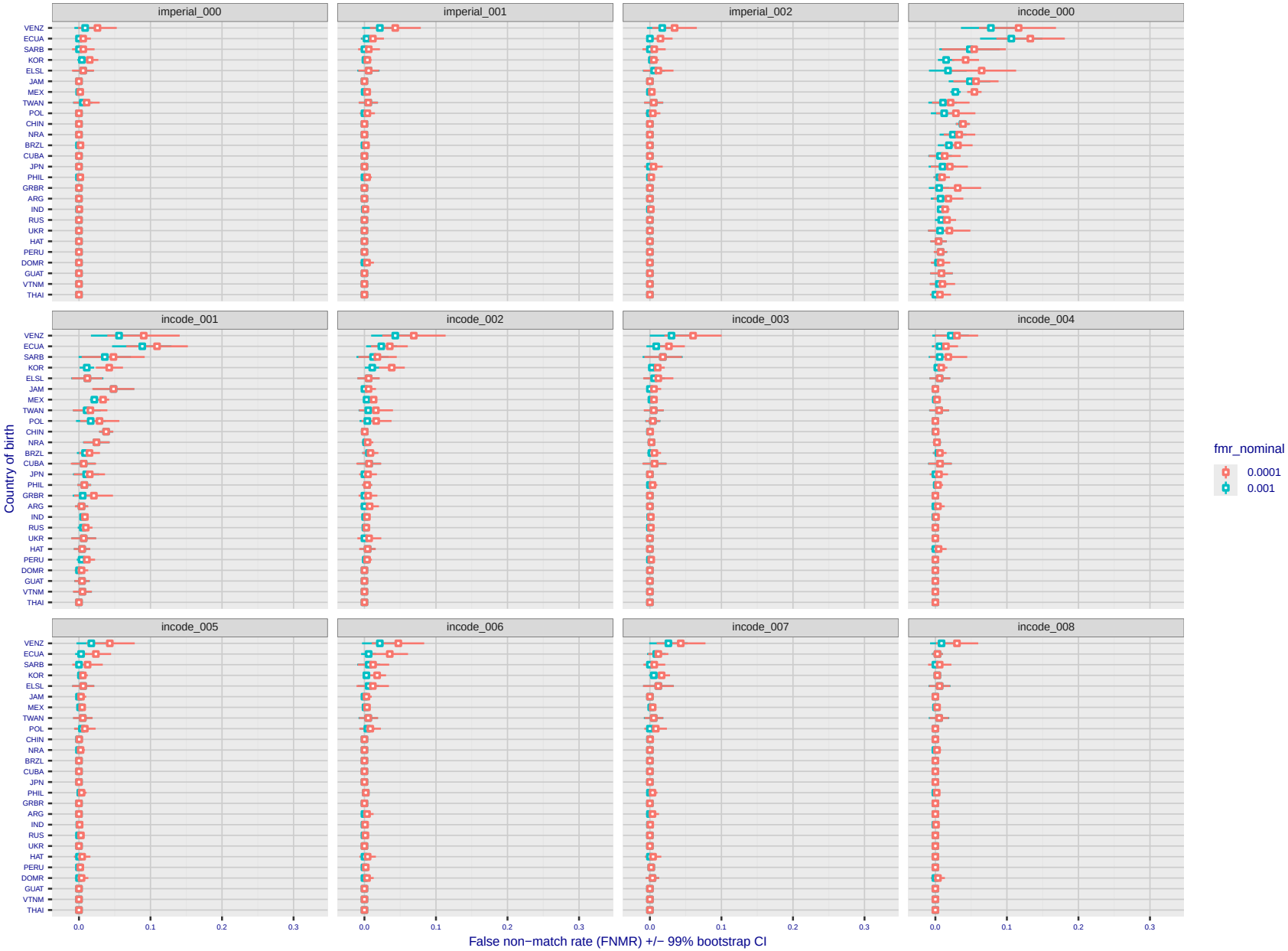

Figure 643: For the visa images, the dots show FNMR by country of birth for two globally set operating thresholds corresponding to FMR = $\{0.001, 0.0001\}$ computed over all on the order of 10^{10} impostor scores. The FMR in each bin will vary also - see subsequent impostor heatmaps in sec. 3.6.1. The figures shows an order of magnitude variation in FNMR across country of birth; these effects are likely due quality variations, then demographics like age and race. The error rates in some cases are zero, and in others the DET is flat so the error rates at the two thresholds are identical. The lines span 1% and 99% of boostrap replicated FNMR estimates.

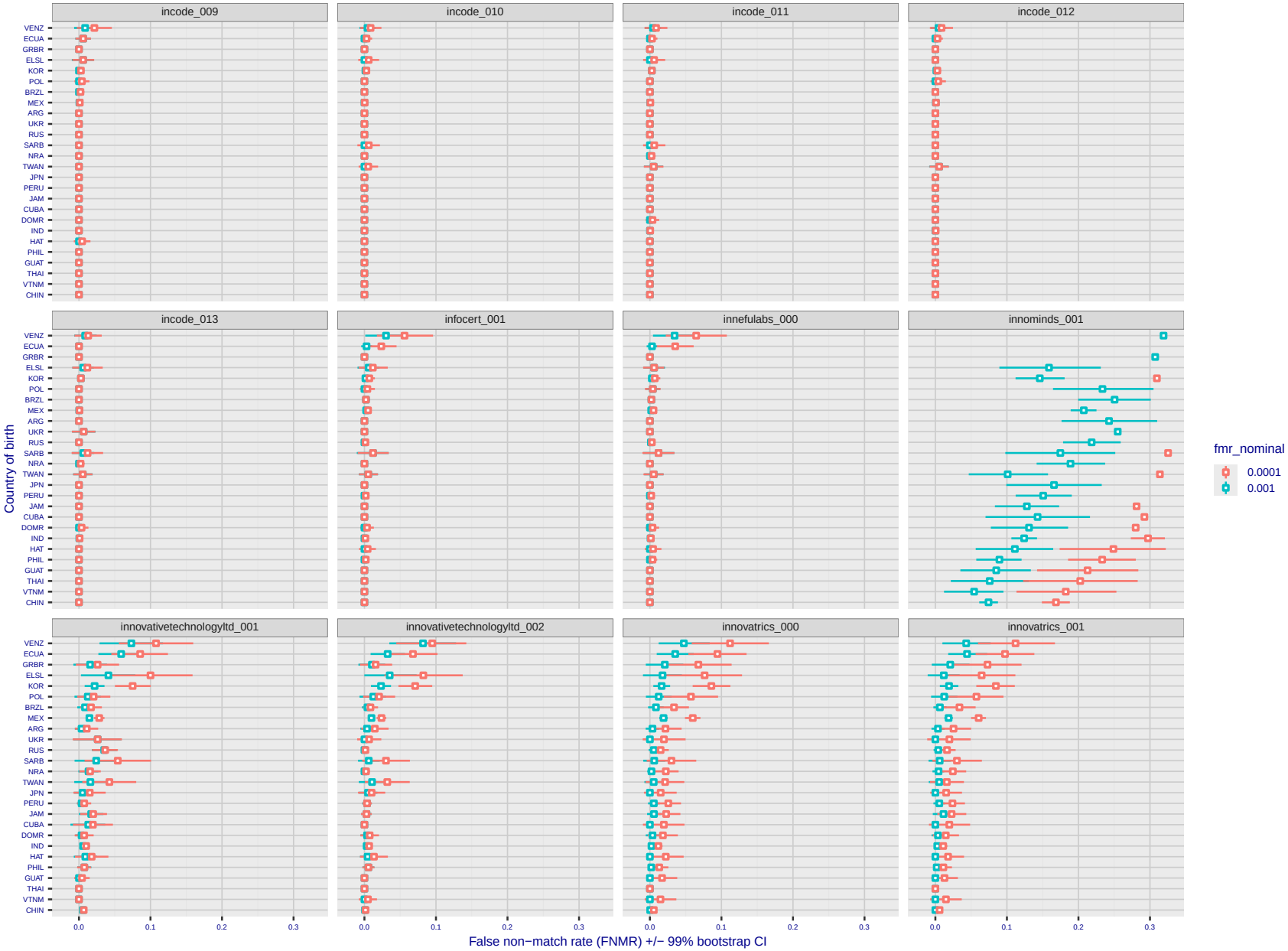

Figure 644: For the visa images, the dots show FNMR by country of birth for two globally set operating thresholds corresponding to FMR = $\{0.001, 0.0001\}$ computed over all on the order of 10^{10} impostor scores. The FMR in each bin will vary also - see subsequent impostor heatmaps in sec. 3.6.1. The figures shows an order of magnitude variation in FNMR across country of birth; these effects are likely due quality variations, then demographics like age and race. The error rates in some cases are zero, and in others the DET is flat so the error rates at the two thresholds are identical. The lines span 1% and 99% of boostrap replicated FNMR estimates.

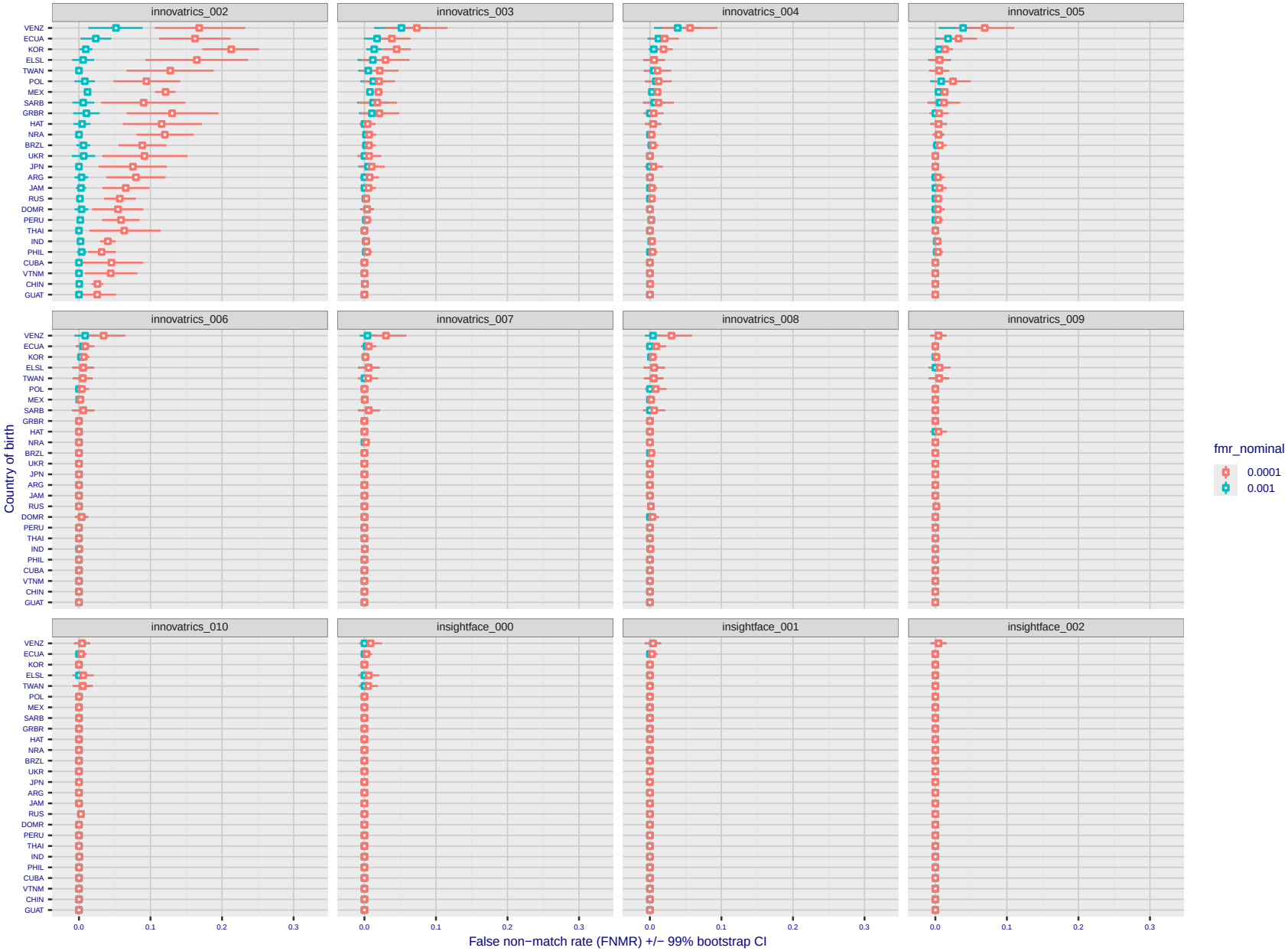

Figure 645: For the visa images, the dots show FNMR by country of birth for two globally set operating thresholds corresponding to FMR = $\{0.001, 0.0001\}$ computed over all on the order of 10^{10} impostor scores. The FMR in each bin will vary also - see subsequent impostor heatmaps in sec. 3.6.1. The figures shows an order of magnitude variation in FNMR across country of birth; these effects are likely due quality variations, then demographics like age and race. The error rates in some cases are zero, and in others the DET is flat so the error rates at the two thresholds are identical. The lines span 1% and 99% of boostrap replicated FNMR estimates.

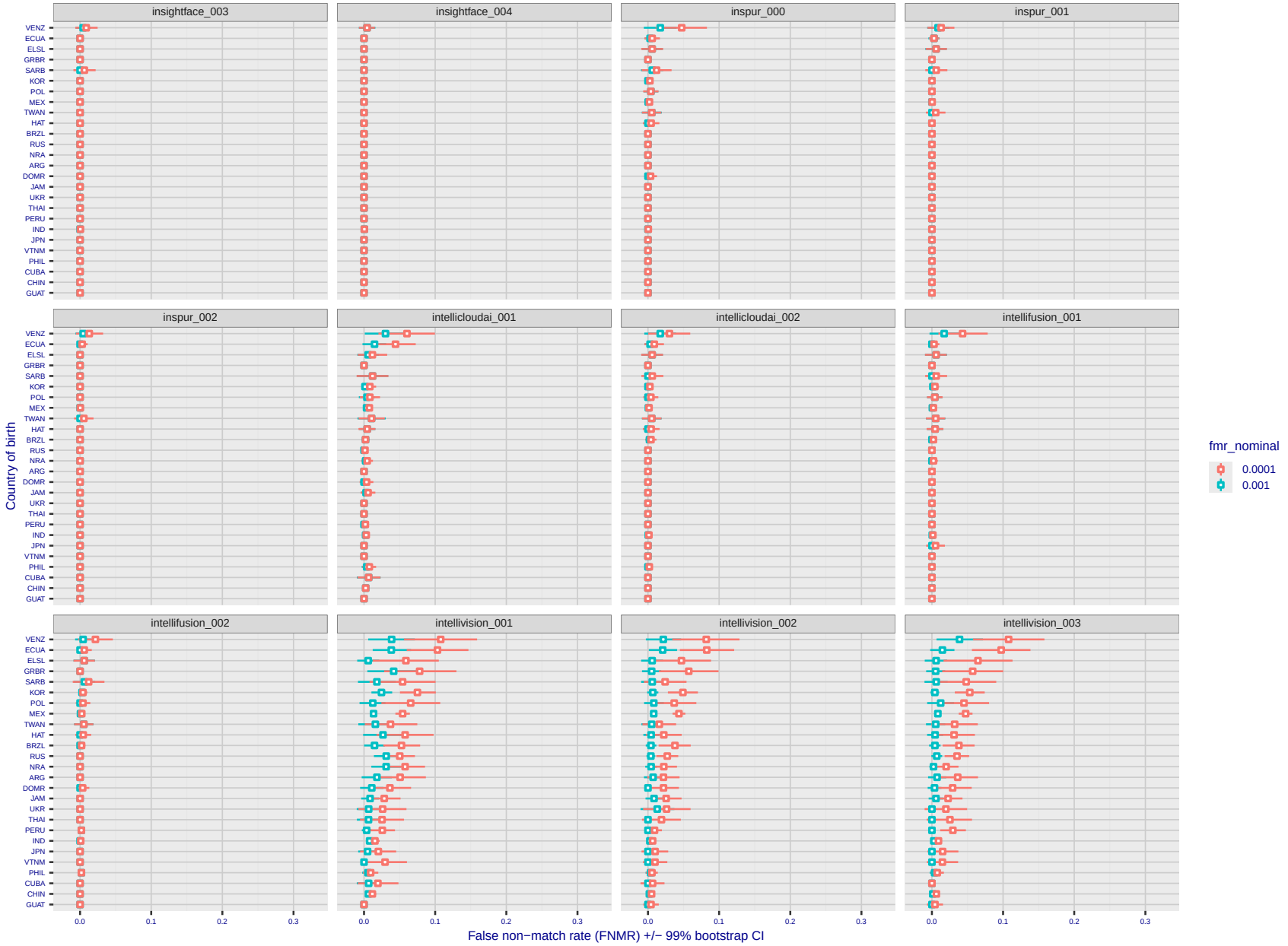

Figure 646: For the visa images, the dots show FNMR by country of birth for two globally set operating thresholds corresponding to FMR = $\{0.001, 0.0001\}$ computed over all on the order of 10^{10} impostor scores. The FMR in each bin will vary also - see subsequent impostor heatmaps in sec. 3.6.1. The figures shows an order of magnitude variation in FNMR across country of birth; these effects are likely due quality variations, then demographics like age and race. The error rates in some cases are zero, and in others the DET is flat so the error rates at the two thresholds are identical. The lines span 1% and 99% of boostrap replicated FNMR estimates.

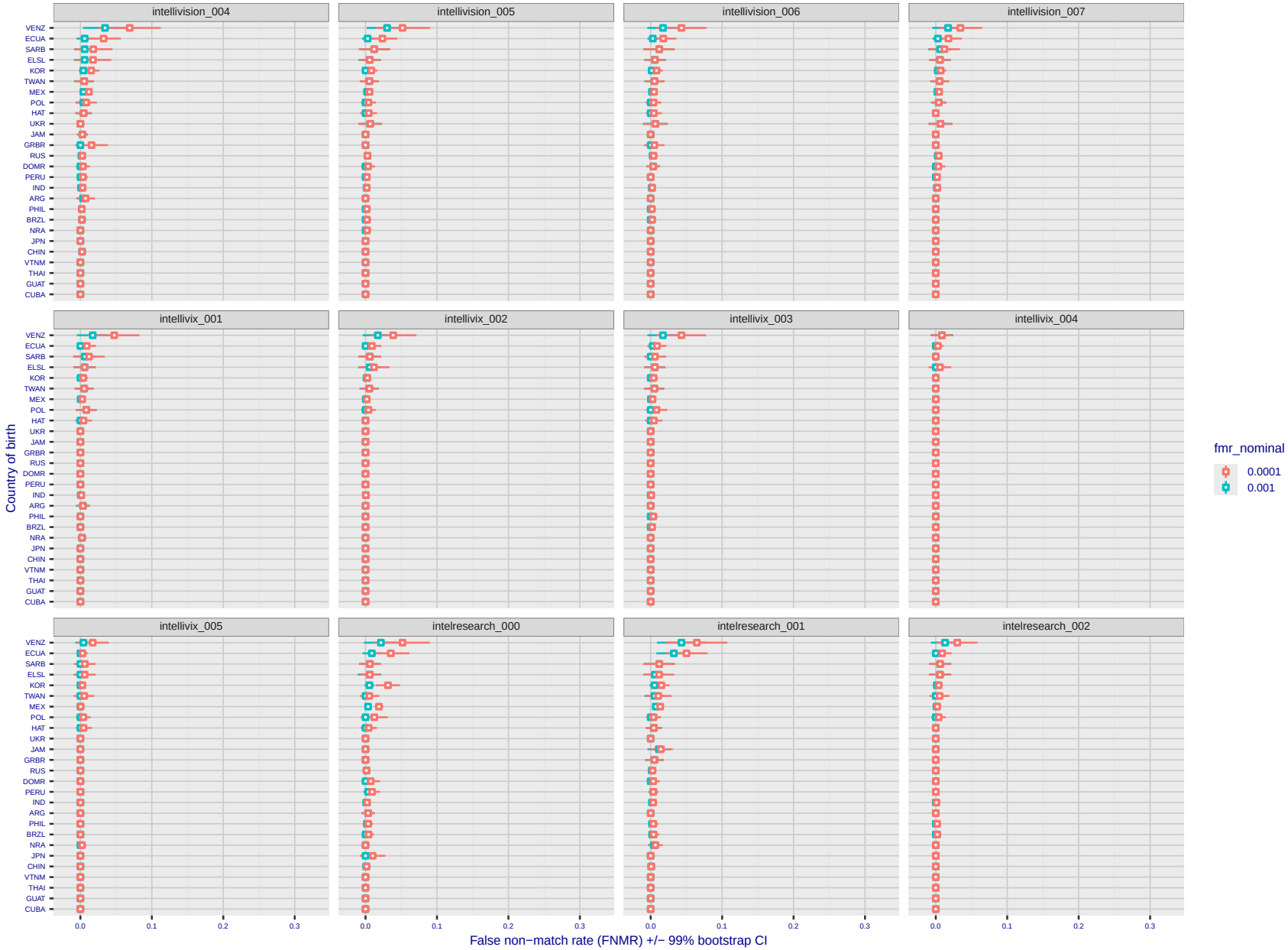

Figure 647: For the visa images, the dots show FNMR by country of birth for two globally set operating thresholds corresponding to FMR = $\{0.001, 0.0001\}$ computed over all on the order of 10^{10} impostor scores. The FMR in each bin will vary also - see subsequent impostor heatmaps in sec. 3.6.1. The figures shows an order of magnitude variation in FNMR across country of birth; these effects are likely due quality variations, then demographics like age and race. The error rates in some cases are zero, and in others the DET is flat so the error rates at the two thresholds are identical. The lines span 1% and 99% of boostrap replicated FNMR estimates.

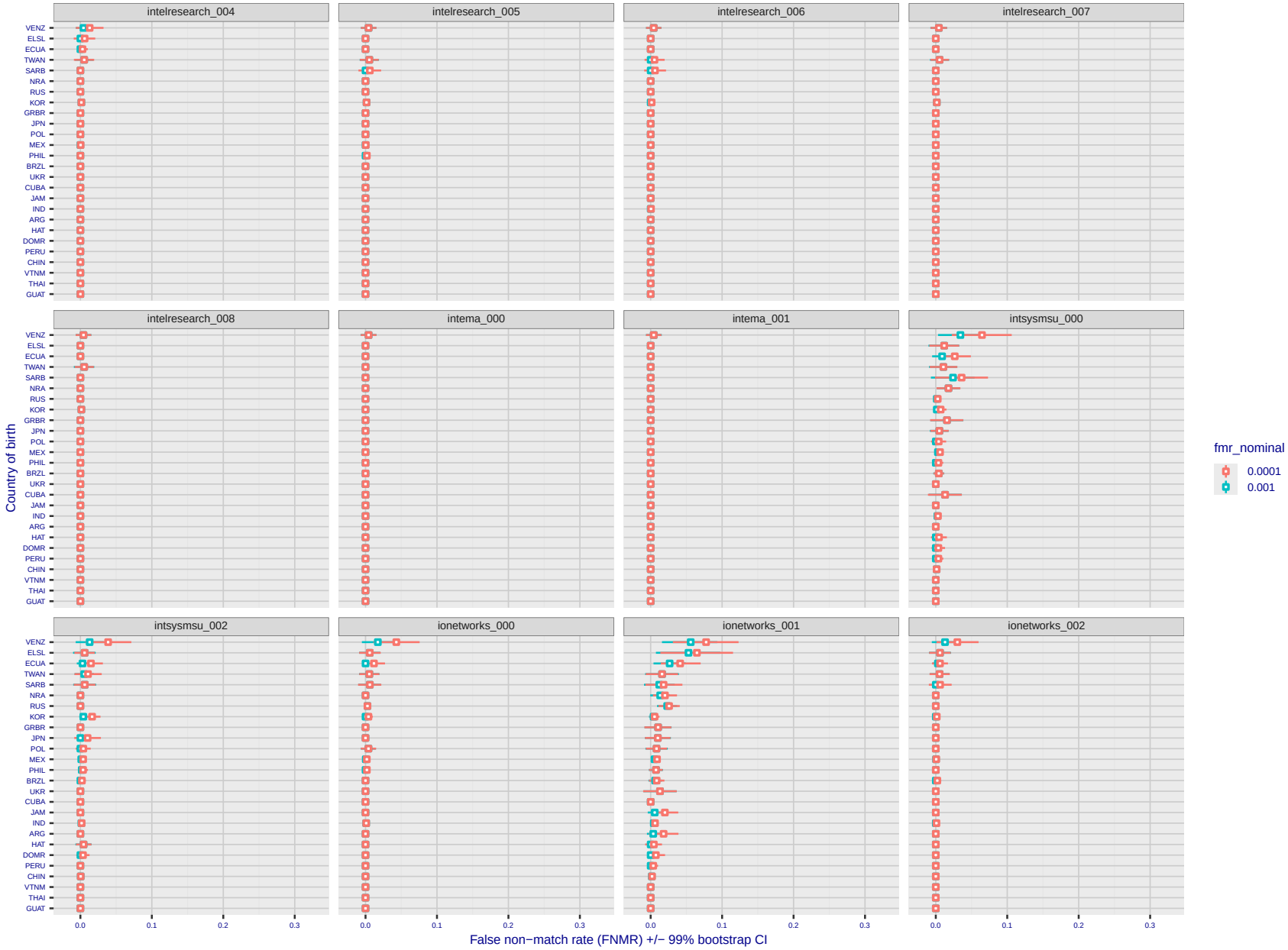

Figure 648: For the visa images, the dots show FNMR by country of birth for two globally set operating thresholds corresponding to FMR = $\{0.001, 0.0001\}$ computed over all on the order of 10^{10} impostor scores. The FMR in each bin will vary also - see subsequent impostor heatmaps in sec. 3.6.1. The figures shows an order of magnitude variation in FNMR across country of birth; these effects are likely due quality variations, then demographics like age and race. The error rates in some cases are zero, and in others the DET is flat so the error rates at the two thresholds are identical. The lines span 1% and 99% of boostrap replicated FNMR estimates.

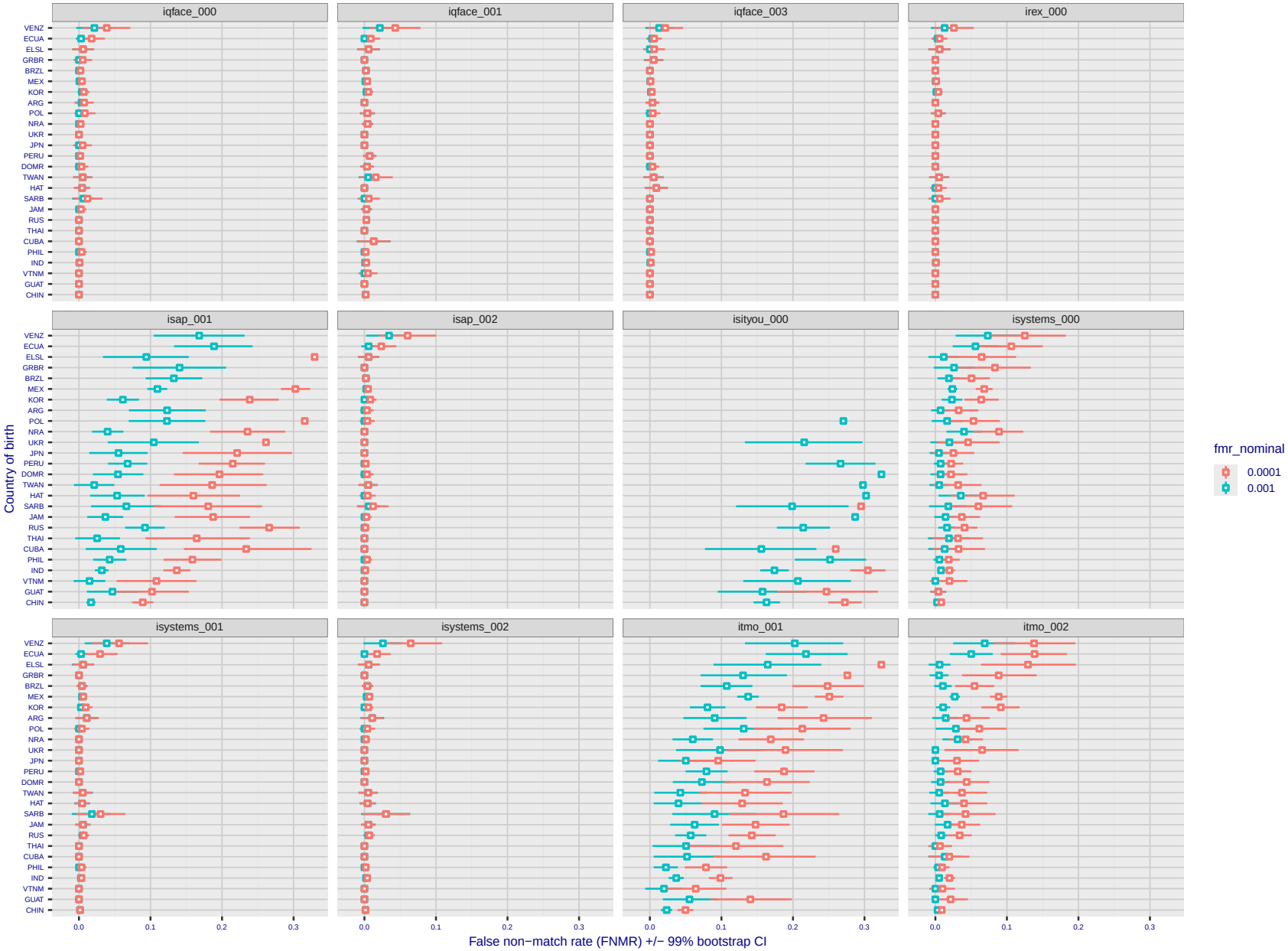

Figure 649: For the visa images, the dots show FNMR by country of birth for two globally set operating thresholds corresponding to FMR = $\{0.001, 0.0001\}$ computed over all on the order of 10^{10} impostor scores. The FMR in each bin will vary also - see subsequent impostor heatmaps in sec. 3.6.1. The figures shows an order of magnitude variation in FNMR across country of birth; these effects are likely due quality variations, then demographics like age and race. The error rates in some cases are zero, and in others the DET is flat so the error rates at the two thresholds are identical. The lines span 1% and 99% of boostrap replicated FNMR estimates.

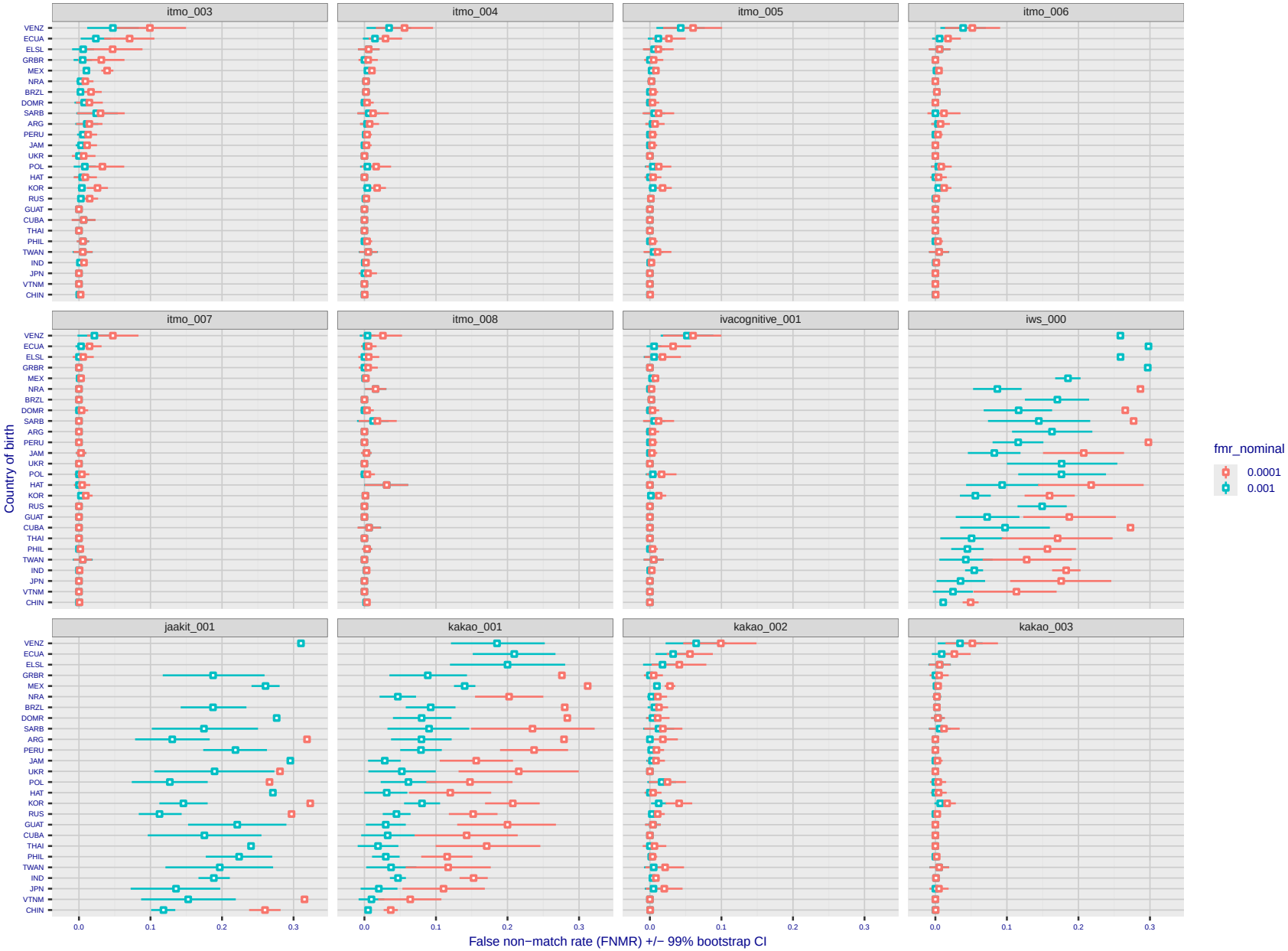

Figure 650: For the visa images, the dots show FNMR by country of birth for two globally set operating thresholds corresponding to FMR = $\{0.001, 0.0001\}$ computed over all on the order of 10^{10} impostor scores. The FMR in each bin will vary also - see subsequent impostor heatmaps in sec. 3.6.1. The figures shows an order of magnitude variation in FNMR across country of birth; these effects are likely due quality variations, then demographics like age and race. The error rates in some cases are zero, and in others the DET is flat so the error rates at the two thresholds are identical. The lines span 1% and 99% of boostrap replicated FNMR estimates.

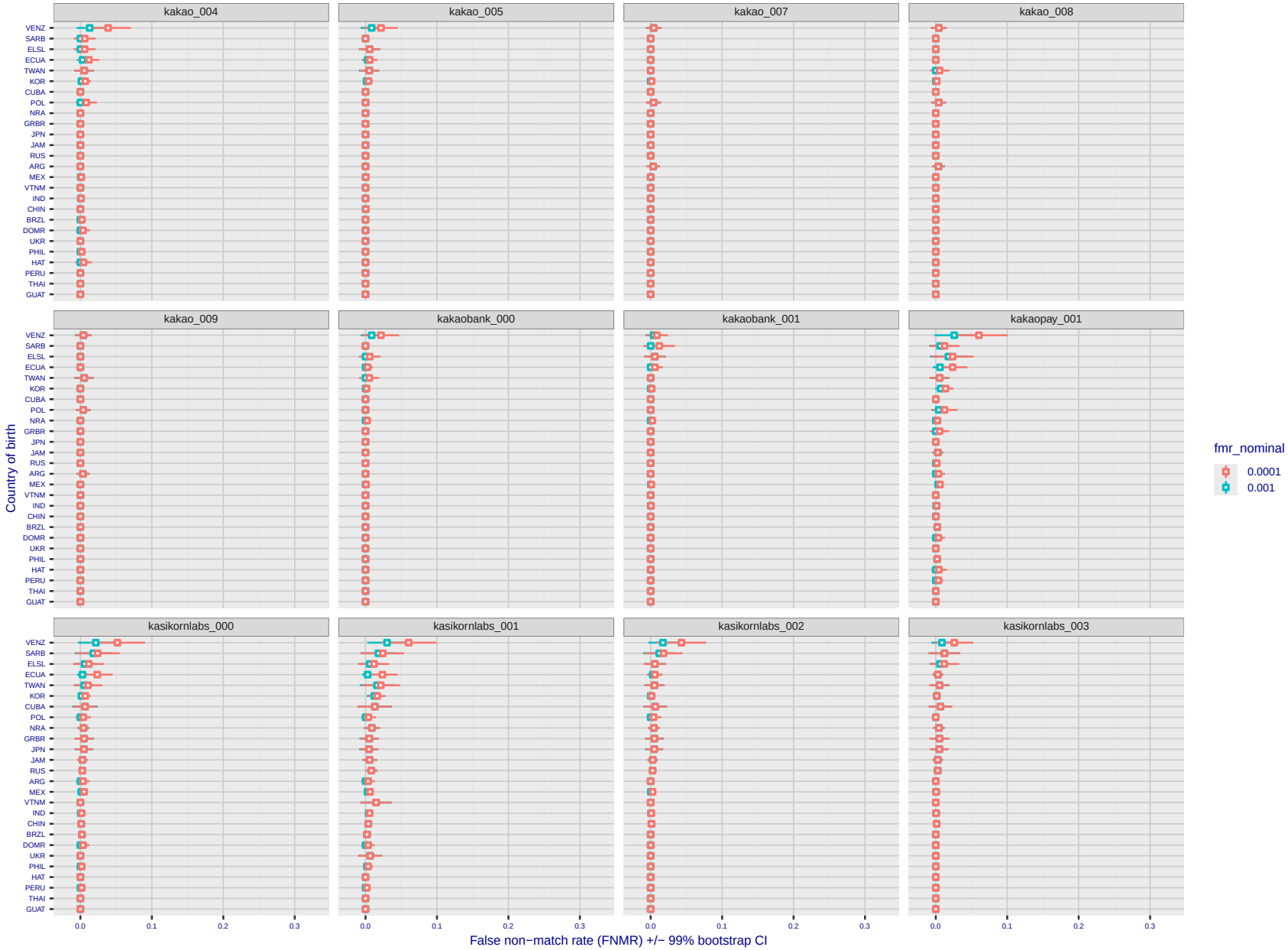

Figure 651: For the visa images, the dots show FNMR by country of birth for two globally set operating thresholds corresponding to FMR = $\{0.001, 0.0001\}$ computed over all on the order of 10^{10} impostor scores. The FMR in each bin will vary also - see subsequent impostor heatmaps in sec. 3.6.1. The figures shows an order of magnitude variation in FNMR across country of birth; these effects are likely due quality variations, then demographics like age and race. The error rates in some cases are zero, and in others the DET is flat so the error rates at the two thresholds are identical. The lines span 1% and 99% of boostrap replicated FNMR estimates.

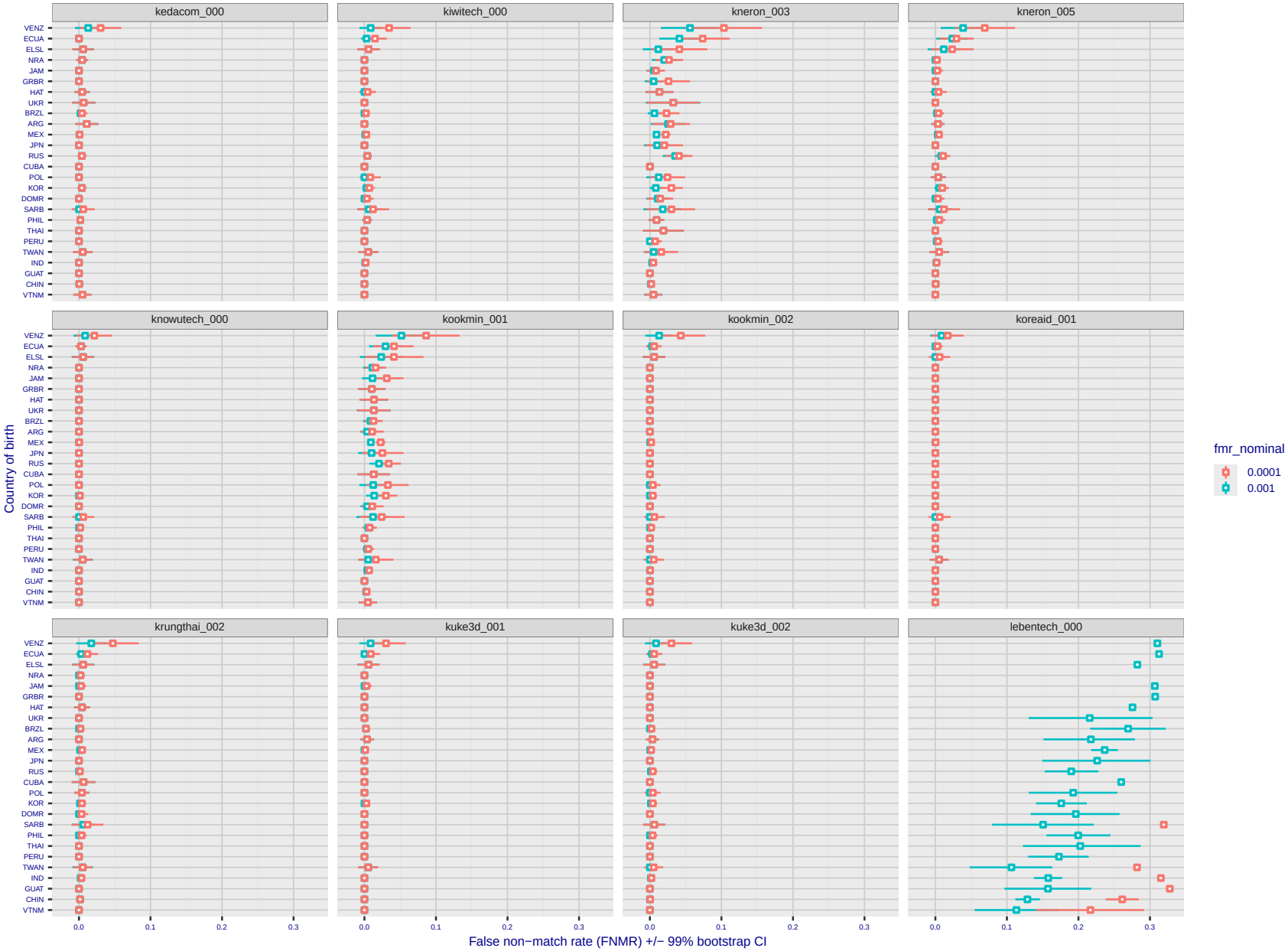

Figure 652: For the visa images, the dots show FNMR by country of birth for two globally set operating thresholds corresponding to FMR = $\{0.001, 0.0001\}$ computed over all on the order of 10^{10} impostor scores. The FMR in each bin will vary also - see subsequent impostor heatmaps in sec. 3.6.1. The figures shows an order of magnitude variation in FNMR across country of birth; these effects are likely due quality variations, then demographics like age and race. The error rates in some cases are zero, and in others the DET is flat so the error rates at the two thresholds are identical. The lines span 1% and 99% of boostrap replicated FNMR estimates.

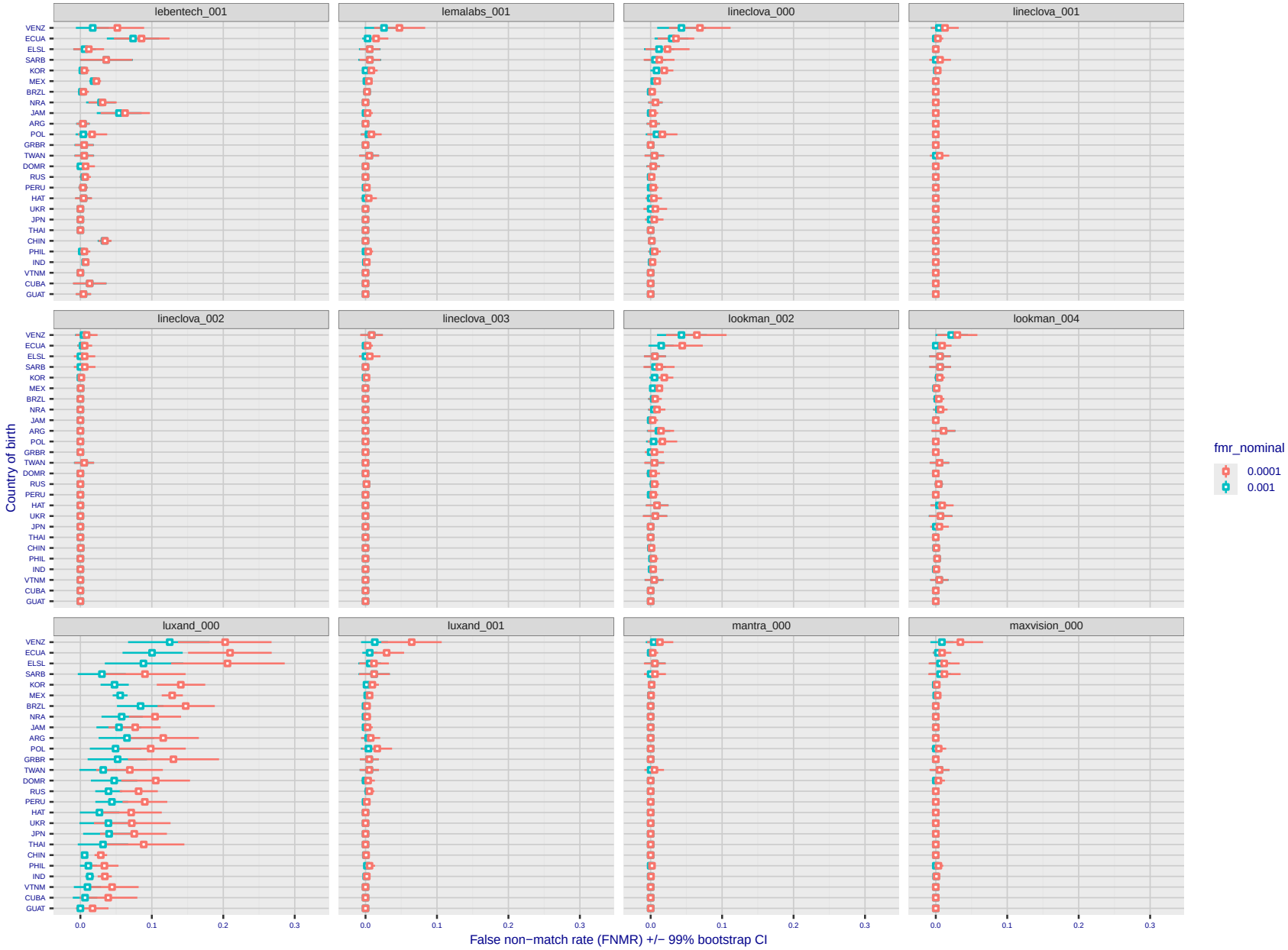

Figure 653: For the visa images, the dots show FNMR by country of birth for two globally set operating thresholds corresponding to FMR = $\{0.001, 0.0001\}$ computed over all on the order of 10^{10} impostor scores. The FMR in each bin will vary also - see subsequent impostor heatmaps in sec. 3.6.1. The figures shows an order of magnitude variation in FNMR across country of birth; these effects are likely due quality variations, then demographics like age and race. The error rates in some cases are zero, and in others the DET is flat so the error rates at the two thresholds are identical. The lines span 1% and 99% of boostrap replicated FNMR estimates.

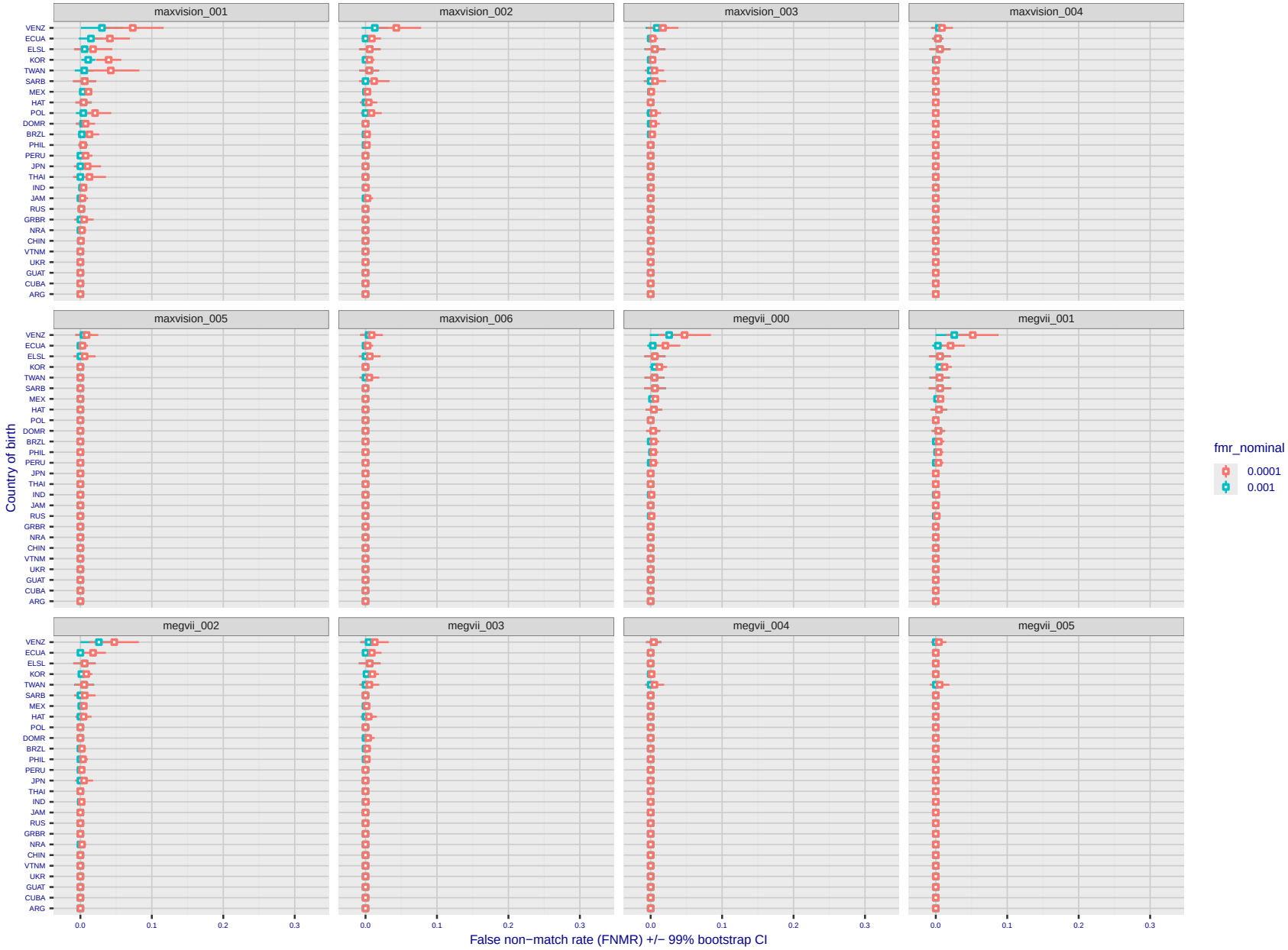

Figure 654: For the visa images, the dots show FNMR by country of birth for two globally set operating thresholds corresponding to FMR = $\{0.001, 0.0001\}$ computed over all on the order of 10^{10} impostor scores. The FMR in each bin will vary also - see subsequent impostor heatmaps in sec. 3.6.1. The figures shows an order of magnitude variation in FNMR across country of birth; these effects are likely due quality variations, then demographics like age and race. The error rates in some cases are zero, and in others the DET is flat so the error rates at the two thresholds are identical. The lines span 1% and 99% of boostrap replicated FNMR estimates.

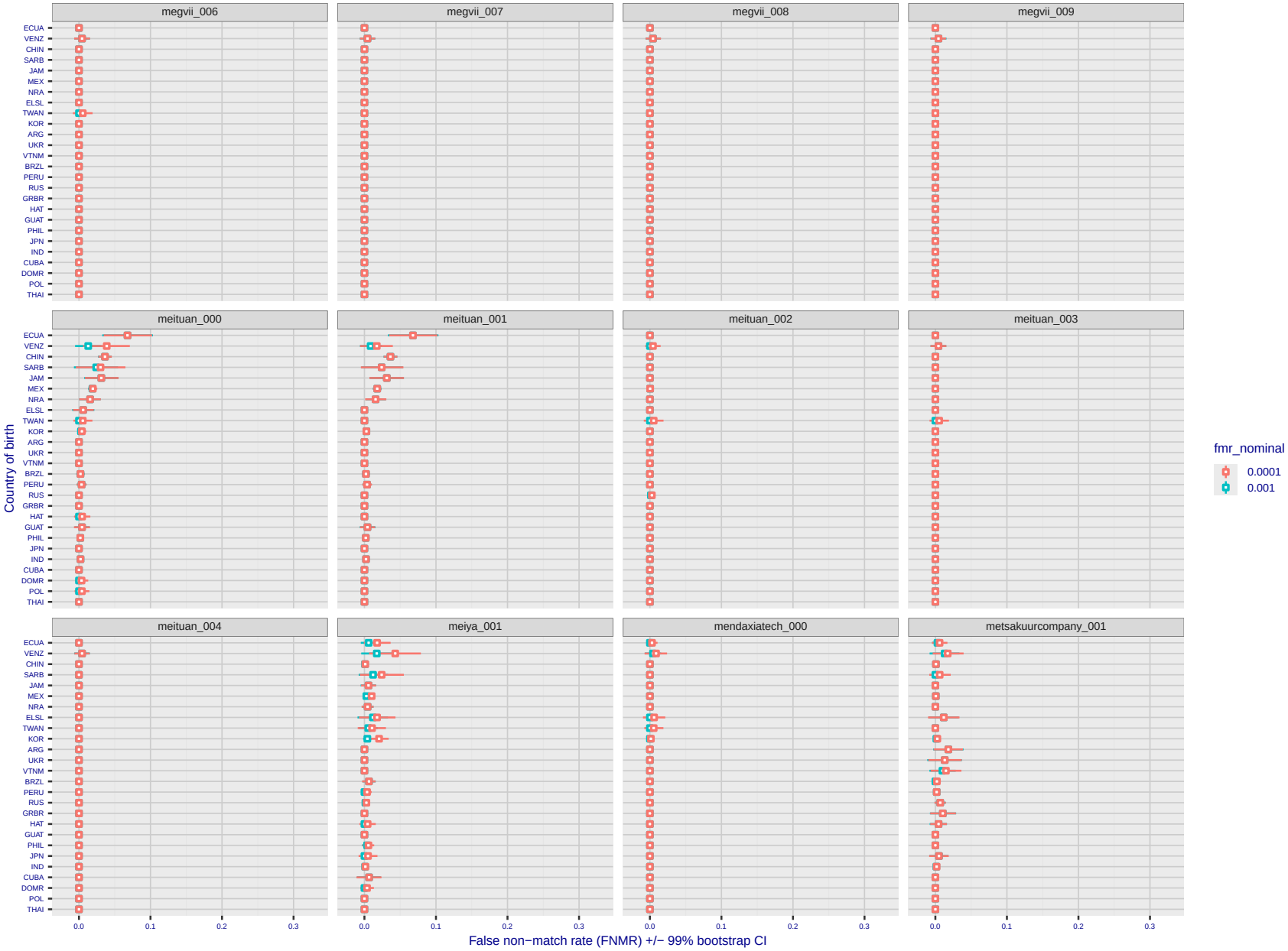

Figure 655: For the visa images, the dots show FNMR by country of birth for two globally set operating thresholds corresponding to FMR = $\{0.001, 0.0001\}$ computed over all on the order of 10^{10} impostor scores. The FMR in each bin will vary also - see subsequent impostor heatmaps in sec. 3.6.1. The figures shows an order of magnitude variation in FNMR across country of birth; these effects are likely due quality variations, then demographics like age and race. The error rates in some cases are zero, and in others the DET is flat so the error rates at the two thresholds are identical. The lines span 1% and 99% of boostrap replicated FNMR estimates.

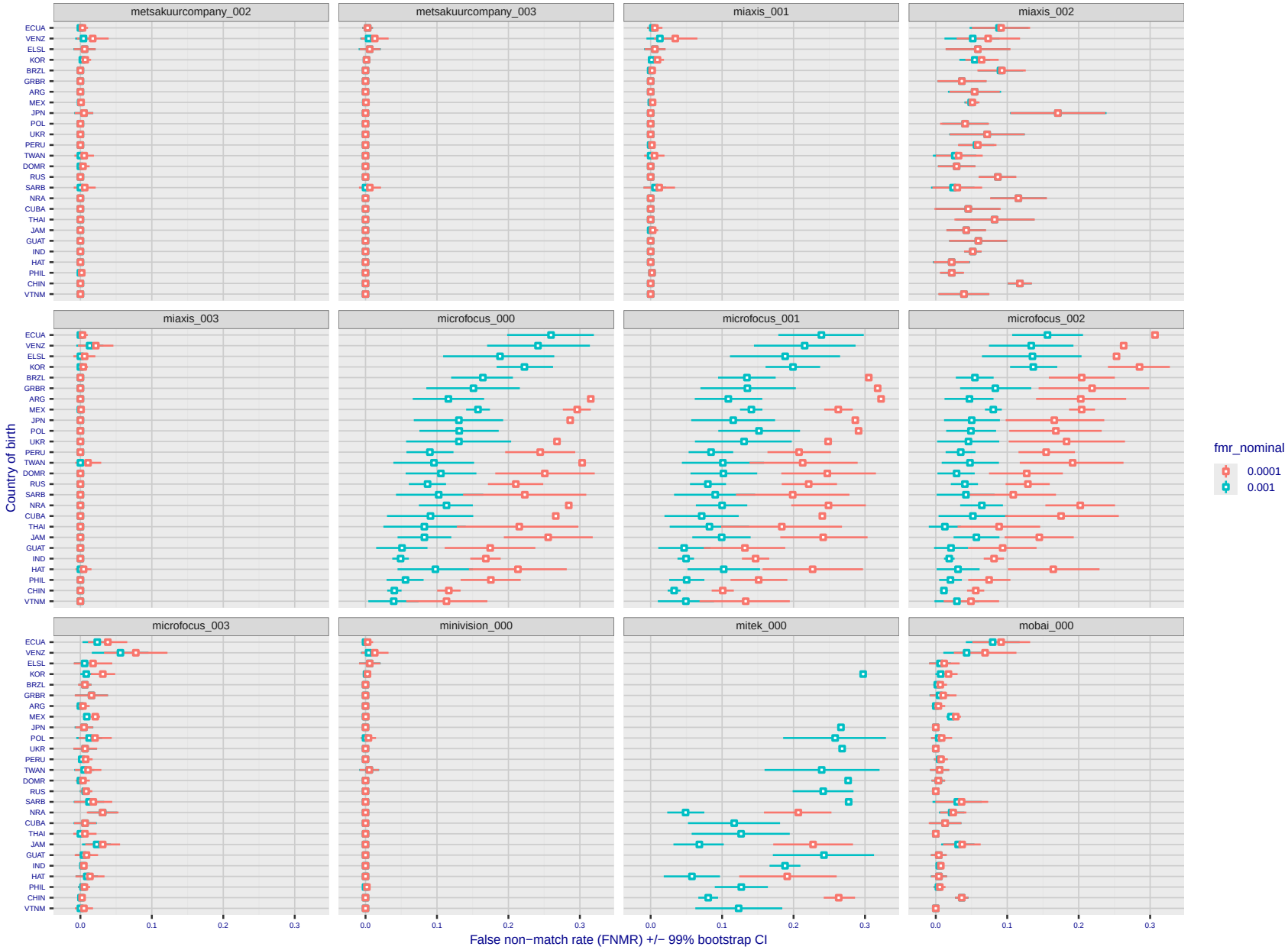

Figure 656: For the visa images, the dots show FNMR by country of birth for two globally set operating thresholds corresponding to FMR = $\{0.001, 0.0001\}$ computed over all on the order of 10^{10} impostor scores. The FMR in each bin will vary also - see subsequent impostor heatmaps in sec. 3.6.1. The figures shows an order of magnitude variation in FNMR across country of birth; these effects are likely due quality variations, then demographics like age and race. The error rates in some cases are zero, and in others the DET is flat so the error rates at the two thresholds are identical. The lines span 1% and 99% of boostrap replicated FNMR estimates.

Figure 657: For the visa images, the dots show FNMR by country of birth for two globally set operating thresholds corresponding to FMR = $\{0.001, 0.0001\}$ computed over all on the order of 10^{10} impostor scores. The FMR in each bin will vary also - see subsequent impostor heatmaps in sec. 3.6.1. The figures shows an order of magnitude variation in FNMR across country of birth; these effects are likely due quality variations, then demographics like age and race. The error rates in some cases are zero, and in others the DET is flat so the error rates at the two thresholds are identical. The lines span 1% and 99% of boostrap replicated FNMR estimates.

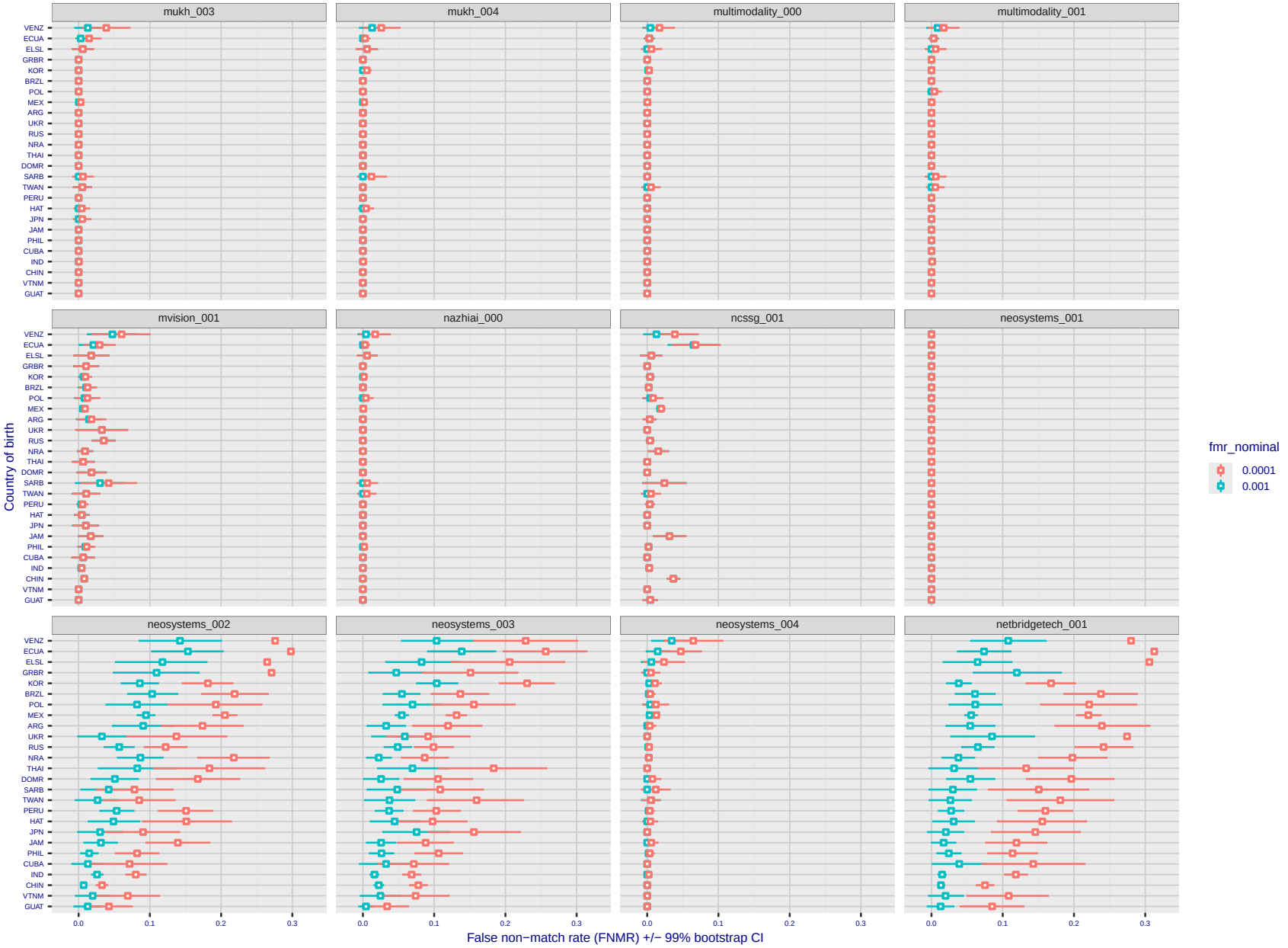

Figure 658: For the visa images, the dots show FNMR by country of birth for two globally set operating thresholds corresponding to FMR = $\{0.001, 0.0001\}$ computed over all on the order of 10^{10} impostor scores. The FMR in each bin will vary also - see subsequent impostor heatmaps in sec. 3.6.1. The figures shows an order of magnitude variation in FNMR across country of birth; these effects are likely due quality variations, then demographics like age and race. The error rates in some cases are zero, and in others the DET is flat so the error rates at the two thresholds are identical. The lines span 1% and 99% of boostrap replicated FNMR estimates.

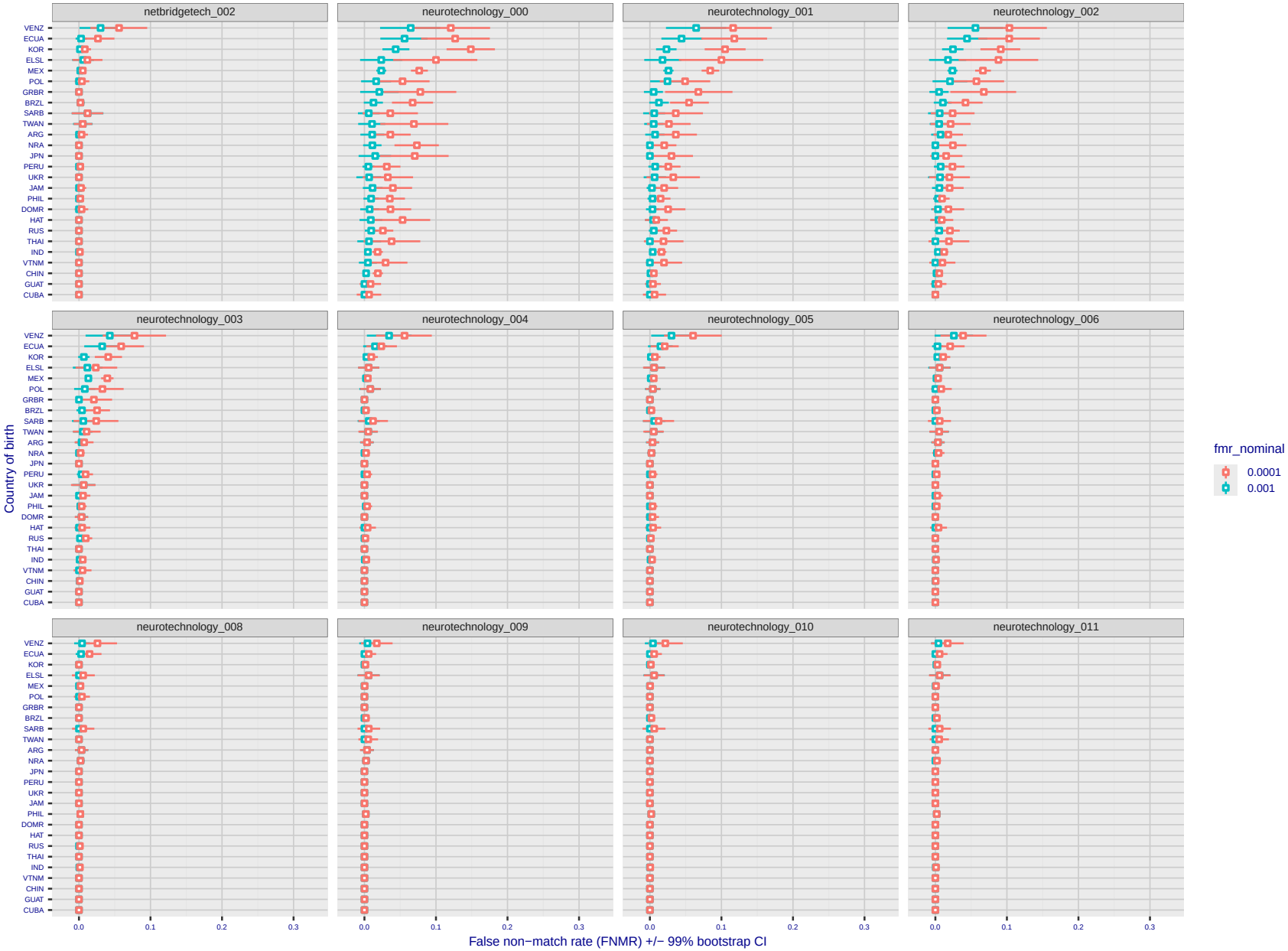

Figure 659: For the visa images, the dots show FNMR by country of birth for two globally set operating thresholds corresponding to FMR = $\{0.001, 0.0001\}$ computed over all on the order of 10^{10} impostor scores. The FMR in each bin will vary also - see subsequent impostor heatmaps in sec. 3.6.1. The figures shows an order of magnitude variation in FNMR across country of birth; these effects are likely due quality variations, then demographics like age and race. The error rates in some cases are zero, and in others the DET is flat so the error rates at the two thresholds are identical. The lines span 1% and 99% of boostrap replicated FNMR estimates.

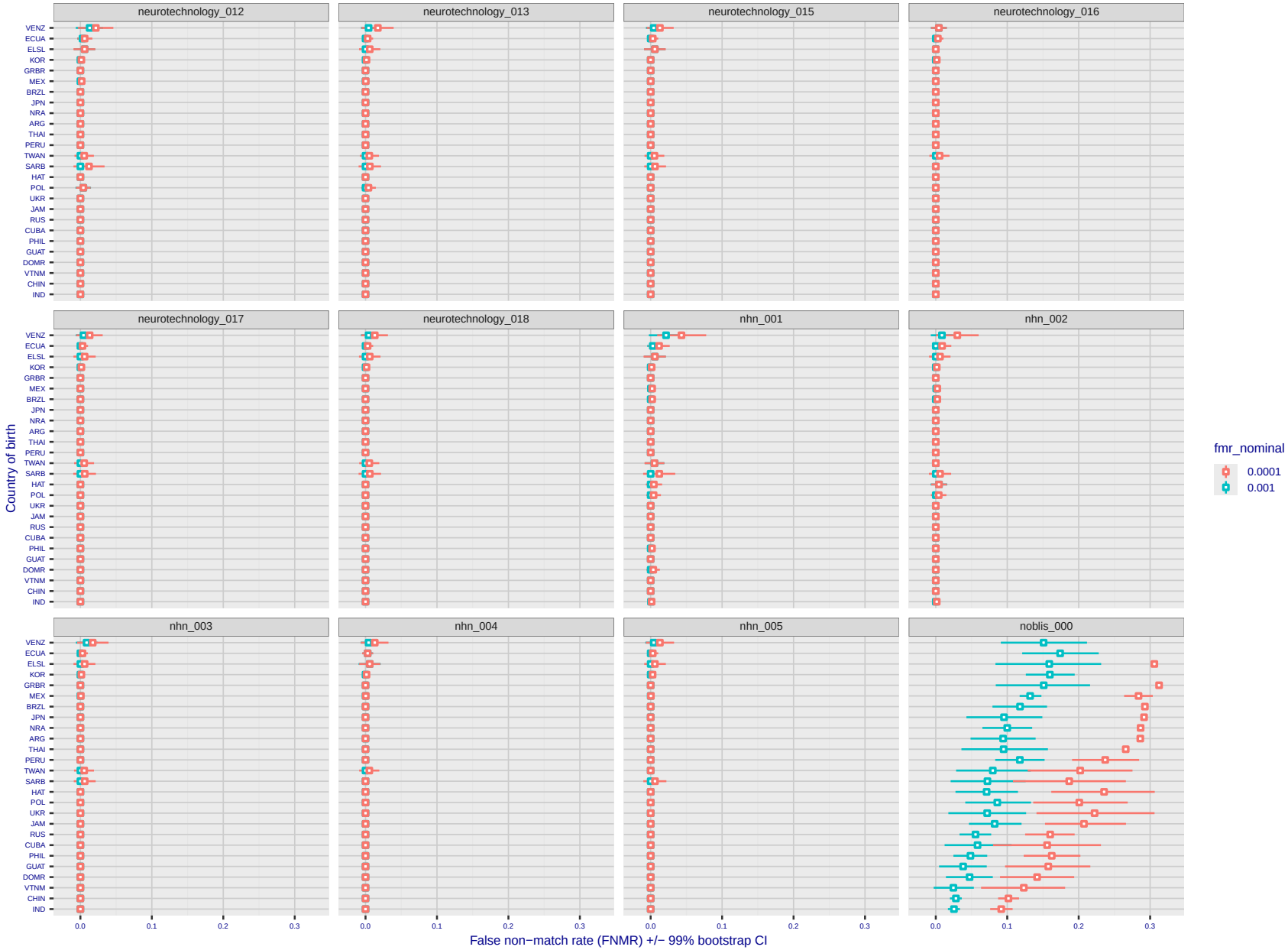

Figure 660: For the visa images, the dots show FNMR by country of birth for two globally set operating thresholds corresponding to FMR = $\{0.001, 0.0001\}$ computed over all on the order of 10^{10} impostor scores. The FMR in each bin will vary also - see subsequent impostor heatmaps in sec. 3.6.1. The figures shows an order of magnitude variation in FNMR across country of birth; these effects are likely due quality variations, then demographics like age and race. The error rates in some cases are zero, and in others the DET is flat so the error rates at the two thresholds are identical. The lines span 1% and 99% of boostrap replicated FNMR estimates.

Figure 661: For the visa images, the dots show FNMR by country of birth for two globally set operating thresholds corresponding to FMR = $\{0.001, 0.0001\}$ computed over all on the order of 10^{10} impostor scores. The FMR in each bin will vary also - see subsequent impostor heatmaps in sec. 3.6.1. The figures shows an order of magnitude variation in FNMR across country of birth; these effects are likely due quality variations, then demographics like age and race. The error rates in some cases are zero, and in others the DET is flat so the error rates at the two thresholds are identical. The lines span 1% and 99% of boostrap replicated FNMR estimates.

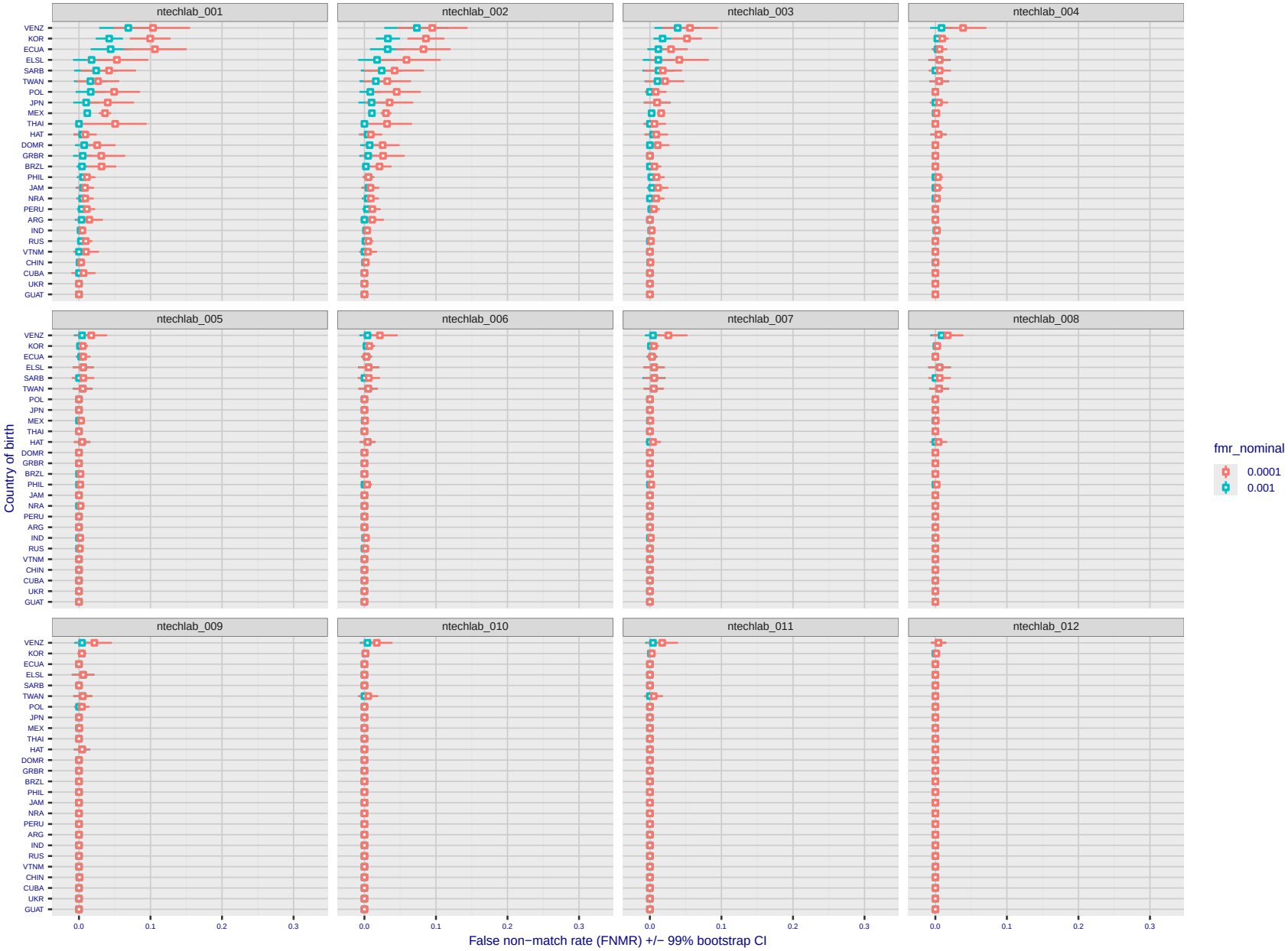

Figure 662: For the visa images, the dots show FNMR by country of birth for two globally set operating thresholds corresponding to FMR = $\{0.001, 0.0001\}$ computed over all on the order of 10^{10} impostor scores. The FMR in each bin will vary also - see subsequent impostor heatmaps in sec. 3.6.1. The figures shows an order of magnitude variation in FNMR across country of birth; these effects are likely due quality variations, then demographics like age and race. The error rates in some cases are zero, and in others the DET is flat so the error rates at the two thresholds are identical. The lines span 1% and 99% of boostrap replicated FNMR estimates.

Figure 663: For the visa images, the dots show FNMR by country of birth for two globally set operating thresholds corresponding to FMR = $\{0.001, 0.0001\}$ computed over all on the order of 10^{10} impostor scores. The FMR in each bin will vary also - see subsequent impostor heatmaps in sec. 3.6.1. The figures shows an order of magnitude variation in FNMR across country of birth; these effects are likely due quality variations, then demographics like age and race. The error rates in some cases are zero, and in others the DET is flat so the error rates at the two thresholds are identical. The lines span 1% and 99% of boostrap replicated FNMR estimates.

Figure 664: For the visa images, the dots show FNMR by country of birth for two globally set operating thresholds corresponding to FMR = $\{0.001, 0.0001\}$ computed over all on the order of 10^{10} impostor scores. The FMR in each bin will vary also - see subsequent impostor heatmaps in sec. 3.6.1. The figures shows an order of magnitude variation in FNMR across country of birth; these effects are likely due quality variations, then demographics like age and race. The error rates in some cases are zero, and in others the DET is flat so the error rates at the two thresholds are identical. The lines span 1% and 99% of boostrap replicated FNMR estimates.

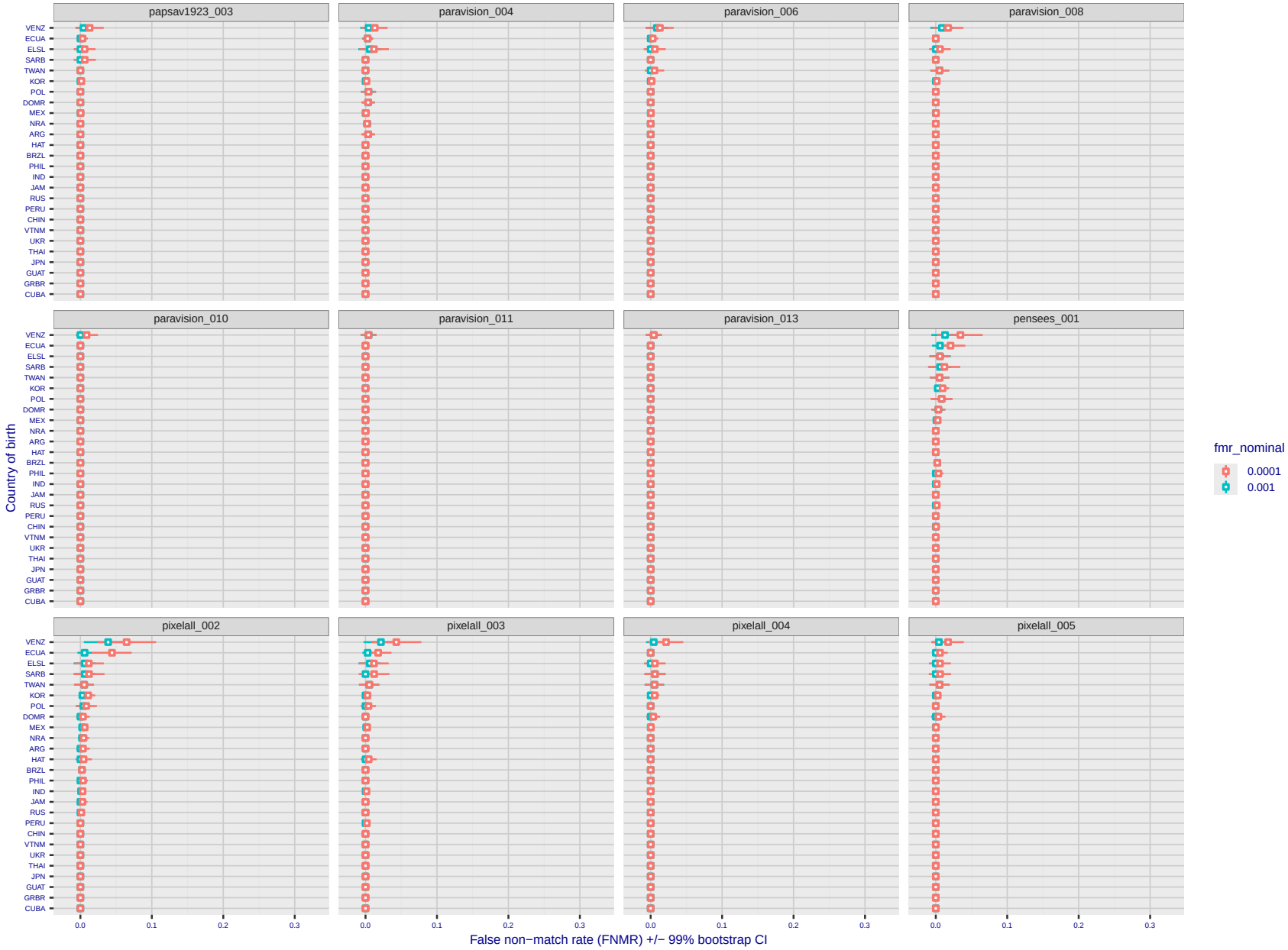

Figure 665: For the visa images, the dots show FNMR by country of birth for two globally set operating thresholds corresponding to FMR = $\{0.001, 0.0001\}$ computed over all on the order of 10^{10} impostor scores. The FMR in each bin will vary also - see subsequent impostor heatmaps in sec. 3.6.1. The figures shows an order of magnitude variation in FNMR across country of birth; these effects are likely due quality variations, then demographics like age and race. The error rates in some cases are zero, and in others the DET is flat so the error rates at the two thresholds are identical. The lines span 1% and 99% of boostrap replicated FNMR estimates.

Figure 666: For the visa images, the dots show FNMR by country of birth for two globally set operating thresholds corresponding to FMR = $\{0.001, 0.0001\}$ computed over all on the order of 10^{10} impostor scores. The FMR in each bin will vary also - see subsequent impostor heatmaps in sec. 3.6.1. The figures shows an order of magnitude variation in FNMR across country of birth; these effects are likely due quality variations, then demographics like age and race. The error rates in some cases are zero, and in others the DET is flat so the error rates at the two thresholds are identical. The lines span 1% and 99% of boostrap replicated FNMR estimates.

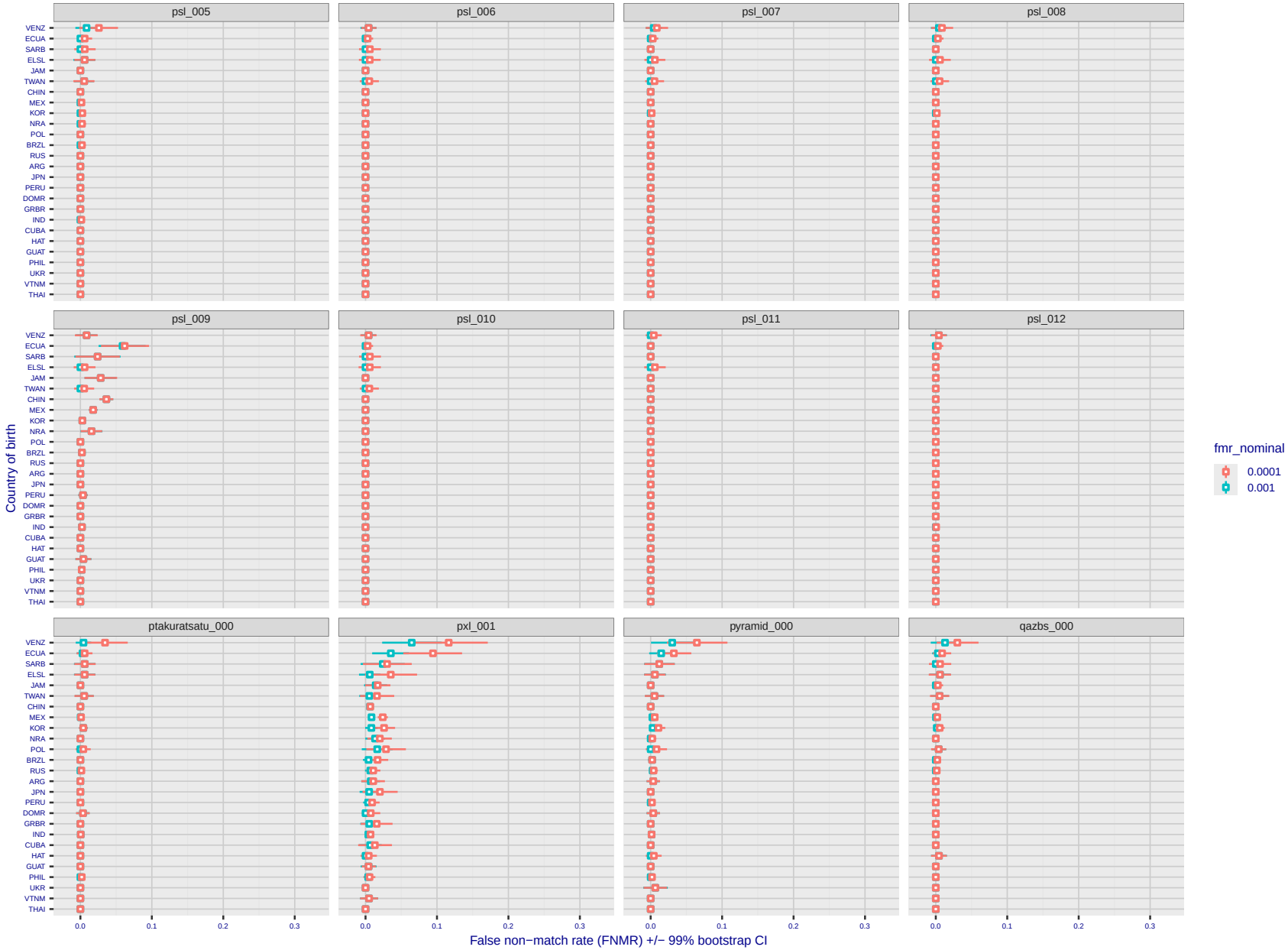

Figure 667: For the visa images, the dots show FNMR by country of birth for two globally set operating thresholds corresponding to FMR = $\{0.001, 0.0001\}$ computed over all on the order of 10^{10} impostor scores. The FMR in each bin will vary also - see subsequent impostor heatmaps in sec. 3.6.1. The figures shows an order of magnitude variation in FNMR across country of birth; these effects are likely due quality variations, then demographics like age and race. The error rates in some cases are zero, and in others the DET is flat so the error rates at the two thresholds are identical. The lines span 1% and 99% of boostrap replicated FNMR estimates.

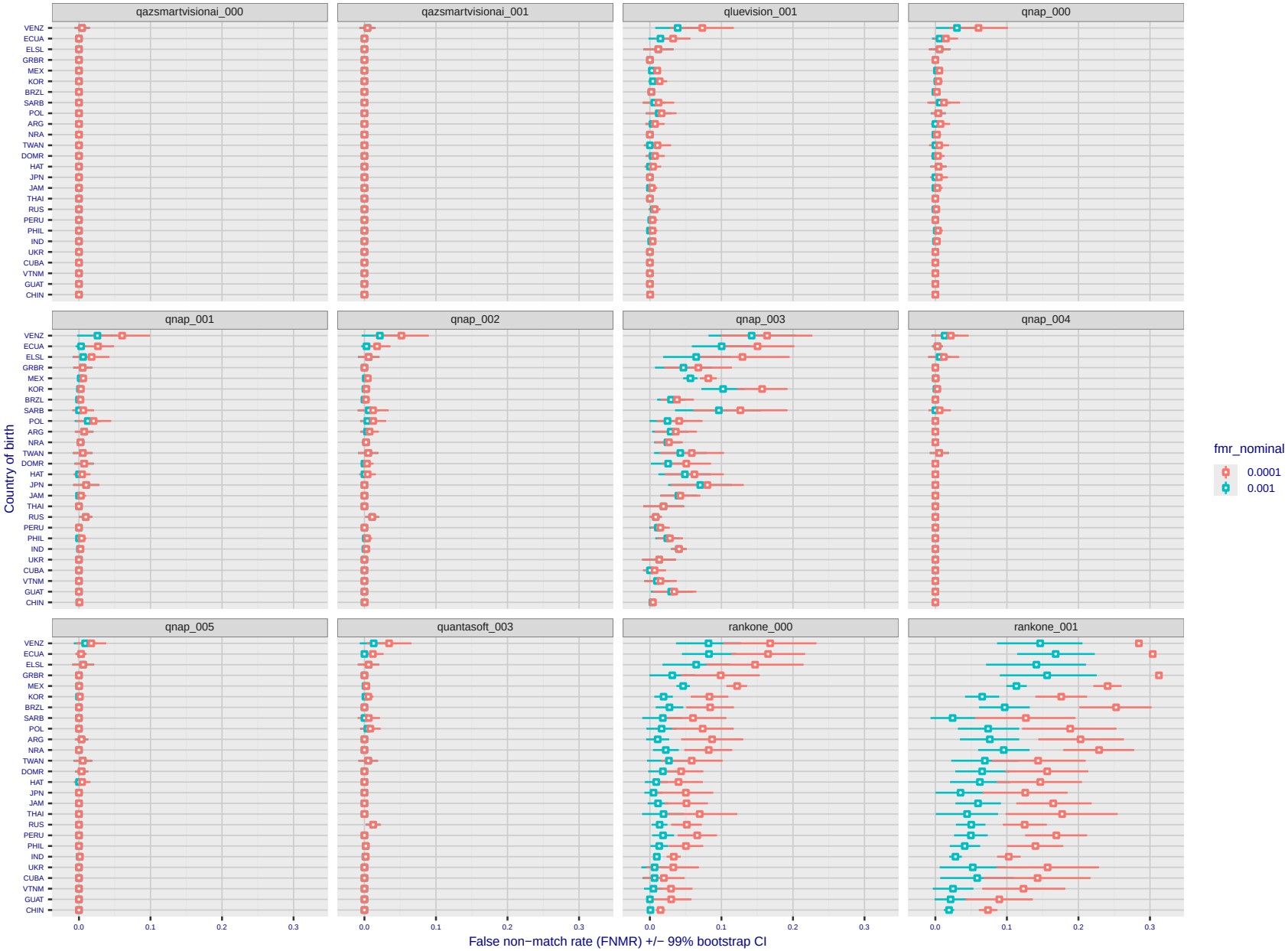

Figure 668: For the visa images, the dots show FNMR by country of birth for two globally set operating thresholds corresponding to FMR = $\{0.001, 0.0001\}$ computed over all on the order of 10^{10} impostor scores. The FMR in each bin will vary also - see subsequent impostor heatmaps in sec. 3.6.1. The figures shows an order of magnitude variation in FNMR across country of birth; these effects are likely due quality variations, then demographics like age and race. The error rates in some cases are zero, and in others the DET is flat so the error rates at the two thresholds are identical. The lines span 1% and 99% of boostrap replicated FNMR estimates.

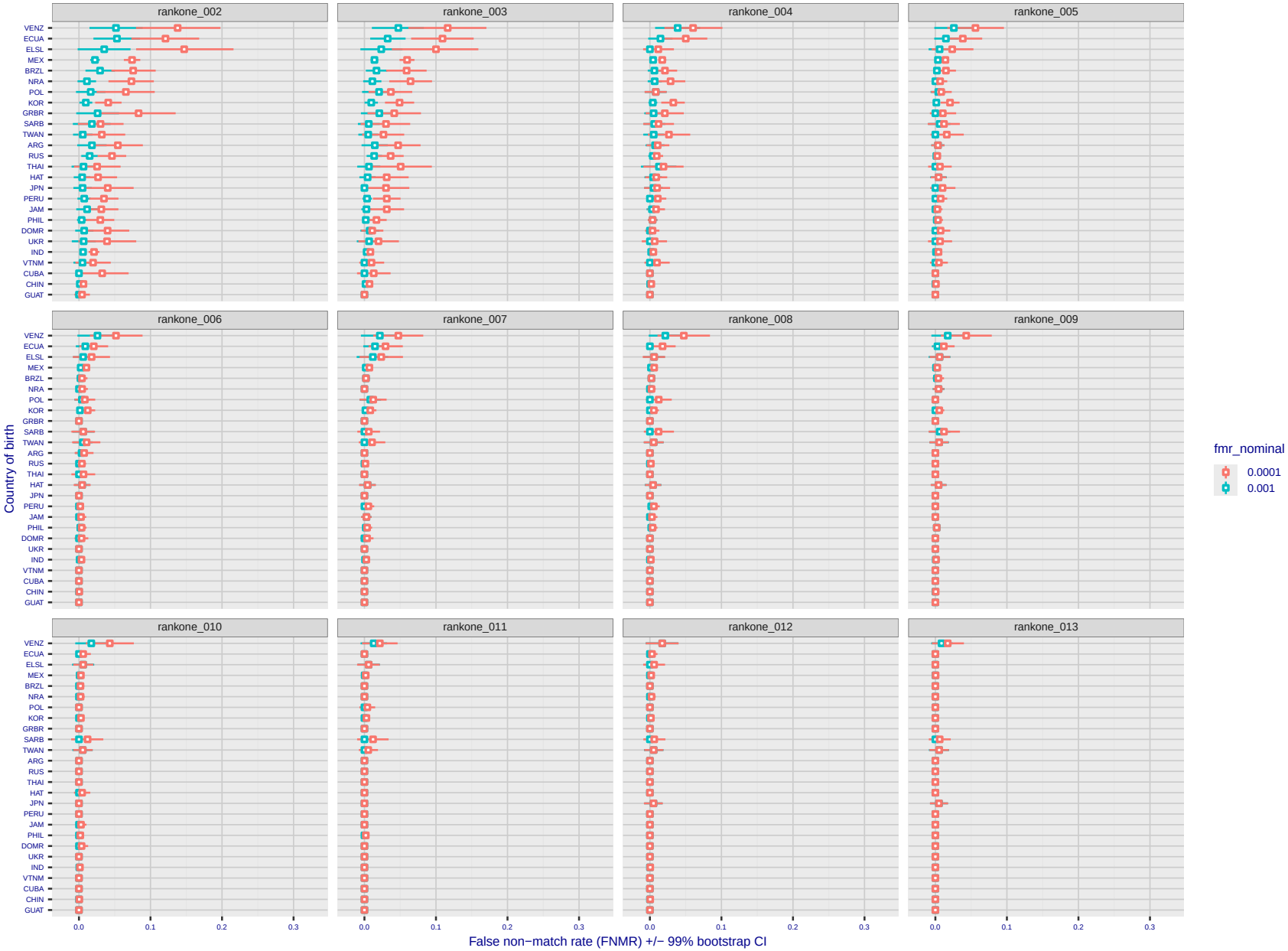

Figure 669: For the visa images, the dots show FNMR by country of birth for two globally set operating thresholds corresponding to FMR = $\{0.001, 0.0001\}$ computed over all on the order of 10^{10} impostor scores. The FMR in each bin will vary also - see subsequent impostor heatmaps in sec. 3.6.1. The figures shows an order of magnitude variation in FNMR across country of birth; these effects are likely due quality variations, then demographics like age and race. The error rates in some cases are zero, and in others the DET is flat so the error rates at the two thresholds are identical. The lines span 1% and 99% of boostrap replicated FNMR estimates.

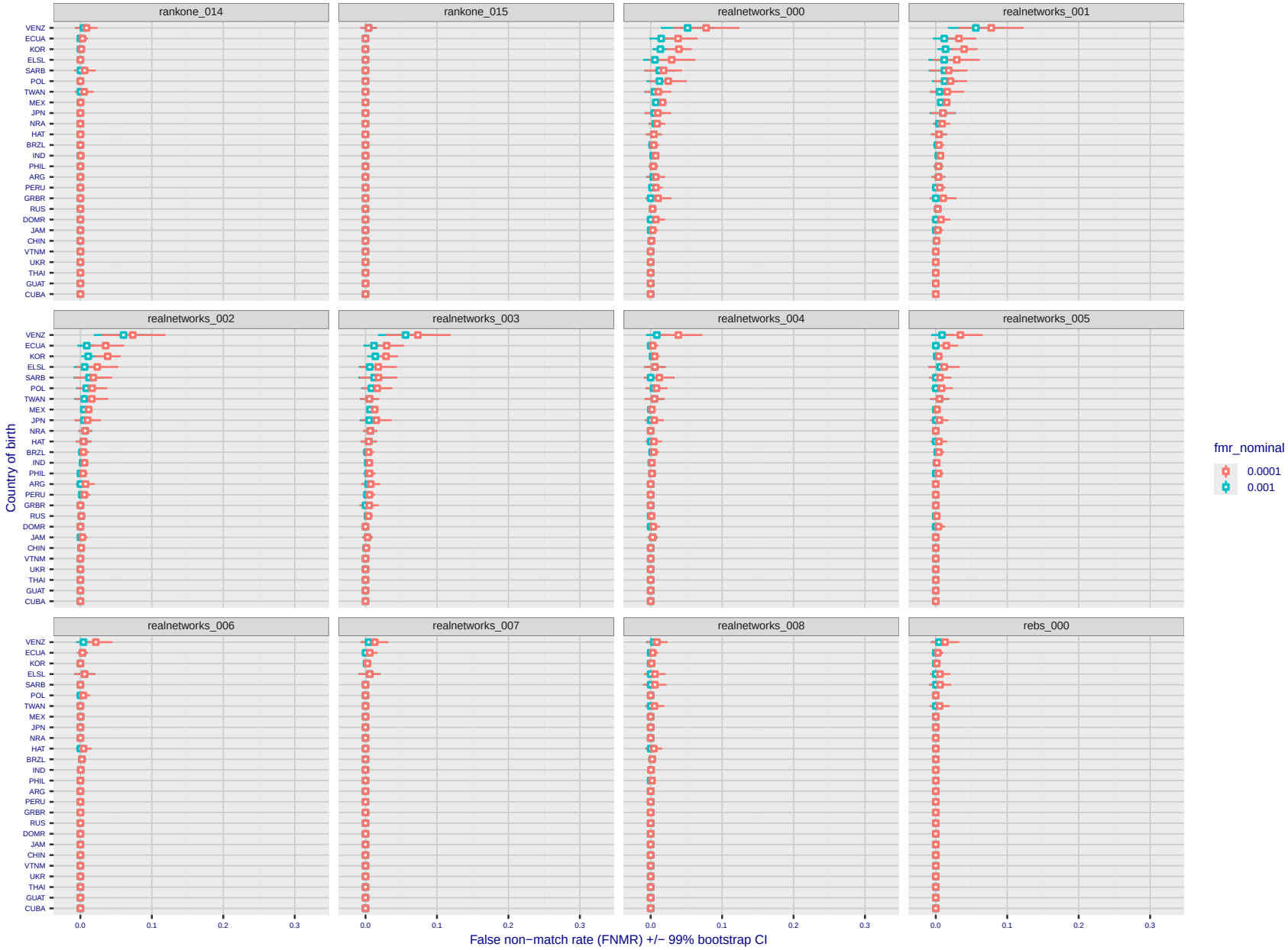

Figure 670: For the visa images, the dots show FNMR by country of birth for two globally set operating thresholds corresponding to FMR = $\{0.001, 0.0001\}$ computed over all on the order of 10^{10} impostor scores. The FMR in each bin will vary also - see subsequent impostor heatmaps in sec. 3.6.1. The figures shows an order of magnitude variation in FNMR across country of birth; these effects are likely due quality variations, then demographics like age and race. The error rates in some cases are zero, and in others the DET is flat so the error rates at the two thresholds are identical. The lines span 1% and 99% of boostrap replicated FNMR estimates.

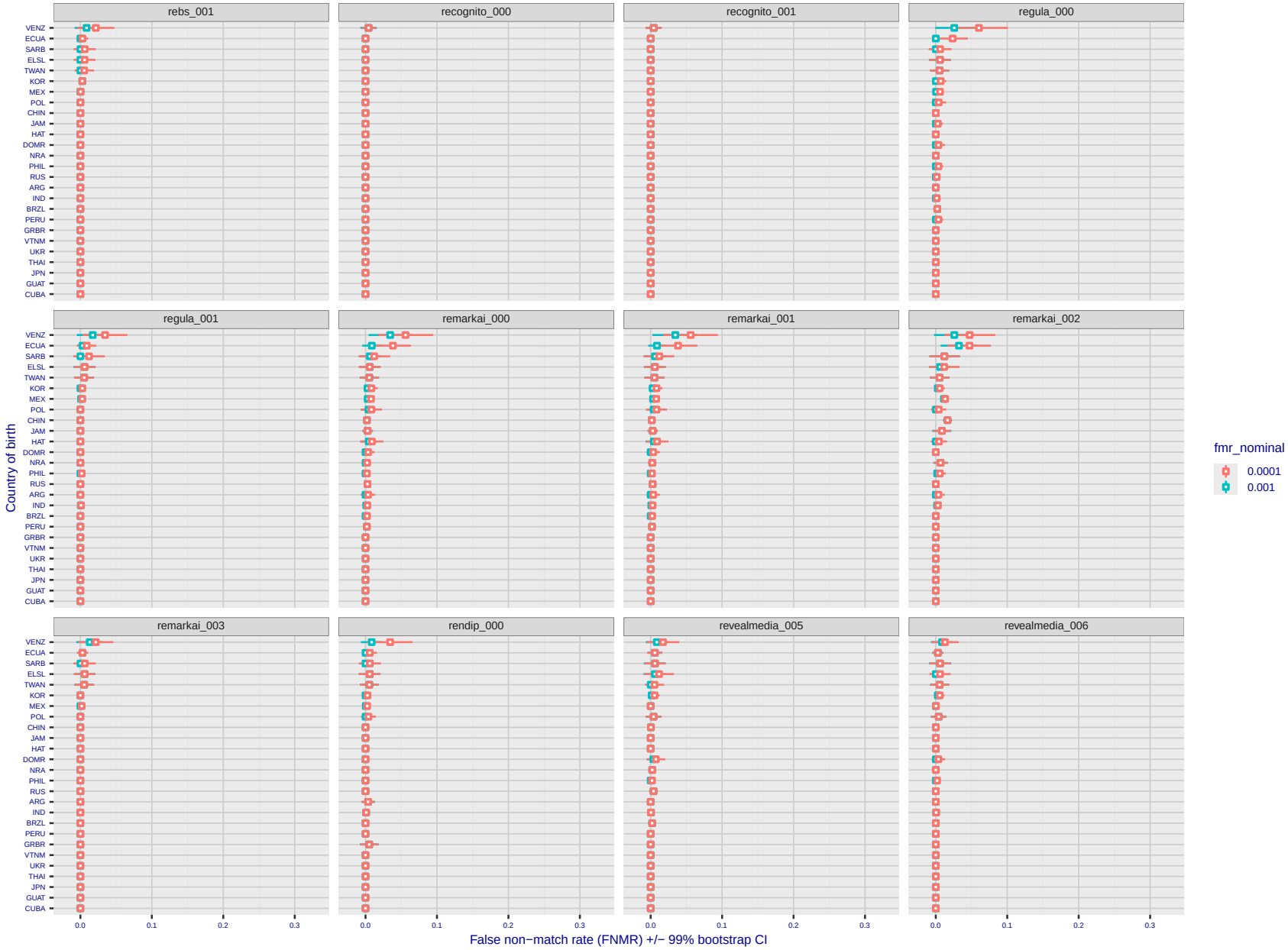

Figure 671: For the visa images, the dots show FNMR by country of birth for two globally set operating thresholds corresponding to FMR = $\{0.001, 0.0001\}$ computed over all on the order of 10^{10} impostor scores. The FMR in each bin will vary also - see subsequent impostor heatmaps in sec. 3.6.1. The figures shows an order of magnitude variation in FNMR across country of birth; these effects are likely due quality variations, then demographics like age and race. The error rates in some cases are zero, and in others the DET is flat so the error rates at the two thresholds are identical. The lines span 1% and 99% of boostrap replicated FNMR estimates.

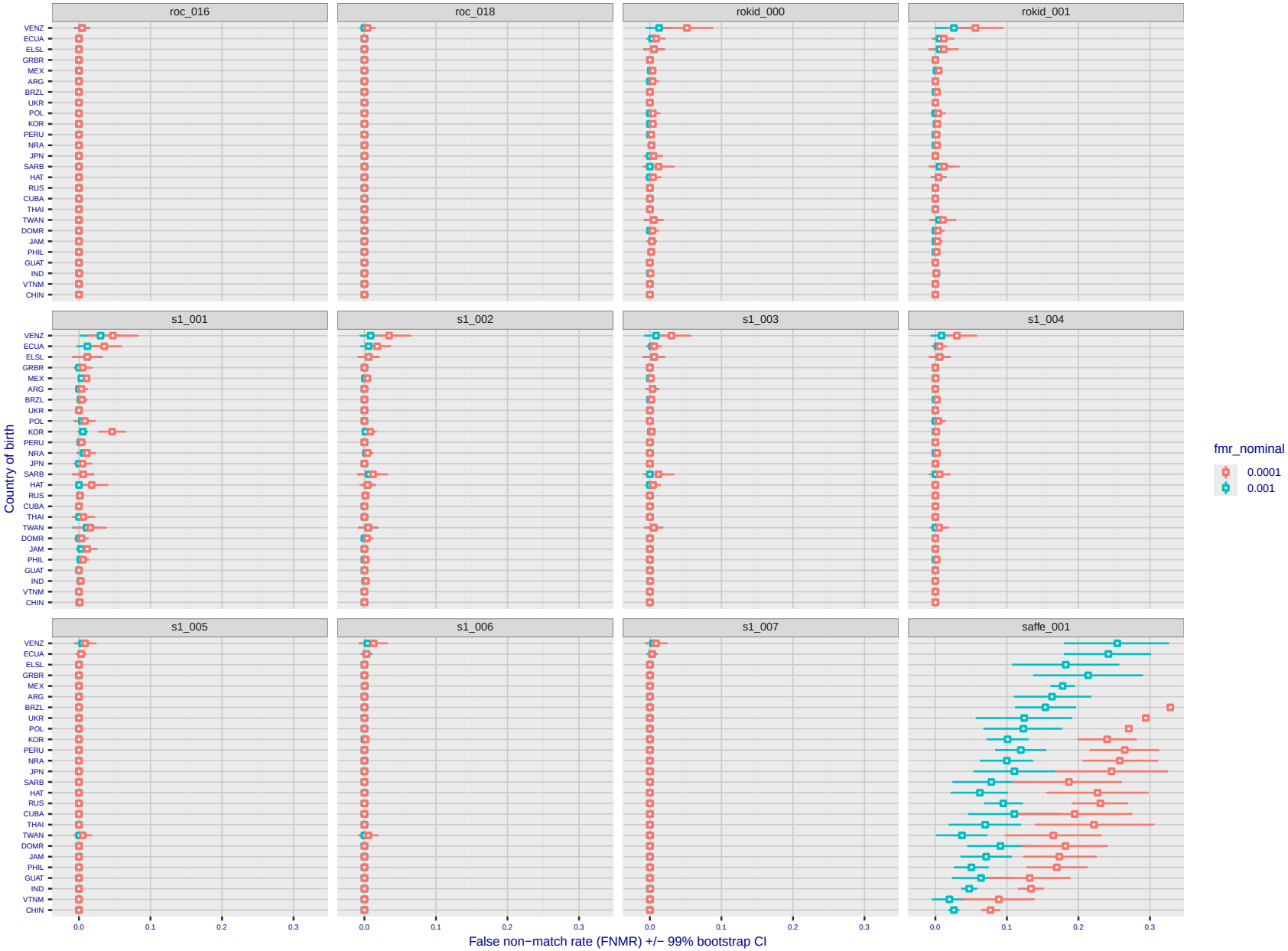

Figure 672: For the visa images, the dots show FNMR by country of birth for two globally set operating thresholds corresponding to FMR = $\{0.001, 0.0001\}$ computed over all on the order of 10^{10} impostor scores. The FMR in each bin will vary also - see subsequent impostor heatmaps in sec. 3.6.1. The figures shows an order of magnitude variation in FNMR across country of birth; these effects are likely due quality variations, then demographics like age and race. The error rates in some cases are zero, and in others the DET is flat so the error rates at the two thresholds are identical. The lines span 1% and 99% of boostrap replicated FNMR estimates.

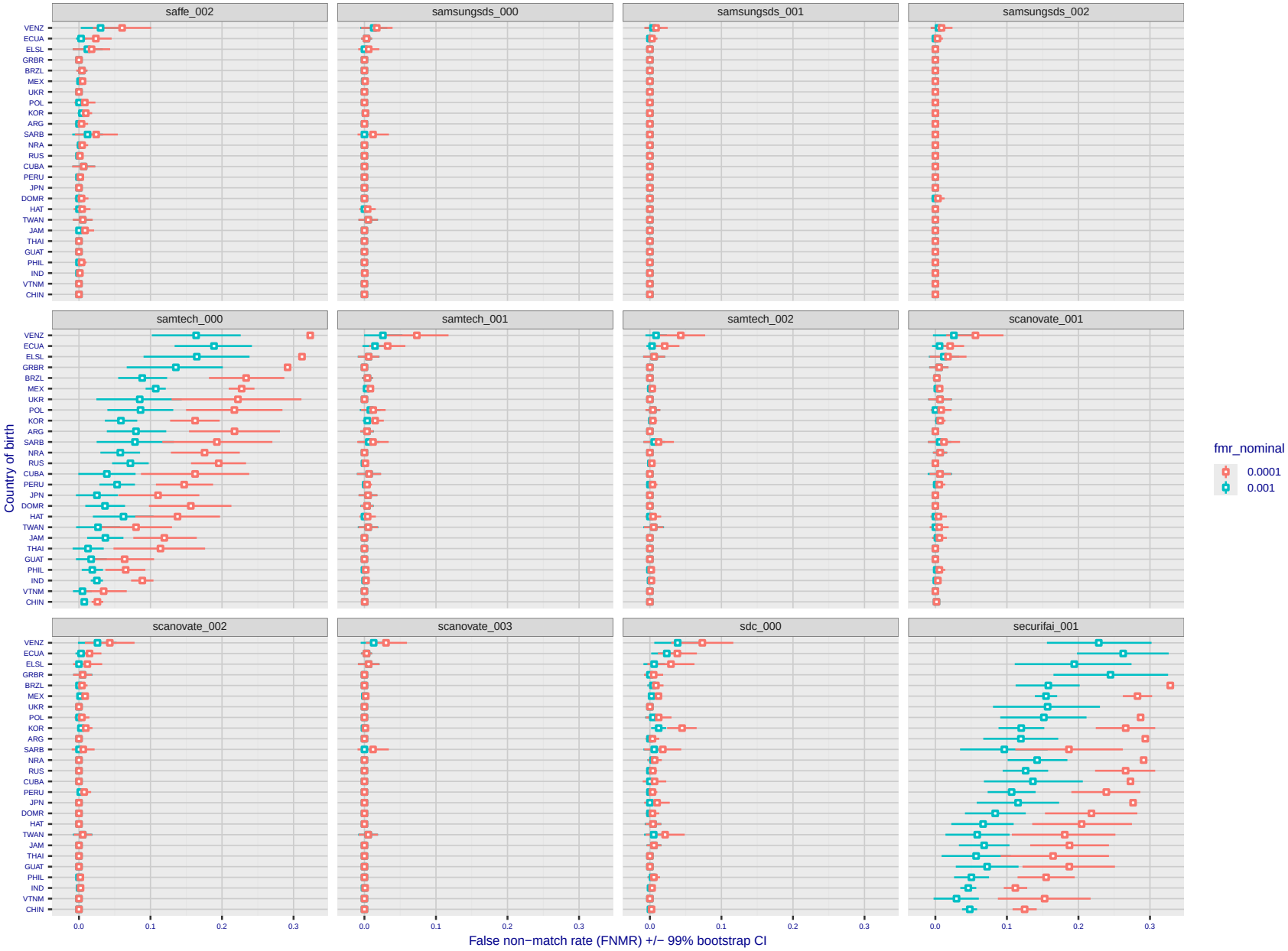

Figure 673: For the visa images, the dots show FNMR by country of birth for two globally set operating thresholds corresponding to FMR = $\{0.001, 0.0001\}$ computed over all on the order of 10^{10} impostor scores. The FMR in each bin will vary also - see subsequent impostor heatmaps in sec. 3.6.1. The figures shows an order of magnitude variation in FNMR across country of birth; these effects are likely due quality variations, then demographics like age and race. The error rates in some cases are zero, and in others the DET is flat so the error rates at the two thresholds are identical. The lines span 1% and 99% of boostrap replicated FNMR estimates.

Figure 674: For the visa images, the dots show FNMR by country of birth for two globally set operating thresholds corresponding to FMR = $\{0.001, 0.0001\}$ computed over all on the order of 10^{10} impostor scores. The FMR in each bin will vary also - see subsequent impostor heatmaps in sec. 3.6.1. The figures shows an order of magnitude variation in FNMR across country of birth; these effects are likely due quality variations, then demographics like age and race. The error rates in some cases are zero, and in others the DET is flat so the error rates at the two thresholds are identical. The lines span 1% and 99% of boostrap replicated FNMR estimates.

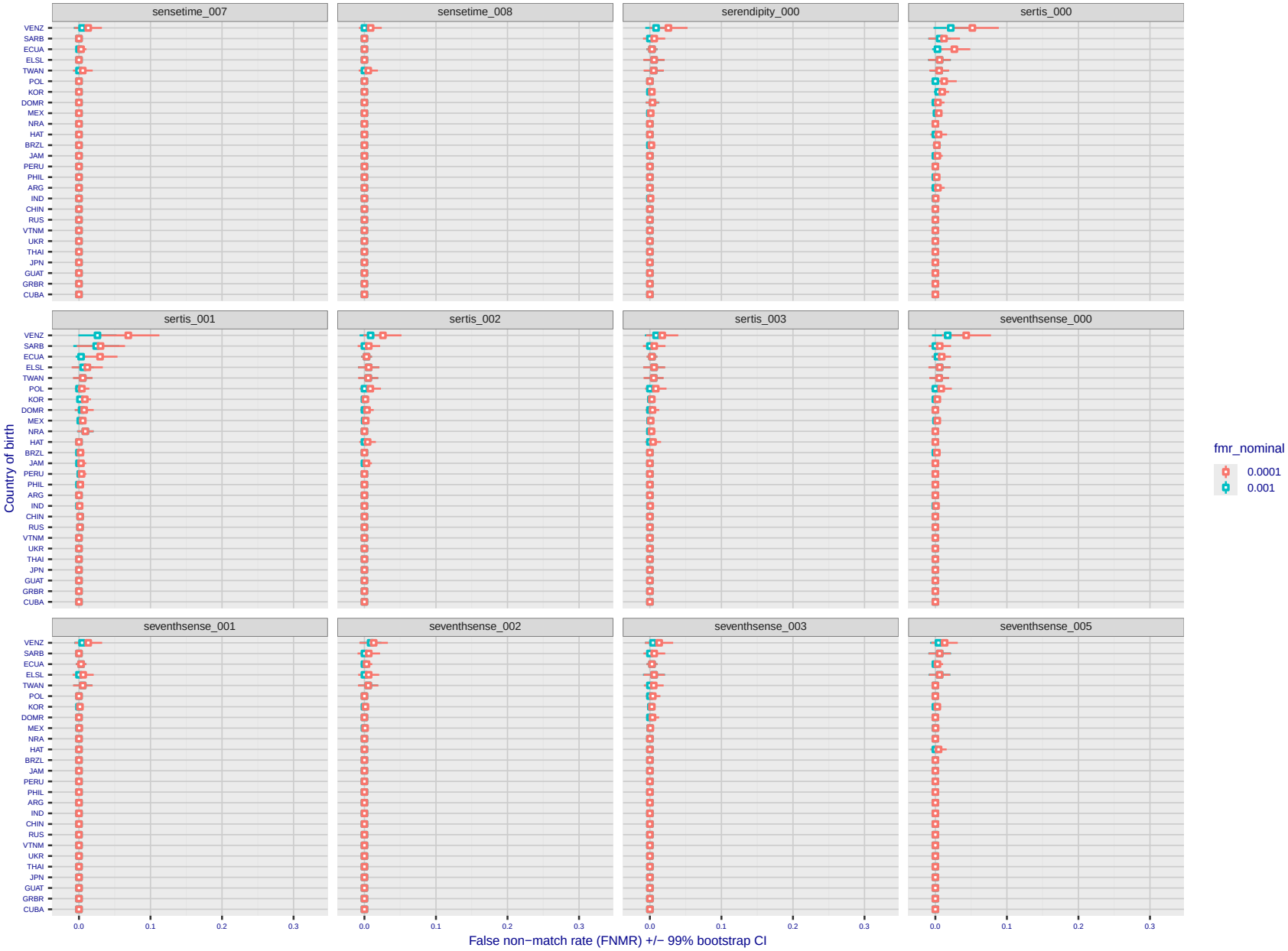

Figure 675: For the visa images, the dots show FNMR by country of birth for two globally set operating thresholds corresponding to FMR = $\{0.001, 0.0001\}$ computed over all on the order of 10^{10} impostor scores. The FMR in each bin will vary also - see subsequent impostor heatmaps in sec. 3.6.1. The figures shows an order of magnitude variation in FNMR across country of birth; these effects are likely due quality variations, then demographics like age and race. The error rates in some cases are zero, and in others the DET is flat so the error rates at the two thresholds are identical. The lines span 1% and 99% of boostrap replicated FNMR estimates.

Figure 676: For the visa images, the dots show FNMR by country of birth for two globally set operating thresholds corresponding to FMR = $\{0.001, 0.0001\}$ computed over all on the order of 10^{10} impostor scores. The FMR in each bin will vary also - see subsequent impostor heatmaps in sec. 3.6.1. The figures shows an order of magnitude variation in FNMR across country of birth; these effects are likely due quality variations, then demographics like age and race. The error rates in some cases are zero, and in others the DET is flat so the error rates at the two thresholds are identical. The lines span 1% and 99% of boostrap replicated FNMR estimates.

Figure 677: For the visa images, the dots show FNMR by country of birth for two globally set operating thresholds corresponding to FMR = $\{0.001, 0.0001\}$ computed over all on the order of 10^{10} impostor scores. The FMR in each bin will vary also - see subsequent impostor heatmaps in sec. 3.6.1. The figures shows an order of magnitude variation in FNMR across country of birth; these effects are likely due quality variations, then demographics like age and race. The error rates in some cases are zero, and in others the DET is flat so the error rates at the two thresholds are identical. The lines span 1% and 99% of boostrap replicated FNMR estimates.

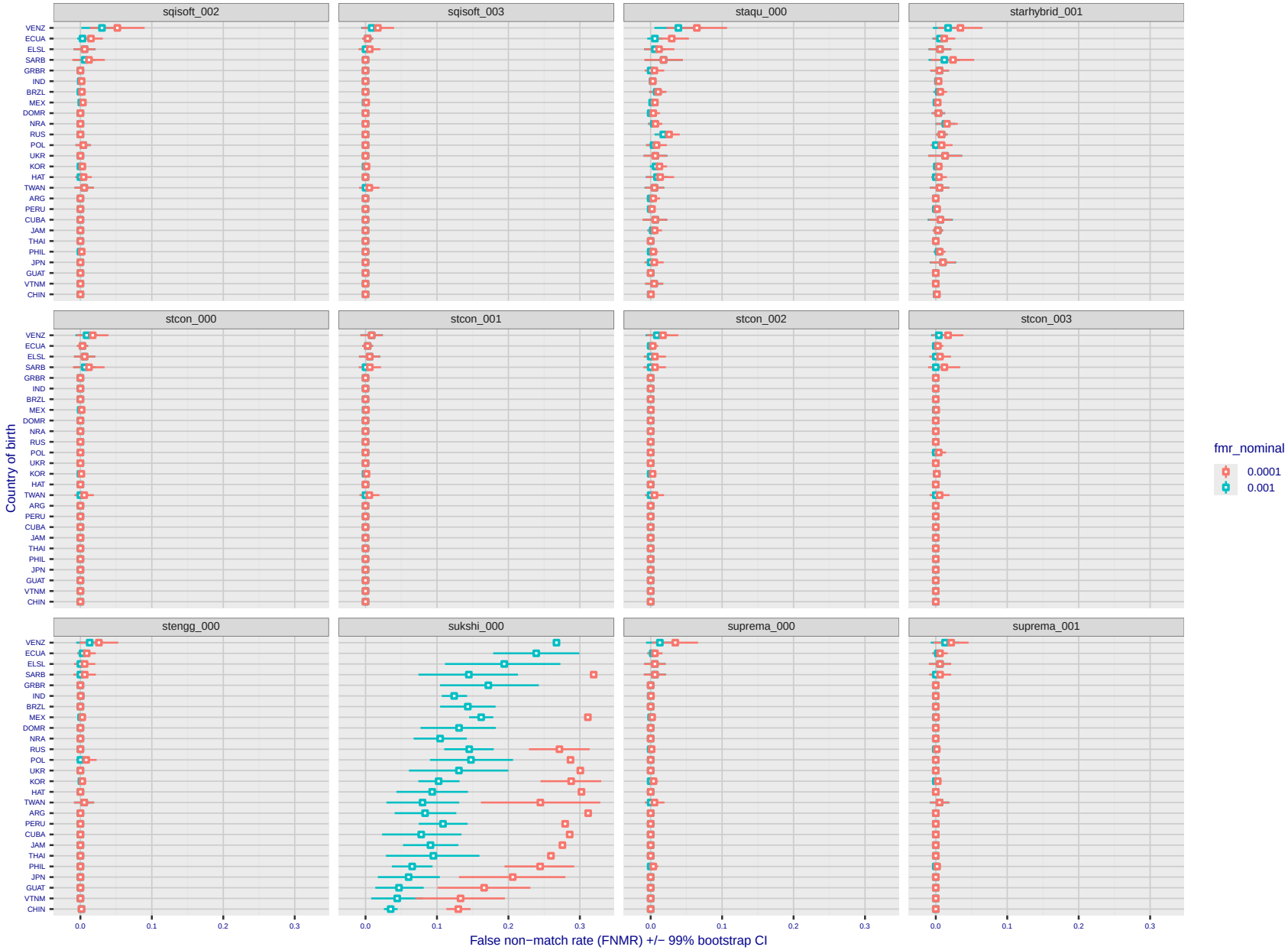

Figure 678: For the visa images, the dots show FNMR by country of birth for two globally set operating thresholds corresponding to FMR = $\{0.001, 0.0001\}$ computed over all on the order of 10^{10} impostor scores. The FMR in each bin will vary also - see subsequent impostor heatmaps in sec. 3.6.1. The figures shows an order of magnitude variation in FNMR across country of birth; these effects are likely due quality variations, then demographics like age and race. The error rates in some cases are zero, and in others the DET is flat so the error rates at the two thresholds are identical. The lines span 1% and 99% of boostrap replicated FNMR estimates.

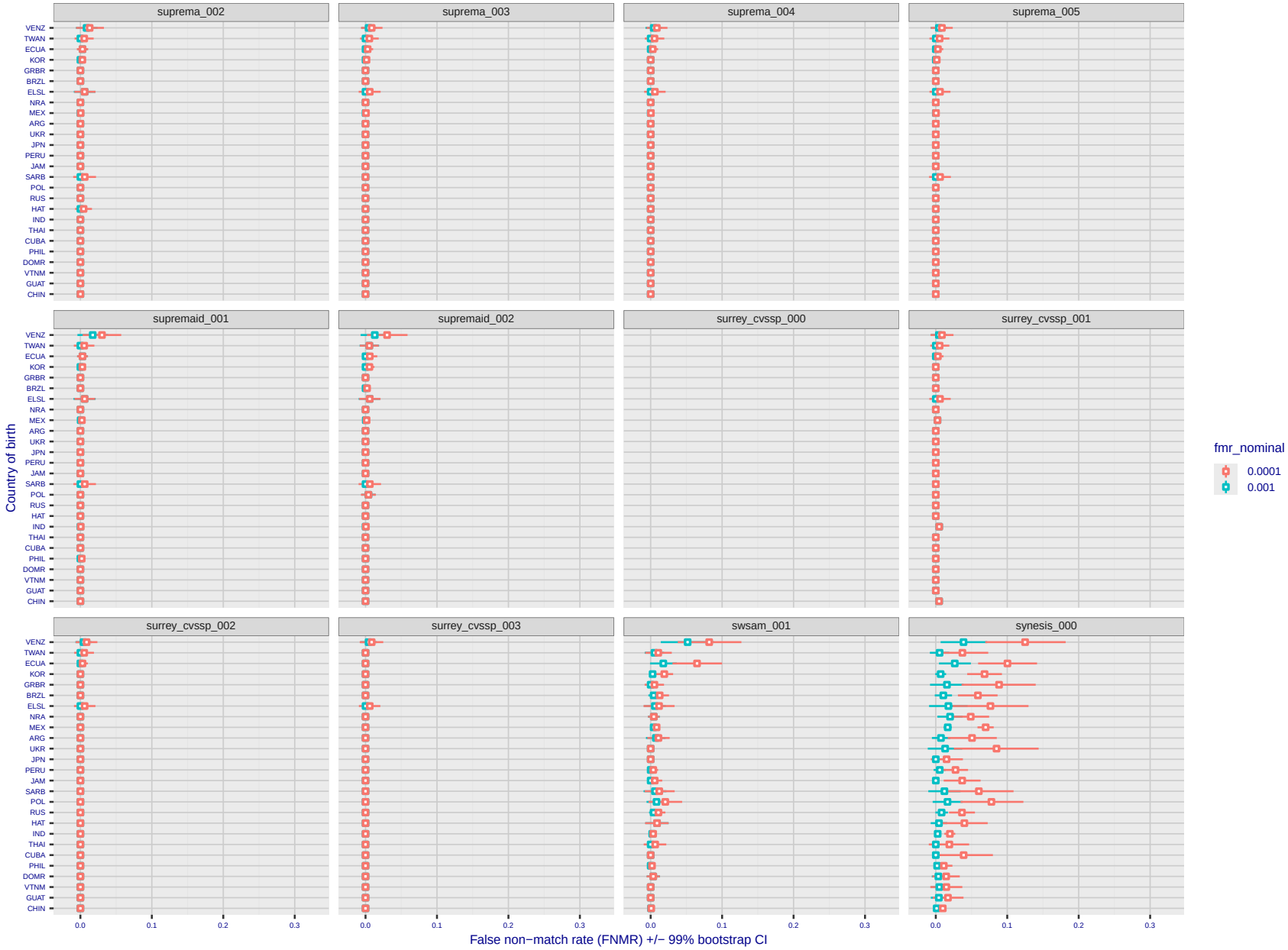

Figure 679: For the visa images, the dots show FNMR by country of birth for two globally set operating thresholds corresponding to FMR = $\{0.001, 0.0001\}$ computed over all on the order of 10^{10} impostor scores. The FMR in each bin will vary also - see subsequent impostor heatmaps in sec. 3.6.1. The figures shows an order of magnitude variation in FNMR across country of birth; these effects are likely due quality variations, then demographics like age and race. The error rates in some cases are zero, and in others the DET is flat so the error rates at the two thresholds are identical. The lines span 1% and 99% of boostrap replicated FNMR estimates.

Figure 680: For the visa images, the dots show FNMR by country of birth for two globally set operating thresholds corresponding to FMR = $\{0.001, 0.0001\}$ computed over all on the order of 10^{10} impostor scores. The FMR in each bin will vary also - see subsequent impostor heatmaps in sec. 3.6.1. The figures shows an order of magnitude variation in FNMR across country of birth; these effects are likely due quality variations, then demographics like age and race. The error rates in some cases are zero, and in others the DET is flat so the error rates at the two thresholds are identical. The lines span 1% and 99% of boostrap replicated FNMR estimates.

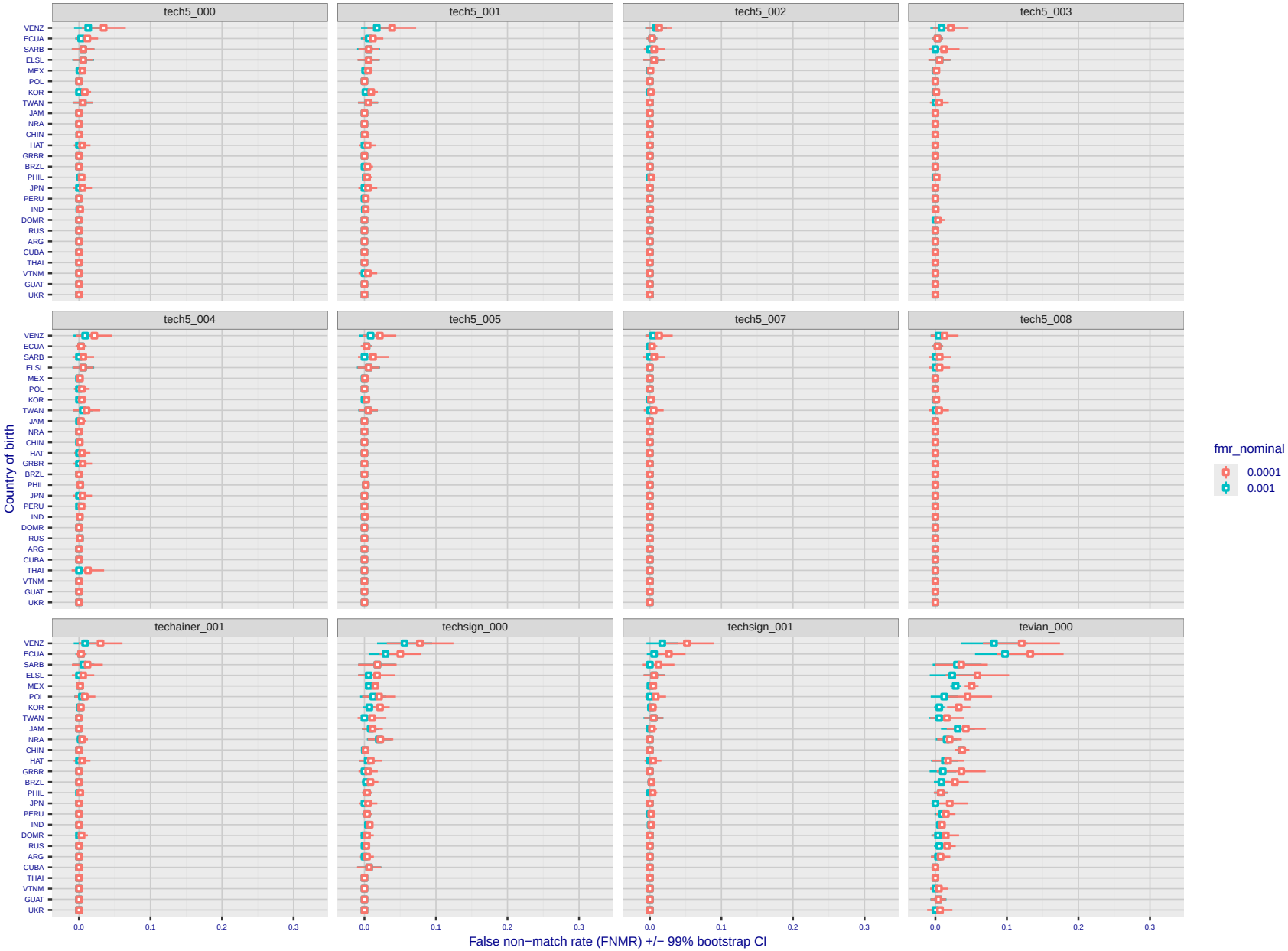

Figure 681: For the visa images, the dots show FNMR by country of birth for two globally set operating thresholds corresponding to FMR = $\{0.001, 0.0001\}$ computed over all on the order of 10^{10} impostor scores. The FMR in each bin will vary also - see subsequent impostor heatmaps in sec. 3.6.1. The figures shows an order of magnitude variation in FNMR across country of birth; these effects are likely due quality variations, then demographics like age and race. The error rates in some cases are zero, and in others the DET is flat so the error rates at the two thresholds are identical. The lines span 1% and 99% of boostrap replicated FNMR estimates.

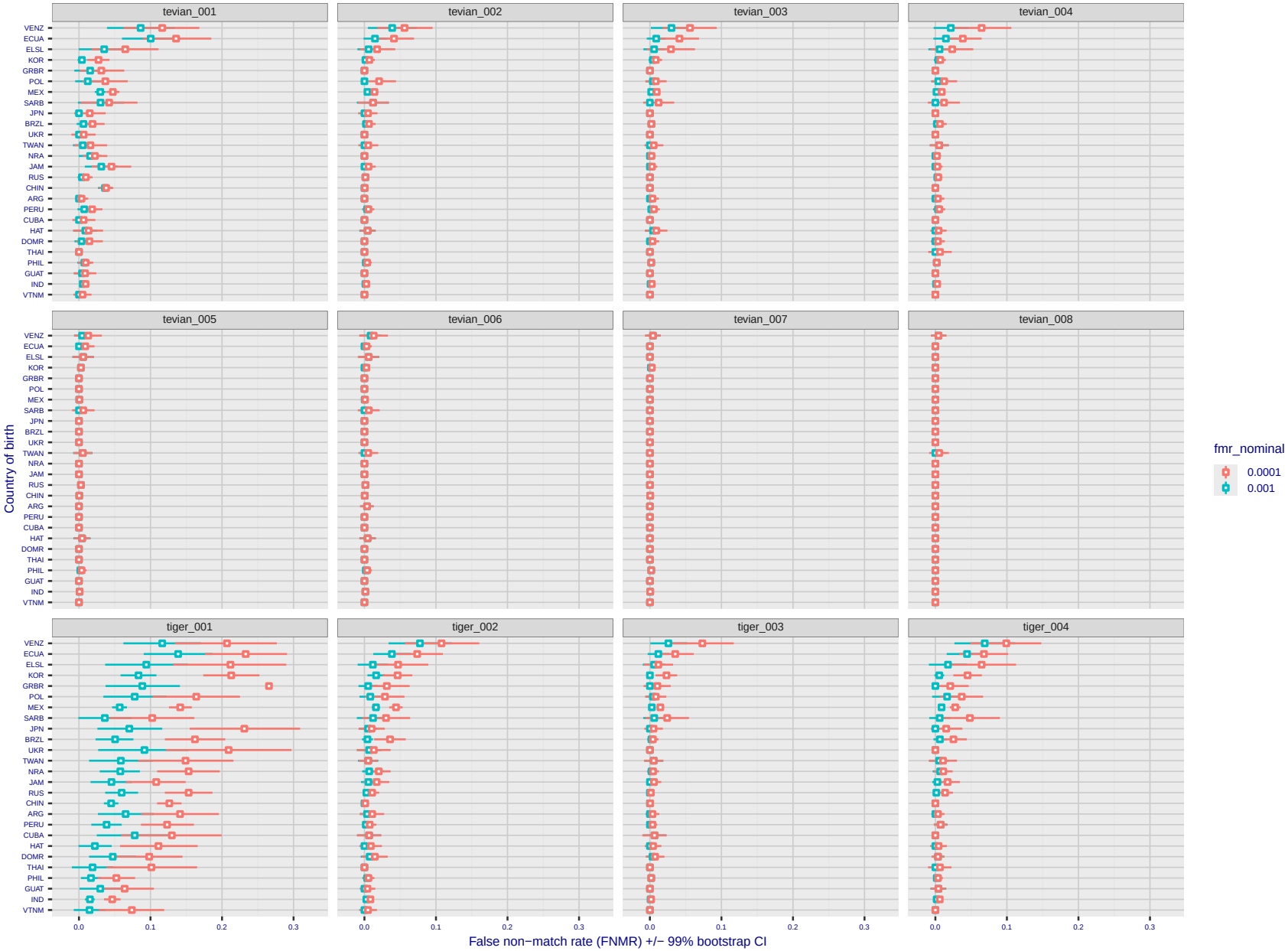

Figure 682: For the visa images, the dots show FNMR by country of birth for two globally set operating thresholds corresponding to FMR = $\{0.001, 0.0001\}$ computed over all on the order of 10^{10} impostor scores. The FMR in each bin will vary also - see subsequent impostor heatmaps in sec. 3.6.1. The figures shows an order of magnitude variation in FNMR across country of birth; these effects are likely due quality variations, then demographics like age and race. The error rates in some cases are zero, and in others the DET is flat so the error rates at the two thresholds are identical. The lines span 1% and 99% of boostrap replicated FNMR estimates.

Figure 683: For the visa images, the dots show FNMR by country of birth for two globally set operating thresholds corresponding to FMR = $\{0.001, 0.0001\}$ computed over all on the order of 10^{10} impostor scores. The FMR in each bin will vary also - see subsequent impostor heatmaps in sec. 3.6.1. The figures shows an order of magnitude variation in FNMR across country of birth; these effects are likely due quality variations, then demographics like age and race. The error rates in some cases are zero, and in others the DET is flat so the error rates at the two thresholds are identical. The lines span 1% and 99% of boostrap replicated FNMR estimates.

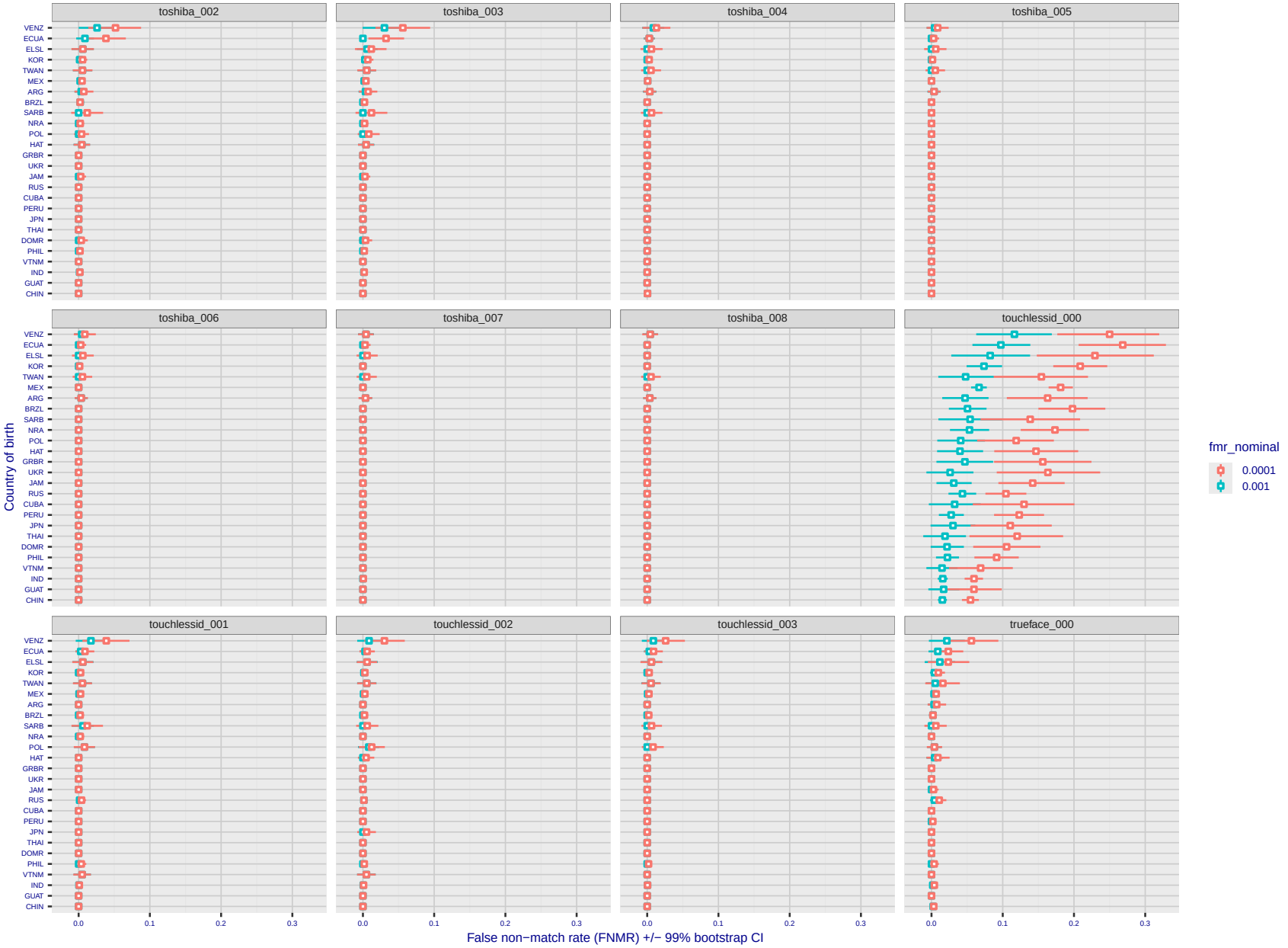

Figure 684: For the visa images, the dots show FNMR by country of birth for two globally set operating thresholds corresponding to FMR = $\{0.001, 0.0001\}$ computed over all on the order of 10^{10} impostor scores. The FMR in each bin will vary also - see subsequent impostor heatmaps in sec. 3.6.1. The figures shows an order of magnitude variation in FNMR across country of birth; these effects are likely due quality variations, then demographics like age and race. The error rates in some cases are zero, and in others the DET is flat so the error rates at the two thresholds are identical. The lines span 1% and 99% of boostrap replicated FNMR estimates.

Figure 685: For the visa images, the dots show FNMR by country of birth for two globally set operating thresholds corresponding to FMR = $\{0.001, 0.0001\}$ computed over all on the order of 10^{10} impostor scores. The FMR in each bin will vary also - see subsequent impostor heatmaps in sec. 3.6.1. The figures shows an order of magnitude variation in FNMR across country of birth; these effects are likely due quality variations, then demographics like age and race. The error rates in some cases are zero, and in others the DET is flat so the error rates at the two thresholds are identical. The lines span 1% and 99% of boostrap replicated FNMR estimates.

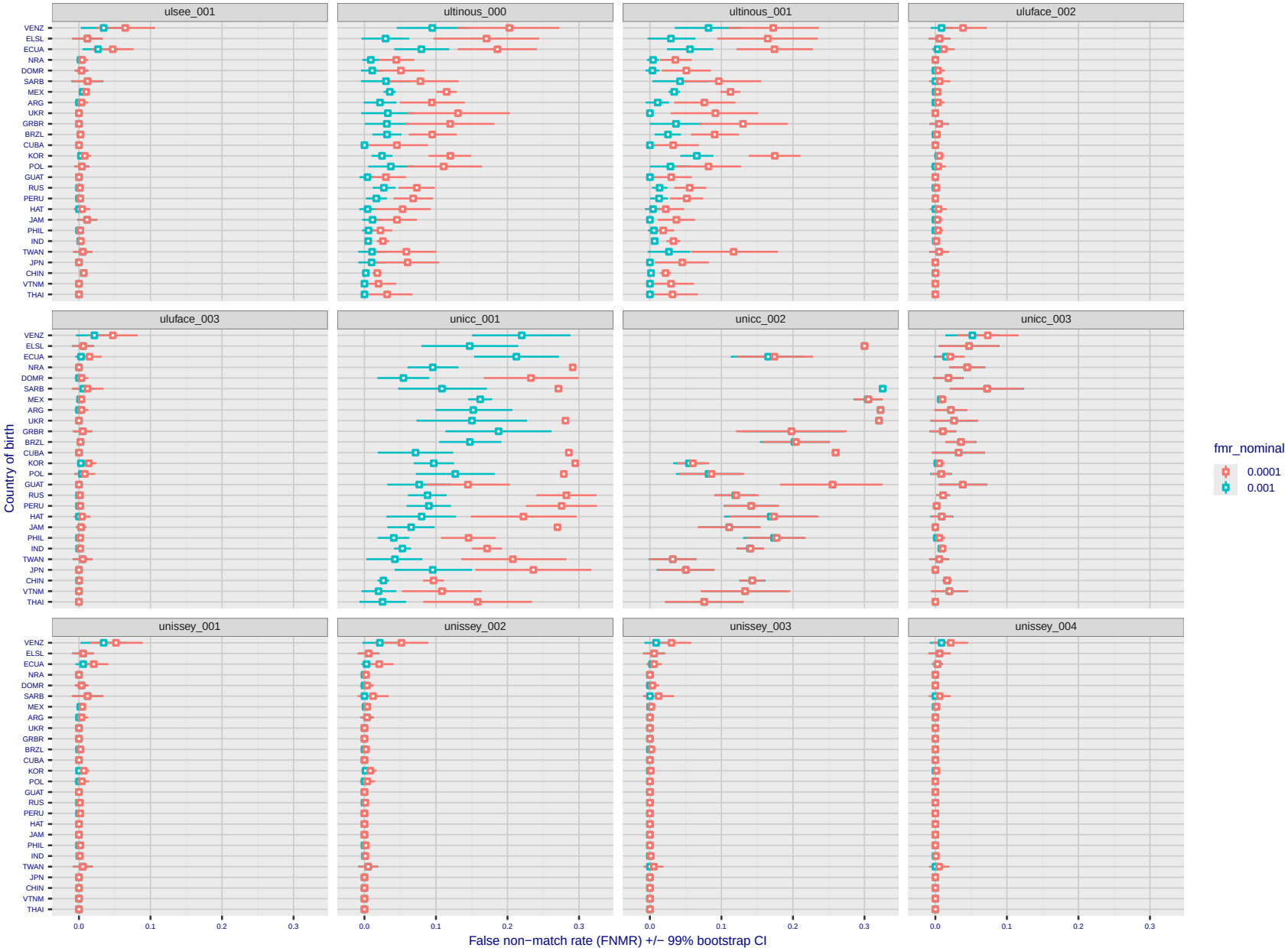

Figure 686: For the visa images, the dots show FNMR by country of birth for two globally set operating thresholds corresponding to FMR = $\{0.001, 0.0001\}$ computed over all on the order of 10^{10} impostor scores. The FMR in each bin will vary also - see subsequent impostor heatmaps in sec. 3.6.1. The figures shows an order of magnitude variation in FNMR across country of birth; these effects are likely due quality variations, then demographics like age and race. The error rates in some cases are zero, and in others the DET is flat so the error rates at the two thresholds are identical. The lines span 1% and 99% of boostrap replicated FNMR estimates.

Figure 687: For the visa images, the dots show FNMR by country of birth for two globally set operating thresholds corresponding to FMR = $\{0.001, 0.0001\}$ computed over all on the order of 10^{10} impostor scores. The FMR in each bin will vary also - see subsequent impostor heatmaps in sec. 3.6.1. The figures shows an order of magnitude variation in FNMR across country of birth; these effects are likely due quality variations, then demographics like age and race. The error rates in some cases are zero, and in others the DET is flat so the error rates at the two thresholds are identical. The lines span 1% and 99% of boostrap replicated FNMR estimates.

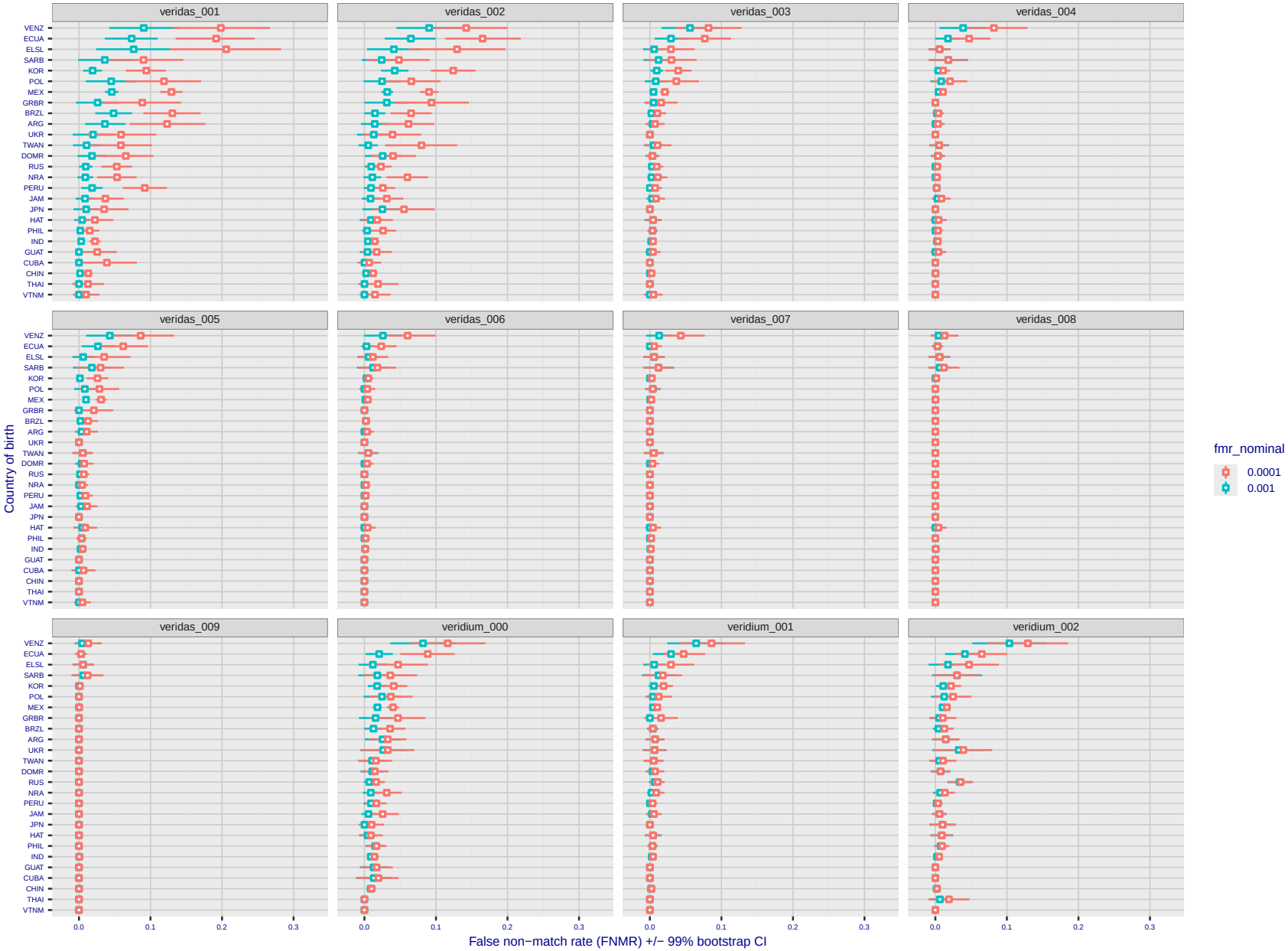

Figure 688: For the visa images, the dots show FNMR by country of birth for two globally set operating thresholds corresponding to FMR = $\{0.001, 0.0001\}$ computed over all on the order of 10^{10} impostor scores. The FMR in each bin will vary also - see subsequent impostor heatmaps in sec. 3.6.1. The figures shows an order of magnitude variation in FNMR across country of birth; these effects are likely due quality variations, then demographics like age and race. The error rates in some cases are zero, and in others the DET is flat so the error rates at the two thresholds are identical. The lines span 1% and 99% of boostrap replicated FNMR estimates.

Figure 689: For the visa images, the dots show FNMR by country of birth for two globally set operating thresholds corresponding to FMR = $\{0.001, 0.0001\}$ computed over all on the order of 10^{10} impostor scores. The FMR in each bin will vary also - see subsequent impostor heatmaps in sec. 3.6.1. The figures shows an order of magnitude variation in FNMR across country of birth; these effects are likely due quality variations, then demographics like age and race. The error rates in some cases are zero, and in others the DET is flat so the error rates at the two thresholds are identical. The lines span 1% and 99% of boostrap replicated FNMR estimates.

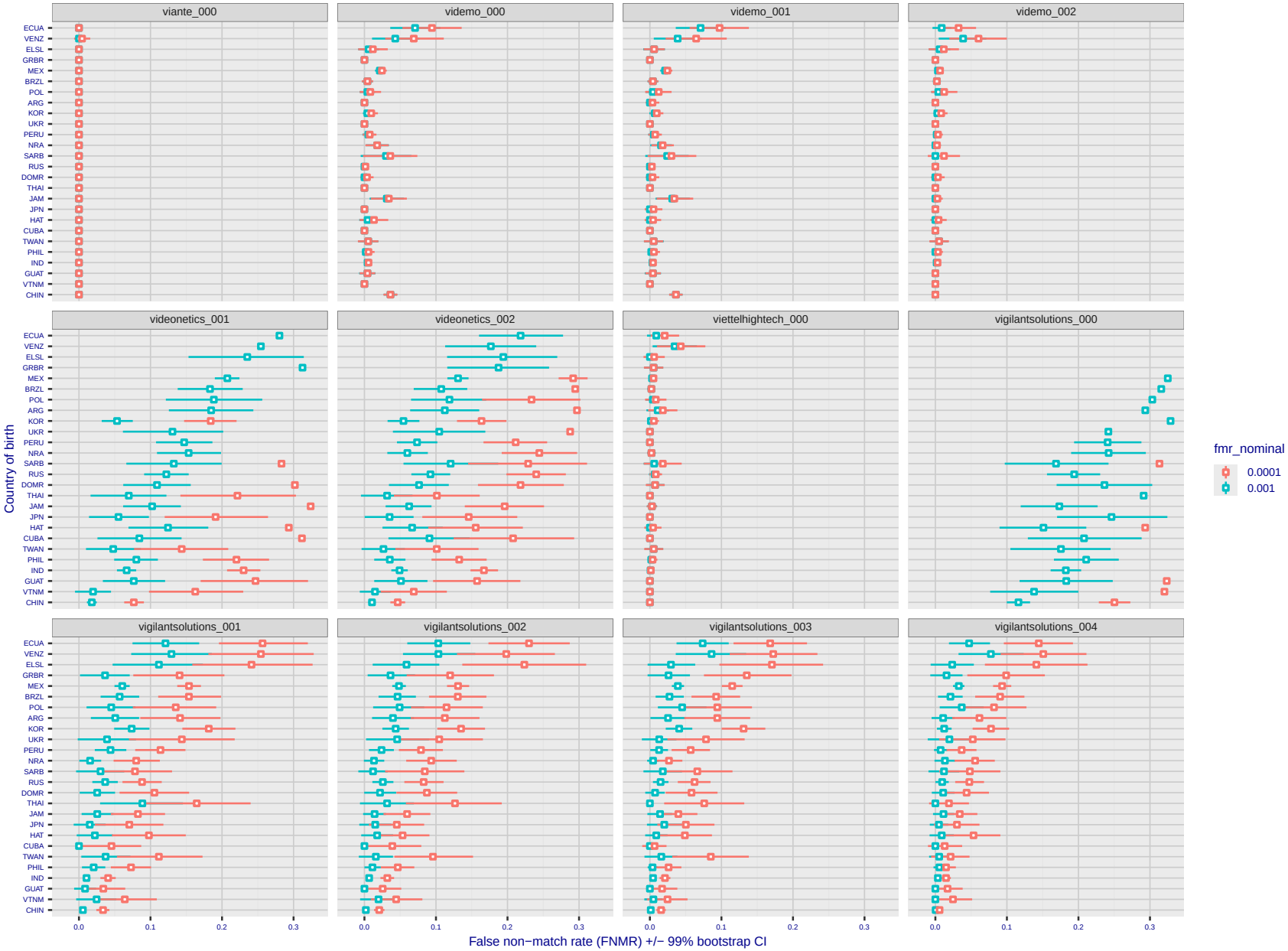

Figure 690: For the visa images, the dots show FNMR by country of birth for two globally set operating thresholds corresponding to FMR = $\{0.001, 0.0001\}$ computed over all on the order of 10^{10} impostor scores. The FMR in each bin will vary also - see subsequent impostor heatmaps in sec. 3.6.1. The figures shows an order of magnitude variation in FNMR across country of birth; these effects are likely due quality variations, then demographics like age and race. The error rates in some cases are zero, and in others the DET is flat so the error rates at the two thresholds are identical. The lines span 1% and 99% of boostrap replicated FNMR estimates.

Figure 691: For the visa images, the dots show FNMR by country of birth for two globally set operating thresholds corresponding to FMR = $\{0.001, 0.0001\}$ computed over all on the order of 10^{10} impostor scores. The FMR in each bin will vary also - see subsequent impostor heatmaps in sec. 3.6.1. The figures shows an order of magnitude variation in FNMR across country of birth; these effects are likely due quality variations, then demographics like age and race. The error rates in some cases are zero, and in others the DET is flat so the error rates at the two thresholds are identical. The lines span 1% and 99% of boostrap replicated FNMR estimates.

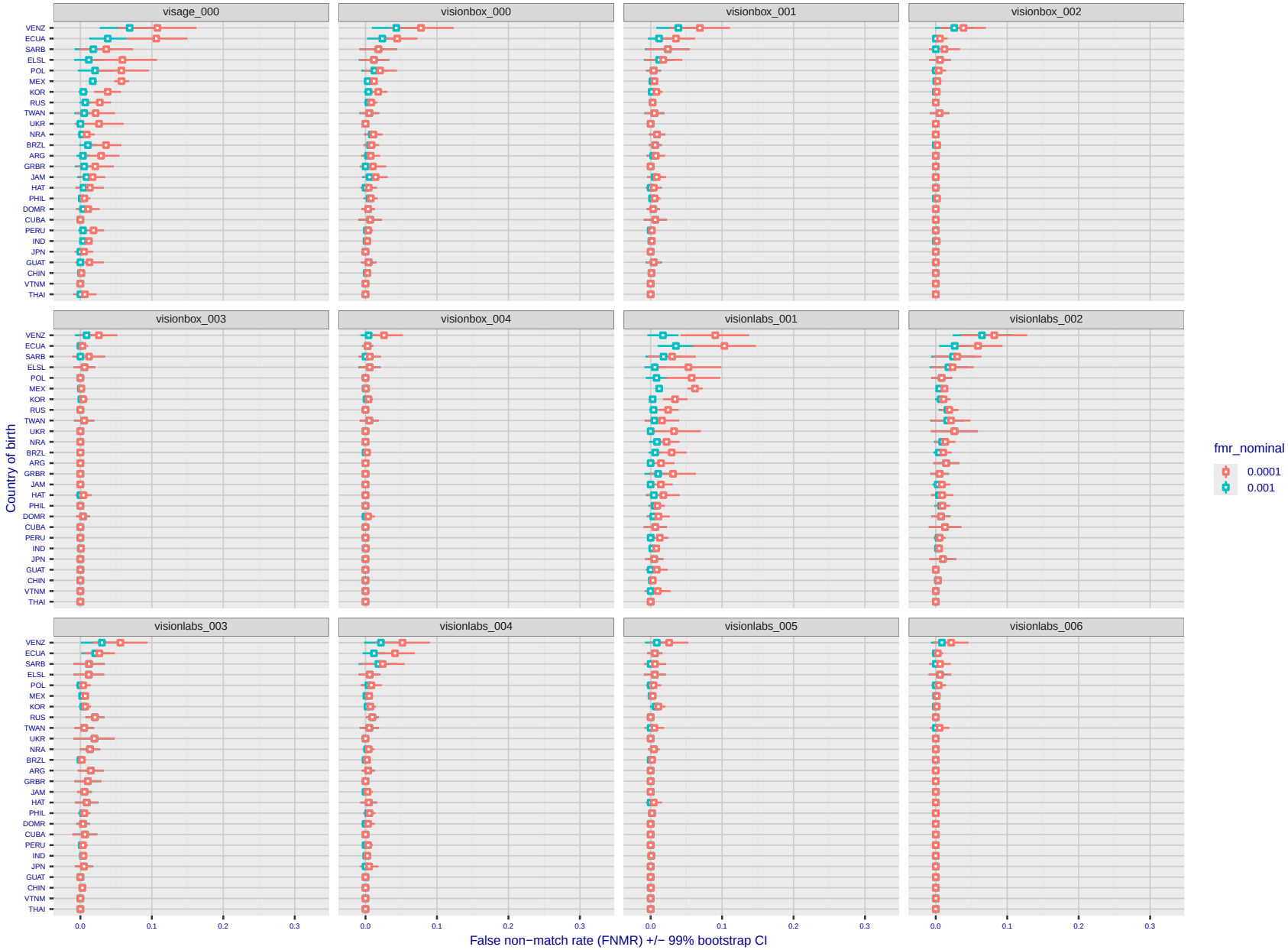

Figure 692: For the visa images, the dots show FNMR by country of birth for two globally set operating thresholds corresponding to FMR = $\{0.001, 0.0001\}$ computed over all on the order of 10^{10} impostor scores. The FMR in each bin will vary also - see subsequent impostor heatmaps in sec. 3.6.1. The figures shows an order of magnitude variation in FNMR across country of birth; these effects are likely due quality variations, then demographics like age and race. The error rates in some cases are zero, and in others the DET is flat so the error rates at the two thresholds are identical. The lines span 1% and 99% of boostrap replicated FNMR estimates.

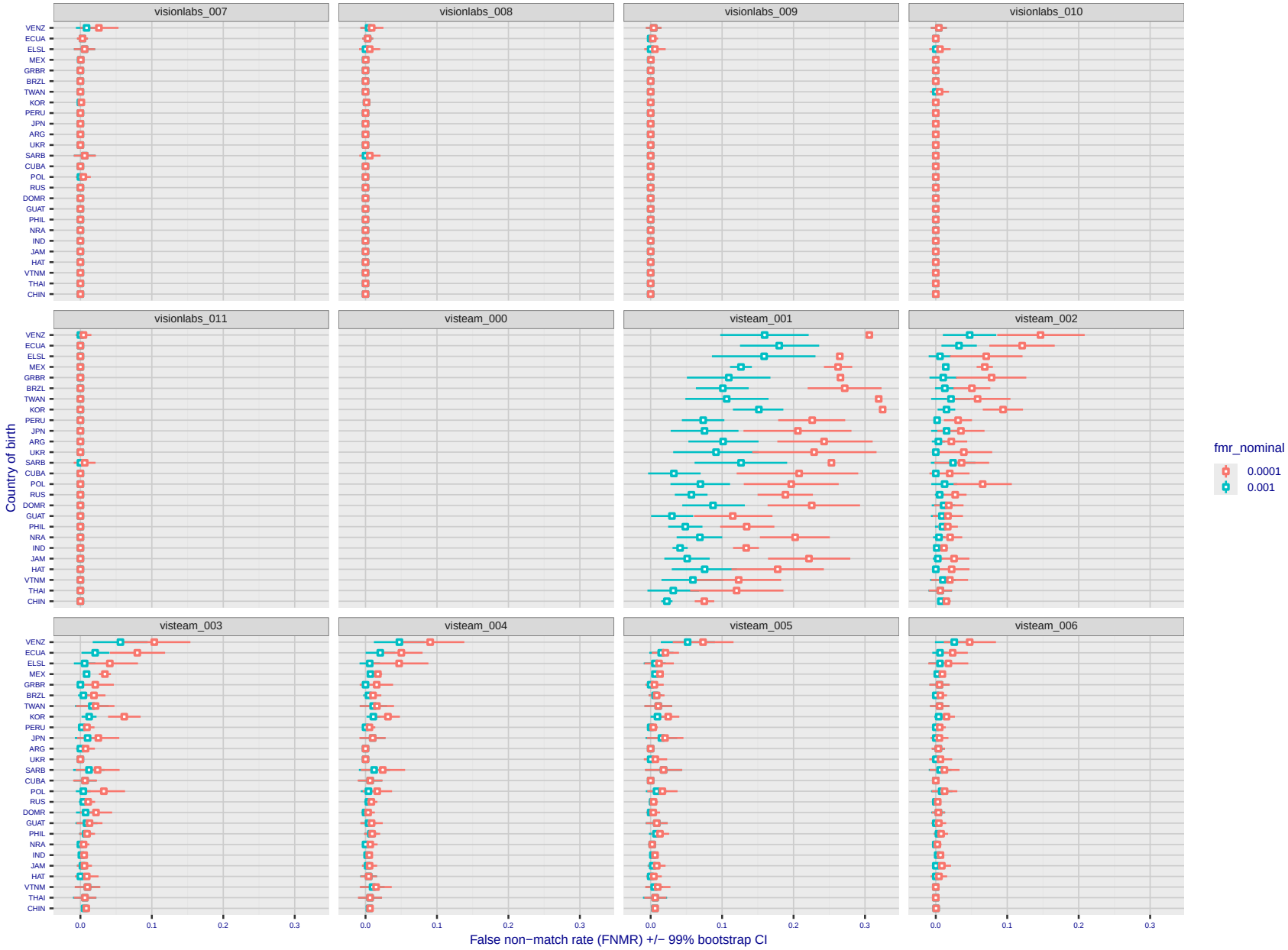

Figure 693: For the visa images, the dots show FNMR by country of birth for two globally set operating thresholds corresponding to FMR = $\{0.001, 0.0001\}$ computed over all on the order of 10^{10} impostor scores. The FMR in each bin will vary also - see subsequent impostor heatmaps in sec. 3.6.1. The figures shows an order of magnitude variation in FNMR across country of birth; these effects are likely due quality variations, then demographics like age and race. The error rates in some cases are zero, and in others the DET is flat so the error rates at the two thresholds are identical. The lines span 1% and 99% of boostrap replicated FNMR estimates.

Figure 694: For the visa images, the dots show FNMR by country of birth for two globally set operating thresholds corresponding to FMR = $\{0.001, 0.0001\}$ computed over all on the order of 10^{10} impostor scores. The FMR in each bin will vary also - see subsequent impostor heatmaps in sec. 3.6.1. The figures shows an order of magnitude variation in FNMR across country of birth; these effects are likely due quality variations, then demographics like age and race. The error rates in some cases are zero, and in others the DET is flat so the error rates at the two thresholds are identical. The lines span 1% and 99% of boostrap replicated FNMR estimates.

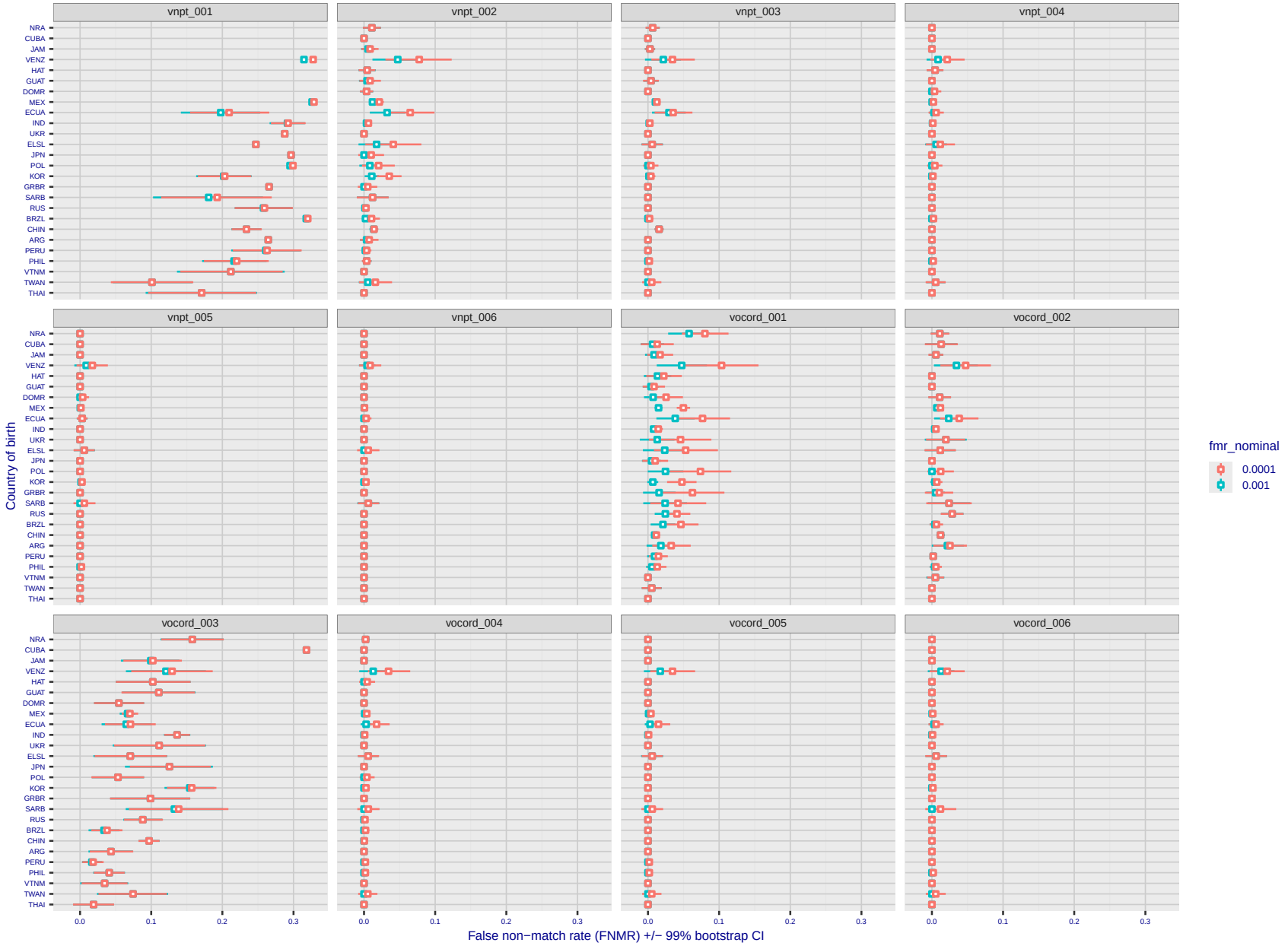

Figure 695: For the visa images, the dots show FNMR by country of birth for two globally set operating thresholds corresponding to FMR = $\{0.001, 0.0001\}$ computed over all on the order of 10^{10} impostor scores. The FMR in each bin will vary also - see subsequent impostor heatmaps in sec. 3.6.1. The figures shows an order of magnitude variation in FNMR across country of birth; these effects are likely due quality variations, then demographics like age and race. The error rates in some cases are zero, and in others the DET is flat so the error rates at the two thresholds are identical. The lines span 1% and 99% of boostrap replicated FNMR estimates.

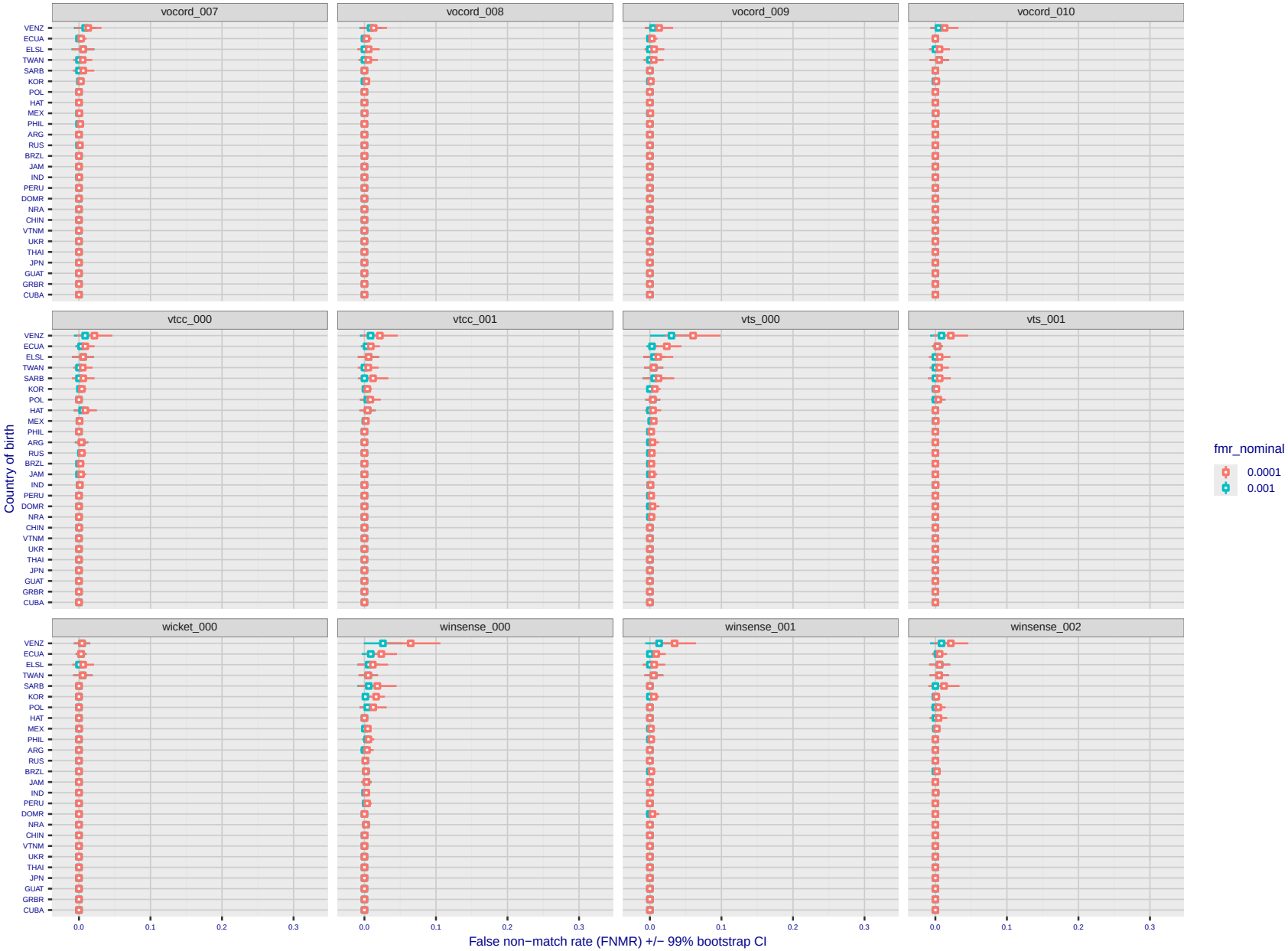

Figure 696: For the visa images, the dots show FNMR by country of birth for two globally set operating thresholds corresponding to FMR = $\{0.001, 0.0001\}$ computed over all on the order of 10^{10} impostor scores. The FMR in each bin will vary also - see subsequent impostor heatmaps in sec. 3.6.1. The figures shows an order of magnitude variation in FNMR across country of birth; these effects are likely due quality variations, then demographics like age and race. The error rates in some cases are zero, and in others the DET is flat so the error rates at the two thresholds are identical. The lines span 1% and 99% of boostrap replicated FNMR estimates.

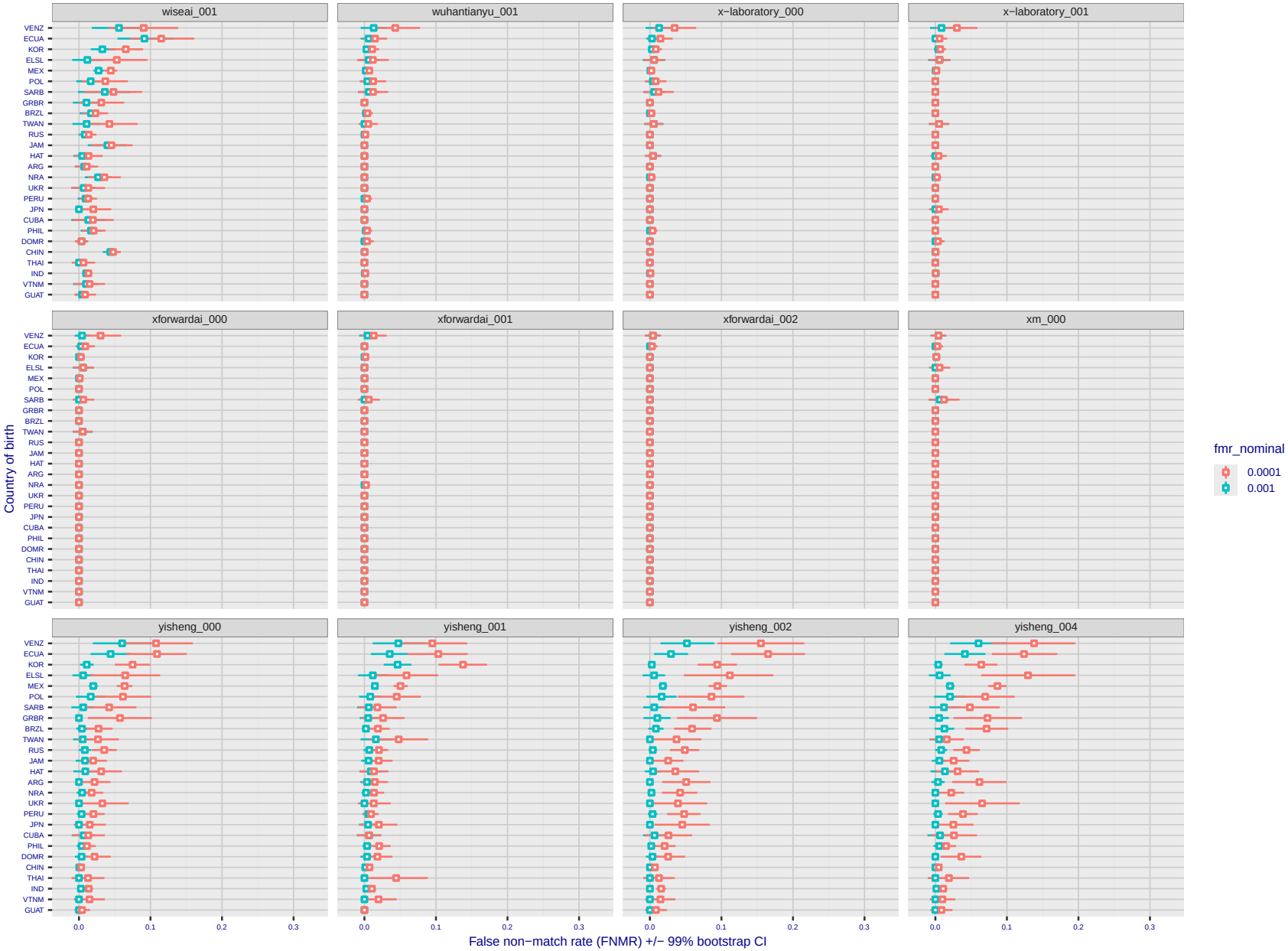

Figure 697: For the visa images, the dots show FNMR by country of birth for two globally set operating thresholds corresponding to FMR = $\{0.001, 0.0001\}$ computed over all on the order of 10^{10} impostor scores. The FMR in each bin will vary also - see subsequent impostor heatmaps in sec. 3.6.1. The figures shows an order of magnitude variation in FNMR across country of birth; these effects are likely due quality variations, then demographics like age and race. The error rates in some cases are zero, and in others the DET is flat so the error rates at the two thresholds are identical. The lines span 1% and 99% of boostrap replicated FNMR estimates.

Figure 698: For the visa images, the dots show FNMR by country of birth for two globally set operating thresholds corresponding to FMR = $\{0.001, 0.0001\}$ computed over all on the order of 10^{10} impostor scores. The FMR in each bin will vary also - see subsequent impostor heatmaps in sec. 3.6.1. The figures shows an order of magnitude variation in FNMR across country of birth; these effects are likely due quality variations, then demographics like age and race. The error rates in some cases are zero, and in others the DET is flat so the error rates at the two thresholds are identical. The lines span 1% and 99% of boostrap replicated FNMR estimates.

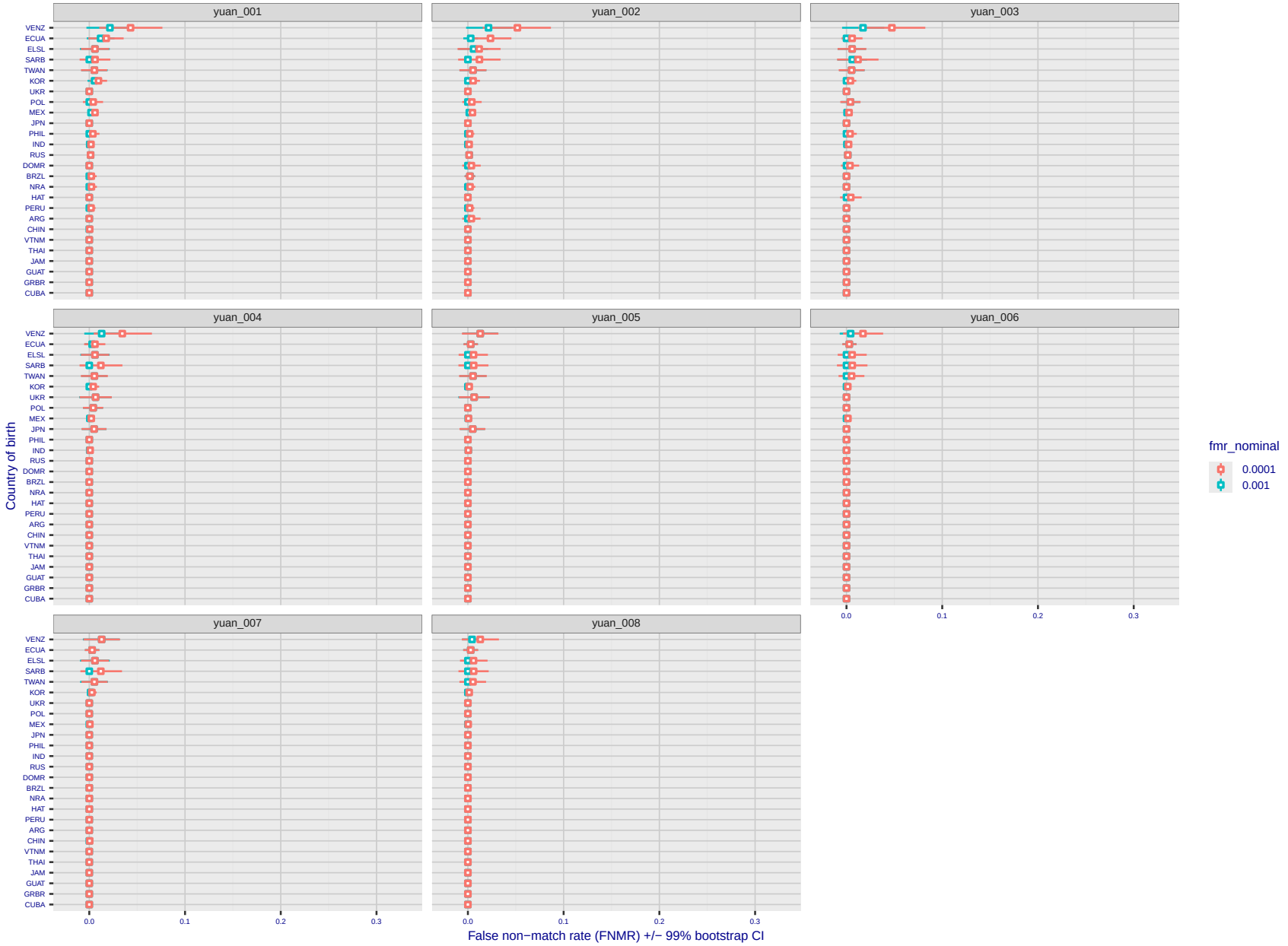

Figure 699: For the visa images, the dots show FNMR by country of birth for two globally set operating thresholds corresponding to FMR = $\{0.001, 0.0001\}$ computed over all on the order of 10^{10} impostor scores. The FMR in each bin will vary also - see subsequent impostor heatmaps in sec. 3.6.1. The figures shows an order of magnitude variation in FNMR across country of birth; these effects are likely due quality variations, then demographics like age and race. The error rates in some cases are zero, and in others the DET is flat so the error rates at the two thresholds are identical. The lines span 1% and 99% of boostrap replicated FNMR estimates.

Caveats: The results may not relate to subject-specific properties. Instead they could reflect image-specific quality differences, which could occur due to collection protocol or software processing variations.

3.5.2 Effect of ageing

Background: Faces change appearance throughout life. This change gradually reduces similarity of a new image to an earlier image. Face recognition algorithms give reduced similarity scores and more frequent false rejections.

Goal: To quantify false non-match rates (FNMR) as a function of elapsed time in an adult population.

Methods: Using the mugshot images, a threshold is set to give FMR = 0.00001 over the entire impostor set. Then FNMR is measured over 1000 bootstrap replications of the genuine scores.

Results: For the visa images, Figure 781 shows how false non-match rates for genuine users, as a function of age group.

FNMR(T) "False non-match rate"
FMR(T) "False match rate"

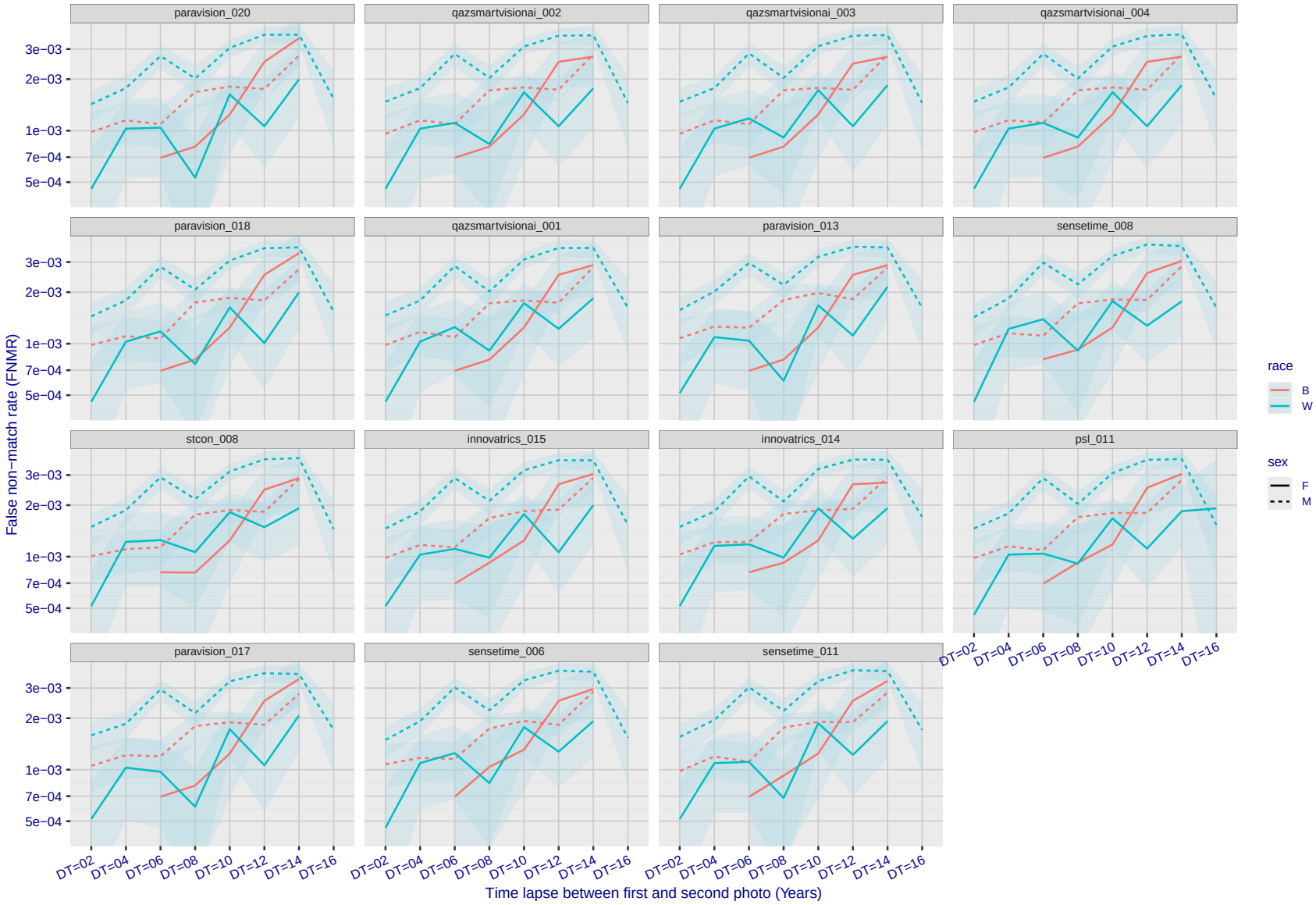

Figure 700: For the mugshot images, FNMR *as a function of elapsed time between initial enrollment and second verification images. The panels appear most accurate first, and vertical scale changes on each page. The four traces correspond to images annotated with codes for black female, black male, white female, white male. The threshold is fixed for each algorithm to give FMR = 0.00001 over all ($\widetilde{10}^8$) impostor comparisons. For short time-lapses, the most accurate algorithms give very few errors (FNMR < 0.001) so that the uncertainty estimates are high.*

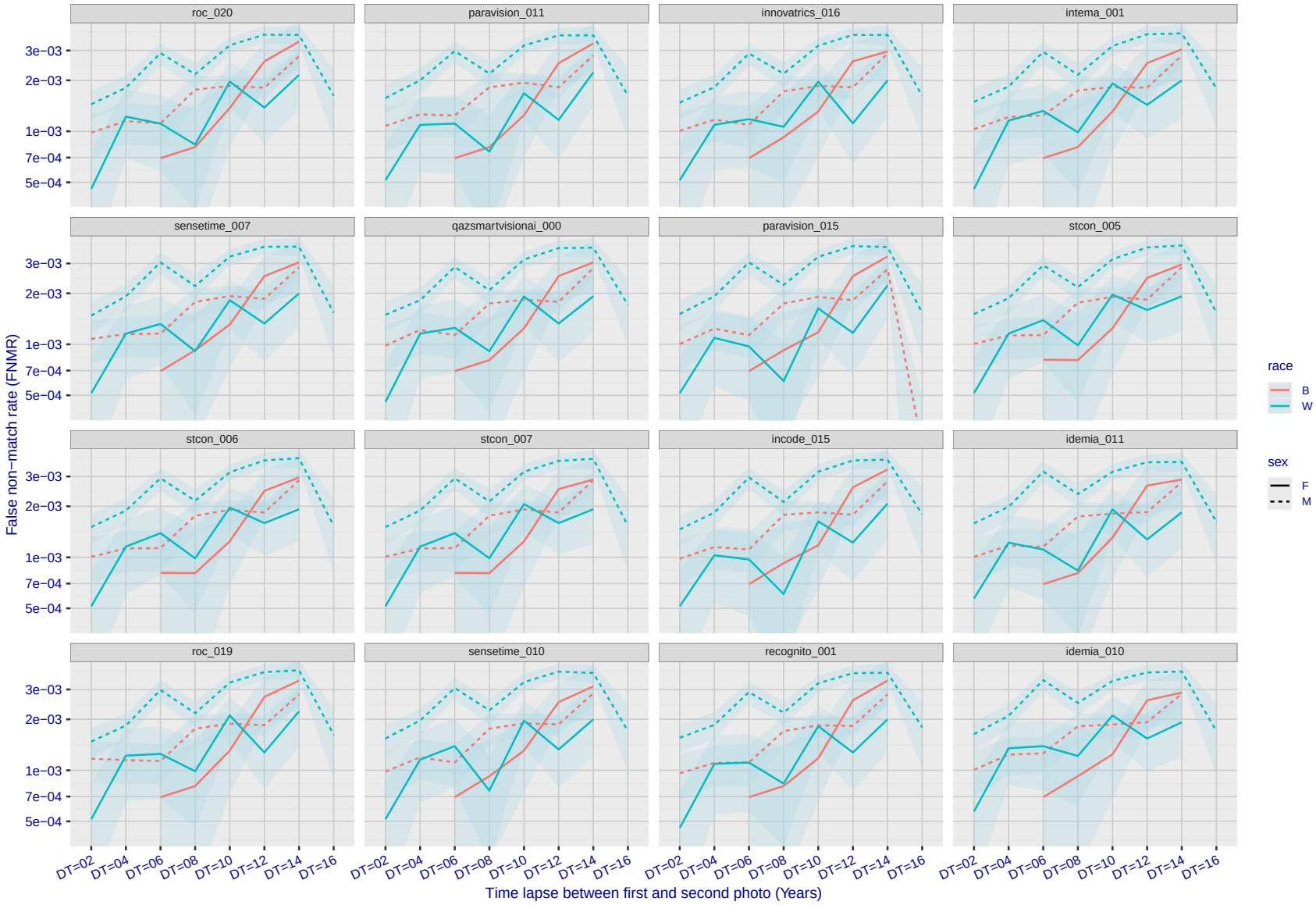

Figure 701: For the mugshot images, FNMR *as a function of elapsed time between initial enrollment and second verification images. The panels appear most accurate first, and vertical scale changes on each page. The four traces correspond to images annotated with codes for black female, black male, white female, white male. The threshold is fixed for each algorithm to give FMR = 0.00001 over all (10^8) impostor comparisons. For short time-lapses, the most accurate algorithms give very few errors (FNMR < 0.001) so that the uncertainty estimates are high.*

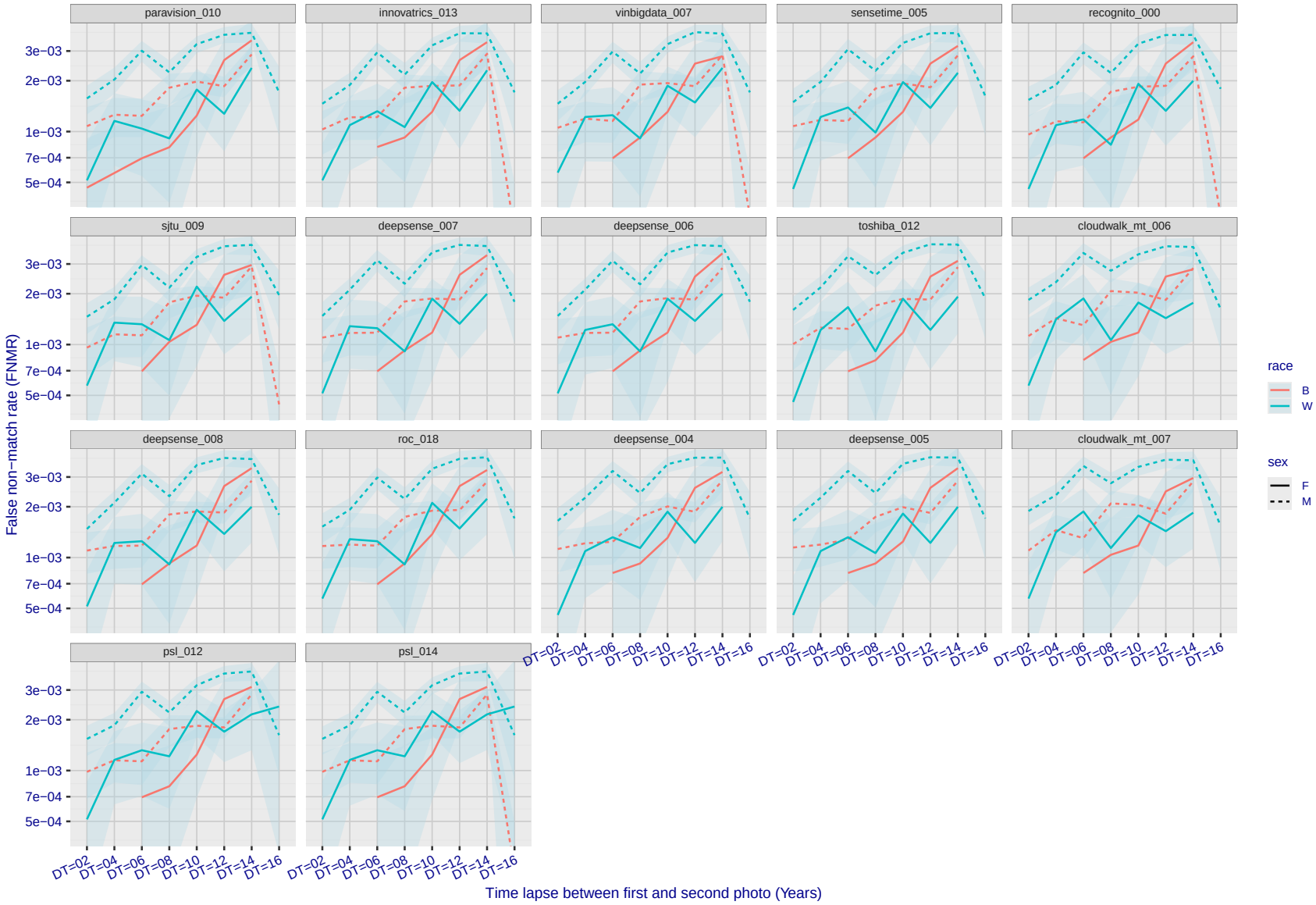

Figure 702: For the mugshot images, FNMR *as a function of elapsed time between initial enrollment and second verification images. The panels appear most accurate first, and vertical scale changes on each page. The four traces correspond to images annotated with codes for black female, black male, white female, white male. The threshold is fixed for each algorithm to give FMR = 0.00001 over all (10^8) impostor comparisons. For short time-lapses, the most accurate algorithms give very few errors (FNMR < 0.001) so that the uncertainty estimates are high.*

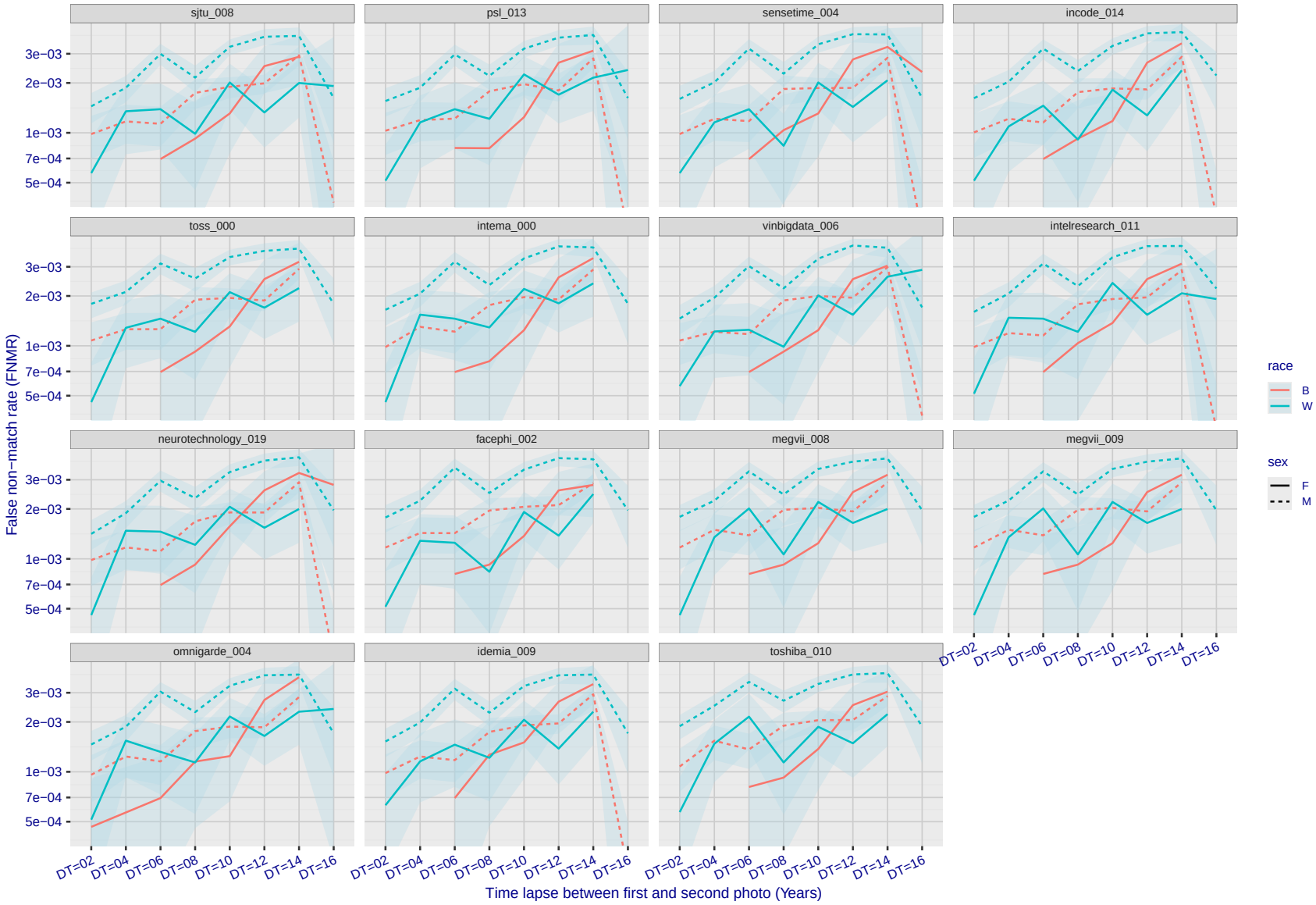

Figure 703: For the mugshot images, FNMR *as a function of elapsed time between initial enrollment and second verification images. The panels appear most accurate first, and vertical scale changes on each page. The four traces correspond to images annotated with codes for black female, black male, white female, white male. The threshold is fixed for each algorithm to give FMR = 0.00001 over all ($\widetilde{10}^8$) impostor comparisons. For short time-lapses, the most accurate algorithms give very few errors (FNMR < 0.001) so that the uncertainty estimates are high.*

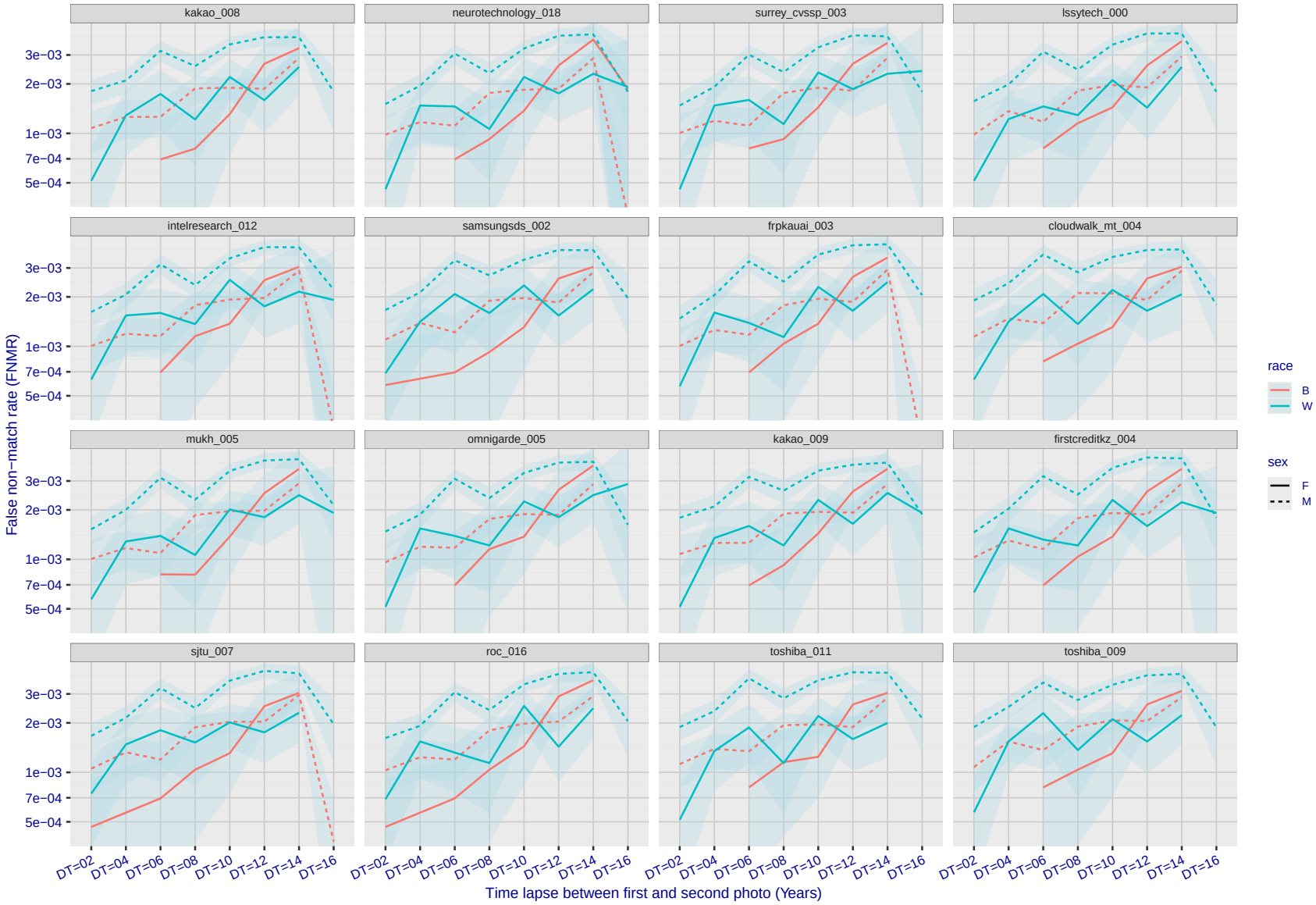

Figure 704: For the mugshot images, FNMR *as a function of elapsed time between initial enrollment and second verification images. The panels appear most accurate first, and vertical scale changes on each page. The four traces correspond to images annotated with codes for black female, black male, white female, white male. The threshold is fixed for each algorithm to give FMR = 0.00001 over all ($\widetilde{10}^8$) impostor comparisons. For short time-lapses, the most accurate algorithms give very few errors (FNMR < 0.001) so that the uncertainty estimates are high.*

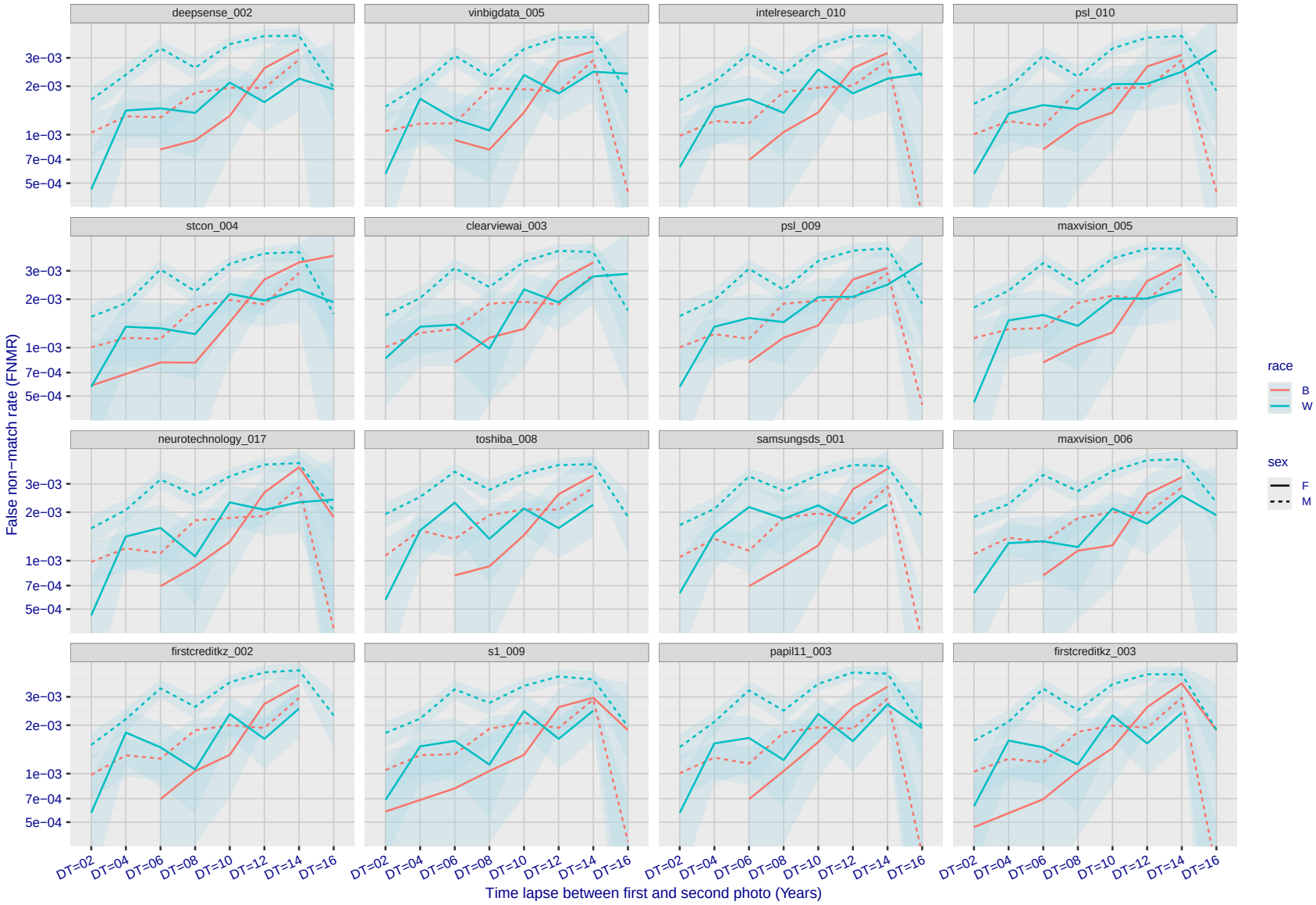

Figure 705: For the mugshot images, FNMR *as a function of elapsed time between initial enrollment and second verification images. The panels appear most accurate first, and vertical scale changes on each page. The four traces correspond to images annotated with codes for black female, black male, white female, white male. The threshold is fixed for each algorithm to give FMR = 0.00001 over all (10^8) impostor comparisons. For short time-lapses, the most accurate algorithms give very few errors (FNMR < 0.001) so that the uncertainty estimates are high.*

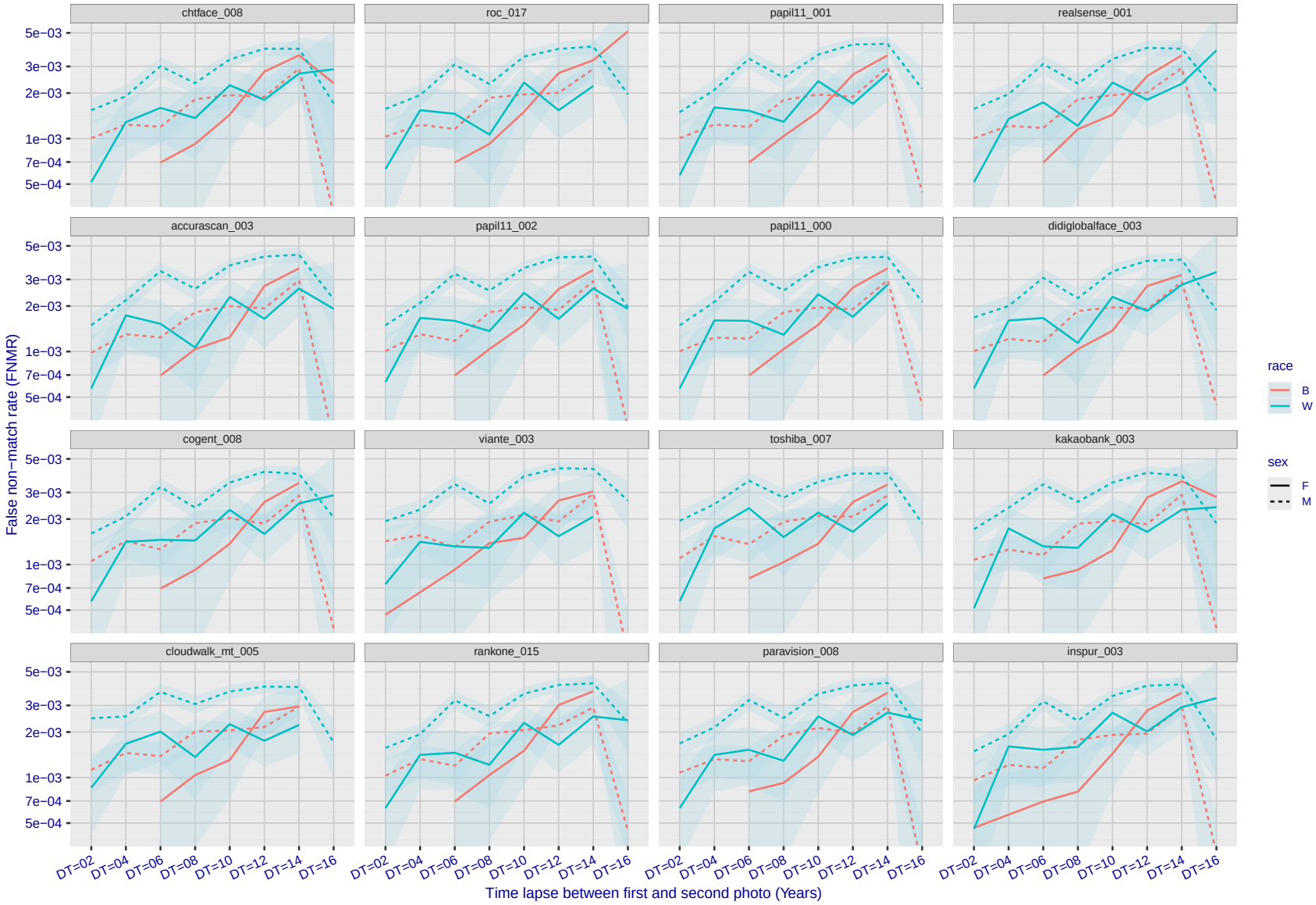

Figure 706: For the mugshot images, FNMR *as a function of elapsed time between initial enrollment and second verification images. The panels appear most accurate first, and vertical scale changes on each page. The four traces correspond to images annotated with codes for black female, black male, white female, white male. The threshold is fixed for each algorithm to give FMR = 0.00001 over all (10^8) impostor comparisons. For short time-lapses, the most accurate algorithms give very few errors (FNMR < 0.001) so that the uncertainty estimates are high.*

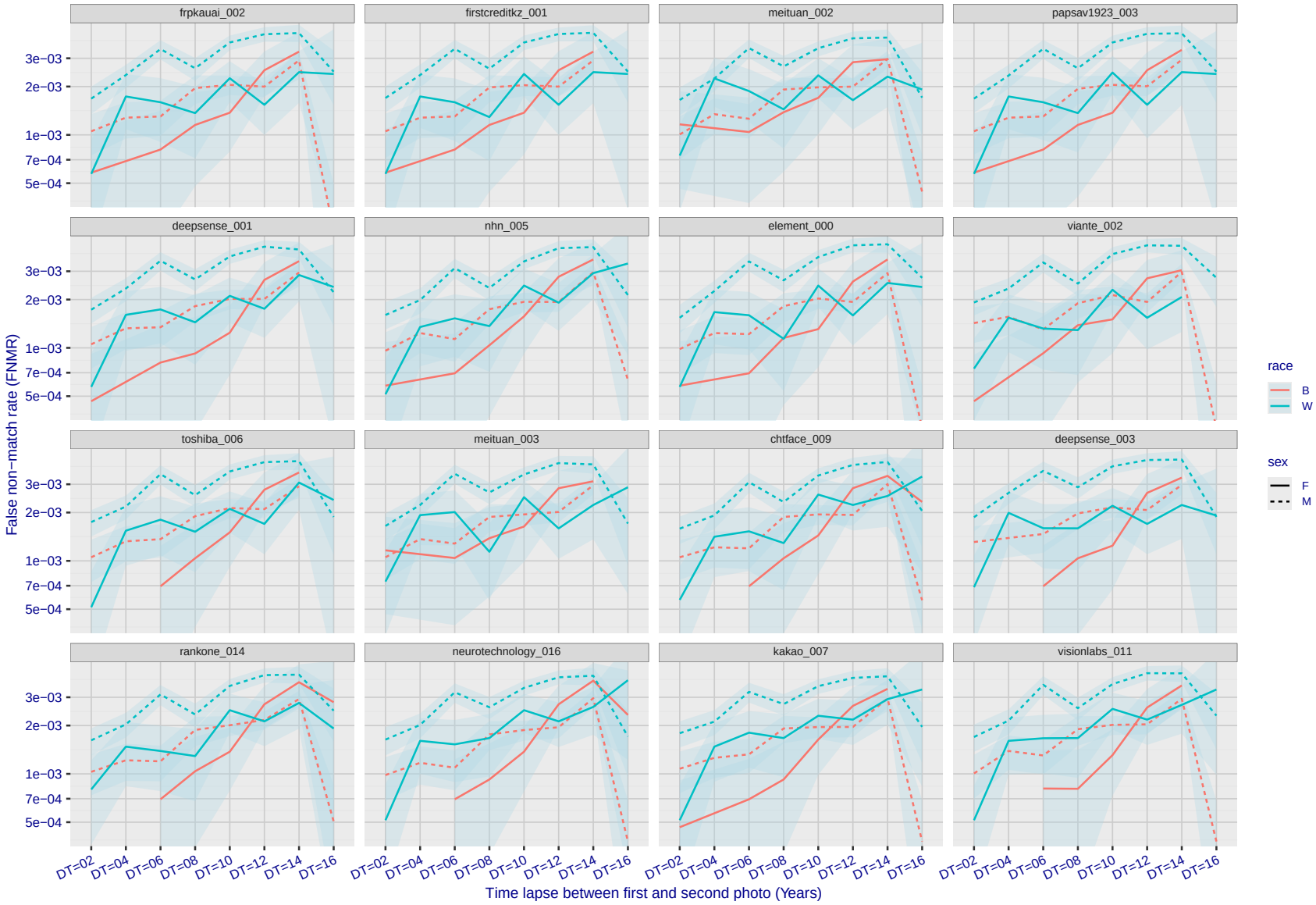

Figure 707: For the mugshot images, FNMR *as a function of elapsed time between initial enrollment and second verification images. The panels appear most accurate first, and vertical scale changes on each page. The four traces correspond to images annotated with codes for black female, black male, white female, white male. The threshold is fixed for each algorithm to give FMR = 0.00001 over all (10^8) impostor comparisons. For short time-lapses, the most accurate algorithms give very few errors (FNMR < 0.001) so that the uncertainty estimates are high.*

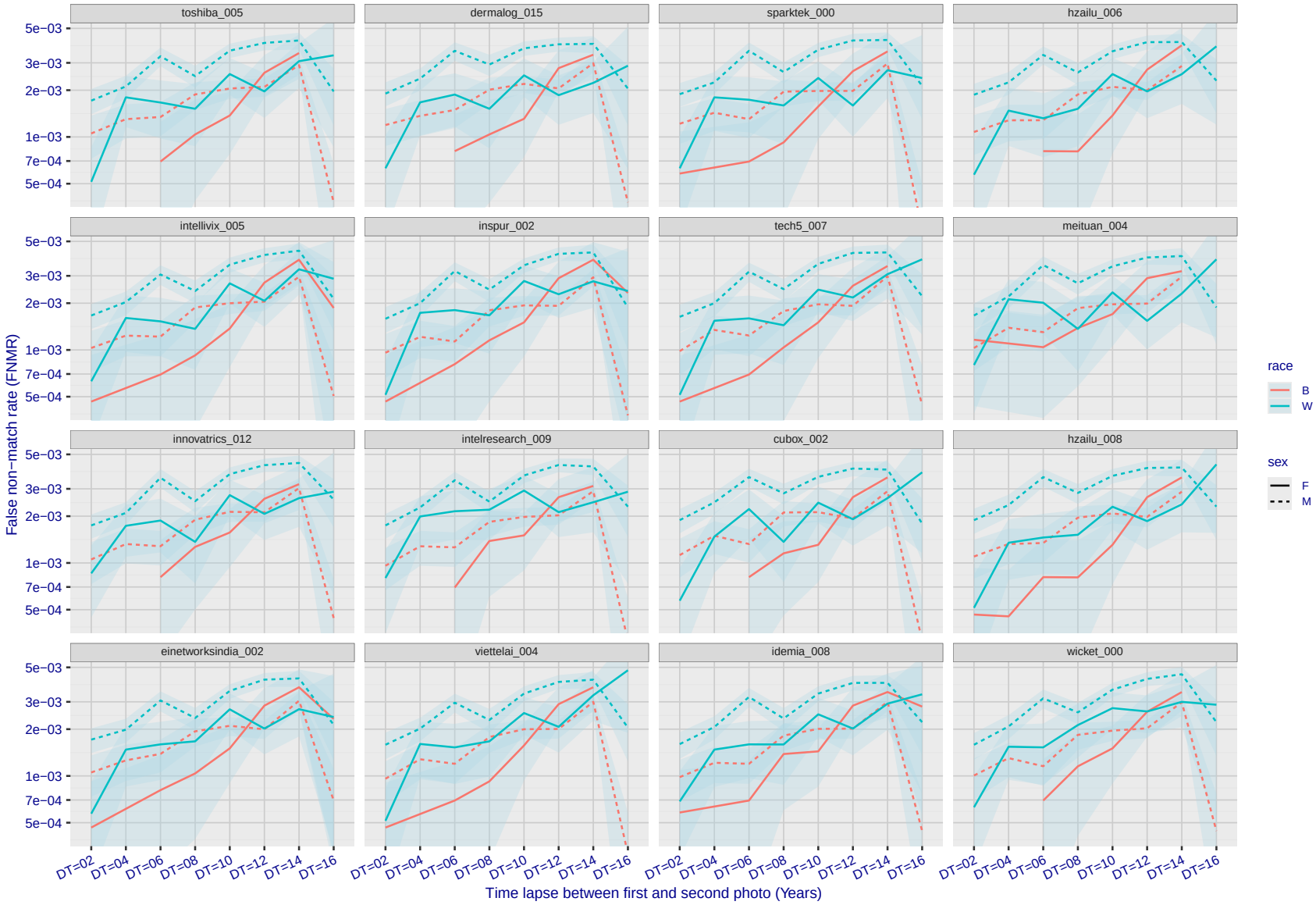

Figure 708: For the mugshot images, FNMR *as a function of elapsed time between initial enrollment and second verification images. The panels appear most accurate first, and vertical scale changes on each page. The four traces correspond to images annotated with codes for black female, black male, white female, white male. The threshold is fixed for each algorithm to give FMR = 0.00001 over all ($\widetilde{10}^8$) impostor comparisons. For short time-lapses, the most accurate algorithms give very few errors (FNMR < 0.001) so that the uncertainty estimates are high.*

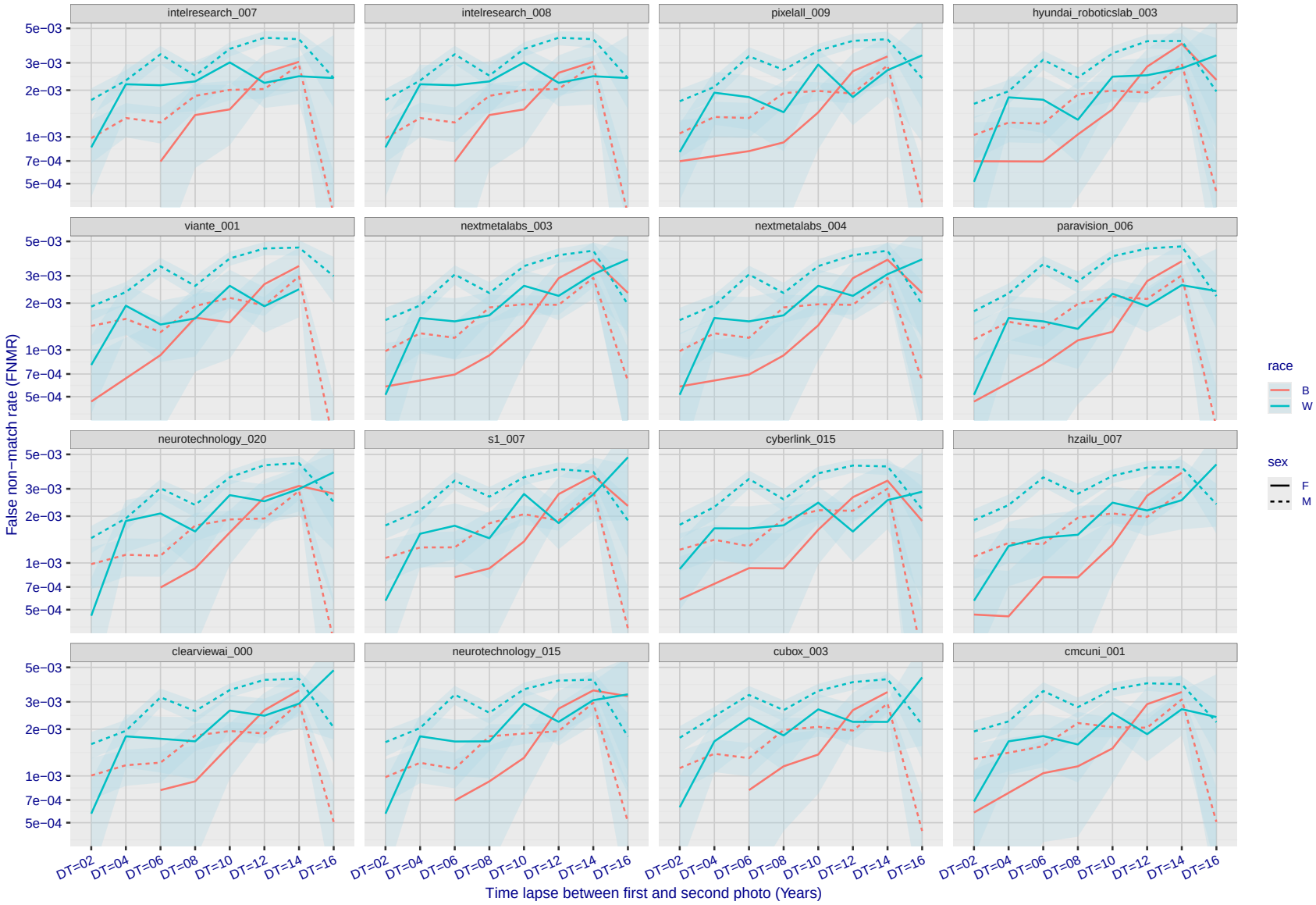

Figure 709: For the mugshot images, FNMR *as a function of elapsed time between initial enrollment and second verification images. The panels appear most accurate first, and vertical scale changes on each page. The four traces correspond to images annotated with codes for black female, black male, white female, white male. The threshold is fixed for each algorithm to give FMR = 0.00001 over all (10^8) impostor comparisons. For short time-lapses, the most accurate algorithms give very few errors (FNMR < 0.001) so that the uncertainty estimates are high.*

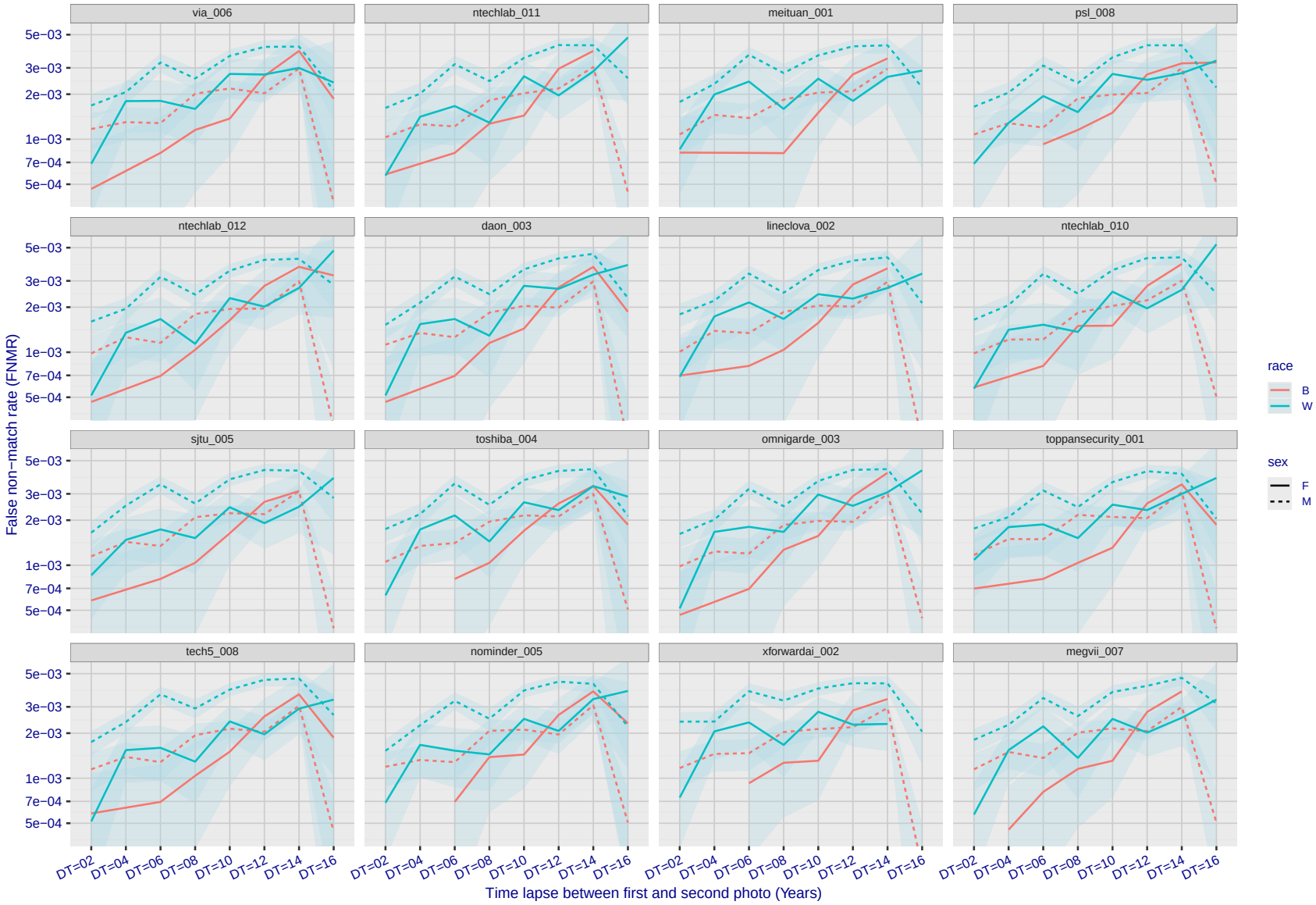

Figure 710: For the mugshot images, FNMR *as a function of elapsed time between initial enrollment and second verification images. The panels appear most accurate first, and vertical scale changes on each page. The four traces correspond to images annotated with codes for black female, black male, white female, white male. The threshold is fixed for each algorithm to give FMR = 0.00001 over all ($\widetilde{10}^8$) impostor comparisons. For short time-lapses, the most accurate algorithms give very few errors (FNMR < 0.001) so that the uncertainty estimates are high.*

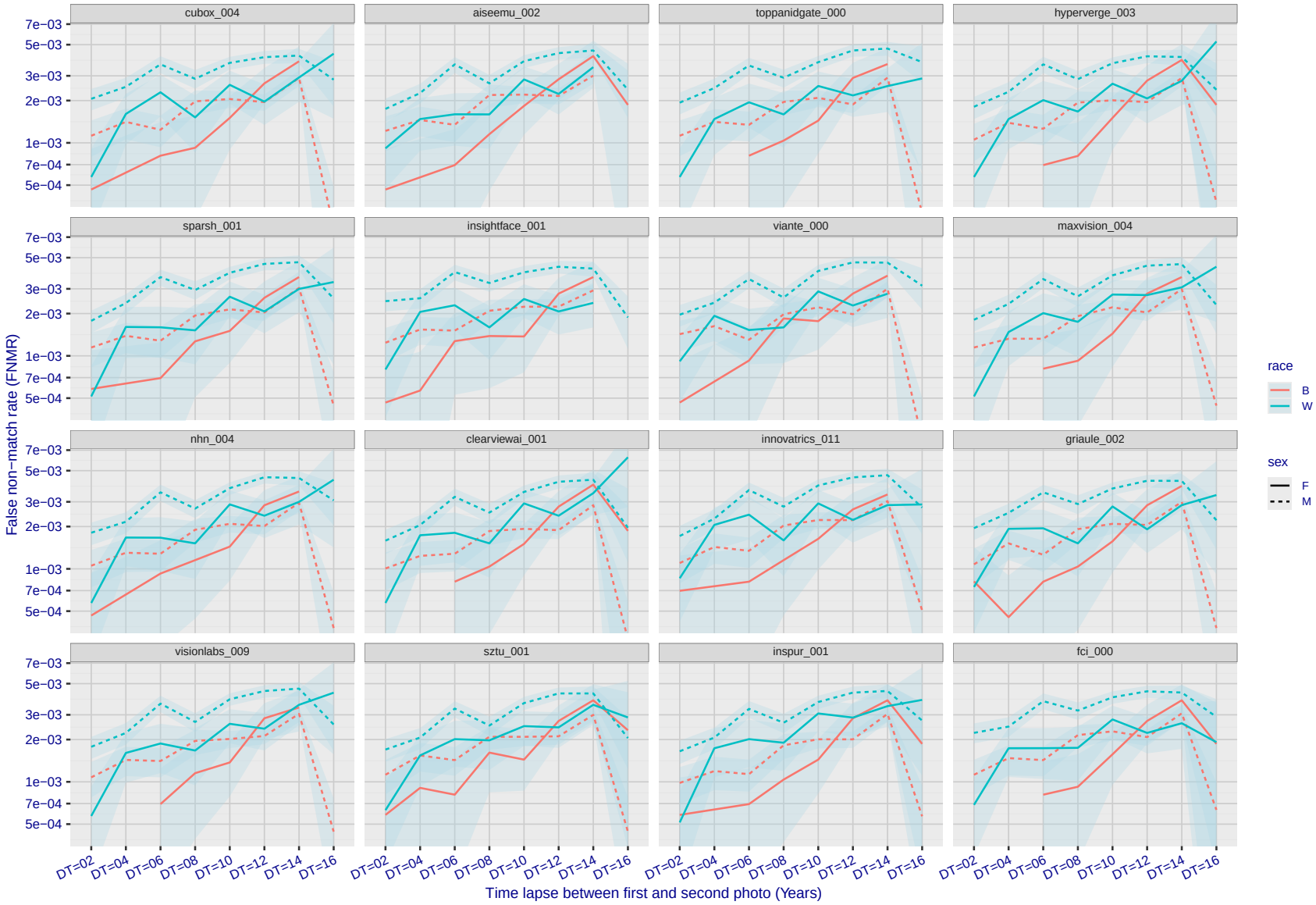

Figure 711: For the mugshot images, FNMR *as a function of elapsed time between initial enrollment and second verification images. The panels appear most accurate first, and vertical scale changes on each page. The four traces correspond to images annotated with codes for black female, black male, white female, white male. The threshold is fixed for each algorithm to give FMR = 0.00001 over all ($\widetilde{10}^8$) impostor comparisons. For short time-lapses, the most accurate algorithms give very few errors (FNMR < 0.001) so that the uncertainty estimates are high.*

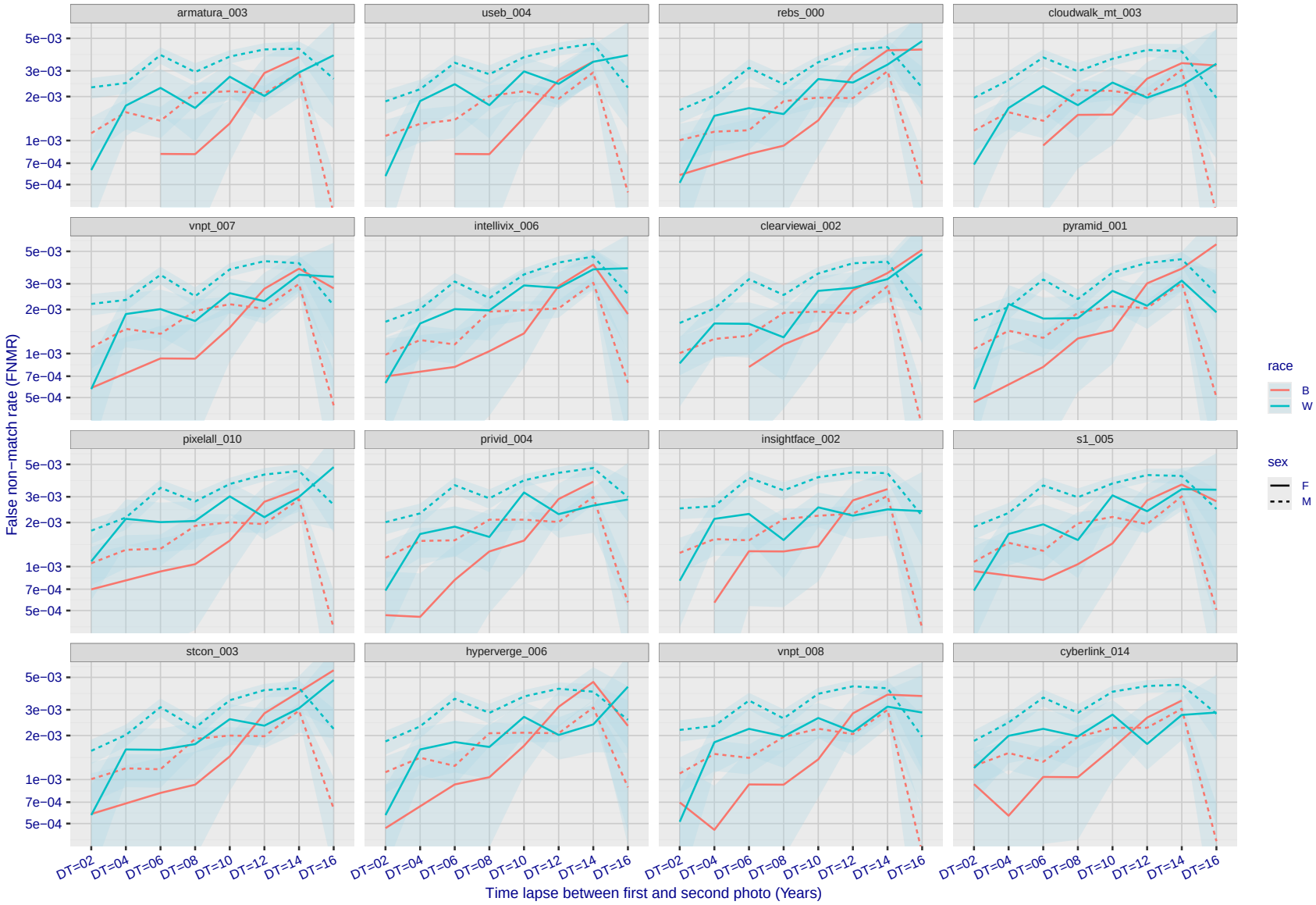

Figure 712: For the mugshot images, FNMR *as a function of elapsed time between initial enrollment and second verification images. The panels appear most accurate first, and vertical scale changes on each page. The four traces correspond to images annotated with codes for black female, black male, white female, white male. The threshold is fixed for each algorithm to give FMR = 0.00001 over all (10^8) impostor comparisons. For short time-lapses, the most accurate algorithms give very few errors (FNMR < 0.001) so that the uncertainty estimates are high.*

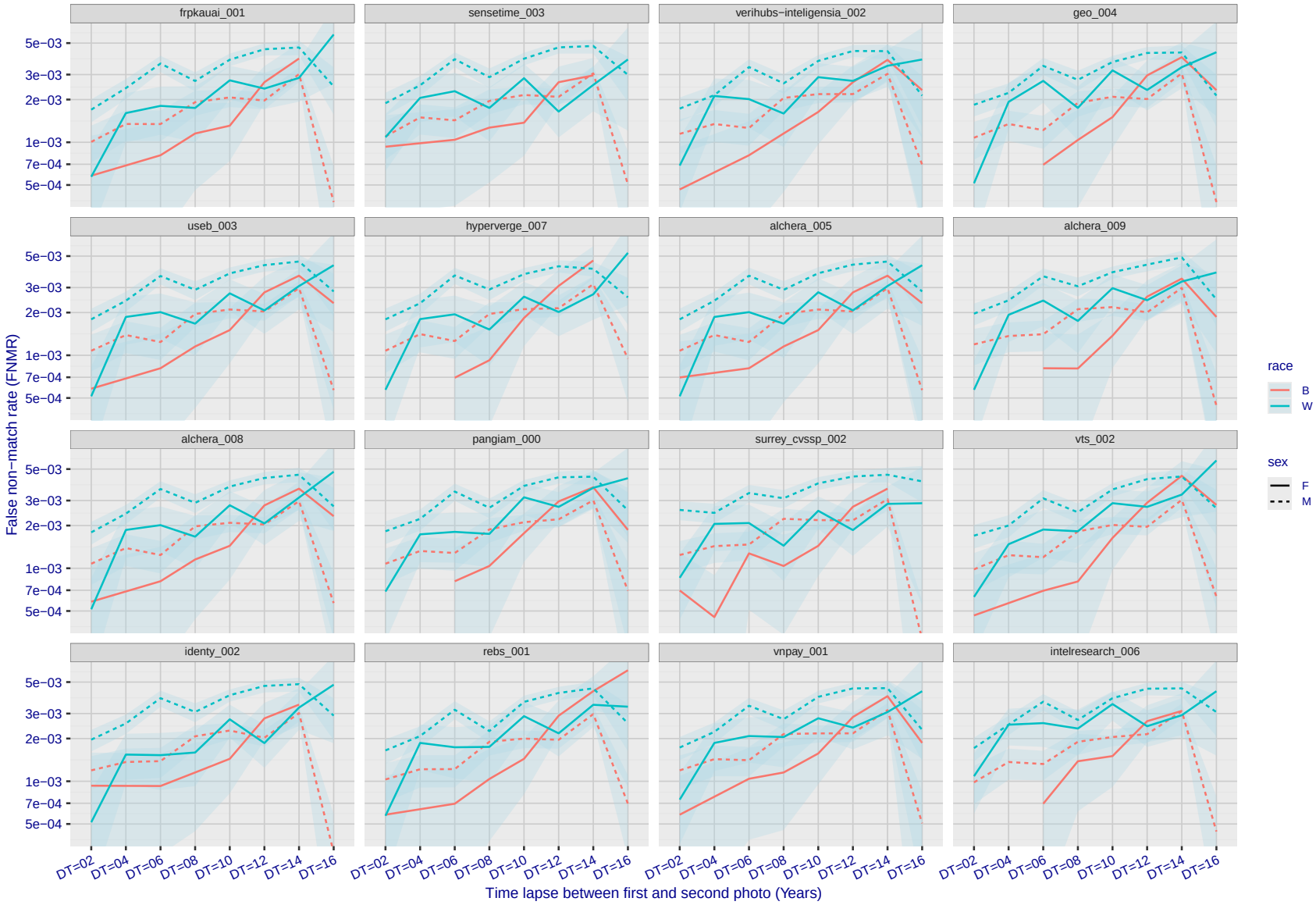

Figure 713: For the mugshot images, FNMR *as a function of elapsed time between initial enrollment and second verification images. The panels appear most accurate first, and vertical scale changes on each page. The four traces correspond to images annotated with codes for black female, black male, white female, white male. The threshold is fixed for each algorithm to give FMR = 0.00001 over all ($\widetilde{10}^8$) impostor comparisons. For short time-lapses, the most accurate algorithms give very few errors (FNMR < 0.001) so that the uncertainty estimates are high.*

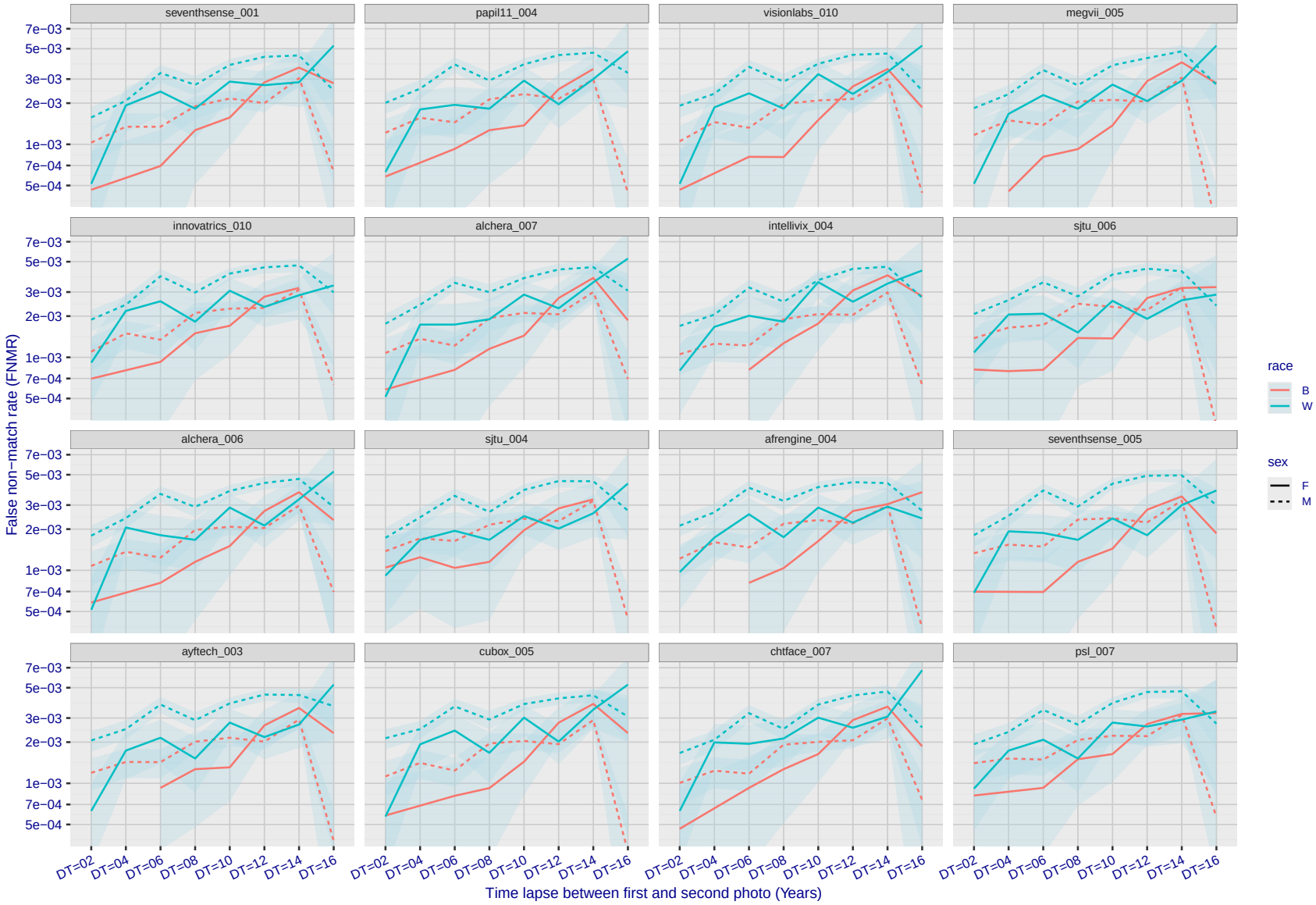

Figure 714: For the mugshot images, FNMR *as a function of elapsed time between initial enrollment and second verification images. The panels appear most accurate first, and vertical scale changes on each page. The four traces correspond to images annotated with codes for black female, black male, white female, white male. The threshold is fixed for each algorithm to give FMR = 0.00001 over all ($\widetilde{10}^8$) impostor comparisons. For short time-lapses, the most accurate algorithms give very few errors (FNMR < 0.001) so that the uncertainty estimates are high.*

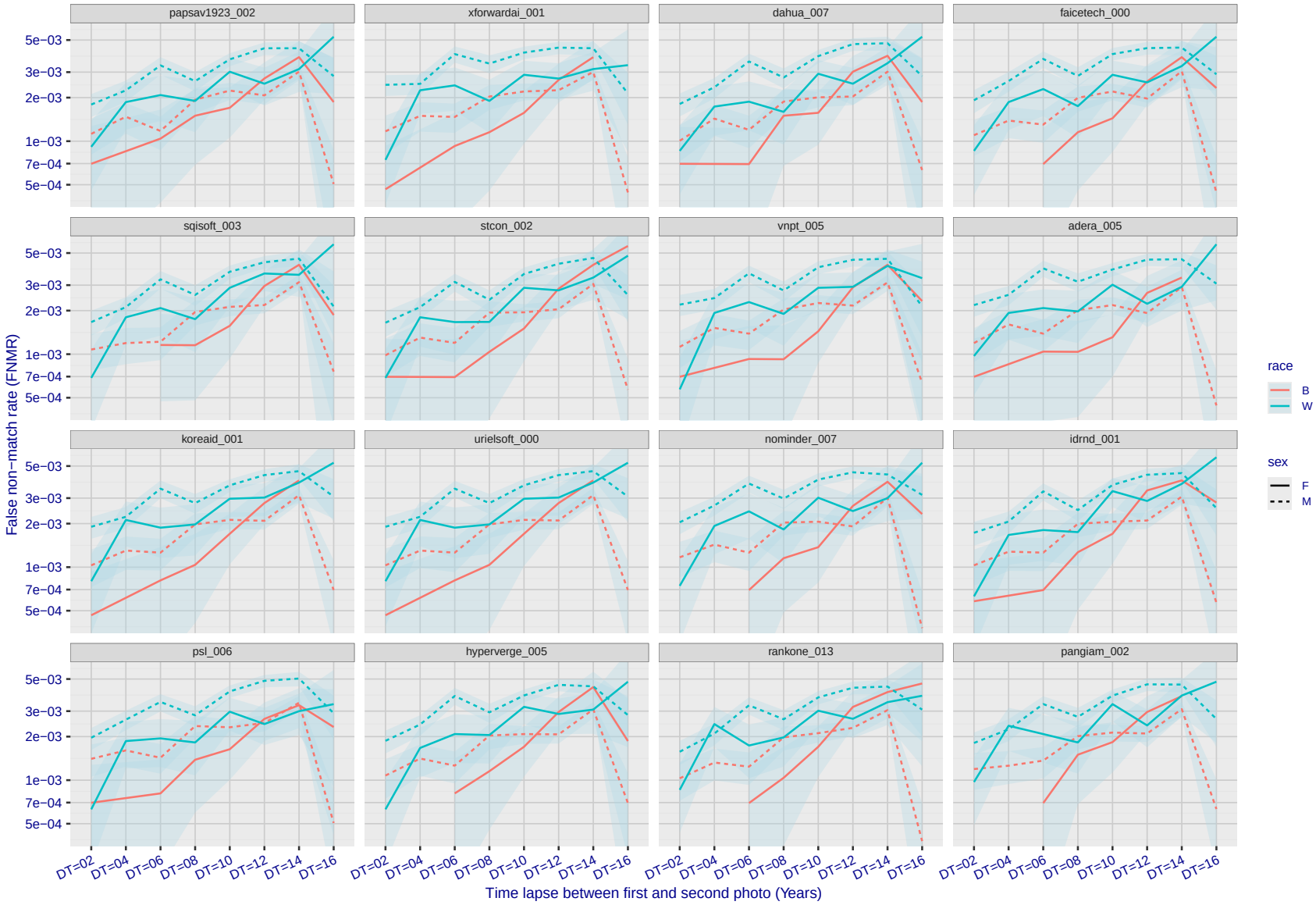

Figure 715: For the mugshot images, FNMR *as a function of elapsed time between initial enrollment and second verification images. The panels appear most accurate first, and vertical scale changes on each page. The four traces correspond to images annotated with codes for black female, black male, white female, white male. The threshold is fixed for each algorithm to give FMR = 0.00001 over all (10^8) impostor comparisons. For short time-lapses, the most accurate algorithms give very few errors (FNMR < 0.001) so that the uncertainty estimates are high.*

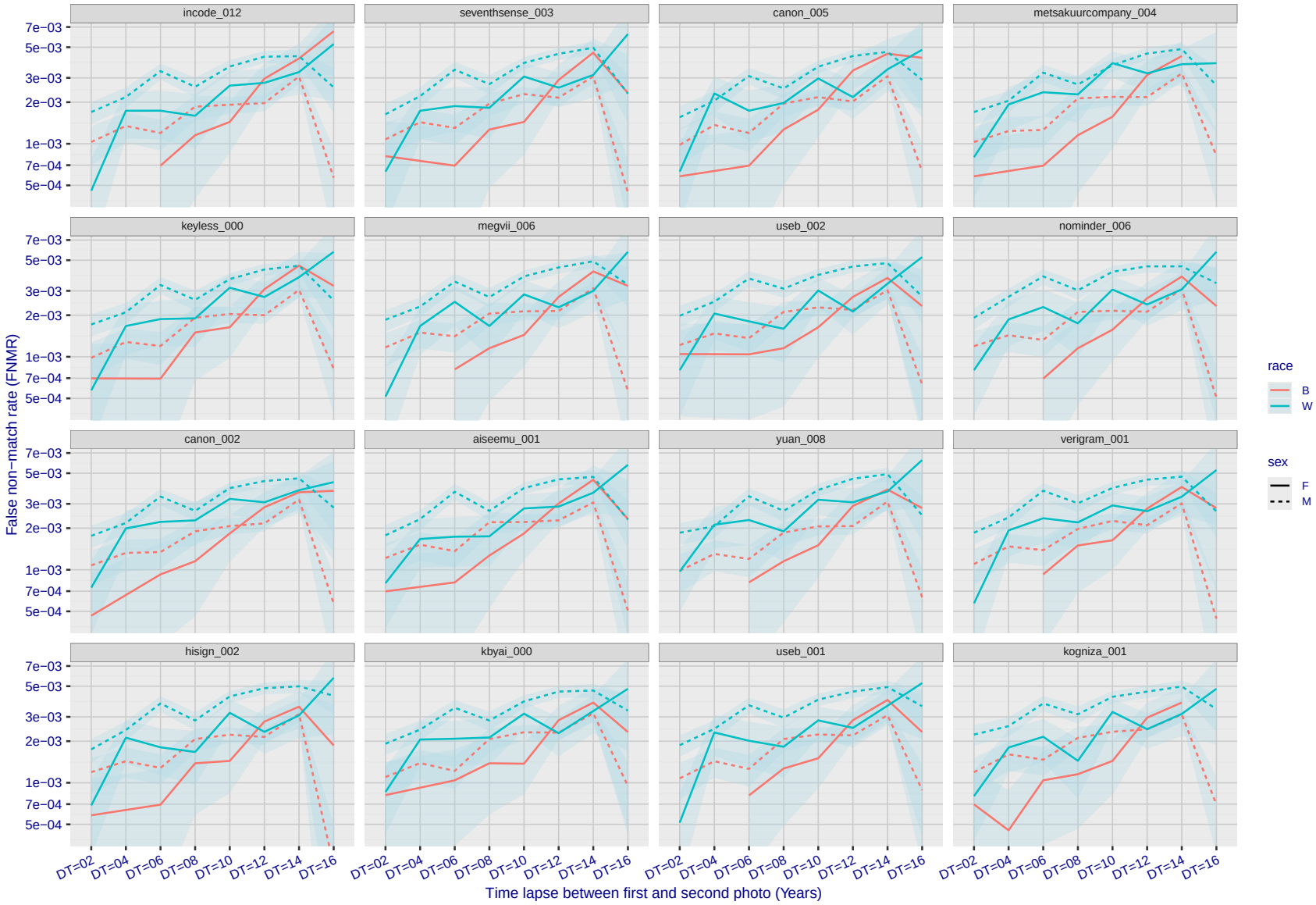

Figure 716: For the mugshot images, FNMR *as a function of elapsed time between initial enrollment and second verification images. The panels appear most accurate first, and vertical scale changes on each page. The four traces correspond to images annotated with codes for black female, black male, white female, white male. The threshold is fixed for each algorithm to give FMR = 0.00001 over all (10^8) impostor comparisons. For short time-lapses, the most accurate algorithms give very few errors (FNMR < 0.001) so that the uncertainty estimates are high.*

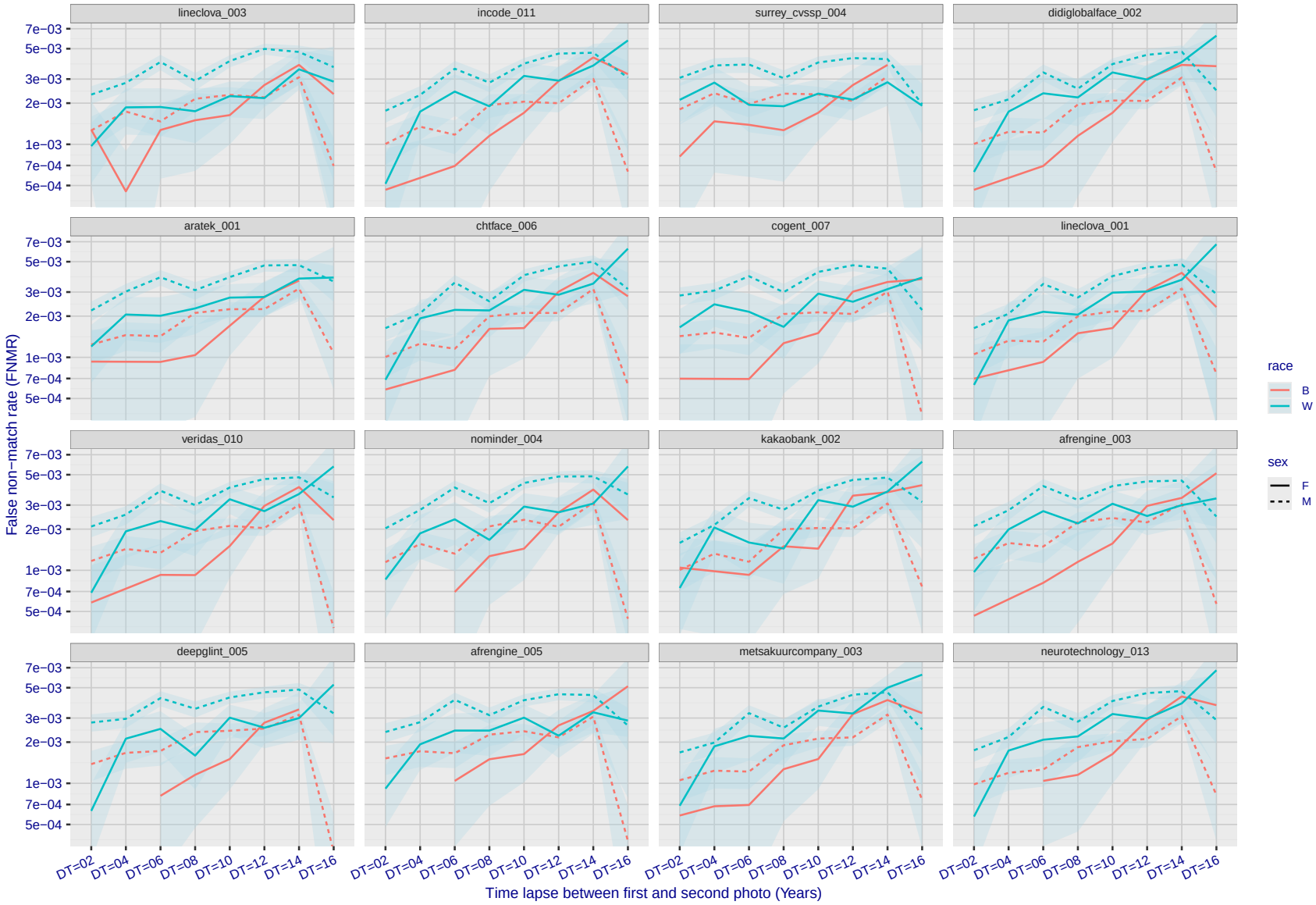

Figure 717: For the mugshot images, FNMR *as a function of elapsed time between initial enrollment and second verification images. The panels appear most accurate first, and vertical scale changes on each page. The four traces correspond to images annotated with codes for black female, black male, white female, white male. The threshold is fixed for each algorithm to give FMR = 0.00001 over all (10^8) impostor comparisons. For short time-lapses, the most accurate algorithms give very few errors (FNMR < 0.001) so that the uncertainty estimates are high.*

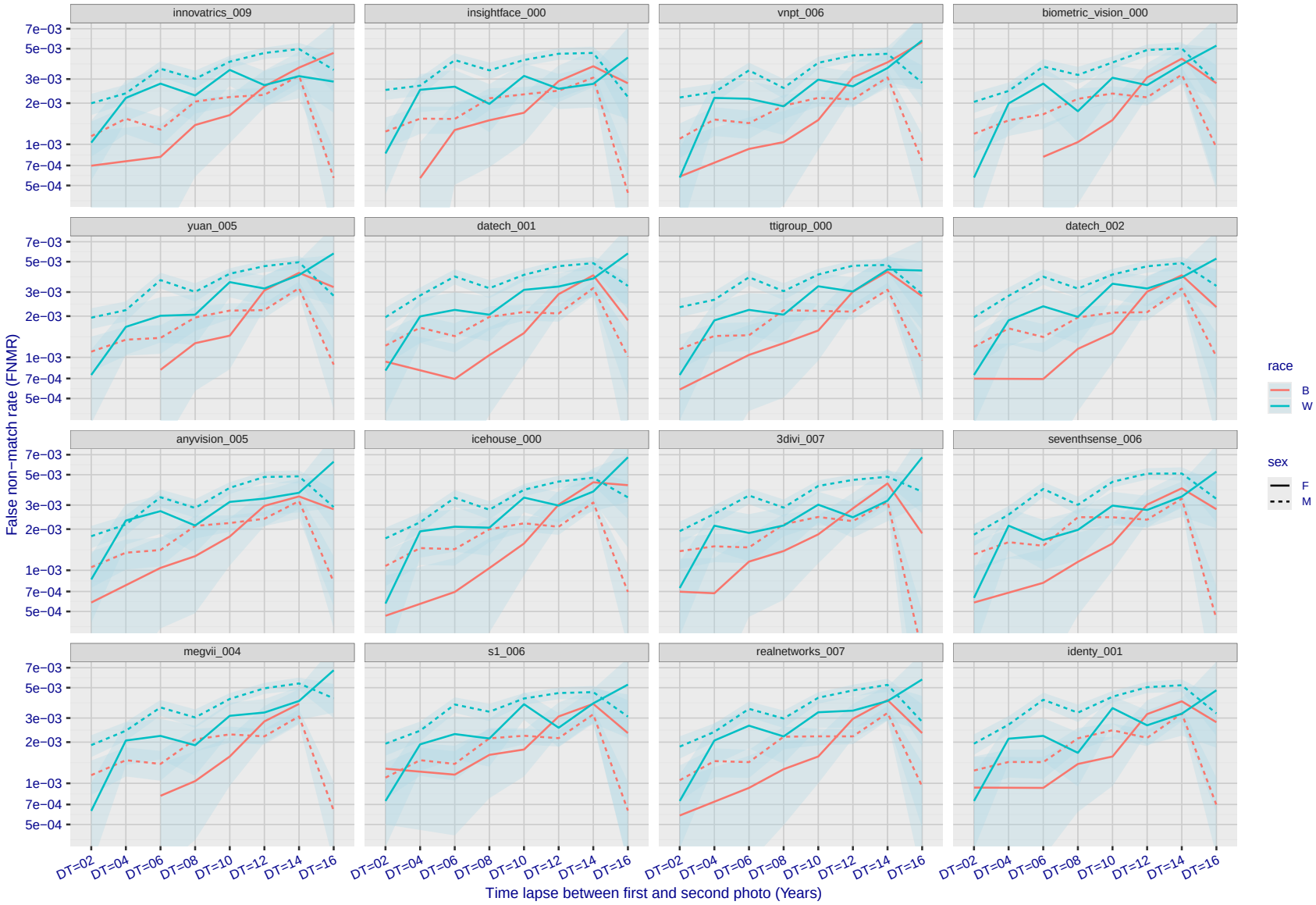

Figure 718: For the mugshot images, FNMR *as a function of elapsed time between initial enrollment and second verification images. The panels appear most accurate first, and vertical scale changes on each page. The four traces correspond to images annotated with codes for black female, black male, white female, white male. The threshold is fixed for each algorithm to give FMR = 0.00001 over all (10^8) impostor comparisons. For short time-lapses, the most accurate algorithms give very few errors (FNMR < 0.001) so that the uncertainty estimates are high.*

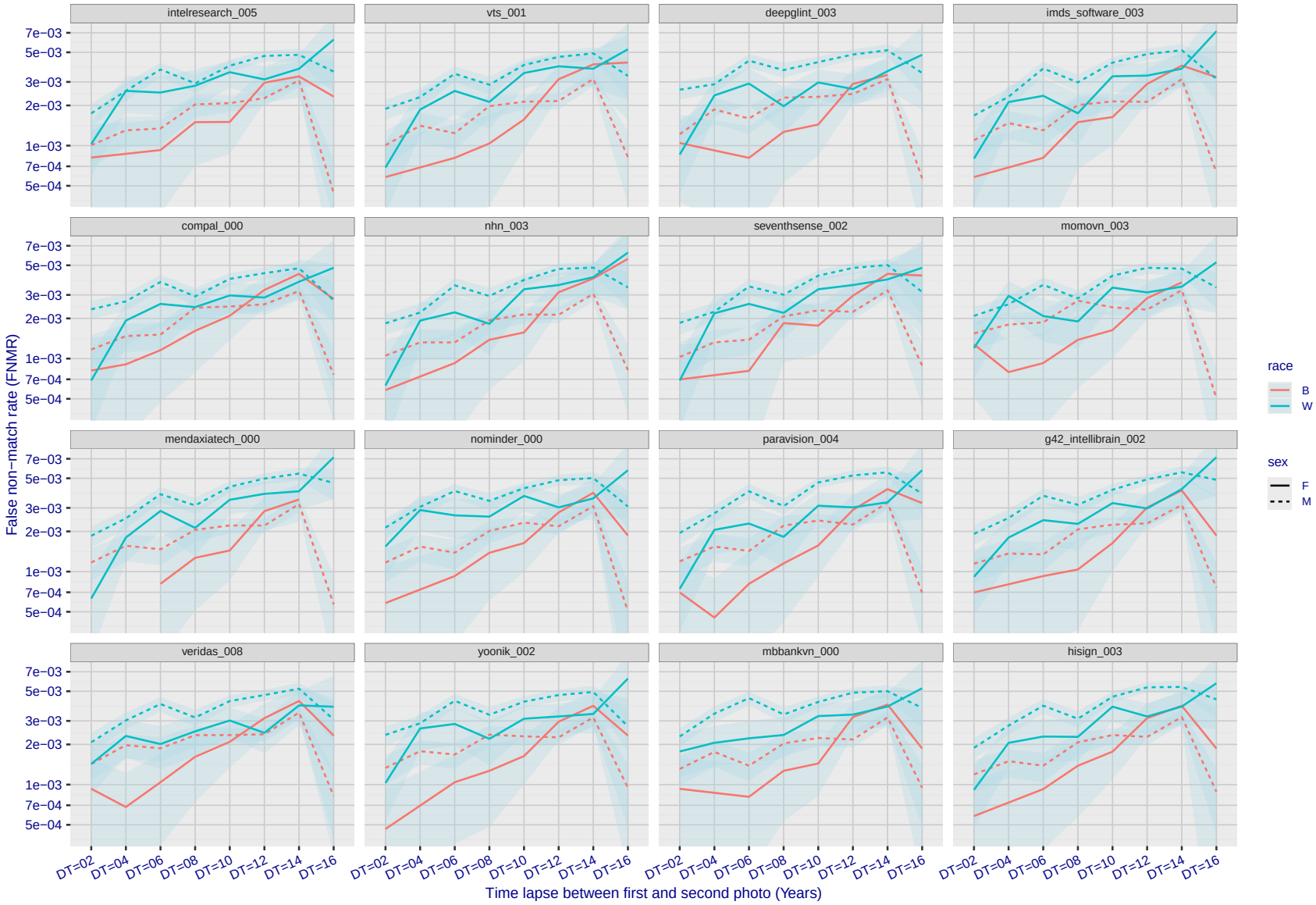

Figure 719: For the mugshot images, FNMR *as a function of elapsed time between initial enrollment and second verification images. The panels appear most accurate first, and vertical scale changes on each page. The four traces correspond to images annotated with codes for black female, black male, white female, white male. The threshold is fixed for each algorithm to give FMR = 0.00001 over all ($\widetilde{10}^8$) impostor comparisons. For short time-lapses, the most accurate algorithms give very few errors (FNMR < 0.001) so that the uncertainty estimates are high.*

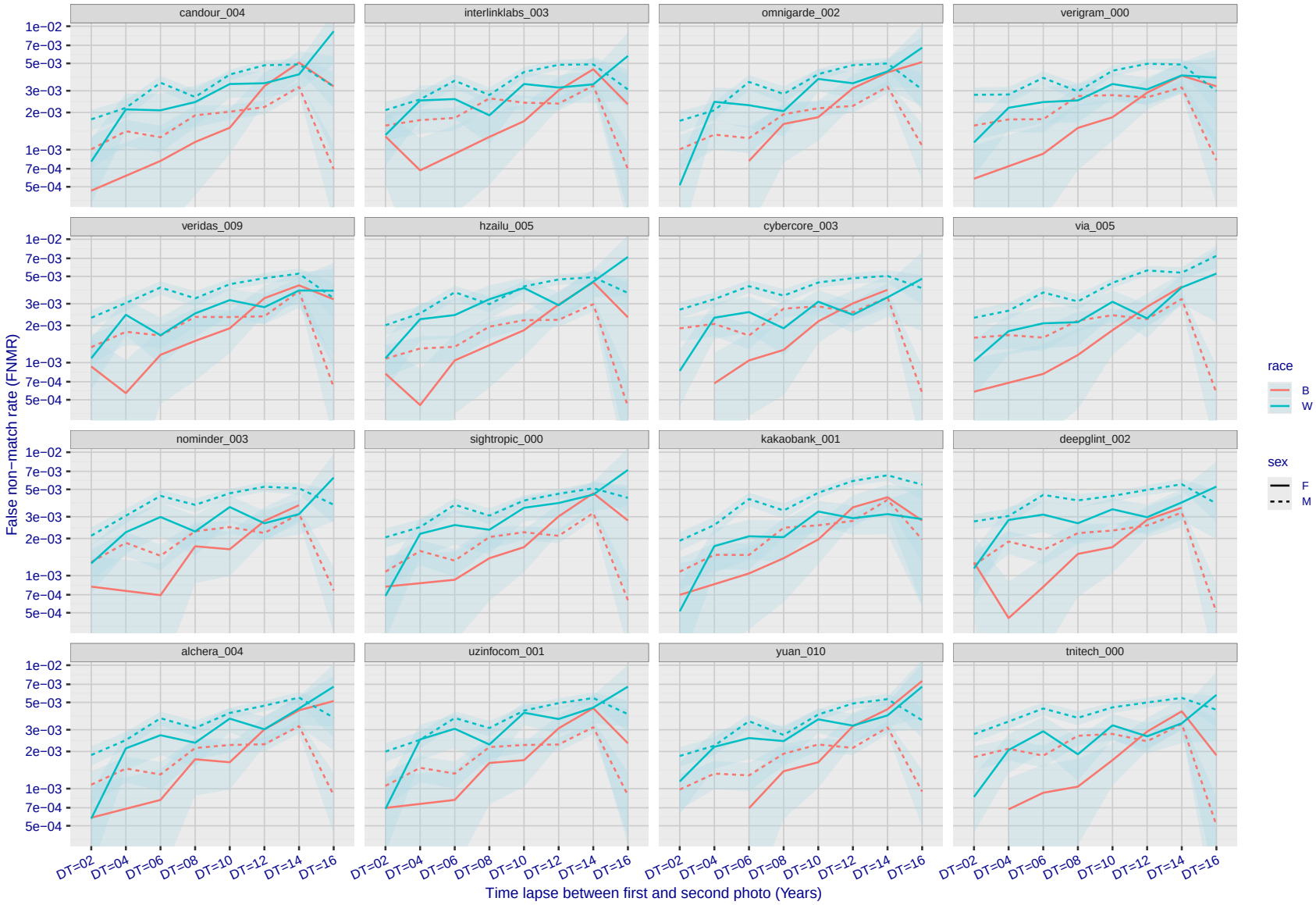

Figure 720: For the mugshot images, FNMR *as a function of elapsed time between initial enrollment and second verification images. The panels appear most accurate first, and vertical scale changes on each page. The four traces correspond to images annotated with codes for black female, black male, white female, white male. The threshold is fixed for each algorithm to give FMR = 0.00001 over all (10^8) impostor comparisons. For short time-lapses, the most accurate algorithms give very few errors (FNMR < 0.001) so that the uncertainty estimates are high.*

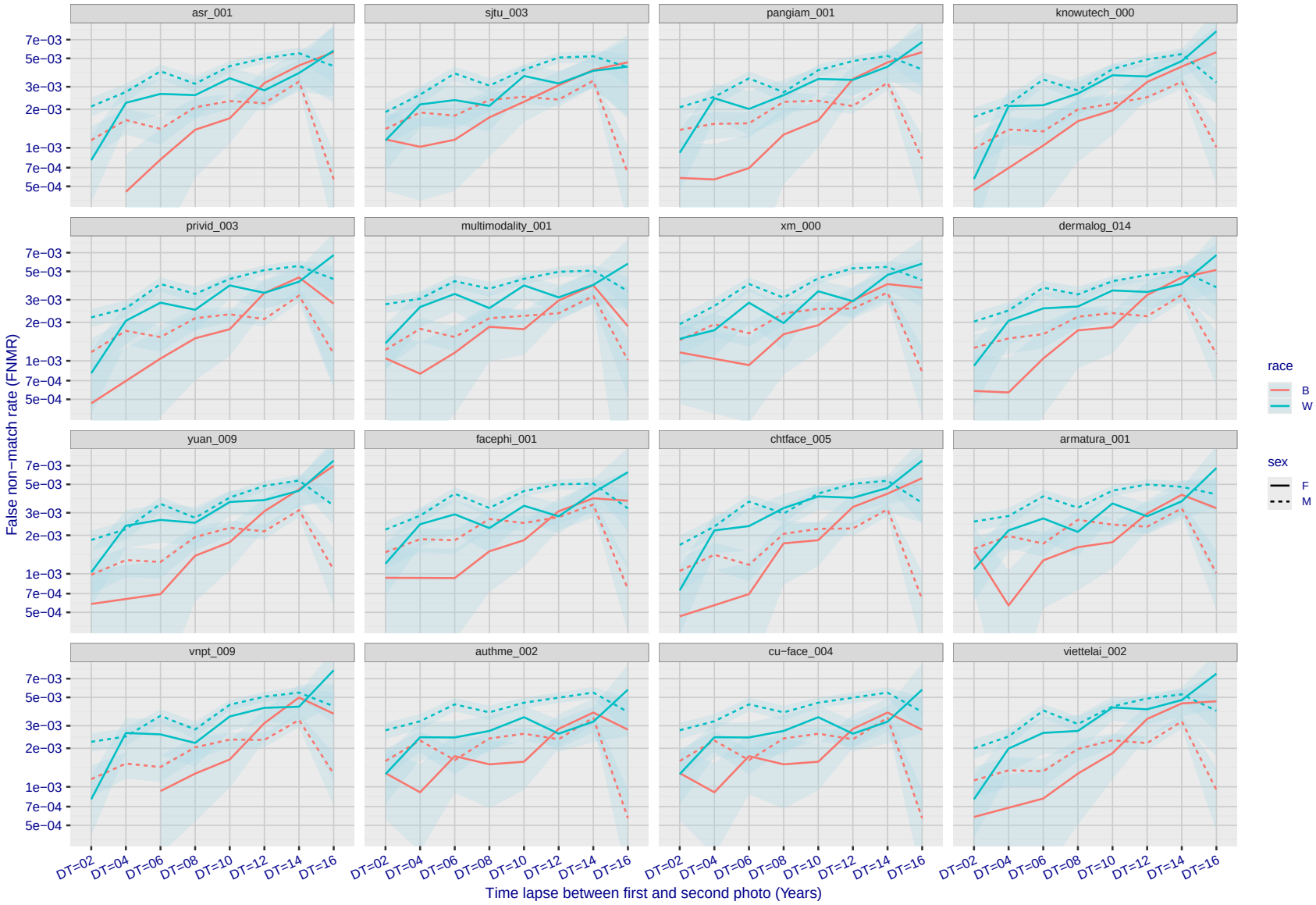

Figure 721: For the mugshot images, FNMR *as a function of elapsed time between initial enrollment and second verification images. The panels appear most accurate first, and vertical scale changes on each page. The four traces correspond to images annotated with codes for black female, black male, white female, white male. The threshold is fixed for each algorithm to give FMR = 0.00001 over all (10^8) impostor comparisons. For short time-lapses, the most accurate algorithms give very few errors (FNMR < 0.001) so that the uncertainty estimates are high.*

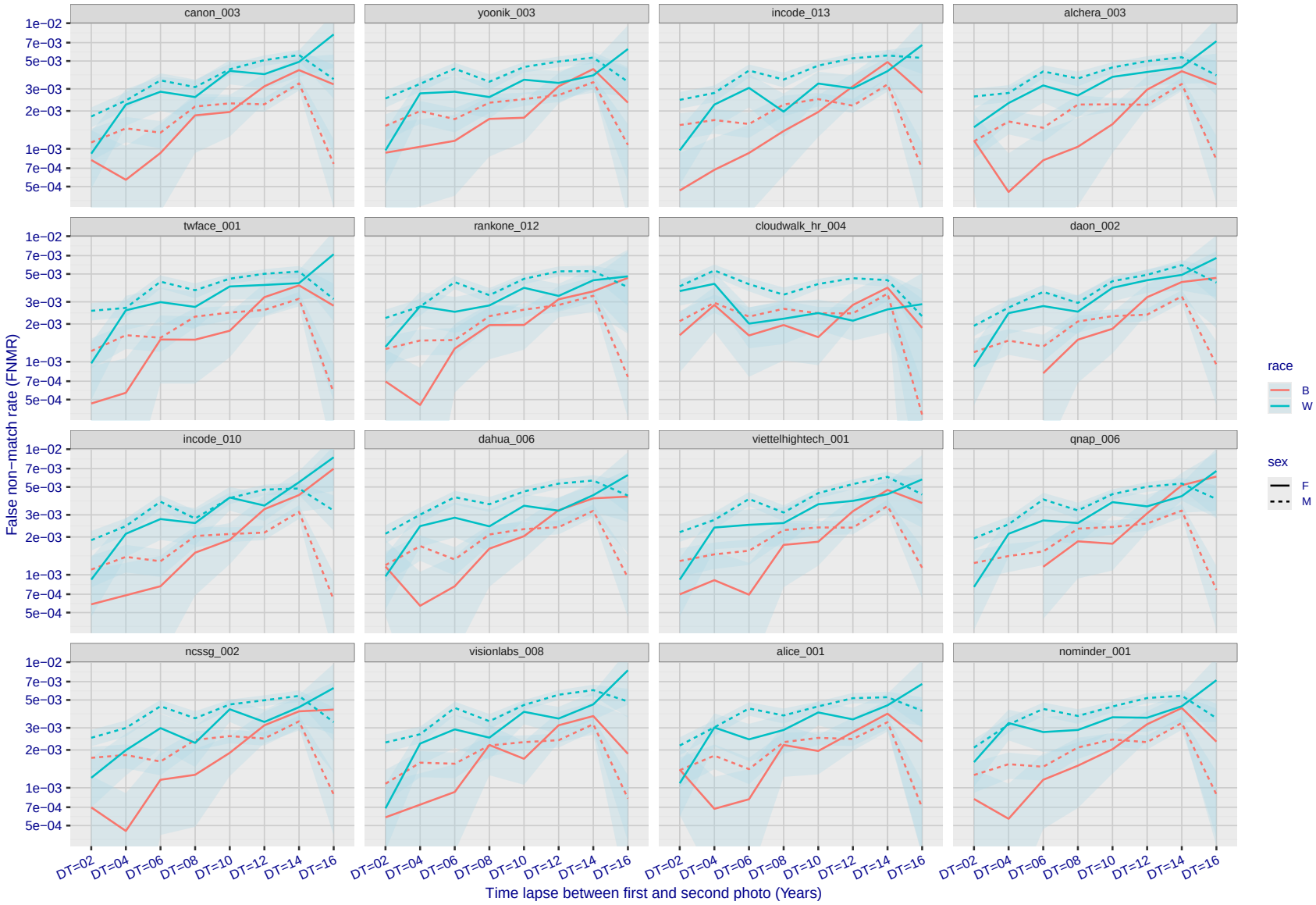

Figure 722: For the mugshot images, FNMR *as a function of elapsed time between initial enrollment and second verification images. The panels appear most accurate first, and vertical scale changes on each page. The four traces correspond to images annotated with codes for black female, black male, white female, white male. The threshold is fixed for each algorithm to give FMR = 0.00001 over all (10^8) impostor comparisons. For short time-lapses, the most accurate algorithms give very few errors (FNMR < 0.001) so that the uncertainty estimates are high.*

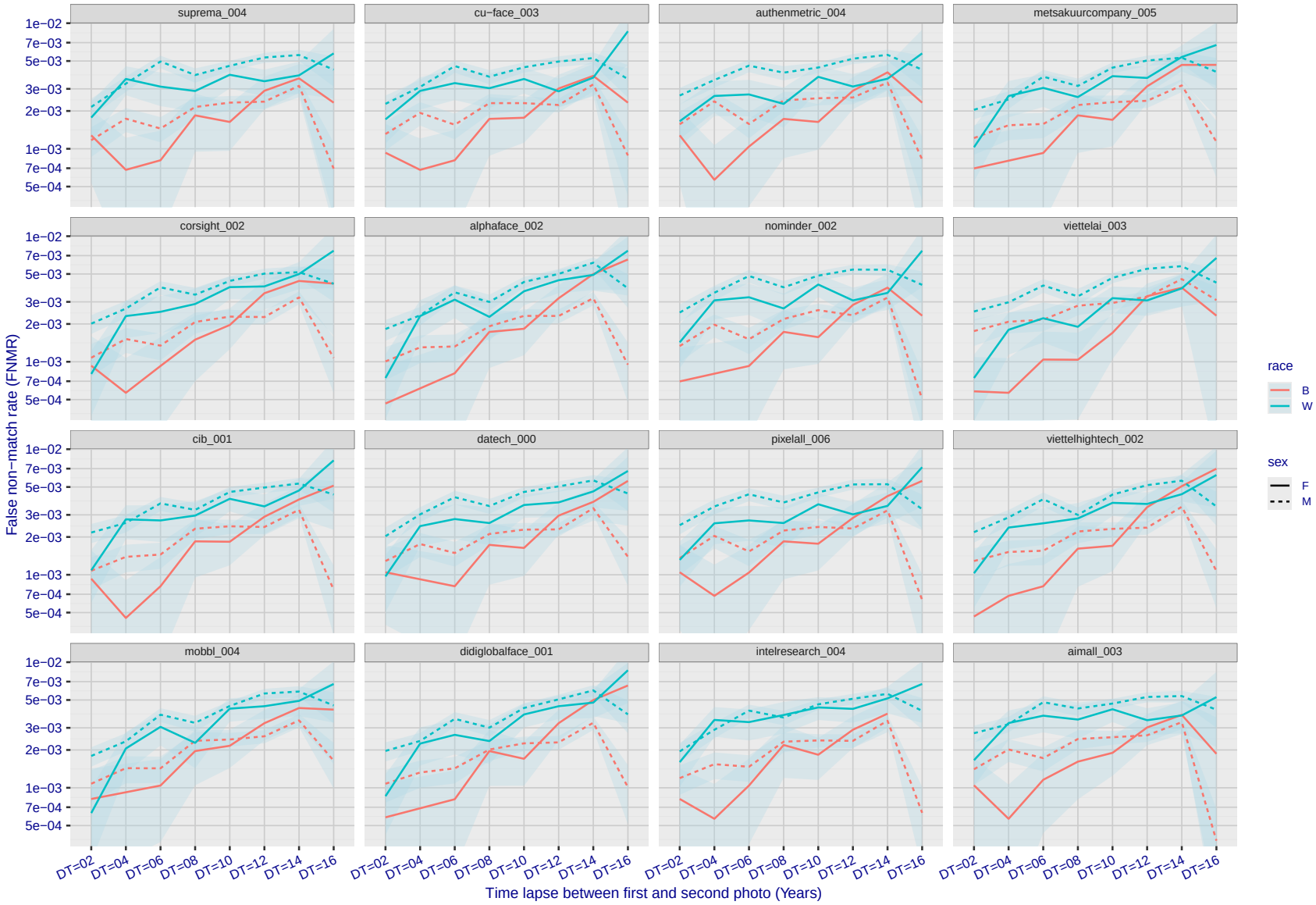

Figure 723: For the mugshot images, FNMR *as a function of elapsed time between initial enrollment and second verification images. The panels appear most accurate first, and vertical scale changes on each page. The four traces correspond to images annotated with codes for black female, black male, white female, white male. The threshold is fixed for each algorithm to give FMR = 0.00001 over all (10^8) impostor comparisons. For short time-lapses, the most accurate algorithms give very few errors (FNMR < 0.001) so that the uncertainty estimates are high.*

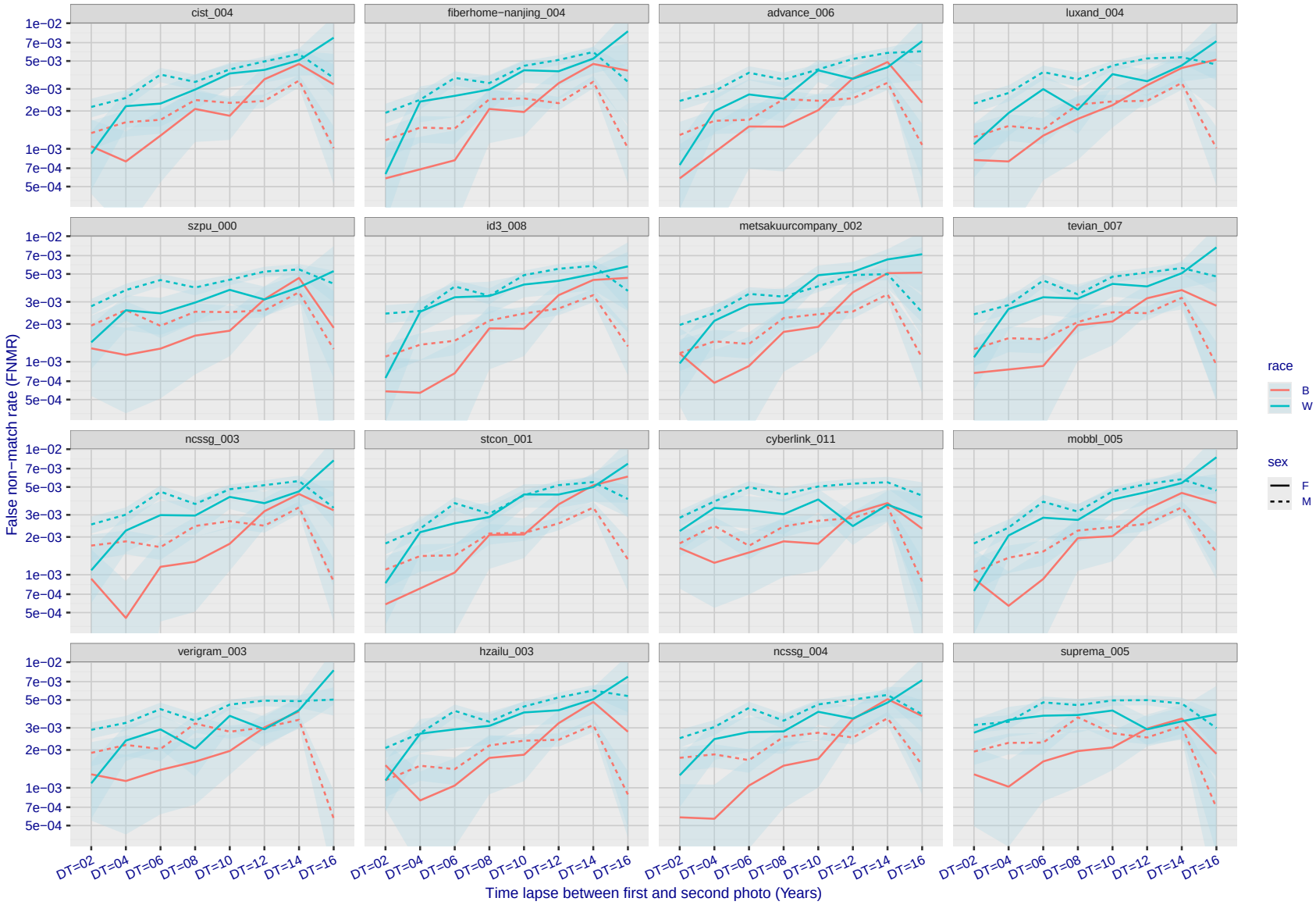

Figure 724: For the mugshot images, FNMR *as a function of elapsed time between initial enrollment and second verification images. The panels appear most accurate first, and vertical scale changes on each page. The four traces correspond to images annotated with codes for black female, black male, white female, white male. The threshold is fixed for each algorithm to give FMR = 0.00001 over all (10^8) impostor comparisons. For short time-lapses, the most accurate algorithms give very few errors (FNMR < 0.001) so that the uncertainty estimates are high.*

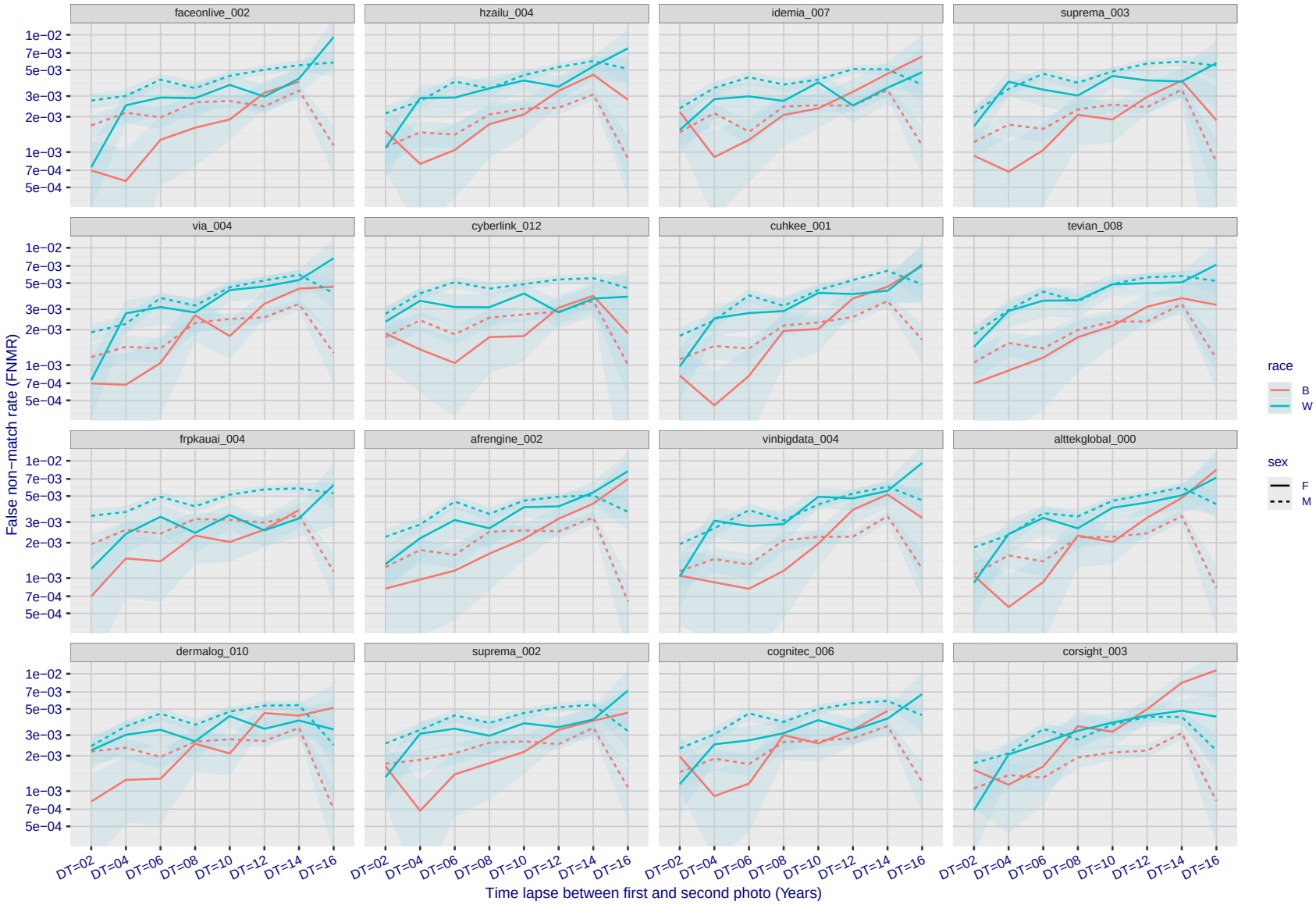

Figure 725: For the mugshot images, FNMR *as a function of elapsed time between initial enrollment and second verification images. The panels appear most accurate first, and vertical scale changes on each page. The four traces correspond to images annotated with codes for black female, black male, white female, white male. The threshold is fixed for each algorithm to give FMR = 0.00001 over all (10^8) impostor comparisons. For short time-lapses, the most accurate algorithms give very few errors (FNMR < 0.001) so that the uncertainty estimates are high.*

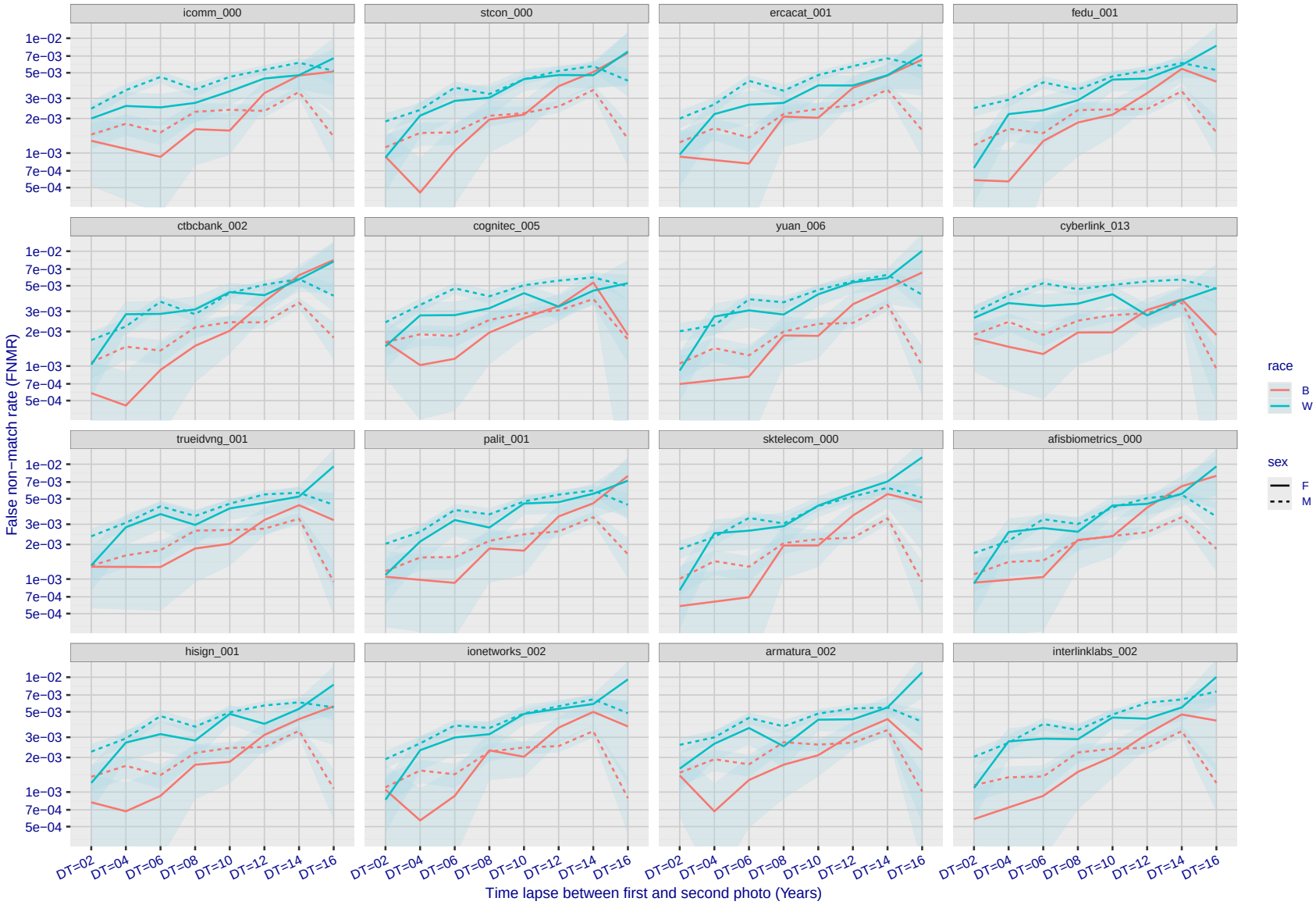

Figure 726: For the mugshot images, FNMR *as a function of elapsed time between initial enrollment and second verification images. The panels appear most accurate first, and vertical scale changes on each page. The four traces correspond to images annotated with codes for black female, black male, white female, white male. The threshold is fixed for each algorithm to give FMR = 0.00001 over all ($\widetilde{10}^8$) impostor comparisons. For short time-lapses, the most accurate algorithms give very few errors (FNMR < 0.001) so that the uncertainty estimates are high.*

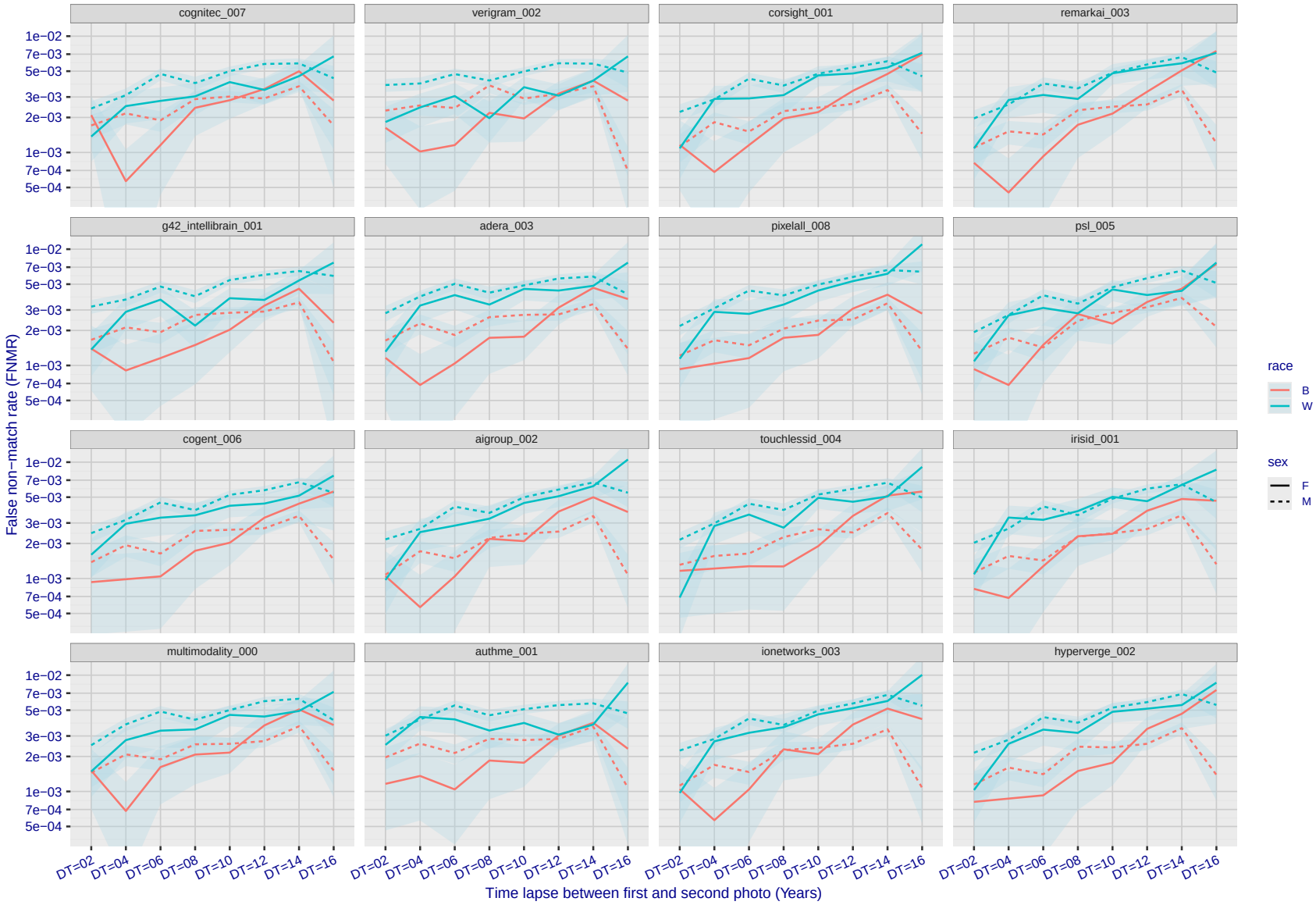

Figure 727: For the mugshot images, FNMR *as a function of elapsed time between initial enrollment and second verification images. The panels appear most accurate first, and vertical scale changes on each page. The four traces correspond to images annotated with codes for black female, black male, white female, white male. The threshold is fixed for each algorithm to give FMR = 0.00001 over all ($\widetilde{10}^8$) impostor comparisons. For short time-lapses, the most accurate algorithms give very few errors (FNMR < 0.001) so that the uncertainty estimates are high.*

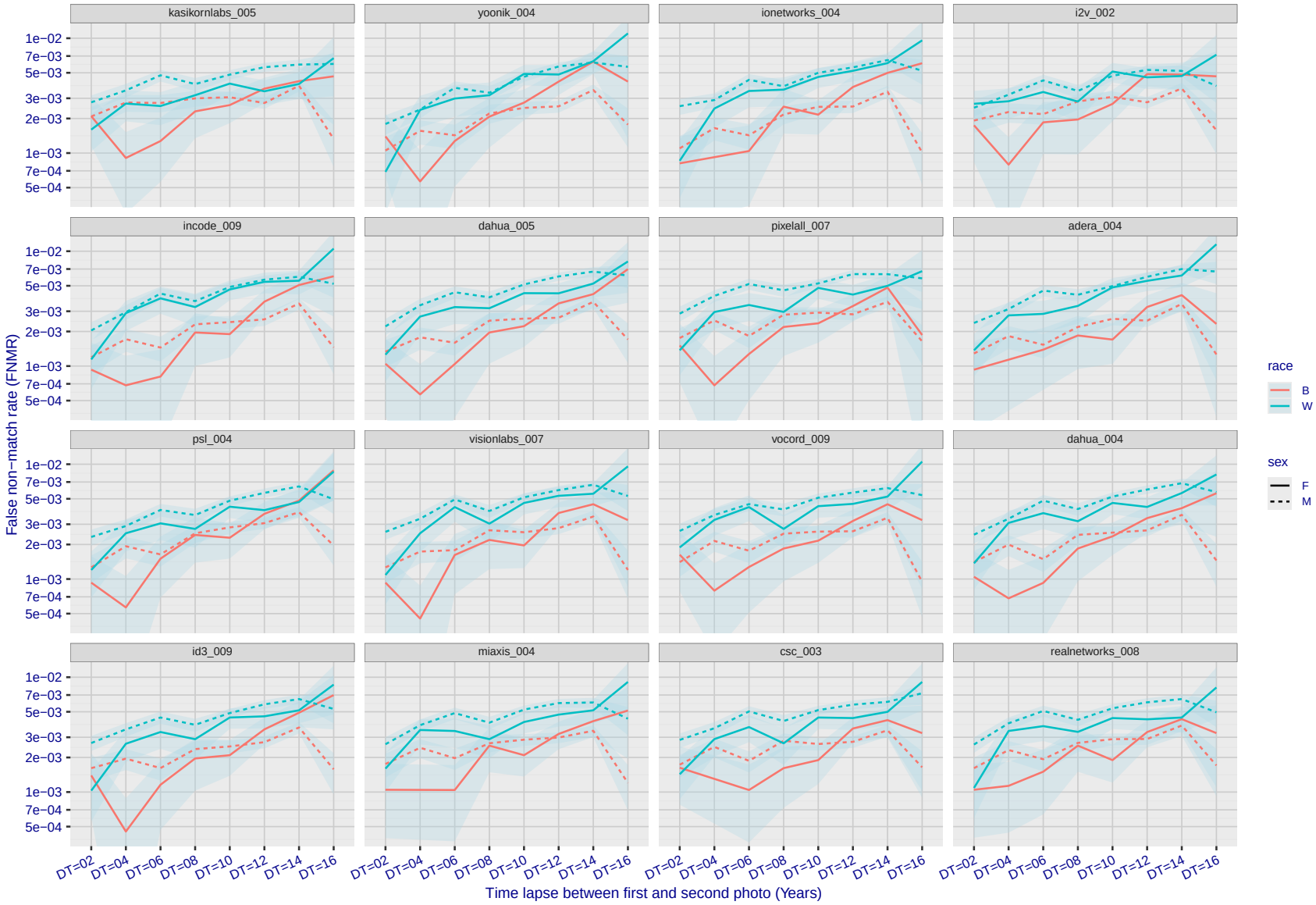

Figure 728: For the mugshot images, FNMR *as a function of elapsed time between initial enrollment and second verification images. The panels appear most accurate first, and vertical scale changes on each page. The four traces correspond to images annotated with codes for black female, black male, white female, white male. The threshold is fixed for each algorithm to give FMR = 0.00001 over all (10^8) impostor comparisons. For short time-lapses, the most accurate algorithms give very few errors (FNMR < 0.001) so that the uncertainty estimates are high.*

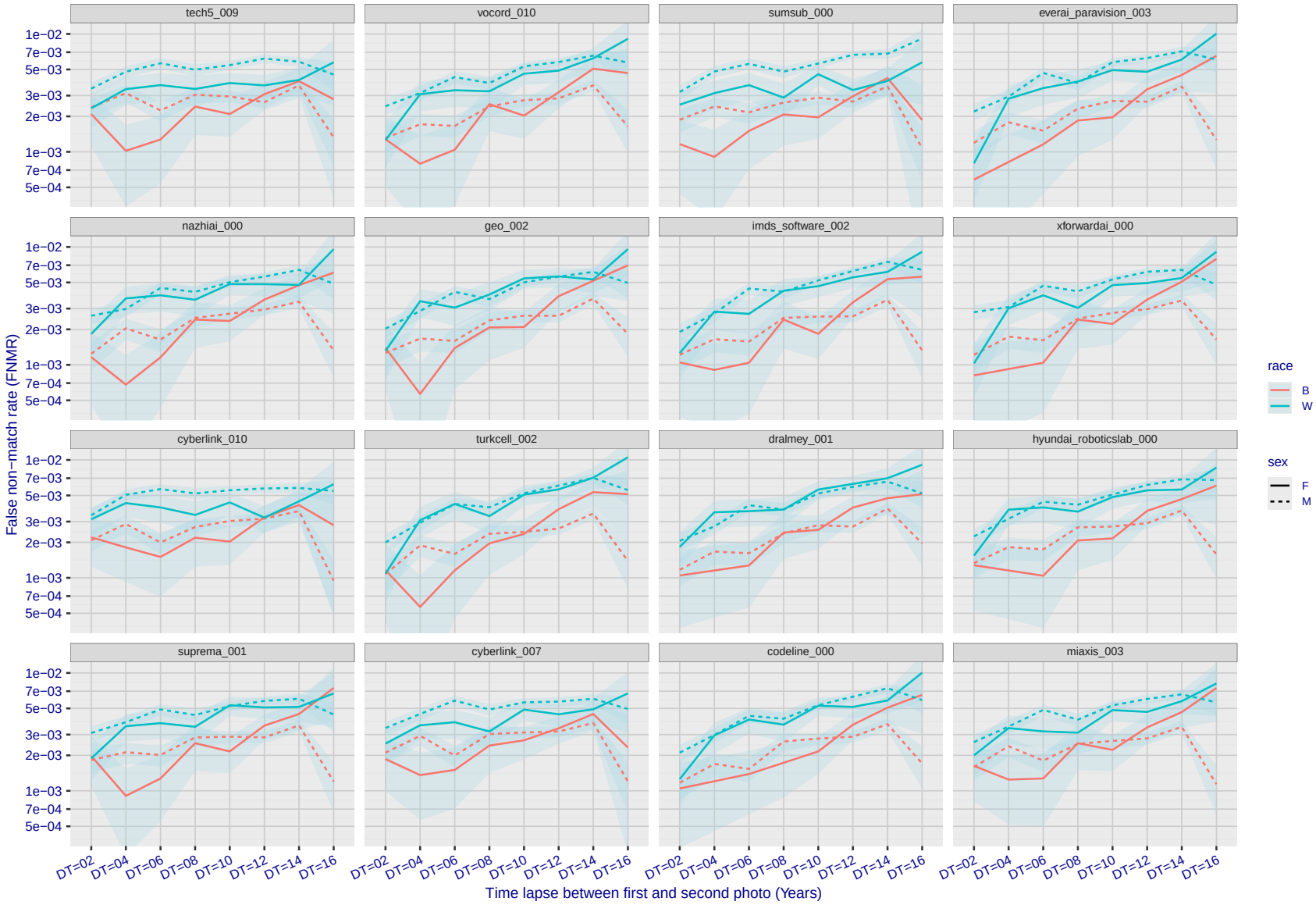

Figure 729: For the mugshot images, FNMR *as a function of elapsed time between initial enrollment and second verification images. The panels appear most accurate first, and vertical scale changes on each page. The four traces correspond to images annotated with codes for black female, black male, white female, white male. The threshold is fixed for each algorithm to give FMR = 0.00001 over all (10^8) impostor comparisons. For short time-lapses, the most accurate algorithms give very few errors (FNMR < 0.001) so that the uncertainty estimates are high.*

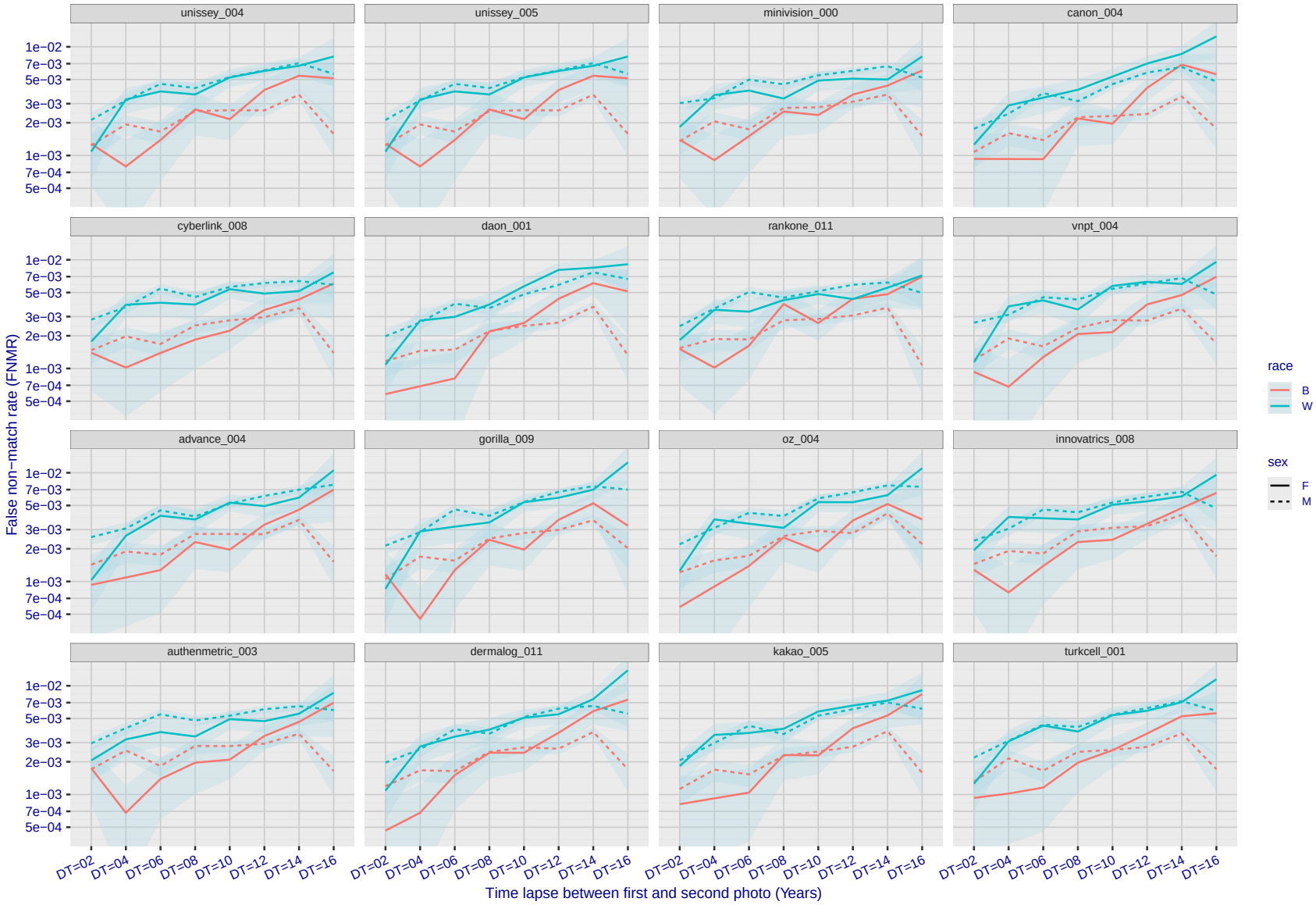

Figure 730: For the mugshot images, FNMR *as a function of elapsed time between initial enrollment and second verification images. The panels appear most accurate first, and vertical scale changes on each page. The four traces correspond to images annotated with codes for black female, black male, white female, white male. The threshold is fixed for each algorithm to give FMR = 0.00001 over all ($\widetilde{10}^8$) impostor comparisons. For short time-lapses, the most accurate algorithms give very few errors (FNMR < 0.001) so that the uncertainty estimates are high.*

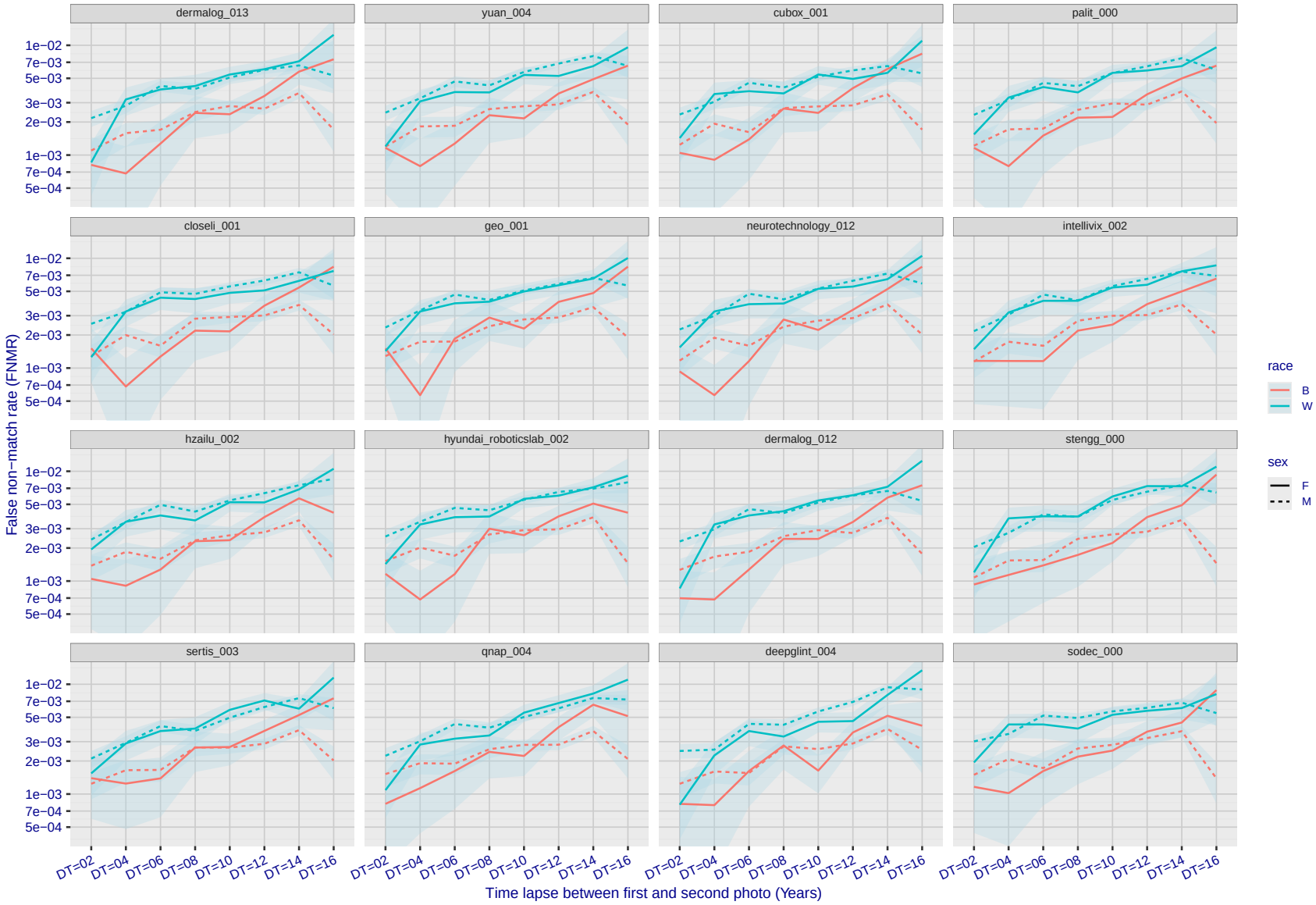

Figure 731: For the mugshot images, FNMR *as a function of elapsed time between initial enrollment and second verification images. The panels appear most accurate first, and vertical scale changes on each page. The four traces correspond to images annotated with codes for black female, black male, white female, white male. The threshold is fixed for each algorithm to give FMR = 0.00001 over all (10^8) impostor comparisons. For short time-lapses, the most accurate algorithms give very few errors (FNMR < 0.001) so that the uncertainty estimates are high.*

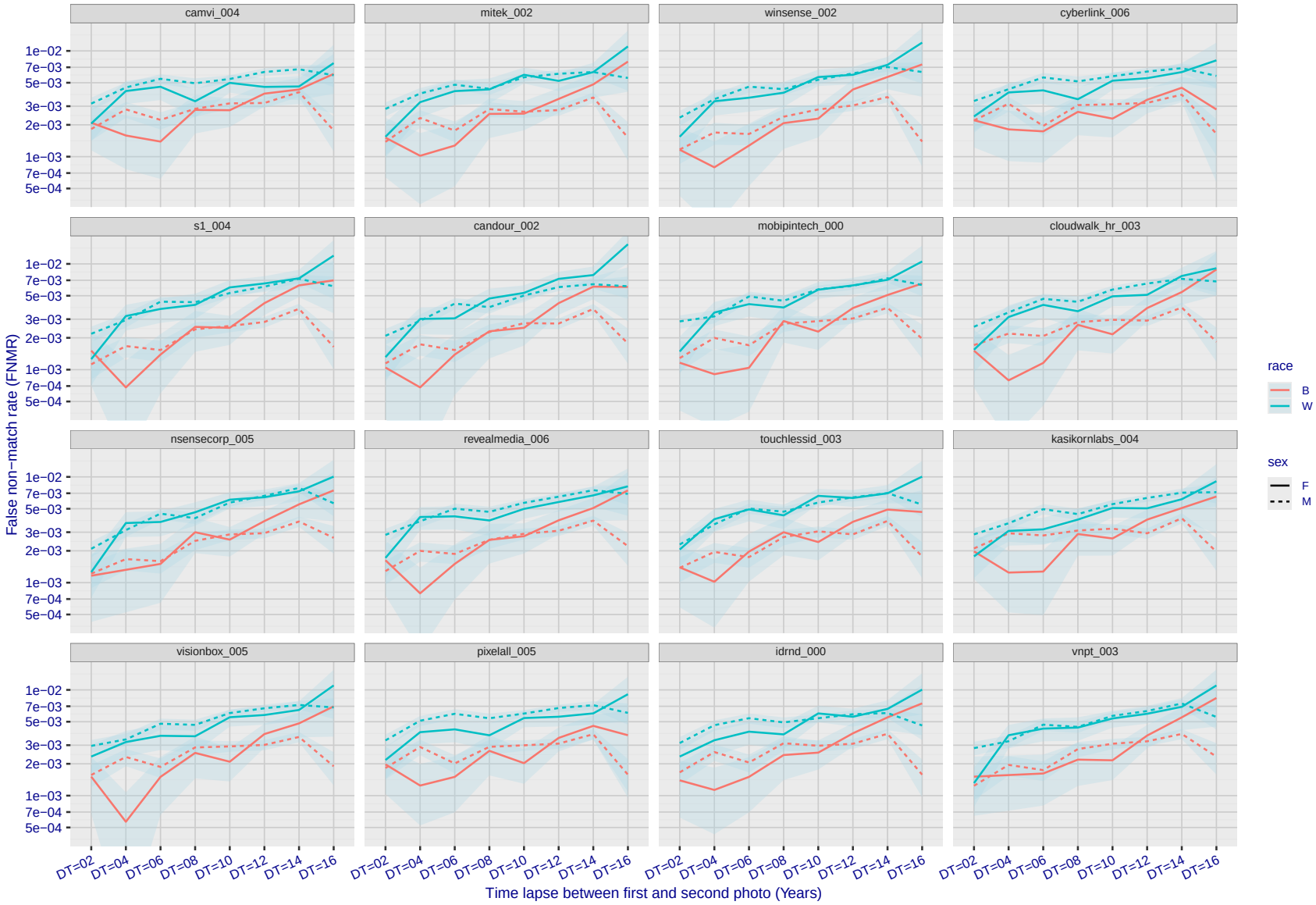

Figure 732: For the mugshot images, FNMR *as a function of elapsed time between initial enrollment and second verification images. The panels appear most accurate first, and vertical scale changes on each page. The four traces correspond to images annotated with codes for black female, black male, white female, white male. The threshold is fixed for each algorithm to give FMR = 0.00001 over all (10^8) impostor comparisons. For short time-lapses, the most accurate algorithms give very few errors (FNMR < 0.001) so that the uncertainty estimates are high.*

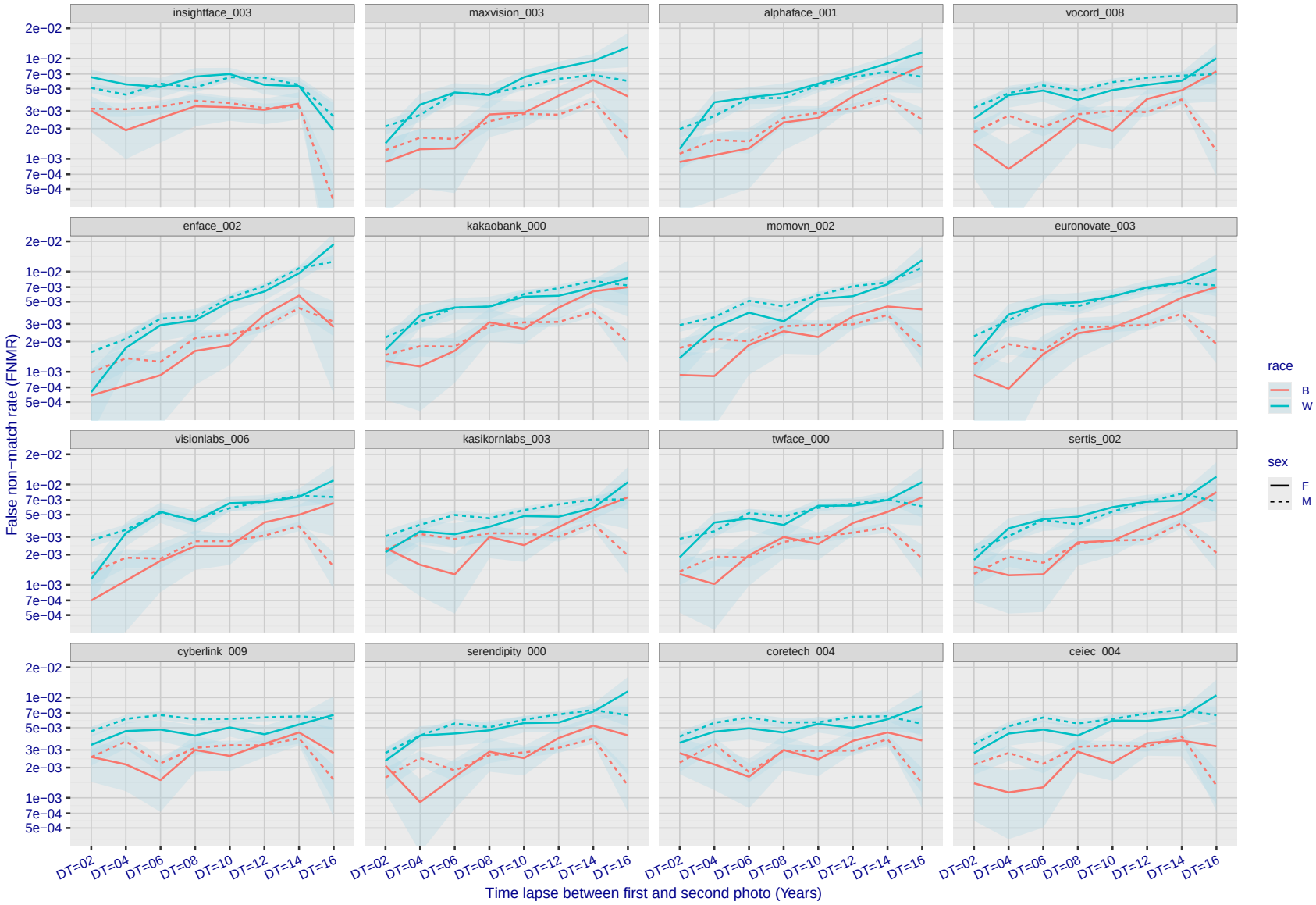

Figure 733: For the mugshot images, FNMR *as a function of elapsed time between initial enrollment and second verification images. The panels appear most accurate first, and vertical scale changes on each page. The four traces correspond to images annotated with codes for black female, black male, white female, white male. The threshold is fixed for each algorithm to give FMR = 0.00001 over all ($\widetilde{10}^8$) impostor comparisons. For short time-lapses, the most accurate algorithms give very few errors (FNMR < 0.001) so that the uncertainty estimates are high.*

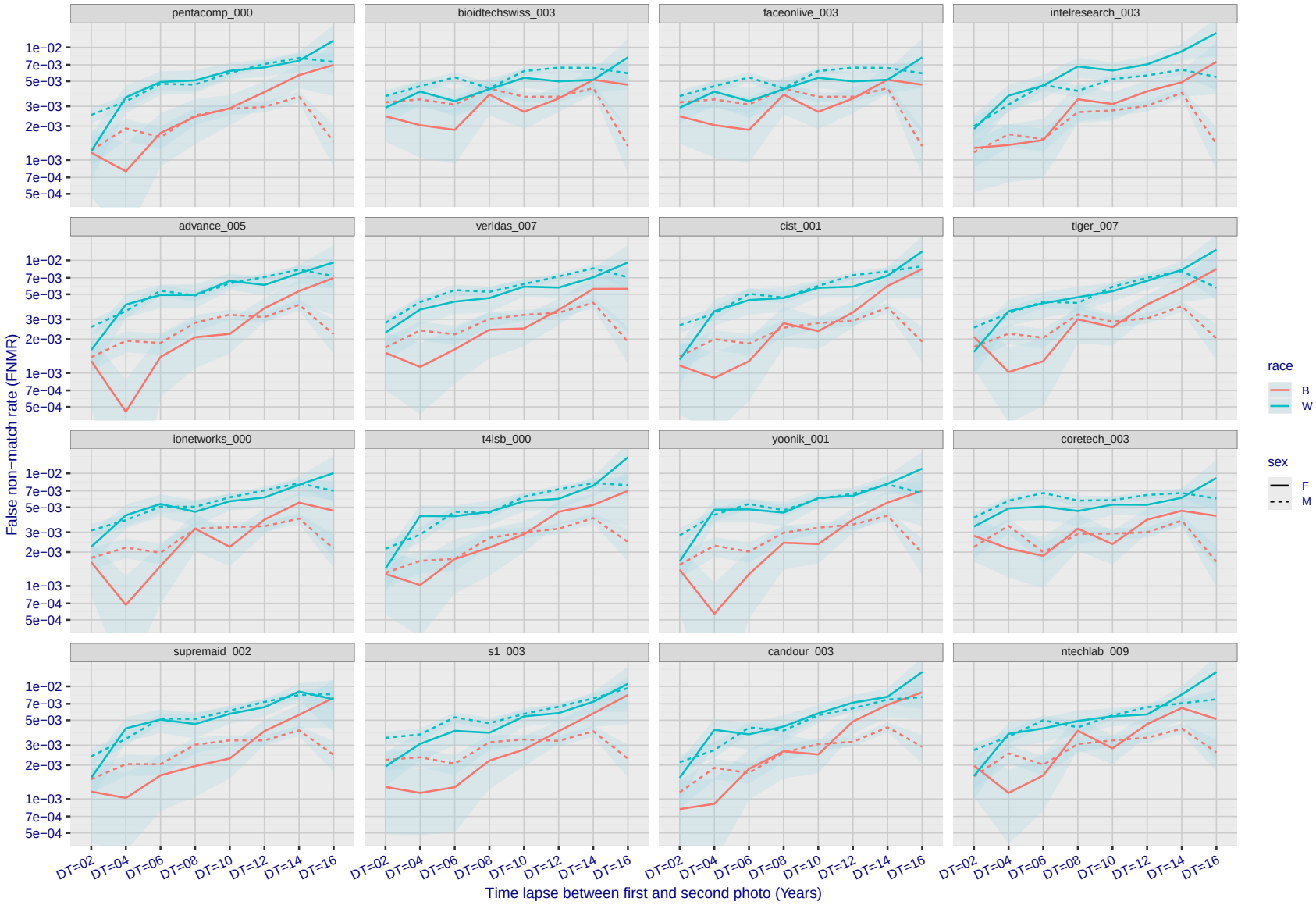

Figure 734: For the mugshot images, FNMR *as a function of elapsed time between initial enrollment and second verification images. The panels appear most accurate first, and vertical scale changes on each page. The four traces correspond to images annotated with codes for black female, black male, white female, white male. The threshold is fixed for each algorithm to give FMR = 0.00001 over all (10^8) impostor comparisons. For short time-lapses, the most accurate algorithms give very few errors (FNMR < 0.001) so that the uncertainty estimates are high.*

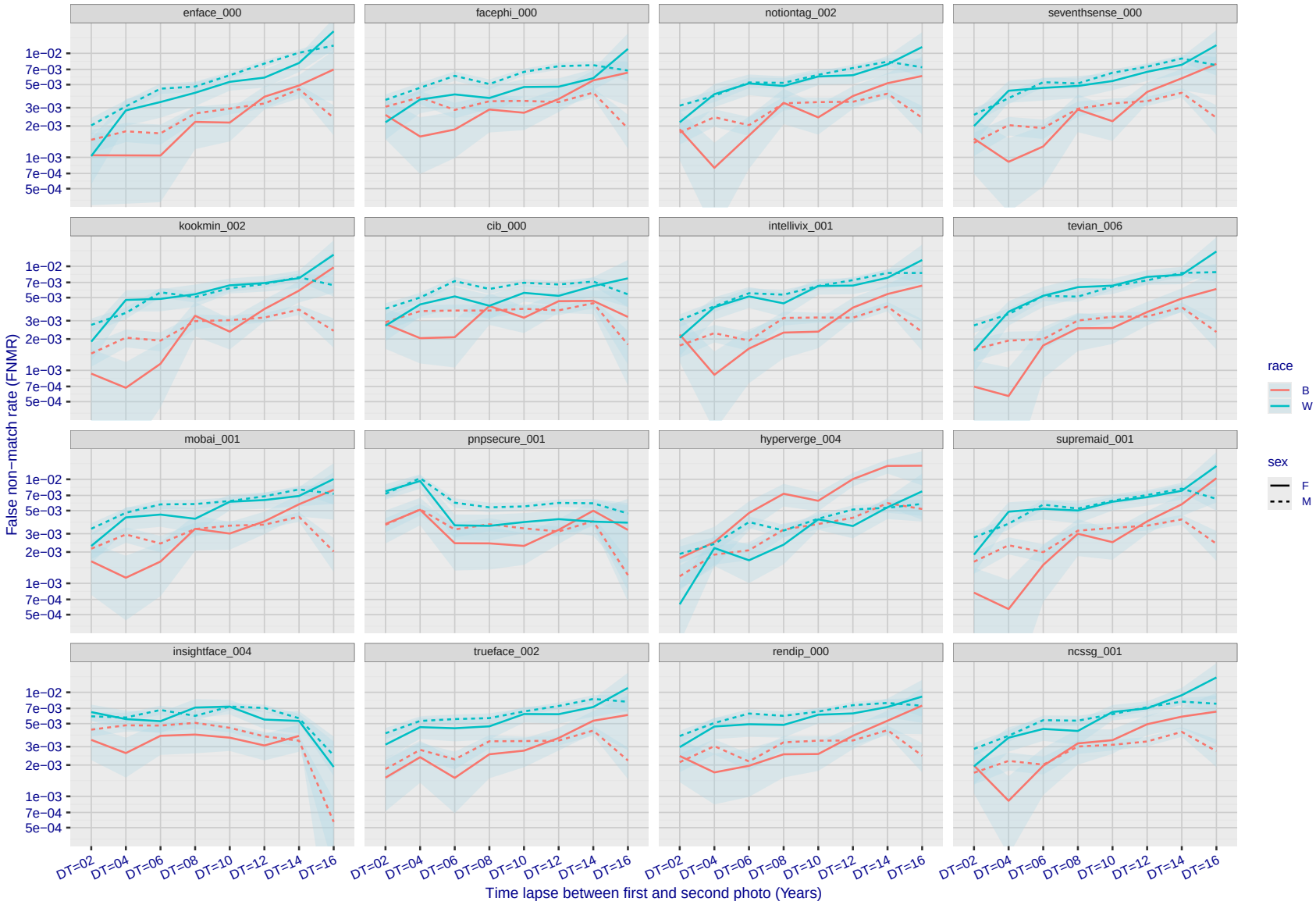

Figure 735: For the mugshot images, FNMR *as a function of elapsed time between initial enrollment and second verification images. The panels appear most accurate first, and vertical scale changes on each page. The four traces correspond to images annotated with codes for black female, black male, white female, white male. The threshold is fixed for each algorithm to give FMR = 0.00001 over all (10^8) impostor comparisons. For short time-lapses, the most accurate algorithms give very few errors (FNMR < 0.001) so that the uncertainty estimates are high.*

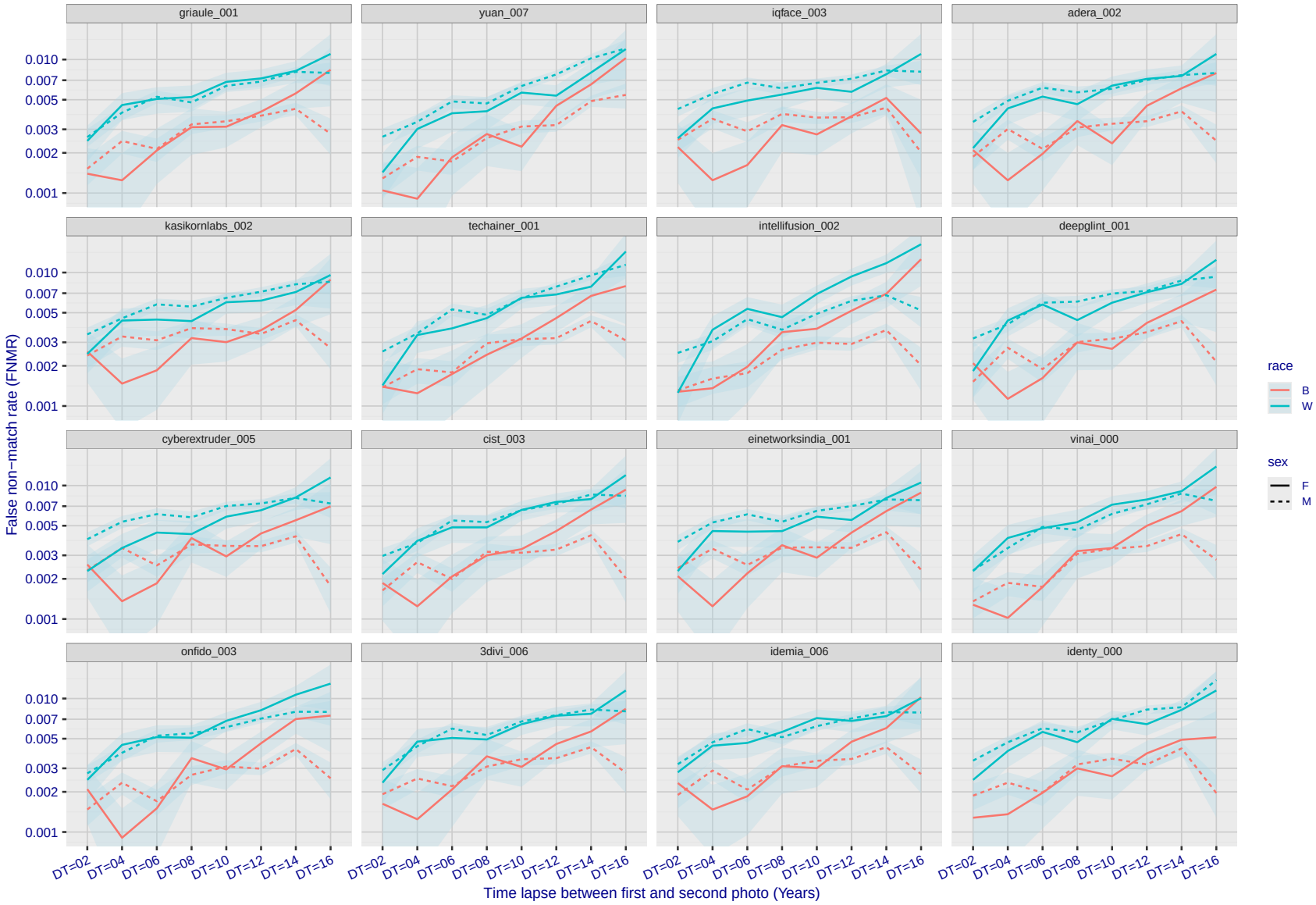

Figure 736: For the mugshot images, FNMR *as a function of elapsed time between initial enrollment and second verification images. The panels appear most accurate first, and vertical scale changes on each page. The four traces correspond to images annotated with codes for black female, black male, white female, white male. The threshold is fixed for each algorithm to give FMR = 0.00001 over all ($\widetilde{10}^8$) impostor comparisons. For short time-lapses, the most accurate algorithms give very few errors (FNMR < 0.001) so that the uncertainty estimates are high.*

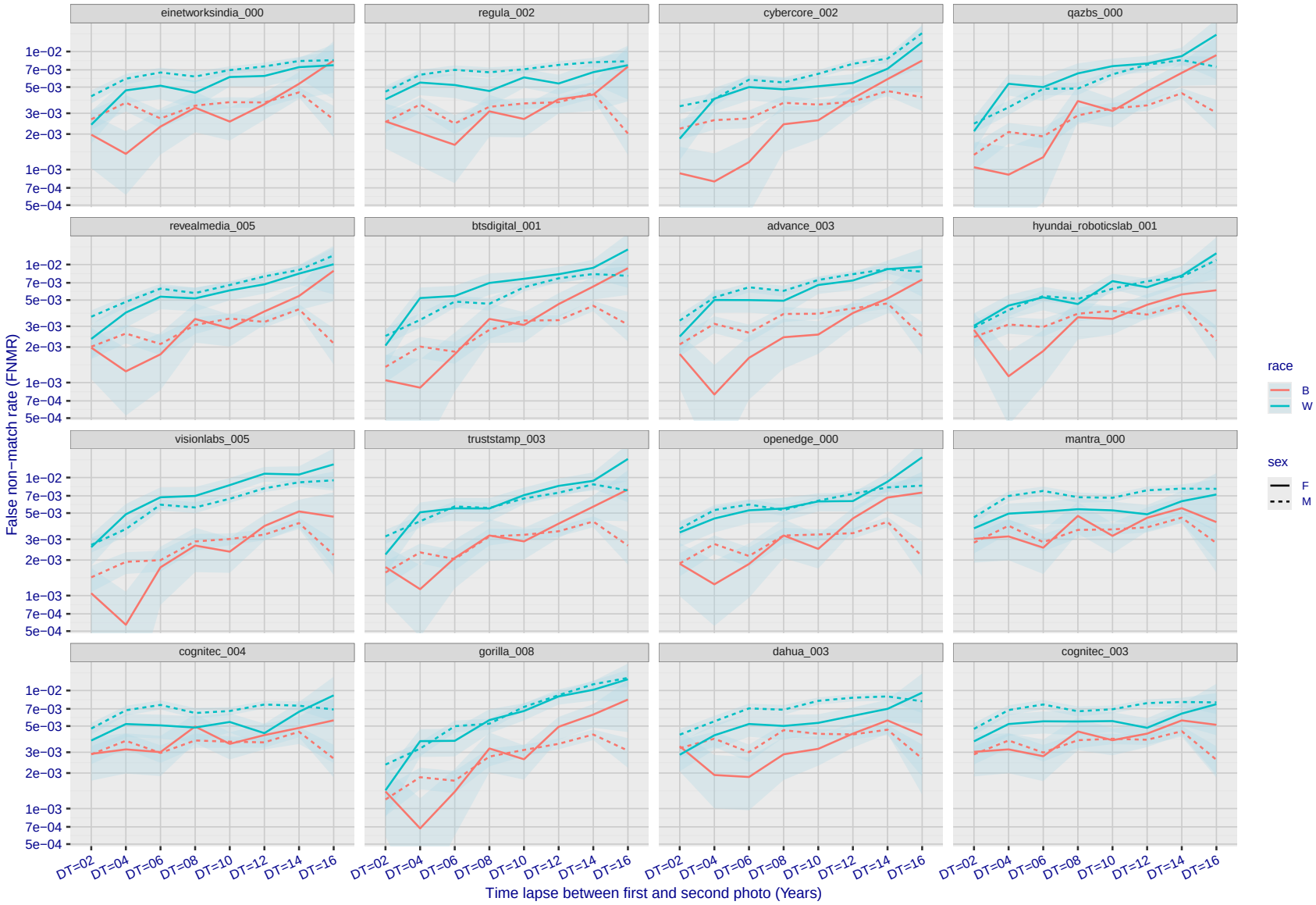

Figure 737: For the mugshot images, FNMR *as a function of elapsed time between initial enrollment and second verification images. The panels appear most accurate first, and vertical scale changes on each page. The four traces correspond to images annotated with codes for black female, black male, white female, white male. The threshold is fixed for each algorithm to give FMR = 0.00001 over all ($\widetilde{10}^8$) impostor comparisons. For short time-lapses, the most accurate algorithms give very few errors (FNMR < 0.001) so that the uncertainty estimates are high.*

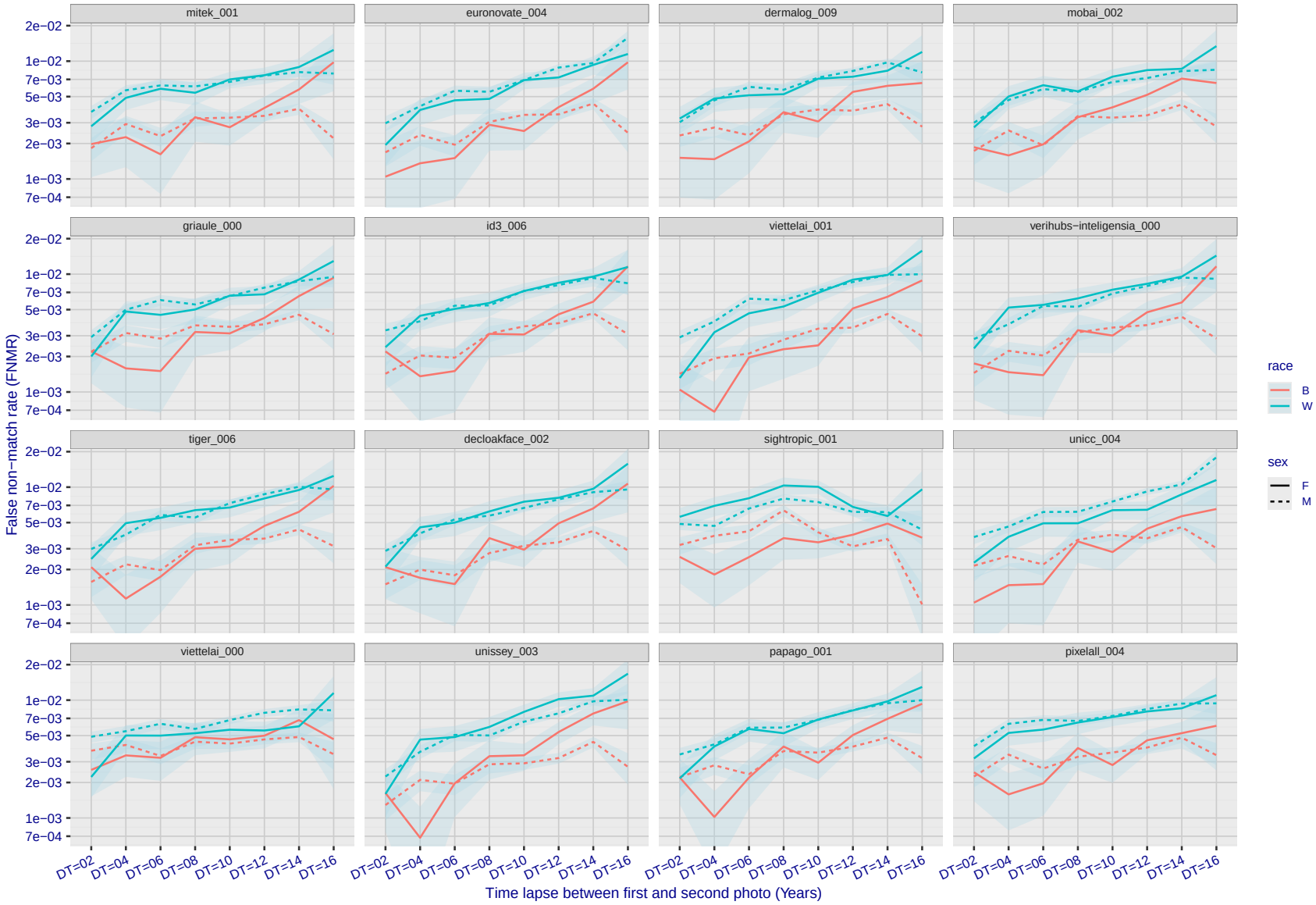

Figure 738: For the mugshot images, FNMR *as a function of elapsed time between initial enrollment and second verification images. The panels appear most accurate first, and vertical scale changes on each page. The four traces correspond to images annotated with codes for black female, black male, white female, white male. The threshold is fixed for each algorithm to give FMR = 0.00001 over all (10^8) impostor comparisons. For short time-lapses, the most accurate algorithms give very few errors (FNMR < 0.001) so that the uncertainty estimates are high.*

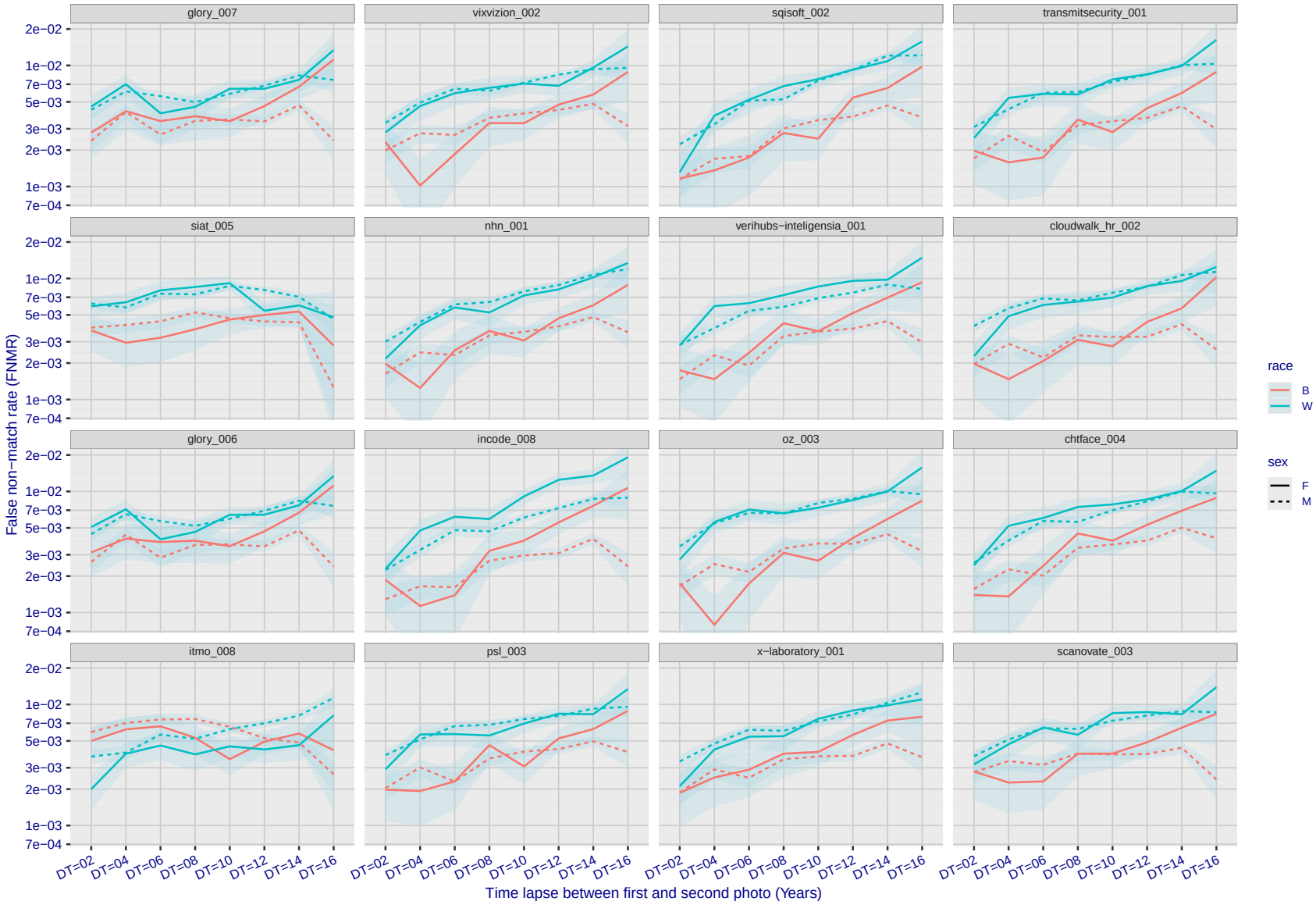

Figure 739: For the mugshot images, FNMR *as a function of elapsed time between initial enrollment and second verification images. The panels appear most accurate first, and vertical scale changes on each page. The four traces correspond to images annotated with codes for black female, black male, white female, white male. The threshold is fixed for each algorithm to give FMR = 0.00001 over all ($\widetilde{10}^8$) impostor comparisons. For short time-lapses, the most accurate algorithms give very few errors (FNMR < 0.001) so that the uncertainty estimates are high.*

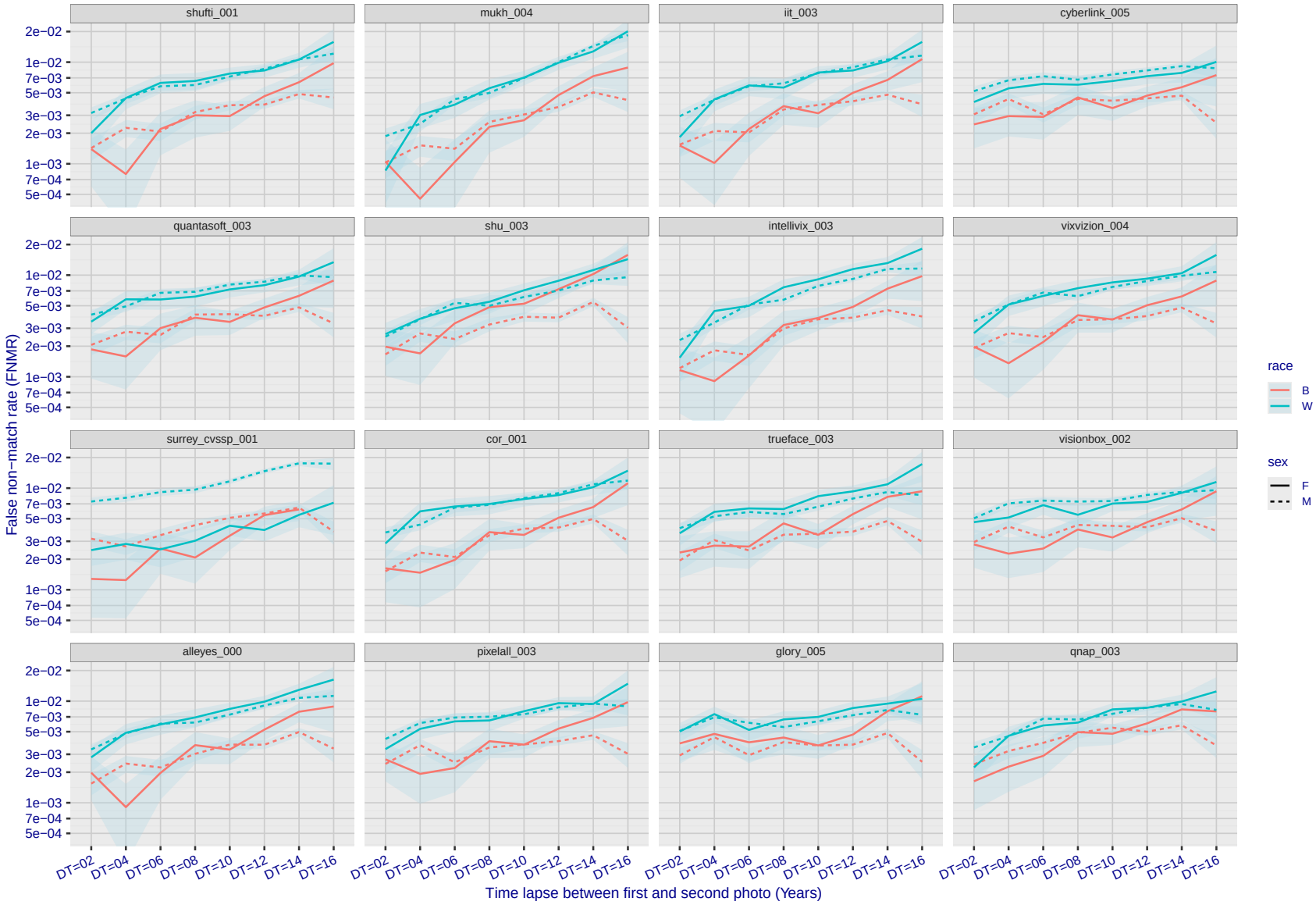

Figure 740: For the mugshot images, FNMR *as a function of elapsed time between initial enrollment and second verification images. The panels appear most accurate first, and vertical scale changes on each page. The four traces correspond to images annotated with codes for black female, black male, white female, white male. The threshold is fixed for each algorithm to give FMR = 0.00001 over all (10^8) impostor comparisons. For short time-lapses, the most accurate algorithms give very few errors (FNMR < 0.001) so that the uncertainty estimates are high.*

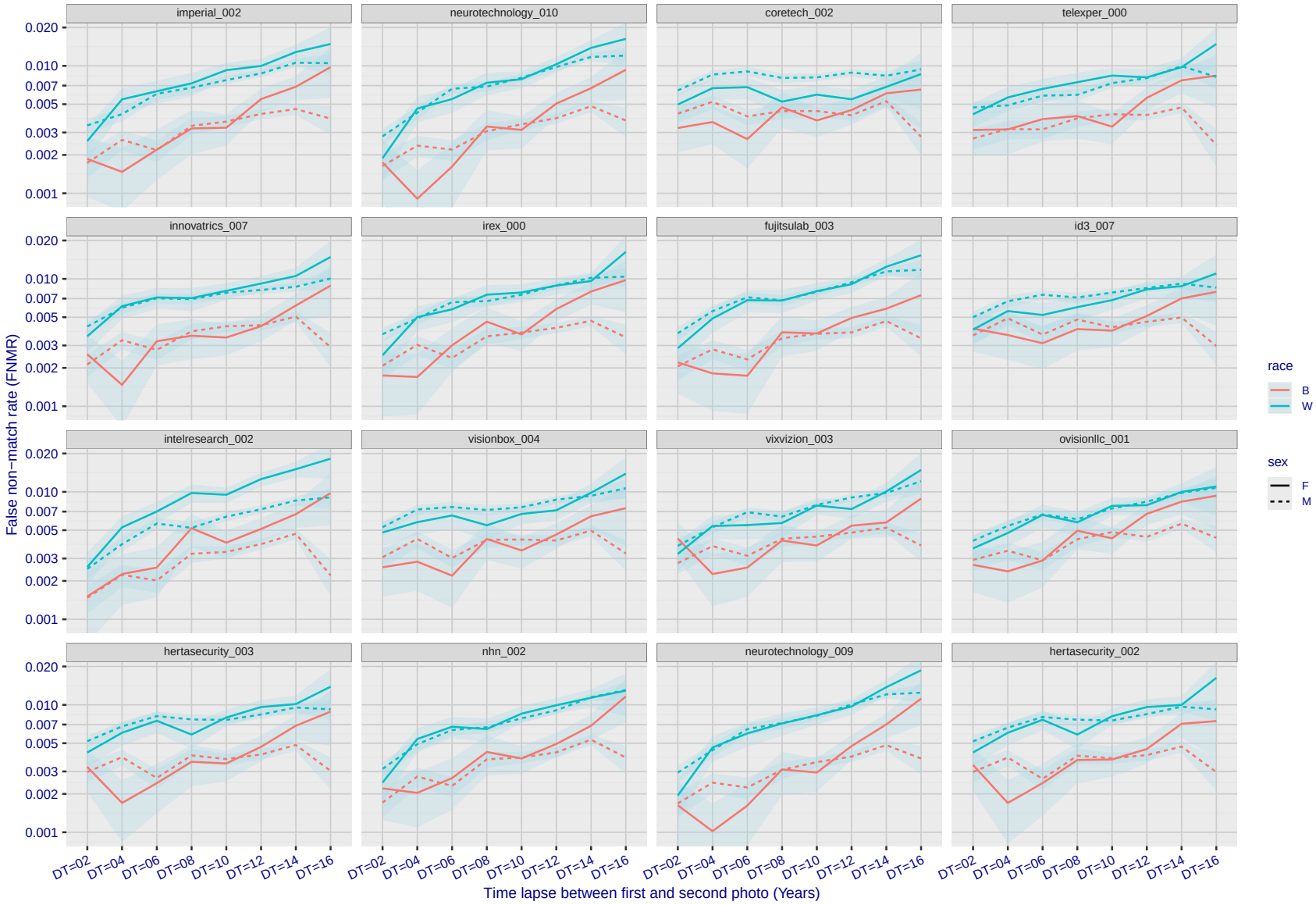

Figure 741: For the mugshot images, FNMR *as a function of elapsed time between initial enrollment and second verification images. The panels appear most accurate first, and vertical scale changes on each page. The four traces correspond to images annotated with codes for black female, black male, white female, white male. The threshold is fixed for each algorithm to give FMR = 0.00001 over all ($\widetilde{10}^8$) impostor comparisons. For short time-lapses, the most accurate algorithms give very few errors (FNMR < 0.001) so that the uncertainty estimates are high.*

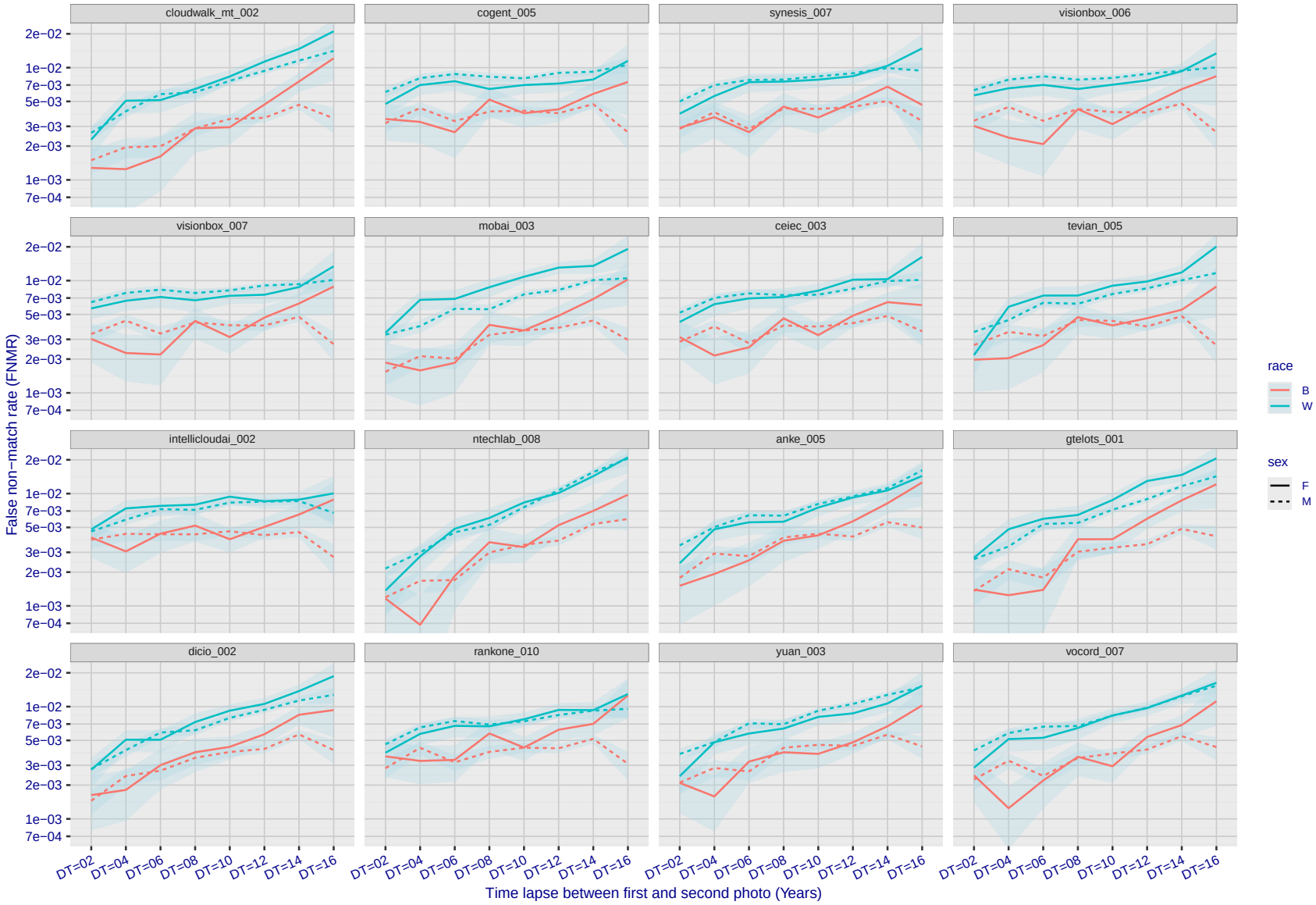

Figure 742: For the mugshot images, FNMR *as a function of elapsed time between initial enrollment and second verification images. The panels appear most accurate first, and vertical scale changes on each page. The four traces correspond to images annotated with codes for black female, black male, white female, white male. The threshold is fixed for each algorithm to give FMR = 0.00001 over all (10^8) impostor comparisons. For short time-lapses, the most accurate algorithms give very few errors (FNMR < 0.001) so that the uncertainty estimates are high.*

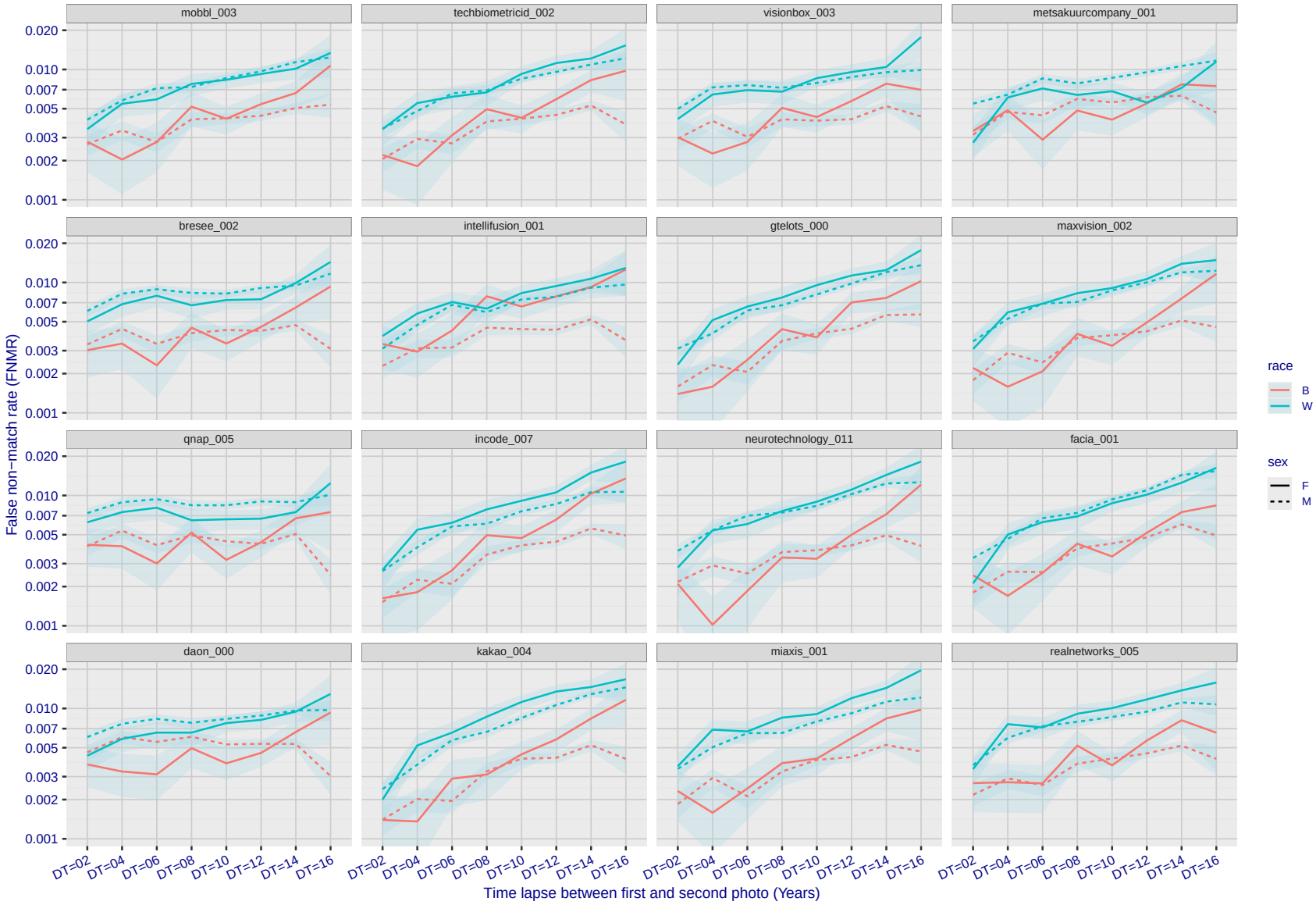

Figure 743: For the mugshot images, FNMR *as a function of elapsed time between initial enrollment and second verification images. The panels appear most accurate first, and vertical scale changes on each page. The four traces correspond to images annotated with codes for black female, black male, white female, white male. The threshold is fixed for each algorithm to give FMR = 0.00001 over all (10^8) impostor comparisons. For short time-lapses, the most accurate algorithms give very few errors (FNMR < 0.001) so that the uncertainty estimates are high.*

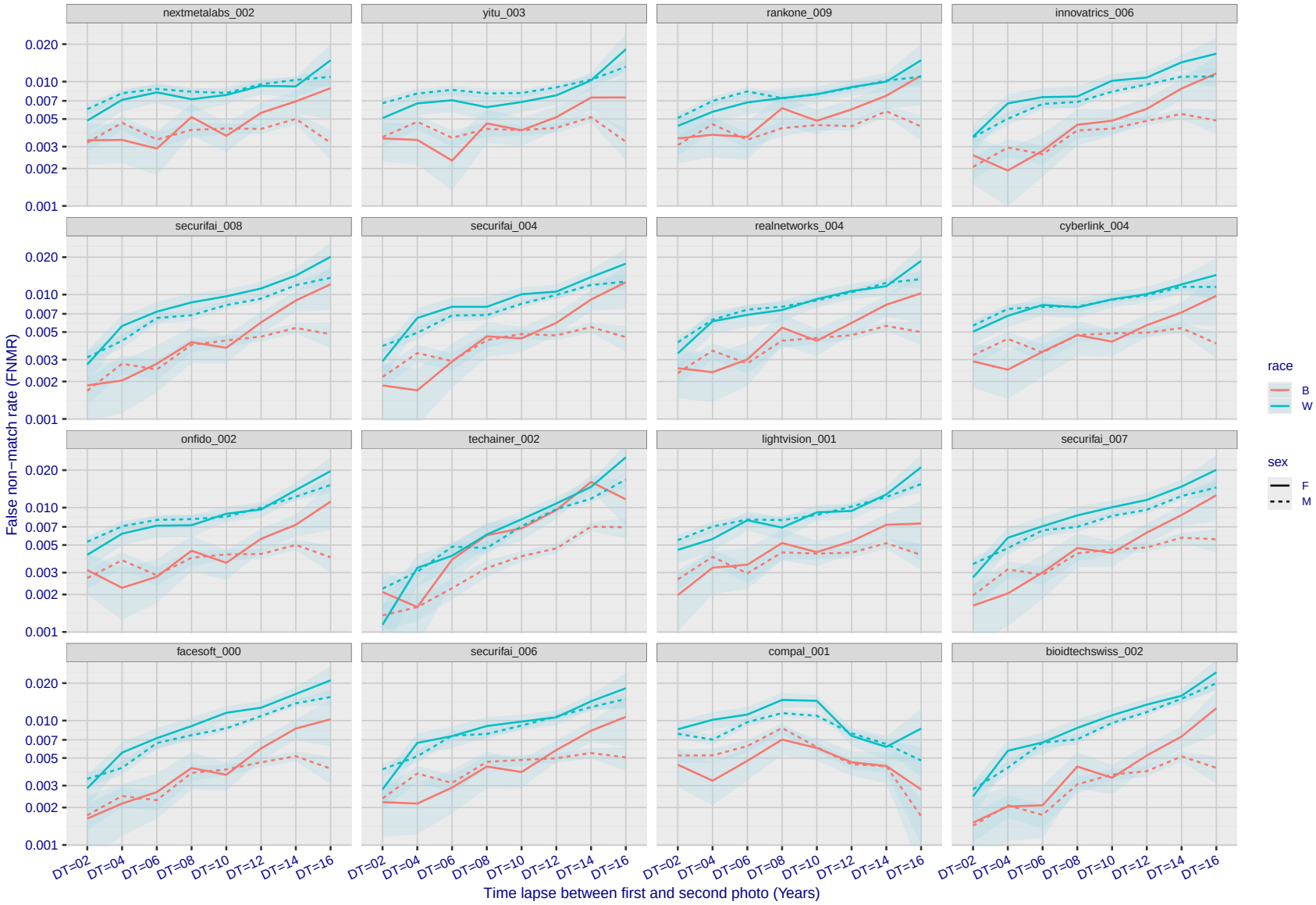

Figure 744: For the mugshot images, FNMR *as a function of elapsed time between initial enrollment and second verification images. The panels appear most accurate first, and vertical scale changes on each page. The four traces correspond to images annotated with codes for black female, black male, white female, white male. The threshold is fixed for each algorithm to give FMR = 0.00001 over all ($\widetilde{10}^8$) impostor comparisons. For short time-lapses, the most accurate algorithms give very few errors (FNMR < 0.001) so that the uncertainty estimates are high.*

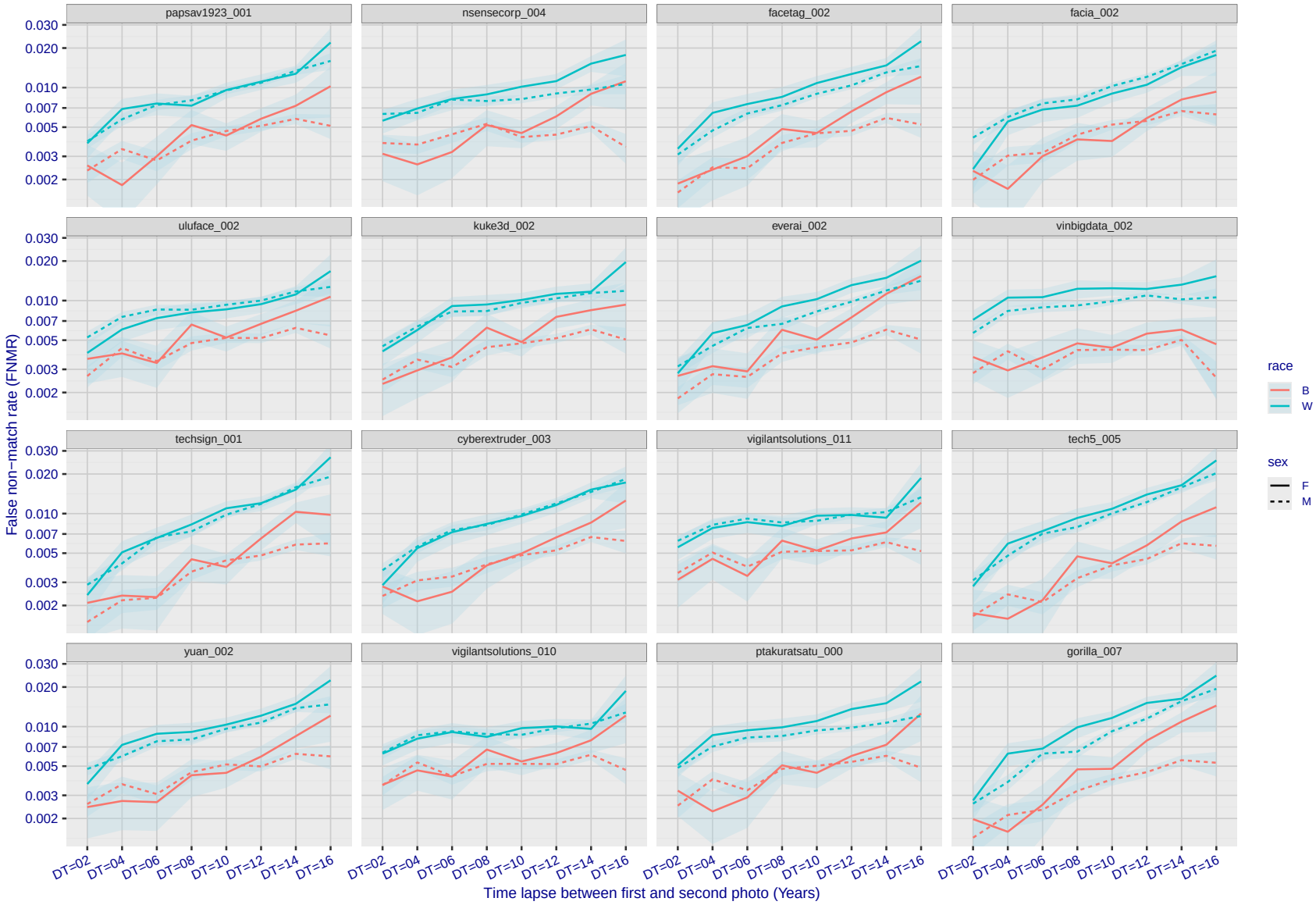

Figure 745: For the mugshot images, FNMR *as a function of elapsed time between initial enrollment and second verification images. The panels appear most accurate first, and vertical scale changes on each page. The four traces correspond to images annotated with codes for black female, black male, white female, white male. The threshold is fixed for each algorithm to give FMR = 0.00001 over all ($\tilde{10}^8$) impostor comparisons. For short time-lapses, the most accurate algorithms give very few errors (FNMR < 0.001) so that the uncertainty estimates are high.*

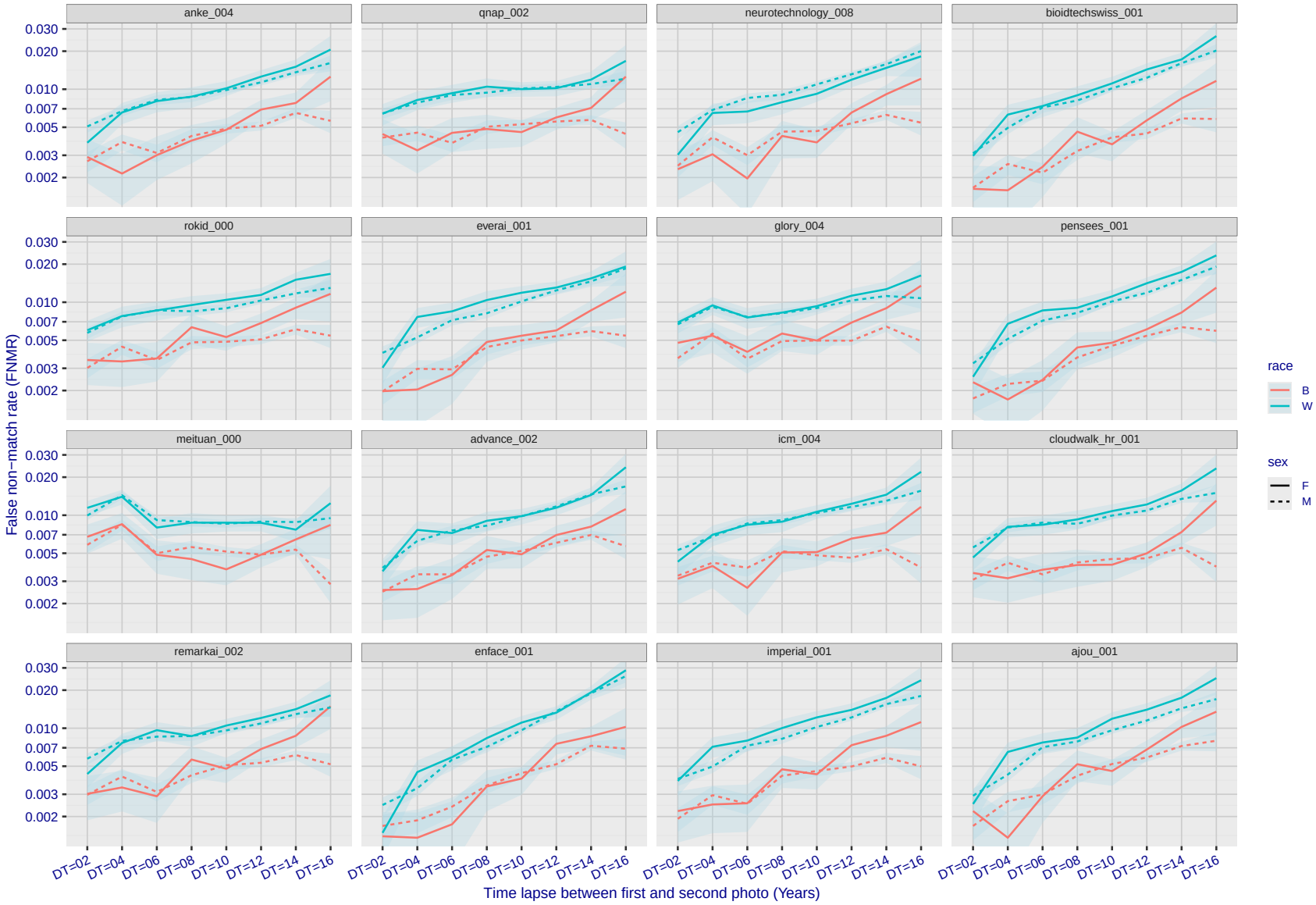

Figure 746: For the mugshot images, FNMR *as a function of elapsed time between initial enrollment and second verification images. The panels appear most accurate first, and vertical scale changes on each page. The four traces correspond to images annotated with codes for black female, black male, white female, white male. The threshold is fixed for each algorithm to give FMR = 0.00001 over all ($\tilde{10}^8$) impostor comparisons. For short time-lapses, the most accurate algorithms give very few errors (FNMR < 0.001) so that the uncertainty estimates are high.*

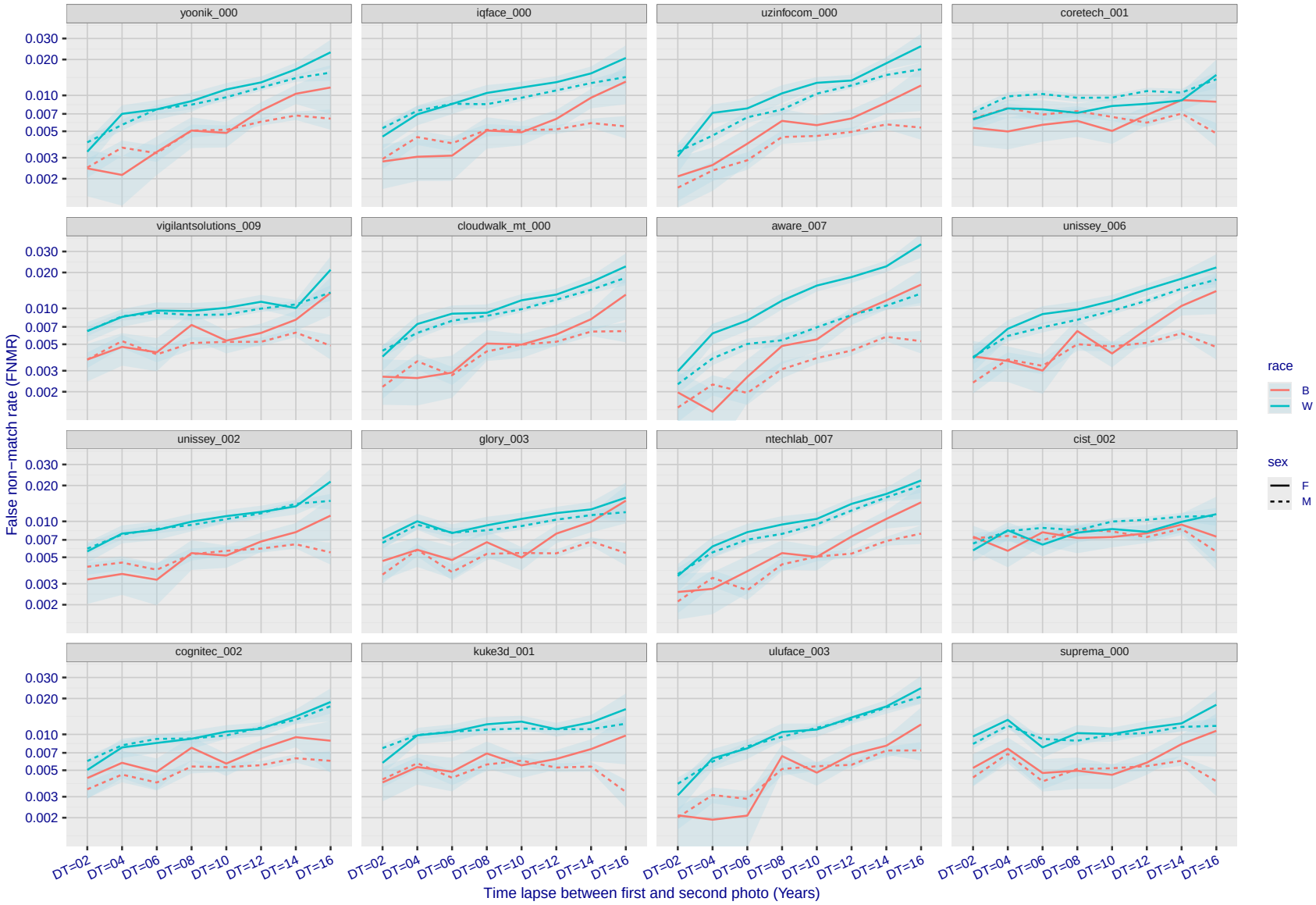

Figure 747: For the mugshot images, FNMR *as a function of elapsed time between initial enrollment and second verification images. The panels appear most accurate first, and vertical scale changes on each page. The four traces correspond to images annotated with codes for black female, black male, white female, white male. The threshold is fixed for each algorithm to give FMR = 0.00001 over all (10^8) impostor comparisons. For short time-lapses, the most accurate algorithms give very few errors (FNMR < 0.001) so that the uncertainty estimates are high.*

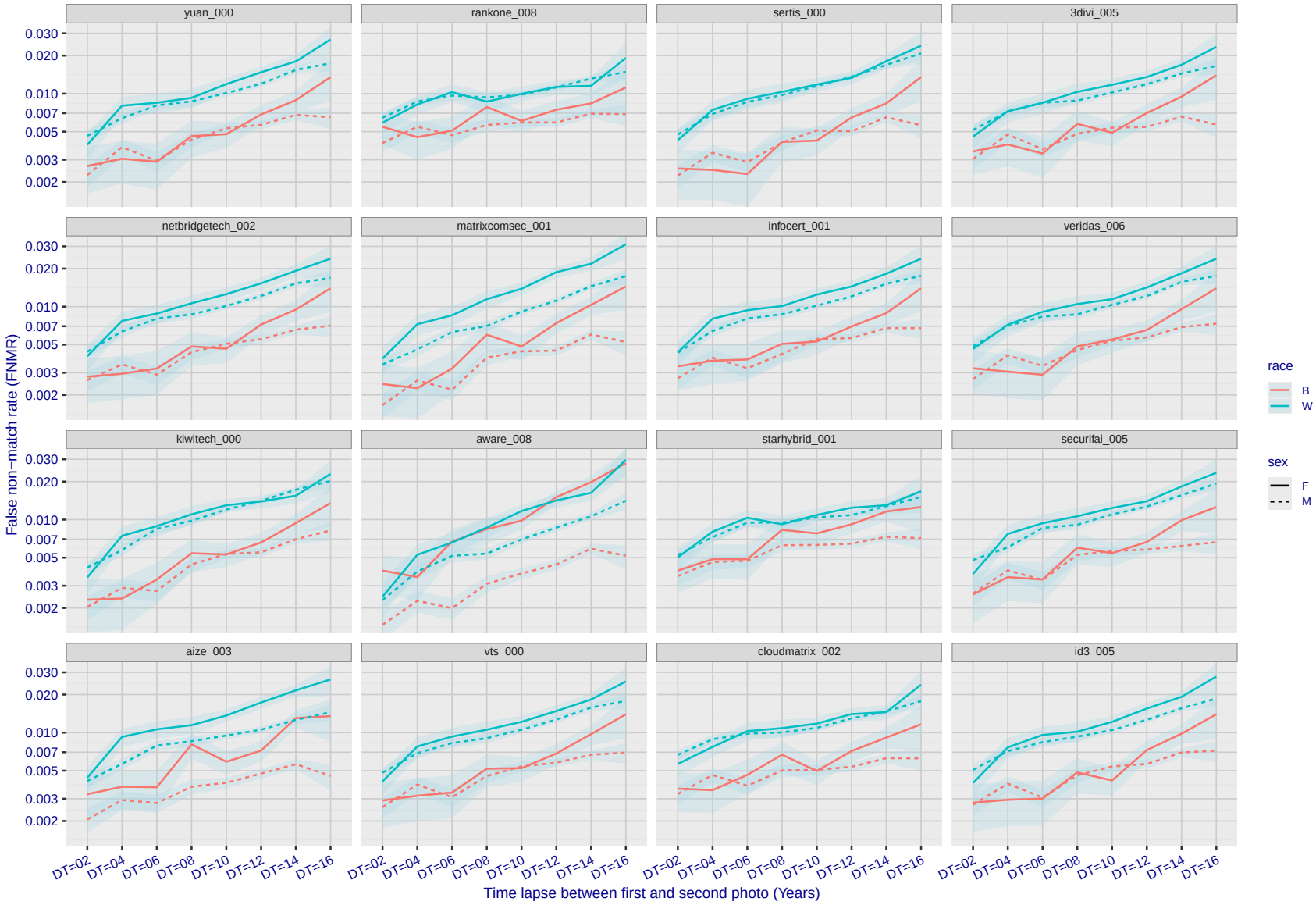

Figure 748: For the mugshot images, FNMR *as a function of elapsed time between initial enrollment and second verification images. The panels appear most accurate first, and vertical scale changes on each page. The four traces correspond to images annotated with codes for black female, black male, white female, white male. The threshold is fixed for each algorithm to give FMR = 0.00001 over all ($\tilde{10}^8$) impostor comparisons. For short time-lapses, the most accurate algorithms give very few errors (FNMR < 0.001) so that the uncertainty estimates are high.*

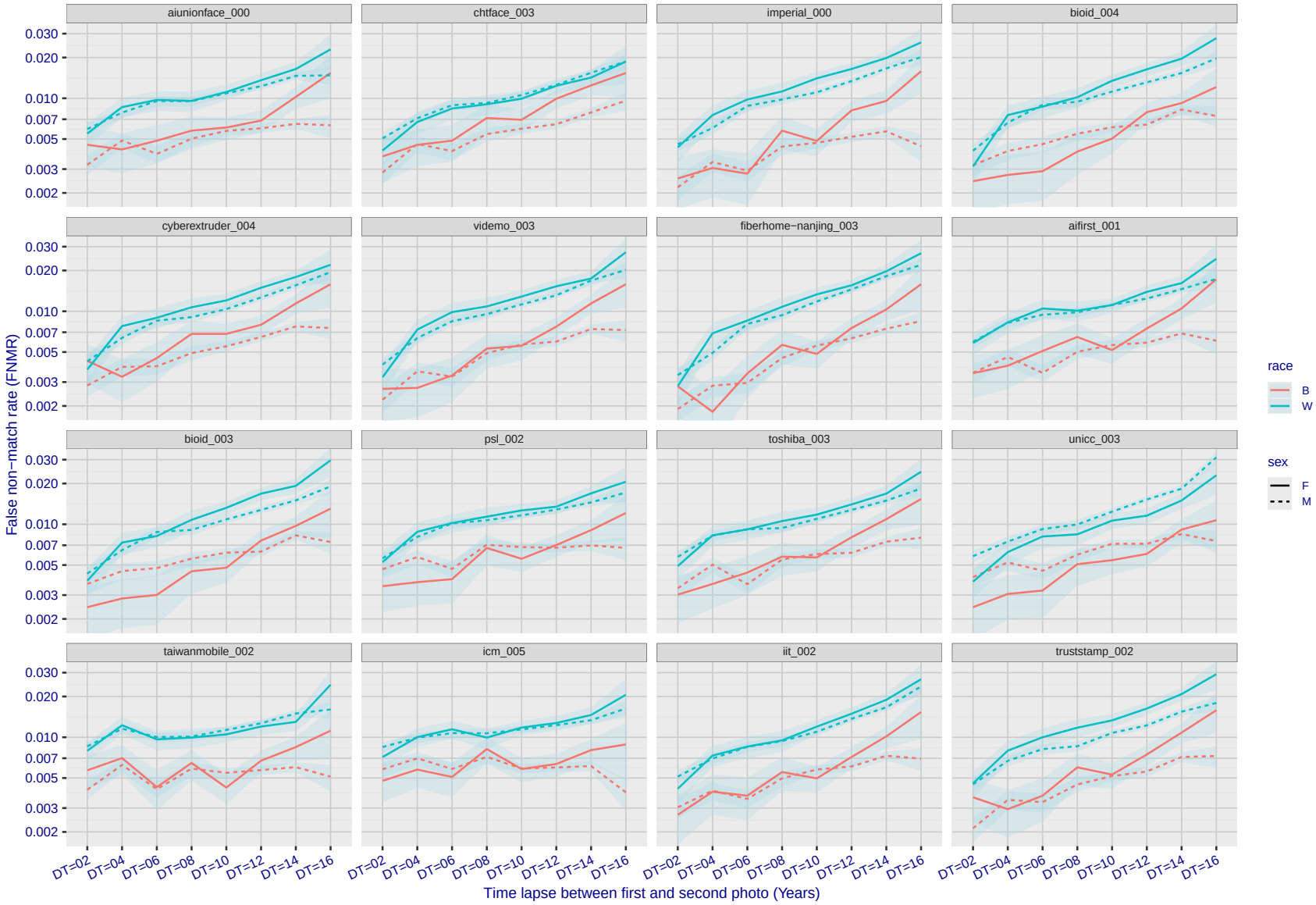

Figure 749: For the mugshot images, FNMR *as a function of elapsed time between initial enrollment and second verification images. The panels appear most accurate first, and vertical scale changes on each page. The four traces correspond to images annotated with codes for black female, black male, white female, white male. The threshold is fixed for each algorithm to give FMR = 0.00001 over all (10^8) impostor comparisons. For short time-lapses, the most accurate algorithms give very few errors (FNMR < 0.001) so that the uncertainty estimates are high.*

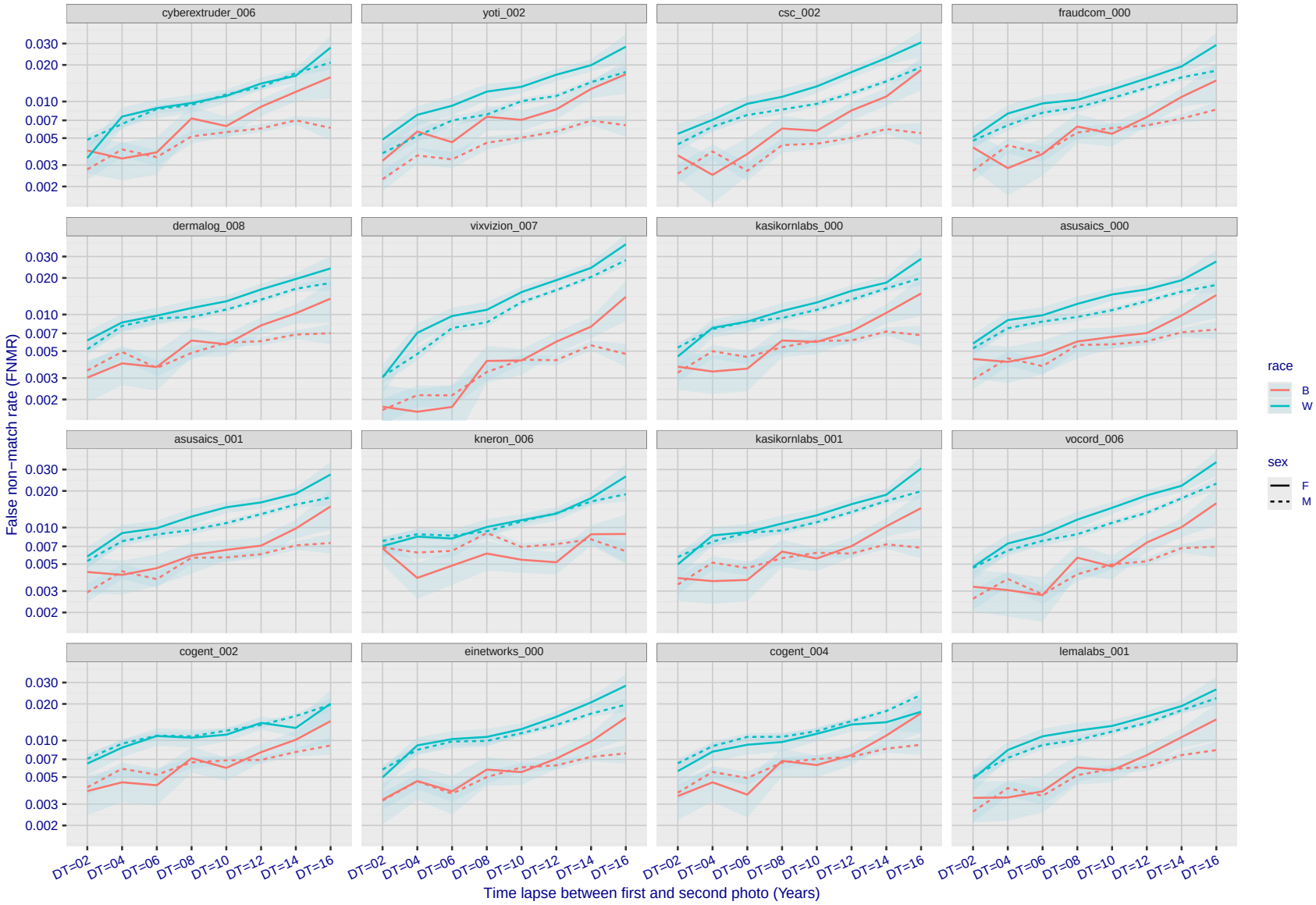

Figure 750: For the mugshot images, FNMR *as a function of elapsed time between initial enrollment and second verification images. The panels appear most accurate first, and vertical scale changes on each page. The four traces correspond to images annotated with codes for black female, black male, white female, white male. The threshold is fixed for each algorithm to give FMR = 0.00001 over all (10^8) impostor comparisons. For short time-lapses, the most accurate algorithms give very few errors (FNMR < 0.001) so that the uncertainty estimates are high.*

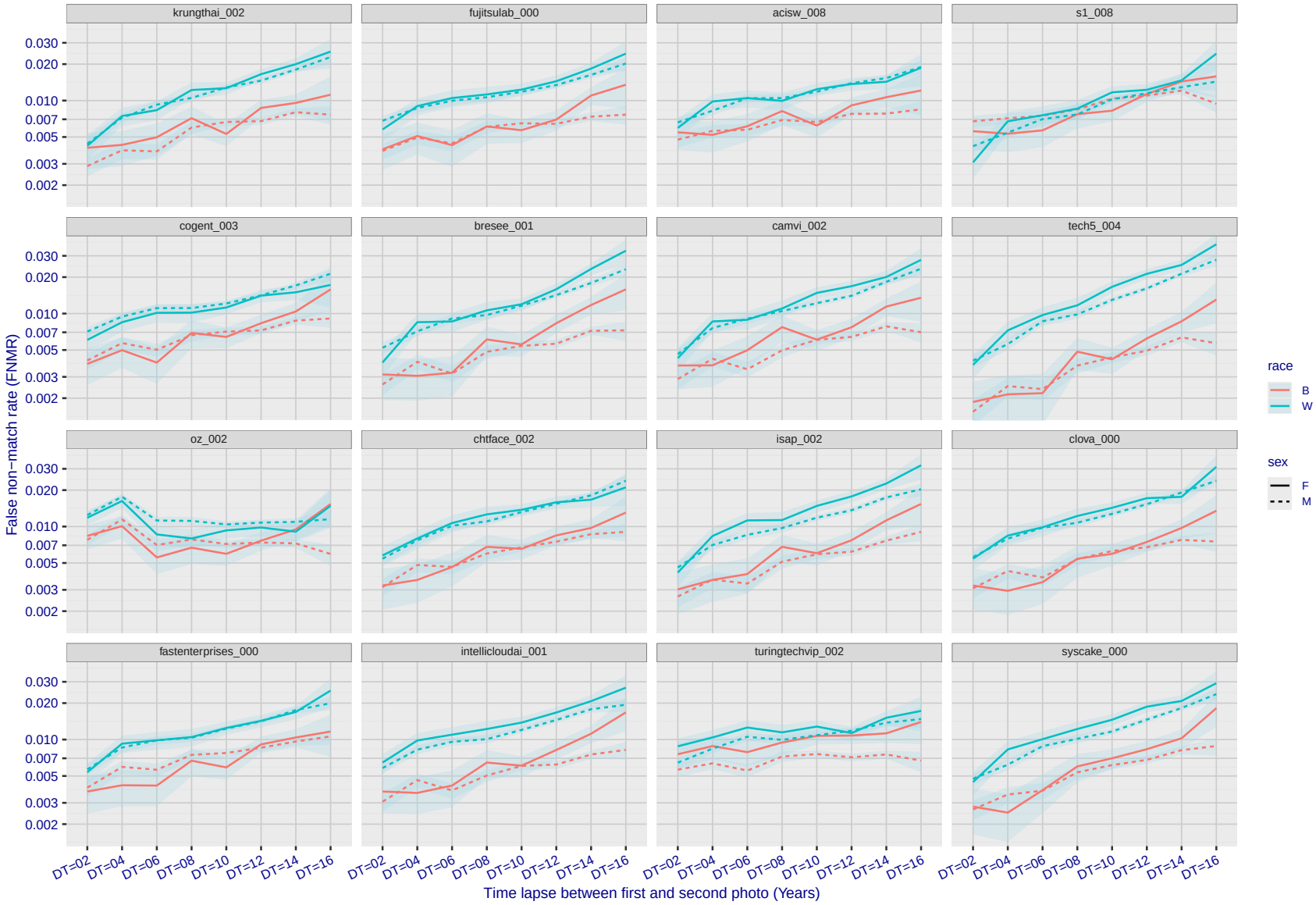

Figure 751: For the mugshot images, FNMR *as a function of elapsed time between initial enrollment and second verification images. The panels appear most accurate first, and vertical scale changes on each page. The four traces correspond to images annotated with codes for black female, black male, white female, white male. The threshold is fixed for each algorithm to give FMR = 0.00001 over all (10^8) impostor comparisons. For short time-lapses, the most accurate algorithms give very few errors (FNMR < 0.001) so that the uncertainty estimates are high.*

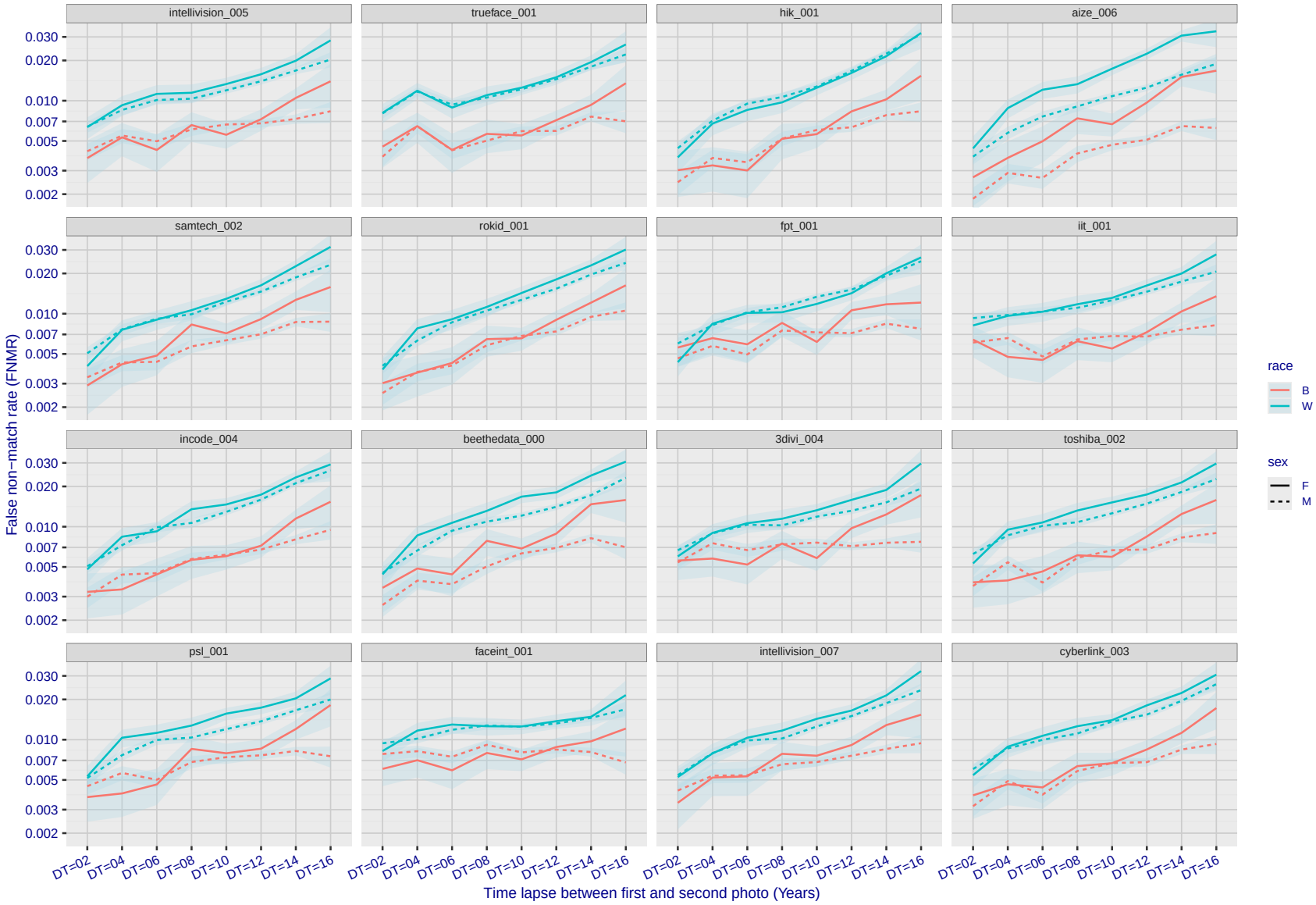

Figure 752: For the mugshot images, FNMR *as a function of elapsed time between initial enrollment and second verification images. The panels appear most accurate first, and vertical scale changes on each page. The four traces correspond to images annotated with codes for black female, black male, white female, white male. The threshold is fixed for each algorithm to give FMR = 0.00001 over all ($\widetilde{10}^8$) impostor comparisons. For short time-lapses, the most accurate algorithms give very few errors (FNMR < 0.001) so that the uncertainty estimates are high.*

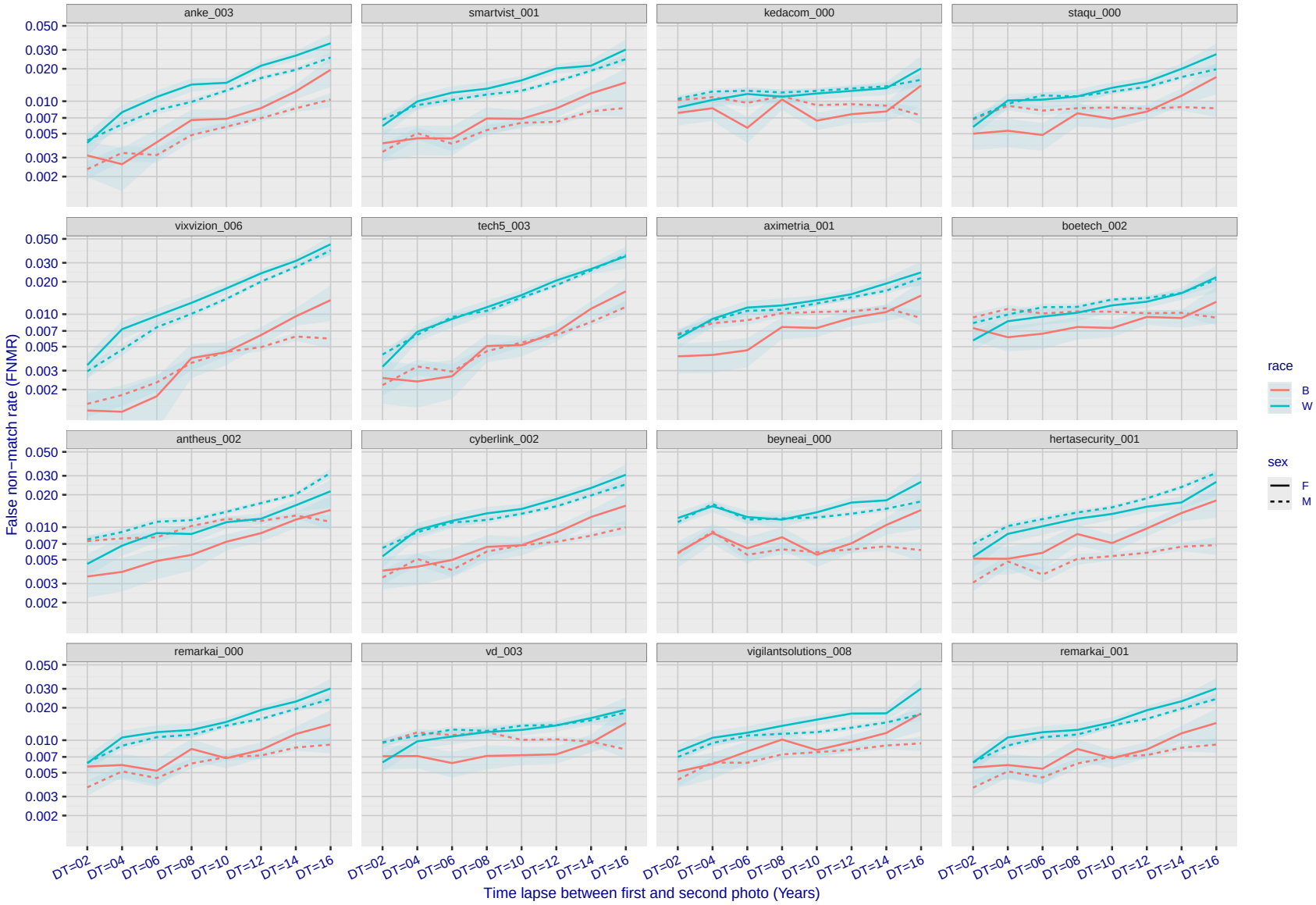

Figure 753: For the mugshot images, FNMR *as a function of elapsed time between initial enrollment and second verification images. The panels appear most accurate first, and vertical scale changes on each page. The four traces correspond to images annotated with codes for black female, black male, white female, white male. The threshold is fixed for each algorithm to give FMR = 0.00001 over all ($\widetilde{10}^8$) impostor comparisons. For short time-lapses, the most accurate algorithms give very few errors (FNMR < 0.001) so that the uncertainty estimates are high.*

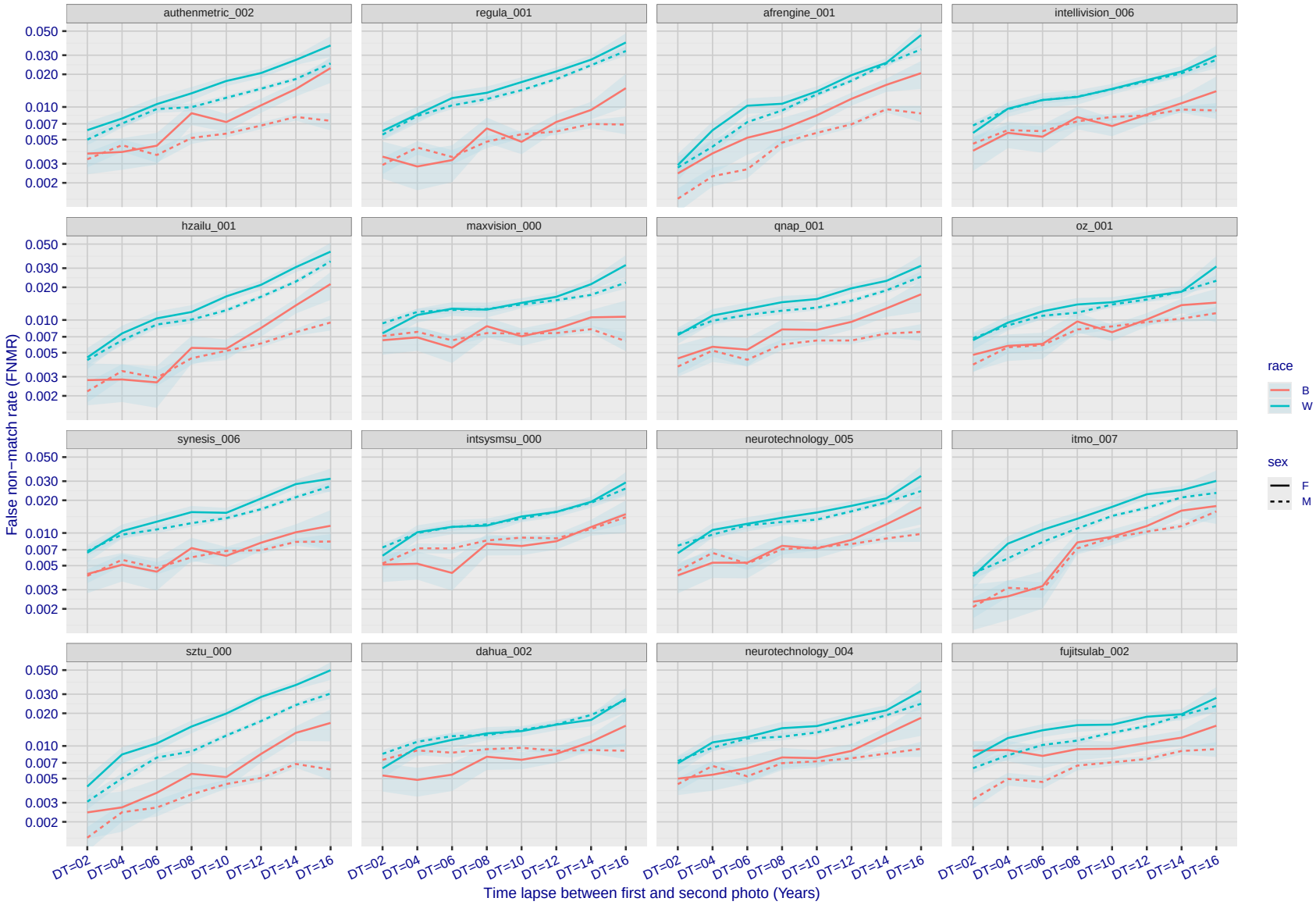

Figure 754: For the mugshot images, FNMR *as a function of elapsed time between initial enrollment and second verification images. The panels appear most accurate first, and vertical scale changes on each page. The four traces correspond to images annotated with codes for black female, black male, white female, white male. The threshold is fixed for each algorithm to give FMR = 0.00001 over all ($\widetilde{10}^8$) impostor comparisons. For short time-lapses, the most accurate algorithms give very few errors (FNMR < 0.001) so that the uncertainty estimates are high.*

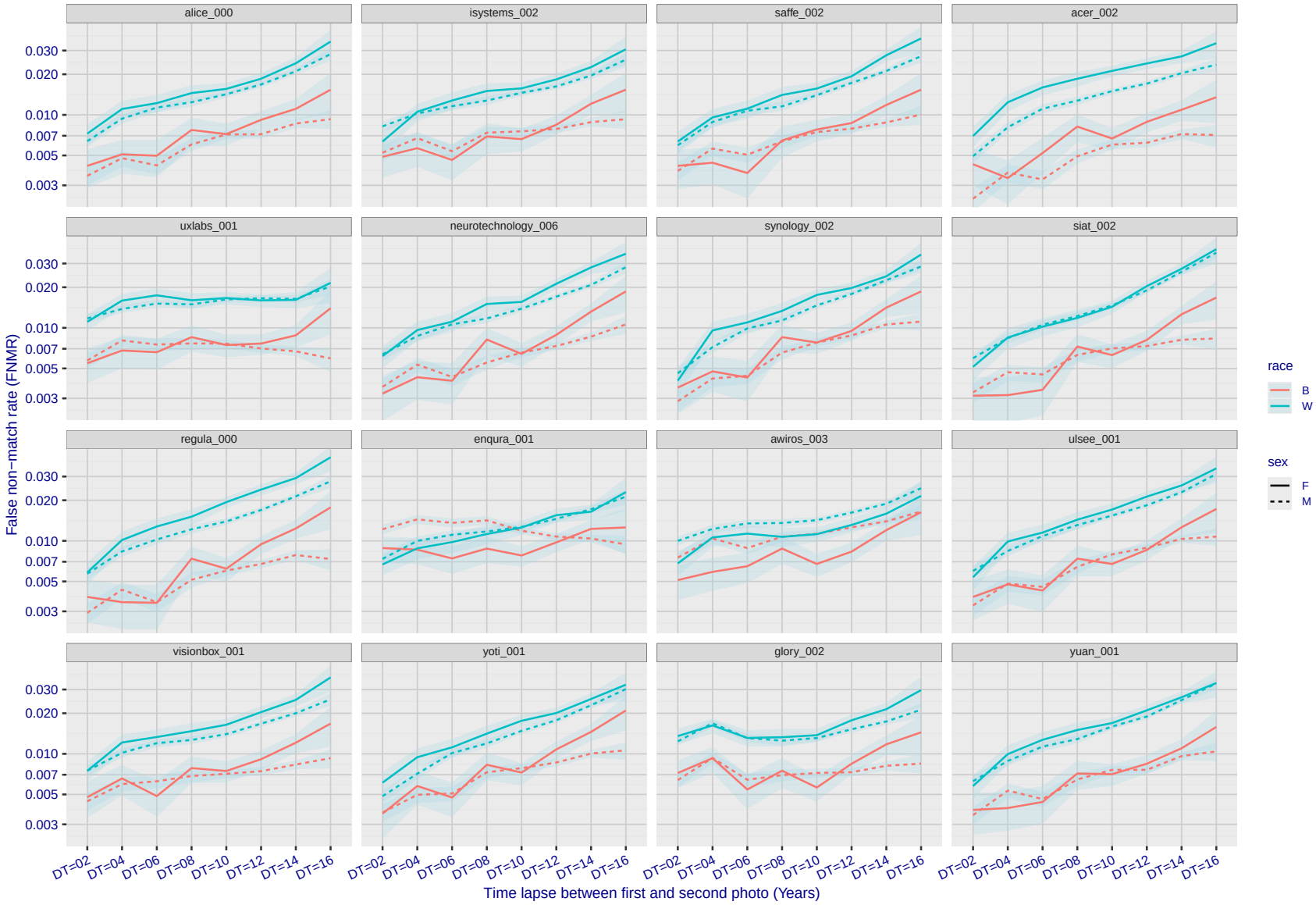

Figure 755: For the mugshot images, FNMR *as a function of elapsed time between initial enrollment and second verification images. The panels appear most accurate first, and vertical scale changes on each page. The four traces correspond to images annotated with codes for black female, black male, white female, white male. The threshold is fixed for each algorithm to give FMR = 0.00001 over all ($\widetilde{10}^8$) impostor comparisons. For short time-lapses, the most accurate algorithms give very few errors (FNMR < 0.001) so that the uncertainty estimates are high.*

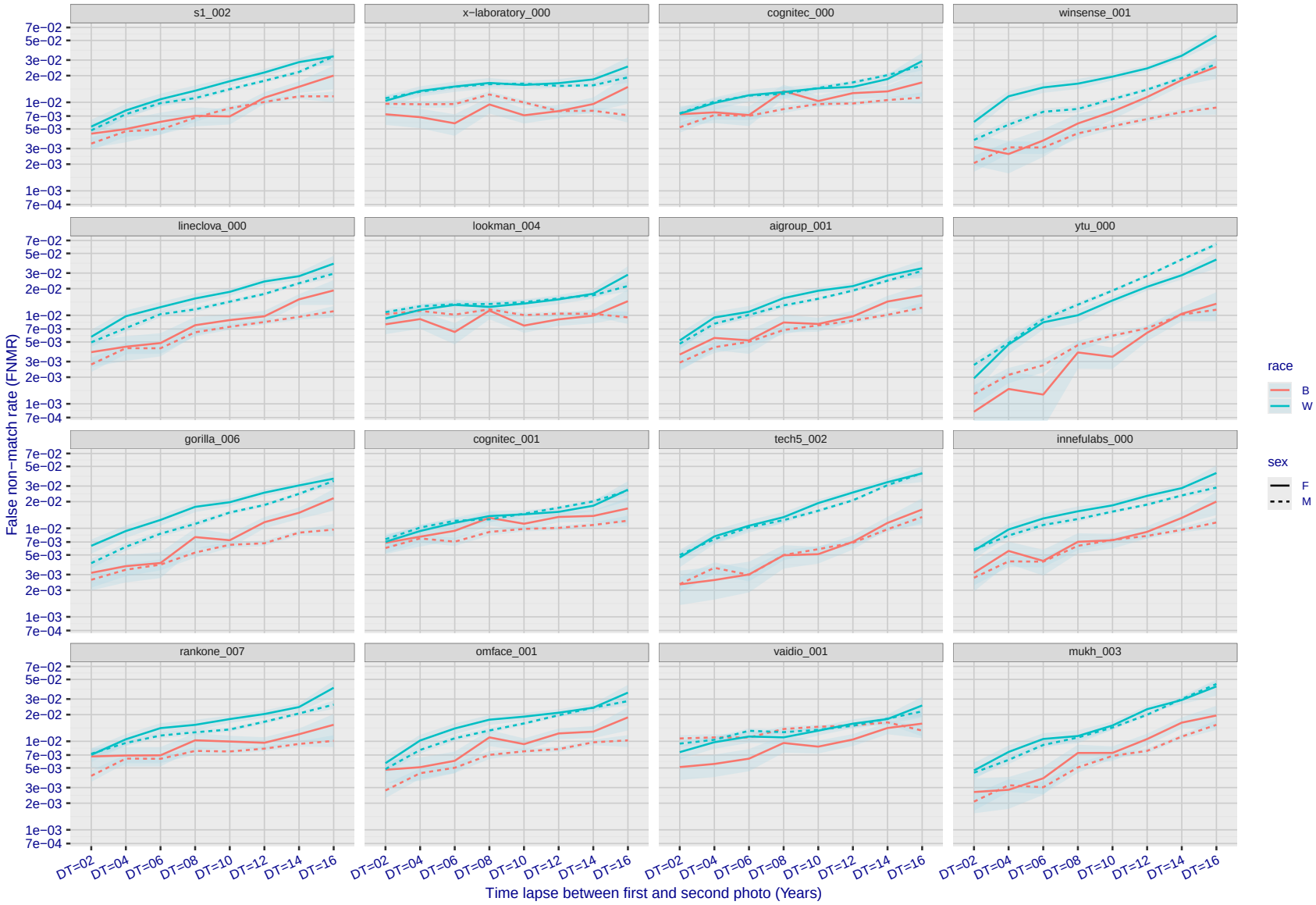

Figure 756: For the mugshot images, FNMR *as a function of elapsed time between initial enrollment and second verification images. The panels appear most accurate first, and vertical scale changes on each page. The four traces correspond to images annotated with codes for black female, black male, white female, white male. The threshold is fixed for each algorithm to give FMR = 0.00001 over all (10^8) impostor comparisons. For short time-lapses, the most accurate algorithms give very few errors (FNMR < 0.001) so that the uncertainty estimates are high.*

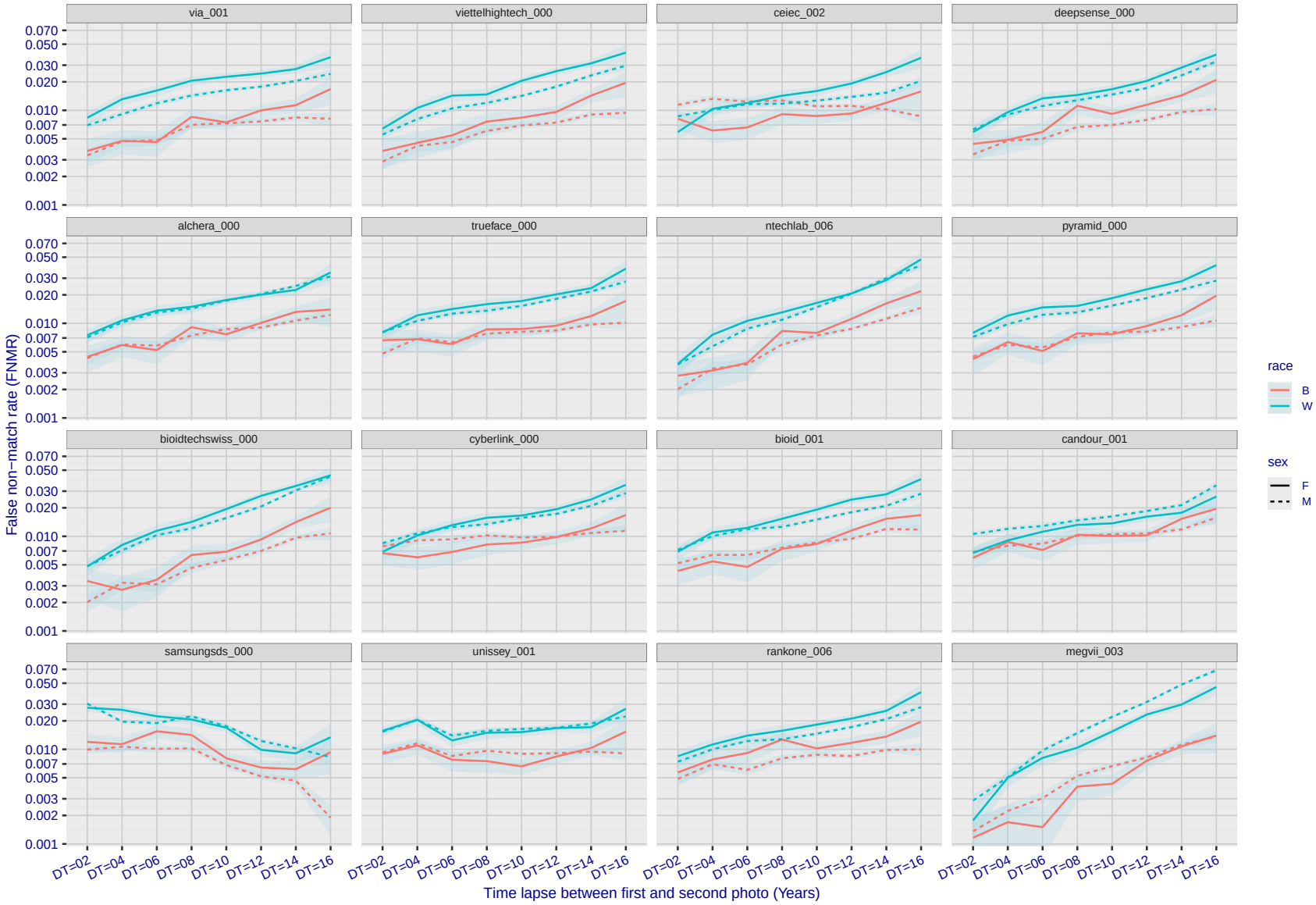

Figure 757: For the mugshot images, FNMR *as a function of elapsed time between initial enrollment and second verification images. The panels appear most accurate first, and vertical scale changes on each page. The four traces correspond to images annotated with codes for black female, black male, white female, white male. The threshold is fixed for each algorithm to give FMR = 0.00001 over all ($\widetilde{10}^8$) impostor comparisons. For short time-lapses, the most accurate algorithms give very few errors (FNMR < 0.001) so that the uncertainty estimates are high.*

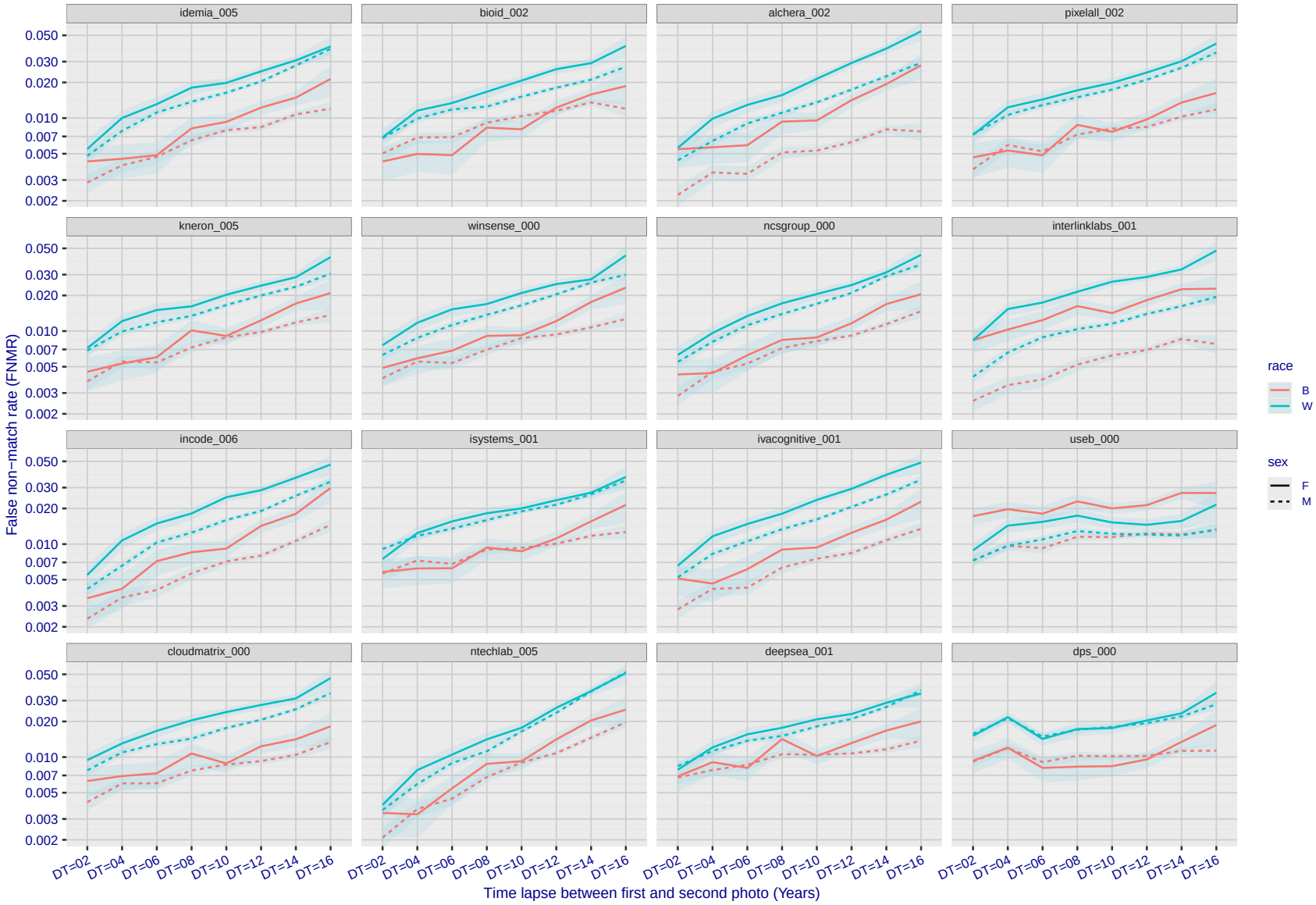

Figure 758: For the mugshot images, FNMR *as a function of elapsed time between initial enrollment and second verification images. The panels appear most accurate first, and vertical scale changes on each page. The four traces correspond to images annotated with codes for black female, black male, white female, white male. The threshold is fixed for each algorithm to give FMR = 0.00001 over all (10^8) impostor comparisons. For short time-lapses, the most accurate algorithms give very few errors (FNMR < 0.001) so that the uncertainty estimates are high.*

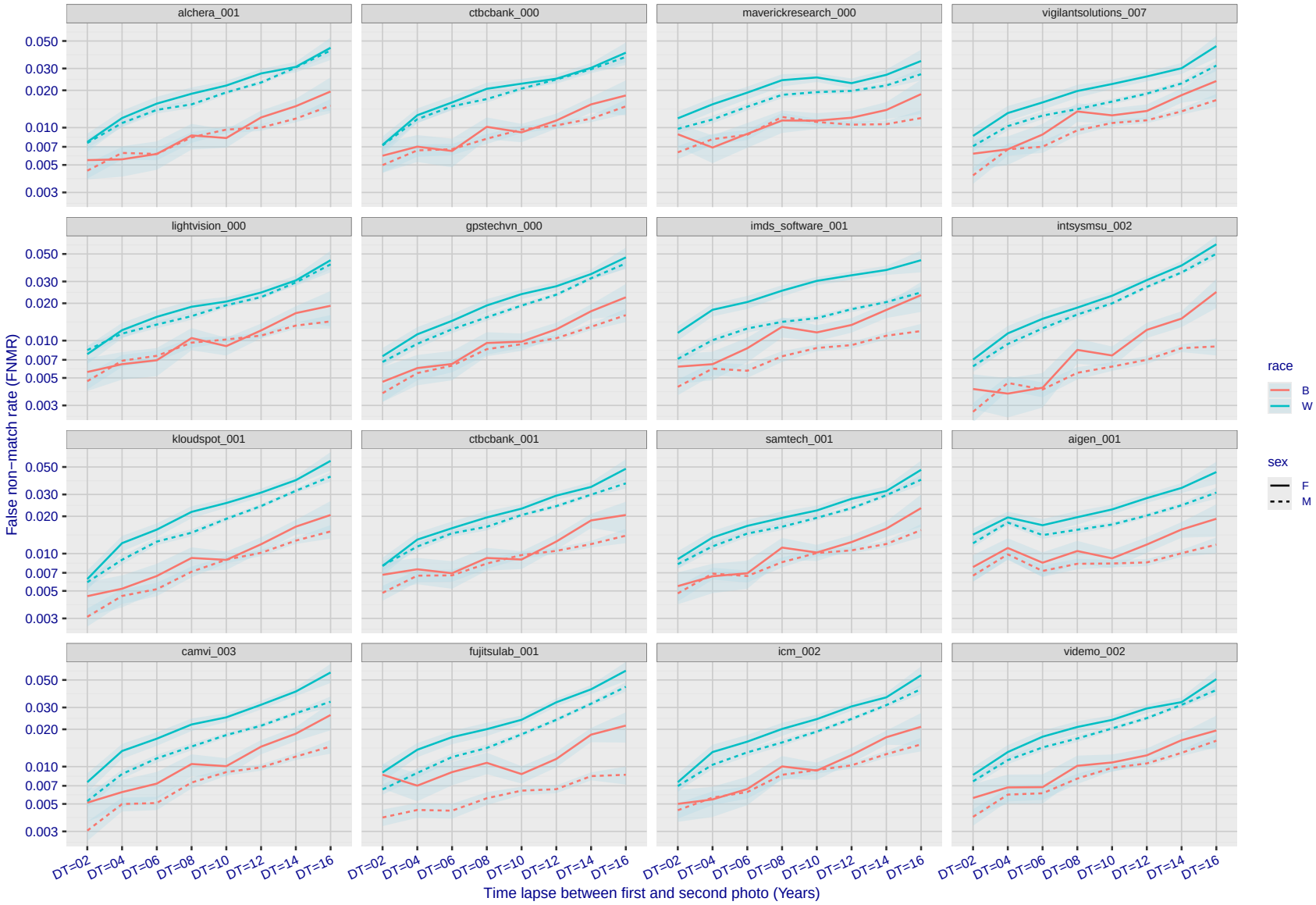

Figure 759: For the mugshot images, FNMR *as a function of elapsed time between initial enrollment and second verification images. The panels appear most accurate first, and vertical scale changes on each page. The four traces correspond to images annotated with codes for black female, black male, white female, white male. The threshold is fixed for each algorithm to give FMR = 0.00001 over all ($\widetilde{10}^8$) impostor comparisons. For short time-lapses, the most accurate algorithms give very few errors (FNMR < 0.001) so that the uncertainty estimates are high.*

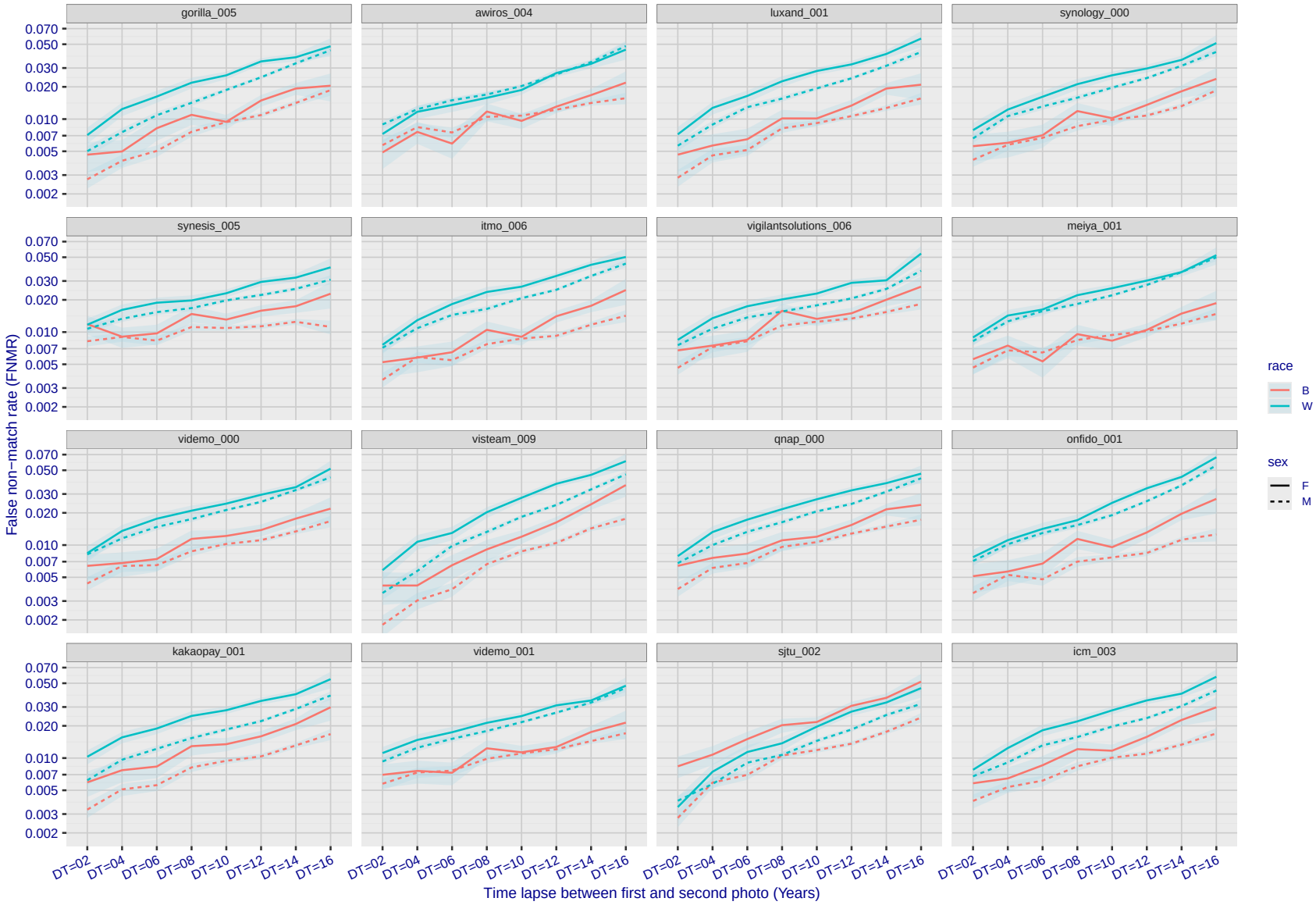

Figure 760: For the mugshot images, FNMR *as a function of elapsed time between initial enrollment and second verification images. The panels appear most accurate first, and vertical scale changes on each page. The four traces correspond to images annotated with codes for black female, black male, white female, white male. The threshold is fixed for each algorithm to give FMR = 0.00001 over all ($\widetilde{10}^8$) impostor comparisons. For short time-lapses, the most accurate algorithms give very few errors (FNMR < 0.001) so that the uncertainty estimates are high.*

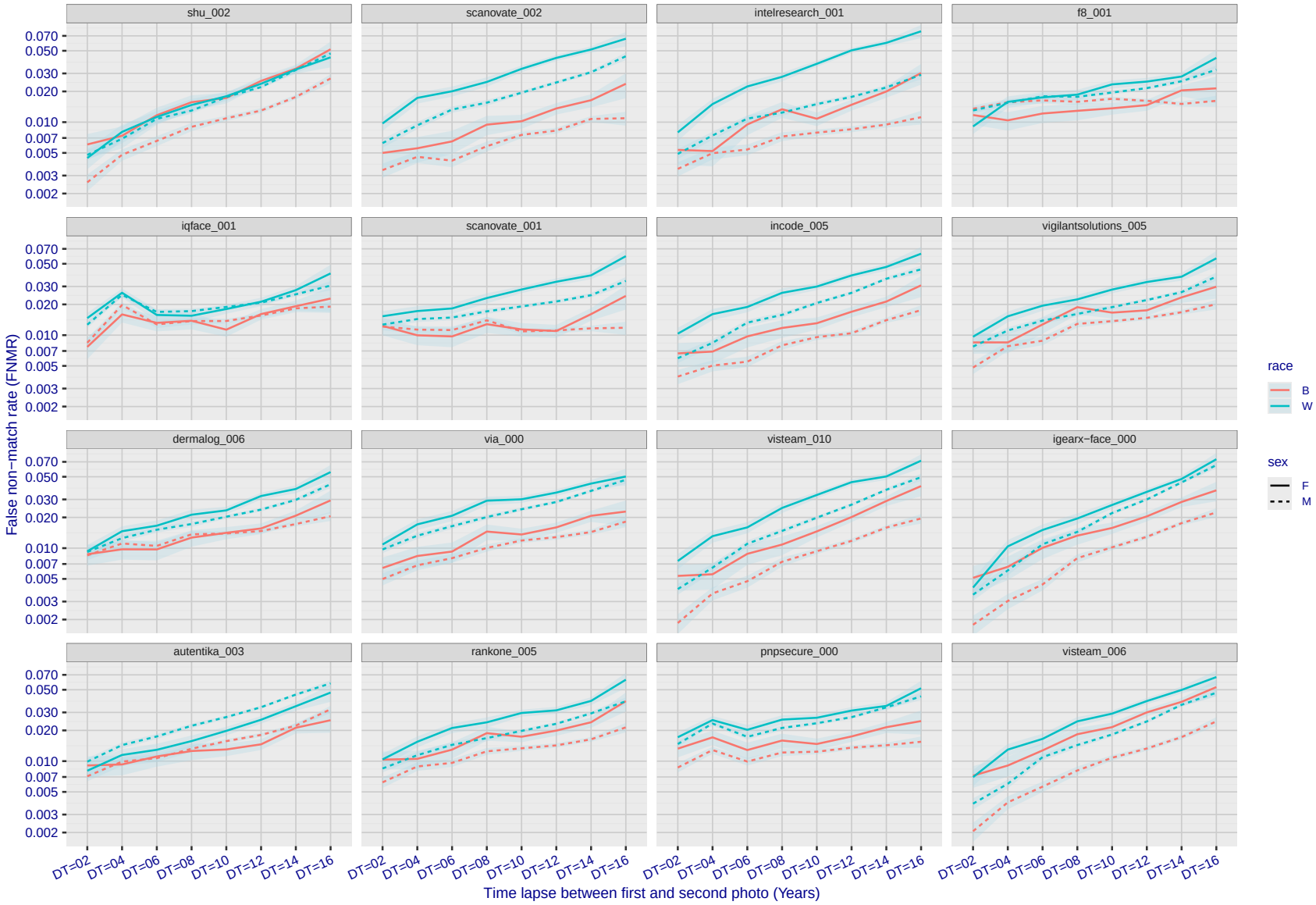

Figure 761: For the mugshot images, FNMR *as a function of elapsed time between initial enrollment and second verification images. The panels appear most accurate first, and vertical scale changes on each page. The four traces correspond to images annotated with codes for black female, black male, white female, white male. The threshold is fixed for each algorithm to give FMR = 0.00001 over all ($\widetilde{10}^8$) impostor comparisons. For short time-lapses, the most accurate algorithms give very few errors (FNMR < 0.001) so that the uncertainty estimates are high.*

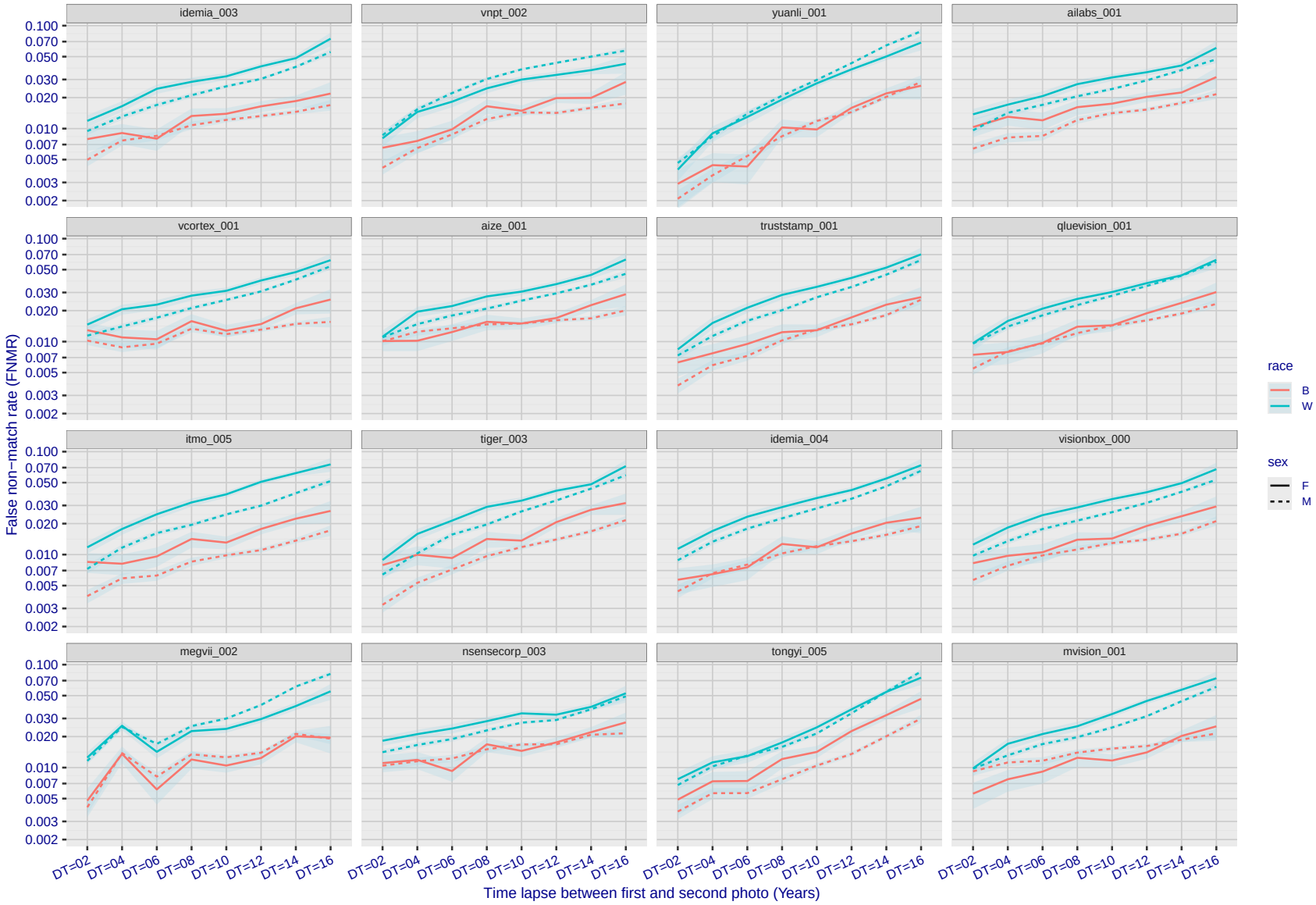

Figure 762: For the mugshot images, FNMR *as a function of elapsed time between initial enrollment and second verification images. The panels appear most accurate first, and vertical scale changes on each page. The four traces correspond to images annotated with codes for black female, black male, white female, white male. The threshold is fixed for each algorithm to give FMR = 0.00001 over all ($\tilde{10}^8$) impostor comparisons. For short time-lapses, the most accurate algorithms give very few errors (FNMR < 0.001) so that the uncertainty estimates are high.*

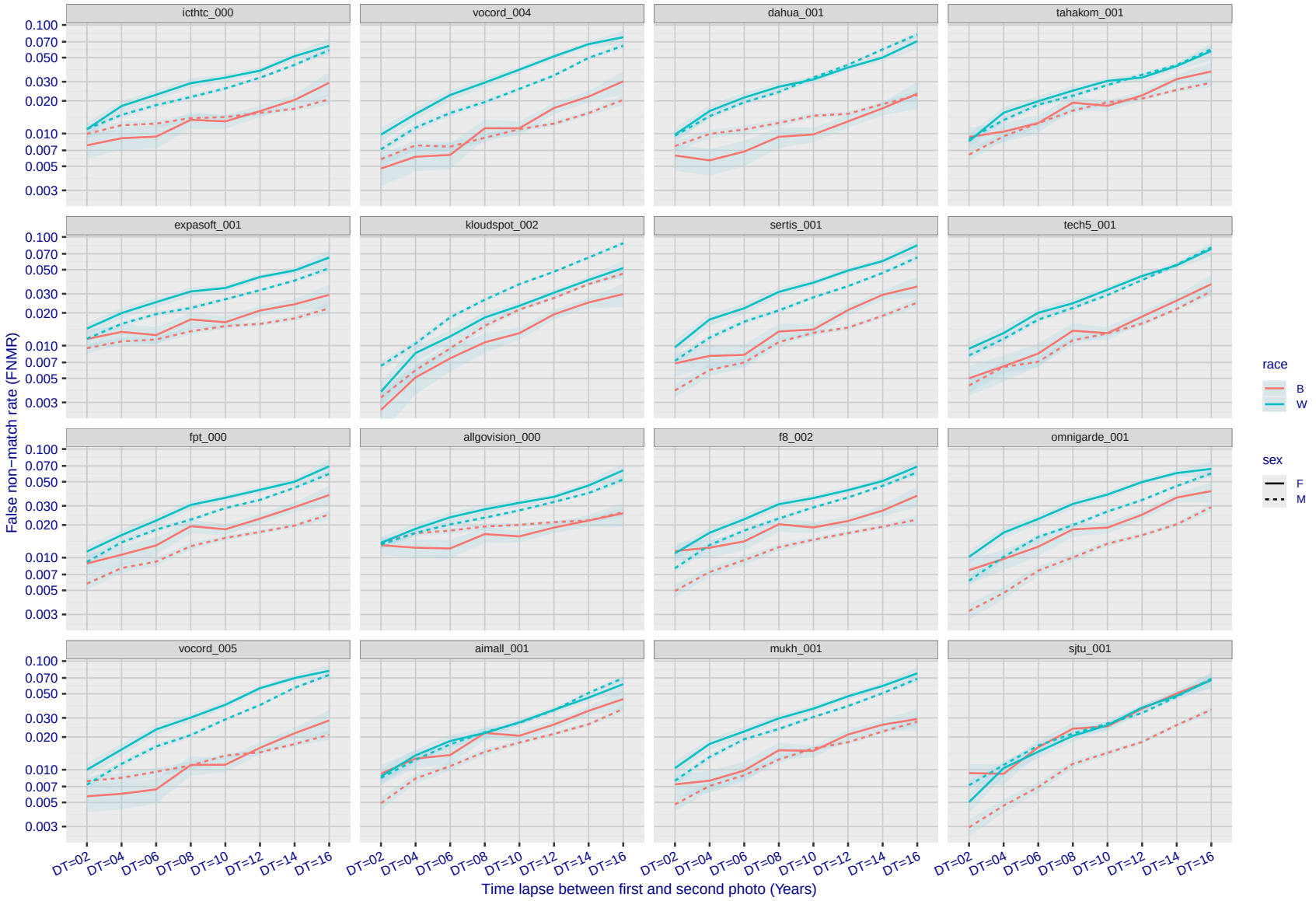

Figure 763: For the mugshot images, FNMR *as a function of elapsed time between initial enrollment and second verification images. The panels appear most accurate first, and vertical scale changes on each page. The four traces correspond to images annotated with codes for black female, black male, white female, white male. The threshold is fixed for each algorithm to give FMR = 0.00001 over all (10^8) impostor comparisons. For short time-lapses, the most accurate algorithms give very few errors (FNMR < 0.001) so that the uncertainty estimates are high.*

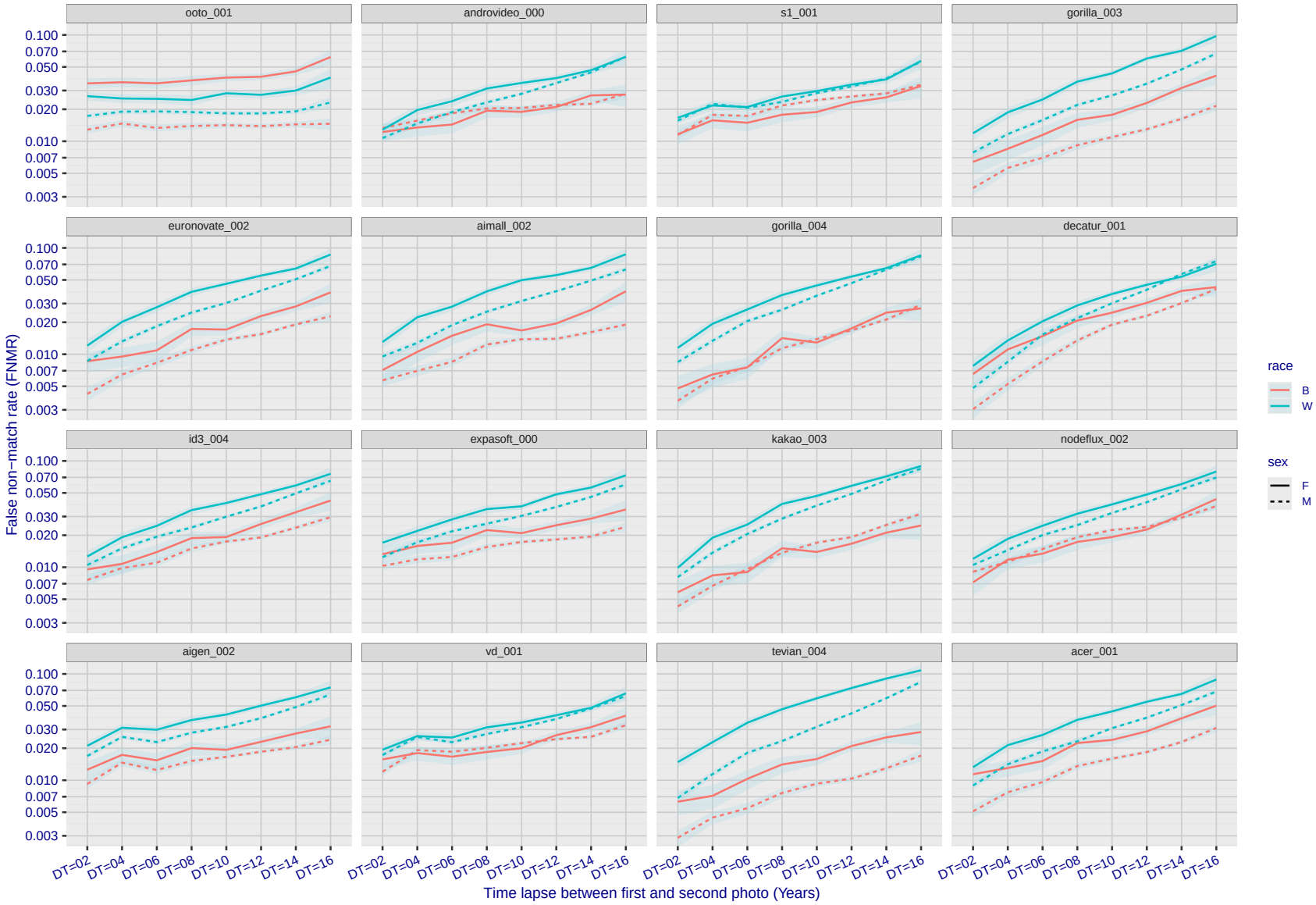

Figure 764: For the mugshot images, FNMR *as a function of elapsed time between initial enrollment and second verification images. The panels appear most accurate first, and vertical scale changes on each page. The four traces correspond to images annotated with codes for black female, black male, white female, white male. The threshold is fixed for each algorithm to give FMR = 0.00001 over all (10^8) impostor comparisons. For short time-lapses, the most accurate algorithms give very few errors (FNMR < 0.001) so that the uncertainty estimates are high.*

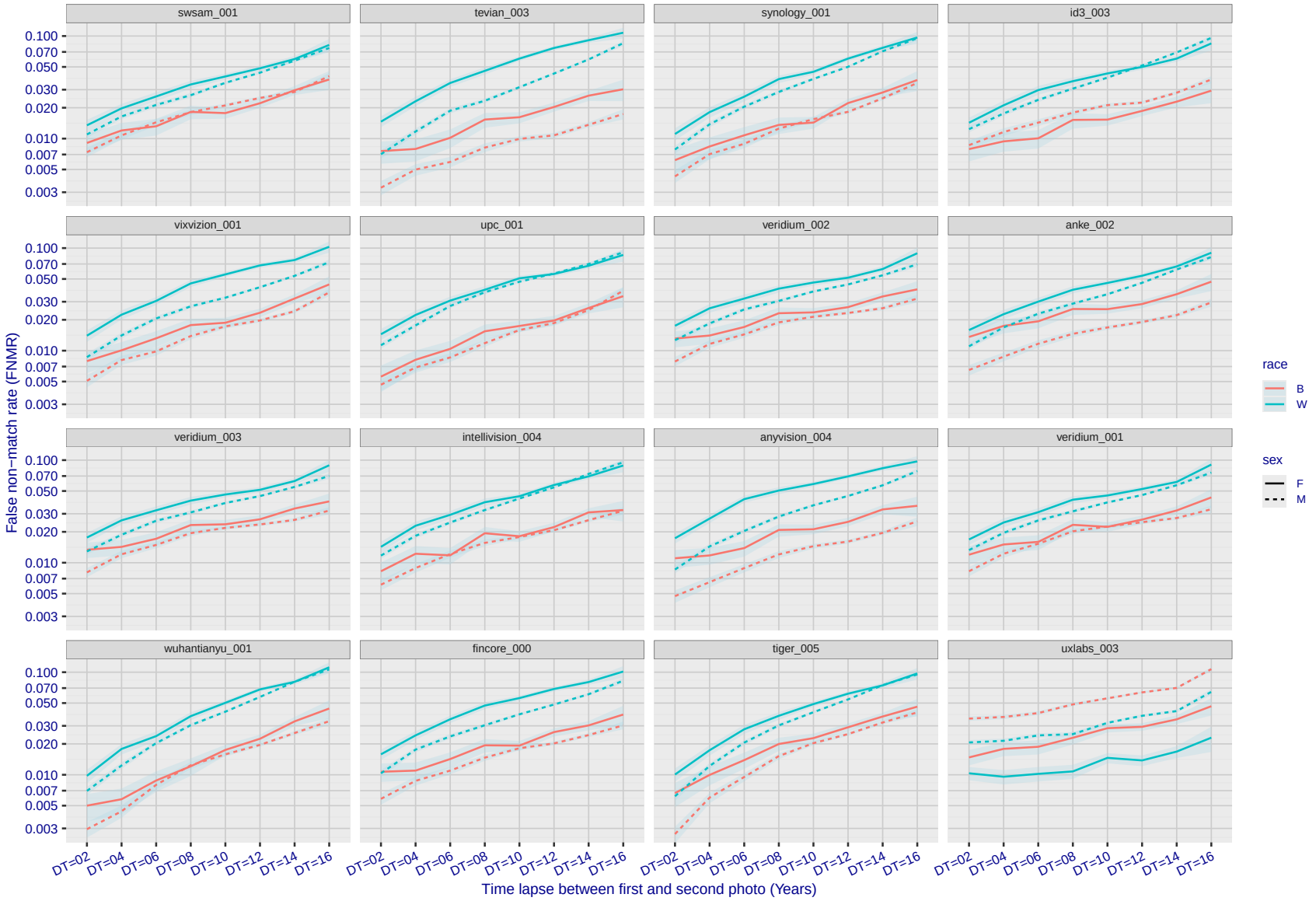

Figure 765: For the mugshot images, FNMR *as a function of elapsed time between initial enrollment and second verification images. The panels appear most accurate first, and vertical scale changes on each page. The four traces correspond to images annotated with codes for black female, black male, white female, white male. The threshold is fixed for each algorithm to give FMR = 0.00001 over all ($\widetilde{10}^8$) impostor comparisons. For short time-lapses, the most accurate algorithms give very few errors (FNMR < 0.001) so that the uncertainty estimates are high.*

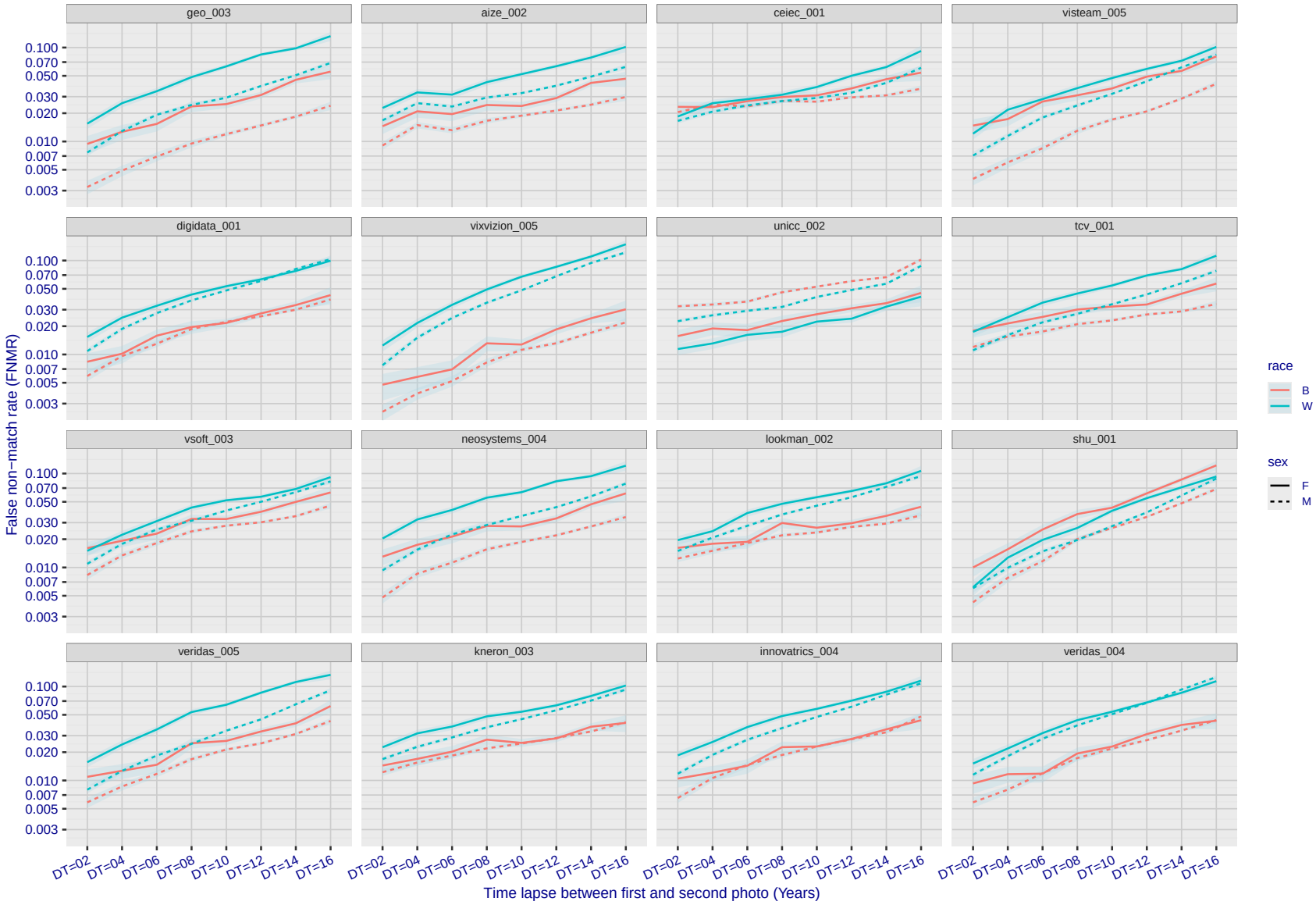

Figure 766: For the mugshot images, FNMR *as a function of elapsed time between initial enrollment and second verification images. The panels appear most accurate first, and vertical scale changes on each page. The four traces correspond to images annotated with codes for black female, black male, white female, white male. The threshold is fixed for each algorithm to give FMR = 0.00001 over all ($\widetilde{10}^8$) impostor comparisons. For short time-lapses, the most accurate algorithms give very few errors (FNMR < 0.001) so that the uncertainty estimates are high.*

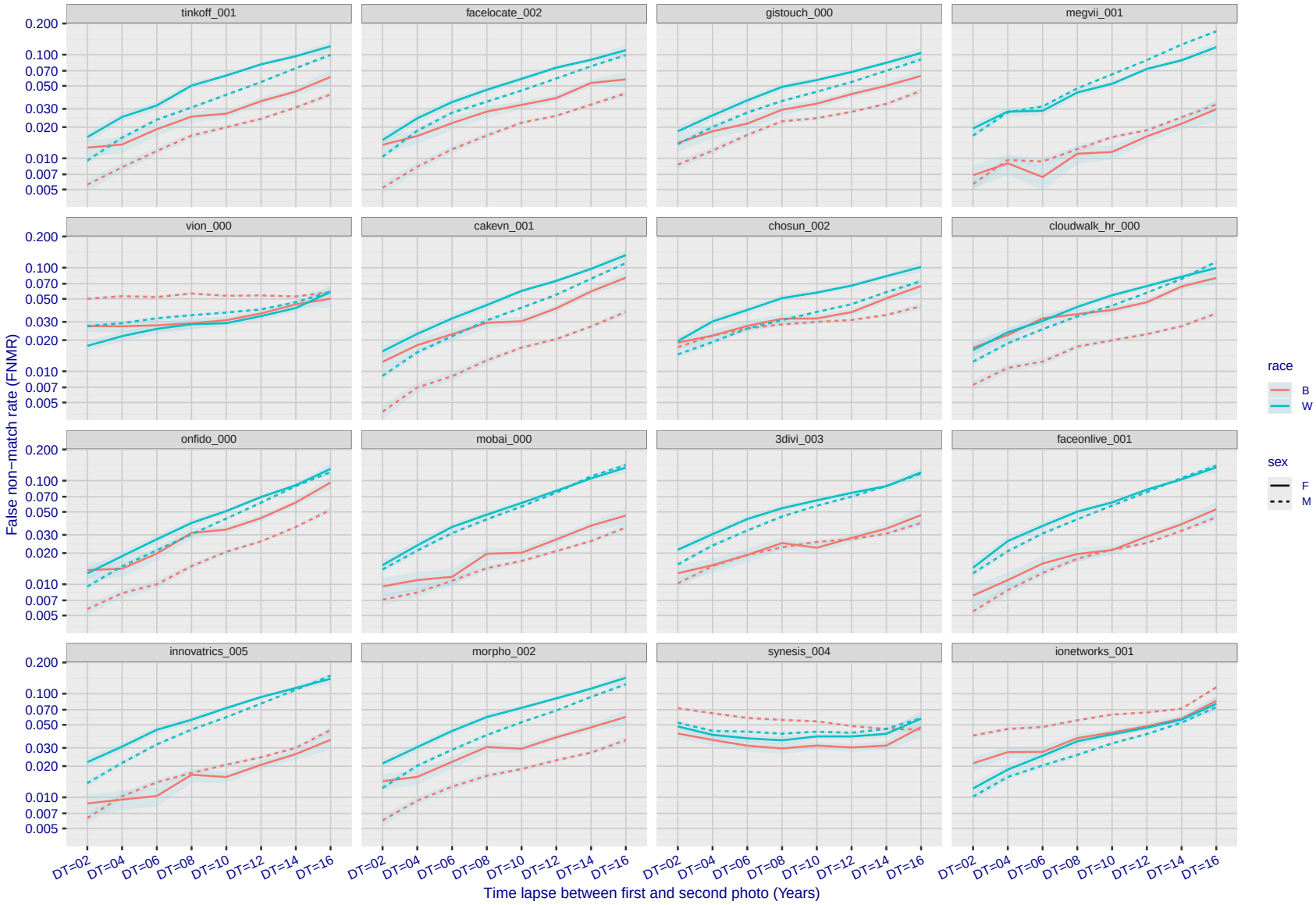

Figure 767: For the mugshot images, FNMR *as a function of elapsed time between initial enrollment and second verification images. The panels appear most accurate first, and vertical scale changes on each page. The four traces correspond to images annotated with codes for black female, black male, white female, white male. The threshold is fixed for each algorithm to give FMR = 0.00001 over all (10^8) impostor comparisons. For short time-lapses, the most accurate algorithms give very few errors (FNMR < 0.001) so that the uncertainty estimates are high.*

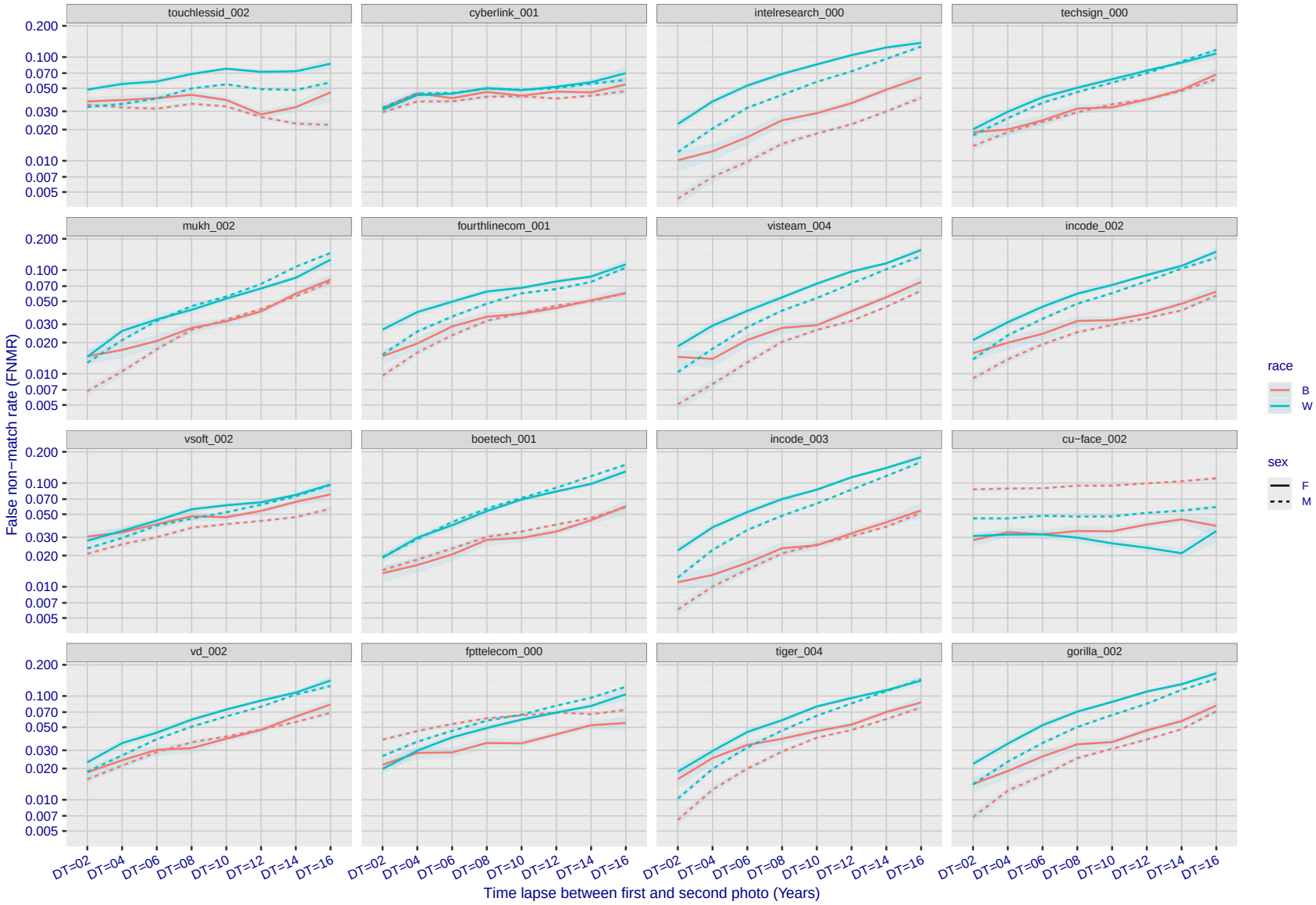

Figure 768: For the mugshot images, FNMR *as a function of elapsed time between initial enrollment and second verification images. The panels appear most accurate first, and vertical scale changes on each page. The four traces correspond to images annotated with codes for black female, black male, white female, white male. The threshold is fixed for each algorithm to give FMR = 0.00001 over all ($\widetilde{10}^8$) impostor comparisons. For short time-lapses, the most accurate algorithms give very few errors (FNMR < 0.001) so that the uncertainty estimates are high.*

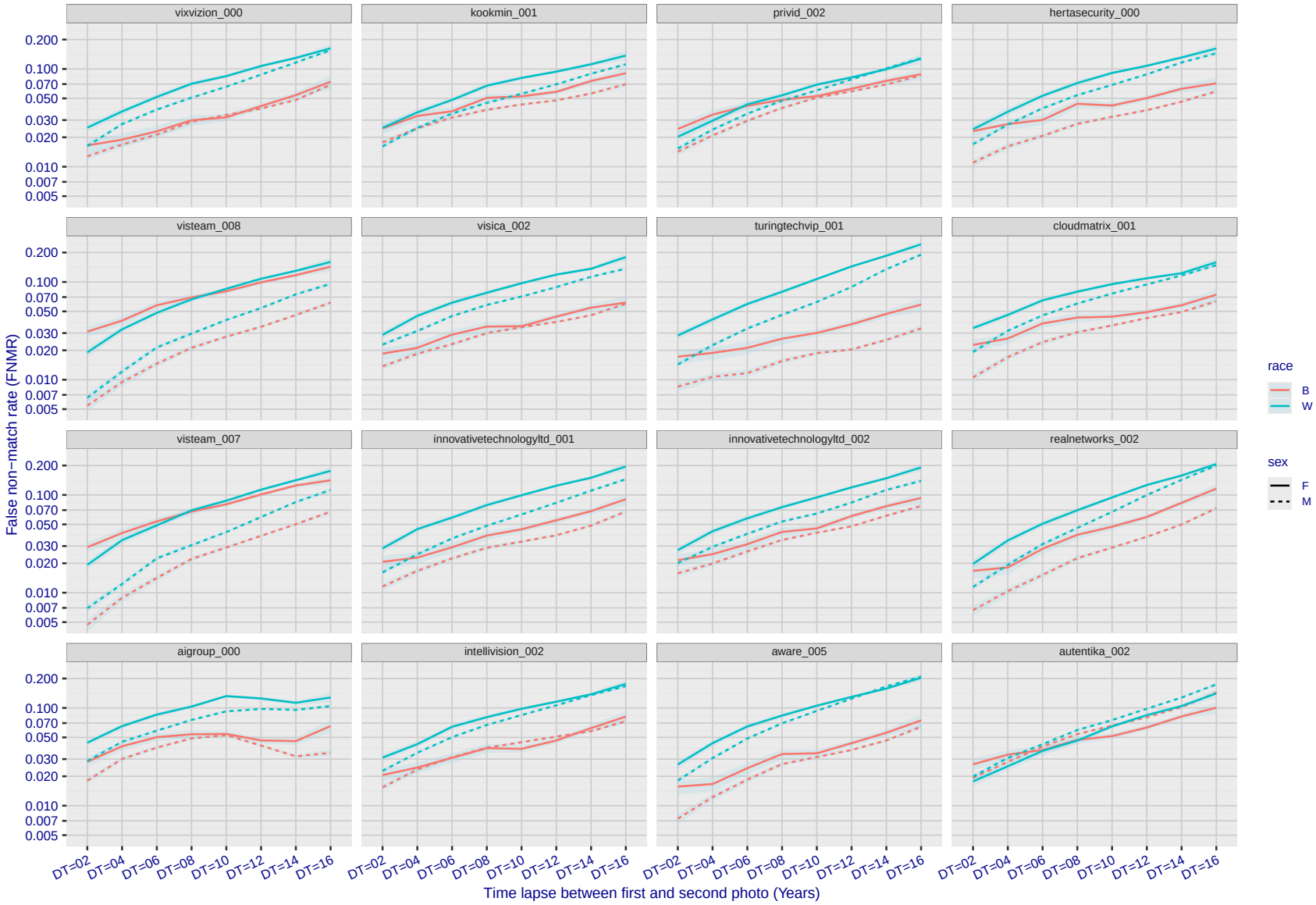

Figure 769: For the mugshot images, FNMR *as a function of elapsed time between initial enrollment and second verification images. The panels appear most accurate first, and vertical scale changes on each page. The four traces correspond to images annotated with codes for black female, black male, white female, white male. The threshold is fixed for each algorithm to give FMR = 0.00001 over all ($\widetilde{10}^8$) impostor comparisons. For short time-lapses, the most accurate algorithms give very few errors (FNMR < 0.001) so that the uncertainty estimates are high.*

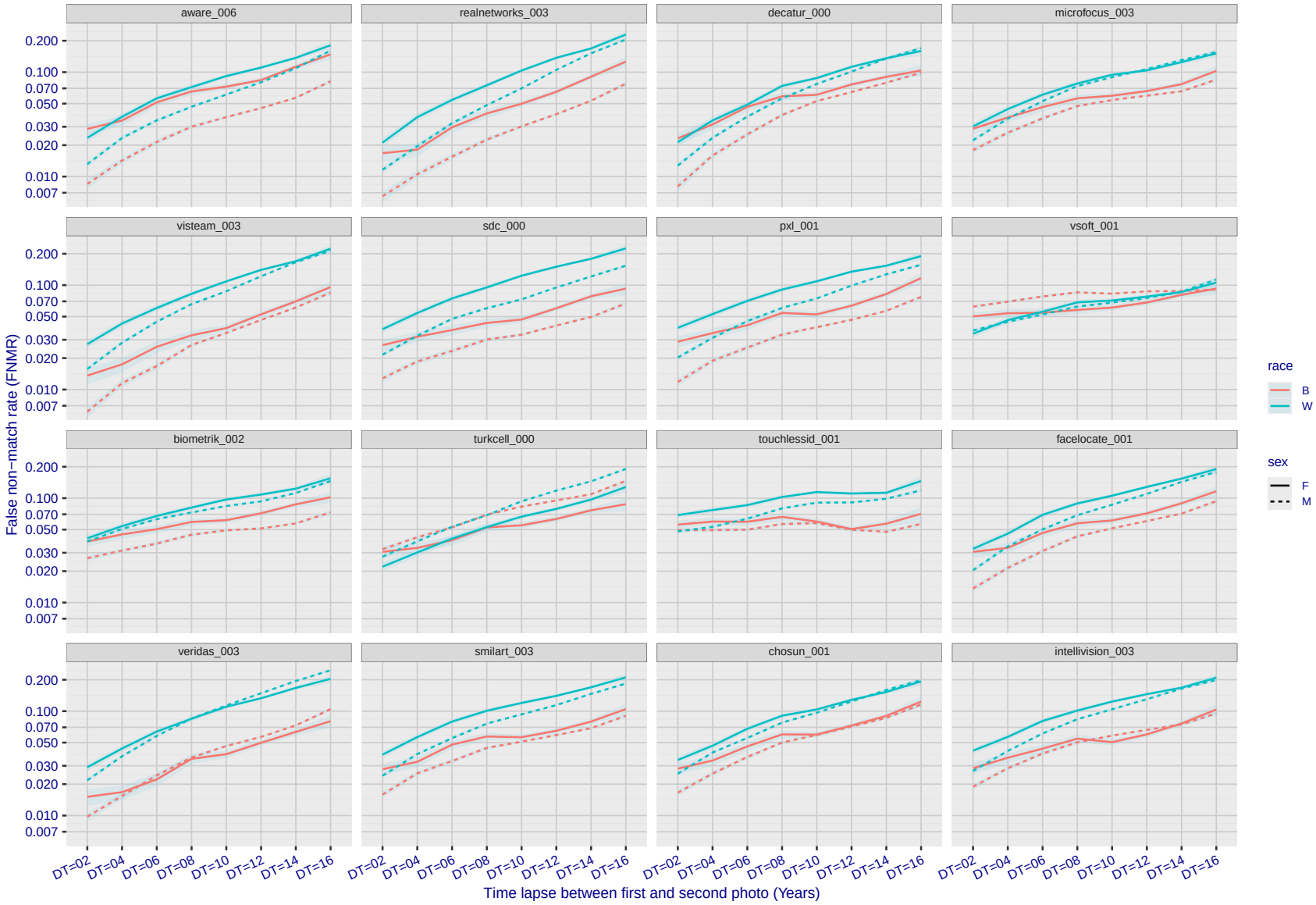

Figure 770: For the mugshot images, FNMR *as a function of elapsed time between initial enrollment and second verification images. The panels appear most accurate first, and vertical scale changes on each page. The four traces correspond to images annotated with codes for black female, black male, white female, white male. The threshold is fixed for each algorithm to give FMR = 0.00001 over all (10^8) impostor comparisons. For short time-lapses, the most accurate algorithms give very few errors (FNMR < 0.001) so that the uncertainty estimates are high.*

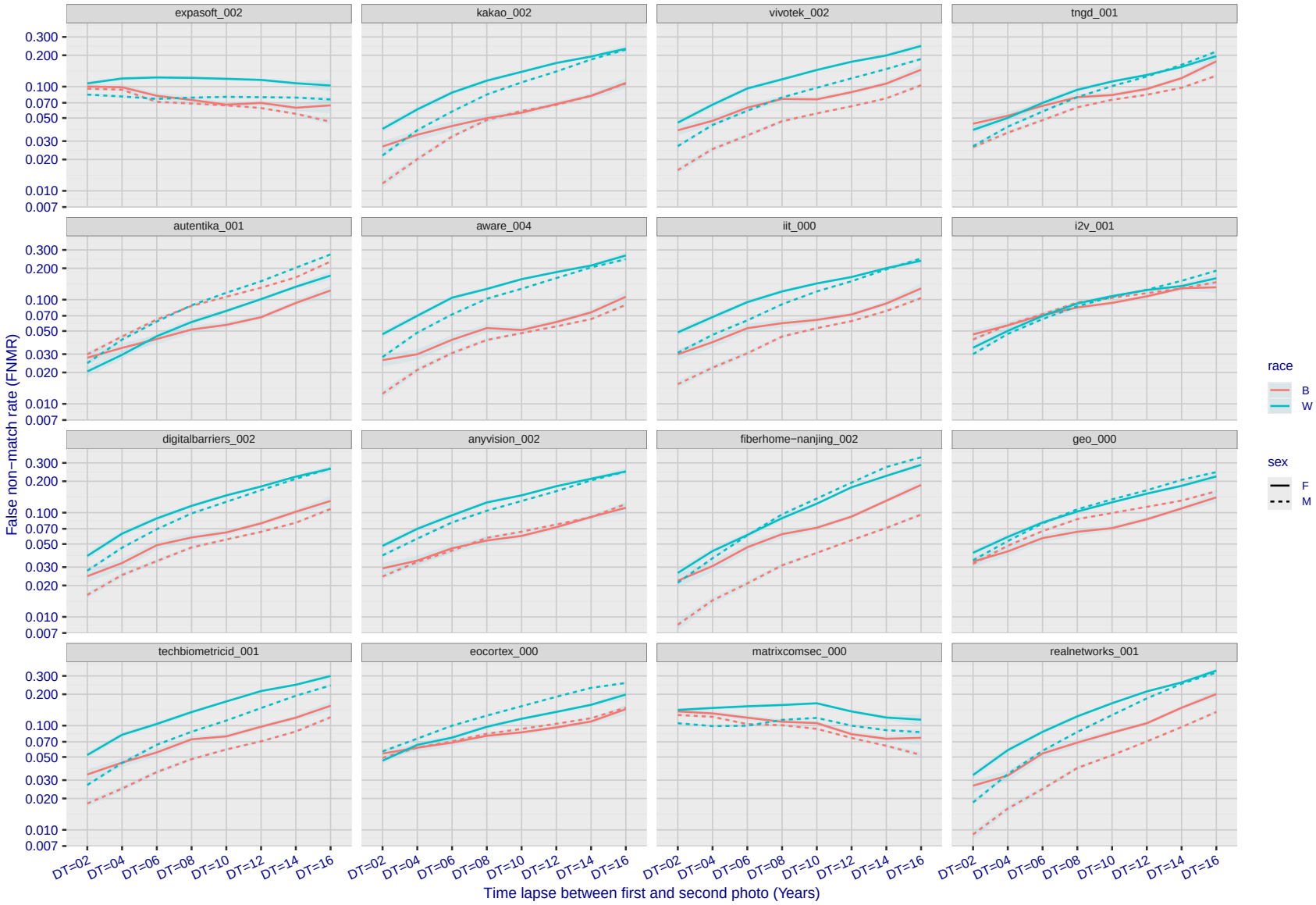

Figure 771: For the mugshot images, FNMR *as a function of elapsed time between initial enrollment and second verification images. The panels appear most accurate first, and vertical scale changes on each page. The four traces correspond to images annotated with codes for black female, black male, white female, white male. The threshold is fixed for each algorithm to give FMR = 0.00001 over all (10^8) impostor comparisons. For short time-lapses, the most accurate algorithms give very few errors (FNMR < 0.001) so that the uncertainty estimates are high.*

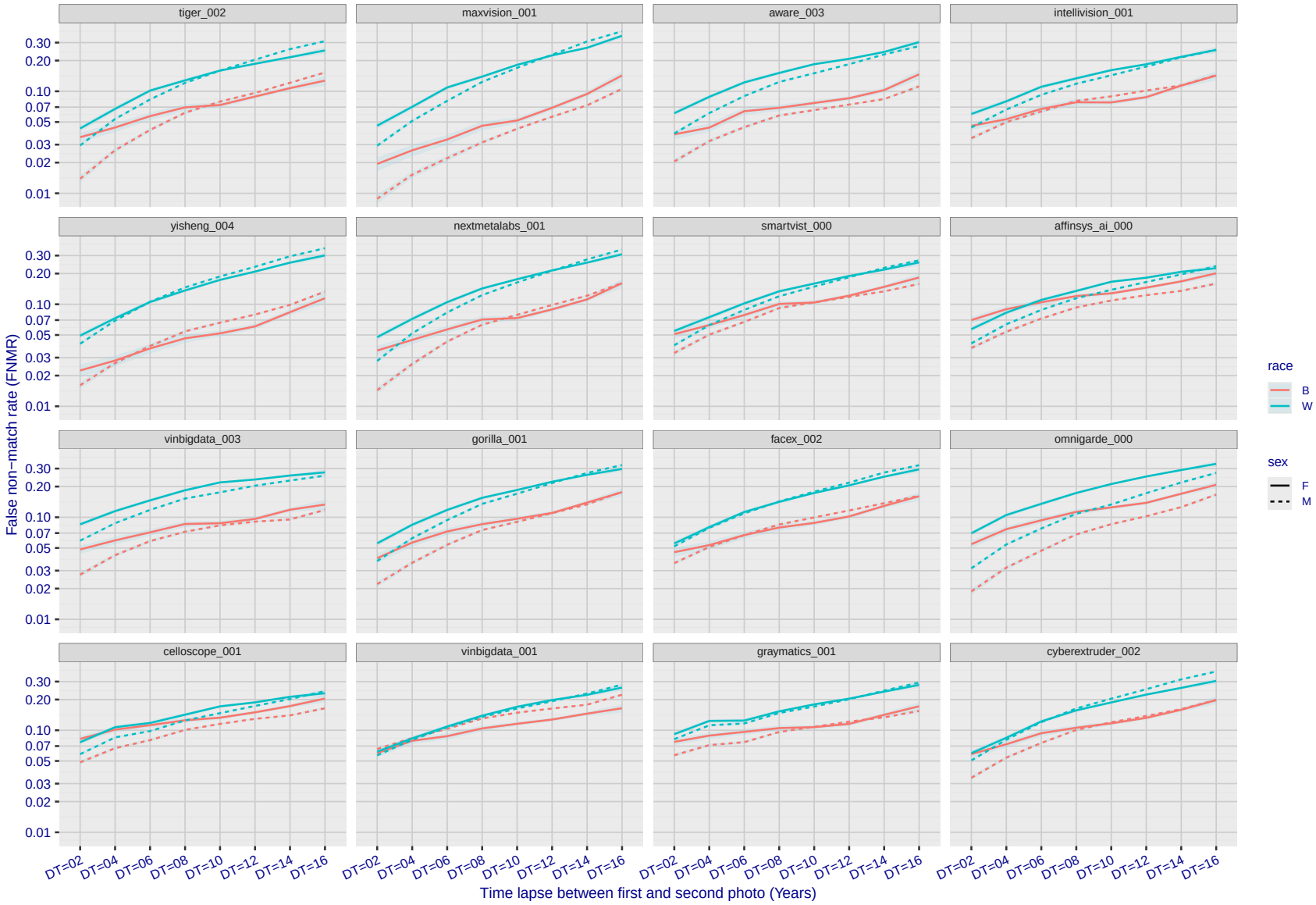

Figure 772: For the mugshot images, FNMR *as a function of elapsed time between initial enrollment and second verification images. The panels appear most accurate first, and vertical scale changes on each page. The four traces correspond to images annotated with codes for black female, black male, white female, white male. The threshold is fixed for each algorithm to give FMR = 0.00001 over all (10^8) impostor comparisons. For short time-lapses, the most accurate algorithms give very few errors (FNMR < 0.001) so that the uncertainty estimates are high.*

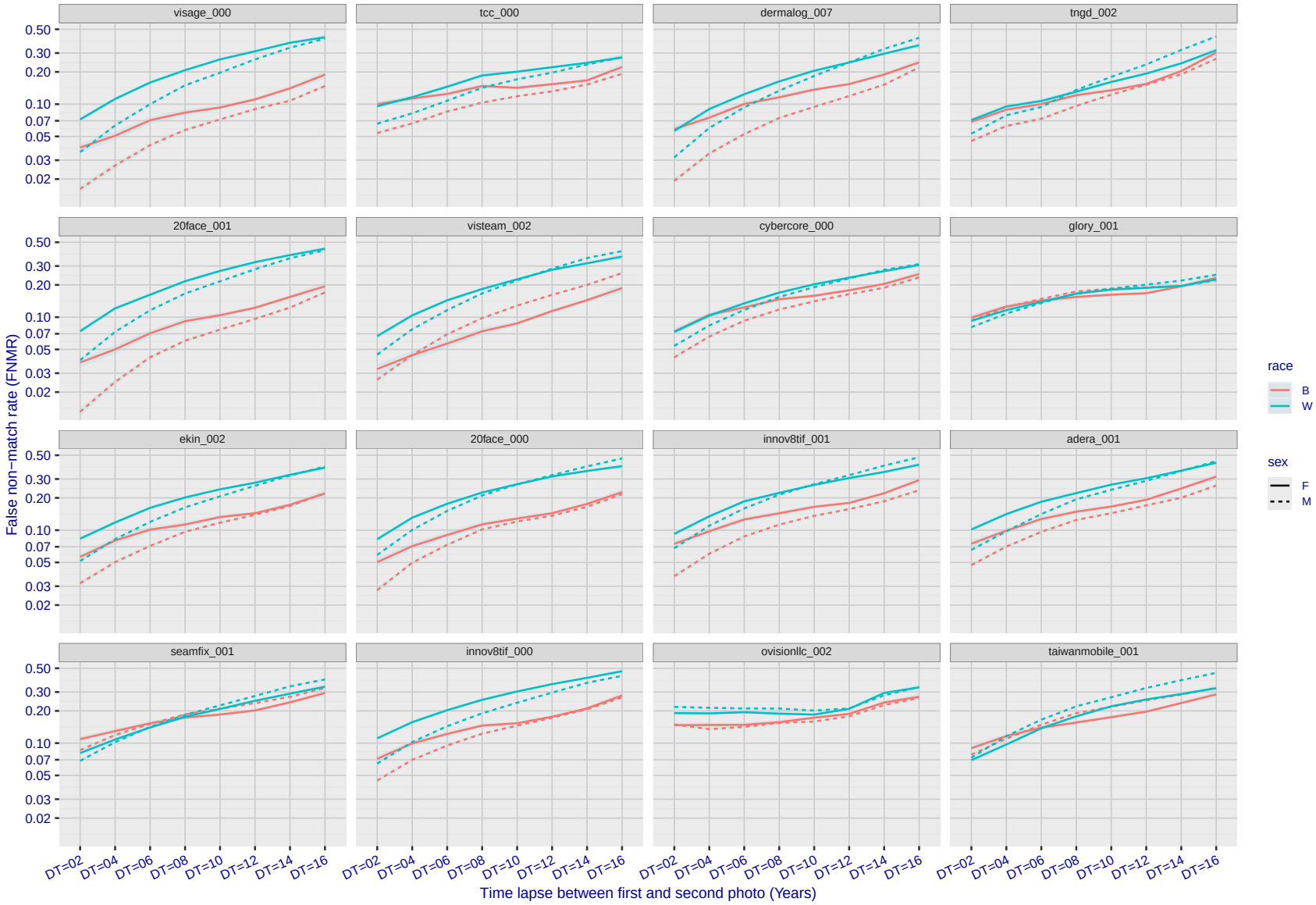

Figure 773: For the mugshot images, FNMR *as a function of elapsed time between initial enrollment and second verification images. The panels appear most accurate first, and vertical scale changes on each page. The four traces correspond to images annotated with codes for black female, black male, white female, white male. The threshold is fixed for each algorithm to give FMR = 0.00001 over all (10^8) impostor comparisons. For short time-lapses, the most accurate algorithms give very few errors (FNMR < 0.001) so that the uncertainty estimates are high.*

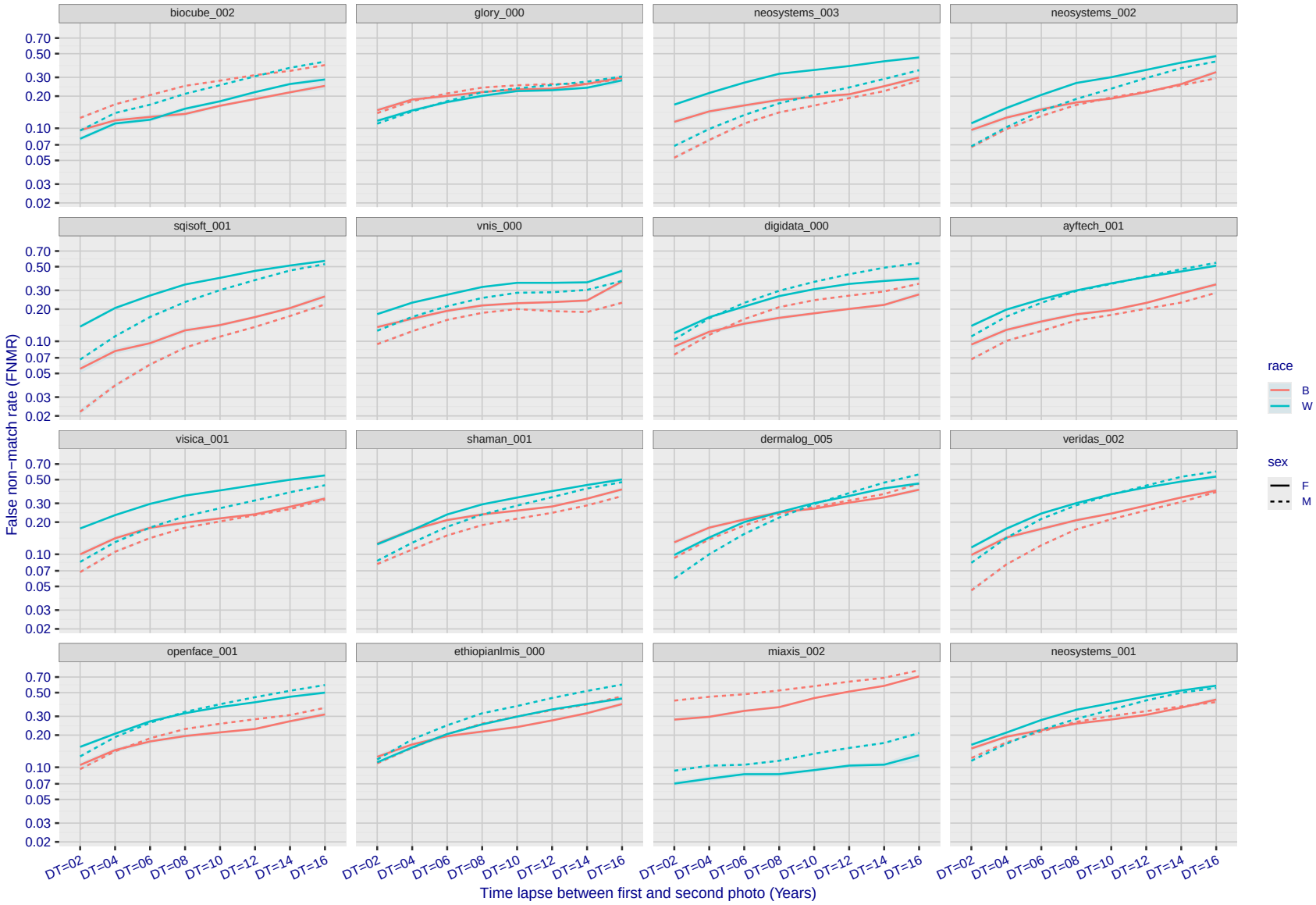

Figure 774: For the mugshot images, FNMR *as a function of elapsed time between initial enrollment and second verification images. The panels appear most accurate first, and vertical scale changes on each page. The four traces correspond to images annotated with codes for black female, black male, white female, white male. The threshold is fixed for each algorithm to give FMR = 0.00001 over all (10^8) impostor comparisons. For short time-lapses, the most accurate algorithms give very few errors (FNMR < 0.001) so that the uncertainty estimates are high.*

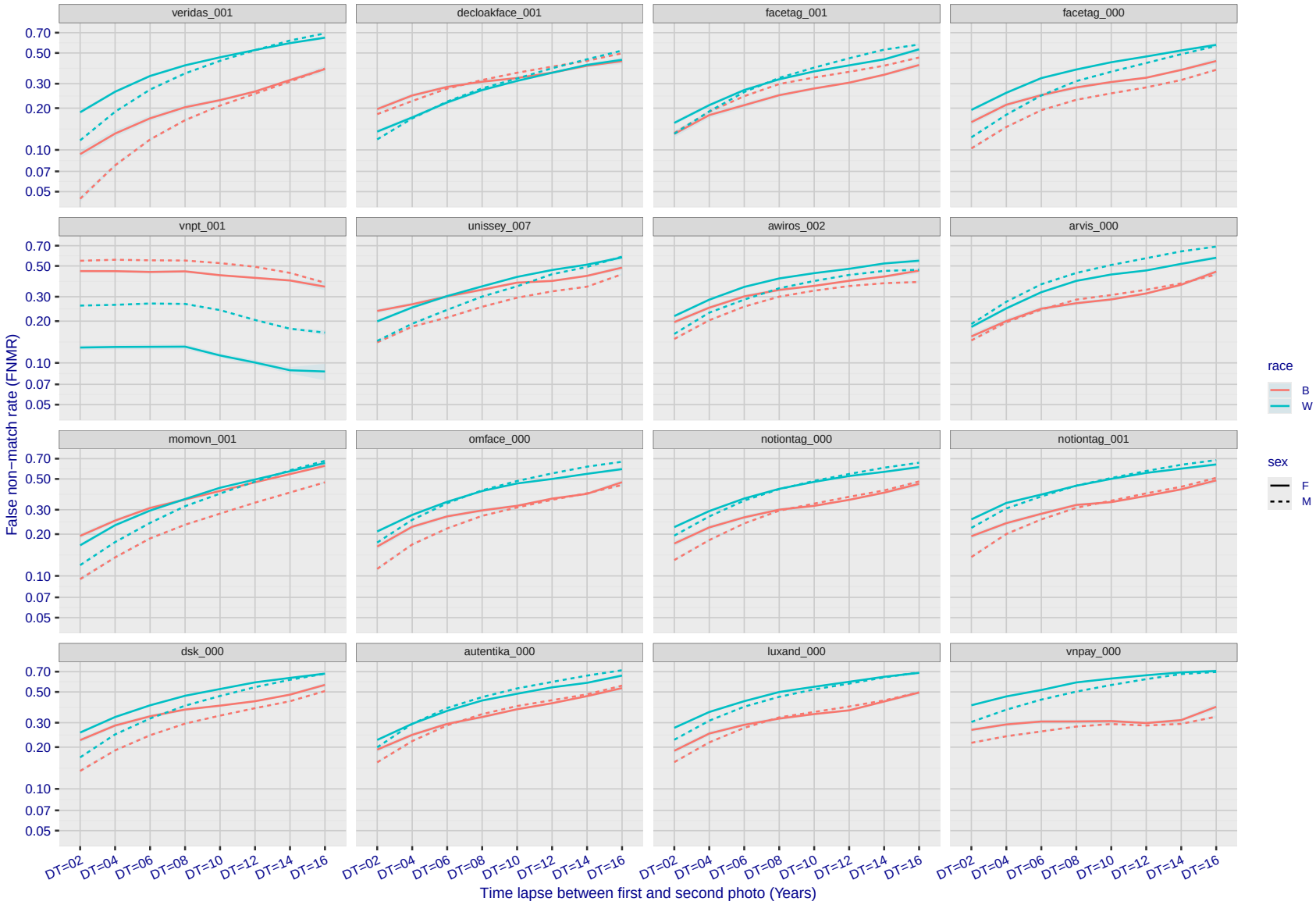

Figure 775: For the mugshot images, FNMR *as a function of elapsed time between initial enrollment and second verification images. The panels appear most accurate first, and vertical scale changes on each page. The four traces correspond to images annotated with codes for black female, black male, white female, white male. The threshold is fixed for each algorithm to give FMR = 0.00001 over all ($\widetilde{10}^8$) impostor comparisons. For short time-lapses, the most accurate algorithms give very few errors (FNMR < 0.001) so that the uncertainty estimates are high.*

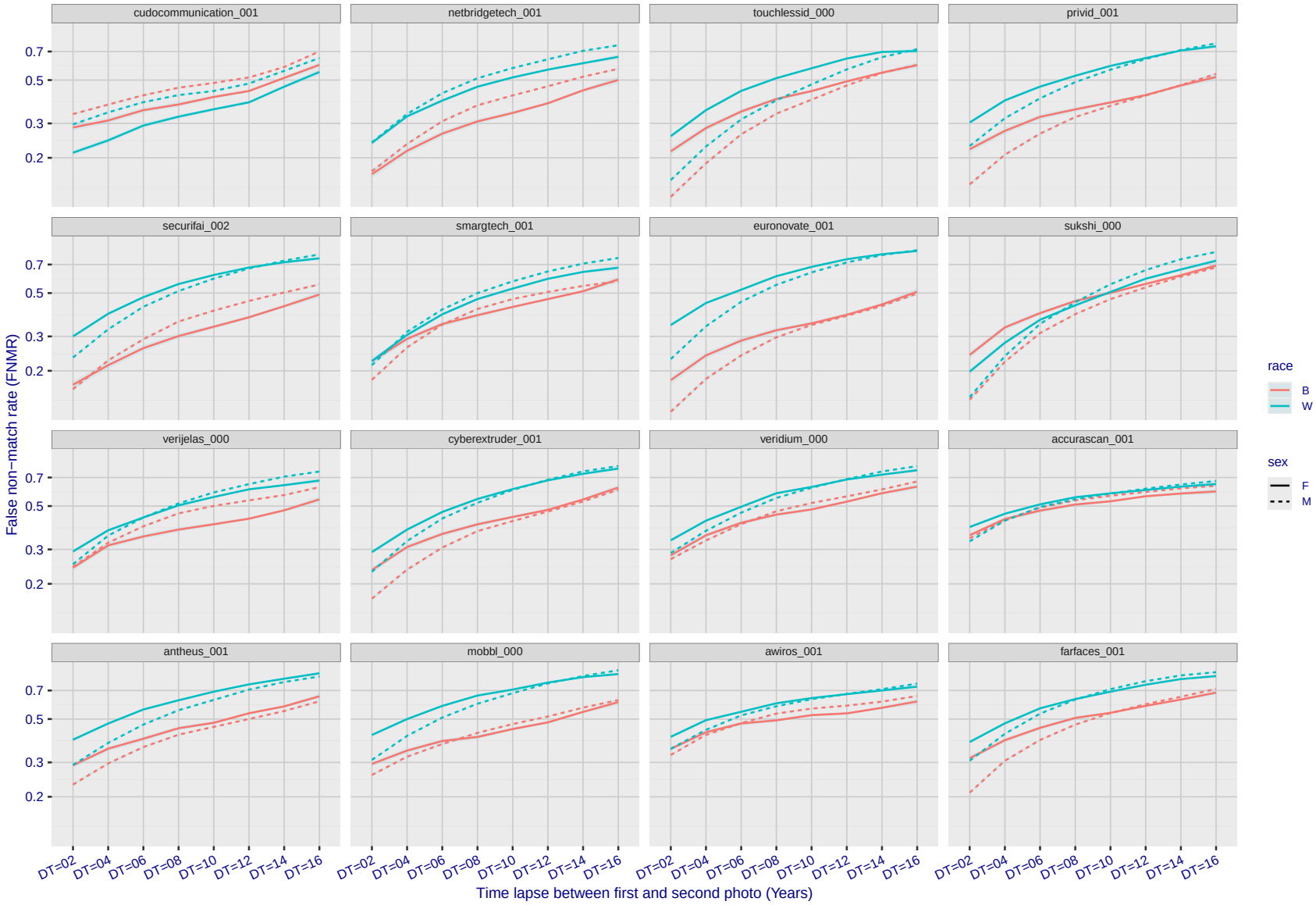

Figure 776: For the mugshot images, FNMR *as a function of elapsed time between initial enrollment and second verification images. The panels appear most accurate first, and vertical scale changes on each page. The four traces correspond to images annotated with codes for black female, black male, white female, white male. The threshold is fixed for each algorithm to give FMR = 0.00001 over all (10^8) impostor comparisons. For short time-lapses, the most accurate algorithms give very few errors (FNMR < 0.001) so that the uncertainty estimates are high.*

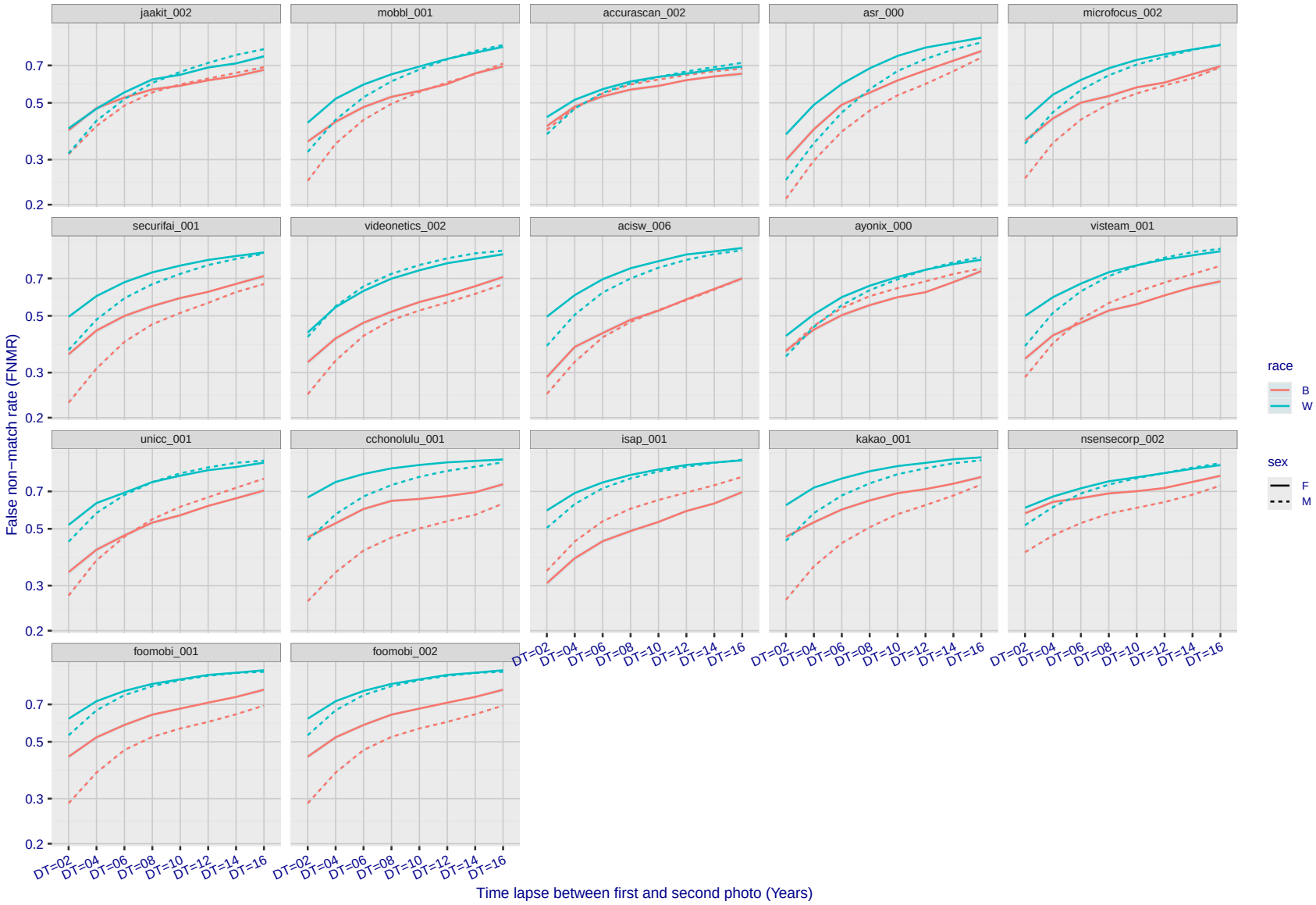

Figure 777: For the mugshot images, FNMR *as a function of elapsed time between initial enrollment and second verification images. The panels appear most accurate first, and vertical scale changes on each page. The four traces correspond to images annotated with codes for black female, black male, white female, white male. The threshold is fixed for each algorithm to give FMR = 0.00001 over all (10^8) impostor comparisons. For short time-lapses, the most accurate algorithms give very few errors (FNMR < 0.001) so that the uncertainty estimates are high.*

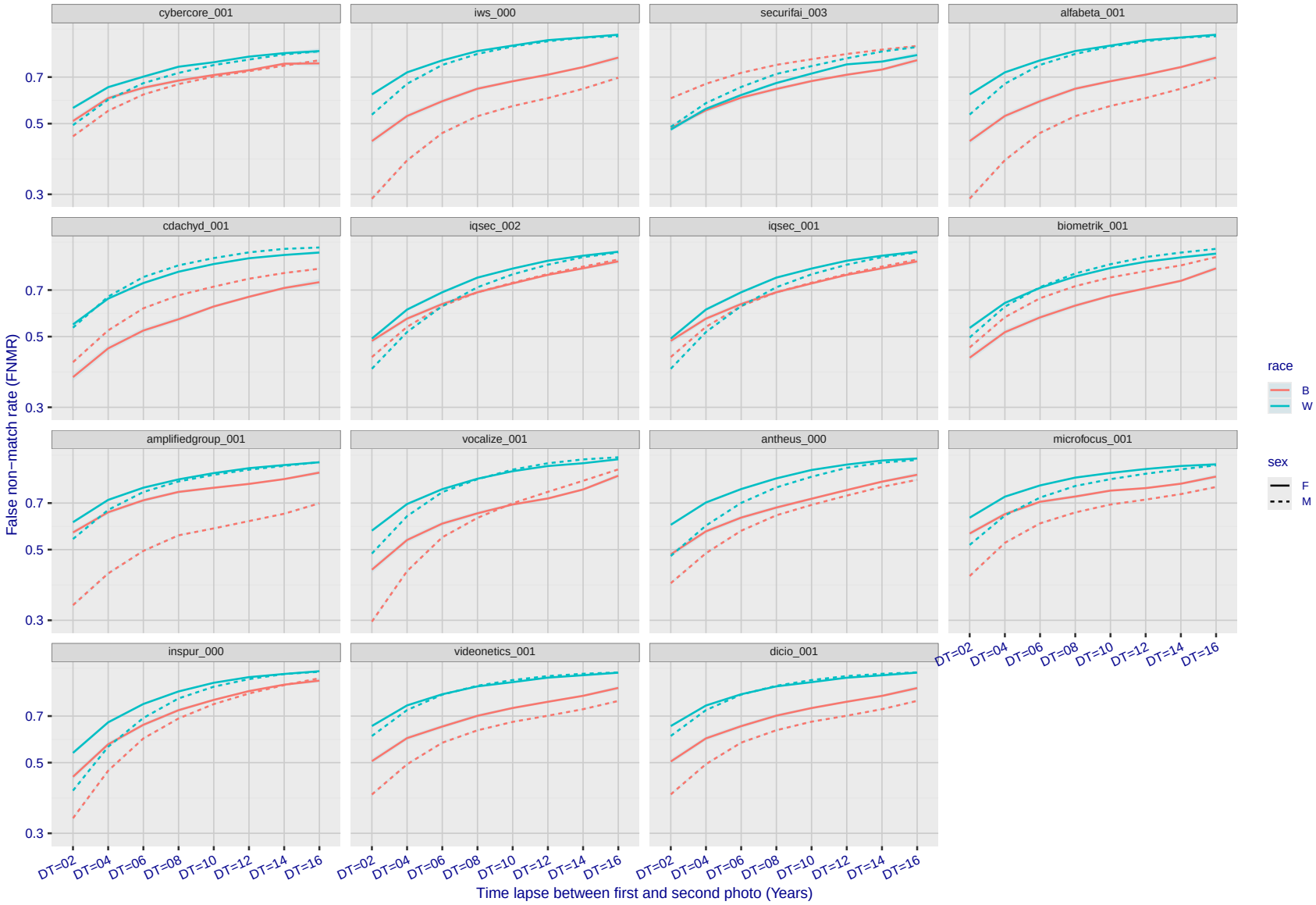

Figure 778: For the mugshot images, FNMR *as a function of elapsed time between initial enrollment and second verification images. The panels appear most accurate first, and vertical scale changes on each page. The four traces correspond to images annotated with codes for black female, black male, white female, white male. The threshold is fixed for each algorithm to give FMR = 0.00001 over all ($\widetilde{10}^8$) impostor comparisons. For short time-lapses, the most accurate algorithms give very few errors (FNMR < 0.001) so that the uncertainty estimates are high.*

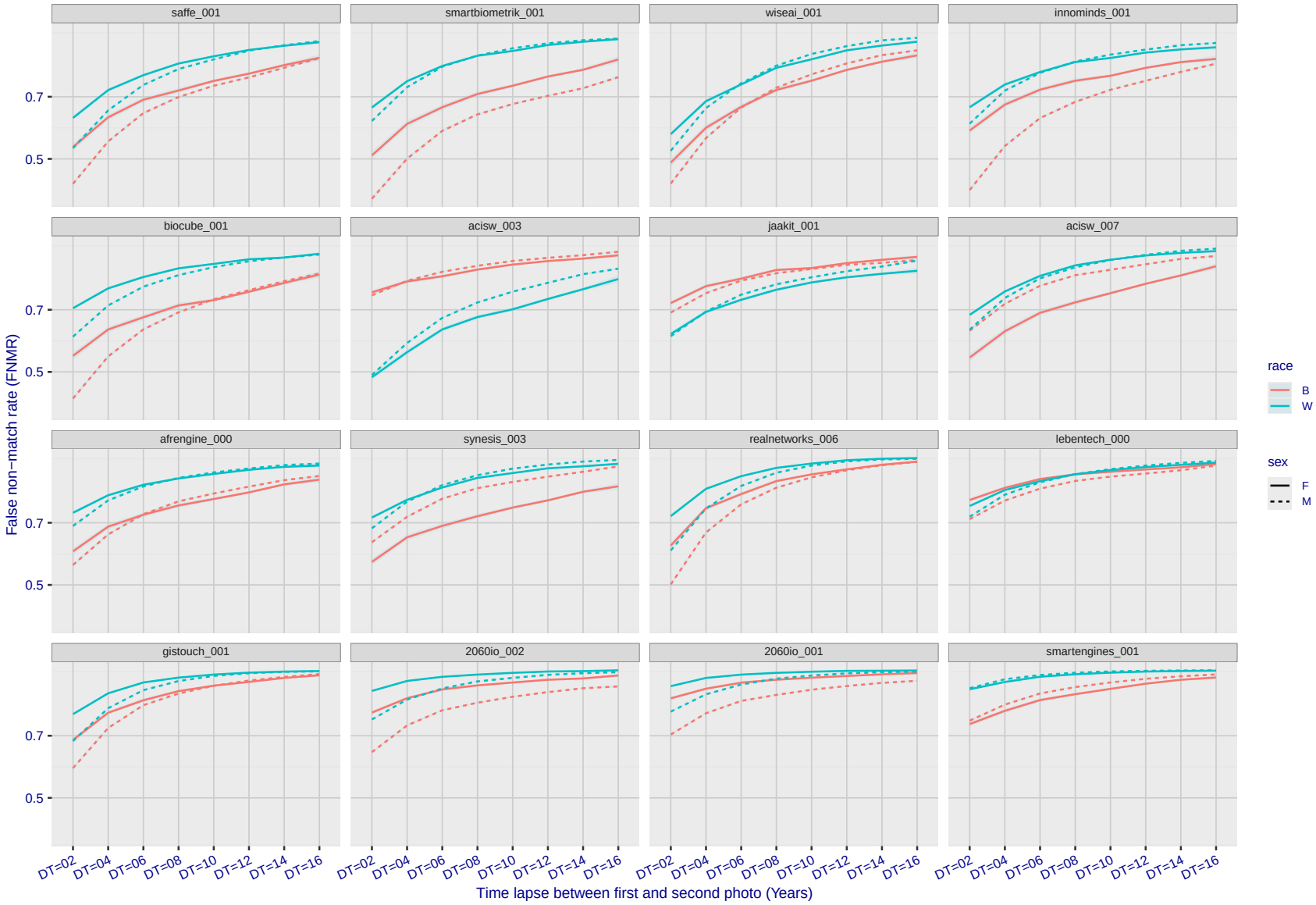

Figure 779: For the mugshot images, FNMR *as a function of elapsed time between initial enrollment and second verification images. The panels appear most accurate first, and vertical scale changes on each page. The four traces correspond to images annotated with codes for black female, black male, white female, white male. The threshold is fixed for each algorithm to give FMR = 0.00001 over all ($\widetilde{10}^8$) impostor comparisons. For short time-lapses, the most accurate algorithms give very few errors (FNMR < 0.001) so that the uncertainty estimates are high.*

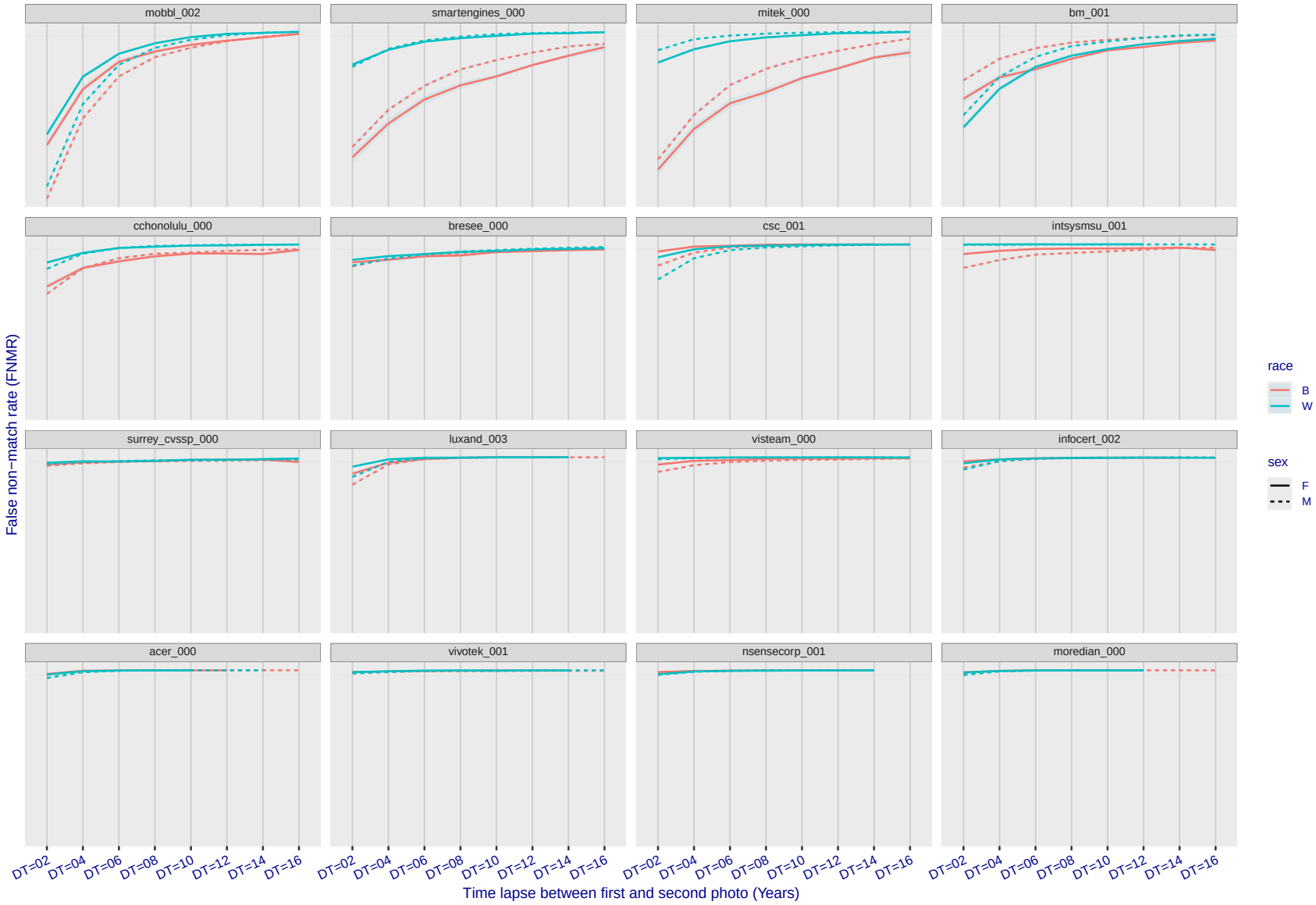

Figure 780: For the mugshot images, FNMR *as a function of elapsed time between initial enrollment and second verification images. The panels appear most accurate first, and vertical scale changes on each page. The four traces correspond to images annotated with codes for black female, black male, white female, white male. The threshold is fixed for each algorithm to give FMR = 0.00001 over all ($\widetilde{10}^8$) impostor comparisons. For short time-lapses, the most accurate algorithms give very few errors (FNMR < 0.001) so that the uncertainty estimates are high.*

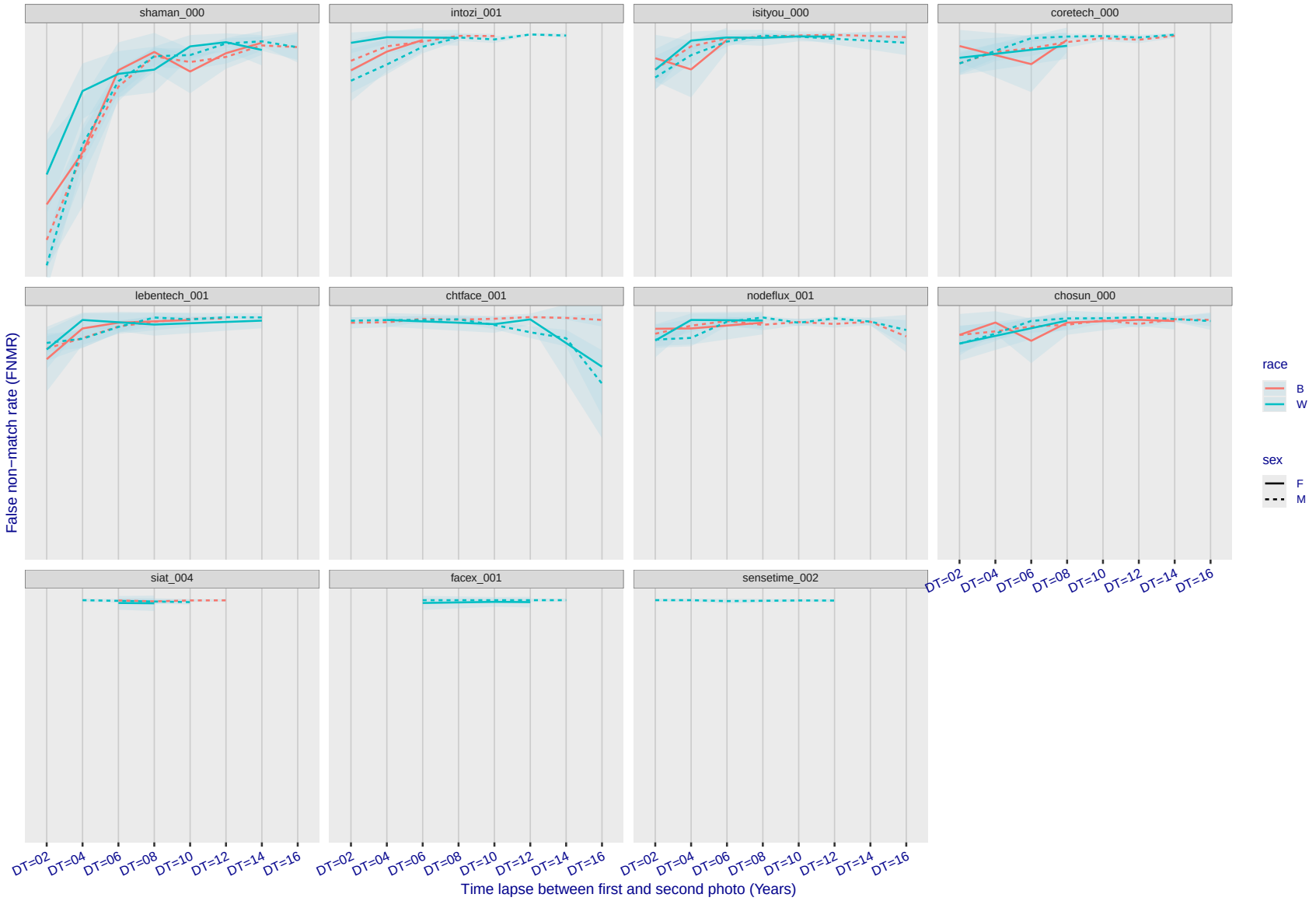

Figure 781: For the mugshot images, FNMR *as a function of elapsed time between initial enrollment and second verification images. The panels appear most accurate first, and vertical scale changes on each page. The four traces correspond to images annotated with codes for black female, black male, white female, white male. The threshold is fixed for each algorithm to give FMR = 0.00001 over all (10^8) impostor comparisons. For short time-lapses, the most accurate algorithms give very few errors (FNMR < 0.001) so that the uncertainty estimates are high.*

3.5.3 Effect of age on genuine subjects

Background: Faces change appearance throughout life. Face recognition algorithms have previously beeen reported to give better accuracy on older individuals (See NIST IR 8009).

Goal: To quantify false non-match rates (FNMR) as a function of age, without an ageing component.

Methods: Using the visa images, which span fewer than five years, thresholds are determined that give FMR = 0.001 and 0.0001 over the entire impostor set. Then FNMR is measured over 1000 bootstrap replications of the genuine scores.

Results: For the visa images, Figure 872 shows how false non-match rates for genuine users, as a function of age group.

The notable aspects are:

- ▷ Younger subjects give considerably higher FNMR. This is likely due to rapid growth and change in facial appearance.
- ▷ FNMR trends down throughout life. The last bin, AGE $>$ 72, contains fewer than 140 mated pairs, and may be affected by small sample size.

FNMR(T) "False non-match rate"
FMR(T) "False match rate"

Figure 782: For the visa images, the dots show FNMR by age group for two operating thresholds corresponding to FMR = $\{0.001, 0.0001\}$ computed over all on the order of 10^{10} impostor scores. The FMR in each bin will vary also - see subsequent impostor heatmaps in sec. 3.6.2. Given a pair of face images taken at different times, we assign the comparison to the bin that is the arithmetic average of the subject's ages. This plot shows only the effect of age, not ageing. The number of comparisons in each bin is generally in the thousands, however the first and last bins are computed over 149 and 124 respectively. The error rates in some (adult) cases are zero, and in others the DET is flat so the error rates at the two thresholds are identical. The lines span 1% and 99% of boostrap replicated FNMR estimates.

Figure 783: For the visa images, the dots show FNMR by age group for two operating thresholds corresponding to FMR = $\{0.001, 0.0001\}$ computed over all on the order of 10^{10} impostor scores. The FMR in each bin will vary also - see subsequent impostor heatmaps in sec. 3.6.2. Given a pair of face images taken at different times, we assign the comparison to the bin that is the arithmetic average of the subject's ages. This plot shows only the effect of age, not ageing. The number of comparisons in each bin is generally in the thousands, however the first and last bins are computed over 149 and 124 respectively. The error rates in some (adult) cases are zero, and in others the DET is flat so the error rates at the two thresholds are identical. The lines span 1% and 99% of boostrap replicated FNMR estimates.

Figure 784: For the visa images, the dots show FNMR by age group for two operating thresholds corresponding to FMR = $\{0.001, 0.0001\}$ computed over all on the order of 10^{10} impostor scores. The FMR in each bin will vary also - see subsequent impostor heatmaps in sec. 3.6.2. Given a pair of face images taken at different times, we assign the comparison to the bin that is the arithmetic average of the subject's ages. This plot shows only the effect of age, not ageing. The number of comparisons in each bin is generally in the thousands, however the first and last bins are computed over 149 and 124 respectively. The error rates in some (adult) cases are zero, and in others the DET is flat so the error rates at the two thresholds are identical. The lines span 1% and 99% of boostrap replicated FNMR estimates.

Figure 785: For the visa images, the dots show FNMR by age group for two operating thresholds corresponding to FMR = $\{0.001, 0.0001\}$ computed over all on the order of 10^{10} impostor scores. The FMR in each bin will vary also - see subsequent impostor heatmaps in sec. 3.6.2. Given a pair of face images taken at different times, we assign the comparison to the bin that is the arithmetic average of the subject's ages. This plot shows only the effect of age, not ageing. The number of comparisons in each bin is generally in the thousands, however the first and last bins are computed over 149 and 124 respectively. The error rates in some (adult) cases are zero, and in others the DET is flat so the error rates at the two thresholds are identical. The lines span 1% and 99% of boostrap replicated FNMR estimates.

Figure 786: For the visa images, the dots show FNMR by age group for two operating thresholds corresponding to FMR = $\{0.001, 0.0001\}$ computed over all on the order of 10^{10} impostor scores. The FMR in each bin will vary also - see subsequent impostor heatmaps in sec. 3.6.2. Given a pair of face images taken at different times, we assign the comparison to the bin that is the arithmetic average of the subject's ages. This plot shows only the effect of age, not ageing. The number of comparisons in each bin is generally in the thousands, however the first and last bins are computed over 149 and 124 respectively. The error rates in some (adult) cases are zero, and in others the DET is flat so the error rates at the two thresholds are identical. The lines span 1% and 99% of boostrap replicated FNMR estimates.

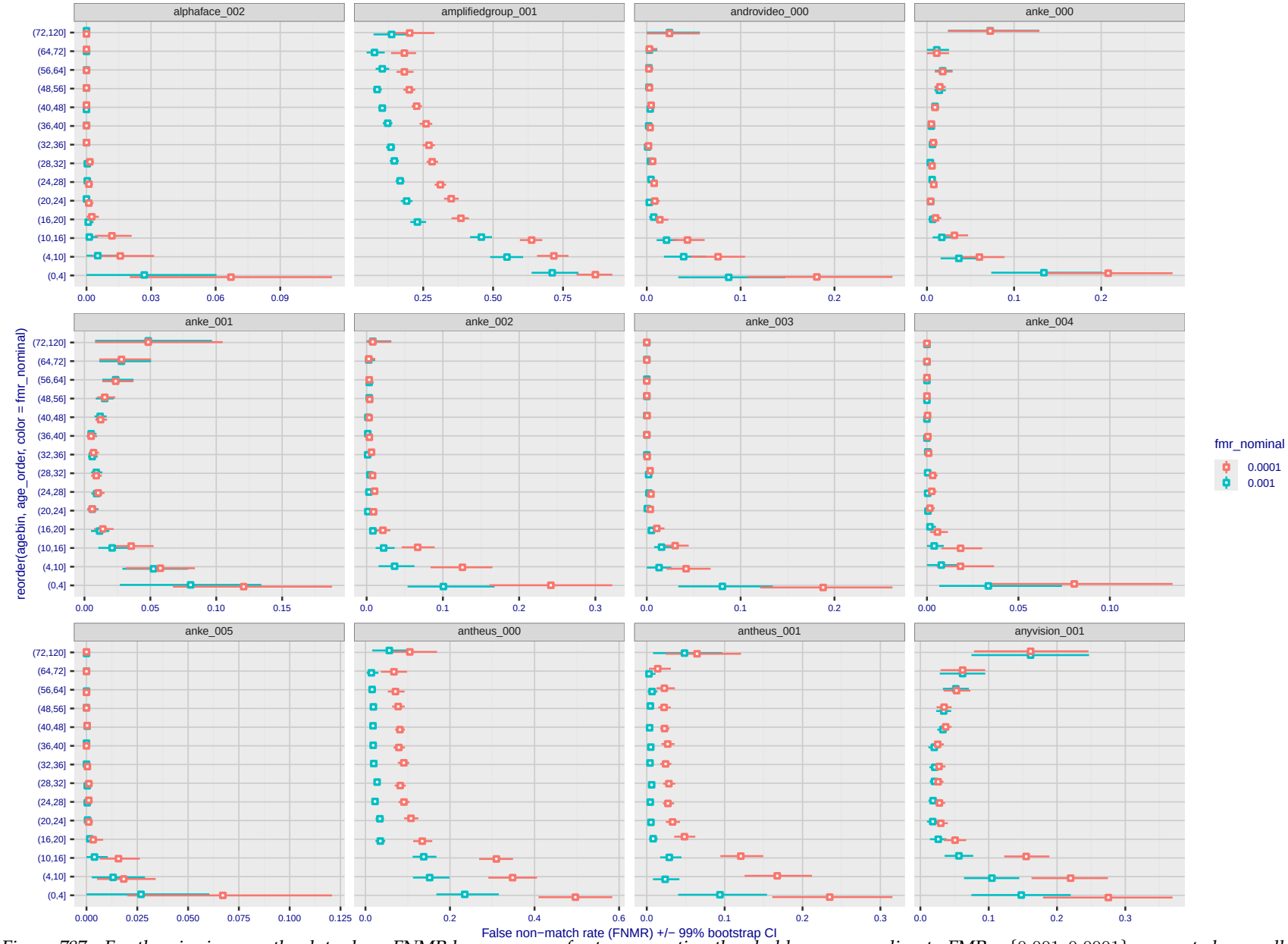

Figure 787: For the visa images, the dots show FNMR by age group for two operating thresholds corresponding to FMR = $\{0.001, 0.0001\}$ computed over all on the order of 10^{10} impostor scores. The FMR in each bin will vary also - see subsequent impostor heatmaps in sec. 3.6.2. Given a pair of face images taken at different times, we assign the comparison to the bin that is the arithmetic average of the subject's ages. This plot shows only the effect of age, not ageing. The number of comparisons in each bin is generally in the thousands, however the first and last bins are computed over 149 and 124 respectively. The error rates in some (adult) cases are zero, and in others the DET is flat so the error rates at the two thresholds are identical. The lines span 1% and 99% of boostrap replicated FNMR estimates.

Figure 788: For the visa images, the dots show FNMR by age group for two operating thresholds corresponding to FMR = $\{0.001, 0.0001\}$ computed over all on the order of 10^{10} impostor scores. The FMR in each bin will vary also - see subsequent impostor heatmaps in sec. 3.6.2. Given a pair of face images taken at different times, we assign the comparison to the bin that is the arithmetic average of the subject's ages. This plot shows only the effect of age, not ageing. The number of comparisons in each bin is generally in the thousands, however the first and last bins are computed over 149 and 124 respectively. The error rates in some (adult) cases are zero, and in others the DET is flat so the error rates at the two thresholds are identical. The lines span 1% and 99% of boostrap replicated FNMR estimates.

Figure 789: For the visa images, the dots show FNMR by age group for two operating thresholds corresponding to FMR = $\{0.001, 0.0001\}$ computed over all on the order of 10^{10} impostor scores. The FMR in each bin will vary also - see subsequent impostor heatmaps in sec. 3.6.2. Given a pair of face images taken at different times, we assign the comparison to the bin that is the arithmetic average of the subject's ages. This plot shows only the effect of age, not ageing. The number of comparisons in each bin is generally in the thousands, however the first and last bins are computed over 149 and 124 respectively. The error rates in some (adult) cases are zero, and in others the DET is flat so the error rates at the two thresholds are identical. The lines span 1% and 99% of boostrap replicated FNMR estimates.

Figure 790: For the visa images, the dots show FNMR by age group for two operating thresholds corresponding to FMR = $\{0.001, 0.0001\}$ computed over all on the order of 10^{10} impostor scores. The FMR in each bin will vary also - see subsequent impostor heatmaps in sec. 3.6.2. Given a pair of face images taken at different times, we assign the comparison to the bin that is the arithmetic average of the subject's ages. This plot shows only the effect of age, not ageing. The number of comparisons in each bin is generally in the thousands, however the first and last bins are computed over 149 and 124 respectively. The error rates in some (adult) cases are zero, and in others the DET is flat so the error rates at the two thresholds are identical. The lines span 1% and 99% of boostrap replicated FNMR estimates.

Figure 791: For the visa images, the dots show FNMR by age group for two operating thresholds corresponding to FMR = $\{0.001, 0.0001\}$ computed over all on the order of 10^{10} impostor scores. The FMR in each bin will vary also - see subsequent impostor heatmaps in sec. 3.6.2. Given a pair of face images taken at different times, we assign the comparison to the bin that is the arithmetic average of the subject's ages. This plot shows only the effect of age, not ageing. The number of comparisons in each bin is generally in the thousands, however the first and last bins are computed over 149 and 124 respectively. The error rates in some (adult) cases are zero, and in others the DET is flat so the error rates at the two thresholds are identical. The lines span 1% and 99% of boostrap replicated FNMR estimates.

Figure 792: For the visa images, the dots show FNMR by age group for two operating thresholds corresponding to FMR = $\{0.001, 0.0001\}$ computed over all on the order of 10^{10} impostor scores. The FMR in each bin will vary also - see subsequent impostor heatmaps in sec. 3.6.2. Given a pair of face images taken at different times, we assign the comparison to the bin that is the arithmetic average of the subject's ages. This plot shows only the effect of age, not ageing. The number of comparisons in each bin is generally in the thousands, however the first and last bins are computed over 149 and 124 respectively. The error rates in some (adult) cases are zero, and in others the DET is flat so the error rates at the two thresholds are identical. The lines span 1% and 99% of boostrap replicated FNMR estimates.

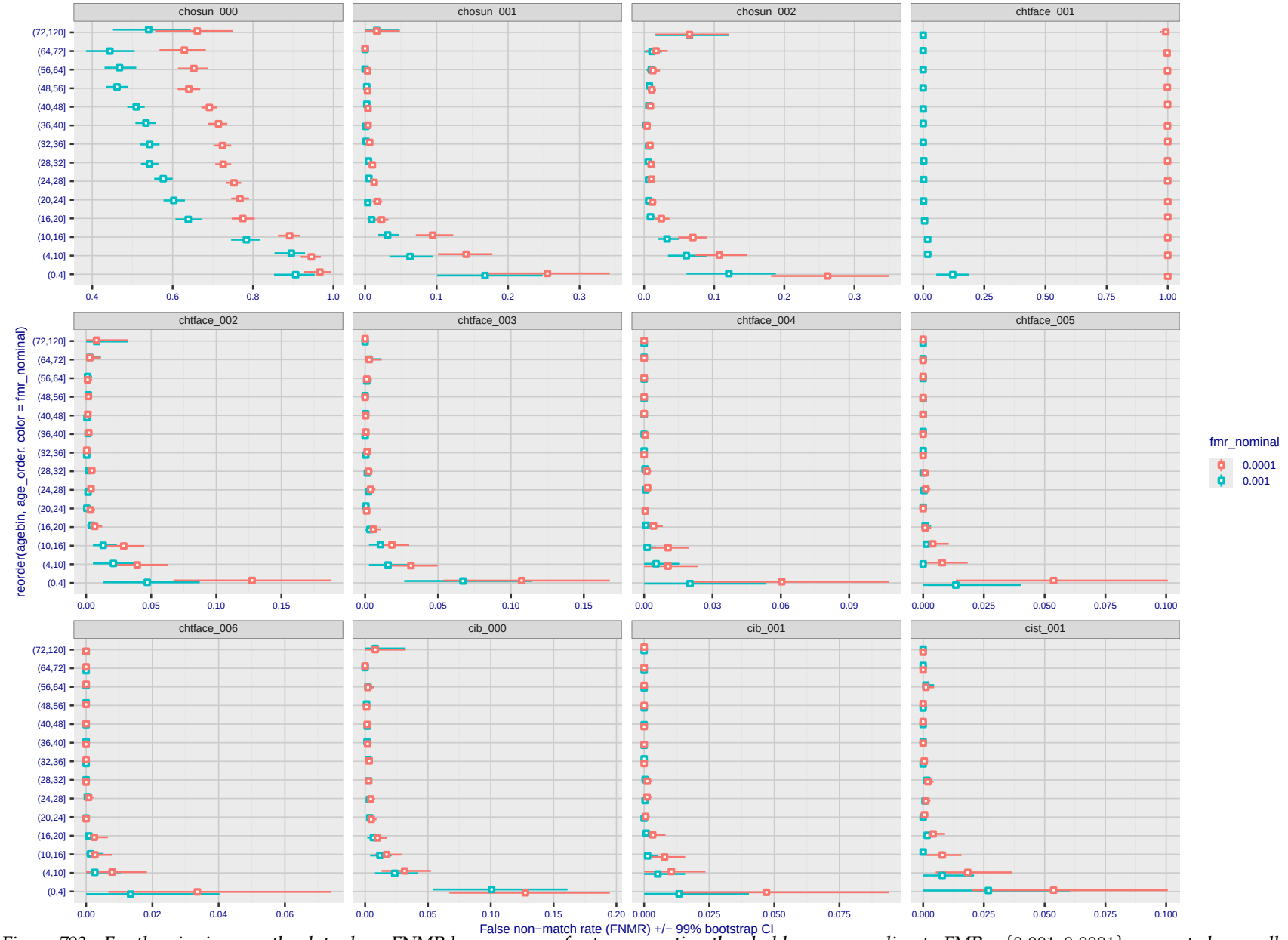

Figure 793: For the visa images, the dots show FNMR by age group for two operating thresholds corresponding to FMR = $\{0.001, 0.0001\}$ computed over all on the order of 10^{10} impostor scores. The FMR in each bin will vary also - see subsequent impostor heatmaps in sec. 3.6.2. Given a pair of face images taken at different times, we assign the comparison to the bin that is the arithmetic average of the subject's ages. This plot shows only the effect of age, not ageing. The number of comparisons in each bin is generally in the thousands, however the first and last bins are computed over 149 and 124 respectively. The error rates in some (adult) cases are zero, and in others the DET is flat so the error rates at the two thresholds are identical. The lines span 1% and 99% of boostrap replicated FNMR estimates.

Figure 794: For the visa images, the dots show FNMR by age group for two operating thresholds corresponding to FMR = $\{0.001, 0.0001\}$ computed over all on the order of 10^{10} impostor scores. The FMR in each bin will vary also - see subsequent impostor heatmaps in sec. 3.6.2. Given a pair of face images taken at different times, we assign the comparison to the bin that is the arithmetic average of the subject's ages. This plot shows only the effect of age, not ageing. The number of comparisons in each bin is generally in the thousands, however the first and last bins are computed over 149 and 124 respectively. The error rates in some (adult) cases are zero, and in others the DET is flat so the error rates at the two thresholds are identical. The lines span 1% and 99% of boostrap replicated FNMR estimates.

Figure 795: For the visa images, the dots show FNMR by age group for two operating thresholds corresponding to FMR = $\{0.001, 0.0001\}$ computed over all on the order of 10^{10} impostor scores. The FMR in each bin will vary also - see subsequent impostor heatmaps in sec. 3.6.2. Given a pair of face images taken at different times, we assign the comparison to the bin that is the arithmetic average of the subject's ages. This plot shows only the effect of age, not ageing. The number of comparisons in each bin is generally in the thousands, however the first and last bins are computed over 149 and 124 respectively. The error rates in some (adult) cases are zero, and in others the DET is flat so the error rates at the two thresholds are identical. The lines span 1% and 99% of boostrap replicated FNMR estimates.

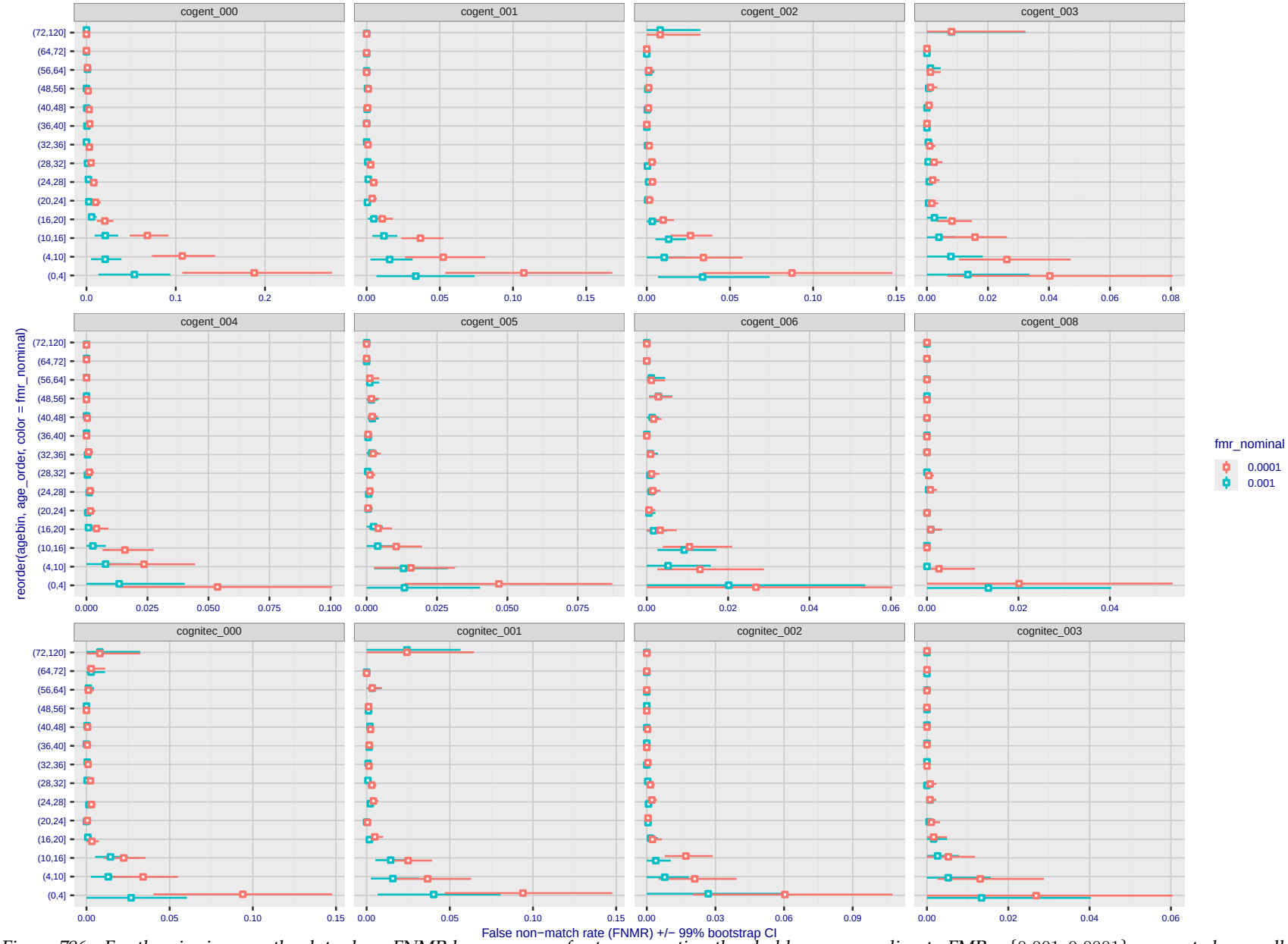

Figure 796: For the visa images, the dots show FNMR by age group for two operating thresholds corresponding to FMR = $\{0.001, 0.0001\}$ computed over all on the order of 10^{10} impostor scores. The FMR in each bin will vary also - see subsequent impostor heatmaps in sec. 3.6.2. Given a pair of face images taken at different times, we assign the comparison to the bin that is the arithmetic average of the subject's ages. This plot shows only the effect of age, not ageing. The number of comparisons in each bin is generally in the thousands, however the first and last bins are computed over 149 and 124 respectively. The error rates in some (adult) cases are zero, and in others the DET is flat so the error rates at the two thresholds are identical. The lines span 1% and 99% of boostrap replicated FNMR estimates.

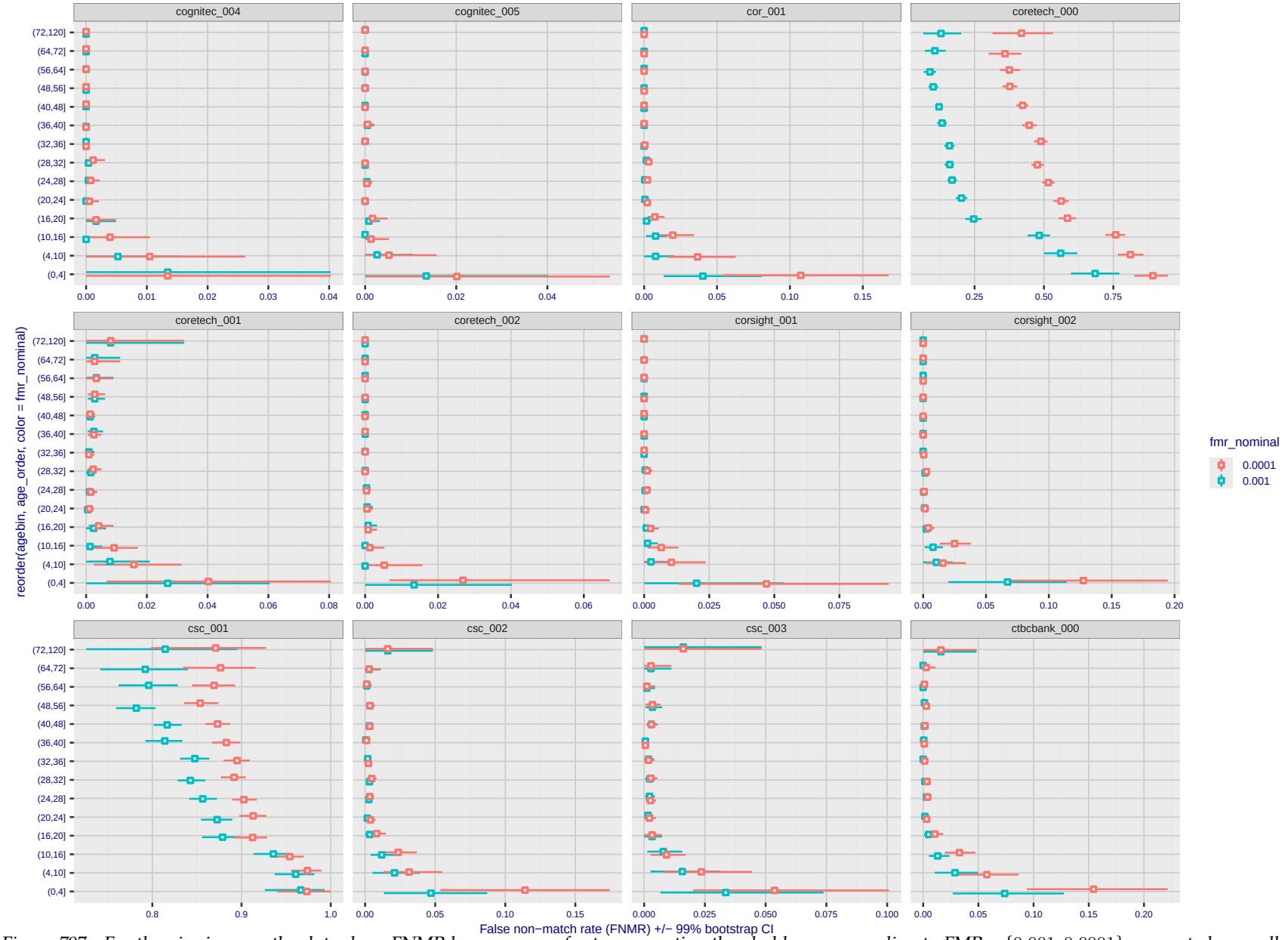

Figure 797: For the visa images, the dots show FNMR by age group for two operating thresholds corresponding to FMR = $\{0.001, 0.0001\}$ computed over all on the order of 10^{10} impostor scores. The FMR in each bin will vary also - see subsequent impostor heatmaps in sec. 3.6.2. Given a pair of face images taken at different times, we assign the comparison to the bin that is the arithmetic average of the subject's ages. This plot shows only the effect of age, not ageing. The number of comparisons in each bin is generally in the thousands, however the first and last bins are computed over 149 and 124 respectively. The error rates in some (adult) cases are zero, and in others the DET is flat so the error rates at the two thresholds are identical. The lines span 1% and 99% of boostrap replicated FNMR estimates.

Figure 798: For the visa images, the dots show FNMR by age group for two operating thresholds corresponding to FMR = $\{0.001, 0.0001\}$ computed over all on the order of 10^{10} impostor scores. The FMR in each bin will vary also - see subsequent impostor heatmaps in sec. 3.6.2. Given a pair of face images taken at different times, we assign the comparison to the bin that is the arithmetic average of the subject's ages. This plot shows only the effect of age, not ageing. The number of comparisons in each bin is generally in the thousands, however the first and last bins are computed over 149 and 124 respectively. The error rates in some (adult) cases are zero, and in others the DET is flat so the error rates at the two thresholds are identical. The lines span 1% and 99% of boostrap replicated FNMR estimates.

Figure 799: For the visa images, the dots show FNMR by age group for two operating thresholds corresponding to FMR = $\{0.001, 0.0001\}$ computed over all on the order of 10^{10} impostor scores. The FMR in each bin will vary also - see subsequent impostor heatmaps in sec. 3.6.2. Given a pair of face images taken at different times, we assign the comparison to the bin that is the arithmetic average of the subject's ages. This plot shows only the effect of age, not ageing. The number of comparisons in each bin is generally in the thousands, however the first and last bins are computed over 149 and 124 respectively. The error rates in some (adult) cases are zero, and in others the DET is flat so the error rates at the two thresholds are identical. The lines span 1% and 99% of boostrap replicated FNMR estimates.

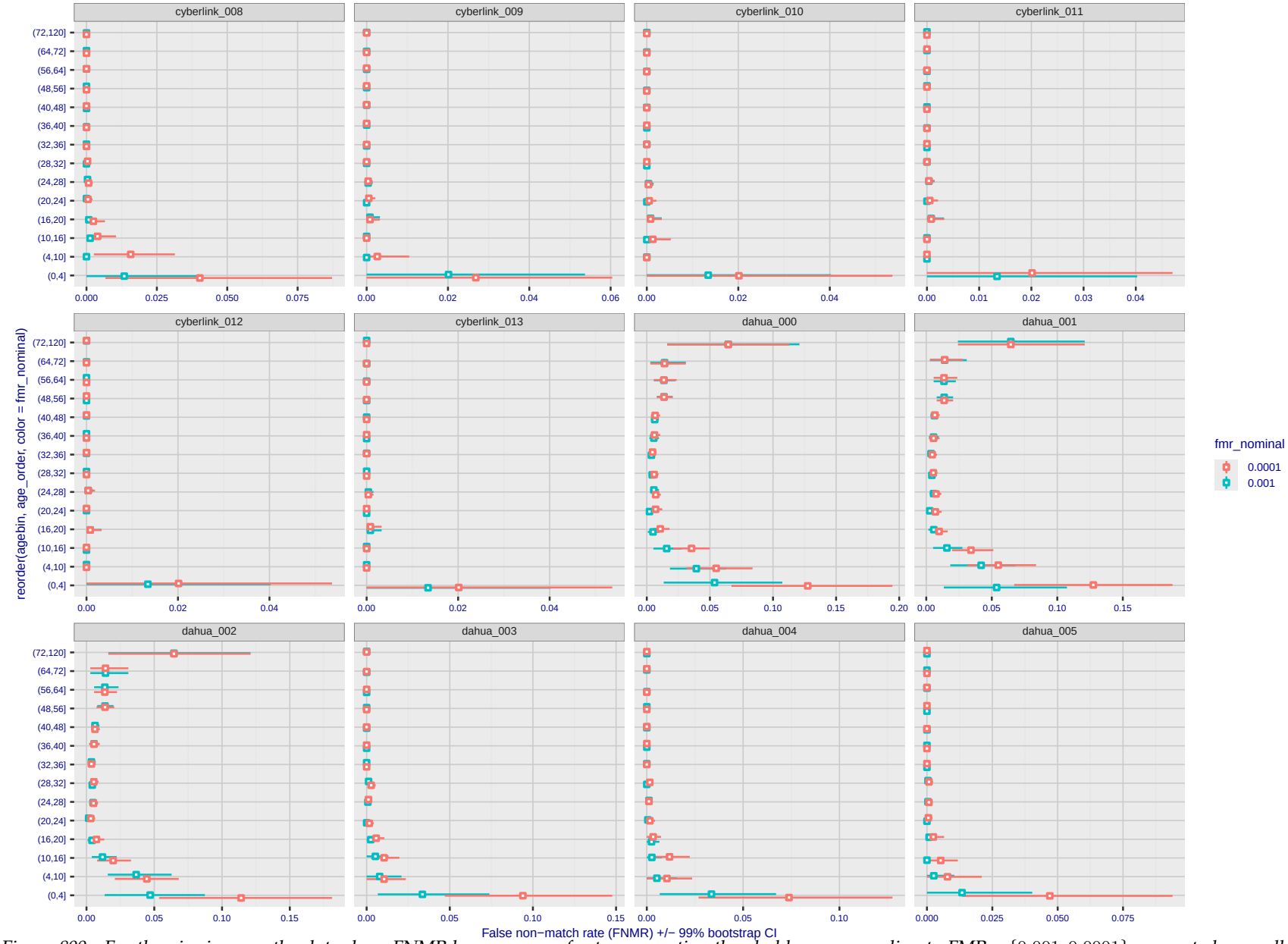

Figure 800: For the visa images, the dots show FNMR by age group for two operating thresholds corresponding to FMR = $\{0.001, 0.0001\}$ computed over all on the order of 10^{10} impostor scores. The FMR in each bin will vary also - see subsequent impostor heatmaps in sec. 3.6.2. Given a pair of face images taken at different times, we assign the comparison to the bin that is the arithmetic average of the subject's ages. This plot shows only the effect of age, not ageing. The number of comparisons in each bin is generally in the thousands, however the first and last bins are computed over 149 and 124 respectively. The error rates in some (adult) cases are zero, and in others the DET is flat so the error rates at the two thresholds are identical. The lines span 1% and 99% of boostrap replicated FNMR estimates.

Figure 801: For the visa images, the dots show FNMR by age group for two operating thresholds corresponding to FMR = $\{0.001, 0.0001\}$ computed over all on the order of 10^{10} impostor scores. The FMR in each bin will vary also - see subsequent impostor heatmaps in sec. 3.6.2. Given a pair of face images taken at different times, we assign the comparison to the bin that is the arithmetic average of the subject's ages. This plot shows only the effect of age, not ageing. The number of comparisons in each bin is generally in the thousands, however the first and last bins are computed over 149 and 124 respectively. The error rates in some (adult) cases are zero, and in others the DET is flat so the error rates at the two thresholds are identical. The lines span 1% and 99% of boostrap replicated FNMR estimates.

Figure 802: For the visa images, the dots show FNMR by age group for two operating thresholds corresponding to FMR = $\{0.001, 0.0001\}$ computed over all on the order of 10^{10} impostor scores. The FMR in each bin will vary also - see subsequent impostor heatmaps in sec. 3.6.2. Given a pair of face images taken at different times, we assign the comparison to the bin that is the arithmetic average of the subject's ages. This plot shows only the effect of age, not ageing. The number of comparisons in each bin is generally in the thousands, however the first and last bins are computed over 149 and 124 respectively. The error rates in some (adult) cases are zero, and in others the DET is flat so the error rates at the two thresholds are identical. The lines span 1% and 99% of boostrap replicated FNMR estimates.

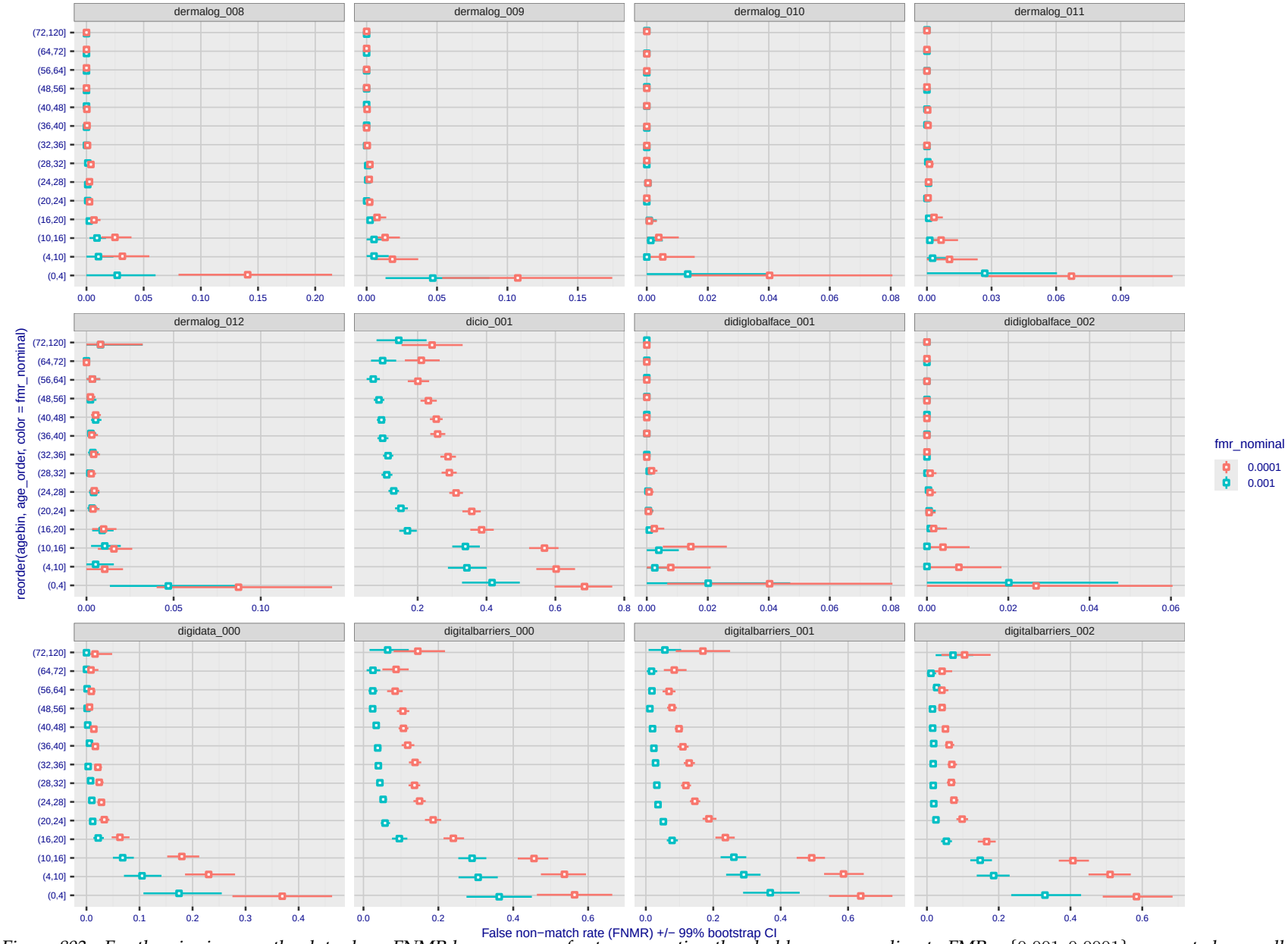

Figure 803: For the visa images, the dots show FNMR by age group for two operating thresholds corresponding to FMR = $\{0.001, 0.0001\}$ computed over all on the order of 10^{10} impostor scores. The FMR in each bin will vary also - see subsequent impostor heatmaps in sec. 3.6.2. Given a pair of face images taken at different times, we assign the comparison to the bin that is the arithmetic average of the subject's ages. This plot shows only the effect of age, not ageing. The number of comparisons in each bin is generally in the thousands, however the first and last bins are computed over 149 and 124 respectively. The error rates in some (adult) cases are zero, and in others the DET is flat so the error rates at the two thresholds are identical. The lines span 1% and 99% of boostrap replicated FNMR estimates.

Figure 804: For the visa images, the dots show FNMR by age group for two operating thresholds corresponding to FMR = $\{0.001, 0.0001\}$ computed over all on the order of 10^{10} impostor scores. The FMR in each bin will vary also - see subsequent impostor heatmaps in sec. 3.6.2. Given a pair of face images taken at different times, we assign the comparison to the bin that is the arithmetic average of the subject's ages. This plot shows only the effect of age, not ageing. The number of comparisons in each bin is generally in the thousands, however the first and last bins are computed over 149 and 124 respectively. The error rates in some (adult) cases are zero, and in others the DET is flat so the error rates at the two thresholds are identical. The lines span 1% and 99% of boostrap replicated FNMR estimates.

Figure 805: For the visa images, the dots show FNMR by age group for two operating thresholds corresponding to FMR = $\{0.001, 0.0001\}$ computed over all on the order of 10^{10} impostor scores. The FMR in each bin will vary also - see subsequent impostor heatmaps in sec. 3.6.2. Given a pair of face images taken at different times, we assign the comparison to the bin that is the arithmetic average of the subject's ages. This plot shows only the effect of age, not ageing. The number of comparisons in each bin is generally in the thousands, however the first and last bins are computed over 149 and 124 respectively. The error rates in some (adult) cases are zero, and in others the DET is flat so the error rates at the two thresholds are identical. The lines span 1% and 99% of boostrap replicated FNMR estimates.

Figure 806: For the visa images, the dots show FNMR by age group for two operating thresholds corresponding to FMR = $\{0.001, 0.0001\}$ computed over all on the order of 10^{10} impostor scores. The FMR in each bin will vary also - see subsequent impostor heatmaps in sec. 3.6.2. Given a pair of face images taken at different times, we assign the comparison to the bin that is the arithmetic average of the subject's ages. This plot shows only the effect of age, not ageing. The number of comparisons in each bin is generally in the thousands, however the first and last bins are computed over 149 and 124 respectively. The error rates in some (adult) cases are zero, and in others the DET is flat so the error rates at the two thresholds are identical. The lines span 1% and 99% of boostrap replicated FNMR estimates.

Figure 807: For the visa images, the dots show FNMR by age group for two operating thresholds corresponding to FMR = $\{0.001, 0.0001\}$ computed over all on the order of 10^{10} impostor scores. The FMR in each bin will vary also - see subsequent impostor heatmaps in sec. 3.6.2. Given a pair of face images taken at different times, we assign the comparison to the bin that is the arithmetic average of the subject's ages. This plot shows only the effect of age, not ageing. The number of comparisons in each bin is generally in the thousands, however the first and last bins are computed over 149 and 124 respectively. The error rates in some (adult) cases are zero, and in others the DET is flat so the error rates at the two thresholds are identical. The lines span 1% and 99% of boostrap replicated FNMR estimates.

Figure 808: For the visa images, the dots show FNMR by age group for two operating thresholds corresponding to FMR = $\{0.001, 0.0001\}$ computed over all on the order of 10^{10} impostor scores. The FMR in each bin will vary also - see subsequent impostor heatmaps in sec. 3.6.2. Given a pair of face images taken at different times, we assign the comparison to the bin that is the arithmetic average of the subject's ages. This plot shows only the effect of age, not ageing. The number of comparisons in each bin is generally in the thousands, however the first and last bins are computed over 149 and 124 respectively. The error rates in some (adult) cases are zero, and in others the DET is flat so the error rates at the two thresholds are identical. The lines span 1% and 99% of boostrap replicated FNMR estimates.

Figure 809: For the visa images, the dots show FNMR by age group for two operating thresholds corresponding to FMR = $\{0.001, 0.0001\}$ computed over all on the order of 10^{10} impostor scores. The FMR in each bin will vary also - see subsequent impostor heatmaps in sec. 3.6.2. Given a pair of face images taken at different times, we assign the comparison to the bin that is the arithmetic average of the subject's ages. This plot shows only the effect of age, not ageing. The number of comparisons in each bin is generally in the thousands, however the first and last bins are computed over 149 and 124 respectively. The error rates in some (adult) cases are zero, and in others the DET is flat so the error rates at the two thresholds are identical. The lines span 1% and 99% of boostrap replicated FNMR estimates.

Figure 810: For the visa images, the dots show FNMR by age group for two operating thresholds corresponding to FMR = $\{0.001, 0.0001\}$ computed over all on the order of 10^{10} impostor scores. The FMR in each bin will vary also - see subsequent impostor heatmaps in sec. 3.6.2. Given a pair of face images taken at different times, we assign the comparison to the bin that is the arithmetic average of the subject's ages. This plot shows only the effect of age, not ageing. The number of comparisons in each bin is generally in the thousands, however the first and last bins are computed over 149 and 124 respectively. The error rates in some (adult) cases are zero, and in others the DET is flat so the error rates at the two thresholds are identical. The lines span 1% and 99% of boostrap replicated FNMR estimates.

Figure 811: For the visa images, the dots show FNMR by age group for two operating thresholds corresponding to FMR = $\{0.001, 0.0001\}$ computed over all on the order of 10^{10} impostor scores. The FMR in each bin will vary also - see subsequent impostor heatmaps in sec. 3.6.2. Given a pair of face images taken at different times, we assign the comparison to the bin that is the arithmetic average of the subject's ages. This plot shows only the effect of age, not ageing. The number of comparisons in each bin is generally in the thousands, however the first and last bins are computed over 149 and 124 respectively. The error rates in some (adult) cases are zero, and in others the DET is flat so the error rates at the two thresholds are identical. The lines span 1% and 99% of boostrap replicated FNMR estimates.

Figure 812: For the visa images, the dots show FNMR by age group for two operating thresholds corresponding to FMR = $\{0.001, 0.0001\}$ computed over all on the order of 10^{10} impostor scores. The FMR in each bin will vary also - see subsequent impostor heatmaps in sec. 3.6.2. Given a pair of face images taken at different times, we assign the comparison to the bin that is the arithmetic average of the subject's ages. This plot shows only the effect of age, not ageing. The number of comparisons in each bin is generally in the thousands, however the first and last bins are computed over 149 and 124 respectively. The error rates in some (adult) cases are zero, and in others the DET is flat so the error rates at the two thresholds are identical. The lines span 1% and 99% of boostrap replicated FNMR estimates.

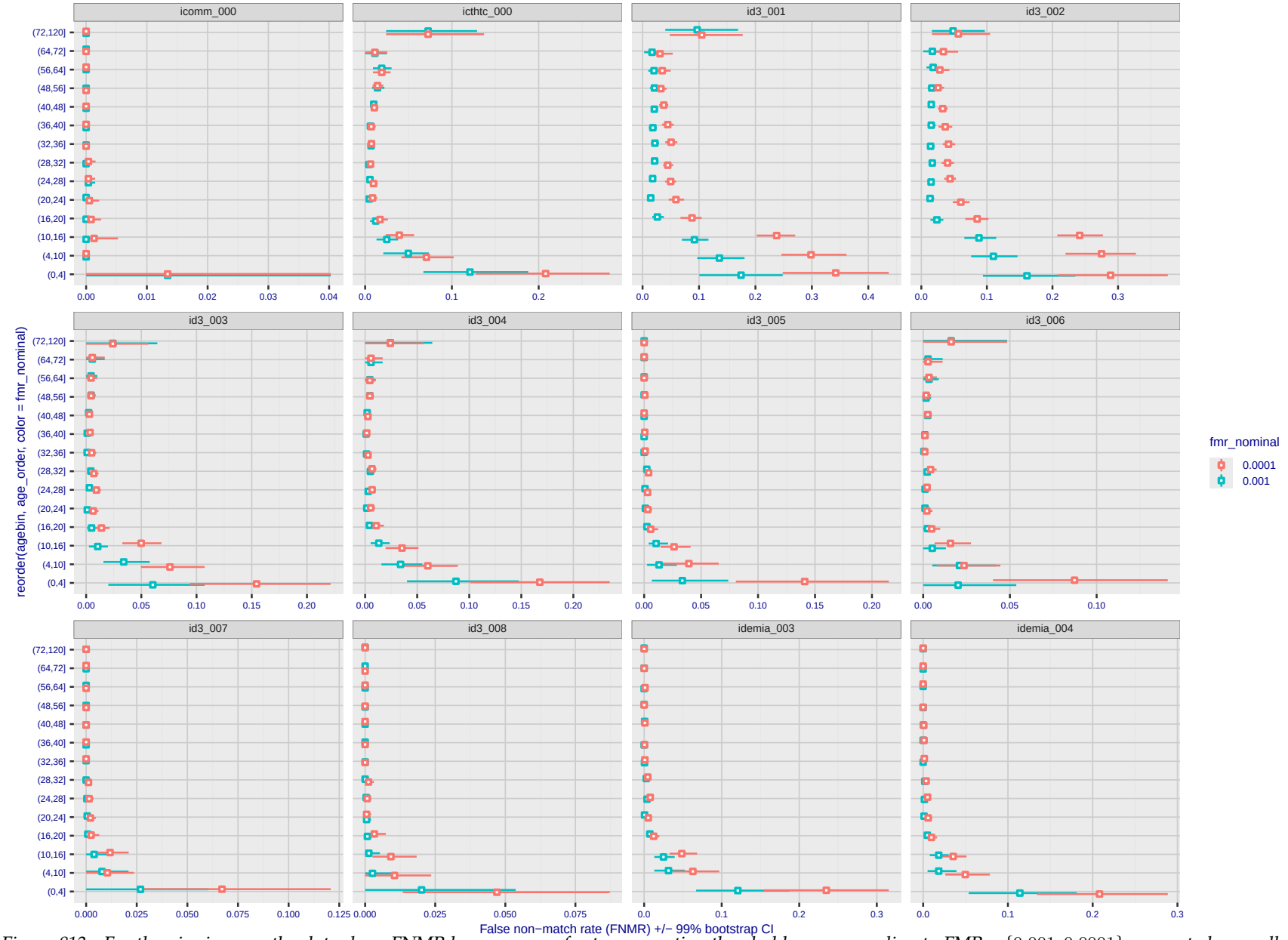

Figure 813: For the visa images, the dots show FNMR by age group for two operating thresholds corresponding to FMR = $\{0.001, 0.0001\}$ computed over all on the order of 10^{10} impostor scores. The FMR in each bin will vary also - see subsequent impostor heatmaps in sec. 3.6.2. Given a pair of face images taken at different times, we assign the comparison to the bin that is the arithmetic average of the subject's ages. This plot shows only the effect of age, not ageing. The number of comparisons in each bin is generally in the thousands, however the first and last bins are computed over 149 and 124 respectively. The error rates in some (adult) cases are zero, and in others the DET is flat so the error rates at the two thresholds are identical. The lines span 1% and 99% of boostrap replicated FNMR estimates.

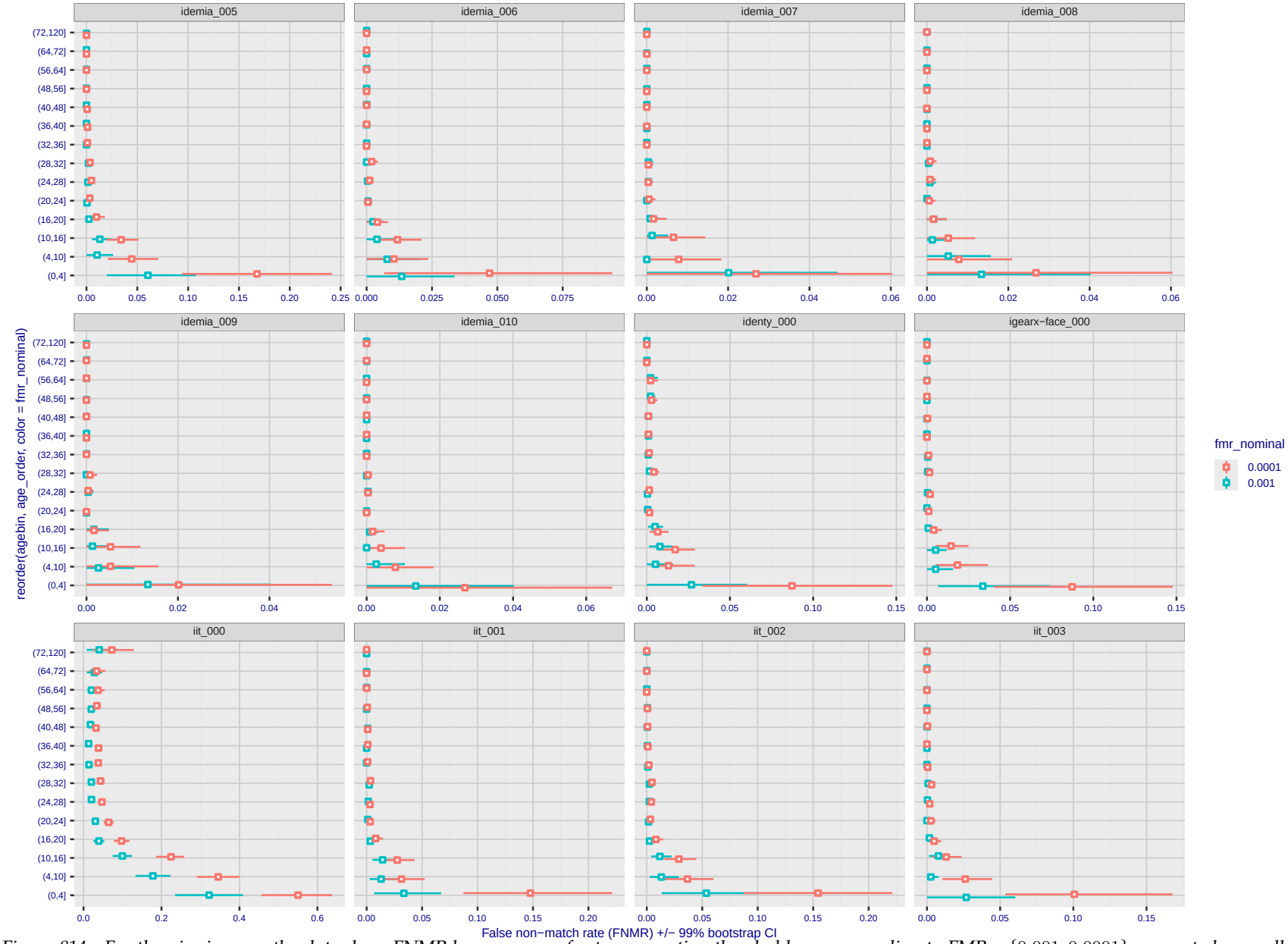

Figure 814: For the visa images, the dots show FNMR by age group for two operating thresholds corresponding to FMR = $\{0.001, 0.0001\}$ computed over all on the order of 10^{10} impostor scores. The FMR in each bin will vary also - see subsequent impostor heatmaps in sec. 3.6.2. Given a pair of face images taken at different times, we assign the comparison to the bin that is the arithmetic average of the subject's ages. This plot shows only the effect of age, not ageing. The number of comparisons in each bin is generally in the thousands, however the first and last bins are computed over 149 and 124 respectively. The error rates in some (adult) cases are zero, and in others the DET is flat so the error rates at the two thresholds are identical. The lines span 1% and 99% of boostrap replicated FNMR estimates.

Figure 815: For the visa images, the dots show FNMR by age group for two operating thresholds corresponding to FMR = $\{0.001, 0.0001\}$ computed over all on the order of 10^{10} impostor scores. The FMR in each bin will vary also - see subsequent impostor heatmaps in sec. 3.6.2. Given a pair of face images taken at different times, we assign the comparison to the bin that is the arithmetic average of the subject's ages. This plot shows only the effect of age, not ageing. The number of comparisons in each bin is generally in the thousands, however the first and last bins are computed over 149 and 124 respectively. The error rates in some (adult) cases are zero, and in others the DET is flat so the error rates at the two thresholds are identical. The lines span 1% and 99% of boostrap replicated FNMR estimates.

Figure 816: For the visa images, the dots show FNMR by age group for two operating thresholds corresponding to FMR = $\{0.001, 0.0001\}$ computed over all on the order of 10^{10} impostor scores. The FMR in each bin will vary also - see subsequent impostor heatmaps in sec. 3.6.2. Given a pair of face images taken at different times, we assign the comparison to the bin that is the arithmetic average of the subject's ages. This plot shows only the effect of age, not ageing. The number of comparisons in each bin is generally in the thousands, however the first and last bins are computed over 149 and 124 respectively. The error rates in some (adult) cases are zero, and in others the DET is flat so the error rates at the two thresholds are identical. The lines span 1% and 99% of boostrap replicated FNMR estimates.

Figure 817: For the visa images, the dots show FNMR by age group for two operating thresholds corresponding to FMR = $\{0.001, 0.0001\}$ computed over all on the order of 10^{10} impostor scores. The FMR in each bin will vary also - see subsequent impostor heatmaps in sec. 3.6.2. Given a pair of face images taken at different times, we assign the comparison to the bin that is the arithmetic average of the subject's ages. This plot shows only the effect of age, not ageing. The number of comparisons in each bin is generally in the thousands, however the first and last bins are computed over 149 and 124 respectively. The error rates in some (adult) cases are zero, and in others the DET is flat so the error rates at the two thresholds are identical. The lines span 1% and 99% of boostrap replicated FNMR estimates.

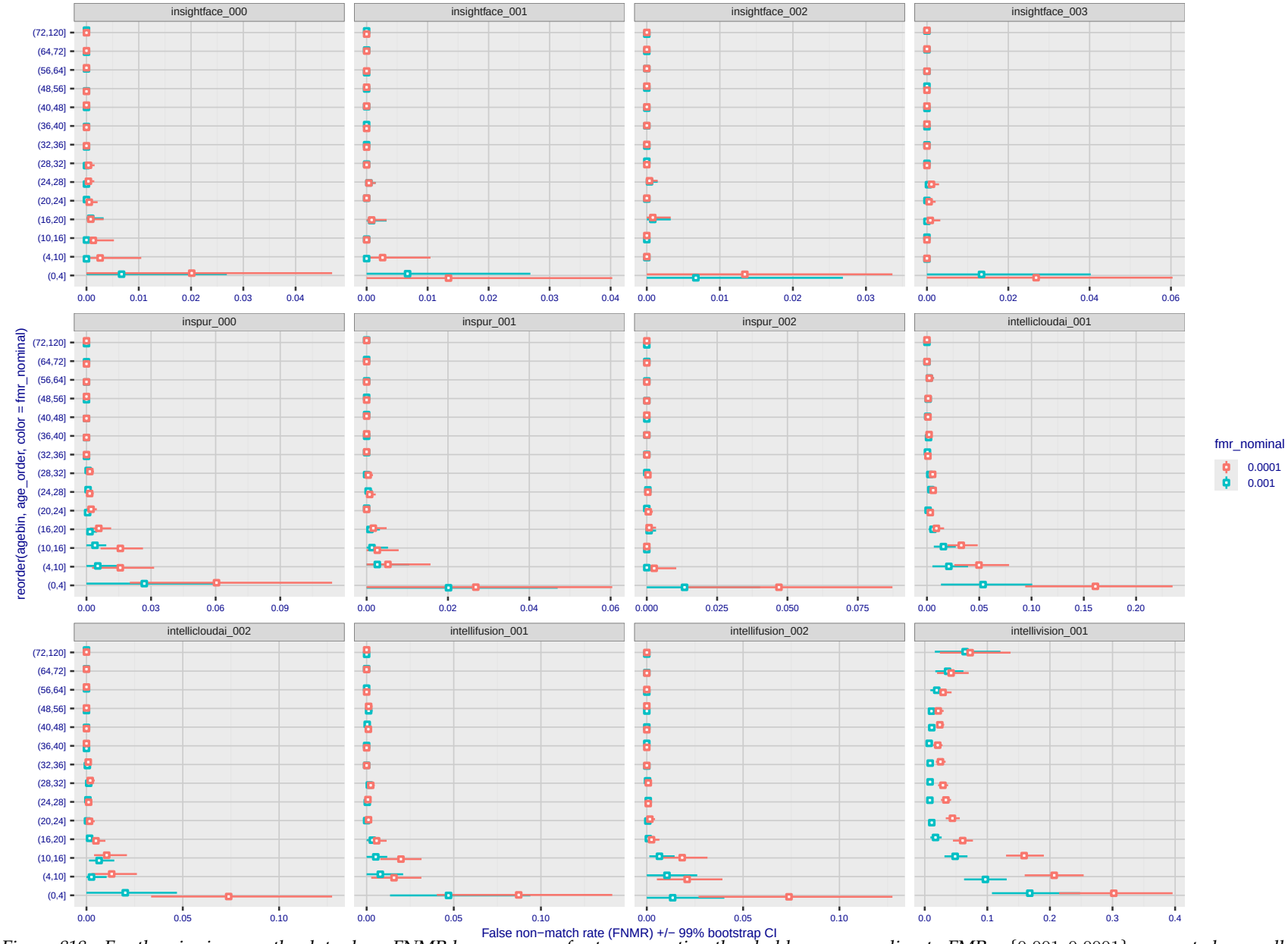

Figure 818: For the visa images, the dots show FNMR by age group for two operating thresholds corresponding to FMR = $\{0.001, 0.0001\}$ computed over all on the order of 10^{10} impostor scores. The FMR in each bin will vary also - see subsequent impostor heatmaps in sec. 3.6.2. Given a pair of face images taken at different times, we assign the comparison to the bin that is the arithmetic average of the subject's ages. This plot shows only the effect of age, not ageing. The number of comparisons in each bin is generally in the thousands, however the first and last bins are computed over 149 and 124 respectively. The error rates in some (adult) cases are zero, and in others the DET is flat so the error rates at the two thresholds are identical. The lines span 1% and 99% of boostrap replicated FNMR estimates.

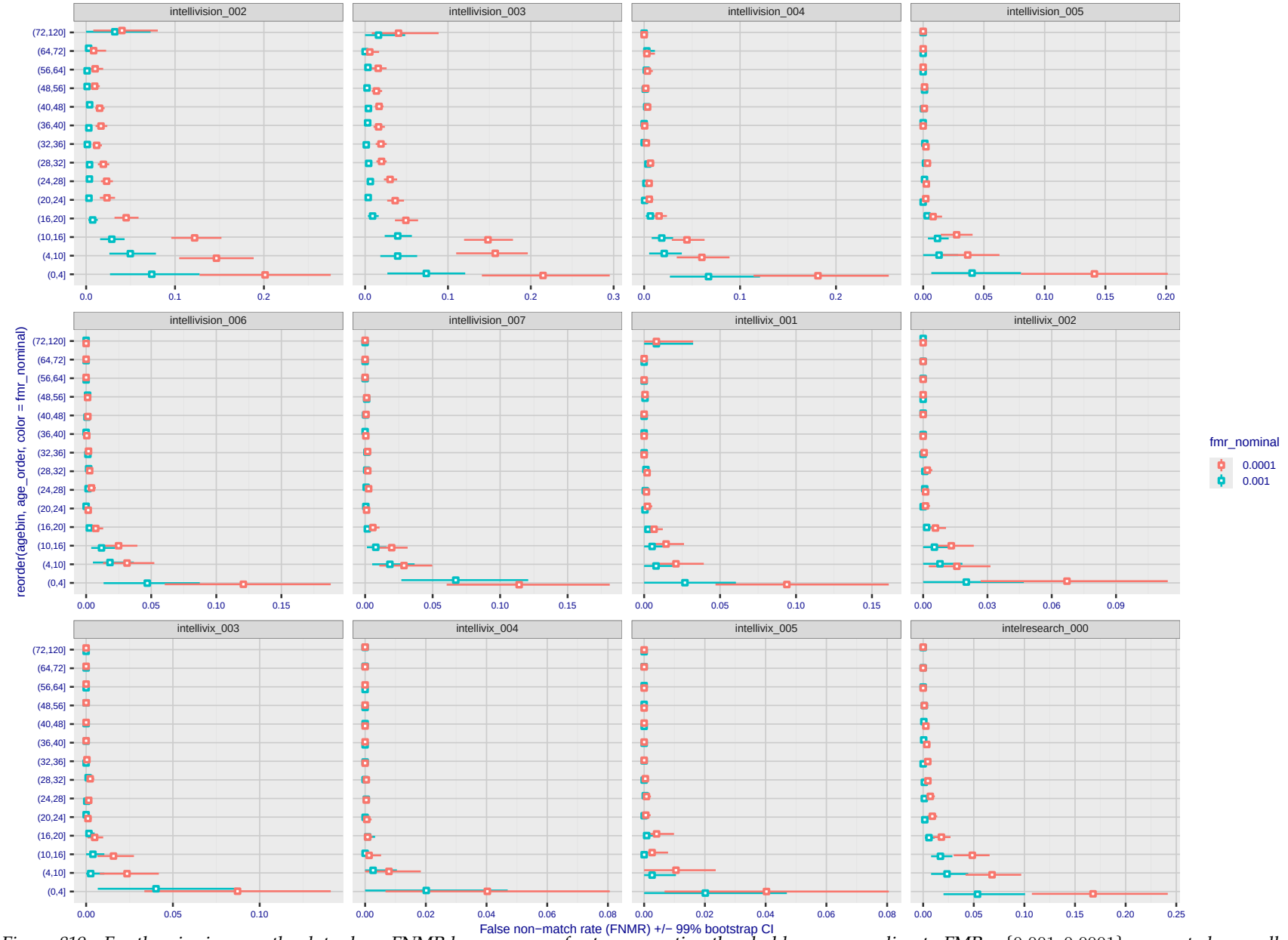

Figure 819: For the visa images, the dots show FNMR by age group for two operating thresholds corresponding to FMR = $\{0.001, 0.0001\}$ computed over all on the order of 10^{10} impostor scores. The FMR in each bin will vary also - see subsequent impostor heatmaps in sec. 3.6.2. Given a pair of face images taken at different times, we assign the comparison to the bin that is the arithmetic average of the subject's ages. This plot shows only the effect of age, not ageing. The number of comparisons in each bin is generally in the thousands, however the first and last bins are computed over 149 and 124 respectively. The error rates in some (adult) cases are zero, and in others the DET is flat so the error rates at the two thresholds are identical. The lines span 1% and 99% of boostrap replicated FNMR estimates.

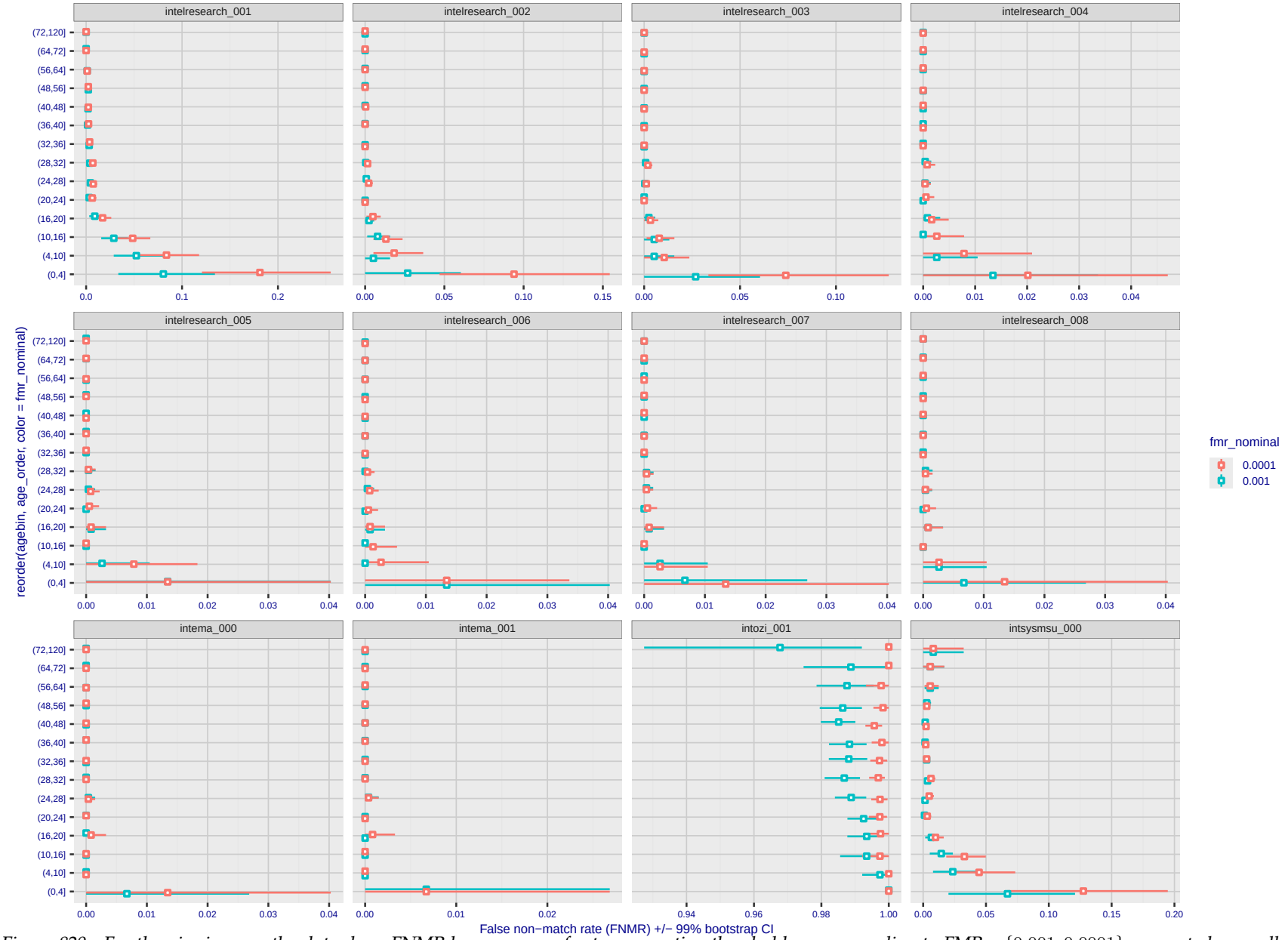

Figure 820: For the visa images, the dots show FNMR by age group for two operating thresholds corresponding to FMR = $\{0.001, 0.0001\}$ computed over all on the order of 10^{10} impostor scores. The FMR in each bin will vary also - see subsequent impostor heatmaps in sec. 3.6.2. Given a pair of face images taken at different times, we assign the comparison to the bin that is the arithmetic average of the subject's ages. This plot shows only the effect of age, not ageing. The number of comparisons in each bin is generally in the thousands, however the first and last bins are computed over 149 and 124 respectively. The error rates in some (adult) cases are zero, and in others the DET is flat so the error rates at the two thresholds are identical. The lines span 1% and 99% of boostrap replicated FNMR estimates.

Figure 821: For the visa images, the dots show FNMR by age group for two operating thresholds corresponding to FMR = $\{0.001, 0.0001\}$ computed over all on the order of 10^{10} impostor scores. The FMR in each bin will vary also - see subsequent impostor heatmaps in sec. 3.6.2. Given a pair of face images taken at different times, we assign the comparison to the bin that is the arithmetic average of the subject's ages. This plot shows only the effect of age, not ageing. The number of comparisons in each bin is generally in the thousands, however the first and last bins are computed over 149 and 124 respectively. The error rates in some (adult) cases are zero, and in others the DET is flat so the error rates at the two thresholds are identical. The lines span 1% and 99% of boostrap replicated FNMR estimates.

Figure 822: For the visa images, the dots show FNMR by age group for two operating thresholds corresponding to FMR = $\{0.001, 0.0001\}$ computed over all on the order of 10^{10} impostor scores. The FMR in each bin will vary also - see subsequent impostor heatmaps in sec. 3.6.2. Given a pair of face images taken at different times, we assign the comparison to the bin that is the arithmetic average of the subject's ages. This plot shows only the effect of age, not ageing. The number of comparisons in each bin is generally in the thousands, however the first and last bins are computed over 149 and 124 respectively. The error rates in some (adult) cases are zero, and in others the DET is flat so the error rates at the two thresholds are identical. The lines span 1% and 99% of boostrap replicated FNMR estimates.

Figure 823: For the visa images, the dots show FNMR by age group for two operating thresholds corresponding to FMR = $\{0.001, 0.0001\}$ computed over all on the order of 10^{10} impostor scores. The FMR in each bin will vary also - see subsequent impostor heatmaps in sec. 3.6.2. Given a pair of face images taken at different times, we assign the comparison to the bin that is the arithmetic average of the subject's ages. This plot shows only the effect of age, not ageing. The number of comparisons in each bin is generally in the thousands, however the first and last bins are computed over 149 and 124 respectively. The error rates in some (adult) cases are zero, and in others the DET is flat so the error rates at the two thresholds are identical. The lines span 1% and 99% of boostrap replicated FNMR estimates.

Figure 824: For the visa images, the dots show FNMR by age group for two operating thresholds corresponding to FMR = $\{0.001, 0.0001\}$ computed over all on the order of 10^{10} impostor scores. The FMR in each bin will vary also - see subsequent impostor heatmaps in sec. 3.6.2. Given a pair of face images taken at different times, we assign the comparison to the bin that is the arithmetic average of the subject's ages. This plot shows only the effect of age, not ageing. The number of comparisons in each bin is generally in the thousands, however the first and last bins are computed over 149 and 124 respectively. The error rates in some (adult) cases are zero, and in others the DET is flat so the error rates at the two thresholds are identical. The lines span 1% and 99% of boostrap replicated FNMR estimates.

Figure 825: For the visa images, the dots show FNMR by age group for two operating thresholds corresponding to FMR = $\{0.001, 0.0001\}$ computed over all on the order of 10^{10} impostor scores. The FMR in each bin will vary also - see subsequent impostor heatmaps in sec. 3.6.2. Given a pair of face images taken at different times, we assign the comparison to the bin that is the arithmetic average of the subject's ages. This plot shows only the effect of age, not ageing. The number of comparisons in each bin is generally in the thousands, however the first and last bins are computed over 149 and 124 respectively. The error rates in some (adult) cases are zero, and in others the DET is flat so the error rates at the two thresholds are identical. The lines span 1% and 99% of boostrap replicated FNMR estimates.

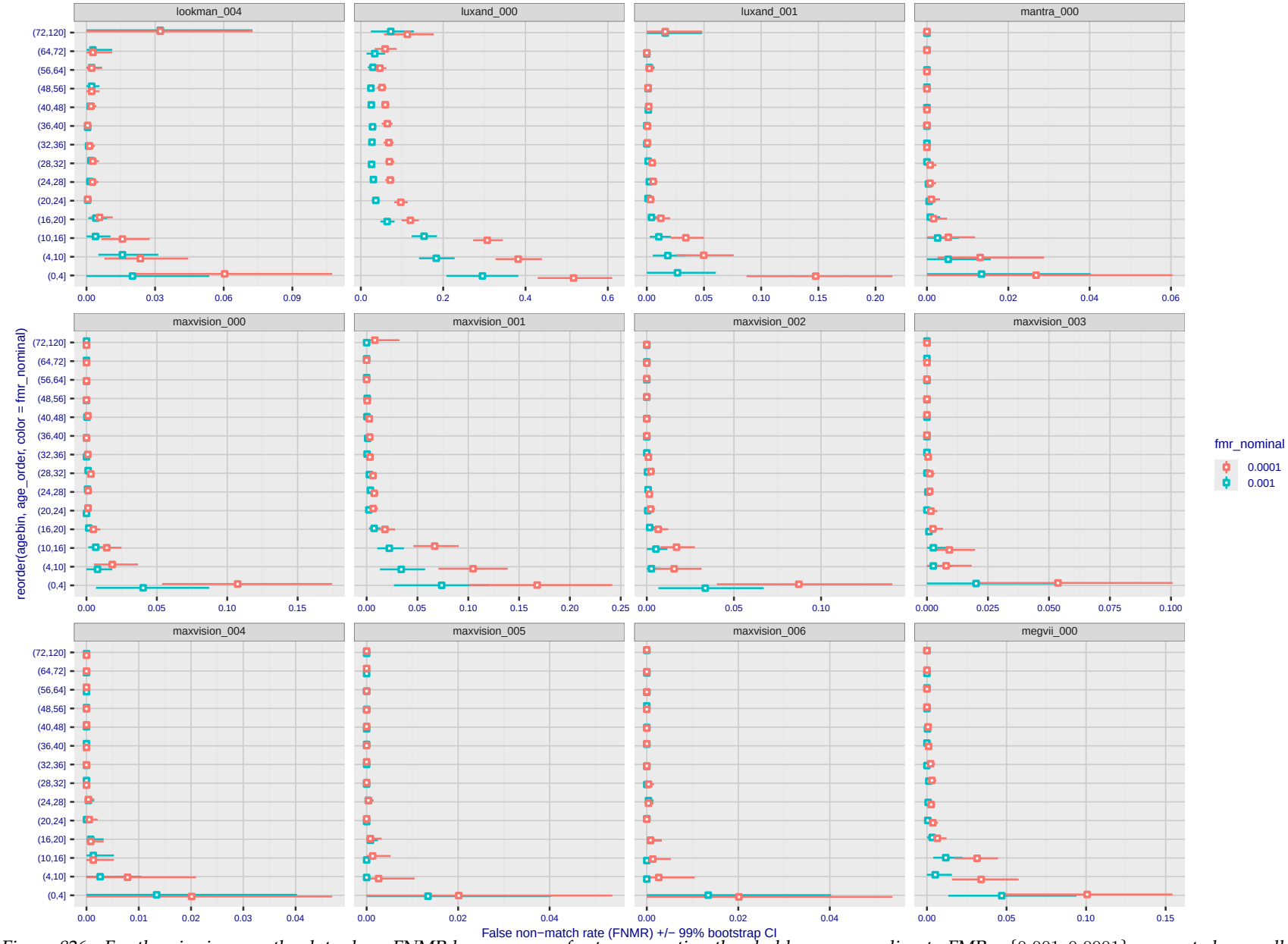

Figure 826: For the visa images, the dots show FNMR by age group for two operating thresholds corresponding to FMR = $\{0.001, 0.0001\}$ computed over all on the order of 10^{10} impostor scores. The FMR in each bin will vary also - see subsequent impostor heatmaps in sec. 3.6.2. Given a pair of face images taken at different times, we assign the comparison to the bin that is the arithmetic average of the subject's ages. This plot shows only the effect of age, not ageing. The number of comparisons in each bin is generally in the thousands, however the first and last bins are computed over 149 and 124 respectively. The error rates in some (adult) cases are zero, and in others the DET is flat so the error rates at the two thresholds are identical. The lines span 1% and 99% of boostrap replicated FNMR estimates.

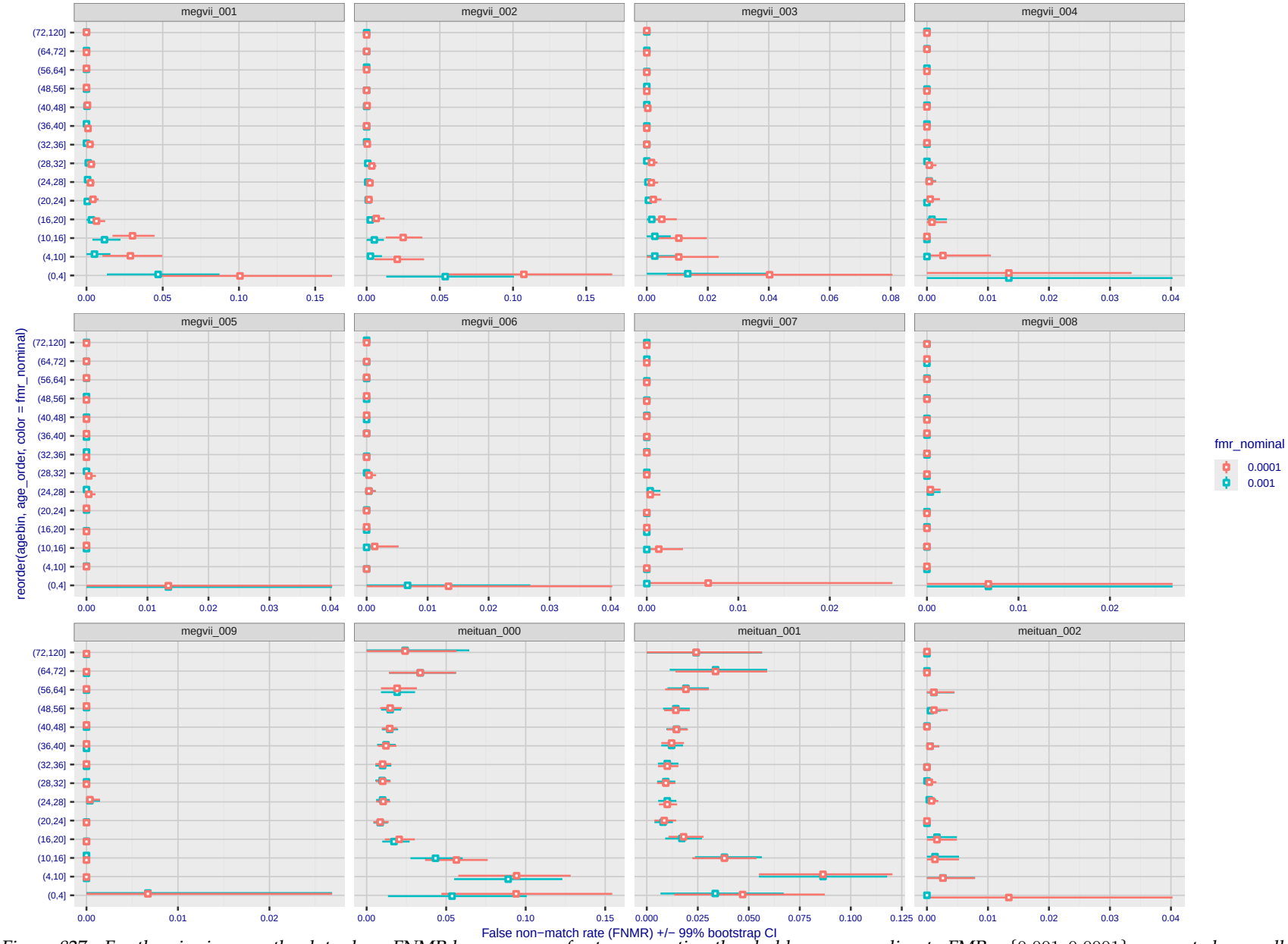

Figure 827: For the visa images, the dots show FNMR by age group for two operating thresholds corresponding to FMR = $\{0.001, 0.0001\}$ computed over all on the order of 10^{10} impostor scores. The FMR in each bin will vary also - see subsequent impostor heatmaps in sec. 3.6.2. Given a pair of face images taken at different times, we assign the comparison to the bin that is the arithmetic average of the subject's ages. This plot shows only the effect of age, not ageing. The number of comparisons in each bin is generally in the thousands, however the first and last bins are computed over 149 and 124 respectively. The error rates in some (adult) cases are zero, and in others the DET is flat so the error rates at the two thresholds are identical. The lines span 1% and 99% of boostrap replicated FNMR estimates.

Figure 828: For the visa images, the dots show FNMR by age group for two operating thresholds corresponding to FMR = $\{0.001, 0.0001\}$ computed over all on the order of 10^{10} impostor scores. The FMR in each bin will vary also - see subsequent impostor heatmaps in sec. 3.6.2. Given a pair of face images taken at different times, we assign the comparison to the bin that is the arithmetic average of the subject's ages. This plot shows only the effect of age, not ageing. The number of comparisons in each bin is generally in the thousands, however the first and last bins are computed over 149 and 124 respectively. The error rates in some (adult) cases are zero, and in others the DET is flat so the error rates at the two thresholds are identical. The lines span 1% and 99% of boostrap replicated FNMR estimates.

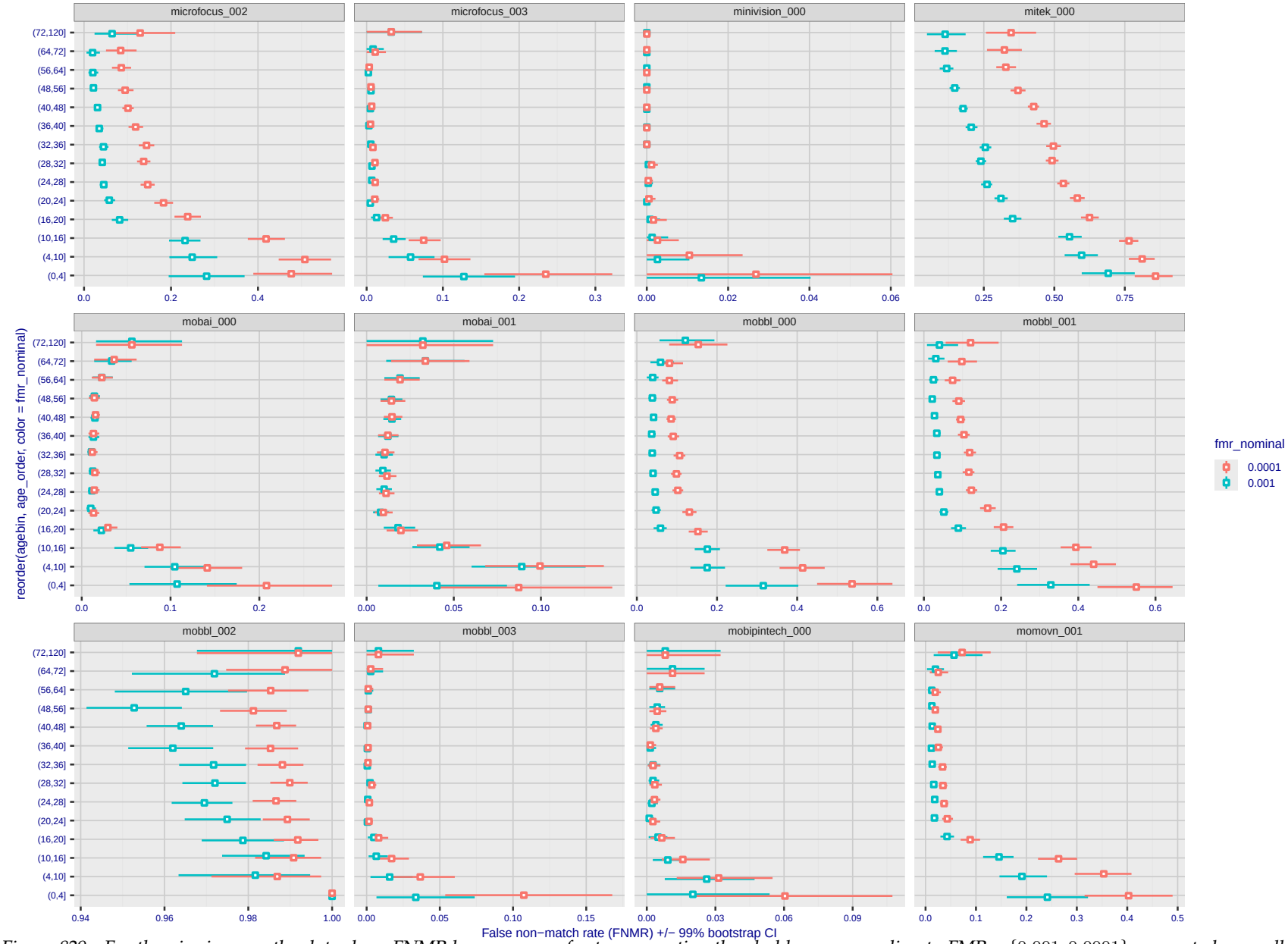

Figure 829: For the visa images, the dots show FNMR by age group for two operating thresholds corresponding to FMR = $\{0.001, 0.0001\}$ computed over all on the order of 10^{10} impostor scores. The FMR in each bin will vary also - see subsequent impostor heatmaps in sec. 3.6.2. Given a pair of face images taken at different times, we assign the comparison to the bin that is the arithmetic average of the subject's ages. This plot shows only the effect of age, not ageing. The number of comparisons in each bin is generally in the thousands, however the first and last bins are computed over 149 and 124 respectively. The error rates in some (adult) cases are zero, and in others the DET is flat so the error rates at the two thresholds are identical. The lines span 1% and 99% of boostrap replicated FNMR estimates.

Figure 830: For the visa images, the dots show FNMR by age group for two operating thresholds corresponding to FMR = $\{0.001, 0.0001\}$ computed over all on the order of 10^{10} impostor scores. The FMR in each bin will vary also - see subsequent impostor heatmaps in sec. 3.6.2. Given a pair of face images taken at different times, we assign the comparison to the bin that is the arithmetic average of the subject's ages. This plot shows only the effect of age, not ageing. The number of comparisons in each bin is generally in the thousands, however the first and last bins are computed over 149 and 124 respectively. The error rates in some (adult) cases are zero, and in others the DET is flat so the error rates at the two thresholds are identical. The lines span 1% and 99% of boostrap replicated FNMR estimates.

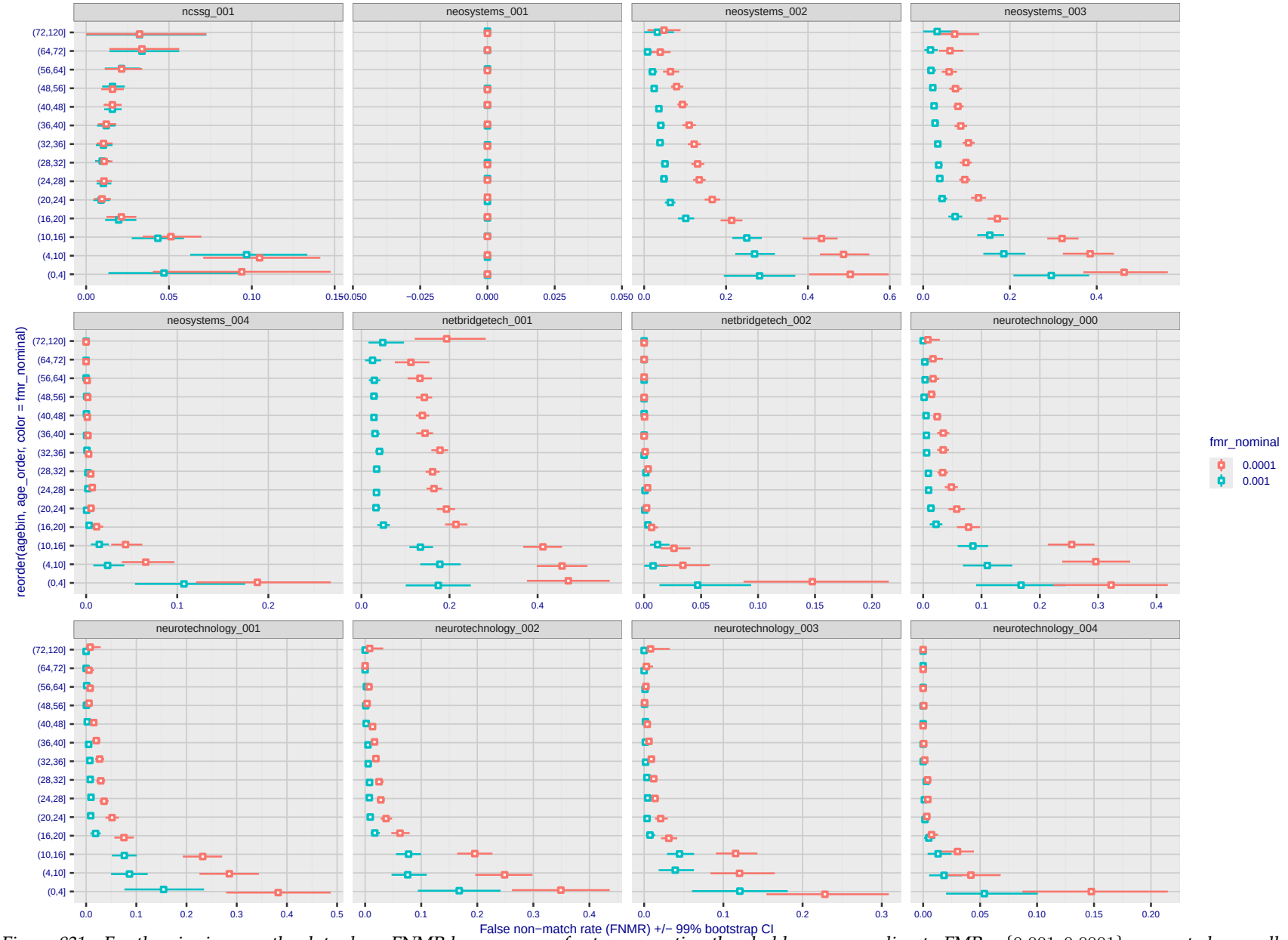

Figure 831: For the visa images, the dots show FNMR by age group for two operating thresholds corresponding to FMR = $\{0.001, 0.0001\}$ computed over all on the order of 10^{10} impostor scores. The FMR in each bin will vary also - see subsequent impostor heatmaps in sec. 3.6.2. Given a pair of face images taken at different times, we assign the comparison to the bin that is the arithmetic average of the subject's ages. This plot shows only the effect of age, not ageing. The number of comparisons in each bin is generally in the thousands, however the first and last bins are computed over 149 and 124 respectively. The error rates in some (adult) cases are zero, and in others the DET is flat so the error rates at the two thresholds are identical. The lines span 1% and 99% of boostrap replicated FNMR estimates.

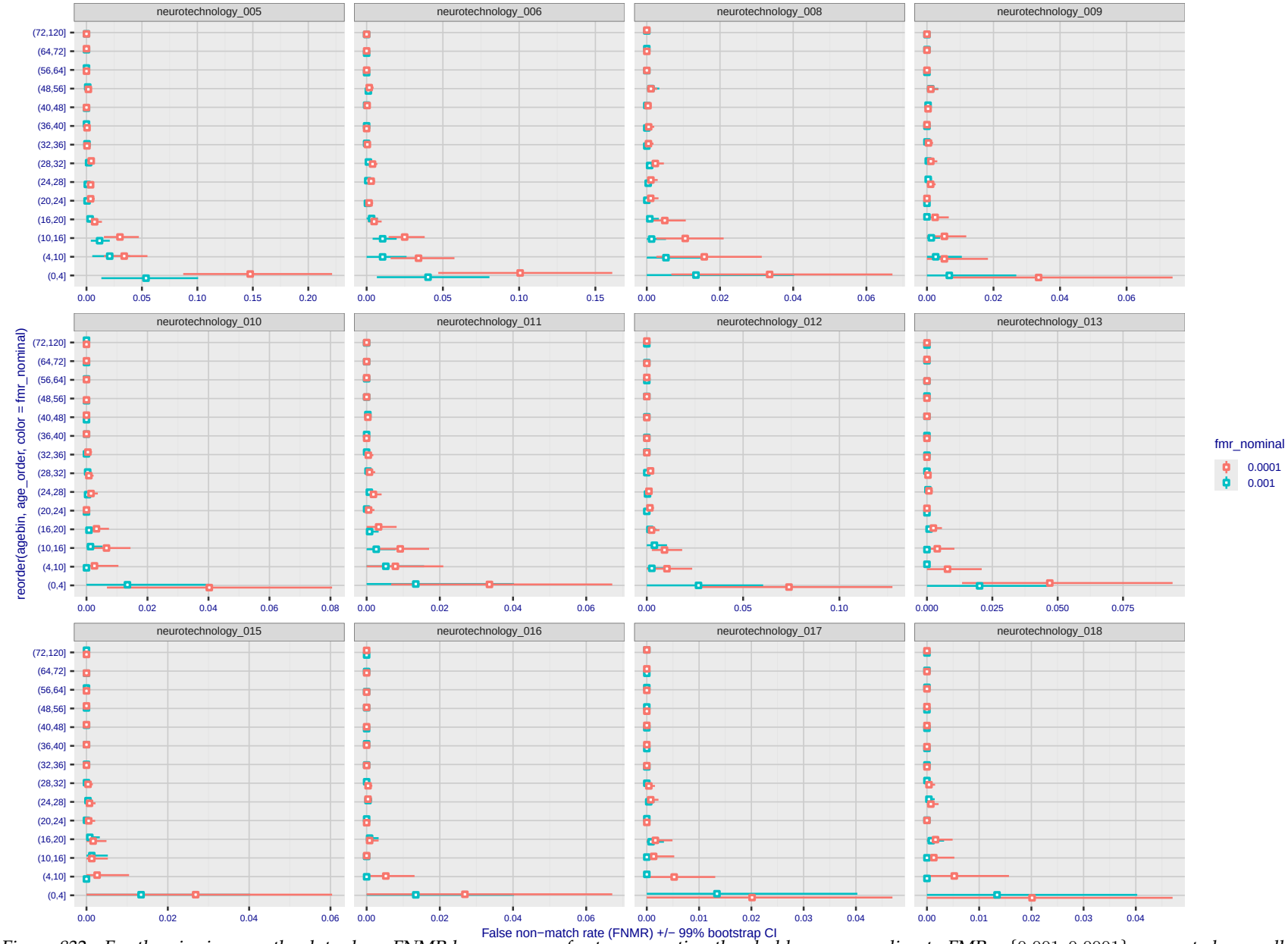

Figure 832: For the visa images, the dots show FNMR by age group for two operating thresholds corresponding to FMR = $\{0.001, 0.0001\}$ computed over all on the order of 10^{10} impostor scores. The FMR in each bin will vary also - see subsequent impostor heatmaps in sec. 3.6.2. Given a pair of face images taken at different times, we assign the comparison to the bin that is the arithmetic average of the subject's ages. This plot shows only the effect of age, not ageing. The number of comparisons in each bin is generally in the thousands, however the first and last bins are computed over 149 and 124 respectively. The error rates in some (adult) cases are zero, and in others the DET is flat so the error rates at the two thresholds are identical. The lines span 1% and 99% of boostrap replicated FNMR estimates.

Figure 833: For the visa images, the dots show FNMR by age group for two operating thresholds corresponding to FMR = $\{0.001, 0.0001\}$ computed over all on the order of 10^{10} impostor scores. The FMR in each bin will vary also - see subsequent impostor heatmaps in sec. 3.6.2. Given a pair of face images taken at different times, we assign the comparison to the bin that is the arithmetic average of the subject's ages. This plot shows only the effect of age, not ageing. The number of comparisons in each bin is generally in the thousands, however the first and last bins are computed over 149 and 124 respectively. The error rates in some (adult) cases are zero, and in others the DET is flat so the error rates at the two thresholds are identical. The lines span 1% and 99% of boostrap replicated FNMR estimates.

Figure 834: For the visa images, the dots show FNMR by age group for two operating thresholds corresponding to FMR = $\{0.001, 0.0001\}$ computed over all on the order of 10^{10} impostor scores. The FMR in each bin will vary also - see subsequent impostor heatmaps in sec. 3.6.2. Given a pair of face images taken at different times, we assign the comparison to the bin that is the arithmetic average of the subject's ages. This plot shows only the effect of age, not ageing. The number of comparisons in each bin is generally in the thousands, however the first and last bins are computed over 149 and 124 respectively. The error rates in some (adult) cases are zero, and in others the DET is flat so the error rates at the two thresholds are identical. The lines span 1% and 99% of boostrap replicated FNMR estimates.

Figure 835: For the visa images, the dots show FNMR by age group for two operating thresholds corresponding to FMR = $\{0.001, 0.0001\}$ computed over all on the order of 10^{10} impostor scores. The FMR in each bin will vary also - see subsequent impostor heatmaps in sec. 3.6.2. Given a pair of face images taken at different times, we assign the comparison to the bin that is the arithmetic average of the subject's ages. This plot shows only the effect of age, not ageing. The number of comparisons in each bin is generally in the thousands, however the first and last bins are computed over 149 and 124 respectively. The error rates in some (adult) cases are zero, and in others the DET is flat so the error rates at the two thresholds are identical. The lines span 1% and 99% of boostrap replicated FNMR estimates.

Figure 836: For the visa images, the dots show FNMR by age group for two operating thresholds corresponding to FMR = $\{0.001, 0.0001\}$ computed over all on the order of 10^{10} impostor scores. The FMR in each bin will vary also - see subsequent impostor heatmaps in sec. 3.6.2. Given a pair of face images taken at different times, we assign the comparison to the bin that is the arithmetic average of the subject's ages. This plot shows only the effect of age, not ageing. The number of comparisons in each bin is generally in the thousands, however the first and last bins are computed over 149 and 124 respectively. The error rates in some (adult) cases are zero, and in others the DET is flat so the error rates at the two thresholds are identical. The lines span 1% and 99% of boostrap replicated FNMR estimates.

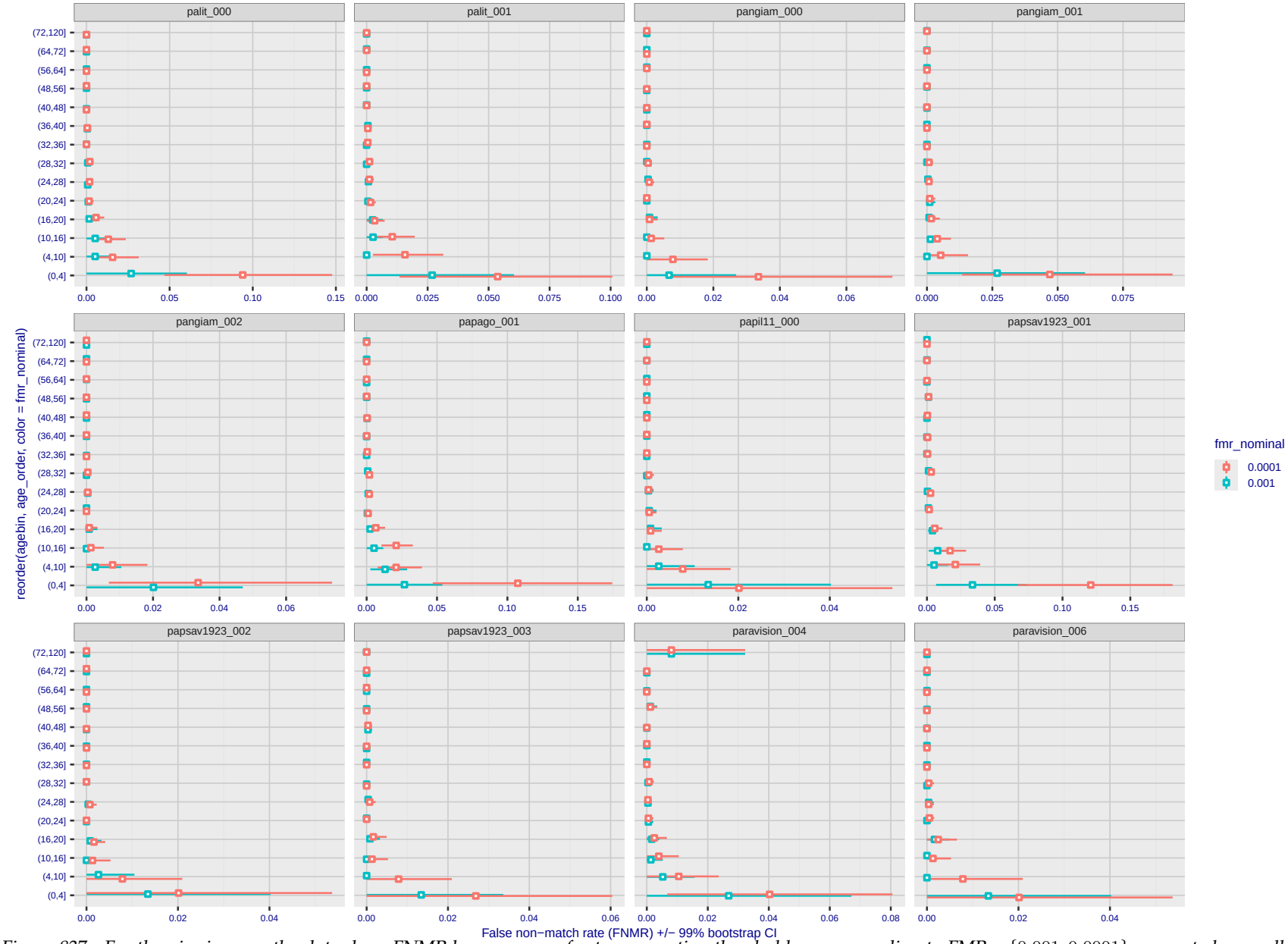

Figure 837: For the visa images, the dots show FNMR by age group for two operating thresholds corresponding to FMR = $\{0.001, 0.0001\}$ computed over all on the order of 10^{10} impostor scores. The FMR in each bin will vary also - see subsequent impostor heatmaps in sec. 3.6.2. Given a pair of face images taken at different times, we assign the comparison to the bin that is the arithmetic average of the subject's ages. This plot shows only the effect of age, not ageing. The number of comparisons in each bin is generally in the thousands, however the first and last bins are computed over 149 and 124 respectively. The error rates in some (adult) cases are zero, and in others the DET is flat so the error rates at the two thresholds are identical. The lines span 1% and 99% of boostrap replicated FNMR estimates.

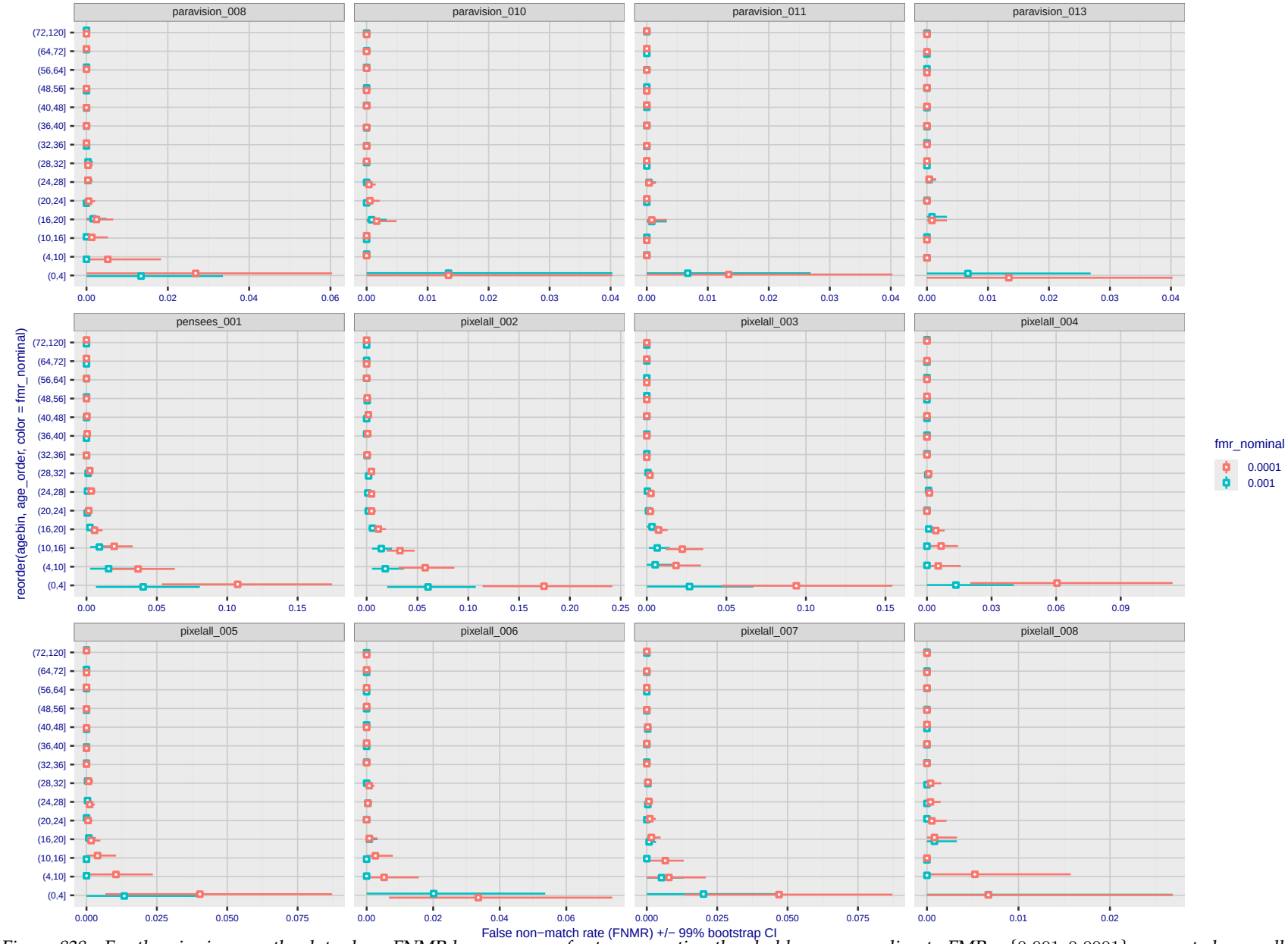

Figure 838: For the visa images, the dots show FNMR by age group for two operating thresholds corresponding to FMR = $\{0.001, 0.0001\}$ computed over all on the order of 10^{10} impostor scores. The FMR in each bin will vary also - see subsequent impostor heatmaps in sec. 3.6.2. Given a pair of face images taken at different times, we assign the comparison to the bin that is the arithmetic average of the subject's ages. This plot shows only the effect of age, not ageing. The number of comparisons in each bin is generally in the thousands, however the first and last bins are computed over 149 and 124 respectively. The error rates in some (adult) cases are zero, and in others the DET is flat so the error rates at the two thresholds are identical. The lines span 1% and 99% of boostrap replicated FNMR estimates.

Figure 839: For the visa images, the dots show FNMR by age group for two operating thresholds corresponding to FMR = $\{0.001, 0.0001\}$ computed over all on the order of 10^{10} impostor scores. The FMR in each bin will vary also - see subsequent impostor heatmaps in sec. 3.6.2. Given a pair of face images taken at different times, we assign the comparison to the bin that is the arithmetic average of the subject's ages. This plot shows only the effect of age, not ageing. The number of comparisons in each bin is generally in the thousands, however the first and last bins are computed over 149 and 124 respectively. The error rates in some (adult) cases are zero, and in others the DET is flat so the error rates at the two thresholds are identical. The lines span 1% and 99% of boostrap replicated FNMR estimates.

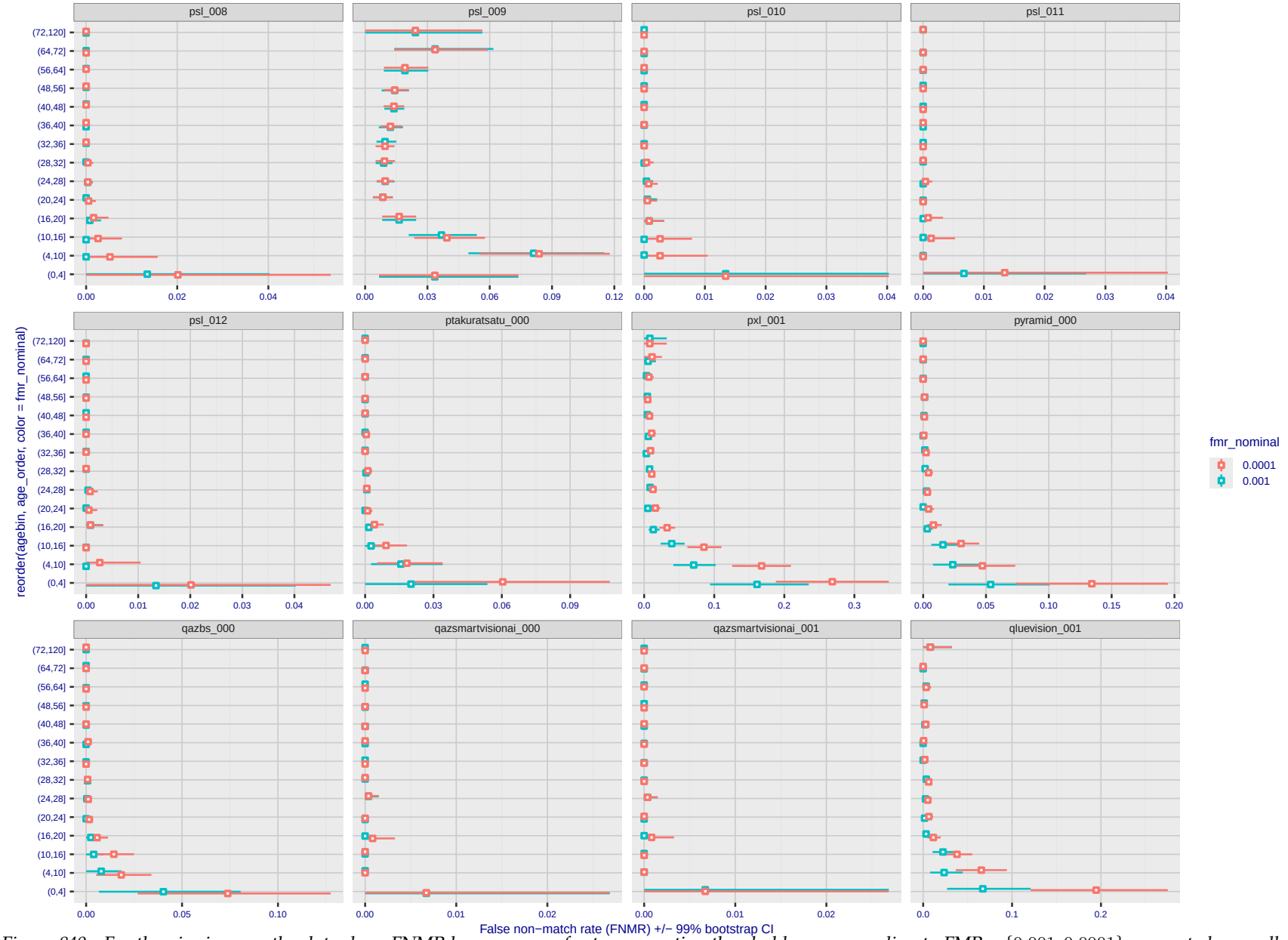

Figure 840: For the visa images, the dots show FNMR by age group for two operating thresholds corresponding to FMR = $\{0.001, 0.0001\}$ computed over all on the order of 10^{10} impostor scores. The FMR in each bin will vary also - see subsequent impostor heatmaps in sec. 3.6.2. Given a pair of face images taken at different times, we assign the comparison to the bin that is the arithmetic average of the subject's ages. This plot shows only the effect of age, not ageing. The number of comparisons in each bin is generally in the thousands, however the first and last bins are computed over 149 and 124 respectively. The error rates in some (adult) cases are zero, and in others the DET is flat so the error rates at the two thresholds are identical. The lines span 1% and 99% of boostrap replicated FNMR estimates.

Figure 841: For the visa images, the dots show FNMR by age group for two operating thresholds corresponding to FMR = $\{0.001, 0.0001\}$ computed over all on the order of 10^{10} impostor scores. The FMR in each bin will vary also - see subsequent impostor heatmaps in sec. 3.6.2. Given a pair of face images taken at different times, we assign the comparison to the bin that is the arithmetic average of the subject's ages. This plot shows only the effect of age, not ageing. The number of comparisons in each bin is generally in the thousands, however the first and last bins are computed over 149 and 124 respectively. The error rates in some (adult) cases are zero, and in others the DET is flat so the error rates at the two thresholds are identical. The lines span 1% and 99% of boostrap replicated FNMR estimates.

Figure 842: For the visa images, the dots show FNMR by age group for two operating thresholds corresponding to FMR = $\{0.001, 0.0001\}$ computed over all on the order of 10^{10} impostor scores. The FMR in each bin will vary also - see subsequent impostor heatmaps in sec. 3.6.2. Given a pair of face images taken at different times, we assign the comparison to the bin that is the arithmetic average of the subject's ages. This plot shows only the effect of age, not ageing. The number of comparisons in each bin is generally in the thousands, however the first and last bins are computed over 149 and 124 respectively. The error rates in some (adult) cases are zero, and in others the DET is flat so the error rates at the two thresholds are identical. The lines span 1% and 99% of boostrap replicated FNMR estimates.

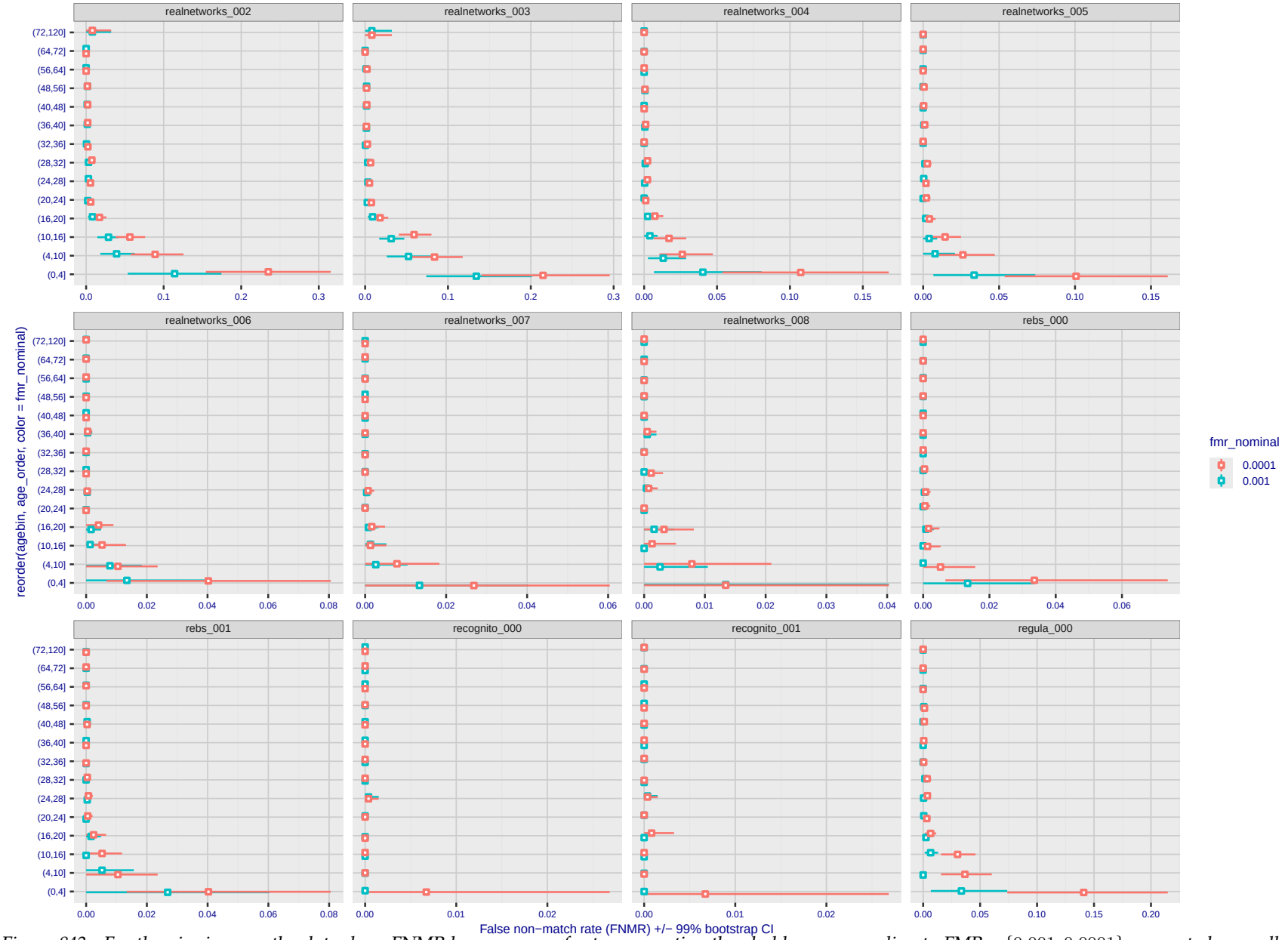

Figure 843: For the visa images, the dots show FNMR by age group for two operating thresholds corresponding to FMR = $\{0.001, 0.0001\}$ computed over all on the order of 10^{10} impostor scores. The FMR in each bin will vary also - see subsequent impostor heatmaps in sec. 3.6.2. Given a pair of face images taken at different times, we assign the comparison to the bin that is the arithmetic average of the subject's ages. This plot shows only the effect of age, not ageing. The number of comparisons in each bin is generally in the thousands, however the first and last bins are computed over 149 and 124 respectively. The error rates in some (adult) cases are zero, and in others the DET is flat so the error rates at the two thresholds are identical. The lines span 1% and 99% of boostrap replicated FNMR estimates.

Figure 844: For the visa images, the dots show FNMR by age group for two operating thresholds corresponding to FMR = $\{0.001, 0.0001\}$ computed over all on the order of 10^{10} impostor scores. The FMR in each bin will vary also - see subsequent impostor heatmaps in sec. 3.6.2. Given a pair of face images taken at different times, we assign the comparison to the bin that is the arithmetic average of the subject's ages. This plot shows only the effect of age, not ageing. The number of comparisons in each bin is generally in the thousands, however the first and last bins are computed over 149 and 124 respectively. The error rates in some (adult) cases are zero, and in others the DET is flat so the error rates at the two thresholds are identical. The lines span 1% and 99% of boostrap replicated FNMR estimates.

Figure 845: For the visa images, the dots show FNMR by age group for two operating thresholds corresponding to FMR = $\{0.001, 0.0001\}$ computed over all on the order of 10^{10} impostor scores. The FMR in each bin will vary also - see subsequent impostor heatmaps in sec. 3.6.2. Given a pair of face images taken at different times, we assign the comparison to the bin that is the arithmetic average of the subject's ages. This plot shows only the effect of age, not ageing. The number of comparisons in each bin is generally in the thousands, however the first and last bins are computed over 149 and 124 respectively. The error rates in some (adult) cases are zero, and in others the DET is flat so the error rates at the two thresholds are identical. The lines span 1% and 99% of boostrap replicated FNMR estimates.

Figure 846: For the visa images, the dots show FNMR by age group for two operating thresholds corresponding to FMR = $\{0.001, 0.0001\}$ computed over all on the order of 10^{10} impostor scores. The FMR in each bin will vary also - see subsequent impostor heatmaps in sec. 3.6.2. Given a pair of face images taken at different times, we assign the comparison to the bin that is the arithmetic average of the subject's ages. This plot shows only the effect of age, not ageing. The number of comparisons in each bin is generally in the thousands, however the first and last bins are computed over 149 and 124 respectively. The error rates in some (adult) cases are zero, and in others the DET is flat so the error rates at the two thresholds are identical. The lines span 1% and 99% of boostrap replicated FNMR estimates.

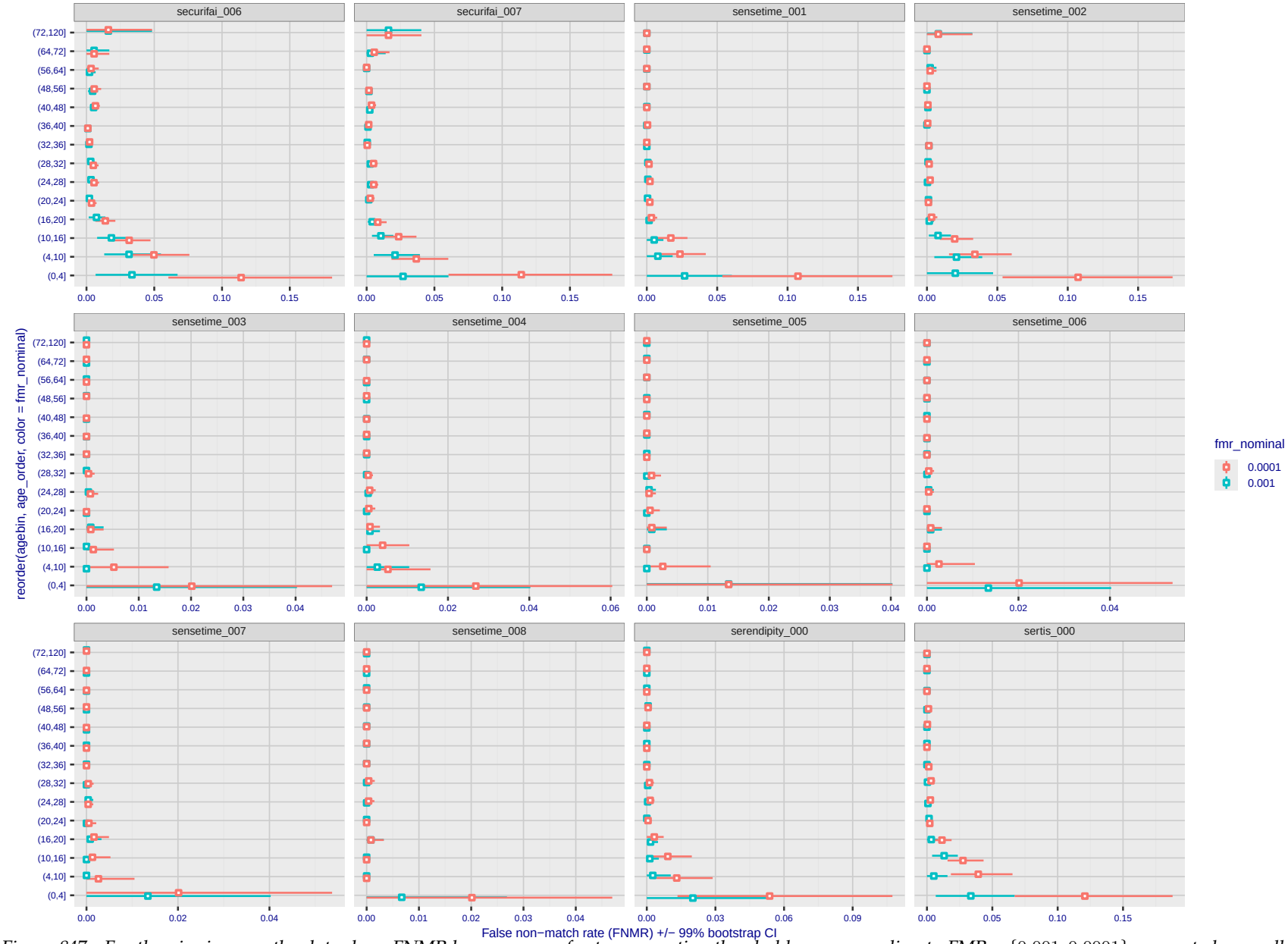

Figure 847: For the visa images, the dots show FNMR by age group for two operating thresholds corresponding to FMR = $\{0.001, 0.0001\}$ computed over all on the order of 10^{10} impostor scores. The FMR in each bin will vary also - see subsequent impostor heatmaps in sec. 3.6.2. Given a pair of face images taken at different times, we assign the comparison to the bin that is the arithmetic average of the subject's ages. This plot shows only the effect of age, not ageing. The number of comparisons in each bin is generally in the thousands, however the first and last bins are computed over 149 and 124 respectively. The error rates in some (adult) cases are zero, and in others the DET is flat so the error rates at the two thresholds are identical. The lines span 1% and 99% of boostrap replicated FNMR estimates.

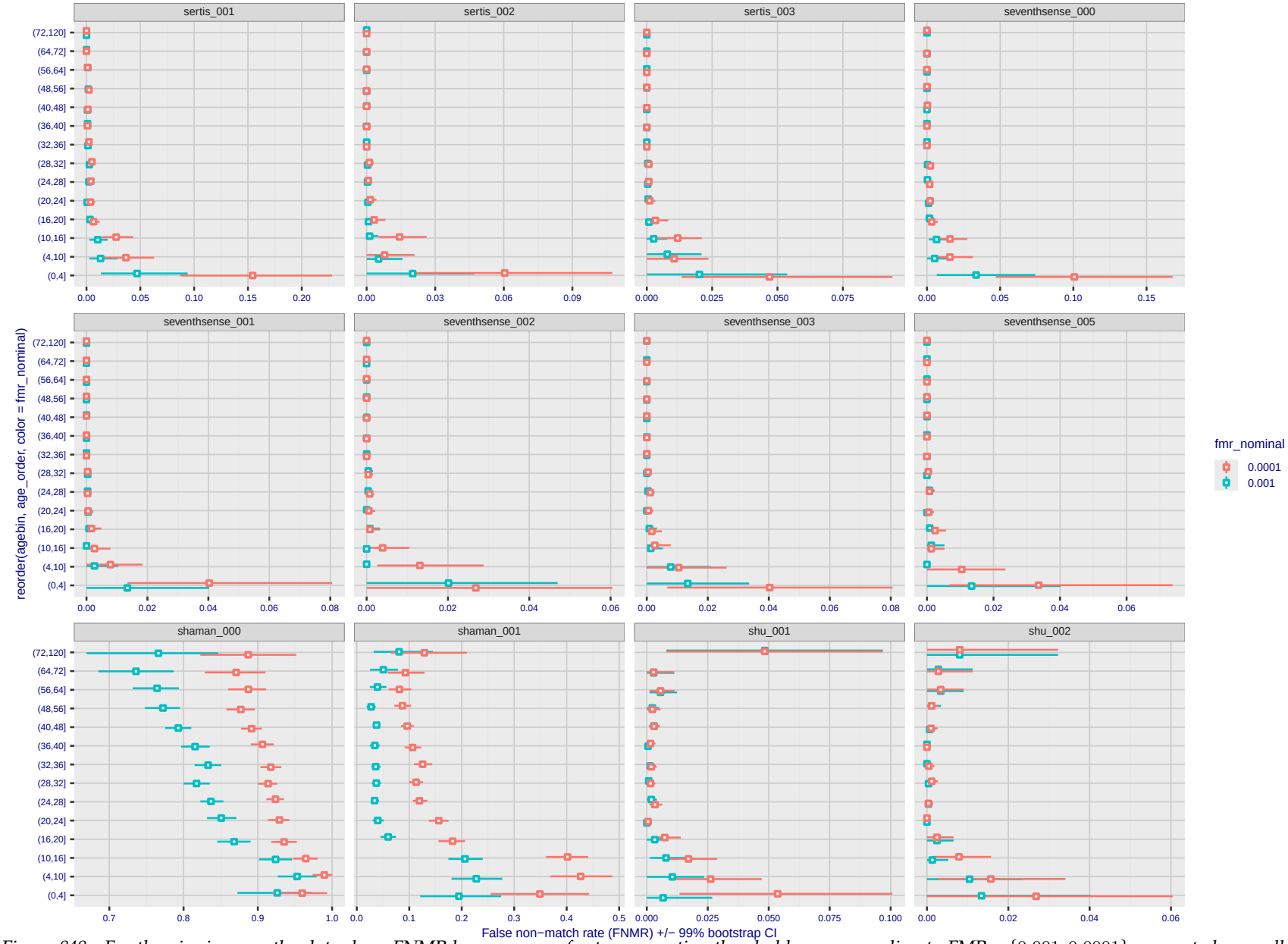

Figure 848: For the visa images, the dots show FNMR by age group for two operating thresholds corresponding to FMR = $\{0.001, 0.0001\}$ computed over all on the order of 10^{10} impostor scores. The FMR in each bin will vary also - see subsequent impostor heatmaps in sec. 3.6.2. Given a pair of face images taken at different times, we assign the comparison to the bin that is the arithmetic average of the subject's ages. This plot shows only the effect of age, not ageing. The number of comparisons in each bin is generally in the thousands, however the first and last bins are computed over 149 and 124 respectively. The error rates in some (adult) cases are zero, and in others the DET is flat so the error rates at the two thresholds are identical. The lines span 1% and 99% of boostrap replicated FNMR estimates.

Figure 849: For the visa images, the dots show FNMR by age group for two operating thresholds corresponding to FMR = $\{0.001, 0.0001\}$ computed over all on the order of 10^{10} impostor scores. The FMR in each bin will vary also - see subsequent impostor heatmaps in sec. 3.6.2. Given a pair of face images taken at different times, we assign the comparison to the bin that is the arithmetic average of the subject's ages. This plot shows only the effect of age, not ageing. The number of comparisons in each bin is generally in the thousands, however the first and last bins are computed over 149 and 124 respectively. The error rates in some (adult) cases are zero, and in others the DET is flat so the error rates at the two thresholds are identical. The lines span 1% and 99% of boostrap replicated FNMR estimates.

Figure 850: For the visa images, the dots show FNMR by age group for two operating thresholds corresponding to FMR = $\{0.001, 0.0001\}$ computed over all on the order of 10^{10} impostor scores. The FMR in each bin will vary also - see subsequent impostor heatmaps in sec. 3.6.2. Given a pair of face images taken at different times, we assign the comparison to the bin that is the arithmetic average of the subject's ages. This plot shows only the effect of age, not ageing. The number of comparisons in each bin is generally in the thousands, however the first and last bins are computed over 149 and 124 respectively. The error rates in some (adult) cases are zero, and in others the DET is flat so the error rates at the two thresholds are identical. The lines span 1% and 99% of boostrap replicated FNMR estimates.

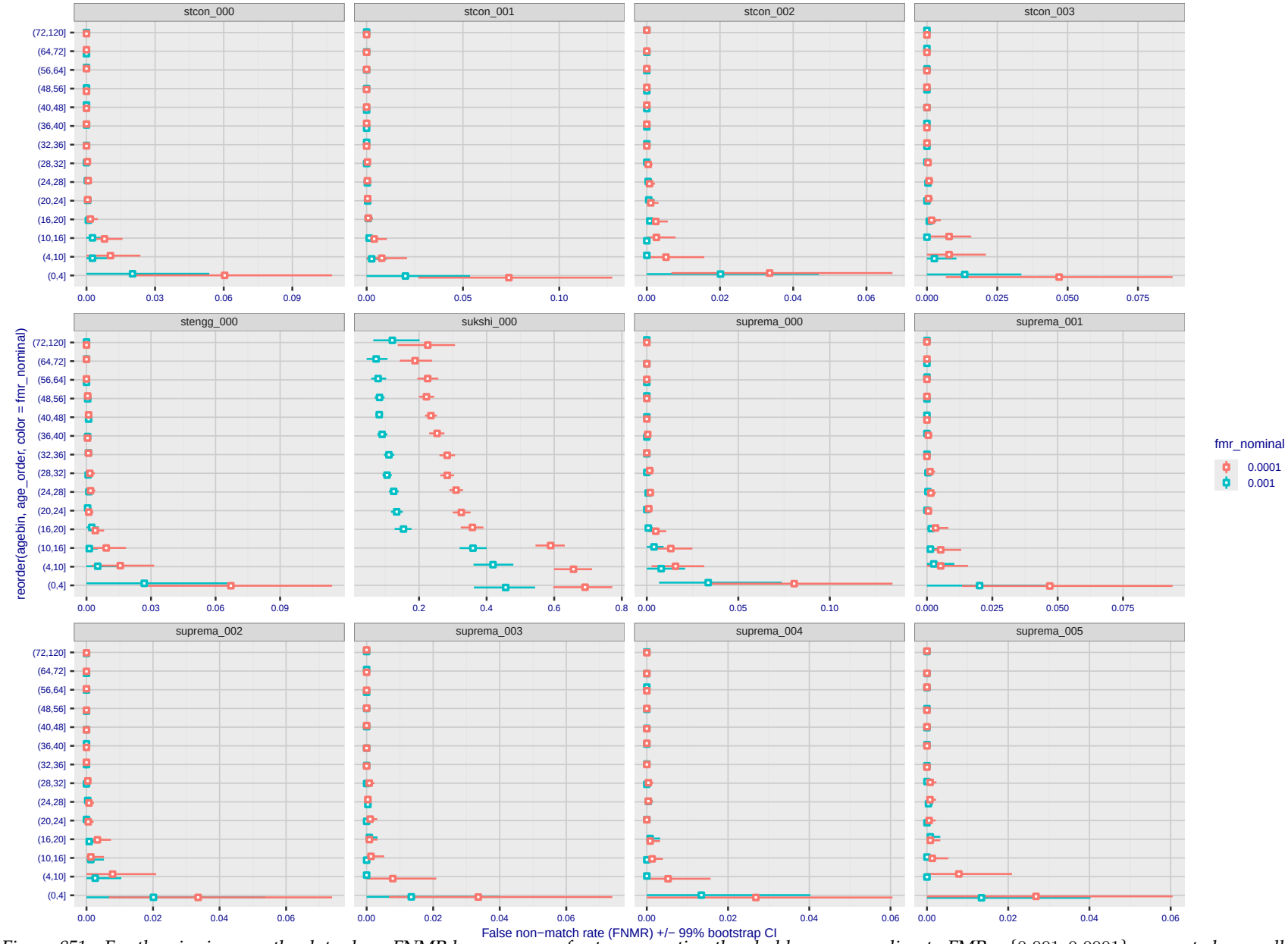

Figure 851: For the visa images, the dots show FNMR by age group for two operating thresholds corresponding to FMR = $\{0.001, 0.0001\}$ computed over all on the order of 10^{10} impostor scores. The FMR in each bin will vary also - see subsequent impostor heatmaps in sec. 3.6.2. Given a pair of face images taken at different times, we assign the comparison to the bin that is the arithmetic average of the subject's ages. This plot shows only the effect of age, not ageing. The number of comparisons in each bin is generally in the thousands, however the first and last bins are computed over 149 and 124 respectively. The error rates in some (adult) cases are zero, and in others the DET is flat so the error rates at the two thresholds are identical. The lines span 1% and 99% of boostrap replicated FNMR estimates.

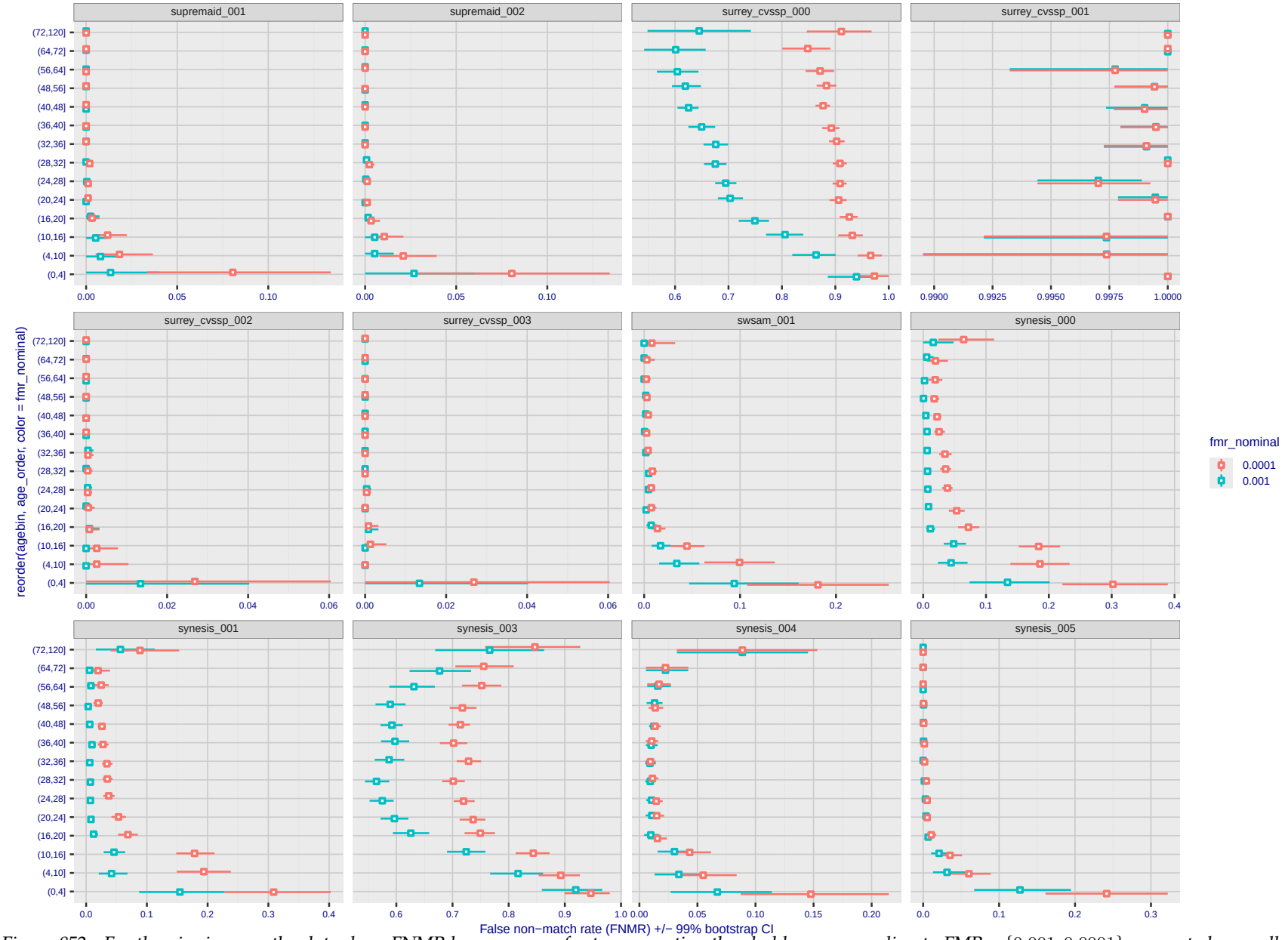

Figure 852: For the visa images, the dots show FNMR by age group for two operating thresholds corresponding to FMR = $\{0.001, 0.0001\}$ computed over all on the order of 10^{10} impostor scores. The FMR in each bin will vary also - see subsequent impostor heatmaps in sec. 3.6.2. Given a pair of face images taken at different times, we assign the comparison to the bin that is the arithmetic average of the subject's ages. This plot shows only the effect of age, not ageing. The number of comparisons in each bin is generally in the thousands, however the first and last bins are computed over 149 and 124 respectively. The error rates in some (adult) cases are zero, and in others the DET is flat so the error rates at the two thresholds are identical. The lines span 1% and 99% of boostrap replicated FNMR estimates.

Figure 853: For the visa images, the dots show FNMR by age group for two operating thresholds corresponding to FMR = $\{0.001, 0.0001\}$ computed over all on the order of 10^{10} impostor scores. The FMR in each bin will vary also - see subsequent impostor heatmaps in sec. 3.6.2. Given a pair of face images taken at different times, we assign the comparison to the bin that is the arithmetic average of the subject's ages. This plot shows only the effect of age, not ageing. The number of comparisons in each bin is generally in the thousands, however the first and last bins are computed over 149 and 124 respectively. The error rates in some (adult) cases are zero, and in others the DET is flat so the error rates at the two thresholds are identical. The lines span 1% and 99% of boostrap replicated FNMR estimates.

Figure 854: For the visa images, the dots show FNMR by age group for two operating thresholds corresponding to FMR = $\{0.001, 0.0001\}$ computed over all on the order of 10^{10} impostor scores. The FMR in each bin will vary also - see subsequent impostor heatmaps in sec. 3.6.2. Given a pair of face images taken at different times, we assign the comparison to the bin that is the arithmetic average of the subject's ages. This plot shows only the effect of age, not ageing. The number of comparisons in each bin is generally in the thousands, however the first and last bins are computed over 149 and 124 respectively. The error rates in some (adult) cases are zero, and in others the DET is flat so the error rates at the two thresholds are identical. The lines span 1% and 99% of boostrap replicated FNMR estimates.

Figure 855: For the visa images, the dots show FNMR by age group for two operating thresholds corresponding to FMR = $\{0.001, 0.0001\}$ computed over all on the order of 10^{10} impostor scores. The FMR in each bin will vary also - see subsequent impostor heatmaps in sec. 3.6.2. Given a pair of face images taken at different times, we assign the comparison to the bin that is the arithmetic average of the subject's ages. This plot shows only the effect of age, not ageing. The number of comparisons in each bin is generally in the thousands, however the first and last bins are computed over 149 and 124 respectively. The error rates in some (adult) cases are zero, and in others the DET is flat so the error rates at the two thresholds are identical. The lines span 1% and 99% of boostrap replicated FNMR estimates.

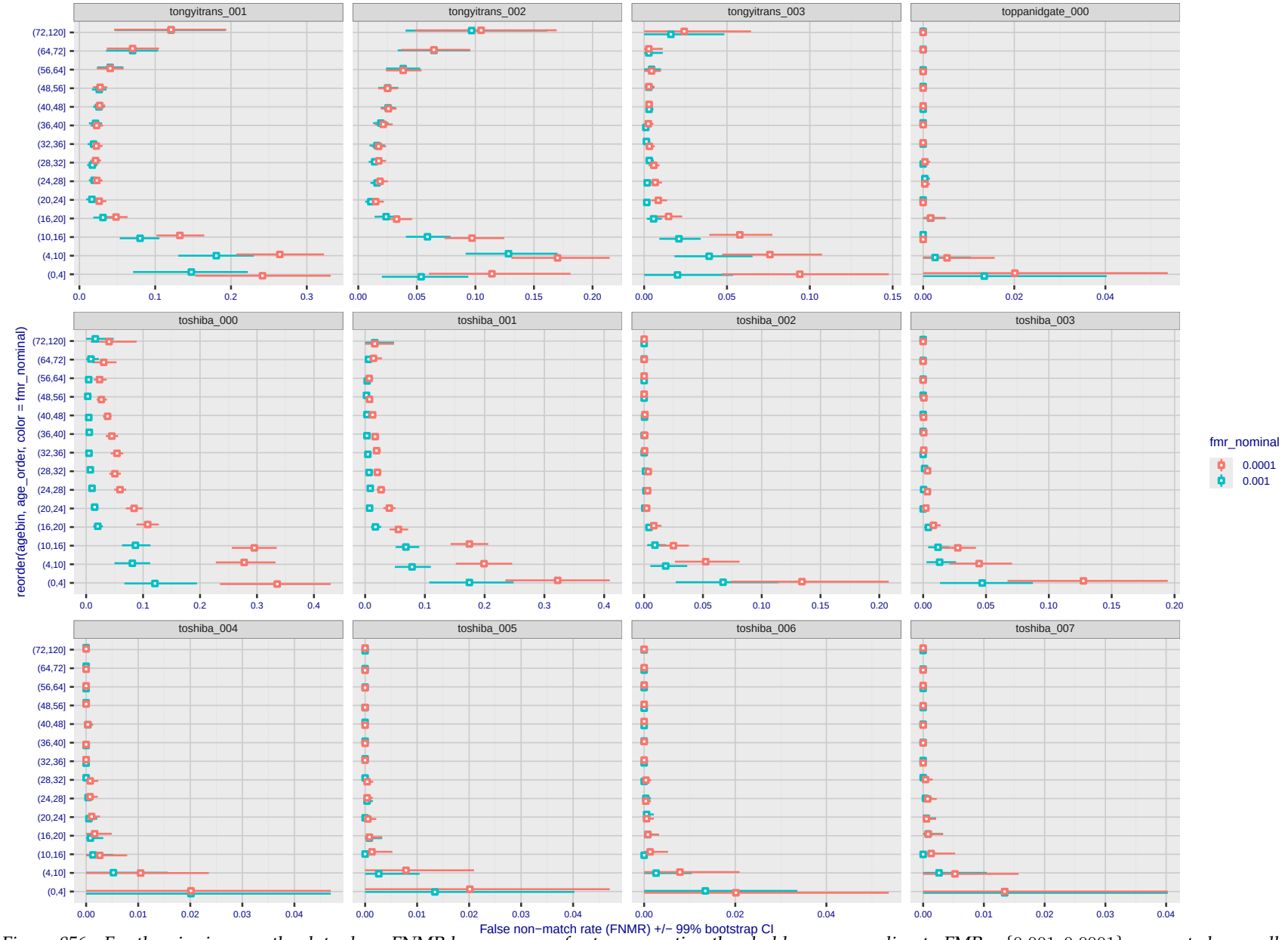

Figure 856: For the visa images, the dots show FNMR by age group for two operating thresholds corresponding to FMR = $\{0.001, 0.0001\}$ computed over all on the order of 10^{10} impostor scores. The FMR in each bin will vary also - see subsequent impostor heatmaps in sec. 3.6.2. Given a pair of face images taken at different times, we assign the comparison to the bin that is the arithmetic average of the subject's ages. This plot shows only the effect of age, not ageing. The number of comparisons in each bin is generally in the thousands, however the first and last bins are computed over 149 and 124 respectively. The error rates in some (adult) cases are zero, and in others the DET is flat so the error rates at the two thresholds are identical. The lines span 1% and 99% of boostrap replicated FNMR estimates.

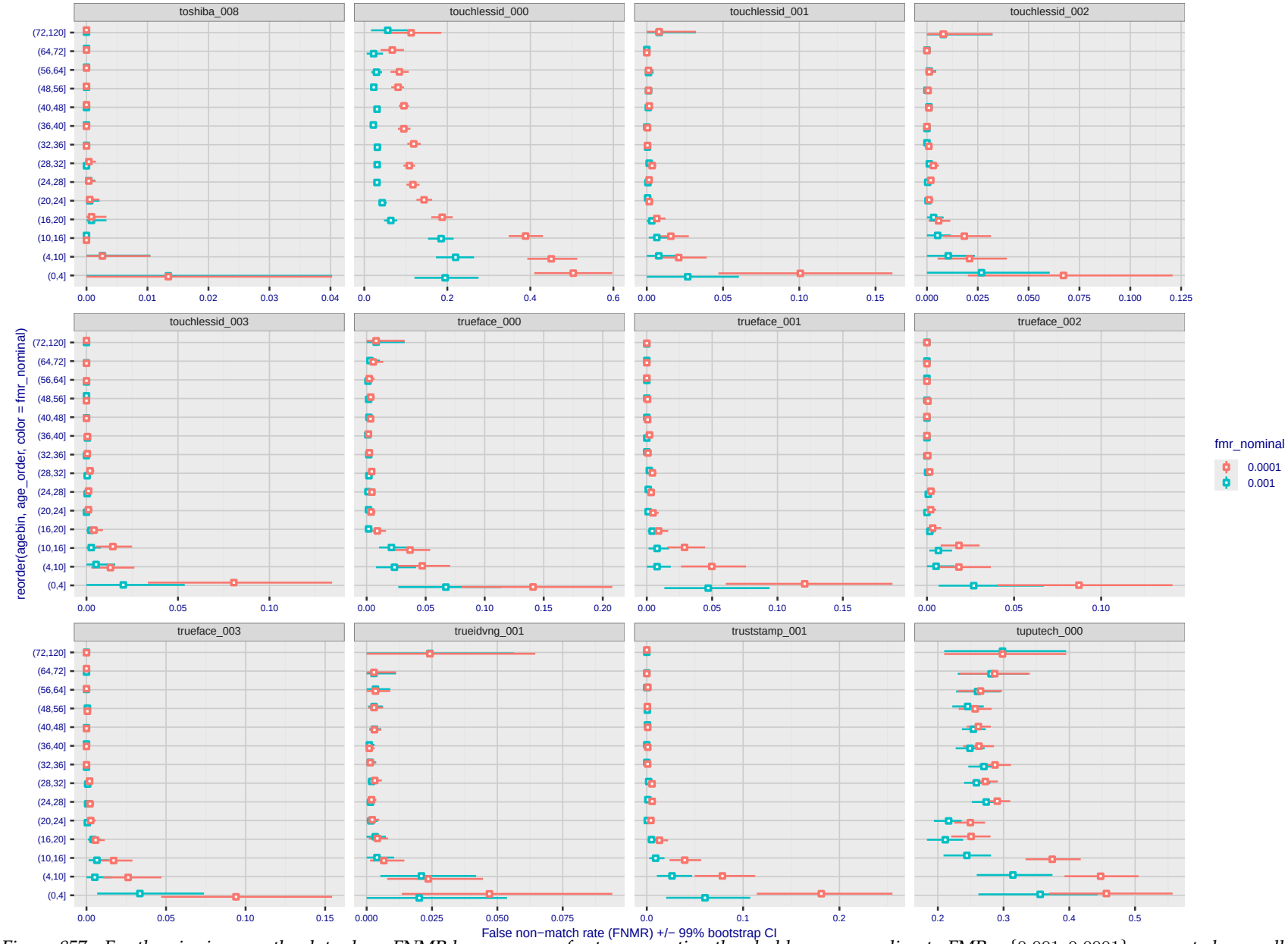

Figure 857: For the visa images, the dots show FNMR by age group for two operating thresholds corresponding to FMR = $\{0.001, 0.0001\}$ computed over all on the order of 10^{10} impostor scores. The FMR in each bin will vary also - see subsequent impostor heatmaps in sec. 3.6.2. Given a pair of face images taken at different times, we assign the comparison to the bin that is the arithmetic average of the subject's ages. This plot shows only the effect of age, not ageing. The number of comparisons in each bin is generally in the thousands, however the first and last bins are computed over 149 and 124 respectively. The error rates in some (adult) cases are zero, and in others the DET is flat so the error rates at the two thresholds are identical. The lines span 1% and 99% of boostrap replicated FNMR estimates.

Figure 858: For the visa images, the dots show FNMR by age group for two operating thresholds corresponding to FMR = $\{0.001, 0.0001\}$ computed over all on the order of 10^{10} impostor scores. The FMR in each bin will vary also - see subsequent impostor heatmaps in sec. 3.6.2. Given a pair of face images taken at different times, we assign the comparison to the bin that is the arithmetic average of the subject's ages. This plot shows only the effect of age, not ageing. The number of comparisons in each bin is generally in the thousands, however the first and last bins are computed over 149 and 124 respectively. The error rates in some (adult) cases are zero, and in others the DET is flat so the error rates at the two thresholds are identical. The lines span 1% and 99% of boostrap replicated FNMR estimates.

Figure 859: For the visa images, the dots show FNMR by age group for two operating thresholds corresponding to FMR = $\{0.001, 0.0001\}$ computed over all on the order of 10^{10} impostor scores. The FMR in each bin will vary also - see subsequent impostor heatmaps in sec. 3.6.2. Given a pair of face images taken at different times, we assign the comparison to the bin that is the arithmetic average of the subject's ages. This plot shows only the effect of age, not ageing. The number of comparisons in each bin is generally in the thousands, however the first and last bins are computed over 149 and 124 respectively. The error rates in some (adult) cases are zero, and in others the DET is flat so the error rates at the two thresholds are identical. The lines span 1% and 99% of boostrap replicated FNMR estimates.

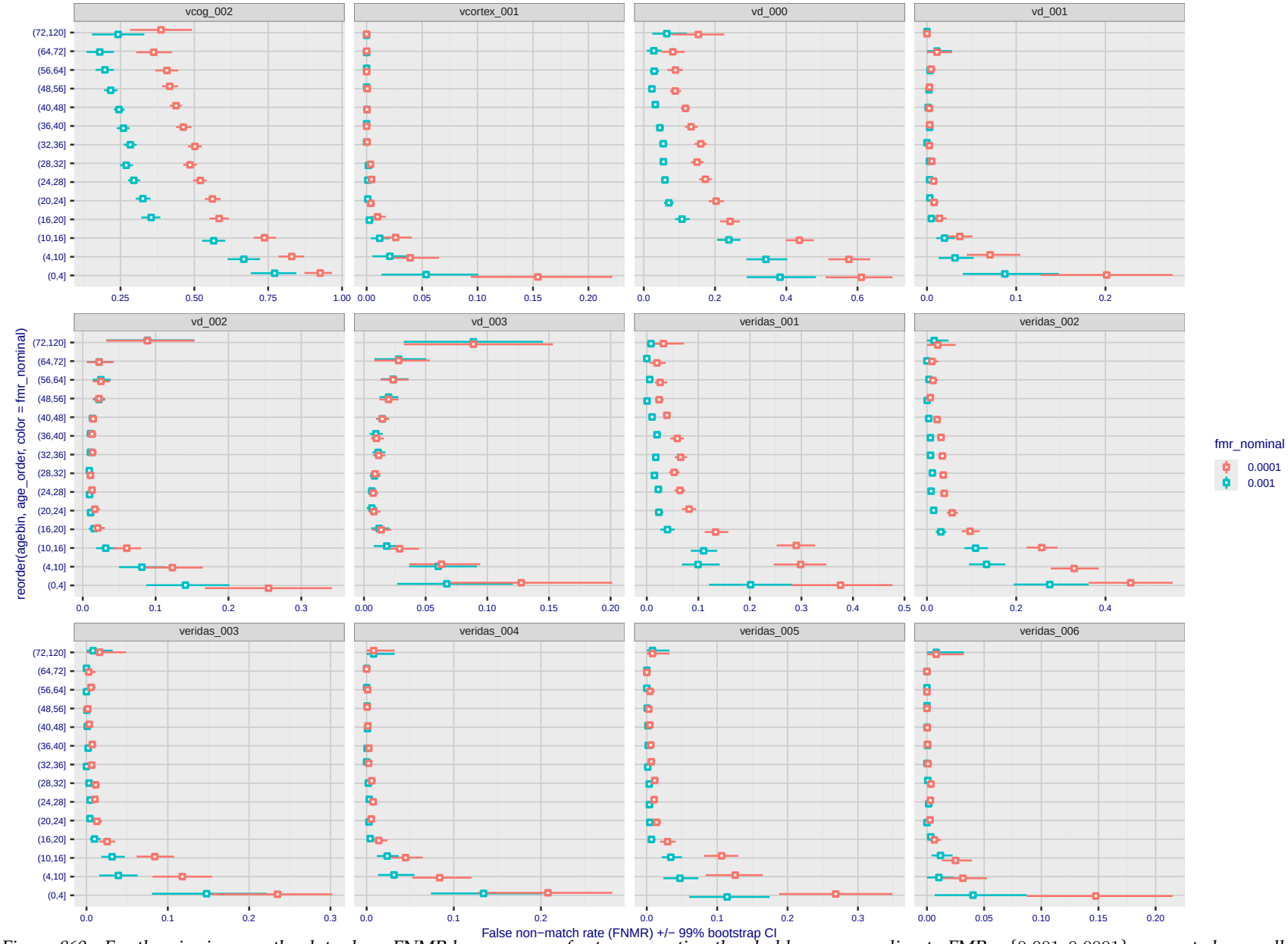

Figure 860: For the visa images, the dots show FNMR by age group for two operating thresholds corresponding to FMR = $\{0.001, 0.0001\}$ computed over all on the order of 10^{10} impostor scores. The FMR in each bin will vary also - see subsequent impostor heatmaps in sec. 3.6.2. Given a pair of face images taken at different times, we assign the comparison to the bin that is the arithmetic average of the subject's ages. This plot shows only the effect of age, not ageing. The number of comparisons in each bin is generally in the thousands, however the first and last bins are computed over 149 and 124 respectively. The error rates in some (adult) cases are zero, and in others the DET is flat so the error rates at the two thresholds are identical. The lines span 1% and 99% of boostrap replicated FNMR estimates.

Figure 861: For the visa images, the dots show FNMR by age group for two operating thresholds corresponding to FMR = $\{0.001, 0.0001\}$ computed over all on the order of 10^{10} impostor scores. The FMR in each bin will vary also - see subsequent impostor heatmaps in sec. 3.6.2. Given a pair of face images taken at different times, we assign the comparison to the bin that is the arithmetic average of the subject's ages. This plot shows only the effect of age, not ageing. The number of comparisons in each bin is generally in the thousands, however the first and last bins are computed over 149 and 124 respectively. The error rates in some (adult) cases are zero, and in others the DET is flat so the error rates at the two thresholds are identical. The lines span 1% and 99% of boostrap replicated FNMR estimates.

Figure 862: For the visa images, the dots show FNMR by age group for two operating thresholds corresponding to FMR = $\{0.001, 0.0001\}$ computed over all on the order of 10^{10} impostor scores. The FMR in each bin will vary also - see subsequent impostor heatmaps in sec. 3.6.2. Given a pair of face images taken at different times, we assign the comparison to the bin that is the arithmetic average of the subject's ages. This plot shows only the effect of age, not ageing. The number of comparisons in each bin is generally in the thousands, however the first and last bins are computed over 149 and 124 respectively. The error rates in some (adult) cases are zero, and in others the DET is flat so the error rates at the two thresholds are identical. The lines span 1% and 99% of boostrap replicated FNMR estimates.

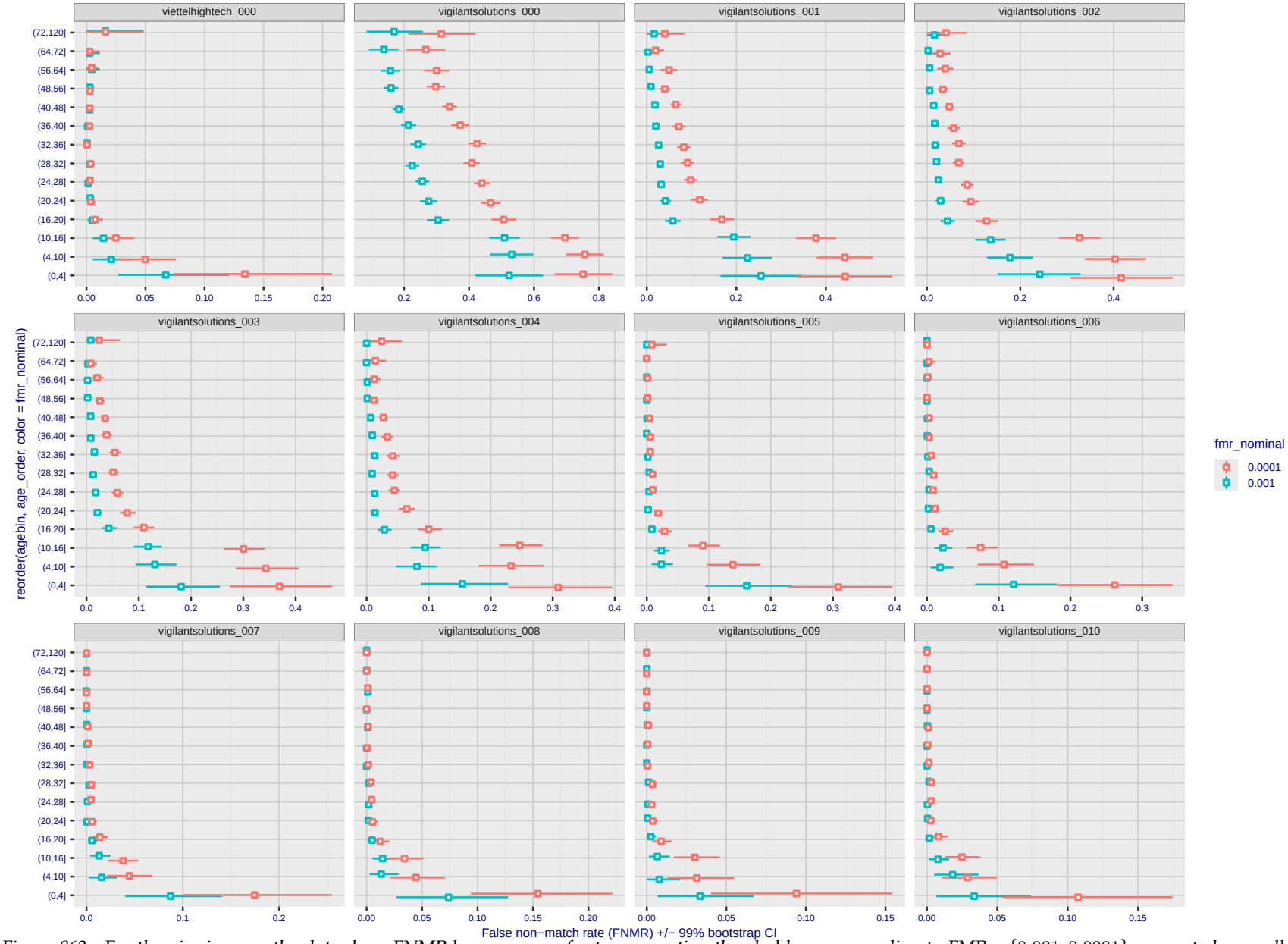

Figure 863: For the visa images, the dots show FNMR by age group for two operating thresholds corresponding to FMR = $\{0.001, 0.0001\}$ computed over all on the order of 10^{10} impostor scores. The FMR in each bin will vary also - see subsequent impostor heatmaps in sec. 3.6.2. Given a pair of face images taken at different times, we assign the comparison to the bin that is the arithmetic average of the subject's ages. This plot shows only the effect of age, not ageing. The number of comparisons in each bin is generally in the thousands, however the first and last bins are computed over 149 and 124 respectively. The error rates in some (adult) cases are zero, and in others the DET is flat so the error rates at the two thresholds are identical. The lines span 1% and 99% of boostrap replicated FNMR estimates.

Figure 864: For the visa images, the dots show FNMR by age group for two operating thresholds corresponding to FMR = $\{0.001, 0.0001\}$ computed over all on the order of 10^{10} impostor scores. The FMR in each bin will vary also - see subsequent impostor heatmaps in sec. 3.6.2. Given a pair of face images taken at different times, we assign the comparison to the bin that is the arithmetic average of the subject's ages. This plot shows only the effect of age, not ageing. The number of comparisons in each bin is generally in the thousands, however the first and last bins are computed over 149 and 124 respectively. The error rates in some (adult) cases are zero, and in others the DET is flat so the error rates at the two thresholds are identical. The lines span 1% and 99% of boostrap replicated FNMR estimates.

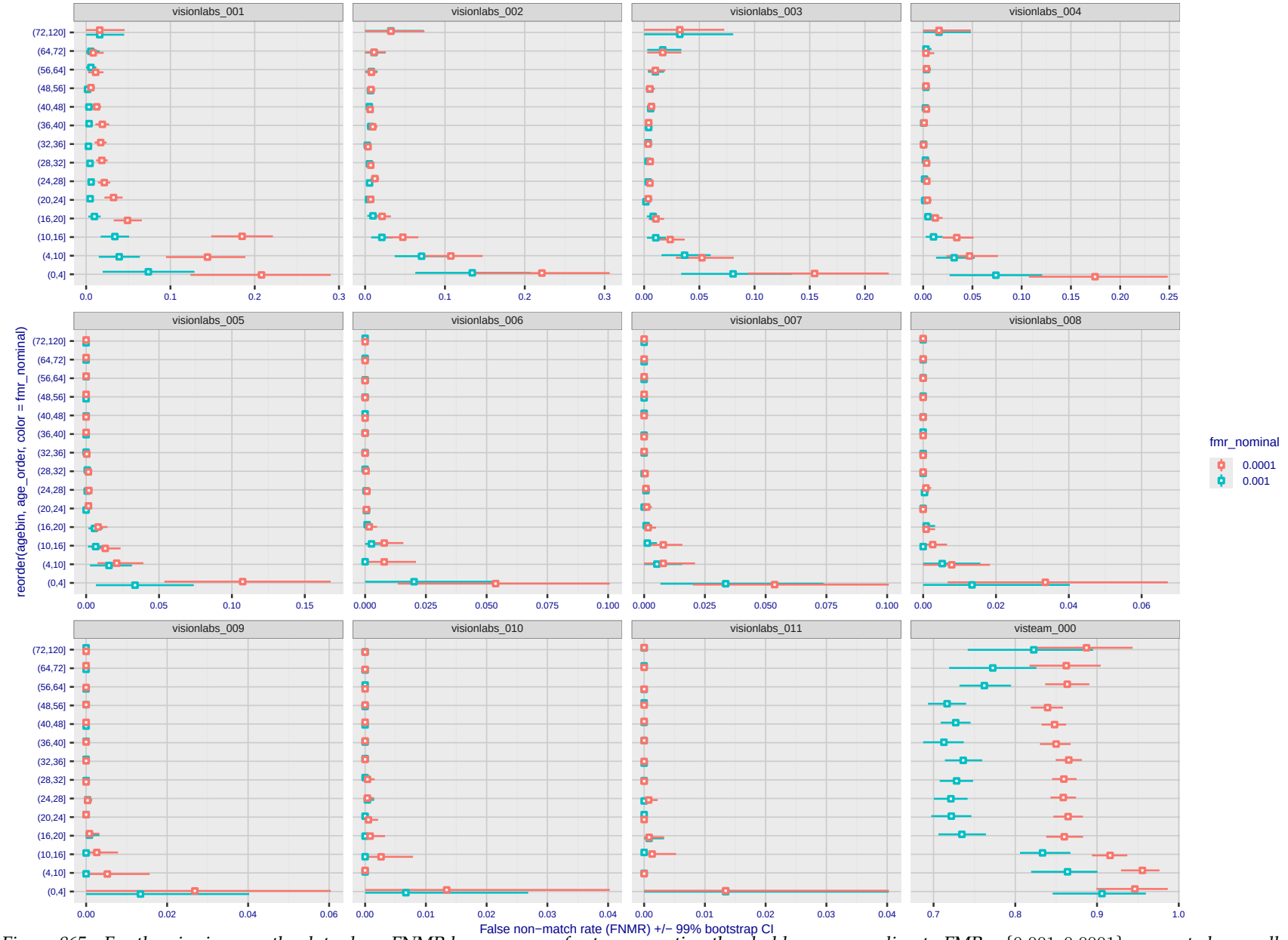

Figure 865: For the visa images, the dots show FNMR by age group for two operating thresholds corresponding to FMR = $\{0.001, 0.0001\}$ computed over all on the order of 10^{10} impostor scores. The FMR in each bin will vary also - see subsequent impostor heatmaps in sec. 3.6.2. Given a pair of face images taken at different times, we assign the comparison to the bin that is the arithmetic average of the subject's ages. This plot shows only the effect of age, not ageing. The number of comparisons in each bin is generally in the thousands, however the first and last bins are computed over 149 and 124 respectively. The error rates in some (adult) cases are zero, and in others the DET is flat so the error rates at the two thresholds are identical. The lines span 1% and 99% of boostrap replicated FNMR estimates.

Figure 866: For the visa images, the dots show FNMR by age group for two operating thresholds corresponding to FMR = $\{0.001, 0.0001\}$ computed over all on the order of 10^{10} impostor scores. The FMR in each bin will vary also - see subsequent impostor heatmaps in sec. 3.6.2. Given a pair of face images taken at different times, we assign the comparison to the bin that is the arithmetic average of the subject's ages. This plot shows only the effect of age, not ageing. The number of comparisons in each bin is generally in the thousands, however the first and last bins are computed over 149 and 124 respectively. The error rates in some (adult) cases are zero, and in others the DET is flat so the error rates at the two thresholds are identical. The lines span 1% and 99% of boostrap replicated FNMR estimates.

Figure 867: For the visa images, the dots show FNMR by age group for two operating thresholds corresponding to FMR = $\{0.001, 0.0001\}$ computed over all on the order of 10^{10} impostor scores. The FMR in each bin will vary also - see subsequent impostor heatmaps in sec. 3.6.2. Given a pair of face images taken at different times, we assign the comparison to the bin that is the arithmetic average of the subject's ages. This plot shows only the effect of age, not ageing. The number of comparisons in each bin is generally in the thousands, however the first and last bins are computed over 149 and 124 respectively. The error rates in some (adult) cases are zero, and in others the DET is flat so the error rates at the two thresholds are identical. The lines span 1% and 99% of boostrap replicated FNMR estimates.

Figure 868: For the visa images, the dots show FNMR by age group for two operating thresholds corresponding to FMR = $\{0.001, 0.0001\}$ computed over all on the order of 10^{10} impostor scores. The FMR in each bin will vary also - see subsequent impostor heatmaps in sec. 3.6.2. Given a pair of face images taken at different times, we assign the comparison to the bin that is the arithmetic average of the subject's ages. This plot shows only the effect of age, not ageing. The number of comparisons in each bin is generally in the thousands, however the first and last bins are computed over 149 and 124 respectively. The error rates in some (adult) cases are zero, and in others the DET is flat so the error rates at the two thresholds are identical. The lines span 1% and 99% of boostrap replicated FNMR estimates.

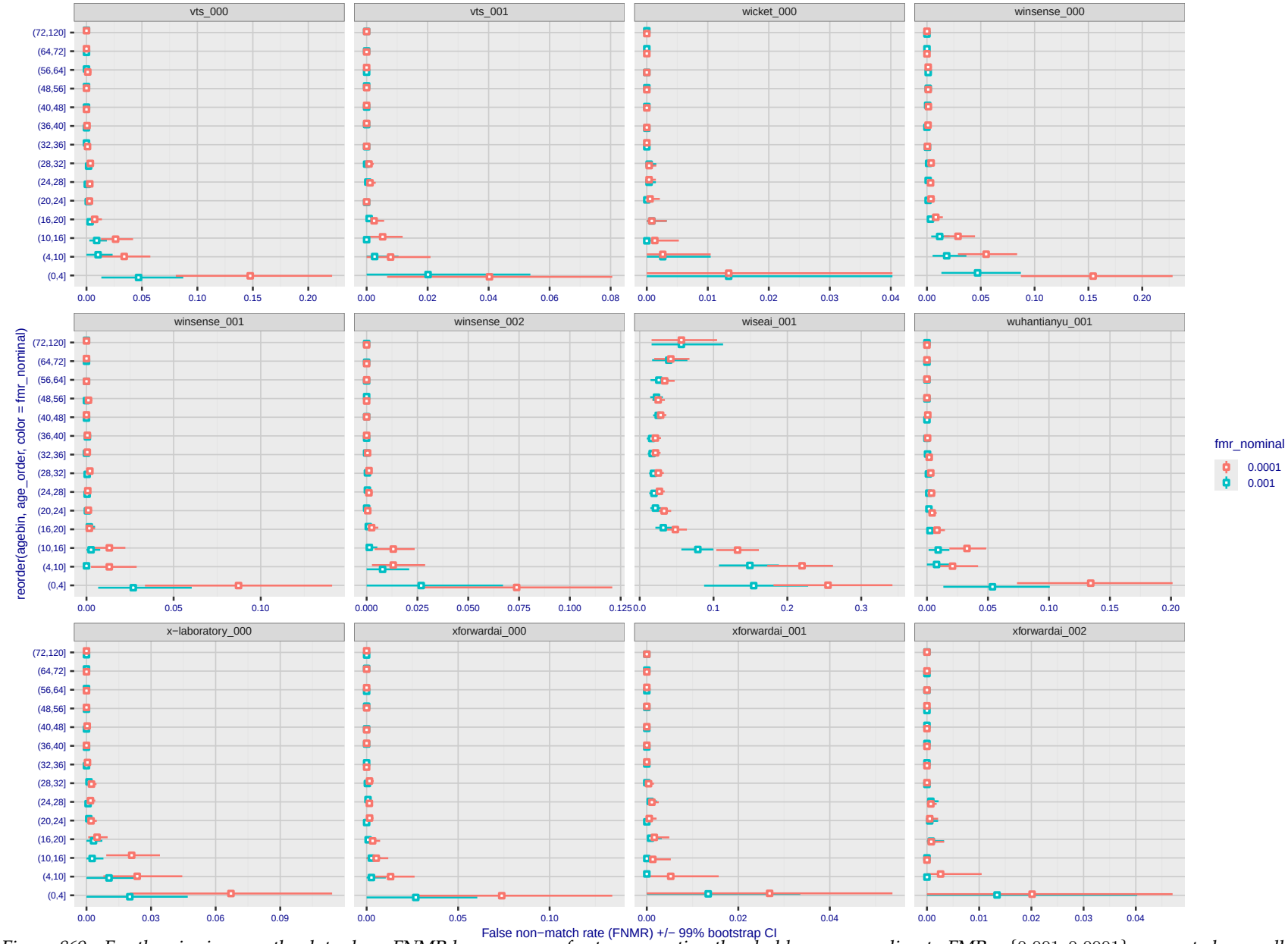

Figure 869: For the visa images, the dots show FNMR by age group for two operating thresholds corresponding to FMR = $\{0.001, 0.0001\}$ computed over all on the order of 10^{10} impostor scores. The FMR in each bin will vary also - see subsequent impostor heatmaps in sec. 3.6.2. Given a pair of face images taken at different times, we assign the comparison to the bin that is the arithmetic average of the subject's ages. This plot shows only the effect of age, not ageing. The number of comparisons in each bin is generally in the thousands, however the first and last bins are computed over 149 and 124 respectively. The error rates in some (adult) cases are zero, and in others the DET is flat so the error rates at the two thresholds are identical. The lines span 1% and 99% of boostrap replicated FNMR estimates.

Figure 870: For the visa images, the dots show FNMR by age group for two operating thresholds corresponding to FMR = $\{0.001, 0.0001\}$ computed over all on the order of 10^{10} impostor scores. The FMR in each bin will vary also - see subsequent impostor heatmaps in sec. 3.6.2. Given a pair of face images taken at different times, we assign the comparison to the bin that is the arithmetic average of the subject's ages. This plot shows only the effect of age, not ageing. The number of comparisons in each bin is generally in the thousands, however the first and last bins are computed over 149 and 124 respectively. The error rates in some (adult) cases are zero, and in others the DET is flat so the error rates at the two thresholds are identical. The lines span 1% and 99% of boostrap replicated FNMR estimates.

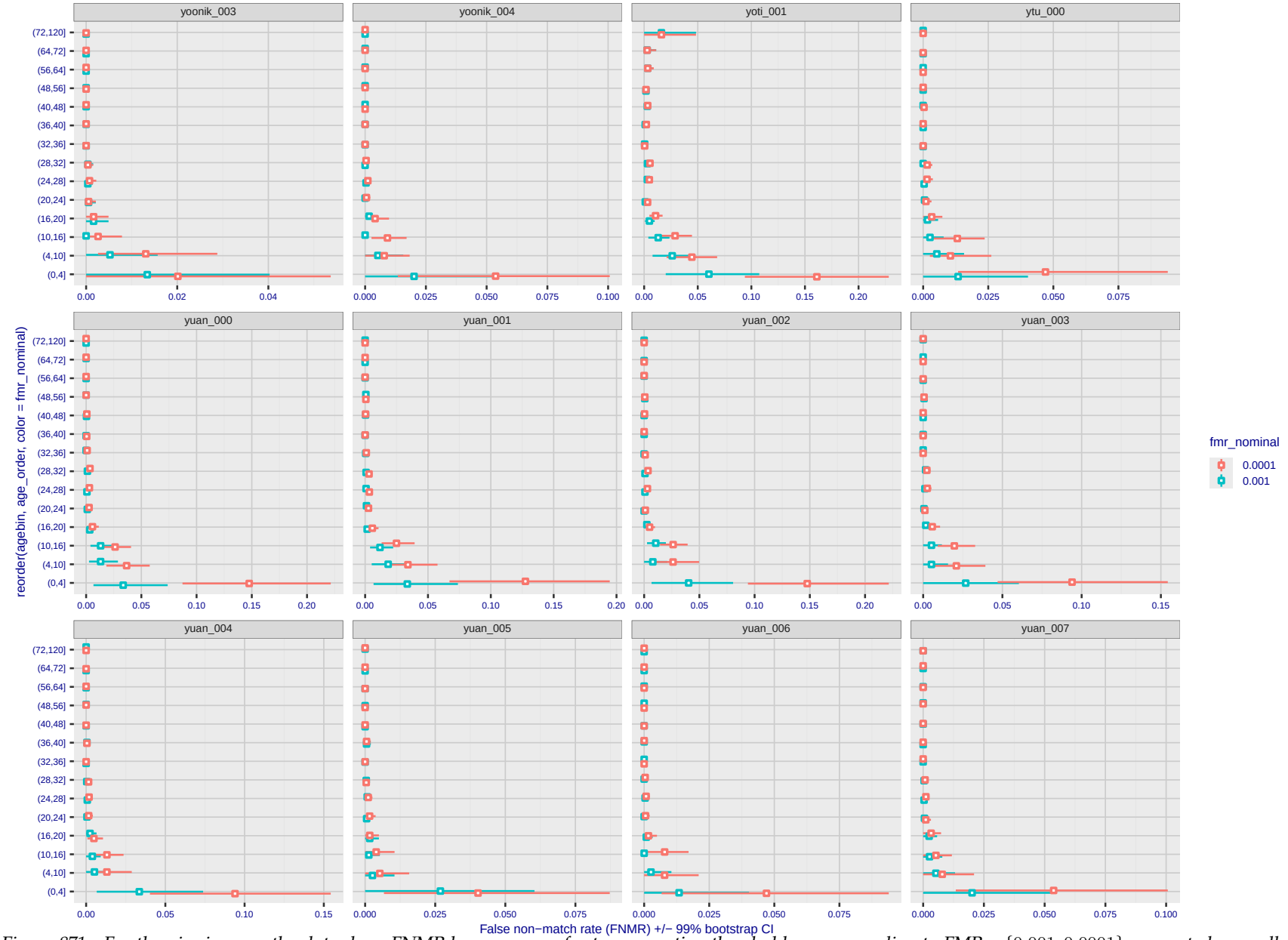

Figure 871: For the visa images, the dots show FNMR by age group for two operating thresholds corresponding to FMR = $\{0.001, 0.0001\}$ computed over all on the order of 10^{10} impostor scores. The FMR in each bin will vary also - see subsequent impostor heatmaps in sec. 3.6.2. Given a pair of face images taken at different times, we assign the comparison to the bin that is the arithmetic average of the subject's ages. This plot shows only the effect of age, not ageing. The number of comparisons in each bin is generally in the thousands, however the first and last bins are computed over 149 and 124 respectively. The error rates in some (adult) cases are zero, and in others the DET is flat so the error rates at the two thresholds are identical. The lines span 1% and 99% of boostrap replicated FNMR estimates.

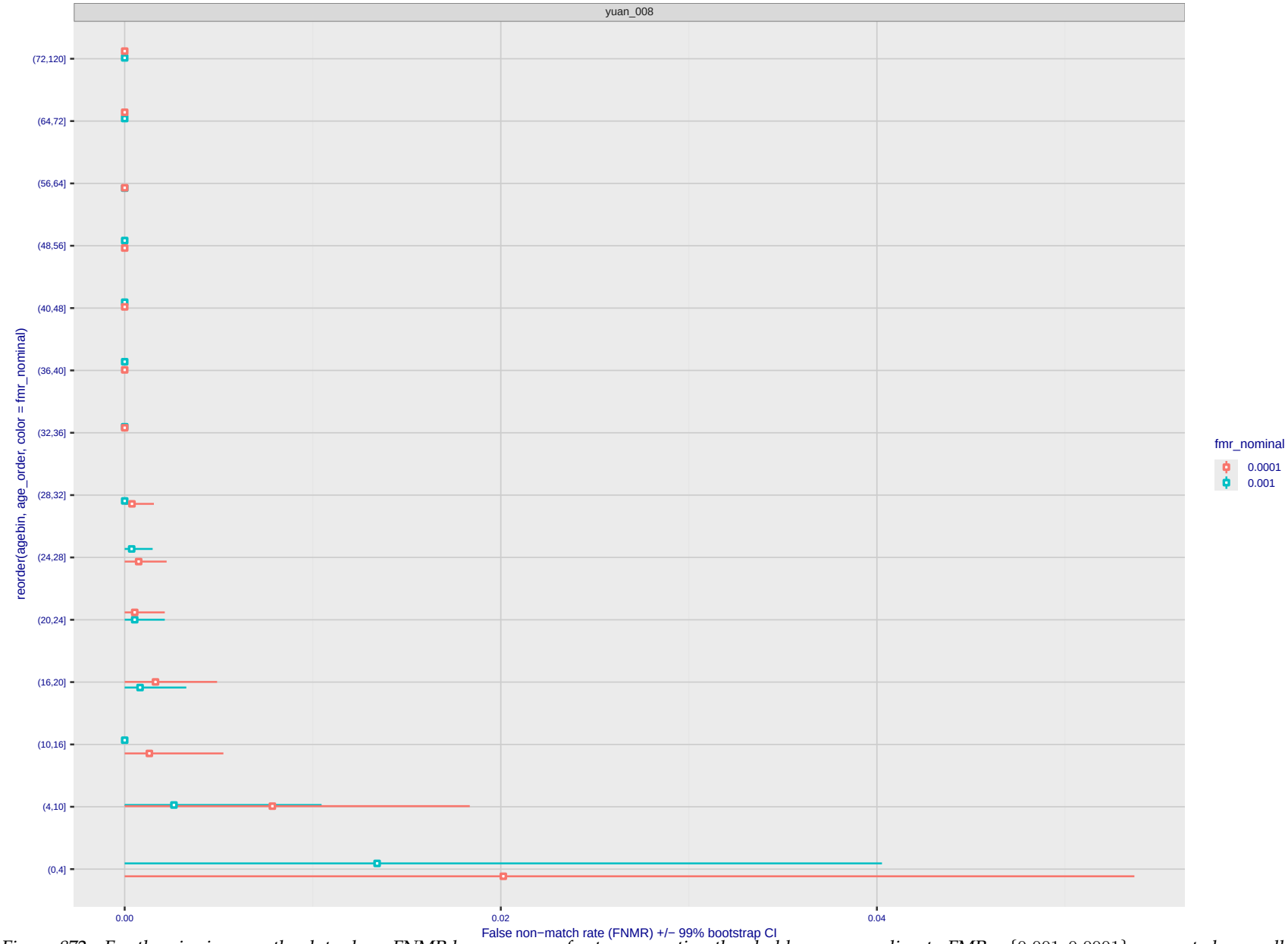

Figure 872: For the visa images, the dots show FNMR by age group for two operating thresholds corresponding to FMR = $\{0.001, 0.0001\}$ computed over all on the order of 10^{10} impostor scores. The FMR in each bin will vary also - see subsequent impostor heatmaps in sec. 3.6.2. Given a pair of face images taken at different times, we assign the comparison to the bin that is the arithmetic average of the subject's ages. This plot shows only the effect of age, not ageing. The number of comparisons in each bin is generally in the thousands, however the first and last bins are computed over 149 and 124 respectively. The error rates in some (adult) cases are zero, and in others the DET is flat so the error rates at the two thresholds are identical. The lines span 1% and 99% of boostrap replicated FNMR estimates.

Caveats: None.

FNMR(T) "False non-match rate"
FMR(T) "False match rate"

3.6 Impostor distribution stability

3.6.1 Effect of birth place on the impostor distribution

Background: Facial appearance varies geographically, both in terms of skin tone, cranio-facial structure and size. This section addresses whether false match rates vary intra- and inter-regionally.

Goals:

- ▷ To show the effect of birth region of the impostor and enrollee on false match rates.
- ▷ To determine whether some algorithms give better impostor distribution stability.

Methods:

- ▷ For the visa images, NIST defined 10 regions: Sub-Saharan Africa, South Asia, Polynesia, North Africa, Middle East, Europe, East Asia, Central and South America, Central Asia, and the Caribbean.
- ▷ For the visa images, NIST mapped each country of birth to a region. There is some arbitrariness to this. For example, Egypt could reasonably be assigned to the Middle East instead of North Africa. An alternative methodology could, for example, assign the Philippines to *both* Polynesia and East Asia.
- ▷ FMR is computed for cases where all face images of impostors born in region r_2 are compared with enrolled face images of persons born in region r_1.

$$\text{FMR}(r_1, r_2, T) = \frac{\sum_{i=1}^{N_{r_1,r_2}} H(s_i - T)}{N_{r_1,r_2}} \tag{5}$$

  where the same threshold, T, is used in all cells, and H is the unit step function. The threshold is set to give FMR(T) = 0.001 over the entire set of visa image impostor comparisons.
- ▷ This analysis is then repeated by country-pair, but only for those country pairs where both have at least 1000 images available. The countries[1] appear in the axes of graphs that follow.
- ▷ The mean number of impostor scores in any cross-region bin is 33 million. The smallest number of impostor scores in any bin is 135000, for Central Asia - North Africa. While these counts are large enough to support reasonable significance, the number of individual faces is much smaller, on the order of $N^{0.5}$.
- ▷ The numbers of impostor scores in any cross-country bin is shown in Figure 873.

Results: Subsequent figures show heatmaps that use color to represent the base-10 logarithm of the false match rate. Red colors indicate high (bad) false match rates. Dark colors indicate benign false match rates. There are two series of graphs corresponding to aggregated geographical regions, and to countries. The notable observations are:

- ▷ The on-diagonal elements correspond to within-region impostors. FMR is generally above the nominal value of FMR = 0.001. Particularly there is usually higher FMR in, Sub-Saharan Africa, South Asia, and the Caribbean. Europe and Central Asia, on the other hand, usually give FMR closer to the nominal value.
- ▷ The off-diagonal elements correspond to across-region impostors. The highest FMR is produced between the Caribbean and Sub-Saharan Africa.
- ▷ Algorithms vary.

[1] These are Argentina, Australia, Brazil, Chile, China, Costa Rica, Cuba, Czech Republic, Dominican Republic, Ecuador, Egypt, El Salvador, Germany, Ghana, Great Britain, Greece, Guatamala, Haiti, Hong Kong, Honduras, Indonesia, India, Israel, Jamaica, Japan, Kenya, Korea, Lebanon, Mexico, Malaysia, Nepal, Nigeria, Peru, Philippines, Pakistan, Poland, Romania, Russia, South Africa, Saudi Arabia, Thailand, Trinidad, Turkey, Taiwan, Ukraine, Venezuela, and Vietnam.

- We computed the same quantities for a global FMR = 0.0001. The effects are similar.

Caveats:

- The effects of variable impostor rates on one-to-many identification systems may well differ from what's implied by these one-to-one verification results. Two reasons for this are a) the enrollment galleries are usually imbalanced across countries of birth, age and sex; b) one-to-many identification algorithms often implement techniques aimed at stabilizing the impostor distribution. Further research is necessary.
- In principle, the effects seen in this subsection could be due to differences in the image capture process. We consider this unlikely since the effects are maintained across geography - e.g. Caribbean vs. Africa, or Japan vs. China.

FNMR(T) "False non-match rate"
FMR(T) "False match rate"

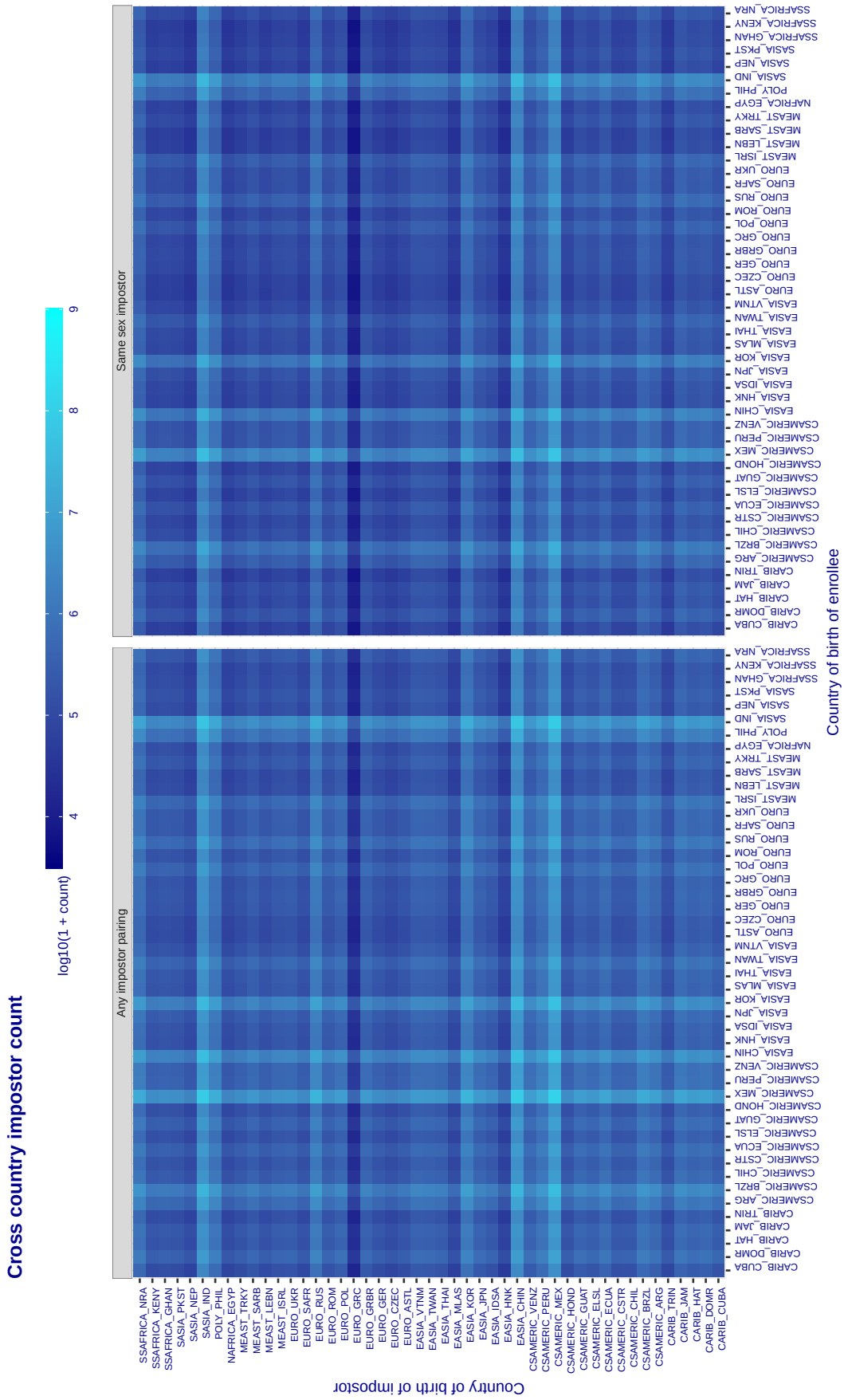

Figure 873: For visa images, the heatmap shows the count of impostor comparisons of faces from different individuals who were born in the given country pair. The FMR heatmaps themselves appear in the 1:1 report cards, for example, this one.

FNMR(T) "False non-match rate"
FMR(T) "False match rate"

3.6.2 Effect of age on impostors

Background: This section shows the effect of age on the impostor distribution. The ideal behaviour is that the age of the enrollee and the impostor would not affect impostor scores. This would support FMR stability over sub-populations.

Goals:

- To show the effect of relative ages of the impostor and enrollee on false match rates.
- To determine whether some algorithms have better impostor distribution stability.

Methods:

- Define 14 age group bins, spanning 0 to over 100 years old.
- Compute FMR over all impostor comparisons for which the subjects in the enrollee and impostor images have ages in two bins.
- Compute FMR over all impostor comparisons for which the subjects are additionally of the same sex, and born in the same geographic region.

Results:

The notable aspects are:

- Diagonal dominance: Impostors are more likely to be matched against their same age group.
- Same sex and same region impostors are more successful. On the diagonal, an impostor is more likely to succeed by posing as someone of the same sex. If $\Delta \log_{10} \text{FMR} = 0.2$, then same-sex same-region FMR exceeds the all-pairs FMR by factor of $10^{0.2} = 1.6$.
- Young children impostors give elevated FMR against young children. Older adult impostor give elevated FMR against older adults. These effects are quite large, for example if $\Delta \log_{10} \text{FMR} = 1.0$ larger than a 32 year old, then these groups have higher FMR by a factor of $10^1 = 10$. This would imply an FMR above 0.01 for a nominal (global) FMR = 0.001.
- Algorithms vary.
- We computed the same quantities for a global FMR = 0.0001. The effects are similar.

Note the calculations in this section include impostors paired across all countries of birth.

FNMR(T) "False non-match rate"
FMR(T) "False match rate"

Accuracy Terms + Definitions

In biometrics, Type II errors occur when two samples of one person do not match – this is called a **false negative**. Correspondingly, Type I errors occur when samples from two persons do match – this is called a **false positive**. Matches are declared by a biometric system when the native comparison score from the recognition algorithm meets some **threshold**. Comparison scores can be either **similarity scores**, in which case higher values indicate that the samples are more likely to come from the same person, or **dissimilarity scores**, in which case higher values indicate different people. Similarity scores are traditionally computed by **fingerprint** and **face** recognition algorithms, while dissimilarities are used in **iris recognition**. In some cases, the dissimilarity score is a distance; this applies only when **metric** properties are obeyed. In any case, scores can be either **mate** scores, coming from a comparison of one person's samples, or **nonmate** scores, coming from comparison of different persons' samples. The words **genuine** or **authentic** are synonyms for mate, and the word **impostor** is used a synonym for nonmate. The words mate and nonmate are traditionally used in identification applications (such as law enforcement search, or background checks) while genuine and impostor are used in verification applications (such as access control).

A **error tradeoff** characteristic represents the tradeoff between Type II and Type I classification errors. For verification this plots false non-match rate (FNMR) vs. false match rate (FMR) parametrically with T.

The error tradeoff plots are often called **detection error tradeoff (DET)** characteristics or **receiver operating characteristic** (ROC). These serve the same function but differ, for example, in plotting the complement of an error rate (e.g. TMR = 1 – FNMR) and in transforming the axes most commonly using logarithms, to show multiple decades of FMR. More rarely, the function might be the inverse Gaussian function.

More detail and generality is provided in formal biometrics testing standards, see the various parts of ISO/IEC 19795 Biometrics Testing and Reporting. More terms, including and beyond those to do with accuracy, see ISO/IEC 2382-37 Information technology -- Vocabulary -- Part 37: Harmonized biometric vocabulary

FNMR(T) "False non-match rate"
FMR(T) "False match rate"

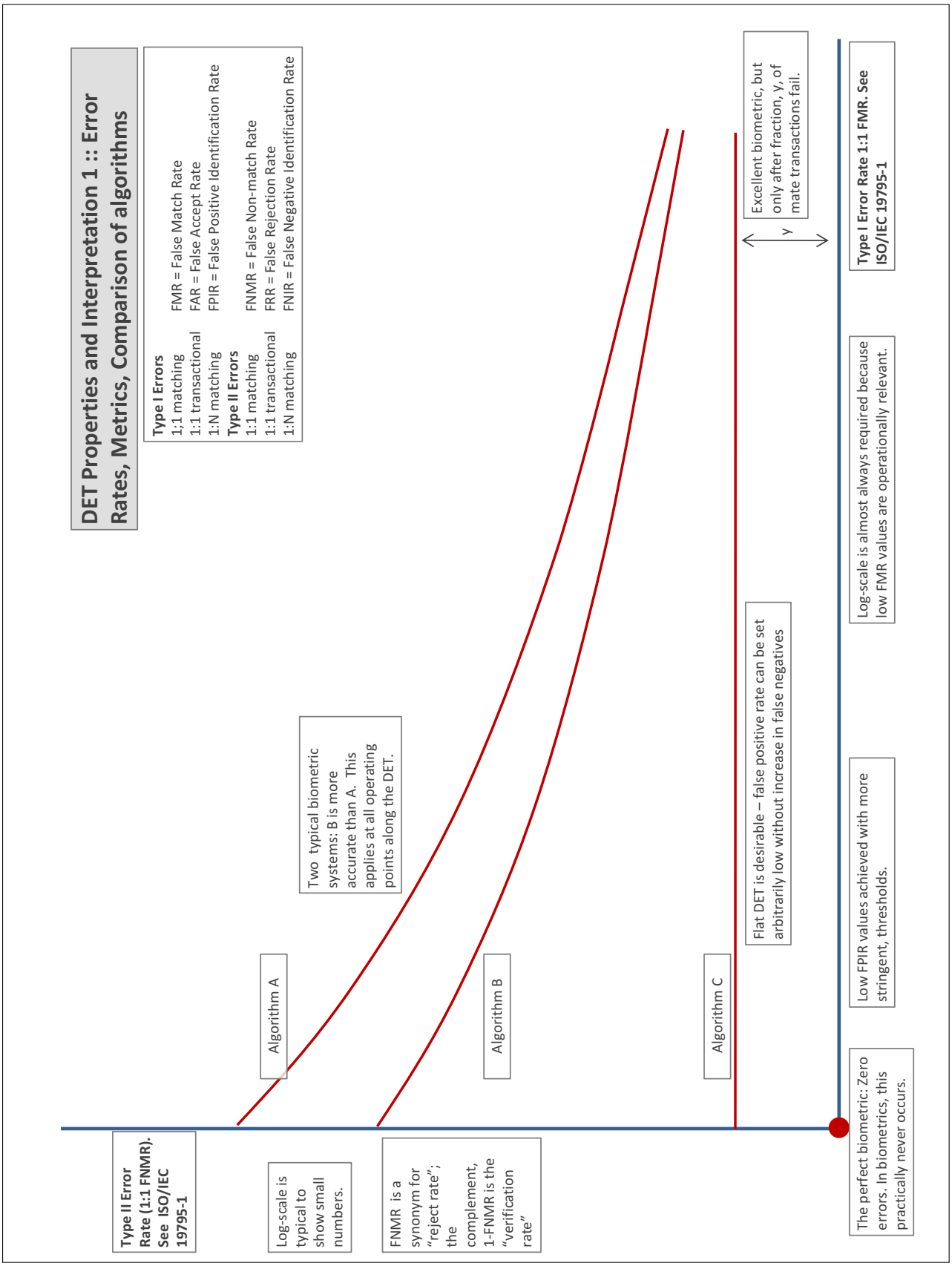

FNMR(T) "False non-match rate"
FMR(T) "False match rate"

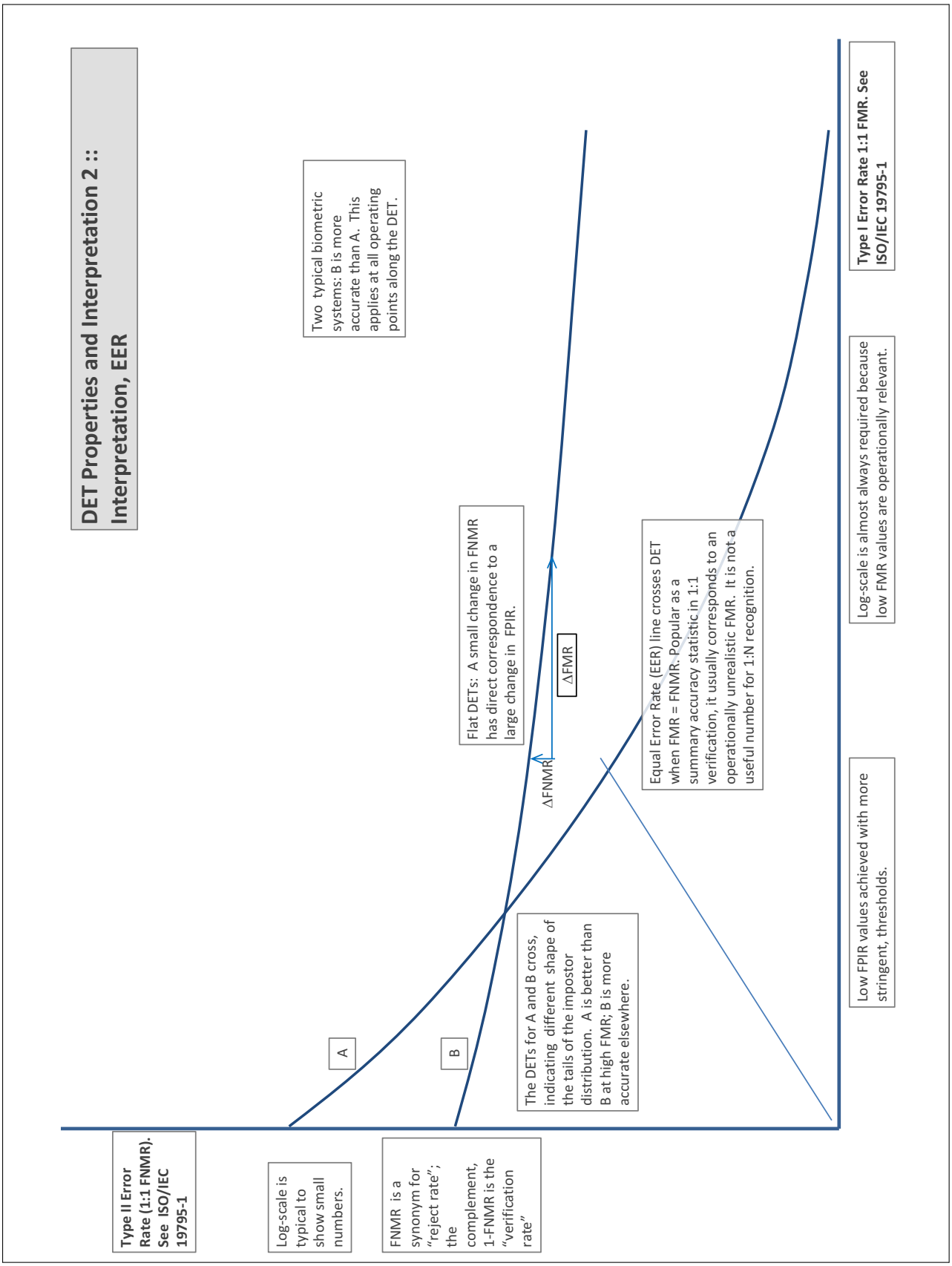

FNMR(T) "False non-match rate"
FMR(T) "False match rate"

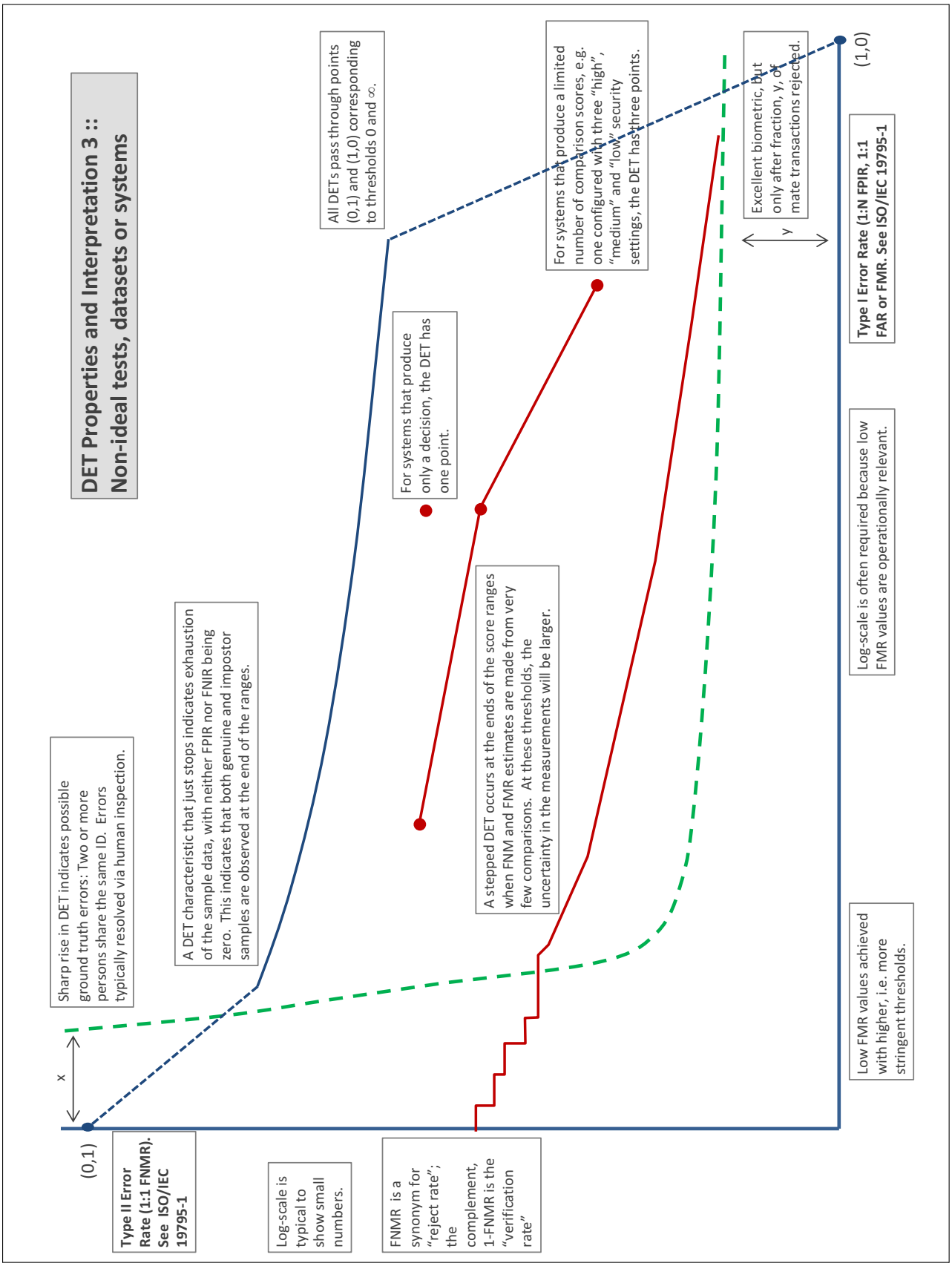

FNMR(T) "False non-match rate"
FMR(T) "False match rate"

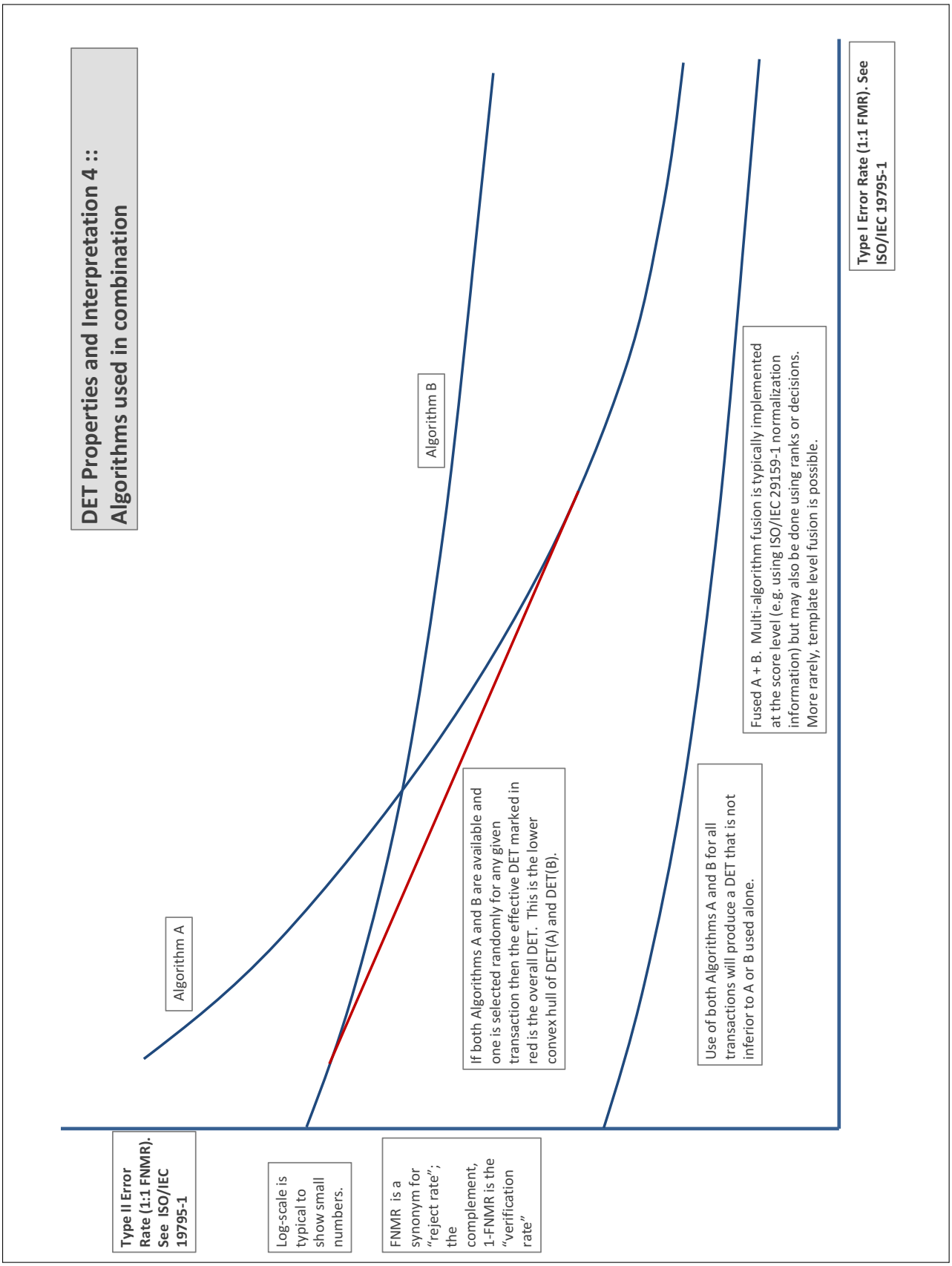

FNMR(T) "False non-match rate"
FMR(T) "False match rate"

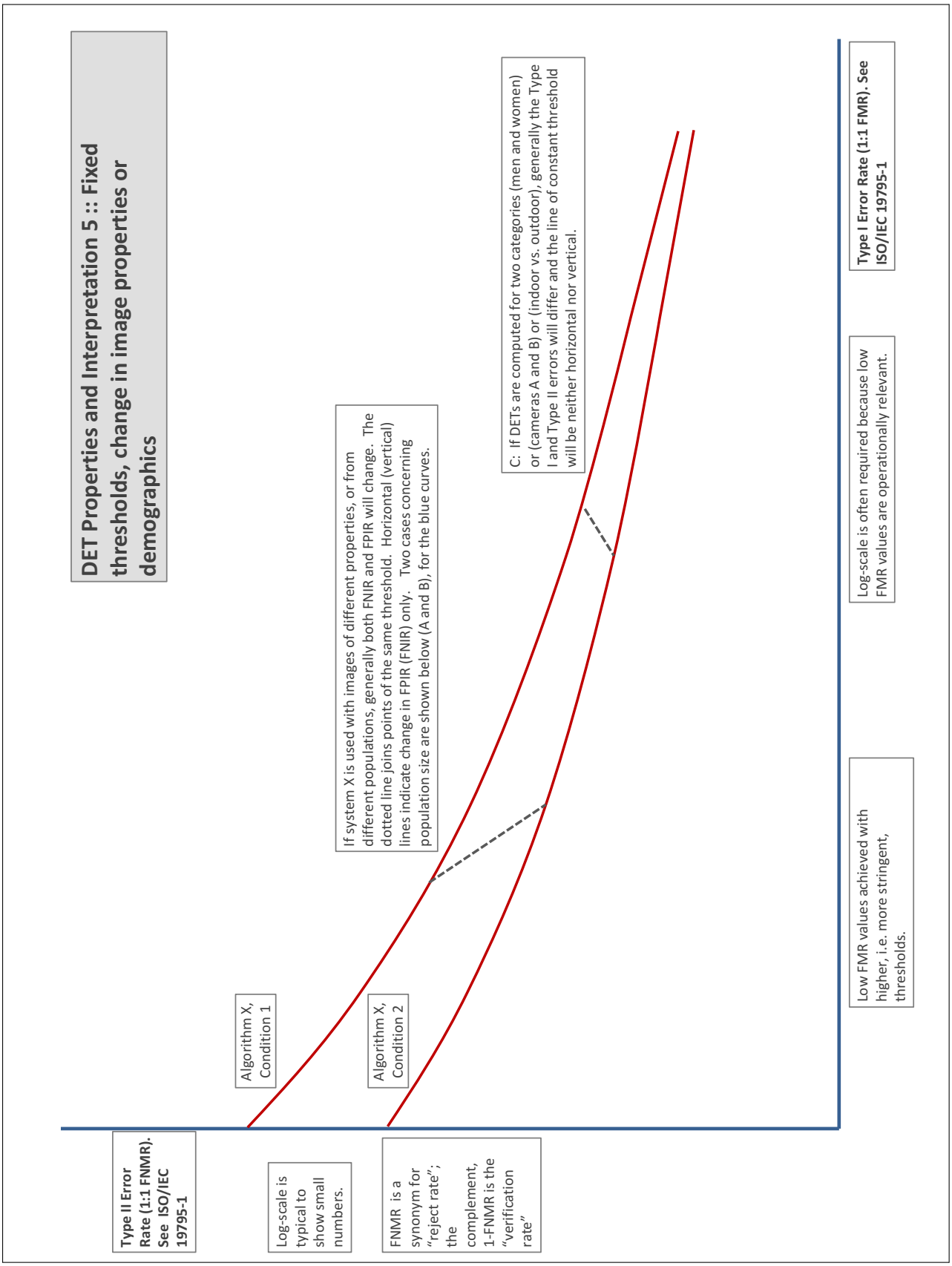

FNMR(T) "False non-match rate"
FMR(T) "False match rate"

References

[1] P. Jonathon Phillips, Amy N. Yates, Ying Hu, Carina A. Hahn, Eilidh Noyes, Kelsey Jackson, Jacqueline G. Cavazos, Géraldine Jeckeln, Rajeev Ranjan, Swami Sankaranarayanan, Jun-Cheng Chen, Carlos D. Castillo, Rama Chellappa, David White, and Alice J. O'Toole. Face recognition accuracy of forensic examiners, superrecognizers, and face recognition algorithms. *Proceedings of the National Academy of Sciences*, 115(24):6171–6176, 2018.

FNMR(T) "False non-match rate"
FMR(T) "False match rate"